

NIST PUBLICATIONS NIST Special Publication 305 Supplement 21

Publications of the National Institute of Standards and Technology 1989 Catalog

PUBLICATIONS

QC 100 .U57 #305 Suppl.21 1990

C.2



United States Department of Commerce National Institute of Standards and Technology

NATIONAL INSTITUTE OF STANDARDS & TECHNOLOGY Research Information Center Gaithersburg, MD 20899

NIST Special Publication 305 Supplement 21 111513

Publications of the National Institute of Standards and Technology 1989 Catalog

Rebecca J. Pardee and Ernestine T. Gladden, Editors

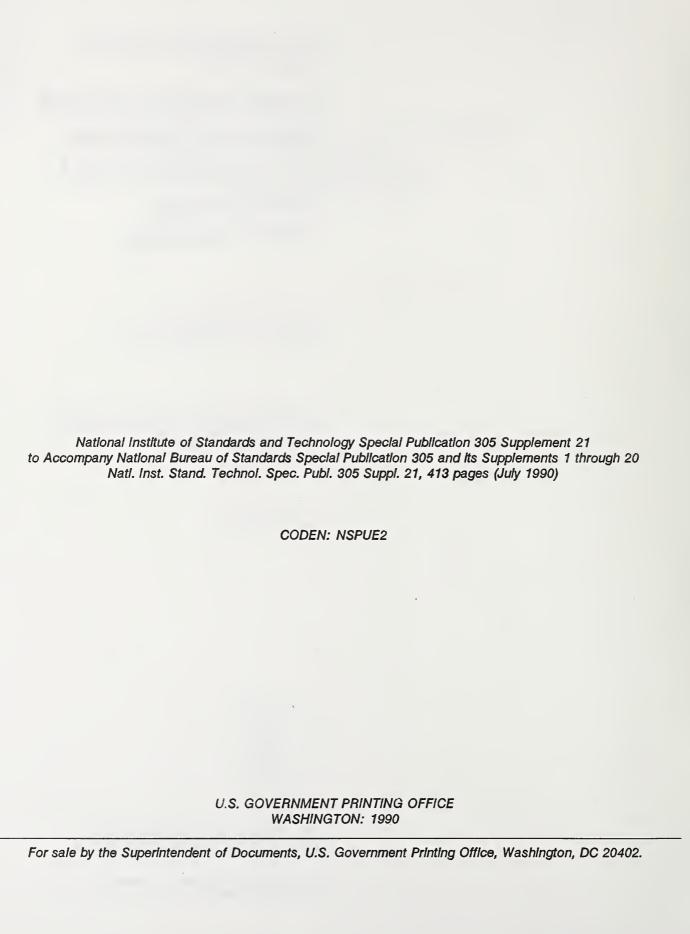
Information Resources and Services Division National Institute of Standards and Technology Gaithersburg, MD 20899

Issued July 1990



U.S. Department of Commerce Robert A. Mosbacher, Secretary

National Institute of Standards and Technology John W. Lyons, Director



CONTENTS

About the National Institute of Standards and Technology	inside front cover
Catalog structure and use	lv
Availability and ordering information	lv
NIST publications announcements	1
Indexes Personal author Keyword. Title. NTIS order/report number.	KW-1
Appendixes A List of depository libraries in the United States	A-1 B-1
Order forms	F-1
NIST technical publications program	inside back cover
NTIS subject categories	hack cover

CATALOG STRUCTURE AND USE

Full bibliographic citations including keywords and abstracts for National Institute of Standards and Technology (NIST) (formerly National Bureau of Standards (NBS)) papers published and entered into the National Technical Information Service (NTIS) collection are cited in the "NIST Publications Announcements" section of this catalog. (Also included are papers published prior to 1989 but not reported in previous supplements of this annual catalog.) Entries are arranged by NTIS subject classifications which consist of 38 broad subject categories (see back cover) and over 350 subcategories. Within a subcategory, entries are listed alphanumerically by NTIS order number.

Four indexes are included to allow the user to identify papers by personal author, keywords, title, and NTIS order/report number. Each entry lists the appropriate title, the NTIS order number, and the abstract number.

Papers may also be identified by searching the NTIS database either online via commercially available systems such as DIALOG, or in the issues of NTIS's Government Reports Announcements and Index and its Government Reports Annual Index.

AVAILABILITY AND ORDERING INFORMATION

The highest quality and least expensive copies of NIST publications published as Government documents are available from the Superintendent of Documents, U.S. Government Printing Office, Washington, DC 20402. Publications cited with stock numbers (SN) should be ordered by these numbers. GPO will accept payment by check, money order, VISA, MasterCard, or deposit account. For availability and price, write to the GPO or telephone (202) 783-3238. Should an NIST publication be out of print at the GPO, its continued availability is assured at NTIS which sells publications in microfiche or paper copy reproduced from microfiche.

If an entry has a price code, such as PC A04/MF A01, the publication may be ordered from NTIS In paper copy (PC) or microfiche (MF) or both if both codes are given. Order from the National Technical Information Service, 5285 Port Royal Road, Springfield, VA 22161. A copy of the latest price code schedule is available from NTIS. NTIS will accept payment by check, money order, VISA, American Express, MasterCard, or deposit account. NTIS is the sole source of Federal Information Processing Standards (FIPS), Interagency Reports (IRs), and Grant/Contract Reports (GCRs). For more information call (703) 487-4650.

Papers noted "Not Available NTIS" may be obtained directly from the author or from the external publisher

cited. Such papers are not for sale by either the GPO or NTIS.

Two other sources for NIST publications are depository libraries (libraries designated to receive Government publications) and Department of Commerce District Offices. The depository libraries listed in Appendix A receive selected NIST publications (see inside back cover for a description of the various NIST publication series). While not every Government publication is sent to all depository libraries, certain depositories designated as Regional Depositories receive and retain one copy of all Government publications made available. Contact the depository library in your area to obtain information on what is available and where.

Department of Commerce District Offices listed in Appendix B provide ready access at the local level to publications, statistical data and summaries, and surveys. Each District Office serves as an official sales agency of the Superintendent of Documents, U.S. Government Printing Office. A wide range of Government publications can be purchased from these offices. In addition, the reference library of each District Office contains review copies of many Government publications.

NIST PUBLICATIONS ANNOUNCEMENTS

SAMPLE ENTRY

COMPUTERS, CONTROL & INFORMATION THEORY

NTIS Subject Category

Computer Software 900,654 PB90-111683

PC A03/MF A01

National Inst. of Standards and Technology (NCSL), Gaithersburg, MD.

Computer Viruses and Related Threats: A Management Guide

J. P. Wack, and L. J. Carnahan. Aug 89, 46p NIST/SP-500/166 Contract F-000000

Keywords: *Computer security, *Instructions, Computer software management, Computer networks . . .

The document contains guidance for managing the threats of computer viruses and related software and unauthorized use.

NTIS Subcategory Abstract Number

NTIS order number Availability Price Codes

Corporate or performing organization

Report Title

Personal authors

Report date

Page count

Report Number

Contract or grant number

Keywords: * Indicates keyword Index entry

Abstract

ADMINISTRATION & MANAGEMENT

Public Administration & Government

900,001
PB89-161905
PC A04/MF A01
National Inst. of Standards and Technology (NEL),
Gaithersburg, MD. Center for Computing and Applied
Mathematics.

Internal Revenue Service Post-of-Duty Location Modeling System: Programmer's Manual for PASCAL Solver.

P. D. Domich, R. H. F. Jackson, M. A. McClain, and D. M. Tate. Feb 89, 66p NISTIR-86/3472-1
See also PB87-165171 and PB89-161913. Sponsored by Internal Revenue Service, Washington, DC.

Keywords: *Facilities management, *Programming manuals, Mathematical models, Computer programs,

Heuristic methods, Lagrangian functions, *Internal Revenue Service, *Site selection, User manuals(Computer programs), PASCAL subroutines.

The report is a programmer's manual for a microcomputer system designed at the National Institute of Standards and Technology for selecting optimal locations of IRS posts-of-duty. The mathematical model is the uncapacitated, fixed charge, facility location model which minimizes travel and facility costs. The package consists of two sections of code, one in FORTRAN and the other in PASCAL. The FORTRAN driver handles graphics displays and controls input and output for the solution procedure. The report discusses the mathematical techniques used to solve the mathematical techniques used to solve the mathematical model developed and includes a Greedy procedure, an Interchange procedure, and a Lagrangian approach to the related linear program. A description of these PASCAL routines and definitions of key data structures and variables are provided.

900,002

PB89-161913 PC A04/MF A01 National Inst. of Standards and Technology (NEL), Gaithersburg, MD. Center for Computing and Applied Mathematics. Internal Revenue Service Post-of-Duty Location Modeling System: Programmer's Manual for FORTRAN Driver Version 5.0.

P. D. Domich, R. H. F. Jackson, and M. A. McClain. Feb 89, 68p NISTIR-86/3473-1

See also PB89-161905. Sponsored by Internal Revenue Service, Washington, DC.

Keywords: *Facilities management, Regional planning, Cost engineering, Computer graphics, *Internal Revenue Service, *Site selection, Fortran subroutines, Input output processing.

The report is a programmer's manual for a microcomputer package which was designed by the National Institute of Standards and Technology to assist the Internal Revenue Service in choosing locations for its posts-of-duty which will minimize costs to the IRS and to the taxpayer. The package was written in two sections of code, one in FORTRAN and the other in PASCAL. The manual describes the FORTRAN driver which handles graphics displays and controls input and output for the solution procedure.

Research Program Administration & Technology Transfer

Research Program Administration & **Technology Transfer**

PC A06/MF A01 PB89-166094 PC A06/MF A01 National Inst. of Standards and Technology (IMSE), Gaithersburg, MD. Polymers Div. Institute for Materials Science and Engineering, Polymers: Technical Activities 1988.
Annual rept. 1 Oct 87-30 Sep 88.
L. E. Smith, and B. M. Fanconi. Nov 88, 120p
NISTIR-88/3842

See also PB87-136693.

Keywords: *Research program administration, *Polymers, Chemical properties, Mechanical properties, Standards, Composite materials, Processing, Durability, Blends, National Institute of Standards and Technology, Technical activities.

The Technical Activities of the Polymers Division for FY 88 are reviewed in the report. Included are descriptions of the 6 Tasks of the Division, project reports, publications, and other technical activities.

900,004 PB89-189294

PC A03/MF A01 National Inst. of Standards and Technology, Gaithers-

National Inst. of Standards and Technology, Gaithersburg, MD.
National Engineering Laboratory's 1989 Report to the National Research Council's Board on Assessment of NIST (National Institute of Standards and Technology) Programs.
Rept. for Apr 88-Apr 89.
G. Ehrlich. Mar 89, 45p NISTIR-89/4060

Keywords: *Research management, *Technology innovation, Manufacturing, Buildings, Chemical engineering, Computers, Measurements, Application of mathematics, Energy methods, Law(Jurisdiction), Standards, Inventions, *National Institute of Standards and Technology.

The 1989 report to the National Research Council's (NRC's) Board on Assessment of the National Institute of Standards and Technology (NIST) programs provides an overview of the National Engineering Laboratory (NEL). It describes the climate that influences NEL's work, program and budget trends, and the external interactions with industry, academia, and trade and professional organizations. Descriptions of NEL's program activities with accompanying lists of recent accomplishments, trends, and significant budget changes are also included. The programs described are Electronic and Electrical Measurements, Manufacare Electronic and Electrical Measurements, Manulacturing Research and Standards, Building Research, Fire Research, Chemical Engineering Metrology, Mathematical Sciences, Computing Support, Energy Related Inventions, and Law Enforcement Standards. The impact of the recently enacted Omnibus Trade and Competitiveness Act of 1988 is discussed.

900,005 PB89-189310 PC A03/MF A01 National Inst. of Standards and Technology, Gaithers-

NIST (National Institute of Standards and Technology, Reach Reports, March 1989.

Special pub. 1989, 36p NIST/SP-761 See also PB89-133565.

Keywords: *Research projects, *Technology innova-tion, Electrooptics, Telecommunication, Manufacturing, Commerce, Government policies, Quality control, Adhesive bonding, Temperature measurement, Lasers, Clocks, Neutrons, Diamonds, Dental materials, *National Institute of Standards and Technology, Photonics, Small businesses.

The report contains a number of articles which discuss the following subjects: Research update; Light: The wave of the future; New centers to aid industry; Commercialization of technology: Whose job; NIST 1990 budget proposed; Quest for quality; Too hot to handle, but not to measure; The beauty of time; Cold neutron facility dedicated; Diamond films: new gems in advanced materials; Fracture test on thick steel plate sets U.S. record; New dental bonding system licensed; New publications; and Conference calendar.

900,006 PB89-218382 PC A15/MF A01 National Inst. of Standards and Technology, Gaithers-burg, MD. Information Resources and Services Div. Publications of the National Institute of Standards and Technology, 1988 Catalog.

Rept. for Jan-Dec 88.

R. J. Pardee. Jun 89, 348p NIST/SP-305-SUPPL-20 Also available from Supt. of Docs. as SN003-003-02940-8. See also PB88-240007. Library of Congress catalog card no. 48-47112.

Keywords: *Catalogs(Publications), *Bibliographies, Science, Technology, Research management, *National Institute of Standards and Technology.

The 20th Supplement to Special Publication 305 contains full bibliographic citations including keywords and abstracts for National Institute of Standards and Technology (NIST) (formerly National Bureau of Standards (NBS)) 1988 papers published and entered into the National Technical Information Service (NTIS) collec-tion. Also included are NBS/NIST papers published tion. Also included are NBS/NIST papers published prior to 1988 but not reported in previous supplements of this annual catalog. Four indexes are included to allow the user to identify NBS/NIST papers by author, keywords, title, and NTIS order/report number.

900,007

PB89-235113 PC A03/MF A01 National Inst. of Standards and Technology, Gaithersburg, MD. NIST (National Institute of Standards and Technol-

ogy) Research Reports, June 1989.

Special pub.

Jun 89, 36p NIST/SP-765

Also available from Supt. of Docs. as SN003-003-02956-4. See also PB89-189310.

Keywords: *Research projects, *Reviews, Fatigue(Materials), Aircraft, Hot pressing, Isostatic pressing, Geology, Composite materials, Time measurement, Sterilization, Smoke abatement, *National Institute of Standards and Technology, Technology transfer, Computer security, Materials science, Computer aided manufacturing.

Contents: Computer security: protection is the name of the game; 'Standard crack' helps detect metal fatigue in aircraft, Building quality into advanced materials during processing; 'HIPing': from metal powders to reliable materials; Exploring earth's formation; NIST: helping industry to compete; Tracking time; Movies reveal secrets of materials; Technique sterilizes clinical instruments in seconds; and Can smoke control systems save lives and property.

General

900,008

PB89-221147 PC A19/MF A01 National Inst. of Standards and Technology, Gaithersburg, MD. Office of Standards Code and Information. Directory of International and Regional Organizations Conducting Standards-Related Activities. Final rept.

M. Breitenberg, May 89, 443p NIST/SP-767 Also available from Supt. of Docs. as SN003-003-02937-8. Supersedes PB84-203439. Library of Congress catalog card no. 89-600735.

Keywords: *Directories, *Standardization, *Organizations, Standards, Trade associations, Technical societies, *International organizations.

The directory contains information on 338 international and regional organizations which conduct standardization, certification, laboratory accreditation, or other standards-related activities. The volume describes their work in these areas, the scope of each organiza-tion, national affiliations of members, U.S. participants, restrictions on membership, as well as the availability of any standards in English. The volume is designed to serve the needs of federal agencies and standards writers for information on international and regional organizations involved in standardization and related activities. It may also be useful to manufacturers, engineers, purchasing agents, and others.

AERONAUTICS & AERODYNAMICS

Aeronautics

National Bureau of Standards (NEL), Gaithersburg, MD. Center for Fire Research. Ignition and Flame Spread Measurements of Air-

Craft Lining Materials.

M. Harkleroad. May 88, 64p NBSIR-88/3773
Sponsored by Federal Aviation Administration Technical Center, Atlantic City, NJ.

Keywords: *Ignition, *Linings, *Flammability, *Aircraft, Measurement, Test methods, Composite materials, Heat transfer, Panels, Epoxy resins, Fiberglass reinforced plastics, Aircraft interiors.

Experimental tests were conducted to study the lateral Experimental tests were conducted to study the lateral and upward flame spread behavior of eight aircraft lining materials. The results are tabulated in terms of parameters useful in predicting ignition and flame spread in the presence of an ignition source under exposure to an external radiant source. Experimental and derived results are graphically compared. Derived material properties related to and indicative of the propentic sity to support flame spread are presented.

Test Facilities & Equipment

900,010 PB89-175293

(Order as PB89-175194, PC A06) European Molecular Biology Lab., Heidelberg (Germa-

Computational Analysis of Protein Structures: Sources, Methods, Systems and Results. Bi-monthly rept. A. M. Lesk, and A. Tramontano. 1989, 9p

Prepared in cooperation with Medical Research Council, Cambridge (England). Lab. of Molecular Biology. Sponsored by Istituto Internazionale di Genetica e Biofisica, Naples (Italy). Included in Jnl. of Research of the National Institute of

Standards and Technology, v94 n1 p85-93 Jan-Feb

Keywords: *Proteins, *Molecular structure, Informa-tion retrieval, Information systems, Models, *Proteins conformation, Molecular biology, Data banks, Computer graphics.

Computational molecular biology is a relatively new specialty that has arisen in response to the very large amount and quality of data currently being produced, including gene and protein sequences and nucleic acid and protein structures. Many important biological in-vestigations can be carried out only through effective computational access to the entire corpus of data. This has stimulated the development of data banks and information retrieval systems. The article describes the kinds of inferences that are possible if such a relationship is found.

AGRICULTURE & FOOD

Food Technology

900,011 PB89-186399

Not available NTIS

National Bureau of Standards (NML), Gaithersburg, MD. Ionizing Radiation Physics Div.

Comprehensive Dosimetry for Food Irradiation. Final rept.

W. L. McLaughlin. 1988, 16p

Pub. in Health Impact, Identification, and Dosimetry of Irradiated Foods, p384-399 Jun 88.

Keywords: *Food processing, *Ionizing radiation, *Food irradiation, Quality control, Radiation protection, Dosimetry, *Gamma dosimetry, *G Gamma radiation, Reprints.

When ionizing radiation is used to process food of many kinds, comprehensive dosimetry is the most expeditious method of assuring that the process has been accomplished within specifications and without excess energy deposition. The term 'comprehensive dosimetry' then implies that, before, during, and after the radiation process, a number of modifying factors with some complexity must be considered and applied. This is particularly the case with the radiation food processing, where achieving success and maintaining wholesomeness and health and safety of the consumer are paramount. The main steps and considerations for practical and relevant food irradiation dosimetry and documentation are reviewed, which will satisfy regulatory authorities and encourage successful trade and safe marketing of food commodities. The process properly controlled with the aid of good dosimetry gives the opportunity to circumvent unsafe chemical additives and treatments to enable means of meeting legal requirement of quarantines and to improve public health through improved diets.

900,012

PB90-107046 PC A03/MF A01 National Inst. of Standards and Technology, Gaithers-

Glass Bottles for Carbonated Soft Drinks: Voluntary Product Standard PS73-89.

Product std.

B. M. Meigs. Jul 89, 18p

Also available from Supt. of Docs. as SN003-003-02958-1. Sponsored by Glass Packaging Inst., Inc., Washington, DC.

Keywords: *Food packaging, *Packaging materials, *Bottles, Design standards, Silica glass, Manufacturing, Carbonation, Defects, Impact strength, ing, Carbonation, Defects, Tolerances(Mechanics).

The Voluntary Product Standard covers conventional refillable and nonrefillable glass bottles that are manufactured from soda-lime-silica glass that have a nominal capacity of up to and including 36 fluid ounces, and that are intended for use in the packaging of soft drinks carbonated to a maximum of five volumes. Manufacturing requirements for bottles are provided for temper number, thermal shock resistance, internal pressure, strength, impact resistance, abrasion resistance, detection of visual defects, wall thickness, dimensional tolerances for height and maximum outside diameter, tolerances for capacity and mass (weight), perpendicularity, bottom characteristics, and bottle identification. A model statement is included for use on manufacturing orders and invoices specifying the maximum carbonation volumes intended for the bottles. Terms are defined or described that include trade terms and methods for identifying bottles that conform to the Standard.

ASTRONOMY & ASTROPHYSICS

Astronomy & Celestial Mechanics

900.013

PB89-171268 Not available NTIS National Bureau of Standards (NML), Boulder, CO. Quantum Physics Div.

Microarcsecond Optical Astrometry: An Instrument and its Astrophysical Applications. Final rept.

R. D. Reasenberg, R. W. Babcock, J. F. Chandler, M. V. Gorenstein, J. P. Huchra, M. R. Pearlman, I. I. Shapiro, R. S. Taylor, R. Bender, A. Buffington, B. Carney, J. A. Hughes, K. J. Johnston, B. F. Jones, and L. E. Matson. 1988, 15p

Grants NSF-PHY84-09671, NSF-AST85-19763 Sponsored by National Science Foundation, Washington, DC., and National Aeronautics and Space Administration, Washington, DC.
Pub. in Astronomical Jnl. 96, n5 p1731-1745 Nov 88.

Keywords: *Astrometry, *Optical interferometers, Gravitation, Reprints, Laser metrology, POINTS interferometer.

POINTS, an optical astrometric interferometer to be operated in space, would be a means of performing a wide variety of astrophysical studies, including a vastly improved deflection test of general relativity, a precise and direct calibration of the Cepheid distance scale, and the determination of stellar masses. The nominal 5 microarcsecond uncertainty in the measurement of the angular separation of two stars in the sky and the estimated measurement rate of 60 star pairs per day would support a rich mixture of scientific projects during the nominal mission life of ten years. Useful results would be available after less than a year. The key to the instrument's success is the control of systematic error, which is addressed by instrumentation and pos-tanalysis of the astrometric data.

Astrophysics

900,014 N89-16535/1 PC A19/MF A01

European Space Agency, Paris (France).

Proceedings of the Celebratory Symposium on a Decade of UV (Ultraviolet) Astronomy with the IUE Satellite, Volume 2.

E. J. Rolfe, cJun 88, 427p ESA-SP-281-V-2 Symposium Held in Greenbelt, MD, 12-15 Apr. 1988; Sponsored by NASA, Esa, the United Kingdom Science and Engineering Research Council, and the American Astronomical Society.

Keywords: *Conferences, *IUE, *Spaceborne astronomy, *Ultraviolet astronomy, *Ultraviolet spectra, Active galactic nuclei, Data bases, Planetary nebulae, Pre-main sequence stars, Quasars, Star formation, Stellar winds, *Foreign technology, *Meetings.

No abstract available.

900,015 PB89-149199 Not available NTIS National Bureau of Standards (NML), Boulder, CO. Quantum Physics Div.

Doppler Imaging of AR Lacertae at Three Epochs. F. M. Walter, J. E. Neff, J. L. Linsky, and M. Rodono.

1988, 3p Pub. in A Decade of UV Astronomy with the IUE Satel-

Keywords: Stellar atmospheres, Doppler effect, Ultraviolet spectra, Magnesium, Reprints, *AR Lacertae star, *Stellar chromospheres, Image analysis, Late

Doppler imaging analysis allows use of the information contained in a time sequence of spectral line profiles to deduce the size, location, and surface flux of rejoins of contrasting brightness on rotating stars. The authors have used IUE observations to study the structure of the lower chromosphere of AR Lacertae in the light of Mg II k. They have obtained sequences of LWR/P-HI images distributed around the binary period at three epochs. Discrete plage-like regions of en-hanced Mg II surface flux in this system were identified. Even with the limited S/N attainable with the IUE, one can map the gross structures of active stellar at-mospheres. With such information, one can begin to study the true 3-D structure of the atmospheres of latetype stars.

900,016 PB89-149207 Not available NTIS National Bureau of Standards (NML), Boulder, CO. Quantum Physics Div.

Late Stages of Close Binary Systems-Clues to Common Envelope Evolution.

Final rept.

R. F. Webbink. 1985, 44p Pub. in Proceedings of Beijing Colloquium on Models for Close Binary Systems, Beijing, China, November 7-13, 1985, p397-440.

Keywords: *Binary stars, Mass flow, Planetary nebulae, *Stellar envelopes, Cataclysmic variables, Symbiotic stars. Barium stars.

Those circumstances are outlined which theoretically lead to engulfment of one star by its companion, creating a common envelope binary. This evolutionary course is believed to lead to the formation of cataclysmic binaries, and other very compact systems containing degenerate components. The implications of these and other evolved binaries which, directly or indirectly, provide insight into the occurrence and nature of common envelope evolution, are examined.

900,017

PB89-157663 Not available NTIS National Bureau of Standards (NEL), Boulder, CO. Sci-

entific Computing Div.

Proper Motion vs. Redshift Relation for Superluminal Radio Sources.

Final rept.

B. W. Rust, S. G. Nash, and B. J. Geldzahler. 1989, 30p

Pub. in Astrophysics Space Science 152, p141-170 1989.

Keywords: *Radio sources(Astronomy), *Red shift, *Quasars, Reprints, *Proper motion, Superluminal motion, Astronomical models.

Two models for superluminal radio sources predict sharp lower bounds for the apparent velocities of separation. The light echo model predicts a minimum velocity v(min) = 2c, and the dipole field model predicts v(min) = 4.446c. Yahil (1979) has suggested that, if either of these models is correct, then v(min) provides a 'standard velocity' which can be used to determine the cosmological parameters H and q sub 0. This is accomplished by estimating a lower envelope for the proper motion vs redshift relation. Yahil also argued that the procedure could easily be generalized to include a nonzero cosmical constant Lambda. The authors derive the formulas relating the proper motion theta dot to the redshift z in a Friedmann universe with a nonzero Lambda. They show that the determination of a lower envelope for a given sample of measured points (z sub i, theta dot sub i) yields an estimate of the angle of inclination phi sub i for each source in the sample. The authors formulate the estimation of the lower envelope as a constrained maximum likelihood problem with the constraints specified by the expected value of the largest order statistic for the estimated phi sub i. The authors solve this problem numerically using an off-the-shelf nonlinearly constrained nonlinear optimization program from the NAg library.

900.018

PB89-171573 Not available NTIS National Bureau of Standards (NML), Boulder, CO. Quantum Physics Div.

Computer Program for Calculating Non-LTE (Local Thermodynamic Equilibrium) Model Stellar Atmos-

pheres. Final rept.

Hubeny. 1988, 30p Pub. in Computer Physics Communications 52, p103-132 1988.

Keywords: *Stellar atmospheres, *Thermodynamic equilibrium, Astrophysics, Spectral lines, Reprints, Radiative transfer.

The program calculates model stellar atmospheres, assuming plane-parallel, horizontally homogeneous atmosphere in radiative and hydrostatic equilibrium and allowing for departures from local thermodynamic equilibrium (LTE) for a set of occupation numbers of selected atomic and ionic energy levels. The program is very flexible as to the choice of chemical.

900,019

PB89-171615 Not available NTIS National Bureau of Standards (NML), Boulder, CO. Quantum Physics Div.

ASTRONOMY & ASTROPHYSICS

Astrophysics

Rotational Modulation and Flares on RS CVn and BY Dra Stars IX. IUE (International Ultraviolet Explorer) Spectroscopy and Photometry of II Peg and V711 Tau during February 1983.

Final rept.

Final rept.
A. D. Andrews, C. J. Butler, M. Rodono, S. Catalano, J. L. Linsky, A. Brown, F. Scaltriti, M. Busso, I. S. Nha, J. Y. Oh, M. C. D. Henry, J. L. Hopkins, H. J. Landis, and S. Engelbreklso. 1988, 16p Contract NASA-NAG5-82
See also PB88-189055. Sponsored by National Aeronautics and Space Administration, Washington, DC. Pub. in Astronomy and Astrophysics 204, p177-192 1988.

Keywords: *Binary stars, Stellar atmospheres, Ultraviolet spectra, Reprints, Stellar flares, Starspots, Faculae, IUE.

Evidence is presented for spots, plages and flares on the non-eclipsing RS CVn system II Peg and V711 Tau, based on sixty spectra obtained with the IUE satellite between 2-7 February 1983 and on supporting ground-based photometry. The large spot originally found on II Peg in 1981.8 could still be identified in 1983. Two spectroscopic flares of II Peg were detected. On V711 Tau at least two flares were observed. For both stellar restorms the fluxes from the higher temperature emissystems the fluxes from the higher temperature emission lines showed the greatest variations. The ratio of the Mg II k and h fluxes was the same for the active component in each stellar system and was closely similar to the solar chromospheric value.

900,020
PB89-202592
Not available NTIS
National Bureau of Standards (NML), Boulder, CO. Quantum Physics Div.

Photospheres of Hot Stars. 3. Luminosity Effects at Spectral Type 09.5. Final rept.

S. A. Voels, B. Bohannan, D. C. Abbott, and D. G.

Hummer. 1989, 18p Grants NSF-AST85-05919, NAGW-766 See also PB87-153680. Sponsored by National Science Foundation, Washington, DC., and National Aeronautics and Space Administration, Washington, DC. Pub. in Astrophysical Jnl. 340, p1073-1090, 15 May 89.

Keywords: *Stellar atmospheres, Line spectra, Hydrogen, Helium, Luminosity, Reprints, *Hot stars, Early stars, Stellar winds, O stars.

The authors have obtained hydrogen and helium line profiles with high signal-to-noise ratios for four stars of spectral type 09/5 (alpha Cam, xc' Ori A, delta Ori A, AE Aur) that form a sequence in luminosity: la, lb, ll, V. The basic stellar parameters of these stars are determined by fitting the observed line profiles of weak pho-tospheric absorption lines with profiles from models which include the effect of radiation scattered back onto the photosphere from their stellar winds, an effect referred to as wind blanketing. The stellar parameters denived for these four O9.5-type stars vary in a mono-tonic way with luminosity class. The authors argue that helium enrichment, and by implication CNO processed material as well, is probably a general characteristic of stars with Of and O Ia spectral classifications.

900,021 PB89-202618 Not available NTIS National Bureau of Standards (NML), Boulder, CO.

Quantum Physics Div.

Rotational Modulation and Flares on RS Canum Venaticorum and BY Draconis Stars X: The 1981 October 3 Flare on V711 Tauri (=HR 1099).

Final rept. J. L. Linsky, J. E. Neff, A. Brown, B. D. Gross, T. Simon, A. D. Andrews, M. Rodono, and P. A. Feldman. 1989, 14p See also PB89-171615.

Pub. in Astronomy and Astrophysics 211, p173-186

Keywords: Stellar spectra, Ultraviolet spectra, Microwave spectra, Binary stars, Reprints, *Stellar flares, Stellar chromospheres, Starspots, IUE.

A unique set of high resolution spectra of V711 Tauri = HR 1099 (G5V + K1IV) is presented, obtained with both the SWP and LWR cameras of IUE, together with simultaneous 6.4 GHz microwave emission and optical photometry, during a bright flare on 3 October 1981.

900,022 PB89-202626 Not available NTIS National Bureau of Standards (NML), Boulder, CO. Quantum Physics Div.

Stellar Winds of 203 Galactic O Stars: A Quantitative Ultraviolet Survey.

Final rept. I. D. Howarth, and R. K. Prinja. 1989, 66p Pub. in Astrophysical Jnl. Supplement Series 69, p527-

Keywords: Ultraviolet spectra, Reprints, *Stellar winds, *O stars, Early stars, IUE.

The paper presents a homogeneous set of column densities and maximum observed velocities derived from the C IV, N V, and Si IV resonance doublets of the 203 O stars observed at high resolution with IUE prior to 1987 January 1. In addition, fundamental parameters (T(eff), L(*), M(*)) are estimated for 201 of these The relationships between observed velocities and physically relevant velocities in the wind and be-tween column densities and mass-loss rates are dis-

900,023 PB89-212054 Not available NTIS National Bureau of Standards (NML), Boulder, CO. Quantum Physics Div.

Interpretation of Emission Wings of Balmer Lines in Luminous Blue Variables.

Final rept.

I. Hubeny, and C. Leitherer. 1989, 4p Grants NSF-AST85-20278, NSF-AST88-02937 Sponsored by National Science Foundation, Washing-

Pub. in Publications of the Astronomical Society of the Pacific 101, n635 p114-117 Jan 89.

Keywords: *Variable stars, Line spectra, Stellar atmospheres, Reprints, *Balmer lines, Blue stars, Stellar

The authors discuss H(alpha) line profiles calculated with plane-parallel, hydrostatic NLTE model atmospheres. In their lowest log g models the profiles show extended emission wings. Qualitatively, these wings are similar to the extended wings generated by electron scattering of line photons in the stellar wind. It is proposed that the line wings observed in luminous blue profibles may be didned to expense the NLTE. variables may be due to a combination on the NLTE effect discussed here and the traditional scattering mechanism.

900,024 PB89-228373 Not available NTIS National Bureau of Standards (NML), Boulder, CO. Quantum Physics Div. IUE Observation of the Interstellar Medium
Toward Beta Geminorum.

Final rept. J. Murthy, J. B. Woffard, R. C. Henry, H. W. Moos, A. Vidal-Madjar, J. L. Linsky, and C. Gry. 1989, 5p Pub. in Astrophysical Jnl. 336, p949-953, 15 Jan 89.

Keywords: *Interstellar matter, Ultraviolet spectra, Reprints, Galactic center, IUE.

The authors present a high-dispersion (Delta lambda = 0.1A) IUE spectrum of the hydrogen Ly(alpha) emission line of the nearby late-type star beta Gem from which they have derived the density, velocity dispersion and bulk velocity of the interstellar H1 in that dispersion. rection. While interstellar deuterium Ly(alpha) is clearly seen in absorption in the line profile, the authors do not obtain a useful limit on the ratio. The present result is important in confirming the generality of the 'emptiness' of the interstellar medium away from the Galactic center.

900,025 PB89-228506 Not available NTIS National Inst. of Standards and Technology (NML), Gaithersburg, MD. Molecular Spectroscopy Div.

Laboratory Measurement of the 1(sub 01)-0(sub 00) Transition and Electric Dipole Moment of SIC2. Final rept.

R. D. Suenram, F. J. Lovas, and K. Matsumura. 1989, 3p

Pub. in Astrophysical Jnl. 342, pL103-L105, 15 Jul 89.

Keywords: *Interstellar matter, *Silicon carbides, Microwave spectroscopy, Reprints, *Electric dipole

The 1(sub01)-0(sub00) transitions of (28)SiC2, (29)SiC2, and (30)SiC2 have been measured in the laboratory using a laser-ablation source coupled to a pulsed nozzle Fabry-Perot Fourier transform microwave spectrometer. The measured frequencies are

23600.242(4) MHz, 23257.511(8) MHz and 22937.583(8) MHz, respectively. The electric dipole moment for (28)SiC2 has been measured to be mu = mu sub alpha = 2.393(6) debye. Using this value for the dipole moment, the column density of SiC2 in IRC + 10216 has been recalculated to be 2.7x10 to the 14th power/sq cm(-2). which is approximately a factor of 2 larger than the previous estimate for which a theoretical value of the dipole moment was used.

900.026

PB89-234298 Not available NTIS National Inst. of Standards and Technology (NML), Boulder, CO. Quantum Physics Div. Rotational Modulation and Flares on RS Canum

Venaticorum and BY Draconis Stars. XI. Ultraviolet Spectral Images of AR Lacertae In September 1985. Final rept

J. E. Neff, F. M. Walter, M. Rodono, and J. L. Linsky.

See also PB89-202618.
Pub. in Astronomy and Astrophysics 215, p79-91

Keywords: *Binary stars, Ultraviolet spectra, Red shift, Reprints, *AR Lacertae stars, Stellar chromospheres, Stellar flares, Faculae.

Using a series of high-resolution ultraviolet spectra, the authors have derived a series of images of the chromosphere of AR Lacertae. In September 1985, chromosphere of AR Lacertae. In September 1985, neither star in this system was uniformly bright. The trailing hemisphere of the KOIV star was globally brighter than the leading hemisphere. The position, size, and surface flux of three distinct plage regions on the K star were measured with the spectral imaging procedure. The factor of 3 variability in total emission from the G2IV star was interpreted as due to a large chromospherically inactive region on its surface. The authors were able to constrain the position, size, and surface flux of a flaring region on the G star and to measure a significant redshift and broadening of the line emission from the flaring region. They used the rotational modulation of the integrated low-resolution line fluxes to determine the far-ultraviolet spectra of the global K and G stars and of the plage and flare regions alone. regions alone.

900.027

PB90-118118 Not available NTIS National Inst. of Standards and Technology (NML), Boulder, CO. Quantum Physics Div. Solar and Stellar Magnetic Fields and Structures: Observations.

Final rept.

J. L. Linsky. 1989, 10p Grant NGL-06-003-057, Contract NAG5-82 Sponsored by National Aeronautics and Space Administration, Washington, DC. Pub. in Solar Physics 121, p187-196 1989.

Keywords: *Solar magnetic fields, *Stellar magnetic fields, Zeeman effect, Circular polarization, Reviews, Reprints, Linear polarization.

The review of stellar magnetic field measurements is both a critique of recent spectral diagnostic techniques and a summary of important trends now appearing in the data. Both the Zeeman broading techniques that have evolved from Robinson's original approach, and techniques based on circular and linear polarization data are discussed. The review concludes with an ambitious agenda for developing self-consistent models of the magnetic atmosphere of active stars.

900,028

PB90-118142 Not available NTIS National Inst. of Standards and Technology (NML), Boulder, CO. Quantum Physics Div. Hellum Resonance Lines In the Flare of 15 June

1973.

Final rept. J. G. Porter, K. B. Gebbie, and L. J. November.

1989, 33p Contract AFOSR-ISSA-79-0002 Sponsored by Air Force Office of Scientific Research, Bolling AFB, DC.

Pub. in Solar Physics 120, p309-341 1989.

Keywords: *Solar flares, *Helium, Solar spectrum, Line spectra, Far ultraviolet radiation, Solar ultraviolet radiation, Reprints.

Time sequences of Hel and Hell resonance line intensities at several sites within the flare of 15 June 1973 are derived from observations obtained with the Naval Research Laboratory's Slitless Spectrohellograph on Skylab. The data are compared with predictions in six model flare atmospheres based on two values for the heating rate and three for the flux of photolonizing coronal X-rays and EUV. A peak ionizing flux more than 1000 times that in the quiet Sun is Indicated. Implications for the common practice of deriving stellar coro-nal fluxes from HeII 1640 A fluxes are indicated, assuming dominance of the recombination mechanism.

900,029

PB90-123787 Not available NTIS National Inst. of Standards and Technology (NML), Gaithersburg, MD. Molecular Spectroscopy Div. Millimeter- and Submillimeter-Wave Surveys of

Orion A Emission Lines in the Ranges 200.7-202.3, 203.7-205.3, and 330-360 GHz.

Final rept.

P. R. Jewell, J. M. Hollis, F. J. Lovas, and L. E. Snyder. 1989, 32p

Pub. in the Astrophysical Jnl. Supplement Series 70, n4 p833-864 Aug 89.

Keywords: Radio astronomy, Millimeter waves, Sub-millimeter waves, Emission spectra, Microwave spectra, Molecular spectra, Spectral lines, Surveys, Reprints, *Orion A, *Interstellar radiation.

The authors have conducted a continuous spectral line survey of the Orion A position from 330.5 to 360.1 GHz. This survey covers nearly the entire 870 micromcartz. This survey covers nearly the entire 670 micrometer atmospheric window accessible from ground-based observations. Approximately 160 distinct spectral features composed of about 180 lines were detected, 29 of which could not be readily identified. In addition, they also surveyed Orion A from 200.7 to 202.3 GHz and from 203.7 to 205.3 GHz and detected 42 distinct, new spectral lines, including four that are understants. identified at present. These data sets are the first thorough survey results in these spectral regions. The new interstellar lines in the survey bands are tabulated and displayed graphically. Moreover, the data are being made available to the Astronomical Data Center at the Goddard Space Flight Center for distribution by request to the astronomical community.

ATMOSPHERIC SCIENCES

Meteorological Instruments & **Instrument Platforms**

900.030

PB90-163882

(Order as PB90-163874, PC A04) National Inst. of Standards and Technology, Gaithersburg, MD.

Reduction of Uncertainties for Absolute Piston Gage Pressure Measurements in the Atmospheric Pressure Range.

Pressure nange.

B. W. Welch, R. E. Edsinger, V. E. Bean, and C. D. Ehrlich. 5 Sep 89, 4p
Included in Jnl. of Research of the National Institute of Standards and Technology, v94 n6 p343-346 1989.

Keywords: *Manometers, *Atmospheric pressure, *Nitrogen, Measurement, Calibrating, Metrology, Gas thermometry.

NIST pressure calibration services with nitrogen are now based on two transfer standard piston gages for which the effective areas have been determined by calibration with the manometer developed at NIST for gas thermometry. Root-sum-squared three sigma un-certainties for the areas for the two gages are 3.05 ppm and 4.18 ppm.

Physical Meteorology

900,031 PB90-118035 Not available NTIS National inst. of Standards and Technology (NEL), Gaithersburg, MD. Electrosystems Div. Interactions between Two Dividers Used in Simultaneous Comparison Measurements.

Final rept. Y. X. Zhang, R. H. McKnight, and R. E. Hebner.

Sponsored by Department of Energy, Washington, DC. Pub. in IEEE (Institute of Electrical and Electronics En-gineers) Transactions on Power Delivery 4, n3 p1586-1594 Jul 89.

Keywords: *Standards, *Lightning, *Measurement, Electric current, Regulations, Atmospheric electricity, Thunderstorms, Specifications, Reprints.

A revised international standard for the measurement of lightning and front-chopped lightning impulses is presently under consideration. The standard states that the accuracy of these measuring systems is to be determined by comparison to reference systems maintained by appropriate national laboratories. Investigations have been made of the interactions between two systems configured for simultaneous measurements and of methods for minimizing these interactions. Step responses were measured for different configurations and a model developed to predict divider response. Simultaneous measurements were made of full and chopped lightning impulses using different divider systems to determine the effects of divider interactions on measurements.

900,032 PB90-123951 Not available NTIS Not available NTIS
National Inst. of Standards and Technology (NML),
Gaithersburg, MD. Gas and Particulate Science Div.
High-Accuracy Gas Analysis via Isotope Dilution
Mass Spectrometry: Carbon Dioxide in Air.

Final rept. R. M. Verkouteren, and W. D. Dorko. 1989, 7p Pub. in Analytical Chemistry 61, n21 p2416-2422, 1

Keywords: *Gas analysis, *Carbon dioxide, *Mass spectroscopy, Error analysis, Temperature control, Performance evaluation, Concentration(Composition), Reprints, *Atmospheric chemistry, *Isotope dilution.

An absolute method, based on isotope dilution mass spectrometry, is described for the determination of at-mospheric concentrations of carbon dioxide (CO2) in dry air. In the study, the relative amounts of sample and spike gases are measured manometrically under temperature control before blending. In the study, the major contributors to uncertainty and imprecision are the predetermination of the gas volume ratio and the measurement of the isotopic composition of the blended CO2, respectively.

BIOMEDICAL **TECHNOLOGY & HUMAN FACTORS** ENGINEERING

Biomedical Instrumentation & Bioengineering

PATENT-4 832 745 Not available NTIS Department of Health and Human Services, Washington, DC.

Non-Aqueous Dental Cements Based on Dimer and Trimer Acids. Patent.

J. M. Antonucci. Filed 16 Oct 86, patented 23 May 89, 11p PB89-219281, PAT-APPL-6-922 811 See also PB85-203628. Prepared in cooperation with National Inst. of Standards and Technology, Gaithersburg, MD.

This Government-owned invention available for U.S. Il-censing and, possibly, for foreign licensing. Copy of patent available Commissioner of Patents, Washington, DC 20231 \$1.50.

Keywords: *Patents, *Dental materials, *AcId bonded reaction cements, Polymerization, Crosslinking(Chemistry), Cations, Carboxylic acids, PAT-CL-106-35.

Non-aqueous polycarboxylic acids such as dimer and trimer acids are reacted with a variety of polyvalent metal bases to yield a new, versatile class of cements. Many of these cements have unique energy-absorbing properties and excellent dimensional stability yielding mechanically tough and ductile materials. They also do not inhibit the polymerization of resin-based dental materials and thus can be formulated to yield hybrid resincomposite-cement materials. The bulky, hydrophobic nature of these acids with their relatively low carboxylic content results in cements that are low shrinking, hydrolytically resistant and biocompatible.

900,034 PB89-146716 Not available NTIS National Bureau of Standards (IMSE), Gaithersburg, MD. Polymers Div.

Effects of Purified Ferric Oxalate/Nitric Acid Solutions as a Pretreatment for the NTG-GMA and PMDM Bonding System.

Final rept.
R. L. Blosser, and R. L. Bowen. 1988, 7p
Sponsored by American Dental Association Health
Foundation, Chicago, IL. Pub. in Dental Materials 4, p225-231 1988.

Keywords: *Dental materials, *Acid bonded reaction cements, *Nitric acid, Dentin, Adhesives, Oxalates, Iron, Bonding strength, Electron microscopy, Reprints.

Nitric acid, found to be a contaminant left over from the synthesis of ferric oxalate, has been shown by this in vitro study to be responsible for the cleansing effect previously associated with ferric oxalate pretreatments. When 2.5% (w/w) nitric acid solution was substituted for ferric oxalate solution and then used in conjunction with the experimental dental bonding system junction with the experimental dental bonding system of NTG-GMA (the adduct of Ntp-tolyl)glycine and glycidyl methacrylate) and PMDM (the adduct of pyromellitic acid dianhydride and 2-hydroxyethyl methacrylate), the result was strong adhesion of both dentin and enamel surfaces to Adaptic (registered trademark) Dental Restorative. When a solution containing 3.4% (w/w) purified ferric oxalate was used with this system, the average bond strengths on both dentin and enamel decreased (p is less than 0.001) as compared with 3.4% (w/w) ferric oxalate solution containing 2.5% (w/w) nitric acid. The effects of pretreatment solutions containing 2.5% (w/w) nitric acid and varying concentrations of purified ferric oxalate on dentin and enamel were demonstrated by adhesion testing and scanning electron microscopy.

900 035 PB89-146732 Not available NTIS National Bureau of Standards (IMSE), Gaithersburg, MD. Polymers Div.

Bonding Agents and Adhesives: Reactor Response. Final rept.

R. L. Bowen. 1988, 3p Sponsored by American Dental Association Health Foundation, Chicago, IL.

Pub. in Advances in Dental Research 2, n1 p155-157

Keywords: *Dental materials, *Acid bonded reaction cements, Dentin, Adhesives, Composite materials, Dimensional stability, Polymers, Reprints.

Adhesive materials must form multiple bonds with sound tooth substrates for maximum adhesion. Adhesive resins can be applied in incremental layers to bond composite materials to enamel and dentin. Hardening shrinkage and stress concentrations are factors that have detrimental effects on adhesive bonding with resins and composites. Improvements in dimensional stability of composites can therefore allow for better bonding and sealing of preventive and restorative materials.

900.036 Not available NTIS PB89-146757 Mational Bureau of Standards (NML), Gaithersburg, MD. Organic Analytical Research Div.

BIOMEDICAL TECHNOLOGY & HUMAN FACTORS ENGINEERING

Biomedical Instrumentation & Bioengineering

Liposome-Enhanced Flow Injection Immunoanaly-Final rept

N. A. Durst, L. Locascio-Brown, A. L. Plant, and M. V. Brizgys. 1988, 2p See also PB88-217914.

Pub. in Clinical Chemistry 34, n9 p1700-1701 1988.

Keywords: Antibodies, Fluorescein, Bioassay, Feedback control, Antigens, Reprints, *Immunoassay, *Biomedical engineering, Liposomes, Immobilized cells.

The development of a repetitive immunoassay is important for monitoring and feedback control in bioprocessing. The assay should be fast and the immunoreactor, which uses immobilized antibodies, regenerable. The automated system employs flow injection analysis for solution manipulation and contains an immunoreactor column with covalently bound Fab' fragments. Recognition of the antigen is through competitive binding on this column of sample antigen and anti-gen contained in the membrane of liposomes. The concentration of sample antigen is proportional to the amount of liposomes competitively excluded from the column. Liposomes are spherical structures composed of a phospholipid bilayer, and are detectable through the marker species which is entrapped inside their aqueous compartment. Detection is through a fluorescent marker, carboxyfluorescein. Liposomes ex-cluded from the column in the competitive assay flow downstream where they are chemically disrupted, and the contents measured. The signal enhancement provided by the liposome marker is approximately 100,000 per analyte binding event making this technique competitive in sensitivity with radioimmunoassays.

900,037 PB89-157127 PB89-157127 Not available NTIS National Bureau of Standards (IMSE), Gaithersburg, MD. Polymers Div.

Interaction of Cupric Ions with Calcium Hydroxylapatite. Final rept.

D. N. Misra. 1988, 5p

Sponsored by American Dental Association Health Foundation, Chicago, IL.
Pub. in Materials Research Bulletin 23, n11 p1545-

Keywords: *Copper, *Calcium, *Dental materials, lons Phosphates, Hydroxides, X-ray analysis, Chemical composition, Bonding, Reprints.

The interaction of aqueous cupric ions with calcium hydroxylapatite produces cupric orthophosphate, Cu3(PO4)2 times 3H2O, and libethenite, Cu2(OH)PO4. The latter product was identified and characterized by chemical analysis and powder X-ray diffraction. The orthophosphate itself changes to libethenite under various experimental conditions. Contrary to a published report, it was not cupric hydroxylapatite that was previously identified. These findings are important to understand the chemistry of and composite bonding to bone and teeth.

900 038 PB89-157150 Not available NTIS National Bureau of Standards (IMSE), Gaithersburg, MD. Polymers Div.

Biological Evaluations of Zinc Hexyl Vanillate Cement Using Two In vivo Test Methods. Final rept.

J. C. Keller, B. D. Hammond, K. K. Kowalyk, and G. M. Brauer. 1988, 10p Contract PHS-DE-06675

Sponsored by National Institutes of Health, Bethesda,

Pub. in Dental Materials 4, p341-350 1988

Keywords: *Dental materials, *Adhesives, *Histology, *Pathology, Tissue extracts, Cells(Biology), Implantation, Peritoneum, Connective tissue, Inflammation, Zinc oxides, Phosphates, Vanillin, In vivo analysis, Reprints, Eugenol.

The cellular and tissue responses to 3 dental cements were studied by 2 methodologies, the connective tissue implantation technique (CTI), recommended by the ADA, and the peritoneal cavity implantation technique (PCI), which has emerged as a method to quantitatively study the cellular response to implanted materials. While similar histopathological results were obtained for the implantation of cements using both methodologies, the PCI technique offers a more thorough investigation of cellular and tissue responses to implanted materials. In addition to histopathological evaluation, the PCI technique allows quantitative investigation of the specific cells responding to the implants, and provides a mechanism, using chemical analysis techniques, to quantify the concentration of specific degradative products within the retrieved cells and host tissue. Finally, the results from these 2 meth-odologies demonstrated the acceptable biological performance of zinc hexyl vanillate cement compared with the clinically acceptable zinc phosphate and zinc oxide-eugenol cement formulations.

900,039 PB89-157168 Not available NTIS National Bureau of Standards (IMSE), Gaithersburg, MD. Polymers Div.

Adhesion to Dentin by Means of Gluma Resin. Final rept.

E. Asmussen, J. M. Antonucci, and R. L. Bowen. 1988, **6**p

Sponsored by American Dental Association Health Foundation, Chicago, IL. Pub. in Scandinavian Jnl. of Dental Research 96,

p584-589 1988

Keywords: *Dental materials, *Resins, *Bonding strength, *Dentin, *Adhesives, Composite materials, Pyruvates, Enamels, Amino acids, Camphor, Quinones, Methacrylic acid, Glycine, Glutarates, Reprints.

In its present version, the Gluma system for bonding restorative resin to dentin involves the application of an enamel bonding agent prior to the composite resin. Conceivably, pretreating the dentin with solutions of amino acids, and incorporating camphorquinone and selected methacrylic monomers into the Gluma adhesive would nullify the need for the enamel bonding agent. A bond strength to dentin of 13.4 MPa was obtained in the control experiment. Using a solution of pyruvic acid and glycine as pretreatment, and an optimized adhesive mixture containing glutaraldehyde, HEMA, BIS-GMA, camphorquinone, and water, bond strengths to dentin of 14.5 MPa and to enamel of 23.3 MPa were obtained. Thus, the new Bluma bonding system gave acceptable bond strengths without the prior application of enamel bonding agents.

900,040 PB89-176077 Not available NTIS National Bureau of Standards (IMSE), Gaithersburg, MD. Polymers Div. Mesh Monitor Casting of Ni-Cr Alloys: Element Ef-

fects. Final rept.

J. A. Tesk, O. Okuno, and R. Penn. 1986, 1p Pub. in Jnl. of Dental Research 65, p301 1986.

Keywords: *Dental materials, *Castings, *Chromium, Metal alloys, Computerized simulation, Temperature, Silicon, Beryllium, Solidus, Design, Mo-lybdenum, Niobium, Boron, Aluminum, Reprints.

A mesh monitor is used for quantitatively evaluating the casting of dental alloys. A castability value, C(sub v), is defined as the fraction of completely cast grid segments. For statistical analysis, a transformed casstability value, C(sub vt), is used and one equation for C(sub vt) was found to fit all of the Ni-Cr alloy data at the 95% confidence level: C(sub vt) = a + bT(sub A)(sup 1/2) T(sub M)(sup 2) where, C(sub vt) = In (2/3) Al(sup 1/2) (Sub M)(sup 2) where, C(sub V) = In (2/2) + the square root of C(sub V))/(2/3 + the square root of 1 - C(sub V)) - a and b are characteristic constants for each alloy. T(sub A) = T(sub c) - T(sub s), with T(sub c) the casting temperature, T(sub s) the solidus temperature, and T(sub M) the mold temperature. A series of alloys were selected to determine effects of critical elements on casting. Compositions were chosen to assure the avoidance of correlated effects. Assuming a linear dependence, the following equation was found to describe C(sub vt): C(sub vt) = K(sub o) Ni/Cr + K(sub 1)(Mo) + K(sub 2)(Si) + K(sub 3)(Nb) + K(sub 4)4(B) + K(sub 5)(Al) + K(sub 6)(Be) + K(sub 7)(Be x Si) where () are elemental concentrations in weight percent, and K(sub i) is a coefficient for the ith term. Because composition is constant for each alloy, $K(sub\ i) = f(sub\ i)$ ($T(sub\ A)$, $T(sub\ M)) = g(sub\ i)$ ($T(sub\ C)$, $T(sub\ M)$). The temperature dependent coefcients were determined for seven elements and the (Ni)/(Cr) ratio. It was also found that Si and Be produce a synergistic effect. The results can be used in computer aided design of Ni-Cr alloys.

900,041 PB89-179220 Not available NTIS National Bureau of Standards (IMSE), Gaithersburg, MD. Polymers Div.

Adsorption of 4-Methacryloxyethyi Trimellitate Anhydride (4-META) on Hydroxyapatite and Its Role in Composite Bonding. Final rent

D. N. Misra, 1989, 6p

Sponsored by American Dental Association Health Foundation, Chicago, IL.

Pub. in Jnl. of Dental Research 68, n1 p42-47 Jan 89.

Keywords: Adsorption, Dental materials, Reprints, *Hydroxyapatite, *Composite bonding, *Methacryloxyethyl trimellitate anhydride, Absorption isotherm.

The adsorption of 4-methacryloxyethyl trimellitate anhydride (4-META) was studied from ethanol and dichloromethane onto synthetic hydroxyapatite (containing about 1.5 monolayers of physisorbed water) in order to study its role in restorative composite bonding to teeth. The adsorption isotherm of 4-META was S-shpaed and reversible from ethanol and followed the Langmuir plot at lower concentrations. The isotherm was irreversible from dichloromethane and a constant amount of adsorbate was removed from the solutions above a certain concentration. The irreversibly adsorbed compound was completely removed by washing with ethanol. Therefore, the bonding between teeth and the re-storative resin containing 4-META as a coupling agent is micromechanical and not chemical in nature. An analysis of isotherms showed that the benzene rings of the adsorbate molecules lie flat on the surface for both solvents.

900,042 PB89-179253 Not available NTIS National Bureau of Standards (IMSE), Gaithersburg,

MD. Polymers Div.
Oligomers with Pendant Isocyanate Groups as Adhesives for Dentln and Other Tissues.

Final rept.

C. H. Lee, and G. M. Brauer. 1989, 5p Pub. in Jnl. of Dental Research 68, n3 p484-488 Mar

Keywords: *Dentin, *Adhesives, Dental materials, Bonding strength, Isocyanates, Reprints, *Oligomers, Isocyanic acid/dimethylbenzyl-isopropenyl, Methacrylate/isocyanatoethyl.

Oligomers containing pendant isocyanate groups were synthesized from various vinyl monomers, m-isopropenyldimethylbenzyl isocyanate (TMI), and 2-isocyanatoethyl methacrylate (IEM). The liquids were characterized by their refractive indices, infrared spectra, and percentage of isocyanate groups in the molecule. Adhesive properties of these compounds were compared with those of oligomers prepared from methacrylate esters, IEM, and/or TMI, which had been synthesized previously. These adhesive compositions, especially formulations synthesized from vinyl monomers, adhered at least as well to dentin as did other dentin bonding agents. Oligomers synthesized with methac-rylate esters bonded more strongly to bone than did other hard-tissue adhesives. These oligomeric compositions are also excellent soft-tissue adhesives. Provided that their biological properties prove satisfactory, these compositions could find many applications as hard-and soft-tissue adhesives in clinical dentistry.

PB89-228068 Not available NTIS National Bureau of Standards (NEL), Boulder, CO. Thermophysics Div.

Thermophysical Properties for Bioprocess Engineering.

Final rept. N. A. Olien. 1987, 4p Pub. in Chemical Engineering Progress, p45-48 Oct

Keywords: *Thermophysical properties, Solutions, Biological products, Reprints, *Biotechnology, Data

The commercialization of biotechnology requires the development of techniques for routine, scientifically-based scaleup of bioprocesses. Many of the engineering problems associated with scaleup are in downstream processing, which is comprised primarily of separation and purification. In traditional process in-dustries, accurate data and predictive models for the thermophysical properties of fluid mixtures play significant roles in the design and operation of separation processes. In a workshop it was concluded that several steps must be taken: develop experimental capability for obtaining thermophysical property data on bio-

BIOMEDICAL TECHNOLOGY & HUMAN FACTORS ENGINEERING

Biomedical Instrumentation & Bioengineering

logical solutions; begin theoretical studies which can lead to the development of predictive models; identify candidate biomolecules for experimental measurements and begin acquisition of a database for their solution properties.

900,044 PB89-229256 Not available NTIS Not available NTIS
National Inst. of Standards and Technology (IMSE),
Gaithersburg, MD. Polymers Div.
Simplified Shielding of a Metallic Restoration
during Radiation Therapy.

Final rept.

Final rept.
Fi. C. Eichmiller, and R. A. Schrack. 1989, 1p
Sponsored by American Dental Association Health
Foundation, Chicago, IL.
Pub. in Jnl. of Prosthetic Dentistry 61, n5 p640 May 89.

Keywords: *Radiation protection, *Protective equipment, Radiation shielding, Radiotherapy, Dental equipment, Reprints, Dental restorations.

Radiation-induced lesions directly adjacent to large metallic restorations have been associated with scatmetallic restorations have been associated with scat-ter of low energy electrons and positrons generated within the restorative material by high energy incident beams. These normally self-resolving lesions very often result in the interruption of the normal course and timing of the radiation treatment. Demonstrated is a simple absorptive intra-oral shield utilizing materials and techniques adaptable to any dental office or radiotherapy treatment facility. The use of the shielding technique can attenuate the low energy scatter to a level where damage to surface tissues can be avoided. The simple intraoral shielding technique utilizes readily available commercial impression materials and can be easily adapted to any radiotherapy treatment setting or dental office. The elimination of the painful and debilitating side effect or radiotherapy will allow for adherence to the most effective therapy course and improvement in the patient's quality of life.

900,045 PB89-229272 Not available NTIS National Inst. of Standards and Technology (IMSE), Gaithersburg, MD. Polymers Div. Ferric Oxalate with Nitric Acid as a Conditioner In an Adhesive Bonding System.

Final rept.

E. N. Cobb, R. L. Blosser, R. L. Bowen, and A. D. Johnston, 1989, 9p

Pub. in Jrl. of Adhesion 28, p41-49 1989. Keywords: *Dental materials, *Acid bonded reaction cements, *Nitric acid, *Oxalates, Dentin, Iron, Enamels, Composite materials, Tensile strength, Adhesive strength, Surface finishing, Resin cements, Reprints.

Strong adhesive bonding of composite resins to dentin and enamel is obtained by conditioning the surface and applying adhesion-promoting compounds. The study examines tensile adhesive bond strengths and effects of the conditioners having various concentrations of ferric oxalate (FO) and nitric acid. In the first part of the study, the average tensile bond strengths increased with concentrations of commercial FO as received up to about 6.8% and averaged no higher with higher concentrations. After the first part of the testing had been completed, it was discovered that the FO as received contained a small amount of nitric acid. Use of solutions having from 6.8% to 20% ferric oxalate as received yielded bonds with strengths that averaged about 13 MPa psi) to dentin and 16 MPa (2,400 psi) to enamel. In the second part of the study, the FO was stripped of the fortuitous nitric acid and, based on results from the first part of the study, solutions were made up to contain a fixed concentration of purified FO (6.8% Fe2(C2O4)3) and various known concentrations of nitric acid. The highest bond strengths to dentin and enamel were obtained with the purified FO solution which contained approximately 2.5% nitric

900,046 PB89-229298 PB89-229298 Not available NTIS National Inst. of Standards and Technology (IMSE), Gaithersburg, MD, Polymers Div. Transient and Residual Stresses In Dental Porce-

lains as Affected by Cooling Rates. Final rept.

K. Asaoka, and J. A. Tesk. 1989, 17p Pub. in Dental Materials Jnl. 8, n1 p9-25 Jun 89.

Keywords: *Dental materials, Cooling rate, Residual stress, Computerized simulation, Reprints, *Dental porcelain.

The development of either transient or residual stress in a slab of dental porcelain during cooling was simulated by use of a super-computer. The temperature dependences of the elastic modulus, the thermal expansion coefficient, the shear viscosity, and the cooling rate dependence of the glass transition temperature were considered in the calculation. Internal stress and viscoelastic creep were computed for several cooling rates. Calculated results display stress profiles which agree reasonably well with reported measured profiles in quenched, tempered glasses. The method by which residual stress develops is also discussed. The discussion suggests a method for strengthening of the porcelain by the development of high-compressive residual stress on the surface.

900,047 PB89-231278 Not available NTIS

National Inst. of Standards and Technology (IMSE), Gaithersburg, MD. Polymers Div. Development of a Microwave Sustained Gas Plasma for the Steriiization of Dental Instruments. Final rept.

W. G. de Rijk, and L. L. Forsythe. 1988, 3p Pub. in Proceedings of Southern Biomedical Engineering Conference (7th), Greenville, SC., October 27-28, 1988, p189-191.

Keywords: *Microwaves, *Plasmas(Physics), *Sterili-

The development of a low temperature gas plasma sterilizing process was sought using electromagnetic radiation from a conventional microwave oven providing energy for both igniting and sustaining the plasma. It was found that a gas plasma readily ignites, but causes rapid heating of the vacuum chamber contents and its walls. Bacterial spore strips showed that sterilization can be achieved with the gas plasma.

900.048 PB90-117375 Not available NTIS National Inst. of Standards and Technology (IMSE), Gaithersburg, MD. Polymers Div.
Use of N-Phenyigiycine in a Dental Adhesive System. Final rept.

R. S. Chen, and R. L. Bowen. 1989, 6p Sponsored by American Dental Association Health Foundation, Chicago, IL. Pub. in Jnl. Adhesion Sci. Technol. 3, n1 p49-54 1989.

Keywords: *Dental materials, *Adhesive bonding, Bonding strength, Performance evaluation, Substitutes, Reprints, *Glycine/N-phenyl.

A dentin and enamel bonding procedure that used an acidic solution (aqueous ferric oxalate), a surface-active co-monomer (NTG-GMA, the reaction product of N(p-tolyl)glycine and glycidyl methacrylate), and a dimethacrylate (PMDM, the reaction product of hydroxyethyl methacrylate and pyromellitic dianhydride) was described earlier. The present paper reveals the discovery that a much more simple and available compound, N-phenylglycine, can be substituted for NTG-GMA without a sacrifice in bond strength.

900,049 PB90-117516 Not available NTIS National Inst. of Standards and Technology (IMSE), Gaithersburg, MD. Polymers Div.

In vitro Investigation of the Effects of Glass Inserts on the Effective Composite Resin Polymerization Shrinkage. Final rept.

K. J. Donly, T. W. Wild, R. L. Bowen, and M. E.

Sensen. 1989, 4p
Sponsored by American Dental Association Health
Foundation, Chicago, IL.
Pub. in Jnl. of Dental Research 68, n8 p1234-1237 Aug

Keywords: *Dental materials, *Glass, *Composite materials, *Resins, *Polymerization, *Shrinkage, In vitro analysis, Strain gages, Reprints.

An MOD preparation was placed in each of 12 permanent molars, then each tooth was restored with a posterior composite resin by means of six different application techniques: I-polymerization as one complete unit; II-polymerization as one complete unit with glass inserts; III-polymerization in gingivo-occlusal incre-ments; IV-polymerization in gingivo-occlusal incre-ments with glass inserts; V-polymerization in bucco-lin-gual increments; and VI-polymerization in a gingival in-crement with glass inserts, then bucco-lingual increments. After each increment was polymerized, the strain appearing on the strain gauge indicator was recorded. Results demonstrated the average microstrain units to be 127-1, 102-II, 105-III, 86-IV, 72-V, and 66-VI. A randomized block design was the format used for data evaluation. Scheffe's Test indicated that composite resin placement and polymerization in bucco-lingual increments (V) created significantly less cuspal deflection than polymerization as one complete unit, with or without glass inserts (I and II), p < 0.001, and gingivo-occlusal increments (III), p < 0.05).

900.050

Not available NTIS PB90-123696 National Inst. of Standards and Technology (IMSE), Gaithersburg, MD. Polymers Div. Adhesive Bonding of Composites.

Final rept.

R. L. Bowen, F. C. Eichmiller, W. A. Marjenhoff, and N. W. Rupp. 1989, 4p Sponsored by American Dental Association Health Foundation, Chicago, IL.

Pub. in Jnl. of the American College of Dentists 56, n2 p10-13 1989.

Keywords: *Adhesive bonding, *Dental materials, *Composite materials, Adhesive strength, Enamels, Dentin, Teeth, Dentistry, Reprints.

Although the strength and durability of adhesive bonds to enamel have been adequate for numerous clinical procedures for many years, commercial products that demonstrate a range of effectiveness of adhesion to dentin are relatively new. The paper discusses several of the more popular commercial dentin and enamel bonding systems, noting differences in the chemical components and instructions for use. Since simple technique errors can lead to failure, it is important that practitioners understand not just the sequence of pro-tocol steps, but the function of each system component. Dentists are encouraged to try dentin and enamel adhesives supported by research literature in referred journals to determine which works best for them, and to provide feedback to dental manufacturers and researchers so that the materials and clinical techniques can be further improved.

900,051

PB90-123795 Not available NTIS National Inst. of Standards and Technology (IMSE), Gaithersburg, MD. Polymers Div.

Substitutes for N-Phenylglycine in Adhesive Bonding to Dentin.

Final rept.

A. D. Johnston, E. Asmussen, and R. L. Bowen. 1989, 8p

Sponsored by American Dental Association Health Foundation, Chicago, IL.

Pub. in Jnl. of Dental Research 68, n9 p1337-1344 Sep

Keywords: *Adhesive bonding, *Dentin, *Surfactants, Surface reactions, Glycine, Reprints.

A number of related compounds were investigated using bond strength measurements in order to elucidate the role of the surface-active ingredient N-phenylglycine (NPG) in experimental two-step and threestep bonding protocols resulting in adhesive bonding to dentin. All active compounds identified for the twostep or the three-step protocol were N-aryl-alpha-amino acids, and the results delineate some of the key features of the NPG molecule for bonding. For the three-step protocol, there was a requirement for a secondary or tertiary aromatic amino group, a carboxylic acid group, and a single (secondary or tertiary) methylene unit between those two functional groups of the amino acid. For the two-step protocol, additional substitutions at the para position of the phenyl ring on the amine improved the bond strength. In both protocols, para-methyl- and para-chloro-substituted NPG analogues ranked higher than NPG. A 'catalytic' effect of the aromatic tertiary amino group on the polymeriza-tion of the adhering resin in both procedures could not be ruled out.

900,052

PB90-128711 Not available NTIS National Inst. of Standards and Technology (IMSE), Gaithersburg, MD. Polymers Div.

BIOMEDICAL TECHNOLOGY & HUMAN FACTORS ENGINEERING

Biomedical Instrumentation & Bioengineering

Dental Materials and Technology Research at the National Bureau of Standards: A Model for Government-Private Sector Cooperation. Final rept.

J. A. Tesk. 1989, 8p Pub. in Materials Research Society Symposia Proceedings, v110 p177-184 1989.

Keywords: *Dental materials, *Technical societies, *Research, Composite materials, Acid bonded reaction cements, X ray apparatus, Resins, Prosthetic devices, Weibull density functions.

In 1919 the United States Army commissioned the National Bureau of Standards (NBS) to develop a federal specification for dental amalgam. In 1928, the American Dental Association (ADA) joined forces with the NBS for dental research and in 1964 the National Institute of Dental Research (NIDR) initiated support. Today, the program involves personnel from the NBS, ADA, NIDR, two dental companies and numerous re-searchers from around the world. Major advances in dentistry have emanated from the collaborative effort; among them are the panoramic x-ray unit, the high speed, turbine, contra-angle handpiece, numerous cements, and the basic formulation of modern composite restoratives. The latter alone has been estimated at saving the American public an annual amount that exceeds the current, combined, appropriated budgets of the NIDR, NBS and the ADA. Current efforts are focussing on tissue adhesives, biocompatible cements, atherosclerotic plaque, new resins for composites, characterization of materials via Weibull Statistics and reliability analysis of dental prosthetic systems.

Prosthetics & Mechanical Organs

900,053 PB89-150890 Not available NTIS National Bureau of Standards (IMSE), Gaithersburg,

MD. Metallurgy Div.
Corrosion of Metallic Implants and Prosthetic Devices.

Final rept. A. C. Fraker. 1987, 12p

Pub. in Metals Handbook (9th Edition), v13 p1324-1335 1987.

Keywords: *Corrosion resistance, *Metals, *Implanta-*Prosthetic devices, Stainless steels, Titanium, Cobalt, Surgery, Alloys, Reprints.

The paper deals with the corrosion of metallic surgical implants. The history of the development of the use of metals as implants and the associated research are given. The metals and alloys are described in detail with the intent of emphasizing effects of composition, microstructure and other metallurgical factors on the corrosion resistance. Basic principles of corrosion processes, corrosion problems occurring with surgical implants and corrosion test procedures are discussed.

900,054 PB89-157143 Not available NTIS National Bureau of Standards (IMSE), Gaithersburg, MD. Polymers Div.

Casting Metals: Reactor Response.

Final rept.

J. A. Tesk. 1988, 3p Pub. in Advances in Dental Research 2, n1 p44-46 Aug

Keywords: *Dental materials, *Prosthetic devices, *Castings, *Metals, Palladium alloys, Titanium, Waxes, Sintering, Reprints. A commentary on the paper given by Dr. Asgar is presented. Agreement with that paper's contents on the trend toward palladium-based and other lower-cost

alloys is rendered. However, with a view toward future competitiveness and quality of prosthetic restorations, the commentary looks for the application of new and emerging technologies. To implement these developments, the National Institute of Dental Research is urged to find avenues to support applications for dentistry in selected instances, despite adverse reviews from an entrenched establishment.

900.055 PB89-202212 Not available NTIS National Bureau of Standards (IMSE), Gaithersburg, MD. Polymers Div.

Oligomers with Pendant Isocyanate Groups as Tissue Adhesives. 1. Synthesis and Characterization.

G. M. Brauer, and C. H. Lee. 1989, 15p See also PB89-179253. Pub. in Jnl. of Biomedical Materials Research 23, p295-309 1989.

Keywords: Synthesis(Chemistry), Methacrylates, Reprints, *Tissue adhesives, *Biocompatible materials, Oligomers.

A series of methacrylate oligomers containing pendant isocyanate groups were synthesized by reacting 2-isocyanatoethyl methacrylate (IEM) and/or m-isopropenyl-alpha, alpha-dimethylbenzyl isocyanate (TMI) in ethoxyethyl acetate with metacrylates ranging from methyl to stearyl methacrylate or allyl-, cyclohexyl-, glycidyl-, i-bornyl-, or dicyclopentenyloxyethyl methacrylate. The oligomers which are stable at room temperrylate. The originals which are stable at room temperature were characterized by IR for NCO, ester, and C=C groups and by their refractive indices. HPLC showed no residual monomer. GPC and intrinsic viscosity of selected oligomers indicated a molecular weight range from 1400 to 2600. Isocyanate groups were determined titrimetrically and ranged from 15.9% to 5.1%. Concurrent studies have demonstrated that these oligomers bond strongly to hard and soft tissues. Thus, subject to their biocompatibility, they could find many applications as tissue adhesives.

900,056 PB89-231245 Not available NTIS National Inst. of Standards and Technology (IMSE),

Gaithersburg, MD. Polymers Div.
Oligomers with Pendant Isocyanate Groups as
Tissue Adhesives. 2. Adhesion to Bone and Other

Final rept.

G. M. Brauer, and C. H. Lee. 1989, 11p See also Part 1, PB89-202212. Pub. in Jnl. of Biomedical Materials Research 23,

p753-763 1989.

Keywords: *Methacrylates, *Isocyanates, *Bones, Tissues(Biology), Materials tests, Tensile strength, Reprints, *Tissue adhesives, Biocompatible materials, prints, *Tissue Dental cements.

The adhesive properties of a series of oligomers pre-pared from 2-isocyanatoethyl methacrylates (IEM) and/or m-isopropenyl-alpha, alpha-dimethylbenzyl isocyanate (TMI) and various acrylates or methacrylates were studied. The bond strength of bone, dentin, or soft tissue specimens joined with these oligomers respectively to bone, dental composite restorative, or denture base resin were determined by tensile adhesion or shear tests. These oligomers are more effective in forming stronger bonds to bone than are other tissue adhesives. Fracture occurs cohesively, usually within the bone. Thermocycling in water for 1 week between 5 C and 55 C did not decrease adhesion indicating that exposure to water or thermal shock produced no deterioration of the bond. Tensile adhesion of bovine or human dentin joined to composite restorative resin by means of the oligomers is similar to that of the best dental bonding agents such as Gluma (glutaraldehyde and 2-hydroxy-ethyl methacrylate) or ferric oxalate + N-phenylglycine + dimethylacryloxyethyl-pyromellitate. These oligomers also strongly bond soft tissues and calfskin and to acrylic resins and compos-

BUILDING INDUSTRY TECHNOLOGY

Architectural Design & Environmental Engineering

900,057

PB89-150783 Not available NTIS National Bureau of Standards (NEL), Gaithersburg, MD. Building Physics Div.

Experimental Validation of a Mathematical Model for Predicting Moisture Transfer in Attics.

Final rept. D. M. Burch. 1985, 10p

Sponsored by Department of Energy, Washington, DC. Pub. in Proceedings of International Symposium on Moisture and Humidity, Washington, DC., April 15-18, 1985, p287-296.

Keywords: *Mathematical models, *Moisture content, *Residential buildings, *Wood, *Roofs, Proving, Predictions, Heating, Test chambers, Climate, Ventilation, Water vapor, Adsorption, Condensing, Static tests, Dynamic tests, Dew point, Environment simulation, Attics.

A small test house having a pitched roof/ventilated attic was installed in a high-bay environmental chamber. The test house and its attic were extensively instrumented for measuring heat and moisture transfer. The test house was subsequently exposed to a series of steady diurnal outdoor climatic conditions. Representative conditions of a residence were simulated within the test house. A mathematical model was developed that included the adsorption of water vapor at wood surfaces in the attic. This model closely predicted the attic dewpoint temperatures for both the steady and dynamic outdoor cycle tests. The model showed that wood surfaces of the attic at a moisture content of 12.5% (by weight) adsorbed water vapor and maintained the wood surface dewpoint temperature below the roof sheathing temperature, thereby preventing condensation.

900,058

PB89-151765 PC A03/MF A01 National Inst. of Standards and Technology (NEL), Gaithersburg, MD. Center for Computing and Applied Mathematics

Mathematics.
ZIP: The ZIP-Code Insulation Program (Version 1.0)
Economic Insulation Levels for New and Existing
Houses by Three-Digit ZIP Code. Users Guide and
Reference Manual.

S. R. Petersen. Jan 89, 42p NISTIR-88/3801 Contract DE-AC05-84OR21400

Also pub. as Oak Ridge National Lab., TN. rept. no. ORNL/TM-11009. Prepared in cooperation with Oak Ridge National Lab., TN. Sponsored by Department of Energy, Washington, DC. Office of Buildings and Community Systems.

Keywords: *Computer systems programs, *Operating systems(Computers), *Residential buildings, *Thermal insulation, Cost engineering, Zip codes, Microcomput-

ZIP (the ZIP Code Insulation Program) is a computer program developed to support the DoE 'Insulation Fact Sheet' by providing users with customized estimates of economic levels of residential insulation for any location in the United States, keyed to the first three digits of its ZIP Code. The program and supporting files are contained on a single 5-1/4 in, diskette for use with microcomputers having an MS-DOS operating system capability. The ZIP program currently calculates economic levels of insulation for attic floors, exterior wood-frame and masonry walls, floors over un-heated areas, slab floors, and basement and crawl-space walls. The economic analysis can be conducted for either new or existing houses. Climate parameters are contained in a file on the ZIP diskette and automatically retrieved when the program is run. Regional renergy and insulation price data are also retrieved from the ZIP diskette, but these can be overridden to more closely correspond to local prices. ZIP can be run for a single ZIP Code and specified heating and cooling system. It can also be run in a 'batch' mode for any number of consecutive ZIP Codes in order to provide a table of economic insulation levels for use at the state or national level.

900,059

PB89-157267 PB89-157267 Not available NTIS National Bureau of Standards (NEL), Gaithersburg, MD. Fire Science and Engineering Div.

Computer Model of Smoke Movement by Air Con-

ditioning Systems (SMACS).

Final rept. J. H. Klote. 1988, 13p

See also PB88-159462. Pub. in Fire Technology 24, n4 p299-311 Nov 88.

Keywords: *Air conditioning equipment, *Smoke, *Computerized simulation, *Air circulation, Mass flow,

Architectural Design & Environmental Engineering

Mass transfer, Fans, Ducts, Cooling systems, Mathematical models, Reprints.

A computer model for simulation of smoke movement through air conditioning systems is described. A brief overview of air conditioning systems is presented. The methods of calculation of mass flow, smoke transport, fan flow, and duct and fitting resistances are presented along with a general description of the program logic.

900,060 PB89-159446 **CP D01** National Inst. of Standards and Technology (NCTL), Gaithersburg, MD. ZIP: ZIP-Code Insulation Program (for Microcom-

puters). Software. S. R. Petersen. Jan 89, 1 diskette NBS/SW/DK-89/

003

The software is contained on 5 1/4-inch diskettes, double density (360K), compatible with the COMPAQ Portable II microcomputer. The diskettes are in the ASCII format. Price includes documentation, PB89-

Keywords: *Software, *Thermal insulation, *Residenrespectively. Terminal institution, Tessional tital buildings, *Economics, Engineering costs, Climate, Prices, Diskettes, Energy conservation, Energy accounting, Costs, Zip codes, L=BASIC, H=COMPAQ Portable II.

ZIP (the ZIP code Insulation Program) is a computer program developed to support the DoE 'Insulation Fact Sheet' by providing users with customized estimates of economic levels of residential insulation for any location in the United States, keyed to the first three digits of its ZIP Code. The ZIP program currently calculates economic levels of insulation for attic floors, exterior wood-frame and masonry walls, floors over unheated areas, slab floors, and basement and crawl-space walls. The economic analysis can be conducted for either new or existing houses. Climate parameters are contained in a file on the ZIP diskette and automatically retrieved when the program is run. Regional energy and insulation price data are also retrieved from the ZIP diskette, but these can be overridden to more closely correspond to local prices. ZIP can be run for a single ZIP Code and specified heating and cooling system. It can also be run in a 'batch' mode for any number of consecutive ZIP Codes in order to provide a table of economic insulation levels for use at the state or national level. Software Description: The software is written in the Basic programming language for implementation on the COMPAQ Portable II or compatible machines using MS DOS operating system.

900,061 PB89-172340 Not available NTIS National Bureau of Standards (NEL), Gaithersburg, MD. Building Environment Div. Control Strategles and Building Energy Consumption.

Final rept.

J. Y. Kao. 1985, 8p Pub. in ASHRAE (American Society of Heating, Refrig-erating and Air-Conditioning Engineers) Transactions 91, pt2 p810-817 1985.

Keywords: *Buildings, *Energy consumption, *Control equipment, *Environmental engineering, Temperature control, Cooling systems, Heating, Ventilation, Management methods, Economic analysis, Air conditioning, Reprints, HVAC systems.

A summary report of building energy studies on basic control strategies applied to air-handling systems of four different buildings in six climatic regions is presented. The building energy program BLAST is used to simulate commonly used air-handling systems for two office buildings, a school, and a retail store. The results of the cooling and the heating energy consumption of these buildings are presented and compared. The energy effects of various economy cycles and temperature resetting strategies applied to reheat, variable air volume, dual-duct, and other systems are discussed.

900,062 PB89-173926 Not available NTIS National Bureau of Standards (NEL), Gaithersburg, MD. Building Environment Div.

Developments In the Heat Balance Method for Simulating Room Thermal Response.

Final rept.
G. N. Walton. 1985, 18p
Pub. in Proceedings of Workshop on HVAC (Heating, Ventilation, and Air Conditioning) Controls Modeling

and Simulation, Atlanta, GA., February 2-3, 1984, 18p

Keywords: *Ventilation, *Heat balance, *Buildings, Computerized simulation, Air flow, Conduction, Heat

The paper reviews recent developments in the heat balance method for the thermal simulation of the non-mechanical components of buildings. These develop-ments include: improved methods for computing response factors, simplified radiant interchange analysis, and detailed calculations for interroom airflows. Further developments are anticipated in the use of response factors for short time step simulation and multidimensional conduction and more detailed simulation of the room air through the concept of ventilation effectiveness.

PB89-174114 Not available NTIS
National Bureau of Standards (NEL), Gaithersburg,
MD. Center for Building Technology.
Design Quality through the Use of Computers.
Final rept

Final rept. R. N. Wright. 1988, 7p

Sponsored by American Society of Civil Engineers. New York. Pub. in Manual of Professional Practice for Quality in

the Constructed Project, Chapter 11, v1, p66-72 1988.

Keywords: *Civil engineering, *Construction, Quality, Design, Reprints, *Computer aided design.

The American Society of Civil Engineers is developing an authoritative and comprehensive guide for quality in construction called the Manual of Professional Practice for Quality in the Constructed Project. The goals for the Manual are to clarify greatly the roles in the construction process and to outline proper procedures construction process and to outline proper procedures and responsibilities for each member of the construction team. Chapter 11 'Design Quality through Use of Computers' describes typical activities and flows of information in design, provides general considerations for quality in the use of computers in design and construction, and gives guidance for the use of computers in each stage of the design process. The designer in each stage of the design process. The designer must use the computer effectively to be competitive both economically and in the quality of his work. The designer must use the computer responsibly to maintain full professional control of his decisions.

900,064 PB89-175905 Not available NTIS National Bureau of Standards (NEL), Gaithersburg, MD. Office of Energy-Related Inventions

Field Measurement of Thermal and Solar/Optical Properties of Insulating Glass Windows.

M. E. McCabe, and D. Hill. 1987, 16p Sponsored by Department of Energy, Washington, DC.

Solar Buildings Technology Div.
Pub. in ASHRAE (American Society of Heating, Refrigerating and Air-Conditioning Engineers) Transactions 93, pt1 p1409-1424 1987.

Keywords: *Calorimeters, *Heating load, *Optical properties, *Window glass, Insulation, Transmittance, Coatings, Leakage, Measurement, Emittance, Re-

The thermal performance of windows with alternative glazing systems were compared by field testing in a side-by-side arrangement using portable calorimeters. Existing double-hung windows installed in an NBS test building were replaced with new sash and insulating glazings provided by the original window manufacturer. Two of the new glazing units had insulating glass with The other two glazing units had insulating glass wiface. The other two glazing units were identical except there was no coating present. Portable calorimeters were placed on the interior of the two northfacing windows, which included a low-emittance and an uncoated control window. Comparative measurements of air leakage, heat loss and solar transmittance were made for these windows. Nighttime heat loss for the uncoated window was approximately 23% greater then that of the low-emittance window, although the U-values for both windows were greater than indicated by the manufacturer's laboratory test results. Possible causes for the discrepancy between laboratory and field test data are evaluated and the potential use of portable calori-meters for both comparative and absolute measurements of windows is discussed.

900,065 PB89-176127

Not available NTIS

National Bureau of Standards (NEL), Gaithersburg, MD. Building Physics Div. Indoor Air Quality.

Final rept.

P. E. McNall. 1986, 7p

Pub. in ASHRAE (American Society of Heating, Refrigerating and Air-Conditioning Engineers) Jnl. 28, n6 p39-42, 44, 46, 48 Jun 86.

Keywords: *Buildings, *Ventilation, Design, Air conditioning, Environmental engineering, Maintenance, Air filters, Efficiency, Quality control, Heat recovery, Reprints, *HVAC systems, *Air Quality, *Indoor air pollu-

The paper outlines in a general way, the methods which are available to the HVAC engineer in the practical design, operation and maintenance of systems which impact the air quality in buildings. The general control methods are: exclude the pollutant source; prevent the source from emanating pollutants into the air; dilute the air with purer air (ventilation); remove pollutants from the air (air cleaners); provide other ventilation strategies (ventilation effectiveness, local exhaust, etc.); discuss occupant actions which reduce their exposure. Strategies which can be used now are: ventilation quantities (ASHRAE Standard 62-1981 and vertilation (quantiles (AGRINAE Statistian and besting and balancing; exhaust air reentry; heat recovery; system design for less contamination; particulate filtering; gaseous filtering; local exhaust. Strategies which are under development or need further application knowledge are: use of ventilation effectiveness; better gaseous removal standards; air washers; air ionization; differential pressure control.

900.066

PB89-176499 Not available NTIS National Bureau of Standards (NEL), Gaithersburg, MD. Building Equipment Div.
Interzonal Natural Convection for Various Aper-

ture Configurations.

Final rept.

B. M. Mahajan, and D. D. Hill. 1986, 7p

Sponsored by Department of Energy, Washington, DC. Passive and Hybrid Solar Energy Div. Pub. in Proceedings of ASME (American Society of Mechanical Engineers) Winter Annual Meeting, Anaheim, CA., December 7-12, 1986, 7p.

Keywords: *Air flow, *Buildings, Doors, Heating, Heat transmission, Walls, Mathematical models, Mass flow, *Natural convection, *Aperture shape.

Experiments were conducted to study the interzonal natural convection for different aperture configurations for a two-zone set-up. The following four aperture configuration were studied: a center door, a side door, a window; and (4) a split window, i.e., two small windows situated symmetrically about the horizontal bisector of the common wall. One of the two zones was heated with baseboard electric heaters placed adjacent to the floor and the wall opposite to the common wall. For each aperture configuration, tests were conducted with various heat inputs to the warmer of the two zones. The data indicate that the discharge coefficient used in a simple one-dimensional model for interzonal airflow varies with the aperture configuration and status of heat input to the warmer zone. The variations in the discharge coefficient are apparently due to the different flow fields and temperature distributions for each aperture configuration.

900,067

PB89-176614 Not available NTIS National Bureau of Standards (NEL), Gaithersburg, MD. Building Physics Div.

Ventilation Effectiveness Measurements in an

Office Building. Final rept.

A. K. Persily. 1986, 11p

Sponsored by Department of Energy, Washington, DC. Pub. in Proceedings of ASHRAE (American Society of Heating, Refrigerating and Air-Conditioning Engineers) Conference on IAO (Indoor Air Quality): Managing Indoor Air for Health and Energy Conservation, Atlanta, GA., April 20-23, 1986, p548-558.

Keywords: "Ventilation, "Commercial buildings, Air flow, Distribution systems, Environmental engineering, Performance evaluation, Draft(Gas flow), Efficiency, Quality control, Reprints, "Air quality, "HVAC systems, Tracer studies.

Architectural Design & Environmental Engineering

To evaluate the impact of ventilation on air quality within mechanical ventilated office buildings, one must examine both the outside air intake or ventilation rate and the performance of the air distribution system in delivering this outside air to the building occupants. Inadequate air distribution may lead to air quality problems, even if a building's total ventilation rate is adequate. Tracer gas measurement procedures have been developed to evaluate these air distribution characteristics of mechanical ventilation systems or their ventilation effectiveness. The paper examines the use of one such technique, tracer gas measurement employing age distribution analysis in modern, mechanically ventilated office buildings. The measurement and analysis techniques are described, along with those features of the building type which impact on their application. The results of the measurements indicate that there is good mixing in a whole building scale, but also provide evidence of local, stagnant zones in the occupied space. These apparently contradictory results are suspected to be due to the fact that the layout of an actual building is much more complex than the measurement theory assumes.

900,068
PB89-177141
Not available NTIS
National Bureau of Standards (NEL), Gaithersburg,
MD. Building Environment Div.
Application of Direct Digital Control to an Existing

Building Air Handler.

Final rept.
G. E. Kelly, W. B. May, and C. Park. 1985, 26p
Sponsored by Department of Energy, Washington, DC.
Office of Buildings and Community Systems, and
Naval Civil Engineering Lab., Port Hueneme, CA.
Pub. in Performance of HVAC (Heating, Ventilating
and Air Conditioning) Systems and Controls in Buildings, Proceedings of CIB International Symposium at
the Building Research Establishment, Garston, England, June 18-19, 1984, p3-28 1985.

Keywords: *Buildings, *Automatic control equipment, *Digital systems, Dynamic response, Systems engineering, Management systems, Environmental engineering, *HVAC systems.

In order to gather reliable information on the dynamic performance of heating, ventilating and air conditioning systems and their controls in buildings, the Center for Building Technology (CBT) at the National Bureau of Standards (NBS) has developed a Building Management and Controls Laboratory. The Laboratory consists of a distributed computerized Energy Management and Control System (EMCS) developed at NBS and used to control a number of different experiments. These experiments currently include the control of an eleven-story office building on the NBS site, a thoroughly instrumented air handler in a laboratory environment, and a large air handler used to condition part of the perimeter of the building housing the Center for Building Technology.

900,069
PB89-177158
Not available NTIS
National Bureau of Standards (NEL), Gaithersburg,
MD. Building Environment Div.
Flow Coefficients for Interzonal Natural Convection for Various Apertures.
Final rept.

B. M. Mahajan, and D. D. Hill. 1987, 7p
Sponsored by Department of Energy, Washington, DC.
Office of Solar Heat Technologies

Office of Solar Heat Technologies.
Pub. in Proceedings of ASME-JSME-JSES (American Society of Mechanical Engineers-Japan Society of Mechanical Engineers-Japanese Solar Energy Society) Solar Energy Conference, Honolulu, HI., March 22-27, 1987, p300-306.

Keywords: *Convection, *Air flow, *Heat transfer coefficient, Temperature distribution, Heat measurement, Environmental engineering, Thermal expansion, Tests, Temperature control, Energy conservation.

Experiments to determine the flow coefficients for interzonal natural convection were carried out at the National Bureau of Standards' Passive Solar Test Facility. Interzonal natural convection was studied for ten different apertures. One of the two zones was heated with baseboard electric heaters placed adjacent to the floor along the wall opposite to the common wall. Experiments were conducted with various heat inputs to the warmer of the two zones. The flow coefficients used in simple one-dimensional models for interzonal airflow varies with the aperture configurations, aperture to wall area ratio, and the level of heat input to the warmer zone. Variations in the flow coefficients are ap-

parently due to the different flow fields and temperature distributions for each aperture configuration.

900,070
PB89-177166
Not available NTIS
National Bureau of Standards (NEL), Gaithersburg,
MD. Building Environment Div.
HVACSIM+, a Dynamic Bullding/HVAC/Control
Systems Simulation Program.

Final rept. G. E. Kelly, C. Park, D. R. Clark, and W. B. May. 1985, 19p

1985, 19p
Sponsored by Department of Energy, Washington, DC.
Office of Buildings and Community Systems, and
Naval Civil Engineering Lab., Port Hueneme, CA.
Pub. in Proceedings of Workshop on HVAC (Heating,
Ventilating and Air Conditioning) Controls Modeling
and Simulation, Atlanta, GA., February 2-3, 1984, p119 1985.

Keywords: *Buildings, *Control equipment, *Con,puterized simulation, Dynamic response, Design, Architecture, Systems engineering, Environmental engineering, Performance evaluation, *HVAC systems.

The dynamic performance of buildings and the service systems within them is becoming more and more important as the use of computerized building management systems become less expensive and increasingly popular. In an effort to understand the dynamic interactions between the building shell, the HVAC system, and building controls, the National Bureau of Standards (NBS) has begun work on a non-proprietary building system simulation program. Called HVACSIM+, which stands for HVAC SIMulation PLUS other systems, this program employs advanced equation solving techniques and a hierarchical, modular approach to simulate the dynamic performance of entire building/HVAC/control systems. The paper discusses the architecture of HVACSIM+, the HVAC component models and building shell model being developed, and other important features of the program. A brief status report on the development of HVACSIM+ and a timetable for completing various portions of the program are also presented.

900,071

PB89-177174

Not available NTIS
National Bureau of Standards (NEL), Gaithersburg,
MD. Building Environment Div.
Simulation of a Large Office Building System Using

Simulation of a Large Office Building System Using the HVACSIM+ Program.

Final rept.
C. Park, S. T. Bushby, and G. E. Kelly. 1989, 10p
Sponsored by Department of Energy, Washington, DC.
Pub. in ASHRAE (American Society of Heating, Refigerating and Air-Conditioning Engineers) Transactions, v95 ot1 10p 1989.

Keywords: *Buildings, *Computerized simulation, Systems analysis, Design, Dynamic response, Systems engineering, Environmental engineering, Control equipment, *HVAC systems.

A large office building system located in Gaithersburg, MD was simulated using the HVACSIM+ computer program. A typical floor of this 11-story building was selected and divided into four zones, with one air-handling unit serving each zone. Dynamic interactions between the building zones and the HVAC and control system were studied for several different control strategies during the cooling season. Simulations were performed using the building shell and zone models along with the air handler and control system models. Simulation results are presented and compared with experimental measurements. The effects of three different control schemes on energy consumption are compared with each other. These schemes are: the start/stop control without purging cycle, the start/stop control without purging cycle, the start/stop control with purging, and continuous operation.

900,072

PB89-179667

Not available NTIS

National Bureau of Standards (NEL), Gaithersburg,
MD. Building Physics Div.

Performance Measurements of Infrared Imaging

Performance Measurements of infrared imaging Systems Used to Assess Thermal Anomalies.

Y. M. Chang, and R. A. Grot. 1986, 14p
Pub. in Proceedings of SPIE (Society of Photo-Optical Instrumentation Engineers), Thermal Imaging, v636
p17-30 1986.

Keywords: *Infrared thermal detectors, *Temperature measuring instruments, *Temperature distribution,

Performance evaluation, Thermal stability, Environmental engineering, Buildings, Spatial distribution, Imaging techniques, Energy conservation.

An evaluation of various infrared imaging systems was performed to determine their abilities to identify thermal anomalies in buildings. The systems were tested under environmental temperatures from -20 C to 25 C for their minimum resolvable temperature differences (MRTD) at spatial frequencies between 0.03 to 0.25 cy/mrad. The temperature dependence of MRTD was analyzed and compared with the predicted values in ASHRAE Standard 101-83 for thermal imaging systems. The temperature dependence of infrared systems object temperature calibrations was investigated. The signal transfer functions (SiTF) of infrared sensors are generated to verify and calibrate the dynamic range of each sensor. Also discussed are the results of measurements of modulation transfer function (MTF) of infrared imaging systems, which are based on Fourier Transforms of the line spread function (LSF). It is shown that the results of the MTF calculations can be correlated with their MRTD measurements.

900.073

PB89-189153 PC A07/MF A01 National Inst. of Standards and Technology, Gaithersburg. MD.

Evaluating Office Lighting Environments: Second Level Analysis.
B. L. Collins, W. S. Fisher, G. L. Gillette, and R. W. Marans. Apr 89, 143p NISTIR-89/4069

See also PB88-164512. Prepared in cooperation with Lighting Research Inst., New York, and Michigan Univ., Ann Arbor. Sponsored by International Council for Educational Development, New York, and New York State Energy Research and Development Authority, Albany.

Keywords: *Office buildings, *Lighting equipment, Lamps, Energy consumption, Energy conservation, Evaluation, Illuminance, Luminance.

Data from a post-occupancy evaluation (POE) of 912 work stations with lighting power density (LPD), photometric, and occupant response measures were examined in a detailed, second-level analysis. Seven types of lighting systems were identified with different combinations of direct and indirect ambient lighting, and task lighting and daylight. The mean illuminances at the primary task location were within the IES target values for office task with a range of mean illuminances from 32 to 75 fc, depending on the lighting system. The median LPD was about 2.36 watts/sq ft, with about one-third the work stations having LPD's at or below 2.0 watts/sq ft. Although a majority of the occupants (69%) were satisfied about their lighting, the highest percentage of those expressing dissatisfaction (37%) with lighting had an indirect fluorescent furniture mounted (IFFM) system. The negative reaction of so many people to the IFFM system suggests that the combination of task lighting with an indirect ambient system had an important influence on lighting satisfaction, even though task illuminances tended to be higher with the IFFM system. Concepts of lighting quality, visual health, and control were explored, as well as average luminance to explain the negative reactions to the combination of indirect lighting with furniture mounted lighting.

900,074

PB89-189237 PC A04/MF A01 National Inst. of Standards and Technology (NEL), Gaithersburg, MD. Center for Building Technology, illumination Conditions and Task Visibility In Daylit Spaces. S. J. Treado. Mar 89, 55p NISTIR-88/4014

Keywords: *Buildings, *Daylighting, *Architecture, *Windows, Design, Illuminating, Computerized simulation, Light(Visible radiation), Brightness, Environmental engineering, Electric lighting, Comparisons, Graphs(Charts), Energy conservation.

Illumination conditions are evaluated in typical building spaces based on detailed computer simulations, in order to characterize and quantify the effects of daylighting on task visibility. Examined are the effects of fenestration location and type on task contrast under daylit, electric-lit and combined conditions. The implications of the illumination conditions with daylighting on lighting and daylighting system design are discussed.

Architectural Design & Environmental Engineering

900.075 PC A03/MF A01 PB89-193247 National Inst. of Standards and Technology, Gaithersburg, MD.

Rating Procedure for Mixed Air-Source Unitary Air Conditioners and Heat Pumps Operating in the

Cooling Mode. Revision 1.

P. A. Domanski. May 89, 25p NISTIR-89/4071 See also PB86-166279. Sponsored by Department of Energy, Washington, DC. Office of Buildings and Community Systems.

Keywords: *Heat pumps, *Air conditioners, *Residential buildings, Cooling systems, Cooling rate, Standards, Evaporators, Condensing, Efficiency.

A procedure is presented for rating split, residential air conditioners and heat pumps operating in the cooling mode which are made up of an evaporator unit com-bined with a condensing unit which has been rated under current procedures in conjunction with a different evaporator unit. The procedure allows calculation of capacity at the 95 F rating point and seasonal energy efficiency ratio without performing laboratory tests of the complete system. The procedure has been prepared for the Department of Energy for consideration in the rule making process. It is a revised version of the original version of the procedure published in 1986

900,076 PC A05/MF A01 PB89-193254 National Inst. of Standards and Technology (NEL), Gaithersburg, MD. Building Environment Div.

AIRNET: A Computer Program for Building Airflow Network Modeling. G. N. Walton. Apr 89, 85p NISTIR-89/4072 Contract DE-Al01-36CE2101-3

Sponsored by Department of Energy, Washington, DC.

Keywords: *Air flow, *Buildings, *Models, Ventilation, Ventilation fans, Ducts, Air conditioning, Infiltration, Computer applications, User manuals(Computer programs).

In spite of its importance, the analysis of airflows has significantly lagged the modeling of other building features because of limited data, computational difficul-ties, and incompatible methods for analyzing different flows. Methods have been developed to analyze airflows in HVAC ducts and to estimate infiltration, but the interaction between building HVAC systems and infiltration airflows has seldom been studied. The report describes a computer program for modeling networks of airflow elements such as openings, ducts, and fans. It emphasizes the numerical aspects of an airflow network method which would provide a unified approach to building airflow calculations. It also discusses the limitations of the method and poorly understood factors that could profit from further research.

900.077 PB89-206833 PC A03/MF A01 National Inst. of Standards and Technology (NEL), Gaithersburg, MD. Building Environment Div. Integral Mass Balances and Pulse Injection Tracer

Techniques.

J. Axley, and A. Persily. Oct 88, 40p NISTIR-88/3855 Presented at the Air Infiltration and Ventilation Centre Conference, Effective Ventilation held at Novotel Gent, Belgium, September 12-15, 1988. Sponsored by Department of Energy, Washington, DC.

Keywords: *Air flow, *Ventilation, *Buildings, Ducts, Environmental engineering, Air circulation, Measuring instruments, Air quality, *Tracer techniques, *HVAC systems, Energy conservation.

Tracer gas techniques for measuring airflow rates in building systems are considered. These techniques are classified in terms of tracer gas injection strategy employed and mass balance relationships used to analyze measured tracer concentration data. The discussion focuses on one class of tracer techniques, the pulse injection techniques, based upon pulse injection strategies and integral mass balance relationships. These pulse injection techniques have not been commonly used in the past yet they provide practically useful means for the determination of airflow rates in building systems. Pulse injection techniques are presented for measuring airflows in ducts, and for studying single-zone and multi-zone building airflow sys-tems. Experimental procedures for these three cases are discussed, and preliminary results from field appli-cations of these techniques are presented. The possibility of flow variation is accounted for in all cases, and the sensitivity of the single-zone pulse injection technique to these flow variations is compared to that of the single-zone constant injection technique. This companson leads to integral formulations of the constant injection technique for duct, single-zone, and multi-zone situations that may provide means to improve the accuracy of the commonly used constant injection tracer technique.

900,078 PB89-211858 Not available NTIS National Bureau of Standards (NEL), Gaithersburg, MD. Fire Safety Technology Div. Outline of a Practical Method of Assessing Smoke

Hazard. Final rept.

A. J. Fowell. 1986, 7p

Pub. in Proceedings of Joint Meeting on Progress in Fire Safety - Society of the Plastics Industry and Fire Retardant Chemical Association, Washington, DC., March 19-21, 1986, p139-145.

Keywords: *Buildings, *Fires, *Smoke, Safety engineering, Computer systems programs, Building codes, Fire prevention, Assessments.

The document outlines the form, content, and capabilities of a practical method for assessing smoke haz-ards planned for delivery by the National Bureau of Standards, Center for Fire Research before the end of 1986. The method will contain a step-by-step procedure, description of generic fires and buildings, data for using with computer programs, and worked examples.

900,079 PB89-228977 PC A07/MF A01 PC A07/MF A01
National Inst. of Standards and Technology (NEL),
Gaithersburg, MD. Center for Building Technology.
Air Quality Investigation in the NiH (National Institutes of Health) Radiation Oncology Branch.
A. Persily, W. S. Dols, S. J. Nabinger, and D. A.
VanBronkhorst. Aug 89, 132p NISTIR-89/4145
Sponsored by National Institutes of Health Pothocology Sponsored by National Institutes of Health, Bethesda,

Keywords: *Ventilation, *Air flow, *Radioactive contaminants, Human factors engineering, Design standards, Safety engineering, Gas flow, Graphs(Charts), Recommendations, *National Institutes of Health Radiation Oncology Branch, *Air quality, *HVAC systems, *Indoor air pollution, Building technology, Office build-

The Radiation Oncology Branch (ROB) is located in the Clinical Center of the National Institutes of Health (NIH). The occupants of the ROB facility have expressed dissatisfaction with the air quality within the facility for several years. To identify the sources of the air quality problems in the ROB facility and to obtain recommendations for their solution, the Center for Building Technology at the National Institute of Standards and Technology (NIST, formerly The National Bureau of Standards) conducted an indoor quality investigation of the ROB facility. Results revealed several deficiencies in the design and current condition of the ROB ventilation system, such as significant differences between the design airflow rates and those recommended in current standards and guidelines. The airflow measurements showed many instances in which measured airflow rates were different from their design values and revealed the existence of airflows leading to the potential for pollutant transport within the building. The contaminant measurements fell generally well below the maximum values in the ASHRAE air quality standard. Thermal comfort measurements revealed instances when the temperature and relative humidity were outside of ASHRAE comfort limits. Recommendations are made to remedy the deficiencies noted and to control the conditions contributing to the building's air quality problems.

Not available NTIS PB89-229157 National Bureau of Standards (NEL), Gaithersburg, MD. Fire Safety Technology Div.

Capabilities of Smoke Control: Fundamentals and Zone Smoke Control.

J. H. Klote, and E. K. Budnick. 1989, 10p Pub. in Jnl. of Fire Prot. Engr. 1, n1 p1-10 1989.

Keywords: *Smoke abatement, *Air flow, Ventilation, Fire protection, Safety engineering, Fire alarm systems, Buildings, Fire safety, Reprints, *HVAC systems, Smoke detectors.

The paper discusses the principles of smoke control and the practical application of these principles to zoned smoke control systems. Zoned smoke control can use dedicated fans or the fans of a building's heating, ventilating and air conditioning systems. The paper discusses concerns with systems that only purge in an attempt to control smoke movement. Considerations of system activation and acceptance testing are presented.

900,081 PB89-230361 Not available NTIS National Inst. of Standards and Technology (NEL), Gaithersburg, MD. Building Environment Div. Investigation of a Washington, DC Office Building. Final rept.

A. K. Persily, W. A. Turner, H. A. Burge, and R. A. Grot. 1989, 16p

Sponsored by Department of Energy, Washington, DC. Pub. in Design and Protocol for Monitoring Indoor Air Quality, p35-50 1989.

Keywords: *Commercial buildings, Human factors encommercial buildings, Huffian factors engineering, Temperature control, Air flow, Ventilation, Monitors, Measuring instruments, Reprints, *Indoor air pollution, *Air quality, *Office buildings, *Sick building syndrome, *HVAC systems, Building technology.

The paper describes the techniques used to study a Washington, D.C. office building with a long history of indoor air quality and thermal comfort complaints. More than twenty investigations, mostly relatively short term, have been conducted since 1978 to determine the causes of the building's problems and to recom-mend corrective actions. More recently a long term, intensive study of the building has been undertaken to study the building more thoroughly and to investigate the application of several techniques for studying office building air quality. These techniques include tracer gas measurements of air exchange rates, ventilation system performance and ventilation effectiveness, and measurements of the levels of various indoor pollutants including bioaerosols. The paper reviews the previous investigations of the building and describes the procedures used in the current study. Some preliminary results of the current effort are pre-

900.082 PB89-230379 Not available NTIS National Inst. of Standards and Technology (NEL), Gaithersburg, MD. Building Environment Div. Airflow Network Models for Element-Based Bulld-Ing Airflow Modeling.

Final rept. G. N. Walton. 1989, 10p Sponsored by Department of Energy, Washington, DC. Office of Buildings and Community Systems. Pub. in ASHRAE (American Society of Heating, Refrigerating and Air Conditioning Engineers) Transactions, v95 pt2 10p Jul 89.

Keywords: *Buildings, *Airflow, Ventilation, Air circulation, Ducts, Temperature control, Reprints, *HVAC

systems, *Air quality, Building technology.

In spite of its importance, the analysis of airflows has significantly lagged behind the modeling of other building features because of limited data, computational difficulties, and incompatible methods for analyzing different flows. Methods have been developed to analyze airflows in HVAC ducts and to estimate infiltration, but the interaction between building HVAC systems and infiltration airflows has seldom been studied. The paper emphasizes the numerical aspects of an airflow network method that would provide a unified approach to building airflow calculations. It also discusses the limitations of the method and poorly understood factors that could profit from further research.

900,083 PB89-231005 Not available NTIS National Inst. of Standards and Technology (NEL), Gaithersburg, MD. Office of Energy-Related Inven-

Origins of ASHRAE (American Society of Heating, Refrigerating and Air-Conditioning Engineers) Window U-Value Data and Revisions for the 1989 Handbook of Fundamentals. Final rept.

M. E. McCabe. 1989, 5p

Pub. in Proceedings of the Annual Conference of the Solar Energy Society of Canada (15th), Penticton, B. C., June 19-21, 1989, p273-277.

Architectural Design & Environmental Engineering

Keywords: *Windows, Architecture, Solar energy, Heat transfer, Buildings, Research projects, *U values, Energy conservation, Building technology.

The ASHRAE Handbook of Fundamentals and its predecessor, the ASHVE Guide, have been the authoritative source of technical information on window U-values since the 1920s. The paper discusses the U-values since the 1920s. The paper discusses mo-historical origins of window U-values beginning with re-search conducted in the last century. The technical basis for the modern form of the ASHRAE U-value table, which appeared at about 1950, is described. Re-visions to the U-value table are traced during the ensuvisions to the o'value used and the case during in easily ing years, concluding with a discussion of the current concerns over the data and the changes that will appear in the 1989 ASHRAE Handbook.

900,084 PB89-231047 Not available NTIS National Inst. of Standards and Technology (NEL), Gaithersburg, MD. Building Environment Div. Considerations for Advanced Building Thermal Simulation Programs. Final rept.

G. N. Walton, 1989, 6p Solution (1989, op Sponsored by Department of Energy, Washington, DC. Pub. in Proceedings of Building Simulation '89 Conference, Vancouver, B.C., Canada, June 23-24, 1989, p155-160.

Keywords: *Buildings, *Thermal analysis, Heat loss, Air flow, Ventilation, Environment simulation, Matrix methods, Thermal measurement, *Energy audits, Energy conservation.

In order to assess the applicability of a more modular approach to the development of building thermal analysis programs, the paper begins with a review of some of the basic numerical methods used in simulation. These are discussed with some observations from other fields of study besides building simulation. Two
major examples of advanced simulation methods are presented: the use of sparse matrix methods for heat transfer simulation and a modular calculation of building airflows. Their implications on the development of the next generation of building thermal analysis programs are discussed.

900,085 PB89-231161 Not available NTIS National Bureau of Standards (NEL), Gaithersburg, MD. Fire Safety Technology Div.

Analysis and Prediction of Air Leakage through
Door Assemblies.

Final rept. D. Gross, and W. L. Haberman. 1989, 10p Pub. in Proceedings of International Symposium on Fire Safety Science (2nd), Tokyo, Japan, June 13-17, 1988, p169-178 1989.

Keywords: *Air flow, *Doors, *Heat loss, Flow rate, Flow measurement, Leakage, Energy dissipation, Comparisons, *Energy conservation.

A generalized relationship is presented for determining air flow rates through narrow gaps around door edges. The relationship provides values of leakage rates for steady laminar flow through gaps over a wide range of pressure difference and eliminates approximations associated with the often inappropriate use of discharge coefficients and exponents in the flow equation Q = C A(delta p)n. The analysis covers straight-through, single bend and double bend gaps of constant thickness, as well as connected gaps of constant thicknesses. Comparison of measured flow rates for installed stairwell door assemblies with those predicted by use of the relationship shows agreement within 20%. The volumetric flow of heated air through simple door gaps has been calculated by use of the relation-ship. The results show that the flow rate may increase or decrease with temperature depending on gap size and flow region.

900,086 PB89-235881 PC A07/MF A01 National Inst. of Standards and Technology, Gaithersburg, MD.
EVSIM: An Evaporator Simulation Model Account-

ing for Refrigerant and One Dimensional Air Distribution.

P. A. Domanski. Aug 89, 142p NISTIR-89/4133 Sponsored by Department of Energy, Washington, DC. Office of Buildings and Community Systems.

Keywords: *Computerized simulation, *Air conditioning equipment, *Evaporators, Air conditioners, Heat

exchanges, Refrigerants, Air circulation, Thermodynamics, Models, Computer programs.

The report describes a computer model, EVSIM, of a refrigerant-to-air heat exchanger of the type used in residential air conditioning as an evaporator. The model provides performance predictions of a one-slab or two-slab evaporator for a given refrigerant enthalpy at the coil inlet, saturation temperature and superheat at the coil outlet, and at imposed one dimensional air mass flow distribution over the coil face. The model accounts for air distribution and for complex refrigerant circuitry designs by simulating refrigerant distribution. Performance of the coil is calculated employing a tubeby-tube scheme. The report includes a User's Guide and a listing written in FORTRAN 77.

900.087

PB90-112368 PC A06/MF A01 National Inst. of Standards and Technology (NEL), Gaithersburg, MD. Center for Building Technology. Proposed Methodology for Rating Air-Source Heat Pumps That Heat, Cool, and Provide Domestic Water Heating.

B. P. Dougherty Aug 89, 108p NISTIR-89/4154, EPRI-RP-2033-26

Sponsored by Electric Power Research Inst., Palo Alto, CA., and Department of Energy, Washington, DC.

Keywords: *Residential buildings, *Hot water heating, Ratings, Performance standards, Heat exchangers, Air conditioning, Heating, Seasonal variations, Mathematical models, *Air source heat pumps.

The work at NIST has centered upon developing a proposed rating methodology for integrated appliances that heat water in a water heating only mode or while simultaneously air conditioning or space heating. De-spite the emphasis, the proposed methodology pro-vides a framework for rating other types of integrated heat pump/water heating appliances. The laboratory testing, the calculation procedure, and the method for reporting performance are described. The testing is an adaptation of the laboratory tests conducted when rating conventional heat pumps and water heaters. Seasonal estimates of energy consumption rates are calculated using a bin type approach. Combined performance factors and operating costs are used for reporting performance.

900,088 PC A08/MF A01 PB90-112384 National Inst. of Standards and Technology (NEL), Gaithersburg, MD. Center for Building Technology. Post-Occupancy Evaluation of Several U.S. Government Buildings.

ernment Buildings.

B. L. Collins, G. L. Gillette, M. S. Dahir, and P. J. Goodin. Sep 89, 159p NISTIR-89/4175

Sponsored by Army Communications-Electronics Support Facility, Vint Hill Farms Station, VA.

Keywords: *Public buildings, *Office buildings, *Human factors engineering, *Environmental engineering, *Comfort, Assessments, Noise(Sound), Performance evaluation, Questionnaires, Lighting equipment, Air quality, Indoor air pollution, HVAC systems.

A post-occupancy evaluation was performed on five small, low-rise U.S. government buildings at a site south of Washington, D.C. to evaluate environmental conditions including lighting, space, noise, and indoor air quality, and provide recommendations for change. In addition, a comparison was made of environmental conditions before and after renovation of one of the buildings. The study employed a questionnaire about buildings. The study employed a questionnaire about the environmental conditions, physical measures of the space (lighting, space, noise, temperature, etc.) and interviews with personnel at the site. A total of 308 people participated (including measures before and after the renovation) and physical measures were taken at 92 work stations. Analysis of the physical measurement data indicated problems with limited space, lack of adjustable task lighting, and perceptions of poor indoor air quality in two of the buildings. The renovation was perceived to have improved the aprenovation was perceived to have improved the appearance of one building substantially, however. Suggestions for improvements to the buildings at the site were also made.

900,089

PB90-118043 Not available NTIS National Inst. of Standards and Technology (NEL), Gaithersburg, MD. Mathematical Analysis Div.

Advanced Heat Pumps for the 1990's Economic Perspectives for Consumers and Electric Utilities.

Final rept. S. R. Petersen. 1989, 6p Sponsored by Electric Power Research Inst., Palo

Pub. in ASHRAE (American Society of Heating, Refrigerating and Air-Conditioning Engineers) Jnl., p36, 38, 40, 42, 44, and 46, Sep 89.

Keywords: *Heat pumps, *Electric power demand, Hot water heating, Electric utilities, Economic analysis, Air conditioning equipment, Heating, Cooling systems,

Advanced heat pumps promise improved energy efficiency and reduced peak-power demand for space heating, space cooling and water heating in houses. Economic analysis shows that they can be cost effective in much of the United States, both for consumers and electric utilities. Consumers will benefit from greatly reduced electric bills; utilities will benefit from improved load management and the increased competi-tiveness of electric heating. A new program, HPEAK (Heat Pump/Economic Analysis of Kilowatt-hours), developed at the National Institute of Standards and Technology, evaluates the hourly performance of conventional and advanced heat pump systems, both from consumer and utility perspectives. HPEAK analyses demonstrate the economic benefits of an advanced air-source heat pump with adjustable-speed control and integrated water-heating capability in five locations in the United States.

900.090 PB90-128158 Not available NTIS National Inst. of Standards and Technology (NEL), Gaithersburg, MD. Building Environment Div. Measured Air infiltration and Ventilation Rates in Eight Large Office Buildings.

Final rept. R. A. Grot, and A. K. Persily. 1986, 33p Pub. in Measured Air Leakage of Buildings, ASTM STP 904. p151-183 1986.

Keywords: *Office buildings, *Ventilation, *Air flow, *Flow measurement, Safety engineering, Human factors engineering, Measuring instruments, Design standards, Building codes, Environmental engineering,

Air infiltration and ventilation rate measurements were made during all seasons of the year in eight federal office buildings using an automatic air infiltration system designed at the National Bureau of Standards. system designed at the National Bureau of Standards. The eight federal office buildings were located in Anchorage, Alaska; Ann Arbor, Michigan; Columbia, South Carolina; Fayetteville, Arkansas; Huron, South Dakota; Norfolk, Virginia; Pittsfield, Massachusetts; and Springfield, Massachusetts. These buildings ranged in size from 1730 sq m (18,600 sq ft) for the building in Pittsfield to 45,500 sq m (490,000 sq ft) for the Anchorage federal building. All were constructed within the last 10 years. Air infiltration rates were found to vary from 0.2 to 0.7 air changes per hour and constituted from 23% to 61% of the building design load. Minimum ventilation rates in the tighter buildings were found to be less than what would be recommended for found to be less than what would be recommended for occupied offices.

Building Equipment, Furnishings, & Maintenance

900.091 PB89-157010 Not available NTIS National Bureau of Standards (NEL), Gaithersburg, MD. Building Environment Div. Control System Simulation in North America.

Final rept. G. E. Kelly. 1988, 10p Pub. in Energy and Buildings 10, p193-202 1988.

Keywords: *Control equipment, *Buildings, *Simulation, Systems engineering, Industrial buildings, Commercial buildings, Management systems, Research projects, Maintenance management, Reviewing, Evaluation, Reprints.

The paper presents a historical review of control system simulation in North America from around 1970 until the present. The subject is divided into the topics

Bullding Equipment, Furnishings, & Maintenance

of Regulation, Supervisory Control, and Optimized Building Controls. Different research efforts and simulation programs that have made a significant contribution to advancing the state of the art are reviewed. The current emphasis and what the author believes will be some future trends in this important field are also dis-

900.092 PB89-189146 PC A04/MF A01
National Inst. of Standards and Technology (NEL),
Gaithersburg, MD. Center for Building Technology.
Assessment of Robotics for Improved Building Operations and Maintenance.

B. M. Mahajan, J. M. Evans, and J. E. Hill. Nov 88, 56p NISTIR-88/4006

Portions of this document are not fully legible. Pre-pared in cooperation with Transitions Research Corp., Hartford, CT. Sponsored by General Services Administration, Washington, DC.

Keywords: *Buildings, *Maintenance, *Operations, Automation, Robots, Cleaning, Delivery, Security, Services, Barriers, *Robotics.

The report provides a state-of-the-art survey of robotic technology useful for building operation and maintenance. Floor cleaning, mail delivery, security, and storage facility operations represent current and near term opportunities for robotic application. Likely future applications may include: bathroom, office and window cleaning; lawn mowing; trash handling; wall painting; and miscellaneous material handling. Potential barriers to the use of robotics within buildings are identified. Amendments to the GSA Handbook on 'Quality Standards for Design and Construction' to accommodate the use of service robots in Federal buildings are suggested. The suggested amendments are not exhaustive and as the knowledge base expands, should be refined and augmented.

900,093 PC A11/MF A01
National Inst. of Standards and Technology (NEL),
Gaithersburg, MD. Center for Fire Research.
False Alarm Study of Smoke Detectors in Department of Veterans Affairs Medical Centers (VAMCS).

P. M. Dubivsky, and R. W. Bukowski. May 89, 235p NISTIR-89/4077

Sponsored by Department of Veterans Affairs, Washington, DC., Department of the Air Force, Washington, DC., and Underwriters' Labs., Inc., Northbrook, IL.

Keywords: *Fire alarm systems, *Smoke, *False alarms, *Hospitals, *Military facilities, Warning systems, Medical centers, Veterans Administration.

A study of 133 VA Medical Centers (VAMC) out of a total of 172 throughout the U.S. coupled with visits to 20 facilities was conducted to gather data on false alarms of smoke detectors. Data collected included name of the detector manufacturer and model number, control unit manufacturer and model number, number and type of detectors installed, where installed, number of false and real alarms for preceding year, date of installation, and policies on smoking, testing, cleaning, and maintenance. VAMC personnel involved with the installations were requested to indicate the maximum level of false alarms that could be tolerated and to provide any recommendations to reduce their occurrence. The study included a total of approximateoccurrence. The study included a total of approximately 37,000 system type smoke detectors of which 69%
were of ionization (ion) type and 31% photoelectric,
3000 duct detectors (90% ion and 10% photo), and
1100 smoke detector modules (80% ion and 20%
photo) integral with door holder closers. Also included
are approximately 100 single station smoke alarms.
Analysis of data collected from operating facilities
through forces site visities and staff intentious resulted. through forms, site visits, and staff interviews resulted in a series of recommendations which could result in a substantial reduction in observed false alarms.

900.094 PB89-229009 PC A03/MF A01 National Inst. of Standards and Technology (NEL), Gaithersburg, MD. Center for Fire Research.
Estimating the Environment and the Response of
Sprinkler Links in Compartment Fires with Draft
Curtains and Fusible Line-Actuated Ceiling Vents.

Part 2. User Guide for the Computer Code Lavent. W. D. Davis, and L. Y. Cooper. Aug 89, 43p NISTIR-89/4122

See also PB88-215462. Sponsored by American Architectural Mfrs. Association, Des Plaines, IL.

Keywords: *Fires, *Bulldings, *Sprinkler systems, Ventilation, Ducts, Computer systems programs, Computerized simulation, Safety engineering, Environment simulation, Fire safety, Graphs(Charts).

Presented Is a User Gulde for the computer code LAVENT (Link-Actuated VENTs) and an associated graphics code GRAPH. LAVENT has been developed to simulate the environment and the response of sprinkler links in compartment fires with draft curtains and fusible-link-actuated ceiling vents. The use of LAVENT is presented by a series of exercises in which the reader reviews and modifies a default input data file which describes vent and sprinkler actuation during fire growth in an array of wood pallets located in a curtained warehouse-type of configuration. Results of the default simulation are discussed. LAVENT is written in FORTRAN 77. The executable code operates on PCcompatible computers and requires a minimum of 252 kilobytes of memory.

900,095 PB89-231187 PB89-231187 Not available NTiS National Inst. of Standards and Technology (NEL), Gaithersburg, MD. Fire Safety Technology Div. Test Results and Predictions for the Response of Near-Celling Sprinkler Links in a Full-Scale Com-partment Fire. Final rept.

L. Y. Cooper, and D. W. Stroup. 1989, 10p See also PB88-113741. Sponsored by Fire Administra-

rion, Emmitsburg, MD.
Pub. in Proceedings of International Symposium Fire Safety Science (2nd), Tokyo, Japan, June 13-17, 1988,

p623-632, 1989, Keywords: *Sprinkler systems, *Fire tests, *Safety engineering, Fire prevention, Smoke, Heat transfer, Buildings, Fire detection systems, Comparisons, De-

Data acquired during tests involving full-scale, sprink-lered compartment fires are presented and analyzed.

Attention is focused on key features of the typical sprinker link deployment/response problem. It is found that the elevated-temperature smoke layer which develops inevitably in compartment fires can have a major impact on the thermal response of sprinkler links. It is shown that traditionally accepted methods of predicting sprinkler link response which do not ac-count for this upper layer can be totally inadequate. Link response predictions used here involve a method of calculation which does take account of the smoke layer. Favorable comparisons between predictions and experiment are obtained and further validation of the method is recommended. Finally, it is found that sprinkler link-to-ceiling spacing can have a significant effect on the thermal response of links and it is recommended that a method which accounts for this effect be developed and validated.

900,096 PB89-235873 PC A04/MF A01 National Inst. of Standards and Technology (NEL), Gaithersburg, MD. Center for Fire Research. Development of a Multiple Layer Test Procedure for Inclusion in NFPA (National Fire Protection Association) 701: Initial Experiments.

S. Davis, and K. M. Villa. Aug 89, 63p NISTIR-89/

Keywords: *Curtains, *Flammability testing, Fire tests, Fabrics, Textiles, Tables(Data), Graphs(Charts).

The research program investigated the flammability behavior of multiple layer fabric assemblies used for draperies and developed a laboratory-scale test proto-col for predicting full-scale fire behavior. The need for such a study arose from recent findings that showed multiple layers of fabrics, comprised of individual fabrics which meet the requirements of National Fire Protection Association (NFPA) 701, may present a serious fire hazard. Eight combinations of four drapery fabrics and two lining fabrics were examined using variants of two established test procedures for single layers: the ASTM D3659 Semi-Restraint Test Method and the NFPA 701 Large-Scale Test Method. The study concludes that neither of the methods, as currently written, adequately predict the full-scale fire behavior of multiple layer fabric assemblies. Based on the results of the study, it is too early to recommend any test pro-tocol for inclusion in NFPA 701.

900,097 PB90-117813

Not available NTIS

National inst. of Standards and Technology (NEL), Gaithersburg, MD. Fire Science and Engineering Div. Experimental Fire Tower Studies of Elevator Pressurization Systems for Smoke Control.

Final rept. G. T. Tamura, and J. H. Klote. 1989, 10p Pub. In Elevator World 37, n6 p80-89 Jun 89.

Keywords: *Elevators(Lifts), *Fire safety, *Smoke abatement, *Pressure control, Pneumatic valves, Relief valves, Ventilation, Fire tests, Air flow, Safety engineering, Buildings, Reprints.

Tests were conducted in the experimental fire tower at the National Research Council of Canada to study smoke movement caused a large fire and to determine the effectiveness of mechanical pressurization in keeping the elevator shaft and lobbies tenable for evacuation of the handicapped and fire-fighting. The tests indicated that pressure control is required to cope with loss of pressurization due to open doors. Equations were developed to assist in designing pres-sure control systems involving either a variable supply air rate with feedback control or relief dampers in the walls of the elevator shaft or lobbies. Tests conducted in the tower indicated that for both methods of pressure control, comparison of measured and calculated values of supply air rates and pressure differences are in good agreement.

Building Standards & Codes

900,098 PB89-149132 Not available NTIS National Bureau of Standards (NEL), Gaithersburg, MD. Structures Div.

Earthquake Hazard Mitigation through Improved

Selsmic Design. Final rept.

C. G. Culver. 1984, 6p Sponsored by Geological Survey, Reston, VA. Pub. in Proceedings of Conference of a Workshop on Geologic Hazards in Puerto Rico (24th), San Juan, Puerto Rico, April 4-6, 1984, p125-130.

Keywords: *Earthquake resistant structures, *Structural design, Design standards, Safety engineering, Structural engineering, Concrete construction, Steel construction, Collapse, Failure.

Buildings and other structures represent a substantial portion of a nation's wealth. For example, the total construction value of buildings and other structures in the United States was estimated at \$2.3 Trillion in 1980. These facilities support a variety of activities ranging from providing basic shelter to facilities housing commercial and industrial functions. Safety and economy are two important factors that must be considered in the design and construction of buildings. Most deaths and injuries during earthquakes result from the failure of man-made structures. Building collapse, falling debris within and around buildings, and the loss of life support systems represent significant hazards. Immediate and long-term economic losses are a direct consequence.

900,099 PB89-149140 Not available NTIS National Bureau of Standards (NEL), Gaithersburg, MD. Structures Div. Earthquake Resistant Design Criteria.

Final rept. G. Culver. 1984, 5p Sponsored by Geological Survey, Reston, VA.
Pub. in Proceedings of Workshop on Earthquake Hazards in the Virgin Islands Region (25th), St. Thomas,
U.S. Virgin Islands, April 9-10, 1984, p103-107.

Keywords: *Earthquake resistant structures, *Design criteria, Building codes, Specifications, Regulations, Concrete construction, Steel construction.

History shows that properly designed and constructed facilities can withstand earthquakes. The design and construction of ordinary buildings are governed by building codes, which are legal documents that specify minimum standards of construction and are adopted by government agencies. A summary of design requirements for earthquake resistant construction in-cluded in the building regulations of various countries throughout the world is available. It is important that

Building Standards & Codes

such design requirements be reviewed periodically and updated to incorporate the results of research and knowledge gained from the performance of buildings in earthquakes.

900,100 PB89-186894 PB89-186894 Not available NTIS
National Bureau of Standards (NEL), Gaithersburg, MD. Structures Div.

Probabilistic Models for Ground Snow Accumulation.

Final rept.

B. Ellingwood. 1984, 10p Pub. in Proceedings of Eastern Snow Conference, v41

p49-58 1984.

Keywords: *Roofs, *Design standards, *Snow, *Loads(Forces), *Meteorological data, Buildings, Structural design, Probability theory, Statistical distribution, Climatology.

Snow loads specified in modern structural design standards, e.g., American National Standard A58 and the National Building Code of Canada, are calculated as the product of a ground snow load and a ground-to-roof conversion factor. The design-basis ground snow loads are sensitive to the choice of probability distribution, since they must be obtained by extrapolating into tion, since they must be obtained by extrapolating into the upper tail of the distribution beyond the range covered by the historical data. The paper considers the selection of probability distributions for modeling annual extreme ground loads, sampling errors caused by limitations in the data, and the sensitivity of nominal design-basis snow loads to these factors. Extensive water-equivalent data from weather stations in the northern United States and Canada are analyzed. The analysis strongly suggests that the log-normal probaextraction of the control of the con

900,101 PB89-231062 Not available NTIS National Inst. of Standards and Technology (NEL), Gaithersburg, MD. Center for Building Technology. Research as the Technical Basis for Standards Used in Building Codes. Final rept.

J. G. Gross. 1989, 6p

Pub. in Proceedings of Pacific Rim Conference of Building Officials, Honolulu, HI, April 9-13, 1989, p51-

Keywords: *Building codes, *Design standards, *Government policies, Regulations, Construction industry, Research, *Center for Building Technology.

Most of the technical requirements in building codes find their basis in national standards which may be adopted by reference or incorporated directly into the adopted by reference or incorporated directly into the body of building codes. National Consensus Standards, which are most widely used and accepted, have their technology based on experience and research. The primary activity of the Center for Building Technology (CBT) at the National Institute of Standards and Technology is research. The research results are provided to standards committees which use the findings for the preparation of National Consensus Standards. Such standards are widely used by the building community for both construction specifications and regula-tory requirements. CBT does not directly produce standards, nor does it have any regulatory authority. This is left to other agencies of federal, state, and local government.

Construction Management & **Techniques**

900,102 PB89-172399 Not available NTIS National Bureau of Standards (NEL), Gaithersburg, MD. Mathematical Analysis Div.

Building Economics in the United States.

H. E. Marshall. 1987, 10p Sponsored by Foras Forbartha Teoranta, Dublin (Ireland).

Pub. in Construction Management and Economics 5, pS43-S52 1987.

Keywords: *Investments, *Construction industry, Benefit cost analysis, Cost engineering, Management methods, Project planning, Thermal efficiency, Cost effectiveness, Return on investment, Reprints.

Building economics is described in the narrow context methods of capital investment analysis applied to building investments in the United States. The common characteristic of all the methods described is that they consider benefits (savings) and costs over the project's life cycle or study period. Eight steps in-volved in making an economic evaluation are present-ed. The process is illustrated with a problem in choosing the economically efficient thermal resistance level of attic insulation. Appropriate applications are described for the following methods: life-cycle cost; net benefits; benefit-to-cost and savings-to-investment ratios; and internal rate of return. Federal and state agencies that use these methods are identified. The role of standards societies and professional organiza-tions in encouraging the use of these methods is de-scribed. Three projects in which these methods have been used are examined briefly in terms of methodology to illustrate the use of building economics methods. A description of difficulties in applying the methods concludes the paper.

900,103 PB89-173819 Not available NTIS MD. Mathematical Analysis Div.

Survey of Selected Methods of Economic Evaluation for Building Decisions.

Final rept. H. E. Marshall. 1987, 35p Pub. in Proceedings of CIB International Symposium on Building Economics (4th), Copenhagen, Denmark, September 14-17, 1987, p23-57.

Keywords: *Construction industry, Technology assessment, Economic analysis, Return on investment, Decision making, Benefit cost analysis, *Building technology nology, Life cycle costs.

The building community needs technically correct, but practical, methods and guidelines for evaluating the economic performance of alternative building technologies. Some of the methods described in the literature and used in practice do not provide the technically correct economic measure. Improved methods help the building community achieve building performance objectives at affordable costs. The paper provides formulas for computing and guidelines on the appropriate use of life-cycle costing, net benefits, benefit-to-cost use of life-cycle costing, net benefits, benefit-to-cost ratio, internal-rate-of-return, and payback methods. These methods are evaluated for making building decisions on accepting or rejecting a given building investment, the cost-effective design or size of a building or component, and the economically efficient combination of projects competing for a limited budget. Techniques available for measuring uncertainty and risk these sets into the methods are surveyed. Some even when applying the methods are surveyed. Some experiences of the United States in applying these methods are described.

900, 104 PB89-174106 PB89-174106 Not available NTIS
National Bureau of Standards (NEL), Gaithersburg, MD. Center for Building Technology.

Trends for Building Technology in North America.

Final rept.
R. N. Wright. 1988, 4p
Pub. in Proceedings of Canadian Building and Construction Congress (5th), Montreal, Canada, November 27-29, 1988, p303-306.

Keywords: *North America, *Construction industry, *Trends, Automation, Forecasting, Competition, Design criteria, Management methods.

Trends in building technology for North America will be dominated by advances in building process technologies: advanced computation and automation. These will facilitate effective responses to demands for increasing the international competitiveness of North American commerce and industry, supporting new industries, commerce and life styles, improving safety and health, and conserving energy and the environment. Advanced information technologies will affect organization of the building process to allow better attention in design to issues such as constructability, maintainability, and productivity of constructed facilities. Automation will advance in design, construction and operation (intelligent buildings) of constructed fa900.105 PB89-191670 PC A03/MF A01 National Bureau of Standards (NEL), Gaithersburg, MD. Center for Building Technology.

Potential Applications of a Sequential Construction Analyzer.

L. W. Masters. May 87, 24p NBSIR-87/3599 Sponsored by Construction Engineering Research Lab. (Army), Champaign, IL.

Keywords: *Sequential analysis, *Construction industry, *Quality assurance, *Construction management, Management methods, Computer systems programs, Maintenance management, Tables(Data).

The need exists in construction applications for improved methods by which (1)quality can be assured throughout the construction process, (2)the degree of construction progress can be assessed and documented and (3)the performance of systems and materials. rials can be assessed over time to aid in maintenance decision-making. Although these aspects of construc-tion processes have traditionally been addressed empirically, recent advances in computer technology have provided new opportunities for improving upon the traditional methods. The Construction Engineering Research Laboratory (CERL) of the U.S. Army's Corps of Engineers, for example, is exploring the use of a sequential construction analyzer to aid in quality assurance, tracking construction progress, and obtaining data for maintenance decision-making. The study was carried out to identify potential applications of the sequential construction analyzer in three areas of construction, buildings, construction sites and paving.

900, 106 PB89-191985 PC A05/MF A01 National Bureau of Standards (NEL), Gaithersburg, MD. Center for Building Technology.

Use of Artificial intelligence Programming Techniques for Communication between Incompatible Building Information Systems.
W. F. Danner. Apr 87, 100p NBSIR-87/3529

Keywords: *Construction industry, *Information systems, *Communicating, *Computer programming, Compatibility, Artificial intelligence, Design, Construction, Data base management systems, Data bases, Protocols, Knowledge representation, *Data transfer protocols.

A communication capability between incompatible information systems is presented. The research develops an interface based on a format for the exchange of ops an interface based on a format for the exchange of knowledge needed by each system to understand the other and a format for the exchange of information in the context of that knowledge. Particular emphasis has been placed on developing protocols supporting the transfer of analytical data. These data are seen as comprising not only facts but also the semantics associated with those facts. Two artificial intelligence programming techniques have been employed: frame-based knowledge representation and object-oriented programming capabilities as an integral part of the frame-based representation. These techniques make self-descriptive formats possible that provide for a virself-descriptive formats possible that provide for a vir-tual extension of an information management system. Such an extension provides access to information without requiring a detailed understanding of specific system operations.

900,107 PB90-112376 PC A03/MF A01 National Inst. of Standards and Technology (NEL), Gaithersburg, MD. Center for Building Technology. Report_of_Roof_Inspection:_Characterization_of Newly-Fabricated Adhesive-Bonded Seams at an

Army Facliity.
W. J. Rossiter, J. F. Seiler, and P. E. Stutzman. Oct 89, 31p NISTIR-89/4155

See also PB89-131916. Sponsored by Corps of Engineers, Baltimore, MD. Baltimore District.

Keywords: *Roofs, *Adhesive bonding, Strength, Seams(Joints), Elastomers, Membranes, Tests, Evaluation, Military facilities, Inspection, Maryland, Aberdeen Proving Ground.

The investigation was a limited study of seams in an EPDM rubber membrane of the roof of the new Wheeled Vehicle Facility' Building at Aberdeen Proying Ground, Maryland. The study was initiated at the request of the Corps of Engineers (CoE) to provide data that could contribute to a data base on the char-

Construction Management & Techniques

acterization of newly-prepared field seams. The investigation was beneficial to the National Institute of Standards and Technology (NIST) because it complemented laboratory research on test methods for evaluating seams of vulcanized rubber roof membranes.

Construction Materials, Components, & Equipment

900,108

PB89-148126 PC A03/MF A01 National Bureau of Standards (NEL), Gaithersburg, MD. Center for Fire Research.

Calculating Flows through Vertical Vents In Zone

Fire Models under Conditions of Arbitrary Cross-Vent Pressure Difference.

L. Y. Cooper. May 88, 17p NBSIR-88/3732

Keywords: *Mathematical models, *Air flow, Algorithms, Pressure gradients, Pressure vessels, Fires, Buildings, Fire safety, *Fire studies.

In typical compartment fire scenarios, ratios of cross-vent absolute pressures are close to 1. When such is the case, algorithms are available to predict the resulting cross-vent room-to-room flows. There are, however, important situations where this pressure condition does not prevail, for example, in fire scenarios involving relatively small penetrations in otherwise hermetically-sealed compartments of fire origin. It is important for a versatile compartment fire model to have a capability of predicting vent flows for the entire range of possible cross-vent pressure conditions. The paper develops a unified analytic description for flows through vertical vents between pairs of two-layer room fire environments under conditions of arbitrary crossvent pressure difference. The analysis, which takes advantage of generally useful modeling approxima-tions, leads to a concise result which is not significantly more complicated than the result for simple, low-pressure-difference cases.

900.109

PC A08/MF A01 PR89-148514 National Inst. of Standards and Technology (NEL), Gaithersburg, MD. Building Environment Div.
Prellminary Performance Criteria for Building Materials, Equipment and Systems Used in Detention

and Correctional Facilities. R. D. Dikkers, R. J. Husmann, J. H. Webster, J. P.

Sorg, and R. A. Holmes. Jan 89, 157p NISTIR-89/4027

Prepared in cooperation with Omni Signal, Inc., Capitola, CA., Webster (James H.), Arlington, VA., Sorg (John P.), Annandale, VA., and Sure-Lock Holmes, Inc., Albany, NY.

Keywords: *Construction materials, *Materials specifications, Performance standards, Criteria, Security, Internal security, Design standards, Facilities management, Planning, Site surveys, Warning systems, Communications equipment, *Correctional institutions.

In a National Institute of Corrections (NIC) sponsored study, many important criteria and standards which need to be developed for improving the selection of materials, equipment and systems for use in detention and correctional facilities were identified. The preliminary performance criteria for materials, equipment, and systems contained in the report have the following objectives: establish performance levels which are consistent with the security and custody levels used in detention and correctional facilities; and establish standard performance measures with regard to securiby, safety and durability. Part I contains general criteria pertaining to the overall facility. Part II contains requirements and criteria relating to the perimeter security of the facility. Part III includes requirements and criteria pertaining to structural systems, doors, windows, glazing, locks, control center, alarms and communica-tion systems.

900,110

PB89-150734 Not available NTIS National Bureau of Standards (NEL), Gaithersburg, MD. Building Materials Div.

Knowledge Based System for Durable Reinforced Concrete.

Final rept. J. R. Clifton, 1986, 6p. Pub. in Proceedings of Corrosion/86 Symposium on Computers in Corrosion Control, Houston, TX., p110-115 1986.

Keywords: *Reinforced concrete, *Concrete durability, Durability, Corrosion, Reinforcing steel, Cement aggregate reactions, Sulfate resisting cements, Recommendations, Industrial engineering, Systems engineering, Expert systems.

DURCON is a prototype expert system being developed to give recommendations on the selection of constituents for durable concrete. Four major concrete deterioration problems are being covered by DURCON: corrosion of reinforcing steel, freeze-thaw, sulfate attack, and cement-aggregate reactions. In this report, the portion of DURCON dealing with corrosion of reinforcing steel is discussed. The factual knowledge based for DURCON is based on the American Concrete Institute Guide to Durable Concrete. Heuristic knowledge is being obtained from experts on the durability of concrete. The approach taken in developing DURCON is discussed. Then a model expert system for the corrosion of reinforcing steel is described.

900,111 PB89-157275 Not available NTIS Mational Bureau of Standards (NEL), Gaithersburg, MD. Fire Science and Engineering Div. Analytical Methods for Firesafety Design. Final rept.

J. G. Quintiere. 1988, 20p See also PB88-153333.

Pub. in Fire Technology 24, n4 p333-352 Nov 88.

Keywords: *Fire safety, *Building codes, Fire prevention, Fires, Safety engineering, Mathematical models, Design criteria, Building, Standards, Reprints.

The ability to predict aspects of fire and its impact on a building's structure, contents, and people is discussed in terms of its application to safety design. It is presented from the perspective of how research has addressed the prediction of fire phenomena. A review of the state of the art on the capability for predicting the fire, its impact and response, is given. Examples are cited to illustrate the scope and accuracy of predictive methods and how they are being incorporated into some codes and standards.

PB89-158000 Not available NTIS National Bureau of Standards (NEL), Gaithersburg, MD. Building Materials Div.

Prediction of Service Life of Building Materials and

Components.

L. W. Masters. 1986, 6p Pub. in Mater. Struct. 19, n114 p417-422 Nov/Dec 86.

Keywords: *Construction materials, *Service life, Predictions, Estimates, Maintenance, Selection, Durability, Research projects, Degradation, Reprints.

Data on service life are essential to the effective selection, use and maintenance of materials and components used in buildings. Changing technologies and re-quirements in recent years have re-emphasized the need to advance the state of knowledge of service life prediction, resulting in a number of new internationally sponsored activities including a joint Technical Committee of CIB and RILEM. In the paper, recent activities of the CIB/RILEM committee are described by summarizing the technical barriers to service life prediction and outlining courses of direction and types of research which can help overcome the barriers.

900,113 PB89-162580 PC A06/MF A01 National Inst. of Standards and Technology (NEL), Gaithersburg, MD. Center for Building Technology.

Corrosion of Metallic Fasteners In Low-Sloped Roofs: A Review of Available Information and Identification of Research Needs.

W. J. Rossiter, M. A. Streicher, and W. E. Roberts. Feb 89, 105p NISTIR-88/4008

Prepared in cooperation with Webster Farm, Wilmington, DE. Sponsored by Department of Energy, Washington, DC.

Keywords: *Fasteners, *Corrosion, *Roofs, Joining, Durability, Deterioration, Roofing, Research projects.

The paper presents the results of a study conducted to summarize available information on the corrosion issue, and to identify research needed to correct problems. In particular, the incidence of loss of fastener se-curement due to corrosion could not be established because of the inaccessibility of installed fasteners within roofs. In reviewing factors affecting fastener corrosion, water was the only one that stood out on the basis of the information obtained. Uniform corrosion (rust on some or all of the surface) was the predominant type that inspectors have observed in service. Nevertheless, some evidence of localized corrosion processes (e.g., crevice corrosion) has also been observed. Both types of corrosion may lead to loss of fastener securement in service. The results of the study indicated that there are three major gaps in the knowledge base: (1) evaluation test procedures for the corrosion resistance of fasteners are limited and need to be improved; (2) a data base on field performance of fasteners is lacking, and; (3) non-destructive diagnostic procedures for assessing the condition of inplace fasteners are not available.

900.114

PB89-168025 PC A04/MF A01 National Inst. of Standards and Technology (NEL), Gaithersburg, MD. Building Materials Div.

Interim Criteria for Polymer-Modified Bituminous Roofing Membrane Materials.

Final rept.

W. J. Rossiter, and J. F. Seiler. Feb 89, 52p NIST/ BSS-167

Also available from Supt. of Docs. as SN003-003-02922-0. Library of Congress catalog card no. 89-600702. Sponsored by Tri-Service Building Materials Committee, Washington, DC.

Keywords: *Roofing, *Bituminous coatings, *Polymers, Bitumens, Stability, Fire resistance, Viscosity, Mechanical properties, Absorption, Moisture content, Performance standards, Military facilities.

The report presents the results of a study to develop interim criteria for the selection of polymer-modified bituminous roofing membrane materials. The criteria are based on a review of existing standard specifications and related documents. They are intended for use by the construction agencies of the Department of Defense in specifying polymer-modified bituminous roofing membrane materials until voluntary consensus standards are developed in the United States. The suggested interim criteria are generally presented using a performance criteria format. The membrane characteristics for which performance criteria are sug-gested are: dimensional stability, fire, flow resistance, hail impact, moisture content and absorption, pliability, strain energy, uplift resistance, and weathering resistance (heat exposure). Prescriptive criteria for five membrane characteristics are used to complement the suggested performance criteria. The approach of using complementary prescriptive criteria is taken to incorporate in the performance criteria test methods which can be relatively rapidly performed for characterization or identification of the membrane material.

900,115

PB89-171748 Not available NTIS National Bureau of Standards (NEL), Gaithersburg, MD. Structures Div.

Damage Accumulation in Wood Structural Members Under Stochastic Live Loads.

Final rept. J. Murphy, B. Ellingwood, and E. Hendrickson. 1987, 11p Pub. in Wood and Fiber Science 19, n4 p453-463

Keywords: *Structural forms, *Construction materials, *Loads(Forces), *Wood products, *Damage, *Creep rupture tests, Stochastic processes, Stress concentra-

tion, Specifications, Reprints.

Damage accumulation in wood structural members is assessed using realistic stochastic models of live load. It is found that practically all damage occurs at times when the live load intensity is equal, or nearly equal to the nominal live load, L sub n, required by codes for design. The time spent at or above the nominal life load, L sub n, is about 40 days during a reference period of 50 years, and not the presently assumed time of 10 years. Using 10 years as the basis for setting allowable stresses for wood should be reexamined.

Construction Materials, Components, & Equipment

900.116

PB89-172514 Not available NTIS National Bureau of Standards (NEL), Boulder, CO. Chemical Engineering Science Div.

Specific Heat of Insulations. Final rept.

J. G. Hust, J. E. Callanan, and S. A. Sullivan. 1985, 18p

Sponsored by Oak Ridge National Lab., TN. Pub. in Thermal Conductivity 19, p533-550 1985.

Keywords: *Thermal insulation, *Specific heat, Thermophysical properties, Latent heat, Heat of vaporization, Moisture content, Temperature, Thermal conductivity, Measurement, Thermal diffusivity, Reprints, *Standard Reference Materials.

The specific heats of insulation Standard Reference Materials(SRMs) have been measured for tempera-tures from 250 to 400 K for both dry and moist specimens. Measurements were performed on SRM 1450b, SRM 1451, a high temperature SRM candidate, and on specimens of the phenolic binder used in SRM 1451. The measured specific heats of moist specimens are significantly larger than the specific heats of dry speci-mens due to the effect of latent heat of vaporization and desorption of the moisture. These results are analyzed in terms of the differences that may be observed between steady-state and transient thermal conductance measurements.

900.117

PB89-172548 Not available NTIS National Bureau of Standards (NEL), Boulder, CO. Chemical Engineering Science Div.
Insulation Standard Reference Materials of Ther-

mal Resistance.

Final rept.

J. G. Hust. 1985, 9p Pub. in Thermal Conductivity 19, p261-269 1985.

Keywords: *Thermal insulation, *Thermal resistance, Heat transmission, Thermophysical properties, Thermal conductivity, Fiberboards, Low temperature tests, Measurement, Thermal diffusivity, Reprints, *Standard Reference Materials.

The National Bureau of Standards recently established two insulation Standard Reference Materials(SRMs) of thermal resistance. These SRMs are available from the Office of Standard Reference Materials. The paper provides a brief description of these SRMs and provides comparisons to similar materials for tempera-tures from 100 to 330 K. A brief description of present and planned research for the establishment of further SRMs is also provided.

900.118

PB89-173454 Not available NTIS National Bureau of Standards (NEL), Gaithersburg, MD. Electrosystems Div.

Coupling, Propagation, and Side Effects of Surges in an Industrial Building Wiring System. Final rept.

Final rept.
F. D. Martzloff. 1988, 10p
Pub. in Conference Record of the IEEE (Institute of Electrical and Electronics Engineers)-IAS (Industry Applications Society) Annual Meeting, Pittsburgh, PA., October 3-6, 1988, p1467-1476.

Keywords: *Surges, *Industrial buildings, *Power lines, Measurement, Electric wire, Electromagnetic interference, Electromagnetic radiation, Coupling circuits, Wave propagation.

Measurements were made in an industrial building to determine the propagation characteristics of surges in the AC power wiring of the facility. The surges, of the unidirectional type or the ring-wave type described in ANSI/IEEE C62.41-1980, were injected at one point of the system and the resulting surges arriving at other points were measured. The results show how unidirectional surges couple through transformers and produce a ring wave component in the response of the system. An unexpected side effect of these surges, applied to the power lines only, was apparent damage suffered by the data line input components of some computer-driven printers.

PB89-174916 Not available NTIS National Bureau of Standards (NEL), Gaithersburg, MD. Building Environment Div.

Thermal Resistance Measurements and Calculations of an Insulated Concrete Block Wall. Final rept.

D. M. Burch, B. A. Licitra, D. F. Ebberts, and R. R.

D. M. Burch, B. A. Licita, D. P. Ebberts, and R. H. Zarr. 1989, 7p Sponsored by Department of Energy, Washington, DC. Pub. in ASHRAE (American Society of Heating, Refrigerating and Air-Conditioning Engineers) Transactions 95, pt1 7p 1989.

Keywords: *Concrete blocks, *Thermal resistance, *Thermal insulation, *Thermal measurements, *Walls, Temperature gradients, Polystyrene, Temperature, Reprints.

Thermal resistance measurements of an insulated concrete block wall were conducted using a calibrated hot box at four different mean temperatures. The hollow concrete block wall was insulated by installing hollow concrete block wall was insulated by installing partial-size inserts composed of expanded polystyrene insulation with reflective air spaces into the cores of the blocks. The thermal resistance measurements were compared with the ASHRAE isothermal plane and parallel path methods. The isothermal plane method was subsequently used to calculate the thermal resistance of uninsulated concrete block, concrete block with full-size insulation inserts, and concrete block with partial-size insulation inserts. Both ways of insulating the concrete block increased the thermal resistance of the uninsulated block by more than a factor

PB89-175848 Not available NTIS Not available N15
National Bureau of Standards (NEL), Gaithersburg,
MD. Building Materials Div.

Prediction of Service Life of Construction and

Other Materials.

Final rept.

G. Frohnsdorff, and L. W. Masters. 1986, 4p Pub. in Communications on the Materials Science and Engineering Study, p61-64 1986.

Keywords: *Construction materials, *Service life, Durability, Design criteria, Reliability, Forecasting, Quality control, Maintenance, Standards, Cost engineering,

A major need in construction technology is to be able to predict the service lives of materials. The need is shared with other technologies, and prediction of the service life of construction materials can use techniques of reliability engineering used in other industries. In the last decade, several important steps have been taken toward development and standardization of a methodology for service life prediction of con-struction materials and components. These activities have influenced the way service lives of construction materials are evaluated, but more needs to be done. It is recommended that the materials science and engineering community encourage the development of improved methodologies for service life prediction and provide guidance on how the methodologies should be applied.

900.121

Not available NTIS National Bureau of Standards (NEL), Gaithersburg, MD. Office of Energy-Related Inventions.

U-Value Measurements for Windows and Movable

Insulations from Hot Box Tests in Two Commercial Laboratories.

M. E. McCabe, W. Ducas, R. W. Cholvibul, and P. Wormser. 1986, 21p

Sponsored by Department of Energy, Washington, DC.

Office of Solar Heat Technologies.
Pub. in ASHRAE (American Society of Heating, Refrigerating and Air-Conditioning Engineers) Transactions 92, pt1A p453-473 1986.

Keywords: *Windows, *Thermal insulation, Solar energy, Design, Architecture, Tests, Wind velocity, Performance evaluation; Simulation, Comparisons, Reprints, *Energy conservation.

Different laboratory test procedures (ASTM 236, ASTM C976 and AAMA 1503.1) are discussed in the context of measuring the U-Value of direct gain fenestration (DGF) components. Four representative DGF components, including a multiple-glazed window and a single-glazed window with movable insulation systems, were purchased and prepared for testing. U-Values were measured for each test article at two commercial testing laboratories, using the ASTM 236 and AAMA 1502.6 test methods for a range of simulated outdoor conditions. For the three movable insulation test articles, manufacturer's claims for energy sav-ings were also overstated, suggesting the need for a standard method for estimating energy performance. Test results between individual laboratories are compared and significant differences are noted where wind speeds of 6.7 m/s (15 mph) were simulated. The differences are attributed to the different directions (parallel and perpendicular) used by each laboratory for simulating wind. The suitability of a single test condi-tion for measuring U-Value is discussed in relation to the use of that test data for estimating seasonal thermal performance.

900.122

PB89-176168 Not available NTIS National Bureau of Standards (NEL), Gaithersburg, MD. Fire Safety Technology Div. Fundamentals of Enclosure Fire 'Zone' Models.

Final rept. J. G. Quintiere. 1988, 47p

Pub. in Proceedings of National Fire Protection Association Annual Meeting for Society of Fire Protection Engineers, Cincinnati, OH., May 18, 1988, 47p.

Keywords: *Fires, *Enclosures, Fire protection, Safety engineering, Model tests, Open channel flow, Fire control.

The conservation laws are presented in control volume form and applied to the behavior of fire in enclosures. The behavior of enclosure fires are discussed and the assumptions for justifying the use of the control volume or 'zone' modeling approach are presented. The governing equations are derived and special solutions are given. Flow through wall vents, room filling, and growing fires are analyzed.

900,123

PB89-176309 Not available NTIS National Bureau of Standards (NEL), Gaithersburg,

MD. Building Materials Div.

Thermographic Imaging and Computer Image Processing of Defects in Building Materials.

J. W. Martin, M. E. McKnight, and D. P. Bentz. 1986,

Pub. in Proceedings of SPIE (Society of Photo-Optical Instrumentation Engineers) International Conference on Thermal Infrared Sensing for Diagnostics and Control, Cambridge, MA., September 17-20, 1985, p152-155 1986.

Keywords: *Construction materials, *Defects, *Thermography, Degradation, Nondestructive tests, *Image processing, Image enhancement, Image analysis.

An image processing system has been coupled to either a thermographic or a video camera for quantifying defects in images of building materials. Several applications to building materials are presented including the detection of delaminations in single-ply roofing membrane seams, the characterization of the extent of corrosion under pigmented organic coatings on metal-lic substrates, the determination of the fractal dimensions of a sandblasted metallic substrate, and the de-termination of the percent porosity in hydrated cement. It is concluded that infrared thermography and image processing are useful analysis tools in detecting and quantifying defects in building materials.

900,124

Not available NTIS PB89-180004 MD. Fire Science and Engineering Div.

Recent Activities of the American Society for Test-

ing and Materials Committee on Fire Standards. Final rept.

D. Gross. 1985, 2p Pub. in Fire and Materials 9, n2 p109-110 1985.

Keywords: *Fires, *Fire tests, Fire protection, Fire prevention, Fire safety, Standards, Flammability tests, Reprints.

A brief summary of selected actions and activities at the recent meeting of ASTM Committee E5 on Fire Standards is presented.

900,125

PB89-184527 PC A08/MF A01 California Univ., Los Angeles. Dept. of Mechanical, Aerospace and Nuclear Engineering.

Construction Materials, Components, & Equipment

Fire Risk Analysis Methodology: Initiating Events. Final rept.

M. D. Brandyberry, and G. E. Apostolakis. Mar 89, 165p NIST/GCR-89/562

Grant NANB-6-D0649

Sponsored by National Inst. of Standards and Technology (NEL), Gaithersburg, MD. Center for Fire Research.

Keywords: *Fires, *Ignition, *Space heaters, *Upholstery, Heat transfer, Drawings, Tables(Data), Models, Probability distribution functions, *Risk assessment.

The report outlines a method for assessing the frequency of ignition of a consumer product in a building and shows how the method would be used in an example scenario utilizing upholstered furniture as the product and radiant auxiliary heating devices (electric heaters, wood stoves) as the ignition source. Deterministic thermal models of the heat transport processes are coupled with parameter uncertainty analysis of the models and with a probabilistic analysis of the events involved in a typical scenario. This leads to a distribution for the frequency of ignition for the product.

900,126
PB89-188635
PC A04/MF A01
National Inst. of Standards and Technology (NEL),
Gaithersburg, MD. Center for Fire Research.
Fire Properties Database for Textile Wall Cover-

Ings.
M. F. Harkleroad. Apr 89, 54p NISTIR-89/4065
Sponsored by American Textile Manufacturers Inst.,
Washington, DC.

Keywords: *Data bases, *Fire safety, *Textiles, *Walls, Flammability, Materials, Physical properties, Ignition, Flame propagation, Polyester fibers, Nylon fibers, Rayon, Polypropylene fibers, Charring, Wall coverings.

A technical basis for linking small scale fire property test data to realistic performance has been initiated by the establishment of a small scale fire property database for some textile wall covering materials. The properties are obtained from experimental small-scale tests of materials in a vertical orientation. They include tests of materials in a vertical orientation. They include tests of materials in a vertical orientation. They include tests from the Lateral Ignition and Flame spread Test (LIFT) apparatus and energy release rate measure (LIFT) apparatus and energy release rate measure ments from the Cone Calorimeter. The database includes fire properties for woven, knit and needle punched polyesters, woven cotton/rayon and wool/nylon blends, nylon and polypropylene wall covering materials.

900,127
PB89-189187
PC A09/MF A01
Michigan State Univ., East Lansing. Dept. of Mechanical Engineering.

Effect of Water on Piloted Ignition of Cellulosic Materials.

Doctoral thesis.

M. Abu-Zaid, and A. Atreya. Feb 89, 187p NIST/ GCR-89/561

Grant NANB-5DO578

See also PB87-127732. Sponsored by National Inst. of Standards and Technology (NEL), Gaithersburg, MD. Center for Fire Research.

Keywords: *Water, *Ignition, *Fire protection, Pyrolysis, Fire extinguishing agents, Wood, Flame propagation, Drops(Liquids), Graphs(Charts), Flammability testing, Heat transfer, Porous materials, *Cellulosic materials.

The experimental study is an attempt to quantify the effect of water on extinguishment; thermal decomposition and piloted ignition of wood. In the extinguishment part, cooling of hot porous and non-porous ceramic solids by water droplets was studied. These solids were used to simulate low thermal diffusivity porous and non-porous combustible building materials and were instrumented by several surface and in-depth thermocouples. Temperature measurements in the solid were used to quantify the heat transfer during droplet evaporation. Thermal decomposition of wood in air was also studied as a function of sample moisture content and externally applied radiation prior to the ignition experiments. Simultaneous measurements of weight loss rate; surface, bottom and in-depth temperatures; O2 depletion and production of CO2, CO, total hydrocarbons and water were made. It was found that the presence of moisture delayed the decomposition process and diluted the decomposition products. Piloted ignition experiments were conducted on Doug-

las fir for four different moisture contents and at different levels of externally applied radiation. It was found that the presence of moisture increases the ignition time, surface temperature and the evolved mass flux at ignition. A single equation was derived to correlate all the ignition data. This correlation accounts for the moisture dependent thermal properties and the heat loss from the sample surface.

900,128
PB89-189252
PC A03/MF A01
National Inst. of Standards and Technology (NEL),
Gaithersburg, MD. Center for Fire Research.
Calculation of the Flow Through a Horizontal Cell-

Ing/Floor Vent.
L. Y. Cooper. Mar 89, 31p NISTIR-89/4052
Sponsored by Naval Research Lab., Washington, DC.

Keywords: *Air flow, *Vents, *Fire safety, *Buildings, Algorithms, Mathematical models, Pressure gradients, Fires, Temperature.

Calculation of the flow through a horizontal vent located in a ceiling or floor of a multi-room compartment is considered. It is assumed that the environments of the two, vent-connected spaces near the elevation of the vent are of arbitrary relative buoyancy and cross-vent pressure difference, delta p. An anomaly of the standard vent flow model, which uses delta p to predict stable uni-directional flow according to Bernoulli's equation is discussed. The problem occurs in practical vent configurations of unstable hydrostatic equilibrium, where, for example, one gas overlays a relatively less-dense gas, and where delta p is relatively small. In such configurations the cross-vent flow is not uni-directional. Also, it is not zero at delta p = 0. Previously published experimental data on a variety of related flow configurations are used to develop a completely general flow model which does not suffer from the standard model anomaly. The model developed leads to a uniformly valid algorithm, called VENTCL, for horizontal vent flow calculations suitable for general use in zone-type compartment fire models.

900,129
PB89-189260
PC A03/MF A01
National Inst. of Standards and Technology (NEL),
Gaithersburg, MD. Center for Fire Research.
Fire Induced Flows in Corridors: A Review of Efforts to Model Key Features.
K. D. Steckler. Feb 89, 26p NISTIR-89/4050

K. D. Steckler. Feb 89, 25p NISTH-8974050 Sponsored by General Services Administration, Washington, DC.

Keywords: *Buildings, *Fire tests, Gas flow, Directional measurement, Fire safety, Mathematical models, *Corridors.

A literature review was undertaken to identify engineering formulas or models which can be used to predict key features of the corridor-filling process. The results of that review are presented and assessed. The filling process is viewed as a series of three events: a forward gravity current moving away from the fire source, a reflected or return gravity current moving toward the source, followed by uniform filling of the entire corridor. Recommendations for estimating the filling during each of these stages are presented.

900,130
PB89-189328
PC A04/MF A01
National Inst. of Standards and Technology (NEL),
Gaithersburg, MD. Center for Building Technology.
Frlability of Spray-Applied Fireproofing and Thermal Insulations: Field Evaluation of Prototype Test
Devices.

W. J. Rossiter, W. E. Roberts, and R. G. Mathey. Mar 89, 64p NISTIR-88/4012 See also PB89-131924. Sponsored by General Services Administration, Washington, DC.

Keywords: *Thermal insulation, *Fire resistant materials, *Friability, Mechanical tests, Brittleness, Toughness, Shear, Tests, Abrasion, Compressive strength.

The report describes results of the third and final phase of a study conducted for the General Services. Administration (GSA) to develop a field test method to measure the friability of spray-applied fireproofing and thermal insulation materials. Field tests were conducted on 17 fibrous and 2 cementitious spray-applied materials to assess surface and bulk compression/shear, indentation, abrasion, and impact properties. The tests were performed using prototype devices developed in an earlier phase of the study. As expected, the field specimens displayed varying response to dislodgment

or indentation in the tests. The field tests confirmed that the goal of the study had been achieved.

900,131
PB89-193213
PC A05/MF A01
National Inst. of Standards and Technology (NEL),
Gaithersburg, MD. Center for Building Technology.
Building Technology Project Summarles 1989.
N. J. Raufaste. Apr 89, 86p NISTIR-89/4068
See also PB88-215512.

Keywords: *Construction industry, *Construction materials, *Project management, Research management, Cost engineering, Contract administration, Performance analysis, *Building technology.

The Center for Building Technology (CBT) of the National Institute of Standards and Technology (NIST) is the national building research laboratory. CBT works cooperatively with other organizations, private and public, to improve building practices. It conducts laboratory, field, and analytical research to predict, measure, and test the performance of building materials, components, systems, and practices. CBT's technologies are widely used in the building industry and adopted by governmental and private organizations that have standards and codes responsibilities. The report summarizes the research underway in the Center during 1989.

900,132
PB89-193304
PC A03/MF A01
National Inst. of Standards and Technology (NEL),
Gaithersburg, MD. Center for Fire Research.
Fire Research Publications, 1988.
N. H. Jason. May 89, 42p NISTIR-89/4081
See also PB88-199641.

Keywords: *Fire safety, *Bibliographies, Safety engineering, Burning rate, Smoke, Ventilation, Sprinkler systems, Flame propagation, Fire resistant materials, Heat measurement.

The document is a supplement to previous editions. Only publications prepared by members of the Center for Fire Research (CFR), by other National Institute of Standards and Technology (NIST) (formerly National Bureau of Standards (NBS)) personnel for CFR, or by external laboratories under contract or grant from the CFR are cited.

900,133
PB89-195671
PC A05/MF A01
National Inst. of Standards and Technology (NEL),
Gaithersburg, MD. Center for Fire Research.
Considerations of Stack Effect In Bullding Fires.
J. H. Klote. May 89, 83p NISTIR-89/4035
Sponsored by Fire Administration, Emmitsburg, MD.

Keywords: *Fire safety, *Fires, *Buildings, Smoke, Air flow, Convection, Mathematical models, Elevators, Combustion, Vents.

The following driving forces of smoke movement in buildings are discussed: stack effect, buoyancy of combustion gases, expansion of combustion gases, wind effect, and elevator piston effect. Based on an analysis of elevator piston effect, it is concluded that the likelihood of smoke being pulled into an elevator shaft due to elevator car motion is greater for single car shafts than for multiple car shafts. Methods of evaluating the location of the neutral plane are presented. It is shown that the neutral plane between a vented shaft and the outside is located between the neutral plane height for an unvented shaft and the vent elevation.

900,134

PB89-200091

National Inst. of Standards and Technology (NEL), Gaithersburg, MD. Center for Fire Research.

Executive Summary for the Workshop on Developing a Predictive Capability for CO Formation in

W. M. Pitts. Apr 89, 72p NISTIR-89/4093

Keywords: *Fires, *Carbon monoxide, *Meetings, Combustion, Gases, Fire hazards, Toxicity.

The proceedings and recommendations of a workshop entitled 'Workshop on Developing a Predictive Capability for CO Formation in Fires' are summarized. The meeting took place on December 3-4, 1988 in Clearwater, Florida. Several brief technical presentations are critiqued. Short summaries for each talk are includ-

Construction Materials, Components, & Equipment

ed in an appendix. Findings of two working groups constituted to address the fundamental and engineering aspects of the workshop topic are discussed. The most important areas of research required to fulfill the workshop topic are provided as final recommenda-tions. Six specific areas are listed. Many workshop details are included in appendices.

900,135 PB89-201149 PB89-201149 Not available NTIS National Bureau of Standards (NEL), Gaithersburg, MD. Statistical Engineering Div.

Statistical Analysis of Experiments to Measure ig-nition of Cigarettes.

Final rept.

Final Top.

K. R. Eberhardt. 1988, 10p

Pub. in Jnl. of the Washington Academy of Sciences 78, n4 p323-332 Dec 88.

Keywords: *Ignition, *Statistical analysis, *Flammability testing, Combustion, Experimental data, Chi square test, Probability theory, Reprints, *Cigarettes.

Under the Cigarette Safety Act of 1984, NIST was given the task of studying several types of commercial and experimental cigarettes to determine their relative propensities to ignite soft furnishings. The analysis of the data came under close scrutiny by the Technical Study Group appointed to oversee the research. In one experiment where the usual chi-squared test could not be readily justified, an extension of Fisher's Exact Test to 2 x 12 contingency tables was adopted. In another experiment, a modification of the angular transformation for count data was used along with normal probability plots of the effects to analyze a 2(sup 5) factorial experiment.

PB89-209316 PC A03/MF A01 National Inst. of Standards and Technology (NEL), Gaithersburg, MD. Center for Building Technology. Results of a Survey of the Performance of EPDM (Ethylene Propylene Diene Terpolymer) Roofing at Army Facilities. W. J. Rossiter, and J. F. Seiler. Jun 89, 28p NISTIR-

89/4085

Sponsored by Construction Engineering Research Lab. (Army), Champaign, IL.

Keywords: *Roofs, *Ethylene copolymers, *Performance evaluation, Maintenance, Military facilities, Mechanical properties, Weathering, Seams(Joints), Sur-

The report presents a summary of a survey to obtain information on the performance of EPDM roofing at Army facilities. Emphasis in the survey was on the performance of seams fabricated with unaged rubber and also patches made on existing, aged rubber. The results are intended to help provide guidelines for the maintenance of EPDM roofs at Army facilities, as well as to define research needs to overcome problems identified. Based on the results of the survey, it is recommended that studies be carried out to provide the technical basis for preparing the surfaces of aged rubber membranes before making seams or patches. The effect of aging on the surface characteristics of EPDM rubber has received little attention in the roofing literature.

900,137 PB89-212005 Not available NTIS National Bureau of Standards (NEL), Gaithersburg, MD. Fire Science and Engineering Div.

Refinement and Experimental Verification of a

Model for Fire Growth and Smoke Transport. Final rept.

W. W. Jones, and R. D. Peacock. 1989, 10p Pub. in Proceedings of International Symposium on Fire Safety Science (2nd), Tokyo, Japan, June 13-17, 1988, p897-906 1989.

Keywords: *Fires, Ignition, Fire safety, Fire tests, Experimental data, Algorithms, Numerical analysis, Verifying, *Fire models.

There is considerable interest in modeling the growth of fires and the spread of toxic gases in multicompartment structures. Much of the attention is focused on the development of numerical models which are fast and robust, but able to make reasonably accurate pre-dictions from the onset of ignition. The authors have constructed such a model (FAST) and performed a series of validation experiments to test it. The paper discusses some of the improvements which have been made to physical algorithms and the underlying numerical basis of the model, a description of some of the experiments used to verify the refined model, and of some additions which the authors intend to incorpo-

900,138 PB89-212120 Not available NTIS National Bureau of Standards (NEL), Gaithersburg, MD. Building Materials Div.

Tests of Adhesive-Bonded Seams of Single-Ply

Rubber Membranes.

Final rept.

W. J. Rossiter. 1987, 10p

Pub. in Proceedings of ASTM (American Society for Testing and Materials) Symposium on Roofing Research and Standards Developn

t, New Orleans, 14, December 2, 1987, 1982, 1982, 1982 LA., December 3, 1986, p53-62 1987.

Keywords: *Roofing, *Ethylene copolymers, *Membranes, *Mechanical tests, Elongation, Loads(Forces), High temperature tests, Shear properties, Stress relaxation, Seams(Joints), Failure.

Commercially-available ethylene propylene diene ter-polymer (EPDM), neoprene, and chlorosulphonated polyethylene (CSME) roofing membrane specimens with adhesive-bonded seams were tested in tension in lap-shear configuration. Some T-peel tests of an a lap-shear configuration. Some 1-peel tests of an EPDM material were also conducted. The lap-shear tests were conducted at temperatures ranging from -20 to 75 C (-4 to 167 F), and at rates of loading from 0.05 to 50 cm/min (0/02 to 20 in/min). In most cases, the EPDM and neoprene specimens failed by seam delamination; otherwise, they failed by membrane rupture with partial delamination of the seam. The CSME represence always failed by membrane rupture without specimens always failed by membrane rupture without seam delamination. In general, the results indicated that, as the temperature of the test increased, the ultimate load and elongation at failure decreased. Also, at a given temperature, the ultimate load and elongation general decreased, for most specimens, as the rate of loading decreased. For stress relaxation experiments, specimens strained to 15% remained intact for over 15 months, whereas other specimens strained to 30% failed in about five weeks. The results of the tests are discussed with regard to the development of tests for seams in single-ply membranes.

900,139 PB89-212203 PB89-212203 Not available NTIS National Bureau of Standards (NEL), Gaithersburg,

MD. Building Materials Div.
Strain Energy of Bituminous Built-Up Membranes:
A New Concept in Load-Elongation Testing.

Final rept. W. J. Rossiter, and D. P. Bentz. 1987, 10p See also P887-138376.

Pub. in Proceedings of Conference on Roofing Technology (8th) 'Applied Technology for Improving Roof Performance', Gaithersburg, MD., April 16-17, 1987, p40-49.

Keywords: *Roofing, *Bitumens, *Strain energy methods, *Tensile strength, Elongation, Mechanical properties, Loads(Forces), Polyester fibers, Performance standards, Mechanical tests.

The study was conducted to revise the performance criterion for tensile strength of bituminous built-up membranes. Bituminous membrane samples, fabricated from polyester fabric, polyester-glass composite fabric, and single plies of APP- and SBS-modified bitumen, were tested in tension to determine their loadelongation properties and to measure their strain energy. The results of the tensile tests of the new bitu-minous membranes indicated wide variability of load minous membranes indicated wide variability of load and elongation among the different types of materials. As an alternative to the criterion that a bituminous built-up membrane have a tensile strength of 200 lbf/ in (35 kN/m), it was recommended that the strain energy should be a minimum of 3 lbf/in/in (14 N/m/m), when tested at 0 F (-18 C) in the weaker direction.

900,140 PB89-212260 PB89-212260
Not available NTIS
National Bureau of Standards (NEL), Gaithersburg,
MD. Building Materials Div.
ASTM (American Society for Testing and Materials) Committee Completes Work on EPDM Specification

cation.

W. J. Rossiter. 1987, 4p Pub. in Handbook of Commercial Roofing Systems, p26-29 1987.

Keywords: *Roofing, *Materials specifications, *Membranes, Ethylene copolymers, Bitumens, Design

standards, Waterproofing, Construction materials, Reprints.

The use of single-ply membrane materials as the waterproofing component of low-sloped roofing systems has become commonplace in the United States, The growth in their use has not been without concern. One of the key issues confronting the roofing industry since the single-ply materials first appeared has been a lack of standard specifications to aid material selection as of standard specifications to aid material selection as well as roofing systems design. ASTM Committee D08 on Roofing, Waterproofing, and Bituminous Materials is the lead organization to which the U.S. roofing industry turns for guidance in developing voluntary standards. The paper presents an update of the latest developments at ASTM regarding single-ply standards, and in particular, details concerning the expected appearance of the long-awaited specification for EPDM.

900.141

PB89-214787 PC A04/MF A01 Pennsylvania State Univ., University Park. Dept. of Mechanical Engineering.
Upward Flame Spread on Vertical Walls.

Final rept.

A. K. Kulkarni. Jun 89, 70p NIST/GCR-89/565 Grant NANB-4-D0037 Sponsored by National Inst. of Standards and Tech-nology (NEL), Gaithersburg, MD. Center for Fire Re-

Keywords: *Walls, *Pyrolysis, *Flame propagation, Burning rate, Particle boards, Fire safety, Fires, Mathematical models.

Reported is a study of upward flame spread on vertical walls. First, a detailed review of literature on upward flame spread is presented. A 'complete procedure' for predicting upward flame spread on practical materials, which can be used in a global fire hazard assessment model, is then described. Experimental results on upward flame spread on various materials are obtained and the validity of the model is established.

900,142

PB89-215354 PC A05/MF A01
Dayton Univ., OH. Research Inst.
Validated Furniture Fire Model with FAST (HEM-FAST).

Technical rept. Jul 87-Sep 88. M. A. Dietenberger. Dec 88, 90p UDR-TR-88-136, NIST/GCR-89/564

Grant NANB-S-D0556

Sponsored by National Inst. of Standards and Technology (NEL), Gaithersburg, MD. Center for Fire Re-

Keywords: *Furniture, *Fire safety, *Models, Burning rate, Fires, Computer program applications, Upholstery, *Validation.

The technical document reports on the validation of the furniture fire model with the furniture calorimeter data and on the restructure of the program 'HEM-FAST. Significant restructuring of the model and its code resolve various problems associated with the first version of HEMFAST. Comprehensive descriptions of the current model and its code structure bene-fit the HEMFAST users. The descriptions include: data processing of the bench scale fire tests database, effective time integrations of surface temperatures, flame spreads, and burn time, effective couple solutions of pyrolysis rates, burnrates, soot production, and thermal radiation, and the effective interfacing be-tween the furniture fire model and FAST. The model is validated with fire tests for a 4-cushion mockup fire with three different fabric/foam cushion types. The comparisons include: burn area fractions of each cushion as a function of time, burnrate of the mockup as a function of time with fire test data from the furniture calorimeter, mass loss rate of the furniture as a function of time, and the overall levels of soot production.

900,143

PB89-215404 **CP D05** National Inst. of Standards and Technology (NEL), Gaithersburg, MD. Center for Fire Research. HAZARD I Fire Hazard Assessment Method. Software.

R. W. Bukowski, R. Peacock, and W. Jones. May 89, 11 diskettes NBS/SW/DK-89/005 The software is contained on 3 1/2 and 5 1/4-inch dis-

kettes, double density (360K and 720K), compatible

Construction Materials, Components, & Equipment

with the IBM PC XT/AT microcomputer. The diskettes are in the ASCII format.

Keywords: *Software, *Fire hazards, *Fire losses, Fires, Fire damage, Fire safety, Models, Evacuating(Transportation), Human behavior, Diskettes, L=Fortran;Basic;Assembly;Clipper, H=IBM PC/XT/AT;IBM PS2.

The Center for Fire Research has developed HAZARD 1, a method for predicting the hazards to building occupants from a fire. Within prescribed limits, HAZARD 1 allows the user to predict the outcome of a fire in a building populated by a representative set of occupants in terms of which persons successfully escape and which are killed, including the time, location, and likely cause of death for each. Specifically, the microcomputer program involves four procedures that combine expert judgment and calculations to estimate the consequences of a specified fire. Software description: The software is written in Fortran, Basic, Assembly and Clipper programming languages for implementation on an iBM-PC (XT, AT, PS/2) microcomputer under MS-DOS 3.0 (or higher). Memory requirement is 640K. A math co-processor (8087, 80287, or 80387) and a 2Mb hard disk drive are required to operate the system.

900,144
PB89-218325 PC A03/MF A01
National Inst. of Standards and Technology (NEL),
Boulder, CO. Chemical Engineering Science Div.
Interlaboratory Comparison of Two Types of LineSource Thermal-Conductivity Apparatus Measuring Five Insulating Materials.
J. G. Hust, and D. R. Smith. Jan 89, 25p NISTIR-89/

Keywords: *Thermal conductivity, *Thermal insulation, *Thermal measurements, Heat transmission, Thermophysical properties, Thermal resistance, Test facilities, Comparison, Standard deviation.

Sponsored by Oak Ridge National Lab., TN.

Measurements of apparent thermal conductivity performed by five different laboratories are compared. Subcommittee C-16.30 (Thermal Measurements) of the American Society for Testing and Materials (ASTM) sponsored the interlaboratory comparison. Two different types of line-source apparatus were used: the needle and the hot wire. The five laboratories measured thermal conductivity of Ottawa silica sand, paraffin wax, and three insulating materials (fibrous glass, expanded polystyrene, and extruded polystyrene). Comparison of the test results illustrates the interlaboratory reproducibility. The standard deviation of the thermal conductivity results for the needle apparatus is 26%, whereas the standard deviation of the results for the hot-wire apparatus is 17%.

900,145
PB89-229215
Not available NTIS
National Inst. of Standards and Technology (NEL),
Gaithersburg, MD. Office of Energy-Related Inventions

Window U-Values: Revisions for the 1989 ASHRAE (American Society of Heating, Refrigerating and Air-Conditioning Engineers) Handbook - Fundamentals.

Final rept. M. E. McCabe. 1989, 7p

Pub. in ASHRAE (American Society of Heating, Refrigerating and Air-Conditioning Engineers) Jnl. 31, n6 p56-62-Jun 89.

Keywords: *Window glazing, *Thermal insulation, *Heat transfer, *Storm windows, Solar energy, Temperature control, Solar radiation, Performance evaluation, Reprints, *U values, Energy conservation.

Recently, high-performance insulated glass has been introduced into the window market. However, with reduced heat flow in the central glazed portion of a window, heat conduction in the edge spacer and in the frame and sash members has become more important in determining the overall U-Value of the system. Characterization of frame heat transfer coefficients is complicated by the variety of frame configurations for operable windows, the different materials, and the different product sizes available. Standard methods for measuring frame heat transfer are not generally available. Chapter 27 in the ASHRAE Handbook of Fundamentals is the authoritative source of technical information on fenestration products such as windows, patio doors, skylights, shading devices, etc. The ASHRAE Handbook is revised every four years based on updat-

ed technical information. A number of changes have been made to the window U-Value table appearing in the 1989 Handbook. The article discusses the technical basis for the changes to appear in the 1989 Handbook and compares data with that from the 1985 Handbook.

900,146
PB90-111667
PC A04/MF A01
National Inst. of Standards and Technology (NEL),
Gaithersburg, MD.
Robot Crane Technology.
Tochnical Late (Final)

Technical note (Final).

N. G. Dagalakis, J. S. Albus, K. R. Goodwin, J. D. Lee, T. M. Tsai, H. Abrishamian, R. Bostelman, and C. Yancey. Jul 89, 65p NIST/TN-1267
Also available from Supt. of Docs. as SN003-00302953-0. Sponsored by Defense Advanced Research Projects Agency, Arlington, VA.

Keywords: *Cranes(Hoists), *Robots, *Automation, Construction equipment, Kinematics, Dynamics, Stiffness, Stability, Constraints, Hoisting, Models, Tests.

The effort to develop kinematically constrained, dynamically stabilized, robot cranes capable of lifting, moving and positioning heavy loads over large volumes, capable of supporting fabrication tools and the inspection of large size and difficult to reach structures, is described in the report. The approach taken was to build on previous work at the NIST Robot Systems Division which has analyzed and measured the stiffness of a small model six-cable suspension system. The system is a modified Stewart platform. Under DARPA sponsorship, the author has: Extended the work to measure and optimize the stiffness of full-size models; Actively damped oscillations in a small scale six-cable suspension platform; Constructed an intermediate sized six-cable suspension platform for an industrial robot.

900,147
PB90-117573
Not available NTIS
National Inst. of Standards and Technology (NEL),
Gaithersburg, MD. Fire Science and Engineering Div.
Note on Calculating Flows Through Vertical Vents
in Zone Fire Models Under Conditions of Arbitrary
Cross-Vent Pressure Difference.
Final rept.

L. Y. Cooper. 1989, 8p Pub. in Combustion Science and Technology 64, n1-3 p43-50 1989.

Keywords: *Vents, *Pressure gradients, *Airflow, *Fire tests, Ventilation, Algorithms, Pressure, Fluid flow, Reprints.

in typical compartment fire scenarios, ratios of cross-vent absolute pressure are very close to 1. When such is the case, algorithms are available to predict the resulting cross-vent room-to-room flows. There are, however, important situations where this pressure condition does not prevail. For example, in fire scenarios involving relatively small penetrations in otherwise heretically-sealed compartments of fire origin, cross-penetration pressure differences can be of the order of an atmosphere and pressure ratios, outside-to-insider, can be several tenths less than one. It is important for a versatile compartment fire model to have a capability of predicting vent flows for the entire range of possible cross-vent pressure conditions. The paper presents a unified analytic description of flows through uniform-width vertical vents connecting pairs of two-layer room fire environments under conditions of arbitrary cross-vent pressure difference. The algorithm presented is not significantly more complicated than previously-available algorithms which are restricted to low-pressure-difference cases.

900,148

PB90-118050

Not available NTIS
National Inst. of Standards and Technology (NEL),
Gaithersburg, MD. Fire Science and Engineering Div.
Upward Turbulent Flame Spread on Wood under
External Radiation.

Final rept. K. Saito, F. A. Williams, I. S. Wichman, and J. G. Quintiere. 1989, 8p

Grant NSF-INT84-03848
See also PB87-128005. Sponsored by National Science Foundation, Washington, DC.
Pub. in Jnl. of Heat Transfer - Transactions of the

ASME (American Society of Mechanical Engineers) 111, p438-445 May 89.

Keywords: *Fire tests, *Douglas fir wood, *Flame propagation, *Turbulence, *Thermal radiation, Burning

rate, Temperature, Combustion, Ignition, Experimental data, Thermal measurement, Reprints.

Experiments were performed to obtain histories of surface temperatures and rates of upward flame spread for vertically oriented, thermally thick wood slabs exposed to surface fluxes of thermal radiation up to 2.6 W/sq cm. Above a critical irradiance sustained upward flame spread occurred for Douglas-fir particle board with pilot initiation at the base of the fuel face. Data obtained included temperatures, flame heights, pyrolysis-front heights, combustion duration, and char-layer thickness for various irradiances and preheat times. The measurements were compared with theory.

900,149

PB90-118068

Not available NTIS
National Inst. of Standards and Technology (NEL),
Gaithersburg, MD. Fire Science and Engineering Div.
Scaling Applications in Fire Research.
Final rept.

J. G. Quintiere. 1989, 27p Pub. in Fire Safety Jnl. 15, p3-29 1989.

Keywords: *Fires, *Fire safety, *Scale(Ratio), Models, Fire tests, Froude number, Pressure, Analogs, Reprints

The principles for scaling fire phenomena are examined from the dimensionless groups derived from the governing differential equations. A review of the literature shows examples of where correlations have been successfully developed for a wide range of fire phenomena in terms of the significant dimensionless groups. Scaling techniques based on Froude modeling, pressure modeling and analog modeling are described and illustrated. The use of small geometric models ranging from fire plumes to enclosure fires are illustrated.

900,150

PB90-118076
Not available NTIS
National Inst. of Standards and Technology (NEL),
Gaithersburg, MD. Fire Science and Engineering Div.
Heat Transfer in Compartment Fires Near Regions
of Ceiling-Jet Impingement on a Wall.

Final rept. L. Y. Cooper. 1989, 6p

Pub. in Jnl. of Heat Transfer 111, p455-460 May 89.

Keywords: *Fire tests, *Fires, *Heat transfer, *Jet flow, Ceilings(Architecture), Walls, Enthalpy, Two dimensional flow, Flux(Rate), Impingement, Momentum, Reprints.

The problem of heat transfer to walls from fire-plume-driven ceiling jets during compartment fires is introduced. Estimates are obtained for the mass, momentum, and enthalpy flux of the ceiling jet immediately upstream of the ceiling-wall function. An analogy is drawn between the flow dynamics and heat transfer at ceiling-jet/wall impingement and at the line impingement of a wall and a two-dimensional plane free jet. Using the analogy, results from the literature on plane free-jet flows and corresponding wall-stagnation heat transfer rates are recast into a ceiling-jet/wall-impingement-problem formulation. This leads to a readily usable estimate for the heat transfer from the ceiling jet as it turns downward and begins its initial descent as a negatively buoyant flow along the compartment walls. Available data from a reduced-scale experiment provide some limited verification of the heat transfer estimate.

900,151
PB90-128232
Not available NTIS
Notional Inst. of Standards and Technology (NEL),
Gaithersburg, MD. Fire Measurement and Research

Effects of Thermal Stability and Melt Viscosity of Thermoplastics on Piloted Ignition. Final rept.

T. Kashiwagi, and A. Omori. 1989, 10p Pub. in Proceedings of International Symposium on Combustion (22nd), Seattle, WA., August 14-19, 1988, p1329-1338 1989.

Keywords: *Ignition, *Flammability, *Thermoplastic resins, Polystyrene, Polymethyl methacrylate, Fire tests, Temperature, Flux(Rate), Radiant flux density.

The effects of material characteristics on piloted ignition were studied by using two different polystyrene, PS, samples and two different poly(methyl methacrylate), PMMA, samples. The difference between the

Construction Materials, Components, & Equipment

two PS samples was melt viscosity due to two different Initial molecular weights and that between the two PMMA samples was thermal stability and melt viscoslty also due to two different initial molecular weights. Ignition delay times and time histories of surface temperature and sample weight changes were measured in the external radiant flux range of 0.9-3.0 W/sq cm. A comparison of results between the two PS samples and between the two PMMA samples was made. The comparison indicates that the transport process of in-depth degradation products through the molten poly-mer layer to the sample surface has negligible effects on piloted ignition. However, the thermal stability of the material has significant effects on the piloted ignition delay time and the surface temperature at ignition.

Not available NTIS National Inst. of Standards and Technology (NEL), Gaithersburg, MD. Fire Science and Engineering Div. Fire Growth and Development.

Pinal rept.
J. G. Quintiere. 1989, 24p
Pub. in Proceedings of International Symposium on
Fire Safety and Engineering, Sydney and Melbourne,
Australia, April 27, 1989, p1-24.

Keywords: *Fire tests, *Furniture, *Fires Fire resistance, Fire safety, Fire hazards, Flammability, Flashover, Combustion.

The phenomena of fire initiation and development is described and discussed. Fire behavior in closed and vented compartments is considered along with the factors important to spread beyond the compartment. The role of furnishings and contents is reviewed and fla-shover is found to be principally responsible for haz-ardous conditions, both thermal and toxic. Exceptions to this are discussed. The use of current and emerging test methods are described. Emphasis is on the interpretation and use of engineering measurements needed in innovative design hazard assessment, in constrast to the conventional practice of performance rankings of materials by a test method.

900,153 PB90-130311 PC A04/MF A01 National Inst. of Standards and Technology (NEL), Boulder, CO. Chemical Engineering Science Div. Microporous Fumed-Silica Insulation as a Stand-ard Reference Material of Thermal Resistance at

High Temperature.
D. R. Smith. Aug 89, 65p NISTIR-89/3919
See also PB89-148373. Sponsored by Oak Ridge National Lab., TN.

Keywords: *Silicon dioxide, *Insulating boards, *Standards, *Porosity, *Thermal conductivity, Fumes, Measurement, High temperature tests, Air pressure, Density, Atmospheric pressure, Graphs(Charts), Standard reference materials.

Measurements of apparent thermal conductivity of mi-croporous fumed-silica insulation board, already certified as a Standard Reference Material (SRM) of therfied as a Standard Reference Material (SRM) of thermal resistance, are reported here to extend the range of certification of the material to higher temperatures and lower pressures. Apparent thermal conductivities of five different pairs of specimens ranging in mean density from 300 to 348 kg/cu m were measured with a high-temperature guarded hot plate 25 cm in diameter. The measurements cover a range of mean spectrent temperatures from 318 to 733 K (45 to 460C), and of environmental air pressures from 26.7 to 83.5 kPa (200 to 626 Torr). Detailed analyses are given. The microporous furned silica (41 an ambient pressure of 83 roporous fumed silica (at an ambient pressure of 83 kPa and a density of 300 kg/cu m) has an apparent thermal conductivity of 19.8 mW/(m K) at 300 K and is suitable for use as an SRM of very low conductivity from 297 to 735 K (24 to 460C). Adsorbed moisture within the material must be driven off by prolonged heating at 110C before its conductivity is measured.

PB90-132705 PC A03/MF A01 National Inst. of Standards and Technology (NEL), Gaithersburg, MD. Center for Building Technology. Gypsum Wallboard Formaldehyde Sorption Model. S. Silberstein. Nov 89, 22p NISTIR-89/4028

Keywords: *Gypsum, *Wallboard, *Formaldehyde, *Houses, Sorption, Safety engineering, Human factors engineering, Air entrainment, engineering, Air entrainment, Concentration(Composition), Contaminants, Environmental engineering, *Indoor air pollution. Gypsum wallboard was shown to absorb formaldehyde in a prototype house and in a measuring chamber, as reported previously by researchers at Oak Ridge National Laboratory (ORNL). Also as reported previously, formaldehyde concentrations attained equilibrium in two phases in response to a change in the air exchange rate or to the removal of the formal-dehyde source. A rapid initial phase was followed by a slow phase lasting several days. A formaldehyde sorp-tion model that accounts for the biphasic concentra-tion pattern is presented here. Experiments for testing the predictability of the model are proposed.

PB90-136805
National Inst. of Standards and Technology (NEL), Gaithersburg, MD. Fire Measurement and Research Flammability of Uphoistered Furniture with Flam-

Ing Sources. Final rept.

V. Babrauskas. 1989, 27p Pub. in Cellular Polymers 8, p198-224 1989.

Keywords: *Furniture, *Upholstery, *Flammability testing, Fire tests, Ignition, Fire safety, Fire resistance, Calonmeters, Reprints.

A number of countries and localities have either re-cently adopted furniture flammability regulations, or are actively considering them. In addition, a number of furniture flammability test methods have been developed in recent years in the course of research. Some of the methods share certain similarities; but, even so, many different testing philosophies exist. The paper compares the more widely used of the methods and examines their advantages and limitations. The impact of some recent research results on test method design is also considered. The methods are discussed only on is also considered. The flethous are discussed only of their technical features and not on their regulatory aspects. The scope is limited to methods for testing the behavior under flaming fire conditions, and excludes tests for determining the cigarette ignition resistance. Some unresolved areas where further research is decirable areas as a few forms. sirable are also cited.

Structural Analyses

900.156 PB89-148092 PC A03/MF A01 National Bureau of Standards (NEL), Gaithersburg,

MD. Center for Building Technology.

Guidelines and Procedures for Implementation of
Executive Order on Seismic Safety.

C. W. C. Yancey, and J. Greenberg. Jan 88, 32p
NBSIR-88/3711

Also pub. as Interagency Committee on Seismic Safety in Construction rept. no. ICSSC/RP-2. Prepared in cooperation with Interagency Committee on Seismic Safety in Construction. Sponsored by Federal Emergency Management Agency, Washington, DC.

Keywords: *Earthquakes, *Safety engineering, *Earthquake resistant structure, Design criteria, Specifications, Concrete construction, Construction management, Readiness, Accident prevention, Project management, Guidelines, Earthquake Hazards Reduction

The 'Earthquake Hazards Reduction Act of 1977,' Public Law 95-125, was passed by Congress to foster the reduction of life and property risks from future earthquakes in the United States through the establishment and maintenance of an effective earthquake hazards reduction program. A proposed Executive Order on Seismic Safety has been drafted that would implement the provisions of the Act by requiring Federal preparedness and mitigation activities to be implemented. The required activities would include the development and promulgation of specifications, building standards, design criteria, and construction practices for new and existing buildings and lifelines. The guidelines and procedures described herein have been pre-pared to support the implementation of the Executive Order on Seismic Safety. It is recommended that each agency concerned with buildings and lifeline that are Federally owned, leased, assisted, or regulated designate an individual or an operating unit as the Agency Seismic Coordinator. It would be the responsibility of the Agency Seismic Coordinator to coordinate all aspects of the agency seismic safety program.

900.157 PB89-154835 PC A21/MF A01
National Inst. of Standards and Technology (NEL),
Gaithersburg, MD. Center for Building Technology.
Wind and Selsmic Effects. Proceedings of the
Joint Meeting of the U.S.-Japan Cooperative Program in Natural Resources Panel on Wind and
Selsmic Effects (20th) Held in Galthersburg, MaryJapan on May 17-20, 1988

land on May 17-20, 1988.

Final rept. N. J. Raufaste. Jan 89, 486p NIST/SP-760 Also available from Supt. of Docs. as SN003-003-02917-3. See also PB88-183983. Library of Congress catalog card no. 88-600610.

Keywords: *Meetings, *Bridges(Structures), *Buildings, *Earthquakes, *Wind pressure, *Ocean waves, Tsuamis, Forecasting, Seismic waves, Earth movements, Dynamic structural analysis, Storm surges, Design criteria, Dynamic loads, Soil mechanics, Standards, Structural engineering, *Seismic design, *Earthquake engineering, Ground motion, Risk assessments.

The 20th Joint Meeting of the U.S.-Japan Panel on Wind and Seismic Effects was held at the National Bureau of Standards, Gaithersburg, Maryland from May 17-20, 1988. The proceedings of the Joint Meeting 17-20, 1988. ing, includes the program, list of members, panel resolutions, task committee reports, and technical papers. The papers covered five themes: Wind engineering, Storm Surge and Tsunamis, Summary of U.S.-Japan Cooperative Research Program, and Two decades of accomplishments and challenges for the future.

900,158 PB89-175715 Not available NTIS National Bureau of Standards (NEL), Gaithersburg,

MD. Structures Div.
Progressive Collapse: U.S. Office Building in Moscow.

Final rept. F. Y. Yokel, R. N. Wright, and W. C. Stone. 1989,

Pub. in Jnl. of Performance of Constructed Facilities 3, n1 p57-76 Feb 89.

Keywords: *Structural analysis, *Loads(Forces), *Collapse, Dynamic response, Failure, Supports, Structural members, Stress analysis, Structural design, Reprints, *Office buildings.

As part of a structural assessment of the new U.S. Embassy Office Building being constructed in Moscow, United Soviet Socialist Republics, the National Bureau of Standards determined the susceptibility of the buildof Standards determined the susceptibility of the building to progressive collapse, which might be triggered by a local failure of a primary load supporting structural member. The building is a precast concrete structure that uses a standardized Soviet building system. The paper discusses criteria for the progressive collapse analysis, mechanisms for alternative load paths, analysis techniques used, and recommended retrofit measurements. ures. Although the building system was not designed to provide continuity in structural connections, it is possible to protect the building against progressive collapse with relatively modest retrofit measures.

900.159 PB89-175723 Not available NTIS National Bureau of Standards (NEL), Gaithersburg,

MD. Structures Div.
Pore-Water Pressure Bulldup In Clean Sands Because of Cyclic Straining.

Final rept. R. S. Ladd, R. Dobry, P. Dutko, F. Y. Yokel, and R. M. Chung. 1989, 10p Pub. in Geotechnical Testing Jnl. 12, n1 p77-86 Mar

Keywords: *Pore pressure, *Water pressure, *Sands, *Liquefication, Shear strain, Soil properties, Mechanical tests, Dynamic response, Reprints, *Earthquake

The prediction of pore-water pressure buildup in sands caused by undrained cyclic loading is one of the key items in evaluating the potential for liquefaction of sandy sites during earthquakes. Presented herein are data indicating that, in strain-controlled tests, there is a predictable correlation between cyclic shear strain, number of cycles, and pore-water pressure buildup; this correlation is much less sensitive to factors, such as relative density and fabric than comparable results

Structural Analyses

obtained from stress-controlled tests. The data indicate that, for clean sands, this threshold shear strain, as well as the pore-water pressure buildup for strains slightly above the threshold, are basically independent of relative density, grain size distribution, fabric, and method of testing (triaxial and direct simple shear). However, both threshold shear strain and pore-water pressure buildup do depend on the overconsolidation

900,160 PB89-187504 PB89-187504 Not available NTIS National Bureau of Standards (NEL), Gaithersburg, MD. Center for Building Technology.

Brick Masonry: U.S. Office Building in Moscow.

Final rept. J. G. Gross, R. G. Mathey, C. Scribner, and W. C. Stone. 1989, 22p
Pub. in Jnl. of Performance of Constructed Facilities 3,

n1 p35-56 Feb 89.

Keywords: *Brick structures, *Structural analysis, *Walls, Lateral stability, Cracks, Defects, Masonry, Mechanical properties, Assessments, Reprints, *Office buildings.

The National Bureau of Standards conducted a structural assessment of the new U.S. Embassy Office Building being built in Moscow. The paper reports the portion of the assessment dealing with the brick masonry walls. It describes the walls and provides sumptions of the city with the proton tradical deals are provided as a standard of the city with the proton tradical and are standard and the city with the proton tradical and a standard and the city was the proton to the city of the maries of two site visits, laboratory studies, and an analysis of the exterior walls, parapet walls, perthouse walls, and interior brick masonry core walls. Numerous cracks were found in exterior walls, incomplete construction of interior core walls was documented, and inadequate lateral strength of parapet walls was identified. Remedial measures were recommended for correction of deficiencies. Companion papers provide background information about the structure, the investigation, the assessment of the primary structural system, and the potential for progressive collapse.

900,161 **PB89-188627** PC A03/MF A01 National Inst. of Standards and Technology (NEL), Gaithersburg, MD. Center for Building Technology. Guidelines for Identification and Mitigation of Selsmically Hazardous Existing Federal Buildings.
H. S. Lew. Mar 89, 17p NISTIR-89/4062
Also pub. as Interagency Committee on Seismic Safety in Construction rept. no. ICSSC/RP-3. Prepared

in cooperation with Interagency Committee on Seismic Safety in Construction. Sponsored by Federal Emergency Management Agency, Washington, DC.

Keywords: *Hazards, *Buildings, *Earthquakes, Identifying, Safety, Instructions, Requirements, Vulnerability, Evaluation, Federal agencies, Earthquake Hazards Reduction Act of 1977.

The report includes Guidelines for Identification and Mitigation of Seismically Hazardous Existing Federal Buildings, and was prepared by the Interagency Committee on Seismic Safety in Construction in support of the National Earthquake Hazards Reduction Program, the President's plan to implement the Earthquake Hazards Reduction Act of 1977 (Public Law 95-124). The Guidelines are intended for consideration and use, as appropriate, by Federal agencies in their plans for mitigation of seismic hazards in existing buildings. Some Federal agencies have their mitigation plan in oper-

900,162 PB89-235865 PB89-235865 PC A04/MF A01
National Inst. of Standards and Technology (NEL),
Gaithersburg, MD. Center for Building Technology.
Sensors and Measurement Techniques for As-

Sensors and Measurement Techniques for Assessing Structural Performance.
R. D. Marshall. Aug 89, 67p NISTIR/89-4153
Proceedings of an International Workshop held in Gaithersburg, MD. on September 8-9, 1988. Sponsored by National Science Foundation, Washington, DC., United States-Japan Cooperative Program in Natural Resources. Panel on Wind and Seismic Effects, and American Society of Civil Engineers, New York. Performance of Structures Research Council.

Keywords: *Meetings, *Structural analysis, Loads(Forces), Detectors, Measurement, Research, Structural engineering, Earthquake engineering.

The report identifies research and development efforts needed to advance the state-of-the-art in instrumentation and measurement techniques for assessing struc-

tural performance. Four topic areas consisting of selsmic effects; wind effects; effects due to occupancy, traffic, snow and other loads; and sensor technology were addressed by respective task groups during a two-day meeting of international experts. The fortyeight specific recommendations presented in the report are intended to serve as a research agenda for use by universities, research establishments and funding agencies.

900,163 PB90-117631 Not available NTIS National Inst. of Standards and Technology (IMSE), Boulder, CO. Fracture and Deformation Div. PB90-117631 Measurement of Applied J-Integral Produced by Residual Stress. Final rept.

D. T. Read. 1989, 7p Sponsored by Naval Sea Systems Command, Washington, DC.

Pub. in Engineering Fracture Mechanics 32, n1 p147-153 1989.

Keywords: *Plates(Structural members), *Strain measurement, *Determination of stress, *Welded joints, *Stress analysis, Mechanical properties, Bending, Elasticity, Cracks, Surface defects, Fractures(Materials), Reprints.

An approximate method for measuring the applied Jintegral produced by residual stresses was developed and applied to four wide plates. The technique uses multiple strain measurements during the cutting of a notch in the weld. Results for welded and post-weld-heat-treated (PWHT) plates with semi-elliptical surface cracks and tube hole ligament cracks were compared. The PWHT plates had much lower J levels. Comparisons with the Newman-Raju linear elastic calculation for surface cracks in bending indicated that the present results are reasonable. Comparison of the present result for the ratio of stress intensity factor to crack mouth-opening displacement with values calculated for through and surface cracks provides additional confidence in the correctness of the present results.

General

900.164 PB89-173983 Not available NTIS National Bureau of Standards (NEL), Gaithersburg, MD. Fire Measurement and Research Div. Hand Calculations for Enclosure Fires. Final rept.

Find 1991. E. K. Budnick, and D. D. Evans. 1986, 6p Pub. in Fire Protection Handbook (16th Edition), Sec-tion 21, Chapter 3, p21-19-21-24 1986.

Keywords: *Enclosures, *Fire protection, *Mathematical models, Containers, Expansion, Growth, Forecast-

In the chapter, a brief discussion of enclosure fire effects is presented, along with equations that can be evaluated using hand calculators to provide estimates of particular effects. Generally, the equations presented are well documented and are widely used for such estimates. However, the user is cautioned that most of esumates. However, the user is cautioned that most of the equations were developed based on data from ex-periments that were conducted for very specific, and sometimes idealized, conditions. Therefore, some judgment must be exercised when applying these equations to complex conditions occurring in enclo-sure fires of general interest.

900.165 PB89-173991 Not available NTIS Mational Bureau of Standards (NEL), Gaithersburg, MD. Fire Measurement and Research Div.

Final rept.

E. K. Budnick, and W. D. Walton. 1986, 6p Pub. in Fire Protection Handbook (16th Edition), Section 21, Chapter 4, p21-25-21-30 1986.

Keywords: *Mathematical models, *Fire protection, *Computerized simulation, Fire safety, Building codes, Fire prevention, Regulations, Design standards, Re-

In recent years, Increasing attention has been given to the development and use of computer fire models.

They have been used by engineers and architects for building design, by building officials for plan review, by the fire service for prefire planning, by investigators for post fire analysis, by groups writing fire codes, and by materials manufacturers, fire researchers, and educators. While these models are not a replacement for the building and fire codes they can be a valuable tool for fire professionals. The report focuses on a representative selection of models. At the end of the chapter an in-depth review of models is given.

900,166 PB89-174130
Not available NTIS
National Bureau of Standards (NEL), Gaithersburg,
MD. Fire Science and Engineering Div.
Creation of a Fire Research Bibliographic Data-

Final rept.

N. H. Jason. 1986, 6p

Pub. in Proceedings of International Meeting of Fire
Research and Test Centres, Avila, Spain, October 7-9, 1986, p669-674.

Keywords: *Bibliographies, *Information retrieval, *Information systems, Data retrieval, Indexes (Documentation), Fire protection, Fire prevention, Fire hazards, Fire resistant materials, *Fire research information services, *Data bases.

It is difficult to perform a comprehensive literature survey in several technical fields, and in fire research the problem is compounded by the diverse nature of the field. Fire research cuts across many boundaries, e.g., chemistry, physics, fluid mechanics, mechanical engineering. In an effort to enhance the retrieval rate of information from the Fire Research Information Services (FRIS) collection, the Center for Fire Research, National Bureau of Standards decided to automate its literature collection. Using available supermi-cro hardware and software, FIREDOC was created as the on-line bibliographic database for the FRIS collection. Analysis of the alternatives which led to the creation of FIREDOC will be discussed, as well as some retrieval methods to locate relevant information in the database.

900.167 PB89-183222 PC A03/MF A01 National Inst. of Standards and Technology (NEL), Gaithersburg, MD. Center for Fire Research. Engineering View of the Fire of May 4, 1988 in the First Interstate Bank Building, Los Angeles, California. H. E. Nelson, Mar 89, 40p NISTIR-89/4061

Keywords: *Fires, *Banks(Buildings), Flame propagation, Safety, Fire damage, Burning rate, Diagrams, Investigations, Smoke, Office buildings, Case studies.

The course of the fire is traced in terms of developing fire phenomena. Special emphasis is given to burning rate of building furnishings, smoke layer temperature, layer level, oxygen consumption, combustion efficiency, flashover, exterior fire propagation, detector response, sprinkler operation, smoke movement and some contamination.

900,168 PB89-202584 Not available NTIS National Bureau of Standards (NEL), Gaithersburg, MD. Center for Building Technology.

Effects of Research on Bullding Practice.

Final rept. R. N. Wright. 1989, 8p Pub. in Construction Specifier 42, n5 p98-105 May 89.

Keywords: *Research management, *Safety engineering, *Building codes, *Economic analysis, International relations, Trends, Competition, Construction industry, Value engineering, Reprints, *Center for Building Technology.

The Center for Building Technology of the National In-The Center for Building I echnology of the National Institute of Standards and Technology (formerly the National Bureau of Standards) is the U.S. national building research laboratory. The Center collaborates with other organizations of the building community to advance building technology to increase the usefulness, safety and economy of buildings and to enhance the international competitiveness of U.S. building products and services. Benefits of research, development and application efforts are described by examples of successful programs with which the Center has been associated. Trends requiring building research and appli-

General

cation are noted and corresponding aspects of the Center's current and planned programs are cited.

900,169 PB90-112327 PC A03/MF A01 National Inst. of Standards and Technology, Gaithers-burg, MD. National Voluntary Lab. Accreditation Pro-

gram.
NVLAP (National Voluntary Laboratory Accredita-tion Program) Program Handbook Construction Testing Services. Requirements for Accreditation. R. L. Gladhill. Mar 89, 48p NISTIR-89/4039

Keywords: *Construction industry, *Laboratories, Test facilities, Performance evaluation, Professional Keywords: personnel, Systems analysis, Scientists, Concretes, *Accreditation, Certification.

The document explains the operation and technical requirements of the Laboratory Accreditation Program for Construction Testing Services. All of the steps leading to accreditation are discussed. Technical requirements are explained indicating how the National Voluntary Laboratory Accreditation Program criteria are applied. It is intended for use by staff of accredited laboratories, those seeking accreditation, other laboratory accreditation systems, and others needing infor-mation on the requirements for NVLAP accreditation.

Not available NTIS
National Inst. of Standards and Technology (NEL),
Gaithersburg, MD. Fire Science and Engineering Div.
Comparisons of NBS/Harvard VI Simulations and
Full-Scale, Multiroom Fire Test Data.
Final rept. 900,170 PB90-128620

J. A. Rockett, M. Morita, and L. Y. Cooper. 1989, 10p

Pub. in Proceedings of International Symposium on Fire Safety Science (2nd), Tokyo, Japan, June 13-17, 1988, p481-490 1989.

Keywords: *Fire tests, *Computerized simulation, *Buildings, Safety engineering, Fire safety, Model tests, Environmental engineering, Comparisons.

The NBS/Harvard VI multi-room fire model was used to simulate results of previously reported full-scale multi-room fire experiments. The tests and simulations involved: four different compartment configurations of two or three rooms connected by open doorways, four different fire types generated by a methane burner and up to four different doorway openings between the burn room and adjacent space. A total of nineteen different tests were carried out and simulated. Selected comparisons between simulated and measured parameters of the fire-generated environments are reviewed. While the computer code is found to provide generally favorable simulations for the entire range of tests, several areas of modeling detail are identified for further improvement.

BUSINESS & ECONOMICS

Domestic Commerce, Marketing, & **Economics**

900,171 PB90-120742 PC A05/MF A01 National Governors' Association, Washington, DC.
Promoting Technological Excellence: The Role of
State and Federal Extension Activities. M. K. Clarke, and E. N. Dobson. c1989, 89p ISBN-1-55877-069-0, NIST/GCR-89-567 Grant NANB-8-D0868

Sponsored by National Inst. of Standards and Technology (NEL), Gaithersburg, MD. Center for Fire Re-

Keywords: *Technology transfer, *Businesses, Surveys, State government, National government, Organizations, Improvement, Extension services.

The report presents the findings of a Nationwide survey of state and federal organizations providing

business and technology assistance to small and medium-sized businesses. Information was collected on the nature of the services provided by these organizations, the type of firms being assisted, and methods used to reach potential clients. In addition, the survey solicited the views of program managers regarding the needs of small and medium-sized businesses for information on new and existing technologies and ways to improve the transfer of federal technology to potential users in the small business community. The report also contains short descriptions of specialized technology extension services in seven states. Finally, the report recommends actions states should take in expanding their technology assistance efforts and the federal government should take to support these efforts.

International Commerce, Marketing, & **Economics**

900,172 PB89-166128 PC A03/MF A01 National Inst. of Standards and Technology, Gaithersburg, MD. Office of the Associate Director for Industry and Standards.

Effect of Chinese Standardization on U.S. Export Opportunities. Y. Lin. Dec 88, 16p NISTIR-88/4000

Keywords: *China, *International trade, *Standards, Requirements, Electric devices, Economic develop-ment, Technology transfer, Exports, Information ex-

The paper describes the standardization system as it exists in the Peoples Republic of China and identifies the role of the China State Bureau of Standards (CSBS) in the standards coordination process. The standards development and approval process is also described. The implementation of the IECQ program in China for producing electronic products in conformance with internationally recognized quality requirements is explained and the organizations responsible for the several aspects of the system are identified. The paper advocates technical information exchange programs between the U.S. and the Peoples Republic of China and more U.S. trade missions to China to encourage the adoption of U.S. standards as well as to increase trade between the two countries.

900,173 PB89-191977 PC A03/MF A01 National Inst. of Standards and Technology, Gaithersburg, MD. Office of the Associate Director for Industry and Standards.

GATT (General Agreement on Tariffs and Trade) Standards Code Activities of the National Institute of Standards and Technology 1988.

J. R. Overman. Mar 89, 39p NISTIR-89/4074 See also PB88-201611.

Keywords: *Standards, Notifications, Regulations, Foreign countries, *GATT standards code, Technical

The report describes the GATT Standards Code activities conducted by the Office of Standards Code and Information, National Institute of Standards and Technology (NIST), for calendar year 1988. NIST responsi-bilities include operating the U.S. GATT inquiry point for information on standards and certification activities; notifying the GATT Secretariat of proposed U.S. Fed-eral government standards-based rules that might sig-nificantly affect trade; assisting U.S. industry with standards-related trade problems; and responding to inquiries about proposed foreign and U.S. regulations.

CHEMISTRY

Analytical Chemistry

900,174 PB89-146807

Not available NTIS

National Bureau of Standards (IMSE), Gaithersburg, MD. Ceramics Div.

Speciation Measurements of Butyitins: Application to Controlled Release Rate Determination and Production of Reference Standards.

Final rept. W. R. Blair, G. J. Olson, and F. E. Brinckman. 1986,

Sponsored by Civil Engineering Lab. (Navy), Port Hue-

neme, CA.
Pub. in Oceans 86--Conference Record, Washington, DC., September 23-25, 1986, p1141-1145.

Keywords: *Chemical analysis, *Gas chromatography, *Wooden piles, Standards, Extraction, Hydridization, Tin organic compounds, Reprints, *Tin/butyl, *Tin/dibutyl, *Tin/tinbutyl, *Tin/tetrabutyl, *Flame photome-

The paper describes methods and results of the determination of release rates for organotin species re-leased from organotin impregnated wood pilings. The analytical method consists of simultaneous extraction/ hydridization of aqueous lechate samples, with organ-otin speciation by gas chromatography coupled with tin selective flame photometric detection. The sensitivtin selective flame photometric defection. The sensitivity of the flame photometric detector to the butyltin family of organotins is 0.1 to 0.2 ng, depending on the species. Chromatographic separation of the butyltins provides speciation of mono-through tetrabutyltin within a 15 min chromatogram, with the additional capability of identifying any methylbutyltin compounds that may be present in the sample. Water samples were collected from the piling leaching tanks immediately upon immersion of the pilings and continued to be collected for approximately 1 year. Speciation and release rate data were obtained on both the early, first order stage of release, and the latter, zeroth order order stage of release, and the latter, zeroth order phase of controlled release. Instrument calibrations were performed using a specially prepared organotin research material.

900,175 PB89-146906 Not available NTIS National Bureau of Standards (NML), Gaithersburg, MD. Inorganic Analytical Research Div.

Determining Picogram Quantitles of U in Human Urine by Thermai ionization Mass Spectrometry.

Final rept. W. R. Kelly, J. D. Fassett, and S. A. Hotes. 1987, 6p Pub. in Health Physics 52, n3 p331-336 Mar 87.

Keywords: *Uranium 238, *Quantitative analysis, *Urine, Ionization, Mass spectroscopy, Isotope separation, Health physics, Reprints.

The U concentration in SRM 2670, Toxic Metals in Freeze-Dried Urine, and the urine of two pre-school age children was determined by measuring the chemi-cally separated U by isotope dilution thermal ionization mass spectrometry using ion counting detection. This procedure can detect about 1% of the atoms in the sample and has a total chemical blank of about 5 pg U. The U concentration in SRM 2670 was found to be 113 The U concentration in SHM 2670 was found to be 113 plus or minus 2 pg (sup 238) U/ml (1s). At this level a 1 ml sample is sufficient for a determination with a total uncertainty of less than 5%. The U concentration in the two children was 3.1 plus or minus 0.9 and 3.6 plus or minus 0.9 pg (sup 238) U/g. These low values suggest that the U concentration in urine of unexposed persons may be at this level or lower.

PB89-150858 Not available NTIS National Bureau of Standards (NML), Gaithersburg, MD. Inorganic Analytical Research Div.

Comparison of Detection Limits in Atomic Spectroscopic Methods of Analysis.

Final rept.
M. S. Epstein. 1988, 17p
Pub. in ACS (American Chemical Society) Symposium
Series 361, p109-125 1988.

Keywords: *Quantitative analysis, *Atomic spectroscopy, Detectors, Lasers, Fluorescence, Absorption, Plasma radiation, Accuracy, Reprints.

The comparison of detection limits is a fundamental part of many decision-making processes for the analytical chemist. Despite numerous efforts to standard-ize methodology for the calculation and reporting of detection limits, there is still a wide divergence in the way they appear in the literature. The paper discusses valid and invalid methods to calculate, report, and compare detection limits using atomic spectroscopic

Analytical Chemistry

techniques. 'Noises' which limit detection are discussed for analytical methods such as plasma emis-sion spectroscopy, atomic absorption spectroscopy and laser excited atomic fluorescence spectroscopy.

900.177 PB89-151773 PC A09/MF A01 Mational Inst. of Standards and Technology (NML), Gaithersburg, MD. Center for Analytical Chemistry. Technical Activities, 1988, Center for Analytical

B. I. Diamondstone, R. A. Durst, and H. S. Hertz. Nov 88, 178p NISTIR-88/3875

See also report for 1985, PB86-178902.

Keywords: *Chemical analysis, *Research projects, Standards, Inorganic compounds, Organic compounds, Particles, Gases, Standards, Biological extracts, *Standard reference materials.

The report summarizes the technical activities of the Center for Analytical Chemistry at the National Institute of Standards and Technology. It emphasizes activities over the Fiscal Year 1988 in the Inorganic Analytical Research Division, the Organic Analytical Research Division, and the Gas and Particulate Science Division. In addition, it describes certain special activities in the Center including quality assurance and vol-untary standardization coordination.

900,178 PB89-156889 Not available NTIS National Bureau of Standards (NML), Gaithersburg, MD. Organic Analytical Research Div. Standard Reference Materials for the Determination of Polycycilc Aromatic Hydrocarbons.

Final rept.
S. A. Wise, L. R. Hilpert, R. E. Rebbert, L. C. Sander, M. M. Schantz, S. N. Chesler, and W. E. May. 1988, 10_D

Pub. in Fresenius' Zeitschrift fuer Analytische Chemie 332, p573-582 1988.

*Aromatic polycyclic hydrocarbons, Kevwords: *Chemical analyses, *Spectrum analyses, Standards, Gas chromatography, Concentration(Composition), Reprints, *Standard reference materials, Certification, Air pollution detection.

Since 1980 a number of Standard Reference Materials (SRMs) have been issued by the National Bureau of Standards (NBS) to assist in validating measurements for the determination of polycyclic aromatic hydrocarbons (PAH) and other polycyclic aromatic compounds (PAC). These SRMs are certified for selected PAC and range in analytical difficulty from calibration solutions to complex natural matrix materials, such as air and diesel particulate matter, shale oil, and crude oil. In the past year three new SRMs have been introduced: (1) SRM 1647a 'Priority Pollutant PAH in Acetonitrile'; (2) SRM 1491 'Aromatic Hydrocarbons in Hexane/Toluene'; and (3) SRM 1597 'Complex Mixture of PAH from Coal Tar.' The SRMs available from NBS for use in the determination of PAC are described and the concentrations of PAC determined in the natural matrix SRMs are summarized and compared. The primary analytical techniques used for the measurement of PAC in these SRMs were gas chromatography, liquid chromatography, and gas chromatography/mass spectrometry.

900,179 PB89-156913 Not available NTIS National Bureau of Standards (NML), Gaithersburg, MD. Inorganic Analytical Research Div.

Radiochemical Procedure for Ultratrace Determi-

nation of Chromlum in Bloiogleai Materials. Final rept.

R. R. Greenberg, and R. Zeisler. 1988, 16p Pub. in Jnl. of Radioanalytical and Nuclear Chemistry 124, n1 p5-20 1988.

Keywords: *Chromium, *Biological surveys, *Neutron activation analysis, Chemical analysis, Radiochemistry, Concentration(Composition), Separation, Blood analysis, Solvent extraction, Trace elements, Reprints, Standard reference materials.

Chromium is one of the most difficult elements to accurately determine at the naturally occurring, ultratrace levels normally found in uncontaminated biological samples. In view of the importance of Cr, both as an essential and as a toxic element, efforts have focused on developing a simple, yet reliable, radiochemical procedure for Cr determination using neutron activation analysis. A number of problem areas have been identified in earlier methods, and an improved radiochemical separation procedure, based upon the liquid/liquid extraction of Cr(VI) into a solution of tribenzylamine/chloroform, has been developed. The fast neutron interference from Fe has been evaluated for the highly thermal FT-4 facility of the NBS Research Reactor, and Cr concentrations have been determined in samples of whole human blood collected under clean conditions and in two certified reference materials.

900,180 PB89-156921 900, 180
PB89-156921
Not available NTIS
National Bureau of Standards (NML), Gaithersburg,
MD. Inorganic Analytical Research Div.
Neutron Activation Analysis of the NIST (National
Institute of Standards and Technology) Bovine
Serum Standard Reference Material Using Chemi-

cai Separations.

Final rept. R. R. Greenberg, R. Zeisler, H. M. Kingston, and T. M. Sullivan. 1988, 5p Pub. in Fresenius' Zeitschrift fuer Analytische Chemie

332, p652-656 1988.

Keywords: *Neutron activation analysis, *Chemical analysis, *Separation, *Biological surveys, Standards, Trace elements, Toxicology, Human nutrition, Reprints, *Standard reference materials, Certification.

The U.S. National Institute of Standards and Technology is currently in the process of certifying a Bovine Serum Standard Reference Material. In addition to elements normally considered to be of clinical interest, a number of other elements, which are analytically more difficult to determine yet are of importance from either a nutritional or toxicological viewpoint, are being determined by a variety of analytical techniques. Neutron activation analysis in combination with appropriate pre- or post-irradiation chemical separations has been used to determine many of these difficult elements.

900,181 PB89-156939 PB89-156939 Not available NTIS National Bureau of Standards (NML), Gaithersburg, MD. Inorganic Analytical Research Div. Long-Term Stability of the Elemental Composition

in Biologicai Materiais.

Final rept. R. Zeisler, R. Greenberg, S. Stone, and T. Sullivan. 1988, 4p

Sponsored by Environmental Protection Agency, Washington, DC.
Pub. in Fresenius' Zeitschrift fuer Analytische Chemie

332, p612-615 1988.

Keywords: *Chemical analysis, *Biological surveys, *Tissue extracts, Standards, Concentration(Composition), Chemical stabilization, Neutron activation analysis, Zinc, Selenium, Arsenic, Trace elements, Liver extracts, Reprints, *Standard reference materials.

Lyophilized and radiation sterilized biological certified reference materials (CRMs) are believed to be stable in their chemical composition. Generally, the certifying agencies consider the certificates of these biological CRMs valid for a 5-year shelf life, i.e., apart from measurable moisture content, the chemical composition should not change during that time. The long-term behavior of fresh frozen material is not known. In the study the elemental compositions of the Bovine Liver Standard Reference Material (SRM 1577) and human liver tissue samples are evaluated over a time period of more than 7 years. The concentrations of selected elements were determined by neutron activation analysis at various times. The initial evaluation of zinc, selenium and arsenic results gives no indication of changes during 7 years storage of fresh frozen tissues, however, a trend towards lower arsenic concentrations has been observed in SRM 1577 during a 10-year

900,182 PB89-156947 Not available NTIS National Bureau of Standards (NML), Gaithersburg,

MD. Inorganic Analytical Research Div.

High-Accuracy Differential-Pulse Anodic Stripping
Voltammetry with Indium as an Internal Standard.

Final rept. K. W. Pratt, and W. F. Koch. 1988, 8p Pub. in Analytica Chimica Acta 215, p21-28 1988.

Keywords: *Indium, *Standards, *Cadmium, *Copper, *Lead, *Voltmeters, Anodic polarization, Chemical analysis, Reprints.

Indium (III) is used as an internal standard for the determination of cadmium, copper and lead at the 20 ng/

g level by using differential-pulse anodic stripping vol-tammetry; the supporting electrolyte is 1.0 mol/l am-monium bromide/0.25 mol/l nitric acid. For each solution, each stripping peak of interest is normalized to the corresponding peak height obtained in the same voltammogram for a known, added concentration of indium (III). A calibration curve is prepared for each element by using these normalized peak heights. The technique is demonstrated for NBS SRM 1643b (Trace Elements in Water). The relative standard deviations for six independent determinations of Cd, Cu, and 7b at the 20 ng/g level are 1.9%, 5.4%, and 1.2%, 1espectively. The imprecision for copper is limited by the sloping baseline at its stripping potential. The detection limit for each element is less than 1 ng/g.

900, 183

PB89-156970 Not available NTI National Bureau of Standards (NML), Gaithersburg, MD. Inorganic Analytical Research Div.

Activation Analysis Opportunities Using Cold Neutron Beams.

Final rept.

R. M. Lindstrom, R. Zeisler, and M. Rossbach. 1987,

Pub. in Jnl. of Radioanalytical and Nuclear Chemistry 112, n2 p321-330 1987.

Keywords: *Radioactivation analysis, Neutron beams, Reprints, *Activation analysis, *Cold neutrons, Neutron capture, Prompt gamma radiation.

Guided beams of cold neutrons being installed at a number of research reactors may become increasingly available for analytical research. A guided cold beam will provide higher neutron fluence rates and lower background interferences than in present facilities. In an optimized facility, fluence rates of one billion n/sq cm/sec are readily obtainable. Focusing a large area beam onto a small target will further increase the neutron intensity. In addition, the shift to lower energies will increase the effective cross sections. The absence of fast neutrons and gamma rays permit detectors to be placed near the sample without intolerable background, and thus the efficiency for counting prompt gamma rays can be much higher than in present systems.

900,184

PB89-157085 Not available NTIS National Bureau of Standards (IMSE), Gaithersburg, MD. Polymers Div.

Trace Speciation by HPLC-GF AA (High-Performance Liquid Chromatography-Graphite Furnace Atomic Absorption) for Tin- and Lead-Bearing Organometallic Compounds, with Signal Increases induced by Transition-Metal ions. Final rept.

E. J. Parks, F. E. Brinckman, K. L. Jewett, W. R. Blair, and C. S. Weiss. 1988, 10p

Pub. in Applied Organometallic Chemistry 2, p441-450 1988

Keywords: *Chromatography, *Quantitative analysis, *Environmental tests, *Organometallic compounds, Atomic spectra, Tin, Lead, Metals, Tungsten, Chromium, Manganese, Volatility, Chlorides, Oxides, Ligands, Metal complexes, Trace elements, Effluents, Liquid phases, Absorption spectra, Reprints.

High-performance liquid chromatography coupled with graphite furnace atomic absorption spectroscopy (HPLC-GF AA) gives element-specific detection of environmental samples containing trace amounts of or-ganotin or organolead species. The analyte and a modifier are co-pipetted into a conventional furnace tube, from either a solution of analyte or an HPLC effluent. Oxides of transition metals (e.g., chromium, manganese, or tungsten) are shown to enhance both tin and lead signals, whereas chlorides do not, suggesting the low-temperature formation of relatively involatile metal oxides or volatile metal chlorides, respectively.

900,185

PB89-157739 Not available NTIS National Bureau of Standards (NML), Gaithersburg,

MD. Gas and Particulate Science Div.

Preparation of Accurate Multicomponent Gas
Standards of Volatile Toxic Organic Compounds in the Low-Parts-per-Billion Range.

Final rept. G. C. Rhoderick, and W. L. Zielinski. 1988, 7p Pub. in Analytical Chemistry 60, n22 p2454-2460 1988.

CHEMISTRY

Analytical Chemistry

Keywords: *Standards, *Chemical analysis, Mixtures, Calibrating, Concentration(Composition), Chemical stabilization, Gravimetric analysis, Microanalysis, Reprints, *Volatile organic compounds, *Standard reference materials, *Air pollution detection, Toxic materials.

Methodology is described for the microgravimetric preparation and analytical evaluation of accurate, stable multicomponent gas standards in compressed gas cylinders containing volatile toxic organic com-pounds in pure nitrogen at the mid- to low-parts-perbillion (ppb) level. Standard mixtures have been prepared containing up to nine organic compounds at concentrations ranging from 1 to 1000 ppb by mole. Current indications are that the number of organic compounds in a single mixture is more limited by analytical capability than by the preparation methodology. Over 100 standards, of which several will be discussed in the paper, have been prepared and evaluated for long-term stability and internal consistency. Over 25 different volatile organic compounds spanning three concentration decades have been studied. The sum of preparative and analytical error compounds spanning three concentration decades have been studied. The sum of preparative and analytical error components of the uncertainty associated with the concentration of the organic analytes at the 95% confidence level typi-cally ranges from 3 to 10% relative, depending upon the compound and its concentration. Intercomparative analyses of new and previously prepared standards have verified that such mixtures are stable for several vears.

900,186 PB89-157747 Not available NTIS National Bureau of Standards (NML), Gaithersburg, MD. Gas and Particulate Science Div.

Moydite, (Y, REE) (B(OH)4)(CO3), a New Mineral
Species from the Evans-Lou Pegmatite, Quebec.

J. D. Gnce, J. Van Velthuizen, P. J. Dunn, D. E. Newbury, E. S. Etz, and C. H. Nielsen. 1986, 9p Pub. in Canadian Mineralogist 24, p665-673 Dec 86.

Keywords: *Carbonate minerals, *Qualitative analysis, *Yttrium, *Rare earth minerals, *Borate minerals, Crystal structure, Raman spectroscopy, X-ray analysis, Popular structure. Reprints, *Moydite.

The complete mineralogy of a newly discovered mineral, recently named moydite, is reported from the appli-cation of classical techniques of mineral characteriza-tion supported by the results of modern microanalytical methods. The mineral is described as a yttrium/rare earth element tetrahydroxoborate carbonate of ideal empirical formula (Y, REE) (B(OH4)) (CO3). The chemical composition and formula of moydite were derived from elemental analysis and x-ray crystal structure determination. The microanalytical techniques employed include electron and ion probe microanalysis, as well as Raman microprobe spectroscopy to infer molecular and vibrational structure relationships. The data on the new mineral are presented and its properties dis-cussed to illustrate the advantages of applying a range of synergistic analytical techniques to the comprehensive characterization of a new mineral species.

900,187 PB89-157879 Not available NTIS Not available NTIS
National Bureau of Standards (NML), Gaithersburg,
MD. Inorganic Analytical Research Div.
Role of Neutron Activation Analysis In the Certification of NBS (National Bureau of Standards)
Standard Reference Materials.

Final rept.

R. R. Greenberg. 1987, 15p Pub. in Jnl. of Radioanalytical and Nuclear Chemistry 113, n1 p233-247 1987.

Keywords: *Neutron activation analysis, Standards, Chemical analysis, Spectrum analysis, Performance evaluation, Quality assurance, Reprints, *Standard reference materials, Certification.

Neutron activation analysis (NAA) is extensively used at the National Bureau of Standards as one of the analytical techniques in the certification of Standard Reference Materials (SRMs). Characteristics of NAA which make it valuable in this role are: inherent accuracy; multielemental capability, especially in the instrumental mode; ability to assess homogeneity; high sensitivity for many elements, and essentially blank-free nature. Examples of recent SRM analyses illustrating these characteristics are described.

900,188 PB89-157994 Not available NTIS National Bureau of Standards (NML), Gaithersburg,

MD. Inorganic Analytical Research Div.

Voltammetric and Liquid Chromatographic Identification of Organic Products of Microwave-Assisted Wet Ashing of Biological Samples.

Final rept. K. W. Pratt, H. M. Kingston, W. A. MacCrehan, and W. F. Koch. 1988, 4p Pub. in Analytical Chemistry 60, n19 p2024-2027, 1

Oct 88.

Keywords: *Liver extracts, *Biological surveys, *Chemical analysis, *Coulometers, *Spectrophotometry, *Nitric acid, Spectrum analysis, Digestion(Decomposition), Polarographic analysis, Reprints, *Wet methods, *Voltammetry, *Liquid column chromatography, Benzoic acid/nitro, Standard reference materials.

Residual organic species in nitric acid digests of freeze-dried bovine liver (NBS SRM 1577a) have been identified by use of voltammetry, liquid chromatography, spectrophotometry, and classical chemical tests. Data from these techniques show that major products of microwave-assisted dissolution by nitric acid include o-, m-, and p-nitrobenzoic acids (NBA). In addition to these compounds, other organic species present in these digests irreversibly complex copper, but not zinc, and result in low values for copper by polarography. and result in low values for copper by polarography. The NBAs and these other organic species are all eliminated by refluxing the nitric acid digest in perchloric acid at atmospheric pressure. Polarographic results obtained for copper following treatment with perchloric acid agree with the certified value. The use of voltammetry in the evaluation of wet ashing procedures is discussed. dures is discussed.

900,189 PB89-161590 Not available NTIS National Bureau of Standards (NML), Gaithersburg, MD. Inorgana Analytical Research Div. Analytical Applications of Resonance Ionization Mass Spectrometry (RIMS). Final rept.

J. D. Fassett, and J. C. Travis. 1988, 14p Pub. in Spectrochimica Acta 43B, n713 p1409-1422

Keywords: *Chemical analysis, *Inorganic compounds, Performance evaluation, Rare gases, Mass spectroscopy, Sampling, Solids, Reprints, *Resonance ionization mass spectroscopy, State of the art, Isotope dilution.

A perspective on the role of resonance ionization mass spectrometry illustrate these capabilities and define the potential of RIMS in the generalized field of chemical analysis. Three areas of application are reviewed here: (1) noble gas measurements; (2) materials analysis using isotope dilution (IDMS); and, (3) solids analysis using direct sampling. The role of RIMS is discussed relative to the more traditional mass spectrometric methods of analysis in these areas. The applications are meant to illustrate the present state-ofthe-art as well as point to the future state-of-the-art of RIMS in chemical analysis.

PB89-171763 Not available NTIS National Bureau of Standards (IMSE), Gaithersburg, MD. Ceramics Div.

Standard X-ray Diffraction Powder Patterns from the JCPDS (Joint Committee on Powder Diffrac-tion Standards) Research Associateship. Final rept.

H. F. McMurdie, M. C. Morris, E. H. Evans, B. Paretzkin, W. Wong-Ng, Y. Zhang, and C. R. Hubbard. 1986, 12p See also PB87-119756. Sponsored by JCPDS-Interna-

tional Centre for Diffraction Data, Swarthmore, PA. Pub. in Powder Diffraction 1, n4 p334-345 Dec 86.

Keywords: *X ray diffraction, *Powder(Particles), *Standards, Calibrating, Crystal structure, Reprints.

Standard x-ray powder diffraction patterns are presented for 17 substances. These patterns, useful for identification, were obtained by automated diffractometer methods. The lattice constants from the experimental work were refined by least-squares methods, and reflections were assigned hkl indices consistent with space group extinctions. Relative intensities, calculated densities, literature references, and other relevant data are included.

PB89-171938 Not available NTIS National Bureau of Standards (NML), Gaithersburg, MD. Inorganic Analytical Research Div. Chemical Calibration Standards for Molecular Ab-

sorption Spectrometry. Final rept.

Pilla Tept.

R. Mavrodineanu, and R. W. Burke. 1987, 50p

Pub. in Advances in Standards and Methodology in Spectrophotometry, p125-174 1987.

Keywords: *Chemical analysis, *Spectrophotometry, Calibrating, Molecular spectroscopy, Design criteria, Performance evaluation, Reprints, *Standard reference materials.

The publication describes activities undertaken since 1969 within the Center for Analytical Chemistry of the National Bureau of Standards (NBS) in the field of high-accuracy spectrophotometry. It presents a summary of the Standard Reference Materials that have been developed for checking the proper functioning of ultraviolet and visible spectrophotometers and includes a brief description of the high-accuracy spectro-photometer constructed in the Center for Analytical Chemistry and subsequently used for performing all of the transmittance measurements.

900,192

PB89-172498 Not available NTIS National Bureau of Standards (NML), Gaithersburg,

MD. Gas and Particulate Science Div.
Strategy for Interpretation of Contrast Mechanisms in Scanning Electron Microscopy: A Tutorlal. Final rept.

D. E. Newbury. 1986, 5p Pub. in Microbeam Analysis - 1986, p1-5 1986.

Keywords: *Laboratory equipment, Performance evaluation, Design criteria, Topography, Images, Reprints, *Scanning light microscopy.

The interpretation of images in the scanning electron microscope is based upon prior knowledge of the characteristics of the contrast mechanism coupled with knowledge of the response of the electron detector. Pertinent contrast and detector properties include the mechanism of contrast encoding by signal carrier, number, trajectory, or energy effects and detector sensitivity to these factors. Examples of the interpretation of images of specimens which have compositional and topographic features are given. Compositional fea-tures are best visualized with a number-sensitive and trajectory-insensitive detector, while topographic fea-tures are detected best with a trajectory-sensitive detector.

900.193

PB89-173843 Not available NTIS National Bureau of Standards (NML), Gaithersburg, MD. Gas and Particulate Science Div.

Comparison of a Cryogenic Preconcentration Technique and Direct Injection for the Gas Chromatographic Analysis of Low PPB (Parts-per-Billion) (NMOL/MOL) Gas Standards of Toxic Organic

Compounds. Final rept.

G. C. Rhoderick. 1988, 6p

G. C. Hnodenck. 1988, 6p Sponsored by Environmental Protection Agency, Washington, DC. Pub. in Proceedings of EPA/APCA (Environmental Protection Agency/Air Pollution Control Association) International Symposium on Measurement of Toxic and Related Air Pollutants, Research Triangle Park, NC., May 2-4, 1988, p259-264.

Keywords: *Gas analyses, *Gas chromatography, Halogen organic compounds, Performance evaluation, Cryogenics, Emission spectroscopy, *Air pollution detection, *Volatile organic compounds, *Toxic substances, *Standard reference materials, Environment tal monitoring, Electron capture detectors, Flame ioni-

There is an increasing need for multicomponent gas standards containing volatile toxic organic compounds at the low parts-per-billion level for use in environmental monitoring programs. Standards containing many organic compounds, both halogenated and nonhalogenated acceptance within the second control of the control of organic compounds, both natiogenated and normalicy genated species within the same mixture, can be very difficult to analyze at the 1-15 ppb concentration level. Analyses of low level multicomponent mixtures have been done using several different techniques. Gas chromatography has been used to separate com-

Analytical Chemistry

pounds in simple and complex mixtures. Original work was done using packed columns with a flame-ioniza-tion detector (FID) and large sample volumes, 10 mL and an electron-capture detector (ECD) to analyze for halogenated compounds at low ppb levels. Therefore, to measure all the compounds in a single analysis, a cryogenic preconcentration technique was developed to increase the sensitivity of both types of compounds to the FID. Temperature programming was coupled with this cryogenic preconcentration technique to increase the quality of baseline separations.

900,194 PB89-175236

(Order as PB89-175194, PC A06) National Inst. of Standards and Technology, Gaithers-

bura, MD. Numeric Databases for Chemical Analysis.

Bi-monthly rept. S. G. Lias. 1989, 11p Included in Jnl. of Research of the National Institute of Standards and Technology, v94 n1 p25-34 Jan-Feb

Keywords: *Chemical analysis, Nuclear magnetic resonance, Infrared spectroscopy, Mass spectroscopy, Evaluation, Identifying, Chemical compounds, *Nu-merical data bases, Analytical chemistry, Computer applications.

Databases for use with analytical chemistry instrumental techniques are surveyed, with attention to existing databases and collection efforts now underway, as well as needs for new databases. Collections of spectra for use in Nuclear Magnetic Resonance Spectroscopy, infrared spectroscopy, and mass spectroscopy are described. Using mass spectral databases as an example, a critique is presented of automated quality control procedures used to evaluate individual spectra in large collections; the kinds of problems which have been encountered in using these procedures are discussed. Finally, a brief critical review is presented covering the application of computers to the identification of unknown compounds using spectral databases; again, algorithms used with mass spectrometry are taken as the example.

900,195 PB89-175863 Not available NTIS National Bureau of Standards (NML), Gaithersburg, MD. Organic Analytical Research Div.

Development of Electrophoresis and Electrofo-

cusing Standards.

Final rept.

D. J. Reeder. 1987, 15p Pub. in ACS (American Chemical Society) Symposium Series, v335 p102-116 1987.

Keywords: *Standards, *Electrophoresis, Separation, Quality assurance, Comparison, Reviews.

The work reviews some of the approaches to standardization in several different areas of electrophoretic separations. While no definitive standards have been established, some practical standards have been reported and are being used by researchers. Standards usage is part of quality assurance programs and is necessary for interlaboratory comparison studies.

900,196 PB89-175962 Not available NTIS National Bureau of Standards (IMSE), Gaithersburg, MD. Ceramics Div.

Characterization of Organolead Polymers in Trace Amounts by Element-Specific Size-Exclusion Chromatography.

E. J. Parks, F. E. Brinckman, and L. B. Kool. 1986,

4p Pub. in Jnl. of Chromatography 370, n1 p206-209, 26

Keywords: *Chromatographic analysis, *Size separation, *Exclusion, *Lead organic compounds, *Polymers, Spectroscopy, Detectors, Graphite, spectra, Absorption spectra, Molecular weight, Methacrylates, Organometallic compounds, Ultraviolet spectroscopy, Reprints.

Size exclusion chromatography (SEC), coupled with lead-specific graphite furnace atomic absorption (GFAA) spectroscopy and ultraviolet spectroscopy (UV) detectors was applied to the characterization of a 5:1 copolymer of 4-vinylphenyl, triphenyllead and octadecylmethacrylate. Less than 1.0 micrograms of the polymer, dissolved and injected in tetrahydrofuran

(THF), provided sufficient data to determine the number- and weight-average molecular weights as well as monomer conversion, with approximately 100% recovery of the injected lead. The method is uniquely capable of characterizing trace quantities of organometallic polymers such as may be obtained in preliminary stages of synthetic research, provided the polymers are soluble in column-compatible solvents.

900,197 PB89-176143 Not available NTIS National Bureau of Standards (NML), Gaithersburg, MD. Gas and Particulate Science Div.

Role of Standards in Electron Microprobe Technlaues. Final rept.

D. E. Newbury. 1986, 26p Pub. in Jnl. of Trace Microprobe Tech. 4, n3 p103-128 1986

Keywords: *Quantitative analysis, *X ray spectroscopy, *Standards, *Chemical composition, *Electron microscopy, Reprints, *Electron microprobe analysis.

Standards play a vital role in quantitative analysis techniques based upon electron excitation of x-rays. In the technique of electron probe x-ray microanalysis (EPMA), the description of the interaction of electrons and x-rays is sufficiently well known to permit quantitative analysis with a suite of pure element standards and calculated matrix corrections. Such a scheme provides flexibility in responding to problems in analyzing unknowns of arbitrary composition. In analytical electron microscopy (AEM), constraints on the specimen force reliance on an internal reference through the use of relative sensitivity factors coupled with matrix corrections. AEM standards must consist at least of two components and be in the form of thin foils, and each sensitivity factor requires a separate standard, making the standards suite more difficult to obtain.

900,198 PB89-176267 Not available NTIS National Bureau of Standards (NML), Gaithersburg, MD. Inorganic Analytical Research Div.

High-Accuracy Differential-Pulse Anodic Stripping
Voltammetry Using Indium as an Internal Standard.

Final rept.

K. W. Pratt, and W. F. Koch. 1986, 1p Pub. in Abstracts of Papers of the American Chemical Society 192, p98 Sep 86.

Keywords: *Coulometers, *Indium, Chemical analysis, Performance evaluation, Standards, Cadmium, Copper, Lead(Metal), Reprints, *Anodic stripping, *Standard reference materials.

In(III) is employed as an internal standard for the determination of Cd, Cu, and Pb at the 20 micrograms/g level using differential pulse anodic stripping voltammetry. A multi-point calibration curve is prepared for each element using these normalized peak heights. The technique is demonstrated using NBS Standard Reference Material 1643b.

900.199 PB89-176275 Not available NTIS National Bureau of Standards (NEL), Gaithersburg, MD. Statistical Engineering Div.

Tests of the Recalibration Period of a Drifting In-

strument.

Final rept.
W. Liggett. 1986, 6p
Sponsored by Environmental Monitoring Systems
Lab., Research Triangle Park, NC.
Pub. in Proceedings of Oceans 86, Conference
Record on National Monitoring Strategies, Washington, DC., September 23-25, 1986, p923-928.

Keywords: *Continuous sampling, *Samplers, *Calibrating, *Statistical analysis, *Drift(Instrumentation), Sulfur dioxide, Performance evaluation, Quality assurance, Reliability, *Air pollution detection, *Air pollution

The use of a drifting instrument requires that an adequately short recalibration period be chosen. After several periods, the calibration data can be used to test the adequacy of the choice. The paper discusses sta-tistical tests of the recalibration period and applies these tests to continuous analyzers for sulfur dioxide. The paper presents two tests, a test of the second differences of the calibration sequence for normality and a test of the upper part of the spectrum for flatness. The paper illustrates these tests with two sequences

each consisting of about fifty recalibrations of a sulfur dioxide analyzer. Also, the power of the tests and some approximations made in their formulation are investigated by Monte Carlo experiments.

PB89-176887 Not available NTIS National Bureau of Standards (NML), Gaithersburg, MD. Gas and Particulate Science Div.

Comparison of Two Translent Recorders for Use

with the Laser Microprobe Mass Analyzer.

R. A. Fletcher, and D. S. Simons. 1985, 3p Pub. in Microbeam Analysis, p319-321 1985.

Keywords: *Laboratory equipment, *Mass spectroscopy, Performance evaluation, Comparison, Reprints, *Data acquisition systems, *Laser microprobe mass analyzers, Laser spectroscopy.

Two transient recorders have been utilized as data acquisition systems for the Laser Microprobe Mass Analyzer (LAMMA). Past work has shown that one transient recorder degrades from about 8 to 4 bit resolution when subjected to high frequency signals. This contributes to errors quantification of peak intensities. The dynamic precision of the two recorders will be compared, analyzing the bit degradation with rapidly varying waveforms. Spectral quality of the two recorders and the precision and accuracy of isotopic ratios from standard samples will be examined. The advantages and disadvantages of each device will be report-

900,201 PB89-184105

(Order as PB89-184089, PC A04) National Inst. of Standards and Technology, Boulder, CO.

Supercritical Fluid Chromatograph for Physicochemical Studies.

Bi-monthly rept. T. J. Bruno. 1989, 8p

Included in Jnl. of Research of the National Institute of Standards and Technology, v94 n2 p105-112 Mar-Apr

Keywords: *Chromatography, Chromatographic analysis, Chemical analysis, Physicochemical properties, Diffusion coefficient, Molecular weight, Polymers, Solubility, *Supercritical fluid chromatography, *Supercritical fluids.

A supercritical fluid chromatograph has been designed and constructed to make physicochemical measure-ments, while retaining the capability to perform chemi-cal analysis. The physicochemical measurements in-clude diffusion coefficients, capacity ratios, partition coefficients, partial molar volumes, virial coefficients, solubilities, and molecular weight distributions of polymers. In the paper, the apparatus will be described in detail, with particular attention given to its unique features and capabilities. The instrument has recently been applied to the measurement of diffusion coefficients of toluene in supercritical carbon dioxide at a temperature of 313 K, and pressures from 133 to 304 bar (13.3-30.4 MPa). The data are discussed and compared with previous measurements on similar systems.

900,202 PB89-186357 Not available NTIS National Bureau of Standards (NML), Gaithersburg, MD. Inorganic Analytical Research Div. Analysis of Ultrapure Reagents from a Large Sub-

Bolling Still Made of Teflon PFA.

Final rept. P. J. Paulsen, E. S. Beary, D. S. Bushee, and J. R. Moody. 1989, 4p

Pub. in Analytical Chemistry 61, n8 p827-830, 15 Apr 89.

Keywords: *Chemical analysis, *Mass spectroscopy, Distillates, Purity, Reprints, *Teflon, *Sub-boiling stills, Polytetra-fluoroethylene.

Inductively coupled plasma mass spectrometry was applied to the analysis of distillates of ultrahigh purity from quartz sub-boiling stills, a sub-boiling still made of Teflon TFE, and a sub-boiling still made of Teflon PFA. Although these studies were originally intended to prove the purity of distillates from the PFA still, comparison of distillates from the various stills has led to an interesting observation about the suitability of TFE for these reagents.

CHEMISTRY

Analytical Chemistry

900.203 PB89-186795 Not available NTIS National Bureau of Standards (NML), Gaithersburg, MD. Temperature and Pressure Div.

Preparation of Multistage Zone-Refined Materials for Thermochemical Standards.

Final rept. E. Rubinstein, M. E. Glicksman, B. W. Mangum, Q. T.

Sponsored by National Aeronautics and Space Administration, Washington, DC.

Pub. in Jnl. of Crystal Growth 89, p101-110 1988.

Keywords: *Calibrating, *Standards, *Purity, *Thermal analysis, *Nitriles, Measurement, Phase diagrams, Critical temperature, Hermetic compressors, Crystal structure, Zone melting, Melting points, Chemical equilibrium, Solids, Liquids, Gases, Reprints, Succinoni-

The melting, boiling, and triple points of materials have long served to define the International Practical Temperature Scale (IPTS), which is the embodiment of the thermodynamic temperature scale as 13 well-defined fixed points along with interpolative schemes for standardized instruments used for temperature measstandardized instruments used for temperature measurement. Techniques have evolved over the past seven years in the laboratory for preparing and characterizing ultra-pure organic compounds by multistage hermetic zone-refining. Methods have matured to the point where high-purity succinonitrile (SCN) now provides the triple-point equilibrium defining 58.0796 + or -0.0015 C relative to the IPTS of 1968. Most recently, the National Bureau of Standards, through its office of Standard Reference Materials, has issued certification for Standard Reference Material 1970, which is offered as an evacuated minicell containing approximately 60 g of double-stage hermetically zone-purified SCN. The steps that lead up to the completed minicells filled with SCN are discussed in detail. Since the cells are evacuated prior to the purification process, the succinonitrile is under its own vapor pressure. The solid/liquid equilibrium, as determined by melting and freezing point measurements, is therefore considered to be equivalent to the triple-point. A compilation of recently ac-quired performance data which assess the statistical properties of over 100 SCN triple-point cells is presented and discussed. These data firmly establish the reliability of multistage zone-refining methods for achieving reliable thermometric standards using solid/liquid/ vapor thermochemical equilibria.

PB89-187520 Not available NTIS National Bureau of Standards (NML), Gaithersburg, MD. Organic Analytical Research Div. Recent Advances in Bonded Phases for Liquid Chromatography.

L. C. Sander, and S. A. Wise. 1987, 117p Pub. in CRC Critical Reviews in Analytical Chemistry 18, n4 p299-415 1987.

Keywords: Chromatography, Chromatographic analysis, Substrates, Reprints, *Liquid chromatography, Void volume, Bonded phases, Retention.

Theoretical and practical aspects of bonded phase research are reviewed for work carried out over the last 5-10 years. Included in the review is research concerning liquid chromatographic substrates, bonded phase syntheses, novel bonded phases, methods used in the characterization of these materials, and progress in the development of retention theory. Not included is work dealing with ion exchange chromatography, immobilized enzymes, size exclusion chromatography, or purely mechanical aspects of liquid chromatography. An effort was made to include studies representative of the more important ongoing research in bonded phase technology.

900,205 PB89-187538 Not available NTIS National Bureau of Standards (NML), Gaithersburg, MD. Organic Analytical Research Div

Determination of Hydrocarbon/Water Partition
Coefficients from Chromatographic Data and
Based on Solution Thermodynamics and Theory.

Final rept. M. M. Schantz, and D. E. Martire. 1987, 17p Pub. in Jnl. of Chromatography 391, n1 p35-51 1987.

Keywords: *Chromatographic analysis, *Alcohols, *Water, Chemical analysis, Aromatic monocyclic hydrocarbons, Alkane compounds, Alkenes, Bromine,

Reprints, *Partition coefficients, Octanol, Hexadecane, Bromoalkanes, Alkylbenzenes.

The octanol/water and hexadecane/water partition coefficients for series of alkylbenzenes, alkanes, al-kenes, alcohols, and bromoalkanes were determined by the generator column technique and compared fato those calculated from the activity coefficients in each phase. A lattice-model theory suggested and the data confirmed that the logarithms of the partition coefficients and solute molar volume were the same for all homologous series studied. Furthermore, the logarithms of the octanol/water partition coefficients were linearly related (r(sup 2) = 0.993) to the logarithms of the reversed phase liquid chromatographic adjusted retention volumes determined by extrapolation to 100% water as the mobile phase for a variety of the solutes.

PB89-187546 Not available NTIS National Bureau of Standards (NML), Gaithersburg, MD. Organic Analytical Research Div. Preparation of Glass Columns for Visual Demonstration of Reversed Phase Liquid Chromatogra-

L. C. Sander, 1988, 2p Pub. in Jnl. of Chemical Education 65, n4 p373-374

Keywords: Separation, Dyes, Education, Colors(Materials), Reprints, *Reverse phase liquid chromatography, *Column packings, Glass column.

The preparation of a reversed phase glass column is described for demonstration of chromatographic principles. The column is prepared from large diameter particles of the type used in solid phase extraction. A simple demonstration is outlined for the separation of various food color dyes.

900,207 PB89-187553 Not available NTIS National Bureau of Standards (NML), Gaithersburg, MD. Inorganic Analytical Research Div Design Principles for a Large High-Efficiency Sub-**Boiling Stlii.** Final rept.

J. R. Moody, C. E. Wissink, and E. S. Beary. 1989, Pub. in Analytical Chemistry 61, n8 p823-827, 15 Apr

Keywords: *Distillation equipment, *Acid treatment, *Purification, Condensers(Liquefiers), Tetrafluoroethylene resins, Trace elements, Metals, Stills, Chemical analysis, Reprints, *Sub-boiling stills.

The sub-boiling method of acid purification for low trace element blank has now been in use for about 20 years. However, to achieve commercially useful yields distillates must be produced at approximately 25-100 L/day. Aspects of still design that include throughput have been examined, including variables such as condenser area, temperatures, distance between the condenser and the liquid in the still pot, and coolant temperature. Designs for several new stills are given and compared to those of prior sub-boiling stills. Perfluoroalkoxy resin construction was used both for ease of fabrication and for the distinct distillate purity.

900,208 Not available NTIS National Bureau of Standards (NML), Gaithersburg, MD. Gas and Particulate Science Div. High-Purity Germanium X-ray Detector on a 200 kV Analytical Electron Microscope. Final rept. E. B. Steel. 1986, 10p Pub. in Microbeam Analysis - 1986, p439-448 1986.

Keywords: *Electron microscopes, Thin films, Reprints, *High-purity Ge detectors, *X-ray detection, Lidrifted Si detectors.

JEOL 200CX AEM with a zero-take-off-angle germanium detector and with a high-take-off-angle Be window Si(Li) detector was used to collect data for the paper. The window thicknesses were 13 micrometers Be on the Si(Li), and 50 micrometers Be on the HPGE. The detectors were connected to either a TN-2000 with a PDP-11 or a multiplexed Ortec 918 multichannel analyzer connected to a VAX 11/730. NBS synthetic glasses, natural minerals, and pure metals were examined at an accelerating potential of 200 kV. The specimens were prepared as particles or sputtered films on thin carbon films supported by 200 mesh copper grids.

900.209

PB89-201610 Not available NTIS National Bureau of Standards (NML), Gaithersburg,

MD. Gas and Particulate Science Div.

Continuum Radiation Produced in Pure-Element
Targets by 10-40 keV Electrons: An Empirical Modei.

Final rept J. A. Small, S. D. Leigh, D. E. Newbury, and R. L.

Myklebust. 1986, 3p Pub. in Microbeam Analysis - 1986, p289-291 1986.

Keywords: *X ray analysis, *Microanalysis, *Bremsstrahlung, Electron beams, Mathematical models, Targets, Reprints, KeV range 10-100.

A new global relation has been developed for predicting electron-excited continuum intensities over a wide range of accelerating voltages 10-40 keV, atomic num-bers 4-92, and x-ray energies 1.5-20 keV. The new re-lation was determined empirically from the mathematical modeling of extensive data and is designed for calculating continuum intensities in analytical procedures, such as those requiring peak-to-background measure-ments, where the direct measurement of the continuum intensities is impracticable. The distribution of errors between the data and the model is symmetrical, centered around zero error with 63% of the values falling between plus or minus 10% relative error.

900.210

PB89-201628 Not available NTIS National Bureau of Standards (NML), Gaithersburg, MD. Gas and Particulate Science Div.

Laser Microprobe Mass Spectrometry: Description and Selected Applications.

D. S. Simons. 1988, 15p See also PB86-193232.

Pub. in Appl. Surf. Sci. 31, n1 p103-117 1988.

Keywords: *Mass spectroscopy, Particles, Aerosols, Surfaces, Reprints, *Laser microprobe mass spectroscopy, Time-of-flight spectrometers.

Laser microprobe mass spectrometry (LMMS) uses a high power density pulsed laser beam to ablate a microvolume of material. The fraction of this material that is ionized can be detected using a time-of-flight mass spectrometer. Two different instrumental configurations, 'transmission' and 'reflection,' that satisfy different analytical requirements are characterized by the geometry of ion collection from the specimen. The fea-tures of LMMS include a spatial resolution of about 1 micrometer, high mass range, isotopic selectivity, ppm detection limits for many elements from picograms of material, and molecular structure information from or-ganic materials. The major application areas for this technique are in the analysis of biological tissues and cells, organic materials, particles and aerosols, and surfaces of metals, semiconductors, and dielectric ma-

900,211

PB89-201651 Not available NTIS National Bureau of Standards (NML), Gaithersburg, MD. Gas and Particulate Science Div. Performance Standards for Microanalysis.

Final rept. E. Steel, A. Hartman, G. Hembree, P. Sheridan, and J. Small. 1986, 15p

Pub. in Jnl. of Trace Microprobe Tech. 4, n3 p147-161

Keywords: *Microanalysis, *Standards, *Electron microscopy, *Asbestos, Optical microscopes, Magnification, Performance, Polystyrene, Spheres, Shape, Size determination, Reprints, Scanning electron microscopy, Transmission electron microscopy.

Several standards for characterizing the performance of microanalysis procedures and instruments that are not directly related to chemical analysis are described. These standards may help analysts in calibration and quality assurance procedures in a wide variety of appli-cations. The magnification, particle size and shape, microscope performance, and asbestos analysis standards discussed are standards developed and characterized at NBS that are specifically designed for electron and light microscopy.

Analytical Chemistry

900.212 PB89-201677 Not available NTIS National Bureau of Standards (NML), Gaithersburg, MD. Gas and Particulate Science Div.
Uncertainties In Mass Absorption Coefficients In

Fundamental Parameter X-ray Fluorescence Anal-

B. A. R. Vrebos, and P. A. Pella. 1988, 10p Pub. in X-ray Spectrometry 17, n1 p3-12 1988.

Keywords: Reprints, *X-ray fluorescence analysis, Mass absorption coefficients, Intercomparison, Uncertainty.

Various compilations of mass absorption coefficients are currently used in fundamental parameter computer programs for correction of interelement effects in quantitative x-ray fluorescence analysis. Statistically significant differences in results of analysis were observed for certain sample types when three most commonly used compilations were compared, especially when only pure element standards were used for calibration. When type standards combined with a second degree polynomial fit to the standards are used for calibration, differences between compilations become negligible in the analysis results.

900 213 PB89-202063 Not available NTIS National Bureau of Standards (NML), Gaithersburg,

MD. Inorganic Analytical Research Div. Quality Assurance in Metals Analysis Using the Inductively Coupled Plasma.

Final rept. R. L. Watters. 1987, 20p

Pub. in ASTM (American Society for Testing and Materials) Special Technical Publication 944, p108-127

Keywords: *Quality assurance, *Chemical analysis, *Metals, Accuracy, Precision, Reprints, *Inductively coupled plasma.

The inductively coupled plasma (ICP) technique is a useful approach for multielement analysis of a wide vaniety of materials. Published reports have described the successful application of the ICP technique for the analysis of trace, minor, and major elements in metal alloys. When assessing the quality of analytical results using the ICP or any other technique, one must consider the contribution of various parts of the measurement process to the total random error. In addition, a careful evaluation of sources of systematic error must be undertaken, so that the appropriate corrections may be applied to the analytical results. The inherent linearity of the ICP technique offers a corrections scheme for dealing with spectral interferences, but the method of measuring correction factors and accounting for their variability warrants close examination. Most descriptions of ICP applications report relative freedom from matrix effects. Although the magnitude of systematic errors may be less than for other spectrometric techniques, such errors can cause analytical bias which can appreciably affect the final results. For example, it has been shown that differences in final acid concentration between pure element standards and the sample can cause systematic error. This type of problem can occur when complex alloys are dis-solved for ICP analysis. Examples of these kinds of errors and approaches to correcting for them will be

Not available NTIS PB89-202246 National Bureau of Standards (IMSE), Gaithersburg, MD. Ceramics Div.

Standard X-ray Diffraction Powder Patterns from the JCPDS (Joint Committee on Powder Diffraction Standards) Research Association. Final rept.

H. F. McMurdie, M. C. Morris, E. H. Evans, B. Paretzkin, W. Wong-Ng, and C. R. Hubbard. 1986,

See also PB89-171763. Sponsored by JCPDS-International Centre for Diffraction Data, Swarthmore, PA. Pub. in Powder Diffraction 1, n3 p265-275 Sep 86.

Keywords: *X ray diffraction, *Powder(Particles), *Standards, Qualitative analysis, Crystal structure, Lattice parameters, Reprints.

Standard x-ray powder diffraction patterns are presented for 15 substances. The patterns, useful for identification, were obtained by automated diffractom-

eter methods. The lattice constants from the experimental work were refined by least-squares methods, and reflections were assigned hk(sub I) indices consistent with space group extinctions. Relative intensities, calculated densities, literature references, and other relevant data are included.

900,215 PB89-211940 Not available NTIS National Bureau of Standards (NML), Gaithersburg, MD. Gas and Particulate Science Div. Preparation of Standards for Gas Analysis.

G. C. Rhoderick, and E. E. Hughes. 1987, 10p Sponsored by Institute of Gas Technology, Chicago,

Final rept.

Pub. in Natural Gas Energy Measurement, p45-54

Keywords: *Gas analysis, *Gravimetric analysis, Concentration(Composition), Chemical analysis, Natural gas, Methane, Reprints, *Standard reference mate-

A primary standard is prepared by an absolute method with the gravimetric method being the preferred technique. The basic method can be modified to prepare samples at very low concentrations (parts per trillion) and containing very specific and complex mixtures such as hydrocarbons. As will be illustrated, it is very important to have standards which are very close and bracket the concentration of the unknown in question. This is especially important when analyzing natural gas. In this case, two methods may be used to determine the concentration of methane in natural gas. However, one method will lead to a much lower uncertainty and thus, a lower uncertainty in the BTU value of the natural gas.

900 216 PB89-229108 Not available NTIS National Bureau of Standards (NML), Gaithersburg,

MD. Inorganic Analytical Research Div.

Expert-Database System for Sample Preparation by Microwave Dissolution. 1. Selection of Analytical Descriptors.

Final rept. F. A. Settle, B. I. Diamondstone, H. M. Kingston, and M. A. Pleva. 1989, 7p Grant NSF-CHE85-17147

Sponsored by National Science Foundation, Washing-

Pub. in Jnl. of Chemical Information and Computer Sciences 29, p11-17 1989.

Keywords: *Chemical analysis, Dissolving, Microwaves, Samples, Reprints, *Computer applications, waves, Samples, Reprints, Expert systems, Data bases.

A hybrid expert-database system is being developed to provide advice on the preparation of samples for elemental analysis. The paper describes an expert system component that is designed to assist the analyst in the identification of four analytical descriptors necessary to develop procedures for sample prepara-tion. When completed, the system will be able to furnish information on the dissolution of the sample. Future versions of the system will also provide advice on separations that may be required prior to the analytical measurement. A PC-AT microcomputer and commercially available software were used to develop the system. A compiled version of the system will run on PC-compatible computers.

900,217 PB89-229116 Not available NTIS National Bureau of Standards (NML), Gaithersburg, MD. Inorganic Analytical Research Div.

Microwave Digestion of Biological Samples: Selenium Analysis by Electrothermal Atomic Absorption Spectrometry.

Final rept. K. Y. Patterson, C. Veillon, and H. M. Kingston. 1988, 12p

Pub. in Introduction to Microwave Sample Preparation, Chapter 7, p155-166 1988.

Keywords: *Atomic absorption, *Selenium, *Analytical chemistry, *Microwaves, Zeeman effect, Tissues(Biology), Isotopic labelling, Standards, Temperature, Pressure, Reprints.

Closed vessel, microwave-heated digestions are used to rapidly destroy the organic matrix of biological samples with nitric acid at elevated temperatures and pressures. The system allows controlled, uniform applica-

tion of microwave power and monitoring of temperature and pressure, and permits reproducible conditions while not exceeding the pressure or temperature limitations of the container. Samples are digested and analyzed for selenium by electrothermal atomic absorption spectrometry using matrix modification and Zeeman background correction. Analyte recoveries are established by using a radiotracer (75)Se and accuracy is verified with standard reference materials of biological origin.

900,218 PB89-229173 Not available NTIS National Bureau of Standards (NML), Gaithersburg, MD. Radiation Physics Div.
Improved Low-Energy Diffuse Scattering Electron-Spin Polarization Analyzer.

Final rept.

M. R. Scheinfein, D. T. Pierce, J. Unguris, J. J.

McClelland, and R. J. Celotta. 1989, 11p

Sponsored by Office of Naval Research, Arlington, VA. Pub. in Review of Scientific Instruments 60, n1 p1-11 Jan 89.

Keywords: *Electron spin, *Polarization(Spin alignment), *Measurement instruments, Diffusion, Energy, Gold, Polycrystalline, Asymmetry, Trajectories, Re-

An improved low-energy diffuse scattering electron-spin polarization analyzer is described. It is based on the low-energy (150eV) diffuse scattering of polarized electrons from polycrystalline evaporated Au targets. By collecting large solid angles and efficiently energy filtering the scattered electrons, a maximum figure of merit, FOM = S sup 2 I/I sub o = 2.3 x 10(sub -4) is achieved. Maximum measured values of the Sherman function were S = 0.15. Further, the instrumental (false) asymmetry due to changes in the trajectory of the incident electron beam has been minimized by balancing the angular and displacement asymmetries. A total residual scan asymmetry as low as 0.0035/mm has been measured over 4-mm scan fields at the Au target in the detector. This instrumental asymmetry would produce a maximum error in the polarization in a SEMPA experiment of less than 0.3% for a 100-micron full-field scan. Details of the design and performance of the new detector are given.

900.219 PB89-230312 Not available NTIS National Inst. of Standards and Technology (NML), Gaithersburg, MD. Inorganic Analytical Research Div. Introduction to Supercritical Fluid Chromatography, Part 2. Applications and Future Trends.

M. D. Palmieri. 1989, 7p Pub. in Jnl. of Chemical Education 66, n5 pA141-A147 May 89.

Keywords: *Chromatographic analysis, Chemical analysis, Bioassay, Organic compounds, Separation, Trends, Forecasting, Reprints, *Supercritical fluid chromatography.

The article describes applications and future trends of supercritical fluid chromatography in analytical chemistry. Examples are given showing the types of organic and biological compounds which can be separated using supercritical fluid chromatography. Present and future areas of research in supercritical fluid chromatography are described.

900,220 PB89-230338 Not available NTIS National Inst. of Standards and Technology (NML), Gaithersburg, MD. Inorganic Analytical Research Div. Isotope Dilution Mass Spectrometry for Accurate Elemental Analysis. Final rept.

Final rept.

J. D. Fassett, and P. J. Paulsen. 1989, 7p

Pub. in Analytical Chemistry, p643A-649A, 15 May 89.

Keywords: *Chemical analysis, *Mass spectroscopy, *Inorganic compounds, Reviews, Reprints, *Isotope

The technique of isotope dilution mass spectrometry (IDMS) as it is applied to inorganic analysis is reviewed. The principles of isotopic spiking are discussed as well as the possibilities of high accuracy, high precision measurement. Recent improvements in instrumentation are cited and special mention is made of the use of IDMS with inductively coupled plasma mass spectrometry. The present role of IDMS in ana-

CHEMISTRY

Analytical Chemistry

lytical chemistry is assessed and a future, expanded role promoted.

900,221 PB89-231070 PB89-231070 Not available NTIS National Inst. of Standards and Technology (NML), Gaithershurg MD Journapie Application (NML) Gaithersburg, MD. Inorganic Analytical Research Div. Development of the NBS (National Bureau of Standards) Beryllium Isotopic Standard Reference Material.

Final rept. J. D. Fassett, K. G. W. Inn, and R. Watters. 1988, 4p. See also DE88002671.

Pub. in RIS 88, Institute of Physics, Conference Series No. 94: Section 11, Gaithersburg, MD, April 10-15, 1988, p379-382.

Keywords: *Beryllium isotopes, *Mass spectroscopy, *Atomic spectroscopy, Spectrum analysis, Chemical analysis, *Standard reference materials, National Institute of Standards and Technology.

A beryllium isotopic standard is being developed for the Accelerator Mass Spectrometry community. A criti-cal aspect in this exercise is the evaluation of the iso-topic composition of the (10)Be enriched source mate-rial. A procedure is presented here for the indirect de-termination of mass spectrometric isotopic discrimination, a potential systematic error in this evaluation. The procedure is demonstrated through the combined application of resonant ionization mass spectrometry and inductively coupled plasma atomic spectroscopy.

900,222 PB89-235642

(Order as PB89-235634, PC A04) National Inst. of Standards and Technology, Gaithersburg, MD.

Determination of Trace Level Iodine in Biological and Botanical Reference Materials by Isotope Dilution Mass Spectrometry. Bi-monthly rept.

J. W. Gramlich, and T. J. Murphy. 1989, 6p Included in Jnl. of Research of the National Institute of Standards and Technology, v94 n4 p215-220 Jul/Aug

Keywords: *lodine, *Trace elements, *Mass spectrometry, Chemical analysis, Milk, Plants(Biology), Isotopes, Lanthanum compounds, *Standard reference materials.

A method has been developed for the determination of trace level iodine in biological and botanical materials. The method consists of spiking a sample with (129)I, equilibration of the spike with the natural iodine, wet ashing under carefully controlled conditions, and separation of the iodine by co-precipitation with silver chlo-nde. Measurement of the (129)I/(127)I ratio is accom-plished by negative thermal ionization mass spectrometry using LaB6 for ionization enhancement. The application of the method to the certification of trace iodine in two Standard Reference Materials is described.

900,223 PB89-235659

(Order as PB89-235634, PC A04) National Inst. of Standards and Technology, Gaithersburg, MD.

Spectrum of Doubly Ionized Tungsten (W III).

Bl-monthly rept.
L. Iglesias, M. I. Cabeza, F. R. Rico, and O. Garcia-Riquelme. and V. Kaufman. 1989, 38p
Prepared in cooperation with Consejo Superior de Investigaciones Cientificas, Madrid (Spain). Inst. de Optica.

Included in Jnl. of Research of the National Institute of Standards and Technology, v94 n4 p221-258 Jul/Aug

Keywords: *Tungsten, *Spectroscopy, *Ionization, Tables(Data).

The spectrum of doubly ionized tungsten (W III) was produced in a sliding-spark discharge and recorded photographically on the NIST 10.7-m normal-incidence vacuum spectrograph in the 600-2680 A spectral region. The analysis has led to the establishment of 71 levels of interacting 5d(4), 5d(3)6s(2) even configurations and 164 levels of the interacting 5d(3)6p and 5d(2)6s6p odd ones. A total of 2636 lines have been classified as transisions between the 235 experimental statements. tally determined levels. Comparison between the observed levels and those calculated from matrix diagonalizations with least-squares fitted parameters shows an rms deviation of + or - 87/cm for the even configurations and + or - 450/cm for the odd ones.

900,224 PB90-117300 PB90-117300 Not available NTIS National Inst. of Standards and Technology (NEL), Gaithersburg, MD. Semiconductor Electronics Div. Interlaboratory Determination of the Calibration Factor for the Measurement of the Interstitial Oxygen Content of Silicon by Infrared Absorption. Final rept.

A. Baghdadi, W. M. Bullis, M. C. Croarkin, Y. Li, R. I. Scace, R. W. Series, P. Stallhofer, and M. Watanabe.

1989, 10p Pub. in Jnl. of the Electrochemical Society 136, n7 p2015-2024 Jul 89.

Keywords: *Silicon, *Quantitative analysis, *Calibrating, *Oxygen, *Infrared spectroscopy, *Interstitials, Reproducibility, Accuracy, Reprints.

An international interlaboratory dual experiment was performed to determine the calibration factor used to calculate the interstitial oxygen content of silicon from room-temperature (300 K) infrared (IR) absorption measurements. Round robins were conducted for both the infrared and the absolute measurements on the same or equivalent specimens. The calibration factor for computing the oxygen content of silicon in parts per million atomic (ppma) from a room-temperature measurement of the absorption coefficient at 1107/cm was determined to be 6.28 + or - 0.18 ppma/cm. The IR round robin showed a reproducibility on the order of

900,225 PB90-117912 Not available NTIS National Inst. of Standards and Technology (NML), Gaithersburg, MD. Chemical Thermodynamics Div. Differential Scanning Calorimetric Study of Brain Clathrin. Final rept

F. P. Schwarz, C. J. Steer, and W. H. Kirchhoff.

1989, 7p Pub. in Archives of Biochemistry and Biophysics 273, n2 p433-439 Sep 89.

Keywords: *Brain, *Chemical analysis, Cattle, Enthalpy, Reprints, *Cell membrane coated pits, *Clathrin, *Differential scanning calorimetry.

The thermal denaturation of clathrin-coated vesicles isolated from bovine brain tissue has been studied by differential scanning calorimetry and has been com-pared to basket structures reformed from isolated tris-kelion trimers of clathrin and to isolated triskelions. The coated vesicles and reformed vesicles exhibited a single denaturation transition peak at 55.9 + or - 0.1 C, skewed to low temperatures whereas the thermograms for the reformed baskets exhibited a broad trangrams for the reformed baskets exhibited a broad transition peak at 53.1 + or - C and a peak at 56.3 + or - 0.1 C. Neither transition was reversible. The specific transition enthalpy was 11.5 + or 1.0 J/g for the coated vesicles and the total transition enthalpy was 9.1 + or - 0.3 J/g for the reformed baskets. In contrast, isolated triskelions showed no thermal transition between 15 and 90 C. Although the coated vesicles and the reformed baskets have similar stability reflection their similar structures the coated vesicles appear ing their similar structures, the coated vesicles appear to be marginally more stable than the reformed bas-kets. The complexity of the transition profiles and their lack of symmetry suggest the existence of several, somewhat independent, domains unique to the cage-like structure of the coated vesicles and reformed bas-

900,226 PB90-118175 Not available NTIS National Inst. of Standards and Technology (NML), Gaithersburg, MD. Inorganic Analytical Research Div. Preconcentration of Trace Transition Metal and Rare Earth Elements from Highly Saline Solutions. Final rept.

D. M. Strachan, S. Tymochowicz, P. Schubert, and H. M. Kingston. 1989, 7p Contract DE-AC06-76RL01830

Sponsored by Department of Energy, Washington, DC. Pub. in Analytica Chimica Acta 220, p243-249 1989.

Keywords: *Quantitative analysis, *Brines, *Transition metals, *Rare earth elements, Concentration(Composition), Chelation, Reprints, Trace amounts.

Quantitative recovery and preconcentration of trace amounts of Ce(III), Co(III), Eu(III), Fe(III), Gd(III), Mn(II), Y(III) and Zn(II) lons from nearly saturated brines on the chelating resin Chelex-100 are described. Carrierfree radioactive isotopes were used. Only manganese was significantly affected by the high ionic strength of the brines. Chromium(III) was retained quantitatively by the resin but not eluted quantitatively. The results indicate that transition metal and rare earth ions can be quantitatively preconcentrated from solutions of low and high ionic strength.

PB90-118191 Not available NTIS National Inst. of Standards and Technology (NML), Gaithersburg, MD. Inorganic Analytical Research Div. Introduction to Microwave Acid Decomposition. Final rept.

L. B. Jassie, and H. M. Kingston. 1988, 6p Pub. in Introduction to Microwave Acid Decomposition. Chapter 1, p1-6 1988.

Keywords: *Acid treatment, *Decomposition, *Microwave equipment, Chemical analysis, Reviews, Reprints, *Sample preparation.

A chronological review of the literature on microwaveassisted sample preparations is presented. Temperature measurements and other innovations in the field of sample decomposition using microwave systems are surveyed.

PB90-123399 Not available NTIS National Inst. of Standards and Technology (IMSE), Gaithersburg, MD. Polymers Div. Calclum Hydroxyapatite Precipitated from an

Aqueous Solution: An International Multimethod Analysis.

Final rept. Third Tept.

J. Arends, J. Christoffersen, M. R. Christoffersen, H. Eckert, B. O. Fowler, J. C. Heughebaert, G. H. Nancollas, J. P. Yesinowski, and S. J. Zawacki.

1987, 18p Pub. in Jnl. of Crystal Growth 84, n3 p515-532 1987.

Keywords: *Chemical analysis, *Precipitation(Chemistry), Synthesis(Chemistry), Infrared spectroscopy, Nuclear magnetic resonance, Differential thermal analysis, Area, Crystal growth, X-ray diffraction, Reprints, *Standard reference materials, *Apatite/(calcium-salt)-hydroxyl, Scanning electron microscopy.

Calcium hydroxylapatite (Ca10(PO4)6(OH)2), pared for use as a standard reference material from aqueous solutions at 70 C, was analyzed by various techniques in six different Institutes to determine its purity and composition. The techniques employed were: chemical analyses, x-ray diffraction, infrared analysis, magic angle spinning nuclear magnetic reso-nance, differential thermal analysis, scanning electron microscopy, surface area and crystal size distribution measurements, crystal growth and crystal dissolution measurements.

900,229

PB90-123464 Not available NTIS
National Inst. of Standards and Technology (NML),
Gaithersburg, MD. Inorganic Analytical Research Div.
Comparison of Microwave Drying and Conventional Drying Techniques for Reference Materials.

Final rept. E. S. Beary. 1988, 5p Pub. in Analytical Chemistry 60, n8 p742-746 1988.

Keywords: *Ovens, *Microwave equipment, Substitutes, Comparison, Performance evaluation, Laboratory equipment, Chemical analysis, Reprints, *Sample preparation, *Standard reference materials.

A microwave drying oven was evaluated for potential use as an alternate method of sample pre-treatment in an analytical laboratory. The high precision drying data an analytical laboratory. The high precision drying data achieved suggests that this instrumer is well suited to industrial applications such as quality control and merits further study. However, differences in conventional drying and microwave drying makes the current implementation of the microwave drying oven unfeasible in a reference laboratory. In addition, a stable sample composition must be confirmed before the method could be recommended as a drying procedure preceding sample analysis. preceeding sample analysis.

900,230

PB90-123472 Not available NTIS National Inst. of Standards and Technology (NML), Galthersburg, MD. Inorganic Analytical Research Div. Determination of Selenium and Tellurium in Copper Standard Reference Materials Using Stable Isotope Dilution Spark Source Mass Spectrometry. Final rept.

E. S. Boary, P. J. Paulsen, and G. M. Lambert. 1988,

Pub. in Analytical Chemistry 60, n7 p733-736 1988.

Keywords: *Selenium, *Tellurium, *Mass spectrosco-py, *Chemical analysis, Copp, Reprints, *Isotope dilu-tion, *Standard reference materials, Tracer studies, Selenium 75.

The concentration of Se and Te have been determined by isotope dilution spark source mass spectrometry (ID SSMS). Discrepancies in Se concentrations prompted an extensive evaluation of the copper benchmarks series. Because certain forms of Se are volatile, a (75)Se tracer study aided in the identification of areas where Se losses could occur. In isotope dilution, slight losses of Se after equilibration of the natural and enriched isotopes would not alter the calculated concentrations. They are based on data generated from the measured isotopic ratio which is established during equilibration. Agreement of Se concentrations between copper samples dissolved in covered teflon beakers with those dissolved in carius tubes assured that no Se was volatilized prior to equilibration. The Cu samples analyzed had Se and Te concentration ranging from 0.59-480 micrograms/g and 0.29-196 micro-grams/g respectively with about a 2% relative stand-ard deviation. The blank contribution was negligible.

900.231 PB90-128539 Not available NTIS National Inst. of Standards and Technology (NML), Gaithersburg, MD. Organic Analytical Research Div. Comparison of Liquid Chromatographic Selectivity for Polycyclic Aromatic Hydrocarbons on Cyclodextrin and C18 Bonded Phases.

Final rept. M. Olsson, L. C. Sander, and S. A. Wise. 1989, 14p Pub. in Jnl. of Chromatography 477, p277-290 1989.

Keywords: *Aromatic polycyclic hydrocarbons, *Chemical analysis, *Chromatographic analysis, *Dextrins, Comparison, Separation, Performance evaluation, Molecular structure, Reprints, *Liquid chromatography, Retention, Selection rules.

Selectivity towards polycyclic aromatic hydrocarbons (PAHs) was studied on cyclodextrin bonded phases and compared to selectivity observed on C18 phases. The study included the separation of eleven five-ring PAH isomers on each of three phase types; monomeric C18, polymeric C18 and cyclodextrin. Retention of PAHs ranging in size from three to six condensed rings was also investigated. Retention on the cyclodextrin phase is based on inclusion complexing between the solute and cyclodextrin cavity, resulting in a strong shape dependence. However, the shape selectivity exhibited by the cyclodextrin phase is different from that exhibited by either the monomenic or polymeric C18 phases; retention on the cyclodextrin phase is strongly dependent on the shape and shows very little molecular weight dependence. Calculations of solute molecular widths were performed to predict the isomers' ability to enter the cyclodextrin cavity. The effect of sample solvent and injection volume was also investigated for the cyclodextrin phase. A retention model based on the solute shape is proposed for PAH isomers on Betacyclodextrin phase.

900.232 PB90-128653 Not available NTIS National Inst. of Standards and Technology (NML), Gaithersburg, MD. Gas and Particulate Science Div. Determination of Experimental and Theoretical k(sub ASI) Factors for a 200-kV Analytical Electron Microscope.

Final rept.

P. J. Sheridan. 1989, 21p Pub. in Jnl. of Electron Microscopy Technique 11, p41-

Keywords: *Quantitative analysis, *Electron microscopy, Glass, X ray analysis, Grinding(Comminution), Standards, Particle size, Reprints.

The relative sensitivity of an analytical electron microscope and energy-dispersive x-ray detector to x-rays of various elements is investigated through an extensive k(sub ASi) factor study. Elemental standards, primarily National Bureau of Standards multielement research glasses, were dry-ground into submicrometer-

sized particles and analyzed at 200 kV accelerating potential. The effect of self-absorption of x-rays by the particle has been corrected for, allowing the experimental k(sub ASi) factors from the study to approximate those that could be obtained from 'infinitely thin' specimens. Whenever possible, elemental k-factors were determined by the analysis of many (up to a maximum of nine) different standard materials. Experimental k(sub ASi) factors were calculated for a wide range of K(sub alpha), L(sub alpha), and M(sub alpha) x-ray lines. For companison, theoretical k(sub ASi) factors, employing a variety of ionization cross sections, were computed. Good agreement is obtained between several of the theoretical k-factor models and the experimental results. Mass volatilization of Na and K from the small glass particles during analysis is discussed, as are observations that the grinding and/or dispersing of standard materials in a liquid (such as ethanol) may promote leaching of certain elements from the particle matrix.

900,233 PB90-128695 Not available NTIS National Inst. of Standards and Technology (NML), Gaithersburg, MD. Organic Analytical Research Div. Synthesis and Characterization of Novel Bonded Phases for Reversed-Phase Liquid Chromatogra-

Phys. Final rept.
A. M. Stalcup, D. E. Martire, L. C. Sander, and S. A. Wise. 1989, 7p

Pub. in Chromatographia 27, n9/10 p405-411 May 89.

Keywords: *Chromatographic analysis, *Aromatic polycyclic hydrocarbons, *Synthesis(Chemistry), *Chemical analysis, Comparison, Chemical bonds, Separation, Reprints, *Liquid chromatography, Retention, Selection rules.

The results of a chromatographic comparison of newly synthesized reversed-phase bonded stationary phases incorporating various degrees of unsaturation or ngidity are presented. The phases studied included monomeric n-decyl, polymeric n-decyl, adamantyl, norpinyl, decadiynyl, phenylbutyl and Beta-naphthyl bonded phases. The effect of bonded phase structure on retention is discussed for selected aromatic so-

900.234 PB90-128786 Not available NTIS National Inst. of Standards and Technology (NML), Gaithersburg, MD. Ionizing Radiation Physics Div. Pattern Recognition Approach in X-ray Fiuorescence Analysis.

L. I. Yin, J. I. Trombka, and S. M. Seltzer. 1989, 8p Pub. in Nuclear Instruments and Methods in Physics Research A277, p619-626 1989.

Keywords: *Pattern recognition, Alloys, Computation, Reprints, *X-ray fluorescence analysis.

In many applications of X-ray fluorescence (XRF) analysis, quantitative information on the chemical components of the sample is not of primary concern. Instead, the XRF spectra are used to monitor changes in the composition among samples, or to select and classify samples with similar compositions. The authors propose in this paper that the use of pattern recognition technique in such applications may be more convenient than traditional quantitative analysis. The pattern recognition technique discussed here involves only one parameter, i.e., the normalized correlation coefficient and can be applied directly to raw data. Its computation is simple and fast, and can be easily carried out on a personal computer. The efficacy of this pattern recgnition approach is luuustrated withthe anaylsis of experimental XRF spectra obtained from geological and alloy samples.

900,235 PB90-135922 Not available NTIS National Inst. of Standards and Technology (NML), Gaithersburg, MD. Gas and Particulate Science Div. Low Pressure, Automated, Sample Packing Unit for Diffuse Reflectance Infrared Spectrometry. Final rept.

A. A. Christy, J. E. Tvedt, T. V. Karstang, and R. A. Velapoldi. 1988, 4p
Pub. in Review of Scientific instruments 59, n3 p423-

426 Mar 88.

Keywords: *Sample preparation, *Infrared spectroscopy, Chemical analysis, Low pressure tests, Solids, Design criteria, Particle size distribution, Performance evaluation, Automatic control equipment, Reprints, *Fourier transform spectroscopy, *Packing.

The authors have designed and built an automatic, low pressure packing unit to prepare ground, solid samples for diffuse reflectance infrared Fourier transform spectroscopy (DRIFTS). Use of this unit coupled with sample rotation during measurement, and control of time, pressure, particle size and size distribution provides excellent precision in obtaining DRIFTS spectra. Thus representative DRIFTS spectra can be obtained quickly and efficiently, with a single spectrum as op-posed to previous efforts requiring the averaging of several spectra.

900.236

PB90-136540 Not available NTIS National Inst. of Standards and Technology (NML), Gaithersburg, MD. Gas and Particulate Science Div. Identification of Carbonaceous Aerosols via C-14 Accelerator Mass Spectrometry, and Laser Microprobe Mass Spectrometry. Final rept.

L. A. Currie, R. A. Fletcher, and G. A. Klouda. 1987,

Pub. in Nuclear Instruments and Methods in Physics Research Section B - Beam Interactions with Materials and Atoms 29, n1-2 p346-354 1987.

Keywords: *Chemical analysis, *Aerosols, *Carbon 12, *Carbon 14, *Mass spectroscopy, Particles, Sampling, Performance evaluation, Reprints, *Laser spectroscopy, Atmospheric chemistry.

Carbon isotopic measurements ((12)C, (14)C), derived from chemical measurements of total carbon plus AMS measurements of (14)C/(12)C have become an accepted means for estimáting fóssil and contemporary carbon source contributions to atmospheric carbon. Because of the limited sensitivity of these techniques, however, such measurements are restricted to 'bulk' samples comprising at least 10 - 100 mi-crograms of carbon. Laser mass spectrometry offers an important complementary opportunity to investigate the chemical nature of individual particles as small as 0.1 micrometers in diameter. Although there is little hope to measure (14)C/(12)C in such small samples, the compositional and structural information available with the laser microprobe is of interest for possible source discrimination. Also, the analysis of individual particles, which may reflect individual sources, yields significant potential increases in spatial, temporal and source resolution, in comparison to bulk sample analy-

900,237

PB90-136979 Not available NTIS National Inst. of Standards and Technology (NML), Gaithersburg, MD. Organic Analytical Research Div. Spectroelectrochemistry of a System involving Two Consecutive Electron-Transfer Reaction. Final rept.

W. T. Yap, G. Marbury, E. A. Blubaugh, and R. A. Durst. 1989, 5p

Pub. in Jnl. of Electroanalytical Chemistry 271, p325-329 1989.

Keywords: *Spectrum analysis, *Electrochemistry, *Electron transfer, Nernst effect, Nonlinear systems, Numerical analysis, Chemical reactions, Separation, Chemical analysis, Reprints, Potentials.

Analysis of the spectroelectrochemistry of a multi-step electrochemical process in a thin layer cell is presented. Typical characteristic Nernst plots for various formal potential separations and various extinction coefficients of the species are illustrated. A method for calculating the formal potentials from these non-linear Nernst plot is suggested, and an illustrative application is given.

Basic & Synthetic Chemistry

900,238

PB89-146963 Not available NTIS National Bureau of Standards (NEL), Gaithersburg, MD. Building Materials Div.

Basic & Synthetic Chemistry

Synthesis and Characterization of Ettringite and Related Phases.

Final rept. L. Struble. 1986, 7p

Sponsored by Department of Energy, Washington, DC.

Passive and Hybrid Solar Energy Div.
Pub. in Proceedings of International Congress on the
Chemistry of Cement (8th), Rio de Janeiro, Brazil, September 22-27, 1986, p582-588.

Keywords: *Dehydration, *Phase diagrams, *Energy storage, Synthesis, Enthalpy, Compositions, Assess-ments, Evaluation, Reprints, *Ettringite, *Energy storage materials.

Ettringite and related phases were studied to assess their performance as energy storage materials, utiliz-ing the dehydration reaction. Ettringite and four isosing the dehydration reaction. Ettringite and four isostructural phases were synthesized and characterized, particularly with regard to thermal properties, to study the effect of chemical composition on such thermal parameters as the temperature and the enthalpy change of the dehydration reaction. Synthesis procedures were developed for following phases: (Ca3AI(OH)6)2(SO4)3x26 H2O (ettringite), (Ca3Cr(OH)6)2(SO4)3x26H2O, (Ca3Cr(OH)6)2(SO4)3x26H2O, (Ca3Si(OH)6)2(SO4)3x26H2O, and (Ca3Si(OH)6)2(SO4)2(CO3)2x24H2O (thaumasite). Each synthesized material was examined for bulk

Each synthesized material was examined for bulk chemical composition, phase composition, unit cell parameters, morphology, and thermal properties. Each phase showed a low-temperature dehydration with initial temperature ranging from 6 C to 33 C. The change in enthalpy associated with the dehydration ranged from 60 to 200 cal/g sample. Thus both the dehydration temperature and the enthalpy change varied significantly for the isostructural phases studied.

900,239 PB89-228423 Not available NTIS Not available NTIS
National Inst. of Standards and Technology (NML),
Gaithersburg, MD. Surface Science Div.
Cr(110) Oxidation Probed by Carbon Monoxide
Chemisorption. Final rept.

N. D. Shinn. 1989, 13p Sponsored by Department of Energy, Washington, DC. Pub. in Surface Science 214, p174-186 1989.

Keywords: *Oxidation reduction reactions, *Chromium oxides, "Chemisorption, "Carbon monoxide, Electron energy, Annealing, Oxygen, Vibrational spectra, Surface chemistry, Reprints, Binding sites.

High resolution electron energy spectroscopy of chemisorbed carbon monoxide is used to distinguish be-tween an annealed, oxidized Cr(110) surface, an intermediate, subsurface Cr(110) oxide, and oxygen-dosed Cr(110). On the annealed oxide, weak signals are observed from both the dissociation-precursor (alpha 1-CO) and the terminally-bonded (alpha 2-CO) molecular CO binding states, but only after relatively high CO exposures, reflecting greatly reduced sticking probabilities. On the surface with subsurface oxygen, both binding states are sequentially populated with sticking probabilities comparable to that of clean Cr(110); also, an increase in nuCO from approximately 1975 to 2035/cm is observed at high coverages of terminally-bonded alpha sub 2-CO. Both the annealed-oxide and subsurface-oxide CO chemisorption results are in contrast to the selective poisoning of only alpha sub 1-CO by chemisorbed atomic oxygen on Cr(110). Comparisons among the three oxygen containing surfaces show how vibrational spectroscopy of chemically-inequivalent molecular binding states may be used as a probe of surface oxidation and provide insights into the oxygen-CO surface chemistry.

900,240 PB90-123753 Not available NTIS National Inst. of Standards and Technology (NML), Gaithersburg, MD. Organic Analytical Research Div. Facile Synthesis of 1-Nitropyrene-d9 of High isotopic Purity. Final rept.

Pillai rept. A. J. Fatiadi, and L. R. Hilpert. 1989, 8p Pub. in Jnl. of Labelled Compounds and Radiopharma-ceuticals XXVII, n2 p129-136 1989.

Keywords: *Chemical reactions, *Isotopes, Aromatic polycylic hydrocarbons, Gas chromatography, Mass spectroscopy, Reprints, *Standard reference materi-als, *Nitropyrenes, Llquid chromatography.

1-Nitropyrene-d9, 1,3-dinitropyrene-d8, 1-6-dinitropyrene-d8, and 1,8-dinitropyrene-d8, used as internal

standards for the determination of nitro-polycyclic aromatic hydrocarbons in simple and complex mixtures and required for GC/MS measurements used in the certification of NBS Standard Reference Material 1596 (a mixture of nitropyrenes), were synthesized in one step from commercially available pyrene-d10 and nitric acid-d1. The electron impact mass spectra and isotopic punity of 1-nitropyrene-d9 and the deuterated dinitro-pyrenes were determined; the compounds were char-acterized by gas chromatography-mass spectrometry and by high performance liquid chromatography.

Industrial Chemistry & Chemical Process Engineering

900,241 PB89-156376 PC A08/MF A01 National Inst. of Standards and Technology (NML), Gaithersburg, MD. Center for Chemical Technology. Center for Chemical Technology: 1988 Technical

Summary rept. 1 Oct 87-30 Sep 88. J. Hord. Dec 88, 162p NISTIR-88/3907 See also PB88-164272.

*Chemical *Research Keywords: engineering, rojects, Measurement, Thermophysical properties, Standards, Reaction kinetics, Proteins, Calibrating, Fluid mechanics, Separation, Thermodynamics, Biotechnology.

Technical research activities performed by the Center for Chemical Technology during the Fiscal Year 1988 are summarized herein. These activities include work in the general categories of measurements (standards, processes, and equipment design), properties (thermophysical, thermochemical, and kinetic), and biotechnology (protein engineering and separations). They embody: development and improvement of measurement standards, measurement principles, and calibration services for pressure, temperature, volumetric and mass flow rates, liquid volume and density, humidity, and airspeed; generation (via accurate measurements and advanced predictive models) of reliable reference data for thermophysical, thermochemical, and kinetic properties of pure fluids, fluid mixtures, and solids of industrial and environmental importance; provision of fundamental understanding of protein structure-function and advanced technology for commercial scale separation of proteins; and development of improved correlations, models, and measurement techniques for complex flows, heat and mass transport, mixing, and chemically reacting flows of interest in modern unit operations.

900,242
PB89-174908
Not available NTIS
National Bureau of Standards (NEL), Boulder, CO.
Chemical Engineering Science Div.
Latent Heats of Supercritical Fluid Mixtures.

Final rept. M. C. Jones, and P. J. Giarratano. 1988, 4p Pub. in AlChE (American Institute of Chemical Engineers) Jnl. 34, n12 p2059-2062 Dec 88.

Keywords: *Latent heat, *Decanes, Equations of state, Aliphatic hydrocarbons, Mixtures, Enthalpy, Carbon dioxide, Reprints, *Supercritical fluids, Heat of condensation, Supercritical pressures.

The Peng-Robinson equation of state was used to calculate partial molar enthalpies for coexisting vapor and liquid phases in the mixture N-decane-CO2 above the critical pressures of the pure components. From these, the heats of condensation in the retrograde region could be calculated.

900,243 PB89-176416 Not available NTIS MD. Chemical Process Metrology Div.
Laser Excited Fluorescence Studies of Black Liquor.

Final rept.
J. J. Horvath, and H. G. Semerjian. 1986, 7p
Pub. in Proceedings of SPIE (Society of Photo-Optical
Instrumentation Engineers)-Optical Techniques for Industrial Inspection, v665 p258-264 1986.

Keywords: *Black liquors, *Pulping, Near ultraviolet radiation, Process control, Papers, Pulps, Inspection, Lignin, *Laser induced fluorescence.

Laser excited fluorescence of black liquor was investi-gated as a possible monitoring technique for pulping processes. A nitrogen pumped dye laser was used to examine the fluorescence spectrum of black liquor solutions. Various excitation wavelengths were used be-tween 290 and 403 nm. Black liquor fluorescence spectra were found to vary with both excitation wavelength and black liquor concentration. Laser excited fluorescence was found to be a sensitive technique for measurement of black liquor with good detection limits and linear response over a large dynamic range.

900,244

PB89-176481 Not available NTIS National Bureau of Standards (NEL), Boulder, CO. Chemical Engineering Science Div.

influence of Reaction Reversibility on Continuous-Flow Extraction by Emulsion Liquid Membranes. Final rept.

D. L. Reed, A. L. Bunge, and R. D. Noble. 1987, 21p Grant EPA-R-811247

Sponsored by Environmental Protection Agency, Washington, DC. Grants Administration Div.

Pub. in ACS (American Chemical Society) Symposium Series 347, p62-82 1987.

Keywords: *Solvent extraction, *Mathematical models, *Liquid filters, *Membranes, *Chemical reactivity, *Chemical equilibrium, Performance evaluation, Irreversible processes, Emulsions, Continuum mechanics, Reprints.

The paper examines theoretically the continuous flow extraction by emulsion globules in which the transferring solute reacts with an internal reagent. The reversi-ble reaction model is used to predict performance. These results are compared with advancing front calculations which assume an irreversible reaction. A simple criterion which indicates the importance of re-action reversibility on performance is described. Calcu-lations show that assuming an irreversible reaction can lead to serious underdesign when low solute concentrations are required. For low solute concentrations are exact analytical solution to the reversible reaction problem is possible. For moderate solute concentra-tions, the authors have developed an easy parameter adjustment of the advancing front model which rea-sonably approximates expected extraction rates.

900.245

PB89-176739 Not available NTIS National Bureau of Standards (NEL), Gaithersburg, MD. Thermophysics Div. Modelling of impurity Effects in Pure Fluids and

Fluid Mixtures.

Final rept.

J. S. Gallagher. 1986, 20p
Pub. in Proceedings of American Institute of Chemical
Engineers Spring National Meeting and Petroleum
Expo'86, New Orleans, LA., April 6-10, 1986, 20p.

Keywords: *Impurities, Mixtures, Ethylene, Thermodynamic properties, *Fluid modelling, *Impurity effects, Isobutane, Isopentane.

An extended corresponding-states model for the Helmholtz free energy for two-component mixtures, based upon existing accurate representations of the principal component as the reference function, has been used to model the effects of impurities. The results give a clearer and more accurate view of the errors caused in the measurement of thermodynamic properties by small amounts of impurity than was previously obtained with simplifying approximations. The model is also extended to include three-component mixtures to allow the estimation of the effects of impurities in two-component mixtures. The model is applied to two systems of practical importance: methane as an impurity in ethylene, and n-butane as an impurity in iso-butane-isopentane mixtures. Both of these systems are of commercial importance and commonly used in their critical regions where the impurities can cause large errors in the thermodynamic properties used and where existing procedures for the estimation of the impurity effects break down.

900,246

Not available NTIS PB89-179584 National Bureau of Standards (NEL), Gaithersburg, MD. Chemical Process Metrology Div.

Industrial Chemistry & Chemical Process Engineering

Dynamic Light Scattering and Angular Dissymmetry for the In situ Measurement of Sillcon Dioxide Particle Synthesis in Flames.

Final rept.

M. R. Zachariah, D. Chin, H. G. Semerjian, and J. L. Katz. 1989, 7p

Pub. in Applied Optics 28, n3 p530-536, 1 Feb 89.

Keywords: *Silicon dioxide, *Particle size, *Light scattering, Diffusion flames, Optical measurement, Process control, Reprints, *Synthesis(Chemistry).

Particle size measurements have been made of silica formation in a counterflow diffusion flame reactor using dynamic light scattering and angular dissymmetry methods. The results suggest that the techniques compare quite favorably in conditions of high signal to noise. However, the dynamic light scattering technique degrades rapidly as the signal strength declines, resulting in erroneously small particle diameters. As a general rule, dynamic light scattering does not seem to possess the versatility and robustness of the classical techniques as a possible on-line diagnostic for process control. The drawbacks and limitations of the two techniques are also discussed.

Photo & Radiation Chemistry

PB89-146682 Not available NTIS National Bureau of Standards (IMSE), Gaithersburg, MD. Polymers Div.

Radiation-Induced Crosslinks between Thymine and 2-D-Deoxyerythropentose.

Final rept.

M. Farahani, and W. L. McLaughlin. 1988, 4p Pub. in Radiation Physics and Chemistry 32, n6 p731-

Keywords: *Crosslinking, *Molecular structure, *Radiation chemistry, Free radicals, Gas chromatography, Mass spectroscopy, Deoxyribonucleic acids, Reprints, *Hydroxyl radicals, *Erythropentose/deoxy, *Thymine, Chemical reaction mechanisms.

Hydroxyl radicals generated by ionizing radiation in aqueous solutions of thymine (Thy) and 2-D-deoxyerythropentose (dR) induce crosslinking between Thy and dR. The crosslinked products were identified by gas chromatography-mass spectrometry (GC-MS) and their yields determined by GC. The mechanisms of their formation are discussed and may serve as a model for radiation-induced or free-radical induced intra-DNA crosslinks.

900.248

Not available NTIS PB89-147490 National Bureau of Standards (NML), Gaithersburg, MD. Ionizing Radiation Physics Div.

Dichromate Dosimetry: The Effect of Acetic Acid on the Radiolytic Reduction Yield. Final rept.

M. Al-Sheikhly, M. H. Hussmann, and W. L. McLaughlin. 1988, 7p Pub. in Radiation Physics and Chemistry 32, n3 p545-

Keywords: *Reduction(Chemistry), *Potassium chromates, *Gamma irradiation, *Visible spectrum, Acetic acid, Nitrogen, Oxygen, Dosimetry, Silver, Hydrogen peroxide, Reprints.

The radiation chemical yield for the reduction of di-chromate, Cr(VI) to Cr(III), in an acidic aqueous perch-loric acid solution of potassium dichromate, may be increased from 0.04 to greater than 0.2 micro mol(J sub -1) by adding acetic acid. The increased yield, G, is about the same in N(sub 2-) and O(sub 2-) saturated solutions. The molar linear absorption coefficient at 350 n also is the same in both solutions. Epsilon sub m = 2800 M(sup -1)cm(sup -1) at pH 0.4. The proposed mechanism to explain the enhanced response in N(sub 2-) saturated solutions involves the efficient reaction of acetic acid with hydroxyl radicals by the abstraction of H from the methyl group; the resulting acid straction of a norm the menting group, the resulting acid radicals react with relatively high yield to reduce Cr(VI). In O(sub 2-) saturated solution, the acetic acid radical apparently goes through an acetic acid peroxyl radical by a bimolecular reaction to the tetroxide intermediate of acetic acid, which releases H2O2 with relatively high yield by a Bennett-type reaction. This additional H2O2, as a reducing agent, reacts slowly with dichromate and

boosts the value of G. The negative slope of the response continues to increase during the period immediately after irradiation of oxygenated solution, due to slow reaction of radiolytically-produced H2O2 with di-chromate. There is also in both O(sub 2-) and N(sub 2-) saturated solution a long-term slow reaction involving oxidation of the organic substrate (in this case, acetic acid). Because of these instabilities, the solutions cannot readily be used for dosimetry without the presence of silver ions, which in the oxidized state, Ag(sup 2+), act to stabilize the solution after irradiation.

Not available NTIS PB89-156954 National Bureau of Standards (NML), Gaithersburg, MD. Inorganic Analytical Research Div.

High Accuracy Determination of (235)U in Nondestructive Assay Standards by Gamma Spectrometry. Final rept.

R. R. Greenberg, and B. S. Carpenter. 1987, 21p Pub. in Jnl. of Radioanalytical and Nuclear Chemistry 111, n1 p177-197 Apr 87.

Keywords: *Uranium 235, *Chemical analysis, *Assaying, *Gamma ray spectroscopy, *Accountability, Nondestructive tests, Standards, Accuracy, Uranium oxides, Radioactive isotopes, Mineral deposits, Resident prints.

High precision gamma spectrometry measurements have been made on five sets of uranium isotope abundance reference materials for nondestructive assay (NDA). These sets are intended for international safeguards use as primary reference materials for the de-termination of the 235U abundance in homogeneous uranium bulk material by gamma spectrometry. The measurements were made to determine the count rate uniformity of the 235U 185.7 keV gamma-ray as well as the 235U isotope abundance for each sample. Since the samples were packaged such that the U308 is infinitely thick for the 185.7 keV gamma-ray, the measured count rate was not dependent on the material density. In addition, the activity observed by the detector was collimated to simulate calibration conditions used to measure bulk material in the field. The results of the study indicate that accuracy of 235U determination via gamma spectrometry, in the range of few hundredths of a percent (2 sigma), is achievable. The main requirement for achieving this level of accuracy is a set of standards whose 235U isotope abundances are known to within 0.01% (2 sigma).

Not available NTIS PB89-157135 National Bureau of Standards (IMSE), Gaithersburg,

MD. Polymers Div.

Effect of pH on the Emission Properties of Aqueous tris (2,6-dipicolinato) Terbium (III) Complexes. Final rept.

Pinta Tept., T. K. Trout, J. M. Bellama, R. A. Faltynek, E. J. Parks, and F. E. Brinckman. 1989, 3p Pub. in Inorganica Chimica Acta 155, p13-15 1989.

Keywords: *Metal complexes, *Terbium, *Luminosity, Emissivity, Pyridines, Carboxylic acid esters, pH, Ligands, Dissociation, Reprints.

Emission characteristics of the complexes formed between terbium(III) and pyridine-2,6-dicarboxylic acid have been measured as a function of solution pH and the molar ratio of ligand to metal present. The liability of these complexes was clearly demonstrated via cor-relation of solution pH to the pKa values of the complexes and the non-coordinated ligand.

900,251 PB89-157556 Not available NTIS National Bureau of Standards (NML), Gaithersburg, MD. Chemical Kinetics Div.

Dehydrogenation of Ethanol in Dilute Aqueous Solution Photosensitized by Benzophenones.

Pinal rept.
P. Green, W. A. Green, A. Harriman, M. C. Richoux, and P. Neta. 1988, 19p
Pub. in Jnl. of the Chemical Society, Faraday Transactions I 84, pt6 p2109-2127 1988.

Keywords: *Ethyl alcohol, *Dehydrogenation, *Photochemical reactions, *Benzophenones, Solutions, Chemical properties, Molecular energy levels, Free radicals, Radiolysis, Catalysts, Reaction kinetics, Reprints, *Hydrogen production.

The photochemical properties of a series of watersoluble benzophenones have been evaluated in dilute

aqueous solution. The compounds possess lowest energy singlet and triplet excited states demonstrating considerable n, *character. As such, irradiation of the compounds in aqueous solution containing ethanol (2% v/v) results in pinacol formation via a triplet state hydrogen abstraction process. In the presence of a colloidal Pt catalyst, the intermediate ketyl and 1methyl-1-hydroxyethyl radicals can be used to reduce water to H2. The rate of H2 formation and its total yield depend upon the nature of the substituent used to solubilize the benzophenone. The rate at which the ketyl radical transfers an electron to the Pt particles can be rationalized in terms of thermodynamic and electrostatic factors.

900.252 PB89-157697 Not available NTIS National Bureau of Standards (NML), Gaithersburg, MD. Surface Science Div.

Synchrotron Radiation Study of BaO Films on W(001) and Their Interaction with H2O, CO2, and O2.

Final rept.

900,253

D. R. Mueller, A. Shih, E. Roman, T. E. Madey, R. Kurtz, and R. Stockbauer. 1988, 5p Sponsored by Office of Naval Research, Arlington, VA. Pub. in Jnl. of Vacuum Science and Technology A 6, n3 p1067-1071 May/Jun 88.

Keywords: *Oxygen, *Carbon dioxide, *Water, *Barium oxides, *Adsorption, *Tungsten, *Photoelectric emission, Ultraviolet spectroscopy, Hydroxides, Carbonates, Thin films, Cathodes, Radiation effects, Synchrotrons, Substrates, Reprints

The interaction of O2, CO2, and H2O with bulk BaO and BaO adlayers adsorbed on W(001) has been examined using ultraviolet photoelectron spectroscopy. H2O reacts with bulk BaO to form Ba(OH)2, while CO2 forms a surface layer of BaCO3. Water and carbon dioxide also react with a (2 sup(1/2))R 45-BaO monolayer adsorbed on W(001) to produce adsorbed OH and CO3 species bound to the tungsten substrate. The interaction of O2 with W(001) is enhanced by the presence of a BaO monolayer on the substrate. The observations are compared with the results of previous stud-

PB89-171193 Not available NTIS National Bureau of Standards (NML), Boulder, CO. Quantum Physics Div. Photodissociation of Methyl lodide Clusters. Final rept. D. J. Donaldson, S. Sapers, V. Vaida, and R. Naaman. 1987, 11p Pub. in Large Finite Systems, p253-263 1987.

Keywords: *Dissociation, *Photochemical reactions, *Iodoalkanes, Absorption spectra, Rare gases, Dimerization, Clustering, Ionization, Reprints, Methyl iodide, Rydberg states.

The dissociation of methyl iodide molecules 'solvated' in clusters has been investigated using both direct absorption spectroscopy and multiphoton ionization methods. Clusters of both neat methyl iodide and of methyl iodide with rare gases were studied in a molecular jet. It was found that dimerization slows the predis-sociation rate from the Rydberg states of CH3I, where-as in large clusters the direct dissociation from the valence state is slowed. A model is presented that explains the effect of CH3I dimer formation on the predissociation dynamics. Evidence is also presented for electron delocalization in higher clusters after excitation into the Rydberg states.

900,254 PB89-171201 Not available NTIS National Bureau of Standards (NML), Boulder, CO. Quantum Physics Div.

Production of 0.1-3 eV Reactive Molecules by Laser Vaporization of Condensed Molecular Films: A Potential Source for Beam-Surface Interactions. Final rept.

L. M. Cousins, and S. R. Leone. 1988, 11p Contract DAAG29-85-K-0033

Sponsored by Army Research Office, Arlington, VA. Pub. in Jnl. of Materials Research 3, n6 p1158-1168 Nov/Dec 88.

Keywords: *Laser beams, *Vaporizing, *Thin films, Molecular theory, Pulse generators, Radiation effects, Cryogenics, Substrates, Condensing, Chlorine, Nitro-

Photo & Radiation Chemistry

gen oxide(NO), Energy levels, Microelectronics, Re-

A versatile, repetitively pulsed source of translationally fast, reactive molecules suitable for materials process ing experiments is described. The pulsed beams are generated by excimer laser vaporization of cryogenic molecular films that are continuously condensed on transparent substrates. The generation of fast, energy variable pulsed molecular sources of Cl2 and NO is demonstrated. The most probable translational ener-gies of Cl2 and NO molecules can be reproducibly yaried monotonically by adjusting the laser fluence or film thickness. Here, the most probable translational energy is quoted as the energy corresponding to the maximum of the time-of-flight trace. Using laser fluences of 2-25 mJ/sq cm from a 193 nm excimer laser, the most probable translational energies of Cl2 laser, the most probable translational energies of Cl2 are 0.4-2 eV. Significant fractions of molecules with translational energies greater than 3 eV are observed at the leading edges of the distributions. Very similar results are obtained by vaporizing Cl2 with 248 and 351 nm radiation. Pulses of translationally fast NO molecules are generated in a similar manner; most probable energies from 0.1-0.4eV, with the fastest molecules up to 0.8 eV, are obtained using laser fluences of 1-11 mJ/sq cm at 193 nm. Approximately 10 sup 13 to 10 sup 14 molecules per sq cm of the film are vaporized per laser pulse, depending on film thickness and laser fluence.

900,255 PB89-172423 PB89-172423 Not available NTIS National Bureau of Standards (NML), Gaithersburg,

MD. Molecular Spectroscopy Div.
Picosecond Laser Study of the Collisionless Photodissociation of Dimethylnitramine at 266 nm. Final rept.

J. C. Mialocq, and J. C. Stephenson. 1986, 4p Pub. in Chemical Physics Letters 123, n5 p390-393, 24 Jan 86.

Keywords: *Nitramines, *Photolysis, Near ultraviolet radiation, Nitrogen dioxide, Reprints, *Photodissociation, Laser induced fluorescence, Picosecond pulses.

A picosecond pump-probe study of the uv photolysis of gaseous dimethylnitramine is reported. After photolysis by picosecond laser pulses at 266 nm, efficient monophotonic collision-free photodissociation occurs within 6 ps. NO2 fragments are formed in the ground electronic state and in a fluorescent excited state; the quantum yields for both of these channels are estimat-

900,256 PB89-176754 Not available NTIS National Bureau of Standards (NML), Gaithersburg, MD. Chemical Kinetics Div.
Chemical Kinetics of Intermediates In the Autoxi-

dation of SO2.

Final rept.
R. E. Huie. 1986, 9p
Pub. in ACS (American Chemical Society) Symposium
Series 319, p284-292 1986.

Keywords: *Kinetics, *Oxidation, *Sulfur dioxide, *Free radicals, *Acidity, *Rainfall, Sulfites, Scrubbers, Flue gases, Peroxy esters, Sulfuric acid, Reprints, Acid

The autoxidation of SO2 solutions is known to involve free radicals. Recent work on the reaction of free radicals with sulfite and bisulfite and on the reaction of the sulfite and peroxysulfite radicals is beginning to allow the complex system to be understood better. It is par-ticularly true for the effect of added chemicals on SO2 autoxidation and chemical transformations induced by the system.

Not available NTIS PB89-176945 National Bureau of Standards (NML), Gaithersburg, MD. Radiometric Physics Div.

Vibrationally Resolved Photoelectron Studies of the 7(sigma) (-1) Channel In N2O. Final rept.

T. A. Ferrett, A. C. Parr, S. H. Southworth, J. E. Hardis, and J. L. Dehmer. 1989, 6p Contract W-31109-eng-38 Sponsored by Department of Energy, Washington, DC. Pub. in Jnl. of Chemical Physics 90, n3 p1551-1556, 1

Keywords: *Nitrogen oxide(N2O), *Vibrational spectra, *Photoelectrons, Energy, Fluorescence, Molecular structure, Synchrotron radiation, Molecular spectra,

Vibrationally resolved photoelectron studies of the 000, 100, 200, and 001 modes of the A state (7sigma(-1)) of N2O+ in the 17.4-26 eV photon-energy range were performed. The vibrational branching ratios sigma(100)/sigma(000) and sigma(001)/sigma(000) sigma(100)/sigma(000) and sigma(001)/sigma(000) agree very well with fluorescence measurements by Kelly et al. and qualitatively with recent theoretical predictions of Braunstein and McKoy. The large non-Franck-Condon variations in the sigma(100)/sigma(000) and sigma(200)/sigma(000) branching ratios are associated with a predicted 7 sigma -> Epsilon sigma shape resonance near 20 eV. Overall, the vibrational branching ratios imply lower resonant energies for the stretching modes (100 and 200) and a similar resonant energy for the asymmetric stretch (001), compared with the 000 mode. The vibrational asymmetry parameters (beta) display a strong variation with energy which is qualitatively reproduced by theory; however, the experimental values for beta(100) and beta(001) exhibit additional structure around 20 eV. When combined with theory and recent fluorescence data, these results help to demonstrate a correlation of shape resonance energy with overall molecular length (RN-N) + R(N-O); this important result implies a resonant state which is localized on the entire triatomic molecular frame rather than on the N-N or N-O components.

PB89-179782 Not available NTIS National Bureau of Standards (NML), Boulder, CO. Quantum Physics Div.

Photodissociation Dynamics of C2H2 at 193 nm: Vibrational Distributions of the CCH Radical and the Rotational State Distribution of the A(010) State by Time-Resolved Fourier Transform Infrared Emission.

T. R. Fletcher, and S. R. Leone. 1989, 9p Contract DE-AC02-79ER10396

Sponsored by Department of Energy, Washington, DC. Pub. in Jnl. of Chemical Physics 90, n2 p871-879, 15

Keywords: *Acetylene, *Chemical radicals, Carbon, Hydrogen, Reprints, *Photodissociation, Rotational states, Vibrational states, Fourier transform infrared

Time-resolved Fourier transform infrared (FTIR) emission is used to study the formation of CCH in the photodissociation of C2H2 at 193 nm. Excitation of C2H2 at 193 nm is known to populate the 10 mu sub 3 level of the trans-bent electronically excited state of acetylene, which undergoes decomposition. State-resolved infrared emission is obtained from the CCH radicals that are produced. Only vibronic levels which originate or borrow oscillator strength from the low-lying elec-tronically excited state of CCH, A(doublet Pi), are ob-served in the study. The relative intensities of these bands are measured and the rotational state distribution for the A(010) state is obtained. A kinematic model which can account for a rotational cooling effect in A(010) state is described.

PB89-201222 Not available NTIS National Bureau of Standards (NML), Gaithersburg, MD. Surface Science Div. Bond Selective Chemistry with Photon-Stimulated

Final rept.

J. A. Yarmoff, and S. A. Joyce. 1989, 6p Pub. in Materials Research Society Symposia Proceedings, v143 p91-96 1989.

Keywords: *Desorption, *Fluorine, *Ions, *Synchrotrons, *Silicon, Photons, Electron transitions, Surface chemistry, Irradiation.

Photon stimulated desorption of fluorine ions from sili-con surfaces was studied via excitation of the Si 2p core level with synchrotron radiation. The results showed that the process is chemically selective in that the removal of a fluorine ion from a silicon species in a given oxidation state can be enhanced by tuning the photon energy to the excitation wavelength corresponding to a transition from the 2p core level of the bonding atom to the conduction band minimum. The process was studied as a possible means for the production of surfaces with selected compositions of species. The results of selective exposures of fluorinated surfaces to monochromatized radiation indicated that secondary desorption processes and the inherent chemistry of the surface reactions can override the effects of selective desorption. Other possibilities for se-lective surface reactions via core-level excitations are

900.260

PB89-202634 Not available NTIS National Bureau of Standards (NML), Boulder, CO.

Cuantum Physics Div.

Time-of-Flight Measurements of Hyperthermal Cl(sub 2) Molecules Produced by UV Laser Vaporlation of Cryogenic Chlorine Films.

Final rept. L. M. Cousins, and S. R. Leone. 1989, 6p

Contract DAAG29-85-K-003

Sponsored by Army Research Office, Washington, DC. Pub. in Chemical Physics Letters 155, n2 p162-167, 24 Feb 89.

Keywords: *Chlorine, *Vaporizing, *Thin films, Ultraviolet lasers, Condensates, Cryogenics, Time, Re-

Time-of-flight distributions are obtained for the repetitive, unfocused laser vaporization of cryogenic CI2 films condensed on a transparent substrate held at 25-110K. Translationally fast molecules are observed using 193, 248, 351 and 355 nm, but no vaporization occurs for 532 or 1064 nm. The most probable kinetic energies of the CI2 molecules, estimated from the maxima of the Cl2 time-of-flight traces, range from 0.4 to 2 eV for 193 nm vaporization at laser powers of 0.2-2 MW/sq cm. The energies increase monotonically with increasing laser fluence and film thickness. Less than 7% of the desorbed flux is due to Cl atoms formed by dissociation in the desorption process. Energies above 5 eV are obtained with focused 355 nm radiation.

900,261

PB89-202642 Not available NTIS National Bureau of Standards (NML), Boulder, CO. Quantum Physics Div. Time-Resolved FTIR Emission Studies of Molecu-

lar Photofragmentation.

Final rept. S. R. Leone. 1989, 6p Grants NSF-PHY86-04504, NSF-CHE84-08403 Sponsored by National Science Foundation, Washington, DC., and Department of Energy, Washington, DC. Pub. in Accounts of Chemicals Research 22, n4 p139-

Keywords: *Infrared spectroscopy, *Polyatomic mole-cules, *Photochemical reactions, Vibrational spectra, Rotational spectra, Excitation, Chemical bonds, Fouri-er transformation, Molecular structure, Photolysis, Steric hindrance, Reprints.

A number of dynamical experiments were conducted in which low resolution, time-resolved infrared fluorescence detection was employed. The experiments used 30-60/cm resolution tunable interference filters for wavelength selectivity. The lack of rotational resolution in those experiments sometimes limited the dynamical detail. In the present account, new experiments are described which utilize a high resolution, time-resolved FTIR emission method to study photofragmentation dynamics of large polyatomic molecules. The capability to obtain vibrational and rotational state details of the excited dynamics of simple bond-breaking proc-esses. The results include information about the times-cales for breaking several bonds in a single molecule and the constraints on rotational motion due to steric hindrance and energy and angular momentum considerations.

900.262

PB89-231336
Not available NTIS
National Inst. of Standards and Technology (NML),
Gaithersburg, MD. Surface Science Div.
Synchrotron Photoemission Study of CO Chemis-

orption on Cr(110).

Final rept. N. D. Shinn. 1988, 11p

N. D. Shillin, 1960, 11p Sponsored by Office of Naval Research, Arlington, VA., and Department of Energy, Washington, DC. Pub. in Physical Review B 38, n17 p12248-12258, 15

Keywords: *Carbon monoxide, *Chemisorption, *Photoelectric emission, *Ultraviolet radiation, *Chemical

Photo & Radiation Chemistry

bonds, Dipole moments, Chromium, Iron, Molybdenum, Synchrotron radiation, Reprints.

Angle-integrated ultraviolet photoemission studies of carbon monoxide chemisorption on Cr(110) confirm the sequential population of two electronically inequivalent molecular binding states (alpha 1-CO and alpha 2-CO) at 90 K. They are distinguished by differences in the CO 4 sigma binding energies (0.8 eV) and photoemission cross sections. Work-function measurements indicate that the surface dipole moment associated with alpha 1-CO is significantly less than that for alpha 2-CO. CO/O interaction data exhibit oxygen-induced alpha 1-CO site blocking and alpha 1-CO alpha 2-CO binding mode conversion. The results support current models for the CO binding geometries on Cr(110) and related binding states on Fe(100) and

900,263 PB90-117425 Not available NTIS Not available N11 National Inst. of Standards and Technology (NML), Gaithersburg, MD. Molecular Spectroscopy Div. Dissociation Lifetimes and Level Mixing in Overtone-Excited HN3 (X tilde (sup 1) A'). Final rept.

Final rept.

B. R. Foy, M. P. Casassa, J. C. Stephenson, and D. S. King. 1989, 9p

Sponsored by Air Force Office of Scientific Research, Bolling AFB, DC.

Pub. in Jnl. of Chemical Physics 90, n12 p7037-7045,

15 Jun 89.

Keywords: *Photochemical reactions, *Dissociation, *Nitrides, *Hydrides, Vibrational spectra, Molecular spectroscopy, Electron transitions, Reprints.

Vibrational overtone photodissociation is used to exvibrational overtone protoclissociation is used to examine the spectroscopy and vibrational predissociation lifetimes of HN3 in its ground electronic state. Direct overtone pumping of the N-H stretching levels 5v(sub NH) and 6v(sub NH) prepares molecules in selected states (v,J,K) near 15,100 and 17,700/cm of vibrational energy; spin-forbidden NH dissociation fragments are detected by laser-induced fluorescence. Photodissociation spectra of beam-cooled HN3 display mixing of individual rotational levels of the nv(sub NH) vibrations with several background states, with derived coupling matrix elements in the range 0.01derived coupling matrix elements in the range 0.01-cm. Vibrational predissociation lifetimes of mixed components of 5v(sub NH) are state specific, with variations of a factor of 2 for only 0.1/cm energy differences. Average lifetimes for low J, K are 210 ns for 5v(sub NH) and 0.95 ns for 6v(sub NH). The ratio of decay rates for the two overtone levels, k(6v(sub NH))/k(5v(sub NH)) = 220, is much greater than predicted by statistical theory, which gives a ratio of 4.

900,264
PB90-123498
Not available NTIS
National Inst. of Standards and Technology (NML),
Gaithersburg, MD. Chemical Kinetics Div.
Reaction of (Ir(C(3), N bpy)(bpy)2)(2+) with OH
Radicals and Radiation induced Covalent Binding

of the Complex to Several Polymers in Aqueous Solutions. Final rept.

D. Behar, P. Neta, J. Silverman, and J. Rabani. 1987,

Pub. in Radiation Physics and Chemistry 29, n4 p253-260 1987.

Keywords: *Polymers, Polyelectrolytes, Radiolysis, Reprints, *Iridium complexes, *Hydroxyl radicals, Radiation binding, Aqueous solutions, Covalence.

Irradiation of aqueous solutions of (Ir(C sup 3, N bpy)(bpy)2)(2+) (IrP) produces a variety of OH adducts to IrP. The OH adducts decay by two second order processes separated in time. In the presence of both IrP and a soluble polymer, the OH radicals are shared between the IrP and the polymer, simultaneously producing OH adducts and polymer radicals. This is followed by radical-radical reactions. The rate constants of the various reactions between the OH adducts and the polymer radicals have been determined. The products of reactions of the OH adducts are discussed. IrP behaves similarly to Ru(bpy)3(2+) which was studied before. This indicates that the radiation method may have a general use in the preparation of polymers with pendant bpy complexes.

900,265 PB90-123704 Not available NTIS National Inst. of Standards and Technology (NML), Gaithersburg, MD. Chemical Kinetics Div. Fluid Flow in Pulsed Laser irradiated Gases; Modeling and Measurement. Final rept.

W. Braun, T. J. Wallington, and R. J. Cvetanovic.

1988, 15p Pub. in Jnl. of Photochemistry and Photobiology A-Chemistry 42, n2-3 p207-221 1988.

Keywords: *Gases, *Fluid flow, Energy transfer, Irradiation, Light pulses, Mixtures, Mercury, Mathematical models, Computerized_simulation, Temperature, Reprints, Laser radiation, Tracer techniques, Density.

Fluid flow processes following laser irradiation of gaseous mixtures have been modeled in order to facilitate quantitative interpretation of experimental observa-tions. Results of computer simulations are compared with experimental measurements of the temporal the recently developed Hg tracer technique. The model outlined in the work accurately reproduces the experimentally observed changes in temperature and density in pulsed laser irradiated gas mixtures using a variety of cell and laser irradiation geometries. Com-parison of the model result with experimental data shows how Hg tracer technique measurements may be influenced by fluid flow.

900,266 PB90-136680 Not available NTIS National Inst. of Standards and Technology (NML), Roulder CO Quantum Physics Dis-PB90-136680 Boulder, CO. Quantum Physics Div.
Time-Resolved FTIR Emission Studies of Molecu-

lar Photofragmentation initiated by a High Repetition Rate Excimer Laser. Final rept.

T. R. Fletcher, and S. R. Leone. 1987, 4p Pub. in Proceedings of International Laser Science Conference (3rd), Atlantic City, NJ., p595-598 Nov 87.

Keywords: *Photolysis, Acetylene, Emission spectra, *Fourier transform infrared spectroscopy, Eximer

The availability of high repetition rate (>300 Hz) excimer lasers provides new opportunities for studies of molecular processes by time-resolved FTIR spectros-copy. An overview of the technique is given and state resolved infrared emission results are presented for the triatomic radical, C2H, generated by photolysis of C2H2 at 193 nm. Electronic emission from the low lying (A tilde) doublet Pi state of C2H is observed, along with high vibrational levels of the ground state which gain intensity by coupling with the vibrationless level of (A tilde) doublet Pi.

Physical & Theoretical Chemistry

900,267 AD-A202 820/7 PC A03/MF A01 Colorado Univ. at Boulder. Dept. of Chemistry.

Alignment Effects in Electronic Energy Transfer and Reactive Events. S. R. Leone. 1988, 20p AFOSR-TR-88-1316 Grant AFOSR-86-0018 Pub. in Selectivity in Chemical Reactions, p245-263

Keywords: Accuracy, Alignment, *Atomic orbitals, *Calcium, *Pumping(Electronics), Crossings, Dynamics, Electron energy, *Electronic states, *Energy transfer, Graphs, *Lasers, Rare gases, Reactivities, Reprints, *Strontium.

The rates of electronic curve crossing processes depend critically on the alignment of atomic orbitals, which determine the symmetries of the electronic potentials participating in the reaction or energy transfer event. Recent work from our laboratory is presented on the effect of orbital alignment in near resonant energy transfer processes of electronically excited Ca and Sr atoms. Several energy transfer events are carded at the several energy transfer events. ried out on aligned p-states in collisions with rare gases. The simplicity of the rare gas systems in terms of their symmetry and nonreactive nature is advantageous for comparison to accurate theoretical treatment. In the context of understanding chemical phenomena, collisions of these atoms with molecular partners are also investigated. This opens the possibility to study the correlation of alignment dependent effects in competing reactive and energy transfer pathways. Remarkably state-specific alignment effects are also observed when two or more independent energy transfer pathways are accessible. Keywords: Pumping (electronics); alignment; Energy transfer; Laser; Reaction dynamics; Calcium; Strontium; Reprints. (JHD)

900,268 PB89-145114 Not available NTIS American Chemical Society, Washington, DC.

Journal of Physical and Chemical Reference Data, Volume 17, Number 4, 1988. Quarterly rept.

Quarterly rept. c1988, 468p
See also PB89-145122 through PB89-145189 and PB88-156435. Prepared in cooperation with American Inst. of Physics, New York. Sponsored by National Bureau of Standards (ICST), Gaithersburg, MD. Available from American Chemical Society, 1155 Sixteenth St., NW, Washington, DC 20036.

Keywords: *Physical properties, *Chemical properties, Data.

Contents: Evaluated chemical kinetic data for the reactions of atomic oxygen O(3P) with sulfur containing compounds; New international skeleton tables for the compounds; New International skeleton tables for the thermodynamic properties of ordinary water substance; Benzene thermophysical properties from 279 to 900 K at pressures to 1000 bar; Estimation of the thermodynamic properties of hydrocarbons at 298.15 K; Wavelengths and energy level classifications of scandium spectra for all stages of ionization; Atomic weights of the elements 1987; The 1986 CODATA recommended values of the fundamental physical constants. (Copyright (c) by the U.S. Secretary of Commerce, 1988.)

900,269 PB89-145122 Not available NTIS National Research Council of Canada, Ottawa (Ontario). Div. of Chemistry.

Evaluated Chemical Kinetic Data for the Reactions

of Atomic Oxygen O(3P) with Sulfur Containing Compounds.

Quarterly rept.
D. L. Singleton, and R. J. Cvetanovic. c1988, 60p
Sponsored by National Inst. of Standards and Technology (NML), Gaithersburg, MD. Chemical Kinetics

Included in Jnl. of Physical and Chemical Reference Data, v17 n4 p1377-1437 1988. Available from American Chemical Society, 1155 Sixteenth St., NW, Washington, DC 20036.

Keywords: *Reaction kinetics, *Oxygen, *Sulfur compounds, Chemical reactions, Arrhenuis parameters.

Chemical kinetic data for reactions of O(3P) atoms with sulfur containing compounds are compiled and critically evaluated. Specifically, the reactions considcritically evaluated. Specifically, the reactions considered include the interactions of the ground electronic state of oxygen atoms, O(3P), with S2, SF2, SF5, SOF, S2O, SO2, SO3, SH, H2S, D2S, H2SO4, CS, CS2, COS, CH3SH, C2H5SH, C3H7SH, C4H9SH, C5H11SH, CH3SCH3, cy-CH2SCH2, cy-CH2SCH2, CH3SCH3, SCF2, SCCI2, and cy-CF2SCF2S. With one exception, the liquid phase reaction O(3P) + H2SO4 -> products, all the data considered were for gas phase reactions. Where possible, 'Recommended' values of the rate parameters have been assessed and conservative uncertainty limits asbeen assessed and conservative uncertainty limits assigned to them.

900.270 PB89-145130 Not available NTIS Keio Univ., Yokohama (Japan). Dept. of Mechanical Engineering.

New International Skeleton Tables for the Thermodynamic Properties of Ordinary Water Substance.

Quarterly rept. H. Sato, M. Uematsu, K. Watanabe, A. Saul, and W.

Wagner. c1988, 100p
Prepared in cooperation with Ruhr Univ., Bochum (Germany, F.R.). Inst. fuer Thermo- und Fluiddynamik. Included in Jnl. of Physical and Chemical Reference Data, v17 n4 p1439-1540 1988. Available from Ameri-can Chemical Society, 1155 Sixteenth St., NW, Washington, DC 20036.

Keywords: Thermodynamic properties, *Water, Enthalpy, Density(Mass/volume), Steam, Vapor pres-

The current knowledge of thermodynamic properties of ordinary water substance is summarized in a condensed form of a set of skeleton steam tables, where

the most probable values with the reliabilities on specific volume and enthalpy are provided in the range of temperatures from 273 to 1073 K and pressures from 101. 325 kPa to 1 GPa and at the saturation state from the triple point to the critical point. About 17,000 experimental thermodynamic data were assessed and classified previously by Working Group 1 of IAPS. About 10,000 experimental data were collected and evaluated in detail and especially about 7000 specific-volume data among them were critically analyzed with respect to their errors using the statistical method originaly developed at Keio University by the first three authors. As a result, specific volume and enthalpy values with as-sociated reliabilities were determined at 1455 grid points of 24 isotherms and 61 isobars in the single-fluid phase state and at 54 temperatures along the saturation curve. The background, analytical procedure, and reliability of IST-85 as well as the assessment of the existing experimental data and equations of state are also discussed in the paper.

900,271
PB89-145148
Not available NTIS
National Inst. of Standards and Technology (NEL),
Boulder, CO. Thermophysics Div.
Benzene Thermophysical Properties from 279 to
900 K at Pressures to 1000 Bar.

Quarterly rept.

R. D. Goodwin. c1988, 96p Included in Jnl. of Physical and Chemical Reference Data, v17 n4 p1541-1636 1988. Available from Ameri-can Chemical Society, 1155 Sixteenth St., NW, Washington, DC 20036.

Keywords: *Thermodynamic properties, *Benzene, Enthalpy, Density, Entropy, Vapor pressure, Equations of state, Joule-Thompson effect, Heat of vaporization, Specific heat.

The thermodynamic data for benzene have been eval-uated and fit to a highly constrained, nonanalytic equation of state. Comparisons of the equation with the selected PVT and derived property data are given. Extensive tables are presented providing tabular values for coexisting liquid and vapor as well as for the single phase along isobars. The equation state and tables cover the range from the triple point (278.68 K) to 900 K, with pressures to 1000 bar.

900,272 PB89-145155 PB89-145155 Not available NTIS National Inst. of Standards and Technology (NML), Gaithersburg, MD. Chemical Thermodynamics Div. Estimation of the Thermodynamic Properties of Hydrocarbons at 298.15 K.

Quarterly rept. E. S. Dorralski, and E. D. Hearing. c1988, 42p Included in Jnl. of Physical and Chemical Reference Data, v17 n4 p1637-1678 1988. Available from American Chemical Society, 1155 Sixteenth St., NW, Washington, DC 20036.

Keywords: *Thermodynamic properties, *Hydrocarbons, Liquid phases, Solid phases, Enthalpy, Entropy.

An estimation method developed by S.W. Benson and coworkers, for calculating the thermodynamic properties of organic compounds in the gas phase, has been extended to the liquid and solid phases for hydrocarbon compounds at 298.15 K. The second order approach which includes nearest neighbor interactions has been applied to the condensed phase. A total of 1311 comparisons are made between experimentally determined values and those calculated using additive group values. The good agreement between experimental and calculated values shows that the Benson group additivity approach to the estimation of thermodynamic properties of organic compounds is applica-ble to the liquid and solid phases as well as the gas phase. Appendices provide example calcuations of the thermodynamic properties selected hydrocarbon compounds, total symmetry numbers, and methyl repulsion corrections.

900,273 PB89-145163 Not available NTIS Not available NTIS National Inst. of Standards and Technology (NML), Gaithersburg, MD. Atomic and Plasma Radiation Div. Wavelengths and Energy Level Classifications of Scandium Spectra for All Stages of Ionization. Quarterly rept.

N. Kaufman, and J. Sugar. c1988, 111p Included in Jnl. of Physical and Chemical Reference Data v17 n4 p1679-1790 1988. Available from Ameri-can Chemical Society, 1155 Sixteenth St., NW, Wash-ington, DC 20036.

Keywords: *Energy levels, *Wavelengths, *Scandium, Ionization, Spectra, Atomic energy levels.

Wavelengths and their classifications are compiled for the spectra of scandium, Sc I through Sc XXI. Selec-tions of data are based on the critical evaluations in compilation of energy levels by Sugar and Corliss. These are updated by a thorough search of the subsequent literature. All classifications are verified with predictions made by differencing the energy levels. Spectra are ordered by ionization stage and listed by wavelength. Two finding lists are included, one containing Sc I to Sc III and the other Sc IV to Sc XXI.

900,274
PB89-145171
Curtin Univ. of Technology, Bentley (Australia).
Atomic Weights of the Elements 1987. Not available NTIS Quarterly rept.

Oldarterly rept.

J. R. De Laeter. c1988, 3p
Included in Jnl. of Physical and Chemical Reference
Data, v17 n4 p1791-1793 1988. Available from American Chemical Society, 1155 Sixteenth St., NW, Washiston DC 20036 ington, DC 20036.

Keywords: *Atomic mass, Transuranium elements, Isotopes, Atomic weights.

The International Union of Pure and Applied Chemistry Commission on Atomic Weights and Isotopic Abundances has reviewed recent literature and confirmed the atomic weight values published in 1985, with one minor change. The current table of standard atomic weights are called the control of the current table. weights is presented.

900.275 PB89-145189 Not available NTIS Rockwell International, Thousand Oaks, CA. Science

CODATA (Committee on Data for Science and Technology) Recommended Values of the Fundamental Physical Constants, 1986.

Cuarterly rept.
E. R. Cohen, and B. N. Taylor. c1988, 9p
Included in Jnl. of Physical and Chemical Reference
Data, v17 n4 p1795-1803 1988. Available from American Chemical Society, 1155 Sixteenth St., NW, Washington, DC 20036. Sponsored by National Inst. of
Standards and Technology, Gaithersburg, MD.

Keywords: *Physical properties, Physics, Chemistry, *Physical constants, CODATA, Task Group of Fundamental Constants.

Presented here are the values of the basic constants and conversion factors of physics and chemistry resulting from 1986 least-squares adjustment of the fundamental physical constants as published by the CODATA (Committee on Data for Science and Technology) Task Group on Fundamental Constants and recommended for international use by CODATA. The 1986 CODATA set of values replaces its predecessor published by the Task Group and recommended for international use by CODATA in 1973.

900,276 PB89-145197 Not available NTIS PB89-143197

American Chemical Society, Washington, DC.

Journal of Physical and Chemical Reference Data,
Volume 17, 1988, Supplement No. 3. Atomic Transition Probabilities Scandium through Manganese. Quarterly rept.

G. A. Martin, J. R. Fuhr, and W. L. Wiese. c1988, 531p ISBN-0-88318-585-7 See also PB89-145205 and PB89-135735. Library of

Congress catalog Card no. 88-72277. Prepared in co-operation with American Inst. of Physics, New York. Sponsored by National Bureau of Standards, Gaithers-

burg, MD. Available from American Chemical Society, 1155 Sixteenth St., NW, Washington, DC 20036.

Keywords: *Atomic spectra, *Scandium, *Titanium, *Vanadium, *Chromium,*Manganese,*Electron transitions, *Transition probabilities, Dipoles, Ionization, Quantum interactions, Accuracy, Tables(Data), Selections tion rules(Physics).

Atomic transition probabilities for about 8,800 spectral lines of five iron-group elements, Sc(Z = 21) to Mn(Z = 25), are critically compiled, based on all available literature sources. The data are presented in separate tables for each element and stage of ionization and are further subdivided into allowed (i.e., electric dipole—E1) and forbidden (magnetic dipole—M1, electric quadrupole—M2). drupole--E2, and magnetic quadrupole--M2) transitions. Within each data table the spectral lines are grouped into multiplets, which which are in turn arranged according to parent configurations, transition arrays, and ascending quantum numbers. For each line the transition probability for spontaneous emission and the line strength are given, along with the spectroscopic designation, the wavelength, the statistical weights and the energy levels of the upper and levels. weights, and the energy levels of the upper and lower states. For allowed lines the absorption oscillator strength is listed, while for forbidden transitions the type of transition is identified (M1, E2, etc.). In addition, the estimated accuracy and the source are indicated. In short introductions, which precede the tables for each ion, the main justifications for the choice of the adopted data and for the accuracy rating are discussed.(Copyright (c) 1988 by the U.S. Secretary of Commerce.)

900,277

PB89-145205 Not available NTIS Rensselaer Polytechnic Inst., Troy, NY. Dept. of Chemistry.

Journal of Physical and Chemical Reference Data, Journal of Physical and Chemical Reference Data, Volume 17, 1988, Supplement No. 2. Thermodynamic and Transport Properties for Molten Salts: Correlation Equations for Critically Evaluated Density, Surface Tension, Electrical Conductance, and Viscosity Data.

Viscosity Data.
Quarterly rept.
G. J. Janz. c1988, 327p ISBN-0-88318-587-3
See also PB89-145197. Library of Congress catalog card no. 88-82581. Prepared in cooperation with American Chemical Society, Washington, DC., and American Inst. of Physics, New York. Sponsored by National Bureau of Standards, Gaithersburg, MD. Available from American Chemical Society, 1155 Sixteenth St., NW, Washington, DC 20036.

Keywords: *Thermodynamics, *Tables(Data), *Fused salts, Interfacial tension, Density, Viscosity, Electrical resistance.

Critically evaluated results for two thermodynamic properties (density and surface tension) and two transport properties (electrical conductance and viscosity) are reported for one and two component salt systems in the molten state. For each system, the recommended results are reported in the form of equations, together with uncertainty estimates, and flagged comments on value judgments and related matters. Results for a limited number of higher multi-component systems are included. The NSRDS-NBS critically evaluated data series have been upgraded as part of the work, and the collection and evaluations of the available experimental data have been systematically extended to 1988. (Copyright (c) 1988 by the U.S. Secretary of Commerce.)

900,278

PB89-146658 Not available NTIS National Bureau of Standards (NML), Gaithersburg,

MD. Chemical Kinetics Div.

Rate Constants for the Reaction HO2+NO2+N2>HO2NO2+N2: The Temperature Dependence of the Fall-Off Parameters.

Final rept. M. J. Kurylo, and P. Ouellette. 1987, 4p Pub. in Jnl. of Physical Chemistry **91**, n12 p3365-3368 1987.

Keywords: *Reaction kinetics, *Hydroperoxides, *Nitrogen, *Nitrogen dioxide, Ultraviolet spectroscopy, Low pressure research, Reprints, Temperature dependence.

Rate constants for the title reaction were measured via flash photolysis UV absorption spectroscopy at N2 pressures of 25, 50, and 100 Torr over the temperature range 288 - 358K. The data of the study were at low enough pressure to yield a precise determination of n (which describes the temperature dependence of the low pressure limiting third-order rate constant) but were less sensitive to the determination of m (associthis reason, the final analysis utilizes a composite fit of the temperature dependent data along with similar data at 100 and 700 Torr of N2 obtained by Sander and Peterson.

900.279

PB89-146666 Not available NTIS National Bureau of Standards (NML), Gaithersburg, MD. Chemical Kinetics Div.

Multiphoton Ionization Spectroscopy and Vibrational Analysis of a 3p Rydberg State of the Hydroxymethyl Radical.

Final rept. C. S. Dulcey, and J. W. Hudgens. 1986, 9p Pub. in Jnl. of Chemical Physics 84, n10 p5262-5270, 15 May 86.

Keywords: *Energy levels, *Vibrational spectra, *Spectrum analysis, Free radicals, Excitation, Deuterium compounds, Isomerization, Reprints, *Hydroxymethyl radicals, *Rydberg states, *Resonance enhanced multiphoton ionization spectroscopy, Electronic structure.

The resonance enhanced multiphoton ionization (REMPI) spectra of CH2OH, CH2OD, CD2OH, and CD2OD between 420-495 nm are reported. Analysis of the excited state vibrational band progressions shows that the spectrum originates from simultaneous two photon absorption to form a 3p Rydberg state (v(sub 00) = 40,064/cm) of the radical. Absorption of a third photon ionized the radical. A normal mode analysis of the REMPI spectra enabled assignments of six active vibrational modes in the excited state. The rate that methoxy radicals isomerize into hydroxymethyl radicals was estimated to be less than 2.9/sec at 300K.

900,280 PB89-146674 Not available NTIS National Bureau of Standards (NML), Gaithersburg, MD. Chemical Kinetics Div.

Gas Phase Proton Affinities and Basicities of Molecules: A Comparison between Theory and Experiment.

Final rept.

D. A. Dixon, and S. G. Lias. 1987, 46p Pub. in Molecular Structure and Energetics, v2 p269-314 1987.

Keywords: Heat of formation, Vapor phases, Thermochemistry, Alkalinity, Comparison, Gases, Reviews, Reprints, *Proton affinity, Ion molecule interactions.

A review is presented of a recently-published evaluation of the scale of gas phase proton affinities (S. G. Lias, J. F. Liebman, and R. D. Levin, J. Phys. Chem. Ref. Data, 13, 695 (1984)). The discussion includes (1) a description of the rationale used in evaluating different data sets from the literature, and (2) detailed evaluations of the heats of formation of MH(1+) ions used in the assignment of absolute values to the relative thermodynamic ladder which constitutes the gas phase proton affinity scale.

900,281 PB89-146864 Not available NTIS National Bureau of Standards (NML), Gaithersburg, MD. Surface Science Div. Adsorption Properties of Pt Films on W(110).

Final rept. R. A. Demmin, S. M. Shivaprasad, and T. E. Madey.

1988, 5p Sponsored by Department of Energy, Washington, DC. Pub. in Langmuir 4, n5 p1104-1108 1988.

Keywords: *Platinum, *Thin films, *Tungsten, *Carbon monoxide, *Chemisorption, Desorption, Reprints.

The surface chemistry of ultrathin Pt films on a W(110) substrate has been investigated by using CO chemis-orption. Carbon monoxide temperature-programmed desorption experiments show that molecular CO is more weakly bound to a monolayer Pt film deposited at 90 K than to either bulk Pt or the W substrate, similar to conclusions drawn from experiments on other metal thin films. Carbon monoxide is also weakly adsorbed on films annealed to 1500 K, even for initial Pt coverages much greater than one monolayer. This has been interpreted as strong evidence for substantial thermally induced structural changes in multilayer films that result in a W surface that is covered by a monolayer Pt film with unique CO chemisorption properties. Platinum films of at least one monolayer also prevent the disso-ciative adsorption of CO normally occurring on the W(110) surface. For submonolayer films annealed to 1500 K, the total amount of dissociative adsorption of CO decreases linearly with increasing Pt coverage, reaching zero at one monoplayer of Pt. This implies that the inhibition of CO dissociation by Pt is very localized. Previously proposed explanations for CO adsorption behavior common to a variety of overlayer-substrate systems are discussed.

900,282 PB89-146898

Not available NTIS

National Bureau of Standards (NML), Gaithersburg, MD. Surface Science Div.

Core-Level Binding-Energy Shifts at Surfaces and in Solids.

Final rept. W. F. Egelhoff. 1986, 163p Pub. in Surface Science Reports 6, n6-8 p253-415 1986.

Keywords: *X-ray analysis, *Energy levels, *Photoe-lectrons, Cores, Surfaces, Solids, Spectroscopy, Re-

The review presents an overview of the theory and of various successful approaches to the interpretation of core-level binding-energy shifts observed in photoe-lectron spectroscopy. The review specially concen-trates on shifts since most of the chemical and physical insights provided by core levels are derived not from the core-level binding energies themselves but from shifts they exhibit. The theoretical background is presented at a level readily accessible to the general reader. Particular attention is paid to relative merits of the two basically different conceptual frameworks for interpreting core-level binding-energy shifts, the initial-state-final approach and the equivalent-core approach.

900,283 PB89-146922 Not available NTIS Motional Bureau of Standards (NEL), Gaithersburg, MD. Semiconductor Electronics Div.

Multiple Scattering in the X-ray-Absorption Near-Edge Structure of Tetrahedral Ge Gases.

Final rept.

C. E. Bouldin, G. Bunker, D. A. McKeown, R. A. Forman, and J. J. Ritter. 1988, 4p Pub. in Physical Review B 38, n15 p10 816-10 819, 15 Nov 88.

Keywords: *X-ray analysis, *Germanium halides, *Germanium hydrides, Scattering, Gases, Absorption spectrum, Molecular structure, Reprints.

X-ray absorption fine-structure (XAFS) measurements of GeCl4, GeH3Cl, and GeH4 were experimentally isolated by comparison of the spectra of the three compounds. The multiple-scattering (MS) amplitude is comparable to the single-scattering (SS) amplitude only within 15 eV of the edge. Beyond 40 eV the MS to SS amplitude ratio is less than 0.06. Calculations are in qualitative agreement with the experiment. Results suggest that XAFS data in the range 1 less than k less than 3 reciprocal Angstroms can be analyzed in a SS picture in many cases.

900,284 PB89-147011 Not available NTIS National Bureau of Standards (NML), Gaithersburg, MD. Atomic and Plasma Radiation Div. Fundamental Configurations in Mo IV Spectrum.

Final rept. M. T. Fernandez, I. Cabeza, L. Iglesias, O. Garcia-Riquelme, F. Rico, and V. Kaufman. 1987, 8p Pub. in Physica Scripta 35, n6 p819-826 1987.

Keywords: *Molybdenum, *Energy levels, *Line spectra, Spectrum analysis, Spectral energy distribution, Reprints, Configurations.

The spectrum of Mo 4 was produced in a sliding-spark discharge and photographed with the 10.7m normalincidence vacuum spectrograph at the NBS in the 600 - 3200 A spectral region. All but one of the 35 levels of the 4d(3) and 4d(2)5S even configurations and all 45 of the levels of the 4d(2)5P odd configuration have been established from the 514 line classifications in the 800 - 3150 A region. Parametric calculations have been made for the even level systems with configuration interaction and for the odd configuration.

900,285 PB89-147060 PB89-147060 Not available NTIS National Bureau of Standards (NEL), Boulder, CO. Chemical Engineering Science Div.

Thermodynamics of Ammonium Scheelites. 6. An Analysis of the Heat Capacity and Ancillary Values for the Metaperiodates KIO4, NH4IO4, and ND4IO4. Final rept.

R. J. C. Brown, J. E. Callanan, R. D. Weir, and E. F. Westrum. 1987, 10p See also PB88-238498.

Pub. in Jnl. of Chemical Thermodynamics 19, p1173-1182 1987

Keywords: *Specific heat, Scheelites, Thermodynamic properties, Anisotropy, Thermal expansion, Computation, Rotation, Deuterium compound, Reprints, *Ammonium scheelites, Ammonium periodate, Deuterated ammonium compounds.

An analysis of the heat capacity of NH4IO4, ND4IO4, and KIO4 has been carried out in which the effects of the anisotropy of the thermal expansion have been considered, an approach hitherto used successfully for the perrhenates KReO4, NH4ReO4, and ND4ReO4. In the ammonium scheelites, the axial expansivities are very large, but of opposite sign, and as a result the molar volume of the scheelite lattice is nearly independent of temperature. It is shown that the correction from constant stress to constant strain results in a major contribution to the heat capacity of this highly anisotropic lattice. The difference between the experimental and calculated heat capacities, referred to as Delta C P.M, is expressed as the sum of the contributions from the anisotropy and the rotational heat capacity. The results of the analysis show that the rotational contribution is much smaller than had previously been thought. However, the exact contribution of the anisotropy cannot yet be calculated because the elastic constants are not known. In calculating the heat capacity, maximum use has been made of external optical-mode frequencies derived from spectroscopic measurements

900,286

PB89-147110 Not available NTIS National Bureau of Standards (NML), Gaithersburg,

National Bureau of Standards (NML), Gaithersburg, MD. Molecular Spectroscopy Div.

Unimolecular Dynamics Following Vibrational Overtone Excitation of HN3 v1=5 and v1=6:HN3(x tilde;v,J,K,)-> HN((X sup 3)(Sigma (1-));v,J,Omega) + N2(x sup 1)(Sigma sub g (1+)).

Final rept.

B. B. Foy M. P. Casassa J. C. Stanbards and D.

B. R. Foy, M. P. Casassa, J. C. Stephenson, and D. S. King. 1988, 2p Sponsored by Air Force Office of Scientific Research, Bolling AFB, DC.

Pub. in Jnl. of Chemical Physics 89, n1 p608-609, 1 Jul

Keywords: *Hydrazoic acid, Reprints, *Hydrogen azides, Laser induced fluorescence, Predissociation, Vibrational states, Unimolecular structures. Lifetime.

Excitation of the NH-stretch overtone transitions of HN3 to v1 = 5 and 6 resulted in predissociation to HN(X) and N2(X) with lifetimes of 80(+60,-30) and less than or = 3 ns, respectively. Following excitation of either overtone, the HN-fragments were formed pre-dominantly in the symmetric E1, F3 spin-rotation states, with less than 4% population in the anti-sym-metric F2 levels. Fragment Doppler profiles confirmed that most of the available energy (greater than 96%) went into translational motion.

900,287

PB89-147128 Not available NTIS National Bureau of Standards (NML), Gaithersburg, MD. Molecular Spectroscopy Div.

Electronic Structure of Diammine (Ascorbato)

Platinum(II) and the Trans influence on the Ligand

Dissociation Energy. Final rept.

H. Basch, M. Krauss, and W. J. Stevens. 1986, 3p Pub. in Inorganic Chemistry 25, n26 p4777-4779 1986.

Keywords: *Platinum, *Ligands, *Reaction kinetics, *Ascorbic acid, *Ammonia, Complex compounds, Molecular orbitals, Electrons, Dissociation energy, Reprints.

The electronic structure of the cis-Pt(ammonia)sub 2 (ascorbate) molecule has been studied by valence electron self-consistent-field calculations. A simpler molecule is used to model the ascorbate in a calculation of ligand binding energies. A comparison of localized ligand bonding orbital charge centroids and density plots supports the validity of the model compound to represent the bonding in the ascorbate. The Pt-C bond energy is calculated to exceed that for Pt-O by about 40 kcal/mole. The dissociation energies for the ammonia ligands exhibit a strong trans-influence with a low dissociation energy for the ammonia trans to the Pt-C bond. These results suggest that this ammonia ligand and the Pt-O bond are suitable for exchange in these molecules.

900 288 PB89-147375

Not available NTIS

National Bureau of Standards (NML), Gaithersburg, MD. Molecular Spectroscopy Div. Electric-Dipole Moments of H2O-Formamide and

CH3OH-Formamide.

Final rept. G. T. Fraser, R. D. Suenram, and F. J. Lovas. 1988,

Pub. in Jnl. of Molecular Structure 189, p165-172

Keywords: *Dipole moments, *Water, *Formamides, *Carbinols, *Microwave spectroscopy, Hydrogen bonds, Electric charge, Reprints.

Electric-dipole moments have been determined for water-formamide and methanol-formamide by pulsednozzle Fourier-transform microwave spectroscopy. For water-formamide mu sub a = 1.050(1) D and mu sub b = 2.135(3) D while for methanol-formamide mu sub a = 1.0666(1) D and mu sub b = 2.091(2) D. The corresponding complexation-induced moments are estimated as 0.55 D and 0.34 D for water-formamide and 0.58 D and 0.10 D for methanol-formamide. The results are compared with theoretical calculations.

900.289

PB89-147417 Not evailable NTIS National Bureau of Standards (NML), Gaithersburg, MD. Molecular Spectroscopy Div.

Vibrational Predissociation of the Nitric Oxide Dimer.

Final rept. M. P. Casassa, J. C. Stephenson, and D. S. King.

1986, 10p See also PB87-128294.

Pub. in Faraday Discussions of the Chemical Society 82, p251-260 1986.

Keywords: *Nitrogen oxides, *Vibrational spectra, *Dissociation energy, Reaction kinetics, Lasers, Re-

Details of experimental measurements of the total energy distribution and time dependence of the vibrapredissociation of the nitric oxide dimer excited to v1 are presented. Energy-disposal measurements indicated the fragments are described by an average rotational energy (E sub R) = 75 cm(sup -1), full equilibration of the lambda doublet species, approximately equal populations in both spin-orbit states, no signifi-cant degree of alignment, an isotropic flux distribution and an average kinetic energy of (E sub K) = 400 cm(sup -1) per fragment. Although about 75% of the available energy went into the fragment translation, the predissociation proceeded at a rate greater than 10(sup 8)s(sup -1).

900,290

PB89-147441 Not available NTIS National Bureau of Standards (NEL), Gaithersburg, MD. Thermophysics Div.

Molecular Dynamics Study of a Dipolar Fluid be-

tween Charged Plates.

Final rept. S. H. Lee, J. C. Rasaiah, and J. B. Hubbard. 1986,

Pub. in Jnl. of Chemical Physics 85, n9 p5232-5237 1986.

Keywords: Polarization(Charge separation), Electric fields, Thin films, Autocorrelation, Dipoles, Reprints, *Dipolar fluids, Dielectric saturation.

Recent experiments and computer simulations of thin films have observed the segregation of nonpolar molecules into layers or sheets parallel to the confining walls. The authors discuss a molecular dynamics study of a thin film of Stockmayer molecules between Lennard-Jones plates and find that, in the absence of an electric field, the dipoles are mainly oriented parallel to the plates in each layer. The polarization density pro-file, with an electric field perpendicular to the plates, is also studied, and is found to oscillate from layer to layer, with a magnitude that is in excess of that predicted by the Debye theory of dielectric saturation by a factor nearly equal to the ratio of the local density to the average bulk density.

900,291

PB89-147458 Not available NTIS National Bureau of Standards (NEL), Gaithersburg, MD. Thermophysics Div.

Microwave Measurements of the Thermal Expansion of a Spherical Cavity.

Final rept. M. B. Ewing, J. B. Mehl, M. R. Moldover, and J. P. M. Trusler. 1988, 9p Sponsored by North Atlantic Treaty Organization,

Brussels (Belgium). Pub. in Metrologia 25, p211-219 1988.

Keywords: *Gases, *Microwaves, *Measurement, *Volume, *Spherical shells, Expansion, Heating, Water, Gallium, Resonance, Temperature, Reprints.

Microwave resonances have been used to measure the volumetric thermal expansion of a spherical cavity the volumetric thermal expansion or a spherical cavity between the temperature of the triple point of water (T sub t) and the temperature of the triple point of gallium (T sub g). Using the TM 1,1 and TM 1,2 modes, we find 10 sup 6(V(T sub g)/V(T sub t)-1) = 1418.5 plus or minus 1.0 and 1418.1 plus or minus 0.6, respectively. These results are in agreement with the value 1416.6 plus or minus 1.5 obtained by filling the cavity with mercury and using it as a dilatometer. The microwave cury and using it as a dilatometer. The microwave measurements are sufficiently accurate that they can be used for primary gas or acoustic thermometry and for measuring the changes in volume standards with temperature, pressure, or time. There is evidence that microwave measurements can be used to determine microwave measurements can be used to determine the volume of a spherical cavity with an uncertainty of the order of 30 ppm and further improvements are

900,292

PB89-147474 Not available NTIS National Bureau of Standards (NML), Boulder, CO. Time and Frequency Div.

Far-Infrared Laser Magnetic Resonance Spectrum

of Vibrationally Excited C2H(1). Final rept.

J. M. Brown, and K. M. Evenson. 1988, 11p Pub. in Jnl. of Molecular Spectroscopy 131, p161-171 1988.

Keywords: *Laser beams, *Magnetic resonance, *Methane, *Molecular vibration, *Far infrared radiation, Spectrum analysis, Fluorine, Excitation, Electronic spectra, Reprints.

Some previously observed but unassigned lines in the laser magnetic resonance spectrum of the F + CH4 flame at 490.4 micro m have been assigned to the N = 6 to 7, - to + transition of the C2H radical in its (010) vibrational level. The spectrum is an interesting example of a magnetic resonance spectrum of a radical dis-ples of a magnetic resonance spectrum of a radical dis-playing Hund's case (b) coupling and arises because the laser frequency. The measured resonances are com-bined with recently available millimeter-wave observa-tions of C2H in the same vibrational level to give an improved set of molecular parameters.

900,293

PB89-148407 PC A04/MF A01 PB89-148407 PC A04/MF A01
National Inst. of Standards and Technology (NEL),
Boulder, CO. Thermophysics Div.
Experimental Thermal Conductivity, Thermal Diffusivity, and Specific Heat Values of Argon and Ni-

trogen. Final rept.

H. M. Roder, R. A. Perkins, and C. A. Nieto de Castro. Oct 88, 54p NISTIR-88/3902

Keywords: *Thermal conductivity, *Thermal diffusivity, *Specific heat, *Argon, *Nitrogen, Hot wire anemometers, Tables(Data), Temperature, Pressure.

Experimental measurements of thermal conductivity and thermal diffusivity as obtained in a transient hotwire apparatus for argon and nitrogen are reported. Values of the specific heat are calculated from these measured values and the density associated with each measurement. The measurements were made at temperatures between 80 and 320 K with pressures between 0.1 and 70 MPa. The density range is 0 to 36 mol/L for argon and 0 to 32 mol/L for nitrogen. The total number of points recorded is 1484 for argon and 1423 for nitrogen.

900.294

PB89-149256 Not available NTIS National Bureau of Standards (NML), Galthersburg, MD. Organic Analytical Research Div.

Optical Rotation.

Final rept.

B. Coxon. 1987, 8p Pub. in Recommended Reference Materials for the Realization of Physicochemical Properties, Chapter 14, p419-426 1987.

Keywords: *Optical activity, Optical properties, Polarimetry, Utilization, Sources, Sucrose, Glucose, Quartz, Light sources, Physicochemical properties, Reprints, *Reference materials.

An introduction to polarimetry is given, including the application of manual and automatic polarimeters and laser light sources. Definitions of specific optical rotation and specific rotatory power are given and the units of these quantities are discussed. Reference materials for the measurement of optical rotation are discussed, including the usage, sources of supply, and pertinent polarimetric data for sucrose, anhydrons dextrose, and quartz control plates.

900,295

PB89-150767 Not available NTIS National Bureau of Standards (NML), Gaithersburg, MD. Radiation Physics Div.

Autodetaching States of Negative Ions.

Final rept. C. W. Clark. 1986, 6p

Sponsored by Air Force Office of Scientific Research, Arlington, VA.

Pub. in Proceedings of International Laser Science Conference Advances in Laser Science-1 (1st), Dallas, TX., p379-384 1986.

Keywords: *Anions, *Resonance absorption, Stability, Laser spectroscopy, Rare gases, Alkalinity, Ions, *Electron-atom collisions.

Autodetaching states (or resonances) of negative ions are very sensitive to electron correlation effects, and the general rules which determine their energetics and stability are not well understood. The experimental techniques used to study them depend strongly on ele-mental species. For instance, laser photodetachment spectroscopy is one of the preferred ways of investi-gating alkali negative ions, whereas negative ion resonances of noble gases can only be produced by par-ticle impact. This tends to obscure possible corre-spondences between the resonance spectra of different elements. However, evidence of common proper-ties of certain classes of autodetaching states is accu-mulating. The paper describes a few simple examples.

900.296

Not available NTIS
National Bureau of Standards (NML), Gaithersburg,
MD. Radiation Physics Div.
Resonance Instantian M

Resonance Ionization Mass Spectrometry of Mg: The 3pnd Autoionizing Series.

Final rept. R. E. Bonanno, C. W. Clark, J. D. Fassett, and T. B.

Lucatorto. 1986, 2p Pub. in Proceedings of International Laser Science Conference (1st), Dallas, TX., November 18-22, 1985, p409-410 1986.

Keywords: *Magnesium, *Ionization, Mass spectroscopy, Photons, Excitation, Rydberg series.

Stepwise multiphoton excitation was utilized to observe autoionizing Rydberg states of magnesium. The 3pad series which converges to the 3p2P0 limits of the Mg ion was observed. Measurements extended up to n-40. A preliminary quantum defect analysis is presented.

900,297

PB89-150908 Not available NTIS National Bureau of Standards (NML), Gaithersburg, MD. Chemical Kinetics Div.

Reactions of Phenyl Radicals with Ethene, Ethyne, and Benzene.

Final rept. A. Fahr, W. G. Mallard, and S. E. Stein. 1986, 7p Sponsored by Gas Research Inst., Chicago, IL. Pub. in Proceedings of International Symposium on Combustion (21st), Munich, West Germany, August 3-8, 1986, p825-831.

Keywords: *Reaction kinetics, *Ethylene, *Benzene, Displacement reactions, Deuterium compounds, Chemical reactions, *Phenyl radicals, *Ethyne.

In a low pressure flow reactor, rates for the displacement of H atoms from unsaturated molecules by phenyl radicals have been measured relative to phenyl phenyl radicals have been measured relative to phenyl radical recombination. Assuming a rate constant for the latter process of 10(sup 0.3)/M/s, the rate constants at 1030 K for displacement reaction from ethyne, ethene, and benzene, respectively, are: Ph* + C2H4 = PhC2H3 + H, where k = 1.2 x 10(sup 8)/M/s; Ph* + C2H2 = PhC2H + H, where k = 1.6 x 10(sup 8)/M/s; Ph* + PhH = Ph-Ph + H, where k = 3.0 x 10(sup 7)/M/s. The role of the reversibility of the formation of the initial radical-molecule complex is information of the initial radical-molecule complex is investigated by determining D-displacement rates for deuterated ethyne and benzene. Reversibility is Important in the latter case, but not in the former.

900,298 PB89-150916 PB89-150916 Not available NTIS National Bureau of Standards (NML), Gaithersburg, MD, Molecular Spectroscopy Div. Final-State-Resolved Studies of Molecule-Surface Interactions.

Final rept.
D. S. King, and R. R. Cavanagh. 1986, 59p
Contract DE-Al05-84ER13150

Sponsored by Department of Energy, Washington, DC. Pub. in Chemistry and Structure at Interfaces: New Laser and Optical Techniques, Chapter 2, p25-83

Keywords: Desorption, Fluorescence, Molecular beams, Ionization, Scattering, Platinum, Ruthenium, Silver, Repnnts, *Surface reactions, Molecule collisions, Nitric oxide, Laser applications.

A critical review is provided of recent experimental research in the area of final state resolved studies of molecule surface interactions.

PB89-150981 Not available NTIS National Bureau of Standards (NML), Gaithersburg, MD. Chemical Kinetics Div.
Relative Acidities of Water and Methanol and the Stabilities of the Dimer Anions.

Final rept. M. Mautner, and L. W. Sieck. 1986, 4p Pub. in Jnl. of Physical Chemistry 90, n25 p6687-6690

Keywords: *Water, *Anions, *Acidity, *Dimenzation, *Chemical stabilization, pH, Dissociation energy, Temperature, Mass spectroscopy, Chemical bonds, Enthalpy, Reprints, *Methyl alcohol.

The difference between delta H(sub acid)(600) of H2O The difference between delta H(sub acid)(600) of H2O and CH3OH was directly measured to be 9.6 + or -.2 kcal/mol using variable-temperature pulsed high pressure mass spectrometry. This result defines delta H(sub acid)(CH3OH) at 300 K as 381.6 + or -.7 kcal/mol and also confirms published values of EA(CH3O2H and delta H(sub D)(CH3O-H). H2O was also used as a reference to measure delta H(sub acid)(C6H6) as 400.7 + or -.8 kcal/mol. The dissociation energies of the hydrogen bonded dimers OH(sup-1) H2O (26.8 kcal/mol), CH3O(sup-1):H2O (23.9 kcal/mol) and CH3O(sup-1):CH3OH (28.8 kcal/mol) were found to be in very good agreement with published ab found to be in very good agreement with published ab initio results of Ikuta.

900,300 PB89-150999 Not available NTIS National Bureau of Standards (NML), Gaithersburg, MD. Chemical Kinetics Div.

Redox Chemistry of Water-Soluble Vanadyl Por-

Phylins.
Final rept.
P. Hambright, P. Neta, M. C. Richoux, Z. Abou-Gamra, and A. Harriman. 1987, 11p
Pub. in Jnl. of Photochemistry 36, n3 p255-265 1987.

Keywords: *Oxidation reduction reactions, Porphyrins, Photochemical reactions, Radiolysis, Anions, Cations, Reprints, *Porphyrin/vanadyl, *Vanadium porphyrin, Pulsed radiation, Chemical reaction mechanisms.

In aqueous solution, pulse radiolytic studies have shown that vanadyl porphyrins undergo redox reac-tions only at the porphyrin ring. The resultant porphyrin radical anions and cations are unstable with respect to radical anions and cations are unstable with respect to disproportionation. Steady-state reduction, both radiolytic and photochemical, of the vanadyl porphyrins results in formation of phlorins, porphodimethenes, and chlorins depending upon pH and the nature of the porphyrin periphery groups. There is no evidence to show formation of products in which the central vanadyl ion has been reduced. has been reduced.

PB89-151005 Not available NTIS National Bureau of Standards (NML), Gaithersburg, MD. Chemical Kinetics Div.

Reactions of Magnesium Prophyrin Radical Ca-tions in Water. Disproportionation, Oxygen Pro-duction, and Comparison with Other Metalloporphyrins. Final rept.

A. Harriman, P. Neta, and M. C. Richoux. 1986, 5p Pub. in Jnl. of Physical Chemistry 90, n15 p3444-3448

Keywords: *Oxidation reduction reactions, *Cations, *Water, *Oxygen, Porphynns, Companson, Radiolysis, pH, Chemical stabilization, Disproportionation, Reaction kinetics, Reprints, *Magnesium porphyrin, Pulsed radiation

Under pulse radiolytic conditions, B22(sup -1) oxidases water-soluble magnesium porphyrins. The stability of the resultant porphyrin radical cations depends upon the relative electron density residing on the por-phyrin ring, which is controlled by the nature of the water-solubilizing groups. Decreasing the electron density on the porphyrin ring by attaching N-methyl-4pyridyl groups at the meso positions or by replacing the central Mg(II) ion with a cation possessing a higher ionization potential renders the radical cation unstable with respect to disproportionation. The rate and total yield of evolved O2 reach a maximum at pH 12.

Not available NTIS PB89-151013 National Bureau of Standards (NML), Gaithersburg, M.D. Chemical Kinetics Div.

Rate Constants for One-Electron Oxidation by Methylperoxyl Radicals in Aqueous Solutions.

Final rept. R. E. Huie, and P. Neta. 1986, 7p Pub. in International Jnl. of Chemical Kinetics 18, n10 p1185-1191 1986.

Keywords: *Reaction kinetics, *Oxidation, Radiolysis, Substitution reactions, Solutions, Reprints, *Peroxylmethyl radicals, Pulsed radiation.

Rate constants for one-electron oxidation by the methylperoxyl radicals, CH3O2, HOCH2O2, (sup 1)O2CCH2O2, and CCl3O2, in aqueous solutions have been measured by pulse radiolysis and found to be in the range of 3x10 to the 5th power to 6x10 to the 8th power/M/s for compounds with redox potentials between 0.6 and 0.1 V. Substitution on the methylperoxyl radical OH or CO2(sup -1) has only a minor effect on the rate of oxidation but substitution with three chlorines increases the rate constants by two orders of magnitude. The redox potential of the CH3O2 radical is estimated to be 0.6-0.7 V.

900.303 Not available NTIS National Bureau of Standards (NML), Gaithersburg, MD. Chemical Kinetics Div.

Qualitative MO Theory of Some Ring and Ladder Polymers.

J. P. Lowe, S. A. Kafafi, and J. P. LaFemina. 1986,

Pub. in Jnl. of Physical Chemistry 90, n25 p6602-6610

Keywords: *Substitution reactions, *Aromatic polycyclic hydrocarbons, *Aliphatic acyclic hydrocarbons, *Polymers, *Band spectra, Polyphenyl hydrocarbons, Thermodynamics, Reprints, *Molecular orbital theory, *Band theory, Polyphenylene, Polypyrrole, Polyacety-

The authors apply qualitative molecular orbital techniques to the electronic pi-band structure of substitu-tionally related ring and ladder polymers of the types represented by poly(paraphenylene), poly(pyrrole), and poly(acene). They show how the band structure for a polymer can be qualitatively constructed from a knowledge of the MOs and energies of the monomer, and then go on to show how the band structure is altered by chemical substitution. There are numerous bands whose edge energies should be insensitive to chemical substitution in certain positions. Relative band gap changes resulting from chemical substitution can be understood as well, although this sometimes requires consideration of orbital mixing. They show how qualitative theory gives insight into the relative thermodynamic stabilities of isomeric polymers and also Into the structures of polarons. In general, qualitative techniques account well for band structures compared at the level of extended Huckel theory and are relevant to results of ab Initio calculations as well.

900.304

PB89-156731 Not available NTIS National Bureau of Standards (NML), Gaithersburg, MD. Chemical Kinetics Div.

New Photolytic Source of Dioxymethylenes: Criegee Intermediates Without Ozonolysis.

Final rept.

R. I. Martinez. 1987, 2p Pub. in Jnl. of Physical Chemistry 91, n6 p1345-1346 1987.

Keywords: *Photochemistry, *Oxidation, Alkenes, Reprints, *Chemical reaction mechanisms, *Criegee intermediates, *Dioxymethylenes.

The work of Akimoto and coworkers on the matrix photoxidation of alkenes in O2 matrices at 10K is reinterpreted in terms of a generalized mechanism for a new photolytic source of dioxymethylenes.

900.305

PB89-156749 Not available NTIS National Bureau of Standards (NML), Gaithersburg, MD. Chemical Kinetics Div.

Kinetics of Electron Transfer from Nitroaromatic Radical Anions in Aqueous Solutions. Effects of Temperature and Steric Configuration.

Final rept.

M. Mautner, and P. Neta. 1986, 3p Pub. in Jnl. of Physical Chemistry 90, n19 p4648-4650

Keywords: *Reaction kinetics, *Anions, *Nitrogen organic compounds, *Electron transfer, Solutions, Molecular structure, Temperature, Aromatic compounds, Radiolysis, Spectrophotometry, Reprints, *Molecular configurations.

Rate constants for electron transfer from various nitroaromatic radical anions to other nitroaromatic compounds in aqueous solutions have been determined by kinetic spectrophotometric pulse radiolysis. In general, nitroaromatic radical anions donate electrons much more slowly than other radical anions, in reactions with similar driving forces, due to low self-exchange rates for ArNO2/ArNO2(sup -1). The kinetics show no anomalies in supercooled solutions.

900,306

Not available NTIS PB89-156756 National Bureau of Standards (NML), Gaithersburg, MD. Chemical Kinetics Div.

Hyperconjugation: Equilibrium Secondary Isotope Effect on the Stability of the t-Butyl Cation. Kinet-lcs of Near-Thermoneutral Hydride Transfer. Final rent.

M. Mautner. 1987, 4p Pub. in Jnl. of the American Chemical Society 109, n26 p7947-7950 1987.

Keywords: *Reaction kinetics, *Cations, *Thermochemistry, *Isotope effect, *Deuterium compounds, *Hydrides, Temperature, Mass spectroscopy, Entropy, Enthalpy, Gibbs free energy, Chemical equilibrium, Reprints, *Butyl ions, *Hyperconjugation.

The thermochemistry of the hydride transfer equilibrithe thermochemistry of the hydride transfer equilibrium (CD3)3C(sup +1) + (CH3)3CH yields (CH3)3C(sup +1) + (CD3)3CH was measured by pulsed high pressure mass spectrometry. The direction of the observed isotope effect is consistent with C-H bond weakening in the ion due to hyperconjugation. The kinetics of the reaction show a slow rate and a large negative temperature coefficient, with K(300) = 0.36 and k(600) = 0.00625 x 10 to the -10th power cu cm/sec, i.e., reaction efficiencies of about 0.03 to 0.0005. The observed negative temperature coefficient, k = AT(sup -5.8) is larger than those observed for more exothermic hydride transfer reactions. The approach to collision rate with decreasing temperature is abrupt.

900,307

Not available NTIS PB89-156764 National Bureau of Standards (NML), Gaithersburg, MD. Chemical Kinetics Div.

CHEMISTRY

Physical & Theoretical Chemistry

Detection of Gas Phase Methoxy Radicals by Resonance Enhanced Multiphoton ionization Spectroscopy.

G. R. Long, R. D. Johnson, and J. W. Hudgens.

1986, 3p

Pub. in Jnl. of Physical Chemistry 90, n21 p4901-4903

Keywords: *Deuterium compounds, Free radicals, Mass spectroscopy, Ultraviolet spectroscopy, Reprints, *Methyl alcohol, *Resonance ionization mass spectroscopy, *Hydroxylmethyl radicals.

Resonance enhanced multiphoton ionization spectra of CH3O and CD3O between 317-331 nm are reported. Methoxy radicals were generated by the reaction of F atoms with CH3OH, CH3OD, and CD3OD in a flow reactor. The most prominent band of these spectra resided of 2324 are in CH3O and 2324 are in CH3O sides at 324.3 nm in CH3O and 323.2 nm in CD3O.

Mass spectra of both isotopic analogues showed that methoxy molecular ions do not fragment.

900,308

PB89-156772 Not available NTIS National Bureau of Standards (NML), Gaithersburg, MD. Chemical Kinetics Div.

Decay of High Valent Manganese Porphyrins in Aqueous Solution and Catalyzed Formation of

Oxygen. Final rept.

A. Harriman, P. A. Christensen, G. Porter, K. Morehouse, P. Neta, and M. C. Richoux. 1986, 17p Pub. in Jnl. of the Chemical Society, Faraday Transactions 1 82, n10 p3215-3231 1986.

Keywords: *Oxidation reduction reactions, *Reaction kinetics, *Oxygen, Porphyrins, Catalysts, Radiolysis, Catalysis, Chemical stabilization, pH, Reprints, *Manganese porphyrin, *Chemical reaction mechanisms, Pulsed radiation.

Manganese (III) porphyrins (Mn(III)Ps) are easily oxidized to the corresponding Mn(IV)Ps in alkaline aqueous solution. At pH<5, the oxidation product is a Mn(III)P pi-radical cation. These oxidized metalloporphyrins have limited stability in water and they revert to the original Mn(III)P upon standing in the dark. The rate and mechanism of this inherent reduction process depends upon pH, with lower pH giving the higher rates. The inherent reduction appears to involve disproportionation and rearrangement of the Mn(IV)Ps but it does not lead to formation of molecular O2. Addition of olloidal RuO2.2H2O, a good O2-evolving catalyst, has a pronounced effect upon the reduction process. The oxidized metalloporphyrin is bound to the catalyst particles by electrostatic forces and, at pH<11, the bound material decays more slowly than the free company of the process of the bound material decays. pound. For 8 < pH < 11, decay of the bound metallo-porphyrin involves oxidation of water to O2 but the yield of O2 is much less than the stoichiometric values.

900,309

Not available NTIS National Bureau of Standards (NML), Gaithersburg, MD. Chemical Thermodynamics Div.

Analytical Expression for Describing Auger Sput-

ter Depth Profile Shapes of Interfaces.

Final rept.

W. H. Kirchhoff, G. P. Chambers, and J. Fine. 1986,

Pub. in Jnl. of Vacuum Science and Technology A 4, n3 p1666-1670 1986.

Keywords: *Interfaces, Width, Least squares method, Mathematical models, Reprints, Logistic functions, Depth profiles, Auger electron spectroscopy, Computer applications.

The composition versus depth distribution of a solid/ solid interface as determined by Auger sputter depth profiling can be described by a logistic function. A least squares fitting program has been written which fits measured Auger spectral intensities to the above equation to within measurement error (approximately 1%). The statistics associated with the least squares fit allow confidence limits to be placed on the measured widths of interface regions and on the asymmetry associated with each such region.

900 310

PB89-157192 Not available NTIS National Bureau of Standards (NEL), Boulder, CO. Thermophysics Div.

PVT of Toluene at Temperatures to 673 K.

Final rept. G. C. Straty, M. J. Ball, and T. J. Bruno. 1988, 3p Pub. in Jnl. of Chemical and Engineering Data 33, n2 p115-117 1988.

Keywords: *Pressure, *Compressing, *Gas laws, *Toluene, *Liquid phases, Volume, Temperature, Density(Mass/volume), Reprints.

Measurements of the PVT behavior of compressed Measurements of the PVT behavior of compressed gaseous and liquid toluene are reported. Pressure versus temperature observations were made along paths of very nearly constant density (pseudoioschores) in the temperature range from about 348 to over 673 K and at pressures to about 35 MPa. Twenty-seven pseudoisochores were determined ranging in density from about 1.7 to pear 9 mol/dm sun 3. density from about 1.7 to near 9 mol/dm sup 3.

900,311 PB89-157200 PB89-157200 Not available NTIS National Bureau of Standards (NEL), Boulder, CO. Thermophysics Div.

PVT Measurements on Benzene at Temperatures to 723 K.

Final rept.
G. C. Straty, M. J. Ball, and T. J. Bruno. 1987, 4p
Pub. in Jnl. of Chemical and Engineering Data 32, n2

Keywords: *Pressure, *Gas laws, *Benzene, *Liquid phases, Volume, Temperature, Compressing, Density(Mass/volume), Reprints.

Measurements of the PVT behavior of compressed gaseous and liquid benzene are reported. Pressure vs. temperature observations were made along paths of very nearly constant density (pseudoisochores) in the temperature range from about 425 K to over 720 K and at pressures to about 35 MPa. Twenty-four pseudoisochores were determined ranging in density from about 1 mol/dm sup 3 to over 9 mol/dm sup 3.

900,312 PB89-157218 PB89-157218 Not available NTIS National Bureau of Standards (NEL), Gaithersburg,

MD. Thermophysics Div.

Molecular Dynamics Study of a Dipolar Fluid between Charged Plates. 2. Final rept.

S. H. Lee, J. C. Rasaiah, and J. B. Hubbard. 1987,

See also PB89-147441. Pub. in Jnl. of Chemical Physics 86, n4 p2383-2393

Keywords: Polarization(Charge separation), Electric fields, Thin films, Dipoles, Reprints, *Dipolar fluids, Stockmayer fluids.

Further molecular dynamics simulations of thin films of Stockmayer molecules between Lennard-Jones plates are discussed when the distance h between the plates ranges from 2.25 sigma to 9.5 sigma, where sigma is the molecular diameter, and the electric field E ranges between 0 and 10 billion V/m. The solvation force is calculated as a function of the plate separation h when E=0 and E= one billion V/m and as a function of the field E= when h= 4.0 sigma and 7.5 sigma. While, in the absence of a field, the molecules tend to form loops and chain-like structures with the dipoles parallel to the wall, a strong external field orients the dipoles along the field so that the long-range repulsive interacalong the field so that the long-range repulsive interac-tion appears to induce a transition to an imperfect (two-dimensional) triangular lattice at low temperature. In between these states, at low temperatures and high fields, the molecules are packed in parallel chains with their moments perpendicular to the field and in 'ferro-electric domains' of opposite polarization.

PB89-157226 Not available NTIS National Bureau of Standards (NEL), Boulder, CO. Thermophysics Div.
Local Order in a Dense Liquid.

Final rept.
H. J. M. Hanley, T. R. Welberry, D. J. Evans, and G. P. Morriss. 1988, 4p
Sponsored by Department of Energy, Washington, DC. Pub. in Physical Review A 38, n3 p1628-1631, 1 Aug

Keywords: *Liquids, Hexagonal lattices, Relaxation time, Anisotropy, Disks(Shapes), Reprints, Order parameters, Structure factors, Transients.

Transient local hexagonal order in a dense liquid is observed in a molecular-dynamics simulation of two-di-

mensional soft disks. Instantaneous local structure factors at a particular density are obtained using an optical transform of the particle coordinates for a single configuration. Local hexagonal order is quantified using an order parameter, and its lifetime charac-terized by the decay of the order-parameter autocorre-lation function. This type of transient structure is significant at densities greater than 7/10 of the freezing density, and becomes persistent near the freezing density.

PB89-157242 Not available NTIS National Bureau of Standards (NEL), Gaithersburg, MD. Thermophysics Div.

Hydrodynamics of Magnetic and Dielectric Colioidai Dispersions. Final rept.

J. B. Hubbard, and P. J. Stiles. 1986, 14p Pub. in Jnl. of Chemical Physics 84, n12 p6955-6968, 15 Jun 86.

Keywords: *Hydrodynamics, Brownian movement, Magnetic fields, Electric fields, Anisotropy, Reprints, Colloidal dispersions.

The hydrodynamic behavior of colloidal suspensions is considered, the particles of which possess electric or magnetic moments. Particular attention is given to the case where an external electric or magnetic field acts on a system in which the polarization does not relax instantaneously, so that reorientational Brownian motion is coupled to both the field and to hydrodynamic degrees of freedom. Magnetosonic and magnetoviscous effects are derived, with emphasis on anisotropy with respect to the external field.

900,315 PB89-157291 Not available NTIS National Bureau of Standards (NML), Gaithersburg, MD. Molecular Spectroscopy Div.

Population Relaxation of CO(v=1) Vibrations in

Solution Phase Metai-Carbonyi Complexes.

Final rept. E. J. Heilweil, R. R. Cavanagh, and J. C.

Stephenson. 1987, 8p Pub. in Chemical Physics Letters 134, n2 p181-188 1987.

Keywords: *Vibrational spectra, *Infrared analysis, Metal complexes, "Carbonyl compounds, Carbon monoxide, Tungsten, Carbon tetrachloride, Chloroform, Hexanes, Benzene, Chromium, Rhodium, Phosphines, Iridium, Chloromethanes, Chemical bonds, Molecular structure, Solvents, Chlorides, Reprints.

Picosecond infrared saturation-recovery experiments were performed to obtain measurements of the vibrational energy lifetimes (T1) of CO(v=1) vibrations (v approximately = 1920 - 1985 cm(sup -1)) of carbonyl-containing metal complexes in dilute, room temperature solutions. For relaxation of the F(1u) CO-stretching vibration of W(CO)6 in CCI4, CHCl3, n-hexane and benzene, T1 was found to be T1(ps) = 800 plus or minus 200, 480 plus or minus 50, 140 plus or minus 15 and 60 plus or minus 6, respectively, while the same mode of Cr(CO)6 in these solvents gave T1(ps) = 440 plus or minus 70, 295 plus or minus 30, 145 plus or minus 25 and 59 plus or minus 6. Monocarbonyl complexes with coordinated triphenylphospine groups (TPP) have shorter CO(v=1) lifetimes: T1(ps) = 71 plus or minus 12, 50 plus or minus 13 and 29 plus or minus 6 for Rh(CO)C(TPP)2, Ir(CO)C(TPP)2, and Ir(CO)H(TPP)3 in CHCI3; T1 = 37 (+20, -10) ps for Ir(CO)H(TPP)3 and T1 less than or equal to 20 ps for Rh(CO)H(TPP)3 in CH2CI2. These observations are rationalized in terms of molecular structure, intramole-cular bonding, solvent interaction, and energy accept Picosecond infrared saturation-recovery experiments cular bonding, solvent interaction, and energy accepting vibrational modes.

900,316 PB89-157309 Not available NTIS National Bureau of Standards (NML), Gaithersburg, MD. Molecular Spectroscopy Div. Plcosecond Studies of Vibrational Energy Transfer

in Moiecules on Surfaces. Final rept.

E. J. Heilweil, M. P. Casassa, R. R. Cavanagh, and J. C. Stephenson. 1986, 2p Pub. in Jnl. of the Optical Society of America B-Optical Physics 3, n8 p140-141 1986.

Keywords: *Surface chemistry, *Chemisorption, *Infrared spectroscopy, Energy transfer, Infrared lasers,

Silicon dioxide, Colloids, Reprints, Vibrational spectra, Picosecond pulses, Tunable lasers, Zeolites.

Pump-probe experiments using tunable infrared picosecond pulses measured vibrational energy relaxation times, T sub 1, for bonds of chemisorbed molecules. The results have important implications for surface chemistry and spectroscopy. Damping mechanisms determining T sub 1 are discussed.

PB89-157317 Not available NTIS National Bureau of Standards (NML), Gaithersburg,

MD. Molecular Spectroscopy Div.

Picosecond Study of the Population Lifetime of CO(v=1) Chemisorbed on SiO2-Supported Rhodlum Particles.

Final rept. E. J. Heilweil, R. R. Cavanagh, and J. C. Stephenson. 1988, 2p

Sponsored by Air Force Office of Scientific Research, Arlington, VA

Pub. in Jnl. of Chemical Physics 89, n8 p5342-5343, 15

Keywords: *Carbon monoxide, *Electron transitions, *Metals, *Infrared spectroscopy, *Chemisorption, Particle size, Rhodium, Reprints.

Infrared pump-probe characterization of the excited state lifetime reveals that CO bound to isolated metal sites (T1 = 140 plus or minus 20 ps) persists longer than the signal observed for CO bound to approximately 35 Angstroms diameter metal particles (less than or equal to 18 ps), suggesting participation of electron-hole excitations in the larger metal particles.

Not available NTIS PB89-157325 National Bureau of Standards (NML), Gaithersburg,

MD. Molecular Spectroscopy Div.

Microwave Spectrum, Structure, and Electric
Dipole Moment of the Ar-Formamide van der Waals Complex.

Final rept. R. D. Suenram, G. T. Fraser, F. J. Lovas, C. W. Gillies, and J. Zozom. 1988, 6p Pub. in Jnl. of Chemical Physics 89, n10 p6141-6146,

15 Nov 88. Keywords: *Formamides, Microwave spectra, Dipole

moments, Molecular structure, Reprints, *Argon complexes, Electric dipoles, Fourier transform spectrosco-

The microwave spectrum of the Ar-formamide van der Waals complex has been obtained using a pulsednozzle Fourier-transform microwave spectrometer. The rotational constants of the complex are: A=10725.7524(48) MHz, B=1771.0738(22) MHz, and C=1548.9974(16) MHz. The complex is shown to be nonplanar. The Ar atom is located at 3.62 A from the center of mass of the formamide unit at Ar-O, Ar-N, and Ar-C distances of 3.55, 3.79, and 3.93 A, respectively. The shortest Ar-H distance is 3.25 A which is similar to that observed for Ar-vinyl cyanide (3.21 A). Stark effect and hyperfine analyses yield values for the electric dipole moment components and (14)N quadru-pole coupling constants for the complex.

900.319 Not available NTIS PB89-157333 National Bureau of Standards (NML), Gaithersburg, MD. Molecular Spectroscopy Div.
Microwave Spectrum and (14)N Quadrupole Cou-

pling Constants of Carbazole. Final rept.

R. D. Suenram, F. J. Lovas, G. T. Fraser, and P. S. Marfey. 1988, 7p Pub. in Jnl. of Molecular Structure 190, p135-141 1988.

Keywords: *Microwave spectroscopy, *Carbazoles, *Molecular structure, *Rotational spectra, *Electron transitions, Spectra, Pyrroles, Indoles, Quadrupole transitions, Spectra, Pyrroles, Indoles, Quamoment, Nitrogen, Molecular beams, Reprints.

The microwave spectrum of carbazole was observed and analyzed in the 8-14 GHz region using a pulsed molecular-beam Fabry Perot microwave spectrometer. Carbazole was vaporized in a heated nozzle source and was entrained in neon carrier gas before expansion into the Fabry Perot cavity. The rotational transitions were fitted using a rigid rotor Hamiltonian without centrifugal distortion parameters. The rotational constants are A = 2253.1985(2) MHz, B = 594.1861(2)

MHz and C = 470.3503(1) MHz. The inertial defect is small (-0.36 micro Angstroms sup 2) and consistent with a planar molecule. The high resolution available with the instrument (approximately 10 kHz allowed the determination of the N14 nuclear quadrupole coupling constants as chi sub aa = 2.0697(40) MHz, chi sub bb = 1.8719(35) MHz and chi sub cc = -3.9416(35) MHz. A comparison of the electronic environment of the nitrogen atom was made for the series pyrrole, indole and carbazole.

900,320 PB89-157341 Not available NTIS National Bureau of Standards (NML), Gaithersburg, MD. Molecular Spectroscopy Div.
Infrared and Microwave Investigations of Inter-

conversion Tunneling in the Acetylene Dimer.

G. T. Fraser, R. D. Suenram, F. J. Lovas, A. S. Pine, J. T. Hougen, W. J. Lafferty, and J. S. Muentor. 1988, 18p Grant NSF-CHE87-20139

Sponsored by National Science Foundation, Washing-

Pub. in Jnl. of Chemical Physics 89, n10 p6028-6045 Nov 88.

Keywords: *Acetylene, Infrared spectroscopy, Microwave spectroscopy, Hydrogen bonds, Electron tunneling, Reprints, Dimers.

A sub-Doppler infrared spectrum of (HCCH)2 has been obtained in the region of the acetylene C-H stretching fundamental using an optothermal molecular-beam color-center laser spectrometer. Microwave spectra were obtained for the ground vibrational state using a pulsed-nozzle Fourier transform microwave spectrometer. In the infrared spectrum, both a parallel and perpendicular band are observed with the parallel band being previously assigned to a T-shaped C(2 mu) com-plex by Prichard, Nandi, and Muenter and the perpen-dicular band to a C(2h) complex by Bryant, Eggers, and Watts.

900,321 PB89-157374 900,327 PB89-157374 Not available NTIS National Bureau of Standards (NEL), Boulder, CO.

Chemical Engineering Science Div.
CO2 Separation Using Facilitated Transport Ion Exchange Membranes. Final rept.

R. D. Noble, J. J. Pellegrino, E. Grosgogeat, D. Sperry, and J. D. Way. 1988, 15p Contract DE-Al21-86MC23120

Sponsored by Department of Energy, Morgantown,

Pub. in Separation Science and Technology 23, n12-13 p1595-1609 1988.

Keywords: *Carbon dioxide, *Separation, *Ion exchange resins, Performance evaluation, Membranes, Transport properties, Thin films, Reprints, *Gas transport, Sulfonic acid/fluoro, Polybenzimidazoles, port, Sulfo Sodium ions.

The use of ion-exchange membranes as supports for facilitated transport of CO2 is demonstrated. Two different ionomer films were evaluated. The ionomers were a perfluorosulfonic acid film and a sulfonated polybenzimidazole film. Sodium (Na(sup +1)) was exchanged into the membrane for diffusion experiments and ethylenediamine (EDA) was exchanged for facilitated transport experiments. The results indicate that thin perfluorosulfonic acid membranes provide the best CO2 flux and can also provide exceptionally high selectivity.

900,322 PB89-157416 PB89-157416 Not available NTIS National Bureau of Standards (NML), Boulder, CO. Time and Frequency Div.

Calibration Tables Covering the 1460- to 1550-cm(-

1) Region from Heterodyne Frequency Measurements on the nu(sub 3) Bands of (12)CS2 and (13)CS2. Final rept.

J. S. Wells, M. Schneider, and A. G. Maki. 1988, 7p Sponsored by National Aeronautics and Space Admin-istration, Washington, DC.

Pub. in Jnl. of Molecular Spectroscopy 132, p422-428

Keywords: *Carbon disulfide, *Frequency measurement, Infrared spectra, Band spectra, Carbon 12, Tables(Data), Heterodyning, Reprints, Carbon 13, Calibration.

Heterodyne frequency measurements have been made on the nu sub 3 band of both (12)CS2 and (13)CS2 near 1500/cm. The data were fitted and new molecular constants determined. Values for the constants and newly calculated frequency calibration tables are presented. The calibration tables cover the range from 1460 to 1550/cm.

900.323

PB89-157440 Not available NTIS National Bureau of Standards (NML), Gaithersburg, MD. Molecular Spectroscopy Div.

Ozonolysis of Ethylene. Microwave Spectrum, Mo-

lecular Structure, and Dipole Moment of Ethylene Primary Ozonide (1,2,3-Trioxolane).

Final rept.

J. Z. Gillies, C. W. Gillies, R. D. Suenram, and F. J. Lovas. 1988, 9p

Pub. in Jnl. of the American Chemical Society 110, n24 p7991-7999 1988.

Keywords: *Molecular structure, *Dipole moments, *Spectrum analysis, *Microwave spectroscopy, *Ozonization, *Ethylene, Formaldehyde, Stereochemistry, Deuterium compounds, Reprints, *Trioxolane, Molecular conformation, Chemical reaction mechanisms. Dioxirane.

The gas-phase structure of ethylene primary ozonide (CH2CH2O3) has been determined from millimeter wave spectra of five isotopic species. The electric dipole moment of the normal isotopic species is 3.43 (4) D. The barrier to pseudorotation is estimated to be high (greater than 300 to 400/cm) in agreement with ab initio MO calculations. Ethylene primary ozonide, dioxirane, formaldehyde, and ethylene secondary ozonide (CH2OCH2O2) are observed as products of the ozone-ethylene reaction in the low-temperature microwave cell. A mechanism of the ozonolysis of ethylene is presented which suggests that the reaction occurs primarily in the condensed phase on the surface of the cell. Microwave techniques utilizing cis- and trans- C2H2D2 show that ozone adds stereospecifically to ethylene in the formation of ethylene primary ozonide.

900,324

PB89-157499 Not available NTIS National Bureau of Standards (IMSE), Gaithersburg, MD. Reactor Radiation Div.

Neutron Vibrational Spectroscopy of Disordered

Metal Hydrogen Systems.

Final rept.

R. Hemplemann, and J. J. Rush. 1986, 20p Pub. in Hydrogen in Disordered and Amorphous Solids, p283-302 1986.

Keywords: *Neutron spectroscopy, *Vibrational spectroscopy, *Hydrides, Inelastic scattering, Neutron scattering, Physical properties, Chemical bonds, Hydrogen bonds, Reprints, *Metallic glasses, *Metal hydrides.

A review is presented of some recent applications of neutron vibrational spectroscopy to the study of disordered metal-hydrogen systems. The examples discussed cover a range of systems from 'simple' dilute solutions in bcc or fcc metals to amorphous alloy hydrides. It is shown that neutron inelastic scattering studies of the vibrational density of states provide a powerful and sensitive probe of the local potentials and bonding sites of hydrogen in metals and often reveal critical information on the novel microscopic physical properties and behavior of disordered metalshydrogen systems, including those influenced by interstitial or substitutional defects.

900,325

PB89-157507 Not available NTIS National Bureau of Standards (NML), Gaithersburg,

MD. Chemical Kinetics Div.

Validation of Absolute Target Thickness Calibrations In a QQQ Instrument by Measuring Absolute Total Cross-Sections of NE(1+) (NE,NE)NE(1+). Final rept.

R. I. Martinez, and S. Dheandhanoo. 1986, 10p Sponsored by Georgetown Univ., Washington, DC. Dept. of Chemistry.

Pub. in International Jnl. of Mass Spectrometry and Ion Processes 74, n2-3 p241-250 1986.

Keywords: *Mass spectroscopy, *Targets, Thickness, Total cross sections, Dissociation, Reprints, eV range 01-10, eV range 100-100, Calibration, Neon ions.

A methodology has been developed for the measurement of total reaction cross-sections sigma(E) in the range of collision energies E(coll) approx = 5-60 eV (LAB) used for collision-induced dissociation (CID) in triple-quadrupole (QQQ) tandem mass spectrometers. triple-quadrupole (QQQ) tandem mass spectrometers. This methodology has been calibrated by making pseudo-first order kinetics measurements of the symmetric (resonant) charge transfer cross-sections sigma(E) for Ne(1+) (Ne,Ne)Ne(1+). The sigma(E), for E approx = 5-60 eV and P approx = 0.04-1 mtorr, agree with the Rapp-Francis theory to within 15%. The authors measured identical sigma(E) from both the rate of reactant decay and the rate of product formation. Hence, it should be possible to readily determine tion. Hence, it should be possible to readily determine branching ratios for different reactive channels. The methodology provides a means whereby the absolute target thickness ((actual path length traversed by the ion) x (effective number density of the CID target)) of gas targets can be accurately calibrated in-situ for collision energies in the range of ca. 5-60 eV (LAB).

900,326 PB89-157515 PB89-157515 Not available NTIS National Bureau of Standards (NML), Gaithersburg, MD. Chemical Kinetics Div.

Stopped-Flow Studies of the Mechanisms of Ozone-Alkene Reactions In the Gas Phase: Tetramethylethylene.

Final rept. R. I. Martinez, and J. T. Herron. 1987, 8p Pub. in Jnl. of Physical Chemistry 91, n4 p946-953

Keywords: *Ozonation, Mass spectroscopy, Ozone, Reprints, *Chemical reaction mechanisms, *Acetone/hydroxy, *Glyoxal/methyl, Ethylene/tetramethyl.

The reaction of ozone with tetramethylethylene has been studied in the gas phase at 294K and 530 Pa (4 torr) using a stopped-flow reactor coupled to a photoionization mass spectrometer. The concentrations of reactants and products were determined as a function reactions and products were determined as a function of reaction time. The major products were (CH3)2CO, H2CO, CH3C(O)CH2OH (hydroxyacetone) and CH3C(O)C(O)H (methylglyoxal). On the basis of computer modeling calculations, the mechanism was pro-

900,327 PB89-157523 Not available NTIS National Bureau of Standards (NML), Gaithersburg, MD. Chemical Kinetics Div.

S2F10 Formation in Computer Simulation Studies of the Breakdown of SF6.

Final rept.

J. T. Herron. 1987, 3p
Pub. in IEEE (Institute of Electrical and Electronics Engineers) Transactions on Electrical Insulation 22, n4

Keywords: *Sulfur fluorides, *Reaction kinetics, *Mathematical models, *Dielectric breakdown, Sulfur hexafluoride, Water vapor, Reprints, *Di(sulfur penta-

The chemistry subsequent to the dielectric breakdown of SF6 under 'mild' conditions has been modeled on the basis of known or estimated chemical kinetic data for the neutral reactive species postulated to be formed in the breakdown process. The emphasis is on the significance of S2F10 as an end product of dielections. tric breakdown and on the role of water vapor in S2F10 formation.

900.328 PB89-157531 Not available NTIS Mational Bureau of Standards (NML), Gaithersburg, MD. Chemical Kinetics Div.

lonic Hydrogen Bond and Ion Solvation. 5. OH...(1-)O Bonds. Gas Phase Solvation and Clustering of Alkoxide and Carboxylate Anions. Final rept.

M. Mautner, and L. W. Sieck. 1986, 5p

See also PB88-238829.
Pub. in Jnl. of American Chemical Society 108, n24 p7525-7529 1986.

Keywords: *Chemical bonds, *Hydrogen bonds, *Anions, *Dissociation energy, *Dimerization, Enthalpy, Temperature, Solvation, Reprints.

Dissociation energies delta H(sub D) of RO(sup -1 HOR, RCOO(sup -1) HOR and RCOO(sup -1) HOCR range from 14 to 29 kcal/mol. Large values of delta H(sub D) are observed for the symmetric dimers CH3O(sup -1) HOCH3 (28.8 kcal/mol) and

CH3COO(sup -1) HOOCCH3 (29.3 kcal/mol). Delta H(sub D) decreases as the difference between the acidities of the components increase; e.g., for dimers with large delta H(sub acid) such as CH3O(sup -1) - H2O and HCOO(sup -1) - H2O (delta H(sub acid) = 42.2 and 45.5 kcal/mol, respectively), delta H(sub D) = 16.0 kcal/mol. For 13 dimers, a linear correlation of the form delta H(sub D) = 28.4 - 0.29 delta H(sub acid)

900,329 PB89-157549 Not available NTIS
National Bureau of Standards (NML), Gaithersburg,
MD. Chemical Kinetics Div.
Filling of Solvent Shells About Ions. 1. Thermoche-

mical Criteria and the Effects of Isomeric Clusters. Final rept.

M. Mautner, and C. V. Speller. 1986, 9p See also AD-A176 006.

Pub. in Jnl. of Physical Chemistry 90, n25 p6616-6624

Keywords: *Solvation, Temperature, Enthalpy, Entropy, Clustering, Ammonium, Water, Anions, Cations, Reprints, *Electronic structure, *Ion pairs, Hydroxyl radicals, Peroxy radicals.

Solvent shells can build up by the stepwise attachment of solvent molecules to gas-phase ions. The filling of a solvent shell by the s-th solvent molecule is indicated solvent snein by the s-th solvent molecule is indicated by a discontinuous drop in the attachment energy at the s+1-th solvent molecule, i.e., a discontinuous drop in the plots of $H(\sup n-1, n)$ vs. n (i.e., enthalpy sequences) after n=s. Another indication is a gap in the spacing of consecutive van't Hoff plots after n=s. Thermochemical criteria based on enthalpy sequences and the spacing of consecutive van't Hoff plots are developed quantitatively and applied to data on clustering about metal ions and onlimin jons. Satison clustering about metal ions and onium ions. Satisfactory evidence for the distinct filling of shells is found in 11, and tentative evidence is found in another 15 out of the 45 systems where data were examined.

PB89-157580 Not available NTIS National Bureau of Standards (IMSE), Gaithersburg,

MD. Metallurgy Div.

Phase Equilibrium in Two-Phase Coherent Solids. Final rept

W. C. Johnson, and P. W. Voorhees. 1987, 16p Pub. in Metallurgical Transactions A-Physical Metallurgy and Materials Science 18, n7 p1213-1228 1987.

Keywords: *Phase diagrams, *Metals, *Thermody-namic equilibrium, Metastable state, Coherence, Solid phases, Stresses, Elastic properties, Free energy, Reprints, Bifurcation theory.

Phase equilibrium in a two-phase coherent solid is analyzed using the conditions necessary for thermody-namic and mechanical equilibrium in nonhydrostatically stressed coherent solids. Subject to the constraints of constant temperature and external pressure, a bulk alloy composition is chosen and the corresponding volume fractions and phase compositions that satisfy the equilibrium conditions are obtained. It is demonstrated that is the corresponding to the corresponding volume fractions are obtained. strated that, unlike fluids, a number of equilibrium states (volume fractions) may exist that yield energy minima for a given temperature, pressure and alloy composition and that these multiple metastable states may lead to a nonuniqueness in the observed physical state of the system. These results are a consequence of the elastic and system energies being a function of the volume fraction in a field of two-phase coexistence in coherent solids. As it is difficult to display these effects on a coherent phase diagram, the concept of a phase stability diagram is introduced for both displaying and analyzing the equilibrium conditions in coherent solids. The influence of elastic inhomogeneity and the form of the free energy curves as a function of composition in the absence of stress on phase equilibrium is examined.

PB89-157689 Not available NTIS National Bureau of Standards (NML), Gaithersburg, MD. Surface Science Div. Theoretical Study of the Vibrational Lineshape for CO/Pt(111).

Final rept. T. S. Jones, J. W. Gadzuk, and S. Holloway. 1987,

Pub. in Jnl. of Surface Science 184, n3 pL421-L430

Keywords: *Vibrational spectra, *Carbon monoxide, *Adsorbates, Platinum, Adsorption, Reprints, Potential energy surfaces, Chaos.

The spectral analysis method of obtaining vibrational spectra for adsorbates using a classical trajectory approach is presented. A potential-energy-surface (PES) is proposed, which includes anharmonic coupling be-tween the C-O stretching mode and the CO-surface hindered translation. The various dynamical conse-quences of this PES topology are discussed by examining trajectories, surfaces of section, and the resulting vibrational spectra.

900,332

PB89-157705 Not available NTIS National Bureau of Standards (NML), Gaithersburg,

MD. Surface Science Div.
Status of Reference Data, Reference Materials and Reference Procedures in Surface Analysis. Final rept.

J. T. Grant, P. Williams, J. Fine, and C. J. Powell.

1988, 5p Pub. in Surface and Interface Analysis 13, p46-50

Keywords: *Surface properties, Assessments, Experimental data, Experimental design, Reprints, *Standard reference materials.

A brief synopsis is given of recent developments and current needs for reference data, reference materials and reference procedures in surface analysis. This assessment is based largely on three presentations and related discussion at the Second Topical Conference on Quantitative Surface Analysis held at Monterey, California on 30-31 October, 1987. While a reasonable start has been made in recent years in providing needed data, materials, and procedures, many important needs remain.

900.333

PB89-157713 PB89-157713 Not available NTIS National Bureau of Standards (NML), Gaithersburg, MD. Surface Science Div. Semiclassical Way to Molecular Dynamics at Sur-

faces. Final rept.

J. W. Gadzuk. 1988, 30p Pub. in Annual Review of Physical Chemistry 39, p395-424 1988.

Keywords: *Molecular energy levels, *Surface chemistry, *Photoelectric emission, Dynamics, Spectra, Desorption, Wave equations, Reprints.

Time-dependent molecular dynamics at surfaces is considered within the framework of semiclassical wave packet dynamics of Heller. Aspects of photo-emission spectroscopy, stimulated desorption, electron energy loss spectroscopy and molecule/surface collisions are considered within a unified picture.

900,334

PB89-157762 Not available NTIS
National Bureau of Standards (NEL), Gaithersburg,
MD. Semiconductor Electronics Div.
Application of Multiscattering Theory to Impurity

Bands in Si:As.

Final rept.
J. R. Lowney. 1988, 5p
Pub. in Jnl. of Applied Physics 64, n9 p4544-4548, 1 Nov 88.

Keywords: *Additives, *Silicon, *Arsenic, *Electron transitions, Impurities, Computation, Electron scattering, Reprints.

Impurity bands in arsenic-doped silicon have been calculated for doping densities of 3.3 x 10(sup 17), 1.2 x(10 sup 18), and $8.0 \times 10(\text{sup } 18)$ cm(sup -3). A multiscattering approach is used with a model potential which provides both electronic screening and the proper bound-state energy for the isolated center. The results are in good agreement with previous calculations based on electron hopping among hydrogenic centers. An advantage of the multiscattering approach is that it treats the conduction-band states as well and shows the loss of these states to the formation of the impurity band. This is a new result and affects the density for the Mott transition. Calculations are also performed for the states associated with the binding of an extra electron to unionized arsenic centers, the so-called D sup minus band. The overall results are in

good agreement with the observed Mott transition in Si:As near 8 x 10 (sup 18) cm(sup -3).

900,335 PB89-157846 Not available NTIS National Bureau of Standards (NML), Gaithersburg, MD. Office of Standard Reference Data. Shimanouchi, Takehiko and the Codification of Spectroscopic Information.

Final rept. D. R. Lide. 1986, 7p

Pub. in Jnl. of Molecular Structure 146, p1-7 Aug 86.

Keywords: *Spectrum analysis, *Molecular structure, *Spectroscopic analysis, Molecular vibration, Tables(Data), Forms(Paper), Information systems, Data acquisition, Reviews, Reprints, Standardized terminology.

The contributions of Takehiko Shimanouchi to the compilation of spectroscopic and structural data and to the adoption of standard terminology and formats for reporting data are reviewed. Included are his work on the Tables of Molecular Vibrational Frequencies, spectral database projects, and international organizations concerned with scientific information.

900,336 PB89-157853 Not available NTIS National Bureau of Standards (IMSE), Gaithersburg, MD. Office of Nondestructive Evaluation.

Infrared Absorption of SF6 from 32 to 3000 cm(-1) in the Gaseous and Liquid States. Final rept.

C. Chapados, and G. Birnbaum. 1988, 29p Pub. in Jnl. of Molecular Spectroscopy 132, p323-351

Keywords: *Sulfur hexafluoride, *Infrared spectra, Gases, Liquids, Pressure, Vibrational spectra, Reprints.

Infrared spectra from 32 to 3000/cm of SF sub 6 were recorded at several pressures from below atmospheric pressure up to 20 atm and in the liquid phase at tem-peratures from 228 to 284 K. The infrared active fun-damentals, difference bands, combination and har-monic bands, and the collision-induced band in the farinfrared region were observed. Integrated intensities of 37 bands were measured at several densities. In the gas phase, a weak band containing v2 + v6 was always found at higher frequencies than the much stronger bands containing v3. In the liquid phase, the positions of these bands are lowered in frequency and the intensities tend toward equalization. The pair v3 and v2 + v6 itself is the exception: while the v3 band is displaced and its intensity lowered, the v2 + v6 band is practically not modified. A possible explanation of the modification in the intensity of the bands in passing from the gas to the liquid is the effect of the interaction with the liquid environment on the Fermi resonance connecting v3 and v2 \pm v6. Within experimental error no collision-induced component was identified in the mid-infrared region in the gas phase. In the liquid phase, the integrated absorption of the bands increases with temperature, surpassing in many cases the gas-phase values.

PB89-157929 Not available NTIS National Bureau of Standards (NML), Gaithersburg, MD. Surface Science Div. Secondary-Electron Effects in Photon-Stimulated Desorption.

Final rept. D. E. Ramaker, T. E. Madey, R. L. Kurtz, and H. Sambe. 1988, 13p Pub. in Physical Review B 38, n3 p2099-2111, 15 Jul

Keywords: *Desorption, Chemisorption, X rays, Reprints, *Electron stimulated desorption, *Photon stimulated desorption, *Secondary electrons, Oxygen ions, Hydrogen ions, Nitrogen ions.

The magnitude of secondary-electron contributions to electron- or photon-stimulated desorption (ESD) or (PSD) yields is considered. In particular, the authors have reexamined three systems where a dominant x-ray-induced ESD (XESD) effect has been postulated. Recent ESD ion-angular-distribution data on the NH3/ Ni system and a detailed determination of the mechanisms involved in H(1+) desorption indicate that all of the features previously attributed to the XESD effect may in fact arise from direct core-level processes. A reexamination of the PSD N(1+) and O(1+) yields

from condensed N2-O2 reveals that the indirect XESD mechanism contributes just one-third of the N(1+) yield, but dominates the O(1+) desorption. This arises because the direct Auger-stimulated desorption (ASD) process following core-hole excitation is inactive for O(1+) desorption, but remains active for N(1+). Finally, a detailed interpretation of H(1+) desorption from OH/Ti and OH/Cr, and comparison with the system OH/TbO-Sm indicates that the direct ASD process is also inactive in the latter case.

900,338

National Bureau of Standards (NML), Gaithersburg, MD. Surface Science Div.

Optically Driven Surface Reactions: Evidence for the Role of Hot Electrons. Final rept.

S. A. Buntin, L. J. Richter, R. R. Cavanagh, and D. S. King. 1988, 4p Contract DE-Al05-84ER13150

Sponsored by Department of Energy, Washington, DC. Pub. in Physical Review Letters 61, n11 p1321-1324, 12 Sep 88.

Keywords: *Desorption, *Nitrogen oxide(NO), Platinum, Reprints, *Laser induced desorption, Hot elec-

Evidence is presented for the role of excited conduction electrons in the laser-induced desorption of NO from Pt(111). State-specific detection of the desorbed NO establishes that the rotational distributions are non-Boltzmann, that the spin-orbit population is inverted, and that both the translational and vibrational dis-tributions are uncorrelated with the laser-induced surface-temperature jump. The role of optically excited substrate electrons in driving the desorption process is evidenced by a dramatic dependence of the vibrational and translation energy distributions on the desorptionlaser wavelength.

900,339

PB89-157945 Not available NTIS National Bureau of Standards (NML), Gaithersburg,

MD. Surface Science Div.
Universality Class of Planar Self-Avoiding Surfaces with Fixed Boundary. Final rept.

U. Glaus, and T. L. Einstein. 1987, 7p Pub. in Jnl. of Physics A 20, n2 pL105-L111, 1 Feb 87.

Keywords: *Surfaces, Monte Carlo method, Polymers, Reprints, *Self avoiding surfaces.

Using a modified version of a Monte Carlo algorithm proposed by Sterling and Greensite, the authors obtain the exponents theta = 1.51 plus or minus 0.25 and mu = 0.502 plus or minus 0.024 for planar self-avoiding surfaces with fixed boundary in three dimensions, con sistent with the conjectured exact values for branched polymers. It is shown how the modifications are needed to obtain a viable distribution of surfaces.

900,340

PB89-157952 Not available NTIS National Bureau of Standards (NML), Gaithersburg, MD. Surface Science Div.

Non-Boitzmann Rotational and inverted Spin-Orbit State Distributions for Laser-Induced Desorption of NO from Pt(111).

Final rept. L. J. Richter, S. A. Buntin, R. R. Cavanagh, and D. S. King. 1988, 2p Contract DE-AI05-84ER13150

Sponsored by Department of Energy, Washington, DC. Pub. in Jnl. of Chemical Physics 89, n8 p5344-5345, 15

Keywords: *Desorption, *Nitrogen oxide(NO), Platinum, Near infrared radiation, Near ultraviolet radiation, Reprints, Laser induced desorption, Laser induced fluorescence, Visible radiation.

The internal state distributions of NO desorbed from a Pt(111) surface by visible and near-visible laser radiation (355, 532 and 1064 nm) were measured by laserinduced fluorescence. Non-Boltzmann rotational state distributions and inverted spin-orbit populations were observed and were found to be relatively insensitive to the desorption-laser wavelength. This is in contrast with the kinetic energy distributions and the vibrational state populations, both of which exhibit a significant dependence on desorption-laser wavelength.

900.341

Not available NTIS PB89-157978 National Bureau of Standards (NML), Gaithersburg, MD. Surface Science Div.

Calculations of Electron Inelastic Mean Free Paths for 31 Materials.

Final rept.

S. Tanuma, C. J. Powell, and D. R. Penn. 1988, 13p Pub. in Surface and Interface Analysis 11, p577-589

Keywords: *Mean free path, *Elastic properties, *Electrons, *Surface properties, Ceramics, Metals, Scattering, Energy dissipation, Dielectric properties, Algorithms, Gases, Reprints.

New calculations of electron inelastic mean free paths (IMFPs) for 200-2000 eV electrons in 27 elements (C, Mg, Al, Si, Ti, V, Cr, Fe, Ni, Cu, Y, Zr, Nb, Mo, Ru, Rh, Pd, Ag, Hf, Ta, W, Re, Os, Ir, Pt, Au and Bi) and four compounds (LiF, SiO2, ZnS and Al2O3) are presented. These calculations are based on an algorithm due to Penn which makes use of experimental optical data (to represent the dependence of the inelastic scattering probability on energy loss) and the theoretical Lindhard dielectric function (to represent the dependence of the scattering probability on momentum transfer). Our calculated IMFPs were fitted to the Bethe equation for inelastic electron scattering in matter; the two parameters in the Bethe equation were then empirically related to several material constants. The resulting general IMFP formula is believed to be useful for predicting the IMFP dependence on electron energy for a given material and the material-dependence for a given energy. The new formula also appears to be a reasonable but more approximate guide to electron attenuation lengths.

900,342 PB89-158026 Not available NTIS National Bureau of Standards (IMSE), Gaithersburg, MD. Ceramics Div.

Effects of Pressure on the Vibrational Spectra of Liquid Nitromethane.

Final rept.

Pinal rept.
P. J. Miller, S. Block, and G. J. Piermarini. 1989, 5p
Sponsored by Army Research Office, Arlington, VA.,
and Naval Surface Warfare Center, Silver Spring, MD.
Pub. in Jnl. of Physical Chemistry 93, n1 p462-466, 12 Jan 89.

*Vibrational spectra, Keywords: *Nitromethane. *Spectrum analysis, *Deuterium compounds, Pressure, Intermolecular forces, Pyrolysis, Decomposition reactions, Reprints, Chemical shifts.

A complete normal-coordinate calculation for nitromethane is given using the vibrational frequencies measured from the three isotopes CH3NO2, CD3NO2, and CH3(sup 15)NO2. Pressure effects on the vibrational normal modes of the superpressed liquid to 2.0 GPa also were measured. A softening of the frequency of the asymmetric stretching mode of NO2 with increasing pressure indicated a strong intermolecular interaction. By calculating a minimum energy pair configuration and applying two-site exiton theory, the au-thors calculated the shifts of the normal modes of the NO2 stretching vibrations as a function of density and pressure and found them to agree qualitatively with the experimentally measured shifts. The results support the bimolecular nature of the mechanism for the ther-mal decomposition of nitromethane under pressure.

900,343

PB89-158083 Not available NTIS National Bureau of Standards (NML), Gaithersburg, MD. Atomic and Plasma Radiation Div.

Stark Broadening of Spectral Lines of Homologous, Doubly ionized Inert Gases.

Final rept.

N. Konjevic, and T. L. Pittman. 1987, 8p Pub. in Jnl. of Quantitative Spectroscopy and Radi-

ative Transfer 37, n3 p311-318 Mar 87.

Keywords: *Spectral lines, *Stark effect, *Line width, *Rare gases, *Line spectra, Spectrum analysis, Argon, Numerical analysis, Ionization, Experimental design, Comparison, Reprints.

In the paper the authors report electron impact widths of 36 lines that belong to the sequence of homologous, doubly ionized atoms of inert gases. Only four Ar Ill lines in this sequence were previously measured and they are in good agreement with the present re-

CHEMISTRY

Physical & Theoretical Chemistry

sults. Good agreement is also found between these experimental results and the theoretical calculations using a modified semiempirical approach. Average ratio between experiment and theory is 1.06 with maximum deviation not exceeding + or - 20%. They used present results to investigate trends of the Stark widths of analogous lines.

PB89-158125 Not available NTIS National Bureau of Standards (NML), Gaithersburg, MD. Atomic and Plasma Radiation Div.

Atomic Transition Probabilities of Argon: A Con-

tinulng Challenge to Plasma Spectroscopy. Final rept.

W. L. Wiese. 1988, 7p Pub. in Jnl. of Quantitative Spectroscopy and Radiative Transfer 40, n3 p421-427 1988.

Keywords: *Argon, *Spectrum analysis, *Spectral lines, *Emission spectroscopy, Performance evaluation, Atomic properties, Reviews, Reprints, *Atom transport.

Determination of the atomic transition probabilities for prominent spectral lines of Ar I and II are classical cases for testing the capabilities of the emission spec-troscopy method. Despite numerous attempts to measure these data accurately, differences of about 30-40% remain in the numerical results, and the available material actually suggests two scales for the transition probabilities, differing by about 30%, as has been pointed out repeatedly. A critical analysis of all emission experiments undertaken in the study is able to remove these differences satisfactorily. A single transition probability value with an error estimated of only + or - 5% is established for a typical Ar I transition; however, discrepancies for the Ar II data are not removed and remain as a challenge to future experiments

900.345 PB89-158133 Not available NTIS National Bureau of Standards (NEL), Gaithersburg, MD. Thermophysics Div.

Van der Waals Equation of State Around the Van

Laar Point.

Final rept. P. H. E. Meijer. 1989, 9p Pub. in Jnl. of Chemical Physics 90, n1 p448-456, 1

Keywords: *Van der Waals equation, *Equations of state, *Binary systems(Materials), *Critical points, Phase diagrams, Separation, Thermodynamic properties, Reprints, *Van Laar point.

The discovery of van Laar that the van der Waals equation of state for binary mixtures can be solved analytically at the double point on the critical line, provided one introduces the geometric-mean condition on the interaction parameters, is used to obtain the explic-it expression for the critical line for this case. The critical line is expressed as a function of the density variables, and the origin is shifted to this double point: the van Laar point. By doing so it is possible to show that this double point is also a tricritical point. This is different from the lattice gas, where the double point is always a tricritical point. Small deviations from this point in parameter space induce very different phase diagrams. The influence of excursions from the van Laar point is expressed as a function of the state variables. Both the k factor (the deviation from the geometric-mean rule) and the 'asymmetry' coefficient e (the deviation from the crossing point) are introduced. The results are given in the form of polynomials in local co-ordinates in density space. Conditions under which the double point is maintained are given and the differences between the Scott and van Konynenburg classes II, III, IV, and IV* are explained.

900.346 PB89-161574 Not available NTIS National Bureau of Standards (NML), Gaithersburg, MD. Molecular Spectroscopy Div.

Far-Infrared Spectrum of Methyl Amine. Assignment and Analysis of the First Torsional State.

N. Ohashi, K. Takagi, J. Hougen, W. Olson, and W. Lafferty. 1988, 19p Pub. in Jnl. of Molecular Spectroscopy 132, p242-260 1988.

Keywords: *Methylamine, *Spectrum analysis, *Infra-red spectroscopy, *Molecular rotation, *Stress relax-

ation tests, Electron tunneling, Far infrared radiation, Deformation, Reprints.

The far-infrared spectrum of methyl amine has been studied in the 40- to 350/cm region with a resolution of 0.005/cm or better. The pure rotational spectrum in the first excited torsional state, as well as the fundamental torsional band, has been assigned. The data obtained have been combined with microwave data from the literature, and a global fit has been carried out, based on a group theoretical formalism developed previously. Some aspects of the torsional potential function and inversion potential function in this molecule are briefly discussed.

900,347 PB89-161582 Not available NTIS National Bureau of Standards (NML), Gaithersburg, MD. Chemical Kinetics Div.

Critical Review of the Chemical Kinetics of Sulfur Tetrafluoride, Sulfur Pentafluoride, and Sulfur Sul-oride (S2F10) in the Gas Phase.

Final rept.

J. T. Herron. 1987, 14p Pub. in International Jnl. of Chemical Kinetics 19, n2 p129-142 1987.

Keywords: *Sulfur fluorides, *Reaction kinetics, *Gases, *Dielectric breakdown, Pyrolysis, Reprints.

The gas phase chemical kinetics of SF4, SF5 and S2F10 are reviewed with particular emphasis on relevance to the general problem of the dielectric breakdown of SF6. Specific reaction systems treated are SF4 + F2, SF5 + SF5 and the pyrolysis of S2F10. Computer modeling calculations were carried out to arrive at best estimates of rate parameters. Based on the results of these calculations, sets of recommended rate parameters are provided. The major discrepancies and problems in establishing the kinetic data base are described. Thermochemical consequences of different model calculations are given.

900,348 PB89-161608 Not available NTIS National Bureau of Standards (NML), Gaithersburg,

MD. Chemical Kinetics Div.
Rate Constants for Hydrogen Abstraction by Resonance Stabilized Radicals In High Temperature

Final rept.

M. J. Manka, R. L. Brown, and S. E. Stein. 1987, 15p Pub. in International Jnl. of Chemical Kinetics 19, n10 p943-957 1987.

Keywords: *Reaction kinetics, *High temperature tests, *Free radicals, Transfer characteristics, Chemical equilibrium, Recombination reactions, Energy levels, Reprints, *Hydrogen transfer.

Benzylic H-atom abstraction rates by diphenylmethyl radicals from a series of donors were determined in nonpolar liquids at elevated temperatures. Relative rates were converted to absolute rates via available equilibrium constant data. Abstraction by diphenyl-methyl from 1,2,3,4-tetrahydronaphthalene (tetralin) was studied over the temperature range 489-573K. Similar reactions with the fluorenyl radical were also studied. In this case, relative rates were converted to absolute rates with an equilibrium constant determined from the observed homolysis rate of the dimer and an assumed recombination rate. In addition, forward and reverse rate measurements yielded the equilibrium constant for hydrogen transfer between fluorenyl and diphenylmethyl.

PB89-161889 PC A07/MF A01 National Inst. of Standards and Technology (NML), Gaithersburg, MD. Surface Science Div. Technical Activities 1988, Surface Science Divi-

C. J. Powell. Jan 89, 142p NISTIR-89/4025 See also report for 1987, PB88-169453.

Keywords: *Surface chemistry, Standards, Surface properties, Catalysts, Electron spectra, Atomic structure, Adsorption, Surface physics.

The report summarizes technical activities of the NIST Surface Science Division during Fiscal Years 1987 and 1988. These activities include surface-standards work, experimental and theoretical research in surface science, the development of improved measurement methods, and applications to important scientific and national problems. A listing is given of publications,

talks, professional committee participation, and professional interactions by the Division staff.

900,350 PB89-171219 PB89-171219 Not available NTIS National Bureau of Standards (NML), Boulder, CO. Quantum Physics Div.

infrared Spectrum of D2HF. Final rept.

C. M. Lovejoy, D. D. Nelson, and D. J. Nesbitt. 1988,

Grants NSF-CHE86-05970, NSF-PHY86-04504 Sponsored by National Science Foundation, Washing-

Pub. in Jnl. of Chemical Physics 89, n12 p7180-7188, 15 Dec 88.

Keywords: *Infrared spectra, *Hydrogen, *Fluorine, Deuterium, Isotopic labeling, Lasers, Vibration, Energy levels, Gases, Reprints.

Ultrasensitive infrared laser absorption spectroscopy Ultrasensitive infrared laser absorption spectroscopy in a slit supersonic expansion is used to obtain the spectrum of the HF stretching fundamental of D2HF. Both a Pi to Pi band due to para-D2HF and a Sigma to Sigma band due to ortho-D2HF are observed, in contrast to the H2HF spectrum which consists of the Pi to Pi band alone. Analysis of the spectrum indicates that the D2HF Pi states are more strongly bound than the Sigma states. Doublet splittings in the Pi to Pi band are analyzed to determine barriers to internal rotation of D2 within the complex. The vibrational predissociation rate of D2HF is approximately 25 times faster than that of H2HF, suggesting the opening of a channel which of H2HF, suggesting the opening of a channel which results in vibrational excitation of the D2 fragment.

900.351 PB89-171227 Not available NTIS National Bureau of Standards (NML), Boulder, CO. Quantum Physics Div.

infrared Spectrum of NeHF.

Final rept.
D. C. Clary, C. M. Lovejoy, S. V. ONeil, and D. J.
Nesbitt. 1988, 4p
Sponsored by National Science Foundation, Washing-

ton, DC. Pub. in Physical Review Letters 61, n14 p1576-1579, 3 Oct 88.

Keywords: *Neon, *Hydrogen, *Fluonne, *Molecular orbitals, Gases, Quantum theory, Vibration, Infrared spectra, Absorption spectra, Computation, Reprints.

The infrared-absorption spectrum of the previously un-The infrared-absorption spectrum of the previously unobserved NeHF molecule has been predicted from an ab initio quantum-mechanical calculation and subsequently determined for the first time by direct measurement. The two procedures yield remarkable agreement in the positions, widths, and intensities of the infrared spectral lines. The calculations predict, and the experiments confirm, highly unusual vibrational dynamics namics.

Not available NTIS
National Bureau of Standards (NML), Boulder, CO.
Quantum Physics Div.
Laser Probing of Ion Velocity Distributions in Drift
Fields: Parallel and Perpendicular Temperatures
and Mobility for Ba(1+) in He.
Final rept.

R. A. Dressler, J. P. M. Beijers, H. Meyer, S. M. Penn, V. M. Bierbaum, and S. R. Leone. 1988, 9p Grant AFOSR-84-0272

Sponsored by Air Force Office of Scientific Research, Bolling AFB, DC. Pub. in Jnl. of Chemical Physics 89, n8 p4707-4715, October 15, 1988.

Keywords: *Barium, *Helium, *Electric fields, *Ionic mobility, Ions, Dnft, Velocity, Lasers, Fluorescence, Doppler tracking, Transport properties, Probes, Re-

Measurements of ion velocity distributions are presented for Ba + drifted in helium under well characterized conditions using single-frequency laser-induced fluorescence probing. The reduced mobilities and the Doppler profiles parallel and perpendicular to the electric field vector as a function of the ratio of the field strength (E) to the buffer gas density (N) up to 33.5 Td are presented. The reduced mobility decreases monotonically with increasing E/N from the zero-field value of 16.7 plus or minus 0.4 sq cm/V/S at 313 K. The parallel and perpendicular ion temperatures are in very Doppler profiles parallel and perpendicular to the elec-

good agreement with both a repulsive Maxwell model good agreement with both a repulsive Maxwell model and a parametrized version of the three-temperature theory of Lin et al. The parallel temperature is always higher than the perpendicular one. Effects of optical pumping on the Doppler profiles are also presented.

900,353 PB89-171250 PB89-171250

Not available NTIS
National Bureau of Standards (NML), Boulder, CO.
Quantum Physics Div.
Laser Probing of Product-State Distributions In
Thermal-Energy Ion-Molecule Reactions.
Final rept

Final rept.

S. R. Leone, and V. M. Bierbaum. 1987, 11p Grants NSF-PHY86-04504, NSF-CHE86-08043 Sponsored by National Science Foundation, Washington, DC., and Air Force Office of Scientific Research, Bolling AFB, DC. Pub. in Faraday Discussions of the Chemical Society

84, p253-263 1987.

Keywords: *Molecular rotation, *Molecular vibration, *Electron transfer, Ionization, Nitrogen, Carbon monoxide, Molecular energy levels, Reprints, *lon-molecule collisions, *Laser induced fluorescence, Franck-Condon principle.

Vibrational and rotational product-state distributions are determined for thermal-energy charge-transfer re-actions and Penning ionization processes using laserinduced fluorescence detection in both a flowing afterglow apparatus and a single-collision molecular beam device. The reactions investigated are the charge transfers between N(+)+CO, A(+)+N2, Ar(+)+CO, and the Penning ionization of N2 by Ne(3P2). Vibration of N2 by Ne(3P2). and the Penning Ionization of N2 by Ne(3P2). Vibrational distributions provide direct information on major features of the dynamics, such as whether a Franck-Condon mechanism is dominant, whether collision complex formation is important, or if selective vibrational passageways exist between the electronic potential-energy surfaces. The rotational distributions show a variety of additional discrimination distributions. show a variety of additional discriminating dynamical effects, including corroborating evidence for Franck-Condon channels, pinpointing separate mechanisms for different vibrational product states and detecting microscopic bimodalities within individual vibrational levels, which are indicative of multiple entrance- or exit-channel pathways.

900,354 PB89-171284 PB89-171284 Not available NTIS National Bureau of Standards (NML), Gaithersburg, MD. Temperature and Pressure Div. Three-State Lattice Gas as Model for Binary Gas-

Liquid Systems.

Final rept.
P. H. E. Meijer, and M. Napiorkowski. 1987, 7p
Pub. in Jnl. of Chemical Physics 86, n10 p5771-5777

Keywords: *Binary systems(Materials), *Phase diagrams, *Critical field, Gases, Liquids, Lattice parameters, Clustering, Reprints.

The paper deals with the three-state lattice model as applied to binary liquid-gas systems. Schouten, ten Seldam and Traeppeniers (Physica 73,556 (1974)) used this model to describe the transition between the liquid phases as well as the gas-gas separation when varying the interaction parameters of the model. The analysis is aimed at the behavior of the system in the vicinity of its tricritical point in the generalized field space. Different shapes of the critical lines are calculated by using the molecular field method as well as by using the lowest approximation of the cluster variation method. The equivalence between the two approaches is demonstrated. In the immediate neighborhood of the tricritical point, the shapes of the critical lines are also determined analytically.

900,355 PB89-171292 Not available NTIS National Bureau of Standards (NML), Gaithersburg, MD. Temperature and Pressure Div. High Resolution Inverse Raman Spectroscopy of the CO Q Branch. Final rept.

Final rept.
G. J. Rosasco, L. A. Rahn, W. S. Hurst, R. E.
Palmer, J. P. Looney, and J. W. Hahn. 1988, 13p
Sponsored by Department of Energy, Washington,
DC., and Army Research Office, Arlington, VA.
Pub. in Pulsed Single-Frequency Lasers: Technology
and Applications, v912 p171-183 1988.

Keywords: *Vibrational spectra, *Raman spectrosco-py, *Carbon monoxide, *Pressure, Gases, Lasers, Repy, *Co

Preliminary results of a high resolution spectroscopic study of the pressure dependence of the Raman vibrational Q-branch spectrum of pure CO are reported. Measurements are made at room temperature over the pressure range 0.5 to 6 atm. The technique of quasi-cw inverse Raman spectroscopy utilizing a pulsed single-frequency laser source is employed. This approach gives enhanced sensitivity compared to ear-lier work which employed cw lasers, allowing exten-sion of that work to higher accuracy, higher J states, and higher pressure. The goal of this work is to test the accuracy of a modified exponential-gap rate law model which is used to predict the pressure dependent spec-

900,356 PB89-171300 Not available NTIS National Bureau of Standards (NML), Gaithersburg, MD. Temperature and Pressure Div. Dynamics of a Spin-One Model with the Pair Correlation.

M. Keskin, and P. H. E. Meijer. 1986, 10p Pub. in Jnl. of Chemcial Physics 85, n12 p7324-7333 1986.

Final rept.

Keywords: *Phase diagrams, *Transition temperature, spin interactions. Metastable state. Quenching(Cooling), Reprints.

A spin-1 or three state system will undergo a first or second order phase transition depending on the ratio of coupling parameter alpha. Using the pair correlation approximation, the transition temperature is determined in order to obtain the unstable, the metastable, as well as the stable states of this cooperative system. The dynamics of the system is studied by means of the most probable path method and the flow lines and fixed points of the system are given for zero field. The choice of possible initial conditions is discussed. The role of the unstable points in the phase diagram, as separators between the stable and metastable points, is described and they are computed for a number of

900,357 PB89-171532 Not available NTIS National Bureau of Standards (NML), Gaithersburg, MD. Chemical Kinetics Div.

Absolute Rate Constants for Hydrogen Abstraction from Hydrocarbons by the Trichloromethylperoxyl Radical. Final rept.

S. Mosseri, Z. B. Alfassi, and P. Neta. 1987, 9p Pub. in International Jnl. of Chemical Kinetics 19, n4 p309-317 1987.

Keywords: *Reaction kinetics, *Hydrogen, *Spectro-photometry, *Free radicals, Cyclohexane, Cyclohex-ene, Oxidation, Metal containing organic compounds, Porphyrins, Hydrocarbons, Reprints, *Peroxyl radicals, Benzene/hexamethyl.

Absolute rate constants have been measured for the reactions of trichloromethyperoxyl radicals with cyclohexane, cyclohexene, and hexamethylbenzene. The CCl3O2 radicals contained various amounts of the hydrocarbons. The rate constants were determined by competition with the one-electron oxidation of metalloporphyrins, using the rate of formation of the metallo-porphyrin radical cation absorption to monitor the re-action by kinetic spectrophotometry.

PB89-171920 Not available NTIS National Bureau of Standards (NEL), Gaithersburg, MD. Scientific Computing Div.

Modeling Chemical Reaction Systems on an IBM

Final rept. W. Braun, J. Herron, and D. Kahaner. 1988, 4p Pub. in ACCESS, the Jnl. of Microcomputer Applica-tions 7, n4 p45-48 Jul/Aug 88.

Keywords: *Chemical reactions, *Reaction kinetics, Reprints, Microcomputers, Computer applications.

The paper provides an informal description of a pair of computer programs, AC40 and ACPLOT, for the efficient solution of reaction rate problems in chemical kinetics.

900,359 PB89-171961 Not available NTIS National Bureau of Standards (NML), Gaithersburg, MD. Inorganic Analytical Research Div.

Microwave Energy for Acid Decomposition at Elevated Temperatures and Pressures Using Biological and Botanical Samples. Final rept.

H. M. Kingston, and L. B. Jassie. 1986, 8p Pub. in Analytical Chemistry 58, n12 p2534-2541 1986.

Keywords: *Bioassay, *High temperature tests, *High pressure tests, "Microwave equipment, "Acid treatment, "Digesters, Sampling, Digestion(Decomposition), Nitric acid, Sulfuric acid, Hydrochloric acid, Hydrofluoric acid, Comparison, Reprints. Standard reference materials.

A closed vessel microwave digestion system is described. In situ measurement of elevated temperatures and pressures in closed Teflon PFA vessels during acid decomposition of organic samples is demonstrated. Temperature profiles for the acid decomposition of biological and botanical standard reference materials are modeled by the dissolving acid. Microwave power absorption of nitric, hydrofluoric, sulfuric, and hydrochloric acids is compared. An equation is applied to acid microwave interactions to predict the time needed to reach target temperatures during sample dissolu-tions. Reaction control techniques and safety precautions are recommended.

900,360

PB89-172365 Not available NTIS National Bureau of Standards (NML), Gaithersburg, MD. Atomic and Plasma Radiation Div.

Aluminumlike Spectra of Copper through Molybdenum.

J. Sponsored by Department of Energy, Washington, DC. Office of Magnetic Fusion Energy, and Naval Research Lab., Washington, DC.

Pub. in Jnl. of the Optical Society of America B 5, n10 p2183-2189 Oct 88.

Keywords: *Copper, *Spectrum analysis, Molybde-num, Rubidium, Strontium, Experimental design, Com-parison, Numerical analysis, Dirac equation, Hartree-Fock approximation, Reprints, Isoelectronic atoms.

Spectra of copper through molybdenum were generated in a tokamak plasma and were photographed with a 2.2-m grazing-incidence spectrograph. The doublet system of the AI I isoelectronic sequence was derived from these data and compared with Dirac-Fock calculations of the wavelengths. The smooth variation of the differences was used to improve the wavelengths and to predict those of rubidium and strontium, which were not observed.

900.361

PB89-172373 Not available NTIS National Bureau of Standards (NML), Gaithersburg, PB89-172373 MD. Atomic and Plasma Radiation Div.

Spectrum and Energy Levels of Singly Ionized Cesium. 2. Interpretation of Fine and Hyperfine Structures.

Final rept. C. J. Sansonetti, K. L. Andrew, and J. F. Wyart.

1988, 11p See also PB86-200979. Pub. in Jnl. of the Optical Society of America B 5, n10 p2076-2086 Oct 88.

Keywords: *Atomic structure, *Cesium, Molecular orbitals, Hyperfine structure, Electron transitions, Eigenvectors, Reprints.

The theoretical interpretation of Cs II has been extended and now includes the $5p(\sup 5)$ ns (n=6-12), $5p(\sup 5)$ nf (n=6-8), $5p(\sup 5)$ nd (n=5-11), $5p(\sup 5)$ nf (n=4-8), $5p(\sup 5)$ ng (n=5-10), and $5p(\sup 5)$ nh (n=6-8) configurations. Most levels are well represented in the single configuration approximation when sented in the single configuration approximation when far configuration interactions are included through effective electrostatic parameters. Explicit interactions of low-lying 5p(sup 5)nd + 5p(sup 5)(n+1)s configurations have been determined. For most configurations, good jik coupling is found. Purities of the levels in jik coupling and the LS composition of the eigenvectors are given. The intermediate-coupling eigenvectors have been used to calculate magnetic disable base. have been used to calculate magnetic-dipole hyperfine-splitting factors, and these are compared with 167 experimentally determined values from earlier work.

900,362

PB89-172415

Not available NTIS

National Bureau of Standards (NML), Gaithersburg, MD. Molecular Spectroscopy Div. infrared Spectrum of the nu6, nu7, and nu8 Bands

of HNO3. Final rept. A. G. Maki, and W. B. Olson. 1989, 11p Pub. in Jnl. of Molecular Spectroscopy 133, p171-181

Keywords: *Infrared spectroscopy, *Spectrum analysis, *Nitric acid, *Band spectra, Bandwidth, Molecular spectroscopy, Molecular rotation, Numerical analysis, Reprints.

The high-resolution spectrum of nitric acid (HNO3) has been measured from 500 to 800/cm. The nu8 band is a C-type out-of-plane vibration and both nu6 and nu7 are in-plane vibrations giving rise to A-type bands. The band centers are at 580.3035(5)/cm for nu7, 646.8262(5)/cm for nu6, and 763.1543(5)/cm for nu8. Constants are given that allow one to accurately calculated to the state of the state late the infrared line positions for all three bands. The intensity of the nu8 band is anomalous with an R branch that is much stronger than the P branch. Effective rotational intensity correction terms are given for both the nu8 and the nu6 band. An estimate is given for the relative transition moments for the nu6 and nu7 bands.

900,363 PB89-172431 Not available NTIS National Bureau of Standards (IMSE), Gaithersburg, MD. Reactor Radiation Div.

Neutron Powder Diffraction Structure and Electrical Properties of the Defect Pyrochlores Pb1.5M2O6.5 (M=Nb, Ta).

Final rept.

Final rept.
F. W. Beech, W. M. Jordon, C. R. A. Catlow, A. Santoro, and B. C. H. Steele. 1988, 14p
Pub. in Jnl. of Solid State Chemistry 77, p322-335
1988.

Keywords: *Crystal structure, *Neutron diffraction, *Electrical properties, Minerals, Lead inorganic compounds, Reprints, *Lead niobates, *Lead tantalates, *Pyrochlore.

Powder neutron diffraction and Rietveld analysis were Powder neutron diffraction and Hierveid analysis were used to investigate the crystal structures of the defective pyrochlores Pb1.5Nb2O6.5 and Pb1.5Ta2O6.5. Both materials crystallize with the symmetry of space group Fd3m, with lattice parameters a = 10.5647(2) and a = 10.55458(2) A, respectively. No evidence has been observed of oxygen or lead vacancy ordering in these compounds. This result is interpreted in terms of smedd in which all lead recent in the structure has a model in which all lead present in the structure has sevenfold pyramidal coordination and forms domains separated by regions of lead vacancies with hexagonal or bipyramidal configurations of the oxygen atoms. or bipyramidal configurations of the oxygen atoms. This model, built on the assumption that the driving force in the formation of this type of defect pyrochlore is the coordination of lead, leads us to conclude that the system Pb(1+2)M2O(6+x)(M=Nb, Ta) may exist over a range of compositions with 0.33 < or = x < or = 0.6, and may also explain results obtained in other studies of related materials. The electric measurements about that both compounds are predesting urements show that both compounds are predominantly electronic conductors and that the ionic contribution to the total conductivity is very small even at the highest temperatures used in the study.

900.364

PB89-172506 Not available NTIS National Bureau of Standards (NML), Gaithersburg, MD. Gas and Particulate Science Div. Dependence of Interface Widths on Ion Bombard-

ment Conditions in SIMS (Secondary Ion Mass Spectrometry) Analysis of a NI/Cr Multilayer Structure.

M. Moens, F. C. Adams, and D. S. Simons. 1987,

Pub. in Analytical Chemistry 59, n11 p1518-1529 1987.

Keywords: *Chromium, *Nickel, *Mass spectroscopy, *Spectrum analysis, Secondary emission, Ion beams, Ion irradiation, Surface chemistry, Interfaces, Reprints, *Secondary Ion mass spectroscopy, Scanning electroscopy tron microscopy.

The effect of varying ion bombardment conditions on interface widths in a Ni/Cr multilayer structure is described. SIMS depth profiles of the structure were obtained using different primary ions, accelerating voltages and ambient oxygen pressures. The depth profiles are displayed together with scenarios deletion miles. files are displayed together with scanning electron mi-

crographs of the craters formed in an effort to relate the induced surface roughness to the interface widths obtained. Secondary ion yield variations, especially at the interfaces, have been studied.

Not available NTIS National Bureau of Standards (NML), Gaithersburg, MD. Inorganic Analytical Research Div.

Twenty Five Years of Accuracy Assessment of the Atomic Weights.

Final rept 900,365 PB89-174007

Final rept.

L. Barnes, and H. S. Peiser. 1986, 10p Pub. in Proceedings of Workshop and Symposium Na-tional Conference of Standards Laboratories, Gaith-ersburg, MD., October 6-9, 1986, p22-1-22-10.

Keywords: *Atomic mass, *Chemical elements, *Minerals, *Accuracy, Isotopes, Abundance.

The atomic weights of the chemical elements in their natural terrestrial occurrences are among the most widely used measurement data affecting science, technology, and commerce. Uncertainties in these values arise not only from the remaining experimental imprecision and bias in determining these values, but also from variations between different sources of a given element. In the tables of the Standard Atomic Weights revised biennially by the International Union of Pure and Applied Chemistry, an attempt is made to publish a single value for each atomic weight with the largest number of significant figures that can be stated with a single digit uncertainty. In this way users can, at a glance, perceive the atomic weight to the highest precision that is safely applicable to any source and corresponding to the best current knowledge as assessed by the Commission on Atomic Weights and Isotopic Abundances. In the paper the steps are traced by which this procedure has been developed.

900,366 PB89-174015 PB89-174015 Not available NTIS National Bureau of Standards (NEL), Boulder, CO. Thermophysics Div.

High Temperature Thermal Conductivity Apparatus for Fiulds.

Final rept.
H. M. Roder. 1987, 8p
Sponsored by Department of Energy, Washington, DC.

Engineering and Geosciences Div.
Engineering and Geosciences Div.
Pub. in Proceedings of DOE (Department of Energy)
Symposium on Energy Engineering Science (5th),
Boulder, CO., p61-68 1987.

Keywords: *High temperature tests, *Thermal measuring instruments, *Thermal conductivity, *Thermal diffusion, *Fluids, Performance evaluation, Design criteria,

A new apparatus for measuring both thermal conductivity and thermal diffusivity of fluids at high temperatures is described. The technique employed is that of the transient hot wire. Measurements are made with a 12.7 micrometer diameter platinum wire at times of up to 1 second. The data acquisition system is controlled by a microcomputer and includes several programmable digital voltmeters. The hot wire and a shorter com-pensating hot wire are arranged in different arms of a Wheatstone bridge. The cell containing the core of the Wheatstone bridge. The cell containing the core of the apparatus is designed to accommodate pressures from near zero to 70 MPa and temperatures form 0 to 500 C. For thermal conductivity, the precision of the new system is expected to be around 0.3% and the accuracy 1.0%. For thermal diffusivity the accuracy is estimated to be around 5%. From the two variables measured, the author can obtain values of the specific heat, Cp, of the fluid, provided that the density is either measured, or available through an equation of state.

900,367 PB89-174098 PB89-174098 Not available NTIS
National Bureau of Standards (NML), Boulder, CO.
Time and Frequency Div.
Study of Long-Term Stability of Atomic Clocks.

Final rept.

D. W. Allan. 1987, 5p Pub. in Proceedings of Annual Precise Time and Time Interval (PTTI) Applications and Planning Meeting (19th), Redondo Beach, CA., December 1-3, 1987,

Keywords: *Frequency standards, *Atomic clocks, Time measurement, Masers, Hydrogen, Cesium, Mercury(Metal), Beams(Radiation), Tracking(Position), Frequency stability, Pulsation, Spacecraft tracking,

The importance of long-term frequency stability has increased significantly in recent years because of the discovery of the millisecond pulsar, PSR 1937 + 21. In addition, long-term stability is extremely useful not only in evaluating primary frequency standards and the per-formance of national timing centers, but also in addressing questions regarding autonomy for the Global Positioning System (GPS) and syntonization for Jet Propulsion Laboratory's (JPL) Deep Space Tracking Network. Over the last year, NBS has carried out several studies addressing questions regarding the long-term frequency stability of different kinds of atomic clocks as well as of principal timing centers. These analyses cover commercial and primary cesium-beam frequency standards, active hydrogen master frequen-cy standards and the new commercial mercury-ion frequency standards at United States Naval Observatory (USNO). Fractional frequency stabilities of parts in 10 sup 14 down to parts in 10 sup 15 were observed for various of these standards. It is believed that frequency stabilities on the order of a part in 10 sup 15 will be necessary to measure the effects of gravity waves on frequency stability between millisecond pulsars and atomic clocks on or near the earth.

900,368 PB89-174932 Not available NTIS National Bureau of Standards (NEL), Boulder, CO. Thermophysics Div.
Vapor-Liquid Equilibrium of Nitrogen-Oxygen Mixtures and Air at High Pressure.

Final rept.

J. C. Rainwater, and R. T. Jacobsen. 1988, 10p

Pub. in Cryogenics 28, p22-31 Jan 88.

Keywords: *High pressure tests, *Nitrogen, *Oxygen, *Binary systems(Materials), *Mathematical models, *Thermodynamic equilibrium, *Phase diagrams, Phase transformations, Vapor phases, Liquid phases, Citical paint Programs Critical point, Reprints.

The vapor-liquid equilibrium surface of the binary mixture nitrogen-oxygen is correlated over an extended critical region with the Leung-Griffiths model as modified by Rainwater and Moldover. No single comprehensive experimental measurement of the coexistence surface is available. However, several different experiments along isopleths, isotherms and isobars collectively provide enough data to make possible the development of a reasonable correlation. The model is optimized to modern data and is shown to be consistent with pioneering measurements done before 1930 to within experimental and temperature-scale uncertainties. It is shown that air in the critical region can be accurately modelled as a nitrogen-oxygen binary mixture by including the small argon component with oxygen. Ancillary equations for the saturation proper-ties of air as functions of temperature are also constructed.

900,369 National Bureau of Standards (NEL), Gaithersburg, MD. Thermophysics Div. Non-Equilibrium Theories of Electrolyte Solutions.

Final rept.
J. B. Hubbard. 1987, 34p
Pub. in Physics and Chemistry of Aqueous Ionic Solutions, p95-128 1987.

Keywords: *Aqueous electrolytes, *Nonequilibrium flow, Mathematical models, Light scattering, Electrical resistance, Friction, Ions, Reprints, Space-time model, Solvent properties, Ion-ion collisions, Debye Falkenhagen Onsager method, Laser spectroscopy.

Dynamic aspects of electrolyte solution theory are explored through a generalized Langevin approach as well as through a van Hove/Smoluchowski description. The classical theory of ion-ion dynamical interac-tions is presented at the Debye-Falkenhagen-Onsager level, while the non-equilibrium ion-solvent interaction is analyzed from both a microscopic and a continuum viewpoint. Emphasis is placed on understanding the physics of simple models on which explicit calculations can be performed. These include electrical conductance, ionic friction coefficients, space-time correlation functions, and laser light scattering spectra for simple electrolytes and charged macromolecules.

900.370 PB89-174957 Not available NTIS National Bureau of Standards (NEL), Gaithersburg, MD. Thermophysics Div.

Molecular Dynamics investigation of Expanded Water at Elevated Temperatures.

Final rept.

R. D. Mountain. 1989, 5p

Pub. In Jnl. of Chemical Physics 90, n3 p1866-1870, 1
Feb 89.

Keywords: *High temperature tests, *Water, *Dynamic structural analysis, Molecular structure, Hydrogen bonds, Density(Mass/volume), Thermodynamic propertles, Reprints, Expansion.

The structure of expanded states of TIP4P water has been examined over a range of densities running from 1000 to 100 kg/cu m and for a range of temperatures running from the coexistence temperature up to supercritical temperatures. The main result is that hydrogen bonding, as evidenced by the maximum in g(sub OH) (R) at 0.18 nm, persists to supercritical temperatures over the entire density range examined. For most liquid densities, the number of hydrogen bonds per molecule scales as a single function of the temperature but does not scale for dense vapor densities.

900,371 PB89-175228

(Order as PB89-175194, PC A06)
National Inst. of Standards and Technology (NML),
Gaithersburg, MD. Chemical Thermodynamics Div.
Numeric Databases in Chemical Thermodynamics
at the National Institute of Standards and Technol-

ogy. Bi-monthly rept. M. W. Chase. 1989, 4p

Included in Jnl. of Research of the National Institute of Standards and Technology, v94 n1 p21-24 Jan-Feb

Keywords: *Thermodynamics, *Thermochemical properties, Chemical elements, Specific heat, Enthalpy, Vapor pressure, Phase transformations, Bibliographies, Oxides, *Numerical data bases.

During the past year the activities of the Chemical Thermodynamics Data Center and the JANAF Thermochemical Tables project have been combined to obtain an extensive collection of thermodynamic information for many chemical species, including the elements. Currently available are extensive bibliographic collections and data files of heat capacity, enthalpy, vapor pressure, phase transitions, etc. Future plans re lated to materials science are to improve the metallic oxide temperature dependent tabulations, upgrade the recommended values periodically, and maintain the bibliographic citations and the thermochemical data current. The recommended thermochemical information is maintained on-line and tied to the calculational routines within the data center. Recent thermodynamic evaluations on the elements and oxides will be discussed, as well as studies in related activities at the National Institute of Standards and Technology.

900,372 PB89-175418 PC A07/MF A01 National Inst. of Standards and Technology (NML), Gaithersburg, MD. Center for Atomic, Molecular and Optical Physics.

Technical Activities 1986-1988, Molecular Spectroscopy Division.

A. Weber. Mar 89, 136p NISTIR-89/4051
See also PB87-140224.

Keywords: *Molecular spectroscopy, *Research programs, Experimental design, Numerical analysis, Van der Waals equation, Environmental surveys, Mathematical models, Reaction kinetics, Surface chemistry, Standards, Molecular structure, Hydrogen bonds, Thermodynamics, Chemical reactions, *National Institute of Standards and Technology, State of the art, Molecular conformation.

The report summarizes the technical activities of the NIST Molecular Spectroscopy Division for the Fiscal Year 1987 and 1988. The activities span experimental and theoretical research in high resolution molecular spectroscopy, quantum chemistry, and laser photo-chemistry, and include the development of frequency standards, critically evaluated spectral data, applica-tions of spectroscopy to important scientific and technological problems, and the advancement of spectroscopy measurement methods and techniques. A listing is given of publications and talks by the Division staff.

900,373 PB89-175681 Not available NTIS National Bureau of Standards (NEL), Boulder, CO. Thermophysics Div.

Decorated Lattice Gas Model for Supercritical Soiubility. Final rept.

G. C. Nielson, and J. M. H. Levelt Sengers. 1987,

10p Pub. in Jnl. of Physical Chemistry 91, n15 p4078-4087

Keywords: *Solubility, *Thermodynamic equilibrium, *Supercritical flow, Phase diagrams, Solutes, Solvents, Temperature, Experimental design, Phase transformations, Solid phases, Liquid phases, Re-

The authors describe a self-consistent nonclassical model for supercritical solubility enhancement near the solvent's critical point. A Widom-Wheel-MermIn decorated lattice gas transformation is used to obtain properties of a dilute supercritical solution from known properties of the pure solvent. Phase equilibria between the solution and the additional solid or liquid phase are described. A semiquantitative representa-tion of solubility data for three different solute-solvent pairs at several temperatures was obtained. Infinite-dilution partial molal volumes based on parameter sets obtained from fits to solubility data did not agree very well with experiment,

900.374

PB89-175707 Not available NTIS National Bureau of Standards (NML), Gaithersburg, MD. Temperature and Pressure Div. Low Range Flowmeters for Use with Vacuum and

Leak Standards. Final rept.

K. E. McCulloh, C. D. Ehrlich, F. G. Long, and C. R.

Tilford. 1987, 6p Pub. in Jnl. of Vacuum Science and Technology A-Vacuum Surfaces and Films 5, n3 p376-381 1987.

Keywords: *Flowmeters, *Standards, *Pressure sensors, "Gas flow, Calibrating, Comparison, Performance evaluation, Leakage, Vacuum apparatus, Re-

Vacuum pressure standards of the orifice-flow type require known gas flows of .00001 mol/s (.01 stid cc/s) and less. Known gas flows can also be used to calibrate 'standard' leaks by comparing the pressures generated when flows from the leak and the flowmeter are alternately passed through a constant conduct-ance. Described here are two constant-pressure, piston displacement flowmeters developed at NBS that can generate flows between .000001 and 10 to the -10th power mol/s with an estimated uncertainty of 0.8 to 2%. Comparisons of the flowmeters with alternate calibration techniques, and repeated low range leak and vacuum gage calibrations, have been used to confirm the estimated uncertainty and random errors of the flowmeter.

900,375

Not available NTIS PB89-175996 National Bureau of Standards (NML), Gaithersburg, MD. Surface Science Div.

Dynamics of Molecular Collisions with Surfaces: Excitation, Dissociation, and Diffraction. Final rept.

S. Holloway, M. Karikorpi, and J. W. Gadzuk. 1987.

Pub. in Nuclear Instruments and Methods in Physics Research B27, n1 p37-54 1987.

Keywords: Excitation, Dissociation, Diffraction, Scattering, Reprints, *Molecular collisions, *Surface reactions, Charge transfer, EV range 01-10, Vibrational

Aspects of molecular collisions with surfaces are dis-Aspects of molecular collisions with surfaces are discussed which are important in the chemically relevant energy range of 1-10 eV. In particular, the role of charge transfer, potential energy surface topology and intra-molecular ground and excited-state potential curves are investigated as they pertain to internal vibrational excitation, dissociative absorption or scattering, and diffractive scattering. The modeling and analysis is based on classical trajectories and semi-classical wavenedet dynamics, both for intra-molecular, and wavepacket dynamics, both for intra-molecular and translational motion.

900,376

PB89-176093 Not available NTIS National Bureau of Standards (NML), Gaithersburg, MD. Chemical Kinetics Div.

One-Electron Transfer Reactions of the Couple SO2/SO2(1-) in Aqueous Solutions. Pulse Radiolytic and Cyclic Voltammetric Studies. Final rept.

P. Neta, A. Harriman, and R. E. Hule. 1987, 6p Pub. In Jnl. of Physical Chemistry 91, n6 p1606-1611

Keywords: *Reaction kinetics, *Sulfur dioxide, *Free radicals, *Radiolysis, *Reduction(Chemistry), pH, Porphyrins, Reprints, *Pulse techniques, *Voltammetry,

Rate constants for one-electron reduction of SO2 by several radicals and for reduction of several com-pounds by SO2(sup -1) radicals were determined by pulse radiolysis at pH 1. The reduction potentials for SO2 and for porphyrins were determined by cyclic voltammetry under identical conditions. These reduction potentials were used along with the rate constants and previously reported self-exchange rates to estimate the self-exchange rate for the couple SO2/SO2(sup 1) in acidic solutions. The calculated values were found to vary over many orders of magnitude, similar to the situation reported before for the O2/O2(sup -1) couple.

900.377

PB89-176101 Not available NTIS National Bureau of Standards (NML), Gaithersburg, MD. Chemical Kinetics Div. ion Kinetics and Energetics.

Final rept.

Pub. in Encyclopedia of Physical Science and Technology, v7 p1-18 1987.

Keywords: *lons, *Reaction kinetics, *lonization, Vapor phases, Reviews, Chemical reactions, Thermodynamics, Reprints.

The article, written for a non-specialist audience (undergraduate and graduate students, scientists and en-gineers from other specialties), presents a broad review of the thermodynamics of ions in the gas phase, as well as the unimolecular and bimolecular kinetics of the chemical reactions of ions in the gas phase.

900,378

PB89-176150 Not available NTIS National Bureau of Standards (NML), Gaithersburg, MD. Gas and Particulate Science Div.

Defocus Modeling for Compositional Mapping with Wavelength-Dispersive X-ray Spectrometry. Final rept.

R. L. Myklebust, D. E. Newbury, R. B. Marinenko, and D. S. Bright. 1986, 3p Pub. in Microbeam Analysis - 1986, p495-497 1986.

Keywords: *X ray spectroscopy, *Molecular structure, *Chemical composition, *Quantitative analysis, Spectrochemical analysis, Numerical analysis, Reprints, *Electron microprobe analysis.

Quantitative compositional mapping by electron probe microanalysis requires the use of corrections for spectrometer defocusing when wavelength-dispersive is employed. A correction procedure has been developed which is based on calculating a synthetic map of the standard from an angular scan across the peak. Equations have been developed which relate the distance in a matrix scan from the line-of-best-focus of the spectrometer to the equivalent angular position in a peak scan. The transmission of the spectrometer can be directly determined from the peak scan and appropriate corrections can be applied to the intensity map of an unknown. The method is effective down to magnifications as low as 150x, where statistical considerations become limiting.

900.379

PB89-176242 Not available NTIS National Bureau of Standards (NML), Gaithersburg, MD. Chemical Kinetics Div.
Rate Constants for Reactions of Nitrogen Oxide

(NO3) Radicals In Aqueous Solutions.

Final rept.

P. Neta, and R. E. Huie. 1986, 5p Pub. in Jnl. of Physical Chemistry 90, n19 p4644-4648

Keywords: *Chemical radicals, *Nitrogen oxides, Chemical reactions, Radiolysis, Reprints, *Rate constants, *Nitrate radicals, *Aqueous solutions, Hydroxyl radicals, Sulfate radicals.

Bate constants for reactions of NO3 radicals in neutral and acidic aqueous solutions were determined by pulse radiolysis. The values for hydrogen abstraction from several organic compounds were in the range of 10(5) - 10(7)/Ms and were dependent on the C-H bond strength. The rate constants for addition to double bonds ranged up to 5x10(7)/Ms. Rate constants for the one-electron oxidation of several organic comthe one-electron oxidation of several organic com-pounds and inorganic ions varied over a wide range. From these, it was possible to estimate the redox po-tential for the NO3/NO3 couple to be 2.3-2.6U. Sever-al rate constants for SO4(2-) were measured as well and the behavior of NO3, SO4(2-), and OH radicals are compared.

900,380 PB89-176408 Not available NTIS National Bureau of Standards (NML), Gaithersburg,

MD. Molecular Spectroscopy Div.

Plcosecond Coherent Anti-Stokes Raman Scattering (CARS) Study of Vibrational Dephasing of Carbon Disulfide and Benzene in Solution. Final rept.

J. W. Perry, A. M. Woodward, and J. C. Stephenson.

1986, 8p Pub. in Proceedings of SPIE (Society of Photo-Optical Instrumentation Engineers), Laser Applications in Chemistry and Biophysics, v620 p7-14 1986.

Keywords: *Raman spectra, *Coherent scattering, *Vibrational spectra, *Carbon disulfide, *Benzene, *Lasers, Phases, Mixtures, Carbon tetrachloride, Nitrobenzenes, Ethanols, Dilution, Polarization, Solarization, S vents, Mathematical models.

The vibrational dephasing of the 656 cm(-1) mode (nu1,a1g) of carbon disulfide and the 991 cm(-1) mode (nu2, a1g) of benzene have been studied as a function of concentration in mixtures with a number of solvents using a picosecond time-resolved coherent anti-Stokes Raman scattering (CARS) technique. The tech-nique employs two tunable synchronously-pumped model-locked dye lasers in a stimulated Raman pump, coherent anti-Stokes Raman probe time-resolved experiment. Results are obtained for CS2 in carbon tetrachloride, benzene, nitrobenzene and ethanol, and for benzene nu2 in CS2. The dephasing rates of CS2 nu1 increase on dilution with the polar solvents and decrease or remain constant on dilution with the nonpolar solvents. The CS2/benzene solutions show a contrasting behavior with the CS2 nu1 dephasing rate being nearly independent of concentrations whereas the benzene nu2 dephasing rate decreases on dilution. These results are compared to theoretical models for vibrational dephasing of polyatomic molecules in solution.

900.381 PB89-176473 Not available NTIS National Bureau of Standards (NML), Gaithersburg, MD. Surface Science Div.

Influence of Electronic and Geometric Structure on Desorption Kinetics of Isoelectronic Polar Molecules: NH3 and H2O. Final rept.

T. E. Madey, C. Benndorf, and S. Semancik. 1987,

Pub. in Springer Ser. Surf. Sci. 8, p175-181 1987.

Keywords: *Water, *Ammonia, *Reaction kinetics, *Desorption, Chemisorption, Surface chemistry, Chemical bonds, Adsorption, Polarity, Dipoles, Reprints, *Electronic structure, Isoelectronic atoms.

The thermal desorption kinetics of isoelectronic NH3 and H2O from surfaces provide an interesting con-trast, due to geometrical and electronic structural effects in the adsorbed layers. Both NH3 and H2O are polar molecules bonded to the surface via lone pair orbitals on N and O, respectively. Hydrogen-bonding attractive interactions between neighboring H2O molecules lead to formation of 2-d and 3-d clusters; thermal desorption kinetics of H2O are characterized by sharp desorption peaks over narrow temperature ranges (delta T less than 10 K in some cases). In distinction, lateral interactions between neighboring NH3 molecules are largely repulsive (dipole-dipole interactions) and the thermal desorption spectra are considerably broader in temperature than for H2O (delta T approximates 80 K to 180 K, depending on substrate).

900.382 PB89-176523 Not available NTIS National Bureau of Standards (NML), Gaithersburg, MD. Center for Basic Standards.

Near-Threshold X-ray Fluorescence Spectroscopy of Moiecules.

Final rept. Final rept.
D. W. Lindle, P. L. Cowan, R. E. LaVilla, T. Jach, R. D. Welling, P. L. Cowan, R. E. LaVilla, T. Jach, R. D. Deslattes, R. C. C. Perera, and B. Karlin. 1988, 5p Sponsored by Department of Energy, Washington, DC. Pub. in Proceedings of SPIE (Society of Photo-Optical Instrumentation Engineers), X-ray and VUV Interaction Data Bases, Calculations, and Measurements, v911 p54-58 1988.

Keywords: *Molecular energy levels, *X ray spectroscopy. *Spectrum analysis, *Emission_spectroscopy, copy, *Spectrum analysis, *Emission spectroscopy, *X ray fluorescence, X ray absorption, Excitations, Ionization, *X-ray fluorescence analysis.

The coupling of high-energy-resolution x-ray absorp-The coupling of high-energy-resolution x-ray absorption and emission spectroscopies with a high-intensity and high-resolution synchrotron-radiation beamline has opened up several new avenues of research in inner-shell molecular physics. Of particular importance is the ability to tune the incident photon energy throughout the near-threshold region for the atomic core levels of the molecules. All of these phenomena have the product some can be used in a complementary way to uncover some of the underlying molecular dynamics which occur upon inner-shell excitation and ionization. Some of the latest results from the NBS X-Ray Spectroscopy Beamline at NSLS will be presented to highlight these

900,383 PB89-176598 Not available NTIS National Bureau of Standards (NML), Gaithersburg, MD. Gas and Particulate Science Div.

Luminescence Standards for Macro- and Micro-

spectrofluorometry.
Final rept.
R. A. Velapoldi, and M. S. Epstein. 1989, 29p
Pub. in ACS (American Chemical Society) Symposium Series 383, Chapter 7, p98-126 1989.

Keywords: *Fluorimeters, *Spectrum analysis, *Luminescence, Standards, Calibrating, Assessments, Performance evaluation, Quantum efficiency, *Standard reference materials.

Requirements for standards used in macro- and microspectrofluorimetry differ, depending on whether they are used for instrument calibration, standardization, or are used for instrument calibration, standardization, or assessment of method accuracy. Specific examples are given of standards for quantum yield, number of quanta, and decay time, and for calibration of instrument parameters, including wavelength, spectral responsivity (determining correction factors for luminescence spectra), stability, and linearity. Differences in requirements for macro- and micro-standards are considered, and specific materials used for each are compared. Pure compounds and matrix-matched standards. pared. Pure compounds and matrix-matched standards are listed for standardization and assessment of method accuracy and existing Standard Reference Materials are discussed.

900,384 PB89-176788 Not available NTIS Mational Bureau of Standards (NML), Gaithersburg, MD. Radiometric Physics Div.

Feasibility of Detector Self-Calibration In the Near

Final rept.
J. Geist, M. J. Nofziger, and G. H. Olsen. 1986, 2p
Pub. in CPEM 86 Digest, Proceedings of Conference on Precision Electromagnetic Measurements, Gaithersburg, MD., June 23-27, 1986, p138-139.

Keywords: *Photodiodes, *Semiconductor devices, *Indium phosphides, Feasibility, Performance evaluation, Near infrared radiation, Indium arsenides, Gallium arsenides, Calibrating, Gallium indium arsenides.

A recent study of the self-calibration of InP/InGaAs heterodiodes in the 1000 to 1600 nm spectral region is reported.

900 385 Not available NTIS PB89-176952 National Bureau of Standards (NML), Gaithersburg, MD. Radiometric Physics Div.

MD. Radiometric Physics Div.
Vibrationally Resolved Photoelectron Angular Distributions for H2 in the Range 17
eV<or=h(nu)<or=39 eV.
Final rept.
A. C. Parr, J. E. Hardis, S. H. Southworth, C. S.
Feigerle, T. A. Ferrett, D. M. P. Holland, F. M. Quinn,
B. R. Dobson, J. B. West, G. V. Marr, and J. L.

Dehmer. 1988, 7p Sponsored by Department of Energy, Washington, DC.

Pub. in Physical Review A 37, n2 p437-443, 15 Jan 88.

Keywords: *Hydrogen, Far ultraviolet radiation, Reprints, *Photoelectron spectroscopy, *Photoionization, Autoionization, eV range 10-100, Extreme ultraviolet radiation, Angular distribution.

Vibrationally resolved photoelectron angular distributions have been measured for photoionization of H2 over the range 17 eV = or < h(mu) = or < 39 eV using independent instrumentation at two synchrotron radiation facilities. The present data greatly extend and add vibrational resolution to earlier variable-wavelength measurements. The average magnitude of the asymmetry parameter continues to lie lower than the best independent-electron calculations. Broad structure is observed for the first time, possibly indicating the effects of channel interaction with dissociative. doubly excited states of H2. Neither the average magnitude nor the gross wavelength-dependent structure vary strongly with the final vibrational channel.

900.386

PB89-176960 Not available NTIS National Bureau of Standards (NML), Gaithersburg, MD. Radiometric Physics Div.

Autolonization Dynamics in the Valence-Shell Pho-

tolonization Spectrum of CO. Final rept.

J. E. Hardis, T. A. Ferrett, S. H. Southworth, A. C. Parr, P. Roy, J. L. Dehmer, P. M. Dehmer, and W. A. Chupka. 1988, 8p

Grant NSF-CHE83-18419, Contract W-31109-eng-38 Sponsored by Department of Energy, Washington, DC., and National Science Foundation, Washington, DC.

Pub. in Jnl. of Chemical Physics 89, n2 p812-819, 15 Jul 88.

Keywords: *Carbon monoxide, Far ultraviolet radiation, Reprints, *Photoionization, *Autoionization, Photoelectron spectroscopy, Rydberg states, Ionization cross sections, Angular distribution, eV range 10-

Autoionizing Rydberg series in the valence-shell spectrum of CO have been studied by determining the high resolution relative photoionization cross section of cooled CO in the energy region 14.0-20.0 eV and by determining the vibrational branching ratios and the determining the vibrational branching ratios and the photoelectron angular distributions for production of CO(1+) X doublet Sigma (+), vu+ = 0-2 in the energy region 16.75-18.75 eV. Of particular interest are three prominent spectral features between 17.0 and 17.5 eV that result from interactions involving Rydberg series converging to the excited A doublet Pi and R doublet Sigma (1) between 5 the ion. The results are B doublet Sigma (+) states of the ion. The results are discussed in the context of recent two-step multichannel quantum defect theory calculations by Leyh and

900,387

PB89-179105 Not available NTIS National Bureau of Standards (NML), Gaithersburg, MD. Atomic and Plasma Radiation Div. Spectra and Energy Levels of the Galliumlike Ions

Rb VII-Mo XII. Final rept.

U. Litzen, and J. Reader. 1989, 8p Sponsored by Department of Energy, Washington, DC. Pub. in Physica Scripta 39, p73-80 1989.

Keywords: *Gallium, *Ultraviolet spectra, *Plasmas(Physics), *Ions, *Electron transitions, Rubidium, Strontium, Yttnum, Zirconium, Niobium, Molybdenum, Reprints.

Spectra of the galliumlike ions Rb VII, Sr VIII, Y IX, Zr X, Nb XI, and Mo XII emitted from sparks and laser-produced plasmas have been recorded in the region 235-665 Angstroms. All levels of 4s(sup2)4p, 4s(sup2)4d, 4s(sup2)4d, 4s4p(sup2), 4p3 and, in Rb VII, Sr VIII and Y IX, 4s(sup2)4f have been established. The level structure has been studied by means of ab initio and parametric calculations.

900.388

Not available NTIS PB89-179113 National Bureau of Standards (NML), Gaithersburg, MD. Molecular Spectroscopy Div.

Vibrational Exchange upon Interconversion Tunneling in (HF)2 and (HCCH)2.

G. T. Fraser. 1989, 12p Pub. in Jnl. of Chemical Physics 90, n4 p2097-2108, 15 Feb 89.

Keywords: *Acetylene, *Hydrogen fluoride, Hydrogen bonds, Infrared spectra, Reprints, Vibrational states, Selection rules, Dimers.

Model calculations are presented to interpret the large H-F and C-H stretching vibrational dependencies of the interconversion tunneling splittings and the corre-sponding infrared vibrational-tunneling state selection rules in (HF)2 and (HCCH)2. The model consists of two potential curves in the tunneling coordinate, coupled by an interaction term that allows the vibrational excitation to be exchanged between the two monomer units, permitting tunneling to occur. The interaction term is approximated by resonant infrared transitiondipole coupling. The magnitudes of the calculated vibrational dependencies, their isotopic shifts, and the predicted selection rules are in agreement with previous ous experimental observations.

900,389 PB89-179121 Not available NTIS National Bureau of Standards (NML), Gaithersburg, MD. Molecular Spectroscopy Div.
infrared and Microwave Spectra of OCO-HF and SCO-HF.

Final rept.

G. T. Fraser, A. S. Pine, R. D. Suenram, D. C. Dayton, and R. E. Miller. 1989, 7p Pub. in Jnl. of Chemical Physics 90, n3 p1330-1336, 1 Feb 89.

Keywords: *Complex compounds, *Infrared spectra, *Microwave spectra, Hydrogen bonds, Hydrogen fluo-ride, Carbon dioxide, Bolometers, Molecular beams, Reprints, Vibrational states, Fourier transform microwave spectroscopy.

The H-F stretching bands of the OCO-HF and SCO-HF complexes have been studied by optothermal (bolometer-detected) molecular-beam spectroscopy. Both species exhibit spectra of a quasilinear molecule red shifted from free HF by 52.1 and 57.5/cm, respectively. The principal band in both molecules is accompanied by a slightly red-shifted doublet-type subsidiary band that can be interpreted as a hot band of a low frequency bending vibration or a K = 1 subband of a bent molecule. Accurate doublet splittings in the ground H-F vibrational state have been measured by pulsed-nozzle Fourier-transform microwave spectros-CODY.

900,390 PB89-179154 PB89-179154 Not available NTIS National Bureau of Standards (NML), Gaithersburg,

MD. Gas and Particulate Science Div.
Wheatleyite, Na2Cu(C2O4)2 . 2H2O, a Natural
Sodium Copper Salt of Oxalic Acid.

Final rept. R. C. Rouse, D. R. Peacor, P. J. Dunn, W. B.

Simmons, and D. Newbury. 1986, 3p Pub. in American Mineralogist 71, n9-10 p1240-1242

Keywords: *Sodium, *Copper, *Oxalates, *Crystal structure, *X ray diffraction, Mohs hardness, Synthesis(Chemistry), Triclinic lattices, Galena, Sphalerite, Powder(Particles), Minerals, Reprints, Wheat-

Wheatleyite, Na2Cu(C2O4)2 . 2H2O, occurs as aggregates of blue acicular crystals associated with galena and sphalerite at the Wheatley mine, near Phoenixville, Pennsylvania. It is triclinic P1, with a=7.559(3), b=9.665(4), c=3.589(1) angstroms, alpha =76.65(2) degrees, beta =103.67(2) degrees, gamma =109.10(2) degrees, and Z=1. The strongest powder 10 $\bar{5}$, 10(2) degrees, and Z = 1. The strongest powder X-ray diffraction lines are (dobs, lobs, hkl) 7.04(8)(100), 6.539(10)(110), 3.655(5)(210), 3.169(9)(121), 2.799(4)(221), 2.538(3)(021), 2.497(3)(231), and 2.344(3)(300). Measured and calculated densities are 2.27(4) and 2.250 g/cu m, respectively. The Mohs hardness is 1 to 2, and there is a perfect (100) cleavage. Optically, wheatleyite is biaxial positive with indices alpha = 1.400(4), beta = 1.499(2), gamma = 1.667(2), and 2V = 83(5) degrees. Dispersion is r < v; pleochroism is X equal colorless, Y = pale blue, Z equal dark blue; absorption is Z > Y > X. A crystal-structure determination shows wheatleyite to be identical to synthetic Na2Cu(C2O4)2.2H2O. 900,391 Not available NTIS PB89-179196 National Bureau of Standards (NML), Gaithersburg, MD. Temperature and Pressure Div. Effects of Velocity and State Changing Collisions on Raman Q-Branch Spectra.

Final rept.

G. J. Rosasco, and W. S. Hurst. 1987, 33p Sponsored by Army Research Office, Research Trian-

gle Park, NC. Pub. in Spectral Line Shapes, p535-567 1987.

Keywords: *Raman spectroscopy, *Molecular vibration, *Line width, *Molecular energy levels, *Velocity, *Molecular rotation, Temperature, Pressure, Performance evaluation, Spectral lines, Reprints, *High resolu-

Recent progress in both the experimental characterization and theoretical understanding of Raman vibrational Q-branch spectra is reviewed. Nonlinear Raman spectroscopy, in particular stimulated Raman gain/ loss spectroscopy, has produced high resolution (1-150 MHz) spectra for many systems over quite large ranges of temperature and pressure. The high resolution capability allows testing theoretical predictions to a previously unattainable level of accuracy. In turn, the use of nonlinear Raman spectroscopies for optical measurements of temperature, pressure, and species concentration in hostile environments requires very accurate prediction of spectra as functions of these variables. The level of current understanding and ability to predict these diagnostic spectra is reviewed. Emphasis is placed on the role of velocity and state changing collisions, since these primarily determine the shapes and widths of Raman Q-branch spectra.

900.392 PB89-179568 Not available NTIS National Bureau of Standards (NEL), Gaithersburg, MD. Chemical Process Metrology Div.

Remote Sensing Technique for Combustion Gas

Temperature Measurement In Black Liquor Recovery Boilers. Final rept.

S. R. Charagundla, and H. G. Semerjian. 1986, 8p Contract DE-AI01-76PR06010 Sponsored by Department of Energy, Washington, DC.

Sponsored by Department of Energy, Washington, DC. Office of Industrial Programs. Pub. in Proceedings of SPIE (Society of Photo-Optical Instrumentation Engineers), Optical Techniques for Industrial Inspection, v665 p298-305 1986.

Keywords: *Remote sensing, *Emission spectroscopy, *Black liquors, *Combustion products, *Gas analysis, *Temperature measurement, Potassium, Boilers, Materials recover, Spectral lines.

A remote sensing technique, based on the principles of emission spectroscopy, is being developed for ap-plication to temperature measurement in black liquor recovery boilers. Thus far, several tests have been carried out, both in the laboratory and at a number of re-covery boilers, to characterize the emission spectra in the wavelength range of 300 micrometers to 800 micrometers. These tests pointed out the potential for the line intensity ratio technique based on a pair of emission lines at 404.4 micrometers and 766.5 micrometers observed in the recovery boiler combustion zone; these emission lines are due to potassium, a common constituent found in all the black liquors. Accordingly, a fiber optics based four-color system has been developed. The in-situ, nonintrusive technique together with some of the results obtained are described in the paper.

900.393 PB89-179576 Not available NTIS National Bureau of Standards (NEL), Gaithersburg, MD. Chemical Process Metrology Div. Surface Properties of Clean and Gas-Dosed SnO2 (110).

Final rept.

D. F. Cox, T. B. Fryberger, J. W. Erickson, and S. Semancik. 1987, 2p

Pub. in Jnl. of Vacuum Science and Technology A 5, n4 pt2 p1170-1171 Jul/Aug 87.

Keywords: *Band spectra, *Tin oxides, *Photoelectric emission, Hydrogen, Oxygen, Water, Gases, Adsorption, Ultraviolet detection, Electron diffraction, Surface properties, Desorption, Reprints.

Surface-sensitive techniques have been used to investigate the mechanisms responsible for gas-induced changes in the electronic behavior of tin oxide (SnO2). Analytical measurements were made before and after dosing a crystalline specimen to controlled amounts of H2, O2, and H2O. Data are presented and discussed which illustrate band bending and band gap emission effects produced by adsorption.

900,394

PB89-179600 Not available NTIS National Bureau of Standards (NEL), Boulder, CO.

Chemical Engineering Science Div.
Thermal Conductivity of Liquid Argon for Temperatures between 110 and 140 K with Pressures to 70 MPa.

Final rept.
H. M. Roder, C. A. Nieto de Castro, and U. V. Mardolcar. 1987, 20p
See also PB87-203725.

Pub. in International Jnl. of Thermophysics 8, n5 p521-540 1987.

Keywords: *Argon, *Thermal conductivity, *High pressure tests, *Cryogenics, Gases, Liquids, Density(Mass/volume), Standards, Reprints.

The paper presents new experimental measurements of the thermal conductivity of liquid argon for four temperatures between 110 and 140 K with pressures to 70 MPa and densities between 23 and 36 mol/L. The measurements were made with a transient hot wire apparatus. A curve fit of each isotherm allows comparison of the present results to those of others and to correlations. The results are sufficiently detailed to illustrate several features of the liquid thermal conductivity surface. If these details are taken into account, the comparisons show the accuracy of the present results to be 1%. The present results along with several other sets of data are recommended for selection as standard thermal conductivity data along the saturated liquid line of argon, extending the standards into the cryogenic temperature range. The results cover a fairly wide range of densities. A hard sphere model cannot represent the data within the estimated experimental accuracy.

900,395

PB89-179618 Not available NTIS National Bureau of Standards (NEL), Boulder, CO. Chemical Engineering Science Div.

Facilitated Transport of CO2 through Highly Swolien ion-Exchange Membranes: The Effect of Hot Glycerine Pretreatment.

Final rept. J. J. Pellegrino, R. Nassimbene, and R. D. Noble.

1988, 5p See also PB87-233532.

Pub. in Gas Separation and Purification 2, p126-130 Sep 88.

Keywords: *Carbon dioxide, *Gases, *Swelling, *Ion exchange membrane electrolytes, *Separation, Glycerol, Hydration, Ethylenediamine, Transport properties, Hydrogen sulfide, Carriers, Diffusion, Permeability, Reprints.

pretreatment for perfluorosulphonic acid ion-exchange films, using glycerine and heating, causes the membranes to swell and imbibe greater (up to threefold) amounts of water than obtained using standard membrane hydration techniques. The permeation of CO, CO2 and H2S has been tested for these membranes in the diffusive transport mode and with carriermediated (facilitated) transport, using ethylenediamine (EDA). When compared to 'normally' hydrated membranes the results indicate that these membranes are up to 50% thicker; have four to six times higher flux in both diffusive and facilitated transport; maintain a high degree of facilitation for CO2 and H2S; and maintain similar selectivity versus non-carrier reactive gases as previously observed. Experimental results show the effects of pretreatment temperature on the CO2 flux.

900.396 PB89-179659 Not available NTIS National Bureau of Standards (IMSE), Gaithersburg, MD. Reactor Radiation Div. Chemical Physics with Emphasis on Low Energy

Excitations. Final rept.

J. J. Rush, and J. M. Rowe, 1986, 14p. Pub. in Physica B+C 137, n1-3 p169-182 1986.

Keywords: *Neutron spectroscopy, Neutron scattering, Cyanides, Reprints, Chemical physics, Low

energy, High resolution, Molecular dynamics, Ionic conductivity, Clathrates, Milli EV range.

Some examples of recent applications of low energy and high resolution neutron spectroscopy in chemical physics are discussed. These include brief descriptions of research on translation-rotation coupling in solids, focused on alkali cyanides and alkali cyanide mixed salts, a discussion of the problem of non-bonded potentials in molecular solids by a study of rotational modes and tunnel splittings, and the use of low energy neutrons to probe the mechanism of translational diffusion and reorientation in molecular complexes, ionic conductors and intercalation compounds. The illustrative examples described demonstrate the application of modern neutron scattering methods to low energy spectroscopy over five orders of magnitude in time and energy (0.1-10,000 (micro)eV). The importance of future research using neutron methods to study molecular dynamics in dilute and low-dimensional systems is stressed.

900,397
PB89-179691
National Bureau of Standards (NEL), Boulder, CO.

Thermophysics Div.
Second Viscosity and Thermal-Conductivity Virlal
Coefficients of Gases: Extension to Low Reduced
Temperature.
Final rept.

J. C. Rainwater, and D. G. Friend. 1987, 5p Pub. in Physical Review A 36, n8 p4062-4066, 15 Oct 87.

Keywords: *Gases, Thermal conductivity, Viscosity, Benzene, Reprints, Virial coefficients, Methanol, Density dependence.

A recent theory of the initial density dependences of both viscosity and thermal conductivity has been extended to include lower reduced temperatures. New data on the second viscosity virial coefficients of some organic vapors are found to be in substantial agreement with the theory even at the lowest temperatures. The authors present in tabular form the numerical values for both transport virial coefficients in the reduced temperature range $0.5 = \text{or less than } T^{\star} = \text{or less than } 100$ and include values for the constituent two-monomer, three-monomer, and monomer-dimer contributions. A brief discussion of the theoretical approach and calculational methods is also given.

900,398
PB89-179758
Not available NTIS
National Bureau of Standards (NML), Gaithersburg,
MD. Chemical Kinetics Div.
Mechanism and Rate of Hydrogen Atom Attack on

Toluene at High Temperatures. Final rept. D. Robaugh, and W. Tsang. 1986, 5p Pub. in Jnl. of Physical Chemistry 90, n17 p4159-4163

Keywords: *Reaction kinetics, *High temperature tests, *Decomposition reactions, Toluene, Methane, Ethane, Butenes, Reprints, *Chemical reaction mechanisms, *Ethane/hexamethyl, *Hydrogen atoms.

Hexamethylethane has been decomposed in the presence of large excesses of toluene and methane/toluene mixtures in single pulse shock tube experiments in the temperature range of 950-1100K and at 2-5 atm. Methane, ethane, isobutene and benzene are the main light hydrocarbon reaction products. In the presence of sufficiently large excess of methane, benzene yields are reduced. This is due to the competitive process.

900,399
PB89-179766
National Bureau of Standards (NML), Boulder, CO. Quantum Physics Div.

Quenching and Energy Transfer Processes of Single Rotational Levels of Br2 B triplet Pi(O(subu)(+)) v'= 24 with Ar under Single Collision Conditions.

Final rept.
K. Yamasaki, and S. R. Leone. 1989, 13p
Grants NSF-CHE84-04803, NSF-CHE86-04504
Sponsored by National Science Foundation, Washington, DC.

Pub. in Jnl. of Chemical Physics 90, n2 p964-976, 15 Jan 89.

Keywords: *Bromine, *Molecular energy levels, Argon, Energy transfer, Fluorescence, Reprints, Atom-molecule collisions, Rotational states, Vibrational states, Dye lasers, Quenching. State-specific total quenching rate constants are measured for selected rotational levels of Br2 under single collision conditions with argon at 296 K. A strict criterion is used to obtain single collision conditions in a cell experiment. A 0.04/cm bandwidth, etalon-narrowed pulsed dye laser excites single rovibronic transitions of the B triplet Pi((O sub u)(+)) state. Fluorescence decay traces with and without the argon collision partner are analyzed at early times to extract total quenching rate constants.

900,400
PB89-179790
Not available NTIS
National Bureau of Standards (NML), Boulder, CO.
Quantum Physics Div.
Alignment Effects in Ca-He(5(sup 1)P(sub 1) F(sup 1)P(sub 1)P(sub 1)P(sub 1) F(sup 1)P(sub 1)P(

5(sup 3)P(sub J)) Energy Transfèr Collisions by Far Wing Laser Scattering. Final rept.

K. C. Lin, P. D. Kleiber, J. X. Wang, W. C. Stwalley, and S. R. Leone. 1988, 6p Grant NSF-CHE86-15118

Sponsored by National Science Foundation, Washington, DC. Pub. in Jnl. of Chemical Physics 89, n8 p4771-4776, 15

Oct 88.

Keywords: *Calcium, Absorption spectra, Alignment

Keywords: *Calcium, Absorption spectra, Alignment, Energy transfer, Helium, Reprints, *Atom-atom collisions.

The far wing absorption profiles for excitation on the Ca(4s sup 2 singlet S sub 0-4s5p singlet p (sup 0, sub 1)) atomic transition, broadened in collisions with He are measured. Strong absorption was observed in both wings and a blue wing satellite was observed near the delta approx. $125/\mathrm{cm}$. This satellite was tentatively identified as due to a maximum in the CaHe(4s sup 2 singlet Sigma(+) - 4s5p singlet Sigma(+)) difference potential. These line-broadening techniques are used to study electronic energy transfer in the spinchanging collisions of Ca with He: Ca(5p singlet p(sup 0, sub 1)) + He yields Ca(5p triplet p(sup 0, sub J)) + He + delta E.

900,401
PB89-185755
Not available NTIS
National Bureau of Standards (NEL), Gaithersburg,
MD. Thermophysics Div.
Van der Waals Fund, Van der Waals Laboratory
and Dutch High-Pressure Science.
Final rept

J. M. H. Levelt Sengers, and J. V. Sengers. 1989, 14p

Pub. in Physica A 156, p1-14 1989.

Keywords: Fluids, Light scattering, Molecular theory, Nuclear magnetic resonance, Phase transformations, Transport properties, Netherlands, Reprints, *Foreign technology, *Van der Waals Fund, *High pressure, Calibration, Diamond anvils.

The history of the van der Waals Fund is traced from events in the late 19th century leading to its establishment in 1898 to the present time. The impact of the fund on the development of high-pressure science and industry in the Netherlands is discussed. The course of high-pressure research at the University of Amsterdam is sketched in the period of van der Waals and Kohnstamm, 1898 to 1920; that of Michels, 1920 to 1961; and that of Trappeniers, 1961 to 1987. The themes are: test of molecular theories at high pressures; quest for accuracy; high-pressure design; impact on Dutch industry; expanding the ranges of pressure and temperature; expanding the capabilities of property measurement; international recognition; and funding, including industrial support.

900,402
PB89-185888
Not available NTIS
National Bureau of Standards (NML), Boulder, CO.
Quantum Physics Div.

One Is Not Enough: Intra-Cavity Spectroscopy with Multi-Mode Lasers.

Final rept.

P. E. Toschek, and V. M. Baev. 1987, 89p Pub. in Laser Spectroscopy and New Ideas, A Tribute to Arthur L. Shawlow, 89p Sep 87.

Keywords: *Spectrum analyses, Multiplexing, Design criteria, Performance evaluation, Quantum chemistry, Quantum interactions, Reprints, *Laser spectroscopy, *Intercavity spectroscopy, Mode selection.

The scope of the presentation is necessarily limited: the authors have not aspired to offer a complete ac-

count of work on or with intra-cavity spectroscopy (ICS). In particular, attempting to cover all the pertinent work that has been done in molecular spectroscopy and chemical kinetics would far exceed the limits of the spectroscopy and chemical kinetics would far exceed the limits of the article. Instead, the authors have tried to point out two facts that are, it seems, not fully appreciated by the broader spectroscopists' community. First, the considerable measure of understanding they now have of the fundamentals that underlie ICS, and second, the level of sophistication and maturity the field has acquired recently. In adaptation of, but also challenging Arthur Schawlow's popular definition of a diatomic molecule, the authors claim that there indeed exist niches in physics where ONE is not enough. Eventually, what is lost in precious simplicity of the system under scrutiny is, perhaps, more than regained with inherent features that allow the spectroscopists to sometimes extend spectacularly the limits previously put on their techniques.

900.403

PB89-185896 Not available NTIS National Bureau of Standards (NML), Boulder, CO. Quantum Physics Div

Quantum Physics Div.
Structure and Dynamics of Molecular Clusters via
High Resolution IR Absorption Spectroscopy.
Final rept.

D. J. Nesbitt. 1987, 5p Grant NSF-PHY86-04504

Sponsored by National Science Foundation, Washington, DC.

Pub. in Proceedings of SPIE (Society of Photo-Optical Instrumentation Engineers), Laser Applications to Chemical Dynamics, Los Angeles, CA., January 13-14, 1987, v742 p16-20.

Keywords: *Infrared spectroscopy, *Absorption spectra, *Molecular structure, *Complex compounds, *Chemical dynamics, *Spectrum analysis, Molecular vibration, Molecular rotation, Hydrogen bonds, Van der Waals equation, Clustering, *High resolution, *Laser spectroscopy.

The combination of high resolution (.001/cm) cw tunable difference frequency generation (2.2-4.2 micrometers) with high sensitivity .0000017((Hz))1/2) long path length absorption methods in pulsed slit supersonic jets has permitted spectroscopic investigation of many weakly bound molecular complexes. Discussion focuses on three complementary areas of experimentation. Cluster formation in the molecular beam is probed via sub-Doppler, velocity resolved absorption profiles of monometer species. Spatially dependent beam clustering is strongly manifested through loss of monometer absorption intensity at line center. IR spectra of simple van der Waals molecules such as ArHF are obtained in the nu1 HF stretching region. Information on all modes in the complex is extracted. IR spectra of hydrogen bonded complexes such as HFCO2 are observed which exhibit large changes in average molecular geometry as a function of vibrational state. Surprisingly low intermolecular bending frequencies are evidenced in the spectra via hot bands and provide dynamical information on coupled vibrational-rotational motion in floppy molecular systems.

900.404

PB89-185938 Not available NTIS
National Bureau of Standards (NML), Boulder, CO.
Quantum Physics Div.

High Resolution Optical Multiplex Spectroscopy. Final rept.

K. P. Dinse, M. P. Winters, and J. L. Hall. 1987, 2p Pub. in Proceedings of International Conference on Laser Spectroscopy (8th), Are, Sweden, June 22-26, 1987, p388-389.

Keywords: *Spectrum analysis, *Doppler effect, *Optical spectra, Calibrating, Excitation, Performance evaluation, Multiplexing, *High resolution, *Laser spectroscopy.

Cross correlation techniques using stochastic sources have been applied in many fields to determine the impulse response functions of a system. The work applies such noise-based techniques for the first time in the optical domain to obtain high resolution sub-Doppler spectra. Interesting advantages of the method include a spectral multiplex advantage which can be a few powers of 10 relative to sequentially-scanned spectroscopy as well as absolute calibration of the frequency axis of the spectrum.

900,405 PB89-185946 PB89-185946 Not available NTIS National Bureau of Standards (NML), Boulder, CO. Quantum Physics Div.

Laser Spectroscopy of Inelastic Collisions. Final rept.

A. Gallagher. 1987, 11p Pub. in Proceedings of Symposium on Laser Spectroscopy (1st), Pecs, Hungary, August 28-30, 1986, p19-29

Keywords: *Inelastic cross sections, *Doppler effect, Experimental design, Inelastic scattering, *Atom-atom collisions, *Electron-atom collisions, *Laser spectroscopy.

The potential for wing recoil Doppler spectroscopy to measure differential inelastic collision cross sections is described. Experiments in the author's laboratory, investigating atom-atom and electron-atom collisions by that technique, are discussed.

900,406 PB89-185961 PB89-185961 Not available NTIS National Bureau of Standards (NML), Boulder, CO. Quantum Physics Div.

Surface Reactions in Sliane Discharges. Final rept.

A. Gallagher. 1986, 9p

A. Gallagner. 1996, Sp. Sponsored by Scientific Energy Research Inst., Golden, CO. Pub. in Proceedings of International Symposium on the Physics of Ionized Gases, Sibernik, Yugoslavia, September 1-5, 1986, p229-237.

Keywords: *Surface chemistry, *Silane, *Silicon hydrides, Experimental design, Sputtering, Thin films, lonization, Discharges.

A qualitative model for the gas and surface reactions in silane discharges leading to a-Si:H films and gas constituents is presented. Several experiments on which this is based are then described.

900,407

PB89-186415 Not available NTIS National Bureau of Standards (NML), Gaithersburg, MD. Atomic and Plasma Radiation Div.

Scheme for a 60-nm Laser Based on Photopumping of a High Level of Mo(6+) by a Spectral Line of Mo(11+).Final rept.

U. Feldman, and J. Reader. 1989, 3p Sponsored by Department of Energy, Washington, DC. Pub. in Jnl. of the Optical Society of America B 6, n2 p264-266 Feb 89.

Keywords: *Spectrum analysis, *Atomic energy levels, *Molecular energy levels, *Molybdenum, *Ultraviolet spectroscopy, Ions, Plasmas(Physics), Excitation, Reprints, *Laser spectroscopy.

A near coincidence between lines of two molybdenum ions at 13.650 nm creates conditions that satisfy re-

ions at 13.650 nm creates conditions that satisfy requirements for producing a short-wavelength photopumped laser in a plasma containing ions of Mo(6+). The scheme is based on the use of radiation from the 4s(doublet)4p(doublet)P(3/2)-4s(doublet)5s(doublet)S(1/2) transition of galliumlike MO(11+) to pump the 4s(doublet)4p(hexlet)(1)S(0)-4s(doublet)4p(heplet)6s 1/2(1/2)1 transition of kryptonlike Mo(6+). The Mo(6+) ion would then lase through several possible 4s(doublet)4p(heplet)5p-4s(doublet)4p(heplet)6s transitions near 60 nm.

900,408 PB89-186449 Not available NTIS American Chemical Society, Washington, DC.

Journal of Physical and Chemical Reference Data,
Volume 17, Number 1, 1988.

Quarterly rept.

D. R. Lide. c1988, 269p See also PB89-186456 through PB89-186480 and PB89-145114. Errata sheet inserted. Prepared in co-operation with American Inst. of Physics, New York. Sponsored by National Bureau of Standards (ICST), Gaithersburg, MD.

Available from American Chemical Society, 1155 16th St., NW, Washington, DC 20036.

Keywords: *Physical properties, *Chemical properties, *Experimental data, Vapor pressure, Density(Mass/volume), Equations of state, Steam, Numerical analysis, Cross section, Ionization, Photochemical reactions, Absorption, Molecular energy levels, Molybdenum, Thermodynamic properties, Aromatic polycyclic hydrocarbons, Isomerization, Atomic energy levels,

Contents: Pressure and density series equations of state for steam as derived from the Haar-Gallagher-Kell formulation; Absolute cross sections for molecular photoabsorption, partial photoionization, and ionic photofragmentation processes; Energy levels of molybdenum, Mo I through Mo XLII; Standard chemical thermodynamic properties of polycyclic aromatic hydrocarbons and their isomer groups I. Benzene series. (Copyright (c) by the U.S. Secretary of Commerce, 1988.)

900,409 PB89-186456 Brown Univ., Providence, RI. Not available NTIS Pressure and Density Series Equations of State for Steam as Derived from the Haar-Gallagher-Kell Formulation.

Quarterly rept. R. A. Dobbins, K. Mohammed, and D. A. Sullivan.

c1988, 8p

Included in Jnl. of Physical and Chemical Reference Data, v17 n1 p1-8 1988. Available from American Chemical Society, 1155 16th St., NW, Washington, DC

Keywords: *Vapor pressure, *Density(Mass/volume), *Steam, *Experimental data, Physical properties, Equations of state, Numerical analysis, Thermodynamic properties, Metastable state, Comparison, Virial co-

Two equations of state for the properties of steam, which are in the form of power series in pressure and density, are developed from the HGK84 formulation. These equations are of high accuracy in the equilibrium region where extensive measurements exist. They also accurately represent the extrapolated data in the metastable region between the vapor saturation and spinodal lines. The accuracy of the representations as a function of the number of terms of the series is presented. Their greatest utility is their use for high accuracy calculations that involve small to moderate departures from ideal-gas behavior. Conversion relationships for the second through the tenth coefficients of the pressure and density series, which apply to the corresponding virial coefficients, are presented. The pressure and density expansions are advantageous for efficient numerical calculations of water vapor properties in the equilibrium and metastable regions.

900,410 PB89-186464 Not available NTIS Joint Inst. for Lab. Astrophysics, Boulder, CO.
Absolute Cross Sections for Molecular Photoabsorption, Partial Photoionization, and Ionic Photofragmentation Process. Quarterly rept.

Quarterly rept.

J. W. Gallagher, C. E. Brion, J. A. R. Samson, and P. W. Langhoff. c1988, 145p
Prepared in cooperation with British Columbia Univ., Vancouver. Dept. of Chemistry, Nebraska Univ.-Lincoln. Dept. of Physics and Astronomy, and Florida State Univ., Tallahassee. Sponsored by National Bureau of Standards (ICST), Gaithersburg, MD. Included in Jnl. of Physical and Chemical Reference Data, v17 n1 p9-149 1988. Available from American Chemical Society, 1155 16th St., NW, Washington, DC 20036.

20036.

Keywords: *Experimental data, *Cross sections, *Ionization, *Photochemical reactions, *Absorption, *Fragmentation, Physical properties, dipole moments, Molecular energy levels, Numerical analysis, Electronic spectra, Graphs(Charts).

A compilation is provided of absolute total photoabsorbion and partial-channel photoionization cross sections for the valence shells of selected molecules, including diatomics (H2, N2, O2, CO, NO) and triatomics (CO2, N2O), simple hydrides (H2O, NH3, CH4), hydrogen halides (HF, HCI, HBr, HI), sulfur compounds (H2S, CS2, OCS, SO2, SF6), and chlorine compounds (Cl2, CCl4). The partial-channel cross sections presented refer to are dustine of the individual set serior sented refer to production of the individual electronic states of molecular ions and also to production of parent and specific fragment ions, as functions of incident photon energy, typically from approximately 20 to 100 eV. Photoelectron anisotropy factors, which together with electronic partial cross sections provide cross sections differential in photon energy and in ejection angle, are also reported. There is generally good agreement between cross sections measured by

the physically distinct optical and dipole electron-impact methods. The cross sections and anisotropy factors also compare favorably with selection ab initio and model potential (X-alpha) calculations which provide a basis for interpretation of the measurements.

900.411

PB89-186472 Not available NTIS National Bureau of Standards (NML), Gaithersburg, MD. Center for Radiation Research.

Energy Levels of Molybdenum, Mo 1 through 42.

J. Sugar, and A. Musgrove. c1988, 85p

Sponsored by National Bureau of Standards (ICST),

Gaithersburg, MD.

Included in Jnl. of Physical and Chemical Reference Data, v17 n1 p155-239 1988. Available from American Chemical Society, 1115 16th St., NW, Washington, DC 20036.

Keywords: *Atomic energy levels, *Molybdenum, *Experimental data, *Molecular energy levels, Ionization, Tables(Data), Isoelectronic atoms, Magnetic dipoles, Physical properties, Excitation.

The energy levels of the molybdenum atom, in all stages of ionization for which experimental data are available, have been compiled. Ionization energies, either experimental or theoretical, and experimental gfactors are given. Leading components of calculated eigenvectors are listed.

900.412

PB89-186480 Not available NTIS Massachusetts Inst. of Tech., Cambridge. Dept. of Chemistry

Standard Chemical Thermodynamic Properties of Polycyclic Aromatic Hydrocarbons and Their isomer Groups 1. Benzene Series.

Quarterly rept.

R. A. Alberty, and A. K. Reif. c1988, 13p Sponsored by National Bureau of Standards (ICST), Gaithersburg, MD.

Included in Jnl. of Physical and Chemical Reference Data, v17 n1 p241-253 1988. Available from American Chemical Society, 1155 16th St., NW, Washington, DC

Keywords: *Experimental data, *Standards, *Thermodynamic properties, *Aromatic polycyclic hydrocarbons, *Benzene, *Isomerization, Chemical properties, Numerical analysis, Enthalpy, Specific heat, Entropy, Gibbs free energy, Tables(Data), Molecular structure.

The polycyclic aromatic hydrocarbons can be organized into an infinite number of series in each of which successive isomer groups differ by C4H2. The first series starts with benzene, and chemical thermodynamic tables are presented here for C6H6, C10H8, C14H10, C18H12, C22H14, and C26H16 in the ideal gas phase. Since chemical thermodynamic properties are known for only several polycyclic aromatic hydro-carbons, the properties of individual species have been estimated using Benson group values of Stein and Fahr for temperatures from 298.15 to 3000 K. Values of Cp, S, delta H, and delta G have been calculated in joules for a standard state pressure of 1 bar. The chemical thermodynamic properties of the isomer groups have also been calculated. This provides a basis for extrapolating to higher carbon numbers where it is not feasible to consider individual molecular species.

900.413 PB89-186746 Not available NTIS National Bureau of Standards (NML), Gaithersburg, MD. Chemical Thermodynamics Div.

Water Structure in Crystalline Solids: ices to Proteins.

Final rept.

H. Savage. 1986, 82p

Sponsored by National Inst. of Arthritis, Diabetes, and Digestive and Kidney Diseases, Bethesda, MD. Pub. in Water Science Reviews 2, p67-148 1986.

Keywords: *Molecular structure, *Water, Hydrogen bonds, Crystal structure, Neutron diffraction, Reprints, *Crystalline hydrates, Non-bonded interactions.

The water structure in hydrate crystals ranging from the ice polymorphs to complicated macromolecular protein systems is reviewed with respect to analyzing the solvent using neutron and X-ray diffraction methods and understanding the resulting experimental structures. Detailed characteristics of water structure (ordered and disordered) are discussed with respect to

CHEMISTRY

Physical & Theoretical Chemistry

the more repulsive interactions that overall appear to control the actual geometries present within each system. The repulsive regularities may be used as a set of restraints in analyzing the possible water structure(s) around larger protein systems and also in computer simulations of water and aqueous systems.

900.414

Not available NTIS PB89-186753 MD. Chemical Thermodynamics Div.

Repulsive Regularities of Water Structure in Ices

and Crystalline Hydrates.

Final rept. H. F. J. Savage, and J. L. Finney. 1986, 4p Pub. in Nature 322, n6081 p717-720 1986.

Keywords: *Water, *Liquids, *Neutron diffraction, *Hydrogen bonds, *Crystal structure, Mathematical models, Solvents, Stereochemistry, Water of hydration, Reprints.

Hydrogen bonded structures display wide ranges of the various angles (e.g., O-H. . . O) and distances (e.g., H. . . O) used to describe their intermolecular geometry. For example, O. . O distances are found to vary be-tween -2.5 and 3.2A, while the hydrogen bond angles normally occur within the 120-180 range. Moreover, al-though many potential functions exist for describing water-water interactions, none of them are totally satisfactory in reproducing experimental results even for pure water. The initial results of an analysis of water structures in high resolution neutron crystal structures are presented and are dramatically more successful in rationalizing the stereochemistry of water interactions. Rather than considering the structures in terms of weak orientation-dependent attractions, a concentration on the repulsive interactions leads to a set of very much stronger stereochemical constraints which not only rationalize the structures but appear largely to control the orientational correlations in aqueous systems. Looked at in this way, water network structures in crystal hydrates and probably in the liquid itself become for the first time comprehensible. The approach provides a much firmer base from which to build realistic potential functions to model and simulate solvent structure(s).

900,415

PB89-186779 Not available NTIS National Bureau of Standards (NML), Gaithersburg, MD. Chemical Thermodynamics Div.

MD. Chemical Thermodynamics Div.
Biological Standard Reference Materials for the
Calibration of Differential Scanning Calorimeters:
Di-alkylphosphatidylcholine in Water Suspensions. Final rept.

F. Schwarz, 1986, 13p

Pub. in Thermochimica Acta 107, p37-49 1986.

Keywords: *Calibrating, *Heat measurement, Enthalpy, Thermodynamic properties, Reprints, *Phosphatidylcholine/dialkyl, *Standard reference materials, Differential scanning calorimeters.

The temperatures and enthalpies of the phase transitions of suspensions of di-alkylphosphatidylcholines in water solutions, prepared and stored under a variety of experimental conditions, were determined in a differential scanning calorimeter (DSC) to evaluate their potential as standard reference materials for the calibration of DSCs. The di-alkylphosphatidylcholine suspensions were 10 mass % 1,2-ditetradecanoyl-sn-glycero-3-phosphocholine (DTPC), and 1,2-dihexadecanoyl-sn-glycero-3-phosphocholine in aqueous buffered solutions at pH 7.0. A subtransition at 8.5 deg C with an enthalpy of 15.5 kJ/mole was observed in the DTPC suspensions after storage of the sample at -5.5 deg C for 2 days. The appearance and the temperature and enthalpy values of the subtransition, the pretransition, and the ice peaks of the suspensions depended on the preparation and storage conditions of the samples. An imprecision of 10% was observed for the values of the main transition and an imprecision of 0.03 deg C for the main transition temperature. Transition tempera-tures and enthalpies were also determined for suspensions of other di-alkylphosphatidylcholines in buffered water solutions.

900.416

PB89-186910 Not available NTIS National Bureau of Standards (NML), Boulder, CO. Quantum Physics Div.

Towards the Uitimate Laser Resolution.

J. L. Hall, D. Hils, C. Salomon, and J. M. Chartier.

1987, 5p Pub. in Proceedings of International Conference on Laser Spectroscopy (8th), Are, Sweden, June 22-26, 1987, p376-380.

Keywords: *Optical spectra, Metastable state, Quantum interactions, Performance evaluation, Calibrating, Iodine, Standards, *Laser spectroscopy, *High resolu-

It is indeed possible to lock to a reference cavity with a reproducibility 10 to the -15th power fringe widths and a stability a decade or so better producing a laser linewidth of 50 milliHertz. Heterodyne tests against an 12-stabilized reference show a frequency drift rate of +6100 Hz/hr stable to .001 per day and 1% for a week. Feed-forward compensation for the smooth drift then offers a source for spectroscopy with a frequency uncertainty 100 milliHertz for about one minute; as will be appropriate to scan over the 'quantum telegraph' optical resonances of single trapped ions with long metastable lifetimes.

PB89-187561 Not available NTIS National Bureau of Standards (NML), Gaithersburg, MD. Gas and Particulate Science Div.

High Resolution Spectrum of the nu(sub 1) + nu(sub 2) Band of NO2. A Spin induced Perturbation in the Ground State.

Final rept. R. L. Sams, and W. J. Lafferty. 1987, 16p Pub. in Jnl. of Molecular Spectroscopy 125, n1 p99-

Keywords: *Nitrogen dioxide, *Rotational spectra, *Electron energy, Ground state, Infrared spectra, Resolution, Vibration, Reprints, Spin orbit interactions.

The spectrum of the nu(sub 1) + nu(sub 2) band of NO2 has been studied with a resolution of 0.025 cm(sup -1). Spin-rotation constants and rotational constants are reported. An interesting perturbation has been found in the ground state of the molecule which occurs when the K(sub a)=0 and K(sub a)=2 levels become accidentally nearly degenerate around N=42. An explanation of this interaction is presented.

900,418

PB89-189351 PC A05/MF A01 National Inst. of Standards and Technology (NML), Gaithersburg, MD. Chemical Thermodynamics Div. Logistic Function Data Analysis Program: LOGIT. W. H. Kirchhoff. Mar 89, 95p NISTIR-88/3803

Keywords: *Hyperbolic functions, *Statistical analysis, *Potential Processing, Computer programs, Graphs(Charts), Tests, Data, Comparison, Experimental data, Chronium, Nickel, Interfaces, *Logistic functions, *Autocatalysis, *Computer applications, Computer programs, Fortran programming language.

A FORTRAN program has been written for the statistical analysis of experimental data in terms of an extended logistic function that includes non-horizontal asymptotes and asymmetry in the pre- and post-transition portions of growth and decay curves. The program is robust in that situations in which few or no data fall within the transition interval can be analyzed by the program. Individual weighting of the data is allowed for situations where the errors in experimental data are not uniform. The primary parameters describing the transition region include a location parameter, a width parameter, and an asymmetry parameter. Six more paparameters describe the two quadratic asymptotic re-gions. Sufficient information is given to allow the devel-opment of companion subroutines for the graphing of the function and its standard deviations as well as for displaying the original data with error bars. The program provides a means for systematically parameteriz-ing sigmoidal profiles for the comparison of measure-ments made with different instruments on different systems and for the comparison of measurements with simulation models. The program is extensively documented.

900,419

PB89-189815 Not available NTIS National Bureau of Standards (IMSE), Gaithersburg, MD. Ceramics Div.

Phase Equilibria and Crystal Chemistry in the Ternary System BaO-TiO2-Nb2O5. Part 2. New Barium Polytlanates with <5 mole % Nb2O5. Final rept.

R. S. Roth, L. D. Ettlinger, and H. S. Parker. 1987,

See also Part 1, PB89-171797. Pub. in Jnl. of Solid State Chemistry 68, n2 p330-339

Keywords: *Barium titanates, *Crystal structure, Titanium oxides, Barium oxides, Niobates, Niobium oxides, Orthorhombic lattices, Monoclinic lattices, Phase diagrams, Ceramics, Reprints, *Phase equilibria.

Four new compounds were found in the BaO-TiO2-Nb2O5 system, each containing <5 mole percent Nb2O5. Ba6Ti14Nb2O39 is an 8-layer orthorhombic phase, Cmcm, with a=17.138(.011), b=9.868(.011), c=18.759(.010)angstroms. The other three phases have similar a and b parameters (a(mon) approximately = b(orth) approximately = 9.9 angapproximately = 0,0rm) approximately = 9.9 ang-stroms, b(mon) approximately = 4,0rth) approximately = 17 angstroms). Ba14Ti40Nb2O99 is a 20-layer orth-orthombic phase, Cmc* with c approximately = 46.86 angstroms. Ba10Ti28Nb2O72 is a 7-layer monoclinic phase, C2/m, c approximately = 16.72 angstroms, beta approximately = 101.2 deg. Ba18Ti54Nb2O132 is a 13-layer monoclinic phase, C2/m, c approximately = 20.65 angstroms, bota approximately = 0.6 deg. = 30.65 angstroms, beta approximately = 96 deg. The compositions were derived by analogy to the layers in Ba4Ti13O30 and Ba6Ti17O40 and are consistent with limited phase equilibria data.

900,420

PB89-189823 Not available NTIS National Bureau of Standards (NML), Boulder, CO.

Quantum Physics Div.

Laser-induced Fluorescence Study of Product Rotational State Distributions in the Charge Transfer Reaction: $Ar(1+)((\sup 2P)(\sup 3/2)) + N2-> Ar+N2(1+)(X)$ at 0.28 and 0.40 eV. Final rept.

D. M. Sonnenfroh, and S. R. Leone, 1989, 9p Grants NSF-PHY86-04504, NSF-CHE83-08403 Sponsored by National Science Foundation, Washington, DC., and Air Force Office of Scientific Research, Bolling AFB, DC.

Pub. in Jnl. of Chemical Physics 90, n3 p1677-1685, 1

Keywords: *Rotational spectra, *Nitrogen, Ground state, Fluorescence, Boltzmann equation, Charged particles, Reprints, *Argon ion, *Charge transfer.

The nascent rotational state distributions of N2(+) produced in the charge transfer reaction of Ar+(doublet P(sub 3/2)) with N2 at 0.28 and 0.40 are remeasured by laser-induced fluorescence. A supersonic expansion is used to reduce the initial rotational angular momentum of the N2. The N2(+) product rotational distributions, in both V=O and V=1, have low and high energy components. For ease of reference, each distribution is described as a summation of two Boltzmann distributions . At a relative collision energy of 0.28 eV, the Boltzmann temperatures are 100 + or20 K and 745 + or - 120 K for N2(+) (V=0) and 80 + or - 10 K and 680 + or - 30 K for N2(+) (V= 1). Adiabatic potential energy curves for the lowest vibronic states are calculated and a simple curve hopping model is presented. Applying the model to the production of N2(+) (V = 1), for example, those reactants that charge transfer on the outgoing leg of a reactive trajectory interact with a deep potential well in the entrance channel for collinear geometry. It is postulated that rotationally excited products result. In comparison, reactants that charge transfer on the ingoing leg (or in perpendicular geometry) do not sample the collinear potential well and the resulting products are less rotationally excited.

900.421

PB89-201081 Not available NTIS National Bureau of Standards (NML), Gaithersburg, MD. Surface Science Div.

Interaction of Water with Solid Surfaces: Fundamentai Aspects.

Final rept. P. A. Thiel, and T. E. Madey. 1987, 175p Pub. in Surface Science Reports 7, n6-8 p211-385

Keywords: *Surface chemistry, *Water, *Chemisorption, Adsorption, Surface properties, Reprints.

The review compares and discusses recent experimental and theoretical results in the field of H2O-solid interactions. The authors emphasize studies per-formed on well-characterized, single crystal surfaces of metals, semiconductors and oxides. The authors discuss the factors which influence dissociative vs. associative adsorption pathways. When H2O adsorbs molecularly, it tends to form three-dimensional hydrogen-bonded clusters, even at fractional monolayer coverages, because the strength of the attractive interaction between two molecules is comparable to that of the substrate-H2O bond. The template effect of the substrate is important in determining both the local and long-range order of H2O molecules in these clusters. influence of surface additive atoms (e.g., O, Br Na, K) and also surface imperfections (e.g., steps and defects) on the surface structure and chemistry of H2O is examined in detail. Results on single crystal substrates are compared with earlier measurements of H2O adsorption on high-area materials, where available.

900.422

Not available NTIS PB89-201115 National Bureau of Standards (NEL), Gaithersburg,

MD. Thermophysics Div.

Simple Apparatus for Vapor-Liquid Equilibrium Measurements with Data for the Binary Systems of Carbon Dioxide with n-Butane and Isobutane.

Final rept. L. A. Weber. 1989, 5p Pub. in Jnl. of Chemical and Engineering Data 34, n2 p171-175 Apr 89.

Keywords: *Test equipment, *Vapor phases, *Liquids, *Equilibrium, *Gases, Measurement, High pressure tests, Carbon dioxide, Butanes, Henrys Law, Reprints.

The design, construction, and testing of a simple vapor-liquid equilibrium apparatus designed for measurements in the range 300-500 K at pressures to 150 bar are described. Data are given for measurements of P, T, x, and y for binary systems of carbon dioxide with n-butane and isobutane in the range 310-394 K.

Not available NTIS PB89-201123 National Bureau of Standards (NEL), Gaithersburg, MD. Chemical Process Metrology Div.
NO/NH3 Coadsorption on Pt(111): Kinetic and Dy-

namical Effects in Rotational Accommodation. Final rept.

D. Burgess, R. R. Cavanagh, and D. S. King. 1989,

Contract DE-Al05-84ER13150

Sponsored by Department of Energy, Washington, DC. Pub. in Surface Science 214, p358-376 1989.

Keywords: *Adsorbates, *Ammonia, *Nitrogen oxide, *Platinum, Mass spectroscopy, Lasers, Fluorescence, Desorption, Dissociation, Reaction kinetics, Reprints.

The strongly interacting coadsorbate system of ammonia/nitric oxide on Pt(111) has been examined using both quadrupole mass spectrometer (QMS) and laser-induced fluorescence (LIF) detected temperature pro-grammed desorption (TPD) methods. The QMS/TPD experiments show simultaneous desorption of NO and NH3 as reaction-limited products from the dissociation of an adsorbed NO-NH3 complex. Although NO TPD kinetics are altered by the formation of the complex, LIF/TPD results show that the rotational accommodation, spin-orbit temperature, lambda doublet popula-tions, and molecular alignment of desorbed NO are insensitive to the attractive interaction. It suggests that, following decomposition of the NO-NH3 species, NO resides on the surface sufficiently long that it has no memory of being complexed.

900,424 PB89-201735 Not available NTIS National Bureau of Standards (NML), Gaithersburg,

MD. Molecular Spectroscopy Div.

Microwave Spectrum and Molecular Structure of the Ethylene-Ozone van der Waals Complex. Final rept.

J. Z. Gillies, C. W. Gillies, R. D. Suenram, F. J. Lovas, and W. Stahl. 1989, 2p

Pub. in Jnl. of the American Chemical Society 111, p3073-3074 1989.

Keywords: *Molecular structure, *Ethylene, *Ozone, Rotational spectra, Ground state, Excitation, Reprints, *Microwave spectra, Reaction kinetics, Dipole mo-ments, Van der Waals complex.

The rotational spectrum of CH2=CH2 ... 03 complex was observed using a pulsed beam Fabry-Perot cavity Fourier transform microwave spectrometer. Internal motions in the complex produced two components for each transition. The two sets of lines were independently fit to a Watson Hamiltonian to give the rotational constants (in MHZ): Ground State - A 8246.841 (2), B 2518.972 (4), C 2044.248 (5); Excited State - A 8241.897 (4), B 2518.941 (9), C 2044.872 (11). Dipole moment measurements determine mu sub c = mu sub total = 0.461 (2) D. The complex structure is described by two parallel planes containing ethylene and ozone in which the two centers of mass are connected by a 3.30 A line perpendicular to the planes. 1,3-dipolar cycloaddition theory and orbital symmetry rules are used in conjunction with ab initio calculations to argue that the CH2=CH2 ... 03 complex lies in a small minimum on the reaction coordinate prior to the transition state which produces ethylene primary ozonide.

900,425 PB89-201743 Not available NTIS National Bureau of Standards (NML), Gaithersburg, MD. Molecular Spectroscopy Div.

Heterodyne Measurements on OCS Near 1372 cm(-

M. Schneider, A. G. Maki, M. D. Vanek, and J. S. Wells. 1989, 5p Sponsored by National Aeronautics and Space Admin-

istration, Washington, DC. Pub. in Jnl. of Molecular Spectroscopy 134, p349-353 1989.

Keywords: *Demodulation, *Molecular structure, Carbonyl compounds, Reprints, *Carbonyl sulfide, Frequency standards.

Heterodyne frequency measurements are given for the 01 (sup 1)1 - 00 (sup) 0 and 02 (sup 0)1 - 01 (sup 1)0 bands of OCS between 1363 and 1398/cm. These measurements were combined with heterodyne measurements on the 01 (sup 1)1 - 01 (sup 1)0 and 02 (sup 0)1 - 00 (sup 0)0 bands to obtain frequencies for the 01 (sup 1)0 - 00 (sup 0)0 transitions by two independent paths. A table of wavenumbers is given for the nu(sub 2) band of OCS from 488 to 557/cm.

900,426 PB89-201750 Not available NTIS National Bureau of Standards (NEL), Gaithersburg, MD. Semiconductor Electronics Div.

Infrared Absorption Cross Section of Arsenic in Silicon in the Impurity Band Region of Concentration.

Final rept.

Pub. in Applied Optics 28, n6 p1193-1199, 15 Mar 89.

Keywords: *Arsenic, *Silicon, *Infrared spectra, Adsorption, Spectral lines, Reprints.

The spectral dependence of the infrared absorption cross section of As in Si near O K has been determined from infrared transmission measurements for three As concentrations (5.3, 8.4, and 15.9 \times 10 to the 17th power cm sup -3) in the impurity band regime. The results demonstrate some features of physical interest. With increasing As concentration, the lines associated with the intra-atomic transitions broaden asymmetrically, while the integral of the total absorption cross section over photon energy is conserved as required by the oscillator strength sum rule. It thus appears that the cross section of the intra-atomic transitions is conserved as the lines hybridize with the continuum. Comparison of results with photoionization cross-sectional data suggests that the lines contribute to the cross section for photoionization through field and thermally assisted transitions when they are near the threshold for photoionization.

900.427 PB89-201800 Not available NTIS National Bureau of Standards (IMSE), Gaithersburg,

MD. Office of Nondestructive Evaluation.

Analysis of Roto-Translational Absorption Spectra Induced in Low Density Gases of Non-Polar Molecules: The Methane Case. Final rept.

P. Dore, M. Moraldi, J. D. Poll, and G. Birnbaum.

Pub. in Molecular Physics 66, n2 p355-373 1989.

Keywords: *Methane, *Absorption spectra, Far infra-red radiation, Reprints, *Nonpolar gases, Temperature dependence.

A new analysis is given of the roto-translational absorption spectrum of gaseous methane for which experimental data are available at different temperatures. The authors consider components of the induced dipole associated at long range with induction by the octopole and hexadecapole multipole moments together with components associated with the gradient of both the octopolar and hexadecapolar fields. A satisfactory description of experimental data is obtained only if short range anisotropic overlap is included with the octopolar and hexadecapolar induction. A better description of the experimental absorption bands is obtained if, in addition, the intensity of the double transitions is slightly increased with increasing temperature. This increase is attributed to anisotropic overlap effects on the double transition spectrum, which have not been explicitly taken into account.

900.428 PB89-202022 Not available NTIS National Bureau of Standards (NML), Gaithersburg,

MD. Radiometric Physics Div.

Exploratory Research in Reflectance and Fluorescence Standards at the National Bureau of Stand-

Final rept. V. R. Weidner, J. J. Hsia, and K. L. Eckerle. 1986, 3p Pub. in Optics News 12, n11 p18-20 Nov 86.

Keywords: *Standards, *Spectrophotometry, Carbon black, Fluorescence, Reflectance, Reprints, Polytetrafluoroethylene.

The paper describes current research relating to the development of spectrophotometric standards of NBS. The results of some experimental work on the preparation and analysis of a gray scale for diffuse reflectance, and materials for possible use as fluorescence stand-ards are reviewed. The gray scale for diffuse reflec-tance was prepared by sintering mixtures of carbon black and polytetrafluoroethylene (PTFE) resin. These are durable solid disks that vary in reflectance from about 3% to over 90%, depending on the concentra-tion of carbon black. The fluorescent samples are prepared by sintering mixtures of inorganic phosphors in the same PTFE resin. These phosphors provide highly stable specimens with blue, green, yellow, and orange emission spectra.

900.429 PB89-202055 Not available NTIS National Bureau of Standards (NML), Boulder, CO.

Time and Frequency Div.

Pure Rotational Far Infrared Transitions of (16)02 in Its Electronic and Vibrational Ground State.

Final rept.

R. Zink, and M. Mizushima. 1987, 5p Pub. in Jnl. of Molecular Spectroscopy 125, n1 p154-158 1987.

Keywords: *Oxygen, *Vibrational spectra, Rotational spectra, Molecular spectroscopy, Spectral lines, Infra-red spectra, Ground state, Adsorption, Reprints, Electron states

Five lines in the far infrared region, due to N(+2) < N (Delta J=0) transitions of the (16)02 molecule in its (X (sup 3)Sigma (sub g))-state are measured at 773.839691, 1466.807133, 1812.405539, 2157.577773, and 2502.323923 GHz, using our new tunable FIR spectrometer. The spectral line shape of the 2.50 THz line is analyzed and the pressure selfbroadening parameter of 18.2(32) kHz/Pa (2.43(43) MHz/torr) is obtained.

900,430 PB89-202071 Not available NTIS National Bureau of Standards (NML), Gaithersburg, MD. Inorganic Analytical Research Div.

Three-Dimensional Atomic Spectra in Flames Using Stepwise Excitation Laser-Enhanced Ionization Spectroscopy.

Final rept. G. C. Turk, F. C. Ruegg, J. C. Travis, and J. R.

DeVoe. 1986, 7p Pub. in Jnl. of Applied Spectroscopy 40, n8 p1146-1152 1986.

Keywords: *Atomic spectroscopy, Spectroscopic analysis, Atomic spectra, Excitation, Reprints, Laser enhanced ionization.

Stepwise excitation laser-enhanced ionization spectroscopy utilizes two independently tunable dye lasers to populate high lying excited states of atoms in

CHEMISTRY

Physical & Theoretical Chemistry

flames. Two atomic resonances are required, with the upper level of the first step transition coinciding with the lower level of the second step transition. Efficient population of a high lying atomic level is achieved from which a high rate of collisional ionization can take place. The double resonance aspect of such excitation adds an extra dimension of spectroscopic selectivity to the measurement. A computer controlled dual wavelength LEI spectrometer, including a Dizeau waveme-ter for wavelength verification, is used to record three-dimensional spectra-ionization signal as a function of both first and second step wavelengths. Examples illustrate the accuracy advantage accorded by the three-dimensional survey.

900 431

PB89-202121 Not available NTIS National Bureau of Standards (NML), Gaithersburg, MD. Atomic and Plasma Radiation Div.

Accurate Energles of nS, nP, nD, nF and nG Levels of Neutral Cesium. Final rept.

K. H. Weber, and C. J. Sansonetti. 1987, 11p Pub. in Physical Review A-General Physics 35, n11 p4650-4660 1987.

Keywords: *Cesium, *Ionization potentials, Interferometers, Lasers, Electron transitions, Energy levels, Reprints, Fabry-Perot spectrometers.

Extensive measurements have been performed to de-Extensive measurements have been performed to de-termine the absolute energies of the n doublet \$(1/2)\$ (n=8-31), n doublet P(1/2) (n=6,9-80), n doublet D(5/2) (n=5,7-36), n doublet F(5/2) (n=6-65) and n doublet G(7/2) (n=6-54) levels of Cs by using non-resonant and resonantly enhanced Doppler-free two-photon spectroscopy. The excitation mechanisms em-ployed include resonantly enhanced dipole-guadruployed include resonantly enhanced dipole-quadru-pole and quadrupole-quadrupole transitions. All energies were measured directly with respect to the n=6 doublet S(1/2) ground state. The laser wavelengths were measured by high-precision Fabry-Perot interferometry yielding an uncertainty of 0.0002/cm for most Cs levels, lonization energies derived by fitting the modified Ritz formula to each of the five series observed coincide within 0.00005/cm. Taking account of possible systematic errors, the Cs ionization energy is 31406.46766(15)/cm.

900,432

PB89-202139 Not available NTIS National Bureau of Standards (NML), Gaithersburg, MD. Chemical Kinetics Div.
Pi-Electron Properties of Large Condensed Po-

Iyaromatic Hydrocarbons. Final rept.

S. E. Stein, and R. L. Brown. 1987, 9p

Pub. in Jnl. of the American Chemical Society 109, n12 p3721-3729 1987. Keywords: *Aromatic polycyclic hydrocarbons, *Electron density(Concentration), Electron distribution, Res-

onance, Energy levels, Heat of formation, Reprints, Bond orders, Hueckel theory.

Hueckel molecular orbital(HMO) theory has been used to calculate energy level density bond orders, electron distributions, free valence, resonance energies, and heats of formation for several homologous series of large, hexagonally symmetric benzenoid polyaromatic molecules with well-defined edge structures containing up to 2300 carbon atoms. When extrapolated to the infinite limit, values for all properties converge to reasonable values. This is in contrast to several other pi-electron theories which do not yield correct graphite limits. Carbon atoms at the edges of such large molecules are predicted to behave like those in small polynuclear aromatic molecules, with properties strongly de-pendent on local structure. Regardless of edge struc-ture, interior carbons several bond lengths from an edge have properties similar to those in an infinite graphite sheet. Edge structure has a larger influence graphite sheet. Edge structure has a larger influence on heats of formation than that predicted by group additivity methods. Only a weak correlation was found between the position of the highest occupied molecular orbital and the reactivity of the most reactive positions. tion.

900.433

Not available NTIS PB89-202162 National Bureau of Standards (NML), Gaithersburg, MD. Molecular Spectroscopy Div.

Nonadiabatic Theory of Fine-Structure Branching Cross-Sections for Sodium-Hellum, Sodium-Neon, and Sodium-Argon Optical Collisions. Final rept.

L. L. Vahala, P. S. Julienne, and M. D. Havey. 1986,

13p Pub. in Physical Review A: General Physics 34, n3

Keywords: *Collision cross sections, *Helium, *Neon, *Sodium, *Argon, Rare gases, Atomic energy levels, Quantum interactions, Electron transitions, Photons, Optical spectra, Reprints, Branching ratio, Fine struc-

The nonadiabatic close-coupled theory of atomic collisions in a radiation field is generalized to include elecrare gas (RG) optical collision. Na(doublet S(1/2)) + RG + nh(nu) yields Na(doublet P(j) + RG + (n-1)h(nu). The effects of detuning and incident energy on the branching into the atomic Na 3p doublet P(3/2) and 3p doublet(1/2) states are examined. The cross sections sigma(j) are found to have a strong asymmetry between red and blue detuning as well as a comtry between red and blue detuning as well as a complex threshold and resonance structure dependence on energy. A partial cross-section analysis of sigma(j) shows a significant difference between contributions from states of e and f molecular parity. The theoretically calculated detuning dependence of the branching ratio into each fine structure state is in good agree-ment with available experimental data for NaAr, NaNe, and NaHe, as well as the total absorption coefficient for the production of Na 3p atoms. The fine structure branching ratio for thermal energy collisions shows considerable variation with rare gas collision partner, due to the different interaction potentials. For sufficiently high collision energy, the branching approaches a recoil limit which is independent of collision part-

900 434 PB89-202485 Not available NTIS National Bureau of Standards (NEL), Gaithersburg, MD. Thermophysics Div.

Gas Solubility and Henry's Law Near the Solvent's Critical Point. Final rept.

M. L. Japas, and J. M. H. Levelt Sengers. 1989, 9p Pub. in AIChE Jnl. 35, n5 p705-713 May 89.

Keywords: *Gases, *Henrys law, *Critical point, *Solvents, "Solubility, High temperature tests, Thermody-namic properties, Water, Benzene, Mathematical models, Fugacity, Reprints.

It has been experimentally observed, for water and nonaqueous solvents alike, that Henry's constant passes through a maximum and then declines as the temperature is raised from the triple point to the critical point. Exact relations for the value of Henry's constant and its temperature dependence at the solvent's critical point are developed from classical and nonclassical models showing that the decline of the constant is a universal phenomenon. The limiting temperature dependence of Henry's constant can be predicted from the thermodynamic properties of the pure solvent and the initial slope of the critical line. The validity of the prediction is tested by comparing it with experimental solubility data for several gases in high-temperature water and benzene. The predictive model appears valid over a temperature range of at least 15% in temperature below the critical point of the solvent.

900,435 PB89-202493 Not available NTIS National Bureau of Standards (NEL), Boulder, CO.

Thermophysics Div.
Isochoric (p,v,T) Measurements on CO2 and (0.98
CO2 + 0.02 CH4) from 225 to 400 K and Pressures to 35 MPa. Final rept.

J. W. Magee, and J. F. Ely. 1988, 11p Pub. in International Jnl. of Thermophysics 9, n4 p547-

Keywords: *Carbon dioxide, *Methane, *Density(Mass/volume), *High pressure tests, *Temperature, Measurement, Purity, Gas laws, Mixtures, Volume, Reprints.

Comprehensive isochoric (p, v, T) measurements have been obtained for (0.98 OC2 \pm 0.02 CH4) at densities from 1 to 26 mol x dm(sup -3). Supplemental isochoric (p, v, T) measurements have been obtained for high-purity CO2 at densities from 12 to 24 mol x dm(sup -3).

Measurements of p(T) cover a broad range of temperature, 225 to 400 K, at pressures to 35 MPa. Compansons have been made with independent sources and with a predictive method based on corresponding

900,436 PB89-202519 Not available NTIS National Bureau of Standards (NEL), Gaithersburg, MD. Thermophysics Div.

NaCl-H2O Coexistence Curve Near the Critical Temperature of H2O. Final rept.

A. H. Harvey, and J. M. H. Levelt Sengers. 1989, 3p Pub. in Chemical Physics Letters 156, n4 p415-417, 7 Apr 89.

Keywords: *Sodium chloride, *Water, *Solubility, Phase transformations, Concentration(Composition), Critical temperature, Reprints, Temperature dependence, Pressure dependences.

Recent high-temperature data on coexisting vapor-liquid compositions as a function of pressure in the CaC1-H2O system have been interpreted as implying a higher-than-expected value of the critical exponent beta. It is suggested that the observed behavior is a consequence of the fact that, as the solvent's critical point is approached, the coexistence curve in pres-sure-composition coordinates ceases to behave in the same manner as the pressure-density coexistence curve, which is always characterized by the exponent beta. At the critical temperature of the solvent, the pressure-composition coexistence curve is characterized by the much larger exponent beta \pm 1.

PB89-202527 Not available NTIS
National Bureau of Standards (NML), Gaithersburg,
MD. Chemical Kinetics Div.
Thermochemistry of Solvation of SF6(1-) by
Simple Polar Organic Molecules in the Vapor

Phase.

Final rept. L. W. Sieck. 1986, 4p

Pub. in Jnl. of Physical Chemistry 90, n25 p6684-6687 1986

Keywords: *Solvation, *Sulfur halides, *Thermochemistry, *Dissociation, Electron beams, Mass spectroscopy, Ligands, Complex ions, Kinetics, Reprints, Temperature dependence, Binding energy, Sulfur fluorides.

The stabilities of SF6(-).HR association ions, where HR is a simple aliphatic alcohol, H20, or Me2SO, have been investigated by the technique of pulsed electron beam high pressure mass spectrometry. Equilibrium constants were determined as a function of temperature in order to define delta H and delta S values for solvation. The binding energies are quite low, ranging from 10.5 kcal mol for SF6(-).H2O to 14.7 kcal/mol for SF6(-).Me2SO. For ligands in which the nature of the bonding is expected to be similar, the binding energies increase nonlinearly with increasing acid strength of the ligand. On the basis of additional measurements involving I(-).HR complexes, as well as existing literature values, the binding energies in SF6(-).HR ions are found to be slightly higher than those for I(-)HR. The SF6(-).HR complexes are less stable, however, due to their more positive dissociation entropies. Some comments are also included concerning the SF6(-).SF6 dimer ion.

900,438 PB89-202543 Not available NTIS National Bureau of Standards (NEL), Gaithersburg, MD. Electrosystems Div.

Drift Tubes for Characterizing Atmospheric Ion Mobility Spectra Using AC, AC-Pulse, and Pulse Time-of-Flight Measurement Techniques. Final rept.

M. Misakian, W. E. Anderson, and O. Laug. 1989,

Pub. in Review of Scientific Instruments 60, n4 p720-729 Apr 89.

Keywords: *Ionic mobility, *Atmospheric pressure, *Measurement, *Test equipment, Spectra, Time, Alternating current, Tubes, Drift(Instrumentation), Re-

Two drift tubes constructed of insulating cylinders with conductive guard rings on the inside walls are examined to determine their suitability for measuring ion mobility spectra at atmospheric pressure. One drift tube is

of the pulse time-of-flight (TOF) type with adjustable drift distance, and the other is an ac-TOF drift tube similar in principle to devices reported by Tyndall and Powell. The latter drift tube is evaluated using sinusoidal and alternating-polarity pulse-voltage waveforms for gating the shutters. Methods for determining the drift velocity of an ion from theoretical fits of the TOF spectrum are described for drift tubes of fixed length exhibiting 'end effects.' Mobility values with uncertainties less than + or - 1% can be obtained with the pulse-TOF drift tube. Comparable results are obtained with the ac drift tube if an alternating-polarity pulsevoltage waveform is used for gating the shutter.

900,439 PB89-202568 Not available NTIS National Bureau of Standards (NEL), Gaithersburg, MD. Fire Measurement and Research Div. Component Spectrum Reconstruction from Partially Characterized Mixtures.

M. R. Nyden, and K. Chittur. 1989, 6p

Pub. in Applied Spectroscopy 43, n1 p123-128 1989.

Keywords: *Proteins, Electromagnetic radiation, Infrared radiation, Mathematical models, Reprints, *Infrared absorption.

A mathematical analysis of some existing approaches to component spectrum reconstruction is presented. The analysis leads to the derivation of a generalization of the cross-correlation technique. The effectiveness of these methods is assessed from the quality of the reconstructions obtained with the use of synthetic mixture spectra. Reconstructions of the spectra of the components of aqueous mixtures of immunoglobulin G and albumin are compared to the corresponding spectral reconstructions of the pure proteins in buffer.

900,440 PB89-202956 Not available NTIS National Bureau of Standards (NEL), Gaithersburg, MD. Chemical Process Metrology Div.

Coadsorption of Water and Lithlum on the Ru(001)

Surface. Final rept. S. Semancik, D. L. Doering, and T. E. Madey. 1986,

18p Sponsored by Department of Energy, Washington, DC. Pub. in Surface Science 176, p165-182 1986.

Keywords: *Surface chemistry, *Adsorption, *Water, *Lithium, *Ruthenium, Single crystals, Desorption, Spectroscopy, Auger electrons, Reprints.

The interactions between water and lithium have been studied on the surface of a Ru(001) crystal using ther-mal desorption spectroscopy electron stimulated desorption ion angular distributions (ESDIAD), Auger spectroscopy and LEED. The presence of Li was found to influence strongly the H+ ESD yield and the ESDIAD patterns from adsorbed water even at Li coverages of 0.02 monolayer; changes in the thermal desorption states for water were also observed at low Li coverages. For coadsorbed Li coverages above 0.05, ESDIAD measurements provided clear evidence of water decomposition, even at surface temperatures near 80 K; evidence for dissociation was also obtained from thermal desorption and Auger measurements. The present results are compared and contrasted to those reported previously for the H2O/Na/Ru(001) system.

900,441 PB89-202980 Not available NTIS National Bureau of Standards (NML), Gaithersburg, MD. Surface Science Div.

Oxygen Chemisorption on Cr(110): 1. Dissociative Adsorption. Final rept.

N. D. Shinn, and T. E. Madey. 1986, 16p See also PB89-202998.

Pub. in Surface Science 173, n2-3 p379-394 1986.

Keywords: *Chemisorption, *Chromium, *Oxygen, Electron diffraction, Auger electrons, Metals, Vibrational spectra, Reprints.

The initial stages of oxygen chemisorption on Cr(110) at 300K have been investigated using high resolution electron energy loss spectroscopy (HREELS), elec-tron stimulated desorption ion angular distributions (ESDIAD), low energy electron diffraction (LEED), and Auger electron spectroscopy (AES). Dissociative chemisorption occurs with near unit sticking probability, leading to an ordered p(4x2)O overlayer at theta(sub

0) approximately equals 1/8. A model with atomic oxygen located in the two-fold symmetric hollow sites is proposed. The previously reported c(3x1)0 overlayer was not observed in the study. A disordered oxygen adlayer is found as theta(sub 0) increases. ESDIAD and HREELS data suggest that chemisorbed oxygen atoms occupy inequivalent local binding sites for theta(sub 0) > 0.25; subsurface oxygen is not found under these mild oxidation conditions

900,442 PB89-202998 Not available NTIS National Bureau of Standards (NML), Gaithersburg, MD. Surface Science Div. Oxygen Chemisorption on Cr(110): 2. Evidence for

Molecular O2(ads).

Final rept. N. D. Shinn, and T. E. Madey. 1986, 18p

See also PB89-202980. Pub. in Surface Science 176, n3 p635-652 1986.

Keywords: *Chemisorption, *Chromium, *Oxygen, Electron diffraction, Auger electrons, Metals, Vibrational spectra, Reprints.

Oxygen chemisorption and dissociation on Cr(110) at 120K have been studied using high resolution electron energy loss spectroscopy (HREELS), electron stimulated desorption ion angular distribution (ESDIAD), low energy electron diffraction (LEED) and Auger electron spectroscopy (AES). Dissociative adsorption domi-nates although vibrational and stimulated desorption data provide evidence for a coexisting minority molecular binding state. An O2(ads) vibrational frequency of 1020/cm and a six beam ESDIAD pattern are suggestive of super-oxo O2(ads) bonding at six local sites each with the 0-0 molecular axis tilted away from the surface normal. These results are compared with data for chemisorbed oxygen on other transition metal sur-

PB89-203004 Not available NTIS National Bureau of Standards (NML), Gaithersburg, MD. Surface Science Div. Stimulated Desorption from CO Chemisorbed on Cr(110).

Final rept. N. D. Shinn, and T. E. Madey, 1987, 18p Pub. in Surface Science 180, n2-3 p615-632 1987.

Keywords: *Chemisorption, *Carbon monoxide, *Chromium, *Desorption, Oxygen, Ions, Potassium, Ruthenium, Iron, Reprints.

Electron stimulated desorption (ESD) experiments using a time-of-flight pulse counting method are reported for molecular CO chemisorbed on the Cr(110) surface at 80K. Consistent with previous qualitative observations, negligible CO+ and O+ desorption sigservations, negligible CO+ and O+ desorption signals were measured from the alpha(1)CO overlayer which saturates at 1/4 monolayer. For theta(CO) 0.25, a terminally-bonded (alpha(2)CO) binding mode is populated in addition to the existing alpha(1)CO binding mode and the ion yield sharply increases. For alpha(2)CO, both O and CO+ ions are observed; the CO+ ions desorb with characteristically lower kinetic energies than O+ ions. Near saturation coverages of CO(ads), an observed decrease in the O+ yield is attributed to adsorbate-adsorbate interactions which reduce the ion desorption probability, as seen in ESD studies of terminally-bonded CO on other metals. These results are considered in the context of two possible models proposed for the alpha(1)CO binding state and related ESD observations for CO chemisorbed on potassium-promoted Ru(001) and Fe(001).

900,444 PB89-203012 Not available NTIS National Bureau of Standards (NML), Gaithersburg, MD. Surface Science Div.
Time Resolved Studies of Vibrational Relaxation

Dynamics of CO(v=1) on Metal Particle Surfaces.

J. D. Beckerle, M. P. Casassa, R. R. Cavanagh, E. J. Heilweil, and J. C. Stephenson. 1989, 2p Pub. in Jnl. of Chemical Physics 90, n8 p4619-4620, 15 Apr 89.

Keywords: *Vibrational spectra, *Molecular relaxation, *Carbon monoxide, *Chemisorption, *Catalysts, *Metal carbonyls, Infrared radiation, Bleaching, Temperature, Polarization, Silicon dioxide, Surface chemistry, Platinum, Rhenium, Hole mobility, Supports, Re-

The vibrational relaxation dynamics of CO chemisorbed on small Pt and Rh particles supported on SiO2 has been investigated by picosecond time-resolved infrared transient bleaching experiments. A vibrational T1 lifetime of 7 + or - 1 ps has been observed for several different samples, independent of polarization, pump intensity, and sample temperature from 100-400K. A 1:3 isotopic dilution has no effect upon T1. The T1 lifetime is a factor of 10-50 times shorter than T1 reported for metal carbonyl cluster compounds in solution and on SiO2 supports. Two possible mechanisms are considered to account for the rapid decay; redistribution of the energy throughout the broad CO vibrational band, and relaxation directly to electron-hole pairs in the metal particles.

900,445

PB89-212013 Not available NTIS
National Bureau of Standards (NML), Gaithersburg, MD. Surface Science Div.

Chemisorption of HF (Hydrofiuoric Acid) on Silicon Surfaces.

Final rept.

S. A. Joyce, J. A. Yarmoff, A. L. Johnson, and T. E.

Madey, 1989, 6p
Sponsored by Department of Energy, Washington, DC.
Pub. in Proceedings of Materials Research Society
Pub. in Proceedings of Materials Research Society Symposium on Chemical Perspectives of Microelectronic Materials, Boston, MA., December 1988, v131 p185-190 1989.

Keywords: *Chemisorption, *Silicon, *Surface properties, *Hydrogen fluoride, *Gases, *Chemical bonds, Single crystals, X ray analysis, Spectroscopy, Dissociation, Photoelectric emission, Microelectronics, Va-

The interaction of gaseous hydrofluoric acid (HF) with single crystal silicon surfaces was investigated using soft x-ray photoemission spectroscopy and Electron Stimulated Desorption Ion Angular Distributions Stimulated Desorption Ion Angular Distributions (ESDIAD). Examination of the Si(2p) core level for surfaces saturated with HF shows the formation of siliconfluoride bonds indicating the dissociative chemisorption of HF on both Si(111) and Si(100) surfaces. Inspection of the F(2s) and F(2p) valence levels at saturation coverage indicate that only one-half monolayer of fluorine bonds to the silicon. The primary ion desorbed by electron bombardment of these surfaces is F+ with only a minor contribution from H+ ESDIAD images from a saturation coverage of HF on stepped Si(100) surfaces reveal F+ desorption primarily along the direction of the terrace dimers. The ESDIAD patterns from HF adsorbed on Si(111) are characterized by strong normal F+ emission with a weak back-ground component of off-normal emission. The results are consistent with the dissociative chemisorption of HF where the ion emission direction is determined by the Si-F bond directions.

900.446

PB89-212153 Not available NTIS National Bureau of Standards (NML), Gaithersburg, MD. Office of Standard Reference Data. Activities of the international Association for the

Properties of Steam between 1979 and 1984.

H. J. White. 1986, 9p

Pub. in Proceedings of International Conference on the Properties of Steam (10th), Moscow, USSR, Sep-tember 3-7, 1984, 9p 1986.

*Steam. *Thermodynamic properties, Keywords: Steam tables, Enthalpy, Entropy, Thermodynamics, Transport properties, *International Association for the Properties of Steam.

The paper reviews the activities of the International Association for the Properties of Steam (IAPS) in the interval between the 9th International Conference on the Properties of Steam held in Munich in 1979 and the 10th Conference held in Moscow, 1984. A brief review of the purpose and organization of IAPS is given to place its latest activities in a broader and perhaps more meaningful context. Some of the activities during the period 1979 to 1984 represent the culmination of a program which began with the 8th Conference, which was held in Giens, France, in 1974.

900.447

PB89-212229 Not available NTIS National Bureau of Standards (NEL), Gaithersburg, MD. Electrosystems Div.

Measurement of Electrical Breakdown in Liquids.

Final rept. R. E. Hebner, 1988, 19p

Pub. in NATO Advanced Study Institute on the Liquid State and Its Electrical Properties, Sintra, Portugal, July 5-17, 1987, p519-537 1988.

Keywords: *Liquids, *Electrical properties, *Electrical faults, Measuring instruments, Additives, Particle density(Concentration), Pressure, Viscosity, Voltage gain, Cathodes, Anodes, Reprints.

The continuing development of light sources, high speed cameras, and high speed electronic measuring systems have made it possible to study the breakdown process in increasing detail. The four measurements described are high speed photography of the break-down process, measurement of the voltage and cur-rent, optical spectroscopy, and the measurement of acoustic emission. Having developed a battery of acoustic emission. Having developed a battery of measurement techniques, understanding of the break-down process is gained by changing the system in known ways and determining the effect of these changes on the measured results. Parameters which have been investigated include types of liquids, chemical additives, particle density, pressure, viscosity, and the rate of rise of the applied voltage. These investigations have led to the identification of tour mode of tions have led to the identification of four modes of growth when the streamer initiates at a cathode and three modes when it initiates at an anode.

PB89-222525 Not available NTIS American Chemical Society, Washington, DC. Journal of Physical and Chemical Reference Data, Volume 18, Number 2, 1989.

Quarterly rept.
D. R. Lide. c1989, 548p
See also PB89-222533 through PB89-222582 and PB89-135685. Prepared in cooperation with American Inst. of Physics, New York. Sponsored by National Inst. of Standards and Technology, Gaithersburg, MD. Available from American Chemical Society, 1155 16th St., NW, Washington, DC 20036.

Keywords: *Thermodynamic properties, Graphs(Charts), Reaction kinetics, Photochemical reactions, Thermal conductivity, Nitrogen, Carbon monoxide, Density(Mass/volume), Methane, Thermophysical properties oxide, Density (Mass/Volume), Methane, Thermophysical properties, Hexoses, Pertoses, Argon, Pressure, Phase transformations, Transport properties, Standards, Tables (Data), Carbohydrates, Organic phosphates, Triplet point, Difluoride/dioxy, Fluoride/dioxy, Atmospheric chemistry.

Contents: The Thermal Conductivity of Nitrogen and Carbon Monoxide in the Limit of Zero Density; Thermophysical Properties of Methane; Thermodynamic Properties erties of Argon from the Triple Point to 1200 K with Pressures to 1000 MPa; Thermodynamic Properties of Dioxygen Difluoride (O2F2) and Dioxygen Fluroide (O2F); Thermodynamic and Transport Properties of Carbohydrates and their Monophosphates: The Pentoses and Hexoses; Evaluated Kinetic and Photochemical Data for Atmospheric Chemistry: Supplement III. (Copyright (c) by the U.S. Secretary of Commerce, 1989.)

900,449 PB89-222533 (Not available NTIS) International Union of Pure and Applied Chemistry, London (England). Projects Centre.

Thermal Conductivity of Nitrogen and Carbon Monoxide in the Limit of Zero Density.

J. Millat, and W. A. Wakeham. c1989, 17p
Prepared in cooperation with American Chemical Society, Washington, DC., and American Inst. of Physics New York. Sponsored by National Inst. of Standards and Technology, Gaithersburg, MD. Included in Jnl. of Physical and Chemical Reference Data, v18 n2 p565-581 1989.

Keywords: *Thermal conductivity, *Nitrogen, *Carbon monoxide, Density(Mass/Volume), Tables(Data), Reaction kinetics, Numerical analysis, Experimental design, Cross sections, Specific heat, Thermodynamic properties.

The paper presents accurate representations for the thermal conductivity of the diatomic gases nitrogen and carbon monoxide in the limit of zero density. These gases were studied because they have nearly the same molecular mass and viscostities. In contrast, the new analysis confirms that the thermal conductivities of the two gases differ remarkably, especially at

low temperatures. The theoretically-based correlations provided are valid for the temperature range 220-2100 K and have associated uncertainties of + or - 1% between 300 and about 500 K, rising to + or - 2.5% at the low- and high-temperature extremes. A comparison with some empirical and semiempirical correla-tions is given. (Copyright (c) by the U.S. Secretary of Commerce, 1989.)

900,450

PB89-222541 (Not Available NTIS) National Inst. of Standards and Technology (NEL), Boulder, CO. Thermophysics Div.

Thermophysical Properties of Methane.

Ouarterly rept.
D. G. Friend, J. F. Ely, and H. Ingham. c1989, 56p
Prepared in cooperation with American Chemical Society, Washington, DC., and American Inst. of Physics,
New York.

Included in Jnl. of Physical and Chemical Reference Data, v18, n2 p583-638 1989.

Keywords: *Thermophysical properties, *Methane, Numerical analysis, Experimental design, Liquid phases, Equations of state, Specific heat, Graphs(Charts), Transport properties, Pressure, Thermospheres, Pressure, Pressure, Thermospheres, Pressure, Pres mal conductivity, Viscosity, Comparison, Virial coeffi-

New correlations for the thermophysical properties of fluid methane are presented. The correlations are based on a critical evaluation of the available experimental data and have been developed to represent these data over a broad range of the state variables. Estimates for the accuracy of the equations and comparisons with measured properties are given. The reasons for the new study of methane include significant new and more accurate data, and improvements in the correlation functions which allow increased accuracy of the correlations especially in the extended critical region. For the thermodynamic properties, a classical equation for the molar Helmholtz energy, which contains terms multiplied by the exponential of the quadratic and quartic powers of the system density, is used. Tables of coefficients and equations are presented to allow the calculation of these and other thermodynamic quantities. (Copyright (c) by the U.S. Secretary of Commerce, 1989.)

900,451

PB89-222558 (Not Available NTIS) Idaho Univ., Moscow. Center for Applied Thermodynamic Studies

Thermodynamic Properties of Argon from the Triple Point to 1200 K with Pressures to 1000 MPa.

Riple Point to 1200 k with Pressures to 1000 MPa. Quarterly rept.

R. B. Stewart, and R. T. Jacobsen. c1989, 160p
Prepared in cooperation with American Chemical Society, Washington, DC., and American Inst. of Physics, New York. Sponsored by National Inst. of Standards and Technology, Gaithersburg, MD.
Included in Jnl. of Physical and Chemical Reference

Data, v18 n2 p639-798 1989.

*Thermodynamic properties, Keywords: Helmholtz free energy, Pressure, Equations of state, Enthalpy, Entropy, Specific heat, Tables(Data), Experi-mental design, Numerical analysis, Comparison, Liquid phases, Vapor phases, *Triple point.

A new thermodynamic property formulation for argon is presented. The formulation includes a fundamental equation explicit in Helmholtz energy, a vapor pressure equation, and estimating functions for the densities of saturated liquid and vapor states. The coefficients of the fundamental equation and ancillary functions were determined by a weighted least-squares fit of selected experimental data using a statistical procedure to select the terms for the equation most appropriate for the representation of the data. The fundamental equation is valid for liquid and vapor phases except near the critical point. Comparisons between the data used to determine the fundamental equation and values calculated from the formulation are given to verify the accuracy of the fundamental equation. Tables of thermodyanmic properties of argon calculated with the formulation presented here are given for fluid states within the range of validity of the correlation. (Copyright (c) by the U.S. Secretary of Commerce, 1989.)

900,452

PB89-222566 (Not Available NTIS) Los Alamos National Lab., NM.

Thermodynamic Properties of Dioxygen Difluoride (O2F2) and Dioxygen Fluoride (O2F). Quarterly rept.
J. L. Lyman. c1989, 9p
Prepared in cooperation with American Chemical Soci-

ety, Washington, DC., and American Chemical Society, Washington, DC., and American Inst. of Physics, New York. Sponsored by National Inst. of Standards and Technology, Gaithersburg, MD. Included in Jnl. of Physical and Chemical Reference Data, v18 n2 p799-807 1989.

Keywords: *Thermodynamic properties, Gibbs free energy, *Specific heat, Entropy, Enthalpy, Tables(Data), Fluorimation, Experimental data, Numerical analysis, *Difluoride/dioxy, *Fluoride/dioxy, Oxygluorides.

Recent spectroscopic and chemical kinetic studies have provided sufficient data for construction of reliable thermodynamic tables for both dioxygen defluoride (O2F2; Chemical Abstracts Registry Number, 7783-44-0) and dioxygen fluoride (O2F; Chemical Abstracts Registry Number, 15499-23-7). The paper contains those tables for these species in both SI units (0.1 MPa standard state) and cal K mol units (1.0 atm standard state). The experimental basis includes three recent assignments of the fundamental vibrational frequencies for O2F2, a new set of rotational constants for O2F, an ethalpy change for dissociation of O2F, and an updated standard enthalpy of formation for O2F2. (Copyright (c) by the U.S. Secretary of Commerce, 1989.)

900,453

PB89-222574 (Not available NTIS) National Inst. of Standards and Technology (NML), Gaithersburg, MD. Chemical Thermodynamics Div.
Thermodynamic and Transport Properties of Carbohydrates and Their Monophosphates: The Pentoses and Hexoses.

Quarterly rept.
R. N. Goldberg, and Y. B. Tewari. c1989, 72p
Prepared in cooperation with American Chemical Society, Washington, DC., and American Inst. of Physics,

Included in Jnl. of Physical and Chemical Reference Data, v18 n2 p809-880 1989.

Keywords: *Thermodynamic properties, *Transport properties, *Pentoses, *Hexoses, *Carbohydrates, *Organic phosphates, Gibbs free energy, Specific heat, Viscosity, Phase diagrams, Enthalpy, Entropy, Tables(Data), Reviews, Transition temperature.

The review contains recommended values of the thermodynamic and transport properties of the five and six membered ring carbohydrates and their phosphates in both the condensed and aqueous phases. Equilibrium data, enthalpies, heat capacities, and entropies have been collected from the literature. The accuracy of these data have been assessed, adjusted to 298.15 K and to common standard state, and entered into a catalog of thermochemical reactions. The solution of the reaction catalog yields a set of recommended values for the formation properties of these sub-stances. The volumetric data have also been critically stances. The volumetric data have also been critically evaluated. Recommended values are presented for standard state molar volumes and the temperature and pressure derivatives of the molar volume, i.e., the expansivity and the compressibility. The excess property data of aqueous solutions of theses substances have been correlated to yield recommended values of the parameters of the virial expansion model used to represent the data. The transport data considered here includes both viscosity and diffusion data of aqueous solutions of the carbohydrates. The available phase diagram data and transition temperatures are summarized. (Copyright (c) by the U.S. Secretary of Commerce, 1989.)

900,454

PB89-222582 (Not Available NTIS) California Univ., Riverside. Statewide Air Pollution Research Center.

Evaluated Kinetic and Photochemical Data for Atmospheric Chemistry. Supplement 3.

Quarterly rept.
R. Atkinson, D. L. Baulch, R. A. Cox, R. F. Hampson, J. A. Kerr, and J. Troe. c1989, 217p
Prepared in cooperation with American Chemical Society, Washington, DC., American Inst. of Physics, New York, and Leeds Univ. (England). Sponsored by Natical Let of Standard and Technology Guithous. tional Inst. of Standards and Technology, Gaithersburg, MD.

Included in Jnl. of Physical and Chemical Reference Data, v18 n2 p881-1097 1989.

Keywords: *Reaction kinetics, *Photochemical reactions, Tables(Data), Enthalpy, Thermodynamic properties, Dissociation, *Atmospheric chemistry.

The paper updates and extends previous critical evaluations of the kinetics and photochemistry of gas phase chemical reactions of neutral species involved in atmosphere chemistry (J. Phys. Chem. Ref. Data 9, 295 (1980); 11, 327 (1982); 13, 1259 (1984)). The work has been carried out by the authors under the auspecies of the IUPAC Subcommittee on Gas Phase Kinetic Data Evaluation for Atmosphereic Chemistry. Data sheets have been prepared for 360 thermal and photochemical reactions, containing summaries of the avail-able experimental data with notes giving details of the experimental procedures. For each reaction, a preferred value of the rate coefficient at 298 K is given together with a temperature dependence where possible. The selection of the preferred value is discussed; and estimates of the accuracies of the rate coefficients and temperature coefficients have been made for each reaction. The data sheets are intended to provide the basic physical chemical data needed as input for calculations which model atmospheric chemistry. A table summarizing the preferred rate data is provided, together with an appendix listing the available data on enthalpies of formation of the reactant and product species. (Copyright (c) by the U.S. Secretary of Commerce, 1989.)

900,455 PB89-226559 Not available NTIS American Chemical Society, Washington, DC.

Journal of Physical and Chemical Reference Data, Volume 18, Number 1, 1989. Quarterly rept.

D. R. Lide. c1989, 567p See also PB89-226567 through PB-226609, PB89-227797, and PB89-222525. Prepared in cooperation with American Inst. of Physics, New York. Sponsored by National Inst. of Standards and Technology, Gaith-

ersburg, MD. Available from American Chemical Society, 1155 16th St., NW, Washington, DC 20036.

Keywords: *Thermodymanic properties, Water, Electrode potentials, Temperature coefficient, Cross sections, Oxygen, Thermal conductivity, Molecular energy levels, Excitation, Reaction kinetics, X rays, Refriger ants, Pressure, Aromatic polycyclic hydrocarbons, Isomers, Pyrenes, Tables(Data), Metal complexes, Helium ions, Hydrogen ions, Coronenes, Electron-molecule collisions, Photon-molecule collisions, Ion-atom collisions. K shell.

Contents: Standard Electrode Potentials and Temperature Coefficients in Water at 298.15 K; Cross Sections for Collisions of Electrons and Photon with Oxygen Molecules; Thermal Conductivity of Refriger-Oxygen Molecules, Thermal Condictivity of Herriger-ants in a Wide Range of Temperature and Pressure; Standard Chemical Thermodynamic Properties of Po-lycyclic Aromatic Hydrocarbons and Their Isomer Groups. II. Pyrene Series, Naphthopyrene Series, and Coronene Series; Cross Sections for K-Shell X-Ray Production by Hydrogen and Helium lons in Elements from Berylium to Uranium; Rate Constants for the Quenching of Excited States of Metal Complexes in Fluid Solution. (Copyright (c) by the U.S. Secretary of Commerce, 1989.)

900,456 PB89-226567 PB89-226567 (Not available NTIS) Southwest Texas State Univ., San Marcos. Dept. of Chemistry.
Standard Electrode Potentials and Temperature
Coefficients in Water at 298.15 K.

S. G. Bratsch. c1989, 21p Prepared in cooperation with American Chemical Society, Washington, DC., and American Inst. of Physics, New York. Sponsored by National Inst. of Standards

and Technology, Gaithersburg, MD.
Included in Jnl. of Physical and Chemical Reference
Data, v18 n1 p1-21 1989. Available from American
Chemical Society, 1155 16th St., NW, Washington, DC

Keywords: *Electrode potentials, *Temperature coefficient, *Water, Solvents, Electrochemical cells, Tables(Data), Standards, Thermodynamic properties, pH, Enthalpy, Entropy, Gibbs free energy.

A great deal of solution chemistry can be summarized in a table of standard electrode potentials of the ele-

ments in the solvent of interest. In the work, standard electrode potentials and temperature coefficients in water at 298.15 K, based primarily on the 'NBS Tables of Chemical Thermodynamic Properties,' are given for nearly 1700 half-reactions at pH = 0.000 and pH = 13.996. The data allow the calculation of the thermodynamic changes and equilibrium constants associated with approximately 1.4 million complete cell reac-tions over the normal temperature range of liquid water. Estimated values are clearly distinguished from experimental values, and half-reactions involving doubtful chemical species are duly noted. General and specific methods of estimation of thermodynamic quantities are summarized. (Copyright (c) by the U.S. Secretary of Commerce, 1989.)

900,457 PB89-226575 (Not available NTIS) Institute of Space and Astronautical Science, Tokyo

Cross Sections for Collisions of Electrons and Photons with Oxygen Molecules. Quarterly rept.

Cularterly rept.
Y. Itikawa, A. Ichimura, K. Onda, K. Sakimoto, K.
Takayanagi, Y. Hatano, M. Hayashi, H. Nishimura,
and S. T. Tsurubuchi. c1989, 20p
Prepared in cooperation with Tokyo Inst. of Tech.

(Japan), Nagoya Inst. of Tech. (Japan), and American Chemical Society, Washington, DC. Sponsored by National Inst. of Standards and Technology, Gaithers-

tional list of Standard Surg MD.
Included in Jnl. of Physical and Chemical Reference Data, v18 n1 p23-42 1989. Available from American Chemical Society, 1155 16th St., NW, Washington, DC

Keywords: *Cross sections, *Oxygen, Tables(Data), Graphs(Charts), Photochemical reactions, Ionization, Dissociation, Spectrum analysis, Thermodynamic properties, Molecular rotation, Molecular vibration, *Electron-molecule collisions, *Photon-molecule collisions

Data have been compiled on the cross sections for collisions of electrons and photons with oxygen molecules (O2). For electron collisions, the processes included are: total scattering, elastic scattering, momentum transfer, excitations of rotational, vibrational, and electronic states, dissociation, ionization, and attachment. Ionization and dissociation processes are considered for photon impact. Cross-section data selected are presented graphically. Spectroscopic and other properties of the oxygen molecule are summarized for understanding of the collision processes. The literature was surveyed through August 1987, but some more recent data are included when available to the authors. (Copyright (c) by the U.S. Secretary of Commerce, 1989.)

PB89-226583 (Not available NTIS) Stuttgart Univ. (Germany, F.R.).
Thermal Conductivity of Refrigerants in a Wide Range of Temperature and Pressure.

Quarterly rept. R. Krauss, and K. Stephan. c1989, 32p

Prepared in cooperation with American Chemical Society, Washington, DC., and American Inst. of Physics, New York. Sponsored by National Inst. of Standards and Technology, Gaithersburg, MD. Included in Jnl. of Physical and Chemical Reference Data, v18 n1 p43-76 1989. Available from American

Chemical Society, 1155 16th St., NW, Washington, DC 20036.

Keywords: *Thermal conductivity, *Refingerants, *Temperature, *Pressure, Thermodynamic properties, Tables(Data), Graphs(Charts), Fluorohydrocarbons, Dichlorodifluoromethane, Gas dynamics, Comparison, Freons, Ethane/dichloro-tetral fluoro, Ethane/trichloro-trifluoro. Ethane/dichloro-tetrafluoro, Cyclobutane/

Thermal conductivities of refrigerant 12 (dichlorodifluoromethane), refrigerant 114 (1,1,2-trichloro-1,2,2-tri-fluoroethane), refrigerant 114 (1,2-dichloro-1,1,2,2-te-trafluoroethane), and refrigerant C318 (Perfluorocyclobutane) were critically evaluated and correlated on the basis of a comprehensive literature survey. Recommended values were established for a wide range of temperatures and pressures, extending up to three times the critical density and excluding the critical region. Using the residual concept, a dilute-gas function and an excess function of simple form were developed for each refrigerant. The average accuracy obtained is approximately 6%. (Copyright (c) by the U.S. Secretary of Commerce, 1989.) 900 459

PB89-226591 (Not available NTIS) Massachusetts Inst. of Tech., Cambridge. Dept. of

Standard Chemical Thermodynamic Properties of Polycyclic Aromatic Hydrocarbons and Their Isomer Groups. 2. Pyrene Series, Naphthopyrene Series, and Coronene Series.

Quarterly rept. R. A. Alberty, M. B. Chung, and A. K. Reif. c1989,

Prepared in cooperation with American Chemical Soci Prepared in cooperation with American Chemical Society, Washington, DC., and American Inst. of Physics. New York. Sponsored by National Inst. of Standards and Technology, Gaithersburg, MD. Included in Jnl. of Physical Chemical Reference Data, v18 n1 p77-110 1989. Available from American Chemical Society, 1155 16th St., NW, Washington, D

20036.

Keywords: *Thermodynamic properties, *Aromatic polycyclic hydrocarbons, *Isomers, *Pyrenes, Standards, Enthalpy, Specific heat, Gibbs free energy, Entropy, Tables(Data), *Coronenes.

The tables in our first paper on polycyclic aromatic hydrocarbons (J. Phys. Chem. Ref. Data 17, 241 (1988)) have been extended by calculating thermodynamic properties for the first four isomer groups in the pyrene series, the first three isomer groups in the naphthopyrene series, and the first three isomer groups in the coronene series. Successive isomer groups in each series differ by C4H2. Since chemical thermodynamic properties are known for only a limited number of polycyclic aromatic hydrocarbons, the properties of individual species have been estimated using Benson group values of Stein and Fahr for temperatures from 298.15 to 3000 K. Values of C(sub p), S, delta(sub f), H, and delta(sub f)G have been calculated in joules for a standard state pressure of 1 bar. The chemical thermodynamic properties of the individual species have also been calculated. The isomer group values provide a basis for extrapolating to higher carbon numbers where it is not feasible to consider individual molecular species. (Copyright (c) by the U.S. Secretary of Commerce, 1989.)

900.460

East Carolina Univ., Greenville, NC.

Cross Sections for You will No.

Cross Sections for K-Shell X-ray Production by Hydrogen and Helium Ions in Elements from Beryllium to Uranium. Quarterly rept.

G. Lapicki. c1989, 108p

Prepared in cooperation with American Chemical Society, Washington, DC., and American Inst. of Physics, New York. Sponsored by National Inst. of Standards and Technology, Gaithersburg, MD. Included in Jnl. of Physical Chemical Reference Data,

v18 n1 p111-218 1989. Available from American Chemical Society, 1155 16th St., NW, Washington, DC 20036.

Keywords: *X rays, *Scattering cross sections, Thermodynamic properties, Tables(Data), Fluorescence, lonization, Numberical analysis, Data processing, Experimental design, Alkaline earth metals, Actinide series, *K shell, *Ion-atom collisions, *Hydrogen ions, *Helium ions.

Experimental cross sections for K-shell x-ray production by hydrogen and helium ions (Z1 = 1,2) in target atoms from beryllium to uranium (Z2 = 4.92) are tabulated as compiled 7418 cross sections) from the literature (161 references were found) with the search for the data terminated in January 1988. These cross sections are compared with predictions of the first Born approximation and ECPSSR theory for inner-shell ionization. The ECPSSR accounts for the energy loss (E) and Coulomb deflection (C) of the projectile ion as well as for the perturbed stationary state (PSS) and relativistic (R) nature of the target's inner-shell electron. While the first Born approximation generally overestimates the data by orders of magnitude, the ECPSSR theory is confirmed to be, on the average, in agreement with the experiment to within 10%-20%. (Copyright (c) by the U.S. Secretary of Commerce, 1989.)

900.461

PB89-227797 (Not available NTIS) Boston Univ., MA. Dept. of Chemistry.

Rate Constants for the Quenching of Excited States of Metal Complexes in Fluid Solution.

M. Z. Hoffman, F. Bolletta, L. Moggi, and G. L. Hug.

c1989, 324p

Prepared in cooperation with Bologna Univ. (Italy), Notre Dame Univ., IN. Radiation Lab., and American Chemical Society, Washington, DC. Sponsored by National Inst. of Standards and Technology, Gaithers-

Included in Jnl. of Physical Chemical Reference Data, v18 n1 p219-543 1989. Available from American Chemical Society, 1155 16th St., NW, Washington, DC

20036.

Keywords: *Reaction kinetics, *Metal complexes, Mo-lecular energy levels, Thermodynamic properties, Ex-citation, Solutions, Quenching media, Tables(Data).

The rate constants for the quenching of the excited states of metal ions and complexes in homogeneous fluid solution are reported in this compilation. Values of K(sub q) for dynamic, collisional processes between excited species and quenchers have been critically evaluated, and are presented with the following information, among others, from the original publications, when available: description of the solution medium, temperature at which K(sub q) was determined, experimental method, range of quencher concentration used, lifetime of the exited state in the absence of quencher, activation parameters, quenching mechanism. Data collection is complete through the end of 1986, and covers the coordination compounds of 26 metals, including the ions and complexes of the innerand outer-transition metals, and porphyrin complexes of nontransition metals. The introduction to the work contains a discussion of the conceptual background to quenching, including a general treatment of the kinetics, an explanation of the tables, and a list of recent review articles. Uncommon kinetics mechanisms and equations, used to obtain the reported values of K(sub q) are discussed in detail as part of the notes to the tables. Indexes of excited states, quenchers, and authors are appended. (Copyright (c) by the U.S. Secretary of Commerce, 1989.)

900,462

PB89-227896 Not available NTIS National Inst. of Standards and Technology (NML), Gaithersburg, MD. Chemical Thermodynamics Div. Second Virial Coefficients of Aqueous Alcohols at Elevated Temperatures: A Calorimetric Study. Final rept.

D. G. Archer. 1989, 8p

Pub. in Jnl. of Physical Chemistry 93, n1 p5272-5279, 29 Jun 89.

Keywords: *Gibbs free energy, *Enthalpy, *Dilution, *Cyclohexanols, *Sugar alcohols, *Water, Heat measurement, Butanols, Propanols, Specific heat, Antifreezes, High temperature tests, Gas laws, Reprints.

Enthalpies of dilution of cyclohexanol (aq) to 448 K and of myo-inositol (aq) and of cyclohexanol + myo-inositol (aq) to 398 K are reported. The results, along with enthalpies of dilution for 1-butanol (aq) to 448 K and for 2-methyl-2-propanol (aq) to 423 K, were combined with freezing point depression measurements and ambient-temperature enthalpy of dilution and heat capacity measurements in order to provide the excess Gibbs energy for the aqueous solutes from 273 to 523 K. The excess Gibbs energies were then used to pro-vide parameters for an additivity scheme that permits an approximation of the excess Gibbs energy, and thus the solute and solvent activity coefficients, for dilute aqueous alcohols for which high-temperature data do not exist. The excess Gibbs energies were also used to estimate the aqueous-solution second virial coefficients of the alcohols and of cyclohexane (aq), 1-butane (aq), and 2-methylpropane (aq) in the McMillan-Mayer convention. These virial coefficients for the aqueous hydrocarbons, when compared to gasphase virial coefficients for the hydrocarbons, suggest that the effect of low-temperature (298 K) water is to lessen the pairwise attraction of aqueous hydrocarbon over that found in the gas phase at the same temperature and that the lessening of the pairwise attraction diminishes at higher temperatures.

900.463

PB89-227912 Not available NTIS National Inst. of Standards and Technology (NML), Boulder, CO. Quantum Physics Div. Absolute Infrared Transition Moments for Open Shell Diatomics from J Dependence of Transition Intensities: Application to OH.

Final rept. D. D. Nelson, A. Schiffman, D. J. Nesbitt, and D. J.

Yaron. 1989, 12p Grant AFOSR-84-0272

Sponsored by Air Force Office of Scientific Research, Bolling AFB, DC. Pub. in Jnl. of Chemical Physics 90, n10 p5443-5454,

15 May 89.

Keywords: *Dipole moments, Vibrational spectra, Diatomic molecules, Reprints, *Hydroxyl radicals, Infrared absorption, Herman Wallis effect.

A general approach to the determination of the dipole moment function and of the absolute vibrational transition moments for diatomic molecules is presented. The method utilizes the variation of intensity with J within a vibrational transition, together with permanent dipole moment information, to extract the absolute transition moments. An essential feature of the model is its use of algebraic expressions for calculating vibration-rotation line intensities. These expressions can be rapidly evaluated in a least squares fit which determines the dipole moment function. This approach is general in that it is not limited to (sup 1)Sigma state molecules, nor to the simplest of Hund's case couplings of spin, orbital and mechanical angular momentum. It is also not limited to molecules with essentially linear dipole moment functions. The model is successfully applied to the OH molecule which violates each of these restrictions. In the accompanying work the authors report experimental measurements of relative infrared absorption intensity measurements for OHmu = 1 <- 0 transitions and the extraction of an experimental mu(r) using the approach presented here.

PB89-227920 Not available NTIS National Inst. of Standards and Technology (NML), Boulder, CO. Quantum Physics Div.
Dipole Moment Function and Vibrational Transition Intensities of OH. Final rept. D. D. Nelson, A. Schiffman, and D. J. Nesbitt. 1989,

Grant AFOSR-84-0272

Sponsored by Air Force Office of Scientific Research, Bolling AFB, DC. Pub. in Jnl. of Chemical Physics 90, n10 p5455-5465,

15 May 89.

Keywords: *Dipole moments, Vibrational spectra, Electron transitions, Infrared spectroscopy, Reprints, *Hydroxyl radicals, Infrared absorption, Flash kinetic spectroscopy.

The relative intensities of nine pairs of rovibrational transitions of OH in the nu $= 1 < \cdot$ 0 fundamental have been measured by flash kinetic infrared absorption spectroscopy. Each pair of transitions originates from a common rotational and spin-orbit state, so that relative intensities are independent of the OH number density and quantum state distribution. The relative intensities are strongly J dependent and this dependence provides detailed information about the shape of the OH dipole moment function, mu(f), and hence the absolute infrared transition strengths. In an accompanying paper, the authors present the theoretical basis for extracting mu(r) for an open shell diatomic like OH from relative infrared intensities and permanent dipole moment measurements and determine the OH dipole moment function.

900,465 PB89-227953 Not available NTIS National Inst. of Standards and Technology (NML), Roulder, CO. Quantum Physics Div.

Rydberg-Klein-Rees Inversion of High Resolution van der Waals Infrared Spectra: An Intermolecular

Potential Energy Surface for Ar + HF (v = 1).

Final rept.
D. J. Nesbitt, M. S. Child, and D. C. Clary. 1989, 10p
Grants NSF-CHE86-05970, NSF-PHY86-04504 Sponsored by National Science Foundation, Washington, DC.

Pub. in Jnl. of Chemical Physics 90, n9 p4855-4864, 1 May 89.

Keywords: *Infrared spectroscopy, *Potential energy, *Molecular rotation, *Hydrogen fluoride, *Argon, Molecular energy levels, Intermolecular forces, Molecular vibration, Experimental design, Numerical analysis, Reprints, *Van der Waals forces, *Rydberg-Klein-Rees method, *Laser spectroscopy.

A method is described for extraction of two-dimensional (angular and radial) potential energy surfaces for triatomic rare gas-hydrogen halide van der Waals complexes. The approach relies on extensive J rotational term values obtained by high resolution infrared laser jet spectroscopy for a family of bending vibrational states to deduce the radial and angular dependence of the intermolecular potential. First, effective 1D radial potentials for series of bend states are obtained by rotational RKR analysis of experimentally observed rotational recommendations. tional progressions. These 1D potentials, which represent vibrational averages over different bending wave functions, are then inverted to determine the radially dependent coefficients of a Legendre expansion to the full surface. This relies on adiabatic angular motion with respect to radial degrees of freedom, the validity of which is discussed. This approach is tested with experimental data. The accuracy of the resulting surface is verified by exact quantum bound state calculations which quantitatively reproduce the rovibrational input data, as well as predict the spectroscopic properties of five other vibrational states observed in the Ar+HF(v = 1) system but not used in the fitting procedure.

900.466

PB89-227961 Not available NTIS
National Inst. of Standards and Technology (NML), Boulder, CO. Quantum Physics Div.

Three Dimensional Quantum Reactive Scattering Study of the I + HI Reaction and of the IHI(1-) Photodetachment Spectrum.

Final rept. G. C. Schatz. 1989, 8p Grant NSF-CHE87-15581

Sponsored by National Science Foundation, Washington, DC.

Pub. in Jnl. of Chemical Physics 90, n9 p4847-4854, 1 May 89.

Keywords: *Hydrogen iodide, *Iodine, Quantum interactions, Resonance, Reprints, *Reactive scattering, *Photodetachment, Coupled channel theory, Hyperspherical coordinates.

The author presents results of coupled channel hyperspherical reactive scattering calculations on the reaction I + HI -> IH + I using a semiempirical potential surface. Only the J = O partial wave is considered. Franck-Condon factors associated with photodetachment of IHI(1-) have also been calculated, and these show mainly direct scattering threshold behavior at low energies (E<0.30 eV), with the (100) and (200) resonances contributing only slightly. Resonant behavior is dominant at higher energies (0.3-0.4 eV) where the (002) resonance especially contributes.

900,467

Not available NTIS
National Bureau of Standards (NML), Boulder, CO.
Quantum Physics Div.

Spectroscopic Signatures of Floppiness in Molecular Complexes.

Final rept

D. J. Nesbitt. 1988, 10p Grants NSF-CHE83-05970, NSF-PHY86-04504 Sponsored by National Science Foundation, Washington, DC.

Pub. in Structure of Small Molecules and Ions, p49-58 1988.

Keywords: *Molecular structure, Molecular spectroscopy, Molecular rotation, Molecular vibration, Rigidity, Reprints, *Molecular complexes, Van der Waal forces, Supersonic jet flow.

The challenge of correctly inferring even the qualitative features of the potential energy hypersurface from spectroscopic measurements is heightened dramatically in studies of weakly bound molecular complexes where large amplitude motion is present. This is especially true for data obtained from low temperature, supersonic expansions where Boltzmann distributions limit the range of internally excited states that can be investigated. To stress this point, the author presents simulated spectra for two model triatomic systems, a 'pinwheel' and a 'hinge,' with nearly flat potentials that support extremely large amplitude internal rotation and bending, respectively. The results indicate that simple eigenvalue analysis of jet cooled molecular spectra in the absence of hyperfine resolution may not be suffi-ciently sensitive to large amplitude angular motion, and that data from a variety of techniques may prove necessary to assess the degree of molecular rigidity.

900.468 PB89-228001 Not available NTIS National Bureau of Standards (NEL), Gaithersburg, MD. Thermophysics Div.

Low-Q Neutron Diffraction from Supercooled D-

Final rept.
H. J. M. Hanley, G. C. Straty, C. J. Glinka, and J. B. Hayter. 1987, 10p
Sponsored by Department of Energy, Washington, DC. Div. of Materials Sciences, and Martin Marietta Energy Systems, Inc., Oak Ridge, TN.
Pub. in Molecular Physics 62, n5 p1165-1174 1987.

Keywords: *Glycerol, *Neutron diffraction, Supercooling, Scattering cross sections, Hydrogen bonds, Reprints, *Structure factors, Vanadium fluorides.

Neutron diffraction measurements of the structure factor of supercooled liquid D-glycerol are reported for the range 0.03 approx = or < Q = or < 4.0/A at temperatures between 300 and 175 K. It was found that the structure is essentially unchanged over this entire range. The authors expected some evidence of increased hydrogen bonding at the lower tempera-tures, but no direct evidence for any strong oriented density correlation at low-Q due to a hydrogen bond is observed. To provide a contrast, the structure factor of vanadium pentafluoride is discussed briefly because vanadium pentafluoride is known to form fluorine-fluorine bridges in the dense state. The authors equate loosely this bridging with a hydrogen bond. In that compound there is evidence for F-F bonding at low-Q. Small angle Placzek corrections to the D-glycerol scattering cross section data are estimated.

900,469 Not available NTIS PB89-228043 National Bureau of Standards (NEL), Boulder, CO. Thermophysics Div.

Shear-Induced Angular Dependence of the Liquid Pair Correlation Function.

Final rept.

H. J. M. Hanley, J. C. Rainwater, and S. Hess. 1987,

Sponsored by Department of Energy, Washington, DC. Pub. in Physical Review A 36, n4 p1795-1802 Aug 87. Keywords: *Liquids, Couette flow, Relaxation time,

Spherical harmonics, Tensors, Simulation, Reprints, Correlation functions, Molecular dynamics.

A formal expansion in spherical harmonics or Cartesian tensors of the pair correlation function of a liquid subjected to a shear rate is discussed. Expressions for the coefficients to tensor rank 4 are evaluated via a nonequilibrium molecular-dynamics simulation of an inverse twelve soft-sphere liquid undergoing Couette flow. It is shown that the expansion converges slowly if the product tau gamma 0.05, where tau is the Maxwell relaxation time and gamma is the shear rate. Further, the fourth-rank coefficient that represents cubic symmetry is significant for the model system. The microstructure of a shear liquid is demonstrated by intensity plots of particles around a given central particle. Expressions were derived for the expansion coefficients using a relaxation-time model, and the comparison between them and simulations is generally very good.

Not available NTIS PB89-228092 National Bureau of Standards (NML), Boulder, CO. Quantum Physics Div.

Quantum Mechanical Calculations on the Ar(1+) + N2 Charge Transfer Reaction.

Final rept.

D. C. Clary, and D. M. Sonnenfroh. 1989, 8p Pub. in Jnl. of Chemical Physics 90, n3 p1686-1693 Feb 89

Keywords: *Nitrogens, Reprints, *Change-exchange reactions, *Argon ions, Quantum mechanics, Rotational states, Born approximations.

Calculations of cross sections for the charge transfer reaction Ar(1+) (doublet P(3/2)) + N2(v=0,j) -> Ar + N2+(1+)(v'=1,j') are reported for thermal collision energies. A three-dimensional quantum-mechanism cal method is used in which separate rotational closecoupling calculations are performed for the Ar(1+) + N2(v=0) -> Ar + N2(1+)(v'=0) and Ar(2+) + N2(v=1) -> Ar + N2(1+)(v'=1) channels, and the cross sections for the v=0 -> v'=1 channel are computed using a coupled channel-distorted wave Born approximation. Potential energy surfaces and couplings are taken from ab initio data. The predicted rotational product distributions for N2(1+)(v'=1,j') agree fairly well with those measured in a molecular beam laser-induced fluorescence experiment.

900,471 PB89-228399 Not available NTIS National Inst. of Standards and Technology (NML), Boulder, CO. Quantum Physics Div. Infrared Spectra of Nitrous Oxide-HF Isomers. Final rept.

C. M. Lovejoy, and D. J. Nesbitt. 1989, 10p Grants NSF-PHY86-04504, NSF-CHE86-05970 Sponsored by National Science Foundation, Washing-

Pub. in Jnl. of Chemical Physics 90, n9 p4671-4680, 1 May 89.

*infrared spectroscopy, *Nitrogen Keywords: oxide(N2O), *Hydrogen fluoride, Dissociation, Complex compounds, Hydrogen binds, Molecular isomerism, Molecular vibration, Reprints, *Laser spectroscopy.

Two spectroscopically distinct isomers of a hydrogen bonded complex between nitrous oxide and hydrogen fluoride are observed by direct infrared laser absorp-tion detection in a slit supersonic expansion. The linear isomer FH-NNO contains a relatively rigid hydrogen bond to the nitrogen end of NNO. The bent isomer NNO-HF has a stronger hydrogen bond to the oxygen end of NNO, but this bond is characterized by a softer bending potential and thus the complex exhibits evidence of large amplitude bending motion. Rapid vibrational predissociation, as determined from the homo-geneous broadening of the rovibrational absorption structure, is evidenced in both isomers. The linear isomer exhibits predissociation lifetimes which show structure as a function of the upper J' rotational level. including narrow resonances which suggest excitation of NNO fragment vibrational modes.

900,472 PB89-228407 Not available NTIS National Bureau of Standards (NML), Boulder, CO. Quantum Physics Div. Dynamical Simulation of Liquid- and Soiid-Metai

Self-Sputtering.

Final rept.

W. L. Morgan, 1989, 5p

Pub. in Jnl. of Applied Physics 65, n3 p1265-1269, 1 Feb 89.

Keywords: *Liquid metals, Surfaces, Simulation, Reprints, *Self sputtering, Molecular dynamics.

Molecular dynamics simulations of self-sputtering are performed using the recent picture of a stratified liquidmetal surface as a model. These results are compared to those obtained from a liquid model having uniformly distributed atoms and a crystalline solid model. The stratified liquid-metal model shows an enhanced lowenergy sputter yield, which falls below those of the other models for ion-impact energies above several hundred electron volts. These results are discussed in light of various published measurements of sputter yields of metals in their liquid and solid phases.

900,473 PB89-228415 Not available NTIS National Bureau of Standards (NML), Boulder, CO. Quantum Physics Div.

Calculation of Vibration-Rotation Spectra for Rare Gas-HCi Complexes.

Final rept. D. C. Clary, and D. J. Nesbitt. 1989, 14p Grants NSF-PHY86-04504, NSF-CHE86-05970 Sponsored by National Science Foundation, Washing-

Pub. in Jnl. of Chemical Physics 90, n12 p7000-7013, 15 Jun 89.

Keywords: *Complex compounds, *Rotational spec-*Vibrational spectra, *Hydrogen chloride, Infrared spectra, Schrodinger equation, Computation, Reprints, *Chemical complexes, *Argon complexes, *Krypton complexes, *Neon complexes, *Xenon complexes, Van der Waals forces.

Calculations are described of spectra for the excitation of the bending and stretching vibrational-rotational energy levels in the van der Waals complexes of HCI with the rare gases Ne, Ar, Kr, and Xe. The calculations are performed using a basis set method, with dis-tributed Gaussian functions being employed for the co-ordinate associated with the stretching of the rare gas atom. Intensities of combination and fundamental transitions for each of the low frequency modes are calculated for total angular momentum up to J=25. Surprisingly large intensities are predicted for transitions to states with multiple vibrations excited in the bending mode. Promising comparisons are obtained with infrared spectra measured recently for the complexes of HCI with Ne and Ar at low temperatures.

PB89-228480 PB39-228480 Not available NTIS National Inst. of Standards and Technology (NEL), Gaithersburg, MD. Semiconductor Electronics Div. Multiple Scattering in the X-ray Absorption Near Edge Structure of Tetrahedral Germanium Gases. Final rept.

Ritter, and G. Bunker. 1989, 3p See also PB89-146922.

Pub. in Physica B 158, p362-364 1989.

Keywords: *Germanium halides, *Germanium hydrides, *X-ray absorption, *Molecular structure, Gases, Electron scattering, Reprints.

X-ray absorption fine structure (XAFS) measurements of GeCl4, GeH3Cl, and GeH4 are reported. Since wide-angle multiple scattering involving H atoms is negligible, the single and multiple scattering (MS) are isolated. Components terms in the XAFS of GeCl4 by comparison of the spectra of the three compounds. It is found that multiple scattering is nowhere dominant over single scattering (SS), although within 15 eV of the edge the two are comparable in size. However, the multiple scattering damps out very quickly with increasing energy above the absorption edge. Beyond 40 eV past the edge the MS/SS ratio is less than 0.06. The calculations are found to be in qualitative agreement with the experiment, but overestimate the size and energy range of the MS. The results suggest that SFS data in the range 1 < K < 3 A sup -1 can be analyzed in an SS picture in many cases, as long as good standard compounds are used, and calculations are used to estimate possible errors due to neglect of MS. The first evidence of single scattering observed from H atoms is also reported.

900.475 PB89-228514 Not available NTIS National Inst. of Standards and Technology (NML), Gaithersburg, MD. Molecular Spectroscopy Div. infrared Spectrum of the 1205-cm(-1) Band of HNO3.

Final rept

A. G. Maki. 1989, 4p

Sponsored by National Aeronautics and Space Administration, Washington, DC. Pub. in Jnl. of Molecular Spectroscopy 136, p105-108

Keywords: *Infrared spectroscopy, *Nitric acid, Molecular rotation, Molecular vibration, Reprints.

The high-resolution spectrum of the 1205/cm band of HNO3 has been measured. It is shown that this is an A-type band and must be due to the nu8 + nu9 combination. The band is relatively unperturbed and effective rovibrational constants are given that can be used to calculate the spectrum between 1183 and 1225/

900,476 PB89-228555 Not available NTIS National Inst. of Standards and Technology (NEL), Gaithersburg, MD. Thermophysics Div. Capillary Waves of a Vapor-Liquid Interface Near

the Critical Temperature. Final rept.

J. V. Sengers, and J. M. J. van Leeuwen. 1989, 10p Pub. in Physical Review A 39, n12 p6346-6355, 15 Jun

Keywords: Critical temperature, Liquid phases, Vapors, Interfaces, Interfacial tension, Reflectivity, Reprints, *Capillary waves, Surface tension.

An attempt is made to develop the picture of an interface near the critical temperature as an intrinsic Fisk-Widom interface broadened by capillary waves. The authors propose a method for determining the free parameters appearing in the capillary-wave theory by requiring that the capillary waves smoothly renormalize the surface tension from the bare to the experimental value. They evaluate the effect of the capillary waves on the width of the interface and make a comparison

with experimental reflectivity measurements obtained by Wu and Webb for SF6 and also with the renormalization results of Jasnow and Rudnick.

PB89-228563 Not available NTIS National Bureau of Standards (NEL), Boulder, CO. Thermophysics Div.

improved Conformal Solution Theory for Mixtures with Large Size Ratios.

M. L. Huber, and J. F. Ely. 1987, 17p Sponsored by Department of Energy, Washington, DC. Pub. in Fluid Phase Equilibria 37, p105-121 1987.

Keywords: *Mixtures, *Perturbation theory, Statistics, Molecules, Potential theory, Reprints, *Lennard-Jones gas, Gas viscosity, Gas density.

Previous studies on model Lennard-Jones systems have shown that conformal solution theories fend to fall when mixtures contain molecules with large size differences. This failure can be attributed to deficiencies in the underlying mean density approximation (MDA) for the mixture's radial distribution functions which was originally proposed by Leland and coworkers. An improved mean density approximation is pre-sented which is obtained from a straightforward application of statistical mechanical perturbation theory. Comparisons of the new theory with simulation PV data for systems with large size ratios show it to be far superior to van der Waals one-fluid and MDA n-fluid theories and an improvement upon hard sphere expansion and perturbation theories as well. Comparisons are also made with chemical potential simulation data, and for these data the new theory is competitive with perturbation theory.

900,478 PB89-229181

Not available NTIS National Inst. of Standards and Technology (NEL),

Boulder, CO. Thermophysics Div.
PVT Relationships in a Carbon Dioxide-Rich Mixture with Ethane.

G. J. Sherman, J. W. Magee, and J. F. Ely. 1989,

Pub. in International Jnl. of Thermophysics 10, n1 p47-59 Jan 89.

Keywords: *Thermochemistry, *Carbon dioxide, *Ethane, Mixtures, Temperature, Isotherms, Pressure, Keywords: Volume, Reprints.

Comprehensive isochoric PVT measurements have been obtained for the system (0.99 CO2 + 0.01 C2H6). The range of state points studied includes those with densities from 2 to 24 mol times dm(sup -3), temperatures from 245 to 400 K, and pressures to 35 MPa. Extensive comparisons have been made with two predictive conformal solution models, one which uses the 32-term BWR-type equation of Stewart and Jacobsen as a reference and the other using the newer Schmidt-Wagner functional form. Results obtained with the Schmidt-Wagner equation are better in the near-critical region owing to the flatter critical isotherm associated with this functional form.

900,479 PB89-230288 Not available NTIS National Inst. of Standards and Technology (NML), Gaithersburg, MD. Molecular Spectroscopy Div. Structure of the CO2-CO2-H2O van der Waals Complex Determined by Microwave Spectroscopy. Final rept.

K. I. Peterson, R. D. Suenram, and F. J. Lovas. 1989,

Pub. in Jnl. of Chemical Physics 90, n11 p5964-5970, 1 Jun 89.

Keywords: *Molecular structure, *Microwave spectroscopy, *Van der Waals equation, *Carbon monoxide, *Water, *Deuterium compounds, Molecular rotation, Dipole moments, Chemical bonds, Reprints, *Fourier transform spectroscopy.

spectra of CO2-CO2-H2O,CO2-CO2-D2O,(13)CO2-(13)CO2-H2O and CO2-CO2-H2(18)O have been measured using a pulsed-molecular-beam Fabry-Perot Fourier-transform microwave spectrometer. An asymmetric top spectrum is observed with rotational constants. The dipole moment was obtained. The orientation of the CO2 subunits in CO2-CO2-H2O is very similar to that observed in CO2-CO2 although the C-C bond length is 0.19 A shorter in the trimer. The

hydrogens of the H2O subunit are directed away from the CO2-CO2 plane although their angular orientation around the b axis is not well determined.

PB89-230296 Not available NTIS National Inst. of Standards and Technology (NML), Gaithersburg, MD. Molecular Spectroscopy Div. Infrared Spectrum of Sodium Hydride.

A. G. Maki, and W. B. Olson. 1989, 6p Pub. in Jnl. of Chemical Physics 90, n12 p6887-6892

Keywords: *Infrared spectroscopy, *Sodium hydrides, Molecular rotation, Molecular vibration, Molecular spectroscopy, Reprints.

The infrared spectrum of gaseous NaH from 886 to 1245/cm has been measured with a resolution of 0.015/cm at temperatures between 670 to 720 C. The v = 1 <- 0, 2 <- 1, and 3 <- 2 transitions have been observed and combined with rotational transitions measured by others to obtain appropriate rovibrational constants and Dunham potential constants. The Herman-Wallis intensity effect has been measured in order to estimate a transition moment of 0.31 + or -0.05 D for the v = 1 < 0 transition.

900,481 PB89-230320 Not available NTIS National Inst. of Standards and Technology (NML), Gaithersburg, MD. Inorganic Analytical Research Div. Determination of the Absolute Specific Conduct-

ance of Primary Standard KCi Solutions.

Final rept. Y. C. Wu, K. W. Pratt, and W. F. Koch. 1989, 14p Pub. in Jnl. of Solution Chemistry 18, n6 p515-528

Keywords: *Potassium chloride, *Solutions, *Resistance, *Primary standards, Electrolytes, Performance evaluation, Concentration(Composition), Reprints, Specificity.

A determination of the absolute specific conductance of KCl solutions is demonstrated. The measurement is based on the conductance cell with a well defined geometry, having a difference in the removable center tube of accurately measured dimensions. The specific conductance of the solution is obtained from the measured resistances of the cell with and without the center tube and the measured I/A ratio of the center tube. Specific conductances obtained using the cell agree with the previously accepted standards for 0.1 demal and 0.01 demal solutions within 0.02%. Results are also presented for solutions based on molality. The temperature control, bridge, and detector technology used to obtain results of this accuracy are described.

900,482 PB89-231054 Not available NTIS National Inst. of Standards and Technology (NEL), Gaithersburg, MD. Building Environment Div. Thermophysical-Property Needs for the Environ-

mentally Acceptable Halocarbon Refrigerants.

M. O. McLinden, and D. A. Didion. 1989, 14p Pub. in International Jnl. of Thermophysics 10, n3, p563-576, May 89.

Keywords: *Refrigerants, *Thermodynamic properties, *Halohydrocarbons, Transport properties, Mixtures, Environmental impacts, Reprints, *Working fluids.

The need for and uses of thermodynamic and transport properties in the selection of working fluids for the vapor compression cycle and in equipment design are reviewed. A list of hydrogen-containing halocarbons, as well as their mixtures, is presented as alternatives to the environmentally harmful, fully halogenated chlorofluorocarbons. These fluids range from wellcharacterized, widely available refngerants to materials available only by custom synthesis about which very little is known. Data priorities for these fluids are presented; most essential are critical point, vapor pressure, liquid density, ideal-gas heat capacity, and vapor p-V-T data. A critical need exists for these data on a number of candidate working fluids in order not to lose the opportunity to select the best set of future refrigerants.

PB89-231138 Not available NTIS National Inst. of Standards and Technology (NML), Gaithersburg, MD. Temperature and Pressure Div.

Pressure Fixed Points Based on the Carbon Dioxide Vapor Pressure at 273.16 K and the H2O(i) - H2O(ii) - H2O(L) Tripie-Point.

Final rept.

N. Bignell, and V. E. Bean. 1988, 10p Pub. in Proceedings of Seminar on High Pressure Standards, Paris, France, May 24-25, 1988, p175-184.

Keywords: *Pressure measurement, *Carbon dioxide, *Vapor pressure, *Water, *Ice, Metrology, *Triple point, Fixed points.

The vapor pressure of carbon dioxide in equilibrium with the liquid at 273.16 K has been measured and found to be 3.48608 + or - .00017 MPa. Results were found to depend upon the purity of the carbon dioxide. Samples prepared by heating analytical reagent quality sodium bicarbonate were of sufficient purity to be suitable for use as a pressure fixed point. The pressure of the H20(U)-H20(III)-H2)(L) triple-point has also been measured and found to be 208.829 + or - 0.025 MPa.

900,484 PB89-231252 PB89-231252 Not available NTIS National Inst. of Standards and Technology (NML), Gaithersburg, MD. Molecular Spectroscopy Div. Stabilization and Spectroscopy of Free Radicals and Reactive Molecules in Inert Matrices.

Final rept.

M. E. Jacox. 1989, 31p Pub. in Chemistry and Physics of Matrix-Isolated Species, p75-105 1989.

Keywords: *Free radicals, Infrared spectra, Ultraviolet spectra, Stabilization, Photolysis, Spectroscopy, Reprints, *Matrix isolation, Atom-molecule collisions.

Characteristics of the infrared and ultraviolet spectra of free radicals isolated in inert matrices are surveyed. Technique by which free radicals have been stabilized in matrices in concentration sufficient for optical spectroscopic detection are reviewed and are illustrated by recent studies. Emphasis is placed on the characteris-tics of atomic diffusion in rare gas matrices and on the consequences of the occurrence of cage recombination in the photolytic generation of free radicals in mat-nces. The stabilization of free radicals by matrix isola-tion sampling of discharge systems is discussed. The role of atom-molecule reactions in free radical stabilization is illustrated by specific consideration of reactions involving H, various metal atoms, C, Si, O, S, and

900,485

PB89-231294 Not available NTIS National Inst. of Standards and Technology (NML), Gaithersburg, MD. Surface Science Div. Electron Transmission Through NiSi2-Si inter-

Final rept. M. Stiles, and D. R. Hamann. 1989, 4p Pub. in Physical Review B 40, n2 p1349-1352, 15 Jul

Keywords: *Electron mobility, *Silicon, *Nickel, *Interfaces, Computation, Epitaxy, Orientation, Surface chemistry, Reprints, *Nickel silicides.

Calculations of electron transmission through epitaxial NiSi2/Si(111) interfaces illustrate the versatility of a newly developed first-principles technique. The transmission is poor and very dependent on the interface structure; of the electrons of primary importance for transport, more than 50% are reflected by the type-A orientation interface and more than 80% by the type B.

Not available NTIS PB89-231310 PB89-231310
National Inst. of Standards and Technology (NML), Gaithersburg, MD. Surface Science Div.
Methodology for Electron Stimulated Desorption ion Angular Distributions of Negative ions.

Final rept.

S. A. Joyce, A. L. Johnson, and T. E. Madey. 1989, Sponsored by Department of Energy, Washington, DC. Pub. in Jnl. of Vacuum Science and Technology A7, n3

p2221-2226 May/Jun 89.

Keywords: *Desorption, Nitrogen fluorides, Acetone, Ruthenium, Surfaces, Reprints, *Negative ions, Electron stimulated desorption, Phosphorus fluorides, Time-of-flight method, Angular distribution, Hexafluoroacetone.

The electron stimulated desorption angular distributions technique has been extended to measure the angular distributions of negative ions desorbing from sur-faces. The apparatus is a modification of an existing display-type detector. Time-of-flight methods have been employed to separate the negative ions from the large background of electrons and to permit mass-re-solved measurements of both positive and negative ions. General trends in negative ion desorption from a series of fluorinated molecules (PF3, NF3, and hexa-fluoroacetone) adsorbed on Ru(0001) are presented. In these systems, negative ions arise primarily from molecularly intact adsorbates while positive ions can arise from both intact and dissociated species with similar probability.

900,487 PB89-234199 Not available NTIS National Inst. of Standards and Technology (NML), Gaithersburg, MD. Molecular Spectroscopy Div.

Vibrational Spectra of Molecular Ions Isolated In Solid Neon. I. CO(sub 2, sup +) and CO(sub 2, sup -

Final rept.
M. E. Jacox, and W. E. Thompson. 1989, 7p
Sponsored by Army Research Office, Research Triangle Park, NC. Pub. in Jnl. of Chemical Physics 91, n3 p1410-1416, 1 Aug 89.

Keywords: *Vibrational spectra, Infrared spectra, Absorption spectra. Solidified gases, Neon, Reprints, *Carbon dioxide ions, Neon atoms, Photoionization, Photodetachment, Matrix isolation, Molecular ions.

When a Ne:CO2 sample was codeposited at approximately 5 K with a beam of neon atoms that had been excited in a microwave discharge, an absorption appeared at 1421.7/cm very near the gas-phase band center for the antisymmetric stretching fundamental (nu sub 3) of CO2(1+). Detailed isotopic substitution studies support the assignment of this absorption to that fundamental of CO2(1+), as well as of an absorption at 1658.3/cm to nu sub 3 of CO2(1-). In earlier studies of the charge transfer interaction of an alkali metal with CO2, this vibration of CO2(1-) had been strongly perturbed by coordination with the alkali metal cation. In the present experiments, the threshold for electron photodetachment from CO2(1-) was observed in the visible spectral region. Evidence was also obtained for the stabilization of the O2C...OCO(1-) cluster anion.

900,488 PB89-234207 Not available NTIS National Inst. of Standards and Technology (NML), Gaithersburg, MD. Molecular Spectroscopy Div. Vibrational Predissociation in the H-F Stretching Mode of HF-DF.

Final rept.
G. T. Fraser, and A. S. Pine. 1989, 4p
Pub. in Jnl. of Chemical Physics 91, n2 p633-636, 15

Keywords: *Hydrogen fluoride, Deuterium compounds, Infrared spectra, Hydrogen bonds, Molecular beams, Vibrational spectra, Reprints, *Complexes, Color center lasers, Laser spectroscopy, Predissociation,

The high-resolution infrared spectrum of the K=1-0 subband of the H-F stretching vibrational band of the hydrogen-bonded HF-DF complex has been recorded using a molecular-beam electric resonance optother-mal color-center-laser spectrometer. The spectrum exhibits minor perturbations and vibrational predissocia-tion linewidths of 23 + or - 2 MHz full width at halfmaximum for comparison to the 11 + or - 1 MHz widths found for the corresponding mode of the homonuclear HF-HF dimer.

900,489 PB89-234215 PB89-234215
Not available NTIS
National Inst. of Standards and Technology (NML),
Gaithersburg, MD. Molecular Spectroscopy Div.
Microwave and Infrared Electric-Resonance Optothermal Spectroscopy of HF-HCl and HCl-HF. Final rept.

G. T. Fraser, and A. S. Pine, 1989, 9p. Pub. in Jnl. of Chemical Physics 91, n2 p637-645, 15

Keywords: *Hydrogen chloride, *Hydrogen fluoride, Infrared spectroscopy, Microwave spectroscopy, Hydrogen bonds, Reprints, *Complexes, Van der Waals forces, Isomers.

Microwave and infrared spectra of HF-HCl and HCl-HF have been obtained using a molecular-beam electricresonance optothermal spectrometer, which operates by quadrupole-field focusing of polar molecules onto a bolometer detector. The HF-HCI microwave measurements extend to K(alpha)=1, the previous K(alpha)=0 results of Janda, Steed, Novick, and Klemperer, allowing the determination of the K(alpha) dependence and asymmetry of the CI quadrupole coupling constant. For the metastable HCI-HF isomer no previous spectroscopic measurements have been re-ported. Here, microwave spectra are observed for the K(alpha) = 0 and K(alpha) = 1 states and interpreted in terms of an L-shaped hydrogen-bonded structure for the complex, with a 3.235 A center-of-mass separation between the HF and HCl subunits.

900,490

PB89-234256 Not available NTIS Not available NTS
National Inst. of Standards and Technology (NML),
Boulder, CO. Quantum Physics Div.
High-Resolution, Slit Jet Infrared Spectroscopy of
Hydrocarbons: Quantum State Specific Mode

Mixing In CH Stretch-Excited Propyne. Final rept.

A. McIroy, and D. J. Nesbitt. 1989, 10p Grants NSF-PHY86-04504, NSF-CHE86-05970 Sponsored by National Science Foundation, Washington, DC.

Pub. in Jnl. of Chemical Physics 91, n1 p104-113, 1 Jul

Keywords: *Hydrocarbons, *Infrared spectroscopy, Reprints, *Propyne, Laser spectroscopy, High resolution, Vibrational states, Supersonic jet flow.

A direct absorption, difference frequency, infrared laser spectrometer with 0.0001/cm resolution combined with slit supersonic jet optical pathlengths is presented as a tool for the study of mode-mode vibrational coupling in laser-excited hydrocarbons. These weak mode-mode couplings are evidenced in frequency domain studies by virtue of transitions to isolated upper J states that are split into multiplets under sub-Doppler resolution. Instrument performance is demonstrated by investigating vibrational coupling in the 3000-3300/cm C-H stretch fundamental region of (12)C3 propyne, as well as the (12)C2(13)C propynes observed in natural isotopic abundance. The implications of apharmacia coupling partial planets of the tions of anharmonic coupling matrix elements of the magnitude found in the study, in overtone vibrational dynamics, are discussed.

900.491

PB89-234264 Not available NTIS National Inst. of Standards and Technology (NML), Boulder, CO. Quantum Physics Div. Observation of Translationally Hot, Rotationally

Cold NO Molecules Produced by 193-nm Laser Vaporization of Multilayer NO Films. Final rept.

L. M. Cousins, R. J. Levis, and S. R. Leone. 1989, 4p

Sponsored by Army Research Office, Research Triangle Park, NC Pub. in Jnl. of Physical Chemistry 93, n14 p5325-5328

Keywords: *Nitrogen oxide(NO), Spin orbit interactions, Far ultraviolet radiation, Surfaces, Films, Cryogenics, Reprints, Rotational states, Laser heating, Vaporization, Multilayers.

Results are presented for the rotational and spin-orbit state excitation of NO molecules which are ejected at hyperthermal velocities by 193-nm laser vaporization of cryogenic multilayer NO films condensed on MgF2. For molecules with translational energies of 0.14 and 0.56 eV, the average rotational energies are 0.014 and 0.50 eV, the average rotational energies are 0.014 and 0.017 eV, corresponding to temperatures of 160 and 180 K, respectively. The spin-orbit population ratio for the 0.14-eV molecules is 0.35 (T approx = 170 K); however, the population ratio for the 0.56-eV molecules is higher, 0.7 (T approx = 500 K). The disequilibrium between translation and rotation may be due in part to a collisional cooling mechanism (adiabatic expansion) which occurs immediately following varorizapansion) which occurs immediately following vaporization. Other dynamical ejection mechanisms are also discussed.

900.492

PB89-234280 Not available NTIS National Inst. of Standards and Technology (NML), Boulder, CO. Quantum Physics Div.

Reduced Dimensionallty Quantum Reactive Scattering Study of the Insertion Reaction O(1D) + H2 - > OH + H. Final rept.

J. K. Badenhoop, H. Koizumi, and G. C. Schatz. 1989. 8p

Pub. in Jnl. of Chemical Physics 91, n1 p142-149, 1 Jul

Keywords: Hamiltonian furictions, Oxygen, Hydrogen, Reprints, *Insertion reactions, Quantum reactive scattering, Hyperspherical coordinates, Hydroxyl radicals, Two degrees of freedom.

The paper presents a two degree of freedom model for describing the quantum dynamics of the insertion reaction O(singlet D)+H2 in which bend motions are treated with a sudden approximation. Comparison of product state vibrational distributions from a classical version of the model with three dimensional trajectory results indicates that the model is realistic. Quantum/ classical comparisons for the model Hamiltonian indicate that recrossing is more important in the quantum dynamics, and as a result, the quantum reaction probability from ground state reagents is lower by as much as 40%. In addition, the quantum vibrational state dis-tribution shows higher excitation than its classical counterpart. This difference in excitation is due to trajectories that produce vibrationally cold products, and it is found that these trajectories always cross the deepest part of the H20 well.

900 493

PB89-235204 PC A19/MF A01 National Inst. of Standards and Technology (NEL), Gaithersburg, MD. Thermophysics Div.

Properties of Lennard-Jones Mixtures at Various Temperatures and Energy Ratios with a Size Ratio of Two.

Technical note.

M. L. Huber, and J. F. Ely. May 89, 429p NIST/TN-

Also available from Supt. of Docs. as SN003-003-02952-1.

Keywords: *Mixtures, Computerized simulation, Distribution functions, Tables(Data), *Lennard-Jones fluids, Lennard-Jones potential, Molecular dynamics, Mean density approximation, Correlation functions.

Results are presented of molecular dynamics computer simulations for binary Lennard-Jones mixtures with a size ratio of two. A total of 84 state points were investigated at seven compositions ranging from 5% to 95% of the small molecule energy ratios from 0.5 to 3.0 and three reduced temperatures. In addition to the thermodynamic results, extensive tabular data are given for the radial distribution functions, local compositions and the direct correlation functions. The authors also discuss several theories of dense fluid mixtures and give a new approximation for the radial distribution function of a pair in a mixture, which they call the modified mean density approximation. The predictions of various thermodynamic quantities from the different liquid mixture models are compared with simula-tion results. For mixtures with large size differences, the modified mean density approximation was found to be competitive with first order, Lee-Levesque type statistical mechanical perturbation theory.

900,494

PB90-117318 Not available NTIS National Inst. of Standards and Technology (NEL), Gaithersburg, MD. Thermophysics Div.
Application of the Gibbs Ensemble to the Study of Symmetric Non-Additive Hard Spheres.

J. G. Amar. 1989, 7p Pub. in Molecular Physics 67, n4 p739-745 1989.

Keywords: *Fluids, Monte Carlo method, Spheres, Separation, Reprints, *Phase studies, Binary mixtures, Gibbs ensemble.

The 'Gibbs' Monte Carlo method introduced by Pana-The 'Gibbs' Monte Carlo method introduced by Pana-giotopoulos to study coexisting phases is applied to the study of fluid-fluid phase equilibrium in a binary system of symmetric, non-additive hard spheres. It was found that the method is generally applicable, al-though requiring a significantly larger number of inser-tions per Monte Carlo step at higher densities than in the previously studied cases of gas-liquid binary mixtures. Also studied was the effects of different initial

conditions in the simulations and the effects of varying system size (number of particles) on the results.

900,495
PB90-117342
Not available NTIS
National Inst. of Standards and Technology (NML),
Boulder, CO. Time and Frequency Div.
Detection of the Free Radicals FeH, CoH, and NIH

by Far Infrared Laser Magnetic Resonance. Final rept. S. P. Beaton, K. M. Evenson, T. Nelis, and J. M.

Brown. 1988, 3p Pub. in Jnl. of Chemical Physics 89, n7 p4446-4448, 1

Keywords: *Interstellar matter, Rotational spectra, Free radicals, Far infrared radiation, Stellar spectra, Infrared detection, Reprints, *Cobalt hydrides, *Iron hydrides, *Nickel hydrides, Laser magnetic resonance, Infrared astronomy.

The authors report the detection of rotational transitions of the free radicals FeH, CoH, and NiH. The measurements were made in the far infrared (FIR) between 50-90/cm using laser magnetic resonance. Signal-to-noise ratios of over 1000 with a 1 s time constant were obtained on the strongest lines of all three species. These metal hydrides are expected to be abundant in the interstellar medium, and optical emission spectra of FeH have been detected in many stellar spectra. Precise ground state rotational transition frequencies are needed for radio and FIR astronomical searches and will be provided from an analysis of the authors' spectra.

900,496
PB90-117359
Not available NTIS
National Inst. of Standards and Technology (NML),
Boulder, CO. Time and Frequency Div.
Far-Infrared Laser Magnetic Resonance Spectrum
of the CD Radical and Determination of Ground
State Parameters.
Final rept.

J. M. Brown, and K. M. Evenson. 1989, 18p Contracts NASW-15, NASW-047 Sponsored by National Aeronautics and Space Administration. Washington DC

istration, Washington, DC. Pub. in Jnl. of Molecular Spectroscopy 136, p68-85

Keywords: Far infrared radiation, Deuterium compounds, Infrared spectra, Free radicals, Ground state, Reprints, *Carbon hydrides, Laser magnetic resonance.

The far-infrared laser magnetic resonance spectrum of the CD radical in the nu=0 level of the X doublet pi state has been studied in detail. Twelve transitions which are accessible with currently available laser lines have been recorded. The measurements have been analyzed and subjected to a single least-squares fit using an effective Hamiltonian. The data provide primary information on the rotational and fine-structure intervals between the lowest rotational intervals. They also yield values for the Lambda-type doubling and deuteron hyperfine splittings in the same levels. Combination of the measurements with the corresponding data for CH allows the two parameters, gamma and A sub D, to be determined separately.

900,497
PB90-117433
Not available NTIS
National Inst. of Standards and Technology (NML),
Gaithersburg, MD. Molecular Spectroscopy Div.
Electric-Resonance Optothermal Spectrum of
(H2O)2: Microwave Spectrum of the K=1-0 Subband for the E((+ or -)2) States.
Final rept.

G. T. Fraser, R. D. Suenram, L. H. Coudert, and R. S. Frye. 1989, 4p Pub. in Jnl. of Molecular Spectroscopy 137, p244-247 1989.

Keywords: *Microwave spectroscopy, *Molecular spectroscopy, *Water, Hydrogen bonds, Dimerization, Electron transitions, Reprints, *Electron tunneling.

Microwave spectra of (H2O)2 have been obtained using an electric-resonance optothermal spectrometer (EROS). The microwave measurements extend previous results on the K=0-0 and K=1-0 bands for the A2(+/-) and B2(+/-) rotational-tunneling states and include the first observations of the weak c-type K=1-0 band for the E2(+/-) states. The results allow a near direct determination of the h2v tunneling matrix element that is associated with the tunneling motion

which interchanges the two hydrogens on the acceptor H2O molecule and the two hydrogens on the donor H2O molecule. It was found that $h2v = 743 \, \text{MHz}$.

900.498
PB90-117441
Not available NTIS
National Inst. of Standards and Technology (NML),
Gaithersburg, MD. Molecular Spectroscopy Div.
Rotational Energy Levels and Line Intensities for (2S+1)Lambda-(2S+1) Lambda and (2S+1)(Lambda + or -)-(2S+1)Lambda Transitions in a Diatomic Molecule van der Waals Bonded to a Closed Shell Partner.
Final rept.

W. M. Fawzy, and J. T. Hougen. 1989, 12p Pub. in Jnl. of Molecular Spectroscopy 137, p154-165 1989.

Keywords: Spin orbit interactions, Diatomic molecules, Hamiltonian functions, Spectral lines, Rare gases, Reprints, *Complexes, *Rotational states, Van der Waals forces, Matrices, Renner-Teller splitting.

Hamiltonian matrix elements needed for calculating rotational energy levels are derived for a planar complex consisting of an open-shell diatomic molecule and a closed-shell partner. These matrix elements take account of spin-orbit interaction and a Renner-Teller-like splitting term, but not of the effects of large-amplitude internal rotation of the diatomic fragment within the complex. Transition-moment matrix elements needed for calculating intensities in spin and orbitally allowed transitions in the open-shell diatomic sup (2S+1)Lambda - sup (2S+1) and sup (2S+1)(Lambda plus or minus 1) sup (2S+1)Lambda, where Lambda = Sigma, Pi, Delta, Phi, eta. A brief discussion of how to use the Hamiltonian and transition-moment matrix elements in a computer program is given.

900,499
PB90-117557
National Inst. of Standards and Technology (IMSE),
Boulder, CO. Fracture and Deformation Div.
Ultrasonic Separation of Stress and Texture Effects in Polycrystalline Aggregates.
Final rept.

P. P. Delsanto, R. B. Mignogna, and A. V. Clark. 1987, 8p

Sponsored by Office of Naval Research, Arlington, VA. Pub. in Review of Progress in Quantitative Nondestructive Evaluation, v6B p1533-1540 1987.

Keywords: *Aggregates, *Polycrystalline, *Determination of stress, *Texture, Plates(Structural members), Rayleigh waves, Metal plates, Error analysis, Nondestructive tests, Alloys, Reprints, *Ultrasonic testing.

The general perturbation formalism for the propagation of Rayleigh waves on the surface of initially deformed anisotropic material plates is applied to the problem of separation of material texture and stress. The preferential alignment of crystallographic axes in a polycrystalline material is described in terms of their orientation distribution function. The authors considered explicitly the case of an orthotropic distribution of cubic crystallites, which occurs, for example, in aluminum and steel alloys. The measured values of the Rayleigh wave phase velocity at different angles on the material plate can be used for the determination, in a reference plate with similar texture, of the three coefficients W(400), W(420) and W(440), which characterize the orientation distribution. An extension of the formalism separates the acoustoelastic effects of the initial stresses. An error analysis and a comparison with similar textuniques using grazing SH-waves complete the discussion.

900,500
PB90-117656
Not available NTIS
National Inst. of Standards and Technology (NML),
Gaithersburg, MD. Molecular Spectroscopy Div.
Photoacoustic Measurement of Differential Broadening of the Lambda Doublets in NO(X (2)PI 1/2,
V=2-0) by Ar.

Final rept.
A. S. Pine. 1989, 8p
Sponsored by National Aeronautics and Space Administration, Washington, DC.
Pub. in Jnl. of Chemical Physics 91, n4 p2002-2009, 15
Aug 89.

Keywords: *Nitrogen oxide(NO), Ground state, Argon, Reprints, *Nitric oxide, Photoacoustic spectroscopy, Pressure broadening, Color center lasers, Tunable lasers.

A differential broadening of the Lambda doublets in the v=2-0 overtone band of the doublet Pi(1/2) ground electronic state of NO in an Ar buffer gas has been observed by photoacoustic spectroscopy using a tunable color-center laser. The broadening coefficients for the f symmetry components are larger than for the e symmetry components by up to about 6% for J about 16.5. The differential depends on J and vanishes at low J, implicating the anisotropy of the unpaired electron Pi orbital in the plane of rotation. The doublet Pi(3/2) transitions are slightly broader than the doublet Pi(1/2) as a result of spin-flipping collisional relaxation. The observed line shapes also exhibit collisional or Dicke narrowing due to velocity-changing collisions.

900.501

PB90-117706 Not available NTIS National Inst. of Standards and Technology (NML), Gaithersburg, MD. Atomic and Plasma Radiation Div. Chlorine-Ilke Spectra of Copper to Molybdenum. Final rept.

V. Kaufman, J. Sugar, and W. L. Rowan. 1989, 3p Sponsored by Department of Energy, Washington, DC. Pub. in Jnl. of the Optical Society of America B 6, n8 p1444-1446 Aug 89.

Keywords: *Spectrum analysis, *Atomic energy levels, *Chlorine, Comparison, Dirac equation, Hartree-Fock approximation, Arsenic, Bromine, Copper, Gallium, Germanium, Krypton, Niobium, Molybdenum, Rubidium, Selenium, Strontium, Yttnium, Zinc, Zirconium, Reprints, *Laser spectroscopy, *Tokamak devices.

Spectra of Cu to Mo (except for Rb and Sr) were generated in tokamak and laser-produced plasmas and observed photographically. Six lines have been identified in each of the spectra as Cl-like 3s(sub 2)3p(sup 5)-3s(sup 2)3p(sup 4)3d transitions. Wavelengths in the range of 75-150 A, measured with an uncertainty of + or -0.005 A, are given. Line classifications were made by comparing the observed wavelengths and relative intensities with those calculated using the relativistic average-of-configuration Hartree-Fock code of Cowan. Predicted values for the corresponding wavelengths of Cl-like Rb and Sr were obtained from these comparisons, with an uncertainty of + or -0.010 A.

900.502

PB90-117714 Not available NTIS National Inst. of Standards and Technology (NML), Gaithersburg, MD. Ionizing Radiation Physics Div. Mechanistry of Benzene.

Final rept.

L. R. Karam, and M. G. Simic. 1989, 5p Pub. in Environmental Health Perspectives 82, p37-41 1989.

Keywords: *Benzene, *Tyrosine, *Biochemistry, Gas chromatography, Mass spectroscopy, Muscles, Tissue(Biology), Laboratory animals, Reprints, *Chemical reaction mechanisms, *Hydroxyl radicals, *Biological indicators, Free radicals.

o-Tyrosine (o-Tyr) was used as a specific biomarker for OH radicals generated in biosystems. Specificity of o-Tyr as an OH biomarker was based on previous studies in systems exposed to ionizing radiations. Fresh muscle tissue incubated with benzene for 1 hr at 38 C exhibits formation of o-Tyr as seen in the cases of ethanol- and carbon tetrachloride-exposed systems. Gas chromatography/mass spectrometry selective ion monitoring measurements of o-Tyr yields in chicken breast muscle incubated with water or benzene indicate levels of less than 0.1 ppm and 3.0 + or - 0.5 ppm of o-Tyr, respectively. Formation of OH is presumed to originate via a Haber-Weiss reaction of H2O2 with Fe(II) preceded by the formation of O2 and H2O2 from distorted mitochondria.

900,503

PB90-117748 Not available NTIS National Inst. of Standards and Technology (NML), Gaithersburg, MD. Molecular Spectroscopy Div. Production and Spectroscopy of Molecular Ions Isolated in Solid Neon.

Final rept. M. E. Jacox, and W. E. Thompson. 1989, 24p Sponsored by Army Research Office, Research Triangle Park, NC.

gle Park, NC. Pub. in Research on Chemical Intermediates 12, p33-56 1989.

Keywords: "Chemical stabilization, "Infrared spectroscopy, "Neon, "Ionization, "Chemical analysis, Molecular structures, Molecular energy levels, Reviews, Carbon dioxide, Oxygen, Carbonyl compounds, Photochemical reactions, Reprints, "Matrix isolation technique, "Fourier transform spectroscopy.

The paper reviews recent studies of the stabilization and infrared spectra of small molecular ions and cluster ions in a neon matrix. The products of the interac-tion between the molecule of interest and a beam of excited neon atoms are trapped in an excess of solid neon, and their Fourier transform infrared spectrum is obtained. Detailed isotopic substitution studies aid in product identification, as does the study of infrared spectra obtained after exposure of the sample to filfor CO2+, CO2-, O4+, O4-, N4+, (CO)2+, and (CO)2- demonstrate the usefulness of the technique and yield new information on the structures and molecular energy levels of these species.

900,504

PB90-117763 Not available NTIS National Inst. of Standards and Technology (IMSE), Gaithersburg, MD. Metallurgy Div. Formation of the Al-Mn Icosahedral Phase by Elec-

trodeposition. Final rept.

B. Grushko, and G. R. Stafford. 1989, 6p

Grant N00014-88-F-0091 Sponsored by Office of Naval Research, Arlington, VA. Pub. in Scripta Metallurgica 23, n7 p1043-1048 1989.

Keywords: *Electrodeposition, *Crystal structures, *Aluminum manganese alloys, Temperature, Fused salts, Diffusion, Metastable state, Repnits, *Icosahedrons, Amorphous state, Quasi-steady states.

Amorphous, quasicrystalline and metastable crystal-line structures have been observed in binary alumiine structures have been observed in binary auminum-manganese alloys electrodeposited from chloroaluminate electrolytes. During electrodeposition, the extent of the deviation from equilibrium as well as the degree of ordering is defined by the concurrent processes of new layer formation and surface diffusion. The metastable arnorphous phase can be formed quite easily by low temperature electrodeposition. The direct formation of quasicrystals, having a level of free energy between that of an amorphous and a stable crystalline phase, can be achieved by an increase in deposition temperature in a manner somewhat analogous to that which has been reported for sputter deposition. An increase in the temperature causes a gradual increase in the size of icosahedral regions.

900,505

PB90-117771 Not available NTIS National Inst. of Standards and Technology (NML), Gaithersburg, MD. Radiation Physics Div. Resonance Enhanced Electron Stimulated Desorp-

tion.

Final rept.

J. W. Gadzuk, and C. W. Clark. 1989, 8p Pub. in Jnl. of Chemical Physics 91, n5 p3174-3181, 1 Sep 89.

Keywords: Resonance scattering, Palladium, Reprints, *Electron stimulated desorption, Oxygen atoms.

A theory is presented which accounts for giant enhancements in electron stimulated desorption (ESD) yields from adsorbate-covered surfaces if the incident electrons become trapped in a shape or Feshbach resonance associated with the adsorbate. The resulting temporary negative ion is displaced inwards towards the surface as a result of the force provided by the image screening charge. Upon reneutralization, the desorbate can be returned high on the dissociative repulsive wall of the neutral-surface potential curve. The process has been modeled within the context of semi-classical Gaussian wave packet dynamics. Recent ob-servations of such giant enhancements in the ESD yields for the system O(alpha)/Pd(111) are explained in terms of the model, and an atomic physics basis for the resonance in atomic oxygen is proposed.

900.506

PB90-117797 PB90-117797 Not available NTIS National Inst. of Standards and Technology (NML), Boulder, CO. Time and Frequency Div.

Heterodyne Measurements on N2O Near 1635 cm(-

1). Final rept. Van M. D. Vanek, M. Schneider, J. S. Wells, and A. G.

Maki. 1989, 5p
Sponsored by National Aeronautics and Space Administration, Washington, DC.
Pub. in Jnl. of Molecular Spectroscopy 134, p154-158

1989.

Keywords: *Nitrogen oxide(N2O), *Infrared spectroscopy, *Molecular spectroscopy, Calibrating, Reprints, Heterodyning.

Heterodyne frequency measurements have been made on eight lines of the 10(sup 0)0-01(sup 1)0 band N2O between 1591 and 1673/cm. These measurements were combined with other heterodyne frequency measurements to obtain improved frequency values for the 01(sup 1)0-00(sup 0)0 transitions from 520 to 660/cm

900,507 PB90-117805 Not available NTIS National Inst. of Standards and Technology (NML), Boulder, CO. Time and Frequency Div.
Heterodyne Frequency and Fourler Transform
Spectroscopy Measurements on OCS Near 1700 cm(-1).

Final rept. J. S. Wells, M. D. Vanek, and A. G. Maki. 1989, 5p Sponsored by National Aeronautics and Space Administration, Washington, DC. Pub. in Jnl. of Molecular Spectroscopy 135, p84-88

Keywords: *Infrared spectroscopy, *Fourier transfor-mation, Demodulation, Calibrating, Molecular spectroscopy, Spectrum analysis, Microwave spectroscopy, Repnits *Carbon oxysulfide, *Heterodyning.

Heterodyne frequency measurements are given for carbonyl sulfide in the 1700/cm region. The measurements were combined with Fourier transform spectroscopy measurements of the same bands and with other measurements in the literature (microwave, submillimeter wave, and other infrared measurements) in a least-squares fit. The combined data and fit result in improved frequency calibration values for the 1700/ cm region and also allow the determination of calibration values for the 00(sup 0)3-00(sup 0)0 band near 2550/cm from application of the Ritz principle.

PB90-117821

Not available NTIS National Inst. of Standards and Technology (NML), Gaithersburg, MD. Atomic and Plasma Radiation Div. Analysis of Magnesiumlike Spectra from Cu XVIII to Mo XXXI.

Rowan. 1989, 7p Pub. in Jnl. of the Optical Society of America B 6, n8

p1437-1443 Aug 89.

Keywords: *Spectrum analysis, *Atomic energy levels, *Magnesium; Comparison, Dirac equation, Hartree-Fock approximation, Arsenic, Strontium, Selenium, Rubidium, Niobium, Molybdenum, Bromine, Copper, Gal-lium, Germanium, Krypton, Yttnum, Zinc, Zirconium, Reprints, *Laser spectroscopy, *Tokamak devices.

The magnesium like spectra of Cu to Mo have been observed with laser- and tokamak-generated plasmas in the range of 1000-300 A. The authors give wave-lengths accurate to + or -0.005 A and classifications of transitions among the 3s doublet, 3p doublet, 3d doublet, 3s3p, 3s3d, and 3p3d configurations. Com-parisons with Dirac-Fock calculations of the wavelengths are presented.

900,509 PB90-117839 Not available NTIS Not available NTIS.

National Inst. of Standards and Technology (NML),
Gaithersburg, MD. Molecular Spectroscopy Div.

Microwave Spectrum of Methyl Amine: Assignment and Analysis of the First Torsional State. Final rept.

N. Ohashi, S. Tsunekawa, K. Takagi, and J. T. Hougen. 1989, 14p Pub. in Jnl. of Molecular Spectroscopy 137, p33-46

Keywords: *Microwave spectroscopy, *Spectrum analysis, *Torsional strength, Molecular rotation, Electron tunneling, Stark effect, Reprints, *Amine/methyl.

The microwave absorption spectrum of methyl amine has been reinvestigated in the range from 7 to 90 GHz, with the aim of analyzing the first torsional state in more detail. By combining the newly obtained micro-wave data with the far-infrared and microwave data already available, it was possible to make an analysis of the tunneling-rotational levels of the first torsional state in which three types of delta K=+ or - 1 elements were introduced into the Hamiltonian matrix described in the group-theoretical formalism developed previously. Stark effect data, remeasured during the present study, are also examined in connection with the delta K = + or - 1 interaction.

900.510

Not available NTIS
National Inst. of Standards and Technology (NML),
Gaithersburg, MD. Molecular Spectroscopy Div.
Microwave Spectrum, Structure, and Electric
Dipole Moment of Ar-Ch3OH.
Final rept.

R. D. Suenram, F. J. Lovas, G. T. Fraser, J. Z. Gillies, C. W. Gillies, and M. Onda. 1989, 11p Pub. in Jnl. of Molecular Spectroscopy 137, p127-137

Keywords: Microwave spectra, Deutenum compounds, Dipole moments, Stark effect, Molecular structure, Reprints, *Argon complexes, Fourier transform spectros-copy, Van der Waals forces, Electric dipoles, Metha-

Microwave spectra of Ar-CH3OH, Ar-CD3OH, and Ar-(13)CH3OH have been measured between 7 and 25 GHz using a pulsed-nozzle Founer transform microwave spectrometer. Two tunneling states are ob-served which correlate to the A and E internal-rotor states of free methanol. The electric-dipole-moment components are determined. The structure of the complex is found to be T-shaped with an Ar to CH3OH center-of-mass separation of 3.684(14) A. A number of transitions are observed which do not appear to fit an asymmetrical-top Hamiltonian. These are assigned to an E tunneling state of the complex.

900,511

PB90-117862 Not available NTIS National Inst. of Standards and Technology (NEL), Gaithersburg, MD. Electrosystems Div. Collisional Electron Detachment and Decomposi-

tion Rates of SF6(1-), SF5(1-), and F(1-) in SF6: im-plications for ion Transport and Electrical Discharges.

Final rept. Champion, and L. D. Doverspike. 1989, 8p Sponsored by Department of Energy, Washington, DC. Pub. in Jnl. of Chemical Physics 91, n4 p2261-2268, 15

Keywords: *Sulfur hexafluoride, *Sulfur fluorides, Electric discharges, Decomposition, Reaction kinetics, Reprints, *Fluorine ions, *Electron detachment, Charge transfer, Negative ions, Ion mobility.

Measured cross sections for prompt collisional detachment and decomposition of SF6(1-), SF5(1-), and F(1-) in SF6 are used to calculate detachment coefficients and ion-conversion reaction coefficients as functions of electric field-to-gas density ratio (E/N) for ion drift in SF6. The calculated detachment and reaction coefficients are used in a model which invokes detachment from long-lived energetically unstable states of colli-sionally excited SF6(1-) to explain the pressure de-pendence of previously measured detachment coeffi-cients and the high detachment thresholds implied by analysis of electrical-breakdown probability data for

900,512

PB90-117870 Not available NTIS Mational Inst. of Standards and Technology (NEL), Gaithersburg, MD. Electrosystems Div. Electron-Energy Dependence of the S2F10 Mass Spectrum.

Final rept. J. K. Olthoff, R. J. Van Brunt, and I. Sauers. 1989, 3p Sponsored by Department of Energy, Washington, DC. Pub. in Jnl. of Physics D: Applied Physics 22, p1399-1401 1989.

Keywords: *Sulfur fluorides, *Mass spectra, Sulfur hexafluoride, Gas ionization, Detection, Reprints, Electron impact, Positive ions, eV range 10-100.

The positive-ion mass spectrum of S2F10 has been measured as a function of electron-impact energy in the range 20-70 eV using quadrupole mass spectrom-eter. Contrary to recent results from mass spectromet-ric analysis of arc-decomposed SF6 there was no evidence of S2F9(1+) or S2F10(1+) ion formation from S2F10 at any energy. The largest ion observed at all electron energies is SF5(1+). It was found, however, that the appearance potentials for SF5(1+) and SF3(1+), the two most prominent ions from S2F10, are significantly lower than the appearance potentials of the same ions from SF6. The differences between the mass spectra of S2F10 and SF6 are delineated and the implications for detection of S2F10 in the presence of SF6 are discussed.

900,513 PB90-117920 Not available NTIS National Inst. of Standards and Technology (NML), Gaithersburg, MD. Chemical Thermodynamics Div. Biological Thermodynamic Data for the Calibration of Differential Scanning Calorimeters: Heat Capac-Ity Data on the Unfolding Transition of Lysozyme in Solution.

Final rept. F. P. Schwarz. 1989, 21p Pub. in Thermochimica Acta 147, p71-91 1989.

Keywords: *Thermodynamics, Enthalpy, Chemical analysis, Reprints, *Differential scanning calonmetry,

Differential scanning calorimetry measurements of the unfolding transition of lysozyme in HCl-glycine buffer solutions were performed over a temperature range from 326 K at pH 2.3 to 349 K at pH 3.9. Van't Hoff transition enthalpies were calculated from the fit of a two-state transition model to the heat capacity measurements. urements (Delta Hvf), from the van't Hoff plot of In(1/K) vs. 1/T where K is the transition equilibrium constant, and from the ratio of the transition peak height to the area under the transition peak. The best linear fit of the van't Hoff enthalpies to the transition temperatures Tm was obtained with Delta Hvf and was Delta Hvf (kJ/mol)=432.7 + or - 1.7 + or - 5.81 + or - 0.24 (Tm-337.2). Calorimetric transition enthalpies were determined from the transition peak area using an extrapolated sigmoidal baseline (Delta Hs) and an extrapolated straight linear baseline. The best linear dependence of the calorimetric enthalpy on Tm was obtained with Delta Hs (kJ/mol) = 434.7 + or - 4.1 + 6.39 + or - 0.60 (Tm-337.2). Linear least-squares fits of Delta Hvf and Delta Hs to Tm were independent of the DSC scan rate, the source of the lysozyme, the buffer concentration from 0.1 to 0.2 M and the concentration of lyso-zyme from 0.26 to 2.8 mM. The transition temperature exhibited a linear dependence on pH and concentra-tion. Cooperativities of the transition ranged from 0.988 + or - 0.0007 at 326 K to 1.012 + or - 0.007 at 349K.

900.514 PB90-117987 Not available NTIS

National Inst. of Standards and Technology (NEL), Gaithersburg, MD. Thermophysics Div. Vapor Pressures and Gas-Phase PVT Data for 1,1,1,2-Tetrafluoroethane.

L. A. Weber. 1989, 11p Sponsored by Department of Energy, Washing.on, DC., and Environmental Protection Agency, Washing-

ton, DC. Pub. in International Jnl. of Thermophysics 10, n3 p617-627 May 89.

Keywords: *Refrigerants, *Vapor pressure, Thermodynamic properties, Pressure, Volume, Reprints, Virial equations, Temperature dependence, Density.

New data is presented for the vapor pressure and PVT surface of 1,1,1,2-tetrafluoroethane (Refrigerant 134a) in the temperature range 40C (313 K) to 150C (423 K). The PVT data are for the gas phase at densities up to one-half critical. Densities of the saturated vapor are derived at five temperatures from the intersections of the experimental isochores with the vapor pressure curve. The data are represented analytically in order to demonstrate experimental precision and to facilitate calculation of thermodynamic properties.

PB90-117995 Not available NTIS National Inst. of Standards and Technology (IMSE), Gaithersburg, MD. Reactor Radiation Div.

Structure of V9Mo6O40 Determined by Powder **Neutron Diffraction.**

Final rept. R. C. T. Slade, A. Ramanan, B. C. West, and E. Prince. 1989, 5p

Pub. in Jnl. of Solid State Chemistry 82, p65-69 1989.

Keywords: *Crystal structure, *Neutron diffraction, *Vanadium oxides, *Molybdenum oxides, Chemical bonds, Crystallography, Powder(Particles), Repnnts, Bond lengths.

The crystal structure of V9Mo6O40 has been determined by Rietveld profile analysis of neutron powder diffraction data. The structure is a monoclinically distorted variant of Nb3O7F (space group C2) consisting of ReO3-type slabs three octahedra thick connected by edge sharing of component octahedra. The octahedra are considerably distorted due to off-center dis-placement of the metal atoms. Metal-oxygen bond lengths conform with lengths of similar compounds.

900,516 PB90-118001 Not available NTIS Not available NTIS National Inst. of Standards and Technology (IMSE), Gaithersburg, MD. Reactor Radiation Div.

Neutron Diffraction Determination of Full Structures of Anhydrous LI-X and LI-Y Zeolites.

Final rept. Andersen, R. C. T. Slade, E. K. Andersen, I. G. K. Andersen, and E. Prince. 1989, 8p Pub. in Jnl. of Solid State Chemistry 82, p95-102 1989.

Keywords: *Crystal structure, Neutron diffraction, Ion exchange resins, Lithium inorganic compounds, Sodium inorganic compounds, Aluminum inorganic compounds, Silicates, Reprints, *Zeolites.

Virtually monoionic Li-X and Li-Y zeolites have been prepared by LIOH titration of parent NH4 zeolites. Structural studies have been performed at room temperature on the anhydrous ze Li(80.7)H(4.9)Na(0.4)Al(86)Si(106)O(384) Li(46.0)H(5.8)Na(5.1)K(0.1)Al(57)Si(135)O(384) zeolites. powder neutron diffraction profile refinement in order to locate Li(+1) cations. The cell parameters are 24.6716(10) and 24.4498(12) A for Li-X and Li-Y, respectively. Three positions have been found for Li(+1) sites I' and II in the six-ring windows of the sodalite unit and site III' in the supercage for the additional Li(+1)

900,517 PB90-118027 Not available NTIS National Inst. of Standards and Technology (NML), Gaithersburg, MD. Surface Science Div.
Photon-Stimulated Desorption of Fluorine from Silicon via Substrate Core Excitations. Final rept.

J. A. Yarmoff, and S. A. Joyce. 1989, 8p Pub. in Physical Review B 40, n5 p3143-3150, 15 Aug 89.

Keywords: *Silicon, *Desorption, Resonance, Reponts, Photon stimulated desorption, *Fluorine ions, Surface reactions.

Photon-stimulated desorption (PSD) of F(1+) was performed for silicon (111) surfaces terminated with fluorine atoms. The surfaces were prepared by exposure of clean silicon to XeF2. The onset for PSD at the Si 2p edge correlated with the transition from the 2p level of the bonding silicon atom to the conduction-band minimum and west that a function of the sind time of the side side size of the side side size of the size of the side size of the size of the side size of the side size of the side size of the siz mum, and was thus a function of the oxidation state of the bonding atom. The ions originating from a SiF species described along the surface normal while the ions from a SiF3 group described in off-normal directions. from a SiF3 group desorbed in oft-normal directions. Localized 3s and 3p Rydberg-like resonances were observed in the quasimolecular SiF3 moieties. The ion kinetic-energy distributions were measured as an aid to elucidating the desorption mechanism. Measurements of the PSD of F(1+) at the Si 2s edge were used to confirm the 3s and 3p character of the measured resonances. ured resonances.

PB90-118092 Not available NTIS National Inst. of Standards and Technology (NEL), Gaithersburg, MD. Thermophysics Div. Measures of Effective Ergodic Convergence in Liquids. Final rept. R. D. Mountain, and D. Thirumalai. 1989, 5p Grant NSF-CHE86-57356 Sponsored by National Science Foundation, WashingPub. in Jnl. of Physical Chemistry 93, n19 p6975-6979

Keywords: *Liquids, Ergodic processes, Dielectric properties, Computenzed simulation, Water, Convergence, Diffusion, Reprints, Binary mixtures, Molecular dynamics

The recently introduced measure for ergodic convergence is used to illustrate the time scales needed for effective ergadicity to be obtained in various liquids. The cases considered are binary mixtures of soft spheres, two-component Lennard-Jones systems, and liquid water. It is shown that various measures obey a dynamical scaling law which is characterized by a single parameter, namely, a novel diffusion constant. The time scales for ergodic behavior are found to be dependent on the particular observable being considered. For example, in water, the diffusion constants for the translational and rotational kinetic energies and for the laboratory frame dipole moments are very different. The implications of these results for the calculation of the dielectric constant of polar liquids by computer simulations are discussed.

Not available NTIS
National Inst. of Standards and Technology (NML),
Boulder, CO. Quantum Physics Div.
Weakly Bound NeHF. 900,519

S. V. O'Neil, D. J. Nesbitt, P. Rosmus, H. J. Werner, and D. C. Clary. 1989, 11p Grants NSF-PHY86-04504, NSF-CHE86-05970 Sponsored by National Science Foundation, Washing-

Pub. in Jnl. of Chemical Physics 91, n2 p711-721, 15 Jul 89.

Keywords: *Hydrogen fluoride, Far infrared radiation, Infrared spectra, Deutenum compounds, Reprints, *Neon complexes, Van der Waals forces, Potential energy surfaces, Predissociation.

The authors have used ab initio methods to characterize the Ne-HF van der Waals complex. The interaction energy was determined using size consistent, correlated CEPA wave functions expanded in a Gaussian basis chosen to represent both intraatomic effects and the low order multipole moments and polarizabilities of the low order multipole moments and polarizabilities of Ne and HF. Converged variational and close-coupling calculations using the ab initio potential surface reveal three bound levels of the Ne-HF stretch mode, and several metastable levels correlating asymptotically with rotationally excited HF(j=1). From the calculated line positions, widths, and intensities, the authors have synthesized far infrared and infrared spectra of Ne-HF and Ne-DF and Ne-DF.

Not available NTIS PB90-118126 National Inst. of Standards and Technology (NML), Boulder, CO. Quantum Physics Div. Slit Jet Infrared Spectroscopy of NeHF Complexes: internal Rotor and J-Dependent Predissociation Dynamics.

Tion Dynamics.
Final rept.
D. J. Nesbitt, C. M. Lovejoy, T. G. Lindemann, S. V. ONeil, and D. C. Clary. 1989, 10p
Grants NSF-CHE86-05970, NSF-PHY86-04504 Sponsored by National Science Foundation, Washing-

Pub. in Jnl. of Chemical Physics 91, n2 p722-731, 15 Jul 89.

Keywords: *Hydrogen fluonde, Infrared spectroscopy, Reprints, *Neon complexes, Van der Waals forces, Potential energy surfaces, Supersonic jet flow, Predissociation.

Direct absorption tunable difference frequency IR spectroscopy in a slit jet supersonic expansion has been used to observe complexes of Ne with HF for the first time. Spectra of both the weak HF stretch fundamental and the 10-20 fold more intense bend and mental and the 10-20 fold more intense bend and stretch combination band transitions are observed, and illustrate several interesting dynamical features. The large ratio of combination band to fundamental intensity is evidence for a highly isotropic potential with respect to HF rotation. The HF bend vibration is thus better thought of as nearly free internal rotor motion with a nearly good space fixed quantum number.

900,521 PB90-118209

900.520

Not available NTIS

National Inst. of Standards and Technology (NML), Roulder, CO. Quantum Physics Div.
Intramolecular Dynamics of van der Waals Molecules: An Extended Infrared Study of ArHF.

Final rept. C. M. Lovejoy, and D. J. Nesbitt. 1989, 18p Grants NSF-CHE86-05970, NSF-PHY86-04054 Sponsored by National Science Foundation, Washing-

Pub. in Jnl. of Chemical Physics 91, n5 p2790-2807, 1

Keywords: *Hydrogen fluoride, Near infrared radiation, Infrared spectra, Reprints, *Argon complexes, Van der Waals forces, Molecular dynamics, Supersonic expansion, Laser spectroscopy, Potential energy surfaces.

The near-infrared spectrum of ArHF prepared in a slit supersonic expansion is recorded with a difference frequency infrared laser spectrometer. By virtue of the high sensitivity of the technique, and the lack of appreciable spectral congestion at the 10 K jet temperature, the authors observe 9 of the 11 vibrational states with energies below the Ar+HF(nu=1,j=0) dissociation limit. The spectroscopic information is quite sensitive to the Ar + HF potential energy surface away from the equilibrium configuration, and thus provides a rigorous test of trial potential energy surfaces. Excellent agreement is obtained between experiment and the predictions of a recently reported Ar+HF(nu=1) potential.

Not available NTIS National Inst. of Standards and Technology (NML), Gaithersburg, MD. Surface Science Div.

Adsorption of Water on Clean and Oxygen-Predosed Nickel(110).

Final rept. 900,522 PB90-123555

Final rept.

C. Benndorf, and T. E. Madey. 1988, 29p Pub. in Surface Science 194, n1-2 p63-91 1988.

Keywords: *Adsorption, *Water, *Surface properties, *Nickel, Hydrogen bonds, Dissociation, Isotopic labeling, Desorption, Chemisorption, Oxygen, Dimerization, Reprints, Electron stimulated desorption ion angular distribution, Thermal desorption spectroscopy, Low energy electron diffraction.

The adsorption of H2O on both clean and modified Ni(110) surface has been studied using a variety of methods: electron stimulated desorption ion angular distribution (ESDIAD), thermal desorption spectroscopy (TDS), and low energy electron diffraction (LEED). Fractional monolayers, of H2O on clean Ni(110) are associated with a four-spot ESDIAD pattern suggesting that the HO ligands are in specific registry with the substrate. The authors postulate the formation of H2O dimers bound via oxygen lone pair orbitals to Ni sub-strate atoms and oriented with the O...H-O axis in 001 strate atoms and oriented with the O...H-O axis in Our azimuthal directions. Upon heating to greater than or equal to 200K, a fraction of the H2O dissociates, forming OH(ad). TDS of H2O from clean Ni(110) reveals four binding states. They are related to multilayer desorption (155K), desorption from larger bilayer clusters (210K), desorption from larger blaster which might be stabilized by OH (245K), and recombination of OH to yield H2O (g) (370K). Isotopic exchange of H2(16)0 with (18)O(ad) is observed even for binding states in which dissociation is believed not to occur and is related to a proton exchange involving H2O(ad) hydrogen bonded to O(ad).

900,523 PB90-123563 Not available NTIS Not available NTIS
National Inst. of Standards and Technology (NML),
Gaithersburg, MD. Surface Science Div.
Ammonia Adsorption and Dissociation on a
Stepped Iron(s) (100) Surface.

Final rept. C. Benndorf, T. E. Madey, and A. L. Johnson. 1987,

Pub. in Surface Science 187, n2-3 p434-444 1987.

Keywords: *Ammonia, *Adsorption, *Dissociation, *Iron, *Surface properties, Single crystals, Desorption, Crystal structure, Chemisorption, Reprints, Electron stimulated desorption ion angular distribution.

The purpose of the present letter is to provide new information about the molecular structure and configuration of NH3 on Fe single crystal surfaces and to provide insight into the influence of steps of NH3 orientation and dissociation. Information about the NH3 orientation on flat Fe(100) terraces and changes induced by steps were gained in the present study from ESDIAD (Electron Stimulated Desorption Ion Angular Distribution). The results provide evidence that at low NH3 coverages adsorption takes place primarily at step sites. The adsorbed species stabilized at step sites are believed to include oriented NHx fragments as well as 'inclined' NH3. The molecular NH3 dipoles are believed to be tilted due to the electrostatic field at steps. For higher coverages NH3 adsorption sites on the Fe(100) terraces are populated; from ESDIAD data the authors conclude that NH3 is bonded mainly to terrace sites via the N atom and the H-atoms are pointed away from the surface, with no azimuthal ordering.

900,524

Not available NTIS PB90-123597 National Inst. of Standards and Technology (NEL), Gaithersburg, MD. Thermophysics Div.

Quantitative Characterization of the Viscosity of a Microemulsion. Final rept.

R. F. Berg, M. R. Moldover, and J. S. Huang. 1987,

Contract NASA-C-86129-D

Sponsored by National Aeronautics and Space Administration, Cleveland, OH. Lewis Research Center. Pub. in Jnl. of Chemical Physics 87, n6 p3687-3691

Keywords: *Quantitative analysis, *Viscosity, Temperature, Volume, Drops(Liquids), Critical point, Water, Decanes, Electrical resistivity, Reprints, *Microemulsions, *Ternary systems, AOT.

The authors measured the viscosity of the 3-component microemulsion water/decane/AOT as a function of temperature and droplet volume fraction. At temperatures well below the critical temperature the viscosity is described by treating the droplets as hard spheres suspended in decane. Upon approaching the 2-phase region from low temperature, there is a large (as much a factor of 4) smooth increase of the viscosity which may be related to the percolation-like transition observed in the electrical conductivity. This increase in viscosity is not completely consistent with either a naive electroviscous model or a simple clustering model. The divergence of the viscosity near the critical point (39 C) is superimposed upon the smooth increase. The magnitude and temperature dependence of the critical divergence are similar to that seen near the critical points of binary liquid mixtures.

900.525

PB90-123852 Not available NTIS National Inst. of Standards and Technology (NML), Boulder, CO. Quantum Physics Div.

Sub-Doppler Infrared Spectroscopy in Slit Supersonic Jets: A Study of all Three van der Waals Modes in v1-Excited ArHCl.

D. J. Nesbitt, and C. M. Lovejoy. 1988, 8p Grants NSF-PHY86-04504, NSF-CHE86-05970 Sponsored by National Science Foundation, Washing-

Pub. in Faraday Discussions of the Chemical Society 86, p13-20 1988.

Keywords: *Hydrogen chloride, Infrared spectroscopy, Far infrared radiation, Reprints, *Argon complexes, Van der Waals forces, Laser spectroscopy, Vibrational states, Supersonic jet flow, High resolution.

Direct absorption tunable difference frequency infrared radiation laser spectroscopy has been used to study the vibrational dynamics of ArHCl complexes cooled in a slit supersonic jet expansion. As a result of large-amplitude vibrational motion in these weakly bound complexes, transitions to each of the three van der Waals modes are observed as combination bands built on the fundamental HCl stretch, thus permitting detailed study of low-frequency, intermolecular modes with a near-infrared laser source. The molecular constants are in excellent agreement with both far-infrared radiation experimental results and semiempirical predictions for the Ar+HCI(v=0) surface, indicating only a small change in the intermolecular potential upon vibrational excitation of the HCl.

900.526

PB90-123860 Not available NTIS National Inst. of Standards and Technology (NML), Boulder, CO. Quantum Physics Div. Apparent Spectroscopic Rigidity of Floppy Molecular Systems.

Final rept.

D. J. Nesbitt, and R. Naaman. 1989, 9p Grants NSF-CHE86-05970, NSF-PHY86-04504 Sponsored by National Science Foundation, Washing-

Pub. in Jnl. of Chemical Physics 91, n7 p3801-3809, 1 Oct 89.

Keywords: Hydrogen bonds, Quantum theory, Hamiltonian functions, Infrared spectroscopy, Reprints, *Complexes, Van der Waals forces, High resolution, Supersonic jet flow.

There has been a wealth of recent infrared experimental data on van der Waals and hydrogen bonded com-plexes obtained under cooled, supersonic jet condi-tions where only a small fraction of the total bound quantum states can be elucidated. This partial set of data can often be well fit to a traditional Watson Hamiltonian derived from a rigid rotor perspective with low order centrifugal distortion effects included. In the paper, the authors show that even in extremely floppy molecular systems with wide amplitude vibrational motion, the quantum term values are very well fit by a rigid or semirigid rotor Hamiltonian over the limited range of energy states accessible in a cooled beam. The authors provide explicit examples of this behavior by full quantum solutions in two extremes of floppy motion: a symmetric triatonic with a square well bending potential ('hinge') and a nearly free internal rotor ('pinwheel'). These results show that potentials with fundamentally different topologies can be consistent with same data, and indicate that even the limits of nearly rigid and floppy internal motion may be difficult to distinguish from a limited set of rovibrational eigen-

900,527 PB90-126236 Not available NTIS American Chemical Society, Washington, DC.

Journal of Physical and Chemical Reference Data, Volume 18, Number 3, 1989.

Quarterly rept.

D. R. Lide. c1989, 426p See also PB90-126244 through PB90-126269 and PB89-222525. Prepared in cooperation with American Inst. of Physics, New York. Sponsored by National Inst. of Standards and Technology, Gaithersburg, MD. Available from American Chemical Society, 1155 16th St., NW, Washington, DC 20036.

Keywords: *Physical properties, *Chemical properties, Water, Organic compounds, Solubility, High termperature tests, Heavy water, Gases, Hydrocarbons, Microwave spectroscopy, Tables(Data), Henrys law, Molecular rotation, Octanols, Distribution(Property).

Contents: Octanol water partition coefficients of simple organic compounds; Evaluation of data on solubility of simple apolar gases in light and heavy water at high temperature; Microwave spectral tables. III. Hydrocarbons, CH to C10H10; Cumulative listing of reprints and supplements. (Copyright (c) by the U.S. Secretary of Commerce, 1989.)

900.528

PB90-126244 Not available NTIS Sangster Research Labs., Montreal (Quebec). Octanol-Water Partition Coefficients of Simple Or-Octanoi-water Partition Coefficients of Shiple Signate Compounds.

Quarterly rept.

J. Sangster. c1989, 118p

Prepared in cooperation with American Chemical Social Machinery (Compound American Line).

Prepared in cooperation with American Chemical Society, Washington, DC., and American Inst. of Physics, New York. Sponsored by National Inst. of Standards and Technology, Gaithersburg, MD. Included in Jnl. of Physical and Chemical Reference Data, v18 n3 p1111-1228 1989. Available from American Chemical Society, 1155 16th St., NW, Washington DC 20036

ton, DC 20036.

Keywords: *Organic compounds, Tables(Data), Physical properties, Data processing, Environmental surveys, Thermodynamics, Experimental design, *Octanols, *Water, *Distribution(Property), Biological effects.

Octanol-water partition coefficients (log P) for 611 simple organic compounds representing all principal classes have been retrieved from the literature. Available experimental details of measurement are documented from original articles. Pertinent thermodynamic relations are presented, with a discussion of direct and indirect methods of measurement. Reported log P

CHEMISTRY

Physical & Theoretical Chemistry

data for each compound have been evaluated according to stated criteria, and recommended values (with uncertainty) are given.

PB90-126251 Not available NTIS Comision Nacional de Energia Atomica, Buenos Aires (Argentina). Dept. de Quimica de Reactores.

Evaluation of Data on Solubility of Simple Apolar Gases in Light and Heavy Water at High Tempera-

Quarterly rept.

R. F. Prini, and R. Crovetto. c1989, 13p

H. F. Prini, and R. Crovetto. c1989, 13p Prepared in cooperation with Delaware Univ., Newark. Dept. of Chemistry, American Chemical Society, Washington, DC., and American Inst. of Physics, New York. Sponsored by National Inst. of Standards and Technology, Gaithersburg, MD. Included in Jnl. of Physical and Chemical Reference Data, v18 n3 p1231-1243 1989. Available from Ameri-can Chemical Society, 1155 16th St., NW, Washing-ton, DC 20036.

ton, DC 20036.

Keywords: *Solubility, *Heavy water, *Water, *Gases, Deuterium, Chemical properties, Thermodynamic properties, Henrys law, Data processing, Ethane, Nitrogen, Oxygen, Hydrogen, Tables(Data), High temperature tests, Rare gases, Methane.

The solubility data of apolar gases in light and heavy water over the temperature range covered experimentally have been evaluated, laying particular emphasis to the region above the normal boiling points of the solvents. The systems that have been included in the solvents. The systems that have been included in the work are the inert gases and CH4 in light water and heavy water, H2, O2, N2 and C2H6 in light water and D2 in heavy water. Data in the original sources have been brought to the same footing by calculating from the raw experimental data P, T, and x when they were not reported by the author. The step is considered necessary to assess critically the available sets of data. The temperature dependence of Henry's constants for all the binary systems have been expressed in terms of two different polynomial equations. The formulations presented are discussed and the limits of application given.

900,530

PB90-126269 Not available NTIS National Inst. of Standards and Technology (NML), Gaithersburg, MD.

Microwave Spectral Tables. 3. Hydrocarbons, CH to C10H10.

New York.

Quarterly rept. F. J. Lovas, and R. D. Suenram. c1989, 27p Prepared in cooperation with American Chemical Society, Washington, DC., and American Inst. of Physics,

Included in Jnl. of Physical and Chemical Reference Data, v18 n3 p1245-1524 1989. Available from American Chemical Society, 1155 16th St., NW, Washington, DC 20036.

Keywords: *Microwave spectroscopy, *Hydrocarbons, *Molecular rotation, Physical properties, Tables(Data), Data processing, Dipole moments, Hyperfine struc-ture, Spectral lines, Isotopes.

All of the rotational spectral lines observed and reported in the open literature for 91 hydrocarbon molecules have been tabulated. The isotopic molecular species, assigned quantum numbers, observed frequency, estimated measurement uncertainty and reference are given for each transition reported. In addition to correcting a number of misprints and errors in the litera-ture cited, the spectral lines for many normal isotopic species have been refit to produce a comprehensive and consistent analysis of all the data extracted from various literature sources. The derived molecular prop-erties, such as rotational and centrifugal distortion constants, hyperfine structure constants, electric dipole moments, and rotational g-factors are listed.

900,531

PB90-128141 Not available NTIS
National Inst. of Standards and Technology (NML),
Gaithersburg, MD. Molecular Spectroscopy Div.
Microwave Electric-Resonance Optothermal Spectroscopy (MC) troscopy of (H2O)2.

Final rept. G. T. Fraser, R. D. Suenram, and L. H. Coudert. 1989, 9p

Pub. in Jnl. of Chemical Physics 90, n11 p6077-6085, 1

Keywords: *Microwave spectroscopy, Hydrogen bonds, Molecular beams, Reprints, *Water dimers, Dimers, *Complexes.

The microwave spectrum of (H2O)2 has been measured between 14 and 110 GHz using a newly developed electric-resonance optothermal spectrometer (EROS) described here. The reported measurements (ÉROS) described here. The reported measurements extend previous results on the a-type K sub a = 0-0 and 1-1 bands for the (A sub 2, sup (+-)), B sup 2, sup (+-)), and E sup (+-) rotational-tunneling states and include the first observations of the c-type K sub a = 1-0 band for the (A sub 2, sup (+-)) and (B sup 2, sup +-)) states and the a-type K sub a = 0-0 band for the (A sub 1, sup (+-1)) states. For the (A sub 1, sup (+-1)) states an interconversion tunneling splitting of 22.6 GHz is obtained, compared to the 19.5 GHz value found previously for the K sub a = O (A sub 2, sup (+-)) and (B sup 2, sup (+-)) states.)) and (B sup 2, sup (+-)) states.

900,532 PB90-128547 PB90-128547 Not available NTIS National Inst. of Standards and Technology (NML), Boulder, CO. Quantum Physics Div.

Interaction of In Atom Spin-Orbit States with Si(100) Surfaces.

Final rept.

D. J. Oostra, R. V. Smilgys, and S. R. Leone. 1989,

Sponsored by Weapons Lab., Kirtland AFB, NM.
Pub. in Materials Research Society Symposia Proceedings Chemical Perspectives of Microelectronic Materials, v131 p239-244 1989.

Keywords: *Indium, *Silicon, *Desorption, Spin orbit interactions, Scattering, Reprints, Laser induced fluorescence, Auger electron spectroscopy, Surface reactions, Binding energy, Semiconductors.

Scattering and desorption of In from Si (100) is investigated. Laser induced fluorescence is used to probe the desorbing and or scattered species. Auger Electron Spectroscopy is used to study the composition on the surface. The results show that at surface temperatures below 820 K atwo dimensional layer of In desorbs by a half order mechanism. This is explained by assuming two dimensional In islands on the surface. Above 820 K, desorption takes place by a first order mechanism. The desorption parameters appear to be spin-orbit state specific. The desorption energy for In doublet P(3/2) is 2.8 plus or minus 0.4 eV and for In doublet P(1/2) 2.5 plus or minus 0.2 eV. The difference is equal to the difference in the spin-orbit energy. So far no specular scattering of In is observed, suggesting that the sticking coefficients are unity.

900,533 PB90-128729 Not available NTIS National Inst. of Standards and Technology (NML), Gaithersburg, MD. Molecular Spectroscopy Div. Vibrational Spectra of Molecular Ions Isolated in Solid Neon. 2. O4(1+) and O4(1-).

W. E. Thompson, and M. E. Jacox. 1989, 12p Sponsored by Army Research Office, Research Triangle Park, NC.
Pub. in Jnl. of Chemical Physics 91, n7 p3826-3837, 1

Oct 89.

Keywords: *Vibrational spectra, *Infrared spectra, Neon, Molecular structure, Photochemical reactions, lonization, Absorption, Solids, Reprints, *Matrix isolation technique, *Oxygen ions, Chemical reaction mechanisms.

When a relatively concentrated Ne:O2 sample is codewhen a relatively concentrated Ne:O2 sample is code-posited at approximately 5 K with a beam of excited neon atoms, prominent infrared absorptions appear which are assigned to O4(+) and O4(-). Absorptions of O3 and O3(-) are also present, and their product distributions in isotopic substitution experiments indicate that O-atom production and reaction is a minor channel in this experimental system. Detailed isotopic substitution experiments require that both O4(+) and O4(-) possess two equivalent O2 units. Analysis of the isotopic shifts strongly favors a planar trans configuration (C(2h)) for both molecules. Several combination bands of O4(+) are observed, and give evidence regarding the position of Nu(sub 1)(a(sub g)), which is infrared inactive, and regarding perturbations by combinations of low-frequency fundamentals. The mechanism of photodestruction of the ions in this system is also considered.

900,534 PB90-136375

Not available NTIS

National Inst. of Standards and Technology (NML), Gaithersburg, MD. Chemical Kinetics Div.

Temperature Dependence of the Rate Constant for the Hydroperoxy + Methylperoxy Gas-Phase Reaction.

Final rept. P. Dagaut, T. J. Wallington, and M. J. Kurylo. 1988,

Pub. in Jnl. of Physical Chemistry 92, n13 p3833-3836

Keywords: *Reaction kinetics, *Photolysis, *Absorption spectra, Ultraviolet spectroscopy, Flash point, Temperature, Spectrum analysis, Vapor phases, Reprints, *Hydroperoxy radicals, *Methylperoxy radicals, Arrhenius equation, Chemical reaction mechanisms, Peroxy radicals.

The temperature dependence of the reaction between hydroperoxy and methylperoxy radicals was measured in a flash photolysis ultraviolet absorption apparatus over the temperature range 228 - 380 K. (HO2 + CH3O2 -> products.) The data represented by the Arrhenius expression are compared to earlier results and discussed in terms of the reaction mechanism. Due to overlapping absorptions of the two radicals and deviations of the complex reaction system from both pseudo-first and -second order behavior, the rate con-stants were determined from a detailed modeling of the radical decay curves. A sensitivity analysis of the rate constant determination procedure to the assumed radical absorption cross-sections and correlated changes in the rate constants for the HO2 and CH3O2 self-reactions was performed and the results are reported.

900,535

PB90-136474 Not available NTIS National Inst. of Standards and Technology (NML), Gaithersburg, MD. Electricity Div. Fundamental Physical Constants - 1986 Adjust-

Final rept.
E. R. Cohen, and B. N. Taylor. 1987, 4p
Sponsored by Rockwell International, Thousand Oaks,
CA. Science Center.

Pub. in Europhysics News 18, n5 p65-68 May 87.

Keywords: *Fundamental constants, Reviews, Physical properties, Least square method, Revisions, Tables(Data), Comparison, Reprints.

The 1986 adjustment of the fundamental constants, just completed under the aegis of the CODATA Task Group on Fundamental Constants, is reviewed and compared with the previous recommendations pub-lished in 1973. The precision of the recommended values for the physical constants has improved by an order of magnitude. Summary tables of these values and associated data are presented.

900.536

PB90-136565 Not available NTIS Not available NTIS
National Inst. of Standards and Technology (NML),
Gaithersburg, MD. Chemical Kinetics Div.
Flash Photolysis Kinetic Absorption Spectroscopy
Study of the Gas Phase Reaction HO2 + C2H5O2
Over the Temperature Range 228-380 K.

Final rept.

P. Dagaut, T. J. Wallington, and M. J. Kurylo. 1988,

Pub. in Jnl. of Physical Chemistry 92, n13 p3836-3839 1988.

Keywords: *Reaction kinetics, *Photolysis, *Absorption spectra, Flash point, Temperature, Spectrum analysis, Vapor phases, Reprints, *Hydroperoxy radicals, *Ethylperoxy radicals, Peroxy radicals, Arrhenius equation.

Flash photolysis kinetic absorption spectroscopy was used to investigate the gas phase reaction between hydroperoxy and ethylperoxy radicals between 228 and 380K in the pressure range 25-400 Torr. (HO2 + C2H5O2 -> products). Due to the large difference be-tween the self reactivities of the two radicals, first or second order kinetic conditions could not be maintained for either species. Thus, the rate constant was determined from computer modeled fits of the radical absorption decay curves recorded at wavelengths between 230 and 280 nm. A reanalysis of earlier measurements of the C2H5O2 self-reaction (C2H5O2 + C2H5O2 -> products) using this expression for k1 resulting in the revised Arrhenius equation produced k2.

900,537 PB90-136573 Not available NTIS National Inst. of Standards and Technology (NML), Gaithersburg, MD. Molecular Spectroscopy Div. Picosecond Vibrational Energy Transfer Studies of Surface Adsorbates.

E. J. Heilweil, M. P. Casassa, R. R. Cavanagh, and J. C. Stephenson. 1989, 29p Sponsored by Air Force Office of Scientific Research, Bolling AFB, DC. Pub. in Annual Review of Physical Chemistry 40, p143-171, 1989. 171 1989.

Keywords: *Adsorbates, *Molecular relaxation, *Surface chemistry, Infrared spectroscopy, Metals, Dielectrics, Reprints, *Picosecond pulses, Laser applications.

Recent measurements of vibrational relaxation for adsorbates at dielectric and metal particle surfaces are reviewed. The vibrational lifetime (T (sub 1)) for various surface and model liquid and solid systems are also tabulated. Transient infrared picosecond laser methods are described as are relevant theories pertinent to adsorbate vibrational (v=1) relaxation mechanisms at surfaces.

Not available NTIS National Bureau of Standards (NML), Gaithersburg, MD. Chemical Thermodynamics Div.

Use of an Imaging Proportional Counter in Macromolecular Crystallography.

Final rept. 900,538

A. J. Howard, G. L. Gilliland, B. C. Finzel, T. L. Poulos, D. H. Ohlendorf, and F. R. Salemme. 1987,

5p Pub. in Jnl. of Applied Crystallography 20, pt5 p383-387, 1 Oct 87.

Keywords: *Proportional counters, *Crystallography, *X ray diffraction, *Molecule structure, Data acquisition, Performance evaluation, Reprints, Fournier analy-

A multiwire proportional chamber known as an Imaging Proportional Counter has been used to collect X-ray intensity data for the determination of several structures by molecular replacement or difference Fourier analysis and has provided data for numerous other macromolecular crystallographic projects. Results obtained with an Imaging Proportional Counter mounted on a rotating anode X-ray generator indicate that the detector produces accurate intensity information and that its reliability is high.

900,539 PB90-136755 Not available NTIS National Inst. of Standards and Technology (IMSE), Gaithersburg, MD. Office of Nondestructive Evalua-

Triplet Dipoles in the Absorption Spectra by Dense Rare Gas Mixtures. 1. Short Range Interactions. Final rept.

B. Guillot, R. D. Mountain, and G. Birnbaum. 1989,

13p Pub. in Jnl. of Chemical Physics 90, n2 p650-662, 15

Keywords: *Rare gases, *Dipole moments, Far infra-red radiation, Absorption spectra, Liquefied gases, Mixtures, Argon, Krypton, Helium, Hydrogen, Reprints, Molecular dynamics.

A theory is proposed to evaluate the induced-dipole moment occurring when three dissimilar atoms are mutually interacting. Based on the one-effective electron model, the theory predicts that, at short and intermediate distances, the triatomic dipole moment origi-nates from three different processes, namely, overlap, quadrupole-induced, and dipole-induced. These threebody dipoles have then been implemented into a molecular dynamics simulation in order to generate the collision-induced absorption spectra by rare-gas mixtures. For Ar-Kr liquid mixtures, the irreducible threebody contributions to the spectral density are found so important that they exceed two-body contributions. This is due to a profound cancellation between twobody dipoles which does not occur between irreducible three-body dipoles. However, the comparison with experimental data is poor because of a shortcoming of the model calculation which does not take into account long-range dispersion interactions. On the contrary, a quantitative agreement is obtained for the fundamental vibration band of compressed H2-He mixtures, indicating that exchange overlap, three-body dipoles play the leading role for such light systems.

900,540 PB90-136904 PB90-136904 Not available NTIS National Bureau of Standards (IMSE), Gaithersburg, MD. Metallurgy Div.

Laser Induced Vaporization Time Resolved Mass Spectrometry of Refractories.

Final rept.

D. W. Bonnell, P. K. Schenck, and J. W. Hastie. 1988, 13p Pub. in Proceedings of the Electrochemical Society,

v88-10 p82-94 1988.

Keywords: *Vaponizing, *Mass spectroscopy, *Spectrum analysis, *Refractory materials, Chemical analysis, Boron nitrides, Graphite, High temperature tests, Thermodynamic equilibrium, Surface temperature, *Laser-radiation heating.

An experimental approach is described which can yield information about refractory surfaces by examining the time history of the gas-dynamic process occurring during pulsed Nd/YAG laser induced vaporization. Specific examples consider BN and graphite vaporization. Time resolved mass spectrometric measurements of evolved species permit direct determination of gas species identities and concentration, independent of mass spectral cracking problems. Of particular interest is the observation of local thermodynamic equilibrium for the observed laser vaporized gas species in both systems from surface temperatures of 2900 K (BN) and 4000 K (graphite). Indirect methods of determining surface temperature as alternatives to of determining surface temperature as alternatives to direct measurement of radiance temperature are presented. Also, a preliminary analysis of the convolution problem to eliminate amplifier RC response delays and to extract true species velocity distributions is discussed.

900,541 PB90-136946 Not available NTIS Not available NTIS National Inst. of Standards and Technology (NML), Boulder, CO. Time and Frequency Div.

Frequency Measurements of High-J Rotational Transitions of OCS and N2O.

Final rept.

M. D. Vanek, D. A. Jennings, and J. S. Wells. 1989,

5p Pub. in Jnl. of Molecular Spectroscopy 138, p79-83

Keywords: *Nitrogen oxide(N2O), *Infrared spectroscopy, *Molecular vibration, *Thiocarbamates, *Frequency measurement, Molecular energy levels, Molecular rotation, Far infrared radiation, Performance evaluation, Reprints.

A metal-insulator-metal diode has been used to generate far-infrared radiation as the difference between two CO2 lasers. With this technique rotational transi-tions of all the vibrational states below 2000/cm have been measured for the normal isotopic species of OCS with an accuracy of 200 kHz or better.

900,542 PB90-163874 **PC A04** National Inst. of Standards and Technology, Gaithers-

burg, MD. Journal of Research of the National Institute of Standards and Technology. November-December 1989. Volume 94, Number 6.

1989, 69p See also PB90-163882 through PB90-163932 and Volume 94, Number 4, PB89-235634. Also available from Supt. of Docs. SN703-027-00031-8.

Keywords: *Atmospheric pressure, *Metrology, *Radioactive isotopes, *Metals, Radioactivity, Nickel isotopes, Standards, Measurement, Waveforms, Ionizing radiation, Atomic mass, Manometers, Mass spectrom-

Contents: The reduction of uncertainties for absolute piston gage pressure measurements in the atmospheric pressure range; Absolute isotopic abundance ratios and atomic weight of a reference sample of nickel; The absolute isotopic composition and atomic weight of terrestrial nickel; Report on the 1989 meeting of the radionuclide measurements section of the consultative committee on standards for the measurement of ionizing radiations; On measuring the root-mean-square value of a finite record length periodic waveform; A search for optical molasses in a vapor cell: General analysis and experimental attempt.

900,543 PB90-163890

(Order as PB90-163874, PC A04) National Inst. of Standards and Technology, Gaithers-

burg, MD.

Absolute Isotopic Abundance Ratios and Atomic

Weight of a Reference Sample of Nickel.
J. W. Gramlich, L. A. Machlan, I. L. Barnes, and P. J. Paulsen. 1989, 10p Prepared in cooperation with Curtin Univ. of Technolo-

gy, Bentley (Australia). Included in Jnl. of Research of the National Institute of Standards and Technology, v94 n6 p347-456 1989.

Keywords: *Nickel isotopes, *Atomic weight, Calibrating, Mass spectrometers, Assay.

Absolute values have been obtained for the isotopic abundance ratios of a reference sample of nickel (Standard Reference Material 986), using thermal ionization mass spectrometry. Samples of known isotopic composition, prepared from nearly isotopically pure separated nickel isotopes, were used to calibrate the mass spectrometers.

900,544 PB90-163908

(Order as PB90-163874, PC A04) National Inst. of Standards and Technology, Gaithers-

Absolute Isotopic Composition and Atomic Weight of Terrestrial Nickel.

J. W. Gramlich, E. S. Beary, L. A. Machlan, and I. L. Barnes. 1989, 6p Included in Jnl. of Research of the National Institute of

Standards and Technology, v94 n6 p357-362 1989.

Keywords: *Nickel isotopes, *Atomic weight, Concentration(Composition), Mass spectrometers, Standards, Accuracy.

Twenty-nine samples of high-purity nickel metals, reagent sales and minerals, collected from worldwide sources, have been examined by high-precision iso-tope ratio mass spectrometry for their nickel isotopic composition. These materials were compared directly with SRM 986, certified isotopic standard for nickel, using identical measurement techniques and the same instrumentation.

900 545 PB90-163916

(Order as PB90-163874, PC A04) National Inst. of Standards and Technology, Gaithersburg, MD.

Report on the 1989 Meeting of the Radionuclide Measurements Section of the Consultative Com-mittee on Standards for the Measurement of Ioniz-Ing Radiations: Special Report on Standards for Radioactivity.
D. D. Hoppes. 1989, 4p
Included in Jnl. of Research of the National Institute of

Standards of Technology, v94 n6 p363-366 1989.

Keywords: *Radioactivity, *Radioactive isotopes, *Ionizing radiation, Standards, Measurement.

The report describes the activities discussed at the 10th meeting of Section II of the Consultative Committee on Standards for the Measurement of Ionizing Radiations held in May 1989 at Sevres (France). Topics included present and future international comparisons of activity measurements, the status and possible ex-tension of the International reference system for activity measurements of gamma-ray emitting nuclides, reports from other working groups, accomplishments at the International Bureau of Weights and Measures.

Polymer Chemistry

900.546 PB89-146724 Not available NTIS National Bureau of Standards (IMSE), Gaithersburg, MD. Polymers Div.

Effect of Crosslinks on the Phase Separation Behavior of a Miscible Polymer Blend.

Final rept.

R. M. Briber, and B. J. Bauer. 1988, 8p Pub. in Macromolecules 21, n11 p3296-3303 Nov 88.

Polymer Chemistry

Keywords: *Irradiation, *Crosslinking, *Polystyrene, *Vinyl ether resins, Phase diagrams, Neutron scattering, Solubility, Blending, Polymers, Reprints.

The effect of radiation cross-linking on the phase diagram and scattering function for a compatible polymer blend of deuterated polystyrene and poly(vinyl methyl ether) has been examined by small angle neutron scattering. The scattering curves for the cross-linked blends exhibit a maximum at a nonzero q vector, the position of which depends linearly on the square root of the radiation dose or inversely on the square root of the number of repeat units between cross-links. This dependence was predicted by de Gennes, but the measured position of the maximum is smaller than predicted. The spinodal temperature can be determined dicted. The spinodal temperature can be determined by plotting the inverse of the scattered intensity at the maximum, S(q sub *) sup minus one, versus inverse temperature and extrapolating to the point where S(q sub *) sup minus one = 0. The inverse of the measured spinodal temperature depends linearly with radiation dose or with N sup minus one as predicted. This increases the size of the single phase region of the phase diagram with the extrapolated spinodal temperature increasing from 149 deg C for the uncross-linked blend to 430 deg C for the blend with a radiation dose of 125 Mrad. The theory by de Gennes predicts that the scattered intensity at q = 0 equals 0 for the cross-linked blends which is not observed experimentally.

900,547 **PB8**9**-14702**9 PB89-147029 Not available NTIS National Bureau of Standards (NML), Gaithersburg, MD. Ionizing Radiation Physics Div. Hydroxyl Radical Induced Cross-Linking between Phenylalanine and 2-Deoxyribose.

Final rept. M. Farahani, and M. G. Simic. 1988, 4p Pub. in Biochemistry 27, n13 p4695-4698, 28 Jun 88.

Keywords: *Chemical reactions, *Crosslinking, *Phen-ylalanine, Chemical radicals, Oxygen, Free radicals, Separation, Gas chromatography, Mass spectroscopy, Models, Deoxyribonucleic acids, Proteins, Amino acids, Radiation chemistry, Reprints, *Deoxyribose, Oxygen radicals.

Hydroxy radicals induce cross-linking between pheny-lalanine (Phe) and 2-deoxyribose (dR) via formation of corresponding free radical intermediates. The crosslinked products were separated and identified by capillary gas chromatography-mass spectrometry. When phenylalanine and 2-deoxyribose radicals were generated in a 1:1 ratio, the predominant interaction was be-tween Phe and dR radicals while the Phe-Phe and dR-dR cross-links were less abundant. The newly discovered cross-link between 2-deoxyribose and phenylalanine may serve as a model for radiation or free radical induced cross-linking between DNA and proteins and in general between sugar moieties and amino

PB89-157093 Not available NTIS National Bureau of Standards (IMSE), Gaithersburg, Resonant Raman Scattering of Controlled Molecular Weight Polyacetylene.

Final rept. M. A. Schen, J. C. W. Chien, E. Perrin, S. Lefrant, and E. Mulazzi. 1988, 6p Pub. in Jnl. of Chemical Physics 89, n12 p7615-7620,

15 Dec 88.

Keywords: *Acetylene, *Molecular weight, *Catalysts, *Polymers, Titanium, Synthesis, Organometallic compounds, Metal complexes, Aluminum, Raman spectra, Oxidation, Isomerization, Electrical resistivity, Reprints.

Polyacetylene, (CH) sub x, films of 500, 5300, 10,500, and 100,000 Daltons number average molecular weights (M sub n) were synthesized using the titanium tetra-n-butoxide/triethyl aluminum-catalyst/cocatalyst system and examined using resonant Raman scattering techniques. Before isomerization, trans segments are found to exist mainly as short, isolated sequences independent of M sub n. After thermal isomerization, theoretical analysis of the RRS spectra using the Brivio, Mulazzi model indicate the ratio of long trans conjugated segments (N is greater than or equal to 30) to short trans conjugated segments (N is less than or equal to 30) is significantly larger for 100,000 Dalton polymer in comparison to polymer of 10,500 M sub n and below. For samples below 10,500 Daltons, no clear relationship between actual polymer molecular

weight and G is observed. Optimization of the isomerization conditions for 100,000 Dalton polymer results in trans-(CH) sub x with a G=0.80. These results suggest that not until very long molecular chains are obtained can samples composed principally of long conjugated segments be obtained. It is proposed that defects which arise during and after the polymerization limit the content of long segments. Ambient, short term oxidation of 100,000 M sub n polymer shows a decrease in G from 0.80 to 0.70. Low-level chain oxidation or doping is shown to preferentially occur within long conjugated segments.

900,549 PB89-157465 Not available NTIS National Bureau of Standards (NEL), Gaithersburg, MD. Building Materials Div. Thermal Degradation of Poly (methyl methacry-

late) at 50 C to 125 C.

Final rept. Final rept.

J. W. Martin, D. P. Bentz, W. E. Byrd, B. Dickens, E. Embree, W. E. Roberts, and D. Waksman. 1987, 17p Sponsored by Department of Energy, Washington, DC. Pub. in Jnl. of Applied Polymer Science 34, n1 p377-393 1987

Keywords: *Chemical bonds, *Cleavage, *Polymers, *Polymethyl methacrylate, Thin films, Temperature, Free radicals, Oxidation, Reprints.

Small but significant numbers of chain scissions occur in a commercial poly (methyl methacrylate) film exposed to temperatures between 50 and 125 C. The scission rate is initially rapid and then slows down to a constant rate. The initial rate of chain scissions is temperature dependent, while the long-term rate of chain scissions appears to be temperature independent. Four modes of failure are proposed to explain the results: (1) the presence of unreacted initiators of polymerization; (2) free radicals generated from additives in the commercial film; (3) weak links in the polymer chain; and (4) free radicals generated in the thermal decomposition of an oxidation product of the monomer methyl methacrylate. The mode of failure which is most consistent with the experimental results is the one involving free radicals generated from an oxidation product of monomer.

900,550 PB89-157473 Not available NTIS National Bureau of Standards (IMSE), Gaithersburg,

MD. Polymers Div.
Temperature, Composition and Molecular-Weight
Dependence of the Binary Interaction Parameter
of Polystyrene/Poly(vinylmethylether) Blends. Final rept

M. Okada, Q. Tran-Cong, and T. Chang. 1988, 13p Pub. in Polymer 29, p2002-2014 Nov 88.

Keywords: *Polystyrene, *Polymers, *Neutron scattering, *Free energy, *Vinyl ether resins, Isotopic labelling, Deuterium, Molecular weight, Temperature, Chemical composition, Mixtures, Reprints.

The binary interaction parameter has been obtained for deuterated polystyrene/poly(vinyl methyl ether) blends as a function of temperature, composition and molecular weight from small-angle neutron scattering experiments. The consistency of the correlation length epsilon, the zero-wavenumber scattering intensity S(0) and the chi sub eff parameter with the mean-field prediction has been demonstrated by the q dependence of the static structure factor S(q) and the 1/T dependence of epsilon sup -2, S(0) sup -1 and chi sub eff. The effective interaction parameter chi sub eff can be related to the Flory-Huggins interaction parameter chi sub F. The free-energy function as well as the spinodal curve and cloud-point curve have been constructed.

PB89-161616 Not available NTIS National Bureau of Standards (IMSE), Gaithersburg, MD. Polymers Div. Characterization

Synthesis and Poly(vinylmethyl ether). Final rept.

J. Bauer, B. Hanley, and Y. Muroga. 1989, 3p Pub. in Polymer Communications 30, p19-21 Jan 89.

Keywords: *Polymerization, *Molecular weight, Reprints, *Poly(ether/vinylmethyl).

High molecular weight poly(vinylmethyl ether) has been produced by cationic polymerization with boron trifluoride ethyl ether complex as an initiator. The polymer has a broad molecular weight distribution, but multiple fractionations with toluene as solvent and hep-tane as non-solvent produced samples with M(sub w)/ M(sub n) as low as 1.2.

900 552 PB89-172449 Not available NTIS National Bureau of Standards (IMSE), Gaithersburg, MD. Polymers Div.

Concentration Dependence of the Compression Modulus of Isotactic Polystyrene/Cis-Decalin

J. M. Guenet, and G. B. McKenna. 1986, 10p Pub. in Jnl. of Polymer Science 24, n11 p2499-2508 Nov 86

Keywords: *Polystyrene, *Decalin, *Gels, *Compressing, *Quenching(Cooling), *Micelles, Polymers, Modulus of elasticity, Phase diagrams, Reprints.

New results for isotactic polystyrene/cis-decalin gels are presented which suggest that a simple fringed micellar model of the gel may not be appropriate. In measuring the room temperature compressive modulus of gels formed at -20C, it was found that, not only are the gols time decadent but sleet that the incoher are the gels time dependent but also that the isochro-nal modulus-concentration diagrams exhibit sharp features reminiscent of a phase diagram rather than the smooth curves (straight lines) typical of swollen rubber and fringed micellar gels.

900,553 PB89-172456 Not available NTIS National Bureau of Standards (IMSE), Gaithersburg, MD. Polymers Div.

Effects of Solvent Type on the Concentration Dependence of the Compression Modulus of Thermoreversible Isotactic Polystyrene Gels.

G. B. McKenna, and J. M. Guenet. 1988, 10p Pub. in Jnl. of Polymer Science B, Polymer Physics 26, n2 p267-276 Feb 88.

Keywords: *Polymers, *Polystyrene, *Decalin, *Gels, *Compression, Quenching(Cooling), Chlorohydrocarbons, Modulus of elasticity, Relaxation(Mechanics), Stresses, Reprints

Solutions of isotactic polystyrene in either trans-decalin or 1-chlorodecane were transformed into gels by quenching from a high temperature (approximately 180 C) to -20 C. The relaxation modulus in compression of these gels was measured over a range of concentrations of from 0.04 g/g to 0.40 g/g. At 22 C the gels show a double logarithmic stress relaxation rate, m, which is higher than for polyvinylchloride and gelatin gel systems. 120s isochronal modulus concentration diagrams exhibit non-power law behavior, i.e., not only is the general trend such that the double logarith-mic slope decreases with increasing concentration, but there are also regions in which abrupt changes in modulus occur over narrow ranges in concentrations. These features in the concentration dependence of the modulus are less pronounced than those found previously in isotactic polystyrene/cis-decalin gels. The behavior is interpreted to be inconsistent with a fringed micelle picture of the gel structure.

Not available NTIS National Bureau of Standards (IMSE), Gaithersburg, MD. Polymers Div.

Measurement of the Torque and Normal Force In Torsion in the Study of the Thermoviscoelastic Properties of Polymer Glasses. Final rept.

G. B. McKenna. 1985, 15p Pub. in Relaxations in Complex Systems, p129-143

Keywords: *Torsion tests, *Polymers, *Glass, *Aging tests(Materials), *Volume, *Polymethyl methacrylate, Torque, Viscoelasticity, Thermal properties, Normal strain, Strain measurement, Reprints.

The simultaneous measurement of the torque and normal force responses in torsion experiments on vis-coelastic materials provides multidimensional (multiaxial) data from a single simple test geometry. Data are presented which support the important theoretical prediction that in two step torsional deformations where the magnitude of the second step is one-half the magnitude of the first step, the normal stress response is predicted to be independent of the duration of the first

Polymer Chemistry

step and equal to the single step response to a deformation of the same magnitude as the second step. The second program involves a study of physical aging in a freshly quenched polymer glass of polymethyl methacrylate.

Not available NTIS PB89-172480 National Bureau of Standards (IMSE), Gaithersburg, MD. Polymers Div.

Viscosity of Blends of Linear and Cyclic Molecules of Similar Molecular Mass.

Final rept.

G. B. McKenna, and D. J. Plazek. 1986, 3p Pub. in Polymer Communications 27, n10 p304-306

Keywords: *Polymers, *Molecular weight, *Polystyrene, *Melt viscosity, Contamination, Chains, Rings, Linearity, Cyclization, Reprints, Reptation.

Narrow fractions of linear polystyrene were added to cyclic polystyrenes of similar molecular weights. For weight concentrations, theta sub c, of the cyclic polymers from 0.85 to 1.0, it is found that the zero shear viscosity varies as theta sub c sup (-5.6). These results suggest that discrepancies between reports in the literature for the molecular weight dependence of the melt viscosity of cyclic polymers can only be partially ac-counted for by contamination of the rings with linear

PB89-173801 Not available NTIS National Bureau of Standards (NEL), Gaithersburg,

MD. Building Materials Div.
Preliminary Stochastic Model for Service Life Prediction of a Photolytically and Thermally Degraded Polymeric Cover Plate Material.

Final rept.

Final rept.

J. Martin, D. Waksman, D. Bentz, J. A. Lechner, and B. Dickens. 1984, 20p

Pub. in Proceedings of International Conference on the Durability of Building Materials and Components. (3rd), Espoo, Finland, August 12-15, 1984, v3 p549-568

Keywords: *Plates(Structural members), *Durability, *Service life, *Thin films, *Polymethyl methacylate, Stochastic processes, Mathematical model, Forecasting, Thermal degradation, Photodegradation, Failure, Polymers, Molecular weight, Oxidation.

A preliminary stochastic model has been developed and partially validated for predicting the service life of a polymeric film, such as poly(methyl methacrylate) (PMMA), which is subjected to both thermal and photolytic degradation. The exposure conditions under which degradation is induced simulate those expected for a polymeric cover plate material in an active solar collector. Service life for a population of films is defined as that time beyond which an unacceptable portion of the population fails. The criterion used for failure of a film is that its number average molecular weight has fallen below a specified threshold value.

PB89-176028 Not available NTIS National Bureau of Standards (IMSE), Gaithersburg, MD. Polymers Div.

Theory of Microphase Separation in Graft and Star Copolymers.

Final rept.
M. O. de la Cruz, and I. C. Sanchez. 1986, 8p
Pub. in Macromolecules 19, n10 p2501-2508 1986.

Keywords: *Polymers, *Graft polymerization, *Phases, *Separation, Radius of gyration, Critical point, Re-

Phase stability criteria and static structure factors have been calculated for simple AB graft copolymers, for star copolymers with equal number of A and B arms, and for n arm star diblock copolymers. The A-B interactions are characterized by the usual chi parameter. The fraction of A monomer in the graft copolymer is denoted as f and the fractional position along the A chain backbone at which the B graft is chemically linked is denoted as tan. When tan equals 0 or 1 the graft copolymer degenerates to a simple diblock co-polymer. Leibler previously calculated that the critical value, (chi N)c, at which a AB diblock copolymer containing N monomer units undergoes microphase separation is 10.5. The critical value occurs at f equals 0.5 and is the only composition for which the transition is second order. According to the present theory, a graft copolymer (0 < tau < 1) does not have a critical point for any f; i.e. all transitions are first order.

Not available NTIS National Bureau of Standards (IMSE), Gaithersburg, MD. Polymers Div.
Solid State (13)C NMR Investigation in Polyoxe-

tanes. Effect of Chain Conformation. Final rept.

E. Perez, and D. L. VanderHart. 1987, 6p. Pub. in Polymer 28, n5 p733-738 1987.

Keywords: *Polymers, *Nuclear magnetic resonance, *Carbon, Solids, Amorphous materials, Crystal structure, Reprints, Carbon 13, Polyoxetanes, Conformational changes.

Carbon-13 nuclear magnetic resonance (NMR) in the solid state has been applied to the study of poly(oxetane) and poly(3,3-dimethyloxetane). Two different crystalline modifications, with T2G2 and T3G conformations, have been prepared for each of the polymers. The corresponding (13)C chemical shifts for each sample, both amorphous and crystalline, have been determined. Single resonances for the methylene carbons alpha to the oxygens, are observed for the crystal having T2G2 conformation. Two reson-ances are observed for these carbons in crystals having T3G conformation. The equivalence of these carbons in the T2G2 conformation and their inequivalence, within the same monomer unit, in the T3G conformation is a property of the isolated chain.

900 559 PB89-176044 Not available NTIS National Bureau of Standards (IMSE), Gaithersburg,

MD. Polymers Div.

Polymer Localization by Random Fixed Impurities: Gaussian Chains.

Final rept.

J. Douglas. 1988, 5p Pub. in Macromolecules 21, n12 p3515-3519 Dec 88.

Keywords: *Polymers, *Monte Carlo method, *Chains, Impurities, *Molecular structure, Scalars, Surface chemistry, Electron distribution, Interactions, Random processes, Position(Location), Reprints.

Simple dimensional analysis is employed to discuss the relevance of impurity interactions on the molecular dimensions of flexible polymers in the limits of highand low-impurity densities. Scaling arguments account for the universal behavior of static properties observed by Baumgartner and Muthukumar in their recent Monte Carlo simulations. An approximate model of the random impurity interaction is introduced by considering the random impurities as being analogous to an effective surface with which the polymer interacts. Qualitatively the same conclusions are obtained as in the scaling arguments except that the effective surface analogy provides closed form scaling functions de-scribing the variation of the molecular dimensions as a function of the dimensionless disorder interaction. The transition to a collapsed state is found to be characterized by a critical impurity density which is a function of the chain length.

900,560 PB89-176051 Not available NTIS National Bureau of Standards (IMSE), Gaithersburg,

MD. Polymers Div.

Morphological Partitioning of Ethyl Branches in Polyethylene by (13)C NMR.

Final rept.

ration, Reprints.

E. Perez, B. Crist, P. R. Howard, and D. L. Vanderhart. 1987, 10p Pub. in Macromolecules 20, n1 p78-87 1987.

Keywords: *Proton magnetic resonance, *Polybutadiene, *Polyethylene, Carbon 13, Hydrogen, Alkanes, Crystallinity, Morphology, Polarization, Diffusion, Sepa-

A combination of (13)C and proton magnetic reso nance experiments has been performed on a model ethylene copolymer (hydrogenated polybutadiene) of about 100,000 molecular weight and 17 ethyl branches per 1000 total carbons. The fraction of ethyl branches found in the crystal in this 41%-crystalline sample was 0.06 + or - 0.02, and the ratio of concentrations between the crystalline and non-crystalline regions was correspondingly about 1:10. For reasons of best integrability, the methyl resonance of the ethyl branches was used to deduce the concentrations in each morphological phase. The same resonance is rather ill-behaved in cross-polarization experiments so that several auxiliary experiments were undertaken to deduce the true concentrations attributed to each phase. The experimental technique utilizes cross-polarization as a probe of proton polarization levels; moreover, the success of the method relies on local proton spin diffu-

900.561

PB89-176069 Not available NTIS National Bureau of Standards (IMSE), Gaithersburg, MD. Polymers Div.

Microphase Separation in Blockcopolymer/Homopolymer. Final rept.

M. O. de la Cruz, and I. C. Sanchez. 1987, 4p Pub. in Macromolecules 20, n2 p440-443 1987.

Keywords: *Phases, *Separation, *Polymerization, Scattering, Mixtures, Chemical analysis, Reprints.

Microphase separation in an A-B blockcopolymer with B homopolymer blend is analyzed. Let theta be the concentration of homopolymer, f the fraction component A along the blockcopolymer, N the degree of po-lymerization of the blockcopolymer and r the ratio of the blockcopolymer to homopolymer degree of polymerization. The scattering function for such a system is obtained. The variations of the spinodal temperature (chi N)s and the wave vector at which the scattering function diverges, q*, are obtained as a function of f, theta, and r in the vicinity of the critical point of a pure blockcopolymer melt (q-o, f=0.5). It is found that (chi N)s and q^* can increase or decrease with respect to the values at theta = zero.

900,562 PB89-176085 Not available NTIS National Bureau of Standards (IMSE), Gaithersburg, MD. Polymers Div.

Crazes and Fracture in Polymers.

Final rept.

E. Passaglia. 1987, 26p

Pub. in Jnl. of Physics and Chemistry of Solids 48, n11 p1075-1100 1987.

Keywords: *Crazing, *Microstructure, *Thermoplastic resins, *Fractures(Materials), *Crack propagation, Polymers, Surveys, Stress analysis, Bursting, Reprints,

A review of crazes in glassy thermoplastic polymers is presented with particular emphasis on those aspects of craze properties that influence and control fracture behavior. Both crazes as they normally occur and crazes at the tip of cracks are covered. The occurrence of crazes, their microstructure, the stress distribution within them and the nature of craze fibrils are discussed. Theoretical treatments of the effect of crazes on polymer fracture are reviewed.

900,563 PB89-176424 Not available NTIS National Bureau of Standards (NEL), Gaithersburg, MD. Chemical Process Metrology Div.

Polymeric Humidity Sensors for Industrial Process Applications. Final rept.

P. H. Huang. 1988, 11p Pub. in Proceedings of Annual Sensors Expo Interna-tional (3rd), Chicago, IL., September 13-15, 1988, p106B-1-106B-16.

Keywords: *Detectors, *Humidity, *Polymers, Measurement, Moisture meters, Thermoplastic resins, Thermoset resins, Industrial engineering, Process control.

Humidity/moisture sensing and measurement techniques are summarized as an introduction. Various commercially available sensors for the on-line determination of humidity/moisture in gases, liquids and solids are described. The advantages and disadvantages of the individual sensor types are listed. Polymeric humidity sensors are now finding increasing use in industrial process applications. This is made possible by the recent advances in polymer science and technology. The paper deals with the current status of research in polymeric humidity sensors which are based on the use of thermoplastics and thermosets.

900,564

PB89-179246 Not available NTIS National Bureau of Standards (IMSE), Gaithersburg, MD. Polymers Div.

CHEMISTRY

Polymer Chemistry

Influence of Molecular Weight on the Resonant Raman Scattering of Polyacetylene.

M. A. Schen, S. Lefrant, E. Perrin, J. C. W. Chien, and E. Mulazzi. 1989. 8p Pub. in Synthetic Metals 28, pD287-D294 1989

Keywords: *Polymers, *Acetylene, *Molecular weight, *Oxidation, *Raman spectra, Catalysis, Titanium, Aluminum, Mathematical models, Resonance, Reprints.

For the first time, polyacetylene, (CH)x, films of known number average molecular weights, Mn, have been examined using Resonance Raman Scattering techniques. (CH)x samples of 500, 5300, 10500, and 100,000 Daltons were synthesized using the classical titanium tetra-n-butoxide/triethyl aluminum catalyst/ cocatalyst system. After thermal isomerization, model-ing of the RRS spectra using the Brivio, Mulazzi model indicate that the 100,000 Dalton polymer is composed principally of long transconjugated segments. In contrast, polymers of 10500 Mn and below are seen to contain significantly larger fractions of short trans conjugated segments. For samples below 10500, no clear relationship between actual polymer molecular weight relationship between actual polymer molecular weight and G, the ratio of long to short segments, is observed. These results suggest that not until very long chains are obtained can samples containing a large fraction of long conjugated segments be obtained. Ambient, short term oxidation of 100,000 Mn polymer shows an increase in satellite band intensities at omega (c-c) and omega (c=c), where omega is frequency, which corresponds to a decrease in G. Low level chain oxidation or doping is shown to preferentially occur within long conjugated segments.

900,565 PB89-186365 Not available NTIS National Bureau of Standards (IMSE), Gaithersburg,

MD. Polymers Div. Deuterium Magnetic Resonance Study of Orientation and Poling in Poly(Vinylidene Fluoride) and Poly(Vinylidene Fluoride-Co-Tetrafluoroethylene). Final rept.

M. A. Doverspike, M. S. Conradi, A. S. DeReggi, and R. E. Cais. 1989, 7p

Pub. in Jnl. of Applied Physics 65, n2 p541-547, 15 Jan

Keywords: *Tetrafluoroethylene resins, *Nuclear magnetic resonance, Vinyl copolymers, Orientation, Deuterium, Molecular structure, Reprints, *Vinylidene fluonde polymers, Poling.

Deuteron nuclear magnetic resonance line shapes are reported for oriented samples of poly(vinylidene fluo-ride) and an (80-20) copolymer of vinylidene fluonde and tetrafluoroethylene. For stretched samples the orientation of the chain axes with respect to the stretch direction is given by a Gaussian distribution of width about 20 degrees. The width of the distribution was slightly smaller in the more highly stretched copolymer. Surprisingly, as the magnetic field is rotated in the plane perpendicular to the stretch direction, the deute-rium spectra of the poled copolymer sample do not change. The occurrence of electrical polarization in the absence of orientation dependence of the deuterium line shape indicates molecular reorientation through 180 degrees in the copolymer.

900,566 PB89-188601 PC A06/MF A01 National Bureau of Standards (IMSE), Gaithersburg, MD. Polymers Div.

institute for Materials Science and Engineering,

Polymers: Technical Activities 1987. Annual rept. 1 Oct 86-30 Sep 87. L. E. Smith, and B. M. Fanconi. Nov 87, 104p NBSIR-87/3614 See also PB89-166094.

Keywords: *Polymers, *Research program administra-tion, Chemical properties, Mechanical properties, Standards, Composite materials, Blends, Durability, Processing, Technical activities, National Institute of Standards and Technology.

Technical Activities of the Polymers Division for FY 87 are reviewed. Included are descriptions of the 6 Tasks of the Division, project reports, publications, and other technical activities.

900,567 PB89-200430 Not available NTIS National Bureau of Standards (IMSE), Gaithersburg, MD. Polymers Div.

Dielectric Measurements for Cure Monitoring. Final rept.

F. I. Mopsik, S. S. Chang, and D. L. Hunston. 1989,

7p Pub. in Materials Evaluation 47, n4 p448-453, 465 Apr

Keywords: *Measurement, *Curing, *Epoxy resins, *Monitors, *Dielectric properties, Spectroscopy, Resistance, Viscosity, Ultrasonics, Reprints.

The use of dielectric measurements to monitor the cure of epoxy resins is investigated. Time-domain spectroscopy and an automated wide-dynamic-range AC-conductance measuring system show that dielectric loss and conductance measurements follow the entire cure cycle with good sensitivity and resolution. Comparisons with viscosity, differential scanning calorimetry (DSC) exotherm, and shear-mode ultrasonic attenuation measurements made simultaneously on the same sample show that dielectric methods compare very favorably with the others. In addition, a limit to the validity of a direct, simple relation between viscosity and dielectric loss is discussed. The conditions necessary for meaningful measurements are considered along with possible implementations of the method.

900.568 PB89-201487 Not available NTIS National Bureau of Standards (IMSE), Gaithersburg, MD. Polymers Div.

Thermal Analysis of VAMAS (Versailles Project on Advanced Materials and Standards) Polycarbonate-Polyethylene Blends.

Final rept.

S. S. Chang. 1989, 13p Pub. in Thermochimica Acta 139, p313-325 1989.

Keywords: *Thermogravimetry, *Polycarbonate resins, *Polyethylene, *Thermodynamic properties, Differential thermal analysis, Solubility, Melting points, Glass transition temperature, Specific heat, Heat of fusion, Compositions, Blends, Reprints.

Differential scanning calorimetry and thermogravimetric analysis were performed on a series of polycarbon-ate-polyethylene (PC-PE) blends, which were provided by the Technical Working Party of Polymer Blends, Versailles Project on Advanced Materials and Standards (VAMAS). Detailed comparison of results from cooperating laboratories were summarized. The PC-PE blends were found to be immiscible. Intensive properties such as melting points and glass transition tem-peratures were found to be independent of the compoperatures were found to be independent of the compo-sition. Extensive properties such as specific heat, heat of fusion and delta C(sub p); of glass transition were found to be nearly proportional to the composition. Onset and residues of degradation at different stages in thermogravimetric analysis were also found to be a function of the composition. Multiple melting peaks of low density polyethylene and relaxation peaks of annealed PC glass transition were also studied.

900,569 PB89-202451 Not available NTIS National Bureau of Standards (IMSE), Gaithersburg,

MD. Polymers Div.
13C NMR Method for Determining the Partitioning
of End Groups and Side Branches between the
Crystalline and Non-Crystalline Regions in Polyethylene.

Final rept. D. L. VanderHart, and E. Perez. 1986, 8p Pub. in Macromolecules 19, n7 p1902-1909 1986.

Keywords: *Carbon 13, *Nuclear magnetic resonance, *Crystal defects, *Polyethylene, Polymers, Butenes, Ethylene, Morphology, Separation, Spin lattice relaxation, Molecular structure, Reprints.

A butene-ethylene linear copolymer (BELC) is shown to give rise to a solid-state 13C spectrum, which contains resolvable resonances from vinyl and methyl end groups as well as ethyl side-branches. In contrast to the backbone methylene resonance which shows shifted, separable signals arising from the crystalline and non-crystalline regions, these weak 'defect' resonances show corresponding shifts too small to be definitive. Therefore, the problem of determining the particular tioning of defects between the crystalline and noncrystalline regions of polyethylene must be approached indirectly. The method for identifying the morphological origin of defect signals is based on the concept that 13C CP signals are proportional to the local spin polarization levels, which, in turn, are kept

quite uniform over distances of nearest neighbors because of proton spin diffusion. Thus, defect signal intensities are argued to be proportional to backbone signal intensities within a given morphological region. By isolating the backbone resonances corresponding to the pure crystalline and non-crystalline compo-nents, one thereby isolates the defect resonances.

900.570

Not available NTIS PB89-202923 National Bureau of Standards (IMSE), Gaithersburg, MD. Polymers Div.
Polymer Phase Separation.

Final rept.

I. C. Sanchez. 1987, 18p Pub. in Encyclopedia of Physical Science and Technology, v11 p1-18 1987.

Keywords: *Polymers, *Liquid phases, Thermodynamics, Separation, Agglomeration, Entropy, Reaction kinetics, Reprints.

A homogeneous polymer solution or mixture under certain thermodynamic conditions will separate into two or more liquid phases that differ in composition. Polymer solutions as a rule are very viscous and the time scales required to effect phase separation are much longer than for analogous mixtures involving only small molecules. In addition to kinetic differences, phase separation in polymer solutions differs qualita-tively in other important respects. In particular, polymer solutions are more susceptible, especially at elevated temperatures, to phase separation. The propensity for phase separation is related to the small entropy of mixing intrinsic to polymer solutions and a concomitant instability with respect to volume fluctuations. In a so-lution very dilute in polymer, phase separation can pro-ceed by the development of a polymer rich phase formed by intermolecular aggregation of the polymer chains. However, intramolecular aggregation will pre-cede the intermolecular aggregation process and cause a partial collapse of a coiling polymer chain. The latter process represents phase separation of isolated polymer chains.

900,571

PB89-202949 Not available NTIS National Bureau of Standards (IMSE), Gaithersburg, MD. Polymers Div.

Surface-interacting Polymers: An Integral Equation and Fractional Calculus Approach. Final rept.

J. F. Douglas. 1989, 12p

Pub. in Macromolecules 22, n4 p1786-1797 Apr 89.

Keywords: *Polymers, *Surface properties, Integral calculus, Friction, Eigenvalues, Reprints.

A method due to Feynman and Kac is used to convert the path integral formulation of surface (variable sur-face dimension) interacting polymers into an equiva-lent integral equation approach. The integral equation for the surface-interacting chain partition function is determined to be the Volterra analogue of the Fred-holm integral equation describing the friction coefficient in the preaveraged Kirkwood-Riseman theory. The approach to surface interacting polymers thus clarifies the close interconnection between the surface interaction and Kirkwood-Riseman theories noted in previous renormalization group calculations. An exact solution of the surface-interacting chain partition function is obtained by using the Riemann-Liouville fractional calculus. Finally, the integral equation and fractional calculus methods are combined to explain some of the most conspicuous features of the renormalization group theory--the mathematical significance of the 'crossover exponent,' 'infrared fixed point,' nontrivial 'critical exponents,' and the pole structure found in the interaction perturbation theory. The integral equation-fractional calculus formalism is also used to examine a point of 'critical instability' defining the adsorption threshold and to examine the failure of the renormalization group and eigenfunction expansion methods to describe scaling functions for values of the interaction near the instability point. The critical instability is readily understood on the basis of the Fredholm alternative. tional calculus methods are combined to explain some

900,572

Not available NTIS PB89-212021 National Bureau of Standards (NEL), Gaithersburg, MD. Fire Measurement and Research Div. Effects of Material Characteristics on Flame Spreading.

rina rept.
Tkashiwagi, A. Omori, and J. Brown. 1989, 11p
Pub. in Proceedings of International Symposium on
Fire Safety Science (2nd), Tokyo, Japan, June 13-17,
1989, p107-117. Final rept.

Keywords: *Polystyrene, *Polymethyl methacrylate, *Flame propagation, Molecular weight, Thermal stability, Melt viscosity, Spreading, Polymers.

Effects of initial molecular weight and thermal stability of polymer samples on horzontal flame spreading behavior and spread rate were studied by comparing results between two polystyrene (PS) samples with different initial molecular weights and between two poly(methylmethacrylate) (PMMA) samples with differ-ent thermal stability and initial molecular weights. The flame spread rate of the higher molecular weight PS sample was about 25% larger than that for the low mo-lecular weight PS sample and the flame spread rate of the higher molecular weight PMMA sample was about four times larger than that for the low molecular weight four times larger than that for the low molecular weight sample. The sample with high initial molecular weight does not form molten polymer near the flame front and the flame spreads steadily. However, the sample with low initial molecular weight forms molten polymer and the opposed slow fluid motion of molten polymer along the inclined vaporizing surface against the traveling flame significantly affects flame spreading behavior

900,573

PB89-228589 Not available NTIS National Inst. of Standards and Technology (IMSE), Gaithersburg, MD. Ceramics Div.

Reevaluation of Forces Measured Across Thin

Polymer Films: Nonequilibrium and Pinning Effects.

Final rept.

Final rept.

R. G. Horn, S. J. Hirz, G. Hadziioannou, C. W. Frank, and J. M. Catala. 1989, 8p

Sponsored by Office of Naval Research, Arlington, VA. Pub. in Jnl. of Chemical Physics 90, n11 p6767-6774, 1 Jun 89.

Keywords: *Polymers, *Fluid friction, *Thin films, *Siloxanes, *Interfacial tension, Measurement, Surface properties, Drag, Viscosity, Molecular structure, Liquid phases, Reprints, *Pinning.

Forces between molecularly smooth solid surfaces separated by thin films of molten polydimethylsiloxane have been measured. A long-range repulsion reported in earlier work is not an equilibrium force, but can be attributed to viscous drag effects. Consistent with pre-vious results, the viscosity of the film can be modeled by assuming that a layer of polymer molecules is im-mobilized or pinned at each surface for a time longer than the time scale of the measurements. The pinning is a result of entanglement-like effects in the vicinity of a wall.

900,574

PB89-229264 Not available NTIS National Inst. of Standards and Technology (IMSE),

Gaithersburg, MD. Polymers Div.
Shear Effects on the Phase Separation Behaviour of a Polymer Blend in Solution by Small Angle Neutron Scattering.

A. I. Nakatani, H. Kim, Y. Takahashi, and C. C. Han.

1989, 4p Pub. in Polymer Communications 30, p143-146 May

Keywords: *Polymers, *Blends, *Boundary layer separation, *Neutron scattering, Polystyrene, Poly butadiene, Plastics, Elastomers, Phthalates, Shear rate, Phase, Settling, Reprints.

The phase separation behavior of polystyrene and polybutadiene in dioctyl phthalate has been examined as a function of shear rate by small angle neutrons scattering. A couette geometry shear cell was used to apply a shear field to the solution at various temperatures. Differences in the correlation lengths parallel and perpendicular to the flow direction were observed by assuming mean field behavior of the solution. Dramatic decreases in the spinodal temperature were ob-served as a function of shear rate in the direction of flow. The results are consistent with the notion of shear stabilization and decoupling of the flow field in orthogonal directions.

900,575 PB89-231286 Not available NTIS National Inst. of Standards and Technology (IMSE), Gaithersburg, MD. Polymers Div.

Polymerization of a Novei Liquid Crystailine Diacetviene Monomer.

Final rept. M. A. Schen. 1988, 8p

Pub. in Proceedings of SPIE (Society of Photo-Optical Instrumentation Engineers) - Nonlinear Optical Proper-ties of Organic Materials, San Diego, CA., August 17-19, 1988, v971 p178-185.

Keywords: *Liquid crystals, *Polymers, *Acetylene, *Reaction kinetics, *Activation energy, *Order disorder transformation, Microscopy, Temperature, Heat

The polymerization of a liquid crystalline diacetylene monomer, 1,6 bis-(N-4-oxybenzylidene 4'-n-octylaniline) 2,4-hexadiyne, 1-OBOA, is reported both within the crystal and liquid crystal phases. The monomer exhibits smectic phase polymorphism at temperatures below the cleaning temperature as show by small angle C-ray scattering and optical microscopy. Polymerization kinetic results show first-order disappearance of monomer as seen by differential scanning calorimetry with a thermal activation energy of 31 kcal/mol. in the liquid crystal phase and approximately 71 kcal/mol. in the crystal phase. Poly(1-OBOA) exhibits a 'soft' lamellar-like layer structure reminiscent of the monomer when polymerized within a low temperature liquid crystal phase. Consequently, the topochemical polymerization of diacetylene monomers within a liquid crystal phase to give ordered polymer structures is reported for the first time.

900.576 PB90-117524 Not available NTIS National Inst. of Standards and Technology (IMSE),

Gaithersburg, MD. Polymers Div.
Off-Lattice Simulation of Polymer Chain Dynamics.

D. Eichinger, D. Kranbuehl, and P. Verdier. 1989, 2p Pub. in Polymer Preprints 30, p45-46 1989.

Keywords: *Polymers, *Computerized simulation, *Lattice parameters, Mathematical models, Monte Carlo method, Coils, Molecular structure, Reprints.

The use of lattice model chains and Monte Carlo techniques has been the basis of numerous studies on the dynamics of random coil polymer chains. The majority of papers have focused on the effect of excluded volume and its associated effects of chain connectivity-entanglement on the dynamic properties of poly-mer chains as a function of chain length and segment density. At the same time, the increasing use of lattice models and the disagreement generated by the predictions have heightened concern about the possibility of anomalous effects due to the lattice constraints and the choices of bead movement rules. In order to study the effects of both the lattice constraints and the bead movement rules on chain dynamics, simulations in which no lattice constraints are present have been carried out. Overall the off lattice results, as did the recent SC, BCC and FCC simulations show with remarkable consistency that excluded volume can cause an additional lengthening of a single chain's longest relaxation time well beyond the value observed for equilibrium properties.

900,577 PB90-123456 Not available NTIS Not available (MSE),
National Inst. of Standards and Technology (IMSE),
Gaithersburg, MD. Polymers Div.
Small Angle Neutron Scattering Studies of Single

Phase interpenetrating Polymer Networks. Final rept.

B. J. Bauer, R. M. Briber, and C. C. Han. 1987, 2p. Pub. in Polymer Preprints 28, n2 p169-170 1987.

Keywords: *Polymers, *Networks, *Neutron scattering, Vinyl ether resins, Polystyrene, Crosslinking, Deuteration, Phase transformations, Deformation, Stability, Compressing, Solubility, Reprints, ty, Compressing Synthesis(Chemistry).

Compatible semi-interpenetrating polymer networks (IPN) have been synthesized from linear poly(vinylmethylether) and deuterated poly(styrene) crosslinked with divinyl benzene. The phase separation behavior of the IPNs has been studied by small angle neutron scattering. At the temperature of synthesis increasing the PSD crosslink density decreases

the miscibility of the system. However, once a compatible IPN has been formed, the presence of the crosslinks increases the single phase stability as the tem-perature is raised. The influence of deformation on phase separation behavior of the samples was also studied. A sample was deformed to 2.5 times the original length by compressing the sample and constraining it to elongate in one direction only. The scattering data indicate that the miscibility is decreased significantly along the deformation direction when compared to the undeformed sample.

900,578

PB90-136813 PB90-136813 Not available NTIS National Bureau of Standards (IMSE), Gaithersburg, MD. Polymers Div.

Charging Behavior of Polyethylene and ionomers. Final rept.

M. G. Broadhurst, A. S. DeReggi, G. T. Davis, and F. I. Mopsik. 1987, 6p

Pub. in Proceedings of Conference on Electrical Insulation and Dielectric Phenomena, Gaithersburg, MD., October 18-22, 1987, p313-318.

Keywords: *Charging, *Polyethylene, *Ions, Electric charge, Polymeric films, Plastics, Zinc, Methacrylic acid, Copolymers, Dielectric properties, Electrical insulation, Temperature.

The charging behaviors of films of polyethylene and zinc ionomers of polyethylene methacrylic acid copolymers are reported. Charge distributions across the thickness were measured with the thermal pulse method. Charging variables included applied fields from 0 to 50 V/micro, temperatures from 20 to 80 C, times unto account and legical differs. times up to one week and electrode metal. Initial differences in the signs and distributions of charge between nominally similar films were related to differences in the mechanical and thermal histories. At long charging times all films approach a steady state, nearly uniform distribution of negative charge. In the steady state the field due to the space charge was found to be a significant fraction of the applied charging field. The results are compatible with a model of homopolar injection of the applied that the control of the section of the sectio negative charge at the cathode and conduction of the injected charge through the film.

General

900.579

PB89-180038 Not available NTIS National Bureau of Standards (NML), Gaithersburg, MD. Office of Standard Reference Data Chemical and Spectral Databases: A Look into the

Future. Final rept

J. R. Rumble, and D. R. Lide. 1985, 5p Pub. in Jnl. of Chemical Information and Computer Sciences 25, p231-235 1985.

Keywords: *Chemistry, Chemical engineering, Information systems, Spectra, Reprints, *Data bases, Expert systems.

Over 50 databases of chemical and spectral information are now available, and in the coming years many more will be built. The paper discusses some of the current trends in the use of these databases and how such databases might affect chemistry.

CIVIL ENGINEERING

Construction Equipment, Materials, & **Supplies**

900.580

PB89-146971 Not available NTIS National Bureau of Standards (NEL), Gaithersburg, MD. Building Materials Div.

CIVIL ENGINEERING

Construction Equipment, Materials, & Supplies

interpretation of the Effects of Retarding Admixtures on Pastes of C3S, C3A plus Gypsum, and Portland Cement. Final rept.

H. M. Jennings, H. Taleb, G. Frohnsdorff, and J. R. Clifton. 1986, 5p

Pub. in Proceedings of International Congress on the Chemistry of Cement (8th), Rio de Janeiro, Brazil, September 22-27, 1986, p239-243.

Keywords: *Cements, *Hydration, *Retardants, Portland cements, Gypsum cements, Coagulation, Setting time, Reprints, Induction period, Tricalcium aluminate, Tricalcium silicate hydration.

From studies of the effects of a range of organic re-tarders on pastes of C3S and of C3A-gypsum, it may be concluded that the two systems have different, possibly independent, influences on the concentrations of retarders in the aqueous phase of a portland cement paste. In the case of C3S, some of the retarder is incorporated into the layer of product which forms around the grains during the early stages of reaction. It appears that a process which controls the induction period occurs within this C-S-H layer and that the incorporation of a retarder in it somehow slows the proccorporation or a retarder in it somenow slows the proc-ess. It may be that a phase change, or other reaction which ends the induction period by making the layer more permeable, is poisoned by the retarder which is incorporated into the layer. The C3A-gypsum-water system removes a large amount of retarder from the aqueous phase during the early stages of hydration, with the rate of removal falling with time. Delaying retarder addition, therefore, decreases the amount of re-tarder which can be incorporated into a C-S-H layer. Thus these systems affect, in separate ways, a retarder's ability to extend the induction period of a portland cement. There is a delay time after initial mixing, when it is most efficient to add a retarder. It seems probable that, at least for some organic retarders, the effects on the portland cement reaction may be considered to be a combination of separate processes occuring in the C3S-water and C3A-gypsum-water subsystems.

900,581
PB89-146989
Not available NTIS
National Bureau of Standards (NEL), Gaithersburg, MD. Building Materials Div.

implications of Computer-Based Simulation Models, Expert Systems, Databases, and Networks for Cement Research.

G. Frohnsdorff, J. Clifton, H. Jennings, P. Brown, L. Struble, and J. Pommershein. 1986, 5p Pub. in Proceedings of International Congress on the Chemistry of Cement (8th), Rio de Janeiro, Brazil, September 22-27, 1986, p598-602.

Keywords: *Cements, *Computer networks, *Research management, Chemical properties, Concretes, Hydration, Mathematical models, Decision making, Expenses, Physical management, *Data bases.

The simulation models, expert systems, and data-bases will complement each other to make possible improved predictions of performance of cements and concretes under diverse conditions, and improved decisions on selection of concrete materials; they will also facilitate identification of research needed to fill gaps in the knowledge base. More sharply focused statements of research needs should help improve decisions on research expenditures and lead to accelerated progress in cement research. Also, cooperative research efforts should become easier to carry out, thereby further contributing to the rate of progress. Examples from the authors' laboratory are used to illustrate some areas where computers are changing the direction of research related to cement hydration. They are: (1) modeling of microstructure development, (2) use of knowledge-based expert systems, and (3) storage, retrieval and transmission of knowledge needed for modeling and for expert system develop-ment. The implications of the growing ease of collec-tion, storage, retrieval, and sharing of knowledge, and the possible use of knowledge, probably by teams, in the development of interconnected computer-based knowledge systems are discussed. It is concluded that these developments provide new opportunities for collaboration among cement researchers. If exploited, these opportunities will accelerate progress in cement and concrete science and technology.

900,582 PB89-176119 Not available NTIS National Bureau of Standards (NEL), Gaithersburg, MD. Building Materials Div.

Integrated Knowledge Systems for Concrete and Other Materials. Final rept.

G. Frohnsdorff, H. Jennings, L. Struble, P. Brown, and J. Clifton. 1986, 4p

Pub. in Communications on the Materials Science and Engineering Study, p57-60 1986.

Keywords: *Concretes, *Materials, Information systems, Mathematical models, Simulation, Materials tests, Reprints, *Expert systems, *Data bases, Knowledge bases(Artificial intelligence).

Advances in understanding and the ability to predict the performance of concrete and other materials will result from the development of 'integrated materials knowledge systems' composed of expert systems, simulations models (and other mathematical models), and databases.

900.583 PB90-124306 PC A03/MF A01 National Inst. of Standards and Technology (NEL), Gaithersburg, MD. Center for Building Technology. Adsorption of High-Range Water-Reducing Agents on Selected Portland Cement Phases and Related Materials.

D. R. Rossington, and L. J. Struble. Sep 89, 27p NISTIR-89/4172

Prepared in cooperation with New York State Coll. of Ceramics, Alfred.

Keywords: *Portland cements, *Plasticizers, *Water reducing agents, *Adsorption, Concretes, Silicate cements, Chemical reactions, Silica materials, Slumping, Hydration, Chemical analysis.

The quantities of high-range water-reducing agents (superplasticizer) absorbed from their aqueous solutions by portland cement, tricalcium silicate, silica fume, wollastonite, and calcium silicate hydrate gel were determined using an ultraviolet spectrophoto-meter. The two superplasticizers (sulfonated melamine formaldehyde and sulfonated naphthalene formaldehyde) produced generally similar results. Wollastonite, a calcium silicate that does not react with water, produced no measurable adsorption of superplasticizer. The adsorption of superplasticizer by tricalcium silicate was similar to the adsorption by portland cement. From these results, it appears that superplas-ticizer is not absorbed by anhydrous silica or anhydrous calcium silicate, but rather by calcium silicate hydrate gel. Additional studies are recommended for im-proving the understanding of the absorption of superplasticizer by portland cement.

Highway Engineering

900,584 PB89-174924 PC A12/MF A01 National Inst. of Standards and Technology (NEL), Gaithersburg, MD. Center for Building Technology, Inelastic Behavior of Full-Scale Bridge Columns Subjected to Cyclic Loading.

W. C. Stone, and G. S. Cheok. Jan 89, 265p NIST/ BSS-166

Also available from Supt. of Docs. as SN003-003-O2925-4. Library of Congress catalog card no. 88-600600. Errata sheet inserted. on National Science Foundation, Washington, DC., Federal Highway Administration, Washington, DC., and California State Dept. of Transportation, Sacramento.

Keywords: *Bridges(Structures), *Columns(Supports), Cyclic loads, *Concrete structures, Elastic properties, Energy absorption, Failure, Dynamic structural analysis, Loading rate, Mechanical tests.

Circular, spirally reinforced concrete bridge columns were subjected to cyclic loading (representing seismic loads) in the laboratory. The test articles were proto-type columns designed in accordance with recent (1983) California Department of Transportation (CAL-TRANS) specifications. Two full-scale columns, each measuring 5 feet (1.52 m) in diameter with aspect ratios (height/width) of 3 and 6, were subjected to slow reversed cyclic lateral load with constant axial load to simulate the gravity weight of the bridge superstruc-ture. Details are presented concerning the design of the special test apparatus required to conduct the project as well as recommendations for future improvements in test procedures. Results from the tests are presented in the form of energy absorption graphs and bar charts, load-displacement hysteresis curves, longitudinal and confining steel strains, and curvature profiles. Comparisons of the ultimate moment capacities, measured displacement ductilities, plastic hinge lengths, cyclic energy absorption capacity and the fail-ure modes of the full-scale specimens are made with those observed from 1/6-scale model tests.

Soil & Rock Mechanics

900,585 PB89-147045 Not available NTIS National Bureau of Standards (IMSE), Gaithersburg, MD. Ceramics Div. Prediction of Tensile Behavior of Strain Softened Composites by Flexural Test Methods.

Final rept. T. J. Chuang, and Y. W. Mai. 1987, 11p Contract DE-Al05-80OR20679 Sponsored by Department of Energy, Oak Ridge, TN.

Oak Ridge Operations Office.
Pub. in Advanced Composite Materials and Structures, p647-657 1987.

Keywords: *Composite materials, *Tensile properties, *Fiber reinforced concretes, Bend test, Flexural strength, Loads(Forces), Tensile strength, Bending, Fiber composites, Reprints, Polymer concrete, Strain softening.

A simple scheme of predicting tensile properties of a composite exhibiting strain-softening behavior from flexural tests is developed based on establishment of a relationship between bending and tensile properties. It is shown that strain-softening materials give higher bending strengths than tensile strengths, a result consistent with experimental observation. Also, given the load-displacement diagram obtained from a flexural test, it is possible to predict the entire tensile response. Bending data of polymer concrete are used to demonstrate the strength of strate the principles.

COMBUSTION, **ENGINES**, & **PROPELLANTS**

Combustion & Ignition

900.586 PB89-147482 Not available NTIS National Bureau of Standards (NEL), Gaithersburg, MD. Fire Science and Engineering Div.

Aerodynamics of Agglomerated Soot Particles.

H. R. Baum, D. M. Corley, and A. F. Rabb. 1987, 4p Sponsored by Defense Nuclear Agency, Washington,

Pub. in Proceedings of Fall Technical Meeting--Chemical and Physical Processes in Combustion, San Juan, PR., December 15-17, 1986, p52.1-52.4 1987.

Keywords: *Combustion, *Soot, *Aerodynamic forces, Agglomeration, Kinetic theory, Numerical analysis, Particles.

Most studies of the effects of soot particles on combustion phenomena assume that the aerodynamic forces on an individual particle can be calculated as if forces on an individual particle can be calculated as if the particle were a sphere. However, for particles of sizes significantly larger than 10(sup -2) microM, most of the growth comes from agglomoration of individual spheres of approximately this diameter into long irregular chains. These chains of reasonably distinct spheres form the characteristic open shapes of large soot particles which range up to several microns in overall length. Under combustion conditions it is apparent that any registic analysis must recognize the parent that any realistic analysis must recognize the

Combustion & Ignition

chainlike shapes of the soot particles, and must be based on the kinetic theory of gases. The present study describes an analysis which satisfies these re-

900,587 PB89-149173 Not available NTIS Mational Bureau of Standards (NEL), Gaithersburg, MD. Fire Science and Engineering Div.

Combustion of Oil on Water.

Final rept.

D. Evans, H. Baum, B. McCaffrey, G. Mulholland, M. Harkleroad, and W. Manders. 1986, 36p Pub. in Proceedings of Annual Arctic and Marine Oilspill Program (9th), Edmonton, Alberta, Canada, Jun 10-12, 1986, p 301-336.

Keywords: *Fires, *Oil spills, *Combustion products, *Water, *Crude oil, *Air pollution, Water pollution, Aerosols, Carbon monoxide, Carbon dioxide, Particle size distribution, Xylenes, Toluene, Smoke, Electron microscopy, Aromatic compounds, Alkanes, Benzene, *Environmental monitoring.

The report contains the results of measurements performed on both 0.4 m and 0.6 m diameter pool fires produced by burning a layer of Prudhoe Bay crude oil supported by a thermally deep layer of water. Both steady and vigorous burning caused by boiling of the water sublayer were observed. The measured energy release rate for steady burning was about 640 kW/sq m. The emission rate, the size distribution, and specific extinction coefficient were measured for the smoke aerosol produced by the fires. Data were also obtained on the structure of the smoke aerosol by electron microscopy and on emission of CO and CO2. Analysis of the crude oil burn residue indicated selected depletion of the short chain alkanes and cycloalkanes when compared to the fresh oil. Mono-ring aromatics includ-ing benzene, toluene, and xylenes present in the fresh crude were absent in the burn residue. Calculations of the induced air flow into a stimulated distribution of 20 fires over a 100 m x 100 m area showed that the maximum inflow velocity near the largest size fire (2.5 m diameter, 3.2 MW) was 1.1 m/s.

900,588 PB89-157234 Not available NTIS National Bureau of Standards (NEL), Gaithersburg, MD. Thermophysics Div.

Light Scattering from Simulated Smoke Agglomer-

Final rept.

R. D. Mountain, and G. W. Mulholland. 1988, 6p Pub. in Langmuir 4, n6 p1321-1326 Nov/Dec 88.

Keywords: *Smoke, *Light scattering, Agglomerates, Computerized simulation, Reprints, Langevin formula, Fractal dimensions.

The computer simulation technique of Langevin dynamics is used to simulate the growth of smoke agglomerates. Clusters consisting of between 10 and 700 primary particles are generated, and the light scattering from these clusters is calculated in the Rayleigh-Debye limit. The results of these calculations are then used to illustrate how light-scattering measurements can be used to infer the concentration, the size, the radius of gyration (R sub g), and the fractal dimension of the agglomerates. The pair distribution function for these agglomerates is shown to be a scaled function of r/R sub g, and the cutoff function describing large separations of particles in the clusters has the form exp(-c(r/R sub g) to the 2.5 power).

900,589 PB89-157572 Not available NTIS National Bureau of Standards (NEL), Gaithersburg, MD. Fire Science and Engineering Div.

Structure and Radiation Properties of Large-Scale

Natural Gas/Air Diffusion Flames. Final rept.

Plantage. J. P. Gore, G. M. Faeth, D. Evans, and D. B. Pfenning. 1986, 9p Pub. in Fire and Materials 10, n3-4 p161-169 Sep-Dec

Keywords: *Diffusion flames, Mathematical models, Natural gas, Heat flux, Heat transfer, Combustion, Temperature, Thermal measurements, Soot, Reprints, *Flame radiation, *Flame structure, Radiative heat transfer.

Recent data from large-scale turbulent natural gas/air diffusion flames (135-210 MW) were used to evaluate analysis of flame structure and radiation properties.

The conserved-scalar formalism, in conjunction with the laminar flamelet concept, was used to estimate flame structure. The discrete-transfer method, in conjunction with a narrow-band radiations model, was used to predict radiative heat fluxes. The narrow-band model considered the nonluminous gas bands of water vapor, carbon dioxide, methane and carbon monoxide in the 1000 - 6000 nm wavelength range. Structure predictions were encouraging, with discrepancies for mean temperatures comparable to experimental un-certainties (ca. 200 K in the hottest portions of the flames). Radiative heat flux predictions were also reasonably good, e.g., predictions based on mean scalar properties were generally 15% lower than the measurements. The findings also suggest that continuum radiation from soot is negligible for these flames.

P689-171904

Not available NTIS
National Bureau of Standards (NEL), Gaithersburg,
MD. Fire Measurement and Research Div.
Chemical Structure of Methane/Air Diffusion
Flames: Concentrations and Production Rates of
Intermediate Hydrocarbons.
Final rept.

Pub. in Preprints of Papers, American Chemical Society, Division of Fuel Chemistry 31, n2 p105-111 1986.

Keywords: *Molecular structure, *Combustion prod-ucts, *Diffusion flames, *Methane, Aromatic polycyclic bydrocarhons. Concentration(Composition), Public hydrocarbons, Concentration(Composition), Public health, Acetylene, Hydrocarbons, Soot, Benzene, *Air pollution effects(Humans).

The production of intermediate and large hydrocarbon species is common to most combustion systems. These products range in size from acetylene, benzene and polynuclear aromatic hydrocarbons (PAH) to very large soot particles. Radiation from particles is the dominant mode of heat transfer in large fires. In addition, sampled particles often have PAH adsorbed onto them. Many of these molecules are known carcino-gens and their presence on inhalable soot particles poses an obvious long-term health hazard. Despite the important role that such species play in flames and the danger they present as combustion byproducts, the mechanism for their formation is as yet unknown.

900,591 PB89-171912 Not available NTIS Mational Bureau of Standards (NEL), Gaithersburg, MD. Fire Measurement and Research Div. Methyl Radical Concentrations and Production Rates in a Laminar Methane/Air Diffusion Flame.

Final rept. J. H. Miller, and P. M. Taylor. 1987, 11p Pub. in Combustion Science and Technology 52, n1-3 p139-149 1987.

Keywords: *Diffusion flames, *Reaction kinetics, *Combustion products, *Concentration(Composition), Combustion, Mass spectroscopy, Temperature, Velocity, Ionization, Reprints, *Methyl radicals.

Methyl radicals have been observed in a laminar methane/air diffusion flame via an application of the scav-enger probe technique. In these experiments, a quartz microprobe was modified such that iodine vapor was pumped from a storage side arm into the inside tip of the probe. Sampled methyl radicals react quantitatively with iodine to product methyl iodide which was de-tected by an on-line mass spectrometer. These quanti-tative profiles are compared to profiles of stable intermediate hydrocarbons which have been observed in this flame, as well as profile signals which are due to methyl radical ionization by laser radiation. The concentration of methyl is combined with velocity and temperature data to calculate the net rates of chemical reactions of methyl in the flame. The use of methyl concentration and rate data to estimate the concentra-tions of other reactive species is discussed.

900,592 PB89-173850 Not available NTIS National Bureau of Standards (NEL), Boulder, CO. Chemical Engineering Science Div. Development of Combustion from Quasi-Stable Temperatures for the Iron Based Alloy UNS S66286.

J. W. Bransford, P. A. Billiard, J. A. Hurley, K. M. McDermott, and I. Vazquez. 1988, 12p Sponsored by National Aeronautics and Space Administration, Huntsville, AL. George C. Marshall Space

Flight Center.

Pub. in Flammability and Sensitivity of Materials in Oxygen-Enriched Atmospheres, ASTM STP 986, v3 p146-157 1988.

Keywords: *Iron alloys, *Combustion, Ignition, Exothermic reactions, Endothermic reactions, Temperature, Carbon dioxide lasers, Ignition temperature, Oxidation, Reprints.

The development of ignition and subsequent combustion from quasi-stable temperatures was studied for several iron, nickel, and cobalt-based alloys. The quasi-stable temperature was produced by heating a specimen with a continuous wave carbon dioxide laser. Endothermic and exothermic transitions appear to play an important role in the development of thermal runaway, ignition, and combustion. The apparent effect of the endothermic transitions was to accelerate the rate of oxidation of the alloy, which produced abrupt changes in surface temperature as well as increasing the rate of increase in surface temperature. In the final stages of the thermal runaway phase, endothermic and exothermic events forced the alloy surface rapidly into combustion. Total destruction of the specimen followed immediately. The results for the iron-based alloy UNS S66286, which represent the phenomena observed, are presented. A spontaneous ignition temperature, enhanced oxidation temperature and ignition temperature for the solid alloy have been defined. Data are presented for the oxygen pressure range of 1.7 to 13.8 MPa.

900,593

PB89-175913 Not available NTIS National Bureau of Standards (NEL), Gaithersburg, MD. Fire Safety Technology Div. Very Large Methane Jet Diffusion Flames. Final rept.

B. J. McCaffrey, and D. D. Evans. 1988, 7p Pub. in Proceedings of International Symposium on Combustion 21, p25-31 1988.

Keywords: *Diffusion flames, *Methane, *Jet flow, Combustion, Flame propagation, Subsonic flow, Temperature, Radiation, Heat transfer.

Methane jet diffusion flames with heat release approaching to 350 MW in both subsonic and supercriti-cal configurations have been studied regarding lift-off height and flame height, absolute flame stability, radi-ative characteristics, and for an evaluation of their propensity for extinguishment using water sprays. Flames from orifices up to 38 mmD could be blown off with sufficient gas pressure. For $D=51\,$ mm the flame could not be blown off even for stagnation pressures to 2300 kPa. The data point at 38 mm allows a more accurate extrapolation, in the manner of Kalghatgi, leading to a predicted critical orifice size of 48 mm for absolute flame stability for CH4. Failure to ignite gas from a 1 mm diameter aperture in a reservoir at 12,000 kPa is consistent with the shape of the upper portion of the locus of the derived stability curve. Wide-band radi-ation measurements coupled with flame temperature measurements confirm small scale absorptivity determinations for use in simple flame radiation models.

900,594

Not available NTIS PB89-176622 National Bureau of Standards (NEL), Gaithersburg, MD. Mathematical Analysis Div. Solution for Diffusion-Controlled Reaction in a Vortex Field.

Final rept.

Pub. in Chemical and Physical Processes in Combustion 1986, p3.1-3.4 1987.

Keywords: *Combustion, *Diffusion, *Vortices, Convection, Mixing, Mathematical models, Reaction kinetics, Turbulence, Navier-Stokes equations, Reprints.

A mathematical model of local, transient, constant-density diffusion-controlled reaction between unmixed species initially occupying adjacent half-spaces is analyzed. An axisymmetric viscous vortex field satisfying the Navier-Stokes equations winds up the interface be-tween the species as they diffuse together and react. A flame-sheet approximation of the rapid reaction is made using Shvab-Zeldovich dependent variables. The model was originally proposed by F. Marble, who performed a local analysis of consumption rates along the flame sheet. The present paper describes a global similarity solution to the problem which is Fourier analyzed in a Lagrangian coordinate system.

COMBUSTION, ENGINES, & PROPELLANTS

Combustion & Ignition

900,595 PB89-176762 Not available NTIS MD. Fire Measurement and Research Div.

Cigarette as a Heat Source for Smolder Initiation in

Upholstery Materials.

Final rept. T. Ohlemiller, and R. Breese. 1987, 4p

Pub. in Chemical and Physical Processes in Combustion 1986, p6.1-6.4 1987.

Keywords: *Flammability testing, *Upholstery, Ignition, Fire resistant materials, Flammability, Fabrics, Reprints, *Cigarettes.

Cigarettes, which themselves undergo smoldering combustion, are prone to induce smoldering in upholstery materials with which they make accidental con-A set of 32 experimental cigarettes with five varied design parameters is being tested for lesser tendency to ignite such substrates. Heat flux scans show cigarettes with lessened ignition tendencies do yield a lesser heat input.

PB89-179261 Not available NTIS National Bureau of Standards (NEL), Gaithersburg, MD. Fire Science and Engineering Div.

Fire Safety Science-Proceedings of the First international Symposium. Final rept.

B. J. McCaffrey. 1987, 1p Pub. in Combustion and Flame 69, p369 1987.

Keywords: *Meetings, *Fire safety, Fires, Fire protection, Fire tests, Fire prevention, Reprints.

The proceedings of the first meeting of the International Association for Fire Safety Science, dedicated to the improvement of man's understanding of fire phenomena, is presented. By bringing together practitioners of fire research -- physicists, chemists, engineers, architects, codes-and-standards, and insurance people -- it is hoped that effective information exchange might result, leading to more focused fire problem definitions and ultimate solutions. This multidisciplinary group with over 300 registrants from 17 countries met at NBS in October 1985.

900,597 PB89-188577

PC A03/MF A01 California Univ., Berkeley. Dept. of Mechanical Engineerina

Fire Propagation in Concurrent Flows.
Final rept. 1 Aug 87-31 Jul 88.
A. C. Fernandez-Pello. Aug 88, 42p NIST/GCR-89/ 560

See also PB87-140190. Sponsored by National Inst. of Standards and Technology (NEL), Gaithersburg, MD. Center for Fire Research.

Keywords: *Flame propagation, *Fire tests, Air flow, Combustion, Fuels, Flow rate, Gas flow, Ignition, Turbulence, Diffusion, Pyrolysis, Numerical analysis,

The research tasks completed during the reporting period include an experimental study of the effect on the spread of flames of the turbulence intensity of an opposed air flow, and a theoretical analysis of the concurrent spread of flames over thin fuels. Both studies are, in the author's opinion, important contributions in the study of the flame spread process. The results of the experimental study show that the flame spread process is significantly affected by the flow turbulence intensity for flames spreading over both thin and thick fuels. The results of the theoretical analysis, which are in good agreement with previous experimental meas-urements, give detailed information about the flame structure and mechanisms of flame spread.

900,598 PB89-201172 Not available NTIS

Not available NTIS
National Bureau of Standards (NEL), Gaithersburg,
MD. Fire Measurement and Research Div.
Importance of Isothermal Mixing Processes to the
Understanding of Lift-Off and Blow-out of Turbulent Jet Diffusion Flames.

Final rept. W. M. Pitts. 1989, 16p

Sponsored by Air Force Office of Scientific Research, Bolling AFB, DC.
Pub. in Combustion and Flame 76, p197-212 1989.

Keywords: *Diffusion flames, *Jet flow, *Fuel sprays, *Turbulent flow, *Mixing, Two phase flow, Flame propagation, Reprints.

Many different theoretical analyses have been developed to predict the lift-off and blowout behaviors of axisymmetric, turbulent jet diffusion flames. Past theoretical production of the control of the retical and experimental work is summarized. It is then shown that these flame stability properties can be pre-dicted using the known time-averaged concentration and velocity profiles of the corresponding nonreacting jet flows of the fuels into air. In contrast to past theoretical treatments of these processes, it is not necessary to consider interactions of the turbulent concentration and/or velocity fluctuations with the combustion process. Possible physical mechanisms that can lead to such a finding are discussed.

900,599 PB89-201966 Not available NTIS National Bureau of Standards (NEL), Gaithersburg, MD. Fire Measurement and Research Div. Soot Inception in Hydrocarbon Diffusion Flames.

K. C. Smyth, and J. H. Miller. 1987, 13p Pub. in Chemical and Physical Processes in Combustion 1986, pC.1-C.13 1987.

Keywords: *Diffusion flames, *Soot, *Hydrocarbons, Combustion, Spectrometers, Chemical reactions, Reaction kinetics, Flame propagation, Combustion products, Reprints.

In the last two years detailed species concentration measurements have been made in hydrocarbon diffusion flames for the first time. Far from being hopelessly complex (as many had thought), the interplay between chemical and transport processes can now be unrav-elled. In addition, questions about the chemical growth processes leading to polycyclic aromatic hydrocarbon and soot formation can be addressed. The results thus far reveal striking parallels with premixed flame stud-

900,600 PB89-211866 Not available NTIS MD. Chemical Process Metrology Div.

FT-IR (Fourier Transform-Infrared) Emission/

Transmission Spectroscopy for in situ Combustion Diagnostics. Final rept.

P. R. Solomon, P. E. Best, R. M. Carangelo, J. R. Markham, P. Chien, R. J. Santoro, and H. G. Semerijan, 1988, 9p

Pub. in Proceedings on International Symposium of Combustion (21st), p1763-1771 1988.

Keywords: *Combustion products, Infrared spectroscopy, Temperature, Soot, Optical measurement, Particles, Diffusion flames, Gases, Emission, Transmission, *Fourier transform spectrometers, *In-situ combus-

An infrared emission/transmission (E/T) technique (a method previously used as an in-situ diagnostic for gases and soot using dispersive infrared) has been implemented with a Fourier Transform Infrared (FT-IR) spectrometer and extended to include measurements on particles, as well as gases and soot. The method on particles, as well as gases and soot. The method can measure both the concentration and temperature of each of the phases. The paper presents the applications of FT-IR E/T spectroscopy to gases, soot and particles in reacting flows. Several examples are presented including a coannular laminar diffusion flame. The results for soot temperature and concentration in this flame are in conditional statements. this flame are in good agreement with measurements reported by other investigators.

900.601 PB89-212096 Not available NTIS National Bureau of Standards (NML), Gaithersburg, MD. Chemical Kinetics Div.

Evaluated Kinetics Data Base for Combustion Chemistry.

Final rept. W. Tsang, and J. T. Herron. 1987, 6p

Pub. in Proceedings of the International CODATA Conference on Comput. Handl. Dissemination Data (10th), p229-234 1987.

Keywords: *Reaction kinetics, *Combustion, *Methane, Computerized simulation, Gases, Hydrocarbons, Chemical reactions.

continuing effort at developing a chemical kinetic data base for the computer simulation of hydrocarbon combustion is described. Because of the complexity of the problem present efforts are directed towards providing data related to the initial stages of methane combustion are considered. The reactions are a key subset of all hydrocarbon combustion processes and the rate expressions form the basis for predictive methods for larger compounds. A key factor in the work is the necessity of interpolating and extrapolating experimental data so as to derive rate constant expressions valid over temperature and pressure ranges of 300-2500K and 10(sup 16)-10(sup21) particles/cu cm, respectively. Unimolecular reactions pose special problems, and the methodology for treating and presenting the data is discussed.

900,602

PB89-218366 PC A07/MF A01 National Inst. of Standards and Technology (NEL), Gaithersburg, MD. Center for Fire Research.

Technical Reference Gulde for FAST (Fire and Smoke Transport) Version 18.

Technical note

W. W. Jones, and R. D. Peacock. May 89, 130p NIST/TN-1262

Also available from Supt. of Docs. as SN003-003-02944-1.

Keywords: *Mathematical models, *Computer programs, *Fires, Algorithms, Differential equations, Compartment analysis, Heating, Radiation, Convection, Conduction, Venting, Smoke, Plumes.

FAST is a model to describe fire growth and smoke transport in multi-compartment structures. The implementation consists of a set of programs to describe the structure to be modeled, run the model and produce usable output. The reference guide describes the equations which constitute the model, data which are used by the model and explains how to operate the model. The physical basis of zone models, their limitations, and development of the predictive equations are described elsewhere and therefore are only summa-rized in the reference guide. The intent of the guide is to provide a complete description of the way the model is structured. In particular the relationship between the equations and the numerical implementation of the equations is laid out. It is intended as a complete description of the parameters and key words available to control various aspects of a simulation. It is hoped that there is sufficient information provided to adapt the model for specialized applications.

900.603

PB89-231096 Not available NTIS National Inst. of Standards and Technology (NEL), Gaithersburg, MD. Fire Measurement and Research

Assessment of Theories for the Behavior and Blowout of Lifted Turbulent Jet Diffusion Flames. Final rept.

W. M. Pitts, 1989, 8p

Pub. in Proceedings of International Symposium on Combustion (22nd), Seattle, WA., August 14-19, 1988, p809-816 1989.

Keywords: *Diffusion flames, *Turbulent flow, *Jet flow, Mixing, Combustion stability, Flame photometry.

Many competing theories have been published to describe the characteristics and blowout of lifted turbu-lent jet diffusion flames. The assumptions which are made as to the physical processes responsible for these behaviors vary widely. In the paper these as-sumptions are summarized for each model and com-pared with the actual turbulent behaviors of unignited fuel jets. As part of this discussion, recent unpublished measurements of real-time concentration fluctuations along a line in a turbulent fuel jet are introduced. To the extent possible, each theory is also assessed as to its capabilities to accurately predict experimentally ob-served lift off and blowout behaviors. The conclusion of these analyses is that none of the currently available theories for flame stabilization are satisfactory. Further experimentation is required before the actual physical processes responsible for flame stabilization can be identified and models which are capable of accurate prediction of lift off heights and blowout velocities developed.

900,604

Not available NTIS PB89-231179 National Bureau of Standards (NEL), Gaithersburg, MD. Fire Safety Technology Div.

Combustion Efficiency, Radiation, CO and Soot Yield from a Variety of Gaseous, Liquid, and Solid Fueled Buoyant Diffusion Flames.

Final rept.

B. J. McCaffrey, and M. F. Harkleroad. 1988, 11p
Sponsored by Defense Nuclear Agency, Washington,
DC., and Department of the Interior, Washington, DC.

Pub. in Proceedings of International Symposium on Combustion (22nd), Seattle, WA., August 14-19, 1988, p1251-1261 1989.

Keywords: *Combustion efficiency, *Diffusion flames, *Combustion products, *Radiation, Carbon monoxide, Soot, Thermal measurements, Heptane, Propane, Wood, Crude oil.

The following compilation of data describes combustion conditions for the free burning of propane, heptane, 3 crude oils, wood and polyurethane cribs in fuel package sizes less than a meter, having heat release rates up to 1/2 MW. Measurements include heat re-lease rate from 02 depletion calorimetry, mass loss rate, incident radiative flux to nearby targets, flame and liquid interface temperatures and overall major gase-ous species yield including soot. The information con-tained herein provides a data base for buoyant diffu-sion flame modelling regarding radiation and elementary chemical characterization. There appears to be a one-to-one correspondence between a fuels radiative behavior and its soot and CO yield. Urethanes and crude oil have significantly higher values for all these parameters as compared to propane, heptane and wood. No correlation was found between these measurements and time-averaged thermocouple readings of temperature.

900,605 PB90-127101 PC A10/MF A02 National Inst. of Standards and Technology (NEL), Gaithersburg, MD. Center for Fire Research. Summaries of Center for Fire Research in-House Projects and Grants: 1989.

Final rept. S. M. Cherry. Oct 89, 214p NISTIR-89/4188 See also PB89-127302.

Keywords: *Combustion, Fire prevention, Research projects, Grants, Soot, Polymers, Carbon monoxide, Flame propagation, Toxicity, Furniture, Charring, Models, Ignition, Hazards, *Fire research, Fire models, Building fires, National Institute of Standards and Technology.

The report describes the research projects performed The report describes the research projects performed in the Center for Fire Research and under its grants program during FY1989. Topics considered include the following: Turbulent combustion, Soot formation, CO prediction, Polymer gasification, Flame spread, Toxic potency, Furniture flammability, Building fire modeling and smoke transport, Fire hazard assessment, Engineering analysis system and fire reconstruction, Suppression, Cone calorimeter, Technology transfer, Fire/modeling interactions, and Fire protection technology. tion technology.

900,606 PB90-136821 Not available NTIS National Inst. of Standards and Technology (NEL), Gaithersburg, MD. Fire Science and Engineering Div.
Summary of the Assumptions and Limitations in Hazard I.

R. W. Bukowski. 1989, 15p Pub. in Proceedings of Fire Retardant Chemicals Association Spring Conference, Baltimore, MD., June 7-8, 1989, p1-15

Keywords: *Fire extinguishing agents, Toxicity, Computer systems programs, Documentation, *Risk as-

A brief description of the function, major assumptions and limitations of the programs and procedures which comprise the prototype Hazard Assessment Method-Hazard I is presented. The method consists of a large software package and three volume report.

Reciprocation & Rotating Combustion Engines

900,607 PB89-147094

Not available NTIS

National Bureau of Standards (NEL), Gaithersburg, MD. Chemical Process Metrology Div.
Thin Film Thermocouples for Internal Combustion

Engines.

Final rept. K. G. Kreider. 1986, 6p Contract DE-Al05-83OR21375 Sponsored by Oak Ridge National Lab., TN. Pub. in Jnl. of Vacuum Science and Technology A 4,

n6 p2618-2623 Nov/Dec 86.

Keywords: *Thermocouples, *Internal combustion engines, *Fabrication, *Measurement, *Temperature, *Coatings, Thin films, Valves, Cylinders, Pistons, Combustion chambers, Aluminum oxide, Iron alloys, Sputering, Adhesion, Platinum alloys, Aluminum alloys, Chromium alloys, Microscopy, Stainless steels, Electrical properties, Reprints.

The feasibility of fabricating thin film thermocouples on internal combustion engine hardware was investigated. The goal was to find a procedure that would be useful for the measurement of the metal temperature of valve, valve seats, combustion chamber surface, cylinder walls, and piston heads during engine operation. The approach pursued was to coat the engine hardware material with an aluminum-containing, oxidation-resistance ferrous alloy (FeCrAlY) which forms an oxide layer with good electrical resistance. This there mal oxide was coated with a thin layer of reactively sputtered aluminum oxide and sputtered thin film type S thermocouple legs of platinum and platinum plus rhodium. This project was used to investigate the materials problems related to obtaining good adhesion in the metal metal-oxide-oxide-metal laminate and the electrical insulating properties of the oxide. Thermal oxidation, reactive sputtering of Al2O3 and platinum alloy sputtering were investigated using optical microscopy, x-ray photoemission spectroscopy (XPS), laminar adhesion testing, and the evaluation of high temperature electrical properties.

Rocket Engines & Motors

900,608 PB90-128661 Not available NTIS National Bureau of Standards (NEL), Boulder, CO. Chemical Engineering Science Div.

Vortex Shedding Flowmeter for Fluids at High Flow Velocitles. Rept. for 1984-86.

J. D. Siegwarth. 1986, 15p Sponsored by National Aeronautics and Space Administration, Huntsville, AL. George C. Marshall Space Flight Center.

Pub. in Advanced Earth-to-Orbit Propulsion Technology, NASA Conference Publication 2437, v2 p139-153

Keywords: *Flowmeters, Liquid oxygen, Hydrogen, Reprints, *Space shuttle main engine, Vortex shedding, Cryogenic fluids.

Vortex shedding flowmeter designs developed for this project are capable of measuring water flowrates at velocities above the liquid oxygen (LOX) flow velocities encountered in the space shuttle main engines (SSME). These meters have been tested in two sections of actual SSME ducts with high velocity water flow. The results show that a meter vane fitted through a pair of appropriately located standard 11.2 mm diameter instrument ports can be used to measure flow without any upstream conditioning. The vortex shedding flowmeter with a 41 mm (1.61 in) bore has undergone preliminary testing with air at SSME fuel-flow densities. In spite of the much lower sound velocity of air, a strong vortex-generated spectrum line has been observed up to 180 m/s (590 ft/s). Successful meter designs suitable for high-pressure cryogenic flow measurement have been built and tested.

Rocket Propellants

900,609 PB89-146278 PC A03/MF A01 National Inst. of Standards and Technology (IMSE), Gaithersburg, MD. Polymers Div.

In Situ Fiuorescence Monitoring of the Viscosities of Particle-Filled Polymers In Flow.

Annual rept.

A. J. Bur, F. W. Wang, A. Lee, R. E. Lowry, S. C. Roth, and T. K. Trout. Nov 88, 37p NISTIR-88/3892 Grant N00014-86-F-0115 See also FY 87, PB88-157698. Sponsored by Office of Naval Research, Arlington, VA.

Keywords: *Laminar flow, *Propellants, *Binders, *Polymers, Fluorometers, *Fluorescence, Monitoring, Spectroscopy, Mixing, Rheology, Viscosity, Polybutadiene, Aluminum oxide, Measuring instruments, Synthesis(Chemistry).

Work during FY 88 has focused on three areas: the chemical synthesis of a polymeric chromophore; the design of experiments to measure fluorescence anisotropy and non-Newtonian viscosity as a function of shear rate; and, measuring the quality-of-mix of a two component material using a fluorescence microscope. Significant results from these areas of work are: (a) a polymeric chromophore, consisting of anthracene co-valently bonded to polybutadiene, has been synthevariety borload to polybududier, has been syntressized and characterized by gel permeation chromatography and infrared observations. The number average molecular weight is 12,000 which is above the entanglement molecular weight for polybutadiene; (b) experiments using the polymeric chromophore as a deposit in a Noutonia third you low resident. dopant in a Newtonian fluid, very low molecular weight polybutadiene, show that fluorescence anisotropy cor-relates with the viscosity, i.e., it remains constant as a function of shear rate; and (c) using a fluorescence microscope, the authors have measured optical transmittance and near neighbor distances between particles in a matrix/particle mixing experiment and correlated these data with fluorescence intensity fluctuations.

COMMUNICATION

Common Carrier & Satellite

900,610 PB89-166086 PC A09/MF A01 National Inst. of Standards and Technology, Gaithersbura, MD.

Ongoing Implementation Agreements for Open Systems interconnection Protocols: Continuing Agreements.

T. Boland. Dec 88, 176p NISTIR-88/3824-2 See also PB89-132351. Proceedings of the NIST/OSI Implementor's Workshop Plenary Assembly, held in Gaithersburg, MD. on December 16, 1988.

Keywords: Standards, Tests, *Open Systems Interconnections, *Protocol(Computers), Computer networks, Channels(Data transmission).

The document records current agreements on implementation details of Open Systems Interconnection Protocols among the organizations participating in the National Institute of Standards and Technology (NIST)/OSI Workshop Series for Implementors of OSI Protocols. These decisions are documented to facilitate organizations in their understanding of the status of agreements. The standing document is updated after each workshop (about 4 times a year).

PB89-171326 Not available NTIS National Bureau of Standards (ICST), Gaithersburg, MD. Systems and Network Architecture Div. PB89-171326 Transport Layer Performance Tools and Measure-

ment.

Final rept

R. Aronoff, K. Mills, and M. Wheatley. 1987, 11p Pub. in IEEE (Institute of Electrical and Electronics Engineers) Network 1, n3 p21-31 Jul 87.

Keywords: *Performance tests, Delay time, Reprints, *Computer networks, *Computer systems performance, Distributed computer systems, Throughput, iNA-960 computers.

The paper describes the function, design and implementation of a Transport Experiment Control System (TECS) that enables transport layer performance ex-

COMMUNICATION

Common Carrier & Satellite

periments between stations on a local area network. The TECS is applied to evaluate the performance of Intel's INA-960 transport service including profiles of throughput, delay and multiple applications. The re-sults define an upper bound on throughput and a lower bound on delay. A problem is described involving flow control interactions between the transport and link layers. The effect of taut flow control on transport connections is investigated. The suitability of iNA-960 for real-time applications is evaluated.

900,612 PB89-171334 Not available NTIS National Bureau of Standards (ICST), Gaithersburg, MD. Systems and Network Architecture Div.

Prediction of Transport Protocol Performance through Simulation.

Final rept.
K. Mills, M. Wheatley, and S. Heatley. 1986, 9p
Pub. in Computer Communication Review 16, n3 p75-83 Aug 86.

Keywords: *Data transmission, *Computerized simulation, Manufacturing, Automation, Reaction time, Reprints, *Protocol(Computers), *Computer networks.

A five-layer simulation model of OSI protocols is described and applied to predict transport user performance on a local area network (LAN). Emphasis is placed on time-critical applications typical of a small, flexible manufacturing system. The results suggest that, with current technology, OSI protocols can prode 1.5 Mbps throughputs, one-way delays between 6 and 10 ms, and response time between 15 and 25 ms. The results also demonstrate that CSMA/CD is a reasonable access method for time-critical applications on small factory LANS.

PB89-172357 Not available NTIS National Bureau of Standards (NEL), 'Gaithersburg, MD. Building Environment Div. Standardizing EMCS Communication Protocols

rınaı rept. S. T. Bushby, and H. M. Newman. 1989, 4p Pub. in ASHRAE (American Society of Heating, Refrig-erating and Air-Conditioning Engineers) Jnl. 31, n1 p33-36 Jan 89. Final rept.

Keywords: *Telecommunication, *Standards, Reprints, *Protocols, *Communication networks, Computer architecture, Open System Interconnection.

The article summarizes the approach to standardizing EMCS communication protocols being taken by ASHRAE Standards Project Committee 135P. The advantages of a layered architecture based on the international standard for Open System Interconnection (OSI) and the possibility of a collapsed architecture are discussed. The structure of the Standards Project Committee along with the progress of its first year of activities are described.

900 614 PB89-174064 Not available NTIS National Bureau of Standards (NML), Boulder, CO. Time and Frequency Div.

Dual Frequency P-Code Time Transfer Experiment.

Final rept. J. R. Clynch, B. W. Tolman, M. A. Weiss, D. W. Allan, and D. Davis. 1987, 8p Pub. in Proceedings of Annual Precise Time and Time Interval (PTTI) Applications and Planning Meeting (19th), Redondo Beach, CA., December 1-3, 1987,

Keywords: *Atomic clocks, Performance evaluation, Time measuring instruments, Frequency standards, Experimental data, *Global positioning system, Autonomous spacecraft clocks, Cesium oscillators.

The Clock Evaluation and Time Keeping Experiment was the cooperative effort of Applied Research Lab-oratories, the National Bureau of Standards, and the United States Naval Observatory. It was designed to collect a dense Global Positioning System (GPS) data set for evaluating methods of monitoring a ground-based atomic clock with on-site data alone, and of inbased atomic clock with on-site data alone, and or in-vestigating improved methods of time setting and time transfer using GPS data. The experiment collected two-frequency, P-code, pseudorange and Doppler data for five weeks at three sites: Austin, Texas; Boul-der, Colorado; and Washington, D.C. All sites used two-frequency receivers on cesium oscillators. A time history of the cesium oscillators against hydrogen

masters also was recorded at two of the sites. The behavior of the cesium oscillators was well tracked by the range residuals over the five weeks of the experiment. Residuals of Doppler data were strongly correlated across stations. This implies that time transfer with acacross stations. This implies that time transfer with ac-curacy approaching 1 ns looks promising over the time period of one satellite pass. With a full GPS constella-tion, continuous use of phase data could significantly improve time transfer via GPS.

900,615 PB89-177125 PB89-177125 Not available NTIS National Bureau of Standards (ICST), Gaithersburg, MD. Systems and Network Architecture Div. Automatic Generation of Test Scenario (Skeletons) from Protocol-Specifications Written in Es-

Final rept.

J. P. Favreau, and R. J. Linn. 1987, 12p Pub. in Proceedings of IFIP (International Federation Full International Federation for Information Processing) WG 6.1 International Workshop on Protocol Specification, Testing, and Verification (6th), Montreal, Quebec, Canada, June 10-13, 1986, p191-202 1987.

Keywords: *Standards, Tests, Automation, Proving, Specifications, *Protocols, *Computer communications, Protocol(Computers).

Estelle is a new formal description technique developed by the International Organization for Standardization for the description of computer communication protocols destined to become international standards. Specification, validation and testing computer communication protocols are all complex issues. The paper focuses on methods for generating test sequences for communication protocols and describes a model and method for partially automated generation of test skel-etons for protocols written in Estelle.

900,616 PB89-177133 Not available NTIS National Bureau of Standards (ICST), Gaithersburg, MD. Systems and Network Architecture Div.

Application of the ISO (International Standards Organization) Distributed Single Layer Testing Method to the Connectionless Network Protocol.

Final rept.

J. S. Nightingale. 1987, 12p

Pub. in Proceedings of IFIP (International Federation for Information Processing) WG 6.1 International Workshop on Protocol Specification, Testing, and Veriginal Conference Con fication (6th), Montreal, Quebec, Canada, June 10-13, 1986, p123-134 1987.

Keywords: *Tests, Conformity, *Protocols, *Communication networks, Protocol(Computers), Computer networks, Connectionless Network Protocol.

An architecture for testing implementations of the ISO Connectionless Network Protocol is described. After a brief description of the Connectionless Network Protocol, or Internet, the architectures for both end system and intermediate system testing are motivated through a set of design principles. The design uses a test maragement protocol which is explained herein. Syntactic constructs within the test language are given. The final section highlights some reactions which have been received concerning the test system.

Not available NTIS National Bureau of Standards (ICST), Gaithersburg, MD. Systems and Network Architecture Div. Simplified Discrete Event Simulation Model for an IEEE (Institute of Electrical and Electronics Engl-

neers) 802.3 Local Area Network.

Final rept. S. K. Heatley. 1986, 7p Pub. in Proceedings of GLOBECOM '86: IEEE (Institute of Electrical and Electronics Engineers) Global Telecommunications Conference Communications Broadening Technology Horizons, Houston, TX., December 1-4, 1986, v1 p143-149.

Keywords: *Models, *Computerized simulation, *Computer networks, *Protocols, Computer performance evaluation, Computer communications, Throughput.

In the Protocol Performance Group at the National Bureau of Standards, the performance of multi-layered ISO protocols is under study. The paper describes a simplified model of the IEEE 802.3 Local Area Network which was developed to serve the lowest layer in a discrete simulation model of multilayered ISÓ proto-cols. In the paper, throughput and delay measurements obtained from the simplified model are compared to measurements from a more detailed model of 802.3. Execution times of the simplified and detailed model are also compared. Sample execution times from the integrated, multi-layered model are present-

900,618 PB89-193312 PC A22/MF A01 National Inst. of Standards and Technology, Gaithers-

Stable Implementation Agreements for Open Systems Interconnection Protocols. Version 2, Edition 1. December 1988.

Final rept.

Final rept.
T. Boland. Feb 89, 511p NIST/SP-500/162
Also available from Supt. of Docs. as SN003-003-02921-1. See also PB88-168331. Library of Congress catalog card no. 89-600726. Based on the Proceedings of the NIST (National Institute of Standards and Technology) Workshop for Implementors of OSI Held at Gaithersburg, Maryland.

Keywords: *Protocols, *Open systems interconnection, *Computer networks, National Institute for Standards and Technology, Computer communications.

The document records current stable agreements for Open Systems Interconnection (OSI) Protocols among the organizations participating in the National Institute of Standards and Technology (NIST)/OSI Workshop Series for Implementors of OSI Protocols.

900.619 PB89-196158 PC A05/MF A01 National Inst. of Standards and Technology (NCSL), Gaithersburg, MD. Systems and Network Architecture

User Gulde for the NBS (National Bureau of Standards) Prototype Compller for Estelle (Revised).

Technical rept. (Final). J. P. Favreau, M. Hobbs, B. Strausser, and A. Weinstein. Feb 89, 79p ICST/SNA-87/3, NBS/SW/

MT-89/004A Supersedes PB88-124185. For system on magnetic tape, see PB89-196141.

Keywords: *Compilers, Prototypes, Computerized simulation, Syntax, Computer programs, Documentation, *Open Systems Interconnection, *Estelle, Software tools, Debugging(Computers), User manuals(Computer programs), Protocols, Computer communications.

The NBS Prototype Compiler for Estelle describes an implementation model for Estelle, the output of the compiler, the run-time library of support routines, and the syntax of Estelle used by the compiler. Instructions are provided for installing the compiler, executing it and providing the necessary implementation environment. Complete source is provided for a practical example of a simple protocol simulation; the report describes this example in some detail.

900,620 PB89-196166 PC A03/MF A01 National Inst. of Standards and Technology (NCSL), Gaithersburg, MD. Systems and Network Architecture

User Gulde for Wise: A Simulation Environment for Estelle. Technical rept.

R. Sijelmassi. Feb 89, 26p NCSL/SNA-89/6, NBS/ SW/MT-89/004B

For system on magnetic tape, see PB89-196141.

Keywords: *Computerized simulation, Semantics, Models, Documentation, *Computer communications, *Protocols, Wise system, Software tools, Estelle, User manuals (Computer programs).

The Wise software system provides a simulation environment for Estelle, which is a formal description technique for specifying computer communication proto-cols. The Wise tool is based on a model of Estelle semantics that is implemented as a collection of classes in the object-oriented language Smalltalk. For simulation, these classes are augmented with control and observation capabilities and the ability to simulate a distributed environment. The report describes how to use the Wise tool, particularly the observation and control features. A comparison document describes the underlying model. The Wise tool works together with the Wizard tool, a syntax-directed editor and translator, which also has a User Guide.

Common Carrier & Satellite

900,621 PB89-196174 PB89-196174 PC A03/MF A01 National Inst. of Standards and Technology (NCSL), Gaithersburg, MD. Systems and Network Architecture

User Guide for Wizard: A Syntax-Directed Editor and Translator for Estelle.

Technical rept.
B. Strausser. Feb 89, 13p NCSL/SNA-89/5, NBS/SW/MT-89/004C

For system on magnetic tape, see PB89-16141.

Keywords: *Editing routines, *Translator routines, Syntax, Documentation, *Computer communications, *Protocols, Wizard system, Estelle, Software tools, User manuals(Computer programs).

The Wizard editor and translator provides syntax-directed editing for Estelle, which is a formal description technique for specifying computer communication protocols. The Wizard also translates an Estelle specification into code in the object-oriented language Small-talk for use with the Wise tool. The report describes some of the editor's features. The Wizard tool was de-veloped with the Cornell Synthesizer Generator; documentation of editor operation from Cornell is desirable.

900,622 PB89-196182 PC A04/MF A01 National Inst. of Standards and Technology (NCSL), Gaithersburg, MD. Systems and Network Architecture

Free Value Tool for ASN.1.

Technical rept.
P. Gaudette, S. Trus, and S. Collins. Feb 89, 71p
NCSL/SNA-89/1, NBS/SW/MT-89/004D For system on magnetic tape, see PB89-196141.

Keywords: *Syntax, Data, Models, Coding, Documentation, *Computer communications, *Protocols, Software tools, Open Systems Interconnection, Data

The Free Value Tool provides the ability to manipulate data values described with Abstract Syntax Notation One (ASN.1). ASN.1 is a non-procedural notation for describing data objects at the application and presentation layers of computer communication protocols in the Open Systems Interconnection model. An abstract syntax in ASN.1 that does not use the macro feature is converted into data structures that capture the type information from the input. Values of those types can then be manipulated in an interpretive style, with transformations among printable value notation, encoded transfer values, and other forms of values. The report describes how to use the Free Value Tool and some of the implementation details. It includes a tutorial on ASN.1.

900,623 PB89-196190 PB89-196190 PC A05/MF A01 National Inst. of Standards and Technology (NCSL), Gaithersburg, MD. Systems and Network Architecture

Object-Oriented Model for Estelie and Its Smalltalk

Implementation. Technical rept. R. Sijelmassi. Feb 89, 81p NCSL/SNA-89/7, NBS/ SW/MT-89/004E

For system on magnetic tape, see PB89-196141.

Keywords: *Computerized simulation, Semantics, Models, Documentation, *Computer communications, *Protocols, Wise system, Estelle, Software tools.

The Wise software system provides a simulation environment for Estelle, which is a formal description technique for specifying computer communication protocols. The Wise tool is based on a model of Estelle semantics that is implemented as a collection of classes in the object-oriented language Smalltalk. The report describes the model and the Smalltalk implementation in some detail, which is useful background for extending or modifying the Wise tool. A companion report, the User Guide for Wise, describes how to use the tool.

900,624 PB89-221196 PC A10/MF A01 National Inst. of Standards and Technology (NCSL), Gaithersburg, MD. Working Implementation Agreements for Open Systems Interconnection Protocols.

Final rept. T. Boland. May 89, 213p NISTIR-89/4082 Proceedings of the NIST (National Institute of Standards and Technology) Workshop for Implementors of OSI Plenary Assembly; Gaithersberg, MD, March 17,

Keywords: *Agreements, Security, Digital systems, Specifications, Meetings, *Protocols, *Computer networks, *Communication networks, National Institute of Standards and Technology.

The document records current agreements on implementation details for Open Systems Interconnection Protocols among the organizations participating in the NIST/OSI Workshop Series for Implementors of OSI Protocols. These decisions are documented to facilitate organizations in their understanding of the status of agreements. This is a standing document that is updated after each workshop (about 4 times a year).

PB89-235576 PC A03/MF A01 National Inst. of Standards and Technology (NCSL), Gaithersburg, MD.
Trial of Open Systems Interconnection (OSI) Pro-

tocols Over Integrated Services Digital Network (ISDN). C. A. Edgar. Aug 89, 21p NISTIR-89/4160

Keywords: Information retrieval, Compatibility, *Computer networks, *Computer communications, *Protocols, Electronic mail, Integrated systems, File management systems, Computer architecture, Workstations.

Presented are the results of the National Institute of Standards and Technology Open Systems Interconnection/Integrated Services Digital Network (OSI/ISDN) Trial. The trial was organized to demonstrate the use of ISDN as a lower layer technology for OSI application. The document addresses the trial's topology, hardware/software configuration, parameters, and results.

PB90-100736 PC A03/MF A01 National Inst. of Standards and Technology (NEL), Boulder, CO. Electromagnetic Fields Div.

X-Band Atmospheric Attenuation for an Earth Terminal Measurement System.

M. H. Francis. Jul 89, 46p NISTIR-89/3918

Keywords: *Atmospheric attenuation, *Satellite antennas, Measurement, Antennas, Gain, Spacecraft communication, Errors, Sky brightness, Heat transfer, X-Band, Tipping curve method.

The National Institute of Standards and Technology has developed an Earth Terminal Measurement System to be used by the Camp Parks Communications Annex in determining satellite effective isotropic radiated power and antenna gain. In determining these quantities the effect of atmospheric attenuation must be taken into account. The paper provides an overview of the methods used for determining atmospheric attenuation with emphasis on a tipping-curve method. An error analysis is also provided.

Graphics

900,627 FIPS PUB 152 National Inst. of Standards and Technology (NCSL), Gaithersburg, MD. Standard Generalized Markup Language (SGML).
Federal information processing standards (Final).
L. A. Welsch. c26 Sep 88, 174p
Three ring vinyl FIPS binder also available, North
American Continent price \$7.00; all others write for

Keywords: Documents, Publishing, *Federal information processing standards, *High level languages, *Text processing.

The publication announces the adoption of the International Standards Organization Standard Generalracional Standards Organization Standard General-ized Markup Language (SGML), ISO 8879-1986, as a Federal Information Processing Standard (FIPS). ISO 8879-1986 specifies a language for describing docu-ments to be used in office document processing, interchange between authors and between authors and publishers, and publishing. The language provides a coherent and unambiguous syntax for describing the elements within a document. (Copyright (c) International Standards Organization, 1986.)

Policies, Regulations, & Studies

900.628 PB89-174072 Not available NTIS National Bureau of Standards (NML), Boulder, CO. Time and Frequency Div.

Comparison of Time Scales Generated with the NBS (National Bureau of Standards) Ensembling

Algorithm.

Final rept.
F. B. Varnum, D. R. Brown, D. W. Allan, and T. K. Peppler. 1987, 11p Pub. in Proceedings of Annual Precise Time and Time

Interval (PTTI) Applications and Planning Meeting (19th), Redondo Beach, CA., December 1-3, 1987, p13-23.

Keywords: *Time standards, *Algorithms, Time measurement, Time measuring instruments, Clocks, Cesium, Weighting functions.

The National Bureau of Standards (NBS), Boulder, Colorado, uses an algorithm which generates UTC(NBS) from its ensemble of clocks and automatically, optimally, and dynamically weights each clock in the ensemble. The same algorithm was used at the Master Control Station (MCS) of the Global Positioning System (GPS) to generate a time scale from a small ensemble of cesium clocks. Time transfer employing the GPS common view technique between NBS (Boulder) and MCS (Colorado Springs) was used to evaluate the stability of the MCS ensemble relative to UTC(NBS). The results demonstrate the power of the NBS algorithm in providing a stable time scale from a small ensemble of clocks. The resulting scale is, in principle, more stable than the best clock and a poor clock need not degrade the ensemble.

900,629 PB89-185722 Not available NTIS National Bureau of Standards (NML), Boulder, CO. Time and Frequency Div.
Millisecond Pulsar Rivals Best Atomic Clock Stabil-

D. W. Allan. 1987, 10p See also PB88-138821. Pub. in Proceedings of Annual Symposium on Fre-quency Control (41st), Philadelphia, PA., May 27-29, 1987, p2-11.

Keywords: *Atomic clocks, *Stability, Comparison, Orbits, Time measuring instruments, Signal to noise ratios, Dispersions, Ephemerides, Interplanetary medium, Interstellar matter, Gravity waves, *Millisecond pulsar.

The measurement time residuals between the millisecond pulsar PSR 1937+21 and atomic time have been significantly reduced. Analysis of data for the most recent 865 period indicates a fractional frequency stability (square root of the modified Allan variance) of less than 2 x 10 to the (-14) power for integration times of about 1/3 year. Analysis of the measurements taken in two frequency bands revealed a random walk behavior for dispersion along the 12,000 to 15,000 light year path from the pulsar to the earth. The random walk accumulates to about 1,000 nanose-conds (ns) over 265 days. The final residuals are nominally characterized by a white phase noise at a level of 369 ns. Following improvement of the signal-to-noise ratio, evidence was found for a residual modulation. Possible explanations for the modulation include: a binary companion to the pulsar with approximate period(s) of 120 days and with a mass of the order of 1 to the pulsar with a period (s) period (s) of 120 days and with a mass of the order of 1 to the pulsar with a period (s) of 120 days and with a mass of the order of 1 to the pulsar irregular mass. x 10 to the (-9) power that of the pulsar; irregular magnetic drag in the pulsar; unaccounted delay variations in the interstellar medium; modeling errors in the earth's ephemeris; reference atomic clock variations in excess of what are estimated; or gravity waves. For gravity waves, the amplitude of the length modulation would be about 5 parts in 10 to the (19) power. Further study is needed to determine which is the most probable explanation.

900,630 PB89-212070 Not available NTIS National Inst. of Standards and Technology (NML), Not available NTIS Boulder, CO. Time and Frequency Div.

Callbration of GPS (Global Positioning System) Equipment In Japan.

Final rept.
M. A. Weiss, and D. D. Davis. 1988, 10p
See also PB88-122023.

COMMUNICATION

Policies, Regulations, & Studies

Pub. in Proceedings of Annual Precise Time and Time Interval (PTTI) Applications and Planning Meeting (20th), Vienna, VA., November 29-December 1, 1988, p101-110.

Keywords: *Calibrating, *Time standards, *Frequency standards, Japan, Telecommunication, Time measure ment, Frequency measurement, Receivers, Synchronism, *Global positioning systems, Time transfer.

With the development of common view time comparisons using Global Positioning System (GPS) satellites the Japanese time and frequency standards laboratories have been able to contribute with more weight to the international unification of time under the coordina-tion of the Bureau International de Poids et Measures. During the period from June 1 through June 11, 1988, the differential delays of time transfer receivers of the GPS were calibrated at three different laboratories in Japan, linking them for absolute time transfer with previously calibrated labs of Europe and North America. The differential delay between two receivers was first calibrated at the National Institute of Standards and Technology (NIST)(formerly the National Bureau of Standards) in Boulder, Colorado, USA. Then one of Standards) in Boulder, Colorado, USA. Then one of these receivers was carried to each of the three laboratories: the Tokyo Astronomical Observatory, the Communications Research Laboratory, both in Tokyo, and the National Research Laboratory of Metrology in Tsukuba City. At each lab data was taken comparing receivers. Finally the traveling receiver was taken back to NIST for closure of the calibration. On the way back the GPS receiver at the WWVH radio station of NIST in Hawaii was also calibrated. The results of the calibrated. Hawaii was also calibrated. The results of the calibration trip are reported, along with some interesting problems that developed concerning the technique.

PB89-212211 Not available NTIS National Bureau of Standards (NML), Boulder, CO.

Time and Frequency Div.

NBS (National Bureau of Standards) Calibration
Service Providing Time and Frequency at a
Remote Site by Weighting and Smoothing of GPS
(Global Positioning System) Common View Data. inal rept.

M. A. Weiss, and D. W. Allan. 1986, 2p Pub. in Proceedings of Conference on Precision Elec-tromagnetic Measurements, Gaithersburg, MD., June 23-27, 1986, p125-126.

Keywords: *Calibrating, *Time standards, *Frequency standards, Time measurement, Frequency measurement, Synchronism, Data smoothing, Data processing, Global positioning systems, Kalman filtering.

The National Bureau of Standards Time and Frequency Division now performs precision time and frequency cy Division now performs precision time and frequency transfer using common view measurements of Global Positioning System (GPS) satellites as a calibration service. Using the service the authors have been able to transfer time with time stabilities of a few nanoseconds, time accuracies of the order of 10 ns, and frequency stabilities of a part in 10 to the 14th power and better for measurement times of about four days and better for measurement times of about four days and longer. The paper describes the technique used for weighting and smoothing the data to produce this level of stability and accuracy.

PB90-117367 Not available NTIS National Inst. of Standards and Technology (NML), Boulder, CO. Time and Frequency Div. in Search of the Best Clock.

Final rept. D. W. Allan, M. A. Weiss, and T. K. Peppler. 1989,

7p
Pub. in IEEE (Institute of Electrical and Electronics Engineers) Transactions on Instrumentation and Measurement 38, n2 p624-630 Apr 89.

Keywords: *Atomic clocks, *Stability, Time standards, Frequency meters, Time measuring instruments, Frequency standards, Time measurement, Chronometers, Timing devices, Gravitational fields, Reprints.

There is an increased need for better clock performance than is currently available. Past work has focused on developing better clocks to meet the increased need. Significant gains have been and can be obtained through the algorithms which optimize the clock readings and through international comparisons now available via satellite. Algorithms for processing are more important than the proportionate attention generally given them. In fact, to date, one of the main ways to investigate some of the long-term performance aspects of the millisecond pulsar, PSR 1937 + 21, is by using such optimization algorithms. Since there are indications in the pulsar data of variations which could be explained as arising from the influence of gravita-tional waves, these long-term stability studies take on a new importance. Improved long-term stability of earth-bound clock systems will significantly assist the study of the incredibly stable spin rates of these neu-

Verbal

900,633

PB89-176713 Not available NTIS National Bureau of Standards (ICST), Gaithersburg, ystems Components Div.

PCM/VCR Speech Database Exchange Format. Final rent.

D. S. Pallett. 1986, 4p Pub. in Proceedings of IEEE-IECEJ-ASJ International Conference on Acoustics, Speech, and Signal Processing, Tokyo, Japan, April 7-11, 1986, p317-320.

Keywords: *Speech, Speech recognition, Data storage, Acoustics, *Data bases, Computer applications, Format, Information transfer.

The use of PCM/VCR technology is described for use as a storage and exchange medium for speech databases. In order to provide a limited amount of digital data, use is made of a recorded modern signal for ASCII character string headers associated with the speech tokens. The format can be used to store field recordings of speech material for subsequent digitization, for transfer of speech database material between laboratories, and in implementing automated testing of speech recognition devices.

900.634

PB89-176721 Not available NTIS National Bureau of Standards (ICST), Gaithersburg, MD, Systems Components Div.
Compensating for Vowel Coarticulation in Continuous Speech Recognition.

J. L. Hieronymus, and W. J. Majurski. 1986, 4p Pub. in Proceedings of ICASSP, IEEE (Institute of Electrical and Electronics Engineers) International Conference on Acoustics, Speech and Signal Processing, Tokyo, Japan, April 7-11, 1986, p2787-2790.

Keywords: *Speech recognition, Speech articulation,

Seven English monothong vowels were studied in continuous sentences. The study determined what methods are likely to be successful in compensating for coarticulation in all vowel and consonantal contexts. A method by Kuwahara is examined in detail. The Kuwahara compensation improves the separation of the vowel regions in a space composed of the first and second formant. Important issues are where to meas-ure the formant target frequencies, how to obtain good formant tracks, measuring speaking rate accurately, and how to label vowels accurately.

COMPUTERS, CONTROL & INFORMATION THEORY

Computer Hardware

900,635

PB89-162614 PC A03/MF A01 National Inst. of Standards and Technology (NEL), Boulder, CO. Center for Computing and Applied MathAnalysis of Computer Performance Data. J. C. M. Wang, J. M. Gary, and H. K. Iyer. Jan 89, 45p NISTIR-88/4019

Prepared in cooperation with Colorado State Univ., Fort Collins. Dept. of Statistics.

Keywords: *Data reduction, Statistics, Computer systems hardware, Computer systems programs, Tables(Data), Bench marks, *Computer performance evaluation, *Data analysis.

The paper is devoted to an analysis of the data from the Livermore loops benchmark. It will be shown that in a general predictive sense the dimension of this data is rather small; perhaps between two and five. Two techniques are used to reduce the 72 loop timings for each machine to a few scores which characterize the machine. The first is based on a principal component analysis, the second on a cluster analysis of the loops. The validity of the reduction of the data to a lesser dimension is checked by various methods.

900,636

PB89-173793 Not available NTIS National Bureau of Standards (ICST), Gaithersburg, MD. Advanced Systems Div.

Performance Measurement of a Shared-Memory Multiprocessor Using Hardware instrumentation. Final rept.

A. Mink, and G. Nacht. 1989, 10p Sponsored by Defense Advanced Research Projects

Agency, Arlington, VA.
Pub. in Proceedings of Annual Hawaii International
Conference on System Sciences (22nd), Kailua-Kona,
Hl., January 3-6, 1989, p267-276.

Keywords: Parallel processors, *Multiprocessors, *Computer performance evaluation, Microprocessors, Parallel computers.

A hardware approach is presented for the design of performance measurement instrumentation for a shared-memory, tightly coupled MIMD multiprocessor. The Resource Measurement System (REMS) is a non-intrusive, hardware measurement tool used to obtain both trace measurement and resource utilization information. This approach provides more detailed and ex-tensive measurement information than alternative software or hybrid approaches without introducing artifacts into the test results. This is accomplished at a significantly higher tool cost than the alternative soft-ware or hybrid approaches. Certain features of today's nicroprocessors limit the applicability of such a hard-ware tool. Measurements obtained using this hardware tool on two kernel (small benchmark) routines are presented.

900.637

Not available NTIS PB89-186845 National Bureau of Standards (ICST), Gaithersburg, MD. Systems Components Div.

Design Factors for Parallel Processing Bench-

marks. Final rept.

G. Lyon. 1988, 12p Sponsored by Defense Advanced Research Projects Agency, Arlington, VA. Pub. in High Performance Computer Systems, p103-114 1988.

Reprints, Keywords: Models, *Parallel processing(Computers), *Computer performance evaluation, Computer architecture, Computer systems

Performance benchmarks should be embedded in comprehensive frameworks that suitably set their context of use. One universal framework is beyond reach, since distinct clusters of use are emerging with sepa-rate emphases. Large application benchmarks are most successful when they run well on a machine, and thereby demonstrate economic compatibility of job and architecture. The present value of smaller benchmarks is diagnostic, although sets of them would encourage the parametric study of architectures and applications.

900,638

PB89-186852 Not available NTIS National Bureau of Standards (ICST), Gaithersburg, MD. Systems Components Div.

COMPUTERS, CONTROL & INFORMATION THEORY

Computer Hardware

Hardware Instrumentation Approach for Performance Measurement of a Shared-Memory Muitiprocessor. Final rept.

G. Nacht, and A. Mink. 1988, 17p Sponsored by Defense Advanced Research Projects

Agency, Arlington, VA. Pub. in Proceedings of International Conference on Modelling Techniques and Tools for Computer Performance Evaluation (4th), Palma de Mallorca, Spain, September 14-16, 1988, v2 p321-337.

Keywords: Computer systems hardware, *Computer performace evaluation, *Multiprocessors, Parallel computers, Hardware.

A hardware approach is presented for the design of performance measurement instrumentation for a shared memory, tightly coupled MIMD multiprocessor. The Resource Measurement System (REMS) is a non-intrusive hardware measurement. intrusive, hardware measurement tool used to obtain both trace measurement and resource utilization information. The approach provides more detailed and extensive measurement information than alternative software or hybrid approaches without introducing arti-facts into the test results. This is accomplished at a significantly higher cost than the alternative software or hybrid approaches. When access to pertinent signals is restricted, the applicability of such a hardware tool is limited.

900,639 PB89-189161 PC A03/MF A01 National Inst. of Standards and Technology (ICST), Gaithersburg, MD. Advanced Systems Div. Hybrid Structures for Simple Computer Performance Estimates.

G. E. Lyon, Mar 89, 25p NISTIR-89/4063

G. E. Lyon. Mar 89, 25p NISTIR-89/4063 Sponsored by Defense Advanced Research Projects Agency, Arlington, VA., Bureau of Export Administra-tion, Washington, DC., and Department of Energy, Washington, DC.

Keywords: Computer systems hardware, Computer components, *Computer architecture, *Computer performance evaluation, Computer applications.

Even the coarsest performance estimators for a modern computer must account for architectural dependencies and variabilities. For example, average execution rate is rather sensitive to the match between machine and application workload. Computing can be viewed as computational components that are loaded by demands of an application, or alternately, as an application workload partitioned by system components. Models based upon these simple perspectives help organize simple performance measurements. Several examples demonstrate strengths of a straight-forward flexible partitioning scheme based upon tree graphs. Quite explicit, the graphs promote a more critical view of measurements and support multiple interpretations.

900,640 PB89-216477 PC A03/MF A01 National Inst. of Standards and Technology (NCSL), Gaithersburg, MD. Advanced Systems Div. Architecturally-Focused Benchmarks with a Com-

munication Example.
G. E. Lyon, and R. D. Snelick. Mar 89, 39p NISTIR-

89/4053 Sponsored by Defense Advanced Research Projects Agency, Arlington, VA.

Keywords: *Performance evaluation, Performance tests, Measurement, Computer systems hardware, Comparison, *Computer architecture, Computer communications, Parallel processing, Vector processing.

The discussion first sketches a framework of modalities for an architecturally-focused performance evaluation. The result is a hybrid of benchmarking and modeling: elements of capacity-and-use trees (CUTs) are explored as a simplified notation. There follows a description of the structure and preliminary results from a practical benchmark set for process communication. Argument is given that performance within a class of architecture is often dominated by unavoidable competitions within distinct machine modalities, such as scalar-vector. A k-alternative, forced choice defines a dimension of comparison equally well in SI- or MIMD architectures. Performance estimators are interpolations between values from basis benchmarks for modes; ideally in the two-alternative forced choice only two benchmark measurements are needed. Re-finements in basis benchmarks support CUT-based estimates of performance.

900,641

PB89-229017 PC A03/MF A01 National Inst. of Standards and Technology (ICST), Gaithersburg, MD. Advanced Systems Div.

Processing Rate Sensitivities of a Heterogeneous Multiprocessor.

G. E. Lyon. Aug 89, 12p NISTIR-89/4128 Sponsored by Defense Advanced Research Projects Agency, Arlington, VA., and Department of Energy, Washington, DC.

Keywords: *Multiprocessors, Mathematical models, Performance evaluation, Parallel processing, Capacity, Computer architecture, Sensitivity.

A recent trend in multiprocessor evaluation has been to seek fundamental but easily parameterized performance characterizations. Freed of specialized detail, simplified models can convey good insight while applying easily and widely. A simple performance estimator and alternate scheduling schemes can, from very modest effort, highlight some first-order improvement tradeoffs in multiprocessors. An application example of a quicksort is used to demonstrate the approach.

900,642

PB89-235931 PC A16/MF A01 National Inst. of Standards and Technology (NCSL), Gaithersburg, MD.

Working implementation Agreements for Open Systems interconnection Protocols. T. Boland. Aug 89, 374p NISTIR-89/4140 See also PB89-221196.

Keywords: *Computer networks, Tests, Standards, Data processing security, *National Institute of Standards and Technology, *Open systems interconnection, *Protocols, Local area networks, Message processing, File maintenance, Data base management.

The document records current agreements on implementation details of Open Systems Interconnection Protocols among the organizations participating in the NIST/OSI Workshop Series for Implementors of OSI Protocols. The decisions are documented to facilitate organizations in their understanding of the status of agreements. It is a standing document that is updated after each workshop (about 4 times a year).

900.643

PB90-112418 PC A07/MF A01 National Inst. of Standards and Technology (NEL), Gaithersburg, MD. Building Environment Div.
Guideline for Work Station Design.

A. Rubin, and G. Gillette. Sep 89, 150p NISTIR-89/ 4163

Sponsored by Public Buildings Service, Washington,

Keywords: *Ergonomics, *Design, *Office equipment, Furniture, Human factors engineering, Acoustics, Illu-minating, Wiring, *Workstations, Man machine sys-

The report describes a workstation design process, starting with an analysis of the activities performed, then deals with environmental, building design, space planning and furniture issues required for designing workstations suitable for a range of office activities. A limited number of generic workstations are presented, as examples of types of configurations that might meet specific office requirements. The examples are illustrative of the results of following the design process sug-gested and are not intended as recommended approaches for particular workstation designs. Technological, ergonomic, and organizational factors are considered from the standpoint of their design implications for automated workstations. Criteria and checklists are included as an aid to making workstation design decisions.

900 644

Not available NTIS PB90-117672 National Inst. of Standards and Technology (NCSL), Gaithersburg, MD. Advanced Systems Div. Design Factors for Parailei Processing Benchmarks. Final rept.

G. Lyon. 1989, 15p

See also PB89-186845. Sponsored by Defense Advanced Research Projects Agency, Arlington, VA. Pub. in Theoretical Computer Science 64, p175-189

Keywords: *Parallel processors, Models, Measurement, Reprints, *Computer performance evaluation, Computer architecture.

Performance benchmarks should be embedded in comprehensive frameworks that suitably set their context of use. One universal framework appears beyond reach, since distinct architectural clusters are emerg-ing with separate emphases. Large application benchmarks are most successful when they run well on a machine, and thereby demonstrate the economic compatibility of job and architecture. The present value of smaller benchmarks is diagnostic, although sets of them would encourage the parametric study of architectures and applications; an extended example illustrates the last aspect.

900.645

PB90-129891 PC A03/MF A01 National Inst. of Standards and Technology (NEL), Boulder, CO. Center for Computing and Applied Math-

Allocating Staff to Tax Facilities: A Graphics-Based Microcomputer Allocation Model. P. D. Domich. Jun 89, 18p NISTIR-89/4059

Keywords: *Microcomputers, *Allocation models, Taxes, Mathematical models, Computer graphics, Facilities, Stuffing.

The paper presents a computer model to allocate Internal Revenue Service staff to field offices so to satisfy a user-defined level of workload. The system is microcomputer-based and uses menus and graphically displayed zip code maps of IRS districts for interactive inputs and solution outputs. The level of workload is interactively specified and a detailed report of work-load and staff assignments is automatically generated.

Computer Software

900.646 PB89-151807 PC A04/MF A01 National Inst. of Standards and Technology (ICST), Gaithersburg, MD. Advanced Systems Div.
Wavefront Matrix Multiplication on a Distributed-

Memory Multiprocessor.
J. R. Nechvatal. Jan 89, 71p NISTIR-88/4001

Sponsored by Defense Advanced Research Projects Agency, Arlington, VA.

Keywords: *Matrices(Mathematics), *Multiplication, Algorithms, *Multiprocessors, Distributed computer systems, Computer networks.

The report considers the problem of efficiently multiplying matrices on distributed-memory, messagepassing computers. Block decomposition and wavefront computing are employed to yield a communica-tion-efficient solution. It also explores interconnections between distributed data structures, physical networks of nodes and virtual networks of nodes and processes. The notion of wavefront computing is extended to include pipelining of data between nodes of networks of processes as well as physical networks of nodes. Algorithms are developed in layers to facilitate porting between topologies and programming environments. The authors show how different topologies can be employed in a single application. A mathematical characterization of data-routing for efficient matrix multiplication on distributed-memory machines is developed, which exhibits a wavefront version of the Dekel/Nassimi/Sahni algorithm as a special case. The authors discuss the notion of granularity in this context and use it to distinguish between algorithms on grounds of communication complexity.

900 647 PB89-176226 PB89-176226 Not available NTIS National Bureau of Standards (NEL), Boulder, CO. Electromagnetic Fields Div. Creating CSUBs in BASIC.

Final rent.

E. J. Vanzura. 1988, 5p Pub. in HP Design and Automation, pt1 p18-21 Oct 88 and HP Design and Automation, pt2 p25 Nov 88.

Keywords: *Subroutines, Operating systems(Computers), Compilers, Reprints, *Basic programming language, *Fortran programming language,

COMPUTERS, CONTROL & INFORMATION THEORY

Computer Software

PASCAL programming language, Computer software, Precompilers, Input output processing.

CSUBs are compiled subprograms created using the Pascal operating system which run in the BASIC envi-ronment. A new technique is described in which programs written in FORTRAN can be turned into CSUBs. Thus, powerful, well-documented FORTRAN routines become accessible to the BASIC-language programmer. I/O and variable interfacing are discussed, and a comprehensive example is provided.

900,648 PB89-177000 PB89-177000 Not available NTIS National Bureau of Standards (NEL), Gaithersburg, MD. Factory Automation Systems Div. Incrementor: A Graphical Technique for Manipulat-Inc Parameters

Ing Parameters. Final rept.

Pub. in ACM (Association for Computing Machinery)
Transactions on Graphics 6, n1 p74-78 Jan 87.

Keywords: Reprints, *Interactive graphics, *Man computer interface, Man machine systems, Computer graphics, Input output processing.

A visually compact technique for manipulating variables is presented. The technique uses both a mouse and keyboard for redundant entry methods.

Not available NTIS National Inst. of Standards and Technology (ICST), Gaithersburg, MD. Systems and Network Architecture

Object-Orlented Model for ASN.1 (Abstract Syntax Notation One).

Final rept.

P. Gaudette, S. Trus, and S. Collins. 1988, 14p Pub. in Proceedings of International Conference on Formal Description Techniques (1st), Stirling, Scotland, September 6-9, 1988, p121-134.

Keywords: Models, *Data definition languages, *ASN.1 data definition language, High level languages, Abstract Syntax Notation One, Protocols, Protocol(Computers).

ASN.1 is a data definition language associated with the OSI Presentation Layer. The model of ASN.1 provides an object-oriented definition of types and values, the most basic concepts of ASN.1. The model is both a target for syntax-directed translation and an input to several tools for working with ASN.1. One tool allows evaluation of an abstract syntax in ASN.1 by providing a collection of transformations of values. Some difficult problems of ASN.1 tools, such as macros, are also discussed

900,650 PB89-180012 Not available NTIS National Bureau of Standards (ICST), Gaithersburg, MD. Systems Components Div. Definitions of Granularity.

Final rept. C. P. Kruskal, and C. H. Smith. 1988, 12p Pub. in High Performance Computer Systems, p257-268 1988

Keywords: Parallel processors, Reprints, *Granularity, *Parallel processing, Parallel computers, Computations, Balance.

'Granularity' is a well known concept in parallel proceranularity is a well known concept in parallel processing. While intuitively, the distinction between coarse grain and fine grain parallelism is clear, there is no rigorous definition. The paper develops two notions of granularity, each defined formally and represented the control of the c sented by a single rational number. The two notions are compared and contrasted with each other and with previously proposed definitions of granularity.

900,651 PB89-193833 PC A03/MF A01 National Inst. of Standards and Technology (NCSL), Gaithersburg, MD.
Software Configuration Management: An Over-

vlew.

W. M. Osborne. Mar 89, 34p NIST/SP-500/161
W. M. Osborne. Mar 89, 34p NIST/SP-500/161
Also available from Supt. of Docs. as SN003-003-02927-1. See also AD-A130 109. Library of Congress catalog card no. 89-600728.

Keywords: Revisions, Quality assurance, *Software configuration management, *Software engineering,

*Computer software management, *Computer program reliability, Reusable software, Computer software maintenance, Computer program verification, Software tools, Life cycles.

The guide provides an overview of software configuration management, a support function dedicated to making both the technical and managerial software ac-tivities more effective. It addresses the problems associated with managing software changes; the importance of implementing software configuration management (SCM) procedures early; and the application of those procedures throughout the software lifecycle. A brief summary of SCM tools and their applicable func-tionality is provided. SCM extends to more than just the code (source, relocatable, executable) and docu-mentation (e.g., system and software requirements and design specifications). It also covers control files, test data, test suites, support tools, and other compo-nents used to develop and maintain the software prod-

900,652 PB89-211908 Not available NTIS National Inst. of Standards and Technology (ICST), Gaithersburg, MD. Systems and Network Architecture

Application of Formal Description Techniques to Conformance Evaluation. Final rept.

J. P. Favreau, R. J. Linn, and P. Gaudette. 1988, 15p Pub. in Proceedings of International Conference on Formal Description Techniques (1st), Stirling, Scotland, September 6-9, 1988, p295-309.

Keywords: Tests, Systems engineering, *Protocols, *Communication networks, Software tools, Estelle, Abstract Syntax Notation One, Electronic mail

Formal description techniques, and software tools based on them, are applied successfully in the development of test systems for OSI protocols. The test system architecture uses reference implementations augmented with test features in a manner that facilitates multi-layer testing and minimizes the effort necessary to develop test cases. The designs for test systems in general and for a specific gateway are described, focusing on the use of Estelle and ASN.1.

900,653 PB89-211916 Not available NTIS National Inst. of Standards and Technology (ICST), Gaithersburg, MD. Systems and Network Architecture

Object-Orlented Model for Estelle.

Final rept.

R. Sijelmassi, and P. Gaudette. 1988, 15p See also PB89-196190.

Pub. in Proceedings of International Conference on Formal Description Techniques (1st), Stirling, Scotland, September 6-9, 1988, p91-105.

Keywords: Models, *Protocols, *Communication networks, Protocol(Computers), Estelle, Translators, Distributed computer systems, Finite state machines.

Estelle is a formal description technique for specifying OSI communication protocols. An object-oriented model for Estelle is presented that is concrete enough to allow execution but abstract enough to remain concise and workable. A synchronization protocol cap-tures the subtleties of parallelism in the semantics of Estelle and allows module instances to execute as if they were asynchronous. The remainder of the basic model defines objects that are very close to the entities defined by Estelle semantics. The model constitutes an excellent specification of the output of a translator. It has been extended to allow appropriate observation and user control of the objects that simulate an Estelle formal description of a protocol. The combination of translation into an implementation of the model provides a powerful tool for specifying, studying, and debugging distributed systems.

900,654 PB90-111683 PC A03/MF A01
National Inst. of Standards and Technology (NCSL),
Gaithersburg, MD.
Computer Viruses and Related Threats: A Management Guide.

Special pub. (Final). J. P. Wack, and L. J. Carnahan. Aug 89, 46p NIST/ SP-500/166

Also available from Supt. of Docs. as SN003-003-02955-6. Library of Congress catalog card no. 89-

Keywords: *Computer security, *Instructions, Computer software management, Computer networks, Contingency, Copyrights, Vulnerability, Trojan horses, Personal computers, *Computer viruses.

The document contains guidance for managing the threats of computer viruses and related software and unauthorized use. The document emphasizes that organizations cannot effectively reduce their vulnerabili-ties to viruses and related threats unless the organiza-tion commits to a virus prevention program, involving the mutual cooperation of all computer managers and users. The guidance is aimed at helping managers prevent and deter virus attacks, detect when they occur or are likely to occur, and then to contain and recover from any damage caused by the attack. The document contains an overview of viruses and related software, and several chapters of guidance for managers of multi-user computers, managers and users of personal computers, managers of wide and local area networks including personal computer networks, and managers of end-user groups.

900,655

PB90-111691 PC A03/MF A01 National Inst. of Standards and Technology (NCSL), Gaithershurg MD

Gaithersburg, MD.
Software Verification and Validation: Its Role in Computer Assurance and Its Relationship with Software Project Management Standards.

Special pub. Jul 88-May 89. D. R. Wallace, and R. U. Fujii. Sep 89, 40p NIST/SP-

500/165

Also available from Supt. of Docs. as SN003-003-02959-9. Library of Congress catalog card no. 89-600754. Prepared in cooperation with Logicon, Inc., San Pedro, CA.

Keywords: *Computer software management, *Software engineering, Computer software maintenance, Computer program verification, Computer security, Computer performance evaluation, Software valida-

The report describes how the software verification and validation methodology and V&V standards provide a strong framework for developing quality software. First, the report describes software V&V, its objectives, recommended tasks, and guidance for selecting techniques to perform V&V. It explains the difference between V&V and quality assurance, development system engineering, and user organization functions. The report explains that V&V produces maximum benefits when it is performed independent of development functions and provides a brief discussion of how V&V benefits change when embedded in quality assurance, development systems engineering, and user organizations. An analysis of two studies of V&V's cost-effec-tiveness concludes that cost benefits of V&V's early error detection outweigh the cost of performing V&V.

900.656

PB90-128752 Not available NTIS National Inst. of Standards and Technology (NEL), Boulder, CO. Electromagnetic Fields Div. Creating CSUBs Written in FORTRAN That Run In BASIC.

Final rept.
E. J. Vanzura. 1988, 18p
Pub. in Proceedings of Conference on HP Technical
Computer Users, Orlando, FL., August 7-12, 1988, p1-

*Subroutines, Operating systems(Computers), Computer programming, *Basic programming language, *Fortran programming language, Pascal programming language.

CSUBs are compiled subprograms created using the Pascal operating system and which run in the BASIC environment. A new technique in which programs written in FORTRAN can be turned into CSUBs is described. Thus, powerful, well-documented FORTRAN routines become accessible to the BASIC-language programmer. I/O and variable interfacing are discussed, and a comprehensive example is provided.

900.657

PB90-130253 PC A03/MF A01 National Inst. of Standards and Technology (NEL), Gaithers Durg, MD. Applied and Computational Mathe-

Supercomputers Need Super Arithmetic. Final rept.

D. W. Lozier, and P. R. Turner. Oct 89, 31p NISTIR-89/4135

Prepared in cooperation with Naval Academy, Annapolis, MD. Dept. of Mathematics.

Keywords: Algorithms, Parallel processors, Error analysis, *Supercomputers, *Floating point arithmetic, Arithmetic units, Vector processing, Symmetric levelindex system.

The paper discusses the parallel computation of vector norms and inner products in floating-point for vector and parallel computers. It concentrates on the vectorization of algorithms for the operations and proposes a new form of computer arithmetic, the symmetric level-index system.

900,658

PB90-133091 PC A03/MF A01 National Inst. of Standards and Technology (NCSL), Gaithersburg, MD.

Graphics Application Programmer's Interface Standards and CALS (Computer-Aided Acquisition

and Logistic Support).
S. J. Kemmerer, and M. W. Skall. Oct 89, 17p
NISTIR-89/4199

Keywords: *Computer graphics, *Standards, Interfaces, Computer aided design, Computer programs.

The principal purpose of a graphics Application Programmer's Interface (API) standard is to provide portability for an application program across a wide range of computers, operating systems, programming languages, and interactive graphics devices. The graphics API's are represented by four major standards' projects: Graphical Kernel System (GKS), GKS-3D, Programmer's Hierarchical Interactive Graphics System (PHIGS), and Programmer's Imaging Kernel (PIK) (PIK).

Control Systems & Control Theory

900.659

PB89-151815 PC A06/MF A01 National Inst. of Standards and Technology (ICST), Gaithersburg, MD. Advanced Systems Div. Small Computer System Interface (SCSI) Com-mand System: Software Support for Control of Small Computer System Interface Devices. J. Gorczyca, and E. S. Villagran. Jan 89, 125p NISTIR-89/4023

Keywords: Systems engineering, Computer programs, *Command and control systems, *Computer software, *Small Computer System Interface (SCSI) devices, Microcomputers, C programming language, User manuals(Computer programs).

The Small Computer System Interface (SCSI) Command System was created by the National Computer and Telecommunications Laboratory of the National Institute of Standards and Technology (NCTL/NIST) personnel for the control of SCSI devices from a microcomputer equipped with a SCSI host adapter. The Command Interfacing Function permits all SCSI standard and manufacturer unique commands to be sent to external devices. The system allows two levels of user programming. The upper and lower levels offer the ability to utilize libraries of commands, and the abilthe ability to utilize libraries of commands, and the ability to edit system parameters and commands directly by using the system's variables. Programming for the system is done in the 'C' language. Also included with the documentation are references, which provide additional information that may be of reader interest.

Information Processing Standards

900,660

FIPS PUB 134-1 PC A03/MF A01 National Inst. of Standards and Technology (NCSL), Gaithersburg, MD.

Coding and Modulation Requirements for 4,800 Blt/Second Modems, Category: Telecommunications Standard.

Federal information processing standards (Final). S. M. Radack, 4 Nov 88, 19p

Supersedes FIPS PUB 134.

Three ring vinyl binder also available, North American Continent price \$7.00; all others write for quote.

*Standards, *Information processing, Coding, Modulation, Communication equipment, Computer communications, *Federal Information Processing Standards.

The standard establishes coding and modulation requirements for 4,800 bit/s modems owned or leased by the Federal government for use over analog transmission channels. It is based upon techniques described in CCITT Recommendations V.27 bis, V.27 ter, and V.32. The standard supersedes former Federal Standard (FED-STD) 1006 in its entirety.

900.661

FIPS PUB 149 **PC E08** National Inst. of Standards and Technology (NCSL), Gaithersburg, MD.

General Aspects of Group 4 Facsimile Apparatus, Category: Telecommunications Standard. Federal information processing standards (Final).

S. M. Radack. 4 Nov 88, 7p
Three ring vinyl binder also available, North American
Continent price \$7.00; all others write for quote.

Keywords: *Standards, *Information Coding, Computer communication, Data transmission, Communication equipment, *Federal Information Processing Standards, Facsimile coding.

The standard adopts Electronic Industries Association (EIA) Standard EIA-536-1988, which defines the facsimile coding schemes and their control functions for Group 4 facsimile apparatus.

900.662

FIPS PUB 150 PC **E08** National Inst. of Standards and Technology (NCSL),

Gaithersburg, MD.
Facsimile Coding Schemes and Coding Control
Functions for Group 4 Facsimile Apparatus, Cate-

gory: Telecommunications Standard.
Federal information processing standards (Final).
S. M. Radack. 4 Nov 88, 7p
Three ring vinyl binder also available North American

Continent price \$7.00; all others write for quote.

Keywords: *Standards, *Information processing, Computer communication, Coding, Communication equipment, *Federal Information Processing Standards, Facsimile coding.

The standard adopts Electronic Industries Association (EIA) Standard EIA-538-1988, which defines the facsimile coding schemes and their control functions for Group 4 facsimile apparatus.

900,663

FIPS PUB 154 PC **E09** National Inst. of Standards and Technology (NCSL), Gaithersburg, MD. High Speed 25-Position Interface for Data Termi-

nal Equipment and Data Circuit-Terminating Equipment, Category: Telecommunications Standard. Federal information processing standards (Final). S. M. Radack. 4 Nov 88, 8p

Three ring vinyl binder also available, North American

Continent price \$7.00; all others write for quote.

Keywords: *Standards, *Information processing, Computer communication, Communication equipment, Data processing terminals, Interfaces, Data transmission, *Federal Information Processing Standards.

The standard adopts Electronic Industries Association (EIA) Standard EIA-530-1987, which specifies the interconnection of data terminal equipment (DTE) and data circuit-terminating equipment (DCE) employing serial binary data interchange circuits with control information exchanged on separate control circuits. In particular, the standard defines the signal characteristics, interface mechanical characteristics, functional description of interchange circuits, and standard inter-faces for selected communication system configurations. The electrical characteristics of the interchange circuits are specified by reference to Elec-tronic Industries Association (EIA) standard EIA-422-A (FED-STD-1020A) and EIA-423-A (FED-STD-1030A). 900.664

FIPS PUB 155 PC E11 National Inst. of Standards and Technology (NCSL), Gaithersburg, MD.

Data Communication Systems and Services User-Oriented Performance Measurement Methods, Category: Telecommunications Standard.

Federal information processing standards (Final). S. M. Radack. 4 Nov 88, 7p

Three ring vinyl binder also available, North American Continent price \$7.00; all others write for quote.

Keywords: *Standards, *Information processing, Computer communications, Data transmission systems, Performance tests, Services, *Federal Information Processing Standards.

The standard adopts American National Standard X3.141-1987, which specifies uniform methods of measuring the performance of data communication services at digital interfaces between data communication systems and their users. These methods may be used to characterize the performance of any data communication service in accordance with the useroriented performance parameters defined in a companion standard, American National Standard X3.102-1983, which has been adopted as FIPS 144 (former Federal Standard 1033).

900.665

PB89-149116 Not available NTIS
National Bureau of Standards (ICST), Gaithersburg,
MD. Systems and Software Technology Div.
Case History: Development of a Software Engi-

neering Standard. Final rept.

T. Daughtrey, R. Fujii, and D. Wallace. 1986, 5p Pub. in Proceedings of Computer Standards Conference: Striking a Balance between Technology, Economics, Politics, and Reality, San Francisco, CA., May 13-15, 1986, p21-25.

Keywords: *Standards, Verifying, Proving, Quality assurance, *Software engineering, Electronic mail.

The IEEE Standard for Verification and Validation Plans (SVVP) (1012) has been under development since March 1983. The paper presents the case history of the development of the SVVP Standard. The history characterizes the development based on the purpose of the Standard, the schedule for its development, the issues resolved for the content of the document, and the working group members. The history in-cludes the results of using electronic mail to aid in the standards development process.

900,666

PB89-211965 Not available NTIS National Bureau of Standards (ICST), Gaithersburg, MD. Systems and Software Technology Div. Federal Software Engineering Standards Program. Final rept

D. R. Wallace, 1986, 11p

Pub. in Proceedings of Concepts and Principles for the Validation of Computer Systems Used in the Manufacture and Control of Drug Products, Chicago, IL., April 20-23, 1986, p103-113 1986.

Keywords: *Standards, Data processing, Tests, Proving, Verifying, *Software engineering, *National Institute of Standards and Technology, Federal information processing standards, Computer software maintenance, Computer software management.

The National Bureau of Standards, through its Institute for Computer Science and Technology (ICST), develops standards and guidelines to aid Government agencies in their effective use of automatic data processing resources. The paper describes the Federal computer software standards program at ICST in general and the program of its Software Engineering Group in detail.

900,667

PB90-111212 PC A07/MF A01 National Inst. of Standards and Technology (NCSL),

Gaithersburg, MD.
Government Open Systems Interconnection Profile Users' Guide.

T. Boland. Aug 89, 149p NIST/SP-500/163 See also FIPS PUB 146. Also available from Supt. of Docs. Library of Congress catalog card no. 89-600749.

COMPUTERS, CONTROL & INFORMATION THEORY

Information Processing Standards

Keywords: Computer networks, Standardization, Government procurement, *Government Open Systems Interconnection Profile, *Federal information processing standards, *Computer communications, Computer architecture, Protocols.

The document provides guidance to users concerning implementation of the Government Open Systems Interconnection Profile (GOSIP) Federal Information Processing Standard (FIPS). Information in the document will help users to better understand and employ the GOSIP FIPS. The document will be updated annu-

Pattern Recognition & Image **Processing**

900.668

PB89-148415 PC A04/MF A01 National Inst. of Standards and Technology, Gaithersburg, MD.

Standards for the Interchange of Large Format **Tiled Raster Documents.**

F. E. Spielman. Dec 88, 72p NISTIR-88/4017

Keywords: *Standards, Sweep generators, Documents, *Image processing, *Computer graphics, Raster graphics, Information processing, Computer ar-

The document is a compilation of five separately prepared, but interrelated, reports which discuss aspects of raster image processing, primarily as they relate to a standard tiling scheme being developed to support the interchange of large raster images. The first report provides the reader with a brief introduction to raster graphics and the current standards used to support raster graphics applications. The second provides the reader with a non-technical overview of the tiling scheme. The third report describes the user's requirements for tiling that were identified by an ad hoc Tiling Task Group (TTG). The fourth report, a Document Application Profile, presents information about all the attributes pertaining to a tiling application. The fifth report is a proposed addendum to an ANSI standard which is required to support the tiling scheme.

General

900.669 PB89-157366 Not available NTIS National Bureau of Standards (NEL), Gaithersburg,

MD. Robot Systems Div.

Automated Analysis of Operators on State Tables:

A Technique for Intelligent Search.

Final rept. T. R. Kramer. 1986, 27p

Pub. in Jnl. of Autom. Reasoning 2, n2 p127-153 1986.

Keywords: *Search structuring, *Searching, *Artificial intelligence, Selection, Tables(Data), Objectives, Operators(Mathematics), Reprints.

In one approach to the artificial intelligence problem of searching, the current situation is represented by a state table which gives the set of current conditions. Changes in the situation are brought about by opera-tors which create a new state by adding some condi-tions to the table and deleting others. The search pro-ceeds by applying operators one after another to the current state until the current state is identical to the goal state. The paper describes a technique for helping select operators. The technique is based on the fact that, during a search in which a partial sequence of operators has been selected, if the last operator or two are known, only a limited group of operators will be sensible to try next, and this group may be selected without prior knowledge of operators most recently tried. The output of the technique is a table that gives, for each feasible partial sequence of one or two operators, a list of operators that might be tried next.

900.670 PB89-168009 PC A09/MF A01 National Inst. of Standards and Technology (NCSL), Gaithersburg, MD. Computer Security Div.

Report of the Invitational Workshop on Integrity Policy In Computer Information Systems (WIPCIS). Final rept.

S. W. Katzke, and Z. G. Ruthberg. Jan 89, 196p NIST/SP-500/160

and National Computer Security Center, Fort George G. Meade, MD.

Keywords: *Meetings, Policies, Standards, *Information systems, *Computer information security, *Data integrity, Computer privacy.

Reported is the Invitational Workshop on Integrity Policy in Computer Information Systems. The work-Policy in Computer Information Systems. The workshop established a foundation for further progress in defining a model for information integrity. The workshop was held in response to the paper by David Clark of M.I.T. and David Wilson of Ernst and Whinney entitled 'A Comparison of Military and Commercial Data Security Policy.' The report's 10 sections contain an introduction, the composition of the organizing committee with a list of participants and a workshop agenda, a summary report by Don Parker and Peter Neumann of SRI International, the reports of the five working groups, a response by Clark and Wilson, and a proposal by the National Bureau of Standards for continuing the effort to define an integrity policy. The appendices include a copy of the original Clark-Wilson pendices include a copy of the original Clark-Wilson

PB89-231021 Not available NTIS National Bureau of Standards (ICST), Gaithersburg, MD. Systems Components Div.

National Bureau of Standards Message Authentication Code (MAC) Validation System.

M. E. Smid, E. B. Barker, and D. M. Balenson. 1986,

Sponsored by National Computer Security Center, Fort George G. Meade, MD. Pub. in Proceedings of National Computer Security Conference (9th), September 15-18, 1986, p99-107.

Keywords: *Standards, Authentication, Cryptology, Reprints, *National Institute of Standards and Technology, *Data encryption, *Computer information security, Computer privacy, Validation.

The paper describes the National Bureau of Standards Message Authentication Code (MAC) Validation System (MVS) for testing the conformance of vendor devices to Federal and commercial data authentica-tion standards. Topics which are covered include the events which led to the development of the MVS, the standards it validates, its design philosophy, the re-quirements it places on vendors validating their de-vices, its performance characteristics, and the results of the validations performed to date.

900,672 PB89-235675

(Order as PB89-235634, PC A04) National Inst. of Standards and Technology (NCSL),

Gaithersburg, MD.
Conference Reports: National Computer Security Conference (11th). Held in Baltimore, MD. on October 17-20, 1988. E. B. Lennon. 1989, 5p Included in Jnl. of Research of the National Institute of

Standards and Technology, v94 n4 p263-267 Jul/Aug

Keywords: *Meetings, Auditing, Models, Information systems, Networks, *Computer security.

The Eleventh National Computer Security Conference held in Baltimore, Maryland on October 17-20, 1988 is summarized. The theme of the conference was the future of computer security. More than 1600 attendees from government, industry and academics partipated. Issues addressed included models and modeling integrity, risk management, audit and intrusion detection, security applications, verification, database management security, networking, system security requirements, automated tools and security architecture.

PB90-213687 PC A04 National Inst. of Standards and Technology, Gaithersburg, MD.

Journal of Research of the Institutes of Standards

Journal of Hesearch of the Institutes of Standards and Technology. September-October 1989. Volume 94, Number 5. 1989, 70p See also PB90-213695 through PB90-213711 and Volume 94, Number 4, PB89-235634. Also available from Supt. of Docs. as SN7003-027-00030-0.

Contents: Instrument-Independent MS/MS Database for XQQ Instruments: A Kinetics-Based Measurement Protocol; A Cotinine in Freeze-Dried Urine Reference Material; The NIST Automated Computer Time Serv-

900,674

PB90-213695

(Order as PB90-213687, PC A04) National Inst. of Standards and Technology, Gaithers-

burg, MD.
Instrument-Independent MS/MS Database for XQQ Instruments: A Kinetics-Based Measurement Protocol.

R. I. Martinez. 1989, 24p

Included in Jnl. of Research of the National Institute of Standards and Technology, v94 n5 p281-304 Sep/Oct

Keywords: *CAD, CBRIS, Characteristic branching ratios of ionic substructures, Collisionally-activated dissociation, Database, Ion-molecule kinetics, Measurement protocol, MS/MS, NIST-EPA International Round Robin, Spectral library, Standardization, Tandem mass spectrometers, XQQ instruments (QQQ, BEQQ, etc).

A detailed kinetics-based measurement protocol is proposed for the development of a standardized MS/ MS database for XQQ tandem mass spectrometers. The technical basis for the protocol is summarized. A CAD database format is proposed.

900,675 PB90-213703

(Order as PB90-213687, PC A04) National Inst. of Standards and Technology, Gaithersburg, MD.

Cotinine in Freeze-Dried Urine Reference Materi-

L. C. Sander, and G. D. Byrd. 1989, 5p Included in Jnl. of Research of the National Institute of Standards and Technology, v94 n5 p305-309 Sep/Oct

Keywords: *Cotinine, Cotinine perchlorate, GC-MS, Passive smoking, Side stream smoke, Standards, To-

A cotinine in freeze-dried urine reference material (RM 8444) was prepared at three concentrations: (1) a 'blank' level typical of nonsmokers with no exposure to cigarette smoke, (2) a 'low' level corresponding to nonsmokers with passive exposure to side-stream smoke, and (3) a 'high' level typical of smokers. Low- and high-level materials were prepared gravimetrically from pooled urine by the addition of appropriate amounts of continine perchlorate. Cotinine was determined by GC-MS using continine-d3 as an internal standard. No evidence for sample inhomogeneity was observed. This reference material will fulfill a need for a urine-based standard to assist in the validation of field methods used for assessing exposure to cigarette smoke.

900.676 PB90-213711

(Order as PB90-213687, PC A04) National Inst. of Standards and Technology, Gaithersburg, MD.
NIST Automated Computer Time Service.

J. Levine, M. H. Weiss, D. D. Davis, D. W. Allan, and D. B. Sullivan. 1989, 11p Included in Jnl. of Research of the National Institute of

Standards and Technology, v94 n5 p311-321 Sep/Oct

Keywords: *Automation, Computers, Delay, Digital systems, Frequency, Propagation delay, Telephone, Synchronization, Time.

The NIST Automated Computer Time Service (ACTS) is a telephone time service designed to provide computers with telephone access to time generated by the National Institute of Standards and Technology at accuracies approaching 1 ms. Features of the service include automated estimation by the transmitter of the telephone-line delay, advanced alert for changes to and from daylight saving time, and advanced notice of insertion of leap seconds. The ASCII-character time code operates with most standard modems and computer systems. The system can be used to set computer clocks and simple hardware can also be developed to set non-computer clock systems.

900,677 PB90-780172 PC A03/MF A01 National Inst. of Standards and Technology (NCSL), Gaithersburg, MD.
Computer Security Training Guidelines.

Final rept.

M. A. Todd, and C. Guitian. Nov 89, 41p NIST/SP-500/172

Also available from Supt. of Docs. as SN003-003-02975-1. Library of Congress catalog card no. 89-

Keywords: Standards, Objectives, Computer personnel, *Computer security, *Training, Computer information security, Computer privacy.

The guidelines describe what should be the learning objectives of agency security training programs. They focus on what the employee should know, and what they should be able to direct or perform. This allows agencies to design training programs that fit their environments and to clearly state the purpose of the training. Effectiveness can be measured by determining how many of the learning objectives were met. and Characterization, Hamburg, FRG, September 19-21, 1988, v1009 p281-289.

Keywords: *Ultrasonic frequencies, *Detectors, *Surface roughness, Acoustics, Sound ranging, Surface properties, Topography, Metal plates, Measurement, Process control, Quality control.

Ultrasonic reflectance/scattering measurements have been made on metal samples possessing a large range of surface roughness values. The root-mean-square roughnesses R(q) ranged from 0.3 to nearly 40 micrometers on the mostly periodic surfaces. The echo amplitude from short incident pulses of ultrasound in the frequency range of 1 to 30 MHz was used, in the manner of a comparator, to measure relative roughnesses with an area-averaging approach defined by the ultrasonic beam spot size. Ultrasonic wave-lengths ranged from about 50 to 300 micrometers at these frequencies, and the beam spot sized varied from 0.2 to 5 mm in diameter. Both air and fluid coupling techniques were used between the sensor (transducer) and surface, on both static and rapidly (in excess of 5 m/sec surface speed) moving parts. On static surfaces, a resolution of better than 1.0 micrometers R(q) was achieved at the higher ultrasonic frequencies. By focusing the ultrasonic beam at 30 MHz, a profilometry capability was demonstrated on a 1 micrometer R(q) sinusoidal specimen of 800 micrometers wavelength.

Electromagnetic & Acoustic DETECTION & Countermeasures COUNTERMEASURES

900.680 PB89-161525 Not available NTIS National Bureau of Standards (NEL), Boulder, CO. Electromagnetic Fields Div. Techniques for Measuring the Electromagnetic Shielding Effectiveness of Materials. Part 1. Far-

Field Source Simulation.

Final rept. P. F. Wilson, M. T. Ma, and J. W. Adams. 1988, 12p

See also Part 2, PB89-161533.
Pub. in IEEE (Institute of Electrical and Electronics Engineers) Transactions on Electromagnetic Compatibility 30, n3 p239-250 Aug 88.

Keywords: *Materials tests, *Electromagnetic shielding, *Coastal cables, Radiation shielding, Far field, Electromagnetic fields, Simulation, Effectiveness, Plane waves, Transmission lines, Time domain sys-

Shielding effectiveness relates to the ability of a material to reduce the transmission of propagating fields in order to electromagnetically isolate one region from another. Because the shielding capability of a complex material is difficult to predict, it often must be measured. A number of approaches to simulating a far-field source are studied, including the use of coaxial trans-mission-line holders and a time-domain system. In each case the authors consider the system frequency range, test sample requirements, test field type, dynamic range, measurement time required, and analytical background, and present data taken on a common set of materials.

900.681 PB89-161533 Not available NTIS National Bureau of Standards (NEL), Boulder, CO. Electromagnetic Fields Div.

Techniques for Measuring the Electromagnetic Shielding Effectiveness of Materials. Part 2. Near-Field Source Simulation.

Final rept. P. F. Wilson, and M. T. Ma. 1988, 9p See also Part 1, PB89-161525.

Pub. in IEEE (Institute of Electrical and Electronics Engineers) Transactions on Electromagnetic Compatibility 30, n3 p251-259 Aug 88.

Keywords: *Materials tests, *Electromagnetic shielding, *Measurement, Radiation shielding, Electromagnetic fields, Antennas, Simulation, Effectiveness.

The paper continues to discuss the topic of measurements of electromagnetic shielding effectiveness of materials by simulating a near-field source. Two specific measurement approaches, the use of a dual TEM cell and the application of an apertured TEM cell in a reverberating chamber, are studied. In each case the

system frequency range, test sample requirements, test field type, dynamic range, measurement time re-quired, analytical background, and present data are considered taken on a common set of materials.

900.682 PB89-173769 Not available NTIS Not available NTIS
National Bureau of Standards (NEL), Boulder, CO.
Electromagnetic Fields Div.
Automated TEM (Transverse Electromagnetic)
Ceil for Measuring Unintentional EM Emissions.

M. T. Ma, and W. D. Bensema. 1987, 12p Pub. in Proceedings of International Conference on Electromagnetic Compatibility, EMC Expo 1987, San Diego, CA., May 19-21, 1987, pT11.1-T11.12.

Keywords: *Electromagnetic radiation detection, Automatic control, Remote control, Leakage, Electromagnetic fields, Emission, Dipole moments, Electric moments, Magnetic moments, Adaptive systems, *Transverse electromagnetic cells.

The paper summarizes the basic electrical properties of a transverse electromagnetic (TEM) cell, and the underlying theoretical background, based on which a TEM cell is used to measure accurately the emission of an unknown, unintentional leakage source. The theory and measurements have been verified by the results of a simulated example and two experiments using a spherical dipole radiator and a small loop antenna. Recent development of an automated measurement system is also included.

900,683 PB89-176184 Not available NTIS National Bureau of Standards (NEL), Boulder, CO. Electromagnetic Fields Div. Photonic Electric Field Probe for Frequencies up

to 2 GHz. Final rept.

Final rept.

K. Masterson. 1987, 5p

Pub. in Proceedings of SPIE (Society of Photo-Optical Instrumentation Engineers), High Bandwidth Analog Applications of Photonics, September 23-24, 1986, Cambridge, MA., v720 p100-104

Keywords: *Electric fields, Electromagnetic radiation, Frequencies, Birefringence, Electrooptics, Measurement, Electromagnetic properties, Optical properties, Photonic probes.

A photonic electric field probe using the Pockel's effect in bulk LINbO3 is described. It was used to measure electromagnetic fields from 10 to 100 V/m. The observed frequency response was flat up to 1.6 GHz and extended beyond 2 GHz. Over the majority of the frequency range field strengths down to about 6 V/ m would be detectable above the noise floor when using a 10 kHz detection bandwidth. Present experimental results indicate a linear dynamic range for the probe of approximately 30 dB. Increasing the optical carrier power and lowering the system noise floor is expected to improve the dynamic range to above 50

Acoustic Detection

PB89-173488 Not available NTIS Notional Bureau of Standards (NEL), Gaithersburg, MD. Automated Production Technology Div. Higher-Order Crossings: A New Acoustic Emission Signai Processing Method. Final rept.

N. N. Hsu, and D. G. Eitzen. 1988, 8p Pub. in Proceedings of International Acoustic Emission Symposium (9th), Kobe, Japan, November 14-17, p59-66 1988.

Keywords: Acoustic measurement, Signal processing, Spectrum analysis, Data reduction, Data smoothing, Fatigue tests, Crack propagation, *High order crossing, *Acoustic emission, Failure analysis, Stress waves.

A new signal processing technique has been developed called the higher-order crossings (HOC) technique. It is intuitively simple yet efficient and useful in many spectral analysis and data reduction applications. Some feasibility studies of the adaptation of HOC for acoustic emission (AE) signal discrimination are reported. First introduced are the mathematical concept and the physical significance of HOC, and then the experience on using the HOC technique to classify some simulated AE, AE during fatigue testing of pre-cracked aluminum specimens, impact-echo sig-nals, and signals from machine tool monitoring is reported. It was found that the first few order crossings are sufficient to distinguish different types of AE, but specific pattern recognition schemes must be devised based on specific applications. To encourage others to experiment with these techniques, a scheme of modifying a conventional multi-channel AE system to do real time AE signal processing using higher-order crossings is presented.

900,679 PB89-211809 Not available NTIS MD. Automated Production Technology Div.

Ultrasonic Sensor for Measuring Surface Roughness.

Final rept.
G. V. Blessing, and D. G. Eitzen. 1988, 9p
Pub. in Proceedings of SPIE (Society of Photo-Optical Instrumentation Engineers): Surface Measurement

Infrared & Ultraviolet Detection

900,684 PB90-117458 Not available NTIS National Inst. of Standards and Technology (NML), Boulder, CO. Time and Frequency Div. Coherent Tunable Far Infrared Radiation.

Final rept. D. A. Jennings. 1989, 3p Contracts NASW-15, NASW-047

Sponsored by National Aeronautics and Space Administration, Washington, DC

Pub. in Applied Physics B 48, p311-313 1989.

Keywords: *Far infrared radiation, *Coherent radiation, Electromagnetic radiation, Continuous radiation, Carbon dioxide lasers, Tuned circuits, Beams(Radiation), Reprints, Metal insulator metal diodes.

Tunable, cw, far infrared (FIR) radiation has been generated by nonlinear mixing of radiation from two CO2 lasers in a metal-insulator-metal (MIM) diode. The FIR difference-frequency power was radiated from the MIM diode antenna to a calibrated indium antimonide

DETECTION & COUNTERMEASURES

Infrared & Ultraviolet Detection

bolometer. Two-tenths of a microwatt of FIR power was generated by 250 mW from each of the CO2 lasers. Using the combination of lines from a wave-guide CO2 laser, with its larger tuning range, with lines from CO2, N2O, and CO2 isotope lasers promises complete coverage of the entire far infrared band from 100 to 5000 GHz (3-200/cm) with stepwise-tunable cw radiation.

Magnetic Detection

900,685 PB89-148365 PC A03/MF A01 PBB9-148365 PC A03/MF A01 National Inst. of Standards and Technology (NEL), Boulder, CO. Electromagnetic Fields Div. Magnetostatic Measurements for Mine Detection. R. G. Geyer. Oct 88, 35p NISTIR-88/3098 Sponsored by U.S. Army Belvoir Research and Development Center, Fort Belvoir, VA.

Keywords: *Magnetic detection, *Land mine detection, *Magnetic measurement, Magnetic permeability, Magnetostatics, Electromagnetic induction.

Magnetic susceptibility measurements are applied to the passive magnetometric detection problem of an arbitrarily shaped susceptible (metallic) mine buned in a magnetically permeable earth. For analysis purposes a conservative susceptibility contrast between a typical metallic mine and host soil having the same measured magnetic characteristics as the U.S. Army Belvoir Research and Development Center (BRDC) magnetitesand mine lane mixture was assumed. Anomalous de-tection limits were then calculated for various total field intensity (Proton precession) sensor head heights and offset distances, given miné dimensions as small as 7.6 cm on a side.

Optical Detection

900,686 PB90-128281 PB90-128281 Not available NTIS National Inst. of Standards and Technology (NEL), Boulder, CO. Electromagnetic Fields Div.

Broadband, isotropic, Photonic Electric-Field

Meter for Measurements from 10 kHz to above 1 GHz.

Final rept. K. D. Masterson, and L. D. Driver. 1989, 12p Sponsored by Army Aviation Systems Command, St. Louis, MO.

Pub. in Proceedings of SPIE (Society of Photo-Optical Instrumentation Engineers) High Bandwidth Analog Applications of Photonics II, Boston, MA., September 8-9, 1988, v987 p107-118 1989.

Keywords: *Electric fields, *Electron probes, Field strength, Measurement, Electromagnetic fields, Detectors, Isotropy, Field emission, Fiber optics, Electrooptics, Crystals, Dipoles.

An isotropic, photonic electric-field meter (PEFM-15) having 15 cm resistively tapered dipole elements and Pockels effect electro-optic modulators is used to measure electric fields of 10 to 100 V/m from 10 kHz to beyond 1 GHz. The probe's frequency response is flat within +1-dB from 30 kHz to 100 MHz except for a region between 1 and 10 MHz where acoustic resonregion between 1 and 10 MHz where account resonances occur in the LiNbO3 modulator crystals. For a 3 kHz detection bandwidth, the noise equivalent field is approximately 7 V/m, thereby giving a calculated linear dynamic range of 68 dB in field power density. The probe's isotropic response is flat within +1-dB, and the response of each dipole closely follows the curve predicted by theory. An optical-beam switch that connects the individual dipoles to a laser source and optical receiver is also described.

Radiofrequency Detection

900,687 PB89-149272 Not available NTIS National Bureau of Standards (NEL), Boulder, CO Electromagnetic Fields Div.

Microwave Power Standards.

Final rept.

T. Larsen. 1987, 7p

Pub. in Proceedings of NCSL Workshop and Symposium 'Innovation: Key to the Future,' Denver, CO., July 12-16, 1987, p34-1-34-7.

Keywords: *Microwaves, *Standards, Calorimeters, Measuring instruments, Calibrating, National Institute for Standards and Technology.

A general review of the history and present status of the microwave power standards in use at the National Bureau of Standards (NBS) is presented. The standards are calorimeters, and the quantity measured is effective efficiency.' The calibration services are based on these standards. The design and evaluation of these standards are discussed.

900,688 PB89-229678 PC A03/MF A01 National Inst. of Standards and Technology (NEL), Boulder, CO. Electromagnetic Fields Div. Ciutter Modeis for Subsurface Electromagnetic Applications.

D. A. Hill. Feb 89, 46p NISTIR-89/3909 Sponsored by Army Belvoir Research Development and Engineering Center, Fort Belvoir, VA.

Keywords: *Subsurface investigations, *Tunnel detection, Magnetic dipoles, Remote sensing, Clutter, Electric dipoles, Born approximation.

Clutter models for subsurface electromagnetic applications are discussed with emphasis on tunnel detection applications. Random medium models are more versatile and require less detailed information than deterministic models. The Born approximation is used to derive expressions for the incoherent field, and electric and magnetic dipoles are treated in detail. When random inhomogeneities are located in the near field of the dipole source, an electric dipole radiates a larger incoherent field than a magnetic dipole because of its larger reactive electric field.

900.689 PB90-118167 Not available NTIS National Inst. of Standards and Technology (NML), Gaithersburg, MD. Inorganic Analytical Research Div. Safety Guidelines for Microwave Systems in the Analytical Laboratory.

Final rept.
H. M. Kingston, and L. B. Jassie. 1988, 13p
Pub. in Introduction to Microwave Sample Preparation-Theory and Practice, Chapter 11, p231-243 1988.

Keywords: *Microwave equipment, *Electronics laboratories, *Safety, Regulations, Laboratory equipment, Accident prevention, Electromagnetic radiation, Safe handling, Instructions, Reprints.

Safety considerations for working with microwave systems in the laboratory are discussed. The regulatory implications of modifying microwave equipment are presented. Guidelines for the selection and use of common laboratory equipment and materials are ex-

900,690 PB90-118183 Not available NTIS National Inst. of Standards and Technology (NML), Gaithersburg, MD. Inorganic Analytical Research Div.
Monitoring and Predicting Parameters in Microwave Dissolution.

Final rept. H. M. Kingston, and L. B. Jassie. 1988, 62p Pub. in Introduction to Microwave Sample Preparation-Theory and Practice, Chapter 6, p93-154 1988.

Keywords: *Microwaves, *Decomposition reactions, *Pressure measurement, *Temperature measurement, Dissolving, Thermal measurement, Predictions, Numerical analysis, Catalysts, Reducing agents, Monitoring, Reprints, Standard reference materials

Procedures are described for the real-time measurement of temperature and pressure during closed-vessel microwave sample decomposition. Pressure and temperature profiles of biological Standard Reference Materials and solitary as well as mixed acids are given to illustrate unique advantages that are available with the closed-vessel technique. A set of equations that permits prediction of target temperatures and times is derived from the fundamental heat capacity relationship for absorptive materials. From a series of fundamental measurements, original equations are introduced that permit the power consumption of common mineral acids to be calculated. The method is proposed as a model to approximate the thermal behavior of reagents intended for microwave use. The fundamental degradation patterns of biological matrices are presented for model compounds.

900.691

PB90-128588 Not available NTIS National Inst. of Standards and Technology (NEL), Boulder, CO. Electromagnetic Fields Div.

Thermo-Optic Designs for Microwave and Millimeter-Wave Electric-Field Probes.

Final rept

J. Randa, M. Kanda, D. Melquist, and R. D. Orr. 1989, 5p

Sponsored by Naval Ocean Systems Center, San Diego, CA.

Pub. in Proceedings of IEEE (Institute of Electrical and Electronics Engineers) Symposium on Electromagnetic Compatibility, Denver, CO., May 23-25, 1989, p7-11.

Keywords: *Electron probes, *Microwaves, *Millimeter waves, Design, Electric fields, Electromagnetic radiation, Radio waves, Extremely high frequency, Temperature measuring instruments, *Thermo-optics.

The authors have considered various thermo-optic designs for electric-field probes for the approximate fre-quency range of 1-110 GHz. The designs are all based on using an optically sensed thermometer to measure the temperature rise of a resistive material in an electric field. The paper presents calculations of the sensitivities of the different designs, measurement results for the most easily fabricated design, and a discussion of possible improvements. The results indicate that a probe based on the design could detect a minimum electric field of about 30-50 V/m.

General

900,692

PB89-176705 Not available NTIS National Bureau of Standards (ICST), Gaithersburg, MD. Systems Components Div.

Standard Format for the Exchange of Fingerprint information.

Final rept.

R. T. Moore, and R. M. McCabe. 1986, 4p Pub. in Proceedings of Carnahan Conference on Secu-

rity Technology, Lexington, KY., May 14-16, 1986, p13-16.

Keywords: *Identification systems, *Standards, Data, Images, *Fingerprints, Format.

There are a number of automatic or semiautomatic identification systems which may be used to extract information from fingerprint images. The information extracted generally relates to discrete features, such as minutiae (ridge endings and bifurcations), cores, deltas, and ridge features, such as tracings or counts, and to their spatial and/or topological relationships with each other. The details of these features and the way that information about them is measured, described, and presented varies from system to system. As a consequence, fingerprint information read on one system cannot be searched directly against the files of fingerprint information read on another system. To cope with this problem, an American National Standard is being developed to define a format that the fingerprint information can be converted into, or from, to provide a mechanism for the exchange of data. This requires that each system have only a single set of data conversion programs to exchange data with any other system rather than a separate set of data conversion routines for each different system. An overview of the standard and the development process is presented.

ELECTROTECHNOLOGY

Antennas

900,693 PB89-149280 Not available NTIS National Bureau of Standards (NEL), Boulder, CO.

Electromagnetic Fields Div.
Calibrating Antenna Standards Using CW and Pulsed-CW Measurements and the Planar Near-Field Method.

Final rept.

D. P. Kremer, and A. G. Repjar. 1988, 9p Pub. in Proceedings of Annual Antenna Measurement Techniques Association (10th), Atlanta, GA., Septem-ber 12-16, 1988, p13-21-13-29.

Keywords: *Antennas, *Continuous radiation, Coherent radiation, Near fields, Measurements, Gain, Calibrating, Cross polarization, Sidelobes.

The National Bureau of Standards (NBS) has calibrated an antenna to be used to evaluate both a near-field range and a compact range. These ranges are to be used to measure an electronically-steerable antenna which transmits only pulsed-CW signals. The antenna calibrated by NBS was chosen to be similar in physical size and frequency of operation to the array and was also calibrated with the antenna transmitting pulsed-CW. The calibration included determining the effects of using different power levels at the mixer, the accuracy of the receiver in making the amplitude and phase measurements, and the effective dynamic range of the receiver. Comparisons were made with calibration results obtained for the antenna transmitting CW and for the antenna receiving CW. The parameters compared include gain, sidelobe and cross polarization levels. The measurements are described and some results are presented.

900,694 PB89-150726 Not available NTIS National Bureau of Standards (NEL), Boulder, CO. Electromagnetic Fields Div.

Antenna Measurements for Millimeter Waves at

the National Bureau of Standards.

Final rept. M. H. Francis, A. G. Repjar, and D. P. Kremer. 1988,

Pub. in Proceedings of Annual Antenna Measurement Techniques Association (10th), Atlanta, GA., September 12-16, 1988, p13-13-17.

Keywords: *Antennas, *Millimeter waves, *Error analysis, Amplification, Insertion loss, Extremely high frequencies, Polarized electromagnetic radiation, Power loss, Waveguides, Near fields, Radiation patterns.

For the past two years the National Bureau of Standards (NBS) has been developing the capability to perform on-axis gain and polarization measurements at millimeter wave frequencies from 33-65 GHz. The paper discusses the error analysis of antenna measurements at these frequencies. The largest source of error is insertion loss measurements. In order to make accurate insertion loss measurements, flanges on antennas need to be flat and perpendicular to the wave-guide axis to within approximately 0.001 cm (0.0005 in). In addition, waveguide screws need to be tightened with a device that supplies constant torque. NBS is continuing development of its measurement capabilities including measuring probe corrections coefficients. ties, including measuring probe correction coefficients required in planar near-field processing, in order to provide accurate pattern measurements at these frequencies.

900,695 PB89-153886 PC A03/MF A01 National Inst. of Standards and Technology (NEL), Roulder, CO. Electromagnetic Fields Div.
Iterative Technique to Correct Probe Position
Errors in Planar Near-Field to Far-Field Transfor-

mations. Technical note. L. A. Muth, and R. L. Lewis. Oct 88, 19p NIST/TN-

1323 Also available from Supt. of Docs. as SN0003-003-

Keywords: *Antennas, *Electrostatic probes, *Electromagnetic fields, Correction, Taylors series, Integral equations, Analysis(Mathematics), Electromagnetic radiation, Field strength, Measurement, *Position

The authors have developed a general theoretical procedure to take into account probe position errors when planar near-field data are transformed to the far field. If the probe position errors are known, measured data can be represented as a Taylor series, whose terms contain the error function and the ideal spectrum of the antenna. Then the ideal spectrum can be solved in terms of the measured data and the measured position errors by inverting the Taylor series. This is complicated by the fact that the derivatives of the ideal data are unknown; that is, they can only be approximated by the derivatives of the measured data. This introduces additional computational errors, which must be properly taken into account. The authors have shown that the first few terms of the inversion can be easily obtained by simple approximation techniques, where the order of the approximation is easily specified. A more general solution can also be written by formulating the prob-lem as an integral equation and using the method of successive approximations to obtain a general solution. An important criterion that emerges from the condition of convergence of the solution to the integral equation is that the total averaged position error must be less than some fraction of the sampling criterion for the antenna under test.

900.696

PB89-156798 Not available NTIS National Bureau of Standards (NEL), Boulder, CO.

Electromagnetic Fields Div.

Spherical-Wave Source-Scattering Matrix Analysis of Coupled Antennas: A General System Two-Port Solution.

Final rept.

R. L. Lewis. 1987, 6p
Pub. in IEEE (Institute of Electrical and Electronics Engineers) Transactions on Antennas and Propagation AP-35, n12 p1375-1380 Dec 87.

Keywords: *Coupled antennas, *S matrix theory, Spherical waves, Elastic waves, Wave propagation, Backscattering, Waveguides, Reprints.

Expressions are given for the coupling between two antennas in terms of each antenna's spherical-wave source-scattering matrix. A comparison with the 'classical' scattering matrix representation is given in sufficient detail to permit conversion back and forth between the source-scattering matrix and the classical scattering matrix. Expressions for the transmission formulas, showing two different expressions corresponding to reversing the direction of propagation are given. However, if both antennas are reciprocal with equal characteristic waveguide impedances, then the twoport scattering matrix is a symmetric matrix.

900,697

PB89-156806 Not available NTIS National Bureau of Standards (NEL), Boulder, CO. Electromagnetic Fields Div.
Improved Spherical and Hemispherical Scanning

Aigorithms.

Pilia rept.

R. L. Lewis, and R. C. Wittmann. 1987, 8p

Pub. in IEEE (Institute of Electrical and Electronics Engineers) Transactions on Antennas and Propagation AP-35, n12 p1381-1388 Dec 87.

Keywords: *Algorithms, *Antennas, Electrostatic probes, Surveillance, Electromagnetic fields, Reprints, Spherical scanning.

A probe-corrected hemispherical-scanning algorithm has been developed which is applicable when the antenna under test radiates negligibly into its rear hemisphere. For a hundred-wavelengths diameter antenna, hemispherical scanning would be about three times more efficient computationally than prior full-sphere scanning algorithms. Improvements have also been made to full-sphere scanning, significantly increasing that algorithm's computational efficiency.

900,698

Not available NTIS PB89-156814 National Bureau of Standards (NEL), Boulder, CO. Electromagnetic Fields Div.

improved Polarization Measurements Using a Modified Three-Antenna Technique.

Final rept. A. C. Newell. 1988, 3p

Pub. in IEEE (Institute of Electrical and Electronics Engineers) Transactions on Antennas and Propagation 36, n6 p852-854 Jun 88.

Keywords: *Antennas, *Electromagnetic fields, *Polarization(Waves), Measurement, Electromagnetic radiation, Calibrating, Standards, Electrostatic probes, Wave phases, Reprints.

An improved three-antenna measurement of polarization that greatly reduces the uncertainty due to phase measurement errors is described. The technique is used to calibrate polarization standards and probes used in near-field antenna measurements.

900.699

PB89-156822 Not available NTIS National Bureau of Standards (NEL), Boulder, CO. Electromagnetic Fields Div. Gain and Power Parameter Measurements Using

Pianar Near-Field Techniques.

Final rept.

A. C. Newell, R. Ward, and E. McFarlane, 1988, 12p. Pub. in IEEE (Institute of Electrical and Electronics Engineers) Transactions on Antennas and Propagation 36, n6 p792-803 Jun 88.

Keywords: *Antennas, *Electromagnetic fields, Field strength, Measurement, Far field, Amplification, Flux density, Reprints, Effective radiated power, Intelsat

Equations are derived and measurement techniques described for obtaining gain, effective radiated power, and saturating flux density using planar near-field measurements. These are compared with conventional far-field techniques, and a number of parallels are evident. These give insight to the theory and help to identify the critical measurement parameters. Applica-tions of the techniques to the INTELSAT VI satellite are described.

900,700 PB89-156830 Not available NTIS National Bureau of Standards (NEL), Boulder, CO. Electromagnetic Fields Div.

Fields of Horizontal Currents Located Above the Earth.

Final rept.

D. A. Hill. 1988, 7p
Pub. in IEEE (Institute of Electrical and Electronics Engineers) Transactions on Geoscience and Remote Sensing 26, n6 p726-732 Nov 88.

Keywords: *Dipole antennas, *Electromagnetic fields, Far field, Electromagnetic radiation, Field strength, Plane waves, Reprints, Fast fourier transforms, Integral transforms.

The plane-wave spectrum technique is used to derive the fields of horizontal currents located in a horizontal plane above the earth. The far field is derived asymptotically, and the near field is computed by two-dimensional fast Fourier transform. Specific numerical results are presented for a pair of oppositely directed dipoles, and the results have application to detection of buried objects. When the antenna is located at low heights, the field is enhanced in the earth and decreased in air.

900.701

PB89-156848 Not available NTIS National Bureau of Standards (NEL), Boulder, CO. Electromagnetic Fields Div.

Error Analysis Techniques for Planar Near-Field Measurements.

Final rept.

A. C. Newell. 1988, 15p
Pub. in IEEE (Institute of Electrical and Electronics Engineers) Transactions on Antennas and Propagation 36, n6 p754-768 Jun 88.

Keywords: *Antennas, *Electromagnetic fields, *Error analysis, Measurements, Numerical analysis, Electromagnetic radiation, Computerized simulation, Re-

The results of an extensive error analysis on planar near-field measurements are described. The analysis provides ways for estimating the magnitude of each individual source of error and then combining them to

ELECTROTECHNOLOGY

Antennas

estimate the total uncertainty in the measurement. Mathematical analysis, computer simulation, and measurement tests are all used where appropriate.

900,702 PB89-156855 Not available NTIS National Bureau of Standards (NEL), Boulder, CO.

Electromagnetic Fields Div.

Comparison of Measured and Calculated Antenna Sidelobe Coupling Loss in the Near Field Using Approximate Far-Field Data.

inal rept. M. H. Francis, and C. F. Stubenrauch. 1988, 4p Pub. in IEEE (Institute of Electrical and Electronics En-gineers) Transactions on Antennas and Propagation 36, n3 p438-441 Mar 88.

Keywords: *Antennas, *Far field, *Computer systems programs, Transmission loss, Attenuation, Reprints, *Coupling(Interaction).

Computer programs are presently in existence to cal-culate the coupling loss between two antennas provid-ed that the amplitude and phase of the far field are available. However, for many antennas the complex far field is not known accurately.

900,703 PB89-156863 PB89-156863 Not available NTIS National Bureau of Standards (NEL), Boulder, CO.

Electromagnetic Fields Div.

Brief History of Near-Field Measurements of Antennas at the National Bureau of Standards. Final rept.

R. C. Baird, A. C. Newell, and C. F. Stubenrauch.

1988, 7p Pub. in IEEE (Institute of Electrical and Electronics Engineers) Transactions on Antennas and Propagation 36, n6 p727-733 Jun 88.

Keywords: *Microwave antennas, *Electromagnetic fields, *Light(Visible radiation), Velocity measurement, Light pulses, Speed indicators, Solar radiation, Cylin-drical antennas, Spherical antennas, Reprints.

The National Bureau of Standards (NBS) played a pioneering role in the development of practical planar near-field antenna measurement techniques. A brief history is presented of that role, which began with theoretical studies to determine corrections for diffraction in a microwave measurement of the speed of light. NBS contributions to the development of nonplanar near-field measurement theory and practice are also described.

900,704 PB89-156871 Not available NTIS National Bureau of Standards (NEL), Boulder, CO.

Electromagnetic Fields Div.

Accurate Determination of Planar Near-Field Correction Parameters for Linearly Polarized Probes.

Final rept. A. G. Repjar, A. C. Newell, and M. H. Francis. 1988,

Pub. in IEEE (Institute of Electrical and Electronics Engineers) Transactions on Antennas and Propagation 36, n6 p855-868 Jun 88.

Keywords: *Antenna radiation patterns, *Electromagnetic fields, *Electrostatic probes, Plane waves, Far field, Correction, Accuracy, Measurements, Reprints.

The receiving patterns (both amplitude and phase) of two probes must be known and utilized to determine accurately the complete far field of an antenna under test from near-field measurements. The process is called probe correction. When the antenna to be tested is nominally linearly polarized, the measurements are more accurate and efficient if nominally linearly polarized. early polarized probes are used. Further efficiency is obtained if only one probe which is dual polarized is used instead of two probes to allow for simultaneous measurements of both components. It should be noted, however, that a single-port probe can be rotated by 90 deg (in effect, the second probe) to obtain the second component. A procedure used by the National Bureau of Standards (NBS) for accurately determining the plane-wave receiving parameters of both single-and dual-port linearly polarized probes is described. Examples are presented, and the effect of these probe receiving characteristics in the calculation of the parameters for the antenna under test is demonstrated using the required planar near-field theory.

900,705 PB89-157036

Not available NTIS

National Bureau of Standards (NEL), Boulder, CO. Electromagnetic Technology Div.

SIS Quasiparticle Mixers with Bow-Tie Antennas.

Final rept.

Grant AFOSR-85-0230
Sponsored by Air Force Office of Scientific Research, Bolling AFB, DC.

Pub. in International Jnl. of Infrared and Millimeter Waves 9, n2 p101-133 1988.

Keywords: *Biconical antennas, Elementary excitations, Antenna couplers, Gain, Electromagnetic noise, Repnints, *Quasiparticle mixers, Microstrip transmis-

The authors have designed and evaluated planar lithographed W-band SIS mixers with bow-tie antennas and several different RF coupling structures. Both Pb-In-Au/Pb-Bi and Nb/Pb-In-Au junctions were used, each with omega times (R sub N) times C>>1. Single junctions and series arrays of five junctions directly attached to bow-tie antennas with no additional coupling structure gave poor performance, as expected. Single junctions with inductive microstrips and five-junction arrays with parallel wire inductors gave good coupling over bandwidths of approximately 5 and 25% respectively. Good agreement was found between design calculations based on a simple equivalent circuit and measurements of the frequency dependence of the mixer gain. When good coupling was achieved, typical values of mixer gain G sub M(DSB) approximately equal to 0 dB, noise T sub M(DSB) approximately equal to 150 K, and receiver noise approximately 200 K were observed.

900,706 PB89-157051 Not available NTIS National Bureau of Standards (NEL), Boulder, CO. Electromagnetic Technology Div.

Measurement of Integrated Tuning Elements for

SIS Mixers with a Fourier Transform Spectrometer.

Final rept. Q. Hu, C. A. Mears, P. L. Richards, and F. L. Lloyd. 1988, 18p Grant AFOSR-85-0230

Grant AFOSH-85-0230
Sponsored by Air Force Office of Scientific Research, Bolling AFB, DC.
Pub. in International Jnl. of Infrared and Millimeter Waves 9, n4 p303-320 1988.

Keywords: *Biconical antennas, *Spectrometers, *Mixing circuits, *Tuners, Optical measuring instruments, Antenna couplers, Lithography, Reprints, Fast fourier transforms.

Planar lithographed quasioptical mixers can profit from the use of integrated tuning elements to improve the coupling between the antenna and the SIS mixer junctions. The authors have used a Fourier transform spec-trometer with an Hg-arc lamp source as an RF sweep-er to measure the frequency response of such inter-grated tuning elements. The SIS junction connected to the tuning element served as the direct detector for the spectrometer. This relatively quick, easy experiment can give enough information over a broad range of millimeter and submillimeter wavelengths to test both design concepts and success in fabrication. One type of tuning element, an inductive wire connected in parallel with a series array of 5 SIS junctions across the terminals of a bow-tie antenna, shows a resonant response peak at 100 GHz with a 30% bandwidth.

900,707 PB89-157457 Not available NTIS National Bureau of Standards (NEL), Boulder, CO. Electromagnetic Fields Div.

Efficient and Accurate Method for Calculating and Representing Power Density in the Near Zone of

Microwave Antennas. Final rept.

R. L. Lewis, and A. C. Newell. 1988, 12p

n. L. Lewis, and A. C. Newell. 1988, 12p See also PB86-181963. Pub. in IEEE (Institute of Electrical and Electronics Engineers) Transactions on Antennas and Propagation 36, n6 p890-901 Jun 88.

Keywords: *Microwave antennas, Electromagnetic fields, Plane waves, Traveling waves, Wave diffraction, *Fresnel integrals, Power density, Fast fourier trans-

An efficient and reliable method has been developed for computing and exhibiting Fresnel-region fields radiated by microwave antennas using plane-wave scattering matrix analysis. That is, near fields are calculated by numerically integrating the complex far-field antenna pattern. The predicted near-fields are exhibited as relative power-density contours lying in a longitudinal plane bisecting the antenna's aperture. The crux of the analysis consists of handling a numerical instability which arises from integrating discrete data. A criterion is developed for excluding highly oscillatory regions of the integrand. In turn, this leads to restricting the output domain where the near field computations are valid. With the numerical instability problem resolved. valid. With the numerical instability problem resolved, the fast Fourier transform is used for efficient numerical integration. The predicted near fields have been compared against both measured and theoretical data, confirming that the authors' near-field computation algorithm is capable of extremely high accuracy.

900.708 PB89-171839 Not available NTIS National Bureau of Standards (NEL), Boulder, CO. Electromagnetic Fields Div. Effect of Random Errors In Planar Near-Field

Measurement.

Final rept.
A. C. Newell, and C. F. Stubenrauch. 1988, 5p
See also PB87-233896.
Pub. in IEEE (Institute of Electrical and Electronics Engineers) Transactions on Antennas and Propagation 36, n6 p769-773 Jun 88.

Keywords: *Antenna radiation patterns, *Electromagnetic fields, *Signal to noise ratio, Far field, Attenuation, Electromagnetic interference, Electromagnetic noise, Transmitter characteristics, Random error, Re-

Expressions which relate the signal-to-noise ratio in the near field to the signal-to-noise ratio in the far field are developed. The expressions are then used to predict errors in far-field patterns obtained from near-field data. A technique to measure the noise in the far-field pattern is also given.

900.709 National Bureau of Standards (NEL), Boulder, CO. Experimental Study (NEL)

Experimental Study of Interpanel Interactions at 3.3 GHz.

Final rept.

. A. Muth. 1987, 5p

Sponsored by Rome Air Development Center, Hanscom AFB, MA. Electromagnetics Directorate.
Pub. in Proceedings of Antenna Measurement Technique Association (AMTA) Annual Meeting and Symposium (9th), Seattle, WA., September 28-October 2, 1987, p25-29.

Keywords: *Antenna arrays, *Electric fields, *Electromagnetic scattering, Reflections, Strip transmission lines, Backscattering, Scattering loss, Deflection, Electromagnetic radiation.

A general theoretical approach is formulated to describe the complex electromagnetic environment of an N-element array. The theory reveals the element-to-element interactions and multiple reflections within the element interactions and multiple reflections within the array. To experimentally verify some features of the theory, measurements on experimental array panels in various configurations were made. The array panels consisted of 256 microstrip radiating elements. In each of the configurations both the near-field and portside signals were measured to study the interactions between these panels. In particular, the effects of open-circuited array pagels on the radiation pattern of a circuited array panels on the radiation pattern of a single panel are observed both in the near field and in the far field. It is found that internal scattering is the main mechanism of interaction between panels, rather than reradiation of signals received from adjacent panels. The effects of scattering are observable at the -50 dB level.

900.710 PB89-179857 Not available NTIS National Bureau of Standards (NEL), Boulder, CO. Electromagnetic Fields Div. Antennas for Geophysical Applications.

Pinal rept.
D. A. Hill. 1988, 26p
Pub. in Antenna Handbook: Theory, Applications, and Design, Chapter 23, p23-1-23-26 1988.

Keywords: *Loop antennas, *Subsurface investigations, Extremely low radio frequencies, Geophysical prospecting, Geologic investigations, Excitation, Surges, Stimulation, Reprints, Grounded wire antennas.

The book chapter is one of approximately forty chapters which will appear in the handbook. It is in the section on Applications, and the other handbook sections are Fundamentals, Antenna Theory, and Related Topics. The chapter discusses a number of antennas which are used for subsurface probing of the earth. The two most commonly used antennas are grounded wires and loops, and they are covered in detail for both time-harmonic and transient excitations. Emphasis is placed on the extremely low frequency (ELF) portion of the spectrum where it is possible to probe the earth to depths of several hundred meters.

900,711 PB89-185623 PC A03/MF A01
National Bureau of Standards (NEL), Gaithersburg,
MD. Center for Electronics and Electrical Engineering.
Center for Electronics and Electrical Engineering Technical Publication Announcements Covering Center Programs, April-June 1986 with 1987 CEEE Events Calendar. E. J. Walters. Jun 87, 20p NBSIR-87/3578 See also PB89-136311.

Keywords: *Electronics, *Electrical engineering, *Research, *Abstracts, Semiconductor devices, Semiconductors(Materials), Metrology, Waveforms, Antennas, Microwaves, Lasers, Fiber optics, Electric power, Electromagnetic interference, Superconduc-

The report is the ninth issue of a quarterly publication providing information on the technical work of the National bureau of Standards Center for Electronics and Electrical Engineering. The Center for Electronics and Electrical Engineering Technical Publication Announcement covers the second quarter of calendar year 1986. Abstracts are provided by technical area for papers published this quarter.

900,712 PB89-187595 Not available NTIS National Bureau of Standards (NEL), Boulder, CO.

Clectromagnetic Fields Div.

Optically Linked Electric and Magnetic Field Sensor for Poynting Vector Measurements in the Near Fields of Radiating Sources.

L. Driver, and M. Kanda. 1988, 9p See also PB89-132773.

Pub. in IEEE (Institute of Electrical and Electronics Engineers) Transactions on Electromagnetic Compatibility 30, n4 p495-503 Nov 88.

Keywords: *Electromagnetic fields, *Radiation patterns, Antennas, Vector analysis, Differential equations, Near fields, Measurement, Detectors, Electrofields, Magnetic fields, Electrooptics, Reprints, *Poynt-

unique, single-element antenna measurement scheme that can simultaneously measure the electric, scheme that can simultaneously measure the electric, magnetic, and time-dependent Poynting vectors of electromagnetic (EM) fields is described. The electric and magnetic responses of the antenna sensor are separated by a 0 degree/180 degree hybrid junction. The resulting two radio frequency (RF) voltages, along with relative phase and frequency information, are transmitted to a remotely located vector analyzer by a pair of well-matched fiber optic downlinks. The remote receiver measures and displays the electric dipole response, the magnetic loop response, and the time phase difference between the two. The information is sufficient to determine the time-dependent Poynting vector. Both a theoretical analysis and a discussion of experimental measurements performed, which describe the capabilities and performance of a working prototype of the antenna measurement scheme, are presented. The results demonstrate that a three-axis (isotropic) version of the system could be used to measure the near fields of EM sources, as well as to completely describe the resultant flow of energy.

900,713 PB90-128208 PB90-128208 Not available NTIS National Inst. of Standards and Technology (NEL), Boulder, CO. Electromagnetic Fields Div. Near-Fleid Detection of Buried Dielectric Objects.

Final rept.
D. A. Hill. 1989, 5p
Pub. in IEEE (Institute of Electrical and Electronics Engineers) Transactions on Geoscience and Remote Sensing 27, n4 p364-368 Jul 89. Keywords: *Antennas, *Electromagnetic fields, *Dielectrics, *Detection, Electric fields, Lossy materials, Di-poles, S matrix theory, Scattering cross sections, Sub-surface investigations, Reprints.

The plane-wave scattering-matrix method is used to compute the response of a detector to a buned dielectric scatterer. The Born approximation is used to derive the scattering matrix for scatterers of small dielectric contrast, but the general theory is not limited to such cases. Specific numerical results are generated for a UHF dipole detector swept over a buried dielectric cube. The maximum response is obtained when the detector is located at the air-earth interface, and the response decays rapidly with detector height. The sweep curves are symmetrical in the horizontal direction and have a null when the detector is directly over the object. An experimental curve for a free-space environment has the same qualitative features.

Circuits

900,714 PB89-171649 Not available NTIS National Bureau of Standards (NML), Boulder, CO.

Time and Frequency Div.
New Cavity Configuration for Cesium Beam Primary Frequency Standards. Final rept.

A. DeMarchi, J. Shirley, D. Glaze, and R. Drullinger.

Pub. in IEEE (Institute of Electrical and Electronics Engineers) Transactions on Instrumentation and Measurement 37, n2 p185-190 Jun 88.

Keywords: *Cesium frequency standards, *Cavity resonators, Oscillators, Resonant frequency, Microwaves, Waveguides, Mathematical models, Reprints.

In the design of cesium beam frequency standards, the presence of distributed cavity-phase-shifts (associated with residual running waves) in the microwave cavity, due to the small losses in the cavity walls, can become a significant source of error. To minimize such errors in future standards, it has been proposed that the long Ramsey excitation structure be terminated with ring-shaped cavities in place of the conventional shorted waveguide. The ring cavity will minimize distributed cavity-phase-variations at the position of the atomic beam, provided only that the two sides of the ring and the T-junction feeding the ring are symmetric. In the paper, a model is developed to investigate the validity of the concept in the presence of the small asymmetries that inevitably accompany the fabrication of such a cavity. The model, partially verified by laboratory tests, predicts that normal tolerances will allow the frequency shifts due to distributed cavity-phase-variations to be held at the 10 to the negative 15th power level for a beam tube with a Q of 10 to the 8th power.

PB89-173777 Not available NTIS National Bureau of Standards (NEL), Boulder, CO. Electromagnetic Fields Div.

ANA (Automatic Network Analyzer) Measurement Results on the ARFTG (Automatic RF Techniques Group) Traveling Experiment.

L. F. Saulsbery, and R. T. Adair. 1987, 14p Pub. in ARFTG (Automatic RF Techniques Group) Conference Digest (28th), St. Petersburg, FL., December 4-5, 1986, p65-78 1987.

Keywords: *Measuring instruments, Reflectivity, Attenuation, Standing wave ratios, Assessments, Phase shift, *Automatic network analyzers.

The Automatic RF Techniques Group (ARFTG) Executive Committee has assembled two traveling measure-ment assessment kits. Each of these kits consists of: 1-dB, 20-dB, 40-dB, and 60-dB attenuators; a 50-ohm termination; a 10-centimeter air line; 1.2-VSWR and 2.0-VSWR mismatched terminations; and a short circuit termination. These devices are equipped with precision 7-mm coaxial connectors. The traveling kits are being circulated among measurement laboratories that wish to assess their ability to measure reflection coefficient, attenuation, and phase shift from 300 MHz to 17 GHz. The results obtained on ten different automated measurement systems are presented.

900,716 PB89-174056

Not available NTIS

National Bureau of Standards (NML), Boulder, CO. Time and Frequency Div.

Low Noise Frequency Synthesis.

Final rept.

F. L. Walls, and C. M. Felton. 1987, 7p Pub. in Proceedings of Annual Symposium on Frequency Control (41st), Philadelphia, PA., May 27-29,

1987, p512-518.

Keywords: *Frequency synthesizers, *Electromagnetic noise, Microwave oscillators, Crystal oscillators, Signal generators, Frequency converters, Frequency multipliers, Frequency dividers.

The paper reviews the various definitions of phase noise and changes in the phase noise of a signal under noiseless multiplication, division, and translation. Next the phase noise in selected noncryogenic rf and microwave oscillators is reviewed. Using a systems ap-proach one can synthesize a microwave signal where the close in phase noise is controlled by a low frequency crystal oscillator while the high frequency phase noise is controlled by a microwave source. The approach yields a phase noise performance that is superior to that possible with a single source. Finally the phase noise of various amplifiers, multipliers, and dividers is compared. The phase noise of dividers while generally inferior to that of the best multipliers, is often sufficient for most applications.

900.717

PB89-201537 Not available NTIS National Bureau of Standards (NEL), Gaithersburg, MD. Electrosystems Div.

Audio-Frequency Current Comparator Power Bridge: Development and Design Considerations. Final rept.

N. M. Oldham, O. Petersons, and B. C. Waltrip.

1989, 5p See also PB88-239561.

Pub. in IEEE (Institute of Electrial and Electronics Engineers) Transactions on Instrumentation and Measurement 38, n2 p390-394 Apr 89.

Keywords: *Comparator circuits, *Power measurement, Design, Calibrating, Wattmeters, Electric power meters, Electric measurement, Electric bridges, Re-

The development, design, construction, and partial evaluation of a system for performing active and reactive power measurement from 50 to 20 kHz is described. The technique is an extension of a power bridge based on a current comparator capacitance bridge that was originally restricted to power frequencies. The design features and component characteristics for wide-band operations are emphasized. A digitally synthesized, dual-channel signal source provides the required voltage and current signals.

PB89-201545 Not available NTIS National Bureau of Standards (NEL), Gaithersburg, MD. Electrosystems Div. International Comparison of Power Meter Calibrations Conducted in 1987.

Final rept.

W. J. M. Moore, E. So, N. M. Oldham, P. N. Miljanic,

and R. Bergeest. 1989, 7p See also PB88-239546. Pub. in IEEE (Institute of Electrical and Electronics En-

gineers) Transactions on Instrumentation and Measurement 38, n2 p395-401 Apr 89.

Keywords: *Power meters, *Calibrating, Comparison, Power measurement, Watt meters, Electrical measurement, Evaluation, International trade, Reprints.

The results of an intercomparison of power meter cali-The results or an intercomparison of power meter calibrations conducted during 1987 among the National Research Council(Ottawa), the National Bureau of Standards(Gaithersburg), The Physikalisch-Technische Bundesanstalt(Braunschweig), and the Institut Mihailo Pupin(Belgrade), are described. The comparison was implemented by a transfer standard consistent of the division published the standard due. ing of a time-division multiplier watt-converter developed at the Institut Mihailo Pupin. The measurements were made at 120 V, 5 A, 50 and 60 Hz, at power factors of 1.0, 0.5 lead and lag, and 0.0 lead and lag. An agreement between the laboratories of better than 20 ppm is indicated.

900.719 PB89-228597

Not available NTIS

Circuits

National Inst. of Standards and Technology (NEL), Gaithersburg, MD. Determination of AC-DC Difference in the 0.1 - 100

MHz Frequency Range.

Final rept.

J. R. Kinard, and T. X. Cai. 1989, 8p Pub. in IEEE (Institute of Electrical and Electronics Engineers) Transactions on Instrumentation and Measurement 38, n2 p360-367 Apr 89.

Keywords: *AC to DC converters, Differences, Frequencies, Reprints, Voltage converters(AC to AC), Voltage converters(DC to DC).

Thermal voltage converter structures have been modeled theoretically and studied experimentally to determine their ac-dc differences in the 0.1-100 MHz frequency range. Estimated uncertainties, corresponding to the one standard deviation confidence level, for these ac-dc differences vary from 20 ppm at 1 MHz to 2000 ppm at 100 MHz.

900,720 PB89-230452 Not available NTIS National Bureau of Standards (NML), Gaithersburg, MD. Electricity Div.
Recharacterization of Thermal Voltage Converters

After Thermoelement Replacement.

J. R. Kinard, and T. E. Lipe. 1989, 6p
Pub. in IEEE (Institute of Electrical and Electronics Engineers) Transactions on Instrumentation and Measurement 38, n2, p351-356, Apr 89.

Keywords: *Electrical measurement, *Electric converters, AC to DC converters, Standards, Impedance, Analyzing, Reprints, *Thermal voltage converters, *Thermoelements, Replacing.

The relationship between the characteristics of various thermoelements (TEs) as voltage or current converters and the overall ac-dc differences of a voltage range in a coaxial thermal voltage converter (TVC) set is described. An algorithm to predict the relationships between the ac-dc differences of individual voltage ranges with different TEs is presented, and a method for recharacterizing a TVC containing a replacement TE is given. The measured results show that for most applications a complete recharacterization of the TVC set is unnecessary.

900,721 PB90-117854 Not available NTIS National Bureau of Standards (NEL), Boulder, CO. Electrosystems Div.

Calculable, Transportable Audio-Frequency AC Reference Standard.

N. M. Oldham, P. S. Hetrick, and X. Zeng. 1989, 4p Sponsored by Instrumentation and Measurement Society (IEEE), New York.

Pub. in IEEE (Institute of Electrical and Electronics En-

gineers) Transactions on Instrumentation and Measurement 38, n2 p368-371 Apr 89.

Keywords: *AC generators, *Electric potential, Alternating current, Digital techniques, Periodic functions, Electric power generation, Power supply circuits, Time standards, Synthesis, Reprints.

A transportable ac voltage source is described, in which sinusoidal signals are synthesized digitally in the which shrusoidal sightais are synthesized upitally in the audio-frequency range. The rms value of the output waveform may be calculated by measuring the dc level of the individual steps used to generate the waveform. The uncertainty of the calculation at the 7-V level is typically less than +/-5 ppm from 60 Hz to 2 kHz and less than +/-10 ppm from 30 Hz to 15 kHz.

900,722 PB90-128703 PB90-128703

Not available NTIS
National Inst. of Standards and Technology (NEL),
Gaithersburg, MD. Electrosystems Div.
Amblguity Groups and Testabliity.
Final rept.
G. N. Stenbakken, T. M. Souders, and G. W.
Stewart 1989

Stewart. 1989, 7p

Pub. in IEEE (Institute of Electrical and Electronics Engineers) Transactions on Instrumentation and Measurement 38, n5 p941-947 Oct 89.

Keywords: *Sensitivity, *Tests, Analog systems, Performance evaluation, Precision, Transient response, Acuity, Accuracy, Reprints, *Circuit analysis.

An efficient method has been developed for determining component ambiguity groups which arise in analog circuit testing. The method makes use of the sensitivity model of the circuit. The ambiguity groupings are shown to depend on the test points selected and the measurement accuracy, and is, therefore, a useful tool for determining where to add or delete test points. The concept of ambiguity groups can be used to refine the testability measure of a circuit.

Electromechanical Devices

900,723 PB89-146930 Not available NTIS National Bureau of Standards (NEL), Boulder, CO. Electromagnetic Fields Div.

Simple Technique for investigating Defects in Co-

axial Connectors.
Final rept.
W. C. Daywitt. 1987, 5p
Pub. in IEEE (Institute of Electrical and Electronics Engineers) Transactions on Microwave Theory and Techniques MTT-35, n4 p460-464 Apr 87.

Keywords: *Electric connectors, *Coaxial cables, *Error analysis, Frequency analyzers, Reprints, Sweep frequency, Automatic Network Analyzer.

The paper describes a technique that uses swept-frequency automatic network analyzer (ANA) data for investigating electrical defects in coaxial connectors. The technique will be useful to connector and ANA manufacturers and to engineers interested in determining connector characteristics for error analyses. A simplified theory is presented and the technique is il-lustrated by applying it to perturbations caused by the center conductor gap in a 7-mm connector pair.

Optoelectronic Devices & Systems

900,724 PB89-171722 PB89-171722 Not available NTIS National Bureau of Standards (NEL), Boulder, CO. Electromagnetic Technology Div. Effect of Multiple Internal Reflections on the Sta-

bliity of Electrooptic and Magnetooptic Sensors.

Final rept. K. S. Lee, and G. W. Day. 1988, 3p Pub. in Applied Optics 27, n22 p4609-4611, 15 Nov 88.

Keywords: *Reflection, *Electrooptics, *Magnetooptics, *Detectors, Optical measurement, Reflectance, Electromagnetic radiation, Stability, Transient response, Reprints.

The effects of multiple internal reflections are evaluated analytically. Response functions showing changes in shape as a function of optical path length are computed. The variation in sensitivity is obtained as a func-tion of the reflectance of the sensing element and is found to be significant (several tenths of a percent) even when the reflectance is reduced to 0.1 percent.

900,725 PB89-173967 PB89-173967 Not available NTIS National Bureau of Standards (NEL), Boulder, CO.

Electromagnetic Technology Div.

Optical Fiber Sensors for Electromagnetic Quanti-

Final rept.
G. W. Day, K. S. Lee, A. H. Rose, L. R. Veeser, B. J. Papatheofanis, and H. K. Whitesel. 1988, 39

Washington Sponsored by Department of Defense, Washington, DC., and Department of Energy, Washington, DC. Pub. in Proceedings of International Instrumentation Symposium (34th), Albuquerque, NM., May 2-6, 1988, p205-207.

Keywords: *Optical measuring instruments, *Fiber optics, Alternating current, Magnetic fields, Electrical measurement, *Optical fibers, Sensors, Voltage.

Several sensors used for the measurement of both pulsed and ac current, voltage, and magnetic field are described. Design considerations, including the choice of components and configurations, and performance achievements, are discussed.

900,726 PB89-176200

Not available NTIS

National Bureau of Standards (NEL), Boulder, CO.

Electromagnetic Technology Div.

NBS (National Bureau of Standards) Standards for Optical Power Meter Calibration.

Optical Fower Misco Final rept. T. R. Scott. 1988, 14p Pub. in Proceedings of DOD/ANSI/EIA Fiber Optics Standardization Symposium, Arlington, VA., December 7-10, 1987, p224-237 1988.

Keywords: *Calibrating, *Power meters, *Lasers, Measuring instruments, Power measurement, Calorimeters, Frequency standards, Performance standards ards, Beam splitters.

The measurement of optical power in the microwatt to milliwatt power range at NBS is based upon a standard reference laser calorimeter called the C-series calorimeter. The C-series calorimeter, which is used as a national standard for the measurement of laser power or energy, was designed to be rugged, easy to use, and capable of measuring energy over a wide range of laser wavelengths. The calorimeter, in conjunction with various laser sources and a calibrated beamsplitter measurement system, is used to calibrate transfer standards which are, in turn, used to calibrate other optical power meters. The paper will review the operation and capabilities of the standard calorimeter and associated measurement system, and will summarize the uncertainties associated with these energy calibration measurements.

900,727 PB89-176689

Not available NTIS
National Bureau of Standards (NEL), Boulder, CO.
Electromagnetic Technology Div.
Picosecond Pulse Response from Hydrogenated
Amorphous Silicon (a-SI:H) Optical Detectors on
Channel Waveguides.
Final rept.

Final rept.

D. R. Larson, and R. J. Phelan. 1987, 5p Pub. in Proceedings of SPIE (Society of Photo-Optical Instrumentation Engineers) Integrated Optical Circuit Engineering V, San Diego, CA., August 17-20, 1987, v835 p59-63.

Keywords: Photodiodes, *Optical detectors, Integrated optics, Amorphous silicon, Optical waveguides, Lithium niobates, Picosecond pulses.

The authors have fabricated high speed optical detectors on channel waveguides formed by both potassium ion-exchange in glass and titanium diffusion in lithium niobate. These new waveguide detectors show re-sponse times of 200 ps full width at half maximum am-plitude (FWHM) when illuminated with subpicosecond optical pulses. The detectors consist of back-to-back Schottky photodiodes formed by chromium-gold metal contacts on hydrogenated amorphous silicon (a-Si:H). When interdigitated metal contacts with the contact separation and semiconductor film thickness dimensions close to one micrometer are used, the detectors are both fast and efficient.

900,728 PB89-176697 Not available NTIS
National Bureau of Standards (NEL), Boulder, CO.
Electromagnetic Technology Div.
Potential Errors in the Use of Optical Fiber Power

Meters.

Final rept

Final rept.
X. Li, and R. L. Gallawa. 1988, 3p
Pub. in Proceedings of SPIE (Society of Photo-Optical
Instrumentation Engineers) Fiber Optic Networks and
Coherent Technology in Fiber Optic Systems II, San
Diego, CA., August 17-19, 1987, v841 p231-233 1988.

Keywords: *Power measurement, Power meters, Errors, Fiber optics, Optical fibers, Optical connectors, Calibration.

The authors discuss the potential errors associated with the measurement of optical power in a field environment. The potential errors arise because field use is often inconsistent with the calibration method. Errors may be due to the use of connectors of different types and due to variation among vendors for a given connector type. The authors consider potential errors in power measurements due to the variation in a connector type among vendors.

900,729 Not available NTIS National Bureau of Standards (NML), Gaithersburg, MD. Radiometric Physics Div.

Optoelectronic Devices & Systems

Characteristics of Ge and InGaAs Photodiodes. Final rept.

Zalewski. 1989, 8p

Pub. in Proceedings of International Conference on Optical Radiometry, NPL (National Physical Laboratory), London, April 12-13, 1988, p47-54 1989.

Keywords: *Photodiodes, *Infrared detectors, Quantum efficiency, Indium phosphides, Near infrared radiation, Radiometry, *Ge semiconductor detectors, Gallium indium arsenides.

Measurements of the internal quantum efficiency of re-cently developed near infrared (1 to 1.6 micrometers) photodiodes show that considerable improvement has been made in the radiometric quality of these devices. Among commercially available devices, the newer InGaAs/InP photodiodes exhibit better characteristics than the Ge devices that have been traditionally used for near infrared radiometry. However, experimental induced junction Ge photodiodes produced at Purdue University have been observed to have nearly ideal internal quantum efficiency.

PB89-212161 Not available NTIS National Bureau of Standards (NEL), Gaithersburg, MD. Semiconductor Electronics Div. **Blocked Impurity Band and Superlattice Detectors:**

Prospects for Radiometry. Final rept.

J. Geist. 1989, 12p

Pub. in Proceedings of International Conference on Optical Radiometry, London, UK, April 12-13, 1988, p99-110 1989.

Keywords: *Radiometry, Infrared detectors, Ultraviolet detectors, Gallium arsenides, Cadmium tellurides, Mercury tellurides, Standards, *Optical detectors, Quantum wells, Superlattices, Aluminum gallium ar-senides, Blocked impurity band detectors.

Blocked impurity band detectors and photomultipliers, which have been described by Petroff and Stapelbroek, may be suitable for use as high-accuracy standards for low background optical radiation measurements extending from the near ultraviolet to beyond 25 micrometers in the infrared. The current status of their development from the point of view of standards appli-cations is reviewed. Superlattice technology offers new materials properties, new degrees of freedom, and new possibilities for optical radiation detectors displaying a large range of tailorability and tunability. GaAs/AlGaAs superlattices are used to illustrate new properties, HgTe/CdTe superlattices are used to illustrate new properties, HgTe/CdTe superlattices are used to illustrate new degrees of freedom, and GaAs-doping superlattices are used to illustrate tailorability and tunability.

900,731 PB89-228498 Not available NTIS National Inst. of Standards and Technology (NEL), Gaithersburg, MD. Semiconductor Electronics Div. Silicon Photodiode Detectors for EXAFS (Extended X-ray Absorption Fine Structure). Final rept.

C. E. Bouldin, and A. C. Carter. 1989, 3p Pub. in Physica B 158, p339-341 1989.

Keywords: *Photodiodes, *Silicon, X ray absorption, Fluorescence, Vacuum, Cryogenics, Linearity, Photons, Flux, Reprints.

Results are shown of using a large-area silicon diode as a fluorescence detector for EXAFS measurements. A direct comparison of this diode detector relative to a gas ionization fluorescence detector is made. Advantages of the diode detector include: higher signal for a given photon flux (due to higher quantum efficiency), vacuum and cryogenic compatibility, freedom from microphonic noise, good linearity, extremely wide dy-namic range, operation without high voltage or gas connections, very simple electronics, and low cost. Use of photodiodes for transmission EXAFS is dis-

900,732 PB89-229207 PB89-229207 Not available NTIS National Bureau of Standards (NEL), Boulder, CO. Electromagnetic Fields Div.

Photonic Electric-Field Probe for Frequencies up to 2 GHz.

Final rept.

K. D. Masterson. 1986, 5p See also PB89-176184. Sponsored by Army Aviation Systems Command, St. Louis, MO.

Pub. in Proceedings of SPIE (Society of Photo-Optical Instrumentation Engineers) High Bandwidth Analog Applications of Photonics, v720 p100-104 1986.

Keywords: *Electric fields, Microwave equipment, Birefringence, Measurement, *Optoelectronic devices, Lithium niobates, Probes(Electromagnetic).

A photonic electric field probe using the Pockels effect in bulk LiNbO3 is used to measure electromagnetic fields from 10 to 100 V/m. The observed frequency response is flat up to 1.6 GHz and extends beyond 2.0 kg. and 2.0 kg. a GHz. Over the majority of the frequency range, field strengths down to about 6 V/m would be detectable above the noise floor when using a 3 kHz detection bandwidth. Present experimental results indicate a linear dynamic range of 30 dB for the probe. Increasing the optical carrier power and lowering the noise floor are expected to improve the dynamic range to above

PB90-117599 Not available NTIS National Inst. of Standards and Technology (NEL), Gaithersburg, MD. Semiconductor Electronics Div. High Accuracy Modeling of Photodlode Quantum Efficiency. Final rept.

J. Geist, and H. Baltes. 1989, 11p Pub. in Applied Optics 28, n18 p3929-3939, 15 Sep 89.

*Quantum efficiency, *Photodiodes, 'Mathematical models, Diffusion theory, Silicon, Accuracy, Reprints.

A new silicon photodiode model is proposed which is optimized for high-accuracy measurement usage. The new model differs from previous models in that the contribution to the quantum efficiency from the diode front region is described by an integral transform of the equilibrium minority carrier concentration. The description is accurate as long as the recombination of excess minority carriers in the front region occurs only at the front surface and the diode is operating linearly.

900,734 PB90-118159 Not available NTIS Not available NTIS
National Inst. of Standards and Technology (NEL),
Gaithersburg, MD. Semiconductor Electronics Div. Silicon Photodiode Self-Calibration.

Final rept.

Pub. in Theory and Practice of Radiation Thermometry, Chapter 14, p821-838 1988.

Keywords: *Photodiodes, *Calibrating, *Silicon, Thermal radiation, Temperature measurement, Blackbody radiation, Reprints.

A new and rapidly evolving technique for radiometric calibrations that is of considerable potential interest to radiation thermometry is considered. Although the method is not yet fully developed, it has already demonstrated an accuracy that is superior to that of all other methods in the spectral region traditionally used for high-precision radiation thermometry (650 nm). Through a simple experimental procedure using relatively inexpensive equipment that is widely available. the quantum efficiency and the spectral reflectance of a high-quality shallow-junction silicon photodiode can be readily determined.

900,735 PB90-128059 Not available NTIS National Inst. of Standards and Technology (NML), Gaithersburg, MD. Radiation Physics Div.

Stability and Quantum Efficiency Performance of Silicon Photodlode Detectors in the Far Ultraviolet. Final rept.

. R. Canfield, J. Kerner, and R. Korde. 1989, 4p Pub. in Applied Optics 28, n18 p3940-3943, 15 Sep 89.

Keywords: *Ultraviolet detectors, *Photodiodes, Far ultraviolet radiation, Quantum efficiency, Silicon dioxide, Radiometry, Stability, Reprints.

Recent improvements in silicon photodiode fabrication technology have resulted in the production of photo-diodes which are stable after prolonged exposure to short wavelength radiation and which have efficiencies in the far ultraviolet close to those predicted using a value of 3.63 eV for electron-hole pair production in Si. Quantum efficiency and stability data are presented in the 6-124-eV region for several variations on the basic successful design and on devices with extremely thin silicon dioxide antireflecting/passivating layers. The

results indicate that the oxide is dominant in determining many of the performance parameters and that a stable efficient far ultraviolet diode can be fabricated by careful control of the Si-SiO2 interface quality.

900 736

PB90-130303 PC A03/MF A01 National Inst. of Standards and Technology (NEL), Boulder, CO. Electromagnetic Technology Div. Improved Low-Level Silicon-Avalanche-Phot diode Transfer Standards at 1.064 Micrometers. A. L. Rasmussen, P. A. Simpson, and A. A. Sanders. Aug 89, 40p NISTIR-89/3917 Sponsored by Aerospace Guidance and Metrology Center, Newark AFS, OH.

Keywords: *Photodiodes, *Avalanche diodes, *Standards, Semiconductor devices, Voltage regulators, De tectors, Lasers, Numerical analysis, Calibrating, Impulse response.

Three silicon-avalanche-photodiode (APD) transfer standards were calibrated from approximately 10(-8) to approximately 10(-5) W/sq cm peak power density at approximately 10 percent uncertainty. The calibrations are for 1.064 micrometer wavelength pulses of 10 to 100 ns duration. For the calibration, an acoustooptically modulated laser beam generated alternately equal levels of pulsed power and cw power into a lowlevel beam splitter. The cw power measured by a transfer standard in the transmitted beam of the splitter was used to determine the pulsed power into the APD transfer standard in one of the low-level reflected beams of the splitter. To increase the sensitivity, one or two 20 dB, 500 MHz bandwidth amplifiers followed the preamplifier. With very low pulsed power, a 30 MHz low-pass filter with Gaussian roll-off was attached to the amplifier output to reduce the noise. A transient digitizer recorded the impulse responses of the APD detectors at 1.064 micrometer. The data were read into computer programs that convolved the unit-area impulse response with unit-height Gaussian pulses. From the data, correction factors of the pulse peak for observed pulse durations from 10 to 100 ns were determined. Instructions, calibrations, error budgets, and system descriptions are included.

Power & Signal Transmission Devices

900.737

PB89-149264 Not available NTIS National Bureau of Standards (NEL), Boulder, CO. Electromagnetic Fields Div.

Mode-Stirred Chamber for Measuring Shielding Effectiveness of Cables and Connectors: An Assessment of MIL-STD-1344A Method 3008.

Final rept. M. L. Crawford, and J. M. Ladbury. 1988, 7p Pub. in Proceedings of IEEE (Institute of Electrical and Electronics Engineers) International Symposium on Electromagnetic Compatibility, Seattle, WA., August 2-4, 1988, p30-36.

Keywords: *Electromagnetic shielding, *Communication cables, Standing wave ratios, Measurements, Specifications, Electric wire, Electric connectors, An-

The mode-stirred method for measuring the shielding effectiveness (SE) of cables and connectors as specified in MIL-STD-1344A Method 3008 is examined. Problems encountered in applying the method are identified and recommendations to improve the measurement results are provided. These include chamber design, type and placement of transmitting and reference receiving antenna, determination and correction for VSWR of the reference antenna and equipment under test (EUT), and the measurement approach to use at specified test frequencies. Design and measurement setups for a small mode-stirred chamber suitable for performing SE measurements in the frequency range 1 - 18 GHz with dynamic ranges up to 130 dB are given along with SE measurement results of some sample EUTs.

900,738

PB89-156780 Not available NTIS National Bureau of Standards (NEL), Boulder, CO. Electromagnetic Fields Div.

ELECTROTECHNOLOGY

Power & Signal Transmission Devices

Two-Layer Dielectric Microstrip Line Structure: SiO2 on Si and GaAs on Si; Modeling and Measurement.

Final rept.

R. A. Lawton, and W. T. Anderson. 1988, 5p Sponsored by Naval Research Lab., Washington, DC. Pub. in IEEE (Institute of Electrical and Electronics Engineers) Transactions on Microwave Theory and Techniques 36, n4 p785-789 Apr 88.

Keywords: *Backscattering, *Dielectrics, Characteristic impedance, Gallium arsenides, Lossy materials, Silicon dioxide, Sensitivity, Reflection, Measurement, Reprints, *Microstrip transmission lines,

Further development is reported of the modeling of the two-layer dielectric microstrip line structure by comput-ing the scattering parameter S sub 21 derived from the model and comparing the computed value with the measured value over the frequency range from 90 MHz to 18 GHz. The sensitivity of the phase of S sub 21 and the magnitude of the characteristic impedance to various parameters of the equivalent circuit is deter-

900,739 PB89-157028 Not available NTIS National Bureau of Standards (NEL), Boulder, CO. Electromagnetic Technology Div. Waveguide Loss Measurement Using Photother-

mal Deflection.

Final rept. R. K. Hickernell, D. R. Larson, R. J. Phelan, and L. E. Larson, 1988, 3p

Pub. in Applied Optics 27, n13 p2636-2638, 1 Jul 88.

Keywords: *Optical communication, *Transmission loss, *Waveguides, Transmission lines, Backscattering, Telecommunication, Lasers, Refractivity, Reprints, *Photothermal deflection.

Photothermal deflection (PTD) is introduced as a technique for measuring propagation loss in optical channel waveguides. A probe laser beam is deflected by the thermally-induced refractive-index gradient due to the absorption of guided pump light. The technique is non-contact and is applicable to a wide range of channel waveguide geometries and materials, including buried guides. Scattering centers and unguided back ground light affect the measurement only indirectly, since the PTD signal depends on the gradient of the local temperature and not the light intensity directly. Scans of the PTD signal as a function of distance along the waveguide yielded propagation loss measurements with lower uncertainty than scans of the scattered light intensity. The PTD technique should be useful in the study of waveguide loss mechanisms.

900,740 PB89-157861 PB89-157861 Not available NTIS National Bureau of Standards (NEL), Boulder, CO. Electrosystems Div.

Tiger Tempering Tampers Transmissions. Final rept.

F. D. Martzloff. 1988, 2p Pub. in BICSI Newsletter, p3 and p10 Dec 88.

Keywords: *Surges, *Wire lines, *Transmission lines, Buildings, Overcurrent, Overvoltage, Retarding, Reprints.

The article is the second of a two-part update on progress at the National Institute of Standards and Technology in a study on the propagation of surges in building wiring systems. In the first part, the problems associated with surge propagation in building wiring systems were described and classified as pussycation. (they can just purr or they can scratch you and make you bleed) or tigers (they can eat you alive). Fast transients were shown to be pussycats. In the article, tests on the propagation of slower surges are cited; an important finding is that attempts at suppressing surges (tempering or taming tigers) on the power lines can have unexpected effects on the data transmission lines of an electronic data processing system.

900 741 PB89-162572 PC A04/MF A01 National Inst. of Standards and Technology (NEL), Gaithersburg, MD. Center for Fire Research. Flammability Characteristics of Electrical Cables

Using the Cone Calorimeter.
E. Braun, J. R. Shields, and R. H. Harris. Jan 89, 63p NISTIR-88/4003

Sponsored by Naval Sea Systems Command, Washington, DC.

Keywords: *Electric wire, *Flammability testing, Ignition, Combustion, Fire safety, Fire tests, Ignition delay, Smoking, Thermal measurements, *Cone calori-Smoking, Thermal mea meters, Heat release rate.

Cone calorimeter tests were performed on eight multi-conductor electrical cables. Measurements of ignition delay time, heat release rate, mass loss rate, and gas and smoke generation rates were made in the vertical (2 irradiance levels) and horizontal (3 irradiance levels) (2 irradiance levels) and nonzontal (3 irradiance levels) orientations. It was found that comparable ignition delay times were observed for all of the cross-linked polyolefin jacketed cables. The PVC jacketed cable had a substantially lower ignition delay time. All of the cables exhibited an ignition delay time dependence on external irradiance proportional to 1/q2. Sample orientation did not significantly affect the ignition delay time. Heat release rate measurements showed that cables burned in multiple stages. Each stage of burning was associated with the decomposition of a different layer of the cable assembly. For some cables, at low external irradiances (25 kW/m2) only the outer jacket burst open exposing the interior cable materials and secondary heat release rate peaks resulted. Changes in the cable components actually burning were reflected in variations in mass loss, gas, and smoke generation rates as well as small changes in the effective heat of combustion.

900,742 PB89-171664 Not available NTIS National Bureau of Standards (NEL), Boulder, CO. Electromagnetic Fields Div.

Magnetic Dipole Excitation of a Long Conductor in

Magnetic Dipole Exercises

a Lossy Medium.

Final rept.

D. A. Hill. 1988, 6p

Pub. in IEEE (Institute of Electrical and Electronics Engineers) Transactions on Geoscience and Remote Sensing 26, n6 p720-725 Nov 88.

Keywords: *Transmission lines, *Magnetic dipoles, *Excitation, Electric current, Polarized electromagnetic radiation, Stimulation, Emission, Electric discharges, Reprints, *Electric dipoles.

Formulations for the excitation of currents on an infinitely long conductor by electric or magnetic dipoles of arbitrary orientation are presented. The conductor can be either insulated or bare to model ungrounded or grounded conductors. Specific calculations are presented for a vertical magnetic dipole source because the source produces the appropriate horizontal polarization and could be used in a borehole-to-borehole configuration. Numerical results for the induced current and secondary magnetic field indicate that long conductors produce a strong anomaly over a broad frequency range. The secondary magnetic field decays slowly in the direction of the conductor and eventually becomes larger than the dipole source field.

900,743 PB89-171706 Not available NTIS National Bureau of Standards (NEL), Boulder, CO. Electromagnetic Technology Div.

Fast Optical Detector Deposited on Dielectric

Channel Waveguides.

Final rept. D. R. Larson, and R. J. Phelan, 1988, 4p

Pub. in Optical Engineering 27, n6 p503-506 Jun 88.

Keywords: *Waveguides, *Optical communication, Detectors, Thin films, Transmission lines, Dielectric films, Silicon, Hydrogeneration, Amorphous materials, Reprints.

A thin-film optical detector has been fabricated for detecting short optical pulses propagating in channel waveguides. The detectors show response times of 200 ps full width at half maximum amplitude when illuminated by guided, subpicosecond optical pulses. The detectors are formed by depositing hydrogenated amorphous silicon (a-Si:H) directly on the dielectric channel waveguides. Back-to-back Schottky photodiodes are then formed when interdigitated chrome-gold metal contacts are deposited on the a-Si:H.

900,744 PB89-173413 Not available NTIS
National Bureau of Standards (NEL), Gaithersburg,
MD. Electrosystems Div.
Measuring Fact Pierre Measuring Fast-Rise Impulses by Use of E-Dot Sensors.

Final rept.

R. H. McKnight. 1988, 3p

Sponsored by Department of Energy, Washington, DC.

Pub. in Proceedings of International Symposium on High Voltage Engineering (5th), Braunschweig, Federal Republic of Germany, August 24-28, 1987, v2 p1-3

Keywords: *Transmission lines, *High voltage, *Electromagnetic pulses, Calibrating, Frequencies, Pulsation, Electromagnetic radiation, Measurement, Power lines, *E-dot detectors.

Field coupled sensors such as capacitive dividers, derivative (E-dot or B-dot) sensors and Rogowski coils are commonly used in pulse power applications. Measurement devices using E-dot sensors in combination with passive or active integrators provide broadband capability, but with limited sensitivity. The use of this category of sensor in measurements of fast use pulses, such as a nuclear electromagnetic pulse (EMP), in power system equipment offers some advantages, such as ease of construction and versatility in installation.

900.745 PB89-173439 Not available NTIS National Bureau of Standards (NEL), Gaithersburg,

MD. Electrosystems Div.

Measurement of Electrical Parameters Near AC and DC Power Lines.

Final rept.

M. Misakian, 1988, 1p

Pub. in Proceedings of IEEE (Institute of Electrical and Electronics Engineers) Instrumentation and Measurement Technology Conference, San Diego, CA., April 20-22, 1988, p114.

Keywords: *Power lines, *Power measurement, *Elecfields, Transmission lines, Electric wire, Power meters, Calibrating, Charge density, Ion currents, Current density, Magnetic fields.

The presentation surveys the instrumentation, calibration procedures, measurement techniques, and measurement standards which can be used for characteriz-ing fields near AC power lines, and the electric field strength, ion current density, monopolar charge densi-ty, and net space charge near DC power lines.

900,746 PB89-173470 Not available NTIS National Bureau of Standards (NEL), Gaithersburg, MD. Electrosystems Div.

AC Electric and Magnetic Field Meter Fundamen-

Final rept.

M. Misakian. 1988, 23p
Pub. in Proceedings EPRI (Electric Power Research
Institute) Utility Seminar: Power-Frequency Electric
and Magnetic Field Exposure Assessment, Colorado
Springs, CO, October 12-14, 1988, p1-23.

Keywords: *Power lines, *Electric fields, *Magnetic fields, Measurement, Calibrating, Standards, Power meters, Transmission lines.

Questions raised in the early 1970s regarding possible adverse environmental effects due to high-voltage AC transmission line fields focused attention on the need for accurate measurements of the power-frequency electric and magnetic fields. Following a brief descrip-tion of the fields near AC power lines, the paper will survey the instrumentation, calibration procedures, measurement techniques and standards that have been developed since the early 1970s to characterize the electric and magnetic fields near AC power lines.

900,747 PB89-176176 Not available NTIS National Bureau of Standards (NEL), Boulder, CO. Electromagnetic Fields Div. Some Questions and Answers Concerning Air

Lines as Impedance Standards.

Final rept.
C. A. Hoer. 1987, 13p
Pub. in Proceedings of ARFTG (Automatic RF Techniques Group) Conference (29th), Las Vegas, NV.,
June 12-13, 1987, p161-173.

Keywords: *Characteristic impedance, *Transmission lines, Calibrating, Standards, Electric conductors, Reflection, Measurement, *Automatic network analyzers, Scattering parameters.

The paper attempts to answer a number of questions that arise when using one or more lengths of precision coaxial transmission line to calibrate a dual 6-port

ELECTROTECHNOLOGY

Power & Signal Transmission Devices

automatic network analyzer, questions such as: how important is the quality of the test port relative to that of the line; what type connectors should the line standards have; what are the advantages of using two lines instead of one line and a through connection when test port imperfections are considered; and how many lines are optimum from a quality control point of view and what should the lengths be. The answers to these questions appear to be: (1) The quality of the line is much more important than that of the test port. A perfect line will calibrate out most imperfections in the test port. An example is given where 75-omega test ports are calibrated with 50-omega lines, and then used to measure reflection coefficient relative to 50 omega with very little error. (2) Greatest accuracy is achieved with line standards having male connectors. (3) Two lines get rid of many test port imperfections that one line cannot. Three lines will show up a problem if one line is bad. Five lines will identify which line is bad. Five is probably optimum. (4) There may not be an optimum for the actual lengths of a set of lines, but there does appear to be an optimum difference in the lengths.

900,748
PB89-176671
National Bureau of Standards (NEL), Boulder, CO. Electromagnetic Technology Div.
Optical Fiber Sensors for the Measurement of Electromagnetic Quantities.

A. H. Rose, G. W. Day, K. S. Lee, D. Tang, L. R. Vesser, B. J. Paptheofanis, and H. R. Whitesel.

1988, 3p Pub. in Proceedings of Sensors Expo, Chicago, IL., September 13-15, 1988, p209A-1-209A-3.

Keywords: *Optical detection, *Electromagnetic interferences, Fiber optics, Electromagnetic compatibility, Magnetic fields, Electric current, Electric potential, Measurement.

Sensors used for the measurement of pulsed and AC current, voltage, and magnetic fields are described. current, voltage, and magnetic fields are described. Design considerations, including the choice of components and configurations, and performance achievements are discussed. The paper describes several sensor configurations presently being used to measure current, voltage, and magnetic fields in environments where electromagnetic interference is a problem. The current and magnetic field sensors are based on the Faraday effect either in single mode optical fiber or in bulk glass or polycrystalline materials. The voltage sensors are based on the linear electro-optic (Pockels) effect in cubic crystalline materials.

900,749 PB89-179816 PB89-179816 Not available NTIS
National Bureau of Standards (NEL), Boulder, CO.
Electromagnetic Technology Div.
Profile Inhomogeneity In Multimode Graded-Index

Fibers.

Final rept.

C. W. Oates, and M. Young. 1989, 3p Pub. in Jnl. of Lightwave Technology 7, n3 p530-532

Keywords: *Fiber optics, *Heterogeneity, *Profiles, Optical communication, Impurities, Inclusions, Gradients, Optical materials, Reprints, *Multimode fiber, *Graded index fibers.

The authors have measured the profile parameters (g) of several multimode graded index fibers and found that g may vary azimuthally by + or - 0.15 or more in fibers for which the average value is between 1.8 and

900,750 PB89-184121

(Order as PB89-184089, PC A04) National Inst. of Standards and Technology, Boulder,

Scattering Parameters Representing Imperfections in Precision Coaxial Air Lines.

Bi-monthly rept.
D. R. Holt. 1989, 17p
Included in Jnl. of Research of the National Institute of Standards and Technology, v94 n2 p117-133 Mar-Apr

Keywords: *Coaxial cables, *Pneumatic lines, *Skin effect, *Surface roughness, Scattering, Measurement, Conformal mapping.

Scattering parameter expressions are developed for the principal mode of a coaxial air line. The model

allows for skin-effect loss and dimensional variations in the inner and outer conductors. Small deviations from conductor circular cross sections are conformally mapped by the Bergman kernel technique. Numerical results are illustrated for a 7 mm air line. An error analysis reveals that the accuracy of the scattering parameters is limited primarily by the conductor radii measurement precision.

900,751 PB89-188593 PB89-188593 PC A04/MF A01 National Bureau of Standards (NEL), Boulder, CO. Center for Electronics and Electrical Engineering. System for Measuring Optical Waveguide Intensity Profiles.

L. E. Larson, D. R. Larson, and R. J. Phelan. Aug 88, 67p NBSIR-88/3092

Keywords: *Waveguides, *Optical communication, *Luminous intensity, Directional couplers, Fiber optics, Telecommunication, Measurement, Profiles, Gradi-ents, Radiance, Brightness, *Computer control.

A computer controlled system has been developed to measure the intensity profile of optical waveguides. Knowledge of the intensity profile provides an indication of the shape of the waveguide, and therefore the degree to which light can be coupled to the guide from an optical fiber. The report describes the construction and operation of the system.

PB89-189179 PC A03/MF A01 National Bureau_of Standards (NEL), Boulder, CO. Group Index and Time Delay Measurements of a

Standard Reference Fiber.

B. L. Danielson, and C. D. Whittenberg. Jul 88, 20p NBSIR-88/3091

Sponsored by Naval Weapons Center Corona Annex,

Keywords: *Optical materials, *Standards, *Calibrating, *Fiber optics, Measurement, Interferometers, Reflectometers, Time lag, Length.

Measurement techniques for establishing a standard reference fiber with well characterized group index and time or group delay are described. Evaluation of an in-terferometric method indicates that fiber group index can be determined with a total estimated uncertainty of about 0.03% in small samples. Group delay of the reference fiber was measured with an overall uncertainty less than 0.004% in a 7 km waveguide. The applica-tion of a standard reference fiber to calibration of the distance measurement accuracy of an optical time-domain reflectometer (OTDR) is discussed.

900,753 PB89-201057 Not available NTIS National Bureau of Standards (NEL), Boulder, CO. Electromagnetic Fields Div.

Reflection Coefficient of a Wavegulde with Slightly Uneven Walls.

Final rept.

D. A. Hill. 1989, 9p Pub. in IEEE (Institute of Electrical and Electronics En-gineers) Transactions on Microwave Theory and Techniques 37, n1 p244-252 Jan 89.

Keywords: *Waveguides, Shape, Asymmetry, Numerical analysis, Transmission lines, Coaxial cables, Telecommunication, Electromagnetic radiation, Reflectivity, Reprints, *Reflection coefficient.

First-order results are derived for the reflection coeffi-cient of a waveguide with slightly uneven walls. Specif-ic analytical and numerical results are given for rectangular waveguides and coaxial transmission lines. Simple upper bounds are given for reflection coeffi-cients in terms of the maximum deviation of the waveguide. For typical tolerances the reflection coefficients are very small (less than .01), but the results are important in precise six-port measurements.

PB89-237986 PC A02 National Inst. of Standards and Technology, Gaithersburg, MD.
National Institute of Standards and Technology
(NIST) Information Poster on Power Quality.

B. F. Field. Jul 89, 12p NIST/SP-768 See also PB83-245068. Also available from Supt. of Docs. as SN003-003-02957-2.

Keywords: *Power lines, *Disturbances, Electric power failures, Outages, Protection, Reliability(Electronics), Cost analysis, Voltage regulators, Dictionaries.

The poster answers seven questions about power quality that should help one pinpoint problems and so-lutions related to power disturbances; describes the types of power disturbances, the equipment affected, the types of protection equipment that is effective against the disturbance; contains a glossary of common power terms.

900.755

PB90-117326 Not available NTIS Not available NTS
National Inst. of Standards and Technology (NEL),
Gaithersburg, MD. Electrosystems Div.
Discussion of Steep-Front Short-Duration Voltage
Surge Tests of Power Line Filters and Translent

Voltage Suppressors.'.

Final rept.

Pilla rept.
P. R. Barnes, and T. L. Hudson. 1989, 2p
Pub. in IEEE (Institute of Electrical and Electronics Engineers) Transactions on Power Delivery 4, n2 p1035-1036 Apr 89.

Keywords: *Power lines, *Electric filters, *Surges, *Suppressors, Overvoltage, Transmission lines, Electric wire, Voltage regulators, Retarding, Damping, Inhibitors, Reprints.

The authors report interesting results of their tests on commercial filters (presumably consisting of linear ele-ments), enhanced by two types of nonlinear surge-pro-tective devices. While there is no problem with the reported performance per se, the wording of the report summary is likely to cause ambiguities when the paper appears in literature abstracts.

900.756

PB90-117474 Not available NTIS National Inst. of Standards and Technology (NEL), Boulder, CO. Electromagnetic Technology Div.
Comparison of Far-Field Methods for Determining
Mode Field Diameter of Single-Mode Fibers Using
Both Gaussian and Petermann Definitions.

Final rept. T. J. Drapela, D. L. Franzen, A. H. Cherin, and R. J.

Smith. 1989, 5p Pub. in Jnl. of Lightwave Technology 7, n8 p1153-1157

Keywords: *Far field, *Fiber optics, Electromagnetic fields, Electromagnetic radiation, Normal density functions, Optical communication, Transmission lines, Reprints, *Single mode fibers, *Mode field diameters.

An interlaboratory comparison of far-field measurement methods to determine mode field diameter of single-mode fibers was conducted among members of the Electronic Industries Association. Measurements were made on dispersion unshifted and shifted fibers at 1300 and 1550 nm. Results were calculated using both Petermann and Gaussian definitions. The Petermann definition gave better agreement than the Gaussian in all cases. A systematic offset of 0.52 micro m was observed between methods when applied to dispersion shifted fibers. Such an offset may be caused by limited angular collection.

900.757 PB90-117482 Not available NTIS National Inst. of Standards and Technology (NEL), Boulder, CO. Electromagnetic Technology Div. Numerical Aperture of Multimode Fibers by Several Methods: Resolving Differences.

Final rept.

D. Franzen, M. Young, A. Cherin, E. Head, M. Hackert, K. Raine, and J. Baines. 1989, 6p Pub. in Jnl. of Lightwave Technology 7, n6 p896-901

Keywords: *Fiber optics, *Apertures, Electric fields, Optical communication, Far field, Electromagnetic fields, Reprints, *Multimode fibers, Gradient index optics, Index profiles.

An industry-wide study among members of the Electronic Industries Association was conducted to document differences among three numerical aperture measurement methods. Results on 12 multi-mode graded index fibers indicate systematic differences exist among commonly used far-field and index profile techniques. Differences can be explained by a wave-length dependent factor and choice of definitions.

Power & Signal Transmission Devices

Conversion factors may be used to relate the various methods.

Resistive, Capacitive, & Inductive Components

900,758 PB89-171805 Not available NTIS
National Bureau of Standards (IMSE), Gaithersburg, MD. Ceramics Div.

Fracture Behavior of Ceramics Used in Muitilayer Capacitors.

Final rept. T. L. Baker, and S. W. Freiman. 1986, 10p Pub. in Materials Research Society Symposium Proceedings on Electronic Packaging Materials Science 72, n2 p81-90 1986.

Keywords: *Ceramics, *Crack propagation, *Aging tests(Materials), *Capacitors, *Dielectric breakdown, Microstructure, Chemical composition, Toughness, Fracturing, Stress corrosion, Indentation, Fatigue (Materials), Dynamic loads, Strength, Reprints.

The study involved the determination of the effects of composition and microstructure on the fracture toughness and susceptibility to environmentally enhanced crack growth of several ceramic materials used in multilayer capacitors. Indentation-fracture procedures were used to measure K(IC) as well as to assess the possible effects of internal stresses on the fracture behavior of these materials and to correlate dielectric aging phenomena with strength. The environmentally enhanced crack growth behavior of these material was determined by conducting dynamic fatigue tests in water.

900.759 PB89-173785 Not available NTIS National Bureau of Standards (NEL), Boulder, CO. Electromagnetic Fields Div.

Transient Response Error in Microwave Power

Meters Using Thermistor Detectors.

Final rept.
F. R. Clague, and N. T. Larsen. 1987, 11p
Pub. in ARFTG (Automatic RF Techniques Group)
Conference Digest (28th), St. Petersburg, FL., December 4-5, 1986, p79-89 1987.

Keywords: *Thermistors, *Transient response, Dynamic response, Amplification, Power measurement, Semiconductor devices, Variable resistors, Microwave frequencies, Bolometers, Electric power meters.

Broadband coaxial thermistor mounts are commonly used in automated precision microwave measurement systems such as six-port networks. To reduce the effect of temperature drift and to decrease the total measurement time, it is desirable to measure the DC bias voltage on the thermistor mount very quickly after turning the rf on or off. However, investigation has re-vealed that a coaxial mount may take much longer to settle to a stable DC bias voltage than the thermistor element time constant or the associated power meter servo bandwidth would indicate. If the bias voltage is measured before this transient ends, the error in the calculated if power can be very large; as much as 1.4% has been observed. The paper describes these transients and gives measured durations and maximum error for a number of different bolometer mounts.

900,760 PB89-176648 PB89-176648 Not available NTIS
National Bureau of Standards (NEL), Gaithersburg, MD. Electrosystems Div.

Selecting Varistor Clamping Voltage: Lower is Not Better.

Final rept.

F. D. Martzloff, and T. F. Leedy. 1989, 6p Pub. in Proceedings of Zurich International EMC (Electromagnetic Compatibility) Symposium, Zurich, Switzerland, March 7-9, 1989, p137-142.

Keywords: *Protectors, *Varistors, *Surges, Overcurrent, Semiconductor devices, Thermistors, Variable resistors, Overvoltage, Power lines, Clamping circuits, Electric potential, Premature aging.

Surge protective devices, such as varistors, are applied to protect sensitive load equipment against power-line surges. The need to provide low clamping

voltage for protection of equipment with low inherent immunity must be balanced against the risk of premature aging of the protective device. Lower clamping voltage causes more frequent interventions of the pro-tective device, accelerating its aging. The paper de-scribes four possible causes of such premature aging, calling for a more careful and thus more reliable application of protective devices.

900,761 PB89-193890 PC A03/MF A01 National Inst. of Standards and Technology (NEL), Boulder, CO. Electromagnetic Fields Div. Theory and Measurements of Radiated Emissions Using a TEM (Transverse Electromagnetic) Celi. Technical note.

G. H. Koepke, M. T. Ma, and W. D. Bensema. Jan 89, 40p NIST/TN-1326

Also available from Supt. of Docs. as SN003-003-

Keywords: *Electromagnetic radiation, Measurement, Antennas, Emission, Test equipment, *Transverse electromagnetic cells.

The transverse electromagnetic cell is widely used to evaluate the electromagnetic characteristics of electrically small devices. The paper reviews the theoretical basis for a technique to quantify the radiated emissions from any such device in the cell. The technique is well suited to an automated test system provided that the mechanical motions required can be controlled by a computer. The difficulties associated with these mechanical motions are discussed and possible solutions are proposed. The measurement technique is also expanded to include multiple-frequency sources in addition to single-frequency sources.

900,762 PB89-200505 Not available NTIS National Inst. of Standards and Technology (NEL), Boulder, CO. Electromagnetic Technology Div. Superconducting Kinetic Inductance Bolometer.

Sponsored by Redstone Arsenal, AL., and Aerospace Guidance and Metrology Center, Newark AFS, OH. Pub. in IEEE (Institute of Electrical and Electronics Engineers) Transactions on Magnetics 25, n2 p1331-1334 Mar 89.

Keywords: *Bolometers, Temperature measuring instruments, Inductance, Niobium, Silicon, Substrates, Reprints, *Superconducting devices, *Thermometers, SQUID (Detectors).

The authors are developing a bolometer with a temperature sensor based on the temperature dependence of the inductance of a superconducting microstrip line. As a first step in exploring this idea, they have designed experiments to test only the temperature sensor. The experimental devices are all-niobium inductance thermometers fabricated on silicon substrates which have been deeply etched to provide areas of relative ther-mal isolation. The ground plane superconductor is thin enough that its kinetic inductance dominates the audio frequency impedance of the stripline near its critical temperature, at 0.09(T sub c). This differential thermometer uses a commercial SQUID as the preamplifier. Preliminary results demonstrate a proof-of-principle for the thermometer design.

900,763 PB89-201032 Not available NTIS National Bureau of Standards (NEL), Boulder, CO. Electromagnetic Technology Div.

Noise in DC SQUIDS with Nb/Ai-Oxide/Nb Josephson Junctions.

Final rept.

M. W. Cromar, J. A. Beall, D. Go, K. A. Masarie, and R. H. Ono. 1989, 3p

Pub. in IEEE (Institute of Electrical and Electronics Entertains).

gineers) Transactions on Magnetics 25, n2 p1005-1007 Mar 89.

Keywords: *Electromagnetic noise, Josephson junctions, Direct current, Aluminum oxide, Niobium, Reprints, *SQUID devices.

The authors have developed a process which incorporates very high quality Nb/Al-oxide/Nb Josephson junctions. The junctions had low subgap conductance yielding (V sub m) greater than 50 mV for critical current densities of 1000 A/sq cm. Low inductance SQUIDs made with these junctions were apparently free from junction conductance fluctuations, at least

for frequencies above 1 Hz. The SQUIDs exhibited flux noise of currently unknown origin.

900.764

PB89-201719 Not available NTIS National Bureau of Standards (NML), Gaithersburg, MD. Temperature and Pressure Div. Impedance of Radio-Frequency Blased Resistive Superconducting Quantum Interference Devices.

R. J. Soulen, and D. Van Vechten. 1987, 27p Pub. in Physical Review B-Condensed Matter 36, n1 p239-265 1987.

Keywords: *Electrical impedance, Josephson junctions, Electrical measurement, Radio frequencies, Reprints, *SQUID devices, Noise thermometers.

The authors have measured with high accuracy (100 ppm) and high precision (5-10 ppm) the impedance of an rf-driven resistive SQUID as a function of the amplitude and frequency of the radio-frequency (rf) bias, as a function of the current bias, and as a function of sev-eral other circuit parameters. They have developed the coupled differential equations for the resistive SQUID and for the rf tank circuit. The fit of the solutions of these equations to the data for non-hysteretic junctions is excellent. The authors were unable to develop solutions for the hysteretic case and thus compare them to the data obtained. The relationship of the study to noise thermometry using resistive SQUIDs is indicated.

900,765

PB89-202014 Not available NTIS National Bureau of Standards (IMSE), Gaithersburg, MD. Metallurgy Div.

Vector Calibration of Ultrasonic and Acoustic Emission Transducers.

Final rept. J. A. Simmons, C. D. Turner, and H. N. G. Wadley.

1987, 9p Pub. in Jnl. of the Acoustical Society of America 82, n4 p1122-1130 1987.

Keywords: *Sound transducers, *Transient response, Electric converters, Dynamic responses, Damping, Impedance, Vectors(Mathematics), Vector analysis, Calibrating, Reprints.

The independent transient response of a transducer to displacements polarized in each of the three orthogonal directions have been determined using a new method which assumes only linearity of transducer re-sponse and circular symmetry of both the transducer and the source. The method forms the basis for vector calibration of acoustic emission and ultrasonic transducers.

900.766

PB89-211114

(Order as PB89-211106, PC A04) National Inst. of Standards and Technology, Gaithers-

burg, MD.

Calibration of Voltage Transformers and High-Voltage Capacitors at NIST.
W. E. Anderson. 1989, 17p
Included in Jnl. of Research of the National Institute of

Standards and Technology, v94 n34 p179-195 May-

Keywords: *Calibration, Capacitors, Dissipation factor, Electric power, Electrical standards, NIST services, Voltage transformers.

The National Institute of Standards and Technology (NIST) calibration service for voltage transformers and (NIST) calibration service for voltage transformers and high-voltage capacitors is described. The service for voltage transformers provides measurements of ratio correction factors and phase angles at primary voltages up to 170 kV and secondary voltages as low as 10 V at 60 Hz. Calibrations at frequencies from 50-400 Hz are available over a more limited voltage range. The service for high-voltage capacitors provides measurements of capacitance and dissipation factor at applied voltages ranging from 100 V to 170 kV at 60 Hz depending on the nominal capacitance. Calibrations over a reduced voltage range at other frequentions over a reduced voltage range at other frequencies are also available. As in the case with voltage transformers, these voltage constraints are determined by the facilities at NIST.

Semiconductor Devices

Semiconductor Devices

900,767 PB89-146880 Not available NTIS National Bureau of Standards (NEL), Gaithersburg, MD. Semiconductor Electronics Div.

Analytical Model for the Steady-State and Translent Characteristics of the Power Insulated-Gate Bipolar Transistor.

A. R. Hefner, and D. L. Blackburn. 1988, 20p Pub. in Solid-State Electronics 31, n10 p1513-1532

Keywords: *Field effect transistors, *Models, Waveforms, Electric potential, Unsteady flow, Steady state, Electric current, Reprints, Ambipolar MOSFET.

An analytical model for the power Insulated-Gate Bipolar Transistor (IGBT) is developed. The model consistently describes the IGBT steady-state current-voltage characteristics and switching transient current and voltage waveforms for all loading conditions. The model is based on the equivalent circuit of a MOSFET which supplies the base current to a low-gain, highlevel injection, bipolar transistor with its base virtual contact at the collector end of the base. The basic element of the model is a detailed analysis of the bipolar transistor which uses ambipolar transport theory and does not assume the quasi-static condition for the transient analysis. This analysis differs from the previous bipolar transistor theory in that (1) the relatively large base current which flows from the collector end of the base is properly accounted for, and (2) the component of current due to the changing carrier distribution under the condition of a moving collector-base de-pletion edge during anode voltage transitions is ac-counted for. Experimental verification of the model using devices with different base lifetimes is presented for the on-state current-voltage characteristics, the steady-state saturation current, and the current and voltage waveforms for the constant voltage transient, the inductive load transient, and the series resistor-inductor load transient.

900,768 PB89-146955 Not available NTIS National Bureau of Standards (NEL), Gaithersburg, MD. Semiconductor Electronics Div.

Use of Artificial Intelligence and Microelectronic Test Structures for Evaluation and Yield Enhancement of Microelectronic Interconnect Systems. Final rept.

M. W. Cresswell, N. Pessall, L. W. Linholm, and D. J.

Radack. 1986, 10p Pub. in Proceedings of International IEEE (Institute of Electrical and Electronics Engineers) VLSI (Very Large Scale Integration) Multilevel Interconnection Conference (3rd), Santa Clara, CA., June 9-10, 1986, p331-

Keywords: *Circuit interconnections, *Integrated circuits, *Test equipment, Tests, Artificial intelligence, Very large scale integration, Expert systems.

A major factor limiting the production and performance of high-density VLSI integrated circuits is the fabrica-tion of reliable interconnect systems. Properly de-signed microelectronic test structures and appropriate test methods can be used to characterize the processes used to fabricate these systems. However, the computer-controlled testing of comprehensive process evaluation and diagnosis structures often results in large quantities of data which cannot be readily or effectively interpreted by the user. As a result, important features of the data are often overlooked or not considered in the evaluation of the fabrication processes. The paper describes an expert system for assisting the user to interpret test results associated with fabricating selected aspects of VLSI interconnect systems.

900,769 PB89-146997 Not available NTIS National Bureau of Standards (IMSE), Gaithersburg,

Stress Effects on III-V Solid-Liquid Equilibria. Final rept. F. C. Larche, and J. W. Cahn. 1987, 8p

Pub. in Jnl. of Applied Physics 62, n4, p1232-1239, 15 Aug 87.

Keywords: *Epitaxy, *Thermodynamic equilibrium, Phase diagrams, Compositions, Stresses, Reprints, *III-V compounds.

The equilibrium of an epitaxial layer grown from the melt is analyzed in detail. The stresses produced by lattice mismatch with the substrate interact with the chemistry of the process. The general equilibrium equations are derived for 3-5 compounds. The stress field, and its approximations for thin layers are obtained. An expression for the composition of the epilayer as a function of liquid composition, valid in the vicinity of the lattice matching composition, is derived. Very good agreement is found between calculated values and measured results from LPE growth. Properties of systems that would present lattice latching phenomena are quantitatively discussed. It is shown that epitaxial equilibrium also affects the results of several methods of phase diagram determination, which are discussed in light of the preceeding results.

PB89-150825 Not available NTIS Motional Bureau of Standards (NEL), Gaithersburg, MD. Semiconductor Electronics Div. Review of Thermal Characterization of Power

Transistors.

Final rept.

Pub. in Proceedings of Annual IEEE (Institute of Electrical Electronics Engineers) Semiconductor Thermal and Temperature Measurement Symposium (SEMI-THERM) (4th), San Diego, CA., February 10-12, 1988, p1-7.

Keywords: *Thermal measurements, *Transistors, Thermal environments, Power supplies, Surges, Switching circuits, Field effect transistors, Darlington transistors.

The thermal characteristics of power transistors and their measurement are discussed. Topic areas addressed include general methods for measuring device temperature, control of the thermal environment, selection of a temperature-sensitive electrical parameter, measurement of temperature-sensitive electrical parameters, reasons for measuring temperature, and temperature measurement of integrated power devices. Procedures for detecting nonthermal switching transients, extrapolation of the measured temperature to the instant of switching, and for measuring the temperature of Darlington transistors are in-

900,771

Final rept.

PB89-150973 Not available NTIS National Bureau of Standards (NEL), Gaithersburg, MD. Precision Engineering Div. Submicrometer Optical Metrology.

R. D. Larrabee. 1988, 2p See also PB87-201646.

Pub. in Proceedings of Annual Meeting of the Electron Microscopy Society of America (46th), Milwaukee, WI., August 7-12, 1988, p50-51.

Keywords: *Standards, *Metrology, *Optical measurements, *Line width, *Integrated circuits, Performance evaluation, Pitch(Inclination), Critical dimensions.

The National Bureau of Standards (NBS) has developed optical linewidth standards for the integrated circuit industry for over 10 years. The past work has concentrated on the development and the certification of photomask linewidth and pitch standards. The recent work is directed at extending the feature sizes on these standards to cover the range from 0.5 to 30 micrometers, and at doubling the certification accuracy to 0.025 micrometers. Features with heights larger than approximately 1/4 wavelength of light cannot be modeled as zero-thickness layers as is done for photomasks. The development of models to handle this thick-layer case and to develop practical edge-detection criteria are currently under development at NBS. It is generally not possible to interpret the image profiles of thick features and thereby measure an accurate linewidth. The basic obstacles that must be overcome to achieve accurate submicron feature size measurements are reviewed and the prospects for future NBS optical standards for features such as photoresist lines on silicon wafers are assessed. Some suggestions about what to do until these standards become available are given.

900,772 PB89-151831 PC A04/MF A01 National Inst. of Standards and Technology (NEL), Gaithersburg, MD. Semiconductor Electronics Div. Semiconductor Measurement Technology: Automatic Determination of the Interstitlal Oxygen Content of Silicon Wafers Polished on Both Sides. Final rept.

W. K. Gladden, S. R. Slaughter, W. M. Duncan, and A. Baghdadi. Nov 88, 73p NIST/SP-400/81 Also available from Supt. of Docs. as SN003-003-02915-7. Library of Congress catalog card no. 88-600601. Prepared in cooperation with Texas Instruments, Inc., Dallas,

Keywords: *Semiconductor devices, *Interstitials, *Silicon, *Computer systems programs, *Infrared spectra, *Oxygen, Computerized simulation, Tests, Automatic control, Wafers, Algorithms.

The Special Publication contains FORTRAN and PASCAL computer programs which implement an ASTM test method for the automatic determination of the interstitial oxygen content of silicon. The programs are to be used as illustrative examples by programmers wishing to implement the ASTM algorithm on their computers. The Publication also includes sample data that can be used to test the computer programs. The sample data are included in two forms: in print, and on an MS-DOS floppy disk.

900.773

PB89-157655 Not available NTIS National Bureau of Standards (NEL), Gaithersburg, MD. Semiconductor Electronics Div. Effect of Neutrons on the Characteristics of the In-

sulated Gate Bipolar Transistor (IGBT). Final rept.

A. R. Hefner, D. L. Blackburn, and K. F. Galloway. 1986, 7p

Pub. in IEEE (Institute of Electrical and Electronics Engineers) Transactions on Nuclear Science NS-33, n6 p1428-1434 Dec 86.

Keywords: *Neutron irradiation, Mathematical models, Field effect transistors, Reprints, *Bipolar transistors, *Insulated gate bipolar transistors, *Physical radiation effects, MOSFET, Carrier lifetime.

The effects of neutrons on the operating characteristics of Insulated Gate Bipolar Transistors (IGBT) are described. Experimental results are presented for devices that have been irradiated up to a fluence of 10 to the 13th power neutrons/c sq cm, and an analytical model is presented which explains the observed effects. The effects of neutrons on the IGBT are compared with the known effects on power MOSFETs, and it is shown that the IGBT characteristics begin to degrade at a fluence that is an order of magnitude less than the fluence at which the power MOSFET begins to degrade. At high fluences, the IGBT takes on the characteristics of a power MOSFET.

900,774

Not available NTIS PB89-158042 National Bureau of Standards (NEL), Gaithersburg, MD. Center for Electronics and Electrical Engineering. Standards and Test Methods for VLSI (Very Large Scale Integration) Materials.

Final rept.

R. I. Scace. 1985, 5p
Pub. in Technical Program: Proceedings of Semiconductor Technology Symposium, Tokyo, Japan, December 7-8, 1984, p4-1-4-5 1985.

Keywords: *Semiconductors(Materials), *Standards, Integrated circuits, Specifications, Tests, Standardization, Reprints, *Very large scale integration.

Standard measurement methods and specifications for the semiconductor industry will be reviewed and discussed with emphasis on applications to VLSI processes. These standards are well accepted in the U.S. and in Europe, but are not so well known in Japan. The standards development process is an excellent way for material producers and users to develop good working relations and to solve their shared measurement problems; this process will be described in some detail. Because the semiconductor industry is an international one, serious efforts have been made for a number of years to rationalize the technical differences between test method standards in Europe and the U.S. with considerable success. The present state of such cooperative activity with Japan, which as a more recent origin, will also be reported.

900,775 PB89-168033

PC A03/MF A01

Semiconductor Devices

National Inst. of Standards and Technology (NEL), Gaithersburg, MD. Center for Electronics and Electro-

cal Engineering.
Center for Electronics and Electrical Engineering Technical Progress Bulletin Covering Center Programs, July to September 1988, with 1989 CEEE Events Calendar.

E. J. Walters. Jan 89, 40p NISTIR-88/4020 See also PB88-130315.

Keywords: *Semiconductor devices, *Electric devices, *Electromagnetic interference, Silicon, Photodetectors, Packaging, Metrology, Superconductors, Millimeter waves, Microwaves, Fiber optics, Electrooptics, Antennas, *Signal acquisition.

The report is the twenty-fourth issue of a quarterly publication providing information on the technical work of the National Institute of Standards and Technology (formerly the National Bureau of Standards) Center for Electronics and Electrical Engineering. The topics discussed are semiconductor technology; first signal acquisition, processing and transmission; electrical systems; and electromagnetic interference.

900,776 PB89-172555 PC A03/MF A01 National Inst. of Standards and Technology (NEL), Gaithersburg, MD. Precision Engineering Div. Approach to Accurate X-Ray Mask Measurements in a Scanning Electron Microscope.

M. T. Postek, R. D. Larrabee, and W. J. Keery. Jan 89, 14p NISTIR-89/4047

Sponsored by Naval Research Lab., Washington, DC.

Keywords: *Dimensional measurement, *Integrated circuits, *Masking, *Lithography, Metrology, Accuracy, *X ray lithography, Scanning electron microscopes.

The paper presents the concept and some preliminary experimental data on a new method for measuring critical dimensions on masks used for x-ray lithography. The method uses a scanning electron microscope (SEM) in a transmitted-scanning electron microscope (TSEM) imaging mode and can achieve nanometer precision. Use of this technique in conjunction with measurement algorithms derived from electron beam interaction modeling may ultimately enable measurements of these masks to be made to nanometer accu-

900,777 PB89-176259 Not available NTIS National Bureau of Standards (NEL), Gaithersburg,

MD. Semiconductor Electronics Div.

Analytical Modeling of Device-Circuit Interactions for the Power Insulated Gate Bipolar Transistor

Final rept.

A. R. Hefner. 1988, 9p Pub. in Conference Record 1988, IEEE (Institute of

Electrical and Electronics Engineers) Industry Applica-tions Society Annual Meeting, Pittsburgh, PA., October 2-7, 1988, p606-614.

Keywords: *Field effect transistors, *Mathematical models, Simulation, Semiconductor devices, Transient response, Impedance, Surges, Protection, Ratings, Performance standards, *Bipolar transistors, Snub-

The device-circuit interactions of the power Insulated Gate Bipolar Transistor (IGBT) for a series resistor-inductor load, both with and without a snubber, are simulated. An analytical model for the transient operation of the IGBT is used in conjunction with the load circuit state equations for the simulations. The simulated results are compared with experimental results for all conditions. Devices with a variety of base lifetimes are studied. For the fastest devices studied, the voltage overshoot of the series resistor-inductor load circuit approaches the device voltage rating for load inductances greater than 1 microHenrys. For slower devices, the voltage overshoot is much less and a larger induct-ance can therefore be switched without a snubber circuit. In the study, the simulations are used to determine the conditions for which the different devices can be switched safely without a snubber protection circuit. Simulations are also used to determine the required values and ratings for protection circuit components when protection circuits are necessary.

900,778 PB89-179675 Not available NTIS National Bureau of Standards (NML), Gaithersburg, MD. Electricity Div.

Quantized Hall Resistance Measurement at the NML (National Measurement Laboratory). Final rept.

B. W. Ricketts, and M. E. Cage. 1987, 4p
Pub. in IEEE (Institute of Electrical and Electronics Engineers) Transactions on Instrumentation and Measurement 36, n2 p245-248 1987.

Keywords: *Gallium arsenides, *Electrical resistance, Semiconductors, Quantum interactions, Impedance, Measurement, Standards, Reprints, *Hall effect, Heterostructures

An automatic measurement system has been developed to determine the values of quantized Hall resistances of two GaAs/AlGaAs heterostructures. The n=2 step of one heterostructure and the n=4 step of the other were measured over a seven-month period. A weighted mean of these determinations gives a SI value for the quantity h/e squared of 0.47 ppm (0.11 ppm 1 sigma uncertainty) above the nominal 25812.80 ohm value.

900,779 Not available NTIS
National Bureau of Standards (NEL), Gaithersburg,
MD. Semiconductor Electronics Div.
Correlation between CMOS (Co.

Oxide Semiconductor) Transistor and Capacitor Measurements of interface Trap Spectra. Final rept.

and P. Roitman. 1986, 6p Sponsored by Defense Nuclear Agency, Washington, DC. T. J. Russell, H. S. Bennett, M. Gaitan, J. S. Suehle,

Pub. in IEEE (Institute of Electrical and Electronics En-

gineers) Transactions on Nuclear Science NS-33, n6 p1228-1233 Dec 86.

Keywords: *Silicon dioxide, *Radiation effects, *Capacitors, *Transistors, Interfacial tension, Energy, Spectra, Semiconductor devices, Charging, Reprints.

The radiation induced change in the energy spectra of SiO2-Si interface traps as determined using the charge-pumping and weak-inversion techniques on complementary metal oxide semiconductors (CMOS) transistors and using the quasi-static capacitance voltage (C-V) and detailed model techniques on CMOS capacitors are compared. Over the range of approximately 10(sup 10) to 10(sup 12)/cm/ev, good quantitative agreement is obtained between these methods.

900,780 PB89-180426 PB89-180426 Not available NTIS National Bureau of Standards (NEL), Boulder, CO. Electromagnetic Fields Div. Electromagnetic Fields In Loaded Shielded

Rooms. Final rept.

. Vanzura, and J. W. Adams. 1987, 7p Pub. in Test and Measurement World, p72, 74, 76, 78, 80, 82, 83 Nov 87.

Keywords: *Electromagnetic fields, *Field strength, *Feedback amplifiers, Electromagnetic shielding, Ra-diation shielding, Feedback control, Automatic control, Electromagnetic interference, Cybernetics, Magnetic permeability, Reprints, *Shielded rooms.

The paper describes a computer-controlled feedback system that can maintain field strength levels within moderate bounds inside a partially-loaded shielded room. The levels are relatively uniform over a large enough volume to allow radiated immunity testing of moderate-sized objects. The frequency range depends on the characteristics of the transmit antenna; 50 to 200 MHz was used, which is a difficult range to cover because of limitations of other EMC susceptibility test facilities. The measurement system consists of a computer, signal generator, amplifier, biconical antenna and an isotropic probe system.

900,781 PB89-186837 Not available NTIS National Bureau of Standards (NEL), Gaithersburg, MD. Semiconductor Electronics Div.
Numerical Analysis for the Small-Signal Response
of the MOS (Metal Oxide Semiconductors) Capaci-

M. Gaitan, and I. Mayergoyz. 1989, 7p Pub. in Solid-State Electronics 32, n3 p207-213 1989.

Keywords: *Metal oxide semiconductors, *Capacitors, *Frequency response, Quantum statistics, Numerical

analysis, Continuity equation, Surface properties, Poisson density functions, Reprints, Bulk trap dynamics.

Simulation results for the small-signal sinusoidal steady-state response of the MOS capacitor using time perturbation analysis of the basic semiconductor equations are presented. The effects of interface and bulk trap dynamics are included. The model uses Fermi-Dirac statistics and Shockley-Read-Hall recombination to describe the trape. The analysis is an imbination to describe the traps. The analysis is an improvement over previous techniques since it can simulate the effect of trap dynamics on the small-signal sinusoidal steady-state response of a semiconductor device with arbitrary geometry, doping and trap distributions.

900,782 PB89-189344

PB89-189344 PC A06/MF A01
CD Metrology, Inc., Germantown, MD.
Narrow-Angle Laser Scanning Microscope System
for Linewidth Measurement on Wafers.
D. Nyyssonen. Apr 89, 111p NISTIR-88/3808
Sponsored by National Inst. of Standards and Technology (NEL), Gaithersburg, MD. Precision Engineering Div.

Keywords: *Measuring instruments, *Semiconductors(Materials), *Integrated circuits, *Coherence, Scanning, Lasers, Line width, Computer systems programs, Thin films, Optical properties, tems programs, Thin film Graphs(Charts), Microscopy.

The integrated-circuit industry in its push to finer and finer line geometries approaching submicrometer di-mensions has created a need for ever more accurate and precise feature-size measurements to establish tighter control of fabrication processes. In conjunction with the NBS Semiconductor Linewidth Metrology Program, a unique narrow-angle laser measurement system was developed. The report describes the theory, optical design, and operation of the system and includes computer software useful for characterizing the pertinent optical parameters and images for patterned thin layers. For thick layers, the physics is more complex and only elements of the theory are included. For more detail the reader is referred to several related reports listed in the references.

900.783

PB89-201156 Not available NTIS National Bureau of Standards (NEL), Gaithersburg, MD. Statistical Engineering Div.

Graphical Analyses Related to the Linewidth Calibration Problem.

Final rept.

M. C. Croarkin. 1986, 8p Pub. in Proceedings of Measurement Science Conference, Irvine, CA., January 23-24, 1986, p159-166.

Keywords: *Graphic methods, *Calibrating, *Integrated circuits, Metrology, Line width, Statistical tests, Measurement, Control charts.

The paper demonstrates that graphical analyses, when properly understood, can often supplant more formal statistical analyses, and in all cases enhance such analyses. Statistical tests, which reduce the information in the data to a one line 'yes' or 'no' finding, are referenced to support the graphical findings. The power of the approach is illustrated with a measure-ment problem that led to the development of Standard Reference Material SRM-475. Assessment of the extent of the measurement problem in the integrated circuit industry and procedures for evaluating system performance are discussed.

900.784

PB89-201974 Not available NTIS National Bureau of Standards (NEL), Gaithersburg, MD. Semiconductor Electronics Div. Radiation-induced interface Traps in Power MOS-

G. Singh, K. F. Galloway, and T. J. Russell. 1986, 6p Pub. in IEEE (Institute of Electrical and Electronics En-gineers) Transactions on Nuclear Science NS-33, n6 p1454-1459 Dec 86.

Keywords: *Field effect transistors, *Radiation effects, Irradiation, Gamma rays, Transconductance, Reprints, MOSFET.

Methods for estimating values of radiation-induced interface trapped charge from the current-voltage (I-V) characteristics of MOSFETs are described and applied

Semiconductor Devices

to commercially available power MOSFETs. The power MOSFETs show severe degradation on radiation exposure with the effects of positive oxide trapped charge dominating; however, interface trap buildup is significant. The results are compared to experimental measurements available on other technol-

900.785 Not available NTIS PR89-202964 National Bureau of Standards (NEL), Gaithersburg, MD. Chemical Process Metrology Div.
Fundamental Characterization of Clean and Gas-

Dosed Tin Oxide. Final rept.

S. Semancik, and D. F. Cox. 1987, 6p Pub. in Sensors and Actuators 12, n2 p101-106 1987.

Keywords: *Tin oxides, *Single crystals, *Water, *Oxygen, *Adsorption, Surface chemistry, High pressure tests, Semiconductors(Materials), Defects, Sensors, Photoelectric emission, Reprints.

The chemical, electronic and structural properties of a SnO2(110) crystal have been studied before and after exposure to H2O and O2. The results show that the initial stages of water adsorption on SnO2(110) can be influenced by structural factors and/or the concentration level of surface defects. The degree of surface oxidation has also been demonstrated to have an observable effect on the nature of water adsorption at higher pressures. These results relate both to basic gas sensing mechanisms for SnO2 and to the influence of humidity on tin oxide.

900,786

PB89-209225 PC A03/MF A01 National Inst. of Standards and Technology (NEL), Gaithersburg, MD. Center for Electronics and Electrical Engineering.

Center for Electronics and Electrical Engineering: Center for Electronics and Electrical Engineering: Technical Progress Bulletin Covering Center Pro-grams, January to March 1989, with 1989 CEEE Events Calendar. E. J. Walters. Jun 89, 27p NISTIR-89/4095

See also PB89-168033.

Keywords: *Semiconductor devices, *Signal processing, *Metrology, Photodetectors, Electric devices, Radiation effects, Waveforms, Lasers, Fiber optics, Electrooptics, Electric power, Superconductors, Electromagnetic interference, Signals and systems, Cryoelectromagnetic

The report is the twenty-sixth issue of a quarterly publication providing information on the technical work of the National Institute of Standards and Technology (formerly the National Bureau of Standards) Center for Electronics and Electrical Engineering. The issue of the CEEE Technical Progress Bulletin covers the first quarter of calendar year 1989.

900 787

PB89-209241 PC A03/MF A01 National Inst. of Standards and Technology (NEL), Gaithersburg, MD. Center for Electronics and Electrical Engineering.

Center for Electronics and Electrical Engineering Technical Publication Announcements. Covering Center Programs, October/December 1988, with 1989 CEEE Events Calendar. E. J. Walters. May 89, 30p NISTIR-89/4096 See also PB89-189302.

Keywords: *Semiconductor devices, *Signal processing, *Metrology, Silicon, Photodetectors, Electric devices, Waveforms, Lasers, Antennas, Microwaves, Millimeter waves, Fiber optics, Electrooptics, Electric power, Superconductors, Electromagnetic interference, Signals and systems, Cryoelectronics.

The report is the nineteenth issue of a quarterly publication providing information on the technical work of the National Institute of Standards and Technology (formerly the National Bureau of Standards) Center for Electronics and Electrical Engineering. The issue of the Center for Electronics and Electrical Engineering Technical Publication Announcements covers the fourth quarter of calendar year 1988.

900,788

PB89-212187 Not available NTIS National Bureau of Standards (NEL), Gaithersburg, MD. Semiconductor Electronics Div. Neural Network Approach for Classifying Test Structure Results. Final rept.

D. Khera, M. E. Zaghloul, L. W. Linholm, and C. L.

Wilson, 1989, 4p
Pub, in Proceedings of IEEE (Institute of Electrical and Electronics Engineers) International Conference on Microelectronic Test Structures, Edinburgh, Scotland, March 13-14, 1989, v2 n1 p201-204.

Keywords: *Integrated circuits, *Manufacturing, *Neural nets, Artificial intelligence, Algorithms, Learn-Tests. *Semiconductors, ing machines, Chips(Electronics).

The paper describes a new approach for identifying and classifying semiconductor manufacturing process variations using test structure data. The technique described employs a machine-learning algorithm based on neural networks to train computers to detect pat-terns associated with test structure results. The objective of the work is to develop more reliable machinelearning classification procedures using test structure data from a semiconductor manufacturing environ-ment. An example based on characterizing the per-formance of a 1 micro m lithography process is pre-sented as well as description of the test chip.

PB89-228308 PC A03/MF A01 National Inst. of Standards and Technology (NEL), Gaithersburg, MD. Center for Electronics and Electrical Engineering.

Center for Electronics and Electrical Engineering Technical Publication Announcements. Covering Center Programs, January-March 1989, with 1989 **CEEE Events Calendar.**

E. J. Walters. Jul 89, 20p NISTIR-89/4118 See also PB89-209241.

Keywords: *Semiconductor devices, *Metrology, Electrical engineering, Integrated circuits, Photodetectors, Electrical insulators, Waveforms, Lasers, Fiber optics, Electrooptics, Superconductors, Electromagnetic interference, Abstracts, *Signals and systems, Cryoe-

The report is the twentieth issue of a quarterly publication providing information on the technical work of the National Institute of Standards and Technology (for-merly the National Bureau of Standards) Center for Electronics and Electrical Engineering. The issue covers the first quarter of calendar year 1989. Ab-stracts are provided by technical area for papers published during the quarter.

900.790

PB89-228530 Not available NTIS National Inst. of Standards and Technology (NEL), Gaithersburg, MD. Semiconductor Electronics Div. Machine-Learning Classification Approach for IC Manufacturing Control Based on Test Structure Measurements.

Final rept. M. E. Zaghloul, D. Khera, L. W. Linholm, and C. P. Reeve. 1989, 7p

Pub. in IEEE (Institute of Electrical and Electronics Engineers) Transactions on Semiconductor Manufacturing 2, n2 p47-53 May 89.

Keywords: *Integrated circuits, *Manufacturing, Semiconductor devices, Learning machines, Classifying, Artificial intelligence, Reprints, *Chips(Electronics), Expert systems.

The paper describes the use of a machine-learning method for classifying electrical measurement results from a custom-designed test chip. The techniques are used for characterizing the performance of a 1 mi-crometer integrated circuit lithographic process. The focus of the work is to develop a method for producing reliable classification rules from data bases containing large samples of measurement data. The paper describes a test chip, data-handling methods, rule gen-eration techniques, and statistical data reduction and parameter extraction techniques. An analysis of error introduced by noise in the rule formation process is presented.

900,791

PB89-230460 Not available NTIS National Inst. of Standards and Technology (NEL), Gaithersburg, MD. Center for Mfg. Engineering. High-Mobility CMOS (Complementary Metal Oxide Semiconductor) Transistors Fabricated on Very Thin SOS Films.

Final rept. D. J. Dumin, S. Dabral, M. Freytag, P. J. Robertson, G. P. Carver, and D. B. Novotny. 1989, 3p Pub. in IEEE (Institute of Electrical and Electronics En-

gineers) Transactions on Electron Devices 36, n3, p596-598, Mar 89.

Keywords: *Metal oxide transistors, *Thin films, Semi-conducting films, Semiconductor devices, Carrier mo-bility, Reprints, *CMOS, *Complementary metal oxide semiconductors, Silicon films.

The increased emphasis on submicrometer geometry CMOS/SOI devices has created a need for high-mobility CMOS transistors fabricated on high-quality SOI films with thicknesses of the order of 0.1 to 0.2 micro m. To date, the only demonstrated way of producing high-mobility transistors on very thin high-quality SOS films in this thickness range has been to apply recrystallizations and regrowths to the films prior to transistor fabrication. It has been found that the mobility of CMOS transistors fabricated on very thin SOS films is a function of the film growth rate. Transistors with mobilities nearly as high as those obtained on 1.0-micro m-thick films have been fabricated on SOS films 0.2 micro m thick that have been grown at growth rates above 4 mícro m/min.

900.792

PB89-231195 Not available NTIS National Inst. of Standards and Technology (NEL), Gaithersburg, MD. Semiconductor Electronics Div. IEEE (Institute of Electrical and Electronics Engineers) IRPS (International Reliability Physics Symposium) Tutorial Thermal Resistance Measurements, 1989.

Final rept.
F. F. Oettinger. 1989, 33p
Pub. in Proceedings of International Reliability Physics
Phonix A7 April 10, 1989, p7.1-7.33.

Keywords: *Thermal resistance, *Integrated circuits, *Transistors, Thermal conductivity, Thermal stability, Temperature, Thermal measuring instruments, Junctions, Measurement.

The tutorial reviews the thermal properties of power transistors and to discuss methods for characterizing these properties. The devices discussed include bipolar transistors and metal-oxide-semi-conductor field-effect-transistors (MOSFETs). Measurement problems common to these devices, such as deciding the reason a particular measurement is required, adequate reference temperature control, selection of a temperature-sensitive electrical parameter, and separation of electrical and thermal effects during measurement are addressed. The thermal characterization of the packaged integrated circuit chip surface/junction for the new generation of VLSI devices generally takes one of three forms: indirect (i.e., electrical) measurements, direct (e.g., infrared), or computer simulations of the surface/junction temperatures. Due to the inherent difficulties in measuring and analyzing the thermal properties of active integrated circuits, an approach using specifically designed thermal test chips for evaluation of new die attachment and packaging schemes is finding wide acceptance in the industry.

900,793

PB89-231203 Not available NTIS National Inst. of Standards and Technology (NEL), Gaithersburg, MD. Semiconductor Electronics Div. AC Impedance Method for High-Resistivity Measurements of Sliicon.

Final rept. W. R. Thurber, J. R. Lowney, R. D. Larrabee, P. Talwar, and J. R. Ehrstein. 1989, 2p Sponsored by Air Force Systems Command, Washing-

Pub. in Proceedings of Electrochemical Society Meeting, Los Angeles, CA., May 7-12, 1989, p365-366.

Keywords: *Impedance, *Alternating current, *Silicon, Semiconductors(Materials), Electrical resistance, Electron probes, Frequencies.

An AC impedance method for measuring the average bulk resistivity of ingots and slices of high-resistivity sli-icon is described. Easily removable contacts, such as silver paste, are applied to the end faces of the sample and the impedance of the resulting capacitive sandwich is measured as a function of frequency. The resis-

ELECTROTECHNOLOGY

Semiconductor Devices

tivity can be calculated from the frequency of the nega-tive peak in the imaginary part of the impedance and model consistency can be checked by comparison of values of resistance obtained from real and imaginary parts at this peak. Comparisons with van der Pauw and four-probe measurements are consistent with the im-

900,794 PB89-231211 Not available NTIS National Inst. of Standards and Technology (NEL), Gaithersburg, MD. Semiconductor Electronics Div. Experimental Verification of the Relation between Two-Probe and Four-Probe Resistances. Final rept.

J. J. Kopanski, J. H. Albers, and G. P. Carver. 1989,

Pub. in Proceedings of Electrochemical Society Meeting, Los Angeles, CA., May 7-12, 1989, p367-368.

Keywords: *Electron probes, *Electrical resistance, Measurement, Wafers, Test equipment, Measurement, equipment, Semiconductors(Materials).

Recent innovations in the measurement of two-probe (spreading) resistance and four-probe resistance using an array of lithographically fabricated, geometrically well-defined contacts have enabled the measurement of the quantities with high accuracy and reproducibility. It has permitted experimental verification of the relationship between the two-probe resistances and the four-probe resistance. Verification was also made of the predicted dependence of the four-probe resistance on the ratio of wafer thickness to probe spacing for inline and square probe configurations.

900,795 PB89-231229 Not available NTIS National Inst. of Standards and Technology (NEL), Gaithersburg, MD. Semiconductor Electronics Div.
Improved Understanding for the Transient Operation of the Power Insulated Gate Bipolar Transis-Final rept.

Final rept.

A. R. Hefner. 1989, 11p

Pub. in Proceedings of IEEE (Institute of Electrical and Electronics Engineers) Power Electronics Specialists

Conference (20th) - PESC '89, Milwaukee, WI., June 26-29, 1989, p303-313.

Keywords: *Field effect transistors, *Electric current, *Waveforms, Models, Comparison, Capacitance, Electric potential, Analyzing.

It is shown that a non-quasi-static analysis must be used to describe the transient current and voltage waveforms of the Insulated Gate Bipolar Transistor (IGBT). The non-quasi-static analysis is necessary because the transport of electrons and holes are coupled for the low-gain, high-level injection conditions, and because the quasi-neutral base width changes faster than the base transit speed for typical load circuit con-ditions. To verify that both of these non-quasi-static effects must be included, the predictions of the quasistatic and non-quasi-static models are compared with measured current and voltage switching waveforms. The comparisons are performed for different load circuit conditions and for different device base lifetimes.

PB89-231237 Not available NTIS
National Inst. of Standards and Technology (NEL),
Gaithersburg, MD. Semiconductor Electronics Div.
Power MOSFET Failure Revisited.

Final rept. D. L. Blackburn. 1988, 8p
Pub. in IEEE (Institute of Electrical and Electronics Engineers) Power Electronics Specialists Conference -PESC '88, Kyoto, Japan, April 11-14, 1988, p681-688.

Keywords: *Field effect transistors, *Failure, Avalanche breakdown, Electrical faults, Nondestructive tests, Energy dissipation, *MOSFET semiconductors.

The failure of power MOSFETs during avalanche breakdown is discussed. A theory is presented that relates the failure to the temperature rise of the chip during the avalanche breakdown and to a critical curtreat for failure. It is shown that the energy that can be safely dissipated during avalanche breakdown decreases as the starting current increases or as the case temperature increases. Thus, if power MOSFETs are to be rated for their energy dissipation capability during avalanche breakdown, both the starting current and temperature must be specified as it is these two parameters that determine the failure limits and not the energy.

900,797 PB90-123589 PB90-123589 Not available NTIS
National Inst. of Standards and Technology (NEL),
Gaithersburg, MD. Semiconductor Electronics Div.
Numerical Simulations of Neutron Effects on Bipolar Transistors.

Final rept.

H. S. Bennett. 1987, 4p Sponsored by Defense Nuclear Agency, Washington,

Pub. in IEEE (Institute of Electrical and Electronics Engineers) Transactions on Nuclear Science NS-34, n6 p1372-1375 Dec 87.

Keywords: *Neutron irradiation, *Radiation effects, Carrier mobility, Concentration(Composition), Mathe-matical models, Reprints, *Bipolar transistors, Carrier lifetime, Numerical solution.

A detailed device model that has been verified by comparisons with experimental measurements on unirra-diated, state-of-the-art bipolar devices has been modified to include the effects of neutron radiation on carrier lifetimes, concentrations, and mobilities. Numerical experiments on the degradation due to neutron fluences in the dc common emitter gains for bipolar transistors with submicrometer emitter and base widths are given and compared in general terms with the few published measurements.

900,798 PB90-128109 Not available NTIS Not available NTS
National Inst. of Standards and Technology (NEL),
Gaithersburg, MD. Semiconductor Electronics Div.
Growth and Properties of High-Quality Very-Thin
SOS (Silicon-on Sapphire) Films.

D. J. Dumin, S. Dabral, M. Freytag, P. J. Robertson, G. P. Carver, and D. B. Novolny. 1989, 5p Pub. in Jnl. of Electronic Materials 18, n1 p53-57 1989.

Keywords: *Thin films, *Crystal growth, Thickness, Quality control, Reprints, *SOS(Semiconductors), CMOS.

The increased emphasis on submicron geometry CMOS/SOS devices has created a need for high qual-CMOS/SOS devices has created a need for high quality silicon-on-sapphire films with thicknesses of the order of 0.1 to 0.2 microns. To date the only viable way of producing high quality SOS films with the thicknesses has been through the application of recrystallization and regrowth techniques. The need for asgrown, high-quality, very-thin SOS films has prompted a study of film quality growth rate for films with thicknesses in the 0.1 to 0.2 micron range as a possible way of producing thin high-quality SOS films. It has been found that film quality increased as the growth rate increased. It was possible to produce films as thin as 0.1 micron with mobilities nearly as high as 1 micron as 0.1 micron with mobilities nearly as high as 1 micron films, if the film growth rate was higher than 4 micron/

900,799 PB90-128182 PB90-128182 Not available NTIS National Inst. of Standards and Technology (NEL), Gaithersburg, MD. Semiconductor Electronics Div. Silicon and GaAs Wire-Bond Cratering Problem. Final rept. Final rept.

G. G. Harman. 1989, 6p Pub. in Proceedings of VLSI and GaAs Chip Packaging Workshop, Santa Clara, CA., September 12-14, 1988, p65-70 1989.

Keywords: *Integrated circuits, *Cratering, Electric wires, Bonding, Gallium arsenides, Silicon, Microelectronics, *Very large scale integration, Fracture me-

The complex synergystic cratering effects of the VLSI era involve not only bonding parameters, but also Au-Al compound-induced stress, silicon nodules in the metallization, plastic package stress, and surface mount stress. The situation is even worse in GaAs.

900,800 PB90-128224 Not available NTIS National Inst. of Standards and Technology (NML),
Boulder, CO. Time and Frequency Div.
Very Low-Noise FET Input Amplifier.
Final rept.

S. R. Jefferts, and F. L. Walls. 1989, 3p Grant NSF-PHY86-04504

Sponsored by National Science Foundation, Washing-

ton, DC. Pub. in Review of Scientific Instruments 60, n6 p1194-1196 Jun 89.

Keywords: *Field effect transistors, *Low noise amplifiers, Semiconductor devices, Transistor amplifiers, Design, Schematic diagrams, Performance evaluation, Reprints, *Cascade amplifiers.

The design, schematics, and performance of a very low-noise FET cascode input amplifier are described. The amplifier has noise performance of less than 1.2 nV/square root(Hz) and 0.25 fA/square root(Hz) over the 500 Hz to 500 kHz frequency range. With modest changes it could be extended to a wide variety of uses requiring low-noise gain in the 1 Hz to 30 MHz frequency range.

General

900.801 PB89-149058 Not available NTIS National Bureau of Standards (NML), Gaithersburg, MD. Electricity Div.

Possible Quantum Hall Effect Resistance Stand-

Final rept.

Final rept.

M. E. Cage, R. F. Dziuba, and B. F. Field. 1982, 15p. Sponsored by Naval Research Lab., Washington, DC., and Department of Defense, Washington, DC. Pub. in Proceedings of NCSL Workshop and Symposium Metrology Management and Technology-A Scientific Approach, Gaithersburg, MD., October 4-7, 1982, 1811.15 pB1-1-B1-15.

Keywords: *Hall effect, *Standards, Semiconductor devices, Metrology, Fundamental constants, Cryogenics, *Quantum Hall effect, *Resistance standards.

The discovery of the quantum Hall effect by K. v. Klitzing, using semiconductor devices that are cryogenically cooled in large applied magnetic fields, has opened up the exciting possibility that this effect could stimu-late the discipline of electrical metrology to an extent analogous to that of the Josephson effect. The paper describes the quantum Hall effect, and explains how it is being used in experiments at NBS in an attempt to achieve a new resistance standard accurate to a few parts in 100 million, in which the resistance is defined in terms of fundamental constants of nature.

PB89-149066 Not available NTIS National Bureau of Standards (NML), Gaithersburg, MD. Electricity Div.

NBS (National Bureau of Standards) Ohm: Past-Present-Future.

Final rept.

R. F. Dziuba. 1987, 13p Pub. in Proceedings of Measurement Science Conference, Irvine, CA., January 29-30, 1987, pVI-A(15)-VI-A(27).

Keywords: *Electrical measurement, Electrical resistance, Units of measurement, Hall effect, Measuring instruments, *Absolute Ohm, *Resistance standards.

A brief history is given of the NBS Ohm commencing from the establishment of the NBS in 1901 to the present. It includes a description of the resistance standards and measurement methods used to maintain the NBS Ohm during its 85-year history. Indications of the drift of the NBS Ohm based on absolute-Ohm determinations and quantized-Hall effect measurements are presented. The results of these measurements may lead to an adjustment of the value of the NBS Ohm in 1990.

900,803 PB89-149074 Not available NTIS National Bureau of Standards (NEL), Gaithersburg, MD. Electrosystems Div.

Thermal-Expansive Growth of Prebreakdown

Streamers in Liquids. Final rept.

C. Fenimore, 1988, 4p Sponsored by Office of Naval Research, Arlington, VA. Pub. in Proceedings of Conference Record IEEE (Institute of Electrical and Electronics Engineers) International Symposium on Electrical Insulation, Boston, MA., June 5-8, 1988, p27-30.

Keywords: *Dielectric breakdown, *Electric discharges, *Liquids, Electrical insulation, Mathematical models, Bubbles, Pressure effects.

The growth of electrically conductive, low-density regions has been observed in dielectric breakdown in a variety of liquids. This phenomenon motivates the development of the present theory for coupling thermal effects with fluid mechanical effects in the dynamics of elongated, impulsively-driven bubbles. The model explicitly describes the time-dependent dimensions of a growing ellipsoidal bubble. In previous work, a model for such effects associated with the growth of a bubble about an arc in a liquid was developed. In the case of about all all it a liquid was developed. If the case we the prebreakdown streamer, the geometry is not as simple as for an arc, and the evolution of the bubble is found in ellipsoidal coordinates. The effect of pressure is to shorten the time scale of the bubble dynamics.

900,804 PB89-170872 PB89-170872 PC A04/MF A01 National Inst. of Standards and Technology (NEL), Gaithersburg, MD. Center for Electronics and Electri-

Gal Engineering.
High-Current Measurement Techniques. Part II.
100-kA Source Characteristics and Preliminary Shunt and Rogowski Coll Evaluations.

J. D. Ramboz. Mar 89, 52p NISTIR-89/4040 See also PB85-100444. Sponsored by Sandia National Labs., Albuquerque, NM.

Keywords: *Electrical measurement, Electric current, Calibrating, Bypasses, Circuits, Alternating currents, Electric coils, Rogowski coils.

The characterization of a 100-kA current source is discussed. The source is intended for use in the calibration of high-current sensors such as shunts and Rogowski coils commonly employed in resistance welders. The output current from the source is derived from SCR-gated signals in the form of bursts of 'chopped' 60-Hz sinsusoidal waveforms. These waveforms and their spectral content were investigated. The near-field magnetic field strength was mapped. Initial calibrations were performed on a 30-kA, 10 microohms shunt. Preliminary results indicate a temperature coefficient of about 130 ppm/deg which is thought to be related to a thermally induced strain. Several Rogowski coil type current sensors were evaluated and calibrated. Each of the coils measured had outputs which were sensitive to the rotational position about the current carrying conductor. The calibration philosophy and approach is discussed and estimates of measurement uncertainty are given. Suggested improvements for the measure-ment process are offered. Planned efforts are outlined.

PB89-171656 Not available NTIS National Bureau of Standards (NEL), Gaithersburg, MD. Electrosystems Div.

Power Quality Site Surveys: Facts, Fiction, and Fallacies.

Final rept. F. D. Martzloff, and T. M. Gruzs. 1988, 14p See also PB87-201679.

Pub. in IEEE (Institute of Electrical and Electronics Engineers) Transactions on Industry Applications 24, n6 p1005-1018 Nov/Dec 88.

Keywords: *Site surveys, *Power supplies, Quality assurance, Reliability, Reprints, *Electronic equipment, Power losses.

The quality of the power supplied to sensitive electronic equipment is an important issue. Monitoring disturbances of the power supply has been the objective of various site surveys, but results often appear to be instrument-dependent or site-dependent, making com-parisons difficult. After a review of the origins and types of disturbances, the types of monitoring instru-ments are described. A summary of nine published surveys reported in the last 20 years is presented, and a close examination of underlying assumptions allows meaningful comparisons which can reconcile some of the differences. Finally, the paper makes an appeal for improved definitions and applications in the use of monitoring instruments.

900,806 PB89-173447 Not available NTIS National Bureau of Standards (NEL), Gaithersburg, MD. Electrosystems Div.
Estimates of Confidence Intervals for Divider Dis-

torted Waveforms.

Final rept.
R. H. McKnight, and J. Lagnese. 1988, 4p
Pub. in Proceedings of International Symposium on High Voltage Engineering (5th), Braunschweig, Federal Republic of Germany, August 24-28, 1987, v3 p1-4

Keywords: *Confidence limits, *High voltage, *Frequencies, Statistical analysis, Pulsation, Measurement, Stochastic processes, Errors.

The paper describes a method for computing confidence intervals for a high voltage impulse distorted by a divider system. The technique is based on a recent algorithm designed to calculate confidence intervals for solutions to ill-posed problems subject to inequality constraints. Applications of the method to measurements made with a resistive divider illustrate its value for obtaining useful stochastic error bounds for high voltage impulse restoration.

900,807

PB89-176192 Not available NTIS National Inst. of Standards and Technology (NEL), Boulder, CO. Electromagnetic Fields Div.

NIST (National Institute of Standards and Technology) Automated Coaxial Microwave Power Standard.

Final rent.

F. R. Clague. 1989, 14p

Pub. in Proceedings of Measurement Science Conference, Anaheim, CA., January 26-27, 1989, p1C-1-1C-

Keywords: *Microwaves, *Frequency standards, *Calorimeters, *Bolometers, Measuring instruments, Performance standards, Automatic control, Electrical measurement, Adaptive systems, Electronic control.

The national microwave power standards consist of two parts: a microcalorimeter and a bolometer mount used as the transfer standard. In the past, operation of the microcalonmeter has been slow and complicated, and required skilled personnel. The paper details the automation of the 0.1 to 18 GHz coaxial microcalorimeter and the design of a new coaxial transfer standard. Together, these have reduced measurement time by a factor of 10. A highly skilled operator is no longer required and largely unattended operation 24 hours a day is possible. The basic theory of operation of both devices, design considerations, some error evaluation problems, and performance results are included.

900.808

PB89-184097

(Order as PB89-184089, PC A04) National Inst. of Standards and Technology, Gaithersburg, MD.

New Internationally Adopted Reference Standards of Voltage and Resistance.

Bi-monthly rept.

B. N. Taylor, 1989, 9p

Included in Jnl. of Research of the National Institute of Standards and Technology, v94 n2 p95-103 Mar-Apr

Keywords: *Electrical measurement, *Standards, Voltage measurement, Electrical resistance, Voltmeters, Ohmmeters, Hall effect, Units of measurement, Calibrating, Consultative Committee on Electricity(CCE), International Committee of Weights and Measures(CIPM), International System of Units(SI).

The report provides the background for and summarizes the main results of the 18th meeting of the Consultative Committee on Electricity (CCE) of the International Committee of Weights and Measures (CIPM) held in September 1988. The principal recommendations originating from the meeting, which were subsequently adopted by the CIPM, establish new interna-tional reference standards of voltage and resistance based on the Josephson effect and the quantum Hall effect, respectively. The new standards, which are to come into effect starting January 1, 1990, will result in improved uniformity of electrical measurements worldwide and their consistency with the International System of Units or SI. The CCE also recommended a particular method, affirmed by the CIPM, of reporting calibration results obtained with the new reference standards that is to be used by all national standards laboratories.

900.809

PB89-186423 Not available NTIS National Bureau of Standards (NEL), Gaithersburg, MD. Electrosystems Div.

International Comparison of HV Impulse Measuring Systems. Final rept.

T. R. McComb, R. C. Hughes, H. A. Lightfoot, K. Schon, R. Schulte, R. McKnight, and Y. X. Zhang.

Pub. in IEEE (Institute of Electrical and Electronics Engineers) Transactions on Power Delivery 4, n2 p906-915 Apr 89.

Keywords: *High voltage, Comparison, Measurement, Standards, Reprints, *Impulses.

Present standards for qualifying high voltage (HV) impulse measuring systems by unit-step-response parameters are complex and difficult to apply and some systems which have response parameters within the limits of the standards have unacceptable errors. The paper takes the first step in providing a simplified method based on simultaneous measurements of an HV impulse by a reference system and the system under test. Comparative measurements have been made in four National Laboratories and the relative differences are reported. The results are discussed and the further work which is required is outlined.

900.810

PB89-189211 PC A06/MF A01 National Inst. of Standards and Technology (NEL),

Boulder, CO. Electromagnetic Fields Div.

Bibliography of the NIST (National Institute of Standards and Technology) Electromagnetic Fields Division Publications.

A. M. Reidy, and K. A. Gibson. Sep 88, 112p NISTIR-88/3900

Supersedes PB86-191947. See also PB89-147847.

Keywords: *Bibliographies, *Electromagnetic fields, Antennas, Dielectrics, Electromagnetic interference, Electrical measurement, Microwaves, Metrology, Electromagnetic noise, Remote sensing, Wave Time domain.

The bibliography lists the publications by the staff of the Electromagnetic Fields Division of the National Institute of Standards and Technology for the period January 1970 through August 1988. Selected earlier publications from the Division's predecessor organizations are included.

900.811

PB89-189245 PC A05/MF A01 National Inst. of Standards and Technology (NEL), Gaithersburg, MD. Center for Electronics and Electri-

cal Engineering.
Emerging Technologies in Electronics and Their Measurement Needs.

Mar 89, 79p NISTIR-89/4057

Keywords: *Electric security, *Electrical measurement, *Metrology, Semiconductor devices, Microwaves, Magnetic measurement, Superconductors, Fiber optics, Optical communication, Television systems, Bioelectricity, *Emerging technologies, Smart systems, Light waves.

The report identifies emerging technologies in electronics that the Center for Electronics and Electrical Engineering (CEEE) believes will require increased measurement support from CEEE in coming years. The emerging technologies described here are new to the marketplace or are experiencing major technological advances. The occument is designed to stimulate feedback that CEEE needs to refine its plans for developing measurement capability to support emerging electronic technologies that are important to the national interest.

900.812

PB89-189302 PC A03/MF A01 National Inst. of Standards and Technology (NEL), Gaithersburg, MD. Center for Electronics and Electrical Engineering.
Center for Electronics and Electrical Engineering

Technical Publication Announcements: Covering Center Programs, July/September 1988, with 1989

CEEE Events Calendar. E. J. Walters. Mar 89, 24p NISTIR-89/4067 See also PB89-136311.

Keywords: *Electrical engineering, *Bibliographies, Semiconductors(Materials), Metrology, Integrated circuits, Signal processing, Transmission, Waveforms, Antennas, Microwaves, Fiber optics, Superconductors, Electric power, Electromagnetic interference,

ELECTROTECHNOLOGY

General

Electronics, Dimensional measurement, Cryoelectron-

The eighteenth issue of a quarterly publication providing information on the technical work of the National Institute of Standards and Technology (formerly the National Bureau of Standards) Center for Electronics and Electrical Engineering. The issue of the Center for Electronics and Electrical Engineering Technical Publi-cation Announcements covers the third quarter of calendar year 1988.

900,813 PB89-193270 PC A03/MF A01 National Inst. of Standards and Technology (NEL), Gaithersburg, MD. Center for Electronics and Electri-

cal Engineering.
Center for Electronics and Electrical Engineering Technical Progress Bulletin Covering Center Programs, October to December 1988, with 1989 CEEE Events Calendar. E. J. Walters. May 89, 44p NISTIR-89/4076 See also PB89-168033.

Keywords: *Electrical engineering, *Semiconductor devices, *Signal processing, *Systems, Metrology, Silicon, Photodetectors, Interfaces, Lasers, Microwaves, Millimeter waves, Fiber optics, Electrooptics, Super-conductors, Electromagnetic interference, Signal acquisition, Cryoelectronics.

The report is the twenty-fifth issue of a quarterly publication providing information on the technical work of the National Institute of Standards and Technology (formerly The National Bureau of Standards) Cente for Electronics and Electrical Engineering. The issue of the CEEE Technical Progress Bulletin covers the fourth quarter of calendar year 1988. Abstracts are provided by technical area for both published papers and papers approved by NIST for publication.

900,814 PB89-193916 PC A07/MF A01 National Inst. of Standards and Technology (NEL), Boulder, CO. Electromagnetic Fields Div. Performance Evaluation of Radiofrequency, Microwave, and Millimeter Wave Power Meters.

Technical note. E. M. Livingston, and R. T. Adair. Dec 88, 149p NIST/TN-1310

Also available from Supt. of Docs. as SN003-003-02931-9.

Keywords: *Power measurement, *Electrical measurement, *Power meters, Thermistors, Wattmeters, Measuring instruments, Radio waves, Performance evaluation, Microwaves, Millimeter waves, Electromagnetic radiation, Calibrating, Temperature.

Measurement techniques are described for the evaluation of the electrical performance of commercially available radiofrequency (rf), microwave (mw), and millimeter wave (mmw) power meters which use bolometric power sensors and typically operate from 10 MHz to 26.5 GHz for an average power range of 10 microW to 10 mW with appropriate attenuation for higher power ranges. Techniques are described for analysis of: ranges of frequency and power, operating tempera-ture, stability, response time, calibration factor, ex-tended power measurement, overload protection, and characteristics of the internal power reference source. Some automated methods are discussed. Block diagrams of test setups are presented. Sources of uncertainty in the bolometric method are analyzed.

Not available NTIS PB89-201552 National Bureau of Standards (NEL), Gaithersburg,

MD. Electrosystems Div.

Accurate RF Voltage Measurements Using a Sampling Voltage Tracker.
Final rept.

T. M. Souders, and P. S. Hetrick. 1989, 6p See also PB88-239579.

Pub. in IEEE (Institute of Electrical and Electronics Engineers) Transactions on Instrumentation and Measurement 38, n2 p451-456 Apr 89.

Keywords: *Electrical measurement, *Electric potential, Electrical properties, Voltmeters, Calibrating, Radio frequencies, Step response, Ramp response, Reprints.

The RF voltage measurement capability of an equivalent-time sampling system has been investigated over the frequency range of 1-100 MHz. The system is easily calibrated from step response measurements, independent of thermal transfer standards. Comparison measurements made with NBS-calibrated thermal converters show agreement generally within the stated uncertainties presently provided by NBS for such calibrations. The system offers several advantages over conventional thermal transfer techniques; ac/dc transfers are not required, loading and transmission line problems are reduced, and direct measurement of vol-tages from 2 V to as low as 10 mV are possible. In addition, other waveform characteristics are readily obtained, e.g., average and peak values, harmonic distortion, etc.

900,816

Not available NTIS PB89-201560 National Bureau of Standards (NML), Gaithersburg, MD. Electricity Div.

AC-DC Difference Calibrations at NBS (National Bureau of Standards).

Final rept. J. R. Kinard. 1986, 6p

Pub. in Proceedings of Measurement Science Conference, Irvine, CA., January 23-24, 1986, p3-8.

Keywords: *Calibrating, *AC to DC converters, Electric potential, Electric current, Electric converters, Rectifiers, Standards, National Institute of Standards and Technology.

The NBS calibration service for thermal voltage and current converters relies on a group of primary multi-junction thermal converters and sets of reference and working standards for extending their ranges and frequencies. The converter sets which constitute the NBS standards--primary, reference and working--as well as the build-up and bootstrap techniques used in their characterization over the full ranges of voltage, current, and frequency are described briefly. Routine NBS uncertainties for ac-dc difference calibrations are given as well as a summary of current activities and plans.

900.817

PB89-214761 PC A05/MF A01 National Inst. of Standards and Technology (NML), Gaithersburg, MD. Electricity Div. Guidelines for Implementing the New Representa-tions of the Volt and Ohm Effective January 1,

1990.

Technical note (Final).

N. B. Belecki, R. F. Dziuba, B. F. Field, and B. N. Taylor. Jun 89, 76p NIST/TN-1263

Also available from Supt. of Docs as SN003-003-02941-6.

Keywords: *Electrical measurement, *Electrical resistance, *Electric potential, Standards, Voltage measuring instruments, Impedance, Electrical measuring instruments, *Calibration standards.

The document provides general guidelines and de-tailed instructions on how to bring laboratory reference standards of voltage and resistance and related instrumentation into conformity with newly established and internationally adopted representations of the volt and ohm. Based on the Josephson and quantum Hall effects, respectively, the new representations are to come into effect worldwide starting on January 1, 1990. Their implementation in the U.S. will result in in-1990. Their implementation in the U.S. will result in increases in the values of the national volt and ohm representations maintained at the National Institute of Standards and Technology (NIST, formerly the National Bureau of Standards or NBS) of 9.264 parts per million (ppm) and 1.69 ppm, respectively. The resulting increase in the value of the U.S. representation of the ampere will be 7.57 ppm and in the U.S. electrical representation of the watt, 16.84 ppm. Also discussed are the effects on electrical standards of the January 1, 1990, replacement of the International Practical Temperature Scale of 1968 by the International Temperature Scale of 1990, and of the January 1, 1990, approximate 0.14 ppm decrease in the U.S. representation of the farad. the farad.

900,818

PB89-222616 PC A14/MF A01 National Inst. of Standards and Technology (NML), Gaithersburg, MD. Center for Basic Standards. NIST (National Institute of Standards and Technology) Measurement Services: AC-DC Difference Calibrations.

Calibrations.
Final rept.
J. R. Kinard, J. R. Hastings, T. E. Lipe, and C. B.
Childers. May 89, 311p NIST/SP-250/27
Also available from Supt. of Docs. as SN003-00302950-5. See also PB89-201560. Library of Congress catalog card no. 89-600736.

Keywords: *Electrical measurement, *Test facilities, Electric current, Direct current, Alternating current, Electric potential, Mathematical models, *Calibration standards.

The publication collects and summarizes the specialized information needed to operate the ac-dc difference laboratory and calibration service at the National ence laboratory and calibration service at the National Institute of Standards and Technology (NIST) in Gaithersburg. It also serves as a convenient reference source for the users of this calibration service and other interested people by documenting the service and its underlying background in considerable detail. It contains the following: an annotated table of contents, a topical index, and a glossary of common ac-dc acronyms; an overview of the service; selected published papers; instructions for the operation of the comparator systems; a schedule for the recalibration and periodic checks of the NIST thermal converters; and a sample report of calibration.

PB89-230387 Not available NTIS National Bureau of Standards (NML), Gaithersburg, MD. Electricity Div.

Determination of the Time-Dependence of ohm NBS (National Bureau of Standards) Using the Quantized Hall Resistance.

Final rept. M. E. Cage, R. F. Dziuba, C. T. Van Degrift, and D.

Yu. 1989, 7p
Pub. in IEEE (Institute of Electrical and Electronics Engineers) Transactions on Instrumentation and Measurement 38, n2, p263-269, Apr 89.

Keywords: *Electrical resistance, *Standards, Electrical measurement, Precision, Reprints, *Resistance standards, *Quantum Hall effect, *Ohm, Temperature

The Quantum Hall effect is being used to monitor the U.S. legal representation of the ohm, or as-maintained ohm, ohm(NBS). Measurements have been made on a regular basis since August 1983. Individual transfers between the quantized Hall resistance, R(H) and the five 1-ohm resistors which comprise ohm(NBS) can five 1-ohm resistors which comprise ohm(NBS) can now be made with a total one standard deviation (1 sigma) uncertainty of + or - 0.014 ppm. This uncertainty is the root-sum-square of 32 individual components. The time-dependent expression for T(H) in terms of ohm(NBS) is: R(H) = 25 812.8 (1 + (1.842 + or -0.012) x 10 to the -6th power + (0.0529 + or -0.0040) (t - 0.7785) x 10 to the -6th power/year) ohm(NBS), where t is measured in years from January 1, 1987. The value of ohm(NBS) is, therefore, decreasing at the rate of (0.0529 + or -0.0040) ppm/year.

900,820 PB89-230403 PB89-230403 Not available NTIS National Bureau of Standards (NML), Gaithersburg,

MD. Electricity Div.

Josephson Array Voltage Calibration System:
Operational Use and Verification. Final rept.

R. L. Steiner, and B. F. Field. 1989, 6p Pub. in IEEE (Institute of Electrical and Electronics En-gineers) Transactions on Instrumentation and Measurement 38, n2, p296-301, Apr 89.

Keywords: *Electric potential, *Standards, Josephson junctions, Arrays, Reprints, *Voltage standards, *Calibration bration.

A new Josephson array system now maintains the U.S. A new Josephson array system now maintains the U.S. Legal Volt. This system is almost fully automated, operates with a typical precision of 0.009 microV, and readily allows U.S. Legal Volt measurements weekly, or more frequently if desired. The system was compared to the previous volt maintenance system, and agreement was made to within 0.03 ppm. This verification is limited by uncertainties in the resistive divider instruments of the previous system. instruments of the previous system.

900.821 PB89-230429

Not available NTIS

National Bureau of Standards (NML), Gaithersburg,

MD. Electricity Div.

Measurement of the NBS (National Bureau of Standards) Electrical Wattin SI Units.

Final rept. P. T. Olsen, R. E. Elmquist, W. D. Phillips, E. R. Williams, G. R. Jones, and V. E. Bower. 1989, 7p Pub. in IEEE (Institute of Electrical and Electronics Engineers) Transactions on Instrumentation and Measurement 38, n2, p238-244, Apr 89.

Keywords: *Electric power, *Standards, Reprints, *Watt, Ampere, Josephson effect.

The authors have measured the NBS electric watt in SI units to be: $W(NBS)/W = K(w) = 1 \cdot (16.69 + or - 1.33)$ ppm. The uncertainty of 1.33 ppm has the significance of a standard deviation and includes their best estimate of random and known or suspected systematic uncertainties. The mean time of the measurement is May 15, 1988. Combined with the recent measurement of the NBS ohm in SI units: ohm(NBS)/ohm = K(ohm) = 1 - (1.593 + or - 0.022) ppm, this leads to a Josephson frequency/voltage quotient of E(J) =((0)(1 + (7.94 + or - 0.67) ppm)) where E(0) = 483594 GHz/V.

PB89-231039 Not available NTIS National Inst. of Standards and Technology (NEL), Gaithersburg, MD. Electrosystems Div. Production and Stability of S2F10 in SF6 Corona Discharges.

Final rept.

I. Sauers, M. C. Siddagangappa, G. Harman, R. J. Van Brunt, and J. T. Herron. 1989, 4p
Sponsored by Department of Energy, Washington, DC. Office of Energy Storage and Distribution.
Pub. in Proceedings of International Symposium on High Voltage Engineering (6th), New Orleans, LA., August 28-September 1, 1989, p1-4.

Keywords: *Sulfur hexafluoride, Decomposition reactions, Gas chromatography, Mass spectroscopy, Water vapor, Production, Stability, *Corona dis-

The authors report the yield of S2F10 produced in corona discharges in SF6 and the dependence of the S2F10 yield on various parameters. The data were obtained from two experimental systems, both employing point-to-plane geometry, a small corona cell (200-ml in volume) with a gas chromatograph-thermal conductivity analyzer (GC-TCD) at ORNL and a large (3.7-1) corona cell with a gas chromatograph-mass spectrom-eter (GC-MS) analyzer at NIST (formerly NBS). The GC-MS technique was found to be quite sensitive to S2F10 when the mass analyzer was tuned to mass 86 (SOF2(1+)).

PB89-231153
Not available NTIS
National Bureau of Standards (NEL), Boulder, CO.
Electromagnetic Technology Div.
Faraday Effect Sensors: The State of the Art.

Final rept.
G. W. Day, and A. H. Rose. 1988, 13p
Sponsored by Department of Energy, Washington,
DC., Electric Power Research Inst., Palo Alto, CA.,
Empire State Electric Energy Research Corp., New
York, and Department of Defense, Washington, DC.
Pub. in Proceedings of SPIE (Society of Photo-Optical
Instrumentation Engineers), Fiber Optic and Laser
Sensors VI, v985, p138-150 1988.

Keywords: *Faraday effect, Electric current, Magnetic fields, Electrical measurement, Magnetic measurement, Optical measurement, Sensitivity, Stability, Detectors, Reviews, Reprints, State of the art, Sensors.

The Faraday effect is becoming widely used as an optical method of measuring electric current or magnetic cal method of measuring electric current or magnetic field. It is particularly advantageous where the measurements must be made at high voltage or in the presence of electromagnetic interference, and where speed or stability are considerations. The paper reviews the development of the technology over the last twenty years, with an emphasis on the basic principles, design considerations, and performance capabilities of senerar that represent the last technology. sensors that represent the latest achievements. Faraday effect current sensors are now used routinely in the measurement of large current pulses and are start-ing to become available for ac current measurements in the power industry. Recent developments include their extension to the measurement of currents in the milliampere range and substantial reductions in size.

Similar devices, in slightly different configurations, can be used for magnetic field measurements. Further improvements, based on new fiber types and new materials, are projected.

PB90-116195 PC A03/MF A01
National Bureau of Standards (NEL), Gaithersburg,
MD. Center for Electronics and Electrical Engineering.
Center for Electronics and Electrical Engineering
Center for Electronics and Electrical Engineering
Center Programs, October to December 1986, with
1987 CEEE Events Calendar.
E. J. Walters. Aug 87, 17p NBSIR-87/3620
See also PB87-226890.

Kenwoods * Elizabeta Standard Responses St 900,824 PB90-116195

Keywords: *Electronics, *Electrical engineering, Abstracts, Metrology, Signal processing, Electromagnetic interference, Semiconductor devices, Catalogs(Publications), *Center for Electronics and Electrical Engineering.

The report is a quarterly publication providing information on the technical work of the National Bureau of Standards Center for Electronics and Electrical Engineering. The issue of the CEEE Technical Publication Announcements covers the fourth quarter of calendar year 1986. The issue contains citations and abstracts for Center papers published in the quarter. Entries are arranged by technical topic as identified in the table of contents and alphabetically by first author within each topic. Following each abstract is the name and telephone number of the individual to contact for more information on the topic (usually the first author).

PB90-117680 Not available NTIS National Inst. of Standards and Technology (NEL), Boulder, CO. Electromagnetic Fields Div. Callbrating Network Analyzers with Imperfect Test PB90-117680 Ports.

Final rept. J. R. Juroshek, C. A. Hoer, and R. F. Kaiser. 1989,

4p
Pub. in IEEE (Institute of Electrical and Electronics Engineers) Transactions on Instrumentation and Measurement 38, n4 p898-901 Aug 89.

Keywords: *Calibrating, *Network analyzers, Transmission lines, Test equipment, Frequency analyzers, Electric analyzers, Measuring instruments, Test sets, Reprints, *Test ports.

The test ports on automatic network analyzers are generally built with an impedance that matches the impedance of the calibration standards. The paper gives experimental evidence that substantial impedance discontinuities can be tolerated at the test port interface if proper calibration procedures are observed. The 50-Omega test port on one of the six-ports in a dual six-port network analyzer was replaced with a 75-Omega test port. The test port was then calibrated to look like a 50-Omega test port. Measurements on various devices showed that indeed it was possible to make a 75-Omega test port indistinguishable from a 50-Omega test port.

900,826 PB90-117953 Not available NTIS National Inst. of Standards and Technology (NEL), Boulder, CO. Electromagnetic Fields Div.

Hybrid Representation of the Green's Function in an Overmoded Rectangular Cavity. Final rept.

D. I. Wu, and D. C. Chang. 1988, 9p Pub. in IEEE (Institute of Electrical and Electronics En-gineers) Transactions on Microwave Theory and Techniques 36, n9 p1334-1342 Sep 88.

Keywords: *Electromagnetic waves, *Greens function, Cavities, Computation, Reprints, Point sources, Rectangular configuration, Numerical solution, Modes.

A hybrid ray-mode representation of the Green's function in a rectangular cavity is developed using the finite Poisson summation formula. In order to obtain a numerically efficient scheme for computing the field generated by a point source in a large rectangular cavity, the conventional modal representation of the Green's function is modified in such a way that all the modes near resonance are retained while the truncated remainder of the mode series is expressed in terms of a weighted contribution of rays. For an electrically large cavity, the contribution of rays from distant images becomes small; therefore the ray sum can be approximated by one or two dominant terms without a loss of

numerical accuracy. To illustrate the accuracy and the computational simplification of this ray-mode representation, numerical examples are included with the conventional mode series (summed at the expense of long computation time) serving as a reference.

900.827 PB90-128190 Not available NTIS National Inst. of Standards and Technology (NEL), Boulder, CO. Electromagnetic Fields Div. Electromagnetic Detection of Long Conductors In

Tunnels.

D. A. Hill. 1988, 20p Pub. in Proceedings of Technical Symposium on Tunnel Detection (3rd), Golden, CO., January 12-15, 1988, p518-537.

Keywords: *Tunnel detection, *Electromagnetic induction, Magnetic dipoles, Magnetic fields, Transmission lines, Electric dipoles.

Formulations for the excitation of currents on an infinitely long conductor by electric or magnetic dipoles of arbitrary orientation are presented. The conductor can be either insulated or bare to model ungrounded or grounded conductors. Specific calculations are presented for a vertical magnetic dipole source because this source produces the appropriate horizontal polarization and could be used in a borehole-to-borehole configuration. Numerical results for the induced current and secondary magnetic field indicate that long conductors produce a strong anomaly over a broad frequency range. The secondary magnetic field decays slowly in the direction of the conductor and eventually becomes larger than the dipole source field.

900,828 Not available NTIS National Inst. of Standards and Technology (NEL), Gaithersburg, MD. Electrosystems Div.

Effect of Pressure on the Development of Prebreakdown Streamers.

Final rept

Final rept. . J. McKenny, E. O. Forster, E. F. Kelley, and R. E.

Hebner, 1988, 6p Pub. in Annual Report of Conference on Electrical Insulation and Dielectric Phenomena, Ottawa, Canada, October 16-20, 1988, p263-268.

Keywords: Liquids, *Breakdown(Electronic threshold), *Prebreakdown, Pressure effects.

The initiation of streamers in a liquid under the application of negative impulse voltages applied to a needle-sphere gap is investigated. A square pulse is applied so that the prebreakdown streamer will not grow to breakdown. With the application of pressure the initial streamer is observed to collapse and disappear while the voltage remains on the tip. When the voltage is chopped, a new streamer appears which resembles the structure of the anode streamers. The branches of the new streamer do not strictly follow the previous branches of the cathode streamer which injected the charge in the liquid. Using a simple model, approximately 11 nC is estimated to be injected into the liquid producing a charge density of 49 microC/cc.

900 829 PB90-128745 Not available NTIS National Inst. of Standards and Technology (NEL), Gaithersburg, MD. Electrosystems Div.

Method for Measuring the Stochastic Properties of
Corona and Partial-Discharge Pulses.

Final rept.

R. J. Van Brunt, and S. V. Kulkarni. 1989, 12p Sponsored by Department of Energy, Washington, DC. Div. of Electric Energy Systems.

Pub. in Review of Scientific Instruments 60, n9 p3012-3023 Sep 89.

Keywords: *Electric corona, *Gas discharges, Electrical measurement, Stochastic processes, Nitrogen, Oxygen, Mixtures, Pulse height analyzers, Markov processes, Reprints.

A new method is described for measuring the stochastic behavior of corona and partial-discharge pulses which uses a pulse selection and sorting circuit in conjunction with a computer-controlled multichannel analysis of the stock of the sto lyzer to directly measure various conditional and un-conditional pulse-height and pulse-time-separation distributions. From these measured distributions it is possible to determine the degree of correlation be-tween successive discharge pulses. Examples are

ELECTROTECHNOLOGY

General

given of results obtained from measurements on negative, point-to-plane (Trichel-type) corona pulses in a N2/O2 gas mixture which clearly demonstrate that the phenomenon is inherently stochastic in the sense that development of a discharge pulse is significantly af-fected by the amplitude of and time separation from the preceding pulse. It is found, for example, that corona discharge pulse amplitude and time separation from an earlier pulse are not independent random vari-ables. Discussions are given about the limitations of the method, sources of error, and data analysis procedures required to determine self-consistency of the various measured distributions.

900,830 PB90-128794 Not available NTIS National Inst. of Standards and Technology (NEL), Gaithersburg, MD. Electrosystems Div.

Method for Fitting and Smoothing Digital Data.

Y. X. Zhang, R. H. McKnight, and C. Fenimore. 1989,

Pub. in Proceedings of International Symposium on High Voltage Engineering (6th), New Orleans, LA., August 28-September 1, 1989, p1-4.

Keywords: *Lightning, *Digital systems, *Data smoothing, *Splines, Cubic equations, Data processing, Data reduction, Numerical analysis, Electric discharges, Static electricity, Step response.

Measurements of the full-lightning or chopped-lightning waveforms or of the step response are confounded by noise, radiated electro-magnetic interference, and high frequency oscillations. Before the advent of digitizers, these effects were minimized by filtering in hardware and fitting photographic data by hand. Unfortunately, unacceptably large errors may be introduced by the process. A method has been developed and evaluated to fit and smooth digital data using cubic splines. These are piecewise cubic polynomials. Their advantage is that the spline and its first two derivatives are continuous, including at the knots (where two polynomials are joined). It is important because the first derivative is used in calculating the unit-step response-time. The location of the knots may be freely chosen. In the case of oscillatory data the choice is critical. A selection criterion is given and evaluated.

900,831 PB90-130899 PB90-130899 PC A03/MF A01 National Inst. of Standards and Technology (NEL), Gaithersburg, MD.

Report on interactions between the National Institute of Standards and Technology and the Institute of Electrical and Electronic Engineers. G. K. Ehrlich. Feb 89, 43p NISTIR-89/4037

Keywords: Technology transfer, Standards, Computers, Electrical engineering, Reliability, Ultrasonic frequencies, *National Institute of Standards and Technology, *Institute of Electrical and Electronic Enginology, *Institut neers, Robotics.

The report highlights examples of interactions between the National Institute of Standards and Technology (NIST) and the Institute of Electrical and Electronic Engineers (IEEE) since October 1, 1987. It is meant to be representative, not all-inclusive. The interactions are organized by discipline in the following categories: IEEE honors and awards, editors, committee memberships and contribution to standards, conferences and workshops, publications, and other interactions. The report illustrates many activities which are designed to disseminate NIST's most recent technical advances and to learn of the technical challenges facing engineers in industry.

900,832 PB90-130907 PC A03/MF A01 National Inst. of Standards and Technology (NEL), Boulder, CO. Electromagnetic Fields Div. Radiometer Equation and Analysis of Systematic Errors for the NIST (National Institute of Standards and Technology) Automated Radiometers.

Technical note.

W. C. Daywitt. Mar 89, 27p NIST/TN-1327

Also available from Supt. of Docs. as SN003-003-

Keywords: *Radiometers, *Microwaves, *Millimeter waves, Noise analyzers, Radiation measuring instru-ments, Waveguides, Coaxial cables, Calibrating, Temperature measurement. Error analysis.

Equations used in the NIST coaxial and waveguide automated radiometers to estimate the noise temperature and associated errors of a single-port noise source are derived in the report. The equations form the foundation upon which the microwave and millimeter wave noise calibration and special test services are performed. Results from the 1-12 GHz coaxial radiometer are presented.

ENERGY

Batteries & Components

900,833 PB89-173421 Not available NTIS Mational Bureau of Standards (NEL), Gaithersburg, MD. Electrosystems Div. Measurement of Partial Discharges in Hexane Under DC Voitage. Final rept.

F. Kelley, M. Nehmadi, R. E. Hebber, M. O. Pace, L. Wintenberg, T. V. Blalock, and J. V. Foust. 1988, 9p

Sponsored by Department of Energy, Washington, DC. Pub. in Proceedings of Annual Report Conference on Electrical Insulation and Dielectric Phenomena, Ottawa, Canada, October 16-20, 1988, p394-402

Keywords: *Electrical phenomena, *Measurement, *Electrodes, *High speed photography, Hexanes, Timing devices, Direct current, Liquids, Dielectric properties, Electronic photography.

The very first stages of the low density region (LDR) at an electrode in hexane are recorded by high-magnification, high-speed photography and low-noise electronics to determine the relationship between the in-ception and growth of the LDR and the current. Obser-vations of the initiation phase of the LDR are made by an image-preserving optical delay which permits photography of unpredictable events after their occur-rence. The current is monitored by a special low-noise preamplifier which also provides timing signals to the photographic system. Here with DC, the current pro-ducing the LDR is in the form of a growing pulse train which is in contrast to the linear growth observed in the

Electric Power Transmission

PB89-173462 Not available NTIS National Bureau of Standards (NEL), Gaithersburg, MD. Electrosystems Div. Characterizing Electrical Parameters Near AC and DC Power Lines.

Final rept.

Final rept.

M. Misakian. 1988, 12p
Sponsored by Department of Energy, Washington, DC.
Pub. in Proceedings of United States-Japan Seminar
on Electromagnetic Interference in Highly Advanced
Social Systems, Honolulu, HI., August 1-4, 1988, p6-

Keywords: *High voltage, *Power transmission lines, *Electric fields, *Magnetic fields, Measuring instruments, lon currents, lon density(Concentration), Charge density.

In the mid-1970s there were no standards which provided guidance for the measurement of fields near power lines or for the calibration of instrumentation used for such measurements. Today an ANSI/IEEE standard exists for measurements of electric and magnetic fields near AC power lines. An IEC standard exists for measuring power-frequency electric fields. In addition, an IEEE standard is currently being prepared for the measurement of DC electric fields and ion related parameters near DC power lines. The paper briefly surveys the instrumentation currently in use for characterizing fields near AC power lines and the electric field, and ion current density and monopolar charge density near DC power lines.

900,835 PB89-176630

Not available NTIS

National Bureau of Standards (NEL), Gaithersburg,

MD. Electrosystems Div.

Power Frequency Electric and Magnetic Field
Measurements: Recent History and Measurement Final rept.

M. Misakian. 1986, 16p

Sponsored by Department of Energy, Washington, DC. Pub. in Proceedings of Workshop and Symposium of the National Conference of Standards Laboratories, Gaithersburg, MD., October 6-9, 1986, p5-1-5-16.

Keywords: *Electric fields, *Magnetic fields, *Standards, *Power transmission lines, Calibrating, Measurement, Wirelines, Electric wire, Substations, Electric

During the early 1970s reports appeared in the literature which raised questions regarding possible biologi-cal effects from exposure to power frequency electric and magnetic fields in the vicinity of high voltage trans-mission lines and in substations. Today a U.S. (IEEE) standard exists for measurement of AC power line fields and an NBS technical note is available which describes the measurement of electrical parameters in biological exposure systems. The paper focuses on selected results of NBS studies which have been in-corporated into the U.S. standard for measurement of power frequency electric and magnetic fields or included in the NBS technical note for measuring electrical parameters in bioeffects exposure systems.

Fuel Conversion Processes

PB90-110065 PC A07/MF A01 National Bureau of Standards (IMSE), Gaithersburg, MD Ceramics Div Effect of Siag Penetration on the Mechanical Prop-

erties of Refractories: Final Report.
S. M. Wiederhorn, and R. F. Krause. Jun 87, 145p

NBSIR-87/3584 Contract DE-Al05-83OR21349 Sponsored by Oak Ridge National Lab., TN.

Keywords: *Refractories, *Slags, *Coal gasification, *Corrosion, Ceramics, Mechanical properties.

The problem of selecting refractory insulation is the result of refractory lining exposure to the gasifier environment and to slag present in that environment. The ronment and to slag present in that environment. The lifetime of the refractory depends on the temperature of operation and the composition of slag at the hot face of the refractory. Higher temperatures (1500 C to 1700 C) and more corrosive slags (high alkali; high Fe) reduce the lifetime of refractories. Since slag is a unique that the refractories all refractories explain. versal solvent for refractories, all refractories eventually dissolve in coal slag. However, by appropriate materials design, the resistance of the refractory to dissolu-tion (and hence lifetime) can be increased.

Fuels 900,837

PB89-148100 PC A03/MF A01 National Bureau of Standards (NEL), Boulder, CO. Chemical Engineering Science Div.

Development of Standard Measurement Tech-

Development of Standard Measurement Techniques and Standard Reference Materials for Heat Capacity and Heat of Vaporization of Jet Fuels.
Final rept. Aug 87-May 88.
J. E. Callanan. Aug 88, 33p NBSIR-88/3093
Contract F33615-85-C-2508
Sponsored by Air Force Wright Aeronautical Labs., Wright-Patterson AFB, OH. Aero-Propulsion Lab.

Keywords: *Jet engine fuels, *Specific heat, *Heat of vaporization, Measurement, Standards, Thermogravimetry, Temperature, Heat measurement, Calorimeters, JP-4, JP-7, JP-8x.

Procedures developed in the NBS-Boulder Laboratory for heat capacity measurements of solids have been adapted successfully for the determination of liquid heat capacities. Heptane was used as a standard in the measurement of the heat capacity of three jet fuels, JP-4, JP-7, and JP-8x, from 220 to 360 K. Transi-

tions were observed in these fuels as follows (fuel, temperature): JP-4, 320 K; JP-7, 220-230 K; JP-8x, 220-240 K. Combined thermogravimetric and scanning calorimetric techniques were used successfully to measure heats of vaporization of cyclohexane, cisdecalin, and heptane. The precision of these measurements was better than 0.9 percent; agreement with literature values was satisfactory in view of small differences between the measuring temperature and the literature values for the boiling points.

900,838 PB89-173868 PB89-173868 Not available NTIS
National Bureau of Standards (NEL), Boulder, CO. Chemical Engineering Science Div. Enthalples of Desorption of Water from Coal Sur-

faces. Final rept.

J. E. Callanan, B. J. Filla, K. M. McDermott, and S.

A. Sullivan, 1987, 4p Pub. in Proceedings of ACS (American Chemical Society) Symposium, Division of Fuel Chemistry, Denver, CO., April 5-10, 1987, p185-188.

Keywords: *Enthalpy, *Desorption, *Water, *Coal, *Calorimeters, Surface properties, Exothermic reactions, Oxidizers, Porosity, Measurement, Outgassing.

An exotherm observed on the initial heating of coal, but not on subsequent heating, has been attributed to the interaction of moisture with the oxidized coal surface. This enthalpy difference has been evaluated as a function of specimen size, coal oxidation, and atmosphere within the cell. A simple procedure has been devised which uses a commercially available calorimeter, for measurement of enthalpies of desorption of water on coal. The method is useful, not only for coal-water interactions, but also for solvent-porous solid interactions in general.

900.839 PB89-173900 Not available NTIS

National Bureau of Standards (NEL), Boulder, CO. Chemical Engineering Science Div. Specific Heat Measurements of Two Premium

Coals. Final rept.

J. E. Callanan, and K. M. McDermott. 1988, 6p Pub. in Proceedings of ACS (American Chemical Society) National Meeting (194th), New Orleans, LA., August 31-September 4, 1987, p237-242 1988.

Keywords: *Coal, *Specific heat, Volatility, Thermophysical properties, Exothermic reactions, Measurement.

Specific heats of high volatile and medium volatile coals from the Argonne Premium Coal Sample Program were measured from 300 to 520 K. The results for the premium coals did not manifest the exothermic behavior on initial runs shown by weathered coals. Qualitative and quantitative differences in the behavior of the premium coals, by comparison with oxidized coals, will be presented.

900,840 PB89-174031 Not available NTIS National Bureau of Standards (NEL), Boulder, CO. Thermophysics Div.
Speed of Sound in Natural Gas Mixtures.

Final rept.

R. D. McCarty. 1986, 7p

Sponsored by Gas Research Inst., Chicago, IL.
Pub. in Proceedings of International Symposium on Fluid Flow Measurement, November 16-19, 1986, 7p.

Keywords: *Natural gas, *Acoustic velocity, *Sound transmission, Flow measurement, Equations of state, Mathematical models, Density(Mass/volume), Pressure, Temperature, Sound waves, Mixtures.

Accurate values for the speed of sound in natural gas mixtures are important in the application of sonic me-tering devices and in many design applications. In the case of mixtures, it is not possible to obtain experimentally determined speed of sound data for all possible compositions of the pure components found in natural gases. The alternative is a mathematical model of acceptable accuracy which allows the prediction of the speed of sound at an arbitrary state point and compo-sition. The paper describes the 'state of the art' for the prediction of the speed of sound for natural gases.

900,841 PB89-176747

Not available NTIS

National Bureau of Standards (NEL), Boulder, CO. Thermophysics Div.

Comprehensive Study of Methane + Ethane System.

W. M. Haynes, and R. D. McCarty. 1986, 16p Pub. in Proceedings of International Symposium on Fluid Flow Measurement, Washington, DC., November 16-19, 1986, p14-27.

Keywords: *Methane, *Ethane, Mixtures, Thermodynamic properties, Transport properties, Thermal conductivity Specific heat, Viscosity, Acoustic velocity.

The paper reports on the use of the methane-ethane system as a model for developing and testing predictive techniques for mixtures. Comprehensive data have been obtained for both thermodynamic (PVT, heat capacity, sound velocity) and transport (viscosity, thermal conductivity) properties of three mixtures of methane and ethane, as well as for both components. The sound velocity and heat capacity data serve as extremely stringent tests for evaluating the performance of calculational techniques, as well as providing key information essential for optimizing the models. A critical enhancement in the thermal conductivity was observed for the system; current theory does not predict such behavior for mixtures.

900,842 PB89-195663 PC A10/MF A01 National Inst. of Standards and Technology (NEL), Gaithersburg, MD. Center for Fire Research. Alaska Arctic Offshore Oil Spill Response Technol-

ogy Workshop Proceedings.

Special pub.

N. H. Jason. Apr 89, 211p NIST/SP-762 Also available from Supt. of Docs. Library of Congress catalog card no. 89-600731. Sponsored by Minerals Management Service, Herndon, VA. Held at Anchorage, Alaska on November 29-December 1, 1988.

Keywords: *Offshore drilling, *Oil pollution, *Proceedings, *Alaska, Combination, Ignition, Artic regions, Water pollution, *Oil spills, *Alaska, *Emergency planning, Chemical treatments, In situ burning, Mechanical containment, Mechanical recovery.

The Proceedings of the Alaska Arctic Offshore Oil Spill Response Technology Workshop contains papers by keynote speakers on the following topics: Mechanical Containment and Recovery; Chemical Treatment; In-Situ Burning; Readiness; the Technology Assessment and Research Program and the OHMSETT Program; the Arctic and Marine Oil Spill Program; the Canadian Environmental Science Revolving Fund; the Alaskan Clean Seas Research and Development Program; the NOFO Program. These papers served as a stimulus to the discussions that followed in the various Panel sessions. The Panels were organized into broad research areas: Mechanical Containment; Mechanical Recov-ery; Chemical Treatment; In-Situ Burning; Readiness. Each Panel summary is included in the Proceedings and these recommendations reflect the combined input from experts in the field. The Proceedings will serve as a working document to the Minerals Manage-ment Service (MMS) to identify their future research

900,843 PB89-222608 PC A21/MF A01 National Inst. of Standards and Technology (NEL), Boulder, CO. Thermophysics Div. Tables for the Thermophysical Properties of Meth-

Technical note. D. G. Friend, J. F. Ely, and H. Ingham. Apr 89, 489p NIST/TN-1325

Also available from Supt. of Docs. as SN003-003-

Keywords: *Methane, *High pressure tests, *Low temperature tests, *Equations of state, Thermodynamic properties, Tables(Data), Specific heat, Viscosity, Thermal conductivity, Computer programs.

The thermophysical properties of methane are tabulated for a large range of fluid states based on recently formulated correlations. For the thermodynamic properties, temperatures from 91 to 600 K at pressures less than 100 MPa are included. For the viscosity, the corresponding range is 91 - 400 K with pressures to 55MPa, while for the thermal conductivity the range is 91 - 600 K with pressures to 100 MPa. In addition to the tables of properties, algebraic expressions and associated tables of coefficients are given to allow addi-

tional property calculations. Tables of comparisons between experimental property determinations and the correlations are also given both for primary data used in the formulation of the correlations and for additional data. A listing of a FORTRAN program for the evaluation of methane thermophysical properties using the Schmidt-Wagner equation of state is included.

900.844

Not available NTIS PB90-117896 National Inst. of Standards and Technology (NEL), Gaithersburg, MD. Thermophysics Div. Measurements of Molar Heat Capacity at Constant

Volume: Cv,m(xCH4+(1-x)C2H6'T = 100 to 320 K,

p < or = 35 MPa). Final rept. J. E. Mayrath, and J. W. Magee. 1989, 15p Sponsored by Gas Research Inst., Chicago, IL Pub. in Jnl. of Chemical Thermodynamics 21, p499-513 1989.

Keywords: *Specific heat, *Thermal measurement, *Thermophysical properties, *Methane, *Ethane, Mixtures, Temperature, Density, Volume, Calorimeters,

Measurements of the molar heat capacity at constant volume Cv,m(XCH4+(1-X)C2H6, X=0.35, 0.50, 0.68) at temperatures from 100 K to 320 K and at pressures to 35 MPa are reported. Heat capacities have been measured for 626 state conditions and these measure-ments complement thermodynamic and transport-property measurements previously reported for the same mixtures. The measurements were made on samples of constant mass contained by a calorimeter vessel of nearly constant volume. Uncertainties of the heat-capacity measurements are estimated to be less than 2.0%. Critical enhancement of heat capacity for each mixture is apparent in the critical-temperature region for constant density and similarly in the critical-density region for constant temperature. Liquid heat capacities at saturation, obtained by extrapolation at constant density, have a minimum for each composition occurring at twice the estimated critical density.

900.845

PB90-136839 Not available NTIS Mational Bureau of Standards (NML), Gaithersburg, MD. Chemical Thermodynamics Div.

Evaluation of Data on Higher Heating Values and Elemental Analysis for Refuse-Derived Fuels.

T. J. Buckley, and E. S. Domalski. 1988, 8p Sponsored by Department of Energy, Washington, DC. Biofuels and Municipal Waste Technology Div. Pub. in Proceedings of National Waste Processing Conference, Philadelphia, PA., May 1-4, 1988, p77-84.

Keywords: Experimental design, Numerical analysis, Error analysis, *Refuse derived fuels, *Heating rate, *Multi-element analysis, Waste utilization, Data bases, Interlaboratory comparisons.

Elemental analyses and higher heating values taken from ASTM Round Robin Testing of RDF-3 have been evaluated. The data base was composed of five rounds of tests with eight to twelve laboratories performing four tests each. The authors found that established formulas can be used to calculate higher heating values on a moisture free basis (HHV2) from elemental analysis. A comparison is made between several methods of calculating HHV2. The Dulong formula and Institute of Gas Technology formula can predict HHV2 to within 3%.

Heating & Cooling Systems

900.846

PB89-150924 Not available NTIS National Bureau of Standards (NEL), Washington, DC. Building Equipment Div. Combustion Testing Methods for Catalytic Heat-

ers.

E. R. Kweller. 1986, 19p Sponsored by Department of Energy, Washington, DC. Pub. in ASHRAE (American Society of Heating, Refrigerating and Air-Conditioning Engineers) Transactions, v92 pt2B p239-257 1986.

Heating & Cooling Systems

Keywords: *Test facilities, Natural gas, Propane, Fuel consumption, Standards, Tests, Thermal efficiency, Reprints, *Catalytic heaters, *Combustion tests, Appliance Efficiency Test Procedures.

Both vented and unvented designs of catalytic heaters using natural gas and propane as the fuel were tested by three test methods. The objective of the study was to determine an appropriate laboratory test method for determining the percentage of unreacted fuel during typical heater use. Results of the study are expected to be useful for manufacturers who are currently developing an ANSI standard for catalytic heaters and by the Department of Energy for their Appliance Efficiency Test Procedures. Results showed that an analytical approach of calculating unreacted fuel using a carbon balance was equivalent to an empirical method. Results of tests in two open-room test methods and one closed room test method showed that the methods to use will depend on whether the heater is vented or unvented. A closed room method was shown to yield results consistent with those obtained by open-room methods for the unvented heater, and may be used in place of an open-room method if the room oxygen is not depleted below 19% as an end-point of the test. A completely sealed test room was found to be unnecessary for this closed room test.

900,847 PB89-188619 PC A04/MF A01 National Bureau of Standards (NEL), Gaithersburg,

Thermal and Economic Analysis of Three HVAC (Heating, Ventilating, and Air Conditioning) System Types in a Typical VA (Veterans Administration) Patient Facility.

G. N. Walton, and S. R. Petersen. Aug 87, 59p NBSIR-87/3619

Sponsored by Veterans Administration, Washington, DC. Office of Facilities.

Keywords: *Thermal analysis, *Economic analysis, *Hospitals, *Military facilities, Computerized simulation, Radiant heating, Environmental engineering, Tables(Data), *Energy analysis, *HVAC systems, Energy demand, Variable air volume systems, Fan coil systems, Life cycle costs.

Thermal and economic analyses were performed for Inermai and economic analyses were performed for three different types of heating, ventilating, and cooling systems for a patient room in a typical VA patient facility in each of four locations. Thermal analysis was done with the U.S. Army's Building Loads Analysis and System Thermodynamics (BLAST) energy analysis system infermodynamics (bLAST) energy analysis program. Radiant panel, variable air volume (VAV), and fan coil systems were simulated. Some subroutines were developed and added to the BLAST program in order to simulate the radiant panel system. The predicted energy requirements, energy cost protesties and several series and several series. jections, and system costs were then evaluated using the NBS Federal Building Life-Cycle Cost (FBLCC) program to determine the 20-year life-cycle cost of each system in each location.

900,848 PB89-212146 Not available NTIS National Bureau of Standards (NEL), Gaithersburg, MD. Building Equipment Div.
Part Load, Seasonal Efficiency Test Procedure
Evaluation of Furnace Cycle Controllers.

Final rept.

R. A. Wise, and E. R. Kweller. 1986, 11p Sponsored by Department of Energy, Washington, DC. Pub. in ASHRAE (American Society of Heating, Refrigerating and Air-Conditioning Engineers) Transactions, v92 pt2B p674-684 1986.

Keywords: *Furnaces, *Performance standards, Thermostats, Thermal efficiency, Heating load, Tests, Temperature control, Reprints, Energy consumption, Energy conservation.

Claims of energy savings of 20 to 40% for space heating have been made by marketers of rapid cycling furnace controllers (cyclers). The present testing method of ANSI/ASHRAE 103-1982 can not be used to evaluate the heating seasonal efficiency of furnaces or boilers should they be installed using cyclers. To develop a test method that will reflect possible changes in effi-ciency, NBS has tested a furnace under various cycling conditions. A supply air temperature based cycler was tested, time based unit was simulated, and the test results were compared to results using simulated standard thermostat control. The comparisons were made using cycles corresponding to the average outdoor air temperatures of four weather condition bins of

approximately the same total heating hours. A test method has been developed which can evaluate the effect of cyclers on furnace efficiency. No proposal is made to use this method because: the test is more difficult to perform and replicate, change would require retesting of all furnaces and destroy the present data base of past test results, and changes in furnace efficiency attributable to cyclers were too small to justify a

Policies, Regulations & Studies

900,849 PB89-151211 National Center for Health Statistics, Hyattsville, MD. NBS (National Bureau of Standards) Life-Cycle Cost (NBSLCC) Program (for Microcomputers). Software

S. R. Petersen, and R. T. Ruegg. 21 Dec 88, 1 diskette NBS/SW/DK-89/001

The software is contained on 5 1/4-inch diskettes, double density (360K), compatible with the IBM PC microcomputer. The diskettes are in the ASCII format. Price includes documentattion, PB87-180253.

Keywords: *Software, *Public buildings, Economic analysis. Benefit cost analysis, Diskettes, *National Inanalysis, Benefit cost analysis, Diskettes, *National Institute of Standards and Technology, *Life-cycle cost, Energy conservation, L=BASIC, H=IBM PC/XT/AT.

The diskette provides the National Bureau of Standards Life-Cycle Cost (BNSLCC) programs and related files referenced in NBS SP 709, Comprehensive Guide for Least-Cost Energy Decisions. The NBSLCC programs perform economic analysis of buildings, building systems and components with special emphasis on energy conservation projects. Software description: The software is written in BASIC for implementation on IBM-PC/XT/AT microcomputers using the MS-DOS operating system. A minimum of 128 K of memory is required.

PB89-153860 PC A04/MF A01 National Inst. of Standards and Technology (NEL), Gaithersburg, MD. Center for Computing and Applied Mathematics.

Energy Prices and Discount Factors for Life-Cycle Cost Analysis 1988: Annual Supplement to NBS (National Bureau of Standards) Handbook 135 and NBS Special Publication 709.

Annual rept. B. C. Lippiatt, and R. T. Ruegg. Nov 88, 61p NISTIR-85/3273-3

See also PB88-109913. Sponsored by Department of Energy, Washington, DC. Assistant Secretary for Conservation and Renewable Energy.

Keywords: *Cost analysis, *Energy management systems, *Federal buildings, Prices, Heating fuels, Investments, Energy conservation, *Life cycle costs, Federal Energy Management and Planning Program, Discount factors

The 1988 energy prices and discount factors for lifecycle cost analysis are reported as established by the U.S. Department of Energy. The data are provided as an aid to implementing life-cycle cost evaluations of potential energy conservation and renewable energy investments in existing and new federally owned and leased buildings.

Solar Energy

900,851 PB89-229058 PC A05/MF A01
National Inst. of Standards and Technology (NML),
Gaithersburg, MD. Electricity Div.
Lightning and Surge Protection of Photovoltalc Installations. Two Case Histories: Vulcano and Kyth-

F. D. Martzloff. Jun 89, 78p NISTIR-89/4113 Sponsored by Sandia National Labs., Albuquerque,

Keywords: *Photovoltaic cells, *Lightning, *Surges, *Circuit protection, Overvoltage, Overcurrent, Light-ning protection, *Solar cell arrays.

Two installations of photovoltaic systems were damaged during lightning storms. The two sites were visited and the damaged equipment that was still available on the site was examined for analysis of the suspected occurrence. The evidence, however, is insufficient to conclude that all the observed damage was caused by the direct effect of a lightning flash. A possible scenario may be that lightning-induced overvoltages caused insulation breakdown at the edges of the photovoltaic modules, with subsequent damage done by the dc current of the array. Other surge protection considerations are also addressed, and suggestions presented for further investigations.

General

900.852 PB89-175897 Not available NTIS National Bureau of Standards (NEL), Gaithersburg, MD. Office of Energy-Related Inventions.

Periodic Heat Conduction in Energy Storage Cylinders with Change of Phase.

Final rept. M. E. McCabe. 1986, 9p Sponsored by Department of Energy, Washington, DC. Office of Solar Heat Technologies. Pub. in Proceedings of Joint AlAA/ASME (American

Institute of Aeronautics and Astronautics/American Society of Mechanical Engineers) Thermophysics and Heat Transfer Conference, Boston, MA., June 2-4, 1986, 9p.

Keywords: *Conduction, *Heat transmission, *Phase transformations, *Cylinders, Flux(Rate), Thermophysical properties, Heat of fusion, Diurnal variations, Enthalpy, Specific heat, Solar heating, *Thermal energy storage equipment.

The thermal performance of an energy storage system subjected to a time dependent flux representing the 24-hour diurnal cycle of the sun is discussed. The governing mathematical equations are presented for a cylindrical configuration and a numerical solution based on the enthalpy model is used to obtain the temperature distribution and phase interface location phase change energy storage system. The steady-periodic solution is investigated to determine the effects of cylinder size, fusion temperature and thermophysical properties on the thermal performance of a radiatively charged/convectively discharged energy storage system in a passive solar heated building. The relationship between fusion temperature and the mean surface temperature is shown to be critical for storage of energy. The numerical results show that maximum energy storage and minimum surface temperature variation occur when the cyclic mean surface temperature equals the fusion temperature.

900,853 PB90-112442 PC A06/MF A01 National Inst. of Standards and Technology (NEL), Gaithersburg, MD. Electrosystems Div. Research for Electric Energy Systems: An Annual Report.

R. J. Van Brunt. Oct 89, 109p NISTIR-89/4167 See also rept. for 1987, PB89-132310. Sponsored by Department of Energy, Washington, DC. Div. of Electric Energy Systems.

Keywords: *Potential energy, *lons, Research projects, Electric fields, Activity coefficients, Charged particles, Transmission lines, Atmospheric pressure, Measurements, Charge density, Gas cylinders, Stochastic processes, Dielectrics, Hydrostatic pressure, Transients.

Reported is technical progress in four investigations conducted at NIST and supported by the U.S. Department of Energy under Task Order Number 137. The first investigation is concerned with the measurements of electric fields and ions in the vicinity of high-voltage transmission lines and biological exposure facilities. Results are reported on evaluations of two methods for measuring monopolar charge densities in air. The second investigation is concerned with development of advanced diagnostics for compressed gas-insulated power systems. Results are reported on measure-ments of collisional electron detachment and negative ion conversion reactions in SF6 and on a new technique for measuring the stochastic behavior of partial discharges. The third investigation is concerned with

measurement of prebreakdown phenomena at solidliquid dielectric interfaces. Results are presented here from optical observations of the influence of hydrostatic pressure on prebreakdown partial discharge development and measurement of nano-second impulse breakdown at liquid-solid interfaces. The fourth area of research is concerned with electrical measurement of fast transient phenomena. Results are presented from an investigation into the interactions between two dividers used simultaneously to measure fast impulse voltages.

ENVIRONMENTAL POLLUTION & CONTROL

Air Pollution & Control

900,854
PB89-148134
PC A03/MF A01
National Bureau of Standards (NEL), Gaithersburg,
MD. Center for Building Technology.
Predicting Formaldehyde Concentrations in Manu-

Predicting Formaldehyde Concentrations in Manufactured Housing Resulting from Medium-Density Fiberboard.

S. Silberstein. Apr 88, 19p NBSIR-88/3761 Sponsored by Department of Housing and Urban Development, Washington, DC.

Keywords: *Formaldehyde, *Fumes, *Air pollution, Fiberboards, Houses, Emission, Particle boards, Plywood, Panels, Temperature, Humidity, Urea-formaldehyde resins, Forecasting.

HUD previously issued Manufactured Home Construction and Safety Standards limiting formaldehyde emissions of particleboard and plywood paneling that were manufactured using urea-formaldehyde resins for use in manufactured homes. The report uses indoor air quality models to predict how much medium-density fiberboard(mdf) may be added to manufactured homes already containing maximum loadings of particleboard and plywood paneling, without raising the formaldehyde concentration beyond 400 ppb. It was found that any combination of mdf that results in a chamber-test concentration of 300 ppb may be added to such a home. A sensitivity analysis was done to predict how this formaldehyde concentration limit is affected by variations in temperature, relative humidity, and air exchange rate. It was concluded that limiting chamber concentrations to 200 ppb would allow for small errors in temperature, relative humidity, and air exchange rate that might be expected to arise in practice.

900,855
PB89-150775
Not available NTIS
National Bureau of Standards, Gaithersburg, MD.
Office of Standards Management.
Draft International Document on Gulde to Portable

Draft International Document on Guide to Portable Instruments for Assessing Airborne Pollutants Arising from Hazardous Wastes.
Draft rept.

S. Chappell, J. Driscoll, G. Flanagan, S. Levine, K. Leichnitz, P. Lillienfeld, and R. Turpin. 1988, 26p Pub. in Draft International Document on Guide to Portable Instruments for Assessing Airborne Pollutants Arising from Hazardous Wastes, p1-26 1988.

Keywords: *Hazardous materials, *Guidelines, *Portable equipment, *Waste disposal, Assessments, Sites, Concentration(Composition), Performance equipment, Sampling, Calibrating, Reprints, *Environmental monitoring, *Air pollution sampling.

The document provides definitions and guidelines for selecting portable monitoring instruments to measure airborne pollutants at hazardous waste sites. A brief description of six types of instruments, including some important metrological and technical characteristics, is given. The document also provides background and literature references on the application of these instruments. Emphasis is placed on methods and requirements for testing and calibrating instruments. Specifics of sampling methods and of instrument type evaluation are not addressed.

900,856

PB89-214779

PC A03/MF A01

National Inst. of Standards and Technology (NEL),
Gaithersburg, MD. Center for Fire Research.

Synergistic Effects of Nitrogen Dioxide and
Carbon Dioxide Following Acute Inhalation Expo-

sures In Rats. B. C. Levin, M. Paabo, L. Highbarger, and N. Eller. May 89, 45p NISTIR-89/4105

Sponsored by Society of the Plastics Industry, Inc., New York.

Keywords: *Air pollution, *Carbon dioxide, *Nitrogen dioxide, *Rats, Toxicology, Respiratory diseases, Oxidizers, Hemoglobins, Exposure, Blood, Mortality, Air pollution control, Standards, Methemoglobins, Fire gases.

All fires occurring in air produce carbon dioxide (CO2). Fire involving nitrogen-containing products will also generate nitrogen dioxide (NO2), a pulmonary irritant. In Fischer 344 male rats, the LC50 (30 minute exposure plus 14 day post-exposure observation period) for NO2 was 200 ppm (with 95% confidence limits of 43 to 51%); whereas, the LC50 for NO2 in the presence of 5% CO2 was 90 ppm (with 90% confidence limits ranging from 70-120 ppm). Exposure to NO2 increased the methemoglobin (MetHb) levels in the arterial blood. At the end of the 30 minute exposures, the MetHb levels were 2-3 times higher in the animals exposed to the combination of NO2 (200 ppm) and CO2 (5%) than in those exposed to NO2 only. Deaths from NO2 were all post-exposure and occurred earlier in the presence of NO2 plus 5% CO2 than in the absence of the CO2. The time of death was concentration-dependent when both gases were present. At death, evidence of hemorrage and extensive edema was observed in the lungs. The mean lung wet weight/body weight ratio from rats exposed to 200 ppm NO2 with and without 5% CO2 was 3-4 times that of non-exposed rats. More edema was noted with NO2 and CO2 than with NO2 alone.

900,857
PB89-229686
PC A03/MF A01
National Inst. of Standards and Technology (NEL),
Gaithersburg, MD. Building Environment Div.
Ventilation and Air Quality Investigation of the U.S.
Geological Survey Building.
W. S. Dols, and A. Persily. Jul 89, 44p NISTIR-89/

4126 Sponsored by Geological Survey, Reston, VA.

Keywords: *Ventilation, *Buildings, *Air quality, *Laboratories, Odors, Air flow, Heating, Measurement, Carbon dioxide, Carbon monoxide, Radon, Concentration(Composition), Formaldehyde, Standards, Recommendations, Improvement, Graphs(Charts), *Indoor air pollution, Tracer gas tests.

The National Center of the U.S. Geological Survey in suburban Washington, DC is a seven story building containing both office and laboratory space. Based on a history of occupant complaints regarding the air quality within the building, an investigation was conducted by the National Institute of Standards and Technology to quantify the ventilation characteristics of the building and to determine the indoor levels of selected indoor pollutants. The investigation of the building included measurements of air exchange rates using the tracer gas decay technique and measurements of indoor concentrations of carbon dioxide, carbon monoxide, radon, formaldehyde and particulates. The measurement results are compared to appropriate standards and guidelines in order to investigate the role of ventilation and pollutant concentrations in the indoor air quality complaints. Based on the investigation, several recommendations are made to improve the environmental conditions within the building.

900,858
PB89-235899
PC A04/MF A01
National Inst. of Standards and Technology (NEL),
Gaithersburg, MD. Building Environment Div.
Method for Measuring the Effectiveness of Gaseous Contaminant Removal Filters.

B. M. Mahajan, Aug 89, 549, NISTIR-89/4119

ous Contaminant Removal Filters.

B. M. Mahajan. Aug 89, 54p NISTIR-89/4119
See also PB88-155882. Sponsored by Consumer Product Safety Commission, Washington, DC.

Keywords: *Air pollution abatement, *Air filters, Ventilation, Air conditioning equipment, Effectiveness, Gases, Activated carbon, Adsorbents, Performance evaluation, Contaminants, *Indoor air pollution. The report presents a brief review of the gas adsorption kinetics theory applicable to adsorption of gaseous contaminants by filter media, and an algorithm for assessing the effectiveness of filtering devices with flow bypass. It briefly describes the selected testing technique for measuring the effectiveness of filter media, and presents experimental data for adsorption of n-butane, toluene, and carbon monoxide.

900,859

PB90-123571 Not available NTIS National Inst. of Standards and Technology (NML), Gaithersburg, MD. Organic Analytical Research Div. Mobile Sources of Atmospheric Polycyclic Aromatic Hydrocarbons: A Roadway Tunnel Study. Final rept.

B. A. Benner, G. E. Gordon, and S. A. Wise. 1989, 10p

Pub. in Environmental Science and Technology 23, n10 p1269-1278 1989.

Keywords: *Aromatic polycyclic hydrocarbons, *Exhaust emissions, *Chemical analysis, *Particles, *Motor vehicles, Chromatographic analysis, Gas analysis, Gasoline engines, Diesel engines, Tunnels, Reprints, *Air pollution sampling, *Air pollution detection, Heavy duty vehicles, Light duty vehicles.

Suspended particulate matter samples were collected by high-volume samplers in a heavily traveled roadway tunnel to characterize the mobile source emissions (diesel- and gasoline-fueled vehicles) for polycyclic aromatic hydrocarbons (PAHs). Liquid and gas chromatographic techniques were employed to isolate and quantify individual PAHs in dichloromethane extracts of Teflon and glass-fiber filters. Mobile-source PAH emission estimates were generated from the particleand vapor-phase samples collected in the tunnel and agree with emission estimates reported previously for roadway tunnels in Japan. Factor analysis of PAH concentrations from 47 filter samples yielded two factors; one which possibly represented the diesel-fueled vehicles (heavy-duty trucks) and the other, either gasoline-fueled vehicles or a composite of the gasoline and diesel sources.

900,860

PB90-128166
Not available NTIS
National Inst. of Standards and Technology (NML),
Gaithersburg, MD. Organic Analytical Research Div.
Residential Wood Combustion: A Source of Atmospheric Polycyclic Aromatic Hydrocarbons.
Final rept.

F. R. Guenther, S. N. Chesler, G. E. Gordon, and W. H. Zoller. 1988, 6p

Pub. in Jnl. of High Resolution Chromatography and Chromatography Communications 11, p761-766 Nov 88.

Keywords: *Aromatic polycyclic hydrocarbons, *Particles, *Combustion products, *Stoves, Sources, Residential building, Exhaust emissions, Automobiles, Chemical analysis, Chromatographic analysis, Atmospheric composition, Reprints, *Air pollution detection, *Air pollution sampling, *Wood burning appliances, Coal combustion, Fairbanks(Alaska).

Samples were taken of the atmospheric particulate matter over Fairbanks Alaska in the winter of 1985, and from wood stoves burning the major wood types locally available. These samples were then analyzed for polycyclic aromatic hydrocarbon (PAH). A PAH emission profile was determined from the wood stove samples and applied to the atmospheric samples to determine the residential wood combustion contribution to the local atmospheric particulate burden. Emission profiles for coal burning and automobile emissions for PAH were also used to estimate their relative contributions.

Solid Wastes Pollution & Control

900,861

PB89-212104 Not available NTIS National Bureau of Standards (NML), Gaithersburg, MD. Chemical Kinetics Div.

ENVIRONMENTAL POLLUTION & CONTROL

Solid Wastes Pollution & Control

Fundamental Aspects of Key Issues In Hazardous Waste Incineration.

Final rept.

W. Tsang. 1986, 6p
Pub. in Proceedings of ASME (American Society of Mechanical Engineers) Winter Annual Meeting, Anaheim, CA., December 7-12, 1986, 6p.

Keywords: *Hazardous materials, *Waste disposal, *Incineration, *Pyrolysis, Reaction kinetics, Oxidation, Chemical reactions, Performance evaluation.

The incineration of hazardous waste is considered from the point of view of its important chemical reactions. The authors begin with a bnef review of the earlier work on destruction mechanisms and expand it by allowing for regions where pyrolytic reactions are important. The authors then discuss the quantitative relationship between destruction efficiency and the appropriate rate constants for hazardous waste destruction. This leads into considerations of the products of incomplete combustion and the author describe in qualitative terms the type of compounds that can be expected. The concept of surrogates is discussed. The authors consider recent results on OH attack on organics near levels of CO usually observed in various types of incinerators, and conclude that there is a high probability that the organics in the incineration effluent stream are formed by pyrolysis mechanism. Finally the authors suggest a number of measures for validating proper incinerator operation.

Water Pollution & Control

900.862 Not available NTIS PB89-173827 National Bureau of Standards (NEL), Gaithersburg, MD. Statistical Engineering Div.

Designs for Assessment of Measurement Uncer-

tainty: Experience in the Eastern Lake Survey.

Final rept.
W. S. Liggett. 1986, 15p
Sponsored by Corvallis Environmental Research Lab.,

Pub. in Proceedings of International Biometric Conference: Invited Papers (13th), Seattle, WA., July 27-August 1, 1986, p1-15.

Keywords: *Lakes, *Error analysis, *Environmental surveys, Quality assurance, Statistical analysis, Assessments, Probability theory, Chromatographic analysis, Inorganic nitrates, Sulfates, Performance evaluation, United States, *Water pollution sampling.

As is typical of environmental studies, the Eastern Lake Survey generated data that reflect both properties of the environment and properties of the sampling and measurement procedures. Thus, environmental conclusions cannot be drawn from these data without assessment of the sampling and measurement error. The paper shows how the properties of ion chromatography affect the nitrate and sulfate measurements in the survey. The investigation, which is based on measurements of routine-duplicate samples, field blanks, and field audit samples, is interesting because of its complexity. The measurement error has a within-day component and a day-to-day component. The variance of the within-day component increases linearly with concentration except near zero where the algorithm used to interpret the chromatographs seems to behave poorly. The day-to-day component depends on the calibration procedure. As an example, this in-vestigation illustrates the strengths and weaknesses of some common designs for uncertainty assessment.

900,863 PB89-185581 PC A04/MF A01

National Bureau of Standards (NEL), Gaithersburg, MD. Center for Fire Research.
Combustion of Oil on Water. November 1987.
D. Evans, H. Baum, B. McCaffrey, G. Mulholland, M. Harkleroad, and W. Manders. Nov 87, 56p NBSIR-86/3420

See also PB89-149173. Sponsored by Minerals Management Service, Reston, VA.

Keywords: *Fuel oil, *Combustion products, *Water pollution, *Fires, *Aerosols, Tanker ships, Measurement, Smoke, Aromatic hydrocarbons, Air flow, Offshore drilling, Graphs(Charts).

The report contains the results of measurements per-formed on both 0.4 m and 0.6 m diameter pool fires

produced by burning a layer of Prudhoe Bay crude oil supported by a thermally deep layer of water. Both steady and vigorous burning caused by boiling of the water sublayer were observed. The measured energy release rate for steady burning was about 640 kW per sq meter. The emission rate, the size distribution, and specific extinction coefficient were measured for the smoke aerosol produced by the fires. Data were also obtained on the structure of the smoke aerosol by electron microscopy and on emission of CO and CO2. Analysis of the crude oil burn residue indicated selected depletion of the short chain alkanes and cycloalkanes when compared to the fresh oil. Mono-ring aro-matics including benzene, toluene, and xylenes present in the fresh crude were absent in the burn residue. Calculations of the induced air flow into a simulated distribution of 20 fires over a 100 m x 100 m area showed that the maximum inflow velocity near the largest size fire (2.5 m diameter, 3.2 MW) was 1.1 m/s.

900,864 PB89-229280
Not available NTIS
National Inst. of Standards and Technology (IMSE),
Gaithersburg, MD. Polymers Div.
Biotransformation of Mercury by Bacteria Isolated
from a River Collecting Cinnabar Mine Waters.
Final rent

F. Baldi, M. Filippelli, and G. J. Olson. 1989, 12p Pub. in Microbial Ecology 17, p263-274 1989.

Keywords: *Aerobic bacteria, *Mercury inorganic compounds, *Water pollution, Mercury ore deposits, Rivers, Reprints, *Mine waters, *Biotransformation, Resistance(Biology).

One hundred six strains of aerobic bacteria were isolated from the Fiora River which drains an area of cinnabar deposits in southern Tuscany, Italy. Thirty-seven of the strains grew on an agar medium containing 10 microg/ml Hg (as HgCl2) with all of these strains producing elemental mercury. Seven of the 37 strains also degraded methylmercury. None of 106 sensitive and resistant strains produced detectable monomethylmercury although 15 strains produced a benzene-soluble mercury species. Two strains of alkylmercury. ble mercury species. Two strains of alkylmercury (methyl-, ethyl- and phenylmercury) degrading bacteria were tested for the ability to degrade several other analogous organometals and organic compounds, but no activity was detected toward these compounds. Mercury methylation is not a mechanism of Hg resistance in aerobic bacteria from this environment. Growth of bacteria on the agar medium containing 10 microg/ml HgCl2 was diagnostic for Hg detoxification based on reduction.

General

900,865 PB89-150940 PB89-150940 Not available NTIS National Bureau of Standards (NML), Gaithersburg, MD. Office of Standard Reference Data Environmental Standard Reference Materials -Present and Future Issues.

Final rept. S. D. Rasberry, 1988, 9p

Pub. in Proceedings of International Symposium on Trace Analysis in Environmental Samples and Stand-ard Reference Materials, Honolulu, HI., January 6-8,

1988, p62-66-4.

Keywords: *Environmental surveys, *Chemical analysis, Measurement, Chemical properties, Physical properties, Quality assurance, Forecasting, *Standard reference materials, Certified reference materials.

Accurate measurements are an important consideration in environmental analysis. The National Bureau of Standards (NBS) provides several types of services or Standards (NBS) provides several types of services to aid analysts in obtaining accurate measurements and in validating the accuracy of measurement methods and measurement systems. The most well known of these services is Standard Reference Materials (SRMs), which are well-characterized, homogeneous materials or simple artifacts with specific chemical or physical properties certified by NBS. There are several hundred SRMs in support of environmental chemists covering inorganic and organic constituents in water covering inorganic and organic constituents in water, air, sediments, rocks, plant and animal materials. Attention is given to providing SRMs which closely approximate the matrix being analyzed in a specific environmental application. The extremely wide range of environmental matrices makes it economically unfeaenvironmental matrices makes it economically unfea-sible for the NBS to offer nearly exact matches to every matrix. For this reason, analysts frequently should use more than one SRM in a 'benchmark-bracketing' way to validate their analytical methods. Non-matrix specific SRMs, such as single element spectrometric solutions, are also available for instru-ment calibration or validation.

900.866

PB90-123969 Not available NTIS National Inst. of Standards and Technology (NML), Gaithersburg, MD. Organic Analytical Research Div. Experiences in Environmental Specimen Banking.

Experience in Land Paris, M. M. Schantz, S. A. Wise, B. J. Koster, R. M. Parris, M. M. Schantz, S. F. Stone, and R. Zeisler. 1989, 16p Pub. in International Jnl. of Environmental Analytical

Keywords: *Chemical analysis, Shelf life, Reprints, *National Institute of Standards and Technology, *Environmental monitoring, *Sample preparation, *Environmental specimen banking.

For the past 10 years, the National Institute of Standards and Technology has been involved in environmental specimen banking activities. These activities have resulted in the development of collection, storage, processing, and analysis procedures for long-term archiving of a variety of environmental specimens including human liver, fish muscle and liver, oysters, mussels, sediment, and seal tissues. In the paper, the authors describe some of the experiences and results from these efforts as related to environmental trend monitoring and the potential value of a specimen bank for future retrospective analyses.

INDUSTRIAL & MECHANICAL ENGINEERING

Industrial Safety Engineering

900.867

PB89-151781 PC A04/MF A01 California Univ., Berkeley. Dept. of Mechanical Engi-

Fire Propagation in Concurrent Flows. Final rept.

A. C. Fernandez-Pello. Jan 89, 67p NIST/GCR-89/ 557

Grant NANB-7-D0737

See also PB86-181849. Sponsored by National Inst. of Standards and Technology (NEL), Gaithersburg, MD. Center for Fire Research.

Keywords: *Air flow, *Flame propagation, *Fire tests, Flames, Heat transfer, Combustion, Turbulence, Fuels, Gases, Flammability, *Rooms.

The research tasks completed during this reporting period include an experimental study of the effect on the spread of flames of the turbulence intensity of an opposed air flow, and a theoretical analysis of the con-current spread of flames over thin fuels. Both studies are in the authors opinion important contributions in the study of the flame spread process. The results of the experimental study show that the flame spread process is significantly affected by the flow turbulence intensity for flames spreading over both thin and thick fuels. For a fixed flow velocity, the spread rate de-creases as the turbulent intensity is increased. This appears to be due to the turbulent convective cooling of the fuel surface and gas in the vicinity of the flame front. Also observed is that extinction of the flames occurs at lower velocities as the turbulent intensity increases. The results of the theoretical analysis, which are in good agreement with previous experimental measurements, give detailed information about the flame structure and mechanisms of flame spread. It is shown that the flame length and consequently the rate

of flame spread, are strongly dependent on the interaction between the pyrolysis and burn-out fronts.

900,868 PB89-174890 Not available NTIS National Bureau of Standards (NEL), Gaithersburg, MD. Fire Measurement and Research Div.

Smoke and Gas Evolution Rate Measurements on Fire-Retarded Plastics with the Cone Calorimeter. Final rept.

V. Babrauskas. 1989, 8p Pub. in Fire Safety Jnl. 14, p135-142 1989.

Keywords: *Plastics, *Flammability testing, *Fire resistant materials, Smoke, Reprints, *Cone calorimeter.

The cone calorimeter was developed originally for making improved rate of heat release measurements. The basic design has proved to be highly versatile, allowing it to become a suitable test bed for making smoke and gas evolution studies. The smoke measurement procedures with the cone calorimeter have recently been published by ASTM as a proposed method. Gas evolution measurements are still at the research laboratory stage, but are being actively developed, with a strong role being seen in the near future for both fire modeling and combustion toxicity. The techniques evolved are seen to be especially useful for comparing fire-retarded materials to non-retarded

900.869 PB89-212047 Not available NTIS National Bureau of Standards (NEL), Gaithersburg, MD. Fire Measurement and Research Div. Toxicity of Mixed Gases Found in Fires.

B. C. Levin, M. Paabo, J. L. Gurman, and S. E.

B. C. Levin, M. Paabo, J. L. Gurman, and S. E. Harris. 1986, 18p Sponsored by Army Medical Research Inst. of Chemical Defense, Aberdeen Proving Ground, MD., and Society of the Plastics Industry, Washington, DC. Pub. in Proceedings of SPI and FRCA Joint Meeting, Washington, DC., March 19-21, 1986, p71-88.

Keywords: *Toxicity, *Fires, *Gases, Fire hazards, Carbon dioxide, Carbon monoxide, Hydrogen cyanide, Concentration(Composition), Lethal dose 50.

The Center for Fire Research is developing a computer model to predict the toxic hazard that people will experience under various fire scenarios. The toxicity of single and multiple fire gases is being studied to deter-mine whether the toxic effects of a material's combustion products can be explained by the biological interactions of the primary fire gases or, if minor, more obscure gases need to be considered. LC50 values for Fisher 344 rats have been calculated for carbon monoxide (CO) in air for 2, 5, 10, 30, and 60 minute exposures using the NBS Toxicity Test Method. LC50 values have also been calculated for hydrogen cyanide (HCN) in air for similar time periods, plus one minute exposures. Combination experiments with CO and HCN indicate that they act in an addictive manner. A preliminary comparison of the concentrations of the major combustion products generated from some ma-terials tested at their LC50 values with the combined gas results indicates that the observed toxicity for these materials appear to be explained by the biologi-cal interactions of the primary toxic fire gases.

Laboratory & Test Facility Design & Operation

900,870 PB89-147086 Not available NTIS National Bureau of Standards (NEL), Gaithersburg, MD. Chemical Process Metrology Div. Economical Ultrahigh Vacuum Four-Point Resistiv-

Ity Probe. Final rept.

Pub. in Jnl. of Vacuum Science and Technology A 5, n1 p115-117 Jan/Feb 87.

Keywords: *Electric measuring instruments, *Ultrahigh vacuum, Semiconductors(Materials), Oxides, Measurement, Reprints, *Resistivity probes, Metal oxides.

An economical four-point probe has been built to measure changes in the surface resistivity of metal oxide semiconductors. Its fabrication from ultra-highvacuum-compatible parts is described.

900,871 PB89-147847 PB89-147847 PC A04/MF A01 National Bureau of Standards (NEL), Boulder, CO. Electromagnetic Technology Div.

Metrology for Electromagnetic Technology: A Bibllography of NBS (National Bureau of Standards)
Publications.

M. E. DeWeese. Aug 88, 63p NBSIR-88/3097 Supersedes PB88-123682.

Keywords: *Metrology, *Electromagnetic properties, *Bibliographies, Superconductors, Magnetic measurement, Lasers, Optical fibers, Cryoelectronics.

The bibliography lists the publications of the personnel of the Electromagnetic Technology Division of NBS in the period from January 1970 through publication of the report. A few earlier references that are directly related to the present work of the Division are also in-

900,872 PB89-149108 Not available NTIS National Bureau of Standards (NML), Gaithersburg, MD. Length and Mass Div. Interpretation of a between-Time Component of

Error in Mass Measurements. Final rept.

B(7) 1987.

R. S. Davis. 1987, 7p Pub. in Proceedings of Measurement Science Conference, Irvine, CA., January 29-30, 1987, pIII-B(1)-III-

Keywords: *Error analysis, *Reliability, Measuring instruments, Metrology, Random error, Mathematical models, *Between-time error, *Calibration errors, Mass measurement.

Detection of a between-time component of error in a calibration process involves analysis of a lengthy record of data. An individual object or device which is being calibrated must be returned to the customer in a timely way. Therefore, evidence of a between-time component of error can only be inferred from studies of standards which are internal to the calibration facility. If study of internal standards reveals such an error component, it then becomes necessary to propagate this error to the reported calibration uncertainty. Because sophisticated calibrations usually involve measurement designs which are solved by least squares techniques, the propagation of a between-time error component is obscured. In order to examine such propagation it is necessary to choose a mathematical model which can account for the observed effects. Since choice of this model has a profound effect on the analysis, the metrologist must be aware of its implications. These considerations are illustrated by a real example from precision mass metrology.

900.873 PB89-149215 Not available NTIS National Bureau of Standards (NML), Gaithersburg, MD. Gas and Particulate Science Div. Special Calibration Systems for Reactive Gases

and Other Difficult Measurements. Final rept. W. D. Dorko, and E. E. Hughes. 1987, 6p

Pub. in ASTM (American Society for Testing and Materials) Special Technical Publication 957, p132-137

Keywords: *Measuring instruments, *Gas analysis, Gas chromatography, Measurement, Reliability, *Reactive gases, *Calibration standards.

The most popular method for analyzing a component of interest in a gas mixture is to use a detector which responds to the analyte and is calibrated directly with a cylinder gas mixture containing the analyte at the ap-proximate concentration of interest. In many in-stances, however, this cannot be achieved; cylinder calibration mixtures may be unstable or the direct response detector may not be sensitive enough. The unstable cylinder mixture can be replaced by a dynamic dilution gas calibration system where the analyte can be introduced to any one of several means including permeation devices, or a higher concentration gas mixture which can be more easily stabilized. If the detector for the analyte is insensitive or difficult to calibrate then the analyte can be converted to another compound for which there is a detector which is sufficiently sensitive and easy to calibrate. Any system which will produce a mixture of the required concentration, of acceptable uncertainty, and of stability sufficient for the analysis at hand can be a special calibration system.

900.874

PR89-153894 PC A05/MF A01 National Bureau of Standards (NEL), Gaithersburg, MD. Precision Engineering Div.

NIST (National Institute of Standards and Technology) Measurement Services: Mass Calibrations. Final rept.

R. S. Davis. Jan 89, 76p NIST/SP-250/31

Also available from Supt. of Docs. as SN003-003-02919-0. Library of Congress catalog card no. 88-600608.

Keywords: Calibrating, Density, Mass, Least squares method, Measurement, Primary standards, method, Measurement, Primary standards, Setting(Adjusting), *Mass calibration, National Institute for Standards and Technology.

The NIST calibration service for standard masses is described. Weights which are accepted for calibration range in nominal values from 1 mg to 13,600 kg (30,000 pounds). Weights used to generate standard pressures in piston gages are also accepted. Cleaning procedures used on weights prior to calibration are described. The measurement algorithms (including density determinations of single-piece kilogram weights) and the uncertainties assigned to calibrated weights are discussed. The system now in place to monitor the quality of calibrations is described. Finally, the limitations of the present controls on measurement quality and outline improvements which are underway are assessed.

900.875

PB89-157184 Not available NTIS National Bureau of Standards (NEL), Gaithersburg, MD. Thermophysics Div.
Semi-Automated PVT Facility for Fluids and Fluid

Mixtures. Final rept.

D. Linsky, J. M. H. L. Sengers, and H. A. Davis.

1987, 5p Pub. in Review of Scientific Instruments 58, n5 p817-821 1987.

Keywords: *Automatic control equipment, *Mixtures, *Fluids, *Supercritical flow, Geothermal prospecting, Boiling points, Capacitance bridges, Dew point, Gas laws, Measurement, Pressure, Volume, Temperature, Bubbles, Density(Mass/volume), Reprints.

A manually-operated Burnett PVT apparatus has been converted into a semi-automated Burnett-isochoric facility. An automated pressure injector with dedicated control logic nulls a sensitive differential pressure indicator. A microcomputer is used in setting the control temperature, monitoring equilibration, measuring temperature and pressure, processing the raw data and storing the information. The quality of the apparatus is demonstrated by means of a low-density and a highdensity isochore obtained for a geothermal working fluids mixture in one-phase, two-phase and supercritical regimes, including a dew and a bubble point.

900 876 PB89-162234 PC A13/MF A01 National Inst. of Standards and Technology, Gaithersburg, MD.

Electrical Performance Tests for Hand-Held Digital Multimeters. Final rept.

T. F. Leedy, K. J. Lentner, O. B. Laug, and B. A. Bell.

Jan 89, 290p NISTIR-88/4021 Sponsored by Army Communications-Electronics Command, Fort Monmouth, NJ.

Keywords: *Performance tests, *Standards, *Multimeters, Electric measuring instruments, Electrical measurement, Reliability, Voltmeters, Ammeters, Digital systems.

Electrical performance test procedures for battery-powered, hand-held digital multimeters were developed for the purpose of evaluating samples submitted by electronic instrument manufacturers in response to specifications issued by the U.S. Army Communica-tions-Electronics Command. The detailed, step-bystep test procedures are based on the Army specifications and include sample data sheets and tables for the recording of interim data and final test results. The report discusses the measurement principles and techniques underlying each of the procedures. In addi-

Laboratory & Test Facility Design & Operation

tion, the sources of measurement uncertainty are dis-

900,877 PB89-173496 Not available NTIS National Bureau of Standards (NML), Gaithersburg, MD. Ionizing Radiation Physics Div.
Computer Program for Instrument Calibration at State-Sector Secondary-Level Laboratories.

Final rept.

H. T. Heaton. 1988, 13p Pub. in Proceedings of Midyear Health Physics Society Topical Meeting on Instrumentation (22nd), San Antonio, TX., December 4-8, 1988, 13p.

Keywords: *Calibrating, *Measuring instruments, Standardization, X rays, Gamma rays, Quality control, *Instrument compensation, Computer software.

To provide the quality assurance necessary for secondary-level laboratories, a computer program has been developed for use by state-sector laboratories calibrating instruments used in x-ray and gamma-ray fields. Although specific to the equipment in statesector laboratories, the basic procedures are also applicable to secondary-level laboratories in the private and federal sectors. The program is written in a compiled BASIC. After the initial program selection, options are menu driven. There are specific programs for each of the classes of instruments calibrated by these lab-oratories. They perform the routine quality control on all of the pertinent equipment used for calibrations and make the measurements to characterize the laboratory, which are necessary for the uncertainty analysis and generation of the final report.

PB89-173934 Not available NTIS National Bureau of Standards, Gaithersburg, MD. Associate Director of Industry and Standards.

NBS (National Bureau of Standards) Calibration Services: A Status Report.

Final rept.

Pilia rept.

G. A. Uriano. 1984, 24p

Pub. in Proceedings of Workshop and Symposium of the National Conference of Standards Laboratories, Gaithersburg, MD., October 1-4, 1984, p35-1-35-24.

Keywords: *Standards, *Metrology, Documentation, National government, *National Institute of Standards and Technology, *Calibration, Standard reference materials, Federal agencies.

A status report is given for NBS calibration service and related activities. Discussed are recent and pending administrative changes in the program, and the budget/resource outlook for the next several years. A budget/resource outlook for the next several years. A description is given of a number of recent NBS publications aimed at improving the quality and quantity of information available to users of NBS measurement services. Highlights of new NBS technical services recently initiated are also described. These include (1) a new MAP for the measurement coefficient of luminous intensity of retroreflectors, (2) the reestablishment of the calibration services for odd decade electrical resistors, (3) new NBS capabilities in x-ray dosimetry, (4) new NBS capabilities and services for microwave and antenna measurements, (5) improvements in dimensional metrology and pressure/vacuum services, (6) several new SRMs for use in measurement of temperature, the dimensions of fine particles, and for the evaluation of the performance of coordinate measuring machines.

PB89-173975 Not available NTIS National Bureau of Standards (NML), Gaithersburg, MD. Electron Physics Div.

Precision Weight Calibration with a Specialized

Final rept.
R. D. Cutkosky. 1988, 6p
Pub. in Proceedings of Measurement Science Conference, Long Beach, CA., January 29-30, 1988, p1-6.

Keywords: *Weight measurement, *Automation, *Robots, Calibrating, Weight indicators, Automatic control, Balance.

A selected commercial top-loading balance with a range of 200 grams and a resolution of 10 micrograms has been adapted for use in conjunction with a specially designed robot arm configured to load and unload the balance in accordance with established weighing designs. The complete system includes a personal computer for control of the robot and the balance, a 6axis stepper motor controller, and a system for maintaining the balance, the robot, and the stored weights at a constant temperature.

900,880 PB89-175699 Not available NTIS National Bureau of Standards (NML), Gaithersburg, MD. Temperature and Pressure Div.

NBS (National Bureau of Standards) Orifice-Flow

Primary High Vacuum Standard.

Final rept. K. E. McCulloh, C. R. Tilford, S. D. Wood, and D. F.

Martin. 1986, 1p Pub. in Jnl. of Vacuum Science and Technology A 4, n3 pt1 p362 May/Jun 86.

Keywords: *Standards, Oriface flow, Vacuum gages, Pressure, Reprints, *High vacuum, Spinning rotor gages, Molecular drag gages.

The National Bureau of Standards has constructed a primary high vacuum standard of the orifice-flow type that currently covers the range 10 to the -6 power to 10 to the -1 power Pa. The uncertainty of the standard is 3.4% at 10 to the -6 power pa, 1.4% at 10 to the -4 power pa, and 2.5% at 10 to the -1 power pa.

900,881 PB89-176135 Not available NTIS National Bureau of Standards (NEL), Gaithersburg, MD. Building Physics Div.

Circular and Square Edge Effect Study for Guard-

ed-Hot-Plate and Heat-Flow-Meter Apparatuses.

B. Peavy, and B. Rennex. 1986, 7p Pub. in Jnl. of Thermal Insulation 9, p254-300 Apr 86.

Keywords: *Heat flow meters, *Size determination, *Shape, *Heat transmission, Circles(Geometry), Squares(Geometry), Thermal insulation, Thermal resistance, Thermal conductivity, Mathematical models, Reprints, *Edge effect, *Guarded hot plate.

The guarded-hot-plate apparatus measures thermal resistance across thermal insulation specimens. The measurement of very thick specimens results in an edge error due to the loss of some of the centrally metered heat to the peripheral ambient surrounding the specimen. To choose the appropriately sized appara-tus for a particular test, it is important to know the order of magnitude of this edge error as a function of specimen thickness. The report defines the edge effect, derives a model for its calculation for both circular and square geometries, and indicates graphically the sensitivity of the edge-effect curves (as a function of thickness) with respect to the following parameters: the ratio of the guard to metered sizes, the metered size itself, the ratio of the surface heat transfer coefficient to the specimen apparent conductivity, and the apparent-thermal-conductivity anisotropy. The results of the square metered area are compared with those of the circular metered area, and the theoretical results are compared with experimental results for a circular geometry (using a 1-m guarded hot plate).

900,882 PB89-176432 Not available NTIS National Bureau of Standards, Gaithersburg, MD. Office of Product Standards Policy

Laboratory Accreditation Systems in the United States, 1984. Final rept.

J. W. Locke. 1984, 13p Pub. in Proceedings of Workshop and Symposium of the National Conference of Standards Laboratories, Gaithersburg, MD., October 1-4, 1984, p29-1-29-13.

Keywords: *Laboratories, *Test facilities, Measurement, Standards, *Accreditation, Calibration.

Laboratory accreditation in the United States is growing as is demonstrated by the comparison of the newest survey conducted for the NBS Office of Product Standards Policy by the Marley Organization with the original study completed in 1979. The largest interest in accreditation comes from administrators of government funded programs (e.g. health care and depand where accurate measurement is peeded to justice the programs of the program of the programs of the program of the programs of the programs of the programs of the program of fense) where accurate measurement is needed to justify payment of fees or contracts. There is a growing interest in accreditation by some product marketeers since the use of test data from accredited testing laboratories in specific areas can help sell products. There is little thrust toward developing a coordinated accreditation system to serve all users, although the continuing increase in the number of accreditation systems and laboratories seeking accreditation and the

expansion of export markets will tend to encourage such coordination. Verification of calibrations is important in most accreditation systems and is emphasized in defense systems, but in no case is the identification of uncertainties throughout the chain of measurement

900,883

Not available NTIS
National Bureau of Standards (NML), Gaithersburg,
MD. Gas and Particulate Science Div.
Trace Gas Calibration Suckey

Devices.

rinal rept. G. D. Mitchell. 1987, 11p Pub. in ASTM (American Society for Testing and Materials) Special Technical Publication 957, p110-120 1987.

Keywords: *Permeameters, *Flow measurement, Temperature control, Stability, Gas analysis, Diffusion, Solubility, Reprints, *Calibration, *Trace gases.

The paper describes trace calibration systems and the factors that influence their operation. COGAS, a dynamic trace calibration system that serves as both a permeation device and an instrument calibration system, is presented. Such a system improves precision, reduces manpower requirements, and is versatile in its application.

900,884 PB89-176606 PB89-176606 Not available NTIS National Bureau of Standards (NEL), Gaithersburg,

MD. Building Physics Div.

Summary of Circular and Square Edge Effect
Study for Guarded-Hot-Plate and Heat-Flow-Meter Apparatuses.

B. Peavy, and B. Rennex. 1988, 26p Pub. in Thermal Conductivity 19, p173-198 1988.

Keywords: *Heat flow meters, *Size determination, *Shape, *Thermal measuring instruments, *Heat transmission, Circles(Geometry), Squares(Geometry), Thermal insulation, Thermal resistance, Thermal conductivity, Mathematical models, Reprints, *Edge effect.

The report provides the information necessary to choose the appropriate apparatus size for a measurement of thermal resistance of a specimen of insulation material of a particular thickness. The information consists of the order of magnitude of apparatus edge error as a function of specimen thickness. The report defines the edge effect; derives a model for its calculation for both circular and square geometries, and indi-cates graphically the sensitivity of the edge-effect curves (as a function of thickness) with respect to the following parameters: the ratio of the guard to metered sizes, the metered size itself, the ratio of the surface heat transfer coefficient to the specimen apparent conductivity, and the apparent-thermal-conductivity anisotropy. The results of the square metered area are compared with those of the circular metered area, and the theoretical results are compared with the expenmental results for a circular geometry (using a 1-m guarded hot plate).

900,885 PB89-177190

Not available NTIS
National Bureau of Standards (NEL), Gaithersburg,
MD. Automated Production Technology Div.
Automated Fringe Counting Laser Interferometer
for Low Frequency Vibration Measurements.
Final rept

Final rept.

Pub. in Proceedings of International Instrumentation Symposium on Instrumentation in the Aerospace Industry (32nd), Seattle, WA., May 5-8, 1986, p1-7.

Keywords: *Accelerometers, *Vibration meters, *Transducers, Automation, *Laser interferometers, *Calibration, Computerized control systems.

Low frequency accelerometers and velocity transducers are widely used for vibration investigations on structures such as buildings, bridges, aircraft, ships, power plant equipment, and seismic applications. Previous work in this area has focused on the development of accurate calibration methods for transducers by optical methods in the frequency range of 2-100 Hz. The paper describes a computer-controlled fringe counting system for transducer calibration. The calibration system uses digital signal analysis for accurate

Laboratory & Test Facility Design & Operation

low frequency voltage measurements. The measurement procedures are fully automated, with menu driven programs using the computer soft keys for controlling the test frequencies, acceleration levels, set-ting test parameters, collecting and storing data and producing reports and graphs. An error analysis is given and experimental data are presented for transducer calibrated on this system.

900,886 PB89-179162 Not available NTIS National Bureau of Standards (NML), Gaithersburg, MD. Gas and Particulate Science Div.

Precision and Accuracy Assessment Derived from

Calibration Data.

Pub. in ASTM (American Society for Testing and Materials) Special Technical Publication 957, p81-86 1987.

Keywords: *Precision, *Accuracy, *Assessments, Data processing, Error analysis, Bias, Standards, Reprints, *Calibration.

During the past ten years, the importance of assessing the precision and the accuracy of data derived from standard methods has become recognized. Both ASTM and EPA have developed policies requiring pre-cision and accuracy assessment for methods before they are designated as standard methods or reference methods. The difficulty in implementing these policies is not in developing a meaningful error estimate for a given method, it is in separating the random from the systematic components of the error. In the paper, a method of separating error components into precision and bias is given. The method uses calibration data taken repeatedly at a fixed point using a standard whose total uncertainty is small compared to the uncertainty of the measurement method.

900,887 PB89-184089 PC A04 National Inst. of Standards and Technology, Gaithers-

Journal of Research of the National Institute of Standards and Technology. Volume 94, Number 2, March-April 1989.

Bi-monthly rept. 1989, 58p

Also available from Supt. of Docs. as SN703-027-00027-0. See also PB89-184097 through PB89-184121 and PB89-133367.

Keywords: *Measurement, *Standards, Electrical measurement, Chromatography, Termal conductivity, Coaxial cables, Pneumatic lines, Spectroscopy, Supercritical fluids, Hot-wire flowmeters.

The journal contains the following articles: New international adopted reference standards of voltage and resistance; A supercritical fluid chromatograph for physicochemical studies; Relation between wire resistance and fluid pressure in the transient hot-wire method; and Scattering parameters representing imperfections in precision coaxial air lines.

900,888 PB89-186381 Not available NTIS National Bureau of Standards (NEL), Boulder, CO. Statistical Engineering Div.

Calibration with Randomly Changing Standard Curves. Final rept. D. F. Vecchia, H. K. Iyer, and P. L. Chapman. 1989,

Pub. in Technometrics 31, n1 p83-90 Feb 89.

Keywords: *Measuring instruments, Statistical samples, Regression analysis, Calibrating, ples, Regression analysis, Calibra Curves(Graphs), Reprints, *Calibration standards.

Changes in calibration curves from one time to the next caused by drift often require measuring devices to be recalibrated at frequent intervals. In such situations, the usual practice is to estimate the unknown values of test samples using only data from the corresponding calibration period. Under a random coefficient regression model for the different calibration curves, however, it can be shown that it is more efficient to combine the data from all calibration periods to estimate the unknowns. The authors consider a particular class of point estimators obtained by inverting suitable prediction functions and show that the estimator obtained from a best prediction function is optimal in a sense defined by Godambe and Durbin in the context of unbiased estimating equations. The small sample performance of the estimator is compared with the usual estimator using the Pitman closeness criterion.

900,889

PB89-186787 Not available NTIS National Bureau of Standards (NEL), Boulder, CO. Chemical Engineering Science Div

NBS (National Bureau of Standards)-Boulder Gas Flow Facility Performance.

S. E. McFaddin, J. A. Brennan, and C. F. Sindt. 1988, 4p

Sponsored by Gas Research Inst., Chicago, IL. Pub. in American Gas Association Operating Section Proceedings, Toronto, Canada, May 16-18, 1988, p492-495

Keywords: *Gas flow, *Test facilities, *Flow measurement, Performance, Efficiency, Gas pipelines, Temperature, Flowmeters, Precision, Reprints.

Major modifications have been made to the gas flow facility at the National Bureau of Standards in Boulder, Colorado. Significant improvements in steady state operation and overall efficiency have resulted. Variability in the gas temperature has been decreased by a factor of five and the precision of performance data on flowmeters has increased by a factor of two. The massbased facility provides the gas industry with an accurate, efficient, and precise research facility operating at pipeline conditions.

900,890

PB89-189278 PC A04/MF A01 National Inst. of Standards and Technology, Gaithers-

burg, MD.
NVLAP (National Voluntary Laboratory Accreditation Program) Directory of Accredited Laboratory

J. L. Donaldson, and J. Horlick. 1 Apr 89, 57p NISTIR-89/4056 See also PB88-169529.

Keywords: *Directories, *Laboratories, Fields, Test facilities, Tests, Accreditation.

The 1989 NVLAP Directory of Accredited Laboratories provides information on the activities of the National Institute of Standards and Technology in administering the National Voluntary Laboratory Accreditation Program (NVLAP) during calendar year 1989. The status of current programs is briefly described and a summary of laboratory participation is provided. Indexes cross reference the laboratories by name, NVLAP Lab Code Number, accreditation program, and geographical lo-cation and cross reference NVLAP code numbers with test method designations. The scope of accreditation of each laboratory, listing the test methods for which it is accredited, is provided.

900.891

PB89-193841 PC A04/MF A01 National Inst. of Standards and Technology (NML), Gaithersburg, MD. Center for Basic Standards. NIST (National Institute of Standards and Technology) Measurement Services: High Vacuum Standard and Its Use.

Interim rept. S. Dittmann. Mar 89, 71p NIST/SP-250/34 Also available from Supt. of Docs as SN003-003-02934-3. Library of Congress catalog card no. 88-600605.

Keywords: *Standards, *High vacuum, *Pressure measurement, Vacuum gages, Test facilities, Flow-meters, Ionization, Resistance, Pressure, Orifices, Calibration standards.

The document presents an in-depth discussion of the National Institute of Standards and Technology primary high vacuum standard, used between 10 to the minus 6th power and .01 Pa. Included are discussions of the theory, design, and construction of the standard. The systematic and random errors in the standard and the methods used to check the accuracy of the standard are presented. Also included is a brief discussion of the molecular drag gage and its use as a transfer standard between .0001 and .1 Pa.

900.892

PB89-201164 Not available NTIS National Bureau of Standards (NML), Gaithersburg, MD. Office of Standard Reference Data.

Standard Reference Materials for Dimensional and Physical Property Measurements.

Final rept.

L. J. Kieffer. 1986, 6p

Pub. in Proceedings of Measurement Science Conference, Irvine, CA., January 23-24, 1986, p167-172.

Keywords: *Standards, *Mechanical properties, *Measurement, Measuring instruments, Test facilities, *Standard Reference Materials.

An overview of Standard Reference Materials (SRMs) distributed by the National Bureau of Standards for use in standardizing physical property measurements is presented. In addition some reference materials (artifacts) to be used in standardizing dimensional metrology measurements are discussed in some detail.

900,893

PB89-201180 Not available NTIS National Bureau of Standards (NML), Gaithersburg, MD. Temperature and Pressure Div. Development of New Standard Reference Materials for Use in Thermometry.

Final rept.

B. W. Mangum, 1986, 11p

Pub. in Proceedings of Measurement Science Conference, Irvine, CA., January 23-24, 1986, p148-158.

Keywords: *Temperature measurement, *Standards, *Thermodynamic properties, Temperature measuring instruments, *Standard Reference Materials.

In recent years, several SRMs have been developed for use in thermometry. These cover the range from 0.015 K to 2326 K. The article will review the use and importance of thermometric fixed points in precision thermometry and discuss new developments in SRMs related to those fixed points.

900,894 PB89-201818 Not available NTIS National Bureau of Standards (NML), Gaithersburg, MD. Length and Mass Div.

Stability of the SI (International System) Unit of Mass as Determined from Electrical Measurements.

Final rept.

R. S. Davis. 1989, 2p

Pub. in Metrologia 26, p75-76 1989.

Keywords: *Mass, *Standards, *Electrical measurement, Precision, Test facilities, Stability, Reprints, Calibration standards.

The apparatus developed by Kibble at the National Physical Laboratory has recently achieved an uncertainty smaller than 1 x 10 to the minus seventh power in measuring the ratio between the electrical watt as maintained and the watt as defined in the International System (SI). Since there is reason to anticipate further experimental improvements, the possibility of monitoring the stability of the SI unit of mass (the kilogram) through such an apparatus is being seriously discussed. The kilogram is the only remaining base unit of the SI still defined by an artifact. The letter points out that electrical measurements even now provide the most critical test of the long-term stability of the SI unit of mass.

900 895 PB89-209266 PC A04/MF A01 National Bureau of Standards (NEL), Gaithersburg, MD. Precision Engineering Div. Length Scale Measurement Procedures at the Na-

tional Bureau of Standards J. S. Beers. Sep 87, 72p NBSIR-87/3625

Keywords: *Interferometers, *Measurement, *Length, Optical measuring instruments, Performance, Calibrating, Precision, Test facilities.

Precision graduated length scales have been measured by interferometry at NBS since 1965. An instrument called the Line Scale Interferometer was designed for this purpose. The history, development, improvement, operation and evaluation of the line scale interferometer are described. Special emphasis is given to detailed operating procedures to provide guidance in the use of the instrument. Evaluating performance through a measurement assurance program is also emphasized.

900,896 PB89-209324

PC A07/MF A01

Laboratory & Test Facility Design & Operation

Virginia Polytechnic Inst. and State Univ., Blacksburg. Dept. of Mechanical Engineering. Development of an Automated Probe for Thermal

Final rept.

Conductivity Measurements.

B. P. Dougherty, and W. C. Thomas. May 89, 131p NIST/GCR-89/563 Grant NSNB-6-D0642

Sponsored by National Inst. of Standards and Technology (NEL), Gaithersburg, MD. Center for Building Technology.

Keywords: *Temperature measuring instruments, *Thermistors, *Thermal conductivity, Thermal resistance, Thermophysical properties, Liquids, Thermal measurements, Mathematical models, Calibrating.

A transient technique was validated for making thermal conductivity measurements. The technique incorporated a small, effectively spherical, heat source and temperature sensing probe. The actual thermal conductivity measurements lasted 30 seconds. After approximately 15 minutes of data reduction, a value for thermal conductivity was obtained. The probe yielded local thermal conductivity measurements. Spherical sample volumes less than 8 cu cm were required for the materials tested. Thermal conductivity (and moisture) distributors can be measured for relatively dry or wetted samples.

900,897 PB89-209340 PC A10/MF A01 National Inst. of Standards and Technology (NML), Gaithersburg, MD. Temperature and Pressure Div. NIST (National Institute of Standards and Technology) Measurement Services: The Calibration of Thermocouples and Thermocouple Materials.

Final rept. G. W. Burns, and M. G. Scroger. Apr 89, 204p NIST/

Also available from Supt. of Docs. as. SN003-003-02939-4. Library of Congress catalog card no. 89-600732.

Keywords: *Thermocouples, Test facilities, Platinum, Temperature measurement, Thermal measurements, Quality control, Mathematical models, Thermophysical properties, Rhodium, Statistics, Accuracy, *Calibration

The document describes the calibration services for thermocouples and thermocouple materials presently thermocouples and thermocouple materials presently provided by the NIST at temperatures from -210 to 2100 C. Three general calibration methods used at NIST, which provide traceability to the International Practical Temperature Scale of 1968, are outlined in detail. Consideration is given primarily to the calibration of type S (platinum-10% rhodium versus platinum) thermocouples at defining fived points of the IPTS-68 thermocouples at defining fixed points of the IPTS-68 as standard instruments, and to the calibration of other letter-designated type thermocouples (types B, R, S, E, J, K, N, and T) by comparison with a calibrated reference thermocouple and by comparison with a standard platinum resistance thermometer. The procedures followed to maintain internal quality control of appara-tus and standards in the NIST thermocouple calibration laboratories are covered, and statistical assess-ments of the uncertainties involved in the calibrations of type S thermocouples by the fixed-point method and by the comparison method are presented.

900.898

Not available NTIS National Inst. of Standards and Technology (NEL), Gaithersburg, MD. Chemical Process Metrology Div. Gas Flow Measurement Standards. Final rept.

Pub. in Proceedings of AIChE (American Institute of Chemical Engineers) Meeting, Houston, TX., April 1989, 20p.

Keywords: *Gas flow, *Flow measurement, *Standards, Air flow, Test facilities, Errors, Pressure, Temperature, Precision.

The National Institute of Standards and Technology The National Institute of Standards and Technology (NIST), formerly the National Bureau of Standards, maintains the U.S. standards for gas flow measurement. These consist of a number of flow facilities that enable the arrangements and measurement of a wide range of fluid and flow conditions. In the paper, descriptions are given for the air flow-rate facilities at NIST-Gaithersburg, MD. The air flow measurement facilities maintained at NIST-Gaithersburg include a variation of fluid technique that the pared. ety of timed-collection of fluid techniques that are used

to calibrate flowmeters and transfer standards. As well, these facilities are available for establishing and well, trese facilities are available for establishing and maintaining the different types of traceability needed by U.S. industry and other government agencies, etc. These needs are based upon the increased concerns for improved gas flow measurements because of the increasing values of the materials involved. Higher actualists and provision levels are being actually as curacies and precision levels are being sought not only in custody transfer between buyer and seller but also in the continuous process industries where optimal control can only be attained via precise measure-

900,899 PB89-211882 PB69-211882 Not available NTIS
National Bureau of Standards (NEL), Gaithersburg, MD. Chemical Process Metrology Div. Prediction of Flowmeter Installation Effects.

Fried rept.
T. T. Yeh, and G. E. Mattingly. 1989, 32p
Pub. in Proceedings of AlChE (American Institute of Chemical Engineers) Spring National Meeting, Houston, TX., April 1989, p1-32.

Keywords: *Flowmeters, *Pipe flow, Fluid flow, Turbulent flow, Flow measurement, Pipes(Tubes), Velocity, Orifice flow, Laser doppler velocimeters.

The research program described is intended to improve flow meter performance in 'non-ideal' installation conditions. The program involves a procedure through which a strategy is proposed and evaluated for predicting flowmeter performance when the meter is installed too near elbows, reducers, flow conditioning elements, etc. The strategy is based upon understand-ing and parameterizing the salient features of the pipe flows produced by selected piping configurations and understanding how specific meters perform in these flows. The results described include: laser Doppler velocimetry (LDV) measurements of the mean and the turbulence velocities for the pipe flows produced by single and double elbow configurations -- the elbows-out-of-plane with different spacings between the elbows, the quantification of these secondary flows in the downstream piping, and the demonstration that the flowmeter prediction strategy works for selected tur-bine-type and orifice-type flowmeters in these flows.

PB89-211890 Not available NTIS National Bureau of Standards (NEL), Gaithersburg, MD. Chemical Process Metrology Div.

Prediction of Flowmeter Installation Effects. Final rept.

Final rept.
T. T. Yeh, and G. E. Mattingly, 1989, 32p
Pub. in Proceedings of Institute of Gas Technology
Symposium, Chicago, IL., June 1989, p1-32.

Keywords: *Flowmeters, *Pipe flow, Fluid flow, Turbulent flow, Flow measurement, Pipes(Tubes), Velocity, Orifice flow, Laser doppler velocimeters.

The research program described is intended to improve flow meter performance in 'non-ideal' installation conditions. The program involves a procedure through which a strategy is proposed and evaluated for predicting flowmeter performance when the meter is installed too near elbows, reducers, flow conditioning elements, etc. The strategy is based upon understanding and parameterizing the salient features of the pipe flows produced by selected piping configurations and understanding how specific meters perform in these flows. The results described include: laser Doppler velocimetry (LDV) measurements of the mean and the turbulence velocities for the pipe flows produced by single and double elbow configurations -- the elbowsout-of-plane with different spacings between the elbows, the quantification of these secondary flows in the downstream piping, and the demonstration that the flowmeter prediction strategy works for selected turbine-type and orifice-type flowmeters in these flows.

PC A03/MF A01 National Inst. of Standards and Technology (NEL), Gaithersburg, MD. Applied and Computational Mathe-

Mechanism for Shear Band Formation in the High Strain Rate Torsion Test. T. J. Burns. Jun 89, 46p NISTIR-89/4121

Keywords: *Torsion tests, Plastic flow, Shear flow, Shear properties, Strains, Conduction, Numerical analysis, Mathematical models.

An asymptotics argument is given, which shows that rigid unloading from the ends of the thin-walled tubular

specimen, enhanced by conductive heat transfer, is a plausible mechanism for adiabatic shear band formation during the high strain rate torsion test. The argument assumes that thickness variations, as well as elastic and dynamic effects in the tube, can be ignored, but that heat conduction and heat-sink thermal boundary conditions must be included. The proposed mechanism is supported by a numerical analysis of a mathematical model of the torsion test, which is based on recent torsional Kolsky bar experimental work of Marchand and Duffy (1988), on a physical model of thermoelastic-plastic flow due to Wallace (1985), and on a phenomenological Arrhenius model of the plastic flow surface. The numerical technique used is the semi-discretization method of lines.

900.902

PB89-228282 PC A03/MF A01 National Bureau of Standards, Gaithersburg, MD. Associate Director of Industry and Standards.

Update of U.S. Participation in International Standards. ards Activities.

P. W. Cooke. Jul 89, 25p NISTIR-89/4124 See also PB88-164165.

Keywords: *Standards, *United States, Standardization, Industrial engineering, *International Standards Organization, *International Electrotechnical Commission, International organizations.

The report presents updated information on the current level of U.S. participation in the two major international standardization bodies, International Standards Organization and International Electrotechnical Com-mission. Data on the new ISO/IEC Joint Technical Committee 1 on Information Technology are also presented.

PB89-228324 PC A03/MF A01 National Inst. of Standards and Technology, Gaithers-burg, MD. National Voluntary Lab. Accreditation Pro-

orgam.

NVLAP (National Voluntary Laboratory Accreditation Program) Assessment and Evaluation Manual.

R. L. Gladhill. Jul 89, 20p NISTIR-88/3853 See also PB85-200079.

Keywords: *Laboratories, Test facilities, Standards, Evaluation, Test facilities, Manuals, *Accreditation, *National Voluntary Laboratory Accreditation Program.

The National Voluntary Laboratory Accreditation Program (NVLAP), established in 1976, is administered by the National Institute of Standards and Technology (NIST) formerly the National Bureau of Standards (NBS). NVLAP is a voluntary system for assessing and evaluating testing laboratories and accrediting those found competent to perform specific test methods or these of that methods of the program of the pro types of test methods. Laboratory accreditation pro-grams are established for specified product or service areas in response to requests and demonstrated need. The publication, intended for the NVLAP technical experts who serve as assessors and evaluators, describes general policies and practices of NVLAP assessment and evaluation. The specific technical critena for assessing and evaluating laboratories are pro-vided elsewhere, in NVLAP Handbooks and checklists for each technical area.

PB89-231104 Not available NTIS National Inst. of Standards and Technology (NML), Gaithersburg, MD. Temperature and Pressure Div. InSb as a Pressure Sensor.

V. E. Bean. 1988, 7p Pub. in Proceedings of Seminar on High Pressure Standards, Paris, France, May 24-25, 1988, p125-131.

Keywords: *Indium antimonides, Pressure sensors, Pressure measurement, Semiconductor devices, Sensitivity, Performance, Standards, *Pressure transduc-

The resistivity of InSb increases exponentially with pressure. A pressure transducer was made, based on InSb, that has nearly 70 times the sensitivity at 645 MPa of a manganin pressure transducer. The trans-ducer has adequate sensitivity and short term stability to be used to measure the change of pressure generated by a controlled-clearance piston gage resulting from a change of jacket pressure from which the cylin-der distortion coefficient can be determined. The long term performance data necessary to evaluate the suit-

INDUSTRIAL & MECHANICAL ENGINEERING Laboratory & Test Facility Design & Operation

ability of the transducer as a transfer standard for laboratory intercomparison is not yet available.

900,905

PB89-231112 Not available NTIS National Inst. of Standards and Technology (NML), Gaithersburg, MD. Temperature and Pressure Div. Non-Geometric Dependencies of Gas-Operated Piston Gage Effective Areas.

Final rept. C. R. Tilford, R. W. Hyland, and S. Yi-Tang. 1988, 9p Pub. in Proceedings of Seminar on High Pressure Me-trology, Paris, France, May 24-25, 1988, p105-113.

Keywords: *Pressure measurement, Manometers, Standards, Gases, *Piston gages, Effective area.

Using a mercury manometer, the authors determined the effective areas of different gas-operated piston gages as a function of pressure, mode of operation (absolute or differential), and gas species. They have observed changes in the effective area of individual gages that vary from zero to 25 ppm as these parameters are changed. Over the 5-160 kPa range of these experiments, changes in the geometry of the pistons and cylinders cannot explain these effects. These results demonstrate the need for a more refined theory of the pistons of the pi of the interaction of the pressure fluid and the piston cylinder. Until that is available, effective areas of primary standard piston gages calculated on the basis of geometric factors alone can have significant uncertainties.

900.906

PB89-231120 Not available NTIS National Inst. of Standards and Technology (NML), Gaithersburg, MD. Temperature and Pressure Div. Observations of Gas Species and Mode of Operation Effects on Effective Areas of Gas-Operated Piston Gages.

Final rept.

B. E. Welch, R. E. Edsinger, V. E. Bean, and C. D. Ehrlich. 1988, 14p

Pub. in Proceedings of Seminar on High Pressure

Standards, Paris, France, May 24-25, 1988, p81-94.

Keywords: *Pressure measurement, Helium, Neon, Nitrogen, Argon, Krypton, Carbon dioxide, *Piston gages, Effective area.

The effective areas of four gas-operated piston gages have been determined by the pressure calibration technique with a state-of-the-art manometer using both helium and nitrogen in the absolute mode. For all four gages, the effective areas with nitrogen are greater than the effective areas using helium. The differer than the effective areas using helium. The differences range from 4 to 28 parts-per-million. Pairs of these gages have been cross-floated in both the gage and the absolute modes with helium, neon, nitrogen, argon, carbon dioxide, and krypton. For a given gas, the effective area in the absolute mode is greater than that for the gage mode. The magnitude of the difference is dependent upon the species of gas.

900.907

PB89-231146 PB89-231146 Not available NTIS National Inst. of Standards and Technology (NEL), Boulder, CO. Electromagnetic Fields Div.

Advances in NIST (National Institute of Standards and Technology) Dielectric Measurement Capability Using a Mode-Filtered Cylindrical Cavity. Final rept.

Pinal rept.

E. J. Vanzura, and W. A. Kissick. 1989, 4p

Pub. in Proceedings of IEEE (Institute of Electrical and Electronics Engineers) MTT-S International Microwave Symposium, Long Beach, CA., p901-904 Jun 89.

Keywords: *Measuring instruments, *Cavity resonators, Microwave frequencies, Design, Performance evaluation.

A 60-mm diameter cylindrical cavity resonator has been constructed for performing high-accuracy permittivity measurements on low-loss materials at microwave frequencies. The cavity's design and evaluation are described. Estimated errors in seven parameters result in approximately 0.2% uncertainty in permittivity and 6% uncertainty in loss tangent for a fused silica measurement.

PB89-235634 **PC A04** National Inst. of Standards and Technology, Gaithersburg, MD.

Journal of Research of the National institute of Standards and Technology, Volume 94, Number 4, July-August 1989.

Bi-monthly rept.

1989, 73p

See also PB89-235642 through PB89-235675 and Volume 94, Number 3, PB89-211106. Also available from Supt. of Docs. as SN703-027-00029-6.

Keywords: *Spectroscopy, *Standards, *Measurement, Iodine, Tungsten, Fluids, Computer security.

Contents: Determination of trace level iodine in biological and botanical reference materials by isotope dilu-tion mass spectrometry; The spectrum of doubly ionized tungsten (W III); Apparatus for neturon scattering measurements on sheared fluids; Eleventh National Computer Security Conference.

900.909

PB89-235915 PC A06/MF A01 National Inst. of Standards and Technology (NEL), Gaithersburg, MD. Automated Production Technology

intercomparison of Load Ceii Verification Tests Performed by National Laboratories of Five Countries.

Final rept.

R. A. Mitchell, S. L. Yaniv, K. Yee, and O. K. Warnlof. Aug 89, 124p NISTIR-89/4101

Keywords: *Load cells, *Verifying, Measuring instruments, Temperature, Weight indicators, Mass, Test facilities, Metrology, *Calibration standards, International cooperation.

A round-robin intercomparison of OILM IR 60 load cell verification tests, as performed by national laboratones of five countries, is reported. The five participating countries were Australia, the Federal Republic of Germany, the Netherlands, the United Kingdom, and the United States. Six OIML Class C load cells, ranging in United States, Six Olimic Class C load cells, ranging in capacity from 18 kg to 25000 kg, were tested by the five laboratories. The objective was to determine the comparability of the results from the verification test processes of the five laboratories, so that the laboratories could accept the results from any one laboratory and avoid the cost of retesting. Overall, the test results indicate reasonably good agreement among the five laboratories in the measurement of most of the characteristics of the six load cells. The degree and pattern of the differences in the results can serve as a guide to making refinements in the verification test processes.

900,910

PB90-111220 PC A05/MF A01 National Inst. of Standards and Technology (NEL), Gaithersburg, MD. Fluid Flow Group.

NBS' (National Bureau of Standards) industry; Government Consortium Research Program on Flowmeter Installation Effects: Summary Report with Emphasis on Research July-December 1987. Summary rept.

G. E. Mattingly, and T. T. Yeh. Nov 88, 82p NISTIR-88/3898

See also PB89-189120.

Keywords: *Flowmeters, *Pipe flow, *Turbulence, Flow distribution, Fluid flow, Pipe bends, Secondary flow, Flow measurement, Research projects, *Installa-

The objective of the research program is to produce improved flowmeter performance when meters are installed in 'non-ideal' conditions. This objective is being attained via a strategy to measure, understand, and quantify the 'non-ideal' pipeflows from such pipeline elements as elbows, reducers, valves, or combinations of these; for selected types of flowmeters, correlate meter factor 'shifts' relative to the features of these 'non-ideal' installations; and disseminate the resulting technology through appropriate channels such as publishing results in pertinent journals and upgrading 'paper' standards for flow measurement.

900,911

PB90-111675 PC A05/MF A01 National Inst. of Standards and Technology (NEL), Boulder, CO. Chemical Engineering Science Div.

Optimum Location of Flow Conditioners in a 4-inch Orifice Meter. Technical note.

S. E. McFaddin, C. F. Sindt, and J. A. Brennan. Jul 89, 84p NIST/TN-1330

Contract GRI-5088-271-1680 Also available from Supt. of Docs. as SN003-003-02961-1. Sponsored by Gas Research Inst., Chicago,

Keywords: *Flow measurement, *Orifice meters, *Position(Location), *Standards, Flow rate, Flow-meters, Pressure measurement, Flow distribution, Experimental data, Test facilities.

Two orifice flow measurement standards are presently used, one in the United States (ANSI/API 2530) and another in Europe (ISO 5167). These two standards have significantly different specifications for installations. One important specification is the location of the flow conditioner relative to the orifice plate.

900,912

PB90-117938 Not available NTIS National Inst. of Standards and Technology (NML), Gaithersburg, MD. Radiation Physics Div.

Use of Thorium as a Target in Electron-Spin Anaiyzers. Final rept.

J. J. McClelland, M. R. Scheinfein, and D. T. Pierce.

Sponsored by Department of Energy, Washington, DC. Pub. in Review of Scientific Instruments 60, n4 p683-687 Apr 89.

Keywords: *Electron spin, *Analyzers, Electron scattering, Gold, Thin films, Reprints, *Thorium 230 target, Mott scattering, Sherman tables.

Measurements of the effective Sherman function have been carried out for 10-100-keV spin-polarized electrons scattering from a thick thorium target in a retarding Mott analyzer. At 20 and 100 keV the dependence on the maximum energy loss accepted by the detector has been measured. Comparison is made with scattering from a 1250 A gold film. Thorium is seen to have a S(eff) up to 30% higher than gold. The higher S(eff) can not only improve the figure of merit of a spin detector, but also lessen its sensitivity to instrumental asymmetries. Comparison is also made with preliminary theoretical results. Good agreement between theory and experiment is seen in the thorium Sherman function relative to that of gold.

900.913

PB90-127820 PC A04/MF A01 National Inst. of Standards and Technology (NML), Gaithersburg, MD. Office of Physical Measurement Services.

NIST (National Institute of Standards and Technology) Calibration Services, Users Guide: Fee Schedule.

Special pub. Mar 89, 70p NIST/SP-250-APP/89ED

Keywords: *Fees, *Metrology, Measuring instruments, Test facilities, Measurement, Setting(Adjusting), Standards, *Calibration, *National Institute of Standards and Technology.

The physical measurement services of the National Institute of Standards and Technology are designed to help the makers and users of precision instruments achieve the highest possible levels of measurement quality and productivity. The hundreds of individual services listed in the Fee Schedule constitute the highest-order calibration services available in the United States. They directly link a customer's precision equipment or transfer standards to national measurement standards. These services are offered to public and private organizations and individuals alike.

900.914

PB90-128273 Not available NTIS National Inst. of Standards and Technology (NEL), Gaithersburg, MD. Statistical Engineering Div. Bootstrap Inference for Replicated Experiments. Final rept

W. Liggett. 1988, 6p
Pub. in Computing Science and Statistics, Proceedings
of Symposium on the Interface (20th), Fairfax, VA., p68-73 Apr 88.

Laboratory & Test Facility Design & Operation

Keywords: *Experimental design, *Replicating, *Statistical inference, Error analysis, Estimating, Robustness(Mathematics).

Inference methods valid for nonnormal error are proposed for experiments in which each design point is replicated three or more times. Differences between the replicates provide the data needed for a pooled estimate of the error density, and the density forms the basis for the bootstrap. The density estimator is specifield for symmetric error, and the symmetric estimator has been generalized to asymmetric error. In the paper, the application of the density estimator to designed experiments is considered. The lack-of-fit test is of particular interest. The extension of the density estimator to data requiring a blocking variable and to data with dispersion effects is discussed. The bootstrap based on the density estimator is shown to be valid for smaller sample sizes when the test statistics are robust. Estimation of the error density is illustrated with measurements replicated at different laboratories.

Manufacturing Processes & Materials Handling

900,915 PB89-147003 Not available NTIS Not available NTIS
National Bureau of Standards (ICST), Gaithersburg,
MD. Advanced Systems Div.
Notion of Granularity.

Final rept. C. P. Kruskal, and C. H. Smith. 1988, 14p Pub. in Jnl. of Superconducting 1, p395-408 1988.

Keywords: *Grain size, Definitions, Fineness, Comparison, Metal industry, Reprints, Parallel processing.

Granularity is a well known concept in parallel processing. While intuitively, the distinction between coarse-grain and fine-grain paralellism is clear, there is no rigorous definition. The paper develops two notions of granularity, each defined formally and represented by a single rational number. The two notions are com-pared and contrasted with each other and with previously proposed definitions of granularity.

PB89-156384 PC A03/MF A01 PB89-156384 PC A03/MF A01 National Bureau of Standards (NEL), Gaithersburg, MD. Factory Automation Systems Div. Integrated Manufacturing Data Administration System (IMDAS) Operations Manual. D. A. Nickerson. 21 Apr 88, 21p NBSIR-88/3743 See also PB88-177290.

Keywords: *Data administration, Manufacturing, Planning, Manuals, *Automated manufacturing.

The report is an operator's manual for the Integrated Manufacturing Data Administration System (IMDAS) of the Automated Manufacturing Research Facility (AMRF). The IMDAS is designed to provide the control systems of the AMRF access to the data necessary to support the design, planning, manufacturing, and in-spection of parts. The manual describes the necessary steps to place the IMDAS into service within the

Nondestructive Testing

900,917 PB89-151625 PC A04/MF A01 National Inst. of Standards and Technology, Gaithers-

burg, MD.
Institute for Materials Science and Engineering,
Nondestructive Evaluation: Technical Activities 1988.

Annual rept. H. T. Yolken. Oct 88, 72p NISTIR-88/3839 See also PB88-153655.

Keywords: *Nondestructive tests, *Ceramics, *Metals, *Powder(Particles), *Reviews, Fabrication, Consolidation, Formability, Composite materials, Processing, Interfaces, Standards, Graphs(Charts), Ultrasonics, Thermal properties, Radiography.

The report provides brief reviews of technical activities in nondestructive evaluation (NDE) that were carried out by or for the National Institute of Standards and Technology (NIST--formerly the National Bureau of Standards) in fiscal year 1988 (October 1, 1987, through September 30, 1988). The reviews in the annual report are arranged in the following sections that reflect the NDE Program's four major activity areas: NDE for Ceramic and Metal Powder Production and Consolidation; NDE for Formability of Metals; NDE for Composites Processing and Interfaces; and NDE Standards and Methods. Each of the sections is preceded by an introduction. ceded by an introduction.

900,918 **PB8**9-**18757**9 PB69-187579
Not available NTIS
National Inst. of Standards and Technology (NEL),
Boulder, CO. Electromagnetic Technology Div.
Optical Power Measurements at the National Institute of Standards and Technology.
Final rept. Final rept.

T. R. Scott. 1989, 11p Pub. in Proceedings of Measurement Science Conference, Anaheim, CA., January 26-27, 1989, p3C-19-3C-

Keywords: *Fiber optics, *Power measurement, *Calorimeters, Lasers, Thermal measurements, Standards, Detectors, Calibrating, Telecommunications, Light transmission, Optical communication.

The measurement of optical power (that is, laser power or energy at wavelengths and power levels of interest to the fiber optic community) at NIST is based upon a standard reference calorimeter called the Cseries calorimeter. The C-series calorimeter is a national reference standard for measuring absolute energy and power levels of cw laser sources over a wide range of wavelengths. Various infrared laser sources and a calibrated beamsplitter measurement system are used to compare an electrically calibrated pyroelectric radiometer (ECPR) to the C-series calo-rimeter. The calibrated ECPR is then used as a laboratory standard for the calibration of measurement of optical power. The measurement of optical power at NIST is reviewed starting with a discussion of the primary reference standard and the associated measurement system. The system used for calibrating optical power detectors is discussed and the associated uncertainties are identified.

900,919 PB89-193866 PC A03/MF A01 National Inst. of Standards and Technology (NEL), Gaithersburg, MD. Center for Mfg. Engineering. Acoustical Technique for Evaluation of Thermal insulation.

D. R. Flynn, D. J. Evans, and T. W. Bartel. Apr 89, 47p NISTIR-88/3882 Sponsored by Department of Energy, Washington, DC. Building Systems Div., and Mineral Insulation Mfrs. Association, Alexandria, VA.

Keywords: *Thermal insulation, *Acoustic measurement, Thermal resistance, Sound transmission, Heat transfer, Evaluation, Cellulose, Houses, Thermal efficiency, Fiberglass, Rockwool, Blown-in-place attic in-

A laboratory apparatus has been constructed that enables rapid measurement of the sound insertion loss of a sample of insulation as a function of frequency. An extensive series of measurements of the sound inser-tion losses associated with blown samples of fiberglass, rockwool, and cellulose has been completed. The results of these acoustical measurements are highly correlated with coverage (mass per unit area) and thermal resistance (R-value). An investigation is planned to extend the acoustical techniques used in the laboratory apparatus to in-situ determination of the sound transmission loss through thermal insulation installed in attics. Two possible approaches to such field measurements are described.

900,920 PB89-202006 PB89-202006 Not available NTIS National Bureau of Standards (IMSE), Gaithersburg, MD. Metallurgy Div. Sensors for Intelligent Processing of Materials.

Final rept. H. N. G. Wadley. 1986, 5p Pub. in Jnl. of Metals 38, n10 p49-53 1986.

Keywords: *Process control, *Sensors, *Nondestructive tests, Ultrasonic frequencies, Eddy current tests, Acoustics, Mathematical models, Reprints.

To implement new process control strategies including Intelligent Processing of Materials strategies ad-

vanced sensors are required to nonintrusively evaluate process and microstructure variables. Examples of emerging sensors based upon ultrasonics, eddy currents and acoustic emission and other new nondestructive evaluation methods are described. In general, it is becoming evident that sophisticated sensor can reduce the dependence upon quantitative process models and vice versa. It is advisable therefore to assess sensor needs and process models together when developing the control scenario for a new proc-

900,921

PB89-211924 Not available NTIS National Bureau of Standards (IMSE), Gaithersburg, MD. Metallurgy Div.

Acoustic Emission: A Quantitative NDE Technique

for the Study of Fracture.

Final rept.
H. N. G. Wadley. 1987, 16p
Pub. in Proceedings of ONR Symposium on Solid Mechanics Research for QNDE, Evanston, IL., September 18-20, 1985, p25-40 1987.

Keywords: *Nondestructive tests, *Acoustic absorption, *Emission, *Crack propagation, Structural forms, Wave propagation, Mechanics, Dislocations(Materials).

Acoustic emission, an NDE technique that shows promise for detecting and locating cracks in engineering structures, has been used as an experimental technique for the basic study of fracture. Examples of the use of acoustic emission for the latter purpose are reviewed, and future research opportunities are identi-

900.922

PB90-123415 Not available NTIS National Inst. of Standards and Technology (IMSE), Gaithersburg, MD. Metallurgy Div.

Mossbauer imaging: Experimental Results. Final rept.

U. Atzmony, S. J. Norton, L. J. Swartzendruber, and L. H. Bennett. 1987, 2p Pub. in Nature 330, n6144 p153-154 1987.

Keywords: *Mossbauer effect, Nondestructive tests, Reprints, *Imaging techniques, Iron 57.

The letter reports the first experimental demonstration of the concept of Mossbauer imaging. For simplicity, a one-dimensional imaging experiment is described; however, the fundamental imaging principle thus demonstrated has obvious extensions to high dimensions. Finally, speculations on some possible applications of the technique in materials science are made.

900,923

PB90-128679 Not available NTIS National Inst. of Standards and Technology (IMSE), Roulder CO. Fracture and Deformation Pine. Boulder, CO. Fracture and Deformation Div. improved Standards for Real-Time Radioscopy. Final rept.

T. A. Siewert, 1989, 3p Pub. in Proceedings of Nondestructive Evaluation NDE Planning and Application Conference, Honolulu, Hl., July 23-27, 1989, p95-97.

Keywords: *Standards, *Radiology, Questionnaires, Nondestructive tests, Fracture tests, Deformation methods, *Real-time radioscopy.

The National Institute of Standards and Technology is assisting in the development of a radiation transfer standard for real-time radioscopy (RTR). The report describes and discusses the replies to a questionnaire which was developed to quantify the parameters with which RTR systems are used, and to identify the appropriate features of such a transfer standard.

900.924

PB90-128687 Not available NTIS National Inst. of Standards and Technology (IMSE), Boulder, CO. Fracture and Deformation Div. Standards for Real-Time Radioscopy. Final rept.

T. Siewert. 1988, 5p

Pub. in Proceedings of Defense Conference on Non-destructive Testing (37th), Jacksonville, FL., Novem-ber 1-3, 1988, p161-165.

Keywords: *Radiology, *Standards, Questionnaires, Nondestructive tests, Fracture tests, Deformation methods, *Real-time radioscopy.

Standards developed to measure the quality of film radiographs are unable to evaluate all the features of real-time systems. Particularly, problems exist when the specimen is rotated to a degree where the image quality indicators are no longer orthogonal to the beam or when the evaluation is performed while the specimen is in motion. The report describes the develop-ment of new standards that will allow quantitative evaluation of real-time systems under these conditions. Other NBS activities, such as a survey of real-time usage and the development of a 150 kV radiation transfer standard, will also be presented.

900,925

PB90-132739 PC A05/MF A01 National Inst. of Standards and Technology (IMSE), Gaithersburg, MD.

Institute for Materials Science and Engineering, Nondestructive Evaluation: Technical Activities, 1989.

Annual rept. H. T. Yolken. Nov 89, 77p NISTIR-89/4147 See also PB89-151625.

Keywords: *Nondestructive tests, Ceramics, Powder metallurgy, Sintering, Machined, Formability, Ultrasonic tests, Surface finishing, Polymers, Composite materials, Standards, Eddy currents, Research, Radiogra-phy, Thermal analysis, National Institute of Standards and Technology, Acoustic emission.

A review of the Nondestructive Evaluation Program at NIST for fiscal year 1989 is presented in the annual report. Topics include the following: Intelligent processing of rapidly solidified metal powders; Nondestructive characterization of ceramic sintering; Monitoring of tive characterization of ceramic sintering; Monitoring of machined ceramic surfaces by thermal waves; Eddy current temperature sensing; Ultrasonic sensor for sheet metal formability; Ultrasonic metrology for surface finish and part thickness; Measurement and control of polymer processing parameters using fluorescence spectroscopy; Nondestructive evaluation of diamond films; Transient elastic waves in laminates; Intelligent processing of solder joint connections for printed wiring assemblies: Ultrasonics and acoustic emission: ligent processing of solder joint connections for printed wiring assemblies; Ultrasonics and acoustic emission; Real-time x-ray radioscopy; Magnetic methods and standards for NDE; Eddy current techniques; New standard test methods for characterizing performance of thermal imaging systems; and Capacitive array research for characterization of ceramics.

Quality Control & Reliability

900.926

PB89-200216 PC A10/MF A01 National Inst. of Standards and Technology (NML), Gaithersburg, MD. Office of Physical Measurement

NIST (National Institute of Standards and Technology) Calibration Services Users Guide. 1989 Edition.

Special pub.

J. D. Simmons. Jan 89, 212p NIST/SP-250/89ED Also available from Supt. of Docs. as SN003-003-02909-2. See also PB87-174041.Color illustrations reproduced in black and white.

Keywords: *Calibration, *Measurement, Standards, Services, Quality assurance, Tests, Fees.

The National Institute of Standards and Technology (NIST) Calibration Services Users Guide provides detailed descriptions of currently available NIST calibration services, measurement assurance programs, and special-test services. The following measurement areas are covered: (1) dimensional; (2) mechanical, including flow, acoustic, and ultrasonic; (3) thermodynamic; (4) optical radiation; (5) ionizing radiation; and (6) electromagnetic, including dc, ac, rf, and microwave. A separate Fee Schedule is issued as required, providing current prices for the services offered, up-dates on points-of-contact, and information on measurement seminars.

LIBRARY & INFORMATION **SCIENCES**

Information Systems

900.927 PB89-170864 PC A04/MF A01 National Inst. of Standards and Technology (NEL), Gaithersburg, MD. Center for Computing and Applied Mathematics.

Internal Structure of the Gulde to Available Mathe-

matical Software.
R. F. Boisvert, S. E. Howe, and J. L. Springmann.
Mar 89, 55p NISTIR-89/4042
See also PB84-171305.

Keywords: *Catalogs(Publications), *Mathematics, *Statistical analysis, *Applications of mathematics, *Computer software, *Computer software catalog, *Scientific data, *On line systems, *Classification, *Data base management systems.

The purpose of the NIST Guide to Available Mathematical Software (GAMS) project is to provide convenient documentation tools for users and maintainers of scientific computer software. The main components of this effort are a detailed tree-structured, problem-ori-ented classification scheme for mathematical and statistical software, a printed catalog based upon this classification scheme which integrates information about all available software, an on-line interactive version of this catalog, and a relational database containing all information upon which the on-line and off-line catalogs rely, along with associated maintenance programs. The report presents a detailed specification of the internal structure of the GAMS database and the programs used to manipulate it. The information is useful to those who wish to implement the GAMS systems on their own computer systems.

900.928 PB89-193874 PC A03/MF A01 National Inst. of Standards and Technology (NCTL), Gaithersburg, MD. Office Systems Engineering Group. Document Interchange Standards: Description and Status of Major Document and Graphics Standards. J. Moline. Sep 88, 37p NISTIR-88/3851

Keywords: *Documents, *Standards, *Document circulation, Information retrieval, Document storage, Computer graphics. Document interchange standards have emerged in response to two distinct needs. First, there is the need to

interchange documents among workstations and tools in the office environment. Second, there is the need to exchange versions of a document between an author and a publisher. The document describes standards which attempt to satisfy those needs. Each relevant standard is presented in summary form and includes following information: standard name, standard number, status, scope, description, use, and references.

900.929 PB89-228993 PC A04/MF A01 National Inst. of Standards and Technology (NCSL), Gaithersburg, MD. Information Systems Engineering

Detailed Description of the Knowledge-Based System for Physical Database Design. Volume 1. Internal rept. Jul 85-Dec 88. C. E. Dabrowski. Aug 89, 63p NISTIR-89/4139/1 See also Volume 2, PB89-229033.

Keywords: *Data base management systems, Factor analysis, Data structures, Information systems, Artificial intelligence, Mathematical models, Design, Knowledge-based systems.

A knowledge-based system for physical database design has been developed at the National Computer Systems Laboratory. The system was previously described in NIST Special Publication 500-151. The report is a follow-up report to that publication which describes the knowledge base for the system in detail The description includes a complete explanation of each component of the knowledge base together with the actual rules used by the system.

900,930 PB89-229033 PC A09/MF A01 National Inst. of Standards and Technology (NCSL), Gaithersburg, MD. Information Systems Engineering

Detailed Description of the Knowledge-Based System for Physical Database Design. Volume 2. Internal rept. Jul 85-Dec 88.

C. E. Dabrowski. Aug 89, 177p NISTIR-89/4139/2 See also Volume 1, PB89-228993.

Keywords: *Data base management systems, Instructions, Information systems, Artificial intelligence, Mathematical models, *Knowledge-based systems.

A knowledge-based system for physical database design has been developed at the National Computer Systems Laboratory. The system was previously described in NIST Special Publication 500-151. The report is a follow-up report to that publication which describes the knowledge base for the system in detail. The description includes a complete explanation of each component of the knowledge base together with the actual rules used by the system.

900,931 PB90-112467 PC A03/MF A01 National Inst. of Standards and Technology (NCSL),

Gaithersburg, MD.

Use of the IRDS (Information Resource Dictionary System) Standard In CALS (Computer-Alded Acquisition and Logistic Support).

D. K. Jefferson, and C. M. Furlani. Sep 89, 16p

NISTIR-89/4169

Keywords: *Information systems, *Data management systems, Dictionaries, Architecture(Computers), Distributed data bases, Standards, Models, Information processing languages, *Computer-aided Acquisition and Logistic Support.

The objective of the point paper is to show how the Information Resource Dictionary System (IRDS) can fulfill critical design and operational requirements for CALS Phase II. First, a series of assumptions are made about the data management services which are needed by CALS Phase II. Next, these assumptions are used to develop a series of requirements for a dictionary system. The structure of the IRDS family of standards is then described. Examples are provided to illustrate how the IRDS could meet the requirements. A schedule is presented to show that the IRDS and other data management standards will be available when needed to meet the immediate requirements of CALS. An architecture is presented to illustrate additional standards required to achieve longer-range goals of distributed database. Finally, development tasks are

Reference Materials

900,932 PB89-160014 PC A06/MF A01 National Inst. of Standards and Technology, Gaithersburg, MD. Information Resources and Services Div. Data Bases Available at the National Institute of Standards and Technology Research Information Center.

Special pub. (Final). D. Cunningham. Nov 88, 117p NIST/SP-753
Supersedes PB88-153754. Also available from Supt. of Docs. as SN003-003-02903-3. Library of Congress catalog card no. 88-600602.

Keywords: *Information systems, *Directories, Information centers, *Bibliographic data bases, *National Institute of Standards and Technology, *Data bases.

Data bases available online at the National Institute of Standards and Technology (NIST) Research Information Center are listed by acronym and by full title. In addition, descriptions of the data bases, periods of coverage, producers, corresponding hard copy titles and principal sources and vendors are listed. A general

LIBRARY & INFORMATION SCIENCES

Reference Materials

subject index and a cross reference index are also supplied.

900.933

PB89-185599 PC A05/MF A01 National Bureau of Standards, Gaithersburg, MD. Directory of NVLAP (National Voluntary Laboratory Accreditation Program) Accredited Laboratory ries, 1986-87.

H. W. Berger, Jan 87, 99p NBSIR-87/3519 See also PB88-169529.

Keywords: *Directories, *Laboratories, Tests. Projects, Position(Location), Accreditation.

The report lists laboratories accredited under the procedures of the National Voluntary Laboratory Accreditation Program (NVLAP) as of January 1, 1987. Indexes cross reference the laboratories by name, NVLAP Lab Code Number, test method, accreditation program, and geographical location. The scope of accreditation of each laboratory, listing the test methods for which it is accredited, is provided along with a tabulation of test methods and the laboratories accredited for those test methods.

General

900,934

PB89-147052 Not available NTIS National Bureau of Standards (NEL), Gaithersburg, MD. Statistical Engineering Div.

Theory and Practice of Paper Preservation for Ar-

Final rept.

A. Calmes, R. Schofer, and K. Eberhardt. 1988, 16p Pub. in Restaurator: International Jnl. for the Preservation of Library and Archival Material 9, p96-111 1988.

Keywords: *Documents, Papers, *Archives, Operations research, Reprints, *Preservation.

The task of preserving huge quantities of paper records may appear so overwhelming that an archivist may not know where to begin or how best to use his limited resources. The paper addresses those difficulties and offers suggestions and a model for reducing the overall paper preservation problem into managea-ble and efficient subtasks. Based on a National Archives/National Bureau of Standards study, the archival/conservation principles employed are: sample surveying, careful planning, protective packaging, use of copies instead of originals, monitoring the condition of records as they are being used, and professional conservation treatment.

900,935

PC A03/MF A01 PB89-214753 National Inst. of Standards and Technology (NCSL), Gaithersburg, MD.

Electronic Publishing: Guide to Selection. Final rept.

L. S. Rosenthal. Jun 89, 39p NIST/SP-500/164 Also available from Supt. of Docs. as SN003-003-02938-6. Library of Congress catalog card no. 89-600734.

Keywords: *Publishing, *Composition, *Documentation, Computer applications, Printing, Instructions, Documents, Fonts, Typography, Data processing, *Electronic publishing.

The purpose of the report is to assist managers and users in making informed decisions on which systems are best for them. The report presents the technical and managerial choices and implications associated with selecting and using electronic publishing systems. A matrix of publishing capabilities and features is presented in the appendix to illustrate one method of comparing and selecting a publishing system.

MANUFACTURING **TECHNOLOGY**

Computer Aided Design (CAD)

900.936 PB89-151799 PC A06/MF A01 Catholic Univ. of America, Washington, DC. Design Protocoi, Part Design Editor, and Geometry Library of the Vertical Workstation of the Automated Manufacturing Research Facility at the National Bureau of Standards.

T. R. Kramer, and J. S. Jun. 28 Jan 88, 113p NISTIR-88/3717

Grant NANB-5-D0522

Sponsored by National Bureau of Standards, Gaithersburg, MD.

Keywords: Design, Machining, Planning, *Computer aided design, *Computer aided manufacturing, Interactive systems, Workstations, Automated Manufacturing Research Facility.

In the Vertical Workstation (VWS) of the NBS Automated Manufacturing Research Facility, metal parts are machined automatically from a feature-based design. A simple two-and-a-half dimensional part may be designed and machined within an hour, allowing half the time for design input. Workstation activity may be divided into design, process planning, data execution, and physical execution stages. The design of a part is expressed as a list of features on a block-shaped workpiece. Each feature is a removed volume. A feature is expressed by giving the name of the feature type and values for several parameters appropriate to that feature type. The design editor is an interactive system that runs on a Sun computer which is used to create or change designs. The system engages the user in a dialog to determine what the user wants to do, and prepares a design according to the user's instructions. The editor draws a three-view picture of the part being edited. The geometry library is a set of LISP functions. that do geometric calculations to support the operation of the design editor and other modules of the VWS

900,937

PC A06/MF A01
National Inst. of Standards and Technology (NEL),
Gaithersburg, MD. Center for Building Technology.
Guidelines for the Specification and Validation of IGES (Initial Graphics Exchange Specification) Ap-

plication Protocols. R. J. Harrison, and M. E. Palmer. Jan 89, 111p NISTIR-88/3846

Prepared in cooperation with Sandia National Labs., Albuquerque, NM.

Keywords: *Data converters, *Standards, Proving, *Computer aided design, *Initial Graphics Exchange Specification, Data management, Computer applica-

The document provides a background discussion of product data, describes the concept of IGES (Initial Graphics Exchange Specification) application protocols, specifies the technical content of an IGES application protocol describes a united to the protocol describes a united to the protocol describes and the protocol describes and the protocol describes and the protocol describes and the protocol describes a protocol describes a protocol describes and the protocol describes a protocol de cation protocol, describes a validation methodology for these application protocols, and provides guide-lines for the implementation of an IGES application protocol. A key conclusion of the background discussion of product data is that IGES application protocols must be developed in order to achieve consistent and reliable exchanges of product data within specified application areas. The technical content of an IGES application protocol includes a conceptual information model for the application area with its supporting documentation, an application protocol format specification with a protocol usage guide, and a set of application protocol format test cases. These test cases must be used in concert with a well-defined testing methodology. Since no complete IGES application protocols currently exist, the document describes a current implementation of an application protocol process that is based on a partially complete application protocol.

900.938 PB90-112426 PC A03/MF A01 National Inst. of Standards and Technology (NEL), Gaithersburg, MD. Factory Automation Systems Div. Product Data Exchange: The PDES Project-Status

and Objectives.

B. M. Smith. Sep 89, 12p NISTIR-89/4165 See also PB89-144794.

Keywords: *Data, *Standardization, Product development, Standards, Mathematical models, *Computer aided design, *Product Data Exchange Specification,

The paper details the strategy behind the development of the Product Data Exchange Specification (PDES) project, identifies the various technical resources that have been brought together to develop, standardize and use PDES technology, gives the status of the effort as of early 1989 and enumerates project plans for the balance of the year.

900,939

PB90-112434 PC A03/MF A01 National Inst. of Standards and Technology (NEL), Gaithersburg, MD. Factory Automation Systems Div. External Representation of Product Definition

B. M. Smith. Sep 89, 11p NISTIR-89/4166

Keywords: *Data, *Standards, Standardization, Product development, *Computer aided design, Computer aided manufacturing, International Organization for Standardization.

The ability to exchange product data files among a variety of different vendor CAD/CAM systems is critical to both a company's internal plans for integration and its external relationships with contractors and customers. Therefore, several national projects are being co-ordinated through the International Organization for Standardization (ISO) to develop a single world standard for data exchange. In addition to geometry, the standard will support a wide range of non-geometry data such as features, tolerance specifications, material properties and surface finish specifications. The geometry model will include solid representations for both boundary and constructive solid geometry forms. The geometry model coupled with the non-geometric data and the relationship information preserved from the sending system will enable the standard to communicate a complete product model. The paper details the strategy behind the development of the ISO project, identifies the various technical resources that have been brought together to develop, standardizes and uses product data technology, gives the status of the effort as of early 1989 and enumerates project plans for the balance of 1989.

Computer Aided Manufacturing (CAM)

900.940 PB89-144794 PC A99/MF E16 National Inst. of Standards and Technology (NEL), Gaithersburg, MD. Factory Automation Systems Div. Product Data Exchange Specification: First Working Draft.

Interim rept B. Smith, and G. Rinaudot. Dec 88, 2513p NISTIR-88/4004

Portions of this document are not fully legible.

Keywords: *Product development, *Data, *Standardization, Standards, *Product Data Exchange Specification, Computer aided manufacturing.

The document contains a neutral format for the representation and communication of product data. Known as the Product Data Exchange Specification (PDES), the document had been developed by the IGES/PDES Organization with active cooperation from the Working Group 1 of ISO/TC184/SC4. It represents the first working draft of PDES for presentation to the international community.

PB89-150809

Not available NTIS National Bureau of Standards (NEL), Gaithersburg, MD. Factory Automation Systems Div.

Computer Aided Manufacturing (CAM)

Automated Documentation System for a Large Scale Manufacturing Engineering Research Project.

Final rept.

H. M. Bloom, and C. E. Wenger. 1983, 10p Pub. in Proceedings of International Conference on Systems Documentation (2nd), Seattle, WA., April 29-

30, 1983, 10p.

Keywords: Data storage, *Automated Manufacturing Research Facility, *Computer aided manufacturing, *Software engineering, Information processing, Computer communications, Data management systems.

The Automated Manufacturing Research Facility (AMRF) being implemented at the National Bureau of Standards (NBS) will involve the development of a software manufacturing system integrating the various information processing, communications and data storage functions required in a totally automated environment. For such a research environment, there ronment. For such a research environment, there exists a need to develop an automated system for generating documentation for the software life cycle that could be used for the following purposes: (1) tracking progress of individual module development; (2) allowing for the availability of up-to-date information on module description to other members of the project who need to interface to a given module; (3) develop-ing a cross reference of module and data element relationships; and (4) generating working level documenta-tion that can be easily modified and serve as information to be given to any one with interest in the project.
The paper describes the structure of a software development system that will function in a research environment.

900,942 PB89-151823 PC A04/MF A01 National Inst. of Standards and Technology (IMSE), Gaithersburg, MD. Office of Nondestructive Evalua-

Intelligent Processing of Materials: Report of an Industrial Workshop Conducted by the National Institute of Standards and Technology.

H. T. Yolken, and L. Mordfin. Jan 89, 51p NISTIR-

89/4024

Keywords: *Materials, *Processing, *Artificial intelligence, Plastics processing, Detectors, Nondestructive tests, Polymers, Ceramics, Metallurgy, Isostatic pressing, *Expert systems, Thermomechanical treatment, National Institute of Standards and Technology.

Intelligent processing of materials has been established as a major new program area in the Institute for Materials Science and Engineering, National Institute of Standards and Technology (NIST). The goal of the program is to develop some of the generic scientific and technological bases for intelligent processing and, by means of selected pilot or demonstration projects, to encourage American industry to pursue and to adopt this powerful new approach to materials procadopt this powerful new approach to materials processing. In developing the new program, NIST cooperated in organizing two national workshops in 1985-86 to help identify the principal industrial needs in this field of technology and to solicit guidance for program planning activities. On August 30 and September 1, 1988, NIST convened a third workshop in this series. This one was comprised primarily of selected industrial specialists and was designed to define the specific materials processes upon which the NIST program should focus, and to discuss suitable approaches for accomplishing the work. The report documents the results of that workshop.

900.943 PB89-159636 PC A04/MF A01 National Bureau of Standards, Gaithersburg, MD.

Data Handling In the Vertical Workstation of the
Automated Manufacturing Research Facility at the
National Bureau of Standards.

Grants NANB-5-D0522, NANB-7-H0716 Sponsored by Catholic Univ. of America, Washington, DC.

Keywords: Machining, Tooling, Tables(Data), *Automated Manufacturing Research Facility, *Data management systems, Computer aided manufacturing, Workstations, Data base management, Automatic pro-

In the Vertical Workstation (VWS) of the NBS Automated Manufacturing Research Facility, metal parts are machined automatically from a feature-based design. A simple two-and-a-half dimensional part may be de-

signed and machined within an hour, allowing half the time for design input. Workstation activity may be divided into design, process planning, data execution, and physical execution stages. The VWS requires data for: features, machining operations, tooling, fixturing, work-pieces, trays and other items. Hierarchical LISP property lists are used to store most of this data. The VWS also exchanges data with a global database. A local database manager is used to handle all exchanges with the global database and also to emulate the global database. Data exchanges take place through structured reports. The VWS system includes a sub-system which automatically writes LISP functions to read and write reports.

900,944 PB89-160634 PB89-160634 PC A03/MF A01 Catholic Univ. of America, Washington, DC. Parser That Converts a Boundary Representation Into a Features Representation Into a Features Representation.
T. R. Kramer. Feb 89, 22p NISTIR 88/3864
Grant NANB7H0716

Sponsored by National Inst. of Standards and Technology (NEL), Gaithersburg, MD. Center for Mfg. Engi-

Keywords: Pattern recognition, Boundaries, *Automated Manufacturing Research Facility, *Computer aided manufacturing, Parsing algorithms, Computer aided design, Workstations, Feature extraction.

The VWS2 B-rep Parser is a computer program written in LISP that takes a file giving the boundary representation of a part as input and produces a file giving a feature-based representation of the part as output. The format of the input file is a Product Data Exchange Specification (PDES)/Standard for The Exchange of Product data (STEP) boundary representation, and the format of the output file is that required by the VWS2 output of the National Institute of Standard and system of the National Institute of Standards and Technology (NIST) Automated Manufacturing Research Facility (AMRF). The parser deals with a limited range of two-and-a-half dimensional parts. The general approach to parsing is to expect that the part is parsable and look for arrangements of faces which are the signatures of features. The initial implementation of the approach recognizes five feature types. The approach is extendible to a wider range of feature and subfeature types, and to parts which have features made from several sides. Parts having features which intersect in a complex manner are likely to test the limits of this approach, or be beyond the limits. With the addition of this parser, the AMRF Vertical Workstation is capable of making a part from a PDES/STEP file without human intervention.

900,945 PB89-172571 PC A03/MF A01 National Inst. of Standards and Technology (NEL), Gaithersburg, MD. Center for Mfg. Engineering.

Artificial Intelligence Techniques in Real-Time Production Scheduling.

W. J. Davis, and A. T. Jones. Feb 89, 20p NISTIR-

Prepared in cooperation with Illinois Univ. at Urbana-Champaign. Dept. of General Engineering.

Keywords: *Production planning, *Scheduling, *Artificial intelligence, Decision making, Automation, *Computer aided manufacturing, Real time.

The paper addresses the real-time production sched-uling problem as a special case of a much larger class of real-time decision-making/control problems. The paper first reviews the definition of the scheduling problem, and then reviews an earlier algorithm proposed by the authors to address this problem. It then concentrates on the possible application of various Al techniques to many of the functions that make up that algorithm.

900,946 PB89-172589 PC A03/MF A01 National Inst. of Standards and Technology (NEL), Gaithersburg, MD. Center for Mfg. Engineering. Functional Approach to Designing Architectures for Computer Integrated Manufacturing. W. J. Davis, and A. T. Jones. Feb 89, 30p NISTIR-

88/3872

Prepared in cooperation with Illinois Univ. at Urbana-Champaign. Dept. of General Engineering.

Keywords: *Production planning, *Scheduling, *Manufacturing, *Automation, Mathematical models, Design, Hierarchies, *Computer integrated manufacturing, Computer systems design.

Developing effective CIM architecture is hampered by automation and integration problems. The key to resolving these problems lies in a better understanding of each manufacturing function and how it is related to other manufacturing functions. The authors view is that mathematical models can provide this understanding. The paper presents the results of their initial efforts to develop such models. They can be used to guide the development of the technology needed for automation. They also specify the inputs, outputs, and interrelations needed for integration, regardless of the specific CIM architecture used.

900.947

PB89-172597 PC A03/MF A01 National Inst. of Standards and Technology (NEL), Gaithersburg, MD. Center for Mfg. Engineering.

Real-Time Optimization in the Automated Manufacturing Research Facility. W. J. Davis, R. H. F. Jackson, and A. T. Jones. Feb

89, 27p NISTIR-88/3865

Prepared in cooperation with Illinois Univ. at Urbana-Champaign. Dept. of General Engineering.

Keywords: *Scheduling, *Routing, *Hierarchical control, Optimization, *Factory automation, *Automated Manufacturing Research Facility, *Flexible manufacturing, Real time.

A major manufacturing research facility has been established at the National Institute of Standards and Technology. The Automated Manufacturing Research Facility has been designed to address the standards and measurement needs for the factory of the future. A five-layer hierarchical planning/control architecture is under development to manage production and support activities. A three layer architecture is being developed to manage the data requirements of the modules within that hierarchy. Each of these architectures contain functions that require the solution to one or more optimization problems. The paper describes both the production planning/control and the data management architectures being developed at NBS. It emphasizes the optimization problems contained within those architectures. It also discusses the work underway at NBS to address some of those problems.

900,948

PB89-172605 PC A03/MF A01 National Inst. of Standards and Technology (NEL), Gaithersburg, MD. Center for Mfg. Engineering. On-Line Concurrent Simulation in Production Scheduling.

W. J. Davis, and A. T. Jones. Feb 89, 27p NISTIR-

Prepared in cooperation with Illinois Univ. at Urbana-Champaign. Dept. of General Engineering.

Keywords: *Production control, *Computerized simulation, Scheduling, Industrial engineering, Computer programming, Numerical control, *Computer aided manufacturing, *On-line programming, *Flexible manufacturing systems, *Automated Manufacturing Research Facility.

Flexible manufacturing systems (FMS) have been installed in many factories around the world. Production scheduling is the function responsible for assigning FMS resources to various manufacturing tasks. On-line simulation is being used as an analysis tool to choose among several candidate scheduling rules. The paper defines on-line simulation, and describes the inputs to and outputs from the on-line simulation trails. It also addresses the statistical analysis of those outputs to determine the 'best' compromise scheduling rule. Finally, it presents results from some preliminary scheduling experiments on the Automated Manufacturing Research Facility (AMRF) at the National Bureau of Standards.

900.949

PB89-172613 PC A03/MF A01 National Inst. of Standards and Technology (NEL), Gaithersburg, MD. Center for Mfg. Engineering Hierarchies for Computer-Integrated Manufactur-

ing: A Functional Description.
W. J. Davis, and A. T. Jones. Feb 89, 30p NISTIR-88/3744

Prepared in cooperation with Illinois Univ. at Urbana-Champaign. Dept. of General Engineering.

Keywords: *Automatic control, *Hierarchical control, Decision making, Mathematical models, *Computer in-

Computer Aided Manufacturing (CAM)

tegrated manufacturing, *Hierarchies, Organizational

In the recent past, several hierchies have been proposed as candidate models for the integration of decision and control functions within a Computer-Integrated Manufacturing environment. A common theme in to manufacturing environment. A common theme in the definition of these models is to construct an analog to managerial hierarchies that are currently employed in many corporate settings. The paper will adopt an alternate approach. Rather than defining a hierarchy, the paper will discuss the manufacturing functions that a CIM hierarchy must address. Whenever possible, mathematical formulations for the functions will be given with consideration for the stochastic environ-ment in which they will function. The conclusion outlines several concerns arising in the definition of a generic CIM hierarchy and associated research topics that must be addressed.

900,950 PB89-176663 PB89-176663 Not available NTIS National Bureau of Standards (NEL), Gaithersburg,

MD. Precision Engineering Div.

Vertical Machining Workstation of the AMRF (Automated Manufacturing Research Facility): Equipment Integration.

Final rept. E. B. Magrab. 1986, 18p See also PB87-218368.

Pub. in Proceedings of ASME (American Society of Mechanical Engineers) Winter Annual Meeting on Integrated and Intelligent Manufacturing, Anaheim, CA., December 7-12, 1986, p83-100.

Keywords: *Machining, Automation, Robots, Manipulators, *Automated Manufacturing Research Facility, Workstations.

The integration and automation of the equipment comprising the vertical machining workstation (VMW) of the Automated Manufacturing Research Facility are presented. The workstation consists of a CNC vertical machining center, robot, vacuum chip removal system, robot cart delivery system, NBS designed grippers and modified pneumatic vise, and a hydraulic clamping system. In conjunction with the workstation controller, this VMW has attained a high level of sophistication and flexibility. Described in detail are the rules and assumptions governing the workstation's equipment operation, its equipment control software structure, the operations of the various pieces of equipment and the placement and type of sensors used to ensure proper execution of its command sets.

900.951 PB89-177083 Not available NTIS Mational Bureau of Standards (NEL), Gaithersburg, MD. Robot Systems Div.

Real-Time Control System Software: Some Prob-

lems and an Approach.

Final rept. L. S. Haynes, and A. J. Wavering. 1986, 12p
Pub. in Proceedings of IEEE (Institute of Electrical and Electronics Engineers) International Conference on Robotics and Automation, San Francisco, CA., p1705-1716 1986

Keywords: Computer systems programs, Robots, *Automated Manufacturing Research Facility, *Computer aided control systems, *Computer software, Real time systems, Robotics, Software engineering.

The Automated Manufacturing Research Facility (AMRF) is currently composed of six workstations, six robots, an automated material handling system, buffer storage, a networking system for communication, a database system to support the needs of the facility and over 100 sensors throughout the facility to provide continued monitoring of all processes. One of the major challenges of the facility is to implement a realtime control system which continually reads the sensors within portions of the facility, interprets those readings, makes decisions as to required actions or changes, and then effects the required change via commands to actuators, manipulators, or subsystems. During development of the AMRF it became clear that real-time control software is fundamentally different, and more complex than scientific or business type systems. The paper discusses the reasons why this is true and describes the NBS Real-Time Control System, a system designed to help deal with these problems.

900,952 PB89-177091

Not available NTIS

National Bureau of Standards (NEL), Gaithersburg,

MD. Factory Automation Systems Div.

AMRF (Automated Manufacturing Research Facility) Material Handling System Architecture. Final rept.

Pub. in Proceedings of Annual Control Engineering Conference (5th), Rosemont, IL., May 6-8, 1986, p40-

Keywords: *Materials handling, Materials handling equipment, Computer systems hardware, *Automated Manufacturing Research Facility, *Computer aided manufacturing, Workstations, Computer software, Data bases.

The paper describes the architecture of the Automated The paper describes the architecture of the Automated Manufacturing Research Facility (AMRF) Material Handling Workstation and interface techniques that are used to integrate the system with other factory components. The material handling system (MHS) is comprised of two automatically guided vehicles, tray roller tables, a storage and retrieval system, control computers, and a tender terminal to coordinate manual support services. These services include: kitting, tray loading, tool setup, and raw material prepara-tion. The architectural aspects of the system that are presented include: the hardware components of the system, a description of major software modules, material handling work element definitions, the programming of handling operations via process plans, the execution of these plans by the workstation controller, database structures and communications interfaces.

900,953

PB89-177109 Not available NTIS National Bureau of Standards (NEL), Gaithersburg, MD. Factory Automation Systems Div. Software for an Automated Machining Worksta-

tion.

T. R. Kramer, and J. S. Jun. 1986, 36p
Pub. in Proceedings of Biennial International Machine Tool Technical Conference (3rd), McLean, VA., September 3-10, 1986, p12-9-12-44.

Keywords: *Machining, *Automation, Computer systems programs, Manufacturing, *Workstations, *Computer software, Computer aided manufacturing, Computer aided design, Control systems.

Software written in LISP is used to control the activities of a workstation developed at the National Bureau of Standards. The controlled activities include the design-using parametric programming, process planning, and data and physical execution.

900,954

PB89-185607 PC A10/MF A01 National Bureau of Standards, Gaithersburg, MD.
Turning Workstation in the AMRF (Automated Manufacturing Research Facility). Manufacturing Research Facility).
A. Donmez, R. Gavin, L. Greenspan, K. Lee, V. Lee, J. Peris, E. Reisenauer, C. Shoemaker, and C. Yang. 20 Apr 88, 207p NBSIR-88/3749
See also PB87-218368. Sponsored by Naval Research Lab., Washington, DC. Navy Manufacturing Technology Program.

Keywords: *Manufacturing, *Automatic control equipment, *Turning(Machining), Components, Loading, Revisions, Robots, Detection, Failure, Controllers, Manipulators, *Flexible manufacturing workstation, Collet changing.

The Turning Workstation is a flexible manufacturing workstation developed in the Automated Manufacturing Research Facility (A.M.R.F.) at the National Bureau of Standards. The development of the workstation addressed some of the problems associated with an un-attended turning operation which include tool chang-ing, collet loading, collet changing, flexible robot end-effectors, and machine malfunction detection. The document describes the components of the Turning Workstation and its relationship to the A.M.R.F.

900.955

PB89-189286 PC A04/MF A01 National Inst. of Standards and Technology, Gaithers-

Workstation Controller of the Cleaning and Debur-ring Workstation.
R. J. Norcross. 16 Feb 89, 70p NISTIR-89/4046 See also PB88-194279.

Keywords: Metal cleaning, Deburring, Robots, Automation, *Automated Manufacturing Research Facility, *Workstations, *Control systems.

The Cleaning and Deburring Workstation at NIST's Automated Manufacturing Research Facility employs two robots and numerous supporting equipment to wash, buff, and deburr discreet metal workpieces. The manual describes the workstation controller for perspective users and for researchers interested in ex-panding the workstation's capabilities. The manual specifies the general control problem and provides the theoretical foundation of the solution along with specific implementation details. These details include impor-tant data structures, programming formats, interfaces, and the current operation of the controller and workstation.

900.956

PB89-193882 PC A06/MF A01 National Inst. of Standards and Technology, Gaithers-

burg, MD. NBS AMRF (National Bureau of Standards) (Automated Manufacturing Research Facility) Process Planning System: System Architecture. P. F. Brown, and S. R. Ray. Mar 89, 117p NISTIR-

See also PB87-234050.

Keywords: Process control, Automation, Research projects, Control systems, Architecture, Research facilities, *Process planning, *Automated Manufacturing Research Facility, Computerized control systems.

The purpose of the document is to provide a general description of design and implementation of the Automated Manufacturing Research Facility (AMRF) Process Planning System. The document should provide the reader with an understanding of the concepts behind the work in the process planning project as well as on the approach adopted. Details on system implementation are provided.

900,957

PB89-201727 Not available NTIS National Bureau of Standards (IMSE), Gaithersburg, MD. Office of Nondestructive Evaluation

Automated Processing of Advanced Materials. The Path to Maintaining U.S. Industrial Competitiveness in Materials.

Final rept. H. T. Yolken, and L. Mordfin. 1986, 4p Pub. in ASTM (American Society for Testing and Mate-

rials) Standardization News 14, n10 p32-35 Oct 86.

Keywords: *Process control, Powder metals, Production controls, Mechanical properties, Process variables, Reprints, *Computer-aided manufacturing, Nondestructive analysis.

Automation of materials processing offers a path to maintaining U.S. industrial competitiveness in materials. The key components of a systems approach to automating materials processing are discussed. These components included the process, a process model, NDE sensors for materials properties and process variable sensors, process controllers, and an expert computer system to integrate and control the oper-ation of the system. An example is present of a model systems approach at the National Bureau of Standards (NBS) involving the production of rapidly solidified metal powders by high pressure gas atomization. NBS invites joint sponsorship and active participation by a consortium of industrial firms.

900,958

PB89-209233 PC A03/MF A01 National Inst. of Standards and Technology, Gaithersburg, MD.

Inventory of Equipment in the Cleaning and Deburring Workstation.

F. M. Proctor, and R. Russell. 11 May 89, 16p NISTIR-89/4092

See also PB89-176663.

Keywords: *Machining, *Inventories, *Control equipment, Cleaning, Deburring, Computer software, Robots, *Workstations, *Automated Manufacturing Research Facility, Computer hardware.

The manual provides a complete inventory of equipment in the Cleaning and Deburring Workstation of the Automated Manufacturing Research Facility of the National Institute of Standards and Technology.

Computer Aided Manufacturing (CAM)

900.959 PC A03/MF A01 PB89-209258 National Inst. of Standards and Technology (NEL), Gaithersburg, MD. Center for Mfg. Engineering.

Data Management Strategles for Computer Integrated Manufacturing Systems.

W. Davis, A. Jones, and S. Ram. Jun 89, 25p

NISTIR-88/4002

Prepared in cooperation with Illinois Univ. at Urbana-Champaign. Dept. of General Engineering, and Arizo-na Univ., Tucson. Dept. of Management Information

Keywords: Automation, Marketing, Sales, Production engineering, Scheduling, Planning, Inventory control, Quality assurance, Models, *Computer aided manu-facturing, *Data management, Data bases, Data base

A recent worldwide trend to improve productivity in manufacturing has centered around the adoption of computer technology. Efforts are underway in many plants to use that technology to automate and integrate all manufacturing functions. This is transforming those plants into computer integrated manufacturing (CIM) systems. The paper addresses some of the special problems that have been and will be encountered in designing data management strategies for CIM. It describes both the major manufacturing functions themselves and the data required to carry out those functions. It also includes discussions on the various alternatives for data placement, data modeling, data administration, and data communications for CIM.

900,960

PC A03/MF A01 PB89-215198 National Inst. of Standards and Technology (NEL), Gaithersburg, MD. Factory Automation Systems Div. Use of GMAP (Geometric Modeling Applications Interface Program) Software as a PDES (Product Data Exchange Specification) Environment in the National PDES Testbed Project.

K. L. Perlotto. Jun 89, 26p NISTIR-89/4117

Prepared in cooperation with Pratt and Whitney Aircraft Group, East Hartford, CT. Sponsored by Department of Energy, Washington, DC. Office of Buildings and Community Systems.

Keywords: *Production models, *Test facilities, Specifications, Manufacturing, Computer programs, *Computer aided manufacturing, GMAP programming language, Computer architecture, Computer applications, National Institute of Standards and Technology, Automated Manufacturing Research Facility.

The report is a basic guide to the use of the GMAP System Architecture as installed on the NIST AMRF VAX as part of the National PDES Testbed Project. An vAX as part of the National PDES Testibed Project. An overview of the GMAP System Architecture is provided. The use of the GMAP software to create an implementation environment for the PDES Draft Proposal Specification (February 1989) is outlined. The software organization on the NIST AMRF VAX and the development of test and validation applications are described. The GMAP System Architecture consists of software system components which meet the three basic requirements of an automated product data environment. The requirements are data definition, application support, and data exchange. The system components are defined and the role they play is described.

900.961

PB89-215339 PC A03/MF A01 National Inst. of Standards and Technology (NEL), Gaithersburg, MD. Automated Production Technology Div.

Inventory of Equipment In the Turning Workstation of the AMRF (Automated Manufacturing Re-

K. Lee. Jun 89, 12p NISTIR-88/3810
See also PB89-185607 and PB89-215347. Sponsored by Naval Research Lab., Washington, DC. Navy Manufacturing Technology Program.

Keywords: *Computer aided Manufacturing, *Turning(Machining), *Automatic control equipment, *Robots, Manipulators, Components, Detectors, Controllers, Loading, Microcomputers, *Flexible manufacturing workstation, Collect changing.

The manual serves as an inventory guide to all electronic and mechanical systems in the Automated Turning Workstation at the Automated Manufacturing Research Facility (AMRF).

900.962 PB89-215347 PC A03/MF A01 National Inst. of Standards and Technology (NEL), Gaithersburg, MD. Automated Production Technology

Recommended Technical Specifications for Pro-

curement of Equipment for a Turning Workstation.
K. Lee. Jun 89, 49p NISTIR-88/3811
See also PB89-215339. Sponsored by Naval Research Lab., Washington, DC. Navy Manufacturing Technology Program.

Keywords: *Turning(Machinery), *Specifications, *Robots, Machine tools, Procurement, Nuclear powered ships, Submarines, *Workstations, *Computer aided manufacturing, Automated Manufacturing Research Facility.

The manual serves as a technical guide to the specifications required to procure commercially available, major components such as a turning center and a robot system for an automated turning workstation.

900.963

PB89-221873 PC A03/MF A01 National Inst. of Standards and Technology (NEL), Gaithersburg, MD. Center for Computing and Applied Mathematics.

AutoMan: Decision Support Software for Automated Manufacturing investments. User's Manual. Final rept.

S. F. Weber, B. C. Lippiatt, and K. S. Johnson. Aug 89, 45p NISTIR-89-4116, NBS/SW/DK-89/006A For system on diskette, see PB89-221741. Sponsored by Office of the Assistant Secretary of the Navy, Washington, DC. Mfg. Technology Program.

Keywords: *Investments, *Fixed investment, Cost effectiveness, Economic analysis, Benefit cost analysis, Automation, Performance evaluation, Documentation, *Computer aided manufacturing, *Decision support systems, Microcomputers, User manuals(Computer programs).

The manual documents AutoMan, a microcomputer program designed to support multi-criteria decisions about automated manufacturing investments. The program permits users to combine quantitative and quali-tative criteria in evaluating investment alternatives. Quantitative criteria could include such traditional financial measures as Life-Cycle Cost and Net Present Value as well as such engineering performance measures as throughput and setup time. Qualitative criteria could include flexibility and product quality. AutoMan combines ratings with criteria weights into an overall rating for each investment alternative and then ranks alternatives. AutoMan comes with sample decision models and a manual that includes a detailed tutorial, a glossary of evaluation criteria, a bibliography, and an index.

900,964

PB90-112350 PC A03/MF A01 National Inst. of Standards and Technology (NEL), Gaithersburg, MD. Factory Automation Systems Div. Experience with IMDAS (Integrated Manufacturing Data Administration System) in the Automated Manufacturing Research Facility.
E. Barkmeyer, and J. Lo. Sep 89, 23p NISTIR-89/

Keywords: Automation, *Automated Manufacturing Research Facility, *Distributed computer systems, *Data base management systems, Computer aided manufacturing, National Institute of Standards and Technology.

The National Institute of Standards and Technology has been operating a locally-developed distributed data management system in its Automated Manufacturing Research Facility (AMRF) since mid-1987. The system, called the Integrated Manufacturing Data Administration System (IMDAS), front-ends existing databases and database management systems with a unified conceptual model and a common data manipula-tion language and interface. The paper first describes the AMRF, a totally automated manufacturing plant in microcosm, using commercially available equipment for the most part, and its data and data repositories. It then describes the operation and performance of IMDAS in the AMRF. Finally, it looks at areas for performance improvement in the IMDAS and draws conclusions about the usage of IMDAS for production manufacturing.

900,965

PB90-112459 PC A03/MF A01 Mational Inst. of Standards and Technology (NEL), Gaithersburg, MD. Factory Automation Systems Div.

Generic Architecture for Computer Integrated Manufacturing Software Based on the Product Data Exchange Specification.
J. E. Fowler. Sep 89, 29p NISTIR-89/4168

Keywords: *Computer aided manufacturing, *Computer graphics, *Architecture(Computers), Computer software, Programming languages, Data bases, Data processing systems, Interfaces, Specifications, *Computer integrated manufacturing.

The Product Data Exchange Specification (PDES) is an emerging standard that is intended to address the problems of data exchange and representation for a variety of manufacturing enterprises. The National Institute of Standards and Technology (NIST) has a long-standing research program that addresses the problems of integration and development of automated manufacturing systems. The document presents a software architecture that forms the basis for the incorporation of PDES into the software applications that are part of NIST's work in Computer Integrated Manufacturing (CIM).

900.966

PB90-128596 Not available NTIS National Inst. of Standards and Technology (NEL), Gaithersburg, MD. Factory Automation Systems Div. Modular Process Planning System Architecture. Final rept.

S. R. Ray. 1989, 5p Sponsored by Department of Defense, Washington,

Pub. in Proceedings of IIE Integrated Systems Conference, Atlanta, GA., November 12-15, 1989, p1-5.

Keywords: *Planning, Systems engineering, Automation, *Computer aided manufacturing, *Computer architecture, integrated systems.

A general purpose architecture for a modular process planning system is presented. Based upon emerging national standards in manufacturing, it offers easy integration among planning subsystems.

900.967

PB90-129446 PC A03/MF A01 National Inst. of Standards and Technology, Gaithersburg, MD.

AMRF Part Model Extensions.

A. Barnard. 5 Oct 89, 32p NISTIR-89/4189

Keywords: Standards, Specifications, Mathematical models, Topology, *Automated Manufacturing Research Facility, *Data management, *Computer aided manufacturing, Product Data Exchange Specification, Format, Data base management systems.

The document specifies the addition of ellipses, hyperbolas, parabolas, and b-splines to the AMRF Part Model Report Format. The reports are used through-out the AMRF to communicate part model data be-tween application processes and the global AMRF database. Part model data consists of geometry, topology, features, and tolerances. The document is intended to be used by programmers implementing systems that make use of AMRF part model data. While the report is a complete description of the extensions, the document 'AMRF Database Report Format: Part Model' by T.H. Hopp is also required to complete the grammar.

900.968

PB90-132713 PC A04/MF A01 Catholic Univ. of America, Washington, DC.
Enhancements to the VWS2 (Vertical Workstation
2) Data Preparation Software.
T. R. Kramer. 1 Nov 89, 68p NISTIR-89/4201

Sponsored by National Inst. of Standards and Technology, Gaithersburg, MD.

Keywords: *Computer software, *Data processing, *Manufacturing, Automatic control, Computer aided manufacturing, Automatic programming, Algorithms, Vertical workstation.

In the Vertical Workstation (VWS) of the NIST Automated Manufacturing Research Facility, metal parts are machined automatically from a feature-based design. Workstation activity may be divided into

Computer Aided Manufacturing (CAM)

design, process planning, data execution, and physical execution stages. The first three of these are data preparation stages. Major enhancements to the VWS2 data preparation software included: Development of new methods for creating contour outlines; Complete rebuilding of the text system; Introduction of tolerance information; A parser that extracts features from a boundary representation; Improvements in the Part Design Editor; An algorithm for the three-dimensional sculpting of contour grooves.

Engineering Materials

900.969 PB89-201768 Not available NTIS National Bureau of Standards (IMSE), Gaithersburg,

Versailles Project on Advanced Materials and Standards Evolution to Permanent Status.

Final rept.

L. Schwartz, and B. Steiner. 1986, 5p Pub. in ASTM (American Society for Testing and Mate-nals) Standardization News 14, n10 p40-44 Oct 86.

Keywords: *Ceramics, *Standardization, *Polymers, Cryogenics, Superconductors, Composite materials, International relations, Corrosion, Creep properties, Reprints, *Versailles Project on Advanced Materials and Standards.

The international activities in advanced materials started at the Versailles Heads of State meeting is described. The motivation for the collaboration, the various technical activities under way, and the organizational structure are summarized.

900 970

PB90-136672 Not available NTIS National Inst. of Standards and Technology (IMSE), Boulder, CO. Fracture and Deformation Div.

Measuring in-Plane Elastic Moduli of Composites with Arrays of Phase-insensitive Ultrasound Receivers.

D. W. Fitting, R. D. Kriz, and A. V. Clark. 1989, 8p Sponsored by National Research Council, Washing-

Pub. in Review of Progress in Quantitative Nonde-structive Evaluation, v8B p1497-1504 1989.

Keywords: *Composite materials, *Phased arrays, *Modulus of elasticity, *Ultrasonic tests, Nondestructive tests, Measurement, Wave phases, Oriented fiber composites, Velocity, Anisotropy, Reprints, Graphiteepoxy composites.

Ultrasonic measurements of elastic moduli of composite materials have traditionally been made on either small specimens cut from a larger component or by using a scanning technique with the specimen immersed in a water bath. A phase-insensitive array has been developed for rapid nondestructive measurement of in-plane elastic moduli. The array characteristics allow for determination of energy flux deviation angle in the composite, as well as measurement of group and phase velocity. Techniques for computing the phase velocity from array measurements are described. Energy flux deviation in unidirectional graphite-epoxy specimens has been determined with the array. Comparisons are made herein of results with analytical (bulk wave) predictions.

Job Environment

PB89-161897 PC A04/MF A01 Maryland Univ., College Park. Dept. of Mechanical Engineering.

Translent Cooling of a Hot Surface by Dropiets

Evaporation. Final rept.

M. di Marzo, F. Kavoosi, and M. Klassen. Nov 88, 65p NIST/GCR-89/559 See also PB87-145421. Sponsored by National Inst. of Standards and Technology (NEL), Gaithersburg, MD. Center for Fire Research.

Keywords: *Evaporative cooling, *Drops(Liquids), *Extinguishing, Fire protection, Metal plates, Fire safety, Aluminum, Computerized simulation, Interfaces, Va-

The report describes the research performed during the period March 1987 - July 1988 under a joint re-search program between the Mechanical Engineering Department of the University of Maryland and the Center for Fire Research of the National Bureau of Standards. The formulation of a model for the prediction of the cooling induced by an evaporating droplet impinging a semi-infinite solid is the subject of the report. The thermal interactions during the evaporation of a liquid droplet deposited on a low conductivity semi-infinite solid are complex because the evaporative process is coupled to the solid intense local cool-Numerical techniques based on finite difference methods have failed to provide meaningful results. This is due to the sharp temperature gradients in the proximity of the droplet edge which cause instabilities in the solution for reasonable time steps due to the explicit coupling of the liquid-vapor regions. An integral method was proposed by Dr. Baum (CFR-NBS) in order to overcome difficulties. The methodology and the application to this specific problem is described in its application to this specific problem is described in

Joining

900,972 PB90-117391 Not available NTIS National Inst. of Standards and Technology (IMSE), Boulder, CO. Fracture and Deformation Div.
On-Line Arc Welding: Data Acquisition and Analysis Using a High Level Scientific Language.

G. Adam, and T. A. Siewert. 1989, 7p
Pub. in Intelligent Instruments and Computers, p14-20 Jan/Feb 89.

Keywords: *Gas metal arc welding, *Welding, Data acquisition, Electrical measurement, Electric current, Electric potential, Reprints, *Data analysis, Personal computers.

A personal computer was used to monitor and record the current and voltage during gas metal arc welding experiments. These data were then evaluated by signal analysis techniques to characterize the welding transfer modes. The necessary hardware for high acquisition rates (up to 90kHz), as well as the software which was written to drive the equipment and to analyze the results, are described.

Manufacturing, Planning, Processing & Control

PB89-183214 PC A03/MF A01 National Inst. of Standards and Technology, Gaithersburg, MD. Operations Manual for the Automatic Operation of

the Vertical Workstation. F. F. Rudder. 12 Jan 89, 38p NISTIR-89/4031

Keywords: *Automation, *Manufacturing, Operations, Manuals, *Automated Manufacturing Research Facility, Workstations, Man machine systems.

The Vertical Workstation (VWS) is located in the Automated Manufacturing Research Facility at the National Institute of Standards and Technology. The manual is for those individuals who wish to use the VWS equipment and control it from the workstation controller. Anyone possessing the ability to flip a switch, press a button, turn a valve, and operate a personal computer can follow these steps and place the VWS under command of the workstation controller. Only the steps re-quired to configure the VWS for automatic operation are presented. The hardware details are contained in the VWS Operator's Manual.

900,974 PB89-183230 PC A03/MF A01 National Inst. of Standards and Technology (NEL), Gaithersburg, MD. Center for Mfg. Engineering.

Reai-Time Simulation and Production Scheduling Systems.

J. Davis, and A. T. Jones, Apr 89, 20p NISTIR-89/4070

Prepared in cooperation with Illinois Univ. at Urbana-Champaign.

Keywords: *Production control, *Scheduling, *Simulation, *Real time operations, Production planning, Automation, Manufacturing, Statistical analysis, Flexible manufacturing systems, Concurrent processing.

The efficient scheduling of resources in a flexible manufacturing system (FMS) has a direct impact on the company's goal of increased profits. Many techniques, including mathematical programming, expert systems, and discrete event simulation have been used to solve these scheduling problems. However, they have all been ineffective in dealing with the unexpected delays that occur on the shop floor. The paper deals with a new approach to address production scheduling prob-lems in an FMS - real-time, concurrent simulations. These simulations can be initialized to the current system state and run any time a new schedule is needed.

900.975

PB89-201495 Not available NTIS National Bureau of Standards (IMSE), Gaithersburg, MD. Polymers Div. Necking Phenomena and Cold Drawing.

Final rept. L. J. Zapas, and J. M. Crissman. 1985, 23p Pub. in Viscoelasticity and Rheology, Chapter 4, p81-103 1985.

Keywords: *Cold drawing, *Necking, *Tensile properties, Stresses, Strains, Loading rate, Elastic properties, Reprints.

The various experimental results presented suggest strongly that the instability leading to neck formation is associated with the nonlinearity of the mechanical behavior coupled with the time dependence. In experiments involving constant rate of clamp separation, necking occurs well beyond the point where the stress-strain curve goes through a maximum, and the amount beyond depends on the rate of strain. For polypropylene, at the lowest rate of clamp separation shown, the strain at which the neck became visible was about three times the value at which the maximum in the stress occurred. At constant rate of loading, the stress-strain behavior is monotonically increasing up to the point of necking where immediately thereafter the specimens break. To describe the instability behavior in a hard device one might in some way use elastic behavior. However for a soft device it becomes very clear that one needs to consider the viscoelastic behavior of the material.

Quality Control & Reliability

900.976

PB89-146740 Not available NTIS National Bureau of Standards (IMSE), Gaithersburg, MD. Office of Nondestructive Evaluation Optical Nondestructive Evaluation at the National

Bureau of Standards. Final rept.

G. Birnbaum, D. Nyyssonen, C. M. Vest, and T. Vorburger, 1986, 17p

Pub. in Proceedings of SPIE (Society of Photo-Optical Instrumentation Engineers), v604 p1-17 1986.

Keywords: *Nondestructive tests, *Optical measurement, Light scattering, Holography, Standards, Surfaces, Microscopy, Scratches, Inspection, Reviews, Reprints, Optical fibers, Calibration.

The report reviews recent and current work on a variety of optical techniques applied to nondestructive eval-uation (NDE) carried out by the National Bureau of Standards. The optical methods discussed include holography, scattering from surfaces, microscopy, scat-tering from particles, and methods employing optical fibers. Much of this work is aimed at the development of accurate measurement methods for in-service inspection and process monitoring in manufacturing, and the development of standards and calibration pro-

Quality Control & Reliability

900.977 Not available NTIS PB89-150874 National Bureau of Standards (NEL), Gaithersburg, MD. Automated Production Technology Div.

Generalized Mathematical Model for Machine Tool

Errors.

13p

M. A. Donmez, C. R. Liu, and M. M. Barash. 1986,

Pub. in Proceedings of ASME (American Society of Mechanical Engineers) Winter Annual Meeting - Modeling, Sensing, and Control of Manufacturing Processes, Anaheim, CA., December 7-12, 1986, p231-243.

Keywords: *Mathematical models, *Machine tools, *Errors, Accuracy, Compensation, Turning(Machining), Deflections, Wear, Positioning error, Coordinate transformations, Turning center, Thermally-induced errors.

In the paper, the authors describe a general mathematical model, which is able to incorporate the error sources to determine the positional error vector of the cutting tool with respect to the workpiece. In the process of the development of the model, the authors first represent individual elements in the machine tool-fixrepresent individual elements in the machine tool-lik-ture-workpiece system by assigning a homogeneous coordinate transformation matrix to each element. This matrix describes the position and orientation of a body in space, and can incorporate the error motions of the body in six degrees of freedom. The machine tool-fixture-workpiece system is then considered as a chain of linkages, and the relationships between these linkages are determined by matrix multiplications. Based on this idea, a matrix equation corresponding to the structural loop of the machine tool-fixture-workpiece system is constructed, and solved for the error vector. Although this model is applied to a turning center, it can easily be modified for any type of machine tools, coordinate measuring machines, and robots.

900,978

PC E06/MF E01 PB89-154322 National Inst. of Standards and Technology, Gaithers-burg, MD. Office of Standards Code and Information. Organizations Represented in the Collection of Voluntary Standards.

Jan 89, 46p Supersedes PB88-145560.

Contains (Ten sheets of 48X reduction microfiche). A supplementary document, U.S. Organizations Represented in the Collection of Voluntary Standards, accompanies this index.

Keywords: *Standards, Indexes(Documentation), Subject index terms, Specifications, Tests, United States, Engineering standards, Product standards.

The list contains the names of U.S. organizations which develop standards or provide technical information on standards-related activities. The standards-developing organizations are represented in the National Center for Standards and Certification Information (NCSCI) reference collection (in microform or hard copy) and are listed in the Key-Word-In-Context (KWIC) index of U.S. voluntary industry standards. The acronym list (Contents) is listed in alphabetical order by acronym. The organization names, address and telephone numbers are listed in alphabetical order by organization name.

PB89-176655 Not available NTIS National Bureau of Standards (NEL), Gaithersburg, MD. Precision Engineering Div.

Optical Roughness Measurements for Industrial

Surfaces. Final rept.

rinai rept.
D. Gilsinn, T. Vorburger, L. X. Cao, C. Giauque, F. Scire, and E. C. Teague. 1986, 9p
Pub. in Proceedings of SPIE (Society of Photo-Optical Instrumentation Engineers) Optical Techniques for Industrial Inspection, Quebec City, Canada, June 4-6, 1986, p8-16.

Keywords: *Optical measurement, *Surface roughness, *Nondestructive tests, Optical measuring instruments, Light scattering, Diffraction, Mathematical models.

The paper reviews the effort to develop the theory and instrumentation needed to measure surface roughness of manufactured surfaces by optical scattering methods. Three key problems are addressed: developing a valid and sufficient optical scattering theory for the roughness range; applying appropriate mathemati-cal inversion techniques so that practical roughness parameters can be calculated from scattering distributions; and evaluating a compact commercial instru-ment that is easy to align on a wide variety of part ge-ometries. Recent results suggest that the simple phase screen approximation model of optical scatter-ing theory validly describes light scattering from ma-chined metal surfaces with a predominant surface lay in the 0.01 Ra to 3.0 Ra range. New measurements of light scattered out of the plane-of-incidence are discussed. A model for scattering in the entire far-field hemisphere and observations on the inverse problem is given.

900,980 PB89-177018 Not available NTIS National Bureau of Standards (NEL), Gaithersburg, MD. Factory Automation Systems Div. CAD (Computer Alded Design)-Directed Inspec-

tion. Final rept.

T. H. Hopp. 1984, 15p Pub. in Annals of the CIRP 33, n1 p1-15 1984.

Keywords: *Inspection, Automation, Measuring instruments, Artificial intelligence, Quality assurance, Reprints, *Computer aided design, *Computer aided manufacturing, Control systems.

The paper describes a control system architecture, based on hierarchical task-decomposition techniques, for multi-axis coordinate measuring machines. An in-spection program consists of a series of high level goals to be satisfied. Goals are satisfied when speci-fied information has been obtained regarding the part. There is a decision hierarchy, each level of which provides logic for partially decomposing goals into simpler goals. The control system executes the inspection program by interpreting the decision hierarchy logic. A world model hierarchy executing in parallel with the task decomposition hierarchy provides information which aids in the decomposition decisions at each level. Artificial intelligence techniques will allow the convenient incorporation of quality assurance standards into inspection tasks.

900.981

PB89-187587 Not available NTIS National Bureau of Standards (NEL), Boulder, CO. Electromagnetic Technology Div.

New Standard Test Method for Eddy Current Probes.

Final rept.

L. L. Dulcie, and T. E. Capobianco. 1987, 7p Sponsored by Army Materials Technology Lab., Watertown, MA.

Pub. in Proceedings of Defense Conference on Non-destructive Testing (36th), St. Louis, MO., October 27-29, 1987, p154-160.

Keywords: *Eddy current tests, *Standards, Test equipment, Electrical impedance, Electrical properties, Eddy currents, Nondestructive tests, Electrical measurement, Equipment specifications, *Military equip-

Recently, a draft military standard for the characterization of eddy current probes was submitted to the U.S. Army Materials Technology Laboratory by the National Bureau of Standards. The development of a standard test set and future plans for a round robin study for evaluating the draft standard in a controlled study are discussed. The test set will be used to determine impedance measurement capability and consists of two parts; a prototype test block set as specified by the draft standard and a specially designed and characterized probe set. A round robin survey will be conducted to determine ease of use, repeatability of characterization measurements, and impedance measurement precision when using the test blocks as specified in the standard.

900,982

PB89-193296 PC A06/MF A01 National Inst. of Standards and Technology, Gaithersburg, MD. Progress Report of the Quality In Automation

Project for FY88.

C. D. Lovett. Apr 89, 108p NISTIR-89/4045 Prepared in cooperation with Department of the Navy, Washington, DC., and Department of Energy, Washington, DC. Keywords: *In-process quality control, *Automation, Verification inspection, Process control, Monitors,

The document describes a quality control architecture that uses real-time sensing, deterministic metrology methods, machine tool characterization, process-intermittent gauging, and process certification to control the machining process with the objective of reducing the reliance on traditional post-process inspections methods and moving toward greater reliance on in-process verification. The 'Quality In Automation' project is developing a computer-based system that includes real-time sensors, a quality database, quality monitors, quality controllers, an inspection station, and a communication network which allows data to flow among components of the quality system. The quality architecture includes control loops such as post-proc-essing characterization, pre-processing characteriza-tion, process intermittent gauging, and real-time sensing. The sensors for temperature, force and ultrasonic may result in a command signal to the machine tool controller to alter its pre-programmed positions, to change its manipulative variables (speed and feed), and to modify the NC code. The corrective action will depend on the time varying nature of the errors and the predictions derived from the analysis models.

900 983

PB89-228290 PC A03/MF A01 National Inst. of Standards and Technology (IMSE),

National Inst. of Standards and Technology (IMSE), Gaithersburg, MD.

Computer-Controlled Test System for Operating Different Wear Test Machines.

E. P. Whitenton, and A. W. Ruff. Jul 89, 50p NISTIR-

Grant N00014-89-F-0021

Sponsored by Office of Naval Research, Arlington, VA.

Keywords: *Wear tests, Computer systems hardware, Computer programs, *Tribology, *Computer aided control systems, Computer architecture, File struc-

The report discusses a wear tester control system, where the same computer and software runs three dif-ferent wear test machines; a commercial crossed-cylinder, a commercial block-on-ring, and an in-house designed controlled-atmosphere tribometer. The computer hardware, the interface to the wear test ma-chines, and the aspects that make the machines func-tionally similar are examined. The program itself, its use, and the data file structure are also explored.

900,984

PB89-229025 PC A03/MF A01 National Inst. of Standards and Technology (IMSE), Gaithersburg, MD. Office of Nondestructive Evalua-NDE (Nondestructive Evaluation) Publications,

1985.

L. Mordfin. Aug 89, 43p NISTIR-89/4131 See also PB87-201406.

Keywords: *Nondestructive tests, *Bibliographies, Radiography, Thermography, Ultrasonic tests, Acoustic measurement, Magnetic tests, Optical measurement, Leak detectors, Nondestructive analysis.

The report provides bibliographic citations, with selected abstracts, for 131 publications that appeared in the open literature, primarily during calendar year 1985. A detailed subject index is included as well as information on how copies of many of the publications may be obtained.

900 985

PR89-229199 Not available NTIS National Inst. of Standards and Technology (IMSE), Gaithersburg, MD. Metallurgy Div. Quantitative Problems in Magnetic Particle Inspec-

tion. Final rept.

L. J. Swartzendruber. 1989, 8p

Pub. in Review of Progress in Quantitative Nonde-structive Evaluation, v8B p2133-2140 1989.

Keywords: *Magnetic particle tests, *Reproducibility, *Quantitative analysis, Magnetic properties, Steels, Quality control, Nondestructive tests, Defects, Inspection, Reprints.

Although long considered a mature technology, a number of questions remain on how to best control the magnetic particle inspection process to obtain repro-

Quality Control & Reliability

ducible, quantitative results. The primary factors that must be controlled to obtain reproducible and predictable results are briefly discussed, followed by a detailed discussion of the magnetic leakage field from defects and a proposed method for determining the applied field necessary to detect defects of a given ge-

PC A03/MF A01
National Inst. of Standards and Technology, Gaithersburg, MD. Office of Standards Code and Information.
Glossary of Standards-Related Terminology.

D. R. Mackay. Oct 89, 29p NISTIR-89/4194 Library of Congress catalog card no. 89-600767.

Keywords: *Dictionaries, *Standards, Definitions, Terminology, Quality control, Tests, *Standardization, Accreditation, Certification.

The glossary provides definitions of 95 terms that are commonly used in standardization, certification, laboratory accreditation, and quality control activities. Multiple definitions are provided in some cases to identify organizational differences in the use of terms. In each case the source of the definition is indicated. The terms are presented in a logically structured format, beginning with general terms and moving to more specific terms.

Robotics/Robots

ann as 7 PB89-157358 Not available NTIS National Bureau of Standards (NEL), Gaithersburg, MD. Robot Systems Div. Optical Sensors for Robot Performance Testing and Calibration.

Final rept. N. Dagalakis, and K. C. Lau. 1988, 5p

Pub. in Vision 5, n3 p10-14 1988.

Keywords: *Robots, *Optical measuring instruments, *Metrology, Performance evaluation, Performance tests, Calibrating, Reprints.

The article presents a brief review of robot performance measurements which may use optical metrology sensors. The desired optical metrology sensors performance characteristics are also discussed. Finally, a brief description of the available optical robot metrology sensors is provided.

900,988 PB89-159644 PC A04/MF A01 National Bureau of Standards, Gaithersburg, MD. Material Handling Workstation Implementation.
C. E. Wenger. 19 May 88, 55p NBSIR-88/3784

Keywords: *Materials handling, *Robots, *Manufacturing, *Workstations, Automation, Work place layout, Operations, Instructions, Machining, Buffing, Hydraulic power pumps, Computers, *Automated Manufacturing Research Facilities, *AMRF material handling workstations, Roller tables, Automatic storage and retrieval systems. systems, Automatic guided vehicles.

The purpose of the document is to provide a general description of design and implementation of the AMRF Material Handling Workstation (MHWS). The MHWS equipment includes two Automatic Guided Vehicles (AGVs), an Automatic Storage and Retrieval System (ASRS), and roller tables at other workstations. The document should provide the reader with an understanding of concepts used to implement the MHWS.

900,989 PC A03/MF A01 PB89-159651 National Bureau of Standards, Gaithersburg, MD. Material Handling Workstation: Operator Manual. C. E. Wenger. 19 May 88, 18p NBSIR-88/3785 See also PB89-159644.

Keywords: *Materials handling, *Robots, *Manufacturing, "Workstations, Automation, Work place layout, Operations, Instructions, Machining, Buffing, Hydraulic power pumps, Computers, "Automated Manufacturing Research Facilities, "AMRF material handling workstations, Roller tables, Automatic storage and retrieval systems, Automatic guided vehicles.

The purpose of the document is to provide operating instructions for the AMRF Material Handling Workstation (MHWS). The material handling equipment includes Automatic Guided Vehicles (AGV) and an Automatic Storage and Retrieval System (ASRS). The document includes operating instructions to startup and shutdown the material handling system. Also included are instructions to operate the AGV in its manual operating mode.

900.990

PB89-159669 PC A03/MF A01 National Bureau of Standards, Gaithersburg, MD.
Real-Time Control System Modifications for a Deburring Robot. User Reference Manual.
K. N. Murphy. 4 Aug 88, 43p NBSIR-88/3832

Keywords: *Control equipment, *Real time operations, *Robots, Deburring, Cleaning, *Automated Manufacturing Research Facility, Computer aided manufacturing, Computer aided design, Workstations, User ing, Computer aided design manuals (Computer programs).

At the National Bureau of Standards' Automated Manufacturing Research Facility a PUMA 760 robot deburrs metal parts at the Cleaning and Deburring Workstation. The robot is controlled by the NBS developed Real-Time Control System (RCS). The basic RCS was extended to meet the needs of the workstation and the manual explains these additions.

PB89-177059 Not available NTIS National Bureau of Standards (NEL), Gaithersburg, MD. Robot Systems Div. **Building Representations from Fusions of Multiple**

Views.

E. W. Kent, M. O. Shneier, and T. H. Hong. 1986, 6p Pub. in Proceedings of IEEE (Institute of Electrical and Electronics Engineers) International Conference on Robotics and Automation, San Francisco, CA., April 7-10, 1986, p1634-1639.

Keywords: *Robots, Pattern recognition, Models, *Computer vision, Position sensing, Spatial resolution,

A robot sensing system is described that uses multiple sources of information to construct an internal representation of its environment. Initially, object models are used to form the basic representations. These are modified by processes that operate on sequences of sensory information which is obtained from sensors that move about in the environment. Two representations are constructed. One is a description of the spatial layout of the environment, represented as an octree. The other is an object- and feature-based representation. The system handles both expected and unexpected objects, and attempts to register its internal representation with the external world using a variety of predictive, sensory-processing, and matching procedures.

900 992

PB89-177067 Not available NTIS National Bureau of Standards (NEL), Gaithersburg, MD. Robot Systems Div. Fast Path Planning in Unstructured, Dynamic, 3-D

Worlds. Final rept.

M. Herman. 1986, 8p

Pub. in Proceedings of SPIE (Society of Photo-Optical Instrumentation Engineers), Applications of Artificial Intelligence III, v635 p505-512 1986.

Keywords: *Paths, *Planning, Collision avoidance, Search structuring, Algorithms, *Robotics, Obstacle avoidance.

Issues dealing with fast motion planning in unstructured, dynamic 3-D worlds are discussed and a fast path planning system under development at NBS is described. It is argued that an octree representation of the obstacles in the world leads to fast path planning algorithms. The system performs the path search in an octree space and uses a hybrid search technique that combines hypothesis and test, hill climbing, A*, and multiresolution grid search.

900,993

PB89-181739 PC A03/MF A01 National Inst. of Standards and Technology (NEL), Gaithersburg, MD. Robot Systems Div. Interfaces to Teleoperation Devices.

Technical note (Final). J. C. Fiala. Oct 88, 16p NIST/TN-1254 Also available from Supt. of Docs. as SN003-003-

Keywords: *Control equipment, *Robots, Servome-chanisms, Interfaces, *Teleoperators, Active control.

The document describes a basic logical architecture for teleoperation control devices and interfaces for integrating these devices with a telerobot control system architecture. The interfaces described are for manipulator control only. The discussion will consider teleo-peration devices as divided into two classes. Section 2 describes the interfaces for joint-space teleoperation devices. The interface requirements for Cartesian teleoperation devices are detailed in section 3.

900,994

PB89-221188 PC A04/MF A01 National Inst. of Standards and Technology (NEL), Gaithersburg, MD. Center for Mfg. Engineering. Visual Perception Processing In a Hierarchical

Control System: Level 1. Technical note (Final).

K. Chaconas, and M. Nashman. Jun 89, 53p NIST/ TN-1260

Also available from Supt. of Docs. as SN003-003-02949-1.

Keywords: *Robotics, *Control systems, *Visual perception, Image processing, Interfaces, Models, Algorithms, *Architecture(Computers).

The document describes the interfaces and functionality of the first level of the visual perception branch of a real time hierarchical manipulator control system. It includes a description of the scope of the processing performed and the outputs generated. It defines the interfaces and the information exchanged between the modules at this level, as well as interfaces to a camera, a human operator, and to higher levels of the system.

Tooling, Machinery, & Tools

900.995

PATENT-4 838 145 Not available NTIS Department of Commerce, Washington, DC.

Multiple Actuator Hydraulic System and Rotary Control Valve Therefor.

Patent.

A. H. Slocum, and J. P. Peris. Filed 18 Jun 87 patented 13 Jun 89, 11p PB89-222368, PAT-APPL-7-063 558

Supersedes PB87-218384. Sponsored by National Inst. of Standards and Technology, Gaithersburg, MD. This Government-owned invention available for U.S. licensing and, possibly, for foreign licensing. Copy of patent available Commissioner of Patents, Washington, DC 20231 \$1.50.

Keywords: *Hydraulic equipment, *Rotary valves, *Actuators, *Patents, Control equipment, Fluidic control devices, Creep strength, Phased arrays, PAT-CL-91-

The present invention provides a rotary hydraulic valve and a multiple hydraulic actuator system which, together, offer a truly practical solution to the problem of automating machine-tool parts fixtures. The control valve of the invention is capable of carrying out the complex logic required for multiple actuator control but is nonetheless both simple and compact. The actuator system is designed to incorporate a rotary valve but avoids the problem of creep which is characteristic of prior rotary-valve controlled actuators. The valve design of the invention also prevents thrust loads on the rotary valve member and thus avoids the need for heavy duty thrust bearings even in high pressure applications.

900,996

Not available NTIS PB89-146781 National Bureau of Standards (NEL), Gaithersburg, MD. Automated Production Technology Div.

Tooling, Machinery, & Tools

General Methodology for Machine Tool Accuracy Enhancement by Error Compensation. Final rept.

A. Donmez, D. S. Blomquist, R. J. Hocken, C. R. Liu, and M. M. Barash. 1986, 10p Pub. in Precision Engineering 8, n4 p187-196 Oct 86.

Keywords: *Machine tools, *Accuracy, Calibrating, Tolerances(Mechanics), Temperature, Errors, Least squares method, Compensation, Reprints.

The methodology introduces a general mathematical model, which relates the error in the position of the cutting tool with respect to the workpiece to the errors of the individual machine elements are then decom-posed into geometric and thermally-induced compo-nents. A predictive machine calibration procedure to predict the geometric and thermally-induced errors of the machine slides is described. Based on the calibration data, empirical models for the error components are generated and valves for the parameters in these models are obtained using least-squares curve fitting techniques. A flexible, modular, and structured soft-ware system compensates for the predicted errors in real-time. The compensation system monitors the tem-peratures on the machine tool structure and the nominal axes positions, and then uses this information to predict the errors. The software is written in high level language and implemented in a dedicated, low cost, single-board microcomputer. The cutting tests carried out under transient thermal conditions have shown that the accuracy enhancement of up to 20 times is achievable using the methodology described in the paper, without a machine warm-up period.

900,997 PB89-150841 Not available NTIS National Bureau of Standards (NEL), Gaithersburg,

MD. Precision Engineering Div.
Preliminary Experiments with Three Identical Uitraprecision Machine Tools. Final rept.

C. Evans, P. Hannah, and R. Rhorer. 1989, 10p Pub. in Proceedings of SPIE (Society of Photo-Optical Instrumentation Engineers), v996 10p.

Keywords: *Machine tools, Precision, Mirrors, Optical equipment, Comparison, *Ultraprecision machine tools, *Precision machining, Diamond turning ma-

The paper outlines the underlying philosophy of, and reports preliminary results from, experiments with three nominally identical diamond turning machines. Identical tools, specially fabricated from the same diamond, were used to machine mirrors from blanks cut from the same base material using previously specified process parameters; parts produced are compared.

900,998 PB89-162564 PC A03/MF A01 National Bureau of Standards, Gaithersburg, MD.

Material Handling Workstation, Recommended
Technical Specifications for Procurement of Commercially Available Equipment. C. E. Wenger. 19 May 88, 32p NBSIR-88/3786

Keywords: *Materials handling equipment, *Procurement, Specifications, Manufacturing, Requirements, Inspection, *Automated Manufacturing Research Facility, *Workstations.

The purpose of the document is to provide specifications to be used in the procurement of material handling equipment to be used in an automated facility. The equipment specified includes Automatic Guided Vehicles (AGV) and an Automatic Storage and Retrieval System (ASRS).

900,999 PB89-201198 Not available NTIS National Bureau of Standards (NML), Gaithersburg, MD. Temperature and Pressure Div.

Progress In Vacuum Standards at NBS (National Bureau of Standards). Final rept.

C. R. Tilford. 1986, 14p Pub. in Proceedings of Measurement Science Conference, Irvine, CA., January 23-24, 1986, p94-107.

Keywords: *Vacuum apparatus, *Standards, Vacuum gages, Pressure measurement, Ionization gages, Leakage, Test facilities, Calibration, National Institute of Standards and Technology.

The increasing reliance of American industry and science on vacuum technology has generated a continu-

ing demand for improved vacuum measurement accuand germand for improved vacuum fleasurement accuracy. The National Bureau of Standards has responded with a vacuum and leak standards program. The article describes the goals of the NBS program, the current state of vacuum standards and calibration services at NBS, and the operation of the U.S. voluntary standards program. Information is contained on the performance of vacuum instruments that might be used in an industrial vacuum calibration laboratory.

901.000 PB89-216469 PC A04/MF A01 National Inst. of Standards and Technology (NEL), Gaithersburg, MD. Center for Building Technology. Static Tests of One-third Scale Impact Limiters. L. T. Phan, and H. S. Lew. May 89, 56p NISTIR-89/ 4089

Keywords: *Impact tests, *Shock absorbers, Energy absorption, Test facilities, Mechanical shock, Stresses, Vibration damping, Shock resistance.

The National Institute of Standards and Technology carried out four tests of one-third scale impact limiters for Transnuclear, Inc. The impact limiters were tested under static load in a 12-million pound capacity universal testing machine. Energy absorbed by the impact limiters, as indicated by the area under the load-deformation curve, was computed and compared with the required value which was specified for each specimen by Transnuclear, Inc. The testing was terminated when the absorbed energy value exceeded the required

Tribology

901.001 PB89-147391 Not available NTIS National Bureau of Standards (IMSE), Gaithersburg,

MD. Metallurgy Div.

Metallographic Evidence for the Nucleation of Subsurface Microcracks during Unlubricated Sild-Ing of Metais. Final rept.

P. J. Blau, and E. D. Doyle. 1987, 7p Pub. in Wear 117, n3 p381-387 1987.

Keywords: *Wear, *Crack propagation, Sliding, Crack initiation, Nucleation, Coalescing, Metallography, Re-

The location, surface or subsurface, for nucleation and propagation of microcracks during sliding wear has been a continuing source of discussion and controversy in the tribology community. Rather than to suggest that there is only one correct answer to this question, the authors propose that depending on the contract conditions and materials involved, several preferred sites for microcrack nucleation can exist. The present paper provides metallographic evidence in support of a model which involves nucleation ahead of the slider, crack closure, and reopening after the slider passes. Once microcracks nucleate, subsequent slider passes can cause crack propagation, coalescence, and the eventual formation of wear debris particles. Observations of uplifted flakes are similar to those of the 'delamination theory of wear,' but the mechanism proposed for crack nucleation differs from that originally proposed based on the subsurface stress analysis from the 'delamination theory.'

901.002 PB89-228274 PC A14/MF A01 National Bureau of Standards (NEL), Gaithersburg, Development and Use of a Tribology Research-In-

Progress Database. S. Jahanmir, and M. B. Peterson. Jul 89, 316p

NISTIR-89/4112 Portions of this document are not fully legible.

Keywords: *Databases, *Management information systems, Data processing, Mechanical engineering, Research management, Lubricants, Components, Systems engineering, Friction, Wear, *Tribology.

Preliminary efforts leading to the development of a re-search-in-progress database on tribology are de-scribed. The database contains brief abstracts of current tribology research being conducted by industry, universities, research institutes and government lab-

oratories based on a survey of active researchers. It also contains information on the types of activities, general areas of interest, program objectives, and tribology applications. The primary program objectives cited in connection with the tribology activities include long life, low maintenance, failure-free machinery, fundamental understanding, and materials development for improved performance.

901,003 PB90-130295 PC A05/MF A01 National Inst. of Standards and Technology, Gaithers-

burg, MD. Tribiology Group.

Measurements of Tribological Behavior of Advanced Materials: Summary of U.S. Results on VAMAS (Versailles Advanced Materials and Standards) Round-Robin No. 2. A. W. Ruff, and S. Jahanmir. Sep 89, 76p NISTIR-

89/4170

Keywords: *Wear, *Sliding friction, *Materials tests, Measurement, Tables(Data), Standards, Ceramics, Tribology, Interlaboratory comparisons, International cooperation, Coordinated research programs.

An interlaboratory comparison of tribological measurements was carried out among 16 U.S. laboratories as part of a large world effort involving six countries within the VAMAS (Versailles Advanced Materials and Standards) activity. Results for friction and wear of five material pairs are described in the report, along with a statistical analysis of the data, and interpretation of some of the findings.

General

901.004 PB89-172563 PC A03/MF A01 National Inst. of Standards and Technology (NEL), Gaithersburg, MD.

Report on Interactions between the National insti-tute of Standards and Technology and the American Society of Mechanical Engineers. G. K. Ehrlich. Feb 89, 32p NISTIR-89/4038

Keywords: *Technology transfer, *Mechanical engineering, *Industrial engineering, *Standards, Computers, Heat transfer, Pressure vessels, Solar energy, Tribology, Meetings, *American Society of Mechanical Engineers(ASME), *National Institute of Standards and Technology (NIST).

The report highlights examples of interactions between the National Institute of Standards and Technology (NIST) and the American Society of Mechanical Engineers (ASME) over the past several years. It is meant to be representative, not all-inclusive. The interactions are organized by discipline in the following cat-egories: Conferences, Committee memberships and contribution to standards, Editors, Publications which are designed to disseminate NIST's most recent technical advances and to learn of the technical chal-

901,005 PB89-173876 Not available NTIS Notional Bureau of Standards (NEL), Boulder, CO. Chemical Engineering Science Div. Ineffectiveness of Powder Regenerators in the 10

K Temperature Range.

Final rept.

lenges facing engineers in industry.

R. Radebaugh. 1987, 19p Sponsored by Air Force Flight Dynamics Lab., Wright-Patterson AFB, OH.

Pub. in Proceedings of Interagency Meeting on Cryocoolers (2nd), Easton, MD., September 24, 1986, p145-163 1987.

Keywords: *Regenerators, *Low temperature tests, *Effectiveness, Mechanical refrigeration, Cryogenics, Performance tests, Powder(Particles), Specific heat, Phase angle, Test facilities, Measurement.

Regenerators for temperatures around 10 K usually have rather high values of ineffectiveness because of a lack of matrix heat capacity. The paper describes various models used to predict regenerator performance and shows how the pressure oscillation and flow through a temperature gradient affect the overall heat transfer in the regenerator. These two effects can par-tially cancel each other and reduce the regenerator

General

loss when the phase angle between the displacer and compressor is less than 90 degrees. The paper also describes an apparatus used to measure the ineffectiveness under realistic operating conditions and gives results of measurements on two powder materials with different heat capacities - Pb and GdRh. The effect of the phase angle between mass flow rate and pressure are examined and are shown to have a strong effect.

901,006 PB89-173884 Not available NTIS
National Bureau of Standards (NEL), Boulder, CO. Mational Burgineering Science Div.

Measurement of Regenerator Ineffectiveness at

Low Temperatures. Final rept.

R. Radebaugh, B. Louie, and D. Linenberger. 1987,

Sponsored by Air Force Flight Dynamics Lab., Wright-Patterson AFB, OH.
Pub. in Proceedings of Interagency Meeting on Cryocoolers (2nd), Easton, MD., September 24, 1986, p69-

93 1987.

Keywords: *Regenerators, *Low temperature tests, *Measurement, *Effectiveness, Heat exchangers, Cryogenics, Helium, Test facilities, Pressure, Temperature, Phase angle, Flow rate, Mass flow.

The low temperature limit of regenerative-cycle cryocoolers is usually determined by the ineffectiveness of the regenerator for temperatures below approximately the regenerator for temperatures below approximately 20 K. It is also this temperature range that the energy stored in the void volume gas becomes significant, which makes regenerator modeling much more difficult compared with regenerators operating at higher temperatures. The paper describes an experimental apparatus for measuring the ineffectiveness of regenerators in the temperature range 4-40 K. All operating parameters, such as mass flow, pressure, tempera-ture, and phase angle can be measured and controlled independently of each other. A discussion of materials and geometries to be tested in the apparatus is given and estimates of performance of refrigerators with improved regenerators are made.

901,007

PB89-173892 Not available NTIS National Bureau of Standards (NEL), Boulder, CO.

Chemical Engineering Science Div.

Refrigeration Efficiency of Pulse-Tube Refrigerators.

R. Radebaugh, and S. Herrmann. 1987, 15p Sponsored by Department of the Navy, Washington, DC., and National Aeronautics and Space Administration, Moffett Field, CA. Ames Research Center. Pub. in Proceedings of International Cryocoolers Conference (4th), Easton, MD., September 25-26, 1986, p119-133 1987.

Keywords: *Low temperature tests, *Thermal efficiency, Cryogenics, Refrigerating machinery, Mass flow, Regenerators, Heat transfer, Performance tests, Power, Test facilities, *Pulse tube refrigerators.

The report describes measurements of the refrigera-The report describes measurements of the refrigera-tion capacity per unit mass flow as well as the thermo-dynamic efficiency of the cooling process which occurs within these pulse tubes. The effect of tube di-ameter, tube length, orifice setting and frequency were investigated. Efficiencies as high as 90% of Carnot ef-ficiency were measured in some cases when compres-sor and regenerator losses were neglected. Gross rerigeration power at the optimum orifice setting was as high as 10 W at 80 K for a tube 12.7 mm O.D. by 240 mm long. It is shown that the performance of orifice pulse tubes is dependent on the tube volume and not on diameter and length, and heat transfer to the tube walls is detrimental to the performance. The regenerator losses can be relatively large since high mass-flow rates occur in these devices.

901,008

PB89-185748 Not available NTIS National Bureau of Standards (NML), Boulder, CO.

Time and Frequency Div.

Analysis of High Performance Compensated Thermal Enclosures.

Final rept. F. L. Walls. 1987, 5p

Pub. in Proceedings of Annual Symposium on Frequency Control (41st), Philadelphia, PA., May 27-29, 1987, p439-443.

Keywords: *Cryostats, *Ovens, *Thermal measurements, *Temperature control, Low temperature tests, Thermostats, Errors, Thermal analysis.

Approximate analysis of the conventional thermal en-Approximate analysis of the conventional thermal en-closures such as ovens and cryostats reveals that the limitation to achievable thermal regulation is in many cases not the gain of the thermal servo loop, but rather the fact that the experiment under observation within the thermal enclosure is still coupled to the outside temperature. So, even if the thermal enclosure is perfectly stable in temperature, the experiment is not. A new configuration is suggested which uses an additional sensor to measure changes in the outside temperature and compensate the temperature set point of the thermal enclosure in order to just correct for the temperature error induced by the coupling to the out-

901,009 PB89-186720 Not available NTIS National Bureau of Standards (NEL), Gaithersburg, MD. Chemical Process Metrology Div.

Measurement of Shear Rate on an Agitator in a Fermentation Broth.

Final rept.

B. Robertson, and J. J. Ulbrecht. 1987, 5p Pub. in Biotechnology Processes, p31-35 1987.

Keywords: *Shear rate, *Turbine blades, *Fermentation, *Vats, Strain rate, Shear properties, Food processing, Electrochemistry, Reprints.

The shear rate was measured on the front face of a Rushton turbine blade rotating in an aqueous polyox solution that models a fermentation broth. The measurements agree with the theory of stagnation flow on the blade. A formula is given for use in scaling the results up to larger-diameter fermentation vats.

901,010 PB89-189120 PC A04/MF A01 National Inst. of Standards and Technology (NEL), Gaithersburg, MD. Fluid Flow Group. NBS' (National Bureau of Standards) Industry; Government Consortium Research Program on

Flowmeter installation Effects: Summary Report with Emphasis on Research January-July 1988. Summary rept.

G. E. Mattingly, and T. T. Yeh. Apr 89, 75p NISTIR-

Keywords: *Fluid flow, *Pipe flow, *Flowmeters, *Pipe bends, *Installing, Turbulent flow, Pressure, Measurement, Graphs(Charts), Vortices.

The report presents results produced in a consortiumsponsored research program on Flowmeter Installa-tion Effects. The project is a collaborative one that has been underway for three years; it is supported by an industry-government consortium that meets twice yearly to review and discuss results and to plan subsequent phases of the work. The report contains the results and conclusions of the recent meeting of the con-sortium at NIST-Gaithersburg, MD in August 1988. Specific results included in the report include the following research results for the pipe flow from a conventional, long radius elbow: the distributions of the mean and the turbulence velocities in the axial and vertical directions; the pressure loss measurements; the performance of selected types of flowmeter in-stalled downstream of the elbow; and the demonstra-tion that satisfactory performance for the selected meters can be predicted using the research results of the study.

PB89-218341 PC A03/MF A01 PB89-218341

National Inst. of Standards and Technology (NEL),
Boulder, CO. Chemical Engineering Science Div.
Interlaboratory Comparison of the Guarded Horizontal Pipe-Test Apparatus: Precision of ASTM
(American Society for Testing and Materials)
Standard Test Method C-335 Applied to Mineral-Fiber Pipe Insulation.

D. R. Smith. Apr 89, 47p NISTIR-89/3913 Sponsored by Oak Ridge National Lab., TN.

Keywords: *Thermal conductivity, *Pipes(Tubes), *Mineral wool, Comparison, Measurement, Methodology, Accuracy, Insulation, Heat transfer, Refractory materials, Graphs(Charts).

Apparent thermal conductivity of refractory pipe insulation from the same production lot was measured by seven different laboratories. The companson assessed the precision and bias of the ASTM Test for Measurement of Steady-State Heat-Transfer Properties of Horizontal Pipe Insulation (C 335). For all test results from all seven participants, the standard deviation was 5%. This value is offered as the estimated precision of the horizontal pipe-test method. The accuracy of the pipe-test method cannot be estimated from the data obtained in the intergence process. the data obtained in the intercomparison.

PB90-130568 PC A07/MF A01 National Inst. of Standards and Technology (NEL), Gaithersburg, MD. Center for Mfg. Engineering. Publications of the Center for Manufacturing Engineering Covering the Period January 1978-December 1988.

P. Nanzetta, A. Weaver, J. Wellington, and L. Wood. Sep 89, 141p NISTIR-89/4180

Keywords: *Manufacturing, *Production engineering, *Bibliographies, Automation, Artificial intelligence, Operations research, Robots, Information systems.

A list of publications by staff of the Center for Manufacturing Engineering for the period 1978-1988, indexed by subject area. Publications cover research done by by subject area. Publications cover research done by the Center in the areas of high precision dimensional measurement and precision engineering; robotics and intelligent machines; manufacturing data description, data administration, and information processing; and sensors for manufacturing processes.

901,013 PB90-132747 PC A04/MF A01 National Inst. of Standards and Technology (NEL), Gaithersburg, MD. Center for Mfg. Engineering. Emerging Technologies in Manufacturing Engineering. Oct 89, 51p NISTIR-89/4187

Keywords: *Production engineering, *Manufacturing, *Technology assessment, *Industrial engineering, Production methods, Robots, Artificial intelligence, Industrial plants, *Computer aided manufacturing, Native Computer aided manufact tional Institute for Standards and Technology.

This is an internal report produced by the managers and staff of the Center for Manufacturing Engineering for planning purposes only. It represents current best thinking about emerging technologies in manufacturtrining about emerging technologies in manufacturing engineering, the impact these technologies will have on the Center's programs, and the directions the Center's programs will go if sufficient resources are available. The emerging technologies discussed are those that the Center believes will require increased support and leadership in coming years.

MATERIALS SCIENCES

Ceramics, Refractories, & Glass

PB89-146823 Not available NTIS National Bureau of Standards (IMSE), Gaithersburg, Defect Intergrowths in Barlum Polytitanates. 1. Ba2Ti9O20. Final rept. P. K. Davies, and R. S. Roth. 1987, 13p

See also PB89-146831. Pub. in Jnl. of Solid State Chemistry 71, n2 p490-502

Keywords: *Barium titanates, *Defects, *Electron microscopy, Microwaves, Dielectrics, Crystal structure, Stoichiometry, Reprints.

Using high-resolution transmission electron microscopy, the mechanisms of defect formation in samples of the microwave dielectric material, Ba(sub 2)Ti(sub 9)O(sub 20) were investigated. Materials prepared by a variety of different techniques show considerable structural disorder. The most prevalent intergrowth involved formation of a new triclinic polytype with an ionic arrangement closely related to that in the accepted structure. Defects also resulted from considerable

Ceramics, Refractories, & Glass

microtwinning and were observed mainly in the samples prepared from a vanadate flux. The degree of nonstoichiometric defect formation was small in comparison to the stoichiometric intergrowths. In this case defects appeared to result from the incorporation of excess vacancies into the close-packed layers of the structure. Barium-deficient surface phases were also formed via a similar mechanism.

PB89-146831 Not available NTIS National Bureau of Standards (IMSE), Gaithersburg, MD. Ceramics Div.

Defect Intergrowths in Barium Polytitanates. 2. BaTI5011.

Final rept. P. K. Davies, and R. S. Roth. 1987, 10p

See also PB89-146823.

Pub. in Jnl. of Solid State Chemistry 71, n2 p503-512 1987.

Keywords: *Barium titanates, *Defects, *Electron microscopy, Crystal lattices, Diffraction, Reprints.

High resolution electron microscopy has been used to investigate the structure of BaTi(sub 5)O(sub 11). Single phase materials were prepared from alkoxide precursors and studied using lattice imaging and microdiffraction techniques. Considerable structural disorder was observed in all the samples investigated. In general, isolated defects were observed. These resulted from a displacement of the close-packed layers of the structure giving some face-sharing of the Ti octahedra. However, in several regions of the samples, systematic stacking faults lead to the formation of a new polytypic structure. The paper describes the defect mechanisms, and relates these to the structure of the new polytype.

901,016 PB89-146849 Not available NTIS National Bureau of Standards (IMSE), Gaithersburg, MD. Ceramics Div.

Critical Assessment of Requirements for Ceramic Powder Characterization.

Final rept. A. L. Dragoo, C. R. Robbins, and S. M. Hsu. 1987,

4p Pub. in Advances in Ceramics 21, p711-720 1987.

Keywords: *Ceramics, *Powder(Particles), *Microstructure, *Particle size distribution, *Quality control, Measurement, Standards, Sampling, Reprints.

The detailed characterization of ceramic powders is very important for the reproducible manufacture of advanced ceramics which will perform reliably in service. The basic issues are: what to measure, how to measure it and how to assure quality in analytical measure-ments by all laboratories. 'What to measure' involves understanding the relationship between powder characteristics and ceramic microstructures. 'How to measure it' requires the development of measurement methods and the determination of repeatability and reproducibility. Standard Reference Materials (SRMs) are required to assure the quality of measurements and the comparability of measurements between different laboratories and techniques. From considerations of the distributed nature of powder and ceramic properties, new SRMs are proposed which will certify distributed properties. As an example of such SRMs, technical requirements are developed for the production of an SRM with a certified particle size distribution for ceramic powders. Factors which enter the certifica-tion of a particle size distribution for a ceramic powder include the approximate mathematical representation of the distribution, weighting of the distribution by the measurement technique, the particle shape distribu-tion, and statistical variances introduced by the powder, the sampling methods, and the methods of measurement.

901,017 PB89-146856 Not available NTIS National Bureau of Standards (IMSE), Gaithersburg, MD. Ceramics Div.

Application of SANS (Small Angle Neutron Scatter-

Ing) to Ceramic Characterization.

Final rept. K. G. Frase, K. A. Hardman-Rhyne, and N. F. Berk.

1986, 8p Pub. in Materials Research Society Symposia Pro-ceedings Better Ceram. Chem. 73, n2 p179-186 1986.

Keywords: *Neutron scattering, *Ceramics, *Defects, *Nondestructive tests, Spinel, Porosity, Particle size,

Agglomeration, Sintering, Precipitation(Chemistry), Microstructure, Reprints.

Traditionally, small angle neutron scattering (SANS) has been used to study dilute concentrations of defects 1 - 100 nm in size. Recent extensions of the scattering theory have allowed the expansion of the technique to include larger sizes through the use of multiple scattering. With multiple small angle neutron scattering, defects (pores, microcracks, precipitates) up to 10 micro ra in size can be studied. SANS is inherently a non-destructive, bulk probe of microstructure, with wide applications in the characterization of materials. A number of studies of ceramic materials using multiple and traditional (single particle diffraction) small angle neutron scattering will be discussed. The emphasis will be on the strength of the technique in the characterization of materials. Particular examples will include: the assessment of pore size distributions in spinel compacts as a function of sintering and agglomeration, the characterization of primary and secondary particle sizes in precipitated aggregates, and the de-termination of microporosity in MDF cements.

PB89-148373 PC A03/MF A01 National Inst. of Standards and Technology (NEL), Boulder, CO. Chemical Engineering Science Div. Microporous Fumed-Silica Insulation Board as a Candidate Standard Reference Material of Thermal Resistance.

D. R. Smith, and J. G. Hust. Oct 88, 25p NISTIR-88/

Sponsored by Oak Ridge National Lab., TN.

Keywords: *Thermal conductivity, *Insulating boards, *Silicon dioxide, Microporosity, Vapor deposition, Temperature, Standards, Pressure, Tables(Data), *Standard Reference Materials.

Measurements of apparent thermal conductivity of microporous fumed-silica insulation board are reported in order to provide a basis for certifying it as a Standard Reference Material (SRM) of thermal resistance. These data, for a pair of specimens having a mean density of 301 kg/m sup 3, encompass a range of tem-perature from 321 to 723 K and environmental gas pressures at and below ambient atmospheric pressure (40 to 83.7 kPa). Detailed analyses and intercomparisons of previously published data are given. Correlations of thermal conductivity with temperature and with pressure are given which represent the data within a standard deviation of 0.2%. This fumed-silica material has a thermal conductivity of 19.68 mW/(mK) at 300 K and is suitable for use as an SRM of very low conductivity from room temperature up to temperatures beyond 720 K (450 deg C). Great care in handling this material is necessary because of its fragility.

PB89-148381 PC A05/MF A01 National Inst. of Standards and Technology (IMSE), Gaithersburg, MD. Ceramics Div. Institute for Materials Science and Engineering, Ceramics: Technical Activities 1988. S. M. Hsu. Feb 88, 92p NISTIR-88/3840 See also PB86-196771.

Keywords: *Ceramics, *Superconductors, *Phase diagrams, *Images, Composite materials, Tensile properties, Lubrication, Grain boundaries, Raman spectroscopy, Synchrotron radiation, Topography.

Current programs of the Ceramics Division are reviewed. Programs include: grain boundary chemistry and structure of YBaCuO superconductors; compilation of phase diagrams for salt systems; diamond film synthesis; tribology; composites; wear maps; tensile tests; time resolved micro RAMAN analysis; typographic imaging (synchrotron radiation analysis).

901,020 PB89-149231 PB89-149231 Not available NTIS National Bureau of Standards (NML), Gaithersburg, MD. Gas and Particulate Science Div.

Stokes and Anti-Stokes Fluorescence of Er(3+) In the Raman Spectra of Erbium Oxide and Erbium Glasses.

Final rept E. Etz, and J. Travis. 1986, 2p Pub. in Proceedings of International Conference on Raman Spectroscopy (10th), Eugene, OR., August 31-September 5, 1986, p11/67-11/68.

Keywords: *Erbium oxides, *Glass, *Fluorescence, *Raman spectra, *Lasers, *Excitation, *Energy levels, Silicate minerals, Energy absorption.

The Abstract reports new observations on the laserexcited visible fluorescence in the micro-Raman spectra of erbium oxide and erbium-bearing silicate glasses. These results relate to the unusual optical behavior of rare-earth ions in solid phase matrices attributed to certain energy transfer reactions, proceeding by various upconversion mechanisms, when stimulated by infrared or visible radiation. The results reported here include the observation of anti-Stokes fluorescence from Er3 + when excited with 568.2 nm laser light.

901.021

PB89-150742 Not available NTIS National Bureau of Standards (NEL), Gaithersburg, MD. Building Materials Div.

Standard Specifications for Cements and the Role In Their Development of Quality Assurance Systems for Laboratories.

Final rept.

G. Frohnsdorff, P. W. Brown, and J. H. Pielert. 1986, 5n

Pub. in Proceedings of International Congress on the Chemistry of Cement (8th), Rio de Janeiro, Brazil, September 22-27, 1986, p316-320.

Keywords: *Cements, *Specifications, *Standards, Portland cements, Quality assurance, Performance standards, Durability, Laboratories, Test facilities, Performance evaluation.

Standard specifications for portland and related cements contain both prescriptive and performance cri-teria. Prescriptive criteria may hinder innovation by placing unnecessary limits on composition. Performance specifications define the performance required of a cement in terms which are closely related to the performance characteristics required in service. Performance tests may take too long to carry out to be suitable as acceptance tests. For this reason cement specifica-tions must continue to include both prescriptive and performance components. It should be practical for a specification to be structured to consist of a complete performance specification supplemented by prescriptive criteria to be developed by the manufacturer according to specified rules. New factors affecting cement specifications may include computer-aided checks for logical consistency, and the needs for precise chemical and physical information for use in mathematical models of cement performance and in integrated project information systems.

901,022

PB89-150759 Not available NTIS National Bureau of Standards (NEL), Gaithersburg, MD. Building Materials Div.

Implications of Phase Equilibria on Hydration in the Tricalcium Silicate-Water and the Tricalcium Aluminate-Gypsum-Water Systems.

Final rept.

P. W. Brown. 1986, 8p

Pub. in Proceedings of International Congress on the Chemistry of Cement (8th), Rio de Janeiro, Brazil, September 22-27, 1986, p231-238.

Keywords: *Cements, *Phase transformations, *Reaction kinetics, *Setting time, Hydration, Calcium silicates, Aluminates, Gypsum, Morphology, Hardening(Materials).

The mechanisms and kinetics of hydration in the C3S-H2O and C3A-gypsum-H2O systems are discussed within the context of the relevant phase equilibria. The development of a layer of C-S-H of variable composition results in the onset of the induction period. The composition gradient in this layer causes a morphological transformation leading to the onset of the acceleratory period. The first-formed aluminate-containing phase in the C3A-gypsum-H2O system may be AH3 or ettringite, depending on the initial solution composition. The rate of early C3A hydration is lowest when ettringite is the first-formed phase. This suggests that initial AH3 formation does not have a major influence on retardation.

901.023

PR89-156350 PC A03/MF A01 National Bureau of Standards, Gaithersburg, MD. Ceramics Div.

Ceramics, Refractories, & Glass

Structural Reliability and Damage Tolerance of Ceramic Composites for High-Temperature Applications. Semi-Annual Progress Report for the Period Ending September 30, 1987.

E. R. Fuller, T. W. Coyle, and R. F. Krause. Feb 88, 27p NBSIR-88/3710

See also P887-208310. Sponsored by Department of Energy, Oak Ridge, TN. Advanced Research and Technology Fossil Energy Materials Program.

Keywords: *Engines, *Thermal efficiency, *Ceramics, High temperature tests, Composite materials, Microstructure, Mechanical properties, Corrosion resistance, Heat recovery, Structural members, Compressing, Sili-con carbides, Strength, Fibers, Shear strength, Damage, Graphs(Charts), Whisker composites, Crack propagation, Creep strength.

The achievement of higher efficiency heat engines and heat recovery systems requires the availability of high-temperature, high-performance structural materials. Structural ceramics, and more recently, ceramic matrix composites have received particular attention for these applications due to their high strength and resistance to corrosion and thermal shock. Even with these positive attributes, improved reliability and extended lifetime under service conditions are necessary for structural ceramics to gain industrial acceptance. The problems with these materials are mechanical and chemical in nature and are enhanced by the fact that they are subjected to high temperatures, reactive envi-ronments and extreme thermal gradients. With an objective of improved performance for heat engine/heat recovery applications, the NBS program on structural ceramics and ceramic composites addresses these problems through the determination of critical factors that influence mechanical and microstructural behavior. The activities of the program are grouped under two major subtasks, each designed to develop key data, associated test methods and companion predictive models. The status of the subtasks for the period ending September 30, 1987 are provided.

901,024

National Inst. of Standards and Technology (IMSE), Gaithersburg, MD. Ceramics Div.

Structural Reliability and Damage Tolerance of Ceramic Composites for High-Temperature Applications. Semi-Annual Progress Report for the Period

tions. Semi-Annual Progress Report for the Period Ending March 31, 1988.
E. R. Fuller, T. W. Coyle, T. R. Palamides, and R. F. Krause. Aug 88, 18p NISTIR-88/3817
See also PB89-156350. Sponsored by Department of Energy, Oak Ridge, TN. Advanced Research and Technology Fossil Energy Materials Program.

Keywords: *Engines, *Thermal efficiency, *Ceramics, High temperature tests, Composite materials, Microstructure, Mechanical properties, Corrosion resistance, Heat recovery, Structural members, Compressing, Silicon carbides, Fibers, Shear strength, Damage, Graphs(Charts), Whisker composites, Crack propagation, Creen strength tion, Creep strength.

The achievement of higher efficiency heat engines and heat recovery systems requires the availability of high-temperature, high-performance structural materials. Structural ceramics, and more recently, ceramic matrix composites have received particular attention for these applications due to their high strength, and resistance to corrosion and thermal shock. Even with these positive attributes, improved reliability and extended lifetime under service conditions are necessary for structural ceramics to gair: industrial acceptance.
The problems with these materials are mechanical and chemical in nature and are enhanced by the fact that they are subjected to high temperatures, reactive envi-ronments and extreme thermal gradients. With an ob-jective of improved performance for heat engine/heat recovery applications, the NBS program on structural ceramics and ceramic composites addresses these problems through the determination of critical factors that influence mechanical and microstructural behavior. The activities of the program are grouped under two major subtasks, each designed to develop key data, associated test methods and companion predictive models. The status of the subtasks for the period ending March 31, 1988 are provided.

901.025

Not available NTIS PB89-157044 National Bureau of Standards (NEL), Boulder, CO. Electromagnetic Technology Div.

Oxygen Isotope Effect in the Superconducting Bi-Sr-Ca-Cu-O System. Final rept.

H. Katayama-Yoshida, T. Hirooka, A. Oyamada, Y. Okabe, T. Takashashi, T. Sasaki, A. Ochiai, T. Suzuki, A. J. Mascarennas, J. I. Pankove, T. F. Ciszek, S. K. Deb, R. B. Goldfarb, and Y. Li. 1988,

4p Contract DE-AC02-83CH10093 Sponsored by Department of Energy, Washington, DC. Pub. in Physica C 156, p481-484 1988.

Keywords: *Superconductors, *Oxygen, *Isotopic labeling, *Copper oxides, Bismuth, Strontium, Calcium, Electrical resistivity, Magnetic permeability, Phonons, Reprints.

An oxygen isotope effect is observed in mixed-phase Bi-Sr-Ca-Cu-O superconductors when O18 is substituted for O16. The superconducting transition temperature Tc, measured by electrical resistivity and magnetic susceptibility, is lowered by about 0.32 K for the higher-Tc (110 K) phase and by about 0.34 K for the lower Tc (75 K) phase. These results suggest a measurable contribution to the superconductivity from phonurable contribution to the superconductivity from phon-

901,026

PB89-157564 PB89-157564 Not available NTIS National Bureau of Standards (IMSE), Gaithersburg. MD. Ceramics Div.

Small Angle Neutron Scattering from Porosity in Sintered Alumina. Final rept.

K. A. Hardman-Rhyne, and N. F. Berk. 1986, 3p Pub. in Jnl. of the American Ceramic Society 69, n11 pC.285-C.287 Nov 86.

Keywords: *Aluminum oxide, *Neutron scattering, *Sintering, *Porosity, Microstructure, Nondestructive tests, Ceramics, Voids, Reprints.

Large voids (approximately 0.2 micrometers and larger) can remain in the ceramic material after the sintering process is over. Often sintered ceramic materials are quite thick as well. Larger volume fraction and pore sizes are not seen with traditional single particle diffraction techniques in small angle neutron scattering. Multiple scattering methods were employed to elu-cidate microstructural information relating to pore size and porosity.

901.027

PB89-158034 Not available NTIS National Bureau of Standards (IMSE), Gaithersburg, MD. Ceramics Div.

Effect of Coal Slag on the Microstructure and Creep Behavior of a Magnesium-Chromite Refractory Final rept.

S. M. Wiederhorn, R. F. Krause, and J. Sun. 1988, 10p

Sponsored by Department of Energy, Washington, DC.
Pub. in American Ceramic Society Bulletin 67, n7 p1201-1210 Jul 88.

Keywords: *Slags, *Refractory materials, *Ceramics, Microstructure, Creep tests, Magnesium, Chromites, Bricks, Aggregates, Viscosity, Penetration, Reprints.

As slag penetrates magnesium chromite refractory, ion As slag penetrates magnesium chromite refractory, ion exchange between the refractory and the slag changes the composition of the slag from anorthite-like to diopside-like. This modification of the slag composition is believed to reduce its viscosity and enhance its reactivity. The creep rate of the refractory brick is increased by a factor of about 3 when slag penetrates into the brick. Creep behavior is rationalized in terms of the spacing and size of the aggregate particles within the refractory, and the structure and composition of the material bonding the aggregate particles together. It is suggested that refractory disintegration involves creep deformation at the hot face of the brick caused by mechanical loading and stresses due to ion exchange within the brick. The results of the present paper suggest that refractory performance can be improved by chemical modification of the brick to prevent a reduction slag viscosity during penetration.

901.028

PB89-162606 PC A03/MF A01 National Inst. of Standards and Technology (IMSE), Gaithersburg, MD. Ceramics Div. Toughening Mechanisms in Ceramic Composites: Semi-Annual Progress Report for the Period Ending September 30, 1988.

Interim rept.

Interim rept.
E. R. Fuller, R. F. Krause, M. D. Vaudin, and T. R. Palamides. Feb 89, 24p NISTIR-88/4018
Sponsored by Department of Energy, Oak Ridge, TN. Advanced Research and Technology Fossil Energy Materials Program.

Keywords: *Ceramics, *Compression tests, *Fractures(Materials), *Crack propagation, Silicon carbides, Borosilicate glass, Toughness, Fiber composites, Aluminum oxide, Creep properties, Bursting, Graphs(Charts).

A fracture mechanics specimen known as the doublecleavage drilled-compression (DCDC) specimen has been used to study crack-fiber interactions and tough-ening increments in a model composite system of SiC monofilaments in a borosilicate glass matrix. The toughening increments were measured from changes in applied stress intensity factor as a function of crack length and number of monofilament fibers. Both the fiber-matrix debond strength and the interfacial fric-tional shear resistance, which influence these tough-ening increments, were measured independently by a single fiber pull-out test and were correlated with the toughness increases measured by the DCDC specimen. A ceramic composite material that has received much attention because of its increased toughness and creep resistance compared with alumina is aluminated as increased with alumina is aluminated. num oxide reinforced with silicon carbide whiskers. In the study, the creep and creep rupture behavior of a 25 wt% SiC whisker-reinforced alumina ceramic with 4.9% porosity were measured at temperature between 100 deg C and 1300 deg C and at applied stresses between 55 and 306 MPa, although the applied stresses at each temperature varied over a much narrower range. Creep strains were determined from loading-point displacement measurements in four-point flexure.

901,029

PB89-165427 Not available NTIS National Bureau of Standards (NEL), Gaithersburg, MD. Chemical Process Metrology Div. Sputtered Thin Film Ba2YCu3On.

Final rept.

Pub. in Proceedings of Colloquium High Temperature Superconductivity: Prospects and Challenges, Washington, DC., October 9, 1987, p51-53 1988.

Keywords: "Thin films, "Sputtering, "Barium oxides, "Oxidation, "Perovskites, "Superconductors, Yttrium, Copper, Zirconium, Aluminum, Sapphire, Magnesium, Silver, Silicon, Crystallization, High temperature tests, Targets, Ceramics, Reprints.

Thin sputtered films were produced from premixed targets of Ba2Y Cu3 O with a planar magnetron. The films were deposited on ZrO2(Y), Al2O3, sapphire, MgO, Ag, and Si. The ZrO2(Y) and MgO enabled crystallization and oxidation of the thin films at 800C into perovskite. Copper loss was observed in films produced at elevated temperatures and with target heating. The sputtering and thermal processing parameters are discussed.

901,030

PB89-171730 Not available NTIS National Bureau of Standards (IMSE), Gaithersburg, MD. Reactor Radiation Div. Not available NTIS

Crystal Chemistry of Superconductors: A Guide to the Tailoring of New Compounds.

Final rept.

A. Santoro, F. Beech, M. Marezio, and R. J. Cava. 1988, 8p Pub. in Physica C 156, p693-700 1988.

Keywords: *Superconductivity, *Copper oxides, *Crystal defects, Perovskites, Lanthanum, Calcium, Thallium, Bismuth, Barium, Strontium, Yttrium, Shearing, Reprints

The crystal structures of the known superconducting copper oxides can be described in terms of two basic copper oxides can be described in terms of two basic structural types. The series La2Ca(n-1)CunO(2n+2), (TI,Bi)2(Ba,Sr)2Ca(n-1)CunO(2n+4) and TIBa2Ca(n-1)CunO(2n+3) can be viewed as made of alternating slices having the rock salt and perovskite structure. The compounds Ba2YCu4O8 and Ba4Y2Cu7O(14+x), on the other hand, are comprised of perovskite blocks alternating with blocks in which a

Ceramics, Refractories, & Glass

crystallographic shear is present. The effect of this shear is that of forming double chains of edge sharing squares with oxygen atoms at the corners and copper atoms at the center. The superconductor Ba2YCu3O7 can be described in terms of both structural types and may be considered as an intermediate type between the other two. The basic building blocks of these su-perconducting materials can be further broken down into constituent nets (or meshes). This description allows one to envisage new structures built from these meshes containing the key structural elements present in the currently known superconductors. As such, the structural schemes used in this description may be used as a guide in the preparation of new materials with interesting electronic properties.

901,031

PB89-171771 Not available NTIS National Bureau of Standards (IMSE), Gaithersburg, PB89-171771

MD. Ceramics Div.
RIsing Fracture Toughness from the Bending Strength of Indented Alumina Beams.

Final rept. R. F. Krause. 1988, 6p

Pub. in Jnl. of the American Ceramic Society 71, n5 p338-343 May 88.

Keywords: *Crack propagation, *Ceramics, *Fracturing, *Aluminum oxide, *Indentation, Defects, Tensile properties, Optical microscopes, Surface properties, Vickers hardness, Impact tests, Loads(Forces), Bending, Toughness, Annealing, Residual stress, Polishing, Beams(Supports), Reprints.

The analytical function of crack extension to a fractional power is used to represent the fracture resistance of a vitreous-bonded 96% alumina ceramic. A varying flaw size, controlled by Vickers indentation loading between 3 and 300 N, was placed on the prospective tensile surfaces of four-point bend specimens, previously polished and annealed. The lengths of surface cracks were measured by optical microscopy. Straight lines were fitted to the logarithmic functions of observed bending strength versus indentation load in two series of experiments, including the residual stress due to indentation and having the residual stress annealed out at an elevated temperature. Within the precision of measurement these lines have the same slope, being about 32% less than the slope which a fracture toughness independent of crack extension would indicate.

901,032

PB89-171789 Not available NTIS National Bureau of Standards (IMSE), Gaithersburg, MD. Ceramics Div.

Phase Relations between the Polytltanates of Barium and the Barium Borates, Vanadates and Molybdates.

Final rept. J. M. Millet, R. S. Roth, and H. S. Parker. 1986, 4p Pub. in Jnl. of the American Ceramic Society 69, n11 p811-814 Nov 86.

Keywords: *Ceramics, *Barium oxides, *Phase diagrams, Barium titanates, Vanadates, Molybdates, Chemical equilibrium, Borates, Ternary systems, X ray diffraction, Liquids, Melting, Reprints.

Phase equilibria in ternary systems involving Ba0, Ti02, and the low melting oxides B203, V205 and Mo03 are reported. Alternative ways to synthesize BaTi409 have been found. These compounds can be obtained by heating at relatively low temperature appropriate com-positions in the system Ba0-Ti02-V205 or Ba0-Ti02-M003 and dissolving the excess phases in dilute HC1. Ba2Ti9020 can also be prepared at low temperature in the Ba0-Ti02-B203 system, in which it may show a limited solid solution, offering the possibility of obtaining dense ceramics at low temperature. The low temperature phase BaTi5011 has not been obtained in equilibrium in any of the studied systems. It has been found that the compound reported with the composition Ba3Ti3V4015 has in fact the composition Ba3Ti3V4014. It decomposes at 995 + or - 5 C (Ba3TiV4013 yields liq + Ba2V207). A ternary compound Ba2Ti2B209 which decomposes into BaTi03 and a liquid at approximately 950 C was also found.

901,033

PB89-171797 Not available NTIS National Bureau of Standards (IMSE), Gaithersburg, MD. Ceramics Div.

Phase Equilibria and Crystal Chemistry in the Ternary System BaO-TiO2-Nb2O5: Part 1.

Final rept.

J. M. Millet, L. D. Ettlinger, H. S. Parker, and R. S. Roth. 1987, 12p

Pub. in Jnl. of Solid State Chemistry 67, n2 p259-270

Keywords: *Phase diagrams, *Ternary system, *Barium titanates, Single crystals, Barium oxides, Titanium, Niobium, Solid solutions, Diffraction, Ceramics,

A partial subsolidus phase diagram is presented of the Ba0-Ti02-Nb205 ternary system. Eight new com-pounds or solid solutions in the ternary system are de-scribed and the existence of three solid solutions previously reported are confirmed and further studied.

901,034 PB89-171813 PB89-171813 Not available NTIS National Bureau of Standards (IMSE), Gaithersburg,

MD. Ceramics Div.
Effect of Lateral Crack Growth on the Strength of Contact Flaws in Brittle Materials.

R. F. Cook, and D. H. Roach. 1986, 12p Sponsored by IBM Thomas J. Watson Research Center, Yorktown Heights, NY. Pub. in Jnl. of Materials Research 1, n4 p589-600 Jul/

Aug 86.

Keywords: *Ceramics, *Glass, *Brittle fracturing, *Crack propagation, *Impact tests, Defects, Single crystals, Contacting, Elastic properties, Plastic properties, Residual stress, Indentation, Radial stress, Lateral pressure, Failure, Fatigue(Materials), Strength, Loads(Forces), Reprints, Fracture mechanics.

The effect of lateral cracks on strength controlling contact flaws in brittle materials is examined. Inert strength studies using controlled indentation flaws on a range of ceramic, glass and single crystal materials reveal significant increases in strength at large contact loads, above the predicted load dependence extrapolated from strength measurements at low indentation loads. The increases are explained by the growth of loads. The increases are explained by the growth of ateral cracks decohesing the plastic deformation zone associated with the contact from the elastically restraining matrix, thereby reducing the residual stress field driving the strength controlling radial cracks. A strength formulation is developed from indentation fracture mechanics which permits inert strengths to be described over the full range of contact loads. The formulation takes account of the decreased constraint of the plastic deformation zone by lateral crack growth as well as post-contact non-equilibrium growth of the radial cracks. Simple extensions permit the strengths of specimens controlled by impact flaws to be de-scribed, as well as those failing under non-equilibrium (fatigue) conditions. The work reinforces the conclusion that a full understanding of the residual stress field at dominant contact flaws is necessary to describe the strength of brittle materials.

901,035 PB89-171821 PB89-171821 Not available NTIS National Bureau of Standards (IMSE), Gaithersburg, MD. Ceramics Div. Densification, Susceptibility and Microstructure of Ba2YCu3O(6+x).

Final rept. 7. E. Blendell, and L. C. Stearns. 1988, 10p Pub. in Ceramic Transactions 1, ptB p1146-1155 1988.

Keywords: *Ceramics, *Microstructure, *Densification, *Magnetic permeability, *Sintering, *Superconductivity, Measurement, Pressure, Temperature, Porosity, Chemical composition, Grain boundaries, Barium oxides, Yttrium, Copper, Compacting, Atmospheres, Pagniste.

The densification of Ba2YCu30(6+x) for different sintering conditions has been measured. The effects of compaction pressure, atmosphere and temperature have been investigated. Measurements of the AC magnetic susceptibility have been used to determine magnetic susceptibility have been used to determine the superconducting properties. Dense samples were found to have less superconducting material as compared to porous samples. Compositional mapping of the samples showed variations in composition in the samples, corresponding to Cu-rich regions and Y-poor regions. Sinter-forging was done in order to align the grains grains.

901,036 PB89-175244

(Order as PB89-175194, PC A06) National Inst. of Standards and Technology (IMSE), Gaithersburg, MD. Ceramics Div.
Structural Ceramics Database: Technical Founda-

tions.

Bi-monthly rept. R. G. Munro, F. Y. Hwang, and C. R. Hubbard. 1989,

Included in Jnl. of Research of the National Institute of Standards and Technology, v94 n1 p37-46 Jan-Feb

Keywords: *Ceramics, Thermodynamic properties, Materials specifications, Thermal expansion, Thermal conductivity, Thermal diffusivity, Specific heat, Shock resistance, Thermal resistance, Bibliographics, Systems engineering, *Numerical data bases, Structural ceramics data base system, User requirements.

The development of a computerized database on advanced structural ceramics can play a critical role in fostering the widespread use of ceramics in industry and in advanced technologies. A preliminary system has been completed as phase one of an ongoing program to establish the Structural Ceramics Database system. The system is designed to be used on personal computers. Developed in a modular design, the pre-liminary system is focused on the thermal properties of monolithic ceramics. The initial modules consist of mamononitric ceramics. The initial modules consist of ma-terials specification, thermal expansion, thermal con-ductivity, thermal diffusivity, specific heat, thermal shock resistance, and a bibliography of data refer-ences. Query and output programs also have been de-veloped for use with these modules. Three primary veloped to use with triese inflowers. Thee primary considerations provide the guidelines to the system's development: (1) The user's needs; (2) The nature of materials properties; and (3) The requirements of the programming language. The repport discusses the manner and rationale by which each of these considerations leads to provide a provider the second to the second th ations leads to specific features in the design of the system.

901,037

PB89-175939 Not available NTIS National Bureau of Standards (IMSE), Gaithersburg. MD. Ceramics Div.

Pore Morphology Analysis Using Small Angle Neu-tron Scattering Techniques.

Final rept.

K. A. Hardman-Rhyne. 1987, 12p Pub. in Advanced Ceramics 21, p767-778 1987.

Keywords: *Ceramics, *Porosity, *Compacting, *Powder(Particles), *Neutron scattering, Aluminum oxide, Microstructure, Green strength, Reprints.

Unfired ceramics are very difficult to characterize due to the often fragile nature of the compacted powder and the high concentration of pores. Furthermore, these pores can have a wide distribution in sizes depending on the size and nature of the particles and the compaction procedure used to form the compacts. Small angle neutron scattering techniques are used to study alumina compacts. Various microstructural phe-nomena, generally in the size range of 1 to 10,000 nm, are discussed including pore size and distribution, pore fraction and surface area.

901,038

PB89-175954 Not available NTIS National Bureau of Standards (IMSE), Gaithersburg, MD. Ceramics Div. Creep Cavitation in Liquid-Phase Sintered Alumi-

R. A. Page, K. S. Chan, K. Hardman-Rhyne, J. Lankford, and S. Spooner. 1987, 9p Pub. in Jnl. of the American Ceramic Society 70, n3

p137-145 1987.

Keywords: *Aluminum oxide, *Ceramics, *Creep tests, *Cavitation, *Grain boundaries, *Sintering, Phases, Liquids, Neutron scattering, Stress analysis, Strain rate, Nucleation, Reprints.

The early stages of creep cavitation in a liquid-phase sintered alumina have been characterized using small-angle neutron scattering. Grain boundary cavities were found to nucleate throughout creep, although at a steadily decreasing rate. The cavities were located on steadily declaring rate. The cavities were located who-two-grain junctions as well as triple points and were spaced approximately 100 to 200 nm apart. Cavity nu-cleation was also found to be relatively independent of the applied stress. The behavior has been rationalized based on the decreasing ratio of epsilon(gbs)/

Ceramics, Refractories, & Glass

epsilon(t), where epsilon(gbs) is the strain due to grain boundary sliding and epsilon(t) is the total strain, at in-creasing stresses. Cavity growth, on the other hand, was highly stress dependent. Above a certain 'threshold' stress cavity growth was observed. In all cases, however, the observed growth was transient, i.e., the cavity growth rate decreased with time. Lowering the stress below the 'threshold' resulted in a condition in which cavities nucleated but continued growth of the cavities did not occur. In all cases the cavities nucleated and grew, when growth did occur, with relatively equiaxed shapes.

901,039 PB89-177182 Not available NTIS National Bureau of Standards (NEL), Gaithersburg, MD. Automated Production Technology Div. Dynamic Poisson's Ratio of a Ceramic Powder dúring Compaction. Final rept.

M. P. Jones, and G. V. Blessing. 1987, 4p Pub. in Proceedings of IEEE (Institute of Electrical and Electronics Engineers) Ultrasonics Symposium, Denver, CO., October 14-16, 1987 p587-590.

Keywords: *Ceramics, *Powder testing, *Elastic properties, *Ultrasonic tests, Compacting, Poisson ratio, Pressure, Secondary waves, Longitudinal waves, Green strength.

Shear and longitudinal wave transit times were measured in a ceramic powder during its compaction. These transit times were used to calculate the dynamic Poisson's ratio of the powder. The goal of the work was to better understand the particles' interaction and rear-rangement under pressure. It was shown that Pois-son's ratio depended upon the type of powder evaluated and the loading path. Information obtained from this technique could be used as real-time feedback to control and monitor the quality of ceramic parts.

901,040 PB89-179717 Not available NTIS National Bureau of Standards (IMSE), Gaithersburg,

MD. Ceramics Div. Syntheses and Unit Cell Determination of Low- and High-Temperature Ba3V4O13 and Ba3P4O13. Final rept.

J. M. Millet, H. S. Parker, and R. S. Roth. 1986, 3p Pub. in Jnl. of the American Ceramic Society 69, n5 pC103-C105 May 86.

Keywords: *Ceramics, *Barium oxides, *Crystal structure, *X ray diffraction, Vanadates, Phosphate deposition, Crystal lattices, Triclinic lattices, Monoclinic lattices, Orthorhombic lattices, Reprints.

Syntheses and unit cell determination of Ba3V4O13 and the two forms (low and high) of Ba3V4O13 are presented. Ba3V4O13 crystallizes in the monoclinic system, space group Cc or C2/c with unit cell dimensions a = 16.087, b = 8.948, c = 10.159 nm x 10, beta = 114.52 degrees. Low-Ba3P4O13 crystallizes in the triclinic system, space group P1 or P-1 with unit cell dimensions, a = 7.240, b = 8.011, c = 5.689 nm x 10, alpha = 104.02 degrees, beta = 109.510, gamma = 83.62 degrees. Low Ba3V4O13 transforms at 870 degrees C into high Ba3P4O13 which crystallizes in the orthorhombic system, space group Pbcm (No. 57) (or Pbc2, No. 29) with unit cell dimensions, a = 7.107, b = 13.883, c = 19.219 nm x 10. No relations have been found between the structures of the tri-barium tetravanadate and the tri-barium tetraphosphate.

901,041 PB89-179741 Not available NTIS National Bureau of Standards (IMSE), Gaithersburg, MD. Ceramics Div. Synthesis, Stability, and Crystal Chemistry of Dibarlum Pentatitanate.

R. S. Roth, J. J. Ritter, H. S. Parker, and D. B. Minor.

1986, 5p Pub. in Jnl. of the American Ceramic Society 69, n12 p858-862 Dec 86.

Keywords: *Ceramics, *Synthesis(Chemistry), *Barium oxides, *Titanates, *Phase transformations, Niobium, Tin, Zirconium, Stability, Triclinic lattices, Orthorhombic lattices, X ray diffraction, Single crystals, Metastable state, Reprints.

A metastable phase corresponding to the previously reported Ba2Ti5O12 was found to form between 650-675 C from hydrolized ethoxide precursors. The stabili-

ty was increased to approximately 850 C by the addition of 1-2 mole% Nb2O5 to the precursor solutions. Addition of 5 mole% SnO2 failed to yield any sign of Addition of 5 miole% ShOz failed to yield any sign of this phase in solid state preparations, contrary to the previous report. Addition of 8 mole% ZrO2, however, did produce the desired phase as reported, both with and without additional Nb2O5, apparently stable to greater than 1300 C. Small single crystals, picked from greater than 1300 C. Small single crystals, picked from a ZrO2 stabilized specimen with one mole% Nb2O5, showed the compound Ba2Ti(5-x)ZrxO12 to be a 10-layer structure, triclinic, pseudo-orthorhombic with Acentered symmetry and a = 9.941(5), b = 11.482(4), c = 23.528(10) nm x 10. The corresponding reduced triclinic unit cell has a equal 9.941, b = 11.482, c = 13.090 nm x 10, alpha = 116.01 degrees, beta = 90.0 degrees, gamma = 90.0 degrees.

901,042 PB89-185573 PC A03/MF A01 National Bureau of Standards (NEL), Gaithersburg, MD. Center for Building Technology. Epoxy Impregnation of Hardened Cement Pastes for Characterization of Microstructure.

L. Struble, and E. Byrd. Nov 86, 22p NBSIR-87/3504 Sponsored by Air Force Office of Scientific Research, Bolling AFB, DC.

Keywords: *Cements, *Hardening(Materials), *Polishing, *Impregnating, *Epoxy resins, *Ethanols, Tests, Microstructure, Crack propagation, Drying, Methodology, Electron microscopy.

Methods were explored for drying of hardened cement paste prior to impregnation with epoxy, in order to polish for microscopic examination. All were shown to cause microcracking of the paste. An alternative method involves replacing pore water with ethanol, then replacing ethanol with epoxy. The method appears to minimize the occurrence of microcracks associated with drying.

901,043 PB89-186290 PB89-186290 Not available NTIS National Bureau of Standards (IMSE), Gaithersburg, MD. Ceramics Div. Computer Graphics for Ceramic Phase Diagrams.

Final rept. P. K. Schenck, and J. R. Dennis. 1987, 5p. Pub. in Computer Handling and Dissemination of Data,

p184-188 1987. Keywords: *Ceramics, *Phase diagrams, Reprints, *Interactive graphics, Computer graphics, Computer applications, Data bases, Computer software.

Specialized graphics software has been written in support of the NBS-ACerS Phase Diagrams for Ceramists Data Base Program. The software runs on a stand alone desk top computer and allows both binary and ternary ceramic phase diagrams to be entered into a graphics data base. The phase diagrams may be entered by keyboard, direct digitization of a published diagram, or from properly formatted data files. The software allows for dynamic on-screen editing of the diagrams and includes many special features to en-hance the appearance and the accuracy of the figures. The rapid generation of uniform, camera-ready copy for inclusion in subsequent volumes of Phase Diagrams for Ceramists has allowed the Data Center to accelerate publication of critically evaluated phase diagrams. In addition, the graphics data base will eventu-ally be integrated with other data bases under development in the Data Center.

901.044 PB89-186308 PB89-186308 Not available NTIS National Bureau of Standards (IMSE), Gaithersburg, MD. Ceramics Div. Phase Diagrams for High Tech Ceramics.

S. J. Schneider, J. W. Hastie, and W. P. Holbrook. 1987, 16p

Pub. in Mater. Sci. Monogr. 38A, p59-74 1987.

Keywords: *Ceramics, *Phase diagrams, *Data processing, Mathematical models, Reprints.

Chemical behavior is the foundation from which advanced ceramics are designed, processed and used; it sets properties, dictates reliable manufacture and ultimately determines performance and lifetimes. Predictive and descriptive chemistry is required and the basis for this is phase equilibria and its graphical expression -- the phase diagram. Ceramic phase equilibria re-search is literally exploding with literature growth out-

stripping the capacity of any single company, or even nation, to compile, evaluate and disseminate the available phase diagram information. Cooperative efforts able phase diagram Information. Cooperative efforts worldwide are needed and in recognition of this, the American Ceramic Society (ACerS) and the National Bureau of Standards (NBS) have initiated a program to expand their previous data effort to develop a comprehensive Phase Diagram Data System. The paper summarizes the status of the development program to achieve more focused and us to data compilerize of achieve more frequent and up-to-date compilations of critically evaluated phase diagrams, expanded cover-age for high technology ceramics and computer serv-ices for data base management, graphics and phase diagram modeling.

901.045 PB89-188569 PC A06/MF A01 National Inst. of Standards and Technology (IMSE), Gaithersburg, MD. Ceramics Div. Advanced Ceramics: A Critical Assessment of

Wear and Lubrication.

wear and Lubrication.

R. G. Munro, and S. M. Hsu. Jan 89, 109p NISTIR-88/3722, GRI-88/0290, CAM-8901
Contract GRI-5084-238-1302
See also PB88-215447. Sponsored by Gas Research Inst., Chicago, IL., and Pennsylvania State Univ., University Park. Center for Advanced Materials.

Keywords: *Wear, *Ceramics, *Gas engines, *Surreywords: wear, "Ceramics, "Gas engines, "Surveys, Thermal properties, Mechanical properties, Lubrication, Reciprocating engines, Gas turbine engines, Rotary combustion engines, Methane, Engine primers, Graphs(Charts), "Tribology.

A critical assessment of the state of the art of the tribo-A crucal assessment of the state of the art of the tribo-logy of ceramics is made. To identify the critical techni-cal barriers confronting the utilization of advanced gas-fired engines, data were gathered specifically on the tribology of materials for gas-fired engine applications. Site visits and discussions with a number of GRI con-tractors in industry were conducted as the first step in identifying critical issues. Then, an extensive review of the technical literature was made to determine what information was available to resolve those issues, and, more importantly, what critical information was not yet available. These data were used to examine the issues for each of the principal engine types (rotary, recipro-cating, and turbine). Materials property data for ceram-ics were then reviewed in the context of the operating environments and conditions for these engines. There mal, mechanical, and tribological properties were examined, along with the important considerations for luarmined, along with the important considerations for in-bricating ceramics in engine applications. The analysis of these data considered the impact and relative merits of using various advanced materials and result-ed in recommendations for research activities that could have a significant impact on the development of gas-fired prime movers.

901,046 PB89-193221 PC A03/MF A01 National Inst. of Standards and Technology (NEL), Gaithersburg, MD. Center for Building Technology. Standard Aggregate Materials for Alkali-Silica Reaction Studies. L. Struble, and M. Brockman. May 89, 39p NISTIR-

Keywords: *Alkali aggregate reactions, *Silicon oxides, *Expansion, *Concretes, Cements, Mortars(Materials), Opal, Quartzites, Rhyolite, Flint glass, Limestone, Graphs(Charts).

89/4058

Preliminary studies have been carried out to identify candidate materials for use as a standard reactive aggregate in alkali-silica investigations. The materials studied included several commercial glasses, an opal, a quartzite, a rhyolite and a calcined flint. Candidate materials were tested for their expansion in mortars prepared using either a high-alkali or a low-alkali cement, a nonreactive limestone sand, and some proportion of reactive material. Tests were carried out according to ASTM C441-81, Standard Test Method for Effectiveness of Mineral Admixtures in Preventing Exercisive Expansion of Congreta Due to the Alkali Agreement. cessive Expansion of Concrete Due to the Alkali-Aggregate Reaction, and ASTM C227-87, Standard Test Method for Potential Alkali Reactivity of Cement-Agregate Combinations (Mortar-Bar Method). The proportion of limestone replaced by each reactive material was varied so as to bracket the pessimum proportion of incomplete of the combination of the combinat the highest level of expansion). Mortar-bar expansion levels were measured throughout reaction periods of approximately 6 months to 1 year. Expansion results are presented and discussed. Based on the studies,

Ceramics, Refractories, & Glass

the Vycor, fused quartz, fused silica, and calcined flint appear suitable as standard reactive materials; the calcined flint appears especially promising.

901,047 PB89-201636 Not available NTIS National Bureau of Standards (NML), Gaithersburg, MD. Gas and Particulate Science Div. Methods for the Production of Particle Standards.

Final rept. J. A. Small, J. J. Ritter, P. J. Sheridan, and T. R. Pereles. 1986, 21p

Pub. in Jnl. of Trace Microprobe Tech. 4, n3 p163-183

Keywords: *Metal particle composites, *Standards, *Ceramics, *Glass particle composites, Particle size, Production, Fiber composites, Spheres, Microstructure, Granular materials, Reprints, National Institute of Standards and Technology.

The microanalysis group at the National Bureau of Standards (NBS) has been studying three different methods of fabricating microscopic and submicroscopic particle standards. These methods include the manufacture of ground glass shards, fibers, and mi-crospheres from the NBS analytical glass standards, the manufacture of metal and metal alloy particles in the spark source emission spectrometer, and the manufacture of doped ceramic particles by alkoxide synthesis. Preliminary studies of these methods indicate that they can be used to produce particle standards which have a wide variety of elemental compositions and sizes.

901,048 PB89-201776 Not available NTIS National Bureau of Standards (IMSE), Gaithersburg,

Commercial Advanced Ceramics.

Final rept.
S. J. Schneider. 1986, 4p
Pub. in ASTM (American Society for Testing and Materials) Standardization News, p36-39 Oct 86.

Keywords: *Ceramics, Standards, Construction materials, Electronics, Engine blocks, Reprints.

Advanced ceramics represent a newer generation of high-performance materials that collectively are viewed as an enabling technology, development and exploitation of which are critical to advances in a host of high-technology applications ranging between modern microelectronic components to futuristic auto engines. New products are in the offing that could impact whole industrial segments including transportation, communications, computers, energy conversion and major defense systems. Even though products are being developed, diffusion to the marketplace is severely inhibited by the lack of commercial standards the test methods, the classification system, the standard reference materials and the like. The standards needs have been identified and include requirements in the areas of: processing, characterization, proper-ties, performance, statistical procedures and terminology.

901,049 PB89-202097 Not available NTIS National Bureau of Standards (IMSE), Gaithersburg, MD. Ceramics Div.

Electron Microscopy Studies of Diffusion-Induced Grain Boundary Migration in Ceramics. Final rept.

M. D. Vaudin, C. A. Handwerker, and J. E. Blendell.

1988, 6p Pub. in Jnl. de Physique 49, n10 pC5-687-C5-692 Oct

Keywords: *Ceramics, *Grain boundaries, Electron microscopy, Diffusion, Sintering, Crystal structure, Magnesium oxides, Annealing, Nickel oxides, Microstructure, Temperature, Surface properties, Interfaces, Strains, Reprints.

The stability of grain boundaries during the uptake of solute into polycrystalline MgO has been investigated by exposing sintered, well-annealed MgO specimens to NiO at various temperatures for different times, and observing their microstructure both before and after this exposure. Electron and optical microscopy techniques have been used to characterize the specimen surface morphology, and the variation in composition and elastic and plastic strains in the interface regions. The spatial distribution of nickel at various depths below the original specimen surface was determined

using electron microprobe analysis. The observations are discussed in terms of the coherency strain theory.

901,050 PB89-202105 Not available NTIS National Bureau of Standards (IMSE), Gaithersburg,

MD. Ceramics Div.

Green Function Method for Calculation of Atomistic Structure of Grain Boundary Interfaces in Ionic Crystals.

Final rept. V. K. Tewary, E. R. Fuller, and R. M. Thomson. 1986,

10p
Pub. in Ceramic Microstructures '86 Role of Interfaces, p167-176.

Keywords: *Atomic structure, *Crystal lattices, *Ceramics, Greens function, Microstructure, Grain boundaries, Interfaces, Ions, Polarity, Coulomb interactions, Crystal defects, Reprints.

A lattice statics Green function method is described for calculating the atomistic structure of grain boundary interfaces in ionic crystals. The grain boundary is taken along coincidence lattice sites of the two crystallites. The periodicity of the coincidence lattice is exploited by taking a partial Fourier transform of the Green function. It is also shown that the Coulomb interaction between ions across the grain boundary line can be represented in terms of effective dipolar and higher order polar interactions which makes them relatively short

PB89-211817 Not available NTIS National Bureau of Standards (IMSE), Gaithersburg,

MD. Ceramics Div.
Crack-Interface Traction: A Fracture-Resistance Mechanism In Brittle Polycrystals.

Final rept.

P. L. Swanson. 1988, 23p Pub. in Proceedings of Conference on the Fractogra-phy of Glasses and Ceramics, Alfred, NY., August 3-6, 1986, p135-155 1988.

Keywords: *Ceramics, *Glass, *Interfaces, *Crack propagation, Fractures(Materials), Microscopy, Traction, Aluminum oxide, Resistance.

Crack-interface tractions have been identified as a source of increasing resistance to fracture with crack extension, or rising R-curve behavior, in previous studies on coarse-grained alumina. Real time in situ microscopy observations are used in the present study to investigate the generality of crack-interface tractions as a crack-resistance mechanism in three alumina and three glass-ceramics with varying R-curve characteristics. Interface tractions are found to operate to varying degrees in each material. Ligamentary-bridge formation is compared with the development of twist hackle, inclusion/wake hackle and cleavage hackle in simple material systems. Both sources of interface traction remain active as far as 100 particle dimensions behind the primary crack tip and, with sufficient crack-opening displacement, are eventually overcome by interface-localized microfracturing. Simple analytical fracture mechanics concepts are used to assess the influence of interface tractions on macroscopic fracture behavior. Because of the observed crack-history dependence of the interface-traction crack-tip shielding, it is suggested that neither R-curve behavior nor applied-K(sub I)/subcritical crack velocity relationships are unique properties of these and similar materials.

PB89-211833 Not available NTIS National Bureau of Standards (IMSE), Gaithersburg, MD. Ceramics Div.

Design Criteria for High Temperature Structural Applications.

Final rept. S. M. Wiederhorn, and E. R. Fuller. 1986, 19p Sponsored by Department of Energy, Oak Ridge, TN. Pub. in Proceedings of International Symposium on Ceramic Materials and Components for Éngines (2nd), Luebeck-Travemuende, West Germany, April 14-17, 1986, p911-929.

Keywords: *Structural forms, *High temperature tests, *Fractures(Materials), *Crack propagation, *Ceramics, Creep rupture tests, Nucleation, Initiation, Damage,

Current methods of assessing high temperature, structural reliability of ceramics are fracture mechanics based, in the sense that failure is assumed to originate

from pre-existing flaws that grow until they reach a critical size for rupture. Recent data on structural ceramics at elevated temperatures suggest that the view may be over-simplified and that flaw initiation and damage accumulation may be important factors to consider in the design of ceramic materials for high temperature applications. The techniques that are currently being used for structural design are summarized and the limits of their application at elevated temperatures are defined. The need for incorporating information on flaw nucleation and damage accumulation into methods of structural design is emphasized.

PB89-211841 Not available NTIS National Bureau of Standards (IMSE), Gaithersburg, MD. Ceramics Div.

PC-Access to Ceramic Phase Diagrams. Final rept. P. K. Schenck, and J. R. Dennis, 1989, 12p.

Pub. in ASTM (American Society for Testing and Materials) Special Technical Publication 1017, p292-303 1989.

Keywords: *Phase diagrams, *Ceramics, Computer systems programs, Data retrieval, Reprints, Computer

A personal computer (PC)-based version of Phase Diagrams for Ceramists has been demonstrated by the joint National Bureau of Standards/American Ceramic Society Phase Diagrams for the Ceramists Data Center. A selection of phase diagrams from the nearly 1100 diagrams of Volume 6 has been transferred from the Data Center's graphics workstations to a PC. Demonstration software has been developed for retrieving and plotting the phase diagrams on the PC's monitor from the PC-based Phase Diagram Data Base. In addition, the software allows the operator to retrieve data from the diagram by means of an interactive graphics cursor whose location is displayed digitally on the monitor in a choice of user units (for example, C, F, K). Areas of the phase diagram can be magnified and replotted to clarify features. The operator can also overlay a second diagram for comparison purposes, reverse the diagram, magnify or rescale the diagram, and apply an electronic lever rule or curve-tracking mode. Future refinements include conversions between weight and mole percent and retrieval of ternary or higher-order phase diagrams.

901,054

PB89-221170 PC A09/MF A01 National Inst. of Standards and Technology (NEL), Gaithersburg, MD. Semiconductor Electronics Div. Semiconductor Measurement Technology: Database for and Statistical Analysis of the Interlaboratory Determination of the Conversion Coefficient for the Measurement of the Interstitial Oxygen Content of Silicon by Infrared Absorption.

Special pub. (Final).

A. Baghdadi, R. I. Scace, and E. J. Walters. Jul 89, 183p NIST/SP-400/82

Also available from Supt. of Docs. as SN003-003-02943-2. Library of Congress catalog card no. 89-600739

Keywords: *Semiconductors(Materials), *Oxygen, *Interstitials, *Silicon, *Infrared radiation, Quantitative analysis, Statistical analysis, Radioactivation analysis, Charged particles, Photons, Conversion, Tables(Data), Graphs(Charts), Electromagnetic absorption, Round robin tests.

The Special Publication contains the data collected for the worldwide, double-round-robin determination of the conversion coefficient used to calculate the interstitial oxygen content of silicon from infrared absorption measurements. It also contains detailed statistical analyses of the data. The approach taken to determine the conversion coefficient was to conduct inter-laboratory round robins for both the infrared measurements and the absolute measurements. The infrared measurements were carried out at 18 laboratories in China, Europe, Japan, and the United States, using either dispersive infrared or Fourier transform infrared spectrometers. The absolute measurements were carried out at eight laboratories in Europe, Japan, and the United States, using either charged-particle activation analysis, photon activation analysis, or inert gas fusion analysis.

901,055 PB89-229074

PC A08/MF A01

Ceramics, Refractories, & Glass

National Inst. of Standards and Technology (IMSE),

Gaithersburg, MD. Ceramics Div.
NBS/BAM (National Bureau of Standards/Bundesanstalt fur Materialprufung) 1986 Symposium on Advanced Ceramics.

Special pub. (Final). S. M. Hsu, and H. Czichos. May 89, 171p NIST/SP-

Also available from Supt. of Docs. as SN003-003-02936-0. Library of Congress catalog card no. 89-600737. Prepared in cooperation with Bundesanstalt fuer Materialpruefung, Berlin (Germany, F.R.).

Keywords: *Meetings, *Ceramics, Fabrication, Standards, Defects, Quality control, Sintering, International relations, Graphs(Charts), Manufacturing, Reliability, Microstructure, Wear, Fretting, Nondestructive tests.

dvanced ceramics offer many advantages that other materials do not possess. They have high strength, dimensional stability, are chemically inert, lightweight, wear resistant, and have desirable properties in electrical, optical, and thermal applications. At high temperatures, they are the only class of material with reasonable properties. Worldwide production of advanced ceramics is growing rapidly. Since ceramics are based on alumina and silica, the most abundant minerals on earth, effective utilization of ceramics carries implications into the next several centuries. One of the major technical barriers to widespread use of ceramics is the inability of industry to manufacture reliable ceramics reproducibly and economically. Advanced ceramics are sensitive to small defects introduced during processing and generated during use. The symposium provides timely exchange of technical information on a very significant subject area of achieving reliable manufacturing through standards.

901,056 PB89-229231

Not available NTIS National Inst. of Standards and Technology (IMSE),

Gaithersburg, MD. Ceramics Div.
Effect of Heat Treatment on Crack-Resistance
Curves in a Liquid-Phase-SIntered Alumina. Final rept.

S. J. Bennison, H. M. Chan, and B. R. Lawn. 1989, 3р

Sponsored by Air Force Office of Scientific Research, Bolling AFB, DC.

Pub. in Jnl. of the American Ceramic Society 72, n4 p677-679 Apr 89.

Keywords: *Aluminum oxide, *Crack propagation, *Heat treatment, *Liquid phases, *Sintering, *Indentation hardness tests, Microstructure, Defects, Design criteria, Ceramics, Reprints.

The effects of heat treatment on the R-curve (crackresistance) behavior of a commercial liquid-phase-sintered (LPS) alumina have been studied using the indentation-strength test. An enhancement of the Recurve characteristic of this LPS alumina is obtained by a treatment that increases the scale of the microstruc-ture. The enhanced R-curve characteristics leads to the desirable property of flaw tolerance, albeit at the expense of a diminished strength at small crack sizes The implications of the findings are discussed with reference to processing and design strategy.

901.057

PB90-111238 PC A09/MF A02 National Inst. of Standards and Technology (NEL), Gaithersburg, MD. Center for Building Technology. Set Time Control Studies of Polymer Concrete. R. G. Mathey, and J. M. Pommersheim. Sep 89, 195p NISTIR-89/4026

Prepared in cooperation with Bucknell Univ., Lewisburg, PA. Sponsored by Air Force Engineering and Services Center, Tyndall AFB, FL.

Keywords: *Concretes, *Polymers, *Setting time, Polyurethane resins, Temperature, Catalysts, Water, Pilot plants, Flexural strength, Mathematical models.

Set time data were obtained for polymer concrete made with a proprietary polyurethane resin for a wide range of aggregate and resin temperatures. Catalyst range of aggregate and resin temperatures. Catalyst concentrations were adjusted so that setting occurred within a required time range. The effects of the presence of water and ice on set time were also studied. Set time data were also obtained from pilot tests using another polyurethane and catalyst for various aggregate and resin temperatures and moisture conditions. Considerably more catalyst was required in the pilot tests to obtain comparable set times. The impact of temperature variations on flexural strength was investi-

gated. The flexural strength and failure mechanism at early ages depended on the temperature of aggregate and resin at the time of casting the polymer concrete. Using the model, a series of design charts were preosing the model, a series of design charts were pre-pared which can be used to predict set time when cat-alyst concentration and initial aggregate and resin tem-peratures are given, or to determine the catalyst con-centration needed to assure set time corresponding to specified aggregate and resin temperatures.

901,058 **PB90-117**3**8**3 Not available NTIS

National Inst. of Standards and Technology (IMSE), Gaithersburg, MD. Ceramics Div. Grain-Size and R-Curve Effects in the Abrasive Wear of Alumina.

Final rept. S. J. Cho, B. J. Hockey, B. R. Lawn, and S. J.

Sension. 1969, 4p Sponsored by Air Force Office of Scientific Research, Bolling AFB, DC., Gas Research Inst., Chicago, IL., and Korea Science and Engineering Foundation. Pub. in Jnl. of the American Ceramic Society 72, n7 p1249-1252 1989.

Keywords: *Ceramics, *Aluminum oxides, *Wear, *Abrasion tests, *Grain size, Crack propagation, Brittleness, Sliding friction, Fracture strength, Microstructure, Reprints.

Results of sliding wear tests on three alumina ceramics with different grain sizes are discussed in the light of crack-resistance (R-curve, or T-curve) characteristics. The degree of wear increases abruptly after a criti-cal sliding period, reflecting a transition from deforma-tion-controlled to fracture-controlled surface removal. The transition occurs at earlier sliding times for the aluminas with the coarser-grained microstructures, indicative of an inherent size effect in the wear process. A simplistic fracture mechanics model, incorporating the role of internal thermal expansion mismatch stresses in the crack-resistance characteristic, is developed. The results suggest an inverse relation between wear resistance and large-crack toughness for ceramics with pronounced R-curve behavior.

901,059 PB90-117722 Not available NTIS National Inst. of Standards and Technology (IMSE), Gaithersburg, MD. Ceramics Div.

Tribochemical Mechanism of Alumina with Water.

Final rept.

R. S. Gates, S. M. Hsu, and E. E. Klaus. 1989, 7p
Sponsored by Department of Energy, Washington, DC.
Pub. in Tribology Transactions 32, n3 p357-363 1989.

Keywords: *Aluminum oxide, *Water, Reaction kinetics, Wear tests, X ray diffraction, Thermal analysis, Surface chemistry, Phase transformations, Aluminum hydroxides, Rubbing, Reprints, *Tribology.

Water has been found to exhibit significant effects on the tribological behavior of alumina. A film-like sub-stance was found on the surfaces of water lubricated alumina wear surfaces, suggesting the possibility of tribochemical reaction between water and alumina in the contact junction. The paper describes an investigation of the alumina/water tribosystem to determine the chemical interaction between the two materials under rubbing conditions. A combination of x-ray powder diffraction and thermogravimetric analysis (TGA) has been used to investigate the kinetics of aluminal/water reactions. The experiments have determined that transition (gamma) alumina reacts with water to form hydroxides of aluminum. At high temperature (approximately 200 C) aluminum oxide hydroxide (boehmite - AIO(OH) is formed, while at lower temperature (approximately 100 C) the formation of aluminum trihy-droxide (bayerite-Al(OH)3) is favored. A mechanism for lubrication of alumina with water is proposed whereby stresses and temperatures in the contact junction case phase transformation from alpha alumi-na to a transition alumina. The transition alumina sub-sequently reacts with water to form a lubricious hydroxide layer and reduce friction and wear.

901,060 PB90-128026 Not available NTIS National Inst. of Standards and Technology (IMSE), Gaithersburg, MD. Ceramics Div. Flaw Tolerance in Ceramics with Rising Crack Resistance Characteristics.

S. J. Bennison, and B. R. Lawn. 1989, 7p Sponsored by Air Force Office of Scientific Research, Washington, DC.

Pub. in Jnl. of Materials Science 24, p3169-3175 1989.

Keywords: *Ceramics, *Crack propagation, *Defects, Toughness, Aluminum oxide, Polycrystalline, Brittleness, Stresses, Reprints, Closures.

The stabilizing influence of increasing toughness with crack size associated with a cumulative closure-stress process (R-curve, or T-curve) on the strength properties of brittle ceramic materials is analyzed. Three strength-controlling flaw types are examined in quantitative detail: microcracks with closure-stress history through both the initial formation and the extension in subsequent strength testing; microcracks with closure stresses active only during the subsequent extension; stresses active only during the subsequent extension; spherical pores. Using a polycrystalline alumina with pronounced T-curve behavior as a case study, it is demonstrated that the strength is insensitive to a greater or lesser extent on the initial size of the flaw, i.e. the material exhibits the quality of 'flaw tolerance'. The insensitivity is particularly striking for the flaws with full closure-stress history, with virtually total independence on initial size up to some 100 microns, for the flaws with only post-evolutionary exposure to the closure elements the effect is less dramatic, but the strength characteristics are nevertheless significantly. strength characteristics are nevertheless significantly more insensitive to initial flaw size than the counterparts for materials with single-value toughnesses. The implications of the results to engineering design methodologies, as expressed in conventional R-curve constructions, and to processing strategies for tailoring materials with optimal crack resistance properties, are discussed.

901,061

PB90-128638 Not available NTIS
National Inst. of Standards and Technology (IMSE),
Boulder CO Freeture and Defermation Reports (IMSE) Boulder, CO. Fracture and Deformation Div.

Low Temperature Mechanical Property Measurements of Silica Aerogel Foam.

Final rept. . L. Scull, and J. M. Arvidson. 1988, 6p Sponsored by Lawrence Livermore National Lab., CA.

Pub. in Advances in Cryogenic Engineering Materials, v34 p413-418 1988.

Keywords: *Cryogenics, *Mechanical properties, *Silicon oxides, *Aerogels, *Foam, *Measurement, Colloids, Ultimate strength, Thermal conductivity, Insulation, Reprints.

Silica aerogel is a low-density foam material produced by supercritically extracting the solvent from a colloidal suspension of silica in solution. The process produces a transparent, open-cell foam structure that possesses a transparent, open-cell foam structure that possesses an extremely small cell size (approximately 60 nm) with a total porosity in excess of 90% by volume. The morphology gives the aerogel a large strength to density ratio with excellent insulating properties (thermal conductivity of 0.02 - 0.05 w/m/k in N2 gas). Also, the material has refractive index less than 1.10. The properties measured in the study include Young's modulus, proportional limit, yield strength and strain in compression. Other properties measured were Poisson's ratio sion. Other properties measured were Poisson's ratio and ultimate tensile strength.

901.062

PB90-136847 Not available NTIS Model for Particle Size and Phase Distributions in

Ground Cement Clinker.

Final rept. P. W. Brown, and K. G. Galuk. 1987, 8p Pub. in Materials Research Society Symposia Proceedings 85, p83-90 1987.

Keywords: *Mathematical models, *Particle size distribution, *Phase transformations, *Portland cements, *Grinding(Comminution), *Clinker, Hydration, Chemical analysis, Physical properties.

Relationships between the phase distributions in portland cement clinker and the phase and particle size distributions in the ground clinker are not well understood. Little experimental work to characterize the distribution of phases in ground clinker seems to have been done. As a result of the factors, it is difficult to develop physically significant, predictive mathematical models for cement hydration. It is the objective of the paper to describe a computer model that relates the phase and particle size distributions of the ground cement clinker to physical and chemical composition of unground clinker.

Coatings, Colorants, & Finishes

Coatings, Colorants, & Finishes

901,063 PB89-162598 PC A04/MF A01 National Inst. of Standards and Technology (NEL), Gaithersburg, MD. Building Materials Div. Relationship between Appearance and Protective Durability of Coatings: A Literature Review. T. Nguyen, B. Collins, L. Kaetzel, J. Martin, and M. McKnight. Dec 88, 57p NISTIR-88/4010 Sponsored by Civil Engineering Lab. (Navy), Port Hueneme, CA.

Keywords: *Protective coatings, *Forecasting, *Service life, *Discoloration, *Paints, Reviews, Construction materials, Fading, Weathening.

For coatings, improved service life prediction aids in the effective selection and use of materials and in the development of cost-effective maintenance strategies. However, quantitative measures of degradation are essential in predicting service life. Standard proceessential in predicting service life. Standard procedures are available to quantitatively measure small changes in the appearance properties of coatings, one of the two primary functions of coatings, the other being protection. However, quantitative measurements of early changes associated with the protective function usually are not possible. Hence, the objective of the report is to ascertain, based upon the literature, whether changes in appearance properties of coatings can be used to predict changes in the protective properties of the film. It was concluded, that for the most part, changes in appearance properties are not related to changes in the protective properties of a coating

901,064 PB89-201040 Not available NTIS National Bureau of Standards (IMSE), Gaithersburg, MD. Metallurgy Div.

Structural Study of a Metastable BCC Phase in Ai-Mn Alloys Electrodeposited from Moiten Saits. Final rept.

B. Grushko, and G. R. Stafford. 1989, 6p Pub. in Scripta Metallurgica 23, n4 p557-562 1989.

Keywords: *Electrodeposition, *Aluminum alloys, *Manganese, *Crystal structure, *Molten salt electrolytes, Body centered cubic lattices, Metastable state, Electron microscopy, X ray diffraction, Copper, Zinc,

The structure of aluminum-manganese alloys electro-deposited from molten salt electrolytes at 150 C were characterized by transmission electron microscopy and x-ray diffraction. Electrodeposits containing 24-27 at .% Mn contain a crystalline phase co-existing with an amorphous phase. Ring electron diffraction data an amorphious phase. Hing electron diffraction data from the crystalline phase is very similar to that reported for the 'F' phase in this system. Selected area electron diffraction confirms the bcc structure but the appearance of additional weak reflections indicates that the structure should be indexed to a lattice which is 3 times larger. Such a unit cell is consistent with the Cu5Zn8 structure and suggests that the crystalline phase is Al8Mn5 with a cubic gamma-brass structure.

901.065 PB89-209290 PC A03/MF A01 National Inst. of Standards and Technology (NEL), Gaithersburg, MD. Chemical Process Metrology Div.
Thin Film Thermocouples for High Temperature Measurement. K. G. Kreider. May 89, 26p NISTIR-89/4087

Keywords: *Thin films, *Thermocouples, *Vacuum de-posited coatings, High temperature tests, Graphs(Charts), Platinum, Rhodium, Measurement,

Engines, Turbines.

Thin film thermocouples have unique capabilities for measuring surface temperatures at high temperatures (above 800K) under harsh conditions. Their low mass, approximately 2x10(sup-5) g/mm permits very rapid response and very little disturbance of heat transfer to the surface being measured. This has led to applications inside gas turbine engines and diesel engines measuring the surface temperature of first stage turbine blades and vanes and ceramic liners in diesel cyl-inders. The most successful high temperature (up to 1300K) thin film thermocouples are sputter deposited from platinum and platinum-10% rhodium targets although results using base metal alloys, gold, and platinel will also be presented. The paper reviews the fabrication techniques used to form the thermocouples,

approaches used to solve the high temperature insulation and adherence problems, current applications, and test results using the thin film thermocouples. In addition a discussion will be presented on the current problems and future trends related to applications of thin film thermocouples at higher temperatures up to

901,066 PB89-212112 Not available NTIS National Bureau of Standards (NEL), Gaithersburg, MD. Building Materials Div.

Quantitative Studies of Coatings on Steel Using Reflection/Absorption Fourier Transform infrared

Spectroscopy. Final rept.

T. Nguyen, D. Bentz, and E. Byrd. 1986, 1p Pub. in Abstracts of Papers, 1p 1986.

Keywords: *Infrared spectroscopy, *Thin films, *Steels, *Absorption, Reflection, Epoxy resins, Coatings, Quantitative analysis, Nondestructive tests, Reprints.

Reflection/absorption infrared spectroscopy (RAS), commonly referred to as external reflection infrared spectroscopy, has become a powerful, nondestructive technique for studies of thin and thick films on metal surfaces. The intensity and shape of the absorption bands obtained by the technique are different from those obtained by the conventional transmission technique and are a complex function of numerous parameters. The theory of RAS is valid only for very thin films and for a particular substrate/film system; for thick films, the theory deviates from experimental data. In the paper, the relationships between band intensities, angles of incidence, and film thicknesses of an aminecured epoxy coating on cold-rolled steel are examined using reflection/absorption Fourier transform infrared spectroscopy. Mathematical expressions are developed to describe the relationships for thick films of a steel/epoxy system.

901,067 PB89-228571 Not available NTIS National Inst. of Standards and Technology (IMSE), Gaithersburg, MD. Ceramics Div.
Fiber Coating and Characterization.

Final rept.

D. C. Cranmer. 1989, 5p Sponsored by Strategic Defense Initiative Organiza-tion, Washington, DC. Innovative Science and Tech-

nology. Pub. in American Ceramic Society Bulletin 68, n2 p415-419 Feb 89.

Keywords: *Coatings, *Ceramic fibers, *Carbon fibers, *Thickness, Monitors, Dimensional measurement, Re-

A variety of techniques exist for depositing coatings on ceramic and carbon fibers. The paper reviews several of the techniques and discusses the advantages and disadvantages. It also points out several deficiencies in the ability to uniformly and reproducibly coat fibers, especially multifilament tows. One of the most significant problems is the inability to monitor the coating composition and thickness in real-time, i.e., as it is deposited. Characterization techniques are currently limted to the examination of small amounts of fiber at a time and can not readily be adapted to continuous processing.

901,068 PB90-112343 PC A03/MF A01 National Inst. of Standards and Technology (IMSE), Gaithersburg, MD. Polymers Div. Design and Synthesis of Prototype Air-Dry Resins for Use in BEP (Bureau of Engraving and Printing) Intaglio Ink Vehicles.

Annual rept.

B. Dickens, B. J. Bauer, W. R. Blair, and E. J. Parks.
Sep 89, 44p NISTIR-89/4110
Sponsored by Bureau of Engraving and Printing,
Washington, DC.

Keywords: *Alkyd resins, *Synthesis(Chemistry), *Inks, Polymers, Drying oils, Pentaerythritol esters, Air, Dispersing, Water, Oxidation, *Synthetic resins, *In-

Over 60 air-dry resins were designed and synthesized to provide prototype resins for intaglio inks used in the Bureau of Engraving and Printing for printing currency. Most of the resins contain linseed oil fatty acids as the air-dry part. The polysols used are trimethylol propane, pentaerythritol, dipentaerythritol, and tripentaerythritol. In other cases, 'super drying oil' resins were synthesized from tripentaerythritol and linseed oil fatty acids. Inks made from the resins must disperse in 1% aqueous alkali. Acids groups were introduced into the resins using trimellitic anhydride, phthalic anhydride or succinic anhydride. The inks must pass two preliminary tests, one for dispersion in aqueous alkali before curing and one for resistance to the same solution after curing. Two resins, one a super-drying-oil type molecule based on tripentaerythritol and one a more typical alkyd based on pentaerythritol, passed these tésts.

901,069

PB90-117961 Not available NTIS National Inst. of Standards and Technology (IMSE), Gaithersburg, MD. Ceramics Div.
Cathodoluminescence of Defects in Diamond

Films and Particles Grown by Hot-Filament Chemicai-Vapor Deposition.

Final rept. L. H. Robins, L. P. Cook, E. N. Farabaugh, and A. Feldman. 1989, 11p

Pub. in Physical Review B 39, n18 p13 367-13 377, 15 Jun 89.

Keywords: *Cathodoluminescence, *Diamonds, *Thin films, *Defects, Crystal structure, Surface properties, Microstructure, Reprints, *Chemical vapor deposition, Scanning electron microscopy.

Point defects, impurities, and defect-impurity complexes in diamond particles and polycrystalline films were investigated by cathodoluminescence (CL) imaging and spectroscopy in a scanning electron microscope. The diamond films and particles were grown by hotfilament methane-hydrogen chemical-vapor deposi-tion at several different temperatures; the nominal deposition temperature (Td) ranged from 600 to 850 C. Electron-beam energies used to excite the CL were 10-30 keV. By companing the CL spectra to spectra of known defects in natural and synthetic diamond, the following luminescence centers were identified: 2.156-eV center attributed to a nitrogen-vacancy complex; 2.326-eV center, also thought to be a nitrogen-vacancy complex; violet-emitting center (observed peak position at 2.82 eV), associated with dislocation line defects, whose atomic structure is uncertain; 3.188-eV center, attributed to interstitial nitrogen or a nitrogen-(carbon-interstitial) complex; isolated neutral vacancy denoted the general radiation center) with principal zero-phonon line at 1.673 eV. The luminescence from each center displayed a different dependence on Td and film morphology.

Composite Materials

901.070

PB89-147078 Not available NTIS National Bureau of Standards (NEL), Boulder, CO.

Chemical Engineering Science Div.
Performance of Alumina/Epoxy Thermal isolation

R. D. Kriz, and L. L. Sparks. 1988, 8p Sponsored by Ball Aerospace Systems Div., Boulder,

Pub. in Advances in Cryogenic Engineering, v34 p107-114 1988

Keywords: *Composite materials, *Aluminum oxide, *Epoxy resins, *Straps, *Mechanical properties, Keywords: Compactive Property of the Conductivity, Loads(Forces), Fatigue (Materials), Pagaints conductivity, Loads(Forces) Fractures(Materials), Reprints.

A study of advanced fiber-reinforced composites indicates improved thermal-mechanical performance for straps fabricated with alumina fiber over conventional fiber/epoxy systems. In particular, the study compared identical thermal-isolation strap configurations but with different fiber-reinforcement: S2-glass and alumina. Static and cyclic mechanical tests and thermal conductivity measurements indicate superior performance of straps with alumina fibers. Here a popular cryogenic grade resin was used in both configurations. Results of the study indicate that failure initiates in a region where the load is transferred by shear and compression.

Composite Materials

901,071 PB89-148399 PC A05/MF A01 National Inst. of Standards and Technology (IMSE), Boulder, CO. Fracture and Deformation Div.
Institute for Materials Science and Engineering,
Fracture and Deformation: Technical Activities

H. I. McHenry. Feb 89, 85p NISTIR-88/3841 See also report for 1987, PB88-153622.

Keywords: *Fractures(Materials), *Deformation, *Composite materials, *Metals, *Ceramics, Nondestructive tests, Cryogenics, Service life, Mathematical models, Superconductors, Microstructure, Welding.

The report describes the 1988 fiscal-year programs of the Fracture and Deformation Division of the Institute for Materials Science and Engineering. It summarizes the principal accomplishments in three general re-search areas: materials performance, properties, and processing. The Fracture Mechanics, Fracture Physics, Nondestructive Evaluation, and Composite Materials Groups work together to detect damage in metals and composite materials and to assess the signifiand composite materials and to assess the signifi-cance of the damage with respect to service perform-ance. The Cryogenic Materials and Physical Properties Groups investigate the behavior of materials at low temperature and measure and model the physical properties of advanced materials, including compos-ites, ceramics and the new high-critical-temperature superconductors. The Welding and Thermomechani-cal Processing Groups investigate the nonequilibrium metallurgical changes that occur during processing metallurgical changes that occur during processing and affect the quality, microstructure, properties and performance of metals. The report lists the division's professional staff, their research areas, publications, leadership in professional societies, and collaboration in research programs with industries and universities.

901,072 PB89-149165 PB89-149165 Not available NTIS National Bureau of Standards (NEL), Gaithersburg, MD. Fire Science and Engineering Div.

Cone Calorimeter Method for Determining the Flammability of Composite Materials.

Final rept.

J. E. Brown. 1988, 10p Sponsored by Naval Sea Systems Command, Wash-

Spotisoica by reach of the proceedings of Annual Conference on Advanced Composites 'How to Apply Advanced Composites Technology' (4th), Dearborn, MI., September 13-15, 1988, p141-150.

Keywords: *Composite materials, *Calorimeters, *Flammability testing, Heat measurement, Ignition, Radiance, Fiberglass reinforced plastics, Epoxy resins, Combustion, Sensitivity, Phenylene sulfide resins.

A study was undertaken to evaluate the fire performance of composite materials using the cone calonime-ter as the bench-scale method of test simulating the thermal irradiance from fires of various magnitudes. Parameters were derived from the calonmetry measurements to characterize the ignitability and flammability of the composite materials. The parameters are, to some extent, empirical since radiative heat losses from the samples were unknown. These parameters are: (1) minimum external radiant flux (MERF) required are: (1) minimum external radiant flux (MERF) required to produce pilot ignition in a predetermined exposure time; (2) thermal sensitivity index (TSI) which indicates the burning intensity dependence on external heat flux; and (3) extinction sensitivity index (ESI) which indicates the propensity for continued flaming combustion without an external heat flux. MERF values at 300 s for 3 mm composite panels of a FR epoxy resin and of a poly(phenylene sulfide) (PS) resin were about 18 and 28 kW/sq m, respectively. The TSI of the PPS resin composite revealed that it had the greatest dependency on external flux. Additionally, the FSI of the resin composite revealed that it had the greatest de-pendency on external flux. Additionally, the ESI of the PPS composites was the only one to indicate an exter-nal flux requirement to sustain combustion during the first 60 s after ignition.

901,073 PB89-157754 Not available NTIS National Bureau of Standards (NML), Gaithersburg, MD. Gas and Particulate Science Div. Computer-Aided Imaging: Quantitative Compositional Mapping with the Electron Probe Microana-

lyzer. Final rept.

D. E. Newbury, R. B. Marinenko, D. S. Bright, and R. L. Myklebust. 1988, 13p Pub. in Scanning 10, p213-225 1988.

Keywords: *Electron probes, *Microanalysis, Composite materials, Quantitative analysis, Mapping, Reprints, Image processing

X-ray area scanning ('dot mapping') is a technique widely used in electron probe microanalysis for determining the spatial distribution of elemental constituents. Although powerful, this technique is subject to significant limitations on concentration sensitivity and significant limitations on concentration sensitivity and flexibility for subsequent processing. The new technique of compositional mapping overcomes these limitations. In compositional mapping, a complete quantitative electron probe analysis is carried out at each point of a matrix scan. The resulting matrices of concentration values can be assembled into images in a digital image processor by assigning gray or color intensities to the actual concentrations rather than the raw spectral intensities. Digital compositional maps raw spectral intensities. Digital compositional maps can be readily manipulated by a wide variety of image processing techniques to improve the visibility of features of interest.

901,074 PB89-179733 Not available NTIS National Bureau of Standards (IMSE), Gaithersburg, MD. Ceramics Div.
Novel Process for the Preparation of Fiber-Reinforced Ceramic-Matrix Composites. Final rept. W. Haller, U. V. Deshmukh, and S. W. Freiman. W. Hailer, U. V. Deshinukh, and S. W. Freiman. 1988, 3p Grant N00014-86-F-0046 Sponsored by Strategic Defense Initiative Organiza-tion, Washington, DC. Pub. in Jnl. of the American Ceramic Society 71, n12 pC-498-C-500 Dec 88.

Keywords: *Ceramics, *Coatings, *Silicon carbides, *Glass Fibers, Monofilaments, Powder(Particles), Composite materials, Ultraviolet radiation, Curing, Reinforcing materials, Reprints.

A procedure for the reproducible production of monofilament/powder composites has been developed. The process consists of making a slurry of the powder in a process consists of making a surry of the powder in a solventiess ultraviolet-curing resin, and coating the fiber with this surry in a continuous process whereby the coating solidifies immediately after leaving the coater. The fast curing prevents the breakup of coating into globules, which usually occurs with monofilaments. This technique can be applied to any composite using continuous filaments and matrices available to the form of patients of the form of patients of the surrors. in the form of particulate precursors. The application of the technique for preparing a silicon carbide monofila-ment/glass composite is demonstrated.

PB89-180376 PC A04/MF A01 National Inst. of Standards and Technology (IMSE), Gaithersburg, MD. Polymers Div. Composites Databases for the 1990's.
D. H. Reneker, J. M. Crissman, and D. L. Hunston.
Feb 89, 62p NISTIR-88/4016

Keywords: *Composite materials, *Standards, *Polymers, *Tables(Data), Matrix methods, Tests, Data, Composite structures, Surveys.

The report contains a draft standard for identification of polymer matrix composite materials and for reporting test results. The draft standard is based on a comprehensive description of the flow of data through the polymer matrix composites community. Two essentially different kinds of data bases are required, one oriented toward a particular group of data users, and one designed to make the collection of all kinds of data straightforward. An interactive dictionary to serve as a tool in the development of the best names is described. Relationships of the draft standard to various groups concerned with composites are noted.

901,076 PB89-189138 PB69-189138 PC A05/MF A01
National Inst. of Standards and Technology (IMSE),
Gaithersburg, MD. Ceramics Div.
Mechanical Property Enhancement In Ceramic Matrix Composites.
Interim rept. 1 Jan-31 Dec 88.
S. W. Freiman, D. C. Cranmer, E. R. Fuller, W. Haller, M. J. Koczak, M. Barsoum, T. Palamides, and U. V. Deshmukh. Apr 89, 80p NISTIR-89/4073
Contract N00014-86-F-0096 See also PB88-232863. Prepared in cooperation with Drexel Univ., Philadelphia, PA. Dept. of Materials Engi-neering. Sponsored by Office of Naval Research, Ar-lington, VA. Keywords: *Ceramics, *Composite materials, *Monofilaments, *Interfaces, *Borosilicate glass, Silicon carbides, Fibers, Indentation hardness tests, Bonding strength, Carbon, Equipment, Mechanical properties, Graphs(Charts), Surface chemistry.

The fiber-matrix interfacial properties of several glass and ceramic matrix composites have been determined using two indentation techniques and a single fiber pull-out technique. An instrumented indenter was developed to improve the acquisition and analysis of the data. The effects of thermal expansion mismatch were determined from three model composite systems containing large SiC monofilaments using the single fiber pull-out test. An indentation push-out test was successfully used to determine the debond strength of a borosilicate matrix/SiC monofilament/carbon core material. A companson of the vanous techniques for determining the fiber-matrix interfacial properties was conducted.

901.077 PB89-211825
National Bureau of Standards (IMSE), Gaithersburg, MD. Ceramics Div. Creep Rupture of a Metal-Ceramic Particulate Composite.
Final rept.

T. J. Chuang, D. F. Carroll, and S. M. Wiederhorn.

1989, 12p Contract DE-A105-85OR21569 Sponsored by Department of Energy, Oak Ridge, TN. Pub. in Proceedings of International Conference on Fracture (ICF7) (7th), Houston, TX., March 20-24, 1989, v1 p2965-2976.

Keywords: *Creep rupture tests, *Composite materials, *Particulate composites, *Silicon carbides, Crack propagation, Ceramics, Metals, Tensile properties, Flexural strength, Loads(Forces), Deformation, Strains, Coalescing, Fractures(Materials), Failure, Rending Septice life. Bending, Service life.

The creep rupture behavior of a ceramic particulate composite system was studied under tensile and flexural loading. The rupture process commences from the heterogeneous formation of cavities at particle interfaces in the tensile stress field. As deformation proceeds, a critical strain is reached whereupon cavity proceeds, a critical strain is reached whereupon cavity coalescence takes place forming large microcracks. Ultimately, rupture occurs when one of these microcracks reaches a critical length and the remaining ligament cannot sustain the applied load. On the assumption that microcracks grow to a critical size through the coalescence of cavities, a new rupture criterion is proposed based upon a critical strain concept of failure. Using the criterion for fracture, together with a detailed creen mechanics analysis; theoretical predictions are creep mechanics analysis; theoretical predictions are made of lifetime under both bending and simple tension. Creep and creep rupture data for a grade of siliconized silicon carbide tested at 1300 C are collected and compared with the proposed theory. Reasonable agreement between theory and experiment were obtained in both modes of loading.

PB89-218358 PC A04/MF A01
National Inst. of Standards and Technology (NEL),
Boulder, CO. Chemical Engineering Science Div.
Low-Temperature Thermal Conductivity of Composites: Alumina Fiber/Epoxy and Alumina Fiber/PEEK.

D. L. Rule, and L. L. Sparks. May 89, 58p NISTIR-89/3914

Sponsored by National Aeronautics and Space Administration, Moffett Field, CA. Ames Research Center.

Keywords: *Composite materials, *Thermal conductivity, *Thermal cycling tests, Plastics, Polymers, Aluminum oxide, Epoxy resins, Ceramic fibers, Orientation, Low temperature tests, Graphs(Charts), Tables(Data), Fiber laminates, Polyetheretherketone.

The thermal conductivities of poly-ether-ether-ketone (PEEK), of alumina fiber in a matrix of PEEK, and of alumina fiber in a matrix of epoxy, were determined along with the effects of fiber orientation and thermal cycling. Thermal conductivity was measured over the temperature range of 4.2 to 310 K using a steady-state apparatus. Data are presented and discussed relative to specimen characteristics. It appears that after accounting for different fiber fractions in the specimens, the thermal conductivity of the PEEK composite mate-rial is less than that of the epoxy composite material in particular temperature ranges.

901,079 PB89-234223 Not available NTIS Not available (IMSE),
National Inst. of Standards and Technology (IMSE),
Gaithersburg, MD. Polymers Div.
Comparison of Microleakage of Experimental and

Selected Commercially Available Bonding Systems.

Final rept.

A. A. Chohayeb, and N. W. Rupp. 1989, 3p Sponsored by American Dental Association Health Foundation, Chicago, IL. Pub. in Dental Materials 5, p241-243 Jul 89.

Keywords: *Dentistry, *Dental materials, *Bonding, *Composites, Cavities, Leakage, Aluminum oxide, Ferric compounds, Reprints, Permanent dental resto-

The study observed microleakages of composite restorations bonded with two commercial and two experimental systems. A high-viscosity condensable com-posite and a low-viscosity composite were used as the restorative materials. The bonding systems used were two widely accepted commercial brands and two experimental systems, one containing ferric oxalate and the other aluminum oxalate. Restorations were placed in cavities prepared in extracted human teeth, then stored in 37 C water for 24 hours and then polished. The restored teeth were subjected to seven days of thermocycling (5 C-55 C for 540 cycles per day). Microleakage was detected and scored from 0-4 according to the degree of stain penetration. The experimental systems had lower scores than the commercial systems. The high-viscosity composite restorations had microleakage scores higher than those of the lower-viscosity composite restorations.

PB89-235907 PC A03/MF A01 National Inst. of Standards and Technology (IMSE),

Gaithersburg, MD. Ceramics Div.
Toughening Mechanisms in Ceramic Composites.
Semi-Annual Progress Report for the Period
Ending March 31, 1989.

Interim rept.

The Hiller, E. P. Butler, R. F. Krause, and M. D. Vaudin. Jul 89, 29p NISTIR-89/4111
Contract DE-Al05-800R20679 See also PB99-162606. Sponsored by Department of Energy, Oak Ridge, TN. Advanced Research and Technology Fossil Energy Materials Program.

Keywords: *Silicon carbides, *Fiber composites, *Borosilicate glass, "Fracture strength, Aluminum oxides, Coatings(Materials), Creep tests, Strain rate, Stresses, Microstructure, Ceramics, Whisker composites.

A silicon carbide fiber used as reinforcement in a borosilicate glass matrix has been shown to enhance the fracture toughness of the glass by as much as 22%. A ductile nickel coating on the fiber was found to reduce the interfacial shear strength and the frictional sliding between the fibers and the glass matrix, but any influ-ence that the thickness of the nickel coating has on toughening was not conclusive. Time functions of creep strain and creep times to failure were measured for a 25 wt% SiC whisker-reinforced Al203 composite with 4.9% porosity. Beam specimens were used in four-point flexure with variously fixed bending moments and fixed temperatures between 1100 and 1300 C. The secondary creep-strain rates of specimens tested at lower stresses did not follow a power-law function of stress which was fitted to the high stress data. The microstructure of as-received specimens and specimens crept to failure were studied using optical and electron microscopy to determine the mechanisms of creep in the two stress regimes. Both kind of specimens contained cavitation at the whisker/Al203 grain boundary intersections to varying degrees. How-ever, high stress specimens contained broken whisk-ers whereas those from the low stress regime did not.

901,081 PB90-112996 PB90-112996 PC A03/MF A01 National Inst. of Standards and Technology (NEL), Gaithersburg, MD. Center for Fire Research. Assessing the Flammability of Composite Materials. ais.

T. Ohlemiller. Jan 89, 27p NISTIR-89/4032 Sponsored by David W. Taylor Naval Ship Research and Development Center, Annapolis, MD.

Keywords: *Flammability testing, *Composite materials, Ignition, Flame propagation, Heat measurement, Polymers, Test equipment, Ship structural components, Honeycomb laminates.

A comprehensive approach to properly characterizing the flammability of composite materials is outlined. Laboratory-scale tests are described which provide measures of material ignitability, flame spread rate and heat release rate. Rather than expressing the measures as arbitrary indices, they are interpreted in terms of models of the controlling phenomena designed to provide information that can be generalized to full scale contexts, particularly compartment fires.

901,082

PB90-128265 Not available NTIS National Inst. of Standards and Technology (IMSE), Boulder, CO. Fracture and Deformation Div. Edge Stresses in Woven Laminates at Low Tem-

peratures.

Final rept.

R. D. Kriz. 1989, 12p

Sponsored by Department of Energy, Washington, DC. Office of Fusion Energy.

Pub. in Composite Materials: Fatigue and Fracture,

ASTM STP 1012, p150-161 1989.

Keywords: *Laminates, *Woven fiber composites, *Stress analysis, Epoxy resins, Composites, Delaminating, Glass fibers, Cryogenics, Thermonuclear energy, Reprints, *Edges, Glass fiber reinforced

Woven glass-epoxy laminates are used as nonmetallic components at low temperatures in magnetic fusion energy structures. Previous damage studies on G-10CR and G-11CR cryogenic grade woven laminates revealed that most of the damage occurred in the laminates nated interior. An existing, generalized plane strain, finite element model was modified to predict stress states at the laminate interior and free edges. Finite element results demonstrated that the weave geometry reduces edge stresses at low temperatures. Delamination edge stresses in woven laminates are more sensitive to small changes in temperature than those in nonwoven laminates.

901,083

PB90-128646 Not available NTIS National Inst. of Standards and Technology (IMSE), Boulder, CO. Fracture and Deformation Div.

Tensile and Fatigue-Creep Properties of a Copper-Stainiess Steel Laminate.

Final rept.

L. L. Scull, and R. P. Reed. 1988, 7p Sponsored by Department of Energy, Washington, DC. Pub. in Advances in Cryogenic Engineering Materials,

v34 p397-403 1988.

Keywords: *Tensile strength, *Fatigue(Materials), *Creep strength, *Copper, *Stainless steels, *Laminates, Composite materials, Electrical resistivity, Thermal conductivity, Magnets, Reprints.

The design of compact ignition magnets uses a highconductivity copper alloy. However, the large magnetic fields cause large stresses in the coil. The application may require a conductor with higher strength than that of the copper alloys and equally high electrical and thermal conductivity. A candidate material was produced by reinforcing the copper alloy with a stainless-steel alloy. The steel is roll-bonded as the midplane between two copper sheets. The material has the high thermal and electrical conductivity of the copper alloy and, possibly, sufficient strength to be used in compact ignition magnets. Tests were conducted at 295 and 76 K to characterize the tensile and creep-fatigue behavior of the laminated composite material in three rollfor or the laminated composite material in three roll-bonded conditions. The conditions correspond to a bulk reduction of 40, 50, and 60% cold work in the laminate as a whole. A mixing rule was used to predict the tensile behavior of the composite on the basis of the individual tensile properties of copper and stainless steel.

Corrosion & Corrosion Inhibition

901.084

PB89-176291 Not available NTIS National Bureau of Standards (NEL), Gaithersburg, MD. Building Materials Div. Corrosion Induced Degradation of Amine-Cured Epoxy Coatings on Steel. Final rept.

T. Nguyen, and E. Byrd. 1987, 1p Pub. in Abstracts of Papers of the American Chemical Society 193, p133 Apr 87.

Keywords: *Protective coatings, *Degradation, *Epoxy resins, *Amines, *Corrosion, *Curing agents, Interfaces, Steels, Aging tests(Materials), Oxidation, Alkalinity, Infrared spectroscopy, Reprints.

Organic protective coatings on metal can undergo physical and chemical changes under service condi-tions. The paper differentiates the interfacial degradation due to corrosion processes from that due to thermal oxidative reactions of an amine-cured epoxy coating on steel substrate exposed to corrosive environ-ment. Relatively thin films of 40 and 400 nm of an amine cured-epoxy coating on well-prepared cold-rolled steel substrate aged in corrosive and thermal oxidative environments were studied by reflection/absorption Fourier Transform Infrared Spectroscopy. The results obtained showed degradation of the coating exposed to corrosive environment but not that exposed to thermal oxidative environment, suggesting that the corrosion reaction products, which are highly alkaline, are responsible for the degradation of the coating.

901.085

PB89-235345 PC A03/MF A01 National Inst. of Standards and Technology (NEL), Gaithersburg, MD. Center for Building Technology. Development of a Method to Measure in situ Chioride at the Coating/Metal interface.

Technical note (Final).

T. Nguyen, and C. Lin. Jul 89, 20p NIST/TN-1266 Also available from Supt. of Docs. as SN003-003-02960-2. Prepared in cooperation with Xiamen Univ. (China).

Keywords: *Chlorides, *Coatings, *Metals, *Corrosion, *Blistering, *Electrodes, Methodology, Interfaces, Electric potential, Microelectronics, Measurement, Graphs(Charts).

One of the main reasons for the lack of a complete understanding of corrosion and adhesion failures of a coated metal is the lack of analytical instrumentation to probe the behaviors of corrosive agents at the coating/steel interface. A procedure has been developed based in microelectrodes for studying in situ the be-haviors of potential and chloride ions in blister and at a naviors of potential and chloride forts in bister and at-coating/metal interface. The procedure requires an at-tachment of a double-barred Cl(-1) selective microe-lectrode at the coating/metal interface, thus allowing direct measurements of Cl(-1) concentration and cor-rosion potential changes at localized areas under a coating. Although it is intricate to prepare the microelectrodes, the procedure provided very useful informa-tion for mechanistic studies of corrosion under coatings, as well as for transport studies of Cl(-1) ions through a coating on metal. The procedure should also be very useful for studying the roles of Cl(-1) in localized corrosion. The utility of an inverted electrode microsampling method for studies of Cl(-1) in very small volumes such as blisters was also demonstrated.

901,086 PB90-131152 PC A03/MF A01 National Inst. of Standards and Technology (IMSE), Gaithersburg, MD. Metallurgy Div.
Corrosion Behavior of Mild Steel in High pH Aque-

ous Media. A. C. Fraker, and J. S. Harris. Sep 89, 20p NISTIR-89/4173

Sponsored by Nuclear Regulatory Commission, Washington, DC. Office of Nuclear Material Safety and Safeguards.

Keywords: *Corrosion resistance, *Alkalinity, *Low alloy steels, Basalt, Ground water, Pitting tests, Passivity, Ferrite, Pearlite, Packaging materials, Aqueous electrolytes, Steel-ASTM-A27, Radioactive waste electrolytes, Steel-ASTM-A27, Ra management, Underground disposal.

The paper reports on a study of the corrosion behavior and localized corrosion susceptibility of mild steel in a simulated ground water with a pH of 9.75 and a temperature of 95C. The steel used in the study was A27, ASTM Grade 60-30. The steel did not passivate in the aqueous environment used. The corrosion rate decreased with exposure time. Corrosion occurred in an uneven form over the surface and eithers a correct in the surface and either a cor uneven form over the surface, and although some pit-

Corrosion & Corrosion Inhibition

ting may have been present, no deep pits were observed. The amount and distribution of the areas of ferrite and pearlite as well as the impurities were determined to be important as related to uneven corrosion and to localized attack.

Elastomers

901,087 PB89-148118 PC A03/MF A01 National Bureau of Standards (IMSE), Gaithersburg, MD. Polymers Div.

Flow of Molecules Through Condoms.

Annual rept. 1 Mar-1 May 87 (Final).

C. M. Guttman. Oct 87, 47p NBSIR-88/3721 Contract FDA-224-79-5023

Sponsored by Food and Drug Administration, Rock-ville, MD. Office of Science and Technology.

Keywords: *Elastomers, *Contraceptives, *Diffusion, Latex, Pin holes, Molecular flow, *Condoms.

An apparatus for the measurement of flux of small molecules through whole condoms has been developed. It is shown that the experiment can measure diffusion constants as low as 10(sup -13) cm(sup 2)/s or a single pinhole as small as .4 micrometers in the condom. For pinhole measurements this is shown to be a factor of 10 better than current ASTM testing methods on the basis of flow considerations only. Analysis of the experimental data show the difficulties in making unambiguous determinations on the mechanisms of flow. Further experiments are necessary to distinguish between large holes and small holes and fluxes due to diffusion and those due to pinholes. The results suggest a more careful study of fluxes through condoms is necessary to assure that a particle about 1 micrometer cannot pass through the condom.

901,088 PB89-175830 Not available NTIS National Bureau of Standards (IMSE), Gaithersburg, MD. Polymers Div.

MIJ. Polymers DIV.

Uniaxial Deformation of Rubber Network Chains by Small Angle Neutron Scattering.

Final rept.

H. Yu, T. Kitano, C. Y. Kim, E. J. Amis, T. Chang, M. R. Landry, J. A. Wesson, C. C. Han, T. P. Lodge, and C. J. Glinka. 1986, 14p

Pub in Advanced Electomers Bubber Clasticity at 477

Pub. in Advanced Elastomers Rubber Elasticity, p407-

420 1986

Keywords: *Polyisoprene, *Neutron scattering, Deformation, Elastomers, Natural rubber, Isocyanates, Crosslinking, Strains, Molecular weight, Extensibility, Contraction, Radius of gyration, Elastic properties, Reprints.

Small angle neutron scattering (SANS) measurements were performed on poly(isoprene) networks at different uniaxial strains, i.e., 1.0 less than lambda (extension ratio) less than 2.1. The networks were prepared from anionically polymerized, alpha, mu-dihydroxypoly(isoprene) precursors (H-chains) and the corresponding poly(isoprene-d8) isotopic counterparts (D-chains). Two molecular weights of D-chains 26.000 chains). Two molecular weights of D-chains, 26,000 and 64,000, crosslinked with approximately the same molecular weight H-chains (29,000 and 68,000 respectively) were examined for the deformation behaviors. The chain extensive deformation is found to follow a behavior intermediate between the junction affine model and the phantom network model which allows unrestricted fluctuations of network junctions. The chain contractive deformation follows closely the chain affine model, indicating an asymmetry between extensive and contractive chain deformation. In either case, the deformation behavior is found to be the same for the two molecular weights.

901.089 PB89-209308 PC A03/MF A01 National Inst. of Standards and Technology (IMSE), Gaithersburg, MD. Polymers Div. Studies on Some Failure Modes In Latex Barrier

Annual rept. (Final).
C. M. Guttman, G. B. McKenna, K. M. Flynn, and T. K. Trout. May 88, 50p NISTIR-89/4084
Contract FDA-224-79-5023

Sponsored by Food and Drug Administration, Rockville, MD. Office of Science and Technology.

Keywords: *Latex, *Thin films, *Barrier materials, *Liquid permeability, *Failure, *Crosslinking, Body fluids, Simulation, Prophylaxis, Natural rubber, Surgical gloves, Swelling, Graphs(Charts), Condoms.

The report covers work on a 1988 contract with the FDA to study failure modes of latex barrier films in their use as condoms or medical gloves. Two areas are re-ported on: The change in the failure of latex barrier films as a result of swelling in bodily fluid simulants and the cross-link density variation in condoms on the 0.1

901.090

search

PC A07/MF A01 PB89-228316 Brown Univ., Providence, RI. Div. of Engineering.
Experimental Study of the Pyrolysis of Pure and Fire Retarded Cellulose. Doctoral thesis.

Y. Chen. Jun 89, 147p NIST/GCR-89/566 Grants NANB-8-D0851, NANB-6-D0629 Sponsored by National Inst. of Standards and Technology (NEL), Gaithersburg, MD. Center for Fire Re-

Keywords: *Pyrolysis, *Cellulose, *Fire resistant coatings, *Sodium hydroxide, Catalysts, Combustion products, Heat of vaporization, Nitrogen, Graphs(Charts), Vapors, Volatility, Theses.

The pyrolysis of pure and fire retarded bulk cellulose samples in a nitrogen atmosphere is studied. The study is directed toward determining the effects of the solid phase fire retardant (sodium hydroxide) on the burning of cellulose. The material property of pure and fire retarded cellulose which most directly affects its burning behavior, the heat of gasification, is measured by using a specially designed pyrolyzing chamber. Theoretical results are obtained for a one-dimensional pyrolysis wave propagating into cellulose by using a finite-difference calculation. The experimental data show that sodium hydroxide acts as a catalyst in the pyrolysis of cellulose. Its addition leads to decreases in the heat of gasification and the mass fraction of non-combustible volatiles in the total volatiles and to increases in stoichiometric ratio and the heat of combustion of combustible volatiles, and thereby has a dual effect on cellulose burning.

Fibers & Textiles

901.091

PB89-174122 PB89-174122 Not available NTIS National Bureau of Standards (NEL), Gaithersburg, MD. Fire Science and Engineering Div. Flammability Tests for Industrial Fabrics: Relevance and Limitations.

Final rept. K. M. Villa, and J. F. Krasny. 1988, 16p Pub. in Proceedings of Annual Conference of the Industrial Fabrics Association International (76th), Chicago, IL., November 9-12, 1988, p119-134.

Keywords: *Flammability testing, *Industrial fabrics, *Fire resistant textiles, Criteria.

Flammability tests applicable to industrial fabrics, including tents and other outdoor equipment, inflatable structures, etc., are discussed briefly. These tests were designed to assure self-extinguishment after ex-posure to small flames. The specimens are generally held vertically in a U-shaped steel frame and ignited at the bottom. Most of these tests were developed when only char-forming materials like flame retardant cotton were available. The criteria chosen for the tests were char length, and afterflame and afterglow time. The applicability of these tests and criteria to both charforming and thermoplastic fabrics is critically reviewed.

Iron & Iron Alloys

901.092

PB89-149082 Not available NTIS National Bureau of Standards (IMSE), Boulder, CO. Fracture and Deformation Div.

Local Brittle Zones in Steel Weldments: An Assessment of Test Methods.

Final rept.

R. Denys, and H. I. McHenry. 1988, 7p Pub. in Proceedings of International Conference on Offshore Mechanics and Arctic Engineering (7th), Houston, TX., February 7-12, 1988, p379-385.

Keywords: *Steels, *Weldments, *Fractures(Materials), *Offshore structures, *Plates(Structural member), *Nondestructive tests, Brittleness, Microstructure, Heating, Quality control, Toughness, Structural analysis.

Local brittle zones (LBZs) are regions of brittle microstructure within the heat affected zones (HAZs) of steel weldments that can initiate brittle fracture at low toughness levels. The paper describes the metallurgical nature of LBZs, reviews the various test methods used to detect and evaluate LBZs, and recommends test methods for controlling LBZs in offshore structures. The recommended tests and their specific functions are: (1) For pre-production qualification of steel plates, CTOD tests evaluate the susceptibility of steels to the formation of LBZs; (2) For quality control of steel plates, drop weight NDT tests evaluate the tolerance for LBZs of the steels used for offshore structures; (3) For qualification of welding materials and procedures, Charpy V-notch tests verify that the HAZ toughness exceeds the minimum toughness specified for the steel; (4) For fitness for purpose evaluations, wide plate tests assess the significance of LBZs in existing structures.

PB89-149090 Not available NTIS National Bureau of Standards (IMSE), Boulder, CO. Fracture and Deformation Div.

J-Integral Values for Small Cracks in Steel Panels.

Final rept.
D. T. Read. 1988, 13p
Sponsored by Naval Sea Systems Command, Washington, DC., and David W. Taylor Naval Ship Research

and Development Center, Annapolis, MD.
Pub. in Fracture Mechanics: Eighteenth Symposium,
ASTM STP 945, p151-163 1988.

Keywords: *Steels, *Fractures(Materials), Toughness, Defects, Loads(Forces), Strains, Crack propagation, Plates(Structural members), Tearing, Reprints, *J-integral, Steel A710.

For a quantitative relationship between fracture toughness, flaw size, and applied loading for small flaws, be used for fitness-for-service assessment, applied J-integral was measured as a function of applied strain in eight 14-mm-thick specimens of ASTM A710 Grade A Class 3 steel plate. All the edge cracks had lengths less than 3% of the specimen width of 82 mm. Six specimens were tested in tension; two were loaded by specimens were tested in tension, two were loaded by four-point-bending in the plane of the plate. One single-edge-cracked, transversely oriented specimen was tested at -30 deg C. Electrical resistance strain gage and clip-gage crack mouth opening displacement measurements were used to obtain quantities inside the J-integral. The J-integral was calculated by trape-zoidal rule integration. Unloading crack mouth compliance measurements were used to obtain crack length values so that tearing effects could be observed. Lueder's strains occurring right after yield caused rapid increases in the applied J-integral values for the ten-sion specimens. Except for the Lueder's strain effect, the behavior of the applied J-integral in bending was similar to that in tension. Tearing caused a smooth ex-ponential rise in applied J as strain increased beyond the point of initiation. The initiation toughness and tearing resistance of the panels with short cracks were equal to or greater than those of conventional threepoint-bend specimens of the same thickness.

901.094 PC A04/MF A01 PB89-156160 National Bureau of Standards (IMSE), Gaithersburg, MD. Fracture and Deformation Div.

Postweld Heat Treatment Criteria for Repair Welds in 2-1/4Cr-1Mo Superheater Headers: An Experimental Study.

D. T. Read, and H. I. McHenry. Aug 88, 60p NBSIR-87/3075

Sponsored by Naval Sea Systems Command, Washington, DC. Keywords: *Weldments, *Maintenance, *Superheater headers, Boilers, Ships, Steels, Heat Treatment, Shielded metal arc welding, Bending,

128

Cracking(Fracturing), Toughness, Residual stress, Strain gages, Pressure vessels, Hydrostatics, Chromium, Molybdenum.

Wide-plate and standard-size specimens cut from repair welds in 2-1/4Cr-1Mo plate were tested as-welded and after post-weld heat treatment (PWHT). Three-point-bend specimens with cracks oriented in the TS direction were used to measure weld-metal and heat-affected-zone (HAZ) toughness values. Results of direct measurements of the applied J-integral on the wide plates were compared with critical J-value measwrote plates were compared with critical 3-value rileasurements of three-point-bend specimens. The comparison indicated that PWHT was highly beneficial, because it reduced the crack-driving force from residual stresses and increased the weld-metal and HAZ toughness. In the as-welded condition, very low toughness values were measured at the HAZ. These low toughness values, together with the measured crackdriving forces, indicated critical crack depths of a few millimeters. To extend the usefulness of these results, a new approach to the problem of the applied J-integral produced by residual stresses is being explored: strain-gage measurements made during notching are analyzed to obtain an applied J-integral as a function of crack depth. The preliminary results are encouraging. The residual-stress-produced J-value is roughly equivalent to that produced by a remote elastic loading to the same stress level.

PB89-157796 Not available NTIS National Bureau of Standards (IMSE), Boulder, CO. Fracture and Deformation Div.

Molybdenum Effect on Volume in Fe-Cr-NI Alloys.

H. M. Ledbetter, and M. W. Austin. 1988, 5p Sponsored by Department of Energy, Washington, DC. Pub. in Jnl. of Materials Science 23, p3120-3124 1988.

Keywords: *Face centered cubic lattices, *Ray diffraction, *Iron alloys, *Compressibility, Crystallography, Chromium, Nickel, Molybdenum, Atomic properties, Atomic orbitals, Reprints.

The unit-cell size for six face-centered-cubic Fe-Cr-Ni alloys, nominally Fe-19Cr-12Ni (at%) were determined alloys, normany re-1907-12Ni (at %) were determined by x-ray diffraction on powder specimens. In these alloys, the molybdenum content ranged up to 2.4 at %. Molybdenum increases volume: 0.45% per at %. Usual models based on atomic volumes and elastic compressibilities fail to explain the large volume increase. The discrepancy was ascribed to changes in interatomic bonding, which are described in terms of 3d-electron models.

901.096

PB89-158018 Not available NTIS National Bureau of Standards (NEL), Gaithersburg, MD. Building Materials Div.

Fractal-Based Description of the Roughness of Blasted Steel Panels.

Final rept.

J. W. Martin, and D. P. Bentz. 1987, 7p Sponsored by Federal Highway Administration, Washington, DC.

Pub. in Jnl. of Coatings Technology 59, n745 p35-41 1987.

Keywords: *Steels, *Roughness, *Thermography, *Images, Panels, Blasting, Fractography, Cameras, Surface properties, Reprints.

The fractal dimensions of a standard series of blasted steel panels are shown to correlate very well with their perceived roughness. This occurs because the roughness of a blasted panel dictates the roughness of its image, and hence, its fractal dimension. The blasted steel panels are imaged with a thermographic camera, as opposed to a visual camera, because a thermo-graphic image better delineates the peak-to-valley heights of the crater-like structures; it minimizes imag-ing problems due to light reflectance; and it eliminates most of the imaging problems associated with surface discoloration. It is concluded that the fractal dimension of a blasted steel surface captures most of the perceptually relevant shape structures on an abraded sur-face, and thus, provides a good quantitative representation of surface roughness.

901,097

Not available NTIS National Bureau of Standards (IMSE), Boulder, CO. Fracture and Deformation Div.

Loading Rate Effects on Discontinuous Deformation in Load-Control Tensile Tests. Final rept.

Ogata, K. Ishikawa, R. P. Reed, and R. P. Walsh. 1988, 8p

Sponsored by Department of Energy, Washington, DC.

Office of Fusion Energy.
Pub. in Advances in Cryogenic Engineering Materials, v34 p233-240 1988.

Keywords: *Tension tests, *Loading rate, *Load control, *Austenitic steels, *Deformation, Tensile properties, Strains, Ultimate strength, Low temperature tests, Cryogenics, Loads(Forces), Reprints.

In load-control tensile tests at liquid helium tempera-ture, an abrupt and large discontinuous deformation occurs, which differs from the discontinuous deformation obtained from displacement-control tests. We investigated the effects of loading rate, varied from 0.5 to 5000 N/s, on the tensile properties of AlSI 304L, 310, and 316LN steels at 4 K. A large deformation, near 40% strain, occurred in AlSI 310. At the high loading rates, the ultimate strength of these materials was 65% of the strength obtained in displacement-control tests; the initiation strength of discontinuous deformation was also less.

901,098 PB89-172621 PC A06/MF A01 National Inst. of Standards and Technology (IMSE), Gaithersburg, MD. Metallurgy Div. Elevated Temperature Deformation of Structural Steel.

B. A. Fields, and R. J. Fields. Mar 89, 121p NISTIR-88/3899

Sponsored by American Iron and Steel Inst., Washington, DC.

Keywords: *High temperature tests, *Creep tests, *Tensile strength, *Computation, *Deformation, *Construction materials, *Steels, Elastic properties, Plastic properties, Equations, Graphs(Charts), Steel ASTM

The results of tensile and creep tests on steels close to the American specification for ASTM A36 have been used to formulate an equation from which elastic, plastic, creep and total strains can be calculated. Correlations between measured and predicted strains for Australian AS A149 and Japanese SS41 steels, both close to the A36 specification, are shown and good agreement is found. The above mentioned equation is also used to construct deformation mechanism (i.e., elastic, plastic, or creep) maps for times of 2 minutes to 4 hours at temperature. From these maps the defor-mation mechanisms operating at a given temperature and stress can be seen. The dominant mechanism for each set of conditions is given. In addition the maps show contours of total strain values 1, 2, and 5%.

901,099 PB89-173**504** Not available NTIS National Bureau of Standards (IMSE), Boulder, CO. Fracture and Deformation Div. Role of Inclusions in the Fracture of Austenitic

Stainless Steel Welds at 4 K.

Final rept.

T. A. Siewert, and C. N. McCowan. 1987, 11p
Sponsored by Department of Energy, Washington, DC.
Pub. in Welding Metallurgy of Structural Steels, p415-425 1987.

Keywords: *Inclusions, *Austenitic stainless steels, *Weldments, *Impact tests, *Toughness, *Cryogenics, Yield strength, Shielded metal arc welding, Gas metal arc welding, Fractures(Materials), Surface properties, Morphology, Ductility, Reprints.

Inclusion densities were measured for three types of austenitic stainless steel welds and compared to the 4-K yield strengths, 76-K Charpy V-notch absorbed energiés, and the ductile dimple densities on the respective fracture surfaces. The welds included shielded metal arc (SMA) welds and gas metal arc (GMA) welds. The arc (SMA) welds and gas metal arc (GMA) welds. The inclusion density was consistently a factor of 8 to 10 less than the fracture surface dimple density. Inclusion and dimple densities ranged from 3.9 x 10 sup 4 inclusions per sq mm and 3.2 x 10 sup 5 dimples per sq mm for one SMA specimen to 1.1 x 10 sup 4 inclusions per sq mm and 1.2 x 10 sup 5 dimples per sq mm for the fully austentitic GMA specimen. Both ductile dimple density and dimple morphology varied with specimen type. The inclusion data for the welds agreed with a linear relationship between fracture touchness and inlinear relationship between fracture toughness and in-clusion spacing that had been developed for base metals.

901,100

PB89-173512 Not available NTIS National Bureau of Standards (IMSE), Boulder, CO. Fracture and Deformation Div.

Influence of Molybdenum on the Strength and

Toughness of Stainless Steel Welds for Cryogenic

Final rept. C. N. McCowan, T. A. Siewert, and E. Kivineva. 1987, 12p

Sponsored by Department of Energy, Washington, DC. Pub. in Proceedings of International Symposium on Welding Metallurgy of Structural Steels, Denver, CO., February 22-26, 1987, p427-438.

Keywords: *Molybdenum, *Austenitic stainless steels, *Additives, *Toughness, *Impact tests, *Cryogenics, Yield strength, Chromium alloys, Nickel, Manganese, Nitrogen, Weldments, Inclusions.

Molybdenum additions to austenitic stainless welds were found to increase the 4-K yield strength by approximately 30 MPa per weight percent. Molybdenum additions had little effect on the 76-k Charpy V-Notch impact energy, with one exception: when the molybde-num content was raised from 1.7 to 3.8 wt. % in an otherwise equivalent stainless steel composition of apotherwise equivalent stainless steel composition of approximately 17Cr-9Ni-6.6Mn-0.17N, the absorbed energy decreased from 33 to 16 J. At a nickel content of 14 wt. %, the higher molybdenum contents did not reduce the impact toughness. The loss in impact toughness for the 9 wt.% nickel, 3.8 wt. % molybdenum composition was linked to an increased number of both small and large inclusion sizes in the weld. The effects of nickel and manganese on the cryogenic strength and toughness are also reported.

901,101

PB89-173835 Not available NTIS National Bureau of Standards (IMSE), Boulder, CO. Fracture and Deformation Div.

Failure Analysis of an Amine-Absorber Pressure

Final rept.

H. I. McHenry, and D. T. Read. 1986, 17p See also PB89-126783. Sponsored by Occupational Safety and Health Administration, Chicago, IL.

Pub. in Proceedings of International Conference on Structural Failure, Product Liability and Technical In-surance (2nd), Vienna, Austria, July 1-3, 1986, p141-

Keywords: *Pressure vessels, *Bursting, *Refineries, *Stress corrosion tests, Failure, Fractures(Materials), Microstructure, Hydrogen, Crack propagation, Pressure, Embrittlement, Petroleum products, Toughness, Weldments, Maintenance, Structural forms, Steels, Reprints.

In 1984, a pressure vessel ruptured at a petroleum refinery causing an explosion and fire. It fractured along a path that was weakened by extensive cracking adja-cent to a repair weld joining a replacement section to the vessel. These pre-existing cracks initiated in areas the vessel. These pre-existing cracks initiated in areas of a hard microstructure due to hydrogen stress cracking. The cracks grew through the vessel wall due to hydrogen pressure cracking. When the depth of the largest of these cracks exceeded 90% of the wall thickness, the remaining ligament ruptured resulting in a through crack about 800 mm long. This crack triggered final fracture at the operating stress level of 35 MPa because the toughness of the vessel steel was reduced nearly 3-fold by hydrogen embrittlement. reduced nearly 3-fold by hydrogen embrittlement.

901,102

PB89-174882 Not available NTIS National Bureau of Standards (IMSE), Boulder, CO. Fracture and Deformation Div.

Tensile Strain-Rate Effects in Liquid Hellum. Final rept.

R. P. Reed, and R. P. Walsh. 1988, 10p Pub. in Advances in Cryogenic Engineering: Materials, v34 p199-208 1988.

Keywords: *Tensile strength, *Strain rate, *Liquids, *Helium, *Austenitic stainless steels, Cryogenics, Heat transfer, Dislocations(Materials), Surface properties, Adiabatic conditions, Reprints.

The effects of strain rate on tensile properties of three austenitic stainless steels at 4 K were examined. Strain rates ranged from 4.4 x 10 sup(-6) s sup(-1) to 8.8 x 10 sup(-3) s sup(-1). Strain rates less than 2.2 x 10 sup(-3) s sup(-1) had no effect on tensile properties. Strain

Iron & Iron Alloys

rates of 4.4 x 10 sup(-3) s sup(-1) or larger reduced the ultimate tensile strength, and stress-strain curves and temperature measurements indicated specimen warming to 100 K. Calculations are presented to estimate the work put into the specimen during deformation, stored energy in terms of dislocations and dislocation interactions, and dissipated heat. The reduction of tensile strength was associated with specimen warming which was caused by the transition from nucleate to film-boiling heat transfer on the specimen surface.

901,103

PR89-189195 PC A03/MF A01 National Inst. of Standards and Technology (IMSE), Boulder, CO. Fracture and Deformation Div. Fracture Behavior of a Pressure Vessel Steel in the

Ductile-to-Brittle Transition Region.
J. Heerens, and D. T. Read. Dec 88, 44p NISTIR-88/

Prepared in cooperation with GKSS - Forschungszentrum Geesthacht G.m.b.H., Geesthacht-Tesperhude (Germany, F.R.).

Keywords: *Fractures(Materials), *Steels, *Pressure vessels, *Ductile brittle transition, *Cleavage, Manganese, Initiation, Crack propagation, Nickel, Molybdenum. Metal allovs.

The reasons for the scatter of fracture toughness in the ductile-to-brittle transition region, as well as the mechanisms leading to cleavage fracture, have been investigated for a quenched and tempered pressure vessel steel, DIN 20 MnMoNi 55. The fracture surfaces indicate that cleavage fracture starts at one small area in the ligament, the cleavage initiation site. Cleavage initiation occurs ahead of the crack tip at the location of the maximum normal stresses. Fractography and metallography show four different types of initiation sites. The mechanisms which may trigger cleavage fracture at these initiation sites are discussed. The results indicate that the scatter of fracture toughness is due to the scatter in the distance between the cleavage initiation site and the fatigue crack tip.

901.104

PB89-189336 PC A03/MF A01
National Inst. of Standards and Technology (NEL),
Boulder, CO. Chemical Engineering Science Div.
Ignition Characteristics of the Iron-Based Alloy
UNS S66286 in Pressurized Oxygen.
J. W. Bransford, P. A. Billiard, J. A. Hurley, K. M.
McDermott, and I. Vazquez. Nov 88, 50p NISTIR-88/

Sponsored by National Aeronautics and Space Administration, Huntsville, AL. George C. Marshall Space Flight Center.

Keywords: *Metal alloys, *Ignition, *Combustion, *Oxygen, *High pressure tests, *Iron alloys, Carbon dioxide lasers, Heat treatment, Solidus, Endothermic reactions, Surface properties, Oxidation, Tables(Data), Graphs(Charts), Alloy UNS S66286.

The development of ignition and combustion in pressurized oxygen atmospheres was studied for the iron based alloy UNS S66286. Ignition of the alloy was achieved by heating the top surface of a cylindrical specimen with a continuous wave CO2 laser. Two heating procedures were used. In the first, laser power was adjusted to maintain an approximately linear increase in surface temperature. In the second, laser power was periodically increased until autoheating (self-heating) was established. It was found that the alloy would autoheat to destruction from temperatures below the soliding temperatures. below the solidus temperature. In addition, endothermic events occurred as the alloy was heated, many at reproducible temperatures. Many endothermic events occurred prior to abrupt increases in surface temperature and appeared to accelerate the rate of increase in specimen temperature to rates greater than what would be expected from increased temperature alone. It is suggested that the source of these endotherms may increase the oxidation rate of the alloy. Ignition parameters are defined and the temperatures at which these parameters occur are given for the oxygen pres-sure range of 1.72 to 13.8 MPa (25 to 2000 psia).

901.105

PB89-193262 PC A03/MF A01 National Inst. of Standards and Technology (IMSE), Gaithersburg, MD. Metallurgy Div.

Metallurgical Evaluation of 17-4 PH Stainless Steel Castings.
G. E. Hicho, and J. H. Smith, May 89, 35p NISTIR-

89/4075

Sponsored by Naval Ordnance Station, Indian Head,

Keywords: *Castings, *Stainless steels, *Heat treatment, *Microscopy, *Hardness, *Missile warheads, *Microstructure, Specifications, Metallography, Measurement, Temperature, Solution annealing, tests (Materials), Tables (Data), Homoge Graphs (Charts), Weapons, Head Caps. Homogenizing,

A metallurgical evaluation was conducted to determine if selected castings of 17-4 PH stainless steel used in head caps on missile weapon systems had been prop-erly heat treated as required by SAE specification AMS-5355D. Optical metallographic analysis and hardness measurements were made on four samples of as-received castings and on selected samples that were homogenized, solution annealed and aged at various temperatures.

901,106 PB89-201586 PB89-201586 Not available NTIS National Bureau of Standards (IMSE), Boulder, CO. Fracture and Deformation Div. Ferrite Number Prediction to 100 FN in Stainless

Steel Weld Metal. Final rept.
T. A. Siewert, C. N. McCowan, and D. L. Olson.

1988, 10p Pub. in Welding Research Supplement, p289-s-298-s

Keywords: *Weldments, *Stainless steels, *Ferrite, Manganese, Molybdenum, Nitrogen, Silicon, Solidifica-tion, Surveys, Reprints, Stainless steel 309, Data

To improve the accuracy of ferrite number (FN) prediction in stainless steel weld metal, a new diagram has been developed using a database containing more than 950 alloy compositions from worldwide sources. In accuracy, the diagram surpasses the DeLong diagram for the low-FN austenitic stainless steel compositions of the 300 series, and it corrects a 2 FN bias detected for Type 309 stainless steel. The diagram is more accurate than the Schaeffler diagram for duplex stainless steel alloys and ferrite contents to 100 FN. It is most accurate when the Mn content is restricted to 10 wt-%, Mo content is restricted to 3 wt-%, N content is restricted to 0.2 wt-%, and Si content is restricted to 1 wt-%. Changes in the primary solidification mode are indicated on the diagram, and they appear to affect the FN response. Transitions in iso-FN line spacings may be caused by these mode changes.

901,107 PB89-231260 Not available NTIS National Inst. of Standards and Technology (IMSE), Boulder, CO. Fracture and Deformation Div. Stainless Steel Weld Metal: Prediction of Ferrite Content.

Final rept. Jan-Oct 88. C. N. McCowan, T. A. Siewert, and D. L. Olson.

Keywords: *Stainless steels, *Weldments, Diagrams, Ferrite, Solidification, Data, Solid phases, Reprints.

A new diagram to predict the ferrite number (FN) in stainless steel welds is proposed. The diagram has a range from 0 to 100 FN, and the primary solidification zones are indicated. The diagram more accurately predicts the ferrite content for welds having FN less than 18 than existing diagrams. It corrects overestimates made by the DeLong diagram for AWS type 309 stainless steel and it predicts the FN of duplex stainless less steel and it predicts the FN of duplex statistics steel more accurately than the Schaeffler diagram. Weld compositions used to develop the diagram ranged (in wt.%) from 0.01 to 0.2 C, 0.4 to 12 Mn, 0.1 to 1.3 Si, 15 to 32 Cr, 5 to 25 Ni, 0 to 7 Mo, 0.02 to 0.3 N, 0 to 0.9 Nb, and 0 to 0.1 Ti. The database contained over 950 welds and is included in Appendix I and II to the report.

901,108 PB90-117623 Not available NTIS National Inst. of Standards and Technology (IMSE), Boulder, CO. Fracture and Deformation Div.

Linear-Elastic Fracture of High-Nitrogen Austenitic Stainless Steels at Liquid Hellum Temperature. Final rept.

R. L. Tobler, R. P. Reed, and P. T. Purtscher, 1989.

Jan 89

Sponsored by Department of Energy, Washington, DC. Office of Fusion Energy.
Pub. in Jnl. of Testing and Evaluation 17, n1 p54-59

Keywords: *Austenitic stainless steels, *Chromium nickel alloys, *Cryogenics, *Fractography, Fracture strength, Brittleness, Reprints, *Nitrogen additions, Manganese additions, Thermonuclear reactors

Four commercial Fe-Cr-Ni-Mn austenitic stainless steels containing 0.14, 0.26, and 0.37 wt% N were fractured in liquid helium at 4 K, and measurements of the linear-elastic plane-strain stress-intensity factor, K(sub 1c), were made. Interstitial nitrogen significantly strengthens these steels at low temperatures so that brittle fractures occur under plane strain conditions at 4 K despite moderate ductility in uniaxial tension. The brittle fracture mechanism at 4 K involves a form of cleavage or slip-band cracking as evidenced by the formation of transgranular facets on (111) planes

901.109 PB90-117649 Not available NTIS National Inst. of Standards and Technology (IMSE), Boulder, CO. Fracture and Deformation Div. Nitrogen in Austenltic Stainless Steels. Final rept. R. P. Reed. 1989, 6p Pub. in Jnl. of Metals 41, n3 p16-21 Mar 89.

Keywords: *Austenitic stainless steels, Corrosion resistant steels, Austenite, Mechanical properties, Toughness, Reprints, *Nitrogen additions.

Nitrogen alloyed in austenitic stainless steels improves austenitie stability, mechanical properties and corrosion resistance. Steels supersaturated with nitrogen ('super-nitrogen steels') have been investigated, which rival the latest ferritic steels in strength but have potentially greater toughness.

901,110 PB90-128554 Not available NTIS Not available NTIS
National Inst. of Stanoards and Technology (IMSE),
Boulder, CO. Fracture and Deformation Div.
Effect of Chemical Composition on the 4 K Mechanical Properties of 316LN-Type Alloys. Final rept.

P. T. Purtscher, R. P. Walsh, and R. P. Reed. 1988,

Pub. in Advances in Cryogenic Engineering Materials, v34 p191-198 1988.

Keywords: *Chemical composition, *Cryogenics, *Mechanical properties, *Austenitic stainless steels, Liquid helium, Toughness, Yield strength, Crack propagation, Molybdenum containing alloys, Nickel containing alloys, Microstructure, Annealing, Reprints, *Stainless-steel-316LN, Molybdenum additions, Nickel additions.

A series of eight austenitic stainless steels was tested in liquid helium to determine the effect of Mo and Ni variations on the strength and toughness. The Mo convariations of the steeping and toughness. The Mo content ranged from 0 to 4 wt.%; the Ni content varied from 11 and 14 wt.%. The microstructure of the alloys depended upon the composition and annealing temperature. Higher alloy content and lower annealing temperatures, 1000 to 1050 C, resulted in a nonuniform structure. The higher temperature 1150 C proform structure. The higher temperature, 1150 C. produced a uniform austenitic structure. The mechanical test results showed that Mo additions increased the yield strength (to a maximum at 3 wt.%) and decreased the K sub (Ic)(J) values, so that there was no improvement in the strength-toughness relationship. Increasing the Ni content decreased the strengthening effect of Mo and increased K sub (Ic)(J). It supports earlier work that showed that Ni does improve the strength-toughness relationship.

PB90-128562 Not available NTIS National Inst. of Standards and Technology (IMSE), Boulder, CO. Fracture and Deformation Div. Fracture Behavior of 316LN Alloy in Uniaxial Tension at Cryogenic Temperatures. Final rept.

P. T. Purtscher, R. P. Walsh, and R. P. Reed. 1988,

Sponsored by Department of Energy, Washington, DC.

Pub. in Advances in Cryogenic Engineering Materials, v34 p379-386 1988.

Keywords: *Fractures(Materials), *Cryogenics, *Austenitic stainless steels, *Tension tests, Axial stress, Inclusions, Surface properties, Microstructure, Nucleation, Reprints, *Stainless-steel-316LN, Maganese sul-

The fracture behavior of an austenitic stainless steel, commercial-grade 316LN alloy, at cryogenic temperatures is studied by careful examination of the fracture surfaces and polished cross-sections through the frac-ture surfaces of round tensile specimens. The fracture is ductile (a dimpled rupture process) and is controlled by inclusions in the structure, MnS stringers and smaller spherical particles. The main effect of the MnS stringers was to decrease the percent reduction in area in the tensile test at 4K. The true stress and strain at fracture vary as a function of test temperature and are shown to be related to the nucleation of microvoids around the spherical particles.

901,112 PB90-130287 PB90-130287 PC A03/MF A01
National Inst. of Standards and Technology (IMSE),
Gaithersburg, MD. Metallurgy Div.
Tensile Tests of Type 305 Stainless Steel Mine
Sweeping Wire Rope.
T. R. Shives, and S. R. Low. Oct 89, 29p NISTIR-89/
4174 PC A03/MF A01

Keywords: *Tension tests, *Minesweepers(Ships), *Wire rope, Graphs(Charts), Tensile stress, Naval mine detection, *Stainless steel-305.

The Naval Coastal Systems Center submitted to the National Institute of Standards and Technology (NIST) approximately 360 feet of each of two different AISI 305 stainless steel wire ropes for testing. Both wire ropes were nominally 5/8 inch in diameter. One was stated as having a 6 x 19 configuration and the other a 7 x 7 configuration. The first number in such a designation indicates the number of strands in the wire rope and the second number indicates how many wires there are per strand. For example, the wire rope with a 6 x 19 configuration consists of six strands of 19 wires each. As shown later, the wire rope stated to have a 7 x7 configuration actually had a 6 x 7 configuration with an independent wire rope core (IWRC). The core is one of the three basic parts of a wire rope. The other two are the wires and the strands. The core may be comprised of steel or fiber. In the case of both of the submitted wire rope samples, the core consisted of an independent wire rope.

901,113 PB90-136771 Not available NTIS National Inst. of Standards and Technology (IMSE), Boulder, CO. Fracture and Deformation Div. Low-Temperature Phase and Magnetic Interactions in fcc Fe-Cr-Ni Alloys.

Final rept. C. Almasan, T. Datta, R. D. Edge, E. R. Jones, J. W. Cable, and H. M. Ledbetter. 1989, 10p Pub. in Jnl. of Magnetism and Magnetic Materials 80, p329-338 1989.

Keywords: *Low temperature tests, *Phase transformations, *Antiferromagnetism, *Face centered cubic lattices, *Nickel chromium steels, *Iron alloys, Neutron diffraction, Ultrasonic tests, Elastic scattering, Magnetic measurement, Interactions, Cryogenics, Neel temperature perature, Cry SQUID(Detectors). Crystal structure, Reprints.

The low-temperature (5 K < T < 300 K) magnetic properties of a set of nine isostructural fcc Fe-Cr-Ni Froperties of a set of nine isostructural rcc Fe-Cr-Ni (Fe approximately 68 at %, Cr approximately 20 at %, Ni approximately 9 at %) alloys were studied by SQUID magnetometry, neutron diffraction and ultrasonic tech-niques. Type-1 antiferromagnetic (AF) ordering was observed below the Neel temperature, T (sub N). The dc susceptibility, X(T), did not exhibit a simple Curie-Weiss dependence. Above T (sub N), a temperature independent component was observed. T (sub N) was externatically influenced by the lattice parameter. independent component was observed. T (sub N) was systematically influenced by the lattice parameter, a, decreasing from (47.9 + or - 0.5) K to (35.0 + or - 0.5) K as a increased by only 0.25%. The average magnetic moment of approximately 0.6 obtained from neutron scattering was lower than the approximately 1 obtained from the SQUID data. Mean field estimates of antiferromagnetic nearest-neighbors exchange interantiferromagnetic nearest-neighbors exchange interaction (J1) and ferromagnetic second-nearest-neighbors interaction (J2) indicate that (J2/J1) is approximately 1.5, evidence of the RKKY interaction. Only the

external d electrons are responsible for the localized average moment. It may mean that s-d hybridization of the external electrons is weak in the alloys.

Lubricants & Hydraulic Fluids

901,114 PB89-175921 Not available NTIS National Bureau of Standards (IMSE), Gaithersburg, MD. Ceramics Div. Preparative Liquid Chromatographic Method for the Characterization of Minor Constituents of Lu-

bricating Base Olls. Final rept. P. Pei, and S. M. Hsu. 1986, 35p

Pub. in Jnl. of Liquid Chromatography 9, n15 p3311-3345 Nov 86.

Keywords: *Lubricating oils, *Chromatography, *Polarity, *Hydrocarbons, Methodology, Liquids, Separation, Synthesis(Chemistry), Friction, Wear, Oxidation, Molecular structure, Reprints.

In an effort to isolate, identify, and measure the properties of the active ingredients in a lubricating base oil, a high performance liquid chromatography (HPLC) separation scheme has been developed. The preparative mode of production is necessary to yield sufficient amounts of minor constituents for property measurements in terms of friction, wear, and oxidation characteristics in frictions and uncorrected the property of the teristics. In friction and wear control, the polarity of the molecular species is more important than the functional groups in the species. Therefore the design of the separation scheme is based on the relative polarity of separation scientifies based on the relative polarity of various functional groupings. Because the effort is directed towards identifying key components rather than analysis of the major compositions, mass recovery requirement is critical. The separation scheme is divided into two stages. The base oil first undergoes a clay-gel separation to yield the saturates, aromatics, and the polar fractions. The polar fraction then is separated further using a neutral alumina column and the sequential solvent extractions into molecular compound classes of varying polarity. The paper describes the separation scheme and the detailed chemical characterization of the fractions.

Materials Degradation & Fouling

901,115

PB89-147409 Not available NTIS National Bureau of Standards (IMSE), Gaithersburg, MD. Metallurgy Div.
Ultrasonic Characterization of Surface Modified

Layers.

Final rept. B. J. Elkind, M. Rosen, and H. N. G. Wadley. 1987,

Contract DARPA Order-4275

Sponsored by Defense Advanced Research Projects Agency, Arlington, VA. Pub. in Metallurgical Transactions A-Physical Metallur-gy and Materials Science 16, n3 p473-480 1987.

Keywords: *Nondestructive tests, *Solidification, *Steels, *Radiation effects, Surface properties, Martensite, Pearlite, Rayleigh waves, Penetration, Hardness, Depth, Electron beams, Ultrasonic tests, Process control, Monitors, Quench hardening, Reprints.

Nondestructive techniques are required for the in-process characterization of rapidly solidified and sur-face modified layers to fulfill the role of sensors in emerging intelligent materials processing technologies. In steels, where surface modification via directed high energy sources is being investigated for surface hardening, it has been found that a difference race narcening, it has been found that a difference exists in the Rayleigh wave velocity of martensite and pearlite. The difference in velocity can be used to characterize the hardness of a surface modified layer on a pearlite substrate. By varying the Rayleigh wave frequency (and thus the depth of wave penetration) and measuring velocity dispersion, it has also been possible to non-destructively determine the depth of modified surface layers on both AISI 1053 and 1044 steels produced by electron beam melting. produced by electron beam melting.

901.116

PB89-157960 Not available NTIS National Bureau of Standards (NML), Gaithersburg, MD. Surface Science Div.

Electron and Photon

Stimulated Desorption: Probes of Structure and Bonding at Surfaces. Final rept.

T. E. Madey. 1986, 7p Pub. in Science 234, n4774 p316-322 1986.

Keywords: *Surface properties, *Solids, *Radiation damage, *Molecular structure, Photons, Quantitative analysis, Simulation, Chemical bonds, Sorption, Reprints.

Techniques for analyzing the structure and composition of solid surfaces using electron and photon beams often suffer from interferences due to radiation damage. Damage-producing processes compete with information-producing events during measurements, and beam damage can be a serious perturbation in and beam damage can be a serious perturbation in quantitative surface analysis. However, there are also substantial benefits of electron and photon stimulated damage processes for studying molecules on surfaces. Direct information about the geometrical structure of adsorbed species can be obtained from measurements of the angular distributions of ions released by electron or photon stimulated desorption. The distributions of ion processing and determined the release the process. rections of ion emission are determined by orientations of the surface bonds which are ruptured by beam irra-diation. The method of Electron Simulated Desorption Ion Angular Distributions (ESDIAD) has proven particularly useful as a direct tool for characterizing local molecular structure at surfaces. Moreover, photon stimulated desorption studies using synchrotron radiation are revealing the fundamental electronic excitations which lead to bond-breaking processes at surfaces.

Miscellaneous Materials

901.117

PB89-186407 Not available NTIS National Bureau of Standards (NEL), Gaithersburg, MD. Building Environment Div.

Experimental Determination of Forced Convection Evaporative Heat Transfer Coefficients for Non-Azeotropic Refrigerant Mixtures.

Rinal rept.

R. Radermacher, H. Ross, and D. Didion. 1983, 7p

Pub. in Proceedings of Winter Annual Meeting of the

American Society of Mechanical Engineers, Boston,

MA., November 13-18, 1983, p1-7.

Keywords: *Refrigerants, *Test facilities, *Heat transfer coefficient, Convection, Mixtures, Evaporators, Two phase flow.

Recently energy conservation requirements spurred interest in nonazeotropic refrigerant mixtures, because such mixtures can improve theoretically the COP of certain refrigerant cycles. The two phase heat transfer coefficient of such mixtures under forced convection conditions is virtually unknown. An experimental rig has been constructed to investigate whether it is possible to predict the heat transfer coefficient of the mixture based on the coefficients of the components. Initially data was taken on R-22 and compared to literature data and to existing predictive correlations. Good agreement was found with the literature's data on forced convection, single phase heat transfer correlations, and some two phase evaporative correlations.

901.118

PB89-229041 PC A06/MF A01 National Inst. of Standards and Technology (NEL), Gaithersburg, MD. Center for Building Technology.

Experimental Investigation and Modeling of the Flow Rate of Refrigerant 22 Through the Short Tube Restrictor.
D. A. Aaron, and P. A. Domanski. Jul 89, 102p
NISTIR-89/4120

Sponsored by Department of Energy, Washington, DC. Office of Buildings and Community Systems.

Keywords: *Refrigerants, *Models, *Flow rate, *Tubes, Air conditioners, Heat pumps, Constrictions, Flow measurement, Experimental data, Pressure, Chamfering.

Miscellaneous Materials

Refrigerant flow through the short tube expansion device was theoretically and experimentally investigated. The analysis was limited to initially subcooled R22 flowing through short tubes with 5 L/D 20. Flow dependency upon upstream subcooling, upstream pres-sure, downstream pressure, length, diameter, en-trance chamfering and exit chamfering was deter-mined. A flow model and flow charts were developed.

Nonferrous Metals & Alloys

901,119 PATENT-4 804 446 Not available NTIS National Bureau of Standards, Gaithersburg, MD. Electrodeposition of Chromium from a Trivalent Electrolyte. Patent.

D. S. Lashmore, I. Weisshaus, and E. NamGoong. Filed 19 Sep 86, patented 14 Feb 89, 14p PB89-160592, PAT-APPL-6-909 433

This Government-owned invention available for U.S. licensing and, possibly, for foreign licensing. Copy of patent available Commissioner of Patents, Washington, DC 20231 \$1.50.

Keywords: *Chromium, *Coatings, *Patents, Electrodeposition, Electrodes, Electrolytes.

An electrodeposition process and a bath therefore are disclosed for performing the electrodeposition of hard smooth coatings of trivalent chromium. The electrodeposition process is accomplished energy efficiently.

The bath includes chromium chloride as a source of chromium, citric acid to complex the chromium, and a wetting agent which is preferably Triton x-100. Preferably, bromide is also provided in the solution to maintain the hexavalent chromium production at the anode at a low level. Ammonium chloride is also preferably provided to improve the conductivity and also the curprovided to improve the conductivity and also the current distribution in the bath. Boric acid is provided to advance the reaction kinetics. The pH of the bath is maintained at approximately 4.0 and the temperature is maintained at approximately 35 C. Either a direct current or pulsed current is used for the deposition process. Hard smooth coatings of trivalent chromium are deposited through use of the process and the bath of the claimed invention.

901,120 PB89-146690 Not available NTIS National Bureau of Standards (IMSE), Gaithersburg,

MD. Polymers Div.
Electronic, Magnetic, Superconducting and Amorphous-Forming Properties Versus Stability of the Ti-Fe, Zr-Ru and Hf-Os Ordered Alloys.

Final rept.

R. Kuentzler, and R. M. Waterstrat. 1986, 15p Sponsored by American Dental Association Health Foundation, Chicago, IL.

Pub. in Jnl. of Less-Common Met. 125, p261-275 Nov

Keywords: *Intermetallics, *Superconductivity, *Magnetic susceptibility, Titanium, Iron, Zirconium, Ruthenium, Hafnium, Osmium, Magnesium, Zinc, Phase transformations, Specific heat, Electron transitions, Reprints, Ordered alloys.

The electronic, magnetic, and superconducting properties of the Ti-Fe, Zr-Ru and Hf-Os ordered alloys of the B2-type and MgZn sub 2-type structures are described using original low temperature specific heat and susceptibility results and known magnetization data. The stability of the B2-type ordered alloys, including that of Ti-Fe, ZrRu and HfOs is discussed. The high stability of the B2-type ordered alloys having an average number of 'd' electrons, N sub d, equal or nearly equal to 5 (which corresponds to a Fermi level ying in a deep valley of the band structure) is accomnearly equal to 5 (which corresponds to a Fermi level lying in a deep valley of the band structure) is accompanied by a low electronic specific heat coefficient gamma, no magnetic order, no superconductivity and poor glass-forming ability. On the other hand, deviations from N sub d = 5 produce a decrease of the stability, high gamma values, appearance of magnetic order and martensitic transformations leading to superconductivity and good classe forming ability. perconductivity and good glass-forming ability.

901,121 PB89-146948 Not available NTIS National Bureau of Standards (IMSE), Boulder, CO. Fracture and Deformation Div.

Ultrasonic Texture Analysis for Polycrystalline Aggregates of Cubic Materials Displaying Orthotropic Symmetry.

Final rept. P. P. Delsanto, R. B. Mignogna, and A. V. Clark. 1986, 9p

Sponsored by Naval Research Lab., Washington, DC. Pub. in Nondestructive Characterization of Materials II, p535-543 1986.

Keywords: *Nondestructive tests, *Ultrasonic frequencies, *Steels, *Aluminum alloys, Texture, Crystal structure, Reprints, *Raleigh waves.

The general perturbation formalism for the propagation of Raleigh waves on the surface of initially deformed anisotropic material plates is applied to the investigation of material texture. The preferential alignment of crystallographic axes in a polycrystalline material can be conveniently described in terms of their orientation distribution function. The case of an orthotro-pic distribution of cubic crystallites, which occurs, for example, in aluminum and steel alloys is considered. It was shown that the measured values of the Raleigh wave phase velocity at these different angles on the material plate can be used for the determination of the three coefficients W sub 400, W sub 420 and W sub 400 was a sub-440 which completely characterize the orientation distribution in the case considered.

901.122

PB89-147102 Not available NTIS National Bureau of Standards (NEL), Gaithersburg, MD. Chemical Process Metrology Div.

Sputter Deposition of Icosahedral Al-Mn and Al-Mn-SI. Final rept

K. G. Kreider, F. S. Biancaniello, and M. J. Kaufman.

1987, 6p Pub. in Scripta Metallurgica 21, n5 p657-662 May 87.

Keywords: *Thin films, *Sputtering, *Crystals, *Intermetallics, Aluminum, Manganese, Microscopy, X-ray analysis, Hexagonal lattices, Morphology, Fabrication, Reprints, Icosahedral.

Thin-film sputtered deposits of AI with 17.4% (atomic) Mn and AI with 20.2% Mn plus 4.7% Si were produced Mn and AI with 20.2% Mn plus 4.7% SI were produced at temperatures ranging from -80 deg C to 420 deg C from prealloyed targets. These films were analyzed using electron microscopy and x-ray diffraction to determine their structures and compositions. The Icosahedral quasicrystalline phase was observed in the films produced at the lower temperatures whereas a mixture of the quasicrystal and the hexagonal Al10Mn3 (Al9Mn3Si) was observed at the higher temperatures. The fabrication technique as well as the physical characterization of the films are described.

901,123

PB89-147383 Not available NTIS National Bureau of Standards (IMSE), Gaithersburg, MD. Metallurgy Div.

Quasicrystals with 1-D Translational Periodicity

and a Ten-Fold Rotation Axis.

Final rept. L. Bendersky. 1986, 4p Pub. in Rapidly Solidified Alloys and Their Mechanical and Magnetic Properties, p237-240 1986.

Keywords: *Quench hardening, *Intermetallics, *Aluminum alloys, *Manganese alloys, *Crystal lattices, Microscopy, Mechanical properties, Reprints, Icosahe-

Studies of phase formation in rapidly solidified Al-Mn alloys (composition range 18-22 at % Mn) show that an icosahedral phase is replaced by another noncrystallographic phase, a decagonal phase. The decagonal phase is another example of quasicrystal: It has a noncrystallographic point group (10/m or 10/mmm) together with long-range orientational order and one-dimensional symmetry. The decagonal phase is an intermediate phase between an icosahedral phase and a crystal both from the symmetry and from the solidifia crystal both from the symmetry and from the solidifi-cation condition points of view.

901.124

PB89-150957 Not available NTIS National Bureau of Standards (IMSE), Boulder, CO. Fracture and Deformation Div.

Ultrasonic Determination of Absolute Stresses in Aluminum and Steel Alloys.

Final rept.
A. V. Clark, J. C. Moulder, R. B. Mignogna, and P. P. Delsanto. 1986, 8p
Sponsored by Naval Sea Systems Command, Wash-

ington, DC.

Pub. in Residual Stresses in Science and Technology, Garmisch-Partenkirchen, Federal Republic of Germany, v1 p207-214 1986.

Keywords: *Ultrasonic tests, *Weldments, *Aluminum, *Steels, *Plates(Structural members), *Residual stress, Strain gages, Piezoelectricity, Electromagnetic fields, Transducers, Measurement, Acoustics, Residual

Components of plane stress have been measured with ultrasonic techniques for welded aluminum and steel alloy plates. Measurements of the difference of princi-pal stresses were performed using both a piezoelectric transducer and an electromagnetic acoustic transducer (EMAT) with good agreement. The EMAT was used to measure arrival times of ultrasonic shear waves along the centerline of baseplates before and after welding. Subject to certain assumptions, changes in arrival times, at a given location, are due to principal stresses at that location. For the aluminum alloy plates these EMAT measurements of principal stresses were within 20 MPa of strain gage values. For the steel plates, the difference between EMAT and strain gage results was about 20%. A second technique used to obtain the normal stress in welded aluminum alloy plates is described.

PB89-157432 Not available NTIS National Bureau of Standards (IMSE), Gaithersburg, MD. Metallurgy Div. Stable and Metastable TI-Nb Phase Diagrams.

Final rept. D. L. Moffat, and U. R. Kattner. 1988, 9p Pub. in Metallurgical Transactions A 19A, p2389-2397

Keywords: *Titanium alloys, *Niobium, *Phase transformations, Thermal degradation, Chemical composition, Thermodynamics, Metastable state, Equilibrium, Vanadium, Molybdenum, Zirconium, Reprints.

The phase transformations which occur in the Ti-Nb binary alloy system have been discussed in two recent papers. The phase relationships were investigated by varying alloy composition and thermal history. In the paper, these results are summarized in complete and thermodynamically consistent calculations of the stable and metastable phase diagrams. The calculations of the metastable equilibria are relevant to the Ti-V and Ti-Mo systems, as well as to several other titanium and zirconium-based transition metal alloy sys-

901,126 PB89-157598 Not available NTIS National Bureau of Standards (IMSE), Gaithersburg,

MD. Metallurgy Div.
Ostwald Ripening in a System with a High Volume
Fraction of Coarsening Phase.

Final rept.

Final rept.

S. C. Hardy, and P. W. Voorhees. 1988, 9p
Sponsored by National Aeronautics and Space Administration, Washington, DC.
Pub. in Metallurgical Transactions A 19A, p2713-2721

Nov 88.

Keywords: *Lead alloys, *Tin, *Particle size distribution, *Sintering, Kinetics, Eutectics, Liquid phases, Reprints, Ostwald ripening.

Experiments on the coarsening behavior of two-phase mixtures in a model Pb-Sn system are reported. This system fulfills most of the assumptions of theory and has the particular advantage that all the materials parameters necessary for a comparison between the ex-perimentally measured and theoretically predicted coarsening kinetics are known. The coarsening of Snrich and Pb-rich solid phases was examined in contact with eutectic liquid in the volume fraction solid range above approximately 0.6 where the development of a solid skeletal structure inhibits sedimentation. Particle intercept distributions are measured and found to be time independent when scaled by the average inter-cept. This invariance is interpreted as evidence that scale factor coarsening is present. The intercept distri-butions are in good agreement with the predictions of

Nonferrous Metals & Allovs

theory. Measurements of average intercept diameter as a function of time establish unambiguously that the coarsening follows the theoretically predicted t sup(1/3) kinetics. The coarsening rate constants are measurements. ured as a function of volume fraction solid and are found to exceed the values calculated from theory using the known thermophysical properties of the Pb Sn system by factors ranging from approximately 2 to

901,127 PB89-157606 PB89-157606 Not available NTIS National Bureau of Standards (IMSE), Gaithersburg, MD.

Observations on Crystal Defects Associated with Diffusion induced Grain Boundary Migration in Cu-

S. A. Hackney, F. S. Biancaniello, D. N. Yoon, and C. A. Handwerker, 1986, 6p Pub. in Scripta Metallurgica 20, n6 p937-942 Jun 86.

Keywords: *Copper, *Crystal defects, *Zinc, *Electron microscopy, Diffusion, Grain boundanes, Brasses, Transmission, Migrations, Dislocations(Materials), Gases, Reprints.

High purity copper foils (.025 mm thick) have been exposed to zinc vapor from an 11 at% zinc brass at 360 deg C. Standard transmission electron microscopy reveals that diffusion induced grain boundary migration (DIGM) has occurred at an average rate of 1.85 x 10(sup -11) m/s over the first 30 hours. The grain boundary structure, grain boundary morphology, and matrix dislocations associated with the DIGM phenomena have been studied in detail. The following general observations have been made: (1) the region over which the grain boundary has migrated is alloyed with zinc; (2) a 'wall' of dislocations marks the original position of the grain boundary; (3) the grain boundary structure includes a high density of defects with a step character having a maximum height of 3 nm; and (4) the matrix dislocation density is highest directly in front of the migrated grain boundary.

901,128 PB89-157614 PB89-157614 Not available NTIS National Bureau of Standards (IMSE), Gaithersburg,

MD. Metallurgy Div.
Migration of Liquid Film and Grain Boundary in MoNi Induced by W Diffusion.

Final rept.

H. K. Kang, S. Hackney, and D. N. Yoon. 1988, 5p Pub. in Acta Metallurgica 36, n3 p695-699 1988.

Keywords: *Liquids, *Migrations, *Grain boundaries, *Nickel alloys, Molybdenum, Diffusion, Heat treatment, Sintenng, Tungsten, Solid solutions, Coherence,

The liquid films and grain boundaries in liquid phase sintered Mo-Ni alloy are observed to migrate during heat-treatment after adding W to the liquid matrix. Behind the migrating boundaries form Mo-Ni-W solid solution with the W concentration decreasing with the migration distance because of W depletion in the liquid matrix. The migration rate during the heat-treatment at 1540 deg C after adding W decreases with the decreasing pretreatment sintering temperature. When the sintering temperature is 1420 deg C, the migration rate is almost reduced to 0. Under this condition, the coherency strain due to the simultaneous diffusion of W and Ni into the grain surfaces is estimated to be almost 0. The results thus lead to the conclusion that the coherency strain due to lattice diffusion is the driving force for the liquid film and grain boundary migra-

901,129 PB89-157622 PB89-157622 Not available NTIS
National Bureau of Standards (IMSE), Gaithersburg,
MD. Metallurgy Div.
Metastable Phase Production and Transformation

in Al-Ge Alloy Films by Rapid Crystallization and Annealing Treatments.

Final rept. M. J. Kaufman, J. E. Cunningham, and H. L. Fraser.

1987, 12p Pub. in Acta Metallurgica 35, n5 p1181-1192 1987.

Keywords: *Crystallization, *Aluminum alloys, *Germanium, *Quenching(Cooling), *Electron beam, Transmission, Electron microscopy, Films, Annealing, Metastable state, Nucleation, Kinetics, Reprints.

Metastable crystalline phases have been produced in Al-Ge alloy films which initially were either entirely or

partially amorphous by rapid crystallization and subsequent annealing treatments. The studies were conducted directly in a transmission electron microscope where the electron beam was used as a local heating source to effect the reactions. The types and se-quences of transformations are described and discussed in terms of competitive nucleation and growth kinetics. In addition, the results are related to those previously obtained on similar alloys subjected to rapid quenching and high undercooling treatments.

PB89-157630 Not available NTIS National Bureau of Standards (IMSE), Gaithersburg, MD. Metallurgy Div.

Experimental Observations on the Initiation of

DIGM (Diffusion Induced Grain Boundary Migration).

Final rept.

Pub. in Scripta Metallurgica 20, n10 p1385-1388 Oct

Keywords: *Microstructure, *Grain boundaries, *Diffusion, *Copper, *Zinc, Migrations, Kinetics, Crystal, Initiation, Dislocations (Materials), Reprints.

Diffusion induced grain boundary migration (DIGM) is now a well recognized phenomena which occurs during multi-component diffusion in many systems. Kinetic theories of diffusional mixing in crystalline solids will have to be modified to include the contributions of DIGM and the related process of diffusion induced recrystallization. The underlying driving force for this important process has been the topic of a great deal of speculation. The theoretical approach to the process has far outstripped the necessary experimental observations. One critical area of experimentation which has been neglected is the microstructural observations of the physical processes involved in the initiation of DIGM. The early observations from a study of DIGM initiation are presented for the Cu-Zn system.

PB89-157648 Not available NTIS Mational Bureau of Standards (NEL), Gaithersburg, MD. Semiconductor Electronics Div. Structural Unit in Icosahedral MnAISI and MnAI.

Final rept. Y. Ma, E. A. Stern, and C. E. Bouldin. 1986, 4p Pub. in Physical Review Letters 57, n13 p1611-1614, 29 Sep 86.

Keywords: *X ray analysis, *Manganese, *Aluminum alloys, *Silicon, *Crystallization, Orthorhombic lattices, Quenching(Cooling), Reprints.

EXAFS measurements were made on icosahedral MnAl and MnSiAl, and on the standards alpha-phase of MnSiAl and orthorhombic phase of MnAl6. Experimental evidence is presented that a cage of Mn atoms at the vertices of an icosahedron is the structural unit in the icosahedral MnSiAl and MnAl phases. The connections among these icosahedral units and between them and the Al atoms are different in the icosahedral phases and in the alpha-phase. As in the alpha-phase, the Mn icosahedra do not share vertices in the icosahedral phases; i.e., they are separated from one another. It is suggested that the i-phase grows by randomly nucleating together Mn icosahedra along their 20 threefold directions, as allowed by local steric con-

901,132 PB89-157671 Not available NTIS National Bureau of Standards (NEL), Gaithersburg, MD. Automated Production Technology Div. Dynamic Young's Modulus Measurements in Metallic Materials: Results of an Interlaboratory Test-

ing Program.

Final rept. A. Wolfenden, M. R. Harmouche, G. V. Blessing, Y. T. Chen, P. Terranova, V. Dayal, V. K. Kinra, J. W. Lemmens, R. R. Phillips, J. S. Smith, P. Mahmoodi, and R. J. Wann. 1989, 12p Pub. in Jnl. of Testing and Evaluation 17, n1 p2-13 Jan

Keywords: *Modulus of elasticity, *Test facilities, *Nickel alloys, Metals, Measurement, Comparison, Reprints.

The results of a round-robin testing study are presented for measurements of dynamic Young's modulus in two nickel-based alloys. The Interlaboratory Testing Program involved six types of apparatus, six different

organizations, and specimens from a well-documented source. All the techniques yielded values of dynamic Young's modulus that agreed within 1.6% of each other. For Incone alloy 600 the dynamic modulus was 213.5 GPa with a standard deviation of 3.6 GPa; for Incoloy alloy 907 the corresponding values were 158.6 and 2.2 GPa, respectively. No significant effect of frequency over the range 780 Hz to 15 MHz was found.

901,133 PB89-157804 Not available NTIS National Bureau of Standards (IMSE), Boulder, CO. Fracture and Deformation Div.

Influence of Dislocation Density on the Ductile-Brittle Transition in bcc Metals. Final rept.

I. H. Lin, and R. Thomson. 1986, 4p Pub. in Scripta Metallurgica 20, n10 p1367-1370 Oct 86.

Keywords: *Body centered cubic lattices, *Ductile brittle transition, *Crack propagation, *Dislocations(Materials), *Metals, Emission, Fractures(Materials), Reprints.

The purpose of the paper is to show that the local k-field at the crack tip at which dislocation emission takes place is lowered by the action of external dislocation sources, and that this mechanism leads to the result that sufficiently high concentrations of dislocations and their sources in the influence field of the crack tip will limit the ability of the crack to cleave.

Not available NTIS PB89-157911 National Bureau of Standards (IMSE), Gaithersburg,

MD. Metallurgy Div.
Directional invariance of Grain Boundary Migration in the Pb-Sn Cellular Transformation and the Tu-Turnbuii Hysteresis.

Final rept. S. A. Hackney, and F. S. Biancaniello. 1986, 6p Pub. in Scripta Metallurgica 20, n10 p1417-1422 Oct

Keywords: *Lead alloys, *Tin, *Grain boundaries, *Migrations, Solid solutions, Thermodynamic properties, Hysteresis, Cellular materials, Porosity, Diffusion, Dissolving, Reprints.

The cellular dissolution process in Pb-5.5% Sn first studied by Tu and Turnbull has been reexamined using instrumental techniques. It has been determined that cell dissolution by grain boundary migration does not cell dissolution by grain boundary migration does not recreate a homogeneous solid solution. This observation has been interpreted in terms of a thermodynamic hysteresis. The driving force for dissolution first proposed by Tu and Turnbull has been modified to include the macroscopic grain boundary curvature term. This allows a direct contrast between the forced oscillation of the grain boundary in the cellular transformation and that studied in DIGM. A simple thermodynamic evolution criteria reveals that the difference in behavior tion criteria reveals that the difference in behavior during dissolution between the two phenomena may be due to the presence of the precipitate phase rather than a difference in migration mechanism.

901,135 PB89-157986 Not available NTIS Not available N16
National Bureau of Standards (NEL), Gaithersburg,
MD. Mathematical Analysis Div.
ASM/NBS (American Society for Metals/National
Bureau of Standards) Numerical and Graphical Da-

tabase for Binary Alloy Phase Diagrams. Final rept.

J. S. Sims, D. F. Redmiles, and J. B. Clark, 1988. 16p

Pub. in Computerized Metallurgical Databases, p119-134 1988.

Keywords: *Alloys, *Metals, *Data retrieval, *Phase diagrams, Surveys, Crystal structure, Reprints.

Under the ASM/NBS program on alloy phase diagrams, a comprehensive relational database of binary alloy phase diagrams has been developed. The phase diagrams, critical numerical data and crystal structure data of the phases of nearly 1600 binary alloy systems can be accessed by a user friendly database management program. Important features of the database program are: (a) Search and display of all phase diagram graphics prepared for the 'Bulletin of Alloy Phase Diagrams'; (b) Search and display of the critical numerical data summarizing the 'structure' of the phase diagram - the phase reactions, the reaction temperatures, the

Nonferrous Metals & Alloys

compositions of the reacting phases, and the crystal structure data of the solid phases.

901,136 PB89-172324 Not available NTIS National Bureau of Standards (IMSE), Gaithersburg, MD. Metallurgy Div. Stable and Metastable Phase Equilibria in the Al-Mn System.

Final rept. J. L. Murray, L. A. Bendersky, F. S. Biancaniello, A. J. McAlister, D. L. Moffat, and R. J. Schaefer. 1987,

Pub. in Metallurgical Transactions A-Physical Metallurgy and Materials Science 18, n3 p385-392 1987.

Keywords: *Aluminum, *Manganese, *Phase diagrams, Thermodynamics, Mathematical models, Equilibrium, Stoichiometry, Liquidus, Quenching(Cooling), Stability, Metastable state, Thermal analysis, Reprints.

The aim of the present investigation was resolution of certain obscure features of the Al4Mn phase diagram. The experimental approach was guided by assessment of the previous literature and modeling of the thermodynamics of the system. It has been shown that the places of approximate, strainburgets, Al4Mn two phases of approximate stoichiometry Al4Mn (lambda and mu) are present in stable equilibrium, lambda forming by a peritectoid reaction at 693 + or C. The liquidus and invariant reactions as proposed by Goedecke and Koester have been verified. A map has been made of the successive non-equilibrium phase transformations of as-splat-quenched alloys. Finally, the thermodynamic calculation of the phase diagram allows interpretation of complex reaction sequences during cooling in terms of a catalog of all the metastable invariant reactions involving (Al), Al6Mn, lambda, mu, theta, and Al11Mn4 phases.

901,137 PB89-172332 PB69-172332 Not available NTIS
National Bureau of Standards (IMSE), Gaithersburg, MD. Metallurgy Div.
Solidification of Aluminum-Manganese Powders.

B. A. Mueller, R. J. Schaefer, and J. H. Perepezko.

1987, 9p Pub. in Jnl. of Materials Research 2, n6 p809-817 Nov/Dec 87.

Keywords: *Aluminum, *Manganese, *Powder(Particles), *Quenching(Cooling), Phase Diagrams, Metastable state, Nucleation, Temperature, Crystallization, Reprints.

The solidification behavior of Al-Mn powders was studied as a function of cooling rate and Mn content. It was found that the phases present in the powder differed from those expected at equilibrium. The Al6Mn phase was absent due to its failure to nucleate, and in the more concentrated and rapidly cooled powders the metastable quasicrystal phases were present. Nucleation temperatures measured in alloys cooled at 25 C/ sec are believed to represent formation of the icosahedral phase, which subsequently transforms to the decagonal phase.

Not available NTIS PB89-176457 National Bureau of Standards (IMSE), Gaithersburg, MD. Metallurgy Div.
Kinetics of Resolidification.

J. H. Perepezko, and W. J. Boettinger. 1987, 40p Pub. in Proceedings of ASM (American Society for Metals) Materials Science Seminar: Surface Alloying by Ion, Electron, and Laser Beams, Toronto, Ontario, Canada, October 12-13, 1985, p51-90 1987.

Keywords: *Solidification, *Kinetics, *Surface finishing, *Metal alloys, *Lasers, *Ion beams, *Electron beams, *Microstructure, Solubility, Metastable state, Free energy, Morphology, Heat transfer, Phase dia-

While ion, laser and electron beam surface treatments involve a variety of experimental conditions, they share some important common kinetic and thermodynamic features. The alloy additions that are incorporated into the surface modified solid region by the various processes are often in metastable states of relatively high free energy. An examination of the metastable equilibrium features of phase diagrams can identify the possi-ble choice of product structures depending on the particular constraints imposed on the system and the controlling phase selection kinetics during nucleation.

Under rapid rates the analysis of resolidification involves the use of response functions to treat the liquidsolid interface conditions during solute trapping. These functions, when combined with solute redistribution and heat flow analysis, provide a basis for the prediction and analysis of microstructural evolution in sur-face treated layers in terms of size scale and morphol-ogy. The application of metastable equilibna and kinetics analysis offers an effective strategy for the genera-tion of tailored microstructures to optimize the results of surface treatments.

901,139 PB89-176465 PB89-176465 Not available NTIS National Bureau of Standards (IMSE), Gaithersburg, MD. Metallurgy Div.
Undercooling and Microstructural Evolution in
Glass Forming Alloys.

M. J. Kaufman, and H. L. Fraser. 1987, 20p Pub. in Undercooled Alloy Phases, Proceedings of Hume-Rothery Memorial Symposium, p249-268 1987.

Keywords: *Aluminum, *Amorphous materials, *Glass, *Solidification, *Nucleation, *Recalescence, Powder(Particles), Forecasting, Computation, Crystallization, Germanium, Metal alloys, Microstructure.

The microstructural evolution of highly undercooled submicron powders of a glass forming alloy (Al-30Ge) is considered. A simple calculation is developed for predicting the number of alpha-Al crystals that form during solidification using classical nucleation and growth equations appropriate for glass forming systems. In addition, a reasonable agreement between theory and experiment is achieved only when a solidliquid temperature gradient, generated by recalescence effects, is considered.

901,140 PB89-176911 Not available NTIS National Bureau of Standards (IMSE), Gaithersburg, MD. Metallurgy Div.

Dynamic MicroIndentation Apparatus for Materials Characterization. Final rept.

R. S. Polvani, A. W. Ruff, and E. P. Whitenton. 1988,

5p Pub. in Jnl. of Testing and Evaluation 16, n1 p12-16

Keywords: *Indentation hardness tests, *Aluminum, *Composite materials, *Equipment, Dynamic tests, Loads(Forces), Penetration, Wear, Mechanical properties, Time, Reprints.

A microindentation system is described that provides a new approach to dynamic mechanical testing. The in-dentation is characterized in terms of continuous measurements of applied load and penetration depth. The indentation can be performed over a wide range of loading times from hours down to milliseconds. The shape of the loading waveform can also be selected. The deformation energy can be measured and partitioned into elastic, plastic, and anelastic components. The apparatus is also able to perform conventional hardness testing and can be used to determine conventional mechanical properties.

901,141 PB89-177026 PB89-177026 Not available NTIS National Bureau of Standards (NML), Gaithersburg, MD. Radiation Physics Div.
Electron Mean Free Path Calculations Using a Model Dielectric Function.

Final rept.

D. R. Penn. 1987, 5p Pub. in Physical Review B-Condensed Matter 35, n2 p482-486 1987.

Keywords: *Electrons, *Mean free path, *Computation, Dielectric properties, Copper, Silver, Gold, Aluminum, Energy, Gas laws, Reprints.

The anelastic electron mean free path as a function of energy is calculated for Cu, Ag, Au, and Al. The calculations are based on a model dielectric function, epsilon(q,w), which is obtained from a modification of the statistical approximation. In this approach epsilon(o,w) is determined by the experimentally measured optical dielectric function. Calculated mean free paths are compared to experimental data and to other theories.

901,142 PB89-179170

Not available NTIS

National Bureau of Standards (IMSE), Gaithersburg, MD. Metallurgy Div.

Process Control during High Pressure Atomization.

Final rept.
S. D. Ridder, and F. S. Biancaniello. 1988, 5p
Pub. in Materials Science and Engineering 98, p47-51

Keywords: *Liquid metals, *Powder(Particles), *Process control, *High pressure tests, *Atomizing, *Rare gases, Metal alloys, Solidification, Particle size, Drops (Liquids), High speed photography, Lasers, Tin alloys Poports alloys, Reprints.

High Pressure Inert Gas Atomization (HPIGA) has been studied using various metal alloy systems. The high yield of ultrafine (less than 45 micrometers) powder produced using HPIGA makes it an ideal test system for rapidly solidified metal powder. High speed photography and laser scattering techniques have been applied to study droplet formation and measure powder size with the intent of future feedback and control of particle size during atomization. Liquid metal droplet formation will be discussed as well as on-line particle size measurement and control. particle size measurement and control.

901.143 PB89-179840 Not available NTIS Not available NTIS
National Bureau of Standards (NEL), Boulder, CO.
Electromagnetic Fields Div.
Transmission Loss through 6061 T-6 Aluminum
Using a Pulsed Eddy Current Source.

Final rept. K. H. Cavcey. 1989, 3p Pub. in Materials Evaluation 47, p216-218 Feb 89.

Keywords: *Aluminum, *Aircraft, *Nondestructive tests, *Eddy currents, *Electric conductors, Pulse analyzers, Electromagnetic testing, Thickness, Frequency analyzers, Reprints, Aluminum T-6.

One method of nondestructive testing in conductors is one inetriod of nondestructive testing in conductors in that of pulsed eddy currents (PEC). The method involves the propagation of a modified electromagnetic field through the medium, resulting in attenuation and time delay of the pulse. The paper outlines work that was done to determine the frequency response for seven different thicknesses of aircraft-grade 6061 T-6 aluminum using a PEC source. aluminum using a PEC source.

901,144 PB89-186316 Not available NTIS National Bureau of Standards (IMSE), Gaithersburg,

MD. Metallurgy Div.

Formation and Stability Range of the G Phase in the Aluminum-Manganese System.

Final rept. R. J. Schaefer, F. S. Biancaniello, and J. W. Cahn.

1986, 6p Pub. in Scripta Metallurgica 20, n10 p1439-1444 1986.

Keywords: *Aluminum alloys, *Manganese, *Phase transformation, *Solidification, Metastable state, Crystal structure, Nucleation, Eutectics, Stability, Microstructure, Quenching(Cooling), Reprints.

The G phase of Al-Mn, which has until now been considered to be metastable, is demonstrated to actually be a stable phase forming by a pentectoid reaction be-tween 490 and 550 C. The growth of the G phase is extremely slow, but by rapid solidification the rate of nucleation of the G phase is greatly increased so that the transformation is almost complete after 1000 hours at 400 C. The G phase contains icosahedral clusters of atoms similar to those proposed in some models of the Al-Mn icosahedral phase.

901.145

PB89-186324 Not available NTIS National Bureau of Standards (IMSE), Gaithersburg, MD. Metallurgy Div. Nucleation and Growth of Aperiodic Crystals In

Aluminum Alloys.

Rinal rept.
R. J. Schaefer, L. A. Bendersky, and F. S.
Biancaniello. 1986, 10p
Pub. in Jnl. de Physique 47, nC-3 p311-320 1986.

Keywords: *Aluminum alloys, *Manganese, *Nucleation, *Solidification, Microstructure, Eutectics, Silicon, Crystal structure, Dendritic crystals, Phase transformation, Quenching(Cooling), Reprints.

Nonferrous Metals & Allovs

The icosahedral and decagonal aperiodic phases dominate the microstructures of rapidly solidified Al-Mn alloys because of their nucleation and growth behavior, which differs substantially from that of the equilibrium phases. Electron beam surface melting can be used to produce a wide range of solidification conditions, in which the different stages of the nucleation and growth processes can be observed. It is found that the icosahedral phase nucleates abundantly in supercooled Al-Mn melts, and that the decagonal phase is subsequently nucleated by the icosahedral phase. Addition of Si to the Al-Mn alloys suppresses formation of the decagonal phase, but in these alloys the hexagonal beta phase can grow rapidly.

901,146 PB89-186332 Not available NTIS National Bureau of Standards (IMSE), Gaithersburg, MD. Metallurgy Div.

Replacement of Icosahedral Al-Mn by Decagonal Phase.

Final rept.

R. J. Schaefer, and L. Bendersky. 1986, 6p Pub. in Scripta Metallurgica 20, n5 p745-750 May 86.

Keywords: *Aluminum alloys, *Manganese, *Microstructure, *Solidification, *Crysta! structure, Phase transformation, Nucleation, Quenching(Cooling), Re-

It is concluded from microstructural evidence that the decagonal T phase is nucleated epitaxially by the icosahedral phase. At low cooling rates, the T phase grows and completely replaces the icosahedral phase, while at high cooling rates the icosahedral phase is preserved. Even in samples where none of the icosa-hedral phase is found, its presence at an early stage of solidification is revealed by the specific geometrical arrangement and orientational variants of the T phase crystals.

901,147 PB89-201321 PC A06/MF A01 National Inst. of Standards and Technology (IMSE),

Gaithersburg, MD. Metallurgy Div.
Institute for Materials Science and Engineering:
Metallurgy, Technical Activities 1988.

Annual rept.

G. N. Pugh, and J. H. Smith. Dec 88, 121p NISTIR-88/3843

See also report for 1987, PB88-157722.

Keywords: *Metallurgy, *Corrosion, Processing, Metals, Alloys, Mechanical properties, Chemical properties, Wear, Electrodeposition, Magnetic materials, Detectors, Technical activities, Metals processing.

The report summarizes the FY 1988 activities of the Metallurgy Division of the National Institute of Standards and Technology (NIST). The research centers upon the structure-processing-properties relations of metals and alloys and on the methods of their measurement. The activities also include the generation and evaluation of critical materials data. Efforts comprise studies of metallurgical processing, corrosion, me-chanical properties, electrodeposition, process sensors, high temperature reactions and magnetic materials. The work described also includes four cooperative programs with American professional societies and inprograms with American professional societies and in-dustry: the National Association of Corrosion Engi-neers (NACE) - NIST Corrosion Data Program, the Alu-minum Association - NIST Temperature Sensor Pro-gram, the American Iron and Steel Institute (AISI) -NIST Steel Sensor Program, and the ASM INTERNA-TIONAL (ASM) - NIST Alloy Phase Diagram Program.

PB89-201693 Not available NTIS National Bureau of Standards (IMSE), Gaithersburg, MD. Reactor Radiation Div.

Magnetic Correlations in an Amorphous Gd-Al Spin Glass.

Final rept.

M. L. Spano, R. J. Gambino, S. K. Hasanain, T. R. McGuire, S. J. Pickart, and J. J. Rhyne. 1987, 3p Pub. in Jnl. of Applied Physics 61, n8 p3639-3641

Keywords: *Neutron scattering, *Thin films, *Gadolinium, *Aluminum alloys, Sputtering, Lorentz transformations, Ferromagnetism, Spin orbit interactions, Temperature, Rare earth elements, Reprints.

Small angle neutron scattering (SANS) as well as magnetization measurements have been made on a sputtered film of Gd43Al57. The low field susceptibility

peaks at a freezing temperature, T sub f, of 33 K. It agrees well with the SANS data, which shows a peak in the intensity at this temperature for the lowest Qs measured. The SANS lineshapes are unusual in that they can be fitted with a Lorentzian-squared cross section with dissimilar correlation lengths. The Lorentzian correlation length peaks near 35 K at a value of approximately 14 angstroms, while the Lorentziansquared correlation length exhibits a large, essentially resolution-limited value up to temperatures several times T sub f. These results are consistent with the coexistence of finite static spin clusters with relatively long range ferromagnetic correlations.

901,149 PB89-201701 Not available NTIS National Bureau of Standards (IMSE), Gaithersburg, MD. Reactor Radiation Div.
Neutron Scattering Study of the Spin Ordering in Amorphous Tb45Fe55 and Tb25Fe75.

Final rept.

M. L. Spano, and J. J. Rhyne. 1987, 3p Pub. in Jnl. of Applied Physics 61, n8 p4100-4102 1987.

Keywords: "Neutron scattering, "Spin orbit interactions, "Terbium, "Iron, "Ferromagnetism, Glass, Metal alloys, Temperature, Lorentz transformations, Rare earth elements, Phase transformations, Reprints.

Small angle neutron scattering measurements (SANS) have been made on Tb45Fe55 and Tb25Fe75 as a function of temperature. The SANS results show that long range ferromagnetic order is quenched in the alloys and is replaced by a spin glass-like state. For T greater than T(c), where T(c) is the transition temperature, both samples exhibit a conventional Lorentzian lineshape (in q), but they depart from the form below T(c). The low temperature lineshapes have been fitted with the Lorentzian plus Lorentzian-squared form appropriate for random field systems. As the temperature of the Tb45Fe55 alloy is lowered, the correlation length rises to a rounded maximum of 80 angstroms at 250 K (T(c) = 298 K) and decreases to about 60 ang-stroms at low T. In both alloys the coefficient of the Lorentzian term rises sharply as T approaches 0, whereas the Lorentzian-squared coefficient follows approximately the square of the order parameter divided by the correlation length. Both systems thus lend support to the suppression of long range order by the random anisotropy field.

PB89-201784 Not available NTIS National Bureau of Standards (IMSE), Gaithersburg,

MD. Ceramics Div.

Grain Boundary Structure in Ni3Al. Final rept.

R. A. D. Mackenzie, M. D. Vaudin, and S. L. Sass. 1988, 6p

Contract DE-FG02-85ER45211 Sponsored by Department of Energy, Washington, DC. Pub. in Jnl. de Physique 49, n10 pC5-227-C5-232 Oct

Keywords: *Nickel alloys, *Aluminum, *Boron, *Grain boundaries, Separation, Stoichiometry, Electron mi-croscopy, Single crystals, Additives, Diffraction, Crystal structure, Dislocations(Materials), Reprints.

The influence of boron segregation and non-stoichiometry on grain boundary structure in Ni3Al was studied by transmission and scanning electron microscopy techniques. Small angle twist and tilt boundaries were produced by hot pressing misoriented single crystals of both doped and undoped material. Dislocation structures were observed in both bicrystal and polycrystal grain boundaries. In most cases the grain boundary dislocations were found to have the expected a <100> Burgers vector, however in one case dislocations with Burgers vector a/2<110> have been observed. Using a SEM diffraction technique the frequency of occurrence of grain boundary types was examined and found to be unchanged by the addition of boron.

901.151 Not available NTIS PB89-201982 National Bureau of Standards (IMSE), Gaithersburg, MD. Metallurgy Div.
In situ Observation of Particle Motion and Diffu-

sion Interactions during Coarsening.

Final rept. P. W. Voorhees, and R. J. Schaefer. 1987, 13p Pub. in Acta Metallurgica 35, n2 p327-339 1987.

Keywords: *Metals, *Phase transformations, Drops(Liquids), Diffusion, Particles, Reprints, *Ostwald ripening, Coarsening. *Phase

In situ observation of the growth and Ostwald ripening of spherical second phase domains in a solid is reported. It was found that at relatively low (3%) volume fractions of coarsening phase, diffusional interactions be-tween particles were sufficiently strong to alter significantly the individual particle coarsening rates from the theoretical predictions of Lifshitz and Slyozov and Wagner (LSW). As a result, the LSE theory was found to be an inadequate description of the coarsening behavior of the low volume fraction system. In addition, particle migration in the solid matrix during coarsening was observed. The experimental results were found to be qualitatively consistent with a theoretical analysis of particle migration due to interparticle diffusional interactions or nonuniform matrix concentration fields. The generality of the mechanism responsible for the particle migration implies that particle motion, and thus a time dependent spatial correlation function, during coarsening will occur to some extent in all systems undergoing first order phase transformations.

901 152

PB89-201990 PB89-201990 Not available NTIS National Bureau of Standards (IMSE), Gaithersburg. MD. Metallurgy Div.

Numerical Simulation of Morphological Develop-ment during Ostwald Ripening.

Final rept. P. W. Voorhees, G. B. McFadden, R. F. Boisvert, and

D. Meiron. 1988, 16p Pub. in Acta Metallurgica 36, n1 p207-222 1988.

Keywords: *Metals, *Microstructure, *Particles, *Spatial distribution, Diffusion, Separation, Interfaces, Sintering, Liquids, Reprints, *Ostwald ripening, Coarsen-

A boundary integral technique is employed to determine the morphological evolution of small number of particles during Ostwald ripening in two dimensions. The approach specifically allows the bodies to change shape consistent with interparticle diffusional interactions and the interfacial concentrations as given by the Gibbs-Thomson equation. It is shown that the strong interparticle diffusional interactions which occur at small interparticle separations can induce significant motions of the centers of mass of the particles. Such motion is shown to be a strong function of the spatial distribution of particles. The generality of the mechanism responsible for the particle migration suggests that particle motion is a generic aspect of the ripening process at high volume fractions of coarsening phase. It was found that significant shape distortions of particles during ripening requires particle arrangements which induce significant diffusional screening of regions of interface. Through particle arrangements similar to those found in solid-liquid systems during liquid phase sintering, it is shown that the formation regions of flat interface between particles is completely consistent with an Ostwald ripening mechanism.

901,153

PB89-202089 Not available NTIS National Bureau of Standards (IMSE), Gaithersburg, MD. Ceramics Div.

Diffraction Effects Along the Normal to a Grain Boundary.

Final rept. J. M. Vitek, M. D. Vaudin, M. Ruhle, and S. L. Sass.

1989, 5p Sponsored by Department of Energy, Washington, DC. Pub. in Scripta Metallurgica 23, p349-353 1989.

Keywords: *Metals, *Grain boundaries, Interfaces, Diffraction, Crystal structure, Separation, Kinematics, Grain structure, Reprints.

Much work has been done in recent years on studying the structure and properties of grain boundaries and interfaces in general in metals. Included in the studies is work done by the present authors on diffraction effects from grain boundaries along the reciprocal lattice direction passing through the origin normal to a planar boundary. The studies considered the simplified case of kinematical diffraction effects caused by distortions normal to the planar interface in the boundary region. It has been noted both in the literature and in personal communications that discrepancies existed between the results of Vaudin, Sass et al., and Vitek and Ruhle. It was felt that the most appropriate action would be to discuss these differences in a joint paper. The paper

Nonferrous Metals & Alloys

clarifies and resolves many of these differences, including some issues that have not been raised previously in the literature, and identifies the remaining areas of disagreements.

901,154 PB89-218333 PB89-218333 PC A03/MF A01 National Inst. of Standards and Technology (NEL), Boulder, CO. Chemical Engineering Science Div. Ignition Characteristics of the Nickel-Based Alloy UNS N07718 in Pressurized Oxygen.
J. W. Bransford, P. A. Billiard, J. A. Hurley, K. M. McDermott, and I. Vazquez. Apr 89, 50p NISTIR-89/

Sponsored by National Aeronautics and Space Administration, Huntsville, AL. George C. Marshall Space Flight Center.

Keywords: *Nickel alloys, *Combustion, *Ignition, Critical temperature, Flammability tests, Graphs(Charts), Tables(Data), UNS NO7718, Pressurized oxygen.

The development of ignition and combustion in pressurized oxygen atmospheres was studied for the nickel-based alloy UNS N07718. Ignition of the alloy was achieved by heating the top. It was found that the alloy would autoheat to destruction from temperatures below the solidus temperature. In addition, endothermic events occurred as the alloy was heated, many at reproducible temperatures. Many endothermic events occurred prior to abrupt increases in surface temperature and appeared to accelerate the rate of increase in specimen temperature. It appeared that the source of some endotherms may increase the oxidation rate of the alloy. Ignition parameters are defined and the temperatures at which these parameters occur are given for the oxygen pressure range of 1.72 to 13.8 MPa (250 to 2000 psia).

901,155 PB89-228985 PC A03/MF A01 National Inst. of Standards and Technology (NEL), Gaithersburg, MD. Applied and Computational Mathe-

Galliersburg, M.D. Applied and Computational Maintenantics Div.

Effect of Anisotropic Thermal Conductivity on the Morphological Stability of a Binary Alloy.

S. R. Coriell, G. B. McFadden, and R. F. Sekerka. Aug 89, 24p NISTIR-89/4143

Prepared in cooperation with Carnegie-Mellon Univ., Pittsburgh, PA.

Keywords: *Bismuth alloys, *Tin alloys, *Anisotropy, *Thermal conductivity, *Crystal growth, *Solidification, Microstructure, Dispersions, Stability, Orientation, Oscillations, Graphs(Charts), Equations.

A linear morphological stability analysis of a planar interface during unidirectional solidification of a binary alloy was performed for the case of a crystal having an anisotropic thermal conductivity. A dispersion relation was calculated which shows that the onset of instability depends on the orientation of the growth direction with respect to crystallographic axes and on the orientation of the wave vector of the perturbation. The onset of instability can be either oscillatory (travelling waves) or non-oscillatory in time. For growth along a principal axis of the crystal there is an exchange of stabilities, and the onset of instability is non-oscillatory. The dispersion relation for a uniaxial crystal was explored in detail. Numerical results for the case of an alloy of 0.78 at % bismuth in tin are given.

901,156 PB89-229306 Not available NTIS National Bureau of Standards (IMSE), Gaithersburg, MD. Ceramics Div.

Grain Boundary Characterization in Ni3Al.

Final rept.

R. A. D. Mackenzie, M. D. Vaudin, and S. L. Sass. 1988, 6p Contract DE-FG02-85ER45211

See also DE88009169. Sponsored by Department of Energy, Washington, DC. Pub. in Materials Research Society Symposia Pro-

ceedings 122, p461-466 1988.

Keywords: *Nickel alloys, *Intermetallics, *Boron, *Additives, *Grain boundaries, *Electron microscopy, Polycrystals, Bicrystals, Aluminum, Crystal dislocations, Nickel aluminides.

Grain boundaries in both pure and boron doped Ni3AI have been studied using a variety of electron micros-copy techniques. Small angle boundary structures were examined in both bicrystal and polycrystalline specimens. Dislocations with Burgers vector a/

2<110> are observed in the presence of boron, while dislocations with Burgers vector a<100> are observed in the absence of boron. A possible explanation for the behavior is the presence of a disordered layer at the interface in boron doped Ni3Al. The addition of boron to Ni3Al was seen to induce faceting of grain boundaries, and to afford the boundaries some protection from etching. Using electron backscatter diffrac-tion patterns, the frequency of occurrence of grain boundary types was found to be unchanged by the addition of boron.

PB89-229314 PB89-229314 Not available NTIS National Bureau of Standards (IMSE), Gaithersburg, MD. Ceramics Div.

Grain Boundary Structure in Ni3Al.

Final rept.

R. A. D. Mackenzie, M. D. Vaudin, and S. L. Sass. 1988, 2p See also DE88009164.

Pub. in Proceedings of the Annual Meeting of the Electron Microscopy Society of America (46th), San Francisco, CA., p602-603 Aug 88.

Keywords: *Nickel alloys, *Intermetallics, *Boron, *Ductility, *Bicrystals, *Aluminum, Intergranular corrosion, Transgranular corrosion, Polycrystals, Grain boundaries, Additives, Nickel aluminides, Flat sur-

Ni3Alk is a potentially useful high temperature alloy. In its single crystal form it exhibits good ductility; however in polycrystalline form the pure alloy is highly prone to intergranular failure. It has been seen that in slightly nickel-rich alloys the addition of small amounts of boron has the effect of dramatically increasing the ma terial ductility and of changing the failure mode from intergranular to transgranular. In alloys which have been ductilitized by boron addition, atom probe investigation has shown the boron to be segregated to grain boundaries. The segregation may induce a change in the boundary structure as has been seen by Sickafus and Sass in gold doped iron bicrystals.

901,158 PB89-231302 PB89-231302 Not available NTIS National Inst. of Standards and Technology (NML), Gaithersburg, MD. Surface Science Div. Interaction of Oxygen and Platinum on W(110). Final rept

Final Tept.

R. A. Demmin, and T. E. Madey. 1989, 7p
Sponsored by Department of Energy, Washington, DC.
Pub. in Jnl. of Vacuum Science and Technology A7, n3 p1954-1960 May/Jun 89.

Keywords: *Tungsten, *Platinum, *Adsorption, *Oxygen, *Thin films, *Annealing, Desorption, Electron diffraction, Auger electrons, Spectroscopy, Monomolecular films, Reprints.

Low-energy electron diffraction (LEED) and Auger spectroscopy have been used to characterize Pt overlayers coadsorbed with oxygen on W(110). Previous work has shown that multilayers of Pt alone will cluster into three-dimensional crystallites of bulk Pt when annealed, leaving a pseudomorphic monolayer of Pt covering the W(110) surface. When oxygen is present on the surface, the monolayer of Pt is no longer stable. Annealing a W(110) surface on which both Pt and oxygen are adsorbed causes nearly all of the Pt to agglomerate into clusters as the oxygen largely replaces the monolayer on the surface. The presence of the Pt the monolayer on the surface. The presence of the Pt clusters reduces the temperature required for desorption of oxygen, however, and the Pt spreads across the W surface as the oxygen is removed. The complex LEED patterns observed when coadsorbed oxygen and Pt are annealed and the changes in the temperature required for desorption of oxygen suggest that there is an interaction between the two adsorbates and that there is not complete phase separation; i.e., some Pt remains dispersed on the W surface within the oxygen phase.

901,159 PB90-117409 Not available NTIS National Inst. of Standards and Technology (IMSE), Boulder, CO. Fracture and Deformation Div.

Texture Monitoring In Aluminum Alloys: A Comparison of Ultrasonic and Neutron Diffraction Measurements.

Final rept.
A. V. Clark, R. C. Reno, R. B. Thompson, J. F. Smith, G. V. Blessing, R. J. Fields, P. P. Delsanto, and R. B. Mignogna. 1988, 9p
Sponsored by Office of Naval Research, Arlington, VA.

Pub. in Ultrasonics 26, p189-197 Jul 88.

Keywords: *Aluminum alloys, *Texture, *Monitors, Ultrasonic tests, Neutron diffraction, Metal sheets, Reprints, Piezoelectric transducers, Electroacoustic transducers.

Theories have been developed by several authors to calculate velocities of bulk, guided and surface waves in polycrystalline aggregates of cubic metals. The theories can be used to predict the effect of texture on ultrasonic velocity in rolled aluminum and steel sheet, provided that the effects of dislocations, secondprovided that the effects of dislocations, second-phase particles, inclusions, etc. can be ignored. The theories predict that ultrasonic velocities will be influ-enced by three orientation distribution coefficients (ODCs). The ODCs are quantitative measures of the texture in the material. In the work, the texture of thin sheets of a commercial grade aluminum alloy was measured with both ultrasonics and neutron diffraction. Several ultrasonic techniques were employed, using bulk, guided and surface waves. Both piezoelectric and electromagnetic-acoustic transducers (EMATs) were used. Quantitative measurements of texture made with different ultrasonic techniques were in good agreement. The ultrasonic measurements also agreed with neutron diffraction measurements, indicating that the dominant features of the effect of texture on wave propagation have been modelled with sufficient accuracy.

901,160 PB90-117607 Not available NTIS National Inst. of Standards and Technology (IMSE), Boulder, CO. Fracture and Deformation Div. Fourth-Order Elastic Constants of beta-Brass.

R. R. Rao, and H. Ledbetter. 1989, 4p Pub. in International Jnl. of Thermophysics 10, n4 p899-902 Jul 89.

Keywords: *Brasses, *Elastic properties, Strains, Cauchy problem, Partial differential equations, Elastic theory, Crystal structure, Reprints, *Brass-beta.

Combinations of the fourth-order elastic constants of beta-brass were calculated using the measured second-order and third-order elastic constants and the expressions for the effective elastic constants of a cubic crystal obtained from finite-strain theory. The present calculations show that the Cauchy relations for the fourth-order elastic constants in beta-brass are not satisfied. This implies that noncentral or many-body forces occur in this material. The authors considered two alloys. The higher-Zn alloy shows lower mag-nitudes of the fourth-order elastic constants and a larger Cauchy discrepancy.

901.161 PB90-117664 Not available NTIS National Inst. of Standards and Technology (IMSE), Boulder, CO. Fracture and Deformation Div.

Typical Usage of Radioscopic Systems: Replies to a Survey. Final rept.

T. A. Siewert. 1989, 5p Pub. in Materials Evaluation 47, p701-705 Jun 89.

Keywords: Real time operations, Aluminum, Steels, Surveys, Reprints, *Radioscopy, Image quality.

program has been initiated at the National Institute of Standards and Technology to develop image quality indicators for real-time radioscopic systems. A survey was conducted to obtain some general parameters to guide the development; the report presents the results of the survey.

901.162 PB90-117755 Not available NTIS National Inst. of Standards and Technology (IMSE), Gaithersburg, MD. Metallurgy Div.

Equilibrium Crystal Shapes and Surface Phase Diagrams at Surfaces in Ceramics. Final rept.

C. A. Handwerker, M. D. Vaudin, and J. E. Blendell. 1988, 7p

Sponsored by Office of Naval Research, Arlington, VA. Pub. in Jnl. de Physique 49, n10 pC5-367-C5-373 Oct

Keywords: *Ceramics, *Surface properties, *Crystal structure, *Shape, *Thermodynamic equilibrium, Free energy, Phase transformations, Magnesium oxides, Nickel oxides, Reprints.

Nonferrous Metals & Alloys

The equilibrium shape of a crystal is the shape that minimizes the total surface free energy of the crystal and may contain any or all of the following: facets, sharp edges, smoothly curved surfaces, and corners. The relationship between the surface free energy per unit area, gamma, and the equilibrium crystal shape is seen straightforwardly from the Wulff plot, the polar straightforwardly from the Wulff plot, the polar straightforwardly grow the contraction of the seen straightforwardly from the Wulff plot, the polar plot of gamma as a function of orientation of the normal vectors, n. The boundaries between surfaces on the equilibrium crystal (for example, between adjacent facet planes) have been described as surface phase transitions. If gamma(n) changes with temperature, pressure, or chemical potentials of the components, the equilibrium shape of the crystal may change. The change in equilibrium shape can be represented by a surface phase diagram with axes of surface orientation, in terms of angle from an arbitrary or chemical comparature, and temperature, pressure or chemical comparature, or chemical comentation, and temperature, pressure, or chemical com-position. The surface phase transitions of MgO have been determined as a function of NiO solute concentration and surface phase diagrams have been constructed.

901,163 PB90-118084 Not available NTIS National Inst. of Standards and Technology (IMSE), Gaithersburg, MD. Metallurgy Div. Magnetic Behavior of Compositionally Modulated

Ni-Cu ThIn Films.

Final rept. L. H. Bennett, L. J. Swartzendruber, D. S. Lashmore, R. Oberle, U. Atzmony, M. P. Dariel, and R. E. Watson. 1989, 5p Pub. in Physical Review B 40, n7 p4633-4637, 1 Sep

Keywords: *Copper nickel alloys, *Thin films, *Magnetic properties, Composition(Property), Measurement, Electrodeposition, Reprints, Compositional modulation.

Magnetic measurements on Ni-Cu compositionally modulated multilayers prepared by electrodeposition indicate less diffusion of Cu into the Ni than previously obtained by either electrodeposition or other means. The samples exhibit magnetic behavior much more closely resembling that of bulk Ni than has been seen previously for Ni-Cu multilayers. No dead layer is found.

901,164 PB90-123423 Not available NTIS Not available NTIS
National Inst. of Standards and Technology (IMSE),
Gaithersburg, MD. Metallurgy Div.
Temperature Hysteresis in the Initial Susceptibility
of Rapidly Solidified Monel.

Final rept. U. Atzmony, L. J. Swartzendruber, and L. H. Bennett. 1988, 4p Pub. in Scripta Metallurgica 22, n5 p721-724 May 88.

Keywords: *Hysteresis, *Solidification, *Monel, *Alternating current, Thermal cycling tests, Annealing, Temperature, Magnetic permeability, Reprints, *Rapid quenching(Metallurgy), AC losses.

The temperature dependence of the ac susceptibility for a Cu-Ni allo y near the monel composition (28 at .% Cu) has been measured over temperature cycles of cooling down and warming up, for both the as-spun an after-thermal-annealing condition. A time-dependent temperature hysteresis was observed. A transforma-tion between the two values can be abruptly induced by external disturbance.

901,165 PB90-123431 PB90-123431 Not available NTIS
National Inst. of Standards and Technology (IMSE),
Gaithersburg MD Matelland D

Gaithersburg, MD. Metallurgy Div.
Magnetization and Magnetic Aftereffect In Textured NI/Cu Compositionally-Modulated Alloys.

U. Atzmony, L. J. Swartzendruber, L. H. Bennett, M. P. Dariel, D. Lashmore, M. Rubinstein, and P. Lubitz. 1987, 10p
Pub. in Jnl. of Magnetism and Magnetic Materials 69,

n3 p237-246 1987.

Keywords: *Magnetization, *Copper nickel alloys, Resonance absorption, Ferromagnetism, Magnetic measurement, Texture, Reprints, Aftereffect.

The magnetic properties of Ni/Cu compositionallymodulated alloys with (100), (110) and (111) textures were measured by magnetometry and ferromagnetic resonance. Unexpectedly, a magnetic aftereffect was

901,166 PB90-123514 Not available NTIS National Inst. of Standards and Technology (IMSE), Gaithersburg, MD. Metallurgy Div. TEM Observation of Icosahedral, New Crystalline

and Giassy Phases in Rapidly Quenched Cd-Cu Allovs.

Final rept.

L. A. Bendersky, and F. S. Biancaniello. 1987, 6p Pub. in Scripta Metallurgica 21, n4 p531-536 Apr 87.

Keywords: *Cadmium alloys, *Copper containing alloys, *Solidification, *Phase diagrams, Intermetallics, Crystal structure, Microstructure, Metastable state, Reprints, *Rapid quenching(Metallurgy), *Transmission electron microscopy, *Icosahedrons, Metallic glasses.

Since the discovery of an icosahedral phase in rapidly snice the discovery of an icosanieural phase in rapidly solidified Al-Mn alloys, similar phases have been found in many other systems. Generally, a successful approach was to rapidly solidify alloys known to form equilibrium intermetallic compounds with structure exhibiting extensive icosahedral (or polytetrahedral) clustering. For example, Frank-Kasper phases have entirely tetrahedral bonding of atoms with coordination numbers 12, 14, 15 and 16. According to the criteria the Cd-Cu system seems to be appropriate for forming the icosahedral phase. The central portion of the Cd-Cu phase diagram consists of three intermetallic phases with unit cells containing the icosahedral clusters. In the present work the microstructure of the rapidly so-lidified Cu-Cd alloys was studied by means of transmission electron microscopy. The purpose was to explore:
(1) a possibility of the icosahedral and other metastable phase formation; and (2) solidification of complex crystal structures under conditions of rapid freezing.

PB90-123522 Not available NTIS National Inst. of Standards and Technology (IMSE), Gaithersburg, MD. Metallurgy Div.

Amorphous Phase Formation in Al70Si17Fe13 Alloy.

Final rept.

L. A. Bendersky, F. S. Biancaniello, and R. J. Schaefer. 1987, 4p

Pub. in Jnl. of Materials Research 2, n4 p427-430 Jul/

Keywords: *Aluminum alloys, *Phase transformations, *Silicon containing alloys, *Iron containing alloys, Microstructure, Solidification, Reprints, *Amorphous state, *Rapid quenching(Metallurgy).

The alloy Al70Si17Fe13 was subjected to a range of rapid solidification conditions and the resulting microstructures were evaluated. It was found that when solidification was sufficiently rapid to bypass the formation of primary intermetallic phases, the alloy consisted of spherical regions of amorphous (or micro-quasicrystalline) material surrounded by a crystalline phase(s). The microstructure is interpreted as the result of solidification of the amorphous phase from the melt by a first-order transformation. The structure of the amorphous phase is different from that of a liquid (or usual metallic glass).

901,168 PB90-123530 Not available NTIS National Inst. of Standards and Technology (IMSE), Gaithersburg, MD. Metallurgy Div. Solidification of an 'Amorphous' Phase in Rapidiy Solidified Al-Fe-SI Alloys.

Final rept.
L. A. Bendersky, M. J. Kaufman, W. J. Boettinger, and F. S. Biancaniello. 1988, 4p
Pub. in Materials Science and Engineering 98, p213-

216 Feb 88.

Keywords: *Solidification, *Aluminum alloys, *Iron containing alloys, *Silicon containing alloys, Crystal structure, Phase transformations, Microstructure, Metastable state, Reprints, *Amorphous state, *Rapid quenching(Metallurgy).

The focus of the work is the amorphous phase formation in Al-Fe-Si alloys. Depending on the concentration of Fe and Si, the phase appears either as an intercellular constituent or as primary phase with globular morphology. Thus the amorphous phase acts like a normal crystalline phase. The globular morphology of the amorphous phase suggests the possibility of a metastable liquid miscibility gap. However there is no ther-modynamic evidence to support a positive heat of

mixing for the liquid phase. Another possibility suggests crystallization of a phase structurally different from liquid but at the same time being neither crystalline nor quasicrystalline. A possible structural relationship among the amorphous phase, the cubic alpha(AIFeSi) and te quasicrystalline phases is discussed.

901,169

PB90-123548 Not available NTIS National Inst. of Standards and Technology (IMSE), Gaithersburg, MD. Metallurgy Div. Quasicrystals and Quasicrystal-Related Phases in the Al-Mn System.

Final rept.

L. A. Bendersky. 1988, 4p Pub. in Materials Science and Engineering 99, p331-334 Mar 88.

Keywords: *Aluminum manganese alloys, *Crystal structure, *Phase transformations, Electron diffraction, Reprints, Icosahedrons, Amorphous state.

The Al-Mn system is very rich in phases with composition close to Al4Mn. As solidification conditions change from very slow (casting) to extremely fast (atomized submicron size droplets) the following phases will form: hexagonal mu phase (a = 1.995 nm, c = 2.452 nm), hexagonal lambda phase (a = 2.841 nm, c = 1.238 nm), decagonal quasicrystal, icosahedral quasicrystal, and microquasicrystalline or 'amorphous' phase. In the present work, the potential interrelationship between the structures of the crystalline, quasicrystalline and amorphous Al4Mn phases is investigated by a systematic study of electron diffraction intensities. Analysis of electron diffraction intensity modulations and the spatial relationships suggests that the phases have a structural skeleton of icosane-dral units, possibly of Mackay icosahedron type. Differ-ent crystalline and quasiperiodic phases can be formed by different stackings of the same icosahedral clusters and they are not necessarily in a single orientation. The amorphous structure can be described as a network of randomly oriented clusters.

901,170

PB90-123621 Not available NTIS National Inst. of Standards and Technology (IMSE), Gaithersburg, MD. Metallurgy Div. Microstructural Variations in Rapidly Solidified

Final rept.

W. J. Boettinger. 1988, 8p Pub. in Materials Science and Engineering 98, p123-

Keywords: *Microstructure, *Alloys, *Solidification, Surface reactions, Powder metals, Atomizing, Reprints, *Rapid quenching(Metallurgy).

Depending on alloy composition and cooling conditions, rapid solidification can produce a wide variety of microstructures. Examples are presented from material produced by three common methods of rapid solidification: surface melting and resolidification, substrate quenching, and powder atomization. The examples illustrate the microstructural similarities and differences that can occur using the methods.

901.171

PB90-123639 Not available NTIS National Inst. of Standards and Technology (IMSE), Gaithersburg, MD. Metallurgy Div. Rapid Solidification and Ordering of B2 and L2 (sub 1) Phases in the NiAl-NiTi System.

Final rept.

W. J. Boettinger, L. A. Bendersky, F. S. Biancaniello, and J. W. Cahn. 1988, 4p
Pub. in Materials Science and Engineering 98, p273-276 1988.

Keywords: *Nickel alloys, *Aluminides, *Titanium intermetallics, *Phase transformations, *Solidification, Thermodynamics, Metastable state, Reprints, Heusler alloys, Rapid quenching(Metallurgy).

Evidence is presented for the direct solidification of the B2 phase in the NiAl-NiTi system at some compositions where the L2sub1 phase is stable at the melting point. Subsequent continuous ordering produces the equilibrium phase. The metastable continuous ordering curve is used to discuss the result.

Nonferrous Metals & Alloys

PB90-123647 Not available NTIS National Inst. of Standards and Technology (IMSE), Gaithersburg, MD. Metallurgy Div.

Formation of Dispersolds during Rapid Solidifica-tion of an Al-Fe-Ni Alloy.

Final rept.

Final rept.
W. J. Boettinger, L. A. Bendersky, R. J. Schaefer, and F. S. Biancaniello. 1988, 7p
Pub. in Metallurgical Transactions A-Physical Metallurgy and Materials Science 19, n4 p1101-1107 1988.

Keywords: *Dispersions, *Aluminum alloys, *Iron containing alloys, *Nickel containing alloys, *Solidification, Microstructure, Eutectics, Cells, Velocity, Reprints, *Rapid quenching(Metallurgy).

Examination of the effect of rapid solidification velocity on the microstructure of Al-3.7 wt% Ni-1.5 wt% Fe has revealed a new mechanism for the formation of dis-crete second phase particles in rapidly solidified alloys. Cellular growth of alpha-Al occurs with the intercellular phase, Al9(Fe,Ni)2 in two distinct morphologies. At low velocity (<50 cm) the phase is continuous in the growth direction while at higher velocity discrete rounded particles are observed. Analysis of the orientation relationship and the number of variants that exists between phases leads to a mechanism where liquid droplets are deposited by the moving cellular interface. The droplets solidified subsequently to form the rounded second phase particles.

901,173 PB90-123779 Not available NTIS National Inst. of Standards and Technology (IMSE), Gaithersburg, MD. Metallurgy Div.

Pathways for Microstructural Development in TIAI. Final rept.

J. A. Graves, L. A. Bendersky, F. S. Biancaniello, J. H. Perepezko, and W. J. Boettinger. 1988, 4p Pub. in Materials Science and Engineering 98, p265-268 Feb 88.

Keywords: "Microstructure, "Titanium intermetallics, "Aluminides, Alloys, Solidification, Crystal structure, Phase diagrams, Transmission electron microscopy, Powder metallurgy, Metastable state, Reprints, "Rapid quenching(Metallurgy).

Rapid solidification processing (RSP) of intermetallic alloys can provide alternative solidification paths and alloys can provide alternative solidification paths and lead to the formation of metastable products. For the intermetallic TiAl with an equilibrium Li sub 0 structure RSP has yielded a metastable hcp (alpha-Ti) phase in both fine powder and melt spun ribbon. Based upon transmission electron microscopy (TEM) observations of a fine anti-phase domain structure the hcp phase orders to the Ti3Al (DO sub 19) structure following so ridiffication. A metastable phase discrete page these significants are producted in the control of th lidification. A metastable phase diagram analysis indicates that a melt undercooling of about 100 C is required for partitionless formation of a hcp phase from an equiatomic melt and reveals other possible solidifi-cation pathways including the nucleation of metastable disordered bcc and fcc phases. Each of the potential pathways offers further opportunity for microstructural modification by solid state annealing treatments.

PB90-128125
Not available NTIS
National Inst. of Standards and Technology (NML),
Gaithersburg, MD. Surface Science Div.
Role of Adsorbed Gases in Metal on Metal Epitaxy.
Final role

W. F. Egelhoff, and D. A. Steigerwald. 1989, 7p Pub. in Jnl. of Vacuum Science and Technology A 7, n3 p2167-2173 May/Jun 89.

Keywords: *Adsorption, *Gases, *Transition metals, *Epitaxy, Surface properties, Thin films, Carbon monoxide, Water, Copper, Nickel, Iron, Silver, Monomolecular films, Reprints.

It is found that a variety of (deliberately) adsorbed gases influence in some manner the epitaxial growth of metals on metals. The adsorbed gases investigated included molecularly adsorbed CO and H2O and dissociatively adsorbed H, O, N, C, and S. The effects of adsorbed gases have been investigated in metal-onmetal epitaxial systems including Cu/Cu(100), Ni/Ni(100), Cu/Ni(100), Ni/Cu(100), Fe/Cu(100), Cu/Fe(100), Fe/Ag(100), and Fe/Fe(100). Although not all of the possible gas-metal combinations among the systems have been studied, enough have been to make the following generalizations. Around room temperature and above, the gases exhibit a strong tenden-

cy to 'float out' to the growing surface, hardly reducing the extent of epitaxial ordering. All but the most strongly bound, e.g., C or N, have a strong tendency to float ly bound, e.g., C or N, nave a strong tendency to float out even during epitaxy at temperatures as low as 100 K. The most strongly bound, e.g., C, N, or O, tend to suppress the agglomeration or interdiffusion (which otherwise occurs) when a monolayer of a transition metal is deposited on a noble metal at room temperature or above, e.g., Fe/Cu(100) or Ni/Cu(100). In some cases, the effects may be useful as a new tool for gaining improved control over epitaxial growth.

PB90-128174 Not available NTIS National Inst. of Standards and Technology (IMSE), Gaithersburg, MD. Metallurgy Div. Diffusion-Induced Grain Boundary Migration.

C. Handwerker. 1989, 4p Pub. in McGraw-Hill Yearbook of Science and Technology, p155-158 1989.

Keywords: *Diffusion, *Grain boundaries, *Alloying, Metals, Solid solutions, Phase diagrams, Solutes, Polycrystalline, Thin films, Reprints.

When large grain-sized, well-annealed polycrystalline materials are exposed to a solute source and the solute diffuses down the grain boundaries, it is fre-quently observed that grain boundaries migrate, some-times away from the centers of curvature, and alloys form in the regions swept by the moving grain boundaries. This newly recognized phenomenon is known as diffusion-induced grain boundary migration (DIGM) since the solute diffusion induces otherwise stable grain boundaries to move. Grain boundaries are placed in contact with solute sources in most engineering systems, for example, in thin film multi-layer contacts on computer circuit boards. The technological and economic impact of the unexpected break-down of the systems by DIGM is enormous.

901,176 PB90-128604 PB90-128604 Not available NTIS National Inst. of Standards and Technology (IMSE), Boulder, CO. Fracture and Deformation Div. Effects of Grain Size and Cold Rolling on Cryogenlc Properties of Copper.

Final rept. R. P. Reed, R. P. Walsh, and F. R. Fickett, 1988.

Sponsored by Department of Energy, Washington, DC. Pub. in Advances in Cryogenic Engineering Materials, v34 p299-308 1988.

Keywords: *Cryogenics, *Copper, *Grain size, *Cold rolling, Electrical resistivity, Yield strength, Tensile stress, Ultimate strength, Microstructure, Reprints.

The effects of grain size and cold rolling on the tensile properties and electrical resistivity at 295, 76 and 4 K were studied for oxygen-free, high-conductivity copper. Tensile-yield and ultimate strengths increase linearly with increasing 1/sq rt d (d = grain diameter), following the Hall-Petch relationship. At low temperatures the dependence on grain size increases in tures, the dependence on grain size increases. Increasing grain size lowers resistivity slightly at all temperatures. Cold rolling to 10 percent reduction of area significantly increases the yield strength at all temperatures. peratures; subsequent rolling produces smaller strength increases. Resistivity increases with cold roll-

PB90-128737 Not available NTIS
National Inst. of Standards and Technology (IMSE),
Boulder, CO. Fracture and Deformation Div.
Fatlgue Resistance of a 2090-78E41 Aluminum Alloy at Cryogenic Temperatures.

Final rept. R. L. Tobler, J. K. Han, and R. P. Reed. 1989, 10p Sponsored by Martin Marietta Aerospace, New Orleans, LA., and Department of Energy, Washington, DC. Pub. in Proceedings of International Cryogenic Materials Conference (1988), Los Angeles, CA., July 23-28, 1989, v2 p703-712.

Keywords: *Fatigue life, *Cryogenics, *Aluminum alloys, Crack propagation, Lithium containing alloys, Copper containing alloys, *Alloy 2090-T8E41, *Alloy

Smooth-bar axial fatigue-life measurements were performed to evaluate the fatigue resistance of a 2090-T8E41 aluminum-copper-lithium alloy at cryogenic temperatures. Conventional S-N curves with failures occuring between 10(sup 4) and 10(sup 6) cycles are presented with similar data for a 2014-T6 aluminum alloy. For specimens in the longitudinal orientation, the 2090 alloy performed better than 2014 in the low-cycle fatigue range at 295, 76, and 4 K. Factors contributing to the results are discussed.

901.178

PB90-136862 Not available NTIS National Bureau of Standards (NML), Gaithersburg, MD. Inorganic Analytical Research Div.

Technical Examination, Lead Isotope Determination, and Elemental Analysis of Some Shang and Zhou Dynasty Bronze Vessels. Final rept.

I. L. Barnes, W. T. Chase, L. L. Holmes, E. C. Joel, P. Meyers, and E. V. Sayre. 1988, 11p

Pub. in Proceedings of Conference on the Beginning of the Use of Metals and Alloys, Zhengghou, China, October 21-26, 1986, p296-306 1988.

Keywords: *Lead isotopes, *Archaeology, *Mass spectroscopy, *Bronzes, *Containers, China, Microscopy, Age determination, Radiography, Nondestructive tests, Neutron activation analysis, Absorption spectroscopy, Antiquities, Artifacts.

The Arthur M. Sackler Collection of works of art con-The Arthur M. Sackler Collection of works of art contains several hundred fine early ritual bronze vessels. Among the vessels, 106 attributed to the Shang Dynasty, 127 attributed to the Western Zhou and 94 attributed to the Eastern Zhou Dynasty have been given a thorough technical examination. The examination has included x-ray radiography viewing under ultraviolet light, overall visual examination and examination of details under a bisecular missenesse. The metal of details under a binocular microscope. The metal of most of the vessels also has been analyzed for lead isotope ratios by means of mass spectrometry, for the major component by atomic absorption spectrometry, major component by atomic absorption spectrometry, and for some minor and trace elemental concentrations by instrumental neutron activation analysis. The vessels may be divided into 11 groups by one particular statistical analysis of the data. The division may indicate the use of different sources of raw materials, although the locations of the different sources is not known at the present time. Data analysis using both chemical and isotopic information is continuing as is the search for samples from sources of ores which might have been used in ancient times.

Plastics

901,179

PB89-146708 Not available NTIS National Bureau of Standards (IMSE), Gaithersburg, MD. Polymers Div.

Effects of Space Charge on the Poling of Ferro-electric Polymers. Final rept.

A. S. DeReggi, and M. G. Broadhurst. 1987, 11p Pub. in Ferroelectrics 73, n3-4 p351-361 Jun 87.

Keywords: *Ferroelectric materials, *Polymers, *Thermal measurements, *Polarization, Poles, Electrical resistivity, Lasers, Charge density, Reprints, Vinylidene fluoride resins.

Thermal pulse measurements of the polarization distribution in ferroelectric polymers and copolymers after poling give distributions concentrated to one side poling give distributions concentrated to one side when the electrical conductivity under poling conditions is significantly different from zero. These results could be explained if net charge were present in the material during poling. The direct observation of distributed charge in nonpolar polymers after exposure to poling conditions support this explanation. However, high resolution laser thermal pulse measurements on the policy of the policy nominally well poled samples of polyvinylidene fluoride reveal a sharp drop of polarization to near zero value at a depth of about 1 micrometer from the surfaces which is not explained.

901.180

PB89-147821 PC A03/MF A01 National Bureau of Standards (NEL), Gaithersburg, MD. Center for Building Technology.

Epoxy impregnation Procedure for Hardened Cement Samples.

Progress rept. L. Struble, and P. Stutzman. May 88, 19p NBSIR-88/

Sponsored by Air Force Office of Scientific Research, Bolling AFB, DC.

Keywords: *Epoxy resins, *Impregnating, *Cements, *Ethanols, *Curing, Viscosity, Cracks, Microscopy, Porosity, Crosslinking, Plastics processing.

A method was previously developed for epoxy impregnation of hydrated cementitious materials for micronation or nydrated cementitious materials for microscopical examination without drying the samples, by sequentially replacing pore solution with ethanol, then the ethanol with epoxy. During subsequent application of the procedure, many specimens were cured. Studies were carried out to identify the cause of these problems and to modify the procedure for more reliable impregnation. Contamination with low levels (4%) of water or ethanol was found to prevent process. pregnation. Contamination with low levels (4%) or water or ethanol was found to prevent proper curing. Modifications in the procedure to prevent contamination, including monitoring the replacement of pore solution by ethanol, were shown to provide consistent and reliable impregnation.

901,181 Not available NTIS PB89-157101 National Bureau of Standards (IMSE), Gaithersburg,

MD. Polymers Div.
Polymers Bearing Intramolecular Photodimeriza ble Probes for Mass Diffusion Measurements by the Forced Rayleigh Scattering Technique: Syn-thesis and Characterization. Final rept.

Q. Tran-Cong, T. Chang, and C. C. Han. 1988, 10p Pub. in Polymer 29, p2261-2270 Dec 88.

Keywords: *Anthracene, *Photochemical reactions, *Synthesis, *Photochromism, *Probes, *Rayleigh scattering, *Polystyrene, Irradiation, Ultraviolet radiation, Solvents, Carbon tetrachloride, Temperature, Refractivity, Polymers, Mixtures, Diffusion, Dyes, Reprints.

A new photochromic probe, bis(9-anthryl methyl)ether(BAME) derivative, was synthesized and introduced as an effective probe for forced Rayleigh scattering (FRS) measurement. It is shown that BAME and polystyrene labelled with BAME exhibit a large change in refractive index under irradiation of u.v. light (363.8 nm). The self-diffusion of BAME and polystyrene labelled with BAME (363.8 nm). (363.8 nm). The self-diffusion of BAME and polystyrene labelled with BAME (PSA) were measured in various solvents. Results of PSA in good, marginal and poor solvents are consistent with those obtained from quasi-elastic light scattering (OELS). Since the photo-dimerization reaction of anthracene has been extensively studied in solution and crystal as well as in polymer matrix, unfavorable multistep photochemical reac-tions can be avoided. One such unfavorable case, which involves a fluorescence quenching solvent CCI4, is demonstrated. A temperature dependence study of polystyrene in semi-dilute theta solution by FRS has suggested that the non-exponential intensity decay is due to large concentration fluctuations in the solution. The well known photochemistry, large refractive index change and temperature stability have made BAME a very promising probe for FRS measurements.

901,182 PB89-157119 PB89-157119 Not available NTIS National Bureau of Standards (IMSE), Gaithersburg,

MD. Polymers Div.

Phase Contrast Matching in Lamellar Structures
Composed of Mixtures of Labeled and Unlabeled
Block Copolymer for Small-Angle Neutron Scatter-

Final rept.
Y. Matsushita, Y. Nakao, R. Saguchi, K. Mori, H. Choshi, Y. Muroga, I. Noda, M. Nagasawa, T. Chang, C. J. Glinka, and C. C. Han. 1988, 5p
Pub. in Macromolecules 21, n6 p1802-1806 1988.

Keywords: *Polystyrene, *Mixtures, *Neutron scattering, *Lamellar structure, Isotopic labelling, Polymers, Deuterium, Molecular weight, Vinyl resins, Phase, Pyridines, Reprints.

To extract the single-chain scattering function of poly-styrene block chain in lamellar structures of styrene-2-vinylpyridine diblock copolymers, the method of 'phase contrast matching' was studied for small-angle neu-tron scattering from blends of the deuterium-labeled and unlabeled block copolymers. The phase contract matching is successfully applied for the samples with

the lowest molecular weights (3.4 x 10 sup 4 for the labeled portions) but not for the samples with the higher molecular weights (9.2 and 16.2 x 10 sup 4). It is concluded that the mismatching may be caused by concentration fluctuation in the mixture of hydrogenated and deuteriated polystyrenes in domains, as well as by nonuniform distribution of deuteriated species along the direction perpendicular to the lamellae due to the difference in lengths of the labeled and unlabeled blocks.

901,183 PB89-173942 PB89-173942 Not available NTIS National Bureau of Standards (IMSE), Gaithersburg,

MD. Polymers Div.

Dynamics of Concentration Fluctuation on Both Sides of Phase Boundary. Final rept.

C. C. Han, M. Okada, and T. Sato. 1988, 11p Pub. in Dynamics of Ordering Processes in Condensed Matter, p433-443 1988.

Keywords: *Polymers, *Boundary layer flow, *Binary systems(Materials), Concentration(Composition), Temperature, Transition flow, Blends, Diffusion coefficient, Reprints.

The authors have shown for PSD/PVME polymer blend system that interfacial free energy is small and consistent with theoretical prediction, which does not play an important role in the dynamics of concentration fluctuations in either one phase or two phase regions. The interdiffusion coefficient is continuous at the phase separation boundary. Furthermore, the mobility M has been extracted and an Arrhenius type of temperature dependence has been found. To the best of their knowledge, this is the first time that M has been obtained on both sides of the phase boundary, and the static results have been incorporated into the kinetics study for a consistent evaluation of the Cahn-Hilliard-Cook theory.

Wood & Paper Products

PB89-172530 Not available NTIS National Bureau of Standards (NEL), Gaithersburg, MD. Chemical Process Metrology Div.

Laser induced Fluorescence for Measurement of

Lignin Concentrations in Pulping Liquors.

Final rept.
J. J. Horvath, H. G. Semerjian, K. L. Biasca, and R. Attala. 1988, 10p
Pub. in Proceedings of SPIE (Society of Photo-Optical Instrumentation Engineers) Industrial Optical Sensing, Dearborn, MI., June 29-30, 1988, v961 p68-77.

Keywords: *Fluorescence, *Lasers, *Lignin, *Process control, Pulping, Dyes, Absorption spectra.

Laser excited fluorescence of pulping liquors was investigated for use in the pulp and paper industry for process measurement and control applications. A Nd-YAG pumped dye laser was used to generate the excitation wavelength of 280 nm; measurements were also performed using a commercially available fluorometer. Measurements on mill pulping liquors gave strong signals and showed changes in the fluorescence intensity during the cook. Absorption spectra of diluted mill liquor samples showed large changes during the cook. Samples from well controlled and characterized labo-ratory cooks showed fluorescence to be linear with concentration over two decades with an upper limit of approximately 1000 ppm dissolved lignin. At the end of these cooks, a possible chemical change was indicated by an increase in the observed fluorescence intensity. Results indicate that lignin concentrations in pulping liquors can be accurately determined with fluorescence in the linear optical region over a greater dy-namic range than absorption spectroscopy.

Not available NTIS Mational Bureau of Standards (NEL), Gaithersburg, MD. Fire Measurement and Research Div. Prediction of the Heat Release Rate of Douglas Fir. Final rept. W. J. Parker. 1989, 10p

W. J. Falker. 1969, 10p See also PB87-131819. Pub. in Proceedings of International Symposium on Fire Safety Science (2nd), Tokyo, Japan, June 13-17, 1989, p337-346.

Keywords: *Douglas fir wood, *Thermal diffusivity, *Fire tests, Heat of combustion, Heat flux, Specific heat, Thermochemical properties, Combustion.

Measurements have been made on the thermal diffusivity of Douglas fir and its char up to 550 deg C. Its char contraction factors have also been determined. Intercontraction factors have also been determined. Interpretation of some data in the literature has resulted in the establishment of the specific heat as a function of temperature over this range. These thermophysical property data along with some data reported separately on the thermochemical properties of cellulose, mannan, xylan and lignin were used as input to a model for the heat release rate of wood in order to calculate the heat release rate and heat of combustion of Douglas fir exposed to an external radiant flux of 25 kW/sq m. These calculations were compared with measurements made in the Cone calorimeter. The agreement is reasonable at this stage of the model development.

General

901,186 PB89-175194 PC A06 National Inst. of Standards and Technology, Gaithersburg, MD.

Journal of Research of the National Institute of Standards and Technology, Volume 94, Number 1, January-February 1989. Special Issue: Numeric Da-tabases in Materials and Biological Sciences. Bi-monthly rept.

1989, 104p

Also available from Supt. of Docs. as SN703-027-00026-1. See also PB89-175202 through PB89-175293 and PB89-133367.

Keywords: *Biology, Thermodynamics, Chemical analysis, Ceramics, Crystallography, Proteins, Electron diffraction, Mass spectroscopy, Phase diagrams, *Materials science, *Numerical data bases.

The special issue on Numeric Databases in Materials and Biological Sciences includes the following articles: The importance of numeric databases to materials science; NIST/Sandia/ICDD electron diffraction database: A database for phase identification by electron diffraction; Numeric databases in chemical thermodynamics at the National Institute of Standards and Technology; Numeric databases for chemical analysis; The structural ceramics database: technical foundations; Applications of the crystallographic search and analysis system CRYSTDAT in materials science; New directions in bioinformatics; The use of structural templates in protein backbone modeling; Comparative modeling of protein structure--progress and prospects; and The computational analysis of protein structures: Sources, methods, systems, and results.

901.187 PB89-175202

(Order as PB89-175194, PC A06) A.T. and T. Bell Labs., Murray Hill, NJ.

Importance of Numeric Databases to Materials Science.

Bi-monthly rept. R. A. Matula. 1989, 4p

Included in Jnl. of Research of the National Institute of Standards and Technology, v94 n1 p9-14 Jan-Feb 89.

Keywords: *Industries, Fiber optics, Crystallography, Crystal lattices, Ferroelectricity, Superconductivity, *Materials science, *Numerical data bases.

Scientific numeric databases are important research tools for materials scientists. In distinction to bibliographic databases, these numeric databases are useful primarily to provide direct, immediate access to data, often evaluated data. Examples showing the apdata, often evaluated data. Examples showing the application of crystallographic databases are given, including determining candidate materials for certain applications. Thermochemical data useful for optimizing optical fiber processing are discussed showing the importance of high-quality data. In addition, these databases are an important tool that can be utilized in the arraduate education of the part representation of materials. graduate education of the next generation of materials scientists.

901.188 PB89-179683

Not available NTIS

MATERIALS SCIENCES

General

National Bureau of Standards (NEL), Gaithersburg, MD. Thermophysics Div. Computer Model of a Porous Medium. Final rept.

R. A. MacDonald. 1988, 9p

Pub. in International Jnl. of Thermophysics 9, n6 p1061-1069 Nov 88.

Keywords: *Porous materials, *Computer systems programs, Diffusion, Channels, Porosity, Percolation, Random walk, Mathematical models, Reprints.

A computer model has been set up to represent a porous medium. The basis for this model is a two-dimensional square network (100 x 100) of channels that have randomly assigned widths between the value of zero (closed) and the value of one (open, unrestricted flow). of zero (closed) and the value of one (open, unrestricted flow). The channel width assignments have been made by a random selection from five different distributions: f(q) = q, f(q) = si q, f(q) = erf(q), f(q) = 1 - sin q, and f(q) = 1 - erf(q). Diffusion of particles in the network has been studied by a random-walk procedure for each realization of the channel width assignments. The diffusivity is quite sensitive to the distribution of channel widths. The percolation properties of the networks obtained from the three most restrictive distributions have been investigated and the independent, linked clusters within the network have been determined. For clusters sizes that are less than the full width of the network, the network does not percolate and either the flow is not diffusive or the diffusivity is severely reduced. An approximate value for the percolation threshold has been determined in each case and the fractal dimension has been calculated also.

901,189 PB89-211932 Not available NTIS National Bureau of Standards (IMSE), Gaithersburg, MD. Metallurgy Div.

Mossbauer Spectroscopy. Final rept.

. J. Swartzendruber, and L. H. Bennett. 1986, 9p Pub. in Metals Handbook, v10 p287-295 1986.

Keywords: *Mossbauer effect, *Metals, Spectroscopy, Scattering, Gamma rays, Fluorescence, Reprints.

A brief introduction to Mossbauer spectroscopy for the materials engineer is presented.

901,190 PB89-212237 Not available NTIS National Bureau of Standards (IMSE), Gaithersburg,

Materials Fallure Prevention at the National Bureau of Standards.

Final rept.

L. H. Schwartz, and D. B. Butrymowicz. 1986, 14p Pub. in Proceedings of International Conference and Exposition on Fatigue, Corrosion Cracking, Fracture Mechanics and Failure Analysis, Salt Lake City, UT., December 2-6, 1985, p1-14 1986.

Keywords: *Fractures(Materials), Measurement, Failure, Prevention, *Technology transfer, National Institute of Standards and Technology.

As a Commerce Department agency, the National Bureau of Standards (NBS) provides the measurement foundation that the national industrial economy needs. Crucial to the needs are the safe, efficient, and economical use of materials. The NBS programs that support generic technologies in materials and the mechanisms by which fundamental information is transferred are analyzed. Specific examples are drawn from recent developments in fracture of materials.

PB89-228332 PC A13/MF A01 National Inst. of Standards and Technology, Gaithers-International Cooperation and Competition in Ma-

terials Science and Engineering. L. H. Schwartz, and S. J. Schneider. Jun 89, 280p NISTIR-89/4041

Keywords: *Engineering, *Research management, Graphs(Charts), Competition, *Materials science, International cooperation, Coordinated research pro-

In 1986, the National Research Council commissioned a Committee on Materials Science and Engineering (COMMSE) to conduct a comprehensive study of the field, to define its progress, assess needs and opportunities and provide policy guidance at the national level.

A Summary Report of COMMSE was published in 1989; it was based primarily on informational inputs generated by five separate panels, each charged to investigate a different aspect of Materials Science and investigate a different aspect of Materials Science and Engineering (MSE). The report documents the results of the individual study conducted by the COMMSE Panel 3 on International Cooperation and Competition in MSE. It deals with many facets of MSE, as practiced in other countries, and in the United States. It surveys national policies and programs for science and technology and MSE, elaborates on administrative structures to carry out R&D, and provides comparisons between the United States and the major industrial nations of the world. Much of the content revolves tions of the world. Much of the content revolves around the theme of industrial competitiveness as influenced by cooperative R&D.

MATHEMATICAL SCIENCES

Algebra, Analysis, Geometry, & Mathematical Logic

901,192 AD-A201 256/5 PC A03/MF A01 Maryland Univ., College Park. Error Bounds for Linear Recurrence Relations. F. W. Olver. Apr 88, 18p ARO-20606.9-MA Contract DAAG29-84-K-0022, Grant NSF-DMS84-19820

Pub. in Mathematics of Computation, v50 n182 p481-499 Apr 88.

Keywords: Arithmetic, *Numerical analysis, Oscillation, *Statistical processes, Linearity, Monotone functions, *Linear recurrence relations.

Recurrence relations of a certain form are examined in Hecurrence relations or a certain form are examined in two cases. In both cases, a posteriori methods are supplied for constructing strict and realistic error bounds in O (r) arithmetic operations. A priori bounds, also requiring O (r) arithmetic operations, are supplied in Case B. Several illustrative numerical examples are included. Keywords: Numerical analysis, Oscillatory systems, Monotonic systems.

901,193 PB89-143283 PC A03/MF A01 National Inst. of Standards and Technology (NEL), Gaithersburg, MD. Center for Computing and Applied Mathematics. Finite Unions of Closed Subgroups of the n-Dimen-

J. Lawrence. Aug 88, 24p NISTIR-88/3777
Prepared in cooperation with George Mason Univ.,

Keywords: *Lattices(Mathematics), Analytic geometry, Optimization, *Toruses, Polytopes, Subgroups.

Let U be an open subset of the torus group T sup n. We show that the set of maximal subgroups of T sup n which miss U is of finite cardinality. This result is applied to show that the lattice of finite unions of closed subgroups of T sup n is a complete distributive lattice, and to show that, up to unimodular equivalence, there are only finitely many convex polytopes P R sup n having vertices in Z sup n but no interior points in Z sup n and such that each subgroup G of the additive group R sup n which properly contains Z sup n does have points in common with the interior of P.

901,194 PB89-147425 PB89-147425 Not available NTIS National Bureau of Standards (NEL), Gaithersburg, MD. Scientific Computing Div.

Mathematical Software: PLOD. Plotted Solutions of Differential Equations.

Final rept. E. Agron, I. L. Chang, G. Gunaratna, D. K. Kahaner, and M. Reed. 1988, 6p
Pub. in IEEE (Institute of Electrical and Electronics En-

gineers) Micro 8, n4 p56-61 Aug 88.

Keywords: *Ordinary differential equations, *Problem solving, Plotting, Reprints, *Computer software, Interactive systems, IBM-PC computers.

PLOD is an acronym for Plotted solutions of Differential Equations. PLOD can solve up to 25 ordinary differential equations with 10 parameters. It is entirely interactive, requiring very little programming experience. PLOD uses state-of-the-art numerical methods to perfect the state of the programming experience. form the integration. The current version of PLOD has been implemented on the IBM Personal Computer family, including the XT, and AT. PLOD is in the public

901,195 PB89-158166 Not available NTIS National Bureau of Standards (NEL), Gaithersburg, MD. Scientific Computing Div.

Numerical Evaluation of Certain Multivariate Normal Integrals.

Final rept. A. Genz, and D. K. Kahaner. 1986, 4p Pub. in Jnl. of Computational and Applied Mathematics 16, n2 p255-258 Oct 86.

Keywords: Multivariate analysis, Numerical quadrature, Iteration, Computation, Numerical integration, Reprints, *Integrals.

It is shown that a multivariate normal integral with tridiagonal covariance matrix can be computed efficiently using iterated integration.

901.196 PB89-171623 Not available NTIS National Bureau of Standards (NEL), Gaithersburg, MD. Robot Systems Div.
Real Time Generation of Smooth Curves Using Local Cubic Segments. Final rept. M. Roche, and W. Li. 1988, 9p Pub. in ACCESS 7, n6 p23-31 Nov/Dec 88.

Keywords: *Curve fitting, *Real time operations, Algorithms, Interpolation, Coordinates, Reprints, Spline functions.

Computer listings of coded curve fitting algorithms for interpolation of coordinate points as they are generated are presented. As coordinate values are determined, they are added to an array and an interpolation procedure is applied to the new coordinate values of the array. In particular, as the sequence is being in-creased, it will be interpolated by a local cubic fitting procedure. The report exhibits a procedure which limits the cubic construction to be one segment behind the last segment of the sequence. The last input co-ordinate values are not the end points for the cubic segment being constructed. Another procedure will include these last input coordinate values as end coordinate values for the last cubic segment being generated. As will be seen, these methods lend themselves to real time curve generation.

901,197 Not available NTIS PB89-172522 MD. Center for Applied Mathematics.

How to Estimate Capacity Dimension.

F. Sullivan, and F. Hunt. 1988, 4p Pub. in Nuclear Physics B 5A, p125-128 1988.

Keywords: Monte Carlo method, Estimates, Algorithms, Reprints, *Euclidean space, Data compression, Fractal dimensions, Strange attractors, Robustness (Mathematics), Sorting, Chaos.

The authors describe a class of robust, computationally efficient algorithms for estimating capacity dimension and related quantities for compact subsets of (R sup n). The algorithms are based on Monte Carlo quadrature, data compression, and generalized distance functions.

901,198 Not available NTIS PB89-175871 National Bureau of Standards (NEL), Gaithersburg, MD. Scientific Computing Div.

Efficient Algorithms for Computing Fractal Dimen-

sions.

Final rept. F. Hunt, and F. Sullivan. 1986, 8p Pub. in Springer Series Synergetics 32, p74-81 1986.

Keywords: *Dimensions, Dimensional analysis, Algorithms, Monte Carlo method, Point set topology, Reprints, *Fractals, Data structures, Vector processing.

Algebra, Analysis, Geometry, & Mathematical Logic

The purpose is to describe a new class of methods for computing the 'capacity dimension' and related quantities for point-sets. The techniques presented here build on existing work which has been described in the literature. The novelty of the methods lies first in the approach taken to the definition of computation of dimension (namely, via Monte Carlo calculation of the volume of an epsilon-cover of the point-set), and second in the use of data structures which result in extremely efficient codes for vector computers such as the Cyber 205 (the computation is reduced to the sorting and searching of one-dimensional arrays so that a calculation employing one million points requires less than 2 minutes).

901,199 PB89-177034 Not available NTIS National Bureau of Standards (NEL), Gaithersburg, MD. Mathematical Analysis Div.

Note on the Capacitance Matrix Algorithm, Sub-structuring, and Mixed or Neumann Boundary Conditions.

Final rept.

D. P. O'Leary. 1987, 7p Pub. in Applied Numerical Mathematics 3, n4 p339-345 1987.

Keywords: *Matrices(Mathematics), *Elliptic differential equations, Partial differential equations, Algorithms, Reprints.

The paper develops variants of the capacitance matrix algorithm which can be used to solve discretizations of elliptic partial differential equations when either the original system of equations or one which arises from substructuring has a rank deficient matrix.

901,200 PB89-209332 PC A03/MF A01 National Inst. of Standards and Technology (NEL), Gaithersburg, MD. Applied and Computational Mathematics Div. Expected Complexity of the 3-Dimensional Vor-onol Diagram.

J. Bernal. May 89, 23p NISTIR-89/4100

Keywords: *Euclidean geometry, A Cubes(Mathematics), *Voronoi diagrams, drons, Complexity, Flat surfaces, Apexes. Algorithms, ns, *Polyhe-

Let S be a set of n sites chosen independently from a Let S be a set of n sites chosen independently from a uniform distribution in a cube in 3-dimensional Euclidean space. Work by Bentley, Weide and Yao is extended to show that the Voronoi diagram for S has an expected O(n) number of faces. A consequence of the proof of the result is that the Voronoi diagram for S can be constructed in expected O(n) time. Finally, it is shown that with the exception of at most an expected O(n) surg(2/3) number of polyhedra. O(n sup(2/3)) number of polyhedra, each polyhedron in the Voronoi diagram for S has an expected constant number of faces.

901,201 PB90-123654 PB90-123654 Not available NTIS National Bureau of Standards (NEL), Gaithersburg, MD. Scientific Computing Div.

Guide to Available Mathematical Software Adviso-

Final rept.
R. F. Boisvert. 1989, 11p
Pub. in Mathematics and Computers in Simulation 31, p453-463 1989.

Keywords: *Applications of mathematics, *Statistical analysis, Artificial intelligence, Documentation, Reprints, *Computer applications, *Computer software, Expert systems, Interactive systems, On line systems, Data bases.

The primary goal of the Guide to Available Mathematical Software (GAMS) project is to provide convenient access to information about mathematical and statistical software which is available to computer users at the National Institute for Standards and Technology. The principal vehicle through which the information is disseminated is an on-line advisory system called the GAMS Interactive Consultant. The paper describes the current status of the GAMS project. It then enumerates some of the weaknesses of the system and suggests knowledge engineering techniques which may alleviate them.

901,202 PB90-123688 Not available NTIS National Bureau of Standards (NEL), Gaithersburg, MD. Scientific Computing Div.

Shortest Paths in Simply Connected Regions in R2.

Final rept.

R. D. Bourgin, and P. L. Renz. 1989, 36p Pub. in Advances in Mathematics 76, n2 p260-295 1989.

Keywords: Topology, Reprints, *Jordan regions, Shortest paths.

Let R be a Jordan region in R2. A number of questions are settled concerning shortest paths in such regions: If there is a rectifiable path in R joining given points p and q then there is a unique shortest path in R joining these points. This path may be characterized by local geometric conditions. If another path joins p and q within R, a quantitative bound determined solely by the arclengths of this path and of the shortest path is presented which determines a tube about the shortest path guaranteed to contain the other path. When no rectifiable path in R exists joining p and q, there is, nevertheless, a unique locally shortest path in R joining them. Finally, the pathology-free nature of shortest paths is explicitly demonstrated by characterizing their connected sections within the boundary of R as well as within its interior.

901,203
PB90-129982
PC A03/MF A01
National Inst. of Standards and Technology (NEL),
Gaithersburg, MD. Center for Computing and Applied Mathematics.

Polytope Volume Computation.
J. Lawrence. Oct 89, 27p NISTIR-89/4123
Prepared in cooperation with George Mason Univ., Fairfax, VA.

Keywords: *Volume, Algorithms, Simplex method, Linear programming, Linear inequalities, *Polytopes.

A combinatorial form of Gram's relation of convex polytopes can be adapted for use in computing polytope volume. The author presents an algorithm for volume computation based on the observation. The algorithm is useful in finding the volume of a polytope given as the solution set to a system of linear inequalities. As an example of the application of the method, the author computes a formula for the volume of a projective image of the n-cube.

Operations Research

901,204
PB89-174049
National Bureau of Standards (NML), Boulder, CO. Time and Frequency Div.

Variances Based on Data with Dead Time between

the Measurements.

J. A. Barnes, and D. W. Allan. 1987, 8p Pub. in Proceedings of Annual Precise Time and Time Interval (PTTI) Applications and Planning Meeting (19th), Redondo Beach, CA., December 1-3, 1987, D227-234

Keywords: *Variance(Statistics), *Dead time, Bias, Displacement, Errors, Damping, Delay time, Resolution, Sensitivity, Data sampling, Frequency stability.

In 1974 a table of bias functions which related variance estimates with various configurations of number of samples and dead time to the two-sample (or Allan) variance was published. The tables were based on noises with pure power-law power spectral densities. Often situations recur which unavoidably have distributed dead time between measurements, but still the conventional variances are not convergent. Some of these applications are outside of the time and frequency field. Also, the dead times are often distributed throughout a given average, and this distributed dead time is not treated in the 1974 tables. The paper reviews the bias functions B1(N_r,r_mu), and B2(r,r_mu) and introduces a new bias function B3(2,r_mu), to handle the commonly occurring cases of the effect of distributed dead time or the page state. uted dead time on the computed variances. Some convenient and easy ways to interpret asymptotic limits are reported.

901,205 PB89-211957 Not available NTIS National Bureau of Standards (NEL), Gaithersburg, MD. Mathematical Analysis Div.

Electronic Mail and the 'Locator's' Dilemma. Final rept.

. Witzgall, and P. B. Saunders, 1988, 20p Pub. in Applications of Discrete Mathematics, p65-84 1988

Keywords: *Linear programming, *Optimization, Telecommunication, Benefit cost analysis, Return on investment, Reprints, Electronic mail, Communication networks, Cost benefit analysis.

A general methodology for optimally selecting subconfigurations from a given universal configuration is discussed. It is based on a method for assessing the effects of shared fixed costs developed by J. M. W. Rhys and M. L. Balinski. A parametric minimum cost network flow algorithm for solving the resulting optimization problems is described. The problem arose in connection with a cost-benefit model called PAREC whose purpose was to analyze particular configurations of a contemplated electronic mail or message service system.

901,206

PB90-112335 PC A03/MF A01 National Inst. of Standards and Technology (NEL), Gaithersburg, MD. Factory Automation Systems Div. Modeling Dynamic Surfaces with Octrees. D. Libes. Sep 89, 14p NISTIR-89/4055

Keywords: *Mathematical models, Monte Carlo method, *Three dimensional models, *Octrees, Data structures, Dynamic models, Systems simulation.

Octrees in the past have been used to represent static objects. The paper discusses the extensions necessary to model dynamic surfaces. One particularly important aspect is the ability to represent expanding surfaces that grow to be arbitrarily large. The ability to represent dynamic surfaces allows one to apply octrees to new problems which could not previously have been modeled with static octrees. One such problem is the 'entropy of random surfaces.' Using dynamic octrees, a simulation of self-avoiding random surfaces using Monte Carlo techniques is produced.

901,207

PB90-112392 PC A03/MF A01 National Inst. of Standards and Technology (NEL), Gaithersburg, MD. Center for Mfg. Engineering. FACTUNC: A User-Friendly System for Uncon-strained Optimization.

R. H. F. Jackson, G. P. McCormick, and A. Sofer. Aug 89, 37p NISTIR-89/4159

Prepared in cooperation with George Washington Univ., Washington, DC. Dept. of Operations Research, and George Mason Univ., Fairfax, VA. Dept. of Operations Research and Applied Statistics.

Keywords: *Nonlinear programming, Functions(Mathematics), Optimization, Constraints, Mathematical models, Regression analysis. *Nonlinear

FACTUNC is a system for solving unconstrained minimization problems based on the concept of factorable programming. The concept enables the user to pro-vide the problem function and data in a user friendly way and does not require user-supplied derivatives. system utilizes the factorable function concept to obtain the first and second derivatives required for unconstrained optimization. As a system for nonlinear minimization, FACTUNG allows several options. First the user can solve regression (nonlinear least squares) problems by providing the regression equation and the data for the dependent and independent variables. The second option allows for the minimization of the sum of an indexed function. The user provides the function, and the indexed data. The third option is simply to minimize a function supplied by the user. Utilizing barrier function methodology, the third option can sometimes be used to solve constrained prob-

901,208

PB90-123944 Not available NTIS National Bureau of Standards (NEL), Gaithersburg, MD. Scientific Computing Div.

Merit Functions and Nonlinear Programming.

Final rept.

J. W. Tolle, and P. T. Boggs. 1988, 8p Pub. in Proceedings of International Conference on Operational Research (11th), Buenos Aires, Argentina, August 10-14, 1987, p882-889 1988.

MATHEMATICAL SCIENCES

Operations Research

Keywords: *Nonlinear programming, *Algorithms, Optimization, Operations research, Convergence.

In the paper, a ment function for inequality constrained nonlinear programs is proposed. A local convergence theorem is stated for an algorithm using the merit function in conjunction with a sequential quadratic pro-gramming procedure for generating steps. The algo-rithm is shown to permit unit step lengths in the pres-ence of superlinear convergence.

Statistical Analysis

901,209 PB89-157812 PB89-157812 Not available NTIS National Bureau of Standards (NEL), Boulder, CO. Statistical Engineering Div. Problems with Interval Estimation When Data Are

Adjusted via Calibration.

Final rept.

J. M. Mulrow, D. F. Vecchia, J. P. Buonaccorsi, and H. K. Iyer. 1988, 15p Pub. in Jnl. of Quality Technology 20, n4 p233-247 Oct

Keywords: *Confidence limits, Error analysis, Estimates, Measurement, Reprints, *Tolerance limits, mates, Measurement, Reprints, Calibration.

The analysis of adjusted data arising from a linear calibration curve is considered. Although it is obvious that adjusted values contain errors due to estimation of the calibration curve, some investigators may be tempted to analyze such data as if one applies 'naive' analyses to calibrated data. In particular, it is shown that standard one-sample confidence intervals have actual confidence levels that are always less than the nominal value. The authors also propose and evaluate two other methods for constructing confidence intervals.

Tolerance intervals derived from adjusted data also may yield deceiving results, having actual probability levels that are usually greater than the desired level but smaller in some cases.

901,210 PB89-157820 Not available NTIS National Bureau of Standards (NEL), Boulder, CO. Statistical Engineering Div.
Estimation of the Error Probability Density from

Repilcate Measurements on Several items.

Final rept.

W. Liggett. 1988, 11p Pub. in Biometrika 75, n3 p557-567 1988.

Keywords: *Error analysis, Orthogonal functions, Monte Carlo method, Variance(Statistics), Probability density functions, Measurement, Computation, Esti-mates, Reprints, Robustness (Mathematics), Hermite polynomials.

Estimation of the measurement error probability density from data that consist of a few measurements on each of several dissimilar items is investigated. An estimator is proposed for independent and identically distributed measurement error with a symmetric density function. This estimator is based on an orthogonal function expansion. Computation begins with the differences between measurements on the same item and makes use of the fact that the characteristic func-tion of these differences equals the square of the characteristic function of the measurement error. Application to robust inference for items measured in triplicate is considered. The M-estimates of the values of the items are compared on the basis of an estimated standard error computed from the density estimate. The circumstances under which this standard error estimator provides nearly valid inferences are delimited by Monte Carlo experiments.

901,211 PB89-171847 Not available NTIS National Bureau of Standards (NEL), Gaithersburg, MD. Statistical Engineering Div.

Minimax Approach to Combining Means, with Practical Examples.

Final rept. K. R. Eberhardt, C. P. Reeve, and C. H. Spiegelman. 1989, 20p Grant N00014-86-F-0025

Sponsored by Office of Naval Research, Arlington, VA. Pub. in Chemometrics and Intelligent Laboratory Systems 5, p129-148 1989.

Keywords: *Minimax technique, *Mean, Comparison, Estimating, Confidence limits, Statistics, Reprints.

The paper describes a method for combining sample means that accounts for bias in those means. It compares the unweighted mean, the weighted mean using reciprocal estimated variances for weights, and a minimax weighted mean. When the individual means are subject to nontrivial biases, the authors show that the minimax estimator can lead to important decreases in mean squared error and confidence interval width. The recommendations are based on statistical theory and on simulations based on three Standard Reference Material data sets.

901,212 PB89-201131 Not available NTIS National Bureau of Standards (NEL), Gaithersburg, MD. Statistical Engineering Div. Estimation of an Asymmetrical Density from Severai Small Samples.

Final rept. W. Liggett. 1989, 9p Pub. in Biometrika 76, n1 p13-21 1989.

Keywords: *Skewed density functions, *Estimating, Probability density functions, Orthogonal functions, Statistical samples, Monte Carlo method, Least squares method, Reprints, Hermitian polynomial.

A method for estimation of the measurement error probability density from three or more measurements on each of several dissimilar items is presented. Differences between measurements on the same item provide estimates of the densities of the first and second differences between error realizations. The relations between these densities and the error density, ex-pressed in terms of characteristic functions and Her-mite function expansions, are the basis for a nonlinear least-squares algorithm. Estimated percentiles of the error density are investigated by Monte Carlo experi-ments. The method is applied to measurements by several laboratories on an inhomogeneous reference material with asymmetric variability.

901,213 PB89-211130

(Order as PB89-211106, PC A04) National Inst. of Standards and Technology, Gaithersburg, MD.

Consensus Values, Regressions, and Weighting Factors.

Bi-monthly rept. R. C. Paule, and J. Mandel. 1989, 7p Included in Jnl. of Research of the National Institute of Standards and Technology, v94 n3 p197-203 May-Jun

Keywords: Variance(Statistics), Regression analysis, Taylor series, Computation, Convergence, *Consensus values, Weighted average, Iterative methods.

An extension to the theory of consensus values is presented. Consensus values are calculated from averages obtained from different sources of measurement. Each source may have its own variability. For each average a weighting factor is calculated, consisting of contributions from both the within- and the betweensource variability. An iteration procedure is used and calculational details are presented. An outline of a proof for the convergence of the procedure is given. Consensus values are described for both the case of the weighted average and the weighted regression.

901,214 PB89-215321 PC A03/MF A01 National Inst. of Standards and Technology (NEL), Gaithersburg, MD. Applied and Computational Mathematics Div. Computation and Use of the Asymptotic Covar-

lance Matrix for Measurement Error Models P. T. Boggs, and J. R. Donaldson. 26 Jun 89, 30p NISTIR-89/4102

Keywords: *Measurement, *Error analysis, Simultaneous equations, Covariance, Regression analysis, Confidence limits, Monte Carlo method, Matrices(Mathematics), Optimization.

The measurement error model assumes that errors occur in both the response variables and the predictor variables. In using this model, it is of interest to compute confidence regions and intervals for the estima-tors of the model parameters. An asymptotic form for the covariance matrix is used to construct approximate confidence regions and intervals. The solution of the minimization problem resulting from the use of the measurement error model is discussed, and a procedure for accurately computing the covariance matrix is developed. Then the quality of the confidence regions and intervals constructed from this matrix is assessed via a Monte Carlo study.

901,215

PB89-229066 PC A05/MF A01 National Inst. of Standards and Technology (NEL), Gaithersburg, MD. Applied and Computational Mathematics Div.

User's Reference Guide for ODRPACK: Software for Weighted Orthogonal Distance Regression Version 1.7.

Internal rent.

P. T. Boggs, R. H. Byrd, J. R. Donaldson, and R. B. Schnabel. Aug 89, 79p NISTIR-89/4103 Prepared in cooperation with Colorado Univ. at Boul-

der. Dept. of Computer Science.

Keywords: *Curve fitting, *Data smoothing, Orthogonality, Regression analysis, Algorithms, Mathematical models, Errors, Least squares method, Data, *User manuals(Computer programs), Computer applications, Independent variables, Dependent variables.

ORDPACK is a portable collection of NASI 77 Fortran subroutines for fitting a model to data. It is designed primarily for instances when the independent as well as the dependent variables have significant errors, implementing a high efficient algorithm for solving the weighted orthogonal distance regression problem, i.e., for minimizing the sum of the squares of the weighted orthogonal distances between each data point and the curve described by the model equation. It can also be used to solve the ordinary least squares problem where all of the errors are attributed to the observations of the dependent variable. A complete description of the orthogonal distance regression problem and the algorithm and implemented in ORDPACK is given by Boggs et al. ORDPACK is designed to handle many levels of user sophistication and problem difficulty.

MEDICINE & BIOLOGY

Anatomy

901.216

PB89-230478 Not available NTIS National Inst. of Standards and Technology (ICST), Gaithersburg, MD. Advanced Systems Div.

Analysis of Ridge-to-Ridge Distance on Finger-

prints. Final rept.

R. T. Moore, 1989, 8p

Sponsored by Federal Bureau of Investigation, Washington, DC.

Pub. in Jnl. of Forensic Identification 39, n4, p231-238, Jul/Aug 89.

Keywords: Females, Males, Distance, Reprints, *Forensic medicine, *Fingerprints.

The distance from the center of one friction skin ridge to the center of the ridge next to it is quite variable in different regions of a given fingerprint. This distance has been measured on a small sample of fingerprints. The measured value ranged from 0.2 mm to 0.85 mm on fingerprints from male subjects, and from 0.2 mm to 0.75 mm on fingerprints from female subjects. The mean ridge-to-ridge distance for 731 measurements on the fingerprints of ten male subjects was 0.46 mm. For 1,046 measurements on the fingerprints of ten female subjects the mean value was 0.41 mm. A method is described for using these values to calculate ridge counts between near neighboring minutiae. Estimates are made of the errors likely to result from the use of calculated ridge counts.

Biochemistry

901,217 PB89-156897 Not available NTIS National Bureau of Standards (NML), Gaithersburg, MD. Inorganic Analytical Research Div.

Sequential Determination of Biological and Pollutant Elements In Marine Bivalves.

Final rept.

R. Zeisler, S. Stone, and R. Sanders. 1988, 6p Pub. in Analytical Chemistry 60, n24 p2760-2765, 15 Dec 88.

Keywords: *Marine biology, *Mollusca, *Radioassay, *X ray fluorescence, Neutron absorption, Neutron activation analysis, Nondestructive analysis, Trace elements, Sequential analysis, Reprints, *Bivalves.

A unique sequence of instrumental methods has been employed to obtain concentrations for 44 elements in marine bivalves tissue. The techniques used were X-ray fluorescence, prompt gamma activation analysis, and neutron activation analysis. It is possible to use a single subsample and follow it nondestructively through the three instrumental analysis techniques. A final radiochemical procedure for tin was also applied after completing the instrumental analyses. Comparison of results for elements determined by more than one technique in sequence showed good agreement, as did results from certified reference material samples analyzed along with the samples. The concentrations found in the bivalve samples ranged from carbon at more than 50% dry weight down to gold at several microgram per kilogram.

901.218

PB89-156905 Not available NTIS National Bureau of Standards (NML), Gaithersburg,

MD. Inorganic Analytical Research Div.
Sample Valldity in Biological Trace Element and
Organic Nutrient Research Studies.

Final rept.

G. V. lyengar. 1987, 10p Sponsored by Department of Agriculture, Beltsville, MD., and Food and Drug Administration, Washington,

Pub. in Jnl. of Radioanalytical and Nuclear Chemistry 112, n1 p151-160 1987.

Keywords: *Trace elements, *Sampling, *Bioassay, Contamination, Acceptability, Selection, Validity, Standards, Nutrients, Storage, Preservation, Organic compounds, Tissues(Biology), Biological extracts, Re-

The complexities involved in dealing with the requirements of trace element research studies in the life sciences demand a comprehensive planning of the investigations and use of a variety of techniques. It also requires a combination of biological insight and analytical awareness on the part of the investigators in order to obtain valid samples for analysis. Thus, the generation of meaningful conclusions from elemental composition studies on biological systems is vital for the overall success of the investigations. In addition, new initiatives are needed to produce multipurpose biological reference standards to cope with the growing demands of this multifaceted area of research. These aspects are discussed.

901.219

PB89-157770 Not available NTIS Not available NTIS
National Bureau of Standards (NML), Gaithersburg,
MD. Office of Standard Reference Materials.
NBS (National Bureau of Standards) Activities in
Biological Reference Materials.

Final rept.

S. D. Rasberry. 1988, 5p Pub. in Fresenius' Zeitschrift fuer Analytische Chemie 332, p528-532 1988.

Keywords: *Biological products, *Cholesterol, *Vitamins, *Diet, *Nutrition, Reprints, *Standard Reference Materials.

National Bureau of Standards (NBS) activities in biological reference materials during 1986 - 1988 are described with a preview of plans for future certifications of reference materials. During the period, work has been completed or partially completed on about 40 reference materials of importance to health, nutrition, and environmental quality. Some of the reference materials that have been completed during the period and are described include: creatinine (SRM) 914a), bovine serum albumin (SRM 927a), cholesterol in human serum (SRMs 1951 - 1952), aspartate aminotransferase (RM 8430), cholesterol and fat-soluble vitamins in coconut oil (SRM 1563), wheat flour (SRM 1567a), rice flour (SRM 1568a), mixed diet (RM 8431a), dinitropyrene isomers and 1-nitropyrene (SRM 1596), and complex PAHs from coal tar (SRM 1597). Oyster tissue (SRM 1566a) is being analyzed and should be available in 1988. able in 1988.

PB89-177216 Not available NTIS National Bureau of Standards (IMSE), Gaithersburg, MD. Ceramics Div.

Element-Specific Eplfluorescence Microscopy In vivo Monitoring of Metal Biotransformations in Environmental Matrices.

Final rept.

T. K. Trout, G. J. Olson, F. E. Brinckman, J. M. Bellama, and R. A. Faltynek. 1989, 14p Pub. in ACS (American Chemical Society) Symposium Series 383, Chapter 6, p84-97 1989.

Keywords: *In vivo analysis, *Quantitative analysis, *Metals, *Absorption spectra, Bioaccumulation, Chemical analysis, Fluorescence, *Epifluorescence microscopy, Fluorescence spectroscopy

Quantitative measurement of metal ion uptake in living cells is accomplished via staining the biota with an appropriate fluorogenic ligand, determining the emission photon flux by epifluorescence microscopy imaging (EMI), and relating the latter quantity to absolute metal ion concentration by atomic absorption analysis. By thus combining the techniques of element-specific fluorimetry and EMI, it is possible to observe the chemistrations of the second of the contraction of the c istry occurring during redox transformations of ele-ments by colonies of living cells in reactions that have significant economic potential. The strengths, weaknesses, and future directions to be taken in improving this analytical method are discussed.

901,221 PB89-186761 PB89-186761 Not available NTIS National Bureau of Standards (NML), Gaithersburg, MD. Chemical Thermodynamics Div.
Thermodynamics of Hydrolysis of Disaccharides. Final rept.

Y. B. Tewari, and R. N. Goldberg. 1989, 6p Pub. in Jnl. of Biological Chemistry 264, n7 p3966-3971, 5 Mar 89.

Keywords: *Thermodynamics, *Hydrolysis, *Disaccharides, Carbohydrates, Cellobiose, Enzymes, Maltose, Chromatographic analysis. Calonmetry, Enthalpy, Entropy, Reprints, Enzymatic hydrolysis, Gentiobiose, Isomaltose.

The thermodynamics of the enzymatic hydrolysis of The thermodynamics of the enzymatic hydrolysis of cellobiose, gentiobiose, isomaltose, and maltose have been studied using both high pressure liquid chromatography and microcalorimetry. The hydrolysis reactions were carried out in aqueous sodium acetate buffer at a pH of 5.65 and over the temperature range of 286 to 316 K using the enzymes Beta-glucosidase, isomaltase, and maltase. The thermodynamic parameters were obtained for the hydrolysis reactions, disaccharide(aq) + H2O(liq) = 2 glucose(aq), at 298.15 K. The standard state is the hypothetical ideal solution of unit molality. Due to enzymatic inhibition by glucose, it was not possible to obtain reliable values for the equilibrium constants for the hydrolysis of either for the equilibrium constants for the hydrolysis of either cellobiose or maltose. The entropy changes for the hydrolysis reactions are in the range 32 to 43 J/mol K; the heat capacity changes are approximately equal to zero J/mol K. Additional pathways for calculating thermodynamic parameters for these hydrolysis reactions are discussed.

901,222 PB89-186803 Not available NTIS National Bureau of Standards (NML), Gaithersburg, MD. Chemical Thermodynamics Div.
Water Structure In Vitamin B12 Coenzyme Crys-

tals. 1. Analysis of the Neutron and X-ray Solvent Densities. Final rept.

H. Savage. 1986, 19p See also PB89-186811. Pub. in Biophysical Jnl. 50, n5 p947-965 1986.

Keywords: *Water, *Molecular structure, Crystal structure, Neutron diffraction, Vitamin B12, X ray diffraction, Reprints, *Vitamin B 12 coenzymes.

The disordered solvent distribution in crystals of vitamin B12 coenzyme was examined using the methods

of high resolution neutron and X-ray diffraction. One set of neutron (0.95A) and two sets of X-ray (0.94A and 1.1A) data were collected and the resulting models were extensively refined using least squares and Fourier syntheses. The solvent regions were analysed in two changes firstly. lysed in two stages: firstly, 'main' sites were assigned to the well defined regions of solvent density and refined using least squares; secondly, 'continuous' sites were assigned representing the more disordered diffuse and elongated regions of solvent density around and between the main sites. Water networks were for-mulated from the assigned sites in the above three models and also from those assigned in the original structure determination. The well established networks extend throughout all the solvent regions of the crystal with interesting orientational arrangements of the individual waters around both polar and apolar groups of the coenzyme molecule. The networks were seen to be consistent among each of the four models in terms of occupying relatively similar positions, however, the occupancy values of the individual networks varied between the models.

901,223 PB89-186811 Not available NTIS National Bureau of Standards (NML), Gaithersburg, MD. Chemical Thermodynamics Div.

Water Structure In Vitamin B12 Coenzyme Crystals. 2. Structural Characteristics of the Solvent Networks.

Final rept.

H. Savage. 1986, 14p See also PB89-186803.

Pub. in Biophysical Jnl. 50, n5 p967-980 1986.

Keywords: *Water, *Molecular structure, Crystal structure, Vitamin B12, Reprints, *Vitamin B12 coenzymes, Biomolecules, Hydrogen bonding.

The geometrical details of the solvent structure in vitamin B12 coenzyme crystals with respect to hydrogen bonding and non-bonded contacts are described. The individual H-bond geometries varied over wide ranges, similar to those observed in small molecule structures. Large deviations from tetrahedral coordination were found around a majority of the waters. The mutual positions and orientations of the water molecules could not be adequately explained in terms of the H-bonding relationships present in the structure. However, additional investigations which focused on the short range non-bonded contacts around water positions in a variety of crystal hydrates, revealed several structural regularities. These features relate to the non-bonded O...O, H...O and H...H interactions and give rise to a set of repulsive restrictions that are seen to be very much stronger stereochemical restraints than those associated with H-bonding. The repulsive restrictions can be used as stereochemical restraints in the interpretation and refinement of solvent structures within larger hydrate systems such as protein crystals. They may also be included in potential functions used to simulate solvent structures in aqueous solutions and hydrate sys-

901,224 PB89-201594 Not available NTIS National Bureau of Standards (NML), Gaithersburg, MD. Chemical Thermodynamics Div.

Crystal Structure of a Cyclic AMP (Adenosine Monophosphate)-Independent Mutant of Catabolite Gene Activator Protein.

Final rept. I. T. Weber, G. L. Gilliland, J. G. Harman, and A.

Peterkofsky. 1987, 7p Pub. in Jnl. of Biological Chemistry 262, n12 p5630-5636 1987.

Keywords: *Crystal structure, Mutations, Reprints, *Cyclic AMP receptors, *Catabolite gene activator proteins, Genetic mapping, Conformation change.

E. coli NCR91 synthesizes a mutant form of catabolite gene activator protein in which alanine 144 is replaced by threonine. This mutant, which also lacks adenyl cyclase activity, has a crp* prenotype; in the absence of cAMP it is able to express genes that normally require cAMP. CRP91 has been purified and crystallized with cAMP. CRP91 has been purified and crystallized with cAMP under the same conditions as crystals of the wild type GAP-cAMP complex. X-ray diffraction data were measured to 2.3A resolution on a Xentronics area detector and the CAP91 structure was determined using initial model phase from the wild type structure. A difference Fourier map calculated between CAP91 and wild type showed the two alongs. tween CAP91 and wild type showed the two alanine to threonine sequence changes in the dimer and also a

Biochemistry

change in the side chain of cysteine 178 in one of the subunits. The CAP91 coordinates were refined by restrained least-squares to an R factor of 0.186. Small changes in the atomic positions of the wild type and mutant protein structures were analyzed by a local vector average. The change included concerted motions of the small domains, the hinge between the two domains and in an adjacent loop between two beta strands. The mutation apparently caused changes in position of the protein atoms that are distal to the mu-

PB89-202576 Not available NTIS National Bureau of Standards (NEL), Gaithersburg, MD. Fire Measurement and Research Div. Spectroscopic Quantitative Analysis of Strongly Interacting Systems: Human Plasma Protein Mixtures.

Final rept. M. R. Nyden, G. P. Forney, and K. Chittur. 1988, 7p Sponsored by National Institutes of Health, Bethesda,

Pub. in Applied Spectroscopy 42, n4 p588-594 1988.

Keywords: *Spectroscopic analysis, *Humans, *Infra-reo spectra, Proteins, Quantitative analysis, Reprints, *Plasma proteins, Blood proteins.

Blood plasma protein infrared spectra, while qualitatively very similar, display subtle differences in the frequencies and intensities of absorption bands. These small differences are sufficient to permit an accurate quantitative analysis of mixtures of these proteins. In the paper the authors examine the performance of some alternative methods of spectroscopic quantitative analysis in determining the concentrations of pro-teins in aqueous solutions. The widely-used K matrix method, using sloping baselines and intercept func-tions, was found to be inadequate for these determinations. In contrast, a method based on the little-known Q matrix approach, augmented by a robust equation solver, yielded results with a sufficient degree of accuracy to make it a viable tool for use in the study of proteins at solid interfaces and for more general applications in the field of protein chemistry.

901.226 PB89-227888 Not available NTIS National Inst. of Standards and Technology (NML), Gaithersburg, MD. Chemical Thermodynamics Div. Calorimetric and Equilibrium Investigation of the Hydrolysis of Lactose. Final rept.

R. N. Goldberg, and Y. B. Tewari. 1989, 4p Pub. in Jnl. of Biological Chemistry 264, n17 p9897-9900, 15 Jun 89.

Keywords: *Lactose, *Heat measurement, *Chemical equilibrium, Hydrolysis, Catalysis, Thermochemistry, Glucose, Galactose, Hypotheses, Reprints, Beta-ga-

The thermodynamics of the hydrolysis of lactose to glucose and galactose have been investigated using both high pressure liquid chromatography and heat conduction microcalorimetry. The reaction was carried out over the temperature range 282-316 K and in 0.1 M sodium acetate buffer at a pH of 5.65 using the enzyme beta-galactosidase to catalyze the reaction. The standard state is the hypothetical ideal solution of unit molality. Thermochemical cycle calculations using enthalpies of combustion and solution, entropies, solubilities, activity coefficients, and apparent molar heat capacities have also been performed. These calculations indicate large discrepancies which are attributa-ble primarily to errors in literature data on the enthalpies of combustion and/or third law entropies of the crystalline forms of the substrates.

PB89-227904 Not available NTIS National Inst. of Standards and Technology (NML), Gaithersburg, MD. Chemical Thermodynamics Div. Thermodynamics of the Hydrolysis of Sucrose.

Final rept. R. N. Goldberg, Y. B. Tewari, and J. C. Ahluwalia. 1989, 4p

Pub. in Jnl. of Biological Chemistry 264, n17 p9901-9904, 15 Jun 89.

Keywords: *Sucrose, *Thermochemistry, Hydrolysis, Thermodynamics, Heat measurement, Liquid chromatography, Chemical equilibrium, Fructose, Glucose, Solutions, Reprints. A thermodynamic investigation of the hydrolysis of sucrose to fructose and glucose has been performed using microcalorimetry and high-pressure liquid chrousing microcalorimetry and night-pressure liquid chloratography. The calorimetric measurements were carried out over the temperature range 298-316 K and in sodium acetate buffer (0.1 M, pH 5.65). Enthalpy and heat capacity changes were obtained for the hydrolysis of aqueous sucrose (process A). Equilibrium data was obtained from the literature, and was used to calculate a value of the equilibrium constant for the hydrolysis of aqueous sucrose. Additional thermochemical cycles that bear upon the accuracy of these results are examined.

901.228 PB90-117508 Not available NTIS
National Inst. of Standards and Technology (IMSE), Raithersburg, MD. Polymers Div.

Biophysical Aspects of Lipid Interaction with Mineral: Liposome Model Studies. Final rept. E. D. Eanes. 1989, 6p

Sponsored by National Inst. of Dental Research, Bethesda, MD. Pub. in Anatomical Record 224, p220-225 1989.

Keywords: *Lipids, *Minerals, *Biophysics, *Biochemistry, pH, Acidification, Calcification, Electrostatics, Reprints, *Liposomes, Phosphatidylcholines, Artificial membranes.

The paper reviews the use of liposomes as synthetic models for studying various biophysical aspects of matrix vesicle calcification, especially the involvement of acidic phospholipids in the nucleation and growth processes which occur during the initial stages of mineral formation in and around these membrane-bound structures. Recent results showed that acidic phospholipids incorporated into phosphatidylcholine-rich anionic liposome membranes were ineffective in initiat-ing extraliposomal calcium phosphate precipitation from metastable solutions at physiological pH. On the contrary, certain acidic phospholipids such as phosphatidic acid and phosphatidylserine retarded the development of such precipitation when the latter was endogenously induced. The extent of inhibition correlated with the strength of the electrostatic interaction between the polar head group of the acidic phospholipid and the surface of the mineral phase. The results suggest that acidic phospholipids may play an important role in controlling the rate of early mineral development in matrix vesicle calcification.

PB90-123886 Not available NTIS National Inst. of Standards and Technology (NML), Gaithersburg, MD. Organic Analytical Research Div. Generic Liposome Reagent for Immunoassays.

A. L. Plant, M. V. Brizgys, L. Locasio-Brown, and R. A. Durst. 1989, 7p Pub. in Analytical Biochemistry 176, p420-426 1989.

Keywords: *Biochemistry, *Antibodies, Lipids, Vitamin B complex, Antigens, Reprints, *Liposomes, *Immunoassay, Cell membranes, Fluorescence spectrometry, Cross-linking reagents, Avidin.

The report discusses the derivatization of liposomes with antibodies by using avidin to crosslink biotinylated phospholipid molecules in the liposome membranes with biotinylated antibody molecules. A comparison of the biotin binding activity of avidin in solution and avidin associated with liposomes shows that avidin bound to biotinylated phospholipid in liposome membranes retains full binding activity for additional biotin molecules. Changes in the fluorescence spectrum of avidin have been used to characterize the binding capacity of avidin for biotin in solution, and change in intensity of light scattered due to aggregation of lipo-somes was used to measure the biotin binding activity of avidin associated with liposomes. Relative amounts of the biotinylated phospholipid, avidin, and biotinylatof the biotinylated priospholipid, avidint, and biodinylated antibody have been optimized to produce stable liposomes which are derivatized with up to 1.7 nmol of antibody/micromol of lipid. These derivatized liposomes are highly reactive to immunospecific aggregation in the presence of multivalent antigen. A linear increase in light scattering was recorded between 1 and 10 pmol of antigen. The work shows that liposomes containing histinylated phespholipid can be successful. containing biotinylated phospholipid can be successful generic reagent for immunoassays.

901.230 PB90-128117

Not available NTIS

National Inst. of Standards and Technology (IMSE), Gaithersburg, MD. Polymers Div.
Liposome Technology in Biomineralization Re-

search. Final rept.

E. D. Eanes, and B. R. Heywood. 1989, 22p Sponsored by National Inst. of Dental Research, Bethesda, MD.

Pub. in New Biotechnology in Oral Research, Chapter 4, p54-75 1989.

Keywords: *Calcification, Calcium phosphate, Precipitation(Chemistry), Reprints, *Liposomes, *Mineralization, Membrane lipids, Lipid bilayers.

The chapter reviews the preparation and use of artificial lipid vesicles (liposomes) as synthetic models for studying membrane controlled precipitation of calcium phosphate salts in aqueous solutions. The impetus behind the development of liposomes for this purpose is the recognition that naturally occuring bilayer counterparts known as matrix vesicles have a primary role in initiating mineralization in many skeletal and dental tissues. Reviewed in the chapter are some of the lipid combinations, preparation procedures, and methods for characterizing liposomes that are currently used in mineralization studies. Also described is an endogenous reaction procedure which allows precipitations to be carried out in liposomal suspensions which parallel those postulated to occur during matrix visicle calcification. With the use of the technology as currently developed, liposomes have proved to be a useful tool for elucidating in vitro the role membrane lipids possibly play in biocalcification processes.

901.231

PB90-136763 Not available NTIS National Bureau of Standards (NEL), Boulder, CO. Thermophysics Div. Bioseparations: Design and Engineering of Parti-

tioning Systems.

Final rept. M. H. Hariri, J. F. Ely, and G. A. Mansoori. 1989, 3p Pub. in Biotechnology 7, p686-688 Jul 89.

Keywords: *Biochemistry, *Molecules, Extraction, Reprints, *Biotechnology, Equipment design, Separation processes.

Aqueous two-phase extraction offers a potential separation technique for separation of biomacromolecules. The manuscript briefly summarizes an approach to separating biomacromolecules using this technique and discusses requirements for industrial scale-up of this type of process.

901,232

Not available NTIS PB90-136854 National Bureau of Standards (IMSE), Gaithersburg, MD. Ceramics Div.

Global Biomethylation of the Elements - Its Role in the Biosphere Translated to New Organometallic Chemistry and Biotechnology.

Final rept.

F. E. Brinckman, and G. J. Olson. 1988, 29p Pub. in Special Publication - Royal Soc. of Chemistry Biol. Alkylation Heavy Elem. 66, p168-196 1988.

Keywords: *Methylation, *Organometallic compounds, Metals, Environment, Microbiology, Reprints, *Biotechnology, *Biosphere.

The paper reviews important aspects of the field of bioorganometallic chemistry opened over 50 years ago by Professor Frederick Challenger. Considered are the scope and rate of organometallic biogenesis, mechanistic implications for environmental (chemical and biological) processes involving processes involving processes. and biological) processes involving organometals and the prospects for control and manipulation of these processes for new biotechnical approaches to materials acquisition and environmental protection. Methylmetal(loid) species are microbially generated endo- and exocellularly by a variety of enzymatic and non-enzymatic processes. Large quantities of microbi-al metabolites which can act as metal methylating agents are generated in the global environment. Examples include methyl halides, methyl corrinoids and methylated sulfur compounds. Interesting prospects for materials processing arise in considering bioorgan-ometallic chemistry with novel routes to metal dissolution precipitation and reduction being possible.

Clinical Chemistry

901.233

Not available NTIS PB89-146773 National Bureau of Standards (NML), Gaithersburg, MD. Organic Analytical Research Div.

Developing Definitive Methods for Human Serum Analytes.

Final rept.

P. Ellerbe. 1986, 5p Pub. in Pathologist 40, n9 p22, 24-27 1986.

Keywords: *Cholesterol, *Glucose, *Urea, *Uric acid, Reprints, *Mass spectroscopy, *Isotope dilution, *Blood serum, *Creatinine, Tracer techniques, Qualitative chemical analysis, Blood chemistry, Radioassay.

The National Bureau of Standards is actively involved in a program with the CAP to develop definitive methods for constituents of human serum. The author is involved in the effort of the Organic Analytical Research Division of the Center for Analytical Chemistry to develop isotope dilution mass spectrometric (IDMS) definitive methods for organic serum constituents. Analytes that have been examined include cholesterol, glucose, uric acid, urea, and creatinine.

Not available NTIS PB89-149223 National Bureau of Standards (NML), Gaithersburg, MD. Gas and Particulate Science Div.

Micro-Raman Characterization of Atheroscierotic and Bioprosthetic Calcification. Final rept.

E. S. Etz, B. B. Tomazic, and W. E. Brown. 1986, 8p. Pub. in Microbeam Analysis 1986, p39-46.

Keywords: *Raman spectra, *Arteriosclerosis, *Calcium metabolism disorders, *Chemical analysis, Vibrational spectra, Calcium phosphates, Carbonates, Deposits, Microanalysis, Minerals, Reprints, *Bioprosthesis, Aortic diseases, Calcinosis, Plaque formation.

Described is the application of Raman microprobe spectroscopy to the characterization of the mineral phase present in atherosclerotic and bioprosthetic calcified deposits. Examined are human agric plaque and calcific deposits removed from a heart assist device implanted in sheep. The vibrational Raman spectra of these mineralized deposits are interpreted relative to the various types of calcium phosphates known to participate in the formation of the biological mineral. A specific goal is the spatial tracking, in the microscopic domain, of carbonate species associated with the mineral phosphate to determine the type of carbonate substitution (Type A or Type B sites) in the biological apatite. Results are presented from the quantitation of carbonate contents based on an empirical procedure using relative scattering intensities of carbonate and phosphate species. These studies are part of a larger research program on the comprehensive physico-chemical characterization of these pathologic, calcified deposits in animals and in man.

901,235 PB89-151922 Not available NTIS National Bureau of Standards (NML), Gaithersburg,

MD. Ionizing Radiation Physics Div.
Chemical Characterization of Ionizing Radiation-Induced Damage to DNA.

Final rept.

M. Dizdaroglu. 1986, 3p

Pub. in Biotechniques 4, n6 p536-538 1986.

Keywords: *lonizing radiation, *Radiation effects, *Gas chromatography, *Mass spectroscopy, *Deoxyribonucleic acids, Spectroscopic analysis, Chromatographic analysis, Damage assessment, Sugars, Nucleosides, Microanalysis, Reprints, *Genetic effects, Base composition, DNA.

The report reviews the application of the capillary gas chromatography-mass spectrometry (GC-MS) technique to chemical characterization of radiation-induced damage to DNA. Damage to both sugar and base moieties of DNA exposed to ionizing radiation in aqueous solution can be unequivocally characterized by GC-MS. Sugar products released from DNA are reduced by NaBD, to corresponding polyalcohols and analyzed by GC-MS following trimethylsilylation. For those sugar products still bound to the DNA backbone, an additional step, alkaline treatment, following NaBDreduction is required to release them. Incorporation of deuterium atoms into the polyalcohols permits the assessment of the presence and the position of the carbonyl and deoxy groups in the precursor sugar molecules. The t-butyldimethylsilyl derivatives provide a typical (M-57) plus ion, which appears in most instances as the base peak in the mass spectra, and is very useful for diagnostic purposes. The technique of selected-ion monitoring (SIM) permits the unequivocal characterization of the products at very low radiation doses that are considered biologically relevant. The SIM is also used for quantitative measurement of the products at low radiation doses.

901.236

Not available NTIS PB89-171953 National Bureau of Standards (NML), Gaithersburg, MD. Inorganic Analytical Research Div.

Radiochemical and Instrumental Neutron Activation Analysis Procedures for the Determination of Low Level Trace Elements In Human Livers.

R. Zeisler, R. R. Greenberg, and S. F. Stone. 1988,

Sponsored by Environmental Protection Agency, Washington, DC.
Pub. in Jnl. of Radioanalytical and Nuclear Chemistry

124, n1 p47-63 1988.

Keywords: *Trace elements, *Neutron activation analysis, *Liver, Humans, Compton effect, Spectrochemical analysis, Tissues(Biology), Nuclear chemistry, Radiochemistry, Reprints.

A comprehensive approach to the analysis of human livers was developed in a pilot program for the National Environmental Specimen Bank that employed a combination of four analytical techniques. Refinements in this approach were needed for improvement in detection limits, for more effective sample usage, and to reduce the number of analytical steps that were involved. Since neutron activation analysis (NAA) determined most of the elements, expansion of NAA was chosen to achieve these goals. Modifications in the instrumental NAA procedures, including the use of a Compton Suppressor System, gave increased sensitivity for some low level elements, such as arsenic and chromium. Radiochemical procedures that followed the instrumental counts increased the sensitivity for the elements chromium, selenium, arsenic, molybdenum, silver, antimony, and tin. Results are given for two radiochemical procedures that were applied following the modified procedure, either the use of an inorganic ion exchange column or a liquid/liquid extraction, and these are compared to instrumental results.

901.237

Not available NTIS PB89-179279 National Bureau of Standards (NEL), Gaithersburg, MD. Fire Science and Engineering Div.

Stabilization of Ascorbic Acid in Human Plasma,

and Its Liquid-Chromatographic Measurement.

S. A. Margolis, and T. P. Davis. 1988, 7p Pub. in Clinical Chemistry 34, n11 p2217-2223 1988.

Keywords: *Ascorbic acid, *Stabilization, Chromatographic analysis, Standards, Reprints, *Human plasma, *Clinical analysis, High pressure liquid chromatography, Reference materials.

Two independent HPLC procedures are described for the rapid and accurate analysis of ascorbic acid in human plasma. No sample extraction or phase separation is required. The development of a human plasma reference material for clinical laboratory analysis of ascorbic acid is described. The plasma ascorbic acid content can be determined with as little as 50 uL of sample in 15 min. Analytical recoveries are 100% with direct injection of deprotiented plasma. Extensive stability data under several conditions using dithiothreitol as a preservative (antioxidant) indicate that ascorbic acid remains stable for up to 57 weeks. Round robin acid remains stable for up to 57 weeks. Hound folin analysis of 11 normal human blood samples by two independent methods showed a % CV between 0.1 and 5.3. These clinical samples appear to be stable for no less than 60 days under the described conditions of stabilization and sample treatment. By using these methods, a laboratory can easily automate the analysis for up to 24 hours of injections at room temperature (21 deg C).

901.238

PB89-202550 Not available NTIS National Bureau of Standards (NML), Gaithersburg, MD. Temperature and Pressure Div.

New International Temperature Scale of 1990 (ITS-

Final rept. B. W. Mangum. 1989, 3p

Pub. in Clinical Chemistry 35, n3 p503-505 1989.

Keywords: *Temperature measurement, Calibrating, Reprints, *Temperature scales.

A new international temperature scale, the ITS-90, will replace the International Practical Temperature Scale of 1968 (amended edition of 1975), IPTS-68(75), on 1 January 1990. Temperatures on the ITS-90 will agree more closely with thermodynamic temperatures; there-fore, the ITS-90 represents a substantial improvement over the IPTS-68(75). Fortunately for the clinical laboratory community, the change in the scale will be at most only 0.05 C or less in the range from 0 to 60 C, but corrections in primary calibrations should be made so that the calibrations are based on the ITS-9C.

901,239

PB89-234181 Not available NTIS National Inst. of Standards and Technology (NML), Gaithersburg, MD. Organic Analytical Research Div.

Determination of Serum Cholesterol by a Modification of the Isotope Dilution Mass Spectrometric Definitive Method.

Final rept. P. Ellerbe, S. Meiselman, L. T. Sniegoski, M. J.

Welch, and E. White. 1989, 6p Pub. in Analytical Chemistry 61, n15 p1718-1723, 1

Aug 89.

Keywords: *Cholesterol, *Blood, *Carbon 13, *Isotopic labeling, *Mass spectroscopy, *Dilution, Measurement, Standards, Methodology, Gas chromatography,

An isotope dilution mass spectrometric (ID/MS) method for cholesterol is described that uses capillary gas chromatography with cholesterol-(13)C3 as the la-beled internal standard. Labeled and unlabeled cholesterol are converted to the trimethylsilyl ether. Combined capillary column gas chromatography and electron impact mass spectrometry are used to obtain the abundance ratio of the unlabeled and labeled ions from the derivative. Quantitation is achieved by measurement of each sample between measurements of two standards whose unlabeled/labeled ratios bracket that of the sample. Seven pools were analyzed by the method. The method is a modification of the original definitive method for cholesterol.

Clinical Medicine

901,240

PB89-157283 Not available NTIS National Bureau of Standards (NML), Gaithersburg, MD. Molecular Spectroscopy Div.

Two-Photon Laser-Induced Fluorescence of the Tumor-Localizing Photosensitizer Hematoporphyrin Derivative. Final rept.

D. King, D. Heller, J. Krasinski, and R. Bodaness. 1986, 4p

See also PB88-175237.

Pub. in AIP (American Institute of Physics) Conference Proceedings, n146 p694-697 1986.

Keywords: *Photosensitivity, *Neoplasms, *Fluorescent dyes, *Drug therapy, Porphyrins, Photons, Excitation, Beams(Radiation), Lasers, Spectra, Emissivity, Tissues(Biology), Penetration, Free radicals. Position(Location).

The tumor localizing photosensitizer hematoporphyrin derivative (HPD) is shown to undergo simultaneous two-photon excitations upon intense laser irradiation at 750 or 1064 nm, a spectral region where there is no significant HPD one-photon absorbance in aqueous solution. Evidence for the two-photon excitation consists in the observation both of the HPD fluorescence spectrum in the region of 615 nm as a result of 750 or 1064 nm excitations and the quadratic dependence of this fluorescence emission intensity upon the excitation laser intensity. Since the penetration depth of ultraviolet and visible light into tissue varies logarithmically with wavelength (red penetrating more deeply than blue), these studies suggest the possibility that two-photon induced localization of tumor-bound HPD

MEDICINE & BIOLOGY

Clinical Medicine

might facilitate the detection of deeper lying tumors than allowed by the current one-photon photolocalization method.

901.241 PB89-171854 Not available NTIS National Bureau of Standards (NML), Gaithersburg, MD. Ionizing Radiation Physics Div. Basic Data Necessary for Neutron Doslmetry.

Final rept. R. S. Caswell, J. J. Coyne, H. M. Gerstenberg, and

E. J. Axton. 1988, 7p Sponsored by Armed Forces Radiobiology Research Inst., Bethesda, MD., and Department of Energy, Washington, DC. Office of Health and Environmental Research.

Pub. in Radiation Protection Dosimetry 23, n1/4 p11-17 1988.

Keywords: *Dosimetry, *Neutron beams, Carbon, Neutron cross sections, Tissues(Biology), Spectra, Reprints, *Radiation therapy, Kerma factor.

Among many developments in basic data for neutron dosimetry, four are highlighted: improvements in kerma factor data for carbon; the use of common data through unification of the European and American protocols for neutron radiation therapy dosimetry; the tabulation of a set of initial spectra of secondary particles produced in tissue and tissue-like materials; and proposed changes in the magnitude and definition of neutron quality factors, which, while not physical quanti-ties, are nevertheless basic to neutron dosimetry.

PB89-176895 Not available NTIS National Bureau of Standards (IMSE), Gaithersburg, MD. Metallurgy Div. Mossbauer imaging. Final rept.

S. J. Norton. 1987, 3p Pub. in Nature 330, n6144 p151-153 1987.

Keywords: *Mossbauer *Diagnosis, effect. *Tissues(Biology), Gamma rays, Images, Doppler effect, Absorption, Rotation, Electromagnetic noise, Spectroscopy analysis, Reprints, *Tomography.

Recoilless gamma-ray resonance, or the Mossbauer effect, is a well-established spectroscopic tool in materials science. Mossbauer spectroscopy shares some of the fundamental characteristics of nuclear magnetic of the fundamental cnaracteristics or nuclear magnetic resonance (NMR) spectroscopy, since both rely on nuclear resonance phenomena. A significant recent advance in the latter field is NMR imaging in biomedicine. In Mossbauer spectroscopy, a quantity analogous to the NMR magnetic field is the relative velocity between the gamma-ray source and the absorber. This sug-gests that an analogous approach to Mossbauer imaging is possible by imposing a velocity gradient on the absorber. This can be achieved simply by rotating the absorbing object relative to the source, generating line integrals of constant Doppler shift, or equivalently, of constant gamma-energy. From such measurements, a spatial map of the gamma-ray absorption coefficient can, in principle, be tomographically reconstructed. Spatial resolution is directly related to the rate of rotation of the absorber, but ultimately is signal-to-noise

901,243 PB89-193858 PC A04/MF A01 National Bureau of Standards (NML), Gaithersburg,

MD. Center for Radiation Research.
NBS (National Bureau of Standards) Measurement
Services: Calibration of Gamma-Ray-Emitting Brachytherapy Sources.

Final rept. J. T. Weaver, T. P. Loftus, and R. Loevinger. Dec 88, 63p NBS/SP-250/19

Also available from Supt. of Docs. as SN003-003-02923-8. Library of Congress catalog card no. 88-600609.

Keywords: *Cobalt 60, *Cesium 137, *Iridium 192, *lodine 125, *Calibrating, *Standards, Radiology, Dosimetry, Radioactive isotopes, Gamma rays, Air, Measurement, Ionization chambers, Accuracy, Exposure, *Brachytherapy.

The calibration of small radioactive sources used for interstital radiation therapy, short distance therapy (brachytherapy), is performed in terms of the physical quantities exposure or air kerma. (60)Co and (137)Cs sources are calibrated by comparison with NBS work ing standard sources of the same type, while (192)Ir

and (125)I sources are calibrated by measurement in a reentrant ionization chamber that was calibrated using NBS working standard sources of the same type. The working standard sources were calibrated using the NBS graphite cavity ionization chambers except for (125)I, for which the NBS measurement standard was a free-air chamber. The working standard sources of the two long-lived sources have been measured a number of times over the years; the reliability of the reentrant chamber for the two short-lived sources is assured by use of sealed radium sources as a constancy check. The overall uncertainty (considered to have the approximate significance of a 95% confidence limit) is given as 2% for all the sources except for (125)I seeds, for which it is given as 5%, 6%, and 7%, depending on the type of seed. The stated uncertainty for (125) seeds does not include possible errors due to low-energy X rays not recognized at the time the standards were established.

Cytology, Genetics, & Molecular

PB89-157838 Not available NTIS National Bureau of Standards (NML), Gaithersburg, MD. Organic Analytical Research Div. Structure of a Hydroxyi Radical Induced Cross-Link of Thymine and Tyrosine.

Final rept. S. A. Margolis, B. Coxon, E. Gajewski, and M.

Dizdaroglu. 1988, 7p Sponsored by Armed Forces Radiobiology Research Inst., Bethesda, MD.

Pub. in Biochemistry 27, n17 p6353-6359, 23 Aug 88.

Keywords: *Tyrosine, *Proteins, *Crosslinking, *Radiobiology, Microanalysis, Ionizing radiation, Molecular structure, Deoxyribonucleic acids, Alpha amino carboxylic acids, Uracils, Radiation effects, Reprints, *Thymine, *DNA, *Hydroxyl radicals, Hydroxy com-

DNA-protein cross-links are formed when living cells or isolated chromatin is exposed to ionizing radiation. Little is known about the actual cross-linked products of DNA and proteins. In the work, a novel hydroxyl radical induced cross-link of thymine and tyrosine has been isolated along with a tyrosine dimer by high-performance liquid chromatography of aqueous mixtures of tyrosine and thymine that had been exposed to hydroxyl radicals generated by ionizing radiation. The iso-lated compounds have been examined by gas chromatography-mass spectrometry, high-resolution mass spectrometry, and (1)H and (13)C nuclear magnetic resonance spectroscopy. The structure of the thy-mine-tyrosine cross-link has been identified as the product from the formation of a covalent bond between the methyl group of the thymine and carbon 3 of the tyrosine ring. In addition, the 3,3' tyrosine dimer was isolated and characterized. The mechanism of the formation of these compounds is discussed. The work presents the first complete chemical characterization of a hydroxyl radical-induced DNA base-amino acid

901,245 PB89-175269

(Order as PB89-175194, PC A06) Lister Hill National Center for Biomedical Communications, Bethesda, MD.

New Directions in Bioinformatics.

Bi-monthly rept. D. R. Masys. 1989, 5p Included in Jnl. of Research of the National Institute of

Standards and Technology, v94 n1 p59-63 Jan-F-eb

Keywords: *Information systems, Nucleic acids, *Molecular biology, *Biotechnology, *Data base management systems, Communication networks, Computer networks. Medical information systems.

Development of automated methods to sequence DNA, RNA, proteins, and other macromolecules have yielded oceans of cryptic symbols, for which there is an absolute dependence upon computerized factual databases to acquire, store, retrieve, and analyze data. The Human Genome Project has focused attention on the information science aspects of nucleic acid data, yet for the practicing scientist nucleic acids and

other sequence data are just one piece of an increasingly complex biological puzzle whose solution will be expressed in terms of structure and function. Access to and integration of information across multiple related biological databases is a major challenge facing information system builders, a challenge which holds the promise of creating knowledge synergy from what are today disconnected, stand-alone information sources.

PB89-175277

(Order as PB89-175194, PC A06) Allelix Biopharmaceuticals, Mississauga (Ontario). Use of Structural Templates in Protein Backbone

Modeling.
Bi-monthly rept.
L. S. Reid. 1989, 8p
Included in Jnl. of Research of the National Institute of Standards and Technology, v94 n1 p65-72 Jan-Feb

Keywords: *Proteins, Conformation, Data bases, Tem-

Many proteins of interest have low (i.e. less than 50%) sequence similarity to any known structure. In these cases new approaches to prediction of structure are required. The use of sequence profiles which relate sequence to known structure has been proposed as one method to assign local regions of structure. As a first stage, templates or icons' of the many relevant substructural motifs found in proteins must be defined. The sequences which gave rise to these structures are then aligned and a weighted profile obtained. Average structures of the 8 and 12 residue helix-turn and turnhelix motifs have been prepared. These coordinate templates were then used to scan through the Brookhaven protein structural database for similar, superimposable fragments. A composite template of 100 similar fragments for each element was found to be internally consistent. All of the sequences, from these structures, were then used to create an overall sequence profile.

901.247 PB89-175285

(Order as PB89-175194, PC A06) Maryland Univ., Rockville. Center for Advanced Research in Biotechnology.

Comparative Modeling of Protein Structure:

Progress and Prospects.

Bi-monthly rept. J. Moult. 1989, 6p Included in Jnl. of Research of the National Institute of Standards and Technology, v94 n1 p79-84 Jan-Feb

Keywords: *Proteins, *Molecular structure, Amino acids, Models, Electrostatics, Crystallography, Reliability, *Protein conformation, Databases.

Comparative modeling of protein structure is a process which determines the three-dimensional structure of protein molecules on the basis of amino acid sequence similarity to experimentally known structures. The procedure is facilitated by the growing database of protein structures obtained from crystallography. In the review a series of stages in the modeling process are identified and discussed. These are (i) obtaining a reliable amino acid sequence of the structure of interest, (ii) producing a structurally correct sequence of the structure of interest, (ii) producing a structurally correct sequence alignment, (iii) identifying which structural features are conserved between target and parent structures, (iv) modeling the new pieces of structure, and (v) tests of reliability.

901.248 PB89-202204 Not available NTIS National Bureau of Standards (NML), Gaithersburg, MD. Chemical Thermodynamics Div.
Comparison of Two Highly Refined Structures of
Bovine Pancreatic Trypsin inhibitor.

A. Wlodawer, J. Deisenhofer, and R. Huber. 1987;

12p Pub. in Jnl. of Molecular Biology 193, n1 p145-156 1987.

Keywords: *Molecular structure, Enzymes, Crystal structure, Reprints, *Trypsin inhibitors, *Pancreatic

The high resolution structures of bovine pancreatic trypsin inhibitor refined in two distinct crystal forms

Cytology, Genetics, & Molecular Biology

have been compared. One of the structures was a result of new least squares x-ray refinement of data from crystal form I, while the other was the joint x-ray/ neutron structure of crystal form II. After superposition, the molecules show an overall root-mean-squares deviation of 0.40A for the atoms in the main chain, while the deviations for the side chain atoms are 1.53A. The latter number decreases to 0.61A when those side chains which adopted drastically different conforma-tions are excluded from companson. The discrepancy between atomic temperature factors in the two models was 6.7 sq A, while their general trends are highly correlated. About half of the solvent molecules occupy similar positions in the two models, while the others are different. As expected, solvent molecules with the lowest temperature factors are most likely to be common in the two crystal forms. While the two models are clearly similar, the differences are significantly larger than the errors inherent in the structure determination.

901,249 PB90-123407 Not available NTIS National Inst. of Standards and Technology (NEL), Gaithersburg, MD. Chemical Process Metrology Div. Nonlinear Effect of an Oscillating Electric Field on Membrane Proteins.

R. D. Astumian, and B. Robertson. 1989, 11p Pub. in Jnl. of Chemical Physics 91, n8 p4891-4901, 15 Oct 89.

Keywords: *Electric fields, *Nonlinear systems, Catalysis, Electrochemistry, Relaxation, Kinetics, Reprints, *Membrane proteins, Biological transport.

The nonlinear response of a two-state chemical transi-tion to an oscillating electric field is examined. A reaction for which the analysis is particularly relevant is a conformational transition of a membrane protein exposed to an ac electric field. Even a modest externally applied field leads to a very large local field within the membrane. This gives rise to nonlinear behavior. The applied ac field causes harmonics in the polarization and can cause a dc shift in the state occupancy, both of which can be observed and used to determine kinetic parameters. Fourier coefficients are calculated for the enzyme state probability in the ac field, exactly for infinite frequency, and in powers of the field for finite frequency. Kramers-Kronig relations are proved and response functions are given for the leading terms of the harmonics. The results are extended to the spherical symmetry relevant to suspensions of spherical cells, vesicles, or colloidal particles. If the protein catalyzes a reaction, free energy is transduced from the electric field to the output reaction, even if that reaction is electrically silent. Many transport enzymes are ideal examples. The ac field can cause the enzyme to pump ions or molecules through the membrane against an (electro) chemical potential. The efficiency of the energy transduction can be as high as 25%.

901,250 PB90-136722 PB90-136722 Not available NTIS National Inst. of Standards and Technology (NML), Gaithersburg, MD. Chemical Thermodynamics Div.
Biological Macromolecule Crystallization Database: A Basis for a Crystallization Strategy.

G. L. Gilliland. 1988, 9p Pub. in Jnl. of Crystal Growth 90, n1-3 p51-59 Jul 89.

Keywords: *Biochemistry, *Molecules, *Crystallization, Molecular weight, Proteins, Viruses, pH, Temperature, Nucleic acids, Reprints, *Databases, *DNA, Osmolar concentration.

A crystallization database, the Biological Macromole-Crystallization Database, containing crystal data and the crystallization conditions for more than 1000 crystal forms of over 600 biological macromolecules, has been compiled from the scientific literature. Data for proteins, protein:protein complexes, nucleic acids, nucleic-acid:nucleic-acid complexes, protein:nucleicacid complexes and viruses have been included. The general information cataloged for each macromolecule includes the macromolecular name(s), the molecular weight, the subunit composition, the presence of prosthetic group(s), and the source of the macromolecule. The crystal data include the unit cell parameter, space group, crystal density, crystal habit and size, and diffraction limit and lifetime. The crystallization data consist of the crystallization method, chemical additions to the crystal growth medium, macromolecule concentration, temperature, pH, and growth time. A result of the compilation of the crystallization data was the development of a general strategy for the crystallization of soluble proteins.

PB90-136730 Not available NTIS National Inst. of Standards and Technology (NML), Gaithersburg, MD. Chemical Thermodynamics Div. Preliminary Crystallographic Study of Recombinant Human Interleukin 1beta.

Final rept. G. L. Gilliland, E. L. Winborn, Y. Masui, and Y. Hirai.

Pub. in Jnl. of Biological Chemistry 262, n25 p12323-12324 1987.

Keywords: *Crystallography, Escherichia coli, X ray diffraction, Ammonium sulfate, Reprints, *Interleukin 1, Recombinant proteins.

Recombinant human interleukin 1 beta (IL-1 beta) which is expressed in Escherichia coli has been crystallized by the method of vapor diffusion using ammonium sulfate as the precipitant. The space group is P41 or P43 with a=b= 55.0 A and c= 77.1 A and one molecule in the asymmetric unit. The crystals diffract to beyond 2.4 A and are suitable for a three-dimensional X-ray structure determination.

Dentistry

PB89-179238 Not available NTIS National Bureau of Standards (IMSE), Gaithersburg, MD. Polymers Div.

Comparison of Fluoride Uptake Produced by Tray

and Flossing Methods In vitro. Final rept.

M. K. Guo, L. C. Chow, C. T. Schreiber, and W. E. Brown. 1989, 3p

Sponsored by American Dental Association Health Foundation, Chicago, IL., and National Taiwan Univ., Taipei. Coll. of Medicine.

Pub. in Jnl. of Dental Research 68, n3 p496-498 Mar

Keywords: *Fluoride, Trays, Adsorption, Reprints, *Dental enamel, Dicalcium phosphate dihydrate, Dental floss, Fluoroapatite.

The study compares: (i) the fluoride (F) uptake by enamel in approximal areas of teeth when the F agent was applied in vitro via a tray or a flossing technique; and (ii) the effectiveness of two treatments -- acidulated phosphate fluoride (APF) alone and CaHPO4-2H20 (DCPD)-forming pre-treatment followed by APF. Groups of three teeth (one premolar and two molars) were mounted in impression compounds simulating their oral configuration. In the tray group, teeth received one four-minute treatment by means of customformed trays. In the flossing group, the approximal areas of teeth were flossed for 40 sec twice daily for three days with an absorbent floss wetted with the treatment solution. The F uptake was calculated from biopsy data obtained before and after the treatment. The results showed that (i) DCPD-APF produced significantly greater F uptake than APF alone in both the tray and flossing methods, and (ii) that the flossing technique produced significantly greater F uptake in the approximal areas than the tray method for either

901,253 PB89-186373 Not available NTIS National Bureau of Standards (IMSE), Gaithersburg, MD. Polymers Div.

Micro-Analysis of Mineral Saturation Within Enamel During Lactic Acid Demineralization. Final rept.

G. L. Vogel, C. M. Carey, L. C. Chow, T. M. Gregory, and W. E. Brown. 1988, 9p

Sponsored by American Dental Association Health Foundation, Chicago, IL. Pub. in Jnl. of Dental Research 67, n9 p1172-1180 Sep

Keywords: *Microanalysis, *Lactic acid, Dental caries, Concentration(Composition), Calcium, Phosphate, Re-prints, *Dental enamel, Demineralization, Hydroxyapa-

tite, Enamel solubility, Tooth permeability.

In this study, the physicochemical factors responsible for caries-like lesion propagation were investigated by

means of a micro-analytical system used to study the fluid within a lesion during a simulation of the decay process. Four 500-micrometer-thick serial sections prepared from a single human molar were mounted between glass plates with only the natural surface of the tooth exposed. The concentrations of calcium, phosphate, and hydrogen ions of the fluid in the wells were then followed as a function of time as the lesion advanced. The results of this study, in which lactic acid was used to demineralize enamel, were consistent with those previously reported (Vogel et al, 1987a). The solution within the lesion remained saturated during the acid attack. Differences in initial mobilities of the calcium and phosphate and other ions increased the concentrations within the lesion and permanently changed the ratio of these ions in the lesion solution. Based on these results, the authors suggest that the ionic permselectivity of tooth enamel can have a profound effect on the transport of mineral from a caries

901,254 PB89-201503 Not available NTIS National Bureau of Standards (IMSE), Gaithersburg, MD. Polymers Div. Mechanism of Hydrolysis of Octacalcium Phos-

phate. Final rept.

B. B. Tomazic, M. S. Tung, T. M. Gregory, and W. E. Brown. 1989, 9p

Sponsored by American Dental Association Health Foundation, Chicago, IL. Pub. in Scanning Microscopy 3, n1 p119-127 1989.

Keywords: *Hydrolysis, Chemical reactions, Solubility, Transformations, Reprints, *Octacalcium phosphate, Hydroxyapatite.

The chemical and structural properties of hydrolyzed octacalcium phosphate (OCP) appear to be of high relevance to tooth, bone and pathological bioapatites. Hydrolysis of synthetic well-crystallized OCP was studied at constant pH by using the pH stat method over the 6.1 to 8.6 range at 50 C and to a lesser extent at 37 C. Hydrolytic transformation proceeds according to thermodynamic requirements except for some retardation at the highest pH value as a consequence of decreased solubility of OCP which may be rate determining. The product of hydrolysis, OCP-hydrolyzate (OCPH), was characterized by chemical analysis, scanning electron microscopy, x-ray diffraction, electron microprobe (x-ray microanalysis, EDX) and solubility measurement under static and dynamic conditions. Overall findings provide new evidence that OCP may be a precursor phase in the formation of pathologic calcified deposits and normal biomineral, which appear to be complex hydrolyzates of OCP.

901 255 PB89-201511 Not available NTIS National Bureau of Standards (IMSE), Gaithersburg, MD. Polymers Div.

Formation of Hydroxyapatite in Hydrogels from Tetracalcium Phosphate/Dicalcium Phosphate Mixtures. Final rept.

A. Sugawara, J. M. Antonucci, S. Takagi, L. C. Chow, and M. Ohashi. 1989, 10p

Sponsored by American Dental Association Health Foundation, Chicago, IL.
Pub. in Jnl. of the Nihon University School of Dentistry

31, n1 p372-381 Mar 89.

Keywords: Dental materials, Reprints, *Hydroxyapatite, *Apatitic calcium phosphate cements, *Dental ce-

Apatitic calcium phosphate cements, formed by the ambient reaction of tetracalcium phosphate (TTCP) with dicalcium phosphates (DCP), have been recently reported. H20 or dilute aq. H3PO4 (0.2%) is used as the liquid vehicle for this reaction. The study ascertained if hydroxyapatite (HAp) can form in self-cured hydrogel composites containing TTCP/DCP mixes. The setting times (ST) and diametral tensile strengths (DTS) of these hydrogel composites were also determined. The hydrogels were of two types: vinyl thermosets derived from the copolymerization of HEMA (2hydroxyethyl methacrylate) and cross-linking monomers, and polyelectrolyte-based hydrogels formed from aq. poly(alkenoic acids), e.g., poly(acrylic acid). Cylindrical specimens 6 mm D x 3 mm H were prepared and stored in H20 for up to 30 days. The HEMA composites were hardened in 7-15 min by free radical initiation (benzoyl peroxide/tertiary aromatic amine).

MEDICINE & BIOLOGY

Dentistry

After various periods of storage in H20 at 37 C, some of the specimens were examined by X-ray spectroscofor HAp. HAp formation was not observed in the py for HAp. HAp formation was not observed in the HEMA composites even after 30 days of H20 storage but was detected in the polyacid cements. Both the H20 content and pH may thus be factors controlling the rate and extent of HAp formation in hydrogel com-posites containing TTCP/DCP mixtures.

901,256 PB89-201529 PB89-201529 Not available NTIS National Bureau of Standards (IMSE), Gaithersburg, MD. Polymers Div. Detection of Lead in Human Teeth by Exposure to

Aqueous Sulfide Solutions.

Final rept.

A. Sugawara, J. M. Antonucci, G. C. Paffenbarger, and M. Ohashi. 1989, 15p Sponsored by American Dental Association Health Foundation, Chicago, IL. Pub. in Jnl. of the Nihon University School of Dentistry

31, n1 p382-396 Mar 89.

Keywords: *Lead(Metal), *Exposure, *Teeth, *Humans, *Detection, Discoloration, Reprints, Dental cements, Sodium sulfide, Aqueous solutions.

A recent study has shown that the presence of lead (Pb) as well as other base metals in esthetic restorative materials, especially dental cements, is detectable by color shifts induced by exposure of hardened speci-mens to a 0.1% (w/v) aqueous solution of sodium sulfide, Na2S. The present study was initiated to determine the applicability of this simple exposure test to the detection of Pb in human teeth. Extracted whole the detection of Pb in furnant eterth. Extracted whole teeth as well as sectioned, thin specimens were exposed first to either a 0.01% or a 0.001% (w/v) aqueous solution of lead nitrate, Pb(NO3)2 at 37 C for 24 h. After rinsing with distilled H20 and a subsequent 24 h exposure to the 0.1% Na2S solution at 37 C, the tooth specimens were examined visually and by a dental color analyzer for color changes. Neither control speci-mens exposed to distilled H20 only or to 0.1% Na2S only exhibited any significant change in appearance after 24 h of storage at 37 C. However, specimens exposed first to the Pb(NO3)2 solutions showed discernible delta E values after exposure to the Na2S solution. Delta E was greatest for specimens exposed to the more concentrated Pb(NO3)2 solution. Most of the discrete the state of the state coloration in both thin and intact tooth specimens was confined to the outermost layers of the tooth structure. For the intact specimens, the greatest degree of discoloration occurred in the cementum, the most permeable part of the tooth structure.

PB89-202477 Not available NTIS National Bureau of Standards (IMSE), Gaithersburg, MD. Polymers Div. High-Temperature Dental Investments.

Final rept.

J. A. Tesk. 1989, 11p Pub. in Dental Materials: Properties and Selection, Chapter 18, p351-361 1989.

Keywords: *Dental materials, Polymers, Castings, High temperature tests, Reprints, *Dental invest-

High-temperature dental investments are materials used primarily for the casting of high-temperature dental alloys, that is, alloys with casting temperatures greater than 1,300 C. While the casting of these alloys into crowns, inlays, partial dentures (fixed or removable), and other restorative devices is certainly the primary use for the investments, they have other dental applications as well. One such use is as fixtures for holding dental prostheses during soldering operations. Another use is for making dies for the fabrication of porcelain facial tooth veneers. Until recently there have been two basic compositional types: phosphate-bonded and ethyl silicate-bonded. However, due to interest in the casting of titanium prostheses, other sys-tems are now being explored and used. This is neces-sary because the conventional phosphate and ethyl silicate investments react with molten titanium and contaminate the casting. Commercial dental investments used in Japan for titanium are based primarily on magnesium oxide. Investments under development in the United States are based on zirconia. They have been used to make titanium castings for limited clinical evaluations by the Paffenbarger Research Unit at the National Bureau of Standards.

901,258 PB89-202931

Not available NTIS

National Bureau of Standards (IMSE), Gaithersburg, MD. Polymers Div.

Pulpal and Micro-organism Responses to Two Experimental Dental Bonding Systems.
Final rept.

R. L. Blosser, N. W. Rupp, H. R. Stanley, and R. L.

Bowen. 1989, 5p Sponsored by American Dental Association Health Foundation, Chicago, IL. Pub. in Dental Materials 5, p140-144 Mar 89.

*Dental materials, *Dentin, *Bonding, Keywords: Teeth, Reprints, *Biocompatibility, Dental pulp, Micro-

Several new bonding systems have been reported that promote strong adhesion. This in vivo study involves treatment with two experimental bonding systems of Class V cavity preparations in the teeth of three Macaca fascicularis primates and reports the pulpal re-sponses and degree of micro-organism invasion associated with each treatment. The upper and lower left quadrants were treated with clinical materials to establish positive and negative controls. After 4, 25, and 59 days, the teeth were removed and underwent routine histological and bacteriological evaluation. Slight pathological conditions were noted for superficial and deep responses, but all value approached 0.0 by the 59th day. Micro-organisms were seen under only 12% of the restorations. Both experimental systems appear to be safe for human clinical trials.

901,259 PB89-229249 Not available NTIS National Inst. of Standards and Technology (IMSE), Gaithersburg, MD. Polymers Div.

Quasi-Constant Composition Method for Studying the Formation of Artificial Caries-Like Leslons.

Final rept. L. C. Chow, and S. Takagi. 1989, 6p Sponsored by American Dental Association Health Foundation, Chicago, IL.

Pub. in Caries Research 23, p129-134 1989.

Keywords: Demineralizing, Volumetric analysis, Reprints, *Dental caries, *Tooth diseases, Dental enamel solubility.

Caries-like lesions were formed in human tooth enamel in a quasi-constant composition titration system without the use of surface dissolution inhibitors or weak acids. The titration systèm maintained the composition of the demineralizing solution constant to within 6% on the average. Thus, the rate of lesion formation may be quantitatively assessed from the rate of titration. The system has sufficient sensitivity for measuring the rate of lesion formation in a small area, e.g., 15 sq mm, of a single human enamel specimen.

Microbiology

901,260 Not available NTIS PB90-123381 National Inst. of Standards and Technology (NML), Gaithersburg, MD. Chemical Thermodynamics Div. Preliminary Crystal Structure of Acinetobacter glutaminasificans Glutaminase-Asparaginase. Final rept.

H. L. Ammon, I. T. Weber, A. Wlodawer, R. W. Harrison, G. L. Gilliland, K. C. Murphy, L. Sjolin, and J. Roberts. 1988, 7p.

Pub. in Jnl. of Biological Chemistry 263, n1 p150-156

Keywords: *Crystal structure, *Glutaminase, Reprints, *Asparaginase, *Acinetobacter glutaminasificans, Protein conformation, Amino acid sequence.

The preliminary structure of a glutaminase-asparaginase from Acinetobacter glutaminasificans (AgGA) is reported. The structure was determined at 3.0 A resolution with a combination of phase information from multiple isomorphous replacement at 4 - 5 A resolu-tion, and phase improvement and extension by density modification techniques. Initially polyalanine was fit to the electron density map and was subsequently re-placed by a polypeptide with an amino acid sequence in agreement with the sizes and shapes of the side chain electron densities. The crystallographic R-factor is 0.300 following constrained least-squares refinement with data to 2.9 A resolution. The AgGA subunit folds into two domains: the amino-terminal domain

contains a five-stranded beta sheet surrounded by five alpha helices, and the carboxy-terminal domain contains three helices and less regular structure. The connectivity is not fully determined at present, due in part to the lack of a complete amino acid sequence. The AgGA structure has been used successfully to determine the relative orientations of the molecules in crystals of Pseudomonas 7A glutaminase-asparaginase and of Vibrio succinogenes asparaginase, and in a new crystal form of E. coli asparaginase (space group 1222, one subunit per asymmetric unit).

901,261

PB90-123712 Not available NTIS National Inst. of Standards and Technology (IMSE), Gaithersburg, MD. Ceramics Div.

Microbiological Materials Processing.

Final rept. F. E. Brinckman, and G. J. Olson. 1988, 2p Pub. in Jnl. of Metals 40, n9 p60-61 1988.

Keywords: *Microbiology, *Metals, Materials recovery, Metalliferous minerals, Reprints, *Biotechnology, Metal recovery.

Microorganisms are increasingly used as agents for processing and recovery of metals. The paper bnefly reviews the industrial applications of microbial processing of ores and wastes and describes NBS contributions of the technology including new measurement methodology, standards activities and critical data. Potential future developments and research needs are briefly described.

Nutrition

901,262

PB89-234173 Not available NTIS Notional Inst. of Standards and Technology (NML), Gaithersburg, MD. Organic Analytical Research Div. Determination of Total Cholesterol in Coconut Oll: A New NIST (National Institute of Standards and Technology) Cholesterol Standard Reference Material terial.

Final rept. P. Ellerbe, L. T. Sniegoski, M. J. Welch, and E. White V. 1989, 4p

Sponsored by College of American Pathologists, Skokie, IL. Pub. in Jnl. of Agricultural and Food Chemistry 37, n4

p954-957 1989.

Keywords: *Cholesterol, *Human nutrition, Mass spectroscopy, Plant oils, Blood, Fats, Nutrients, Gas chro-matography, Reprints, *Coconut oil, Standard Refer-ence Materials.

A new Standard Reference Material (SRM) consisting of coconut oil with various nutrients added has been developed at the National Institute of Standards and Technology in response to the needs of the food measurement community. SRM 1563 consists of ampules of a coconut oil with added cholesterol and selected fat-soluble vitamins and ampules of the natural coconut oil. Cholesterol has been measured in the material by a modification of the definitive method based on isotope dilution mass spectrometry coupled with gas chromatography, originally developed for the measurement of cholesterol in serum. The cholesterol reasonation of cholesterol in section. The fortified oil was determined to be 64.2 + or - 0.6 mg/100 g of oil. This value, with its precision, complies with the request of the food nutrient measurement community for a standard with an uncertainty within + or - 5% of the certified value at 95% confidence limits. The natural oil was found to contain 0.344 + or - 0.014 mg/100 g of

Pharmacology & Pharmacological Chemistry

901.263 Not available NTIS PB89-171870 National Bureau of Standards (NML), Gaithersburg, MD. Ionizing Radiation Physics Div.

Pharmacology & Pharmacological Chemistry

Intramolecular H Atom Abstraction from the Sugar Molety by Thymine Radicals in Oligo- and Polydeoxynucleotides.

Final rept.

L. R. Karam, M. Dizdaroglu, and M. G. Simic. 1988,

Sponsored by Armed Forces Radiobiology Research Inst., Bethesda, MD.

Pub. in Radiation Research 116, p210-216 1988.

Keywords: *Uracils, *Free radicals, *Hydrogen, *Sugars, Chemical reactions, Hydroxides, Thymidines, Ribose, Gas chromatography, Mass spectroscopy, Reprints.

Hydroxyl radical addition to uracil (U) has been suggested to lead to strand breaks in polyundylic acid, an gésted to lead to strand breaks in polyuridylic acid, an occurrence attributed in part to H atom abstraction by U-OH free radicals from the ribose moiety. The particular reaction is investigated by means of the hydroxyl radical-induced products of thymine (T), pT, TpT, TpTT, polythymidylic acid (poly-T), (T+dR) poly-dA center dot poly-T, and a mixture of T and 2-deoxyribose (dR). The major monomeric product of T-OH radical in TpT, TpTpT, poly-T, and poly-dA center dot poly-T was found to be 5-hydroxy-6-hydrothymine (H-T-OH), while that in T, pT, and T plus dR was thymine glycol (HO-T-OH). These results indicated that the intra-molecular H atom abstraction from a nearby sugar (in this case, deoxyribose) moiety by base radisugar (in this case, deoxyribose) moiety by base radi cals, i.e., T-OH, occurs in oligo- and polydeoxynucleotides of T. In poly-T, the yield of H-T-OH is not much greater than in TpT or TpTpT, indicating that the abstraction of an H atom from the sugar moiety of a number of the structure of the st cleotide subunit further than two nucleotides along the chain may not be significant. Additionally, a corresponding decrease in the yield of HO-T-OH with an increase in the yield of H-T-OH suggests that the formations of these two types of thymine products are competitive.

Radiobiology

901,264 PB89-150791 Not available NTIS Not available N118
National Bureau of Standards (NML), Gaithersburg,
MD. Ionizing Radiation Physics Div.
Refinement of Neutron Energy Deposition and Microdosimetry Calculations.

Final rept.

R. S. Caswell, J. J. Coyne, H. M. Gerstenberg, and R. B. Schwartz. 1986, 13p

Sponsored by Department of Energy, Washington, DC. Office of Health and Environmental Research.

Pub. in Proceedings of International Conference on Fast Neutron Physics, Dubrovnik, Yugoslavia, May 26-31, 1986, p122-134.

Keywords: Monte Carlo method, Energy absorption, Computation, *Microdosimetry, Tissue-equivalent ma-

Calculations describing the deposition of energy by neutrons in tissue-like materials are usually carried out by the 'analytic method' or the 'Monte-Carlo method.' Extensions of the equations of the analytic method to include thin walls as well as thick walls are now available. Furthermore, inclusion of straggling effects in the analytic method is relatively simple and has been programmed for computer calculations. The first step in the analytic method is the calculation of the 'initial' spectra of secondary charged particles generated by the neutrons. The authors are preparing tables of initial spectra below 20 MeV. The calculation of 'lineal energy' or 'y' spectra for neutrons is of interest for microdosimetry. The possibility of carrying out microdosimetry the possibility of carrying out microdosimetry. metric calculations on a nanometer scale using track structure information generated by Wilson and Par-etzke is being pursued. A Monte-Carlo code is being generated using the same data base as the authors' analytic method codes. The chief advantage of the Monte-Carlo code is in the correct handling of events where two or three correlated charged particles are emitted. Some results of microdosimetric calculations including straggling are given.

901.265

PB89-171862 Not available NTIS National Bureau of Standards (NML), Gaithersburg, MD. Ionizing Radiation Physics Div.

Initial Spectra of Neutron-Induced Secondary Charged Particles.

Final rept. H. M. Gerstenberg, R. S. Caswell, and J. J. Coyne. 1988, 4p

Sponsored by Department of Energy, Washington, DC. Office of Health and Environmental Research.

Pub. in Radiation Protection Dosimetry 23, n1/4 p41-44 1988.

Keywords: *Nuclear cross sections, *Neutron reactions, *Computation, *Carbon, *Tissues(Biology), *Charged particles, Spectra, Hydrogen, Helium, Deuterium, Boron, Nitrogen, Oxygen, Beryllium, Radioacterium, Boron, tive decay, lons, Reprints.

Calculations have been made of the initial spectra of secondary charged particles which result from neutron interactions with materials such as tissue. These secondary particles are ions of H, D, He and the heavier recoil ions of Be, B, C, N and O. The spectra of the ions have been determined in 200 keV neutron energy bin sizes between 0 and 20 MeV as well as for 76 almostlogarithmic bins extending from thermal energy to 2 MeV. The primary input for these calculations is the ENDF/B-V nuclear data file from the National Nuclear Data Center at Brookhaven. Additional supplementary information is also needed on the angular distribution of neutron reactions leading to charged particles and on the final excitation of residual nuclei. Recently measured kerma factors in carbon disagree with those calculated using the nuclear cross section data from ENDF/B-V by as much as 25% in the region between 14 MeV and 18 MeV. A recently made evaluation of the carbon cross sections in the energy region between 5 MeV and 32 MeV is used here to calculate kerma and initial spectra at neutron energies of 16.9, 14.9, and 13.9 MeV; the results are then compared with that obtained using the ENDF/B-V data.

Toxicology

901.266 PB90-117888 Not available NTIS National Inst. of Standards and Technology (NML), Gaithersburg, MD. Ionizing Radiation Physics Div. Generation of Oxy Radicals in Biosystems. Final rept.

M. G. Simic, D. S. Bergtold, and L. R. Karam. 1989,

Pub. in Mutation Research 214, p3-12 1989.

Keywords: *Free radicals, *Oxygen, *Toxicity, *Mutations, Reprints, *DNA damage.

Many recent lines of evidence indicate that endogenous free radicals contribute to spontaneous mutagenesis through the direct induction of DNA damage. However, the mechanisms underlying the process are not yet fully understood. A brief overview of the knowledge that is currently available is provided, with emphasis on the generation of oxy radicals in biosystems, the reactions of those radicals with biomolecules, and the induction of oxidative DNA base damage that might lead to mutation.

901.267 PB90-128760 Not available NTIS National Inst. of Standards and Technology (NML), Gaithersburg, MD. Organic Analytical Research Div. Anti-T2 Monoclonal Antibody Immobilization on Quartz Fibers: Stability and Recognition of T2 Mycotoxin.

Final rept.
M. L. Williamson, D. H. Atha, D. J. Reeder, and P. V. Sundaram. 1989, 14p
Pub. in Analytical Letters 22, n4 p803-816 1989.

Keywords: Quartz, Bioinstrumentation, Silane, Reprints, *T-2 toxin, *Monoclonal antibodies, *Optical prints, *T-2 toxin, *M sensors, Binding sites.

Several methods for immobilizing anti-T2 mycotoxin monoclonal antibodies on quartz fibers, for use in optical sensor development, have been evaluated with respect to the surface density and stability of the immo-bilized proteins. The first method activates matrix hy-droxyl groups using p-toluenesulfonyl chloride (TSC). The second method activates these groups using pnitrophenyl chloroformate (NPCF). The third method requires an initial silanization using 3-aminopropyl-triethoxysilane (APTES) followed by carrier activation with glutaraldehyde. The activated carrier in all three methods is then reacted with the amino groups of the protein. The first two non-silanizing coupling methods are simple, inexpensive and non-hazardous compared to the third, more complex method in which an initial silanization step is required. The active antibody surface densities and stabilities were monitored at 4 and 50C. Each of these methods produced active antibody surface densities in the range of 181 - 297 ng/sq cm with half lives ranging from 30 to 80 hours at 50C to several months at 4C.

MILITARY SCIENCES

Antimissile Defense Systems

901,268

Not available NTIS PB89-173405 National Bureau of Standards (NEL), Gaithersburg, MD. Electrosystems Div.

Strategic Defense Initiative Space Power Systems Metrology Assessment.

J. K. Olthoff, and R. E. Hebner. 1989, 4p

Pub. in Transactions of Symposium on Space Nuclear Power Systems (6th), Albuquerque, NM., January 8-12, 1989, p124-127.

Keywords: *Metrology, *Technology assessment, Reliability, Antimissile defense, Measurement, Temperature, Detectors, Calibrating, Reprints, *Strategic Defense Initiative, *Spacecraft power supplies.

A survey of Strategic Defense Initiative (SDI) programs has been performed to determine the measurement requirements of anticipated SDI space power systems. These requirements have been compared to present state-of-the-art metrology capabilities as represented by the calibration capabilities at the National Institute of Standards and Technology. Metrology areas where present state-of-the-art capabilities are inadequate to meet SDI requirements are discussed, and areas of metrology related research which appear promising to meet these needs are examined. Particular attention is paid to the difficulties of long-term, unattended sensor calibrations and measurement reliability.

901,269

PB89-209357 PC A07/MF A01 National Inst. of Standards and Technology (NEL), Gaithersburg, MD. Center for Electronics and Electrical Engineering.

Assessment of Space Power Related Measurement Requirements of the Strategic Defense Initiative.

Technical note (Final).

J. K. Olthoff, and R. E. Hebner. Apr 89, 147p NIST/ TN-1259

Also available from Supt. of Docs. as SN003-003-02930-1. Sponsored by Defense Nuclear Agency, Washington, DC., and Strategic Defense Initiative Organization, Washington, DC.

Keywords: Measurement, Sensors, Electromagnetic fields, Lasers, Vibration, Neutron flux, *Strategic Defense Initiative.

A survey has been performed to determine the measurement requirements of space power related parameters for anticipated SDI systems. These requirements have been compared to present state-of-the-art metrology capabilities as represented by the calibration capabilities of the National Institute of Standards and Technology. Metrology areas where present state-of-the-art capabilities are inadequate to meet SDI requirements are discussed, and areas of metrology-related research which appear promising to meet these needs are examined. Particular attention is paid to the difficulties of long-term, unattended sensor calibrations and long-term measurement reliability.

Logistics, Military Facilities, & Supplies

Logistics, Military Facilities, & Supplies

PB89-150965 Not available NTIS National Bureau of Standards (NML), Gaithersburg, MD. Office of Physical Measurement Services. Measurement Standards for Defense Technology. Final rept.

B. C. Belanger, and L. Vestal. 1985, 8p

Pub. in Proceedings of National Conference of Standards Laboratories Workshop and Symposium, Boulder, CO., July 15-18, 1985, p206-213.

Keywords: *Technological intelligence, *National defense, *Standards, *Measurements, Lasers, Infrared surveillance, Millimeter waves, Radar, Electronic warfare, Spacecraft communication, Ammunition, Homing devices, Range finders, Guidance(Motion).

Over the past few years the state of the art of defense technology has advanced rapidly. Measurement requirements to support this technology are particularly demanding in technical areas such as millimeter waves (for radar, electronic warfare, satellite communications, and munitions guidance), lasers (for target designators, rangefinders, and weapons), and IR (for focal plane array space surveillance sensors and tactical missile homing sensors). The paper reviews how the National Bureau of Standards (NBS) and the De-partment of Defense (DOD) identify measurement and standards requirements and coordinate their planning and describes areas where R&D work is needed to meet future defense needs.

901,271 PB89-177075 Not available NTIS National Bureau of Standards (NEL), Gaithersburg,

MD. Robot Systems Div.
Hierarchically Controlled Autonomous Robot for Heavy Payload Military Field Applications.

H. G. McCain, R. D. Kilmer, S. Szabo, and A.

Abrishamian. 1986, 10p Sponsored by Human Engineering Lab., Aberdeen

roving Ground, MD.

Pub. in Proceedings of International Conference on Intelligent Autonomous Systems, Amsterdam, Netherlands, December 8-11, 1986, p372-381.

Keywords: *Materiel, *Materiels handling, *Robots, Cargo transportation, Research projects, Field Materiel-Handling Robot, Control systems, Real time sys-

The U.S. Army Human Engineering Laboratory, with assistance from the National Bureau of Standards, Robot Systems Division, is developing a heavy-lift pallet handling robotic system designated as the Field Materiel-Handling Robot (FMR). The initial demonstra-tion of the FMR will be the sensor-driven autonomous acquisition and high speed manipulation of pallets of artillery ammunition. The paper describes the FMR research and development project with emphasis on the robot control architecture and the sensor-driven autonomous operational capabilities.

901,272 PB89-235139 PC A03/MF A01 National Inst. of Standards and Technology (NEL), Boulder, CO. Electromagnetic Fields Div. Alternative Techniques for Some Typical MIL-STD-461/462 Types of Measurements.

Technical note. J. E. Cruz, and E. B. Larsen. Mar 89, 43p NIST/TN-1320

Also available from Supt. of Docs. as SN003-003-02946-7. Sponsored by Army Aviation Systems Command, St. Louis, MO.

Keywords: *Antenna radiation patterns, *Standards, *Electromagnetic absorption, *Measurement, Antennas, Electromagnetic radiation, Transmitters, Electromagnetic properties, Electromagnetic fields, *Military equipment.

The report presents antenna factors determined in a screenroom which was partially loaded with radio fre-quency (rf) absorbing material, using the two-antenna insertion-loss technique. These antenna factors are compared with the antenna factors obtained in an unloaded screenroom, a fully loaded screenroom (an-echoic chamber), and at an open field site. In addition, measurements at the eight corners of a cube were made in the partially loaded and fully loaded screen-

room to determine the field deviation at the eight corners of the cube with respect to its center. Also, measurement improvements are quantified for the electric-field strength beneath a single-wire transmission line, in a partially loaded screenroom. Finally, electric-field measurements were made on top of the grounded table in a partially loaded screenroom to determine the field strength variation above the table.

901,273

PB90-128067 Not available NTIS National Inst. of Standards and Technology (NEL), Gaithersburg, MD. Mathematical Analysis Dir Analyzing the Economic Impacts of a Military Mobliization.

Final rept.

R. E. Chapman, C. M. Harris, and S. I. Gass. 1989, 34p

Sponsored by Federal Emergency Management

Agency, Washington, DC.
Pub. in Proceedings of Institute of Cost Analysis National Conference on Cost Analysis Applications of Economics and Operations Research, Washington, DC., July 5-7, 1989, p353-386.

Keywords: *Military mobilizing, *Economic analysis, Economic mobilization, Readiness, National defense, Command and control, Mathematical models.

A military mobilization is a complex series of events, which if modeled adequately, can specify how a national economy makes the transition from a peacetime to a war-time footing. Problems in modeling such situations have highlighted the importance of evaluating large-scale, policy-oriented models prior to their use by decision makers. The current study outlines a generic procedure for conducting such an evaluation. Specifically, macro-economic modeling and a structured sensitivity analysis can be combined to measure and evaluate the economic impacts of a military mobili-

Military Operations, Strategy, & Tactics

901,274

Not available NTIS PB89-176507 National Bureau of Standards (NML), Boulder, CO. Time and Frequency Div.

Secure Military Communications Can Benefit from Accurate Time.

Final rept. D. W. Hanson, and J. L. Jespersen. 1986, 12p Pub. in Proceedings of IEEE (Institute of Electrical and Electronics Engineers) Military Communications Conference, Monterey, CA., October 5-9, 1986, 12p.

Keywords: *Secure communication, *Military communication, Security, Coding, Countermeasures, Detection, Time division multiplexing, Pulse modulation, Interception, Deception, National defense.

Some military communications systems have requirements quite different from civilian systems. Among others there are the necessities to protect military communications from detection, interception, exploitation, or disruption by adversaries particularly during times of hostilities. There are a number of techniques available to protect communications against these threats -- some of them can benefit from unambiguous time information. A hypothetical military communica-tions system is used in the paper to discuss these pro-tection techniques and to illustrate how time may assume a useful role in their operation. The paper will also cover sources external to the communications system from which the necessary time information may be obtained.

Nuclear Warfare

901.275

PB89-188809 PC A05/MF A01 National Bureau of Standards (NML), Gaithersburg, PB89-188809 MD. Center for Radiation Research.

DCTDOS: Neutron and Gamma Penetration in Composite Duct Systems.

L. V. Spencer. Feb 87, 93p NBSIR-87/3534 Sponsored by Federal Emergency Man Agency, Washington, DC. Emergency Management

Keywords: *Radiation shielding, *Neutron absorption, *Nuclear weapons, Neutron albedo, Ducts, Computer programs, *Computer applications, *Gamma ray ab-

The paper describes computer methods for estimating neutron and gamma ray fluence rate, dose, and even spectral features due to penetration through a series of duct segments. The procedure links together data for individual segments -- straight sections and bends -- in arbitrary combinations; and the resulting composite can include computations for a room at the end, if there is one. This particular method was developed for rapid estimates in the protection problems against nuclear weapons, but the concepts which are employed are more broadly applicable.

901,276

PB89-200208 PC A10/MF A01 National Inst. of Standards and Technology (NEL), Gaithersburg, MD. Center for Fire Research. Assessment of Need for and Design Requirements

of a Wind Tunnel Facility to Study Fire Effects of Interest to DNA.
W. M. Pitts. May 89, 209p NISTIR-89/4049

Sponsored by Defense Nuclear Agency, Washington,

Keywords: *Fires, *Wind, Spreading, Dispersing, Urban areas, Nuclear explosions, Nuclear weapons, Wind tunnels.

The objective of the study is to recommend whether or not a new wind tunnel facility should be designed and constructed for the investigation of wind-aided fire spread. The focus is on the types of mass fire which can be expected following a nuclear detonation above an urban environment. The final conclusions of the report are (1) the need for an improved understanding of urban fire spread as it relates to nuclear weapon effects is overwhelming, (2) the authors currently have essentially zero predictive capability for fire damage in an urban environment following a nuclear attack, (3) wind tunnel experiments will not provide all of the required information, but offer the opportunity to substantially improve the understanding of the problem, (4) most existing wind tunnels were designed decades ago and are not well-suited for the required experimentation, and (5) some progress can be and is being made in existing facilities, but substantial improvements in understanding require a new facility and a sustained commitment for support.

NATURAL RESOURCES & EARTH SCIENCES

Geology & Geophysics

Not available NTIS PB89-147037 National Bureau of Standards (NML), Gaithersburg, MD. Gas and Particulate Science Div.

Application of Synergistic Microanalysis Tech-

niques to the Study of a Possible New Mineral Containing Light Elements.

Final rept. E. S. Etz, D. E. Newbury, P. J. Dunn, and J. D. Grice.

1985, 5p Pub. in Microbeam Analysis 1985, p60-64.

Keywords: *Microanalysis, *Minerals, Borate minerals, Carbonate minerals, Electron probes, Chemical elements, Raman spectroscopy, Classifications, Yttrium, Reprints, Light elements, Ion probes.

Complementary microanalysis techniques, including electron probe, ion microprobe and laser-Raman microanalysis, are applied to the compositional and structural characterization of a candidate new mineral containing light elements. The findings from ion probe analysis (SIMS) indicate the presence of boron and carbon as major constituents in addition to yttrium as the chief rare-earth element. The application of Raman microprobe analysis is explored to substantiate the results of optical measurements and x-ray structure determinations concerning the existence of carbonate and borate species. A series of synthetic components and natural minerals are studied by micro-Raman spectroscopy to obtain a spectral data base for structurally complex carbonates, borates, and minerals containing both species. These data are used in the interpretation of the Raman spectrum of the unknown Y/B/C-mineral and its classification as an yttrium carbonborate containing hydrogen-bonded borate group-

901,278 PB89-150882 Not available NTIS National Bureau of Standards (IMSE), Gaithersburg, MD. Metallurgy Div.

Multicritical Phase Relations in Minerals.

Final rept.

B. P. Burton, and P. M. Davidson. 1988, 31p Pub. in Structural and Magnetic Phase Transitions in Minerals, Chapter 4, p60-90 1988.

Keywords: *Crystallization, *Phase diagrams, *Carbonate minerals, Mathematical models, Hematite, Ilmenite, Heat of mixing, Critical point, Topology, Reprints, Diopside, Jadeite.

Models of multicritical phase relations are reviewed and theoretical results pertaining to the rhombohedral carbonates, hematite-ilmenite, and diopside-jadeite systems are discussed. The microscopic interactions that cause ordering and phase separation in these systems are highly anisotropic, such that ordering is favored in one crystallographic direction but clustering is favored in another. Model calculations which incorporate such interactions predict appropriate phase diagram topologies and appreciate composition and temperature dependence for excess heats of mixing.

901,279 PB89-185953 Not available NTIS National Bureau of Standards (NML), Boulder, CO.

Quantum Physics Div. Relationships between Fault Zone Deformation and Segment Obliquity on the San Andreas Fault, California.

Final rept.

R. Bilham, and K. Hurst. 1988, 15p Pub. in Proceedings of China-U.S. Symposium on Crustal Deformation and Earthquakes, Wuhan, Peo-ple's Republic of China, October 29, 1985, p510-524

Keywords: *San Andreas Fault, *Geological faults, *Earthquakes, *Creep rate, Earth movements, California, Numerical analysis, *Geologic structures.

Faults of the San Andreas system are considered as a sequence of contiguous straight segments with lengths from 2-30 km. A dominant length of approximately 12 km appears to exist. The segments are not parallel to each other nor to the plate slip vector calcu-lated from global plate motions. Although it is possible to choose a regional slip vector that will approximate the local strike of the fault by invoking slip on adjacent faults, it is not possible to eliminate oblique slip on all segments simultaneously. The detailed consequences of oblique slip on fault segments are described in terms of their impedance, a measure of the resistance of segment to fault motion. Impedance is defined to be the change of area resulting from slip on the fault. Cir-cumstantial evidence suggests that segments with anomalously large or small impedance may play a role in terminating or initiating earthquake rupture. The inferred instantaneous compression rate of creeping sections of the fault is calculated. It is shown that the present creep rate is insufficient to create the observed transpressive features on the southern San Andreas Fault and that much of the observed deformation must occur during earthquakes.

901,280 PB89-185979 Not available NTIS National Bureau of Standards (NML), Boulder, CO. Quantum Physics Div. Transducers in Michelson Tiltmeters. Final rept.

R. Bilham. 1988, 12p

Pub. in Proceedings of China-U.S. Symposium on Crustal Deformation and Earthquakes, Wuhan, Peo-

ple's Republic of China, October 29, 1985, p264-275 1988

Keywords: *Indicating instruments, *Water distribution, *Earthquakes, *Earth surface, Design criteria, Performance evaluation, Transducers, *Tiltmeters.

A Michelson tiltmeter consists of a horizontal pipe in which a continuous water surface extends from end to end. Tilt of the Earth's surface causes an increase in water depth at one end and a corresponding decrease in water depth at the other. Methods to detect these changes in water level to 0.001 mm accuracy are reviewed and several new methods are discussed. A new transducer is described that senses movements of the image position of a light emitting diode (LED) after it has been reflected from the water surface. The projected image of the LED is followed by a null-seeking servo system based on a silicon photodiode bi-cell whose vertical position is monitored by an LVDT transwhose vertical position's fillolition by all EVDT training ducer. The absolute depth of the water may be measured directly by the LED follower transducer to approximately 1 micrometers accuracy. In a 1km tiltmeter this is equivalent to a long term measurement accuracy of 1 nanoradian/year. System accuracy, however, is only as good as the accuracy with which the water level transducer is indexed to the Earth's surface. The method uses an array of vertical extensometers to identify locally generated signals that are typically of non-tectonic origin.

901,281

PB89-227946 Not available NTIS National Bureau of Standards (NML), Boulder, CO. Quantum Physics Div.

High-Precision Absolute Gravity Observations in the United States.

Final rept.

G. Peter, R. E. Moose, C. W. Wessells, J. Faller, and T. M. Niebauer. 1989, 16p Pub. in Jnl. of Geophysical Research 94, nB5 p5659-5674 May 89.

Keywords: *Gravity, United States, Precision, Measurement, Reprints, Ground motion.

From May 1987 to June 1988 the National Geodetic Survey (NGS) made approximately 50 observations at 30 sites with one of the six absolute gravimeters built by the Joint Institute for Laboratory Astrophysics between 1983 and 1986. Of the 10 sites where two to three observations were made, the scatter about the mean site values ranged from under plus or minus 1 microGal to plus or minus 4.0 microGal. The data correction methods now employed at NGS allow the establishment of high-precision reference gravity sta-tions in the United States and abroad for monitoring the temporal variations of gravity and studying vertical ground motions.

901,282

PB89-234272 Not available NTIS National Inst. of Standards and Technology (NML), Boulder, CO. Quantum Physics Div.

Rate of Change of the Quincy-Monument Peak Baseline from a Translocation Analysis of LAGEOS Laser Range Data.

Final rept. A. Stolz, M. A. Vincent, P. L. Bender, R. J. Eanes, M. M. Watkins, and B. D. Tapley. 1989, 4p Pub. in Geophysical Research Letters 16, n6 p539-542

Keywords: *Geological faults, Geodynamics, Earth-quakes, California, Motion, Reprints, *Plate tectonics, *San Andreas Fault, Laser range finders, Lageos(Satellite).

Translocation studies of LAGEOS laser range data from Quincy and Monument Peak in California observed during 1984-1987 suggest that plate tectonic motion across the San Andreas fault system in the di-rection of the baseline between the two stations is uniform at a rate of -30(+ or - 3) mm/a. Changes in the components of the baseline vector were inferred from repeat determinations using the solutions from suc-cessive half-year intervals. The changes in the vertical and transverse components of the Quincy-Monument and transverse components of the Quincy-Monument Peak baseline are -0.4(+ or -5) mm/a and +14(+ or -5) mm/a respectively. The vertical component deter-minations attest to the height stability of the laser rang-ing method. LAGEOS measurements made from Quincy and Monument Peak before 1984 are inaccurate enough to limit their usefulness for plate tectonic 901,283 PB90-136649 Not available NTIS National Inst. of Standards and Technology (NML),

Boulder, CO. Time and Frequency Div.

Tilt Observations Using Borehole Tiltmeters 1. Analysis of Tidal and Secular Tilt. Final rept.

J. Levine, C. Meertens, and R. Busby. 1989, 13p Contracts F19628-81-K-0040, F19628-78-C-0065 Sponsored by Air Force Geophysics Lab., Hansco

Pub. in Jnl. of Geophysical Research 94, nB1 p574 586, 10 Jan 89.

Keywords: *Boreholes, *Site surveys, Colorado, Wyoming, Yellowstone National Park, Oceans, Topogra-phy, Reprints, *Tiltmeters, *Earth tides, phy, Reprints, *Tiltmeters, Earth tides *Attitude(Inclination), Erie(Colorado), Secular var ations.

The authors have designed a porehole tiltmeter using two horizontal pendulums which have periods of 1 s. They have installed the instruments at seven sites in Colorado and Wyoming to evaluate the secular tilt, the tides, and the coherence between nearby instruments. Using 28 days of data from Boulder, Colorado, the estimates agree with models that include the body tide, the ocean load, and the topographic correction to better than the estimated uncertainty. Tidal measurements at Erie, Colorado, have larger, possibly nonrandom variability that may be caused by a coupling between the tides and long-period tilts. Measurements at Erie, Colorado and in Yellowstone National Park, Wyoming exhibit an annual or biannual periodicity.

Mineral Industries

901.284 PB89-175947 Not available NTIS National Bureau of Standards (IMSE), Gaithersburg, MD. Ceramics Div.
Microbiological Metal Transformations: Biotech-

nological Applications and Potential.

Final rept.

G. J. Olson, and R. M. Kelly. 1986, 15p Pub. in Biotechnol. Prog. 2, n1 p1-15 1986.

Keywords: *Microbiology, *Metals, *Bioengineering, *Mineral deposits, *Copper, *Uranium, Catalysis, Strategic materials, Materials recovery, Hydrometallurgy, Solution mining, Reprints.

The article reviews the recent literature on biological and engineering aspects of biotechnological metals and engineering aspects of biolectrinological installar recovery. Microorganisms catalyze many transforma-tions of metals including solubilization, precipitation and volatilization reactions, often associated with metal reduction, oxidation, alkylation or dealkylation reactions. There is a growing awareness in the microbiological, engineering, and mining fields that such reactions are of importance in metal recovery operations. Currently, copper and uranium are being commercially recovered from ores via biohydrometallurgy, and extension of the technology to other metals, especially precious and strategic, is underway. Efforts to commercialize such activities are hampered by a number of biological and engineering considerations, in part relating to inadequate knowledge of mechanisms of metal solubilization on surfaces by microorganisms and engineering problems related to heterogeneous systems in bioprocessing of solid materials. Various potential process engineering designs are discussed.

901.285 PB89-202113 PB89-202113 Not available NTIS National Bureau of Standards (IMSE), Gaithersburg, MD. Ceramics Div.

Novel Flow Process for Metal and Ore Solubilization by Aqueous Methyl lodide.

Final rept.

J. S. Thayer, G. J. Olson, and F. E. Brinckman. 1987,

Pub. in Appl. Organomet. Chem. 1, n1 p73-79 1987.

Keywords: *Solution mining, *Strategic materials, Metals, Atomic spectra, Absorption spectra, Bioengineering, Iron, Copper, Leaching, Wastes, Liquid flow, Hydrometallurgy, Metal containing organic compounds, Mineral deposits, Reprints, Iodomethanes.

NATURAL RESOURCES & EARTH SCIENCES

Mineral Industries

A novel process for bulk metal and metal ore solubilization by aqueous methyl iodide is described. A flow bioreactor system was developed and used in connection with a graphite furnace atomic absorption spectrometer for continuous, on-line quantitation of dis-solved metals. Dissolution of binary and ternary metal ores as well as bulk metals was enhanced 5-145x by aqueous methyl iodide in the flow system. Repeated alternating cycles of water and aqueous methyl iodide resulted in increasing enhancement of bulk from dissolution apparently due to a uncovering of fresh new reactive surfaces. Films of copper on circuit boards were also dissolved by methyl iodide. The process has many possible uses in mining and metallurgy especial-ly for recovery of precious and/or strategic metals from difficult to reach locations in ores or wastes.

901,286

PB89-221154 PC A04/MF A01 National Inst. of Standards and Technology (NEL), Gaithersburg, MD. Center for Mfg. Engineering. Mining Automation Real-Time Control System Ar-chitecture Standard Reference Model (MASREM).

Trechnical note (Final).

J. Albus, R. Quintero, H. M. Huang, and M. Roche.
May 89, 64p NIST/TN-1261-VOL-1
Also available from Supt. of Docs. as SN003-00302948-3. Sponsored by Bureau of Mines, Pittsburgh,

Keywords: *Real time systems, *Automation, *Mining equipment, *Mining, Models, Control systems, Interfaces, Computer software, Memory devices, Adaptive control systems, Task decomposition, Sensory processina.

The Mining Automation Real-Time Control System Architecture Standards Reference Model (MASREM) defines a logical hierarchical architecture for mining auto-mation. The MASREM architecture defines a set of standard modules and interfaces which facilitates software design, development, validation, and test, and makes possible the integration of software from a wide variety of sources. Standard interfaces also provide the software hooks necessary to incrementally upgrade future mining automation systems as new capabilities develop in computer science, robotics, and autonomous system control.

Natural Resource Surveys

901.287

PB89-201214 Not available NTIS National Bureau of Standards, Gaithersburg, MD. Office of the Director. Environmental Intelligence. Final rept.

B. D. Kraselsky, and C. C. Gravatt. 1989, 13p Pub. in Technology in Society 11, p99-111 1989.

Keywords: *Economic analysis, *Environmental surveys, Data acquisition, Remote sensing, Economic surveys, Land surveys, Commerce, Observation, Examination, Regulations, Reprints, *Satellite surveys,

Satellite remote sensing is being used to obtain a wide range of information about the land, the oceans, the atmosphere and man-made objects. The information, or environmental intelligence, is used to help solve problems that affect the general population, such as the greenhouse effect, the depletion of the ozone layer and land use planning, as well as for specialized com-mercial activities such as agriculture and forestry evaluations, mineral and petroleum exploration. The level of commercial involvement in the use of satellite remote-sensing data is increasing, due to technologi-cal and economic factors. However, commercial involvement in satellite system operations is plagued with economic impediments, is running into conflict with international obligations that regard this activity as a public good, and is being chilled by ambiguous domestic laws and regulations. The paper identifies the trends in commercial development; the legal, political, technical and economic factors that will affect the rate of the development; and the impact that such development will have on the overall conduct of satellite remote sensing activity.

Soil Sciences

901.288 PB89-186431 Not available NTIS National Bureau of Standards (NML), Gaithersburg, MD. Gas and Particulate Science Div.

Pahasapaite, a Beryllophosphate Zeolite Related to Synthetic Zeolite Rho, from the Tip Top Pegmatite of South Dakota.

Final rept. R. C. Rouse, T. J. Campbell, P. J. Dunn, D. Newbury, D. R. Peacor, W. L. Roberts, and F. J. Wicks. 1987,

8p Pub. in Neues Jahrbuch fur Mineralogie Monatshefte, n10 p433-440 1987.

Keywords: *Minerals, *Ion exchange resins, Calcium, Lithium, Potassium, Sodium, Phosphorus, Beryllium, Crystal structure, X ray diffraction, Refractivity, Density(Mass/volume), Beryl, Reprints, *Pahasapaite.

Pahasapaite, (Ca5.5Li3.6K1.2Na0.2 0 13.5) Li8Be24P24O96(center dot)38H20, is a new zeolite mineral associated with roscherite, tiptopite, and englishite at the Tip Top Mine, Custer, South Dakota. It is shite at the IIp Iop Mine, Custer, South Dakota. It is cubic, I23, with a = 13.781(4) angstroms and Z=1. The strongest powder X-ray diffraction lines are (d(angstroms), I,hkl): 9.60, 100, 110; 3.684, 90, 321; 3.248, 90, 411, 330; 2,935, 90, 332; 2.702, 60, 510, 431; 2.237, 40, 611, 532; and 4.35, 40, 310. Pahasapaite occurs as light pink, yellow-green, or colorless crystals, which are 1.0 mm in size and show the forms (110) and (111). There is no experient decrease the (110) and (111). There is no apparent cleavage, the refractive index is 1.523(2), and the observed and calculated densities are 2.28(4) and 2.241 g/cu m, respectively. A crystal structure determination shows pahasapaite to be a beryllophosphate zeolite with a tetrahedral framework configuration like that in systhetic zeolite rho. The name is from the Lakota Sioux word 'Pahasapa,' meaning Black Hills, in allusion to the locality.

901,289 PB89-188585 PC A03/MF A01 National Bureau of Standards (NEL), Boulder, CO. Center for Electronics and Electrical Engineering Dielectric Mixing Rules for Background Test Soils.
R. G. Geyer. Jun 88, 25p NBSIR-88/3095
Sponsored by Army Belvoir Research and Development Center, Fort Belvoir, VA.

Keywords: *Dielectric properties, *Mixing, *Soil tests, Simulation, Electromagnetic absorption, Microwaves, Remote sensing, Estimates, Soil-water mixtures.

The bulk, or effective dielectric constant of any back-ground test medium (whether naturally occurring or synthetic) determines the electromagnetic visibility of buried objects. Heuristic mixing rules are considered that allow the prediction of complex dielectric behavior in linear, homogeneous, isotropic, and lossy multi-phase soil mixtures. Measurement results in bioelectromagnetic and microwave remote sensing suggest a refractive mixing model as that being most suited for dry soils or soil-water mixtures.

901.290 PB89-209274 PC A04/MF A01 National Inst. of Standards and Technology (NEL), Gaithersburg, MD. Center for Building Technology. Site Characterization for Radon Source Potential. F. Y. Yokel. Jun 89, 59p NISTIR-89/4106 Sponsored by Department of Housing and Urban Development, Washington, DC. Innovative Projects and Special Technology Div., New Jersey Div. of Housing and Development, Trenton, and Ryland Group, Inc., Columbia, MD.

Keywords: *Site surveys, *Radon, *Soil analysis, *Buildings, Exploration, Concentration(Composition), Keywords: Soil properties, Moisture content, Permeability, Atmospheric pressure, Wind velocity, Field tests, Gamma ray spectroscopy, Density(Mass/volume), Sources, Numerical analysis, Temperature, Radioactivity, *Soil gases, Environmental transport, Indoor air pollution.

Radon source potential characterization of sites in terms of soil index properties which do not vary with transient conditions such as moisture content, barometric pressure, temperature and wind speed is studied. The invariant index properties which were found to be critical for site characterization are radium activity concentration in the soil, in-place dry density, porosity, and dry gas permeability. These properties can be measured in situ or in the laboratory or estimated on

the basis of other soil index properties such as grainsize distribution and Atterberg limits. Various expressions for radon source potential are reviewed and a new expression is formulated on the basis of data from areas of deep glacial terrace deposits. Site exploration methods proposed include use of the Standard Penetration Test together with a laboratory determination of radium activity concentration, and a rapid field measurement procedure using a portable gamma ray spectrometer, a portable nuclear moisture-density meter and retrieval of a soil sample for laboratory determination of particle-size distribution. A plan to develop ex-ploration protocols, test the effectiveness of the source potential prediction, and prepare a draft exploration standard is proposed.

PB89-211973 Not available NTIS National Bureau of Standards (NEL), Gaithersburg,

MD. Structures Div.
Laboratory Evaluation of an NBS (National Bureau of Standards) Polymer Soil Stress Gage. Final rept.

Final rept.

R. M. Chung, A. J. Bur, and J. R. Holder. 1985, 6p

Pub. in Proceedings of Symposium on the Interaction
of Non-Nuclear Munitions with Structures (2nd),

Panama City Beach, FL., April 15-18, 1985, p296-301.

Keywords: *Soil mechanics, *Stress analysis, *Measuring instruments, Laboratory equipment, Determination of stress, Performance evaluation, *Gages

The NBS polymer gage, which is made of thin sheets of polyvinylidene fluoride (PVDF) sandwiched between polycarbonate sheets, has been tested extensively at the National Bureau of Standards to evaluate its ability to measure soil dynamic stresses due to blast loading.

NAVIGATION, **GUIDANCE, &** CONTROL

Navigation Systems

901,292 PB89-174080 Not available NTIS National Bureau of Standards (NML), Boulder, CO.

Time and Frequency Div.

Apparent Diurnal Effects in the Global Positioning

System.

M. Weiss. 1987, 16p

Pub. in Proceedings of Annual Precise Time and Time Interval (PTTI) Applications and Planning Meeting (19th), Redondo Beach, CA., December 1-3, 1987, p33-48

Keywords: *Diurnal variations, Bias, Displacement, Errors, Delay time, Resolution, Sensitivity, Damping, Periodic variations, *Global positioning system, *Time

Since the Global Positioning System (GPS) has been used for common view time and frequency transfer between remote locations various systematic effects have been observed. These effects have been discussed on various occasions appearing as biases between different daily measurements as well as ob-structing closure in around-the-world time transfer. GPS satellites are examined from several locations around the world, after linking the ground station clocks GPS. The results are that there are apparent diurnal variations in many of the SV clocks. These systematic effects are studied, the biases in common view time transfer, the lack of closure in around-the-world time transfer, and the diurnal variations in the SV clocks. The diurnal effects are primarily due to errors in the transmitted satellite ephemeris and ionospheric model.

901,293 PB89-185730

Not available NTIS

NAVIGATION, GUIDANCE, & CONTROL Navigation Systems

National Bureau of Standards (NML), Boulder, CO.

Time and Frequency Div.

Using Multiple Reference Stations to Separate the Variances of Noise Components in the Global Positioning System.

Final rept.

M. A. Weiss, and D. W. Allan. 1986, 11p Pub. in Proceedings of Annual Symposium on Fre-quency Control (40th), Philadelphia, PA., May 28-30, 1986, p394-404.

Keywords: *Periodic variations, *Electromagnetic noise, Space surveillance(Spaceborne), Divergence, Atmospherics, Natural radio frequency interference, Clocks, Correlation, Variability, *Global positioning system's.

The separation of variance technique has been applied to measurements of a clock against received sigpiled to measurements of a clock against received sig-nals from Global Positioning System (GPS) satellites to separate out various noise components in the system. First, the authors show how measurements can be taken from several different locations to obtain estimates of more components of GPS system and to obtain better estimates of the components previously studied. It is shown how to estimate the variances of the GPS system clock, the error in the transmitted cor-rection term between the satellite clock and the GPS system clock, propagation noise in the measurement including ionospheric and tropospheric modelling errors, error in the transmitted ephemeris for the satellite, and the local reference clock. The authors consider the effects of correlations between elements of the data and analyze the confidence one may have in the estimates in light of those correlations. Finally, the multi-station separation of variance technique is applied to recent GPS data. New insights into the GPS system that have been learned using the technique are discussed.

NUCLEAR SCIENCE & TECHNOLOGY

Isotopes

901,294 Not available NTIS PB89-146872 National Bureau of Standards (NML), Gaithersburg, MD. Inorganic Analytical Research Div. Analytical Applications of Neutron Depth Profiling.

R. G. Downing, J. T. Maki, and R. F. Fleming. 1987, 14p

Pub. in Jnl. of Radioanalytical and Nuclear Chemistry 112, n1 p33-46 1987.

Keywords: *Neutron irradiation, *Depth detectors, Isotopes, Probes, Nondestructive tests, Metals, Ceramics. Reprints.

Using a low-energy neutron beam as an isotopic probe, neutron depth profiling (NDP) provides quantitative depth profiles in nearly all solid matrix materials. Several of the light elements, such as He, Li, B, and N can be non-destructively analyzed by NDP. The information obtained using NDP is difficult if not impossible to determine by non-nuclear techniques. As a result, NDP is used collaboratively with techniques as SIMS, RBS, FTIR, PGAA, and AES. Profiles measured by NDP are given for semiconductor and optical processing materials, and light weight alloys. Improvements in the technique are discussed with emphasis on the use of intense cold neutron beams.

901,295 PB89-171888 PB89-171888 Not available NTIS
National Bureau of Standards (NML), Gaithersburg, MD. Ionizing Radiation Physics Div.

NBS (National Bureau of Standards) Radon-in-Water Standard Generator.

Final rept. J. M. R. Hutchinson, P. A. Mullen, and R. Colle.

1986, 5p Pub. in Nuclear Instruments and Methods in Physics Research A247, n2 p385-389, 15 Jun 86.

Keywords: *Radioactivity, *Standards, Water, Reprints, *Radon 222, Radium 226.

NBS has completed the development of a transfer standard for radon-in-water measurements. This standard can be used to generate and accurately dis-pense radium-free (222)Rn solutions of known con-centration. The present finalized version is based on an earlier and previously described prototype. The standard consists of a polyethylene-encapsulated (226)Ra solution source in a small-volume accumulation chamber and an ancillary mixing and dispensing system which is partially automated with motor-driven syringes. The revised source configuration is more stable than the original prototype and the mixing and dispensing system is more compact, rugged, and convenient. The standard generator was calibrated and certified in terms of the (222)Rn concentration or total activity in an aliquot dispensed from the generator when a detailed operating procedure is adequately followed. The overall uncertainty of the calibration was estimated to be approximately + or - 4%.

901,296 Not available NTIS
National Bureau of Standards (NML), Gaithersburg,
MD. Radiometric Physics Div.
Using 'Resonant' Charge Exchange to Detect
Traces of Noble Gas Atom.

Final rept. J. E. Hardis, W. R. Peifer, C. L. Cromer, A. L. Migdall, and A. C. Parr. 1989, 4p Pub. in Proceedings of International Symposium on

Resonance Ionization Spectroscopy and Its Applica-tions (4th), Gaithersburg, MD., April 10-15, 1988, p237-240 1989

Keywords: *Resonance, *Krypton, *Rubidium, *Mass spectroscopy, *Ionization, Detection, Trace elements, Rare gases, Interferometers, Charge carriers, Cross sections, Isotopic labeling.

An experiment in progress is described to measure the charge-exchange cross sections of ${\rm Kr}+{\rm incident}$ upon Rb. The column density in the Rb cell will be measured using an optical interferometer. The reaction is expected to generate a significant flux of Kr atoms in the 5s (3/2) (J=2) metastable state, which will be useful as a step in RIMS studies of Kr isotope distributions.

901 297 PB89-201669 Not available NTIS National Bureau of Standards (NML), Gaithersburg, MD. Gas and Particulate Science Div.

Single Particle Standards for Isotopic Measure-ments of Uranium by Secondary Ion Mass Spectrometry.

D. S. Simons. 1986, 11p Pub. in Jnl. of Trace Microprobe Tech. 4, n3 p185-195

Keywords: *Uranium, *Radioactive isotopes, *Mass spectroscopy, Glass, Standards, Quantitative analysis, Ions, Reprints.

The isotopic abundance ratios of uranium have been determined from individual glass microparticles using secondary ion mass spectrometry (SIMS). Synthetic glasses were prepared using oxides of known isotopic composition as starting materials. Relative precisions and accuracies of better than 1% could be attained for (235)U/(238)U ratios between 0.0020 and 0.0072. These were primarily limited by counting statistics. Even the abundances of the minor isotopes (234)U and (236)U could be determined since molecular ion interferences were not present at measurable levels.

Nuclear Instrumentation

901.298 PB89-147508 Not available NTIS National Bureau of Standards (NML), Gaithersburg, MD. Ionizing Radiation Physics Div. Measurement Quality Assurance.

Final rept. E. H. Eisenhower. 1988, 7p Pub. in Health Physics 55, n2 p207-213 1988.

Keywords: *Quality assurance, *Measurement standards, *Ionizing radiation, Measurement, Radiation pro-

tection, Health physics, Quality control, Laboratories, Reprints.

The quality of a radiation protection program can be no better than the quality of the measurements made to support it. In many cases that quality is unknown, and is merely assumed on the basis of a calibration of a measuring instrument. If that calibration is inappropriate or is performed improperly, the measurement result will be inaccurate and misleading. Assurance of measurement quality can be achieved if appropriate procedures are followed, including periodic quality control actions that demonstrate adequate performance. Several national measurement quality assurance (MQA) programs are operational or under devel-opment in specific areas. They employ secondary standards laboratories that provide a high-quality link between the National Bureau of Standards and measurements made at the field use level. The procedures followed by these secondary laboratories to achieve MQA will be described, as well as plans for similar tuture programs. A growing general national interest in quality assurance, combined with strong specific motivations for MQA in the area of ionizing radiation, will provide continued demand for appropriate national programs.

901,299 Not available NTIS PB89-176549 National Bureau of Standards (NML), Gaithersburg,

MD. Ionizing Radiation Physics Div.

Monte Carlo Calculated Response of the Dual Thin Scintillation Detector in the Sum Coincidence Mode.

Final rept.

K. C. Duvall, and R. G. Johnson, 1988, 3p Pub. in Proceedings of International Conference on Nuclear Data for Science and Technology, Mito, Japan, May 30-June 3, 1988, p419-421.

Keywords: *Scintillation counters, *Neutron counters, Spectra, Mathematical models, Pulse height analyzers, Monte Carlo method, Neutron flux, Reaction time, Efficiency, Coincidence circuits.

The Dual Thin Scintillator is a unique neutron detector that is being developed for improved fluence and spectrum measurement. Current attention has been directed towards understanding some details of the detector response in the sum coincidence mode of operation where a peaked pulse-height response is exhibited throughout the energy region of interest. As a result of the peaked distribution, the detector efficiency is a weak function of the pulse-height bias, allowing the number of recorded events above the bias to be deternumber of recorded events above the bias to be determined with greater certainty. A Monte Carlo code has been used to calculate the sum coincidence pulseheight response at several energies within the 1 to 15 MeV region. The detector efficiency as a function of neutron energy has also been calculated. The results of the Monte Carlo calculations, which include the effect of multiple scattering on the shape of the response function and efficiency curve are presented.

901,300 PB89-229165 Not available NTIS National Inst. of Standards and Technology (NML), Gaithersburg, MD. Ionizing Radiation Physics Div. International Intercomparison of Neutron Survey Instrument Calibrations.

Final rept. J. B. Hunt, P. Champlong, M. Chemtob, H. Kluge, and R. B. Schwartz. 1989, 8p

Pub. in Radiation Protection Dosimetry 27, n2 p103-110 1989.

Keywords: Reprints, *Neutron monitors, *Survey monitors, Interlaboratory comparisons, Calibration, International separation.

An informal intercomparison of the methods of calibration of neutron area survey meters has been undertak-en by NIST, NPL, PTB and ETCA-CEA. The measurement programming was based upon the calibration of two different types of survey instrument in the neutron fields emitted by bare and by heavy water moderated californium spontaneous fission neutron sources. One of the transfer devices was a conventional spherical survey meter and the other was a new type of monitor which attempts to take the neutron spectral distribu-tion into account through the ratio of responses of two different sized moderating spheres. The results are compared and demonstrate that agreement among the various institutions can be obtained within + or - 3% for conventional instruments, but larger differ-

NUCLEAR SCIENCE & TECHNOLOGY

Nuclear Instrumentation

ences may exist for devices which are new and unconventional.

901,301 PB90-117532 Not available NTIS National Inst. of Standards and Technology (NML), Matther burg, MD. Ionizing Radiation Physics Div.
Method for Evaluating Air Kerma and Directional
Dose Equivalent for Currently Available Multi-Element Dosemeters in Radiation Protection Dosimetry. Final rept.

M. Ehrlich. 1989, 7p Pub. in Radiation Protection Dosimetry 28, n1-2 p89-95 1989.

Keywords: *Radiation protection, Reprints, *Kerma, *Dose equivalents, *Personnel dosimetry, *Dosemeters.

A method is outlined for estimating air kerma and di-rectional dose equivalent from indications on multi-element dosemeters having energy and angle response functions that are different for at least two of the dose-meter's radiation-sensitive elements. The method em-ploys dosemeter calibrations relating response of each element and the corresponding indication ratio(s) to radiation energy and angle of radiation incidence. Indications are measured in the usual way on the elements of each dosemeter irradiated under unknown conditions, and the ratio is formed of the indications of any two elements known to have different response any two elements known to have different response functions. Using the calibration curves, energy-angle pairs are found that correspond to these indication ratios, and are then used to determine the corresponding response values of which there are several per energy-angle pair. Finally, the response values corresponding to any given energy-angle pair are averaged, and air kerma or directional dose equivalent is computed from average response and the measured indications. The method is illustrated for a dosemeter for which photon calibration data were available which photon calibration data were available.

Radioactive Wastes & Radioactivity

901,302 NUREG/CP-0103 PC A10/MF A02 NUREG/CP-0103 PC A10/MF A02
Nuclear Regulatory Commission, Washington, DC.
Office of Nuclear Regulatory Research.
Proceedings of the Workshop on Cement Stabilization of Low-Level Radioactive Waste. Held at Gaithersburg, Maryland on May 31-June 2, 1989.
P. R. Reed. Oct 89, 224p NISTIR-89/4178
Also available from Supt. of Docs. Sponsored by National Inst. of Standards and Technology (NEL), Gaithersburg. MD. Building Materials Div.

Keywords: *Meetings, *Cements, *Solidification, *Stabilization, Leaching, Thermal cycling tests, Biodeterioration, Structural forms, Curing, *Low-level radioactive

ersburg, MD. Building Materials Div.

The workshop on Cement Stabilization of Low-Level Radioactive Waste was co-sponsored by the U.S. Nuclear Regulatory Commission and National Institute of Standards and Technology and held in Gaithersburg, Maryland on May 31-June 2, 1989. The workshop provided a forum for exchanging information on the solidi-fication and stabilization of low-level radioactive waste in cement among federal and state regulators, nuclear in cement among federal and state regulators, nuclear power station operators, cement vendors, national laboratory researchers and consultants. The workshop was structured into a 'Plenary' and four 'Working Group' sessions. Each working group session discussed specific issues: Lessons learned from small-and full-scale waste forms and observations at nuclear power stations; Laboratory test experience and application to problem waste streams; Stabilized waste form testing guidance; and Waste characterization, solidification, and process control programs.

901.303 PB89-215362 PC A07/MF A01 National Inst. of Standards and Technology (NEL), Gaithersburg, MD. Center for Building Technology.

Service Life of Concrete.

J. R. Clifton, and L. I. Knab. Jun 89, 150p NISTIR-

Sponsored by Nuclear Regulatory Commission, Washington, DC.

Keywords: *Concretes, Degradation, Service life, Mathematical models, Corrosion mechanisms, Accelerated tests, Durability, Permeability, *Radioactive waste management, Underground disposal, Low-level radioactive wastes.

The U.S. Nuclear Regulatory Commission (NRC) has the responsibility for developing a strategy for the disposal of low-level radioactive waste (LLW). An approach being considered for their disposal is to place the waste forms in concrete vaults buned in th earth. A service life of 500 years is required for the concrete vaults as they may be left unattended for much of their lives. The report examines the basis for making service life predictions based on accelerated testing and mathematical modeling of factors controlling the durability of concrete buried in the ground. Degradation processes are analyzed based on considerations of their occurrence, extent of potential damage, and mechanisms. A recommended research plan for developing methods for predicting the service life of con-crete is presented. Concepts of quality and factors af-fecting quality of concrete are discussed. Permeability is discussed in terms of the water-to-cement ratio, the pore structure of concrete, and the effects of cracks.

Reactor Engineering & Nuclear Power Plants

PB89-168017 PC A11/MF A01 National Inst. of Standards and Technology (IMSE), Gaithersburg, MD. Reactor Radiation Div. NBS (National Bureau of Standards) Reactor: Summary of Activities July 1987 through June 1988.
Technical note Jul 87-Jun 88.
C. O'Connor. Jan 89, 230p NIST/TN-1257
Also available from Supt. of Docs. as SN003-003-02920-3. See also PB83-218636.

Keywords: *NBSR reactor, Activation analysis, Crystal structure, Isotopes, Diffraction, Neutron, Radiography, Nondestructive tests.

The report summarizes all those programs which use the NBS Reactor. It covers the period for July 1987 through June 1988. The programs range from the use of neutron beams to study the structure and dynamics of materials through nuclear physics and neutron standards to sample irradiations for activation analysis isotrop production poutron reduction and poor sis, isotope production, neutron radiography, and nondestructive evaluation

Reactor Fuels & Fuel Processing

Not available NTIS PB89-176556 National Bureau of Standards (NML), Gaithersburg, MD. Ionizing Radiation Physics Div.

Measurements of the (235)U (n,1) Standard Cross

Section at the National Bureau of Standards

Final rept.

R. G. Johnson, A. D. Carlson, O. A. Wasson, K. C. Duvall, J. W. Behrens, M. M. Meier, B. D. Patrick, and M. S. Dias. 1988, 4p

Pub. in Proceedings of International Conference on Nuclear Data for Science and Technology, Mito, Japan, May 30-June 3, 1988, p1037-1040.

Keywords: *Fissionable materials, *Standards, *Neutron cross sections, *Uranium 235, Nuclear fuels, Linear accelerators, Measurement.

The Neutron Interactions and Dosimetry Group at the National Bureau of Standards (NBS) has had a long-term program for the measurement of standard neutron cross sections. The group has maintained a significant effort on the measurement of one of the most important of these cross sections -- the neutron-induced fission cross section of 235U. Since the ENDF/ B-VI evaluation has been recently released, it is appropriate to review the measurements of the (235)U(n,f) cross section which have been made at the NBS using accelerator-based neutron sources. In the 0.1 to 20 MeV region where the cross section is a standard, six separate measurements of the differential cross section, using a variety of techniques have been made.

Both the NBS 150-MeV Electron Linac and the 3-MV Positive Ion Accelerator have been used as neutron sources. Two of the measurements are relative to the H(n,p) cross section while the remainder are absolute. These measurements will be reviewed and compared to ENDF/B-VI. The current status of the program and possible future improvements will be discussed.

Reactor Physics

901.306 PB89-171946 Not available NTIS National Bureau of Standards (NML), Gaithersburg,

MD. Inorganic Analytical Research Div.
Use of Focusing Supermirror Neutron Guides to
Enhance Cold Neutron Fluence Rates.

M. Rossbach, O. Scharpf, W. Kaiser, W. Graf, A. Schirmer, W. Faber, J. Duppich, and R. Zeisler. 1988, 10p

Pub. in Nuclear Instruments and Methods in Physics Research B35, p181-190 1988.

Keywords: *Neutron beams, *Equipment, *Focusing, *Neutron flux, *Mirrors, Gamma spectrometers, Nickel, Titanium, Radioactivation analysis, Neutron cross sections, Transmissivity, Substrates, Reprints.

A simple neutron focusing system was installed and tested at a neutron guide in the external neutron guide laboratory ELLA at KFA in Juelich. The device uses nickel-titaninum supermirrors. The production of these supermirrors is described together with results and practical hints for improving their behavior for a certain practical limits for improving their behavior for a certain glass substrate with the measured roughness of 18.5 Angstroms. Results of Monte Carlo calculations of the transmission and focusing properties for different wavelengths are given and compared with measured results. The obelisk shaped 150 cm long supermirror coated tube has an average transmission of 62% and a maximum local gain of 3. a maximum local gain of 3.

General

901,307

PB90-130279 PC A09/MF A01 National Inst. of Standards and Technology (NML), Gaithersburg, MD. Center for Radiation Research.
Center for Radiation Research (of the National institute of Standards and Technology) Technical

Activities for 1989. C. E. Kuyatt. Nov 89, 181p NISTIR-89/4183 See also PB89-127294.

Keywords: *Irradiation, *Research projects, *Test fa-cilities, Measurement, Nuclear physics, Radiometry, Ion sources, Ionizing radiation, Instruments, Dosimetry, Calibrating, Standards, Beams(Radiation), Radio-chemistry, *Center for Radiation Research.

The report summarizes research projects, measurement method development, calibration and testing, and data evaluation activities that were carried out during Fiscal Year 1989 in the NIST Center for Radiation Research. The activities fall in the areas of radiometric physics, radiation sources and instrumentation, ionizing radiation, and nuclear physics.

OCEAN TECHNOLOGY & ENGINEERING

Biological Oceanography

901,308 PB89-175855

Not available NTIS

OCEAN TECHNOLOGY & ENGINEERING

Biological Oceanography

National Bureau of Standards (NML), Gaithersburg, MD. Organic Analytical Research Div.

Specimen Banking in the National Status and Trends Program: Development of Protocols and First Year Results. Final rept.

G. G. Lauenstein, M. M. Schantz, S. A. Wise, and R.

Zeisler. 1986, 5p Pub. in Proceedings of Oceans 86, Conference Record, Washington, DC., September 23-25, 1986, p586-590.

Keywords: *Aquatic animals, *Trace elements, *Chemical analysis, *Organic compounds, Sampling, Performance evaluation, Fishes, Mussels, *Environmental monitoring, *Baseline studies, *Water pollution detection.

The National Oceanic and Atmospheric Administration has initiated a Specimen Bank for estuarine and coastal samples as part of its National Status and Trends Program. During the first year, sample collection proto-cols were developed for the collection of benthic fish, bivalve molluscs, and associated sediments. Specimens from over 40 sites nationwide have now been submitted for inclusion in the Specimen Bank which is housed at the National Bureau of Standards in Gaithersburg, Maryland. Specimens are preserved at liquid nitrogen temperature with degradation expected to be minimal for decades. Retrospective analysis of specimens will allow the opportunity to derive baseline values for new environmental contaminants and make historical marine samples available for analysis when new and improved analytical procedures become available. Preliminary analyses of selected samples collected during the first year are presently under way for organic and trace element contaminants.

901,309 PB89-177232 Not available NTIS National Bureau of Standards (IMSE), Gaithersburg, MD. Ceramics Div.

Biodegradation of Tributyitin by Chesapeake Bay Microorganisms.

Final rept. G. J. Olson, and F. E. Brinckman, 1986, 6p

Sponsored by Office of Naval Research, Arlington, VA. Pub. in Proceedings of Oceans 86, Conference Record, Washington, DC., September 23-25, 1986, p1196-1201.

Keywords: *Chesapeake Bay, *Biodeterioration, *Marine microorganisms, *Water analysis, Gas chromatography, Chemical analysis, *Tin/tributyl, Flame photometry.

The authors have been studying microbial resistance to butyltin compounds and the degradation of tributyl-tin spiked into samples of Chesapeake Bay waters. Butyltin species were identified and quantified using a gas chromatograph equipped with a tin-selective flame photometric detector (GC-FPD), providing micrograms/1 detection limits. Incubation of these samples under incandescent lamps accelerated biodegradation, suggesting the involvement of photosynthetic microorganisms. At certain times in these degradation experiments, tetrabutyltin was detected by GC-FPD and confirmed by gas chromatography-mass spectrometry.

Dynamic Oceanography

901,310 PB89-171755 Not available NTIS National Bureau of Standards (NML), Boulder, CO. Time and Frequency Div.

Gravity Tide Measurements with a Feedback Gravity Meter. Final rept.

J. Levine, J. C. Harrison, and W. Dewhurst. 1986, 7p Pub. in Jnl. of Geophysical Research 91, nB12 p12835-12841, 10 Nov 86.

Keywords: *Tides, *Gravimeters, *Measurement, Surface waves, Gravity waves, Tidal currents, Ocean waves, Atmospheric pressure, Amplitude, Reprints.

Gravity-tide data obtained using a calibrated LaCoste and Romberg gravity meter with electrostatic feedback has been analyzed. There is agreement between the measured amplitude and phase of the major semi-diurnal components and the corresponding values to be

expected using current earth models and ocean-load calculations. Both local and global barometric pressure changes make significant contributions to the power in the tidal bands and are included in the fitting function. The admittance estimates at diurnal frequencies can be used to determine the frequency and to set a lower bound on the dissipation of the nearly-diurnal resonance in the tidal response by fitting a resonance function to the observations. These estimates are in reasonable agreement with results obtained by other methods, but are somewhat different from the values to be expected on the basis of more elaborate theoretical estimates.

Physical & Chemical Oceanography

901,311 PB89-177224 Not available NTIS National Bureau of Standards (IMSE), Gaithersburg, MD. Ceramics Div.

Determination of Ultratrace Concentrations of Butyltin Compounds in Water by Simultaneous Hydridization/Extraction with GC-FPD Detection.

Final rept. C. L. Matthias, J. M. Bellama, and F. E. Brinckman. 1986, 6p

Sponsored by Office of Naval Research, Arlington, VA., and David W. Taylor Naval Ship Research and

va., and David w. Taylor Naval Ship Research and Development Center, Annapolis, MD. Pub. in Proceedings of Oceans 86, Conference Record, Washington, DC., September 23-25, 1986, p1146-1151.

Keywords: *Trace elements, *Water analysis, *Marine atmospheres, Gas chromatography, Extraction, pH, Salinity, Chemical stabilization, *Tin/butyl, Flame photometry, Hydridization.

An improved method for the ultratrace determination of butyltins in water by simultaneous hydridization/extraction followed by gas chromotography coupled with a flame photometric detector is reported. Detection limits for the new system are 5 micrograms/L tributyltin cation (TBT(sup +)). Effects of pH and salinity on the procedure are reported and stability of the derived extracts is discussed.

General

PB89-187512 Not available NTIS National Bureau of Standards (NML), Gaithersburg, MD. Office of Standard Reference Data. Computerized Materials Property Data Systems.

J. Rumble, and J. G. Kaufman. 1986, 3p Pub. in Proceedings of Oceans '86 Conference Record, Washington, DC., September 23-25, 1986, p370-372.

Keywords: *Marine engineering, *Materials specifications, Offshore structures, Mechanical properties, Structural design, Corrosion, Failure, *Data bases.

Because of the harshness of the marine environment, the selection of materials for structural and other purposes has always been a demanding task, complicated by the enhancement of mechanical failures by corrosion. Not only are data such as corrosion fatique scarce, locating the available data can be very difficult. The computer offers an opportunity to allow easy and efficient access to technical data. Over the last few years, a comprehensive materials data system has been started to meet the needs of industrial and other materials data users. One result has been to establish the National Materials Property Data Network. Recognizing that databases will be built by the same wide variety of groups that now use only one kind of computer system, the Network plans to offer a gateway service that features a common user interface, a convenient catalog of existing data, and coverage of all types of engineering materials and their properties. Progress towards these goals will be described as well as efforts to make available high-quality data of interest to marine environments.

901,313 PB90-117417

Not available NTIS

National Inst. of Standards and Technology (NEL), Gaithersburg, MD. Structures Div.

Hydrodynamic Forces on Vertical Cylinders and the Lighthiii Correction.

Final rept.

G. R. Cook, and E. Simiu. 1989, 18p

Sponsored by Department of the Interior, Washington,

Pub. in Ocean Engineering 16, n4 p355-372 1989.

Keywords: *Hydrodynamics, *Force, *Offshore structures, Damping, Drag, Water waves, Reprints, *Cylinders, *Lighthill correction, Morison equation.

In the paper the expression for the Lighthill correction was derived for finite water depths. Measurements obtained in periodic wave flow at the Naval Civil Engineering Laboratory and in random wave flow at the Delft Hydraulics Laboratory were subjected to an extensive analysis. The results of the analysis showed that for both the periodic and random wave conditions the addition of the Lighthill correction did not improve the Morison equation significantly and had no significant effect on the estimation of the drag force, including the drag force corresponding to very low Keulegan-Carpenter numbers.

ORDNANCE

Ammunition, Explosives, & **Pyrotechnics**

901,314

PB89-146914 Not available NTIS National Bureau of Standards (NEL), Boulder, CO. Electromagnetic Fields Div.

Measurement Procedures for Electromagnetic Compatibility Assessment of Electroexplosive Devices.

Final rept.

J. W. Adams, and D. S. Friday. 1988, 11p

Sponsored by Army Aviation Systems Command, St. Louis, MO., and Naval Surface Weapons Center, Silver Spring, MD.

Pub. in IEEE (Institute of Electrical and Electronics Engineers) Transactions on Electromagnetic Compatibility 30, n4, p484-494 Nov 88.

Keywords: *Initiators(Explosives), *Electromagnetic compatibility, Electromagnetic interference, Measurement, Mathematical models, Statistical theory, Vulnerability, Electromagnetic fields, Electromagnetic pulses, Nuclear explosion effects, Reprints.

Electroexplosive devices (EEDs) are electrically fired explosive initiators used in a wide variety of applica-tions. The nature of most of these applications requires that the devices function with near certainty when required and otherwise remain inactive. Recent concern with pulsed electromagnetic interference (EMI) and the nuclear electromagnetic pulse (EMP) made apparent the lack of methodology for assessing EED vulnerability. A new and rigorous approach for characterizing EED firing levels is developed in the context of statistical linear models and is demonstrated in the paper. The authors combine statistical theory and methodology with thermodynamic modeling to determine the probability that an EED of a particular type fires when excited by a pulse of a given width and amplitude. The results can be applied to any type of EED for which the hot wire explosive binder does not melt below the firing temperature of the primary explosive.

PHOTOGRAPHY & RECORDING DEVICES

Photographic Techniques & Equipment

901.315 PB89-186340 Not available NTIS National Bureau of Standards (NEL), Gaithersburg, MD. Precision Engineering Div.

Automated Calibration of Optical Photomask Linewidth Standards at the National Institute of

Standards and Technology. Final rept.

J. E. Potzick. 1989, 13p Pub. in Proceedings of SPIE (Society of Photo-Optical Instrumentation Engineers) Symposium on Microlithography, San Jose, CA., February 26-March 3, 1989, 13p.

Keywords: *Calibrating, *Automation, *Line width, Standards, Optical equipment, *Photomasks.

An automated system has been developed at the National Institute of Standards and Technology (NIST), formerly the National Bureau of Standards, for calibrating optical photomask linewidth standards. The system, controlled by a desktop computer, locates each feature to be measured in the field of view of the microscope, centers and focuses the image, scans the image, and calculates the optical linewidth from the scan data. The results are checked for errors and the process repeated until every feature on the photomask has been calibrated. If statistical tests are passed, a calibration certificate is printed.

PHYSICS

Acoustics

901.316 PB89-147839 PC A10/MF A01 National Inst. of Standards and Technology (NEL), Boulder, CO. Electromagnetic Fields Div.

Measurement of Adapter Loss, Mismatch, and Effi-clency Using the Dual Six-Port. G. J. Counas, and B. C. Yates. Jul 88, 209p NBSIR-

88/3096

Sponsored by Aerospace Guidance and Metrology Center, Newark AFS, OH. Metrology Engineering Section.

Keywords: *Acoustic measurement, Measuring instruments, Noise, Standards, Efficiency, Accuracy, Adapters, Temperature, *Dual six-port measurement system.

A noise measurement system is being developed for the U.S. Air Force which uses coaxial cryogenic and ambient noise temperature standards to determine the noise temperature of the device under test. When the device under test has a different connector than those on the noise standards, an adapter has to be used. Adapter loss and complex reflection coefficient must be compensated for or noise measurement accuracy is affected. A technique has been developed which uses a dual six-port measurement system to determine the mismatch, loss, and ultimately the efficiency of the adapter used. This enables correction of measurement results and allows measurements to be made with an adapter with no degradation of accuracy.

901,317 PB89-179709 Not available NTIS National Bureau of Standards (NEL), Gaithersburg, MD. Thermophysics Div.

Spherical Acoustic Resonators in the Undergraduate Laboratory.

Final rept. M. Bretz, M. L. Shapiro, and M. R. Moldover. 1989,

Pub. in American Jnl. of Physics 57, n2 p129-133 Feb

Keywords: *Acoustic resonators, *Acoustic velocity, *Velocity measurement, Gases, Reprints, Temperature dependence, Pressure dependence, Acoustic thermometry.

A spherical acoustic resonator is reported that measures the speed of sound in gases with very high accuracy using comparatively simple instrumentation. The resonator can be used to illustrate, in a quantitative fashion, the temperature and pressure dependence of the speed of sound, the effects of thermal conductivity, and the splitting of nearly degenerate modes.

PB89-179808 Not available NTIS National Bureau of Standards (IMSE), Boulder, CO. Fracture and Deformation Div. Acoustoeiastic Determination Residuai Stresses.

Final rept. Final rept.
P. P. Delsanto, R. B. Mignogna, A. V. Clark, D. Mitrakovic, and J. C. Moulder. 1987, 7p
Sponsored by Office of Naval Research, Arlington, VA., and Office of Nondestructive Evaluation, Arling-

Pub. in Residual Stresses in Science and Technology, v1 p175-181 1987.

Keywords: *Residual stress, *Ultrasonic tests, Acoustic properties, Rayleigh waves, Surface waves, Metal plates, Crystal lattices, Texture, Nondestructive tests, Reprints, *Acoustoelasticity.

A general perturbative formalism for the propagation of Rayleigh waves on the surface of initially deformed anisotropic material plates is applied to the particular case of an orthotropic distribution of cubic crystallites. Applied and residual stresses can be determined from their correlation with the measured Rayleigh waves propagation velocity. A critical problem, especially in the case of residual stresses, is the separation of texture and acoustoelastic effects. Two techniques are proposed for the solution of this problem and their range of validity is discussed.

PB89-202220 Not available NTIS National Bureau of Standards (NML), Gaithersburg, MD. Temperature and Pressure Div.

Speed of Sound in a Mercury Ultrasonic Interferometer Manometer.

C. R. Tilford. 1987, 11p Pub. in Metrologia 24, n3 p121-131 1987.

Keywords: *Acoustic velocity, *Sound transmission, *Interferometers, *Manometers, *Mercury(Metal), *Mercury(Metal), Acoustic measurement, Sound waves, Optical meas-uring instruments, Pressure measurement, Carbon di-oxide lasers, Reprints.

The speed of sound in mercury for frequencies between 9.5 and 10.5 MHz has been measured by comparison with a frequency stabilized infrared laser. The apparatus and techniques used for both the ultrasonic and optical measurements are discussed, along with details of the error analysis.

901.320 PB89-228548 Not available NTIS National Inst. of Standards and Technology (NEL), Gaithersburg, MD. Thermophysics Div. Acoustic and Microwave Resonances Applied to

Measuring the Gas Constant and the Thermodynamic Temperature.

Final rept.
M. R. Moldover. 1989, 8p
Pub. in IEEE (Institute of Electrical and Electronics Engineers) Transactions on Instrumentation and Measurement 38, n2 p217-224 Apr 89.

Keywords: *Ideal gas law, *Temperature measure-ment, *Acoustic resonance, *Microwaves, Thermody-namic properties, Resonant frequency, Resonance, Acoustic velocity, Reprints.

Techniques are being developed for simultaneously measuring the frequencies of microwave and acoustic

resonances in a spherical cavity. They will permit the determination of the thermodynamic temperature with unprecedented accuracy. Progress to date includes: a new value for the universal gas constant: R = 8.314 471 + or - 0.000 014 J/(mol times K) (1.7 ppm) with a five-fold reduction in its standard error, a new value of the thermodynamic temperature of the triple point of gallium (302.9169 + or - 0.0005 K), and a microwave measurement of the volumetric thermal expansion of an acquistic resonator with an error of about + or - 1.5 an acoustic resonator with an error of about + or - 1.5 ppm. Improved values of the Boltzmann constant, (1.38 065 13 + or - 0.000 002 5) x 10(-23) J/K, and the Stefan-Boltzmann constant, (5.670 399 + or - 0.000 038) x 10(-8) W/(m sup 2 times K sup 4), were obtained from R, and further studies of the temperature scale are in progress.

901,321 PB90-128505 Not available NTIS National Inst. of Standards and Technology (NEL), Gaithersburg, MD. Thermophysics Div. Sphericai Acoustic Resonators.

Final rept. J. B. Mehl, and M. R. Moldover. 1989, 23p Pub. in Topics of Current Physics: Photoacoustic, Photothermal and Photochemical Processes in Gases, Chapter 4, p61-83 1989.

Keywords: *Acoustic resonators, *Acoustic velocity, *Thermophysical properties, *Gases, Mathematical models, Acoustic measurement, Reprints, Spherical configuration.

Gas-filled spherical resonators are excellent tools for measurements of the speed of sound. The radially symmetric gas resonances are nondegenerate and have high quality factors (typically 2,000-10,000). These resonances can be used with very simple instrumentation and unsophisticated analysis to measure the speed of sound in a gas with an accuracy on the order of 0.01%. With data analysis based on a complete theoretical model of the acoustical system, the accuracy can be increased to better than one part per million. The model includes the effects of the coupling between acoustic and thermal waves, thermal and vis cous effects at the shell boundary, shell motion, and imperfect shell geometry. Other boundary effects, including the effects of holes in the resonator wall and precondensation effects, have also been considered. The results of the theoretical model are described in detail and compared with experimental results in the chapter. There is also a brief review of the thermophysical importance of acoustic measurements, including a discussion of the determination of ideal-gas specific heats and information about intermolecular interactions.

Fluid Mechanics

901.322 PB89-150932 Not available NTIS National Bureau of Standards (NEL), Gaithersburg, MD. Mathematical Analysis Div. Solutal Convection during Directional Solidification.

G. B. McFadden, and S. R. Coriell, 1988, 7p. Sponsored by National Aeronautics and Space Administration, Washington, DC.
Pub. in Proceedings of National Fluid Dynamics Con-

gress (1st), Cincinnati, OH., July 25-28, 1988, p1572-1578.

Keywords: *Alloys, *Metals, *Solidification, *Crystallization, *Convection, *Fluid dynamics, Buoyancy, Computation, Gravitation, Mathematical models, Melts, Bifurcation.

During directional solidification of a binary alloy at constant velocity, buoyancy-driven fluid flow may occur due to the solute gradients generated by the solidifica-tion process. Numerical calculations of the solute and fluid flow fields in the melt have been carried out using finite differences in a two-dimensional, time-dependent model that assumes a planar crystal-melt interface and allows time-dependent gravitational accelerations. The container walls are rigid and perfectly insulating for solute. For constant vertical gravitational accelerations, as the solutal Rayleigh number is varied, multiple steady states and time-dependent states may occur. The bifurcation from the quiescent state may be sub-

critical or transcritical, depending on the aspect ratio of the container. The maximum variation in the solute concentration at the crystal-melt interface was also calculated for various values of the rotation rate of the gravitational acceleration.

PB89-157259 Not available NTIS National Bureau of Standards (NEL), Gaithersburg, MD. Thermophysics Div.

Effect of Surface Ionization on Wetting Layers.

Final rept. R. F. Kayser. 1986, 4p Pub. in Physical Review Letters 56, n17 p1831-1834 1986.

Keywords: *Ionization, *Liquid phases, *Substrates, *Polarity, *Wetting, *Glass, Langmuir probes, Mathematical models, Mixtures, Carbon disulfide, Dispersants, Reprints.

A generalized surface ionization model of Langmuir's to liquid mixtures of polar and nonpolar components in contact with ionizable substrates is presented. When a predominantly nonpolar mixture is near a miscibility gap, thick wetting layers of the conjugate polar phase form on the substrate. Such charged layers can be much thicker than similar wetting layers stabilized by dispersion forces. The model may explain the 0.4-0.6 micro m thick wetting layers formed by mixtures of nitrogethers and other thinds in the last stabilized by the control with place. tromethane and carbon disulfide in contact with glass.

901,324 PB89-158117 Not available NTIS National Bureau of Standards (NEL), Gaithersburg, MD. Chemical Process Metrology Div.

Numerical Computation of Particle Trajectories: A Model Problem.

Final rept. E. F. Moore, and R. W. Davis. 1986, 6p Pub. in Gas-Solid Flows, p111-116 1986.

Keywords: *Particle trajectones, *Numerical analysis, Mathematical models, Stokes law(Fluid mechanics), Unsteady flow, Incompressible flow, Computenzed simulation, Reprints, *Gas-particle flow.

Computer simulations are useful in gas-solid particle systems where experimental measurements are often difficult. The relative accuracy of various numerical methods becomes important in assessing the significance of results obtained. The note presents a model problem for trajectories of solid particles in a quasisteady, incompressible axisymmetric flowfield and numerical results obtained from three different methods for tracking particles through this flow. The characteristics of the trajectories, with sudden changes in direction, are reminiscent of particle tracks seen in the wake of a bluff body. Thus, this model problem is highly pertinent to numerical simulations of realistic gas-particle flows. The basic parameter involved here is particle Stokes number. Trajectories of a particle are presented for three values of Stokes number. The relative accuracy of the three particle-tracking methods when the flow is either steady or suddenly reversing direction is discussed.

901,325 PB89-158141 Not available NTIS National Bureau of Standards (NEL), Gaithersburg, MD. Thermophysics Div.
Shear Induced Anisotropy in Two-Dimensional

Llaulds.

Final rept. H. J. M. Hanley, G. P. Morriss, T. R. Welberry, and D. J. Evans. 1988, 26p Sponsored by Department of Energy, Washington, DC. Pub. in Physica 149A, p406-431 1988.

Keywords: *Liquids, Shear tests, Photographic techniques, Light scattering, Anisotropy, Reprints, Two dimensional.

The behavior of a dense two-dimensional soft disc liquid under shear is studied via nonequilibrium molecular dynamics. The structure factor for the liquid at a given shear rate is evaluated directly by plotting the particle positions, taken at random from the NEMD simulation at that shear, onto photographic film and using light scattering to obtain a diffraction pattern. The pair correlation function of this system is also extended intention to the pair correlation function of this system is also extended intention. tracted directly by histogramming the particle positions with respect to a given central particle as a function of separation and angle. The pair correlation function is compared to that approximated by a Fourier series expansion to rank ten. Results are reported as a function

of shear rate from a shear rate of 0.1 (when the fluid is essentially Newtonian) to 10 (when the fluid can dis-play a string phase). The appearance of the string phase is discussed and shown to be a consequence of the definition of temperature in the simulation algonthm. A modification of the algorithm is proposed. Comparisons between this work and previous work with three-dimensional liquids are given. The two-dimensional structure factor is compared with that obtained from a real colloidal suspension via light scatter-

901.326 PB89-161871

National Inst. of Standards and Technology (NML),
Gaithersburg, MD. Center for Chemical Technology.
MIxing Motions Produced by Pipe Elbows.
T. T. Yeb, and G. E. Mattington Leading. T. T. Yeh, and G. E. Mattingly. Jan 89, 41p NISTIR-89/4029

Keywords: *Pipe flow, *Mixing, *Elbows(Pipe), Pipes(Tubes), Velocity measurement, Swirling, Vortex flow, Pressure distribution, Turbulent flow, Laser ane-

Experimental measurements have been made, using laser Doppler velocimetry (LDV) of the pipeflows produced by a range of pipe-elbow configurations. The secondary flow characteristics of these pipeflows are described qualitatively and quantitatively together with their decay rates in the downstream piping. The poten-tial these flows have as mixing environments is de-scribed on the basis of the profiles of the mean and scribed on the basis of the profiles of the mean and turbulent velocity components, the change of these with downstream distance, and the pressure losses. Parameters characterizing these flow fields are defined from the measured velocity profiles. It is shown that double elbow 'out-of-plane' combinations where minimal pipelengths separate the elbows can produce very energetic long-lasting, swiring flows that can very energetic, long-lasting, swirling flows that can serve as effective mixers. Such effectiveness suggests that process designers might consider adding an additional elbow (and the slight increase in pressure loss) to pipe turns so as to take advantage of the enhanced mixedness that can be achieved via closecoupled elbows-out-of-plane.

901,327 PB89-173918 Not available NTIS National Bureau of Standards (NEL), Boulder, CO. Chemical Engineering Science Div.
Use of Dye Tracers In the Study of Free Convection in Porous Media.

Final rept.

M. C. Jones, and R. A. Perkins. 1988, 7p Contract DE-AI05-87ER13770

Sponsored by Department of Energy, Washington, DC. Pub. in Proceedings of Symposium on Energy Engineering Sciences (6th), Argonne, IL., May 4-6, 1988, p152-158.

Keywords: *Porous materials, *Fluorescent dyes, Temperature gradients, Fiber optics, Lasers, Three dimensional flow, Porosity, *Free convection, *Tracer techniques

A new experimental approach based on age distribution functions is described for the study of free convection in porous media. Fiberoptic probes are being used to track the dispersion of a fluorescent dye by the convective flow. The initial focus is on three-dimensional flows in rectangular boxes with vertical temperature gradients.

901,328 PB89-174023 Not available NTIS National Bureau of Standards (NEL), Boulder, CO. Thermophysics Div. Shear Dilatancy and Finite Compressibility in a Dense Non-Newtonian Liquid.

Final rept. H. J. M. Hanley, J. C. Rainwater, D. J. Evans, and L. Hood. 1988, 3p

Pub. in Proceedings of International Congress on Rheology (10th), Sydney, Australia, August 14-19, 1988, v1 p386-388.

Keywords: *Non-Newtonian fluids, *Compressible flow, *Shear tests, Rheological properties, Dilatancy, Density(Mass/volume), Viscosity, Dynamic pressure,

Nonequilibrium molecular dynamic (NEMD) simulations of model systems indicate that liquids of spherical particles are non-Newtonian. The authors illustrate here that the shear viscosity coefficient, Eta(sub +) of a liquid of soft spheres is a function of the shear rate, gamma; they show that the liquid is shear dilatant, i.e., that the density, rho, is a decreasing function of gamma at constant pressure, p; they also indicate that the liquid exhibits normal pressure differences. The re-sults are used to analyze fluid behavior in a typical flow problem, namely flow between vertical rotating concentric cylinders.

PB89-179592 Not available NTIS National Bureau of Standards (NEL), Gaithersburg,

MD. Chemical Process Metrology Div.

Application of Magnetic Resonance Imaging to Visualization of Flow in Porous Media. Final rept.

A. K. Gaigalas, A. Van Orden, B. Robertson, T. H. Mareci, and L. A. Lewis. 1989, 6p Sponsored by Nuclear Regulatory Commission, Wash-

ington, DC. Pub. in Nuclear Technology 84, p113-118 Jan 89.

Keywords: *Flow visualization, *Water flow, Porous materials, Aluminum oxide, Bentonite, Kaolin, Absorption, Reprints, *Magnetic resonance imaging.

The flow of water in porous materials has been visualized using nuclear magnetic resonance imaging (MRI). ized using nuclear magnetic resonance imaging (MHI). For flow in an initially dry bed, the water gives a large signal that can be detected directly. Flow in a wet bed is visualized indirectly by displacing the pure water with a dilute solution of paramagnetic ions. The solution does not give an MRI signal and so can be contrasted with pure water. Another use of MRI is to observe the absorption of water by a solid. The MRI technique is sensitive and can give accurate and quantitative results for flow with low Peclet number.

901,330

PC A03/MF A01 PB89-209282 National Inst. of Standards and Technology (NEL), Gaithersburg, MD. Center for Computing and Applied Mathematics

Elimination of Spurious Eigenvalues in the Chebyshev Tau Spectral Method.

G. B. McFadden, B. T. Murray, and R. F. Boisvert. May 89, 19p NISTIR-89/4090

Keywords: *Chebyshev inequality, *Hydrodynamics, *Eigenvalues, Spectrum analysis, Models, *Chebyshev approximation, *Spectral methods, Computational fluid dynamics, Chebyshev tau method, Chebyshev Galerkin method, Orr-Sommerfeld equations, Vorticity equations.

Spectral methods have been used to great advantage in hydrodynamic stability calculations; the concepts are described in Orszag's seminal application of the Chebyshev tau method to the Orr-Sommerfeld equation for plane Poiseuille flow in 1971. Orszag discusses both the Chebyshev Galerkin and the Chebyshev tau methods, but presents results for the tau method, which is easier to implement than the Galerkin method. The tau method has the disadvantage that two unstable eigenvalues are produced that are artifacts of the discretization. The authors present an extremely simple modification to the Chebyshev tau method which eliminates the spunious eigenvalues. They first study a simplified model of the Orr-Sommerfeld equation discussed by Gottlieb and Orszag. They consider the Chebyshev tau method, which has two spurious eigenvalues, and then describe a modification which eliminates them. Finally, they consider results for the Orr-Sommerfeld equation, where the modified tau method also eliminates the spurious eigenvalues. The simplicity of the modification makes it a convenient alternative to other approaches to the problem.

901,331

PB89-227995 PB89-227995 Not available NTIS National Bureau of Standards (NEL), Boulder, CO. Thermophysics Div.

Development of a Field-Space Corresponding-States Method for Fluids and Fluid Mixtures. Final rept.

Fillal rept.

J. R. Fox. 1987, 18p

Sponsored by Department of Energy, Washington, DC.

Pub. in Fluid Phase Equilibria 37, p123-140 1987.

Keywords: *Fluids, *Mixtures, *Phase transformation, Pressure, Temperature, Equations of state, Van der Waals equation, Thermodynamics, Reprints.

Fluid Mechanics

A field-space corresponding-states transformation is one in which the properties of a fluid, or fluid mixture, are related to the properties of a reference fluid, or fluid mixture, by equations which are analytic in the field variables (i.e., the pressure, temperature and chemical potentials). Such transformations are radically different from traditional corresponding states methods. The most useful of these differences is that the presence of phase coexistence in the target system is a direct reflection of phase coexistence in the reference system and never the result of the transformation itself. An immediate consequence of technical interest is that, if the phase transitions of the reference system are tabulated or known analytically, transforming these states maps all of the phase transitions of the target system directly.

901,332 PB89-228050 Not available NTIS National Inst. of Standards and Technology (NEL), Gaithersburg, MD. Thermophysics Div. Simplified Representation for the Thermal Conductivity of Fluids in the Critical Region.

Final rept. G. A. Olchowy, and J. V. Sengers. 1989, 10p Contract DE-FG05-88ER13902

Sponsored by Department of Energy, Washington, DC.
Pub. in International Jnl. of Thermophysics 10, n2 p417-426 Mar 89.

Keywords: *Thermal conductivity, *Fluids, *Critical flow, Ethane, Methane, Carbon dioxide, Thermal diffusivity, Reprints.

A practical representation for the critical thermal conductivity enhancement is developed by incorporating a finite cutoff into the asymptotic mode-coupling inte-grals for the diffusivity associated with the critical fluctuations. This procedure yields a simplified approximation to a more complete nonasymptotic solution of the mode-coupling integrals obtained earlier. A comparison is made with thermal conductivity data for carbon dioxide, ethane, and methane.

901.333 PB89-231484 PC A04/MF A01 National Inst. of Standards and Technology (NEL), Boulder, CO. Chemical Engineering Science Div. Effect of Pipe Roughness on Orifice Flow Meas-

Trechnical note.
J. A. Brennan, S. E. McFaddin, C. F. Sindt, and R. R. Wilson. Jul 89, 66p NIST/TN-1329
Contracts GRI-5081-353-0422, GRI-5081-271-1680
Also available from Supt. of Docs. as SN003-003-02951-3. Sponsored by Gas Research Inst., Chicago,

Keywords: *Orifice flow, *Flow measurement, *Pipes(Tubes), *Roughness, Orifice meters, Surface roughness, Gases, Water, Experimental data.

Flow measurement with orifice flowmeters is simple in concept and can be accurate, but, as demonstrated in flow measurement test facilities, can also result in large errors if any of the significant parameters are not controlled. Many of these parameters are well known and particular care is taken to ensure that they do not cause measurement errors. Others are more subtle and not so easily detected or controlled. One such parameter is the surface finish of the pipe immediately upstream of the orifice plate. Results of an experimental investigation into the effects of this pipe roughness on the orifice discharge coefficient are presented, along with a review of some of the pertinent literature. Measurement errors of approximately 1% can result from using meter tubes that are too rough but still within the specification of the standards.

901.334 PB89-235147 PC A23/MF A01 National Inst. of Standards and Technology (NEL), Gaithersburg, MD.

Measurements of Coefficients of Discharge for

Concentric Flange-Tapped Square-Edged Orifice Meters in Water Over the Reynolds Number Range 600 to 2,700,000.

Technical note (Final). J. R. Whetstone, W. G. Cleveland, G. P. Baumgarten, S. Woo, and M. C. Croarkin. Jun 89, 544p NIST/TN-1264

Also available from Supt. of Docs. as SN003-003-02942-4. Sponsored by American Petroleum Inst., Washington, DC.

Keywords: *Orifice meters, *Flow measurement, *Reynolds number, Fluid flow, Water meters, Standards, Velocity, Pressure, Mathematical models

Presented is a description of the measurement procedures and standards, data acquisition systems, and data bases developed in the American Petroleum Institute-sponsored orifice discharge coefficient data base project performed at the National Bureau of Standards primary water flow rate measurement facility. Measurements were performed on five orifice meter sizes, 2, 3, 4, 6, and 10 inches, over the beta ratio range of 0.08 to 0.75. The measurement systems and procedures were designed to provide full documentation of the relation between the observations comprising the data base developed and U.S. national measurement

901.335 PB89-235667

(Order as PB89-235634, PC A04) Great Lakes Fishery Commission, Ann Arbor, Ml., Apparatus for Neutron Scattering Measurements on Sheared Fluids.

Bi-monthly rept. G. C. Straty. 1989, 3p Included in Jnl. of Research of the National Institute of Standards and Technology, v94 n4 p259-261 Jul/Aug

Keywords: *Neutron scattering, *Fluids, *Shear properties, *Measuring instruments, Torque, Temperature, Computer applications.

The construction of an apparatus to allow neutron scattering measurements on fluids undergoing shear is reported. The apparatus has been used with the cold neutron small-angle-neutron-scattering (SANS) spectrometer at the NIST research reactor and will be made available to users as a permanent part of the NIST facility.

Optics & Lasers

901,336 PB89-156996 Not available NTIS National Bureau of Standards (NML), Gaithersburg, MD. Radiometric Physics Div. Ultrasensitive Laser Spectroscopy and Detection.

Final rept.

R. A. Keller, and J. J. Snyder. 1986, 9p Pub. in Laser Focus/Electro-Optics 22, n3 p86-94 Mar

Keywords: Mass spectroscopy, Fluorescence, Detection, Reprints, *Laser spectroscopy, Resonance ionization spectroscopy, High resolution.

Recent advances in laser technology have led to the development of several techniques for ultrasensitive high resolution spectroscopy and ultrasensitive detection. A recent symposium and a feature issue of the Journal of the Optical Society of America contain a series of papers on the theory and applications of these new techniques. For simplicity, the authors have chosen most examples in the article from these two references, although they are by no means exhaustive of the subject. They have further restricted their attention to three techniques which they find particularly exciting: quantum noise limited absorption measurements, photon burst detection of fluorescence, and resonance ionization mass spectrometry.

901.337 PB89-157069 Not available NTIS National Bureau of Standards (NEL), Boulder, CO. Electromagnetic Technology Div.

Tresnel Lenses Display Inherent Vignetting.

Final rept. M. Young. 1988, 2p

Pub. in Applied Optics 27, n17, p3593-3594, 1 Sep 88. Keywords: *Optical lenses, Photometry, Radiometry, Reprints, *Fresnel lenses, Optical fibers, Vignetting.

Some of the light refracted by a facet of a Fresnel lens impinges on the axial (or horizontal) portion of the facet and is directed away from the focal point. Loss of this light may be significant in applications where precise radiometric measurements are necessary.

901.338

PB89-157382 Not available NTIS National Bureau of Standards (NML), Boulder, CO. Time and Frequency Div.

Thermal Shifts of the Spectral Lines in the (4)F3/2

to (4)I11/2 Manifold of an Nd:YAG Laser. Final rept.

S. Z. Xing, and J. C. Bergquist. 1988, 4p Sponsored by Air Force Office of Scientific Research, Washington, DC., and Office of Naval Research, Ar-lington, VA.

Pub. in IEEE (Institute of Electrical and Electronics Engineers) Jnl. of Quantum Electronics 24, n9 p1829-1832 Sep 88.

Keywords: *Spectral lines, *Line spectra, *Frequency shift, Frequency standards, Near infrared radiation, Reprints, *YAG lasers, Temperature dependence.

The authors report the thermal shifts of eleven of the twelve lines from the quartet F (3/2) Stark energy levels to the quartet I (11/2) energy levels in an Nd:YAG laser for a temperature change from 20-200 C. The thermal shift difference between the Stark sublevels R1, R2 in quartet F (3/2) is found to be about - 0.6 plus or minus 0.6/cm/100 C. Within the experimental uncertainty, all of the lasting lines either moved to longer wavelength or remained unchanged with increasing temperature.

901.339

PB89-157390 Not available NTIS National Bureau of Standards (NML), Boulder, CO. Time and Frequency Div.

Precise Test of Quantum Jump Theory.

R. G. Hulet, D. J. Wineland, J. C. Bergquist, and W.

п. G. Hulet, D. J. Wineland, J. C. Bergquist, and W. M. Itano. 1988, 4р Sponsored by Air Force Office of Scientific Research, Washington, DC., and Office of Naval Research, Arlington, VA. Pub. in Physical Review A 37, n11 p4544-4547 Jun 88.

Keywords: Atomic spectroscopy, Optical pumping, Raman spectra, Fluorescence, Tests, Reprints, *Magnesium ions, *Quantum jumps, Quantum optics, Laser spectroscopy, Trapping(Charged particles), Magnesium 24.

Quantum jumps due solely to spontaneous Raman scattering between the Zeeman sublevels of a single (24)Mg(1+) ion have been observed in the fluorescence emitted by the ion. A theory of quantum jumps for this system predicts that coherences between ex-cited levels cause the ratio of the mean duration of the 'fluorescence-on periods' to the mean duration of the 'fluorescence-off periods' to be independent of laser intensity. The measured value agrees with the predicted one to within the measurement precision of 2%. The distribution of the durations of the off periods also agrees with theory.

901,340 Not available NTIS PB89-157887 National Bureau of Standards (NEL), Gaithersburg, MD. Precision Engineering Div. Resonance Light Scattering from a Liquid Suspen-

sion of Microspheres. Final rept.

T. R. Lettieri, and E. Marx. 1986, 7p Pub. in Applied Optics 25, n23 p4325-4331, 1 Dec 86.

Keywords: *Microscopy, Dielectrics, Mie scattering, Electromagnetic scattering, Diameters, Reprints, *Resonance light scattering, *Microspheres.

Resonance light scattering (RLS) spectra have been obtained from a liquid suspension of dielectric microspheres having a narrow size distribution in order to deduce the mean size and distribution width of the spheres. Comparison with single-particle spectra shows that most peaks in the size-distributed spectra are due to several resonances in the a sub n or b sub n Mie scattering coefficients. A mean diameter for the microspheres, obtained by matching experimental resonance wavelengths with those calculated using a vectorized Mie scattering algorithm, is in excellent agreement with optical microscopy and scanning electrons and scanning electrons are set to the control of th tron microscopy results. However, the measured width of the size distribution is significantly smaller than those from optical microscopy and transmission electron microscopy. Several sources of experimental error which affect the RLS spectra, including angle

misalignment and oversized collection apertures, are

901.341

PB89-158091 Not available NTIS National Bureau of Standards (NML), Gaithersburg, MD. Atomic and Plasma Radiation Div. Recent Progress on Spectral Data for X-ray Lasers

at the National Bureau of Standards.

Final rept.

J. Reader, J. Sugar, and V. Kaufman. 1988, 4p Sponsored by Strategic Defense Initiative Organiza-tion, Washington, DC., and Department of Energy. Washington, DC. Office of Magnetic Fusion Energy. Pub. in IEEE (Institute of Electrical and Electronics Engineers) Transactions on Plasma Science 16, n5 p560-563 Oct 88.

Keywords: Energy levels, Spectrum analysis, Reprints, *X ray lasers, Laser-produced plasma, Isoelectronic sequence, Tokamak devices, Multicharged ions.

Recent work on the spectra of laser-produced plasmas and tokamaks has led to the observation of long sequences of isoelectronic ions extending to very high ionic charge states. The measurements of the wavelengths and energy levels provide data that are impor-lengths and energy levels provide data that are impor-tant for the development of X-ray lasers. In addition to contributing to a knowledge of the energy levels and transitions of possible lasing media, the data provide reference lines for wavelength calibration of X-ray laser experiments and reference data for testing theoretical methods used for predicting the properties of lasing ions.

901.342

PB89-171235 Not available NTIS National Bureau of Standards (NML), Boulder, CO. Quantum Physics Div.

Laser-Nolse-Induced Population Fluctuations in

Two- and Three-Level Systems.

Final rept. T. Haslwanter, H. Ritsch, J. Cooper, and P. Zoller.

1988, 8p Grant NSF-PHY86-04504

Sponsored by National Science Foundation, Washington, DC.

Pub. in Physical Review A 38, n11 p5652-5659, 1 Dec

Keywords: Light scattering, Reprints, *Laser noise, Resonance fluorescence.

Significant fluctuations, above the shot-noise limit, have been observed in the intensity of fluorescent light scattered from atoms excited by an intense noisy laser, where a central role is played by the nonlinearity laser, where a central role is played by the nonlinearity of the atom-field interaction. By considering the variance of the atomic populations, the authors show that noise spectroscopy is sensitive to the field statistics of the laser. They specifically consider the cases of resonance fluorescence (analogous in the weak-field limit to analysis by a Fabry-Perot interferometer), two-photon excitation, and double optical resonance for variable laser intensity and bandwidth. It is shown that large differences in the noise spectra can occur between lasers characterized by a phase diffusion or a tween lasers characterized by a phase-diffusion or a phase-jump model, although these models would give the same values for the mean atomic populations. The authors believe that observation of population fluctua-tions can become a useful method for characterizing laser noise.

901.343

PB89-171276 PB89-171276 Not available NTIS National Bureau of Standards (NML), Boulder, CO. Quantum Physics Div.

One-Photon Resonant Two-Photon Excitation of Rydberg Series Close to Threshold.

Final rept. G. Alber, T. Haslwanter, and P. Zoller, 1988, 7p Pub. in Jnl. of the Optical Society of America B 5, n12 p2439-2445 Dec 88.

Keywords: Reprints, *Rydberg series, Multi-photon processes, Autoionization, Bound state, Ware pack-

One-photon resonant two-photon excitation of autoionizing Rydberg series close to threshold is studied. Analytical expressions for the time evolution of boundstate amplitudes are derived by adapting ideas from quantum-defect theory. The two limiting cases of exci-tation of Rydberg wave packets and AC-Stark splitting close to the threshold are discussed in detail. 901,344
PB89-171607
National Bureau of Standards (NML), Boulder, CO. Quantum Physics Div.

Scattering of Polarized Light in Spectral Lines with Partial Frequency Redistribution: General Redistribution Matrix.

Final rept.

H. Domke, and I. Hubeny. 1988, 12p Pub. in Astrophysical Jnl. 334, p527-538, 1 Nov 88.

Keywords: *Spectral lines, Resonance scattering, Legendre functions, Reprints, *Polarized light, Radiative transfer

The redistribution matrix for resonance scattering of arbitrarily polarized light, described by a vector of Stokes parameters, is derived assuming that the ground state is isotropic (i.e., assuming negligible optical pumping). When specified in the atomic rest frame, the redistribution matrix is found to be composed of several terms with individually separate frequency and angular dependence. The laboratory frame (velocity averaged) redistribution matrix exhibits an analogous structure, but the angular and frequency dependences are intermingled. The authors consider two possibilities for treating the angular dependence in practical applications, namely, an expansion in a series of Legendre polynomials, and an azimuthal expansion. Finally, the concept of azimuthally averaged redistribu-tion matrix is examined, and explicit expressions for resonance lines are given.

PB89-171672 Not available NTIS
National Bureau of Standards (NEL), Boulder, CO.
Electromagnetic Technology Div.
Stability of Birefringent Linear Retarders (Wave-

plates).

Final rept.
P. D. Hale, and G. W. Day. 1988, 8p
Sponsored by Optical Society of America, Washington,

Pub. in Applied Optics 27, n24 p5146-5153, 15 Dec 88.

Keywords: *Retarders(Devices), Birefringence, Stability, Reprints, *Waveplates.

The effects of changes in temperature, wavelength, and direction of propagation (angle of incidence) on the retardance of zero-order, multiple-order, compound zero-order, and temperature-compensated waveplates are described in detail. A disagreement in the literature regarding the properties of a compound zeroorder waveplate is resolved by showing that with respect to temperature and wavelength, it behaves like a true zero-order waveplate, but with respect to angle of incidence it behaves like a multiple-order waveplate. A previously proposed temperature-compensated design is shown to suffer from the same directional limitations. A new design for a retarder consisting of one element of a positive uniaxial crystal and one element of a negative uniaxial crystal is proposed. The retardance of such a waveplate would be much less sensitive to the direction of propagation, but somewhat more sensitive to temperature than a typical compound zero-order waveplate.

PB89-171680 Not available NTIS

National Bureau of Standards (NEL), Boulder, CO. Electromagnetic Technology Div.

NBS (National Bureau of Standards) Laser Power and Energy Measurements.

Final rept. T. R. Scott. 1988, 7p 1. H. Scott. 1988, 7p Pub. in Proceedings of the SPIE (Society of Photo-Optical Instrumentation Engineers), Laser Beam Radiometry, Los Angeles, CA., January 14-15, 1988, v888 p48-54.

Keywords: *Calorimeters, *Laser beams, *Power meters, Measuring instruments, Standards, Calibrating, Optical communications, Power measurement, Thermal measurements.

The National Bureau of Standards (NBS) maintains a set of electrically calibrated calorimeters designed and built specifically for laser energy measurements. These calorimeters are used as national reference standards for the calibration of optical power and energy meters. NBS offers laser measurement services based on the standard calorimeter to the public at a variety of laser wavelengths and power ranges. The uncertainties associated with these measurements have recently been re-evaluated.

901,347

PB89-171698 Not available NTIS National Bureau of Standards (NEL), Boulder, CO. Electromagnetic Technology Div.

Fast-Puise Generators and Detectors for Characterlzing Laser Receivers at 1.06 um.

Final rept.

P. A. Simpson. 1988, 5p

Pub. in Proceedings of the SPIE (Society of Photo-Optical Instrumentation Engineers), Laser Beam Radiometry, Los Angeles, CA., January 14-15, 1988, v888 p43-47.

Keywords: *Detectors, *Generators, *Lasers, Calibrating, Pulsation, Receivers, Optical communication, Pulse amplifiers, Pulse analyzers.

A detector system capable of measuring the waveform of pulses used to calibrate laser receivers at 1.06 micrometers is described. The risetime of the system is 0.8 ns. All parts of the system are available commercially. Also described is an optical impulse generator at 1.06 micrometers with a risetime of less than 100 ps. This impulse generator can be used to measure the impulse response of the detector system and laser re-

901,348

PB89-171714 Not available NTIS National Bureau of Standards (NEL), Boulder, CO.

Electromagnetic Technology Div.
Electrically Calibrated Silicon Bolometer for Low Level Optical Power and Energy Measurements.

Final rept.

R. J. Phelan, and R. M. Craig. 1988, 5p Pub. in Proceedings of the SPIE (Society of Photo-Optical Instrumentation Engineers), Laser Beam Radiometry, Los Angeles, CA., January 14-15, 1988, v888 p38-42.

Keywords: *Bolometers, Power measurement, Silicon on sapphire, Laser radiation.

A cryogenically cooled, silicon on sapphire, electrically calibrated bolometer has been designed and measured to have a noise equivalent power of 3 x 10 to the -11 power watt per root hertz. The electrical calibration of the bolometer has agreed with an electrically calibrated pyroelectric to better than 1%.

PB89-173959 Not available NTIS National Bureau of Standards (NEL), Boulder, CO. Electromagnetic Technology Div.

Interferometric Dispersion Measurements on Small Guided-Wave Structures. Final rept.

B. L. Danielson, and C. D. Whittenberg. 1988, 2p Pub. in Proceedings of Conference on Lasers and Electro-Optics, Anaheim, CA., April 25-29, 1988, p360-

Keywords: Fourier analysis, *Optical waveguides, *Optical fibers, *Dispersion, Coherence domain reflectometry, Time domain reflectometry.

A method is described for obtaining dispersion properties of components in microoptic systems. The technique is based on a Fourier analysis of the reflective signatures obtained from a coherence-domain reflectometer.

901,350

PB89-175731 Not available NTIS National Bureau of Standards (NML), Boulder, CO. Time and Frequency Div.

New FIR Laser Lines and Frequency Measure-

ments for Optically Pumped CD3OH.

Final rept.

R. J. Saykally, K. M. Evenson, D. A. Jennings, L. R. Zink, and A. Scalabrin. 1987, 10p

Pub. in International Jnl. of Infrared and Millimeter Waves 8, n6 p653-662 1987.

Keywords: *Infrared lasers, Far infrared radiation, Deuterium compounds, Optical pumping, Carbon dioxide lasers, Frequency measurement, Continuous radiation, Reprints, *Methyl alcohol lasers, Methanol.

Twenty new cw FIR laser lines in CD3OH, optically pumped by a CO2 laser, are reported. The frequencies of 39 of the stronger laser lines were measured relative to stabilized CO2 lasers with a fractional uncertain-

Optics & Lasers

ty, as determined by the reproducibility of the FIR frequency itself, of 2 parts in 10 million.

901,351 PR89-175749 Not available NTIS National Bureau of Standards (NML), Gaithersburg, MD. Radiation Source and Instrumentation Div.
NBS/NRL (National Bureau of Standards/Naval
Research Laboratory) Free Electron Laser Facility. Final rept.

Final rept.

S. Penner, R. Ayres, R. Cutler, P. Debenham, B. C. Johnson, E. Lindstrom, D. Mohr, J. Rose, M. Wilson, P. Sprangle, and and C. M. Tang. 1988, 8p See also AD-A194 214.

Pub. in Nuclear Instruments and Methods in Physics Research A272, p73-80 1988.

Keywords: Reprints, *Free electron lasers, *Racetrack microtrons, US NBS, National Institute of Standards and Technology.

A free electron laser is being built at the National Bureau of Standards as a joint project with the Naval Research Laboratory. The electron beam source is the 185 MeV CW racetrack microtron (RTM) presently nearing completion. The accelerator is characterized by extremely good emittance and small energy spread. A new photocathode injector operating on the 32nd subharmonic of the 2380 MHz rf frequency is being developed to increase the peak current to approx = or > 2 A in 3 ps micropulses. The wiggler design has 130 periods of (lambda sub w) = 28 mm with rms wiggler parameter K approx = or < 1. Three-dimensional calculations indicated that power gains of 10-30% per pass can be achieved for optical wavelengths in the range 200 nm to 10.0 micrometers. The design of the RTM and FEL will be described. The FEL is intended for use in a broad program of research applications in biomedicine and materials science.

901,352 PB89-176234 Not available NTIS National Bureau of Standards (NEL), Gaithersburg, MD. Precision Engineering Div.

Resonance Light Scattering from a Suspension of

Microspheres.

Final rept.

T. R. Lettieri, and E. Marx. 1987, 3p Pub. in AIP (American Institute of Physics) Conference Proceedings, n160 p523-525 1987.

Keywords: *Resonance scattering, *Light(Visible radiation), *Spectra, Dielectrics, Visible spectrum, Spectrum analysis, Diameters, Dimensions, Mie scattering, Microspheres.

Resonance light scattering spectra have been obtained from a liquid suspension of dielectric microspheres and then used to determine the mean diameter and width of the size distribution of the spheres.

901,353 PB89-176515 Not available NTIS National Bureau of Standards (NML), Gaithersburg, MD. Radiation Source and Instrumentation Div.
NBS (National Bureau of Standards) Free Electron Laser Facility.

B. C. Johnson, P. H. Debenham, S. Penner, C. M. Tang, and P. Sprangle. 1989, 4p

Pub. in Proceedings of International Symposium on

Resonance Ionization Spectroscopy and Its Applica-tions (4th), Gaithersburg, MD., April 10-15, 1989, p247-

Keywords: Continuous radiation, Far ultraviolet radiation, Intermediate infrared radiation, *Research facilities, *Free electron lasers, *Tunable lasers, Picosecond pulses, National Institute of Standards and Technology.

A free electron laser (FEL) user facility is being constructed at the National Bureau of Standards in collaboration with the Naval Research Laboratory. The anticipated performance of the FEL is: (1) wavelength variable from approximately 150 nm to 10 micrometers; (2) continuous train of 3 ps-wide pulses at 74.375 MHz; and (3) average power of 10 W to 200 W. One advantage of the NBS-FEL for RIS schemes is the ability to select the wavelength at will. It is also possible to scan the wavelength. The high repetition rate is an additional attractive feature. an additional attractive feature.

901.354 PB89-176929

Not available NTIS

National Bureau of Standards (IMSE), Gaithersburg, MD. Metallurgy Div.
Computing Ray Trajectories between Two Points:

A Solution to the Ray-Linking Problem. Final rept.

Pub. in Jnl. of the Optical Society of America A-Optics and Image Science 4, n10 p1919-1922 1987.

Keywords: *Ray tracing, *Light transmission, Integral equations, Iteration, Perturbation, Convergence, Reprints, Refractive index, Successive approximations method, Imaging techniques.

The problem of computing the ray trajectory between points a and b, when given the refractive index (or sound velocity) distribution, is complicated by the ignorance of the initial ray direction at the point a, which is needed in defining the path intercepting the end point b when numerically integrating the ray equation. It is shown that this ray-linking problem can be avoided by transforming the ray equation into an implicit integral equation for the true ray path that satisfies the given boundary conditions. The integral equation can be solved for the true path by the method of successive approximations. Simulations suggest that this iterative scheme often converges rapidly to the true path. An explicit expression for a ray path, obeying the boundary conditions, is also derived which is correct to first order in the refractive index perturbation. This path provides an excellent approximation to the true path when the refractive index perturbation is small, and becomes increasingly good as the perturbation goes to

901,355 PB89-177208 Not available NTIS National Bureau of Standards (IMSE), Gaithersburg, MD. Ceramics Div. Photoelastic Properties of Optical Materials.

Final rept.

A. Feldman. 1986, 8p Pub. in Proceedings of SPIE (Society of Photo-Optical Instrumentation Engineers), Laser and Nonlinear Optical Materials, San Diego, CA., August 19-20, 1986, p127-134.

Keywords: *Photoelastic analysis, *Optical properties, *Piezoelectric crystals, Wavelengths, Acoustic measurement, Tensor analysis, Brillouin zones, Interferometers, Birefringence, Polarization(Waves), Refracti-

The tensorial nature of the photoelastic effect in opti-cal materials is discussed. The commonly used phocal materials is discussed. The commonly used price to elastic constants, the piezo-optic and the elasto-optic constants, are defined, and the general form of these tensors is presented. The most commonly used methods for measuring photoelastic constants, inter-ferometry, polarimetry, the acousto-optic effect, and Brillouin scattering are discussed. The effect of wave-length dispersion is discussed.

901,356

Not available NTIS
National Bureau of Standards (NML), Boulder, CO.
Time and Frequency Div.
CO Laser Stabilization

CO Laser Stabilization Using the Optogalvanic Lamb-Dip.

Final rept. M. Schneider, A. Hinz, A. Groh, K. M. Evenson, and W. Urban. 1987, 5p
Pub. in Applied Physics B 44, p241-245 1987.

Keywords: *Frequency stability, Infrared lasers, Intermediate infrared radiation, Stabilization, Reprints, *Carbon monoxide lasers, Optogalvanic spectrosco-

Frequency stabilization of the CO laser using a CO Lamb-dip is achieved in the range from 5.0-6.3 mi-Lamb-dip is achieved in the range from 5.0-6.3 mil-crometers. The CO saturation signal is obtained from a low-pressure discharge in absorption and is detected using optogalvanic detection. The frequency stability and reproducibility has been verified to be better than 100 k Hz, this is an improvement of more than one order of magnitude compared with locking techniques using CO laser gain profiles.

901.357

DV.

PB89-179212 Not available NTIS National Bureau of Standards (NML), Gaithersburg, MD. Temperature and Pressure Div.

Measurements of the Nonresonant Third-Order Susceptibility. Final rept.

G. J. Rosasco, and W. S. Hurst. 1986, 4p Pub. in AIP (American Institute of Physics) Conference Proceedings 146, p261-264 1986.

Keywords: Kerr electrooptical effect, Roman spectroscopy, Hydrogen, Argon, Optical measurement, *Third order susceptibility, Second harmonic generation, Nonlinearity.

The authors advance evidence for the validity of a long-known dispersion formula for the electronic contribution to the third-order nonlinear susceptibility.

PB89-179774 Not available NTIS National Bureau of Standards (NML), Boulder, CO. Quantum Physics Div.
Simple F-Center Laser Spectrometer for Continu-

ous Single Frequency Scans.

Ous Single Frequency Scalis.
Final rept.
D. D. Nelson, A. Schiffman, K. R. Lykke, and D. J.
Nesbitt. 1988, 7p
Sponsored by Air Force Office of Scientific Research,
Bolling AFB, DC.
Pub. in Chemical Physics Letters 153, n2-3 p105-111,

9 Dec 88.

Keywords: Absorption spectra, Solid state lasers, Spin orbit interactions, Reprints, *Laser spectrometers, *Color center lasers, *F center lasers, Tunable lasers,

The authors report a simple and novel scheme for continuous, single frequency scanning of a commercial F-center laser without any computer interfacing. The scheme utilizes galvo tuning of the cavity and intracavity CaF2 Brewster plates with servo loop control of the intracavity etalon. This permits continuous tuning of the F-center frequency over 0.8/cm-1 under com-plete manual control, as well as arbitrarily long, concat-enated scans, and trivial interfacing to a data acquisi-tion system. This scanning spectrometer operation is demonstrated on direct absorption of atomic bromine.

901,359

PB89-186282 Not available NTIS National Bureau of Standards (NML), Gaithersburg, MD. Radiometric Physics Div.

Apparatus Function of a Prism-Grating Double Monochromator. Final rept.

R. D. Saunders, and J. B. Shumaker. 1986, 5p Pub. in Applied Optics 25, n20 p3710-3714 1986.

*Monochromators, Spectroradiometers, Spectrometers, Reprints, Slit functions.

The slit function of a double monochromator has been studied using a dye laser and a few ion laser lines. The value of the slit function is roughly nine orders of magnitude below the peak at 300 nm from the line center. The difference between the slit function obtained by monochromator scanning over a fixed spectral line and that obtained by tuning a spectral line through a fixed monochromator setting is illustrated. Also reported is a prominent structure in the slit function which is attributed to the intermediate slit of the instrument.

901,360

Not available NTIS PB89-192678 Notional Bureau of Standards (NML), Gaithersburg, MD. Radiation Source and Instrumentation Div. Research Opportunities Below 300 nm at the NBS (National Bureau of Standards) Free-Electron Laser Facility.

Laser racing.
Final rept.
P. H. Debenham, and B. C. Johnson. 1988, 4p
Grant N00014-87-F-0066
See also AD-A193 100. Sponsored by Strategic De-

fense Initiative Organization, Washington, DC., and Office of Naval Research, Arlington, VA.

Pub. in Free-Electron Laser Applications in the Ultraviolet Topical Meeting, Cloudcroft, NM., March 2-5, 1988, p76-79.

Keywords: Ultraviolet lasers, Near ultraviolet radiation, Light pulses, Reprints, *Free electron lasers, Picosec-ond pulses, National Institute for Standards and Tech-

Average output power of 25 W in 3 ps pulses at 75 MHz will be available at fundamental wavelengths from 200 to 300 nm beginning in April 1990.

901,361 PB89-193908 PB89-193908 PC A03/MF A01 National Bureau of Standards (NML), Boulder, CO. Time and Frequency Div. (12)C(16)O Laser Frequency Tables for the 34.2 to 62.3 THz (1139 to 2079 cm(-1)) Region.

Technical note.
M. Schneider, K. M. Evenson, M. D. Vanek, D. A. Jennings, and J. S. Wells. Aug 88, 27p NBS/TN-

Also available from Supt. of Docs. as SN003-003-02933-5. Prepared in cooperation with Bonn Univ. (Germany, F.R.).

Keywords: Infrared spectra, Vibrational spectra, Far infrared radiation, Tables(Data), *Carbon monoxide lasers, Laser radiation.

Frequencies for (12)C(16)0 laser transitions are tabulated for the spectral range from 34.2 to 62.3 THz (1139 to 2079/cm). The transition frequencies were calculated using molecular constants which were derived by heterodyne frequency measurements on the (12)C(16)0 laser.

901,362 PB89-201099 PB89-201099 Not available NTIS National Bureau of Standards (NEL), Gaithersburg, MD. Building Physics Div.

Heuristic Analysis of von Kries Color Constancy. Final rept.

J. A. Worthey, and M. H. Brill. 1986, 5p Pub. in Jnl. of the Optical Society of America A 3, n10 p1708-1712 Oct 86.

Keywords: Reflectance, Reprints, *Color constancy, Von Kries adaptation, Robot vision.

The properties of a constancy model based on the proportionality rule of von Kries are examined in a series of simplified examples. It is found that the breadth of receptor sensitivity functions causes metamerism, thwarting color constancy. Overlap of these functions limits the accuracy of von Kries adaptation, for a more subtle reason: it causes non-zero off-diagonal ele-ments in the transformation matrix relating object re-flectance to receptor stimuli. Such off-diagonal elements make von Kries adaptation incorrect even when the illuminant is restricted so as to prevent metamerism.

901,363 PB89-212252 PB89-212252 Not available NTIS
National Bureau of Standards (IMSE), Gaithersburg,
MD. Office of Nondestructive Evaluation.
Collision Induced Spectroscopy: Absorption and

Light Scattering.

Final rept. G. Birnbaum, L. Frommhold, and G. C. Tabisz. 1989,

Sponsored by National Aeronautics and Space Admin-

istration, Washington, DC.
Pub. in Proceedings of International Conference on Spectral Line Shapes (9th), Torun, Poland, July 25-29, 1988, p623-647 1989.

Keywords: *Light scattering, *Hydrogen, *Helium, *Deuterium, Molecular spectroscopy, Infrared spectroscopy, Absorption spectra, Planetary atmospheres, *Molecule collisions, Line shape.

The survey deals with collision (or interaction) induced absorption (CIA) and light scattering (CILS) primarily in gases at low densities where bimolecular collisions predominate. The advances in these fields that have occurred primarily in the last five years are empha-sized. In the area of CIA, these topics include: H2-H2 and H2-He spectra in the far infrared (FIR) and in the fundamental IR bands; dimer features in these spectra; and the role of anisotropic interactions. The effects of the vibrational dependence of the potential function of the H2IR spectra are presented. The interesting line shapes and intensity problems in the FIR and IR spectra of HD due to interference between the collision in duced and allowed transitions is discussed in some detail. Collision induced light scattering from simple isotropic and anisotropic molecules, including H2, is discussed. Another section deals with the onset of three-body collisions in both CIA and CILS.

901,364 PB89-221162

PC A99/MF A01

National Inst. of Standards and Technology, Boulder,

Laser induced Damage in Optical Materials: 1987.

Special pub. (Final). H. E. Bennett, A. H. Guenther, D. Milam, B. E. Newnam, and M. J. Soileau. Oct 88, 653p NIST/SP-756

Also available from Supt. of Docs. as SN003-003-02929-7. See also PB89-129548. Proceedings of a Symposium on 'Optical Materials for High-Power Lasers', Boulder, CO, October 26-28, 1987. Library of Congress catalog card no. 88-600576. Portions of this document are not fully legible. Prepared in cooperation with American Society for Testing and Materials, Philadelphia.

Keywords: *Optical materials, *Radiation damage, *Meetings, Optical coatings, Optical measurement, Thin films, Surfaces, Mirrors, Substrates, *High power lasers, *Laser damage, Laser radiation.

The Nineteenth Annual Symposium on Optical Materials for High-Power Lasers (Boulder Damage Symposium) was divided into sessions concerning Materials and Measurements, Mirrors and Surfaces, Thin Films, and, finally, Fundamental Mechanisms. As in previous years, the emphasis of the papers presented at the Symposium was directed toward new frontiers and new developments. Particular emphasis was given to materials for high power systems. The wavelength range of prime interest was from 10.6 micrometers to the uv region. Highlights included surface character-ization, thin film substrate boundaries, and advances in fundamental laser-matter threshold interactions and mechanisms. The scaling of damage thresholds with pulse duration, focal area, and wavelength was discussed in detail.

901.365 PB89-227938 Not available NTIS National Bureau of Standards (NML), Boulder, CO. Quantum Physics Div. Generation of Squeezed Light by intracavity Fre-

quency Doubling.

Final rept. S. F. Pereira, M. Xiao, H. J. Kimble, and J. L. Hall.

Grant N00014-87-K-0156

Sponsored by Office of Naval Research, Arlington, VA. Pub. in Physical Review A 38, n9 p4931-4934, 1 Nov

Keywords: Frequency multipliers, Reprints, *Squeezed light, Second harmonic generation, Squeezed states(Quantum theory), Quantum optics, Nonlinear

Squeezed states of light are generated by the process of second-harmonic conversion within an optical cavity resonant at both fundamental and harmonic frequencies. Observations of squeezing are made by analyzing the spectral density of photocurrent fluctuations produced by the total field reflected from the nonlinear cavity. Reductions in photocurrent noise of 13% relative to the coherent-state or shot-noise level are achieved for frequency offsets near 4 MHz.

901,366 PB89-228084 Not available NTIS National Inst. of Standards and Technology (NML), Boulder, CO. Quantum Physics Div.
Optical Novelty Filters.

Final rept. D. Z. Anderson, and J. Feinberg. 1989, 13p Pub. in IEEE (Institute of Electrical and Electronics Engineers) Jnl. of Quantum Electronics 25, n3 p635-647 Mar 89.

Keywords: *Optical filters, High-pass filters, Low-pass filters, Bandpass filters, Characteristics, Quantum electronics, Reprints.

A novelty filter detects what is new in a scene and may be likened to a temporal high-pass filter. The report reviews the current status of optical novelty filters and related devices that use four-wave mixing or two-beam coupling in photorefractive media. A detector that shows only what is not new is called a monotony filter and may be likened to a temporal low-pass filter. Demonstrations of high- and low-pass and bandpass temporal image filters are discussed. An analytical treatment of the two-beam coupling devices is given in a Laplace transform framework in the undepleted pump approximation assuming plane wave inputs. This allows a unified treatment of the various filter charac-

901,367 PB89-230304 Not available NTIS National Inst. of Standards and Technology (NML), Gaithersburg, MD. Molecular Spectroscopy Div. Ultrashort-Pulse Multichannel Infrared Spectroscopy Using Broadband Frequency Conversion in Lilo3.

Final rept.

E. J. Heilweil. 1989, 3p Sponsored by Air Force Office of Scientific Research, Bolling AFB, DC.

Pub. in Optics Letters 14, n11 p551-553, 1 Jun 89.

Keywords: *Infrared spectroscopy, Frequency converters, Infrared spectra, Broadband, Reprints, Infrared upconversion, Picosecond pulses, Femtosecond pulses, Lithium iodates, YAG lasers, Dye lasers.

A simple probing method for obtaining broadband multichannel infrared spectra with picosecond or higher time resolution is described. Spectrally broad infrared pulses are produced by difference frequency mixing in LilO3 between the second harmonic of a Nd(+3):YAG laser and the broadband output of a synchronously pumped dye laser. After sample absorption the infra-red pulse is upconverted by a second LilO3 crystal, which yields a visible pulse that is dispersed on a multichannel vidicon detector to obtain transient spectra of 4/cm FWHM resolution.

901,368

PB89-230346 Not available NTIS National Inst. of Standards and Technology (NEL), Boulder, CO. Electromagnetic Technology Div. Spatial Filtering Microscope for the New York Spatial Filtering Microscope for Linewidth Measurements. Final rept.

M. Young. 1989, 7p

Special pub.

Pub. in Applied Optics 28, n8 p1467-1473, 15 Apr 89.

Keywords: *Optical microscopes, *Optical measurement, *Line width, High pass filters, Reprints, Integrated optics, Optical waveguides, Spatial filtering.

High pass filtering has been relatively little used in microscopy, yet it may have application to linewidth measurement and visualization of phase objects. The author has designed and built a spatial filtering microscope entirely of conventional microscope objectives. For linewidth measurement, the spatial filter has an optimum width that allows linewidths to be measured within a few percent. Phase lines can also be examined, but phase contrast microscopy may be more suited to weak phase objects such as integrated-optical waveguides.

901,369 PB89-235923 PC A12/MF A01 National Inst. of Standards and Technology (NEL), Gaithersburg, MD. Semiconductor Electronics Div. Semiconductor Measurement Technology: A Software Program for Aiding the Analysis of Ellipsometric Measurements, Simple Models.

J. F. Marchiando. Jul 89, 256p NIST/SP-400/83 Also available from Supt. of Docs. as SN003-003-02954-8. Library of Congress catalog card no. 89-600743.

Keywords: *Polarimetry, *Ellipsometers, Optical measurement, Least squares method, Iteration, Mathematical models, Computer programs, *Computer calculations, Computer applications.

MAIN1 is a software program for aiding the analysis of ellipsometric measurements. MAIN1 consists of a suite of routines written in FORTRAN that are used to invert the standard reflection ellipsometric equations for simple systems. Here a system is said to be simple if the solid material sample may be adequately charac-terized by models which assume at least the following: materials are nonmagnetic; samples exhibit depth-dependent optical properties, such as one with layered or laminar structure atop a substrate that behaves like a semi-infinite half-space; layers are flat and of uniform thickness; and the dielectric function within each layer/substrate is isotropic, homogeneous, local, and linear. Each layer is characterized in part by a thickness, while the optical properties for a given material and wavelength are expressed in terms of a refractive index and extinction coefficient. The ellipsometric equations are formulated as a standard damped nonlinear least-squares problem and then solved by an iterative method when possible. Estimates of the uncer-

Optics & Lasers

tainties associated with assigning numerical values to the model parameters are calculated as well.

901,370 PB90-118134

901,370
PB90-118134
Not available NTIS
National Inst. of Standards and Technology (NML),
Boulder, CO. Quantum Physics Div.
PrecIse Laser Frequency Scanning Using Frequency-Synthesized Optical Frequency Sidebands: Application to Isotope Shifts and Hyperfine Structure of Mercury. Final rept.

M. D. Rayman, C. G. Aminoff, and J. L. Hall. 1989,

Grant NSF-PHY86-04504

Sponsored by Office of Naval Research, Arlington, VA., and National Science Foundation, Washington,

Pub. in Jnl. of the Optical Society of America B 6, n4 p539-549 Apr 89.

Keywords: *Lasers, *Dyes, *Frequency control, *Scanning, Frequency shift, Spectrometers, Modulators, Optical scanners, Automatic control, Frequency synthesizers, Mercury isotopes, Reprints.

Based on an efficient (30%), broadband (approx. 3-5-GH2) electro-optic modulator producing rf optical sidebands locked to a stable cavity, a tunable dye laser can be scanned under computer control with frequency-synthesizer precision. Cavity drift is suppressed in software by using a strong feature in the spectrum for stabilization. Mercury isotope shifts have been measured with a reproducibility of approx. 50 kHz. This ac-curacy of approx. 1/300 of the linewidth illustrate the power of the technique. Derived hyperfine-structure constants are compared with previous atomic-beam data where available.

901,371 PB90-163932

(Order as PB90-163874, PC A04) National Inst. of Standards and Technology, Gaithersburg, MD.

Search for Optical Molasses in a Vapor Celi: General Analysis and Experimental Attempt.

A. L. Migdall. 1989, 6p Office of Naval Research, Arlington, VA.

Included in Jnl. of Research of the National Institute of Standards and Technology, v94 n6 p373-378.

Keywords: *Lasers, *Cooling, Viscosity, *Optical molasses, *Vapor cells, Cold atoms.

The authors analyze the application of optical molasses to a thermal vapor cell to make and collect cold atoms. Such as arrangement would simplify the production of cold atoms by eliminating the difficulty of first having to produce and slow an atomic beam. The authors present the results of our calculations, computer models, and experimental work.

Plasma Physics

Not available NTIS National Bureau of Standards (NML), Gaithersburg, MD. Atomic and Plasma Radiation Div.

Wavelengths and Energy Levels of the K i isoelectronic Sequence from Copper to Molybdenum. Final rept

V. Kaufman, J. Sugar, and W. L. Rowan. 1989, 4p Pub. in Jul. of the Optical Society of America B 6, n2 p142-145 Feb 89.

Keywords: *Molecular orbitals, *Rubidium, *Strontium, Copper, Molybdenum, Plasmas(Physics), Spectra, Wavelengths, Energy levels, Arsenic, Bromine, Gallium, Germanium, Krypton, Niobium, Potassium, Selenium, Yttrium, Zinc, Zirconium, Reprints.

Seven lines in the K-like transition array 3p63d-3p53d2 were observed for each of the spectra Cu XI to Mo XXIV (except for Rb and Sr) in radiation from impuritydoped tokamak and laser-generated plasmas. Wavelengths in the range of 70-112 angstroms, measured with an uncertainty of + or - 0.005 angstroms, are given. These are compared with calculations obtained with the relativistic Hartree-Fock code of Cowan. From these comparisons, predicted values for the wavelengths of Rb and Sr were obtained, with an uncertainty of the control of the programs of the programs. ty of + or - 0.01 angstroms.

901.373 PB89-185904 Not available NTIS National Bureau of Standards (NML), Boulder, CO. Quantum Physics Div. Atomic internal Partition Function.

D. G. Hummer. 1988, 14p Contract NAGW-766

Sponsored by National Aeronautics and Space Admin-

istration, Washington, DC.
Pub. in Proceedings of Conference on Atomic Processes in Plasmas, Santa Fe, NM., October 1987, p1-14 1988

Keywords: *Atomic energy levels, Equations of state, Thermodynamic equilibrium, *Plasma, Partition functions, Stellar opacity.

Recent work on the evaluation of the atomic internal partition function at densities less than about 0.02 gm/ cc is discussed, in which an attempt is made to identify the physical mechanism responsible for determining the level populations of atoms and ions in dense LTE plasmas. Level populations predicted by a phenomenological theory based on the identification are compared with those obtained by the activity expansion method.

PB89-229223 Not available NTIS National Bureau of Standards (NML), Boulder, CO. Time and Frequency Div.

Heterodyne Frequency Measurements of (12)C(16)O Laser Transitions. Final rept.

M. Schneider, K. M. Evenson, M. D. Vanek, D. A. Jennings, J. S. Wells, A. Stahns, and W. Urban. 1989, 10p

Pub. in Jnl. of Molecular Spectroscopy 135, p197-206

Keywords: *Lasers, *Carbon monoxide, *Frequency measurements, Demodulation, Lamb wave tests, Carbon dioxide, Vibrational spectra, Doppler effect,

The paper reports the first frequency measurements of a Lamb-dip-stabilized (12)C(16)O laser. The laser was stabilized to the optogalvanic Lamb dip of the CO molecule excited in a low-pressure dc discharge. The region of study was for transitions with lower state vibrational quantum numbers ranging from nu = 6 to nu = 16. Supplementary Doppler limited measurements are also reported for the range nu = 16 to nu = 34. The frequencies were directly measured in a heterodyne experiment in which two saturation-stabilized CO2 lasers were used as references. By fitting the transition frequencies to the Dunham expression, new coefficients have been determined which fit the new sub-Doppler data with over an order of magnitude more accuracy than previous coefficients.

Radiofrequency Waves

901 375 PB89-186902 Not available NTIS National Bureau of Standards (NEL), Gaithersburg, MD. Structures Div. Finite Element Studies of Transient Wave Propa-

gation. Final rept.

M. Sansalone, N. J. Carino, and N. N. Hsu. 1987, 9p Pub. in Review of Progress in Quantitative Nondestructive Evaluation, v6A p125-133 1987.

Keywords: *Stress waves, *Elastic shells, Strains, Displacement, Greens function, Differential equations, Impact, Transducers, Reprints, *Finite element

The paper shows the versatility and power of the finite element method for solving stress wave propagation problems and provides background information about the finite element program that was used to carry out wave propagation studies at the National Bureau of Standards. The paper illustrates the use of the method to solve the following three problems: stress and dis-placement fields produced by transient point impact on the surface of an elastic plate; the interaction of transient stress waves produced by point impact with a planar disk-shaped void and a flat-bottom hole within

elastic plates; stress and displacement fields produced by an ultrasonic transducer radiating into an elastic solid. The finite element results are compared to exact Green's function solutions for a point source on an infinite plate, experimentally obtained displacement wave-forms for point impact on a plate containing a planar flaw, and photoelastic pictures of the stress fields produced by an ultrasonic transducer radiating into silica.

901,376 PB90-117466 Not available NTIS National Inst. of Standards and Technology (NML), Boulder, CO. Time and Frequency Div. Improved Rotational Constants for HF.

D. A. Jennings, and J. S. Wells. 1988, 2p Pub. in Jnl. of Molecular Spectroscopy 130, 2p 1988.

Keywords: *High frequencies, *Rotational spectra, *Vibrational spectra, Radio frequencies, Electromagnetic spectra, Electronic spectra, Frequency synthesizers, Radio waves, Radio signals, Reprints.

The J 27 to 26 and J 33 to 32 rotational transition frequencies of the HF ground vibrational state have been measured using frequency synthesis spectroscopy. These new more accurate measurements when combined with recent measurements yield molecular constants with nearly an order of magnitude improvement in accuracy.

901,377 PB90-117698 Not available NTIS Not available NTS
National Inst. of Standards and Technology (NEL),
Boulder, CO. Electromagnetic Fields Div.
Implementation of an Automated System for
Measuring Radiated Emissions Using a TEM Cell.

Final rept.

G. H. Koepke, M. T. Ma, and W. D. Bensema. 1989,

Pub. in IEEE (Institute of Electrical and Electronics Engineers) Transactions on Instrumentation and Measurement 38, n2 p473-479 Apr 8 9.

Keywords: *Transverse waves, *Electromagnetic radiation, *Measurement, Electric fields, Automatic control equipment, Electronic test equipment, Electric analyzers, Frequency analyzers, Measuring instruments, Network analyzers, Reprints.

The transverse electromagnetic (TEM) cell is widely used to evaluate the electromagnetic characteristics of electrically small devices. The paper reviews the theoretical basis for a technique to quantify the radiated emissions from any such device in the cell. The technique is well suited to an automated test system provided that the mechanical motions required can be controlled by a computer. The difficulties associated with these mechanical motions are discussed and possible solutions are proposed. The measurement technique is also expanded to include multiple-frequency sources in addition to single-frequency sources.

901,378 PB90-117946 Not available NTIS National Inst. of Standards and Technology (NEL), Boulder, CO. Electromagnetic Fields Div.

Effect of an Electrically Large Stirrer in a Mode-Stirred Chamber.

Final rept. D. I. Wu, and D. C. Chang. 1989, 6p Pub. in IEEE (Institute of Electrical and Electronics En-

gineers) Transactions on Electromagnetic Compatibility 31, n2 p164-169 May 89.

Keywords: *Electric fields, *Cavity resonators, *Stirrers, *Frequency shift, Apertures, Eigenvectors, Wave dispersion, Oscillations, Pulsation, Frequency stability,

In a mode-stirred chamber, the field in the cavity is perturbed with a stirrer or rotating scatterer so that the time-averaged field is constant. The paper investigates the key factor that governs the effectiveness of a stirrer. By examining the fundamental properties associated with a perturbing body in a cavity, the key to effec-tive field perturbation is found in shifting the eigen-mode frequencies. The phenomenon is illustrated by examining a 2-D cavity with a 1-D perturbing body. Using the Transmission-Line-Matrix method, the shifting of eigenfrequencies is computed and the variation on the magnitude of the fields is examined for different stirrer sizes. From the analysis, insights one draws in-

Radiofrequency Waves

clude an analogy between the action of a large stirrer and a frequency modulator.

901 379

PB90-128042 Not available NTIS National Inst. of Standards and Technology (NML), Boulder, CO. Time and Frequency Div.
Frequency Standards Utilizing Penning Traps.

Final rept.
J. J. Bollinger, S. L. Gilbert, W. M. Itano, and D. J. Wineland. 1989, 7p
Sponsored by Air Force Office of Scientific Research, Bolling AFB, DC., and Office of Naval Research, Arlington, VA.

Pub. in Proceedings of Symposium on Frequency Standards and Metrology (4th), Ancona, Italy, Septem-ber 5-9, 1988, p319-325 1989.

Keywords: *Frequency standards, *Microwaves, *Hyperfine structures, Radiowaves, Atomic spectra, Spectrum analysis, Experimental data, *Penning traps.

lons in a Penning trap provide a promising candidate for a microwave frequency standard. The performance of a frequency standard based on a hyperfine transition in the ground state of a few thousand 9Be + ions stored in a Penning trap is discussed. An inaccuracy of less than 2x10(-13) and fractional frequency stability of 2x10-11 tou(-1/2) were obtained in a first experimental setup. With the use of sympathetic cooling, a 0.9 mHz linewidth and a second order Doppler shift less than 1x10(-14) were obtained on the Be + clock transition. This should enable an order of magnitude improvement in the frequency standard.

901,380

PB90-128521 Not available NTIS

Not available NTIS
National Inst. of Standards and Technology (NEL),
Gaithersburg, MD. Electrosystems Div.
DC Electric Field Effects during Measurements of
Monopolar Charge Density and Net Space Charge
Density Near HVDC Power Lines.

Final rept. M. Misakian, and R. H. McKnight. 1989, 6p Sponsored by Department of Energy, Washington, DC.

Pub. in IEEE (Institute of Electrical and Electronics Engineers) Transactions on Power Delivery 4, n4 p2229-2234 Oct 89.

Keywords: *Direct current, *Electric fields, *Charge density, *High voltage, *Power transmission lines, Measurements, Electric current, Electric charge, Power distribution lines, Field strength, Field emission, Polarity, Reprints.

The influence of a dc electric field on the measurement of monopolar charge densities using an aspirator-type ion counter and the measurement of net space charge density using a Faraday cage or filter is examined. Optimum configurations which minimize the effect of the electric field are identified for each type of instrumentation.

901,381

PB90-128612 Not available NTIS

National Inst. of Standards and Technology (NEL), Boulder, CO. Electromagnetic Fields Div. Proficiency Testing for MIL-STD 462 NVLAP (National Voluntary Laboratory Accreditation Pro-

gram) Laboratories.
Final rept.
G. R. Reeve. 1988, 3p
Sponsored by Naval Air Systems Command, Washing-

Pub. in Proceedings of EMC EXPO 88 International Conference on Electromagnetic Compatibility, Washington, DC., May 10-12, 1988, pT33.13-T33.15.

*Electromagnetic compatibility, Standards, Measurement, Requirements, Electronics laboratories, Electric fields, *National Voluntary Laboratory Accreditation Program, *MIL-STD-462.

Some of the difficulties in obtaining accurate results using MIL-STD 462 test procedures are reviewed. Several devices that could be used for verification of test results are presented along with their application to proficiency testing for NVLAP (National Voluntary Laboratory Accreditation Program) certification.

901,382

PB90-128778 Not available NTIS National Inst. of Standards and Technology (NEL), Boulder, CO. Electromagnetic Fields Div. Fields Radiated by Electrostatic Discharges. Final rept.

P. F. Wilson, M. T. Ma, and A. R. Ondrejka. 1988, 5p Pub. in Proceedings of IEEE (Institute of Electrical and Electronics Engineers) International Symposium on Electromagnetic Compatibility, Seattle, WA., August 2-4, 1988, p179-183.

Keywords: *Electric fields, *Mathematical models, *Dipoles, Electromagnetic theory, Static electricity, Electrostatic charge, Polarity, Electrostatics, Field emission, Field strength, *Electrostatic discharge.

Electrostatic discharge (ESD) can be a serious threat to electronic equipment. To date, metrology efforts have focused primarily on ESD-associated currents in order to develop test simulators. Significantly less work has been done on the ESD radiated fields. The paper examines the fields problem both theoretically and experimentally. Measurements indicate that the electric fields can be quite significant (greater than 150 V/m at a distance of 1.5 m), particularly, for relatively low voltage sparks (less than 6 kV). A theoretical dipole model for the ESD spark is developed to compute the radiated fields. The agreement between theory and experiment is good. The model may be used to predict the fields for a wide range of possible discharge configurations.

Solid State Physics

901.383

PATENT-4 747 684 Not available NTIS Department of the Army, Washington, DC.

Method of and Apparatus for Real-Time Crystallographic Axis Orientation Determination.

Patent.

S. Weiser. Filed 27 Aug 87, patented 31 May 88, 3p PB89-230148, PAT-APPL-7-089 893 Supersedes PB88-221460. Prepared in cooperation

with National Inst. of Standards and Technology, Gaithersburg, MD.

This Government-owned invention available for U.S. licensing and, possibly, for foreign licensing. Copy of patent available Commissioner of Patents, Washington, DC 20231 \$1.50.

Keywords: *Patents, *Crystallography, Orientation, Alignment, Laser beams, PAT-CL-356-31.

A specific small area of a crystal sample is scanned by a laser beam which rotates about an axis substantially perpendicular to the sample surface such that the inter-section of the beam with a plane above and parallel to the surface describes a true spiral or a stepwise spiral pattern. The laser beam is reflected in different amounts for different beam positions to produce a reflectance pattern indicative of crystallographic orienta-

901,384

PB89-146799 Not available NTIS National Bureau of Standards (IMSE), Gaithersburg, MD. Ceramics Div.

Standard Reference Materials for X-ray Diffraction. Part 1. Overview of Current and Future Standard Reference Materials.

Final rept. A. L. Dragoo. 1986, 5p Pub. in Powder Diffr. 1, n4 p294-298 1986.

Keywords: *X-ray diffraction, *Standards, Crystal structure, Lattice parameters, Quartz, Austenite, Silicon, Reprints, *Standard reference materials.

Standard Reference Materials (SRMs) are stable materials which have one or more properties certified by the National Bureau of Standards. A general introduction is given to the types of SRMs and their certifica-tion. SRMs for X-ray diffraction are described in detail, including their intended use and their certified and other properties. New SRMs are under consideration as additional quantitative standards, intensity and line shape standards, and materials properties standards.

901,385

Not available NTIS PB89-146815 National Bureau of Standards (IMSE), Gaithersburg, MD. Ceramics Div.

Magnetic Field Dependence of the Superconductivity in Bi-Sr-Ca-Cu-O Superconductors.

Final rept.

F. J. Adrian, J. Bohandy, B. F. Kim, K. Moorjani, J. S. Wallace, R. D. Shull, L. J. Swartzendruber, and L. H. Bennett. 1988, 5p Pub. in Physica C 156, p184-188 1988.

Keywords: *Superconductivity, Magnetic fields, Reprints, *High temperature superconductors, *Bismuth calcium strontium cuprates, *Barium yttrium cuprates, *Yttrium barium cuprates, Microwave absorption.

The changes in superconducting behavior of Bi-Sr-Ca-Cu-O and Y-Ba-Cu-O high temperature superconductors upon the application of an applied field of 0.5 T are explored, using field-modulated-microwave absorp-tion. Significant differences in the behavior are noted and discussed.

901.386

PB89-147433 Not available NTIS National Bureau of Standards (NML), Gaithersburg, MD. Radiation Physics Div. High Resolution Imaging of Magnetization.

D. T. Pierce, J. Unguris, and R. J. Celotta. 1988, 5p Sponsored by Office of Naval Research, Arlington, VA. Pub. in MRS Bulletin XIII, n6 p19-23 Jun 88.

Keywords: *Magnetic domains, Polarization(Spin alignment), Permalloys, Metal films, Iron, Reprints, Scanning electron microscopy, Imaging techniques, Spin orientation, High resolution.

The paper reviews imaging of magnetic domains using scanning electron microscopy with polarization analysis. The measurement of the spin polarization of the secondary electrons provides a vector image of the magnetization with high contrast and spatial resolution independent of surface topography, which is measured simultaneously. Examples of these features are illustrated by data from an iron-silicon single crystal, a ferromagnetic glass, a permalloy tape head, and an ultra-thin Fe film.

901,387

PB89-149181 Not available NTIS National Bureau of Standards (NML), Boulder, CO. Quantum Physics Div.

Surface Structure and Growth Mechanism of Ga on Si(100).

Final rept.

B. Bourguignon, and S. R. Leone. 1988, 6p Grants AFOSR-84-0272, NSF-CHE84-08403 Sponsored by Air Force Geophysics Lab., Hanscom AFB, MA., and National Science Foundation, Washington, DC.

Pub. in Proceedings of Symposium on Atomic and Surface Physics, LaPlagne, France, January 17-23, 1988, p228-233.

Keywords: *Semiconductors, *Gallium, *Silicon, Crystallization, Surface properties, Spectroscopy, Bonding, Lacors, Fluorescence, Auger electrons, *Molecular beam epitaxy.

The surface structures and growth mechanism of Ga overlayers on Si(100) are important data for the molecular beam epitaxy (MBE) of GaAs on Si(100). Some experimental results are discussed. It is found that Ga forms a well-ordered first layer with a large binding energy to Si(100). Surface structures are proposed where Ga is dimerized below 0.5 ML, while the Si(100) 2 x 1 reconstruction is removed above 0.5 ML. These structures account for an observed change in desorption energy and preexponential factor at $0.5\,ML$. (In the paper, 1 ML refers to Ga:Si = 1:1, or 6.8 x 10(sup 14)cm(sup -2).) From these surface structures, covalent bonding as opposed to metallic bonding between the metal atoms and the semiconductor, and bonding to the substrate as opposed to lateral bonding be-tween adatoms, are inferred to be dominant. Islands start to grow at coverages above 1 ML, which depends on the surface temperature T(sub s). These results are contrasted with other recent results on similar systems, namely In and As on Si(100).

901,388

PB89-150833 Not available NTIS National Bureau of Standards (NEL), Gaithersburg, MD. Semiconductor Electronics Div.

Indirect Energy Gap of Si, Doping Dependence. Final rept.

H. S. Bennett. 1988, 8p

Pub. in Properties of Crystalline Silicon, Electronic Materials Information Services for the Physics and Engineering Communities, p174-181 1988.

Keywords: *Silicon, *Additives, *Energy gap, Optical measurement, Photoluminescence, Electric devices, Superconductivity, Band structure of solids, Reprints.

The doping dependence of the indirect energy gap of silicon is reviewed for the Electronic Materials Information Service of IEE (London). The review is a guide with commentary to assist readers in selecting which values are best for applications. Knowledge in this area is such that intended application for the data on bandgap changes determines in many cases the ap-propriate values to use. Both data from interpreting electrical and optical measurements are given.

PB89-150866 Not available NTIS MD. Surface Science Div.

Angle Resolved XPS (X-ray Photoelectron Spec-

troscopy) of the Epitaxial Growth of Cu on Ni(100). Final rept. W. F. Egelhoff, 1985, 5p

Pub. in Structure of Surfaces, p199-203 1985.

Keywords: *X-ray analysis, *Photoelectrons, *Copper, *Nickel, *Epitaxy, Spectroscopy, Single crystals, Lattice parameters, Reprints.

In angle resolved x-ray photoelectron spectroscopy (XPS) of single crystals the core level peaks exhibit enhanced intensities along major crystal axes. This phenomenon is often referred to as electron channeling (or Kikuchi beams) due to an apparent analogy with effects found in electron microscopy. The present analysis of this phenomenon for epitaxial Cu on Ni(100) demonstrates that the electron channeling (or Kikuchi beams) approach fails completely to describe the data. The actual physical basis for this phenome-non is forward scattering of photoelectrons by overlying atoms in the lattice.

901,390 PC A04/MF A01
National Bureau of Standards (NEL), Gaithersburg,
MD. Precision Engineering Div.
Standard Reference Materials: Description of the

SRM 1965 Microsphere Slide.

Final rept. A. W. Hartman, and R. L. McKenzie. Nov 88, 69p NIST/SP-260/107

Also available from Supt. of Docs. as SN003-003-02911-4. Library of Congress catalog card no. 88-600598.

Keywords: *Microscopy, Polystyrene, Magnification, Spheres, Arrays, Distortion, Crystal structures, Micrometeorology, *Standard reference materials, *Microspheres, Kubitschek effect, Space manufacturing, lmage analysis.

The manual describes a new Standard Reference Material (SRM 1965). The SRM consists of two single-layer groupings of contacting monosize 10-micrometer polystyrene spheres that have been permanently sealed in an air chamber on a microscope slide. One sphere grouping consists of hexagonally ordered arrays, while the other grouping is unordered. The diameter distribution of the sphere material (SRM 1960), ameter distribution of the sphere material (SHM 1960), which was made under microgravity conditions on a Space Shuttle, is accurately known. SRM 1965 has a dual function: supporting measurements involving microscopy and supporting teachings and experiments in micrometrology. The manual describes how to measure microscope magnification and image distortion at levels below 0.5% and describes micrometrology expended they are the 20 for micrometrology. periments at the 0.05 micrometer level.

901,391

PB89-157481 Not available NTIS National Bureau of Standards (IMSE), Gaithersburg, MD. Reactor Radiation Div.

Re-Entrant Spin-Glass Properties of a-(FexCr1x)75P15C10. Final rept.

P. Mangin, D. Boumazouza, R. W. Erwin, J. J. Rhyne, and C. Tete. 1987, 3p Pub. in Jnl. of Applied Physics 61, n8 p3619-3621 1987.

Keywords: Ferromagnetism, Iron, Chromium, Neutron scattering, Reprints, *Spin glass state, Amorphous materials, Spin waves, Order parameters.

The magnetic excitations and instantaneous spatial correlations have been studied in amorphous (Fe(x)Cr(1-x))(75)P(15)C(10) using neutron inelastic scattering and small angle neutron scattering (SANS). The authors report the results for the sample with x The authors report the results for the sample with x = 0.7, which is in the reentrant spin-glass region (RSG) of the magnetic phase diagram. As in other materials displaying RSG properties, the authors found conventional spin-wave behavior for temperatures down to about half the Curie temperature (T(c) = 134 K), but decreasing excitation energies and lifetimes as the temperature is further lowered. They studied the critical scattering near T(c) with SANS, and found that the transverse correlation length 'diverges' provided that the data analysis includes the longitudinal fluctuations.

PB89-157721 Not available NTIS National Bureau of Standards (NML), Gaithersburg, MD. Gas and Particulate Science Div.

Refinement of the Substructure and Superstructure of Romanechite.

Final rept.

S. Turner, and J. E. Post. 1988, 7p

Pub. in American Mineralogist 73, p1155-1161 1988.

Keywords: *Crystal structure, *Electron transitions, Barium oxides, Manganese, Minerals, Cells, Anisotropy, Reprints, *Romanechite.

The substructure and superstructure of romanechite, (Ba,H2O)2Mn5O10, were refined using a crystal from Schneeburg, Germany. The subcell is monoclinic, space group C2/m, with a = 13.929(1) Angstroms, beta = 92.39(1) degrees, Z = 2, and it refined to R = 0.036 for anisotropic temperature factors using 598 refusions. flections. The Mn(2) octahedra of the structure show significant distortion consistent with the concentration of Mn sup 3+ on the Mn(2) site. The supercell consisting of a tripling along b (i.e., the tunnel axis), results from ordering Ba and H2O along the tunnel lengths. Further, long-exposure diffraction patterns show mod-ulated streaks along (201)*, implying only short-range ordering between the tunnels in one direction. A simplest monoclinic unit cell was chosen with space group C2/m and Z = 6. It was refined to R = 0.041 for anisotropic temperature factors using 954 reflections. Ba preferentially occupies the Ba(1) site, and correspondingly the closest framework octahedra (Mn(2) site) are preferentially occupied by Mn sup 3+.

901,393 PB89-158059 Not available NTIS National Bureau of Standards (NML), Gaithersburg, MD. Radiation Physics Div.

Free-Electron-Like Stoner Excitations In Fe.

Final rept. D. R. Penn, and P. Apell. 1988, 4p Pub. in Physical Review B 38, n7 p5051-5054, 1 Sep

Keywords: *Iron, Electron spin, Reprints, Stoner excitations, Spin orientation, Energy losses, Electron

An analysis of spin-polarized electron-energy-loss experiments in Fe is described which identifies the contribution of d-electron Stoner excitations, the usual type of Stoner excitation, suggests that free-electron-like Stoner excitations are more probable than d-electron Stoner excitations, and indicates that exchange events involving large energy losses are as likely as direct scattering.

901,394 Not available NTIS PB89-158067 National Bureau of Standards (NML), Gaithersburg, MD. Radiation Physics Div.

Domain Images of Ultrathin Fe Films on Ag(100).

J. L. Robins, R. J. Celotta, J. Unguris, D. T. Pierce, B. T. Jonker, and G. A. Prinz. 1988, 3p Sponsored by Office of Naval Research, Arlington, VA. Pub. in Applied Physics Letters 52, n22 p1918-1920,

Keywords: *Iron, *Magnetic domains, Metal films, Thin films, Substrates, Silver, Reprints, *Surface magnetism, Electron spin polarization, Scanning electron microscopy.

Scanning electron microscopy with electron polariza-tion analysis has been used to image domains of ul-trathin Fe films grown epitaxially on a Ag(100) sub-strate. Room-temperature measurements show clearly the existence of large domains of in-plane magnetization for film thickness of 3.4 monolayers or more. No in-plane domains were observed for thinner films.

PB89-158075 Not available NTIS National Bureau of Standards (NML), Gaithersburg, MD. Radiation Physics Div.
SpIn-Polarized Electron Microscopy.

Final rept.

D. T. Pierce. 1988, 6p

Sponsored by Office of Naval Research, Arlington, VA. Pub. in Physica Scripta 38, p291-296 1988.

Keywords: Magnetic domains, Microstructure, Reprints, *Electron spin polarization, Scanning electron microscopy, Scanning tunneling microscopy, Secondary electrons, High resolution.

The measurement of the spin polarization of secondary electrons generated by a finely focused (unpolarized) scanning electron microscope (SEM) beam to obtain high-resolution magnetization images is presented. An alternative measurement, using a spin-po-larized incident beam in an SEM, has many difficulties which are discussed. To measure spin configurations with higher spatial resolution, the possibility of intro-ducing electron spin polarization in scanning field-emission and tunneling microscopy is considered. The measurement of the spin polarization of secondary electrons generated by a specially prepared single-atom scanning field-emission tip looks promising. The potential advantages and unsolved problems involved in using a ferromagnetic tip or an optically pumped semiconductor tip are described.

901,396

PB89-158158 Not available NTIS National Bureau of Standards (IMSE), Gaithersburg, MD. Reactor Radiation Div.

Small Angle Neutron Scattering Spectrometer at the National Bureau of Standards.

Final rept. C. J. Glinka, J. M. Rowe, and J. G. LaRock. 1986,

Pub. in Jnl. of Applied Crystallography 19, pt6 p427-439, 1 Dec 86.

Keywords: *Neutron spectrometers, Neutron scattering, Magnetic domains, Crystal structure, Reprints, Small angle scattering, Position sensitive detectors, Neutron detectors, NBSR reactor.

A small angle neutron scattering spectrometer, suitable for the study of structural and magnetic inhomgeneities in materials in the 10 to 1000 A range, has been constructed at the National Bureau of Standards Research Reactor. The instrument is 8 m long and uses a mechanical velocity selector and pinhole collimation to provide a continuous incident beam whose wavelength is variable from 5 to 10 A. The neutron detector is a 65 x 65 sq cm position sensitive proportional counter which pivots about the sample position to extend the angular range of the spectrometer. Features unique to this instrument include a multibeam converging collimation system for high resolution measurements and an interactive color graphics termi-nal with specialized software for the rapid imaging and analysis of data from the two dimensional detector. The design and characteristics of the spectrometer and data acquisition system are described in detail, and examples of data are presented which illustrate its

901,397

PB89-158174 Not available NTIS National Bureau of Standards (NML), Gaithersburg, MD. Chemical Thermodynamics Div.
Sayre's Equation is a Chernov Bound to Maximum

Entropy.

Final rept.
R. W. Harrison. 1987, 3p
Pub. in Acta Crystallographica A43, n3 p428-430 1987.

Keywords: Crystallography, Entropy, Reprints, *Sayre equation.

Sayre's equation is fundamental to a large part of classical direct methods. In the paper, it is shown that this equation can be derived via an integral bound to the

entropy integral. While positivity is implicit in this denvation, atomicity is not used.

901,398 PB89-171318 PB89-171318 Not available NTIS National Bureau of Standards (NML), Gaithersburg, MD. Temperature and Pressure Div. Electronic Structure of the Cd Vacancy in CdTe.

P. H. E. Meijer, P. Pecheur, and G. Toussaint. 1987,

Pub. in Physica Status Solidi B-Basic Research 140, n1 p155-162 1987.

Keywords: *Cadmium tellurides, *Vacancies(Crystal defects), Greens functions, Reprints, *Electronic structure, Tight binding theory, Bound state, Slater

By means of a tight binding parametrization of the band structure of Cadmium Telluride, in conjunction with the Green function method, the authors determine the density of state of the perfect crystal. They compare various parametrizations for this compound. The energy levels for the Cd vacancy are calculated, taking into account the change in the wave functions around the missing atom.

901,399 PB89-171342 PB89-171342 Not available NTIS National Bureau of Standards (NML), Boulder, CO. Quantum Physics Div.

Surface Structures and Growth Mechanism of Ga on Si(100) Determined by LEED (Low Energy Elec-tron Diffraction) and Auger Electron Spectrosco-

py. Final rept. B. Bourguignon, K. L. Carleton, and S. R. Leone.

1988, 18p Grant AFOSR-84-0272 Sponsored by Air Force Office of Scientific Research, Bolling AFB, DC. Pub. in Surface Science 204, p455-472 1988.

Keywords: *Gallium arsenides, *Gallium, *Silicon, *Surfaces, Substrates, Reprints, *Epitaxial growth, Low energy electron diffraction, Auger electron spectroscopy, Temperature dependence, Binding energy.

The surface structures of gallium overlayers on Si(100) are studied using LEED and Auger electron spectros-copy (AES). At 300 K, Ga grows epitaxially up to at least 5 ML. In the range of low surface temperature least 5 ML. In the range of low surface temperature T(s) = 330-600 L, the growth obeys a Stranski-Krastanov mechanism, and the coverage at which island growth begins depends on T(s). Structures are proposed for the observed LEED patterns of Ga on Si(100)(3x2, 5x2, 2x2, 8x1 and 2x1). The existence of well-ordered structures suggests that Ga terminated Si(100) surfaces are suitable for epitaxy of GaAs on Si.

901,400 PB89-171359 Not available NTIS National Bureau of Standards (NML), Gaithersburg,

MD. Surface Science Div.

Progress in Understanding Atomic Structure of the Icosahedral Phase.

A. J. Melmed, M. J. Kaufman, and H. A. Fowler. 1986, 6p

Pub. in Jnl. of Physics Colloquium 47, nC-7 p35-40 Nov

Keywords: *Aluminum-manganese alloys, Electron dif-fraction, Atomic structure, Reprints, *Icosahedral fraction, Atomic structure, Reprints, * phase, Quasicrystals, Field ion microscopy.

Electron diffraction analysis of the icosahedral phase (1-phase) in AlMn alloys (1-AlMn) is presented which shows clearly that, in addition to the sharp diffraction maxima from the i-phase, there is a considerable amount of diffuse intensity indicating the presence of a certain amount of disorder interspersed within this phase. This result correlates well with previous results from both neutron diffraction and field ion microscopy studies and helps to reduce the number of possible structural models of the i-phase. Analysis of FIM images indicates the presence of a hierarchy of cluster sizes with numerous features which appear to agree qualitatively with recently proposed models. A complete quantitative description of the structure of the iphase is being pursued by comparing experimentally observed atomic motifs with computer-simulated model surfaces, and preliminary results are presented.

901,401 PB89-171599 Not available NTIS National Bureau of Standards (NML), Boulder, CO. Quantum Physics Div.

AES and LEED Studies Correlating Desorption Energles with Surface Structures and Coverages for Ga on Si(100). Final rept.

B. Bourguignon, R. V. Smilgys, and S. R. Leone.

1988, 12p Grant AFOSR-84-0272

Sponsored by Air Force Office of Scientific Research, Bolling AFB, DC.

Pub. in Surface Science 204, p473-484 1988.

Keywords: *Gallium, *Silicon, *Auger electrons, *Semiconductors(Materials), *Desorption, *Monomolecular films, Chemical bonds, Temperature, Surface properties, Kinetics, Heat of vaporization, Electrodeposition, Spectroscopy, Energy bands, Reprints.

Gallium interactions with silicon (100) are studied with Auger electron spectroscopy and LEED to correlate the desorption energies with surface coverages and structures in isothermal desorption experiments. Some evidence for a temperature-induced change from a Stranski-Karstanov to a Volmer-Weber growth mode between 600 and 700 K is presented. In the temperature range 800-900 K, three different kinetic regimes are observed. Between 0 and 0.5 monolayers (ML), first-order desorption is observed from a well-ordered Ga overlayer (Si:Ga 2x2), with a desorption energy of 2.9 plus or minus 0.2 eV and a pre-exponential factor of 3x10(sup 16 plus or minus 1)s. Between 0.5 and 1 ML, first-order desorption is also observed from a wellordered Ga layer (Si:Ga 8x1), but the desorption energy decreases to 2.3 plus or minus 0.2 eV with a pre-exponential factor of 8x10(sup 12 plus or minus .2)/s. Above 1 ML, zeroth-order desorption from Ga islands on top of an ordered Ga monolayer is ob-served, and the desorption energy of the combination of surface species is 2.61 plus or minus 0.07 eV with a pre-exponential factor equal to (4 plus or minus 3)x10(sup 13) ML/s. It is suggested that atoms from the islands and the ordered layer are kinetically coupled, and that the islands cover too little of the surface to exhibit the bulk heat of vaporization of liquid Ga, 2.9 eV. The observed kinetic regimes are correlated with the surface structures proposed in the preceding paper.

901.402 PB89-175251

(Order as PB89-175194, PC A06)

A.T. and T. Bell Labs., Murray Hill, NJ.

Applications of the Crystallographic Search and
Analysis System CRYSTDAT in Materials Science. Bi-monthly rept.
T. Siegrist. 1989, 10p
Included in Jnl. of Research of the National Institute of

Standards and Technology, v94 n1 p49-58 Jan-Feb

Keywords: *Crystallography, Super conductors, Search structuring, Data retrieval, X ray diffraction, Qualitative analysis, Quantitative analysis, *Crystallinity, *Numerical data bases, CRYSTDAT system, Materials science.

Numerical database systems have recently become available online. Their enhanced search capabilities and fast retrieval of data make them a valuable tool in research. In particular, CRYSTDAT which is a search and analysis system for NBS CRYSTAL DATA has proven to be powerful in the identification of crystalline materials. In conjunction with a single-crystal x-ray diffractometer, a qualitative as well as quantitative phase determination is easily performed. The use of CRYST-DAT is illustrated in several examples.

PB89-175970 Not available NTIS National Bureau of Standards (NML), Gaithersburg, MD. Surface Science Div.

Superiattice Magnetoroton Bands

H. C. A. Oji, S. M. Girvin, and A. H. MacDonald. 1987, 4p

Pub. in Physical Review Letters 58, n8 p824-827 1987. Keywords: Electron gas, Magnetic fields, Gallium arse-

nide, Reprints, *Magnetorotons, Fractional quantum Hall effect, Superlattices, Wigner crystallization.

A theory is given for the effect of interlayer coupling in a superlattice on the magnetoroton modes of a two-dimensional electron gas in a strong magnetic field. It was found that for typical fields and layer spacings, the modes broaden into bands. For sufficiently small layer spacings, the gap necessary for the occurrence of the fractional quantum Hall effect vanishes. The authors argue that the vanishing of the gap should be associated with an instability toward the state with a two-dimensional Wigner crystal in each layer and that this state is favored by interlayer coupling.

Not available NTIS PB89-175988 National Bureau of Standards (NML), Gaithersburg,

MD. Surface Science Div. Effects of a Gold Shank-Overlayer on the Field ion imaging of Sillcon.

Final rept.
A. J. Melmed, W. A. Schmidt, J. H. Block, M. Naschitzki, and M. Lovisa. 1986, 4p
Pub. in Jnl. of Physics Colloquium 47, nC-7 p333-336 Nov 86

Keywords: *Silicon, Thin films, Covering, Gold, Reprints, *Field ion microscopy, Microprobes, Semicon-

The importance of the specimen shank in determining the magnitude of photo-illumination and field effects observed for Si specimens in field ion microscopy and atom probe mass analysis is established by measurements with and without an Au shank-overlayer. The field strength Au field ionization of hydrogen and argon over Si is shown to be the same as for metals.

901.405 PB89-176564 Not available NTIS National Bureau of Standards (NML), Gaithersburg,

MD. Radiation Physics Div.

Magnetic Properties of Surfaces Investigated by Spin Polarized Electron Beams. Final rept.

D. T. Pierce. 1986, 12p

Pub. in Proceedings of International Workshop on Magnetic Properties of Low-Dimensional Systems, Taxco, Mexico, January 6-9, 1986, p58-69.

Keywords: Electron scattering, Chemisorption, Carbon monoxide, Oxygen, Nickel, Magnetic moments, *Surface magnetism, *Magnetic surfaces, Electron spin polarization, Electronic structure.

A spin polarized electron beam incident on a ferromagnetic surface results in elastically and inelastically scattered electrons and in photons via radiative transitions. The spin dependent intensities of each of these provide a sensitive measure of surface magnetization. comparison between low temperature spin deviations at the surface and in the bulk is given; the varia-tion follows the same power law with temperature but with a larger pre-factor for the surface. The connection between surface electronic structure and surface magnetism and the changes in each induced by chemisorption have been studied by spin polarized inverse photoemission. For oxygen and carbon monoxide on Ni(110), a reduction of the Ni magnetic moment is found, rather than a decrease in exchange coupling and corresponding randomization of the alignment of the moments. Further, in the case of CO, the chemis-orption interaction is non-local with one CO molecule eliminating on the average the magnetic moment of two Ni atoms.

901.406 PB89-176978 Not available NTIS National Bureau of Standards (NEL), Boulder, CO.

National Bureau of Calabata (1997)

Electromagnetic Technology Div.

Josephson-Junction Model of Critical Current in Granular Y1Ba2Cu3O(7-delta) Superconductors. Final rept.

R. L. Peterson, and J. W. Ekin. 1988, 4p Pub. in Physical Review B 37, n16 p9848-9851, 1 Jun

Keywords: *Superconductors, *Josephson junctions, Magnetic fields, Grain boundaries, Reprints, *High temperature superconductors, *Critical current, *Yttrium barium cuprates, *Barium yttrium cuprates.

The authors calculate the transport critical-current density in a granular superconductor in magnetic fields below about 0.005 T. The field dependence in this region is assumed to be controlled by intragranular or intergranular Josephson junctions. Various model calculations are fitted to transport critical-current data on bulk Y1Ba2Cu3O(7-delta) ceramic superconductors, whose average grain size somewhat exceeds 10 micrometers. The results yield an average junction cross-

sectional area (thickness x length) of 4-6 sq micrometers. If the junctions are at the grain boundaries, a London penetration depth of about 150-300 nm is inferred, consistent with other estimates. The authors conclude that Josephson junctions are limiting the transport critical current in the samples and that they lie at the grain boundaries. The parameters of the fit are not consistent with Josephson junctions at twinning boundaries.

901,407 PB89-176994 Not available NTIS National Bureau of Standards (NEL), Boulder, CO. Electromagnetic Technology Div. Bean Model Extended to Magnetization Jumps.

Final rept. R. L. Peterson. 1988, 4p Pub. in Physics Letters A 131, n2 p131-134, 8 Aug 88.

Keywords: *Superconductors, Flux jumping, Magnetization, Reprints, *High temperature superconductors, Bean model.

The author extends the phenomenological Bean model of magnetization in hard superconductors to include the trains of magnetization jumps seen at low temperature in moderate-to-high magnetic fields. As in the original Bean model, no particular mechanisms for flux pinning are invoked. The extended model correctly accounts for the general dependence of the size of the magnetization jumps on sample size and critical current density. The data together with the model show that the shielding fields are approximately equal after each jump.

901,408 PB89-179188 PB89-179188 Not available NTIS National Bureau of Standards (NML), Gaithersburg, MD. Surface Science Div. Temperature-Dependent Radiation-Enhanced Dif-

fusion in Ion-Bombarded Soilds.

Final rept.

D. Marton, J. Fine, and G. P. Chambers. 1988, 4p Pub. in Physical Review Letters 61, n23 p2697-2700, 5 Dec 88.

Keywords: *Silver, *Nickel, *Diffusion, Crystal defects, Reprints, Ion bombardment, Physical radiation effects, Temperature dependence.

Temperature-dependence radiation-enhanced-diffusion rates for Ag in Ni have been found to decrease at elevated temperatures. The observed narrowing of interface interdiffusion regions with increasing temperature depends on both defect concentration and migration processes which occur in ion-bombarded solids. These findings can be interpreted in terms of a general model of radiation-enhanced diffusion that in-volves long-lived complex defects which can migrate for large distances and which are themselves subject to annealing.

901,409 PB89-179626 Not available NTIS National Bureau of Standards (IMSE), Gaithersburg,

MD. Reactor Radiation Div.
Significance of Multiple Scattering in the Interpretation of Small-Angle Neutron Scattering Experiments.

Final rept.

J. R. D. Copley. 1988, 6p Pub. in Jnl. of Appl. Cryst. 21, p639-644 1988.

Keywords: *Neutron scattering, Monte Carlo method, *Computerized simulation, Vacuum, Embedding, Dispersing, Spheres, Wavelengths, Water, Reprints.

The multiple scattering of neutrons in small-angle neutron scattering experiments has been studied using the technique of Monte Carlo simulation. As a test of the approach, investigations have been performed on strongly scattering samples of a system of monodisperse spheres in vacuo: the results are in excellent agreement with semianalytic calculations by Schelten and Schmatz. The scattering by systems of monodisperse spheres embedded in a medium has also been studied: the standard procedure for subtraction of the scattering by the medium slightly oversubtracts the multiple scattering due to the medium alone. The wavelength dependence of the single and multiple scattering in light water has been estimated and com-pared with experimental measurements by groups at the Institut Laue-Langevin, Grenoble, France.

901,410 PB89-179634

Not available NTIS

National Bureau of Standards (IMSE), Gaithersburg,

MD. Reactor Radiation Div.
Occurrence of Long-Range Helical Spin Ordering in Dy-Y Muitilayers. Final rept.

J. J. Rhyne, J. Borchers, R. Du, R. W. Erwin, C. P. Flynn, M. B. Salamon, and S. Sinha. 1987, 6p See also PB89-179642.

Pub. in Jnl. of Applied Physics 61, n8 p4043-4048

Keywords: *Dysprosium, *Yttrium, Neutron diffraction, Metal films, Single crystals, Magnetic fields, Magnons, Ferromagnetism, Reprints, *Magnetic ordering, Magnetic films, Molecular beam epitaxy, Multilayers, Temperature dependence, Band theory, Spin waves.

The magnetic ordering of highly perfect single crystal multilayer films of alternate layers of magnetic Dy and non-magnetic Y prepared by molecular beam epitaxy has been studied by neutron diffraction. Results on a series of films with Dy thicknesses of approximately 16 atomic planes (about 45 A) and Y thicknesses ranging from 10 to 22 planes have confirmed the existence of long-range helimagnetic ordering of the Dy 4f spins which is propagated through the intervening Y layers in phase coherence. The propagation vectors in both Dy and Y layers have been calculated from the wave vector of the magnetic satellites and the intensity of the bilayer harmonics. The application of a field along basal plane directions destroys the helical order and produces a ferromagnetic state with all spins aligned along the field direction.

901,411 PB89-179642 Not available NTIS National Bureau of Standards (IMSE), Gaithersburg, MD. Reactor Radiation Div.

Long-Range Incommensurate Magnetic Order In Dy-Y Multilayers.

Final rept.

J. J. Rhyne, J. Borchers, J. E. Cunningham, R. W. Erwin, C. P. Flynn, M. B. Salamon, and S. Sinha. 1986, 10p See also PB89-179634.

Pub. in Jnl. of the Less Common Metals 126, p53-62 Dec 86.

Keywords: *Dysprosium, *Yttrium, Ferromagnetism, Neutron diffraction, Metal films, Magnetic fields, Reprints, *Magnetic ordering, Superlattices, Molecular beam epitaxy, Temperature dependence, Multilayers.

Neutron diffraction studies have demonstrated the existence of helical magnetic order in a metallic superlat-tice of Dy and Y produced by molecular beam epitaxy. Analysis of the magnetic satellite peak widths indicates that phase coherence of the helix exists over at least five bilayer cells, each consisting of 14 atomic planes of Dy and of non-magnetic Y. The multilayer comprises 64 bilayer cells. Results are given for the temperature dependence of the magnetic intensity and for the effect of an applied magnetic field which continuously converts the helical ordering to ferromagnetism.

PB89-179725 Not available NTIS National Bureau of Standards (IMSE), Gaithersburg, MD. Ceramics Div.

Synthesis and Magnetic Properties of the Bi-Sr-Ca-Cu Oxide 80- and 110-K Superconductors. Final rept

J. S. Wallace, J. J. Ritter, E. Fuller, L. H. Bennett, R. D. Shull, and L. J. Swartzendruber. 1989, 3p Pub. in Physical Review B 39, n4 p2333-2335, 1 Feb

Keywords: *Superconductors, *High temperature, Synthesis(Chemistry), Bismuth, Strontium, Calcium, Copper oxides, Solids, Magnetic properties, Magnetic hysteresis, Meissner effect, Reprints.

The observation of both the 80- and 110-K superconducting transitions in a nominally BiSrCaCu2OX material produced by a new chemical synthesis procedure as well as by solid-state reaction is reported. Also discussed is a method for the confirmation of the presence of superconductivity when only a small amount is present.

901,413 PB89-179824 Not available NTIS National Bureau of Standards (NEL), Boulder, CO. Electromagnetic Technology Div.

High T(sub c) Superconductor/Nobie-Metal Contacts with Surface Resistivities in the (10 to the Minus 10th Power) Omega sq cm Range. Final rept.

Final rept.
J. W. Ekin, T. M. Larson, N. F. Bergren, A. J. Nelson,
A. B. Swartzlander, L. L. Kazmerski, A. J. Panson,
and B. A. Blankenship. 1988, 3p
Pub. in Applied Physics Letters 52, n21 p1819-1821,

23 May 88.

Keywords: *Superconductors, *Electric contacts, Gold, Silver, Indium, Comparison, Electrical resistivity, Reprints, *High temperature superconductors, *Yttnum banium cuprates, *Barium yttrium cuprates.

Contact surface resistivities (product of contact resist-Contact surface resistivities (product of contact resist-ance and area) have been obtained for both silver and gold contacts to high T(sub C) superconductors. This is a reduction by about eight orders of magnitude from the contact resistivity is low enough to be considered for both on-chip and package interconnect applica-tions. The contacts were formed by sputter depositing either silver or gold at low temperatures (< 100 C) on a clean surface of Y1Ba2Cu3O(T-delta) (YBCO) and later annealing the contacts in oxygen. Auger micro-probe analysis shows that indium/YBCO contacts contain a significant concentration of oxygen in the indium layer adjacent to the YBCO interface. Silver and gold contacts, on the other hand, contain almost no oxygen and have favorable interfacial chemistry with low oxygen affinity. Silver also acts as a 'switchable' passivation buffer, allowing oxygen to penetrate to the YBCO interface at elevated temperatures, but protecting the YBCO surface at room temperature.

901.414

PB89-179832 Not available NTIS
National Bureau of Standards (NEL), Boulder, CO.
Electromagnetic Technology Div.
Effect of Room-Temperature Stress on the Critical

Current of NbTi. Final rept.

S. L. Bray, and J. W. Ekin. 1989, 4p Pub. in Jnl. of Applied Physics 65, n2 p684-687, 15 Jan

Keywords: Stresses, Strains, Comparison, Reprints, *Superconducting wires, *Niobium titanium, *Critical current, Room temperature, Temperature depend-

The effect of axial tensile stress, applied at room temperature, on the critical current of NbTi superconducting wire was measured and compared with the effect of tensile stress applied at liquid-helium temperature (about 4 K). The results of these measurements indi-cate that the effect on the critical current is independ-ent of the temperature at which the stress is applied. Thus, the existing 4-K data base can be used to determine I(sub c) degradation from room-temperature fabrication stress, cool-down stress introduced by differential contraction, as well as 4-K stress generated by the Lorentz force when the magnetic is energized. To generalize these results for arbitrary matrix-to-super-conductor volume ratios, the data are presented in terms of the stress on the NbTi portion of the composite conductor. Methods for determining the stress on the NbTi from the total composite load are presented.

901.415

PB89-180046 Not available NTIS National Bureau of Standards (IMSE), Gaithersburg,

Critical and Noncritical Roughening of Surfaces (Comment). Final rept.

C. Rottman, and W. F. Saam. 1987, 1p Pub. in Physical Review Letters 58, n15 p1588 1987.

Keywords: *Surface roughness, *Crystal lattices, *Lattice properties, *Surfaces, Symmetry, Crystals, Re-

The paper comments on 'Critical and Noncritical Roughening of Surfaces,' by Franz S. Rys (Phys. Rev. Lett. 56, 624 (1986)). Rys argues that the special symetry which must be present for the roughening transition of crystal surfaces to occur is broken with twobody interactions. It is pointed out that only three- and higher-odd-order-body forces break this symmetry.

901.416 PB89-186241

Not available NTIS

National Bureau of Standards (IMSE), Gaithersburg, MD. Reactor Radiation Div.

Alternative Approach to the Hauptman-Karle Determinantal Inequalities.

Final rept. E. Prince. 1989, 1p Pub. in Acta Cryst. A45, p144 1989.

Keywords: Crystal structure, Determinants, Inequalities, Reprints, *Structure factors, Electron density, Cholesky factorization, Matrices.

A procedure is described for constructing a series of progressively stronger restrictions on the magnitudes and phases of individual structure factors in terms of sets of other structure factors. The existence of the Cholesky factors of Hauptman-Karle matrices is used to ensure that the electron density is everywhere posi-

Not available NTIS
National Bureau of Standards (IMSE), Gaithersburg,
MD. Reactor Radiation Div.
Maximum Entropy Plants ... 901,417 PB89-186258 MD. Heactor Hadiation DIV.

Maximum Entropy Distribution Consistent with Observed Structure Amplitudes.

Final rept.

E. Prince. 1989, 4p

Pub. in Acta Cryst. A45, p200-203 1989.

Keywords: Fourier series, Crystal structure, Reprints, *Structure factors, Electron density, Maximum entropy method. Iterative methods.

It is shown that an electron density distribution of the form rho sub $k=\exp{(Sigma~(f~sub~y)(r~sub~k)(x~sub~y))}$ has maximum entropy under the constraint that the expected values of a set of functions, f~sub~j(r), are constant. For a Fourier map the functions f~sub~j(r) are the magnitudes of the structure factors for a set of reflec-tions h sub j including F(000). Maximum entropy is an efficient way of expressing the phase implications of a large set of structure amplitudes.

901,418 PB89-186266 Not available NTIS National Bureau of Standards (IMSE), Gaithersburg,

MD. Reactor Radiation Div.

Theoretical Models for High-Temperature Superconductivity.

Final rept. R. C. Casella. 1988, 10p Pub. in Il Nuovo Cimento 10, n12 p1439-1448 Dec 88.

Keywords: *Superconductors, Phonons, Bosons, Reprints, *High temperature superconductors, *Band theory, Yttrium barium cuprates, Barium yttrium cu-

A semi-phenomenological analysis is given of the effects of certain band structure features on the gap ratios 2 Delta/(k sub B)(T sub c) for high (T sub c) superconductors, including multigap systems. In addition to phonons, other intermediate bosons (IB) mediating the superconducting interaction are considered. Interthe superconducting interaction are considered. Inter-esting results emerge when the IB energy exceeds the widths of possible narrow peaks in the density of states associated with subbands presumably belong-ing to substructures such as stacked Cu-O planes. Comparison with experiment is made. In particular, data obtained by Warren et al. via nuclear-spin relax-ation on Ba2YCu3O(7-delta) can be interpreted within the present framework in terms of a model having an IB of energy approx = or > 1 eV, which exceeds the predicted width (approx = or < 0.3 eV) of a peak in the density of states containing the normal-state Fermi level. This suggests that the IB is not a phonon.

901,419 PB89-186274 Not available NTIS National Bureau of Standards (NML), Gaithersburg,

MD. Radiation Physics Div.

Oxygen Partial-Density-of-States Change in the YBa2Cu3Ox Compounds for x(Approx.)6,6.5,7

Measured by Soft X-ray Emission.

Final rept. C. H. Zhang, T. A. Callcott, K. L. Tsang, D. L. Ederer, J. E. Blendell, C. W. Clark, T. Scimeca, and Y. W. Liu. 1989, 4p Contract DE-AC05-84OR21400

Sponsored by Department of Energy, Washington, DC., and Air Force Office of Scientific Research, Bolling AFB, DC.

Pub. in Physical Review B 39, n7 p4796-4799, 1 Mar

Keywords: *Superconductors, Emission spectra, Oxygen, Reprints, *High temperature superconduc-

tors, *Yttrium barium cuprates, *Barium yttrium cuprates, Soft x rays, Density of states, Band theory.

Oxygen K soft x-ray emission spectra are presented for the YBa2Cu3Ox compounds with x nominally equal to 6, 6.5, and 7, and are compared with x-ray emission spectra determined from recent band-structure calculations. The K emission spectrum of O provides a measure of the p-type local partial density of states (p-LPDOS) at the oxygen sites. As x decreases from 7 delta to about 6.5, a chemical shift of the entire spectrum to lower energy indicates that screening is modified for all oxygen sites. The integrated intensity of the spectra is nearly unchanged by oxygen removal, indi-cating an increase in p-LPDOS per oxygen site. These results and changes in the spectral shape suggest that tilnerant electron density near the O atoms is reduced and bound electron density is increased as oxygen is removed.

901,420 PB89-186860 Not available NTIS
National Bureau of Standards (NML), Gaithersburg,
MD. Surface Science Div.
Resonant Excitation Resonant Excitation of an Oxygen Valence Satel-lite in Photoemission from High-T(sub c) Superconductors.

Final rept. R. L. Kurtz, S. W. Robey, R. L. Stockbauer, D. Mueller, A. Shih, and L. Toth. 1989, 4p Sponsored by Office of Naval Research, Arlington, VA. Pub. in Physical Review B 39, n7 p4768-4771, 1 Mar

Keywords: *Superconductors, Excitation, Oxygen, Reprints, *High temperature superconductors, *Yttrium barium cuprates, *Barium yttrium cuprates, *Lanthanum strontium cuprates, *Photoemission.

A detailed analysis of the intensities of valence-band photoelectron YBa2Cu3O(7-x) features of and superconducting semiconducting La(1.85)(Sr(0.05)CuO4 had revealed a resonance in the peak located at a binding energy of about 9.5 eV for photon energies spanning the onset of O 2s excitations. This demonstrates conclusively that the feature is associated with oxygen excitations. The origin of the satellite is described and its disappearance on superconducting surfaces is explained.

901,421 PB89-186886 PB89-186886 Not available NTIS National Bureau of Standards (NML), Gaithersburg, MD. Surface Science Div. Dynamical Diffraction of X-rays at Grazing Angle.

Final rept. T. Jach, P. L. Cowan, Q. Shen, and M. J. Bedzyk.

1989, 9p Pub. in Physical Review B 39, n9 p5739-5747, 15 Mar

Keywords: *X ray diffraction, Germanium, Standing waves, Reprints, *Grazing incidence, KeV range 01-10.

Details are presented of the theory and experimental observation of dynamical diffraction of X rays at grazing angle from crystal planes normal to a surface. The authors are able to associate different features of the authors are able to associate different features of the specularly reflected and diffracted-reflected beam fluxes with the contributions from the alpha and beta branches of the dispersion surfaces. The theory predicts surface propagation modes to which internal and external beams can couple only through the diffraction process. An experiment is described in which the spe-cularly reflected and reflected-diffracted beams were simultaneously observed for 8-keV X rays incident on germanium. The agreement with first-order theory is germanum. The agreement with instruction theory good, but systematic deviations were observed. Calculations are presented that illustrate how eigenstates of the wave fields, which are X ray standing waves with nodal planes normal to the surface of the crystal, can be used to obtain atomic registration at a surface or interface.

901,422
PB89-186928
Not available NTIS
National Bureau of Standards (NML), Boulder, CO.
Quantum Physics Div. Laser Probing of the Dynamics of Ga Interactions on Si(100). Final rept.

Final rept.
K. L. Carleton, B. Bourguignon, R. V. Smilgys, D. J.
Oostra, and S. R. Leone. 1988, 6p
Grant AFOSR-84-0272
Sponsored by Air Force Office of Scientific Research,
Bolling AFB, DC.

Pub. in Proceedings of Materials Research Society Symposium, Reno, NV., p45-50 Apr 88.

Keywords: *Gallium, *Silicon, *Kinetics, *Desorption, *Epitaxy, *Semiconducting films, Lasers, Probes, Fluorescence, Auger electrons, Surface properties, Electron diffraction, Monomolecular films, Temperature, Growth, Gallium arsenides.

The kinetics of desorption and scattering of Ga atoms on Si(100) surfaces are probed by laser-induced fluorescence detection of the gas phase species and by Auger analysis of the surface composition. The kinetic parameters are correlated with the structures deduced by Low Energy Electron Diffraction (LEED) and the by Low Energy Electron Diffraction (LEED) and the coverages determined by Auger spectroscopy. The binding energy of Ga on Si(100) is found to be a function of coverage, starting out at 2.9 eV at low coverages and decreasing to 2.3 eV for coverages between 0.5 and 1 monolayer (ML). Ordered growth is always observed for coverages below 1 ML, but above one monolayer the growth of islands occurs on the well-ordered monolayer. The onset of island formation is a strong function of temperature. A model is proposed for the structures and energetics involved in the growth of Ga on Si(100). The results are discussed in terms of the implications for epitaxial growth of GaAs

901,423

PB89-200448 Not available NTIS National Bureau of Standards (NEL), Boulder, CO.

Electromagnetic Technology Div.

Ag Screen Contacts to Sintered YBa2Cu3Ox

Powder for Rapid Superconductor Characterization.

J. Moreland, and L. F. Goodrich. 1989, 4p Pub. in IEEE (Institute of Electrical and Electronics Engineers) Transactions on Magnetics 25, n2 p2056-2059 Mar 89.

Keywords: *Superconductors, *Electric contacts, Sin-Reywords: Superconductors, Electric contacts, Sintering, Silver, Powder(Particles), Electrical resistivity, Electrical measurement, Reprints, *High temperature superconductors, *Yttrium barium cuprates, *Barium yttrium cuprates, Critical current.

A new method was developed for making current contacts and voltage taps to YBa2Cu3Ox sintered pellets for rapid superconductor characterization. Ag wire screens are interleaved between calcined powder sections and then fired at 930 C to form a composite pellet for resistivity and critical current measurements. The Ag diffuses into the powder during the sintering process forming a proximity contact that is permeable to O2. In this configuration, current can be uniformly injected into the ends of the pellet through the bonded Ag screen electrodes. Also, Ag screen voltage contacts, which span a cross section of the pellet, may provide an ideal geometry for detecting voltage drops along the pellet, minimizing current transfer effects.

901.424

PB89-200463 Not available NTIS
National Bureau of Standards (NEL), Boulder, CO.
Electromagnetic Technology Div.
Chaos and Catastrophe Near the Plasma Frequen-

cy in the RF-Biased Josephson Junction. Final rept. R. L. Kautz, and R. Monaco. 1989, 5p

Grant N00014-88-F-0018

Sponsored by Office of Naval Research, Arlington, VA. Pub. in IEEE (Institute of Electrical and Electronics Engineers) Transactions on Magnetics 25, n2 p1399-1403 Mar 89.

Keywords: *Josephson junctions, *Electric potential, *Plasma frequency, Bessel functions, Cusps(Mathematics), Superconductivity, Bias, Reprints, Chaos, Catastrophe theory.

At bias frequencies much higher than the plasma frequency, the zero-voltage state of the rf-biased Joseph-son junction is known to span a range of dc bias pro-portional to the zero-order Bessel function of the rf amplitude. This pattern is modified at frequencies near the plasma frequency by the onset of chaotic instabilities and by the presence of cusp catastrophes.

901.425

PB89-200489 Not available NTIS National Bureau of Standards (NEL), Boulder, CO. Electromagnetic Technology Div.

Magnetic Evaluation of Cu-Mn Matrix Material for Fine-Filament Nb-Ti Superconductors.

R. B. Goldfarb, D. L. Ried, T. S. Kreilick, and E. Gregory. 1989, 3p Sponsored by Department of Energy, Washington, DC. Pub. in IEEE (Institute of Electrical and Electronics Engineers) Transactions on Magnetics 25, n2 p1953-1955 Mar 89.

Keywords: *Superconductivity, *Copper manganese alloys, Magnetic permeability, Niobium intermetallics, Composite materials, Microstructure, Reprints, Superconducting wires, AC losses, Spin glass.

Copper-manganese alloys have been proposed as matrix material for the reduction of coupling losses in fine-filament Nb-Ti superconductor wires. Magnetization and susceptibility measurements show that adverse magnetic effects arising from the spin-glass properties of this matrix are minimal for concentrations of Mn up to at least 4%.

901,426 PB89-200513 Not available NTIS National Bureau of Standards (NEL), Boulder, CO. Electromagnetic Technology Div.
Swltching Noise in YBa2Cu3Ox 'Macrobridges'.

R. H. Ono, J. A. Beall, M. W. Cromar, P. M. Mankiewich, R. E. Howard, and W. Skocpol. 1989,

Pub. in IEEE (Institute of Electrical and Electronics Engineers) Transactions on Magnetics 25, n2 p976-979 Mar 89.

Keywords: *Superconductors, *Integrated circuits, *Thin films, *Electromagnetic noise, Resistance, Electric bridges, Bias, Switching circuits, Microstructure, Flux density, Reprints, *High temperature superconductors, Magnetic flux, Copper oxide superconductors.

Intermittent switching in the voltage-current characteristics (VIC) of thin film bridges of YBa2Cu3Ox have been observed. At a fixed bias point there are multiple metastable voltage states with lifetimes which depend on the bias current and applied magnetic field. The microbridges are made of thin (<500nm), polycrystalline films of YBa2Cu3Ox which are patterned by liftoff into structures with dimensions ranging from less than 1 micro m to 100 micro m. Details of the fabrication process and the measurements are presented. The results are discussed in the context of fluctuations in the effective resistance of the bridge due to motion of trapped flux.

901,427
PB89-200745
National Bureau of Standards (NML), Gaithersburg, MD. Surface Science Div.

Electron and Photon Stimulated Desorption: Benefits and Difficulties. Final rept.

T. E. Madey, A. L. Johnson, and S. A. Joyce. 1988,

See also PB84-136308. Sponsored by Department of Energy, Washington, DC. Pub. in Vacuum 38, n8-10 p579-583 1988.

Keywords: *Desorption, *lonization, *Surface properties, Photons, Electron impact, X ray spectroscopy, Radiation damage, Silicon, Ruthenium, Reprints, Auger electron spectroscopy, Transmission electron microscopy.

Some of the benefits and pitfalls of electron and photon stimulated (ESD/PSD) processes at surfaces are described. The benefits include useful information about the local structure of surface molecules, provided by electron stimulated desorption ion angular distri-butions (ESDIAD). ESDIAD is an effective surface structural tool because the directions of ion desorption structural tool because the directions of lon description are determined by the orientation of the surface bonds ruptured by electron or photon bombardment. Other benefits of electron and photon-stimulated damage processes at surfaces include electron and photon beam lithography in microelectronics. The pitfalls of ESD/PSD include beam damage in surface analysis (by Auger electron spectroscopy, X-ray photoelectron spectroscopy and high resultation transmission elecspectroscopy and high resolution transmission elec-tron microscopy), the PSD of gases from vacuum walls in fusion reactors and synchrotron radiation sources, and inaccurate pressure readings due to ESD effects in ionization gauges.

901,428 PB89-201107

Not available NTIS

National Bureau of Standards (IMSE), Gaithersburg, MD.

Physics of Fracture, 1987.

Final rept. R. Thomson. 1987, 19p See also PB89-124036.

Pub. in Jnl. of Physics and Chemistry of Solids 48, n11 p965-983 1987.

Keywords: Ductile brittle transition, Crack propagation, Dislocations(Materials), Fracture strength, Brittleness, Reprints, *Fracture mechanics, Crack tips, Atmosphere effects.

The article first presents introductory material which The article first presents introductory material which should make it possible for the person unfamiliar with fracture to read the papers of this series. Then material of a basic physical nature regarding cracks in materials is presented. Emphasis is placed on the effects of chemical attack of bonds at a crack tip, and on the basic physical cause for a material to exhibit a tough (desirable) or a brittle (undesirable) overall aspect.

PB89-201206 Not available NTIS Mossbauer Hyperfine Fleids In RBa2(Cu0.97Fe0.03)3 O(7-x)(R=Y,Pr,Er).

Final rept.

M. Rubinstein, M. Z. Harford, L. J. Swartzendruber, and L. H. Bennett. 1988, 2p Pub. in Jnl. de Physique 49, n12 pC8-2209-C8-2210

Keywords: *Mossbauer effect, Hyperfine structure, Ferrates, Substitutes, Iron, Reprints, *High temperature superconductors, Yttrium barium cuprates, Erbium barium cuprates, Praseodymium barium cuprates.

Room temperature (57)Fe Mossbauer spectra of RBa2 (Cu(0.97)Fe(0.03))3O(7-x) (R = Y, Pr, Er) were obtained from samples with varying x. A magnetically-split hyperfine field spectrum was observed for the most oxygen-deficient Y sample, for all the Pr samples, and for none of the Er samples.

901,430 PB89-201230 PB89-201230 Not available NTIS National Bureau of Standards (NML), Gaithersburg, MD. Surface Science Div.

Electron-Stimulated-Desorption Ion-Angular Distributions. Final rept.

A. L. Johnson, S. A. Joyce, and T. E. Madey. 1988,

Sponsored by Department of Energy, Washington, DC. Pub. in Physical Review Letters 61, n22 p2578-2581, 28 Nov 88

Keywords: *Ionization, *Chemisorption, *Fluorine, *Ruthenium, Anions, Desorption, Surface chemistry,

The first measurements of the electron-stimulated-desorption ion-angular-distributions of negative ions from surface are reported. The angular distribution of F(-) ions for electron-stimulated desorption of PF3, NF3, and (CF3(2)C) on Ru(0001) depend on the molecular geometry and the state of the adsorbed species. The structural information obtained from these negativeion studies complements that from similar positive-ion studies.

901.431 Not available NTIS PB89-201792 National Bureau of Standards (IMSE), Gaithersburg, MD. Ceramics Div. Electron Diffraction Study of the Faceting of Tilt

Grain Boundaries in NiO. Final rept.

J. A. Eastman, M. D. Vaudin, K. L. Merkle, and S. L. Sass. 1989, 13p Contracts W-31109-ENG-38, DE-FG02-85ER45211 Sponsored by Department of Energy, Washington, DC. Pub. in Philosophical Magazine A 59, n3 p465-477

Keywords: *Diffraction, *Grain boundaries, *Crystal dislocations, *Nickel oxides, Crystal lattices, Electron microscopy, Reprints.

The diffraction effects expected from a periodically faceted boundary containing a periodic array of dislo-cations in the long facet have been analyzed. The characteristic manifestation in reciprocal space of peri-

odic faceting was identified as the occurrence of bundles of reciprocal lattice rods; within each bundle the rods are displaced with respect to each other parallel to their length in a manner related to the facet geometry. Electron diffraction and microscopy were used to study the facet structure of tilt boundaries in NiO, and the boundary structure deduced from the observed diffraction effects was in good agreement with the imagtraction effects was in good agreement with the imaging observations. In those cases where there was only one type of dislocation present in the long facet, it was possible to determine the average boundary plane, the dislocation spacing in the long facet, the facet period and the facet height from electron diffraction observations. The technique is especially useful for large-angle boundaries having high-index rotation axes, where little detailed information can be obtained using where little detailed information can be obtained using imaging techniques.

901,432 PB89-201826
Not available NTIS
National Bureau of Standards (IMSE), Gaithersburg,
MD. Reactor Radiation Div.
Statistical Descriptors in Crystallography: Report
of the International Union of Crystallography Subcommittee on Statistical Descriptors.
Final rept.

Final rept.
D. Schwarzenbach, S. C. Abrahams, H. D. Flack, W. Gonschorek, T. Hahn, K. Huml, R. E. Marsh, E. Prince, B. E. Robertson, J. S. Rollett, and A. J. C. Wilson. 1989, 13p Pub. in Acta Crystallographica A45, p63-75 1989.

Keywords: *Crystallography, Definitions, Nomenclature, Statistics, Reprints.

The International Union of Crystallography Subcommittee on Statistical Descriptors has attempted to elu-cidate the nature of problems encountered in the defi-nition and use of statistical descriptors as applied to crystallography and to propose procedural improve-ments. The report contains: (a) a dictionary of statisti-cal terms established for use by experimentalists; (b) a description of the statistical basis for refinement procedures; (c) sections dealing with defects in the physical model used for refinement, and with the choice and significance of weighting schemes; and (d) recommendations, some of which may be readily implemented, while others may require a long-term effort to bring them into general use.

901,433 PB89-202030 Not available NTIS National Bureau of Standards (IMSE), Gaithersburg, MD. Reactor Radiation Div.

Spin-Density-Wave Transition in Dilute YGd Single Crystals. Final rept.

L. E. Wenger, G. W. Hunter, J. A. Mydosh, J. A. Gotaas, and J. J. Rhyne. 1986, 4p Pub. in Physical Review Letters 56, n10 p1090-1093

Keywords: *Yttrium alloys, *Magnons, Gadolinium containing alloys, Neutron diffraction, Specific heat, Single crystals, Phase transformations, Antiferromagnetism, Reprints, *Spin waves, Magnetic susceptibility, Magnetic ordering.

Neutron diffraction, heat capacity, and susceptibility measurements on dilute YGd single crystals with 1.5 to 4.4 at .% Gd show long-range helical magnetic ordering at low temperatures. The neutron data reveal a periodic incommensurate spin structure with the Gd moments in the basal plane and a propagation wave-vector of 0.28c. A semicusp-like behavior is observed in the magnetic specific heats with the maxima occurring at similar temperatures as the susceptibility peaks (H perpendicular to c axis) and the onset of Bragg scattering. These results are quantitatively interpreted within a helical spin-density-wave stabilization of the conduction electrons.

901,434 Not available NTIS PB89-202238 National Bureau of Standards (IMSE), Gaithersburg,

MD. Metallurgy Div.
Roles of Atomic Volume and Disclinations in the
Magnetism of the Rare Earth-3D Hard Magnets. Final rept.

L. H. Bennett, R. E. Watson, and M. Melamud. 1988, See also DE88015197.

Pub. in Jnl. de Physique 49, n12 pC8-537-C8-538 Dec

168

Keywords: *Permanent magnets, *Rare earth elements, Atomic properties, Atomic structure, Reprints, Electron orbitals.

Although no clear pattern exists in the experimental data, structural factors are expected to be important to local 3d magnetism in the hard magnets. A measure of two structural factors (local site volume and the presence of disinclinations) are provided so as to disentangle their role in the local magnetism.

901,435 PB89-202444 Not available NTIS National Bureau of Standards (NEL), Gaithersburg, MD. Thermophysics Div.

Ergodic Behavior in Supercooled Liquids and In

Final rept

D. Thirumalai, R. D. Mountain, and T. R. Kirkpatrick.

Grants NSF-CHE86-09722, NSF-DMR86-07605 Sponsored by National Science Foundation, Washing-

Pub. in Physical Review A 39, n7 p3563-3574, 1 Apr

Keywords: *Ergodic processes, *Glass, *Liquids, *Phase transformations, Supercooling, Statistical mechanics, Correlation, Mathematical models, Symmetry, Vitreous state, Molecular relaxation, Reprints.

Ergodic behavior in liquids, supercooled liquids, and glasses is examined with a focus on the time scale needed to obtain ergodicity. In addition to broken ergodicity, the possibility that a subtle symmetry is broken as the liquid-to-glass transition takes place is examined. It is suggested that a 'discrete' symmetry, to be referred to as the statistical symmetry, is broken in the glassy phase. This is illustrated by analyzing the distri-bution of the energy of the particles. Based on this, long-time dynamics and structural relaxation in glasses will be dominated by fluctuations in domains of finite length within which the particles are highly correlated. This is in accord with the ideas of Adams and Gibbs. All of the above arguments are illustrated with the aid of molecular-dynamics simulations of soft-sphere mix-

901,436 PB89-202501 Not available NTIS National Bureau of Standards (NEL), Gaithersburg, MD. Thermophysics Div.

Liquid, Crystalline and Glassy States of Binary Charged Colloidal Suspensions. Final rept.

R. O. Rosenberg, D. Thirumalai, and R. D. Mountain.

1989, 6p Grant NSF-CHE86-57396

Sponsored by National Science Foundation, Washington, DC.

Pub. in Jnl. of Physics: Condens. Matter 1, p2109-2114

Keywords: *Suspending(Mixing), *Colloids, Polystyrene, Spheres, Liquids, Vitreous state, Crystallization, Computerized simulation, Reprints.

The formation of the liquid, crystalline, and glassy states in binary mixtures of aqueous suspensions of charged polystyrene spheres of different sizes is investigated. It is shown that on merely mixing the particles, crystalline (a substitutional body-centered cubic) and glassy states are readily formed for a 1:1 mixture at appropriate values of the density. These results are in agreement with recent experimental studies. The ease of formation of the crystal and the glassy phases is rationalized by an analysis of the local potential energy profiles calculated using the Hessian (dynamical matrix). It is suggested that the eigenvalues of such a Hessian can be used to define a preferred length in any glassy system.

901,437 PB89-202659 Not available NTIS National Bureau of Standards (IMSE), Gaithersburg, MD. Reactor Radiation Div.

Antiferromagnetic Structure and Crystal Fleld Splittings in the Cubic Heusler Alloys HoPd2Sn and ErPd2Sn.

W. H. Li, J. W. Lynn, H. B. Stanley, T. J. Udovic, R. N. Shelton, and P. Klavins. 1988, 2p Sponsored by National Science Foundation, Washing-

Pub. in Jnl. de Physique 49, n12 pC8-373-C8-374 Dec

Keywords: *Antiferromagnetism, *Holmium compounds, *Erbium compounds, Crystal lattices, Electric fields, Neutron diffraction, Low temperature research, Reprints, *Heusler alloys.

Neutron scattering techniques have been employed to investigate the magnetic properties of the cubic Heusler alloys HoPd2Sn and ErPd2Sn. Both materials exhibit an fcc type-II antiferromagnetic order, with T(sub N)=5.0 and 1.0 K for Ho and Er materials, respectively. However, there is an additional modulation of this basic structure. Inelastic neutron scattering measurements have been performed by time-of-flight techniques to determine the crystal field levels of the rare-earth ions. The (cubic) Lea, Leask, and Wolf crystal field parameters were determined to be W=0.0287(4) meV, x=0.3248(8) for HoPd2Sn, and W=0.0450(4) meV, x=0.3022(6) for ErPd2Sn.

901,438 PB89-202667 Not available NTIS National Bureau of Standards (IMSE), Gaithersburg, MD. Reactor Radiation Div.

Exchange and Magnetostrictive Effects in Rare Earth Superlattices. Final rept.

J. J. Rhyne, R. W. Erwin, J. Borchers, M. B. Salamon, R. Du, and C. P. Flynn, 1989, 17p Pub. in Jnl. of the Less-Common Metals 148, p17-33

Keywords: *Single crystals, *Rare earth elements, *Thin films, *Yttrium, *Neutron diffraction, *Ferromagnetism, Magnetic properties, Dysprosium, Erbium, Crystal structure, Crystal lattices, Reprints.

Single-crystal multilayer films with alternate heavy rare earth and yttrium layers have been shown by neutron diffraction to exhibit long-range magnetic order. Analysis of the neutron results on Dy/Y and Er/Y super-lattices shows that the phase of the modulated magnetic structures in the dysprosium and erbium is preserved across the intervening yttrium non-magnetic layer and corresponds to a 'pseudo turn-angle' near 51 degrees in the yttrium, which is in accord with theoretical calculations from the band structure. The ferromagnetic transitions occurring in the pure elements are completely suppressed in the multilayers as a result of epitaxial 'clamping' by the yttrium layers, which inhibits the development of sufficient magnetostrictive strain to induce the phase transition. The temperature of the intermediate transitions in Er/Y multilayers is also modified by magnetostriction, and evidence is found for different turn-angles for c axis and basal plane moment components.

PB89-202675 Not available NTIS National Bureau of Standards (IMSE), Gaithersburg, MD. Reactor Radiation Div.

Magnetic Structure of Y0.97Er0.03. Final rept.

J. A. Gotaas, J. J. Rhyne, L. E. Wenger, and J. A. Mydosh. 1988, 2p Grant NSF-DMR84-00711

Sponsored by National Science Foundation, Washing-

Pub. in Jnl. de Physique 49, n12 pC8-365-C8-366 Dec 88.

Keywords: *Yttrium alloys, *Erbium containing alloys, Neutron diffraction, Single crystals, Low temperature research, Magnetic moments, Magnetic anisotropy, Reprints, Spin waves, Spin glass.

Neutron diffraction has demonstrated that a single crystal alloy of Y(0.97)ER(0.03) orders below T(sub N)=3.25 K into a sinusoidally modulated slate with a propagation vector along the c-axis. The moments lie predominantly along the c-axis, but a small (< 0.1 mu sub B) basal plane component exhibits the same temperature dependence. Below 2 K, weak third harmonics indicate that the sinusoidal structure is beginning to square up.

901,440 PB89-202972 Not available NTIS National Bureau of Standards (NML), Gaithersburg, MD. Surface Science Div. Cross Sections for Inelastic Electron Scattering In

Final rept. C. J. Powell. 1989, 8p. Pub. in Ultramicroscopy 28, p24-31 1989.

Keywords: *Electron scattering, *Solids, *Inelastic scattering, *Cross sections, Electron energy, Ioniza-

tion, X ray spectroscopy, Radiation damage, Beta particle spectroscopy, Mean free path, Reprints, Auger electron spectroscopy, Energy loss spectroscopy, Electronic structure.

An overview is given of available information on cross-sections for inelastic electron scattering in solids with emphasis on the need for cross-section data in elecemphasis on the fleed for cross-section data in elec-tron energy-loss spectroscopy (EELS), X-ray emission spectroscopy (XES), and Auger-electron spectroscopy (AES). After a brief survey of the relevant theory, infor-mation is given on inelastic mean free paths of 200-2000 eV electrons in solids (AES), total inner-shell ionization cross sections (AES and XES), partial innershell ionization cross section (EELS), and electronbeam-induced damage.

901,441 PB89-211106 PC A04 National Inst. of Standards and Technology, Gaithersburg, MD.

Journal of Research of the National Institute of Standards and Technology, Volume 94, Number 3, May-June 1989.

Bi-monthly rept. 1989 68n

Also available from Supt. of Docs. as SN703-027-00028-8. See also PB89-211114 through PB89-211130 and PB89-175194.

Keywords: *Superconductivity, *Transformers, *Capacitors, *Research, *Consensus values, High voltage, Calibration.

Contents: A brief review of recent superconductivity research at NIST; Calibration of voltage transformers and high-voltage capacitors at NIST; Consensus values, regressions, and weighting factors.

901.442 PB89-211114

(Order as PB89-211106, PC A04) National Inst. of Standards and Technology, Gaithersbura. MD.

Brief Review of Recent Superconductivity Research at NIST (National Institute of Standards and Technology).

Bi-monthly rept. D. R. Lundy, L. J. Swartzendruber, and L. H. Bennett. 1989, 32p

Included in Jnl. of Research of the National Institute of Standards and Technology, v94 n3 p147-178 May-Jun

Keywords: *Superconductivity, Electric contacts, Crystal structures, Phase diagrams, Josephson junctions, Reviews, *High temperature superconductors, Electronic structure, Voltage standards, Yttrium barium cuprates, Barium yttrium cuprates.

A brief overview of recent superconductivity research at NIST is presented. Emphasis is placed on the new high-temperature oxide superconductors, though mention is made of important work on low-temperature superconductors, and a few historical notes are included. For the new high-temperature superconductors, research activities include determination of physical properties such as elastic constants and electronics structure, development of new techniques such as magnetic-field modulated microwave-absorption and determination of phase diagrams and crystal structure. For the low-temperature superconductors, research spans studying the effect of stress on current density to the fabrication of a new Josephson junction voltage standard.

901.443

PB89-212179 Not available NTIS National Bureau of Standards (NEL), Gaithersburg, MD. Semiconductor Electronics Div.

Electromigration Damage Response Time and Implications for dc and Pulsed Characterization. Final rept.

J. S. Suehle, and H. A. Schafft. 1989, 3p Pub. in Proceedings of Annual Reliability Physics Symposium (27th), Phoenix, AZ., April 11-13, 1989, p229-231.

Keywords: *Stress corrosion tests, *Metallizing, Reliability, Reaction time, Vacancies(Crystal defects), Integrated circuits, *Electromigration.

new measurement interference for highly accelerated electromigration stress tests is identified. Measurements of the median-time-to-failure, t(50) for dc and

for pulsed current stress as a function of pulse repetition frequency, reveal that highly accelerated stress tests may overestimate metallization reliability if t(50) is comparable with the response time of the vacancy concentration. Techniques necessary to make reliable wafer-level t(50) measurements are described.

901.444 PB89-212195 Not available NTIS National Bureau of Standards (NEL), Gaithersburg, MD. Semiconductor Electronics Div.
Thermal Conductivity Measurements of Thin-Film

Silicon DloxIde.

Final rept. H. A. Schafft, J. S. Suehle, and P. G. A. Mirel. 1989,

Contract DARPA Order-3882 Sponsored by Defense Advanced Research Projects Agency, Arlington, VA.
Pub. in Proceedings of IEEE (Institute of Electrical and

Electronics Engineers) International Conference on Microelectronic Test Structures, Edinburgh, Scotland, March 13-14, 1989, v2 n1 p121-126.

Keywords: *Silicon dioxide, *Thin films, *Thermal conductivity, *Measurement, *Integrated circuits, *Semiconducting films, Stresses, Thickness, Ohmic dissipa-Temperature, Microelectronics, Accelerated

Measurements of the thermal conductivity of micrometer-thick films of silicon dioxide are reported for the first time. Results show that the thermal conductivity is much lower than the values reported for bulk speci-mens and decreases with decreasing film thickness. It means that healing effects may be much larger than expected in accelerated stress tests and in other cases where Joule heating can be a concern.

901 445

PB89-212245 Not available NTIS National Bureau of Standards (NML), Gaithersburg, MD. Radiometric Physics Div.
Interpolation of Silicon Photodiode Quantum Effi-

ciency as an Absolute Radiometric Standard.

E. F. Zalewski, and W. K. Gladden. 1986, 2p Pub. in Proceedings of Conference on Precision Electromagnetic Measurements, Gaithersburg, MD., June 23-27, 1986, p134-135.

Keywords: *Photodiodes, *Quantum efficiency, Silicon, Interpolation, Standards, Radiometry, Spectral response, Calibration.

The calibration of the external quantum efficiency of silicon photodiodes over the entire silicon spectral range based on quantum efficiency measurements at a few wavelengths is described.

PB89-214738 Not available NTIS
National Bureau of Standards (NEL), Boulder, CO.
Electromagnetic Technology Div.
MM Wave Quasioptical SIS Mixers.

Final rept. Q. Hu, C. A. Mears, P. L. Richards, and F. L. Lloyd.

See also DE89001262. Sponsored by Department of Energy, Washington, DC.
Pub. in IEEE (Institute of Electrical and Electronics En-

gineers) Transactions on Magnetics 25, n2 p1380-1383 Mar 89.

Keywords: *Mixing circuits, *Integrated circuits, *Log periodic antennas, *Josephson junctions, Electromagnetic noise, Niobium oxides, Niobium, Lead, Indium, Gold, Reprints.

The performance of planar SIS mixers was tested with log-periodic antennas at near millimeter and submillimeter wave frequencies from 90 to 360 GHz. The large (omega)(R sub N)(C) product (about 10 at 90 GHz,) of the Nb/Nb(O sub x)/Pb-In-Au junctions requires an in-tegrated inductive tuning element to resonate the junction capacitance at the operating frequencies. Two types of integrated tuning element were designed with the aid of measurements using a Fourier transform the aid of measurements using a Fourier transform spectrometer. Preliminary results indicate that the tuning elements can give very good mixer performance up to at least 200 GHz. The relatively high mixer noise temperatures compared to those of waveguide SIS mixers in a similar frequency range are attributed mainly to the losses in the optical system, which is being improved. being improved.

901.447 PB89-228076 Not available NTIS National Inst. of Standards and Technology (NEL), Boulder, CO. Thermophysics Div. Torsional Plezoelectric Crystal Viscometer for Compressed Gases and Liquids.

Final rept.
D. E. Diller, and N. V. Frederick. 1989, 13p
Sponsored by Department of Energy, Washington, DC.
Pub. in International Jnl. of Thermophysics 10, n1 p145-157 Jan 89.

Keywords: *Piezoelectric crystals, *Viscometers, *Gases, *Liquids, Pressure, Temperature, Impedance, Argon, Methane, Resonance, Repnits.

A torsional piezoelectric crystal viscometer for compressed gases and liquids at temperatures to 600 K and at pressures to 70 MPa has been developed. Several torsional crystals were prepared from swept (electrolyzed) quartz to obtain a good performance a: high temperatures. Measurements of the bandwidth of the crystal resonance curve were automated using an impedance analyzer. The viscometer was tested on compressed gaseous argon and methane at temperatures to 500 K and at pressures to 50 MPa. The measurements differ from accurate wide-range correlating equations by less than 2%.

901,448 PB89-228431 PB89-228431 Not available NTIS National Bureau of Standards (NEL), Boulder, CO. Relationagnetic Technology Div.
Resistance Measurements of High T(sub c) Superconductors Using a Novel 'Bathysphere' Cryostat.

Final rept.

J. Moreland, Y. Li, R. M. Folsom, and T. E. Capobianco. 1989, 3p Pub. in IEEE (Institute of Electrical and Electronics Engineers) Transactions on Magnetics 25, n2 p2560-2562 Mar 89.

Keywords: *Superconductors, *Electrical resistance, *Cryostats, Magnetic fields, Critical temperature, Definitions, Thermodynamics, Reprints, *High temperature superconductors, Temperature dependence, Cryogenics and Parkets and Parket ic equipment, Bathyspheres.

The authors have developed a novel cryostat for variable temperature testing of high temperature super-conductors. The cryostat is a bathysphere consisting of an overturned stainless steel Dewar suspended in liquid helium. Results for resistance versus temperature of some high temperature superconductors in a magnetic field are presented. Also, various definitions for thermodynamic and practical T sub c derived from transport resistance measurements are suggested and discussed. These definitions are based on T sub c midpoint, various relative resistance criteria, or absolute resistivity criteria.

PB89-228449 Not available NTIS National Inst. of Standards and Technology (NEL), Boulder, CO. Electromagnetic Technology Div. Evidence for the Superconducting Proximity Effect in Junctions between the Surfaces of YBa2CU3Ox Thin Films.

Final rept. A. J. Moreland, R. H. Ono, J. A. Beall, M. Madden, and A. J. Nelson. 1989, 3p Contract N00014-88-F-0013

Sponsored by Office of Naval Research, Arlington, VA., and Department of Energy, Washington, DC. Pub. in Applied Physics Letters 54, n15 p1477-1479, 10 Apr 89.

Keywords: Electron tunneling, Thin films, Electrodes, Reprints, "Superconducting junctions, "Superconducting films, "High temperature superconductors, "Yttrium barium cuprates, "Barium yttrium cuprates, Josephson effect, Proximity effect (Electricty).

The authors have used the squeezable electron tunproperties of the surfaces of YBa2Cu3Ox (YBCO) thin-film electrodes. As deposited and annealed, the surfaces of the electrodes were insulating at 4 K. Several methods were used to improve the electrical proper-ties of the electrodes' surfaces including rapid thermal annealing, oxygen sputter etching, and thin Ag coating treatments. The greatest improvement occurred after a deposition of a 5 nm Ag coating and subsequent rapid thermal anneal of one set of YBCO films. Under these conditions it was possible to make a supercon-

ducting Josephson point contact between the surfaces of the electrodes. The authors think that the Ag acts as a normal-metal proximity layer effectively shunting the degraded electrodes' surfaces.

PB89-228456 Not available NTIS National Inst. of Standards and Technology (NEL), Boulder, CO. Electromagnetic Technology Div. Cryogenic Bathysphere for Rapid Variable-Tem-perature Characterization of High-T(sub c) Superconductors.

Final rept. That Tept.

J. Moreland, Y. K. Li, R. Folsom, and T. E.
Capobianco. 1988, 4p

Pub. in Review of Scientific Instruments 59, n12

p2535-2538 Dec 88.

Keywords: *Superconductors, Electrical resistance, Cryostats, Reprints, *High temperature superconductors, Bathyspheres, Cryogenic equipment, Temperature dependence, Yttrum banum cuprates, Banum yttrus and Michigan Standards. trium cuprates, Niobium titanium.

A bathysphere consisting of an inverted Dewar flask for submersible operation in cryogenic fluids is used to ror submersible operation in cryogenic fluids is used to measure the resistance of superconductors, including high T sub c superconducting copper oxides, as a function of temperature from 4 to 300 K. The authors describe the cryostat incorporating the bathysphere and present data on NbTi (44% Ti) and YBa2Cu3O(7-delta) with respective superconducting transitions temperatures of 9.5 and 91.5 K. There are several advantages of the bathysphere method. The except is of tages of the bathysphere method. The cryostat is of simple, compact design, easily adapted to high-field applications where magnet bore size is a limiting factor. The sample and thermometer are thermolyzed in the dry vapor trapped at the top of the bathysphere. Temperature can be varied rapidly from 300 to 4 K at a rate of 1 K/min with less than a 0.1 K thermal lag between the sample and thermometer.

901,451 PB89-228464
Not.available NTIS
National Inst. of Standards and Technology (NEL),
Gaithersburg, MD. Precision Engineering Div.
Specimen Blasing to Enhance or Suppress Secondary Electron Emission from Charging Specimens at Low Accelerating Voltages.
Final rept.

M. T. Postek, W. J. Keery, and R. D. Larrabee. 1989, Pub. in Scanning 11, p111-121 1989.

Keywords: *Transistors, *Electron emission, *Electric potential, Polyethylene, Electron microscopy, Acceleration(Physics), Gallium arsenides, Bias, Silicon, Methylmethacrylates, Reprints.

Biasing of the specimen is shown to produce improved images in the scanning electron microscope at low beam energies (0.8-2.5 keV) when charging effects (induced by the primary electron beam), topographic effects, or detector shadowing effects would otherwise be present. Examples of such improvement are given for gallium arsenide field-effect transistors (positive for gallium arsenide field-effect transistors (positive charging), patterned photoresist layers on silicon wafers (negative charging and shadowing in contact holes), fractured polymethylmethacrylate (negative charging), polyethylene wrapper material (positive charging), and polished diamond tools (positive charging). It is concluded that specimen biasing may be a simpler and more convenient way to achieve some of simpler and more convenient way to achieve some of the advantages of the converted backscattered secondary electron technique for imaging.

901.452 PB89-228472 Not available NTIS
National Inst. of Standards and Technology (NEL),
Gaithersburg, MD. Semiconductor Electronics Div.
EXAFS (Extended X-ray Absorption Fine Structure) Study of Burled Germanium Layer in Sillcon.

Final rept. C. E. Bouldin. 1989, 2p Pub. in Physica B 158, p596-59**7** 1989.

Keywords: *Germanium, *Silicon dioxide, *Single crystals, *Gallium arsenides, Silicon, Thin films, X ray fluorescence, Reprints.

EXAFS measurements are made of a 200 A layer of Ge on a Si substrate. The Ge layer is covered by a 3000 A layer of SiO2. Sensitivity to the buried layer is enhanced through the use of grazing incidence fluorescence detection. A two-channel photodiode detec-

tor is used to detect the fluorescence and to discriminate against Bragg peaks from the single-crystal Si substrate. Since the fluorescence signal is isotropic, while the Bragg peaks are directional, one channel of the detector is always free of Bragg peak interference. The average number of Ge-Ge and Ge-Si neighbors in the buried Ge layer, the distances and disorder in the first-shell were determined. Prospects for studying the buried Ge-SiO2 interface are discussed.

901,453 PB89-228522 Not available NTIS Not available NTIS
National Inst. of Standards and Technology (NEL),
Gaithersburg, MD. Semiconductor Electronics Div.
Effects of Doping-Density Gradients on Band-Gap
Narrowing in Silicon and GaAs Devices. Final rept.

7 III. Teyling. J. R. Lowney, and H. S. Bennett. 1989, 5p Pub. in Jnl. of Applied Physics 65, n12 p4823-4827, 15

Keywords: *Semiconductor devices, *Gallium arsenides, *Silicon, *Energy gap, Semiconductor doping, Reprints, Quantum wells.

The limitations of the theory for band-gap narrowing, which is based on uniform material, are considered in devices that have steep doping gradients. Validity criteria are derived that place upper bounds on the dopant and carrier density gradients for the application of the results from uniform theory. The existence of wave-function tailing beyond the potential barriers that occur in devices is studied. At room temperature the effects due to these tails are usually small, but at low effects due to these tails are usually small, but at low temperatures they can become very significant.

901,454 PB89-229082 Not available NTIS National Bureau of Standards (IMSE), Boulder, CO. Fracture and Deformation Div.

Hysteretic Phase Transition in Y1Ba2Cu3O7-x Su-

perconductors. Final rept. H. M. Ledbetter, and S. A. Kim. 1988, 4p Pub. in Physical Review B 38, n16 p11857-11860, 1

Dec 88.

Keywords: *Superconductors, *Phase transforma-tions, Barium titanates, Hysteresis, Elastic properties, Ultrasonic radiation, Acoustic velocity, Reprints, *High temperature superconductors, *Yttrium barium cuprates, *Barium yttrium cuprates, Holmium barium cuprates, Europium barium cuprates.

The authors studied ultrasonic-wave velocities, both longitudinal and shear, in YBa2Cu3O7-x between 5 and 295 K, during both cooling and warming. Both waves, especially the longitudinal, show thermal hysteresis. The results suggest a hysteretic phase change that occurs between 160 and 170 K during cooling, and between 170 and 260 K during warming. This phase-change hypothesis explains anomalies in several physical properties. The phase change agrees with thermodynamic instability predictions. The authors with thermodynamic instability predictions. with thermodynamic instability predictions. The authors confirmed the hysteresis in Ho-Ba-Cu-O, where it is smaller than in Y-Ba-Cu-O, and in Eu-Ba-Cu-O, where it is larger. In a comparison perovskite, BaTiO3 they observed zero hysteresis. At T(c), 91 K, sound velocities show no measurable change in either magnitude or slope. This continuity disputes the current popular view that, contrary to thermodynamics, elastic stiffness increases upon cooling through T(c) into the superconducting state. The authors believe that stiffening results from the usual thermal effects after a phase transformation from a stiffer phase.

Not available NTIS National Inst. of Standards and Technology (IMSE), Gaithersburg, MD. Reactor Radiation Div. Dependence of T(sub c) on the Number of CuO2 Planes per Cluster in Interplaner-Boson-Exchange Models of High-T(sub C) Superconductivity. Final rept.

Pub. in Solid State Communications 70, n1 p75-77

Keywords: *Superconductors, *Critical temperature, *Copper oxides, Bismuth inorganic compounds, Thallium inorganic compounds, Mathematical models, Cuprates, Bosons, Reprints, *High temperature superconductors.

The critical temperature T sub c(n) of systems, such as the TI and Bi compounds, containing n CuO2 planes per cluster is discussed theoretically within semi-phenomenological models which are based upon the exchange of (unspecified) high-energy bosons (omega > > omega(phonon)) between different CuO2 planes. Applied to representative data for the TI2 compounds, the models predict rapid saturation of T sub c(n) at relatively low n, with the possibility of a diminution beyond n=3. Within the theoretical framework, these qualitative features appear to be quite general for this class of materials.

901,456 PB89-229140 Not available NTIS National Bureau of Standards (IMSE), Gaithersburg, MD. Reactor Radiation Div.

Hydrogen Sites in Amorphous Pd85Si15HX Probed by Neutron Vibrational Spectroscopy. Final rept.

J. J. Rush, T. J. Udovic, R. Hempelmann, D. Richter, and G. Driesen. 1989, 10p Pub. in Jnl. of Physics: Condens. Matter 1, p1061-1070

Keywords: *Hydrogen, Neutron spectroscopy, Vibrational spectre, Crystal structure, Palladium, Silicides, Hydrides, Reprints, Amorphous materials.

In order to clarify the discrepancy between the Gaussian distribution of H-site energies suggested from difsain distribution of H-site energies suggested from different macroscopic measurements and the evidence for two energetically well separated types of H sites obtained from a microscopic H diffusion study of hydrogen in amorphous Pd(85)Si(15)H(x), 0.13 < or = x < or = 8.23. At concentrations below 1% the spectra exhibit distinct features that indicate the occupation of distorted Pd(s) exhabed a league with a repose of the distorted Pd(6) octahedra, along with a range of tetrahedral sites. These observations are consistent with a bimodal distribution of H-site energies in this glassy metal hydride.

901,457 PB89-230353 Not available NTIS Notional Inst. of Standards and Technology (NEL), Boulder, CO. Electromagnetic Technology Div. Flux Creep and Activation Energies at the Grain Boundaries of Y-Ba-Cu-O Superconductors.

M. Nikolo, and R. B. Goldfarb. 1989, 4p Pub. in Physical Review B 39, n10 p6615-6618, 1 Apr

Final rept.

Keywords: *Superconductors, *Flux, *Creep properties, *Activation energy, *Grain boundaries, Magnetic hysteresis, Temperature, Reprints.

The ac susceptibility of sintered YBa2CuO7-delta pellets as a function of temperature and ac magnetic-field amplitude and frequency was measured. The imaginary part of the susceptibility chi double prime exhibits two peaks. A narrow peak is located at the critical temperature of the grains. A broad peak at lower tempera-ture is attributed to hysteresis losses at the grain boundaries. There is a small shift in this coupling peak to higher temperature as the frequency increases from 10 to 1000 Hz. The shift is explained in terms of Anderson flux creep on a time scale of milliseconds. The shift depends on the amplitude of the measuring field. The activation energy for flux creep ranges from 11.9 + or - 1.0 eV in the zero-field limit (0.8 Am(sup -1) (0.01 Oe)) to 1.2 + or - 0.3 eV at 800 Am(sup -1) (10 Oe). The data is extrapolated to find the value for an intergrain decoupling field of 1-2 kAm(sup -1) (13-25 Oe), above which flux creep presumably becomes flux they extra be received. flow at the grain boundaries.

901,458 PB89-231088 Not available NTIS National Inst. of Standards and Technology (IMSE), Gaithersburg, MD. Ceramics Div. Thermomechanical Detwinning of Superconduct-ing YBa2Cu3O7-x Single Crystals. Final rept.

D. L. Kaiser, F. W. Gayle, R. S. Roth, and L. J. Swartzendruber. 1989, 3p Pub. in Jnl. of Materials Research 4, no. 4, p745-747,

Jul/Aug 89.

Keywords: *Single crystals, *Superconductors, *Twinning, *Crystal defects, Yttrium oxides, Barium oxides, Copper oxides, Perovskites, Thermomagnetic effects, Anisotropy, Reprints.

A method for the complete removal of twins from single crystals of superconducting YBa2Cu3O(7-x) is described. The process depends on ferroelastic behavior found to exist in the phase, and should be gen-

erally applicable to the layered perovskite-type phases containing accommodation twins resulting from a tetragonal-to-orthorhombic transformation on cooling. The twin-free, superconducting single crystals will enable investigations of a-b anisotropy of properties as well as crystal structure determination without complication by the presence of microtwins.

901,459

PB89-231328 Not available NTIS National Inst. of Standards and Technology (NML), Gaithersburg, MD. Surface Science Div.

Photon-Stimulated Desorption as a Measure of Surface Electronic Structure.

Final rept.
J. A. Yarmoff, and S. A. Joyce. 1989, 4p
Pub. in Jnl. of Vacuum Science and Technology A7, n3 p2445-2448 May/Jun 89.

Keywords: *Surfaces, Fluorine, Silicon, Adsorption, Reprints, *Photon stimulated desorption, *Electronic structure.

The yield of ions desorbed via excitation of the Si 2p and F 1s levels was measured for fluorine adsorbed on Si(111). These photon-stimulated desorption (PSD) spectra were compared with the absorption measured via secondary or Auger electrons. It was seen that the PSD is dominated by direct excitations, and that the PSD spectra are sensitive to the final-state density at the local atomic site associated with the initial excita-tion. At the Si 2p edge, the PSD is sensitive to the oxidation state of the bonding silicon atom. At the F 1s edge, it is sensitive to the correspondence between the polarization vector of the incident light and the bond direction. Measurements of the kinetic energies of the desorbed ions were used to ascertain details of the desorption mechanism.

901,460 PB89-234314 Not available NTIS National Inst. of Standards and Technology (NML), Boulder, CO. Quantum Physics Div. Universal Resputtering Curve.

Final rept. W. L. Morgan. 1989, 3p Pub. in Applied Physics Letters 55, n2 p106-108, 10 Jul

Keywords: *Sputtering, Monte Carlo method, Deposition, Simulation, Substrates, Reprints, *Resputtering, Universal curves.

The process of resputtering material being sputter deposited onto a substrate is investigated via Monte Carlo simulations and simple analytical models. This resputtering comprises contributions from self-sputter-ing and from neutralized ions reflected from the target being sputtered. The results of these models are in reasonable agreement with recent measurements over a wide variety of gases and metal targets. When plotted versus a dimensionless mass parameter, the intrinsic resputtered fraction lies on a seemingly universal curve. The reason for this becomes clear through the development of simple analytical models.

901,461 PB90-112400 PC A04/MF A01 National Inst. of Standards and Technology, Gaithers-

Directional Solidification of a Planar Interface in the Presence of a Time-Dependent Electric Cur-

L. N. Brush, S. R. Coriell, and G. B. McFadden. Sep 89, 53p NISTIR-89/4161

Keywords: *Crystal growth, *Electric current, Peltier effect, Thermoelectricity, Ohmic dissipation, Resistance heating, Bismuth, Mathematical models, Indium antimonides, Germanium containing alloys, Tin alloys, *Directional solidification(Crystals), Numerical solution, Electromigration.

The paper develops a numerical method to study the motion of a planar crystal-melt interface during the directional solidification of a binary alloy in the presence of a time-dependent electric current. The model in-cludes the Thomson effect, the Peltier effect, Joule heating and electromigration of solute in the coupled set of equations governing heat flow in the crystal and melt, and solute diffusion in the melt. For a variety of time dependent currents, the temperature fields and interface velocity are calculated as functions of time for indium antimonide and bismuth, and for the binary alloys, germanium-gallium and tin-bismuth. For the

alloys, it also calculates the solid composition of a function of position, and thus makes quantitative pre-dictions of the effect of an electrical pulse on the solute distribution in the solidified material. In addition, for a sinusoidal current of small amplitude, it compares the numerical solutions with approximate analytical solutions valid to first order in the current amplitude. By using the numerical approach the specific mechanisms which play dominant roles in interface demarcation by current pulsing can be identified.

901,462 PB90-117334 Not available NTIS National Inst. of Standards and Technology (IMSE), Gaithersburg, MD. Reactor Radiation Div.
Comparison of Interplaner-Boson-Exchange
Models of High-Temperature Superconductivity -

Possible Experimental Tests.

Final rept. R. C. Casella. 1989, 3p

Pub. in Applied Physics Letters 55, n9 p908-910, 28 Aug 89.

Keywords: *Superconductivity, Bismuth inorganic compounds, Thallium inorganic compounds, Copper oxides, Comparison, Reprints, *High temperature superconductors, *Boson-exchange models, Cuprates.

Semiquantitative tests are considered of models in which high T(c) superconductivity follows from the exchange of unspecified intermediate bosons (IB) with omega >> omega(phonon) between fermionic pairs binegary of the dependence of T(c) (a) layers. Earlier predictions of the dependence of T(c) (n) on the number n of layers per cluster and extended to include the possibility that T(c) (n = 1) < about 10K in the TI1201 and 2201 compounds. In common with other authors rapid saturation of T(c)(n) with increasing n is found here. Nonetheless, the experimental value of T(c)(n=1) in the TI and Bi systems can play an important role in discriminating between the various models empirically.

901,463 PB90-117490 Not available NTIS National Inst. of Standards and Technology (NML), Gaithersburg, MD. Radiation Physics Div.
Structure of Cs on GaAs(110) as Determined by Scanning Tunneling Microscopy. Final rept.

Piria rept.
P. N. First, R. A. Dragoset, J. A. Stroscio, R. J.
Celotta, and R. M. Feenstra. 1989, 5p
Sponsored by Office of Naval Research, Arlington, VA.
Pub. in Jnl. of Vacuum Science and Technology A 7,
n4 p2868-2872 Jul/Aug 89.

Keywords: *Cesium, Monomolecular films, Gallium arsenides, Crystal structure, Absorption, Substrates, Reprints, *Surface structure, Scanning tunneling microscopy, Semiconductors, Room temperature.

Submonolayer coverages of Cs adsorbed at room temperature on the GaAs(110) surface are examined with scanning tunneling microscopy. Linear chains, formed by two adjoining rows of Cs atoms, are observed along the (1,-1,0) direction for coverages as low as 0.03 monolayer. The one-dimensional Cs chains are observed to be several hundred A long, and are seen in images of both the occupied and unoccupied electronic states. At higher coverages, approaching 0.15 monolayer, stable linear structures consisting of three neighboring Cs rows have been found.

901,464 PB90-117540 Not available NTIS National Inst. of Standards and Technology (IMSE), Boulder, CO. Fracture and Deformation Div. Reentrant Softening in Perovskite Superconductors.

Final rept. T. Datta, H. M. Ledbetter, C. E. Violet, C. Almasan, and J. Estrada. 1988, 4p Pub. in Physical Review B 37, n13 p7502-7505, 1 May

Keywords: *Superconductors, Elastic properties, Shear modulus, Acoustic velocity, Reprints, *High temperature superconductors, Yttrium barium cuprates, Barium yttrium cuprates, Lanthanum strontium cuprates.

A model of reentrant elastic softening is suggested that achieves three useful results. First, and principally, it reconciles existing sound-velocity-elastic-constant measurements with thermodynamics. Second, it leads to Debye characteristic temperatures that agree with those from specific-heat and phonon density-of-states determinations. Third, it links elastic-constant-temperature behavior in Y-Ba-Cu-O and La-Sr-Cu-O. The model predicts a superconducting-state elastic stiffness lower than the normal state.

901.465

PB90-117615 Not available NTIS National Inst. of Standards and Technology (IMSE), Boulder, CO. Fracture and Deformation Div. Gruneisen Parameter of Y1Ba2Cu3O7. Final rept.

H. Ledbetter. 1989, 3p Pub. in Physica C 159, p488-490 1989.

Keywords: *Superconductors, Bulk modulus, Elastic properties, Reprints, *High temperature superconductors, *Yttrium barium cuprates, *Barium yttrium cu-

prates, *Gruneisen constant. Contrary to reports that the Gruneisen parameter of Y1Ba2Cu3O7 is approximately 3.0, the author argues

that the parameter is approximately 1.5., a value consistent with metal oxides. The author offers three argusistent with metal oxides. The author offers three arguments. One depends on a lower bulk modulus (B), near 101 GPa, than found in high-pressure X-ray diffraction studies, which yield bulk-modulus values up to 200 GPa. The second depends on an ionic-crystal-model calculation of the Gruneisen parameter. The third depends on the Anderson-Gruneisen parameter determined by measuring dB/dT.

901.466

PB90-117789 Not available NTIS National Inst. of Standards and Technology (IMSE), Gaithersburg, MD. Reactor Radiation Div. Magnetic Structure of Cubic Tb0.3Y0.7Ag.

Final rept.

J. A. Gotaas, M. R. Said, J. S. Kouvel, and T. O. Brun. 1988, 2p See also DE89-005783. Pub. in Jnl. de Physique 49, n12 pC8-1103-C8-1104

Keywords: Phase transformations, Terbium alloys, Yttrium alloys, Silver alloys, Cryogenics, Reprints, *Antiferromagnetic materials, Spin glass, Cubic lattices.

Tb(0.3)Y(0.7)Ag undergoes a magnetic phase transi-tion at about 36 K to an antiferromagnetic structure which neutron diffraction has shown to have two components. A commensurate antiferromagnetic component is similar to the (pi pi 0) structure found in TbAg, but with a correlation range of only 42 A at 4 K while an incommensurate modulated component is like that found in HoAg, but with a finite correlation range of 290

901,467

PB90-118019 Not available NTIS National Inst. of Standards and Technology (NML), Gaithersburg, MD. Radiation Physics Div.
Influence of the Surface on Magnetic Domain-Wall

Microstructure. Final rept.

M. R. Scheinfein, J. Unguris, R. J. Celotta, and D. T. Pierce. 1989, 4p Sponsored by Office of Naval Research, Arlington, VA. ub. in Physical Review Letters 63, n6 p668-671, 7 Aug 89.

Keywords: *Magnetic domains, Microstructure, Surfaces, Permalloys, Iron, Reprints, *Domain walls, Magnetic films, Scanning electron microscopy.

The magnetization orientations in domain walls at the surfaces of an Fe crystal, a ferromagnetic glass, and a Permalloy film, measured by scanning electron microscopy with polarization analysis, exhibit asymmetric surface Neel wall profiles which are at least twice as wide as interior Bloch walls in bulk and are described quantitatively by the authors' micromagnetic calculations without assuming any special surface parameters. Mis-interpretation of domain-wall widths, Bitter patterns, and magnetic-force-microscopy images can result from overlooking the extreme effect of the surface on magnetic microstructure.

901.468

PB90-123480 Not available NTIS National Inst. of Standards and Technology (IMSE), Gaithersburg, MD. Ceramics Div. Neutron Study of the Crystal Structure and Vacancy Distribution in the Superconductor Ba2Y Cu3 O(sub g-delta).

Final rept Beech, S. Miraglia, A. Santoro, and R. S. Roth.

1987, 4p Pub. in Physical Review B 35, n16 p8778-8781, 1 Jun

Keywords: *Superconductors, *Crystal structure, Keywords: "Superconductors, "Crystal structure, "Vacancies(Crystal defects), Orthorhombic lattices, Neutron diffraction, Oxygen, Cryogenics, Reprints, "High temperature superconductors, "Banum yttnum cuprates, "Yttrium banum cuprates, Room tempera-

Two samples of the high temperature superconductor Ba2YCu3O(g-delta) with delta=2.0 and 2.2, have been studied at row temperature and at 10K, with the neutron powder diffraction method and profile analysis. The structure of the compound is orthorhombic. In the compound with delta=2.0 all oxygen sites are fully occupied. When delta=2.2 there are oxygen vacancies, but these are confined to one set of positions only, specifically to the oxygen atoms of the chains, located on the b-axis. No detectable change of the structure has been observed between room and low temperature.

901,469 PB90-123613 Not available NTIS National Inst. of Standards and Technology (IMSE), Gaithersburg, MD. Ceramics Div. Bulk Modulus and Young's Modulus of the Super-conductor Ba2Cu3Y07.

Final rept. Wong-Ng. 1987, 5p Pub. in Advanced Ceramic Materials 2, n3B p601-605

Keywords: *Bulk modulus, *Modulus of elasticity, *Superconductors, *Barium oxides, *Copper oxides, *Yttrum oxides, *Ceramics, X ray diffraction, Isotherms, Equations of state, Compressibility, Reprints

The isothermal equation of state of the high tempera-ture superconducting ceramic material Ba2Cu3YO7 has been measured in a diamond anvil pressure cell using an energy dispersive x-ray diffraction method. The unit cell lattice parameters (a,b,c) were found to have compressions of (2.0%, 2.3%, 1.1%), respectively over the pressure range from one atmosphere to 10.6 GPa at room temperature. Subsequent equation of state analysis of the approximately linear compression of the volume determined that the isothermal bulk modulus was 196 + or - 17 GPa. Young's modulus was estimated to be 235 + or - 20 GPa assuming that the Poisson's ratio for Ba2Cu3YO7 was 0.3, which is beined of more compressions. typical of many ceramics.

901.470 PB90-123662 Not available NTIS National Inst. of Standards and Technology (IMSE), Gaithersburg, MD. Reactor Radiation Div. Characterization of Structural and Magnetic Order of Er/Y Superlattices. Final rept.

W. Erwin, and J. J. Rhyne. 1988, 4p Pub. in Superlattices and Microstructures 4, n4 pt5 p439-442 1988.

Keywords: *Erbium, *Ytterbium, Phase transforma-tions, Neutron diffraction, Reprints, *Superlattices, Molecular beam epitaxy, Magnetic ordening, Multi-

Coherent, crystalline superlattices of erbium and yttnum have been prepared by molecular beam epitaxy techniques. Magnetometer measurements indicate that the transition temperatures for the superlattices are significantly lower than those for pure erbium. The ferromagnetic phase observed in erbium is completely supressed. Neutron diffraction studies show that the periodic magnetic order of Er propagates through the Y layers, but has a temperature independent magnetic wavelength. These results suggest that the erbium magneto-elastic energy has been altered in the superlattice samples.

901.471 PB90-123803 Not available NTIS National Inst. of Standards and Technology (IMSE), Gaithersburg, MD. Reactor Radiation Div.

Magnetic Order of Pr in PrBa2Cu3O7.

Final rept. W. H. Li, J. W. Lynn, S. Skanthakumar, T. W. Clinton, A. Kebede, C. S. Jee, J. E. Crow, and T. Mihalisin. 1989, 4p

Pub. in Physical Review B 40, n7 p5300-5303, 1 Sep

Keywords: Specific heat, Neutron diffraction, Magnetic moments, Reprints, *Praseodymium banum cuprates, *Barium praseodymium cuprates, *Magnetic ordering, *Praseodymium ions, Magnetic susceptibility, Antiferromagnetic materials.

The magnetic order of Pr in nonsuperconducting PrBa2CuO7 has been studied by specific-heat, susceptibility, and neutron-diffraction measurements. The basic ordering consists of a simple antiferromagnetic arrangement, with a saturated moment of 0.74 (mu sub s) and a Neel temperature T(N) of about 17 K, which is two orders of magnitude higher than expected from either dipolar or Rudeman-Kittel-Kasuya-Yosida interactions alone. The small moment, along with the large value of the low-temperature electronic specific-heat coefficient gamma of 196 mJ/mole(K squared), suggests that there is substantial f-electron character at the Fermi level.

901,472 PB90-123829 Not available NTIS National Inst. of Standards and Technology (IMSE), Gaithersburg, MD. Reactor Radiation Div.

Pressure Dependence of the Cu Magnetic Order In RBa2Cu3O6+x.

Final rept. J. W. Lynn, W. H. Li, S. F. Trevino, and Z. Fisk. 1989. 4p

Pub. in Physical Review B 40, n7 p5172-5175, 1 Sep

Keywords: Neutron diffraction, Neel temperature, Reprints, *Neodymium banum cuprates, *Barium neodymium cuprates, *Magnetic ordering, *Copper ions, Pressure dependence, Antiferromagnetic materials, High temperature superconductors.

Neutron-diffraction measurements have been carried out as a function of hydrostatic pressure to study the magnetic order of the Cu spins in NdBa2Cu3O(6.35) and NdBa2Cu3O6.1). In the high-temperature phase, where the Cu planes order antiferromagnetically, it is found that the Neel temperature T(N1) is very strongly dependent on pressure, increasing at the rate of about 23 K/kbar. The authors attribute this phenomenal sensitivity to the two-dimensional-like behavior of this magnetic system. In the low-temperature phase, which is associated with magnetic ordering of the chains, only a small change in the ordering temperature T(N2) is observed.

901,473 PB90-123878 Not available NTIS National Inst. of Standards and Technology (NML), Boulder, CO. Quantum Physics Div. Initial Stages of Heteroepitaxial Growth of InAs on

SI(100).

D. J. Oostra, R. V. Smilgys, and S. R. Leone. 1989,

Sponsored by Air Force Office of Scientific Research, Bolling AFB, DC. Pub. in Applied Physics Letters 55, n13 p1333-1335, 25 Sep 89.

Keywords: *Indium arsenides, Silicon, Substrates, Adsorption, Desorption, Reprints, *Epitaxial growth, Auger electron spectroscopy, Laser induced fluorescence, Semiconductor materials.

Adsorption and desorption of In on partially and fully As-terminated Si(100) are investigated by laser-in-duced fluorescence detection and Auger electron spectroscopy using the methods of temperature pro-grammed desorption and isothermal desorption. Desorption measurements show that As is bound to the surface more strongly than In. For In, a 2/3 order kinetic desorption mechanism is observed. This and Si auger intensity attenuation measurements indicate a strong tendency for In to form three-dimensional is-lands on the As-terminated surface. The activation energy for In diffusion from the islands ranges from 1.5 to 1.9 eV, depending on the As coverage. The results have important implications for growth of InAs on Si(100).

901,474 PB90-128133 Not available NTIS National Inst. of Standards and Technology (NEL), Boulder, CO. Electromagnetic Technology Div. Offset Criterion for Determining Superconductor Critical Current.

Final rept. J. W. Ekin. 1989, 3p

Pub. in Applied Physics Letters 55, n9 p905-907, 28 Aug 89.

Keywords: *Superconductors, Standards, Criteria, Reprints, *Critical current, High temperature superconductors.

Critical-current criteria based on electric field or resistivity can present a number of problems in defining critical current, especially for high T(c) superconductors in the vicinity of the critical temperature or upper critical field. The resulting critical-current density J(c) can be quite arbitrary, since it depends strongly on criterion level at high fields and temperatures. These J(c) definitions also create problems in distinguishing between superconductors and high-conductivity normal metals such as copper. They can also bias J(c) data when superconductors are compared that have different values of normal-state resistivity. To minimize these problems, an intrinsic J(c) criterion is proposed, which effectively separates superconducting and normalstate properties. Based on the long-standing concept of a flux-flow resistivity, J(c) is defined as the current where the tangent to the E-J curve at a given electric field level extrapolates to zero electric field. This determines an offset J(c) that minimizes the above problems. The criterion is particularly useful near T(c) or near the effective upper critical field where the E-J characteristic starts to approach ohmic behavior.

901,475 PB90-128216 Not available NTIS National Inst. of Standards and Technology (NML), Gaithersburg, MD. Surface Science Div. Direct Observation of Surface-Trapped Diffracted Waves.

Final rept T. Jach, D. B. Novotny, M. J. Bedzyk, and Q. Shen.

1989, 4p Pub. in Physical Review B 40, n8 p5557-5560, 15 Sep

Keywords: *X ray diffraction, Surface roughness, Germanium, Interfaces, Reprints, Grazing incidence.

The authors have made the first direct observation of a diffracted x-ray beam that occurs only at an interface in the grazing-angle diffraction geometry. The beam, which is unable to propagate into the bulk of either component of the interface, was detected at the surface of a Ge crystal. A roughened area etched into the surface permitted phase matching to a beam in the vacuum. The diffracted beam that is observed to escape in this configuration shows a wave-vector dependence that cannot be qualitatively explained by purely kinematic models of scattering from rough surfaces.

901,476 PB90-128240 Not available NTIS National Inst. of Standards and Technology (NML), Gaithersburg, MD. Radiation Physics Div. Vector Imaging of Magnetic Microstructure. Final rept.

M. H. Kelley, J. Unguris, M. R. Scheinfein, D. T. Pierce, and R. J. Celotta. 1989, 6p Pub. in Microbeam Analysis - 1989, p391-396 1989.

Keywords: *Magnetic domains, Whiskers(Single crystals), Microstructure, Polarization(Spin alignment), Cobalt, Iron, Reprints, *Imaging techniques, Electron spin polarization.

An ability to study the properties of microscopic mag-netic structures and to investigate magnetic properties with submicron spatial resolution is important both for with submicron spatial resolution is important both for its fundamental scientific value and its usefulness in applied magnetic technology. Many current tech-niques for the investigation of magnetic structures suffer either from poor spatial resolution or from the inability clearly to separate contrast due to magnetic structures from that due to topographic or other physical features. The authors describe a method of magnetic imaging that overcomes many of the difficulties of other current techniques and that allows quantitative analysis at high spatial resolution of the vectorial properties of sample magnetization.

901,477 PB90-130261

PC A03/MF A01

National Inst. of Standards and Technology (NEL), Gaithersburg, MD. Applied and Computational Mathe-

Effect of a Crystal-Melt Interface on Taylor-Vortex Flow.

G. B. McFadden, S. R. Coriell, B. T. Murray, M. E. Glicksman, and M. E. Selleck. Oct 89, 22p NISTIR-89/4192

Prepared in cooperation with Rensselaer Polytechnic Inst., Troy, NY. Dept. of Materials Engineering.

Keywords: *Crystal growth, *Hydrodynamics, Solidification, Morphology, Stability, Couette flow, Taylor instability

The linear stability of circular Couette flow between concentric infinite cylinders is considered for the case that the stationary outer cylinder is a crystal-melt inter-face rather than a rigid surface. A radial temperature difference is maintained across the liquid gap, and equations for heat transport in the crystal and melt phases are included to extend the ordinary formulation of the problem. The stability of the two-phase system depends on the Prandtl number. For small Prandtl number the linear stability of the two-phase system is given by the classical results for a rigid-walled system. For increasing values of the Prandtl number, convective heat transport becomes significant and the system becomes increasingly less stable. Previous results in a narrow-gap approximation are extended to the case of a finite gap, and both axisymmetric and non-axisymmetric disturbance modes are considered. The twophase system becomes less stable as the finite gap tends to the narrow-gap limit. The two-phase system is more stable to non-axisymmetric modes with azimuthal wavenumber n=1; the stability of these n=1 modes is sensitive to the latent heat of fusion.

901.478 PB90-136706 Not available NTIS National Inst. of Standards and Technology (IMSE), Gaithersburg, MD. Reactor Radiation Div. Mn-Mn Exchange Constants In Zinc-Manganese

Chalcogenides.

Final rept. T. M. Giebultowicz, J. J. Rhyne, and J. K. Furdyna. 1987, 3p

Pub. in Jnl. of Applied Physics 61, n8 pt2A p3537-3539, 15 Apr 87.

Keywords: Neutron scattering, Inelastic scattering, Single crystals, Polycrystalline, Reprints, *Magnetic semiconductors, *Antiferromagnetic materials, *Manganese zinc sulfides, *Manganese zinc selenides, Manganese zinc tellurides, Exchange interactions.

Excited levels of isolated nearest-neighbor Mn-Mn pairs in Zn(1-x)Mn(x)S, Zn(1-x)Mn(x)Se, and Zn(1-x)Mn(x) x)Mn(x)Te have been studied by inelastic neutron scattering. The measurements have been carried out on several single crystal and polycrystalline samples with x = or < 0.05 at various temperatures. Values obtained for the exchange constants 2J(NN) are -2.78, -2.12, and -1.64 meV for the three studied systems, respectively.

901,479 PB90-136714 Not available NTIS National Inst. of Standards and Technology (IMSE), Rational flist. Of Standards and February (MSE), Gaithersburg, MD. Reactor Radiation Div. Neutron Diffraction Study of the Wurtzite-Struc-ture Dilute Magnetic Semiconductor Zn0.45Mn0.55Se. Final rept. T. M. Giebultowicz, J. J. Rhyne, J. K. Furdyna, and

U. Debska. 1987, 3p Pub. in Jnl. of Applied Physics 61, n8 pt2A p3540-3542, 15 Apr 87.

Keywords: Neutron diffraction, Reprints, *Magnetic semiconductors, *Manganese zinc selenides, *Antiferromagnetic materials, Magnetic ordering, Exchange interactions.

First results are reported of neutron diffraction studies First results are reported of neutron diffraction studies of magnetic ordering phenomena in a wurtzite-structured diluted magnetic (semimagnetic) semiconductor Zn(0.45)Mn(0.55)Te. At low temperatures the system exhibits a short-range antiferromagnetic ordering, closely related to the antiferromagnetic structure seen in the wurtzite form of beta-MnS. This type of ordering indicates short-range and artiferromagnetic solvities. indicates short-range and antiferromagnetic only inter-actions between the Mn spins, in agreement with present theories of exchange mechanism in DMS ma-terials. Similarly as in cubic DMS systems, the magnet-

PHYSICS

Solid State Physics

ic correlation range in Zn(0.45)Mn(0.55)Te exhibits a pronounced anisotropy.

901,480 PB90-136748 Not available NTIS National Inst. of Standards and Technology (NEL), Boulder, CO. Electromagnetic Technology Div. Critical Current Measurements of Nb3Sn Superconductors: NBS (National Bureau of Standards)
Contribution to the VAMAS (Versallies Agreement
on Advanced Materials and Standards) Interlaboratory Comparison.

Final rept. L. F. Goodrich, and S. L. Bray. 1989, 11p Sponsored by Department of Energy, Washington, DC. Pub. in Cryogenics 29, p699-709 Jul 89.

Keywords: *Superconductors, Electrical measurement, Reprints, *Niobium stannides, *Critical current, Interlaboratory comparisons, Comparative evaluations, VAMAS.

Critical current measurements on several Nb3Sn superconductors were made as part of an interlaboratory companson (round robin). These measurements were made in conjunction with twenty-four laboratories from the European Economic Community, Japan and the USA as part of the Versailles Agreement on Advanced Materials and Standards (VAMAS). The results of the NBS measurements, including the effect of sample mounting techniques on the measured critical current, are niver. are given. A systematic study of the effect of measure-ment mandrel (tubular sample-holder made from G10 ment manufer (ubular sample-holder made from G1) fiberglass-epoxy composite) geometry revealed that a seemingly small change in that geometry can result in a 40% change in the measured critical current at a magnetic field of 12 T. Specifically, the radial thermal contraction of the measurement mandrel depends on the send that the contraction of the measurement mandrel depends on its wall thickness and, thus, so does the conductor prestrain (at 4 K) and, ultimately, the measured critical current. Techniques for reducing variation in the measured critical current are suggested.

Structural Mechanics

901 481 PB89-157788 Not available NTIS National Bureau of Standards (IMSE), Boulder, CO.

Fracture and Deformation Div.

Conventional and Quarter-Point Mixed Elements In Linear Elastic Fracture Mechanics.

P. R. Heyliger. 1988, 15p
Pub. in Engineering Fracture Mechanics 31, n1 p157-

Keywords: *Finite element analysis, Displacement, Stress analysis, Numerical analysis, Stiffness methods, Elastic analysis, Reprints, *Elastic fracture mechanics, Quarter-point element, Stress intensity factor, J-integral technique.

The numerical performance of conventionally configured and quarter-point mixed elements is examined for planar problems in linear elastic fracture mechanics. Because of the independent approximations of the displacement and stress components characteristic of the mixed formulation, the shifting of a mid-side node of an element to the quarter-point results in a singular strain but a finite stress at the corner node. For the example problems considered, the conventional and quarter-point mixed elements provide lower and upper bounds, respectively, for the strain energy of a cracked body. Mode I stress intensity factors are computed for several representative geometries using the crack extension, stiffness derivative and J-integral techniques. The quarter-point elements yield superior results only for the J-integral technique, with each of the three techniques giving excellent results for very coarse mesh configurations.

901.482 PB89-157903 Not available NTIS National Bureau of Standards (IMSE), Gaithersburg, MD. Metallurgy Div. Elastic Interaction and Stability of Misfitting Cubol-

dal Inhomogeneities. Final rept.

W. C. Johnson, and P. W. Voorhees. 1987, 10p Pub. in Jnl. of Applied Physics 61, n4 p1610-1619

Keywords: *Elastic analysis, *Stability, Energy methods, Matrix methods, Elastic properties, ods, Matrix methods, Elastic properties, Plates(Structural members), Precipitates, Heterogeneity, Reprints.

The elastic interaction energy between several rectangular parallel-epipeds and the elastic self energy of a cuboid are calculated to first-order in the difference in elastic constants between the precipitate and matrix. The system is assumed to be isotropic and the precipitates to possess a dilatational misfit. The functionality and magnitude of the interaction energy per precipitate is extremely sensitive to the precipitate morphology and number of precipitates considered. The interaction energy between three or more precipitates cannot be accurately estimated by summing the pairwise interactions. The influence of the interaction energy on the stability of precipitate arrays is discussed.

901,483

PB89-166110 PC A03/MF A01 National Inst. of Standards and Technology (NEL), Gaithersburg, MD. Center for Building Technology. Method to Measure the Tensile Bond Strength between Two Weakiy-Cemented Sand Grains.
L. I. Knab, and N. E. Waters. Nov 88, 41p NISTIR-

Sponsored by Air Force Weapons Lab., Kirtland AFB,

Keywords: *Bonding strength, *Sands, *Tension tests, Adhesive strength, Bonding, Cements, Grain structure, Tensile strength, Breaking load, Tensile stress.

A method to measure the tensile bond strength between two weakly-cemented sand grains was developed. Special microloading testing equipment was developed to measure the force required to pull apart two sand grains. To illustrate the method, bond strengths were measured in tension for six pairs of cemented sand grains. A wide range in the bond failure stress occurred and was attributed primarily to (a) difficulties in identifying and measuring the actual bond failure surface area and, (b) eccentricity in the specimens during loading. The method developed is seen as a starting point and can be used as a basis for further development. Improved techniques need to be devel-oped to identify and measure the actual bond failure surface area and to reduce, or at least measure and account for, the eccentricity introduced.

901,484

PB89-229124 Not available NTIS National Bureau of Standards (IMSE), Boulder, CO. Fracture and Deformation Div. Higher Order Beam Finite Element for Bending and Vibration Problems.

Final rept.

P. R. Heyliger, and J. N. Reddy. 1988, 18p Pub. in Jnl. of Sound and Vibration 126, n2 p309-326

Keywords: *Beams (Supports), *Finite element analysis, Vibration, Bending, Shear properties, Deformation, Reprints, Timoshenko beams, Rectangular configuration, Numerical solution.

The finite element equations for a variationally consistent higher order beam theory are presented for the static and dynamic behavior of rectangular beams. The higher order theory correctly accounts for the stress-free conditions on the upper and lower surfaces of the beam while retaining the parabolic shear strain distribution. The need for a shear correction coefficient is therefore eliminated. Full integration of the shear stiffness terms is shown to result in the recovery of the Kirchoff constraint for thin beams without introducing spurious locking constraints. The accuracy of this formulation is demonstrated by using several numerical examples for the cases of small and large displacements. For a hinged-hinged beam, the linear thickness-shear mode frequency can be matched with the Timoshenko frequency to yield a shear coefficient of 0.824. Matching the bending frequencies between the two theories indicates a shear coefficient for the Timoshenko theory that changes with mode number and slenderness ratio. The influence of in-plane inertia and slenderness ratio on the non-linear frequency is examined for beams with a number of different support con-

General

901,485

PB89-147466 Not available NTIS National Bureau of Standards (IMSE), Gaithersburg, MD. Reactor Radiation Div.
Use of Multiple-Slot Multiple Disk Chopper Assem-

blies to Pulse Thermal Neutron Beams.

Final rept.
J. R. D. Copley. 1988, 10p
Pub. in Nuclear Instruments and Methods in Physics
Research A273, p67-76 1988.

Keywords: *Neutron beams, *Thermal neutrons, Neutron scattering, Reprints, *Neutron choppers, Time-of-flight method, High resolution.

Single-slot disk choppers are commonly used to pulse thermal neutron beams, but their use in high resolution applications is limited because the maximum transmitted beam intensity, given that the chopper is rotating at its maximum possible speed, is proportional to the square of the burst time of the chopper, which is itself proportional to the width of the incident beam. The transmitted intensity can be doubled, with no associated transmitted intensity can be doubled, with no associated increase in the burst time, by doubling the beam width and using counter-rotating choppers to double the effective chopping speed. In order to increase the intensity still further, without degrading the resolution, the author proposes the use of multiply-slotted choppers in combination with a multiply-slotted beam mask, the intensity is four times that of the single-slot single chopper arrangement. A further doubling is achieved if a system of three choppers and a mask, each fitted with four slots, is employed. The effects of relative phasing errors in multiple chopper systems are examphasing errors in multiple chopper systems are examined in detail, and the implications of nonzero chopper separation and nonzero radial slot extent are briefly discussed.

901,486 PB89-149124 Not available NTIS National Bureau of Standards (NML), Gaithersburg, MD. Center for Radiation Research. QCD Vacuum.

Final rept.

M. Danos. 1987, 15p
Pub. in Proceedings of NATO (North Atlantic Treaty
Organization) Advanced Study Institute, Maratea, Italy, June 1-4, 1986, p817-831 1987.

Keywords: Quantum electrodynamics, *Quantum chromodynamics, Bose-Einstein condensation, Quasi particles, Vacuum.

QCD is inherently a strong-field system in the infrared. GCD is inherently a strong-field system in the infrared. Hence the physical vacuum itself without external charges is already non-perturbatively polarized, it has an energy density lower than that of the QED-type so-called perturbative vacuum by the amount of the 'bag energy density.' It will be shown that the physical vacuum can be described by an analogue of the BCS-state of superconductivity. This vacuum exhibits color confinement. confinement.

901,487 PB89-149157 Not available NTIS National Bureau of Standards (NEL), Gaithersburg, MD. Fire Science and Engineering Div. Evaporation of a Water Droplet Deposited on a Hot High Thermal Conductivity Solid Surface.

Final rept. M. di Marzo, and D. D. Evans. 1987, 8p See also PB86-247871

Pub. in Proceedings of National Heat Transfer Conference and Exhibition, Heat and Mass Transfer in Fire, (24th), Pittsburgh, PA., August 9-12, 1987, p11-18.

Keywords: *Evaporative cooling, *Drops(Liquids), Thermal conductivity, Thermal diffusivity, Heat transfer, Heat flux, Spray queaching, Models, Interfacial temperature, Semi-infinite body, Molar fraction.

A model is presented that predicts major features of the evaporation of water droplets deposited on a hot non-porous solid surface. In the temperature range of interest, nucleate boiling heat transfer is fully sup-pressed, hence the model is only concerned with the evaporative process. In the model, the solid material is assumed to have high thermal conductivity and diffusi-vity, so that the surface temperature under the water droplet can be considered uniform. The temperature of this portion of a larger solid surface covered by the

liquid is calculated from the classic solution for contact temperature between two semi-infinite bodies. The liquid-vapor interfacial temperature and the watervapor molar fraction in the air at the exposed surface of the water droplet are deduced from the coupled heat and mass transfer energy balance at the interface. Spatial and temporal integration of the overall droplet energy equation is used to predict the droplet evaporation time and the instantaneous evaporation rate. Model predictions for the total evaporation time and temporal variation of the droplet volume agree well with experiments performed using a heated aluminum block.

901.488 PB89-149249 Not available NTIS National Bureau of Standards (NEL), Gaithersburg, MD. Fire Measurement and Research Div. Cooling Effect Induced by a Single Evaporating

Droplet on a Semi-infinite Body. Final rept.

M. di Marzo, and D. D. Evans. 1987, 4p
Pub. in Proceedings of Fall Technical Meeting on
Chemical and Physical Processes in Combustion, San
Juan, PR., December 15-17, 1986, p23.1-23.4 1987.

Keywords: *Heat transfer, *Drops(Liquids), Evaporation, Water, Research projects, *Cooling effect, Solid fuels, Hot metal surfaces, Semi-infinite body.

The publication is an extended abstract of work performed to model the evaporation process of a water droplet deposited on a hot metal surface. This work is the first phase of an extensive research program aimed at developing accurate droplet cooling models of burning solid fuel surfaces.

901.489 PB89-153878 PC A09/MF A01 National Inst. of Standards and Technology (NML), Boulder, CO. Time and Frequency Div. Trapped Ions and Laser Cooling 2: Selected Publi-

cations of the ion Storage Group, Time and Frequency Division, NiST, Boulder, CO.

Quency Division, NIS1, Boulder, CO.
Technical note.
D. J. Wineland, W. M. Itano, J. C. Bergquist, and J. J.
Bollinger. Oct 88, 198p NIST/TN-1324
Also available from Supt. of Docs. as SN003-00302918-1. See also PB86-110855. Sponsored by Office
of Naval Research, Arlington, VA., and Air Force Office
of Scientific Research, Bolling AFB, DC.

Keywords: *Frequency standards, *Atomic spectroscopy, Time standards, Atomic clocks, *lon traps, *Laser cooling, Laser spectroscopy, Trapping(Charged particles), Quantum jumps, Re-

The technical note is a collection of selected reprints of the Ion Storage Group for the period July 1985 to September 1988. Major topics include the following: Spectroscopy and frequency standards; Quantum jumps; Nonneutral plasma studies; General articles; Apparatus.

PB89-156988 Not available NTIS National Bureau of Standards (NEL), Gaithersburg, MD. Electrosystems Div.

Effect of an Oli-Paper Interface Parallel to an Electric Field on the Breakdown Voitage at Elevated Temperatures.

Final rept.
E. F. Kelley, R. E. Hebner, W. E. Anderson, J. A. Lechner, and J. L. Blue. 1988, 11p
Sponsored by Department of Energy, Washington, DC.
Pub. in IEEE (Institute of Electrical and Electronics En gineers) Transactions on Electrical Insulation 23, n2 p249-259 Apr 88.

Keywords: *Electrical faults, *Interfaces, Insulating oil, Weibull density functions, Reprints, *Breakdown, Paper(Material), Finite element method.

The paper reports the measurement of the electrical breakdown location in the vicinity of an oil-paper inter-face over the temperature range from room tempera-ture to 150 deg C. The data indicated that the electrical breakdown occurred at the interface from 15% to 43% of the time, depending on the details of the particular set of measurements. A theoretical analysis shows that this experimental result is consistent with the electric field enhancement, the area over which the en-hancement occurs, and the spread in the breakdown voltages for nominally identical tests.

901,491 PB89-157002 Not available NTIS National Bureau of Standards (NML), Gaithersburg, MD. Electricity Div. U.S. Perspective on Possible Changes in the Electrical Units.

Final rept.

K. Jaeger, and B. N. Taylor. 1987, 4p Pub. in IEEE (Institute of Electrical and Electronics Engineers) Transactions on Instrumentation and Measurement IM-36, n2 p672-675 Jun 87.

Keywords: *Units of measurement, *Electrical potential, *Electrical resistance, Standards, Electrical measurement, Reprints.

The paper summarizes the U.S. view regarding possible changes in the U.S. legal units of voltage and resistance. Such changes, about 9 and 1.5 ppm respectively, would result if the Consultative Committee on Electricity adopted a new value for the Josephson freedom of the quency-voltage ratio and a value for the quantized Hall resistance consistent with the SI and these values were used internationally for defining and maintaining national units of voltage and resistance.

Not available NTIS
National Bureau of Standards (NEL), Boulder, CO.
Electromagnetic Technology Div.
Current Ripple Effect on Superconductive D.C.
Critical Current Measurements.
Final rept. 901.492

Final rept.

L. F. Goodrich, and S. L. Bray. 1988, 7p Sponsored by Department of Energy, Washington, DC. Office of Fusion Energy. Pub. in Cryogenics 28, p737-743 Nov 88.

Keywords: *Superconductors, Titanium alloys, Direct current, Alternating current, Power supplies, Electro-magnetic noise, Reprints, *Critical current, Niobium alloys, Ripples.

The effect of current ripple or noise on d.c. critical current measurements was systematically studied. Measurements were made on multifilamentary Nb-Ti superconductor. A low-noise, battery-powered current supply was required in the study in order to make the pure d.c. critical current measurements. Also, an elec-tronic circuit that stimulates a superconductor's gener-al current-voltage characteristic was developed and used as an analysis tool. In order to make critical current measurements in which current ripple was present, the battery supply was modified to allow the introduction of controlled amounts of a.c. ripple. The results of this work are general and quantitatively applicable to the evaluation of critical current data and measurement systems. A theoretical model was developed to further support and explain the ripple effect.
An unexpected benefit of this work was a more precise method for general critical current data acquisition. Problems common to all large conductor critical current measurements are discussed.

901,493 PB89-157408 Not available NTIS National Bureau of Standards (NML), Boulder, CO. Time and Frequency Div.
Perpendicular Laser Cooling of a Rotating ion
Plasma in a Penning Trap.

Final rept.

W. M. Itano, L. R. Brewer, D. J. Larson, and D. J.

Wineland, 1988, 9p Sponsored by Office of Naval Research, Arlington, VA., Air Force Office of Scientific Research, Washing-ton, DC., and National Science Foundation, Washington, DC.

Pub. in Physical Review A 38, n11 p5698-5706, 1 Dec

Keywords: Temperature measurement, Reprints, *Beryllium ions, Beryllium 9, Laser cooling, Penning traps, Ion storage.

The steady-state temperature of an ion plasma in a Penning trap, cooled by a laser beam perpendicular to the trap axis, has been calculated and measured. The rotation of the plasma, due to crossed E and B fields, strongly affects the minimum attainable temperature. This is because the velocity distribution of the ions, as seen by a laser beam intersecting the plasma at some distance from the axis of rotation, is skewed, and this leads to a change in the velocity distribution (and hence temperature) at which a steady state is attained. The calculated temperature is a function of the intensi-

ty, frequency, and position of the laser beam, and of the rotation frequency of the plasma. Temperatures of (9)Be(1+) plasmas were measured for a wide range of experimental parameters. The lowest and highest temperatures were approximately 40 mK and 2 K. The measured and calculated temperatures are in agree-

PB89-157424 Not available NTIS
National Bureau of Standards (NML), Boulder, CO.
Time and Frequency Div.
Atomic-lon Coulomb Clusters in an Ion Trap. Atomic-Ion Coulomb Clusters in an Ion Trap. Final rept.
D. J. Wineland, J. C. Bergquist, W. M. Itano, J. J. Bollinger, and C. H. Manney. 1987, 4p
Sponsored by Office of Naval Research, Arlington, VA., and Air Force Office of Scientific Research, Washington, DC.
Pub. in Physical Review Letters 59, n26 p2935-2938, 28 Dec 87.

28 Dec 87.

Keywords: Atomic spectroscopy, Reprints, *Mercury ions, Ion traps, Laser cooling, Ion storage, Wigner crystallization.

Small numbers of laser-cooled Hg(1+) ions, which are confined in a Pual radio-frequency ion trap, to crystallize into regular arrays or clusters were observed. The structure of these clusters was investigated by direct imaging, optical spectroscopy, and numerical calcula-tions. The spectroscopy of such 'pseudomolecules' is unique in that individual atoms of the molecule can be probed separately. The ratio of Coulomb potential energy per ion to k(B)T in these clusters is observed to be as high as 120.

PB89-157895 Not available NTIS National Bureau of Standards (NEL), Gaithersburg, MD. Precision Engineering Div.
Electromagnetic Pulse Scattered by a Sphere.

Final rept.

E. Marx. 1987, 6p Pub. in IEEE (Institute of Electrical and Electronics Engineers) Transactions on Antennas and Propagation 35, n4 p412-417 1987.

Keywords: *Electromagnetic pulses, *Electromagnetic scattering, Integral equations, Magnetic fields, Spheres, Reprints, Transient radiation effects.

The magnetic field integral equation for transient electromagnetic scattering by a perfectly conducting sphere is solved by the stepping-in-time procedure. The contribution of the self-patch, where the integrand is singular, and of the neighboring patches to the surface current density are computed separately from the contributions of other patches to correct for inaccuracies. The term of the integrand with the time-derivative of the current density is shown to make a contribution to these corrections that cannot be neglected in calcu-lating the initial (small) values of the surface current density. The improvement in the values of the scat-tered fields due to these corrections is significant but not dramatic.

901.496 PB89-158109 Not available NTIS National Bureau of Standards (NML), Gaithersburg, MD. Atomic and Plasma Radiation Div. Calculation of Tighter Error Bounds for Theoretical Atomic-Oscillator Strengths.

Final rept.

D. V. I. Roginsky, and A. W. Weiss. 1988, 7p Pub. in Physical Review A 38, n4 p1760-1766, 15 Aug

Keywords: Hartree-Fock approximation, Electron transitions, Transition probabilities, Lithium, Sodium, Reprints, *Oscillator strengths, Beryllium ions, Magnesium ions.

The authors report a series of calculations of error bounds to the Hartree-Fock approximation for the 2s-2p and 3s-3p transitions in lithium and sodium, and the singly ionized ions Be(1+) and Mg(1+). The purpose is to test the efficacy of various modifications of Weinhold's effective-bounds formula for several simple but realistic examples of multielectron systems. The authors therefore assume the overlap error epsilon to be known, adopting overlap values from extensive variational calculations. The authors find angular momentum projection of the transition operator to be effective in tightening the bounds, while the variational optimiza-

tion of a mixture of length and velocity operators is not. The authors also found a wave-function projection based on Brillouin's theorem to be especially effective. When used in conjunction with angular momentum projection, this last procedure has yielded bounds for lithium very close to the known Hartree-Fock error.

901,497 PB89-161541 Not available NTIS National Bureau of Standards (NEL), Gaithersburg, MD. Thermophysics Div.
Thermodynamic Values Near the Critical Point of

Final rept.
L. Haar, and J. S. Gallagher. 1986, 3p
Pub. in Proceedings of International Conference on
Properties of Steam (10th), Moscow, USSR, September 3-7, 1984, p167-169 1986.

Keywords: *Thermodynamic properties, *Water, *Critical point, Steam, Equations of state, Specific heat, Temperature, Pressure, Volume, Measurement.

In the immediate neighborhood of the critical point the thermodynamic consistency between very accurate measurements for the heat capacities, the speed of measurements for the neat capacities, the speed of sound, and pressure-volume-temperature values is examined. For this purpose several thermodynamic formulations are employed, including: the Haar, Gallagher, and Kell (HGK) formulation and the Pollak formulation, which everywhere are analytic, and the scaled equation for the critical region reported by Levelt Sengers, and co-workers, which is an expansion about a non-analytic critical point. It is shown that HGK and the scaled equation are in accord with the measurethe scaled equation are in accord with the measurements for the different thermodynamic properties; also, the recent PVT measurements by Hanafusa and co-workers are the most accurate yet made close to the critical point. A description is provided of the HGK formulation and specification of the liquid-vapor co-existence curve.

901.498 PB89-161558 Not available NTIS National Bureau of Standards (NML), Gaithersburg, MD. Ionizing Radiation Physics Div.

NBS (National Bureau of Standards) DecayScheme Investigations of (82)Sr-(82)Rb.

Final rept. D. D. Hoppes, B. M. Coursey, F. J. Schima, and D. Yang. 1987, 9p Pub. in Applied Radiation and Isotopes 38, n3 p195-

203 1987.

Keywords: *Decay schemes, Gamma rays, Positrons, Half life, Gamma ray spectroscopy, Impurities, Standards, Reprints, *Strontium 82, *Rubidium 82, Liquid scintillation detectors, Nuclear medicine, Annihilation, Calibration.

Measurements of photon- and positron-emission rates for equilibrium mixtures of (82)Sr-(82)Rb indicate a gamma-ray probability per decay for the 776-keV gamma ray of 0.152 plus or minus 0.003 if the positron gamma ray of 0.152 plus or minus 0.003 if the positron rate is derived from annihilation-radiation measurements and 0.145 plus or minus 0.002 if positrons are measured in a liquid scintillator. The half life of (82)Sr was measured as 25.36 plus or minus 0.03 days. Methods for measuring a (82)Sr impurity by gamma-ray spectrometry and by liquid-scintillation counting are described.

901,499 PB89-161566 Not available NTIS National Bureau of Standards (NML), Boulder, CO. Time and Frequency Div.

Frequency Measurement of the J=1<-0 Rotational Transition of HD (Hydrogen Deuteride). Final rept.

K. M. Evenson, D. A. Jennings, J. M. Brown, L. R. . Zink, K. R. Leopold, M. D. Vanek, and I. G. Nolt.

Pub. in Astrophysical Jnl. 330, pL135-L136, 15 Jul 88.

Keywords: *Rotational spectra, Far infrared radiation, Planetary atmospheres, interstellar matter, Reprints, Hydrogen deuteride.

The frequency of the astronomically important J = 1<- 0 rotational transition of hydrogen deuteride (HD) at 2.7 THz (90/cm) has been measured with tunable drar-infrared radiation with an accuracy of 150 kHz. This frequency is now known to sufficient accuracy for use</p> in future astrophysical heterodyne observations of HD in planetary atmospheres reported by Bezard et al. in 1986 and the interstellar medium reported by Bussoletti et al. in 1975.

901,500 PB89-171185 Not available NTIS National Bureau of Standards (NML), Boulder, CO. Quantum Physics Div. Systems Driven by Colored Squeezed Noise: The Atomic Absorption Spectrum.

Final rept.

H. Ritsch, and P. Zoller. 1988, 12p Pub. in Physical Review A 38, n9 p4657-4668, 1 Nov

Keywords: *Atomic spectra, *Absorption spectra, Stochastic processes, Reprints, *Squeezed light, chastic processes, Reprints, *Squeezed light, Squeezed states (Quantum theory), Bloch equations, Matrices.

Stochastic density-matrix equations are derived for an atom strongly driven by finite-bandwidth squeezed light. The quantum properties of the light are accounted for by a doubling of dimensions of the stochastic process for c-number electric field amplitudes. Saturation properties and the weak-field absorption spectrum of a two-level atom embedded in finite-bandwidth squeezed light and driven by a coherent field are calculated. The effect of finite bandwidth of the squeezed light in obtaining subnatural linewidth in the atomic absorption spectra is discussed, based on nonperturbative solutions of the stochastic optical Bloch equa-

901,501 PB89-171540 Not available NTIS National Bureau of Standards (NML), Boulder, CO. Quantum Physics Div.
Electron-Transport, Ionization, Attachment, and Dissociation Coefficients in SF6 and Its Mixtures.

A. V. Phelps, and R. J. Van Brunt. 1988, 9p

Sponsored by Department of Energy, Washington, DC. Pub. in Jnl. of Applied Physics 64, n9 p4269-4277, 1

Keywords: *Sulfur hexafluoride, Collision cross sections, Mixtures, Nitrogen, Oxygen, Neon, Gas ionization, Dissociation, Reprints, Electron-molecule colli-

An improved set of electron-collision cross sections is derived for SF6 and used to calculate transport, ionization, attachment, and dissociation coefficients for pure SF6 and mixtures of SF6 with N2, O2, and Ne. Electron kinetic energy distributions computed from numerical solutions of the electron-transport (Boltzmann) equation using the two-term, spherical harmonic ex-pansion approximation were used to obtain electron-transport and reaction coefficients as functions of E/N and the fractional concentration of SF6. Here E is the electric field strength and N is the gas number density. Attachment rate data for low concentrations of SF6 in N2 are used to test the attachment cross sections. Particular attention is given to the calculation of transport and reaction coefficients at the critical E/N = (E/ N) sub c at which the ionization and attachment rates are equal.

901,502 PB89-171557 Not available NTIS National Bureau of Standards (NML), Boulder, CO. Quantum Physics Div.
Electron-Impact Excitation of the Resonance Transition in CA(1+).

Final rept.

J. Mitroy, D. C. Griffin, D. W. Norcross, and M. S. Pindzola. 1988, 12p
Contract DOE-EA-77-A-01-6010

Sponsored by Department of Energy, Washington, DC. Pub. in Physical Review A 38, n7 p3339-3350.

Keywords: Electron irradiation, Perturbation theory, Excitation, Reprints, *Calcium ions, *Electron-ion collisions.

Detailed calculations of the electron-impact excitation of Ca(1+) are performed using both perturbation theory and the close-coupling approach. Particular attention is focused on the resonance (4s-4p) excitation since experimental emission-cross-section data are available for this transition. The results of the most sophisticated model, a six-state (4s, 3d, 4p, 5s, 4d, 5p) close-coupling calculation with semiempirical Hartree-Fock target wave functions and including one- and two-body core-polarization potentials are in better agreement with the experimental cross section and resonance-fluorescence polarization data than any other calculation. At incident electron energies below

the 5s, 4d, and 5p thresholds, the six-state calculations are essentially in agreement with the experimental data, although rich resonance structures predicted by theory are not seen experimentally due to the finite energy resolution. At energies above the 5s, 4d, and 5p thresholds the six-state emission cross sections exceed the experimental cross sections by about 20%, once allowance is made for cascades from the 5s, 4d, and 5p levels.

901,503

PB89-171565 Not available NTIS National Bureau of Standards (NML), Boulder, CO. Quantum Physics Div. Electron-Impact Excitation of Al(2+).

J. Mitroy, and D. W. Norcross. 1989, 8p Contract DOE-EA-77-A-01-6010

Sponsored by Department of Energy, Washington, DC. Pub. in Physical Review A 39, n2 p537-544, 15 Jan 89.

Keywords: Electron irradiation, Approximation, Excitation, Reprints, *Aluminum ions, *Electron-ion collisions, Bound state, Oscillator strengths.

Detailed calculations of the electron-impact excitation of the sodiumlike ion Al(2+) were performed using both the unitarized Coulomb-Born approximation and the close-coupling approach. Calculations were undertaken at both the five-state (3s, 3p, 3d, 4s, and 4p) and nine-state levels of approximation. Calculations using Hamiltonians both with and without (semiempirical) core-polarization potentials were completed. Particular attention was paid to the resonance (3s-3p) excitation. The inclusion of core-polarization potentials resulted in cross sections for the resonance excitation that are 10% smaller in magnitude. As an additional check on the calculations, binding energies of Al(1+) bound states and oscillator strengths for Al(2+) transitions, were also computed and compared with the results of measurements and other calculations.

901,504

PB89-171581 Not available NTIS National Bureau of Standards (NML), Boulder, CO.

Quantum Physics Div.
Comment on 'Possible Resolution of the Brookhaven and Washington Eotvos Experiments'.

T. M. Niebauer, J. E. Faller, and P. L. Bender. 1988,

Pub. in Physical Review Letters 61, n19 p2272, 7 Nov

Keywords: Gravitation, Reprints, *Eotvos experiment, Fifth force.

The comment points out several things that the authors of a recent article (Physical Review Letters 60, 1225 (1988)) overlooked or misinterpreted. Particular emphasis is on the significance of the authors' earlier paper (Physical Review Letters 59, 609 (1987)) to this discussion.

901,505

PB89-171631 Not available NTIS

Time and Frequency Div.

Recoilless Optical Absorption and Doppler Sidebands of a Single Trapped Ion.

Final rept.

J. C. Bergquist, W. M. Itano, and D. J. Wineland. 1987, 3p Sponsored by Air Force Office of Scientific Research, Arlington, VA., and Office of Naval Research, Arling-

Pub. in Physical Review A 36, n1 p428-430, 1 Jul 87.

Keywords: Near ultraviolet radiation, Reprints, *Mercury ions, Trapping(Charged particles), Laser cooling, Laser spectroscopy, High resolution, Quadrupoles,

Doppler sidebands. Spectroscopic measurements of the electric-quadrupole-allowed 5d(10)6s doublet s(1/2) to 5d(9)6s(2) doublet D(5/2) transition near 282 nm on a single,

laser-cooled Hg(1+) ion give a recoil-free absorption line (carrier) and well-resolved motional sidebands. From the intensity ratio of the sidebands to the carrier, the effective temperature of the Hg(1+) ion was determined to be near the theoretical minimum of 1.7 mK. A fraction resolution of better than 3 \times 10 to the -11th power for this ultraviolet transition is achieved.

901,506 PB89-172381 Not available NTIS National Bureau of Standards (NEL), Boulder, CO.

Mathematical Analysis Div.
Classical Chaos, the Geometry of Phase Space, and Semiclassical Quantization.

Final rept.

W. P. Reinhardt. 1985, 77p Grants NSF-CHE80-11442, NSF-PHY82-00805 Sponsored by National Science Foundation, Washing-

Pub. in Mathematical Analysis of Physical Systems, Chapter 8, p169-245 1985.

Keywords: Hamiltonian functions, Schrodinger equation, Reprints, *Chaos, *Phase space, *Quantization, Two degrees of freedom.

Basic concepts relating to the onset of chaos in deterministic dynamics are illustrated using conservative Hamiltonian dynamics in two degrees of freedom--that is, dynamics in a four-dimensional phase space. The correspondence between regular and chaotic dynamics and concepts of integrability and nonintegrability are established, and semiclassical quantization (i.e., determination of estimates of energy eigenvalues of the corresponding Schrodinger operator using only classical dynamical information as input) is carried out utilizing the invariant tori of integrable (regular) classical dynamics. The origins of classical chaos are briefly discussed in terms of orbit bifurcation and in terms of the Painleve analysis of the complex time singularities of the orbits themselves. Expectations of quantum correspondence principle ramifications of classical chaos are discussed in terms of Percival's 'irregular spectrum' and in terms of the statistics of nearest-neighbor level spacings.

901,507 PB89-172407 Not available NTIS National Bureau of Standards (IMSE), Gaithersburg,

Grain Boundaries with Impurities in a Two-Dimensional Lattice-Gas Model.

Final rept.

R. Kikuchi, and J. W. Cahn. 1987, 11p Pub. in Physical Review B 36, n1 p418-428, 1 Jul 87.

Keywords: *Grain boundaries, *Lattice parameters, *Gases, *Impurities, Models, Thermodynamic properties, Statistical mechanics, Temperature, Adsorption.

Grain boundaries are examined between two 2-dimensional two-component square grains. Although the grains are assumed ideal solid solutions, the model grain boundary shows complicated thermodynamic behavior. There are high adsorption regions, both a low temperature and again a high temperature where the grain boundary resembles a molten zone. The sign of the adsorption can be different in these two regions. In between adsorption is low.

901.508 PB89-175210

(Order as PB89-175194, PC A06) National Inst. of Standards and Technology, Gaithers-

NIST (National Institute of Standards and Technology)/Sandla/ICDD Electron Diffraction Database: A Database for Phase Identification by Electron

Diffraction.

Bil-monthly rept.
M. J. Carr, W. F. Chambers, D. Melgaard, V. L.
Himes, J. K. Stalick, and A. D. Mighell. 1989, 7p
Sponsored by Sandia National Labs., Albuquerque,
NM., and Jand M Systems Ltd., Albuquerque, NM. Included in Jnl. of Research of the National Institute of Standards and Technology, v94 n1 p15-20 Jan-Feb

Keywords: *Electron diffraction, Phase, Electron microscopes, Crystallography, Inorganic compounds, Searching, Matching, Data retrieval, X ray spectrosco-py, *Numerical data bases, Search profiles.

A new database containing crystallographic and chemical information designed especially for application to electron diffraction search/match and related problems has been developed. The database described in the report contains what the authors believe to be the only complete collection of inorganic com-pounds data structured for phase identification by electron diffraction available. Nevertheless, the database is small enough to reside on a personal computer or laboratory microcomputer dedicated to electron diffraction and energy dispersive x-ray spectroscopy analysis in an electron microscope laboratory. It is anticipated that many different search/match schemes will be able to use this database.

901.509

PB89-176002 Not available NTIS
National Bureau of Standards (NML), Gaithersburg, MD. Atomic and Plasma Radiation Div.

Spectra and Energy Levels of Br XXV, Br XXIX, Br XXX, and Br XXXI.

Final rept.

U. Feldman, J. F. Seely, C. M. Brown, J. O. Ekberg, M. C. Richardson, W. E. Behring, and J. Reader. 1986, 4p

Pub. in Jnl. of the Optical Society of America B 3, n11 p1605-1608 Nov 86.

Keywords: *Atomic energy levels, *Emission spectra, Reprints, *Bromine ions, Soft x rays, Multicharged ions, M1-transitions.

Emission lines of highly-ionized bromine in the wavelength region 17 A to 93 A have been identified in spectra recorded at the University of Rochester's OMEGA laser facility. The wavelengths of 2s-2p transitions in nitrogenlike Br XXIX, carbonlike Br XXX, and boronlike Br XXXi are presented. The wavelengths of the magnetic dipole transitions within the 2s(2)2p(3) ground configuration of Br XXIX are predicted from the experimental energy levels. Transitions from the n = 4 and 5 levels of sodiumlike Br XXV were also identified, and the ionization energy of Br XXV was determined.

901,510

PB89-176010 Not available NTIS National Bureau of Standards (NML), Gaithersburg, MD. Atomic and Plasma Radiation Div.

Laser-Produced Spectra and QED (Quantum Electrodynamic) Effects for Fe-, Co-, Cu-, and Zn-Like lons of Au, Pb, Bi, Th, and U. Final rept

J. F. Seely, J. O. Ekberg, C. M. Brown, U. Feldman, W. E. Behring, J. Reader, and M. C. Richardson.

1986, 3p Pub. in Physical Review Letters 57, n23 p2924-2926, 8

Keywords: Far ultraviolet radiation, Reprints, *Gold ions, *Lead ions, *Bismuth ions, *Thorium ions, *Uranium ions, *Laser-produced plasma, Isoelectronic sequence, Multicharged ions, Extreme ultraviolet radiation, Quantum electrodynamics.

Transitions in the Fe I, Co I, Cu I, and Zn I isoelectronic sequences of the elements Au, Pb, Bi, Th, and U have been identified in the extreme ultraviolet spectra from laser-produced plasmas. The measured wavelengths are compared with calculated values, and the QED contributions to the CU I transition energies are determined.

901,511

PB89-176440 Not available NTIS National Bureau of Standards (NML), Gaithersburg, MD. Electricity Div.

Laser-Cooling and Electromagnetic Trapping of Neutral Atoms. Final rept.

W. D. Phillips, A. L. Migdall, and H. J. Metcalf. 1986, 4p

See also PB88-175096.

Pub. in AIP (American Institute of Physics) Conference Proceedings, n146 p362-365 1986.

Keywords: Atomic beams, Reviews, *Atom traps, Laser cooling, Magnetic traps, Sodium atoms.

Until recently it has been impossible to confine and trap neutral atoms using electromagnetic fields. While many proposals for such traps exist, the small potential energy depth of the traps and the high kinetic energy of available atoms prevented trapping. The authors review various schemes for atom trapping, the advances in laser cooling of atomic beams which have now made trapping possible, and the successful magnetic trapping of cold sodium atoms.

901.512

PB89-176531 Not available NTIS National Bureau of Standards (NML), Gaithersburg, MD. Ionizing Radiation Physics Div.

2.5 MeV Neutron Source for Fission Cross Section Measurement.

Final rept.

K. C. Duvall, O. A. Wasson, and M. Hongchang. 1988, 4p

Pub. in Proceedings of International Conference on Nuclear Data for Science and Technology, Mito, Japan, May 30-June 3, 1988, p355-358.

Keywords: *Neutron sources, Fission cross sections, Neutron beams, Deutenum target, Deuteron reactions, Uranium 235 target, MeV range 01-10.

A 2.5-MeV neutron source has been established on the beamline of a 100-kV, 0.5-ma ion accelerator. The neutron source is produced by the D(d,n)(3)He reaction with a yield of about 10 million n.sec. A fission chamber containing six uranium tetrafluoride deposits has been designed for use in the (235)U(n,f) cross section measurement at 2.5 MeV. A description of the 2.5-MeV neutron source facility is presented along with de-tails of the associated particle detection and neutron beam characteristics. Preparation for the fission cross section measurement are discussed.

PB89-176572 Not available NTIS National Bureau of Standards (NML), Gaithersburg, MD. Radiation Physics Div.

State Selection in Electron-Atom Scattering: Spin-Polarized Electron Scattering from Optically Pumped Sodium.

Final rept J. J. McClelland, M. H. Kelley, and R. J. Celotta.

1986, 4p Pub. in Proceedings of Symposium on Physics of Ion-ized Gases (13th), Sibenik, Yugoslavia, September 1-5, 1986, p15-18.

*Electron scattering, *Sodium, Polarization(Spin alignment), Optical pumping, *Electron-atom collisions.

When an electron collides with an atom, there are generally many quantum channels through which the scat-tering can take place. These can involve several energetically accessible channels, several angular momentum states degenerate in energy, and several spin states also degenerate in energy. A theoretical calcu-lation of the scattering must examine each of the chan-nels individually, and then perform an average over those not separated in the experiment with which comparison is to be made.

901,514

PB89-176903 Not available NTIS National Bureau of Standards (IMSE), Gaithersburg,

MD. Metallurgy Div.
Fast Magnetic Resonance Imaging with Simultaneously Oscillating and Rotating Field Gradients. Final rept.

S. J. Norton. 1987, 11p

Pub. in IEEE (Institute of Electrical and Electronics Engineers) Transactions on Medical Imaging 6, n1 p21-31 1987.

Keywords: *Nuclear magnetic resonance, Gradients, Magnetic fields, Oscillations, Reprints, *Image reconstruction, Tomography.

The report presents an approach to magnetic resonance imaging employing a magnetic field gradient that rotates 180 degrees in the image plane while the gradient magnitude oscillates rapidly during the rotation. A single free induction decay recorded during this rotation contains all information needed to reconstruct a two-dimensional image. In effect, each sinusoidal oscillation of the gradient provides information corresponding to one projection in more conventional Fourier-projection approaches. Since the data acquisition can be achieved in a period less than T2, the method offers the potential of great speed, which is limited only by the gradient modulation frequency. An explicit image reconstruction formula is derived that gives, when evaluated, a reconstruction of the magnetization equal to the true magnetization convolved with a space-invariant point spread function. This point spread function is derived and characterizes the resolving power and sidelobe response of the technique. Moreover, it derives a similar reconstruction formula which is valid when known inhomogeneities in the static field H0 and T2 are present. Finally, it shows how the general approach can be extended to three dimen-

901,515 PB89-176937 Not available NTIS National Bureau of Standards (NML), Gaithersburg, MD. Electricity Div. Cooling and Trapping Atoms.

Final rept.
W. D. Phillips, and H. J. Metcalf. 1987, 7p
Sponsored by Office of Naval Research, Arlington, VA. Pub. in Scientific American 256, n3 p50-56 1987.

Keywords: Reprints, *Atom traps, *Laser cooling,

Thermal motion of atoms interferes with many measurements of atomic properties. The authors describe techniques whereby lasers are used to cool the atomic motion. Laser-cooled atoms can then be confined in electromagnetic traps for long periods of time.

901,516 PB89-176986 Not available NTIS National Bureau of Standards (NEL), Boulder, CO. Electromagnetic Technology Div. Cool It.

Final rept. J. Lehman, 1988, 4p

Pub. in Science Teacher, p29-32 Mar 88.

Keywords: *Cryogenics, *Education, Instructors, Training devices, Reprints, Instructional materials, Teaching methods, Science instruction.

Sometimes a well-rounded curriculum for the physical sciences is burdened with bringing into the classroom topics that do not necessarily correspond to daily observations and intuition. Heat, energy, resistance, kinetics, and countless other topics challenge not only the student's imagination, but also an instructor's ability to present such topics in realistic and interesting ways. Cryogenics, known informally as the science of cold, offers many avenues for learning beyond the obvious effects of cold temperature. The paper includes some justification, pedagogy, and motivation for use of cryogenics in science curricula.

901,517 PB89-177042 Not available NTIS National Bureau of Standards (NEL), Gaithersburg, MD. Robot Systems Div.

Algebraic Representation for the Topology of Multicomponent Phase Diagrams.

Final rept.

D. J. Orser. 1986, 30p Pub. in Proceedings of Computer Modeling of Phase Diagrams Symposium, Toronto, Ontario, Canada, October 13-17, 1985, p301-330 1986.

Keywords: *Phase diagrams, *Tcµology, Models, Thermodynamics, Incidence matrices, Algebra, Equilibrium, Data bases.

The paper describes a methodology based on treating phase diagrams as topological structures and devel-ops a representation along the following lines: for each topologically distinct phase diagram there exists a finite incidence algebra whose elements correspond to the invariant (vertices), monovariant (edges), bivariant (surfaces), etc., transition equilibria of the diagram. The elements of the incidence algebra are sets for which a relation and two binary operations are defined. This defines a calculus of phase diagram equilibria and provides an efficient method for a computer to retrieve the topological relationships between an equilibrium and the rest of the diagram or between any two equilib-ria. Its application to a multicomponent data base and its potential for qualitative thermodynamic modeling are discussed.

PB89-179147 Not available NTIS National Bureau of Standards (NML), Boulder, CO. Time and Frequency Div.

Laser Cooling. Final rept.

D. J. Wineland, and W. M. Itano. 1987, 8p Sponsored by Office of Naval Research, Arlington, VA., and Air Force Office of Scientific Research, Bolling AFB, DC. Pub. in Physics Today, p1-8 Jun 87.

Keywords: Radiation pressure, Reprints, *Ion traps, *Atom traps, *Laser cooling, *Trapping(Charged particles), lon storage.

Theory and experiments on laser cooling of neutral atoms and atomic ions is presented. A brief history of

the mechanical forces of light is given first. Then, a simple theory of radiation pressure cooling (laser cooling) of free and bound atoms is presented along with the temperature limits imposed by recoil. Experiments on trapped ions and neutral atoms are then described. Finally, the future of laser cooling is briefly discussed.

901,519 PB89-179204 Not available NTIS Mational Bureau of Standards (NML), Gaithersburg, MD. Temperature and Pressure Div. Magnetic Resonance of (160)Tb Oriented in a Ter-

blum Single Crystal at Low Temperatures. Final rept. P. Roman, W. D. Brewer, E. Klein, H. Marshak, K. Freitag, and P. Herzog. 1986, 4p Pub. in Physical Review Letters 56, n18 p1976-1979, 5

May 86.

Keywords: *Nuclear magnetic resonance, Quadrupole moment, Single crystals, Gamma rays, Reprints, *Ter-bium 160, *Oriented nuclei, Ion implantation, Ther-mometers, Terbium 159, Rare earth nuclei.

The first observation of magnetic resonance of oriented rare earth nuclei in a rare earth host is reported. Radioactive 160Tb implanted in a single crystal of ferromagnetic terbium was subjected to magnetic resonance detected by perturbation of the gamma-ray anisotropy. The open Tb 4f shell gives rise to a strong electric quadrupole interaction in addition to the magnetic interaction; the resulting resonance signal has 6 components, of which the first was detected at 480.0(4) MHz. The derived quadrupole interaction frequency is 167.7(2.6) MHz, giving Q=3.56(10) b.

901,520 PB89-184113

(Order as PB89-184089, PC A04) National Inst. of Standards and Technology, Boulder, CO.

Relation between Wire Resistance and Fluid Pressure in the Translent Hot-Wire Method. Bi-monthly rept.

H. M. Roder, and R. A. Perkins. 1989, 4p Included in Jnl. of Research of the National Institute of Standards and Technology, v94 n2 p113-116 Mar-Apr

Keywords: *Thermal conductivity, *Fluids, Plantinum, Electrical resistance, Pressure, Calibrating, Measurement, *Hot wire flowmeters.

The resistance of metals is a function of applied pressure, and the dependence is large enough to be significant in the calibration of transient hot-wire thermal conductivity instruments. For the highest possible accuracy, the instrument's hot wires should be calibrated in situ. If this is not possible, the author recommended that a value of campa, the relative resistance change that a value of gamma, the relative resistance change with pressure, of -2x10 sup (-5) MPa(-1) be used to account for the pressure dependence of the platinum wire's resistance.

National Bureau of Standards (NML), Gaithersburg, MD. Center for Basic Standards.

Technical Activities 1997 Technical Activities 1987, Center for Basic Stand-

P. L. M. Heydemann. Oct 87, 290p NBSIR-87/3587 See also PB86-140043.

Keywords: *Standards, *Physics, *Research management, Electric current, Temperature, Mass, Length, Time, Frequencies, Quantum theory, X rays, *Center for Basic Standards.

The report summarizes the research and technical activities of the Center for Basic Standards during the Fiscal Year 1987. These activities include work in the areas of electricity, temperature and pressure, mass and length, time and frequency, quantum metrology, and quantum physics.

PB89-185912 Not available NTIS National Bureau of Standards (NML), Boulder, CO. Quantum Physics Div.

Current Research Efforts at JILA (Joint Institute for Laboratory Astrophysics) to Test the Equiva-lence Principle at Short Ranges.

Final rept.
J. E. Faller, T. M. Niebauer, M. P. McHugh, and D. A. Van Baak. 1988, 14p
Sponsored by Air Force Geophysics Lab., Hanscom AFB, MA.

Pub. in Proceedings of Moriond Conference 5th Force Neutrino Physics (23rd), Les Arcs, Savoie, France, January 23-30, 1988, p457-470.

Keywords: *Gravitation, Gravity, *Equivalence principle, Fifth force, Free fall.

The authors are presently engaged in three different experiments to search for a possible breakdown of the equivalence principle at short ranges. The first of these experiments, which has been completed, is the socalled Galilean test in which the differential free-fall of two objects of differing composition was measured using laser interferometry. The authors observed that the differential acceleration of two test bodies was less than 5 parts in 10 billion. The experiment set new limits on a suggested baryon dependent Fifth Force at ranges longer than 1 km. With a second experiment, the authors are investigating substance dependent interactions primarily for ranges up to 10 meters using a fluid supported torsion balance; the apparatus has been built and is now undergoing laboratory tests. A proposal has been made to measure the gravitational signal associated with the changing water level at a large pumped storage facility in Ludington, Michigan. Measuring the gravitational signal above and below the pond will yield the value of the gravitational content of stant, G, at ranges from 10-100 m.

901.523 PB89-185920 Not available NTIS National Bureau of Standards (NML), Boulder, CO.

Quantum Physics Div.
Fundamental Tests of Special Relativity and the Isotropy of Space. Final rept.

S. A. Lee, L. U. Andersen, N. Bjerre, O. Poulsen, E. Riis, and J. L. Hall. 1987, 4p Grant NSF-PHY86-04504

Sponsored by National Science Foundation, Washington, DC

Pub. in Proceedings of International Conference on Laser Spectroscopy (8th), Are, Sweden, June 22-26, 1987, p52-55.

Keywords: *Special relativity, Atomic beams, Frequency shift, Anisotropy, Tests, *Two photon absorption, Light speed, Neon atoms, Spectral shift, 1sotropy.

A two-photon absorption experiment was performed using a fast Ne* atom beam merged to be coaxial with a standing wave laser field. Intermediate state resoa standing wave last lifetime late state resor-nance was achieved by controlling the accelerator-de-termined Doppler shift. A diurnal optical frequency shift would be expected if the speed of light were anisotropic. Preliminary measurements relative to an I2 reference line yield a diurnal frequency shift <2 kHz, corresponding to a '1-way' speed of light anisotropy epsilon < 3 x 10 to the -9 power.

901.524 PB89-186738 Not available NTIS National Bureau of Standards (NML), Gaithersburg,

MD. Center for Radiation Research.

Quasifree Electron Scattering on Nucleons In a
Momentum-Dependent Potential.

J. S. O'Connell, and B. Schroder. 1988, 3p Pub. in Physical Review C 38, n5 p2447-2449 Nov 88.

Keywords: *Electron scattering, Momentum transfer, Carbon, Reprints, *Electron-nucleon interactions, Carbon, Reprints, *Electror Energy losses, Effective mass.

Systematics on the location of the quasifree peak observed in electron-nucleus scattering as a function of momentum transfer are related to the momentum-dependent mean field in which the struck nucleon moves. Data on carbon are used as an example.

901,525 PB89-200455 Not available NTIS National Bureau of Standards (NEL), Boulder, CO. Electromagnetic Technology Div. Battery-Powered Current Supply for Supercon-

ductor Measurements.

Final rept.
S. L. Bray, L. F. Goodrich, and W. P. Dube. 1989, 4p
Sponsored by Department of Energy, Washington, DC.
Pub. in Review of Scientific Instruments 60, n2 p261-264 Feb 89

Keywords: *Superconductors, *Power supplies, Electrical measurement, Reprints, *Critical current, Circuit diagrams, Battery operated.

To measure the critical current of superconductors, a high output current supply is required. In addition to high current capability, the supply should be designed to reduce ground loop problems, respond linearly to an input control signal, and minimize output noise. A current supply with these qualifications has been con-structed and tested. Although the supply was originally designed for testing conventional superconductors at high current levels, it has also been successfully used in measurements on the high-critical-temperature ceramic superconductors where the maximum current output was less than 1 A. The supply can produce 1000 A output current with a noise level of approxi-mately 0.05 A peak-to-peak. The specifics of the current supply's design and performance are given.

901.526 PB89-200471 Not available NTIS National Bureau of Standards (NEL), Boulder, CO. Electromagnetic Technology Div.

Current Capacity Degradation in Superconducting

Cable Strands. Final rept.

L. F. Goodrich, and S. L. Bray. 1989, 4p Sponsored by Department of Energy, Washington, DC. Pub. in IEEE (Institute of Electrical and Electronics Engineers) Transactions on Magnetics 25, n2 p1949-1952 Mar 89.

Keywords: Superconducting magnets, Deformation, Degradation, Reprints, *Superconducting cables, Critical current, Superconducting super collider, Niobium titanium, Aspect ratio.

The electromagnetic properties of NbTi strands extracted from Rutherford cables were studied to clarify the effect of mechanical deformation, caused by the cabling process, on the current capacity of the strands. Three different cables were studied, all of which are prototypes for the Superconducting Super Collider's dipole magnets. The extracted cable strands were instrumented to allow measurement of the voltage across several key regions of mechanical deformation as a function of current and the orientation of the applied magnetic field. The resulting data are presented in terms of the strand's voltage profile as well as its critical current in order to more thoroughly characterize the conductor's electromagnetic properties.

901.527 PB89-200497 Not available NTIS National Bureau of Standards (NEL), Boulder, CO. Electromagnetic Technology Div. Nb3Sn Critical-Current Measurements Using Tubu-

lar Fiberglass-Epoxy Mandrels. Final rept.

L. F. Goodrich, S. L. Bray, and T. C. Stauffer. 1989,

Sponsored by Department of Energy, Washington, DC. Pub. in IEEE (Institute of Electrical and Electronics Engineers) Transactions on Magnetics 25, n2 p2375-2378 Mar 89.

Keywords: Superconductors, Strains, Thermal expansion, Contraction, Electrical measurement, Reprints, *Superconducting wires, *Niobium stannides, *Critical current, Fiberglass epoxy composites, Niobium tin.

A systematic study of the effect of sample mounting techniques on the superconducting critical-current measurement was made in conjunction with the VAMAS (Versailles Agreement on Advanced Materials and Standards) interlaboratory comparison (round robin) measurements. A seemingly small change in mandrel geometry can result in a 40% change in the measured critical current of a Nb3Sn sample at 12 T. This is a result of a change in the conductor pre-strain at 4 K caused by variation in thermal contraction between thick- and thin-walled fiberglass-epoxy composite (G-10) tubes.

901,528 PB89-201065 Not available NTIS Mational Bureau of Standards (NML), Gaithersburg, MD. Atomic and Plasma Radiation Div. 4s(2) 4p(2)-4s4p(3) Transition Array and Energy Levels of the Germanium-Like Ions Rb VI - Mo XI.

U. Litzen, and J. Reader. 1989, 6p See also PB87-109666. Sponsored by Department of Energy, Washington, DC. Pub. in Physica Scripta 39, n468-473 1989.

Keywords: *Atomic energy levels, *Ultraviolet spectra, Far ultraviolet radiation, Reprints, *Rubidium ions,

*Strontium ions, *Zirconium ions, *Niobium ions, *Molybdenum ions, *Yttrium ions, Multicharged ions.

Spectra of the germanium-like ions Rb VI, Sr VII, Y VIII, Zr IX, Nb X, and Mo XI have been investigated in the region 280-790 A. Identification of lines of the transition array 4s(2) 4p(2)-4s4p(3) has yielded all levels of the two configurations except 4s 4p(3) quintet S. The level structure has been studied by means of ab initio and parametric calculations.

901,529 PB89-201073 Not available NTIS National Bureau of Standards (NML), Gaithersburg, MD. Atomic and Plasma Radiation Div. Resonance-Enhanced Multiphoton Ionization of

Atomic Hydrogen.

Final rept. L. R. Brewer, F. Buchinger, M. Ligare, and D. E.

L. n. brewer, r. buchinger, M. Ligare, and D. E. Kelleher. 1989, 12p Sponsored by U.S. Air Force Office of Scientific Research, Bolling AFB, DC. Pub. in Physical Review A 39, n8 p3912-3923, 15 Apr

Keywords: Resonance, Reprints, *Hydrogen atoms, *Multi-photon processes, *Photoionization, Laser radiation.

The resonance-enhanced four-photon ionization of atomic hydrogen was measured. The degenerate fourphoton process occurs via a three-photon resonance between the 1s and the 2p levels, with subsequent one-photon ionization near threshold. The highly asymmetric resonance-enhanced profile was studied, i.e., the photo ion yield as a function of laser detuning from three-photon resonance between the 1s and 2p levels. In particular, the authors have determined the width, shift, peak, and asymmetry of the profile as a function of laser intensity. The experimental results are compared to theoretical models. These models involve both the properties of the atom in an intense near-resonant radiative field, and a detailed model for the multimode laser field, particularly the field fluctuations due to mode beating. The asymmetric resonance-enhanced photoionization profile is well reproduced by both a random-phase and a chaotic-light model.

901.530 PB89-201578 Not available NTIS National Bureau of Standards (NML), Gaithersburg, MD. Molecular Spectroscopy Div.

Influence of the ac Stark Effect on Multiphoton Transitions in Molecules.

Final rept.

W. L. Meerts, I. Ozier, and J. T. Hougen. 1989, 8p Pub. in Jnl. of Chemical Physics 90, n9 p4681-4688, 1 May 89.

Keywords: *Molecular beams, *Stark effect, Electronic spectra, Photons, Linear differential equations, Computerized simulation, Resonance absorption, Boundary value problems, Mathematical models, Reprints

A multiphoton mechanism for molecular beam transitions is presented which relies on a large first-order ac Stark effect to modulate the energy separation of the initial and final states of the multiphoton transition, but which does not require the presence of any intermediate level(s). The algebraic formalism is checked by computer solution of an initial value problem involving four real coupled linear differential equations. It is then used to explain the multiphoton transitions previously observed in molecular beam electric resonance studies on the two symmetric top molecules OPF3 and CH3CF3, where the number of photons involved in a given transition varies from 1-40. Application of the analysis to other experiments is briefly discussed.

901 531 PB89-201644 Not available NTIS National Bureau of Standards (NML), Gaithersburg, MD. Gas and Particulate Science Div.

Modeling of the Bremsstrahlung Radiation Produced in Pure Element Targets by 10-40 keV Electrons.

J. A. Small, S. D. Leigh, D. E. Newbury, and R. L.

Myklebust. 1987, 11p Pub. in Jnl. of Applied Physics 61, n2 p459-469 1987.

Keywords: *X ray analysis, *Bremsstrahlung, Mathematical models, Electron irradiation, Microanalysis, Reprints, KeV range 10-100.

A new global relation has been developed for predicting electron-excited bremsstrahlung intensities over a wide range of accelerating voltages, atomic numbers, and x-ray energies. The new relation was determined from the mathematical modeling of extensive data and is designed for calculating bremsstrahlung intensities in analytical procedures, such as those requiring peakto-background measurements, where the direct measurement of the bremsstrahlung intensities is impracti-cable. The distribution of errors between the data and the model is symmetrical, centered around zero error with 63% of the values falling between plus or minus 10% relative error.

901,532 PB89-201685 Not available NTIS National Bureau of Standards (NML), Gaithersburg, MD. Radiometric Physics Div. NBS (National Bureau of Standards) Scale of Spec-

tral Radiance.

Final rept. J. H. Walker, A. T. Hattenburg, and R. D. Saunders. 1987, 10p

Pub. in Metrologia 24, n2 p79-88 1987.

Keywords: *Radiance, *Spectroradiometers, Precision, Blackbody radiation, Measuring instruments, Radiometry, Electromagnetic scattering, Linearity, Reprints, *Calibration standards.

The paper describes the measurement methods and instrumentation used in the realization and transfer of the NBS scale of spectral radiance. The application of the basic measurement equation to both blackbody and tungsten strip lamp sources is discussed. The polarizance, response linearity, spectral responsivity function, and 'size-of-source effect' of the spectrora-diometer are described. The analysis of sources of error and estimates of uncertainty are presented. The assigned uncertainties in spectral radiance range from about 1.75% at 225 nm to 0.25% at 2400 nm.

901,533 PB89-202048 Not available NTIS National Bureau of Standards (NML), Gaithersburg, MD. Office of Standard Reference Data.

Properties of Steam.

Final rept. H. J. White. 1986, 2p Pub. in Mechanical Engineering 108, n8 p36-37 1986.

*Thermodynamic properties, Keywords: *Steam, *Standards, Water vapor, Steam tables(Thermodynamics), Enthalpy, Entropy, Density, Reprints, *International Association for the Properties of Steam.

The paper briefly outlines the activities of the International Association for the Properties of Steam (IAPS) and the ASME Research Committee on the Properties of Steam, which serves as the U.S. National Committee for the Properties of Steam to IAPS. Emphasis is based on the internationally agreed upon reference data published by IAPS in the form of releases. A list of current releases is provided as well as archival papers which back up the releases.

901.534 PB89-202147 Not available NTIS National Bureau of Standards (NEL), Boulder, CO.

Electromagnetic Technology Div.

VAMAS (Versailles Project on Advanced Materials and Standards) Intercomparison of Critical Current Measurement in Nb3Sn Wires.

K. Tachikawa, K. Itoh, H. Wada, D. Gould, H. Jones, C. R. Walters, L. F. Goodrich, J. W. Ekin, and S. L.

Bray. 1989, 7p
Pub. in IEEE (Institute of Electrical and Electronics Engineers) Transactions on Magnetics 25, n2 p2368-2374 Mar 89.

Keywords: Electrical measurement, Reprints, *Superconducting wires, *Niobium stannides, *Critical current, Niobium tin, Interlaboratory comparisons.

The VAMAS (Versailles Agreement on Advanced Materials and Standards) technical working party in the area of superconducting and cryogenic structural materials has recently carried out the first world-wide intercomparison of critical current, I sub c, measurement on multifilamentary Nb3Sn wires. Three sample wires were supplied from each of the European Communities, Japan and USA. The total number of participant labs were 24 (EC 11, Japan 8 and USA 5). There were

PHYSICS

General

few restrictions for the I sub c measurement at participant labs. The standard deviations of the I sub c values reported from these labs varied among test samples and were 6-21% of averaged I sub c values at 12 Tesla.

901.535 PB89-202154 Not available NTIS National Bureau of Standards (NML), Gaithersburg,

MD. Electricity Div.
History of the Present Value of 2e/h Commonly
Used for Defining National Units of Voltage and
Possible Changes in National Units of Voltage and Resistance.

Final rept.

P. N. Taylor. 1987, 6p
Pub. in IEEE (Institute of Electrical and Electronics Engineers) Transactions on Instrumentation and Measurement 36, n2 p659-664 1987.

Keywords: *Electrical measurement, *Electric potential, *Electrical resistance, Metrology, Hall effect, Units of measurement, Reprints.

The national standards laboratories of most major industrialized countries employ the Josephson effect to define and maintain their national or laboratory unit of voltage V(LAB). The value of the Josephson frequency-voltage ratio commonly used for this purpose, 2e/h = 483594 GHz/V(LAB), is now known to be about eight parts-per-million less than the absolute or SI value. Consequently, the different national units of voltage are smaller than the SI unit by the same amount. One of the purposes of the paper is to review how this value of 2e/h was selected and hence the origin of the present inconsistency between national voltage units and the SI unit. The motivation for such an historical study is the hope that it can benefit the selection of a new, more accurate value of 2e/h planned for the near future. Also discussed is the status of national units of resistance and the effect of defining and maintaining such units using a value of the quantized Hall resistance consistent with the SI as may also be suggested in the near future.

901,536 PB89-202170 Not available NTIS National Bureau of Standards (NEL), Boulder, CO. Thermophysics Div.

Determination of Binary Mixture Vapor-Liquid Critical Densities from Coexisting Density Data.

Final rept.

L. J. Van Poolen, and J. C. Rainwater. 1987, 21p Pub. in International Jnl. of Thermophysics 8, n6 p695-715 1987.

Keywords: *Mixtures, *Critical density, Nitrogen, Methane, Thermodynamic equilibrium, Thermodynamic properties, Experimental data, Liquids, Two phase flow, Vapors, Reprints, *Isochoric processes.

Two-phase vapor-liquid equilibrium ((VLE) isochores for binary mixtures are defined as the thermodynamic for binary mixtures are defined as the thermodynamic paths along which the overall density and composition are fixed. Data along such isochores are generated from a modified Leung-Griffiths model fit to experimental data for the binary system nitrogen-methane. The behavior of the liquid volume fraction along these isochores is found to be similar to that for pure fluids. Rectilinear diameters for varying overall densities (fixed composition) are seen to be nearly coincident. Straight-line diameters and the critical liquid volume fraction method are utilized to predict critical densities using data near and removed from the critical point. Both methods give acceptable results but the critical liquid volume fraction method is more accurate. A criti-cal literature review of the need for binary mixture criti-cal densities is presented and a proposed experimental procedure is given for the determination of mixture critical densities.

901.537 PB89-202469 Not available NTIS National Bureau of Standards (IMSE), Gaithersburg, MD. Polymers Div.

Computer Simulation Studies of the Soliton Model. 3. Noncontinuum Regimes and Soliton Interactions.

K. J. Wahlstrand, 1988, 7p

Pub. in Polymer 29, n2 p256-262 1988.

Keywords: *Elementary excitations, *Klein-Gordon equation, Computerized simulation, Correlation, Interactions, Temperature, Field theory(Physics), Energy

levels, Scaling, Phonons, Mathematical models, Reprints, *Solitons, Coupling constants.

The Klein-Gordon soliton model is studied by performing stochastic molecular dynamics computer simula-tions for a wide range of both temperatures and coupling constants. Three general regimes of behavior are found: the continuum limit or non-interacting regime; the pinned or transition state theory limit, where soliton-phonon interactions are important; and the general noncontinuum regime, where soliton-soliton interac-tions or 'multiple soliton effects' are important. In the noncontinuum regime the correlation function changes as a function of temperature and coupling constant. This will lead to deviations from the continuum limit temperature scaling and soliton energy scaling observed in the dynamics of Klein-Gordon systems.

901,538 PB89-202535 Not available NTIS National Bureau of Standards (NML), Gaithersburg, MD. Radiation Physics Div.

Computation of the ac Stark Effect in the Ground State of Atomic Hydrogen.

Final rept.
L. Pan, K. T. Taylor, and C. W. Clark. 1988, 4p
Pub. in Physical Review Letters 61, n23 p2673-2676, 5

Keywords: *Hydrogen, *Stark effect, Perturbation theory, Ground state, Greens function, Reprints, Coulomb potential.

Using a Sturmian function expansion the authors have computed the nth-order coefficients E sub n(omega), for a 2 less than or = n less than or = 22, in the perturbation expansion of the ac Stark effect in the hydrogen 1s state. An effective convergence similar to that in the dc case is observed. A parametrization of these coefficients, based upon the analytic structure of the Coulomb Green's function, separates the rapid oscillatory resonant behavior and the smooth background variation with respect to omega.

901,539 PB89-202600 Not available NTIS National Bureau of Standards (NML), Boulder, CO. Quantum Physics Div.

Quantum-Defect Parametrization of Perturbative Two-Photon Ionization Cross Sections.

Final rept

M. G. J. Fink, and P. Zoller. 1989, 15p Sponsored by National Science Foundation, Washington, DC.

Pub. in Physical Review A 39, n6 p2933-2947, 15 Mar

Keywords: *Hydrogen, Photons, Perturbation theory, Energy levels, Quantum theory, Reprints, *Ionization cross sections, Rydberg states, Coulomb potential.

A multichannel quantum-defect theory (MQDT) parametrization of two-photon ionization (2PI) of atoms, suitable for use with ab initio calculations of perturbative 2PI amplitudes in the presence of intermediateand/or final-state Rydberg resonances is developed. The rapid energy variation of such amplitudes is extracted in terms of elementary functions of energy and a set of MQDT parameters, which are smooth functions of energy. As an example, results of numerical computations of MQDT parameters for 2PI of atomic hydrogen (1s, 2s, and 3s) by circularly polarized light are presented. MQDT parameters for the many-channel case are derived, and an analysis of their phaseshifted Coulomb functions, and simple analytic formulas are given for the energy dependence of the amplitude as a function of a small set of physical parameters.

901,540 PB89-211981 Not available NTIS

National Inst. of Standards and Technology (IMSE), Gaithersburg, MD. Reactor Radiation Div. Applications of Mirrors, Supermirrors and Multi-layers at the National Bureau of Standards Cold Neutron Research Facility.

Final rept. C. F. Majkrzak, C. J. Glinka, and S. K. Satija. 1989,

15p
Pub. in Proceedings of SPIE (Society of Photo-Optical
Instrumentation Engineers) Thin-Film Neutron Optical Devices: Mirrors, Supermirrors, Multilayer Monochro-mators, Polarizers, and Beam Guides, v983, p129-143

Keywords: Neutron spectrometers, Neutron scattering, Polarization(Spin alignment), *Neutron reflectors,

Neutron reflectometers, Supermirrors, Multilayers, Polarized beams.

It is expected that thin-film mirrors, multilayers and supermirrors will play an important role as optical elements to transport, focus, monochromate, and polarize neutrons at the cold neutron research facility which is presently under construction at the National Bureau of Standards. In the paper, specific applications of these reflecting devices to three instruments, a spin-polarized, inelastic scattering spectrometer with novel, adjustable resolution properties, a focusing small angle scattering machine, and a neutron reflectometer are described

901.541 PB89-211999 PB89-211999 Not available NTIS National Bureau of Standards (IMSE), Gaithersburg, MD. Reactor Radiation Div.

Calculations and Measurement of the Perform-

ance of Converging Neutron Guides. Final rept.

Prina rept.
J. R. D. Copley, and C. F. Majkrzak. 1989, 12p
Pub. in Proceedings of SPIE (Society of Photo-Optical Instrumentation Engineers), Thin-Film Neutron Optical Devices: Mirrors, Supermirrors, Multilayer Monochromators, Polarizers, and Beam Guides, v983 p93-104

Keywords: Neutron beams, Convergence, Mirrors, *Neutron guides, Neutron reflectors, Supermirrors.

If properly designed, converging guides may be used to increase the current density of neutrons in a beam from a parallel neutron guide. The disadvantage of this type of device is that there is an increase in beam divergence. The spatial and angular distributions of the beam emerging from a converging guide are generally nonuniform, and the performance of the guide is dependent on the neutron's wavelength. Analytic and numerical methods of calculation are bnefly discussed, and the results of selected Monte Carlo numerical calculations are presented. Measurements on a scaled down version of a converging guide system are reported and found to compare well with calculation.

901.542 PB89-212062 PB89-212062 Not available NTIS National Bureau of Standards (NML), Boulder, CO. Quantum Physics Div.

Liquid-Supported Torsion Balance: An Updated Status Report on Its Potential for Tunnel Detection.

Final rept.

J. E. Faller, P. T. Keyser, and M. P. McHugh. 1988, 22p Sponsored by Air Force Weapons Lab., Kirtland AFB,

NM. Pub. in Proceedings of Technical Symposium on Tunnel Detection (3rd), Golden, CO., January 12-15, 1988, p412-433.

Keywords: *Torsion balances, *Tunnel detection, Variometers, Precision, Measurement, *Gradiometers.

At the Joint Institute for Laboratory Astrophysics, the authors have been developing the liquid-supported torsion balance (LSTB), also known as the fluid-fiber torsion balance, for a variety of precision measurement applications. Recent work has concentrated on curvaapplications. Recent work has concentrated on curve ture variometers and 'split-disc' vertical gradiometers as an auxiliary to 'Fifth-Force' tests. The authors review the history and design of the LSTB and de-scribe the theoretical and experimental progress since the last Symposium on Tunnel Detection. Significant increases in experimental sensitivity to changes in the curvature of the level surface have been made together with advances in understanding and reducing various noise terms. The current limiting noise terms and sensitivity to tunnel evolution are discussed.

901.543 PB89-212138 Not available NTIS National Bureau of Standards (NEL), Gaithersburg, MD. Thermophysics Div.
Simulation Study of Light Scattering from Soot Ag-

glomerates. Final rept.

Pilia repl.

1988, 6p

Pub. in Springer Proceedings in Physics, v33 p49-54

Keywords: *Light scattering, *Agglomeration, Soot, Computerized simulation, Distribution functions, Dynamics.

The article presents an example of current research utilizing Langevin dynamics simulation methods. This technique is used to generate agglomerates with soot-like structures. The light scattering properties of the agglomerates are examined in order to determine the information available in light scattering measurements and how this information relates to the structure of the

PC A04/MF A01 National Inst._of Standards and Technology (NEL), Vapor-Liquid Equilibrium of Binary Mixtures in the Extended Critical Region. i. Thermodynamic

Modei. Technical note.

J. C. Rainwater. Apr 89, 73p NIST/TN-1328
Also available from Supt. of Docs. as SN003-003-02945-9. Sponsored by Department of Energy, Washington, DC. Office of Basic Energy Sciences.

Keywords: *Thermodynamic equilibrium, *Models, Thermodynamics, Density, Vapor phases, Liquids, *Binary mixtures.

The thermodynamic model of Leung and Griffiths for binary mixture vapor-liquid equilibrium near the critical locus, as modified by Moldover, Rainwater and coworkers, is extended to accommodate fluid pairs of greater dissimilarity.

901,545 PB89-227987 Not available NTIS National Inst. of Standards and Technology (NEL), Boulder, CO. Thermophysics Div. Asymptotic Expansions for Constant-Composition

Dew-Bubble Curves Near the Critical Locus. Final rept. J. C. Rainwater. 1989, 12p

Sponsored by Department of Energy, Washington, DC. Pub. in International Jnl. of Thermophysics 10, n2 p357-368 1989.

Keywords: *Critical point, *Bubbles, *Dew, Critical temperature, Critical pressure, Curves(Geometry), Asymptotic series, Approximation, Thermodynamic properties, Reprints, Binary mixtures, Liquid vapor equilibri-

Explicit function representations are developed for constant-composition dew and bubble curves near critical according to the modified Leung-Griffiths theory. The critical point in temperature-density space is shown to be a point of maximum concave upward curvature, rather than an inflection point as previously conjectured.

901,546 PB89-228019 PB89-228019 Not available NTIS
Not available NTIS
Thermorphysis Standards (NEL), Boulder, CO. Thermophysics Div.

Mean Density Approximation and Hard Sphere Ex-pansion Theory: A Review. Final rept.

Fillal 1595. L. J. Chen, J. F. Ely, and G. A. Mansoori. 1987, 27p Sponsored by Gas Research Inst., Chicago, IL. Pub. in Fluid Phase Equilibria 37, p1-27 1987.

Keywords: *Liquids, *Mixtures, Density, Computer simulation, Approximation, Van der Waals equation, Ther-modynamic equilibrium, Thermodynamic properties, Reprints, *Mean density approximation, *Hard sphere expansion theory, Liquid vapor equilibrium.

The review surveys research dealing with the Mean Density Approximation (MDA) and the Hard Sphere Expansion (HSE) theory developed by Leland and coworkers. MDA and its modifications provide a simple way to predict radial distribution functions of inixtures from the pure fluid information. Comparisons with computer simulation data show the MDA to be superior to the van der Waals approximation for mixture radial dis-tribution functions. Derivations of the HSE theory and the HSE Conformal Solution Theory (HSE-CST) are also described. For Lennard-Jones mixtures, the HSE theory is proven to be superior to the van der Waals theory by using a proper method to determine the hard-sphere diameter. The major problem associated with the development of a consistent method to determine the hard-sphere diameter of the HSE-CST and the requirements regarding the extension of the HSE-CST to polar mixtures are discussed.

901,547 PB89-228027

Not available NTIS

National Bureau of Standards (NEL), Boulder, CO. Thermophysics Div.

Method for Improving Equations of State Near the Criticai Point. Final rept.

D. D. Erickson, T. W. Leland, and J. F. Ely. 1987,

Sponsored by Gas Research Inst., Chicago, IL Pub. in Fluid Phase Equilibria 37, p185-205 1987.

Keywords: *Equations of state, *Carbon dioxide, *Pentanes, *Critical point, Thermodynamic properties, Ideal gases, Reprints.

Accurate nonanalytic equations of state have been developed for pentane and carbon dioxide for use as reference equations in the critical region. This was done using a method which transforms any analytic equation of state into a nonanalytic equation of state. For this study, a 32 constant analytic BWR equation of state was transformed into a nonanalytic equation of state. The nonanalytic equation of state is more accurate in the critical region for the prediction of the PVT properties of carbon dioxide than is a Schmidt-Wagner analytic equation of state developed at the National Bureau of Standards. The nonanalytic equation of state is slightly less accurate over the whole PVT surface than the Schmidt-Wagner equation of state, but the predicted nonanalytic surface makes a smooth transition into the classical region. This is an improvement over the scaled fundamental equation of state which breaks down at a small distance away from the critical point.

901,548 PB89-228035 Not available NTIS

Notional Inst. of Standards and Technology (NEL), Boulder, CO. Thermophysics Div.

Prediction of Shear Viscosity and Non-Newtonian Behavior in the Soft-Sphere Liquid. Final rept.

H. J. M. Hanley, J. C. Rainwater, and M. Huber. 1988, 10p

Sponsored by Department of Energy, Washington, DC. Pub. in International Jnl. of Thermophysics 9, n6 p1041-1050 Nov 88.

Keywords: *Non-Newtonian fluids, *Shear properties, Viscosity, Rheological properties, Relaxation time, Molecular relaxation, Liquids, Correlation, Reprints.

It is shown that a shear rate-dependent viscosity coefficient, normal pressure differences, and shear dilatancy can be predicted in a soft-sphere liquid given only the equilibrium radial distribution function and a relax-ation time. Calculations are made using the relaxationtime theory of Hess and Hanley, and the results are compared with simulation data from nonequilibrium molecular dynamics.

901,549 PB89-228100 PB89-228100 Not available NTIS National Bureau of Standards (NML), Boulder, CO. Quantum Physics Div.

Spectroscopic Detection Methods. Final rept.

U. Hefter, and K. Bergmann. 1983, 61p Pub. in Atomic and Molecular Beam Methods, Chapter 9, p193-253 1988.

Keywords: *Atomic energy levels, *Molecular energy levels, Molecular beams, Alignment, Reprints, *Laser induced fluorescence, *Vibrational states, *Rotational states, Multi-photon processes, Raman effect, Optical fibers, Magic angle detectors.

The authors discuss the basic formulae relevant to laser induced fluorescence detection of atomic and molecular level population and alignment as well as velocities. Discussion of other techniques such as twophoton ionization and Raman scattering is also includ-ed. Experimental hardware such as high-speed optical devices and optical fibers are described.

PB89-228118 Not available NTIS National Bureau of Standards (NML), Boulder, CO.

Quantum Physics Div. State Selection via Optical Methods. Final rept.

K. Bergmann, 1988, 52p Pub. in Atomic and Molecular Beam Methods, Chapter 12, p293-344 1988.

Keywords: *Atomic energy levels, *Molecular energy levels, Experimental design, Optical pumping, Selec-

tion, Alignment, Atomic beams, Molecular beams, Reprints, *Rotational states, *Vibrational states, Laser applications.

The author describes the experimental techniques of laser state selection in atomic and molecular beams that have been developed since 1975. The bibliography contains about 200 references concerning selection of rotational-vibrational states as well as alignment in atoms, simple molecules, and molecular ions.

901,551

PB89-228365 Not available NTIS National Bureau of Standards (NML), Boulder, CO. Quantum Physics Div.

Precision Experiments to Search for the Fifth

J. E. Faller, E. Fischbach, Y. Fujii, K. Kuroda, H. J. Paik, and C. C. Speake. 1989, 9p

Sponsored by Department of Energy, Washington, DC. Pub. in IEEE (Institute of Electrical and Electronics Engineers) Transactions on Instrumentation and Measurement 38, n2 p180-188 Apr 89.

Keywords: *Gravitation, Experimental design, Precision, Reprints, *Fifth force, *Basic interactions.

The suggestion of a possible new fifth force of Nature has prompted a large number of high precision experi-ments to search for its presence. After reviewing the motivation for this suggestion, the authors describe some of the experiments that are presently underway and the results that have been obtained to date.

901.552

PB89-228381 Not available NTIS National Inst. of Standards and Technology (NML), Boulder, CO. Quantum Physics Div.

Ionization and Current Growth in N2 at Very High Electric Field to Gas Density Ratios.

Final rept.

V. T. Gylys, B. M. Jelenkovic, and A. V. Phelps. 1989, 12p

Pub. in Jnl. of Applied Physics 65, n9 p3369-3380, 1 May 89.

Keywords: *Nitrogens, *Gas discharges, *Gas ionization, Electric current, Electric fields, Electric measurement, Reprints, Electron impact, Low pressure, High

Measurements and analyses have been made of electron impact ionization and of current growth in pulsed, low-current, prebreakdown discharges in parallelplane geometry in N2 at very high electric field to gas density ratios E/n and low products of the gas density n and electrode separation d. Measurements were made of the transported charge on the tie scales of electron transit, ion transit, and metastable decay. Measurements were also made of the growth of steady-state discharge currents as a function of discharge voltage. The contributions of avalanches resulting from ion and metastable-induced secondary electrons were determined from the ratio of electronexcited N2(1+) 391.4-nm emission integrated over all avalanches to the integrated emission during the laserinitiated electron pulse.

901,553 PB89-229090 Not available NTIS National Bureau of Standards (NEL), Boulder, CO. Chemical Engineering Science Div.

Performance of He ii of a Centrifugal Pump with a

Jet Pump Inducer.

Final rept.

D. E. Daney, P. R. Ludtke, and A. Kashani. 1989, 6p Sponsored by National Aeronautics and Space Admin-istration, Moffett Field, CA. Ames Research Center. Pub. in Cryogenics 29, p563-568 May 89.

Keywords: *Centrifugal pumps, *Jet pumps, Liquid helium, Weightlessness, Superfluidity, Cavitation, Performance, Reprints, Helium II.

The tendency of turbopumps operating in He II to cavitate makes their use in zero gravity questionable betate makes their use in zero gravity questionable be-cause of the zero net positive suction head (NPSH) available at the pump inlet. The authors investigated a jet pump, positioned at the inlet of a centrifugal pump with a screw inducer, as a means of operating a cen-trifugal pump at zero or lower NPSH. Pump perform-ance in He II was measured as a function of NPSH for its six different combinations of primary and secondary six different combinations of primary and secondary nozzles. Suction heads down to -91 mm were meas-

ured for a 3% reduction in developed head. These are referenced to the leading edge of the screw inducer, which is 100 mm above the jet pump inlet. Because cavitation at the primary jet always precedes cavitation in the jet pump secondary nozzle, they also tested reverse (pressure driven) flow through a porous plug as a means of obtaining a subcooled primary jet. These brief tests were inconclusive.

901,554 PB89-230395 Not available NTIS National Bureau of Standards (NML), Gaithersburg, MD. Electricity Div.

improved Transportable DC Voltage Standard.

Final rept. B. F. Field, and M. R. McCaleb. 1989, 6p Sponsored by Department of Defense Calibration Co-

ordination Group, Redstone Arsenal, AL.
Pub. in IEEE (Institute of Electrical and Electronics Engineers) Transactions on Instrumentation and Measurement 38, n2, p324-329, Apr 89.

Keywords: *Electrical measurement, *Standards, *Avalanche diodes, Calibrating, Prototypes, Reprints.

Zener-diode-based dc voltage standards can be excel-lent transport standards for the unit of dc voltage because of their resistance to physical shock and temperature changes. The problems of transporting a unit of voltage and the properties of available Zener standards were studied to develop a set of characteristics considered essential for an optimum transport standard. The report lists some of the results of the require-ments study, explains the design of the improved transport standard, discusses the efforts to select Zener diodes for the standards, and presents data obtained from prototype Zener reference modules to be used in the standard.

901,555 PB89-230411 Not available NTIS National Bureau of Standards (NML), Gaithersburg,

Low Field Determination of the Proton Gyromagnetic Ratio in Water.

Final rept. E. R. Williams, G. R. Jones, S. Ye, R. Liu, H. Sasaki, P. T. Olsen, W. D. Phillips, and H. P. Layer. 1989, 5p Pub. in IEEE (Institute of Electrical and Electronics Engineers) Transactions on Instrumentation and Measurement 38, n2, p233-237, Apr 89.

Keywords: *Fundamental constants, Nuclear magnetic resonance, Electrical resistance, Solenoids, Precision, Reprints, *Gyromagnetic ratio, Quantum Hall effect, Fine structure constant.

The authors measured the proton gyromagnetic ratio in H2O by the low field method, gamma'(p)(low). The result gamma'(p)(low) = 2.67 513 376 10 to the 8th power/s(T(NBS)) (0.11 ppm), leads to a value of the fine structure constant of 1/alpha = 137.0 359 840 (0.037 ppm) and a value for the quantized Hall resistance in SI units of R(H) = 25 812.80460 ohm (0.037 ppm). To apply this result they measured the displacements. ppm). To achieve this result, they measured the dimensions of a 2.1-m solenoid with an accuracy of 0.04 micrometer, and then measured the NMR frequency of a water sample in the field of the solenoid.

901,556 PB89-230437 Not available NTIS National Bureau of Standards (NML), Gaithersburg, MD. Electricity Div.

NBS (National Bureau of Standards) Determination of the Fine-Structure Constant, and of the Quantized Hall Resistance and Josephson Frequencyto-Voltage Quotient in SI Units.

Final rept. M. E. Cage, R. F. Dziuba, R. E. Elmquist, B. F. Field, G. R. Jones, P. T. Olsen, W. D. Phillips, J. Q. Shields, R. L. Steiner, B. N. Taylor, and E. R.

1989, 6p

Williams. 1989, 6p
Pub. in IEEE (Institute of Electrical and Electronics Engineers) Transactions on Instrumentation and Measurement 38, n2, p284-289, Apr 89.

Keywords: *Fundamental constants, Reprints, *Fine structure constant, *Quantum Hall effect, *Josephson effect, *Plancks constant, *Electron charge.

Results from NBS experiments to realize the ohm and the watt, to determine the proton gyromagnetic ratio by the low field method, to determine the time dependence of the NBS representation of the ohm using the quantum Hall effect, and to maintain the NBS representation of the volt using the Josephson effect, are

appropriately combined to obtain an accurate value of the fine-structure constant and of the quantized Hall resistance in SI units, and values in SI units of the Josephson frequency-to-voltage quotient, Planck constant, and elementary charge.

PB89-230445 Not available NTIS National Bureau of Standards (NML), Gaithersburg, MD. Electricity Div.

New Realization of the Ohm and Farad Using the NBS (National Bureau of Standards) Calculable Capacitor. Final rept.

J. Q. Shields, R. F. Dziuba, and H. P. Layer. 1989, 3p Pub. in IEEE (Institute of Electrical and Electronics Engineers) Transactions on Instrumentation and Measurement 38, n2, p249-251, Apr 89.

Keywords: *Electric measuring instruments, Ohmmeters, Electrical measurement, Electrical resistance meters, Capacitors, Reprints, *National Institute of Standards and Technology, *Absolute ohm, *Absolute farad.

Results of a new realization of the ohm and farad using the NBS calculable capacitor and associated apparatus are reported. The results show that both the NBS representation of the ohm and the NBS representation of the farad are changing with time: the ohm at the rate of-0.054 ppm/year and the Farad at the rate of 0.010 ppm/year. The realization of the ohm is of particular significance at this time because of its role in assigning an SI value to the quantized Hall resistance. The estimated uncertainty of the ohm realization is 0.022 ppm while the estimated uncertainty of the farad realization is 0.014 ppm.

901.558

PB89-234165
National Inst. of Standards and Technology (NML), Gaithersburg, MD. Atomic and Plasma Radiation Div. Line Identifications and Radiative-Branching Ratios of Magnetic Dipole Lines in Si-iike Ni, Cu, Zn, Ge, and Se.

Final rept. R. U. Datla, J. R. Roberts, N. Woodward, S. Lippman, and W. L. Rowan. 1989, 4p Sponsored by Department of Energy, Washington, DC. Pub. in Physical Review A 40, n3 p1484-1487, 1 Aug

Keywords: Plasmas(Physics), Line spectra, Reprints, *M1-transitions, Multicharged ions, Branching ratio, Nickel ions, Copper ions, Zinc ions, Germanium ions, Selenium ions, Tokamak devices, Calibration.

Magnetic dipole transitions within the ground-state configuration of Si-like Ni, Cu, Zn, Ge, and Se have been observed. Seven lines have been newly identified. Observations are made on the Texas Experimentied. Observations are made on the Texas Experimental Tokamak by laser-ablation injection of each of these elements into the plasma. The radiative-branching-ratio technique, utilizing lines originating from the same upper level, 3p(2) (1)D2, is used for the radiometric calibration of a 1-m normal-incidence spectrometer. This calibration is in good agreement with the absolute radiometric calibration obtained by using an access minister. argon miniarc.

901.559

Not available NTIS PB89-234306 National Inst. of Standards and Technology (NML), Boulder, CO. Quantum Physics Div. Sodium Doppler-Free Collisional Line Shapes.

Final rept.

M. J. O'Callaghan, and A. Gallagher. 1989, 16p Grant NSF-PHY86-04504 Sponsored by National Science Foundation, Washing-

ton, DC Pub. in Physical Review A 39, n12 p6190-6205, 15 Jun

Keywords: *Sodium, Excitation, Reprints, Atom collisions, Line broadening.

Measurements of resonant, two-step excitation of sodium in the presence of very-low-pressure buffer gases (He, Ar, Xe, and N2) are reported. These data are analyzed to isolate the effects of line broadening and velocity-changing (VC) collisions in the single-col-lision limit. Velocity dependence of the several line broadenings involved is obtained from this data analysis. The inelastic VC kernels are also obtained as a function of initial velocity.

901.560

PB90-117292 Not available NTIS National Inst. of Standards and Technology (NML), Gaithersburg, MD. Center for Radiation Research. Cross Section and Linear Polarization of Tagged Photons. Final rept.

J. Asai, H. S. Caplan, D. M. Skopik, W. Del Bianco, and L. C. Maximon. 1988, 9p Pub. in Canadian Jnl. of Physics 66, p1079-1087 1988.

Keywords: *Bremsstrahlung, *Photon cross sections, *Polarization(Waves), Monochromators, Marking, Reprints, *Tagged photon method, Coordinate transformations, Linear polarization.

Formulae for bremsstrahlung cross sections and po-larizations are usually presented in coordinate systems unsuitable for application by experimental physicists to devices such as photon-tagging monochromators. The paper presented the transformations between the different coordinate systems, along with examples of the calculated cross sections and polarizations in a form convenient from the experimental standpoint. These examples also give the predicted characteristics of the photon tagger currently under construction at the Sas-katchewan Accelerator Laboratory.

901.561

PB90-117565 Not available NTIS National Inst. of Standards and Technology (NML), Gaithersburg, MD. Center for Radiation Research. Intrinsic Sticking in dt Muon-Catalyzed Fusion: Interplay of Atomic, Molecular and Nuclear Phenomena Final rept.

M. Danos, A. A. Stahlhofen, and L. C. Biedenharn. 1989, 46p Pub. in Annals of Physics 192, n1 p158-203, 15 May

Keywords: *Nuclear fusion, Molecules, Atoms, Deuterium, Tritium, Reprints, *Muon-catalyzed fusion, Branching ratio.

comprehensive reaction theory for the resonant muon catalyzed fusion of deuterium and tritium is formulated. Emphasis is put on non-perturbative, many body treatment of the long range Coulomb force and its interference with the nuclear forces, with the aim of providing the theoretical framework for an accurate calculation of the branching ratio dt(mu) -> ((alpha + mu) + n)/(alpha + mu + n) essential for muon catalyzed fusion.

901.562

PB90-117581 Not available NTIS National Inst. of Standards and Technology (NML), Gaithersburg, MD. Quantum Metrology Div. Marked Differences in the 3p Photoabsorption be-tween the Cr and Mn(1+) Isoelectronic Pair: Reasons for the Unique Structure Observed in Cr.

J. W. Cooper, C. W. Clark, C. L. Cromer, T. B. Lucatorto, B. F. Sonntag, E. T. Kennedy, and J. T. Costello. 1989, 4p
Contract AFOSR-ISSA-87-0050

Sponsored by Air Force Office of Scientific Research, Bolling AFB, DC.

Pub. in Physical Review A 39, n11 p6074-6077, 1 Jun

Keywords: *Chromium, *Atomic structure, *Absorption spectra, Atomic energy levels, Reprints, *Manganese ions, *Photoabsorption, Inner-shell excitation, Inner-shell ionization, Giant resonance.

Chromium is the only member of the transition-group elements with a well-developed Rydberg structure appearing in its 3p-absorption spectrum. New high-resolution measurements of Mn, Mn(1+) and Cr have revealed weak Rydberg structure in Mn(1+) and an analysis of the data shows that the anomalous Cr 3p absorption spectra is due to a unique relationship between its energy levels, and not to the previously supposed fact that Cr has an unpaired 4s electron.

901,563

PB90-117730 Not available NTIS National Inst. of Standards and Technology (NML), Gaithersburg, MD. Center for Radiation Research. Comment on 'Feasibility of Measurement of the Electromagnetic Polarizability of the Bound Nucleon'.

Final rept. E. Hayward. 1989, 3p

Pub. in Physical Review C 40, n1 p467-469 1989.

Keywords: *Nucleons, Measurement, Feasibility, Polarization(Spin alignment), Reprints, *Polarizability, Bound state, Total cross sections, Photon absorption, Photon scattering

It is shown that the polarizability of the bound nucleon is, within the errors in the total cross section measurements, the same as that of a free nucleon.

901,564 PB90-123449 Not available NTIS National Inst. of Standards and Technology (NML), Gaithersburg, MD. lonizing Radiation Physics Div. (109)Pd and (109)Cd Activity Standardization and Decay Data. Final rept.

C. Ballaux, B. M. Coursey, and D. D. Hoppes. 1988,

Pub. in Applied Radiation and Isotopes 39, n11 p1131-1139 1988.

Keywords: Radioactive decay, Internal conversion, Beta particles, Radiotherapy, Standardization, Reprints, *Cadmium 109, *Palladium 109, Gamma radiation, Activity levels.

Sources of (109)Cd and (109)Pd were measured with liquid-scintillation counters, a NaI (TI) well detector, a 4 pi(Si(Li)) assembly, a Ge(Li) detector, and ionization chambers. For the 88.034-keV transition, a total internal-conversion coefficient of 26.21 plus or minus 0.14 and a gamma-ray emission probability of 3.675 plus or minus 0.018% were measured. (109)Pd, because of its short half life, 13,404 plus or minus 0.008 h, and high beta-ray energy, has some promise of applications in radiotherapy. The uncertainty in the present activity standardization was only 0.41%.

901,565 PB90-123506 Not available NTIS National Inst. of Standards and Technology (NML), Advances in the Use of (3)He in a Gas Scintillation Counter. Final rept.

J. W. Behrens, H. Ma, and O. A. Wasson. 1986, 1p Pub. in Transactions of the American Nuclear Society 53, p163 1986.

Keywords: *Scintillation counters, *Helium 3, Reprints, *Gas scintillation detectors, *Neutron detectors.

The development of a (3)He gas scintillator for use as a neutron detector is described.

901,566 PB90-123605 Not available NTIS National Inst. of Standards and Technology (NML), Gaithersburg, MD. Ionizing Radiation Physics Div. Electron Stopping Powers for Transport Calculations. Final rept.

M. J. Berger. 1988, 24p

Sponsored by Department of Energy, Washington, DC. Pub. in Monte Carlo Transport of Electrons and Photons, Chapter 3, p57-80 1988.

Keywords: Excitation, Positrons, Reviews, Reprints, *Electron transport, *Electron collisions, *Stopping power.

The paper reviews the calculation and tabulation of collision stopping powers for electrons, mainly at energies above 10 keV. The discussion includes mean excitation energies and the density-effect correction.

901,567 PB90-123670 Not available NTIS National Inst. of Standards and Technology (NML), Gaithersburg, MD. Quantum Metrology Div. Determination of Short Lifetimes with Ultra High Resolution (n,gamma) Spectroscopy. Final rept.

H. G. Borner, J. Jolie, F. Hoyler, S. Robinson, M. S. Dewey, G. Greene, E. Kessler, and R. D. Deslattes. 1988, 5p

Pub. in Physics Letters B 215, n1 p45-49 1988.

Keywords: *Nuclear energy levels, Neutron reactions, Gamma rays, Reprints, *Excited states, *Lifetime,

Gamma spectroscopy, Doppler broadening, High reso-

It is shown how high resolution (n,gamma) spectroscopy allows the determination of lifetimes of nuclear excited levels, through the observation of Doppler broadening. The Doppler broadening of these gamma-rays is due to the recoil from the feeding of gamma-ray transition.

901,568

PB90-123720 Not available NTIS National Inst. of Standards and Technology (NML), Boulder, CO. Quantum Physics Div.

Approximate Formulation of Redistribution In the

Ly(alpha), Ly(beta), H(alpha) System.

Final rept.

J. Cooper, R. J. Ballagh, and I. Hubeny. 1989, 17p Grant NSF-PHY86-04504

Sponsored by National Science Foundation, Washington, DC

Pub. in Astrophysical Jnl. 344, n2 p949-965, 15 Sep

Keywords: *Hydrogen, Absorption spectra, Emission spectra, Approximation, Distribution functions, Reprints, Lyman lines, Line broadening, Redistribution.

Simple approximate formulae are given for the coupled redistribution of Ly(alpha), Ly(beta, and H(alpha), by using well-defined approximations to an essentially exact formulation. These formulae incorporate all the essential physics including Raman scattering, lower state radiative decay, and correlated terms representing emission during a collision which must be retained in order that the emission coefficients are properly behaved in the line wings. Approximate expressions for the appropriate line broadening parameters are collected. Finally, practical expressions for the source functions are given. These are formulated through newly introduced non-impact redistribution functions, which are shown to be reasonably approximated by existing (ordinary and generalized) redistribution functions.

901.569

PB90-123738 Not available NTIS National Inst. of Standards and Technology (IMSE), Gaithersburg, MD. Reactor Radiation Div. Neutron Scattering and Its Effect on Reaction Rates in Neutron Absorption Experiments. Final rept.

J. R. D. Copley, and C. A. Stone. 1989, 12p Pub. in Nuclear Instruments and Methods in Physics Research A281, p593-604 1989.

Keywords: *Neutron absorption, *Neutron scattering, Monte Carlo method, Neutron radiography, Reprints, Activation analysis, Self-shielding.

In general there is a systematic error in the results of any in-beam neutron absorption experiment because of neutron scattering in the sample. The error is largest when scattering predominates over absorption, when the transmission of the sample is small, and when the lateral dimensions of the sample are large compared with its thickness. The ratio of the reaction rate in the sample to the rate calculated ignoring both scattering self-shielding due to absorption may be significantly less than or greater than unity, depending on the scattering properties of the sample and its size and shape. The conclusions are derived from Monte Carlo calculations based on a very general expression for the rate of a neutron absorption reaction in a sample which scatters and absorbs neutrons. The expression for the reaction rate, written as a sum over orders of scattering within the sample, was obtained using the technique adopted by V.F. Sears in his study of multiple scattering effects in neutron scattering experi-ments. The authors' calculations were performed for slab samples placed in a narrow, monoenergetic, monodirectional neutron beam. The assumed scattering cross section was isotropic and also static, meaning that no change in neutron energy was permitted to occur within the sample. The work has potentially important implications in various areas of neutron research including activation analysis and radiography.

901,570

PB90-123746 Not available NTIS National Inst. of Standards and Technology (NML), Gaithersburg, MD. Radiometric Physics Div.

Neonlike Ar and CI 3p-3s Emission from a thetapinch Plasma. Final rept.

R. C. Elton, R. U. Datla, J. R. Roberts, and A. K.

Bhatia. 1989, 3p Pub. in Physical Review A 40, n7 p4142-4144, 1 Oct

Keywords: Spectral lines, Emission spectra, Reprints, *Argon ions, *Chlorine ions, Multicharged ions, Extreme ultraviolet radiation, X ray lasers, Theta pinc

Time-resolved extreme-ultraviolet emission from siteen 3p-3s transitions, some of the type in which lasing has been demonstrated in heavier elements, is measured for neonlike Ar(8+) and Cl(7+). These observa-tions are made on a hydrogen theta-pinch plasma with a 5% admixture of argon or freon (for Cl). Fourteen 3d-3p spectral lines are also detected. The measured in tensities are compared to theoretical predictions. Al. major lines agree within plus or minus 30%. Hence, there is no evidence of anomalously intense lines originating on 2p(5)3p J = 2 upper levels compared to J0, as observed in gain experiments.

901,571 PB90-123761 Not available NTIS National Inst. of Standards and Technology (NML), Boulder, CO. Quantum Physics Div. Exoergic Collisions of Cold Na*-Na.

Final rept. A. Gallagher, and D. Pritchard. 1989, 4p Grant N00014-83-K-0695

Sponsored by Office of Naval Research, Arlington, VA. Pub. in Physical Review Letters 63, n9 p957-960, 28 Aug 89.

Keywords: *Sodium, Reprints, *Atomic traps.

Rates were calculated for two exothermic excitedstate collision processes involving sodium at ultracold temperatures. The authors predict that the rate for fine-structure changing collisions exceeds that of radiative redistribution with release of enough energy to cause loss from current optical traps. A semiclassical treatment is used which accounts for the frequency dependence of absorption and spontaneous emission in midcollision.

901.572 PB90-123837 Not available NTIS National Inst. of Standards and Technology (NML), Boulder, CO. Quantum Physics Div. Spectroscopy of Autoionizing States Contributing

to Electron-Impact ionization of lons. Final rept.

A. Muller, G. Hofmann, K. Tinschert, E. Salzborn, G.

H. Dunn, and R. Becker. 1989, 3p
Pub. in Nuclear Instruments and Methods in Physics Research B40/41, p232-234 1989.

Keywords: Excitation, Reprints, *Electron ion collisions, *Autoionization, Ionization cross sections, Electron impact, Colliding beams.

In electron-ion crossed-beam experiments the authors have used a fast electron-energy scanning technique to detect fine details in ionization cross sections. They obtained data with a relative point to point uncertainty of less than 0.1%. The electron energy spread at 100 eV (15 mA beam current) is 0.4 eV. Thus they were able to measure state-resolved excitation-autoionization contributions and to demonstrate new ionization mechanisms involving dielectronic capture of the pro-jectile electron with subsequent emission of several electrons.

PB90-123845 Not available NTIS National Inst. of Standards and Technology (NML), Boulder, CO. Quantum Physics Div. Electron-Impact Ionization of La(q+) Ions (q = 1,2,3). Final rept.

A. Mueller, K. Tinschert, G. Hofmann, E. Salzborn, G. H. Dunn, S. M. Younger, and M. S. Pindzola. 1989.

Contract DE-AI05-86ER53237

Sponsored by Department of Energy, Washington, DC. Office of Energy Research. Pub. in Physical Review A 40, n7 p3584-3598, 1 Oct

Keywords: Excitation, Reprints, *Electron ion colli-*Lanthanum ions, Ionization cross sections,

Multicharged ions, Colliding beams, Electron impact,

Experimental cross sections for single ionization of La(1+), La(2+), and La(3+) ions as well as for double ionization of La(1+) and La(2+) ions and for triple ionization of La(2+) ions are presented in an electron-impact energy range from threshold up to 1000 eV. By using a fast energy-scanning technique with step widths of about 40 meV and an energy resolution of 0.4 eV, fine details in the cross sections and especially resonant contributions could be observed. Resonant excitation of La(2+) at 95 eV with subsequent emission of three electrons appears in the authors' inter-pretation to account for 30% of the total measured double-ionization cross section. The data are interpreted on the basis of calculations of energy levels and distorted-wave calculations of direct ionization from various electron sub-shells and of excitation-autoionization processes. A detailed analysis of the La(3+ single ionization both for ground-state and 5p(5)4f metastable ions is presented.

PB90-123902 Not available NTIS National Inst. of Standards and Technology (NML), Gaithersburg, MD. Ionizing Radiation Physics Div. Applications of ETRAN Monte Carlo Codes.

Final rept. S. M. Seltzer. 1988, 26p

Sponsored by Department of Energy, Washington, DC. Pub. in Monte Carlo Transport of Electrons and Photons, Chapter 9, p221-246 1988.

Keywords: Monte Carlo method, Bremsstrahlung, Electrons, Radiation shielding, Aerospace environment, Reprints, *ETRAN computer code, *Radiation transport, Electron transport, Gamma detection, Liquid scintillation detectors, Energy losses, Uses.

Some applications of ETRAN Monte Carlo calculations to radiation transport problems are described. These include calculations of the response of gamma-ray detectors, the shielding from the dose due to electrons and bremsstrahlung in space-radiation environments, the characteristics of bremsstrahlung beams for use in radiation processing, and the distortion of energy-loss spectra due to energy lost in the walls of containers used in liquid-scintillation counting of beta emitters.

901,575 PB90-123910 PB90-123910

Not available NTIS
National Inst. of Standards and Technology (NML),
Gaithersburg, MD. Ionizing Radiation Physics Div.
Cross Sections for Bremsstrahlung Production
and Electron-Impact Ionization Final rept.

S. M. Seltzer. 1988, 34p Sponsored by Department of Energy, Washington, DC. Pub. in Monte Carlo Transport of Electrons and Photons, Chapter 4, p81-114 1988.

Keywords: *Bremsstrahlung, *Ionization, Positrons, Reprints, *Electron impact, *Electron transport, Ionization cross sections, Electron-atom collisions, Electronmolecule collisions.

The paper discusses the cross section for two processes that are important in electron transport calculations: bremsstrahlung production by electrons and po-sitrons in the fields of atomic nuclei and orbital electrons, and electron-impact ionization of atoms and molecules. In the discussion of bremsstrahlung, the author outlines the synthesis of various theoretical results that were involved in the development of a comprehensive set of cross sections, differential in emitted photon energy, for the production of bremsstrahlung by electrons, illustrates the generally good agreement between these cross sections and the results of measurement, and indicates the differences in the corresponding positron cross sections. In the case of electron-impact ionization, the author describes exploratory calculations of the shell-by-shell cross section, differential in ejected electron energy, based on a Weizsacker-Williams treatment.

901,576
PB90-123928
National Inst. of Standards and Technology (NML),
Gaithersburg, MD. Ionizing Radiation Physics Div. Overview of ETRAN Monte Carlo Methods. Final rept.

S. M. Seltzer. 1988, 29p Sponsored by Department of Energy, Washington, DC. Pub. in Monte Carlo Transport of Electrons and Photons, Chapter 7, p153-181 1988. Keywords: Monte Carlo method, Bremsstrahlung, Cross sections, Sampling, Reprints, *ETRAN computer code, *Radiation transport, Electron transport.

The paper outlines the sampling methods and the underlying cross sections used in the ETRAN Monte Carlo codes for coupled electron/photon transport calculations. The structure, capabilities, and limitations of current versions are briefly discussed, and some future improvements are indicated.

PB90-123936 Not available NTIS National Inst. of Standards and Technology (NML), Boulder, CO. Quantum Physics Div. Collisional Losses from a Light-Force Atom Trap. Final rept. D. Sesko, T. Walker, C. Monroe, A. Gallagher, and C. Weiman. 1989, 4p Grant NSF-PHY86-04504 Sponsored by National Science Foundation, Washington, DC., and Office of Naval Research, Arlington, VA. Pub. in Physical Review Letters 63, n9 p961-964, 28 Aug 89.

Keywords: Energy transfer, Reprints, *Atom collisions, *Atom traps, Cesium atoms, Energy losses.

The authors have studied the collisional loss rates for very cold cesium atoms held in a spontaneous-force optical trap. In contrast with previous work, it was found that collisions involving excitation by the trapping light fields are the dominant loss mechanism. It was also found that hyperfine-changing collisions between atoms in the ground state can be significant under some circumstances.

PB90-128034 Not available NTIS National Inst. of Standards and Technology (NML), Boulder, CO. Time and Frequency Div. Ion Trapping Techniques: Laser Cooling and Sympathetic Cooling.
Final rept.
J. J. Bollinger, L. R. Brewer, J. C. Bergquist, W. M. Itano, D. J. Larson, S. L. Gilbert, and D. J. Wineland. 1988, 11p Sponsored by Air Force Office of Scientific Research, Bolling AFB, DC., and Office of Naval Research, Arlington, VA.

Pub. in Proceedings of Workshop on Intense Positron Beams, Idahofalls, Idaho, June 18-19, 1987, p63-73

Keywords: Radiation pressure, Positrons, *Ion trapping, *Laser cooling, *Beryllium ions, *Mercury ions, *Sympathetic cooling, Penning traps.

Radiation pressure from lasers has been used to cool and compress (9)Be(1+) ions stored in a combination of static electric and magnetic fields (Penning trap) to temperatures less than 10 mK and densities greater temperatures less than 10 mK and densities greater than 10 to the 7th power/cm(-3) in a magnetic field of 1.4 T. A technique called sympathetic cooling can be used to transfer this cooling and compression to other ion species. An example of (198)Hg(1+) ions sympathetically cooled by laser cooled (9)Be(1+) ions is given. The possibility of making an ultracold positron source via sympathetic cooling is also discussed.

Not available NTIS PB90-128075 National Inst. of Standards and Technology (NML), Boulder, CO. Quantum Physics Div. Redistribution in Astrophysically Important Hydro-

gen Lines. Final rept. J. Cooper, R. J. Ballagh, and I. Hubeny. 1989, 30p Grant NGL-06-003-057

Sponsored by National Aeronautics and Space Administration, Washington, DC.
Pub. in Proceedings of International Conference on Spectral Line Shapes (9th), Torun, Poland, July 25-29, 1988, v5 p275-304 1989.

Keywords: *Hydrogen, Line spectra, Emission spectra, Absorption spectra, *Lyman lines.

Theory is specifically developed for the coupled Lyalpha, Ly-beta, H-alpha system, and equations of statistical equilibrium and absorption and emission coefficients are given. All correlated events are examined cients are given. All correlated events are examined and emission during a collision is found to be important in the line wings. Stimulated emission and absorption is also included within a broadband approximation. The major approximation is also included within a broadband approximation. The major approximation, adopted for convenience, is to ignore lower state interaction. (For H-alpha estimated errors in the redistribu-tion formulae from this approximation are the order of 20% in the line center and the order of 40% in the

901,580 PB90-128083 Not available NTIS National Inst. of Standards and Technology (NML), Gaithersburg, MD. Quantum Metrology Div. Performance of a High-Energy-Resolution, Tender X-ray Synchrotron Radiation Beamline. Final rept.

B. A. Karlin. 1989, 5p Pub. in Review of Scientific Instruments 60, n7 p1603-1607 Jul 89.

Keywords: Reprints, *NSLS, *Beamlines, Synchrotron radiation sources, X-ray sources, High resolution.

Beamline X-24A at the National Synchrotron Light Source was designed for optimal performance in the x-ray spectral region 500-5000eV. This choice of energy range placed a number of constraints on the beamline design, requiring a crystal monochromator in a windowless UHV environment. Although this increased the complexity of the design, there were compelling scientific reasons for the desire to work in this range. In addition to tunability over the selected energy range, a primary goal was to obtain the highest possible energy resolution in the primary beam. The authors have achieved incident energy resolution significantly better than the typical core-level lifetime broadening for this energy range. This has permitted studies of processes that are not broadened by lifetimes, such as resonant scattering and back-reflection x-ray standing-wave effects. In addition to high resolution, it was designed to collect and focus as much flux as possible from the bending magnet source.

PB90-128091 Not available NTIS National Inst. of Standards and Technology (NML), Boulder, CO. Time and Frequency Div. Laser Cooling to the Zero-Point Energy of Motion.

Final rept. Final rept.
F. Diedrich, J. C. Bergquist, W. M. Itano, and D. J. Wineland. 1989, 4p
Pub. in Physical Review Letters 62, n4 p403-406, 23

Jan 89.

Keywords: Atomic spectroscopy, Atomic structure, Reprints, *Laser cooling, *Mercury ions, prints, *Laser cooling, *Mercury ions, Trapping(Charged particles), Laser spectroscopy, High resolution

A single trapped (198)Hg(1+) ion was cooled by scattering laser radiation that was tuned to the resolved lower motional sideband of the narrow doublet S(1/2) doublet D(5/2) transition. The different absorption strengths on the upper and lower sidebands after cooling indicated that the ion was in the ground state of its confining well approximately 95% of the time.

901,582 PB90-128257
National Inst. of Standards and Technology (NML), Gaithersburg, MD. Atomic and Plasma Radiation Div. Branching Ratio Technique for Vacuum UV Radiance Calibrations: Extensions and a Comprehensive Data Set. Final rept.

Pub. in Jnl. of Quantitative Spectroscopy and Radiative Transfer 42, n5 p337-353 1989.

Keywords: Spectral lines, Transition probabilities, Reprints, *Vacuum ultraviolet radiation, *Branching ratio, *Multicharged ions, *Calibration, High temperature, Plasma.

The branching-ratio technique for calibrations in the VUV is reviewed in detail. The basic method is described, followed by extensions and applications. Lists of transitions suitable for the technique are given for H-, He-, Li-, and Be-like ions, along with pertinent data for their application.

901,583 PB90-128299 Not available NTIS National Inst. of Standards and Technology (NML), Gaithersburg, MD. Radiation Physics Div.

Progress on Spin Detectors and Spin-Polarized Electron Scattering from Na at NIST. Final rept.

J. J. McClelland. 1989, 13p

Sponsored by Department of Energy, Washington, DC. Pub. in Proceedings of Symposium on Polarization and Correlation in Electronic and Atomic Collisions, Hoboken, NJ., p1-13 Aug 89.

Keywords: *Electron scattering, *Thonium, Electron spin, Detectors, *Sodium atoms, *Electron spin polarization, Sherman functions, S matrix.

Recent progress in the Electron Physics Group at Hecent progress in the Electron Physics Group at NIST is discussed. Improvements have been made on the low-energy diffuse-scattering spin analyzer, reducing instrumental asymmetries and boosting the effective Sherman function. A figure of merit of0.00023 has been achieved. Thorium has been used as a target in a 100 ke V retarding Mott spin analyzer, resulting in an effective Sherman function as high as 0.40. This ineffective Sherman function as high as 0.49. This increased Sherman function, together with an increase scattering intensity, results in a factor of 2 increase in the figure of merit. Good agreement is seen between experiment and theoretical predictions of the Sherman function for thorium. A hierarchial description of the Tmatrix is discussed as a context for interpreting recent results on spin-polarized electron scattering from opti-cally pumped sodium. Results are presented for elastic and superelastic scattering at 20 eV incident energy.

901,584 PB90-128307 Not available NTIS National Inst. of Standards and Technology (NML), Gaithersburg, MD. Radiation Physics Div.
Superelastic Scattering of Spin-Polarized Elec-

trons from Sodlum. Final rept.

J. J. McClelland, M. H. Kelley, and R. J. Celotta. 1989, 9p

Sponsored by Department of Energy, Washington, DC. Pub. in Physical Review A 40, n5 p2321-2329, 1 Sep 89

Keywords: *Electron scattering, Polarization(Spin alignment), Reprints, *Sodium atoms, *Electron spin polarization, EV range 01-10, EV range 10-100.

Superelastic scattering of spin-polarized electrons Superelastic scattering of spin-polarized electrons from laser-excited sodium atoms has been measured at incident energies of 2.0, 17.9, and 52.3 eV over the angular range 10 deg - 120 deg. Circularly polarized excitation of the sodium atoms was used to produce pure 3 doublet P(3/2) (F=3,Mf=plus or minus 3) states, which are deexcited by collisions with spin-polarized electrons. The spin polarization of both the target electron and the incident electron allows the resolution of triplet and signlet contributions to (11) resolution of triplet and singlet contributions to L(1), the angular momentum transferred in the collision per-pendicular to the scattering plane, and the measure-ment of r, the ratio of triplet to singlet cross sections. At low energy, agreement with theory is good over the entire angular range for r, but only at small angles for L(1). At high energy, agreement is excellent over the full angular range.

901,585 PB90-128513 Not available NTIS National Inst. of Standards and Technology (NML), Gaithersburg, MD. Electricity Div.

Drift Tubes for Characterizing Atmospheric ion

Mobility Spectra.

Final rept.

M. Misakian, W. Anderson, and O. Laug. 1989, 4p
Sponsored by Department of Energy, Washington, DC.
Pub. in Proceedings of International Symposium on
High Voltage Engineering (6th), New Orleans, LA.,
August 28-September 1, 1989, p1-4.

Keywords: *lonic mobility, *Atmospheric pressure, *Spectra, Measurement, Alternating current, Direct current, Transport properties, Atmospheric tides, Electric fields, Spectral emittance, *Drift tubes.

Two drift tubes constructed of insulating cylinders with conductive guard rings on the inside walls are examined to determine their suitability for measuring ion mobility spectra at atmospheric pressure. One drift tube is of the pulse time-of-flight (TOF) type with adjustable drift distance and the other is an ac-TOF drift tube similar in principle to a device reported by Van de Graaff. The latter drift tube is evaluated using sinusoidal and alternating-polarity pulse-voltage waveforms for gating the shutters.

901,586 PB90-133158

PC A16/MF A02

National Inst. of Standards and Technology (NML), Gaithersburg, MD. Center for Atomic, Molecular and Optical Physics.

Center for Atomic, Molecular, and Optical Physics Technical Activities, 1989. K. B. Gebbie. Dec 89, 364p NISTIR-89/4184

See also PB89-132302.

Keywords: *Atomic physics, *Physical chemistry, Fundamental constants, Synchrotron radiation, Plasmas(Physics), Atomic structure, Surface chemistry, Molecular spectroscopy, Quantum theory, Gamma rays, Metrology, Frequency standards, Time standards, Astrophysics, Lasers, Gravity, *Molecular physics, Lasers, Gravity, *Mol ics, Laser cooling, Atom traps, Soft x-rays, Surface reactions Calibration.

The report summarizes the research and technical activities of the Center for Atomic, Molecular and Optical Physics (CAMOP) during the Fiscal Year 1989. The activities include work in the areas of fundamental constants, radiation physics, surface science, molecular spectroscopy, electron and optical physics, atomic and plasma spectroscopy, time and frequency, quantum metrology, and quantum physics.

901.587 PB90-136797 Not available NTIS

National Inst. of Standards and Technology (NML), Gaithersburg, MD. Chemical Thermodynamics Div. Monte Carlo Simulation of Domain Growth in the Kinetic Ising Model on the Connection Machine. Final rept.

J. G. Amar, and F. Sullivan. 1989, 9p Pub. in Computer Physics Communications 55, p287-295 1989

Keywords: *Ferromagnetism, *Computerized simulation, Mathematical models, Monte Carlo method, Algorithms, Reprints, Computer applications, Parallel proc-

A fast multispin algorithm for the Monte Carlo simulation of the two-dimensional spin-exchange kinetic Ising model has been adapted for use on the Connection Machine and applied as a first test in a calculation of domain growth. Features of the code include: the use of demon bits, the simulation of several runs simultaneously to improve the efficiency of the code, the use of virtual processors to simulate easily and efficiently a larger system size, the use of the (NEWS) grid for fast communication between neighboring processors and updating of boundary layers, the implementation of an efficient random number generator much faster than that provided by Thinking Machines Corp., and the use of the LISP function 'funcall' to select which processors to update. Overall speed of the code when run on a (128 X 128) processor machine is about 130 million attempted spin-exchanges per second, about 9 times faster than the comparable code, using hardware vectorized-logic operations and 64-bit multispin coding on the Cyber 205. The same code can be used on a larger machine (65536 processors) and should produce speeds in excess of 500 million attempted spin-exchanges per second.

901.588 PB90-163924

(Order as PB90-163874, PC A04) National Inst. of Standards and Technology, Gaithersburg, MD.

Measuring the Root-Mean-Square Value of a Finite Record Length Periodic Waveform.

E. C. Teague. 1989, 5p

Included in Jnl. of Research of the National Institute of Standards and Technology, v94 n6 p367-371 1989.

Keywords: *Waveforms, *Surface roughness, Measurement, Profiles, Random error, Root mean square value, Uncertainty.

The paper presents a discussion of the uncertainty in measuring the root-mean-square, rms, value of a periodic waveform which results from the use of a finite record length. The analysis was motivated by seeking to understand the source of a random uncertainty component which was present in some measurements of the absolute arithmetic average, R sub a deviation from a mean line of profiles of precision routhness specimens. The profiles of these specimens had an approximately triangular waveform with two wavelengths and amplitudes. For the longer wavelength specimens the random phasing of the waveform with respect to the recording interval proved to be a major source of uncertainty in the measurements.

SPACE TECHNOLOGY

Manned Spacecraft

901,589

PB89-193940 PC A05/MF A01 National Inst. of Standards and Technology (NEL), Gaithersburg, MD. Robot Systems Div. NASA/NBS (National Aeronautics and Space Ad-

ministration/National Bureau of Standards) Standard Reference Model for Telerobot Control System Architecture (NASREM).

Téchnical note (Final). J. S. Albus, H. G. McCain, and R. Lumia. Apr 89, 85p NIST/TN-1235-89

Also available from Supt. of Docs. as SN003-003-02928-9. See also PB88-123773. Sponsored by National Aeronautics and Space Administration, Greenbelt, MD. Goddard Space Flight Center.

Keywords: *Robots, Control systems, Space stations, System analysis, Functional analysis, Computer communications, Interfaces, Memory devices, *Computerized control systems, Hierarchical control, NASA standard reference model.

The document describes the NASA Standard Reference Model (NASREM) Architecture for the Space Station Telerobot Control System. It defines the functional requirements and high level specifications of the control system for the NASA Space Station document for the functional specification, and a guideline for the development of the control system architecture, of the IOC Flight Telerobot Servicer. The NASREM telerobot control system architecture defines a set of standard modules and interfaces which facilitates software design, development, validation, and test, and make possible the integration of telerobotics software from a wide variety of sources. Standard interfaces also provide the software hooks necessary to incrementally upgrade future Flight Telerobot Systems as new capabilities develop in computer science, robotics, and autonomous system control.

901.590

PB89-231013 Not available NTIS National Inst. of Standards and Technology (NEL), Gaithersburg, MD. Center for Fire Research. Expert Systems Applied to Spacecraft Fire Safety. Final rept. R. L. Smith, and T. Kashiwagi. 1989, 12p

Contract NASA-C-32000-M

Sponsored by National Aeronautics and Space Administration, Cleveland, OH. Lewis Research Center. Pub. in NASA Contractor Report 182266, p1-12, Jun

Keywords: *Fire safety, Fire_detection systems, Fire protection, Space stations, Fire extinguishers, Flammability, Reduced gravity, Ventilation, Air Flow, Decisions, Reprints, *Spacecraft electronic equipment, *Expert systems, Knowledge bases(Artificial intelligence).

Expert systems are problem-solving programs that combine a knowledge base and a reasoning mechanism to simulate a human 'expert.' The development of an expert system to manage fire safety in space-craft, in particular the NASA Space Station Freedom, is difficult but clearly advantageous in the long-term. The report discusses some needs in low-gravity flam-mability characteristics, ventilating-flow effects, fire detection, fire extinguishment, and decision models, all necessary to establish the knowledge base for an expert system.

901.591

PB90-123811 Not available NTIS National Inst. of Standards and Technology (NEL), Gaithersburg, MD. Robot Systems Div. Teleoperation and Autonomy for Space Robotics.

Final rept. R. Lumia, and J. S. Albus. 1988, 7p Pub. in Robotics 4, n1 p27-33 Mar 88.

SPACE TECHNOLOGY

Manned Spacecraft

Keywords: *Manned space flight, *Robots, Technology transfer, Standards, Reprints, Teleoperators, Control systems, Autonomy.

A logical enhancement to manned space flight in-A logical ennancement to manned space flight in-cludes the use of robots in space. To achieve this goal, there must be a phased program where the capabili-ties of the robot can evolve as technology advances. The present paper will review some of the ways in which robots can be used in space. Then, a system architecture standard will be suggested which sup-ports the evolution of robot control from teleoperation to autopowe. Finally some areas of technology transto autonomy. Finally, some areas of technology transfer will be discussed which are relevant to land-based robot operation.

Spacecraft Trajectories & Flight Mechanics

901.592

PB89-156962 Not available NTIS National Bureau of Standards (NML), Gaithersburg, MD. Inorganic Analytical Research Div.

Detection of Uranium from Cosmos-1402 in the Stratosphere.

Final rept. R. Leifer, Z. R. Juzdan, W. R. Kelly, J. D. Fassett, and K. R. Eberhardt. 1987, 3p

Pub. in Science 238, n4826 p512-514, 23 Oct 87.

Keywords: *Atmospheric entry, Stratosphere, Uranium, Mass spectroscopy, Ablation, Reprints, *Space power reactors, *Cosmos 1402 satellite, Spacecraft power supplies.

A series of balloon flights were launched in 1984 to A series of balloon flights were launched in 1984 to intercept the debris from the ablation of Cosmos 1402 which unexpectedly re-entered the earth's atmosphere February 7, 1983. Based on isotopic uranium analyses of filters collected between 26 and 36 km in February and March 1984, the authors are able to show unequivocally that the reactor from the Russian satellite cosmos 1402 did in fact burn in the high strategyphore. osphere.

Unmanned Spacecraft

901,593

PB89-156152 PC A05/MF A01 National Bureau of Standards (NEL), Boulder, CO. Center for Electronics and Electrical Engineering. Development of Near-Field Test Procedures for Communication Satellite Antennas, Phase 1, Part

A. C. Newell. Aug 88, 83p NBSIR-87/3081 See also Part 1, PB86-164357.

Keywords: *Spacecraft antennas, Electromagnetic fields, Antennas, Tests, Measurement, Communication satellites, Near field.

The purpose of the program is to define and further develop the capabilities of near-field antenna test techniques, specifically for the requirements associated with the development and verification testing of reconfigurable, multibeam, frequency reuse, commercial satellite antennas. The report, Phase I, Part 2, focuses on the planar near-field measurement method and covers the determination of sampling criteria and scan limits, development of diagnostic and design assist methods, development of beam alignment techniques, development of swept-frequency equivalent tests, and specification of hardware requirements for the measurement system. The basis for the choice of the best measurement technique was established with the planar near-field measurement method receiving the best score for the directive antennas considered.

901,594

Not available NTIS PB89-234231 National Inst. of Standards and Technology (NML), Boulder, CO. Quantum Physics Div.

Antenna for Laser Gravitational-Wave Observations in Space.

J. E. Faller, P. L. Bender, J. L. Hall, D. Hils, R. T. Stebbins, and M. A. Vincent. 1989, 5p Contract NAGW-822

Sponsored by National Aeronautics and Space Admin-

(9)111 1989.

Progress during the past two years on a proposed Laser Gravitational-Wave Observatory in Space (LAGOS) is discussed. Calculated performance for a 1 million km sized antenna over the frequency range of 0.00001 to 1 Hz is given. The sensitivity from 0.001 to 0.1 Hz is expected to be 1 x 10 to the -21st power/(Hz to the 0.5 power). Noise sources such as accelerations of the drag-free test masses by random molecular impacts and by fluctuations in the net thermal radiation pressure will limit the sensitivity at lower frequencies. The scientific objectives are the observation of CW gravitational waves from large numbers of binary systems and the detection of pulses which may have been emitted during the period of galaxy formation.

901,595 PB89-234249 Not available NTIS National Inst. of Standards and Technology (NML), Boulder, CO. Quantum Physics Div. Conceptual Dealer for Conceptual Design for a Mercury Relativity Satel-

lite.

Final rept. P. L. Bender, N. Ashby, M. A. Vincent, and J. M.

Wahr. 1989, 4p Contract NAGW-822

Sponsored by National Aeronautics and Space Admin-

istration, Washington, DC. Pub. in Advances in Space Research 9, n9 p(9)113-(9)116 1989.

Keywords: *Gravitation, *Relativity, Polar orbits, Spacecraft tracking, Celestial mechanics, Mercury(Planet), Doppler effect, Tests, Reprints, *Mercury spacecraft, Orbit calculation, Satellite

It was shown earlier that 1 x 10 to the -14th power It was shown earlier that 1 x 10 to the -14th power Doppler data and 3 cm accuracy range measurements to a small Mercury Relativity Satellite in a polar orbit with 4-hour period can give high-accuracy tests of gravitational theory. A particular conceptual design has been developed for such a satellite, which would take less than 10% of the approach mass for a possible future Mercury Orbiter Mission. The spacecraft is similar to the Pioneer Venus Orbiter, but scaled down by about a factor of 4 in linear dimensions. The orbit parameters for individual eight-hour arcs and the gravi-ty field of Mercury through degree and order 10 are determined mainly from the Doppler data. A 50 MHz K-band sidetone system provides the basic ranging ac-curacy. The spacecraft mass is 50 kg or less.

Final rept.

istration, Washington, DC. Pub. in Advances in Space Research 9, n9 p(9)107-

Keywords: *Astronomical observatories, Continuous radiation, Sensitivity, Reprints, *Gravitational waves, *Gravitational wave antennas, Infrasonic frequencies.

The report is number 18 in a series covering the research performed by the National Institute of Standards and Technology (formerly National Bureau of Standards) for the Federal Railroad Administration. The issue collects seven reprints and preprints of papers written by the Fracture and Deformation Division over the last two years on the ultrasonic nondestructive evaluation of railroad wheels for the presence of residual stress and cracks. All the work concentrated on the use of electromagnetic-acoustic transducers (EMATs). Tensile residual stresses and tread cracks are major factors in wheel failure. Two ultrasonic techare major factors in wheel failure. Two ultrasonic tech-niques are applicable to these wear defects: (1) Bire-fringence: A stress field effects the velocity of a shear horizontal wave depending on its polarization. Precise velocity measurements in a wheel rim may allow calculation of the amount and direction of stresses; (2) Pulse-echo: A Rayleigh (surface) wave transducer mounted inside the rail can introduce a signal to interrogate the circumference of a wheel as it rolls by. An echo indicates a flaw's presence and size.

901,597 PB90-123894 Not available NTIS National Inst. of Standards and Technology (IMSE), Boulder, CO. Fracture and Deformation Div. EMATs (Electromagnetic Acoustic Transducers) for Roll-By Crack Inspection of Rallroad Wheels.

Final rept.

R. E. Schramm, P. J. Shull, A. V. Clark, and D. V. Mitrakovic. 1989, 7p
Sponsored by Federal Railroad Administration, Wash-

Ington, DC.
Pub. in Review of Progress in Quantitative Nonde-structive Evaluation, v8A p1083-1089 1989.

Keywords: *Cracks, Keywords: *Cracks, *Inspection, *Rolling stock, *Wheels, Nondestructive tests, Ultrasonic tests, Railroad cars, Rayleigh waves, Safety, Reprints.

Railroad safety depends on many factors. The integrity of the wheels on rolling stock is one that is subject to nondestructive evaluation. For some years, ultrasonic testing has been applied to the detection of cracks in wheel treads, with particular attention to automatic, in-rail, roll-by methods. A system using relatively low fre-quency Rayleigh waves generated by electromagnet-ic-acoustic transducers (EMATs) is being developed. The current design uses a permanent magnet to maintain a compact structure and minimize the size of the pocket machined into the rail. Measurements thus far indicate a responsiveness, even to small flaws. With the development of a signal processing and analysis system, field tests should soon be possible.

URBAN & REGIONAL TECHNOLOGY & DEVELOPMENT

TRANSPORTATION

Railroad Transportation

901,596 PB89-189229 PC A05/MF A01 National Inst. of Standards and Technology (IMSE), Boulder, CO. Fracture and Deformation Div. Ultrasonic Rallroad Wheel Inspection Using EMATs (Electromagnetic-Accoustic Transducers),

Report No. 18.
R. E. Schramm, and A. van Clark. Dec 88, 86p

See also PB88-194519. Sponsored by Federal Railroad Administration, Washington, DC.

Keywords: *Ultrasonic testing, *Railroad cars, *Wear, Cracks, Nondestructive tests, Transducers, Residual stress, Birefringence, Wheels, EMAT, Roll-by inspec-

Emergency Services & Pianning

901.598

PB89-189203 PC A10/MF A01 National Inst. of Standards and Technology (NEL), Gaithersburg, MD. Center for Computing and Applied

Gathersburg, MD. Center for Computing and Applied Mathematics.

Evaluating Emergency Management Models and Data Bases: A Suggested Approach.

R. E. Chapman, S. I. Gass, J. J. Filliben, and C. M. Harris. Mar 89, 215p NISTIR-88/3826

Prepared in cooperation with George Mason Univ., Fairfax, VA. Dept. of Operations Research and Applied Statistics. Sooppered by Ederal Emergency Manage. Statistics. Sponsored by Federal Emergency Management Agency, Washington, DC.

Keywords: *Mathematical models, Evaluation, Assessments, Management, Tables(Data), Graphs(Charts), *Emergency planning, Emergency preparedness, Crises, Data bases.

Large-scale models and data bases are key informa-tional resources for the Federal Emergency Manage-ment Agency (FEMA). In order to carry out its emer-

URBAN & REGIONAL TECHNOLOGY & DEVELOPMENT

Emergency Services & Planning

gency missions, it is necessary for FEMA to determine which models, modeling techniques and data bases are appropriate for what purposes and which ones need modification, updating and maintenance. The development of evaluation guidelines is therefore of direct benefit to FEMA in discharging its emergency management duties. The purpose of the report is twofold. First, it provides the reader with a generic set of guidelines which can be used to evaluate large-scale, computer-based models and data bases. Second, the guidelines are illustrated through a critical evaluation of the Dynamic General Equilibrium Model (DGEM). DGEM is currently being used by FEMA to analyze a variety of emergency management problems. The evaluation of DGEM serves both as a step-by-step procedure for conducting an indepth model evaluation and as an introduction to a non-proprietary model which has broad applicability to the analysis of macroeconomic issues.

Fire Services, Law Enforcement, & **Criminal Justice**

901,599

PB89-176283 Not available NTIS National Bureau of Standards (NEL), Gaithersburg, MD. Law Enforcement Standards Lab.

ACSB (Amplitude Companded Sideband): What Is Adequate Performance.

Final rept.

W. A. Kissick, and M. J. Treado. 1986, 9p Sponsored by National Inst. of Justice, Washington,

Pub. in Proceedings of International Carnahan Conference on Security Technology: Electronic Crime Countermeasures, Gothenburg, Sweden, August 12-14, 1986, p219-227.

Keywords: *Compandor transmission, *Law enforcement, *Voice communication, Single sideband transmission, Modulation, Speech recognition, Intelligibility, Performance evaluation, Amplitude companded side-

Amplitude companded sideband (ACSB) is a new modulation technique that uses a much smaller channel width than does conventional frequency modulation (FM). ACSB has been proposed for the land mobile communications needs of law enforcement agencies. Among the requirements of such a commuagencies. Allow the equilibrium of sacromatications system is adequate speech intelligibility under a variety of conditions. The paper explores this aspect of 'adequate performance.' First, the basic principles of ACSB are described, with emphasis on those features that affect speech quality. Second, the results of ACSB equipment testing are given. Next, the appropriate performance measures for ACSB are reviewed. Last, a subjective voice quality scoring method is used to determine the values of the performance measures that equate to the minimum level of intelligibility. It is assumed that the intelligibility of an FM system operating at 12 dB SINAD represents that minimum.



SAMPLE ENTRY

Wack, J. P., and Carnahan, L. J.

Computer Viruses and Related Threats: A Management

PB90-111683

900,654

Author name(s) Title

NTIS order number

Abstract number

AA	RON,	D.	Α
----	------	----	---

Experimental Investigation and Modeling of the Flow Rate of Refrigerant 22 Through the Short Tube Restrictor. PB89-229041 901.118

ABBOTT, D. C.

Photospheres of Hot Stars. 3. Luminosity Effects at Spectral Type 09.5. PB89-202592 900.020

ABOU-GAMRA, Z.

Redox Chemistry of Water-Soluble Vanadyl Porphyrins 900,300

ABRAHAMS, S. C.

Statistical Descriptors in Crystallography: Report of the International Union of Crystallography Subcommittee on Statistical Descriptors. PB89-201826

ABRISHAMIAN, A.

Hierarchically Controlled Autonomous Robot for Heavy Payload Military Field Applications. PB89-177075 901,271

ABRISHAMIAN, H.

Robot Crane Technology. PB90-111667

ABU-ZAID, M.

Effect of Water on Piloted Ignition of Cellulosic Materials PB89-189187 900, 900,127

ADAIR, R. T.

ANA (Automatic Network Analyzer) Measurement Results on the ARFTG (Automatic RF Techniques Group) Traveling PB89-173777 900.715

Performance Evaluation of Radiofrequency, Microwave, and Millimeter Wave Power Meters. 900.814

ADAM, G.

On-Line Arc Welding: Data Acquisition and Analysis Using a High Level Scientific Language. PB90-117391 900,972

ADAMS, F. C.

Dependence of Interface Widths on Ion Bombardment Conditions in SIMS (Secondary Ion Mass Spectrometry) Analysis of a Ni/Cr Multilayer Structure.

PB89-172506

ADAMS, J. W.

Electromagnetic Fields in Loaded Shielded Rooms. PB89-180426 900,780

Measurement Procedures for Electromagnetic Compatibility Assessment of Electroexplosive Devices. PB89-146914

Techniques for Measuring the Electromagnetic Shielding Effectiveness of Materials. Part 1. Far-Field Source Simulation. PB89-161525 900,680

ADRIAN, F. J.

Magnetic Field Dependence of the Superconductivity in Bi-Sr-Ca-Cu-O Superconductors. PB89-146815

Mathematical Software: PLOD, Plotted Solutions of Differential Equations PB89-147425 901,194

AHLUWALIA, J. C.

Thermodynamics of the Hydrolysis of Sucrose. PB89-227904 901,227

AL-SHEIKHLY, M.

Dichromate Dosimetry: The Effect of Acetic Acid on the Radiolytic Reduction Yield. PB89-147490 900,248

ALBER, G.

900,146

One-Photon Resonant Two-Photon Excitation of Rydberg Series Close to Threshold. PB89-171276 901,343

ALBERS, J. H.

Experimental Verification of the Relation between Two-Probe and Four-Probe Resistances. PB89-231211 900.794

ALBERTY, R. A.

Standard Chemical Thermodynamic Properties of Polycyclic Aromatic Hydrocarbons and Their Isomer Groups 1. Benzene Series. PB89-186480 900 412

Standard Chemical Thermodynamic Properties of Polycyclic Aromatic Hydrocarbons and Their Isomer Groups.

Pyrene Series, Naphthopyrene Series, and Coronene PB89-226591 900,459

ALBUS, J.

900,364

Mining Automation Real-Time Control System Architecture Standard Reference Model (MASREM). PB89-221154 901.286

ALBUS, J. S.

NASA/NBS (National Aeronautics and Space Administra-tion/National Bureau of Standards) Standard Reference Model for Telerobot Control System Architecture PB89-193940 901,589

Robot Crane Technology. PB90-111667 900,146

Teleoperation and Autonomy for Space Robotics. PB90-123811

Absolute Rate Constants for Hydrogen Abstraction from Hydrocarbons by the Trichloromethylperoxyl Radical. PB89-171532

ALLAN, D. W.

Comparison of Time Scales Generated with the NBS (National Bureau of Standards) Ensembling Algorithm. PB89-174072 900,628

Dual Frequency P-Code Time Transfer Experiment. PB89-174064

900.614 In Search of the Best Clock.

PB90-117367 900,632

Millisecond Pulsar Rivals Best Atomic Clock Stability, PB89-185722 , 900.629

NBS (National Bureau of Standards) Calibration Service Providing Time and Frequency at a Remote Site by Weighting and Smoothing of GPS (Global Positioning System) Common View Data. PB89-212211 900,631

NIST Automated Computer Time Service. PB90-213711 900,676

Study of Long-Term Stability of Atomic Clocks. PB89-174098

900,367

901,591

Using Multiple Reference Stations to Separa iances of Noise Components in the Global		PB89-158059	901,393	PB89-234280	900,49
System. PB89-185730	901,293	APOSTOLAKIS, G. E. Fire Risk Analysis Methodology: Initiating Events		BAEV, V. M. One Is Not Enough: Intra-Cavity Speci	troscopy with Mult
Variances Based on Data with Dead Time b		PB89-184527 ARCHER, D. G.	900,125	Mode Lasers. PB89-185888	900,40
Measurements. PB89-174049	901,204	Second Virial Coefficients of Aqueous Alcohols	at Elevated	BAGHDADI, A.	900,40
ALMASAN, C.		Temperatures: A Calorimetric Study. PB89-227896	900,462	Interlaboratory Determination of the Ca	alibration Factor fo
Low-Temperature Phase and Magnetic Interac Fe-Cr-Ni Alloys.	tions in fcc	ARENDS, J.		the Measurement of the Interstitial Oxycon by Infrared Absorption.	
PB90-136771	901,113	Calcium Hydroxyapatite Precipitated from an Aqu tion: An International Multimethod Analysis.		PB90-117300 Semiconductor Measurement Technolog	900,22 Tv: Automatic Deter
Reentrant Softening in Perovskite Superconduct PB90-117540	901,464	PB90-123399 ARONOFF, R.	900,228	mination of the Interstitial Oxygen Conte Polished on Both Sides.	nt of Silicon Wafer
AMAR, J. G.	dy of Eluid	Transport Layer Performance Tools and Measure	ement.	PB89-151831	900,77
Application of the Gibbs Ensemble to the Stu Fluid Phase Equilibrium in a Binary Mixture of	f Symmetric	PB89-171326 ARVIDSON, J. M.	900,611	Semiconductor Measurement Technol and Statistical Analysis of the Interlabor	ogy: Database for atory Determination
Non-Additive Hard Spheres. PB90-117318	900,494	Low Temperature Mechanical Property Measur	rements of	of the Conversion Coefficient for the Manuel Interstitial Oxygen Content of Silicon by	deasurement of the
Monte Carlo Simulation of Domain Growth in Ising Model on the Connection Machine.	the Kinetic	Silica Aerogel Foam. PB90-128638	901,061	PB89-221170	901,05
PB90-136797	901,587	ASAI, J.	Dhatana	BAINES, J. Numerical Aperture of Multimode Fiber	s by Saveral Meth
AMINOFF, C. G. Precise Laser Frequency Scanning Using Frequency	TUENCY-SVN-	Cross Section and Linear Polarization of Tagged PB90-117292	901,560	ods: Resolving Differences. PB90-117482	900,75
thesized Optical Frequency Sidebands: Applica	ation to Iso-	ASAOKA, K. Transient and Residual Stresses in Dental Borne	laine as Af	BAIRD, R. C.	900,75
tope Shifts and Hyperfine Structure of Mercury. PB90-118134	901,370	Transient and Residual Stresses in Dental Porce fected by Cooling Rates.		Brief History of Near-Field Measureme	nts of Antennas a
AMIS, E. J.	an hii Canall	PB89-229298 ASHBY, N.	900,046	the National Bureau of Standards. PB89-156863	900,70
Uniaxial Deformation of Rubber Network Chair Angle Neutron Scattering.		Conceptual Design for a Mercury Relativity Satell		BAKER, T. L.	
PB89-175830 AMMON, H. L.	901,088	PB89-234249 ASMUSSEN, E.	901,595	Fracture Behavior of Ceramics Used in tors.	Multilayer Capac
Preliminary Crystal Structure of Acinetobacter g	lutaminasifi-	Adhesion to Dentin by Means of Gluma Resin.	200 000	PB89-171805	900,75
cans Glutaminase-Asparaginase. PB90-123381	901,260	PB89-157168 Substitutes for N-Phenylglycine in Adhesive I	900,039	BALDI, F. Biotransformation of Mercury by Bacte	ria Isolated from
ANDERSEN, E. K.		Dentin.		River Collecting Cinnabar Mine Waters. PB89-229280	
Neutron Diffraction Determination of Full Struct hydrous Li-X and Li-Y Zeolites.	ures of An-	PB90-123795 ASTUMIAN, R. D.	900,051	BALENSON, D. M.	900,86
PB90-118001	900,516	Nonlinear Effect of an Oscillating Electric Field	on Mem-	National Bureau of Standards Mess.	age Authentication
ANDERSEN, I. G. K. Neutron Diffraction Determination of Full Struct	ures of An-	brane Proteins. PB90-123407	901,249	Code (MAC) Validation System. PB89-231021	900,67
hydrous Li-X and Li-Y Zeolites. PB90-118001	900,516	ATHA, D. H.	on Ouest	BALL, M. J.	
ANDERSEN, L. U.	000,010	Anti-T2 Monoclonal Antibody Immobilization Fibers: Stability and Recognition of T2 Mycotoxin		PVT Measurements on Benzene at Tem PB89-157200	peratures to 723 K 900,31
Fundamental Tests of Special Relativity and the Space.	s Isotropy of	PB90-128760 ATKINSON, R.	901,267	PVT of Toluene at Temperatures to 673	K.
PB89-185920	901,523	Evaluated Kinetic and Photochemical Data for A	tmospheric	PB89-157192	900,31
ANDERSON, D. Z. Optical Novelty Filters.		Chemistry. Supplement 3. PB89-222582	900,454	BALLAGH, R. J. Approximate Formulation of Redistribution	on in the Ly(alpha)
PB89-228084	901,366	ATREYA, A.		Lý(beta), H(alpha) System. PB90-123720	901,56
NDERSON, W.	on Mobility	Effect of Water on Piloted Ignition of Cellulosic N PB89-189187	900,127	Redistribution in Astrophysically Importar	nt Hydrogen Lines.
Drift Tubes for Characterizing Atmospheric I Spectra.		ATTALA, R.		PB90-128075	901,57
PB90-128513 NDERSON, W. E.	901,585	Laser Induced Fluorescence for Measurement Concentrations in Pulping Liquors.		BALLAUX, C. (109)Pd and (109)Cd Activity Standard	dization and Deca
Calibration of Voltage Transformers and High-	Voltage Ca-	PB89-172530 ATZMONY, U.	901,184	Data. PB90-123449	901,56
pacitors at NIST. PB89-211114	901,442	Magnetic Behavior of Compositionally Modula	ated Ni-Cu	BALTES, H.	ŕ
Drift Tubes for Characterizing Atmospheric I Spectra Using AC, AC-Pulse, and Pulse Til	on Mobility	Thin Films. PB90-118084	901,163	High Accuracy Modeling of Photodiode (PB90-117599	Quantum Efficiency 900,73
Measurement Techniques. PB89-202543		Magnetization and Magnetic Aftereffect in Texts Compositionally-Modulated Alloys.	ured Ni/Cu	BARASH, M. M.	500,70
Effect of an Oil-Paper Interface Parallel to an E	900,438 lectric Field	PB90-123431	901,165	General Methodology for Machine Tool ment by Error Compensation.	Accuracy Enhance
on the Breakdown Voltage at Elevated Tempera PB89-156988		Mossbauer Imaging: Experimental Results. PB90-123415	900,922	PB89-146781	900,99
ANDERSON, W. T.	001,400	Temperature Hysteresis in the Initial Susceptibilit		Generalized Mathematical Model for Mac PB89-150874	chine Tool Errors. 900,97
Two-Layer Dielectric Microstrip Line Structure: and GaAs on Si; Modeling and Measurement.	SiO2 on Si	ly Solidified Monel. PB90-123423	901,164	BARKER, E. B.	200,27
PB89-156780	900,738	AUSTIN, M. W.		National Bureau of Standards Messa Code (MAC) Validation System.	age Authentication
NDREW, K. L. Spectrum and Energy Levels of Singly Ionized	Cosium 2	Molybdenum Effect on Volume in Fe-Cr-Ni Alloys PB89-157796	901,095	PB89-231021	900,67
Interpretation of Fine and Hyperfine Structures.		AXLEY, J.		BARKMEYER, E.	ufacturing Data Au
PB89-172373 ANDREWS, A. D.	900,361	Integral Mass Balances and Pulse Injection Tra niques.	acer Tech-	Experience with IMDAS (Integrated Man ministration System) in the Automated	Manufacturing Re
Rotational Modulation and Flares on RS Can		PB89-206833	900,077	search Facility. PB90-112350	900,96
corum and BY Draconis Stars X: The 1981 Octoon V711 Tauri (= HR 1099).		AXTON, E. J. Basic Data Necessary for Neutron Dosimetry.		BARNARD, A.	
PB89-202618	900,021	PB89-171854	901,241	AMRF Part Model Extensions. PB90-129446	900,96
Rotational Modulation and Flares on RS CVn a Stars IX. IUE (International Ultraviolet Explorer)	Spectrosco-	AYRES, R. NBS/NRL (National Bureau of Standards/Nava	I Research	BARNES, I. L.	550,55
py and Photometry of II Peg and V711 Tau duni 1983.		Laboratory) Free Electron Laser Facility. PB89-175749	901,351	Absolute Isotopic Abundance Ratios and	d Atomic Weight o
PB89-171615 Antonucci, J. M.	900,019	BABCOCK, R. W.	.,	a Reference Sample of Nickel. PB90-163890	900,54
Adhesion to Dentin by Means of Gluma Resin.		Microarcsecond Optical Astrometry: An Instrume Astrophysical Applications.	ent and Its	Absolute Isotopic Composition and Ato restrial Nickel.	mic Weight of Ter
PB89-157168	900,039	PB89-171268	900,013	PB90-163908	900,54
Detection of Lead in Human Teeth by Exposure Sulfide Solutions.		BABRAUSKAS, V. Flammability of Upholstered Furniture with	n Flaming	Technical Examination, Lead Isotope Elemental Analysis of Some Shang a	
PB89-201529 Formation of Hydroxyanatite in Hydrogels from	901,256 m Tetracal	Sources. PB90-136805	900,155	Bronze Vessels. PB90-136862	901,170
Formation of Hydroxyapatite in Hydrogels from Cium Phosphate/Dicalcium Phosphate Mixtures.		Smoke and Gas Evolution Rate Measurements		Twenty Five Years of Accuracy Assessi	
PB89-201511 Non-Aqueous Dental Cements Based on Dimer	901,255 and Trimer	tarded Plastics with the Cone Calorimeter. PB89-174890	900,868	Weights. PB89-174007	900,36
Acids. PATENT-4 832 745	900,033	BADENHOOP, J. K.		BARNES, J. A.	
APELL, P.	200,000	Reduced Dimensionality Quantum Reactive Study of the Insertion Reaction O(1D) + H2 -	Scattering	Variances Based on Data with Dead Measurements.	Time between the
Free-Electron-Like Stoner Excitations in Fe.		H.	J., T	PB89-174049	901,20

		,
BARNES, P. R.	PB90-117342 900,495	PB89-147383 901,123
Discussion of 'Steep-Front Short-Duration Voltage Surge Tests of Power Line Filters and Transient Voltage Suppres-	BECKER, R. Spectroscopy of Autoionizing States Contributing to Elec-	Replacement of Icosahedral Al-Mn by Decagonal Phase. PB89-186332 901,146
sors.' PB90-117326 <i>900,755</i>	tron-Impact Ionization of Ions. PB90-123837 901,572	BENDERSKY, L. A.
BARSOUM, M.	BECKERLE, J. D.	Amorphous Phase Formation in Al70Si17Fe13 Alloy. PB90-123522 901,167
Mechanical Property Enhancement in Ceramic Matrix Composites.	Time Resolved Studies of Vibrational Relaxation Dynamics of CO(v= 1) on Metal Particle Surfaces.	Formation of Dispersoids during Rapid Solidification of an
PB89-189138 901,076 BARTEL, T. W.	PB89-203012 900,444 BEDZYK, M. J.	AI-Fe-Ni Alloy. PB90-123647 901,172
Acoustical Technique for Evaluation of Thermal Insulation.	Direct Observation of Surface-Trapped Diffracted Waves.	Nucleation and Growth of Aperiodic Crystals in Aluminum Alloys.
PB89-193866 900,919 BASCH, H.	PB90-128216 901,475 Dynamical Diffraction of X-rays at Grazing Angle.	PB89-186324 901,145
Electronic Structure of Diammine (Ascorbato) Platinum(II)	PB89-186886 901,421	Pathways for Microstructural Development in TiAl. PB90-123779 901,173
and the Trans Influence on the Ligand Dissociation Energy. PB89-147128 900,287	BEECH, F. Crystal Chemistry of Superconductors: A Guide to the Tai-	Quasicrystals and Quasicrystal-Related Phases in the Al-
BAUER, B. Temperature, Composition and Molecular-Weight Depend-	loning of New Compounds. PB89-171730 901,030	Mn System. PB90-123548 901,169
ence of the Binary Interaction Parameter of Polystyrene/	Neutron Study of the Crystal Structure and Vacancy Distri-	Rapid Solidification and Ordering of B2 and L2 (sub 1) Phases in the NiAl-NiTi System.
Poly(viny!methylether) Blends. PB89-157473 900,550	bution in the Superconductor Ba2Y Cu3 O(sub g-delta). PB90-123480 901,468	PB90-123639 901,171
BAUER, B. J.	BEECH, F. W. Neutron Powder Diffraction Structure and Electrical Proper-	Solidification of an 'Amorphous' Phase in Rapidly Solidified Al-Fe-Si Alloys.
Design and Synthesis of Prototype Air-Dry Resins for Use in BEP (Bureau of Engraving and Printing) Intaglio Ink Vehi-	ties of the Defect Pyrochlores Pb1.5M2O6.5 (M= Nb, Ta). PB89-172431	PB90-123530 901,168
cles. PB90-112343 901,068	BEERS, J. S.	Stable and Metastable Phase Equilibria in the Al-Mn System.
Effect of Crosslinks on the Phase Separation Behavior of a	Length Scale Measurement Procedures at the National Bureau of Standards.	PB89-172324 901,136 TEM Observation of Icosahedral, New Crystalline and
Miscible Polymer Blend. PB89-146724 900,546	PB89-209266 900,895	Glassy Phases in Rapidly Quenched Cd-Cu Alloys.
Small Angle Neutron Scattering Studies of Single Phase Interpenetrating Polymer Networks.	BEHAR, D. Pagetion of (Ir(C(2), N. hpv)(hpv)(2)(2) with OH Padicals	PB90-123514 901,166 BENNDORF, C.
PB90-123456 900,577	Reaction of (Ir(C(3), N bpy)(bpy)2)(2+) with OH Radicals and Radiation Induced Covalent Binding of the Complex to	Adsorption of Water on Clean and Oxygen-Predosed
Synthesis and Characterization of Poly(vinylmethyl ether). PB89-161616 900,551	Several Polymers in Aqueous Solutions. PB90-123498 900,264	Nickel(110). PB90-123555 900,522
BAULCH, D. L.	BEHRENS, J. W.	Ammonia Adsorption and Dissociation on a Stepped Iron(s)
Evaluated Kinetic and Photochemical Data for Atmospheric Chemistry. Supplement 3.	Advances in the Use of (3)He in a Gas Scintillation Counter.	(100) Surface. PB90-123563 900,523
PB89-222582 900,454	PB90-123506 901,565 Measurements of the (235)U (n,f) Standard Cross Section	Influence of Electronic and Geometric Structure on Desorp-
BAUM, H. Combustion of Oil on Water.	at the National Bureau of Standards.	tion Kinetics of Isoelectronic Polar Molecules: NH3 and H2O.
PB89-149173 900,587	PB89-176556 901,305 BEHRING, W. E.	PB89-176473 900,381
Combustion of Oil on Water. November 1987. PB89-185581 900,863	Laser-Produced Spectra and QED (Quantum Electrodynamics) Effects for Eq. Co. Cu. and Zn Like long of Au. Ph. Bi	BENNER, B. A. Mobile Sources of Atmospheric Polycyclic Aromatic Hydro-
BAUM, H. R.	ic) Effects for Fe-, Co-, Cu-, and Zn-Like lons of Au, Pb, Bi, Th, and U.	carbons: A Roadway Tunnel Study. PB90-123571 900,859
Aerodynamics of Agglomerated Soot Particles. PB89-147482 900,586	PB89-176010 901,510 Spectra and Energy Levels of Br XXV, Br XXIX, Br XXX,	BENNETT, H. E.
Solution for Diffusion-Controlled Reaction in a Vortex Field.	and Br XXXI. PB89-176002 901,509	Laser Induced Damage in Optical Materials: 1987.
PB89-176622 900,594 BAUMGARTEN, G. P.	BEIJERS, J. P. M.	PB89-221162 901,364
Measurements of Coefficients of Discharge for Concentric	Laser Probing of Ion Velocity Distributions in Drift Fields: Parallel and Perpendicular Temperatures and Mobility for	BENNETT, H. S. Correlation between CMOS (Complementary Metal Oxide
Flange-Tapped Square-Edged Onfice Meters in Water Over the Reynolds Number Range 600 to 2,700,000.	Ba(1+) in He.	Semiconductor) Transistor and Capacitor Measurements of Interface Trap Spectra.
PB89-235147 901,334 BEALL J. A.	PB89-171243 900,352 BELANGER, B. C.	PB89-180020 900,779
Evidence for the Superconducting Proximity Effect in Junc-	Measurement Standards for Defense Technology. PB89-150965 901,270	Effects of Doping-Density Gradients on Band-Gap Narrowing in Silicon and GaAs Devices.
tions between the Surfaces of YBa2CU3Ox Thin Films. PB89-228449 901,449	BELECKI, N. B.	PB89-228522 901,453
Noise in DC SQUIDS with Nb/Al Oxide/Nb Josephson	Guidelines for Implementing the New Representations of the Volt and Ohm Effective January 1, 1990.	Indirect Energy Gap of Si, Doping Dependence. PB89-150833 901,388
Junctions. PB89-201032 900,763	PB89-214761 900,817	Numerical Simulations of Neutron Effects on Bipolar Transistors.
Switching Noise in YBa2Cu3Ox 'Macrobridges'. PB89-200513 901,426	BELL, B. A. Electrical Performance Tests for Hand-Held Digital Multi-	PB90-123589 <i>900,797</i>
BEAN, V. E.	meters. PB89-162234 900,876	BENNETT, L. H.
InSb as a Pressure Sensor. PB89-231104 900,904	BELLAMA, J. M.	Brief Review of Recent Superconductivity Research at NIST (National Institute of Standards and Technology).
Observations of Gas Species and Mode of Operation Ef-	Determination of Ultratrace Concentrations of Butyltin Compounds in Water by Simultaneous Hydridization/Extraction	PB89-211114 900,766
fects on Effective Areas of Gas-Operated Piston Gages. PB89-231120 900,906	with GC-FPD Detection. PB89-177224 901,311	Magnetic Behavior of Compositionally Modulated Ni-Cu Thin Films.
Pressure Fixed Points Based on the Carbon Dioxide Vapor	Effect of pH on the Emission Properties of Aqueous tris	PB90-118084 901,163 Magnetic Field Dependence of the Superconductivity in Bi-
Pressure at 273.16 K and the H2O(I) - H2O(III) - H2O(L) Triple-Point.	(2,6-dipicolinato) Terbium (III) Complexes. PB89-157135 900,250	Sr-Ca-Cu-O Superconductors. PB89-146815 901,385
PB89-231138 900,483	Element-Specific Epifluorescence Microscopy In vivo Moni-	Magnetization and Magnetic Aftereffect in Textured Ni/Cu
Reduction of Uncertainties for Absolute Piston Gage Pressure Measurements in the Atmospheric Pressure Range.	toring of Metal Biotransformations in Environmental Matri- ces.	Compositionally-Modulated Alloys. PB90-123431 901,165
PB90-163882 900,030 BEARY, E. S.	PB89-177216 <i>901,220</i> BENDER, P.	Mossbauer Hyperfine Fields in RBa2(Cu0.97Fe0.03)3 O(7-
Absolute Isotopic Composition and Atomic Weight of Ter-	Microarcsecond Optical Astrometry: An Instrument and Its	x)(R = Y,Pr,Er). PB89-201206 901,429
restrial Nickel. PB90-163908 900,544	Astrophysical Applications. PB89-171268 900,013	Mossbauer Imaging: Experimental Results.
Analysis of Ultrapure Reagents from a Large Sub-Boiling	BENDER, P. L.	PB90-123415 900,922 Mossbauer Spectroscopy.
Still Made of Teflon PFA. PB89-186357 900,202	Antenna for Laser Gravitational-Wave Observations in Space.	PB89-211932 901,189
Comparison of Microwave Drying and Conventional Drying Techniques for Reference Materials.	PB89-234231 901,594 Comment on 'Possible Resolution of the Brookhaven and	Roles of Atomic Volume and Disclinations in the Magnetism of the Rare Earth-3D Hard Magnets.
PB90-123464 900,229	Comment on 'Possible Resolution of the Brookhaven and Washington Eotvos Experiments'.	PB89-202238 901,434
Design Principles for a Large High-Efficiency Sub-Boiling Still.	PB89-171581 901,504 Conceptual Design for a Mercury Relativity Satellite.	Synthesis and Magnetic Properties of the Bi-Sr-Ca-Cu Oxide 80- and 110-K Superconductors.
PB89-187553 900,207	PB89-234249 901,595	PB89-179725 901,412 Temperature Hysteresis in the Initial Susceptibility of Banida
Determination of Selenium and Tellurium in Copper Standard Reference Materials Using Stable Isotope Dilution	Rate of Change of the Quincy-Monument Peak Baseline from a Translocation Analysis of LAGEOS Laser Range	Temperature Hysteresis in the Initial Susceptibility of Rapidly Solidified Monel.
Spark Source Mass Spectrometry. PB90-123472 900,230	Data. PB89-234272 901,282	PENNISON S I
BEATON, S. P.	BENDERSKY, L.	BENNISON, S. J. Effect of Heat Treatment on Crack-Resistance Curves in a
Detection of the Free Radicals FeH, CoH, and NiH by Far Infrared Laser Magnetic Resonance.	Quasicrystals with 1-D Translational Periodicity and a Ten- Fold Rotation Axis.	Liquid-Phase-Sintered Alumina. PB89-229231 901,056
-		301,000

Flaw Tolerance in Ceramics with Rising Crack Res Characteristics.	sistance	PB89-209332 901,200	
PB90-128026	901,060	BEST, P. E. FT-IR (Fourier Transform-Infrared) Emission/Transmission	Triplet Dipoles in the Absorption Spectra by Dense Rare Gas Mixtures. 1. Short Range Interactions.
Grain-Size and R-Curve Effects in the Abrasive V Alumina.	Vear of	Spectroscopy for In situ Combustion Diagnostics. PB89-211866 900,600	PB90-136755 900,539
PB90-117383	901,058	BHATIA, A. K.	BJERRE, N. Fundamental Tests of Special Relativity and the Isotropy of
BENSEMA, W. D. Automated TEM (Transverse Electromagnetic) C	Cell for	Neonlike Ar and Cl 3p-3s Emission from a theta-pinch Plasma.	Space. PB89-185920 <i>901,523</i>
Measuring Unintentional EM Emissions.	900,682	PB90-123746 901,570	
PB89-173769 Implementation of an Automated System for Measur		BIANCANIELLO, F. S.	Analytical Model for the Steady-State and Transient Char-
diated Emissions Using a TEM Cell.	_	Amorphous Phase Formation in Al70Si17Fe13 Alloy. PB90-123522 901,167	acteristics of the Power Insulated-Gate Bipolar Transistor. PB89-146880 900,767
PB90-117698 Theory and Measurements of Radiated Emissions I	901,377 Using a	Directional Invariance of Grain Boundary Migration in the	
TEM (Transverse Electromagnetic) Cell.	_	Pb-Sn Cellular Transformation and the Tu-Turnbull Hysteresis.	PB89-157655 900 773
PB89-193890 BENTZ, D.	900,761	PB89-157911 901,134	Power MOSFET Failure Revisited.
Preliminary Stochastic Model for Service Life Predic	ction of	Formation and Stability Range of the G Phase in the Alumi- num-Manganese System.	Berlin of Thermal Observator in the Control of Brown Tourist Control of the Control of Brown Tourist Control of the Control of
a Photolytically and Thermally Degraded Polymeric Plate Material.	Cover	PB89-186316 901,144	PB89-150825 900 270
	900,556	Formation of Dispersoids during Rapid Solidification of an Al-Fe-Ni Alloy.	BLAIR, W. R.
Quantitative Studies of Coatings on Steel Using Refl Absorption Fourier Transform Infrared Spectroscopy.	lection/	PB90-123647 901,172	in BER (Bureau of Engraving and Printing) Integlia lak Vohi
PB89-212112	901,066	Nucleation and Growth of Aperiodic Crystals in Aluminum Alloys.	Cles.
BENTZ, D. P.	Disated	PB89-186324 901,145	Speciation Managerements of Butulting Application to Con-
Fractal-Based Description of the Roughness of Steel Panels.		Observations on Crystal Defects Associated with Diffusion Induced Grain Boundary Migration in Cu-Zn.	trolled Release Rate Determination and Production of Ref-
	901,096	PB89-157606 901,127	erence Standards. PB89-146807 900,174
Strain Energy of Bituminous Built-Up Membranes: Concept in Load-Elongation Testing.		Pathways for Microstructural Development in TiAl. PB90-123779 901,173	Trace Speciation by HPLC-GF AA (High-Performance Liquid
	900,139	Process Control during High Pressure Atomization.	Tin- and Lead-Bearing Organometallic Compounds, with
Thermal Degradation of Poly (methyl methacrylate) to 125C.		PB89-179170 901,142	PP90 157095
	900,549	Rapid Solidification and Ordering of B2 and L2 (sub 1) Phases in the NiAl-NiTi System.	BLALOCK, T. V.
Thermographic Imaging and Computer Image Proces Defects in Building Materials.	ssing of	PB90-123639 901,171	Measurement of Partial Discharges in Hexane Under DC
	900,123	Solidification of an 'Amorphous' Phase in Rapidly Solidified AI-Fe-Si Alloys.	Voltage. PB89-173421 900,833
BERG, R. F. Quantitative Characterization of the Viscosity of a	Microe.	PB90-123530 901,168	BLANKENSHIP, B. A.
mulsion.		Sputter Deposition of Icosahedral Al-Mn and Al-Mn-Si. PB89-147102 901,122	High T(sub c) Superconductor/Noble-Metal Contacts with Surface Resistivities in the (10 to the Minus 10th Power)
PB90-123597 BERGEEST, R.	900,524	Stable and Metastable Phase Equilibria in the Al-Mn	Omega sq cm Range.
International Companison of Power Meter Calibration	ns Con-	System. PB89-172324 901,136	PB89-179824 901,413 BLAU, P. J.
ducted in 1987. PB89-201545	900,718	TEM Observation of Icosahedral, New Crystalline and	Metallographic Evidence for the Nucleation of Subsurface
BERGER, H. W.	,	Glassy Phases in Rapidly Quenched Cd-Cu Alloys. PB90-123514 901,166	Microcracks during Unlubricated Sliding of Metals. PB89-147391 901,001
Directory of NVLAP (National Voluntary Laboratory A tation Program) Accredited Laboratories, 1986-87.	Accredi-	BIASCA, K. L.	BLENDELL, J. E.
	900,933	Laser Induced Fluorescence for Measurement of Lignin Concentrations in Pulping Liquors.	
BERGER, M. J.		PB89-172530 901,184	Ba2YCu3O(6+ x). PB89-171821 901,035
Electron Stopping Powers for Transport Calculations. PB90-123605	901,566	BIEDENHARN, L. C.	Electron Microscopy Studies of Diffusion-Induced Grain
BERGMANN, K.		Intrinsic Sticking in dt Muon-Catalyzed Fusion: Interplay of Atomic, Molecular and Nuclear Phenomena.	PB89-202097 901,049
Spectroscopic Detection Methods. PB89-228100	901,549	PB90-117565 901,561 BIERBAUM, V. M.	Equilibrium Crystal Shapes and Surface Phase Diagrams at
State Selection via Optical Methods.		Laser Probing of Ion Velocity Distributions in Drift Fields:	Surfaces in Ceramics. PB90-117755 901,162
	901,550	Parallel and Perpendicular Temperatures and Mobility for Ba(1+) in He.	Oxygen Partial-Density-of-States Change in the
BERGQUIST, J. C. Atomic-lon Coulomb Clusters in an Ion Trap.		PB89-171243 900,352	Out A-lay Lillission.
	901,494	Laser Probing of Product-State Distributions in Thermal- Energy Ion-Molecule Reactions.	PB89-186274 901,419 BLESSING, G. V.
Ion Trapping Techniques: Laser Cooling and Symp Cooling.	pathetic	PB89-171250 900,353	Dynamic Poisson's Ratio of a Ceramic Powder during Com-
PB90-128034	901,578	BIGNELL, N. Pressure Fixed Points Based on the Carbon Dioxide Vapor	paction. PB89-177182 901,039
Laser Cooling to the Zero-Point Energy of Motion. PB90-128091	901,581	Pressure at 273.16 K and the H2O(I) - H2O(III) - H2O(L)	Dynamic Young's Modulus Measurements in Metallic Mate-
Precise Test of Quantum Jump Theory.	,,,,,,,,,,,,,,,,,,,,,,,,,,,,,,,,,,,,,,,	Triple-Point. PB89-231138 900,483	rials: Results of an Interlahoratory Testing Program
	901,339	BILHAM, R.	Texture Monitoring in Aluminum Alloys: A Companison of
Recoilless Optical Absorption and Doppler Sideband Single Trapped Ion.	ds of a	Relationships between Fault Zone Deformation and Seg- ment Obliquity on the San Andreas Fault, California.	Ultrasonic and Neutron Diffraction Measurements. PB90-117409 901,159
PB89-171631	901,505	PB89-185953 901,279	Ultrasonic Sensor for Measuring Surface Roughness.
Thermal Shifts of the Spectral Lines in the (4)F (4)I11/2 Manifold of an Nd:YAG Laser.	3/2 to	Transducers in Michelson Tiltmeters. PB89-185979 901,280	PB89-211809 900,679
PB89-157382	901,338	BILLIARD, P. A.	BLOCK, J. H.
Trapped Ions and Laser Cooling 2: Selected Publica the Ion Storage Group, Time and Frequency Division		Development of Combustion from Quasi-Stable Tempera-	Effects of a Gold Shank-Overlayer on the Field Ion Imaging of Silicon.
Boulder, CO.	901,489	tures for the Iron Based Alloy UNS S66286. PB89-173850 900,592	PB89-175988 901,404
BERGREN, N. F.	001,400	Ignition Characteristics of the Iron-Based Alloy UNS	BLOCK, S. Bulk Modulus and Young's Modulus of the Superconductor
High T(sub c) Superconductor/Noble-Metal Contact	ts with	S66286 in Pressurized Oxygen. PB89-189336 901,104	Page 9VO7
Surface Resistivities in the (10 to the Minus 10th Omega sq cm Range.	Power)	Ignition Characteristics of the Nickel-Based Alloy UNS	Effects of Pressure on the Vibrational Spectra of Liquid Ni-
PB89-179824	901,413	N07718 in Pressunzed Oxygen. PB89-218333 901,154	team ethono
BERGTOLD, D. S. Generation of Oxy Radicals in Biosystems.		BIRNBAUM, G.	RI OMOUIST D. S.
PB90-117888	901,266	Analysis of Roto-Translational Absorption Spectra Induced in Low Density Gases of Non-Polar Molecules: The Meth-	General Methodology for Machine Tool Accuracy Enhance-
BERK, N. F.	ring) to	ane Case. PB89-201800 900,427	ment by Error Compensation.
Application of SANS (Small Angle Neutron Scatte Ceramic Characterization.	-	Collision Induced Spectroscopy: Absorption and Light Scat-	
	901,017 Sintered	tering. PB89-212252 901,363	Automated Documentation System for a Large Scale Manu-
Small Angle Neutron Scattering from Porosity in S Alumina.		Infrared Absorption of SF6 from 32 to 3000 cm(-1) in the	PRO0 150900
	901,026	Gaseous and Liquid States. PB89-157853 900,336	BLOSSER, R. L.
BERNAL, J. Expected Complexity of the 3-Dimensional Voron	oi Dia-	Optical Nondestructive Evaluation at the National Bureau of	Effects of Furfiled Ferric Oxalate/ Willie Acid Soldions as a
gram.		Standards.	System.

PB89-146716 900,034	PB89-153878 901,489	PB89-184527 900,125
Ferric Oxalate with Nitric Acid as a Conditioner in an Adhe-	BONANNO, R. E.	BRANSFORD, J. W.
sive Bonding System. PB89-229272 900,045	Resonance Ionization Mass Spectrometry of Mg: The 3pnd Autoionizing Series.	Development of Combustion from Quasi-Stable Temperatures for the Iron Based Alloy UNS S66286.
Pulpal and Micro-organism Responses to Two Experimental	PB89-150817 900,296	PB89-173850 900,592
Dental Bonding Systems. PB89-202931 901,258	BONNELL, D. W. Laser Induced Vaporization Time Resolved Mass Spec-	Ignition Characteristics of the Iron-Based Alloy UNS S66286 in Pressurized Oxygen.
BLUBAUGH, E. A.	trometry of Refractories.	PB89-189336 901,104
Spectroelectrochemistry of a System Involving Two Con- secutive Electron-Transfer Reaction.	PB90-136904 900,540 BORCHERS, J.	Ignition Characteristics of the Nickel-Based Alloy UNS N07718 in Pressurized Oxygen.
PB90-136979 900,237	Characterization of Structural and Magnetic Order of Er/Y	PB89-218333 901,154
BLUE, J. L.	Superlattices. PB90-123662 901,470	BRATSCH, S. G.
Effect of an Oil-Paper Interface Parallel to an Electric Field on the Breakdown Voltage at Elevated Temperatures.	Exchange and Magnetostrictive Effects in Rare Earth Su-	Standard Electrode Potentials and Temperature Coeffi- cients in Water at 298.15 K.
PB89-156988 901,490	perlattices.	PB89-226567 900,456
IODANESS, R. Two-Photon Laser-Induced Fluorescence of the Tumor-Lo-	PB89-202667 901,438 Long-Range Incommensurate Magnetic Order in Dy-Y Multi-	BRAUER, G. M.
calizing Photosensitizer Hematoporphyrin Derivative.	layers.	Biological Evaluations of Zinc Hexyl Vanillate Cement Using Two In vivo Test Methods.
PB89-157283 901,240 IOETTINGER, W. J.	PB89-179642 901,411 Occurrence of Long-Range Helical Spin Ordering in Dy-Y	PB89-157150 900,038
Formation of Dispersoids during Rapid Solidification of an	Multilayers.	Oligomers with Pendant Isocyanate Groups as Adhesives for Dentin and Other Tissues.
Al-Fe-Ni Alloy. PB90-123647 901,172	PB89-179634 901,410 BORNER, H. G.	PB89-179253 900,042
Kinetics of Resolidification.	Determination of Short Lifetimes with Ultra High Resolution	Oligomers with Pendant Isocyanate Groups as Tissue Adhesives. 1. Synthesis and Characterization.
PB89-176457 901,138	(n,gamma) Spectroscopy. PB90-123670 901,567	PB89-202212 900,055
Microstructural Variations in Rapidly Solidified Alloys. PB90-123621 901,170	BOSTELMAN, R.	Oligomers with Pendant Isocyanate Groups as Tissue Adhesives. 2. Adhesion to Bone and Other Tissues.
Pathways for Microstructural Development in TiAl.	Robot Crane Technology.	PB89-231245 900,056
PB90-123779 901,173	PB90-111667 900,146	BRAUN, E.
Rapid Solidification and Ordering of B2 and L2 (sub 1) Phases in the NiAl-NiTi System.	BOULDIN, C. E. EXAFS (Extended X-ray Absorption Fine Structure) Study of	Flammability Characteristics of Electrical Cables Using the Cone Calorimeter.
PB90-123639 901,171	Buried Germanium Layer in Silicon.	PB89-162572 900,741
Solidification of an 'Amorphous' Phase in Rapidly Solidified Al-Fe-Si Alloys.	PB89-228472 901,452	BRAUN, W.
PB90-123530 <i>901,168</i>	Multiple Scattering in the X-ray-Absorption Near-Edge Structure of Tetrahedral Ge Gases.	Fluid Flow in Pulsed Laser Irradiated Gases; Modeling and Measurement.
OGGS, P. T.	PB89-146922 900,283	PB90-123704 900,265
Computation and Use of the Asymptotic Covariance Matrix for Measurement Error Models.	Multiple Scattering in the X-ray Absorption Near Edge Structure of Tetrahedral Germanium Gases.	Modeling Chemical Reaction Systems on an IBM PC. PB89-171920 900,358
PB89-215321 901,214	PB89-228480 900,474	BRAY, S. L.
Merit Functions and Nonlinear Programming. PB90-123944 901,208	Silicon Photodiode Detectors for EXAFS (Extended X-ray Absorption Fine Structure).	Battery-Powered Current Supply for Superconductor Meas-
User's Reference Guide for ODRPACK: Software for	PB89-228498 900,731	urements. PB89-200455 901,525
Weighted Orthogonal Distance Regression Version 1.7. PB89-229066 901,215	Structural Unit in Icosahedral MnAlSi and MnAl. PB89-157648 901,131	Critical Current Measurements of Nb3Sn Superconductors:
OHANDY, J.	BOUMAZOUZA, D.	NBS (National Bureau of Standards) Contribution to the VAMAS (Versailles Agreement on Advanced Materials and
Magnetic Field Dependence of the Superconductivity in Bi- Sr-Ca-Cu-O Superconductors.	Re-Entrant Spin-Glass Properties of a-(FexCr1-x)75P15C10.	Standards) Interlaboratory Comparison.
PB89-146815 901,385	PB89-157481 <i>901,391</i> BOURGIN, R. D.	PB90-136748 901,480
OHANNAN, B.	Shortest Paths in Simply Connected Regions in R2.	Current Capacity Degradation in Superconducting Cable Strands.
Photospheres of Hot Stars. 3. Luminosity Effects at Spectral Type 09.5.	PB90-123688 901,202	PB89-200471 901,526
PB89-202592 900,020	BOURGUIGNON, B. AES and LEED Studies Correlating Desorption Energies	Current Ripple Effect on Superconductive D.C. Critical Current Measurements.
OISVERT, R. F. Elimination of Spurious Eigenvalues in the Chebyshev Tau	with Surface Structures and Coverages for Ga on Si(100).	PB89-157077 901,492
Spectral Method.	PB89-171599 901,401	Effect of Room-Temperature Stress on the Critical Current of NbTi.
PB89-209282 901,330 Guide to Available Mathematical Software Advisory System.	Laser Probing of the Dynamics of Ga Interactions on Si(100).	PB89-179832 901,414
PB90-123654 901,201	PB89-186928 901,422	Nb3Sn Critical-Current Measurements Using Tubular Fiber- glass-Epoxy Mandrels.
Internal Structure of the Guide to Available Mathematical	Surface Structure and Growth Mechanism of Ga on Si(100). PB89-149181 901,387	glass-Epoxy Mandrels. PB89-200497 901,527
Software. PB89-170864 900,927	Surface Structures and Growth Mechanism of Ga on	VAMAS (Versailles Project on Advanced Materials and Standards) Intercompanson of Critical Current Measure-
Numerical Simulation of Morphological Development during	Si(100) Determined by LEED (Low Energy Electron Diffrac- tion) and Auger Electron Spectroscopy.	ment in Nb3Sn Wires.
Ostwald Ripening. PB89-201990 901,152	PB89-171342 901,399	PB89-202147 901,534 BREESE, R.
OLAND, T.	BOWEN, R. L. Adhesion to Dentin by Means of Gluma Resin.	Cigarette as a Heat Source for Smolder Initiation in Uphol-
Government Open Systems Interconnection Profile Users' Guide.	PB89-157168 900,039	stery Materials. PB89-176762 900,595
PB90-111212 900,667	Adhesive Bonding of Composites.	BREITENBERG. M.
Ongoing Implementation Agreements for Open Systems Interconnection Protocols: Continuing Agreements.	PB90-123696 900,050 Bonding Agents and Adhesives: Reactor Response.	Directory of International and Regional Organizations Con-
PB89-166086 900,610	PB89-146732 900,035	ducting Standards-Related Activities. PB89-221147 900,008
Stable Implementation Agreements for Open Systems Inter-	Effects of Purified Ferric Oxalate/Nitric Acid Solutions as a Pretreatment for the NTG-GMA and PMDM Bonding	BRENNAN, J. A.
connection Protocols. Version 2, Edition 1. December 1988. PB89-193312 900,618	System,	Effect of Pipe Roughness on Orifice Flow Measurement.
Working Implementation Agreements for Open Systems	PB89-146716 900,034	PB89-231484 901,333 NBS (National Bureau of Standards)-Boulder Gas Flow Fa-
Interconnection Protocols. PB89-221196 900,624	Ferric Oxalate with Nitric Acid as a Conditioner in an Adhesive Bonding System.	cility Performance.
Working Implementation Agreements for Open Systems	PB89-229272 900,045	PB89-186787 900,889 Optimum Location of Flow Conditioners in a 4-Inch Orifice
Interconnection Protocols. PB89-235931 900,642	In vitro Investigation of the Effects of Glass Inserts on the Effective Composite Resin Polymerization Shrinkage.	Meter.
BOLLETTA, F.	PB90-117516 900,049	PB90-111675 900,911
Rate Constants for the Quenching of Excited States of Metal Complexes in Fluid Solution.	Pulpal and Micro-organism Responses to Two Experimental Dental Bonding Systems.	BRENNAN, S. Performance of a High-Energy-Resolution, Tender X-ray
PB89-227797 900,461	PB89-202931 901,258	Synchrotron Radiation Beamline.
Atomic-lon Coulomb Clusters in an Ion Tran	Substitutes for N-Phenylglycine in Adhesive Bonding to Dentin.	PB90-128083 <i>901,580</i> BRETZ, M.
Atomic-Ion Coulomb Clusters in an Ion Trap. PB89-157424 901,494	PB90-123795 900,051	Spherical Acoustic Resonators in the Undergraduate Labo-
Frequency Standards Utilizing Penning Traps.	Use of N-Phenylglycine in a Dental Adhesive System. PB90-117375 900,048	ratory. PB89-179709 <i>901,317</i>
PB90-128042 901,379 Ion Trapping Techniques: Laser Cooling and Sympathetic	BOWER, V. E.	BREWER, L. R.
Cooling.	Measurement of the NBS (National Bureau of Standards) Electrical Watt in SI Units.	Ion Trapping Techniques: Laser Cooling and Sympathetic
PB90-128034 901,578 Trapped lons and Laser Cooling 2: Selected Publications of	PB89-230429 900,821	Cooling. PB90-128034 <i>901,578</i>
Trapped Ions and Laser Cooling 2: Selected Publications of the Ion Storage Group, Time and Frequency Division, NIST,	BRANDYBERRY, M. D.	Perpendicular Laser Cooling of a Rotating Ion Plasma in a
Boulder, CO.	Fire Risk Analysis Methodology: Initiating Events.	Penning Trap.

901,578
Perpendicular Laser Cooling of a Rotating Ion Plasma in a Penning Trap.

PB89-157408 901,493 Resonance-Enhanced Multiphoton Ionization of Atomic Hy-	Spectra and Energy Levels of Br XXV, Br XXIX, Br XXX, and Br XXXI.	PB90-136839 900,848 BUDNICK, E. K.
drogen.	PB89-176002 901,509	Capabilities of Smoke Control: Fundamentals and Zone
PB89-201073 901,529	BROWN, D. R. Comparison of Time Scales Generated with the NBS (Na-	Smoke Control.
BREWER, W. D. Magnetic Resonance of (160)Tb Onented in a Terbium	tional Bureau of Standards) Ensembling Algorithm.	PB89-229157 900,086 Computer Fire Models.
Single Crystal at Low Temperatures.	PB89-174072 900,628 BROWN, J.	PB89-173991 900,163
PB89-179204 901,519	Effects of Material Characteristics on Flame Spreading.	Hand Calculations for Enclosure Fires.
BRIBER, R. M.	PB89-212021 900,572	PB89-173983 900,16-
Effect of Crosslinks on the Phase Separation Behavior of a Miscible Polymer Blend.	BROWN, J. E.	BUFFINGTON, A. Microarcsecond Optical Astrometry: An Instrument and Its
PB89-146724 900,546	Cone Calorimeter Method for Determining the Flammability of Composite Materials.	Astrophysical Applications.
Small Angle Neutron Scattering Studies of Single Phase Interpenetrating Polymer Networks.	PB89-149165 901,072	PB89-171268 900,013
PB90-123456 900,577	BROWN, J. M. Detection of the Free Radicals FeH, CoH, and NiH by Far	BUKOWSKI, R. W. False Alarm Study of Smoke Detectors in Department o
BRIGHT, D. S.	Infrared Laser Magnetic Resonance.	Veterans Affairs Medical Centers (VAMCS).
Computer-Aided Imaging: Quantitative Compositional Map- ping with the Electron Probe Microanalyzer.	PB90-117342 900,495	PB89-193288 900,093
PB89-157754 <i>901,073</i>	Far-Infrared Laser Magnetic Resonance Spectrum of the CD Radical and Determination of Ground State Parameters.	HAZARD I Fire Hazard Assessment Method. PB89-215404 900, 143
Defocus Modeling for Compositional Mapping with Wave- length-Dispersive X-ray Spectrometry.	PB90-117359 900,496	Summary of the Assumptions and Limitations in Hazard I.
PB89-176150 900,378	Far-Infrared Laser Magnetic Resonance Spectrum of Vibra- tionally Excited C2H(1).	PB90-136821 900,606
BRILL, M. H.	PB89-147474 900,292	BULLIS, W. M.
Heuristic Analysis of von Kries Color Constancy. PB89-201099 901,362	Frequency Measurement of the $J = 1 < -0$ Rotational Transition of HD (Hydrogen Deutende).	Interlaboratory Determination of the Calibration Factor fo the Measurement of the Interstitial Oxygen Content of Sili
BRINCKMAN, F. E.	PB89-161566 901,499	con by Infrared Absorption. PB90-117300 900,224
Biodegradation of Tributyltin by Chesapeake Bay Microor-	BROWN, P.	BUNGE, A. L.
ganisms. PB89-177232 <i>901,309</i>	Implications of Computer-Based Simulation Models, Expert Systems, Databases, and Networks for Cement Research.	Influence of Reaction Reversibility on Continuous-Flow Ex
Characterization of Organolead Polymers in Trace Amounts	PB89-146989 900,581	traction by Emulsion Liquid Membranes. 900,244
by Element-Specific Size-Exclusion Chromatography. PB89-175962 900,196	Integrated Knowledge Systems for Concrete and Other Materials.	BUNKER, G.
Determination of Ultratrace Concentrations of Butyltin Com-	PB89-176119 900,582	Multiple Scattering in the X-ray-Absorption Near-Edge
pounds in Water by Simultaneous Hydridization/Extraction	BROWN, P. F.	Structure of Tetrahedral Ge Gases. PB89-146922 900,283
with GC-FPD Detection. PB89-177224 901,311	NBS AMRF (National Bureau of Standards) (Automated Manufacturing Research Facility) Process Planning System:	Multiple Scattering in the X-ray Absorption Near Edge
Effect of pH on the Emission Properties of Aqueous tris	System Architecture.	Structure of Tetrahedral Germanium Gases.
(2,6-dipicolinato) Terbium (III) Complexes. PB89-157135 <i>900,250</i>	PB89-193882 900,956 BROWN, P. W.	PB89-228480 900,474
Element-Specific Epifluorescence Microscopy In vivo Moni-	Implications of Phase Equilibria on Hydration in the Trical-	BUNTIN, S. A. Non-Boltzmann Rotational and Inverted Spin-Orbit State
toring of Metal Biotransformations in Environmental Matri-	cium Silicate-Water and the Tricalcium Aluminate-Gypsum- Water Systems.	Distributions for Laser-Induced Desorption of NO from
ces. PB89-177216 <i>901,220</i>	PB89-150759 901,022	Pt(111). PB89-157952 900,340
Global Biomethylation of the Elements - Its Role in the Bio-	Model for Particle Size and Phase Distributions in Ground	Optically Driven Surface Reactions: Evidence for the Role
sphere Translated to New Organometallic Chemistry and Biotechnology.	Cement Clinker. PB90-136847 901,062	of Hot Electrons. PB89-157937 900,338
PB90-136854 901,232	Standard Specifications for Cements and the Role in Their	BUONACCORSI, J. P.
Microbiological Materials Processing.	Development of Quality Assurance Systems for Laborate- nes.	Problems with Interval Estimation When Data Are Adjusted
PB90-123712 901,261 Novel Flow Process for Metal and Ore Solubilization by	PB89-150742 901,021	via Calibration. PB89-157812 901,205
Aqueous Methyl Iodide.	BROWN, R. J. C.	BUR, A. J.
PB89-202113 901,285	Thermodynamics of Ammonium Scheelites. 6. An Analysis of the Heat Capacity and Ancillary Values for the Metaper-	In Situ Fluorescence Monitoring of the Viscosities of Parti
Speciation Measurements of Butyltins: Application to Con- trolled Release Rate Determination and Production of Ref-	iodates KIO4, NH4IO4, and ND4IO4. PB89-147060 900,285	cle-Filled Polymers in Flow. PB89-146278 900,608
erence Standards. PB89-146807 900,174	BROWN, R. L.	Laboratory Evaluation of an NBS (National Bureau o
Trace Speciation by HPLC-GF AA (High-Performance Liquid	Pi-Electron Properties of Large Condensed Polyaromatic	Standards) Polymer Soil Stress Gage. PB89-211973 901,29
Chromatography-Graphite Furnace Atomic Absorption) for	Hydrocarbons. PB89-202139 900,432	BURCH, D. M.
Tin- and Lead-Bearing Organometallic Compounds, with Signal Increases Induced by Transition-Metal Ions.	Rate Constants for Hydrogen Abstraction by Resonance	Experimental Validation of a Mathematical Model for Pre
PB89-157085 900,184	Stabilized Radicals in High Temperature Liquids. PB89-161608 900,348	dicting Moisture Transfer in Attics. PB89-150783 900,05
BRION, C. E.	BROWN. W. E.	Thermal Resistance Measurements and Calculations of ar
Absolute Cross Sections for Molecular Photoabsorption, Partial Photoionization, and Ionic Photofragmentation Proc-	Comparison of Fluoride Uptake Produced by Tray and	Insulated Concrete Block Wall.
ess. PB89-186464 <i>900,410</i>	Flossing Methods In vitro. PB89-179238 901,252	PB89-174916 900,115
BRIZGYS, M. V.	Mechanism of Hydrolysis of Octacalcium Phosphate.	BURGE, H. A. Investigation of a Washington, DC Office Building.
Generic Liposome Reagent for Immunoassays.	PB89-201503 901,254	PB89-230361 900,08
PB90-123886 <i>901,229</i>	Micro-Analysis of Mineral Saturation Within Enamel during Lactic Acid Demineralization.	BURGESS, D.
Liposome-Enhanced Flow Injection Immunoanalysis. PB89-146757 900,036	PB89-186379 901,253	NO/NH3 Coadsorption on Pt(111): Kinetic and Dynamica Effects in Rotational Accommodation.
BROADHURST, M. G.	Micro-Raman Characterization of Atherosclerotic and Bio-	PB89-201123 900,423
Charging Behavior of Polyethylene and Ionomers.	prosthetic Calcification. PB89-149223 901,234	BURKE, R. W.
PB90-136813 900,578	BRUN, T. O.	Chemical Calibration Standards for Molecular Absorption Spectrometry.
Effects of Space Charge on the Poling of Ferroelectric Polymers.	Magnetic Structure of Cubic Tb0.3Y0.7Ag. PB90-117789 901,466	PB89-171938 900,191
PB89-146708 901,179	BRUNO, T. J.	BURNS, G. W.
BROCKMAN, M.	PVT Measurements on Benzene at Temperatures to 723 K.	NIST (National Institute of Standards and Technology Measurement Services: The Calibration of Thermocouples
Standard Aggregate Materials for Alkali-Silica Reaction Studies.	PB89-157200 900,311	and Thermocouple Materials.
PB89-193221 <i>901,046</i>	PVT of Toluene at Temperatures to 673 K. PB89-157192 900,310	PB89-209340 900,897
BROWN, A. Rotational Modulation and Flares on BS Canum Venation	Supercritical Fluid Chromatograph for Physicochemical	BURNS, T. J. Mechanism for Shear Band Formation in the High Strain
Rotational Modulation and Flares on RS Canum Venati- corum and BY Draconis Stars X: The 1981 October 3 Flare	Studies. PB89-184105 900,201	Rate Torsion Test.
on V711 Tauri (= HR 1099). PB89-202618 900,021	BRUSH, L. N.	PB89-215370 900,907
Rotational Modulation and Flares on RS CVn and BY Dra	Directional Solidification of a Planar Interface in the Pres-	BURTON, B. P. Multicritical Phase Relations in Minerals.
Stars IX, IUE (International Ultraviolet Explorer) Spectrosco-	ence of a Time-Dependent Electric Current. PB90-112400 901,461	PB89-150882 901,278
py and Photometry of II Peg and V711 Tau during February 1983.	BUCHINGER, F.	BUSBY, R.
PB89-171615 900,019	Resonance-Enhanced Multiphoton Ionization of Atomic Hy-	Tilt Observations Using Borehole Tiltmeters 1. Analysis of Tidal and Secular Tilt.
BROWN, C. M.	drogen. PB89-201073 901,529	PB90-136649 901,283
Laser-Produced Spectra and QED (Quantum Electrodynamic) Effects for Fe-, Co-, Cu-, and Zn-Like lons of Au, Pb, Bi,	BUCKLEY, T. J.	BUSHBY, S. T.
Th, and U. PB89-176010 901,510	Evaluation of Data on Higher Heating Values and Elemental Analysis for Refuse-Derived Fuels.	Simulation of a Large Office Building System Using the HVACSIM+ Program.

PB89-177174	900,071	CALLANAN, J. E.	CARVER, G. P.	_
Stendardizing EMCS Communication Protocols. PB89-172357 USHEE. D. S.	900,613	Development of Standard Meesurement Techniques a Standard Reference Materials for Heat Capacity and He of Vaporization of Jet Fuels.	at Probe end Four-Probe Resistances. PB89-231211 900	Two- <i>0,794</i>
Anelysis of Ultrapure Reagents from e Lerge Still Made of Teflon PFA.	Sub-Boiling	PB89-148100 900,8 Enthalpies of Desorption of Water from Coal Surfaces. PB89-173868 900,8	con-on Sapphire) Films.	(Sili- 0,798
PB89-186357 USSO, M.	900,202	Specific Heet Measurements of Two Premium Coals. PB89-173900 900,8	High-Mobility CMOS (Complementary Metal Oxide S	Semi-
Rotational Modulation and Flares on RS CVn el Stars IX. IUE (Internetional Ultraviolet Explorer) S py and Photometry of II Peg end V711 Teu durin	pectrosco-	Specific Heat of Insulations. PB89-172514 900,1	PB89-230460 900	0,791
1983. PB89-171615	900,019	Thermodynamics of Ammonium Scheelites. 6. An Analy of the Heat Capecity and Ancillary Values for the Metap	is Dissociation Lifetimes and Level Mixing in Overtone-Ex ir- HN3 (X tilde (sup 1) A').	
UTLER, C. J. Rotational Moduletion and Flares on RS CVn a		iodates KIO4, NH4IO4, and ND4IO4. PB89-147060 900,2	Picosecond Studies of Vibrational Energy Transfer in N	<i>0,263</i> Mole-
Stars IX. IUE (International Ultreviolet Explorer) S py and Photometry of II Peg and V711 Teu durin 1983.	g February	CALLCOTT, T. A. Oxygen Partial-Density-of-States Change in t YBa2Cu3Ox Compounds for x(Approx.)6,6.5,7 Measured		0,316
PB89-171615	900,019	Soft X-ray Emission. PB89-186274 901.4	Adsorbates.	0,537
UTLER, E. P. Toughening Mechanisms in Ceramic Composit		CALMES, A.	Time Resolved Studies of Vibrationel Relaxation Dyna	
Annual Progress Report for the Period Ending 1989. PB89-235907	March 31, 901,080	Theory and Practice of Paper Preservation for Archives. PB89-147052 900,9		0,444
UTRYMOWICZ, D. B.	00.,000	CAMPBELL, T. J. Pahasapaite, e Beryllophosphate Zeolite Related to Sy	Unimolecular Dynamics Following Vibrational Overtone citation of HN3 v1= 5 and v1= 6:HN3(X tilde;v,J,K,)) ->
Materials Failure Prevention at the National Standards. PB89-212237	Bureau of 901,190	thetic Zeolite Rho, from the Tip Top Pegmatite of Sou Dakota.	th sub g (1+)).	Sigma <i>0,286</i>
YRD, E.	001,100	PB89-186431 901,2 CANFIELD, L. R.	Vibrational Predissociation of the Nitric Oxide Dimer.	•
Corrosion Induced Degredation of Amine-Cur Coatings on Steel.		Stability and Ouantum Efficiency Performance of Silic Photodiode Detectors in the Far Ultraviolet.	CASELLA, R. C.	0,289
PB89-176291 Epoxy Impregnation of Hardened Cement Pastes	<i>901,084</i> s for Char-	PB90-128059 900,7 CAO, L. X.	High-Temperature Superconductivity - Possible Expeni	
acterization of Microstructure. PB89-185573	901,042	Optical Roughness Measurements for Industrial Surfaces. PB89-176655 900,9	tal Tests. PB90-117334 90:	1,462
Ouantitative Studies of Coatings on Steel Using F Absorption Fourier Trensform Infrared Spectrosco	py.	CAPLAN, H. S.	Dependence of T(sub c) on the Number of CuO2 PI per Cluster in Interplaner-Boson-Exchange Models of the	anes High-
PB89-212112 YRD, G. D.	901,066	Cross Section end Linear Polarization of Tagged Photons PB90-117292 901,5	T(sub C) Superconductivity.	1,455
Continine in Freeze-Dried Urine Reference Materi	al.	CAPOBIANCO, T. E.	Theoretical Models for High-Temperature Supercond	ducti-
PB90-213703 YRD, R. H.	900,675	Cryogenic Bathysphere for Rapid Variable-Temperatu Characterization of High-T(sub c) Superconductors.	PB89-186266 907	1,418
User's Reference Guide for ODRPACK: So	ftware for	PB89-228456 901,4 New Standard Test Method for Eddy Current Probes.	CASWELL, R. S.	
Weighted Orthogonal Distance Regression Versio PB89-229066	on 1.7. 901,215	PB89-187587 900,9	FB09-171034 901	1,241
YRD, W. E.	4-) -4 500	Resistance Measurements of High T(sub c) Superconductors Using a Novel 'Bathysphere' Cryostat.	ticles	Par-
Thermal Degradation of Poly (methyl methacryla to 125C.		PB89-228431 901,4 CARANGELO, R. M.	PB89-171862 90	1,265
PB89-157465 ABEZA, I.	900,549	FT-IR (Fourier Transform-Infrared) Emission/Transmissi		
Fundamental Configurations in Mo IV Spectrum.	000 004	Spectroscopy for In situ Combustion Diegnostics. PB89-211866 900,6	00	1,264
P889-147011 ABEZA, M. I.	900,284	CAREY, C. M.	CATALA, J. M. Reevaluation of Forces Measured Across Thin Pol	lymer
Spectrum of Doubly Ionized Tungsten (W III). PB89-235659	900,223	Micro-Analysis of Mineral Saturation Within Enamel duri Lactic Acid Demineralization. PB89-186373 901,2	PB89-228589 900	0,573
ABLE, J. W.		CARINO, N. J.	CATALANO, S.	
Low-Temperature Phase and Magnetic Interacti Fe-Cr-Ni Alloys. PB90-136771	ons in fcc 901,113	Finite Element Studies of Transient Wave Propagation. PB89-186902 901,3 CARLETON, K. L.	Rotational Modulation and Flares on RS CVn and BY Stars IX. IUE (International Ultraviolet Explorer) Spectro py and Photometry of II Peg and V711 Tau during Feb 1983	osco-
AGE, M. E.	NOC (No	Laser Probing of the Dynamics of Ga Interactions	DD00 474045	0,019
Determination of the Time-Dependence of ohm tional Bureau of Standards) Using the Ouantize		Si(100). PB89-186928 901,4	CATLOW, C. R. A. Neutron Powder Diffraction Structure and Electrical Properties of the control	
Sistance. PB89-230387 NBS (National Bureau of Standards) Determinal	900,819	Surface Structures and Growth Mechanism of Ga Si(100) Determined by LEED (Low Energy Electron Diffra	on ties of the Defect Pyrochlores Pb1.5M2O6.5 (M= Nb, 1	
Fine-Structure Constant, and of the Ouantized Fance and Josephson Frequency-to-Voltage Ouc	Hall Resist-	tion) and Auger Electron Spectroscopy. PB89-171342 901,3		
Units. PB89-230437	901,556	CARLSON, A. D Measurements of the (235)U (n,t) Standard Cross Secti	Crystal Chemistry of Superconductors: A Guide to the loning of New Compounds.	
Possible Ouantum Hall Effect Resistance Standar	rd.	at the National Bureau of Standards. PB89-176556 901,3	1 803-171700	1,030
PB89-149058 Quantized Hall Resistance Measurement at the	900,801 NML (Na-	CARNAHAN, L. J.	Final-State-Resolved Studies of Molecule-Surface Int	erac-
tional Measurement Laboratory). PB89-179675	900,778	Computer Viruses and Related Threats: A Manageme Guide.	nt tions. PB89-150916 <i>90</i> 0	0,298
AHN, J. W.	,	PB90-111683 900,6	54 NO/NH3 Coadsorption on Pt(111): Kinetic and Dyna Effects in Rotational Accommodation.	.mical
Formation and Stability Range of the G Phase in num-Manganese System.	the Alumi-	CARNEY, B. Microarcsecond Optical Astrometry: An Instrument and	PB89-201123 900	0,423
PB89-186316	901,144	Astrophysical Applications. PB89-171268 900,0	Non-Boltzmann Rotational and Inverted Spin-Orbit Distributions for Laser-Induced Desorption of NO	from
Grain Boundaries with Impurities in a Two-Dimer tice-Gas Model. PB89-172407		CARPENTER, B. S.		0,340
Rapid Solidification and Ordering of B2 and I Phases in the NiAI-NiTi System.	901,507 L2 (sub 1)	High Accuracy Determination of (235)U in Nondestruct Assay Standards by Gamma Spectrometry. PB89-156954 900,2	of Hot Electrons.	Role 0.338
PB90-123639	901,171	CARR, M. J.	Picosecond Studies of Vibrational Energy Transfer in I	
Stress Effects on III-V Solid-Liquid Equilibria. PB89-146997	900,769	NIST (National Institute of Standards and Technolog Sandia/ICDD Electron Diffraction Database: A Database Phase Identification by Electron Diffraction.)/ cules on Surfaces. or PB89-157309 <i>90</i> 0	0,316
AI, T. X. Determination of AC-DC Difference in the 0.1	- 100 MHz	PB89-175210 901,5	Chemisorbed on SiO2-Supported Rhodium Particles.	
Frequency Range. PB89-228597	900,719	CARROLL, D. F. Creep Rupture of a Metal-Ceramic Particulate Composite PB89-211825 901,0	Picosecond Vibrational Energy Transfer Studies of Su	0,317 urface
AIS, R. E. Deuterium Magnetic Resonance Study of Orier	ntation and	CARTER, A. C.	PB90-136573 906	0,537
Poling in Poly(Vinylidene Fluoride) and Poly(Vinyl ride-Co-Tetrafluoroethylene).	idene Fluo-	Silicon Photodiode Detectors for EXAFS (Extended X- Absorption Fine Structure).	Population Relaxation of CO(v= 1) Vibrations in So Phase Metal-Carbonyl Complexes.	lutior
PB89-186365	900,565	PB89-228498 900,7		0,315

Time Resolved Studies of Vibrational Relaxation Dynamics of $CO(v = 1)$ on Metal Particle Surfaces.	PB89-157473 900,550	PB89-211866 900,60
PB89-203012 900,444	Uniaxial Deformation of Rubber Network Chains by Small Angle Neutron Scattering. PB89-175830 901,088	CHILD, M. S. Rydberg-Klein-Rees Inversion of High Resolution van de
CAVCEY, K. H. Transmission Loss through 6061 T-6 Aluminum Using a	PB89-175830 901,088 CHANG, Y. M.	Waals Infrared Spectra: An Intermolecular Potential Energ Surface for Ar+ HF (v= 1).
Pulsed Eddy Current Source. PB89-179840 901,143	Performance Measurements of Infrared Imaging Systems Used to Assess Thermal Anomalies.	PB89-227953 900,46 CHILDERS, C. B.
CELOTTA, R. J.	PB89-179667 900,072	NIST (National Institute of Standards and Technology
Domain Images of Ultrathin Fe Films on Ag(100). PB89-158067 901,394	CHAPADOS, C. Infrared Absorption of SF6 from 32 to 3000 cm(-1) in the	Measurement Services: AC-DC Difference Calibrations. PB89-222616 900,81
High Resolution Imaging of Magnetization. PB89-147433 901,386	Gaseous and Liquid States. PB89-157853 900,336	CHIN, D.
Improved Low-Energy Diffuse Scattering Electron-Spin Po-	CHAPMAN, P. L.	Dynamic Light Scattering and Angular Dissymmetry for the Insitu Measurement of Silicon Dioxide Particle Synthesis in
larization Analyzer. PB89-229173 900,218	Calibration with Randomly Changing Standard Curves. PB89-186381 900,888	Flames. PB89-179584 <i>900,24</i>
Influence of the Surface on Magnetic Domain-Wall Microstructure.	CHAPMAN, R. E.	CHITTUR, K.
PB90-118019 901,467	Analyzing the Economic Impacts of a Military Mobilization. PB90-128067 901,273	Component Spectrum Reconstruction from Partially Characterized Mixtures.
State Selection in Electron-Atom Scattering: Spin-Polarized Electron Scattering from Optically Pumped Sodium.	Evaluating Emergency Management Models and Data Bases: A Suggested Approach.	PB89-202568 900,43 Spectroscopic Quantitative Analysis of Strongly Interactin
PB89-176572 901,513 Structure of Cs on GaAs(110) as Determined by Scanning	PB89-189203 901,598	Systems: Human Plasma Protein Mixtures. PB89-202576 901,22
Tunneling Microscopy. PB90-117490 901,463	CHAPPELL, S. Draft International Document on Guide to Portable Instru-	CHO, S. J.
Superelastic Scattering of Spin-Polarized Electrons from	ments for Assessing Airborne Pollutants Arising from Haz- ardous Wastes.	Grain-Size and R-Curve Effects in the Abrasive Wear of Alumina.
Sodium. PB90-128307 <i>901,584</i>	PB89-150775 900,855 CHARAGUNDLA, S. R.	PB90-117383 901,05
Vector Imaging of Magnetic Microstructure.	Remote Sensing Technique for Combustion Gas Tempera-	CHOHAYEB, A. A. Comparison of Microleakage of Experimental and Selecte
PB90-128240 901,476 CHACONAS, K.	ture Measurement in Black Liquor Recovery Boilers. PB89-179568 900,392	Commercially Available Bonding Systems. PB89-234223 901,07
Visual Perception Processing in a Hierarchical Control System: Level 1.	CHARTIER, J. M.	CHOLVIBUL, R. W.
PB89-221188 900,994	Towards the Ultimate Laser Resolution. PB89-186910 900,416	U-Value Measurements for Windows and Movable Insulations from Hot Box Tests in Two Commercial Laboratories.
CHAMBERS, G. P. Analytical Expression for Describing Auger Sputter Depth	CHASE, M. W. Numeric Databases in Chemical Thermodynamics at the	PB89-175889 900,12
Profile Shapes of Interfaces. PB89-157176 900.309	National Institute of Standards and Technology. PB89-175228 900,371	CHOSHI, H. Phase Contrast Matching in Lamellar Structures Compose
Temperature-Dependent Radiation-Enhanced Diffusion in	CHASE, W. T.	of Mixtures of Labeled and Unlabeled Block Copolymer fo Small-Angle Neutron Scattering.
Ion-Bombarded Solids. PB89-179188 901,408	Technical Examination, Lead Isotope Determination, and Elemental Analysis of Some Shang and Zhou Dynasty	PB89-157119 901,18
CHAMBERS, W. F.	Bronze Vessels. PB90-136862 901,178	CHOW, L. C. Comparison of Fluoride Uptake Produced by Tray and
NIST (National Institute of Standards and Technology)/ Sandia/ICDD Electron Diffraction Database: A Database for	CHEMTOB, M.	Flossing Methods In vitro. PB89-179238 901,25
Phase Identification by Electron Diffraction. PB89-175210 901,508	International Intercomparison of Neutron Survey Instrument Calibrations.	Formation of Hydroxyapatite in Hydrogels from Tetraca cium Phosphate/Dicalcium Phosphate Mixtures.
CHAMPION, R. L.	PB89-229165 901,300	PB89-201511 901,25
Collisional Electron Detachment and Decomposition Rates of SF6(1-), SF5(1-), and F(1-) in SF6: Implications for Ion	CHEN, L. J. Mean Density Approximation and Hard Sphere Expansion	Micro-Analysis of Mineral Saturation Within Enamel durin Lactic Acid Demineralization.
Transport and Electrical Discharges. PB90-117862 900,511	Theory: A Review. PB89-228019 901,546	PB89-186373 901,25
CHAMPLONG, P.	CHEN, R. S.	Quasi-Constant Composition Method for Studying the Formation of Artificial Caries-Like Lesions.
International Intercomparison of Neutron Survey Instrument Calibrations.	Use of N-Phenylglycine in a Dental Adhesive System. PB90-117375 900,048	PB89-229249 901,25 CHRISTENSEN, P. A.
PB89-229165 901,300 CHAN, H. M.	CHEN, Y.	Decay of High Valent Manganese Porphyrins in Aqueou
Effect of Heat Treatment on Crack-Resistance Curves in a	Experimental Study of the Pyrolysis of Pure and Fire Retarded Collulose.	Solution and Catalyzed Formation of Oxygen. PB89-156772 900,30
Liquid-Phase-Sintered Alumina. PB89-229231 901,056	PB89-228316 901,090 CHEN, Y. T.	CHRISTOFFERSEN, J. Calcium Hydroxyapatite Precipitated from an Aqueous Solu
CHAN, K. S. Creep Cavitation in Liquid-Phase Sintered Alumina.	Dynamic Young's Modulus Measurements in Metallic Materials: Results of an Interlaboratory Testing Program.	tion: An International Multimethod Analysis. PB90-123399 900,22
PB89-175954 901,038	PB89-157671 901,132	CHRISTOFFERSEN, M. R.
CHANDLER, J. F. Microarcsecond Optical Astrometry: An Instrument and Its	CHEOK, G. S. Inelastic Behavior of Full-Scale Bridge Columns Subjected	Calcium Hydroxyapatite Precipitated from an Aqueous Solution: An International Multimethod Analysis.
Astrophysical Applications. PB89-171268 900,013	to Cyclic Loading. PB89-174924 900,584	PB90-123399 900,22
CHANG, D. C.	CHERIN, A.	CHRISTY, A. A. Low Pressure, Automated, Sample Packing Unit for Diffusi
Effect of an Electrically Large Stirrer in a Mode-Stirred Chamber.	Numerical Aperture of Multimode Fibers by Several Methods: Resolving Differences.	Reflectance Infrared Spectrometry. PB90-135922 900,23
PB90-117946 901,378	PB90-117482 900,757 CHERIN, A. H.	CHUANG, T. J.
Hybrid Representation of the Green's Function in an Over- moded Rectangular Cavity.	Comparison of Far-Field Methods for Determining Mode	Creep Rupture of a Metal-Ceramic Particulate Composite. PB89-211825 901,07
PB90-117953 900,826 CHANG, I. L.	Field Diameter of Single-Mode Fibers Using Both Gaussian and Petermann Definitions.	Prediction of Tensile Behavior of Strain Softened Compos
Mathematical Software: PLOD. Plotted Solutions of Differ-	PB90-117474 900,756 CHERRY, S. M.	ites by Flexural Test Methods. PB89-147045 900,58
ential Equations. PB89-147425 <i>901,194</i>	Summaries of Center for Fire Research In-House Projects and Grants: 1989.	CHUNG, M. B.
CHANG, S. S. Dielectric Measurements for Cure Monitoring.	PB90-127101 900,605	Standard Chemical Thermodynamic Properties of Polycycli Aromatic Hydrocarbons and Their Isomer Groups. 2
PB89-200430 900,567	CHESLER, S. N. Residential Wood Combustion: A Source of Atmospheric	Pyrene Series, Naphthopyrene Series, and Coronen Series.
Thermal Analysis of VAMAS (Versailles Project on Advanced Materials and Standards) Polycarbonate-Polyethyl-	Polycyclic Aromatic Hydrocarbons. PB90-128166 900.860	PB89-226591 900,45 CHUNG, R. M.
ene Blends. PB89-201487 900,568	Standard Reference Materials for the Determination of Po-	Laboratory Evaluation of an NBS (National Bureau of
CHANG, T.	lycyclic Aromatic Hydrocarbons. PB89-156889 900,178	Standards) Polymer Soil Stress Gage. PB89-211973 901,29
Phase Contrast Matching in Lamellar Structures Composed of Mixtures of Labeled and Unlabeled Block Copolymer for	CHIEN, J. C. W.	Pore-Water Pressure Buildup in Clean Sands Because of Cyclic Straining.
Small-Angle Neutron Scattering. PB89-157119 901,182	Influence of Molecular Weight on the Resonant Raman Scattering of Polyacetylene.	PB89-175723 900,15
Polymers Bearing Intramolecular Photodimerizable Probes	PB89-179246 900,564 Resonant Raman Scattering of Controlled Molecular Weight	CHUPKA, W. A. Autoionization Dynamics in the Valence-Shell Photoioniza
for Mass Diffusion Measurements by the Forced Rayleigh Scattering Technique: Synthesis and Characterization.	Polyacetylene. PB89-157093 900,548	tion Spectrum of CO. PB89-176960 900,38
PB89-157101 901,181 Temperature, Composition and Molecular-Weight Depend-	CHIEN, P.	CISZEK, T. F.
ence of the Binary Interaction Parameter of Polystyrene/ Poly(vinylmethylether) Blends.	FT-IR (Fourier Transform-Infrared) Emission/Transmission Spectroscopy for In situ Combustion Diagnostics.	Oxygen Isotope Effect in the Superconducting Bi-Sr-Ca-Cu O System.

PB89-157044	901,025	PB89-176119	900,582	PB90-128620	900,170
LAGUE, F. R. NIST (National Institute of Standards and Automated Coaxial Microwave Power Standard	Technology)	CLIFTON, J. R. Interpretation of the Effects of Reta Pastes of C3S, C3A plus Gypsum, and		Estimating the Environment and the Links in Compartment Fires with Dra Line-Actuated Ceiling Vents. Part 2	ft Curtains and Fusible
PB89-176192 Transient Response Error in Microwave P	900,807	PB89-146971 Knowledge Based System for Dura	900,580	Computer Code Lavent. PB89-229009	900,094
Using Thermistor Detectors. PB89-173785	900,759	crete. PB89-150734	900,110	Heat Transfer in Compartment Fires ing-Jet Impingement on a Wall. PB90-118076	Near Hegions of Ceil-
LARK, A. V.		Service Life of Concrete. PB89-215362	901,303	Note on Calculating Flows Through	
Acoustoelastic Determination of Residual Stres PB89-179808	901,318	CLINTON, T. W.	901,303	Fire Models Under Conditions of Arb sure Difference.	itrary Cross-Vent Pres-
EMATs (Electromagnetic Acoustic Transducer Crack Inspection of Railroad Wheels. PB90-123894	s) for Roll-By 901,597	Magnetic Order of Pr in PrBa2Cu3O7. PB90-123803	901,471	PB90-117573 Test Results and Predictions for the	
Measuring In-Plane Elastic Moduli of Com Arrays of Phase-Insensitive Ultrasound Receive	posites with	CLYNCH, J. R. Dual Frequency P-Code Time Transfer	Experiment. 900,614	Ceiling Sprinkler Links in a Full-Scale PB89-231187	900,095
PB90-136672	900,970	PB89-174064	900,014	COPLEY, J. R. D. Calculations and Measurement of the	o Portormonoo of Con
Texture Monitoring in Aluminum Alloys: A Co Ultrasonic and Neutron Diffraction Measurement	nts.	COBB, E. N. Ferric Oxalate with Nitric Acid as a Cosive Bonding System.	nditioner in an Adhe-	verging Neutron Guides. PB89-211999	901,541
PB90-117409 Ultrasonic Determination of Absolute Stresses	901,159 In Aluminum	PB89-229272 COHEN, E. R.	900,045	Neutron Scattering and Its Effect Neutron Absorption Experiments.	
and Steel Alloys. PB89-150957	901,124	CODATA (Committee on Data for Scie	nce and Technology)	PB90-123738	901,569
Ultrasonic Separation of Stress and Texture Encrystalline Aggregates.		Recommended Values of the Fundar stants, 1986. PB89-145189	nental Physical Con- 900,275	Significance of Multiple Scattering i Small-Angle Neutron Scattering Expe PB89-179626	n the Interpretation of riments. 901,409
PB90-117557 Ultrasonic Texture Analysis for Polycrystalline	900,499 Aggregates	Fundamental Physical Constants - 198		Use of Multiple-Slot Multiple Disk C Pulse Thermal Neutron Beams.	
of Cubic Materials Displaying Orthotropic Symn PB89-146948	netry. 901,121	PB90-136474 COLLE, R.		PB89-147466	901,485
LARK, C. W.		NBS (National Bureau of Standards) R ard Generator.	adon-in-Water Stand-	CORIELL, S. R. Directional Solidification of a Planar	Interface in the Pres-
Autodetaching States of Negative Ions. PB89-150767	900,295	PB89-171888 COLLINS, B.	901,295	ence of a Time-Dependent Electric C PB90-112400	
Computation of the ac Stark Effect in the Gro Atomic Hydrogen.		Relationship between Appearance and of Coatings: A Literature Review.	Protective Durability	Effect of a Crystal-Melt Interface on PB90-130261	Faylor-Vortex Flow. 901,477
PB89-202535 Marked Differences in the 3p Photoabsorption	901,538 between the	PB89-162598 COLLINS, B. L.	901,063	Effect of Anisotropic Thermal Condulogical Stability of a Binary Alloy.	activity on the Morpho-
Cr and Mn(1+) Isoelectronic Pair: Reasons to Structure Observed in Cr. PB90-117581	or the Unique 901,562	Evaluating Office Lighting Environm Analysis.	ents: Second Level	PB89-228985 Solutal Convection during Directional	901,155 Solidification.
Oxygen Partial-Density-of-States Change	in the	PB89-189153	900,073	PB89-150932	. 901,322
YBa2Cu3Ox Compounds for x(Approx.)6,6.5,7 Soft X-ray Emission.		Post-Occupancy Evaluation of Sever Buildings.		CORLEY, D. M. Aerodynamics of Agglomerated Soot	Particles.
PB89-186274 Resonance Enhanced Electron Stimulated Des	901,419	PB90-112384 COLLINS, S.	900,088	PB69-147482	900,586
PB90-117771	900,505	Free Value Tool for ASN.1.		COSTELLO, J. T. Marked Differences in the 3p Photoa	bsorption between the
Resonance Ionization Mass Spectrometry of Mattoionizing Series.		PB89-196182 Object-Oriented Model for ASN.1 (Abs	900,622 tract Syntax Notation	Cr and Mn(1+) Isoelectronic Pair: F Structure Observed in Cr.	Reasons for the Unique
PB89-150817	900,296	One). PB89-177117	900,649	PB90-117581	901,562
LARK, D. R. HVACSIM+, a Dynamic Building/HVAC/Cor	ntrol Systems	CONRADI, M. S.	300,043	COUDERT, L. H. Electric-Resonance Optothermal S	Spectrum of (H2O)2:
Simulation Program. PB89-177166	900,070	Deutenum Magnetic Resonance Stud Poling in Poly(Vinylidene Fluonde) and	y of Orientation and Poly(Vinylidene Fluo-	Microwave Spectrum of the K= 1-0 or -)2) States.	Subband for the E((+
LARK, J.		nde-Čo-Tetrafluoroethylene). PB89-186365	900,565	PB90-117433 Microwave Electric-Resonance Opto	900,497
Temperature, Composition and Molecular-We ence of the Binary Interaction Parameter of	Polystyrene/	COOK, G. R.		of (H2O)2. PB90-128141	900,531
Poly(vinylmethylether) Blends. PB89-157473	900,550	Hydrodynamic Forces on Vertical Cylin Correction.		COUNAS, G. J.	300,331
LARK, J. B.	and December of	PB90-117417 COOK. L. P.	901,313	Measurement of Adapter Loss, Mis Using the Dual Six-Port.	smatch, and Efficiency
ASM/NBS (American Society for Metals/Nation Standards) Numerical and Graphical Databas Alloy Phase Diagrams.		Cathodoluminescence of Defects in		PB89-147839	901,316
PB89-157986	901,135	Particles Grown by Hot-Filament Che		COURSEY, B. M. (109)Pd and (109)Cd Activity Stand	dardization and Decay
LARKE, M. K.	of State and	PB90-117961	901,069	Data. PB90-123449	901,564
Promoting Technological Excellence: The Role Federal Extension Activities.		COOK, R. F. Effect of Lateral Crack Growth on the	Strength of Contact	NBS (National Bureau of Standards)	
PB90-120742 LARY, D. C.	900,171	Flaws in Brittle Materials. PB89-171813	901,034	tigations of (82)Sr-(82)Rb. PB89-161558	901,498
Calculation of Vibration-Rotation Spectra for F	Rare Gas-HCI	COOKE, P. W.		COUSINS, L. M.	
Complexes. PB89-228415	900,473	Update of U.S. Participation in Internativities.		Observation of Translationally Hot, Molecules Produced by 193-nm Lase	
Infrared Spectrum of NeHF. PB89-171227	900,351	PB89-228282 COOPER, J.	900,902	layer NO Films. PB89-234264	900.491
Quantum Mechanical Calculations on the Ar(Charge Transfer Reaction.		Approximate Formulation of Redistributy(beta), H(alpha) System.	ition in the Ly(alpha),	Production of 0.1-3 eV Reactive Molezation of Condensed Molecular Film	ecules by Laser Vapon-
PB89-228092	900,470	PB90-123720	901,568	for Beam-Surface Interactions. PB89-171201	900,254
Rydberg-Klein-Rees Inversion of High Resolu Waals Infrared Spectra: An Intermolecular Pot Surface for $Ar + HF$ ($v = 1$).		Laser-Noise-Induced Population Fluct Three-Level Systems.		Time-of-Flight Measurements of H Molecules Produced by UV Laser Va	yperthermal Cl(sub 2)
PB89-227953	900,465	PB89-171235 Redistribution in Astrophysically Import	901,342	Chlorine Films.	
Slit Jet Infrared Spectroscopy of NeHF Comple Rotor and J-Dependent Predissociation Dynam	exes: Internal nics.	PB90-128075	901,579	PB89-202634 COWAN, P. L.	900,260
PB90-118126	900,520	COOPER, J. W. Marked Differences in the 3p Photoab		Dynamical Diffraction of X-rays at Gr PB89-186886	azing Angle. 901,421
Weakly Bound NeHF. PB90-118100	900,519	Cr and Mn(1+) Isoelectronic Pair: Re Structure Observed in Cr.	easons for the Unique	Near-Threshold X-ray Fluorescence	
LEVELAND, W. G. Measurements of Coefficients of Discharge for	or Concentric	PB90-117581 COOPER, L. Y.	901,562	cules. PB89-176523	900,382
Flange-Tapped Square-Edged Onfice Meters in the Reynolds Number Range 600 to 2,700,000	n Water Over	Calculating Flows through Vertical		Performance of a High-Energy-Res Synchrotron Radiation Beamline.	solution, Tender X-ray
PB89-235147	901,334	Models under Conditions of Arbitrary Difference.		PB90-128083	901,580
LIFTON, J. Implications of Computer Record Simulation M	adala Evant	PB89-148126	900,108	COX, D. F.	on and Goe Deced T'-
Implications of Computer-Based Simulation M Systems, Databases, and Networks for Cemen	t Research.	Calculation of the Flow Through a Ho Vent.	_	Fundamental Characterization of Cle Oxide.	
PB89-146989 Integrated Knowledge Systems for Concrete a	900,581 and Other Ma-	PB89-189252 Comparisons of NBS/Harvard VI S	900,128 imulations and Full-	PB89-202964 Surface Properties of Clean and Gas	900,785 -Dosed SnO2 (110).
		Scale, Multiroom Fire Test Data.		PB89-179576	900,393

COX, R. A. Evaluated Kinetic and Photochemical Data for A	Atmospheric	PB89-235139 CULVER, C. G.	901,272	PB90-117565 QCD Vacuum.	901,5
Chemistry. Supplement 3. PB89-222582	900,454	Earthquake Hazard Mitigation through	Improved Seismic	PB89-149124	901,4
COXON, B.	300,434	Design. PB89-149132	900,098	DARIEL, M. P.	
Optical Rotation.		Earthquake Resistant Design Criteria.		Magnetic Behavior of Composition Thin Films.	nally Modulated Ni-0
PB89-149256	900,294	PB89-149140	900,099	PB90-118084	901,1
Structure of a Hydroxyl Radical Induced Cross-l mine and Tyrosine.	·	CUNNINGHAM, D. Data Bases Available at the National Inst	titute of Standards	Magnetization and Magnetic Afterer Compositionally-Modulated Alloys.	fect in Textured Ni/0
PB89-157838	901,244	and Technology Research Information Ce	nter.	PB90-123431	. 901,1
COYLE, T. W. Structural Reliability and Damage Tolerance	of Ceramic	PB89-160014 CUNNINGHAM, J. E.	900,932	DATLA, R. U.	anabina Dalina at Ma
Composites for High-Temperature Application	ons. Semi-	Long-Range Incommensurate Magnetic O	rder in Dy-Y Multi-	Line Identifications and Radiative-Br netic Dipole Lines in Si-like Ni, Cu, Z	n, Ge, and Se.
Annual Progress Report for the Period Ending 30, 1987.		layers. PB89-179642	901,411	PB89-234165	901,5
PB89-156350	901,023	Metastable Phase Production and Transi		Neonlike Ar and Cl 3p-3s Emissi Plasma.	on from a theta-pin
Structural Reliability and Damage Tolerance Composites for High-Temperature Application	ns. Semi-	Alloy Films by Rapid Crystallization and ments.	Annealing Treat-	PB90-123746	901,5
Annual Progress Report for the Period Ending 1988.	March 31,	PB89-157622	901,129	DATTA, T. Low-Temperature Phase and Magn	etic Interactions in f
PB89-156368	901,024	CURRIE, L. A.	de O 44 Assertant	Fe-Cr-Ni Alloys.	
COYNE, J. J.		Identification of Carbonaceous Aerosols value tor Mass Spectrometry, and Laser Micro		PB90-136771 Reentrant Softening in Perovskite Si	901,1
Basic Data Necessary for Neutron Dosimetry. PB89-171854	901,241	trometry. PB90-136540	900,236	PB90-117540	901,4
Initial Spectra of Neutron-Induced Secondary Cl	narged Par-	CUTKOSKY, R. D.	5.1,2.1	DAUGHTREY, T.	
ticles. PB89-171862	901,265	Precision Weight Calibration with a Specia		Case History: Development of a Standard.	Software Engineeri
Refinement of Neutron Energy Deposition and	Microdosi-	PB89-173975 CUTLER, R.	900,879	PB89-149116	900,6
metry Calculations. PB89-150791	901,264	NBS/NRL (National Bureau of Standard	s/Naval Research	DAVIDSON, P. M.	-1-
CRAIG, R. M.	,	Laboratory) Free Electron Laser Facility. PB89-175749	901,351	Multicritical Phase Relations in Miner PB89-150882	rais. <i>901,2</i> .
Electrically Calibrated Silicon Bolometer for Low	Level Opti-	CVETANOVIC, R. J.	001,001	DAVIES, P. K.	
cal Power and Energy Measurements. PB89-171714	901,348	Evaluated Chemical Kinetic Data for		Defect Intergrowths in Barium Polytit PB89-146823	
CRANMER, D. C.		Atomic Oxygen O(3P) with Sulfur Containi PB89-145122	ng Compounds. 900,269	Defect Intergrowths in Barium Polytit	<i>901,0</i> 2 PaTi5O11
Fiber Coating and Characterization. PB89-228571	901.067	Fluid Flow in Pulsed Laser Irradiated Gas	ses; Modeling and	PB89-146831	901,0
Mechanical Property Enhancement in Ceramic N	,	Measurement. PB90-123704	900,265	DAVIS, D.	
posites. PB89-189138	901.076	CZICHOS, H.	000,200	Dual Frequency P-Code Time Transf PB89-174064	fer Experiment, 900,6
CRAWFORD, M. L.	301,070	NBS/BAM (National Bureau of Standa		DAVIS, D. D.	
Mode-Stirred Chamber for Measuring Shielding	Effective-	fur Materialprufung) 1986 Symposium on ics.		Calibration of GPS (Global Position	ing System) Equipme
ness of Cables and Connectors: An Assessme STD-1344A Method 3008.	ent of MIL-	PB89-229074	901,055	in Japan. PB89-212070	900,6
PB89-149264	900,737	DABRAL, S. Growth and Properties of High-Quality Ve	ery-Thin SOS (Sili-	NIST Automated Computer Time Se	
CRESSWELL, M. W.	Took Ctrue	con-on Sapphire) Films. PB90-128109	900,798	PB90-213711 DAVIS, G. T.	900,6
Use of Artificial Intelligence and Microelectronic tures for Evaluation and Yield Enhancement of		High-Mobility CMOS (Complementary M		Charging Behavior of Polyethylene a	nd lonomers.
tronic Interconnect Systems. PB89-146955	900,768	conductor) Transistors Fabricated on Very	Thin SOS Films.	PB90-136813	900,5
CRISSMAN, J. M.	•	PB89-230460 DABROWSKI, C. E.	900,791	DAVIS, H. A.	ide and Eluid Midures
Composites Databases for the 1990's.	901,075	Detailed Description of the Knowledge-B	Based System for	Semi-Automated PVT Facility for Flu PB89-157184	900,8
PB89-180376 Necking Phenomena and Cold Drawing.	901,075	Physical Database Design. Volume 1. PB89-228993	900,929	DAVIS, R. S.	
PB89-201495	900,975	Detailed Description of the Knowledge-B		Interpretation of a between-Time (Mass Measurements.	Component of Error
CRIST, B.	Dalvathul	Physical Database Design. Volume 2. PB89-229033	900,930	PB89-149108	900,8
Morphological Partitioning of Ethyl Branches in ene by (13)C NMR.		DAGALAKIS, N.	000,000	NIST (National Institute of Stand Measurement Services: Mass Calibra	
PB89-176051	900,560	Optical Sensors for Robot Performance	Testing and Cali-	PB89-153894	900,8
CROARKIN, M. C. Graphical Analyses Related to the Linewidth	Calibration	bration. PB89-157358	900,987	Stability of the SI (International Sy Determined from Electrical Measurer	stem) Unit of Mass
Problem.		DAGALAKIS, N. G.		PB89-201818	900,8
PB89-201156 Interlaboratory Determination of the Calibration	900,783	Robot Crane Technology. PB90-111667	900,146	DAVIS, R. W.	
the Measurement of the Interstitial Oxygen Con	tent of Sili-	DAGAUT, P.	000,110	Numerical Computation of Particle Problem.	Trajectones: A Mod
con by Infrared Absorption. PB90-117300	900,224	Flash Photolysis Kinetic Absorption Specthe Gas Phase Reaction HO2 + C2H50	troscopy Study of	PB89-158117	901,3
Measurements of Coefficients of Discharge for		perature Range 228-380 K.		DAVIS, S. Development of a Multiple Layer Te	est Procedure for Inc
Flange-Tapped Square-Edged Orifice Meters in the Reynolds Number Range 600 to 2,700,000.		PB90-136565 Temperature Dependence of the Rate Co	900,536	sion in NFPA (National Fire Protection	on Association) 701: In
PB89-235147	901,334	droperoxy + Methylperoxy Gas-Phase R	eaction.	tial Experiments. PB89-235873	900,0
CROMAR, M. W. Noise in DC SQUIDS with Nb/Al-Oxide/Nb	losenhson	PB90-136375	900,534	DAVIS, T. P.	
Junctions.		Post-Occupancy Evaluation of Several	U.S. Government	Stabilization of Ascorbic Acid in H Liquid-Chromatographic Measurement	
PB89-201032 Switching Noise in YBa2Cu3Ox 'Macrobridges'.	900,763	Buildings.		PB89-179279	901,2
PB89-200513	901,426	PB90-112384 DANEY, D. E.	900,088	DAVIS, W.	
CROMER, C. L.		Performance of He II of a Centrifugal	Pump with a Jet	Data Management Strategies for Co ufacturing Systems.	mputer Integrated Ma
Marked Differences in the 3p Photoabsorption b Cr and Mn(1+) Isoelectronic Pair: Reasons for		Pump Inducer. PB89-229090	901,553	PB89-209258	900,9
Structure Observed in Cr. PB90-117581	901,562	DANIELSON, B. L.	507,000	DAVIS, W. D.	Beenonee of Carietal
Using 'Resonant' Charge Exchange to Detect		Group Index and Time Delay Measureme	nts of a Standard	Estimating the Environment and the Links in Compartment Fires with Dra	aft Curtains and Fusit
Noble Gas Atoms.		Reference Fiber. PB89-189179	900,752	Line-Actuated Ceiling Vents. Part Computer Code Lavent.	 User Guide for the control
PB89-176770 CROVETTO, R.	901,296	Interferometric Dispersion Measurements		PB89-229009	900,0
Evaluation of Data on Solubility of Simple Apola	ar Gases in	Wave Structures. PB89-173959	901,349	DAVIS, W. J.	Pool Time Product
Light and Heavy Water at High Temperature. PB90-126251	900,529	DANNER, W. F.		Artificial Intelligence Techniques in Scheduling.	
CROW, J. E.	000,020	Use of Artificial Intelligence Programmir Communication between Incompatible Bu	g Techniques for	PB89-172571	900,9
Magnetic Order of Pr in PrBa2Cu3O7.	004 17	Systems.		Functional Approach to Designing puter Integrated Manufacturing.	
PB90-123803	901,471	PB89-191985 DANOS, M.	900,106	PB89-172589	900,9
CRUZ, J. E. Alternative Techniques for Some Typical MIL-SI	D-461/462	Intrinsic Sticking in dt Muon-Catalyzed F	usion: Interplay of	Hierarchies for Computer-Integrated tional Description.	
Tunos of Monauromonto		Atomic Molecular and Musicar Dhanaman	١٥	DD90 172612	ann a

On-Line Concurrent Simulation in Production Scheduling. PB89-172605 900,94	Ultrasonic Determination of Absolute Stresses in Aldminum	PB90-112343 901,068 Preliminary Stochastic Model for Service Life Prediction of
Real-Time Optimization in the Automated Manufacturin Research Facility.	PB89-150957 901,124	a Photolytically and Thermally Degraded Polymeric Cover Plate Material.
PB89-172597 900,94 Real-Time Simulation and Production Scheduling Systems.	7 Ultrasonic Separation of Stress and Texture Effects in Polycrystalline Aggregates.	PB89-173801 900,556 Thermal Degradation of Poly (methyl methacrylate) at 50C
PB89-183230 900,97		to 125C. PB89-157465 900,549
DAY, G. W. Effect of Multiple Internal Reflections on the Stability of Electrooptic and Magnetooptic Sensors.	of Cubic Materials Displaying Orthotropic Symmetry. PB89-146948 901,121	DIDION, D. Experimental Determination of Forced Convection Evapora-
PB89-171722 900,72 Faraday Effect Sensors: The State of the Art.	DEMARCHI, A. New Cavity Configuration for Cesium Beam Primary Fre-	tive Heat Transfer Coefficients for Non-Azeotropic Refrigerant Mixtures.
PB89-231153 900,82		PB89-186407 901,117 DIDION, D. A.
Optical Fiber Sensors for Electromagnetic Quantities. PB89-173967 900,72		Thermophysical-Property Needs for the Environmentally Acceptable Halocarbon Refrigerants.
Optical Fiber Sensors for the Measurement of Electromagnetic Quantities. PB89-176671 900,74	1 500-140004	PB89-231054 900,482 DIEDRICH, F.
Stability of Birefringent Linear Retarders (Waveplates).	PB89-231302 901,158	Laser Cooling to the Zero-Point Energy of Motion. PB90-128091 901,581
PB89-171672 901,34 DAYAL, V.	Computer Graphics for Ceramic Phase Diagrams.	DIETENBERGER, M. A.
Dynamic Young's Modulus Measurements in Metallic Materials: Results of an Interlaboratory Testing Program.	PC-Access to Ceramic Phase Diagrams.	Validated Furniture Fire Model with FAST (HEMFAST). PB89-215354 900,142
PB89-157671 901,13	PB89-211841 901,053 DENYS, R.	DIKKERS, R. D.
DAYTON, D. C. Infrared and Microwave Spectra of OCO-HF and SCO-HF. PB89-179121 900,38.	Local Brittle Zones in Steel Weldments: An Assessment of Test Methods.	Preliminary Performance Criteria for Building Materials, Equipment and Systems Used in Detention and Correction- al Facilities.
DAYWITT, W. C.	PB89-149082 901,092 DEREGGI, A. S.	PB89-148514 900,109 DILLER. D. E.
Radiometer Equation and Analysis of Systematic Errors for the NIST (National Institute of Standards and Technology	Charging Behavior of Polyethylene and Ionomers. PB90-136813 900,578	Torsional Piezoelectric Crystal Viscometer for Compressed
Automated Radiometers. PB90-130907 900,83		Gases and Liquids. PB89-228076 901,447
Simple Technique for Investigating Defects in Coaxial Connectors.	ride-Co-Tetrafluoroethylene). PB89-186365 900.565	DINSE, K. P. High Resolution Optical Multiplex Spectroscopy.
PB89-146930 900,72. DE LA CRUZ, M. O.	Effects of Space Charge on the Poling of Ferroelectric	PB89-185938 900,404
Microphase Separation in Blockcopolymer/Homopolymer. PB89-176069 900,56	Polymers. PB89-146708 901,179 DESHMUKH, U. V.	DITTMANN, S. NIST (National Institute of Standards and Technology) Measurement Services: High Vacuum Standard and Its
Theory of Microphase Separation in Graft and Star Copoly mers.		Use. PB89-193841 900,891
PB89-176028 900,555	7 PB89-189138 <i>901,076</i>	DIXON, D. A.
DE LAETER, J. R. Atomic Weights of the Elements 1987. PB89-145171 900,27		Gas Phase Proton Affinities and Basicities of Molecules: A Comparison between Theory and Experiment. PBs9-146674 900,280
DE RIJK, W. G.	DESLATTES, R. D. Determination of Short Lifetimes with Ultra High Resolution	DIZDAROGLU, M.
Development of a Microwave Sustained Gas Plasma for the Sterilization of Dental Instruments. PB89-231278 900,04	(n,gamma) Spectroscopy.	Chemical Characterization of Ionizing Radiation-Induced Damage to DNA. PB89-151922 901,235
DEB, S. K.	Near-Threshold X-ray Fluorescence Spectroscopy of Mole- cules.	Intramolecular H Atom Abstraction from the Sugar Moiety by Thymine Radicals in Oligo- and Polydeoxynucleotides.
Oxygen Isotope Effect in the Superconducting Bi-Sr-Ca-Cu O System.	DEVOE I B	PB89-171870 901,263
PB89-157044 901,02. DEBENHA™, P.	Three-Dimensional Atomic Spectra in Flames Using Step- wise Excitation Laser-Enhanced Ionization Spectroscopy.	Structure of a Hydroxyl Radical Induced Cross-Link of Thymine and Tyrosine.
NBS/NRL (National Bureau of Standards/Naval Research Laboratory) Free Electron Laser Facility.	PB89-202071 900,430	PB89-157838 901,244 DOBBINS, R. A.
PB89-175749 901,35	DEWEESE, M. E. Metrology for Electromagnetic Technology: A Bibliography	Pressure and Density Series Equations of State for Steam as Derived from the Haar-Gallagher-Kell Formulation.
DEBENHAM, P. H. NBS (National Bureau of Standards) Free Electron Lase Facility.		BBBY, R.
PB89-176515 901,35	Determination of Short Lifetimes with Ultra High Resolution	Pore-Water Pressure Buildup in Clean Sands Because of
Research Opportunities Below 300 nm at the NBS (Nation al Bureau of Standards) Free-Electron Laser Facility.	PB90-123670 901,567	Cyclic Straining. PB89-175723 900,159
PB89-192678 901,36 DEBSKA, U.	DEWHURST, W. Gravity Tide Measurements with a Feedback Gravity Meter.	DOBSON, B. R. Vibrationally Resolved Photoelectron Angular Distributions
Neutron Diffraction Study of the Wurtzite-Structure Dilute Magnetic Semiconductor Zn0.45Mn0.55Se.	PB89-171755 901,310	for H2 in the Range 17 eV < or = h(nu) < or = 39 eV. PB89-176952 900,385
PB90-136714 901,47. DEHMER, J. L.	Validation of Absolute Target Thickness Calibrations in a QQQ Instrument by Measuring Absolute Total Cross-Sec-	DOBSON, E. N. Promoting Technological Excellence: The Role of State and
Autoionization Dynamics in the Valence-Shell Photoionization Spectrum of CO.		Federal Extension Activities. PB90-120742 990,171
PB89-176960 900,38		DOERING, D. L.
Vibrationally Resolved Photoelectron Angular Distribution for H2 in the Range 17 eV < or = h(nu) < or = 39 eV. PB89-176952	a Semi-Infinite Body.	Coadsorption of Water and Lithium on the Ru(001) Surface. PB89-202956 900,440
Vibrationally Resolved Photoelectron Studies of the 7(sigma) (-1) Channel in N2O.	Thermal Conductivity Solid Surface.	DOLS, W. S. Air Quality Investigation in the NIH (National Institutes of Health) Radiation Oncology Branch.
PB89-176945 900,25 DEHMER, P. M.	Transient Cooling of a Hot Surface by Droplets Evapora-	PB89-228977 900,079
Autoionization Dynamics in the Valence-Shell Photoioniza	tion	Ventilation and Air Quality Investigation of the U.S. Geological Survey Building.
tion Spectrum of CO. PB89-176960 900,38	6 DIAMONDSTONE, B. I.	PB89-229686 900,857 DOMALSKI, E. S.
DEISENHOFER, J. Comparison of Two Highly Refined Structures of Bovin Page 15 Truckin Inhibitor	Expert-Database System for Sample Preparation by Microwave Dissolution. 1. Selection of Analytical Descriptors. PB89-229108 900,216	Estimation of the Thermodynamic Properties of Hydrocarbons at 298.15 K.
Pancreatic Trypsin Inhibitor. PB89-202204 901,24	g Technical Activities, 1988, Center for Analytical Chemistry. PB89-151773 900, 177	PB89-145155 900,272 Evaluation of Data on Higher Heating Values and Elemental
DEL BIANCO, W. Cross Section and Linear Polarization of Tagged Photons.	DIAS, M. S.	Analysis for Refuse-Derived Fuels. PB90-136839 900,845
PB90-117292 901,56	Measurements of the (235)U (n,f) Standard Cross Section	DOMANSKI D A

Measurements of the (235)U (n,f) Standard Cross Section at the National Bureau of Standards.
PB89-176556 901,305

Design and Synthesis of Prototype Air-Dry Resins for Use in BEP (Bureau of Engraving and Printing) Intaglio Ink Vehi-

DICKENS, B.

DELSANTO, P. P.

Acoustoelastic Determination of Residual Stresses. PB89-179808 901,318

Texture Monitoring in Aluminum Alloys; A Comparison of Ultrasonic and Neutron Diffraction Measurements.

DOMANSKI, P. A.

EVSIM: An Evaporator Simulation Model Accounting for Re-frigerant and One Dimensional Air Distribution. PB89-235881 900,086

Experimental Investigation and Modeling of the Flow Rate of Refrigerant 22 Through the Short Tube Restrictor.

PB89-229041	901,118	PB89-146849 901,016	PB89-157747 900,186
Rating Procedure for Mixed Air-Source Unitary tioners and Heat Pumps Operating in the Co		Standard Reference Materials for X-ray Diffraction. Part 1. Overview of Current and Future Standard Reference Materials	Pahasapaite, a Beryllophosphate Zeolite Related to Synthetic Zeolite Rho, from the Tip Top Pegmatite of South
Revision 1. PB89-193247	900,075	rials. PB89-146799 901,384	Dakota. PB89-186431 901,288
OOMICH, P. D.		DRAGOSET, R. A.	Wheatleyite, Na2Cu(C2O4)2 . 2H2O, a Natural Sodium
Allocating Staff to Tax Facilities: A Graphics-B computer Allocation Model.		Structure of Cs on GaAs(110) as Determined by Scanning Tunneling Microscopy.	Copper Salt of Oxalic Acid. PB89-179154 900,390
PB90-129891	900,645	PB90-117490 901,463 DRAPELA. T. J.	DUPPICH, J.
Internal Revenue Service Post-of-Duty Location System: Programmer's Manual for FORTRAN	Driver Ver-	Comparison of Far-Field Methods for Determining Mode	Use of Focusing Supermirror Neutron Guides to Enhance Cold Neutron Fluence Rates.
sion 5.0. PB89-161913	900,002	Field Diameter of Single-Mode Fibers Using Both Gaussian and Petermann Definitions.	PB89-171946 901,306
Internal Revenue Service Post-of-Duty Location		PB90-117474 900,756	DURST, R. A. Generic Liposome Reagent for Immunoassays.
System: Programmer's Manual for PASCAL Solv PB89-161905	900,001	DRESSLER, R. A. Laser Probing of Ion Velocity Distributions in Drift Fields:	PB90-123886 901,229
OMKE, H.		Parallel and Perpendicular Temperatures and Mobility for	Liposome-Enhanced Flow Injection Immunoanalysis. PB89-146757 900,036
Scattering of Polarized Light in Spectral Lines Frequency Redistribution: General Redistribution	with Partial Matrix.	Ba(1+) in He. PB89-171243 900,352	Spectroelectrochemistry of a System Involving Two Con-
PB89-171607	901,344	DRIESEN, G.	secutive Electron-Transfer Reaction. PB90-136979 900,237
Photodissociation of Methyl Iodide Clusters.		Hydrogen Sites in Amorphous Pd85Si15HX Probed by Neutron Vibrational Spectroscopy.	Technical Activities, 1988, Center for Analytical Chemistry.
PB89-171193	900,253	PB89-229140 901,456	PB89-151773 900,177
ONALDSON, J. L. NVLAP (National Voluntary Laboratory Accred	litation Pro-	DRISCOLL, J. Draft International Document on Guide to Portable Instru-	DUTKO, P. Pore-Water Pressure Buildup in Clean Sands Because of
gram) Directory of Accredited Laboratories. PB89-189278		ments for Assessing Airborne Pollutants Arising from Haz- ardous Wastes.	Cyclic Straining. PB89-175723 900,159
ONALDSON, J. R.	900,890	PB89-150775 900,855	DUVALL, K. C.
Computation and Use of the Asymptotic Covan	ance Matrix	DRIVER, L.	2.5 MeV Neutron Source for Fission Cross Section Meas-
for Measurement Error Models. PB89-215321	901,214	Optically Linked Electric and Magnetic Field Sensor for Poynting Vector Measurements in the Near Fields of Radi-	urement. PB89-176531 901,512
User's Reference Guide for ODRPACK: S	oftware for	ating Sources. PB89-187595 900,712	Measurements of the (235)U (n,f) Standard Cross Section
Weighted Orthogonal Distance Regression Versi PB89-229066	on 1.7. 901,215	DRIVER, L. D.	at the National Bureau of Standards. PB89-176556 901,305
ONLY, K. J.		Broadband, Isotropic, Photonic Electric-Field Meter for Measurements from 10 kHz to above 1 GHz.	Monte Carlo Calculated Response of the Dual Thin Scintil-
In vitro Investigation of the Effects of Glass Ins Effective Composite Resin Polymerization Shrink		PB90-128281 900,686	lation Detector in the Sum Coincidence Mode. PB89-176549 901,299
PB90-117516	900,049	DRULLINGER, R.	DZIUBA, R. F.
ONMEZ, A. General Methodology for Machine Tool Accuracy	y Enhance	New Cavity Configuration for Cesium Beam Primary Frequency Standards.	Determination of the Time-Dependence of ohm NBS (Na-
ment by Error Compensation.		PB89-171649 900,714	tional Bureau of Standards) Using the Quantized Hall Resistance.
PB89-146781 Turning Workstation in the AMRF (Automated)	900,996	DU, R. Characterization of Structural and Magnetic Order of Er/Y	PB89-230387 900,819
ing Research Facility).		Superlattices. PB90-123662 901,470	Guidelines for Implementing the New Representations of the Volt and Ohm Effective January 1, 1990.
PB89-185607 ONMEZ, M. A.	900,954	Exchange and Magnetostrictive Effects in Rare Earth Su-	PB89-214761 900,817 NBS (National Bureau of Standards) Determination of the
Generalized Mathematical Model for Machine To		perlattices. PB89-202667 901,438	Fine-Structure Constant, and of the Quantized Hall Resist-
PB89-150874	900,977	Occurrence of Long-Range Helical Spin Ordering in Dy-Y	ance and Josephson Frequency-to-Voltage Quotient in SI Units.
ORE, P. Analysis of Roto-Translational Absorption Spec	tra Induced	Multilayers. PB89-179634 901,410	PB89-230437 901,556
in Low Density Gases of Non-Polar Molecules: ane Case.	The Meth-	DUBE, W. P.	NBS (National Bureau of Standards) Ohm: Past-Present- Future.
PB89-201800	900,427	Battery-Powered Current Supply for Superconductor Meas-	PB89-149066 900,802
ORKO, W. D. High-Accuracy Gas Analysis via Isotope Dili	ution Mace	urements. PB89-200455 901,525	New Realization of the Ohm and Farad Using the NBS (National Bureau of Standards) Calculable Capacitor.
Spectrometry: Carbon Dioxide in Air.		DUBIVSKY, P. M.	PB89-230445 901,557 Possible Quantum Hall Effect Resistance Standard.
PB90-123951 Special Calibration Systems for Reactive Gases	900,032	False Alarm Study of Smoke Detectors in Department of Veterans Affairs Medical Centers (VAMCS).	PB89-149058 900,801
Difficult Measurements. PB89-149215	900,873	PB89-193288 900,093	EANES, E. D.
OUGHERTY, B. P.	300,073	DUCAS, W. U-Value Measurements for Windows and Movable Insula-	Biophysical Aspects of Lipid Interaction with Mineral: Lipo- some Model Studies.
Development of an Automated Probe for Thern	nal Conduc-	tions from Hot Box Tests in Two Commercial Laboratories. PB89-175889 900,121	PB90-117508 901,228
tivity Measurements. PB89-209324	900,896	DULCEY, C. S.	Liposome Technology in Biomineralization Research. PB90-128117 901,230
Proposed Methodology for Rating Air-Source H	leat Pumps	Multiphoton Ionization Spectroscopy and Vibrational Analysis of a 3p Rydberg State of the Hydroxymethyl Radical.	EANES, R. J.
That Heat, Cool, and Provide Domestic Water He PB90-112368	900,087	PB89-146666 900,279	Rate of Change of the Quincy-Monument Peak Baseline from a Translocation Analysis of LAGEOS Laser Range
OUGLAS, J.		DULCIE, L. L.	Data.
Polymer Localization by Random Fixed Impuritie Chains.	s: Gaussian	New Standard Test Method for Eddy Current Probes. PB89-187587 900,981	PB89-234272 901,282 EASTMAN, J. A.
PB89-176044	900,559	DUMIN, D. J.	Electron Diffraction Study of the Faceting of Tilt Grain
OUGLAS, J. F. Surface-Interacting Polymers: An Integral Eq	uation and	Growth and Properties of High-Quality Very-Thin SOS (Sili- con-on Sapphire) Films.	Boundaries in NiO. PB89-201792 901,431
Fractional Calculus Approach. PB89-202949	900,571	PB90-128109 900,798	EBBERTS, D. F.
OVERSPIKE, L. D.	300,377	High-Mobility CMOS (Complementary Metal Oxide Semi- conductor) Transistors Fabricated on Very Thin SOS Films.	Thermal Resistance Measurements and Calculations of an
Collisional Electron Detachment and Decompos		PB89-230460 900,791	Insulated Concrete Block Wall. PB89-174916 900,119
of SF6(1-), SF5(1-), and F(1-) in SF6: Implicati Transport and Electrical Discharges.		DUNCAN, W. M. Semiconductor Measurement Technology: Automatic Deter-	EBERHARDT, K.
PB90-117862	900,511	mination of the Interstitial Oxygen Content of Silicon Wafers	Theory and Practice of Paper Preservation for Archives. PB89-147052 900,934
OVERSPIKE, M. A. Deuterium Magnetic Resonance Study of Orie		Polished on Both Sides. PB89-151831 900,772	EBERHARDT, K. R.
Poling in Poly(Vinylidene Fluoride) and Poly(Viny ride-Co-Tetrafluoroethylene).		DUNN, G. H.	Detection of Uranium from Cosmos-1402 in the Strato-
PB89-186365	900,565	Electron-Impact Ionization of La($q+$) lons ($q=1,2,3$). PB90-123845 901,573	sphere. PB89-156962 <i>901,592</i>
OWNING, R. G. Analytical Applications of Neutron Depth Profiling		Spectroscopy of Autoionizing States Contributing to Elec-	Minimax Approach to Combining Means, with Practical Ex-
PB89-146872	901,294	tron-Impact Ionization of Ions. PB90-123837 901,572	amples. PB89-171847 <i>901,211</i>
OYLE, E. D.	Cubernet	DUNN, P. J.	Statistical Analysis of Experiments to Measure Ignition of Cigarettes.
Metallographic Evidence for the Nucleation of Microcracks during Unlubricated Sliding of Metal	S.	Application of Synergistic Microanalysis Techniques to the Study of a Possible New Mineral Containing Light Ele-	PB89-201149 900,135
PB89-147391 PRAGOO, A. L.	901,001	ments. PB89-147037 901,277	ECKERLE, K. L.
Critical Assessment of Requirements for Cerai	mic Powder	Moydite, (Y, REE) (B(OH)4)(CO3), a New Mineral Species	Exploratory Research in Reflectance and Fluorescence Standards at the National Bureau of Standards.
Characterization.		from the Evans-Lou Pegmatite, Quebec.	PB89-202022 900,428

CKERT, H. Calcium Hydroxyapatite Precipitated from an Aqueous Sc	EKIN, J. W. Effect of Room-Temperature Stress on the Critical Current	PB89-176598 900,38,
tion: An International Multimethod Analysis. PB90-123399 900,2	of NbTi.	Method for Improving Equations of State Near the Critica
DERER, D. L.	High T(sub c) Superconductor/Noble-Metal Contacts with	Point. PB89-228027 901,54.
Oxygen Partial-Density-of-States Change in	Surface Resistivities in the (10 to the Minus 10th Power)	ERICKSON, J.
YBa2Cu3Ox Compounds for x(Approx.)6,6.5,7 Measured Soft X-ray Emission.	Omega sq cm Range. PB89-179824 901,413	Economical Ultrahigh Vacuum Four-Point Resistivity Probe.
PB89-186274 901,4		PB89-147086 900,870
DGAR, C. A.	Y1Ba2Cu3O(7-delta) Superconductors. PB89-176978 901,406	ERICKSON, J. W.
Trial of Open Systems Interconnection (OSI) Protoc	Offset Criterion for Determining Superconductor Critical	Surface Properties of Clean and Gas-Dosed SnO2 (110). PB89-179576 900,39
Over Integrated Services Digital Network (ISDN). PB89-235576 900,6	25 Current.	ERWIN, R. W.
DGE, R. D.	PB90-128133 901,474	Characterization of Structural and Magnetic Order of Er/
Low-Temperature Phase and Magnetic Interactions in	vAMAS (Versailles Project on Advanced Materials and Standards) Intercomparison of Critical Current Measure-	Superlattices. PB90-123662 901,470
Fe-Cr-Ni Alloys. PB90-136771 901,1	ment in Nb3Sn Wires.	Exchange and Magnetostrictive Effects in Rare Earth Su
DSINGER, R. E.	PB89-202147 901,534	perlattices.
Observations of Gas Species and Mode of Operation	ELKIND, B. J. Ultrasonic Characterization of Surface Modified Layers.	PB89-202667 901,430
fects on Effective Areas of Gas-Operated Piston Gages. PB89-231120 900,9	DD00 147400 001 115	Long-Range Incommensurate Magnetic Order in Dy-Y Multi layers.
Reduction of Uncertainties for Absolute Piston Gage Pro	FILED N	PB89-179642 901,41
sure Measurements in the Atmospheric Pressure Range.	Synergistic Effects of Nitrogen Dioxide and Carbon Dioxide	Occurrence of Long-Range Helical Spin Ordering in Dy-
PB90-163882 900,0	PB89-214779 900,856	Multilayers. PB89-179634 901,410
GELHOFF, W. F. Angle Resolved XPS (X-ray Photoelectron Spectroscopy)	of ELLERBE, P.	Re-Entrant Spin-Glass Properties of a-(FexCr1-x)75P15C10
the Epitaxial Growth of Cu on Ni(100).	Determination of Serum Cholesterol by a Modification of	PB89-157481 901,39
PB89-150866 901,3	PB89-234181 901.239	ESTRADA, J.
Core-Level Binding-Energy Shifts at Surfaces and in Solid PB89-146898 900,2	5.	Reentrant Softening in Perovskite Superconductors. PB90-117540 901,46
Role of Adsorbed Gases in Metal on Metal Epitaxy.	NIST (National Institute of Standards and Technology) Cho-	ETTLINGER, L. D.
PB90-128125 901,1	lesterol Standard Reference Material. PB89-234173 901,262	Phase Equilibria and Crystal Chemistry in the Ternar
HRLICH, C. D.	Developing Definitive Methods for Human Serum Analytes.	System BaO-TiO2-Nb2O5: Part 1.
Low Range Flowmeters for Use with Vacuum and Le Standards.		PB89-171797 901,03
PB89-175707 900,3	ELLINGWOOD, B.	Phase Equilibria and Crystal Chemistry in the Ternar System BaO-TiO2-Nb2O5. Part 2. New Banum Polytitan
Observations of Gas Species and Mode of Operation	Damage Accumulation in Wood Structural Members Under Stochastic Live Loads.	ates with < 5 mole % Nb2O5.
fects on Effective Areas of Gas-Operated Piston Gages. PB89-231120 900,5	PB89-171748 900.115	PB89-189815 900,41
Reduction of Uncertainties for Absolute Piston Gage Pro	Probabilistic Models for Ground Snow Accumulation.	ETZ, E. Stokes and Anti-Stokes Fluorescence of Er(3+) in the
sure Measurements in the Atmospheric Pressure Range.	F1 100004 500,700	Raman Spectra of Erbium Oxide and Erbium Glasses.
PB90-163882 900,0	30 ELMQUIST, R. E. Measurement of the NBS (National Bureau of Standards)	PB89-149231 901,020
HRLICH, G.	Electrical Watt in SI Units.	ETZ, E. S.
National Engineering Laboratory's 1989 Report to the National Research Council's Board on Assessment of NI	ST	Application of Synergistic Microanalysis Techniques to the Study of a Possible New Mineral Containing Light Ele
(National Institute of Standards and Technology) Program	s. NBS (National Bureau of Standards) Determination of the	ments.
PB89-189294 900,0	ance and Josephson Frequency-to-Voltage Quotient in SI	PB89-147037 901,27
Report on Interactions between the National Institute	Units. of PB89-230437 901,556	Micro-Raman Characterization of Atherosclerotic and Bio prosthetic Calcification.
Standards and Technology and the American Society	of ELTON, R. C.	PB89-149223 901,23
Mechanical Engineers. PB89-172563 901,0		Moydite, (Y, REE) (B(OH)4)(CO3), a New Mineral Specie
Report on Interactions between the National Institute	Plasma.	from the Evans-Lou Pegmatite, Quebec. PB89-157747 900,18
Standards and Technology and the Institute of Electric	al ELY, J. F.	EVANS, C.
and Electronic Engineers. PB90-130899 900,8	· · · · · · · · · · · · · · · · · · ·	Preliminary Experiments with Three Identical Ultraprecision
HRLICH, M.	tems.	Machine Tools. PB89-150841 900.99
Method for Evaluating Air Kerma and Directional Do	PB90-136763 901,231	·
Equivalent for Currently Available Multi-Element Do	e- Improved Conformal Solution Theory for Mixtures with Large Size Ratios.	EVANS, D. Combustion of Oil on Water.
meters in Radiation Protection Dosimetry. PB90-117532 901,3	DD00 400500	PB89-149173 900,58
HRSTEIN, J. R.	Isochoric (p,v,T) Measurements on CO2 and (0.98 CO2 +	Combustion of Oil on Water. November 1987.
AC Impedance Method for High-Resistivity Measurement	ots 0.02 CH4) from 225 to 400 K and Pressures to 35 MPa. PB89-202493 900,435	PB89-185581 900,86
of Silicon. PB89-231203 900,7		Structure and Radiation Properties of Large-Scale Natura Gas/Air Diffusion Flames.
ICHINGER, D.	Theory: A Review.	PB89-157572 900,58
Off-Lattice Simulation of Polymer Chain Dynamics.	PB89-228019 901,546	EVANS, D. D.
PB90-117524 900,5	Method for Improving Equations of State Near the Critical Point.	Cooling Effect Induced by a Single Evaporating Droplet of
ICHMILLER, F. C.	PB89-228027 901,547	a Semi-Infinite Body. PB89-149249 <i>901,48</i>
Adhesive Bonding of Composites. PB90-123696 900,0	Properties of Lennard-Jones Mixtures at Various Tempera-	Evaporation of a Water Droplet Deposited on a Hot Hig
Simplified Shielding of a Metallic Restoration during Ra	tures and Energy Hatios with a Size Hatio of Two.	Thermal Conductivity Solid Surface.
ation Therapy.	PVT Relationships in a Carbon Diovide-Rich Mixture with	PB89-149157 901,48
PB89-229256 900,0	Luare.	Hand Calculations for Enclosure Fires. PB89-173983 900,16
EINSTEIN, T. L. Universality Class of Planar Self-Avoiding Surfaces v	PB89-229181 900,478	Very Large Methane Jet Diffusion Flames.
Fixed Boundary.	PB89-222608 900,843	PB89-175913 900,59
PB89-157945 900,3	Thermophysical Properties of Methane.	EVANS, D. J.
EISENHOWER, E. H.	PB89-222541 900,450	Acoustical Technique for Evaluation of Thermal Insulation. PB89-193866 900.91
Measurement Quality Assurance. PB89-147508 901,2	EMBREE, E.	PB89-193866 900,91 Local Order in a Dense Liquid.
EITZEN, D. G.	Thermal Degradation of Poly (methyl methacrylate) at 50C to 125C.	PB89-157226 900,31
Higher-Order Crossings: A New Acoustic Emission Sig	DD00 155105	Shear Dilatancy and Finite Compressibility in a Dense Nor
Processing Method. PB89-173488 900,	ENGELBREKLSO, S.	Newtonian Liquid. PB89-174023 901,32
Ultrasonic Sensor for Measuring Surface Roughness.	Rotational Modulation and Flares on RS CVn and BY Dra Stars IX. IUE (International Ultraviolet Explorer) Spectrosco-	Shear Induced Anisotropy in Two-Dimensional Liquids.
PB89-211809	py and Photometry of II Peg and V711 Tau during February	PB89-158141 901,32
EKBERG, J. O.	1983. PB89-171615 <i>900,019</i>	EVANS, E. H.
Laser-Produced Spectra and QED (Quantum Electrodyna ic) Effects for Fe-, Co-, Cu-, and Zn-Like Ions of Au, Pb,	M- FROTEIN M. C	Standard X-ray Diffraction Powder Patterns from the JCPD
Th, and U.	Comparison of Detection Limits in Atomic Spectroscopic	(Joint Committee on Powder Diffraction Standards) Re search Associateship.
PB89-176010 901,	DD00 450050 000 470	PB89-171763 900,19
Spectra and Energy Levels of Dr. YYV Br. YYIY Br. Y	300,770	Standard V ray Diffraction Douglar Pottorns from the ICDD

Luminescence Standards for Macro- and Microspectrofluorometry.

Spectra and Energy Levels of Br XXV, Br XXIX, Br XXX, and Br XXXI. PB89-176002 901,509

Standard X-ray Diffraction Powder Patterns from the JCPDS (Joint Committee on Powder Diffraction Standards) Research Association.

PB89-202246 EVANS, J. M.	900,214	PB89-146682 FASSETT, J. D.	900,247	Vibrationally Resolved Photoelectron Angular Distributions for H2 in the Range 17 eV $<$ or= h(nu) $<$ or= 39 eV.
Assessment of Robotics for Improved Building (Operations	Analytical Applications of Resonance Ionization	Mass Spec-	PB89-176952 900,385 Vibrationally Resolved Photoelectron Studies of the
and Maintenance. PB89-189146	900,092	trometry (RIMS). PB89-161590	900, 189	Vibrationally Resolved Photoelectron Studies of the 7(sigma) (-1) Channel in N2O. PB89-176945 900,257
EVENSON, K. M. (12)C(16)O Laser Frequency Tables for the 34	2 to 62 2	Detection of Uranium from Cosmos-1402 in sphere.	the Strato-	FIALA, J. C.
THz (1139 to 2079 cm(-1)) Region.	901.361	PB89-156962	901,592	Interfaces to Teleoperation Devices. PB89-181739 900,993
PB89-193908 CO Laser Stabilization Using the Optogalvanic La		Determining Picogram Quantities of U in Hum Thermal Ionization Mass Spectrometry. PB89-146906	900,175	FICKETT, F. R.
PB89-179139 Detection of the Free Radicals FeH, CoH, and N		Development of the NBS (National Bureau o Beryllium Isotopic Standard Reference Material	f Standards)	Effects of Grain Size and Cold Rolling on Cryogenic Properties of Copper. PB90-128604 901,176
Infrared Laser Magnetic Resonance. PB90-117342	900,495	PB89-231070	900,221	FIELD, B. F.
Far-Infrared Laser Magnetic Resonance Spectric CD Radical and Determination of Ground State Part PB90-117359	um of the arameters. 900,496	Isotope Dilution Mass Spectrometry for Accura Analysis. PB89-230338	900,220	Guidelines for Implementing the New Representations of the Volt and Ohm Effective January 1, 1990. PB89-214761 900,817
Far-Infrared Laser Magnetic Resonance Spectrum tionally Excited C2H(1).		Resonance Ionization Mass Spectrometry of M Autoionizing Series.	lg: The 3pnd	Improved Transportable DC Voltage Standard. PB89-230395 901,554
PB89-147474	900,292	PB89-150817 FATIADI, A. J.	900,296	Josephson Array Voltage Calibration System: Operational
Frequency Measurement of the $J=1<-0$ Transition of HD (Hydrogen Deutende). PB89-161566	901,499	Facile Synthesis of 1-Nitropyrene-d9 of High Iso PB90-123753	otopic F. vity. 900,240	Use and Venfication. PB89-230403 National Institute of Standards and Technology (NIST) In-
Heterodyne Frequency Measurements of (12)C(1 Transitions.	6)O Laser	FAVREAU, J. P. Application of Formal Description Techniques	to Conform-	formation Poster on Power Quality. PB89-237986 900,754
PB89-229223	901,374	ance Evaluation. PB89-211908	900,652	NBS (National Bureau of Standards) Determination of the
New FIR Laser Lines and Frequency Measure Optically Pumped CD3OH. PB89-175731	901,350	Automatic Generation of Test Scenario (Ske Protocol-Specifications Written in Estelle.		Fine-Structure Constant, and of the Quantized Hall Resist- ance and Josephson Frequency-to-Voltage Quotient in SI Units.
WING, M. B.		PB89-177125	900,615	PB89-230437 901,556
Microwave Measurements of the Thermal Expansion Spherical Cavity.		User Guide for the NBS (National Bureau or Prototype Compiler for Estelle (Revised).		Possible Quantum Hall Effect Resistance Standard. PB89-149058 900,801
PB89-147458 ABER, W.	900,291	PB89-196158 FAWZY, W. M.	900,619	FIELDS, B. A. Elevated Temperature Deformation of Structural Steel.
Use of Focusing Supermirror Neutron Guides to Cold Neutron Fluence Rates.	Enhance	Rotational Energy Levels and Line Intensitie	es for (2S+	PB89-172621 901,098
PB89-171946	901,306	 Lambda-(2S+ 1) Lambda and (2S+ 1)(Lamb (2S+ 1)Lambda Transitions in a Diatomic Mole Waals Bonded to a Closed Shell Partner. 	ecule van der	FIELDS, R. J. Elevated Temperature Deformation of Structural Steel.
AETH, G. M. Structure and Radiation Properties of Large-Sca	le Natural	PB90-117441	900,498	PB89-172621 901,098
Gas/Air Diffusion Flames. PB89-157572	900,589	FEENSTRA, R. M. Structure of Cs on GaAs(110) as Determined	by Scanning	Texture Monitoring in Aluminum Alloys: A Comparison of Ultrasonic and Neutron Diffraction Measurements. PB90-117409 901,159
AHR, A.		Tunneling Microscopy. PB90-117490	901,463	FILIPPELLI, M.
Reactions of Phenyl Radicals with Ethene, Ethe		FEIGERLE, C. S.		Biotransformation of Mercury by Bacteria Isolated from a River Collecting Cinnabar Mine Waters.
PB89-150908 ALLER, J.	900,297	Vibrationally Resolved Photoelectron Angular for H2 in the Range 17 eV < or= h(nu) < or=	39 eV.	PB89-229280 900,864
High-Precision Absolute Gravity Observations in t States.	the United	PB89-176952 FEINBERG, J.	900,385	FILLA, B. J. Enthalpies of Desorption of Water from Coal Surfaces.
PB89-227946	901,281	Optical Novelty Filters.	004.000	PB89-173868 900,838
ALLER, J. E. Antenna for Laser Gravitational-Wave Obsen	rations in	PB89-228084 FELDMAN, A.	901,366	FILLIBEN, J. J. Evaluating Emergency Management Models and Data
Space. PB89-234231	901,594	Cathodoluminescence of Defects in Diamond Particles Grown by Hot-Filament Chemical-Va		Bases: A Suggested Approach." PB89-189203 901,598
Comment on 'Possible Resolution of the Brookh	naven and	tion. PB90-117961	901,069	FINE, J.
Washington Eotvos Experiments'. PB89-171581	901,504	Photoelastic Properties of Optical Materials.		Analytical Expression for Describing Auger Sputter Depth Profile Shapes of Interfaces.
Current Research Efforts at JILA (Joint Institute for Astrophysics) to Test the Equivalence Pr		PB89-177208 FELDMAN, P. A.	901,355	PB89-157176 900,309 Status of Reference Data, Reference Materials and Reference
Short Ranges. PB89-185912	901,522	Rotational Modulation and Flares on RS Ca corum and BY Draconis Stars X: The 1981 Oct	num Venati-	ence Procedures in Surface Analysis. PB89-157705 900,332
Liquid-Supported Torsion Balance: An Update Report on its Potential for Tunnel Detection.		on V711 Tauri (= HR 1099). PB89-202618	900,021	Temperature-Dependent Radiation-Enhanced Diffusion in lon-Bombarded Solids.
PB89-212062 Precision Experiments to Search for the Fifth Force	901,542	FELDMAN, U.		PB89-179188 901,408 FINK, M. G. J.
PB89-228365 ALTYNEK, R. A.	901,551	Laser-Produced Spectra and QED (Quantum El ic) Effects for Fe-, Co-, Cu-, and Zn-Like Ions of Th, and U.	of Au, Pb, Bi,	Quantum-Defect Parametrization of Perturbative Two- Photon Ionization Cross Sections.
Effect of pH on the Emission Properties of Aq (2,6-dipicolinato) Terbium (III) Complexes.	ueous tris	PB89-176010 Scheme for a 60-nm Laser Based on Photop	901,510	PB89-202600 901,539 FINNEY, J. L.
PB89-157135 Element-Specific Epifluorescence Microscopy In v	<i>900,250</i> vivo Moni-	High Level of Mo(6+) by a Spectral Line of Mo PB89-186415	0(11+). 900,407	Repulsive Regularities of Water Structure in Ices and Crystalline Hydrates.
toring of Metal Biotransformations in Environmences.		Spectra and Energy Levels of Br XXV, Br XX and Br XXXI.	XIX, Br XXX,	PB89-186753 900,414
PB89-177216	901,220	PB89-176002	901,509	FINZEL, B. C. Use of an Imaging Proportional Counter in Macromolecular
ANCONI, B. M. Institute for Materials Science and Engineering,	Polymers:	FELTON, C. M. Low Noise Frequency Synthesis.		Crystallography. PB90-136599 900,538
Technical Activities 1987. PB89-188601	900,566	PB89-174056 FENIMORE, C.	900,716	FIRST, P. N. Structure of Cs on GaAs(110) as Determined by Scanning
Institute for Materials Science and Engineering, Technical Activities 1988.		Method for Fitting and Smoothing Digital Data. PB90-128794	900,830	Tunneling Microscopy. PB90-117490 901,463
PB89-166094 FANG, Q. T.	900,003	Thermal-Expansive Growth of Prebreakdown		FISCHBACH, E.
Preparation of Multistage Zone-Refined Materials mochemical Standards.		Liquids. PB89-149074	900,803	Precision Experiments to Search for the Fifth Force. PB89-228365 901,551
PB89-186795	900,203	FERNANDEZ, M. T. Fundamental Configurations in Mo IV Spectrum	l.	FISHER, W. S. Evaluating Office Lighting Environments: Second Level
Cathodoluminescence of Defects in Diamond	Films and	PB89-147011 FERNANDEZ-PELLO, A. C.	900,284	Analysis. PB89-189153 900,073
Particles Grown by Hot-Filament Chemical-Vapo tion.	or Deposi-	Fire Propagation in Concurrent Flows.	000.007	FISK, Z.
PB90-117961 FARAHANI, M.	901,069	PB89-151781 Fire Propagation in Concurrent Flows.	900,867	Pressure Dependence of the Cu Magnetic Order in RBa2Cu3O6+ x.
Hydroxyl Radical Induced Cross-Linking between	Phenyla-	PB89-188577	900,597	PB90-123829 901,472
lanine and 2-Deoxyribose. PB89-147029	900,547	FERRETT, T. A. Autoionization Dynamics in the Valence-Shell	Photoioniza-	FITTING, D. W. Measuring In-Plane Elastic Moduli of Composites with
Radiation-Induced Crosslinks between Thymine Decryen/thropentose	and 2-D-	tion Spectrum of CO. PB89-176960	900.386	Arrays of Phase-Insensitive Ultrasound Receivers. PB90-136672 900,970

FLACK, H. D.	PB89-171359 901,400	PB89-176465 901,139
Statistical Descriptors in Crystallogrephy: Report of the	FOWLER, J. E.	FREDERICK, N. V.
Internetionel Union of Crystallography Subcommittee on Stetisticel Descriptors.	Generic Architecture for Computer Integrated Manufactur	
PB89-201826 901,432	ing Software Besed on the Product Data Exchange Specifi- cation.	Geses end Liquids. PB89-228076 901,447
FLANAGAN, G.	PB90-112459 900,965	FREIMAN, S. W.
Dreft Internetional Document on Guide to Porteble Instru- ments for Assessing Airborne Pollutents Arising from Haz-	FOX, J. R.	Fracture Rehevior of Ceremics Used in Multilaver Conaci-
erdous Wastes.	Development of e Field-Space Corresponding-States Method for Fluids end Fluid Mixtures.	PB89-171805 900 758
PB89-150775 900,855	PB89-227995 901,331	Mechanical Property Enhancement in Ceremic Matrix Com-
FLEMING, R. F.	FOY, B. R.	posites.
Anelyticel Applications of Neutron Depth Profiling. PB89-146872 901,294	Dissociation Lifetimes and Level Mixing in Overtone-Excited HN3 (X tilde (sup 1) A').	
FLETCHER, R. A.	PB90-117425 900,263	Novel Process for the Preperation of Fiber-Reinforced Ceremic-Metrix Composites.
Comperison of Two Transient Recorders for Use with the	Unimolecular Dynemics Following Vibretionel Overtone Excitation of HN3 v1 = 5 end v1 = 6:HN3(X tilde;v,J,K,) ->	PB89-179733 901,074
Laser Microprobe Mass Anelyzer. PB89-176887 900,200	HN((X sup 3)(Sigme (1-));v,J,Omega) + N2(x sup 1)(Sigma	FREITAG, K.
Identification of Cerbonaceous Aerosols vie C-14 Accelera-	sub g (1+)). PB89-147110 900,286	Megnetic Resonance of (160)Tb Oriented in e Terbium Single Crystel et Low Temperatures.
tor Mass Spectrometry, and Leser Microprobe Mass Spec-	FRAKER, A. C.	PB89-179204 901,519
trometry. PB90-136540 900,236	Corrosion Behavior of Mild Steel in High pH Aqueous	FREYTAG, M.
FLETCHER, T. R.	Media. PB90-131152 901,086	Growth end Properties of High-Quelity Very-Thin SOS (Sili-
Photodissocietion Dynemics of C2H2 et 193 nm: Vibretionel	Corrosion of Metellic Implants end Prosthetic Devices.	con-on Sapphire) Films. PB90-128109 900,798
Distributions of the CCH Redicel end the Rotational State Distribution of the A(010) State by Time-Resolved Fourier	PB89-150890 900,053	High-Mobility CMOS (Complementery Metal Oxide Semi-
Transform Infrared Emission.	FRANCIS, M. H.	conductor) Trensistors Fabricated on Very Thin SOS Films.
PB89-179782 900,258	Accurete Determination of Planar Near-Field Correction Parameters for Linearly Polarized Probes.	FRIDAY, D. S.
Time-Resolved FTIR Emission Studies of Molecular Photo- fragmentation Initiated by a High Repetition Rete Excimer	PB89-156871 900,704	Measurement Procedures for Electromagnetic Compatibility
Leser.	Antenna Meesurements for Millimeter Waves at the Nation-	Assessment of Electroexplosive Devices.
PB90-136680 900,266	el Bureau of Standards. PB89-150726 900,694	PB89-146914 901,314
FLYNN, C. P. Characterization of Structural and Magnetic Order of Er/Y	Comperison of Measured end Calculated Antenna Sidelobe	Micho, D. G.
Superlattices.	Coupling Loss in the Near Field Using Approximate Far-	Second Viscosity and Thermal-Conductivity Virial Coeffi- cients of Gases: Extension to Low Reduced Temperature.
PB90-123662 901,470	Field Dete. PB89-156855 900,702	PB89-179691 900.397
Exchenge and Magnetostrictive Effects in Rare Earth Superlattices.	X-Bend Atmospheric Attenuation for an Earth Termina	Tables for the Thermophysical Properties of Methane.
PB89-202667 901,438	Measurement System.	The state of the s
Long-Range Incommensurete Magnetic Order in Dy-Y Multi-	PB90-100736 900,626	PB89-222541 900,450
layers. PB89-179642 901,411	FRANK, C. W. Reevaluation of Forces Measured Across Thin Polymer	FROHNSDORFF, G.
Occurrence of Long-Range Helical Spin Ordering in Dy-Y	Films: Nonequilibrium and Pinning Effects.	Implications of Computer-Based Simulation Models, Expert
Multilayers.	PB89-228589 900,573	Systems, Databases, and Networks for Cement Research. PB89-146989 900,581
PB89-179634 <i>901,410</i> FLYNN, D. R.	FRANZEN, D. Numerical Aperture of Multimode Fibers by Several Meth-	
Acoustical Technique for Evaluation of Thermal Insulation.	ods: Resolving Differences.	terials.
PB89-193866 900,919	PB90-117482 900,757	
FLYNN, K. M.	FRANZEN, D. L. Comparison of Far-Field Methods for Determining Mode	Interpretation of the Effects of Retarding Admixtures on Pastes of C3S, C3A plus Gypsum, and Portland Cement.
Studies on Some Failure Modes in Latex Berner Films. PB89-209308 901,089	Field Diameter of Single-Mode Fibers Using Both Gaussian	900,300
FOLSOM, R.	and Petermann Definitions. PB90-117474 900,756	Prediction of Service Life of Construction and Other Materials.
Cryogenic Bathysphere for Rapid Veriable-Temperature	FRASE, K. G.	PB89-175848 900,120
Characterization of High-T(sub c) Superconductors. PB89-228456 901,450	Application of SANS (Small Angle Neutron Scattering) to	Standard Specifications for Cements and the Role in Their
FOLSOM, R. M.	Ceramic Characterization. PB89-146856 901,017	Development of Quality Assurance Systems for Laborato- ries.
Resistance Measurements of High T(sub c) Superconduc-	FRASER, G. T.	PB89-150742 901,021
tors Using a Novel 'Bathysphere' Cryostat.	Electric-Dipole Moments of H2O-Formamide and CH3OH	
PB89-228431 901,448 FORANO. C.	Formamide. PB89-147375 900,288	Collision Induced Spectroscopy: Absorption and Light Scattering.
Neutron Diffraction Determination of Full Structures of An-	Electric-Resonance Optothermal Spectrum of (H2O)2	DD00 0400E0 004 060
hydrous Li-X and Li-Y Zeolites.	Microwave Spectrum of the K= 1-0 Subband for the E((+	FRYBERGER, T. B.
PB90-118001 900,516	or -)2) States. PB90-117433 900,497	Surface Properties of Clean and Gas-Dosed SnO2 (110). PB89-179576 900,393
FORMAN, R. A. Multiple Scattering in the X-ray-Absorption Near-Edge	Infrared and Microwave Investigations of Interconversion	F B09-119310 900,000
Structure of Tetrahedral Ge Gases.	Tunneling in the Acetylene Dimer.	Florid Bossess Octoberral Constant of (1900)
PB89-146922 900,283	PB89-157341 900,320 Infrared and Microwave Spectra of OCO-HF and SCO-HF.	Microwave Spectrum of the K= 1-0 Subband for the E((+
Multiple Scattering in the X-ray Absorption Near Edge Structure of Tetrahedral Germanium Gases.	PB89-179121 900,385	or -)2) States. PB90-117433 900,497
PB89-228480 900,474	Microwave and Infrared Electric-Resonance Optotherma	
FORNEY, G. P.	Spectroscopy of HF-HCl and HCl-HF. PB89-234215 900,489	Journal of Physical and Chemical Reference Data, Volume
Spectroscopic Quantitative Analysis of Strongly Interacting Systems: Human Plasma Protein Mixtures.	Microwave Electric-Resonance Optothermal Spectroscopy	17, 1988, Supplement No. 3. Atomic Transition Probabilities
PB89-202576 901,225	of (H2O)2.	PB89-145197 900,276
FORSTER, E. O.	PB90-128141 900,53	rodi, r.
Effect of Pressure on the Development of Prebreakdown Streamers.	Microwave Spectrum and (14)N Quadrupole Coupling Con stants of Carbazole.	ease motory: Development of a contrare Engineering
PB90-128315 900,828	PB89-157333 900,315	Standard. PB89-149116 900,665
FORSYTHE, L. L.	Microwave Spectrum, Structure, and Electric Dipole Moment of Ar-Ch3OH.	
Development of a Microwave Sustained Gas Plasma for the	PB90-117847 900,510	Software Verification and Validation: Its Role in Computer
Sterilization of Dental Instruments. PB89-231278 900,047	Microwave Spectrum, Structure, and Electric Dipole	
FOUST, J. V.	Moment of the Ar-Formamide van der Waals Complex. PB89-157325 900,316	PB90-111691 900.655
Measurement of Partial Discharges in Hexane Under DC	Vibrational Exchange upon Interconversion Tunneling in	FUJII, Y.
Voltage. PB89-173421 900,833	(HF)2 and (HCCH)2.	DD90-229265 Oo1 561
FOWELL, A. J.	PB89-179113 900,386	CILLED E
Outline of a Practical Method of Assessing Smoke Hazard.	Vibrational Predissociation in the H-F Stretching Mode of HF-DF.	Synthesis and Magnetic Properties of the Bi-Sr-Ca-Cu
PB89-211858 900,078	PB89-234207 900,48	
FOWLER, B. O.	FRASER, H. L.	301,412

Metastable Phase Production and Transformation in Al-Ge Alloy Films by Rapid Crystallization and Annealing Treatments. PB99-157622 901,129

Undercooling and Microstructural Evolution in Glass Forming Alloys.

FULLER, E. R.

Design Criteria for High Temperature Structural Applications.
PB89-211833 901,052

Green Function Method for Calculation of Atomistic Structure of Grain Boundary Interfaces in Ionic Crystals.

Calcium Hydroxyapatite Precipitated from an Aqueous Solution: An International Multimethod Analysis.
PB90-123399 900,228

Progress in Understanding Atomic Structure of the Icosahedral Phase.

FOWLER, H. A.

PB89-202105 901,050		PB89-189211 900,810
Mechanical Property Enhancement in Ceramic Matrix Com- posites.	GAMBINO, R. J. Magnetic Correlations in an Amorphous Gd-Al Spin Glass.	GIEBULTOWICZ, T. M.
PB89-189138 901,076	PB89-201693 901,148	Mrf-Mn Exchange Constants in Zinc-Manganese Chalco- genides.
Structural Reliability and Damage Tolerance of Ceramic Composites for High-Temperature Applications. Semi-	GARCIA-RIQUELME, O.	PB90-136706 901,478
Annual Progress Report for the Period Ending September 30, 1987.	Fundamental Configurations in Mo IV Spectrum. PB89-147011 900,284	Neutron Diffraction Study of the Wurtzite-Structure Dilute Magnetic Semiconductor Zn0.45Mn0.55Se.
PB89-156350 901,023	Spectrum of Doubly Ionized Tungsten (W III).	PB90-136714 901,475
Structural Reliability and Damage Tolerance of Ceramic Composites for High-Temperature Applications. Semi-	PB89-235659 900,223 GARY, J. M.	GILBERT, S. L.
Annual Progress Report for the Period Ending March 31,	Analysis of Computer Performance Data.	Frequency Standards Utilizing Penning Traps. PB90-128042 901,378
1988. PB89-156368 <i>901,024</i>	PB89-162614 900,635	Ion Trapping Techniques: Laser Cooling and Sympathetic
Toughening Mechanisms in Ceramic Composites. Semi-	GASS, S. I. Analyzing the Economic Impacts of a Military Mobilization.	Cooling. PB90-128034 901,578
Annual Progress Report for the Period Ending March 31, 1989.	PB90-128067 901,273	GILLETTE, G.
PB89-235907 901,080	Evaluating Emergency Management Models and Data Bases: A Suggested Approach.	Guideline for Work Station Design.
Toughening Mechanisms in Ceramic Composites: Semi- Annual Progress Report for the Period Ending September	PB89-189203 901,598	PB90-112418 900,643
30, 1988. PB89-162606 <i>901,028</i>	GATES, R. S.	GILLETTE, G. L. Evaluating Office Lighting Environments: Second Leve
FURDYNA, J. K.	Tribochemical Mechanism of Alumina with Water. PB90-117722 901,059	Analysis. PB89-189153 900,073
Mn-Mn Exchange Constants In Zinc-Manganese Chalco- genides.	GAUDETTE, P.	Post-Occupancy Evaluation of Several U.S. Governmen
PB90-136706 901,478	Application of Formal Description Techniques to Conformance Evaluation.	Buildings. PB90-112384 900,088
Neutron Diffraction Study of the Wurtzite-Structure Dilute	PB89-211908 900,652	
Magnetic Semiconductor Zn0.45Mn0.55Se. PB90-136714 901,479	Free Value Tool for ASN.1. PB89-196182 900,622	GILLIES, C. W. Microwave Spectrum and Molecular Structure of the Ethyl-
FURLANI, C. M.	Object-Oriented Model for ASN.1 (Abstract Syntax Notation	ene-Ozone van der Waals Complex. PB89-201735 900,424
Use of the IRDS (Information Resource Dictionary System) Standard in CALS (Computer-Aided Acquisition and Logistic	One). PB89-177117 900,649	Microwave Spectrum, Structure, and Electric Dipole
Support). PB90-112467 900,931	Object-Oriented Model for Estelle.	Moment of Ar-Ch3OH. PB90-117847 900,510
GADZUK, J. W.	PB89-211916 900,653	Microwave Spectrum, Structure, and Electric Dipole
Dynamics of Molecular Collisions with Surfaces: Excitation,	GAVIN, R. Turning Workstation in the AMRF (Automated Manufactur-	Moment of the Ar-Formamide van der Waals Complex. PB89-157325 900,318
Dissociation, and Diffraction. PB89-175996 900,375	ing Research Facility).	Ozonolysis of Ethylene. Microwave Spectrum, Molecular
Resonance Enhanced Electron Stimulated Desorption.	PB89-185607 900,954 GAYLE, F. W.	Structure, and Dipole Moment of Ethylene Primary Ozonide
PB90-117771 900,505	Thermomechanical Detwinning of Superconducting	(1,2,3-Tnoxolane). PB89-157440 900,323
Semiclassical Way to Molecular Dynamics at Surfaces. PB89-157713 900,333	YBa2Cu3O7-x Single Crystals. PB89-231088 901,458	GILLIES, J. Z.
Theoretical Study of the Vibrational Lineshape for CO/	GEBBIE, K. B.	Microwave Spectrum and Molecular Structure of the Ethyl- ene-Ozone van der Waals Complex.
Pt(111). PB89-157689 900,331	Center for Atomic, Molecular, and Optical Physics Techni-	PB89-201735 900,424
GAIGALAS, A. K.	cal Activities, 1989. PB90-133158 <i>901,586</i>	Microwave Spectrum, Structure, and Electric Dipole
Application of Magnetic Resonance Imaging to Visualization of Flow in Porous Media.	Helium Resonance Lines in the Flare of 15 June 1973.	Moment of Ar-Ch3OH. PB90-117847 900,510
PB89-179592 <i>901,329</i>	PB90-118142 900,028 GEIST, J.	Ozonolysis of Ethylene. Microwave Spectrum, Molecular Structure, and Dipole Moment of Ethylene Primary Ozonide
GAITAN, M. Correlation between CMOS (Complementary Metal Oxide	Blocked Impurity Band and Superlattice Detectors: Pros-	(1,2,3-Trioxolane).
Semiconductor) Transistor and Capacitor Measurements of	pects for Radiometry. PB89-212161 900,730	PB89-157440 900,323
Interface Trap Spectra. PB89-180020 900,779	Feasibility of Detector Self-Calibration in the Near Infrared.	GILLILAND, G. L. Biological Macromolecule Crystallization Database: A Basis
Numerical Analysis for the Small-Signal Response of the	PB89-176788 900,384	for a Crystallization Strategy.
MOS (Metal Oxide Semiconductors) Capacitor. PB89-186837 900,781	High Accuracy Modeling of Photodiode Quantum Efficiency. PB90-117599 900,733	PB90-136722 901,250 Crystal Structure of a Cyclic AMP (Adenosine Monophos-
GAJEWSKI, E.	Infrared Absorption Cross Section of Arsenic in Silicon in	phate)-Independent Mutant of Catabolite Gene Activator
Structure of a Hydroxyl Radical Induced Cross-Link of Thy- mine and Tyrosine.	the Impurity Band Region of Concentration. PB89-201750 900,426	Protein. PB89-201594 901,224
PB89-157838 901,244	GEIST, J. C.	Preliminary Crystal Structure of Acinetobacter glutaminasifi-
GALLAGHER, A. Collisional Losses from a Light-Force Atom Trap.	Silicon Photodiode Self-Calibration. PB90-118159 900,734	cans Glutáminase-Asparaginase. PB90-123381 901,260
PB90-123936 901,577	GELDZAHLER, B. J.	Preliminary Crystallographic Study of Recombinant Human
Exoergic Collisions of Cold Na*-Na. PB90-123761 901.571	Proper Motion vs. Redshift Relation for Superluminal Radio	PB90-136730 901,251
PB90-123761 901,571 Laser Spectroscopy of Inelastic Collisions.	Sources. PB89-157663 900,017	Use of an Imaging Proportional Counter in Macromolecular
PB89-185946 900,405	GENZ, A.	Crystallography. PB90-136599 900,538
Sodium Doppler-Free Collisional Line Shapes. PB89-234306 901,559	Numerical Evaluation of Certain Multivariate Normal Integrals.	GILSINN, D.
Surface Reactions in Silane Discharges.	PB89-158166 901,195	Optical Roughness Measurements for Industrial Surfaces. PB89-176655 900,979
PB89-185961 900,406	GERSTENBERG, H. M. Basic Data Necessary for Neutron Dosimetry.	GIRVIN, S. M.
GALLAGHER, J. S. Modelling of Impurity Effects in Pure Fluids and Fluid Mix-	PB89-171854 901,241	Superlattice Magnetoroton Bands.
tures.	Initial Spectra of Neutron-Induced Secondary Charged Particles.	PB89-175970 901,403
PB89-176739 900,245 Thermodynamic Values Near the Critical Point of Water.	PB89-171862 <i>901,265</i>	GLADDEN, W. K.
PB89-161541 901,497	Refinement of Neutron Energy Deposition and Microdosimetry Calculations.	Interpolation of Silicon Photodiode Quantum Efficiency as an Absolute Radiometric Standard.
GALLAGHER, J. W. Absolute Cross Sections for Molecular Photoabsorption,	PB89-150791 901,264	PB89-212245 901,445
Partial Photoionization, and Ionic Photofragmentation Proc-	GEYER, R. G.	Semiconductor Measurement Technology: Automatic Deter- mination of the Interstitial Oxygen Content of Silicon Wafers
ess. PB89-186464 900,410	Dielectric Mixing Rules for Background Test Soils. PB89-188585 901,289	Polished on Both Sides. PB89-151831 900,772
GALLAWA, R. L.	Magnetostatic Measurements for Mine Detection.	GLADHILL, R. L.
Potential Errors in the Use of Optical Fiber Power Meters. PB89-176697 900,728	PB89-148365 900,685 GIARRATANO, P. J.	NVLAP (National Voluntary Laboratory Accreditation Pro-
GALLOWAY, K. F.	Latent Heats of Supercritical Fluid Mixtures.	gram) Assessment and Evaluation Manual. PB89-228324 900,903
Effect of Neutrons on the Characteristics of the Insulated	PB89-174908 900,242	NVLAP (National Voluntary Laboratory Accreditation Program) Program Handbook Construction Testing Services.
Gate Bipolar Transistor (IGBT). PB89-157655 900,773	GIAUQUE, C. Optical Roughness Measurements for Industrial Surfaces.	Requirements for Accreditation.
Radiation-Induced Interface Traps in Power MOSFETs.	PB89-176655 900,979	PB90-112327 900,169
PB89-201974 900,784 GALUK, K. G.	GIBSON, K. A.	GLAUS, U.
Model for Particle Size and Phase Distributions in Ground	Bibliography of the NIST (National Institute of Standards and Technology) Electromagnetic Fields Division Publica-	Universality Class of Planar Self-Avoiding Surfaces with Fixed Boundary.
Cement Clinker.	tions.	PB89-157945 900,339

		DD00 454045	000.650	DD90 495007	00.054
GLAZE, D. New Cavity Configuration for Cesium Beam Primar	v Fre-	PB89-151815 GORDON, G. E.	900,659	PB89-185607 96 GREGORY, E.	00,954
quency Standards.	00,714	Mobile Sources of Atmospheric Polycyclic Ar carbons: A Roadway Tunnel Study.		Magnetic Evaluation of Cu-Mn Matrix Material for Fin- ment Nb-Ti Superconductors.	
GLICKSMAN, M. E. Effect of a Crystal-Melt Interface on Taylor-Vortex Flo	w.	PB90-123571 Residential Wood Combustion: A Source o	900,859		01,425
PB90-130261 96 Preparation of Multistage Zone-Refined Materials for	01,477	Polycyclic Aromatic Hydrocarbons. PB90-128166	900,860	GREGORY, T. M. Mechanism of Hydrolysis of Octacalcium Phosphate. PB89-201503 90	01,254
mochemical Standards.	00,203	GORE, J. P.		Micro-Analysis of Mineral Saturation Within Enamel	
GLINKA, C. J.	,	Structure and Radiation Properties of Large Gas/Air Diffusion Flames.		Lactic Acid Demineralization. PB89-186373 90	01,253
Applications of Mirrors, Supermirrors and Multilayers National Bureau of Standards Cold Neutron Research	at the	PB89-157572	900,589	GRICE, J. D.	,,
cility.		GORENSTEIN, M. V. Microarcsecond Optical Astrometry: An Instr	ument and its	Application of Synergistic Microanalysis Techniques	
	01,540	Astrophysical Applications.		Study of a Possible New Mineral Containing Ligh ments.	
Low-Q Neutron Diffraction from Supercooled D-Glycer PB89-228001 96	00,468	PB89-171268 GOTAAS, J. A.	900,013		01,277
Phase Contrast Matching in Lamellar Structures Com of Mixtures of Labeled and Unlabeled Block Copolyn	nposed ner for	Magnetic Structure of Cubic Tb0.3Y0.7Ag. PB90-117789	901,466	Moydite, (Y, REE) (B(OH)4)(CO3), a New Mineral Sp from the Evans-Lou Pegmatite, Quebec. PB89-157747 90	pecies 00,186
Small-Angle Neutron Scattering. PB89-157119 99	01,182	Magnetic Structure of Y0.97Er0.03.	204 402	GRIFFIN, D. C.	
Small Angle Neutron Scattering Spectrometer at the	ne Na-	PB89-202675 Spin-Density-Wave Transition In Dilute YGd S	901,439	Electron-Impact Excitation of the Resonance Transit CA(1+).	tion in
tional Bureau of Standards. PB89-158158 96	01,396	PB89-202030	901,433	PB89-171557 90	01,502
Uniaxial Deformation of Rubber Network Chains by	Small	GOULD, D.		GROH, A.	
Angle Neutron Scattering. PB89-175830 90 GO, D.	01,088	VAMAS (Versailles Project on Advanced Standards) Intercomparison of Critical Curr ment in Nb3Sn Wires.			Dip. <i>01,356</i>
Noise in DC SQUIDS with Nb/Al-Oxide/Nb Jose	phson	PB89-202147	901,534	GROSGOGEAT, E. CO2 Separation Using Facilitated Transport Ion Excl	hanne
Junctions.	00,763	GRAF, W.	o to Eshapea	Membranes.	-
GOLDBERG, R. N.	,	Use of Focusing Supermirror Neutron Guide Cold Neutron Fluence Rates.		PB89-157374 96 GROSS, B. D.	00,321
Calonmetric and Equilibrium Investigation of the Hyd	Irolysis	PB89-171946	901,306	Rotational Modulation and Flares on RS Canum V	/enati-
of Lactose. PB89-227888 96	01,226	GRAMLICH, J. W. Absolute Isotopic Abundance Ratios and Ato	mic Weight of	corum and BY Draconis Stars X: The 1981 October 3	
Thermodynamic and Transport Properties of Carbohy		a Reference Sample of Nickel.	900.543	on V711 Tauri (= HR 1099). PB89-202618 90	00,021
and Their Monophosphates: The Pentoses and Hexos PB89-222574 96	ses. 00,453	PB90-163890 Absolute Isotopic Composition and Atomic V	,	GROSS, D.	
Thermodynamics of Hydrolysis of Disaccharides.		restrial Nickel.		Analysis and Prediction of Alr Leakage through Doc semblies.	or As-
	01,221	PB90-163908	900,544		00,085
Thermodynamics of the Hydrolysis of Sucrose. PB89-227904 9/ GOLDFARB, R. B.	01,227	Determination of Trace Level lodine in Biolo tanical Reference Materials by Isotope Dilutio trometry.		Recent Activities of the American Society for Testin Materials Committee on Fire Standards.	•
Flux Creep and Activation Energies at the Grain Boun	ndaries	PB89-235642	900,222	PB89-180004 96 GROSS, J. G.	00,124
of Y-Ba-Cu-O Superconductors.	01.457	GRANT, J. T. Status of Reference Data, Reference Materia	als and Refer-	Brick Masonry: U.S. Office Building in Moscow.	
Magnetic Evaluation of Cu-Mn Matrix Material for Fin		ence Procedures in Surface Analysis.		PB89-187504 90	00,160
ment Nb-Ti Superconductors.	01,425	PB89-157705 GRAVATT, C. C.	900,332	Research as the Technical Basis for Standards Us Building Codes.	sed in
Oxygen Isotope Effect in the Superconducting Bi-Sr-C		Environmental Intelligence.		PB89-231062 90	00,101
O System.	01,025	PB89-201214	901,287	GROT, R. A.	
GONSCHOREK, W.	01,023	GRAVES, J. A. Pathways for Microstructural Development in	ΤίΔΙ	Investigation of a Washington, DC Office Building. PB89-230361	00,081
Statistical Descriptors in Crystallography: Report of		PB90-123779	901,173	Measured Air Infiltration and Ventilation Rates in	Eight
International Union of Crystallography Subcommitte Statistical Descriptors.	ee on	GREEN, P.	0.1.6	Large Office Buildings. PB90-128158 90	00,090
	01,432	Dehydrogenation of Ethanol in Dilute Aqu Photosensitized by Benzophenones.		Performance Measurements of Infrared Imaging Sy	stems
GOODIN, P. J. Post-Occupancy Evaluation of Several U.S. Gover	rnment	PB89-157556	900,251	Used to Assess Thermal Anomalies. PB89-179667 96	00,072
Buildings.	00,088	GREEN, W. A. Dehydrogenation of Ethanol in Dilute Aqu	eous Solution	GRUSHKO, B.	
GOODRICH, L. F.	00,000	Photosensitized by Benzophenones.		Formation of the Al-Mn Icosahedral Phase by Electro sition.	depo-
Ag Screen Contacts to Sintered YBa2Cu3Ox Powo	der for	PB89-157556 GREENBERG, J.	900,251		00,504
Rapid Superconductor Characterization. PB89-200448 90	01,423	Guidelines and Procedures for Implementatio	n of Executive	Structural Study of a Metastable BCC Phase in Alloys Electrodeposited from Molten Salts.	Al-Mn
Battery-Powered Current Supply for Superconductor	Meas-	Order on Seismic Safety. PB89-148092	900,156		01,064
urements. PB89-200455 99	01,525	GREENBERG, R.	ŕ	GRUZS, T. M.	
Critical Current Measurements of Nb3Sn Superconde		Long-Term Stability of the Elemental Compos ical Materials.	sition in Biolog-	Power Quality Site Surveys: Facts, Fiction, and Fallaci PB89-171656 96	ies. <i>00,805</i>
NBS (National Bureau of Standards) Contribution VAMAS (Versailles Agreement on Advanced Materia		PB89-156939	900,181	GRY, C.	
Standards) Interlaboratory Comparison. PB90-136748 96	01,480	GREENBERG, R. R.		IUE Observation of the Interstellar Medium Toward	J Beta
Current Capacity Degradation in Superconducting		High Accuracy Determination of (235)U in I Assay Standards by Gamma Spectrometry.	Nondestructive	Geminorum. PB89-228373 99	00,024
Strands.	01,526	PB89-156954	900,249	GUENET, J. M.	
Current Ripple Effect on Superconductive D.C. Critica		Neutron Activation Analysis of the NIST (Na of Standards and Technology) Bovine Serum		Concentration Dependence of the Compression Mode Isotactic Polystyrene/Cis-Decalin Gels.	ulus of
rent Measurements.	01,492	erence Material Using Chemical Separations. PB89-156921	900,180	PB89-172449 96	00,552
Nb3Sn Critical-Current Measurements Using Tubular		Radiochemical and Instrumental Neutron Ac		Effects of Solvent Type on the Concentration Depen of the Compression Modulus of Thermoreversible Isr	
glass-Epoxy Mandrels.	01,527	sis Procedures for the Determination of Lor Elements in Human Livers.	w Level Trace	Polystyrene Gels.	00,553
VAMAS (Versailles Project on Advanced Material Standards) Intercomparison of Critical Current Me	ls and	PB89-171953 Radiochemical Procedure for Ultratrace De	901,236 etermination of	GUENTHER, A. H.	
ment in Nb3Sn Wires.		Chromium in Biological Materials.		Laser Induced Damage in Optical Materials: 1987. PB89-221162 96	01,364
PB89-202147 <i>9</i> GOODWIN, K. R.	001,534	PB89-156913 Role of Neutron Activation Analysis in the	900,179 Certification of	GUENTHER, F. R.	
Robot Crane Technology.		NBS (National Bureau of Standards) Stand	ard Reference	Residential Wood Combustion: A Source of Atmos Polycyclic Aromatic Hydrocarbons.	spheric
PB90-111667 9 GOODWIN, R. D.	100, 146	Materials. PB89-157879	900,187		00,860
Benzene Thermophysical Properties from 279 to 90	00 K at	GREENE, G.		GUILLOT, B.	
Pressures to 1000 Bar.	000,271	Determination of Short Lifetimes with Ultra F (n,gamma) Spectroscopy.	ligh Resolution	Triplet Dipoles in the Absorption Spectra by Dense Gas Mixtures. 1. Short Range Interactions.	
GORCZYCA, J.		PB90-123670	901,567		00,539

GREENSPAN, L.

Turning Workstation in the AMRF (Automated Manufacturing Research Facility).

Small Computer System Interface (SCSI) Command System: Software Support for Control of Small Computer System Interface Devices.

900,677

GUITIAN, C.

Computer Security Training Guidelines. PB90-780172

GUNAHA INA, G.	PB89-157150 900,038	PB89-146856 901,017
Mathematical Software: PLOD. Plotted Solutions of Differential Equations.	HAMPSON, R. F. Evaluated Kinetic and Photochemical Data for Atmospheric	Pore Morphology Analysis Using Small Angle Neutron Scat- tering Techniques.
PB89-147425 901,194 GUO, M. K.	Chemistry. Supplement 3.	PB89-175939 901,037
Comparison of Fluoride Uptake Produced by Tray and	PB89-222582 900,454 HAN, C.	Small Angle Neutron Scattering from Porosity in Sintered Alumina.
Flossing Methods In vitro. PB89-179238 901,252	Temperature, Composition and Molecular-Weight Depend-	PB89-157564 901,026
GURMAN, J. L.	ence of the Binary Interaction Parameter of Polystyrene/ Poly(vinylmethylether) Blends.	HARDY, S. C.
Toxicity of Mixed Gases Found in Fires. PB89-212047 900,869	PB89-157473 900,550 HAN, C. C.	Ostwald Ripening in a System with a High Volume Fraction of Coarsening Phase.
GUTTMAN, C. M.	Dynamics of Concentration Fluctuation on Both Sides of	PB89-157598 901,126
Flow of Molecules Through Condoms. PB89-148118 901,087	Phase Boundary. PB89-173942 <i>901.183</i>	HARFORD, M. Z. Mossbauer Hyperfine Fields in RBa2(Cu0.97Fe0.03)3 O(7-
Studies on Some Failure Modes in Latex Barrier Films.	Phase Contrast Matching in Lamellar Structures Composed	x)(R= Y,Pr,Er). PB89-201206 901,429
PB89-209308 <i>901,089</i> GYLYS, V. T.	of Mixtures of Labeled and Unlabeled Block Copolymer for Small-Angle Neutron Scattering.	HARIRI, M. H.
Ionization and Current Growth in N2 at Very High Electric	PB89-157119 901,182	Bioseparations: Design and Engineering of Partitioning Sys-
Field to Gas Density Ratios. PB89-228381 901,552	Polymers Bearing Intramolecular Photodimerizable Probes for Mass Diffusion Measurements by the Forced Rayleigh	tems. PB90-136763 901,231
HAAR, L.	Scattering Technique: Synthesis and Characterization. PB89-157101 901,181	HARKLEROAD, M.
Thermodynamic Values Near the Critical Point of Water. PB89-161541 901,497	Shear Effects on the Phase Separation Behaviour of a	Combustion of Oil on Water. PB89-149173 900,587
HABERMAN, W. L.	Polymer Blend in Solution by Small Angle Neutron Scatter- ing.	Combustion of Oil on Water. November 1987.
Analysis and Prediction of Air Leakage through Door Assemblies.	PB89-229264 900,574	PB89-185581 900,863
PB89-231161 900,085	Small Angle Neutron Scattering Studies of Single Phase Interpenetrating Polymer Networks.	Ignition and Flame Spread Measurements of Aircraft Lining Materials.
HACKERT, M. Numerical Aperture of Multimode Fibers by Several Meth-	PB90-123456 900,577	PB89-172886 900,009
ods: Resolving Differences. PB90-117482 900,757	Uniaxial Deformation of Rubber Network Chains by Small Angle Neutron Scattering.	HARKLEROAD, M. F. Combustion Efficiency, Radiation, CO and Soot Yield from
HACKNEY, S.	PB89-175830 901,088	a Variety of Gaseous, Liquid, and Solid Fueled Buoyant Dif-
Migration of Liquid Film and Grain Boundary in Mo-Ni In-	HAN, J. K. Fatigue Resistance of a 2090-T8E41 Aluminum Alloy at	fusion Flames. PB89-231179 900,604
duced by W Diffusion. PB89-157614 901,128	Cryogenic Temperatures. PB90-128737 901,177	Fire Properties Database for Textile Wall Coverings.
HACKNEY, S. A.	HANDWERKER, C.	PB89-188635 900,126 HARMAN, G.
Directional Invariance of Grain Boundary Migration in the Pb-Sn Cellular Transformation and the Tu-Turnbull Hystere-	Diffusion-Induced Grain Boundary Migration.	Production and Stability of S2F10 in SF6 Corona Dis-
sis. PB89-157911 <i>901,134</i>	PB90-128174 901,175 HANDWERKER, C. A.	charges. PB89-231039 900,822
Experimental Observations on the Initiation of DIGM (Diffu-	Electron Microscopy Studies of Diffusion-Induced Grain	HARMAN, G. G.
sion Induced Grain Boundary Migration). PB89-157630 901,130	Boundary Migration in Ceramics. PB89-202097 901,049	Silicon and GaAs Wire-Bond Cratering Problem.
Observations on Crystal Defects Associated with Diffusion	Equilibrium Crystal Shapes and Surface Phase Diagrams at	PB90-128182 900,799
Induced Grain Boundary Migration in Cu-Zn. PB89-157606 901,127	Surfaces in Ceramics. PB90-117755 901,162	HARMAN, J. G. Crystal Structure of a Cyclic AMP (Adenosine Monophos-
HADZIIOANNOU, G.	Observations on Crystal Defects Associated with Diffusion	phate)-Independent Mutant of Catabolite Gene Activator Protein.
Reevaluation of Forces Measured Across Thin Polymer Films: Nonequilibrium and Pinning Effects.	Induced Grain Boundary Migration in Cu-Zn. PB89-157606 901,127	PB89-201594 901,224
PB89-228589 900,573	HANLEY, B.	HARMOUCHE, M. R.
HAHN, J. W. High Resolution Inverse Raman Spectroscopy of the CO Q	Synthesis and Characterization of Poly(vinylmethyl ether). PB89-161616 900,551	Dynamic Young's Modulus Measurements in Metallic Materials: Results of an Interlaboratory Testing Program.
Branch. PB89-171292 900,355	HANLEY, H. J. M.	PB89-157671 901,132
HAHN, T.	Local Order in a Dense Liquid. PB89-157226 900,313	HARRIMAN, A. Decay of High Valent Manganese Porphyrins in Aqueous
Statistical Descriptors in Crystallography: Report of the International Union of Crystallography Subcommittee on	Low-Q Neutron Diffraction from Supercooled D-Glycerol.	Solution and Catalyzed Formation of Oxygen.
Statistical Descriptors. PB89-201826 901,432	PB89-228001 900,468 Prediction of Shear Viscosity and Non-Newtonian Behavior	PB89-156772 900,308 Dehydrogenation of Ethanol in Dilute Agueous Solution
HALE, P. D.	in the Soft-Sphere Liquid.	Photosensitized by Benzophenones. PB89-157556 900,251
Stability of Birefringent Linear Retarders (Waveplates). PB89-171672 901.345	PB89-228035 901,548 Shear Dilatancy and Finite Compressibility in a Dense Non-	One-Electron Transfer Reactions of the Couple SO2/
HALL, J. L.	Newtonian Liquid. PB89-174023 901,328	SO2(1-) in Aqueous Solutions. Pulse Radiolytic and Cyclic Voltammetric Studies.
Antenna for Laser Gravitational-Wave Observations in	Shear-Induced Angular Dependence of the Liquid Pair Cor-	PB89-176093 900,376
Space. PB89-234231 901,594	relation Function. PB89-228043 900,469	Reactions of Magnesium Prophyrin Radical Cations in Water. Disproportionation, Oxygen Production, and Compar-
Fundamental Tests of Special Relativity and the Isotropy of Space.	Shear Induced Anisotropy in Two-Dimensional Liquids.	ison with Other Metalloporphyrins. PB89-151005 900,301
PB89-185920 901,523	PB89-158141 901,325	Redox Chemistry of Water-Soluble Vanadyl Porphyrins.
Generation of Squeezed Light by Intracavity Frequency Doubling.	HANNAH, P. Preliminary Experiments with Three Identical Ultraprecision	PB89-150999 900,300
Doubling. PB89-227938 <i>901,365</i>	Machine Tools. PB89-150841 900,997	HARRIS, C. M. Analyzing the Economic Impacts of a Military Mobilization.
High Resolution Optical Multiplex Spectroscopy. PB89-185938 900,404	HANSON, D. W.	PB90-128067 901,273
Precise Laser Frequency Scanning Using Frequency-Syn-	Secure Military Communications Can Benefit from Accurate	Evaluating Emergency Management Models and Data Bases: A Suggested Approach.
thesized Optical Frequency Sidebands: Application to Iso- tope Shifts and Hyperfine Structure of Mercury.	Time. PB89-176507 <i>901,274</i>	PB89-189203 901,598
PB90-118134 901,370	HARDIS, J. E.	HARRIS, J. S.
Towards the Ultimate Laser Resolution. PB89-186910 900,416	Autoionization Dynamics in the Valence-Shell Photoionization Spectrum of CO.	Corrosion Behavior of Mild Steel in High pH Aqueous Media.
HALLER, W.	PB89-176960 900,386	PB90-131152 901,086
Mechanical Property Enhancement in Ceramic Matrix Composites.	Using 'Resonant' Charge Exchange to Detect Traces of Noble Gas Atoms.	HARRIS, R. H. Flammability Characteristics of Electrical Cables Using the
PB89-189138 901,076	PB89-176770 901,296	Cone Calonmeter.
Novel Process for the Preparation of Fiber-Reinforced Ceramic-Matrix Composites.	Vibrationally Resolved Photoelectron Angular Distributions for H2 in the Range 17 eV< or= h(nu)< or= 39 eV.	PB89-162572 900,741 HARRIS, S. E.
PB89-179733 901,074 HAMANN, D. R.	PB89-176952 900,385	Toxicity of Mixed Gases Found in Fires.
Electron Transmission Through NiSi2-Si Interfaces.	Vibrationally Resolved Photoelectron Studies of the 7(sigma) (-1) Channel in N2O.	PB89-212047 900,869
PB89-231294 900,485 HAMBRIGHT, P.	PB89-176945 900,257 HARDMAN-RHYNE, K.	HARRISON, J. C. Gravity Tide Measurements with a Feedback Gravity Meter
Redox Chemistry of Water-Soluble Vanadyl Porphyrins.	Creep Cavitation in Liquid-Phase Sintered Alumina.	Gravity Tide Measurements with a Feedback Gravity Meter. PB89-171755 901,310
PB89-150999 900,300	PB89-175954 901,038	HARRISON, R. J.
HAMMOND, B. D. Biological Evaluations of Zinc Hexyl Vanillate Cement Using	HARDMAN-RHYNE, K. A. Application of SANS (Small Angle Neutron Scattering) to	Guidelines for the Specification and Validation of IGES (Initial Graphics Exchange Specification) Application Protocols.
Two In vivo Test Methods.	Ceramic Characterization.	PB89-166102 900,937

		, ==
HARRISON, R. W. Preliminary Crystal Structure of Acinetobacter glutaminasifi-	HEBNER, R. E. Assessment of Space Power Related Measurement Re-	PB89-171920 900,358
cans Glutaminase-Asparaginase. PB90-123381 901,260	quirements of the Strategic Defense Initiative. PB89-209357 901,269	HERRON, J. T. Critical Review of the Chemical Kinetics of Sulfur Tetrafluo-
Sayre's Equation is a Chernov Bound to Maximum Entropy. PB89-158174 901,397	Effect of an Oil-Paper Interface Parallel to an Electric Field on the Breakdown Voltage at Elevated Temperatures.	ride, Sulfur Pentafluoride, and Sulfur Fluoride (S2F10) in the Gas Phase. PB89-161582 900,347
ARTMAN, A.	PB89-156988 901,490	Evaluated Kinetics Data Base for Combustion Chemistry.
Performance Standards for Microanalysis. PB89-201651 900,211	Effect of Pressure on the Development of Prebreakdown Streamers. PB90-128315 900,828	PB89-212096 900,601 Production and Stability of S2F10 in SF6 Corona Dis-
IARTMAN, A. W. Standard Reference Materials: Description of the SRM	Interactions between Two Dividers Used in Simultaneous	charges. PB89-231039 900,822
1965 Microsphere Slide. PB89-153704 901,390	Companson Measurements. PB90-118035 900,031	S2F10 Formation in Computer Simulation Studies of the Breakdown of SF6.
IARVEY, A. H.	Measurement of Electrical Breakdown in Liquids. PB89-212229 900,447	PB89-157523 900,327
NaCI-H2O Coexistence Curve Near the Critical Tempera- ture of H2O. PB89-202519 900,436	Strategic Defense Initiative Space Power Systems Metrology Assessment. PB89-173405 901,268	Stopped-Flow Studies of the Mechanisms of Ozone-Alkene Reactions in the Gas Phase: Tetramethylethylene. PB89-157515 900,326
IASANAIN, S. K.	PB89-173405 <i>901,268</i> HEERENS, J.	HERTZ, H. S. Technical Activities, 1988, Center for Analytical Chemistry.
Magnetic Correlations in an Amorphous Gd-Al Spin Glass. PB89-201693 901,148 ASLWANTER, T.	Fracture Behavior of a Pressure Vessel Steel in the Ductile- to-Brittle Transition Region. PB89-189195 901,103	PB89-151773 HERZOG, P.
Laser-Noise-Induced Population Fluctuations in Two- and	HEFNER, A. R.	Magnetic Resonance of (160)Tb Oriented in a Terbium Single Crystal at Low Temperatures.
Three-Level Systems. PB89-171235 901,342	Analytical Model for the Steady-State and Transient Characteristics of the Power Insulated-Gate Bipolar Transistor.	PB89-179204 901,519 HESS, S.
One-Photon Resonant Two-Photon Excitation of Rydberg Series Close to Threshold.	PB89-146880 900,767 Analytical Modeling of Device-Circuit Interactions for the	Shear-Induced Angular Dependence of the Liquid Pair Cor-
PB89-171276 901,343 ASTIE, J. W.	Power Insulated Gate Bipolar Transistor (IGBT). PB89-176259 900.777	relation Function. PB89-228043 900,469
Laser Induced Vaporization Time Resolved Mass Spec-	Effect of Neutrons on the Characteristics of the Insulated	HETRICK, P. S.
trometry of Refractories. PB90-136904 900,540	Gate Bipolar Transistor (IGBT). PB89-157655 900,773	Accurate RF Voltage Measurements Using a Sampling Voltage Tracker.
Phase Diagrams for High Tech Ceramics. PB89-186308 901,044	Improved Understanding for the Transient Operation of the Power Insulated Gate Bipolar Transistor (IGBT).	PB89-201552 900,815 Calculable, Transportable Audio-Frequency AC Reference
ASTINGS, J. R.	PB89-231229 900,795	Standard. PB90-117854 900,721
NIST (National Institute of Standards and Technology) Measurement Services: AC-DC Difference Calibrations.	HEFTER, U. Spectroscopic Detection Methods.	HEUGHEBAERT, J. C.
PB89-222616 900,818 ATANO, Y.	PB89-228100 901,549 HEILWEIL, E. J.	Calcium Hydroxyapatite Precipitated from an Aqueous Solu- tion: An International Multimethod Analysis. PB90-123399 900,228
Cross Sections for Collisions of Electrons and Photons with Oxygen Molecules.	Picosecond Studies of Vibrational Energy Transfer in Mole- cules on Surfaces.	HEYDEMANN, P. L. M.
PB89-226575 900,457 ATTENBURG, A. T.	PB89-157309 900,316	Technical Activities 1987, Center for Basic Standards. PB89-185615 901,521
NBS (National Bureau of Standards) Scale of Spectral Ra-	Picosecond Study of the Population Lifetime of CO(v = 1) Chemisorbed on SiO2-Supported Rhodium Particles. PB89-157317 900,317	HEYLIGER, P. R.
diance. PB89-201685 901,532	Picosecond Vibrational Energy Transfer Studies of Surface	Conventional and Quarter-Point Mixed Elements in Linear Elastic Fracture Mechanics.
AVEY, M. D. Nonadiabatic Theory of Fine-Structure Branching Cross-	Adsorbates. PB90-136573 900,537	PB89-157788 901,481 Higher Order Beam Finite Element for Bending and Vibra-
Sections for Sodium-Helium, Sodium-Neon, and Sodium-Argon Optical Collisions. PB89-202162 900,433	Population Relaxation of CO(v= 1) Vibrations in Solution Phase Metal-Carbonyl Complexes. PB89-157291 900.315	tion Problems. PB89-229124 901,484
AYASHI, M.	Time Resolved Studies of Vibrational Relaxation Dynamics	HEYWOOD, B. R. Liposome Technology in Biomineralization Research.
Cross Sections for Collisions of Electrons and Photons with Oxygen Molecules.	of CO(v= 1) on Metal Particle Surfaces. PB89-203012 900,444	PB90-128117 901,230 HICHO, G. E.
PB89-226575 900,457 AYNES, L. S.	Ultrashort-Pulse Multichannel Infrared Spectroscopy Using Broadband Frequency Conversion in LilO3.	Metallurgical Evaluation of 17-4 PH Stainless Steel Castings.
Real-Time Control System Software: Some Problems and	PB89-230304 901,367 HELLER, D.	PB 89-193262 901,105
an Approach. PB89-177083 900,951	Two-Photon Laser-Induced Fluorescence of the Tumor-Lo-	HICKERNELL, R. K. Waveguide Loss Measurement Using Photothermal Deflec-
AYNES, W. M. Comprehensive Study of Methane + Ethane System.	calizing Photosensitizer Hematoporphynn Derivative. PB89-157283 901,240	tion. PB89-157028 900,739
PB89-176747 900,841	HEMBREE, G. Performance Standards for Microanalysis.	HIERONYMUS, J. L.
AYTER, J. B. Low-Q Neutron Diffraction from Supercooled D-Glycerol.	PB89-201651 900,211	Compensating for Vowel Coarticulation in Continuous Speech Recognition. PB89-176721 900.634
PB89-228001 900,468 AYWARD, E.	HEMPELMANN, R. Hydrogen Sites in Amorphous Pd85Si15HX Probed by Neu-	PB89-176721 900,634 HIGHBARGER, L.
Comment on 'Feasibility of Measurement of the Electro-	tron Vibrational Spectroscopy. PB89-229140 901,456	Synergistic Effects of Nitrogen Dioxide and Carbon Dioxide Following Acute Inhalation Exposures in Rats.
magnetic Polarizability of the Bound Nucleon'. PB90-117730 901,563	HEMPLEMANN, R.	PB89-214779 900,856
EAD, E. Numerical Aperture of Multimode Fibers by Several Meth-	Neutron Vibrational Spectroscopy of Disordered Metal Hydrogen Systems.	HILL, D. Field Measurement of Thermal and Solar/Optical Proper-
ods: Resolving Differences. PB90-117482 900,757	PB89-157499 900,324 HENDRICKSON, E.	ties of Insulating Glass Windows. PB89-175905 900,064
EARING, E. D.	Damage Accumulation in Wood Structural Members Under Stochastic Live Loads.	HILL, D. A.
Estimation of the Thermodynamic Properties of Hydrocarbons at 298.15 K.	PB89-171748 900,115	Antennas for Geophysical Applications. PB89-179857 900,710
PB89-145155 900,272 EATLEY. S.	HENRY, M. C. D. Rotational Modulation and Flares on RS CVn and BY Dra	Clutter Models for Subsurface Electromagnetic Applica- tions.
Prediction of Transport Protocol Performance through Sim-	Stars IX. IUE (International Ultraviolet Explorer) Spectrosco- py and Photometry of II Peg and V711 Tau during February	PB89-229678 900,688 Electromagnetic Detection of Long Conductors in Tunnels.
ulation. PB89-171334 900,612	1983. PB89-171615 <i>900,019</i>	PB90-128190 900,827
EATLEY, S. K. Simplified Discrete Event Simulation Model for an IEEE (In-	HENRY, R. C.	Fields of Honzontal Currents Located Above the Earth. PB89-156830 900,700
stitute of Electroal and Electronics Engineers) 802.3 Local Area Network.	IUE Observation of the Interstellar Medium Toward Beta Geminorum. PB89-228373 900,024	Magnetic Dipole Excitation of a Long Conductor in a Lossy Medium.
PB89-186829 900,617	PB89-228373 900,024 HERMAN, M.	PB89-171664 900,742
Computer Program for Instrument Calibration at State-	Fast Path Planning in Unstructured, Dynamic, 3-D Worlds. PB89-177067 900,992	Near-Field Detection of Buried Dielectric Objects. PB90-128208 900,713
Sector Secondary-Level Laboratories. PB89-173496 900,877	HERRMANN, S.	Reflection Coefficient of a Waveguide with Slightly Uneven Walls.
Measurement of Partial Discharges in Hexane Under DC	Refrigeration Efficiency of Pulse-Tube Refrigerators. PB89-173892 901,007	PB89-201057 <i>900,753</i> HILL, D. D.
Voltage. PB89-173421 900,833	HERRON, J. Modeling Chemical Reaction Systems on an IBM PC.	Flow Coefficients for Interzonal Natural Convection for Various Apertures.
200,000		out a porturos.

DD00 477450	200.000	BB00 40000			
PB89-177158 Interzonal Natural Convection for Various Aper	900,069 ture Configu-	PB90-136862 HOLMES, R. A.	901,178	PB89-202626 HOWE, S. E.	900,02
rations. PB89-176499	900,066	Preliminary Performance Criteria for		Internal Structure of the Guid	e to Available Mathematica
HILL, J. E.	,	Equipment and Systems Used in Detential Facilities. PB89-148514	900,109	Software. PB89-170864	900,92
Assessment of Robotics for Improved Building and Maintenance.	g Operations	HOLT, D. R.	300,103	HOYLER, F.	
PB89-189146	900,092	Scattering Parameters Representing Impaion Coaxial Air Lines.	perfections in Preci-	Determination of Short Lifetime (n,gamma) Spectroscopy.	_
HILPERT, L. R. Facile Synthesis of 1-Nitropyrene-d9 of High Iso		PB89-184121 HONG, T. H.	900,750	PB90-123670 HSIA, J. J.	901,56
PB90-123753	900,240	Building Representations from Fusions of	f Multiple Views	Exploratory Research in Ref	
Standard Reference Materials for the Determin lycyclic Aromatic Hydrocarbons. PB89-156889	900,178	PB89-177059 HONGCHANG, M.	900,991	Standards at the National Bure PB89-202022	au of Standards. 900,42
HILS, D.	300,170	2.5 MeV Neutron Source for Fission Co	ross Section Meas-	HSU, N. N.	
Antenna for Laser Gravitational-Wave Obs	ervations in	urement.		Finite Element Studies of Trans PB89-186902	sient Wave Propagation. 901,37
Space. PB89-234231	901,594	PB89-176531 HOOD, L.	901,512	Higher-Order Crossings: A Ne	
Towards the Ultimate Laser Resolution.	301,334	Shear Dilatancy and Finite Compressibil	ity in a Dense Non-	Processing Method.	_
PB89-186910	900,416	Newtonian Liquid.		PB89-173488	900,67
HIMES, V. L.		PB89-174023 HOPKINS, J. L.	901,328	HSU, S. M. Advanced Ceramics: A Critica	I Assessment of Wear an
NIST (National Institute of Standards and T Sandia/ICDD Electron Diffraction Database: A I	echnology)/ Database for	Rotational Modulation and Flares on R	S CVn and BY Dra	Lubrication.	
Phase Identification by Electron Diffraction.		Stars IX. IUE (International Ultraviolet Ex	plorer) Spectrosco-	PB89-188569	901,04
PB89-175210	901,508	py and Photometry of II Peg and V711 1 1983.	au during rebruary	Critical Assessment of Require Characterization.	ments for Ceramic Powde
HINZ, A. CO Laser Stabilization Using the Optogalvanic I	amb-Din	PB89-171615	900,019	PB89-146849	901,01
PB89-179139	901,356	HOPP, T. H.	Inconction	Institute for Materials Science	and Engineering, Ceramics
HIRAI, Y.		CAD (Computer Aided Design)-Directed PB89-177018	900,980	Technical Activities 1988. PB89-148381	901,01
Preliminary Crystallographic Study of Recombi Interleukin 1beta.	nant Human	HOPPES, D. D.		NBS/BAM (National Bureau	
PB90-136730	901,251	(109)Pd and (109)Cd Activity Standard	lization and Decay	fur Materialprufung) 1986 Symp ics.	osium on Advanced Ceram
HIROOKA, T.		Data. PB90-123449	901,564	PB89-229074	901,05
Oxygen Isotope Effect in the Superconducting O System.	Bi-Sr-Ca-Cu-	NBS (National Bureau of Standards) De	cay-Scheme Inves-	Preparative Liquid Chromatogra	phic Method for the Charac
PB89-157044	901,025	tigations of (82)Sr-(82)Rb. PB89-161558	901,498	terization of Minor Constituents PB89-175921	of Lubricating Base Oils. 901,11
HIRZ, S. J.		Report on the 1989 Meeting of the Rac		Tribochemical Mechanism of Al	
Reevaluation of Forces Measured Across T Films: Nonequilibrium and Pinning Effects.	hin Polymer	ments Section of the Consultative Comm	nittee on Standards	PB90-117722	901,05
PB89-228589	900,573	for the Measurement of Ionizing Radiation on Standards for Radioactivity.	ons: Special Report	HU, Q.	
HOBBS, M.		PB90-163916	900,545	Measurement of Integrated Tur with a Fourier Transform Spect	
User Guide for the NBS (National Bureau of Prototype Compiler for Estelle (Revised).	Standards)	HORD, J.		PB89-157051	900,70
PB89-196158	900,619	Center for Chemical Technology: 1988 T PB89-156376	echnical Activities. 900,241	MM Wave Quasioptical SIS Mix	
HOCKEN, R. J.		HORLICK, J.	000,2	PB89-214738	901,44
General Methodology for Machine Tool Accura- ment by Error Compensation.	cy Enhance-	NVLAP (National Voluntary Laboratory	Accreditation Pro-	HUANG, H. M. Mining Automation Real-Time	Control System Architectur
PB89-146781	900,996	gram) Directory of Accredited Laboratorio PB89-189278	es. <i>900,890</i>	Standard Reference Model (MA	SREM).
HOCKEY, B. J.		HORN, R. G.	000,000	PB89-221154	901,28
Grain-Size and R-Curve Effects in the Abrasi Alumina.	ive Wear of	Reevaluation of Forces Measured Ac		HUANG, J. S.	6 Abr. \
PB90-117383	901,058	Films: Nonequilibrium and Pinning Effect PB89-228589	s. <i>900,573</i>	Quantitative Characterization o mulsion.	
HOER, C. A.		HORVATH, J. J.		PB90-123597	900,52
Calibrating Network Analyzers with Imperfect Te PB90-117680	est Ports. 900.825	Laser Excited Fluorescence Studies of B		HUANG, P. H.	1.1.1.1.1.1.
Some Questions and Answers Concerning Air		PB89-176416	900,243	Polymeric Humidity Sensors fo tions.	Industrial Process Applica
pedance Standards.		Laser Induced Fluorescence for Meas Concentrations in Pulping Liquors.	surement of Lignin	PB89-176424	900,56
PB89-176176	900,747	PB89-172530	901,184	HUBBARD, C. R.	
HOFFMAN, M. Z. Rate Constants for the Quenching of Excite	d States of	HOTES, S. A.		Standard X-ray Diffraction Power (Joint Committee on Powder	
Metal Complexes in Fluid Solution.		Determining Picogram Quantities of U i Thermal Ionization Mass Spectrometry.	n Human Urine by	search Associateship.	
PB89-227797	900,461	PB89-146906	900,175	PB89-171763	900, 19
HOFMANN, G. Electron-Impact Ionization of La(q+) Ions (q=	1 2 3)	HOUGEN, J.		Standard X-ray Diffraction Power (Joint Committee on Powder	
PB90-123845	901,573	Far-Infrared Spectrum of Methyl Amine Analysis of the First Torsional State.	a. Assignment and	search Association. PB89-202246	900,21
Spectroscopy of Autoionizing States Contribut	ing to Elec-	PB89-161574	900,346	Structural Ceramics Database:	
tron-Impact Ionization of Ions. PB90-123837	901,572	HOUGEN, J. T.	internal Transitions	PB89-175244	901,03
HOLBROOK, W. P.		Influence of the ac Stark Effect on Mult in Molecules.	ipnoton Transitions	HUBBARD, J. B.	
Phase Diagrams for High Tech Ceramics.		PB89-201578	901,530	Hydrodynamics of Magnetic an sions.	d Dielectric Colloidal Disper
PB89-186308	901,044	Infrared and Microwave Investigations Tunneling in the Acetylene Dimer.	of Interconversion	PB89-157242	900,31
HOLDER, J. R. Laboratory Evaluation of an NBS (National	Bureau of	PB89-157341	900,320	Molecular Dynamics Study of	a Dipolar Fluid between
Laboratory Evaluation of an NBS (National Standards) Polymer Soil Stress Gage.	Daroud Or	Microwave Spectrum of Methyl Amine	: Assignment and	Charged Plates. PB89-147441	900,29
PB89-211973	901,291	Analysis of the First Torsional State. PB90-117839	900,509	Molecular Dynamics Study of	
HOLLAND, D. M. P. Vibrationally Resolved Photoelectron Angular	Distributions		•	Charged Plates. 2.	
for H2 in the Range 17 eV < or = h(nu) < or = 3	39 eV.	Rotational Energy Levels and Line In 1)Lambda-(2S+ 1) Lambda and (2S+ 1))(Lambda + or -)-	PB89-157218	900,31,
PB89-176952	900,385	(2S+1)Lambda Transitions in a Diatomi Waals Bonded to a Closed Shell Partner		Non-Equilibrium Theories of Ele PB89-174940	900,36
HOLLIS, J. M. Millimeter- and Submillimeter-Wave Surveys	of Orion A	PB90-117441	900,498	HUBENY, I.	
Emission Lines in the Ranges 200.7-202.3,	203.7-205.3,	HOWARD, A. J.		Approximate Formulation of Re	distribution in the Ly(alpha)
and 330-360 GHz. PB90-123787	900,029	Use of an Imaging Proportional Counter Crystallography.	in Macromolecular	Ly(beta), H(alpha) System. PB90-123720	901,56
HOLLOWAY, S.	200,020	PB90-136599	900,538	Computer Program for Calculate	
Dynamics of Molecular Collisions with Surfaces	s: Excitation,	HOWARD, P. R.	noboo in Delucthui	dynamic Equilibrium) Model Ste PB89-171573	
Dissociation, and Diffraction. PB89-175996	900,375	Morphological Partitioning of Ethyl Brai ene by (13)C NMR.		Interpretation of Emission Wing	
Theoretical Study of the Vibrational Linesha		PB89-176051	900,560	nous Blue Vanables.	
Pt(111).		HOWARD, R. E.	vidaos!	PB89-212054	900,02
PB89-157689 HOLMES, L. L.	900,331	Switching Noise in YBa2Cu3Ox 'Macrobi PB89-200513	ridges". 901,426	Redistribution in Astrophysically PB90-128075	Important Hydrogen Lines. 901,57
Technical Examination, Lead Isotope Determ	ination, and	HOWARTH, I. D.		Scattering of Polarized Light in	Spectral Lines with Partia
Elemental Analysis of Some Shang and Zh Bronze Vessels.	ou Dynasty	Stellar Winds of 203 Galactic O Stars: A violet Survey.	Quantitative Ultra-	Frequency Redistribution: Gene PB89-171607	ral Redistribution Matrix. 901,34

HUBER, M.		HURLEY, J. A.		PB90-128091	901,581
Prediction of Shear Viscosity and Non-Newtonian E in the Soft-Sphere Liquid.	Behavior 901,548	Development of Combustion from Quasi-Stab tures for the Iron Based Alloy UNS S66286. PB89-173850	le Tempera- 900,592	Perpendicular Laser Cooling of a F Penning Trap. PB89-157408	Rotating Ion Plasma in a 901,493
HUBER, M. L. Improved Conformal Solution Theory for Mixtur	es with	Ignition Characteristics of the Iron-Based S66286 in Pressurized Oxygen.	•	Precise Test of Quantum Jump The PB89-157390	
Large Size Ratios.	900,477	PB89-189336 Ignition Characteristics of the Nickel-Based	<i>901,104</i> Alloy UNS	Recoilless Optical Absorption and Single Trapped Ion.	• •
Properties of Lennard-Jones Mixtures at Various To tures and Energy Ratios with a Size Ratio of Two.	empera- 900,493	N07718 in Pressurized Oxygen. PB89-218333	901,154	PB89-171631 Trapped lons and Laser Cooling 2:	
HUBER, R.		HURST, K. Relationships between Fault Zone Deformation ment Obliquity on the San Andreas Fault, California (Control of the Control of the Co		the Ion Storage Group, Time and F Boulder, CO. PB89-153878	requency Division, NIST,
Comparison of Two Highly Refined Structures of Pancreatic Trypsin Inhibitor. PB89-202204	901,248	PB89-185953 HURST, W. S.	901,279	ITIKAWA, Y. Cross Sections for Collisions of Ele	
HUCHRA, J. P.		Effects of Velocity and State Changing C	ollisions on	Oxygen Molecules.	
Microarcsecond Optical Astrometry: An Instrument Astrophysical Applications.	and Its 900,013	Raman Q-Branch Spectra. PB89-179196	900,391	PB89-226575 I TOH, K .	900,457
PB89-171268 HUDGENS, J. W.	300,073	High Resolution Inverse Raman Spectroscopy Branch.		VAMAS (Versailles Project on A Standards) Intercomparison of C	dvanced Materials and
Detection of Gas Phase Methoxy Radicals by Res Enhanced Multiphoton Ionization Spectroscopy.		PB89-171292 Measurements of the Nonresonant Third-Order	900,355 Susceptibili-	ment in Nb3Sn Wires. PB89-202147	901,534
	900,307	ty. PB89-179212	901,357	IYENGAR, G. V.	
Multiphoton Ionization Spectroscopy and Vibrationa sis of a 3p Rydberg State of the Hydroxymethyl Rad	lical.	HUSMANN, R. J.		Sample Validity in Biological Trac Nutrient Research Studies.	e Element and Organic
PB89-146666 HUDSON, T. L.	900,279	Preliminary Performance Criteria for Building Equipment and Systems Used in Detention and al Facilities.	g Materials, I Correction-	PB89-156905 IYER, H. K.	901,218
Discussion of 'Steep-Front Short-Duration Voltage Steep Stee	Surge Suppres-	PB89-148514 HUSSMANN, M. H.	900,109	Analysis of Computer Performance PB89-162614	Data. 900,635
sors.' PB90-117326	900,755	Dichromate Dosimetry: The Effect of Acetic Acid	d on the Ra-	Calibration with Randomly Changing	
HUG, G. L. Rate Constants for the Quenching of Excited SI	tates of	diolytic Reduction Yield. PB89-147490	900,248	PB89-186381 Problems with Interval Estimation \	900,888 When Data Are Adjusted
Metal Complexes in Fluid Solution.	900,461	HUST, J. G. Insulation Standard Reference Materials of The	rmal Resist-	via Calibration. PB89-157812	901,209
HUGHES, E. E.		ance. PB89-172548	900,117	JACH, T. Direct Observation of Surface-Trap	ned Diffracted Waves
	900,215	Interlaboratory Companison of Two Types of Thermal-Conductivity Apparatus Measuring Fiv		PB90-128216 Dynamical Diffraction of X-rays at 0	901,475
Special Calibration Systems for Reactive Gases an Difficult Measurements.		Materials. PB89-218325	900,144	PB89-186886	901,421
PB89-149215 HUGHES, J. A.	900,873	Microporous Fumed-Silica Insulation Board as Standard Reference Material of Thermal Resista		Near-Threshold X-ray Fluorescence cules. PB89-176523	e Spectroscopy of Mole-
Microarcsecond Optical Astrometry: An Instrument Astrophysical Applications.	and its	PB89-148373	901,018	Performance of a High-Energy-R	•
	900,013	Specific Heat of Insulations. PB89-172514	900,116	Synchrotron Radiation Beamline. PB90-128083	901,580
HUGHES, R. C. International Comparison of HV Impulse Measurin	na Svs-	HUTCHINSON, J. M. R.		JACKSON, R. H. F.	
tems.	900,809	NBS (National Bureau of Standards) Radon-in-V ard Generator. PB89-171888	901,295	FACTUNC: A User-Friendly System mization.	
HUIE, R. E.		HWANG, F. Y.	001,200	PB90-112392	901,207
Chemical Kinetics of Intermediates in the Autoxida SO2.	ation of	Structural Ceramics Database: Technical Found		Internal Revenue Service Post-of- System: Programmer's Manual for	r FORTRAN Driver Ver-
PB89-176754	900,256	PB89-175244 HYLAND, R. W.	901,036	sion 5.0. PB89-161913	900,002
One-Electron Transfer Reactions of the Couple SO2(1-) in Aqueous Solutions. Pulse Radiolytic and Voltammetric Studies.	d Cyclic	Non-Geometric Dependencies of Gas-Oper- Gage Effective Areas. PB89-231112	ated Piston 900,905	Internal Revenue Service Post-of- System: Programmer's Manual for I PB89-161905	
PB89-176093 Rate Constants for One-Electron Oxidation by Me	900,376	ICHIMURA, A.	900,905	Real-Time Optimization in the A	*
oxyl Radicals in Aqueous Solutions.	900,302	Cross Sections for Collisions of Electrons and I Oxygen Molecules.		Research Facility. PB89-172597	900,947
Rate Constants for Reactions of Nitrogen Oxide	(NO3)	PB89-226575	900,457	JACOBSEN, R. T.	- 6 W 71-1- B. 1-1-1
	900,379	IGLESIAS, L. Fundamental Configurations in Mo IV Spectrum PB89-147011	900,284	Thermodynamic Properties of Argor 1200 K with Pressures to 1000 MP PB89-222558	
HULET, R. G. Precise Test of Quantum Jump Theory.		Spectrum of Doubly Ionized Tungsten (W III).	300,204	Vapor-Liquid Equilibrium of Nitrog	
	901,339	PB89-235659 INDELICATO, P.	900,223	Air at High Pressure. PB89-174932	900,368
Statistical Descriptors in Crystallography: Report	of the	Analysis of Magnesiumlike Spectra from Cu	XVIII to Mo	JACOX, M. E.	falanulas lana lankat in
International Union of Crystallography Subcommi Statistical Descriptors. PB89-201826	ttee on 901,432	XXXI. PB90-117821	900,508	Production and Spectroscopy of N Solid Neon. PB90-117748	900,503
HUMMER, D. G.	301,432	INGHAM, H. Tables for the Thermophysical Properties of Me	thana	Stabilization and Spectroscopy of I	•
Atomic Internal Partition Function.		PB89-222608	900,843	tive Molecules in Inert Matrices. PB89-231252	900,484
Photospheres of Hot Stars. 3. Luminosity Effects a	<i>901,373</i> at Spec-	Thermophysical Properties of Methane. PB89-222541	900,450	Vibrational Spectra of Molecular Neon. I. CO(sub 2, sup +) and CO	lons Isolated in Solid
tral Type 09.5. PB89-202592	900,020	INN, K. G. W.		PB89-234199	900,487
HUNSTON, D. L.		Development of the NBS (National Bureau or Beryllium Isotopic Standard Reference Material.		Vibrational Spectra of Molecular Neon. 2. O4(1+) and O4(1-).	
Composites Databases for the 1990's. PB89-180376	901,075	PB89-231070 ISHIKAWA, K.	900,221	PB90-128729 JAEGER, K.	900,533
Dielectric Measurements for Cure Monitoring. PB89-200430	900,567	Loading Rate Effects on Discontinuous De Load-Control Tensile Tests.		U.S. Perspective on Possible Ch Units.	nanges in the Electrical
HUNT, F.		PB89-171896	901,097	PB89-157002	901,491
	ns. <i>901,198</i>	ITANO, W. M. Atomic-lon Coulomb Clusters in an Ion Trap. PB89-157424	901,494	JAHANMIR, S. Development and Use of a Tribolo	ogy Research-in-Progress
	901,197	Frequency Standards Utilizing Penning Traps. PB90-128042	901,379	Database. PB89-228274	901,002
HUNT, J. B. International Intercompanson of Neutron Survey Ins	strument	Ion Trapping Techniques: Laser Cooling and		Measurements of Tribological Beh rials: Summary of U.S. Results or	avior of Advanced Mate-
Calibrations.	901,300	Cooling. PB90-128034	901,578	vanced Materials and Standards) F PB90-130295	

Laser Cooling to the Zero-Point Energy of Motion.

HUNTER, G. W.

Spin-Density-Wave Transition in Dilute YGd Single Crystals. PB89-202030 901,433 Journal of Physical and Chemical Reference Data, Volume 17, 1988, Supplement No. 2. Thermodynamic and Trans-

JANZ, G. J.

901,518

port Properties for Molten Salts: Correlation Equations for	PB90-136862 <i>901,178</i>	PB89-230411 901,555
Critically Evaluated Density, Surface Tension, Electrical Conductance, and Viscosity Data. PB89-145205 900,277	JOHNSON, A. L. Ammonia description and Dissociation on a Stepped Iron(s)	Measurement of the NBS (National Bureau of Standards) Electrical Watt in SI Units. PB89-230429 900,821
JAPAS, M. L. Gas Solubility and Henry's Law Near the Solvent's Critical	(100) Surface. PB90-123563 Chemisorption of HF (Hydrofluonic Acid) on Silicon Sur-	NBS (National Bureau of Standards) Determination of the Fine-Structure Constant, and of the Quantized Hall Resist-
Point. PB89-202485 900,434	faces. PB89-212013 900,445	ance and Josephson Frequency-to-Voltage Quotient in SI Units.
JASON, N. H. Alaska Arctic Offshore Oil Spill Response Technology	Electron and Photon Stimulated Desorption: Benefits and Difficulties.	PB89-230437 901,556 JONES, H.
Workshop Proceedings. PB89-195663 900,842 Creation of a Fire Research Bibliographic Database.	PB89-200745 901,427 Electron-Stimulated-Desorption Ion-Angular Distributions.	VAMAS (Versailles Project on Advanced Materials and Standards) Intercompanson of Critical Current Measure-
PB89-174130 900,166 Fire Research Publications, 1988.	PB89-201230 901,430 Methodology for Electron Stimulated Desorption Ion Angu-	ment in Nb3Sn Wires. PB89-202147 901,534
PB89-193304 900,132 JASSIE, L. B.	lar Distributions of Negative Ions. PB89-231310 900,486	JONES, M. C. Latent Heats of Supercritical Fluid Mixtures.
Introduction to Microwave Acid Decomposition. PB90-118191 900,227	JOHNSON, B. C. NBS (National Bureau of Standards) Free Electron Laser	PB89-174908 900,242 Use of Dye Tracers in the Study of Free Convection in
Microwave Energy for Acid Decomposition at Elevated Temperatures and Pressures Using Biological and Botanical	Facility. PB89-176515 901,353	Porous Media. PB89-173918 901,327
Samples. PB89-171961 900,359	NBS/NRL (National Bureau of Standards/Naval Research Laboratory) Free Electron Laser Facility. PB89-175749 901,351	JONES, M. P. Dynamic Poisson's Ratio of a Ceramic Powder during Com-
Monitoring and Predicting Parameters in Microwave Dissolution. PB90-118183 900,690	Research Opportunities Below 300 nm at the NBS (National Bureau of Standards) Free-Electron Laser Facility.	paction. PB89-177182 901,039
Safety Guidelines for Microwave Systems in the Analytical Laboratory.	PB89-192678 901,360 JOHNSON, K. S.	JONES, T. S. Theoretical Study of the Vibrational Lineshape for CO/Pt(111).
PB90-118167 <i>900,689</i> JEE, C. S.	AutoMan: Decision Support Software for Automated Manufacturing Investments. User's Manual.	PB89-157689 900,331
Magnetic Order of Pr in PrBa2Cu3O7. PB90-123803 901,471	PB89-221873 900,963 JOHNSON, R. D.	JONES, W. HAZARD I Fire Hazard Assessment Method. PB89-215404 900.143
JEFFERSON, D. K. Use of the IRDS (Information Resource Dictionary System)	Detection of Gas Phase Methoxy Radicals by Resonance Enhanced Multiphoton Ionization Spectroscopy.	PB89-215404 900,143 JONES, W. W.
Standard in CALS (Computer-Aided Acquisition and Logistic support). PB90-112467 900,931	PB89-156764 900,307 JOHNSON, R. G.	Refinement and Experimental Verification of a Model for Fire Growth and Smoke Transport.
JEFFERTS, S. R. Very Low-Noise FET Input Amplifier.	Measurements of the (235)U (n,f) Standard Cross Section at the National Bureau of Standards. PB89-176556 901.305	PB89-212005 900,137 Technical Reference Guide for FAST (Fire and Smoke
PB90-128224 900,800 JELENKOVIC, B. M.	Monte Carlo Calculated Response of the Dual Thin Scintil-	Transport) Version 18. PB89-218366 900,602
Ionization and Current Growth in N2 at Very High Electric Field to Gas Density Ratios.	lation Detector in the Sum Coincidence Mode. PB89-176549 901,299	JONKER, B. T. Domain Images of Ultrathin Fe Films on Ag(100). PB89-158067 901,394
PB89-228381 901,552 JENNINGS, D. A.	JOHNSON, W. C. Elastic Interaction and Stability of Misfitting Cuboidal Inhomogeneities.	PB89-158067 901,394 JORDON, W. M.
(12)C(16)O Laser Frequency Tables for the 34.2 to 62.3 THz (1139 to 2079 cm(-1)) Region.	PB89-157903 901,482 Phase Equilibrium in Two-Phase Coherent Solids.	Neutron Powder Diffraction Structure and Electrical Properties of the Defect Pyrochlores Pb1.5M2O6.5 (M= Nb, Ta). PB89-172431 900,363
PB89-193908 <i>901,361</i> Coherent Tunable Far Infrared Radiation. PB90-117458 <i>900,684</i>	PB89-157580 900,330 JOHNSTON, A. D.	JOYCE, S. A.
Frequency Measurement of the J = 1 < - 0 Rotational Transition of HD (Hydrogen Deutende).	Ferric Oxalate with Nitric Acid as a Conditioner in an Adhesive Bonding System.	Bond Selective Chemistry with Photon-Stimulated Desorption. PB89-201222 900,259
PB89-161566 901,499 Frequency Measurements of High-J Rotational Transitions	PB89-229272 900,045 Substitutes for N-Phenylglycine in Adhesive Bonding to	Chemisorption of HF (Hydrofluoric Acid) on Silicon Surfaces.
of OCS and N2O. PB90-136946 900,541	Dentin. PB90-123795 900,051	PB89-212013 900,445 Electron and Photon Stimulated Desorption: Benefits and
Heterodyne Frequency Measurements of (12)C(16)O Laser Transitions.	JOHNSTON, K. J. Microarcsecond Optical Astrometry: An Instrument and Its	Difficulties. PB89-200745 901,427
PB89-229223 901,374 Improved Rotational Constants for HF. PB90-117466 901,376	Astrophysical Applications. PB89-171268 900,013	Electron-Stimulated-Desorption Ion-Angular Distributions. PB89-201230 901,430
New FIR Laser Lines and Frequency Measurements for Optically Pumped CD3OH.	JOLIE, J. Determination of Short Lifetimes with Ultra High Resolution	Methodology for Electron Stimulated Desorption Ion Angular Distributions of Negative Ions.
PB89-175731 901,350 JENNINGS, H.	(n.gamma) Spectroscopy. PB90-123670 901,567 JONES, A.	PB89-231310 900,486 Photon-Stimulated Description as a Measure of Surface
Implications of Computer-Based Simulation Models, Expert Systems, Databases, and Networks for Cement Research.	Data Management Strategies for Computer Integrated Manufacturing Systems.	Electronic Structure. PB89-231328 901,459
PB89-146989 900,581 Integrated Knowledge Systems for Concrete and Other Ma-	PB89-209258 900,959 JONES, A. T.	Photon-Stimulated Desorption of Fluorine from Silicon via Substrate Core Excitations. PB90-118027 900,517
terials. PB89-176119 900,582	Artificial Intelligence Techniques in Real-Time Production Scheduling.	JULIENNE, P. S.
JENNINGS, H. M. Interpretation of the Effects of Retarding Admixtures on Pastes of C3S, C3A plus Gypsum, and Portland Cement.	PB89-172571 900,945 Functional Approach to Designing Architectures for Com-	Nonadiabatic Theory of Fine-Structure Branching Cross- Sections for Sodium-Helium, Sodium-Neon, and Sodium- Argon Optical Collisions.
PB89-146971 900,580 JENSEN, M. E.	puter Integrated Manufacturing. PB89-172589 900,946	PB89-202162 900,433 JUN, J. S.
In vitro Investigation of the Effects of Glass Inserts on the Effective Composite Resin Polymenzation Shrinkage.	Hierarchies for Computer-Integrated Manufacturing: A Functional Description. PB89-172613 900,949	Design Protocol, Part Design Editor, and Geometry Library of the Vertical Workstation of the Automated Manufacturing
PB90-117516 900,049 JESPERSEN, J. L.	PB89-172613 900,949 On-Line Concurrent Simulation in Production Scheduling, PB89-172605 900,948	Research Facility at the National Bureau of Standards. PB89-151799 900,936
Secure Military Communications Can Benefit from Accurate Time.	Real-Time Optimization in the Automated Manufacturing Research Facility.	Software for an Automated Machining Workstation. PB89-177109 900,953
PB89-176507 901,274 JEWELL, P. R.	PB89-172597 900,947	JUROSHEK, J. R. Calibrating Network Analyzers with Imperfect Test Ports.
Millimeter- and Submillimeter-Wave Surveys of Orion A Emission Lines in the Ranges 200.7-202.3, 203.7-205.3, and 330-360 GHz.	Real-Time Simulation and Production Scheduling Systems. PB89-183230 900,974 JONES, B. F.	PB90-117680 900,825 JUZDAN, Z. R.
PB90-123787 900,029 JEWETT, K. L.	Microarcsecond Optical Astrometry: An Instrument and Its Astrophysical Applications.	Detection of Uranium from Cosmos-1402 in the Stratosphere.
Trace Speciation by HPLC-GF AA (High-Performance Liquid Chromatography-Graphite Furnace Atomic Absorption) for	PB89-171268 900,013 JONES, E. R.	PB89-156962 901,592 KAETZEL, L.
Tin- and Lead-Bearing Organometallic Compounds, with Signal Increases Induced by Transition-Metal Ions. PB89-157085 900,184	Low-Temperature Phase and Magnetic Interactions in fcc Fe-Cr-Ni Alloys. PB90-136771 901,113	Relationship between Appearance and Protective Durability of Coatings: A Literature Review. PB89-162598 901,063
JOEL, E. C. Technical Examination, Lead Isotope Determination, and Elemental Analysis of Some Shang and Zhou Dynasty Bronze Vessels.	JONES, G. R. Low Field Determination of the Proton Gyromagnetic Ratio in Water.	KAFAFI, S. A. Qualitative MO Theory of Some Ring and Ladder Polymers. PB89-156723 900,303

		DD00 457000	201 102	
Modeling Chemical Reaction Systems on an IBM PC PB89-171920). 900,358	PB89-157622 Progress in Understanding Atomic Structure o draft Phase.	901,129 f the Icosahe-	HVACSIM + , a Dynamic Building/HVAC/Control Systems Simulation Program. PB89-177166 900,070
KAHANER, D. K.		PB89-171359	901,400	Simulation of a Large Office Building System Using the HVACSIM+ Program.
Mathematical Software: PLOD. Plotted Solutions of ential Equations. PB89-147425	f Differ- 901,194	Solidification of an 'Amorphous' Phase In Rap Al-Fe-Si Alloys. PB90-123530	oidly Solidified	PB89-177174 900,071
Numerical Evaluation of Certain Multivariate Norm		Sputter Deposition of Icosahedral Al-Mn and A	I-Mn-Si.	KELLY, R. M. Microbiological Metal Transformations: Biotechnological Ap-
grals. PB89-158166	901,195	PB89-147102 Undercooling and Microstructural Evolution in	901,122	plications and Potential. PB89-175947 901,284
KAISER, D. L. Thermomechanical Detwinning of Supercor	nductina	ing Alloys. PB89-176465	901,139	KELLY, W. R.
YBa2Cu3O7-x Single Crystals.	901,458	KAUFMAN, V.	301,133	Detection of Uranium from Cosmos-1402 in the Strato- sphere.
KAISER, R. F.		Aluminumlike Spectra of Copper through Molyl PB89-172365	bdenum. <i>900,360</i>	PB89-156962 901,592 Determining Picogram Quantities of U in Human Urine by
Calibrating Network Analyzers with Imperfect Test Po PB90-117680	orts. <i>900,825</i>	Analysis of Magnesiumlike Spectra from Cu		Thermal Ionization Mass Spectrometry. PB89-146906 900,175
KAISER, W.		XXXI. PB90-117821	900,508	KEMMERER, S. J.
Use of Focusing Supermirror Neutron Guides to E Cold Neutron Fluence Rates.		Chlorine-like Spectra of Copper to Molybdenur PB90-117706	n. <i>900,501</i>	Graphics Application Programmer's Interface Standards and CALS (Computer-Aided Acquisition and Logistic Sup-
PB89-171946 KANDA, M.	901,306	Fundamental Configurations in Mo IV Spectrur	n.	port). PB90-133091 900,658
Optically Linked Electric and Magnetic Field Sen Poynting Vector Measurements in the Near Fields of	nsor for	PB89-147011 Recent Progress on Spectral Data for X-ray	<i>900,284</i> Lasers at the	KENNEDY, E. T.
ating Sources.	900,712	National Bureau of Standards. PB89-158091	901,341	Marked Differences in the 3p Photoabsorption between the Cr and Mn(1+) Isoelectronic Pair: Reasons for the Unique
Thermo-Optic Designs for Microwave and Millimeter		Wavelengths and Energy Level Classifications	•	Structure Observed in Cr. PB90-117581 901,562
Electric-Field Probes. PB90-128588	900,691	Spectra for All Stages of Ionization. PB89-145163	900,273	KENT, E. W.
KANG, H. K.		Wavelengths and Energy Levels of the K I Iso- quence from Copper to Molybdenum.	electronic Se-	Building Representations from Fusions of Multiple Views. PB89-177059 900,991
Migration of Liquid Film and Grain Boundary in Moduced by W Diffusion.		PB89-179097	901,372	KERNER, J.
PB89-157614	901,128	KAUTZ, R. L. Chaos and Catastrophe Near the Plasma Fre-	guency in the	Stability and Quantum Efficiency Performance of Silicon Photodiode Detectors in the Far Ultraviolet.
Control Strategies and Building Energy Consumption	i.	RF-Biased Josephson Junction. PB89-200463	901,424	PB90-128059 900,735
PB89-172340 KARAM, L. R.	900,061	KAVOOSI, F.	301,424	KERR, J. A. Evaluated Kinetic and Photochemical Data for Atmospheric
Generation of Oxy Radicals in Biosystems.	901,266	Transient Cooling of a Hot Surface by Drop tion.	lets Evapora-	Chemistry. Supplement 3. PB89-222582 900,454
Intramolecular H Atom Abstraction from the Sugar	Moiety	PB89-161897	900,971	KESKIN, M.
by Thymine Radicals in Oligo- and Polydeoxynucleot PB89-171870	ides. 901,263	KAYSER, R. F. Effect of Surface Ionization on Wetting Layers.		Dynamics of a Spin-One Model with the Pair Correlation. PB89-171300 900,356
Mechanisms of Free Radical Chemistry and Biochem	nistry of	PB89-157259	901,323	KESSLER, E.
Benzene. PB90-117714	900,502	KAZMERSKI, L. L. High T(sub c) Superconductor/Noble-Metal (Contacts with	Determination of Short Lifetimes with Ultra High Resolution (n,gamma) Spectroscopy.
KARIKORPI, M. Dynamics of Molecular Collisions with Surfaces: Ex-	citation	Surface Resistivities in the (10 to the Minus Omega sq cm Range.		PB90-123670 901,567
Dissociation, and Diffraction.	900,375	PB89-179824	901,413	KEYSER, P. T. Liquid-Supported Torsion Balance: An Updated Status
KARLIN, B.	300,073	KEBEDE, A. Magnetic Order of Pr in PrBa2Cu3O7.		Report on its Potential for Tunnel Detection. PB89-212062 901,542
Near-Threshold X-ray Fluorescence Spectroscopy o cules.	of Mole-	PB90-123803	901,471	KHERA, D.
PB89-176523	900,382	KEERY, W. J. Approach to Accurate X-Ray Mask Measur	rements in a	Machine-Learning Classification Approach for IC Manufacturing Control Based on Test Structure Measurements.
KARLIN, B. A. Performance of a High-Energy-Resolution, Tende	r X-ray	Scanning Electron Microscope. PB89-172555	900,776	PB89-228530 900,790
Synchrotron Radiation Beamline. PB90-128083	901,580	Specimen Biasing to Enhance or Suppress Se	condary Elec-	Neural Network Approach for Classifying Test Structure Results.
KARSTANG, T. V.		tron Emission from Charging Specimens at Ling Voltages.		PB89-212187 900,788
Low Pressure, Automated, Sample Packing Unit for Reflectance Infrared Spectrometry.		PB89-228464 KELLEHER, D. E.	. 901,451	KIEFFER, L. J. Standard Reference Materials for Dimensional and Physical
PB90-135922 KASHANI, A.	900,235	Resonance-Enhanced Multiphoton Ionization	of Atomic Hy-	Property Measurements. PB89-201164 900,892
Performance of He II of a Centrifugal Pump with	n a Jet	drogen. PB89-201073	901,529	KIKUCHI, R.
	901,553	KELLER, J. C.	Coment Heine	Grain Boundaries with Impurities in a Two-Dimensional Lat- tice-Gas Model.
KASHIWAGI, T. Effects of Material Characteristics on Flame Spreadin	00	Biological Evaluations of Zinc Hexyl Vanillate (Two In vivo Test Methods.	•	PB89-172407 901,507
PB89-212021	900,572	PB89-157150 KELLER, R. A.	900,038	KILMER, R. D. Hierarchically Controlled Autonomous Robot for Heavy Pay-
Effects of Thermal Stability and Melt Viscosity of T plastics on Piloted Ignition.		Ultrasensitive Laser Spectroscopy and Detecti PB89-156996	on. <i>901,336</i>	load Military Field Applications. PB89-177075 901,271
PB90-128232 Expert Systems Applied to Spacecraft Fire Safety.	900,151	KELLEY, E. F.	301,330	KIM, B. F.
PB89-231013	901,590	Effect of an Oil-Paper Interface Parallel to an on the Breakdown Voltage at Elevated Tempe	Electric Field	Magnetic Field Dependence of the Superconductivity in Bi- Sr-Ca-Cu-O Superconductors.
KATAYAMA-YOSHIDA, H. Oxygen Isotope Effect in the Superconducting Bi-Sr	-Ca-Cu-	PB89-156988	901,490	PB89-146815 901,385
O System.	901,025	Effect of Pressure on the Development of F Streamers.	Prebreakdown	KIM, C. Y. Uniaxial Deformation of Rubber Network Chains by Small
KATTNER, U. R.	,	PB90-128315	900,828	Angle Neutron Scattering. PB89-175830 901,088
Stable and Metastable Ti-Nb Phase Diagrams. PB89-157432	901,125	Measurement of Partial Discharges in Hexal Voltage.		KIM, H.
KATZ, J. L.		PB89-173421 KELLEY, M. H.	900,833	Shear Effects on the Phase Separation Behaviour of a Polymer Blend in Solution by Small Angle Neutron Scatter-
Dynamic Light Scattering and Angular Dissymmetry In situ Measurement of Silicon Dioxide Particle Synt	thesis in	State Selection in Electron-Atom Scattering: Selectron Scattering from Optically Pumped Society	Spin-Polarized	ing. PB89-229264 <i>900,574</i>
	900,246	PB89-176572	901,513	KIM, S. A.
KATZKE, S. W. Report of the Invitational Workshop on Integrity F	Policy in	Superelastic Scattering of Spin-Polarized E Sodium.	lectrons from	Hysteretic Phase Transition in Y1Ba2Cu3O7-x Superconductors.
Computer Information Systems (WIPCIS).	-	PB90-128307	901,584	PB89-229082 901,454
KAUFMAN, J. G.	900,670	Vector Imaging of Magnetic Microstructure. PB90-128240	901,476	KIMBLE, H. J. Generation of Squeezed Light by Intracavity Frequency
Computerized Materials Property Data Systems. PB89-187512	901,312	KELLY, G. E. Application of Direct Digital Control to an Ex	istina Buildina	Doubling. PB89-227938 901,365
KAUFMAN, M. J.		Air Handler. PB89-177141	-	KINARD, J. R.
Metastable Phase Production and Transformation i Alloy Films by Rapid Crystallization and Annealing		Control System Simulation in North America.	900,068	AC-DC Difference Calibrations at NBS (National Bureau of Standards).
ments.		PB89-157010	900,091	PB89-201560 900,816

Determination of AC-DC Difference in the 0.1 - 100 MHz	PB89-173512 901,100	KARDE B
Frequency Range. PB89-228597 900,719	KLASSEN, M.	KORDE, R. Stability and Quantum Efficiency Performance of Silicon
NIST (National Institute of Standards and Technology)	Transient Cooling of a Hot Surface by Droplets Evapora- tion.	Photodiode Detectors in the Far Ultraviolet. PB90-128059 900,73
Measurement Services: AC-DC Difference Calibrations. PB89-222616 900,818	PB89-161897 900,971 KLAUS, E. E.	KOSTER, B. J. Experiences in Environmental Specimen Benkins
Recharacterization of Thermal Voltage Converters After Thermoelement Replacement.	Tribochemical Mechanism of Alumina with Water.	Experiences in Environmental Specimen Banking. PB90-123969 900,86
PB89-230452 900,720	PB90-117722 901,059 KLAVINS, P.	KOUVEL, J. S. Magnetic Structure of Cubic Tb0.3Y0.7Ag.
KING, D. Two-Photon Laser-Induced Fluorescence of the Tumor-Lo-	Antiferromagnetic Structure and Crystal Field Splittings in	PB90-117789 901,46
calizing Photosensitizer Hematoporphyrin Derivative. PB89-157283 901,240	the Cubic Heusler Alloys HoPd2Sn and ErPd2Sn. PB89-202659 901,437	KOWALYK, K. K. Richarded Evaluations of Zine Hand Varillate Company Hair
KING, D. S.	KLEIBER, P. D.	Biological Evaluations of Zinc Hexyl Vanillate Cement Using Two In vivo Test Methods.
Dissociation Lifetimes and Level Mixing in Overtone-Excited HN3 (X tilde (sup 1) A').	Alignment Effects in Ca-He(5(sup 1)P(sub 1) - 5(sup 3)P(sub J)) Energy Transfer Collisions by Far Wing Laser	PB89-157150 900,036 KRAMER, T. R.
PB90-117425 900,263 Final-State-Resolved Studies of Molecule-Surface Interac-	Scattering. PB89-179790 <i>900,400</i>	Automated Analysis of Operators on State Tables: A Tech
tions. PB89-150916 900,298	KLEIN, E.	nique for Intelligent Search. PB89-157366 900,66
NO/NH3 Coadsorption on Pt(111): Kinetic and Dynamical	Magnetic Resonance of (160)Tb Oriented in a Terbium Single Crystal at Low Temperatures.	Data Handling in the Vertical Workstation of the Automater Manufacturing Research Facility at the National Bureau of
Effects in Rotational Accommodation. PB89-201123 900,423	PB89-179204 <i>901,519</i> KLOSE, J. Z.	Standards. PB89-159636 900,94
Non-Boltzmann Rotational and Inverted Spin-Orbit State	Branching Ratio Technique for Vacuum UV Radiance Cali-	Design Protocol, Part Design Editor, and Geometry Librar
Distributions for Laser-Induced Desorption of NO from Pt(111).	brations: Extensions and a Comprehensive Data Set. PB90-128257 901,582	of the Vertical Workstation of the Automated Manufacturing Research Facility at the National Bureau of Standards.
PB89-157952 900,340 Optically Driven Surface Reactions: Evidence for the Role	KLOTE, J. H.	PB89-151799 900,930
of Hot Électrons. PB89-157937 900,338	Capabilities of Smoke Control: Fundamentals and Zone Smoke Control.	Enhancements to the VWS2 (Vertical Workstation 2) Data Preparation Software.
Unimolecular Dynamics Following Vibrational Overtone Ex-	PB89-229157 900,080	PB90-132713 900,966 Parser That Converts a Boundary Representation into a
citation of HN3 v1= 5 and v1= $6:HN3(X \text{ tilde;v,J,K,}) \rightarrow HN((X \text{ sup 3})(Sigma (1-));v,J,Omega) + N2(x \text{ sup 1})(Sigma$	Computer Model of Smoke Movement by Air Conditioning Systems (SMACS).	Features Representation. PB89-160634 900,944
sub g (1 +)). PB89-147110 900,286	PB89-157267 900,059 Considerations of Stack Effect in Building Fires.	Software for an Automated Machining Workstation.
Vibrational Predissociation of the Nitric Oxide Dimer. PB89-147417 900,289	PB89-195671 900,133	PB89-177109 900,953 KRANBUEHL, D.
KINGSTON, H. M.	Experimental Fire Tower Studies of Elevator Pressurization Systems for Smoke Control.	Off-Lattice Simulation of Polymer Chain Dynamics.
Expert-Database System for Sample Preparation by Microwave Dissolution. 1. Selection of Analytical Descriptors.	PB90-117813 900,097 KLOUDA, G. A.	PB90-117524 900,570 KRASELSKY, B. D.
PB89-229108 900,216	Identification of Carbonaceous Aerosols via C-14 Accelera-	Environmental Intelligence.
Introduction to Microwave Acid Decomposition. PB90-118191 900,227	tor Mass Spectrometry, and Laser Microprobe Mass Spectrometry.	PB89-201214 901,28.
Microwave Digestion of Biological Samples: Selenium Analysis by Electrothermal Atomic Absorption Spectrometry.	PB90-136540 <i>900,236</i> KLUGE, H.	KRASINSKI, J. Two-Photon Laser-Induced Fluorescence of the Tumor-Lo
PB89-229116 900,217	International Intercomparison of Neutron Survey Instrument	calizing Photosensitizer Hematoporphyrin Derivative. PB89-157283 901,240
Microwave Energy for Acid Decomposition at Elevated Temperatures and Pressures Using Biological and Botanical	Calibrations. PB89-229165 901,300	KRASNY, J. F.
Samples. PB89-171961 900,359	KNAB, L. I.	Flammability Tests for Industrial Fabrics: Relevance and Limitations.
Monitoring and Predicting Parameters in Microwave Disso-	Method to Measure the Tensile Bond Strength between Two Weakly-Cemented Sand Grains.	PB89-174122 901,09
lution. PB90-118183 900,690	PB89-166110 901,483 Service Life of Concrete.	KRAUSE, R. F. Effect of Coal Slag on the Microstructure and Creep Behav
Neutron Activation Analysis of the NIST (National Institute of Standards and Technology) Bovine Serum Standard Ref-	PB89-215362 901,303	ior of a Magnesium-Chromite Refractory. PB89-158034 901,023
erence Material Using Chemical Separations. PB89-156921 900,180	KOCH, W. F. Determination of the Absolute Specific Conductance of Pri-	Effect of Slag Penetration on the Mechanical Properties o
Preconcentration of Trace Transition Metal and Rare Earth	mary Standard KCl Solutions. PB89-230320 900,481	Refractories: Final Report. PB90-110065 900,836
Elements from Highly Saline Solutions. PB90-118175 900,226	High-Accuracy Differential-Pulse Anodic Stripping Voltam-	Rising Fracture Toughness from the Bending Strength o Indented Alumina Beams.
Safety Guidelines for Microwave Systems in the Analytical Laboratory.	metry Using Indium as an Internal Standard. PB89-176267 900,198	PB89-171771 901,03
PB90-118167 900,689	High-Accuracy Differential-Pulse Anodic Stripping Voltam-	Structural Reliability and Damage Tolerance of Ceramic Composites for High-Temperature Applications. Semi
Voltammetric and Liquid Chromatographic Identification of Organic Products of Microwave-Assisted Wet Ashing of Bi-	metry with Indium as an Internal Standard. PB89-156947 900,182	Annual Progress Report for the Period Ending Septembe 30, 1987.
ological Samples. PB89-157994 900,188	Voltammetric and Liquid Chromatographic Identification of Organic Products of Microwave-Assisted Wet Ashing of Bi-	PB89-156350 901,023
KINRA, V. K.	ological Samples. PB89-157994 900,188	Structural Reliability and Damage Tolerance of Ceramic Composites for High-Temperature Applications. Semi
Dynamic Young's Modulus Measurements in Metallic Materials: Results of an Interlaboratory Testing Program.	KOCZAK, M. J.	Annual Progress Report for the Period Ending March 31 1988. PB89-156368 901,024
PB89-157671 901,132 KIRCHHOFF, W. H.	Mechanical Property Enhancement in Ceramic Matrix Composites.	PB89-156368 901,024 Toughening Mechanisms in Ceramic Composites. Semi
Analytical Expression for Describing Auger Sputter Depth	PB89-189138 901,076	Annual Progress Report for the Period Ending March 31 1989.
Profile Shapes of Interfaces. PB89-157176 900,309	KOEPKE, G. H. Implementation of an Automated System for Measuring Ra-	PB89-235907 901,080
Differential Scanning Calorimetric Study of Brain Clathrin. PB90-117912 900,225	diated Emissions Using a TEM Cell. PB90-117698 901,377	Toughening Mechanisms in Ceramic Composites: Semi- Annual Progress Report for the Period Ending September
Logistic Function Data Analysis Program: LOGIT.	Theory and Measurements of Radiated Emissions Using a	30, 1988. PB89-162606 <i>901,028</i>
PB89-189351 900,418 (IRKPATRICK, T. R.	TEM (Transverse Electromagnetic) Cell. PB89-193890 900,761	KRAUSS, M.
Ergodic Behavior in Supercooled Liquids and in Glasses.	KOIZUMI, H.	Electronic Structure of Diammine (Ascorbato) Platinum(II) and the Trans Influence on the Ligand Dissociation Energy.
PB89-202444 901,435 KISSICK, W. A.	Reduced Dimensionality Quantum Reactive Scattering Study of the Insertion Reaction O(1D) + H2 -> OH +	PB89-147128 900,287
ACSB (Amplitude Companded Sideband): What Is Adequate Performance.	H. PB89-234280 <i>900,492</i>	KRAUSS, R. Thermal Conductivity of Refrigerants in a Wide Range or
PB89-176283 901,599	KONJEVIC, N.	Temperature and Pressure. PB89-226583 900,458
Advances in NIST (National Institute of Standards and Technology) Dielectric Measurement Capability Using a	Stark Broadening of Spectral Lines of Homologous, Doubly lonized Inert Gases.	KREIDER, K. G.
Mode-Filtered Cylindrical Cavity. PB89-231146 900,907	PB89-158083 900,343 KOOL, L. B.	Sputter Deposition of Icosahedral Al-Mn and Al-Mn-Si. PB89-147102 901,122
KITANO, T.	Characterization of Organolead Polymers in Trace Amounts	Sputtered Thin Film Ba2YCu3On. PB89-165427 901,025
Uniaxial Deformation of Rubber Network Chains by Small Angle Neutron Scattering.	by Element-Specific Size-Exclusion Chromatography. PB89-175962 900,196	Thin Film Thermocouples for High Temperature Measure-
PB89-175830 901,088 (IVINEVA, E.	KOPANSKI, J. J.	ment.` PB89-209290 901,065
Influence of Molybdenum on the Strength and Toughness of Stainless Steel Welds for Cryogenic Service.	Experimental Verification of the Relation between Two- Probe and Four-Probe Resistances. PB89-231211 900.794	Thin Film Thermocouples for Internal Combustion Engines. PB89-147094 900.607
OF CIGHTIESS STEEL TYEIRS IN CITYOUGHIC SETVICE.	1 500.794	, 203-17,007 900,007

					,
REILICK, T. S.	vial for Fire File	PB89-157341	900,320	PB90-123431	901,165
Magnetic Evaluation of Cu-Mn Matrix Mate ment Nb-Ti Superconductors.		LAGNESE, J. Estimates of Confidence Intervals for	Divider Distorted	LASHMORE, D. S. Electrodeposition of Chromium from a Trivaler	nt Electrolyte
PB89-200489 REMER, D. P.	901,425	Waveforms. PB89-173447	900,806	PATENT-4 804 446	901,119
Antenna Measurements for Millimeter Wave	es at the Nation-	LAMBERT, G. M.	550,555	Magnetic Behavior of Compositionally Mod Thin Films.	Julated Ni-Cu
al Bureau of Standards. PB89-150726	900,694	Determination of Selenium and Tellurium and Reference Materials Using Stable		PB90-118084	901,163
Calibrating Antenna Standards Using CW	and Pulsed-CW	Spark Source Mass Spectrometry. PB90-123472	900,230	LAU, K. C. Optical Sensors for Robot Performance Test	ting and Cali-
Measurements and the Planar Near-Field M PB89-149280	lethod. <i>900,693</i>	LANDIS, H. J.	900,230	bration.	
RIZ, R. D.		Rotational Modulation and Flares on RS		PB89-157358 LAUENSTEIN, G. G.	900,987
Edge Stresses in Woven Laminates at Low PB90-128265	Temperatures. 901,082	Stars IX. IUE (International Ultraviolet Expl py and Photometry of II Peg and V711 Tau	during February	Specimen Banking in the National Status and	
Measuring In-Plane Elastic Moduli of C		1983. PB89-171615	900,019	gram: Development of Protocols and First Yea PB89-175855	r Results. <i>901,308</i>
Arrays of Phase-Insensitive Ultrasound Rec PB90-136672	900,970	LANDRY, M. R.	01.1.1.0.11	LAUG, O.	
Performance of Alumina/Epoxy Thermal Iso PB89-147078	olation Straps. 901,070	Uniaxial Deformation of Rubber Network Angle Neutron Scattering.		Drift Tubes for Characterizing Atmospheric Spectra.	Ion Mobility
RUSKAL, C. P.	301,070	PB89-175830 LANGHOFF, P. W.	901,088	PB90-128513	901,585
Definitions of Granularity. PB89-180012	900,650	Absolute Cross Sections for Molecular		Drift Tubes for Characterizing Atmospheric Spectra Using AC, AC-Pulse, and Pulse	
Notion of Granularity.	900,030	Partial Photoionization, and Ionic Photofra ess.	gmentation Proc-	Measurement Techniques. PB89-202543	900,438
PB89-147003	900,915	PB89-186464	900,410	LAUG, O. B.	000,100
UENTZLER, R. Electronic, Magnetic, Superconducting a	nd Amorphous-	LANKFORD, J. Creep Cavitation in Liquid-Phase Sintered A	Alumina.	Electrical Performance Tests for Hand-Held meters.	Digital Multi-
Forming Properties Versus Stability of the	Ti-Fe, Zr-Ru and	PB89-175954	901,038	PB89-162234	900,876
Hf-Os Ordered Alloys. PB89-146690	901,120	LAPICKI, G. Cross Sections for K-Shell X-ray Product	ion by Hydrogen	LAVILLA, R. E.	
ULKARNI, A. K.		and Helium lons in Elements from Berylliun PB89-226609		Near-Threshold X-ray Fluorescence Spectrosc cules.	copy of Mole-
Upward Flame Spread on Vertical Walls. PB89-214787	900,141	LARCHE, F. C.	300,400	PB89-176523	900,382
ULKARNI, S. V.		Stress Effects on III-V Solid-Liquid Equilibri: PB89-146997	a. <i>900,769</i>	LAWN, B. R. Effect of Heat Treatment on Crack-Resistance	e Curves in a
Method for Measuring the Stochastic Prop- and Partial-Discharge Pulses.		LAROCK, J. G.	900,769	Liquid-Phase-Sintered Alumina. PB89-229231	901,056
PB90-128745 URODA, K.	900,829	Small Angle Neutron Scattering Spectron	neter at the Na-	Flaw Tolerance in Ceramics with Rising Crac	
Precision Experiments to Search for the Fift	th Force.	tional Bureau of Standards. PB89-158158	901,396	Characteristics. PB90-128026	901,060
PB89-228365	901,551	LARRABEE, R. D.	Managements	Grain-Size and R-Curve Effects in the Abra	-
JRTZ, R. Synchrotron Radiation Study of BaO Films	on W(001) and	AC Impedance Method for High-Resistivit of Silicon.		Alumina. PB90-117383	901,058
Their Interaction with H2O, CO2, and O2. PB89-157697	900,252	PB89-231203 Approach to Accurate X-Ray Mask Mea	900,793	LAWRENCE, J.	•
URTZ, R. L.	010,232	Scanning Electron Microscope.		Finite Unions of Closed Subgroups of the r Torus.	n-Dimensional
Resonant Excitation of an Oxygen Valence toemission from High-T(sub c) Superconduct	Satellite in Pho-	PB89-172555 Specimen Biasing to Enhance or Suppress	900,776 Secondary Flec-	PB89-143283	901,193
PB89-186860	901,420	tron Emission from Charging Specimens a		Polytope Volume Computation. PB90-129982	901,203
Secondary-Electron Effects in Photon-Stin tion.	nulated Desorp-	ing Voltages. PB89-228464	901,451	LAWTON, R. A.	001,200
PB89-157929	900,337	Submicrometer Optical Metrology. PB89-150973	900,771	Two-Layer Dielectric Microstrip Line Structure	: SiO2 on Si
JRYLO, M. J. Flash Photolysis Kinetic Absorption Spectro	oscopy Study of	LARSEN, E. B.	200,777	and GaAs on Si; Modeling and Measurement. PB89-156780	900,738
the Gas Phase Reaction HO2 + C2H5O2 perature Range 228-380 K.	Over the Tem-	Alternative Techniques for Some Typical N Types of Measurements.	MIL-STD-461/462	LAYER, H. P.	
PB90-136565	900,536	PB89-235139	901,272	Low Field Determination of the Proton Gyrom in Water.	
Rate Constants for the Reaction HO2+ HO2NO2+ N2: The Temperature Depende		LARSEN, N. T. Microwave Power Standards.		PB89-230411 New Realization of the Ohm and Farad Using	901,555
Off Parameters. PB89-146658	900,278	PB89-149272	900,687	tional Bureau of Standards) Calculable Capacit	tor.
Temperature Dependence of the Rate Cons		Transient Response Error in Microwave Using Thermistor Detectors.	Power Meters	PB89-230445 LECHNER, J. A.	901,557
droperoxy + Methylperoxy Gas-Phase Rea PB90-136375		PB89-173785	900,759	Effect of an Oil-Paper Interface Parallel to an	Electric Field
JYATT, C. E.	200,007	LARSON, D. J. Ion Trapping Techniques: Laser Cooling	and Sympathetic	on the Breakdown Voltage at Elevated Temper PB89-156988	ratures. 901,490
Center for Radiation Research (of the Nati Standards and Technology) Technical Activi	ional Institute of	Cooling. PB90-128034		Preliminary Stochastic Model for Service Life	Prediction of
PB90-130279	901,307	Perpendicular Laser Cooling of a Rotating	901,578 Ion Plasma in a	a Photolytically and Thermally Degraded Pol Plate Material.	ymeric Cover
WELLER, E. R. Combustion Testing Methods for Catalytic H	leaters	Penning Trap. PB89-157408	901,493	PB89-173801	900,556
PB89-150924	900,846	LARSON, D. R.	001,400	LEDBETTER, H. Fourth-Order Elastic Constants of beta-Brass.	
Part Load, Seasonal Efficiency Test Proce of Furnace Cycle Controllers.	edure Evaluation	Fast Optical Detector Deposited on Dielec veguides.	tric Channel Wa-	PB90-117607	901,160
PB89-212146	900,848	PB89-171706	900,743	Gruneisen Parameter of Y1Ba2Cu3O7. PB90-117615	901,465
ADBURY, J. M. Mode-Stirred Chamber for Measuring Shi	elding Effectives	Picosecond Pulse Response from Hydr phous Silicon (a-Si:H) Optical Detectors or		LEDBETTER, H. M.	
ness of Cables and Connectors: An Asse STD-1344A Method 3008.	essment of MIL-	guides. PB89-176689	900,727	Hysteretic Phase Transition in Y1Ba2Cu3O7 ductors.	-x Supercon-
PB89-149264	900,737	System for Measuring Optical Waveguide In		PB89-229082	901,454
ADD, R. S.	- d- D	PB89-188593	900,751	Low-Temperature Phase and Magnetic Intera Fe-Cr-Ni Alloys.	actions in fcc
Pore-Water Pressure Buildup in Clean Sa Cyclic Straining.		Waveguide Loss Measurement Using Photition.	tothermal Deflec-	PB90-136771	901,113
PB89-175723 AFEMINA, J. P.	900,159	PB89-157028	900,739	Molybdenum Effect on Volume in Fe-Cr-Ni Allo PB89-157796	oys. 901,095
Qualitative MO Theory of Some Ring and Li	adder Polymers.	LARSON, L. E. System for Measuring Optical Waveguide II		Reentrant Softening in Perovskite Supercondu	ctors.
PB89-156723 AFFERTY, W.	900,303	PB89-188593	900,751	PB90-117540 LEE, A.	901,464
Far-Infrared Spectrum of Methyl Amine.	Assignment and	Waveguide Loss Measurement Using Photion.		In Situ Fluorescence Monitoring of the Viscos	sities of Parti-
Analysis of the First Torsional State. PB89-161574	900,346	PB89-157028 LARSON, T. M.	900,739	cle-Filled Polymers in Flow. PB89-146278	900,609
AFFERTY, W. J.		High T(sub c) Superconductor/Noble-Met	al Contacts with	LEE, C. H.	223,000
High Resolution Spectrum of the nu(sub 1 Band of NO2. A Spin Induced Perturbation	1) + nu(sub 2) n in the Ground	Surface Resistivities in the (10 to the Mi Omega sq cm Range.	nus 10th Power)	Oligomers with Pendant Isocyanate Groups for Dentin and Other Tissues.	as Adhesives
State. PB89-187561	900,417	PB89-179824	901,413	PB89-179253	900,042
Infrared and Microwave Investigations of		LASHMORE, D. Magnetization and Magnetic Aftereffect in	Textured Ni/Cu	Oligomers with Pendant Isocyanate Groups a hesives. 1. Synthesis and Characterization.	s Tissue Ad-
Tunneling in the Acetylene Dimer.		Compositionally-Modulated Alloys.		PB89-202212	900,055

Oligomers with Pendant Isocyanate Groups as Tissue Ad-	PB89-171599 <i>901,401</i>	PB89-171755 901,310
hesives. 2. Adhesion to Bone and Other Tissues. PB89-231245 900,056	Alignment Effects in Ca-He(5(sup 1)P(sub 1) - 5(sup	NIST Automated Computer Time Service.
LEE, J. D.	 P(sub J)) Energy Transfer Collisions by Far Wing Laser Scattering. 	PB90-213711 900,676
Robot Crane Technology. PB90-111667 900,146	PB89-179790 900,400	Tilt Observations Using Borehole Tiltmeters 1. Analysis of Tidal and Secular Tilt.
LEE, K.	Alignment Effects in Electronic Energy Transfer and Reactive Events.	PB90-136649 901,283
Inventory of Equipment in the Turning Workstation of the AMRF (Automated Manufacturing Research Facility).	AD-A202 820/7 900,267	LEVINE, S. Draft International Document on Guide to Portable Instru-
PB89-215339 900,961	Initial Stages of Heteroepitaxial Growth of InAs on Si(100). PB90-123878 901,473	ments for Assessing Airborne Pollutants Arising from Haz- ardous Wastes.
Recommended Technical Specifications for Procurement of Equipment for a Turning Workstation.	Interaction of In Atom Spin-Orbit States with Si(100) Sur-	PB89-150775 900,855
PB89-215347 900,962	faces. PB90-128547 900,532	LEVIS, R. J.
Turning Workstation in the AMRF (Automated Manufacturing Research Escilibit)	Laser-Induced Fluorescence Study of Product Rotational	Observation of Translationally Hot, Rotationally Cold NO Molecules Produced by 193-nm Laser Vaporization of Multi-
ing Research Facility). PB89-185607 900,954	State Distributions in the Charge Transfer Reaction: $Ar(1+)((\sup 2 P)(\sup 3/2)) + N2 \rightarrow Ar + N2(1+)(X)$ at 0.28	layer NO Films.
LEE, K. S.	and 0.40 eV. PB89-189823 900,420	PB89-234264 900,491 LEW, H. S.
Effect of Multiple Internal Reflections on the Stability of Electrooptic and Magnetooptic Sensors.	Laser Probing of Ion Velocity Distributions in Drift Fields:	Guidelines for Identification and Mitigation of Seismically
PB89-171722 900,724	Parallel and Perpendicular Temperatures and Mobility for Ba(1+) in He.	Hazardous Existing Federal Buildings. PB89-188627 900,161
Optical Fiber Sensors for Electromagnetic Quantities. PB89-173967 900,725	PB89-171243 900,352	Static Tests of One-third Scale Impact Limiters.
Optical Fiber Sensors for the Measurement of Electromag-	Laser Probing of Product-State Distributions in Thermal- Energy Ion-Molecule Reactions.	PB89-216469 901,000
netic Quantities. PB89-176671 <i>900,748</i>	PB89-171250 900,353	LEWIS, L. A.
LEE, S. A.	Laser Probing of the Dynamics of Ga Interactions on Si(100).	Application of Magnetic Resonance Imaging to Visualization of Flow in Porous Media.
Fundamental Tests of Special Relativity and the Isotropy of Space.	PB89-186928 901,422	PB89-179592 <i>901,329</i>
PB89-185920 901,523	Observation of Translationally Hot, Rotationally Cold NO Molecules Produced by 193-nm Laser Vaporization of Multi-	LEWIS, R. L. Efficient and Accurate Method for Calculating and Repre-
LEE, S. H.	layer NO Films.	senting Power Density in the Near Zone of Microwave An-
Molecular Dynamics Study of a Dipolar Fluid between Charged Plates.	PB89-234264 900,491	tennas. PB89-157457 <i>900,707</i>
PB89-147441 900,290	Photodissociation Dynamics of C2H2 at 193 nm: Vibrational Distributions of the CCH Radical and the Rotational State	Improved Spherical and Hemispherical Scanning Algo-
Molecular Dynamics Study of a Dipolar Fluid between Charged Plates. 2.	Distribution of the A(010) State by Time-Resolved Fourier Transform Infrared Emission.	rithms. PB89-156806 900,697
PB89-157218 900,312	PB89-179782 900,258	Iterative Technique to Correct Probe Position Errors in
LEE, V. Turning Workstation in the AMRF (Automated Manufactur-	Production of 0.1-3 eV Reactive Molecules by Laser Vapori- zation of Condensed Molecular Films: A Potential Source	Planar Near-Field to Far-Field Transformations. PB89-153886 900,695
ing Research Facility). PB89-185607 900,954	for Beam-Surface Interactions. PB89-171201 900,254	Spherical-Wave Source-Scattering Matrix Analysis of Cou-
LEEDY, T. F.	Quenching and Energy Transfer Processes of Single Rota-	pled Antennas: A General System Two-Port Solution. PB89-156798 900,696
Electrical Performance Tests for Hand-Held Digital Multi-	tional Levels of Br2 B triplet Pi(O(sub u)(+)) v'= 24 with	LI, W.
meters. PB89-162234 900,876	Ar under Single Collision Conditions. PB89-179766 900,399	Real Time Generation of Smooth Curves Using Local Cubic
Selecting Varistor Clamping Voltage: Lower Is Not Better.	Surface Structure and Growth Mechanism of Ga on Si(100).	Segments. PB89-171623 901,196
PB89-176648 900,760 LEFRANT, S.	PB89-149181 901,387 Surface Structures and Growth Mechanism of Ga on	LI, W. H.
Influence of Molecular Weight on the Resonant Raman	Si(100) Determined by LEED (Low Energy Electron Diffrac-	Antiferromagnetic Structure and Crystal Field Splittings in
Scattering of Polyacetylene. PB89-179246 900,564	tion) and Auger Electron Spectroscopy. PB89-171342 901,399	the Cubic Heusler Alloys HoPd2Sn and ErPd2Sn. PB89-202659 901,437
Resonant Raman Scattering of Controlled Molecular Weight	Time-of-Flight Measurements of Hyperthermal CI(sub 2)	Magnetic Order of Pr in PrBa2Cu3O7.
Polyacetylene. PB89-157093 900,548	Molecules Produced by UV Laser Vaporization of Cryogenic Chlorine Films.	PB90-123803 901,471 Pressure Dependence of the Cu Magnetic Order in
LEHMAN, J.	PB89-202634 900,260	RBa2Cu3O6+ x.
Cool It.	Time-Resolved FTIR Emission Studies of Molecular Photo- fragmentation.	PB90-123829 901,472
PB89-176986 901,516 LEICHNITZ, K.	PB89-202642 900,261	LI, X. Potential Errors in the Use of Optical Fiber Power Meters.
Draft International Document on Guide to Portable Instru-	Time-Resolved FTIR Emission Studies of Molecular Photo- fragmentation Initiated by a High Repetition Rate Excimer	PB89-176697 900,728
ments for Assessing Airborne Pollutants Arising from Haz- ardous Wastes.	Laser. PB90-136680 900,266	LI, Y.
PB89-150775 900,855	LEOPOLD, K. R.	Interlaboratory Determination of the Calibration Factor for the Measurement of the Interstitial Oxygen Content of Sili-
LEIFER, R. Detection of Uranium from Cosmos-1402 in the Strato-	Frequency Measurement of the $J = 1 < -0$ Rotational	con by Infrared Absorption. PB90-117300 900,224
sphere.	Transition of HD (Hydrogen Deutende). PB89-161566 901,499	Oxygen Isotope Effect in the Superconducting Bi-Sr-Ca-Cu-
PB89-156962 901,592 LEIGH, S. D.	LESK, A. M.	O System. PB89-157044 901,025
Continuum Radiation Produced in Pure-Element Targets by	Computational Analysis of Protein Structures: Sources, Methods, Systems and Results.	Resistance Measurements of High T(sub c) Superconduc-
10-40 keV Electrons: An Empirical Model. PB89-201610 900,209	PB89-175293 900,010	tors Using a Novel 'Bathysphere' Cryostat. PB89-228431 901,448
Modeling of the Bremsstrahlung Radiation Produced in	LETTIERI, T. R. Resonance Light Scattering from a Liquid Suspension of	Li, Y. K.
Pure Element Targets by 10-40 keV Electrons. PB89-201644 901,531	Microspheres.	Cryogenic Bathysphere for Rapid Variable-Temperature
LEITHERER, C.	PB89-157887 901,340 Resonance Light Scattering from a Suspension of Micros-	Characterization of High-T(sub c) Superconductors. PB89-228456 901,450
Interpretation of Emission Wings of Balmer Lines in Luminous Blue Variables.	pheres.	LIAS, S. G.
PB89-212054 900,023	PB89-176234 901,352 LEVELT SENGERS, J. M. H.	Gas Phase Proton Affinities and Basicities of Molecules: A
LELAND, T. W.	Decorated Lattice Gas Model for Supercritical Solubility.	Comparison between Theory and Experiment. 900,280
Method for Improving Equations of State Near the Critical Point.	PB89-175681 900,373	Ion Kinetics and Energetics.
PB89-228027 901,547	Gas Solubility and Henry's Law Near the Solvent's Critical Point.	PB89-176101 900,377
LEMMENS, J. W. Dynamic Young's Modulus Measurements in Metallic Mate-	PB89-202485 900,434	Numeric Databases for Chemical Analysis. PB89-175236 900,194
nals: Results of an Interlaboratory Testing Program.	NaCI-H2O Coexistence Curve Near the Critical Tempera- ture of H2O.	LIBES, D.
PB89-157671 901,132 LENNON, E. B.	PB89-202519 900,436	Modeling Dynamic Surfaces with Octrees. PB90-112335 901,206
Conference Reports: National Computer Security Confer-	Van der Waals Fund, Van der Waals Laboratory and Dutch High-Pressure Science.	LICITRA, B. A.
ence (11th). Held in Baltimore, MD. on October 17-20, 1988.	PB89-185755 900,401	Thermal Resistance Measurements and Calculations of an
PB89-235675 900,672	LEVIN, B. C. Superpictic Effects of Nitrogen Digwide and Carbon Digwide	Insulated Concrete Block Wall. PB89-174916 900,119
LENTNER, K. J. Electrical Performance Tests for Hand-Held Digital Multi-	Synergistic Effects of Nitrogen Dioxide and Carbon Dioxide Following Acute Inhalation Exposures in Rats.	LIDE, D. R.
meters.	PB89-214779 900,856	Chemical and Spectral Databases: A Look into the Future.
PB89-162234 900,876 LEONE, S. R.	Toxicity of Mixed Gases Found in Fires. PB89-212047 900,869	PB89-180038 900,579 Journal of Physical and Chemical Reference Data, Volume
AES and LEED Studies Correlating Desorption Energies	LEVINE, J.	17, Number 1, 1988.
with Surface Structures and Coverages for Ga on Si(100).	Gravity Tide Measurements with a Feedback Gravity Meter.	PB89-186449 900,408

Journal of Physical and Chemical Reference Data, Volum	Automatic Generation of Test Scenario (Skeletons) from Protocol-Specifications Written in Estelle.	PB89-176432 900,88
18, Number 1, 1989. PB89-226559 900,4.	55 PB89-177125 900,615	LODGE, T. P. Uniaxial Deformation of Rubber Network Chains by Sma
Journal of Physical and Chemical Reference Data, Volun 18, Number 2, 1989.	Semi-Automated PVT Facility for Fluids and Fluid Mixtures.	Angle Neutron Scattering. PB89-175830 901,08
PB89-222525 900,4- Journal of Physical and Chemical Reference Data, Volun	1 200 101.01	LOEVINGER, R.
18, Number 3, 1989. PB90-126236 900,5.	Donnler Imaging of AR Lacertae at Three Enochs	NBS (National Bureau of Standards) Measurement Services: Calibration of Gamma-Ray-Emitting Brachytherap
Shimanouchi, Takehiko and the Codification of Spectrosc		Sources. PB89-193858 901,24
pic Information. PB89-157846 900,3	95 Gemino:um. PB89-228373 900,024	LOFTUS, T. P.
IGARE, M.	Rotational Modulation and Flares on RS Canum Venati-	NBS (National Bureau of Standards) Measurement Serv
Resonance-Enhanced Multiphoton Ionization of Atomic H drogen.	y- corum and BY Draconis Stars X: The 1981 October 3 Flare on V711 Tauri (= HR 1099).	ices: Calibration of Gamma-Ray-Emitting Brachytherap Sources.
PB89-201073 901,5	²⁹ PB89-202618 900,021	PB89-193858 901,24
IGGETT, W.	Rotational Modulation and Flares on RS Canum Venati- corum and E7 Draconis Stars. XI. Ultraviolet Spectral	LONG, F. G.
Bootstrap Inference for Replicated Experiments. PB90-128273 900,9	Images of AR Lacertae in September 1985.	Low Range Flowmeters for Use with Vacuum and Lea Standards.
Estimation of an Asymmetrical Density from Several Smannes.	PB89-234298 900,026 Rotational Modulation and Flares on RS CVn and BY Dra	PB89-175707 900,37
PB89-201131 901,2		LONG, G. R.
Estimation of the Error Probability Density from Replica Measurements on Several Items.	1983.	Detection of Gas Phase Methoxy Radicals by Resonanc Enhanced Multiphoton Ionization Spectroscopy.
PB89-157820 901,2	PB89-171615 900,019 Solar and Stellar Magnetic Fields and Structures: Observa-	PB89-156764 900,30
Tests of the Recalibration Period of a Drifting Instrument. PB89-176275 900,18	tions.	LOONEY, J. P.
IGGETT, W. S.	PB90-118118 900,027 LIPE, T. E.	High Resolution Inverse Raman Spectroscopy of the CO (Branch.
Designs for Assessment of Measurement Uncertainty: E	NIST (National Institute of Standards and Technology)	PB89-171292 900,35
perience in the Eastern Lake Survey. PB89-173827 900,86	Measurement Services: AC-DC Difference Calibrations. PB89-222616 900,818	LOUIE, B.
IGHTFOOT, H. A.	Recharacterization of Thermal Voltage Converters After	Measurement of Regenerator Ineffectiveness at Low Temperatures.
International Comparison of HV Impulse Measuring Sytems.	Thermoelement Replacement. PB89-230452 900,720	PB89-173884 901,00
PB89-186423 900,86		LOVAS, F. J.
ILLIENFELD, P.	AutoMan: Decision Support Software for Automated Manufacturing Investments. User's Manual.	Electric-Dipole Moments of H2O-Formamide and CH3OF Formamide.
Draft International Document on Guide to Portable Instruments for Assessing Airborne Pollutants Arising from Ha		PB89-147375 900,20
ardous Wastes. PB89-150775 900,8	Energy Prices and Discount Factors for Life-Cycle Cost	Infrared and Microwave Investigations of Interconversio Tunneling in the Acetylene Dimer.
IN, C.	Bureau of Standards) Handbook 135 and NBS Special Pub-	PB89-157341 900,32
Development of a Method to Measure In situ Chloride	at lication 709. PB89-153860 900,850	Laboratory Measurement of the 1(sub 01)-0(sub 00) Trans tion and Electric Dipole Moment of SiC2.
the Coating/Metal Interface. PB89-235345 901,00	5 LIPPMAN, S.	PB89-228506 900,02
IN, I. H.	Line Identifications and Radiative-Branching Ratios of Mag- netic Dipole Lines in Si-like Ni, Cu, Zn, Ge, and Se.	Microwave Spectral Tables. 3. Hydrocarbons, CH t C10H10.
Influence of Dislocation Density on the Ductile-Brittle Tra sition in bcc Metals.	PB89-234165 901,558	PB90-126269 900,53
PB89-157804 901,13	33 LITZEN, U. 4s(2) 4p(2)-4s4p(3) Transition Array and Energy Levels of	Microwave Spectrum and Molecular Structure of the Ethy ene-Ozone van der Waals Complex.
IN, K. C. Alignment Effects in Ca-He(5(sup 1)P(sub 1) - 5(sup 1)P(sub 1) - 5(sub 1)P(sub	the Germanium-Like Ions Rb VI - Mo XI.	PB89-201735 900,42
3)P(sub J)) Energy Transfer Collisions by Far Wing Las	PB89-201065 901,528 Spectra and Energy Levels of the Galliumlike Ions Rb VII-	Microwave Spectrum and (14)N Quadrupole Coupling Cor stants of Carbazole.
Scattering. PB89-179790 900,44	00 Mo XII.	PB89-157333 900,31
IN, Y.	PB89-179105 900,387	Microwave Spectrum, Structure, and Electric Dipol Moment of Ar-Ch3OH.
Effect of Chinese Standardization on U.S. Export Opport nities.	General Methodology for Machine Tool Accuracy Enhance-	PB90-117847 900,51
PB89-166128 900,1	72 ment by Error Compensation. PB89-146781 900,996	Microwave Spectrum, Structure, and Electric Dipol Moment of the Ar-Formamide van der Waals Complex.
INDEMANN, T. G. Slit Jet Infrared Spectroscopy of NeHF Complexes: Interr	Generalized Mathematical Model for Machine Tool Errors.	PB89-157325 900,31
Rotor and J-Dependent Predissociation Dynamics. PB90-118126 900,5.	FB03-130074 300,377	Millimeter- and Submillimeter-Wave Surveys of Orion Emission Lines in the Ranges 200.7-202.3, 203.7-205.3
JINDLE, D. W.	Low Field Determination of the Proton Gyromagnetic Ratio	and 330-360 GHz. PB90-123787 900,02
Near-Threshold X-ray Fluorescence Spectroscopy of Mol	in Water. e- PB89-230411 <i>901,555</i>	Ozonolysis of Ethylene. Microwave Spectrum, Molecula
cules. PB89-176523 900,30		Structure, and Dipole Moment of Ethylene Primary Ozonid (1,2,3-Trioxolane).
Performance of a High-Energy-Resolution, Tender X-r.	Oxygen Partial-Density-of-States Change in the YBa2Cu3Ox Compounds for x(Approx.)6,6.5,7 Measured by	PB89-157440 900,32
Synchrotron Radiation Beamline. PB90-128083 901,50	30 Soft X-ray Emission.	Structure of the CO2-CO2-H2O van der Waals Comple Determined by Microwave Spectroscopy.
INDSTROM, E.	PB89-186274 901,419 LIVINGSTON, E. M.	PB89-230288 900,47
NBS/NRL (National Bureau of Standards/Naval Researd Laboratory) Free Electron Laser Facility.	Performance Evaluation of Radiofrequency, Microwave, and	LOVEJOY, C. M.
PB89-175749 901,3	Millimeter Wave Power Meters. PB89-193916 900,814	Infrared Spectra of Nitrous Oxide-HF Isomers. PB89-228399 900,47
INDSTROM, R. M.	LLOYD, F. L.	Infrared Spectrum of D2HF.
Activation A. lysis Opportunities Using Cold Neutro Beams.	with a Fourier Transform Spectrometer	PB89-171219 900,35 Infrared Spectrum of NeHF.
PB89-156970 900, 1. INENBERGER, D.	PB89-157051 900,706	PB89-171227 900,35
Measurement of Regenerator Ineffectiveness at Low Te	MM Wave Quasioptical SIS Mixers. PB89-214738 901,446	Intramolecular Dynamics of van der Waals Molecules: A Extended Infrared Study of ArHF.
peratures. PB89-173884 901,0	CIC Overienstiele Misses with Day Tie Antonnes	PB90-118209 900,52
INHOLM, L. W.	PB89-157036 900,705	Slit Jet Infrared Spectroscopy of NeHF Complexes: International Rotor and J-Dependent Predissociation Dynamics.
Machine-Learning Classification Approach for IC Manufa	C- Experience with IMDAS (Integrated Manufacturing Data Ad-	PB90-118126 900,52
turing Control Based on Test Structure Measurements. PB89-228530 900,7	ministration Contam) in the Automated Manufacturing Do	Sub-Doppler Infrared Spectroscopy in Slit Supersonic Jet- A Study of all Three van der Waals Modes in v1-Excite
Neural Network Approach for Classifying Test Structure F	search Facility. e- PB90-112350 <i>900,964</i>	ArHCI.
sults. PB89-212187 900,7	LOCASCIO-BROWN, L.	PB90-123852 900,52
Use of Artificial Intelligence and Microelectronic Test Stru	Liposome-Enhanced Flow Injection Immunoanalysis. PB89-146757 900,036	LOVETT, C. D. Progress Report of the Quality in Automation Project for
tures for Evaluation and Yield Enhancement of Microele tronic Interconnect Systems.	LOCASIO-BROWN, L.	FY88.
PB89-146955 900,7	68 Generic Liposome Reagent for Immunoassays. PB90-123886 901,229	
LINN, R. J. Application of Formal Description Techniques to Confor	LOOKE LW	LOVISA, M. Effects of a Gold Shank-Overlayer on the Field Ion Imagin
ance Evaluation. PB89-211908 900,6	Laboratory Accreditation Systems in the United States,	of Silicon. PB89-175988 901,40

LOW, S. R.	Fields Radiated by Electrostatic Discharges. PB90-128778 901,382	PB89-203004 900,443
Tensile Tests of Type 305 Stainless Steel Mine Sweeping Wire Rope.	Implementation of an Automated System for Measuring Ra-	Synchrotron Radiation Study of BaO Films on W(001) and Their Interaction with H2O, CO2, and O2.
PB90-130287 901,112	diated Emissions Using a TEM Cell.	PB89-157697 900,252
LOWE, J. P. Overliebling MO Theory of Same Bing and Lodder Polymers	PB90-117698 901,377 Techniques for Measuring the Electromagnetic Shielding	MAGEE, J. W.
Qualitative MO Theory of Some Ring and Ladder Polymers. PB89-156723 900,303	Effectiveness of Materials. Part 1. Far-Field Source Simula-	Isochoric (p,v,T) Measurements on CO2 and (0.98 CO2 + 0.02 CH4) from 225 to 400 K and Pressures to 35 MPa.
LOWNEY, J. R.	tion. PB89-161525 900,680	PB89-202493 900,435
AC Impedance Method for High-Resistivity Measurements of Silicon.	Techniques for Measuring the Electromagnetic Shielding	Measurements of Molar Heat Capacity at Constant Volume: Cv,m(xCH4+ (1-x)C2H6' T = 100 to 320 K, p < or =
PB89-231203 900,793	Effectiveness of Materials. Part 2. Near-Field Source Simulation.	35 MPa).
Application of Multiscattering Theory to Impurity Bands in Si:As.	PB89-161533 900,681	PB90-117896 900,844 PVT Relationships in a Carbon Dioxide-Rich Mixture with
PB89-157762 900,334	Theory and Measurements of Radiated Emissions Using a TEM (Transverse Electromagnetic) Cell.	Ethane.
Effects of Doping-Density Gradients on Band-Gap Narrow-	PB89-193890 900,761	PB89-229181 900,478
ing in Silicon and GaAs Devices. PB89-228522 901,453	MA, Y.	MAGRAB, E. B. Vertical Machining Workstation of the AMRF (Automated
LOWRY, R. E.	Structural Unit in Icosahedral MnAISi and MnAI. PB89-157648 901,131	Manufacturing Research Facility): Equipment Integration.
In Situ Fluorescence Monitoring of the Viscosities of Parti-	MACCREHAN, W. A.	PB89-176663 900,950
cle-Filled Polymers in Flow. PB89-146278 900,609	Voltammetric and Liquid Chromatographic Identification of	MAHAJAN, B. M. Assessment of Robotics for Improved Building Operations
LOZIER, D. W.	Organic Products of Microwave-Assisted Wet Ashing of Bi- ological Samples.	and Maintenance.
Solution for Diffusion-Controlled Reaction in a Vortex Field. PB89-176622 900,594	PB89-157994 900,188	PB89-189146 900,092
Supercomputers Need Super Anithmetic.	MACDONALD, A. H. Superlattice Magnetoroton Bands.	Flow Coefficients for Interzonal Natural Convection for Van- ous Apertures.
PB90-130253 900,657	PB89-175970 901,403	PB89-177158 900,069
LUBITZ, P.	MACDONALD, R. A.	Interzonal Natural Convection for Various Aperture Configu- rations.
Magnetization and Magnetic Aftereffect in Textured Ni/Cu Compositionally-Modulated Alloys.	Computer Model of a Porous Medium. PB89-179683 901,188	PB89-176499 900,066
PB90-123431 901,165	MACHLAN, L. A.	Method for Measuring the Effectiveness of Gaseous Contaminant Removal Filters.
LUCATORTO, T. B.	Absolute Isotopic Abundance Ratios and Atomic Weight of	PB89-235899 900,858
Marked Differences in the 3p Photoabsorption between the Cr and Mn(1+) Isoelectronic Pair: Reasons for the Unique	a Reference Sample of Nickel. PB90-163890 900,543	MAHMOODI, P.
Structure Observed in Cr.	Absolute Isotopic Composition and Atomic Weight of Ter-	Dynamic Young's Modulus Measurements in Metallic Materials: Results of an Interlaboratory Testing Program.
PB90-117581 901,562 Resonance Ionization Mass Spectrometry of Mg: The 3pnd	restrial Nickel. PB90-163908 900,544	PB89-157671 901,132
Autoionizing Series.	MACKAY, D. R.	MAI, Y. W.
PB89-150817 900,296	Glossary of Standards-Related Terminology.	Prediction of Tensile Behavior of Strain Softened Composites by Flexural Test Methods.
LUDTKE, P. R. Performance of He II of a Centrifugal Pump with a Jet	PB90-130246 900,986 MACKENZIE, R. A. D.	PB89-147045 900,585
Pump Inducer.	Grain Boundary Characterization in Ni3Al.	MAJKRZAK, C. F.
PB89-229090 <i>901,553</i> LUMIA, R.	PB89-229306 901,156	Applications of Mirrors, Supermirrors and Multilayers at the National Bureau of Standards Cold Neutron Research Fa-
NASA/NBS (National Aeronautics and Space Administra-	Grain Boundary Structure in Ni3Al. PB89-201784 901,150	cility.
tion/National Bureau of Standards) Standard Reference	Grain Boundary Structure in Ni3Al.	PB89-211981 901,540
Model for Telerobot Control System Architecture (NASREM).	PB89-229314 901,157	Calculations and Measurement of the Performance of Converging Neutron Guides.
PB89-193940 901,589	MADDEN, M.	PB89-211999 901,541
Teleoperation and Autonomy for Space Robotics. PB90-123811 901,591	Evidence for the Superconducting Proximity Effect in Junctions between the Surfaces of YBa2CU3Ox Thin Films.	MAJURSKI, W. J. Compensating for Vowel Coarticulation in Continuous
LUNDY, D. R.	PB89-228449 901,449	Speech Recognition.
Brief Review of Recent Superconductivity Research at	MADEY, T. E. Adsorption of Water on Clean and Oxygen-Predosed	PB89-176721 900,634
NIST (National Institute of Standards and Technology). PB89-211114 900,766	Nickel(110).	MAKI, A. G. Calibration Tables Covering the 1460- to 1550-cm(-1)
LYKKE, K. R.	PB90-123555 900,522 Adsorption Properties of Pt Films on W(110).	Region from Heterodyne Frequency Measurements on the
Simple F-Center Laser Spectrometer for Continuous Single Frequency Scans.	PB89-146864 900,281	nu(sub 3) Bands of (12)CS2 and (13)CS2. PB89-157416 900,322
PB89-179774 901,358	Ammonia Adsorption and Dissociation on a Stepped Iron(s)	Heterodyne Frequency and Fourier Transform Spectrosco-
LYMAN, J. L.	(100) Surface. PB90-123563 900,523	py Measurements on OCS Near 1700 cm(-1). PB90-117805 900,507
Thermodynamic Properties of Dioxygen Difluoride (O2F2) and Dioxygen Fluoride (O2F).	Chemisorption of HF (Hydrofluonc Acid) on Silicon Sur-	Heterodyne Measurements on N2O Near 1635 cm(-1).
PB89-222566 900,452	faces. PB89-212013 900,445	PB90-117797 900,506
LYNN, J. W.	Coadsorption of Water and Lithium on the Ru(001) Surface.	Heterodyne Measurements on OCS Near 1372 cm(-1), PB89-201743 900,425
Antiferromagnetic Structure and Crystal Field Splittings in the Cubic Heusler Alloys HoPd2Sn and ErPd2Sn.	PB89-202956 900,440	Infrared Spectrum of Sodium Hydride.
PB89-202659 901,437	Electron and Photon Stimulated Desorption: Benefits and Difficulties.	PB89-230296 900,480
Magnetic Order of Pr in PrBa2Cu3O7. PB90-123803 901,471	PB89-200745 901,427	Infrared Spectrum of the nu6, nu7, and nu8 Bands of HNO3.
Pressure Dependence of the Cu Magnetic Order in	Electron and Photon Stimulated Desorption: Probes of Structure and Bonding at Surfaces.	PB89-172415 900,362
RBa2Cu3O6 + x. PB90-123829 901,472	PB89-157960 901,116	Infrared Spectrum of the 1205-cm(-1) Band of HNO3. PB89-228514 900,475
LYON, G.	Electron-Stimulated-Desorption Ion-Angular Distributions. PB89-201230 901,430	MAKI, J. T.
Design Factors for Parallel Processing Benchmarks.	Influence of Electronic and Geometric Structure on Desorp-	Analytical Applications of Neutron Depth Profiling.
PB89-186845 900,637	tion Kinetics of Isoelectronic Polar Molecules: NH3 and	PB89-146872 901,294
Design Factors for Parallel Processing Benchmarks. PB90-117672 900,644	H2O. PB89-176473 900,381	MALLARD, W. G.
LYON, G. E.	Interaction of Oxygen and Platinum on W(110).	Reactions of Phenyl Radicals with Ethene, Ethyne, and Benzene.
Architecturally-Focused Benchmarks with a Communication	PB89-231302 901,158	PB89-150908 900,297
Example. PB89-216477 900,640	Interaction of Water with Solid Surfaces: Fundamental Aspects.	MANDEL, J. Consensus Values, Regressions, and Weighting Factors.
Hybrid Structures for Simple Computer Performance Esti-	PB89-201081 900,421	PB89-211130 901,213
mates. PB89-189161 900,639	Methodology for Electron Stimulated Desorption Ion Angular Distributions of Negative Ions.	MANDERS, W.
Processing Rate Sensitivities of a Heterogeneous Multi-	PB89-231310 900,486	Combustion of Oil on Water. PB89-149173 900,587
processor. PB89-229017 900,641	Oxygen Chemisorption on Cr(110): 1. Dissociative Adsorp-	Combustion of Oil on Water. November 1987.
MA, H.	tion. PB89-202980 900,441	PB89-185581 900,863
Advances in the Use of (3)He in a Gas Scintillation	Oxygen Chemisorption on Cr(110): 2. Evidence for Molecu-	MANGIN, P.
Counter. PB90-123506 901,565	lar Ö2(ads). PB89-202998 900,442	Re-Entrant Spin-Glass Properties of a-(FexCr1-x)75P15C10. PB89-157481 901,391
MA, M. T.	Secondary-Electron Effects in Photon-Stimulated Desorp-	MANGUM, B. W.
Automated TEM (Transverse Electromagnetic) Cell for	tion. PB89-157929 <i>900,337</i>	Development of New Standard Reference Materials for Use
Measuring Unintentional EM Emissions. PB89-173769 900,682	Stimulated Desorption from CO Chemisorbed on Cr(110).	in Thermometry. PB89-201180 900,893

				MAXIMON, L. C.
New International Temperature Scale of 1990 (ITS		PB89-235865	900,162	PB89-176184 900,683
PB89-202550 Preparation of Multistage Zone-Refined Materials	901,238	MARTIN, D. F. NRS (National Burgay of Standards) Orific	o Flow Primary	MASTERSON, K. D.
mochemical Standards. PB89-186795	900,203	NBS (National Bureau of Standards) Orific High Vacuum Standard. PB89-175699	900,880	Broadband, Isotropic, Photonic Electric-Field Meter for Measurements from 10 kHz to above 1 GHz. PB90-128281 900,686
IANKA, M. J. Rate Constants for Hydrogen Abstraction by R	esonance	MARTIN, G. A. Journal of Physical and Chemical Reference		Photonic Electric-Field Probe for Frequencies up to 2 GHz. PB89-229207 900,732
Stabilized Radicals in High Temperature Liquids. PB89-161608	900,348	17, 1988, Supplement No. 3. Atomic Transit Scandium through Manganese. PB89-145197	900,276	MASUI, Y.
IANKIEWICH, P. M. Switching Noise in YBa2Cu3Ox 'Macrobridges'.		MARTIN, J.		Preliminary Crystallographic Study of Recombinant Human Interleukin 1beta. PB90-136730 901,251
PB89-200513	901,426	Preliminary Stochastic Model for Service Li a Photolytically and Thermally Degraded F	fe Prediction of Polymeric Cover	MASYS, D. R.
Atomic-lon Coulomb Clusters in an Ion Trap.		Plate Material. PB89-173801	900,556	New Directions in Bioinformatics.
PB89-157424 IANSOORI, G. A.	901,494	Relationship between Appearance and Prote	ective Durability	PB89-175269 901,245
Bioseparations: Design and Engineering of Partition	oning Sys-	of Coatings: A Literature Review. PB89-162598	901,063	MATHEY, R. G. Brick Masonry: U.S. Office Building in Moscow.
tems. PB90-136763	901,231	MARTIN, J. W. Fractal-Based Description of the Roughn	ess of Blasted	PB89-187504 900,160 Friability of Spray-Applied Fireproofing and Thermal Insula-
Mean Density Approximation and Hard Sphere I Theory: A Review.	Expansion	Steel Panels. PB89-158018	901,096	tions: Field Evaluation of Prototype Test Devices. PB89-189328 900,130
PB89-228019	901,546	Thermal Degradation of Poly (methyl metha	•	Set Time Control Studies of Polymer Concrete.
IARANS, R. W. Evaluating Office Lighting Environments: Seco	nd Level	to 125C. PB89-157465	900,549	PB90-111238 901,057
Analysis. PB89-189153	900,073	Thermographic Imaging and Computer Imag	e Processing of	MATSON, L. E. Microarcsecond Optical Astrometry: An Instrument and Its
IARBURY, G.	300,073	Defects in Building Materials. PB89-176309	900,123	Astrophysical Applications. PB89-171268 900,013
Spectroelectrochemistry of a System Involving secutive Electron-Transfer Reaction.	Two Con-	MARTINEZ, R. I. Instrument-Independent MS/MS Database	for XOO Instru-	MATSUMURA, K.
PB90-136979	900,237	ments: A Kinetics-Based Measurement Proto PB90-213695		Laboratory Measurement of the 1(sub 01)-0(sub 00) Transi-
IARCHIANDO, J. F. Semiconductor Measurement Technology: A Soft	ware Pro-	New Photolytic Source of Dioxymethylenes		tion and Electric Dipole Moment of SiC2. PB89-228506 900,025
gram for Aiding the Analysis of Ellipsometric ments, Simple Models.		mediates Without Ozonolysis. PB89-156731	900,304	MATSUSHITA, Y.
PB89-235923	901,369	Stopped-Flow Studies of the Mechanisms o		Phase Contrast Matching in Lamellar Structures Composed of Mixtures of Labeled and Unlabeled Block Copolymer for
IARDOLCAR, U. V. Thermal Conductivity of Liquid Argon for Tempera	atures be-	Reactions in the Gas Phase: Tetramethyleth PB89-157515	900,326	Small-Angle Neutron Scattering. PB89-157119 901,182
tween 110 and 140 K with Pressures to 70 MPa. PB89-179600	900,394	Validation of Absolute Target Thickness C QQQ Instrument by Measuring Absolute To		Temperature, Composition and Molecular-Weight Depend-
IARECI, T. H.	000,007	tions of NE(1+) (NE,NE)NE(1+). PB89-157507	900,325	ence of the Binary Interaction Parameter of Polystyrene/ Poly(vinylmethylether) Blends.
Application of Magnetic Resonance Imaging to Vis of Flow in Porous Media.	sualization	MARTIRE, D. E.	000,020	PB89-157473 900,550 MATTHIAS, C. L.
PB89-179592	901,329	Determination of Hydrocarbon/Water Partit from Chromatographic Data and Based on	ion Coefficients Solution Ther-	Determination of Ultratrace Concentrations of Butyltin Com-
IAREZIO, M. Crystal Chemistry of Superconductors: A Guide to	o the Tai-	modynamics and Theory. PB89-187538	900,205	pounds in Water by Simultaneous Hydridization/Extraction with GC-FPD Detection.
loring of New Compounds. PB89-171730	901,030	Synthesis and Characterization of Novel E	Bonded Phases	PB89-177224 901,311
IARFEY, P. S.		for Reversed-Phase Liquid Chromatography. PB90-128695	900,233	MATTINGLY, G. E. Gas Flow Measurement Standards.
Microwave Spectrum and (14)N Quadrupole Coup stants of Carbazole.	oling Con-	MARTON, D. Temperature-Dependent Radiation-Enhance	ad Diffusion in	PB89-211874 900,898 Mixing Motions Produced by Pipe Elbows.
PB89-157333 IARGOLIS, S. A.	900,319	Ion-Bombarded Solids. PB89-179188	901,408	PB89-161871 901,326
Stabilization of Ascorbic Acid in Human Plasma	a, and Its	MARTZLOFF, F. D.	301,400	NBS' (National Bureau of Standards) Industry; Government Consortium Research Program on Flowmeter Installation
Liquid-Chromatographic Measurement. PB89-179279	901,237	Coupling, Propagation, and Side Effects of S dustrial Building Wiring System.	Surges in an In-	Effects: Summary Report with Emphasis on Research January-July 1988.
Structure of a Hydroxyl Radical Induced Cross-Lin mine and Tyrosine.	nk of Thy-	PB89-173454	900,118	PB89-189120 901,010
PB89-157838	901,244	Lightning and Surge Protection of Photovolt. Two Case Histories: Vulcano and Kythnos. PB89-229058	aic Installations.	NBS' (National Bureau of Standards) Industry; Government Consortium Research Program on Flowmeter Installation Effects: Summary Report with Emphasis on Research July-
IARINENKO, R. B. Computer-Aided Imaging: Quantitative Composition	onal Map-	Power Quality Site Surveys: Facts, Fiction, a	•	December 1987. PB90-111220 900,910
ping with the Electron Probe Microanalyzer. PB89-157754	901,073	PB89-171656	900,805	Prediction of Flowmeter Installation Effects.
Defocus Modeling for Compositional Mapping w length-Dispersive X-ray Spectrometry.	ith Wave-	Selecting Varistor Clamping Voltage: Lower PB89-176648	900,760	PB89-211882 900,899 Prediction of Flowmeter Installation Effects.
PB89-176150	900,378	Tiger Tempering Tampers Transmissions. PB89-157861	900,740	PB89-211890 900,900
IARJENHOFF, W. A. Adhesive Bonding of Composites.		MARX, E.		MATULA, R. A. Importance of Numeric Databases to Materials Science.
PB90-123696	900,050	Electromagnetic Pulse Scattered by a Spher PB89-157895	e. <i>901,495</i>	PB89-175202 901,187
IARKHAM, J. R. FT-IR (Fourier Transform-Infrared) Emission/Tra	nsmission	Resonance Light Scattering from a Liquid Microspheres.	Suspension of	MAUTNER, M.
Spectroscopy for In situ Combustion Diagnostics. PB89-211866	900,600	PB89-157887	901,340	Filling of Solvent Shells About Ions. 1. Thermochemical Criteria and the Effects of Isomeric Clusters.
ARR, G. V.	,	Resonance Light Scattering from a Susper pheres.		PB89-157549 900,329 Hyperconjugation: Equilibrium Secondary Isotope Effect on
Vibrationally Resolved Photoelectron Angular Di for H2 in the Range 17 eV < or = h(nu) < or = 39		PB89-176234 MASARIE, K. A.	901,352	the Stability of the t-Butyl Cation. Kinetics of Near-Thermoneutral Hydride Transfer.
PB89-176952 IARSH, R. E.	900,385	Noise in DC SQUIDS with Nb/Al-Oxide	'Nb Josephson	PB89-156756 900,306
Statistical Descriptors in Crystallography: Repo	ort of the	Junctions. PB89-201032	900,763	lonic Hydrogen Bond and Ion Solvation. 5. OH(1-)C Bonds. Gas Phase Solvation and Clustering of Alkoxide and
International Union of Crystallography Subcom Statistical Descriptors.	mittee on	MASCARENNAS, A. J. Oxygen Isotope Effect in the Superconducti	ing Bi-Sr-Ca-Cu	Carboxylate Anions. PB89-157531 900,328
PB89-201826 MARSHAK, H.	901,432	O System.		Kinetics of Electron Transfer from Nitroaromatic Radical Anions in Aqueous Solutions. Effects of Temperature and
Magnetic Resonance of (160)Tb Oriented in a	Terbium	PB89-157044 MASTERS, L. W.	901,025	Steric Configuration. PB89-156749 900,305
Single Crystal at Low Temperatures. PB89-179204	901,519	Potential Applications of a Sequential Conser.	struction Analyz-	Relative Acidities of Water and Methanol and the Stabilities
MARSHALL, H. E.		PB89-191670	900, 105	of the Dimer Anions. PB89-150981 900,299
Building Economics in the United States. PB89-172399	900,102	Prediction of Service Life of Building Materi nents.		MAVRODINEANU, R.
Survey of Selected Methods of Economic Eval Building Decisions.	luation for	PB89-158000 Prediction of Service Life of Construction ar	900,112 nd Other Materi-	Chemical Calibration Standards for Molecular Absorption Spectrometry.
PB89-173819	900,103	als. PB89-175848	900,120	PB89-171938 900,193
MARSHALL, R. D.			100,120	MAXIMON, L. C.

Sensors and Measurement Techniques for Assessing Structural Performance.

MASTERSON, K.

Photonic Electric Field Probe for Frequencies up to 2 GHz.

Cross Section and Linear Polarization of Tagged Photons. PB90-117292 901,560

MAY, W. B.	PB89-176572 901,513	PB89-156160 901,094
Application of Direct Digital Control to an Existing Building Air Handler.	Superelastic Scattering of Spin-Polarized Electrons from Sodium.	MCHUGH, M. P.
PB89-177141 900,068	PB90-128307 901,584	Current Research Efforts at JILA (Joint Institute for Laboratory Astrophysics) to Test the Equivalence Principle at
HVACSIM+, a Dynamic Building/HVAC/Control Systems Simulation Program.	Use of Thorium as a Target in Electron-Spin Analyzers. PB90-117938 900,912	Short Ranges. PB89-185912 901,522
PB89-177166 900,070	MCCOMB, T. R.	Liquid-Supported Torsion Balance: An Updated Status
MAY, W. E.	International Comparison of HV Impulse Measuring Sys-	Report on its Potential for Tunnel Detection. PB89-212062 901,542
Standard Reference Materials for the Determination of Polycyclic Aromatic Hydrocarbons.	tems. PB89-186423 900,809	MCILROY, A.
PB89-156889 900,178	MCCORMICK, G. P.	High-Resolution, Slit Jet Infrared Spectroscopy of Hydrocar-
MAYERGOYZ, I. Numerical Analysis for the Small-Signal Response of the	FACTUNC: A User-Friendly System for Unconstrained Opti-	bons: Quantum State Specific Mode Mixing in CH Stretch- Excited Propyne.
MOS (Metal Oxide Semiconductors) Capacitor.	mization. PB90-112392 901,207	PB89-234256 900,490
PB89-186837 900,781	MCCOWAN, C. N.	MCKENNA, G. B.
MAYRATH, J. E. Measurements of Molar Heat Capacity at Constant Volume:	Femite Number Prediction to 100 FN in Stainless Steel Weld Metal.	Concentration Dependence of the Compression Modulus of Isotactic Polystyrene/Cis-Decalin Gels.
$Cv_{,m}(xCH4+ (1-x)C2H6' T = 100 to 320 K, p < or =$	PB89-201586 901,106	PB89-172449 900,552
35 MPa). PB90-117896 900,844	Influence of Molybdenum on the Strength and Toughness	Effects of Solvent Type on the Concentration Dependence of the Compression Modulus of Thermoreversible Isotactic
MCALISTER, A. J.	of Stainless Steel Welds for Cryogenic Service. PB89-173512 901,100	Polystyrene Gels.
Stable and Metastable Phase Equilibria in the Al-Mn	Role of Inclusions in the Fracture of Austenitic Stainless	PB89-172456 900,553
System. PB89-172324 <i>901,136</i>	Steel Welds at 4 K. PB89-173504 901,099	Measurement of the Torque and Normal Force in Torsion in the Study of the Thermoviscoelastic Properties of Polymer
MCCABE, M. E.	Stainless Steel Weld Metal: Prediction of Ferrite Content.	Glasses. PB89-172472 900,554
Field Measurement of Thermal and Solar/Optical Proper-	PB89-231260 901,107	Studies on Some Failure Modes in Latex Barrier Films.
ties of Insulating Glass Windows. PB89-175905 900,064	MCCULLOH, K. E. Low Range Flowmeters for Use with Vacuum and Leak	PB89-209308 901,089
Origins of ASHRAE (American Society of Heating, Refriger-	Standards.	Viscosity of Blends of Linear annd Cyclic Molecules of
ating and Air-Conditioning Engineers) Window U-Value Data and Revisions for the 1989 Handbook of Fundamentals.	PB89-175707 900,374	Similar Molecular Mass. PB89-172480 900,555
PB89-231005 900,083	NBS (National Bureau of Standards) Orifice-Flow Primary High Vacuum Standard.	MCKENNY, P. J.
Periodic Heat Conduction in Energy Storage Cylinders with Change of Phase.	PB89-175699 900,880	Effect of Pressure on the Development of Prebreakdown
PB89-175897 900,852	MCDERMOTT, K. M.	Streamers. PB90-128315 900,828
U-Value Measurements for Windows and Movable Insula-	Development of Combustion from Quasi-Stable Tempera- tures for the Iron Based Alloy UNS S66286.	MCKENZIE, R. L.
tions from Hot Box Tests in Two Commercial Laboratories. PB89-175889 900,121	PB89-173850 900,592	Standard Reference Materials: Description of the SRM 1965 Microsphere Slide.
Window U-Values: Revisions for the 1989 ASHRAE (Amen-	Enthalpies of Desorption of Water from Coal Surfaces. PB89-173868 900,838	PB89-153704 901,390
can Society of Heating, Refrigerating and Air-Conditioning Engineers) Handbook - Fundamentals.	Ignition Characteristics of the Iron-Based Alloy UNS	MCKEOWN, D. A.
PB89-229215 900,145	\$66286 in Pressurized Oxygen. PB89-189336 901,104	Multiple Scattering in the X-ray-Absorption Near-Edge Structure of Tetrahedral Ge Gases.
MCCABE, R. M.	Ignition Characteristics of the Nickel-Based Alloy UNS	PB89-146922 900,283
Standard Format for the Exchange of Fingerprint Informa- tion.	N07718 in Pressurized Oxygen.	Multiple Scattering in the X-ray Absorption Near Edge
PB89-176705 900,692	PB89-218333 901,154 Specific Heat Measurements of Two Promium Cools	Structure of Tetrahedral Germanium Gases. PB89-228480 900,474
MCCAFFREY, B.	Specific Heat Measurements of Two Premium Coals. PB89-173900 900,839	MCKNIGHT, M.
Combustion of Oil on Water. PB89-149173 900,587	MCDONALD, D. G.	Relationship between Appearance and Protective Durability
Combustion of Oil on Water, November 1987.	Superconducting Kinetic Inductance Bolometer. PB89-200505 900,762	of Coatings: A Literature Review. PB89-162598 901,063
PB89-185581 900,863 MCCAFFREY, B. J.	MCFADDEN, G. B.	MCKNIGHT, M. E.
Combustion Efficiency, Radiation, CO and Soot Yield from	Directional Solidification of a Planar Interface in the Pres-	Thermographic Imaging and Computer Image Processing of Defects in Building Materials.
a Variety of Gaseous, Liquid, and Solid Fueled Buoyant Dif- fusion Flames.	ence of a Time-Dependent Electric Current. PB90-112400 901,461	PB89-176309 900,123
PB89-231179 900,604	Effect of a Crystal-Melt Interface on Taylor-Vortex Flow.	MCKNIGHT, R.
Fire Safety Science-Proceedings of the First International	PB90-130261 901,477	International Comparison of HV Impulse Measuring Systems.
Symposium. PB89-179261 900,596	Effect of Anisotropic Thermal Conductivity on the Morphological Stability of a Binary Alloy.	PB89-186423 900,809
Very Large Methane Jet Diffusion Flames.	PB89-228985 901,155	MCKNIGHT, R. H.
PB69-175913 900,593	Elimination of Spurious Eigenvalues in the Chebyshev Tau Spectral Method.	DC Electric Field Effects during Measurements of Monopolar Charge Density and Net Space Charge Density Near
MCCAIN, H. G. Hierarchically Controlled Autonomous Robot for Heavy Pay-	PB89-209282 901,330	HVDC Power Lines.
load Military Field Applications.	Numerical Simulation of Morphological Development during Ostwald Ripening.	PB90-128521 901,380 Estimates of Confidence Intervals for Divider Distorted
PB89-177075 901,271 NASA/NBS (National Aeronautics and Space Administra-	PB89-201990 901,152	Waveforms.
tion/National Bureau of Standards) Standard Reference	Solutal Convection during Directional Solidification. PB89-150932 901,322	PB89-173447 900,806
Model for Telerobot Control System Architecture (NASREM).	PB89-150932 901,322 MCFADDIN, S. E.	Interactions between Two Dividers Used in Simultaneous Companison Measurements.
PB89-193940 901,589	Effect of Pipe Roughness on Orifice Flow Measurement.	PB90-118035 900,031
MCCALEB, M. R.	PB89-231484 901,333	Measuring Fast-Rise Impulses by Use of E-Dot Sensors. PB89-173413 900,744
Improved Transportable DC Voltage Standard. PB89-230395 901,554	NBS (National Bureau of Standards)-Boulder Gas Flow Facility Performance.	Method for Fitting and Smoothing Digital Data.
MCCARTY, R. D.	PB89-186787 900,889	PB90-128794 900,830
Comprehensive Study of Methane + Ethane System. PB89-176747 900,841	Optimum Location of Flow Conditioners in a 4-Inch Orifice Meter.	MCLAUGHLIN, W. L. Comprehensive Dosimetry for Food Irradiation.
Speed of Sound in Natural Gas Mixtures.	PB90-111675 900,911	PB89-186399 900,011
PB89-174031 900,840	MCFARLANE, E.	Dichromate Dosimetry: The Effect of Acetic Acid on the Ra-
MCCLAIN, M. A.	Gain and Power Parameter Measurements Using Planar Near-Field Techniques.	diolytic Reduction Yield. PB89-147490 900,248
Internal Revenue Service Post-of-Duty Location Modeling System: Programmer's Manual for FORTRAN Driver Ver-	PB89-156822 900,699	Radiation-Induced Crosslinks between Thymine and 2-D-
sion 5.0. PB89-161913 900,002	MCGUIRE, T. R. Magnetic Correlations in an Amorphous Gd-Al Spin Glass.	Deoxyerythropentose. PB89-146682 900,247
Internal Revenue Service Post-of-Duty Location Modeling	PB89-201693 901,148	MCLEAN, C. R.
System: Programmer's Manual for PASCAL Solver.	MCHENRY, H. I.	AMRF (Automated Manufacturing Research Facility) Material Handling System Architecture
PB89-161905 900,001 MCCLELLAND, J. J.	Failure Analysis of an Amine-Absorber Pressure Vessel. PB89-173835 901,101	al Handling System Architecture. PB89-177091 900,952
Improved Low-Energy Diffuse Scattering Electron-Spin Po-	Institute for Materials Science and Engineering, Fracture	MCLINDEN, M. O.
larization Analyzer. PB89-229173 900,218	and Deformation: Technical Activities 1988. PB89-148399 901,071	Thermophysical-Property Needs for the Environmentally Acceptable Halocarbon Refrigerants.
Progress on Spin Detectors and Spin-Polarized Electron	Local Brittle Zones in Steel Weldments: An Assessment of	PB89-231054 900,482
Scattering from Na at NIST. PB90-128299 901,583	Test Methods. PB89-149082 901,092	MCMURDIE, H. F.
State Selection in Electron-Atom Scattering: Spin-Polarized	Postweld Heat Treatment Criteria for Repair Welds in 2-1/	Standard X-ray Diffraction Powder Patterns from the JCPDS (Joint Committee on Powder Diffraction Standards) Re-
Electron Scattering from Optically Pumped Sodium.	4Cr-1Mo Superheater Headers: An Experimental Study.	search Associateship.

		•
PB89-171763 900,190	PB90-136862 901,178	PB90-123480 901,468
Standard X-ray Diffraction Powder Patterns from the JCPDS (Joint Committee on Powder Diffraction Standards) Re-	MIALOCQ, J. C. Picosecond Laser Study of the Collisionless Photodissocia-	MIREL, P. G. A.
search Association.	tion of Dimethylnitramine at 266 nm.	Thermal Conductivity Measurements of Thin-Film Silicon Di- oxide.
PB89-202246 900,214 ICNALL, P. E.	PB89-172423 900,255 MIGDALL, A. L.	PB89-212195 901,444
Indoor Air Quality.	Laser-Cooling and Electromagnetic Trapping of Neutral	MISAKIAN, M. AC Electric and Magnetic Field Meter Fundamentals.
PB89-176127 900,065	Atoms. PB89-176440 901,511	PB89-173470 900,746
IEARS, C. A.	Search for Optical Molasses in a Vapor Cell: General Anal-	Characterizing Electrical Parameters Near AC and DC
Measurement of Integrated Tuning Elements for SIS Mixers with a Fourier Transform Spectrometer.	ysis and Experimental Attempt. PB90-163932 901,371	Power Lines. PB89-173462 900,834
PB89-157051 900,706	Using 'Resonant' Charge Exchange to Detect Traces of	DC Electric Field Effects during Measurements of Monopo-
MM Wave Quasioptical SIS Mixers. PB89-214738 901,446	Noble Gas Atoms.	tar Charge Density and Net Space Charge Density Near HVDC Power Lines.
EERTENS, C.	PB89-176770 901,296 MIGHELL, A. D.	PB90-128521 901,380
Tilt Observations Using Borehole Tiltmeters 1. Analysis of Tidal and Secular Tilt.	NIST (National Institute of Standards and Technology)/	Drift Tubes for Characterizing Atmospheric Ion Mobility Spectra.
PB90-136649 901,283	Sandia/ICDD Electron Diffraction Database: A Database for Phase Identification by Electron Diffraction.	PB90-128513 901,585
IEERTS, W. L.	PB89-175210 901,508	Drift Tubes for Characterizing Atmospheric Ion Mobility Spectra Using AC, AC-Pulse, and Pulse Time-of-Flight
Influence of the ac Stark Effect on Multiphoton Transitions in Molecules.	MIGNOGNA, R. B.	Measurement Techniques.
PB89-201578 901,530	Acoustoelastic Determination of Residual Stresses. PB89-179808 901,318	PB89-202543 900,438
IEHL, J. B.	Texture Monitoring in Aluminum Alloys: A Companson of	Measurement of Electrical Parameters Near AC and DC Power Lines.
Microwave Measurements of the Thermal Expansion of a Spherical Cavity.	Ultrasonic and Neutron Diffraction Measurements. PB90-117409 901,159	PB89-173439 900,745
PB89-147458 900,291	Ultrasonic Determination of Absolute Stresses in Aluminum	Power Frequency Electric and Magnetic Field Measure- ments: Recent History and Measurement Standards.
Spherical Acoustic Resonators. PB90-128505 901,321	and Steel Alloys. PB89-150957 901,124	PB89-176630 900,835
EIER, M. M.	Ultrasonic Separation of Stress and Texture Effects in Poly-	MISRA, D. N.
Measurements of the (235)U (n,f) Standard Cross Section	crystalline Aggregates. PB90-117557 900,499	Adsorption of 4-Methacryloxyethyl Trimellitate Anhydride (4- META) on Hydroxyapatite and Its Role in Composite Bond-
at the National Bureau of Standards. PB89-176556 901,305	Ultrasonic Texture Analysis for Polycrystalline Aggregates	ing. PB89-179220 <i>900,041</i>
IEIGS, B. M.	of Cubic Materials Displaying Orthotropic Symmetry.	Interaction of Cupric Ions with Calcium Hydroxylapatite.
Glass Bottles for Carbonated Soft Drinks: Voluntary Product	PB89-146948 901,121 MIHALISIN, T.	PB89-157127 900,037
Standard PS73-89. PB90-107046 900,012	Magnetic Order of Pr in PrBa2Cu3O7.	MITCHELL, G. D.
EIJER, P. H. E.	PB90-123803 901,471	Trace Gas Calibration Systems Using Permeation Devices. PB89-176580 900.883
Dynamics of a Spin-One Model with the Pair Correlation. PB89-171300 900,356	MILAM, D. Laser Induced Damage in Optical Materials: 1987.	MITCHELL, R. A.
Electronic Structure of the Cd Vacancy in CdTe.	PB89-221162 901,364	Intercomparison of Load Cell Verification Tests Performed
PB89-171318 901,398	MILJANIC, P. N.	by National Laboratories of Five Countries. PB89-235915 900,909
Three-State Lattice Gas as Model for Binary Gas-Liquid Systems.	International Comparison of Power Meter Calibrations Conducted in 1987.	MITRAKOVIC, D.
PB89-171284 900,354	PB89-201545 900,718	Acoustoelastic Determination of Residual Stresses.
Van der Waals Equation of State Around the Van Laar Point.	MILLAT, J. Thermal Conductivity of Nitrogen and Carbon Monoxide in	PB89-179808 901,318
PB89-158133 900,345	the Limit of Zero Density.	MITRAKOVIC, D. V. EMATs (Electromagnetic Acoustic Transducers) for Roll-By
EIRON, D.	PB89-222533 900,449 MILLER, J. H.	Crack Inspection of Railroad Wheels.
Numerical Simulation of Morphological Development during Ostwald Ripening.	Chemical Structure of Methane/Air Diffusion Flames: Con-	PB90-123894 901,597 MITROY, J.
PB89-201990 901,152	centrations and Production Rates of Intermediate Hydrocar- bons.	Electron-Impact Excitation of Al(2+).
IEISELMAN, S.	PB89-171904 900,590	PB89-171565 901,503
Determination of Serum Cholesterol by a Modification of the Isotope Dilution Mass Spectrometric Definitive Method.	Methyl Radical Concentrations and Production Rates in a Laminar Methane/Air Diffusion Flame.	Electron-Impact Excitation of the Resonance Transition in CA(1 +).
PB89-234181 901,239	PB89-171912 900,591	PB89-171557 901,502
IELAMUD, M. Roles of Atomic Volume and Disclinations in the Magnetism	Soot Inception in Hydrocarbon Diffusion Flames. PB89-201966 900,599	MIZUSHIMA, M.
of the Rare Earth-3D Hard Magnets.	MILLER, P. J.	Pure Rotational Far Infrared Transitions of (16)O2 in Its Electronic and Vibrational Ground State.
PB89-202238 901,434	Effects of Pressure on the Vibrational Spectra of Liquid Ni-	PB89-202055 900,429
IELGAARD, D. NIST (National Institute of Standards and Technology)/	tromethane. PB89-158026 900,342	MOENS, M.
Sandia/ICDD Electron Diffraction Database: A Database for	MILLER, R. E.	Dependence of Interface Widths on Ion Bombardment Con- ditions in SIMS (Secondary Ion Mass Spectrometry) Analy-
Phase Identification by Electron Diffraction. PB89-175210 901,508	Infrared and Microwave Spectra of OCO-HF and SCO-HF. PB89-179121 900,389	sis of a Ni/Cr Multilayer Structure. PB89-172506 900,364
IELMED, A. J.	MILLET, J. M.	MOFFAT, D. L.
Effects of a Gold Shank-Overlayer on the Field Ion Imaging of Silicon.	Phase Equilibria and Crystal Chemistry in the Ternary	Stable and Metastable Phase Equilibria in the Al-Mn
PB89-175988 901,404	System BaO-TiO2-Nb2O5: Part 1. PB89-171797 901,033	System. PB89-172324 901,136
Progress in Understanding Atomic Structure of the Icosahe-	Phase Relations between the Polytitanates of Barium and	Stable and Metastable Ti-Nb Phase Diagrams.
dral Phase. PB89-171359 <i>901,400</i>	the Barium Borates, Vanadates and Molybdates. PB89-171789 901,032	PB89-157432 901,125
IELQUIST, D.	Syntheses and Unit Cell Determination of Ba3V4O13 and	MOGGI, L.
Thermo-Optic Designs for Microwave and Millimeter-Wave Electric-Field Probes.	Low- and High-Temperature Ba3P4O13. PB89-179717 901,040	Rate Constants for the Quenching of Excited States of Metal Complexes in Fluid Solution.
PB90-128588 900,691	MILLS, K.	PB89-227797 900,461
ERKLE, K. L.	Prediction of Transport Protocol Performance through Sim-	MOHAMMED, K. Pressure and Density Series Equations of State for Steam
Electron Diffraction Study of the Faceting of Tilt Grain Boundaries in NiO.	ulation. PB89-171334 900,612	Pressure and Density Series Equations of State for Steam as Derived from the Haar-Gallagher-Kell Formulation.
PB89-201792 901,431	Transport Layer Performance Tools and Measurement.	PB89-186456 900,409
AETCALF, H. J.	PB89-171326 900,611	MOHR, D. NBS/NRL (National Bureau of Standards/Naval Research
Cooling and Trapping Atoms. PB89-176937 901,515	MINK, A. Hardware Instrumentation Approach for Performance Meas-	Laboratory) Free Electron Laser Facility.
Laser-Cooling and Electromagnetic Trapping of Neutral	urement of a Shared-Memory Multiprocessor.	PB89-175749 901,351
Atoms. PB89-176440 901,511	PB89-186852 900,638 Performance Measurement of a Shared-Memory Multi-	MOLDOVER, M. R. Acoustic and Microwave Resonances Applied to Measuring
MEYER, H.	processor Using Hardware Instrumentation.	the Gas Constant and the Thermodynamic Temperature.
Laser Probing of Ion Velocity Distributions in Drift Fields:	PB89-173793 900,636 MINOR, D. B.	PB89-228548 901,320 Microwave Measurements of the Thermal Expansion of a
Parallel and Perpendicular Temperatures and Mobility for Ba(1+) in He.	Synthesis, Stability, and Crystal Chemistry of Dibarium Pen-	Spherical Cavity.
PB89-171243 900,352	tatitanate. PB89-179741 901,041	PB89-147458 900,291 Quantitative Characterization of the Viscosity of a Microe-
RETERO, P.	. 200 1.0111	Sugnificative Characterization of the Viscosity of a Micros.

MIRAGLIA, S.

Neutron Study of the Crystal Structure and Vacancy Distribution in the Superconductor Ba2Y Cu3 O(sub g-delta).

MEYERS, P.

Technical Examination, Lead Isotope Determination, and Elemental Analysis of Some Shang and Zhou Dynasty Bronze Vessels.

900,524

Quantitative Characterization of the Viscosity of a Microemulsion. PB90-123597 900,524

Spherical Acoustic Resonators.

PB90-128505 <i>901,321</i>	PB89-157119 <i>901,182</i>	MULROW, J. M.
Spherical Acoustic Resonators in the Undergraduate Laboratory.	MORITA, M.	Problems with Interval Estimation When Data Are Adjusted via Calibration.
PB89-179709 901,317 MOLINE, J.	Comparisons of NBS/Harvard VI Simulations and Full- Scale, Multiroom Fire Test Data. PB90-128620 900,170	PB9-157812 901,209 MUNRO, R. G.
Document Interchange Standards: Description and Status	MORRIS, M. C.	Advanced Ceramics: A Critical Assessment of Wear and
of Major Document and Graphics Standards. PB89-193874 900,928	Standard X-ray Diffraction Powder Patterns from the JCPDS (Joint Committee on Powder Diffraction Standards) Re-	Lubrication. PB89-188569 901,045
MONACO, R.	search Associateship.	Bulk Modulus and Young's Modulus of the Superconducto
Chaos and Catastrophe Near the Plasma Frequency in the RF-Biased Josephson Junction.	PB89-171763 900,190 Standard X-ray Diffraction Powder Patterns from the JCPDS	Ba2Cu3YO7. PB90-123613 901,469
PB89-200463 901,424	(Joint Committee on Powder Diffraction Standards) Re-	Structural Ceramics Database: Technical Foundations.
MONROE, C. Collisional Losses from a Light-Force Atom Trap.	search Association. PB89-202246 900,214	PB89-175244 901,036
PB90-123936 901,577	MORRISS, G. P.	MUROGA, Y. Phase Contrast Matching in Lamellar Structures Composed
MOODY, J. R.	Local Order in a Dense Liquid. PB89-157226 900,313	of Mixtures of Labeled and Unlabeled Block Copolymer for
Analysis of Ultrapure Reagents from a Large Sub-Boiling Still Made of Teflon PFA.	Shear Induced Anisotropy in Two-Dimensional Liquids.	Small-Angle Neutron Scattering. PB89-157119 901,182
PB89-186357 900,202	PB89-158141 901,325	Synthesis and Characterization of Poly(vinylmethyl ether).
Design Principles for a Large High-Efficiency Sub-Boiling Still.	MOSSERI, S. Absolute Rate Constants for Hydrogen Abstraction from	PB89-161616 900,55 Temperature, Composition and Molecular-Weight Depend
PB89-187553 900,207	Hydrocarbons by the Trichloromethylperoxyl Radical.	ence of the Binary Interaction Parameter of Polystyrene/
MOORE, E. F. Numerical Computation of Particle Trajectories: A Model	PB89-171532 900,357 MOULDER, J. C.	Poly(vinylmethylether) Blends. PB89-157473 900,550
Problem. PB89-158117 901,324	Acoustoelastic Determination of Residual Stresses.	MURPHY, J.
MOORE, R. T.	PB89-179808 901,318	Damage Accumulation in Wood Structural Members Under Stochastic Live Loads.
Analysis of Ridge-to-Ridge Distance on Fingerprints.	Ultrasonic Determination of Absolute Stresses in Aluminum and Steel Alloys.	PB89-171748 900,111
PB89-230478 901,216 Standard Format for the Exchange of Fingerprint Informa-	PB89-150957 901,124	MURPHY, K. C.
tion.	MOULT, J. Comparative Modeling of Protein Structure: Progress and	Preliminary Crystal Structure of Acinetobacter glutaminasifi- cans Glutaminase-Asparaginase.
PB89-176705 900,692 MOORE, W. J. M.	Prospects.	PB90-123381 901,260
International Comparison of Power Meter Calibrations Con-	PB89-175285 901,247 MOUNTAIN, R. D.	MURPHY, K. N.
ducted in 1987. PB89-201545 900,718	Ergodic Behavior in Supercooled Liquids and in Glasses.	Real-Time Control System Modifications for a Deburring Robot. User Reference Manual.
MOORJANI, K.	PB89-202444 901,435	PB89-159669 900,990
Magnetic Field Dependence of the Superconductivity in Bi-	Light Scattering from Simulated Smoke Agglomerates. PB89-157234 900,588	MURPHY, T. J. Determination of Trace Level Iodine in Biological and Bo-
Sr-Ca-Cu-O Superconductors. PB89-146815 901,385	Liquid, Crystalline and Glassy States of Binary Charged	tanical Reference Materials by Isotope Dilution Mass Spec-
MOOS, H. W.	Colloidal Suspensions. PB89-202501 901,436	trometry. PB89-235642 900,222
IUE Observation of the Interstellar Medium Toward Beta Geminorum.	Measures of Effective Ergodic Convergence in Liquids.	MURRAY, B. T.
PB89-228373 900,024	PB90-118092 900,518	Effect of a Crystal-Melt Interface on Taylor-Vortex Flow. PB90-130261 901,477
MOOSE, R. E. High-Precision Absolute Gravity Observations in the United	Molecular Dynamics Investigation of Expanded Water at Elevated Temperatures.	PB90-130261 901,477 Elimination of Spurious Eigenvalues in the Chebyshev Tau
States.	PB89-174957 900,370	Spectral Method.
PB89-227946 901,281 MOPSIK, F. I.	Simulation Study of Light Scattering from Soot Agglomerates.	PB89-209282 901,330 MURRAY, J. L.
Charging Behavior of Polyethylene and Ionomers.	PB89-212138 901,543	Stable and Metastable Phase Equilibria in the Al-Mr
PB90-136813 900,578	Triplet Dipoles in the Absorption Spectra by Dense Rare Gas Mixtures. 1. Short Range Interactions.	System. PB89-172324 901,136
Dielectric Measurements for Cure Monitoring. PB89-200430 900,567	PB90-136755 900,539	MURTHY, J.
MORALDI, M.	MUELLER, A. Electron-Impact Ionization of La(q+) lons (q= 1,2,3).	IUE Observation of the Interstellar Medium Toward Beta
Analysis of Roto-Translational Absorption Spectra Induced in Low Density Gases of Non-Polar Molecules: The Meth-	PB90-123845 901,573	Geminorum. PB89-228373 900,024
ane Case. PB89-201800 900,427	MUELLER, B. A.	MUSGROVE, A.
MORDFIN, L.	Solidification of Aluminum-Manganese Powders. PB89-172332 901,137	Energy Levels of Molybdenum, Mo 1 through 42. PB89-186472 900,411
Automated Processing of Advanced Materials. The Path to	MUELLER, D.	MUTH, L. A.
Maintaining U.S. Industrial Competitiveness in Materials. PB89-201727 900,957	Resonant Excitation of an Oxygen Valence Satellite in Pho- toemission from High-T(sub c) Superconductors.	Experimental Study of Interpanel Interactions at 3.3 GHz.
Intelligent Processing of Materials: Report of an Industrial	PB89-186860 901,420	PB89-176218 900,705
Workshop Conducted by the National Institute of Standards and Technology.	MUELLER, D. R. Synchrotron Radiation Study of BaO Films on W(001) and	Iterative Technique to Correct Probe Position Errors in Planar Near-Field to Far-Field Transformations.
PB89-151823 900,942	Their Interaction with H2O, CO2, and O2.	PB89-153886 900,695
NDE (Nondestructive Evaluation) Publications, 1985. PB89-229025 900,984	PB89-157697 900,252 MUENTOR, J. S.	MYDOSH, J. A. Magnetic Structure of Y0.97Er0.03.
MOREHOUSE, K.	Infrared and Microwave Investigations of Interconversion	PB89-202675 901,439
Decay of High Valent Manganese Porphyrins in Aqueous Solution and Catalyzed Formation of Oxygen.	Tunneling in the Acetylene Dimer. PB89-157341 900,320	Spin-Density-Wave Transition in Dilute YGd Single Crystals. PB89-202030 901,433
PB89-156772 900,308	MULAZZI, E.	MYKLEBUST, R. L.
MORELAND, J. Ag Screen Contacts to Sintered YBa2Cu3Ox Powder for	Influence of Molecular Weight on the Resonant Raman	Computer-Aided Imaging: Quantitative Compositional Map-
Rapid Superconductor Characterization.	Scattering of Polyacetylene. PB89-179246 900,564	ping with the Electron Probe Microanalyzer. PB89-157754 901,073
PB89-200448 901,423 Cryogenic Bathysphere for Rapid Variable-Temperature	Resonant Raman Scattering of Controlled Molecular Weight	Continuum Radiation Produced in Pure-Element Targets by
Characterization of High-T(sub c) Superconductors.	Polyacetylene. PB89-157093 <i>900,548</i>	10-40 keV Electrons: An Empirical Model. PB89-201610 900,209
PB89-228456 901,450	MULHOLLAND, G.	Defocus Modeling for Compositional Mapping with Wave-
Evidence for the Superconducting Proximity Effect in Junctions between the Surfaces of YBa2CU3Ox Thin Films.	Combustion of Oil on Water. PB89-149173 900,587	length-Dispersive X-ray Spectrometry. PB89-176150 900,376
PB89-228449 901,449 Resistance Measurements of High T(sub c) Superconduc-	Combustion of Oil on Water. November 1987.	Modeling of the Bremsstrahlung Radiation Produced in
Resistance Measurements of High T(sub c) Superconductors Using a Novel 'Bathysphere' Cryostat.	PB89-185581 900,863	Pure Element Targets by 10-40 keV Electrons. PB89-201644 901,531
PB89-228431 901,448	MULHOLLAND, G. W. Light Scattering from Simulated Smoke Agglomerates.	NAAMAN, R.
MORGAN, W. L. Dynamical Simulation of Liquid- and Solid-Metal Self-Sput-	PB89-157234 900,588	Apparent Spectroscopic Rigidity of Floppy Molecular Sys-
tering. PB89-228407 900,472	MULLEN, P. A.	tems. PB90-123860 900,526
Universal Resputtering Curve.	NBS (National Bureau of Standards) Radon-in-Water Standard Generator.	Photodissociation of Methyl Iodide Clusters.
PB89-234314 901,460	PB89-171888 901,295	PB89-171193 900,253
MOR!, K. Phase Contrast Matching in Lamellar Structures Composed	MULLER, A. Spectroscopy of Autoionizing States Contributing to Elec-	NABINGER, S. J. Air Quality Investigation in the NIH (National Institutes of
of Mixtures of Labeled and Unlabeled Block Copolymer for	tron-Impact Ionization of Ions.	Health) Radiation Oncology Branch. PB89-228977 900,079
Small-Angle Neutron Scattering.	PB90-123837 901,572	1 200-220077

NACHT, G.	Simple F-Center Laser Spectrometer for Continuous Single Frequency Scans.	PB89-179154 900,390
Hardware Instrumentation Approach for Performance Measurement of a Shared-Memory Multiprocessor.	PB89-179774 901,358	NEWBURY, D. E. Application of Synergistic Microanalysis Techniques to the
PB89-186852 900,638 Performance Measurement of a Shared-Memory Multi-	NELSON, H. E. Engineering View of the Fire of May 4, 1988 in the First	Study of a Possible New Mineral Containing Light Elements.
processor Using Hardware Instrumentation. PB89-173793 900,636	Interstate Bank Building, Los Angeles, California. PB89-183222 900,167	PB89-147037 901,277
NAGASAWA, M.	NESBITT, D. J.	Computer-Aided Imaging: Quantitative Compositional Map- ping with the Electron Probe Microanalyzer.
Phase Contrast Matching in Lamellar Structures Composed of Mixtures of Labeled and Unlabeled Block Copolymer for	Absolute Infrared Transition Moments for Open Shell Diatomics from J Dependence of Transition Intensities: Applica-	PB89-157754 901,073 Continuum Radiation Produced in Pure-Element Targets by
Small-Angle Neutron Scattering. PB89-157119 901,182	tion to OH. PB89-227912 900,463	10-40 keV Electrons: An Empirical Model. PB89-201610 900,209
NAKAO, Y.	Apparent Spectroscopic Rigidity of Floppy Molecular Sys-	Defocus Modeling for Compositional Mapping with Wave-
Phase Contrast Matching in Lamellar Structures Composed of Mixtures of Labeled and Unlabeled Block Copolymer for	tems. PB90-123860 900,526	length-Dispersive X-ray Spectrometry. PB89-176150 900,378
Small-Angle Neutron Scattering. PB89-157119 901,182	Calculation of Vibration-Rotation Spectra for Rare Gas-HCl Complexes.	Modeling of the Bremsstrahlung Radiation Produced in
NAKATANI, A. I.	PB89-228415 900,473	Pure Element Targets by 10-40 keV Electrons. PB89-201644 901,531
Shear Effects on the Phase Separation Behaviour of a Polymer Blend in Solution by Small Angle Neutron Scatter- ing	Dipole Moment Function and Vibrational Transition Intensi- ties of OH. PB89-227920 900,464	Moydite, (Y, REE) (B(OH)4)(CO3), a New Mineral Species from the Evans-Lou Pegmatite, Quebec. PB89-157747 900,186
PB89-229264 900,574	High-Resolution, Slit Jet Infrared Spectroscopy of Hydrocar- bons: Quantum State Specific Mode Mixing in CH Stretch-	Role of Standards in Electron Microprobe Techniques.
NAMGOONG, E. Electrodeposition of Chromium from a Trivalent Electrolyte.	Excited Propyne.	PB89-176143 900,197
PATENT-4 804 446 901,119	PB89-234256 900,490 Infrared Spectra of Nitrous Oxide-HF Isomers.	Strategy for Interpretation of Contrast Mechanisms in Scan- ning Electron Microscopy: A Tutorial.
NANCOLLAS, G. H. Calcium Hydroxyapatite Precipitated from an Aqueous Solu-	PB89-228399 900,471	PB89-172498 900,192 NEWELL, A. C.
tion: An International Multimethod Analysis. PB90-123399 900,228	Infrared Spectrum of D2HF. PB89-171219 900,350	Accurate Determination of Planar Near-Field Correction Pa-
NANZETTA, P.	Infrared Spectrum of NeHF.	rameters for Linearly Polarized Probes. PB89-156871 900,704
Publications of the Center for Manufacturing Engineering	PB89-171227 900,351 Intramolecular Dynamics of van der Waals Molecules: An	Brief History of Near-Field Measurements of Antennas at
Covering the Period January 1978-December 1988. PB90-130568 901,012	Extended Infrared Study of ArHF. PB90-118209 900,521	the National Bureau of Standards. PB89-156863 900,703
NAPIORKOWSKI, M. Three-State Lattice Gas as Model for Binary Gas-Liquid	Rydberg-Klein-Rees Inversion of High Resolution van der	Development of Near-Field Test Procedures for Communication Satellite Antennas, Phase 1, Part 2.
Systems. PB89-171284 900,354	Waals Infrared Spectra: An Intermolecular Potential Energy Surface for Ar+ HF ($v = 1$).	PB89-156152 901,593
NASCHITZKI, M.	PB89-227953 900,465 Simple F-Center Laser Spectrometer for Continuous Single	Effect of Random Errors in Planar Near-Field Measurement. PB89-171839 900,708
Effects of a Gold Shank-Overlayer on the Field Ion Imaging of Silicon.	Frequency Scans. PB89-179774 901,358	Efficient and Accurate Method for Calculating and Representing Power Density in the Near Zone of Microwave An-
PB89-175988 901,404 NASH, S. G.	Slit Jet Infrared Spectroscopy of NeHF Complexes: Internal Rotor and J-Dependent Predissociation Dynamics.	tennas. PB89-157457 900,707
Proper Motion vs. Redshift Relation for Superluminal Radio	PB90-118126 900,520	Error Analysis Techniques for Planar Near-Field Measurements.
Sources. PB89-157663 900,017	Spectroscopic Signatures of Floppiness in Molecular Complexes.	PB89-156848 900,701
NASHMAN, M.	PB89-227979 900,467	Gain and Power Parameter Measurements Using Planar Near-Field Techniques.
Visual Perception Processing in a Hierarchical Control System: Level 1. PB89-221188 900,994	Structure and Dynamics of Molecular Clusters via High Resolution IR Absorption Spectroscopy. PB89-185896 900,403	PB89-156822 900,699 Improved Polarization Measurements Using a Modified
NASSIMBENE, R.	Sub-Doppler Infrared Spectroscopy in Slit Supersonic Jets:	Three-Antenna Technique. PB89-156814 900,698
Facilitated Transport of CO2 through Highly Swollen Ion-Exchange Membranes: The Effect of Hot Glycenne Pretreat-	A Study of all Three van der Waals Modes in v1-Excited ArHCl.	NEWMAN, H. M.
ment. PB89-179618 900,395	PB90-123852 900,525	Standardizing EMCS Communication Protocols. PB89-172357 900,613
NECHVATAL, J. R.	Weakly Bound NeHF. PB90-118100 900,519	NEWNAM, B. E.
Wavefront Matrix Multiplication on a Distributed-Memory	NETA, P.	Laser Induced Damage in Optical Materials: 1987. PB89-221162 901,364
Multiprocessor. PB89-151807 900,646	Absolute Rate Constants for Hydrogen Abstraction from Hydrocarbons by the Trichloromethylperoxyl Radical.	PB89-221162 901,364 NGUYEN, T.
NEFF, J. E.	PB89-171532 900,357 Decay of High Valent Manganese Porphyrins in Aqueous	Corrosion Induced Degradation of Amine-Cured Epoxy
Doppler Imaging of AR Lacertae at Three Epochs. PB89-149199 900,015	Solution and Catalyzed Formation of Oxygen. PB89-156772 900,308	Coatings on Steel. PB89-176291 901,084
Rotational Modulation and Flares on RS Canum Venati- corum and BY Draconis Stars X: The 1981 October 3 Flare	Dehydrogenation of Ethanol in Dilute Aqueous Solution	Development of a Method to Measure In situ Chloride at the Coating/Metal Interface.
on V711 Tauri (= HR 1099). PB89-202618 900,021	Photosensitized by Benzophenones. PB89-157556 900,251	PB89-235345 901,085
Rotational Modulation and Flares on RS Canum Venati-	Kinetics of Electron Transfer from Nitroaromatic Radical Anions in Aqueous Solutions. Effects of Temperature and	Quantitative Studies of Coatings on Steel Using Reflection/ Absorption Fourier Transform Infrared Spectroscopy.
corum and BY Draconis Stars, XI. Ultraviolet Spectral Images of AR Lacertae in September 1985.	Steric Configuration.	PB89-212112 901,066
PB89-234298 900,026	PB89-156749 900,305 One-Electron Transfer Reactions of the Couple SO2/	Relationship between Appearance and Protective Durability of Coatings: A Literature Review. PB89-162598 901.063
NEHMADI, M. Measurement of Partial Discharges in Hexane Under DC	SO2(1-) in Aqueous Solutions. Pulse Radiolytic and Cyclic Voltammetric Studies.	PB89-162598 901,063 NHA, I. S.
Voltage. PB89-173421 900,833	PB89-176093 900,376	Rotational Modulation and Flares on RS CVn and BY Dra
NELIS, T.	Rate Constants for One-Electron Oxidation by Methylper- oxyl Radicals in Aqueous Solutions.	Stars IX. IUE (International Ultraviolet Explorer) Spectrosco- py and Photometry of II Peg and V711 Tau during February
Detection of the Free Radicals FeH, CoH, and NiH by Far Infrared Laser Magnetic Resonance.	PB89-151013 900,302	1983. PB89-171615 900,019
PB90-117342 900,495	Rate Constants for Reactions of Nitrogen Oxide (NO3) Radicals in Aqueous Solutions.	NICKERSON, D. A.
NELSON, A. J. Evidence for the Superconducting Proximity Effect in Junc-	PB89-176242 900,379 Reaction of (Ir(C(3), N bpy)(bpy)2)(2+) with OH Radicals	Integrated Manufacturing Data Administration System (IMDAS) Operations Manual.
tions between the Surfaces of YBa2CU3Ox Thin Films. PB89-228449 901,449	and Radiation Induced Covalent Binding of the Complex to Several Polymers in Aqueous Solutions.	PB89-156384 900,916 NIEBAUER, T. M.
High T(sub c) Superconductor/Noble-Metal Contacts with Surface Resistivities in the (10 to the Minus 10th Power)	PB90-123498 900,264	Comment on 'Possible Resolution of the Brookhaven and
Surface Resistivities in the (10 to the Minus 10th Power) Omega sq cm Range. BP90 170924	Reactions of Magnesium Prophyrin Radical Cations in Water. Disproportionation, Oxygen Production, and Compar-	Washington Eotvos Experiments'. PB89-171581 901,504
PB89-179824 901,413 NELSON, D. D.	ison with Other Metalloporphyrins. PB89-151005 900,301	Current Research Efforts at JILA (Joint Institute for Laboratory Astrophysics) to Test the Equivalence Principle at
Absolute Infrared Transition Moments for Open Shell Diato-	Redox Chemistry of Water-Soluble Vanadyl Porphyrins. PB89-150999 900,300	Short Ranges. PB89-185912 901,522
mics from J Dependence of Transition Intensities: Applica-	PB89-150999 900,300	901,522

Pahasapaite, a Beryllophosphate Zeolite Related to Synthetic Zeolite Rho, from the Tip Top Pegmatite of South Dakota.

Wheatleyite, Na2Cu(C2O4)2 . 2H2O, a Natural Sodium Copper Salt of Oxalic Acid.

NEWBURY, D.

PB89-186431

900,350

NELSON, D. D.

Infrared Spectrum of D2HF. PB89-171219

Absolute Infrared Transition Moments for Open Shell Diatomics from J Dependence of Transition Intensities: Application to OH. PB89-227912

Dipole Moment Function and Vibrational Transition Intensities of OH. PB89-227920 900,464

901,288

NIELSEN, C. H.

High-Precision Absolute Gravity Observations in the United States.
PB89-227946 901,281

Moydite, (Y, REE) (B(OH)4)(CO3), a New Mineral Species from the Evans-Lou Pegmatite, Quebec.
PB89-157747 900,186

NIELSON, G. C. Decorated Lattice Gas Model for Supercritical Solubility.	O'CALLAGHAN, M. J. Sodium Doppler-Free Collisional Line Shapes.	Calculable, Transportable Audio-Frequency AC Reference Standard.
PB89-175681 900,	73 PB89-234306 901,55	
NIETO DE CASTRO, C. A.	O'CONNELL, J. S.	International Comparison of Power Meter Calibrations Conducted in 1987.
Experimental Thermal Conductivity, Thermal Diffusivity, a Specific Heat Values of Argon and Nitrogen.	nd Quasifree Electron Scattering on Nucleons in a Momentum Dependent Potential.	PB89-201545 900,718
PB89-148407 900,	The state of the s	
Thermal Conductivity of Liquid Argon for Temperatures tween 110 and 140 K with Pressures to 70 MPa.	oe- O'CONNOR, C. NBS (National Bureau of Standards) Reactor: Summary	Thermophysical Properties for Bioprocess Engineering. PB89-228068 900,043
PB89-179600 900,	Activities July 1987 through June 1988.	OLSEN, G. H.
NIGHTINGALE, J. S.	PB89-168017 901,30	reasibility of Detector con Cambration in the real inflated.
Application of the ISO (International Standards Organ tion) Distributed Single Layer Testing Method to the C		
nectionless Network Protocol. PB89-177133 900,	and Mixed or Neumann Boundary Conditions.	Low Field Determination of the Proton Gyromagnetic Ratio
NIKOLO, M.	1200 111004	9 in Water. PB89-230411 901,555
Flux Creep and Activation Energies at the Grain Boundar	O'NEIL, S. V: es Weakly Bound NeHF.	Measurement of the NBS (National Bureau of Standards)
of Y-Ba-Cu-O Superconductors. PB89-230353 901,	PB90-118100 900 51	9 Electrical Watt in SI Units.
NISHIMURA, H.	OATES, C. W.	PB89-230429 900,821 NBS (National Bureau of Standards) Determination of the
Cross Sections for Collisions of Electrons and Photons v	ith Profile Inhomogeneity in Multimode Graded-Index Fibers. 900,74	g Fine-Structure Constant, and of the Quantized Hall Resist-
Oxygen Molecules. PB89-226575 900,	57 OBERLE, R.	ance and Josephson Frequency-to-Voltage Quotient in SI Units.
NOBLE, R. D.	Magnetic Behavior of Compositionally Modulated Ni-C	u PB89-230437 <i>901,556</i>
CO2 Separation Using Facilitated Transport Ion Exchain	Thin Films. ge PB90-118084 901,16	OLSON, D. L.
Membranes. PB89-157374 900,	21 OCHIAI, A.	Femite Number Prediction to 100 FN in Stainless Steel Weld Metal.
Facilitated Transport of CO2 through Highly Swollen Ion-	Oxygen Isotope Effect in the Superconducting Bi-Sr-Ca-Ci	
change Membranes: The Effect of Hot Glycerine Pretre	O System. PB89-157044 901,02	Stainless Steel Weld Metal: Prediction of Ferrite Content. PB89-231260 901,107
PB89-179618 900,	95 OETTINGER, F. F.	OLSON, G. J.
Influence of Reaction Reversibility on Continuous-Flow	Ex- IEEE (Institute of Electrical and Electronics Engineers IRPS (International Reliability Physics Symposium) Tutoric	Biodegradation of TributyItin by Chesapeake Bay Microor-
traction by Emulsion Liquid Membranes. PB89-176481 900,2	Thermal Resistance Measurements, 1989.	ganisms. DB90.177222 001.200
NODA, I.	PB89-231195 900,79	Biotransformation of Mercury by Bacteria Isolated from a
Phase Contrast Matching in Lamellar Structures Compos	ed OGATA, T. Loading Rate Effects on Discontinuous Deformation in	River Collecting Cinnabar Mine Waters.
of Mixtures of Labeled and Unlabeled Block Copolymer Small-Angle Neutron Scattering.	Load-Control Tensile Tests.	Florest Occide Follows and Market In 1 and 1
PB89-157119 901,		tonng of Metal Biotransformations in Environmental Matri-
NOFZIGER, M. J.	OH, J. Y. Rotational Modulation and Flares on RS CVn and BY Dr	ces. a PB89-177216 <i>901,220</i>
Feasibility of Detector Self-Calibration in the Near Infrare PB89-176788 900,	84 Stars IX. IUE (International Ultraviolet Explorer) Spectrosco	Global Biomethylation of the Flements - Its Bole in the Bio-
NOLT, I. G.	py and Photometry of II Peg and V711 Tau during Februar 1983.	sphere Translated to New Organometallic Chemistry and Biotechnology.
Frequency Measurement of the J = 1 < - 0 Rotation	nal PB89-171615 900,01	9 PB90-136854 901,232
Transition of HD (Hydrogen Deutende). PB89-161566 901,	gg OHASHI, M.	Microbiological Materials Processing.
NORCROSS, D. W.	Detection of Lead in Human Teeth by Exposure to Aqueou Sulfide Solutions.	
Electron-Impact Excitation of Al(2+). PB89-171565 901,8	PB89-201529 901,25	6 Microbiological Metal Transformations: Biotechnological Applications and Potential.
Electron-Impact Excitation of the Resonance Transition	Formation of Hydroxyapatite in Hydrogeis from Tetraca	PB89-175947 <i>901,284</i>
CA(1 +).	PB89-201511 901,25	Novel Flow Process for Metal and Ore Solubilization by Aqueous Methyl lodide.
PB89-171557 901,	Onashi, N.	PB89-202113 901,285
NORCROSS, R. J. Workstation Controller of the Cleaning and Deburring Wo	Far-Infrared Spectrum of Methyl Amine. Assignment an rk- Analysis of the First Torsional State.	Speciation Measurements of Butyltins: Application to Controlled Release Rate Determination and Production of Ref-
station.	PB89-161574 900,34	erence Standards.
PB89-189286 900,8 NORTON, S. J.	Microwave Spectrum of Methyl Amine: Assignment an Analysis of the First Torsional State.	
Computing Ray Trajectories between Two Points: A So	DD 0 44 = 000 CO	OLSON, W. Far-Infrared Spectrum of Methyl Amine. Assignment and
tion to the Ray-Linking Problem. PB89-176929 901,	OHLEMILLER, T.	Analysis of the First Torsional State.
Fast Magnetic Resonance Imaging with Simultaneously	Assessing the Flammability of Composite Materials.	PB89-161574 900,346
cillating and Rotating Field Gradients.	Cigarette as a Heat Source for Smolder Initiation in Linho	OLGO14, 11. D.
PB89-176903 901,8 Mossbauer Imaging.	74 stery Materials. PB89-176762 900,59	PB89-230296 900,480
PB89-176895 901,	42 OHLENDORF, D. H.	Infrared Spectrum of the nu6, nu7, and nu8 Bands of HNO3.
Mossbauer Imaging: Experimental Results.	Use of an Imaging Proportional Counter in Macromolecula	
PB90-123415 900,8 NOVEMBER, L. J.	²² Crystallography. PB90-136599 <i>900.53</i>	B OLSSON, M.
Helium Resonance Lines in the Flare of 15 June 1973.	OJI, H. C. A.	Comparison of Liquid Chromatographic Selectivity for Polycyclic Aromatic Hydrocarbons on Cyclodextrin and C18
PB90-118142 900,	Superiative magnetoroton bando.	Bonded Phases.
NOVOLNY, D. B.	PB89-175970 901,40	
Growth and Properties of High-Quality Very-Thin SOS (scon-on Sapphire) Films.	illi- OKABE, Y. Oxygen Isotope Effect in the Superconducting Bi-Sr-Ca-Ci	OLTHOFF, J. K. Assessment of Space Power Related Measurement Re-
PB90-128109 900,	98 O System.	quirements of the Strategic Defense Initiative.
NOVOTNY, D. B.	PB89-157044 901,02 OKADA, M.	5 PB89-209357 901,269 Collisional Electron Detachment and Decomposition Rates
Direct Observation of Surface-Trapped Diffracted Waves PB90-128216 901,		of SF6(1-), SF5(1-), and F(1-) in SF6: Implications for Ion
High-Mobility CMOS (Complementary Metal Oxide Se	ni- Phase Boundary.	Transport and Electrical Discharges.
conductor) Transistors Fabricated on Very Thin SOS Film PB89-230460 900,		Floation Francis Dependence of the COF10 Mass Coss
NYDEN, M. R.	ence of the Binary Interaction Parameter of Polystyrene	
Component Spectrum Reconstruction from Partially Char	Poly(vinylmethylether) Blends. PB89-157473 900,55	·
terized Mixtures. PB89-202568 900,		gy Assessment.
Spectroscopic Quantitative Analysis of Strongly Interact	Mesh Monitor Casting of Ni-Cr Alloys: Element Effects.	
Systems: Human Plasma Protein Mixtures. PB89-202576 901,	PB89-176077 900,04 25 OLCHOWY, G. A.	OLVER, F. W. Error Bounds for Linear Recurrence Relations.
NYYSSONEN, D.	Simplified Representation for the Thermal Conductivity	AD-A201 256/5 901 192
Narrow-Angle Laser Scanning Microscope System	Fluida in the Critical Desire	OMORI, A.
Linewidth Measurement on Wafers. PB89-189344 900,		Effects of Material Characteristics on Flame Spreading. PB89-212021 900,572
Optical Nondestructive Evaluation at the National Bureau	of Audio-Frequency Current Comparator Power Bridge: Deve	I- Effects of Thermal Stability and Melt Viscosity of Thermo-
Standards. PB89-146740 <i>900,</i>	opment and Design Considerations.	plastics on Piloted Ignition.
. 555 . 757 75	. 5 . 500-201001 300,71	

ONDA, K.		Toughening Mechanisms in Ceramic Composites: Semi-	Tin- and Lead-Bearing Organometallic Compounds, with
Cross Sections for Collisions of Electrons and Pl Oxygen Molecules.		Annual Progress Report for the Period Ending September 30, 1988. PB89-162606 901,028	Signal Increases Induced by Transition-Metal lons. PB89-157085 900,184
PB89-226575	900,457	PALLETT, D. S.	PARR, A. C.
ONDA, M. Microwave Spectrum, Structure, and Elect Moment of Ar-Ch3OH.	tric Dipole	PCM/VCR Speech Database Exchange Format. PB89-176713 900,633	Autoionization Dynamics in the Valence-Shell Photoioniza- tion Spectrum of CO. PB89-176960 900,386
PB90-117847 ONDREJKA, A. R.	900,510	PALMER, M. E. Guidelines for the Specification and Validation of IGES (Initial Creation Evolution). Application Protocols	Using 'Resonant' Charge Exchange to Detect Traces of Noble Gas Atoms. PB89-176770 901,296
Fields Radiated by Electrostatic Discharges. PB90-128778	901,382	tlal Graphics Exchange Specification) Application Protocols. PB89-166102 900,937 PALMER, R. E.	Vibrationally Resolved Photoelectron Angular Distributions for H2 in the Range 17 eV $<$ or= h(nu) $<$ or= 39 eV.
ONEIL, S. V. Infrared Spectrum of NeHF.		High Resolution Inverse Raman Spectroscopy of the CO Q	PB89-176952 900,385
PB89-171227	900,351	Branch. PB89-171292 900,355	Vibrationally Resolved Photoelectron Studies of the 7(sigma) (-1) Channel in N2O.
Slit Jet Infrared Spectroscopy of NeHF Complex Rotor and J-Dependent Predissociation Dynamics	S.	PALMIERI, M. D.	PB69-176945 900,257
PB90-118126 ONO, R. H.	900,520	Introduction to Supercritical Fluid Chromatography. Part 2. Applications and Future Trends. PB89-230312 900,219	PARRIS, R. M. Experiences in Environmental Specimen Banking.
Evidence for the Superconducting Proximity Effe		PB89-230312 900,219 PAN, L.	PB90-123969 900,866
tions between the Surfaces of YBa2CU3Ox Thin PB89-228449	901,449	Computation of the ac Stark Effect in the Ground State of	PASSAGLIA, E. Crazes and Fracture in Polymers.
Noise in DC SQUIDS with Nb/Al-Oxide/Nb Junctions.	Josephson	Atomic Hydrogen. PB89-202535 901,538	PB89-176085 900,562
PB89-201032	900,763	PANKOVE, J. I.	PATRICK, B. D. Managements of the (235VL) in 9. Standard Cross Section
Switching Noise in YBa2Cu3Ox 'Macrobridges'. PB89-200513	901,426	Oxygen Isotope Effect in the Superconducting Bi-Sr-Ca-Cu-O System.	Measurements of the (235)U (n,f) Standard Cross Section at the National Bureau of Standards.
OOSTRA, D. J.		PB89-157044 901,025 PANSON, A. J.	PB89-176556 901,305 PATTERSON, K. Y.
Initial Stages of Heteroepitaxial Growth of InAs of PB90-123878	n Si(100). <i>901,473</i>	High T(sub c) Superconductor/Noble-Metal Contacts with	Microwave Digestion of Biological Samples: Selenium Anal-
Interaction of In Atom Spin-Orbit States with S faces.	i(100) Sur-	Surface Resistivities in the (10 to the Minus 10th Power) Omega sq cm Range.	ysis by Electrothermal Atomic Absorption Spectrometry. PB89-229116 900,217
PB90-128547	900,532	PB89-179824 901,413 PAPATHEOFANIS, B. J.	PAULE, R. C.
Laser Probing of the Dynamics of Ga Intera Si(100).	actions on	Optical Fiber Sensors for Electromagnetic Quantities.	Conserisus Values, Regressions, and Weighting Factors. PB89-211130 901,213
PB89-186928	901,422	PB89-173967 900,725 PAPTHEOFANIS, B. J.	PAULSEN, P. J.
ORR, R. D. Thermo-Optic Designs for Microwave and Millin	neter-Wave	Optical Fiber Sensors for the Measurement of Electromag-	Absolute Isotopic Abundance Ratios and Atomic Weight of a Reference Sample of Nickel.
Electric-Field Probes. PB90-128588	900,691	netic Quantities. PB89-176671 900,748	PB90-163890 900,543
ORSER, D. J.	,	PARDEE, R. J.	Analysis of Ultrapure Reagents from a Large Sub-Boiling Still Made of Teflon PFA.
Algebraic Representation for the Topology of Mu ent Phase Diagrams.		Publications of the National Institute of Standards and Technology, 1988 Catalog.	PB89-186357 900,202 Determination of Selenium and Tellurium in Copper Stand-
PB89-177042	901,517	PB89-218382 900,006 PARETZKIN, B.	ard Reference Materials Using Stable Isotope Dilution
OSBORNE, W. M. Software Configuration Management: An Overvie	w.	Standard X-ray Diffraction Powder Patterns from the JCPDS	Spark Source Mass Spectrometry. PB90-123472 900,230
PB89-193833	900,651	(Joint Committee on Powder Diffraction Standards) Research Associateship.	Isotope Dilution Mass Spectrometry for Accurate Elemental Analysis.
OUELLETTE, P. Rate Constants for the Reaction HO2+ NO	2+ N2->	PB89-171763 900,190 Standard V van Diffraction Devuder Detterns from the ICPDS	PB89-230338 900,220
HO2NO2 + N2: The Temperature Dependence of Off Parameters.		Standard X-ray Diffraction Powder Patterns from the JCPDS (Joint Committee on Powder Diffraction Standards) Re-	PAYNE, B. F.
PB89-146658	900,278	search Association. PB89-202246 900,214	Automated Fringe Counting Laser Interferometer for Low Frequency Vibration Measurements.
OVERMAN, J. R. GATT (General Agreement on Tariffs and Trade)	Standards	PARK, C.	PB89-177190 900,885
Code Activities of the National Institute of Star Technology 1988.		Application of Direct Digital Control to an Existing Building Air Handler.	PEACOCK, R. HAZARD I Fire Hazard Assessment Method.
PB89-191977	900,173	PB89-177141 900,068 HVACSIM+, a Dynamic Building/HVAC/Control Systems	PB89-215404 900,143
Oyamada, A. Oxygen Isotope Effect in the Superconducting B	i-Sr-Ca-Cu-	Simulation Program. PB89-177166 900,070	PEACOCK, R. D. Refinement and Experimental Verification of a Model for
O System. PB89-157044	901,025	Simulation of a Large Office Building System Using the	Fire Growth and Smoke Transport. PB89-212005 900,137
OZIER, I.	001,020	HVACSIM+ Program. PB89-177174 900,071	Technical Reference Guide for FAST (Fire and Smoke
Influence of the ac Stark Effect on Multiphoton in Molecules.	Transitions	PARKER, H. S.	Transport) Version 18. PB89-218366 900,602
PB89-201578	901,530	Phase Equilibria and Crystal Chemistry in the Ternary System BaO-TiO2-Nb2O5: Part 1.	PEACOR, D. R.
PAABO, M. Synergistic Effects of Nitrogen Dioxide and Carb	on Dioxide	PB89-171797 901,033	Pahasapaite, a Beryllophosphate Zeolite Related to Synthetic Zeolite Rho, from the Tip Top Pegmatite of South
Following Acute Inhalation Exposures in Rats. PB89-214779	900,856	Phase Equilibria and Crystal Chemistry in the Ternary System BaO-TiO2-Nb2O5. Part 2. New Banum Polytitan-	Dakota. PB89-186431 <i>901,288</i>
Toxicity of Mixed Gases Found in Fires.		ates with < 5 mole % Nb2O5. PB89-189815 900,419	Wheatleyite, Na2Cu(C2O4)2 2H2O, a Natural Sodium
PB89-212047 PACE, M. O.	900,869	Phase Relations between the Polytitanates of Barium and	Copper Salt of Oxalic Acid. PB89-179154 900,390
Measurement of Partial Discharges in Hexane	Under DC	the Barium Borates, Vanadates and Molybdates. PB89-171789 901,032	PEARLMAN, M. R.
Voltage. PB89-173421	900,833	Syntheses and Unit Cell Determination of Ba3V4O13 and Low- and High-Temperature Ba3P4O13.	Microarcsecond Optical Astrometry: An Instrument and Its Astrophysical Applications.
PAFFENBARGER, G. C.		PB89-179717 901,040	PB89-171268 900,013
Detection of Lead in Human Teeth by Exposure Sulfide Solutions.	to Aqueous	Synthesis, Stability, and Crystal Chemistry of Dibarium Pentatitanate.	PEAVY, B.
PB89-201529	901,256	PB89-179741 901,041	Circular and Square Edge Effect Study for Guarded-Hot- Plate and Heat-Flow-Meter Apparatuses.
PAGE, R. A. Creep Cavitation in Liquid-Phase Sintered Alumin	na.	PARKER, W. J. Prediction of the Heat Release Rate of Douglas Fir.	PB89-176135 900,881 Summary of Circular and Square Edge Effect Study for
PB89-175954	901,038	PB89-212039 901,185	Guarded-Hot-Plate and Heat-Flow-Meter Apparatuses. PB89-176606 900,884
Precision Experiments to Search for the Fifth For	rce.	PARKS, E. J. Characterization of Organolead Polymers in Trace Amounts	PECHEUR, P.
PB89-228365 PALAMIDES, T.	901,551	by Element-Specific Size-Exclusion Chromatography. PB89-175962 900,196	Electronic Structure of the Cd Vacancy in CdTe. PB89-171318 901,398
Mechanical Property Enhancement in Ceramic M		Design and Synthesis of Prototype Air-Dry Resins for Use	PEI, P.
	Matrix Com-		
posites. PB89-189138	Matrix Com- 901,076	in BEP (Bureau of Engraving and Printing) Intaglio Ink Vehi- cles.	Preparative Liquid Chromatographic Method for the Charac-
PB89-189138 PALAMIDES, T. R.	901,076	in BEP (Bureau of Engraving and Printing) Intaglio Ink Vehicles. PB90-112343 901,068	
PB89-189138 PALAMIDES, T. R. Structural Reliability and Damage Tolerance Composites for High-Temperature Application	901,076 of Ceramic	in BEP (Bureau of Engraving and Printing) Intaglio Ink Vehicles. PB90-112343 901,068 Effect of pH on the Emission Properties of Aqueous tris (2,6-dipicolinato) Terbium (III) Complexes.	Preparative Liquid Chromatographic Method for the Characterization of Minor Constituents of Lubricating Base Oils. PB89-175921 901,114 PEIFER, W. R.
PB89-189138 PALAMIDES, T. R. Structural Reliability and Damage Tolerance	901,076 of Ceramic	in BEP (Bureau of Engraving and Printing) Intaglio Ink Vehicles. PB90-112343 901,068 Effect of pH on the Emission Properties of Aqueous tris	Preparative Liquid Chromatographic Method for the Characterization of Minor Constituents of Lubricating Base Oils. PB89-175921 901,114

PEISER, H. S.	Specification) Environment in the National PDES Testbed Project.	PB89-171706 900,74
Twenty Five Years of Accuracy Assessment of the Atomic Weights.	PB89-215198 900,960	Picosecond Pulse Response from Hydrogenated Amor phous Silicon (a-Si:H) Optical Detectors on Channel Wave
PB89-174007 <i>900,365</i> PELLA, P. A.	PERRIN, E. Influence of Molecular Weight on the Resonant Raman	guides. PB89-176689 900,72
Uncertainties in Mass Absorption Coefficients in Fundamen-	Scattering of Polyacetylene.	System for Measuring Optical Waveguide Intensity Profiles.
tal Parameter X-ray Fluorescence Analysis. PB89-201677 900,212	PB89-179246 900,564 Resonant Raman Scattering of Controlled Molecular Weight	PB89-188593 900,75
PELLEGRINO, J. J.	Polyacetylene. PB89-157093 900,548	Waveguide Loss Measurement Using Photothermal Deflection.
CO2 Separation Using Facilitated Transport Ion Exchange Membranes.	PERRY, J. W.	PB89-157028 900,73 PHELPS, A. V.
PB89-157374 900,321	Picosecond Coherent Anti-Stokes Raman Scattering (CARS) Study of Vibrational Dephasing of Carbon Disulfide	Electron-Transport, Ionization, Attachment, and Dissociation
Facilitated Transport of CO2 through Highly Swollen Ion-Exchange Membranes: The Effect of Hot Glycerine Pretreat-	and Benzene in Solution. PB89-176408	Coefficients in SF6 and Its Mixtures. PB89-171540 901,50
ment. PB89-179618 900,395	PERSILY, A.	Ionization and Current Growth in N2 at Very High Electri
PENN, D. R.	Air Quality Investigation in the NIH (National Institutes of	Field to Gas Density Ratios. PB89-228381 901,55
Calculations of Electron Inelastic Mean Free Paths for 31 Materials.	Health) Radiation Oncology Branch. PB89-228977 900,079	PHILLIPS, R. R.
PB89-157978 900,341 Electron Mean Free Path Calculations Using a Model Di-	Integral Mass Balances and Pulse Injection Tracer Techniques.	Dynamic Young's Modulus Measurements in Metallic Mate rials: Results of an Interlaboratory Testing Program.
electric Function.	PB89-206833 900,077	PB89-157671 901,13
PB89-177026 901,141 Free-Electron-Like Stoner Excitations in Fe.	Ventilation and Air Quality Investigation of the U.S. Geological Survey Building.	PHILLIPS, W. D. Cooling and Trapping Atoms.
PB89-158059 901,393	PB89-229686 900,857	PB89-176937 901,51
PENN, R. Mesh Monitor Casting of Ni-Cr Alloys: Element Effects.	PERSILY, A. K. Investigation of a Washington, DC Office Building.	Laser-Cooling and Electromagnetic Trapping of Neutra Atoms.
PB89-176077 900,040	PB89-230361 900,081	PB89-176440 901,51
PENN, S. M. Laser Probing of Ion Velocity Distributions in Drift Fields:	Measured Air Infiltration and Ventilation Rates in Eight Large Office Buildings.	Low Field Determination of the Proton Gyromagnetic Ration Water.
Parallel and Perpendicular Temperatures and Mobility for Ba(1+) in He.	PB90-128158 900,090	PB89-230411 901,55
PB89-171243 900,352	Ventilation Effectiveness Measurements in an Office Building.	Measurement of the NBS (National Bureau of Standards Electrical Watt in SI Units.
PENNER, S. NBS (National Bureau of Standards) Free Electron Laser	PBS9-176614 900,067 PESSALL, N.	PB89-230429 900,82 NBS (National Bureau of Standards) Determination of the
Facility.	Use of Artificial Intelligence and Microelectronic Test Struc-	Fine-Structure Constant, and of the Quantized Hall Resist ance and Josephson Frequency-to-Voltage Quotient in S
PB89-176515 901,353 NBS/NRL (National Bureau of Standards/Naval Research	tures for Evaluation and Yield Enhancement of Microelec- tronic Interconnect Systems.	Units.
Laboratory) Free Electron Laser Facility. PB89-175749 901,351	PB89-146955 900,768	PB89-230437 901,55
PEPPLER, T. K.	PETER, G. High-Precision Absolute Gravity Observations in the United	Magnetic Correlations in an Amorphous Gd-Al Spin Glass.
Comparison of Time Scales Generated with the NBS (National Bureau of Standards) Ensembling Algorithm.	States. PB89-227946 901,281	PB89-201693 901,144
PB89-174072 900,628	PETERKOFSKY, A.	PIELERT, J. H. Standard Specifications for Cements and the Role in Their
In Search of the Best Clock. PB90-117367 900,632	Crystal Structure of a Cyclic AMP (Adenosine Monophos- phate)-Independent Mutant of Catabolite Gene Activator	Development of Quality Assurance Systems for Laboratories.
PEREIRA, S. F.	Protein.	PB89-150742 901,02
Generation of Squeezed Light by Intracavity Frequency Doubling.	PB89-201594 901,224 PETERSEN, S. R.	PIERCE, D. T. Domain Images of Ultrathin Fe Films on Ag(100).
PB89-227938 901,365	Advanced Heat Pumps for the 1990's Economic Perspectives for Consumers and Electric Utilities.	PB89-158067 901,39
PERELES, T. R. Methods for the Production of Particle Standards.	PB90-118043 900,089	High Resolution Imaging of Magnetization. PB89-147433 901,38
PB89-201636 901,047	NBS (National Bureau of Standards) Life-Cycle Cost (NBSLCC) Program (for Microcomputers).	Improved Low-Energy Diffuse Scattering Electron-Spin Po
PEREPEZKO, J. H. Kinetics of Resolidification.	PB89-151211 . 900,849	larization Analyzer. PB89-229173 900,210
PB89-176457 901,138	Thermal and Economic Analysis of Three HVAC (Heating, Ventilating, and Air Conditioning) System Types in a Typical	Influence of the Surface on Magnetic Domain-Wall Micros
Pathways for Microstructural Development in TiAl. PB90-123779 901,173	VA (Veterans Administration) Patient Facility. PB89-188619 900,847	tructure. PB90-118019 901,46
Solidification of Aluminum-Manganese Powders. PB89-172332 901,137	ZIP: The ZIP-Code Insulation Program (Version 1.0) Eco-	Magnetic Properties of Surfaces Investigated by Spin Polar ized Electron Beams.
PERERA, R. C. C.	nomic Insulation Levels for New and Existing Houses by Three-Digit ZIP Code. Users Guide and Reference Manual.	PB89-176564 901,40
Near-Threshold X-ray Fluorescence Spectroscopy of Mole-	PB89-151765 900,058	Spin-Polarized Electron Microscopy. PB89-158075 901,39
PB89-176523 900,382	ZIP: ZIP-Code Insulation Program (for Microcomputers). PB89-159446 900,060	Use of Thorium as a Target in Electron-Spin Analyzers.
PEREZ, E. 13C NMR Method for Determining the Partitioning of End	PETERSON, K. I.	PB90-117938 900,91. Vector Imaging of Magnetic Microstructure.
Groups and Side Branches between the Crystalline and Non-Crystalline Regions in Polyethylene.	Structure of the CO2-CO2-H2O van der Waals Complex Determined by Microwave Spectroscopy.	PB90-128240 901,476
PB89-202451 900,569	PB89-230288 900,479 PETERSON, M. B.	PIERMARINI, G. J.
Morphological Partitioning of Ethyl Branches in Polyethyl- ene by (13)C NMR.	Development and Use of a Tribology Research-in-Progress	Bulk Modulus and Young's Modulus of the Superconducto Ba2Cu3YO7.
PB89-176051 900,560	Database. PB89-228274 901,002	PB90-123613 901,463 Effects of Pressure on the Vibrational Spectra of Liquid Ni
Solid State (13)C NMR Investigation in Polyoxetanes. Effect of Chain Conformation.	PETERSON, R. L.	tromethane.
PB89-176036 900,558	Bean Model Extended to Magnetization Jumps. PB89-176994 901,407	PB89-158026 900,344 PINDZOLA, M. S.
PERIS, J. Turning Workstation in the AMRF (Automated Manufactur-	Josephson-Junction Model of Critical Current in Granular	Electron-Impact Excitation of the Resonance Transition in
ing Research Facility). PB89-185607 900,954	Y1Ba2Cu3O(7-delta) Superconductors. PB89-176978 901,406	CA(1 +). PB89-171557 901,50
PERIS, J. P.	PETERSONS, O.	Electron-Impact Ionization of La(q+) lons (q= 1,2,3).
Multiple Actuator Hydraulic System and Rotary Control Valve Therefor.	Audio-Frequency Current Comparator Power Bridge: Development and Design Considerations.	PB90-123845 901,573 PINE, A. S.
PATENT-4 838 145 900,995	PB89-201537 900,717 PFENNING, D. B.	Infrared and Microwave Investigations of Interconversion
PERKINS, R. A. Experimental Thermal Conductivity, Thermal Diffusivity, and	Structure and Radiation Properties of Large-Scale Natural	Tunneling in the Acetylene Dimer. PB89-157341 900,320
Specific Heat Values of Argon and Nitrogen. PB89-148407 900,293	Gas/Air Diffusion Flames. PB89-157572 900,589	Infrared and Microwave Spectra of OCO-HF and SCO-HF.
Relation between Wire Resistance and Fluid Pressure in	PHAN, L. T.	PB89-179121 900,389 Microwave and Infrared Electric-Resonance Optotherma
the Transient Hot-Wire Method. PB89-184113 901,520	Static Tests of One-third Scale Impact Limiters. PB89-216469 901,000	Spectroscopy of HF-HCl and HCl-HF. PB89-234215 900,489
Use of Dye Tracers in the Study of Free Convection in	PHELAN, R. J.	Photoacoustic Measurement of Differential Broadening of
Porous Media. PB89-173918 <i>901,327</i>	Electrically Calibrated Silicon Bolometer for Low Level Opti- cal Power and Energy Measurements.	the Lambda Doublets in NO(X (2)Pi 1/2, v= 2-0) by Ar. PB90-117656 900,500
PERLOTTO, K. L.	PB89-171714 901,348	Vibrational Predissociation in the H-F Stretching Mode of
Use of GMAP (Geometric Modeling Applications Interface	Fast Optical Detector Deposited on Dielectric Channel Wa-	HF-DF.

		,,
PITTMAN, T. L.	PB89-230320 900,481	FIPS PUB 134-1 900,660
Stark Broadening of Spectral Lines of Homologous, Doubly lonized Inert Gases.	High-Accuracy Differential-Pulse Anodic Stripping Voltam- metry Using Indium as an Internal Standard.	Data Communication Systems and Services User-Oriented Performance Measurement Methods, Category: Telecom-
PB89-158083 900,343	PB89-176267 900,198	munications Standard. FIPS PUB 155 900,664
PITTS, W. M. Assessment of Need for and Design Requirements of a	High-Accuracy Differential-Pulse Anodic Stripping Voltam- metry with Indium as an Internal Standard.	Facsimile Coding Schemes and Coding Control Functions
Wind Tunnel Facility to Study Fire Effects of Interest to DNA.	PB89-156947 900,182	for Group 4 Facsimile Apparatus, Category: Telecommuni- cations Standard.
PB89-200208 901,276	Voltammetric and Liquid Chromatographic Identification of Organic Products of Microwave-Assisted Wet Ashing of Bi-	FIPS PUB 150 900,662
Assessment of Theories for the Behavior and Blowout of Lifted Turbulent Jet Diffusion Flames.	ological Samples. PB89-157994 <i>900,188</i>	General Aspects of Group 4 Facsimile Apparatus, Category: Telecommunications Standard.
PB89-231096 900,603	PRINCE, E.	FIPS PUB 149 900,661
Executive Summary for the Workshop on Developing a Predictive Capability for CO Formation in Fires.	 Alternative Approach to the Hauptman-Karle Determinantal Inequalities. 	High Speed 25-Position Interface for Data Terminal Equip- ment and Data Circuit-Terminating Equipment, Category:
PB89-200091 900,134	PB89-186241 901,416	Telecommunications Standard. FIPS PUB 154 900,663
Importance of Isothermal Mixing Processes to the Under- standing of Lift-Off and Blow-out of Turbulent Jet Diffusion	Maximum Entropy Distribution Consistent with Observed Structure Amplitudes.	RADEBAUGH, R.
Flames. PB89-201172 900,598	PB89-186258 901,417	Ineffectiveness of Powder Regenerators in the 10 K Tem-
PLANT, A. L.	Neutron Diffraction Determination of Full Structures of Anhydrous Li-X and Li-Y Zeolites.	perature Range. PB89-173876 <i>901,005</i>
Generic Liposome Reagent for Immunoassays.	PB90-118001 900,516	Measurement of Regenerator Ineffectiveness at Low Tem-
PB90-123886 901,229 Liposome-Enhanced Flow Injection Immunoanalysis.	Statistical Descriptors in Crystallography: Report of the International Union of Crystallography Subcommittee on	peratures. PB89-173884 901,006
PB89-146757 900,036	Statistical Descriptors. PB89-201826 901,432	Refrigeration Efficiency of Pulse-Tube Refrigerators. PB89-173892 901,007
PLAZEK, D. J.	Structure of V9Mo6O40 Determined by Powder Neutron	PB89-173892 901,007 RADERMACHER, R.
Viscosity of Blends of Linear annd Cyclic Molecules of Similar Molecular Mass.	Diffraction. PB90-117995 900,515	Experimental Determination of Forced Convection Evapora-
PB89-172480 900,555	PRINI, R. F.	tive Heat Transfer Coefficients for Non-Azeotropic Refriger- ant Mixtures.
PLEVA, M. A. Expert-Database System for Sample Preparation by Micro-	Evaluation of Data on Solubility of Simple Apolar Gases in Light and Heavy Water at High Temperature.	PB89-186407 901,117
wave Dissolution. 1. Selection of Analytical Descriptors. PB89-229108 900,216	PB90-126251 900,529	RAHN, L. A. High Resolution Inverse Raman Spectroscopy of the CO Q
POLL, J. D.	PRINJA, R. K. Stellar Winds of 203 Galactic O Stars: A Quantitative Ultra-	Branch.
Analysis of Roto-Translational Absorption Spectra Induced in Low Density Gases of Non-Polar Molecules: The Meth-	violet Survey. PB89-202626 900,022	PB89-171292 900,355 RAINE, K.
ane Case.	PRINZ, G. A.	Numerical Aperture of Multimode Fibers by Several Meth-
PB89-201800 900,427 POLVANI, R. S.	Domain Images of Ultrathin Fe Films on Ag(100). PB89-158067 901,394	ods: Resolving Differences. PB90-117482 900,757
Dynamic Microindentation Apparatus for Materials Charac-	PRITCHARD, D.	RAINWATER, J. C.
terization. PB89-176911 901,140	Exoergic Collisions of Cold Na*-Na. PB90-123761 901,571	Asymptotic Expansions for Constant-Composition Dew-
POMMERSHEIM, J. M.	PROCTOR, F. M.	Bubble Curves Near the Critical Locus. PB89-227987 901,545
Set Time Control Studies of Polymer Concrete. PB90-111238 901,057	Inventory of Equipment in the Cleaning and Deburring	Determination of Binary Mixture Vapor-Liquid Critical Densities from Coexisting Density Data.
POMMERSHEIN, J.	Workstation. PB89-209233 900,958	PB89-202170 901,536
Implications of Computer-Based Simulation Models, Expert Systems, Databases, and Networks for Cement Research.	PUGH, G. N.	Prediction of Shear Viscosity and Non-Newtonian Behavior in the Soft-Sphere Liquid.
PB89-146989 900,581	Institute for Materials Science and Engineering: Metallurgy, Technical Activities 1988.	PB89-228035 901,548
PORTER, G.	PB89-201321 901,147 PURTSCHER, P. T.	Second Viscosity and Thermal-Conductivity Vinal Coefficients of Gases: Extension to Low Reduced Temperature.
Decay of High Valent Manganese Porphyrins in Aqueous Solution and Catalyzed Formation of Oxygen.	Effect of Chemical Composition on the 4 K Mechanical	PB89-179691 900,397
PB89-156772 900,308	Properties of 316LN-Type Alloys. PB90-128554 <i>901,110</i>	Shear Dilatancy and Finite Compressibility in a Dense Non- Newtonian Liquid.
PORTER, J. G. Helium Resonance Lines in the Flare of 15 June 1973.	Fracture Behavior of 316LN Alloy in Uniaxial Tension at	PB89-174023 901,328
PB90-118142 900,028	Cryogenic Temperatures. PB90-128562 901,111	Shear-Induced Angular Dependence of the Liquid Pair Cor- relation Function.
POST, J. E. Refinement of the Substructure and Superstructure of Ro-	Linear-Elastic Fracture of High-Nitrogen Austenitic Stainless Steels at Liquid Helium Temperature.	PB89-228043 900,469
manechite. PB89-157721 <i>901,392</i>	PB90-117623 901,108	Vapor-Liquid Equilibrium of Binary Mixtures in the Extended Critical Region. I. Thermodynamic Model.
POSTEK, M. T.	QUINN, F. M. Vibrationally Resolved Photoelectron Angular Distributions	PB89-218374 901,544
Approach to Accurate X-Ray Mask Measurements in a	for H2 in the Range 17 eV < or = h(nu) < or = 39 eV.	Vapor-Liquid Equilibrium of Nitrogen-Cxygen Mixtures and Air at High Pressure.
PB89-172555 900,776	PB89-176952 900,385 QUINTERO, R.	PB89-174932 <i>900,368</i> RAM. S.
Specimen Biasing to Enhance or Suppress Secondary Elec-	Mining Automation Real-Time Control System Architecture	Data Management Strategies for Computer Integrated Man-
tron Emission from Charging Specimens at Low Accelerating Voltages.	Standard Reference Model (MASREM). PB89-221154 901,286	ufacturing Systems. PB89-209258 900,959
PB89-228464 901,451 POTZICK, J. E.	QUINTIERE, J. G.	RAMAKER, D. E.
Automated Calibration of Optical Photomask Linewidth	Analytical Methods for Firesafety Design. PB89-157275 900,111	Secondary-Electron Effects in Photon-Stimulated Desorp-
Standards at the National Institute of Standards and Technology.	Fire Growth and Development.	tion. PB89-157929 <i>900,337</i>
PB89-186340 901,315	PB90-128570 900,152 Fundamentals of Enclosure Fire 'Zone' Models.	RAMANAN, A.
POULOS, T. L. Use of an Imaging Proportional Counter in Macromolecular	PB89-176168 900,122	Structure of V9Mo6O40 Determined by Powder Neutron Diffraction.
Crystallography.	Scaling Applications in Fire Research. PB90-118068 900,149	PB90-117995 900,515
PB90-136599 900,538 POULSEN, O.	Upward Turbulent Flame Spread on Wood under External	RAMBOZ, J. D.
Fundamental Tests of Special Relativity and the Isotropy of	Radiation. PB90-118050 <i>900,148</i>	High-Current Measurement Techniques. Part II. 100-kA Source Characteristics and Preliminary Shunt and Rogowski
Space. PB89-185920 <i>901,523</i>	RABANI, J.	Coil Evaluations. PB89-170872 900,804
POWELL, C. J.	Reaction of (Ir(C(3), N bpy)(bpy)2)(2+) with OH Radicals and Radiation Induced Covalent Binding of the Complex to	RANDA, J.
Calculations of Electron Inelastic Mean Free Paths for 31 Materials.	Several Polymers in Aqueous Solutions.	Thermo-Optic Designs for Microwave and Millimeter-Wave Electric-Field Probes.
PB89-157978 900,341	PB90-123498 900,264 RABB, A. F.	PB90-128588 900,691
Cross Sections for Inelastic Electron Scattering in Solids. PB89-202972 901,440	Aerodynamics of Agglomerated Soot Particles.	RAO, R. R.
Status of Reference Data, Reference Materials and Refer-	PB89-147482 900,586 RADACK, D. J.	Fourth-Order Elastic Constants of beta-Brass. PB90-117607 901,160
ence Procedures in Surface Analysis. PB89-157705 900,332	Use of Artificial Intelligence and Microelectronic Test Struc-	RASAIAH, J. C.
Technical Activities 1988, Surface Science Division.	tures for Evaluation and Yield Enhancement of Microelectronic Interconnect Systems.	Molecular Dynamics Study of a Dipolar Fluid between Charged Plates.
PB89-161889 900,349 PRATT, K. W.	PB89-146955 900,768 RADACK, S. M.	PB89-147441 900,290
Determination of the Absolute Specific Conductance of Pri-	Coding and Modulation Requirements for 4,800 Bit/Second	Molecular Dynamics Study of a Dipolar Fluid between Charged Plates. 2.
mary Standard KCI Solutions.	Modems, Category: Telecommunications Standard.	PB89-157218 900,312

RASBERRY, S. D.	PB90-128554 <i>901,110</i>	PB89-149280 900,68
Environmental Standard Reference Materials - Present and Future Issues. PB89-150940 900.865	Effects of Grain Size and Cold Rolling on Cryogenic Properties of Copper.	RESSLER, S. Incrementor: A Graphical Technique for Manipulating P.
NBS (National Bureau of Standards) Activities in Biological	PB90-128604 901,176 Fatigue Resistance of a 2090-T8E41 Aluminum Alloy at	rameters. PB89-177000 900,6-
Reference Materials. PB89-157770 901,219	Cryogenic Temperatures. PB90-128737 901,177	RHODERICK, G. C.
RASMUSSEN, A. L. Improved Low-Level Silicon-Avalanche-Photodiode Transfer	Fracture Behavior of 316LN Alloy in Uniaxial Tension at	Comparison of a Cryogenic Preconcentration Technique
Standards at 1.064 Micrometers. PB90-130303 900,736	Cryogenic Temperatures. PB90-128562 901,111	and Direct Injection for the Gas Chromatographic Analys of Low PPB (Parts-per-Billion) (NMOL/MOL) Gas Standard of Toxic Organic Compounds.
RAUFASTE, N. J.	Linear-Elastic Fracture of High-Nitrogen Austenitic Stainless Steels at Liquid Helium Temperature.	PB89-173843 900,18
Building Technology Project Summaries 1989. PB89-193213 900,131	PB90-117623 901,108 Loading Rate Effects on Discontinuous Deformation in	Preparation of Accurate Multicomponent Gas Standards Volatile Toxic Organic Compounds in the Low-Parts-per-B
Wind and Seismic Effects. Proceedings of the Joint Meeting of the U.SJapan Cooperative Program in Natural Re-	Load-Control Tensile Tests. PB89-171896 901,097	lion Range. PB89-157739 900,18
sources Panel on Wind and Seismic Effects (20th) Held in Gaithersburg, Maryland on May 17-20, 1988.	Nitrogen in Austenitic Stainless Steels.	Preparation of Standards for Gas Analysis. PB89-211940 900,21
PB89-154835 900,157	PB90-117649 901,109 Tensile and Fatigue-Creep Properties of a Copper-Stainless	RHORER, R.
RAY, S. R. Modular Process Planning System Architecture.	Steel Laminate. PB90-128646 901,083	Preliminary Experiments with Three Identical Ultraprecision Machine Tools.
PB90-128596 900,966 NBS AMRF (National Bureau of Standards) (Automated	Tensile Strain-Rate Effects in Liquid Helium. PB89-174882 901,102	PB89-150841 900,98
Manufacturing Research Facility) Process Planning System: System Architecture.	REEDER, D. J.	RHYNE, J. J. Characterization of Structural and Magnetic Order of Er/
PB89-193882 900,956 RAYMAN, M. D.	Anti-T2 Monoclonal Antibody Immobilization on Quartz Fibers: Stability and Recognition of T2 Mycotoxin.	Superlattices. PB90-123662
Precise Laser Frequency Scanning Using Frequency-Syn-	PB90-128760 901,267 Development of Electrophoresis and Electrofocusing Stand-	Exchange and Magnetostrictive Effects in Rare Earth S
thesized Optical Frequency Sidebands: Application to Isotope Shifts and Hyperfine Structure of Mercury. PB90-118134 901,370	ards. PB89-175863 900,195	perlattices. PB89-202667 <i>901,43</i>
PB90-118134 901,370 READ, D. T.	REEVE, C. P.	Long-Range Incommensurate Magnetic Order in Dy-Y Mul layers.
Failure Analysis of an Amine-Absorber Pressure Vessel. PB89-173835 901,101	Machine-Learning Classification Approach for IC Manufac- turing Control Based on Test Structure Measurements.	PB89-179642 901,41
Fracture Behavior of a Pressure Vessel Steel in the Ductile-	PB89-228530 900,790 Minimax Approach to Combining Means, with Practical Ex-	Magnetic Correlations in an Amorphous Gd-Al Spin Glass. PB89-201693 901,14
to-Brittle Transition Region. PB89-189195 901,103	amples. PB89-171847 901,211	Magnetic Structure of Y0.97Er0.03. PB89-202675 901,43
J-Integral Values for Small Cracks in Steel Panels. PB89-149090 901,093	REEVE, G. R.	Mn-Mn Exchange Constants in Zinc-Manganese Chalco
Measurement of Applied J-Integral Produced by Residual Stress.	Proficiency Testing for MIL-STD 462 NVLAP (National Vol- untary Laboratory Accreditation Program) Laboratories.	genides. PB90-136706 <i>901,47</i>
PB90-117631 900,163	PB90-128612 901,381 REHM, R. G.	Neutron Diffraction Study of the Wurtzite-Structure Dilut Magnetic Semiconductor Zn0.45Mn0.55Se.
Postweld Heat Treatment Criteria for Repair Welds in 2-1/4Cr-1Mo Superheater Headers: An Experimental Study.	Solution for Diffusion-Controlled Reaction in a Vortex Field. PB89-176622 900,594	PB90-136714 901,47
PB89-156160 901,094 READER, J.	REID, L. S.	Neutron Scattering Study of the Spin Ordering in Amo phous Tb45Fe55 and Tb25Fe75. PB89-201701 901,14
4s(2) 4p(2)-4s4p(3) Transition Array and Energy Levels of the Germanium-Like Ions Rb VI - Mo XI.	Use of Structural Templates in Protein Backbone Modeling. PB89-175277 901,246	Occurrence of Long-Range Helical Spin Ordering in Dy-
PB89-201065 901,528	REIDY, A. M.	Multilayers. PB89-179634 901,41
Laser-Produced Spectra and QED (Quantum Electrodynamic) Effects for Fe-, Co-, Cu-, and Zn-Like lons of Au, Pb, Bi,	Bibliography of the NIST (National Institute of Standards and Technology) Electromagnetic Fields Division Publica-	Re-Entrant Spin-Glass Properties of a-(FexCr1-x)75P15C10 PB89-157481
Th, and U. PB89-176010 <i>901,510</i>	tions. PB89-189211 900,810	Spin-Density-Wave Transition in Dilute YGd Single Crystals
Recent Progress on Spectral Data for X-ray Lasers at the National Bureau of Standards.	REIF, A. K. Standard Chemical Thermodynamic Properties of Polycyclic	PB89-202030 901,43
PB89-158091 901,341 Scheme for a 60-nm Laser Based on Photopumping of a	Aromatic Hydrocarbons and Their Isomer Groups 1. Benzene Series.	RICHARDS, P. L. Measurement of Integrated Tuning Elements for SIS Mixe
High Level of Mo(6+) by a Spectral Line of Mo(11+). PB89-186415 900,407	PB89-186480 900,412	with a Fourier Transform Spectrometer. PB89-157051 900,70
Spectra and Energy Levels of Br XXV, Br XXIX, Br XXX,	Standard Chemical Thermodynamic Properties of Polycyclic Aromatic Hydrocarbons and Their Isomer Groups. 2.	MM Wave Quasioptical SIS Mixers. PB89-214738 901,44
and Br XXXI. PB89-176002 901,509	Pyrene Series, Naphthopyrene Series, and Coronene Series.	SIS Quasiparticle Mixers with Bow-Tie Antennas.
Spectra and Energy Levels of the Galliumlike Ions Rb VII- Mo XII.	PB89-226591 900,459 REINHARDT, W. P.	PB89-157036 900,70 RICHARDSON, M. C.
PB89-179105 900,387 REASENBERG, R. D.	Classical Chaos, the Geometry of Phase Space, and Semi- classical Quantization.	Laser-Produced Spectra and QED (Quantum Electrodynan
Microarcsecond Optical Astrometry: An Instrument and Its Astrophysical Applications.	PB89-172381 901,506 REISENAUER, E.	ic) Effects for Fe-, Co-, Cu-, and Zn-Like lons of Au, Pb, E Th, and U.
PB89-171268 900,013	Turning Workstation in the AMRF (Automated Manufactur-	PB89-176010 901,51 Spectra and Energy Levels of Br XXV, Br XXIX, Br XXX
REBBERT, R. E. Standard Reference Materials for the Determination of Po-	ing Research Facility). PB89-185607 900,954	and Br XXXI. PB89-176002 901,50
lycyclic Aromatic Hydrocarbons. PB89-156889 900,178	RENEKER, D. H. Composites Databases for the 1990's.	RICHOUX, M. C.
REDDY, J. N. Higher Order Beam Finite Element for Bending and Vibra-	PB89-180376 901,075	Decay of High Valent Manganese Porphyrins in Aqueou Solution and Catalyzed Formation of Oxygen.
tion Problems. PB89-229124 901,484	RENNEX, B. Circular and Square Edge Effect Study for Guarded-Hot-	PB89-156772 900,30 Dehydrogenation of Ethanol in Dilute Aqueous Solution
REDMILES, D. F.	Plate and Heat-Flow-Meter Apparatuses. PB89-176135 900,881	Photosensitized by Benzophenones. PB89-157556 900,25
ASM/NBS (American Society for Metals/National Bureau of Standards) Numerical and Graphical Database for Binary	Summary of Circular and Square Edge Effect Study for Guarded-Hot-Plate and Heat-Flow-Meter Apparatuses.	Reactions of Magnesium Prophyrin Radical Cations i
Alloy Phase Diagrams. PB89-157986 901,135	PB89-176606 900,884	Water. Disproportionation, Oxygen Production, and Compa ison with Other Metalloporphyrins.
REED, D. L. Influence of Reaction Reversibility on Continuous-Flow Ex-	RENO, R. C. Texture Monitoring in Aluminum Alloys: A Comparison of	PB89-151005 900,30 Redox Chemistry of Water-Soluble Vanadyl Porphyrins.
traction by Emulsion Liquid Membranes. PB89-176481 900,244	Ultrasonic and Neutron Diffraction Measurements. PB90-117409 901,159	PB89-150999 900,30
REED, M.	RENZ, P. L. Shortest Paths in Simply Connected Regions in R2	RICHTER, D. Hydrogen Sites in Amerohous Pd85Si15HY Probed by Ne
Mathematical Software: PLOD. Plotted Solutions of Differential Equations.	Shortest Paths in Simply Connected Regions in R2. PB90-123688 901,202	Hydrogen Sites in Amorphous Pd85Si15HX Probed by Nei tron Vibrational Spectroscopy. PB89-229140 901,45
PB89-147425 <i>901,194</i> REED, P. R .	REPJAR, A. G. Accurate Determination of Planar Near-Field Correction Pa-	RICHTER, L. J.
Proceedings of the Workshop on Cement Stabilization of Low-Level Radioactive Waste. Held at Gaithersburg, Mary-	rameters for Linearly Polarized Probes. PB89-156871 900,704	Non-Boltzmann Rotational and Inverted Spin-Orbit Stat Distributions for Laser-Induced Desorption of NO froi
land on May 31-June 2, 1989. NUREG/CP-0103 901,302	Antenna Measurements for Millimeter Waves at the National Bureau of Standards.	Distributions for Laser-induced Desorption of NO from Pt(111). PB89-157952
REED, R. P.	PB89-150726 900,694	Optically Driven Surface Reactions: Evidence for the Rol
Effect of Chemical Composition on the 4 K Mechanical Properties of 316LN-Type Alloys.	Calibrating Antenna Standards Using CW and Pulsed-CW Measurements and the Planar Near-Field Method.	of Hot Electrons. PB89-157937 900,33

RICKETTS, B. W. Quantized Hall Resistance Measurement at the NML (Na-	PB90-123407 901,249 ROBERTSON, B. E.	ROOK, H. L. Precision and Accuracy Assessment Derived from Calibra.
tional Measurement Laboratory). PB89-179675 900,778	Statistical Descriptors in Crystallography: Report of the	tion Data. PB89-179162 900,886
RICO, F.	International Union of Crystallography Subcommittee on Statistical Descriptors.	ROSASCO, G. J.
Fundamental Configurations in Mo IV Spectrum. PB89-147011 900,284	PB89-201826 901,432 ROBERTSON, P. J.	Effects of Velocity and State Changing Collisions or Raman Q-Branch Spectra.
RICO, F. R.	Growth and Properties of High-Quality Very-Thin SOS (Sili-	PB89-179196 900,39
Spectrum of Doubly Ionized Tungsten (W III). PB89-235659 900,223	con-on Sapphire) Films. PB90-128109 900,798	High Resolution Inverse Raman Spectroscopy of the CO C Branch.
RIDDER, S. D.	High-Mobility CMOS (Complementary Metal Oxide Semi- conductor) Transistors Fabricated on Very Thin SOS Films.	PB89-171292 900,355
Process Control during High Pressure Atomization. PB89-179170 901,142	PB89-230460 900,791	Measurements of the Nonresonant Third-Order Susceptibili- ty.
RIED, D. L.	ROBEY, S. W.	PB89-179212 901,357
Magnetic Evaluation of Cu-Mn Matrix Material for Fine-Filament Nb-Ti Superconductors.	Resonant Excitation of an Oxygen Valence Satellite in Photoemission from High-T(sub c) Superconductors.	ROSE, A. H. Faraday Effect Sensors: The State of the Art.
PB89-200489 901,425	PB89-186860 901,420 ROBINS, J. L.	PB89-231153 900,823
RIIS, E. Fundamental Tests of Special Relativity and the Isotropy of	Domain Images of Ultrathin Fe Films on Ag(100).	Optical Fiber Sensors for Electromagnetic Quantities. PB89-173967 900,725
Space. PB89-185920 901,523	PB89-158067 901,394 ROBINS, L. H.	Optical Fiber Sensors for the Measurement of Electromagnetic Quantities.
RINAUDOT, G.	Cathodoluminescence of Defects in Diamond Films and	PB89-176671 900,748
Product Data Exchange Specification: First Working Draft.	Particles Grown by Hot-Filament Chemical-Vapor Deposition.	ROSE, J.
PB89-144794 900,940	PB90-117961 901,069	NBS/NRL (National Bureau of Standards/Naval Research Laboratory) Free Electron Laser Facility.
Laser-Noise-Induced Population Fluctuations in Two- and	ROBINSON, S. Determination of Short Lifetimes with Ultra High Resolution	PB89-175749 901,351
Three-Level Systems. PB89-171235 901,342	(n,gamma) Spectroscopy. PB90-123670 <i>901,567</i>	ROSEN, M. Ultrasonic Characterization of Surface Modified Layers.
Systems Driven by Colored Squeezed Noise: The Atomic	ROCHE, M.	PB89-147409 901,115
Absorption Spectrum. PB89-171185 901,500	Mining Automation Real-Time Control System Architecture	ROSENBERG, R. O.
RITTER, J. J.	Standard Reference Model (MASREM). PB89-221154 901,286	Liquid, Crystalline and Glassy States of Binary Charged Colloidal Suspensions.
Methods for the Production of Particle Standards. PB89-201636 901,047	Real Time Generation of Smooth Curves Using Local Cubic Segments.	PB89-202501 901,436
Multiple Scattering in the X-ray-Absorption Near-Edge	PB89-171623 901,196	ROSENTHAL, L. S. Electronic Publishing: Guide to Selection.
Structure of Tetrahedral Ge Gases. PB89-146922 900,283	ROCKETT, J. A. Comparisons of NBS/Harvard VI Simulations and Full-	PB89-214753 900,935
Multiple Scattering in the X-ray Absorption Near Edge Structure of Tetrahedral Germanium Gases.	Scale, Multiroom Fire Test Data.	ROSMUS, P.
PB89-228480 900,474	PB90-128620 <i>900,170</i> RODER, H. M.	Weakly Bound NeHF. PB90-118100 900,518
Synthesis and Magnetic Properties of the Bi-Sr-Ca-Cu Oxide 80- and 110-K Superconductors.	Experimental Thermal Conductivity, Thermal Diffusivity, and	ROSS, H.
PB89-179725 901,412	Specific Heat Values of Argon and Nitrogen. PB89-148407 900,293	Experimental Determination of Forced Convection Evapora- tive Heat Transfer Coefficients for Non-Azeotropic Refriger-
Synthesis, Stability, and Crystal Chemistry of Dibanum Pentatitanate.	High Temperature Thermal Conductivity Apparatus for Fluids.	ant Mixtures. PB89-186407 901,117
PB89-179741 901,041	PB89-174015 900,366	ROSSBACH, M.
Effect of Lateral Crack Growth on the Strength of Contact	Relation between Wire Resistance and Fluid Pressure in the Transient Hot-Wire Method.	Activation Analysis Opportunities Using Cold Neutron Beams.
Flaws in Brittle Materials. PB89-171813 901,034	PB89-184113 901,520	PB89-156970 900,183
ROBAUGH, D.	Thermal Conductivity of Liquid Argon for Temperatures be- tween 110 and 140 K with Pressures to 70 MPa.	Use of Focusing Supermirror Neutron Guides to Enhance Cold Neutron Fluence Rates.
Mechanism and Rate of Hydrogen Atom Attack on Toluene at High Temperatures.	PB89-179600 900,394	PB89-171946 901,306
PB89-179758 900,398	RODONO, M. Doppler Imaging of AR Lacertae at Three Epochs.	ROSSINGTON, D. R.
ROBBINS, C. R. Critical Assessment of Requirements for Ceramic Powder	PB89-149199 900,015	Adsorption of High-Range Water-Reducing Agents on Selected Portland Cement Phases and Related Materials.
Characterization. PB89-146849 901,016	Rotational Modulation and Flares on RS Canum Venati- corum and BY Draconis Stars X: The 1981 October 3 Flare	PB90-124306 900,583 ROSSITER, W. J.
ROBERTS, J.	on V711 Tauri (= HR 1099). PB89-202618 900,021	ASTM (American Society for Testing and Materials) Com-
Preliminary Crystal Structure of Acinetobacter glutaminasificans Glutaminase-Asparaginase.	Rotational Modulation and Flares on RS Canum Venati-	mittee Completes Work on EPDM Specification. PB89-212260 900,140
PB90-123381 901,260	corum and BY Draconis Stars. XI. Ultraviolet Spectral Images of AR Lacertae in September 1985.	Corrosion of Metallic Fasteners in Low-Sloped Roofs: A
ROBERTS, J. R. Line Identifications and Radiative-Branching Ratios of Mag-	PB89-234298 900,026 Rotational Modulation and Flares on RS CVn and BY Dra	Review of Available Information and Identification of Re- search Needs.
netic Dipole Lines in Si-like Ni, Cu, Zn, Ge, and Se.	Stars IX. IUE (International Ultraviolet Explorer) Spectrosco-	PB89-162580 900,113
PB89-234165 901,558 Neonlike Ar and Cl 3p-3s Emission from a theta-pinch	py and Photometry of II Peg and V711 Tau during February 1983.	Friability of Spray-Applied Fireproofing and Thermal Insula- tions: Field Evaluation of Prototype Test Devices. P889-189328 900,130
Plasma. PB90-123746 <i>901,570</i>	PB89-171615 900,019 ROGINSKY, D. V. I.	PB89-189328 900,130 Interim Criteria for Polymer-Modified Bituminous Roofing
ROBERTS, W. E.	Calculation of Tighter Error Bounds for Theoretical Atomic-	Membrane Materials. PB89-168025 900,114
Corrosion of Metallic Fasteners in Low-Sloped Roofs: A Review of Available Information and Identification of Re-	Oscillator Strengths. PB89-158109 901,496	Report of Roof Inspection: Characterization of Newly-Fabri-
search Needs.	ROITMAN, P.	cated Adhesive-Bonded Seams at an Army Facility. PB90-112376 900,107
PB89-162580 900,113 Friability of Spray-Applied Fireproofing and Thermal Insula-	Correlation between CMOS (Complementary Metal Oxide Semiconductor) Transistor and Capacitor Measurements of	Results of a Survey of the Performance of EPDM (Ethylene
tions: Field Evaluation of Prototype Test Devices. PB89-189328 900,130	Interface Trap Spectra. PB89-180020 900,779	Propylene Diene Terpolymer) Roofing at Army Facilities. PB89-209316 900, 136
Thermal Degradation of Poly (methyl methacrylate) at 50C	ROLFE, E. J.	Strain Energy of Bituminous Built-Up Membranes: A New
to 125C. PB89-157465 900,549	Proceedings of the Celebratory Symposium on a Decade of UV (Ultraviolet) Astronomy with the IUE Satellite, Volume 2.	Concept in Load-Elongation Testing. PB89-212203 900,138
ROBERTS, W. L.	N89-16535/1 900,014	Tests of Adhesive-Bonded Seams of Single-Ply Rubber Membranes.
Pahasapaite, a Beryllophosphate Zeolite Related to Synthetic Zeolite Rho, from the Tip Top Pegmatite of South	ROLLETT, J. S. Statistical Descriptors in Crystallography: Report of the	PB89-212120 900,138
Dakota. PB89-186431 901,288	International Union of Crystallography Subcommittee on	ROTH, R. S.
PB89-186431 901,288 ROBERTSON, B.	Statistical Descriptors. PB89-201826 901,432	Defect Intergrowths in Banum Polytitanates. 1. Ba2Ti9O20. PB89-146823 901,014
Application of Magnetic Resonance Imaging to Visualization	ROMAN, E.	Defect Intergrowths in Barium Polytitanates. 2. BaTi5O11.
of Flow in Porous Media. PB89-179592 901,329	Synchrotron Radiation Study of BaO Films on W(001) and Their Interaction with H2O, CO2, and O2.	PB89-146831 901,015 Neutron Study of the Crystal Structure and Vacancy Distri
Measurement of Shear Rate on an Agitator in a Fermentation Broth.	PB89-157697 900,252 ROMAN, P.	bution in the Superconductor Ba2Y Cu3 O(sub g-delta). PB90-123480 901,466
PB89-186720 901,009	Magnetic Receptors of (150)Th Oriented in a Terhium	Phone Equilibria and Country Chemistry in the Toronto

Magnetic Resonance of (160)Tb Oriented in a Terbium Single Crystal at Low Temperatures. PB89-179204 901,519

Nonlinear Effect of an Oscillating Electric Field on Membrane Proteins.

Phase Equilibria and Crystal Chemistry in the Ternary System BaO-TiO2-Nb2O5: Part 1.
PB89-171797 901,033

Phase Equilibria and Crystal Chemistry in the System BaO-TiO2-Nb2O5. Part 2. New Barium P	Ternary Polytitan-	PB90-130295 901,003 RUHLE, M.	PB90-123845 901,573 Spectroscopy of Autoionizing States Contributing to Elec-
ates with < 5 mole % Nb2O5. PB89-189815	900,419	Diffraction Effects Along the Normal to a Grain Boundary. PB89-202089 901,153	tron-impact lonization of lons. PB90-123837 901,572
Phase Relations between the Polytitanates of Banthe Banum Borates, Vanadates and Molybdates.		RULE, D. L.	SAMBE, H.
	901,032	Low-Temperature Thermal Conductivity of Composites: Alumina Fiber/Epoxy and Alumina Fiber/PEEK.	Secondary-Electron Effects in Photon-Stimulated Desorption.
Syntheses and Unit Cell Determination of Ba3V4C Low- and High-Temperature Ba3P4O13. PB89-179717	901.040	PB89-218358 901,078	PB89-157929 900,337
Synthesis, Stability, and Crystal Chemistry of Dibanu		RUMBLE, J. Computerized Materials Property Data Systems.	SAMS, R. L. High Resolution Spectrum of the nu(sub 1) + nu(sub 2)
tatitanate.	901,041	PB89-187512 <i>901,312</i>	Band of NO2. A Spin Induced Perturbation in the Ground State.
Thermomechanical Detwinning of Supercor		RUMBLE, J. R. Chemical and Spectral Databases: A Look into the Future.	PB89-187561 900,417
YBa2Cu3O7-x Single Crystals.	901,458	PB89-180038 900,579	SAMSON, J. A. R.
ROTH, S. C.	,	RUPP, N. W.	Absolute Cross Sections for Molecular Photoabsorption, Partial Photoionization, and Ionic Photofragmentation Proc-
In Situ Fluorescence Monitoring of the Viscosities of cle-Filled Polymers in Flow.	of Parti-	Adhesive Bonding of Composites. PB90-123696 900,050	ess. PB89-186464 <i>900.410</i>
PB89-146278	900,609	Comparison of Microleakage of Experimental and Selected Commercially Available Bonding Systems.	SANCHEZ, I. C.
ROTTMAN, C. Critical and Noncritical Roughening of Surfaces (Cor	mment)	PB89-234223 901,079	Microphase Separation in Blockcopolymer/Homopolymer.
PB89-180046	901,415	Pulpal and Micro-organism Responses to Two Experimental Dental Bonding Systems.	PB89-176069 900,561 Polymer Phase Separation.
ROUSE, R. C. Pahasapaite, a Beryllophosphate Zeolite Related	to Syn-	PB89-202931 901,258	PB89-202923 900,570
thetic Zeolite Rho, from the Tip Top Pegmatite o		RUSH, J. J. Chemical Physics with Emphasis on Low Energy Excita-	Theory of Microphase Separation in Graft and Star Copolymers.
Dakota. PB89-186431	901,288	tions.	PB89-176028 900,557
Wheatleyite, Na2Cu(C2O4)2 . 2H2O, a Natural Copper Salt of Oxalic Acid.	Sodium	PB89-179659 900,396 Hydrogen Sites in Amorphous Pd85Si15HX Probed by Neu-	SANDER, L. C.
	900,390	tron Vibrational Spectroscopy.	Comparison of Liquid Chromatographic Selectivity for Poly- cyclic Aromatic Hydrocarbons on Cyclodextrin and C18
ROWAN, W. L.		PB89-229140 901,456 Neutron Vibrational Spectroscopy of Disordered Metal Hy-	Bonded Phases. PB90-128539 900,231
Aluminumlike Spectra of Copper through Molybdenu PB89-172365	m. <i>900,360</i>	drogen Systems. PB89-157499 900,324	Continine in Freeze-Dried Urine Reference Material.
Analysis of Magnesiumlike Spectra from Cu XVIII XXXI.	to Mo	PB89-15/499 900,324 RUSSELL, R.	PB90-213703 900,675 Preparation of Glass Columns for Visual Demonstration of
	900,508	Inventory of Equipment in the Cleaning and Deburring	Reversed Phase Liquid Chromatography.
Chlorine-like Spectra of Copper to Molybdenum. PB90-117706	900,501	Workstation. PB89-209233 900,958	PB89-187546 900,206 Recent Advances in Bonded Phases for Liquid Chromatog-
Line Identifications and Radiative-Branching Ratios		RUSSELL, T. J.	raphy.
netic Dipole Lines in Si-like Ni, Cu, Zn, Ge, and Se.	901.558	Correlation between CMOS (Complementary Metal Oxide Semiconductor) Transistor and Capacitor Measurements of	PB89-187520 900,204 Standard Reference Materials for the Determination of Po-
Wavelengths and Energy Levels of the K I Isoelectro	,	Interface Trap Spectra. PB89-180020 900,779	lycyclic Aromatic Hydrocarbons.
quence from Copper to Molybdenum. PB89-179097	901,372	Radiation-Induced Interface Traps in Power MOSFETs.	PB89-156889 900,178 Synthesis and Characterization of Novel Bonded Phases
ROWE, J. M.	,	PB89-201974 900,784	for Reversed-Phase Liquid Chromatography. PB90-128695 900,233
Chemical Physics with Emphasis on Low Energy tions.	Excita-	RUST, B. W. Proper Motion vs. Redshift Relation for Superluminal Radio	SANDERS, A. A.
PB89-179659	900,396	Sources.	Improved Low-Level Silicon-Avalanche-Photodiode Transfer
Small Angle Neutron Scattering Spectrometer at t tional Bureau of Standards.	the Na-	PB89-157663 900,017 RUTHBERG, Z. G.	Standards at 1.064 Micrometers. PB90-130303 900,736
	901,396	Report of the Invitational Workshop on Integrity Policy in	SANDERS, R.
ROY, P. Autoionization Dynamics in the Valence-Shell Phot	oioniza-	Computer Information Systems (WIPCIS). PB89-168009 900,670	Sequential Determination of Biological and Pollutant Elements in Marine Bivalves.
tion Spectrum of CO.	900,386	SAAM, W. F.	PB89-156897 901,217
RUBIN, A.		Critical and Noncritical Roughening of Surfaces (Comment). PB89-180046 901,415	SANGSTER, J.
Guideline for Work Station Design. PB90-112418	900,643	SAGUCHI, R.	Octanol-Water Partition Coefficients of Simple Organic Compounds.
RUBINSTEIN, E.	000,040	Phase Contrast Matching in Lamellar Structures Composed of Mixtures of Labeled and Unlabeled Block Copolymer for	PB90-126244 900,528
Preparation of Multistage Zone-Refined Materials for mochemical Standards.	or Ther-	Small-Angle Neutron Scattering.	SANSALONE, M. Finite Element Studies of Transient Wave Propagation.
	900,203	PB89-157119 901,182 SAID, M. R.	PB89-186902 901,375
RUBINSTEIN, M. Magnetization and Magnetic Aftereffect in Textured	d NE (C)	Magnetic Structure of Cubic Tb0.3Y0.7Ag.	SANSONETTI, C. J.
Compositionally-Modulated Alloys.		PB90-117789 901,466	Accurate Energies of nS, nP, nD, nF and nG Levels of Neutral Cesium.
PB90-123431 Mossbauer Hyperfine Fields in RBa2(Cu0.97Fe0.03	901,165 N3 O(7•	SAITO, K. Upward Turbulent Flame Spread on Wood under External	PB89-202121 900,431
x)(R = Y,Pr,Er).		Radiation. PB90-118050 900,148	Spectrum and Energy Levels of Singly Ionized Cesium. 2. Interpretation of Fine and Hyperfine Structures.
PB89-201206 RUDDER, F. F.	901,429	SAKIMOTO, K.	PB89-172373 900,361
Operations Manual for the Automatic Operation of th	ne Verti-	Cross Sections for Collisions of Electrons and Photons with Oxygen Molecules.	SANTORO, A. Crystal Chemistry of Superconductors: A Guide to the Tai-
cal Workstation. PB89-183214	900,973	PB89-226575 900,457	loring of New Compounds. PB89-171730 901,030
RUEGG, F. C.		SALAMON, M. B.	Neutron Powder Diffraction Structure and Electrical Proper-
Three-Dimensional Atomic Spectra in Flames Usin wise Excitation Laser-Enhanced Ionization Spectrosc	сору.	Characterization of Structural and Magnetic Order of Er/Y Superlattices.	ties of the Defect Pyrochlores Pb1.5M2O6.5 (M = Nb, Ta). PB89-172431 900,363
PB89-202071 RUEGG. R. T.	900,430	PB90-123662 901,470 Evaluation and Magnetostrictive Effects in Page Earth Su-	Neutron Study of the Crystal Structure and Vacancy Distri-
Energy Prices and Discount Factors for Life-Cyc	le Cost	Exchange and Magnetostrictive Effects in Rare Earth Superlattices.	bution in the Superconductor Ba2Y Cu3 O(sub g-delta). PB90-123480 901,468
Analysis 1988: Annual Supplement to NBS (I Bureau of Standards) Handbook 135 and NBS Spec	National	PB89-202667 901,438 Long-Range Incommensurate Magnetic Order in Dy-Y Multi-	SANTORO, R. J.
lication 709.	900,850	layers.	FT-IR (Fourier Transform-Infrared) Emission/Transmission
NBS (National Bureau of Standards) Life-Cycle		PB89-179642 901,411 Occurrence of Long-Range Helical Spin Ordering in Dy-Y	Spectroscopy for In situ Combustion Diagnostics. PB89-211866 900,600
(NBSLCC) Program (for Microcomputers).	900,849	Multilayers. PB89-179634 901,410	SAPERS, S.
RUFF, A. W.	.,	SALEMME, F. R.	Photodissociation of Methyl Iodide Clusters. PB89-171193 900,253
Computer-Controlled Test System for Operating E Wear Test Machines.	Different	Use of an Imaging Proportional Counter in Macromolecular	SASAKI, H.
PB89-228290	900,983	Crystallography. PB90-136599 <i>900,538</i>	Low Field Determination of the Proton Gyromagnetic Ratio in Water.
Dynamic Microindentation Apparatus for Materials terization.	Charac-	SALOMON, C.	PB89-230411 901,555
PB89-176911	901,140	Towards the Ultimate Laser Resolution. PB89-186910 900,416	SASAKI, T.
Measurements of Tribological Behavior of Advance- rials: Summary of U.S. Results on VAMAS (Versail	d Mate- lles Ad-	SALZBORN, E.	Oxygen Isotope Effect in the Superconducting Bi-Sr-Ca-Cu- O System.
vanced Materials and Standards) Round-Robin No. 2		Electron-Impact Ionization of La(q+) lons (q= 1,2,3).	PB89-157044 901,025

SASS, S. L.		py and Photometry of II Peg and V711 Tau d	uring February	Simple F-Center Laser Spectrometer for Cont	inuous Single
Diffrection Effects Along the Normal to a Grain B	oundary. <i>901,153</i>	1983. PB89-171615	900,019	Frequency Scans. PB89-179774	901,35
PB89-202089 Electron Diffraction Study of the Faceting of		SCHAEFER, R. J.		SCHIMA, F. J.	
Boundaries in NiO. PB89-201792	901,431	Amorphous Phase Formation in Al70Si17Fe13 PB90-123522	901,167	NBS (National Bureau of Standards) Decay-Sitigations of (82)Sr-(82)Rb. PB89-161558	cheme Inves
Grain Boundary Characterization in Ni3Al. PB89-229306	901,156	Formation and Stability Range of the G Phese num-Manganese System.	e in the Alumi-	SCHIRMER. A.	301,43
Grain Boundary Structure in Ni3Al.	,	PB89-186316	901,144	Use of Focusing Supermirror Neutron Guides	s to Enhence
PB89-201784 Grain Boundary Structure in Ni3Al.	901,150	Formation of Dispersoids during Rapid Solid Al-Fe-Ni Alloy.		Cold Neutron Flüence Rates. PB89-171946	901,30
PB89-229314	901,157	PB90-123647 In situ Observation of Particle Motion and Dif	901,172	SCHMIDT, W. A.	
SATIJA, S. K.	vers at the	tions during Coarsening.		Effects of a Gold Shank-Overlayer on the Field of Silicon.	d Ion Imagin
Applications of Mirrors, Supermirrors and Multilate National Bureau of Standards Cold Neutron Res	search Fa-	PB89-201982	901,151	PB89-175988	901,40
cility. PB89-211981	901,540	Nucleation and Growth of Aperiodic Crystals Alloys.	s in Aluminum	SCHNABEL, R. B.	0-4
SATO, H.	.,	PB89-186324	901,145	User's Reference Guide for ODRPACK: Weighted Orthogonal Distance Regression Ver	
New International Skeleton Tebles for the Therr	modynamic	Replacement of Icosahedral Al-Mn by Decago PB89-186332	onal Phase. 901,146	PB89-229066	901,21
Properties of Ordinary Water Substance. PB89-145130	900,270	Solidification of Aluminum-Manganese Powde PB89-172332		SCHNEIDER, M. (12)C(16)O Laser Frequency Tables for the	34.2 to 62.
ATO, T. Dynemics of Concentration Fluctuation on Both	Sides of	Stable and Metesteble Phase Equilibrie		THz (1139 to 2079 cm(-1)) Region. PB89-193908	901,36
Phase Boundary.		System.		Calibration Tables Covering the 1460- to	
PB89-173942 SAUERS, I.	901,183	PB89-172324	901,136	Region from Heterodyne Frequency Measurer	ments on the
Electron-Energy Dependence of the S2F10 M	ass Spec-	SCHAFFT, H. A. Electromigration Damage Response Time an	d Implications	nu(sub 3) Bends of (12)CS2 and (13)CS2. PB89-157416	900,32
trum. PB90-117870	900,512	for dc end Pulsed Characterization. PB89-212179	901.443	CO Laser Stabilization Using the Optogalvenic PB89-179139	Lemb-Dlp. 901,35
Production and Stability of S2F10 in SF6 Co	orona Dis-	Thermal Conductivity Measurements of Thin-F	Ilm Silicon Di-	Heterodyne Frequency Measurements of (12)	
charges. PB69-231039	900.822	oxide.	901,444	Transitions.	
AUL, A.	300,022	PB89-212195 SCHANTZ, M. M.	301,444	PB89-229223	901,37
New International Skeleton Tables for the Therr	nodynamic	Determination of Hydrocarbon/Water Pertitio	n Coefficients	Heterodyne Measurements on N2O Near 1635 PB90-117797	o cm(-1). <i>900,50</i>
Properties of Ordinary Water Substance. PB89-145130	900,270	from Chromatogrephic Data and Based on	Solution Ther-	Heterodyne Measurements on OCS Neer 1372	2 cm(-1).
AULSBERY, L. F.	500,270	modynamics and Theory. PB89-187538	900,205	PB89-201743	900,42
ANA (Automatic Network Analyzer) Measureme		Experiences in Environmental Specimen Bank	ing.	SCHNEIDER, S. J.	
on the ARFTG (Automatic RF Techniques Group Experiment.) Traveling	PB90-123969	900,866	Commercial Advanced Ceramics. PB89-201776	901,04
PB89-173777	900,715	Specimen Banking in the National Status an gram: Development of Protocols and First Yea	ar Results.	International Cooperation and Competition in	Materials Sc
SAUNDERS, P. B.		PB89-175855	901,308	ence and Engineering. PB89-228332	901,19
Electronic Meil and the 'Locator's' Dilemme. PB89-211957	901,205	Standard Reference Materials for the Determ lycyclic Aromatic Hydrocarbons.	nination of Po-	Phase Diagrams for High Tech Ceramics.	001,10
AUNDERS, R. D.		PB89-156889	900,178	PB89-186308	901,04
Apparatus Function of a Prism-Grating Double mator.	Monochro-	SCHARPF, O.		SCHOFER, R.	
PB89-186282	901,359	Use of Focusing Supermirror Neutron Guide Cold Neutron Fluence Rates.	s to Enhance	Theory and Practice of Paper Preservation for PB89-147052	900,93
NBS (National Bureau of Standards) Scale of Sp	ectral Ra-	PB89-171946	901,306	SCHON, K.	
diance. PB89-201685	901,532	SCHATZ, G. C.		International Comparison of HV Impulse Me	asuring Sys
AUVAGEAU, J. E.		Reduced Dimensionality Quantum Reactin Study of the Insertion Reaction O(1D) + H		tems. PB89-186423	900,80
Superconducting Kinetic Inductance Bolometer. PB89-200505	900,762	H. PB89-234280	900,492	SCHRACK, R. A.	
SAVAGE, H.	555,152	Three Dimensional Quantum Reactive Scatte		Simplified Shielding of a Metallic Restoration ation Therapy.	during Rad
Water Structure in Crystalline Solids: Ices to Prote	eins.	the I + HI Reaction and of the IHI(1-) Pho		PB89-229256	900,04
PB89-186746	900,413	Spectrum. PB89-227961	900,466	SCHRAMM, R. E.	
Water Structure in Vitamin B12 Coenzyme Crysta ysis of the Neutron and X-rey Solvent Densities.		SCHEINFEIN, M. R.		EMATs (Electromagnetic Acoustic Transducer Crack Inspection of Railroad Wheels.	s) for Roll-B
PB89-186803	901,222	Improved Low-Energy Diffuse Scattering Ele- larization Analyzer.	ctron-Spin Po-	PB90-123894	901,59
Water Structure in Vitamin B12 Coenzyme C Structural Characteristics of the Solvent Networks	irystals. 2. S.	PB89-229173	900,218	Ultrasonic Railroad Wheel Inspection Using I	EMATs (Elec
PB89-186811	901,223	Influence of the Surface on Magnetic Domai	n-Wall Micros-	tromagnetic-Accoustic Transducers), Report N PB89-189229	16. 18. <i>901,59</i>
SAVAGE, H. F. J.	and Cris	tructure. PB90-118019	901,467	SCHREIBER, C. T.	
Repulsive Regularities of Water Structure in Ices talline Hydrates.		Use of Thorium as a Target in Electron-Spin A	Analyzers.	Comparison of Fluoride Uptake Produced	by Tray an
PB89-186753	900,414	PB90-117938	900,912	Flossing Methods In vitro. PB89-179238	901,25
SAYKALLY, R. J. New FIR Laser Lines and Frequency Measure	ements for	Vector Imaging of Magnetic Microstructure. PB90-128240	901,476	SCHRODER, B.	
Optically Pumped CD3OH.		SCHEN, M. A.	.,	Quasifree Electron Scattering on Nucleons in	a Momentum
PB89-175731 SAYRE, E. V.	901,350	Influence of Molecular Weight on the Res	onant Raman	Dependent Potential. PB89-186738	901,52
Technical Examination, Lead Isotope Determin	ation, and	Scattering of Polyacetylene. PB89-179246	900.564	SCHUBERT, P.	
Elemental Analysis of Some Shang and Zho	u Dynasty	Polymerization of a Novel Liquid Crystallin	e Diacetylene	Preconcentration of Trace Transition Metal ar	nd Rare Eart
Bronze Vessels. PB90-136862	901,178	Monomer. PB89-231286	900.575	Elements from Highly Saline Solutions. PB90-118175	900,22
SCACE, R. I.		Resonant Raman Scattering of Controlled Mo	•	SCHULTE, R.	
Interlaboratory Determination of the Calibration the Measurement of the Interstitial Oxygen Con	Factor for tent of Sili-	Polyacetylene.		International Comparison of HV Impulse Me	easuring Sys
con by Infrared Absorption.		PB89-157093 SCHENCK, P. K.	900,548	tems. PB89-186423	900,80
PB90-117300 Semiconductor Measurement Technology: Da	900,224	Computer Graphics for Ceramic Phase Diagra	ams.	SCHWARTZ, L.	
Semiconductor Measurement Technology: Da end Statistical Analysis of the Interlaboratory De	termination	PB89-186290	901,043	Versailles Project on Advenced Materials e Evolution to Permanent Status.	nd Standard
of the Conversion Coefficient for the Measuren Interstitial Oxygen Content of Silicon by Infrared	nent of the Absorption	Laser Induced Vaporization Time Resolved trometry of Refractores.	Mass Spec-	PB89-201768	900,96
PB89-221170	901,054	PB90-136904	900,540	SCHWARTZ, L. H.	
Standards and Test Methods for VLSI (Very Larg tegration) Materials.	e Scale In-	PC-Access to Ceramic Phase Diagrams. PB89-211841	901,053	International Cooperation and Competition in ence and Engineering.	Materials Sc
PB89-158042	900,774	SCHIFFMAN, A.	901,003	PB89-228332	901,19
SCALABRIN, A.		Absolute Infrared Transition Moments for Op-	en Shell Diato-	Materials Failure Prevention at the Nation	al Bureau d
New FIR Laser Lines and Frequency Measur Optically Pumped CD3OH.	ements for	mics from J Dependence of Transition Intention to OH.	sities: Applica-	Standards. PB89-212237	901,19
PB89-175731	901,350	PB89-227912	900,463	SCHWARTZ, R. B.	

Dipole Moment Function and Vibrational Transition Intensities of OH.
PB89-227920 900,464

SCALTRITI, F.

Rotational Modulation and Flares on RS CVn and BY Dra Stars IX. IUE (International Ultraviolet Explorer) Spectrosco-

International Intercomparison of Neutron Survey Instrument Calibrations.
PB89-229165 901,300

Refinement of Neutron Energy Deposition and Microdosimetry Calculations.	PB89-202964 900,785	PB89-186860 901,420
PB89-150791 901,264	Influence of Electronic and Geometric Structure on Desorption Kinetics of Isoelectronic Polar Molecules: NH3 and	Synchrotron Radiation Study of BaO Films on W(001) and Their Interaction with H2O, CO2, and O2.
SCHWARZ, F. Biological Standard Reference Materials for the Calibration	H2O. PB89-176473 <i>900,381</i>	PB89-157697 900,252
of Differential Scanning Calorimeters: Di-alkylphosphatidyl- choline in Water Suspensions.	Surface Properties of Clean and Gas-Dosed SnO2 (110).	SHINN, N. D. Cr(110) Oxidation Probed by Carbon Monoxide Chemisorp-
PB89-186779 900,415	PB89-179576 900,393 SEMERJIAN, H. G.	tion. PB89-228423 900,239
SCHWARZ, F. P. Biological Thermodynamic Data for the Calibration of Differ-	Dynamic Light Scattering and Angular Dissymmetry for the	Oxygen Chemisorption on Cr(110): 1. Dissociative Adsorp-
ential Scanning Calonmeters: Heat Capacity Data on the	In situ Measurement of Silicon Dioxide Particle Synthesis in Flames.	tion. PB89-202980 900,441
Unfolding Transition of Lysozyme in Solution. PB90-117920 900,513	PB89-179584 900,246	Oxygen Chemisorption on Cr(110): 2. Evidence for Molecu-
Differential Scanning Calorimetric Study of Brain Clathrin.	FT-IR (Fourier Transform-Infrared) Emission/Transmission Spectroscopy for In situ Combustion Diagnostics.	lar Ö2(ads). PB89-202998 900,442
PB90-117912 900,225 SCHWARZENBACH, D.	PB89-211866 900,600	Stimulated Desorption from CO Chemisorbed on Cr(110).
Statistical Descriptors in Crystallography: Report of the	Laser Excited Fluorescence Studies of Black Liquor. PB89-176416 900,243	PB89-203004 900,443
International Union of Crystallography Subcommittee on Statistical Descriptors.	Laser Induced Fluorescence for Measurement of Lignin	Synchrotron Photoemission Study of CO Chemisorption on Cr(110).
PB89-201826 901,432 SCIMECA, T.	Concentrations in Pulping Liquors. PB89-17.2530 901,184	PB89-231336 900,262
Oxygen Partial-Density-of-States Change in the	Remote Sensing Technique for Combustion Gas Tempera-	SHIRLEY, J. New Cavity Configuration for Cesium Beam Primary Fre-
YBa2Cu3Ox Compounds for x(Approx.)6,6.5,7 Measured by Soft X-ray Emission.	ture Measurement in Black Liquor Recovery Boilers. PB89-179568 900,392	quency Standards.
PB89-186274 901,419	SENGERS, J. M. H. L.	PB89-171649 900,714 SHIVAPRASAD, S. M.
SCIRE, F.	Semi-Automated PVT Facility for Fluids and Fluid Mixtures. PB89-157184 900,875	Adsorption Properties of Pt Films on W(110).
Optical Roughness Measurements for Industrial Surfaces. PB89-176655 900,979	SENGERS, J. V.	PB89-146864 900,281
SCOTT, T. R.	Capillary Waves of a Vapor-Liquid Interface Near the Criti-	SHIVES, T. R. Tensile Tests of Type 305 Stainless Steel Mine Sweeping
NBS (National Bureau of Standards) Laser Power and Energy Measurements.	cal Temperature. PB89-228555 900,476	Wire Rope.
PB89-171680 <i>901,346</i>	Simplified Representation for the Thermal Conductivity of	PB90-130287 901,112 SHNEIER, M. O.
NBS (National Bureau of Standards) Standards for Optical Power Meter Calibration.	Fluids in the Critical Region. PB89-228050 901,332	Building Representations from Fusions of Multiple Views.
PB89-176200 <i>900,726</i>	Van der Waals Fund, Van der Waals Laboratory and Dutch	PB89-177059 900,991
Optical Power Measurements at the National Institute of Standards and Technology.	High-Pressure Science. PB89-185755 900,401	SHOEMAKER, C. Turning Workstation in the AMRF (Automated Manufactur-
PB89-187579 900,918	SERIES, R. W.	ing Research Facility).
SCRIBNER, C. Brick Masonry: U.S. Office Building in Moscow.	Interlaboratory Determination of the Calibration Factor for the Measurement of the Interstitial Oxygen Content of Sili-	PB89-185607 900,954 SHULL, P. J.
PB89-187504 900,160	con by Infrared Absorption.	EMATs (Electromagnetic Acoustic Transducers) for Roll-By
SCROGER, M. G.	PB90-117300 900,224 SESKO, D.	Crack Inspection of Railroad Wheels. PB90-123894 901,597
NIST (National Institute of Standards and Technology) Measurement Services: The Calibration of Thermocouples	Collisional Losses from a Light-Force Atom Trap.	SHULL, R. D.
and Thermocouple Materials. PB89-209340 900,897	PB90-123936 <i>901,577</i>	Magnetic Field Dependence of the Superconductivity in Bi-
SCULL, L. L.	SETTLE, F. A. Expert-Database System for Sample Preparation by Micro-	Sr-Ca-Cu-O Superconductors. PB89-146815 901,385
Low Temperature Mechanical Property Measurements of Silica Aerogel Foam.	wave Dissolution. 1. Selection of Analytical Descriptors. PB89-229108 900,216	Synthesis and Magnetic Properties of the Bi-Sr-Ca-Cu
PB90-128638 901,061	SHAPIRO, I. I.	Oxide 80- and 110-K Superconductors. PB89-179725 901,412
Tensile and Fatigue-Creep Properties of a Copper-Stainless Steel Laminate.	Microarcsecond Optical Astrometry: An Instrument and Its	SHUMAKER, J. B.
PB90-128646 901,083	Astrophysical Applications. PB89-171268 900,013	Apparatus Function of a Prism-Grating Double Monochro- mator,
SEELY, J. F. Laser-Produced Spectra and QED (Quantum Electrodynam-	SHAPIRO, M. L.	PB89-186282 901,359
ic) Effects for Fe-, Co-, Cu-, and Zn-Like lons of Au, Pb, Bi,	Spherical Acoustic Resonators in the Undergraduate Laboratory.	SIDDAGANGAPPA, M. C.
Th, and U. PB89-176010 901,510	PB89-179709 901,317	Production and Stability of S2F10 in SF6 Corona Discharges.
Spectra and Energy Levels of Br XXV, Br XXIX, Br XXX, and Br XXXI.	SHELTON, R. N. Antiferromagnetic Structure and Crystal Field Splittings in	PB89-231039 900,822
PB89-176002 901,509	the Cubic Heusler Alloys HoPd2Sn and ErPd2Sn.	SIECK, L. W. Ionic Hydrogen Bond and Ion Solvation. 5. OH(1-)O
SEILER, J. F.	PB89-202659 901,437 SHEN, Q.	Bonds. Gas Phase Solvation and Clustering of Alkoxide and
Interim Criteria for Polymer-Modified Bituminous Roofing Membrane Materials.	Direct Observation of Surface-Trapped Diffracted Waves.	Carboxylate Anions. PB89-157531 900,328
PB89-168025 900,114	PB90-128216 901,475	Relative Acidities of Water and Methanol and the Stabilities of the Dimer Anions.
Report of Roof Inspection: Characterization of Newly-Fabricated Adhesive-Bonded Seams at an Army Facility.	Dynamical Diffraction of X-rays at Grazing Angle. PB89-186886 901,421	PB89-150981 900,299
PB90-112376 900,107	SHERIDAN, P.	Thermochemistry of Solvation of SF6(1-) by Simple Polar Organic Molecules in the Vapor Phase.
Results of a Survey of the Performance of EPDM (Ethylene Propylene Diene Terpolymer) Roofing at Army Facilities.	Performance Standards for Microanalysis. PB89-201651 900,211	PB89-202527 900,437
PB89-209316 900,136	SHERIDAN, P. J.	SIEGRIST, T.
SEKERKA, R. F. Effect of Anisotropic Thermal Conductivity on the Morpho-	Determination of Experimental and Theoretical k (sub ASi) Factors for a 200-kV Analytical Electron Microscope.	Applications of the Crystallographic Search and Analysis System CRYSTDAT in Materials Science.
logical Stability of a Binary Alloy. PB89-228985 901,155	PB90-128653 900,232	PB89-175251 901,402
SELLECK, M. E.	Methods for the Production of Particle Standards. PB89-201636 901,047	SIEGWARTH, J. D. Vortex Shedding Flowmeter for Fluids at High Flow Veloci-
Effect of a Crystal-Melt Interface on Taylor-Vortex Flow.	PB89-201636 901,047 SHERMAN, G. J.	ties.
PB90-130261 901,477 SELTZER, S. M.	PVT Relationships in a Carbon Dioxide-Rich Mixture with	PB90-128661 900,608
Applications of ETRAN Monte Carlo Codes.	Ethane. PB89-229181 900,478	SIEWERT, T. Standards for Real-Time Radioscopy.
PB90-123902 901,574 Cross Sections for Bremsstrahlung Production and Elec-	SHIELDS, J. Q.	PB90-128687 900,924
tron-Impact Ionization.	NBS (National Bureau of Standards) Determination of the Fine-Structure Constant, and of the Quantized Hall Resist-	SIEWERT, T. A. Ferrite Number Prediction to 100 FN in Stainless Steel
PB90-123910 901,575 Overview of ETRAN Monte Carlo Methods.	ance and Josephson Frequency-to-Voltage Quotient in SI	Weld Metal.
PB90-123928 901,576	Units. PB89-230437 <i>901,556</i>	PB89-201586 901,106 Improved Standards for Real-Time Radioscopy.
Pattern Recognition Approach in X-ray Fluorescence Analysis	New Realization of the Ohm and Farad Using the NBS (Na-	PB90-128679 900,923
PB90-128786 900,234	tional Bureau of Standards) Calculable Capacitor. PB89-230445 901,557	Influence of Molybdenum on the Strength and Toughness of Stainless Steel Welds for Cryogenic Service.
SEMANCIK, S.	SHIELDS, J. R.	PB89-173512 901,100
Coadsorption of Water and Lithium on the Ru(001) Surface. PB89-202956 900,440	Flammability Characteristics of Electrical Cables Using the Cone Calorimeter.	On-Line Arc Welding: Data Acquisition and Analysis Using a High Level Scientific Language.
Economical Ultrahigh Vacuum Four-Point Resistivity Probe.	PB89-162572 900,741	PB90-117391 900,972
PB89-147086 900,870 Fundamental Characterization of Clean and Gas-Dosed Tin	SHIH, A. Resonant Excitation of an Oxygen Valence Satellite in Pho-	Role of Inclusions in the Fracture of Austenitic Stainless Steel Welds at 4 K.
Oxide.	toemission from High-T(sub c) Superconductors.	PB89-173504 901,099

Stainless Steel Weld Metal: Prediction of Ferrite Content.	SINGH, N. B.	Testing and Materials) Standard Test Method C-335 Ap-
PB89-231260 901,107	Preparation of Multistage Zone-Refined Materials for Ther- mochemical Standards.	plied to Mineral-Fiber Pipe Insulation. PB89-218341 901,011
Typical Usage of Radioscopic Systems: Replies to a Survey.	PB89-186795 900,203	Interlaboratory Comparison of Two Types of Line-Source
PB90-117664 901,161	SINGLETON, D. L.	Thermal-Conductivity Apparatus Measuring Five Insulating
SIJELMASSI, R.	Evaluated Chemical Kinetic Data for the Reactions of	Materials. PB89-218325 900,144
Object-Oriented Model for Estelle. PB89-211916 900,653	Atomic Oxygen O(3P) with Sulfur Containing Compounds. PB89-145122 900.269	Microporous Fumed-Silica Insulation as a Standard Refer-
Object-Oriented Model for Estelle and Its Smalltalk Imple-	SINHA, S.	ence Material of Thermal Resistance at High Temperature.
mentation.	Long-Range Incommensurate Magnetic Order in Dy-Y Multi-	PB90-130311 900,153
PB89-196190 900,623	layers.	Microporous Fumed-Silica Insulation Board as a Candidate Standard Reference Material of Thermal Resistance.
User Guide for Wise: A Simulation Environment for Estelle.	PB89-179642 901,411	PB89-148373 901,018
PB89-196166 900,620	Occurrence of Long-Range Helical Spin Ordering in Dy-Y Multilayers.	SMITH, J. F.
SILBERSTEIN, S.	PB89-179634 901,410	Texture Monitoring in Aluminum Alloys: A Comparison of
Gypsum Wallboard Formaldehyde Sorption Model. PB90-132705 900,154	SJOLIN, L.	Ultrasonic and Neutron Diffraction Measurements.
Predicting Formaldehyde Concentrations in Manufactured	Preliminary Crystal Structure of Acinetobacter glutaminasifi-	
Housing Resulting from Medium-Density Fiberboard.	cans Glutaminase-Asparaginase. PB90-123381 901,260	SMITH, J. H.
PB89-148134 900,854	SKALL. M. W.	Institute for Materials Science and Engineering: Metallurgy, Technical Activities 1988.
SILVERMAN, J.	Graphics Application Programmer's Interface Standards	PB89-201321 901,147
Reaction of (Ir(C(3), N bpy)(bpy)2)(2+) with OH Radicals and Radiation Induced Covalent Binding of the Complex to	and CALS (Computer-Aided Acquisition and Logistic Sup-	Metallurgical Evaluation of 17-4 PH Stainless Steel Cast-
Several Polymers in Aqueous Solutions.	port). PB90-133091 900,658	ings. PB89-193262 <i>901,105</i>
PB90-123498 900,264	SKANTHAKUMAR, S.	SMITH, J. S.
SIMIC, M. G. Generation of Oxy Radicals in Biosystems.	Magnetic Order of Pr in PrBa2Cu3O7.	Dynamic Young's Modulus Measurements in Metallic Mate-
PB90-117888 901,266	PB90-123803 901,471	nals: Results of an Interlaboratory Testing Program.
Hydroxyl Radical Induced Cross-Linking between Phenyla-	SKOCPOL, W.	PB89-157671 901,132
lanine and 2-Deoxyribose.	Switching Noise in YBa2Cu3Ox 'Macrobridges'. PB89-200513 901,426	SMITH, L. E.
PB89-147029 900,547	SKOPIK, D. M.	Institute for Materials Science and Engineering, Polymers: Technical Activities 1987.
Intramolecular H Atom Abstraction from the Sugar Moiety by Thymine Radicals in Oligo- and Polydeoxynucleotides.	Cross Section and Linear Polarization of Tagged Photons.	PB89-188601 900,566
PB89-171870 901,263	PB90-117292 901,560	Institute for Materials Science and Engineering, Polymers:
Mechanisms of Free Radical Chemistry and Biochemistry of	SLADE, R. C. T.	Technical Activities 1988.
Benzene.	Neutron Diffraction Determination of Full Structures of An-	PB89-166094 900,003
PB90-117714 900,502 SIMIU. E.	hydrous Li-X and Li-Y Zeolites. PB90-118001 900,516	SMITH, R. J.
Hydrodynamic Forces on Vertical Cylinders and the Lighthill	Structure of V9Mo6O40 Determined by Powder Neutron	Comparison of Far-Field Methods for Determining Mode Field Diameter of Single-Mode Fibers Using Both Gaussian
Correction.	Diffraction.	and Petermann Definitions.
PB90-117417 901,313	PB90-117995 900,515	PB90-117474 900,756
SIMMONS, J. A.	SLAUGHTER, S. R.	SMITH, R. L.
Vector Calibration of Ultrasonic and Acoustic Emission Transducers.	Semiconductor Measurement Technology: Automatic Deter- mination of the Interstitial Oxygen Content of Silicon Wafers	Expert Systems Applied to Spacecraft Fire Safety. PB89-231013 901,590
PB89-202014 900,765	Polished on Both Sides.	SMYTH, K. C.
SIMMONS, J. D.	PB89-151831 900,772	Chemical Structure of Methane/Air Diffusion Flames: Con-
NIST (National Institute of Standards and Technology) Cali-	SLOCUM, A. H.	centrations and Production Rates of Intermediate Hydrocar-
bration Services Users Guide. 1989 Edition. PB89-200216 900,926	Multiple Actuator Hydraulic System and Rotary Control Valve Therefor.	bons.
SIMMONS, W. B.	PATENT-4 838 145 900,995	
Wheatleyite, Na2Cu(C2O4)2 . 2H2O, a Natural Sodium	SMALL, J.	Soot Inception in Hydrocarbon Diffusion Flames. PB89-201966 900,599
Copper Salt of Oxalic Acid.	Performance Standards for Microanalysis.	SNELICK, R. D.
PB89-179154 900,390	PB89-201651 900,211	Architecturally-Focused Benchmarks with a Communication
SIMON, T.	SMALL, J. A.	Example.
Rotational Modulation and Flares on RS Canum Venati- corum and BY Draconis Stars X: The 1981 October 3 Flare	Continuum Radiation Produced in Pure-Element Targets by 10-40 keV Electrons: An Empirical Model.	PB89-216477 900,640
on V711 Tauri (= HR 1099).	PB89-201610 900,209	SNIEGOSKI, L. T.
PB89-202618 900,021	Methods for the Production of Particle Standards.	Determination of Serum Cholesterol by a Modification of the Isotope Dilution Mass Spectrometric Definitive Method.
SIMONS, D. S.	PB89-201636 901,047	PB89-234181 901,239
Comparison of Two Transient Recorders for Use with the Laser Microprobe Mass Analyzer.	Modeling of the Bremsstrahlung Radiation Produced in	Determination of Total Cholesterol in Coconut Oil: A New
PB89-176887 900,200	Pure Element Targets by 10-40 keV Electrons. PB89-201644 901,531	NIST (National Institute of Standards and Technology) Cho- lesterol Standard Reference Material.
Dependence of Interface Widths on Ion Bombardment Con-	SMID, M. E.	PB89-234173 901,262
ditions in SIMS (Secondary Ion Mass Spectrometry) Analy-	National Bureau of Standards Message Authentication	SNYDER, J. J.
sis of a Ni/Cr Multilayer Structure. PB89-172506 900,364	Code (MAC) Validation System.	Ultrasensitive Laser Spectroscopy and Detection.
Laser Microprobe Mass Spectrometry: Description and Se-	PB89-231021 900,671 SMILGYS, R. V.	PB89-156996 901,336
lected Applications.	AES and LEED Studies Correlating Desorption Energies	SNYDER, L. E.
PB89-201628 900,210	with Surface Structures and Coverages for Ga on Si(100).	Millimeter- and Submillimeter-Wave Surveys of Orion A
Single Particle Standards for Isotopic Measurements of Uranium by Secondary Ion Mass Spectrometry.	PB89-171599 901,401	Emission Lines in the Ranges 200.7-202.3, 203.7-205.3, and 330-360 GHz.
PB89-201669 901,297	Initial Stages of Heteroepitaxial Growth of InAs on Si(100).	PB90-123787 900,029
SIMPSON, P. A.	PB90-123878 901,473	SO, E.
Fast-Pulse Generators and Detectors for Characterizing	Interaction of In Atom Spin-Orbit States with Si(100) Surfaces.	International Comparison of Power Meter Calibrations Con-
Laser Receivers at 1.06 um. PB89-171698 901.347	PB90-128547 900,532	ducted in 1987. PB89-201545 900,718
PB89-171698 901,347 Improved Low-Level Silicon-Avalanche-Photodiode Transfer	Laser Probing of the Dynamics of Ga Interactions on	•
Standards at 1.064 Micrometers.	Si(100).	SOFER, A. FACTUNC: A User-Friendly System for Unconstrained Opti-
PB90-130303 900,736	PB89-186928 901,422 SMITH, B.	mization.
SIMS, J. S.	Product Data Exchange Specification: First Working Draft.	PB90-112392 901,207
ASM/NBS (American Society for Metals/National Bureau of	PB89-144794 900,940	SOILEAU, M. J.
Standards) Numerical and Graphical Database for Binary Alloy Phase Diagrams.	SMITH, B. M.	Laser Induced Damage in Optical Materials: 1987.
PB89-157986 901,135	External Representation of Product Definition Data.	PB89-221162 901,364
SINDT, C. F.	PB90-112434 900,939	SOLOMON, P. R.
Effect of Pipe Roughness on Orifice Flow Measurement. PB89-231484 901,333	Product Data Exchange: The PDES Project-Status and Ob- jectives.	FT-IR (Founer Transform-Infrared) Emission/Transmission Spectroscopy for In situ Combustion Diagnostics.
	PB90-112426 900,938	PB89-211866 900,600
NBS (National Bureau of Standards)-Boulder Gas Flow Fa- cility Performance.	SMITH, C. H.	SONNENFROH, D. M.
PB89-186787 900,889	Definitions of Granularity.	Laser-Induced Fluorescence Study of Product Rotational
Optimum Location of Flow Conditioners in a 4-Inch Orifice	PB89-180012 900,650	State Distributions in the Charge Transfer Reaction: $Ar(1+)((\sup 2 P)(\sup 3/2)) + N2 -> Ar + N2(1+)(X)$ at 0.28
Meter. PB90-111675 900,911	Notion of Granularity. PB89-147003 900,915	and 0.40 eV.
230,377	300,915	PB89-189823 900,420

SMITH, D. R.

Interlaboratory Comparison of the Guarded Horizontal Pipe-Test Apparatus: Precision of ASTM (American Society for

SINGH, G.

Radiation-Induced Interface Traps in Power MOSFETs. PB89-201974 900,784

Quantum Mechanical Calculations on the Ar(1+) + N2 Charge Transfer Reaction. PB69-228092 900,470

SONNTAG, B. F.	STAHNS, A.	PB89-176408 900,3
Marked Differences in the 3p Photoabsorption between the	Heterodyne Frequency Measurements of (12)C(16)O Laser	Picosecond Laser Study of the Collisionless Photodissoci
Cr and Mn(1+) Isoelectronic Pair: Reasons for the Unique	Transitions.	tion of Dimethylnitramine at 266 nm.
Structure Observed in Cr. PB90-117581 901,562	PB89-229223 901,374 STALCUP, A. M.	PB89-172423 900,23
SORG, J. P.	Synthesis and Characterization of Novel Bonded Phases	Picosecond Studies of Vibrational Energy Transfer in Mol cules on Surfaces.
Preliminary Performance Criteria for Building Materials,	for Reversed-Phase Liquid Chromatography.	PB89-157309 900,3
Equipment and Systems Used in Detention and Correctional Facilities.	PB90-128695 900,233	Picosecond Study of the Population Lifetime of CO(v=
PB89-148514 900,109	STALICK, J. K.	Chemisorbed on SiO2-Supported Rhodium Particles. PB89-157317 900.3
SOUDERS, T. M.	NIST (National Institute of Standards and Technology)/ Sandia/ICDD Electron Diffraction Database: A Database for	
Accurate RF Voltage Measurements Using a Sampling Volt-	Phase Identification by Electron Diffraction.	Picosecond Vibrational Energy Transfer Studies of Surface Adsorbates.
age Tracker. PB89-201552 900,815	PB89-175210 901,508	PB90-136573 900,53
	STALLHOFER, P. Interlaboratory Determination of the Calibration Factor for	Population Relaxation of CO(v= 1) Vibrations in Solution
Ambiguity Groups and Testability. PB90-128703 900,722	the Measurement of the Interstitial Oxygen Content of Sili-	Phase Metal-Carbonyl Complexes. PB89-157291 900,3
SOULEN, R. J.	con by Infrared Absorption.	Time Resolved Studies of Vibrational Relaxation Dynamic
Impedance of Radio-Frequency Biased Resistive Supercon-	PB90-117300 900,224 STANLEY, H. B.	of CO(v = 1) on Metal Particle Surfaces.
ducting Quantum Interference Devices. PB89-201719 900,764	Antiferromagnetic Structure and Crystal Field Splittings in	PB89-203012 900,44
SOUTHWORTH, S. H.	the Cubic Heusler Alloys HoPd2Sn and ErPd2Sn.	Unimolecular Dynamics Following Vibrational Overtone E citation of HN3 v1= 5 and v1= 6:HN3(X tilde;v,J,K,) ->
Autoionization Dynamics in the Valence-Shell Photoioniza-	PB89-202659 901,437	HN((X sup 3)(Sigma (1-));v,J,Omega) + N2(x sup 1)(Sigma
tion Spectrum of CO.	STANLEY, H. R.	sub g (1 +)).
PB89-176960 900,386	Pulpal and Micro-organism Responses to Two Experimental Dental Bonding Systems.	PB89-147110 900,28
Vibrationally Resolved Photoelectron Angular Distributions	PB89-202931 901,258	Vibrational Predissociation of the Nitric Oxide Dimer. PB89-147417 900,28
for H2 in the Range 17 eV< or= h(nu)< or= 39 eV. PB89-176952 900,385	STAUFFER, T. C.	STERN, E. A.
Vibrationally Resolved Photoelectron Studies of the	Nb3Sn Critical-Current Measurements Using Tubular Fiber-	Structural Unit in Icosahedral MnAlSi and MnAl.
7(sigma) (-1) Channel in N2O.	glass-Epoxy Mandrels. PB89-200497 901,527	PB89-157648 901, 13
PB89-176945 900,257	STEARNS, L. C.	STEVENS, W. J.
SPANO, M. L.	Densification, Susceptibility and Microstructure of	Electronic Structure of Diammine (Ascorbato) Platinum(
Magnetic Correlations in an Amorphous Gd-Al Spin Glass. PB89-201693 901,148	Ba2YCu3O(6+ x).	and the Trans Influence on the Ligand Dissociation Energy
	PB89-171821 901,035	
Neutron Scattering Study of the Spin Ordering in Amorphous Tb45Fe55 and Tb25Fe75.	STEBBINS, R. T.	STEWART, G. W.
PB89-201701 901,149	Antenna for Laser Gravitational-Wave Observations in Space.	Ambiguity Groups and Testability. PB90-128703 900,72
SPARKS, L. L.	PB89-234231 901,594	STEWART, R. B.
Low-Temperature Thermal Conductivity of Composites: Alu-	STECKLER, K. D.	Thermodynamic Properties of Argon from the Triple Point
mina Fiber/Epoxy and Alumina Fiber/PEEK. PB89-218358 901,078	Fire Induced Flows in Comdors: A Review of Efforts to	1200 K with Pressures to 1000 MPa.
	Model Key Features.	PB89-222558 900,45
Performance of Alumina/Epoxy Thermal Isolation Straps. PB89-147078 901,070	PB89-189260 900,129 STEEL, E.	STILES, M.
SPEAKE, C. C.	Performance Standards for Microanalysis.	Electron Transmission Through NiSi2-Si Interfaces.
Precision Experiments to Search for the Fifth Force.	PB89-201651 900,211	PB89-231294 900,48
PB89-228365 901,551	STEEL, E. B.	STILES, P. J.
SPELLER, C. V.	High-Punty Germanium X-ray Detector on a 200 kV Analyti-	Hydrodynamics of Magnetic and Dielectric Colloidal Dispesions.
Filling of Solvent Shells About Ions. 1. Thermochemical Cri-	cal Electron Microscope. PB89-201602 900,208	PB89-157242 900,3
teria and the Effects of Isomeric Clusters. PB89-157549 900,329	STEELE, B. C. H.	STOCKBAUER, R.
SPENCER, L. V.	Neutron Powder Diffraction Structure and Electrical Proper-	Synchrotron Radiation Study of BaO Films on W(001) ar
DCTDOS: Neutron and Gamma Penetration in Composite	ties of the Defect Pyrochlores Pb1.5M2O6.5 (M = Nb, Ta).	Their Interaction with H2O, CO2, and O2. PB89-157697 900,25
Duct Systems.	PB89-172431 900,363	STOCKBAUER, R. L.
PB89-188809 901,275	STEER, C. J.	Resonant Excitation of an Oxygen Valence Satellite in Pho
SPERRY, D.	Differential Scanning Calorimetric Study of Brain Clathrin. PB90-117912 900,225	toemission from High-T(sub c) Superconductors.
CO2 Separation Using Facilitated Transport Ion Exchange Membranes.	STEIGERWALD, D. A.	PB89-186860 901,42
PB89-157374 900,321	Role of Adsorbed Gases in Metal on Metal Epitaxy.	STOLZ, A.
SPIEGELMAN, C. H.	PB90-128125 901,174	Rate of Change of the Quincy-Monument Peak Baselin
Minimax Approach to Combining Means, with Practical Ex-	STEIN, S. E.	from a Translocation Analysis of LAGEOS Laser Rang Data.
amples. PB89-171847 <i>901,211</i>	Pi-Electron Properties of Large Condensed Polyaromatic	PB89-234272 901,28
SPIELMAN, F. E.	Hydrocarbons. PB89-202139 900,432	STONE, C. A.
Standards for the Interchange of Large Format Tiled Raster	Rate Constants for Hydrogen Abstraction by Resonance	Neutron Scattering and Its Effect on Reaction Rates
Documents.	Stabilized Radicals in High Temperature Liquids.	Neutron Absorption Experiments. PB90-123738 901,56
PB89-148415 900,668	PB89-161608 900,348	•
SPOONER, S.	Reactions of Phenyl Radicals with Ethene, Ethyne, and Benzene.	STONE, S. Long-Term Stability of the Elemental Composition in Biological Composition in Biologi
Creep Cavitation in Liquid-Phase Sintered Alumina. PB89-175954 901,038	PB89-150908 900,297	ical Materials.
SPRANGLE, P.	STEINER, B.	PB89-156939 900,18
NBS (National Bureau of Standards) Free Electron Laser	Versailles Project on Advanced Materials and Standards	Sequential Determination of Biological and Pollutant Ele
Facility.	Evolution to Pérmanent Status. PB89-201768 900,969	ments in Marine Bivalves. PB89-156897 901,2
PB89-176515 901,353	STEINER, R. L.	STONE, S. F.
NBS/NRL (National Bureau of Standards/Naval Research	Josephson Array Voltage Calibration System: Operational	Experiences in Environmental Specimen Banking.
Laboratory) Free Electron Laser Facility. PB89-175749 901,351	Use and Venification.	PB90-123969 900,86
SPRINGMANN, J. L.	PB89-230403 900,820	Radiochemical and Instrumental Neutron Activation Anal
Internal Structure of the Guide to Available Mathematical	NBS (National Bureau of Standards) Determination of the	sis Procedures for the Determination of Low Level Trac
Software.	Fine-Structure Constant, and of the Quantized Hall Resist- ance and Josephson Frequency-to-Voltage Quotient in SI	Elements in Human Livers. PB89-171953 901,23
PB89-170864 900,927	Units.	STONE, W. C.
STAFFORD, G. R.	PB89-230437 901,556	Brick Masonry: U.S. Office Building in Moscow.
Formation of the Al-Mn Icosahedral Phase by Electrodepo- sition.	STENBAKKEN, G. N.	PB89-187504 900,16
PB90-117763 900,504	Ambiguity Groups and Testability. PB90-128703 900,722	Inelastic Behavior of Full-Scale Bridge Columns Subjecte
Structural Study of a Metastable BCC Phase in Al-Mn	STEPHAN, K.	to Cyclic Loading. PB89-174924 900,58
Alloys Electrodeposited from Molten Salts.	Thermal Conductivity of Refrigerants in a Wide Range of	·
PB89-201040 901,064	Temperature and Pressure.	Progressive Collapse: U.S. Office Building in Moscow. PB89-175715 900, 15
STAHL, W.	PB89-226583 900,458	STRACHAN, D. M.
Microwave Spectrum and Molecular Structure of the Ethyl- ene-Ozone van der Waals Complex.	STEPHENSON, J. C. Dissociation Lifetimes and Loyal Mixing in Overtone Excited	Preconcentration of Trace Transition Metal and Rare Ear
PB89-201735 . 900,424	Dissociation Lifetimes and Level MixIng in Overtone-Excited HN3 (X tilde (sup 1) A').	Elements from Highly Saline Solutions.
STAHLHOFEN, A. A.	PB90-117425 900,263	PB90-118175 900,22
Intrinsic Sticking in dt Muon-Catalyzed Fusion: Interplay of	Picosecond Coherent Anti-Stokes Raman Scattering	STRATY, G. C.
Atomic, Molecular and Nuclear Phenomena. PB90-117565 901,561	(CARS) Study of Vibrational Dephasing of Carbon Disulfide and Benzene in Solution.	Apparatus for Neutron Scattering Measurements of Sheared Fluids.

PB89-235667 901,335	Infrared and Microwave Spectra of OCO-HF and SCO-HF. PB89-179121 900,389	PB89-157044 901,025
Low-Q Neutron Diffraction from Supercooled D-Glycerol. PB89-228001 900,468	Laboratory Measurement of the 1(sub 01)-0(sub 00) Transi-	SWANSON, P. L. Crack-Interface Traction: A Fracture-Resistance Mechanism
PVT Measurements on Benzene at Temperatures to 723 K.	tion and Electric Dipole Moment of SiC2. PB89-228506 900,025	in Brittle Polycrystals. PB89-211817 901,05
PB89-157200 900,311 PVT of Toluene at Temperatures to 673 K.	Microwave Electric-Resonance Optothermal Spectroscopy of (H2O)2.	SWARTZENDRUBER, L. J.
PB89-157192 900,310	PB90-128141 900,531	Brief Review of Recent Superconductivity Research a NIST (National Institute of Standards and Technology).
STRAUSSER, B. User Guide for the NBS (National Bureau of Standards)	Microwave Spectral Tables. 3. Hydrocarbons, CH to C10H10.	PB89-211114 900,766
Prototype Compiler for Estelle (Revised). PB89-196158 900,619	PB90-126269 900,530 Microwave Spectrum and Molecular Structure of the Ethyl-	Magnetic Behavior of Compositionally Modulated Ni-Cu Thin Films.
User Guide for Wizard: A Syntax-Directed Editor and Trans-	ene-Ozone van der Waals Complex. PB89-201735 900,424	PB90-118084 901,16
lator for Estelle. PB89-196174 900,621	Microwave Spectrum and (14)N Quadrupole Coupling Con-	Magnetic Field Dependence of the Superconductivity in Bi Sr-Ca-Cu-O Superconductors. PB89-146815 901,38:
STREICHER, M. A. Corrosion of Metallic Fasteners in Low-Sloped Roofs: A	stants of Carbazole. PB89-157333 900,319	PB89-146815 901,389 Magnetization and Magnetic Aftereffect in Textured Ni/Cu
Review of Available Information and Identification of Re-	Microwave Spectrum, Structure, and Electric Dipole	Compositionally-Modulated Alloys. PB90-123431 901,169
search Needs. PB89-162580 900,113	Moment of Ar-Ch3OH. PB90-117847 900,510	Mossbauer Hyperfine Fields in RBa2(Cu0.97Fe0.03)3 O(7
STROSCIO, J. A. Structure of Cs on GaAs(110) as Determined by Scanning	Microwave Spectrum, Structure, and Electric Dipole Moment of the Ar-Formamide van der Waals Complex.	x)(R= Y,Pr,Er). PB89-201206 901,423
Tunneling Microscopy. PB90-117490 901,463	PB89-157325 900,318	Mossbauer Imaging: Experimental Results. PB90-123415 900,922
STROUP, D. W.	Ozonolysis of Ethylene. Microwave Spectrum, Molecular Structure, and Dipole Moment of Ethylene Primary Ozonide	Mossbauer Spectroscopy.
Test Results and Predictions for the Response of Near- Ceiling Sprinkler Links in a Full-Scale Compartment Fire.	(1,2,3-Trioxolane). PB89-157440 900,323	PB89-211932 901,189 Quantitative Problems in Magnetic Particle Inspection.
PB89-231187 900,095	Structure of the CO2-CO2-H2O van der Waals Complex Determined by Microwave Spectroscopy.	PB89-229199 900,988
STRUBLE, L. Epoxy Impregnation of Hardened Cement Pastes for Char-	PB89-230288 900,479	Synthesis and Magnetic Properties of the Bi-Sr-Ca-Ct Oxide 80- and 110-K Superconductors.
acterization of Microstructure. PB89-185573 901,042	SUGAR, J. Aluminumlike Spectra of Copper through Molybdenum.	PB89-179725 901,412
Epoxy Impregnation Procedure for Hardened Cement Sam-	PB89-172365 900,360	Temperature Hysteresis in the Initial Susceptibility of Rapid ly Solidified Monel.
ples. PB89-147821 901,180	Analysis of Magnesiumlike Spectra from Cu XVIII to Mo XXXI. PB90-117821 900,508	PB90-123423 901,16- Thermomechanical Detwinning of Superconducting
Implications of Computer-Based Simulation Models, Expert Systems, Databases, and Networks for Cement Research.	Chlorine-like Spectra of Copper to Molybdenum.	YBa2Cu3O7-x Single Crystals. PB89-231088 901,458
PB89-146989 900,581	PB90-117706 900,501	SWARTZLANDER, A. B.
Integrated Knowledge Systems for Concrete and Other Materials.	Energy Levels of Molybdenum, Mo 1 through 42. PB89-186472 900,411	High T(sub c) Superconductor/Noble-Metal Contacts with Surface Resistivities in the (10 to the Minus 10th Power
PB89-176119 900,582	Recent Progress on Spectral Data for X-ray Lasers at the National Bureau of Standards.	Omega sq cm Range. PB89-179824 901,41.
Standard Aggregate Materials for Alkali-Silica Reaction Studies.	PB89-158091 901,341	SZABO, S.
PB89-193221 901,046 Synthesis and Characterization of Ettringite and Related	Wavelengths and Energy Level Classifications of Scandium Spectra for All Stages of Ionization.	Hierarchically Controlled Autonomous Robot for Heavy Pay load Military Field Applications.
Phases. PB89-146963 900,238	PB89-145163 900,273 Wavelengths and Energy Levels of the K I Isoelectronic Se-	PB89-177075 901,27
STRUBLE, L. J.	quence from Copper to Molybdenum. PB89-179097 901,372	TABISZ, G. C. Collision Induced Spectroscopy: Absorption and Light Scal
Adsorption of High-Range Water-Reducing Agents on Selected Portland Cement Phases and Related Materials.	SUGAWARA, A.	tering. PB89-212252 901,36
PB90-124306 900,583	Detection of Lead in Human Teeth by Exposure to Aqueous Sulfide Solutions.	TACHIKAWA, K.
STUBENRAUCH, C. F. Brief History of Near-Field Measurements of Antennas at	PB89-201529 901,256	VAMAS (Versailles Project on Advanced Materials and Standards) Intercomparison of Critical Current Measure
the National Bureau of Standards. PB89-156863 900,703	Formation of Hydroxyapatite in Hydrogels from Tetracal- cium Phosphate/Dicalcium Phosphate Mixtures. P889-201511 901,255	ment in Nb3Sn Wires. PB89-202147 901,53
Comparison of Measured and Calculated Antenna Sidelobe Coupling Loss in the Near Field Using Approximate Far-	SULLIVAN, D. A.	TAKAGI, K.
Field Data. PB89-156855 900,702	Pressure and Density Series Equations of State for Steam as Derived from the Haar-Gallagher-Kell Formulation.	Far-Infrared Spectrum of Methyl Amine. Assignment and Analysis of the First Torsional State.
Effect of Random Errors in Planar Near-Field Measurement.	PB89-186456 900,409	PB89-161574 900,34
PB89-171839 900,708	SULLIVAN, D. B. NIST Automated Computer Time Service.	Microwave Spectrum of Methyl Amine: Assignment and Analysis of the First Torsional State.
STUTZMAN, P. Epoxy Impregnation Procedure for Hardened Cement Sam-	PB90-213711 900,676 SULLIVAN. F.	PB90-117839 900,500
ples. PB89-147821 901,180	Efficient Algorithms for Computing Fractal Dimensions.	TAKAGI, S. Formation of Hydroxyapatite in Hydrogels from Tetracal
STUTZMAN, P. E.	PB89-175871 901,198 How to Estimate Capacity Dimension.	cium Phosphate/Dicalcium Phosphate Mixtures. PB89-201511 901,25
Report of Roof Inspection: Characterization of Newly-Fabricated Adhesive-Bonded Seams at an Army Facility.	PB89-172522 901,197	Quasi-Constant Composition Method for Studying the Formation of Artificial Caries-Like Lesions.
PB90-112376 900,107 STWALLEY, W. C.	Monte Carlo Simulation of Domain Growth in the Kinetic Ising Model on the Connection Machine. PB90-136797 901.587	PB89-229249 901,25
Alignment Effects in Ca-He(5(sup 1)P(sub 1) - 5(sup	PB90-136797 901,587 SULLIVAN, S. A.	TAKAHASHI, Y. Shear Effects on the Phase Separation Behaviour of
3)P(sub J)) Energy Transfer Collisions by Far Wing Laser Scattering.	Enthalpies of Desorption of Water from Coal Surfaces. PB89-173868 900,838	Polymer Blend in Solution by Small Angle Neutron Scatter
PB89-179790 900,400 SUEHLE, J. S.	Specific Heat of Insulations.	PB89-229264 900,57
Correlation between CMOS (Complementary Metal Oxide Semiconductor) Transistor and Capacitor Measurements of	PB89-172514 900,116 SULLIVAN, T.	TAKASHASHI, T. Oxygen Isotope Effect in the Superconducting Bi-Sr-Ca-Cu
Interface Trap Spectra.	Long-Term Stability of the Elemental Composition in Biolog-	O System.
PB89-180020 900,779 Electromigration Damage Response Time and Implications	ical Materials. PB89-156939 900,181	PB89-157044 901,02 TAKAYANAGI, K.
for dc and Pulsed Characterization. PB89-212179 901,443	SULLIVAN, T. M. Neutron Activation Analysis of the NIST (National Institute	Cross Sections for Collisions of Electrons and Photons wit
Thermal Conductivity Measurements of Thin-Film Silicon Di-	of Standards and Technology) Bovine Serum Standard Reference Material Using Chemical Separations.	Oxygen Molecules. PB89-226575 900,45
oxide. PB89-212195 901,444	PB89-156921 900,180	TALEB, H.
SUENRAM, R. D.	SUN, J. Effect of Coal Slag on the Microstructure and Creep Behav-	Interpretation of the Effects of Retarding Admixtures of Pastes of C3S, C3A plus Gypsum, and Portland Cement.
Electric-Dipole Moments of H2O-Formamide and CH3OH-Formamide.	ior of a Magnesium-Chromite Refractory. PB89-158034 901,027	PB89-146971 900,58 TALWAR, P.
PB89-147375 900,288 Electric-Resonance Optothermal Spectrum of (H2O)2:	SUNDARAM, P. V.	AC Impedance Method for High-Resistivity Measurement
Microwave Spectrum of the $K=1-0$ Subband for the $E((+ \text{ or } -)2)$ States.	Anti-T2 Monoclonal Antibody Immebilization on Quartz Fibers: Stability and Recognition of T2 Mycotoxin.	of Silicon. PB89-231203 900,79
PB90-117433 900,497	PB90-128760 901,267 SUZUKI, T.	TAMURA, G. T.
Infrared and Microwave Investigations of Interconversion Tunneling in the Acetylene Dimer.	Oxygen Isotope Effect in the Superconducting Bi-Sr-Ca-Cu-	Experimental Fire Tower Studies of Elevator Pressurization Systems for Smoke Control.
PB89-157341 900,320	O System.	PB90-117813 900,09

TANG, AND C. M.		00,453	PB89-174064 900,	614
NBS/NRL (National Bureau of Standards/Naval Research Laboratory) Free Electron Laser Facility.	PB89-186761 90	01,221	TOMAZIC, B. B.	
PB89-175749 901,35	Thermodynamics of the Hydrolysis of Sucrose.		Mechanism of Hydrolysis of Octacalcium Phosphate. PB89-201503 901,	254
TANG, C. M. NBS (National Bureau of Standards) Free Electron Lase		01,227	Micro-Raman Characterization of Atherosclerotic and I prosthetic Calcification.	Bio-
Facility. PB89-176515 901,353	Green Eupstion Mothed for Colculation of Atamietic	Struc-	PB89-149223 901,	234
TANG, D.	ture of Grain Boundary Interfaces in Ionic Crystals.	01,050	TOSCHEK, P. E.	
Optical Fiber Sensors for the Measurement of Electromag netic Ouantities.		,	One Is Not Enough: Intra-Cavity Spectroscopy with M Mode Lasers.	ulti-
PB89-176671 900,748	Novel Flow Process for Metal and Ore Solubilization Aqueous Methyl Iodide.	ion by	PB89-185888 900,	402
TANUMA, S.	PB89-202113 90	01,285	TOTH, L. Resonant Excitation of an Oxygen Valence Satellite in P)ha
Calculations of Electron Inelastic Mean Free Paths for 31 Materials.		hal Aa	toemission from High-T(sub c) Superconductors.	
PB89-157978 900,341	pecis.		PB89-186860 901, TOUSSAINT. G.	420
TAPLEY, B. D. Rate of Change of the Quincy-Monument Peak Baseline		00,421	Electronic Structure of the Cd Vacancy in CdTe.	
from a Translocation Analysis of LAGEOS Laser Range Data.	Ergodic Behavior in Supercooled Liquids and in Glasse	es.	PB89-171318 901,	398
PB89-234272 901,282	PB89-202444 90	01,435	TRAMONTANO, A.	
TATE, D. M.	Liquid, Crystalline and Glassy States of Binary Che Colloidal Suspensions.	varged	Computational Analysis of Protein Structures: Source Methods, Systems and Results.	
Internal Revenue Service Post-of-Duty Location Modeling System: Programmer's Manual for PASCAL Solver.		01,436	PB89-175293 900,	010
PB89-161905 900,001	Measures of Effective Ergodic Convergence in Liquids. PB90-118092 90	s. 00,518	TRAN-CONG, Q. Polymers Bearing Intramolecular Photodimenzable Prol	hes
FAYLOR, B. N. CODATA (Committee on Data for Science and Technology)	THOMAS, W. C.		for Mass Diffusion Measurements by the Forced Rayle Scattering Technique: Synthesis and Characterization.	
Recommended Values of the Fundamental Physical Con-		onduc-	PB89-157101 901,	181
stants, 1986. PB89-145189 900,275	PB89-209324 90	00,896	Temperature, Composition and Molecular-Weight Depe ence of the Binary Interaction Parameter of Polystyre	and-
Fundamental Physical Constants - 1986 Adjustments. PB90-136474 900,535	THOMPSON, R. B. Texture Monitoring in Aluminum Alloys: A Companis	on of	Poly(vinylmethylether) Blends.	
Guidelines for Implementing the New Representations of	Ultrasonic and Neutron Diffraction Measurements.		PB89-157473 900,	550
the Volt and Ohm Effective January 1, 1990.		01,159	TRAVIS, J. Stokes and Anti-Stokes Fluorescence of Er(3+) in	the
PB89-214761 900,817 History of the Present Value of 2o/h Commonly Used for	Production and Spectroscopy of Molecular lons Isolat	ted in	Raman Spectra of Erbium Oxide and Erbium Glasses. PB89-149231 901,	
Defining National Units of Voltage and Possible Changes in	Solid Neon.	00,503	TRAVIS, J. C.	UEU
National Units of Voltage and Resistance. PB89-202154 901,535	Vibrational Spectra of Molecular lons Isolated in		Analytical Applications of Resonance Ionization Mass Sp	ec-
NBS (National Bureau of Standards) Determination of the		00,487	trometry (RIMS). PB89-161590 900,	189
Fine-Structure Constant, and of the Quantized Hall Resistance and Josephson Frequency-to-Voltage Ouotient in SI			Three-Dimensional Atomic Spectra in Flames Using St	
Units. PB89-230437 <i>901,556</i>	Neon. 2. O4(1+) and O4(1-). PB90-128729 90	00,533	wise Excitation Laser-Enhanced Ionization Spectroscopy. PB89-202071 900,	430
New Internationally Adopted Reference Standards of Volt-			TREADO, M. J.	
age and Resistance. PB89-184097 900,808	Influence of Dislocation Density on the Ductile-Brittle sition in bcc Metals.	Tran-	ACSB (Amplitude Companded Sideband): What Is A	de-
U.S. Perspective on Possible Changes in the Electrical		01,133	quate Performance. PB89-176283 901,	599
Units. PB89-157002 901,491	Physics of Fracture, 1987. PB89-201107 90	01,428	TREADO, S. J.	
AYLOR, K. T.	THOMSON, R. M.	71,420	Illumination Conditions and Task Visibility in Daylit Space PB89-189237 900,0	
Computation of the ac Stark Effect in the Ground State of Atomic Hydrogen.	Green Function Method for Calculation of Atomistic S	Struc-	TREVINO, S. F.	
PB89-202535 901,538	ture of Grain Boundary Interfaces in Ionic Crystals. PB89-202105 90	1,050	Pressure Dependence of the Cu Magnetic Order	in
TAYLOR, P. M.	THURBER, W. R.		RBa2Cu3O6+ x. PB90-123829 901,4	472
Methyl Radical Concentrations and Production Rates in a Laminar Methane/Air Diffusion Flame.	AC Impedance Method for High-Resistivity Measuren of Silicon.	ments	TROE, J.	
PB89-171912 900,591 FAYLOR, R. S.	. 255 25 .255	00,793	Evaluated Kinetic and Photochemical Data for Atmosphe Chemistry. Supplement 3.	eric
Microarcsecond Optical Astrometry: An Instrument and Its	TILFORD, C. R. Low Range Flowmeters for Use with Vacuum and	Leak	PB89-222582 900,4	454
Astrophysical Applications. PB89-171268 900,013	Standards.	00,374	TROMBKA, J. I.	- 4.
EAGUE, E. C.	NBS (National Bureau of Standards) Orifice-Flow Pri		Pattern Recognition Approach in X-ray Fluorescence Ansis.	
Measuring the Root-Mean-Square Value of a Finite Record	High Vacuum Standard.		PB90-128786 900,2	234
Length Periodic Waveform. PB90-163924 901,588		-	TROUT, T. K. Effect of pH on the Emission Properties of Aqueous	tris
Optical Roughness Measurements for Industrial Surfaces. PB89-176655 900.979	Gage Effective Areas.	00,905	(2,6-dipicolinato) Terbium (III) Complexes. PB89-157135 900,2	
TERRANOVA, P.	Progress in Vacuum Standards at NBS (National Bure		Element-Specific Epifluorescence Microscopy In vivo Mo	
Dynamic Young's Modulus Measurements in Metallic Mate-	Standards). PB89-201198 900	00,999	toring of Metal Biotransformations in Environmental Maces.	atri-
rials: Results of an Interlaboratory Testing Program. PB89-157671 901,132			PB89-177216 901,2	220
TESK, J. A.	nometer.	01,319	In Situ Fluorescence Monitoring of the Viscosities of Pacle-Filled Polymers in Flow.	arti-
Casting Metals: Reactor Response. PB89-157143 900,054		,,,,,,	PB89-146278 900,6	609
Dental Materials and Technology Research at the National	Electron-Impact Ionization of La($q+$) lons ($q=1,2,3$).	01.573	Studies on Some Failure Modes in Latex Barrier Films. PB89-209308 901,0	กคล
Bureau of Standards: A Model for Government-Private Sector Cooperation.	PB90-123845 90 Spectroscopy of Autoionizing States Contributing to		TRUS, S.	
PB90-128711 900,052	tron-Impact Ionization of Ions.		Free Value Tool for ASN.1.	
High-Temperature Dental Investments. PB89-202477 901,257		11,572	PB89-196182 900,6	
Mesh Monitor Casting of Ni-Cr Alloys: Element Effects.	Fatigue Resistance of a 2090-T8E41 Aluminum Allo	loy at	Object-Oriented Model for ASN.1 (Abstract Syntax Notat One).	
PB89-176077 900,040	PB90-128737 90	01,177	PB89-177117 900,6	549
Transient and Residual Stresses in Dental Porcelains as Affected by Cooling Rates.	Linear-Elastic Fracture of High-Nitrogen Austenitic Stair		TRUSLER, J. P. M. Microwave Measurements of the Thermal Expansion o	of a
PB89-229298 900,046	Steels at Liquid Helium Temperature. PB90-117623 90	01,108	Spherical Cavity. PB89-147458 900,2	
FETE, C. Re-Entrant Spin-Glass Properties of a-(FexCr1-x)75P15C10.	TODD, M. A.		TSAI, T. M.	,
PB89-157481 901,391	Computer Security Training Guidelines. PB90-780172 900	00,677	Robot Crane Technology.	
TEWARI, Y. B. Calorimetric and Equilibrium Investigation of the Hydrolysis	TOLLE .I W		PB90-111667 900,	146
of Lactose.	Ment Functions and Nonlinear Programming.	1,208	TSANG, K. L. Oxygen Partial-Density-of-States Change in	the
PB89-227888 901,226 Thermodynamic and Transport Properties of Carbohydrates	TOLMAN D W	.,200	YBa2Cu3Ox Compounds for x(Approx.)6,6.5,7 Measured Soft X-ray Emission.	
and Their Monophosphates: The Pentoses and Hexoses.	Dual Frequency P-Code Time Transfer Experiment.		PB89-186274 901,4	419

TSANG, W.	PB89-202162 900,433	VANZURA, E. J.
Evaluated Kinetics Data Base for Combustion Chemistry. PB89-212096 900,601	VAIDA, V.	Advances in NIST (National Institute of Standards and Technology) Dielectric Measurement Capability Using a
Fundamental Aspects of Key Issues in Hazardous Waste	Photodissociation of Methyl Iodide Clusters. PB89-171193 900,253	Mode-Filtered Cylindrical Cavity. PB89-231146 900.907
Incineration. PB89-212104 900,861	VAN BAAK, D. A.	Creating CSUBs in BASIC.
Mechanism and Rate of Hydrogen Atom Attack on Toluene	Current Research Efforts at JILA (Joint Institute for Labora- tory Astrophysics) to Test the Equivalence Principle at	PB89-176226 900,647
at High Temperatures. PB89-179758 900,398	Short Ranges. PB89-185912 901,522	Creating CSUBs Written in FORTRAN That Run in BASIC. PB90-128752 900,656
TSUNEKAWA, S.	VAN BRUNT, R. J.	VARNUM, F. B.
Microwave Spectrum of Methyl Amine: Assignment and Analysis of the First Torsional State.	Collisional Electron Detachment and Decomposition Rates of SF6(1-), SF5(1-), and F(1-) in SF6: Implications for Ion	Comparison of Time Scales Generated with the NBS (Na-
PB90-117839 900,509	Transport and Electrical Discharges.	tional Bureau of Standards) Ensembling Algorithm. PB89-174072 900,628
TSURUBUCHI, S. T.	PB90-117862 900,511 Electron-Energy Dependence of the S2F10 Mass Spec-	VAUDIN, M. D.
Cross Sections for Collisions of Electrons and Photons with Oxygen Molecules.	trum.	Diffraction Effects Along the Normal to a Grain Boundary. PB89-202089 901,153
PB89-226575 900,457	PB90-117870 900,512 Electron-Transport, Ionization, Attachment, and Dissociation	Electron Diffraction Study of the Faceting of Tilt Grain
TUNG, M. S. Mechanism of Hydrolysis of Octacalcium Phosphate.	Coefficients in SF6 and Its Mixtures.	Boundaries in NiO. PB89-201792 901,431
PB89-201503 901,254	PB89-171540 901,501 Method for Measuring the Stochastic Properties of Corona	Electron Microscopy Studies of Diffusion-Induced Grain
TURK, G. C. Three Dimensional Atomic Spectra in Flamos Heing Stop	and Partial-Discharge Pulses.	Boundary Migration in Ceramics. PB89-202097 901,049
Three-Dimensional Atomic Spectra in Flames Using Step- wise Excitation Laser-Enhanced Ionization Spectroscopy.	PB90-128745 900,829 Production and Stability of S2F10 in SF6 Corona Dis-	Equilibrium Crystal Shapes and Surface Phase Diagrams at
PB89-202071 900,430	charges.	Surfaces in Ceramics. PB90-117755 901,162
TURNER, C. D. Vector Calibration of Ultrasonic and Acoustic Emission	PB89-231039 900,822 Research for Electric Energy Systems: An Annual Report.	Grain Boundary Characterization in Ni3Al.
Transducers. PB89-202014 900,765	PB90-112442 900,853	PB89-229306 901,156
TURNER, P. R.	VAN CLARK, A.	Grain Boundary Structure in Ni3Al. PB89-201784 901,150
Supercomputers Need Super Anthmetic.	Ultrasonic Railroad Wheel Inspection Using EMATs (Electromagnetic-Accoustic Transducers), Report No. 18.	Grain Boundary Structure in Ni3Al.
PB90-130253 900,657 TURNER, S.	PB89-189229 901,596	PB89-229314 901,157 Toughening Mechanisms in Ceramic Composites. Semi-
Refinement of the Substructure and Superstructure of Ro-	VAN DEGRIFT, C. T. Determination of the Time-Dependence of ohm NBS (Na-	Annual Progress Report for the Period Ending March 31,
manechite. PB89-157721 901,392	tional Bureau of Standards) Using the Quantized Hall Resistance.	1989. PB89-235907 <i>901,080</i>
TURNER, W. A.	PB89-230387 900,819	Toughening Mechanisms in Ceramic Composites: Semi-
Investigation of a Washington, DC Office Building. PB89-230361 900,081	VAN LEEUWEN, J. M. J.	Annual Progress Report for the Period Ending September 30, 1988.
PB89-230361 900,081 TURPIN, R.	Capillary Waves of a Vapor-Liquid Interface Near the Criti- cal Temperature.	PB89-162606 901,028
Draft International Document on Guide to Portable Instru-	PB89-228555 900,476	VAZQUEZ, I.
ments for Assessing Airborne Pollutants Arising from Haz- ardous Wastes.	VAN ORDEN, A. Application of Magnetic Resonance Imaging to Visualization	Development of Combustion from Quasi-Stable Tempera- tures for the Iron Based Alloy UNS S66286.
PB89-150775 900,855	of Flow in Porous Media. PB89-179592 901,329	PB89-173850 900,592
TVEDT, J. E. Low Pressure, Automated, Sample Packing Unit for Diffuse	VAN POOLEN, L. J.	Ignition Characteristics of the Iron-Based Alloy UNS S66286 in Pressurized Oxygen.
Reflectance Infrared Spectrometry.	Determination of Binary Mixture Vapor-Liquid Critical Densi-	PB89-189336 901,104 Ignition Characteristics of the Nickel-Based Alloy UNS
PB90-135922 900,235 TYMOCHOWICZ, S.	ties from Coexisting Density Data. PB89-202170 901,536	N07718 in Pressurized Oxygen.
Preconcentration of Trace Transition Metal and Rare Earth	VAN VECHTEN, D.	PB89-218333 901,154
Elements from Highly Saline Solutions. PB90-118175 900,226	Impedance of Radio-Frequency Biased Resistive Superconducting Quantum Interference Devices.	VECCHIA, D. F. Calibration with Randomly Changing Standard Curves.
UDOVIC, T. J.	PB89-201719 900,764	PB89-186381 900,888
Antiferromagnetic Structure and Crystal Field Splittings in	VAN VELTHUIZEN, J. Moydite, (Y, REE) (B(OH)4)(CO3), a New Mineral Species	Problems with Interval Estimation When Data Are Adjusted via Calibration.
the Cubic Heusler Alloys HoPd2Sn and ErPd2Sn. PB89-202659 901,437	from the Evans-Lou Pegmatite, Quebec.	PB89-157812 901,209
Hydrogen Sites in Amorphous Pd85Si15HX Probed by Neutron Vibrational Spectroscopy.	PB89-157747 900,186 VANBRONKHORST, D. A.	VEESER, L. R.
PB89-229140 901,456	Air Quality Investigation in the NIH (National Institutes of	Optical Fiber Sensors for Electromagnetic Quantities. PB89-173967 900,725
UEMATSU, M.	Health) Radiation Oncology Branch. PB89-228977 900,079	VEILLON, C.
New International Skeleton Tables for the Thermodynamic Properties of Ordinary Water Substance.	VANDERHART, D. L.	Microwave Digestion of Biological Samples: Selenium Anal-
PB89-145130 900,270	13C NMR Method for Determining the Partitioning of End Groups and Side Branches between the Crystalline and	ysis by Electrothermal Atomic Absorption Spectrometry. PB89-229116 900,217
ULBRECHT, J. J. Measurement of Shear Rate on an Agitator in a Fermenta-	Non-Crystalline Regions in Polyethylene. PB89-202451 900,569	VELAPOLDI, R. A.
tion Broth. PB89-186720 901,009	Morphological Partitioning of Ethyl Branches in Polyethyl-	Low Pressure, Automated, Sample Packing Unit for Diffuse Reflectance Infrared Spectrometry.
UNGURIS, J.	ene by (13)C NMR. PB89-176051 900,560	PB90-135922 900,235
Domain Images of Ultrathin Fe Films on Ag(100).	Solid State (13)C NMR Investigation in Polyoxetanes. Effect	Luminescence Standards for Macro- and Microspectrofluor- ometry.
PB89-158067 901,394	of Chain Conformation. PB89-176036 900,558	PB89-176598 <i>900,383</i>
High Resolution Imaging of Magnetization. PB89-147433 901,386	VANEK, M. D.	VERDIER, P.
Improved Low-Energy Diffuse Scattering Electron-Spin Po-	(12)C(16)O Laser Frequency Tables for the 34.2 to 62.3	Off-Lattice Simulation of Polymer Chain Dynamics. PB90-117524 900,576
larization Analyzer. PB89-229173 900,218	THz (1139 to 2079 cm(-1)) Region. PB89-193908 901,361	VERKOUTEREN, R. M.
Influence of the Surface on Magnetic Domain-Wall Microstructure.	Frequency Measurement of the J = 1 < - 0 Rotational	High-Accuracy Gas Analysis via Isotope Dilution Mass
PB90-118019 901,467	Transition of HD (Hydrogen Deutende). PB89-161566 901,499	Spectrometry: Carbon Dioxide in Air. PB90-123951 900,032
Vector Imaging of Magnetic Microstructure. PB90-128240 901,476	Frequency Measurements of High-J Rotational Transitions	VESSER, L. R.
URBAN, W.	of OCS and N2O. PB90-136946 900,541	Optical Fiber Sensors for the Measurement of Electromagnetic Quantities.
CO Laser Stabilization Using the Optogalvanic Lamb-Dip.	Heterodyne Frequency and Fourier Transform Spectrosco-	PB89-176671 900,748
PB89-179139 901,356 Heterodyne Frequency Measurements of (12)C(16)O Laser	py Measurements on OCS Near 1700 cm(-1). .PB90-117805 900,507	VEST, C. M.
Transitions.	Heterodyne Frequency Measurements of (12)C(16)O Laser	Optical Nondestructive Evaluation at the National Bureau of Standards.
PB89-229223 901,374 URIANO, G. A.	Transitions. PB89-229223 901,374	PB89-146740 - 900,976
NBS (National Bureau of Standards) Calibration Services: A	Heterodyne Measurements on N2O Near 1635 cm(-1). PB90-117797 900,506	VESTAL, L.
Status Report. PB89-173934 900,878	PB90-117797 900,506 Heterodyne Measurements on OCS Near 1372 cm(-1).	Measurement Standards for Defense Technology. PB89-150965 901,270
VAHALA, L. L.	PB89-201743 900,425	VIDAL-MADJAR, A.
Nonadiabatic Theory of Fine-Structure Branching Cross- Sections for Sodium-Helium, Sodium-Neon, and Sodium-	VANZURA, E. Electromagnetic Fields in Loaded Shielded Rooms.	IUE Observation of the Interstellar Medium Toward Beta Geminorum.
Argon Optical Collisions.	PB89-180426 900,780	PB89-228373 900,024

VILLA, K. M.	PB89-222533	900,449	PB89-185623	900,71
Development of a Multiple Layer Test Procedure for Inclusion in NFPA (National Fire Protection Association) 701: In:	 WAKSMAN, D. Preliminary Stochastic Model for S 	ervice Life Prediction of	Center for Electronics and El Publication Announcements.	ectrical Engineering Technical Covering Center Programs
tial Experiments. PB89-235873 900,09	a Photolytically and Thermally Deg	graded Polymeric Cover	January-March 1989, with 198 PB89-228308	39 CEEE Events Calendar. 900,78
Flammability Tests for Industrial Fabrics: Relevance and	riale Malerial.	900,556	Center for Electronics and El	
Limitations. PB89-174122 901,09	Thermal Degradation of Poly (meth	yl methacrylate) at 50C	Publication Announcements:	Covering Center Programs
VILLAGRAN, E. S.	to 125C. PB89-157465	900,549	July/September 1988, with 19 PB89-189302	900,81
Small Computer System Interface (SCSI) Command System: Software Support for Control of Small Compute			Center for Electronics and El	ectrical Engineering Technica
System Interface Devices.	diance	s) Scale of Spectral Ra-	Publication Announcements. October/December 1988, with	
PB89-151815 900,65	PB89-201685	901,532	dar. PB89-209241	900,78
VINCENT, M. A. Antenna for Laser Gravitational-Wave Observations in	WALKER, T.		Center for Electronics and El	ectrical Engineering Technica
Space. PB89-234231 901,594	DD00 100006	e Atom Trap. <i>901,577</i>	Publication Announcements C tober to December 1986, with	
Conceptual Design for a Mercury Relativity Satellite.	WALLACE, D.		PB90-116195	900,82
PB89-234249 901,599	Standard	Software Engineering	Semiconductor Measuremen and Statistical Analysis of the	
Rate of Change of the Quincy-Monument Peak Baseline from a Translocation Analysis of LAGEOS Laser Range	PB89-149116	900,665	of the Conversion Coefficien	t for the Measurement of the
Data. PB89-234272 901,282	WALLACE, D. R.	arde Brogram	Interstitial Oxygen Content of PB89-221170	901,054
VIOLET, C. E.	PB89-211965	900,666	WALTON, G. N.	
Reentrant Softening in Perovskite Superconductors.	Software Verification and Validation	: Its Role in Computer	Airflow Network Models for E Modeling.	lement-Based Building Airflov
PB90-117540 901,46- /ITEK, J. M.	agement Standards.		PB89-230379	900,082
Diffraction Effects Along the Normal to a Grain Boundary.	PB90-111691	900,655	AIRNET: A Computer Program Modeling.	n for Building Airflow Network
PB89-202089 901,153	WALLACE, J. S. Magnetic Field Dependence of the	Superconductivity in Ri-	PB89-193254	900,076
/OELS, S. A. Photospheres of Hot Stars. 3. Luminosity Effects at Spec	Sr-Ca-Cu-O Superconductors.		Considerations for Advanced	Building Thermal Simulation
tral Type 09.5. PB89-202592 900,020	1 000-140010	901,385	Programs. PB89-231047	900,084
/OGEL, G. L.	Oxide 80- and 110-K Superconducto	ors.	Developments in the Heat B	alance Method for Simulating
Micro-Analysis of Mineral Saturation Within Enamel dunna	PB89-179725 WALLINGTON, T. J.	901,412	Room Thermal Response. PB89-173926	900,062
Lactic Acid Demineralization. PB89-186373 901,253	Flash Photolysis Kinetic Absorption	Spectroscopy Study of	Thermal and Economic Analy	
OORHEES, P. W.	the Gas Phase Reaction HO2 + 0 perature Range 228-380 K.	22H5O2 Over the Tem-	Ventilating, and Air Conditioni VA (Veterans Administration)	
Elastic Interaction and Stability of Misfitting Cuboidal Inhomogeneities.	PB90-136565	900,536	PB89-188619	900,847
PB89-157903 901,482	Fluid Flow in Pulsed Laser Irradiate Measurement.	d Gases; Modeling and	WALTON, W. D. Computer Fire Models.	
In situ Observation of Particle Motion and Diffusion Interac- tions during Coarsening.	PB90-123704	900,265	PB89-173991	900,165
PB89-201982 901,15	Temperature Dependence of the Ra droperoxy + Methylperoxy Gas-Pha		WALTRIP, B. C.	
Numerical Simulation of Morphological Development during Ostwald Ripening.	PB90-136375	900,534	Audio-Frequency Current Con opment and Design Considera	nparator Power Bridge: Devel
PB89-201990 901,152			PB89-201537	900,717
Ostwald Ripening in a System with a High Volume Fraction	Analysis of High Performance Con closures.	pensated Thermal En-	WANG, F. W.	
of Coarsening Phase. PB89-157598 901,126	PB89-185748	901,008	In Situ Fluorescence Monitori cle-Filled Polymers in Flow.	ng of the Viscosities of Parti
Phase Equilibrium in Two-Phase Coherent Solids. PB89-157580 900,330	Low Noise Frequency Synthesis. PB89-174056	900,716	PB89-146278	900,608
/ORBURGER, T.	Very Low-Noise FET Input Amplifier.		WANG, J. C. M.	D-to
Optical Nondestructive Evaluation at the National Bureau of	PB90-128224	900,800	Analysis of Computer Perform PB89-162614	900,635
Standards. PB89-146740 900,976	WALSH, R. P. Effect of Chemical Composition o	n the 4 K Mechanical	WANG, J. X.	
Optical Roughness Measurements for Industrial Surfaces.	Properties of 316LN-Type Alloys.	901,110	Alignment Effects in Ca-He 3)P(sub J)) Energy Transfer	(5(sup 1)P(sub 1) - 5(sup Collisions by Far Wing Lase
PB89-176655 900,975 /REBOS, B. A. R.	Effects of Grain Size and Cold Rollin	•	Scattering. PB89-179790	
Uncertainties in Mass Absorption Coefficients in Fundamen-	tion of Conner	901,176	WANG, Y.	900,400
tal Parameter X-ray Fluorescence Analysis. PB89-201677 900,212			Collisional Electron Detachme	ent and Decomposition Rates
VACK, J. P.	Cryogenic Temperatures.		of SF6(1-), SF5(1-), and F(1- Transport and Electrical Disch) in SF6: Implications for lor
Computer Viruses and Related Threats: A Management Guide.	PB90-128562 Loading Rate Effects on Discont	901,111 inuous Deformation in	PB90-117862	900,51
PB90-111683 900,654	Load-Control Tensile Tests.		WANN, R. J.	
VADA, H. VAMAS (Versailles Project on Advanced Materials and	PB89-171896 Tensile Strain-Rate Effects in Liquid	901,097 Helium.	Dynamic Young's Modulus Me nals: Results of an Interlabora	tory Testing Program.
Standards) Intercomparison of Critical Current Measure-	PB89-174882	901,102	PB89-157671	901,132
ment in Nb3Sn Wires. PB89-202147 901,534	WALTER, F. M. Doppler Imaging of AR Lacertae at	Three Enochs	WARD, R. Gain and Power Parameter	Measurements Using Plana
VADLEY, H. N. G.	PB89-149199	900,015	Near-Field Techniques.	
Acoustic Emission: A Quantitative NDE Technique for the Study of Fracture.		on RS Canum Venati-	PB89-156822 WARNLOF, O. K.	900,698
PB89-211924 900,921		r 1985.	Intercomparison of Load Cell	Verification Tests Performed
Sensors for Intelligent Processing of Materials. PB89-202006 900,920	PB89-234298	900,026	by National Laboratories of Fit PB89-235915	
Ultrasonic Characterization of Surface Modified Layers.	VAMAS (Versailles Project on Ac	Ivanced Materials and	WASSON, O. A.	300,300
PB89-147409 901,115	Standards) Intercomparison of Cri		2.5 MeV Neutron Source for	Fission Cross Section Meas
Vector Calibration of Ultrasonic and Acoustic Emission Transducers.	PB89-202147	901,534	urement. PB89-176531	901,512
PB89-202014 900,765			Advances in the Use of (·
VAGNER, W. New International Skeleton Tables for the Thermodynamic	Center for Electronics and Electrical Progress Bulletin Covering Center	Programs, January to	Counter. PB90-123506	901,565
Properties of Ordinary Water Substance.	March 1989, with 1989 CEEE Event	S Calendar. 900,786	Measurements of the (235)U	(n,f) Standard Cross Section
PB89-145130 900,270 VAHLSTRAND, K. J.	Center for Electronics and Electrica		at the National Bureau of Star PB89-176556	ndards. 901,305
Computer Simulation Studies of the Soliton Model. 3. Non-	Progress Bulletin Covering Center	Programs, July to Sep-	WATANABE, K.	00.,000
continuum Regimes and Soliton Interactions. PB89-202469 901,533	DB80-168033	900,775	New International Skeleton T	
NAHR, J. M.	Center for Electronics and Electrica	Programs October to	Properties of Ordinary Water 5 PB89-145130	Substance. 900,270
Conceptual Design for a Mercury Relativity Satellite.	Progress Bulletin Covering Center December 1988, with 1989 CEEE E	vents Calendar.	WATANABE, M.	
PB89-234249 901,595 WAKEHAM, W. A.	, 200 , 1002, 1	900,813	Interlaboratory Determination the Measurement of the Inter	of the Calibration Factor for
Thermal Conductivity of Nitrogen and Carbon Monoxide in	Center for Electronics and Electrica Publication Announcements Cove	ing Center Programs,	con by Infrared Absorption.	
the Limit of Zero Density.	April-June 1986 with 1987 CEEE Ev	ents Calendar.	PB90-117300	900,224

VATERS, N. E. Method to Measure the Tensile Bond Strength beto	PB89-147060 veen WEISER, S .	900,285	PB89-177091 Automated Documentation System for a Large	900,95
Two Weakly-Cemented Sand Grains.		or Real-Time Crystallographic	facturing Engineering Research Project. PB89-150809	900,94
VATERSTRAT, R. M. Electronic, Magnetic, Superconducting and Amorph	PATENT-4 747 684	901,383	Material Handling Workstation Implementation PB89-159644	
Forming Properties Versus Stability of the Ti-Fe, Zr-Ru Hf-Os Ordered Alloys.	and '	ounds for Theoretical Atomic-	Material Handling Workstation: Operator Man PB89-159651	
	,120 PB89-158109	901,496	Material Handling Workstation, Recommen	
VATKINS, M. M. Rate of Change of the Quincy-Monument Peak Bas	WEISS, C. S.		Specifications for Procurement of Commerce	
from a Translocation Analysis of LAGEOS Laser Ri	nace Speciation by rifecture	F AA (High-Performance Liquid rnace Atomic Absorption) for	Equipment. PB89-162564	900,99
Data. PB89-234272 901	7282 Tin- and Lead-Bearing Organic Signal Increases Induced by	anometallic Compounds, with	WENGER, L. E.	
VATSON, R. E.	PB89-157085	900,184	Magnetic Structure of Y0.97Er0.03. PB89-202675	901,43
Magnetic Behavior of Compositionally Modulated N Thin Films.	,		Spin-Density-Wave Transition in Dilute YGd S	
PB90-118084 901	,163 Apparent Diurnal Effects in th PB89-174080	e Global Positioning System. 901,292	PB89-202030	901,43
Roles of Atomic Volume and Disclinations in the Magne of the Rare Earth-3D Hard Magnets.	tism WEISS, M. A.		WERNER, H. J.	
PB89-202238 901	,434 Calibration of GPS (Global F in Japan.	ositioning System) Equipment	Weakly Bound NeHF. PB90-118100	900,51
VATTERS, R. Development of the NBS (National Bureau of Standa	PB89-212070	900,630	WESSELLS, C. W.	,
Beryllium Isotopic Standard Reference Material.	Dual Frequency P-Code Time	Transfer Experiment.	High-Precision Absolute Gravity Observations	s in the United
	.221 PB89-174064 In Search of the Best Clock.	900,614	States. PB89-227946	901,28
VATTERS, R. L. Quality Assurance in Metals Analysis Using the Induct	DD00 117967	900,632	WESSON, J. A.	
Coupled Plasma.	NBS (National Bureau of S	tandards) Calibration Service y at a Remote Site by Welght-	Uniaxial Deformation of Rubber Network Ch	hains by Smal
VAVERING, A. J.	ing and Smoothing of GPS	(Global Positioning System)	Angle Neutron Scattering. PB89-175830	901,088
Real-Time Control System Software: Some Problems	and Common View Data. PB89-212211	900,631	WEST, B. C.	
an Approach. PB89-177083 900	.951 Using Multiple Reference S	tations to Separate the Var-	Structure of V9Mo6O40 Determined by Po	owder Neutro
VAY, J. D.	iances of Noise Componen System.	ts in the Global Positioning	Diffraction. PB90-117995	900,51
CO2 Separation Using Facilitated Transport Ion Excha Membranes.	nge PB89-185730	901,293	WEST, J. B.	
	321 WEISS, M. H.		Vibrationally Resolved Photoelectron Angula	
/EAVER, A.	NIST Automated Computer Ti PB90-213711	me Service. 900,676	for H2 in the Range 17 eV < or = h(nu) < or = PB89-176952	= 39 6V. 900,385
Publications of the Center for Manufacturing Engine Covering the Period January 1978-December 1988.	WEISSHAUS, I.		WESTRUM, E. F.	
	.012 Electrodeposition of Chromiur PATENT-4 804 446	n from a Trivalent Electrolyte. 901,119	Thermodynamics of Ammonium Scheelites, of the Heat Capacity and Ancillary Values fo	6. An Analysis
/EAVER, J. T. NBS (National Bureau of Standards) Measurement S		301,113	iodates KIO4, NH4IO4, and ND4IO4.	•
ices: Calibration of Gamma-Ray-Emitting Brachythe	rapy Local Order in a Dense Liquid	l	PB89-147060	900,28
Sources. PB89-193858 901	243 PB89-157226	900,313	WHEATLEY, M. Prediction of Transport Protocol Performance	e through Sim
/EBBINK, R. F.	Shear Induced Anisotropy in PB89-158141	901,325	ulation.	_
Late Stages of Close Binary Systems-Clues to Com Envelope Evolution.	WELCH, B. E.		PB89-171334 Transport Layer Performance Tools and Mea	900,61
PB89-149207 900	,016 Observations of Gas Specie fects on Effective Areas of Gas	s and Mode of Operation Ef- as-Operated Piston Gages.	PB89-171326	900,61
VEBER, A. Technical Activities 1986-1988, Molecular Spectroscop	PB89-231120	900,906	WHETSTONE, J. R.	
vision.	WELCH, B. W.	Absolute Distan Cone Dres	Measurements of Coefficients of Discharge Flange-Tapped Square-Edged Orifice Meters	for Concentre
PB89-175418 900 /EBER, I. T.	sure Measurements in the Atr		the Reynolds Number Range 600 to 2,700,00	00.
Crystal Structure of a Cyclic AMP (Adenosine Monop	PB90-163882 hos-	900,030	PB89-235147 WHITE, E.	901,33
phate)-Independent Mutant of Catabolite Gene Active Protein.	ator WELCH, M. J. Determination of Serum Cho	plesterol by a Modification of	Determination of Serum Cholesterol by a l	Modification o
PB89-201594 901	.224 the Isotope Dilution Mass Spe	ectrometric Definitive Method.	the Isotope Dilution Mass Spectrometric Defii PB89-234181	
Preliminary Crystal Structure of Acinetobacter glutamin cans Glutaminase-Asparaginase.	23111-	901,239 esterol in Coconut Oil: A New	WHITE, H. J.	301,23
PB90-123381 <i>901</i>	,260 NIST (National Institute of Sta	andards and Technology) Cho-	Activities of the International Association for	the Properties
VEBER, K. H. Accurate Energies of nS, nP, nD, nF and nG Levels of	lesterol Standard Reference I PB89-234173	waterial. 901,262	of Steam between 1979 and 1984. PB89-212153	900,44
tral Cesium.	WELLINGTON, J.		Properties of Steam.	555,77
PB89-202121 900 VEBER, L. A.	Publications of the Center f Covering the Period January	or Manufacturing Engineering	PB89-202048	901,53
Simple Apparatus for Vapor-Liquid Equilibrium Meas	sure- PB90-130568	901,012	WHITE V, E.	aut Oile A Mar
ments with Data for the Binary Systems of Carbon Did with n-Butane and Isobutane.	xide WELLS, J. S.	Tables for the 34.2 to 62.3	Determination of Total Cholesterol in Cocor NIST (National Institute of Standards and Tec	
PB89-201115 900	THz (1139 to 2079 cm(-1)) Re	egion.	lesterol Standard Reference Material. PB89-234173	901,26
Vapor Pressures and Gas-Phase PVT Data for 1,1,1,2 trafluoroethane.		901,361	WHITENTON, E. P.	,20
PB90-117987 900	Region from Heterodyne Fre	the 1460- to 1550-cm(-1) the 1460- to 1550-cm (-1)	Computer-Controlled Test System for Open	rating Differen
VEBER, S. F.	nu(sub 3) Bands of (12)CS2 a anu- PB89-157416	and (13)CS2. 900,322	Wear Test Machines. PB89-228290	900,98
AutoMan: Decision Support Software for Automated M facturing Investments. User's Manual.	Frequency Measurements of	High-J Rotational Transitions	Dynamic Microindentation Apparatus for Ma	terials Charac
PB89-221873 900 VEBSTER, J. H.	.963 of OCS and N2O. PB90-136946	900.541	terization. PB89-176911	901,14
Preliminary Performance Criteria for Building Mate		Fourier Transform Spectrosco-	WHITESEL, H. K.	,
Equipment and Systems Used in Detention and Correct al Facilities.		ear 1700 cm(-1). 900,507	Optical Fiber Sensors for Electromagnetic Qu	
PB89-148514 900	109	urements of (12)C(16)O Laser	PB89-173967 WHITESEL, H. R.	900,72
VEIDNER, V. R.	Transitions.		Optical Fiber Sensors for the Measurement	of Electromac
Exploratory Research in Reflectance and Fluoresc Standards at the National Bureau of Standards.	Hotorodyno Moogyroments o	<i>901,374</i> n №O Near 1635 cm(-1).	netic Quantities.	
	9,428 PB90-117797	900,506	PB89-176671 WHITTENBERG, C. D.	900,74
VEIMAN, C. Collisional Losses from a Light-Force Atom Trap.	Heterodyne Measurements o PB89-201743	n OCS Near 1372 cm(-1). 900,425	Group Index and Time Delay Measurements	of a Standar
PB90-123936 903	,577 PB89-201743 Improved Rotational Constan		Reference Fiber. PB89-189179	900,75
VEINSTEIN, A. User Guide for the NBS (National Bureau of Stand	PB90-117466	901,376	Interferometric Dispersion Measurements on	
Prototype Compiler for Estelle (Revised).	WELSON, L. A.	Longuago (ECML)	Wave Structures. PB89-173959	901,34
PB89-196158 908 WEIR, R. D.	7,619 Standard Generalized Markup FIPS PUB 152	Language (SGML). 900,627	WICHMAN, I. S.	301,34
Thermodynamics of Ammonium Scheelites. 6. An Ana	llysis WENGER, C. E.		Upward Turbulent Flame Spread on Wood	under Externa

AMRF (Automated Manufacturing Research Facility) Material Handling System Architecture.

Thermodynamics of Ammonium Scheelites. 6. An Analysis of the Heat Capacity and Ancillary Values for the Metaperiodates KIO4, NH4IO4, and ND4IO4.

Upward Turbulent Flame Spread on Wood under External Radiation.
PB90-118050 900,148

WICKS, F. J. Pahasapaite, a Beryllophosphate Zeolite Related to Syn-	Laser Cooling. PB89-179147 901,518	PB90-130568 901,012
thetic Zeolite Rho, from the Tip Top Pegmatite of South Dakota.	Laser Cooling to the Zero-Point Energy of Motion. PB90-128091 901,581	WOOD, S. D. NBS (National Bureau of Standards) Onfice-Flow Primary
PB89-186431 <i>901,288</i>	Perpendicular Laser Cooling of a Rotating Ion Plasma in a	High Vacuum Standard. PB89-175699 900,880
WIEDERHORN, S. M. Creep Rupture of a Metal-Ceramic Particulate Composite.	Penning Trap. PB89-157408 901,493	WOODWARD, A. M.
PB89-211825 901,077	Precise Test of Quantum Jump Theory. PB89-157390 901,339	Picosecond Coherent Anti-Stokes Raman Scattering (CARS) Study of Vibrational Dephasing of Carbon Disulfide
Design Criteria for High Temperature Structural Applica- tions.	PB89-157390 901,339 Recoilless Optical Absorption and Doppler Sidebands of a	and Benzene in Solution. PB89-176408 900,380
PB89-211833 901,052 Effect of Coal Slag on the Microstructure and Creep Behav-	Single Trapped Ion. PB89-171631 901,505	WOODWARD, N.
ior of a Magnesium-Chromite Refractory. PB89-158034 901,027	Trapped Ions and Laser Cooling 2: Selected Publications of	Line Identifications and Radiative-Branching Ratios of Mag- netic Dipole Lines in Si-like Ni, Cu, Zn, Ge, and Se.
Effect of Slag Penetration on the Mechanical Properties of	the Ion Storage Group, Time and Frequency Division, NIST, Boulder, CO.	PB89-234165 901,558
Refractories: Final Report. PB90-110065 900,836	PB89-153878 901,489 WINTENBERG. A. L.	WORMSER, P. U-Value Measurements for Windows and Movable Insula-
WIESE, W. L.	Measurement of Partial Discharges in Hexane Under DC	tions from Hot Box Tests in Two Commercial Laboratories. PB89-175889
Atomic Transition Probabilities of Argon: A Continuing Challenge to Plasma Spectroscopy.	Voltage. PB89-173421 <i>900,833</i>	WORTHEY, J. A.
PB89-158125 900,344	WINTERS, M. P.	Heuristic Analysis of von Kries Color Constancy. PB89-201099 901,362
Branching Ratio Technique for Vacuum UV Radiance Cali- brations Extensions and a Comprehensive Data Set.	High Resolution Optical Multiplex Spectroscopy. PB89-185938 900,404	WRIGHT, R. N.
PB90-128257 901,582 Journal of Physical and Chemical Reference Data, Volume	WISE, R. A.	Design Quality through the Use of Computers.
17, 1988, Supplement No. 3. Atomic Transition Probabilities Scandium through Manganese.	Part Load, Seasonal Efficiency Test Procedure Evaluation of Furnace Cycle Controllers.	PB89-174114 900,063 Effects of Research on Building Practice.
PB89-145197 900,276	PB89-212146 900,848 WISE, S. A.	PB89-202584 900,168
WILD, T. W. In vitro Investigation of the Effects of Glass Inserts on the	Comparison of Liquid Chromatographic Selectivity for Poly-	Progressive Collapse: U.S. Office Building in Moscow. PB89-175715 900,158
Effective Composite Resin Polymerization Shrinkage. PB90-117516 900,049	cyclic Aromatic Hydrocarbons on Cyclodextrin and C18 Bonded Phases.	Trends for Building Technology in North America. PB89-174106 900,104
WILLIAMS, E. R.	PB90-128539 900,231 Experiences in Environmental Specimen Banking.	WU, D. I.
Low Field Determination of the Proton Gyromagnetic Ratio in Water.	PB90-123969 900,866	Effect of an Electrically Large Stirrer in a Mode-Stirred
PB89-230411 901,555	Mobile Sources of Atmospheric Polycyclic Aromatic Hydro- carbons: A Roadway Tunnel Study.	Chamber. PB90-117946 <i>901,378</i>
Measurement of the NBS (National Bureau of Standards) Electrical Watt in SI Units.	PB90-123571 900,859	Hybrid Representation of the Green's Function in an Over- moded Rectangular Cavity.
PB89-230429 900,821	Recent Advances in Bonded Phases for Liquid Chromatography.	PB90-117953 900,826
 NBS (National Bureau of Standards) Determination of the Fine-Structure Constant, and of the Quantized Hall Resist- 	PB9-187520 900,204 Specimen Banking in the National Status and Trends Pro-	WU, Y. C. Determination of the Absolute Specific Conductance of Pri-
ance and Josephson Frequency-to-Voltage Quotient in SI Units.	gram: Development of Protocols and First Year Results. PB89-175855	mary Standard KCI Solutions.
PB89-230437 901,556	Standard Reference Materials for the Determination of Po-	PB89-230320 900,481 WYART, J. F.
WILLIAMS, F. A. Upward Turbulent Flame Spread on Wood under External	lycyclic Aromatic Hydrocarbons. PB89-156889 900,178	Spectrum and Energy Levels of Singly Ionized Cesium. 2.
Radiation. PB90-118050 900,148	Synthesis and Characterization of Novel Bonded Phases	Interpretation of Fine and Hyperfine Structures. PB89-172373 900,361
WILLIAMS, P.	for Reversed-Phase Liquid Chromatography. PB90-128695 900,233	XIAO, M.
Status of Reference Data, Reference Materials and Reference Procedures in Surface Analysis.	WISSINK, C. E.	Generation of Squeezed Light by Intracavity Frequency Doubling.
PB89-157705 900,332	Design Principles for a Large High-Efficiency Sub-Boiling Still.	PB89-227938 901,365
WILLIAMSON, M. L. Anti-T2 Monoclonal Antibody Immobilization on Quartz	PB89-187553 900,207 WITTMANN, R. C.	XING, S. Z. Thermal Shifts of the Spectral Lines in the (4)F3/2 to
Fibers: Stability and Recognition of T2 Mycotoxin. PB90-128760 901,267	Improved Spherical and Hemispherical Scanning Algo-	(4)I11/2 Manifold of an Nd:YAG Laser. PB89-157382 901,338
WILSON, A. J. C.	nithms. PB89-156806 900,697	XIZHI, L.
Statistical Descriptors in Crystallography: Report of the International Union of Crystallography Subcommittee on	WITZGALL, C.	SIS Quasiparticle Mixers with Bow-Tie Antennas. PB89-157036 900,705
Statistical Descriptors. PB89-201826 901,432	Electronic Mail and the 'Locator's' Dilemma. PB89-211957 901,205	YAMASAKI, K.
WILSON, C. L.	WLODAWER, A.	Quenching and Energy Transfer Processes of Single Rotational Levels of Br2 B triplet Pi(O(sub u)(+)) v'= 24 with
Neural Network Approach for Classifying Test Structure Results.	Companson of Two Highly Refined Structures of Bovine Pancreatic Trypsin Inhibitor.	Ar under Single Collision Conditions. PB89-179766 900,399
PB89-212187 900,788	PB89-202204 901,248 Preliminary Crystal Structure of Acinetobacter glutaminasifi-	YANCEY, C.
WILSON, M. NBS/NRL (National Bureau of Standards/Naval Research	cans Glutaminase-Asparaginase.	Robot Crane Technology. PB90-111667 900,146
Laboratory) Free Electron Laser Facility. PB89-175749 901,351	PB90-123381 901,260 WOFFARD, J. B.	YANCEY, C. W. C.
WILSON, P. F.	IUE Observation of the Interstellar Medium Toward Beta Geminorum.	Guidelines and Procedures for Implementation of Executive Order on Seismic Safety.
Fields Radiated by Electrostatic Discharges. PB90-128778 901,382	PB89-228373 900,024	PB89-148092 900,156
Techniques for Measuring the Electromagnetic Shielding	WOLFENDEN, A. Dynamic Young's Modulus Measurements in Metallic Mate-	YANG, C.
Effectiveness of Materials. Part 1. Far-Field Source Simulation.	rials: Results of an Interlaboratory Testing Program.	Turning Workstation in the AMRF (Automated Manufacturing Research Facility).
PB89-161525 900,680	PB89-157671 901,132 WONG-NG. W.	PB89-185607 900,954 YANG, D.
Techniques for Measuring the Electromagnetic Shielding Effectiveness of Materials. Part 2. Near-Field Source Simu-	Bulk Modulus and Young's Modulus of the Superconductor	NBS (National Bureau of Standards) Decay-Scheme Inves-
lation. PB89-161533 <i>900,681</i>	Ba2Cu3YO7. PB90-123613 <i>901,469</i>	tigations of (82)Sr-(82)Rb. PB89-161558 901,498
WILSON, R. R.	Standard X-ray Diffraction Powder Patterns from the JCPDS (Joint Committee on Powder Diffraction Standards) Re-	YANIV, S. L.
Effect of Pipe Roughness on Orifice Flow Measurement. PB89-231484 901,333	search Associateship. PB89-171763 900,190	Intercomparison of Load Cell Verification Tests Performed by National Laboratories of Five Countries.
WINBORN, E. L.	Standard X-ray Diffraction Powder Patterns from the JCPDS	PB89-235915 900,909
Preliminary Crystallographic Study of Recombinant Human Interleukin 1beta.	(Joint Committee on Powder Diffraction Standards) Re- search Association.	YAP, W.T. Spectroelectrochemistry of a System Involving Two Con-
PB90-136730 901,251 WINELAND, D. J.	PB89-202246 900,214	secutive Electron-Transfer Reaction. PB90-136979 900,237
Atomic-lon Coulomb Clusters in an Ion Trap.	WOO, S. Measurements of Coefficients of Discharge for Concentric	YARMOFF, J. A.
PB89-157424 901,494 Frequency Standards Utilizing Penning Traps.	Flange-Tapped Square-Edged Orifice Meters in Water Over the Reynolds Number Range 600 to 2,700,000.	Bond Selective Chemistry with Photon-Stimulated Desorption.
PB90-128042 901,379	PB89-235147 901,334	PB89-201222 900,259
Ion Trapping Techniques: Laser Cooling and Sympathetic Cooling.	WOOD, L. Publications of the Center for Manufacturing Engineering	Chemisorption of HF (Hydrofluoric Acid) on Silicon Surfaces.
PB90-128034 901,578	Covering the Period January 1978-December 1988.	PB89-212013 900,445

Photon-Stimulated Desorption as a Measure of Si	urface	YOON, D. N.		PB89-171953 901,236
Electronic Structure. PB89-231328 90	01,459	Migration of Liquid Film and Grain Boundary in Mo-t duced by W Diffusion.		Radiochemical Procedure for Ultratrace Determination of Chromium in Biological Materials.
Photon-Stimulated Description of Fluorine from Silico	on via		01,128	PB89-156913 900,179
	00,517	Observations on Crystal Defects Associated with Diffinduced Grain Boundary Migration in Cu-Zn.	tusion 01,127	Sequential Determination of Biological and Pollutant Elements in Marine Bivalves.
YARON, D. J.	5	PB89-157606 90 YOUNG. M.	11,127	PB89-156897 901,217
Absolute Infrared Transition Moments for Open Shell mics from J Dependence of Transition Intensities: Aption to OH.		Fresnel Lenses Display Inherent Vignetting.	0 <i>1,337</i>	Specimen Banking in the National Status and Trends Program: Development of Protocols and First Year Results. P889-175855 901,308
PB89-227912 90	00,463	Numerical Aperture of Multimode Fibers by Several M	Meth-	Use of Focusing Supermirror Neutron Guides to Enhance
YATES, B. C. Measurement of Adapter Loss, Mismatch, and Effic	ciency	ods: Resolving Differences. PB90-117482 900	00,757	Cold Neutron Fluence Rates. PB89-171946 901,306
Using the Dual Six-Port.	01,316	Profile Inhomogeneity in Multimode Graded-Index Fiber PB89-179816 900	ers. 20,749	ZENG, X.
YE, S.		Spatial Filtering Microscope for Linewidth Measuremen		Calculable, Transportable Audio-Frequency AC Reference Standard.
Low Field Determination of the Proton Gyromagnetic	Ratio	PB89-230346 90:	01,368	PB90-117854 900,721
in Water. PB89-230411 90	01,555	Electron-Impact Ionization of La(q+) lons (q= 1,2,3).		ZHANG, C. H.
YEE, K.			01,573	Oxygen Partial-Density-of-States Change in the
Intercomparison of Load Cell Verification Tests Perfo	ormed	YU, D.		YBa2Cu3Ox Compounds for x(Approx.)6,6.5,7 Measured by Soft X-ray Emission.
by National Laboratories of Five Countries. PB89-235915 90	00,909	Determination of the Time-Dependence of ohm NBS tional Bureau of Standards) Using the Quantized Hall	all Re-	PB89-186274 901,419
YEH, T. T.		sistance. PB89-230387 900	00,819	ZHANG, Y.
Mixing Motions Produced by Pipe Elbows.	11 226	YU, H.	70,073	Standard X-ray Diffraction Powder Patterns from the JCPDS (Joint Committee on Powder Diffraction Standards) Re-
PB89-161871 90 NBS' (National Bureau of Standards) Industry; Govern	01,326 nment	Uniaxial Deformation of Rubber Network Chains by Sangle Neutron Scattering.	Small	search Associateship. PB89-171763 900,190
Consortium Research Program on Flowmeter Instal Effects: Summary Report with Emphasis on Research	llation		01,088	ZHANG, Y. X.
ary-July 1988.		ZACHARIAH, M. R.		Interactions between Two Dividers Used in Simultaneous
	01,010	Dynamic Light Scattering and Angular Dissymmetry fo In situ Measurement of Silicon Dioxide Particle Synthes	or the	Companson Measurements. PB90-118035 900.031
NBS' (National Bureau of Standards) Industry; Govern Consortium Research Program on Flowmeter Instal		Flames.		PB90-118035 900,031 International Comparison of HV Impulse Measuring Sys-
Effects: Summary Report with Emphasis on Research			00,246	tems.
December 1987. PB90-111220 90	00,910	ZAGHLOUL, M. E.	aufaa	PB89-186423 900,809
Prediction of Flowmeter Installation Effects.	00,899	Machine-Learning Classification Approach for IC Man turing Control Based on Test Structure Measurements. PB89-228530 900		Method for Fitting and Smoothing Digital Data. PB90-128794 900,830
Prediction of Flowmeter Installation Effects.	0,033	Neural Network Approach for Classifying Test Structure	•	ZIELINSKI, W. L
	00,900	sults.	700	Preparation of Accurate Multicomponent Gas Standards of
YESINOWSKI, J. P.		PB89-212187 900 ZALEWSKI, E.	00,788	Volatile Toxic Organic Compounds in the Low-Parts-per-Billion Range.
Calcium Hydroxyapatite Precipitated from an Aqueous	Solu-	Characteristics of Ge and InGaAs Photodiodes.		PB89-157739 900,185
tion: An International Multimethod Analysis. PB90-123399 90	00,228	PB89-176796 900	00,729	ZINK, L. R.
YI-TANG, S.		ZALEWSKI, E. F.		Frequency Measurement of the $J=1<-0$ Rotational Transition of HD (Hydrogen Deutende).
Non-Geometric Dependencies of Gas-Operated I Gage Effective Areas.	Piston	Interpolation of Silicon Photodiode Quantum Efficience an Absolute Radiometric Standard.	•	PB89-161566 901,499
	00,905		01,445	New FIR Laser Lines and Frequency Measurements for Optically Pumped CD3OH.
YIN, L I.		ZAPAS, L J. Necking Phenomena and Cold Drawing.		PB89-175731 901,350
Pattern Recognition Approach in X-ray Fluorescence Asis.	Analy-	PB89-201495 900	00,975	Pure Rotational Far Infrared Transitions of (16)O2 in Its
	00,234	ZARR, R. R.		Electronic and Vibrational Ground State. PB89-202055 900,429
YOKEL, F. Y.		Thermal Resistance Measurements and Calculations of Insulated Concrete Block Wall.		ZOLLER, P.
Pore-Water Pressure Buildup in Clean Sands Becau Cyclic Straining.	use of	PB89-174916 900	00,119	Laser-Noise-Induced Population Fluctuations in Two- and
PB89-175723 90	00,159	ZAWACKI, S. J. Calcium Hydroxyapatite Precipitated from an Aqueous	Solu	Three-Level Systems. PB89-171235 901.342
Progressive Collapse: U.S. Office Building in Moscow. PB89-175715	00,158	tion: An International Multimethod Analysis.	00,228	One-Photon Resonant Two-Photon Excitation of Rydberg Series Close to Threshold.
Site Characterization for Radon Source Potential. PB89-209274 90	01,290	ZEISLER, R.		PB89-171276 901,343
YOLKEN, H. T.	,	Activation Analysis Cpportunities Using Cold Ne Beams.	eutron	Quantum-Defect Parametrization of Perturbative Two- Photon Ionization Cross Sections.
Automated Processing of Advanced Materials. The Pa			00,183	PB89-202600 901,539
Maintaining U.S. Industrial Competitiveness in Material P889-201727 90	ls. <i>00,957</i>	Experiences in Environmental Specimen Banking. PB90-123969 900	00,866	Systems Driven by Colored Squeezed Noise: The Atomic Absorption Spectrum.
Institute for Materials Science and Engineering, N	londe-	Long-Term Stability of the Elemental Composition in Bi	Biolog-	PB89-171185 901,500
structive Evaluation: Technical Activities 1988. PB89-151625 90	00,917	ical Materials. PB89-156939 900	00,181	ZOLLER, W. H.
Institute for Materials Science and Engineering, N		Neutron Activation Analysis of the NIST (National Ins	stitute	Residential Wood Combustion: A Source of Atmospheric Polycyclic Aromatic Hydrocarbons.
structive Evaluation: Technical Activities, 1989.	00,925	of Standards and Technology) Bovine Serum Standard erence Material Using Chemical Separations.		PB90-128166 900,860
Intelligent Processing of Materials: Report of an Ind			00,180	ZOZOM, J.
Workshop Conducted by the National Institute of Stan	ndards	Radiochemical and Instrumental Neutron Activation A	Analy-	Microwave Spectrum, Structure, and Electric Dipole
and Technology. PB89-151823 90	00,942	sis Procedures for the Determination of Low Level 1 Elements in Human Livers.	race	Moment of the Ar-Formamide van der Waals Complex. PB89-157325 900,318



SAMPLE ENTRY

Computer Software

Computer Viruses and Related Threats: A Management

PB90-111683

900.654

Keyword term

Title

NTIS order number

Abstract number

A	3R.	ASI	ON	TE	STS

Grain-Size and R-Curve Effects in the Abrasive Wear of PB90-117383 901,058

ABSOLUTE FARAD

New Realization of the Ohm and Farad Using the NBS (National Bureau of Standards) Calculable Capacitor. PB89-230445 901,557

ABSOLUTE OHM

NBS (National Bureau of Standards) Ohm: Past-Present-900.802

New Realization of the Ohm and Farad Using the NBS (National Bureau of Standards) Calculable Capacitor. PB89-230445 901,557

ABSORPTION

Absolute Cross Sections for Molecular Photoabsorption, Partial Photoionization, and Ionic Photofragmentation PR89-186464

Quantitative Studies of Coatings on Steel Using Reflection/Absorption Fourier Transform Infrared Spectroscopy. PB89-212112 901,066

ABSORPTION SPECTRA

Systems Driven by Colored Squeezed Noise: The Atomic Absorption Spectrum.
PB89-171185
901,500 Element-Specific Epifluorescence Microscopy In vivo Monitoring of Metal Biotransformations in Environmental

Structure and Dynamics of Molecular Clusters via High Resolution IR Absorption Spectroscopy. PB89-185896

Analysis of Roto-Translational Absorption Spectra In-duced in Low Density Gases of Non-Polar Molecules: The Methane Case. PB89-201800 900,427

Marked Differences in the 3p Photoabsorption between the Cr and Mn(1+) Isoelectronic Pair: Reasons for the Unique Structure Observed in Cr.
PB90-117581
901,562

Temperature Dependence of the Rate Constant for the Hydroperoxy + Methylperoxy Gas-Phase Reaction.

PB90-136375

900,534 Flash Photolysis Kinetic Absorption Spectroscopy Study of the Gas Phase Reaction HO2 + C2H5O2 Over the Temperature Range 228-380 K.

PB90-136565 900.536

ABSTRACTS

Center for Electronics and Electrical Engineering Techni-cal Publication Announcements Covering Center Pro-grams, April-June 1986 with 1987 CEEE Events Calen-dar. PB89-185623 900.711 AC GENERATORS

Calculable, Transportable Audio-Frequency AC Reference Standard. PB90-117854 900.721

AC TO DC CONVERTERS AC-DC Difference Calibrations at NBS (National Bureau

of Standards). PB89-201560 900.816 Determination of AC-DC Difference in the 0.1 - 100 MHz Frequency Range. PB89-228597 900.719

ACCELEROMETERS

Automated Fringe Counting Laser Interferometer for Low Frequency Vibration Measurements. PB89-177190 900,885

ACCOUNTABILITY

High Accuracy Determination of (235)U in Nondestructive Assay Standards by Gamma Spectrometry. PB89-156954

ACCREDITATION

Laboratory Accreditation Systems in the United States, 900.882 NVLAP (National Voluntary Laboratory Accreditation Program) Assessment and Evaluation Manual. PB89-228324 900,903

NVLAP (National Voluntary Laboratory Accreditation Program) Program Handbook Construction Testing Services. Requirements for Accreditation. PB90-112327 900,169

ACCURACY

General Methodology for Machine Tool Accuracy Enhancement by Error Compensation.

PB89-146781

900.996

Twenty Five Years of Accuracy Assessment of the Atomic Weights.
PB89-174007 900,365

Precision and Accuracy Assessment Derived from Calibration Data. PB89-179162 900.886

ACETONE/HYDROXY

Stopped-Flow Studies of the Mechanisms of Ozone-Alkene Reactions in the Gas Phase: Tetramethylethy-PB89-157515

ACETYLENE

Resonant Raman Scattering of Controlled Molecular Weight Polyacetylene. PB89-157093

Infrared and Microwave Investigations of Interconversion Tunneling in the Acetylene Dimer. PB89-157341 900,320

Vibrational Exchange upon Interconversion Tunneling in (HF)2 and (HCCH)2. PB89-179113

Influence of Molecular Weight on the Resonant Raman Scattering of Polyacetylene.
PB89-179246 900,564

Photodissociation Dynamics of C2H2 at 193 nm: Vibrational Distributions of the CCH Radical and the Rotational State Distribution of the A(010) State by Time-Resolved Fourier Transform Infrared Emission.

PB89-179782

900,258

Polymerization of a Novel Liquid Crystalline Diacetylene PB89-231286

ACID BONDED REACTION CEMENTS

Non-Aqueous Dental Cements Based on Dimer and Trimer Acids PATENT-4 832 745

Effects of Purified Ferric Oxalate/Nitric Acid Solutions as a Pretreatment for the NTG-GMA and PMDM Bonding PB89-146716 900.034

Bonding Agents and Adhesives: Reactor Response PB89-146732 900.035

KW-1

Force Overlate with Nitrie Acid as a Conditionar in an	. 4.4	ACTIVATION ANALYCIC		PP00 426540
Ferric Oxalate with Nitric Acid as a Conditioner in an hesive Bonding System. PB89-229272 900	7.045	ACTIVATION ANALYSIS Activation Analysis Opportunities Using Cold Net Beams.	eutron A	PB90-136540 900,236 GGLOMERATION
ACID TREATMENT	,040		0,183	Simulation Study of Light Scattering from Soot Agglomer-
Microwave Energy for Acid Decomposition at Elev	ated	ACTIVATION ENERGY		ates. PB89-212138 901,543
Temperatures and Pressures Using Biological and Boical Samples.	otan-	Flux Creep and Activation Energies at the Grain Bo aries of Y-Ba-Cu-O Superconductors.	ound- A	GGREGATES
	,359		1,457	Ultrasonic Separation of Stress and Texture Effects in Polycrystalline Aggregates.
Design Principles for a Large High-Efficiency Sub-Bo Still.	oiling	Polymerization of a Novel Liquid Crystalline Diacety Monomer.	tylene	PB90-117557 900,499
	,207		0,575 A	GING TESTS (MATERIALS)
Introduction to Microwave Acid Decomposition.		ACTUATORS		Fracture Behavior of Ceramics Used in Multilayer Capaci- tors.
	,227	Multiple Actuator Hydraulic System and Rotary Co Valve Therefor.	ontrol	PB89-171805 900,758
ACIDITY Relative Acidities of Water and Methanol and the St.	abili-		0,995	Measurement of the Torque and Normal Force in Torsion
ties of the Dimer Anions.	.299	ADDITIVES		in the Study of the Thermoviscoelastic Properties of Polymer Glasses.
Chemical Kinetics of Intermediates in the Autoxidation		Indirect Energy Gap of Si, Doping Dependence. PB89-150833 901	1,388	PB89-172472 900,554
SO2.		Application of Multiscattering Theory to Impurity Bank	nds in A	GREEMENTS Working Implementation Agreements for Open Systems
	,256	Si:As. PB89-157762 900	0,334	Working Implementation Agreements for Open Systems Interconnection Protocols.
ACINETOBACTER GLUTAMINASIFICANS Preliminary Crystal Structure of Acinetobacter glutan	nina-	Influence of Molybdenum on the Strength and Tough	nness	PB89-221196 900,624
sificans Glutaminase-Asparaginase. PB90-123381 901	,260	of Stainless Steel Welds for Cryogenic Service.	1,100 A	IR CIRCULATION Computer Model of Smoke Movement by Air Conditioning
ACOUSTIC ABSORPTION	,200	Grain Boundary Characterization in Ni3AI.	1,100	Systems (SMACS).
Acoustic Emission: A Quantitative NDE Technique for	r the		1,156	PB89-157267 900,059
Study of Fracture. PB89-211924 900	,921	ADHESIVE BONDING		IR CONDITIONERS Rating Procedure for Mixed Air-Source Unitary Air Condi-
ACOUSTIC EMISSION	,02 ,	Report of Roof Inspection: Characterization of Ne Fabricated Adhesive-Bonded Seams at an Army Faci	lewly- cility.	tioners and Heat Pumps Operating in the Cooling Mode.
Higher-Order Crossings: A New Acoustic Emission Si	ignal	PB90-112376 900	0,107	Revision 1. PB89-193247 900,075
Processing Method. PB89-173488 900	,678	Use of N-Phenylglycine in a Dental Adhesive System. PB90-117375 900	n. 10.048 A	IR CONDITIONING EQUIPMENT
ACOUSTIC MEASUREMENT		Adhesive Bonding of Composites.	0,040	Computer Model of Smoke Movement by Air Conditioning
Measurement of Adapter Loss, Mismatch, and Efficients the Dual Six Post	ency		0,050	Systems (SMACS). PB89-157267 900,059
Using the Dual Six-Port. PB89-147839 901	,316	Substitutes for N-Phenylglycine in Adhesive Bondin Dentin.	ng to	EVSIM: An Evaporator Simulation Model Accounting for
Acoustical Technique for Evaluation of Thermal Ins	sula-		0,051	Refrigerant and One Dimensional Air Distribution. PB89-235881 900,086
tion. PB89-193866 <i>900</i>	.919	ADHESIVES	Α.	IR FILTERS
ACOUSTIC RESONANCE	,	Biological Evaluations of Zinc Hexyl Vanillate Cer Using Two In vivo Test Methods.	ement	Method for Measuring the Effectiveness of Gaseous Con-
Acoustic and Microwave Resonances Applied to Mea			0,038	taminant Removal Filters. PB89-235899 900,858
ing the Gas Constant and the Thermodynamic Temp ture.		Adhesion to Dentin by Means of Gluma Resin. PB89-157168 900	0,039 A	IR FLOW
	,320	Oligomers with Pendant Isocyanate Groups as Adhes		Calculating Flows through Vertical Vents in Zone Fire
ACOUSTIC RESONATORS Spherical Acoustic Resonators in the Undergraduate	i ah-	for Dentin and Other Tissues.		Models under Conditions of Arbitrary Cross-Vent Pressure Difference.
oratory.		PB89-179253 900 ADSORBATES	0,042	PB89-148126 900,108
PB89-179709 901 Spherical Acoustic Resonators.	,317	Theoretical Study of the Vibrational Lineshape for	CO/	Fire Propagation in Concurrent Flows. PB89-151781 900,867
	,321	Pt(111). PB89-157689 900	0,331	Interzonal Natural Convection for Various Aperture Con-
COUSTIC VELOCITY		NO/NH3 Coadsorption on Pt(111): Kinetic and Dynar		figurations. PB89-176499 900,066
Speed of Sound in Natural Gas Mixtures. PB89-174031 900	.840	Effects in Rotational Accommodation.	0,423	Flow Coefficients for Interzonal Natural Convection for
Spherical Acoustic Resonators in the Undergraduate		Picosecond Vibrational Energy Transfer Studies of	•	Various Apertures.
oratory. PB89-179709 <i>901</i>	.317	face Adsorbates.		PB89-177158 900,069 Calculation of the Flow Through a Horizontal Ceiling/
Speed of Sound in a Mercury Ultrasonic Interferom		PB90-136573 900 ADSORPTION	0,537	Floor Vent.
Manometer.		Synchrotron Radiation Study of BaO Films on W((001)	PB89-189252 900,128
PB89-202220 901 Spherical Acoustic Resonators.	,319	and Their Interaction with H2O, CO2, and O2. PB89-157697 900	0,252	AIRNET: A Computer Program for Building Airflow Net- work Modeling.
	,321	Coadsorption of Water and Lithium on the Ru(001)		PB89-193254 900,076
ACOUSTICS & SOUND		face.	0,440	Integral Mass Balances and Pulse Injection Tracer Techniques.
Compensating for Vowel Coarticulation in Continu Speech Recognition.	uous	Fundamental Characterization of Clean and Gas-De	-	PB89-206833 900,077
PB89-176721 900	,634	Tin Oxide.		Air Quality Investigation in the NIH (National Institutes of
Dynamic Poisson's Ratio of a Ceramic Powder do Compaction.	uring	PB89-202964 900 Interaction of Oxygen and Platinum on W(110).	0,785	Health) Radiation Oncology Branch. PB89-228977 900,079
	,039		1,158	Capabilities of Smoke Control: Fundamentals and Zone
Spherical Acoustic Resonators in the Undergraduate oratory.	Lab-	Adsorption of Water on Clean and Oxygen-Pred	dosed	Smoke Control. PB89-229157 900,080
	,317	Nickel(110). PB90-123555 900	0,522	Analysis and Prediction of Air Leakage through Door As-
Finite Element Studies of Transient Wave Propagation		Ammonia Adsorption and Dissociation on a Step	epped	semblies. PB89-231161 900,085
PB89-186902 901 Acoustical Technique for Evaluation of Thermal In:	,375	Iron(s) (100) Surface. PB90-123563 900	0,523	Measured Air Infiltration and Ventilation Rates in Eight
tion.		Adsorption of High-Range Water-Reducing Agents or	n Se-	Large Office Buildings.
	,919	lected Portland Cement Phases and Related Material	als.	PB90-128158 900,090
Vector Calibration of Ultrasonic and Acoustic Emis Transducers.	ssion	Role of Adsorbed Gases in Metal on Metal Epitaxy.	о,ооо д	Predicting Formaldehyde Concentrations in Manufactured
PB89-202014 900	,765		1,174	Housing Resulting from Medium-Density Fiberboard. PB89-148134 900,854
Ultrasonic Sensor for Measuring Surface Roughness. PB89-211809 900	0.679	AEROBIC BACTERIA	rom o	Combustion of Oil on Water.
Acoustic and Microwave Resonances Applied to Mea	,	Biotransformation of Mercury by Bacteria Isolated fro River Collecting Cinnabar Mine Waters.		PB89-149173 900,587
ing the Gas Constant and the Thermodynamic Temp	oera-		0,864	Synergistic Effects of Nitrogen Dioxide and Carbon Diox-
ture. PB89-228548 <i>901</i>	,320	AERODYNAMIC FORCES Aerodynamics of Agglomerated Soot Particles.		ide Following Acute Inhalation Exposures in Rats. PB89-214779 900,856
Texture Monitoring in Aluminum Alloys: A Compariso	on of	PB89-147482 900	0,586 A	IR POLLUTION ABATEMENT
Ultrasonic and Neutron Diffraction Measurements. PB90-117409 901	,159	AEROGELS Low Temperature Mechanical Property Measuremen	nte of	Method for Measuring the Effectiveness of Gaseous Contaminant Removal Filters.
Ultrasonic Separation of Stress and Texture Effect	ts in	Silica Aerogel Foam.		PB89-235899 900,858
Polycrystalline Aggregates. PB90-117557 900	,499		1,061 A	IR POLLUTION DETECTION
Spherical Acoustic Resonators.		AEROSOLS Combustion of Oil on Water. November 1987.		Preparation of Accurate Multicomponent Gas Standards of Volatile Toxic Organic Compounds in the Low-Parts-
PB90-128505 901	,321	PB89-185581 900	0,863	per-Billion Range. PB89-157739 900,185
ACOUSTOELASTICITY Acoustoelastic Determination of Residual Stresses.		Identification of Carbonaceous Aerosols via C-14 A erator Mass Spectrometry, and Laser Microprobe I		Comparison of a Cryogenic Preconcentration Technique
	,318	Spectrometry.		and Direct Injection for the Gas Chromatographic Analy-

ANALYTICAL CHEMISTRY

sis of Low PPB (Parts-per-Billion) (NMOL/MOL) Gas Standards of Toxic Organic Compounds.	PB90-112343 901,068 ALLOCATION MODELS	PB90-123647 901,172 Fatique Resistance of a 2090-T8E41 Aluminum Alloy at
PB89-173843 900,193 Tests of the Recalibration Period of a Drifting Instrument.	Allocating Staff to Tax Facilities: A Graphics-Based Microcomputer Allocation Model.	
PB89-176275 900,199	PB90-129891 900,645	
Mobile Sources of Atmospheric Polycyclic Aromatic Hydrocarbons: A Roadway Tunnel Study. PB90-123571 900.859	ALLOY 2014-T6 Fatigue Resistance of a 2090-T8E41 Aluminum Alloy a	Electron-Impact Excitation of Al(2+). PB89-171565 901,503
Residential Wood Combustion: A Source of Atmospheric	Cryogenic Temperatures. PB90-128737 90,1,177	ALUMINUM-MANGANESE ALLOYS Progress in Understanding Atomic Structure of the Icosa-
Polycyclic Aromatic Hydrocarbons. PB90-128166 900,860	ALLOY 2090-T8E41 Fatigue Resistance of a 2090-T8E41 Aluminum Alloy a	hedral Phase.
R POLLUTION EFFECTS (HUMANS) Chemical Structure of Methane/Air Diffusion Flames:	Cryogenic Temperatures. PB90-128737 901,177	Formation of the Al-Mn Icosahedral Phase by Electrode-
Concentrations and Production Rates of Intermediate Hydrocarbons.	ALLOYING	position. PB90-117763 900,504
PB89-171904 900,590	Diffusion-Induced Grain Boundary Migration. PB90-128174 901,175	Quasicrystals and Quasicrystal-Related Phases in the Al- Mn System.
POLLUTION SAMPLING Draft International Document on Guide to Portable Instru-	ALLOYS Solutal Convection during Directional Solidification.	PB90-123548 901,169
ments for Assessing Airborne Pollutants Arising from Hazardous Wastes. PB89-150775 900,855	PB89-150932 901,322 ASM/NBS (American Society for Metals/National Bureau	Performance of Alumina/Epoxy Thermal Isolation Straps.
Tests of the Recalibration Period of a Drifting Instrument.	of Standards) Numerical and Graphical Database for Binary Alloy Phase Diagrams.	PB89-147078 901,070 Small Angle Neutron Scattering from Porosity in Sintered
PB89-176275 900,199 Mobile Sources of Atmospheric Polycyclic Aromatic Hy-	PB89-157986 901,135	
drocarbons: A Roadway Tunnel Study. PB90-123571 900,859	Microstructural Variations in Rapidly Solidified Alloys. PB90-123621 901,170	Rising Fracture Toughness from the Bending Strength of
Residential Wood Combustion: A Source of Atmospheric Polycyclic Aromatic Hydrocarbons.	ALTERNATING CURRENT AC Impedance Method for High-Resistivity Measure	Indented Alumina Beams. PB89-171771 901,031
PB90-128166 900,860	ments of Silicon. PB89-231203 900,793	Creep Cavitation in Liquid-Phase Sintered Alumina.
R QUALITY Indoor Air Quality.	Temperature Hysteresis in the Initial Susceptibility of	Effect of Heat Treatment on Crack-Resistance Curves in
PB89-176127 900,065 Ventilation Effectiveness Measurements in an Office	Rapidly Solidified Monel. PB90-123423 901,164	· ·
Building. PB89-176614 900,067	ALUMINIDES Rapid Solidification and Ordering of B2 and L2 (sub 1)	Tribochemical Mechanism of Alumina with Water. PB90-117722 901,059
Air Quality Investigation in the NIH (National Institutes of	Phases in the NiAl-NiTi System. PB90-123639 901,173	ALUMINUM OXIDES
Health) Radiation Oncology Branch. PB89-228977 900,079	Pathways for Microstructural Development in TiAl.	Grain-Size and R-Curve Effects in the Abrasive Wear of Alumina.
Ventilation and Air Quality Investigation of the U.S. Geological Survey Building.	PB90-123779 901,173 ALUMINUM	PB90-117383 901,058 AMERICAN SOCIETY OF MECHANICAL ENGINEERS
PB89-229686 900,857 Investigation of a Washington, DC Office Building.	Ultrasonic Determination of Absolute Stresses in Aluminum and Steel Alloys.	Report on Interactions between the National Institute of
PB89-230361 900,081	PB89-150957 901,124 Stable and Metastable Phase Equilibria in the Al-Mr	Standards and Technology and the American Society of
Airflow Network Models for Element-Based Building Airflow Modeling. PB89-230379 900,082	System. PB89-172324 901,136	PB89-172563 901,004
R SOURCE HEAT PUMPS	Solidification of Aluminum-Manganese Powders.	Microwave Spectrum of Methyl Amine: Assignment and
Proposed Methodology for Rating Air-Source Heat Pumps That Heat, Cool, and Provide Domestic Water	PB89-172332 901,137 Undercooling and Microstructural Evolution in Glass	DD00 44 7000 000 500
Heating. PB90-112368 900,087	Forming Alloys. PB89-176465 901,135	AMINES
1 500 1 12000		
RCRAFT	Dynamic Microindentation Apparatus for Materials Char-	Coatings on Steel.
RCRAFT Ignition and Flame Spread Measurements of Aircraft Lining Materials.	Dynamic Microindentation Apparatus for Materials Characterization. PB89-176911 901,140	Coatings on Steel. PB89-176291 901,084 AMMONIA
RCRAFT Ignition and Flame Spread Measurements of Aircraft Lining Materials. PB89-172886 900,009 Transmission Loss through 6061 T-6 Aluminum Using a	Dynamic Microindentation Apparatus for Materials Characterization. PB89-176911 901,140 Transmission Loss through 6061 T-6 Aluminum Using a Pulsed Eddy Current Source.	Coatings on Steel. PB89-176291 AMMONIa Electronic Structure of Diammine (Ascorbato) Platinum(II) and the Trans Influence on the Ligand Dissociation
RCRAFT Ignition and Flame Spread Measurements of Aircraft Lining Materials. PB89-172886 900,009 Transmission Loss through 6061 T-6 Aluminum Using a Pulsed Eddy Current Source. PB89-179840 901,143	Dynamic Microindentation Apparatus for Materials Characterization. PB89-176911 901,140 Transmission Loss through 6061 T-6 Aluminum Using a Pulsed Eddy Current Source. PB89-179840 901,143	Coatings on Steel. PB89-176291 AMMONIa Electronic Structure of Diammine (Ascorbato) Platinum(II) and the Trans Influence on the Ligand Dissociation
RCRAFT Ignition and Flame Spread Measurements of Aircraft Lining Materials. PB89-172886 900,009 Transmission Loss through 6061 T-6 Aluminum Using a Pulsed Eddy Current Source. PB89-179840 RFLOW Airflow Network Models for Element-Based Building Air-	Dynamic Microindentation Apparatus for Materials Characterization. PB89-176911 901,140 Transmission Loss through 6061 T-6 Aluminum Using a Pulsed Eddy Current Source. PB89-179840 901,143 Grain Boundary Structure in Ni3Al. PB89-201784 901,150	Coatings on Steel. PB89-176291 AMMONIA Electronic Structure of Diammine (Ascorbato) Platinum(II) and the Trans Influence on the Ligand Dissociation Energy, PB89-147128 900,287 Influence of Electronic and Geometric Structure on De-
RCRAFT Ignition and Flame Spread Measurements of Aircraft Lining Materials. PB89-172886 900,009 Transmission Loss through 6061 T-6 Aluminum Using a Pulsed Eddy Current Source. PB89-179840 RFLOW 901,143	Dynamic Microindentation Apparatus for Materials Characterization. PB89-176911 901,140 Transmission Loss through 6061 T-6 Aluminum Using a Pulsed Eddy Current Source. PB89-179840 901,140 Grain Boundary Structure in Ni3Al. PB89-201784 901,150 Grain Boundary Structure in Ni3Al. PB89-229314 901,150	Coatings on Steel. PB89-176291 AMMONIA Electronic Structure of Diammine (Ascorbato) Platinum(II) and the Trans Influence on the Ligand Dissociation Energy. PB89-147128 900,287 Influence of Electronic and Geometric Structure on De- sorption Kinetics of Isoelectronic Polar Molecules: NH3
RCRAFT Ignition and Flame Spread Measurements of Aircraft Lining Materials. PB89-172886 900,009 Transmission Loss through 6061 T-6 Aluminum Using a Pulsed Eddy Current Source. PB89-179840 901,143 RFLOW Airflow Network Models for Element-Based Building Airflow Modeling, PB89-230379 Note on Calculating Flows Through Vertical Vents in	Dynamic Microindentation Apparatus for Materials Characterization. PB89-176911 901,140 Transmission Loss through 6061 T-6 Aluminum Using a Pulsed Eddy Current Source. PB89-179840 901,142 Grain Boundary Structure in Ni3Al. PB89-201784 901,150 Grain Boundary Structure in Ni3Al. PB89-229314 901,157	Coatings on Steel. PB89-176291 901,084 AMMONIA Electronic Structure of Diammine (Ascorbato) Platinum(II) and the Trans Influence on the Ligand Dissociation Energy. PB89-147128 900,287 Influence of Electronic and Geometric Structure on Desorption Kinetics of Isoelectronic Polar Molecules: NH3 and H2O. PB89-176473 900,381 NO/NH3 Coadsorption on Pt(1111): Kinetic and Dynamical
RCRAFT Ignition and Flame Spread Measurements of Aircraft Lining Materials. PB89-172886 900,009 Transmission Loss through 6061 T-6 Aluminum Using a Pulsed Eddy Current Source. PB89-179840 RFLOW Airflow Network Models for Element-Based Building Airflow Modeling. PB89-230379 Note on Calculating Flows Through Vertical Vents in Zone Fire Models Under Conditions of Arbitrary Cross- Vent Pressure Difference.	Dynamic Microindentation Apparatus for Materials Characterization. PB89-176911 901,140 Transmission Loss through 6061 T-6 Aluminum Using a Pulsed Eddy Current Source. PB89-179840 901,140 Grain Boundary Structure in Ni3Al. PB89-201784 901,150 Grain Boundary Structure in Ni3Al. PB89-229314 901,150	Coatings on Steel. PB89-176291 901,084 AMMONIA Electronic Structure of Diammine (Ascorbato) Platinum(II) and the Trans Influence on the Ligand Dissociation Energy. PB89-147128 900,287 Influence of Electronic and Geometric Structure on Desorption Kinetics of Isoelectronic Polar Molecules: NH3 and H2O. PB89-176473 900,381 NO/NH3 Coadsorption on Pt(111): Kinetic and Dynamical Effects in Rotational Accommodation.
RCRAFT Ignition and Flame Spread Measurements of Aircraft Lining Materials. PB89-172886 900,009 Transmission Loss through 6061 T-6 Aluminum Using a Pulsed Eddy Current Source. PB89-179840 901,143 RFLOW Airflow Network Models for Element-Based Building Air- flow Modeling. PB89-230379 Note on Calculating Flows Through Vertical Vents in Zone Fire Models Under Conditions of Arbitrary Cross- Vent Pressure Difference. PB90-117573 900,147 LASKA	Dynamic Microindentation Apparatus for Materials Characterization. PB89-176911 901,140 Transmission Loss through 6061 T-6 Aluminum Using a Pulsed Eddy Current Source. PB89-179840 901,143 Grain Boundary Structure in Ni3Al. PB89-201784 901,150 Grain Boundary Structure in Ni3Al. PB89-229314 901,150 ALUMINUM ALLOYS Ultrasonic Texture Analysis for Polycrystalline Aggregates of Cubic Materials Displaying Orthotropic Symmetry. PB89-146948 Quasicrystals with 1-D Translational Periodicity and a	Coatings on Steel. PB89-176291 901,084 AMMONIA Electronic Structure of Diammine (Ascorbato) Platinum(II) and the Trans Influence on the Ligand Dissociation Energy. PB89-147128 900,287 Influence of Electronic and Geometric Structure on Desorption Kinetics of Isoelectronic Polar Molecules: NH3 and H2O. PB89-176473 900,381 NO/NH3 Coadsorption on Pt(111): Kinetic and Dynamical Effects in Rotational Accommodation. PB89-201123 900,423 Ammonia Adsorption and Dissociation on a Stepped Iron(s) (100) Surface.
RCRAFT Ignition and Flame Spread Measurements of Aircraft Lining Materials. PB89-172886 900,009 Transmission Loss through 6061 T-6 Aluminum Using a Pulsed Eddy Current Source. PB89-179840 901,143 RFLOW Airflow Network Models for Element-Based Building Airflow Modeling. PB89-230379 Note on Calculating Flows Through Vertical Vents in Zone Fire Models Under Conditions of Arbitrary Cross- Vent Pressure Difference. PB90-117573 900,147 LASKA Alaska Arctic Offshore Oil Spill Response Technology Workshop Proceedings.	Dynamic Microindentation Apparatus for Materials Characterization. PB89-176911 901,140 Transmission Loss through 6061 T-6 Aluminum Using a Pulsed Eddy Current Source. PB89-179840 901,143 Grain Boundary Structure in Ni3Al. PB89-201784 901,150 Grain Boundary Structure in Ni3Al. PB89-229314 901,150 ALUMINUM ALLOYS Ultrasonic Texture Analysis for Polycrystalline Aggregates of Cubic Materials Displaying Orthotropic Symmetry. PB89-146948 with 1-D Translational Periodicity and a Ten-Fold Rotation Axis. PB89-147383 901,123	Coatings on Steel. PB89-176291 901,084 AMMONIA Electronic Structure of Diammine (Ascorbato) Platinum(II) and the Trans Influence on the Ligand Dissociation Energy. PB89-147128 900,287 Influence of Electronic and Geometric Structure on Desorption Kinetics of Isoelectronic Polar Molecules: NH3 and H2O. PB89-176473 900,381 NO/NH3 Coadsorption on Pt(111): Kinetic and Dynamical Effects in Rotational Accommodation. PB89-201123 900,423 Ammonia Adsorption and Dissociation on a Stepped Iron(s) (100) Surface. PB90-123563 900,523
RCRAFT Ignition and Flame Spread Measurements of Aircraft Lining Materials. PB89-172886 900,009 Transmission Loss through 6061 T-6 Aluminum Using a Pulsed Eddy Current Source. PB89-179840 8FLOW Airflow Network Models for Element-Based Building Airflow Modeling. PB89-230379 Note on Calculating Flows Through Vertical Vents in Zone Fire Models Under Conditions of Arbitrary Cross- Vent Pressure Difference. PB90-117573 900,147 LASKA Alaska Arctic Offshore Oil Spill Response Technology Workshop Proceedings. PB89-195663 900,842 LCOHOLS	Dynamic Microindentation Apparatus for Materials Characterization. PB89-176911 901,140 Transmission Loss through 6061 T-6 Aluminum Using a Pulsed Eddy Current Source. PB89-179840 Grain Boundary Structure in Ni3Al. PB89-201784 901,150 Grain Boundary Structure in Ni3Al. PB89-229314 901,150 ALUMINUM ALLOYS Ultrasonic Texture Analysis for Polycrystalline Aggregates of Cubic Materials Displaying Orthotropic Symmetry. PB89-146948 Quasicrystals with 1-D Translational Periodicity and a Ten-Fold Rotation Axis. PB89-147383 Metastable Phase Production and Transformation in Al Ge Alloy Films by Rapid Crystallization and Annealing	Coatings on Steel. PB89-176291 901,084 AMMONIA Electronic Structure of Diammine (Ascorbato) Platinum(II) and the Trans Influence on the Ligand Dissociation Energy. PB89-147128 900,287 Influence of Electronic and Geometric Structure on Desorption Kinetics of Isoelectronic Polar Molecules: NH3 and H2O. PB89-176473 900,381 NO/NH3 Coadsorption on Pt(111): Kinetic and Dynamical Effects in Rotational Accommodation. PB89-201123 900,423 Ammonia Adsorption and Dissociation on a Stepped Iron(s) (100) Surface. PB90-123563 900,523 AMMONIUM SCHEELITES Thermodynamics of Ammonium Scheelites. 6. An Analy-
RCRAFT Ignition and Flame Spread Measurements of Aircraft Lining Materials. PB89-172886 900,009 Transmission Loss through 6061 T-6 Aluminum Using a Pulsed Eddy Current Source. PB89-179840 901,143 RFLOW Airllow Network Models for Element-Based Building Air- flow Modeling. PB89-230379 Note on Calculating Flows Through Vertical Vents in Zone Fire Models Under Conditions of Arbitrary Cross- Vent Pressure Difference. PB90-117573 900,147 LASKA Alaska Arctic Offshore Oil Spill Response Technology Workshop Proceedings. PB89-195663 900,842 LCOHOLS Determination of Hydrocarbon/Water Partition Coefficients from Chromatographic Data and Based on Solu-	Dynamic Microindentation Apparatus for Materials Characterization. PB89-176911 901,140 Transmission Loss through 6061 T-6 Aluminum Using a Pulsed Eddy Current Source. PB89-179840 901,143 Grain Boundary Structure in Ni3Al. PB89-201784 901,150 Grain Boundary Structure in Ni3Al. PB89-229314 901,150 ALUMINUM ALLOYS Ultrasonic Texture Analysis for Polycrystalline Aggregates of Cubic Materials Displaying Orthotropic Symmetry. PB89-146948 901,120 Quasicrystals with 1-D Translational Periodicity and a Ten-Fold Rotation Axis. PB89-147983 901,120 Metastable Phase Production and Transformation in Al Ge Alloy Films by Rapid Crystallization and Annealing Treatments. PB89-157622 901,128	Coatings on Steel. PB89-176291 901,084 AMMONIA Electronic Structure of Diammine (Ascorbato) Platinum(II) and the Trans Influence on the Ligand Dissociation Energy. PB89-147128 900,287 Influence of Electronic and Geometric Structure on Desorption Kinetics of Isoelectronic Polar Molecules: NH3 and H2O. PB89-176473 900,381 NO/NH3 Coadsorption on Pt(111): Kinetic and Dynamical Effects in Rotational Accommodation. PB89-201123 900,423 Ammonia Adsorption and Dissociation on a Stepped Iron(s) (100) Surface. PB90-123563 900,523 AMMONIUM SCHEELITES Thermodynamics of Ammonium Scheelites. 6. An Analysis of the Heat Capacity and Ancillary Values for the Metaperiodates KIO4, NH4IO4, and ND4IO4.
RCRAFT Ignition and Flame Spread Measurements of Aircraft Lining Materials. PB89-172886 900,009 Transmission Loss through 6061 T-6 Aluminum Using a Pulsed Eddy Current Source. PB89-179840 901,143 RFLOW Airflow Network Models for Element-Based Building Airflow Modeling. PB89-230379 900,082 Note on Calculating Flows Through Vertical Vents in Zone Fire Models Under Conditions of Arbitrary Cross- Vent Pressure Difference. PB90-117573 900,147 LASKA Alaska Arctic Offshore Oil Spill Response Technology Workshop Proceedings. PB99-195663 900,842 LCOHOLS Determination of Hydrocarbon/Water Partition Coeffi-	Dynamic Microindentation Apparatus for Materials Characterization. PB89-176911 901,140 Transmission Loss through 6061 T-6 Aluminum Using a Pulsed Eddy Current Source. PB89-179840 901,143 Grain Boundary Structure in Ni3Al. PB89-201784 901,150 Grain Boundary Structure in Ni3Al. PB89-229314 901,150 ALUMINUM ALLOYS Ultrasonic Texture Analysis for Polycrystalline Aggregates of Cubic Materials Displaying Orthotropic Symmetry. PB89-145945 901,120 Quasicrystals with 1-D Translational Periodicity and a Ten-Fold Rotation Axis. PB89-147383 901,120 Metastable Phase Production and Transformation in Al Ge Alloy Films by Rapid Crystallization and Annealing Treatments.	Coatings on Steel. PB89-176291 AMMONIA Electronic Structure of Diammine (Ascorbato) Platinum(II) and the Trans Influence on the Ligand Dissociation Energy. PB89-147128 John Millian Geometric Structure on Desorption Kinetics of Isoelectronic Polar Molecules: NH3 and H2O. PB89-176473 NO/NH3 Coadsorption on Pt(111): Kinetic and Dynamical Effects in Rotational Accommodation. PB89-201123 Ammonia Adsorption and Dissociation on a Stepped Iron(s) (100) Surface. PB90-123563 AMMONIUM SCHEELITES Thermodynamics of Ammonium Scheelites. 6. An Analysis of the Heat Capacity and Ancillary Values for the Metaperiodates KIO4, NH4IO4, and ND4IO4. PB89-147060 900,285
RCRAFT Ignition and Flame Spread Measurements of Aircraft Lining Materials. PB89-172886 900,009 Transmission Loss through 6061 T-6 Aluminum Using a Pulsed Eddy Current Source. PB89-179840 901,143 RFLOW Airflow Network Models for Element-Based Building Airflow Modeling. PB89-230379 Note on Calculating Flows Through Vertical Vents in Zone Fire Models Under Conditions of Arbitrary Cross-Vent Pressure Difference. PB90-117573 PB90-117573 900,147 LASKA Alaska Arctic Offshore Oil Spill Response Technology Workshop Proceedings. PB89-195663 900,842 LCOHOLS Determination of Hydrocarbon/Water Partition Coefficients from Chromatographic Data and Based on Solution Thermodynamics and Theory. PB89-187538 900,205 LGORITHMS	Dynamic Microindentation Apparatus for Materials Characterization. PB89-176911 901,140 Transmission Loss through 6061 T-6 Aluminum Using a Pulsed Eddy Current Source. PB89-179840 901,143 Grain Boundary Structure in Ni3Al. PB89-201784 901,150 Grain Boundary Structure in Ni3Al. PB89-229314 901,150 ALUMINUM ALLOYS Ultrasonic Texture Analysis for Polycrystalline Aggregates of Cubic Materials Displaying Orthotropic Symmetry. PB89-145948 901,120 Quasicrystals with 1-D Translational Periodicity and a Ten-Fold Rotation Axis. PB89-147383 901,120 Metastable Phase Production and Transformation in Al Ge Alloy Films by Rapid Crystallization and Annealing Treatments. PB89-157622 901,120 Structural Unit in Icosahedral MnAISi and MnAI. PB89-157648 901,137	Coatings on Steel. PB89-176291 901,084 AMMONIA Electronic Structure of Diammine (Ascorbato) Platinum(II) and the Trans Influence on the Ligand Dissociation Energy. PB89-147128 900,287 Influence of Electronic and Geometric Structure on Desorption Kinetics of Isoelectronic Polar Molecules: NH3 and H2O. PB89-176473 900,381 NO/NH3 Coadsorption on Pt(111): Kinetic and Dynamical Effects in Rotational Accommodation. PB89-201123 900,423 Ammonia Adsorption and Dissociation on a Stepped Iron(s) (100) Surface. PB90-123563 900,523 AMMONIUM SCHEELITES Thermodynamics of Ammonium Scheelites. 6. An Analysis of the Heat Capacity and Ancillary Values for the Metaperiodates KIO4, NH4IO4, and ND4IO4. PB89-147060 900,285 AMORPHOUS MATERIALS Undercooling and Microstructural Evolution in Glass Forming Alloys.
RCRAFT Ignition and Flame Spread Measurements of Aircraft Lining Materials. PB89-172886 900,009 Transmission Loss through 6061 T-6 Aluminum Using a Pulsed Eddy Current Source. PB89-179840 901,143 RFLOW Airflow Network Models for Element-Based Building Air- flow Modeling. PB89-230379 900,082 Note on Calculating Flows Through Vertical Vents in Zone Fire Models Under Conditions of Arbitrary Cross- Vent Pressure Difference. PB90-117573 900,147 LASKA Alaska Arctic Offshore Oil Spill Response Technology Workshop Proceedings. PB89-195663 900,842 LCOHOLS Determination of Hydrocarbon/Water Partition Coefficients from Chromatographic Data and Based on Solution Thermodynamics and Theory. PB89-187538	Dynamic Microindentation Apparatus for Materials Characterization. PB89-176911 901,140 Transmission Loss through 6061 T-6 Aluminum Using a Pulsed Eddy Current Source. PB89-179840 901,142 Grain Boundary Structure in Ni3Al. PB89-201784 901,150 Grain Boundary Structure in Ni3Al. PB89-21784 901,150 Ultrasonic Texture Analysis for Polycrystalline Aggregates of Cubic Materials Displaying Orthotropic Symmetry. PB89-146948 901,120 Quasicrystals with 1-D Translational Periodicity and a Ten-Fold Rotation Axis. PB89-147383 901,120 Metastable Phase Production and Transformation in Al Ge Alloy Films by Rapid Crystallization and Annealing Treatments. PB89-157622 Structural Unit in Icosahedral MnAISi and MnAl. PB89-157648 Pontation and Stability Range of the G Phase in the Aluminum-Manganese System. PB89-186316 901,144	Coatings on Steel. PB89-176291 901,084 AMMONIA Electronic Structure of Diammine (Ascorbato) Platinum(II) and the Trans Influence on the Ligand Dissociation Energy. PB89-147128 900,287 Influence of Electronic and Geometric Structure on Desorption Kinetics of Isoelectronic Polar Molecules: NH3 and H2O. PB89-176473 900,381 NO/NH3 Coadsorption on Pt(111): Kinetic and Dynamical Effects in Rotational Accommodation. PB89-201123 900,423 Ammonia Adsorption and Dissociation on a Stepped Iron(s) (100) Surface. PB90-123563 900,523 AMMONIUM SCHEELITES Thermodynamics of Ammonium Scheelites. 6. An Analysis of the Heat Capacity and Ancillary Values for the Metaperiodates KIO4, NH4IO4, and ND4IO4. PB89-147060 900,285 AMORPHOUS MATERIALS Undercooling and Microstructural Evolution in Glass Forming Alloys. PB89-176465 901,139
RCRAFT Ignition and Flame Spread Measurements of Aircraft Lining Materials. PB89-172886 900,009 Transmission Loss through 6061 T-6 Aluminum Using a Pulsed Eddy Current Source. PB89-179840 901,143 RFLOW Airflow Network Models for Element-Based Building Airflow Modeling, PB89-230379 Note on Calculating Flows Through Vertical Vents in Zone Fire Models Under Conditions of Arbitrary Cross- Vent Pressure Difference. PB90-117573 900,147 LASKA Alaska Arctic Offshore Oil Spill Response Technology Workshop Proceedings. PB89-195663 900,842 LCOHOLS Determination of Hydrocarbon/Water Partition Coefficients from Chromatographic Data and Based on Solution Thermodynamics and Theory. PB89-187538 LGORITHMS Improved Spherical and Hemispherical Scanning Algorithms. PB89-156806 900,697 Comparison of Time Scales Generated with the NBS	Dynamic Microindentation Apparatus for Materials Characterization. PB89-176911 901,140 Transmission Loss through 6061 T-6 Aluminum Using a Pulsed Eddy Current Source. PB89-179840 901,140 Grain Boundary Structure in Ni3Al. PB89-201784 901,150 Grain Boundary Structure in Ni3Al. PB89-229314 901,150 ALUMINUM ALLOYS Ultrasonic Texture Analysis for Polycrystalline Aggregates of Cubic Materials Displaying Orthotropic Symmetry. PB89-146948 901,12: Quasicrystals with 1-D Translational Periodicity and a Ten-Fold Rotation Axis. PB89-147383 901,12: Metastable Phase Production and Transformation in Al Ge Alloy Films by Rapid Crystallization and Annealing Treatments. PB89-157622 901,12: Structural Unit in Icosahedral MnAISi and MnAI. PB89-157648 901,13: Formation and Stability Range of the G Phase in the Aluminum-Manganese System. PB89-186316 901,144 Nucleation and Growth of Aperiodic Crystals in Aluminum Alloys.	Coatings on Steel. PB89-176291 901,084 AMMONIA Electronic Structure of Diammine (Ascorbato) Platinum(II) and the Trans Influence on the Ligand Dissociation Energy. PB89-147128 900,287 Influence of Electronic and Geometric Structure on Desorption Kinetics of Isoelectronic Polar Molecules: NH3 and H2O. PB89-176473 900,381 NO/NH3 Coadsorption on Pt(111): Kinetic and Dynamical Effects in Rotational Accommodation. PB89-201123 900,423 Ammonia Adsorption and Dissociation on a Stepped Iron(s) (100) Surface. PB90-123563 900,523 AMMONIUM SCHEELITES Thermodynamics of Ammonium Scheelites. 6. An Analysis of the Heat Capacity and Ancillary Values for the Metaperiodates KIO4, NH4IO4, and ND4IO4. PB89-147060 900,285 AMORPHOUS MATERIALS Undercooling and Microstructural Evolution in Glass Forming Alloys. PB89-176465 901,139 AMORPHOUS STATE Amorphous Phase Formation in Al70Si17Fe13 Alloy.
RCRAFT Ignition and Flame Spread Measurements of Aircraft Lining Materials. PB89-172886 900,009 Transmission Loss through 6061 T-6 Aluminum Using a Pulsed Eddy Current Source. PB89-179840 8FLOW Airflow Network Models for Element-Based Building Air- flow Modeling. PB89-230379 Note on Calculating Flows Through Vertical Vents in Zone Fire Models Under Conditions of Arbitrary Cross- Vent Pressure Difference. PB90-117573 900,147 LASKA Alaska Arctic Offshore Oil Spill Response Technology Workshop Proceedings. PB89-195663 COHOLS Determination of Hydrocarbon/Water Partition Coefficients from Chromatographic Data and Based on Solution Thermodynamics and Theory. PB89-187538 900,205 LGORITHMS Improved Spherical and Hemispherical Scanning Algorithms. PB89-156806 900,697 Comparison of Time Scales Generated with the NBS (National Bureau of Standards) Ensembling Algorithms. PB89-174072	Dynamic Microindentation Apparatus for Materials Characterization. PB89-176911 901,140 Transmission Loss through 6061 T-6 Aluminum Using a Pulsed Eddy Current Source. PB89-179840 901,142 Grain Boundary Structure in Ni3Al. PB89-201784 901,150 Grain Boundary Structure in Ni3Al. PB89-21784 901,150 Ultrasonic Texture Analysis for Polycrystalline Aggregates of Cubic Materials Displaying Orthotropic Symmetry. PB89-146948 901,120 Quasicrystals with 1-D Translational Periodicity and a Ten-Fold Rotation Axis. PB89-147383 901,120 Metastable Phase Production and Transformation in Al Ge Alloy Films by Rapid Crystallization and Annealing Treatments. PB89-157622 Structural Unit in Icosahedral MnAISi and MnAl. PB89-157648 901,130 Formation and Stability Range of the G Phase in the Aluminum-Manganese System. PB89-186316 901,144 Nucleation and Growth of Aperiodic Crystals in Aluminum Alloys. PB89-186324 901,144	Coatings on Steel. PB89-176291 AMMONIA Electronic Structure of Diammine (Ascorbato) Platinum(II) and the Trans Influence on the Ligand Dissociation Energy. PB89-147128 Influence of Electronic and Geometric Structure on Desorption Kinetics of Isoelectronic Polar Molecules: NH3 and H2O. PB89-176473 NO/NH3 Coadsorption on Pt(1111): Kinetic and Dynamical Effects in Rotational Accommodation. PB89-201123 Ammonia Adsorption and Dissociation on a Stepped Iron(s) (100) Surface. PB90-123563 AMMONIUM SCHEELITES Thermodynamics of Ammonium Scheelites. 6. An Analysis of the Heat Capacity and Ancillary Values for the Metaperiodates KIO4, NH4IO4, and ND4IO4. PB89-147060 AMORPHOUS MATERIALS Undercooling and Microstructural Evolution in Glass Forming Alloys. PB89-176465 AMORPHOUS STATE Amorphous Phase Formation in AI70Si17Fe13 Alloy. PB90-123522 901,167 Solidification of an 'Amorphous' Phase in Rapidly Solidi-
RCRAFT Ignition and Flame Spread Measurements of Aircraft Lining Materials. PB89-172886 900,009 Transmission Loss through 6061 T-6 Aluminum Using a Pulsed Eddy Current Source. PB89-179840 8FLOW Airflow Network Models for Element-Based Building Air- flow Modeling. PB89-230379 Note on Calculating Flows Through Vertical Vents in Zone Fire Models Under Conditions of Arbitrary Cross- Vent Pressure Difference. PB90-117573 900,147 LASKA Alaska Arctic Offshore Oil Spill Response Technology Workshop Proceedings. PB89-195663 900,842 LCOHOLS Determination of Hydrocarbon/Water Partition Coefficients from Chromatographic Data and Based on Solution Thermodynamics and Theory. PB89-187538 900,205 LGORITHMS Improved Spherical and Hemispherical Scanning Algo- rithms. PB89-156806 Comparison of Time Scales Generated with the NBS (National Bureau of Standards) Ensembling Algorithm.	Dynamic Microindentation Apparatus for Materials Characterization. PB89-176911 901,14t Transmission Loss through 6061 T-6 Aluminum Using a Pulsed Eddy Current Source. PB89-179840 901,14t Grain Boundary Structure in Ni3Al. PB89-201784 901,15t Grain Boundary Structure in Ni3Al. PB89-229314 901,15t ALUMINUM ALLOYS Ultrasonic Texture Analysis for Polycrystalline Aggregates of Cubic Materials Displaying Orthotropic Symmetry. PB89-146948 901,12t Quasicrystals with 1-D Translational Periodicity and a Ten-Fold Rotation Axis. PB89-147383 901,12t Metastable Phase Production and Transformation in Al Ge Alloy Films by Rapid Crystallization and Annealing Treatments. PB89-157622 901,12t Structural Unit in Icosahedral MnAISi and MnAI. PB89-157648 901,13t Formation and Stability Range of the G Phase in the Aluminum-Manganese System. PB89-186316 901,14t Replacement of Icosahedral Al-Mn by Decagonal Phase. PB89-186332	Coatings on Steel. PB89-176291 AMMONIA Electronic Structure of Diammine (Ascorbato) Platinum(II) and the Trans Influence on the Ligand Dissociation Energy. PB89-147128 Influence of Electronic and Geometric Structure on Desorption Kinetics of Isoelectronic Polar Molecules: NH3 and H2O. PB89-176473 NO/NH3 Coadsorption on Pt(1111): Kinetic and Dynamical Effects in Rotational Accommodation. PB89-201123 Ammonia Adsorption and Dissociation on a Stepped Iron(s) (100) Surface. PB90-123563 AMMONIUM SCHEELITES Thermodynamics of Ammonium Scheelites. 6. An Analysis of the Heat Capacity and Ancillary Values for the Metaperiodates KIO4, NH4IO4, and ND4IO4. PB89-147060 AMORPHOUS MATERIALS Undercooling and Microstructural Evolution in Glass Forming Alloys. PB89-174665 AMORPHOUS STATE Amorphous Phase Formation in AI70Si17Fe13 Alloy. PB90-123522 AMORPHOUS STATE Amorphous Phase Formation in Rapidly Solidified AI-Fe-Si Alloys. PB90-123522
RCRAFT Ignition and Flame Spread Measurements of Aircraft Lining Materials. PB89-172886 900,009 Transmission Loss through 6061 T-6 Aluminum Using a Pulsed Eddy Current Source. PB89-179840 8FLOW Airflow Network Models for Element-Based Building Air- flow Modeling. PB89-230379 Note on Calculating Flows Through Vertical Vents in Zone Fire Models Under Conditions of Arbitrary Cross- Vent Pressure Difference. PB90-117573 900,147 LASKA Alaska Arctic Offshore Oil Spill Response Technology Workshop Proceedings. PB89-195663 COHOLS Determination of Hydrocarbon/Water Partition Coefficients from Chromatographic Data and Based on Solution Thermodynamics and Theory. PB89-187538 900,205 LGORITHMS Improved Spherical and Hemispherical Scanning Algorithms. PB89-156806 900,697 Comparison of Time Scales Generated with the NBS (National Bureau of Standards) Ensembling Algorithm. PB89-174072 Merit Functions and Nonlinear Programming. PB90-123944 LIPHATIC ACYCLIC HYDROCARBONS	Dynamic Microindentation Apparatus for Materials Characterization. PB89-176911 901,14t Transmission Loss through 6061 T-6 Aluminum Using a Pulsed Eddy Current Source. PB89-179840 901,14t Grain Boundary Structure in Ni3Al. PB89-201784 901,15t Grain Boundary Structure in Ni3Al. PB89-229314 901,15t ALUMINUM ALLOYS Ultrasonic Texture Analysis for Polycrystalline Aggregates of Cubic Materials Displaying Orthotropic Symmetry. PB89-146948 901,12t Quasicrystals with 1-D Translational Periodicity and at Ten-Fold Rotation Axis. PB89-147383 901,12t Metastable Phase Production and Transformation in Al Ge Alloy Films by Rapid Crystallization and Annealing Treatments. PB89-157622 901,12t Structural Unit in Icosahedral MnAISi and MnAI. PB89-157648 901,13t Formation and Stability Range of the G Phase in the Aluminum-Manganese System. PB89-186316 901,14t Replacement of Icosahedral Al-Mn by Decagonal Phase. PB89-186332 Structural Study of a Metastable BCC Phase in Al-Mi Alloys Electrodeposited from Molten Salts.	Coatings on Steel. PB89-176291 AMMONIA Electronic Structure of Diammine (Ascorbato) Platinum(II) and the Trans Influence on the Ligand Dissociation Energy. PB89-147128 Influence of Electronic and Geometric Structure on Desorption Kinetics of Isoelectronic Polar Molecules: NH3 and H2O. PB89-176473 NO/NH3 Coadsorption on Pt(1111): Kinetic and Dynamical Effects in Rotational Accommodation. PB89-201123 Ammonia Adsorption and Dissociation on a Stepped Iron(s) (100) Surface. PB90-123563 AMMONIUM SCHEELITES Thermodynamics of Ammonium Scheelites. 6. An Analysis of the Heat Capacity and Ancillary Values for the Metaperiodates KIO4, NH4IO4, and ND4IO4. PB89-147660 AMORPHOUS MATERIALS Undercooling and Microstructural Evolution in Glass Forming Alloys. PB89-176465 AMORPHOUS STATE Amorphous Phase Formation in Al70Si17Fe13 Alloy. PB90-123522 Solidification of an 'Amorphous' Phase in Rapidly Solidified Al-Fe-Si Alloys. PB90-123520 901,168 AMRF MATERIAL HANDLING WORKSTATIONS
RCRAFT Ignition and Flame Spread Measurements of Aircraft Lining Materials. PB89-172886 900,009 Transmission Loss through 6061 T-6 Aluminum Using a Pulsed Eddy Current Source. PB89-179840 901,143 RFLOW Airflow Network Models for Element-Based Building Airflow Modeling. PB89-230379 900,082 Note on Calculating Flows Through Vertical Vents in Zone Fire Models Under Conditions of Arbitrary Cross- Vent Pressure Difference. PB90-117573 900,147 LASKA Alaska Arctic Offshore Oil Spill Response Technology Workshop Proceedings. PB89-195663 900,842 LCOHOLS Determination of Hydrocarbon/Water Partition Coefficients from Chromatographic Data and Based on Solution Thermodynamics and Theory. PB89-187538 900,205 LGORITHMS Improved Spherical and Hemispherical Scanning Algorithms. PB89-156806 900,697 Comparison of Time Scales Generated with the NBS (National Bureau of Standards) Ensembling Algorithm. PB89-174072 900,628 Merit Functions and Nonlinear Programming. PB90-123944 901,208	Dynamic Microindentation Apparatus for Materials Characterization. PB89-176911 901,140 Transmission Loss through 6061 T-6 Aluminum Using a Pulsed Eddy Current Source. PB89-179840 901,142 Grain Boundary Structure in Ni3Al. PB89-201784 901,150 Grain Boundary Structure in Ni3Al. PB89-210144 901,150 Ultrasonic Texture Analysis for Polycrystalline Aggregates of Cubic Materials Displaying Orthotropic Symmetry. PB89-146948 901,120 Quasicrystals with 1-D Translational Periodicity and a Ten-Fold Rotation Axis. PB89-147383 901,120 Metastable Phase Production and Transformation in Al Ge Alloy Films by Rapid Crystallization and Annealing Treatments. PB89-157622 901,120 Structural Unit in Icosahedral MnAISi and MnAI. PB89-157648 901,130 Formation and Stability Range of the G Phase in the Aluminum-Manganese System. PB89-186324 901,140 Nucleation and Growth of Aperiodic Crystals in Aluminum Alloys. PB89-186324 901,141 Structural Study of a Metastable BCC Phase in Al-Mi Alloys Electrodeposited from Molten Salts. PB89-201040 Magnetic Correlations in an Amorphous Gd-Al Spin	Coatings on Steel. PB89-176291 AMMONIA Electronic Structure of Diammine (Ascorbato) Platinum(II) and the Trans Influence on the Ligand Dissociation Energy. PB89-147128 John Millians of Electronic and Geometric Structure on Desorption Kinetics of Isoelectronic Polar Molecules: NH3 and H2O. PB89-176473 NO/NH3 Coadsorption on Pt(111): Kinetic and Dynamical Effects in Rotational Accommodation. PB89-201123 Ammonia Adsorption and Dissociation on a Stepped Iron(s) (100) Surface. PB90-123563 AMMONIUM SCHEELITES Thermodynamics of Ammonium Scheelites. 6. An Analysis of the Heat Capacity and Ancillary Values for the Metaperiodates KIO4, NH4IO4, and ND4IO4. PB89-147060 AMORPHOUS MATERIALS Undercooling and Microstructural Evolution in Glass Forming Alloys. PB89-176465 AMORPHOUS STATE Amorphous Phase Formation in Al70Si17Fe13 Alloy. PB90-123522 Solidification of an 'Amorphous' Phase in Rapidly Solidified Al-Fe-Si Alloys. PB90-123530 AMRF MATERIAL HANDLING WORKSTATIONS Material Handling Workstation Implementation. PB89-159644
RCRAFT Ignition and Flame Spread Measurements of Aircraft Lining Materials. PB89-172886 900,009 Transmission Loss through 6061 T-6 Aluminum Using a Pulsed Eddy Current Source. PB89-179840 8FLOW Airflow Network Models for Element-Based Building Air- flow Modeling, PB89-230379 Note on Calculating Flows Through Vertical Vents in Zone Fire Models Under Conditions of Arbitrary Cross- Vent Pressure Difference. PB90-117573 900,147 LASKA Alaska Arctic Offshore Oil Spill Response Technology Workshop Proceedings. PB89-195663 900,842 LCOHOLS Determination of Hydrocarbon/Water Partition Coefficients from Chromatographic Data and Based on Solution Thermodynamics and Theory. PB89-187538 1GORITHMS Improved Spherical and Hemispherical Scanning Algorithms. PB89-156806 900,697 Comparison of Time Scales Generated with the NBS (National Bureau of Standards) Ensembling Algorithm. PB89-174072 Merit Functions and Nonlinear Programming. PB90-123944 1901,208 LIPHATIC ACYCLIC HYDROCARBONS Oualitative MO Theory of Some Ring and Ladder Polymers. PB89-156723 LKALI AGGREGATE REACTIONS	Dynamic Microindentation Apparatus for Materials Characterization. PB89-176911 901,14t Transmission Loss through 6061 T-6 Aluminum Using a Pulsed Eddy Current Source. PB89-179840 901,14t Grain Boundary Structure in Ni3Al. PB89-201784 901,15t Grain Boundary Structure in Ni3Al. PB89-229314 901,15t ALUMINUM ALLOYS Ultrasonic Texture Analysis for Polycrystalline Aggregates of Cubic Materials Displaying Orthotropic Symmetry. PB89-146948 901,12t Quasicrystals with 1-D Translational Periodicity and a Ten-Fold Rotation Axis. PB89-147383 901,12t Metastable Phase Production and Transformation in Al Ge Alloy Films by Rapid Crystallization and Annealing Treatments. PB89-157622 901,12t Structural Unit in Icosahedral MnAISi and MnAI. PB89-157648 901,13t Formation and Stability Range of the G Phase in the Aluminum-Manganese System. PB89-168316 901,14t Replacement of Icosahedral Al-Mn by Decagonal Phase. PB89-186332 Structural Study of a Metastable BCC Phase in Al-Mi Alloys Electrodeposited from Molten Salts. PB89-201040 901,065	Coatings on Steel. PB89-176291 AMMONIA Electronic Structure of Diammine (Ascorbato) Platinum(II) and the Trans Influence on the Ligand Dissociation Energy. PB89-147128 Influence of Electronic and Geometric Structure on Desorption Kinetics of Isoelectronic Polar Molecules: NH3 and H2O. PB89-176473 NO/NH3 Coadsorption on Pt(1111): Kinetic and Dynamical Effects in Rotational Accommodation. PB89-201123 Ammonia Adsorption and Dissociation on a Stepped Iron(s) (100) Surface. PB90-123563 AMMONIUM SCHEELITES Thermodynamics of Ammonium Scheelites. 6. An Analysis of the Heat Capacity and Ancillary Values for the Metaperiodates KIO4, NH4IO4, and ND4IO4. PB89-147060 AMORPHOUS STATE Amorphous Phase Formation in AI70Si17Fe13 Alloy. PB90-123522 Solidification of an 'Amorphous' Phase in Rapidly Solidified AI-Fe-Si Alloys. PB90-123520 Olidification of an 'Amorphous' Phase in Rapidly Solidified AI-Fe-Si Alloys. PB90-123500 AMRF MATERIAL HANDLING WORKSTATIONS Material Handling Workstation Implementation. PB89-159644 Material Handling Workstation: Operator Manual.
RCRAFT Ignition and Flame Spread Measurements of Aircraft Lining Materials. PB89-172886 900,009 Transmission Loss through 6061 T-6 Aluminum Using a Pulsed Eddy Current Source. PB89-179840 801,143 RIFLOW Airflow Network Models for Element-Based Building Airflow Modeling, PB89-230379 Note on Calculating Flows Through Vertical Vents in Zone Fire Models Under Conditions of Arbitrary Cross- Vent Pressure Difference. PB90-117573 900,147 ASKA Alaska Arctic Offshore Oil Spill Response Technology Workshop Proceedings. PB89-19563 200,842 LOHOLS Determination of Hydrocarbon/Water Partition Coefficients from Chromatographic Data and Based on Solution Thermodynamics and Theory. PB89-187538 Improved Spherical and Hemispherical Scanning Algorithms. PB89-156806 900,697 Comparison of Time Scales Generated with the NBS (National Bureau of Standards) Ensembling Algorithm. PB89-174072 Merit Functions and Nonlinear Programming. PB90-123944 1901,208 LIPHATIC ACYCLIC HYDROCARBONS Qualitative MO Theory of Some Ring and Ladder Polymers. PB89-156723 100,003 LKALI AGGREGATE REACTIONS Standard Aggregate Materials for Alkali-Silica Reaction Studies.	Dynamic Microindentation Apparatus for Materials Characterization. PB89-176911 901,140 Transmission Loss through 6061 T-6 Aluminum Using a Pulsed Eddy Current Source. PB89-179840 901,142 Grain Boundary Structure in Ni3Al. PB89-201649 901,150 Grain Boundary Structure in Ni3Al. PB89-21784 901,150 Grain Boundary Structure in Ni3Al. PB89-229314 901,150 ALUMINUM ALLOYS Ultrasonic Texture Analysis for Polycrystalline Aggregates of Cubic Materials Displaying Orthotropic Symmetry. PB89-146948 901,120 Quasicrystals with 1-D Translational Periodicity and a Ten-Fold Rotation Axis. PB89-147383 901,120 Metastable Phase Production and Transformation in Al Ge Alloy Films by Rapid Crystallization and Annealing Treatments. PB89-157622 Structural Unit in Icosahedral MnAISi and MnAl. PB89-157648 901,130 Formation and Stability Range of the G Phase in the Aluminum-Manganese System. PB89-186324 901,140 Nucleation and Growth of Aperiodic Crystals in Aluminum Alloys. PB89-186324 901,144 Replacement of Icosahedral Al-Mn by Decagonal Phase. PB89-186322 Structural Study of a Metastable BCC Phase in Al-Mi Alloys Electrodeposited from Molten Salts. PB89-201040 Magnetic Correlations in an Amorphous Gd-Al Spin Glass. PB89-201693 901,144 Texture Monitoring in Aluminum Alloys: A Comparison of	Coatings on Steel. PB89-176291 901,084 AMMONIA Electronic Structure of Diammine (Ascorbato) Platinum(II) and the Trans Influence on the Ligand Dissociation Energy. PB89-147128 900,287 Influence of Electronic and Geometric Structure on Desorption Kinetics of Isoelectronic Polar Molecules: NH3 and H2O. PB89-176473 900,381 NO/NH3 Coadsorption on Pt(1111): Kinetic and Dynamical Effects in Rotational Accommodation. PB89-201123 900,423 Ammonia Adsorption and Dissociation on a Stepped Iron(s) (100) Surface. PB90-123563 900,523 AMMONIUM SCHEELITES Thermodynamics of Ammonium Scheelites. 6. An Analysis of the Heat Capacity and Ancillary Values for the Metaperiodates KIO4, NH4IO4, and ND4IO4. PB89-147060 900,285 AMORPHOUS MATERIALS Undercooling and Microstructural Evolution in Glass Forming Alloys. PB89-176465 901,139 AMORPHOUS STATE Amorphous Phase Formation in Al70Si17Fe13 Alloy. PB90-123522 901,167 Solidification of an 'Amorphous' Phase in Rapidly Solidited Al-Fe-Si Alloys. PB90-123530 901,168 AMRF MATERIAL HANDLING WORKSTATIONS Material Handling Workstation Implementation. PB89-159661 ANALYTICAL CHEMISTRY
RCRAFT Ignition and Flame Spread Measurements of Aircraft Lining Materials. PB89-172886 900,009 Transmission Loss through 6061 T-6 Aluminum Using a Pulsed Eddy Current Source. PB89-179840 8FLOW Airflow Network Models for Element-Based Building Air- flow Modeling. PB89-230379 Note on Calculating Flows Through Vertical Vents in Zone Fire Models Under Conditions of Arbitrary Cross- Vent Pressure Difference. PB90-117573 900,147 LASKA Alaska Arctic Offshore Oil Spill Response Technology Workshop Proceedings. PB89-195663 900,842 LCOHOLS Determination of Hydrocarbon/Water Partition Coefficients from Chromatographic Data and Based on Solution Thermodynamics and Theory. PB89-187538 LGORITHMS Improved Spherical and Hemispherical Scanning Algo- rithms. PB89-156806 900,697 Comparison of Time Scales Generated with the NBS (National Bureau of Standards) Ensembling Algorithm. PB89-174072 900,628 Merit Functions and Nonlinear Programming. PB90-123944 901,208 LIPHATIC ACYCLIC HYDROCARBONS Qualitative MO Theory of Some Ring and Ladder Polymers. PB89-156723 900,303 LKALI AGGREGATE REACTIONS Standard Aggregate Materials for Alkali-Silica Reaction	Dynamic Microindentation Apparatus for Materials Characterization. PB89-176911 901,14t Transmission Loss through 6061 T-6 Aluminum Using a Pulsed Eddy Current Source. PB89-179840 901,14t Grain Boundary Structure in Ni3Al. PB89-201784 901,15t Grain Boundary Structure in Ni3Al. PB89-229314 901,15t ALUMINUM ALLOYS Ultrasonic Texture Analysis for Polycrystalline Aggregates of Cubic Materials Displaying Orthotropic Symmetry. PB89-146948 901,12: Quasicrystals with 1-D Translational Periodicity and a Ten-Fold Rotation Axis. PB89-147383 901,12: Metastable Phase Production and Transformation in Al Ge Alloy Films by Rapid Crystallization and Annealing Treatments. PB89-157622 901,12t Structural Unit in Icosahedral MnAISi and MnAI. PB89-157648 901,13t Formation and Stability Range of the G Phase in the Aluminum-Manganese System. PB89-166316 901,14t Replacement of Icosahedral Al-Mn by Decagonal Phase. PB89-186324 901,14t Replacement of Icosahedral Al-Mn by Decagonal Phase. PB89-186332 901,14t Replacement of Icosahedral Al-Mn by Decagonal Phase. PB89-186332 901,14t Structural Study of a Metastable BCC Phase in Al-Mn Alloys Electrodeposited from Molten Salts. PB89-201040 901,06t Magnetic Correlations in an Amorphous Gd-Al Spin Glass. PB89-201693 7exture Monitoring in Aluminum Alloys: A Comparison of Ultrasonic and Neutron Diffraction Measurements. PB90-117409 901,155	Coatings on Steel. PB89-176291 AMMONIA Electronic Structure of Diammine (Ascorbato) Platinum(II) and the Trans Influence on the Ligand Dissociation Energy. PB89-147128 PB89-147128 Jone 200,287 Influence of Electronic and Geometric Structure on Desorption Kinetics of Isoelectronic Polar Molecules: NH3 and H2O. PB89-176473 NO/NH3 Coadsorption on Pt(1111): Kinetic and Dynamical Effects in Rotational Accommodation. PB89-201123 Ammonia Adsorption and Dissociation on a Stepped Iron(s) (100) Surface. PB90-123563 AMMONIUM SCHEELITES Thermodynamics of Ammonium Scheelites. 6. An Analysis of the Heat Capacity and Ancillary Values for the Metaperiodates KIO4, NH4IO4, and ND4IO4. PB89-147060 AMORPHOUS MATERIALS Undercooling and Microstructural Evolution in Glass Forming Alloys. PB89-176465 AMORPHOUS STATE Amorphous Phase Formation in AI70Si17Fe13 Alloy. PB90-123522 AMRF MATERIAL HANDLING WORKSTATIONS Material Handling Workstation Implementation. PB89-159641 Material Handling Workstation: Operator Manual. PB89-159661 ANALYTICAL CHEMISTRY Developing Definitive Methods for Human Serum Analytes.
RCRAFT Ignition and Flame Spread Measurements of Aircraft Lining Materials. PB89-172886 900,009 Transmission Loss through 6061 T-6 Aluminum Using a Pulsed Eddy Current Source. PB89-179840 8FLOW Airflow Network Models for Element-Based Building Air- flow Modeling. PB89-230379 900,082 Note on Calculating Flows Through Vertical Vents in Zone Fire Models Under Conditions of Arbitrary Cross- Vent Pressure Difference. PB30-117573 900,147 LASKA Alaska Arctic Offshore Oil Spill Response Technology Workshop Proceedings. PB89-195663 900,842 LCOHOLS Determination of Hydrocarbon/Water Partition Coefficients from Chromatographic Data and Based on Solution Thermodynamics and Theory. PB89-187538 900,205 LCORITHMS Improved Spherical and Hemispherical Scanning Algorithms. PB89-156806 900,697 Comparison of Time Scales Generated with the NBS (National Bureau of Standards) Ensembling Algorithm. PB89-174072 900,628 Merit Functions and Nonlinear Programming. PB90-123944 LIPHATIC ACYCLIC HYDROCARBONS Qualitative MO Theory of Some Ring and Ladder Poly- mers. PB89-156723 LKALI AGGREGATE REACTIONS Standard Aggregate Materials for Alkali-Silica Reaction Studies. PB89-193221 901,046 LKALINITY Corrosion Behavior of Mild Steel in High pH Aqueous Media.	Dynamic Microindentation Apparatus for Materials Characterization. PB89-176911 901,140 Transmission Loss through 6061 T-6 Aluminum Using a Pulsed Eddy Current Source. PB89-179840 901,142 Grain Boundary Structure in Ni3Al. PB89-201784 901,150 Grain Boundary Structure in Ni3Al. PB89-201784 901,150 Grain Boundary Structure in Ni3Al. PB89-229314 901,150 Ultrasonic Texture Analysis for Polycrystalline Aggregates of Cubic Materials Displaying Orthotropic Symmetry. PB89-146948 901,12: Quasicrystals with 1-D Translational Periodicity and a Ten-Fold Rotation Axis. PB89-147383 901,12: Metastable Phase Production and Transformation in Al Ge Alloy Films by Rapid Crystallization and Annealing Treatments. PB89-157622 Structural Unit in Icosahedral MnAlSi and MnAl. PB89-157648 Formation and Stability Range of the G Phase in the Aluminum-Manganese System. PB89-186316 901,14: Nucleation and Growth of Aperiodic Crystals in Aluminum Alloys. PB89-186324 901,14: Structural Study of a Metastable BCC Phase in Al-Mi Alloys Electrodeposited from Molten Salts. PB89-201040 Magnetic Correlations in an Amorphous Gd-Al Spin Glass. PB89-201693 901,14: Texture Monitoring in Aluminum Alloys: A Comparison of Ultrasonic and Neutron Diffraction Measurements. PB90-117409 901,15.	Coatings on Steel. P89-176291 AMMONIA Electronic Structure of Diammine (Ascorbato) Platinum(II) and the Trans Influence on the Ligand Dissociation Energy. P89-147128 Influence of Electronic and Geometric Structure on Desorption Kinetics of Isoelectronic Polar Molecules: NH3 and H2O. P89-176473 NO/NH3 Coadsorption on Pt(111): Kinetic and Dynamical Effects in Rotational Accommodation. P89-201123 Ammonia Adsorption and Dissociation on a Stepped Iron(s) (100) Surface. P890-123563 AMMONIUM SCHEELITES Thermodynamics of Ammonium Scheelites. 6. An Analysis of the Heat Capacity and Ancillary Values for the Metaperiodates KIO4, NH4IO4, and ND4IO4. P899-147060 AMORPHOUS MATERIALS Undercooling and Microstructural Evolution in Glass Forming Alloys. P899-176465 AMORPHOUS STATE Amorphous Phase Formation in Al70Si17Fe13 Alloy. P890-123522 Solidification of an 'Amorphous' Phase in Rapidly Solidited Al-Fe-Si Alloys. P890-123503 AMRF MATERIAL HANDLING WORKSTATIONS Material Handling Workstation Implementation. P899-159651 ANALYTICAL CHEMISTRY Developing Definitive Methods for Human Serum Analytes. P899-146773 Speciation Measurements of Butyltins: Application to
RCRAFT Ignition and Flame Spread Measurements of Aircraft Lining Materials. PB89-172886 900,009 Transmission Loss through 6061 T-6 Aluminum Using a Pulsed Eddy Current Source. PB89-179840 8FLOW Airflow Network Models for Element-Based Building Air- flow Modeling. PB89-230379 Note on Calculating Flows Through Vertical Vents in Zone Fire Models Under Conditions of Arbitrary Cross- Vent Pressure Difference. PB90-117573 900,147 LASKA Alaska Arctic Offshore Oil Spill Response Technology Workshop Proceedings. PB89-195663 COHOLS Determination of Hydrocarbon/Water Partition Coefficients from Chromatographic Data and Based on Solution Thermodynamics and Theory. PB89-187538 900,205 LGORITHMS Improved Spherical and Hemispherical Scanning Algorithms. PB89-156806 900,697 Comparison of Time Scales Generated with the NBS (National Bureau of Standards) Ensembling Algorithm. PB89-174072 Merit Functions and Nonlinear Programming. PB90-123944 LIPHATIC ACYCLIC HYDROCARBONS Qualitative MO Theory of Some Ring and Ladder Polymers. PB89-156723 900,303 LKALI AGGREGATE REACTIONS Standard Aggregate Materials for Alkali-Silica Reaction Studies. PB89-193221 LKALINITY Corrosion Behavior of Mild Steel in High pH Aqueous Media. PB90-131152 901,086	Dynamic Microindentation Apparatus for Materials Characterization. PB89-176911 901,140 Transmission Loss through 6061 T-6 Aluminum Using a Pulsed Eddy Current Source. PB89-179840 901,142 Grain Boundary Structure in Ni3Al. PB89-201784 901,150 Grain Boundary Structure in Ni3Al. PB89-201693 901,142 ALUMINUM ALLOYS Ultrasonic Texture Analysis for Polycrystalline Aggregates of Cubic Materials Displaying Orthotropic Symmetry. PB89-146948 901,122 Quasicrystals with 1-D Translational Periodicity and a Ten-Fold Rotation Axis. PB89-147383 901,122 Metastable Phase Production and Transformation in Al Ge Alloy Films by Rapid Crystallization and Annealing Treatments. PB89-157622 Structural Unit in Icosahedral MnAISi and MnAI. PB89-157648 901,132 Formation and Stability Range of the G Phase in the Aluminum-Manganese System. PB89-186324 901,143 Replacement of Icosahedral Al-Mn by Decagonal Phase. PB89-186322 Structural Study of a Metastable BCC Phase in Al-Mi Alloys Electrodeposited from Molten Salts. PB89-201040 Magnetic Correlations in an Amorphous Gd-Al Spin Glass. PB89-201693 901,144 Texture Monitoring in Aluminum Alloys: A Comparison of Ultrasonic and Neutron Diffraction Measurements. PB90-117409 901,156 Solidification of an 'Amorphous' Phase in Rapidly Solidified Al-Fe-Si Alloys.	Coatings on Steel. PB89-176291 AMMONIA Electronic Structure of Diammine (Ascorbato) Platinum(II) and the Trans Influence on the Ligand Dissociation Energy. PB89-147128 900,287 Influence of Electronic and Geometric Structure on Desorption Kinetics of Isoelectronic Polar Molecules: NH3 and H2O. PB89-176473 NO/NH3 Coadsorption on Pt(111): Kinetic and Dynamical Effects in Rotational Accommodation. PB89-201123 Ammonia Adsorption and Dissociation on a Stepped Iron(s) (100) Surface. PB90-123563 AMMONIUM SCHEELITES Thermodynamics of Ammonium Scheelites. 6. An Analysis of the Heat Capacity and Ancillary Values for the Metaperiodates KIO4, NH4IO4, and ND4IO4. PB89-147060 AMORPHOUS MATERIALS Undercooling and Microstructural Evolution in Glass Forming Alloys. PB89-176465 AMORPHOUS STATE Amorphous Phase Formation in Al70Si17Fe13 Alloy. PB90-123522 Solidification of an 'Amorphous' Phase in Rapidly Solidified Al-Fe-Si Alloys. PB90-123530 AMRF MATERIAL HANDLING WORKSTATIONS Material Handling Workstation Implementation. PB89-159644 Material Handling Workstation Implementation. PB89-159661 ANALYTICAL CHEMISTRY Developing Definitive Methods for Human Serum Analytes. PB89-146773 Speciation Measurements of Butyltins: Application to Controlled Release Rate Determination and Production of Reference Standards.
RCRAFT Ignition and Flame Spread Measurements of Aircraft Lining Materials. PB89-172886 900,009 Transmission Loss through 6061 T-6 Aluminum Using a Pulsed Eddy Current Source. PB89-179840 8FLOW Airflow Network Models for Element-Based Building Air- flow Modeling. PB89-230379 900,082 Note on Calculating Flows Through Vertical Vents in Zone Fire Models Under Conditions of Arbitrary Cross- Vent Pressure Difference. PB30-117573 900,147 LASKA Alaska Arctic Offshore Oil Spill Response Technology Workshop Proceedings. PB89-195663 900,842 LCOHOLS Determination of Hydrocarbon/Water Partition Coefficients from Chromatographic Data and Based on Solution Thermodynamics and Theory. PB89-187538 900,205 LCORITHMS Improved Spherical and Hemispherical Scanning Algorithms. PB89-156806 900,697 Comparison of Time Scales Generated with the NBS (National Bureau of Standards) Ensembling Algorithm. PB89-174072 900,628 Merit Functions and Nonlinear Programming. PB90-123944 LIPHATIC ACYCLIC HYDROCARBONS Qualitative MO Theory of Some Ring and Ladder Poly- mers. PB89-156723 LKALI AGGREGATE REACTIONS Standard Aggregate Materials for Alkali-Silica Reaction Studies. PB89-193221 901,046 LKALINITY Corrosion Behavior of Mild Steel in High pH Aqueous Media.	Dynamic Microindentation Apparatus for Materials Characterization. PB89-176911 901,14t Transmission Loss through 6061 T-6 Aluminum Using a Pulsed Eddy Current Source. PB89-179840 901,14t Grain Boundary Structure in Ni3Al. PB89-201784 901,15t Grain Boundary Structure in Ni3Al. PB89-229314 901,15t ALUMINUM ALLOYS Ultrasonic Texture Analysis for Polycrystalline Aggregates of Cubic Materials Displaying Orthotropic Symmetry. PB89-146948 901,12: Quasicrystals with 1-D Translational Periodicity and Ten-Fold Rotation Axis. PB89-147383 901,12: Metastable Phase Production and Transformation in Al Ge Alloy Films by Rapid Crystallization and Annealing Treatments. PB89-157622 901,12s Structural Unit in Icosahedral MnAISi and MnAI. PB89-157648 901,13: Formation and Stability Range of the G Phase in the Aluminum-Manganese System. PB89-186316 901,144 Replacement of Icosahedral Al-Mn by Decagonal Phase. PB89-186324 901,144 Replacement of Icosahedral Al-Mn by Decagonal Phase. PB89-186332 901,144 Structural Study of a Metastable BCC Phase in Al-Mi Alloys Electrodeposited from Molten Salts. PB89-201040 901,06: Magnetic Correlations in an Amorphous Gd-Al Spir Glass. PB89-201693 901,144 Texture Monitoring in Aluminum Alloys: A Comparison of Ultrasonic and Neutron Diffraction Measurements. PB90-117409 401,156 Solidification of an 'Amorphous' Phase in Rapidly Solidification of an 'Amorphous' Phase	Coatings on Steel. PB89-176291 AMMONIA Electronic Structure of Diammine (Ascorbato) Platinum(II) and the Trans Influence on the Ligand Dissociation Energy. PB89-147128 Influence of Electronic and Geometric Structure on Desorption Kinetics of Isoelectronic Polar Molecules: NH3 and H2O. PB89-176473 NO/NH3 Coadsorption on Pt(1111): Kinetic and Dynamical Effects in Rotational Accommodation. PB89-201123 Ammonia Adsorption and Dissociation on a Stepped Iron(s) (100) Surface. PB90-123563 AMMONIUM SCHEELITES Thermodynamics of Ammonium Scheelites. 6. An Analysis of the Heat Capacity and Ancillary Values for the Metaperiodates KIO4, NH4IO4, and ND4IO4. PB89-147060 AMORPHOUS MATERIALS Undercooling and Microstructural Evolution in Glass Forming Alloys. PB89-176465 AMORPHOUS STATE Amorphous Phase Formation in AI70Si17Fe13 Alloy. PB90-123522 Solidification of an 'Amorphous' Phase in Rapidly Solidified AI-Fe-Si Alloys. PB90-123500 AMRF MATERIAL HANDLING WORKSTATIONS Material Handling Workstation Implementation. PB89-159651 AMALYTICAL CHEMISTRY Developing Definitive Methods for Human Serum Analytes. PB89-146773 Speciation Measurements of Butyltins: Application to Controlled Release Rate Determination and Production of Reference Standards. P889-146807

Determining Picogram Quantities of U in Human Urine by Thermal Ionization Mass Spectrometry.	PB89-175962 900,196	PB89-230320 900,48
PB89-146906 900,175	Role of Standards in Electron Microprobe Techniques. PB89-176143 900,197	Isotope Dilution Mass Spectrometry for Accurate Elemental Analysis.
Application of Synergistic Microanalysis Techniques to the Study of a Possible New Mineral Containing Light	Defocus Modeling for Compositional Mapping with Wave- length-Dispersive X-ray Spectrometry.	PB89-230338 900,220 Determination of Total Cholesterol in Coconut Oil: A Nev
Elements. PB89-147037 <i>901,277</i>	PB89-176150 <i>900,378</i>	NIST (National Institute of Standards and Technology Cholesterol Standard Reference Material.
Special Calibration Systems for Reactive Gases and Other Difficult Measurements.	High-Accuracy Differential-Pulse Anodic Stripping Voltammetry Using Indium as an Internal Standard. PB89-176267 900,198	PB89-234173 901,26
PB89-149215 900,873 Stokes and Anti-Stokes Fluorescence of Er(3+) in the	Trace Gas Calibration Systems Using Permeation De-	Determination of Serum Cholesterol by e Modification of the Isotope Dilution Mass Spectrometric Definitive
Raman Spectra of Erbium Oxide and Erbium Glasses. PB89-149231 901,020	" vices. PB89-176580 900,883	Method. PB89-234181 901,23
Optical Rotation.	Luminescence Standards for Macro- and Microspectro- fluorometry.	Center for Electronics end Electrical Engineering Technical Publication Announcements Covering Center Pro
PB89-149256 900,294 Companison of Detection Limits in Atomic Spectroscopic	PB89-176598 900,383	grems, October to December 1986, with 1987 CEEL Events Calendar.
Methods of Analysis. PB89-150858 900,176	Companison of Two Transient Recorders for Use with the Laser Microprobe Mass Analyzer.	PB90-116195 900,824
Technical Activities, 1988, Center for Analytical Chemis-	PB89-176887 900,200 Determination of Ultratrace Concentrations of Butyltin	Safety Guidelines for Microwave Systems in the Anelyti cal Laboratory.
try. PB89-151773 900,177	Compounds in Water by Simultaneous Hydridization/Extraction with GC-FPD Detection.	PB90-118167 900,688 Preconcentretion of Trece Transition Metal and Rare
Standard Reference Materials for the Determination of Polycyclic Aromatic Hydrocarbons.	PB89-177224 901,311	Earth Elements from Highly Saline Solutions. PB90-118175 900,220
PB89-156889 <i>900,178</i>	Precision end Accurecy Assessment Derived from Calibretion Data.	Monitoring and Predicting Paremeters in Microwave Dis
Sequential Determination of Biological end Pollutant Elements in Marine Bivalves. PB89-156897 901,217	PB89-179162 900,886 Anelysis of Ultrapure Reagents from e Large Sub-Boiling	solution. PB90-118183 <i>900,69</i> 6
PB89-156897 901,217 Sample Validity in Biological Trece Element end Orgenic	Still Made of Teflon PFA. PB89-186357 900,202	Introduction to Microweve Acid Decomposition. PB90-118191 900,22.
Nutrient Research Studies. PB89-156905 901,218	Penesapeite, a Beryllophosphete Zeolite Releted to Synthetic Zeolite Rho, from the Tip Top Pegmetite of South	Comperison of Microweve Drying and Conventiona
Radiochemical Procedure for Ultratrace Determination of Chromium in Biological Materials.	Dekota. PB89-186431 901,288	Drying Techniques for Reference Meterials. PB90-123464 900,22
PB89-156913 900,179	Recent Advances in Bonded Phases for Liquid Chrome-	Determinetion of Selenium and Tellurium in Coppe Standard Reference Materials Using Stable Isotope Dilu
Neutron Activation Analysis of the NIST (National Insti- tute of Standards and Technology) Bovine Serum Stand-	togrephy. PB89-187520 900,204	tion Spark Source Mess Spectrometry. PB90-123472 900,236
ard Reference Material Using Chemical Separations. PB89-156921 900,180	Determination of Hydrocarbon/Weter Pertition Coeffi- cients from Chrometographic Data and Based on Solu-	Mobile Sources of Atmospheric Polycyclic Arometic Hy
Long-Term Stability of the Elemental Composition in Biological Materials.	tion Thermodynemics and Theory. PB89-187538 900,205	drocarbons: A Roadway Tunnel Study. PB90-123571 900,85
PB89-156939 900,181	Preparation of Glass Columns for Visual Demonstration	Facile Synthesis of 1-Nitropyrene-d9 of High Isotopic Purity.
High-Accuracy Differential-Pulse Anodic Stripping Voltammetry with Indium as an Internal Standard.	of Reversed Phase Liquid Chromatography. PB89-187546 900,206	PB9Ó-123753 900,240
PB89-156947 900,182 Trace Speciation by HPLC-GF AA (High-Performance	Design Principles for a Large High-Efficiency Sub-Boiling Still.	High-Accuracy Gas Analysis via Isotope Dilution Mass Spectrometry: Carbon Dioxide in Air.
Liquid Chromatography-Graphite Furnace Atomic Absorp- tion) for Tin- and Lead-Bearing Organometallic Com-	PB89-187553 900,207	PB90-123951 900,03. Experiences in Environmental Specimen Banking.
pounds, with Signal Increases Induced by Transition- Metal Ions.	High-Purity Germanium X-ray Detector on a 200 kV Analytical Electron Microscope.	PB90-123969 900,860
PB89-157085 900,184 Preparation of Accurate Multicomponent Gas Standards	PB89-201602 900,208 Continuum Radiation Produced in Pure-Element Targets	Residential Wood Combustion: A Source of Atmospheric Polycylic Aromatic Hydrocarbons.
of Volatile Toxic Organic Compounds in the Low-Parts- per-Billion Range.	by 10-40 keV Electrons: An Empirical Model. PB89-201610 900,209	PB90-128166 900,860 Comparison of Liquid Chromatographic Selectivity for Po
PB89-157739 900,185	Laser Microprobe Mass Spectrometry: Description and Selected Applications.	lycyclic Aromatic Hydrocarbons on Cyclodextrin and C18 Bonded Phases.
Computer-Aided Imaging: Quantitative Compositional Mapping with the Electron Probe Microanalyzer.	PB89-201628 900,210	PB90-128539 900,23
PB89-157754 901,073 Role of Neutron Activation Analysis in the Certification of	Methods for the Production of Particle Standards. PB89-201636 901,047	Determination of Experimental and Theoretical k (sub- ASi) Factors for a 200-kV Analytical Electron Microscope
NBS (National Bureau of Standards) Standard Reference Materials.	Performance Standards for Microanalysis. PB89-201651 900,211	PB90-128653 900,23. Synthesis and Characterization of Novel Bonded Phase
PB89-157879 900,187	Single Particle Standards for Isotopic Measurements of	for Reversed-Phase Liquid Chromatography. PB90-128695 900,23
Voltammetric and Liquid Chromatographic Identification of Organic Products of Microwave-Assisted Wet Ashing	Uranium by Secondary Ion Mass Spectrometry. PB89-201669 901,297	Anti-T2 Monoclonal Antibody Immobilization on Quart
of Biological Samples. PB89-157994 900,188	Uncertainties in Mass Absorption Coefficients in Fundamental Parameter X-ray Fluorescence Analysis.	Fibers: Stability and Recognition of T2 Mycotoxin. PB90-128760 901,26.
Analytical Applications of Resonance Ionization Mass Spectrometry (RIMS).	PB89-201677 900,212	Low Pressure, Automated, Sample Packing Unit for Diffuse Reflectance Infrared Spectrometry.
PB89-161590 900,189 Chemical Calibration Standards for Molecular Absorption	Quality Assurance in Metals Analysis Using the Inductive- ly Coupled Plasma. PB89-202063 900,213	PB90-135922 900,23: Identification of Carbonaceous Aerosols via C-14 Accel
Spectrometry. PB89-171938 900,191	Three-Dimensional Atomic Spectra in Flames Using Step-	erator Mass Spectrometry, and Laser Microprobe Mass Spectrometry.
Radiochemical and Instrumental Neutron Activation Anal-	wise Excitation Laser-Enhanced Ionization Spectroscopy. PB89-202071 900,430	PB90-136540 900,236
ysis Procedures for the Determination of Low Level Trace Elements in Human Livers. PB89-171953 901.236	Novel Flow Process for Metal and Ore Solubilization by Aqueous Methyl Iodide.	Technical Examination, Lead Isotope Determination, and Elemental Analysis of Some Shang and Zhou Dynast
PB89-171953 901,236 Microwave Energy for Acid Decomposition at Elevated Temperatures and Pressures Using Biological and Botan-	PB89-202113 901,285 Spectroscopic Quantitative Analysis of Strongly Interact-	Bronze Vessels. PB90-136862 901,178
ical Samples.	ing Systems: Human Plasma Protein Mixtures. PB89-202576 901,225	Absolute Isotopic Abundance Ratios and Atomic Weigh of a Reference Sample of Nickel.
PB89-171961 900,359 Strategy for Interpretation of Contrast Mechanisms in	Preparation of Standards for Gas Analysis.	PB90-163890 900,54
Scanning Electron Microscopy: A Tutonal. PB89-172498 900,192	PB89-211940 900,215 Quantitative Studies of Coatings on Steel Using Reflec-	Absolute Isotopic Composition and Atomic Weight of Ter restrial Nickel. PROJECTOR
Dependence of Interface Widths on Ion Bombardment	tion/Absorption Fourier Transform Infrared Spectroscopy. PB89-212112 901,066	PB90-163908 900,54- ANALYZERS
Conditions in SIMS (Secondary Ion Mass Spectrometry) Analysis of a Ni/Cr Multilayer Structure.	Collision Induced Spectroscopy: Absorption and Light	Use of Thorium as a Target in Electron-Spin Analyzers. PB90-117938 900,912
PB89-172506 900,364 Comparison of a Cryogenic Preconcentration Technique	Scattering. PB89-212252 <i>901,363</i>	ANIONS
and Direct Injection for the Gas Chromatographic Analysis of Low PPB (Parts-per-Billion) (NMOL/MOL) Gas	Expert-Database System for Sample Preparation by Microwave Dissolution, 1. Selection of Analytical Descrip-	Autodetaching States of Negative Ions. PB89-150767 900,29
Standards of Toxic Organic Compounds. PB89-173843 900,193	tors. PB89-229108 900,216	Relative Acidities of Water and Methanol and the Stabili ties of the Dimer Anions.
Numeric Databases for Chemical Analysis. PB89-175236 900,194	Microwave Digestion of Biological Samples: Selenium Analysis by Electrothermal Atomic Absorption Spectrom-	PB89-150981 900,298
Specimen Banking in the National Status and Trends	etry. PB89-229116 900,217	Kinetics of Electron Transfer from Nitroaromatic Radica Anions in Aqueous Solutions. Effects of Temperature and
Program: Development of Protocols and First Year Results.	Introduction to Supercritical Fluid Chromatography. Part	Steric Configuration. PB89-156749 900,303
PB89-175855 901,308 Characterization of Organolead Polymers in Trace	2. Applications and Future Trends. PB89-230312 900,219	lonic Hydrogen Bond and Ion Solvation. 5. OH(1-)C Bonds. Gas Phase Solvation and Clustering of Alkoxide
Amounts by Element-Specific Size-Exclusion Chromatography.	Determination of the Absolute Specific Conductance of Primary Standard KCI Solutions.	and Carboxylate Anions. PB89-157531 900,328

łΥ of

		ATMOSPHERIC CHEMISTRY
ANISOTROPY	Guide to Available Mathematical Software Advisory	Standard Reference Materials for the Determination of
Effect of Anisotropic Thermal Conductivity on the Mor phological Stability of a Binary Alloy.	- System. PB90-123654 901,201	Polycyclic Aromatic Hydrocarbons. PB89-156889 900,178
PB89-228985 901,15 ANNEALING	AQUATIC ANIMALS Specimen Banking in the National Status and Trends	Standard Chemical Thermodynamic Properties of Polycy- clic Aromatic Hydrocarbons and Their Isomer Groups 1.
Interaction of Oxygen and Platinum on W(110).	Program: Development of Protocols and First Year Re-	Benzene Series. PB89-186480 900,412
PB89-231302 901,15 ANODIC STRIPPING	PB89-175855 901,308	Pi-Electron Properties of Large Condensed Polyaromatic
High-Accuracy Differential-Pulse Anodic Stripping Voltammetry Using Indium as an Internal Standard.	AQUEOUS ELECTROLYTES Non-Equilibrium Theories of Electrolyte Solutions.	Hydrocarbons. PB89-202139 900,432
PB89-176267 900,19	PB89-174940 <i>900,369</i>	Standard Chemical Thermodynamic Properties of Polycy-
ANTENNA ARRAYS Experimental Study of Interpanel Interactions at 3.3 GHz.	AQUEOUS SOLUTIONS Rate Constants for Reactions of Nitrogen Oxide (NO3)	clic Aromatic Hydrocarbons and Their Isomer Groups. 2. Pyrene Series, Naphthopyrene Series, and Coronene
PB89-176218 900,70 ANTENNA RADIATION PATTERNS	Radicals in Aqueous Solutions. PB89-176242 900,379	Series. PB89-226591 900,459
Accurate Determination of Planar Near-Field Correction	AR LACERTAE STAR Doppler Imaging of AR Lacertae at Three Epochs.	Mobile Sources of Atmospheric Polycyclic Aromatic Hydrocarbons: A Roadway Tunnel Study.
Parameters for Linearly Polarized Probes. PB89-156871 900,70		PB90-123571 900,859
Effect of Random Errors in Planar Near-Field Measure ment.	AR LACERTAE STARS Rotational Modulation and Flares on RS Canum Venati-	Residential Wood Combustion: A Source of Atmospheric Polycyclic Aromatic Hydrocarbons.
PB89-171839 900,700	corum and BY Draconis Stars. XI. Ultraviolet Spectral	PB90-128166 900,860 Comparison of Liquid Chromatographic Selectivity for Po-
Alternative Techniques for Some Typical MIL-STD-461 462 Types of Measurements.	PB89-234298 900,026	lycyclic Aromatic Hydrocarbons on Cyclodextrin and C18 Bonded Phases.
PB89-235139 <i>901,27.</i> ANTENNAS	P ARCHAEOLOGY Technical Examination, Lead Isotope Determination, and	PB90-128539 900,231
Calibrating Antenna Standards Using CW and Pulsed-CV	Clamental Applysic of Came Chang and They Dynasty	Synthesis and Characterization of Novel Bonded Phases for Reversed-Phase Liquid Chromatography.
Measurements and the Planar Near-Field Method. 900,69.	PB90-136862 <i>901,178</i>	PB90-128695 900,233
Antenna Measurements for Millimeter Waves at the Na tional Bureau of Standards.	illumination Conditions and Lask Visibility in Daylit	ARSENIC Application of Multiscattering Theory to Impurity Bands in
PB89-150726 900,694	PB89-189237 900.074	Si:As. PB89-157762 900,334
Iterative Technique to Correct Probe Position Errors in Planar Near-Field to Far-Field Transformations.	ARCHITECTURE (COMPUTERS)	Infrared Absorption Cross Section of Arsenic in Silicon in
PB89-153886 900,698 Improved Spherical and Hemispherical Scanning Algo	System: Leve! 1.	the Impurity Band Region of Concentration. PB89-201750 900,426
nithms. PB89-156806 900,693	7 200 221100	ARTERIOSCLEROSIS
Improved Polarization Measurements Using a Modified	turing Software Based on the Product Data Exchange	Micro-Raman Characterization of Atherosclerotic and Bio- prosthetic Calcification.
Three-Antenna Technique. PB89-156814 900,698	PB90-112459 900,965	PB89-149223 901,234 ARTIFICIAL INTELLIGENCE
Gain and Power Parameter Measurements Using Plana Near-Field Techniques.	meory and Fractice of Faper Freservation for Archives.	Intelligent Processing of Materials: Report of an Industrial Workshop Conducted by the National Institute of Stand-
PB89-156822 900,698	PB89-147052 900,934 ARGON	ards and Technology.
Error Analysis Techniques for Planar Near-Field Measure ments.	Experimental Thermal Conductivity, Thermal Diffusivity,	PB89-151823 900,942 Automated Analysis of Operators on State Tables: A
PB89-156848 900,70	PB89-148407 900,293	Technique for Intelligent Search. PB89-157366 900,669
Comparison of Measured and Calculated Antenna Side lobe Coupling Loss in the Near Field Using Approximate		Artificial Intelligence Techniques in Real-Time Production
Far-Field Data. PB89-156855 900,702	PB89-158125 900,344	Scheduling. PB89-172571 900,945
Near-Field Detection of Buried Dielectric Objects. PB90-128208 900,713	Thermal Conductivity of Liquid Argon for Temperatures between 110 and 140 K with Pressures to 70 MPa.	ASBESTOS
ANTHRACENE	PB89-1/9600 900,394	Performance Standards for Microanalysis. PB89-201651 900,211
Polymers Bearing Intramolecular Photodimerizable Probes for Mass Diffusion Measurements by the Force	Sections for Sodium-Helium, Sodium-Neon, and Sodium-	ASCORBIC ACID
Rayleigh Scattering Technique: Synthesis and Character ization.	PB89-202162 900,433	Electronic Structure of Diammine (Ascorbato) Platinum(II) and the Trans Influence on the Ligand Dissociation
PB89-157101 901,181	to 1200 K with Pressures to 1000 MPa.	Energy. PB89-147128 900,287
Generic Liposome Reagent for Immunoassays.	PB89-222558 900,451	Stabilization of Ascorbic Acid in Human Plasma, and Its Liquid-Chromatographic Measurement.
PB90-123886 901,228 ANTIFERROMAGNETIC MATERIALS	Waals Infrared Spectra: An Intermolecular Potential	PB89-179279 901,237
Magnetic Structure of Cubic Tb0.3Y0.7Ag. PB90-117789 901,466	Energy Surface for Ar + HF (v = 1). PB89-227953 900,465	ASN.1 DATA DEFINITION LANGUAGE Object-Oriented Model for ASN.1 (Abstract Syntax Nota-
Mn-Mn Exchange Constants in Zinc-Manganese Chalco	ARGON COMPLEXES	tion One). PB89-177117 900.649
genides. PB90-136706 901,478	Moment of the Ar-Formamide van der Waals Complex	ASPARAGINASE
Neutron Diffraction Study of the Wurtzite-Structure Dilute Magnetic Semiconductor Zn0.45Mn0.55Se.	Calculation of Vibration-Rotation Spectra for Rare Gas-	Preliminary Crystal Structure of Acinetobacter glutamina- sificans Glutaminase-Asparaginase.
PB90-136714 901,478	HCI Complexes. PB89-228415 900,473	PB90-123381 901,260 ASSAYING
ANTIFERROMAGNETISM Antiferromagnetic Structure and Crystal Field Splittings in	Microwave Spectrum, Structure, and Electric Dipole Moment of Ar-Ch3OH.	High Accuracy Determination of (235)U in Nondestructive
the Cubic Heusler Alloys HoPd2Sn and ErPd2Sn. PB89-202659 901,433	PB90-117847 900,510	Assay Standards by Gamma Spectrometry. PB89-156954 900,249
Low-Temperature Phase and Magnetic Interactions in for	Intramolecular Dynamics of van der Waals Molecules: An	ASSESSMENTS
Fe-Cr-Ni Álloys. PB90-136771 901,113	PB90-118209 900,521	Precision and Accuracy Assessment Derived from Calibration Data.
APATITE/ (CALCIUM-SALT)-HYDROXYL	Sub-Doppler Infrared Spectroscopy in Slit Supersonic Jets: A Study of all Three van der Waals Modes in v1-Ex-	PB89-179162 900,886 ASTROMETRY
Calcium Hydroxyapatite Precipitated from an Aqueous Solution: An International Multimethod Analysis.	PB90-123852 900,525	Microarcsecond Optical Astrometry: An Instrument and
PB90-123399 900,228 APATITIC CALCIUM PHOSPHATE CEMENTS	ARGON ION Laser-Induced Fluorescence Study of Product Rotational	Its Astrophysical Applications. PB89-171268 900,013
Formation of Hydroxyapatite in Hydrogels from Tetracal cium Phosphate/Dicalcium Phosphate Mixtures.	State Distributions in the Charge Transfer Reaction: Ar(1+)((sup 2 P)(sub 3/2)) + N2 -> Ar + N2(1+	ASTRONOMICAL OBSERVATORIES Antenna for Laser Gravitational-Wave Observations in
PB89-201511 901,255)(X) at 0.28 and 0.40 eV. PB89-189823 900,420	Space. PB89-234231 901,594
APERTURE SHAPE Interzonal Natural Convection for Various Aperture Con		ATMOSPHERIC ATTENUATION
figurations. PB89-176499 900,060	Quantum Mechanical Calculations on the Ar(1+) + N2	X-Band Atmospheric Attenuation for an Earth Terminal Measurement System.
APERTURES	PB89-228092 900,470	PB90-100736 900,626
Numerical Aperture of Multimode Fibers by Several Methods: Resolving Differences.	Plasma.	ATMOSPHERIC CHEMISTRY Evaluated Kinetic and Photochemical Data for Atmos-
PB90-117482 900,75	PB90-123746 <i>901,570</i>	pheric Chemistry. Supplement 3.

AROMATIC POLYCYCLIC HYDROCARBONS
Qualitative MO Theory of Some Ring and Ladder Polymers.
PB89-156723
900,303

APPLICATIONS OF MATHEMATICS
Internal Structure of the Guide to Available Mathematical Software.
PB89-170864
900,927

Evaluated Kinetic and Photochemical Data for Atmospheric Chemistry, Supplement 3.
PB89-222582 900,454

High-Accuracy Gas Analysis via Isotope Dilution Mass Spectromatry: Carbon Dioxide in Air. PB90-123951 900,032

TMOSPHERIC ENTRY	PB89-147011 900,284	PB89-171185 901,50
Detection of Uranium from Cosmos-1402 in the Strato- sphere. PB89-156962 901,592	Unimolecular Dynamics Following Vibrational Overtone Excitation of HN3 v1 = 5 and v1 = 6:HN3(X tilde;v,J,K,) -	Photodissociation of Methyl Iodide Clusters, PB89-171193 900,25
TMOSPHERIC PRESSURE	> HN((X sup 3)(Sigma (1-));v,J,Omega) + N2(x sup 1)(Sigma sub g (1+)).	Production of 0.1-3 eV Reactive Molecules by Laser Va porization of Condensed Molecular Films: A Potentia
Drift Tubes for Characterizing Atmospheric Ion Mobility Spectra Using AC, AC-Pulse, and Pulse Time-of-Flight Measurement Techniques.	PB89-147110 900,286 Electronic Structure of Diammine (Ascorbato) Platinum(II) and the Trans Influence on the Ligand Dissociation	Source for Beam-Surface Interactions. PB89-171201 900,25
PB89-202543 900,438	Energy. PB89-147128 900,287	Infrared Spectrum of D2HF. PB89-171219 900,35
Drift Tubes for Characterizing Atmospheric Ion Mobility Spectra. PB90-128513 901,585	* Electric-Dipole Moments of H2O-Formamide and CH3OH-Formamide.	Infrared Spectrum of NeHF. PB89-171227 900,35
Journal of Research of the National Institute of Stand-	PB89-147375 900,288	Laser Probing of Ion Velocity Distributions in Drift Fields
ards and Technology. November-December 1989. Volume 94, Number 6. PB90-163874 900,542	Vibrational Predissociation of the Nitric Oxide Dimer. PB89-147417 900,289	Parallel and Perpendicular Temperatures and Mobility for Ba(1+) in He. PB89-171243 900,35
Reduction of Uncertainties for Absolute Piston Gage Pressure Measurements in the Atmospheric Pressure Range.	Far-Infrared Laser Magnetic Resonance Spectrum of Vi- brationally Excited C2H(1). PB89-147474 900,292	Laser Probing of Product-State Distributions in Therma Energy Ion-Molecule Reactions. PB89-171250 900,35
PB90-163882 900,030	Thermal-Expansive Growth of Prebreakdown Streamers in Liquids.	One-Photon Resonant Two-Photon Excitation of Rydber
TOM-ATOM COLLISIONS Alignment Effects in Ca-He(5(sup 1)P(sub 1) - 5(sup	PB89-149074 900,803 Autodetaching States of Negative Ions.	Series Close to Threshold. PB89-171276 901,34
(Sub J)) Energy Transfer Collisions by Far Wing Laser Scattering.	PB89-150767 900,295 ·	High Resolution Inverse Raman Spectroscopy of the Co Q Branch.
PB89-179790 900,400 Laser Spectroscopy of Inelastic Collisions.	Resonance Ionization Mass Spectrometry of Mg: The 3pnd Autoionizing Series.	PB89-171292 900,35
PB89-185946 900,405	PB89-150817 900,296 Trapped lons and Laser Cooling 2: Selected Publications	Progress in Understanding Atomic Structure of the Icose hedral Phase.
TOM COLLISIONS Collisional Losses from a Light-Force Atom Trap. PB90-123936 901,577	of the Ion Storage Group, Time and Frequency Division, NIST, Boulder, CO.	PB89-171359 901,40 Electron-Impact Excitation of the Resonance Transition i
TOM TRANSPORT	PB89-153878 901,489 Qualitative MO Theory of Some Ring and Ladder Poly-	CA(1+). PB89-171557 901,50
Atomic Transition Probabilities of Argon: A Continuing Challenge to Plasma Spectroscopy.	mers.	Electron-Impact Excitation of Al(2+).
PB89-158125 900,344	PB89-156723 900,303 High Accuracy Determination of (235)U in Nondestructive	PB89-171565 901,50 Scattering of Polarized Light in Spectral Lines with Partie
TOM TRAPS Laser-Cooling and Electromagnetic Trapping of Neutral	Assay Standards by Gamma Spectrometry. PB89-156954 900,249	Frequency Redistribution: General Redistribution Matrix. PB89-171607
Atoms. PB89-176440 901,511	Population Relaxation of $CO(v=1)$ Vibrations in Solution Phase Metal-Carbonyl Complexes.	Recoilless Optical Absorption and Doppler Sidebands of a Single Trapped Ion.
Cooling and Trapping Atoms. PB89-176937 901,515	PB89-157291 900,315	PB89-171631 901,50
Laser Cooling. PB89-179147 <i>901,518</i>	Picosecond Studies of Vibrational Energy Transfer in Molecules on Surfaces. PB89-157309 900,316	Spectrum and Energy Levels of Singly Ionized Cesium. 2 Interpretation of Fine and Hyperfine Structures. PB89-172373 900,36
Collisional Losses from a Light-Force Atom Trap. PB90-123936 901,577	Picosecond Study of the Population Lifetime of CO(v= 1) Chemisorbed on SiO2-Supported Rhodium Particles.	Infrared Spectrum of the nu6, nu7, and nu8 Bands of
TOMIC ABSORPTION	PB89-157317 900,317	HNO3. PB89-172415 900,36
Microwave Digestion of Biological Samples: Selenium Analysis by Electrothermal Atomic Absorption Spectrom-	Microwave Spectrum, Structure, and Electric Dipole Moment of the Ar-Formamide van der Waals Complex.	Technical Activities 1986-1988, Molecular Spectroscop
etry. PB89-229116 <i>900,217</i>	PB89-157325 900,318	Division. PB89-175418 900,37
TOMIC CLOCKS	Microwave Spectrum and (14)N Quadrupole Coupling Constants of Carbazole.	New FIR Laser Lines and Frequency Measurements for Optically Pumped CD3OH.
Dual Frequency P-Code Time Transfer Experiment. PB89-174064 900,614	PB89-157333 900,319	PB89-175731 901,35
Study of Long-Term Stability of Atomic Clocks.	Infrared and Microwave Investigations of Interconversion Tunneling in the Acetylene Dimer.	Superlattice Magnetoroton Bands. PB89-175970 901,40
PB89-174098 900,367 Millisecond Pulsar Rivals Best Atomic Clock Stability.	PB89-157341 900,320 Thermal Shifts of the Spectral Lines in the (4)F3/2 to	Spectra and Energy Levels of Br XXV, Br XXIX, Br XXX and Br XXXI.
PB89-185722 900,629	(4)I11/2 Manifold of an Nd:YAG Laser. PB89-157382 901,338	PB89-176002 901,50
In Search of the Best Clock. PB90-117367 900,632	Precise Test of Quantum Jump Theory.	Laser-Produced Spectra and QED (Quantum Electrody namic) Effects for Fe-, Co-, Cu-, and Zn-Like Ions of Ai
TOMIC ENERGY LEVELS	PB89-157390 901,339 Calibration Tables Covering the 1460- to 1550-cm(-1)	Pb, Bi, Th, and U. PB89-176010 901,51
Spectra and Energy Levels of Br XXV, Br XXIX, Br XXX, and Br XXXI.	Region from Heterodyne Frequency Measurements on the nu(sub 3) Bands of (12)CS2 and (13)CS2.	Ion Kinetics and Energetics.
PB89-176002 901,509 Atomic Internal Partition Function.	PB89-157416 900,322	PB89-176101 900,37 Picosecond Coherent Anti-Stokes Raman Scattern
PB89-185904 901,373	Atomic-lon Coulomb Clusters in an Ion Trap. 901,494	(CARS) Study of Vibrational Dephasing of Carbon Disu
Scheme for a 60-nm Laser Based on Photopumping of a High Level of $Mo(6+)$ by a Spectral Line of $Mo(11+)$.	Ozonolysis of Ethylene. Microwave Spectrum, Molecular	PB89-176408 900,38
PB89-186415 900,407	Structure, and Dipole Moment of Ethylene Primary Ozon- ide (1,2,3-Trioxolane).	Near-Threshold X-ray Fluorescence Spectroscopy of Mo ecules.
Energy Levels of Molybdenum, Mo 1 through 42. PB89-186472 900,411	PB89-157440 900,323 Molybdenum Effect on Volume in Fe-Cr-Ni Alloys.	PB89-176523 900,38
4s(2) 4p(2)-4s4p(3) Transition Array and Energy Levels of the Germanium-Like Ions Rb VI - Mo XI.	PB89-157796 901,095	State Selection in Electron-Atom Scattering: Spin-Polal ized Electron Scattering from Optically Pumped Sodium. PB89-176572 901,51
PB89-201065 901,528 Spectroscopic Detection Methods.	Infrared Absorption of SF6 from 32 to 3000 cm(-1) in the Gaseous and Liquid States. PB89-157853 900,336	Using 'Resonant' Charge Exchange to Detect Traces of
PB89-228100 901,549 State Selection via Optical Methods.	Non-Boltzmann Rotational and Inverted Spin-Orbit State Distributions for Laser-Induced Desorption of NO from	Noble Gas Atoms. PB89-176770 901,29
PB89-228118 901,550 Chlorine-like Spectra of Copper to Molybdenum.	Pt(111). PB89-157952 900,340	Cooling and Trapping Atoms. PB89-176937 901,51
PB90-117706 900,501	Effects of Pressure on the Vibrational Spectra of Liquid Nitromethane.	Autoionization Dynamics in the Valence-Shell Photoion zation Spectrum of CO.
Analysis of Magnesiumlike Spectra from Cu XVIII to Mo XXXI.	PB89-158026 900,342	PB89-176960 900,38 Vibrational Exchange upon Interconversion Tunneling i
PB90-117821 900,508 TOMIC MASS	Spin-Polarized Electron Microscopy. PB89-158075 901,395	(HF)2 and (HCCH)2. PB89-179113 900,38
Atomic Weights of the Elements 1987. PB89-145171 900,274	Stark Broadening of Spectral Lines of Homologous, Doubly Ionized Inert Gases.	Infrared and Microwave Spectra of OCO-HF and SCO HF.
Twenty Five Years of Accuracy Assessment of the Atomic Weights.	PB89-158083 900,343 Calculation of Tighter Error Bounds for Theoretical	PB89-179121 900,38
PB89-174007 900,365 TOMIC & MOLECULAR STUDIES	Atomic-Oscillator Strengths. PB89-158109 901,496	Effects of Velocity and State Changing Collisions of Raman Q-Branch Spectra. PB89-179196 900,35
Alignment Effects in Electronic Energy Transfer and Re-	Frequency Measurement of the J = 1 < - 0 Rotational	Quenching and Energy Transfer Processes of Single Ro
active Events. AD-A202 820/7 900,267	Transition of HD (Hydrogen Deuteride). PB89-161566 901,499	tational Levels of Br2 B triplet $Pi(O(sub\ u)(+\))\ v'=2$ with Ar under Single Collision Conditions.
Multiphoton Ionization Spectroscopy and Vibrational Analysis of a 3p Rydberg State of the Hydroxymethyl	Far-Infrared Spectrum of Methyl Amine. Assignment and Analysis of the First Torsional State.	PB89-179766 900,39
Radical. PB89-146666 900,279	PB89-161574 900,346	Photodissociation Dynamics of C2H2 at 193 nm: Vibrational Distributions of the CCH Findical and the Rotation
Fundamental Configurations in Mo IV Spectrum.	Systems Driven by Colored Squeezed Noise: The Atomic Absorption Spectrum.	State Distribution of the A(010) State by Time-Resolve Fourier Transform Infrared Emission.

PB89-179782 900,258	PB89-228118 901,556	Stit Jet Infrared Spectroscopy of NeHF Complexes: Inter- nal Rotor and J-Dependent Predissociation Dynamics.
Alignment Effects in Ca-He(5(sup 1)P(sub 1) - 5(sup 3)P(sub J)) Energy Transfer Collisions by Far Wing Laser	Infrared Spectra of Nitrous Oxide-HF Isomers. PB89-228399 900,47	PB90-118126 900,520
Scattering. PB89-179790 <i>900,400</i>	Calculation of Vibration-Rotation Spectra for Rare Gas HCI Complexes.	Extended Infrared Study of ArHF.
Structure and Dynamics of Molecular Clusters via High Resolution IR Absorption Spectroscopy.	PB89-228415 900,473 Laboratory Measurement of the 1(sub 01)-0(sub 00	Approximate Formulation of Redistribution in the
PB89-185896 900,403 Atomic Internal Partition Function.	Transition and Electric Dipole Moment of SiC2. PB89-228506 900,025	Ly(alpha), Ly(beta), H(alpha) System.
PB89-185904 901,373	Infrared Spectrum of the 1205-cm(-1) Band of HNO3.	Exoergic Collisions of Cold Na*-Na.
High Resolution Optical Multiplex Spectroscopy. PB89-185938 900,404	PB89 228514 900,475 Heterodyne Frequency Measurements of (12)C(16)C	Spectroscopy of Autoionizing States Contributing to Elec-
Laser Spectroscopy of Inelastic Collisions. PB89-185946 900,405	Laser Transitions. PB89-229223 901,374	tron-Impact fonization of lons. PB90-123837 901,57^
Resonant Excitation of an Oxygen Valence Satellite in Photoemission from High-T(sub c) Superconductors.	Structure of the CO2-CO2-H2O van der Waals Complex Determined by Microwave Spectroscopy.	Electron-Impact Ionization of La($q+$) Ions ($q=1,2,3$). PB90-123845
PB89-186860 901,420	PB89-230288 900,479	
High Resolution Spectrum of the nu(sub 1) + nu(sub 2) Band of NO2. A Spin Induced Perturbation in the Ground	Infrared Spectrum of Sodium Hydride. PB89-230296 900,480	
State. PB89-187561 900,417	Ultrashort-Pulse Multichannel Infrared Spectroscopy Using Broadband Frequency Conversion in LilO3.	Apparent Spectroscopic Rigidity of Floppy Molecular Sys-
Laser-Induced Fluorescence Study of Product Rotational	PB89-230304 901,367	PR90-123860 900 526
State Distributions in the Charge Transfer Reaction: Ar(1+)((sup 2 P)(sub 3/2)) + N2 -> Ar + N2(1+)(X) at 0.28 and 0.40 eV.	Stabilization and Spectroscopy of Free Radicals and Reactive Molecules in Inert Matrices.	Collisional Losses from a Light-Force Atom Trap.
PB89-189823 900,420	PB89-231252 900,484 Synchrotron Photoemission Study of CO Chemisorption	Ion Trapping Techniques: Laser Cooling and Sympathetic
Influence of the ac Stark Effect on Multiphoton Transitions in Molecules.	on Cr(110). PB89-231336 900,262	Cooling.
PB89-201578 901,530 Modeling of the Bremsstrahlung Radiation Produced in	Vibrational Spectra of Molecular lons Isolated in Solid	Frequency Standards Utilizing Penning Traps.
Pure Element Targets by 10-40 keV Electrons. PB89-201644 901,531	Neon. I. CO(sub 2, sup +) and CO(sub 2, sup -). PB89-234199 900,487	PB90-128042 901,379 Redistribution in Astrophysically Important Hydrogen
NBS (National Bureau of Standards) Scale of Spectral	Vibrational Predissociation in the H-F Stretching Mode of HF-DF.	
Radiance. PB89-201685 <i>901,532</i>	PB89-234207 900,488	Laser Cooling to the Zero-Point Energy of Motion.
Microwave Spectrum and Molecular Structure of the Eth-	Microwave and Infrared Electric-Resonance Optothermal Spectroscopy of HF-HCI and HCI-HF.	Microwaya Floatria Pagananaa Ontothormal Spectrosco
ylene-Ozone van der Waals Complex. PB89-201735 900,424	PB89-234215 900,489 High-Resolution, Slit Jet Infrared Spectroscopy of Hydro-	pv of (H2O)2.
Heterodyne Measurements on OCS Near 1372 cm(-1). PB89-201743 900,425	carbons: Quantum State Specific Mode Mixing in CH Stretch-Excited Propyne.	Branching Ratio Technique for Vacuum UV Radiance
Analysis of Roto-Translational Absorption Spectra In-	PB89-234256 900,490	PB90-128257 901,582
duced in Low Density Gases of Non-Polar Molecules: The Methane Case.	Observation of Translationally Hot, Rotationally Cold NC Molecules Produced by 193-nm Laser Vaporization of	Superelastic Scattering of Spin-Polarized Electrons from
PB89-201800 900,427 Pure Rotational Far Infrared Transitions of (16)O2 in Its	Multilayer NO Films. PB89-234264 900,491	Sodium. PB90-128307 901,584
Electronic and Vibrational Ground State. PB89-202055 900,429	Reduced Dimensionality Quantum Reactive Scattering	Vibrational Construct Adaptation land install in Calif
Accurate Energies of nS, nP, nD, nF and nG Levels of	Study of the Insertion Reaction O(1D) + H2 -> OH + H.	PB90-128729 900,533
Neutral Cesium. PB89-202121 900,431	PB89-234280 900,492 Sodium Doppler-Free Collisional Line Shapes.	nical Activities, 1989.
Nonadiabatic Theory of Fine-Structure Branching Cross-	PB89-234306 901,559	
Sections for Sodium-Helium, Sodium-Neon, and Sodium-Argon Optical Collisions.	Spectrum of Doubly Ionized Tungsten (W III). PB89-235659 900,223	Time-Resolved FTIR Emission Studies of Molecular Photogrammentation Initiated by a High Repetition Rate Ex-
PB89-202162 900,433 Drift Tubes for Characterizing Atmospheric Ion Mobility	Far-Infrared Laser Magnetic Resonance Spectrum of the	
Spectra Using AC, AC-Pulse, and Pulse Time-of-Flight Measurement Techniques.	CD Radical and Determination of Ground State Parameters.	Triplet Dipoles in the Absorption Spectra by Dense Rare
PB89-202543 900,438	PB90-117359 900,496 Dissociation Lifetimes and Level Mixing in Overtone-Ex-	PB90-136755 900.539
Quantum-Defect Parametrization of Perturbative Two- Photon Ionization Cross Sections.	cited HN3 (X tilde (sup 1) A'). PB90-117425 900,263	Frequency Measurements of High-J Rotational Transi-
PB89-202600 901,539	Electric-Resonance Optothermal Spectrum of (H2O)2:	PB90-136946 900,541
Time-of-Flight Measurements of Hyperthermal Cl(sub 2) Molecules Produced by UV Laser Vaporization of Cryo-	Microwave Spectrum of the K= 1-0 Subband for the E((+ or -)2) States.	Spectroelectrochemistry of a System Involving Two Con- secutive Electron-Transfer Reaction.
genic Chlorine Films. PB89-202634 900,260	PB90-117433 900,497	PB90-136979 900,237 ATOMIC ORBITALS
Time-Resolved FTIR Emission Studies of Molecular Photogrammentation.	Rotational Energy Levels and Line Intensities for (2S+1)Lambda-(2S+1) Lambda and (2S+1)(Lambda+or	Alignment Effects in Electronic Energy Transfer and Re-
PB89-202642 900,261	 -)-(2S+ 1)Lambda Transitions in a Diatomic Molecule van der Waals Bonded to a Closed Shell Partner. 	AD-A202 820/7 900,267
Exchange and Magnetostrictive Effects in Rare Earth Superlattices.	PB90-117441 900,498 Improved Rotational Constants for HF.	ATOMIC PHYSICS
PB89-202667 901,438	PB90-117466 901,376	DD00 100150
Cross Sections for Inelastic Electron Scattering in Solids, PB89-202972 901,440	Marked Differences in the 3p Photoabsorption between the Cr and Mn(1+) Isoelectronic Pair: Reasons for the	
Absolute Infrared Transition Moments for Open Shell Diatomics from J Dependence of Transition Intensities: Ap-	Unique Structure Observed in Cr. PB90-117581 901,562	Journal of Physical and Chemical Reference Data,
plication to OH. PB89-227912 900,463	Photoacoustic Measurement of Differential Broadening of the Lambda Doublets in NO(X (2)Pi 1/2, v= 2-0) by Ar.	
Dipole Moment Function and Vibrational Transition Inten-	PB90-117656 900,500	
sities of OH. PB89-227920 900,464	Mechanisms of Free Radical Chemistry and Biochemistry of Benzene.	Absorption Spectrum. PB89-171185 901,500
Rydberg-Klein-Rees Inversion of High Resolution van der	PB90-117714 900,502	ATOMIC SPECTHOSCOPY
Waals Infrared Spectra: An Intermolecular Potential Energy Surface for Ar+ HF (v= 1).	Production and Spectroscopy of Molecular Ions Isolated in Solid Neon.	Methods of Analysis.
PB89-227953 900,465 Three Dimensional Quantum Reactive Scattering Study	PB90-117748 900,503 Heterodyne Measurements on N2O Near 1635 cm(-1).	PB89-150858 900,176 Trapped Ions and Laser Cooling 2: Selected Publications
of the I + HI Reaction and of the IHI(1-) Photodetach- ment Spectrum.	PB90-117797 900,506	of the Ion Storage Group, Time and Frequency Division,
PB89-227961 900,466	Heterodyne Frequency and Fourier Transform Spectros- copy Measurements on OCS Near 1700 cm(-1).	PB89-153878 901,489
Spectroscopic Signatures of Floppiness in Molecular Complexes.	PB90-117805 900,507 Microwave Spectrum of Methyl Amine: Assignment and	Three Difference Atomic opecita in Traines Using Otep-
PB89-227979 900,467 Quantum Mechanical Calculations on the Ar(1+) + N2	Analysis of the First Torsional State. PB90-117839 900,508	PB89-202071 900,430
Charge Transfer Reaction. PB89-228092 900,470	Microwave Spectrum, Structure, and Electric Dipole	Beryllium Isotopic Standard Reference Material.
Spectroscopic Detection Methods.	Moment of Ar-Ch3OH. PB90-117847 900,510	PB89-231070 900,221
PB89-228100 901,549 State Selection via Optical Methods.	Weakly Bound NeHF. PB90-118100 900,515	Spectrum and Energy Levels of Singly Ionized Cesium. 2.
Same School the Option motilous.	. 555 110100	interpretation or rine and rispertite Structures.

PB89-172373 900,361 Green Function Method for Calculation of Atomistic	PB89-172597 900,947 On-Line Concurrent Simulation in Production Scheduling	facturing Research Facility at the National Bureau of Standards. PB89-151799 900,936
Structure of Grain Boundary Interfaces in Ionic Crystals. PB89-202105 Marked Differences in the 3p Photoabsorption between the Cr and Mn(1+) Isoelectronic Pair: Reasons for the	PB89-172605 900,948 Vertical Machining Workstation of the AMRF (Automated Manufacturing Research Facility): Equipment Integration. PB89-176663 900,950	Integrated Manufacturing Data Administration System (IMDAS) Operations Manual. PB89-156384 900,916
Unique Structure Observed in Cr. PB90-117581 901,562	Real-Time Control System Software: Some Problems and an Approach.	Optical Sensors for Robot Performance Testing and Calibration.
ATOMIC TRAPS Excergic Collisions of Cold Na*-Na.	PB89-177083 900,951 AMRF (Automated Manufacturing Research Facility) Ma-	PB89-157358 900,987 Automated Analysis of Operators on State Tables: A
PB90-123761 901,571	terial Handling System Architecture. PB89-177091 900,952	Technique for Intelligent Search. PB89-157366 900,669
Absolute Isotopic Abundance Ratios and Atomic Weight of a Reference Sample of Nickel. PB90-163890 900,543	Operations Manual for the Automatic Operation of the Vertical Workstation. PB89-183214 900.973	Material Handling Workstation Implementation. PB89-159644 900,988
Absolute Isotopic Composition and Atomic Weight of Terrestrial Nickel.	Workstation Controller of the Cleaning and Deburing	Material Handling Workstation: Operator Manual. PB89-159651 900,989
PB90-163908 900,544 ATOMIZING	Workstation. PB89-189286 900,955	Real-Time Control System Modifications for a Debuming Robot. User Reference Manual. PB89-159669 900.990
Process Control during High Pressure Atomization. PB89-179170 901,142	NBS AMRF (National Bureau of Standards) (Automated Manufacturing Research Facility) Process Planning System: System Architecture. PB89-193882 900.956	PB89-159669 900,990 Material Handling Workstation, Recommended Technical Specifications for Procurement of Commercially Available
ATTICS Experimental Validation of a Mathematical Model for Pre-	Inventory of Equipment in the Cleaning and Deburring	Equipment. PB89-162564 900,998
dicting Moisture Transfer in Attics. PB89-150783 900,057	Workstation. PB89-209233 900,958	Artificial Intelligence Techniques in Real-Time Production Scheduling.
ATTITUDE (INCLINATION) Tilt Observations Using Borehole Tiltmeters 1. Analysis of Tidal and Secular Tilt.	Experience with IMDAS (Integrated Manufacturing Data Administration System) in the Automated Manufacturing Research Facility.	PB89-172571 900,945 Functional Approach to Designing Architectures for Com-
PB90-136649 901,283	PB90-112350 900,964 AMRF Part Model Extensions.	puter Integrated Manufacturing. PB89-172589 900,946
AES and LEED Studies Correlating Desorption Energies with Surface Structures and Coverages for Ga on	PB90-129446 900,967 AUTOMATIC CONTROL	Real-Time Optimization in the Automated Manufacturing Research Facility. PB89-172597 900.947
Si(100). PB89-171599 901,401	Hierarchies for Computer-Integrated Manufacturing: A Functional Description.	On-Line Concurrent Simulation in Production Scheduling.
NUSTENITIC STAINLESS STEELS Role of Inclusions in the Fracture of Austenitic Stainless	PB89-172613 900,949 Automated TEM (Transverse Electromagnetic) Cell for	PB89-172605 900,948 Hierarchies for Computer-Integrated Manufacturing: A
Steel Welds at 4 K. PB89-173504 901,099	Measuring Unintentional EM Emissions. PB89-173769 900,682	Functional Description. PB89-172613 900,949
Influence of Molybdenum on the Strength and Toughness of Stainless Steel Welds for Cryogenic Service. PB89-173512 901,100	AUTOMATIC CONTROL EQUIPMENT Semi-Automated PVT Facility for Fluids and Fluid Mixtures.	Vertical Machining Workstation of the AMRF (Automated Manufacturing Research Facility): Equipment Integration. PB89-176663 900,950
Tensile Strain-Rate Effects in Liquid Helium. PB89-174882 901,102	PB89-157184 900,875 Application of Direct Digital Control to an Existing Build-	Building Representations from Fusions of Multiple Views. PB89-177059 900,991
Linear-Elastic Fracture of High-Nitrogen Austenitic Stainless Steels at Liquid Helium Temperature. PB90-117623 901,108	ing Air Handler. PB89-177141 <i>900,068</i>	Fast Path Planning in Unstructured, Dynamic, 3-D Worlds. PB89-177067 900,992
Nitrogen in Austenitic Stainless Steels. PB90-117649 901,109	Turning Workstation in the AMRF (Automated Manufacturing Research Facility). PB89-185607 900,954	Hierarchically Controlled Autonomous Robot for Heavy Payload Military Field Applications.
Effect of Chemical Composition on the 4 K Mechanical Properties of 316LN-Type Alloys.	Inventory of Equipment in the Tuming Workstation of the AMRF (Automated Manufacturing Research Facility).	PB89-177075 901,271 Real-Time Control System Software: Some Problems and
PB90-128554 901,110 Fracture Behavior of 316LN Alloy in Uniaxial Tension at	PB89-215339 900,961 AUTOMATIC NETWORK ANALYZERS	an Approach. PB89-177083 <i>900,951</i>
Cryogenic Temperatures. PB90-128562 901,111 AUSTENITIC STEELS	ANA (Automatic Network Analyzer) Measurement Results on the ARFTG (Automatic RF Techniques Group) Travel- ing Experiment.	AMRF (Automated Manufacturing Research Facility) Material Handling System Architecture. PB89-177091 900,952
Loading Rate Effects on Discontinuous Deformation in Load-Control Tensile Tests.	PB89-173777 900,715 Some Questions and Answers Concerning Air Lines as	Software for an Automated Machining Workstation. PB89-177109 900,953
PB89-171896 <i>901,097</i> UTOCATALYSIS	Impedance Standards. PB89-176176 900,747	Interfaces to Teleoperation Devices. PB89-181739 900,993
Logistic Function Data Analysis Program: LOGIT. PB89-189351 900,418	AUTOMATION Functional Approach to Designing Architectures for Computer Integrated Manufacturing.	Operations Manual for the Automatic Operation of the Vertical Workstation. PB89-183214 900,973
Autoionization Dynamics in the Valence-Shell Photoionization Spectrum of CO.	PB89-172589 900,946 Precision Weight Calibration with a Specialized Robot.	Dielectric Mixing Rules for Background Test Soils.
PB89-176960 900,386 Spectroscopy of Autoionizing States Contributing to Elec-	PB89-173975 900,879 Software for an Automated Machining Workstation.	Workstation Controller of the Cleaning and Deburing
tron-Impact Ionization of Ions. PB90-123837 901,572	PB89-177109 900,953 Operations Manual for the Automatic Operation of the	Workstation. PB89-189286 900,955
AUTOMATED MANUFACTURING Integrated Manufacturing Data Administration System	Vertical Workstation. PB89-183214 900,973	Progress Report of the Quality in Automation Project for FY88. PB89-193296 900,982
(IMDAS) Operations Manual. PB89-156384 900,916	Automated Calibration of Optical Photomask Linewidth Standards at the National Institute of Standards and	NBS AMRF (National Bureau of Standards) (Automated Manufacturing Research Facility) Process Planning
AUTOMATED MANUFACTURING RESEARCH FACILITIES Material Handling Workstation Implementation.	Technology. PB89-186340 901,315	System: System Architecture. PB89-193882 900,956
PB89-159644 900,988 Material Handling Workstation: Operator Manual.	Progress Report of the Quality in Automation Project for FY88. PB89-193296 900,982	NASA/NBS (National Aeronautics and Space Administra- tion/National Bureau of Standards) Standard Reference
PB89-159651 900,989 NUTOMATED MANUFACTURING RESEARCH FACILITY Automated Documentation System for a Large Scale	Mining Automation Real-Time Control System Architecture Standard Reference Model (MASREM).	Model for Telerobot Control System Architecture (NASREM). PB89-193940 901,589
Manufacturing Engineering Research Project. PB89-150809 900,941	PB9-221154 901,286 Robot Crane Technology. PB90-111667 900,146	Inventory of Equipment in the Cleaning and Debuming Workstation.
Data Handling in the Vertical Workstation of the Automat- ed Manufacturing Research Facility at the National Bureau of Standards.	NIST Automated Computer Time Service. PB90-213711 900,676	PB89-209233 900,958 Data Management Strategies for Computer Integrated Manufacturing Systems.
PB89-159636 900,943 Real-Time Control System Modifications for a Deburing Robot. User Reference Manual.	AUTOMATION & ROBOTICS General Methodology for Machine Tool Accuracy Enhancement by Error Compensation.	PB89-209258 900,959 Inventory of Equipment in the Turning Workstation of the AMRF (Automated Manufacturing Research Facility).
PB89-159669 900,990 Parser That Converts a Boundary Representation into a	PB89-146781 900,996 Use of Artificial Intelligence and Microelectronic Test	PB89-215339 900,961 Recommended Technical Specifications for Procurement
Features Representation. PB89-160634 900,944	Structures for Evaluation and Yield Enhancement of Microelectronic Interconnect Systems. PB9-146955 900,768	of Equipment for a Turning Workstation. PB89-215347 900,962
Material Handling Workstation, Recommended Technical Specifications for Procurement of Commercially Available Equipment.	Preliminary Experiments with Three Identical Ultraprecision Machine Tools.	Mining Automation Real-Time Control System Architecture Standard Reference Model (MASREM). PB89-221154 901,286
PB89-162564 900,998 Real-Time Optimization in the Automated Manufacturing	PB89-150841 900,997 Design Protocol, Part Design Editor, and Geometry Li-	Visual Perception Processing in a Hierarchical Control System: Level 1.
Research Facility.	brary of the Vertical Workstation of the Automated Manu-	PB89-221188 900,994

			DIOGNERMOTH
Robot Crane Technology. PB90-111667	900,146	BARIUM TITANATES Defect Intergrowths in Barium Polytitanates. 1.	PB89-157408 901,493
Modeling Dynamic Surfaces with Octrees.		Ba2Ti9O20. PB89-146823 901,014	Ion Trapping Techniques: Laser Cooling and Sympathetic Cooling.
PB90-112335 Experience with IMDAS (Integrated Manufacture)	901,206	Defect Intergrowths in Barium Polytitanates. 2. BaTi5O11.	PB90-128034 901,578 BERYLLIUM ISOTOPES
Administration System) in the Automated Ma	nufacturing	PB89-146831 901,015 Phase Equilibria and Crystal Chemistry in the Ternary	Development of the NBS (National Bureau of Standards)
Research Facility. PB90-112350	900,964	System BaO-TiO2-Nb2O5: Part 1.	Beryllium Isotopic Standard Reference Material. PB89-231070 900,221
FACTUNC: A User-Friendly System for Und Optimization.	constrained	PB89-171797 901,033 Phase Equilibria and Crystal Chemistry in the Ternary	BETWEEN-TIME ERROR
PB90-112392	901,207	System BaO-TiO2-Nb2O5. Part 2. New Barium Polytitan- ates with < 5 mole % Nb2O5.	Interpretation of a between-Time Component of Error in Mass Measurements.
Generic Architecture for Computer Integrated turing Software Based on the Product Data	d Manufac- Exchange	PB89-189815 900,419	PB89-149108 900,872
Specification. PB90-112459	900,965	BARIUM YTTRIUM CUPRATES Magnetic Field Dependence of the Superconductivity in	BIBLIOGRAPHIC DATA BASES Data Bases Available at the National Institute of Stand-
Teleoperation and Autonomy for Space Roboti	ics.	Bi-Śr-Ca-Cu-O Superconductors. PB89-146815 901,385	ards and Technology Research Information Center. PB89-160014 900,932
PB90-123811 Summaries of Center for Fire Research	901,591	Josephson-Junction Model of Critical Current in Granular	BIBLIOGRAPHIES
Projects and Grants: 1989.	900,605	Y1Ba2Cu3O(7-delta) Superconductors. PB89-176978 901,406	Metrology for Electromagnetic Technology: A Bibliogra- phy of NBS (National Bureau of Standards) Publications.
PB90-127101 Modular Process Planning System Architecture		High T(sub c) Superconductor/Noble-Metal Contacts with Surface Resistivities in the (10 to the Minus 10th Power)	PB89-147847 900,871
PB90-128596	900,966	Omega sq cm Range.	Creation of a Fire Research Bibliographic Database. PB89-174130 900,166
AMRF Part Model Extensions. PB90-129446	900,967	PB89-179824 901,413 Oxygen Partial-Density-of-States Change in the	Bibliography of the NIST (National Institute of Standards and Technology) Electromagnetic Fields Division Publica-
Publications of the Center for Manufacturing E Covering the Period January 1978-December 1		YBa2Cu3Ox Compounds for x(Approx.)6,6.5,7 Measured by Soft X-ray Emission.	tions.
PB90-130568	901,012	PB89-186274 901,419	PB89-189211 900,810 Center for Electronics and Electrical Engineering Techni-
Enhancements to the VWS2 (Vertical World Data Preparation Software.	kstation 2)	Resonant Excitation of an Oxygen Valence Satellite in Photoemission from High-T(sub c) Superconductors.	cal Publication Announcements: Covering Center Programs, July/September 1988, with 1989 CEEE Events
PB90-132713	900,968	PB89-186860 901,420	Calendar. PB89-189302 900.812
Emerging Technologies in Manufacturing Engir PB90-132747	neering. <i>901,013</i>	Ag Screen Contacts to Sintered YBa2Cu3Ox Powder for Rapid Superconductor Characterization.	Fire Research Publications, 1988.
ALANCHE DIODES		PB89-200448 901,423 Evidence for the Superconducting Proximity Effect in	PB89-193304 900,132
Improved Transportable DC Voltage Standard. PB89-230395	901,554	Junctions between the Surfaces of YBa2CU3Ox Thin Films.	Publications of the National Institute of Standards and Technology, 1988 Catalog.
Improved Low-Level Silicon-Avalanche-Photodi	iode Trans-	PB89-228449 901,449	PB89-218382 900,006
fer Standards at 1.064 Micrometers. PB90-130303	900,736	Hysteretic Phase Transition in Y1Ba2Cu3O7-x Superconductors.	NDE (Nondestructive Evaluation) Publications, 1985. PB89-229025 900,984
ACKSCATTERING Two-Layer Dielectric Microstrip Line Structure:	SiO2 on Si	PB89-229082 901,454	Publications of the Center for Manufacturing Engineering Covering the Period January 1978-December 1988.
and GaAs on Si; Modeling and Measurement.	900,738	Gruneisen Parameter of Y1Ba2Cu3O7. PB90-117615 901,465	PB90-130568 901,012
PB89-156780	900,730	Neutron Study of the Crystal Structure and Vacancy Dis- tribution in the Superconductor Ba2Y Cu3 O(sub g-delta).	BICONICAL ANTENNAS SIS Ouasiparticle Mixers with Bow-Tie Antennas.
Interpretation of Emission Wings of Balmer Lin nous Blue Variables.	es in Lumi-	PB90-123480 901,468	PB89-157036 900,705
PB89-212054	900,023	BARRIER MATERIALS Studies on Some Failure Modes in Latex Barrier Films.	Measurement of Integrated Tuning Elements for SIS Mixers with a Fourier Transform Spectrometer.
AND SPECTRA Oualitative MO Theory of Some Ring and La	adder Poly-	PB89-209308 901,089	PB89-157051 900,706
mers.	900,303	Specimen Banking in the National Status and Trends	BICRYSTALS Grain Boundary Structure in Ni3Al.
PB89-156723 Infrared Spectrum of the nu6, nu7, and nu8		Program: Development of Protocols and First Year Results.	PB89-229314 901,157
HNO3. PB89-172415	900,362	PB89-175855 901,308	BINARY MIXTURES Vapor-Liquid Equilibrium of Binary Mixtures in the Ex-
Surface Properties of Clean and Gas-Dosed St	nO2 (110).	Precision Experiments to Search for the Fifth Force.	tended Critical Region. I. Thermodynamic Model. PB89-218374 901,544
PB89-179576 AND THEORY	900,393	PB89-228365 901,551 BASIC PROGRAMMING LANGUAGE	BINARY STARS
Oualitative MO Theory of Some Ring and La	adder Poly-	Creating CSUBs in BASIC.	Late Stages of Close Binary Systems-Clues to Common Envelope Evolution.
mers. PB89-156723	900,303	PB89-176226 900,647 Creating CSUBs Written in FORTRAN That Run in	PB89-149207 900,016
Theoretical Models for High-Temperature Supvity.	erconducti-	BASIC. PB90-128752 900,656	Rotational Modulation and Flares on RS CVn and BY Dra Stars IX. IUE (International Ultraviolet Explorer) Spectros-
PB89-186266	901,418	BEAMLINES	copy and Photometry of II Peg and V711 Tau during February 1983.
ANKS (BUILDINGS) Engineering View of the Fire of May 4, 1988	in the First	Performance of a High-Energy-Resolution, Tender X-ray Synchrotron Radiation Beamline.	PB89-171615 900,019 Rotational Modulation and Flares on RS Canum Venati-
Interstate Bank Building, Los Angeles, Californ PB89-183222	ia. <i>900,167</i>	PB90-128083 901,580 BEAMS (SUPPORTS)	corum and BY Draconis Stars. XI. Ultraviolet Spectral
ARIUM	000,707	Higher Order Beam Finite Element for Bending and Vi-	Images of AR Lacertae in September 1985. PB89-234298 900,026
Laser Probing of Ion Velocity Distributions in Parallel and Perpendicular Temperatures and		bration Problems. PB89-229124 901,484	BINARY SYSTEMS (MATERIALS) Van der Waals Equation of State Around the Van Laar
Ba(1 +) in He. PB89-171243	900,352	BENZENE Benzene Thermophysical Properties from 279 to 900 K at	Point.
ARIUM NEODYMIUM CUPRATES	000,002	Pressures to 1000 Bar. PB89-145148 900.271	PB89-158133 900,345 Three-State Lattice Gas as Model for Binary Gas-Liquid
Pressure Dependence of the Cu Magnetic RBa2Cu3O6+ x.	Order in	Reactions of Phenyl Radicals with Ethene, Ethyne, and	Systems. PB89-171284 <i>900,354</i>
PB90-123829	901,472	Benzene. PB89-150908 900,297	Dynamics of Concentration Fluctuation on Both Sides of
ARIUM OXIDES Synchrotron Radiation Study of BaO Films	on W(001)	PVT Measurements on Benzene at Temperatures to 723	Phase Boundary. PB89-173942 901,183
and Their Interaction with H2O, CO2, and O2. PB89-157697	900,252	K. PB89-157200 <i>900,311</i>	Vapor-Liquid Equilibrium of Nitrogen-Oxygen Mixtures and
Sputtered Thin Film Ba2YCu3On.		Picosecond Coherent Anti-Stokes Raman Scattering (CARS) Study of Vibrational Dephasing of Carbon Disul-	Air at High Pressure. PB89-174932 900,368
PB89-165427 Phase Relations between the Polytitanates of	901,029 Barium and	fide and Benzene in Solution. PB89-176408 900,380	BINDERS In Situ Fluorescence Monitoring of the Viscosities of Par-
the Barium Borates, Vanadates and Molybdate PB89-171789		Standard Chemical Thermodynamic Properties of Polycy-	In Situ Fluorescence Monitoring of the Viscosities of Particle-Filled Polymers in Flow.
Syntheses and Unit Cell Determination of Ba3		clic Aromatic Hydrocarbons and Their Isomer Groups 1. Benzene Series.	PB89-146278 900,609 BIOASSAY
Low- and High-Temperature Ba3P4O13. PB89-179717	901,040	PB89-186480 900,412	Sample Validity in Biological Trace Element and Organic
Synthesis, Stability, and Crystal Chemistry of		Mechanisms of Free Radical Chemistry and Biochemistry of Benzene.	Nutrient Research Studies. PB89-156905 901,218
Pentatitanate. PB89-179741	901,041	PB90-117714 900,502 BENZOPHENONES	Microwave Energy for Acid Decomposition at Elevated Temperatures and Pressures Using Biological and Botan-
Bulk Modulus and Young's Modulus of the Su	perconduc-	Dehydrogenation of Ethanol in Dilute Aqueous Solution	ical Samples. PB89-171961 900,359
tor Ba2Cu3YO7. PB90-123613	901,469	Photosensitized by Benzophenones. PB89-157556 900,251	BIOCHEMISTRY
ARIUM PRASEODYMIUM CUPRATES Magnetic Order of Pr in PrBa2Cu3O7.		BERYLLIUM IONS Perpendicular Laser Cooling of a Rotating Ion Plasma in	Biophysical Aspects of Lipid Interaction with Mineral: Liposome Model Studies.
PB90-123803	901,471	a Penning Trap.	PB90-117508 901,228

В

Mechanisms of Free Radical Chemistry and Biochemistry	PB89-175947 <i>901,284</i>	PB89-229264 900,574
of Benzene. PB90-117714 900,502	Water Structure in Vitamin B12 Coenzyme Crystals. 2.	BLISTERING
Generic Liposome Reagent for Immunoassays. PB90-123886 901,229	Structural Characteristics of the Solvent Networks. PB89-186811 901,223 Coastal Structure of a Cyclic AMP (Adopting Management	Development of a Method to Measure In situ Chlonde at the Coating/Metal Interface. PB89-235345 901,085
Biological Macromolecule Crystallization Database: A Basis for a Crystallization Strategy.	Crystal Structure of a Cyclic AMP (Adenosine Monophos- phate)-Independent Mutant of Catabolite Gene Activator Protein.	BLOOD
PB90-136722 901,250 Bioseparations: Design and Engineering of Partitioning	PB89-201594 901,224 Comparison of Two Highly Refined Structures of Bovine	Determination of Serum Cholesterol by a Modification of the Isotope Dilution Mass Spectrometric Definitive Method.
Systems. PB90-136763 <i>901,231</i>	Pancreatic Trypsin Inhibitor. PB89-202204 901,248	PB89-234181 901,239 BLOOD SERUM
BIOCOMPATIBILITY Pulpal and Micro-organism Responses to Two Experi-	Thermophysical Properties for Bioprocess Engineering. PB89-228068 900,043	Developing Definitive Methods for Human Serum Analytes.
mental Dental Bonding Systems. PB89-202931 901,258	Biotransformation of Mercury by Bacteria Isolated from a River Collecting Cinnabar Mine Waters. PB89-229280 900,864	PB89-146773 901,233 BODY CENTERED CUBIC LATTICES
BIOCOMPATIBLE MATERIALS Oligomers with Pendant Isocyanate Groups as Tissue Adhesives. 1. Synthesis and Characterization.	Determination of Trace Level lodine in Biological and Botanical Reference Materials by Isotope Dilution Mass	Influence of Dislocation Density on the Ductile-Brittle Transition in bcc Metals. PB89-157804 901,133
PB89-202212 900,055 BIODETERIORATION	Spectrometry. PB89-235642 <i>900,222</i>	BOLOMETERS Electrically Calibrated Silicon Bolometer for Low Level
Biodegradation of Tributyltin by Chesapeake Bay Microorganisms.	Biophysical Aspects of Lipid Interaction with Mineral: Li- posome Model Studies. PB90-117508 901,228	Optical Power and Energy Measurements. PB89-171714 901,348
PB89-177232 901,309	Generation of Oxy Radicals in Biosystems.	NIST (National Institute of Standards and Technology)
Microbiological Metal Transformations: Biotechnological	PB90-117888 <i>901,266</i>	Automated Coaxial Microwave Power Standard. PB89-176192 900,807
Applications and Potential. PB89-175947 901,284	Differential Scanning Calonmetric Study of Brain Clathrin. PB90-117912 900,225	Superconducting Kinetic Inductance Bolometer. PB89-200505 900,762
BIOLOGICAL INDICATORS	Preliminary Crystal Structure of Acinetobacter glutamina- sificans Glutaminase-Asparaginase.	BONDING
Mechanisms of Free Radical Chemistry and Biochemistry of Benzene. PB90-117714 900,502	PB90-123381 901,260 Microbiological Materials Processing.	Pulpal and Micro-organism Responses to Two Experimental Dental Bonding Systems.
BIOLOGICAL PRODUCTS	PB90-123712 901,261	PB89-202931 901,258 Companson of Microleakage of Experimental and Select-
NBS (National Bureau of Standards) Activities in Biological Reference Materials.	Generic Liposome Reagent for Immunoassays. PB90-123886 901,229	ed Commercially Available Bonding Systems. PB89-234223 901,079
PB89-157770 901,219 BIOLOGICAL SURVEYS	Use of an Imaging Proportional Counter in Macromolecular Crystallography.	BONDING STRENGTH
Radiochemical Procedure for Ultratrace Determination of Chromium in Biological Materials.	PB90-136599 900,538 Biological Macromolecule Crystallization Database: A	Adhesion to Dentin by Means of Gluma Resin. PB89-157168 900,039
PB89-156913 900,179	Basis for a Crystallization Strategy. PB90-136722 901,250	Method to Measure the Tensile Bond Strength between Two Weakly-Cemented Sand Grains.
Neutron Activation Analysis of the NIST (National Insti- tute of Standards and Technology) Bovine Serum Stand-	Preliminary Crystallographic Study of Recombinant	PB89-166110 901,483
ard Reference Material Using Chemical Separations. PB89-156921 900,180	Human Interleukin 1beta. PB90-136730 <i>901,251</i>	BONES Oligomers with Pendant Isocyanate Groups as Tissue
Long-Term Stability of the Elemental Composition in Biological Materials.	Bioseparations: Design and Engineering of Partitioning Systems.	Adhesives. 2. Adhesion to Bone and Other Tissues. PB89-231245 900,056
PB89-156939 900,181	PB90-136763 901,231	BORATE MINERALS
Voltarmetric and Liquid Chromatographic Identification of Organic Products of Microwave-Assisted Wet Ashing of Biological Samples.	Global Biomethylation of the Elements - Its Role in the Biosphere Translated to New Organometallic Chemistry and Biotechnology.	Moydite, (Y, REE) (B(OH)4)(CO3), a New Mineral Species from the Evans-Lou Pegmatite, Quebec. PB89-157747 900,186
December 2004	PB90-136854 901,232	BOREHOLES
PB89-15/994 900,188		
PB89-157994 <i>900,188</i> BIOLOGY	BIOTRANSFORMATION	Tilt Observations Using Borehole Tiltmeters 1. Analysis of
BIOLOGY Journal of Research of the National Institute of Standards and Technology, Volume 94, Number 1, January-		Tilt Observations Using Borehole Tiltmeters 1. Analysis of Tidal and Secular Tilt. PB90-136649 901,283
BIOLOGY Journal of Research of the National Institute of Standards and Technology, Volume 94, Number 1, January-February 1989. Special Issue: Numeric Databases in Materials and Biological Sciences.	BIOTRANSFORMATION Biotransformation of Mercury by Bacteria Isolated from a River Collecting Cinnabar Mine Waters. P89-229280 900,864 BIPOLAR TRANSISTORS	Tilt Observations Using Borehole Tiltmeters 1. Analysis of Tidal and Secular Tilt. PB90-136649 901,283 BORON
BIOLOGY Journal of Research of the National Institute of Standards and Technology, Volume 94, Number 1, January-February 1989. Special Issue: Numeric Databases in Materials and Biological Sciences. PB89-175194 901,186	BIOTRANSFORMATION Biotransformation of Mercury by Bacteria Isolated from a River Collecting Cinnabar Mine Waters. PB89-229280 900,864	Tilt Observations Using Borehole Tiltmeters 1. Analysis of Tidal and Secular Tilt. PB90-136649 901,283 BORON Grain Boundary Structure in Ni3Al. PB89-201784 901,150
BIOLOGY Journal of Research of the National Institute of Standards and Technology, Volume 94, Number 1, January-February 1989. Special Issue: Numeric Databases in Materials and Biological Sciences. PB89-175194 BIOMEDICAL ENGINEERING Liposome-Enhanced Flow Injection Immunoanalysis.	BIOTRANSFORMATION Biotransformation of Mercury by Bacteria Isolated from a River Collecting Cinnabar Mine Waters. PB89-229280 900,864 BIPOLAR TRANSISTORS Effect of Neutrons on the Characteristics of the Insulated Gate Bipolar Transistor (IGBT). PB89-157655 900,773 Analytical Modeling of Device-Circuit Interactions for the	Tilt Observations Using Borehole Tiltmeters 1. Analysis of Tidal and Secular Tilt. PB90-136649 901,283 BORON Grain Boundary Structure in Ni3Al. PB89-201784 901,150 Grain Boundary Characterization in Ni3Al. PB89-229306 901,156
BIOLOGY Journal of Research of the National Institute of Standards and Technology, Volume 94, Number 1, January-February 1989. Special Issue: Numeric Databases in Materials and Biological Sciences. PB89-175194 BIOMEDICAL ENGINEERING Liposome-Enhanced Flow Injection Immunoanalysis. PB89-146757 BIOPHYSICS	BIOTRANSFORMATION Biotransformation of Mercury by Bacteria Isolated from a River Collecting Cinnabar Mine Waters. P89-229280 900,864 BIPOLAR TRANSISTORS Effect of Neutrons on the Characteristics of the Insulated Gate Bipolar Transistor (IGBT). P889-157655 900,773	Tilt Observations Using Borehole Tiltmeters 1. Analysis of Tidal and Secular Tilt. PB90-136649 901,283 BORON Grain Boundary Structure in Ni3Al. PB89-201784 901,150 Grain Boundary Characterization in Ni3Al.
BIOLOGY Journal of Research of the National Institute of Standards and Technology, Volume 94, Number 1, January-February 1989. Special Issue: Numeric Databases in Materials and Biological Sciences. PB89-175194 901,186 BIOMEDICAL ENGINEERING Liposome-Enhanced Flow Injection Immunoanalysis. PB89-146757 BIOPHYSICS Biophysical Aspects of Lipid Interaction with Mineral: Liposome Model Studies.	BIOTRANSFORMATION Biotransformation of Mercury by Bacteria Isolated from a River Collecting Cinnabar Mine Waters. PB89-229280 900,864 BIPOLAR TRANSISTORS Effect of Neutrons on the Characteristics of the Insulated Gate Bipolar Transistor (IGBT). PB89-157655 900,773 Analytical Modeling of Device-Circuit Interactions for the Power Insulated Gate Bipolar Transistor (IGBT). PB89-176259 Numerical Simulations of Neutron Effects on Bipolar	Tilt Observations Using Borehole Tiltmeters 1. Analysis of Tidal and Secular Tilt. PB90-136649 901,283 BORON Grain Boundary Structure in Ni3Al. PB89-201784 901,150 Grain Boundary Characterization in Ni3Al. PB89-229306 901,156 Grain Boundary Structure in Ni3Al. PB89-229314 901,157 BOROSILICATE GLASS
BIOLOGY Journal of Research of the National Institute of Standards and Technology, Volume 94, Number 1, January-February 1989. Special Issue: Numeric Databases in Materials and Biological Sciences. PB89-175194 BIOMEDICAL ENGINEERING Liposome-Enhanced Flow Injection Immunoanalysis. PB89-146757 BIOPHYSICS Biophysical Aspects of Lipid Interaction with Mineral: Liposome Model Studies. PB90-117508 901,228	BIOTRANSFORMATION Biotransformation of Mercury by Bacteria Isolated from a River Collecting Cinnabar Mine Waters. PB89-229280 900,864 BIPOLAR TRANSISTORS Effect of Neutrons on the Characteristics of the Insulated Gate Bipolar Transistor (IGBT). PB89-157655 900,773 Analytical Modeling of Device-Circuit Interactions for the Power Insulated Gate Bipolar Transistor (IGBT). PB89-176259 Numerical Simulations of Neutron Effects on Bipolar Transistors. PB90-123589 900,797	Tilt Observations Using Borehole Tiltmeters 1. Analysis of Tidal and Secular Tilt. PB90-136649 901,283 BORON Grain Boundary Structure in Ni3Al. PB89-201784 901,150 Grain Boundary Characterization in Ni3Al. PB89-229306 901,156 Grain Boundary Structure in Ni3Al. PB89-229314 901,157 BOROSILICATE GLASS Mechanical Property Enhancement in Ceramic Matrix Composites.
BIOLOGY Journal of Research of the National Institute of Standards and Technology, Volume 94, Number 1, January-February 1989. Special Issue: Numeric Databases in Materials and Biological Sciences. PB89-175194 901,186 BIOMEDICAL ENGINEERING Liposome-Enhanced Flow Injection Immunoanalysis. PB89-146757 BIOPHYSICS Biophysical Aspects of Lipid Interaction with Mineral: Liposome Model Studies. PB90-117508 901,228 BIOPROSTHESIS Micro-Raman Characterization of Atherosclerotic and Bio-	BIOTRANSFORMATION Biotransformation of Mercury by Bacteria Isolated from a River Collecting Cinnabar Mine Waters. PB89-229280 900,864 BIPOLAR TRANSISTORS Effect of Neutrons on the Characteristics of the Insulated Gate Bipolar Transistor (IGBT). PB89-157655 900,773 Analytical Modeling of Device-Circuit Interactions for the Power Insulated Gate Bipolar Transistor (IGBT). PB89-176259 Numerical Simulations of Neutron Effects on Bipolar Transistors. PB90-123589 900,797 BISMUTH ALLOYS	Tilt Observations Using Borehole Tiltmeters 1. Analysis of Tidal and Secular Tilt. PB90-136649 901,283 BORON Grain Boundary Structure in Ni3Al. PB89-201784 901,150 Grain Boundary Characterization in Ni3Al. PB89-229306 901,156 Grain Boundary Structure in Ni3Al. PB89-229314 901,157 BOROSILICATE GLASS Mechanical Property Enhancement in Ceramic Matrix Composites. PB89-189138 901,076
BIOLOGY Journal of Research of the National Institute of Standards and Technology, Volume 94, Number 1, January-February 1989. Special Issue: Numeric Databases in Materials and Biological Sciences. PB89-175194 BIOMEDICAL ENGINEERING Liposome-Enhanced Flow Injection Immunoanalysis. PB89-146757 BIOPHYSICS Biophysical Aspects of Lipid Interaction with Mineral: Liposome Model Studies. PB90-117508 BIOPROSTHESIS Micro-Raman Characterization of Atherosclerotic and Bioprosthetic Calcification. PB89-149223 901,234	BIOTRANSFORMATION Biotransformation of Mercury by Bacteria Isolated from a River Collecting Cinnabar Mine Waters. PB89-229280 900,864 BIPOLAR TRANSISTORS Effect of Neutrons on the Characteristics of the Insulated Gate Bipolar Transistor (IGBT). PB89-157655 900,773 Analytical Modeling of Device-Circuit Interactions for the Power Insulated Gate Bipolar Transistor (IGBT). PB89-176259 Numerical Simulations of Neutron Effects on Bipolar Transistors. PB90-123589 900,797	Tilt Observations Using Borehole Tiltmeters 1. Analysis of Tidal and Secular Tilt. PB90-136649 901,283 BORON Grain Boundary Structure in Ni3Al. PB89-201784 901,150 Grain Boundary Characterization in Ni3Al. PB89-229306 901,156 Grain Boundary Structure in Ni3Al. PB89-229314 901,157 BOROSILICATE GLASS Mechanical Property Enhancement in Ceramic Matrix Composites.
BIOLOGY Journal of Research of the National Institute of Standards and Technology, Volume 94, Number 1, January-February 1989. Special Issue: Numeric Databases in Materials and Biological Sciences. PB89-175194 BIOMEDICAL ENGINEERING Liposome-Enhanced Flow Injection Immunoanalysis. PB89-146757 BIOPHYSICS Biophysical Aspects of Lipid Interaction with Mineral: Liposome Model Studies. PB90-117508 BIOPROSTHESIS Micro-Raman Characterization of Atherosclerotic and Bioprosthetic Calcification. PB89-149223 901,234 BIOSPHERE	BIOTRANSFORMATION Biotransformation of Mercury by Bacteria Isolated from a River Collecting Cinnabar Mine Waters. PB89-229280 900,864 BIPOLAR TRANSISTORS Effect of Neutrons on the Characteristics of the Insulated Gate Bipolar Transistor (IGBT). PB89-157655 900,773 Analytical Modeling of Device-Circuit Interactions for the Power Insulated Gate Bipolar Transistor (IGBT). PB89-176259 900,777 Numerical Simulations of Neutron Effects on Bipolar Transistors. PB90-123589 900,797 BISMUTH ALLOYS Effect of Anisotropic Thermal Conductivity on the Morphological Stability of a Binary Alloy. PB89-228985 BISMUTH CALCIUM STRONTIUM CUPRATES	Tilt Observations Using Borehole Tiltmeters 1. Analysis of Tidal and Secular Tilt. PB90-136649 901,283 BORON Grain Boundary Structure in Ni3Al. PB89-201784 Grain Boundary Characterization in Ni3Al. PB89-229306 Grain Boundary Structure in Ni3Al. PB89-229314 901,156 Grain Boundary Structure in Ni3Al. PB89-229314 901,157 BOROSILICATE GLASS Mechanical Property Enhancement in Ceramic Matrix Composites. PB89-189138 901,076 Toughening Mechanisms in Ceramic Composites. Semi-Annual Progress Report for the Period Ending March 31,
BIOLOGY Journal of Research of the National Institute of Standards and Technology, Volume 94, Number 1, January-February 1989. Special Issue: Numeric Databases in Materials and Biological Sciences. PB89-175194 BIOMEDICAL ENGINEERING Liposome-Enhanced Flow Injection Immunoanalysis. PB89-146757 BIOPHYSICS Biophysical Aspects of Lipid Interaction with Mineral: Liposome Model Studies. PB90-117508 BIOPROSTHESIS Micro-Raman Characterization of Atherosclerotic and Bioprosthetic Calcification. PB89-149223 BIOSPHERE Global Biomethylation of the Elements - Its Role in the Biosphere Translated to New Organometallic Chemistry	BIOTRANSFORMATION Biotransformation of Mercury by Bacteria Isolated from a River Collecting Cinnabar Mine Waters. PB89-229280 900,864 BIPOLAR TRANSISTORS Effect of Neutrons on the Characteristics of the Insulated Gate Bipolar Transistor (IGBT). PB89-157655 900,773 Analytical Modeling of Device-Circuit Interactions for the Power Insulated Gate Bipolar Transistor (IGBT). PB89-176259 900,777 Numerical Simulations of Neutron Effects on Bipolar Transistors. PB90-123589 900,797 BISMUTH ALLOYS Effect of Anisotropic Thermal Conductivity on the Morphological Stability of a Binary Alloy. PB89-228985 901,155 BISMUTH CALCIUM STRONTIUM CUPRATES Magnetic Field Dependence of the Superconductivity in Bi-Sr-Ca-Cu-O-O Superconductors.	Tilt Observations Using Borehole Tiltmeters 1. Analysis of Tidal and Secular Tilt. PB90-136649 BORON Grain Boundary Structure in Ni3Al. PB89-201784 Grain Boundary Characterization in Ni3Al. PB89-229306 Grain Boundary Structure in Ni3Al. PB89-229314 BOROSILICATE GLASS Mechanical Property Enhancement in Ceramic Matrix Composites. PB89-189138 701,076 Toughening Mechanisms in Ceramic Composites. Semi-Annual Progress Report for the Period Ending March 31, 1989. PB89-235907 BOSON-EXCHANGE MODELS
BIOLOGY Journal of Research of the National Institute of Standards and Technology, Volume 94, Number 1, January-February 1989. Special Issue: Numeric Databases in Materials and Biological Sciences. PB89-175194 BIOMEDICAL ENGINEERING Liposome-Enhanced Flow Injection Immunoanalysis. PB89-146757 BIOPHYSICS Biophysical Aspects of Lipid Interaction with Mineral: Liposome Model Studies. PB90-117508 BIOPROSTHESIS Micro-Raman Characterization of Atherosclerotic and Bioprosthetic Calcification. PB89-149223 BIOSPHERE Global Biomethylation of the Elements - Its Role in the	BIOTRANSFORMATION Biotransformation of Mercury by Bacteria Isolated from a River Collecting Cinnabar Mine Waters. PB89-229280 900,864 BIPOLAR TRANSISTORS Effect of Neutrons on the Characteristics of the Insulated Gate Bipolar Transistor (IGBT). PB89-157655 900,773 Analytical Modeling of Device-Circuit Interactions for the Power Insulated Gate Bipolar Transistor (IGBT). PB89-176259 900,777 Numerical Simulations of Neutron Effects on Bipolar Transistors. PB90-123589 900,797 BISMUTH ALLOYS Effect of Anisotropic Thermal Conductivity on the Morphological Stability of a Binary Alloy. PB89-228985 BISMUTH CALCIUM STRONTIUM CUPRATES Magnetic Field Dependence of the Superconductivity in Bi-Sr-Ca-Cu-O Superconductors. PB89-146815 901,385	Tilt Observations Using Borehole Tiltmeters 1. Analysis of Tidal and Secular Tilt. PB90-136649 901,283 BORON Grain Boundary Structure in Ni3Al. PB89-201784 Grain Boundary Characterization in Ni3Al. PB89-229306 Grain Boundary Structure in Ni3Al. PB89-229314 901,156 Grain Boundary Structure in Ni3Al. PB89-229314 901,157 BOROSILICATE GLASS Mechanical Property Enhancement in Ceramic Matrix Composites. PB89-189138 901,076 Toughening Mechanisms in Ceramic Composites. Semi-Annual Progress Report for the Period Ending March 31, 1989. PB89-235907 901,080 BOSON-EXCHANGE MODELS Comparison of Interplaner-Boson-Exchange Models of High-Temperature Superconductivity - Possible Experi-
BIOLOGY Journal of Research of the National Institute of Standards and Technology, Volume 94, Number 1, January-February 1989. Special Issue: Numeric Databases in Materials and Biological Sciences. PB89-175194 BIOMEDICAL ENGINEERING Liposome-Enhanced Flow Injection Immunoanalysis. PB89-146757 BIOPHYSICS Biophysical Aspects of Lipid Interaction with Mineral: Liposome Model Studies. PB90-117508 BIOPROSTHESIS Micro-Raman Characterization of Atherosclerotic and Bioprosthetic Calcification. PB89-149223 BIOSPHERE Global Biomethylation of the Elements - Its Role in the Biosphere Translated to New Organometallic Chemistry and Biotechnology. PB90-136854 BIOTECHNOLOGY	BIOTRANSFORMATION Biotransformation of Mercury by Bacteria Isolated from a River Collecting Cinnabar Mine Waters. PB89-229280 900,864 BIPOLAR TRANSISTORS Effect of Neutrons on the Characteristics of the Insulated Gate Bipolar Transistor (IGBT). PB89-157655 900,773 Analytical Modeling of Device-Circuit Interactions for the Power Insulated Gate Bipolar Transistor (IGBT). PB89-176259 900,777 Numerical Simulations of Neutron Effects on Bipolar Transistors. PB90-123589 900,797 BISMUTH ALLOYS Effect of Anisotropic Thermal Conductivity on the Morphological Stability of a Binary Alloy. PB89-228985 901,155 BISMUTH CALCIUM STRONTIUM CUPRATES Magnetic Field Dependence of the Superconductivity in Bi-Sr-Ca-Cu-O Superconductors. PB89-146815 BISMUTH IONS Laser-Produced Spectra and QED (Quantum Electrody-	Tilt Observations Using Borehole Tiltmeters 1. Analysis of Tidal and Secular Tilt. PB90-136649 901,283 BORON Grain Boundary Structure in Ni3Al. PB89-201784 901,150 Grain Boundary Characterization in Ni3Al. PB89-229306 901,156 Grain Boundary Structure in Ni3Al. PB89-229314 901,157 BOROSILICATE GLASS Mechanical Property Enhancement in Ceramic Matrix Composites. PB89-189138 901,076 Toughening Mechanisms in Ceramic Composites. Semi-Annual Progress Report for the Period Ending March 31, 1989. PB89-235907 901,080 BOSON-EXCHANGE MODELS Comparison of Interplaner-Boson-Exchange Models of High-Temperature Superconductivity - Possible Experimental Tests. PB90-117334 901,462
BIOLOGY Journal of Research of the National Institute of Standards and Technology, Volume 94, Number 1, January-February 1989. Special Issue: Numeric Databases in Materials and Biological Sciences. PB89-175194 BIOMEDICAL ENGINEERING Liposome-Enhanced Flow Injection Immunoanalysis. PB89-146757 BIOPHYSICS Biophysical Aspects of Lipid Interaction with Mineral: Liposome Model Studies. PB90-117508 BIOPROSTHESIS Micro-Raman Characterization of Atherosclerotic and Bioprosthetic Calcification. PB89-149223 BIOSPHERE Global Biomethylation of the Elements - Its Role in the Biosphere Translated to New Organometallic Chemistry and Biotechnology. PB90-136654 BIOTECHNOLOGY Liposome-Enhanced Flow Injection Immunoanalysis. PB89-146757 900,036	BIOTRANSFORMATION Biotransformation of Mercury by Bacteria Isolated from a River Collecting Cinnabar Mine Waters. PB89-229280 900,864 BIPOLAR TRANSISTORS Effect of Neutrons on the Characteristics of the Insulated Gate Bipolar Transistor (IGBT). PB89-157655 900,773 Analytical Modeling of Device-Circuit Interactions for the Power Insulated Gate Bipolar Transistor (IGBT). PB89-176259 900,777 Numerical Simulations of Neutron Effects on Bipolar Transistors. PB90-123589 900,797 BISMUTH ALLOYS Effect of Anisotropic Thermal Conductivity on the Morphological Stability of a Binary Alloy. PB89-228985 901,155 BISMUTH CALCIUM STRONTIUM CUPRATES Magnetic Field Dependence of the Superconductivity in Bi-Sr-Ca-Cu-O Superconductors. PB89-146815 BISMUTH IONS Laser-Produced Spectra and QED (Quantum Electrodynamic) Effects for Fe-, Co-, Cu-, and Zn-Like Ions of Au, Pb, Bi, Th, and U	Tilt Observations Using Borehole Tiltmeters 1. Analysis of Tidal and Secular Tilt. PB90-136649 BORON Grain Boundary Structure in Ni3Al. PB89-201784 Grain Boundary Characterization in Ni3Al. PB89-229306 Grain Boundary Structure in Ni3Al. PB89-229314 BOROSILICATE GLASS Mechanical Property Enhancement in Ceramic Matrix Composites. PB89-189138 Toughening Mechanisms in Ceramic Composites. Semi-Annual Progress Report for the Period Ending March 31, 1989. PB89-235907 BOSON-EXCHANGE MODELS Comparison of Interplaner-Boson-Exchange Models of High-Temperature Superconductivity - Possible Experimental Tests. PB90-117334 BOTTLES Glass Bottles for Carbonated Soft Drinks: Voluntary Prod-
BIOLOGY Journal of Research of the National Institute of Standards and Technology, Volume 94, Number 1, January-February 1989. Special Issue: Numeric Databases in Materials and Biological Sciences. PB89-175194 BIOMEDICAL ENGINEERING Liposome-Enhanced Flow Injection Immunoanalysis. PB89-146757 BIOPHYSICS Biophysical Aspects of Lipid Interaction with Mineral: Liposome Model Studies. PB90-117508 BIOPROSTHESIS Micro-Raman Characterization of Atherosclerotic and Bioprosthetic Calcification. PB89-149223 BIOSPHERE Global Biomethylation of the Elements - Its Role in the Biosphere Translated to New Organometallic Chemistry and Biotechnology. PB90-136654 BIOTECHNOLOGY Liposome-Enhanced Flow Injection Immunoanalysis. PB89-146757 900,036 Chemical Characterization of Ionizing Radiation-Induced Damage to DNA.	BIOTRANSFORMATION Biotransformation of Mercury by Bacteria Isolated from a River Collecting Cinnabar Mine Waters. PB69-229280 900,864 BIPOLAR TRANSISTORS Effect of Neutrons on the Characteristics of the Insulated Gate Bipolar Transistor (IGBT). PB89-157655 900,773 Analytical Modeling of Device-Circuit Interactions for the Power Insulated Gate Bipolar Transistor (IGBT). PB89-176259 Numerical Simulations of Neutron Effects on Bipolar Transistors. PB90-123589 900,797 BISMUTH ALLOYS Effect of Anisotropic Thermal Conductivity on the Morphological Stability of a Binary Alloy. PB89-228985 901,155 BISMUTH CALCIUM STRONTIUM CUPRATES Magnetic Field Dependence of the Superconductivity in Bi-Sr-Ca-Cu-O Superconductors. PB89-146815 BISMUTH IONS Laser-Produced Spectra and QED (Quantum Electrodynamic) Effects for Fe-, Co-, Cu-, and Zn-Like Ions of Au, Pb, Bi, Th, and U. PB89-176010 BITUMENS	Tilt Observations Using Borehole Tiltmeters 1. Analysis of Tidal and Secular Tilt. PB90-136649 901,283 BORON Grain Boundary Structure in Ni3Al. PB89-201784 901,150 Grain Boundary Characterization in Ni3Al. PB89-229306 901,156 Grain Boundary Structure in Ni3Al. PB89-229314 901,157 BOROSILICATE GLASS Mechanical Property Enhancement in Ceramic Matrix Composities. PB89-189138 901,076 Toughening Mechanisms in Ceramic Composites. Semi-Annual Progress Report for the Period Ending March 31, 1989. PB89-235907 901,080 BOSON-EXCHANGE MODELS Comparison of Interplaner-Boson-Exchange Models of High-Temperature Superconductivity - Possible Experimental Tests. PB90-117334 901,462
BIOLOGY Journal of Research of the National Institute of Standards and Technology, Volume 94, Number 1, January-February 1989. Special Issue: Numeric Databases in Materials and Biological Sciences. PB89-175194 BIOMEDICAL ENGINEERING Liposome-Enhanced Flow Injection Immunoanalysis. PB89-146757 BIOPHYSICS Biophysical Aspects of Lipid Interaction with Mineral: Liposome Model Studies. PB90-117508 BIOPROSTHESIS Micro-Raman Characterization of Atherosclerotic and Bioprosthetic Calcification. PB89-149223 BIOSPHERE Global Biomethylation of the Elements - Its Role in the Biosphere Translated to New Organometallic Chemistry and Biotechnology. PB90-136654 BIOTECHNOLOGY Liposome-Enhanced Flow Injection Immunoanalysis. PB89-146757 Chemical Characterization of Ionizing Radiation-Induced Damage to DNA. PB89-151922 901,235	BIOTRANSFORMATION Biotransformation of Mercury by Bacteria Isolated from a River Collecting Cinnabar Mine Waters. PB89-229280 900,864 BIPOLAR TRANSISTORS Effect of Neutrons on the Characteristics of the Insulated Gate Bipolar Transistor (IGBT). PB89-157655 900,773 Analytical Modeling of Device-Circuit Interactions for the Power Insulated Gate Bipolar Transistor (IGBT). PB89-176259 900,777 Numerical Simulations of Neutron Effects on Bipolar Transistors. PB90-123589 900,797 BISMUTH ALLOYS Effect of Anisotropic Thermal Conductivity on the Morphological Stability of a Binary Alloy. PB89-228985 901,155 BISMUTH CALCIUM STRONTIUM CUPRATES Magnetic Field Dependence of the Superconductivity in Bi-Sr-Ca-Cu-O-O Superconductors. PB89-146815 901,385 BISMUTH IONS Laser-Produced Spectra and QED (Quantum Electrodynamic) Effects for Fe-, Co-, Cu-, and Zn-Like Ions of Au, Pb, Bi, Th, and U. PB89-176010 901,510 BITUMENS Strain Energy of Bituminous Built-Up Membranes: A New Concept in Load-Elongation Testing.	Tilt Observations Using Borehole Tiltmeters 1. Analysis of Tidal and Secular Tilt. PB90-136649 BORON Grain Boundary Structure in Ni3Al. PB89-201784 Grain Boundary Characterization in Ni3Al. PB89-229306 Grain Boundary Structure in Ni3Al. PB89-229314 BOROSILICATE GLASS Mechanical Property Enhancement in Ceramic Matrix Composites. PB89-189138 Toughening Mechanisms in Ceramic Composites. Semi-Annual Progress Report for the Period Ending March 31, 1989. PB89-235907 BOSON-EXCHANGE MODELS Comparison of Interplaner-Boson-Exchange Models of High-Temperature Superconductivity - Possible Experimental Tests. PB90-117334 BOTTLES Glass Bottles for Carbonated Soft Drinks: Voluntary Product Standard PS73-89. PB90-107046 BOUNDARY LAYER FLOW
BIOLOGY Journal of Research of the National Institute of Standards and Technology, Volume 94, Number 1, January-February 1989. Special Issue: Numeric Databases in Materials and Biological Sciences. PB89-175194 BIOMEDICAL ENGINEERING Liposome-Enhanced Flow Injection Immunoanalysis. PB89-146757 BIOPHYSICS Biophysical Aspects of Lipid Interaction with Mineral: Liposome Model Studies. PB90-117508 BIOPROSTHESIS Micro-Raman Characterization of Atherosclerotic and Bioprosthetic Calcification. PB89-149223 BIOSPHERE Global Biomethylation of the Elements - Its Role in the Biosphere Translated to New Organometallic Chemistry and Biotechnology. PB90-136654 BIOTECHNOLOGY Liposome-Enhanced Flow Injection Immunoanalysis. PB89-146757 Chemical Characterization of Ionizing Radiation-Induced Damage to DNA. PB89-151922 Structure of a Hydroxyl Radical Induced Cross-Link of Thymine and Tyrosine.	BIOTRANSFORMATION Biotransformation of Mercury by Bacteria Isolated from a River Collecting Cinnabar Mine Waters. PB89-229280 900,864 BIPOLAR TRANSISTORS Effect of Neutrons on the Characteristics of the Insulated Gate Bipolar Transistor (IGBT). PB89-157655 900,773 Analytical Modeling of Device-Circuit Interactions for the Power Insulated Gate Bipolar Transistor (IGBT). PB89-176259 Numerical Simulations of Neutron Effects on Bipolar Transistors. PB90-123589 900,777 Numerical Simulations of Neutron Effects on Bipolar Transistors. PB90-123589 900,797 BISMUTH ALLOYS Effect of Anisotropic Thermal Conductivity on the Morphological Stability of a Binary Alloy. PB89-228985 901,155 BISMUTH CALCIUM STRONTIUM CUPRATES Magnetic Field Dependence of the Superconductivity in Bi-Sr-Ca-Cu-O Superconductors. PB89-146815 BISMUTH IONS Laser-Produced Spectra and QED (Quantum Electrodynamic) Effects for Fe-, Co-, Cu-, and Zn-Like Ions of Au, PB, Bi, Th, and U. PB89-176010 BITUMENS Strain Energy of Bituminous Built-Up Membranes: A New Concept in Load-Elongation Testing. PB89-212203 900,139	Tilt Observations Using Borehole Tiltmeters 1. Analysis of Tidal and Secular Tilt. PB90-136649 BORON Grain Boundary Structure in Ni3Al. PB89-201784 Grain Boundary Characterization in Ni3Al. PB89-229306 Grain Boundary Structure in Ni3Al. PB89-229314 BOROSILICATE GLASS Mechanical Property Enhancement in Ceramic Matrix Composites. PB89-189138 Toughening Mechanisms in Ceramic Composites. Semi-Annual Progress Report for the Period Ending March 31, 1989. PB89-235907 BOSON-EXCHANGE MODELS Comparison of Interplaner-Boson-Exchange Models of High-Temperature Superconductivity - Possible Experimental Tests. PB90-117344 BOTTLES Glass Bottles for Carbonated Soft Drinks: Voluntary Product Standard PS73-89. PB90-107046 BOUNDARY LAYER FLOW Dynamics of Concentration Fluctuation on Both Sides of Phase Boundary.
BIOLOGY Journal of Research of the National Institute of Standards and Technology, Volume 94, Number 1, January-February 1989. Special Issue: Numeric Databases in Materials and Biological Sciences. PB89-175194 BIOMEDICAL ENGINEERING Liposome-Enhanced Flow Injection Immunoanalysis. PB89-146757 BIOPHYSICS Biophysical Aspects of Lipid Interaction with Mineral: Liposome Model Studies. PB90-117508 BIOPROSTHESIS Micro-Raman Characterization of Atherosclerotic and Bioprosthetic Calcification. PB89-149223 BIOSPHERE Global Biomethylation of the Elements - Its Role in the Biosphere Translated to New Organometallic Chemistry and Biotechnology. PB90-136654 BIOTECHNOLOGY Liposome-Enhanced Flow Injection Immunoanalysis. PB89-146757 Chemical Characterization of Ionizing Radiation-Induced Damage to DNA. PB89-151922 Structure of a Hydroxyl Radical Induced Cross-Link of Thymine and Tyrosine. PB89-157836 Intramolecular H Atom Abstraction from the Sugar Moiety by Thymine Radicals in Oligo- and Polydeoxynucleotides.	BIOTRANSFORMATION Biotransformation of Mercury by Bacteria Isolated from a River Collecting Cinnabar Mine Waters. PB89-229280 900,864 BIPOLAR TRANSISTORS Effect of Neutrons on the Characteristics of the Insulated Gate Bipolar Transistor (IGBT). PB89-157655 900,773 Analytical Modeling of Device-Circuit Interactions for the Power Insulated Gate Bipolar Transistor (IGBT). PB89-176259 Numerical Simulations of Neutron Effects on Bipolar Transistors. PB90-123589 900,797 BISMUTH ALLOYS Effect of Anisotropic Thermal Conductivity on the Morphological Stability of a Binary Alloy. PB89-228985 BISMUTH CALCIUM STRONTIUM CUPRATES Magnetic Field Dependence of the Superconductivity in Bi-Sr-Ca-Cu-O Superconductors. PB89-146815 BISMUTH IONS Laser-Produced Spectra and OED (Quantum Electrodynamic) Effects for Fe-, Co-, Cu-, and Zn-Like Ions of Au, Pb, Bi, Th, and U. PB89-176010 BITUMENS Strain Energy of Bituminous Built-Up Membranes: A New Concept in Load-Elongation Testing. PB89-212203 900,139 BITUMINOUS COATINGS Interim Criteria for Polymer-Modified Bituminous Roofing Membrane Materials.	Tilt Observations Using Borehole Tiltmeters 1. Analysis of Tidal and Secular Tilt. PB90-136649 901,283 BORON Grain Boundary Structure in Ni3Al. PB89-201784 901,150 Grain Boundary Characterization in Ni3Al. PB89-229306 901,156 Grain Boundary Structure in Ni3Al. PB89-229314 901,157 BOROSILICATE GLASS Mechanical Property Enhancement in Ceramic Matrix Composites. PB89-189138 901,076 Toughening Mechanisms in Ceramic Composites. Semi-Annual Progress Report for the Period Ending March 31, 1989. PB89-235907 901,080 BOSON-EXCHANGE MODELS Comparison of Interplaner-Boson-Exchange Models of High-Temperature Superconductivity - Possible Experimental Tests. PB90-117334 901,462 BOTTLES Glass Bottles for Carbonated Soft Drinks: Voluntary Product Standard PS73-89. PB90-107046 900,012 BOUNDARY LAYER FLOW Dynamics of Concentration Fluctuation on Both Sides of Phase Boundary. PB89-173942 901,183
BIOLOGY Journal of Research of the National Institute of Standards and Technology, Volume 94, Number 1, January-February 1989. Special Issue: Numeric Databases in Materials and Biological Sciences. PB89-175194 BIOMEDICAL ENGINEERING Liposome-Enhanced Flow Injection Immunoanalysis. PB89-146757 BIOPHYSICS Biophysical Aspects of Lipid Interaction with Mineral: Liposome Model Studies. PB90-117508 BIOPROSTHESIS Micro-Raman Characterization of Atherosclerotic and Bioprosthetic Calcification. PB89-149223 BIOSPHERE Global Biomethylation of the Elements - Its Role in the Biosphere Translated to New Organometallic Chemistry and Biotechnology. PB90-136654 BIOTECHNOLOGY Liposome-Enhanced Flow Injection Immunoanalysis. PB89-146757 Chemical Characterization of Ionizing Radiation-Induced Damage to DNA. PB89-151922 Structure of a Hydroxyl Radical Induced Cross-Link of Thymine and Tyrosine. PB89-157838 Intramolecular H Atom Abstraction from the Sugar Moiety by Thymine Radicals in Oligo- and Polydeoxynucleotides. PB89-171870 901,263	BIOTRANSFORMATION Biotransformation of Mercury by Bacteria Isolated from a River Collecting Cinnabar Mine Waters. PB89-229280 900,864 BIPOLAR TRANSISTORS Effect of Neutrons on the Characteristics of the Insulated Gate Bipolar Transistor (IGBT). PB89-157655 900,773 Analytical Modeling of Device-Circuit Interactions for the Power Insulated Gate Bipolar Transistor (IGBT). PB89-176259 900,777 Numerical Simulations of Neutron Effects on Bipolar Transistors. PB90-123589 900,797 BISMUTH ALLOYS Effect of Anisotropic Thermal Conductivity on the Morphological Stability of a Binary Alloy. PB89-228985 901,155 BISMUTH CALCIUM STRONTIUM CUPRATES Magnetic Field Dependence of the Superconductivity in Bi-Sr-Ca-Cu-O Superconductors. PB89-146815 901,385 BISMUTH IONS Laser-Produced Spectra and QED (Quantum Electrodynamic) Effects for Fe-, Co-, Cu-, and Zn-Like Ions of Au, Pb, Bi, Th, and U. PB89-176010 901,510 BITUMENS Strain Energy of Bituminous Built-Up Membranes: A New Concept in Load-Elongation Testing. PB89-212203 900,139 BITUMINOUS COATINGS Interim Criteria for Polymer-Modified Bituminous Roofing Membrane Materials. PB89-168025 900,114	Tilt Observations Using Borehole Tiltmeters 1. Analysis of Tidal and Secular Tilt. PB90-136649 BORON Grain Boundary Structure in Ni3Al. PB89-201784 Grain Boundary Characterization in Ni3Al. PB89-229306 Grain Boundary Structure in Ni3Al. PB89-229314 BOROSILICATE GLASS Mechanical Property Enhancement in Ceramic Matrix Composites. PB89-189138 Grain Boundary Structure in Ni3Al. PB89-229314 BOROSILICATE GLASS Mechanical Property Enhancement in Ceramic Matrix Composites. PB89-189138 GOLOPICATE GLASS Mechanical Property Enhancement in Ceramic Matrix Composites. PB89-189138 GOLOPICATE GLASS Mechanical Property Enhancement in Ceramic Matrix Composites. PB89-189138 GOLOPICATE GLASS Mechanical Property Enhancement in Ceramic Matrix Composites. PB89-189138 GOLOPICATE GLASS Mechanical Property Enhancement in Ceramic Matrix Composites. PB89-189138 901,076 BOSON-EXCHANGE MODELS Comparison of Interplaner-Boson-Exchange Models of High-Temperature Superconductivity - Possible Experimental Tests. PB90-117334 BOTTLES Glass Bottles for Carbonated Soft Drinks: Voluntary Product Standard PS73-89. PB90-107046 BOUNDARY LAYER FLOW Dynamics of Concentration Fluctuation on Both Sides of Phase Boundary. PB89-173942 BOUNDARY LAYER SEPARATION Shear Effects on the Phase Separation Behaviour of a Polymer Blend in Solution by Small Angle Neutron Scat-
BIOLOGY Journal of Research of the National Institute of Standards and Technology, Volume 94, Number 1, January-February 1989. Special Issue: Numeric Databases in Materials and Biological Sciences. PB89-175194 BIOMEDICAL ENGINEERING Liposome-Enhanced Flow Injection Immunoanalysis. PB89-146757 BIOPHYSICS Biophysical Aspects of Lipid Interaction with Mineral: Liposome Model Studies. PB90-117508 BIOPROSTHESIS Micro-Raman Characterization of Atherosclerotic and Bioprosthetic Calcification. PB89-149223 BIOSPHERE Global Biomethylation of the Elements - Its Role in the Biosphere Translated to New Organometallic Chemistry and Biotechnology. PB90-136854 BIOTECHNOLOGY Liposome-Enhanced Flow Injection Immunoanalysis. PB89-146757 Chemical Characterization of Ionizing Radiation-Induced Damage to DNA. PB89-151922 Structure of a Hydroxyl Radical Induced Cross-Link of Thymine and Tyrosine. PB89-157838 901,244 Intramolecular H Atom Abstraction from the Sugar Moiety by Thymine Radicals in Oligo- and Polydeoxynucleotides. PB89-175269 901,245	BIOTRANSFORMATION Biotransformation of Mercury by Bacteria Isolated from a River Collecting Cinnabar Mine Waters. PB89-229280 900,864 BIPOLAR TRANSISTORS Effect of Neutrons on the Characteristics of the Insulated Gate Bipolar Transistor (IGBT). PB89-157655 900,773 Analytical Modeling of Device-Circuit Interactions for the Power Insulated Gate Bipolar Transistor (IGBT). PB89-176259 900,777 Numerical Simulations of Neutron Effects on Bipolar Transistors. PB90-123589 900,797 BISMUTH ALLOYS Effect of Anisotropic Thermal Conductivity on the Morphological Stability of a Binary Alloy. PB89-228985 901,155 BISMUTH CALCIUM STRONTIUM CUPRATES Magnetic Field Dependence of the Superconductivity in Bi-Sr-Ca-Cu-O Superconductors. PB89-146815 901,385 BISMUTH IONS Laser-Produced Spectra and QED (Quantum Electrodynamic) Effects for Fe-, Co-, Cu-, and Zn-Like Ions of Au, Pb, Bi, Th, and U. PB89-176010 901,510 BITUMENS Strain Energy of Bituminous Built-Up Membranes: A New Concept in Load-Elongation Testing. PB89-212203 900,139 BITUMINOUS COATINGS Interim Criteria for Polymer-Modified Bituminous Roofing Membrane Materials. PB89-168025 900,114 BIVALVES Sequential Determination of Biological and Pollutant Elements in Marine Bivalves.	Tilt Observations Using Borehole Tiltmeters 1. Analysis of Tidal and Secular Tilt. PB90-136649 BORON Grain Boundary Structure in Ni3Al. PB89-201784 Grain Boundary Characterization in Ni3Al. PB89-229306 Grain Boundary Structure in Ni3Al. PB89-229314 BOROSILICATE GLASS Mechanical Property Enhancement in Ceramic Matrix Composites. PB89-189138 FB89-189138 FB89-189138 FB89-189138 FB89-189138 FB89-235907 FOUNDARY LAYER FLOW Dynamics of Conebritation Fluctuation on Both Sides of Phase Boundary. PB90-107046 BOUNDARY LAYER SEPARATION Shear Effects on the Phase Separation Behaviour of a Polymer Blend in Solution by Small Angle Neutron Scattering. PB89-229264 900,574
BIOLOGY Journal of Research of the National Institute of Standards and Technology, Volume 94, Number 1, January-February 1989. Special Issue: Numeric Databases in Materials and Biological Sciences. PB89-175194 BIOMEDICAL ENGINEERING Liposome-Enhanced Flow Injection Immunoanalysis. PB89-146757 BIOPHYSICS Biophysical Aspects of Lipid Interaction with Mineral: Liposome Model Studies. PB90-117508 BIOPROSTHESIS Micro-Raman Characterization of Atherosclerotic and Bioprosthetic Calcification. PB89-149223 BIOSPHERE Global Biomethylation of the Elements - Its Role in the Biosphero Translated to New Organometallic Chemistry and Biotechnology. PB90-136854 BIOTECHNOLOGY Liposome-Enhanced Flow Injection Immunoanalysis. PB89-146757 Chemical Characterization of Ionizing Radiation-Induced Damage to DNA. PB89-151922 Structure of a Hydroxyl Radical Induced Cross-Link of Thymine and Tyrosine. PB89-157838 101,244 Intramolecular H Atom Abstraction from the Sugar Moiety by Thymine Radicals in Oligo- and Polydeoxynucleotides. PB89-171870 New Directions in Bioinformatics. PB89-175269 Use of Structural Templates in Protein Backbone Modeling.	BIOTRANSFORMATION Biotransformation of Mercury by Bacteria Isolated from a River Collecting Cinnabar Mine Waters. PB69-229280 BIPOLAR TRANSISTORS Effect of Neutrons on the Characteristics of the Insulated Gate Bipolar Transistor (IGBT). PB89-157655 Analytical Modeling of Device-Circuit Interactions for the Power Insulated Gate Bipolar Transistor (IGBT). PB89-176259 Numerical Simulations of Neutron Effects on Bipolar Transistors. PB90-123589 BISMUTH ALLOYS Effect of Anisotropic Thermal Conductivity on the Morphological Stability of a Binary Alloy. PB89-228985 BISMUTH CALCIUM STRONTIUM CUPRATES Magnetic Field Dependence of the Superconductivity in Bi-Sr-Ca-Cu-O Superconductors. PB89-146815 BISMUTH IONS Laser-Produced Spectra and QED (Quantum Electrodynamic) Effects for Fe-, Co-, Cu-, and Zn-Like Ions of Au, Pb, Bi, Th, and U. PB89-176010 BITUMENS Strain Energy of Bituminous Built-Up Membranes: A New Concept in Load-Elongation Testing. PB89-12203 BITUMINOUS COATINGS Interim Criteria for Polymer-Modified Bituminous Roofing Membrane Materials. PB89-168025 Sequential Determination of Biological and Pollutant Elements in Marine Bivalves. PB89-156897 901,217	Tilt Observations Using Borehole Tiltmeters 1. Analysis of Tidal and Secular Tilt. PB90-136649 901,283 BORON Grain Boundary Structure in Ni3Al. PB89-201784 901,150 Grain Boundary Characterization in Ni3Al. PB89-229306 901,156 Grain Boundary Structure in Ni3Al. PB89-229314 901,157 BOROSILICATE GLASS Mechanical Property Enhancement in Ceramic Matrix Composites. PB89-189138 901,076 Toughening Mechanisms in Ceramic Composites. Semi-Annual Progress Report for the Period Ending March 31, 1989. PB89-235907 901,080 BOSON-EXCHANGE MODELS Comparison of Interplaner-Boson-Exchange Models of High-Temperature Superconductivity - Possible Experimental Tests. PB90-117334 901,462 BOTTLES Glass Bottles for Carbonated Soft Drinks: Voluntary Product Standard PS73-89. PB90-107046 900,012 BOUNDARY LAYER FLOW Dynamics of Concentration Fluctuation on Both Sides of Phase Boundary. PB89-173942 901,183 BOUNDARY LAYER SEPARATION Shear Effects on the Phase Separation Behaviour of a Polymer Blend in Solution by Small Angle Neutron Scattering. PB89-229264 900,574 BRACHYTHERAPY NSS (National Bureau of Standards) Measurement Serv-
BIOLOGY Journal of Research of the National Institute of Standards and Technology, Volume 94, Number 1, January-February 1989. Special Issue: Numeric Databases in Materials and Biological Sciences. PB89-175194 BIOMEDICAL ENGINEERING Liposome-Enhanced Flow Injection Immunoanalysis. PB89-146757 BIOPHYSICS Biophysical Aspects of Lipid Interaction with Mineral: Liposome Model Studies. PB90-117508 BIOPROSTHESIS Micro-Raman Characterization of Atherosclerotic and Bioprosthetic Calcification. PB89-149223 BIOSPHERE Global Biomethylation of the Elements - Its Role in the Biosphero Translated to New Organometallic Chemistry and Biotechnology. PB90-136654 BIOTECHNOLOGY Liposome-Enhanced Flow Injection Immunoanalysis. PB89-146757 Chemical Characterization of Ionizing Radiation-Induced Damage to DNA. PB89-151922 Structure of a Hydroxyl Radical Induced Cross-Link of Thymine and Tyrosine. PB89-157838 Intramolecular H Atom Abstraction from the Sugar Moiety by Thymine Radicals in Oligo- and Polydeoxynucleotides. PB89-175899 New Directions in Bioinformatics. PB89-175279 901,245 Use of Structural Templates in Protein Backbone Modeling. PB89-175277 901,246	BIOTRANSFORMATION Biotransformation of Mercury by Bacteria Isolated from a River Collecting Cinnabar Mine Waters. PB89-229280 900,864 BIPOLAR TRANSISTORS Effect of Neutrons on the Characteristics of the Insulated Gate Bipolar Transistor (IGBT). PB89-157655 900,773 Analytical Modeling of Device-Circuit Interactions for the Power Insulated Gate Bipolar Transistor (IGBT). PB89-176259 Numerical Simulations of Neutron Effects on Bipolar Transistors. PB90-123589 900,797 BISMUTH ALLOYS Effect of Anisotropic Thermal Conductivity on the Morphological Stability of a Binary Alloy. PB89-228985 901,155 BISMUTH CALCIUM STRONTIUM CUPRATES Magnetic Field Dependence of the Superconductivity in BI-Sr-Ca-Cu-O Superconductors. PB89-146815 BISMUTH IONS Laser-Produced Spectra and QED (Quantum Electrodynamic) Effects for Fe-, Co-, Cu-, and Zn-Like Ions of Au, Pb, Bi, Th, and U. PB89-176010 BITUMENS Strain Energy of Bituminous Built-Up Membranes: A New Concept in Load-Elongation Testing. PB89-212203 BITUMINOUS COATINGS Interim Criteria for Polymer-Modified Bituminous Roofing Membrane Materials. PB89-168025 900,114 BIVALVES Sequential Determination of Biological and Pollutant Elements in Marine Bivalves. PB89-156897 901,217 BLACK LIQUORS Laser Excited Fluorescence Studies of Black Liquor.	Tilt Observations Using Borehole Tiltmeters 1. Analysis of Tidal and Secular Tilt. PB90-136649 BORON Grain Boundary Structure in Ni3Al. PB89-201784 Grain Boundary Characterization in Ni3Al. PB89-229306 Grain Boundary Structure in Ni3Al. PB89-229314 BOROSILICATE GLASS Mechanical Property Enhancement in Ceramic Matrix Composites. PB89-189138 Toughening Mechanisms in Ceramic Composites. Semi-Annual Progress Report for the Period Ending March 31, 1989. PB89-235907 BOSON-EXCHANGE MODELS Comparison of Interplaner-Boson-Exchange Models of High-Temperature Superconductivity - Possible Experimental Tests. PB90-117394 BOTILES Glass Bottles for Carbonated Soft Drinks: Voluntary Product Standard P573-89. PB90-107046 BOUNDARY LAYER FLOW Dynamics of Concentration Fluctuation on Both Sides of Phase Boundary. PB89-173942 BOUNDARY LAYER SEPARATION Shear Effects on the Phase Separation Behaviour of a Polymer Blend in Solution by Small Angle Neutron Scattering. PB89-229264 BRACHYTHERAPY NBS (National Bureau of Standards) Measurement Services: Calibration of Gamma-Ray-Emitting Brachytherapy
BIOLOGY Journal of Research of the National Institute of Standards and Technology, Volume 94, Number 1, January-February 1989. Special Issue: Numeric Databases in Materials and Biological Sciences. PB89-175194 BIOMEDICAL ENGINEERING Liposome-Enhanced Flow Injection Immunoanalysis. PB89-146757 BIOPHYSICS Biophysical Aspects of Lipid Interaction with Mineral: Liposome Model Studies. PB90-117508 BIOPROSTHESIS Micro-Raman Characterization of Atherosclerotic and Bioprosthetic Calcification. PB89-149223 BIOSPHERE Global Biomethylation of the Elements - Its Role in the Biosphere Translated to New Organometallic Chemistry and Biotechnology. PB90-136854 BIOTECHNOLOGY Liposome-Enhanced Flow Injection Immunoanalysis. PB89-146757 Chemical Characterization of Ionizing Radiation-Induced Damage to DNA. PB89-151922 Structure of a Hydroxyl Radical Induced Cross-Link of Thymine and Tyrosine. PB89-157838 901,244 Intramolecular H Atom Abstraction from the Sugar Moiety by Thymine Radicals in Oligo- and Polydeoxynucleotides. PB89-171870 New Directions in Bioinformatics. PB89-175269 Use of Structural Templates in Protein Backbone Modeling. PB89-175277 Comparative Modeling of Protein Structure: Progress and Prospects.	BIOTRANSFORMATION Biotransformation of Mercury by Bacteria Isolated from a River Collecting Cinnabar Mine Waters. PB69-229280 BIPOLAR TRANSISTORS Effect of Neutrons on the Characteristics of the Insulated Gate Bipolar Transistor (IGBT). PB89-157655 900,773 Analytical Modeling of Device-Circuit Interactions for the Power Insulated Gate Bipolar Transistor (IGBT). PB89-176259 Numerical Simulations of Neutron Effects on Bipolar Transistors. PB90-123589 900,797 BISMUTH ALLOYS Effect of Anisotropic Thermal Conductivity on the Morphological Stability of a Binary Alloy. PB89-228985 BISMUTH CALCIUM STRONTIUM CUPRATES Magnetic Field Dependence of the Superconductivity in Bi-Sr-Ca-Cu-O Superconductors. PB89-146815 BISMUTH IONS Laser-Produced Spectra and QED (Quantum Electrodynamic) Effects for Fe-, Co-, Cu-, and Zn-Like lons of Au, Pb, Bi, Th, and U. PB89-176010 BITUMENS Strain Energy of Bituminous Built-Up Membranes: A New Concept in Load-Elongation Testing. PB89-176010 BIVALVES Sequential Determination of Biological and Pollutant Elements in Marine Bivalves. PB89-156897 900,243 BLASE Excited Fluorescence Studies of Black Liquor. PB89-176416 900,243	Tilt Observations Using Borehole Tiltmeters 1. Analysis of Tidal and Secular Tilt. PB90-136649 901,283 BORON Grain Boundary Structure in Ni3Al. PB89-201784 901,150 Grain Boundary Characterization in Ni3Al. PB89-229306 901,156 Grain Boundary Structure in Ni3Al. PB89-229314 901,157 BOROSILICATE GLASS Mechanical Property Enhancement in Ceramic Matrix Composites. PB89-189138 901,076 Toughening Mechanisms in Ceramic Composites. Semi-Annual Progress Report for the Period Ending March 31, 1989. PB89-235907 901,080 BOSON-EXCHANGE MODELS Comparison of Interplaner-Boson-Exchange Models of High-Temperature Superconductivity - Possible Experimental Tests. PB90-117334 901,462 BOTTLES Glass Bottles for Carbonated Soft Drinks: Voluntary Product Standard PS73-89. PB90-107046 900,012 BOUNDARY LAYER FLOW Dynamics of Concentration Fluctuation on Both Sides of Phase Boundary. PB89-173942 901,183 BOUNDARY LAYER SEPARATION Shear Effects on the Phase Separation Behaviour of a Polymer Blend in Solution by Small Angle Neutron Scattering. PB89-229264 900,574 BRACHYTHERAPY NES (National Bureau of Standards) Measurement Services: Calibration of Gamma-Ray-Emitting Brachytherapy Sources. PB89-193858 901,243
BIOLOGY Journal of Research of the National Institute of Standards and Technology, Volume 94, Number 1, January-February 1989. Special Issue: Numeric Databases in Materials and Biological Sciences. PB89-175194 BIOMEDICAL ENGINEERING Liposome-Enhanced Flow Injection Immunoanalysis. PB89-146757 BIOPHYSICS Biophysical Aspects of Lipid Interaction with Mineral: Liposome Model Studies. PB90-117508 BIOPROSTHESIS Micro-Raman Characterization of Atherosclerotic and Bioprosthetic Calcification. PB89-149223 BIOSPHERE Global Biomethylation of the Elements - Its Role in the Biosphere Translated to New Organometallic Chemistry and Biotechnology. PB90-136654 BIOTECHNOLOGY Liposome-Enhanced Flow Injection Immunoanalysis. PB89-146757 Chemical Characterization of Ionizing Radiation-Induced Damage to DNA. PB89-151922 Structure of a Hydroxyl Radical Induced Cross-Link of Thymine and Tyrosine. PB89-157838 Intramolecular H Atom Abstraction from the Sugar Moiety by Thymine Radicals in Oligo- and Polydeoxynucleotides. PB89-171870 New Directions in Bioinformatics. PB89-175277 901,245 Comparative Modeling of Protein Structure: Progress and Prospects. PB89-175285 901,247	BIOTRANSFORMATION Biotransformation of Mercury by Bacteria Isolated from a River Collecting Cinnabar Mine Waters. PB89-229280 900,864 BIPOLAR TRANSISTORS Effect of Neutrons on the Characteristics of the Insulated Gate Bipolar Transistor (IGBT). PB89-157655 900,773 Analytical Modeling of Device-Circuit Interactions for the Power Insulated Gate Bipolar Transistor (IGBT). PB89-176259 Numerical Simulations of Neutron Effects on Bipolar Transistors. PB90-123589 900,797 BISMUTH ALLOYS Effect of Anisotropic Thermal Conductivity on the Morphological Stability of a Binary Alloy. PB89-228985 901,155 BISMUTH CALCIUM STRONTIUM CUPRATES Magnetic Field Dependence of the Superconductivity in BI-Sr-Ca-Cu-O Superconductors. PB89-146815 BISMUTH IONS Laser-Produced Spectra and QED (Quantum Electrodynamic) Effects for Fe-, Co-, Cu-, and Zn-Like Ions of Au, Pb, Bi, Th, and U. PB89-176010 BITUMENS Strain Energy of Bituminous Built-Up Membranes: A New Concept in Load-Elongation Testing. PB89-212203 BITUMINOUS COATINGS Interim Criteria for Polymer-Modified Bituminous Roofing Membrane Materials. PB89-168025 900,114 BIVALVES Sequential Determination of Biological and Pollutant Elements in Marine Bivalves. PB89-156897 901,217 BLACK LIQUORS Laser Excited Fluorescence Studies of Black Liquor.	Tilt Observations Using Borehole Tiltmeters 1. Analysis of Tidal and Secular Tilt. PB90-136649 901,283 BORON Grain Boundary Structure in Ni3Al. PB89-201784 901,156 Grain Boundary Characterization in Ni3Al. PB89-229306 901,156 Grain Boundary Structure in Ni3Al. PB89-229314 901,157 BOROSILICATE GLASS Mechanical Property Enhancement in Ceramic Matrix Composites. PB89-189138 901,076 Toughening Mechanisms in Ceramic Composites. PB89-189138 901,076 Toughening Mechanisms in Ceramic Composites. PB89-189138 901,076 BOSON-EXCHANGE MODELS Comparison of Interplaner-Boson-Exchange Models of High-Temperature Superconductivity - Possible Experimental Tests. PB90-117334 901,462 BOTTLES Glass Bottles for Carbonated Soft Drinks: Voluntary Product Standard PS73-89. PB90-107046 900,012 BOUNDARY LAYER FLOW Dynamics of Concentration Fluctuation on Both Sides of Phase Boundary. PB89-173942 901,183 BOUNDARY LAYER SEPARATION Shear Effects on the Phase Separation Behaviour of a Polymer Blend in Solution by Small Angle Neutron Scattering. PB89-229264 BRAIN Differential Scanning Calonmetric Study of Brain Clathrin.
BIOLOGY Journal of Research of the National Institute of Standards and Technology, Volume 94, Number 1, January-February 1989. Special Issue: Numeric Databases in Materials and Biological Sciences. PB89-175194 BIOMEDICAL ENGINEERING Liposome-Enhanced Flow Injection Immunoanalysis. PB89-146757 BIOPHYSICS Biophysical Aspects of Lipid Interaction with Mineral: Liposome Model Studies. PB90-117508 BIOPROSTHESIS Micro-Raman Characterization of Atherosclerotic and Bioprosthetic Calcification. PB89-149223 BIOSPHERE Global Biomethylation of the Elements - Its Role in the Biosphere Translated to New Organometallic Chemistry and Biotechnology. PB90-136854 BIOTECHNOLOGY Liposome-Enhanced Flow Injection Immunoanalysis. PB89-146757 Chemical Characterization of Ionizing Radiation-Induced Damage to DNA. PB89-151922 Structure of a Hydroxyl Radical Induced Cross-Link of Thymine and Tyrosine. PB89-157838 901,244 Intramolecular H Atom Abstraction from the Sugar Moiety by Thymine Radicals in Oligo- and Polydeoxynucleotides. PB89-171870 New Directions in Bioinformatics. PB89-175269 Use of Structural Templates in Protein Backbone Modeling. PB89-175277 Comparative Modeling of Protein Structure: Progress and Prospects.	BIOTRANSFORMATION Biotransformation of Mercury by Bacteria Isolated from a River Collecting Cinnabar Mine Waters. PB89-229280 900,864 BIPOLAR TRANSISTORS Effect of Neutrons on the Characteristics of the Insulated Gate Bipolar Transistor (IGBT). PB89-157655 900,773 Analytical Modeling of Device-Circuit Interactions for the Power Insulated Gate Bipolar Transistor (IGBT). PB89-176259 Numerical Simulations of Neutron Effects on Bipolar Transistors. PB90-123589 900,797 BISMUTH ALLOYS Effect of Anisotropic Thermal Conductivity on the Morphological Stability of a Binary Alloy. PB89-228985 901,155 BISMUTH CALCIUM STRONTIUM CUPRATES Magnetic Field Dependence of the Superconductivity in BI-Sr-Ca-Cu-O Superconductors. PB89-146815 BISMUTH IONS Laser-Produced Spectra and QED (Quantum Electrodynamic) Effects for Fe-, Co-, Cu-, and Zn-Like Ions of Au, Pb, Bi, Th, and U. PB89-176010 BITUMENS Strain Energy of Bituminous Built-Up Membranes: A New Concept in Load-Elongation Testing. PB89-212203 900,139 BITUMINOUS COATINGS Interim Criteria for Polymer-Modified Bituminous Roofing Membrane Materials. PB89-168025 900,114 BIVALVES Sequential Determination of Biological and Pollutant Elements in Marine Bivalves. PB89-156897 901,217 BLACK LIQUORS Laser Excited Fluorescence Studies of Black Liquor. PB89-176416 Remote Sensing Technique for Combustion Gas Temperature Measurement in Black Liquor Recovery Boilers.	Tilt Observations Using Borehole Tiltmeters 1. Analysis of Tidal and Secular Tilt. PB90-136649 BORON Grain Boundary Structure in Ni3Al. PB89-201784 Grain Boundary Characterization in Ni3Al. PB89-229306 Grain Boundary Structure in Ni3Al. PB89-229314 BOROSILICATE GLASS Mechanical Property Enhancement in Ceramic Matrix Composites. PB89-189138 FB89-189138 FB89-189138 FB89-189138 FB89-189138 FB89-235907 BOSON-EXCHANGE MODELS Comparison of Interplaner-Boson-Exchange Models of High-Temperature Superconductivity - Possible Experimental Tests. PB90-117334 FB90-117334 FB90-117334 BOTTLES Glass Bottles for Carbonated Soft Drinks: Voluntary Product Standard P573-89. PB90-107046 BOUNDARY LAYER FLOW Dynamics of Concentration Fluctuation on Both Sides of Phase Boundary. PB89-173942 BOUNDARY LAYER SEPARATION Shear Effects on the Phase Separation Behaviour of a Polymer Blend in Solution by Small Angle Neutron Scattering. PB89-229264 BRACHYTHERAPY NES (National Bureau of Standards) Measurement Services: Calibration of Gamma-Ray-Emitting Brachytherapy Sources. PB89-193858 BRAIN

PB90-128257	901,582			PB89-176291 901,084
BRASS-BETA Fourth-Order Elastic Constants of beta-Brass.		Earthquake Hazard Mitigation through Improved S Design.		Thermographic Imaging and Computer Image Processing of Defects in Building Materials.
PB90-117607 BRASSES	901,160	PB89-149132 96 Earthquake Resistant Design Criteria.		PB89-176309 900,123 nterzonal Natural Convection for Various Aperture Con-
Fourth-Order Elastic Constants of beta-Brass.	004.460	PB89-149140 96	00,099 <u>f</u>	igurations.
PB90-117607 BREAKDOWN	901,160	Knowledge Based System for Durable Reinforced crete.		PB89-176499 900,066 Summary of Circular and Square Edge Effect Study for
Effect of an Oil-Paper Interface Parallel to an Field on the Breakdown Voltage at Elevated		PB89-150734 96 Standard Specifications for Cements and the R	00,110	Guarded-Hot-Plate and Heat-Flow-Meter Apparatuses. PB89-176606 900,884
tures.		Their Development of Quality Assurance System	no for	/entilation Effectiveness Measurements in an Office
PB89-156988 BREAKDOWN (ELECTRONIC THRESHOLD)	901,490	Laboratories. PB89-150742	01.021	Building. PB89-176614 900,067
Effect of Pressure on the Development of Prebi	reakdown	Experimental Validation of a Mathematical Model for dicting Moisture Transfer in Attics.	or Pre-	Application of Direct Digital Control to an Existing Build-
PB90-128315	900,828	PB89-150783 90		ng Air Handler. PB89-177141 900,068
BREMSSTRAHLUNG. Continuum Radiation Produced in Pure-Elemen	t Targets	Combustion Testing Methods for Catalytic Heaters. PB89-150924	00 846 H	IVACSIM+, a Dynamic Building/HVAC/Control Sys-
by 10-40 keV Electrons: An Empirical Model. PB89-201610	900,209	NBS (National Bureau of Standards) Life-Cycle		ems Simulation Program. PB89-177166 900,070
Modeling of the Bremsstrahlung Radiation Pro		(NBSLCC) Program (for Microcomputers). PB89-151211 96		Simulation of a Large Office Building System Using the
Pure Element Targets by 10-40 keV Electrons. PB89-201644	901,531	ZIP: The ZIP-Code Insulation Program (Version 1.0 nomic Insulation Levels for New and Existing House) ECO- E	IVACSIM+ Program. 1889-177174 900,071
Cross Section and Linear Polarization of Tage	ged Pho-	Three-Digit ZIP Code. Users Guide and Refe Manual.	erence E	poxy Impregnation of Hardened Cement Pastes for characterization of Microstructure.
tons. PB90-117292	901,560	PB89-151765 90	<i>00,058</i> F	PB89-185573 901,042
Cross Sections for Bremsstrahlung Production a tron-Impact Ionization.	and Elec-	Wind and Seismic Effects. Proceedings of the Joint ing of the U.SJapan Cooperative Program in Natur		Brick Masonry: U.S. Office Building in Moscow. 989-187504 900,160
PB90-123910	901,575	sources Panel on Wind and Seismic Effects (20th) in Gaithersburg, Maryland on May 17-20, 1988.) Held F	ire Propagation in Concurrent Flows.
BRICK STRUCTURES Brick Masonry: U.S. Office Building in Moscow.		PB89-154835 90	00,137	900,597
PB89-187504	900, 160	Control System Simulation in North America. PB89-157010 90	20.091 ir	hermal and Economic Analysis of Three HVAC (Heating, Ventilating, and Air Conditioning) System Types in a
BRIDGES (STRUCTURES) Wind and Seismic Effects. Proceedings of the Jo		Prediction of Service Life of Building Materials and ponents.		ypical VA (Veterans Administration) Patient Facility. B89-188619 900,847
ing of the U.SJapan Cooperative Program in Na sources Panel on Wind and Seismic Effects (2)				auidelines for Identification and Mitigation of Seismically lazardous Existing Federal Buildings.
in Gaithersburg, Maryland on May 17-20, 1988. PB89-154835	900,157	Fractal-Based Description of the Roughness of B Steel Panels.		B89-188627 900,161
Inelastic Behavior of Full-Scale Bridge Columns	Subject-	PB89-158018 90		OCTDOS: Neutron and Gamma Penetration in Composite duct Systems.
ed to Cyclic Loading. PB89-174924	900,584	ZIP: ZIP-Code Insulation Program (for Microcompute PB89-159446	00,060 P	PB89-188809 901,275
BRINES Preconcentration of Trace Transition Metal a	nd Rare	Corrosion of Metallic Fasteners in Low-Sloped Ro- Review of Available Information and Identification of	O.O. 71	valuating Office Lighting Environments: Second Level nalysis.
Earth Elements from Highly Saline Solutions. PB90-118175	900,226	search Needs.	F	B89-189153 <i>900,073</i>
BRITTLE FRACTURING	300,220	PB89-162580 90 Method to Measure the Tensile Bond Strength be	tween S	lumination Conditions and Task Visibility in Daylit paces.
Effect of Lateral Crack Growth on the Strength tact Flaws in Brittle Materials.	of Con-	Two Weakly-Cemented Sand Grains.	P 400	B89-189237 900,074
PB89-171813	901,034	Interim Criteria for Polymer-Modified Bituminous Re	oofina la	riability of Spray-Applied Fireproofing and Thermal Insu- ations: Field Evaluation of Prototype Test Devices.
BROMINE Quenching and Energy Transfer Processes of S	ingle Ro-	Membrane Materials. PB89-168025 90	20 114	B89-189328 900,130 otential Applications of a Sequential Construction Ana-
tational Levels of Br2 B triplet Pi(O(sub u)(+) with Ar under Single Collision Conditions.) v'= 24	Damage Accumulation in Wood Structural Mer	mbers ly	zer.
PB89-179766	900,399	Under Stochastic Live Loads. PB89-171748 90	20 115	B89-191670 900,105 lse of Artificial Intelligence Programming Techniques for
BROMINE IONS Spectra and Energy Levels of Br XXV, Br XXIX,	Br XXX,	Control Strategies and Building Energy Consumption PB89-172340 90	n. C	communication between Incompatible Building Information Systems.
and Br XXXI. PB89-176002	901,509	Building Economics in the United States.	F	B89-191985 900,106
BRONZES		PB89-172399 90 Preliminary Stochastic Model for Service Life Prediminary Stochastic Model for Service Model for Serv		uilding Technology Project Summaries 1989. B89-193213 • 900,131
Technical Examination, Lead Isotope Determina Elemental Analysis of Some Shang and Zhou	Dynasty	of a Photolytically and Thermally Degraded Poly Cover Plate Material.	ymeric s	tandard Aggregate Materials for Alkali-Silica Reaction
Bronze Vessels. PB90-136862	901,178	PB89-173801 90	<i>00,556</i> p	tudies. B89-193221 <i>901,046</i>
BUBBLES Asymptotic Expansions for Constant Compositi	en Dow	Survey of Selected Methods of Economic Evaluation Building Decisions.	ti	lating Procedure for Mixed Air-Source Unitary Air Condi- oners and Heat Pumps Operating in the Cooling Mode.
Asymptotic Expansions for Constant-Compositi Bubble Curves Near the Critical Locus.		PB89-173819 90	10, 103 F	levision 1.
PB89-227987 BUILDING CODES	901,545	Trends for Building Technology in North America. PB89-174106 90	20 104	B89-193247 900,075 IRNET: A Computer Program for Building Airflow Net-
Analytical Methods for Firesafety Design. PB89-157275	900,111	Thermal Resistance Measurements and Calculation an Insulated Concrete Block Wall.	ons of w	ork Modeling. B89-193254 900,076
Effects of Research on Building Practice.		PB89-174916 90	00,119 ₊	leuristic Analysis of von Kries Color Constancy.
PB89-202584 Research as the Technical Basis for Standards	900,168	Inelastic Behavior of Full-Scale Bridge Columns Su ed to Cyclic Loading.	_	B89-201099 901,362
Building Codes.		PB89-174924 90 Progressive Collapse: U.S. Office Building in Moscov	,,,,,,, p	ffects of Research on Building Practice. B89-202584 900,168
PB89-231062 BUILDING TECHNOLOGY	900,101		00,158 II	ntegral Mass Balances and Pulse Injection Tracer Techiques.
Proceedings of the Workshop on Cement Stabil Low-Level Radioactive Waste. Held at Gait	ization of	Pore-Water Pressure Buildup in Clean Sands Becau Cyclic Straining.		B89-206833 900,077
Maryland on May 31-June 2, 1989.		PB89-175723 90	· P	ite Characterization for Radon Source Potential. B89-209274 901,290
NUREG/CP-0103 Interpretation of the Effects of Retarding Admit	<i>901,302</i> dures on	Prediction of Service Life of Construction and Othe tenals.	erma- F	lesults of a Survey of the Performance of EPDM (Ethyl-
Pastes of C3S, C3A plus Gypsum, and Portland PB89-146971	Cement, 900,580	PB89-175848 90 U-Value Measurements for Windows and Movable II	neula. ti	ne Propylene Diene Terpolymer) Roofing at Army Facilies.
Implications of Computer-Based Simulation	Models,	tions from Hot Box Tests in Two Commercial Lab	orato-	B89-209316 900,136
Expert Systems, Databases, and Networks for Research.			00,121 S	aboratory Evaluation of an NBS (National Bureau of tandards) Polymer Soil Stress Gage.
PB89-146989 Enovy Impregnation Procedure for Hardened	900,581 Cement	Field Measurement of Thermal and Solar/Optical Pities of Insulating Glass Windows.	TOPCI-	B89-211973 901,291 ests of Adhesive-Bonded Seams of Single-Ply Rubber
Epoxy Impregnation Procedure for Hardened Samples.		PB89-175905 90	00,064 <u>N</u>	lembranes. B89-212120 900,138
PB89-147821 Guidelines and Procedures for Implementation of	901,180 of Execu-	Integrated Knowledge Systems for Concrete and Materials.	P	art Load, Seasonal Efficiency Test Procedure Evaluation
tive Order on Seismic Safety. PB89-148092	900,156	PB89-176119 <i>90</i> Indoor Air Quality.	00,582	f Furnace Cycle Controllers. B89-212146 900,848
Predicting Formaldehyde Concentrations in Man	ufactured	PB89-176127 90	00,065 S	train Energy of Bituminous Built-Up Membranes: A New
Housing Resulting from Medium-Density Fiberbook PB89-148134	ard. <i>900,854</i>	Circular and Square Edge Effect Study for Guarder Plate and Heat-Flow-Meter Apparatuses.	d-Hot- C	concept in Load-Elongation Testing. 889-212203 900,139
Preliminary Performance Criteria for Building (Equipment and Systems Used in Detention and	Materials,	PB89-176135 90	00,881 A	STM (American Society for Testing and Materials) Com-
tional Facilities,	- Correc-	Corrosion Induced Degradation of Amine-Cured Coatings on Steel.		nittee Completes Work on EPDM Specification. 900,140

Service Life of Concrete.	PB89-177166 900,070	PB89-179790 900,400
PB89-215362 901,303 Static Tests of One-third Scale Impact Limiters.	Simulation of a Large Office Building System Using the HVACSIM+ Program.	CALCIUM IONS
PB89-216469 901,000	PB89-177174 900,071	Electron-Impact Excitation of the Resonance Transition in CA(1+).
Air Quality Investigation in the NIH (National Institutes of Health) Radiation Oncology Branch. PB89-228977 900,079	Guidelines for Identification and Mitigation of Seismically Hazardous Existing Federal Buildings. PB89-188627 900.161	PB89-171557 901,502 CALCIUM METABOLISM DISORDERS
Experimental Investigation and Modeling of the Flow	Assessment of Robotics for Improved Building Oper-	Micro-Raman Characterization of Atherosclerotic and Bio- prosthetic Calcification.
Rate of Refrigerant 22 Through the Short Tube Restrictor.	ations and Maintenance. PB89-189146 900,092	PB89-149223 901,234
PB89-229041 901,118	Illumination Conditions and Task Visibility in Daylit	CALIBRATING Computer Program for Instrument Calibration at State-
Window U-Values: Revisions for the 1989 ASHRAE (American Society of Heating, Refrigerating and Air-Con-	Spaces. PB89-189237 900,074	Sector Secondary-Level Laboratories.
ditioning Engineers) Handbook - Fundamentals. PB89-229215 900,145	Calculation of the Flow Through a Horizontal Ceiling/	PB89-173496 900,877 NBS (National Bureau of Standards) Standards for Opti-
Ventilation and Air Quality Investigation of the U.S. Geo-	Floor Vent. PB89-189252 900.128	cal Power Meter Calibration. PB89-176200 900.726
logical Survey Building. PB89-229686 900,857	Fire Induced Flows in Corridors: A Review of Efforts to	Tests of the Recalibration Period of a Drifting Instrument.
Investigation of a Washington, DC Office Building. PB89-230361 900.081	Model Key Features. PB89-189260 900,129	PB89-176275 900,199
PB89-230361 900,081 Airflow Network Models for Element-Based Building Air-	AIRNET: A Computer Program for Building Airflow Net-	Automated Calibration of Optical Photomask Linewidth Standards at the National Institute of Standards and
flow Modeling. PB89-230379 900,082	work Modeling. PB89-193254 900,076	Technology. PB89-186340 <i>901,315</i>
Origins of ASHRAE (American Society of Heating, Refrig-	Considerations of Stack Effect in Bullding Fires.	Biological Standard Reference Materials for the Calibra-
erating and Air-Conditioning Engineers) Window U-Value Data and Revisions for the 1989 Handbook of Funda-	PB89-195671 900,133 Integral Mass Balances and Pulse Injection Tracer Tech-	tion of Differential Scanning Calorimeters: Di-alkylphos- phatidylcholine in Water Suspensions.
mentals. PB89-231005 900,083	niques.	PB89-186779 900,415
Considerations for Advanced Building Thermal Simulation	PB89-206833 900,077 Site Characterization for Radon Source Potential.	Preparation of Multistage Zone-Refined Materials for Thermochemical Standards.
Programs. PB89-231047 900,084	PB89-209274 901,290	PB89-186795 900,203
Thermophysical-Property Needs for the Environmentally	Outline of a Practical Method of Assessing Smoke Hazard.	Group Index and Time Delay Measurements of a Stand- ard Reference Fiber.
Acceptable Halocarbon Refrigerants. PB89-231054 900,482	PB89-211858 900,078	PB89-189179 900,752
Research as the Technical Basis for Standards Used in	Estimating the Environment and the Response of Sprin- kler Links in Compartment Fires with Draft Curtains and	NBS (National Bureau of Standards) Measurement Serv- ices: Calibration of Gamma-Ray-Emitting Brachytherapy
Building Codes. PB89-231062 900,101	Fusible Line-Actuated Ceiling Vents. Part 2. User Guide for the Computer Code Lavent.	Sources. PB89-193858 901,243
Sensors and Measurement Techniques for Assessing	PB89-229009 900,094	Graphical Analyses Related to the Linewidth Calibration
Structural Performance. PB89-235865 900,162	Ventilation and Air Quality Investigation of the U.S. Geological Survey Building.	Problem. PB89-201156 <i>900,783</i>
EVSIM: An Evaporator Simulation Model Accounting for	PB89-229686 900,857	International Comparison of Power Meter Calibrations
Refrigerant and One Dimensional Air Distribution. PB89-235881 900,086	Airflow Network Models for Element-Based Building Airflow Modeling.	Conducted in 1987. PB89-201545 900,718
Method for Measuring the Effectiveness of Gaseous Con-	PB89-230379 900,082	AC-DC Difference Calibrations at NBS (National Bureau
taminant Removal Filters. PB89-235899 900,858	Considerations for Advanced Building Thermal Simulation Programs.	of Standards). PB89-201560 900,816
Set Time Control Studies of Polymer Concrete. PB90-111238 901.057	PB89-231047 900,084	Calibration of GPS (Global Positioning System) Equip-
PB90-111238 901,057 Proposed Methodology for Rating Air-Source Heat	Comparisons of NBS/Harvard VI Simulations and Full- Scale, Multiroom Fire Test Data.	ment in Japan. PB89-212070 900,630
Pumps That Heat, Cool, and Provide Domestic Water Heating.	PB90-128620 900,170	NBS (National Bureau of Standards) Calibration Service
PB90-112368 900,087	BULK MODULUS Bulk Modulus and Young's Modulus of the Superconduc-	Providing Time and Frequency at a Remote Site by Weighting and Smoothing of GPS (Global Positioning
Report of Roof Inspection: Characterization of Newly- Fabricated Adhesive-Bonded Seams at an Army Facility.	tor Ba2Cu3YO7. PB90-123613 901,469	System) Common View Data. PB89-212211 900,631
PB90-112376 900,107	BURSTING	Interlaboratory Determination of the Calibration Factor for
Post-Occupancy Evaluation of Several U.S. Government Buildings.	Failure Analysis of an Amine-Absorber Pressure Vessel. PB89-173835 901,101	the Measurement of the Interstitial Oxygen Content of Silicon by Infrared Absorption.
PB90-112384 <i>900,088</i>	PB89-173835 901,101 BUSINESSES	PB90-117300 900,224
Hydrodynamic Forces on Vertical Cylinders and the Lighthill Correction.	Promoting Technological Excellence: The Role of State and Federal Extension Activities.	Calibrating Network Analyzers with Imperfect Test Ports. PB90-117680 900,825
PB90-117417 901,313	PB90-120742 900,171	Silicon Photodiode Self-Calibration.
Advanced Heat Pumps for the 1990's Economic Per- spectives for Consumers and Electric Utilities.	BUTYL IONS	PB90-118159 900,734
PB90-118043 900,089	Hyperconjugation: Equilibrium Secondary Isotope Effect on the Stability of the t-Butyl Cation. Kinetics of Near-	CALIBRATION NBS (National Bureau of Standards) Calibration Services:
Adsorption of High-Range Water-Reducing Agents on Selected Portland Cement Phases and Related Materials.	Thermoneutral Hydride Transfer. PB89-156756 900,306	A Status Report. PB89-173934 900,878
PB90-124306 900,583	CAD	Trace Gas Calibration Systems Using Permeation De-
Measured Air Infiltration and Ventilation Rates in Eight Large Office Buildings.	Instrument-Independent MS/MS Database for XQQ Instruments: A Kinetics-Based Measurement Protocol.	vices. PB89-176580 <i>900,883</i>
PB90-128158 900,090 Gypsum Wallboard Formaldehyde Sorption Model.	PB90-213695 900,674	Automated Fringe Counting Laser Interferometer for Low
PB90-132705 900,154	CADMIUM High-Accuracy Differential-Pulse Anodic Stripping Voltam-	Frequency Vibration Measurements. PB89-177190 900,885
Model for Particle Size and Phase Distributions in Ground Cement Clinker.	metry with Indium as an Internal Standard.	Precision and Accuracy Assessment Derived from Cali-
PB90-136847 901,062	PB89-156947 900,182 CADMIUM 109	bration Data. PB89-179162 900,886
BUILDINGS Wind and Seismic Effects. Proceedings of the Joint Meet-	(109)Pd and (109)Cd Activity Standardization and Decay	NIST (National Institute of Standards and Technology)
ing of the U.SJapan Cooperative Program in Natural Resources Panel on Wind and Seismic Effects (20th) Held	Data. PB90-123449 <i>901,564</i>	Calibration Services Users Guide. 1989 Edition. PB89-200216 900,926
in Gaithersburg, Maryland on May 17-20, 1988.	CADMIUM ALLOYS	Calibration of Voltage Transformers and High-Voltage Ca-
PB89-154835 900,157 Control System Simulation in North America.	TEM Observation of Icosahedral, New Crystalline and Glassy Phases in Rapidly Quenched Cd-Cu Alloys.	pacitors at NIST. PB89-211114 901,442
PB89-157010 900,091	PB90-123514 901,166	Josephson Array Voltage Calibration System: Operational
Control Strategies and Building Energy Consumption. PB89-172340 900,061	CADMIUM TELLURIDES Electronic Structure of the Cd Vacancy in CdTe.	Use and Verification. PB89-230403 900,820
Developments in the Heat Balance Method for Simulating	PB89-171318 901,398	NIST (National Institute of Standards and Technology)
Room Thermal Response. PB89-173926 900,062	CALCIFICATION Liposome Technology in Biomineralization Research.	Calibration Services, Users Guide: Fee Schedule. PB90-127820 900,913
Indoor Air Ouality.	PB90-128117 901,230	Branching Ratio Technique for Vacuum UV Radiance
PB89-176127 900,065	CALCIUM Alignment Effects in Electronic Energy Transfer and Re-	Calibrations: Extensions and a Comprehensive Data Set. PB90-128257 901,582
Interzonal Natural Convection for Various Aperture Configurations.	active Events.	CALIBRATION ERRORS
PB89-176499 900,066 Application of Direct Digital Control to an Evisting Build-	AD-A202 820/7 900,267 Interaction of Cupric Ions with Calcium Hydroxylapatite.	Interpretation of a between-Time Component of Error in Mass Measurements.
Application of Direct Digital Control to an Existing Building Air Handler.	PB89-157127 900,037	PB89-149108 900,872
PB89-177141 900,068 HVACSIM+, a Dynamic Building/HVAC/Control Sys-	Alignment Effects in Ca-He(5(sup 1)P(sub 1) - 5(sup 3)P(sub J)) Energy Transfer Collisions by Far Wing Laser	CALIBRATION STANDARDS Special Calibration Systems for Reactive Gases and
tems Simulation Program.	Scattering.	Other Difficult Measurements.

PB89-149215	900,873	PB89-157374	900,321	CARBONATE MINERALS	
Calibration with Randomly Chang PB89-186381	ging Standard Curves. 900,888	Synchrotron Radiation Study and Their Interaction with H2O,	CO2, and O2.	Multicritical Phase Relations in Miner PB89-150882	901,278
NBS (National Bureau of Stand Radiance.		PB89-157697 Facilitated Transport of CO2 th	900,252 rough Highly Swollen Ion-	Moydite, (Y, REE) (B(OH)4)(CO3), a lifted from the Evans-Lou Pegmatite, Queb	ec.
PB89-201685 NIST (National Institute of Stat	901,532 ndards and Technology)	Exchange Membranes: The Eff treatment.	fect of Hot Glycerine Pre-	PB89-157747 CARBONYL COMPOUNDS	900,186
Measurement Services: The Ca ples and Thermocouple Materials	alibration of Thermocou- s.	PB89-179618 Isochoric (p,v,T) Measurements	s on CO2 and (0.98 CO2	Population Relaxation of CO(v= 1) Phase Metal-Carbonyl Complexes.	
PB89-209340 Guidelines for Implementing the	900,897 New Representations of	+ 0.02 CH4) from 225 to 40 MPa.		PB89-157291 CARBONYL SULFIDE	900,315
the Volt and Ohm Effective Janu PB89-214761	ary 1, 1990. <i>900,817</i>	PB89-202493 Synergistic Effects of Nitrogen		Heterodyne Measurements on OCS P PB89-201743	Near 1372 cm(-1). 900,425
NIST (National Institute of Star Measurement Services: AC-DC D PB89-222616	ndards and Technology) Difference Calibrations. 900,818	ide Following Acute Inhalation E PB89-214779 Method for Improving Equations	900,856	CASCADE AMPLIFIERS Very Low-Noise FET Input Amplifier. PB90-128224	900,800
Intercomparison of Load Cell formed by National Laboratories PB89-235915	Verification Tests Per- of Five Countries. 900,909	Point. PB89-228027 PVT Relationships in a Carbon	901,547	CASTINGS Casting Metals: Reactor Response.	
CALORIMETERS		Ethane. PB89-229181	900,478	PB89-157143 Mesh Monitor Casting of Ni-Cr Alloys	900,054
Cone Calorimeter Method for De ity of Composite Materials. PB89-149165	termining the Flammabil-	Pressure Fixed Points Based Vapor Pressure at 273.16 K at	on the Carbon Dioxide	PB89-176077 Metallurgical Evaluation of 17-4 PH	900,040
NBS (National Bureau of Stand Energy Measurements.		H2O(L) Triple-Point. PB89-231138	900,483	ings. PB89-193262	901,105
PB89-171680	901,346	High-Accuracy Gas Analysis v Spectrometry: Carbon Dioxide in	ria Isotope Dilution Mass n Air.	CATABOLITE GENE ACTIVATOR PROT	EINC
Enthalpies of Desorption of Wate PB89-173868	900,838	PB90-123951 CARBON DIOXIDE IONS	900,032	Crystal Structure of a Cyclic AMP (Ac phate)-Independent Mutant of Catab	denosine Monophos-
Field Measurement of Thermal a ties of Insulating Glass Windows. PB89-175905		Vibrational Spectra of Molecul Neon. I. CO(sub 2, sup +) and	CO(sub 2, sup -).	Protein. PB89-201594	901,224
NIST (National Institute of Star Automated Coaxial Microwave Po	ndards and Technology)	PB89-234199 CARBON DISULFIDE	900,487	CATALOGS (PUBLICATIONS) Internal Structure of the Guide to Av	ailable Mathematical
PB89-176192	900,807	Calibration Tables Covering the Region from Heterodyne Frequency	uency Measurements on	Software. PB89-170864	900,927
Optical Power Measurements at Standards and Technology.		the nu(sub 3) Bands of (12)CS2 PB89-157416	and (13)CS2. 900,322	Publications of the National Institute	e of Standards and
PB89-187579 CAPACITORS	900,918	Picosecond Coherent Anti-St	okes Raman Scattering	Technology, 1988 Catalog. PB89-218382	900,006
Fracture Behavior of Ceramics U tors.	sed in Multilayer Capaci-	(CARS) Study of Vibrational De fide and Benzene in Solution.		CATALYSTS Resonant Raman Scattering of C	controlled Molecular
PB89-171805	900,758	PB89-176408 CARBON FIBERS	900,380	Weight Polyacetylene. PB89-157093	900,548
Correlation between CMOS (Con Semiconductor) Transistor and C		Fiber Coating and Characterizat PB89-228571	ion. <i>901,067</i>	Time Resolved Studies of Vibrationa	Relaxation Dynam-
of Interface Trap Spectra. PB89-180020	900,779	CARBON HYDRIDES Far-Infrared Laser Magnetic Re	sonance Spectrum of the	ics of CO(v= 1) on Metal Particle Sur PB89-203012	900,444
Numerical Analysis for the Small MOS (Metal Oxide Semiconducto	ors) Capacitor.	CD Radical and Determination eters.	of Ground State Param-	CATALYTIC HEATERS Combustion Testing Methods for Cata	
PB89-186837 Journal of Research of the Nat	900,781 rional Institute of Stand-	PB90-117359	900,496	PB89-150924 CATHODOLUMINESCENCE	900,846
ards and Technology, Volume 9 1989.	4, Number 3, May-June	CARBON MONOXIDE Adsorption Properties of Pt Film PB89-146864	s on W(110). 900,281	Cathodoluminescence of Defects in Particles Grown by Hot-Filament Che	Diamond Films and mical-Vapor Deposi-
PB89-211106 CAPILLARY WAVES	901,441	Picosecond Study of the Popula	•	tion. PB90-117961	901,069
Capillary Waves of a Vapor-Liquid ical Temperature.	d Interface Near the Crit-	Chemisorbed on SiO2-Supporte PB89-157317		CATIONS	
PB89-228555 CARBAZOLES	900,476	Theoretical Study of the Vibrat Pt(111).	tional Lineshape for CO/	Reactions of Magnesium Prophyrin Water. Disproportionation, Oxygen Proparison with Other Metalloporphyrins.	oduction, and Com-
Microwave Spectrum and (14)Il Constants of Carbazole.	N Quadrupole Coupling	PB89-157689	900,331	PB89-151005	900,301
PB89-157333 CARBINOLS	900,319	High Resolution Inverse Ramar Q Branch. PB89-171292	900,355	Hyperconjugation: Equilibrium Secon on the Stability of the t-Butyl Cation Thermoneutral Hydride Transfer.	dary Isotope Effect n. Kinetics of Near-
Electric-Dipole Moments of CH3OH-Formamide.	H2O-Formamide and	Autoionization Dynamics in the zation Spectrum of CO.	Valence-Shell Photoioni-	PB89-156756 CAVITATION	900,306
PB89-147375 CARBOHYDRATES	900,288	PB89-176960 Executive Summary for the We	900,386	Creep Cavitation in Liquid-Phase Sinte PB89-175954	ered Alumina. 901,038
Thermodynamic and Transport drates and Their Monophospha	Properties of Carbohy- tes: The Pentoses and	Predictive Capability for CO For PB89-200091		CAVITY RESONATORS New Cavity Configuration for Cesium	•
Hexoses. PB89-222574	900,453	Stimulated Desorption from CO PB89-203004	Chemisorbed on Cr(110). 900,443	quency Standards. PB89-171649	900,714
CARBON Initial Spectra of Neutron-Induc	ed Secondary Charged	Time Resolved Studies of Vibra ics of CO(v= 1) on Metal Partic	le Surfaces.	Advances in NIST (National Institute Technology) Dielectric Measurement	
Particles. PB89-171862	901,265	PB89-203012 Thermal Conductivity of Nitroge	900,444 en and Carbon Monoxide	Mode-Filtered Cylindrical Cavity. PB89-231146	900,907
Solid State (13)C NMR Investi Effect of Chain Conformation. PB89-176036	gation in Polyoxetanes.	in the Limit of Zero Density. PB89-222533	900,449	Effect of an Electrically Large Stirre Chamber.	
CARBON 12	300,330	Cr(110) Oxidation Probed by C orption.	arbon Monoxide Chemis-	PB90-117946 CELL MEMBRANE COATED PITS	901,378
Identification of Carbonaceous A erator Mass Spectrometry, and	Aerosols via C-14 Accel- Laser Microprobe Mass	PB89-228423 Heterodyne Frequency Measi	900,239	Differential Scanning Calorimetric Stu PB90-117912	dy of Brain Clathrin. 900,225
Spectrometry. PB90-136540	900,236	Laser Transitions. PB89-229223	901,374	CELLULOSE	
CARBON 13	on the Postitioning of End	Structure of the CO2-CO2-H2O	van der Waals Complex	Experimental Study of the Pyrolysis of tarded Cellulose.	of Pure and Fire Re-
13C NMR Method for Determinin Groups and Side Branches betw Non-Crystalline Regions in Polyet	veen the Crystalline and	Determined by Microwave Spec PB89-230288		PB89-228316 CELLULOSIC MATERIALS	901,090
PB89-202451	900,569	Synchrotron Photoemission Stu on Cr(110).	udy of CO Chemisorption	Effect of Water on Piloted Ignition of PB89-189187	Cellulosic Materials. 900,127
Determination of Serum Choleste the Isotope Dilution Mass S		PB89-231336	900,262	CEMENTS	000,127
Method. PB89-234181	901,239	CO Laser Stabilization Using the		Proceedings of the Workshop on Cer Low-Level Radioactive Waste. Hel	ment Stabilization of d at Gaithersburg,
CARBON 14	Aerosols via C-14 Accel-	PB89-179139 (12)C(16)O Laser Frequency Ta	901,356	Maryland on May 31-June 2, 1989. NUREG/CP-0103	901,302

(12)C(16)O Laser Frequency Tables for the 34.2 to 62.3 THz (1139 to 2079 cm(-1)) Region. PB89-193908 901,361

Heterodyne Frequency and Fourier Transform Spectroscopy Measurements on OCS Near 1700 cm(-1). PB90-117805 900,507

900,507

CARBON OXYSULFIDE

Identification of Carbonaceous Aerosols via C-14 Accelerator Mass Spectrometry, and Laser Microprobe Mass Spectrometry, PB90-136540

CO2 Separation Using Facilitated Transport Ion Exchange Membranes.

CARBON DIOXIDE

Interpretation of the Effects of Retarding Admixtures on Pastes of C3S, C3A plus Gypsum, and Portland Cement. PB89-146971 900,580

Implications of Computer-Based Simulation Models, Expert Systems, Databases, and Networks for Cement Research.

PB89-146989 <i>900,581</i>	Dynamic Poisson's Ratio of a Ceramic Powder during Compaction.	PB90-128521 901,380
Epoxy Impregnation Procedure for Hardened Cement Samples.	PB89-177182 901,039	CHARGE TRANSFER Laser-Induced Fluorescence Study of Product Rotationa
PB89-147821 901,180	Syntheses and Unit Cell Determination of Ba3V4O13 and Low- and High-Temperature Ba3P4O13.	State Distributions in the Charge Transfer Reaction Ar(1+)((sup 2 P)(sub 3/2)) + N2 -> Ar + N2(1+
Standard Specifications for Cements and the Role in Their Development of Quality Assurance Systems for	PB89-179717 901,040)(X) at 0.28 and 0.40 eV.
Laboratories. PB89-150742 <i>901,021</i>	Novel Process for the Preparation of Fiber-Reinforced Ceramic-Matrix Composites.	PB89-189823 900,420 CHARGED PARTICLES
Implications of Phase Equilibria on Hydration in the Tri-	PB89-179733 901,074 Synthesis, Stability, and Crystal Chemistry of Dibanum	Initial Spectra of Neutron-Induced Secondary Charged Particles.
calcium Silicate-Water and the Tricalcium Aluminate- Gypsum-Water Systems.	Pentatitanate.	PB89-171862 901,263
PB89-150759 901,022 Epoxy Impregnation of Hardened Cement Pastes for	PB89-179741 901,041 Computer Graphics for Ceramic Phase Diagrams.	CHARGING
Characterization of Microstructure. PB89-185573 901,042	PB89-186290 901,043	Charging Behavior of Polyethylene and Ionomers. PB90-136813 900,570
CENTER FOR BASIC STANDARDS	Phase Diagrams for High Tech Ceramics. PB89-186308 901,044	CHEBYSHEV APPROXIMATION Elimination of Spurious Eigenvalues in the Chebyshev
Technical Activities 1987, Center for Basic Standards. PB89-185615 901,521	Advanced Ceramics: A Critical Assessment of Wear and Lubrication.	Tau Spectral Method. PB89-209282 901,330
CENTER FOR BUILDING TECHNOLOGY	PB89-188569 901,045	CHEBYSHEV INEQUALITY
Effects of Research on Building Practice. PB89-202584 900,168	Mechanical Property Enhancement in Ceramic Matrix Composites.	Elimination of Spurious Eigenvalues in the Chebyshev
Research as the Technical Basis for Standards Used in	PB89-189138 901,076	Tau Spectral Method. PB89-209282 901,330
Building Codes. PB89-231062 900,101	Methods for the Production of Particle Standards. PB89-201636 901,047	CHEMICAL ANALYSES
CENTER FOR ELECTRONICS AND ELECTRICAL	Versailles Project on Advanced Materials and Standards	Standard Reference Materials for the Determination o Polycyclic Aromatic Hydrocarbons.
ENGINEERING Center for Electronics and Electrical Engineering Techni-	Evolution to Permanent Status. PB89-201768 900,969	PB89-156889 900,178
cal Publication Announcements Covering Center Programs, October to December 1986, with 1987 CEEE	Commercial Advanced Ceramics. PB89-201776 901,048	CHEMICAL ANALYSIS Speciation Measurements of Butyltins: Application to
Events Calendar. PB90-116195 900,824	Electron Microscopy Studies of Diffusion-Induced Grain	Controlled Release Rate Determination and Production o Reference Standards.
CENTER FOR RADIATION RESEARCH	Boundary Migration in Ceramics. PB89-202097 901.049	PB89-146807 900,17-
Center for Radiation Research (of the National Institute of Standards and Technology) Technical Activities for	Green Function Method for Calculation of Atomistic	Micro-Raman Characterization of Atherosclerotic and Bio prosthetic Calcification.
1989. PB90-130279 <i>901,307</i>	Structure of Grain Boundary Interfaces in Ionic Crystals. PB89-202105 901,050	PB89-149223 901,234
CENTRIFUGAL PUMPS	Crack-Interface Traction: A Fracture-Resistance Mecha-	Environmental Standard Reference Materials - Presen and Future Issues.
Performance of He II of a Centrifugal Pump with a Jet Pump Inducer.	nism in Brittle Polycrystals. PB89-211817 901,051	PB89-150940 900,869 Technical Activities, 1988, Center for Analytical Chemis
PB89-229090 · 901,553	Design (* teria for High Temperature Structural Applications.	try.
CERAMIC FIBERS Fiber Coating and Characterization.	PB89-211833 901,052	PB89-151773 900,173 Neutron Activation Analysis of the NIST (National Insti
PB89-228571 901,067	PC-Access to Ceramic Phase Diagrams. PB89-211841 901,053	tute of Standards and Technology) Bovine Serum Stand ard Reference Material Using Chemical Separations.
CERAMICS Critical Assessment of Requirements for Ceramic Powder	NBS/BAM (National Bureau of Standards/Bundesanstalt	PB89-156921 900,186
Characterization. PB89-146849 901,016	fur Materialprufung) 1986 Symposium on Advanced Ceramics.	Long-Term Stability of the Elemental Composition in Bio logical Materials.
Application of SANS (Small Angle Neutron Scattering) to	PB89-229074 901,055	PBS9-156939 900,183
Ceramic Characterization. PB89-146856 901,017	Grain-Size and R-Curve Effects in the Abrasive Wear of Alumina.	High Accuracy Determination of (235)U in Nondestructive Assay Standards by Gamma Spectrometry.
Institute for Materials Science and Engineering, Ceram-	PB90-117383 901,058 Equilibrium Crystal Shapes and Surface Phase Diagrams	PB89-156954 900,245
ics: Technical Activities 1988. PB89-148381 901,019	at Surfaces in Ceramics.	Preparation of Accurate Multicomponent Gas Standards of Volatile Toxic Organic Compounds in the Low-Parts
Institute for Materials Science and Engineering, Fracture	PB90-117755 901,162 Bulk Modulus and Young's Modulus of the Superconduc-	per-Billion Range. PB89-157739 900,18:
and Deformation: Technical Activities 1988. PB89-148399 901,071	tor Ba2Cu3YO7. PB90-123613 901,469	Voltammetric and Liquid Chromatographic Identification
Institute for Materials Science and Engineering, Nonde-	Flaw Tolerance in Ceramics with Rising Crack Resistance	of Organic Products of Microwave-Assisted Wet Ashing of Biological Samples.
structive Evaluation: Technical Activities 1988. PB89-151625 900,917	Characteristics. PB90-128026 901,060	PB89-157994 900,188 Analytical Applications of Resonance Ionization Mass
Structural Reliability and Damage Tolerance of Ceramic Composites for High-Temperature Applications. Semi-	CESIUM	Spectrometry (RIMS).
Annual Progress Report for the Period Ending September	Spectrum and Energy Levels of Singly Ionized Cesium. 2. Interpretation of Fine and Hyperfine Structures.	PB89-161590 900,189 Chemical Calibration Standards for Molecular Absorption
30, 1987. PB89-156350 <i>901,023</i>	PB89-172373 900,361	Spectrometry. PB89-171938 900,19
Structural Reliability and Damage Tolerance of Ceramic Composites for High-Temperature Applications. Semi-	Accurate Energies of nS, nP, nD, nF and nG Levels of Neutral Cesium.	Numeric Databases for Chemical Analysis.
Annual Progress Report for the Period Ending March 31, 1988.	PB89-202121 900,431 Structure of Cs on GaAs(110) as Determined by Scan-	PB89-175236 900,194
PB89-156368 901,024	ning Tunneling Microscopy. PB90-117490 901,463	Specimen Banking in the National Status and Trends Program: Development of Protocols and First Year Re
Effect of Coal Slag on the Microstructure and Creep Behavior of a Magnesium-Chromite Refractory.	CESIUM 137	sults. PB89-175855 901,308
PB89-158034 901,027	NBS (National Bureau of Standards) Measurement Services: Calibration of Gamma-Ray-Emitting Brachytherapy	Analysis of Ultrapure Reagents from a Large Sub-Boiling
Toughening Mechanisms in Ceramic Composites: Semi- Annual Progress Report for the Period Ending September	Sources.	Still Made of Teflon PFA. PB89-186357 900,20.
30, 1988. PB89-162606 <i>901,028</i>	PB89-193858 901,243 CESIUM FREQUENCY STANDARDS	Quality Assurance in Metals Analysis Using the Inductive
Rising Fracture Toughness from the Bending Strength of	New Cavity Configuration for Cesium Beam Primary Frequency Standards.	ly Coupled Plasma. PB89-202063 900,213
Indented Alumina Beams. PB89-171771 901,031	PB89-171649 900,714	Expert-Database System for Sample Preparation by Microwave Dissolution. 1. Selection of Analytical Descrip
Phase Relations between the Polytitanates of Barium and	CHAINS Polymer Localization by Random Fixed Impunties: Gaus-	tors.
the Barium Borates, Vanadates and Molybdates. PB89-171789 901,032	sian Chains. PB89-176044 900,559	PB89-229108 900,210 Isotope Dilution Mass Spectrometry for Accurate Elemen
Fracture Behavior of Ceramics Used in Multilayer Capaci-	CHANGE-EXCHANGE REACTIONS	tal Analysis. PB89-230338 900,220
tors. PB89-171805 <i>900,758</i>	Quantum Mechanical Calculations on the Ar(1+) + N2 Charge Transfer Reaction.	Production and Spectroscopy of Molecular Ions Isolated
Effect of Lateral Crack Growth on the Strength of Contact Flaws in Brittle Materials.	PB89-228092 900,470	in Solid Neon. PB90-117748 900,503
PB89-171813 901,034	CHAOS Classical Chaos, the Geometry of Phase Space, and	Differential Scanning Calorimetric Study of Brain Clathrin.
Densification, Susceptibility and Microstructure of Ba2YCu3O($6+x$).	Semiclassical Quantization. PB89-172381 901,506	PB90-117912 900,223
PB89-171821 901,035	CHARACTERISTIC IMPEDANCE	Calcium Hydroxyapatite Precipitated from an Aqueous Solution: An International Multimethod Analysis.
Structural Ceramics Database: Technical Foundations. PB89-175244 901,036	Some Questions and Answers Concerning Air Lines as Impedance Standards.	PB90-123399 900,220 Determination of Selenium and Tellurium in Coppe
Pore Morphology Analysis Using Small Angle Neutron Scattering Techniques.	PB89-176176 900,747	Standard Reference Materials Using Stable Isotope Dilu
PB89-175939 <i>901,037</i>	CHARGE DENSITY DC Electric Field Effects during Measurements of Mono-	tion Spark Source Mass Spectrometry. PB90-123472 900,230
Creep Cavitation in Liquid-Phase Sintered Alumina. PB89-175954 901.038	polar Charge Density and Net Space Charge Density Near HVDC Power Lines.	Mobile Sources of Atmospheric Polycyclic Aromatic Hy drocarbons: A Roadway Tunnel Study.

PB90-123571 900,859	PB89-147029 900,547	PB89-234173 901,262
Experiences in Environmental Specimen Banking. PB90-123969 900.866	Modeling Chemical Reaction Systems on an IBM PC. PB89-171920 900,358	Determination of Serum Cholesterol by a Modification of the Isotope Dilution Mass Spectrometric Definitive
PB90-123969 900,866 Comparison of Liquid Chromatographic Selectivity for Po-	Facile Synthesis of 1-Nitropyrene-d9 of High Isotopic	Method.
lycyclic Aromatic Hydrocarbons on Cyclodextrin and C18	Purity.	PB89-234181 901,239
Bonded Phases. PB90-128539 900,231	PB90-123753 900,240 CHEMICAL REACTIVITY	CHROMATOGRAPHIC ANALYSIS Characterization of Organolead Polymers in Trace
Synthesis and Characterization of Novel Bonded Phases	Influence of Reaction Reversibility on Continuous-Flow	Amounts by Element-Specific Size-Exclusion Chromatog-
for Reversed-Phase Liquid Chromatography. PB90-128695 900,233	Extraction by Emulsion Liquid Membranes. PB89-176481 900,244	raphy. PB89-175962 900,196
Identification of Carbonaceous Aerosols via C-14 Accel-	CHEMICAL STABILIZATION	Determination of Hydrocarbon/Water Partition Coeffi-
erator Mass Spectrometry, and Laser Microprobe Mass Spectrometry.	Relative Acidities of Water and Methanol and the Stabili-	cients from Chromatographic Data and Based on Solu- tion Thermodynamics and Theory.
PB90-136540 900,236	ties of the Dimer Anions. PB89-150981 900,299	PB89-187538 900,205
CHEMICAL BONDS Thermal Degradation of Poly (methyl methacrylate) at	Production and Spectroscopy of Molecular lons Isolated	Introduction to Supercritical Fluid Chromatography. Part 2. Applications and Future Trends.
50C to 125C.	in Solid Neon. PB90-117748 900,503	PB89-230312 900,219
PB89-157465 900,549 Ionic Hydrogen Bond and Ion Solvation. 5. OH(1-)O	CHEMICAL VAPOR DEPOSITION	Comparison of Liquid Chromatographic Selectivity for Polycyclic Aromatic Hydrocarbons on Cyclodextrin and C18
Bonds. Gas Phase Solvation and Clustering of Alkoxide	Cathodoluminescence of Defects in Diamond Films and Particles Grown by Hot-Filament Chemical-Vapor Deposi-	Bonded Phases.
and Carboxylate Anions. PB89-157531 900,328	tion.	PB90-128539 900,231
Chemisorption of HF (Hydrofluoric Acid) on Silicon Sur-	PB90-117961 901,069 CHEMISORPTION	Synthesis and Characterization of Novel Bonded Phases for Reversed-Phase Liquid Chromatography.
faces. PB89-212013 900,445	Adsorption Properties of Pt Films on W(110).	PB90-128695 900,233
Synchrotron Photoemission Study of CO Chemisorption	PB89-146864 900,281	CHROMATOGRAPHY Trace Speciation by HPLC-GF AA (High-Performance
on Cr(110). PB89-231336 900,262	Picosecond Studies of Vibrational Energy Transfer in Molecules on Surfaces.	Liquid Chromatography-Graphite Furnace Atomic Absorp-
CHEMICAL COMPLEXES	PB89-157309 900,316	tion) for Tin- and Lead-Bearing Organometallic Com- pounds, with Signal Increases Induced by Transition-
Calculation of Vibration-Rotation Spectra for Rare Gas-	Picosecond Study of the Population Lifetime of CO(v= 1) Chemisorbed on SiO2-Supported Rhodium Particles.	Metal lons. PB89-157085 900,184
HCI Complexes. PB89-228415 900,473	PB89-157317 900,317	Preparative Liquid Chromatographic Method for the Char-
CHEMICAL COMPOSITION	Interaction of Water with Solid Surfaces: Fundamental Aspects.	acterization of Minor Constituents of Lubricating Base
Role of Standards in Electron Microprobe Techniques. PB89-176143 900,197	PB89-201081 900,421	Oils. PB89-175921 901,114
Defocus Modeling for Compositional Mapping with Wave-	Electron-Stimulated-Desorption Ion-Angular Distributions. PB89-201230 901,430	Supercritical Fluid Chromatograph for Physicochemical
length-Dispersive X-ray Spectrometry. PB89-176150 900,378	Oxygen Chemisorption on Cr(110): 1. Dissociative Ad-	, Studies. PB89-184105 900,201
Effect of Chemical Composition on the 4 K Mechanical	sorption.	CHROMIUM
Properties of 316LN-Type Alloys. PB90-128554 901,110	PB89-202980 900,441 Oxygen Chemisorption on Cr(110): 2. Evidence for Mo-	Electrodeposition of Chromium from a Trivalent Electro-
CHEMICAL DYNAMICS	lecular O2(ads).	lyte. PATENT-4 804 446 901,119
Structure and Dynamics of Molecular Clusters via High	PB89-202998 900,442 Stimulated Desorption from CO Chemisorbed on Cr(110).	Journal of Physical and Chemical Reference Data,
Resolution IR Absorption Spectroscopy. PB89-185896 900,403	PB89-203004 900,443	Volume 17, 1988, Supplement No. 3. Atomic Transition Probabilities Scandium through Manganese.
CHEMICAL ELEMENTS	Time Resolved Studies of Vibrational Relaxation Dynam-	PB89-145197 900,276
Twenty Five Years of Accuracy Assessment of the Atomic Weights.	ics of CO(v= 1) on Metal Particle Surfaces. PB89-203012 900,444	Radiochemical Procedure for Ultratrace Determination of Chromium in Biological Materials.
PB89-174007 900,365	Chemisorption of HF (Hydrofluoric Acid) on Silicon Sur-	PB89-156913 900,179
CHEMICAL ENGINEERING Center for Chemical Technology: 1988 Technical Activi-	faces. PB89-212013 900,445	Dependence of Interface Widths on Ion Bombardment Conditions in SIMS (Secondary Ion Mass Spectrometry)
ties. PB89-156376 900,241	Cr(110) Oxidation Probed by Carbon Monoxide Chemis-	Analysis of a Ni/Cr Multilayer Structure.
CHEMICAL EQUILIBRIUM	orption. PB89-228423 900,239	PB89-172506 900,364 Mesh Monitor Casting of Ni-Cr Alloys: Element Effects.
Influence of Reaction Reversibility on Continuous-Flow	Synchrotron Photoemission Study of CO Chemisorption	PB89-176077 900,040
Extraction by Emulsion Liquid Membranes. PB89-176481 900,244	on Cr(110). PB89-231336 900,262	Oxygen Chemisorption on Cr(110): 1. Dissociative Ad-
Calorimetric and Equilibrium Investigation of the Hydroly-	CHEMISTRY	sorption. PB89-202980 900,441
sis of Lactose. PB89-227888 901,226	Chemical and Spectral Databases: A Look into the Future.	Oxygen Chemisorption on Cr(110): 2. Evidence for Mo-
CHEMICAL PROPERTIES	PB89-180038 900,579	lecular O2(ads). PB89-202998 900,442
Journal of Physical and Chemical Reference Data, Volume 17, Number 4, 1988.	CHESAPEAKE BAY Biodegradation of Tributyltin by Chesapeake Bay Microor-	Stimulated Desorption from CO Chemisorbed on Cr(110).
PB89-145114 900,268	ganisms.	PB89-203004 900,443
Journal of Physical and Chemical Reference Data, Volume 17, Number 1, 1988.	PB89-177232 901,309 CHINA	Marked Differences in the 3p Photoabsorption between the Cr and Mn(1+) Isoelectronic Pair: Reasons for the
PB89-186449 900,408	Effect of Chinese Standardization on U.S. Export Oppor-	Unique Structure Observed in Cr. PB90-117581 901,562
Journal of Physical and Chemical Reference Data, Volume 18, Number 3, 1989.	tunities. PB89-166128 900,172	CHROMIUM NICKEL ALLOYS
PB90-126236 900,527	CHIPS (ELECTRONICS)	Linear-Elastic Fracture of High-Nitrogen Austenitic Stain- less Steels at Liquid Helium Temperature.
CHEMICAL RADICALS Rate Constants for Reactions of Nitrogen Oxide (NO3)	Machine-Learning Classification Approach for IC Manufacturing Control Based on Test Structure Measurements.	PB90-117623 901,108
Radicals in Aqueous Solutions. PB89-176242 900,379	PB89-228530 900,790	CHROMIUM OXIDES
Photodissociation Dynamics of C2H2 at 193 nm: Vibra-	CHLORIDES	Cr(110) Oxidation Probed by Carbon Monoxide Chemis- orption.
tional Distributions of the CCH Radical and the Rotational	Development of a Method to Measure In situ Chloride at the Coating/Metal Interface.	PB89-228423 900,239
State Distribution of the A(010) State by Time-Resolved Fourier Transform Infrared Emission.	PB89-235345 901,085	CIGARETTES
PB89-179782 900,258	CHLORINE Time-of-Flight Measurements of Hyperthermal CI(sub 2)	Cigarette as a Heat Source for Smolder Initiation in Up- holstery Materials.
CHEMICAL REACTION MECHANISMS New Photolytic Source of Dioxymethylenes: Criegee In-	Molecules Produced by UV Laser Vaporization of Cryo-	PB89-176762 900,595
termediates Without Ozonolysis. PB89-156731 900,304	genic Chlorine Films. PB89-202634 900,260	Statistical Analysis of Experiments to Measure Ignition of Cigarettes.
Decay of High Valent Manganese Porphyrins in Aqueous	Chlorine-like Spectra of Copper to Molybdenum.	PB89-201149 900,135
Solution and Catalyzed Formation of Oxygen.	PB90-117706 900,501	CIRCUIT ANALYSIS Ambiguity Groups and Testability.
PB89-156772 900,308 Stopped-Flow Studies of the Mechanisms of Ozone-	CHLORINE IONS Neonlike Ar and Cl 3p-3s Emission from a theta-pinch	PB90-128703 900,722
Alkene Reactions in the Gas Phase: Tetramethylethy-	Plasma. PB90-123746 901,570	CIRCUIT INTERCONNECTIONS
lene. PB89-157515 900,326	CHOLESTEROL 901,570	Use of Artificial Intelligence and Microelectronic Test Structures for Evaluation and Yield Enhancement of
Mechanism and Rate of Hydrogen Atom Attack on Tolu-	Developing Definitive Methods for Human Serum Ana-	Microelectronic Interconnect Systems. PB89-146955 900,768
ene at High Temperatures. PB89-179758 900,398	lytes. PB89-146773 901,233	CIRCUIT PROTECTION
Mechanisms of Free Radical Chemistry and Biochemistry	NBS (National Bureau of Standards) Activities in Biologi-	Lightning and Surge Protection of Photovoltaic Installa-
of Benzene. PB90-117714 900,502	cal Reference Materials. PB89-157770 901,219	tions. Two Case Histories: Vulcano and Kythnos. PB89-229058 900,851
CHEMICAL REACTIONS	Determination of Total Cholesterol in Coconut Oil: A New	CIVIL ENGINEERING
Hydroxyl Radical Induced Cross-Linking between Pheny- lalanine and 2-Deoxynbose.	NIST (National Institute of Standards and Technology) Cholesterol Standard Reference Material.	Design Quality through the Use of Computers. PB89-174114 900,063

CLASSIFICATION Internal Structure of the Guide to Available Mathematical	PB90-128604 901,176	PB89-176614 900,067
Software. PB89-170864 900,927	Progressive Collapse: U.S. Office Building in Moscow.	Investigation of a Washington, DC Office Building. 900,081
CLATHRIN	PBĕ9-175715 900,158 COLLISION CROSS SECTIONS	COMMUNICATING Use of Artificial Intelligence Programming Techniques for
Differential Scanning Calorimetric Study of Brain Clathrin. PB90-117912 900,225	Nonadiabatic Theory of Fine-Structure Branching Cross- Sections for Sodium-Helium, Sodium-Neon, and Sodium-	Communication between Incompatible Building Informa- tion Systems.
Thermal Degradation of Poly (methyl methacrylate) at	Argon Optical Collisions. PB89-202162 900,433	PB89-191985 900,108 COMMUNICATION CABLES
50C to 125C. PB89-157465 <i>900,549</i>	COLLOIDAL DISPERSIONS Hydrodynamics of Magnetic and Dielectric Colloidal Dis-	Mode-Stirred Chamber for Measuring Shielding Effective
Fracture Behavior of a Pressure Vessel Steel in the Duc- tile-to-Brittle Transition Region.	persions. PB89-157242 900,314	ness of Cables and Connectors: An Assessment of MIL- STD-1344A Method 3008. PB89-149264 900.733
PB89-189195 901,103 CLINICAL ANALYSIS	COLLOIDS	PB89-149264 900,737 COMMUNICATION NETWORKS
Stabilization of Ascorbic Acid in Human Plasma, and Its	Liquid, Crystalline and Glassy States of Binary Charged Colloidal Suspensions.	Standardizing EMCS Communication Protocols. PB89-172357 900,613
Liquid-Chromatographic Measurement. PB69-179279 901,237	PB89-202501 901,436 COLOR CENTER LASERS	Application of the ISO (International Standards Organiza-
CLINKER Model for Particle Size and Phase Distributions in Ground	Simple F-Center Laser Spectrometer for Continuous Single Frequency Scans.	tion) Distributed Single Layer Testing Method to the Con- nectionless Network Protocol.
Cement Clinker. PB90-136847 901,062	PB89-179774 901,358	PB89-177133 900,616 Application of Formal Description Techniques to Con-
CMOS High-Mobility CMOS (Complementary Metal Oxide Semi-	Heuristic Analysis of von Kries Color Constancy.	formance Evaluation. PB89-211908 900,652
conductor) Transistors Fabricated on Very Thin SOS Films.	PB89-201099 901,362 COLUMN PACKINGS	Object-Oriented Model for Estelle. PB89-211916 900,653
PB89-230460 900,791	Preparation of Glass Columns for Visual Demonstration of Reversed Phase Liquid Chromatography.	Working Implementation Agreements for Open Systems
Enthalpies of Desorption of Water from Coal Surfaces.	PB89-187546 900,206 COLUMNS (SUPPORTS)	Interconnection Protocols. PB89-221196 900,624
PB89-173868 900,838 Specific Heat Measurements of Two Premium Coals.	Inelastic Behavior of Full-Scale Bridge Columns Subject-	COMPACTING Pore Morphology Analysis Using Small Angle Neutron
PB89-173900 <i>900,839</i> COAL GASIFICATION	ed to Cyclic Loading. PB89-174924 900,584	Scattering Techniques. PB89-175939 901,033
Effect of Slag Penetration on the Mechanical Properties of Refractories: Final Report.	COMBUSTION Aerodynamics of Agglomerated Soot Particles.	COMPANDOR TRANSMISSION
PB90-110065 900,836	PB89-147482 900,586	ACSB (Amplitude Companded Sideband): What Is Adequate Performance.
COASTAL CABLES Techniques for Measuring the Electromagnetic Shielding	Development of Combustion from Quasi-Stable Tempera- tures for the Iron Based Alloy UNS S66286. PB89-173850 900,592	PB89-176283 901,598 COMPARATOR CIRCUITS
Effectiveness of Materials. Part 1. Far-Field Source Simulation.	Solution for Diffusion-Controlled Reaction in a Vortex	Audio-Frequency Current Comparator Power Bridge: Development and Design Considerations.
PB89-161525 900,680 COATINGS	Field. PB89-176622 900,594	PB89-201537 900,71
Electrodeposition of Chromium from a Trivalent Electrolyte.	Ignition Characteristics of the Iron-Based Alloy UNS \$66286 in Pressurized Oxygen.	COMPILERS User Guide for the NBS (National Bureau of Standards
PATENT-4 804 446 901,119	PB89-189336 901,104	Prototype Compiler for Estelle (Revised). PB89-196158 900,618
Thin Film Thermocouples for Internal Combustion Engines. PB89-147094 900,607	Evaluated Kinetics Data Base for Combustion Chemistry. PB89-212096 900,601	COMPLEMENTARY METAL OXIDE SEMICONDUCTORS
Novel Process for the Preparation of Fiber-Reinforced	Ignition Characteristics of the Nickel-Based Alloy UNS N07718 in Pressurized Oxygen.	High-Mobility CMOS (Complementary Metal Oxide Semi conductor) Transistors Fabricated on Very Thin SOS
Ceramic-Matrix Composites. PB89-179733 901,074	PB89-218333 901,154 Summaries of Center for Fire Research In-House	Films. PB89-230460 <i>900,79</i> :
Fiber Coating and Characterization. PB89-228571 901,067	Projects and Grants: 1989. PB90-127101 900,605	COMPLEX COMPOUNDS Infrared and Microwave Spectra of OCO-HF and SCO
Development of a Method to Measure In situ Chloride at the Coating/Metal Interface.	COMBUSTION EFFICIENCY	HF. PB89-179121 900,38
PB89-235345 901,085	Combustion Efficiency, Radiation, CO and Soot Yield from a Variety of Gaseous, Liquid, and Solid Fueled	Structure and Dynamics of Molecular Clusters via High Resolution IR Absorption Spectroscopy.
COAXIAL CABLES Simple Technique for Investigating Defects in Coaxial	Buoyant Diffusion Flames. PB89-231179 900,604	PB89-185896 900,403
Connectors. PB89-146930 <i>900,723</i>	COMBUSTION PRODUCTS Combustion of Oil on Water.	Calculation of Vibration-Rotation Spectra for Rare Gas HCI Complexes.
Scattering Parameters Representing Imperfections in Pre- cision Coaxial Air Lines.	PB89-149173 900,587 Chemical Structure of Methane/Air Diffusion Flames:	PB89-228415 900,473 COMPLEXES
PB89-184121 900,750 COBALT 60	Concentrations and Production Rates of Intermediate Hydrocarbons.	Vibrational Predissociation in the H-F Stretching Mode o HF-DF.
NBS (National Bureau of Standards) Measurement Services: Calibration of Gamma-Ray-Emitting Brachytherapy	PB89-171904 900,590	PB89-234207 900,488
Sources. PB89-193858 901,243	Methyl Radical Concentrations and Production Rates in a Laminar Methane/Air Diffusion Flame.	Microwave and Infrared Electric-Resonance Optotherma Spectroscopy of HF-HCl and HCl-HF. PB89-234215 900,48
COBALT HYDRIDES	PB89-171912 900,591 Remote Sensing Technique for Combustion Gas Temper-	Rotational Energy Levels and Line Intensities for (2S+
Detection of the Free Radicals FeH, CoH, and NiH by Far Infrared Laser Magnetic Resonance. PB90-117342 900.495	ature Measurement in Black Liquor Recovery Boilers. PB89-179568 900,392	1)Lambda-(2S+ 1) Lambda and (2S+ 1)(Lambda + o -)-(2S+ 1)Lambda Transitions in a Diatomic Molecule
COCONUT OIL	Combustion of Oil on Water. November 1987. PB89-185581 900,863	van der Waals Bonded to a Closed Shell Partner. PB90-117441 900,498
Determination of Total Cholesterol in Coconut Oil: A New NIST (National Institute of Standards and Technology)	FT-IR (Fourier Transform-Infrared) Emission/Transmis-	Apparent Spectroscopic Rigidity of Floppy Molecular Systems.
Cholesterol Standard Reference Material. PB89-234173 901,262	sion Spectroscopy for In situ Combustion Diagnostics. PB89-211866 900,600	PB90-123860 900,526
COHERENCE Narrow-Angle Laser Scanning Microscope System for	Combustion Efficiency, Radiation, CO and Soot Yield from a Variety of Gaseous, Liquid, and Solid Fueled	Microwave Electric-Resonance Optothermal Spectrosco py of (H2O)2. PB90-128141 900,53
Linewidth Measurement on Wafers. PB89-189344 900,782	Buoyant Diffusion Flames. PB89-231179 900,604	COMPOSITE BONDING
COHERENT RADIATION	Residential Wood Combustion: A Source of Atmospheric Polycyclic Aromatic Hydrocarbons.	Adsorption of 4-Methacryloxyethyl Trimellitate Anhydride (4-META) on Hydroxyapatite and Its Role in Composite
Coherent Tunable Far Infrared Radiation. PB90-117458 900,684	PB90-128166 900,860	Bonding. PB89-179220 900,04
COHERENT SCATTERING Picosecond Coherent Anti-Stokes Raman Scattering	COMBUSTION TESTS Combustion Testing Methods for Catalytic Heaters.	COMPOSITE MATERIALS Prodiction of Teneilo Rehavior of Strain Softened Com
(CARS) Study of Vibrational Dephasing of Carbon Disul- fide and Benzene in Solution.	PB89-150924 900,846 COMFORT	Prediction of Tensile Behavior of Strain Softened Composites by Flexural Test Methods. PB89-147045 900,58:
PB89-176408 900,380 COLD DRAWING	Post-Occupancy Evaluation of Several U.S. Government Buildings.	Performance of Alumina/Epoxy Thermal Isolation Straps.
Necking Phenomena and Cold Drawing. PB89-201495 900,975	PB90-112384 900,088 COMMAND AND CONTROL SYSTEMS	PB89-147078 901,070 Institute for Materials Science and Engineering, Fracture
COLD NEUTRONS	Small Computer System Interface (SCSi) Command	and Deformation: Technical Activities 1988. PB89-148399 901,07
Activation Analysis Opportunities Using Cold Neutron Beams. PRep. 15970	System: Software Support for Control of Small Computer System Interface Devices. PB89-151815 900,659	Cone Calorimeter Method for Determining the Flammabil
PB89-156970 900,183 COLD ROLLING	COMMERCIAL BUILDINGS	ity of Composite Materials. PB89-149165 901,072
Effects of Grain Size and Cold Rolling on Cryogenic Properties of Copper.	Ventilation Effectiveness Measurements in an Office Building.	Dynamic Microindentation Apparatus for Materials Characterization.

			COMPUTER SCIENCE & TECHNOLOGY
PB89-176911 901	1,140	Design Protocol, Part Design Editor, and Geometry Li-	PB90-111212 900,667
Composites Databases for the 1990's.	1,075	facturing Research Facility at the National Bureau of	COMPUTER CONTROL
Mechanical Property Enhancement in Ceramic M		Standards. PB89-151799 <i>900,936</i>	System for Measuring Optical Waveguide Intensity Pro- files. PB89-188593 900,751
Composites. PB89-189138 901	1,076	Parser That Converts a Boundary Representation into a Features Representation.	COMPUTER GRAPHICS
Creep Rupture of a Metal-Ceramic Particulate Compo PB89-211825 901	osite. 1,077	PB89-160634 900,944	Standards for the Interchange of Large Format Tiled Raster Documents.
Low-Temperature Thermal Conductivity of Compos Alumina Fiber/Epoxy and Alumina Fiber/PEEK.	sites: 1,078	Artificial Intelligence Techniques in Real-Time Production Scheduling. PB89-172571 900,945	PB89-148415 900,668 Generic Architecture for Computer Integrated Manufacturing Software Based on the Product Data Exchange
Assessing the Flammability of Composite Materials.	1,081	On-Line Concurrent Simulation in Production Scheduling. PB89-172605 900,948	Specification. PB90-112459 900,965
In vitro Investigation of the Effects of Glass Inserts the Effective Composite Resin Polymerization Shrinka PB90-117516 900	s on age. 2,049	CAD (Computer Aided Design)-Directed Inspection. PB89-177018 900,980	Graphics Application Programmer's Interface Standards and CALS (Computer-Aided Acquisition and Logistic Sup- port).
Adhesive Bonding of Composites.	0,050		PB90-133091 900,658 COMPUTER INFORMATION SECURITY
Measuring In-Plane Elastic Moduli of Composites		AMRF (Automated Manufacturing Research Facility) Material Handling System Architecture. PB89-177091 900,952	Report of the Invitational Workshop on Integrity Policy in Computer Information Systems (WIPCIS).
Arrays of Phase-Insensitive Ultrasound Receivers. PB90-136672 900	0,970	Automated Processing of Advanced Materials. The Path	PB89-168009 900,670
COMPOSITES Comparison of Microleakage of Experimental and Se	elect-	to Maintaining U.S. Industrial Competitiveness in Materials.	National Bureau of Standards Message Authentication Code (MAC) Validation System.
ed Commercially Available Bonding Systems.	1,079	PB89-201727 900,957 Data Management Strategies for Computer Integrated	PB89-231021 900,671 COMPUTER INTEGRATED MANUFACTURING
COMPOSITION Electronic Publishing: Guide to Selection.	,	Manufacturing Systems. PB89-209258 900,959	Functional Approach to Designing Architectures for Computer Integrated Manufacturing.
PB89-214753 900	0,935	Use of GMAP (Geometric Modeling Applications Interface Program) Software as a PDES (Product Data Exchange	PB89-172589 900,946 Hierarchies for Computer-Integrated Manufacturing: A
COMPRESSIBILITY Molybdenum Effect on Volume in Fe-Cr-Ni Alloys.		Specification) Environment in the National PDES Testbed Project.	Functional Description. PB89-172613 900,949
PB89-157796 901	,095	PB89-215198 900,960	Generic Architecture for Computer Integrated Manufac-
COMPRESSIBLE FLOW Shear Dilatancy and Finite Compressibility in a De Non-Newtonian Liquid.	ense	Recommended Technical Specifications for Procurement of Equipment for a Turning Workstation. PB89-215347 900,962	turing Software Based on the Product Data Exchange Specification. PB90-112459 900,965
	,328	AutoMan: Decision Support Software for Automated Manufacturing Investments. User's Manual.	COMPUTER NETWORKS
PVT of Toluene at Temperatures to 673 K.	0,310	PB89-221873 900,963	Implications of Computer-Based Simulation Models, Expert Systems, Databases, and Networks for Cement
Concentration Dependence of the Compression Mod		Generic Architecture for Computer Integrated Manufacturing Software Based on the Product Data Exchange	Research. PB89-146989 900,581
of Isotactic Polystyrene/Cis-Decalin Gels.	0,552	Specification. PB90-112459 <i>900,965</i>	Transport Layer Performance Tools and Measurement. PB89-171326 900,611
COMPRESSION		Modular Process Planning System Architecture. PB90-128596 900,966	Prediction of Transport Protocol Performance through
Effects of Solvent Type on the Concentration Depence of the Compression Modulus of Thermorevers Isotactic Polystyrene Gels.	ena- sible	AMRF Part Model Extensions.	Simulation. PB89-171334 <i>900,612</i>
PB89-172456 900,),553	PB90-129446 900,967	Simplified Discrete Event Simulation Model for an IEEE (Institute of Electrical and Electronics Engineers) 802.3
COMPRESSION TESTS Toughening Mechanisms in Ceramic Composites: S Annual Progress Report for the Period Ending Septen		Emerging Technologies in Manufacturing Engineering. PB90-132747 901,013	Local Area Network. PB89-186829 900,617
30, 1988. PB89-162606 <i>901</i> ,	,028	MPUTER APPLICATIONS DCTDOS: Neutron and Gamma Penetration in Composite Duct Systems.	Stable Implementation Agreements for Open Systems Interconnection Protocols. Version 2, Edition 1. December 1988.
COMPUTATION Initial Spectra of Neutron-Induced Secondary Chai	rged	PB89-188809 901,275	PB89-193312 900,618 Working Implementation Agreements for Open Systems
Particles. PB89-171862 901,	,265	Logistic Function Data Analysis Program: LOGIT. PB89-189351 900,418	Interconnection Protocols. PB89-221196 900,624
Elevated Temperature Deformation of Structural Steel PB89-172621	l. .098	Expert-Database System for Sample Preparation by Microwave Dissolution. 1. Selection of Analytical Descrip-	Trial of Open Systems Interconnection (OSI) Protocols
Electron Mean Free Path Calculations Using a Mode electric Function.	el Di-	tors. PB89-229108 <i>900,216</i>	Over Integrated Services Digital Network (ISDN). PB89-235576 900,625
PB89-177026 901,	,141	Guide to Available Mathematical Software Advisory System.	Working Implementation Agreements for Open Systems Interconnection Protocols.
COMPUTER-AIDED ACQUISITION AND LOGISTIC SUPPORT	CO	PB90-123654 901,201 MPUTER ARCHITECTURE	PB89-235931 900,642 COMPUTER PERFORMACE EVALUATION
Use of the IRDS (Information Resource Diction System) Standard in CALS (Computer-Aided Acquire and Logistic Support).		Hybrid Structures for Simple Computer Performance Esti- mates.	Hardware Instrumentation Approach for Performance Measurement of a Shared-Memory Multiprocessor.
	0,931	PB89-189161 900,639 Architecturally-Focused Benchmarks with a Communica-	PB89-186852 900,638 COMPUTER PERFORMANCE EVALUATION
Real-Time Control System Software: Some Problems an Approach.	s and	tion Example. PB89-216477 900.640	Analysis of Computer Performance Data. PB89-162614 900,635
PB89-177083 900	0,951	Modular Process Planning System Architecture.	Performance Measurement of a Shared-Memory Multi- processor Using Hardware Instrumentation.
Computer-Controlled Test System for Operating Diff- Wear Test Machines.	CO	MPUTER CALCULATIONS	PB89-173793 900,636
PB89-228290 908 COMPUTER AIDED DESIGN	0,983	Semiconductor Measurement Technology: A Software Program for Aiding the Analysis of Ellipsometric Measure-	Design Factors for Parallel Processing Benchmarks. PB89-186845 900,637
Design Protocol, Part Design Editor, and Geometr brary of the Vertical Workstation of the Automated N	∕tanu-	ments, Simple Models. PB89-235923 901,369	Hybrid Structures for Simple Computer Performance Esti- mates.
facturing Research Facility at the National Burea Standards.	au of CO	MPUTER COMMUNICATIONS Automatic Generation of Test Scenario (Skeletons) from	PB89-189161 900,639
PB89-151799 900 Guidelines for the Specification and Validation of	0,936 IGES	Protocol-Specifications Written in Estelle. PB89-177125 900,615	Design Factors for Parallel Processing Benchmarks. PB90-117672 900,644
(Initial Graphics Exchange Specification) Application tocols.	Pro-	User Guide for Wise: A Simulation Environment for Estelle.	COMPUTER PROGRAM RELIABILITY Software Configuration Management: An Overview, DR90,100923
PB89-166102 906 Design Quality through the Use of Computers.	0,937	PB89-196166 900,620	PB89-193833 900,651 COMPUTER PROGRAMMING
	0,063	User Guide for Wizard: A Syntax-Directed Editor and Translator for Estelle. PB89-196174 900,621	Use of Artificial Intelligence Programming Techniques for Communication between Incompatible Building Informa-
PB89-177018 906	0,980	Free Value Tool for ASN.1.	tion Systems. PB89-191985 900,106
Product Data Exchange: The PDES Project-Status Objectives.		PB89-196182 900,622 Object-Oriented Model for Estelle and Its Smalltalk Imple-	COMPUTER PROGRAMS Technical Reference Guide for FAST (Fire and Smoke
PB90-112426 900 External Representation of Product Definition Data.	0,938	mentation. PB89-196190 900,623	Transport Version 18. PB89-218366 900,602
PB90-112434 900	0,939	Trial of Open Systems Interconnection (OSI) Protocols	COMPUTER SCIENCE & TECHNOLOGY

Trial of Open Systems Interconnection (OSI) Protocols Over Integrated Services Digital Network (ISDN). PB89-235576 900,625

Government Open Systems Interconnection Profile Users' Guide.

COMPUTER AIDED MANUFACTURING
Automated Documentation System for a Large Scale
Manufacturing Engineering Research Project.
PB89-150809 900,941

COMPUTER SCIENCE & TECHNOLOGY
Coding and Modulation Requirements for 4,800 Bit/
Second Moderns, Category: Telecommunications Standard.
FIPS PUB 134-1 900,660

		· ·
General Aspects of Group 4 Facsimile Apparatus, Category: Telecommunications Standard.	PB89-177125 900,615	PB90-111691 900,65
FIPS PUB 149 900,661 Facsimile Coding Schemes and Coding Control Functions	Application of the ISO (International Standards Organiza- tion) Distributed Single Layer Testing Method to the Con- nectionless Network Protocol.	Product Data Exchange: The PDES Project-Status an Objectives. PB90-112426 900.93
for Group 4 Facsimile Apparatus, Category: Telecommunications Standard.	PB89-177133 900,616	External Representation of Product Definition Data.
FIPS PUB 150 900,662	Definitions of Granularity. PB89-180012 900,650	PB90-112434 900,93 Use of the IRDS (Information Resource Dictionar
Standard Generalized Markup Language (SGML). FIPS PUB 152 900,627	Composites Databases for the 1990's. PB89-180376 901,075	System) Standard in CALS (Computer-Aided Acquisitio and Logistic Support).
High Speed 25-Position Interface for Data Terminal Equipment and Data Circuit-Terminating Equipment, Cat-	Simplified Discrete Event Simulation Model for an IEEE (Institute of Electrical and Electronics Engineers) 802.3	PB90-112467 900,93
egory: Telecommunications Standard. FIPS PUB 154 900,663	Local Area Network. PB89-186829 900,617	Design Factors for Parallel Processing Benchmarks. PB90-117672 900,64
Data Communication Systems and Services User-Oriented Performance Measurement Methods, Category: Tele-	Design Factors for Parallel Processing Benchmarks.	Creating CSUBs Written in FORTRAN That Run in BASIC.
communications Standard. FIPS PUB 155 900,664	Hardware Instrumentation Approach for Performance	PB90-128752 900,65
Notion of Granularity. PB89-147003 900,915	Measurement of a Shared-Memory Multiprocessor. PB89-186852 900,638	Supercomputers Need Super Arithmetic. PB90-130253 900,65
Mathematical Software: PLOD. Plotted Solutions of Dif-	Hybrid Structures for Simple Computer Performance Estimates.	Graphics Application Programmer's Interface Standard and CALS (Computer-Aided Acquisition and Logistic Sup
ferential Equations. PB89-147425 901,194	PB89-189161 900,639 Logistic Function Data Analysis Program: LOGIT.	port). PB90-133091 900,65
Standards for the Interchange of Large Format Tiled Raster Documents.	PB89-189351 900,418	NIST Automated Computer Time Service. PB90-213711 900,67
PB89-148415 900,668 Case History: Development of a Software Engineering	Stable Implementation Agreements for Open Systems Interconnection Protocols. Version 2, Edition 1. Decem-	Computer Security Training Guidelines.
Standard. PB89-149116 900,665	ber 1988. PB89-193312 900,618	PB90-780172 900,67 COMPUTER SECURITY
Automated Documentation System for a Large Scale	Software Configuration Management: An Overview. PB89-193833	Conference Reports: National Computer Security Confer
Manufacturing Engineering Research Project. PB89-150809 900,941	Document Interchange Standards: Description and Status of Major Document and Graphics Standards.	ence (11th). Held in Baltimore, MD. on October 17-20 1988.
Wavefront Matrix Multiplication on a Distributed-Memory Multiprocessor.	PB89-193874 900,928	PB89-235675 900,67
PB89-151807 900,646 Small Computer System Interface (SCSI) Command	User Guide for the NBS (National Bureau of Standards) Prototype Compiler for Estelle (Revised).	Computer Viruses and Related Threats: A Managemer Guide.
System: Software Support for Control of Small Computer System Interface Devices.	PB89-196158 900,619 User Guide for Wise: A Simulation Environment for Es-	PB90-111683 900,65
PB89-151815 900,659 Data Handling in the Vertical Workstation of the Automat-	telle. PB89-196166 900,620	Computer Security Training Guidelines. PB90-780172 900,67
ed Manufacturing Research Facility at the National Bureau of Standards.	User Guide for Wizard: A Syntax-Directed Editor and Translator for Estelle.	
PB89-159636 900,943	PB89-196174 900,621	COMPUTER SOFTWARE
Parser That Converts a Boundary Representation into a Features Representation.	Free Value Tool for ASN.1. PB89-196182 900,622	Mathematical Software: PLOD. Plotted Solutions of Differential Equations.
PB89-160634 900,944 Ongoing Implementation Agreements for Open Systems	Object-Oriented Model for Estelle and Its Smalltalk Implementation.	PB89-147425 901,19 Small Computer System Interface (SCSI) Comman
Interconnection Protocols: Continuing Agreements. PB89-166086 900,610	PB89-196190 900,623 Application of Formal Description Techniques to Con-	System: Software Support for Control of Small Compute System Interface Devices.
Guidelines for the Specification and Validation of IGES (Initial Graphics Exchange Specification) Application Pro-	formance Evaluation. PB89-211908 900,652	PB89-151815 900,65. Internal Structure of the Guide to Available Mathematica
tocols. PB89-166102 900,937	Object-Oriented Model for Estelle. PB89-211916 900,653	Software. PB89-170864 900,92
Report of the Invitational Workshop on Integrity Policy in Computer Information Systems (WIPCIS).	Federal Software Engineering Standards Program.	Real-Time Control System Software: Some Problems and
PB89-168009 900,670 Internal Structure of the Guide to Available Mathematical	Electronic Publishing: Guide to Selection.	an Approach. PB89-177083 900,95
Software. PB89-170864 900,927	PB89-214753 900,935 Use of GMAP (Geometric Modeling Applications Interface	Software for an Automated Machining Workstation. PB89-177109 900,95
Transport Layer Performance Tools and Measurement.	Program) Software as a PDES (Product Data Exchange Specification) Environment in the National PDES Testbed	Guide to Available Mathematical Software Advisor System.
PB89-171326 900,611 Prediction of Transport Protocol Performance through	Project. PB89-215198 <i>900,960</i>	PB90-123654 901,20
Simulation. PB89-171334 900,612	Architecturally-Focused Benchmarks with a Communication Example.	Enhancements to the VWS2 (Vertical Workstation 2 Data Preparation Software.
Computer Program for Calculating Non-LTE (Local Thermodynamic Equilibrium) Model Stellar Atmospheres.	PB89-216477 900,640	PB90-132713 900,966 COMPUTER SOFTWARE CATALOG
PB89-171573 900,018	Working Implementation Agreements for Open Systems Interconnection Protocols.	Internal Structure of the Guide to Available Mathematica Software.
Modeling Chemical Reaction Systems on an IBM PC. PB89-171920 900,358	PB89-221196 900,624 Detailed Description of the Knowledge-Based System for	PB89-170864 900,92. COMPUTER SOFTWARE MANAGEMENT
Standardizing EMCS Communication Protocols. PB89-172357 900,613	Physical Database Design. Volume 1. PB89-228993 900,929	Software Configuration Management: An Overview.
Performance Measurement of a Shared-Memory Multi- processor Using Hardware Instrumentation.	Processing Rate Sensitivities of a Heterogeneous Multi- processor.	PB89-193833 900,65 Software Verification and Validation: Its Role in Compute
PB89-173793 900,636	PB89-229017 900,641 Detailed Description of the Knowledge-Based System for	Assurance and Its Relationship with Software Project Management Standards.
Design Quality through the Use of Computers. PB89-174114 900,063	Physical Database Design. Volume 2. PB89-229033 900,930	PB90-111691 900,65. COMPUTER SYSTEMS PERFORMANCE
Importance of Numeric Databases to Materials Science. PB89-175202 901,187	National Bureau of Standards Message Authentication	Transport Layer Performance Tools and Measurement. PB89-171326 900,61
Applications of the Crystallographic Search and Analysis System CRYSTDAT in Materials Science.	Code (MAC) Validation System. PB89-231021 900,671	COMPUTER SYSTEMS PROGRAMS
PB89-175251 <i>901,402</i> Creating CSUBs in BASIC.	That of Open Systems Interconnection (OSI) Protocols Over Integrated Services Digital Network (ISDN).	ZIP: The ZIP-Code Insulation Program (Version 1.0) Economic Insulation Levels for New and Existing Houses by
PB89-176226 900,647	PB89-235576 900,625 Conference Reports: National Computer Security Confer-	Three-Digit ZIP Code. Users Guide and Reference Manual.
Standard Format for the Exchange of Fingerprint Informa- tion.	ence (11th). Held in Baltimore, MD. on October 17-20, 1988.	PB89-151765 900,050 Semiconductor Measurement Technology: Automatic De
PB89-176705 900,692 PCM/VCR Speech Database Exchange Format.	PB89-235675 900,672 Working Implementation Agreements for Open Systems	termination of the Interstitial Oxygen Content of Silicon Wafers Polished on Both Sides.
PB89-176713 900,633 Incrementor: A Graphical Technique for Manipulating Pa-	Interconnection Protocols. PB89-235931 900,642	PB89-151831 900,77. Comparison of Measured and Calculated Antenna Side
rameters. PB89-177000 900,648	Government Open Systems Interconnection Profile	lobe Coupling Loss in the Near Field Using Approximate Far-Field Data.
CAD (Computer Aided Design)-Directed Inspection.	Users' Guide. PB90-111212 - 900,667	PB89-156855 900,70
PB89-177018 900,980 Object-Oriented Model for ASN.1 (Abstract Syntax Nota-	Computer Viruses and Related Threats: A Management Guide.	Computer Model of a Porous Medium. PB89-179683 901,186
tion One). PB89-177117 900,649	PB90-111683 900,654 Software Verification and Validation: Its Role in Computer	COMPUTER VIRUSES Computer Viruses and Related Threats: A Management
Automatic Generation of Test Scenario (Skeletons) from	Assurance and its Relationship with Software Project Management Standards	Guide. PR90-111683

COMPUTER VISION	N89-16535/1 900,014	PB89-189286 900,955
Building Representations from Fusions of Multiple Views. PB89-177059 900,991	CONFIDENCE LIMITS Problems with Interval Estimation When Data Are Adjust-	Visual Perception Processing in a Hierarchical Control System: Level 1.
COMPUTERIZED CONTROL SYSTEMS NASA/NBS (National Aeronautics and Space Administra-	ed via Calibration. PB89-157812 901,209	PB89-221188 900,994 CONVECTION
tion/National Bureau of Standards) Standard Reference Model for Telerobot Control System Architecture	Estimates of Confidence Intervals for Divider Distorted Waveforms.	Solutal Convection during Directional Solidification. PB89-150932 901,322
(NASREM). PB89-193940 901,589	PB89-173447 900,806 CONSENSUS VALUES	Flow Coefficients for Interzonal Natural Convection for
COMPUTERIZED SIMULATION Computer Model of Smoke Movement by Air Conditioning	Journal of Research of the National Institute of Standards and Technology, Volume 94, Number 3, May-June	Various Apertures. PB89-177158 900,069
Systems (SMACS). PB89-157267 900,059	1989. PB89-211106 901,441	COOLING
Prediction of Transport Protocol Performance through	Consensus Values, Regressions, and Weighting Factors.	Search for Optical Molasses in a Vapor Cell: General Analysis and Experimental Attempt.
Simulation. PB89-171334 900,612	PB89-211130 901,213 CONSTRUCTION	PB90-163932 <i>901,371</i> COOLING EFFECT
On-Line Concurrent Simulation in Production Scheduling. PB89-172605 900,948	Design Quality through the Use of Computers.	Cooling Effect Induced by a Single Evaporating Droplet on a Semi-Infinite Body.
Developments in the Heat Balance Method for Simulating Room Thermal Response.	PB89-174114 900,063 CONSTRUCTION INDUSTRY	PB89-149249 901,488
PB89-173926 900,062	Building Economics in the United States. PB89-172399 900,102	COPPER Angle Resolved XPS (X-ray Photoelectron Spectroscopy)
Computer Fire Models. PB89-173991 900,165	Survey of Selected Methods of Economic Evaluation for Building Decisions.	of the Epitaxial Growth of Cu on Ni(100). PB89-150866 901,389
HVACSIM+, a Dynamic Building/HVAC/Control Systems Simulation Program.	PB89-173819 900,103	High-Accuracy Differential-Pulse Anodic Stripping Voltam-
PB89-177166 900,070	Trends for Building Technology in North America. PB89-174106 900, 104	metry with Indium as an Internal Standard. PB89-156947 900,182
Simulation of a Large Office Building System Using the HVACSIM+ Program.	Potential Applications of a Sequential Construction Analyzer.	Interaction of Cupric Ions with Calcium Hydroxylapatite. PB89-157127 900,037
PB89-177174 900,071 Significance of Multiple Scattering in the Interpretation of	PB89-191670 900,105	Observations on Crystal Defects Associated with Diffu-
Small-Angle Neutron Scattering Experiments. PB89-179626 901,409	Use of Artificial Intelligence Programming Techniques for Communication between Incompatible Building Informa-	sion Induced Grain Boundary Migration in Cu-Zn. PB89-157606 901,127
Simplified Discrete Event Simulation Model for an IEEE (Institute of Electrical and Electronics Engineers) 802.3	tion Systems. PB89-191985 900,106	Experimental Observations on the Initiation of DIGM (Dif-
Local Area Network. PB89-186829 900,617	Building Technology Project Summaries 1989. PB89-193213 900,131	fusion Induced Grain Boundary Migration). PB89-157630 901,130
User Guide for Wise: A Simulation Environment for Es-	NVLAP (National Voluntary Laboratory Accreditation Pro-	Aluminumlike Spectra of Copper through Molybdenum. PB89-172365 900,360
telle. PB89-196166 900,620	gram) Program Handbook Construction Testing Services. Requirements for Accreditation.	Microbiological Metal Transformations: Biotechnological
Object-Oriented Model for Estelle and Its Smalltalk Implementation.	PB90-112327 900,169 CONSTRUCTION MANAGEMENT	Applications and Potential. PB89-175947 901,284
PB89-196190 900,623	Potential Applications of a Sequential Construction Analyzer.	Wheatleyite, Na2Cu(C2O4)2 . 2H2O, a Natural Sodium Copper Salt of Oxalic Acid.
EVSIM: An Evaporator Simulation Model Accounting for Refrigerant and One Dimensional Air Distribution.	PB89-191670 900,105	PB89-179154 900,390
PB89-235881 900,086 Off-Lattice Simulation of Polymer Chain Dynamics.	Preliminary Performance Criteria for Building Materials,	Effects of Grain Size and Cold Rolling on Cryogenic Properties of Copper.
PB90-117524 900,576 Companisons of NBS/Harvard VI Simulations and Full-	Equipment and Systems Used in Detention and Correctional Facilities.	PB90-128604 901,176 Tensile and Fatigue-Creep Properties of a Copper-Stain-
Scale, Multiroom Fire Test Data. PB90-128620 900,170	PB89-148514 900, 109 Prediction of Service Life of Building Materials and Com-	less Steel Laminate. PB90-128646 901,083
Monte Carlo Simulation of Domain Growth in the Kinetic	ponents. PB89-158000 900,112	COPPER CONTAINING ALLOYS
Ising Model on the Connection Machine. PB90-136797 901,587	Damage Accumulation in Wood Structural Members	TEM Observation of Icosahedral, New Crystalline and Glassy Phases in Rapidly Quenched Cd-Cu Alloys.
ONCENTRATION (COMPOSITION) Methyl Radical Concentrations and Production Rates in a	Under Stochastic Live Loads. PB89-171748 900,115	PB90-123514 901,166
Laminar Methane/Air Diffusion Flame. PB89-171912 900,591	Elevated Temperature Deformation of Structural Steel. PB89-172621 901,098	COPPER IONS Pressure Dependence of the Cu Magnetic Order in
CONCRETE BLOCKS	Prediction of Service Life of Construction and Other Ma-	RBa2Cu3O6 + x. PB90-123829 <i>901,472</i>
Thermal Resistance Measurements and Calculations of an Insulated Concrete Block Wall.	terials. PB89-175848 <i>900,120</i>	COPPER MANGANESE ALLOYS
PB89-174916 900,119 CONCRETE DURABILITY	Thermographic Imaging and Computer Image Processing of Defects in Building Materials.	Magnetic Evaluation of Cu-Mn Matrix Material for Fine- Filament Nb-Ti Superconductors.
Knowledge Based System for Durable Reinforced Concrete.	PB89-176309 900,123 Building Technology Project Summaries 1989.	PB89-200489 901,425 COPPER NICKEL ALLOYS
PB89-150734 900,110	PB89-193213 900,131	Magnetic Behavior of Compositionally Modulated Ni-Cu Thin Films.
Inelastic Behavior of Full-Scale Bridge Columns Subject	CONTAINERS Technical Examination, Lead Isotope Determination, and	PB90-118084 901,163
ed to Cyclic Loading. PB89-174924 900,584	Elemental Analysis of Some Shang and Zhou Dynasty Bronze Vessels.	Magnetization and Magnetic Aftereffect in Textured Ni/ Cu Compositionally-Modulated Alloys.
CONCRETES Integrated Knowledge Systems for Concrete and Other	PB90-136862 901,178 CONTINUOUS RADIATION	PB90-123431 901,165 COPPER OXIDES
Materials. PB89-176119 900,582	Calibrating Antenna Standards Using CW and Pulsed-CW Measurements and the Planar Near-Field Method.	Oxygen Isotope Effect in the Superconducting Bi-Sr-Ca-
Standard Aggregate Materials for Alkali-Silica Reaction Studies.	PB89-149280 900,693 CONTINUOUS SAMPLING	Cu-O System. PB89-157044 901,025
PB89-193221 901,046	Tests of the Recalibration Period of a Drifting Instrument, PB89-176275 900,199	Crystal Chemistry of Superconductors: A Guide to the Tailoring of New Compounds.
Service Life of Concrete. PB89-215362 901,303	CONTRACEPTIVES Flow of Molecules Through Condoms.	PB89-171730 901,030
Set Time Control Studies of Polymer Concrete. PB90-111238 901,057	PB89-148118 901,087	Dependence of T(sub c) on the Number of CuO2 Planes per Cluster in Interplaner-Boson-Exchange Models of
CONDOMS	CONTROL EQUIPMENT Control System Simulation in North America.	High-T(sub C) Superconductivity. PB89-229132 901,455
Flow of Molecules Through Condoms. PB89-148118 901,087	PB89-157010 900,091 Real-Time Control System Modifications for a Deburring	Bulk Modulus and Young's Modulus of the Superconductor Ba2Cu3YO7.
CONDUCTION Periodic Heat Conduction in Energy Storage Cylinders	Robot. User Reference Manual. PB89-159669 900,990	PB90-123613 901,469
with Change of Phase. PB89-175897 900,852	Control Strategies and Building Energy Consumption.	CORONA DISCHARGES Production and Stability of S2F10 in SF6 Corona Dis-
CONE CALORIMETER	PB89-172340 900,061 HVACSIM+ , a Dynamic Building/HVAC/Control Sys-	charges. PB89-231039 900,822
Smoke and Gas Evolution Rate Measurements on Fire- Retarded Plastics with the Cone Calorimeter.	tems Simulation Program. PB89-177166 900,070	CORONENES
PB89-174890 900,868 CONE CALORIMETERS	Interfaces to Teleoperation Devices.	Standard Chemical Thermodynamic Properties of Polycyclic Aromatic Hydrocarbons and Their Isomer Groups. 2.
Flammability Characteristics of Electrical Cables Using the Cone Calorimeter.	PB89-181739 900,993 Inventory of Equipment in the Cleaning and Deburring	Pyrene Series, Naphthopyrene Series, and Coronene Series.
PB89-162572 900,741	Workstation.	PB89-226591 900,459
Proceedings of the Celebratory Symposium on a Decade	CONTROL SYSTEMS	CORRECTIONAL INSTITUTIONS Preliminary Performance Criteria for Building Materials,
of UV (Ultraviolet) Astronomy with the IUE Satellite, Volume 2.	Workstation Controller of the Cleaning and Deburring Workstation.	Equipment and Systems Used in Detention and Correctional Facilities.
		PB89-148514 900,109

CORRIDORS	PB90-123894	901,597	PB89-158133	900,34
Fire Induced Flows in Comidors: A Review of Efforts to Model Key Features.	CRANES (HOISTS)		CRITICAL TEMPERATURE	
PB89-189260 900,129	Robot Crane Technology. PB90-111667	900,146	Dependence of T(sub c) on	the Number of CuO2 Plane
CORROSION	CRATERING	300,140	per Cluster in Interplaner- High-T(sub C) Superconduct	Boson-Exchange Models of ivity.
Corrosion of Metallic Fasteners in Low-Sloped Roofs; A Review of Available Information and Identification of Re-	Silicon and GaAs Wire-Bond Cratering	g Problem.	PB89-229132	901,45
search Needs. PB89-162580 900.113	PB90-128182	900,799	CROSS SECTIONS Absolute Cross Sections fo	r Molecular Photosheomior
Corrosion Induced Degradation of Amine-Cured Epoxy	CRAZING Crazes and Fracture in Polymers.		Partial Photoionization, an	d Ionic Photofragmentatio
Coatings on Steel.	PB89-176085	900,562	Process. PB89-186464	900.41
PB89-176291 901,084	CREATININE	C A	Cross Sections for Inelastic	
Institute for Materials Science and Engineering: Metallurgy, Technical Activities 1988.	Developing Definitive Methods for I lytes.	Human Serum Ana-	PB89-202972	901,44
PB89-201321 901,147	PB89-146773	901,233	Cross Sections for Collision with Oxygen Molecules.	ns of Electrons and Photon
Development of a Method to Measure In situ Chloride at the Coating/Metal Interface.	CREEP PROPERTIES Flux Creep and Activation Energies	at the Grain Bound-	PB89-226575	900,45
PB89-235345 901,085	aries of Y-Ba-Cu-O Superconductors.		CROSSLINKING	
Effect of Slag Penetration on the Mechanical Properties of Refractories: Final Report.	PB89-230353	901,457	Radiation-Induced Crosslinks Deoxyerythropentose.	s between Thymine and 2-D
PB90-110065 900,836	CREEP RATE Relationships between Fault Zone De	eformation and Sec-	PB89-146682	900,24
CORROSION RESISTANCE	ment Obliquity on the San Andreas F PB89-185953	ault, California.	Effect of Crosslinks on the F a Miscible Polymer Blend.	hase Separation Behavior of
Corrosion of Metallic Implants and Prosthetic Devices. PB89-150890 900,053	CREEP RUPTURE TESTS	901,279	PB89-146724	900,54
Corrosion Behavior of Mild Steel in High pH Aqueous	Damage Accumulation in Wood	Structural Members	Hydroxyl Radical Induced C	ross-Linking between Pheny
Media. PB90-131152 901,086	Under Stochastic Live Loads. PB89-171748	900,115	lalanine and 2-Deoxyribose. PB89-147029	900,54
COSMOS 1402 SATELLITE	Creep Rupture of a Metal-Ceramic Pa		Structure of a Hydroxyl Ra	· ·
Detection of Uranium from Cosmos-1402 in the Strato-	PB89-211825	901,077	Thymine and Tyrosine. PB89-157838	901.24
sphere. PB89-156962 <i>901,592</i>	CREEP STRENGTH		Studies on Some Failure Mo	
COST ANALYSIS	Tensile and Fatigue-Creep Properties less Steel Laminate.	s of a Copper-Stain-	PB89-209308	901,08
Energy Prices and Discount Factors for Life-Cycle Cost	PB90-128646	901,083	CRUDE OIL	
Analysis 1988: Annual Supplement to NBS (National Bureau of Standards) Handbook 135 and NBS Special	CREEP TESTS Elevated Temperature Deformation of	Company Const	Combustion of Oil on Water. PB89-149173	900,58
Publication 709. PB89-153860 <i>900,850</i>	PB89-172621	901,098	CRYOGENICS	300,00
7 200-130000	Creep Cavitation in Liquid-Phase Sinto		Role of Inclusions in the Fra	acture of Austenitic Stainles
COTININE	PB89-175954	901,038	Steel Welds at 4 K. PB89-173504	901,09
Cotinine in Freeze-Dried Urine Reference Material. PB90-213703 900,675	CRIEGEE INTERMEDIATES New Photolytic Source of Dioxymeti	hylenes: Criegee In-	Influence of Molybdenum on	
•	termediates Without Ozonolysis.		of Stainless Steel Welds for PB89-173512	Cryogenic Service. 901,10
COULOMETERS Voltammetric and Liquid Chromatographic Identification	PB89-156731	900,304	Cool It.	901,10
of Organic Products of Microwave-Assisted Wet Ashing	CRITICAL CURRENT Current Ripple Effect on Supercond	ductive D.C. Critical	PB89-176986	901,51
of Biological Samples. PB89-157994 900,188	Current Measurements. PB89-157077	901,492	Thermal Conductivity of Lic	uid Argon for Temperature
High-Accuracy Differential-Pulse Anodic Stripping Voltam-	Josephson-Junction Model of Critical		between 110 and 140 K with PB89-179600	Pressures to 70 MPa. 900,39
metry Using Indium as an Internal Standard. 900,198	Y1Ba2Cu3O(7-delta) Superconductors	S.	Linear-Elastic Fracture of H	igh-Nitrogen Austenitic Stair
COUPLED ANTENNAS	PB89-176978	901,406	less Steels at Liquid Helium PB90-117623	Temperature. 901,10
Spherical-Wave Source-Scattering Matrix Analysis of	Effect of Room-Temperature Stress rent of NbTi.	on the Critical Cur-	Effect of Chemical Compos	
Coupled Antennas: A General System Two-Port Solution. PB89-156798 900,696	PB89-179832	901,414	Properties of 316LN-Type Al	loys.
COUPLING (INTERACTION)	Battery-Powered Current Supply 1 Measurements.	for Superconductor	PB90-128554	901,11
Companson of Measured and Calculated Antenna Side-	PB89-200455	901,525	Fracture Behavior of 316LN Cryogenic Temperatures.	
lobe Coupling Loss in the Near Field Using Approximate Far-Field Data.	Nb3Sn Critical-Current Measurement	s Using Tubular Fi-	PB90-128562	901,11
PB89-156855 900,702	berglass-Epoxy Mandrels. PB89-200497	901,527	Effects of Grain Size and Properties of Copper.	Cold Rolling on Cryogeni
CRACK PROPAGATION Metallographic Evidence for the Nucleation of Subsurface	VAMAS (Versailles Project on Adva	nced Materials and	PB90-128604	901,17
Microcracks during Unlubricated Sliding of Metals.	Standards) Intercomparison of Critica ment in Nb3Sn Wires.	al Current Measure-	Low Temperature Mechanic Sitica Aerogel Foam.	al Property Measurements of
PB89-147391 901,001 Influence of Dislocation Density on the Ductile-Brittle	PB89-202147	901,534	PB90-128638	901,06
Transition in bcc Metals.	Offset Criterion for Determining Sup	perconductor Critical	Fatigue Resistance of a 20	90-T8E41 Aluminum Alloy a
PB89-157804 901,133	Current. PB90-128133	901,474	Cryogenic Temperatures. PB90-128737	901,17
Toughening Mechanisms in Ceramic Composites: Semi- Annual Progress Report for the Period Ending September	Critical Current Measurements of N		CRYOSTATS	
30, 1988.	tors: NBS (National Bureau of Standa the VAMAS (Versailles Agreement o		Analysis of High Performand	e Compensated Thermal Er
PB89-162606 901,028 Rising Fracture Toughness from the Bending Strength of	als and Standards) Interlaboratory Co	mparison.	closures. PB89-185748	901,00
Indented Alumina Beams.	PB90-136748	901,480	Resistance Measurements	of High T(sub c) Supercor
PB89-171771 901,031	CRITICAL DENSITY Determination of Binary Mixture Vapo	r-Liquid Critical Den-	ductors Using a Novel 'Bath' PB89-228431	ysphere' Cryostat. 901,44
Fracture Behavior of Ceramics Used in Multilayer Capacitors.	sities from Coexisting Density Data. PB89-202170	901,536	CRYSTAL DEFECTS	507,44
PB89-171805 <i>900,758</i>	CRITICAL FIELD	901,536	Observations on Crystal De	efects Associated with Diffu
Effect of Lateral Crack Growth on the Strength of Contact Flaws in Brittle Materials.	Three-State Lattice Gas as Model for	or Binary Gas-Liquid	sion Induced Grain Boundary PB89-157606	y Migration in Cu-Zn. 901.12
PB89-171813 901,034	Systems. PB89-171284	900,354	Crystal Chemistry of Super	
Crazes and Fracture in Polymers. PB89-176085 900,562	CRITICAL FLOW	300,334	Tailoring of New Compounds PB89-171730	s. <i>901,03</i>
PB89-176085 900,562 Crack-Interface Traction: A Fracture-Resistance Mecha-	Simplified Representation for the The	ermal Conductivity of	13C NMR Method for Deter	
nism in Brittle Polycrystals.	Fluids in the Critical Region. PB89-228050	901,332	Groups and Side Branches	between the Crystalline an
PB89-211817 901,051	CRITICAL POINT		Non-Crystalline Regions in P PB89-202451	olyethylene. <i>900,56</i>
Design Criteria for High Temperature Structural Applica- tions.	Thermodynamic Values Near the Criti		Thermomechanical Detwir	nning of Superconductin
PB89-211833 901,052	PB89-161541	901,497	YBa2Cu3O7-x Single Crystal PB89-231088	ls. 901,45
Acoustic Emission: A Quantitative NDE Technique for the Study of Fracture.	Gas Solubility and Henry's Law Nea cal Point.		CRYSTAL DISLOCATIONS	301,43
PB89-211924 900,921	PB89-202485	900,434	Electron Diffraction Study of	of the Faceting of Tilt Grai
Effect of Heat Treatment on Crack-Resistance Curves in a Liquid-Phase-Sintered Alumina.	Asymptotic Expansions for Constan Bubble Curves Near the Critical Locus		Boundaries in NiO. PB89-201792	901,43
PB89-229231 901,056	PB89-227987	901,545	CRYSTAL GROWTH	231,10
Flaw Tolerance in Ceramics with Rising Crack Resistance	Method for Improving Equations of St	tate Near the Critical	Effect of Anisotropic Therm	nal Conductivity on the Mon
Characteristics. PB90-128026 901,060	Point. PB89-228027	901,547	phological Stability of a Bina PB89-228985	ry Alloy. 901,15
CRACKS	CRITICAL POINTS		Directional Solidification of a	
EMATs (Electromagnetic Acoustic Transducers) for Roll- By Crack Inspection of Ballroad Wheels	Van der Waals Equation of State A	round the Van Laar	ence of a Time-Dependent E PB90-112400	Electric Current. 901.46

Growth end Properties of High-Quality Very-Thin SOS	PB89-201826 901,432	PB89-146989 900,581
(Silicon-on Sapphire) Films. PB90-128109 900,798	Use of an Imaging Proportional Counter in Macromolecu- lar Crystallography.	Data Bases Available at the National Institute of Stand- erds and Technology Research Information Center.
Effect of a Crystal-Melt Interface on Taylor-Vortex Flow. PB90-130261 901,477	PB90-136599 900,538 Preliminary Crystallographic Study of Recombinant	PB89-160014 900,932
CRYSTAL LATTICES	Human Interleukin 1beta. PB90-136730 901,251	Creation of a Fire Research Bibliographic Database. PB89-174130 900,166
Quasicrystals with 1-D Translational Periodicity and a Ten-Fold Rotation Axis.	CRYSTALS	Integrated Knowledge Systems for Concrete and Other Materials.
PB89-147383 901,123	Sputter Deposition of Icosahedral Al-Mn end Al-Mn-Si. PB89-147102 901,122	PB89-176119 900,582
Critical and Noncritical Roughening of Surfaces (Comment).	CURING	PCM/VCR Speech Database Exchange Format. PB89-176713 900,633
PB89-180046 901,415 Green Function Method for Calculation of Atomistic	Epoxy Impregnation Procedure for Hardened Cement Samples.	Chemical and Spectral Databases: A Look into the
Structure of Grain Boundary Interfaces in Ionic Crystals. PB89-202105 901,050	PB89-147821 901,180	Future. PB89-180038 900,579
CRYSTAL STRUCTURE	Dielectric Measurements for Cure Monitoring. PB89-200430 900,567	Computerized Materials Property Data Systems.
Refinement of the Substructure and Superstructure of Romenechite.	CURING AGENTS Corrosion Induced Degradation of Amine-Cured Epoxy	PB89-187512 901,312 Fire Properties Database for Textile Wall Coverings.
PB89-157721 901,392	Coatings on Steel.	PB89-188635 900,126
Neutron Powder Diffrection Structure and Electrical Properties of the Defect Pyrochlores Pb1.5M2O6.5 (M= Nb,	PB89-176291 901,084 CURTAINS	DATA CONVERTERS Guidelines for the Specification and Validation of IGES
Te). PB89-172431 900,363	Development of a Multiple Layer Test Procedure for Inclusion in NFPA (National Fire Protection Association)	(Initial Graphics Exchange Specification) Application Protocols.
Wheatleyite, Na2Cu(C2O4)2 . 2H2O, a Natural Sodium	701: Initial Experiments.	PB89-166102 900,937
Copper Salt of Oxalic Acid. PB89-179154 900,390	PB89-235873 900,096 CURVE FITTING	DATA DEFINITION LANGUAGES Object Oriented Model for ASN 1 (Abstract Supray Notes
Syntheses and Unit Cell Determination of Ba3V4O13 and	Real Time Generation of Smooth Curves Using Local Cubic Segments.	Object-Oriented Model for ASN.1 (Abstract Syntax Notation One).
Low- end High-Temperature Ba3P4O13. PB89-179717 901,040	PB89-171623 901,196	PB89-177117 900,649 DATA ENCRYPTION
Replacement of Icosahedral Al-Mn by Decagonal Phase. PB89-186332 901,146	User's Reference Guide for ODRPACK: Software for Weighted Orthogonal Distance Regression Version 1.7.	National Bureau of Standards Message Authentication
Repulsive Regularities of Water Structure in Ices and	PB89-229066 901,215	Code (MAC) Validation System. PB89-231021 900,671
Crystalline Hydretes. PB89-186753 900,414	CYCLIC AMP RECEPTORS Crystal Structure of a Cyclic AMP (Adenosine Monophos-	DATA INTEGRITY
Phase Equilibria end Crystal Chemistry in the Ternary	phate)-Independent Mutant of Catabolite Gene Activator Protein.	Report of the Invitational Workshop on Integrity Policy in Computer Information Systems (WIPCIS).
System BaO-TiO2-Nb2O5. Part 2. New Barium Polytitanetes with < 5 mole % Nb2O5.	PB89-201594 901,224	PB89-168009 900,670
PB89-189815 900,419 Structural Study of a Metastable BCC Phase in Al-Mn	CYCLIC LOADS Inelastic Behavior of Full-Scale Bridge Columns Subject-	Data Management Strategies for Computer Integrated
Alloys Electrodeposited from Molten Salts.	ed to Cyclic Loading. PB89-174924 900,584	Manufacturing Systems. PB89-209258 900,959
PB89-201040 901,064 Crystal Structure of a Cyclic AMP (Adenosine Monophos-	CYCLOHEXANOLS	AMRF Part Model Extensions.
phate)-Independent Mutant of Catabolite Gene Activator Protein.	Second Virial Coefficients of Aqueous Alcohols at Elevat- ed Temperatures: A Calorimetric Study.	PB90-129446 900,967 DATA MANAGEMENT SYSTEMS
PB89-201594 901,224	PB89-227896 900,462 CYLINDERS	Data Handling in the Vertical Workstation of the Automat-
Equilibrium Crystal Shapes and Surface Phase Diagrams at Surfaces in Ceramics.	Periodic Heat Conduction in Energy Storage Cylinders	ed Manufacturing Research Facility at the National Bureau of Standards.
PB90-117755 901,162	with Change of Phase. PB89-175897 900,852	PB89-159636 900,943
Structure of V9Mo6O40 Determined by Powder Neutron Diffraction.	Hydrodynamic Forces on Vertical Cylinders and the Lighthill Correction.	Use of the IRDS (Information Resource Dictionary System) Standard in CALS (Computer-Aided Acquisition
PB90-117995 900,515 Neutron Diffraction Determination of Full Structures of	PB90-117417 901,313	and Logistic Support). PB90-112467 900,931
Anhydrous Li-X and Li-Y Zeolites. PB90-118001 900,516	Damage Accumulation in Wood Structural Members	DATA PROCESSING
Preliminary Crystal Structure of Acinetobacter glutamina-	Under Stochastic Live Loads. PB89-171748 900,115	Phase Diagrams for High Tech Ceramics. PB89-186308 901,044
sificans Glutaminase-Asparaginase. PB90-123381 901,260	DATA	Logistic Function Data Analysis Program: LOGIT. PB89-189351 900,418
Neutron Study of the Crystal Structure and Vacancy Dis-	Product Data Exchange Specification: First Working Draft.	Enhancements to the VWS2 (Vertical Workstation 2)
tribution in the Superconductor Ba2Y Cu3 O(sub g-delta). PB90-123480 901,468	PB89-144794 900,940	Data Preparation Software. PB90-132713 900,968
Quasicrystals and Quasicrystal-Related Phases in the Al- Mn System.	Product Data Exchange: The PDES Project-Status and Objectives.	DATA REDUCTION
PB90-123548 901,169	PB90-112426 900,938 External Representation of Product Definition Data.	Analysis of Computer Performance Data. PB89-162614 900,635
RYSTAL STRUCTURES Formation of the Al-Mn Icosahedral Phase by Electrode-	PB90-112434 900,939	DATA RETRIEVAL
position. PB90-117763 900,504	DATA ACQUISITION SYSTEMS Comparison of Two Transient Recorders for Use with the	ASM/NBS (American Society for Metals/National Bureau of Standards) Numerical and Graphical Database for
CRYSTALLINE HYDRATES	Laser Microprobe Mass Analyzer. PB89-176887 900,200	Binary Alloy Phase Diagrams. PB89-157986 901,135
Water Structure in Crystalline Solids: Ices to Proteins. PB89-186746 900,413	DATA ADMINISTRATION	DATA SMOOTHING
RYSTALLINITY	Integrated Manufacturing Data Administration System (IMDAS) Operations Manual.	User's Reference Guide for ODRPACK: Software for Weighted Orthogonal Distance Regression Version 1.7.
Applications of the Crystallographic Search and Analysis System CRYSTDAT in Materials Science.	PB89-156384 900,916 DATA ANALYSIS	PB89-229066 901,215
PB89-175251 901,402	Analysis of Computer Performance Data.	Method for Fitting and Smoothing Digital Data. PB90-128794 900,830
CRYSTALLIZATION Multicritical Phase Relations in Minerals.	PB89-162614 900,635 On-Line Arc Welding: Data Acquisition and Analysis	DATA TRANSFER PROTOCOLS
PB89-150882 901,278 Solutal Convection during Directional Solidification.	Using a High Level Scientific Language. PB90-117391 900,972	Use of Artificial Intelligence Programming Techniques for Communication between Incompatible Building Informa-
PB89-150932 901,322	DATA BASE MANAGEMENT SYSTEMS	tion Systems. PB89-191985 900,106
Metastable Phase Production and Transformation in Al- Ge Alloy Films by Rapid Crystallization and Annealing	Internal Structure of the Guide to Available Mathematical Software.	DATA TRANSMISSION
Treatments. PB89-157622 901,129	PB89-170864 900,927	Prediction of Transport Protocol Performance through Simulation.
Structural Unit in Icosahedral MnAISi and MnAI.	New Directions in Bioinformatics. PB89-175269 901,245	PB89-171334 900,612 DATABASES
PB89-157648 901,131 Biological Macromolecule Crystallization Database: A	Detailed Description of the Knowledge-Based System for Physical Database Design. Volume 1.	Development and Use of a Tribology Research-in-
Basis for a Crystallization Strategy.	PB89-228993 900,929	Progress Database. PB89-228274 901,002
PB90-136722 901,250 CRYSTALLOGRAPHY	Detailed Description of the Knowledge-Based System for Physical Database Design. Volume 2.	Biological Macromolecule Crystallization Database: A
Method of and Apparatus for Real-Time Crystallographic Axis Orientation Determination.	PB89-229033 900,930	Basis for a Crystallization Strategy. PB90-136722 901,250
PATENT-4 747 684 901,383	Experience with IMDAS (Integrated Manufacturing Data Administration System) in the Automated Manufacturing	DAYLIGHTING Illumination Conditions and Task Visibility in Daylit
Applications of the Crystallographic Search and Analysis System CRYSTDAT in Materials Science.	Research Facility. PB90-112350 900,964	Spaces.
PB89-175251 901,402 Statistical Descriptors in Crystallography: Report of the	DATA BASES Implications of Computer-Based Simulation Models,	PB89-189237 900,074 DEAD TIME
International Union of Crystallography Subcommittee on Statistical Descriptors.	Expert Systems, Databases, and Networks for Cement Research.	Variances Based on Data with Dead Time between the Measurements.

PP00 174040		
PB89-174049 901,204	PB89-179238 901,252	PB89-231062 900,101
DECALIN Concentration Dependence of the Compression Modulus	Micro-Analysis of Mineral Saturation Within Enamel during Lactic Acid Demineralization.	DESORPTION Secondary-Electron Effects in Photon-Stimulated Desorp-
of Isotactic Polystyrene/Cis-Decalin Gels. PB89-172449 900,552	PB89-186373 901,253 DENTAL INVESTMENTS	tion. PB89-157929 <i>900,337</i>
Effects of Solvent Type on the Concentration Dependence of the Compression Modulus of Thermoreversible	High-Temperature Dental Investments.	Optically Driven Surface Reactions: Evidence for the
Isotactic Polystyrene Gels. PB89-172456 900,553	PB89-202477 901,257 DENTAL MATERIALS	Role of Hot Electrons. PB89-157937 <i>900,338</i>
DECANES 900,333	Non-Aqueous Dental Cements Based on Dimer and Trimer Acids.	Non-Boltzmann Rotational and Inverted Spin-Orbit State Distributions for Laser-Induced Desorption of NO from
Latent Heats of Supercritical Fluid Mixtures. PB89-174908 900,242	PATENT-4 832 745 900,033	Pt(111). PB89-157952 900,340
DECAY SCHEMES	Effects of Purified Ferric Oxalate/Nitric Acid Solutions as a Pretreatment for the NTG-GMA and PMDM Bonding	AES and LEED Studies Correlating Desorption Energies
NBS (National Bureau of Standards) Decay-Scheme Investigations of (82)Sr-(82)Rb.	System. PB89-146716 900,034	with Surface Structures and Coverages for Ga on Si(100).
PB89-161558 901,498 DECISION SUPPORT SYSTEMS	Bonding Agents and Adhesives: Reactor Response. PB89-146732 900,035	PB89-171599 901,401
AutoMan: Decision Support Software for Automated Man-	Interaction of Cupric Ions with Calcium Hydroxylapatite.	Enthalpies of Desorption of Water from Coal Surfaces. PB89-173868 900,838
ufacturing Investments. User's Manual. PB89-221873 900,963	PB89-157127 900,037	Influence of Electronic and Geometric Structure on De- sorption Kinetics of Isoelectronic Polar Molecules: NH3
DECOMPOSITION Introduction to Microwave Acid Decomposition.	Casting Metals: Reactor Response. PB89-157143 900,054	and H2O. PB89-176473 <i>900,381</i>
PB90-118191 900,227	Biological Evaluations of Zinc Hexyl Vanillate Cement Using Two In vivo Test Methods.	Laser Probing of the Dynamics of Ga Interactions on
DECOMPOSITION REACTIONS Mechanism and Rate of Hydrogen Atom Attack on Tolu-	PB89-157150 900,038	Si(100). PB89-186928 <i>901,422</i>
ene at High Temperatures. PB89-179758 900,398	Adhesion to Dentin by Means of Gluma Resin. PB89-157168 900,039	Electron and Photon Stimulated Desorption: Benefits and Difficulties.
Monitoring and Predicting Parameters in Microwave Dis-	Mesh Monitor Casting of Ni-Cr Alloys: Element Effects. PB89-176077 900,040	PB89-200745 901,427
solution. PB90-118183 <i>900,690</i>	High-Temperature Dental Investments.	Bond Selective Chemistry with Photon-Stimulated Desorption.
DEFECTS Defect Intergrowths in Barium Polytitanates. 1.	PB89-202477 901,257 Pulpal and Micro-organism Responses to Two Experi-	PB89-201222 900,259
Ba2Ti9O20. PB89-146823 901,014	mental Dental Bonding Systems. PB89-202931 901,258	Stimulated Desorption from CO Chemisorbed on Cr(110). PB89-203004 900,443
Defect Intergrowths in Barium Polytitanates. 2. BaTi5O11.	Ferric Oxalate with Nitric Acid as a Conditioner in an Ad-	Methodology for Electron Stimulated Desorption Ion Angular Distributions of Negative Ions.
PB89-146831 901,015	hesive Bonding System. PB89-229272 900.045	PB89-231310 900,486
Application of SANS (Small Angle Neutron Scattering) to Ceramic Characterization.	Transient and Residual Stresses in Dental Porcelains as	Photon-Stimulated Desorption of Fluorine from Silicon via Substrate Core Excitations.
PB89-146856 901,017 Thermographic Imaging and Computer Image Processing	Affected by Cooling Rates. PB89-229298 900,046	PB90-118027 900,517
of Defects in Building Materials. PB89-176309 900,123	Comparison of Microleakage of Experimental and Selected Commercially Available Bonding Systems.	Interaction of In Atom Spin-Orbit States with Si(100) Surfaces.
Cathodoluminescence of Defects in Diamond Films and	PB89-234223 901,079	PB90-128547 900,532 DETECTION
Particles Grown by Hot-Filament Chemical-Vapor Deposition.	Use of N-Phenylglycine in a Dental Adhesive System. PB90-117375 900,048	Detection of Lead in Human Teeth by Exposure to Aqueous Sulfide Solutions.
PB90-117961 901,069 Flaw Tolerance in Ceramics with Rising Crack Resistance	In vitro Investigation of the Effects of Glass Inserts on the Effective Composite Resin Polymerization Shrinkage.	PB89-201529 901,256
Characteristics.	PB90-117516 900,049	Near-Field Detection of Buried Dielectric Objects. PB90-128208 900,713
PB90-128026 901,060 DEFORMATION	Adhesive Bonding of Composites. PB90-123696 900,050	DETECTORS
Institute for Materials Science and Engineering, Fracture and Deformation: Technical Activities 1988.	Dental Materials and Technology Research at the National Burgay of Standards: A Model for Covernment Briggs	Fast-Pulse Generators and Detectors for Characterizing Laser Receivers at 1.06 um.
PB89-148399 901,071	al Bureau of Standards: A Model for Government-Private Sector Cooperation.	PB89-171698 901,347 Fast Optical Detector Deposited on Dielectric Channel
Loading Rate Effects on Discontinuous Deformation in	PB90-128711 900,052	Waveguides.
Load-Control Tensile Tests.	DENTAL PORCELAIN	
Load-Control Tensile Tests. PB89-171896 901,097	Transient and Residual Stresses in Dental Porcelains as	PB89-171706 900,743 Effect of Multiple Internal Reflections on the Stability of
Load-Control Tensile Tests. PB89-171896 901,097 Elevated Temperature Deformation of Structural Steel. PB89-172621 901,098	Transient and Residual Stresses in Dental Porcelains as Affected by Cooling Rates. PB89-229298 900,046	PB89-171706 900,743 Effect of Multiple Internal Reflections on the Stability of Electrooptic and Magnetooptic Sensors.
Load-Control Tensile Tests. PB89-171896 901,097 Elevated Temperature Deformation of Structural Steel.	Transient and Residual Stresses in Dental Porcelains as Affected by Cooling Rates. PB89-229298 900,046 DENTIN Adhesion to Dentin by Means of Gluma Resin.	PB89-171706 900,743 Effect of Multiple Internal Reflections on the Stability of Electrooptic and Magnetooptic Sensors. PB89-171722 900,724 Polymeric Humidity Sensors for Industrial Process Appli-
Load-Control Tensile Tests. PB89-171896 901,097 Elevated Temperature Deformation of Structural Steel. PB89-172621 901,098 DEGRADATION Corrosion Induced Degradation of Amine-Cured Epoxy Coatings on Steel.	Transient and Residual Stresses in Dental Porcelains as Affected by Cooling Rates. PB89-229298 900,046 DENTIN Adhesion to Dentin by Means of Gluma Resin. PB89-157168 900,039	PB89-171706 900,743 Effect of Multiple Internal Reflections on the Stability of Electrooptic and Magnetooptic Sensors. PB89-171722 900,724
Load-Control Tensile Tests. PB89-171896 901,097 Elevated Temperature Deformation of Structural Steel. PB89-172621 901,098 DEGRADATION Corrosion Induced Degradation of Amine-Cured Epoxy Coatings on Steel. PB89-176291 901,084 DEHYDRATION	Transient and Residual Stresses in Dental Porcelains as Affected by Cooling Rates. PB89-229298 900,046 DENTIN Adhesion to Dentin by Means of Gluma Resin. PB89-157168 900,039 Oligomers with Pendant Isocyanate Groups as Adhesives for Dentin and Other Tissues.	PB89-171706 900,743 Effect of Multiple Internal Reflections on the Stability of Electrooptic and Magnetooptic Sensors. PB89-171722 900,724 Polymeric Humidity Sensors for Industrial Process Applications. PB89-176424 900,563 Ultrasonic Sensor for Measuring Surface Roughness.
Load-Control Tensile Tests. PB89-171896 PB89-171896 PB89-172621 DEGRADATION Corrosion Induced Degradation of Amine-Cured Epoxy Coatings on Steel. PB89-176291 DEHYDRATION Synthesis and Characterization of Ettringite and Related Phases.	Transient and Residual Stresses in Dental Porcelains as Affected by Cooling Rates. PB89-229298 900,046 DENTIN Adhesion to Dentin by Means of Gluma Resin. PB89-157168 Oligomers with Pendant Isocyanate Groups as Adhesives for Dentin and Other Tissues. PB89-179253 900,042	PB89-171706 900,743 Effect of Multiple Internal Reflections on the Stability of Electrooptic and Magnetooptic Sensors. PB89-171722 900,724 Polymeric Humidity Sensors for Industrial Process Applications. PB89-176424 900,563
Load-Control Tensile Tests. PB89-171896 901,097 Elevated Temperature Deformation of Structural Steel. PB89-172621 901,098 DEGRADATION Corrosion Induced Degradation of Amine-Cured Epoxy Coatings on Steel. PB89-176291 901,084 DEHYDRATION Synthesis and Characterization of Ettringite and Related Phases. PB89-146963 900,238	Transient and Residual Stresses in Dental Porcelains as Affected by Cooling Rates. PB89-229298 900,046 DENTIN Adhesion to Dentin by Means of Gluma Resin. PB89-157168 900,039 Oligomers with Pendant Isocyanate Groups as Adhesives for Dentin and Other Tissues. PB89-179253 900,042 Pulpal and Micro-organism Responses to Two Experimental Dental Bonding Systems.	PB89-171706 900,743 Effect of Multiple Internal Reflections on the Stability of Electrooptic and Magnetooptic Sensors. PB89-171722 Polymeric Humidity Sensors for Industrial Process Applications. PB89-176424 900,563 Ultrasonic Sensor for Measuring Surface Roughness. PB89-211809 DETERMINATION OF STRESS Ultrasonic Separation of Stress and Texture Effects in
Load-Control Tensile Tests. PB89-171896 PB89-171896 Elevated Temperature Deformation of Structural Steel. PB89-172621 DEGRADATION Corrosion Induced Degradation of Amine-Cured Epoxy Coatings on Steel. PB89-176291 DEHYDRATION Synthesis and Characterization of Ettringite and Related Phases. PB89-146963 DEHYDROGENATION Dehydrogenation of Ethanol in Dilute Aqueous Solution	Transient and Residual Stresses in Dental Porcelains as Affected by Cooling Rates. PB89-229298 900,046 DENTIN Adhesion to Dentin by Means of Gluma Resin. PB89-157168 900,039 Oligomers with Pendant Isocyanate Groups as Adhesives for Dentin and Other Tissues. PB89-179253 900,042 Pulpal and Micro-organism Responses to Two Experimental Dental Bonding Systems. PB89-202931 901,258 Substitutes for N-Phenylglycine in Adhesive Bonding to	PB89-171706 Effect of Multiple Internal Reflections on the Stability of Electrooptic and Magnetooptic Sensors. PB89-171722 Polymeric Humidity Sensors for Industrial Process Applications. PB89-176424 Ultrasonic Sensor for Measuring Surface Roughness. PB89-211809 DETERMINATION OF STRESS Ultrasonic Separation of Stress and Texture Effects in Polycrystalline Aggregates. PB90-117557 900,499
Load-Control Tensile Tests. PB89-171896 PB89-171896 PB89-172621 PB89-172621 PB89-172621 DEGRADATION Corrosion Induced Degradation of Amine-Cured Epoxy Coatings on Steel. PB89-176291 PB89-176291 PB99-176291 PB99-1763 Synthesis and Characterization of Ettringite and Related Phases. PB89-146963 DEHYDROGENATION	Transient and Residual Stresses in Dental Porcelains as Affected by Cooling Rates. PB89-229298 900,046 DENTIN Adhesion to Dentin by Means of Gluma Resin. PB89-157168 900,039 Oligomers with Pendant Isocyanate Groups as Adhesives for Dentin and Other Tissues. PB89-179253 900,042 Pulpal and Micro-organism Responses to Two Experimental Dental Bonding Systems. PB89-202931 901,258	PB89-171706 Effect of Multiple Internal Reflections on the Stability of Electrooptic and Magnetooptic Sensors. PB89-171722 Polymeric Humidity Sensors for Industrial Process Applications. PB89-176424 900,563 Ultrasonic Sensor for Measuring Surface Roughness. PB89-211809 PETERMINATION OF STRESS Ultrasonic Separation of Stress and Texture Effects in Polycrystalline Aggregates. PB90-117557 Measurement of Applied J-Integral Produced by Residual Stress.
Load-Control Tensile Tests. PB89-171896 PB89-171896 PB89-171896 PB89-172621 PB89-172621 PB89-172621 PB89-176291 PB89-176291 PB89-176291 PB89-176291 PB89-176291 PB89-176291 PB99-176291 PB99-176596 PB99-176596 PB99-176596 PB99-176596 PB99-176596	Transient and Residual Stresses in Dental Porcelains as Affected by Cooling Rates. PB89-229298 900,046 DENTIN Adhesion to Dentin by Means of Gluma Resin. PB89-157168 900,039 Oligomers with Pendant Isocyanate Groups as Adhesives for Dentin and Other Tissues. PB89-179253 900,042 Pulpal and Micro-organism Responses to Two Experimental Dental Bonding Systems. PB89-202931 901,258 Substitutes for N-Phenylglycine in Adhesive Bonding to Dentin. PB90-123795 900,051	PB89-171706 Effect of Multiple Internal Reflections on the Stability of Electrooptic and Magnetooptic Sensors. PB89-171722 Polymeric Humidity Sensors for Industrial Process Applications. PB89-176424 Ultrasonic Sensor for Measuring Surface Roughness. PB89-211809 DETERMINATION OF STRESS Ultrasonic Separation of Stress and Texture Effects in Polycrystalline Aggregates. PB90-117557 Measurement of Applied J-Integral Produced by Residual Stress. PB90-117631 900,163
Load-Control Tensile Tests. PB89-171896 PB89-171896 PB89-172621 DEGRADATION Corrosion Induced Degradation of Amine-Cured Epoxy Coatings on Steel. PB89-176291 DEHYDRATION Synthesis and Characterization of Ettringite and Related Phases. PB89-146963 DEHYDROGENATION Dehydrogenation of Ethanol in Dilute Aqueous Solution Photosensitized by Benzophenones. PB89-157556 DEMODULATION Heterodyne Measurements on OCS Near 1372 cm(-1). PB89-201743 900,425	Transient and Residual Stresses in Dental Porcelains as Affected by Cooling Rates. PB89-229298 900,046 DENTIN Adhesion to Dentin by Means of Gluma Resin. PB89-157168 900,039 Oligomers with Pendant Isocyanate Groups as Adhesives for Dentin and Other Tissues. PB89-179253 900,042 Pulpal and Micro-organism Responses to Two Experimental Dental Bonding Systems. PB89-202931 901,258 Substitutes for N-Phenylglycine in Adhesive Bonding to Dentin. PB90-123795 900,051 DENTISTRY Comparison of Microleakage of Experimental and Selected Commercially Available Bonding Systems.	PB89-171706 Effect of Multiple Internal Reflections on the Stability of Electrooptic and Magnetooptic Sensors. PB89-171722 Polymeric Humidity Sensors for Industrial Process Applications. PB89-176424 Ultrasonic Sensor for Measuring Surface Roughness. PB89-211809 DETERMINATION OF STRESS Ultrasonic Separation of Stress and Texture Effects in Polycrystalline Aggregates. PB90-117557 Measurement of Applied J-Integral Produced by Residual Stress. PB90-117631 DEUTERIUM Collision Induced Spectroscopy: Absorption and Light
Load-Control Tensile Tests. PB89-171896 PB89-171896 PB89-172621 DEGRADATION Corrosion Induced Degradation of Amine-Cured Epoxy Coatings on Steel. PB89-176291 DEHYDRATION Synthesis and Characterization of Ettringite and Related Phases. PB89-146963 DEHYDROGENATION Dehydrogenation of Ethanol in Dilute Aqueous Solution Photosensitized by Benzophenones. PB89-157556 DEMODULATION Heterodyne Measurements on OCS Near 1372 cm(-1).	Transient and Residual Stresses in Dental Porcelains as Affected by Cooling Rates. PB89-229298 900,046 DENTIN Adhesion to Dentin by Means of Gluma Resin. PB89-157168 900,039 Oligomers with Pendant Isocyanate Groups as Adhesives for Dentin and Other Tissues. PB89-179253 900,042 Pulpal and Micro-organism Responses to Two Experimental Dental Bonding Systems. PB89-202931 901,258 Substitutes for N-Phenylglycine in Adhesive Bonding to Dentin. PB90-123795 900,051 DENTISTRY Comparison of Microleakage of Experimental and Select-	PB89-171706 900,743 Effect of Multiple Internal Reflections on the Stability of Electrooptic and Magnetooptic Sensors. PB89-171722 900,724 Polymeric Humidity Sensors for Industrial Process Applications. PB89-176424 900,563 Ultrasonic Sensor for Measuring Surface Roughness. PB89-211809 DETERMINATION OF STRESS Ultrasonic Separation of Stress and Texture Effects in Polycrystalline Aggregates. PB90-117557 900,499 Measurement of Applied J-Integral Produced by Residual Stress. PB90-117631 900,163
Load-Control Tensile Tests. PB89-171896 PB89-171896 PB89-172621 PB89-172621 PB89-172621 DEGRADATION Corrosion Induced Degradation of Amine-Cured Epoxy Coatings on Steel. PB89-176291 DEHYDRATION Synthesis and Characterization of Ettringite and Related Phases. PB89-146963 DEHYDROGENATION Dehydrogenation of Ethanol in Dilute Aqueous Solution Photosensitized by Benzophenones. PB89-157556 DEMODULATION Heterodyne Measurements on OCS Near 1372 cm(-1). PB89-201743 DENSIFICATION Densification, Susceptibility and Microstructure of Ba2YCu3O(6+ x).	Transient and Residual Stresses in Dental Porcelains as Affected by Cooling Rates. PB89-229298 900,046 DENTIN Adhesion to Dentin by Means of Gluma Resin. PB89-157168 900,039 Oligomers with Pendant Isocyanate Groups as Adhesives for Dentin and Other Tissues. PB89-179253 900,042 Pulpal and Micro-organism Responses to Two Experimental Dental Bonding Systems. PB89-202931 901,258 Substitutes for N-Phenylglycine in Adhesive Bonding to Dentin. PB90-123795 900,051 DENTISTRY Comparison of Microleakage of Experimental and Selected Commercially Available Bonding Systems. PB89-234223 901,079 DEOXYRIBONUCLEIC ACIDS Chemical Characterization of Ionizing Radiation-Induced	PB89-171706 Effect of Multiple Internal Reflections on the Stability of Electrooptic and Magnetooptic Sensors. PB89-171722 Polymeric Humidity Sensors for Industrial Process Applications. PB89-176424 Ultrasonic Sensor for Measuring Surface Roughness. PB89-211809 DETERMINATION OF STRESS Ultrasonic Separation of Stress and Texture Effects in Polycrystalline Aggregates. PB90-117557 Measurement of Applied J-Integral Produced by Residual Stress. PB90-117631 DEUTERIUM Collision Induced Spectroscopy: Absorption and Light Scattering. PB89-212252 DEUTERIUM COMPOUNDS
Load-Control Tensile Tests. PB89-171896 PB89-171896 PB89-172621 DEGRADATION Corrosion Induced Degradation of Amine-Cured Epoxy Coatings on Steel. PB89-176291 DEHYDRATION Synthesis and Characterization of Ettringite and Related Phases. PB99-146963 DEHYDROGENATION Dehydrogenation of Ethanol in Dilute Aqueous Solution Photosensitized by Benzophenones. PB99-157556 DEMODULATION Heterodyne Measurements on OCS Near 1372 cm(-1). PB89-201743 DENSIFICATION Densification, Susceptibility and Microstructure of Ba2YCu3O(6+ x). PB89-171821 DENSIFY (MASS/VOLUME)	Transient and Residual Stresses in Dental Porcelains as Affected by Cooling Rates. PB89-229298 DENTIN Adhesion to Dentin by Means of Gluma Resin. PB89-157168 Oligomers with Pendant Isocyanate Groups as Adhesives for Dentin and Other Tissues. PB89-179253 PB89-179253 900,042 Pulpal and Micro-organism Responses to Two Experimental Dental Bonding Systems. PB89-202931 Substitutes for N-Phenylglycine in Adhesive Bonding to Dentin. PB90-123795 DENTISTRY Comparison of Microleakage of Experimental and Selected Commercially Available Bonding Systems. PB89-234223 DEOXYRIBONUCLEIC ACIDS Chemical Characterization of Ionizing Radiation-Induced Damage to DNA. PB89-151922 901,235	PB89-171706 Effect of Multiple Internal Reflections on the Stability of Electrooptic and Magnetooptic Sensors. PB89-171722 Polymeric Humidity Sensors for Industrial Process Applications. PB89-176424 Ultrasonic Sensor for Measuring Surface Roughness. PB89-211809 DETERMINATION OF STRESS Ultrasonic Separation of Stress and Texture Effects in Polycrystalline Aggregates. PB90-117557 Measurement of Applied J-Integral Produced by Residual Stress. PB90-117631 DEUTERIUM Collision Induced Spectroscopy: Absorption and Light Scattering. PB99-212252 DEUTERIUM COMPOUNDS Hyperconjugation: Equilibrium Secondary Isotope Effect on the Stability of the t-Butyl Cation. Kinetics of Near-
Load-Control Tensile Tests. PB89-171896 PB89-171896 PB89-171896 PB89-172621 PB89-172621 PB89-176291 DEGRADATION Corrosion Induced Degradation of Amine-Cured Epoxy Coatings on Steel. PB89-176291 PB89-176291 PB89-176291 DEHYDRATION Synthesis and Characterization of Ettringite and Related Phases. PB89-146963 DEHYDROGENATION Dehydrogenation of Ethanol in Dilute Aqueous Solution Photosensitized by Benzophenones. PB89-157556 DEMODULATION Heterodyne Measurements on OCS Near 1372 cm(-1). PB89-201743 DENSIFICATION Densification, Susceptibility and Microstructure of Ba2YCu3O(6+ x). PB89-171821 DENSITY (MASS/VOLUME) Pressure and Density Series Equations of State for Steam as Derived from the Haar-Gallagher-Kell Formula-	Transient and Residual Stresses in Dental Porcelains as Affected by Cooling Rates. PB89-229298 900,046 DENTIN Adhesion to Dentin by Means of Gluma Resin. PB89-157168 900,039 Oligomers with Pendant Isocyanate Groups as Adhesives for Dentin and Other Tissues. PB89-179253 900,042 Pulpal and Micro-organism Responses to Two Experimental Dental Bonding Systems. PB89-202931 901,258 Substitutes for N-Phenylglycine in Adhesive Bonding to Dentin. PB90-123795 900,051 DENTISTRY Comparison of Microleakage of Experimental and Selected Commercially Available Bonding Systems. PB89-234223 901,079 DEOXYRIBONUCLEIC ACIDS Chemical Characterization of Ionizing Radiation-Induced Damage to DNA. PB89-151922 901,235 DEOXYRIBOSE	PB89-171706 Effect of Multiple Internal Reflections on the Stability of Electrooptic and Magnetooptic Sensors. PB89-171722 Polymeric Humidity Sensors for Industrial Process Applications. PB89-176424 Ultrasonic Sensor for Measuring Surface Roughness. PB89-211809 DETERMINATION OF STRESS Ultrasonic Separation of Stress and Texture Effects in Polycrystalline Aggregates. PB89-117557 Measurement of Applied J-Integral Produced by Residual Stress. PB90-117631 DEUTERIUM Collision Induced Spectroscopy: Absorption and Light Scattering. PB89-212252 DEUTERIUM COMPOUNDS Hyperconjugation: Equilibrium Secondary Isotope Effect on the Stability of the t-Butyl Cation. Kinetics of Near-Thermoneutral Hydride Transfer. PB89-156756
Load-Control Tensile Tests. PB89-171896 PB89-171896 PB89-171896 PB89-172621 DEGRADATION Corrosion Induced Degradation of Amine-Cured Epoxy Coatings on Steel. PB89-176291 DEHYDRATION Synthesis and Characterization of Ettringite and Related Phases. PB89-146963 DEHYDROGENATION Dehydrogenation of Ethanol in Dilute Aqueous Solution Photosensitized by Benzophenones. PB89-157556 DEMODULATION Heterodyne Measurements on OCS Near 1372 cm(-1). PB89-201743 DENSIFICATION Densification, Susceptibility and Microstructure of Ba2YCu3O(6+ x). PB89-171821 DENSITY (MASS/VOLUME) Pressure and Density Series Equations of State for	Transient and Residual Stresses in Dental Porcelains as Affected by Cooling Rates. PB89-229298 DENTIN Adhesion to Dentin by Means of Gluma Resin. PB89-157168 Oligomers with Pendant Isocyanate Groups as Adhesives for Dentin and Other Tissues. PB89-179253 900,042 Pulpal and Micro-organism Responses to Two Experimental Dental Bonding Systems. PB89-202931 901,258 Substitutes for N-Phenylglycine in Adhesive Bonding to Dentin. PB90-123795 DENTISTRY Comparison of Microleakage of Experimental and Selected Commercially Available Bonding Systems. PB89-234223 DEOXYRIBONUCLEIC ACIDS Chemical Characterization of Ionizing Radiation-Induced Damage to DNA. PB89-151922 901,235 DEOXYRIBOSE Hydroxyl Radical Induced Cross-Linking between Phenylalanine and 2-Deoxyribose.	PB89-171706 Effect of Multiple Internal Reflections on the Stability of Electrooptic and Magnetooptic Sensors. PB89-171722 Polymeric Humidity Sensors for Industrial Process Applications. PB89-176424 Ultrasonic Sensor for Measuring Surface Roughness. PB89-211809 DETERMINATION OF STRESS Ultrasonic Separation of Stress and Texture Effects in Polycrystalline Aggregates. PB90-117557 Measurement of Applied J-Integral Produced by Residual Stress. PB90-117631 DEUTERIUM Collision Induced Spectroscopy: Absorption and Light Scattering. PB99-212252 DEUTERIUM COMPOUNDS Hyperconjugation: Equilibrium Secondary Isotope Effect on the Stability of the t-Butyl Cation. Kinetics of Near-Thermoneutral Hydride Transfer. PB89-156756 Detection of Gas Phase Methoxy Radicals by Resonance Enhanced Multiphoton Ionization Spectroscopy.
Load-Control Tensile Tests. PB89-171896 PB89-171896 PB89-172621 PB89-172621 PB89-176291 DEGRADATION Corrosion Induced Degradation of Amine-Cured Epoxy Coatings on Steel. PB89-176291 PB89-176291 PB89-176291 DEHYDRATION Synthesis and Characterization of Ettringite and Related Phases. PB89-146963 DEHYDROGENATION Dehydrogenation of Ethanol in Dilute Aqueous Solution Photosensitized by Benzophenones. PB89-157556 DEMODULATION Heterodyne Measurements on OCS Near 1372 cm(-1). PB89-201743 DENSIFICATION Densification, Susceptibility and Microstructure of Ba2YCu3O(6+ x). PB89-171821 PRSS-171821 PRSS-17182	Transient and Residual Stresses in Dental Porcelains as Affected by Cooling Rates. PB89-229298 900,046 DENTIN Adhesion to Dentin by Means of Gluma Resin. PB89-157168 900,039 Oligomers with Pendant Isocyanate Groups as Adhesives for Dentin and Other Tissues. PB89-179253 900,042 Pulpal and Micro-organism Responses to Two Experimental Dental Bonding Systems. PB89-202931 901,258 Substitutes for N-Phenylglycine in Adhesive Bonding to Dentin. PB90-123795 900,051 DENTISTRY Comparison of Microleakage of Experimental and Selected Commercially Available Bonding Systems. PB89-234223 901,079 DEOXYRIBONUCLEIC ACIDS Chemical Characterization of Ionizing Radiation-Induced Damage to DNA. PB89-151922 901,235 DEOXYRIBOSE Hydroxyl Radical Induced Cross-Linking between Phenylalanine and 2-Deoxyribose. PB89-147029 900,547 DEPTH DETECTORS	PB89-171706 Effect of Multiple Internal Reflections on the Stability of Electrooptic and Magnetooptic Sensors. PB89-171722 Polymeric Humidity Sensors for Industrial Process Applications. PB89-176424 Ultrasonic Sensor for Measuring Surface Roughness. PB89-211809 DETERMINATION OF STRESS Ultrasonic Separation of Stress and Texture Effects in Polycrystalline Aggregates. PB90-117557 Measurement of Applied J-Integral Produced by Residual Stress. PB90-117631 DEUTERIUM Collision Induced Spectroscopy: Absorption and Light Scattering. PB89-212252 DEUTERIUM COMPOUNDS Hyperconjugation: Equilibrium Secondary Isotope Effect on the Stability of the t-Butyl Cation. Kinetics of Near-Thermoneutral Hydride Transfer. PB89-156756 Detection of Gas Phase Methoxy Radicals by Resonance Enhanced Multiphoton Ionization Spectroscopy. PB89-156764
Load-Control Tensile Tests. PB89-171896 PB89-171896 PB89-172621 PB89-172621 PB89-172621 PB89-172621 PB89-172621 PB89-172621 PB89-170N Corrosion Induced Degradation of Amine-Cured Epoxy Coatings on Steel. PB89-176291 PF89-176291 PF89-1	Transient and Residual Stresses in Dental Porcelains as Affected by Cooling Rates. PB89-229298 900,046 DENTIN Adhesion to Dentin by Means of Gluma Resin. PB89-157168 900,039 Oligomers with Pendant Isocyanate Groups as Adhesives for Dentin and Other Tissues. PB89-179253 900,042 Pulpal and Micro-organism Responses to Two Experimental Dental Bonding Systems. PB89-202931 901,258 Substitutes for N-Phenylglycine in Adhesive Bonding to Dentin. PB90-123795 900,051 DENTISTRY Comparison of Microleakage of Experimental and Selected Commercially Available Bonding Systems. PB89-234223 901,079 DEOXYRIBONUCLEIC ACIDS Chemical Characterization of Ionizing Radiation-Induced Damage to DNA. PB89-151922 901,235 DEOXYRIBOSE Hydroxyl Radical Induced Cross-Linking between Phenylalanine and 2-Deoxyribose. PB89-147029 900,547	PB89-171706 Effect of Multiple Internal Reflections on the Stability of Electrooptic and Magnetooptic Sensors. PB89-171722 Polymeric Humidity Sensors for Industrial Process Applications. PB89-176424 Ultrasonic Sensor for Measuring Surface Roughness. PB89-211809 DETERMINATION OF STRESS Ultrasonic Separation of Stress and Texture Effects in Polycrystalline Aggregates. PB90-117557 Measurement of Applied J-Integral Produced by Residual Stress. PB90-117631 DEUTERIUM Collision Induced Spectroscopy: Absorption and Light Scattering. PB89-212252 DEUTERIUM COMPOUNDS Hyperconjugation: Equilibrium Secondary Isotope Effect on the Stability of the t-Butyl Cation. Kinetics of Near-Thermoneutral Hydride Transfer. PB89-156756 Detection of Gas Phase Methoxy Radicals by Resonance Enhanced Multiphoton Ionization Spectroscopy. PB89-156764 Effects of Pressure on the Vibrational Spectra of Liquid Nitromethane.
Load-Control Tensile Tests. PB89-171896 PB89-171896 PB89-171896 PB89-172621 DEGRADATION Synthesis and Characterization of Ettringite and Related Phases. PB89-146963 DEHYDROGENATION Dehydrogenation of Ethanol in Dilute Aqueous Solution Photosensitized by Benzophenones. PB89-157556 DEMODULATION Heterodyne Measurements on OCS Near 1372 cm(-1). PB89-201743 DENSIFICATION Densification, Susceptibility and Microstructure of Ba2YCu3O(6+ x). PB89-171821 DENSITY (MASS/VOLUME) Pressure and Density Series Equations of State for Steam as Derived from the Haar-Gallagher-Kell Formulation. PB89-186456 J90,409 Isochoric (p.v,T) Measurements on CO2 and (0.98 CO2 + 0.02 CH4) from 225 to 400 K and Pressures to 35	Transient and Residual Stresses in Dental Porcelains as Affected by Cooling Rates. PB89-229298 900,046 DENTIN Adhesion to Dentin by Means of Gluma Resin. PB89-157168 900,039 Oligomers with Pendant Isocyanate Groups as Adhesives for Dentin and Other Tissues. PB89-179253 900,042 Pulpal and Micro-organism Responses to Two Experimental Dental Bonding Systems. PB89-202931 901,258 Substitutes for N-Phenylglycine in Adhesive Bonding to Dentin. PB90-123795 900,051 DENTISTRY Comparison of Microleakage of Experimental and Selected Commercially Available Bonding Systems. PB89-234223 901,079 DEOXYRIBONUCLEIC ACIDS Chemical Characterization of Ionizing Radiation-Induced Damage to DNA. PB89-151922 901,235 DEOXYRIBOSE Hydroxyl Radical Induced Cross-Linking between Phenylalanine and 2-Deoxyribose. PB89-147029 900,547 DEPTH DETECTORS Analytical Applications of Neutron Depth Profiling. PB89-146872 901,294 DESIGN	PB89-171706 Effect of Multiple Internal Reflections on the Stability of Electrooptic and Magnetooptic Sensors. PB89-171722 Polymeric Humidity Sensors for Industrial Process Applications. PB89-176424 Ultrasonic Sensor for Measuring Surface Roughness. PB89-211809 DETERMINATION OF STRESS Ultrasonic Separation of Stress and Texture Effects in Polycrystalline Aggregates. PB90-117557 Measurement of Applied J-Integral Produced by Residual Stress. PB90-117631 DEUTERIUM Collision Induced Spectroscopy: Absorption and Light Scattering. PB89-212252 DEUTERIUM COMPOUNDS Hyperconjugation: Equilibrium Secondary Isotope Effect on the Stability of the t-Butyl Cation. Kinetics of Near-Thermoneutral Hydride Transfer. PB89-156756 Detection of Gas Phase Methoxy Radicals by Resonance Enhanced Multiphoton Ionization Spectroscopy. PB89-156764 Effects of Pressure on the Vibrational Spectra of Liquid
Load-Control Tensile Tests. PB89-171896 PB89-171896 PB89-172621 PB89-172621 PB89-172621 PB89-172621 PB89-172621 PB89-172621 PB89-172621 PB89-176291 PB89-176291 PB89-176291 PB89-176291 PB89-176291 PB89-176291 PB89-176291 PB89-176291 PB89-176291 POLYPRATION Synthesis and Characterization of Ettringite and Related Phases, PB89-146963 PB89-146963 PB89-146963 PB89-157556 PB89-157556 PB89-157556 PB89-157556 PB89-157556 PB89-157556 PB89-171821 PB89-201743 PB89-201743 PB89-201743 PB89-171821 PB89-171821 PR89-171821 PR89-171821 PR89-171821 PS89-186456 Pressure and Density Series Equations of State for Steam as Derived from the Haar-Gallagher-Kell Formulation. PB89-186456 PB89-186456 PB89-202493 PB89-202493 PB89-202493 PBNITAL CARIES Quasi-Constant Composition Method for Studying the	Transient and Residual Stresses in Dental Porcelains as Affected by Cooling Rates. PB89-229298 900,046 DENTIN Adhesion to Dentin by Means of Gluma Resin. PB89-157168 900,039 Oligomers with Pendant Isocyanate Groups as Adhesives for Dentin and Other Tissues. PB89-179253 900,042 Pulpal and Micro-organism Responses to Two Experimental Dental Bonding Systems. P889-202931 901,258 Substitutes for N-Phenylglycine in Adhesive Bonding to Dentin. P890-123795 900,051 DENTISTRY Comparison of Microleakage of Experimental and Selected Commercially Available Bonding Systems. P899-234223 901,079 DEOXYRIBONUCLEIC ACIDS Chemical Characterization of Ionizing Radiation-Induced Damage to DNA. P899-151922 901,235 DEOXYRIBOSE Hydroxyl Radical Induced Cross-Linking between Phenylalanine and 2-Deoxyribose. P889-147029 900,547 DEPTH DETECTORS Analytical Applications of Neutron Depth Profiling. P889-148722 901,294	PB89-171706 Effect of Multiple Internal Reflections on the Stability of Electrooptic and Magnetooptic Sensors. PB89-171722 Polymeric Humidity Sensors for Industrial Process Applications. PB89-176424 Ultrasonic Sensor for Measuring Surface Roughness. PB89-211809 DETERMINATION OF STRESS Ultrasonic Separation of Stress and Texture Effects in Polycrystalline Aggregates. PB90-117557 Measurement of Applied J-Integral Produced by Residual Stress. PB90-117631 DEUTERIUM Collision Induced Spectroscopy: Absorption and Light Scattering. PB89-212252 DEUTERIUM COMPOUNDS Hyperconjugation: Equilibrium Secondary Isotope Effect on the Stability of the t-Butyl Cation. Kinetics of Near-Thermoneutral Hydride Transfer. PB89-156756 Detection of Gas Phase Methoxy Radicals by Resonance Enhanced Multiphoton Ionization Spectroscopy. PB89-156764 Effects of Pressure on the Vibrational Spectra of Liquid Nitromethane. PB89-158026 Structure of the CO2-CO2-H2O van der Waals Complex Determined by Microwave Spectroscopy.
Load-Control Tensile Tests. PB89-171896 PB89-171896 PB89-172621 DEGRADATION Corrosion Induced Degradation of Amine-Cured Epoxy Coatings on Steel. PB89-176291 DEHYDRATION Synthesis and Characterization of Ettringite and Related Phases. PB89-146963 DEHYDROGENATION Dehydrogenation of Ethanol in Dilute Aqueous Solution Photosensitized by Benzophenones. PB89-157556 DEMODULATION Heterodyne Measurements on OCS Near 1372 cm(-1). PB89-201743 DENSIFICATION Densification, Susceptibility and Microstructure of Ba2YCu3O(6+ x). PB89-171821 DENSITY (MASS/VOLUME) Pressure and Density Series Equations of State for Steam as Derived from the Haar-Gallagher-Kell Formulation. PB89-186456 PB89-186456 PB89-202493 DENTAL CARIES Quasi-Constant Composition Method for Studying the Formation of Artificial Caries-Like Lesions. PB89-229249 901,259	Transient and Residual Stresses in Dental Porcelains as Affected by Cooling Rates. PB89-229298 900,046 DENTIN Adhesion to Dentin by Means of Gluma Resin. PB89-157168 900,039 Oligomers with Pendant Isocyanate Groups as Adhesives for Dentin and Other Tissues. PB89-179253 900,042 Pulpal and Micro-organism Responses to Two Experimental Dental Bonding Systems. PB89-202931 901,258 Substitutes for N-Phenylglycine in Adhesive Bonding to Dentin. PB90-123795 900,051 DENTISTRY Comparison of Microleakage of Experimental and Selected Commercially Available Bonding Systems. PB89-234223 901,079 DEOXYRIBONUCLEIC ACIDS Chemical Characterization of Ionizing Radiation-Induced Damage to DNA. PB89-151922 901,235 DEOXYRIBOSE Hydroxyl Radical Induced Cross-Linking between Phenylalanine and 2-Deoxyribose. PB89-147029 900,547 DEPTH DETECTORS Analytical Applications of Neutron Depth Profiling. PB89-146872 DESIGN Guideline for Work Station Design. PB90-112418 900,643 DESIGN CRITERIA	PB89-171706 Effect of Multiple Internal Reflections on the Stability of Electrooptic and Magnetooptic Sensors. PB89-171722 Polymeric Humidity Sensors for Industrial Process Applications. PB89-176424 900,563 Ultrasonic Sensor for Measuring Surface Roughness. PB89-211809 DETERMINATION OF STRESS Ultrasonic Separation of Stress and Texture Effects in Polycrystalline Aggregates. PB90-117557 Measurement of Applied J-Integral Produced by Residual Stress. PB90-117631 DEUTERIUM Collision Induced Spectroscopy: Absorption and Light Scattering. PB89-212252 DEUTERIUM COMPOUNDS Hyperconjugation: Equilibrium Secondary Isotope Effect on the Stability of the t-Butyl Cation. Kinetics of Near-Thermoneutral Hydride Transfer. PB89-156756 Detection of Gas Phase Methoxy Radicals by Resonance Enhanced Multiphoton Ionization Spectroscopy. PB89-156766 Effects of Pressure on the Vibrational Spectra of Liquid Nitromethane. PB89-158026 Structure of the CO2-CO2-H2O van der Waals Complex Determined by Microwave Spectroscopy. PB89-230288 DEW
Load-Control Tensile Tests. PB89-171896 PB89-171896 Elevated Temperature Deformation of Structural Steel. PB89-172621 PB89-172621 PB89-172621 DEGRADATION Corrosion Induced Degradation of Amine-Cured Epoxy Coatings on Steel. PB89-176291 PB89-176291 DEHYDRATION Synthesis and Characterization of Ettringite and Related Phases. PB99-146963 DEHYDROGENATION Dehydrogenation of Ethanol in Dilute Aqueous Solution Photosensitized by Benzophenones. PB89-157556 DEMODULATION Heterodyne Measurements on OCS Near 1372 cm(-1). PB89-201743 DENSIFICATION Densification, Susceptibility and Microstructure of Ba2YCu3O(6+ x). PB89-171821 DENSITY (MASS/VOLUME) Pressure and Density Series Equations of State for Steam as Derived from the Haar-Gallagher-Kell Formulation. PB89-186456 PB89-186456 PB89-202493 DENTAL CARIES Quasi-Constant Composition Method for Studying the Formation of Artificial Caries-Like Lesions. PB89-229249 DENTAL CARIES Formation of Hydroxyapatite in Hydrogels from Tetracal-	Transient and Residual Stresses in Dental Porcelains as Affected by Cooling Rates. PB89-229298 900,046 DENTIN Adhesion to Dentin by Means of Gluma Resin. PB89-157168 900,039 Oligomers with Pendant Isocyanate Groups as Adhesives for Dentin and Other Tissues. PB89-179253 900,042 Pulpal and Micro-organism Responses to Two Experimental Dental Bonding Systems. PB89-202931 901,258 Substitutes for N-Phenylglycine in Adhesive Bonding to Dentin. PB90-123795 900,051 DENTISTRY Comparison of Microleakage of Experimental and Selected Commercially Available Bonding Systems. PB89-234223 901,079 DEOXYRIBONUCLEIC ACIDS Chemical Characterization of Ionizing Radiation-Induced Damage to DNA. PB89-151922 901,235 DEOXYRIBONUCLEIC ACIDS Chemical Characterization of Ionizing Radiation-Induced Damage to DNA. PB89-147029 900,547 DEPTH DETECTORS Analytical Applications of Neutron Depth Profiling. PB89-146872 901,294 DESIGN Guideline for Work Station Design. PB90-112418 900,643 DESIGN CRITERIA Earthquake Resistant Design Criteria. PB89-149140 900,099	Effect of Multiple Internal Reflections on the Stability of Electrooptic and Magnetooptic Sensors. PB89-171722 900,724 Polymeric Humidity Sensors for Industrial Process Applications. PB89-176424 900,563 Ultrasonic Sensor for Measuring Surface Roughness. PB89-211809 900,679 DETERMINATION OF STRESS Ultrasonic Separation of Stress and Texture Effects in Polycrystalline Aggregates. PB90-117557 900,499 Measurement of Applied J-Integral Produced by Residual Stress. PB90-117631 900,163 DEUTERIUM Collision Induced Spectroscopy: Absorption and Light Scattering. PB89-212252 901,363 DEUTERIUM COMPOUNDS Hyperconjugation: Equilibrium Secondary Isotope Effect on the Stability of the t-Butyl Cation. Kinetics of Near-Thermoneutral Hydride Transfer. PB89-156756 Detection of Gas Phase Methoxy Radicals by Resonance Enhanced Multiphoton Ionization Spectroscopy. PB89-156764 Effects of Pressure on the Vibrational Spectra of Liquid Nitromethane. PB89-158026 Structure of the CO2-CO2-H2O van der Waals Complex Determined by Microwave Spectroscopy. PB89-230288 900,479 DEW Asymptotic Expansions for Constant-Composition Dew-Bubble Curves Near the Critical Locus.
Load-Control Tensile Tests. PB89-171896 PB89-171896 PB89-172621 PB89-172621 PB89-172621 DEGRADATION Corrosion Induced Degradation of Amine-Cured Epoxy Coatings on Steel. PB89-176291 PB89-176291 PB89-176291 DEHYDRATION Synthesis and Characterization of Ettringite and Related Phases. PB89-146963 DEHYDROGENATION Dehydrogenation of Ethanol in Dilute Aqueous Solution Photosensitized by Benzophenones. PB89-157556 DEMODULATION Heterodyne Measurements on OCS Near 1372 cm(-1). PB89-201743 DENSIFICATION Densification, Susceptibility and Microstructure of Ba2YCu3O(6+ x). PB89-171821 DENSITY (MASS/VOLUME) Pressure and Density Series Equations of State for Steam as Derived from the Haar-Gallagher-Kell Formulation. PB89-186456 J900,409 Isochoric (p.,T) Measurements on CO2 and (0.98 CO2 + 0.02 CH4) from 225 to 400 K and Pressures to 35 MPa. PB89-202493 DENTAL CARIES Quasi-Constant Composition Method for Studying the Formation of Artificial Caries-Like Lesions. PB89-202499 DENTAL CEMENTS	Transient and Residual Stresses in Dental Porcelains as Affected by Cooling Rates. PB89-229298 900,046 DENTIN Adhesion to Dentin by Means of Gluma Resin. PB89-157168 900,039 Oligomers with Pendant Isocyanate Groups as Adhesives for Dentin and Other Tissues. PB89-179253 900,042 Pulpal and Micro-organism Responses to Two Experimental Dental Bonding Systems. PB89-202931 901,258 Substitutes for N-Phenylglycine in Adhesive Bonding to Dentin. PB90-123795 900,051 DENTISTRY Comparison of Microleakage of Experimental and Selected Commercially Available Bonding Systems. PB89-234223 901,079 DEOXYRIBONUCLEIC ACIDS Chemical Characterization of Ionizing Radiation-Induced Damage to DNA. PB89-151922 901,235 DEOXYRIBOSE Hydroxyl Radical Induced Cross-Linking between Phenylalanine and 2-Deoxyribose. PB89-147029 900,547 DEPTH DETECTORS Analytical Applications of Neutron Depth Profiling. PB89-146872 901,294 DESIGN Guideline for Work Station Design. PB89-14184 900,643 DESIGN CRITERIA Earthquake Resistant Design Criteria. PB89-149140 DESIGN STANDARDS Probabilistic Models for Ground Snow Accumulation.	Effect of Multiple Internal Reflections on the Stability of Electrooptic and Magnetooptic Sensors. PB89-171722 Polymeric Humidity Sensors for Industrial Process Applications. PB89-176424 P00,653 Ultrasonic Sensor for Measuring Surface Roughness. PB89-211809 PB89-211809 PB89-11809 PB89-11809 PB89-117657 Measurement of Stress and Texture Effects in Polycrystalline Aggregates. PB90-117557 Measurement of Applied J-Integral Produced by Residual Stress. PB90-117631 PB90-117631 PB90-117631 PB89-12252 PB90-117631 PB89-12252 PB90-117631 PB89-12255 PB90-117631 PB89-12255 PB90-117631 PB89-12255 PB90-117631 PB89-12255 PB90-117631 PB89-12255 PHyperconjugation: Equilibrium Secondary Isotope Effect on the Stability of the t-Butyl Cation. Kinetics of Near-Thermoneutral Hydride Transfer. PB89-156756 Petection of Gas Phase Methoxy Radicals by Resonance Enhanced Multiphoton Ionization Spectroscopy. PB89-156764 PB89-156766 PB89-158026 PB89-158026 PB89-158026 PB89-158026 PB89-230288 PBW Asymptotic Expansions for Constant-Composition Dew-Bubble Curves Near the Critical Locus. PB89-27987 P00,742
Load-Control Tensile Tests. PB89-171896 PB89-171896 PB89-172621 PB89-172621 DEGRADATION Synthesis and Characterization of Ettringite and Related Phases. PB89-146963 DEHYDROGENATION Dehydrogenation of Ethanol in Dilute Aqueous Solution Photosensitized by Benzophenones. PB89-157556 DEMODULATION Heterodyne Measurements on OCS Near 1372 cm(-1). PB89-201743 DENSIFICATION Densification, Susceptibility and Microstructure of Ba2YCu3O(6 + x). PB89-171821 PB89-171821 DENSITY (MASS/VOLUME) Pressure and Density Series Equations of State for Steam as Derived from the Haar-Gallagher-Kell Formulation. PB89-202493 DENTAL CARIES Quasi-Constant Composition Method for Studying the Formation of Hydroxyapatite in Hydrogels from Tetracal-cium Phosphate/Dicalcium Phosphate Mixtures.	Transient and Residual Stresses in Dental Porcelains as Affected by Cooling Rates. PB89-229298 900,046 DENTIN Adhesion to Dentin by Means of Gluma Resin. PB89-157168 900,039 Oligomers with Pendant Isocyanate Groups as Adhesives for Dentin and Other Tissues. PB89-179253 900,042 Pulpal and Micro-organism Responses to Two Experimental Dental Bonding Systems. PB89-202931 901,258 Substitutes for N-Phenylglycine in Adhesive Bonding to Dentin. PB90-123795 900,051 DENTISTRY Comparison of Microleakage of Experimental and Selected Commercially Available Bonding Systems. PB89-234223 901,079 DEOXYRIBONUCLEIC ACIDS Chemical Characterization of Ionizing Radiation-Induced Damage to DNA. PB89-151922 901,235 DEOXYRIBOSE Hydroxyl Radical Induced Cross-Linking between Phenylalanine and 2-Deoxyribose. PB99-147029 900,547 DEPTH DETECTORS Analytical Applications of Neutron Depth Profiling. PB89-146872 901,294 DESIGN Guideline for Work Station Design. PB90-112418 900,643 DESIGN CRITERIA Earthquake Resistant Design Criteria. PB89-149140 900,099	Effect of Multiple Internal Reflections on the Stability of Electrooptic and Magnetooptic Sensors. PB89-171722 900,724 Polymeric Humidity Sensors for Industrial Process Applications. PB89-176424 900,563 Ultrasonic Sensor for Measuring Surface Roughness. PB89-211809 900,679 DETERMINATION OF STRESS Ultrasonic Separation of Stress and Texture Effects in Polycrystalline Aggregates. PB90-117557 900,499 Measurement of Applied J-Integral Produced by Residual Stress. PB90-117631 900,163 DEUTERIUM Collision Induced Spectroscopy: Absorption and Light Scattering. PB89-212252 901,363 DEUTERIUM COMPOUNDS Hyperconjugation: Equilibrium Secondary Isotope Effect on the Stability of the t-Butyl Cation. Kinetics of Near-Thermoneutral Hydride Transfer. PB89-156756 Detection of Gas Phase Methoxy Radicals by Resonance Enhanced Multiphoton Ionization Spectroscopy. PB89-156764 Effects of Pressure on the Vibrational Spectra of Liquid Nitromethane. PB89-158026 Structure of the CO2-CO2-H2O van der Waals Complex Determined by Microwave Spectroscopy. PB89-230288 900,479 DEW Asymptotic Expansions for Constant-Composition Dew-Bubble Curves Near the Critical Locus.

PB90-128539 900,2 DI (SULFUR PENTAFLUORIDE)	and Dioxygen Fluoride (O2F). PB89-222568	900,452	DISACCHARIDES Thermodynamics of Hydrolysis o	Disaccharides.
S2F10 Formation in Computer Simulation Studies of the Breakdown of SF6.	Microwave Energy for Acid De	ecomposition at Elevated	PB89-186761 DISCOLORATION	901,221
PB89-157523 900,3	27 Temperatures and Pressures Us ical Samples.	sing Biological and Botan-	Relationship between Appearan bility of Coatings: A Literature Re	ce and Protective Dura-
Mossbauer Imaging.	PB89-171961	900,359	PB89-162598	901,063
PB89-176895 901,2	Application of Direct Digital Cor	ntrol to an Existing Build-	DISLOCATIONS (MATERIALS) Influence of Dislocation Densit	y on the Ductile-Brittle
Cathodoluminescence of Defects in Diamond Films a		900,068	Transition in bcc Metals.	
Particles Grown by Hot-Filament Chemical-Vapor Depo- tion.	Method for Fitting and Smoothin	ng Digital Data.	PB89-157804 DISPERSION	901,133
PB90-117961 901,0 DICTIONARIES	69 PB90-128794 DILUTION	900,830	Interferometric Dispersion Me	asurements on Small
Glossary of Standards-Related Terminology. PB90-130246 900,9	Second Virial Coefficients of Aq		Guided-Wave Structures. PB89-173959	_é 901,349
DIELECTRIC BREAKDOWN	ed Temperatures: A Calorimetric PB89-227896	: Study. 900,462	DISPERSIONS	Danid Calidisiansian of an
Thermal-Expansive Growth of Prebreakdown Streams in Liquids.	Determination of Serum Choles the Isotope Dilution Mass	terol by a Modification of	Formation of Dispersoids during Al-Fe-Ni Alloy.	
PB89-149074 900,8	Method.		PB90-123647 DISSOCIATION	901,172
S2F10 Formation in Computer Simulation Studies of the Breakdown of SF6.	PB89-234181 DIMENSIONAL MEASUREMENT	901,239	Photodissociation of Methyl Iodid	
PB89-157523 900,3	Approach to Accurate X-Ray N	Mask Measurements in a	PB89-171193 Thermochemistry of Solvation of	900,253
Critical Review of the Chemical Kinetics of Sulfur Tetral fluoride, Sulfur Pentafluoride, and Sulfur Fluoride (S2F1)		900,776	Organic Molecules in the Vapor F PB89-202527	Phase.
in the Gas Phase. PB89-161582 900,3	DIMENSIONS Efficient Algorithms for Computing	ng Fractal Dimoneione	Dissociation Lifetimes and Level	900,437 Mixing in Overtone-Ex-
Fracture Behavior of Ceramics Used in Multilayer Capa- tors.	PB89-175871	901,198	cited HN3 (X tilde (sup 1) A'). PB90-117425	900,263
PB89-171805 900,73	58 DIMERIZATION Relative Acidities of Water and	Methanol and the Stabili-	Ammonia Adsorption and Diss	-
DIELECTRIC PROPERTIES Dielectric Mixing Rules for Background Test Soils.	ties of the Dimer Anions. PB89-150981	900,299	Iron(s) (100) Surface. PB90-123563	900,523
PB89-188585 901,26	lonic Hydrogen Bond and Ion	· ·	DISSOCIATION ENERGY	000,020
Dielectric Measurements for Cure Monitoring. PB89-200430 900,58	Bonds, Gas Phase Solvation ar	nd Clustering of Alkoxide	Vibrational Predissociation of the PB89-147417	Nitric Oxide Dimer. 900,289
DIELECTRICS	PB89-157531	900,328	lonic Hydrogen Bond and Ion	Solvation. 5. OH(1-)O
Two-Layer Dielectric Microstrip Line Structure: SiO2 on and GaAs on Si; Modeling and Measurement.	Microwave Electric-Resonance	Optothermal Spectrosco-	Bonds. Gas Phase Solvation an and Carboxylate Anions.	d Clustering of Alkoxide
PB89-156780 900,73 Near-Field Detection of Buried Dielectric Objects.	py of (H2O)2. PB90-128141	000 501	PB89-157531	900,328
PB90-128208 900,7		300,307	DISTILLATION EQUIPMENT Design Principles for a Large High	ah-Efficiency Sub-Boiling
NBS (National Bureau of Standards) Activities in Biological Control of Standards (National Bureau of Standards)	New Photolytic Source of Dioxy itermediates Without Ozonolysis.	ymethylenes: Criegee In-	Still. PB89-187553	900,207
cal Reference Materials. PB89-157770 901,2	PB89-156731	900,304	DISTRIBUTED COMPUTER SYSTEM	-
DIFFERENTIAL SCANNING CALORIMETRY	DIPOLAR FLUIDS Molecular Dynamics Study of a	a Dipolar Fluid hetween	Experience with IMDAS (Integra Administration System) in the A	
Differential Scanning Calorimetric Study of Brain Clathrin PB90-117912 900,22	Charged Plates.	900,290	Research Facility. PB90-112350	900,964
Biological Thermodynamic Data for the Calibration of D	if- Molecular Dynamics Study of	·	DISTRIBUTION (PROPERTY)	300,304
ferential Scanning Calorimeters: Heat Capacity Data of the Unfolding Transition of Lysozyme in Solution.	On Charged Plates, 2. PB89-157218	900,312	Octanol-Water Partition Coefficie Compounds.	ents of Simple Organic
PB90-117920 900,5 DIFFRACTION	DIPOLE ANTENNAS		PB90-126244	900,528
Electron Diffraction Study of the Faceting of Tilt Gra	in Fields of Horizontal Currents Loc PB89-156830	ated Above the Earth. 900,700	DISTURBANCES National Institute of Standards an	d Tachpalagy (NIST) In
Boundaries in NiO. PB89-201792 901,43		· ·	formation Poster on Power Qualit	y.
DIFFUSION Flow of Molecules Through Condoms.	Electric-Dipole Moments of CH3OH-Formamide,	H2O-Formamide and	PB89-237986 DIURNAL VARIATIONS	900,754
PB89-148118 901,08	One obtain of Education Mission	900,288	Apparent Diurnal Effects in System.	the Global Positioning
Experimental Observations on the Initiation of DIGM (D fusion Induced Grain Boundary Migration).	Structure, and Dipole Moment of	f Ethylene Primary Ozon-	PB89-174080	901,292
PB89-157630 901,13	PB89-157440	900,323	DNA Structure of a Hydroxyl Radical	Induced Cross Link of
Solution for Diffusion-Controlled Reaction in a Vorte Field.	Absolute Intrared Transition Mon	nents for Open Shell Dia-	Thymine and Tyrosine.	
PB89-176622 900,58 Temperature-Dependent Radiation-Enhanced Diffusion	plication to OH.		PB89-157838 Biological Macromolecule Cryst	901,244 allization Database: A
Ion-Bombarded Solids. PB89-179188 901,40	D: 1 M	900,463 prational Transition Inten-	Basis for a Crystallization Strateg PB90-136722	y. 901,250
Diffusion-Induced Grain Boundary Migration.	sities of OH. PB89-227920		DNA DAMAGE	001,200
PB90-128174 901,17 DIFFUSION FLAMES	Triplet Dipoles in the Absorption	Spectra by Dense Rare	Generation of Oxy Radicals in Bio PB90-117888	systems. 901,266
Structure and Radiation Properties of Large-Scale Natur	Gas Mixtures. 1. Short Range Int PB90-136755	teractions. 900,539	DOCUMENT CIRCULATION	331,233
Gas/Air Diffusion Flames. PB89-157572 900,58	g DIPOLES		Document Interchange Standards of Major Document and Graphics	: Description and Status Standards.
Chemical Structure of Methane/Air Diffusion Flame Concentrations and Production Rates of Intermediate H	s: Fields Radiated by Electrostatic I PB90-128778	901.382	PB89-193874	900,928
drocarbons. PB89-171904 900,58	DIRECT CURRENT		DOCUMENTATION Electronic Publishing: Guide to Se	election.
Methyl Radical Concentrations and Production Rates in	a polar Charge Density and Net	Space Charge Density	PB89-214753	900,935
Laminar Methane/Air Diffusion Flame. PB89-171912 900,58	Near HVDC Power Lines. PB90-128521	901,380	DOCUMENTS Theory and Practice of Paper Pre	servation for Archives.
Very Large Methane Jet Diffusion Flames.	DIRECTIONAL SOLIDIFICATION (C		PB89-147052	900,934
PB89-175913 900,53 Importance of Isothermal Mixing Processes to the Unde	ence of a Time-Dependent Elect	ric Current.	Document Interchange Standards of Major Document and Graphics	Standards.
standing of Lift-Off and Blow-out of Turbulent Jet Diff sion Flames.	PB90-112400 DIRECTORIES	901,461	PB89-193874 DOMAIN WALLS	900,928
PB89-201172 900,58	Data Bases Available at the Na	itional Institute of Stand-	Influence of the Surface on Ma	gnetic Domain-Wall Mi-
Soot Inception in Hydrocarbon Diffusion Flames. PB89-201966 900,58	ards and Technology Research I PB89-160014	nformation Center. 900,932	crostructure. PB90-118019	901,467
Assessment of Theories for the Behavior and Blowout Lifted Turbulent Jet Diffusion Flames.	Directory of NVLAP (National \ creditation Program) Accredited I	/oluntary Laboratory Ac-	DOORS Analysis and Prediction of Air Le	akaga through D *
PB89-231096 900,60	93 PB89-185599	900,933	Analysis and Prediction of Air Le semblies.	
Combustion Efficiency, Radiation, CO and Soot Yie from a Variety of Gaseous, Liquid, and Solid Fuele	ed gram) Directory of Accredited La		PB89-231161 DOPPLER EFFECT	900,085
Buoyant Diffusion Flames. PB89-231179 900,600	PB89-189278	900,890	High Resolution Optical Multiplex PB89-185938	
DIFLUORIDE/DIOXY	Conducting Standards-Related A	ctivities.	Laser Spectroscopy of Inelastic C	900,404 ollisions.
Thermodynamic Properties of Dioxygen Difluoride (O2F2		900,008	PB89-185946	900,405

DOSE EQUIVALENTS Method for Evaluating Air Kerma and Directional Dose	PB89-148092 900,156	PB89-148118 901,08
Equivalent for Currently Available Multi-Element Dose- meters in Radiation Protection Dosimetry.	Earthquake Hazard Mitigation through Improved Seismic	ELBOWS (PIPE) Mixing Motions Produced by Pipe Elbows.
PB90-117532 901,301 DOSEMETERS	Design. PB89-149132 900,098	PB89-161871 901,32 ELECTRIC CONDUCTORS
Method for Evaluating Air Kerma and Directional Dose	Earthquake Resistant Design Criteria. PB89-149140 900,099	Transmission Loss through 6061 T-6 Aluminum Using Pulsed Eddy Current Source.
Equivalent for Currently Available Multi-Element Dosemeters in Radiation Protection Dosimetry.	EAHTHQUAKES	PB89-179840 901,14
PB90-117532 <i>901,301</i> DOSIMETRY	tive Order on Seismic Safety.	ELECTRIC CONNECTORS Simple Technique for Investigating Defects in Coaxi
Basic Data Necessary for Neutron Dosimetry. PB89-171854 901,241	Wind and Seismic Effects, Proceedings of the Joint Meet-	Connectors. PB89-146930 900,72
DOUGLAS FIR WOOD	sources Panel on Wind and Seismic Effects (20th) Held	ELECTRIC CONTACTS
Prediction of the Heat Release Rate of Douglas Fir. PB89-212039 901,185	in Gaithersburg, Maryland on May 17-20, 1988. PB89-154835 <i>900,157</i>	High T(sub c) Superconductor/Noble-Metal Contacts wit Surface Resistivities in the (10 to the Minus 10th Powe
Upward Turbulent Flame Spread on Wood under External Radiation.	Relationships between Fault Zone Deformation and Seg- ment Obliquity on the San Andreas Fault, California.	Omega sq cm Range. PB89-179824 901,41
PB90-118050 900,148	PB89-185953 901,279	Ag Screen Contacts to Sintered YBa2Cu3Ox Powder for Rapid Superconductor Characterization.
DRIFT (INSTRUMENTATION) Tests of Recalibration Period of a Drifting Instrument.	Transducers in Michelson Tiltmeters. PB89-185979 901,280	PB89-200448 901,42 ELECTRIC CONVERTERS
PB89-176275 900,199 DRIFT TUBES	Hazardous Existing Federal Buildings.	Recharacterization of Thermal Voltage Converters After
Drift Tubes for Characterizing Atmospheric Ion Mobility Spectra.	PB89-188627 900,161 ECONOMIC ANALYSIS	Thermoelement Replacement. PB89-230452 900,72
PB90-128513 901,585		ELECTRIC CORONA Method for Measuring the Stochastic Properties
DROPS (LIQUIDS) Evaporation of a Water Droplet Deposited on a Hot High	Typical VA (Veterans Administration) Patient Facility. PB89-188619 900,847	Corona and Partial-Discharge Pulses.
Thermal Conductivity Solid Surface. PB89-149157 901,487	Environmental Intelligence.	PB90-128745 900,82 ELECTRIC CURRENT
Cooling Effect Induced by a Single Evaporating Droplet on a Semi-Infinite Body.	PB89-201214 901,287 Effects of Research on Building Practice.	Improved Understanding for the Transient Operation of the Power Insulated Gate Bipolar Transistor (IGBT).
PB89-149249 901,488	PB89-202584 900,168	PB89-231229 900,79
Transient Cooling of a Hot Surface by Droplets Evapora- tion.	Analyzing the Economic Impacts of a Military Mobiliza- tion.	Directional Solidification of a Planar Interface in the Presence of a Time-Dependent Electric Current.
PB89-161897 900,971 DRUG THERAPY	PB90-128067 901,273 ECONOMICS	PB90-112400 901,46 ELECTRIC DEVICES
Two-Photon Laser-Induced Fluorescence of the Tumor- Localizing Photosensitizer Hematoporphyrin Derivative.	ZIP: ZIP-Code Insulation Program (for Microcomputers). PB89-159446 900,060	Center for Electronics and Electrical Engineering Technical Progress Bulletin Covering Center Programs, July 1
PB89-157283 901,240	EDDY CURRENT TESTS	September 1988, with 1989 CEEE Events Calendar. PB89-168033 900,77
DUAL SIX-PORT MEASUREMENT SYSTEM Measurement of Adapter Loss, Mismatch, and Efficiency	New Standard Test Method for Eddy Current Probes. PB89-187587 900,981	ELECTRIC DIPOLE MOMENTS
Using the Dual Six-Port. PB89-147839 901,316	EDDY CURRENTS Transmission Loss through 6061 T-6 Aluminum Using a	Laboratory Measurement of the 1(sub 01)-0(sub 00 Transition and Electric Dipole Moment of SiC2.
DUCTILE BRITTLE TRANSITION	Pulsed Eddy Current Source. PB89-179840 901,143	PB89-228506 900,02 ELECTRIC DIPOLES
Influence of Dislocation Density on the Ductile-Brittle Transition in bcc Metals.	EDGE EFFECT	Magnetic Dipole Excitation of a Long Conductor in
PB89-157804 901,133 Fracture Behavior of a Pressure Vessel Steel in the Duc-	Circular and Square Edge Effect Study for Guarded-Hot- Plate and Heat-Flow-Meter Apparatuses.	Lossy Medium. PB89-171664 900,74
tile-to-Brittle Transition Region. PB89-189195 901,103	PB89-176135 900,881 Summary of Circular and Square Edge Effect Study for	ELECTRIC DISCHARGES Thermal-Expansive Growth of Prebreakdown Streamer
DUCTILITY	Guarded-Hot-Plate and Heat-Flow-Meter Apparatuses. PB89-176606	in Liquids. PB89-149074 900.80
Grain Boundary Structure in Ni3AI. PB89-229314 901,157	EDGES	ELECTRIC FIELDS
DURABILITY Preliminary Stochastic Model for Service Life Prediction	Edge Stresses in Woven Laminates at Low Temperatures.	Laser Probing of Ion Velocity Distributions in Drift Field: Parallel and Perpendicular Temperatures and Mobility for
of a Photolytically and Thermally Degraded Polymeric Cover Plate Material.	PB90-128265 901,082 EDITING ROUTINES	Ba(1+) in He. PB89-171243 900,35
PB89-173801 900,556	User Guide for Wizard: A Syntax-Directed Editor and Translator for Estelle.	Measurement of Electrical Parameters Near AC and D Power Lines.
DYES Precise Laser Frequency Scanning Using Frequency-Syn-	PB89-196174 900,621	PB89-173439 900,74
thesized Optical Frequency Sidebands: Application to Isotope Shifts and Hyperfine Structure of Mercury.	EDUCATION Cool It.	Characterizing Electrical Parameters Near AC and D Power Lines.
PB90-118134 901,370 DYNAMIC STRUCTURAL ANALYSIS	PB89-176986 901,516 EFFECTIVENESS	PB89-173462 900,83 AC Electric and Magnetic Field Meter Fundamentals.
Molecular Dynamics Investigation of Expanded Water at Elevated Temperatures.	Ineffectiveness of Powder Regenerators in the 10 K	PB89-173470 900,74
PB89-174957 900,370	Temperature Range. PB89-173876 901,005	Photonic Electric Field Probe for Frequencies up to GHz.
DYSPROSIUM Occurrence of Long-Range Helical Spin Ordering in Dy-Y	Measurement of Regenerator Ineffectiveness at Low Temperatures.	PB89-176184 900,68 Experimental Study of Interpanel Interactions at 3.3 GHz
Multilayers. PB89-179634 901,410	PB89-173884 901,006 EIGENVALUES	PB89-176218 900,70
Long-Range Incommensurate Magnetic Order in Dy-Y Multilayers.	Elimination of Spurious Eigenvalues in the Chebyshev Tau Spectral Method.	Power Frequency Electric and Magnetic Field Measurements: Recent History and Measurement Standards.
PB89-179642 <i>901,411</i>	PB89-209282 901,330	PB89-176630 900,83 Photonic Electric-Field Probe for Frequencies up to
E-DOT DETECTORS Measuring Fast-Rise Impulses by Use of E-Dot Sensors.	ELASTIC ANALYSIS Elastic Interaction and Stability of Misfitting Cuboidal In-	GHz. PB89-229207 900,73
PB89-173413 900,744	homogeneities. PB89-157903 901,482	Effect of an Electrically Large Stirrer in a Mode-Stirre
EARTH SURFACE Transducers in Michelson Tiltmeters.	ELASTIC FRACTURE MECHANICS	Chamber. PB90-117946 <i>901,37</i>
PB89-185979 901,280 EARTH TIDES	Conventional and Quarter-Point Mixed Elements in Linear Elastic Fracture Mechanics.	Nonlinear Effect of an Oscillating Electric Field on Membrane Proteins.
Tilt Observations Using Borehole Tiltmeters 1. Analysis of Tidal and Secular Tilt.	PB89-157788 901,481 ELASTIC PROPERTIES	PB90-123407 901,24
PB90-136649 901,283	Calculations of Electron Inelastic Mean Free Paths for 31 Materials.	Broadband, Isotropic, Photonic Electric-Field Meter for Measurements from 10 kHz to above 1 GHz.
EARTHQUAKE ENGINEERING Wind and Seismic Effects. Proceedings of the Joint Meet-	PB89-157978 900,341	PB90-128281 900,68 DC Electric Field Effects during Measurements of Mono
ing of the U.SJapan Cooperative Program in Natural Re- sources Panel on Wind and Seismic Effects (20th) Held	Dynamic Poisson's Ratio of a Ceramic Powder during Compaction.	polar Charge Density and Net Space Charge Densit Near HVDC Power Lines.
in Gaithersburg, Maryland on May 17-20, 1988. PB89-154835 900,157	PB89-177182 901,039 Fourth-Order Elastic Constants of beta-Brass.	PB90-128521 901,38
Pore-Water Pressure Buildup in Clean Sands Because of	PB90-117607 901,160	Fields Radiated by Electrostatic Discharges. PB90-128778 901,38
Cyclic Straining. PB89-175723 <i>900,159</i>	Finite Element Studies of Transient Wave Propagation.	ELECTRIC FILTERS Discussion of 'Steep-Front Short-Duration Voltage Surg
EARTHQUAKE RESISTANT STRUCTURE Guidelines and Procedures for Implementation of Execu-	PB89-186902 901,375 ELASTOMERS	Tests of Power Line Filters and Transient Voltage Sup pressors.
tive Order on Seismic Safety.	Flow of Molecules Through Condoms.	PB90-117326 900,75

	KETWORD INDEX	
		ELECTROMAGNETIC METROLOGY
ELECTRIC MEASURING INSTRUMENTS	PB89-201818 900,894	PB89-156822 900,699
Economical Ultrahigh Vacuum Four-Point Resistivity	History of the Present Value of 2e/h Commonly Used for	Fields of Honzontal Currents Located Above the Earth.
Probe. PB89-147086 900,870	Defining National Units of Voltage and Possible Changes in National Units of Voltage and Resistance.	PB89-156830 900,700
New Realization of the Ohm and Farad Using the NBS (National Bureau of Standards) Calculable Capacitor.	PB89-202154 901,535	Error Analysis Techniques for Planar Near-Field Measure- ments.
PB89-230445 901,557	Guidelines for Implementing the New Representations of the Volt and Ohm Effective January 1, 1990.	PB89-156848 900,701
Chaos and Catastrophe Near the Plasma Frequency in	PB89-214761 900,817 NIST (National Institute of Standards and Technology)	Brief History of Near-Field Measurements of Antennas at the National Bureau of Standards.
the RF-Biased Josephson Junction. PB89-200463 901,424	Measurement Services: AC-DC Difference Calibrations.	PB89-156863 900,703 Accurate Determination of Planar Near-Field Correction
Accurate RF Voltage Measurements Using a Sampling	PB89-222616 900,818 Improved Transportable DC Voltage Standard.	Parameters for Linearly Polarized Probes.
Voltage Tracker. PB89-201552 900,815	PB89-230395 901,554	PB89-156871 900,704 Effect of Random Errors in Planar Near-Field Measure-
History of the Present Value of 2e/h Commonly Used for	Recharacterization of Thermal Voltage Converters After Thermoelement Replacement.	ment. PB89-171839 900,708
Defining National Units of Voltage and Possible Changes in National Units of Voltage and Resistance.	PB89-230452 900,720	Electromagnetic Fields in Loaded Shielded Rooms.
PB89-202154 901,535 Guidelines for Implementing the New Representations of	ELECTRICAL PHENOMENA Measurement of Partial Discharges in Hexane Under DC	PB89-180426 900,780
the Volt and Ohm Effective January 1, 1990. PB89-214761 900,817	Voltage. PB89-173421 900,833	Optically Linked Electric and Magnetic Field Sensor for Poynting Vector Measurements in the Near Fields of Ra-
Specimen Biasing to Enhance or Suppress Secondary	ELECTRICAL POTENTIAL	diating Sources. PB89-187595 <i>900,712</i>
Electron Emission from Charging Specimens at Low Accelerating Voltages.	U.S. Perspective on Possible Changes in the Electrical Units.	Bibliography of the NIST (National Institute of Standards
PB89-228464 901,451	PB89-157002 901,491 ELECTRICAL PROPERTIES	and Technology) Electromagnetic Fields Division Publications.
Josephson Array Voltage Calibration System: Operational Use and Verification.	Neutron Powder Diffraction Structure and Electrical Prop-	PB89-189211 900,810
PB89-230403 900,820	erties of the Defect Pyrochlores Pb1.5M2O6.5 (M= Nb, Ta).	Near-Field Detection of Buried Dielectric Objects. PB90-128208 900,713
Calculable, Transportable Audio-Frequency AC Reference Standard.	PB89-172431 900,363 Measurement of Electrical Breakdown in Liquids.	ELECTROMAGNETIC INDUCTION
PB90-117854 900,721 ELECTRIC POWER	PB89-212229 900,447	Electromagnetic Detection of Long Conductors in Tun- nels.
Measurement of the NBS (National Bureau of Standards)	U.S. Perspective on Possible Changes in the Electrical	PB90-128190 900,827 ELECTROMAGNETIC INTERFERENCE
Electrical Watt in SI Units. PB89-230429 900,821	Units.	Center for Electronics and Electrical Engineering Techni-
ELECTRIC POWER DEMAND	PB89-157002 901,491 Quantized Hall Resistance Measurement at the NML (Na-	cal Progress Bulletin Covering Center Programs, July to September 1988, with 1989 CEEE Events Calendar.
Advanced Heat Pumps for the 1990's Economic Per- spectives for Consumers and Electric Utilities.	tional Measurement Laboratory). PB89-179675 900,778	PB89-168033 900,775
PB90-118043 900,089 ELECTRIC SECURITY	History of the Present Value of 2e/h Commonly Used for	ELECTROMAGNETIC INTERFERENCES Optical Fiber Sensors for the Measurement of Electro-
Emerging Technologies in Electronics and Their Meas-	Defining National Units of Voltage and Possible Changes in National Units of Voltage and Resistance.	magnetic Quantities. PB89-176671 900,748
urement Needs. PB89-189245 900,811	PB89-202154 901,535	ELECTROMAGNETIC METROLOGY
Flammability Characteristics of Electrical Cables Using	Guidelines for Implementing the New Representations of the Volt and Ohm Effective January 1, 1990.	Simple Technique for Investigating Defects in Coaxial Connectors.
the Cone Calorimeter.	PB89-214761 900,817	PB89-146930 900,723
PB89-162572 900,741 ELECTRICAL ENGINEERING	Resistance Measurements of High T(sub c) Superconductors Using a Novel 'Bathysphere' Cryostat.	Mode-Stirred Chamber for Measuring Shielding Effective- ness of Cables and Connectors: An Assessment of MIL-
Center for Electronics and Electrical Engineering Techni- cal Publication Announcements Covering Center Pro-	PB89-228431 901,448 Determination of the Time-Dependence of ohm NBS (Na-	STD-1344A Method 3008. PB89-149264 900,737
grams, April-June 1986 with 1987 CEEE Events Calen-	tional Bureau of Standards) Using the Quantized Hall Re-	Microwave Power Standards.
dar. PB89-185623 900,711	sistance. PB89-230387 900,819	PB89-149272 900,687 Calibrating Antenna Standards Using CW and Pulsed-CW
Center for Electronics and Electrical Engineering Techni- cal Publication Announcements: Covering Center Pro-	Experimental Verification of the Relation between Two- Probe and Four-Probe Resistances.	Measurements and the Planar Near-Field Method.
grams, July/September 1988, with 1989 CEEE Events Calendar.	PB89-231211 900,794	PB89-149280 900,693 Antenna Measurements for Millimeter Waves at the Na-
PB89-189302 900,812	Spectroelectrochemistry of a System Involving Two Con-	tional Bureau of Standards. PB89-150726 900.694
Center for Electronics and Electrical Engineering Techni- cal Progress Bulletin Covering Center Programs, October	secutive Electron-Transfer Reaction. PB90-136979 900,237	Development of Near-Field Test Procedures for Commu-
to December 1988, with 1989 CEEE Events Calendar. PB89-193270 900,813	ELECTRODE POTENTIALS	nication Satellite Antennas, Phase 1, Part 2. PB89-156152 901,593
Center for Electronics and Electrical Engineering Techni-	Standard Electrode Potentials and Temperature Coefficients in Water at 298.15 K.	Two-Layer Dielectric Microstrip Line Structure: SiO2 on Si
cal Publication Announcements Covering Center Programs, October to December 1986, with 1987 CEEE	PB89-226567 900,456	and GaAs on Si; Modeling and Measurement. PB89-156780 900,738
Events Calendar. PB90-116195 900,824	Structural Study of a Metastable BCC Phase in Al-Mn	Spherical-Wave Source-Scattering Matrix Analysis of
ELECTRICAL FAULTS	Alloys Electrodeposited from Molten Salts. PB89-201040 901,064	Coupled Antennas: A General System Two-Port Solution. PB89-156798 900,696
Effect of an Oil-Paper Interface Parallel to an Electric Field on the Breakdown Voltage at Elevated Tempera-	Formation of the Al-Mn Icosahedral Phase by Electrode-	Improved Spherical and Hemispherical Scanning Algorithms.
tures. PB89-156988 901,490	position. PB90-117763 900,504	PB89-156806 900,697
Measurement of Electrical Breakdown in Liquids.	ELECTRODES	Improved Polarization Measurements Using a Modified Three-Antenna Technique.
PB89-212229 900,447 ELECTRICAL IMPEDANCE	Measurement of Partial Discharges in Hexane Under DC Voltage.	PB89-156814 900,698
Impedance of Radio-Frequency Biased Resistive Super-	PB89-173421 900,833	Gain and Power Parameter Measurements Using Planar Near-Field Techniques.
conducting Quantum Interference Devices. PB89-201719 900,764	Development of a Method to Measure In situ Chloride at the Coating/Metal Interface.	PB89-156822 900,699
ELECTRICAL MEASUREMENT NBS (National Bureau of Standards) Ohm: Past-Present-	PB89-235345 901,085 ELECTROMAGNETIC ABSORPTION	Fields of Horizontal Currents Located Above the Earth. PB89-156830 900,700
Future.	Alternative Techniques for Some Typical MIL-STD-461/	Error Analysis Techniques for Planar Near-Field Measure-
PB89-149066 900,802 High-Current Measurement Techniques. Part II. 100-kA	462 Types of Measurements. PB89-235139 901,272	ments. PB89-156848 900,701
Source Characteristics and Preliminary Shunt and Rogowski Coil Evaluations.	ELECTROMAGNETIC COMPATIBILITY Measurement Procedures for Electromagnetic Compat-	Comparison of Measured and Calculated Antenna Side- lobe Coupling Loss in the Near Field Using Approximate
PB89-170872 900,804	ibility Assessment of Electroexplosive Devices.	Far-Field Data.
New Internationally Adopted Reference Standards of Voltage and Resistance.	PB89-146914 901,314 Proficiency Testing for MIL-STD 462 NVLAP (National	PB89-156855 900,702 Brief History of Near-Field Measurements of Antennas at
PB89-184097 900,808	Voluntary Laboratory Accreditation Program) Laboratories.	the National Bureau of Standards. PB89-156863 900,703
Emerging Technologies in Electronics and Their Measurement Needs.	PB90-128612 901,381	Accurate Determination of Planar Near-Field Correction
PB89-189245 900,811 Performance Evaluation of Radiofrequency, Microwave,	ELECTROMAGNETIC FIELDS Iterative Technique to Correct Probe Position Errors in	Parameters for Linearly Polarized Probes. PB89-156871 900,704
and Millimeter Wave Power Meters. PB89-193916 900,814	Planar Near-Field to Far-Field Transformations. PB89-153886 900,695	Effect of an Oil-Paper Interface Parallel to an Electric
Accurate RF Voltage Measurements Using a Sampling	Improved Polarization Measurements Using a Modified	Field on the Breakdown Voltage at Elevated Tempera- tures.
Voltage Tracker. PB89-201552 900,815	Three-Antenna Technique. PB89-156814 900,698	PB89-156988 901,490 U.S. Perspective on Possible Changes in the Electrical

Gain and Power Parameter Measurements Using Planar Near-Field Techniques.

Stability of the SI (International System) Unit of Mass as Determined from Electrical Measurements.

U.S. Perspective on Possible Changes in the Electrical Units. PB89-157002 901,491

Waveguide Loss Measurement Using Photothermal De-	Performance Evaluation of Radiofrequency, Microwave, and Millimeter Wave Power Meters.	PB90-128745 900,829
flection. PB89-157028 <i>900,739</i>	PB89-193916 900,814	Fields Radiated by Electrostatic Discharges. PB90-128778 901,382
Fresnel Lenses Display Inherent Vignetting. PB89-157069 901,337	Battery-Powered Current Supply for Superconductor Measurements. PB89-200455 901,525	Radiometer Equation and Analysis of Systematic Errors for the NIST (National Institute of Standards and Tech-
Current Ripple Effect on Superconductive D.C. Critical Current Measurements. PB89-157077 901,492	Superconducting Kinetic Inductance Bolometer. PB89-200505 900,762	nology) Automated Radiometers. PB90-130907 900,832
Efficient and Accurate Method for Calculating and Representing Power Density in the Near Zone of Microwave	Noise in DC SQUIDS with Nb/Al-Oxide/Nb Josephson Junctions. PB89-201032 900,763	ELECTROMAGNETIC NOISE Low Noise Frequency Synthesis. PB89-174056 900,716
Antennas. PB89-157457 Electromagnetic Pulse Scattered by a Sphere.	Reflection Coefficient of a Waveguide with Slightly Uneven Walls.	Using Multiple Reference Stations to Separate the Variances of Noise Components in the Global Positioning
PB89-157895 901,495	PB89-201057 900,753	System. PB89-185730 <i>901,293</i>
Techniques for Measuring the Electromagnetic Shielding Effectiveness of Materials. Part 1. Far-Field Source Simulation.	Impedance of Radio-Frequency Biased Resistive Super- conducting Quantum Interference Devices. PB89-201719 900,764	Switching Noise in YBa2Cu3Ox 'Macrobridges'. PB89-200513 901,426
PB89-161525 900,680	Assessment of Space Power Related Measurement Re-	Noise in DC SQUIDS with Nb/Al-Oxide/Nb Josephson Junctions.
Techniques for Measuring the Electromagnetic Shielding Effectiveness of Materials. Part 2. Near-Field Source Sim- ulation.	quirements of the Strategic Defense Initiative. PB89-209357 901,269 Calibration of Voltage Transformers and High-Voltage Ca-	PB89-201032 900,763 ELECTROMAGNETIC PROPERTIES
PB89-161533 900,681 Fast Optical Detector Deposited on Dielectric Channel	pacitors at NIST. PB89-211114 90;,442	Metrology for Electromagnetic Technology: A Bibliogra- phy of NBS (National Bureau of Standards) Publications.
Waveguides.	Calibration of GPS (Global Positioning System) Equip-	PB89-147847 900,871
PB89-171706 900,743 Electrically Calibrated Silicon Bolometer for Low Level Optical Power and Energy Measurements.	ment in Japan. PB89-212070 900,630 MM Wave Quasioptical SIS Mixers.	ELECTROMAGNETIC PULSES Electromagnetic Pulse Scattered by a Sphere. PB89-157895 901,495
PB89-171714 901,348	PB89-214738 901,446	Measuring Fast-Rise Impulses by Use of E-Dot Sensors.
Effect of Random Errors in Planar Near-Field Measurement.	Generation of Squeezed Light by Intracavity Frequency Doubling.	PB89-173413 900,744
PB89-171839 900,708	PB89-227938 901,365	ELECTROMAGNETIC RADIATION Theory and Measurements of Radiated Emissions Using
Measuring Fast-Rise Impulses by Use of E-Dot Sensors. PB89-173413 900,744	Cryogenic Bathysphere for Rapid Variable-Temperature Characterization of High-T(sub c) Superconductors. PB89-228456 901,450	a TEM (Transverse Electromagnetic) Cell. PB89-193890 900,761
Measurement of Electrical Parameters Near AC and DC Power Lines.	PB89-228456 901,450 Determination of AC-DC Difference in the 0.1 - 100 MHz	Implementation of an Automated System for Measuring
PB89-173439 900,745	Frequency Range. PB89-228597 900,719	Radiated Emissions Using a TEM Cell. PB90-117698 901,377
Estimates of Confidence Intervals for Divider Distorted Waveforms.	Photonic Electric-Field Probe for Frequencies up to 2	ELECTROMAGNETIC RADIATION DETECTION
PB89-173447 900,806 Characterizing Electrical Parameters Near AC and DC	GHz. PB89-229207 900,732	Automated TEM (Transverse Electromagnetic) Cell for Measuring Unintentional EM Emissions.
Power Lines.	Clutter Models for Subsurface Electromagnetic Applica-	PB89-173769 900,682 ELECTROMAGNETIC SCATTERING
PB89-173462 900,834 Automated TEM (Transverse Electromagnetic) Cell for	tions. PB89-229678 900,688	Electromagnetic Pulse Scattered by a Sphere.
Measuring Unintentional EM Emissions. PB89-173769 900,682	Flux Creep and Activation Energies at the Grain Boundaries of Y-Ba-Cu-O Superconductors.	PB89-157895 901,495 Experimental Study of Interpanel Interactions at 3.3 GHz.
ANA (Automatic Network Analyzer) Measurement Results	PB89-230353 901,457	PB89-176218 900,709
on the ARFTG (Automatic RF Techniques Group) Traveling Experiment. PB89-173777 900,715	Advances in NIST (National Institute of Standards and Technology) Dielectric Measurement Capability Using a Mode-Filtered Cylindrical Cavity.	ELECTROMAGNETIC SHIELDING Mode-Stirred Chamber for Measuring Shielding Effectiveness of Cables and Connectors: An Assessment of MIL-
Transient Response Error in Microwave Power Meters Using Thermistor Detectors.	PB89-231146 900,907 Alternative Techniques for Some Typical MIL-STD-461/	STD-1344A Method 3008. PB89-149264 900,737
PB89-173785 900,759 Interferometric Dispersion Measurements on Small	462 Types of Measurements. PB89-235139 901,272	Techniques for Measuring the Electromagnetic Shielding Effectiveness of Materials. Part 1. Far-Field Source Simu-
Guided-Wave Structures. PB89-173959 901,349	X-Band Atmospheric Attenuation for an Earth Terminal Measurement System.	lation. PB89-161525 900,680
Optical Fiber Sensors for Electromagnetic Quantities.	PB90-100736 900,626	Techniques for Measuring the Electromagnetic Shielding
PB89-173967 900,725 Dual Frequency P-Code Time Transfer Experiment.	Detection of the Free Radicals FeH, CoH, and NiH by Far Infrared Laser Magnetic Resonance.	Effectiveness of Materials. Part 2. Near-Field Source Simulation.
PB89-174064 900,614	PB90-117342 900,495 Calibrating Network Analyzers with Imperfect Test Ports.	PB89-161533 900,681 ELECTROMAGNETIC WAVES
Some Questions and Answers Concerning Air Lines as Impedance Standards. PB89-176176 900,747	PB90-117680 900,825 Implementation of an Automated System for Measuring	Hybrid Representation of the Green's Function in an Overmoded Rectangular Cavity.
Photonic Electric Field Probe for Frequencies up to 2	Radiated Emissions Using a TEM Cell. PB90-117698 901,377	PB90-117953 900,826 ELECTROMIGRATION
GHz. PB89-176184 <i>900,683</i>	Calculable, Transportable Audio-Frequency AC Refer-	Electromigration Damage Response Time and Implica-
NIST (National Institute of Standards and Technology) Automated Coaxial Microwave Power Standard.	ence Standard. PB90-117854 900,721	tions for dc and Pulsed Characterization. PB89-212179 901,443
PB89-176192 900,807	Effect of an Electrically Large Stirrer in a Mode-Stirred Chamber.	ELECTRON-ATOM COLLISIONS Autodetaching States of Negative Ions.
Experimental Study of Interpanel Interactions at 3.3 GHz. PB89-176218 900,709	PB90-117946 <i>901,378</i>	PB89-150767 900,295
Resonance Light Scattering from a Suspension of Microspheres. PB89-176234 901,352	Hybrid Representation of the Green's Function in an Overmoded Rectangular Cavity. PB90-117953 900,826	State Selection in Electron-Atom Scattering: Spin-Polarized Electron Scattering from Optically Pumped Sodium. PB89-176572 901,513
Potential Errors in the Use of Optical Fiber Power Meters. PB89-176697 900,728	Interactions between Two Dividers Used in Simultaneous Comparison Measurements.	Laser Spectroscopy of Inelastic Collisions. PB89-185946 900,405
Profile Inhomogeneity in Multimode Graded-Index Fibers.	PB90-118035 900,031 Millimeter- and Submillimeter-Wave Surveys of Orion A	ELECTRON BEAM
PB89-179816 900,749	Emission Lines in the Ranges 200.7-202.3, 203.7-205.3, and 330-360 GHz.	Metastable Phase Production and Transformation in Al- Ge Alloy Films by Rapid Crystallization and Annealing
High T(sub c) Superconductor/Noble-Metal Contacts with Surface Resistivities in the (10 to the Minus 10th Power)	PB90-123787 900,029	Treatments. PB89-157622 901,129
Omega sq cm Range. PB89-179824 901,413	Electromagnetic Detection of Long Conductors in Tun-	ELECTRON BEAMS
Transmission Loss through 6061 T-6 Aluminum Using a	nels. PB90-128190 <i>900,827</i>	Kinetics of Resolidification. PB89-176457 901,138
Pulsed Eddy Current Source. PB89-179840 901,143	Near-Field Detection of Buried Dielectric Objects. PB90-128208 900,713	ELECTRON CHARGE
Antennas for Geophysical Applications. PB89-179857 900,710	Broadband, Isotropic, Photonic Electric-Field Meter for Measurements from 10 kHz to above 1 GHz. PB90-128281 900,686	NBS (National Bureau of Standards) Determination of the Fine-Structure Constant, and of the Quantized Hall Re- sistance and Josephson Frequency-to-Voltage Quotient
Electromagnetic Fields in Loaded Shielded Rooms. PB89-180426 900,780	Thermo-Optic Designs for Microwave and Millimeter-	in SI Units. PB89-230437 901,556
New Standard Test Method for Eddy Current Probes. PB89-187587 900,981	Wave Electric-Field Probes. PB90-128588 900,691	ELECTRON COLLISIONS
Theory and Measurements of Radiated Emissions Using	Proficiency Testing for MIL-STD 462 NVLAP (National	Electron Stopping Powers for Transport Calculations. PB90-123605 901,566
a TEM (Transverse Electromagnetic) Cell. PB89-193890 900,761	Voluntary Laboratory Accreditation Program) Laboratories.	ELECTRON DENSITY (CONCENTRATION)
(12)C(16)O Laser Frequency Tables for the 34.2 to 62.3	PB90-128612 901,381 Method for Measuring the Stochastic Properties of	Pi-Electron Properties of Large Condensed Polyaromatic Hydrocarbons.
THz (1139 to 2079 cm(-1)) Region.	Corona and Partial-Discharge Pulses.	PB89-202139 900,432

ELECTRON DETACHMENT	PB90-128307 901,584	PB89-147839 <i>901,316</i>
Collisional Electron Detechment and Decomposition Retes of SF6(1-), SF5(1-), end F(1-) in SF6: Implications	ELECTRON SPIN Improved Low-Energy Diffuse Scattering Electron-Spin	Magnetostatic Measurements for Mine Detection. PB89-148365 900,685
for Ion Trensport and Electrical Discherges. PB90-117862 900,511	Polerization Analyzer. PB89-229173 900,218	Review of Thermal Characterizetion of Power Trensistors. PB89-150825 900,770
ELECTRON DIFFRACTION NIST (National Institute of Standerds end Technology)/	Use of Thorium es a Target in Electron-Spin Anelyzers. PB90-117938 900,912	Indirect Energy Gap of Si, Doping Dependence.
Sendia/ICDD Electron Diffraction Detabese: A Detabase for Phase Identification by Electron Diffrection.	ELECTRON SPIN POLARIZATION	PB89-150833 901,388 Submicrometer Opticel Metrology.
PB89-175210 901,508 ELECTRON ENERGY	Spin-Polarized Electron Microscopy. PB89-158075 901,395	PB89-150973 900,771
High Resolution Spectrum of the nu(sub 1) + nu(sub 2) Band of NO2. A Spin Induced Perturbation in the Ground	Progress on Spin Detectors end Spin-Polerized Electron Scettering from Na at NIST. PB90-128299 901,583	Semiconductor Measurement Technology: Automatic De- termination of the Interstitiel Oxygen Content of Silicon Wefers Polished on Both Sides.
State. PB89-187561 900,417	Superelestic Scattering of Spin-Polerized Electrons from	PB89-151831 900,772
Cross Sections for Bremsstrehlung Production end Elec-	Sodium. PB90-128307 <i>901,584</i>	SIS Quesiparticle Mixers with Bow-Tie Antennas. PB89-157036 900,705
tron-Impact Ionization. PB90-123910 901,575	ELECTRON STIMULATED DESORPTION Secondary-Electron Effects in Photon-Stimulated Desorp-	Measurement of Integrated Tuning Elements for SIS Mixers with e Fourier Transform Spectrometer.
LECTRON-ION COLLISIONS	tion. PB89-157929 900,337	PB89-157051 900,706
Electron-Impact Excitetion of the Resonence Trensition in CA(1+).	Resonance Enhenced Electron Stimulated Desorption.	Effect of Neutrons on the Characteristics of the Insulated Gate Bipolar Transistor (IGBT).
PB89-171557 901,502 Electron-Impact Excitetion of AI(2+).	PB90-117771 900,505 ELECTRON TRANSFER	PB89-157655 900,773 Application of Multiscattering Theory to Impurity Bends in
PB89-171565 901,503 Spectroscopy of Autoionizing States Contributing to Elec-	Kinetics of Electron Transfer from Nitroeromatic Radical Anions in Aqueous Solutions. Effects of Temperature and	Si:Às. PB89-157762 <i>900,334</i>
tron-Impact Ionization of Ions. PB90-123837 901,572	Steric Configuration. PB89-156749 900,305	Tiger Tempering Tampers Transmissions. PB89-157861 900,740
Electron-Impact Ionization of La(q+) lons (q= 1,2,3).	Laser Probing of Product-State Distributions in Thermal-	Standards and Test Methods for VLSI (Very Large Scale
PB90-123845 901,573 ELECTRON MICROPROBE ANALYSIS	Energy Ion-Molecule Reections. PB89-171250 900,353	Integration) Materials. PB89-158042 900,774
Role of Standards in Electron Microprobe Techniques. PB89-176143 900,197	Spectroelectrochemistry of a System Involving Two Con- secutive Electron-Transfer Reaction.	Electrical Performance Tests for Hand-Held Digital Multi- meters.
Defocus Modeling for Compositional Mapping with Wave-	PB90-136979 900,237 ELECTRON TRANSITIONS	PB89-162234 900,876
length-Dispersive X-rey Spectrometry. PB89-176150 900,378	Journal of Physical and Chemical Reference Data, Volume 17, 1988, Supplement No. 3. Atomic Transition	Analysis of Computer Performance Data. PB89-162614 900,635
ELECTRON MICROSCOPES High-Purity Germanium X-rey Detector on a 200 kV Ane-	Probebilities Scandium through Manganese. PB89-145197 900,276	Center for Electronics and Electrical Engineering Technical Progress Bulletin Covering Center Programs, July to
lytical Electron Microscope. PB89-201602 900,208	Picosecond Study of the Population Lifetime of CO(v= 1)	September 1988, with 1989 CEEE Events Celendar. PB89-168033
ELECTRON MICROSCOPY	Chemisorbed on SiO2-Supported Rhodium Particles. PB89-157317 900,317	High-Current Measurement Techniques. Part II. 100-kA
Defect Intergrowths in Barium Polytitanates. 1. Ba2Ti9O20. PB89-146823 901,014	Microwave Spectrum and (14)N Quadrupole Coupling Constants of Carbazole.	Source Characteristics and Preliminary Shunt and Rogowski Coil Evaluations.
Defect Intergrowths in Banum Polytitanates. 2. BaTi5O11.	PB89-157333 900,319 Refinement of the Substructure and Superstructure of	PB89-170872 900,804 Power Quality Site Surveys: Facts, Fiction, and Fallacies.
PB89-146831 901,015 Observations on Crystal Defects Associeted with Diffu-	Romanechite. PB89-157721 901,392	PB89-171656 900,805 Strategic Defence Initiative Space Rower Systems Metrol
sion Induced Grain Boundary Migration in Cu-Zn. PB89-157606 901,127	Application of Multiscattering Theory to Impurity Bands in	Strategic Defense Initiative Space Power Systems Metrology Assessment. PB89-173405 901,268
Role of Standards in Electron Microprobe Techniques.	Si:As. PB89-157762 900,334	Measurement of Partial Discharges in Hexane Under DC
PB89-176143 900,197 Performance Standards for Microanalysis.	Spectra and Energy Levels of the Galliumlike Ions Rb VII- Mo XII.	Voltage. PB89-173421 900,833
PB89-201651 900,211 Grain Boundary Characterization in Ni3Al.	PB89-179105 900,387 ELECTRON TRANSPORT	Coupling, Propagation, and Side Effects of Surges in an Industrial Building Wiring System.
PB89-229306 <i>901,156</i>	Electron Stopping Powers for Transport Calculations. PB90-123605 901,566	PB89-173454 900,118
Determination of Experimental and Theoretical k (sub ASi) Factors for a 200-kV Analytical Electron Microscope. PB90-128653 900,232	Cross Sections for Bremsstrahlung Production and Elec-	Low Noise Frequency Synthesis. PB89-174056 900,716
ELECTRON MOBILITY	tron-Impact Ionization. PB90-123910 901,575	Analytical Modeling of Device-Circuit Interactions for the Power Insulated Gate Bipolar Transistor (IGBT).
Electron Transmission Through NiSi2-Si Interfaces. PB89-231294 900,485	ELECTRON TUNNELING Electric-Resonance Optothermal Spectrum of (H2O)2:	PB89-176259 900,777
LECTRON-MOLECULE COLLISIONS	Microwave Spectrum of the K= 1-0 Subband for the E((+ or -)2) States.	Secure Military Communications Can Benefit from Accurate Time. PB89-176507 901,274
Cross Sections for Collisions of Electrons and Photons with Oxygen Molecules.	PB90-117433 900,497	Power Frequency Electric and Magnetic Field Measure-
PB89-226575 900,457 ELECTRON-NUCLEON INTERACTIONS	Power Quality Site Surveys: Facts, Fiction, and Fallacies.	ments: Recent History and Measurement Standards. PB89-176630 900,835
Quasifree Electron Scattering on Nucleons in a Momen- tum-Dependent Potential.	PB89-171656 900,805 ELECTRONIC PUBLISHING	Selecting Varistor Clamping Voltage: Lower Is Not Better. PB89-176648 900,760
PB89-186738 901,524 ELECTRON PROBES	Electronic Publishing: Guide to Selection. PB89-214753 900,935	Picosecond Pulse Response from Hydrogenated Amor-
Computer-Aided Imaging: Quantitative Compositional Mapping with the Electron Probe Microanalyzer.	ELECTRONIC STATES	phous Silicon (a-Si:H) Optical Detectors on Channel Wavegudes.
PB89-157754 901,073	Alignment Effects in Electronic Energy Transfer and Re- active Events.	PB89-176689 900,727 Correlation between CMOS (Complementary Metal Oxide
Experimental Verification of the Relation between Two- Probe and Four-Probe Resistances.	AD-A202 820/7 900,267 ELECTRONIC STRUCTURE	Semiconductor) Transistor and Capacitor Measurements of Interface Trap Spectra.
PB89-231211 900,794 Broadband, Isotropic, Photonic Electric-Field Meter for	Filling of Solvent Shells About Ions. 1. Thermochemical Criteria and the Effects of Isomeric Clusters.	PB89-180020 900,779 Scattering Parameters Representing Imperfections in Pre-
Measurements from 10 kHz to above 1 GHz. PB90-128281 900,686	PB89-157549 900,329 Electronic Structure of the Cd Vacancy in CdTe.	cision Coaxial Air Lines. PB89-184121 900,750
Thermo-Optic Designs for Microwave and Millimeter- Wave Electric-Field Probes.	PB89-171318 901,398	Turning Workstation in the AMRF (Automated Manufac-
PB90-128588 900,691	Influence of Electronic and Geometric Structure on Desorption Kinetics of Isoelectronic Polar Molecules: NH3	turing Řesearch Facility). PB89-185607 900,954
State Selection in Electron-Atom Scattering: Spin-Polar-	and H2O. PB89-176473 900,381	Center for Electronics and Electrical Engineering Technical Publication Announcements Covering Center Pro-
ized Electron Scattering from Optically Pumped Sodium. PB89-176572 901,513	Photon-Stimulated Desorption as a Measure of Surface Electronic Structure.	grams, April-June 1986 with 1987 CEEE Events Calendar.
Quasifree Electron Scattering on Nucleons in a Momentum-Dependent Potential.	PB89-231328 901,459 ELECTRONIC TECHNOLOGY	PB89-185623 900,711
PB89-186738 901,524	Multiple Scattering in the X-ray-Absorption Near-Edge	International Comparison of HV Impulse Measuring Sys- tems. PB89-186423 900,809
Cross Sections for Inelastic Electron Scattering in Solids. PB89-202972 901,440	Structure of Tetrahedral Ge Gases. PB89-146922 900,283	Numerical Analysis for the Small-Signal Response of the
Progress on Spin Detectors and Spin-Polarized Electron Scattering from Na at NIST.	Economical Ultrahigh Vacuum Four-Point Resistivity Probe.	MOS (Metal Oxide Semiconductors) Capacitor. PB89-186837 900,781
PB90-128299 901,583	PB89-147086 900,870	Emerging Technologies in Electronics and Their Meas-

Measurement of Adapter Loss, Mismatch, and Efficiency Using the Dual Six-Port.

Superelastic Scattering of Spin-Polarized Electrons from Sodium.

Emerging Technologies in Electronics and Their Measurement Needs. PB89-189245 900,811

Center for Electronics and Electrical Engineering Technical Publication Announcements: Covening Center Pro-	PB90-117300 900,22	,
grams, July/September 1988, with 1989 CEEE Events Calendar.	Discussion of 'Steep-Front Short-Duration Voltage Surg- Tests of Power Line Filters and Transient Voltage Sup pressors.'	Emerging Technologies in Electronics and Their Meas-
PB89-189302 900,812	PB90-117326 900,75	urement Needs. PB89-189245 900,811
Center for Electronics and Electrical Engineering Techni- cal Progress Bulletin Covering Center Programs, October	High Accuracy Modeling of Photodiode Quantum Efficien	
to December 1988, with 1989 CEEE Events Calendar. PB89-193270 900,813	PB90-117599 900,73	Acoustic Emission: A Quantitative NDE Technique for the Study of Fracture.
Audio-Frequency Current Comparator Power Bridge: Development and Design Considerations.	Electron-Energy Dependence of the S2F10 Mass Spectrum.	- PB89-211924 <i>900,921</i>
PB89-201537 <i>900,717</i>	PB90-117870 900,512	Spectra and Engrav Loyale of Dr VVV Dr VVIV Dr VVV
Infrared Absorption Cross Section of Arsenic in Silicon in the Impurity Band Region of Concentration.	Numerical Simulations of Neutron Effects on Bipola Transistors.	and Br XXXI.
PB89-201750 900,426	PB90-123589 900,791	EMICCION COPOTROCOORY
Radiation-Induced Interface Traps in Power MOSFETs. PB89-201974 900,784 Center for Electronics and Electrical Engineering: Techni-	Stability and Quantum Efficiency Performance of Silicor Photodiode Detectors in the Far Ultraviolet. PB90-128059 900,73:	Atomic Transition Probabilities of Argon: A Continuing Challenge to Plasma Spectroscopy.
cal Progress Bulletin Covering Center Programs, January to March 1989, with 1989 CEEE Events Calendar.	Growth and Properties of High-Quality Very-Thin SOS (Silicon-on Sapphire) Films.	PB89-158125 900,344 Near-Threshold X-ray Fluorescence Spectroscopy of Mol-
PB89-209225 900,786	PB90-128109 900,796	
Center for Electronics and Electrical Engineering Techni- cal Publication Announcements. Covering Center Pro-	Silicon and GaAs Wire-Bond Cratering Problem. PB90-128182 900,799	
grams, October/December 1988, with 1989 CEEE Events Calendar	Effect of Pressure on the Development of Prebreakdown Streamers.	atura Maggurament in Blook Linuar Beauties, Belleve
PB89-209241 900,787 Blocked Impurity Band and Superlattice Detectors: Pros-	PB90-128315 900,826	
pects for Radiometry. PB89-212161 900,730	Drift Tubes for Characterizing Atmospheric Ion Mobility Spectra.	Hand Calculations for Enclosure Fires. PB89-173983 900.164
Electromigration Damage Response Time and Implica-	PB90-128513 901,585	rundamentals of Enclosure File Zone Models.
tions for dc and Pulsed Characterization. PB89-212179 901,443	DC Electric Field Effects during Measurements of Mono polar Charge Density and Net Space Charge Density	
Neural Network Approach for Classifying Test Structure	Near HVDC Power Lines. PB90-128521 901,380	Thermal and Economic Analysis of Three HVAC (Heat-
Results. PB89-212187 900,788	Ambiguity Groups and Testability.	ing, Ventilating, and Air Conditioning) System Types in a Typical VA (Veterans Administration) Patient Facility.
Thermal Conductivity Measurements of Thin-Film Silicon	PB90-128703 900,722	PB89-188619 900,847
Dioxide. PB89-212195 901,444	ELECTRONICS Center for Electronics and Electrical Engineering Techni	
Guidelines for Implementing the New Representations of the Volt and Ohm Effective January 1, 1990.	cal Publication Announcements Covering Center Pro- grams, April-June 1986 with 1987 CEEE Events Calen	Programs
PB89-214761 900,817	dar. PB89-185623 900,711	
Semiconductor Measurement Technology: Database for and Statistical Analysis of the Interlaboratory Determina-	Center for Electronics and Electrical Engineering Techni	U-Value Measurements for Windows and Movable Insula-
tion of the Conversion Coefficient for the Measurement of the Interstitial Oxygen Content of Silicon by Infrared	cal Publication Announcements Covering Center Programs, October to December 1986, with 1987 CEEE	ries.
Absorption.	Évents Calendar.	PB69-175609 900,121
PB89-221170 901,054 Center for Electronics and Electrical Engineering Techni-	PB90-116195 900,824 ELECTRONICS LABORATORIES	semblies.
cal Publication Announcements. Covering Center Programs, January-March 1989, with 1989 CEEE Events Cal-	Safety Guidelines for Microwave Systems in the Analyti-	PB89-231161 900,085
endar.	cal Laboratory. PB90-118167 <i>900,68</i> 5	
PB89-228308 900,789 EXAFS (Extended X-ray Absorption Fine Structure) Study	ELECTRONS	date Standard Reference Material of Thermal Resistance.
of Buried Germanium Layer in Silicon. PB89-228472 901,452	Calculations of Electron Inelastic Mean Free Paths for 31 Materials.	PB89-148373 901,018
Silicon Photodiode Detectors for EXAFS (Extended X-ray	PB89-157978 900,341	Applysic 1099: Applied Supplement to NIPS (National
Absorption Fine Structure). PB89-228498 900,731	Electron Mean Free Path Calculations Using a Model Di electric Function.	Bureau of Standards) Handbook 135 and NBS Special
Effects of Doping-Density Gradients on Band-Gap Nar-	PB89-177026 901,141 ELECTROOPTICS	PB89-153860 900,850
rowing in Silicon and GaAs Devices. PB89-228522 901,453	Effect of Multiple Internal Reflections on the Stability of	Periodic Heat Conduction in Energy Storage Cylinders with Change of Phase.
Machine-Learning Classification Approach for IC Manufacturing Control Based on Test Structure Measurements.	Electrooptic and Magnetooptic Sensors. PB89-171722 900,724	PB89-175897 <i>900,852</i>
PB89-228530 900,790	ELECTROPHORESIS	Performance Measurements of Infrared Imaging Systems Used to Assess Thermal Anomalies.
Lightning and Surge Protection of Photovoltaic Installa- tions. Two Case Histories: Vulcano and Kythnos.	Development of Electrophoresis and Electrofocusing Standards.	1 200 1 1 0001
PB89-229058 900,851	PB89-175863 900,195	Laser Induced Vaporization Time Resolved Mass Spectrometry of Refractories.
High-Mobility CMOS (Complementary Metal Oxide Semi- conductor) Transistors Fabricated on Very Thin SOS	ELECTROSTATIC DISCHARGE Fields Radiated by Electrostatic Discharges.	PB90-136904 900,540
Films. PB89-230460 900,791	PB90-128778 901,382 ELECTROSTATIC PROBES	Control Strategies and Building Energy Consumption.
Production and Stability of S2F10 in SF6 Corona Dis-	Iterative Technique to Correct Probe Position Errors in	PB89-172340 900,061
charges. PB89-231039 900,822	Planar Near-Field to Far-Field Transformations. PB89-153886 900,695	ENERGY GAP Indirect Energy Gap of Si, Doping Dependence.
IEEE (Institute of Electrical and Electronics Engineers) IRPS (International Reliability Physics Symposium) Tutori-	Accurate Determination of Planar Near-Field Correction	PB89-150833 901,388
al Thermal Resistance Measurements, 1989.	Parameters for Linearly Polarized Probes. PB89-156871 900,704	Effects of Doping-Density Gradients on Band-Gap Narrowing in Silicon and GaAs Devices.
PB89-231195 900,792 AC Impedance Method for High-Resistivity Measure-	ELEMENTARY EXCITATIONS	PB89-228522 901,453
ments of Silicon. PB89-231203 900,793	Computer Simulation Studies of the Soliton Model. 3 Noncontinuum Regimes and Soliton Interactions.	Wavelengths and Energy Level Classifications of Scandi-
Experimental Verification of the Relation between Two-	PB89-202469 901,537	um Spectra for All Stages of Ionization. PB89-145163 900,273
Probe and Four-Probe Resistances. PB89-231211 900,794	ELEVATORS (LIFTS) Experimental Fire Tower Studies of Elevator Pressuriza-	
Improved Understanding for the Transient Operation of	tion Systems for Smoke Control. PB90-117813 900,097	Analysis of a 3p Rydberg State of the Hydroxymethyl
the Power Insulated Gate Bipolar Transistor (IGBT). PB89-231229 900,795	ELLIPSOMETERS	PB89-146666 900,279
Power MOSFET Failure Revisited. PB89-231237 900,796	Semiconductor Measurement Technology: A Software Program for Aiding the Analysis of Ellipsometric Measure	
Semiconductor Measurement Technology: A Software	ments, Simple Models. PB89-235923 901,365	PB89-146898 <i>900,282</i>
Program for Aiding the Analysis of Ellipsometric Measurements, Simple Models.	ELLIPTIC DIFFERENTIAL EQUATIONS	Fundamental Configurations in Mo IV Spectrum. PB89-147011 900,284
PB89-235923 901,369	Note on the Capacitance Matrix Algorithm, Substructur- ing, and Mixed or Neumann Boundary Conditions.	Stokes and Anti-Stokes Fluorescence of Er(3+) in the
National Institute of Standards and Technology (NIST) Information Poster on Power Quality.	PB89-177034 901,198	Raman Spectra of Erbium Oxide and Erbium Glasses. PB89-149231 901,020
PB89-237986 900,754	EMERGENCY PLANNING Evaluating Emergency Management Models and Data	ENERGY MANAGEMENT SYSTEMS
Research for Electric Energy Systems: An Annual Report. PB90-112442 900,853	Bases: A Suggested Approach.	Analysis 1988: Annual Supplement to NBS (National
Interlaboratory Determination of the Calibration Factor for the Measurement of the Interstitial Oxygen Content of	PB89-189203 901,598 Alaska Arctic Offshore Oil Spill Response Technology	Bureau of Standards) Handbook 135 and NBS Special
Silicon by Infrared Absorption.	Workshop Proceedings.	PB89-153860 900,850

				DD00 105010	204.50
ENERGY STORAGE	nd Polated	PB90-123969	900,866	PB89-185912	901,52
Synthesis and Characterization of Ettringite at Phases.	iu neialeu	ENVIRONMENTAL SPECIMEN BANKING Experiences in Environmental Specimental Specim		ERBIUM Characterization of Structural and I	Magnetic Order of Er
PB89-146963	900,238	PB90-123969	900,866	Y Superlattices.	Magnetic Order of Er
ENERGY STORAGE MATERIALS		ENVIRONMENTAL STUDIES: POLLUTIO	N MEASUREMENT	PB90-123662	901,47
Synthesis and Characterization of Ettringite at Phases.	nd Related	Draft International Document on Guid	le to Portable Instru-	ERBIUM COMPOUNDS	
PB89-146963	900,238	ments for Assessing Airborne Pol Hazardous Wastes.	utants Arising from	Antiferromagnetic Structure and Cry the Cubic Heusler Alloys HoPd2Sn	
NERGY TRANSFER		PB89-150775	900,855	PB89-202659	901,43
Alignment Effects in Electronic Energy Transfe	er and Re-	Alaska Arctic Offshore Oil Spill Re	esponse Technology	ERBIUM CONTAINING ALLOYS	
active Events. AD-A202 820/7	900,267	Workshop Proceedings. PB89-195663	900,842	Magnetic Structure of Y0.97Er0.03.	
	000,207		900,842	PB89-202675	901,43
ENGINEERING International Cooperation and Competition in	Materials	Environmental Intelligence. PB89-201214	901,287	ERBIUM OXIDES	
Science and Engineering.		ENVIRONMENTAL SURVEYS	· ·	Stokes and Anti-Stokes Fluorescer Raman Spectra of Erbium Oxide an	ice of Er(3+) in the
PB89-228332	901,191	Environmental Standard Reference	Materials - Present	PB89-149231	901,02
NGINEERING/PRODUCT/INFORMATION STAN		and Future Issues.	900,865	ERGODIC PROCESSES	
U.S. Organizations Represented in the Collect untary Standards.	ion or voi-	PB89-150940		Ergodic Behavior in Supercooled Lie	quids and in Glasses.
PB89-154322	900,978	Designs for Assessment of Measu Experience in the Eastern Lake Surve		PB89-202444	901,43
Effect of Chinese Standardization on U.S. Exp	ort Oppor-	PB89-173827	900,862	ERGONOMICS	
tunities.	900,172	Environmental Intelligence.		Guideline for Work Station Design. PB90-112418	900,64
PB89-166128	-	PB89-201214	901,287	ERROR ANALYSIS	500,57
Developments in the Heat Balance Method for Room Thermal Response.	Simulating	ENVIRONMENTAL TESTS		Simple Technique for Investigation	g Defects in Coaxia
PB89-173926	900,062	Trace Speciation by HPLC-GF AA Liquid Chromatography-Graphite Furi		Connectors.	
ACSB (Amplitude Companded Sideband): Wh	at Is Ade-	tion) for Tin- and Lead-Bearing C	rganometallic Com-	PB89-146930	900,72
quate Performance.	001 500	pounds, with Signal Increases Ind	uced by Transition-	Interpretation of a between-Time C	omponent of Error in
PB89-176283	901,599	Metal Ions. PB89-157085	900,184	Mass Measurements. PB89-149108	900,87
Directory of NVLAP (National Voluntary Labo creditation Program) Accredited Laboratories, 1	986-87.	EOTVOS EXPERIMENT		Antenna Measurements for Millime	· ·
PB89-185599	900,933	Comment on 'Possible Resolution of	the Brookhaven and	tional Bureau of Standards.	
NVLAP (National Voluntary Laboratory Accredi	tation Pro-	Washington Eotvos Experiments'.		PB89-150726	900,69
gram) Directory of Accredited Laboratories.	900,890	PB89-171581	901,504	Error Analysis Techniques for Plana	r Near-Field Measure
PB89-189278		EPIFLUORESCENCE MICROSCOPY	diaranana In who	ments. PB89-156848	900,70
GATT (General Agreement on Tariffs and Tra ards Code Activities of the National Institute of	de) Stand- Standards	Element-Specific Epifluorescence I Monitoring of Metal Biotransformation	ns in Environmental	Estimation of the Error Probability I	•
and Technology 1988.	Otarioards	Matrices.		Measurements on Several Items.	rensity from Hopiloat
PB89-191977	900,173	PB89-177216	901,220	PB89-157820	901,21
Directory of International and Regional Organic	ganizations	EPITAXIAL GROWTH	at anima of On an	Designs for Assessment of Meas	
Conducting Standards-Related Activities. PB89-221147	900,008	Surface Structures and Growth Me Si(100) Determined by LEED (Low		Experience in the Eastern Lake Sur PB89-173827	vey. <i>900,86.</i>
Update of U.S. Participation in International		fraction) and Auger Electron Spectros	сору.	Computation and Use of the A	·
Activities.		PB89-171342	901,399	Matrix for Measurement Error Mode	is.
PB89-228282	900,902	Initial Stages of Heteroepitaxial (arowth of InAs on	PB89-215321	<i>901,21</i>
NVLAP (National Voluntary Laboratory Accredi	tation Pro-	Si(100). PB90-123878	901,473	ERRORS	
gram) Assessment and Evaluation Manual. PB89-228324	900,903	EPITAXY		Generalized Mathematical Model Errors.	for Machine Too
Intercomparison of Load Cell Verification		Stress Effects on III-V Solid-Liquid Ed	uilibria.	PB89-150874	900,97
formed by National Laboratories of Five Countr	ies.	PB89-146997	900,769	ERYTHROPENTOSE/DEOXY	,
PB89-235915	900,909	Angle Resolved XPS (X-ray Photoele	ctron Spectroscopy)	Radiation-Induced Crosslinks between	en Thymine and 2-D
Glass Bottles for Carbonated Soft Drinks: Volum	ntary Prod-	of the Epitaxial Growth of Cu on Ni(1 PB89-150866	00). <i>901,389</i>	Deoxyerythropentose.	000.24
uct Standard PS73-89. PB90-107046	900,012	Laser Probing of the Dynamics of		PB89-146682	900,24
NVLAP (National Voluntary Laboratory Accredi		Si(100).	da interacaons on	User Guide for the NBS (National	Purposu of Standards
gram) Program Handbook Construction Testing	Services.	PB89-186928	901,422	Prototype Compiler for Estelle (Revi	ised).
Requirements for Accreditation.		Role of Adsorbed Gases in Metal on		PB89-196158	900,61
PB90-112327	900,169	PB90-128125	901,174	ESTIMATING	
Standards for Real-Time Radioscopy. PB90-128687	900,924	Performance of Alumina/Epoxy There	mal legistion Strane	Estimation of an Asymmetrical I Small Samples.	Density from Severa
Glossary of Standards-Related Terminology.		PB89-147078	901,070	PB89-201131	901,21,
PB90-130246	900,986	Epoxy Impregnation Procedure for	Hardened Cement	ETHANE	
ENGINES		Samples.		Comprehensive Study of Methane -	
Structural Reliability and Damage Tolerance	of Ceramic	PB89-147821	901,180	PB89-176747	900,84
Composites for High-Temperature Application Annual Progress Report for the Period Ending	ns. Semi-	Corrosion Induced Degradation of Coatings on Steel.	Amine-Cured Epoxy	PVT Relationships in a Carbon Dio	xide-Rich Mixture with
30, 1987.	September	PB89-176291	901,084	Ethane. PB89-229181	900,47
PB89-156350	901,023	Epoxy Impregnation of Hardened		Measurements of Molar Heat C	•
Structural Reliability and Damage Tolerance		Characterization of Microstructure.		Volume: Cv,m(xCH4+ (1-x)C2H6'	$\Gamma = 100 \text{ to } 320 \text{ K,}$
Composites for High-Temperature Application Annual Progress Report for the Period Ending		PB89-185573	901,042	< or = 35 MPa). PB90-117896	900,84
1988.		Dielectric Measurements for Cure Mo PB89-200430	nitoring. <i>900,567</i>		900,84
PB89-156368	901,024		300,307	ETHANE/HEXAMETHYL Mechanism and Rate of Hydrogen	Atom Attack on Tole
ENTHALPY		Van der Waals Equation of State A	round the Van Laar	ene at High Temperatures.	
Enthalpies of Desorption of Water from Coal S PB89-173868	urfaces. 900,838	Point.		PB89-179758	900,39
		PB89-158133	900,345	ETHANOLS	
Second Virial Coefficients of Aqueous Alcohols ed Temperatures: A Calorimetric Study.		Tables for the Thermophysical Prope PB89-222608	rties of Methane. 900,843	Epoxy Impregnation Procedure for Samples.	or Hardened Cemer
PB89-227896	900,462			PB89-147821	901,18
ENVIRONMENTAL ENGINEERING		Method for Improving Equations of S Point.	tate Near the Critical	Epoxy Impregnation of Hardened	
Control Strategies and Building Energy Consun	nption. 900,061	PB89-228027	901,547	Characterization of Microstructure.	
PB89-172340		EQUILIBRIUM		PB89-185573	901,04
Post-Occupancy Evaluation of Several U.S. G Buildings.	overnment	Simple Apparatus for Vapor-Liquid		ETHYL ALCOHOL Dehydrogenation of Ethanol in Dil	uto Aguagua Caludia
PB90-112384	900,088	ments with Data for the Binary Syst ide with n-Butane and Isobutane.	ems of Carbon Diox-	Dehydrogenation of Ethanol in Dil Photosensitized by Benzophenones	ute Aqueous Solutio
ENVIRONMENTAL MONITORING		PB89-201115	900,422	PB89-157556	900,25
Combustion of Oil on Water.	000 507	EQUIPMENT		ETHYLENE	
PB89-149173	900,587	Use of Focusing Supermirror Neutro	Guides to Enhance	Reactions of Phenyl Radicals with	Ethene, Ethyne, an
Draft International Document on Guide to Port ments for Assessing Airborne Pollutants A	able instru- rising from	Cold Neutron Fluence Rates. PB89-171946	901,306	Benzene. PB89-150908	900,29
Hazardous Wastes.		Dynamic Microindentation Apparatus		Ozonolysis of Ethylene. Microwave	
PB89-150775	900,855	acterization.		Structure, and Dipole Moment of E	thylene Primary Ozor
Specimen Banking in the National Status a		PB89-176911	901,140	ide (1,2,3-Trioxolane).	
Program: Development of Protocols and Firs sults.	t Year He-	EQUIVALENCE PRINCIPLE	tea te attaca de la companya de la c	PB89-157440	900,32
PB89-175855	901,308	Current Research Efforts at JILA (Jo ratory Astrophysics) to Test the Equ	int institute for Labo-	Microwave Spectrum and Molecula ylene-Ozone van der Waals Comple	i Structure of the Eth ex.
Experiences In Environmental Specimen Banki	ng.	Short Ranges.		PB89-201735	900,42

ETHYLENE COPOLYMERS	Integrated Knowledge Systems for Concrete and Other Materials.	FIPS PUB 134-1 900,660
Results of a Survey of the Performance of EPDM (Ethyl- ene Propylene Diene Terpolymer) Roofing at Army Facili- ties.	PB89-176119 900,582	General Aspects of Group 4 Facsimile Apparatus, Cate gory: Telecommunications Standard.
PB89-209316 900,136	Expert Systems Applied to Spacecraft Fire Safety. PB89-231013 901,590	FIPS PUB 149 900,66: Facsimile Coding Schemes and Coding Control Functions
Tests of Adhesive-Bonded Seams of Single-Ply Rubber Membranes.	EXPOSURE Detection of Lead in Human Teeth by Exposure to Aque-	for Group 4 Facsimile Apparatus, Category: Telecommunications Standard.
PB89-212120 900,138 ETHYLPEROXY RADICALS	ous Sulfide Solutions. PB89-201529 901,256	FIPS PUB 150 900,662
Flash Photolysis Kinetic Absorption Spectroscopy Study of the Gas Phase Reaction HO2 + C2H5O2 Over the	EXTINGUISHING	Standard Generalized Markup Language (SGML). FIPS PUB 152 900,627
Temperature Range 228-380 K. PB90-136565 900,536	Transient Cooling of a Hot Surface by Droplets Evapora- tion. PB89-161897 900,971	High Speed 25-Position Interface for Data Termina Equipment and Data Circuit-Terminating Equipment, Cat-
ETHYNE	PB89-161897 900,971 F CENTER LASERS	egory: Telecommunications Standard. FIPS PUB 154 900,663
Reactions of Phenyl Radicals with Ethene, Ethyne, and Benzene.	Simple F-Center Laser Spectrometer for Continuous Single Frequency Scans.	Data Communication Systems and Services User-Orient ed Performance Measurement Methods, Category: Tele
PB89-150908 900,297 ETRAN COMPUTER CODE	PB89-179774 901,358 FABRICATION	communications Standard. FIPS PUB 155 900,664
Applications of ETRAN Monte Carlo Codes. PB90-123902 901,574	Thin Film Thermocouples for Internal Combustion En-	Government Open Systems Interconnection Profile
Overview of ETRAN Monte Carlo Methods.	gines. PB89-147094 900,607	Users' Guide. PB90-111212 900,667
PB90-123928 <i>901,576</i> ETTRINGITE	FACE CENTERED CUBIC LATTICES Molybdenum Effect on Volume in Fe-Cr-Ni Alloys.	FEEDBACK AMPLIFIERS Electromagnetic Fields in Loaded Shielded Rooms.
 Synthesis and Characterization of Ettringite and Related Phases. 	PB89-157796 901,095 Low-Temperature Phase and Magnetic Interactions in fcc	PB89-180426 900,780
PB89-146963 900,238	Fe-Cr-Ni Alloys. PB90-136771 901,113	NIST (National Institute of Standards and Technology)
EVELIDEAN GEOMETRY Expected Complexity of the 3-Dimensional Voronoi Dia-	FACILITIES MANAGEMENT	Calibration Services, Users Guide: Fee Schedule. PB90-127820 900,913
gram. PB89-209332 901,200	Internal Revenue Service Post-of-Duty Location Modeling System: Programmer's Manual for PASCAL Solver.	FERMENTATION Measurement of Shear Rate on an Agitator in a Fermen-
EUCLIDEAN SPACE How to Estimate Capacity Dimension.	PB89-161905 900,001 Internal Revenue Service Post-of-Duty Location Modeling	tation Broth. PB89-186720 901,009
PB89-172522 901,197	System: Programmer's Manual for FORTRAN Driver Version 5.0.	FERRITE
EVAPORATIVE COOLING Evaporation of a Water Droplet Deposited on a Hot High	PB89-161913 900,002	Femite Number Prediction to 100 FN in Stainless Stee Weld Metal.
Thermal Conductivity Solid Surface. PB89-149157 901,487	FACTORY AUTOMATION Real-Time Optimization in the Automated Manufacturing	PB89-201586 901,108 FERROELECTRIC MATERIALS
Transient Cooling of a Hot Surface by Droplets Evapora- tion.	Research Facility. PB89-172597 900,947	Effects of Space Charge on the Poling of Ferroelectric Polymers.
PB89-161897 900,971 EVAPORATORS	FAILURE Studies on Some Failure Modes in Latex Barrier Films.	PB89-146708 901,175 FERROMAGNETISM
EVSIM: An Evaporator Simulation Model Accounting for	PB89-209308 <i>901,089</i>	Neutron Scattering Study of the Spin Ordering in Amor-
Refrigerant and One Dimensional Air Distribution. PB89-235881 900,086	Power MOSFET Failure Revisited. PB89-231237 900,796	phous Tb45Fe55 and Tb25Fe75. PB89-201701 901,145
Stokes and Anti-Stokes Fluorescence of Er(3+) in the	FAILURE ANALYSIS Influence of Dislocation Density on the Ductile-Brittle	Exchange and Magnetostrictive Effects in Rare Earth Su- perlattices.
Raman Spectra of Erbium Oxide and Erbium Glasses. PB89-149231 901,020	Transition in bcc Metals. PB89-157804 901,133	PB89-202667 901,438 Monte Carlo Simulation of Domain Growth in the Kinetic
Magnetic Dipole Excitation of a Long Conductor in a Lossy Medium.	Failure Analysis of an Amine-Absorber Pressure Vessel. PB89-173835 901,101	Ising Model on the Connection Machine. PB90-136797 901,587
PB89-171664 900,742 EXCITED STATES	Crazes and Fracture in Polymers. PB89-176085 900,562	FIBER COMPOSITES Toughening Mechanisms in Ceramic Composites, Semi-
Determination of Short Lifetimes with Ultra High Resolu-	FALSE ALARMS	Annual Progress Report for the Period Ending March 31, 1989.
tion (n,gamma) Spectroscopy. PB90-123670 901,567	False Alarm Study of Smoke Detectors in Department of Veterans Affairs Medical Centers (VAMCS).	PB89-235907 901,080
EXCLUSION Characterization of Organolead Polymers in Trace	PB89-193288 900,093 FAR FIELD	FIBER OPTICS Optical Fiber Sensors for Electromagnetic Quantities.
Amounts by Element-Specific Size-Exclusion Chromatog- raphy. PB89-175962 900,196	Comparison of Measured and Calculated Antenna Side- lobe Coupling Loss in the Near Field Using Approximate	PB89-173967 900,725 Profile Inhomogeneity in Multimode Graded-Index Fibers.
EXHAUST EMISSIONS	Far-Field Data PB89-156855 900,702	PB89-179816 900,749 Optical Power Measurements at the National Institute of
Mobile Sources of Atmospheric Polycyclic Aromatic Hy- drocarbons: A Roadway Tunnel Study. PB90-123571 900,859	Comparison of Far-Field Methods for Determining Mode Field Diameter of Single-Mode Fibers Using Both Gaussian and Petermann Definitions.	Standards and Technology. PB89-187579 900,918
EXPANSION	PB90-117474 900,756	Group Index and Time Delay Measurements of a Standard Reference Fiber.
Standard Aggregate Materials for Alkali-Silica Reaction Studies.	FAR INFRARED RADIATION Far-Infrared Laser Magnetic Resonance Spectrum of Vi-	PB89-189179 900,752 Comparison of Far-Field Methods for Determining Mode
PB89-193221 901,046 EXPERIMENTAL DATA	brationally Excited C2H(1). PB89-147474 900,292	Field Diameter of Single-Mode Fibers Using Both Gaussian and Petermann Definitions.
Journal of Physical and Chemical Reference Data, Volume 17, Number 1, 1988.	Coherent Tunable Far Infrared Radiation. PB90-117458 900,684	PB90-117474 900,756 Numerical Aperture of Multimode Fibers by Several Meth-
PB89-186449 900,408 Pressure and Density Series Equations of State for	FARADAY EFFECT	ods: Resolving Differences. PB90-117482 900,757
Steam as Derived from the Haar-Gallagher-Kell Formula- tion.	Faraday Effect Sensors: The State of the Art. PB89-231153 900,823	FIBER REINFORCED CONCRETES
PB89-186456 900,409	FASTENERS Corrosion of Metallic Fasteners in Low-Sloped Roofs: A	Prediction of Tensile Behavior of Strain Softened Com- posites by Flexural Test Methods.
Absolute Cross Sections for Molecular Photoabsorption, Partial Photoionization, and Ionic Photofragmentation	Review of Available Information and Identification of Research Needs.	PB89-147045 900,585 FIBERS
Process. PB89-186464 <i>900,410</i>	PB89-162580 <i>900,113</i> FATIGUE LIFE	Performance of Alumina/Epoxy Thermal Isolation Straps. PB89-147078 901,070
Energy Levels of Molybdenum, Mo 1 through 42. PB89-186472 900,411	Fatigue Resistance of a 2090-T8E41 Aluminum Alloy at Cryogenic Temperatures.	FIELD EFFECT TRANSISTORS
Standard Chemical Thermodynamic Properties of Polycy-	PB90-128737 901,177	Analytical Model for the Steady-State and Transient Characteristics of the Power Insulated-Gate Bipolar Tran-
clic Aromatic Hydrocarbons and Their Isomer Groups 1. Benzene Series. PB89-186480 900,412	FATIGUE (MATERIALS) Tensile and Fatigue-Creep Properties of a Copper-Stain-	sistor. PB89-146880 <i>900,767</i>
EXPERIMENTAL DESIGN	less Steel Laminate. PB90-128646 901,083	Analytical Modeling of Device-Circuit Interactions for the Power Insulated Gate Bipolar Transistor (IGBT).
Bootstrap Inference for Replicated Experiments. PB90-128273 900,914	FEDERAL BUILDINGS Energy Prices and Discount Factors for Life-Cycle Cost	PB89-176259 900,777
EXPERT SYSTEMS Knowledge Based System for Durable Reinforced Con-	Analysis 1988: Annual Supplement to NBS (National Bureau of Standards) Handbook 135 and NBS Special	Radiation-Induced Interface Traps in Power MOSFETs. PB89-201974 900,784
crete. PB89-150734 900,110	Publication 709. PB89-153860 900,850	Improved Understanding for the Transient Operation of the Power Insulated Gate Bipolar Transistor (IGBT).
Intelligent Processing of Materials: Report of an Industrial	FEDERAL INFORMATION PROCESSING STANDARDS	PB89-231229 900,795 Power MOSFET Failure Revisited.
Workshop Conducted by the National Institute of Standards and Technology. PB89-151823 900,942	Coding and Modulation Requirements for 4,800 Bit/ Second Modems, Category: Telecommunications Stand-	PB89-231237 900,796
1 555-151025 900,942	ard.	Very Low-Noise FET Input Amplifier.

PB90-128224	900,800	PB89-173983	900, 164	Upward Flame Spread on Vertical Walls. PB89-214787 900,141
FIELD ION MICROSCOPY Effects of a Gold Shank-Overlayer on the Field	Ion Imag-	Computer Fire Models. PB89-173991	900,165	PB89-214787 900,141 Validated Furniture Fire Model with FAST (HEMFAST).
ing of Silicon. PB89-175988	901.404	Flammability Tests for Industrial Fabrics: Re		PB89-215354 900,142
FIELD STRENGTH	301,404	Limitations. PB89-174122	901,091	HAZARD I Fire Hazard Assessment Method. PB89-215404 900,143
Electromagnetic Fields in Loaded Shielded Root PB89-180426	ms. <i>900,780</i>	Creation of a Fire Research Bibliographic Dat		Ignition Characteristics of the Nickel-Based Alloy UNS
FIFTH FORCE	000,700	PB89-174130 Smoke and Gas Evolution Rate Measureme	900,166 Ints on Fire-	N07718 in Pressurized Oxygen. PB89-218333 901,154
Precision Experiments to Search for the Fifth Fo PB89-228365	rce. <i>901,551</i>	Retarded Plastics with the Cone Calorimeter. PB89-174890	900,868	Technical Reference Guide for FAST (Fire and Smoke Transport) Version 18.
FINE STRUCTURE CONSTANT		Very Large Methane Jet Diffusion Flames.	000 500	PB89-218366 900,602
NBS (National Bureau of Standards) Determinat Fine-Structure Constant, and of the Quantized sistance and Josephson Frequency-to-Voltage	Hall Re-	PB89-175913 Fundamentals of Enclosure Fire 'Zone' Model PB89-176168	<i>900,593</i> ls. <i>900,122</i>	Experimental Study of the Pyrolysis of Pure and Fire Retarded Cellulose. PB89-228316 901,090
in SI Units. PB89-230437	901,556	Cigarette as a Heat Source for Smolder Initi holstery Materials.		Estimating the Environment and the Response of Sprin- kler Links in Compartment Fires with Draft Curtains and
FINGERPRINTS Standard Format for the Exchange of Fingerprin	t Informa-	PB89-176762	900,595	Fusible Line-Actuated Ceiling Vents. Part 2. User Guide for the Computer Code Lavent.
tion. PB89-176705	900.692	Computing Ray Trajectories between Two Potion to the Ray-Linking Problem.		PB89-229009 900,094 Capabilities of Smoke Control: Fundamentals and Zone
Analysis of Ridge-to-Ridge Distance on Fingerpr		PB89-176929 Fire Safety Science-Proceedings of the First	901,354 International	Smoke Control. PB89-229157 900,080
PB89-230478 FINITE ELEMENT ANALYSIS	901,216	Symposium. PB89-179261	900,596	Expert Systems Applied to Spacecraft Fire Safety.
Conventional and Quarter-Point Mixed Elements Elastic Fracture Mechanics.	in Linear	Dynamic Light Scattering and Angular Diss	ymmetry for	PB89-231013 901,590
PB89-157788	901,481	the In situ Measurement of Silicon Dioxide F thesis in Flames.	Particle Syn-	Assessment of Theories for the Behavior and Blowout of Lifted Turbulent Jet Diffusion Flames.
Higher Order Beam Finite Element for Bending bration Problems.	g and Vi-	PB89-179584	900,246	PB89-231096 900,603 Analysis and Prediction of Air Leakage through Door As-
PB89-229124	901,484	Novel Process for the Preparation of Fiber Ceramic-Matrix Composites.		semblies. PB89-231161 900,085
FINITE ELEMENT METHOD Finite Element Studies of Transient Wave Propar	gation.	PB89-179733	901,074	Combustion Efficiency, Radiation, CO and Soot Yield
PB89-186902	901,375	Recent Activities of the American Society for Materials Committee on Fire Standards.		from a Variety of Gaseous, Liquid, and Solid Fueled Buoyant Diffusion Flames.
FIRE ALARM SYSTEMS False Alarm Study of Smoke Detectors in Depa	rtment of	PB89-180004 Engineering View of the Fire of May 4, 1988	900,124	PB89-231179 900,604
Veterans Affairs Medical Centers (VAMCS). PB89-193288	900,093	Interstate Bank Building, Los Angeles, Californ PB89-183222		Test Results and Predictions for the Response of Near- Ceiling Sprinkler Links in a Full-Scale Compartment Fire.
FIRE EXTINGUISHING AGENTS		Fire Risk Analysis Methodology: Initiating Ever		PB89-231187 900,095
Summary of the Assumptions and Limitations in PB90-136821	Hazard I. <i>900,606</i>	PB89-184527 Combustion of Oil on Water. November 1987.	900,125	Development of a Multiple Layer Test Procedure for Inclusion in NFPA (National Fire Protection Association)
FIRE HAZARDS		PB89-185581	900,863	701: Initial Experiments. PB89-235873 900,096
HAZARD I Fire Hazard Assessment Method. PB89-215404	900,143	Fire Properties Database for Textile Wall Cove PB89-188635	erings. <i>900,126</i>	Assessing the Flammability of Composite Materials. PB90-112996 901,081
FIRE LOSSES HAZARD I Fire Hazard Assessment Method.		Effect of Water on Piloted Ignition of Cellulosi PB89-189187	c Materials. 900,127	Note on Calculating Flows Through Vertical Vents in Zone Fire Models Under Conditions of Arbitrary Cross-
PB89-215404 FIRE MODELS	900,143	Calculation of the Flow Through a Horizon		Vent Pressure Difference. PB90-117573 900,147
Refinement and Experimental Verification of a I	Model for	Floor Vent. PB89-189252	900,128	Experimental Fire Tower Studies of Elevator Pressuriza-
Fire Growth and Smoke Transport. PB89-212005	900,137	Fire Induced Flows in Corridors: A Review of Model Key Features.	of Efforts to	tion Systems for Smoke Control. PB90-117813 900,097
FIRE PROTECTION Hand Calculations for Enclosure Fires.		PB89-189260	900, 129	Upward Turbulent Flame Spread on Wood under External Radiation.
PB89-173983	900,164	False Alarm Study of Smoke Detectors in De Veterans Affairs Medical Centers (VAMCS).		PB90-118050 900,148
Computer Fire Models. PB89-173991	900,165	PB89-193288 Fire Research Publications, 1988.	900,093	Scaling Applications in Fire Research. PB90-118068 900.149
Effect of Water on Piloted Ignition of Cellulosic N PB89-189187	Materials. 900,127	PB89-193304	900, 132	Heat Transfer in Compartment Fires Near Regions of
FIRE RESEARCH	300,127	Considerations of Stack Effect in Building Fire PB89-195671	s. 900,133	Ceiling-Jet Impingement on a Wall. PB90-118076 900,150
Aerodynamics of Agglomerated Soot Particles. PB89-147482	900,586	Executive Summary for the Workshop on D	eveloping a	Summaries of Center for Fire Research In-House Projects and Grants: 1989.
Calculating Flows through Vertical Vents in 2	one Fire	Predictive Capability for CO Formation in Fires PB89-200091	s. 900,134	PB90-127101 900,605
Models under Conditions of Arbitrary Cross-Vesure Difference.		Assessment of Need for and Design Require Wind Tunnel Facility to Study Fire Effects of		Effects of Thermal Stability and Melt Viscosity of Thermo- plastics on Piloted Ignition.
PB89-148126 Combustion of Oil on Water.	900,108	DNA. PB89-200208	901.276	PB90-128232 900,151 Fire Growth and Development.
PB89-149173	900,587	Importance of Isothermal Mixing Processes to	the Under-	PB90-128570 900,152
Cooling Effect Induced by a Single Evaporating on a Semi-Infinite Body.		standing of Lift-Off and Blow-out of Turbuler sion Flames.		Comparisons of NBS/Harvard VI Simulations and Full- Scale, Multiroom Fire Test Data.
PB89-149249 Fire Propagation in Concurrent Flows.	901,488	PB89-201172 Soot Inception in Hydrocarbon Diffusion Flame	<i>900,598</i> es	PB90-128620 900,170 Flammability of Upholstered Furniture with Flaming
PB89-151781	900,867	PB89-201966	900,599	Sources.
Light Scattering from Simulated Smoke Agglome PB89-157234	rates. <i>900,588</i>	Component Spectrum Reconstruction from Pa acterized Mixtures.	·	PB90-136805 900,155 Summary of the Assumptions and Limitations in Hazard I.
Computer Model of Smoke Movement by Air Co Systems (SMACS).	nditioning	PB89-202568 Development of an Automated Probe for Th	900,439	PB90-136821 900,606
PB89-157267	900,059	ductivity Measurements.		FIRE RESEARCH INFORMATION SERVICES Creation of a Fire Research Bibliographic Database.
Analytical Methods for Firesafety Design. PB89-157275	900,111	PB89-209324 Outline of a Practical Method of Assess	<i>900,896</i> sing Smoke	PB89-174130 900,166 FIRE RESISTANT COATINGS
Structure and Radiation Properties of Large-Scal	e Natural	Hazard. PB89-211858	900,078	Experimental Study of the Pyrolysis of Pure and Fire Retarded Cellulose.
Gas/Air Diffusion Flames. PB89-157572	900,589	FT-IR (Fourier Transform-Infrared) Emissio	n/Transmis-	PB89-228316 901,090
Flammability Characteristics of Electrical Cabl the Cone Calorimeter.	es Using	sion Spectroscopy for In situ Combustion Diag PB89-211866	900,600	FIRE RESISTANT MATERIALS Smoke and Gas Evolution Rate Measurements on Fire-
PB89-162572	900,741	Refinement and Experimental Verification of Fire Growth and Smoke Transport.	a Model for	Retarded Plastics with the Cone Calorimeter. PB89-174890 900.868
Chemical Structure of Methane/Air Diffusion Concentrations and Production Rates of Intermediate	riames: ediate Hy-	PB89-212005	900,137	Friability of Spray-Applied Fireproofing and Thermal Insu-
drocarbons. PB89-171904	900,590	 Effects of Material Characteristics on Flame S PB89-212021 	Spreading. <i>900,572</i>	lations: Field Evaluation of Prototype Test Devices. PB89-189328 900,130
Methyl Radical Concentrations and Production F Laminar Methane/Air Diffusion Flame.	Rates in a	Prediction of the Heat Release Rate of Dougle PB89-212039	as Fir. <i>901,185</i>	FIRE RESISTANT TEXTILES
PB89-171912	900,591	Toxicity of Mixed Gases Found in Fires.		Flammability Tests for Industrial Fabrics: Relevance and Limitations.
Ignition and Flame Spread Measurements o Lining Materials.		PB89-212047 Synergistic Effects of Nitrogen Dioxide and C	900,869 Carbon Diox-	PB89-174122 901,091 FIRE SAFETY
PB89-172886 Hand Calculations for Enclosure Fires.	900,009	ide Following Acute Inhalation Exposures in R PB89-214779		Analytical Methods for Firesafety Design. PB89-157275 900,111
Juliana in Lindigalio I ilos.			220,000	300,111

Fire Safety Science-Proceedings of the First International Symposium.	PB89-229009 900,094 Scaling Applications in Fire Research.	PB90-130253 900,65 FLOW MEASUREMENT
PB89-179261 900,596 Fire Properties Database for Textile Wall Coverings.	PB90-118068 900,149	Trace Gas Calibration Systems Using Permeation De
PB89-188635 900,126 Calculation of the Flow Through a Horizontal Ceiling/	Heat Transfer in Compartment Fires Near Regions of Ceiling-Jet Impingement on a Wall. PB90-118076 900,150	vices. PB89-176580 <i>900,88</i> .
Floor Vent. PB89-189252 900,128	FIRES FIRE RESISTANCE	NBS (National Bureau of Standards)-Boulder Gas Flow Facility Performance.
Fire Research Publications, 1988.	Fire Growth and Development. PB90-128570 900,152	PB89-186787 900,88 Gas Flow Measurement Standards.
PB89-193304 900,132 Considerations of Stack Effect in Building Fires.	FISSIONABLE MATERIALS Measurements of the (235)U (n,f) Standard Cross Sec-	PB89-211874 900,89
PB89-195671 900,133	tion at the National Bureau of Standards. PB89-176556 901,305	Effect of Pipe Roughness on Orifice Flow Measurement. PB89-231484 901,33
Validated Furniture Fire Model with FAST (HEMFAST). PB89-215354 900,142	FIXED INVESTMENT	Measurements of Coefficients of Discharge for Concertric Flange-Tapped Square-Edged Onfice Meters in Water
Expert Systems Applied to Spacecraft Fire Safety. PB89-231013 901,590	AutoMan: Decision Support Software for Automated Man- ufacturing Investments. User's Manual.	Over the Reynolds Number Range 600 to 2,700,000. PB89-235147 901,33
Experimental Fire Tower Studies of Elevator Pressurization Systems for Smoke Control.	PB89-221873 900,963 FLAME PHOTOMETRY	Optimum Location of Flow Conditioners in a 4-Inch Or
PB90-117813 900,097	Speciation Measurements of Butyltins: Application to Controlled Release Rate Determination and Production of	fice Meter. PB90-111675 900,91
Scaling Applications in Fire Research. PB90-118068 900,149	Reference Standards. PB89-146807 900,174	Measured Air Infiltration and Ventilation Rates in Eigh Large Office Buildings.
RE STUDIES Calculating Flows through Vertical Vents in Zone Fire	FLAME PROPAGATION	PB90-128158 900,09
Models under Conditions of Arbitrary Cross-Vent Pressure Difference.	Fire Propagation in Concurrent Flows. PB89-151781 900,867	Experimental Investigation and Modeling of the Flor
PB89-148126 900,108 RE TESTS	Fire Propagation in Concurrent Flows. PB89-188577 900,597	Rate of Refrigerant 22 Through the Short Tube Restrictor.
Fire Propagation in Concurrent Flows.	Effects of Material Characteristics on Flame Spreading.	PB89-229041 901,11. FLOW VISUALIZATION
PB89-151781 900,867 Recent Activities of the American Society for Testing and	Upward Flame Spread on Vertical Walls.	Application of Magnetic Resonance Imaging to Visualization of Flow in Porous Media.
Materials Committee on Fire Standards. PB89-180004 900,124	PB89-214787 900,141 Upward Turbulent Flame Spread on Wood under External	PB89-179592 <i>901,32</i>
Fire Propagation in Concurrent Flows. PB89-188577 900,597	Radiation. PB90-118050 -900,148	FLOWMETERS Low Range Flowmeters for Use with Vacuum and Lea
Fire Induced Flows in Corridors: A Review of Efforts to	FLAME RADIATION	Standards. PB89-175707 <i>900,37</i>
Model Key Features. PB89-189260 900,129	Structure and Radiation Properties of Large-Scale Natural Gas/Air Diffusion Flames.	NBS' (National Bureau of Standards) Industry, Govern
Prediction of the Heat Release Rate of Douglas Fir. PB89-212039 901,185	PB89-157572 900,589 FLAME SPREAD	ment Consortium Research Program on Flowmeter Installation Effects: Summary Report with Emphasis on Re
Test Results and Predictions for the Response of Near- Ceiling Sprinkler Links in a Full-Scale Compartment Fire.	Fire Propagation in Concurrent Flows. PB89-188577 900,597	search January-July 1988. PB89-189120 <i>901,01</i>
PB89-231187 900,095	FLAME STRUCTURE	Prediction of Flowmeter Installation Effects. PB89-211882 900,89
Note on Calculating Flows Through Vertical Vents in Zone Fire Models Under Conditions of Arbitrary Cross-	Structure and Radiation Properties of Large-Scale Natural Gas/Air Diffusion Flames.	Prediction of Flowmeter Installation Effects. PB89-211890 900,90
Vent Pressure Difference. PB90-117573 900,147	PB89-157572 900,589 FLAMMABILITY	NBS' (National Bureau of Standards) Industry; Govern
Upward Turbulent Flame Spread on Wood under External Radiation.	Ignition and Flame Spread Measurements of Aircraft Lining Materials.	ment Consortium Research Program on Flowmeter Installation Effects: Summary Report with Emphasis on Re
PB90-118050 <i>900,148</i>	PB89-172886 900,009	search July-December 1987. PB90-111220 900,91
Heat Transfer in Compartment Fires Near Regions of Ceiling-Jet Impingement on a Wall. PB90-118076 900,150	Effects of Thermal Stability and Melt Viscosity of Thermo- plastics on Piloted Ignition.	Vortex Shedding Flowmeter for Fluids at High Flow Velocities.
Fire Growth and Development.	PB90-128232 900,151 FLAMMABILITY TESTING	PB90-128661 900,60
PB90-128570 900,152 Comparisons of NBS/Harvard VI Simulations and Full-	Cone Calorimeter Method for Determining the Flammability of Composite Materials.	FLUID DYNAMICS Solutal Convection during Directional Solidification.
Scale, Multiroom Fire Test Data. PB90-128620 900,170	PB89-149165 901,072	PB89-150932 901,32 FLUID FLOW
RES	Flammability Characteristics of Electrical Cables Using the Cone Calorimeter. PB89-162572 900,741	NBS' (National Bureau of Standards) Industry; Govern
Combustion of Oil on Water. PB89-149173 900,587	Flammability Tests for Industrial Fabrics: Relevance and	ment Consortium Research Program on Flowmeter Installation Effects: Summary Report with Emphasis on Research Journal Ville 1998
Fundamentals of Enclosure Fire 'Zone' Models. PB89-176168 900,122	Limitations. PB89-174122 901,091	search January-July 1988. PB89-189120 <i>901,01</i>
Recent Activities of the American Society for Testing and Materials Committee on Fire Standards.	Smoke and Gas Evolution Rate Measurements on Fire- Retarded Plastics with the Cone Calorimeter.	Fluid Flow in Pulsed Laser Irradiated Gases; Modelin and Measurement.
PB89-180004 900,124	PB89-174890 <i>900,868</i>	PB90-123704 900,26 FLUID FRICTION
Engineering View of the Fire of May 4, 1988 in the First Interstate Bank Building, Los Angeles, California.	Cigarette as a Heat Source for Smolder Initiation in Up- holstery Materials. PB89-176762 900,595	Reevaluation of Forces Measured Across Thin Polyme
PB89-183222 900,167 Fire Risk Analysis Methodology: Initiating Events.	Statistical Analysis of Experiments to Measure Ignition of	Films: Nonequilibrium and Pinning Effects. PB89-228589 900,57
PB89-184527 900,125 Combustion of Oil on Water. November 1987.	Cigarettes. PB89-201149 900,135	FLUID MODELLING Modelling of Impurity Effects in Pure Fluids and Fluid Mix
PB89-185581 900,863	Development of a Multiple Layer Test Procedure for Inclusion in NFPA (National Fire Protection Association)	tures. PB89-176739 900,24
Considerations of Stack Effect in Building Fires. PB89-195671 900,133	701: Initial Experiments. PB89-235873 900,096	FLUIDS
Executive Summary for the Workshop on Developing a Predictive Capability for CO Formation in Fires.	Assessing the Flammability of Composite Materials.	Semi-Automated PVT Facility for Fluids and Fluid Mix tures.
PB89-200091 900,134 Assessment of Need for and Design Requirements of a	PB90-112996 901,081 Flammability of Upholstered Furniture with Flaming	PB89-157184 900,87. High Temperature Thermal Conductivity Apparatus for
Wind Tunnel Facility to Study Fire Effects of Interest to DNA.	Sources. PB90-136805 900,155	Fluids. PB89-174015 900,36
PB89-200208 901,276	FLEXIBLE MANUFACTURING Real-Time Optimization in the Automated Manufacturing	Relation between Wire Resistance and Fluid Pressure i
Outline of a Practical Method of Assessing Smoke Hazard.	Research Facility.	the Transient Hot-Wire Method. PB89-184113 901,52
PB89-211858 900,078 Refinement and Experimental Verification of a Model for	FLEXIBLE MANUFACTURING SYSTEMS	Development of a Field-Space Corresponding-State Method for Fluids and Fluid Mixtures.
Fire Growth and Smoke Transport. PB89-212005 900,137	On-Line Concurrent Simulation in Production Scheduling. PB89-172605 900,948	PB89-227995 <i>901,33</i>
Toxicity of Mixed Gases Found in Fires.	FLEXIBLE MANUFACTURING WORKSTATION Turning Workstation in the AMRF (Automated Manufac-	Simplified Representation for the Thermal Conductivity of Fluids in the Critical Region. PB89-228050 901,33
PB89-212047 900,869 Technical Reference Guide for FAST (Fire and Smoke	turing Research Facility). PB89-185607 900,954	Apparatus for Neutron Scattering Measurements o
Transport) Version 18. PB89-218366 900,602	Inventory of Equipment in the Turning Workstation of the	Sheared Fluids. PB89-235667 901,33
Estimating the Environment and the Response of Sprin- kler Links in Compartment Fires with Draft Curtains and	AMRF (Automated Manufacturing Research Facility). PB89-215339 900,961	Application of the Gibbs Ensemble to the Study of Fluic Fluid Phase Equilibrium in a Binary Mixture of Symmetri
Fusible Line-Actuated Ceiling Vents. Part 2. User Guide for the Computer Code Lavent.	FLOATING POINT ARITHMETIC Supercomputers Need Super Arithmetic.	Non-Additive Hard Spheres. PB90-117318 900,49

LUIDS: LIQUIDS/GASES/PLASMAS	PB89-173918	901,327	FOURIER TRANSFORM SPECTROMETERS
Molecular Dynamics Study of a Dipolar Fluid between Charged Plates.	FLUORIDE		FT-IR (Fourier Transform-Infrared) Emission/Transmission Spectroscopy for In situ Combustion Diagnostics.
PB89-147441 900,290	Comparison of Fluoride Uptake Producer Flossing Methods In vitro.	d by fray and	PB89-211866 900,600
Semi-Automated PVT Facility for Fluids and Fluid Mix-	PB89-179238	901,252	FOURIER TRANSFORM SPECTROSCOPY
tures. PB89-157184 <i>900,875</i>	FLUORIDE/DIOXY Thermodynamic Properties of Dioxygen Di	fluorido (O2E2)	Structure of the CO2-CO2-H2O van der Waals Complex Determined by Microwave Spectroscopy.
Local Order in a Dense Liquid.	and Dioxygen Fluoride (O2F).		PB89-230288 900,479
PB89-157226 900,313 Thermodynamic Values Near the Critical Point of Water.	PB89-222566	900,452	Production and Spectroscopy of Molecular Ions Isolated in Solid Neon.
PB89-161541 901,497	FLUORIMETERS Luminescence Standards for Macro- and	Microspectro-	PB90-117748 900,503
Mixing Motions Produced by Pipe Elbows.	fluorometry. PB89-176598	900,383	Low Pressure, Automated, Sample Packing Unit for Dif-
PB89-161871 901,326 Shear Dilatancy and Finite Compressibility in a Dense	FLUORINE	900,383	fuse Reflectance Infrared Spectrometry. PB90-135922 900,235
Non-Newtonian Liquid.	Infrared Spectrum of D2HF.		FOURIER TRANSFORMATION
PB89-174023 901,328	PB89-171219	900,350	Heterodyne Frequency and Fourier Transform Spectros-
Solution for Diffusion-Controlled Reaction in a Vortex Field.	Infrared Spectrum of NeHF. PB89-171227	900,351	copy Measurements on OCS Near 1700 cm(-1). PB90-117805 900,507
PB89-176622 900,594	Bond Selective Chemistry with Photon-S	•	FRACTALS
Flow Coefficients for Interzonal Natural Convection for Various Apertures.	sorption. PB89-201222	900,259	Efficient Algorithms for Computing Fractal Dimensions. PB89-175871 901, 198
PB89-177158 900,069	Electron-Stimulated-Desorption Ion-Angular		FRACTOGRAPHY
Measurement of Shear Rate on an Agitator in a Fermentation Broth.	PB89-201230	901,430	Linear-Elastic Fracture of High-Nitrogen Austenitic Stain-
PB89-186720 901,009	FLUORINE IONS Collisional Electron Detachment and	Decomposition	less Steels at Liquid Helium Temperature. PB90-117623 901,108
NBS (National Bureau of Standards)-Boulder Gas Flow Facility Performance.	Rates of SF6(1-), SF5(1-), and F(1-) in SF	6: Implications	FRACTURE MECHANICS
PB89-186787 900,889	for Ion Transport and Electrical Discharges PB90-117862	900,511	Physics of Fracture, 1987.
NBS' (National Bureau of Standards) Industry; Govern-	Photon-Stimulated Description of Fluorine f		PB89-201107 901,428
ment Consortium Research Program on Flowmeter Instal- lation Effects: Summary Report with Emphasis on Re-	Substrate Core Excitations. PB90-118027	900,517	FRACTURE STRENGTH Toughening Mechanisms in Ceramic Composites. Semi-
search January-July 1988. PB89-189120 901,010	FLUX	900,517	Annual Progress Report for the Period Ending March 31,
Determination of Binary Mixture Vapor-Liquid Critical Den-	Flux Creep and Activation Energies at the	Grain Bound-	1989. PB89-235907 <i>901,080</i>
sities from Coexisting Density Data.	aries of Y-Ba-Cu-O Superconductors. PB89-230353	901.457	FRACTURES (MATERIALS)
PB89-202170 901,536 Ergodic Behavior in Supercooled Liquids and in Glasses.	FOAM	301,431	Institute for Materials Science and Engineering, Fracture
PB89-202444 901,435	Low Temperature Mechanical Property Me	asurements of	and Deformation: Technical Activities 1988. PB89-148399 901,071
Gas Solubility and Henry's Law Near the Solvent's Criti-	Silica Aerogel Foam. PB90-128638	901,061	Local Brittle Zones in Steel Weldments: An Assessment
cal Point. PB89-202485 900,434	FOCUSING	,	of Test Methods. PB89-149082 901,092
Gas Flow Measurement Standards.	Use of Focusing Supermirror Neutron Guid	es to Enhance	J-Integral Values for Small Cracks in Steel Panels.
PB89-211874 900,898	Cold Neutron Fluence Rates. PB89-171946	901,306	PB89-149090 901,093
Prediction of Flowmeter Installation Effects. PB89-211882 900,899	FOOD IRRADIATION		Toughening Mechanisms in Ceramic Composites: Semi-
Prediction of Flowmeter Installation Effects.	Comprehensive Dosimetry for Food Irradiat PB89-186399	ion. <i>900,011</i>	Annual Progress Report for the Period Ending September 30, 1988.
PB89-211890 900,900	FOOD PACKAGING	220,077	PB89-162606 901,028
Development of a Field-Space Corresponding-States Method for Fluids and Fluid Mixtures.	Glass Bottles for Carbonated Soft Drinks: \	oluntary Prod-	Crazes and Fracture in Polymers. PB89-176085 900,562
PB89-227995 901,331	uct Standard PS73-89. PB90-107046	900,012	Fracture Behavior of a Pressure Vessel Steel in the Duc-
Low-Q Neutron Diffraction from Supercooled D-Glycerol. PB89-228001 900,468	FOOD PROCESSING		tile-to-Brittle Transition Region. PB89-189195 901,103
Mean Density Approximation and Hard Sphere Expansion	Comprehensive Dosimetry for Food Irradiat PB89-186399	ion. <i>900,011</i>	Design Criteria for High Temperature Structural Applica-
Theory: A Review. PB89-228019 901,546	FORCE	555,577	tions.
Method for Improving Equations of State Near the Critical	Hydrodynamic Forces on Vertical Cylin	ders and the	PB89-211833 901,052
Point. PB89-228027 901,547	Lighthill Correction. PB90-117417	901,313	Materials Failure Prevention at the National Bureau of Standards.
Prediction of Shear Viscosity and Non-Newtonian Behav-	FORECASTING		PB89-212237 901,190
ior in the Soft-Sphere Liquid.	Relationship between Appearance and Pr bility of Coatings: A Literature Review.	otective Dura-	Fracture Behavior of 316LN Alloy in Uniaxial Tension at Cryogenic Temperatures.
PB89-228035 901,548 Shear-Induced Angular Dependence of the Liquid Pair	PB89-162598	901,063	PB90-128562 <i>901,111</i>
Correlation Function.	FOREIGN TECHNOLOGY		FRACTURING
PB89-228043 900,469	Proceedings of the Celebratory Symposiun of UV (Ultraviolet) Astronomy with the		Rising Fracture Toughness from the Bending Strength of Indented Alumina Beams.
Improved Conformal Solution Theory for Mixtures with Large Size Ratios.	Volume 2.		PB89-171771 901,031
PB89-228563 900,477	N89-16535/1	900,014	FRAGMENTATION
Effect of Pipe Roughness on Orifice Flow Measurement. PB89-231484 901,333	Van der Waals Fund, Van der Waals L Dutch High-Pressure Science.	-	Absolute Cross Sections for Molecular Photoabsorption, Partial Photoionization, and Ionic Photofragmentation
Measurements of Coefficients of Discharge for Concen-	PB89-185755	900,401	Process. PB89-186464 900,410
tric Flange-Tapped Square-Edged Orifice Meters in Water Over the Reynolds Number Range 600 to 2,700,000.	FORENSIC MEDICINE Analysis of Ridge-to-Ridge Distance on Fin	gernrints	FREE CONVECTION
PB89-235147 901,334	PB89-230478	901,216	Use of Dye Tracers in the Study of Free Convection in
Optimum Location of Flow Conditioners in a 4-Inch Ori-	FORMALDEHYDE		Porous Media. PB89-173918 <i>901,327</i>
fice Meter. PB90-111675 900,911	Predicting Formaldehyde Concentrations in Housing Resulting from Medium-Density Fil		FREE ELECTRON LASERS
Measures of Effective Ergodic Convergence in Liquids.	PB89-148134	900,854	NBS/NRL (National Bureau of Standards/Naval Re-
PB90-118092 900,518	Gypsum Wallboard Formaldehyde Sorption PB90-132705	Model. 900, 154	search Laboratory) Free Electron Laser Facility. PB89-175749 901,351
Vortex Shedding Flowmeter for Fluids at High Flow Velocities.	FORMAMIDES	000,707	NBS (National Bureau of Standards) Free Electron Laser
PB90-128661 900,608	Electric-Dipole Moments of H2O-For	mamide and	Facility. PB89-176515 901,353
.UORESCENCE In Situ Fluorescence Monitoring of the Viscosities of Par-	CH3OH-Formamide. PB89-147375	900,288	Research Opportunities Below 300 nm at the NBS (Na-
ticle-Filled Polymers in Flow.	Microwave Spectrum, Structure, and E		tional Bureau of Standards) Free-Electron Laser Facility.
PB89-146278 900,609 Stokes and Anti-Stokes Elugrascance of Er/3 L) in the	Moment of the Ar-Formamide van der Waa PB89-157325	ls Complex. 900,318	PB89-192678 901,360
Stokes and Anti-Stokes Fluorescence of Er(3+) in the Raman Spectra of Erbium Oxide and Erbium Glasses.	FORTRAN PROGRAMMING LANGUAGE	230,010	FREE ENERGY Temperature, Composition and Molecular-Weight De-
PB89-149231 901,020	Creating CSUBs in BASIC.	000 - 15	pendence of the Binary Interaction Parameter of Polysty-
Laser Induced Fluorescence for Measurement of Lignin Concentrations in Pulping Liquors.	PB89-176226	900,647	rene/Poly(vinylmethylether) Blends. PB89-157473 900,550
PB89-172530 901,184	Creating CSUBs Written in FORTRAN BASIC.		FREE RADICALS
-UORESCENT DYES Two-Photon Laser-Induced Fluorescence of the Tumor-	PB90-128752	900,656	Rate Constants for Hydrogen Abstraction by Resonance Stabilized Radicals in High Temperature Liquids.
Localizing Photosensitizer Hematoporphyrin Derivative.	FOURIER TRANSFORM INFRARED SPECTRO Time-Resolved FTIR Emission Studies of I		PB89-161608 900,348
PB89-157283 901,240	tofragmentation Initiated by a High Reper		Absolute Rate Constants for Hydrogen Abstraction from
Use of Dye Tracers in the Study of Free Convection in Porous Media.	cimer Laser. PB90-136680	900,266	Hydrocarbons by the Trichloromethylperoxyl Radical. PB89-171532 900,357

Intramolecular H Atom Abstraction from the Sugar Moiety by Thymine Radicals in Oligo- and Polydeoxynucleotides. PB89-171870 901,263	FUNDAMENTAL CONSTANTS Low Field Determination of the Proton Gyromagnetic Ratio in Water.	Preparation of Standards for Gas Analysis. PB89-211940 900,215
One-Electron Transfer Reactions of the Couple SO2/ SO2(1-) in Aqueous Solutions. Pulse Radiolytic and	PB89-230411 901,555 NBS (National Bureau of Standards) Determination of the	High-Accuracy Gas Analysis via Isotope Dilution Mass Spectrometry: Carbon Dioxide in Air. PB90-123951 900,032
Cyclic Voltammetric Studies. PB89-176093 900,376	Fine-Structure Constant, and of the Quantized Hall Re- sistance and Josephson Frequency-to-Voltage Quotient	GAS CHROMATOGRAPHY Speciation Measurements of Butyltins: Application to
Chemical Kinetics of Intermediates in the Autoxidation of SO2. PB89-176754 900.256	in SI Units. PB89-230437 901,556	Controlled Release Rate Determination and Production of Reference Standards. PB89-146807 900,174
Stabilization and Spectroscopy of Free Radicals and Re-	Fundamental Physical Constants - 1986 Adjustments. PB90-136474 900,535	Chemical Characterization of Ionizing Radiation-Induced
active Molecules in Inert Matrices. PB89-231252 900,484	FURNACES Part Load, Seasonal Efficiency Test Procedure Evaluation	Damage to DNA. PB89-151922 901,235
Generation of Oxy Radicals in Biosystems. PB90-117888 901,266	of Furnace Cycle Controllers. PB89-212146 900,848	Comparison of a Cryogenic Preconcentration Technique and Direct Injection for the Gas Chromatographic Analysis of Low PPB (Parts-per-Billion) (NMOL/MOL) Gas
Estimates of Confidence Intervals for Divider Distorted	FURNITURE Validated Furniture Fire Model with FAST (HEMFAST). PB89-215354 900,142	Standards of Toxic Organic Compounds. PB89-173843 900,193
Waveforms. PB89-173447 900,806	Fire Growth and Development. PB90-128570 900,152	GAS DISCHARGES Ionization and Current Growth in N2 at Very High Electric
REQUENCY CONTROL Precise Laser Frequency Scanning Using Frequency-Synthesized Optical Frequency Sidebands: Application to	Flammability of Upholstered Furniture with Flaming	Field to Gas Density Ratios. PB89-228381 901,552
Isotope Shifts and Hyperfine Structure of Mercury. PB90-118134 901,370	Sources. PB90-136805 900,155	Method for Measuring the Stochastic Properties of Corona and Partial-Discharge Pulses.
REQUENCY MEASUREMENT	FUSED SALTS Journal of Physical and Chemical Reference Data,	PB90-128745 900,829 GAS ENGINES
Calibration Tables Covering the 1460- to 1550-cm(-1) Region from Heterodyne Frequency Measurements on the nu(sub 3) Bands of (12)CS2 and (13)CS2. PB89-157416 900,322	Volume 17, 1988, Supplement No. 2. Thermodynamic and Transport Properties for Molten Salts: Correlation Equations for Critically Evaluated Density, Surface Ten- sion, Electrical Conductance, and Viscosity Data.	Advanced Ceramics: A Critical Assessment of Wear and Lubrication. PB89-188569 901,045
Frequency Measurements of High-J Rotational Transitions of OCS and N2O.	PB89-145205 900,277 GADOLINIUM	GAS FLOW Low Range Flowmeters for Use with Vacuum and Leak
PB90-136946 900,541 REQUENCY MEASUREMENTS	Magnetic Correlations in an Amorphous Gd-Al Spin Glass.	Standards. PB89-175707 900,374
Heterodyne Frequency Measurements of (12)C(16)O Laser Transitions.	PB89-201693 901,148 GAGES	NBS (National Bureau of Standards)-Boulder Gas Flow Facility Performance.
PB89-229223 901,374	Laboratory Evaluation of an NBS (National Bureau of Standards) Polymer Soil Stress Gage.	PB89-186787 900,889 Gas Flow Measurement Standards.
REQUENCY RESPONSE Numerical Analysis for the Small-Signal Response of the MOS (Metal Oxide Semiconductors) Capacitor.	PB89-211973 901,291 GALLIUM	PB89-211874 900,898
PB89-186837 900,781	Surface Structure and Growth Mechanism of Ga on Si(100).	GAS IONIZATION Ionization and Current Growth in N2 at Very High Electric Field to Gas Density Ratios.
Thermal Shrifts of the Spectral Lines in the (4)F3/2 to	PB99-149181 901,387 Surface Structures and Growth Mechanism of Ga on	PB89-228381 901,552
(4)111/2 Manifold of an Nd:YAG Laser. PB89-157382 901,338	Si(100) Determined by LEED (Low Energy Electron Dif- fraction) and Auger Electron Spectroscopy.	GAS LAWS PVT of Toluene at Temperatures to 673 K. PB89-157192 900,310
Effect of an Electrically Large Stirrer in a Mode-Stirred Chamber. PB90-117946 901,378	PB89-171342 901,399 AES and LEED Studies Correlating Desorption Energies	PB89-157192 900,310 PVT Measurements on Benzene at Temperatures to 723
REQUENCY STABILITY	with Surface Structures and Coverages for Ga on Si(100).	K. PB89-157200 <i>900,311</i>
CO Laser Stabilization Using the Optogalvanic Lamb-Dip. PB89-179139 901,356	PB89-171599 901,401 Spectra and Energy Levels of the Galliumlike lons Rb VII-	GAS METAL ARC WELDING On-Line Arc Welding: Data Acquisition and Analysis
REQUENCY STANDARDS Trapped Ions and Laser Cooling 2: Selected Publications	Mo XII. PB89-179105 900,387	Using a High Level Scientific Language. PB90-117391 900,972
of the Ion Storage Group, Time and Frequency Division, NIST, Boulder, CO. PB89-153878 901,489	Laser Probing of the Dynamics of Ga Interactions on Si(100).	GAS-PARTICLE FLOW Numerical Computation of Particle Trajectories: A Model
Study of Long-Term Stability of Atomic Clocks.	PB89-186928 901,422 GALLIUM ARSENIDES	Problem. PB89-158117 901,324
NIST (National Institute of Standards and Technology)	Surface Structures and Growth Mechanism of Ga on Si(100) Determined by LEED (Low Energy Electron Dif-	GAS SCINTILLATION DETECTORS Advances in the Use of (3)He in a Gas Scintillation
Automated Coaxial Microwave Power Standard. PB89-176192 900,807	fraction) and Auger Electron Spectroscopy. PB89-171342 901,399	Counter. PB90-123506 901,565
Calibration of GPS (Global Positioning System) Equipment in Japan. PB89-212070 900,630	Quantized Hall Resistance Measurement at the NML (National Measurement Laboratory).	GAS TRANSPORT CO2 Separation Using Facilitated Transport Ion Ex-
NBS (National Bureau of Standards) Calibration Service	PB89-179675 900,778 EXAFS (Extended X-ray Absorption Fine Structure) Study	change Membranes. PB89-157374 900,321
Providing Time and Frequency at a Remote Site by Weighting and Smoothing of GPS (Global Positioning Systein) Common View Data.	of Buned Germanium Layer in Silicon. PB89-228472 901,452	GASES Microwave Measurements of the Thermal Expansion of a
PB89-212211 900,631	Effects of Doping-Density Gradients on Band-Gap Narrowing in Silicon and GaAs Devices.	Spherical Cavity. PB89-147458 900,291
Frequency Standards Utilizing Penning Traps. PB90-128042 901,379	PB89 ⁻ 228522 901,453 GAMMA DOSIMETRY	Critical Review of the Chemical Kinetics of Sulfur Tetra- fluonde, Sulfur Pentafluoride, and Sulfur Fluonde (S2F10)
FREQUENCY SYNTHESIZERS Low Noise Frequency Synthesis.	Comprehensive Dosimetry for Food Irradiation. PB89-186399 900,011	in the Gas Phase. PB89-161582 900,347
PB89-174056 900,716 FRESNEL INTEGRALS	GAMMA IRRADIATION Dichromate Dosimetry: The Effect of Acetic Acid on the	Grain Boundaries with Impurities in a Two-Dimensional Lattice-Gas Model. PB89-172407 901,507
Efficient and Accurate Method for Calculating and Representing Power Density in the Near Zone of Microwave	Radiolytic Reduction Yield. PB89-147490 900,248	Facilitated Transport of CO2 through Highly Swollen Ion-
Antennas. PB89-157457 900,707	GAMMA RAY ABSORPTION DCTDOS: Neutron and Gamma Penetration in Composite	Exchange Membranes: The Effect of Hot Glycerine Pre- treatment. PB89-179618 900,395
FRESNEL LENSES Fresnel Lenses Display Inherent Vignetting. PB89-157069 901,337	Duct Systems. PB89-188809 901,275	Second Viscosity and Thermal-Conductivity Virial Coefficients of Gases: Extension to Low Reduced Tempera-
FRIABILITY	GAMMA RAY SPECTROSCOPY High Accuracy Determination of (235)U in Nondestructive	ture. PB89-179691 900,397
Friability of Spray-Applied Fireproofing and Thermal Insulations: Field Evaluation of Prototype Test Devices. PB89-189328 900,130	Assay Standards by Gamma Spectrometry. PB89-156954 GAS ANALYSES	Simple Apparatus for Vapor-Liquid Equilibrium Measure- ments with Data for the Binary Systems of Carbon Diox- ide with n-Butane and Isobutane.
FUEL OIL Combustion of Oil on Water. November 1987. PB89-185581 900,863	Comparison of a Cryogenic Preconcentration Technique and Direct Injection for the Gas Chromatographic Analysis of Levy RPR (Ports per Billion) (NMO (MOL)). Gas	PB89-201115 900,422 Gas Solubility and Henry's Law Near the Solvent's Criti-
FUEL SPRAYS	sis of Low PPB (Parts-per-Billion) (NMOL/MOL) Gas Standards of Toxic Organic Compounds. PB89-173843 900,193	cal Point. PB89-202485 900,434
Importance of Isothermal Mixing Processes to the Understanding of Lift-Off and Blow-out of Turbulent Jet Diffusion Flames	GAS ANALYSIS	Chemisorption of HF (Hydrofluoric Acid) on Silicon Surfaces.
sion Flames. PB89-201172 900,598	Special Calibration Systems for Reactive Gases and Other Difficult Measurements. PB89-149215 900,873	PB89-212013 900,445 Toxicity of Mixed Gases Found in Fires.
FUMES Predicting Formaldehyde Concentrations in Manufactured Housing Resulting from Medium-Density Fiberboard.	Remote Sensing Technique for Combustion Gas Temperature Measurement in Black Liquor Recovery Boilers.	PB89-212047 900,869 Torsional Piezoelectric Crystal Viscometer for Compressed Gases and Liquids.
PB89-148134 900,854	PB89-179568 900,392	product added and Elquidor

PB89-228076 901,447	PB89-202618 900,021	PB89-146922 900,28
Fluid Flow in Pulsed Laser Irradiated Gases; Modeling and Measurement.	Stellar Winds of 203 Galactic O Stars: A Quantitative Ultraviolet Survey.	Multiple Scattering in the X-ray Absorption Near Edg Structure of Tetrahedral Germanium Gases.
PB90-123704 900,265	PB89-202626 900,022	PB89-228480 900,47
Evaluation of Data on Solubility of Simple Apolar Gases in Light and Heavy Water at High Temperature.	Interpretation of Emission Wings of Balmer Lines in Luminous Blue Variables.	GIBBS FREE ENERGY Second Virial Coefficients of Aqueous Alcohols at Eleval
PB90-126251 900,529 Role of Adsorbed Gases in Metal on Metal Epitaxy.	PB89-212054 900,023 Publications of the National Institute of Standards and	ed Temperatures: A Calorimetric Study. PB89-227896 900,46
PB90-128125 901,174	Technology, 1988 Catalog. PB89-218382 900,006	900,40. GLASS
Spherical Acoustic Resonators. PB90-128505 901,321	IUE Observation of the Interstellar Medium Toward Beta	Stokes and Anti-Stokes Fluorescence of Er(3+) in the
ATT STANDARDS CODE	Geminorum. PB89-228373 900,024	Raman Spectra of Erbium Oxide and Erbium Glasses. PB89-149231 901,02
GATT (General Agreement on Tariffs and Trade) Standards Code Activities of the National Institute of Standards	NDE (Nondestructive Evaluation) Publications, 1985.	Effect of Surface Ionization on Wetting Layers. PB89-157259 901,32:
and Technology 1988. PB89-191977 900,173	PB89-229025 900,984 Rotational Modulation and Flares on RS Canum Venati-	Effect of Lateral Crack Growth on the Strength of Con
E SEMICONDUCTOR DETECTORS	corum and BY Draconis Stars. XI. Ultraviolet Spectral	tact Flaws in Brittle Materials. PB89-171813 901,03
Characteristics of Ge and InGaAs Photodiodes. PB89-176796 900,729	Images of AR Lacertae in September 1985. PB89-234298 900,026	Measurement of the Torque and Normal Force in Torsion
ELS	NIST (National Institute of Standards and Technology) Research Reports, June 1989.	in the Study of the Thermoviscoelastic Properties of Polymer Glasses.
Concentration Dependence of the Compression Modulus of Isotactic Polystyrene/Cis-Decalin Gels.	PB89-235113 900,007	PB89-172472 900,55
PB89-172449 900,552 Effects of Solvent Type on the Concentration Depend-	Typical Usage of Radioscopic Systems: Replies to a Survey.	Undercooling and Microstructural Evolution in Glas: Forming Alloys.
ence of the Compression Modulus of Thermoreversible Isotactic Polystyrene Gels.	PB90-117664 901,161	PB89-176465 901,13.
PB89-172456 900,553	Solar and Stellar Magnetic Fields and Structures: Observations.	Ergodic Behavior in Supercooled Liquids and in Glasses. PB89-202444 901,43.
ENERAL INTEREST Proceedings of the Celebratory Symposium on a Decade	PB90-118118 900,027 Helium Resonance Lines in the Flare of 15 June 1973.	Crack-Interface Traction: A Fracture-Resistance Mechanism in Brittle Polycrystals.
of UV (Ultraviolet) Astronomy with the IUE Satellite, Volume 2.	PB90-118142 900,028	PB89-211817 901,05
N89-16535/1 900,014	Analyzing the Economic Impacts of a Military Mobilization.	In vitro Investigation of the Effects of Glass Inserts of the Effective Composite Resin Polymerization Shrinkage.
Theory and Practice of Paper Preservation for Archives. PB89-147052 900,934	PB90-128067 901,273	PB90-117516 900,04
NBS (National Bureau of Standards) Ohm: Past-Present-	Report on Interactions between the National Institute of Standards and Technology and the Institute of Electrical	GLASS FIBERS Novel Process for the Preparation of Fiber-Reinforcer
Future. PB89-149066 900,802	and Electronic Engineers. PB90-130899 900,831	Ceramic-Matrix Composites. PB89-179733 901,074
Doppler Imaging of AR Lacertae at Three Epochs. PB89-149199 900.015	Tilt Observations Using Borehole Tiltmeters 1. Analysis of	GLASS PARTICLE COMPOSITES
Late Stages of Close Binary Systems-Clues to Common	Tidal and Secular Tilt. PB90-136649 901,283	Methods for the Production of Particle Standards.
Envelope Evolution. PB89-149207 900,016	GENERAL THEORETICAL CHEMISTRY & PHYSICS Electrodeposition of Chromium from a Trivalent Electro-	PB89-201636 901,04. GLOBAL POSITIONING SYSTEM
Center for Chemical Technology: 1988 Technical Activi-	lyte.	Dual Frequency P-Code Time Transfer Experiment.
ties. PB89-156376 900,241	PATENT-4 804 446 901,119 Numerical Computation of Particle Trajectories: A Model	PB89-174064 900,61- Apparent Diurnal Effects in the Global Positioning
Proper Motion vs. Redshift Relation for Superluminal Radio Sources.	Problem. PB89-158117 901,324	System. PB89-174080 901,294
PB89-157663 900,017	Shear Induced Anisotropy in Two-Dimensional Liquids.	GLOBAL POSITIONING SYSTEMS
Shimanouchi, Takehiko and the Codification of Spectroscopic Information. PB89-157846 900,335	PB89-158141 901,325 Three-State Lattice Gas as Model for Binary Gas-Liquid Systems.	Using Multiple Reference Stations to Separate the Variances of Noise Components in the Global Positioning System.
Data Bases Available at the National Institute of Stand-	PB89-171284 900,354	PB89-185730 901,293
ards and Technology Research Information Center. PB89-160014 900,932	Dynamics of a Spin-One Model with the Pair Correlation. PB89-171300 900,356	Calibration of GPS (Global Positioning System) Equip ment in Japan.
Microarcsecond Optical Astrometry: An Instrument and Its Astrophysical Applications.	Non-Equilibrium Theories of Electrolyte Solutions.	PB89-212070 900,636
PB89-171268 900,013	PB89-174940 900,369 One Is Not Enough: Intra-Cavity Spectroscopy with Multi-	NBS (National Bureau of Standards) Calibration Service Providing Time and Frequency at a Remote Site by
Rotational Modulation and Flares on RS CVn and BY Dra Stars IX. IUE (International Ultraviolet Explorer) Spectros-	Mode Lasers. PB89-185888 900,402	Weighting and Smoothing of GPS (Global Positioning System) Common View Data.
copy and Photometry of II Peg and V711 Tau during February 1983.	GENERATORS	PB89-212211 900,63
PB89-171615 900,019	Fast-Pulse Generators and Detectors for Characterizing Laser Receivers at 1.06 um.	GLUCOSE Developing Definitive Methods for Human Serum Ana
Classical Chaos, the Geometry of Phase Space, and Semiclassical Quantization.	PB89-171698 <i>901,347</i>	lytes. PB89-146773 901,233
PB89-172381 901,506 Report on Interactions between the National Institute of	GENETIC EFFECTS Chemical Characterization of Ionizing Radiation-Induced	GLUTAMINASE
Standards and Technology and the American Society of	Damage to DNA. PB89-151922 <i>901,235</i>	Preliminary Crystal Structure of Acinetobacter glutamina sificans Glutaminase-Asparaginase.
Mechanical Engineers. PB89-172563 901,004	GEOLOGIC STRUCTURES	PB90-123381 901,260
Cool It. PB89-176986 901,516	Relationships between Fault Zone Deformation and Seg- ment Obliquity on the San Andreas Fault, California.	GLYCEROL Low-Q Neutron Diffraction from Supercooled D-Glycerol.
Fundamental Tests of Special Relativity and the Isotropy	PB89-185953 901,279	PB89-228001 900,468
of Space. PB89-185920 901,523	GEOLOGICAL FAULTS Relationships between Fault Zone Deformation and Seg-	GLYCINE/N-PHENYL Use of N-Phenylglycine in a Dental Adhesive System,
Relationships between Fault Zone Deformation and Segment Obliquity on the San Andreas Fault, California.	ment Obliquity on the San Andreas Fault, California. PB89-185953 901,279	PB90-117375 900,048
PB89-185953 901,279	Rate of Change of the Quincy-Monument Peak Baseline from a Translocation Analysis of LAGEOS Laser Range	GLYOXAL/METHYL Stopped-Flow Studies of the Mechanisms of Ozone
Bibliography of the NIST (National Institute of Standards and Technology) Electromagnetic Fields Division Publica-	Data.	Alkene Reactions in the Gas Phase: Tetramethylethy lene.
tions. PB89-189211 900,810	PB89-234272 901,282 GERMANIUM	PB89-157515 900,326
National Engineering Laboratory's 1989 Report to the	Metastable Phase Production and Transformation in Al-	GOLD IONS Laser-Produced Spectra and QED (Quantum Electrody
National Research Council's Board on Assessment of NIST (National Institute of Standards and Technology)	Ge Alloy Films by Rapid Crystallization and Annealing Treatments.	namic) Effects for Fe-, Co-, Cu-, and Zn-Like lons of Au
Programs. PB89-189294 900,004	PB89-157622 901,129 EXAFS (Extended X-ray Absorption Fine Structure) Study	Pb, Bi, Th, and U. PB89-176010 <i>901,51</i> 0
NIST (National Institute of Standards and Technology)	of Buried Germanium Layer in Silicon. PB89-228472 901,452	GOVERNMENT OPEN SYSTEMS INTERCONNECTION PROFILE
Research Reports, March 1989. PB89-189310 900,005	GERMANIUM HALIDES	Government Open Systems Interconnection Profile
Versailles Project on Advanced Materials and Standards Evolution to Permanent Status.	Multiple Scattering in the X-ray-Absorption Near-Edge Structure of Tetrahedral Ge Gases.	Users' Guide. PB90-111212 900,66.
PB89-201768 900,969	PB89-146922 900,283	GOVERNMENT POLICIES
Photospheres of Hot Stars. 3. Luminosity Effects at Spectral Type 09.5.	Multiple Scattering in the X-ray Absorption Near Edge Structure of Tetrahedral Germanium Gases.	Research as the Technical Basis for Standards Used in Building Codes.
PB89-202592 900,020	PB89-228480 900,474	PB89-231062 900,10

GERMANIUM HYDRIDES

Multiple Scattering in the X-ray-Absorption Near-Edge Structure of Tetrahedral Ge Gases.

GRADED INDEX FIBERS

Profile Inhomogeneity in Multimode Graded-Index Fibers. PB89-179816 900,749

Rotational Modulation and Flares on RS Canum Venati-corum and BY Draconis Stars X: The 1981 October 3 Flare on V711 Tauri (= HR 1099).

GRADIOMETERS Liquid-Supported Torsion Balance: An Updated Status Report on its Potential for Tunnel Detection.	GRUNEISEN CONSTANT Gruneisen Parameter of Y1Ba2Cu3O7. PB90-117615 901,465	Development of a Microwave Sustained Gas Plasma for the Sterilization of Dental Instruments. PB89-231278 900,047
PB89-212062 901,542 GRAFT POLYMERIZATION	GUARDED HOT PLATE Circular and Square Edge Effect Study for Guarded-Hot-	Comparison of Microleakage of Experimental and Selected Commercially Available Bonding Systems.
Theory of Microphase Separation in Graft and Star Co- polymers.	Plate and Heat-Flow-Meter Apparatuses. PB89-176135 900,881	PB89-234223 901,079 Use of N-Phenylglycine in a Dental Adhesive System.
PB89-176028 900,557	GUIDELINES	PB90-117375 900,048
GRAIN BOUNDARIES Migration of Liquid Film and Grain Boundary in Mo-Ni Induced by W Diffusion. PB89-157614 901,128	Draft International Document on Guide to Portable Instru- ments for Assessing Airborne Pollutants Arising from Hazardous Wastes. PB89-150775 900,855	In vitro Investigation of the Effects of Glass Inserts on the Effective Composite Resin Polymerization Shrinkage. PB90-117516 900,049
Experimental Observations on the Initiation of DIGM (Dif-	GYPSUM	Substitutes for N-Phenylglycine in Adhesive Bonding to Dentin.
fusion Induced Grain Boundary Migration). PB89-157630 901,130 Directional Invariance of Grain Boundary Migration in the	Gypsum Wallboard Formaldehyde Sorption Model. PB90-132705 900,154	PB90-123795 900,051 Liposome Technology in Biomineralization Research.
Pb-Sn Cellular Transformation and the Tu-Turnbull Hysteresis.	GYROMAGNETIC RATIO Low Field Determination of the Proton Gyromagnetic Ratio in Water.	PB90-128117 901,230 Dental Materials and Technology Research at the Nation-
PB89-157911 901,134	PB89-230411 901,555	al Bureau of Standards: A Model for Government-Private Sector Cooperation.
Grain Boundaries with Impurities in a Two-Dimensional Lattice-Gas Model. PB89-172407 901,507	HALL EFFECT Possible Quantum Hall Effect Resistance Standard. PB89-149058 900,801	PB90-128711 900,052 HEAT BALANCE
Creep Cavitation in Liquid-Phase Sintered Alumina. PB89-175954 901,038	Quantized Hall Resistance Measurement at the NML (National Measurement Laboratory).	Developments in the Heat Balance Method for Simulating Room Thermal Response.
Grain Boundary Structure in Ni3Al. PB89-201784 901,150	PB89-179675 900,778 HALOHYDROCARBONS	PB89-173926 900,062 HEAT FLOW METERS
Electron Diffraction Study of the Faceting of Tilt Grain	Thermophysical-Property Needs for the Environmentally	Circular and Square Edge Effect Study for Guarded-Hot- Plate and Heat-Flow-Meter Apparatuses.
Boundaries in NiO. PB89-201792 901,431	Acceptable Halocarbon Refrigerants. PB89-231054 900,482	PB89-176135 900,881
Diffraction Effects Along the Normal to a Grain Boundary. PB89-202089 901,153	HARD SPHERE EXPANSION THEORY Mean Density Approximation and Hard Sphere Expansion	Summary of Circular and Square Edge Effect Study for Guarded-Hot-Plate and Heat-Flow-Meter Apparatuses. PB89-176606 900,884
Electron Microscopy Studies of Diffusion-Induced Grain Boundary Migration in Ceramics.	Theory: A Review. PB89-228019 901,546	HEAT LOSS
PB89-202097 901,049 Grain Boundary Characterization in Ni3Al.	HARDENING (MATERIALS) Epoxy Impregnation of Hardened Cement Pastes for	Analysis and Prediction of Air Leakage through Door Assemblies.
PB89-229306 901,156	Characterization of Microstructure. PB89-185573 901,042	PB89-231161 900,085 HEAT MEASUREMENT
Flux Creep and Activation Energies at the Grain Boundaries of Y-Ba-Cu-O Superconductors. PB89-230353 901,457	HARDNESS Metallurgical Evaluation of 17-4 PH Stainless Steel Cast-	Biological Standard Reference Materials for the Calibration of Differential Scanning Calonmeters: Di-alkylphos-
Diffusion-Induced Grain Boundary Migration.	ings. PB89-193262 <i>901,105</i>	phatidylcholine in Water Suspensions. PB89-186779 900,415
PB90-128174 901,175 GRAIN SIZE	HAZARDOUS MATERIALS	Calonmetric and Equilibrium Investigation of the Hydroly-
Notion of Granularity.	Draft International Document on Guide to Portable Instru- ments for Assessing Airborne Pollutants Arising from	sis of Lactose. PB89-227888 <i>901,226</i>
PB89-147003 900,915 Grain-Size and R-Curve Effects in the Abrasive Wear of	Hazardous Wastes. PB89-150775 <i>900,855</i>	HEAT OF VAPORIZATION
Alumina. PB90-117383 901,058	Fundamental Aspects of Key Issues in Hazardous Waste Incineration.	Development of Standard Measurement Techniques and Standard Reference Materials for Heat Capacity and Heat of Vaporization of Jet Fuels.
Effects of Grain Size and Cold Rolling on Cryogenic	PB89-212104 900,861	PB89-148100 900,837
Properties of Copper. PB90-128604 901,176	HAZARDS Guidelines for Identification and Mitigation of Seismically	HEAT PUMPS Rating Procedure for Mixed Air-Source Unitary Air Condi-
GRANULARITY Definitions of Granularity	Hazardous Existing Federal Buildings. PB89-188627 900,161	tioners and Heat Pumps Operating in the Cooling Mode. Revision 1.
Definitions of Granularity. PB89-180012 900,650	HEALTH & SAFETY	PB89-193247 900,075
GRAPHIC METHODS Graphical Analyses Related to the Linewidth Calibration Problem.	Non-Aqueous Dental Cements Based on Dimer and Trimer Acids. PATENT-4 832 745 900,033	Advanced Heat Pumps for the 1990's Economic Perspectives for Consumers and Electric Utilities. PB90-118043 900,089
PB89-201156 900,783	Micro-Raman Characterization of Atherosclerotic and Bio-	HEAT TRANSFER
GRAVIMETERS Gravity Tide Measurements with a Feedback Gravity	prosthetic Calcification. PB89-149223 901,234	Cooling Effect Induced by a Single Evaporating Droplet on a Semi-Infinite Body.
Meter. PB89-171755 901,310	Corrosion of Metallic Implants and Prosthetic Devices. PB89-150890 900,053	PB89-149249 901,488
GRAVIMETRIC ANALYSIS Preparation of Standards for Gas Analysis.	Interaction of Cupric Ions with Calcium Hydroxylapatite. PB89-157127 900,037	Window U-Values: Revisions for the 1989 ASHRAE (American Society of Heating, Refrigerating and Air-Con- ditioning Engineers) Handbook - Fundamentals.
PB89-211940 900,215	Fast Magnetic Resonance Imaging with Simultaneously	PB89-229215 900,145
GRAVITATION Current Research Efforts at JILA (Joint Institute for Laboratory Astrophysics) to Test the Equivalence Principle at	Oscillating and Rotating Field Gradients. PB89-176903 901,514	Heat Transfer in Compartment Fires Near Regions of Ceiling-Jet Impingement on a Wall. PB90-118076 900,150
Short Ranges. PB89-185912 901,522	Adsorption of 4-Methacryloxyethyl Trimellitate Anhydride (4-META) on Hydroxyapatite and Its Role in Composite	HEAT TRANSFER COEFFICIENT
Precision Experiments to Search for the Fifth Force.	Bonding. PB89-179220 <i>900,041</i>	Flow Coefficients for Interzonal Natural Convection for Various Apertures.
PB89-228365 901,551	Comparison of Fluoride Uptake Produced by Tray and	PB89-177158 900,069
Conceptual Design for a Mercury Relativity Satellite. PB89-234249 901,595 GRAVITATIONAL WAVE ANTENNAS	Flossing Methods In vitro. PB89-179238 901,252 Oligomers with Pendant Isocyanate Groups as Adhesives	Experimental Determination of Forced Convection Evapo- rative Heat Transfer Coefficients for Non-Azeotropic Re- frigerant Mixtures.
Antenna for Laser Gravitational-Wave Observations in Space.	for Dentin and Other Tissues. PB89-179253 900,042	PB89-186407 901,117 HEAT TRANSMISSION
PB89-234231 901,594	Stabilization of Ascorbic Acid in Human Plasma, and Its	Periodic Heat Conduction in Energy Storage Cylinders
GRAVITATIONAL WAVES Antenna for Laser Gravitational-Wave Observations in	Liquid-Chromatographic Measurement. PB89-179279 901,237	with Change of Phase. PB89-175897 900,852
Space. PB89-234231 901,594	Micro-Analysis of Mineral Saturation Within Enamel during Lactic Acid Demineralization.	Circular and Square Edge Effect Study for Guarded-Hot- Plate and Heat-Flow-Meter Apparatuses.
GRAVITY High-Precision Absolute Gravity Observations in the	PB89-186373 901,253 Formation of Hydroxyapatite in Hydrogels from Tetracal-	PB89-176135 900,881 Summary of Circular and Square Edge Effect Study for
United States. PB89-227946 901,281	cium Phosphate/Dicalcium Phosphate Mixtures. PB89-201511 901,255	Summary of Circular and Square Edge Effect Study for Guarded-Hot-Plate and Heat-Flow-Meter Apparatuses. PB89-176606 900,884
GRAZING INCIDENCE Dynamical Diffraction of X-rays at Grazing Angle.	Detection of Lead in Human Teeth by Exposure to Aqueous Sulfide Solutions.	HEAT TREATMENT Metallurgical Evaluation of 17-4 PH Stainless Steel Cast-
PB89-186886 901,421	PB89-201529 901,256	ings. PB89-193262 901,105
GREENS FUNCTION Hybrid Representation of the Green's Function in an	High-Temperature Dental Investments. PB89-202477 901,257	Effect of Heat Treatment on Crack-Resistance Curves in
Overmoded Rectangular Cavity. PB90-117953 900,826	Pulpal and Micro-organism Responses to Two Experimental Dental Bonding Systems.	a Liquid-Phase-Sintered Alumina. PB89-229231 901,056
GRINDING (COMMINUTION) Model for Particle Size and Phase Distributions in Ground	PB89-202931 901,258 Quasi-Constant Composition Method for Studying the	HEATING LOAD Field Measurement of Thermal and Solar/Optical Proper-
Cement Clinker.	Formation of Artificial Caries-Like Lesions.	ties of Insulating Glass Windows.

HEATING RATE Evaluation of Data on Higher Heating Values and Ele-	PB89-202493 900,435	PB89-172621 901,098
mental Analysis for Refuse-Derived Fuels.	Tables for the Thermophysical Properties of Methane. PB89-222608 900,843	High Temperature Thermal Conductivity Apparatus for Fluids.
PB90-136839 900,845 HEAVY WATER	HIGH-PURITY GE DETECTORS	PB89-174015 900,366
Evaluation of Data on Solubility of Simple Apolar Gases in Light and Heavy Water at High Temperature.	High-Purity Germanium X-ray Detector on a 200 kV Analytical Electron Microscope.	Molecular Dynamics Investigation of Expanded Water at Elevated Temperatures.
PB90-126251 900,529	PB89-201602 900,208 HIGH RESOLUTION	PB89-174957 900,370
HELIUM Laser Probing of Ion Velocity Distributions in Drift Fields:	Effects of Velocity and State Changing Collisions on	Mechanism and Rate of Hydrogen Atom Attack on Tolu- ene at High Temperatures.
Parallel and Perpendicular Temperatures and Mobility for	Raman Q-Branch Špectra. PB89-179196 900,391	PB89-179758 900,398 Design Criteria for High Temperature Structural Applica-
Ba(1+) in He. PB89-171243 900,352	Structure and Dynamics of Molecular Clusters via High	tions.
Tensile Strain-Rate Effects in Liquid Helium. PB89-174882 901,102	Resolution IR Absorption Spectroscopy. PB89-185896 900,403	PB89-211833 901,052 HIGH VACUUM
Nonadiabatic Theory of Fine-Structure Branching Cross-	High Resolution Optical Multiplex Spectroscopy. PB89-185938 900,404	NBS (National Bureau of Standards) Orifice-Flow Primary
Sections for Sodium-Helium, Sodium-Neon, and Sodium- Argon Optical Collisions.	Towards the Ultimate Laser Resolution.	High Vacuum Standard. PB89-175699 900,880
PB89-202162 900,433	PB89-186910 900,416	NIST (National Institute of Standards and Technology)
Collision Induced Spectroscopy: Absorption and Light Scattering.	HIGH SPEED PHOTOGRAPHY Measurement of Partial Discharges in Hexane Under DC	Measurement Services: High Vacuum Standard and Its Use.
PB89-212252 901,363 Helium Resonance Lines in the Flare of 15 June 1973.	Voltage. PB89-173421 900,833	PB89-193841 900,891 HIGH VOLTAGE
PB90-118142 900,028	HIGH TEMPERATURE	Measuring Fast-Rise Impulses by Use of E-Dot Sensors.
HELIUM 3 Advances in the Use of (3)He in a Gas Scintillation	Synthesis ano Magnetic Properties of the Bi-Sr-Ca-Cu Oxide 80- and 110-K Superconductors.	PB89-173413 900,744
Counter.	PB89-179725 901,412	Estimates of Confidence Intervals for Divider Distorted Waveforms.
PB90-123506 901,565 HELIUM IONS	HIGH TEMPERATURE SUPERCONDUCTORS Magnetic Field Dependence of the Superconductivity in	PB89-173447 900,806
Cross Sections for K-Shell X-ray Production by Hydrogen	Bi-Sr-Ca-Cu-O Superconductors.	Characterizing Electrical Parameters Near AC and DC Power Lines.
and Helium Ions in Elements from Beryllium to Uranium. PB89-226609 900,460	PB89-146815 901,385 Josephson-Junction Model of Critical Current in Granular	PB89-173462 900,834
HENRYS LAW Gas Solubility and Henry's Law Near the Solvent's Criti-	Y1Ba2Cu3O(7-delta) Superconductors. PB89-176978 901,406	International Comparison of HV Impulse Measuring Systems.
cal Point	Bean Model Extended to Magnetization Jumps.	PB89-186423 900,809
PB89-202485 900,434 HETERODYNING	PB89-176994 901,407	DC Electric Field Effects during Measurements of Mono- polar Charge Density and Net Space Charge Density
Heterodyne Frequency and Fourier Transform Spectros-	High T(sub c) Superconductor/Noble-Metal Contacts with Surface Resistivities in the (10 to the Minus 10th Power)	Near HVDC Power Lines. PB90-128521 901,380
copy Measurements on OCS Near 1700 cm(-1). PB90-117805 900,507	Omega sq cm Range. PB89-179824 901,413	HISTOLOGY
HETEROGENEITY	Theoretical Models for High-Temperature Superconducti-	Biological Evaluations of Zinc Hexyl Vanillate Cement Using Two In vivo Test Methods.
Profile Inhomogeneity in Multimode Graded-Index Fibers. PB89-179816 900,749	vity. PB89-186266 <i>901,418</i>	PB89-157150 900,038
HEUSLER ALLOYS	Oxygen Partial-Density-of-States Change in the	HOLMIUM COMPOUNDS Antiferromagnetic Structure and Crystal Field Splittings in
Antiferromagnetic Structure and Crystal Field Splittings in the Cubic Heusler Alloys HoPd2Sn and ErPd2Sn.	YBa2Cu3Ox Compounds for x(Approx.)6,6.5,7 Measured by Soft X-ray Emission.	the Cubic Heusler Alloys HoPd2Sn and ErPd2Sn. PB89-202659 901,437
PB89-202659 901,437 HEXOSES	PB89-186274 901,419	HOSPITALS
Thermodynamic and Transport Properties of Carbohy-	Resonant Excitation of an Oxygen Valence Satellite in Photoemission from High-T(sub c) Superconductors.	Thermal and Economic Analysis of Three HVAC (Heat-
drates and Their Monophosphates: The Pentoses and Hexoses.	PB89-186860 901,420	ing, Ventilating, and Air Conditioning) System Types in a Typical VA (Veterans Administration) Patient Facility.
PB89-222574 900,453	Ag Screen Contacts to Sintered YBa2Cu3Ox Powder for Rapid Superconductor Characterization.	PB89-188619 900,847
HIERARCHICAL CONTROL Real-Time Optimization in the Automated Manufacturing	PB89-200448 901,423	False Alarm Study of Smoke Detectors in Department of Veterans Affairs Medical Centers (VAMCS).
Research Facility. PB89-172597 900,947	Switching Noise in YBa2Cu3Ox 'Macrobridges'. PB89-200513 901,426	PB89-193288 900,093 HOT STARS
Hierarchies for Computer-Integrated Manufacturing: A	Mossbauer Hyperfine Fields in RBa2(Cu0.97Fe0.03)3 O(7-x)(R = Y,Pr,Er).	Photospheres of Hot Stars. 3. Luminosity Effects at
Functional Description. PB89-172613 900,949	PB89-201206 901,429	Spectral Type 09.5. PB89-202592 900,020
HIERARCHIES	Brief Review of Recent Superconductivity Research at NIST (National Institute of Standards and Technology).	HOT WATER HEATING
Hierarchies for Computer-Integrated Manufacturing: A Functional Description.	PB89-211114 900,766	Proposed Methodology for Rating Air-Source Heat Pumps That Heat, Cool, and Provide Domestic Water
PB89-172613 900,949	Resistance Measurements of High T(sub c) Superconductors Using a Novel 'Bathysphere' Cryostat.	Heating. PB90-112368 900,087
HIGH FREQUENCIES Improved Rotational Constants for HF.	PB89-228431 901,448	HOT WIRE FLOWMETERS
PB90-117466 901,376	Evidence for the Superconducting Proximity Effect in Junctions between the Surfaces of YBa2CU3Ox Thin	Relation between Wire Resistance and Fluid Pressure in the Transient Hot-Wire Method.
HIGH LEVEL LANGUAGES Standard Generalized Markup Language (SGML).	Films. PB89-228449 901,449	PB89-184113 901,520
FIPS PUB 152 900,627 HIGH ORDER CROSSING	Cryogenic Bathysphere for Rapid Variable-Temperature	HOUSES
Higher-Order Crossings: A New Acoustic Emission Signal	Characterization of High-T(sub c) Superconductors. PB89-228456 901,450	Gypsum Wallboard Formaldehyde Sorption Model. PB90-132705 900,154
Processing Method. PB89-173488 900,678	Hysteretic Phase Transition in Y1Ba2Cu3O7-x Supercon-	HUMAN FACTORS ENGINEERING
HIGH POWER LASERS	ductors. PB89-229082 901,454	Post-Occupancy Evaluation of Several U.S. Government Buildings.
Laser Induced Damage in Optical Materials: 1987. PB89-221162 901,364	Dependence of T(sub c) on the Number of CuO2 Planes	PB90-112384 900,088
HIGH PRESSURE	per Cluster in Interplaner-Boson-Exchange Models of High-T(sub C) Superconductivity.	HUMAN NUTRITION Determination of Total Cholesterol in Coconut Oil: A New
Van der Waals Fund, Van der Waals Laboratory and Dutch High-Pressure Science.	PB89-229132 901,455	NIST (National Institute of Standards and Technology) Cholesterol Standard Reference Material.
PB89-185755 900,401 HIGH PRESSURE TESTS	Comparison of Interplaner-Boson-Exchange Models of High-Temperature Superconductivity - Possible Expen-	PB89-234173 901,262
Microwave Energy for Acid Decomposition at Elevated	mental Tests. PB90-117334 901,462	HUMAN PLASMA Stabilization of Ascorbic Acid in Human Plasma, and Its
Temperatures and Pressures Using Biological and Botan- ical Samples.	Reentrant Softening in Perovskite Superconductors.	Liquid-Chromatographic Measurement.
PB89-171961 900,359	PB90-117540 <i>901,464</i> Gruneisen Parameter of Y1Ba2Cu3O7.	PB89-179279 901,237 HUMANS
Vapor-Liquid Equilibrium of Nitrogen-Oxygen Mixtures and Air at High Pressure.	PB90-117615 901,465	Detection of Lead in Human Teeth by Exposure to Aque-
PB89-174932 900,368 Process Control during High Pressure Atomization	Neutron Study of the Crystal Structure and Vacancy Dis- tribution in the Superconductor Ba2Y Cu3 O(sub g-delta).	ous Sulfide Solutions. PB89-201529 901,256
Process Control during High Pressure Atomization. PB89-179170 901,142	PB90-123480 901,468	Spectroscopic Quantitative Analysis of Strongly Interact-
Thermal Conductivity of Liquid Argon for Temperatures between 110 and 140 K with Pressures to 70 MPa.	HIGH TEMPERATURE TESTS Rate Constants for Hydrogen Abstraction by Resonance	ing Systems: Human Plasma Protein Mixtures. PB89-202576 901,225
PB89-179600 900,394	Stabilized Radicals in High Temperature Liquids. PB89-161608 900,348	HUMIDITY Polymorio Humidity Sonore for Industrial Passace April
Ignition Characteristics of the Iron-Based Alloy UNS S66286 in Pressurized Oxygen.	Microwave Energy for Acid Decomposition at Elevated	Polymeric Humidity Sensors for Industrial Process Applications.
PB89-189336 901,104	Temperatures and Pressures Using Biological and Botan- ical Samples.	PB89-176424 900,563
Isochoric (p,v,T) Measurements on CO2 and (0.98 CO2 + 0.02 CH4) from 225 to 400 K and Pressures to 35	PB89-171961 900,359	Indoor Air Quality.
MPa.	Elevated Temperature Deformation of Structural Steel.	PB89-176127 900,065

Ventilation Effectiveness Measurements in an Office	PB89-176952 900,385	PB89-186761 901,221
Building. PB89-176614 900,067	Computation of the ac Stark Effect in the Ground State of Atomic Hydrogen.	Mechanism of Hydrolysis of Octacalcium Phosphate. PB89-201503 901,254
Application of Direct Digital Control to an Existing Building Air Handler. PB89-177141 900,068	PB89-202535 901,538 Ouantum-Defect Parametrization of Perturbative Two-Photon Ionization Cross Sections.	HYDROPEROXIDES Rate Constants for the Reaction HO2+ NO2+ N2->
HVACSIM+, a Dynamic Building/HVAC/Control Systems Simulation Program.	PB89-202600 901,539 Collision Induced Spectroscopy: Absorption and Light	HO2NO2+ N2: The Temperature Dependence of the Fall-Off Parameters. PB89-146658 900,278
PB89-177166 900,070 Simulation of a Large Office Building System Using the	Scattering. PB89-212252 901,363	HYDROPEROXY RADICALS
HVACSIM+ Program. PB89-177174 900,071	Hydrogen Sites in Amorphous Pd85Si15HX Probed by Neutron Vibrational Spectroscopy.	Temperature Dependence of the Rate Constant for the Hydroperoxy + Methylperoxy Gas-Phase Reaction. PB90-136375 900.534
Thermal and Economic Analysis of Three HVAC (Heating, Ventilating, and Air Conditioning) System Types in a	PB89-229140 901,456	Flash Photolysis Kinetic Absorption Spectroscopy Study
Typical VA (Veterans Administration) Patient Facility. PB89-188619 900,847	Approximate Formulation of Redistribution in the Ly(alpha), Ly(beta), H(alpha) System. PB90-123720 901,568	of the Gas Phase Reaction HO2 + C2H5O2 Over the Temperature Range 228-380 K. PB90-136565 900,536
Integral Mass Balances and Pulse Injection Tracer Techniques.	Redistribution in Astrophysically Important Hydrogen	HYDROXYAPATITE
PB89-206833 900,077	Lines. PB90-128075 <i>901,579</i>	Adsorption of 4-Methacryloxyethyl Trimellitate Anhydride (4-META) on Hydroxyapatite and Its Role in Composite
Air Ouality Investigation in the NIH (National Institutes of Health) Radiation Oncology Branch.	HYDROGEN ATOMS Mechanism and Rate of Hydrogen Atom Attack on Tolu-	Bonding. PB89-179220 900,041
PB89-228977 900,079 Capabilities of Smoke Control: Fundamentals and Zone	ene at High Temperatures. PB89-179758 900,398	Formation of Hydroxyapatite in Hydrogels from Tetracal-
Smoke Control. PB89-229157 900,080	Resonance-Enhanced Multiphoton Ionization of Atomic	cium Phosphate/Dicalcium Phosphate Mixtures. PB89-201511 901,255
Investigation of a Washington, DC Office Building.	Hydrogen. PB89-201073 901,529	HYDROXYL RADICALS Radiation-Induced Crosslinks between Thymine and 2-D-
PB89-230361 900,081 Airflow Network Models for Element-Based Building Air-	HYDROGEN AZIDES	Deoxyerythropentose.
flow Modeling.	Unimolecular Dynamics Following Vibrational Overtone Excitation of HN3 v1 = 5 and v1 = 6:HN3(X tilde;v,J,K,) -	PB89-146682 900,247 Structure of a Hydroxyl Radical Induced Cross-Link of
PB89-230379 900,082 YDRATION	> HN((X sup 3)(Sigma (1-));v,J,Omega) + N2(x sup 1)(Sigma sub g (1+)).	Thymine and Tyrosine. PB89-157838 901,244
Interpretation of the Effects of Retarding Admixtures on Pastes of C3S, C3A plus Gypsum, and Portland Cement.	PB89-147110 900,286	Absolute Infrared Transition Moments for Open Shell Dia-
PB89-146971 900,580	HYDROGEN BONDS Ionic Hydrogen Bond and Ion Solvation. 5. OH(1-)O	tomics from J Dependence of Transition Intensities: Ap- plication to OH.
YDRAULIC EQUIPMENT Multiple Actuator Hydraulic System and Rotary Control	Bonds, Gas Phase Solvation and Clustering of Alkoxide and Carboxylate Anions.	PB89-227912 900,463
Valve Therefor. PATENT-4 838 145 900,995	PB89-157531 900,328	Dipole Moment Function and Vibrational Transition Intensities of OH.
YDRAZOIC ACID	Repulsive Regularities of Water Structure in Ices and Crystalline Hydrates.	PB89-227920 900,464 Mechanisms of Free Radical Chemistry and Biochemistry
Unimolecular Dynamics Following Vibrational Overtone Excitation of HN3 v1 = 5 and v1 = 6:HN3(X tilde;v,J,K,) -	PB89-186753 900,414	of Benzene. PB90-117714 900,502
> HN((X sup 3)(Sigma (1-));v,J,Omega) + N2(x sup 1)(Sigma sub g (1+)).	HYDROGEN CHLORIDE Calculation of Vibration-Rotation Spectra for Rare Gas-	Reaction of (Ir(C(3), N bpy)(bpy)2)(2+) with OH Radicals
PB89-147110 900,286	HCI Complexes. PB89-228415 900,473	and Radiation Induced Covalent Binding of the Complex to Several Polymers in Aqueous Solutions.
YDRIDES Hyperconjugation: Equilibrium Secondary Isotope Effect	Microwave and Infrared Electric-Resonance Optothermal Spectroscopy of HF-HCI and HCI-HF.	PB90-123498 900,264
on the Stability of the t-Butyl Cation. Kinetics of Near- Thermoneutral Hydride Transfer.	PB89-234215 900,489	HYDROXYLMETHYL RADICALS Detection of Gas Phase Methoxy Radicals by Resonance
PB89-156756 900,306	Sub-Doppler Infrared Spectroscopy in Slit Supersonic Jets: A Study of all Three van der Waals Modes in v1-Ex-	Enhanced Multiphoton Ionization Spectroscopy. PB89-156764 900,307
Neutron Vibrational Spectroscopy of Disordered Metal Hydrogen Systems.	cited ArHCI. PB90-123852 900,525	HYDROXYMETHYL RADICALS
PB89-157499 900,324 Dissociation Lifetimes and Level Mixing in Overtone-Ex-	HYDROGEN FLUORIDE	Multiphoton Ionization Spectroscopy and Vibrational Analysis of a 3p Rydberg State of the Hydroxymethy
cited HN3 (X tilde (sup 1) A'). PB90-117425 900,263	Vibrational Exchange upon Interconversion Tunneling in (HF)2 and (HCCH)2.	Radical. PB89-146666 900,279
YDROCARBONS	PB89-179113 900,388 Chemisorption of HF (Hydrofluonic Acid) on Silicon Sur-	HYPERBOLIC FUNCTIONS
Estimation of the Thermodynamic Properties of Hydrocarbons at 298.15 K.	faces.	Logistic Function Data Analysis Program: LOGIT. PB89-189351 900,418
PB89-145155 . 900,272	PB89-212013 900,445 Rydberg-Klein-Rees Inversion of High Resolution van der	HYPERCONJUGATION
Preparative Liquid Chromatographic Method for the Characterization of Minor Constituents of Lubricating Base	Waals Infrared Spectra: An Intermolecular Potential Energy Surface for Ar+ HF (v= 1).	Hyperconjugation: Equilibrium Secondary Isotope Effection the Stability of the t-Butyl Cation. Kinetics of Near
Oils. PB89-175921 901,114	PB89-227953 900,465	Thermoneutral Hydride Transfer. PB89-156756 900,306
Soot Inception in Hydrocarbon Diffusion Flames.	Infrared Spectra of Nitrous Oxide-HF Isomers. PB89-228399 900,471	HYPERFINE STRUCTURES
PB89-201966 900,599 High-Resolution, Slit Jet Infrared Spectroscopy of Hydro-	Vibrational Predissociation in the H-F Stretching Mode of	Frequency Standards Utilizing Penning Traps. PB90-128042 901,378
carbons: Ouantum State Specific Mode Mixing in CH Stretch-Excited Propyne.	PB89-234207 900,488	HYSTERESIS Temperature Hysteresis in the Initial Susceptibility o
PB89-234256 900,490	Microwave and Infrared Electric-Resonance Optothermal Spectroscopy of HF-HCI and HCI-HF.	Rapidly Solidified Monel.
Microwave Spectral Tables. 3. Hydrocarbons, CH to C10H10.	PB89-234215 900,489	ICE
PB90-126269 900,530 YDRODYNAMICS	Weakly Bound NeHF. PB90-118100 900,519	Pressure Fixed Points Based on the Carbon Dioxide Vapor Pressure at 273.16 K and the H2O(I) - H2O(III)
Hydrodynamics of Magnetic and Dielectric Colloidal Dis-	Slit Jet Infrared Spectroscopy of NeHF Complexes: Internal Rotor and J-Dependent Predissociation Dynamics.	H2O(L) Triple-Point. PB89-231138 900,483
persions. PB89-157242 900,314	PB90-118126 900,520	ICOSAHEDRAL PHASE
Elimination of Spurious Eigenvalues in the Chebyshev Tau Spectral Method.	Intramolecular Dynamics of van der Waals Molecules: An Extended Infrared Study of ArHF.	Progress in Understanding Atomic Structure of the Icosa hedral Phase.
PB89-209282 901,330	PB90-118209 900,521	PB89-171359 901,400
Hydrodynamic Forces on Vertical Cylinders and the Lighthill Correction.	HYDROGEN IODIDE Three Dimensional Quantum Reactive Scattering Study	ICOSAHEDRONS Formation of the Al-Mn Icosahedral Phase by Electrode
PB90-117417 901,313 Effect of a Crystal-Melt Interface on Taylor-Vortex Flow.	of the I + HI Reaction and of the IHI(1-) Photodetachment Spectrum.	position. PB90-117763 900,50-
PB90-130261 901,477	PB89-227961 900,466	TEM Observation of Icosahedral, New Crystalline and
IYDROGEN Infrared Spectrum of D2HF.	HYDROGEN IONS Cross Sections for K-Shell X-ray Production by Hydrogen	Glassy Phases in Rapidly Ouenched Cd-Cu Alloys. PB90-123514 901,160
PB89-171219 900,350	and Helium Ions in Elements from Beryllium to Uranium. PB89-226609 900,460	IDEAL GAS LAW Acoustic and Microwave Resonances Applied to Measur
Infrared Spectrum of NeHF. PB89-171227 900,351	HYDROGEN PRODUCTION	ing the Gas Constant and the Thermodynamic Tempera
Absolute Rate Constants for Hydrogen Abstraction from Hydrocarbons by the Trichloromethylperoxyl Radical.	Dehydrogenation of Ethanol in Dilute Aqueous Solution Photosensitized by Benzophenones.	ture. PB89-228548 901,320
PB89-171532 900,357	PB89-157556 900,251 HYDROGEN TRANSFER	IDENTIFICATION SYSTEMS Standard Format for the Exchange of Fingerprint Information
Intramolecular H Atom Abstraction from the Sugar Moiety by Thymine Radicals in Oligo- and Polydeoxynucleotides.	Rate Constants for Hydrogen Abstraction by Resonance	tion.
PB89-171870 901,263 Vibrationally Resolved Photoelectron Angular Distribu-	Stabilized Radicals in High Temperature Liquids. PB89-161608 900,348	PB89-176705 900,69.
tions for H2 in the Range 17 eV < or = h(nu) < or = 39	HYDROLYSIS Thermodynamics of Hydrolysis of Disaccharides.	Ignition and Flame Spread Measurements of Aircrai Lining Materials.
eV.	cimodynamics of rigorolysis of bisaconamics.	

PB89-172886	900,009	PB89-193296	900,982	PB89-202972	901,440
Fire Risk Analysis Methodology: Initiating Events. PB89-184527	900,125	IN-SITU COMBUSTION FT-IR (Fourier Transform-II	nfrared) Emission/Transmis-	INFORMATION PROCESSING	Paguiromonto for 4.900 Bit/
Effect of Water on Piloted Ignition of Cellulosic Ma		sion Spectroscopy for In situ	Combustion Diagnostics.	Second Modems, Category	Requirements for 4,800 Bit/ r: Telecommunications Stand-
· -	900,127	PB89-211866 IN VIVO ANALYSIS	900,600	ard. FIPS PUB 134-1	900,660
Ignition Characteristics of the Iron-Based Allo S66286 in Pressurized Oxygen.		Element-Specific Epifluores	cence Microscopy In vivo	General Aspects of Group	4 Facsimile Apparatus, Cate-
PB89-189336 Statistical Analysis of Experiments to Measure Igi	901,104	Matrices.	sformations in Environmental	gory: Telecommunications S FIPS PUB 149	900,661
Cigarettes.		PB89-177216 INCINERATION	901,220		and Coding Control Functions paratus, Category: Telecom-
PB89-201149 Ignition Characteristics of the Nickel-Based Allo	900,135 ov UNS	Fundamental Aspects of Key	/ Issues in Hazardous Waste	munications Standard. FIPS PUB 150	
N07718 in Pressurized Oxygen.	901,154	Incineration. PB89-212104	900,861		900,6്2 Interface for Data Termina
Effects of Thermal Stability and Melt Viscosity of T		INCLUSIONS	sature of Australia's Challeton	Equipment and Data Circuit egory: Telecommunications	t-Terminating Equipment, Cat-
plastics on Piloted Ignition.	900,151	Role of Inclusions in the Fra Steel Welds at 4 K.		FÎPS PUB 154	900,663
III-V COMPOUNDS	,	PB89-173504 INDENTATION	901,099		ms and Services User-Orient- ent Methods, Category: Tele-
Stress Effects on III-V Solid-Liquid Equilibria. PB89-146997	900,769	Rising Fracture Toughness for	rom the Bending Strength of	communications Standard. FIPS PUB 155	900.66
IMAGE PROCESSING		Indented Alumina Beams. PB89-171771	901,031	INFORMATION RETRIEVAL	000,00
Standards for the Interchange of Large Forma Raster Documents.	at Tiled	INDENTATION HARDNESS TES		Creation of a Fire Research PB89-174130	Bibliographic Database. 900,166
PB89-148415	900,668	Dynamic Microindentation Apacterization.	•	INFORMATION SYSTEMS	500,100
Thermographic Imaging and Computer Image Pro of Defects in Building Materials.	cessing	PB89-176911 Effect of Heat Treatment on	901,140	Data Bases Available at th ards and Technology Resea	e National Institute of Stand-
	900,123	a Liquid-Phase-Sintered Alum	nina.	PB89-160014	900,932
IMAGE RECONSTRUCTION Fast Magnetic Resonance Imaging with Simulta	ine Jusly	PB89-229231 INDICATING INSTRUMENTS	901,056	Report of the Invitational W Computer Information Syste	orkshop on Integrity Policy in
Oscillating and Rotating Field Gradients. PB89-176903	901,514	Transducers in Michelson Till PB89-185979	tmeters. 901,280	PB89-168009	900,670
IMAGES	,	INDIUM	901,280	Creation of a Fire Research PB89-174130	Bibliographic Database. 900,166
Institute for Materials Science and Engineering, ics; Technical Activities 1988.	Ceram-	High-Accuracy Differential-Pu metry with Indium as an Inter	ilse Anodic Stripping Voltam-	New Directions in Bioinform	
PB89-148381	901,019	PB89-156947	900,182	PB89-175269 Use of Artificial Intelligence	901,245 Programming Techniques for
Fractal-Based Description of the Roughness of Steel Panels.		High-Accuracy Differential-Pu metry Using Indium as an Inte			ncompatible Building Informa-
	901,096	PB89-176267	900,198	PB89-191985	900,106
Mossbauer Imaging: Experimental Results.		Interaction of In Atom Spin-C faces.	Orbit States with Si(100) Sur-	Use of the IRDS (Information System) Standard in CALS	mation Resource Dictionary (Computer-Aided Acquisition
	900,922	PB90-128547	900,532	and Logistic Support). PB90-112467	900,931
Vector Imaging of Magnetic Microstructure. PB90-128240	901,476	INDIUM ANTIMONIDES InSb as a Pressure Sensor.		INFRARED ABSORPTION	300,331
IMMUNOASSAY	io	PB89-231104	900,904	Component Spectrum Reco acterized Mixtures.	nstruction from Partially Char-
Liposome-Enhanced Flow Injection Immunoanalys PB89-146757	900,036	Initial Stages of Heteroepi	taxial Growth of InAs on	PB89-202568	900,439
Generic Liposome Reagent for Immunoassays. PB90-123886	901,229	Si(100). PB90-123878	901,473	INFRARED ANALYSIS Population Relaxation of CC	O(v= 1) Vibrations in Solution
IMPACT TESTS	007,220	INDIUM PHOSPHIDES		Phase Metal-Carbonyl Comp PB89-157291	
Effect of Lateral Crack Growth on the Strength tact Flaws in Brittle Materials.	of Con-	Feasibility of Detector Self-C red.		INFRARED DETECTORS	900,313
PB89-171813	901,034	PB89-176788 INDOOR AIR POLLUTION	900,384	Characteristics of Ge and In PB89-176796	GaAs Photodiodes.
Role of Inclusions in the Fracture of Austenitic S Steel Welds at 4 K.		Indoor Air Quality.		INFRARED LASERS	300,723
	901,099	PB89-176127 Air Quality Investigation in th	900,065	New FIR Laser Lines and Optically Pumped CD3OH.	Frequency Measurements for
Influence of Molybdenum on the Strength and Tou of Stainless Steel Welds for Cryogenic Service.		Health) Radiation Oncology E	Branch.	PB89-175731	901,350
PB89-173512 Static Tests of One-third Scale Impact Limiters.	901,100	PB89-228977 Ventilation and Air Quality In	900,079 vestigation of the U.S. Geo-	INFRARED RADIATION Semiconductor Measurement	nt Technology: Database for
	901,000	logical Survey Building. PB89-229686	900,857	and Statistical Analysis of t	he Interlaboratory Determina- efficient for the Measurement
IMPEDANCE AC Impedance Method for High-Resistivity M	leasure.	Investigation of a Washingtor	n, DC Office Building.	of the Interstitial Oxygen C Absorption.	Content of Silicon by Infrared
ments of Silicon.	900,793	PB89-230361	900,081	PB89-221170	901,054
IMPLANTATION	300,733	Method for Measuring the Eff taminant Removal Filters.		INFRARED SPECTRA	nt Technology: Automatic De-
Corrosion of Metallic Implants and Prosthetic Devi-	ces. 900,053	PB89-235899 Gypsum Wallboard Formalde	900,858 hyde Sorption Model	termination of the Interstitia	al Oxygen Content of Silicon
IMPREGNATING	20,000	PB90-132705	900, 154	Wafers Polished on Both Sid PB89-151831	des. 900,772
Epoxy Impregnation Procedure for Hardened Samples.	Cement	Quality Assurance in Metals		Infrared Absorption of SF6 f Gaseous and Liquid States.	from 32 to 3000 cm(-1) in the
PB89-147821	901,180	ly Coupled Plasma. PB89-202063	900,213	PB89-157853	900,336
Epoxy Impregnation of Hardened Cement Pas Characterization of Microstructure.	stes for	INDUSTRIAL BUILDINGS	000,210	Infrared Spectrum of D2HF, PB89-171219	900,350
	901,042	Coupling, Propagation, and S Industrial Building Wiring Syst	Side Effects of Surges in an tem.		pectra of OCO-HF and SCO-
IMPULSES International Comparison of HV Impulse Measuring	ng Sys-	PB89-173454	900,118	HF. PB89-179121	900,389
tems. PB89-186423	900,809	Report on Interactions between		Infrared Absorption Cross S the Impurity Band Region of	ection of Arsenic in Silicon in
IMPURITIES		Standards and Technology a Mechanical Engineers.		PB89-201750	900,426
Grain Boundaries with Impurities in a Two-Dime Lattice-Gas Model.		PB89-172563	901,004	Spectroscopic Quantitative ing Systems: Human Plasma	Analysis of Strongly Interact- a Protein Mixtures.
PB89-172407	901,507	Emerging Technologies in Ma PB90-132747	anufacturing Engineering. 901,013	PB89-202576	901,225
Polymer Localization by Random Fixed Impurities sian Chains.		INDUSTRIAL FABRICS	trial Echrica, Delayerse and	Neon. 2. O4(1+) and O4(1-	ecular lons Isolated in Solid
PB89-176044 Modelling of Impurity Effects in Pure Fluids and Fluids	900,559 uid Mix-	Flammability Tests for Indus Limitations.		PB90-128729 INFRARED SPECTROSCOPY	900,533
tures.	900,245	PB89-174122 INDUSTRIES	901,091	Picosecond Studies of Vit	brational Energy Transfer in
IMPURITY EFFECTS	JJU,24J	Importance of Numeric Datab	pases to Materials Science.	Molecules on Surfaces. PB89-157309	900,316
Modelling of Impurity Effects in Pure Fluids and Fluires.	luid Mix-	PB89-175202 INELASTIC CROSS SECTIONS	901,187	Picosecond Study of the Po Chemisorbed on SiO2-Supp	pulation Lifetime of CO(v= 1)
PB89-176739	900,245	Laser Spectroscopy of Inelas PB89-185946	tic Collisions.	PB89-157317	900,317
IN-PROCESS QUALITY CONTROL Progress Report of the Quality in Automation Pro	piect for	INELASTIC SCATTERING	300,403	Far-Infrared Spectrum of Manalysis of the First Torsion	ethyl Amine. Assignment and al State.
FY88.	_,	Cross Sections for Inelastic E	Electron Scattering in Solids.	PB89-161574	900,346

Infrared Spectrum of the nu6, nu7, and nu8 Bands of HNO3.	PB90-130899 900,831 INSTRUCTIONS	lonization and Current Growth in N2 at Very High Electri Field to Gas Density Ratios.
PB89-172415 900,362 Structure and Dynamics of Molecular Clusters via High Resolution IR Absorption Spectroscopy.	Computer Viruses and Related Threats: A Management Guide.	PB89-228381 901,55 Resistance Measurements of High T(sub c) Supercor
PB89-185896 900,403 Time-Resolved FTIR Emission Studies of Molecular Pho-	PB90-111683 900,654 INSTRUMENT COMPENSATION	ductors Using a Novel 'Bathysphere' Cryostat. PB89-228431
tofragmentation. PB89-202642 900,261	Computer Program for Instrument Calibration at State- Sector Secondary-Level Laboratories. PB89-173496 900,877	Specimen Biasing to Enhance or Suppress Secondar Electron Emission from Charging Specimens at Low Ac celerating Voltages.
Quantitative Studies of Coatings on Steel Using Reflec- tion/Absorption Fourier Transform Infrared Spectroscopy. PB89-212112 901,066	INSTRUMENTATION & EXPERIMENTAL METHODS Multiple Actuator Hydraulic System and Rotary Control	PB89-228464 901,45 Spatial Filtering Microscope for Linewidth Measurements
Rydberg-Klein-Rees Inversion of High Resolution van der Waals Infrared Spectra: An Intermolecular Potential	Valve Therefor. PATENT-4 838 145 900,995	PB89-230346 901,36 Improved Transportable DC Voltage Standard.
Energy Surface for Ar + HF (v = 1). PB89-227953 900,465	Thin Film Thermocouples for Internal Combustion Engines. PB89-147094 900,607	PB89-230395 901,55 NBS (National Bureau of Standards) Determination of the
Infrared Spectra of Nitrous Oxide-HF Isomers. PB89-228399 900,471	Development of Standard Measurement Techniques and Standard Reference Materials for Heat Capacity and	Fine-Structure Constant, and of the Quantized Hall Re sistance and Josephson Frequency-to-Voltage Quotier in SI Units.
Infrared Spectrum of the 1205-cm(-1) Band of HNO3. PB89-228514 900,475	Heat of Vaporization of Jet Fuels. PB89-148100 900,837	PB89-230437 901,55 InSb as a Pressure Sensor.
Infrared Spectrum of Sodium Hydride. PB89-230296 900,480	Small Angle Neutron Scattering Spectrometer at the National Bureau of Standards.	PB89-231104 900,90 Non-Geometric Dependencies of Gas-Operated Pisto
Ultrashort-Pulse Multichannel Infrared Spectroscopy Using Broadband Frequency Conversion in LilO3. PB89-230304 901,367	PB89-158158 901,396 New Carty Configuration for Cesium Beam Primary Fre-	Gage Effective Areas. PB89-231112 900,90
High-Resolution, Slit Jet Infrared Spectroscopy of Hydro- carbons: Quantum State Specific Mode Mixing in CH	quency Standards. PB89-171649 900,714	Observations of Gas Species and Mode of Operation Effects on Effective Areas of Gas-Operated Piston Gages.
Stretch-Excited Propyne. PB89-234256 900,490	Fast-Pulse Generators and Detectors for Characterizing Laser Receivers at 1.06 um. PB89-171698 901,347	PB89-231120 900,90 Conceptual Design for a Mercury Relativity Satellite.
Interlaboratory Determination of the Calibration Factor for the Measurement of the Interstitial Oxygen Content of	Approach to Accurate X-Ray Mask Measurements in a Scanning Electron Microscope.	PB89-234249 901,59 Apparatus for Neutron Scattering Measurements of
Silicon by Infrared Absorption. PB90-117300 900,224	PB89-172555 900,776 Higher-Order Crossings: A New Acoustic Emission Signal	Sheared Fluids. PB89-235667 901,33
Production and Spectroscopy of Molecular lons Isolated in Solid Neon. PB90-117748 900,503	Processing Method PB89-173488 900,678	NBS' (National Bureau of Standards) Industry; Govern ment Consortium Research Program on Flowmeter Insta- lation Effects: Summary Report with Emphasis on Re
Heterodyne Measurements on N2O Near 1635 cm(-1). PB90-117797 900,506	Use of Dye Tracers in the Study of Free Convection in Porous Media.	search July-December 1987. PB90-111220 900,91
Heterodyne Frequency and Fourier Transform Spectroscopy Measurements on OCS Near 1700 cm(-1).	PB89-173918 901,327 Precision Weight Calibration with a Specialized Robot.	Coherent Tunable Far Infrared Radiation. PB90-117458 900,68
PB90-117805 900,507 Low Pressure, Automated, Sample Packing Unit for Dif-	PB89-173975 900,879 High Temperature Thermal Conductivity Apparatus for	Very Low-Noise FET Input Amplifier. PB90-128224 900,80
fuse Reflectance Infrared Spectrometry. PB90-135922 900,235	Fluids. PB89-174015 900,366	INSULATED GATE BIPOLAR TRANSISTORS Effect of Neutrons on the Characteristics of the Insulate
Frequency Measurements of High-J Rotational Transitions of OCS and N2O. PB90-136946 900.541	NBS (National Bureau of Standards) Orifice-Flow Primary High Vacuum Standard. PB89-175699 900,880	Gate Bipolar Transistor (IGBT). PB89-157655 900,770
NFRARED THERMAL DETECTORS Performance Measurements of Infrared Imaging Systems	Low Range Flowmeters for Use with Vacuum and Leak Standards.	INSULATING BOARDS Microporous Fumed-Silica Insulation Board as a Cand
Used to Assess Thermal Anomalies. PB89-179667 900,072	PB89-175707 900,374 Preparative Liquid Chromatographic Method for the Char-	date Standard Reference Material of Thermal Resist ance. PB89-148373 901,01.
NITIAL GRAPHICS EXCHANGE SPECIFICATION Guidelines for the Specification and Validation of IGES	acterization of Minor Constituents of Lubricating Base Oils.	Microporous Fumed-Silica Insulation as a Standard Rel erence Material of Thermal Resistance at High Tempera
(Initial Graphics Exchange Specification) Application Protocols. PB89-166102 900,937	Polymeric Humidity Sensors for Industrial Process Appli-	ture. PB90-130311 900,15
NITIATORS (EXPLOSIVES) Measurement Procedures for Electromagnetic Compat-	cations. PB89-176424 900,563 Optical Roughness Measurements for Industrial Surfaces.	INTAGLIO Design and Synthesis of Prototype Air-Dry Resins for Us-
ibility Assessment of Electroexplosive Devices. PB89-146914 901,314	PB89-176655 900,979 Mossbauer Imaging.	in BEP (Bureau of Engraving and Printing) Intaglio Ink Ve hicles.
NKS Design and Synthesis of Prototype Air-Dry Resins for Use	PB89-176895 901,242 Automated Fringe Counting Laser Interferometer for Low	PB90-112343 901,060 INTEGRALS
in BEP (Bureau of Engraving and Printing) Intaglio Ink Vehicles. PB90-112343 901,068	Frequency Vibration Measurements. PB89-177190 900,885	Numerical Evaluation of Certain Multivariate Normal Integrals. PB89-158166 901,19
NORGANIC COMPOUNDS Analytical Applications of Resonance Ionization Mass	Quantized Hall Resistance Measurement at the NML (National Measurement Laboratory).	INTEGRATED CIRCUITS
Spectrometry (RIMS). PB89-161590 <i>900,189</i>	PB89-179675 900,778 Real-Time Simulation and Production Scheduling Sys-	Use of Artificial Intelligence and Microelectronic Tes Structures for Evaluation and Yield Enhancement of Microelectronic Interconnect Systems.
Isotope Dilution Mass Spectrometry for Accurate Elemental Analysis.	tems. PB89-183230 900,974	PB89-146955 900,76 Submicrometer Optical Metrology.
PB89-230338 900,220 INSERTION REACTIONS	Supercritical Fluid Chromatograph for Physicochemical Studies. PB89-184105 900,201	PB89-150973 900,77 Approach to Accurate X-Ray Mask Measurements in a
Reduced Dimensionality Quantum Reactive Scattering Study of the Insertion Reaction O(1D) + H2 -> OH + H.	Relation between Wire Resistance and Fluid Pressure in the Transient Hot-Wire Method.	Scanning Electron Microscope. PB89-172555 900,77
PB89-234280 900,492 NSPECTION	PB89-184113 901,520 Analysis of High Performance Compensated Thermal En-	Narrow-Angle Laser Scanning Microscope System to Linewidth Measurement on Wafers. PB89-189344 900,78.
CAD (Computer Aided Design)-Directed Inspection. PB89-177018 900,980	closures. PB89-185748 <i>901,008</i>	Switching Noise in YBa2Cu3Ox 'Macrobridges'.
EMATs (Electromagnetic Acoustic Transducers) for Roll- By Crack Inspection of Railroad Wheels. PB90-123894 901,597	Transducers in Michelson Tiltmeters. PB89-185979 901,280	PB89-200513 901,42 Graphical Analyses Related to the Linewidth Calibration Problem.
NSTALLATION	Optically Linked Electric and Magnetic Field Sensor for Poynting Vector Measurements in the Near Fields of Ra-	PB89-201156 900,78
NBS' (National Bureau of Standards) Industry; Govern- ment Consortium Research Program on Flowmeter Instal- lation Effects: Summary Report with Emphasis on Re-	diating Sources. PB89-187595 900,712	Neural Network Approach for Classifying Test Structure Results. PB89-212187 900,78
search July-December 1987. PB90-111220 900,910	Narrow-Angle Laser Scanning Microscope System for Linewidth Measurement on Wafers. PB89-189344 900,782	Thermal Conductivity Measurements of Thin-Film Silicol Dioxide.
NSTALLING NBS' (National Bureau of Standards) Industry; Govern-	VAMAS (Versailles Project on Advanced Materials and Standards) Intercomparison of Critical Current Measure-	PB89-212195 901,44- MM Wave Quasioptical SIS Mixers.
ment Consortium Research Program on Flowmeter Instal- lation Effects: Summary Report with Emphasis on Re- search January-July 1988.	ment in NoSh Wires. PB89-202147 901,534	PB89-214738 901,44: Machine-Learning Classification Approach for IC Manu
PB89-189120 901,010 NSTITUTE OF ELECTRICAL AND ELECTRONIC	Calculations and Measurement of the Performance of Converging Neutron Guides.	facturing Control Based on Test Structure Measurements PB89-228530 900,79
Report on Interactions between the National Institute of	PB89-211999 901,541 Torsional Piezoelectric Crystal Viscometer for Com-	IEEE (Institute of Electrical and Electronics Engineers IRPS (International Reliability Physics Symposium) Tutori
Standards and Technology and the Institute of Electrical and Electronic Engineers.	pressed Gases and Liquids. PB89-228076 901.447	al Thermal Resistance Measurements, 1989. PB89-231195 900.79

Silicon and GaAs Wire-Bond Cratering Problem PB90-128182	n. <i>900,799</i>	PB89-228506	900,025		900,438
NTERACTIVE GRAPHICS		Detection of the Free Radicals FeH, Far Infrared Laser Magnetic Resonance	ce.	Drift Tubes for Characterizing Atmospheric Ion I Spectra.	
Incrementor: A Graphical Technique for Manip rameters.	oulating Pa-	PB90-117342 INTERSTELLAR RADIATION	900,495	PB90-128513 <i>S</i>	901,585
PB89-177000	900,648	Millimeter- and Submillimeter-Wave S		Resonance Ionization Mass Spectrometry of M	g: The
Computer Graphics for Ceramic Phase Diagram PB89-186290	ns. <i>901,043</i>	Emission Lines in the Ranges 200.7- and 330-360 GHz.		3pnd Autoionizing Series. PB89-150817	900,296
NTERCAVITY SPECTROSCOPY	, suith Adulti	PB90-123787 INTERSTITIALS	900,029	Effect of Surface Ionization on Wetting Layers.	201 202
One Is Not Enough: Intra-Cavity Spectroscopy Mode Lasers.		Semiconductor Measurement Technol		PB89-157259 Ion Kinetics and Energetics.	901,323
PB89-185888 NTERFACES	900,402	termination of the Interstitial Oxygen Wafers Polished on Both Sides.		PB89-176101	900,377
Effect of an Oil-Paper Interface Parallel to		PB89-151831	900,772	Using 'Resonant' Charge Exchange to Detect Tra Noble Gas Atoms.	aces of
Field on the Breakdown Voltage at Elevated tures.		Semiconductor Measurement Techno and Statistical Analysis of the Interlat	oratory Determina-	PB89-176770	901,296
PB89-156988	901,490	tion of the Conversion Coefficient for of the Interstitial Oxygen Content of		Absolute Cross Sections for Molecular Photoabse Partial Photoionization, and Ionic Photofragme	
Analytical Expression for Describing Auger Sp Profile Shapes of Interfaces.		Absorption. PB89-221170	901.054	Process.	900.410
PB89-157176 Mechanical Property Enhancement in Cera	900,309	Interlaboratory Determination of the Ca	alibration Factor for	Electron and Photon Stimulated Desorption: Benef	
Composites. PB89-189138	901,076	the Measurement of the Interstitial (Silicon by Infrared Absorption.	Oxygen Content of	Difficulties. PB89-200745	901,427
Crack-Interface Traction: A Fracture-Resistan		PB90-117300	900,224	Electron-Stimulated-Desorption Ion-Angular Distribu	utions.
nism in Brittle Polycrystals. PB89-211817	901,051	Inventory of Equipment in the Clear	ning and Deburning		901,430
Electron Transmission Through NiSi2-Si Interfa	aces.	Workstation. PB89-209233	900,958	Spectrum of Doubly Ionized Tungsten (W III). PB89-235659	900,223
PB89-231294	900,485	INVESTMENTS	300,330	Production and Spectroscopy of Molecular lons Is in Solid Neon.	solated
NTERFACIAL TENSION Reevaluation of Forces Measured Across Th	in Polymer	Building Economics in the United State PB89-172399	es. 900,102		900,503
Films: Nonequilibrium and Pinning Effects. PB89-228589	900,573	AutoMan: Decision Support Software f	or Automated Man-	Cross Sections for Bremsstrahlung Production and tron-Impact Ionization.	d Elec-
NTERFEROMETERS	,	ufacturing Investments. User's Manual PB89-221873	900,963		901,575
Speed of Sound in a Mercury Ultrasonic Inte Manometer.	erferometer	IODINE	550,555	IONIZATION CROSS SECTIONS	Tuo
PB89-202220	901,319	Three Dimensional Quantum Reactiv of the I + HI Reaction and of the II		Quantum-Defect Parametrization of Perturbative Photon Ionization Cross Sections.	
Length Scale Measurement Procedures at the Bureau of Standards.		ment Spectrum. PB89-227961	900,466	PB89-202600 9 IONIZATION POTENTIALS	901,539
PB89-209266	900,895	Determination of Trace Level lodine in		Accurate Energies of nS, nP, nD, nF and nG Le	vels of
NTERLEUKIN 1 Preliminary Crystallographic Study of Re	ecombinant	tanical Reference Materials by Isoto Spectrometry.	ope Dilution Mass	Neutral Cesium. PB89-202121 9	900,431
Human Interleukin 1beta. PB90-136730	901,251	PB89-235642	900,222	IONIZING RADIATION	
NTERMETALLICS		NBS (National Bureau of Standards)	Measurement Serv-	Measurement Quality Assurance. PB89-147508	901,298
Electronic, Magnetic, Superconducting and A Forming Properties Versus Stability of the T		ices: Calibration of Gamma-Ray-Emit		Chemical Characterization of Ionizing Radiation-In	nduced
and Hf-Os Ordered Alloys. PB89-146690	901,120	Sources. PB89-193858	901,243	Damage to DNA. PB89-151922 9	901,235
Sputter Deposition of Icosahedral Al-Mn and A		IODOALKANES Photodissociation of Methyl Iodide Clu	etore	Comprehensive Dosimetry for Food Irradiation. PB89-186399	900.011
PB89-147102 Quasicrystals with 1-D Translational Periodi	901,122 city and a	PB89-171193	900,253	Report on the 1989 Meeting of the Radionuclide	-
Ten-Fold Rotation Axis.		ION-ATOM COLLISIONS Cross Sections for K-Shell X-ray Production	uction by Hydrogen	urements Section of the Consultative Committ Standards for the Measurement of Ionizing Rad	tee on
PB89-147383 Grain Boundary Characterization in Ni3Al.	901,123	and Helium lons in Elements from Ber	yllium to Uranium.	Special Report on Standards for Radioactivity.	
PB89-229306	901,156	PB89-226609 ION BEAMS	900,460	IONS	900,545
Grain Boundary Structure in Ni3Al. PB89-229314	901,157	Kinetics of Resolidification. PB89-176457	901,138	Ion Kinetics and Energetics.	900.377
NTERNAL COMBUSTION ENGINES	tiaa Fa	ION EXCHANGE MEMBRANE ELECTROI	•	Spectra and Energy Levels of the Galliumlike lons	
Thin Film Thermocouples for Internal Comb gines.		Facilitated Transport of CO2 through Exchange Membranes: The Effect of	Highly Swollen Ion-	Mo XII.	900.387
PB89-147094 NTERNAL REVENUE SERVICE	900,607	treatment.		Bond Selective Chemistry with Photon-Stimulate	,
Internal Revenue Service Post-of-Duty Location	n Modeling	PB89-179618 ION EXCHANGE RESINS	900,395	sorption. PB89-201222	900,259
System: Programmer's Manual for PASCAL Sc PB89-161905	900,001	CO2 Separation Using Facilitated	Transport Ion Ex-	Research for Electric Energy Systems: An Annual I	Report.
Internal Revenue Service Post-of-Duty Location System: Programmer's Manual for FORTRAN	n Modeling	change Membranes. PB89-157374	900,321	PB90-112442 Charging Behavior of Polyethylene and lonomers.	900,853
sion 5.0.	900.002	Pahasapaite, a Beryllophosphate Zeol thetic Zeolite Rho, from the Tip Top		PB90-136813	900,578
PB89-161913 NTERNATIONAL ASSOCIATION FOR THE PRO		Dakota.	901,288	IRIDIUM 192 NBS (National Bureau of Standards) Measuremen	nt Serve
OF STEAM Properties of Steam.		PB89-186431 ION-MOLECULE COLLISIONS	901,288	ices: Calibration of Gamma-Ray-Emitting Brachy	therapy
PB89-202048	901,533	Laser Probing of Product-State Distril	butions in Thermal-	Sources. PB89-193858	901,243
Activities of the International Association for ties of Steam between 1979 and 1984.	the Proper-	Energy Ion-Molecule Reactions. PB89-171250	900,353	IRIDIUM COMPLEXES	1 - di 1 -
PB89-212153	900,446	ION PAIRS	4. Thermachemical	Reaction of (Ir(C(3), N bpy)(bpy)2)(2+) with OH R and Radiation Induced Covalent Binding of the C	omplex
NTERNATIONAL ELECTROTECHNICAL COMMI Update of U.S. Participation in International		Filling of Solvent Shells About Ions. Criteria and the Effects of Isomeric Clu	usters.	to Several Polymers in Aqueous Solutions. PB90-123498	900,264
Activities. PB89-228282	900,902	PB89-157549 ION TRAPPING	900,329	IRON	
NTERNATIONAL ORGANIZATIONS		Ion Trapping Techniques: Laser Coolin	ng and Sympathetic	Free-Electron-Like Stoner Excitations in Fe. PB89-158059	901,393
Directory of International and Regional Or Conducting Standards-Related Activities.	rganizations	Cooling. PB90-128034	901,578	Domain Images of Ultrathin Fe Films on Ag(100). PB89-158067	901.394
PB89-221147	900,008	ION TRAPS	alastad Dubit of	Neutron Scattering Study of the Spin Ordering in	,
NTERNATIONAL STANDARDS ORGANIZATION Update of U.S. Participation in International		Trapped lons and Laser Cooling 2: So of the Ion Storage Group, Time and		phous Tb45Fe55 and Tb25Fe75.	901,149
Activities. PB89-228282	900,902	NIST, Boulder, CO. PB89-153878	901,489	Ammonia Adsorption and Dissociation on a S	•
NTERNATIONAL TRADE		Laser Cooling.	201.513	Iron(s) (100) Surface.	900,523
Effect of Chinese Standardization on U.S. Ex tunities.		PB89-179147 IONIC MOBILITY	901,518	IRON ALLOYS	, 23
PB89-166128 NTERSTELLAR MATTER	900,172	Laser Probing of Ion Velocity Distribu	tions in Drift Fields:	Molybdenum Effect on Volume in Fe-Cr-Ni Alloys. PB89-157796	901,095
IUE Observation of the Interstellar Medium T	oward Beta	Parallel and Perpendicular Temperatu Ba(1+) in He.		Development of Combustion from Quasi-Stable Te	
Geminorum. PB89-228373	900,024	PB89-171243 Drift Tubes for Characterizing Atmos	900,352 spheric Ion Mobility	tures for the Iron Based Alloy UNS S66286. PB89-173850	900,592

Drift Tubes for Characterizing Atmospheric Ion Mobility Spectra Using AC, AC-Pulse, and Pulse Time-of-Flight Measurement Techniques.

Laboratory Measurement of the 1(sub 01)-0(sub 00) Transition and Electric Dipole Moment of SiC2.

Ignition Characteristics of the Iron-Based Alloy UNS S66286 in Pressurized Oxygen.

	•	
PB89-189336 901,	Ceiling, let Impingement on a Wall	LAKES
Low-Temperature Phase and Magnetic Interactions in Fe-Cr-Ni Alloys.	PB90-118076 900,150	Designs for Assessment of Measurement Uncertainty Experience in the Eastern Lake Survey.
PB90-136771 901, 3	13 JET PUMPS Performance of He II of a Centrifugal Pump with a Jet	PB89-173827 900,86 LAMELLAR STRUCTURE
Amorphous Phase Formation in Al70Si17Fe13 Alloy.	Pump Inducer.	Phase Contrast Matching in Lamellar Structures Corr
PB90-123522 901,1 Solidification of an 'Amorphous' Phase in Rapidly Sol	JORDAN REGIONS	posed of Mixtures of Labeled and Unlabeled Block Co polymer for Small-Angle Neutron Scattering.
fied Al-Fe-Si Alloys.	Shortest Paths in Simply Connected Hegions in H2.	PB89-157119 901,18 LAMINAR FLOW
PB90-123530 901,1 Formation of Dispersoids during Rapid Solidification of	IOCEDICON CECCOT	In Situ Fluorescence Monitoring of the Viscosities of Par
AI-Fe-Ni Alloy. PB90-123647 901, 7	NBS (National Bureau of Standards) Determination of the	ticle-Filled Polymers in Flow. PB89-146278 900,60
RON HYDRIDES	sistance and Josephson Frequency-to-Voltage Quotient in SI Units.	LAMINATES
Detection of the Free Radicals FeH, CoH, and NiH Far Infrared Laser Magnetic Resonance.	by PB89-230437 <i>901,556</i>	Edge Stresses in Woven Laminates at Low Temperatures.
PB90-117342 900,4	95 JOSEPHSON JUNCTIONS Josephson-Junction Model of Critical Current in Granular	PB90-128265 901,08
RRADIATION Effect of Crosslinks on the Phase Separation Behavior	Y1Ba2Cu3O(7-delta) Superconductors.	Tensile and Fatigue-Creep Properties of a Copper-Stair less Steel Laminate.
a Miscible Polymer Blend. PB89-146724 900,5	Chan and Catastrophe Mass the Disease Francisco in	PB90-128646 901,08 LAND MINE DETECTION
Center for Radiation Research (of the National Institu	the HF-Blased Josephson Junction.	Magnetostatic Measurements for Mine Detection.
of Standards and Technology) Technical Activities 1989.	or MM Wave Quasioptical SIS Mixers.	PB89-148365 900,68
PB90-130279 901,3	07 PB89-214738 901,446 K SHELL	LANTHANUM IONS Electron-Impact Ionization of La($q+$) Ions ($q=1,2,3$).
SOCHORIC PROCESSES Determination of Binary Mixture Vapor-Liquid Critical De	n- Cross Sections for K-Shell X-ray Production by Hydrogen	PB90-123845 901,57
sities from Coexisting Density Data. PB89-202170 901,5	and Helium lons in Elements from Beryllium to Uranium.	Resonant Excitation of an Oxygen Valence Satellite i
SOCYANATES	KERMA	Photoemission from High-T(sub c) Superconductors. PB89-186860 901,42
Oligomers with Pendant Isocyanate Groups as Tiss Adhesives. 2. Adhesion to Bone and Other Tissues.	ue Method for Evaluating Air Kerma and Directional Dose Equivalent for Currently Available Multi-Element Dose-	LASER BEAMS
PB89-231245 900,0	56 meters in Radiation Protection Dosimetry. PB90-117532 901,301	Far-Infrared Laser Magnetic Resonance Spectrum of V brationally Excited C2H(1).
SOMERIZATION Standard Chemical Thermodynamic Properties of Poly-	y. KINETICS	PB89-147474 900,29
clic Aromatic Hydrocarbons and Their Isomer Groups Benzene Series.		Production of 0.1-3 eV Reactive Molecules by Laser Va porization of Condensed Molecular Films: A Potenti
PB89-186480 900,4	Offermed Miletics of intermediates in the Autoxidation of	Source for Beam-Surface Interactions. PB89-171201 900,25
SOMERS Standard Chemical Thermodynamic Properties of Poly	SO2. PB89-176754 900,256	NBS (National Bureau of Standards) Laser Power an
clic Aromatic Hydrocarbons and Their Isomer Groups. Pyrene Series, Naphthopyrene Series, and Corone	Laser Probing of the Dynamics of Ga Interactions on	Energy Measurements. PB89-171680 901,34
Series. PB89-226591 900,4	PB89-186928 901,422	LASER COOLING
SOTOPE DILUTION	KLEIN-GORDON EQUATION Computer Simulation Studies of the Soliton Model. 3.	Trapped Ions and Laser Cooling 2: Selected Publication of the Ion Storage Group, Time and Frequency Division
Developing Definitive Methods for Human Serum Ar lytes.	a- Noncontinuum Regimes and Soliton Interactions. PB89-202469 901,537	NIST, Boulder, CO. PB89-153878 901,48
PB89-146773 901,2	KNOWLEDGE-BASED SYSTEMS	Cooling and Trapping Atoms.
Isotope Dilution Mass Spectrometry for Accurate Elemetal Analysis.	Detailed Description of the Knowledge-Based System for Physical Database Design. Volume 1.	PB89-176937 901,51 Laser Cooling.
PB89-230338 900,2	PB89-228993 900,929	PB89-179147 901,51
Determination of Selenium and Tellurium in Copp Standard Reference Materials Using Stable Isotope Di		Ion Trapping Techniques: Laser Cooling and Sympatheti Cooling.
tion Spark Source Mass Spectrometry. PB90-123472 900,2	900,930 PB89-229033 900,930	PB90-128034 901,57
High-Accuracy Gas Analysis via Isotope Dilution Ma	KRYPTON Using 'Resonant' Charge Exchange to Detect Traces of	Laser Cooling to the Zero-Point Energy of Motion. PB90-128091 901,58
Spectrometry: Carbon Dioxide in Air. PB90-123951 900,0	Nebla Goo Atema	LASER DAMAGE
SOTOPE EFFECT Hyperconjugation: Equilibrium Secondary Isotope Effe	KRYPTON COMPLEXES	Laser Induced Damage in Optical Materials: 1987. PB89-221162 901,36
on the Stability of the t-Butyl Cation. Kinetics of Ne	Calculation of Vibration-Rotation Spectra for Rare Gas- HCI Complexes.	LASER INDUCED DESORPTION
Thermoneutral Hydride Transfer. PB89-156756 900,3	900,473 PB89-228415	Optically Driven Surface Reactions: Evidence for th Role of Hot Electrons.
SOTOPES Facile Synthesis of 1-Nitropyrene-d9 of High Isoto	LABORATORIES Laboratory Accreditation Systems in the United States,	PB89-157937 900,33 LASER INDUCED FLUORESCENCE
Purity.	1984.	Laser Probing of Product-State Distributions in Therma
PB90-123753 900,2 SOTOPIC LABELING	Directory of NVLAP (National Voluntary Laboratory Ac-	Energy Ion-Molecule Reactions. PB89-171250 900,35
Oxygen Isotope Effect in the Superconducting Bi-Sr-Cu-O System.	creditation Program) Accredited Laboratories, 1986-87. PB89-185599 900,933	Laser Excited Fluorescence Studies of Black Liquor. PB89-176416 900.24
PB89-157044 901,0	gram) Directors of Approdited Laboratories	PB89-176416 900,24 Spectroscopic Detection Methods.
Determination of Serum Cholesterol by a Modification the Isotope Dilution Mass Spectrometric Definit	DD00 100070 000 000	PB89-228100 901,54
Method. PB89-234181 901,2	NVLAP (National Voluntary Laboratory Accreditation Pro-	LASER INTERFEROMETERS Automated Fringe Counting Laser Interferometer for Lov
UE	PB89-228324 900,903	Frequency Vibration Measurements. PB89-177190 900,88
Proceedings of the Celebratory Symposium on a Deca of UV (Ultraviolet) Astronomy with the IUE Satelli		LASER MICROPROBE MASS ANALYZERS
Volume 2. N89-16535/1 900,0	PB89-229686 900,857	Comparison of Two Transient Recorders for Use with the Laser Microprobe Mass Analyzer.
-INTEGRAL	gram) Program Handbook Construction Testing Services.	PB89-176887 900,20
J-Integral Values for Small Cracks in Steel Panels. PB89-149090 901,0	Requirements for Accreditation. 93 PB90-112327 900,169	LASER MICROPROBE MASS SPECTROSCOPY Laser Microprobe Mass Spectrometry: Description and
ET ENGINE FUELS	LABORATORY EQUIPMENT	Selected Applications. PB89-201628 900.21
Development of Standard Measurement Techniques a Standard Reference Materials for Heat Capacity a	nd Scanning Electron Microscopy: A Lutorial.	LASER NOISE
Heat of Vaporization of Jet Fuels. PB89-148100 900.6	PB89-172498 900,192	Laser-Noise-Induced Population Fluctuations in Two- and Three-Level Systems.
ET FLOW	Laser Microprobe Mass Analyzer.	PB89-171235 901,34
Very Large Methane Jet Diffusion Flames. PB89-175913 900,5	PB89-176887 900,200 93 LACTIC ACID	LASER-PRODUCED PLASMA Laser-Produced Spectra and QED (Quantum Electrody
Importance of Isothermal Mixing Processes to the Und	Micro-Analysis of Mineral Saturation Within Enamel	namic) Effects for Fe-, Co-, Cu-, and Zn-Like lons of Au
standing of Lift-Off and Blow-out of Turbulent Jet Dif sion Flames.	PB89-186373 901,253	Pb, Bi, Th, and U. PB89-176010 <i>901,51</i> 0
PB89-201172 900,5	ENG 100E	LASER-RADIATION HEATING Laser Induced Vaporization Time Resolved Mass Spec
Assessment of Theories for the Behavior and Blowout Lifted Turbulent Jet Diffusion Flames.	sis of Lactose.	trometry of Refractories.

		EINE WIOTH
LASER SPECTROMETERS	Optical Fiber Sensors for the Measurement of Electro- magnetic Quantities,	PB89-209266 900,895
Simple F-Center Laser Spectrometer for Continuous Single Frequency Scans.	PB89-176671 900,748	LENNARD-JONES FLUIDS
PB89-179774 901,358 LASER SPECTROSCOPY	CO Laser Stabilization Using the Optogalvanic Lamb-Dip. PB89-179139 901,356	Properties of Lennard-Jones Mixtures at Various Tem- peratures and Energy Ratios with a Size Ratio of Two. PB89-235204 900,493
Ultrasensitive Laser Spectroscopy and Detection.	Laser Cooling. PB89-179147 901,518	LENNARD-JONES GAS
PB89-156996 901,336 One Is Not Enough: Intra-Cavity Spectroscopy with Multi-	Measurements of the Nonresonant Third-Order Suscepti-	Improved Conformal Solution Theory for Mixtures with Large Size Ratios.
Mode Lasers. PB89-185888 900,402	bility. PB89-179212 <i>901,357</i>	PB89-228563 900,477
Structure and Dynamics of Molecular Clusters via High	Simple F-Center Laser Spectrometer for Continuous	LIFE-CYCLE COST NBS (National Bureau of Standards) Life-Cycle Cost
Resolution IR Absorption Spectroscopy. PB89-185896 900,403	Single Frequency Scans. PB89-179774 901,358	(NBSLCC) Program (for Microcomputers).
High Resolution Optical Multiplex Spectroscopy.	Apparatus Function of a Prism-Grating Double Monochro-	PB89-151211 900,849 LIFE CYCLE COSTS
PB89-185938 900,404	mator. PB89-186282 901,359	Energy Prices and Discount Factors for Life-Cycle Cost
Laser Spectroscopy of Inelastic Collisions. PB89-185946 900,405	Towards the Ultimate Laser Resolution. PB89-186910 900,416	Analysis 1988: Annual Supplement to NBS (National Bureau of Standards) Handbook 135 and NBS Special Publication 709.
Scheme for a 60-nm Laser Based on Photopumping of a High Level of Mo(6+) by a Spectral Line of Mo(11+). PB89-186415 900,407	Laser Induced Damage in Optical Materials: 1987. PB89-221162 901,364	PB89-153860 900,850
Towards the Ultimate Laser Resolution.	Rate of Change of the Quincy-Monument Peak Baseline from a Translocation Analysis of LAGEOS Laser Range	Determination of Short Lifetimes with Ultra High Resolution (n,gamma) Spectroscopy.
PB89-186910 900,416 Rydberg-Klein-Rees Inversion of High Resolution van der	Data.	PB90-123670 901,567
Waals Infrared Spectra: An Intermolecular Potential	PB89-234272 901,282 Numerical Aperture of Multimode Fibers by Several Meth-	LIGANDS
Energy Surface for Ar+ HF (v = 1). PB89-227953 900,465	ods: Resolving Differences. PB90-117482 900,757	Electronic Structure of Diammine (Ascorbato) Platinum(II) and the Trans Influence on the Ligand Dissociation
Infrared Spectra of Nitrous Oxide-HF Isomers.		Energy. PB89-147128 <i>900,287</i>
PB89-228399 900,471 Chlorine-like Spectra of Copper to Molybdenum.	Precise Laser Frequency Scanning Using Frequency-Syn- thesized Optical Frequency Sidebands: Application to Isotope Shifts and Hyperfine Structure of Mercury.	LIGHT SCATTERING
PB90-117706 900,501	PB90-118134 901,370	Light Scattering from Simulated Smoke Agglomerates. PB89-157234 900,588
Analysis of Magnesiumlike Spectra from Cu XVIII to Mo XXXI.	Latent Heats of Supercritical Fluid Mixtures.	Dynamic Light Scattering and Angular Dissymmetry for
PB90-117821 900,508	PB89-174908 900,242	the In situ Measurement of Silicon Dioxide Particle Synthesis in Flames.
Identification of Carbonaceous Aerosols via C-14 Accelerator Mass Spectrometry, and Laser Microprobe Mass	LATEX Studies on Some Failure Modes in Latex Barrier Films.	PB89-179584 900,246
Spectrometry. PB90-136540 900,236	PB89-209308 901,089	Simulation Study of Light Scattering from Soot Agglomerates.
LASERS	LATTICE PARAMETERS Grain Boundaries with Impurities in a Two-Dimensional	PB89-212138 901,543
Alignment Effects in Electronic Energy Transfer and Re-	Lattice-Gas Model.	Collision Induced Spectroscopy: Absorption and Light Scattering.
active Events. AD-A202 820/7 900,267	PB89-172407 901,507 Off-Lattice Simulation of Polymer Chain Dynamics.	PB89-212252 901,363
Stokes and Anti-Stokes Fluorescence of Er(3+) in the	PB90-117524 900,576	LIGHT TRANSMISSION Computing Ray Trajectories between Two Points: A Solu-
Raman Spectra of Erbium Oxide and Erbium Glasses. PB89-149231 901,020	LATTICE PROPERTIES Critical and Noncritical Roughening of Surfaces (Com-	tion to the Ray-Linking Problem. PB89-176929 901,354
Fast-Pulse Generators and Detectors for Characterizing Laser Receivers at 1.06 um.	ment). PB89-180046 901,415	LIGHT (VISIBLE RADIATION)
PB89-171698 901,347	LATTICES (MATHEMATICS)	Brief History of Near-Field Measurements of Antennas at
Laser Induced Fluorescence for Measurement of Lignin Concentrations in Pulping Liquors.	Finite Unions of Closed Subgroups of the n-Dimensional Torus.	the National Bureau of Standards. PB89-156863 900,703
PB89-172530 901,184	PB89-143283 901,193	Resonance Light Scattering from a Suspension of Microspheres.
NBS (National Bureau of Standards) Standards for Opti- cal Power Meter Calibration.	LAW ENFORCEMENT ACSB (Amplitude Companded Sideband): What Is Ade-	PB89-176234 901,352
PB89-176200 900,726	quate Performance.	LIGHTHILL CORRECTION
Picosecond Coherent Anti-Stokes Raman Scattering (CARS) Study of Vibrational Dephasing of Carbon Disul-	PB89-176283 901,599 LEAD	Hydrodynamic Forces on Vertical Cylinders and the Lighthill Correction.
fide and Benzene in Solution. PB89-176408 900,380	High-Accuracy Differential-Pulse Anodic Stripping Voltam- metry with Indium as an Internal Standard.	PB90-117417 901,313 LIGHTING EQUIPMENT
Kinetics of Resolidification.	PB89-156947 900,182	Evaluating Office Lighting Environments: Second Level
PB89-176457 901,138	LEAD ALLOYS Ostwald Ripening in a System with a High Volume Frac-	Analysis. PB89-189153 <i>900,073</i>
Heterodyne Frequency Measurements of (12)C(16)O Laser Transitions,	tion of Coarsening Phase.	LIGHTNING
PB89-229223 901,374	PB89-157598 901,126 Directional Invariance of Grain Boundary Migration in the	Lightning and Surge Protection of Photovoltaic Installa- tions. Two Case Histories; Vulcano and Kythnos.
Precise Laser Frequency Scanning Using Frequency-Synthesized Optical Frequency Sidebands: Application to	Pb-Sn Cellular Transformation and the Tu-Turnbull Hys-	PB89-229058 900,851
Isotope Shifts and Hyperfine Structure of Mercury. PB90-118134 901,370	teresis. PB89-157911 901,134	Interactions between Two Dividers Used in Simultaneous Comparison Measurements.
Search for Optical Molasses in a Vapor Cell: General	LEAD IONS	PB90-118035 900,031
Analysis and Experimental Attempt. PB90-163932 901,371	Laser-Produced Spectra and QED (Quantum Electrody- namic) Effects for Fe-, Co-, Cu-, and Zn-Like lons of Au,	Method for Fitting and Smoothing Digital Data. PB90-128794 900,830
LASERS & THEIR APPLICATIONS	Pb, Bi, Th, and U. PB89-176010 <i>901,510</i>	LIGNIN
Method of and Apparatus for Real-Time Crystallographic Axis Orientation Determination.	LEAD ISOTOPES	Laser Induced Fluorescence for Measurement of Lignin Concentrations in Pulping Liquors.
PATENT-4 747 684 901,383	Technical Examination, Lead Isotope Determination, and Elemental Analysis of Some Shang and Zhou Dynasty	PB89-172530 901,184
Ultrasensitive Laser Spectroscopy and Detection. PB89-156996 901,336	Bronze Vessels. PB90-136862 901,178	LINE SPECTRA Fundamental Configurations in Mo IV Spectrum.
Two-Photon Laser-Induced Fluorescence of the Tumor-	LEAD (METAL)	PB89-147011 900,284
Localizing Photosensitizer Hematoporphyrin Derivative. PB89-157283 901,240	Detection of Lead in Human Teeth by Exposure to Aqueous Sulfide Solutions.	Thermal Shifts of the Spectral Lines in the (4)F3/2 to (4)I11/2 Manifold of an Nd:YAG Laser.
Perpendicular Laser Cooling of a Rotating Ion Plasma in a Penning Trap.	PB89-201529 901,256 LEAD NIOBATES	PB89-157382 901,338 Stark Broadening of Spectral Lines of Homologous,
PB89-157408 901,493	Neutron Powder Diffraction Structure and Electrical Prop-	Doubly Ionized Inert Gases.
Laser-Noise-Induced Population Fluctuations in Two- and Three-Level Systems.	erties of the Defect Pyrochlores Pb1.5M2O6.5 (M = Nb, Ta).	PB89-158083 900,343 LINE WIDTH
PB89-171235 901,342	PB89-172431 900,363	Submicrometer Optical Metrology.
Picosecond Laser Study of the Collisionless Photodisso- ciation of Dimethylnitramine at 266 nm.	Characterization of Organolead Polymers in Trace	PB89-150973 900,771
PB89-172423 900,255	Amounts by Element-Specific Size-Exclusion Chromatog- raphy.	Stark Broadening of Spectral Lines of Homologous, Doubly longed Inert Gases.
NBS/NRL (National Bureau of Standards/Naval Research Laboratory) Free Electron Laser Facility.	PB89-175962 900,196	PB89-158083 900,343 Effects of Velocity and State Changing Collisions on
PB89-175749 901,351	Neutron Powder Diffraction Structure and Electrical Prop-	Raman Q-Branch Spectra.
Laser-Cooling and Electromagnetic Trapping of Neutral Atoms.	erties of the Defect Pyrochlores Pb1.5M2O6.5 (M = Nb, Ta).	PB89-179196 900,391 Automated Calibration of Optical Photomask Linewidth
PB89-176440 901,511	PB89-172431 900,363	Standards at the National Institute of Standards and Technology.
NBS (National Bureau of Standards) Free Electron Laser Facility.	Length Scale Measurement Procedures at the National	PB89-186340 901,315

Length Scale Measurement Procedures at the National Bureau of Standards.

NBS (National Bureau of Standards) Free Electron Laser Facility.
PB89-176515 901,353

Spatial Filtering Microscope for Linewidth Measurements.

PB89-230346 901,368	Measurement of Electrical Breakdown in Liquids. PB89-212229 900,447	PB89-176994 901,407
LINEAR PROGRAMMING Electronic Mail and the 'Locator's' Dilemma.	Mean Density Approximation and Hard Sphere Expansion Theory: A Review.	Second Viscosity and Thermal-Conductivity Virial Coeffi- cients of Gases: Extension to Low Reduced Tempera-
PB89-211957 901,205 LINEAR RECURRENCE RELATIONS	PB89-228019 901,546	ture. PB89-179691 <i>900,397</i>
Error Bounds for Linear Recurrence Relations. AD-A201 256/5 901,192	Shear-Induced Angular Dependence of the Liquid Pair Correlation Function. PB89-228043 900,469	Fracture Behavior of a Pressure Vessel Steel in the Ductile-to-Brittle Transition Region.
LININGS	Torsional Piezoelectric Crystal Viscometer for Com-	PB89-189195 901,103 Ag Screen Contacts to Sintered YBa2Cu3Ox Powder for
Ignition and Flame Spread Measurements of Aircraft Lining Materials. PB89-172886 900,009	pressed Gases and Liquids. PB89-228076 901,447	Rapid Superconductor Characterization. PB89-200448 901,423
LIPIDS Biophysical Aspects of Lipid Interaction with Mineral: Li-	Measures of Effective Ergodic Convergence in Liquids. PB90-118092 900,518	Chaos and Catastrophe Near the Plasma Frequency in the RF-Biased Josephson Junction.
posome Model Studies. PB90-117508 901,228	LITHIUM Coadsorption of Water and Lithium on the Ru(001) Sur-	PB89-200463 901,424 Nb3Sn Critical-Current Measurements Using Tubular Fi-
LIPOSOMES	face. PB89-202956 900,440	berglass-Epoxy Mandrels. PB89-200497 901.527
Biophysical Aspects of Lipid Interaction with Mineral: Liposome Model Studies.	LITHOGRAPHY Approach to Accurate X-Ray Mask Measurements in a	Hysteretic Phase Transition in Y1Ba2Cu3O7-x Supercon-
PB90-117508 901,228 Generic Liposome Reagent for Immunoassays.	Scanning Electron Microscope. PB89-172555 900,776	ductors. PB89-229082 901,454
PB90-123886 901,229 Liposome Technology in Biomineralization Research.	LIVER	Performance of He II of a Centrifugal Pump with a Jet Pump Inducer.
PB90-128117 901,230	Radiochemical and Instrumental Neutron Activation Analysis Procedures for the Determination of Low Level Trace	PB89-229090 901,553 Reentrant Softening in Perovskite Superconductors.
Pore-Water Pressure Buildup in Clean Sands Because of	Elements in Human Livers. PB89-171953 901,236	PB90-117540 901,464
Cyclic Straining. PB89-175723 <i>900,159</i>	LIVER EXTRACTS Voltammetric and Liquid Chromatographic Identification	Edge Stresses in Woven Laminates at Low Tempera- tures.
LIQUID CHROMATOGRAPHY Recent Advances in Bonded Phases for Liquid Chroma-	of Organic Products of Microwave-Assisted Wet Ashing of Biological Samples.	PB90-128265 901,082 Effect of Chemical Composition on the 4 K Mechanical
tography. PB89-187520 <i>900,204</i>	PB89-157994 900,188 LOAD CELLS	Properties of 316LN-Type Alloys. PB90-128554 901,110
Comparison of Liquid Chromatographic Selectivity for Polycyclic Aromatic Hydrocarbons on Cyclodextrin and C18	Intercomparison of Load Cell Verification Tests Performed by National Laboratories of Five Countries.	Fracture Behavior of 316LN Alloy in Uniaxial Tension at Cryogenic Temperatures.
Bonded Phases. PB90-128539 900,231	PB89-235915 900,909	PB90-128562 901,111
Synthesis and Characterization of Novel Bonded Phases	Loading Rate Effects on Discontinuous Deformation in	Effects of Grain Size and Cold Rolling on Cryogenic Properties of Copper.
for Reversed-Phase Liquid Chromatography. PB90-128695 900,233	Load-Control Tensile Tests. PB89-171896 901,097	PB90-128604 901,176 Low Temperature Mechanical Property Measurements of
Voltammetric and Liquid Chromatographic Identification	LOADING RATE Loading Rate Effects on Discontinuous Deformation in	Silica Aerogel Foam. PB90-128638 901,061
of Organic Products of Microwave-Assisted Wet Ashing of Biological Samples.	Load-Control Tensile Tests. PB89-171896 901,097	Tensile and Fatigue-Creep Properties of a Copper-Stainless Steel Laminate.
PB89-157994 900,188 LIQUID CRYSTALS	LOADS (FORCES) Damage Accumulation in Wood Structural Members	PB90-128646 901,083
Polymerization of a Novel Liquid Crystalline Diacetylene Monomer.	Under Stochastic Live Loads. PB89-171748 900,115	Fatigue Resistance of a 2090-T8E41 Aluminum Alloy at Cryogenic Temperatures. PB90-128737 901,177
PB89-231286 900,575 LIQUID FILTERS	Progressive Collapse: U.S. Office Building in Moscow. PB89-175715 900,158	Low-Temperature Phase and Magnetic Interactions in fcc
Influence of Reaction Reversibility on Continuous-Flow Extraction by Emulsion Liquid Membranes.	Probabilistic Models for Ground Snow Accumulation.	Fe-Cr-Ni Alloys. PB90-136771 901,113
PB89-176481 900,244	PB89-186894 900,100 LOG PERIODIC ANTENNA S	LOW TEMPERATURE TESTS Ineffectiveness of Powder Regenerators in the 10 K
Process Control during High Pressure Atomization.	MM Wave Quasioptical SIS Mixers. PB89-214738 901,446	Temperature Range. PB89-173876 <i>901,005</i>
PB89-179170 901,142 Dynamical Simulation of Liquid- and Solid-Metal Self-	LOGISTIC FUNCTIONS Logistic Function Data Analysis Program: LOGIT.	Measurement of Regenerator Ineffectiveness at Low Temperatures.
Sputtering. PB89-228407 900,472	PB89-189351 900,418	PB89-173884 901,006
LIQUID PERMEABILITY Studies on Some Failure Modes in Latex Barrier Films.	Antennas for Geophysical Applications.	Refrigeration Efficiency of Pulse-Tube Refrigerators. PB89-173892 901,007
PB89-209308 901,089	PB89-179857 900,710 LOW ALLOY STEELS	Tables for the Thermophysical Properties of Methane. PB89-222608 900,843
LIQUID PHASES PVT of Toluene at Temperatures to 673 K.	Corrosion Behavior of Mild Steel in High pH Aqueous Media.	Low-Temperature Phase and Magnetic Interactions in fcc Fe-Cr-Ni Alloys.
PB89-157192 900,310 PVT Measurements on Benzene at Temperatures to 723	PB90-131152 901,086 LOW-LEVEL RADIOACTIVE WASTES	PB90-136771 901,113
K. PB89-157200 <i>900,311</i>	Proceedings of the Workshop on Cement Stabilization of	LUBRICATING OILS Preparative Liquid Chromatographic Method for the Char-
Effect of Surface Ionization on Wetting Layers. PB89-157259 901.323	Low-Level Radioactive Waste. Held at Gaithersburg, Maryland on May 31-June 2, 1989. NUREG/CP-0103 901,302	acterization of Minor Constituents of Lubricating Base Oils.
Polymer Phase Separation.	LOW NOISE AMPLIFIERS	PB89-175921 <i>901,114</i> LUMINESCENCE
PB89-202923 900,570 Effect of Heat Treatment on Crack-Resistance Curves in	Very Low-Noise FET Input Amplifier. PB90-128224 900,800	Luminescence Standards for Macro- and Microspectro- fluorometry.
a Liquid-Phase-Sintered Alumina. PB89-229231 901,056	LOW TEMPERATURE SCIENCE & ENGINEERING Performance of Alumina/Epoxy Thermal Isolation Straps.	PB89-176598 900,383 LUMINOSITY
LIQUIDS Thermal Funencias Crouth of Probackdown Strongers	PB89-147078 901,070	Effect of pH on the Emission Properties of Aqueous tris
Thermal-Expansive Growth of Prebreakdown Streamers in Liquids. PB89-149074 900,803	Institute for Materials Science and Engineering, Fracture and Deformation: Technical Activities 1988. PB89-148399 901,071	(2,6-dipicolinato) Terbium (III) Complexes. PB89-157135 900,250
Local Order in a Dense Liquid.	Effect of Multiple Internal Reflections on the Stability of	LUMINOUS INTENSITY System for Measuring Optical Waveguide Intensity Pro-
PB89-157226 900,313 Migration of Liquid Film and Grain Boundary in Mo-Ni In-	Electrooptic and Magnetooptic Sensors. PB89-171722 900,724	files. PB89-188593 <i>900,751</i>
duced by W Diffusion. PB89-157614 901,128	Loading Rate Effects on Discontinuous Deformation in Load-Control Tensile Tests.	LYMAN LINES Redistribution in Astrophysically Important Hydrogen
Shear Induced Anisotropy in Two-Dimensional Liquids. PB89-158141 901,325	PB89-171896 901,097 Ineffectiveness of Powder Regenerators in the 10 K	Lines. PB90-128075 901,579
Tensile Strain-Rate Effects in Liquid Helium.	Temperature Range. PB89-173876 901,005	M1-TRANSITIONS
Repulsive Regularities of Water Structure in Ices and	Measurement of Regenerator Ineffectiveness at Low Temperatures.	Line Identifications and Radiative-Branching Ratios of Magnetic Dipole Lines in Si-like Ni, Cu, Zn, Ge, and Se.
Crystalline Hydrates. PB89-186753 900,414	PB89-173884 901,006	PBB-234165 901,558 MACHINE TOOLS
Simple Apparatus for Vapor-Liquid Equilibrium Measurements with Data for the Binary Systems of Carbon Diox-	Refrigeration Efficiency of Pulse-Tube Refrigerators. PB89-173892 901,007	General Methodology for Machine Tool Accuracy Enhancement by Error Compensation.
ide with n-Butane and Isobutane. PB89-201115 900,422	Josephson-Junction Model of Critical Current in Granular Y1Ba2Cu3O(7-delta) Superconductors.	PBB9-146781 900,996 Prellminary Experiments with Three Identical Ultrapreci-
Ergodic Behavior in Supercooled Liquids and in Glasses. PB89-202444	PB89-176978 901,406 Bean Model Extended to Magnetization Jumps.	sion Machine Tools. PB89-150841 900,997

	MAGNETIC SURFACES	
Generalized Mathematical Model for Machine Tool	Magnetic Properties of Surfaces Investigated by Spin Po-	PB89-202220 901,319
Errors. PB89-150874 900,977	larized Electron Beams.	Reduction of Uncertainties for Absolute Piston Gage
MACHINING	PB89-176564 901,405	Pressure Measurements in the Atmospheric Pressure Range.
Vertical Machining Workstation of the AMRF (Automated	MAGNETIC SUSCEPTIBILITY Electronic, Magnetic, Superconducting and Amorphous-	PB90-163882 900,030
Manufacturing Research Facility): Equipment Integration.	Forming Properties Versus Stability of the Ti-Fe, Zr-Ru	MANUFACTURING
	and Hf-Os Ordered Alloys. PB89-146690 901,120	Material Handling Workstation Implementation.
Software for an Automated Machining Workstation. PB89-177109 900,953	MAGNETIZATION	PB89-159644 900,988
Inventory of Equipment in the Cleaning and Deburring	Magnetization and Magnetic Aftereffect in Textured Ni/	Material Handling Workstation: Operator Manual. PB89-159651 900,989
Workstation.	Cu Compositionally-Modulated Alloys. PB90-123431 901,165	Functional Approach to Designing Architectures for Com-
PB89-209233 900,958	PB90-123431 901,165 MAGNETOOPTICS	puter Integrated Manufacturing.
MAGNESIUM Resonance Ionization Mass Spectrometry of Mg: The	Effect of Multiple Internal Reflections on the Stability of	PB89-172589 900,946
3pnd Autoionizing Series.	Electrooptic and Magnetooptic Sensors.	Operations Manual for the Automatic Operation of the
PB89-150817 900,296	PB89-171722 900,724 MAGNETOROTONS	Vertical Workstation. PB89-183214 900,973
Analysis of Magnesiumlike Spectra from Cu XVIII to Mo	Superlattice Magnetoroton Bands.	Turning Workstation in the AMRF (Automated Manufac-
XXXI. PB90-117821 900,508	PB89-175970 901,403	turing Research Facility).
	MAGNONS	PB89-185607 900,954
MAGNESIUM IONS Precise Test of Quantum Jump Theory.	Spin-Density-Wave Transition in Dilute YGd Single Crystals.	Neural Network Approach for Classifying Test Structure
PB89-157390 901,339	PB89-202030 901,433	Results. PB89-212187 900,788
MAGNESIUM PORPHYRIN	MAINTENANCE	
Reactions of Magnesium Prophyrin Radical Cations in	Postweld Heat Treatment Criteria for Repair Welds in 2-	Machine-Learning Classification Approach for IC Manufacturing Control Based on Test Structure Measurements.
Water. Disproportionation, Oxygen Production, and Com- parison with Other Metalloporphyrins.	1/4Cr-1Mo Superheater Headers: An Experimental Study. PB89-156160 901.094	PB89-228530 900,790
PB89-151005 900,301	Assessment of Robotics for Improved Building Oper-	Publications of the Center for Manufacturing Engineering
MAGNETIC DETECTION	ations and Maintenance.	Covering the Period January 1978-December 1988, PB90-130568 901.012
Magnetostatic Measurements for Mine Detection.	PB89-189146 900,092	
PB89-148365 900,685	MAN COMPUTER INTERFACE	Enhancements to the VWS2 (Vertical Workstation 2) Data Preparation Software.
MAGNETIC DIPOLES	Incrementor: A Graphical Technique for Manipulating Parameters.	PB90-132713 900,968
Magnetic Dipole Excitation of a Long Conductor in a Lossy Medium.	PB89-177000 900,648	Emerging Technologies in Manufacturing Engineering.
PB89-171664 900,742	MANAGEMENT INFORMATION SYSTEMS	PB90-132747 901,013
MAGNETIC DOMAINS	Development and Use of a Tribology Research-in-	MARINE ATMOSPHERES
High Resolution Imaging of Magnetization.	Progress Database. PB89-228274 901,002	Determination of Ultratrace Concentrations of Butyltin
PB89-147433 901,386	MANGANESE	Compounds in Water by Simultaneous Hydridization/Extraction with GC-FPD Detection.
Domain Images of Ultrathin Fe Films on Ag(100). PB89-158067 901,394	Journal of Physical and Chemical Reference Data,	PB89-177224 901,311
Influence of the Surface on Magnetic Domain-Wall Mi-	Volume 17, 1988, Supplement No. 3. Atomic Transition	MARINE BIOLOGY
crostructure.	Probabilities Scandium through Manganese. PB89-145197 900,276	Sequential Determination of Biological and Pollutant Ele-
PB90-118019 901,467	Structural Unit in Icosahedral MnAlSi and MnAl.	ments in Marine Bivalves.
Vector Imaging of Magnetic Microstructure.	PB89-157648 901,131	PB89-156897 901,217
PB90-128240 901,476	Stable and Metastable Phase Equilibria in the Al-Mn	MARINE ENGINEERING
MAGNETIC FIELDS	System.	Computerized Materials Property Data Systems. PB89-187512 901,312
Characterizing Electrical Parameters Near AC and DC Power Lines.	PB89-172324 901,136	MARINE MICROORGANISMS
PB89-173462 900,834	Solidification of Aluminum-Manganese Powders. PB89-172332 901,137	Biodegradation of Tributyltin by Chesapeake Bay Microor-
AC Electric and Magnetic Field Meter Fundamentals.	Formation and Stability Range of the G Phase in the Alu-	ganisms.
PB89-173470 900,746	minum-Manganese System.	PB89-177232 901,309
Power Frequency Electric and Magnetic Field Measure-	PB89-186316 901,144	MASKING
ments: Recent History and Measurement Standards. PB89-176630 900,835	Nucleation and Growth of Aperiodic Crystals in Aluminum	Approach to Accurate X-Ray Mask Measurements in a Scanning Electron Microscope.
MAGNETIC MEASUREMENT	Alloys. PB89-186324 <i>901,145</i>	PB89-172555 900,776
Magnetostatic Measurements for Mine Detection.	Replacement of Icosahedral Al-Mn by Decagonal Phase.	MASS
PB89-148365 900,685	PB89-186332 901,146	Stability of the SI (International System) Unit of Mass as
MAGNETIC ORDERING	Structural Study of a Metastable BCC Phase in Al-Mn	Determined from Electrical Measurements. PB89-201818 900,894
Occurrence of Long-Range Helical Spin Ordering in Dy-Y Multilayers.	Alloys Electrodeposited from Molten Salts. PB89-201040 901,064	MASS CALIBRATION
PB89-179634 901,410	MANGANESE ADDITIONS	NIST (National Institute of Standards and Technology)
Long-Range Incommensurate Magnetic Order in Dy-Y	Linear-Elastic Fracture of High-Nitrogen Austenitic Stain-	Measurement Services: Mass Calibrations.
Multilayers.	less Steels at Liquid Helium Temperature.	PB89-153894 900,874
PB89-179642 901,411	PB90-117623 901,108	MASS MEASUREMENT
Magnetic Order of Pr in PrBa2Cu3O7. PB90-123803 901,471	MANGANESE ALLOYS Quasicrystals with 1-D Translational Periodicity and a	Interpretation of a between-Time Component of Error in
	Ten-Fold Rotation Axis.	Mass Measurements. PB89-149108 900,872
Pressure Dependence of the Cu Magnetic Order in RBa2Cu3O6+ x.	PB89-147383 901,123	MASS SPECTRA
PB90-123829 901,472	MANGANESE IONS	Electron-Energy Dependence of the S2F10 Mass Spec-
MAGNETIC PARTICLE TESTS	Marked Differences in the 3p Photoabsorption between the Cr and Mn(1+) Isoelectronic Pair: Reasons for the	trum.
Quantitative Problems in Magnetic Particle Inspection. PB89-229199 900,985	Unique Structure Observed in Cr.	PB90-117870 900,512
· · · · · · · · · · · · · · · · · · ·	PB90-117581 <i>901,562</i>	MASS SPECTROMETRY
MAGNETIC PERMEABILITY Densification, Susceptibility and Microstructure of	MANGANESE PORPHYRIN	Determination of Trace Level Iodine in Biological and Botanical Reference Materials by Isotope Dilution Mass
Ba2YCu3O(6+ x).	Decay of High Valent Manganese Porphyrins in Aqueous Solution and Catalyzed Formation of Oxygen.	Spectrometry.
PB89-171821 901,035	PB89-156772 900,308	PB89-235642 900,222
MAGNETIC PROPERTIES	MANGANESE ZINC SELENIDES	MASS SPECTROSCOPY
Magnetic Behavior of Compositionally Modulated Ni-Cu	Mn-Mn Exchange Constants in Zinc-Manganese Chalco-	Developing Definitive Methods for Human Serum Ana-
Thin Films. PB90-118084 901,163	genides. PB90-136706 901,478	lytes. PB89-146773 901,233
MAGNETIC RESONANCE	Neutron Diffraction Study of the Wurtzite-Structure Dilute	Chemical Characterization of Ionizing Radiation-Induced
Far-Infrared Laser Magnetic Resonance Spectrum of Vi-	Magnetic Semiconductor Zn0.45Mn0.55Se,	Damage to DNA.
brationally Excited C2H(1).	PB90-136714 901,479	PB89-151922 901,235
PB89-147474 900,292	MANGANESE ZINC SULFIDES	Validation of Absolute Target Thickness Calibrations in a
MAGNETIC RESONANCE IMAGING	Mn-Mn Exchange Constants in Zinc-Manganese Chalco- genides.	QQQ Instrument by Measuring Absolute Total Cross-Sections of NE(1+) (NE,NE)NE(1+).
Application of Magnetic Resonance Imaging to Visualiza-	PB90-136706 901,478	PB89-157507 900,325
tion of Flow in Porous Media.	MANGANESE ZINC TELLURIDES	Dependence of Interface Widths on Ion Bombardment
PB89-179592 <i>901,329</i>	Mn-Mn Exchange Constants in Zinc-Manganese Chalco-	Conditions in SIMS (Secondary Ion Mass Spectrometry)
MAGNETIC SEMICONDUCTORS	genides. PB90-136706 <i>901,478</i>	Analysis of a Ni/Cr Multilayer Structure. PB89-172506 900,364
Mn-Mn Exchange Constants in Zinc-Manganese Chalco-	MANNED SPACE FLIGHT	Using 'Resonant' Charge Exchange to Detect Traces of
genides. PB90-136706 901,478	Teleoperation and Autonomy for Space Robotics.	Noble Gas Atoms.
	PB90-123811 901,591	PB89-176770 901,296
Neutron Diffraction Study of the Wurtzite-Structure Dilute Magnetic Semiconductor Zn0.45Mn0.55Se.	MANOMETERS Speed of Sound in a Morouny Ultrasonic Interferemeter	Comparison of Two Transient Recorders for Use with the Laser Microprobe Mass Analyzer.
PB90-136714 901,479	Speed of Sound in a Mercury Ultrasonic Interferometer Manometer.	PB89-176887 900,200

Analysis of Ultrapure Reagents from a Large Sub-Boiling Still Made of Teflon PFA. PB89-186357 900,202	MATHEMATICAL MODELS	901,271	Comparison of Time Scales Generated with the NBS (National Bureau of Standards) Ensembling Algorithm. PB89-174072 900,628
Laser Microprobe Mass Spectrometry: Description and Selected Applications.	Calculating Flows through Vertical Vents in Zo Models under Conditions of Arbitrary Cross-Ver sure Difference.	nt Pres-	Efficient Algorithms for Computing Fractal Dimensions. PB89-175871 901,198
PB89-201628 900,210 Single Particle Standards for Isotopic Measurements of		900,108 for Pre-	Tests of the Recalibration Period of a Drifting Instrument. PB89-176275 900,199
Uranium by Secondary Ion Mass Spectrometry. PB89-201669 901,297	dicting Moisture Transfer in Attics.	900,057	Electron Mean Free Path Calculations Using a Model Di- electric Function.
Isotope Dilution Mass Spectrometry for Accurate Elemental Analysis.	Generalized Mathematical Model for Machin Errors.	ne Tool	PB89-177026 901,141
PB89-230338 900,220 Development of the NBS (National Bureau of Standards)		900,977	Note on the Capacitance Matrix Algorithm, Substructur- ing, and Mixed or Neumann Boundary Conditions. PB89-177034 901,199
Beryllium Isotopic Standard Reference Material. PB89-231070 900,221	Breakdown of SF6.	900,327	Algebraic Representation for the Topology of Multicomponent Phase Diagrams.
Determination of Serum Cholesterol by a Modification of the Isotope Dilution Mass Spectrometric Definitive	Hand Calculations for Enclosure Fires. PB89-173983	900,164	PB89-177042 901,517
Method. PB89-234181 901,239	Computer Fire Models. PB89-173991	900,165	Millisecond Pulsar Rivals Best Atomic Clock Stability. PB89-185722 900,629
Determination of Selenium and Tellurium in Copper Standard Reference Materials Using Stable Isotope Dilu- tion Spark Source Mass Spectrometry.	Vapor-Liquid Equilibrium of Nitrogen-Oxygen Mixtu Air at High Pressure.	-	Using Multiple Reference Stations to Separate the Variances of Noise Components in the Global Positioning
PB90-123472 900,230		900,368	System. PB89-185730 <i>901,293</i>
High-Accuracy Gas Analysis via Isotope Dilution Mass Spectrometry: Carbon Dioxide in Air. PB90-123951 900,032	Analytical Modeling of Device-Circuit Interactions Power Insulated Gate Bipolar Transistor (IGBT). PB89-176259	900,777	Calibration with Randomly Changing Standard Curves. PB89-186381 900,888
PB90-123951 900,032 Identification of Carbonaceous Aerosols via C-14 Accel-	Influence of Reaction Reversibility on Continuo		Probabilistic Models for Ground Snow Accumulation.
erator Mass Spectrometry, and Laser Microprobe Mass Spectrometry.	Extraction by Emulsion Liquid Membranes.	900,244	PB89-186894 900,100 Evaluating Emergency Management Models and Data
PB90-136540 900,236 Technical Examination, Lead Isotope Determination, and	Evaluating Emergency Management Models ar Bases: A Suggested Approach.		Bases: A Suggested Approach. PB89-189203 901,598
Elemental Analysis of Some Shang and Zhou Dynasty Bronze Vessels. PB90-136862 901,178	PB89-189203 Technical Reference Guide for FAST (Fire and	<i>901,598</i> I Smoke	Estimation of an Asymmetrical Density from Several Small Samples.
Laser Induced Vaporization Time Resolved Mass Spec-	Transport) Version 18. PB89-218366	900.602	PB89-201131 901,212 Statistical Analysis of Experiments to Measure Ignition of
trometry of Refractories. PB90-136904 900,540	Modeling Dynamic Surfaces with Octrees.	901,206	Cigarettes, PB89-201149 900,135
ATERIALS Intelligent Processing of Materials: Report of an Industrial	High Accuracy Modeling of Photodiode Quantum		Graphical Analyses Related to the Linewidth Calibration
Workshop Conducted by the National Institute of Stand-	cy.	900,733	Problem. PB89-201156 900,783
ards and Technology. PB89-151823 900,942	Fields Radiated by Electrostatic Discharges.	901,382	Statistical Descriptors in Crystallography: Report of the International Union of Crystallography Subcommittee on
Integrated Knowledge Systems for Concrete and Other Materials. PB89-176119 900,582	Model for Particle Size and Phase Distributions in Cement Clinker.		Statistical Descriptors. PB89-201826 901,432
ATERIALS HANDLING		901,062	Elimination of Spurious Eigenvalues in the Chebyshev Tau Spectral Method.
Material Handling Workstation Implementation. PB89-159644 900,988	MATHEMATICAL & STATISTICAL METHODS Error Bounds for Linear Recurrence Relations.	221 122	PB89-209282 901,330 Expected Complexity of the 3-Dimensional Voronoi Dia-
Material Handling Workstation: Operator Manual. PB89-159651 900,989	AD-A201 256/5 Finite Unions of Closed Subgroups of the n-Dim	901,192 ensional	gram. PB89-209332 901,200
AMRF (Automated Manufacturing Research Facility) Material Handling System Architecture.	Torus.	901,193	Consensus Values, Regressions, and Weighting Factors.
PB89-177091 900,952 ATERIALS HANDLING EQUIPMENT	Analytical Model for the Steady-State and T Characteristics of the Power Insulated-Gate Bipol	ransient lar Tran-	PB89-211130 901,213 Electronic Mail and the 'Locator's' Dilemma.
Material Handling Workstation, Recommended Technical Specifications for Procurement of Commercially Available	sistor. PB89-146880	900,767	PB89-211957 901,205 Simulation Study of Light Scattering from Soot Agglomer-
Equipment. PB89-162564 900,998	Measurement Procedures for Electromagnetic ibility Assessment of Electroexplosive Devices.	Compat-	ates. PB89-212138 901,543
ATERIALS SCIENCE Journal of Research of the National Institute of Stand-		901,314	NBS (National Bureau of Standards) Calibration Service Providing Time and Frequency at a Remote Site by
ards and Technology, Volume 94, Number 1, January- February 1989. Special Issue: Numeric Databases in Ma-	Errors.	900,977	Weighting and Smoothing of GPS (Global Positioning System) Common View Data.
terials and Biological Sciences. PB89-175194 901,186	Iterative Technique to Correct Probe Position E Planar Near-Field to Far-Field Transformations.		PB89-212211 900,631 Computation and Use of the Asymptotic Covariance
Importance of Numeric Databases to Materials Science. PB89-175202 901,187		900,695	Matrix for Measurement Error Models. PB89-215321 901,214
International Cooperation and Competition in Materials Science and Engineering.	ed via Calibration.	901,209	AutoMan: Decision Support Software for Automated Manufacturing Investments. User's Manual.
PB89-228332 901,191	Estimation of the Error Probability Density from F		PB89-221873 900,963
ATERIALS SPECIFICATIONS Preliminary Performance Criteria for Building Materials,	Measurements on Several Items. PB89-157820	901,210	User's Reference Guide for ODRPACK: Software for Weighted Orthogonal Distance Regression Version 1.7.
Equipment and Systems Used in Detention and Correctional Facilities. PB89-148514 900,109	Numerical Evaluation of Certain Multivariate Norr	mal Inte-	PB89-229066 901,215 Analysis of Ridge-to-Ridge Distance on Fingerprints.
Computerized Materials Property Data Systems.		901,195	PB89-230478 901,216
PB89-187512 901,312 ASTM (American Society for Testing and Materials) Com-	Internal Revenue Service Post-of-Duty Location N System: Programmer's Manual for PASCAL Solve PB89-161905	900,001	Comparison of Far-Field Methods for Determining Mode Field Diameter of Single-Mode Fibers Using Both Gaus- sian and Petermann Definitions.
mittee Completes Work on EPDM Specification. PB89-212260 900,140	Internal Revenue Service Post-of-Duty Location M	Modeling	PB90-117474 900,756
ATERIALS TESTS	System: Programmer's Manual for FORTRAN Dri sion 5.0.		Guide to Available Mathematical Software Advisory System.
Techniques for Measuring the Electromagnetic Shielding Effectiveness of Materials. Part 1. Far-Field Source Simu-	PB89-161913 Real Time Generation of Smooth Curves Usin	900,002	PB90-123654 901,201 Sheetest Batha in Simply Connected Regions in R3
lation. PB89-161525 900,680	Cubic Segments.	901,196	Shortest Paths in Simply Connected Regions in R2. PB90-123688 901,202
Techniques for Measuring the Electromagnetic Shielding Effectiveness of Materials. Part 2. Near-Field Source Sim-	Minimax Approach to Combining Means, with Examples.		Ment Functions and Nonlinear Programming. PB90-123944 901,208
ulation. PB89-161533 900,681	PB89-171847	901,211	Bootstrap Inference for Replicated Experiments. PB90-128273 900,914
Measurements of Tribological Behavior of Advanced Materials: Summary of U.S. Results on VAMAS (Versailles	How to Estimate Capacity Dimension. PB89-172522	901,197	Method for Fitting and Smoothing Digital Data. PB90-128794 900,830
Advanced Materials and Standards) Round-Robin No. 2. PB90-130295 901,003	Laser Induced Fluorescence for Measurement of Concentrations in Pulping Liquors. PB89-172530	of Lignin 901,184	Allocating Staff to Tax Facilities: A Graphics-Based Microcomputer Allocation Model.
ATERIEL Hierarchically Controlled Autonomous Robot for Heavy	Designs for Assessment of Measurement Und		PB90-129891 900,645
Payload Military Field Applications. PB89-177075 901,271	Experience in the Eastern Lake Survey. PB89-173827	900,862	Polytope Volume Computation. PB90-129982 901,203
ATERIELS HANDLING	Variances Based on Data with Doad Time between		Monte Carlo Simulation of Domain Growth in the Kinetic
Hierarchically Controlled Autonomous Robot for Heavy Payload Military Field Applications.	Measurements. PB89-174049	901,204	Ising Model on the Connection Machine. PB90-136797 901,587

MECHANICAL ENGINEERING

		MECHANICAL ENGINEERING
Measuring the Root-Mean-Square Value of a Finite	PB90-118035 900,031	PB89-227946 901,281
Record Length Periodic Waveform. PB90-163924 901,588	Low Temperature Mechanical Property Measurements of	Precision Experiments to Search for the Fifth Force. PB89-228365 901,551
MATHEMATICS	Silica Aerogel Foam. PB90-128638 901,061	Determination of the Time-Dependence of ohm NBS (Na-
Internal Structure of the Guide to Available Mathematical Software.	MEASUREMENT INSTRUMENTS Improved Low-Energy Diffuse Scattering Electron-Spin	tional Bureau of Standards) Using the Quantized Hall Resistance.
PB89-170864 900,927	Polarization Analyzer.	PB89-230387 900,819
MATRICES (MATHEMATICS) Wavefront Matrix Multiplication on a Distributed-Memory	PB89-229173 900,218 MEASUREMENT SCIENCE & TECHNOLOGY	Measurement of the NBS (National Bureau of Standards) Electrical Watt in SI Units.
Multiprocessor. PB89-151807 900,646	CALIBRATION	PB89-230429 900,821
Note on the Capacitance Matrix Algorithm, Substructur-	NIST (National Institute of Standards and Technology) Measurement Services: Mass Calibrations.	New Realization of the Ohm and Farad Using the NBS (National Bureau of Standards) Calculable Capacitor.
ing, and Mixed or Neumann Boundary Conditions. PB89-177034 901,199	PB89-153894 900,874 NBS (National Bureau of Standards) Measurement Serv-	PB89-230445 901,557
MATRIX ISOLATION	ices: Calibration of Gamma-Ray-Emitting Brachytherapy	Antenna for Laser Gravitational-Wave Observations in Space.
Stabilization and Spectroscopy of Free Radicals and Reactive Molecules in Inert Matrices.	Sources. PB89-193858 901,243	PB89-234231 901,594
PB89-231252 900,484	NIST (National Institute of Standards and Technology)	Determination of Short Lifetimes with Ultra High Resolution (n,gamma) Spectroscopy.
Production and Spectroscopy of Molecular Ions Isolated	Calibration Services Users Guide. 1989 Edition. PB89-200216 900,926	PB90-123670 901,567
in Solid Neon.	International Comparison of Power Meter Calibrations Conducted in 1987.	Offset Criterion for Determining Superconductor Critical Current.
PB90-117748 900,503 Vibrational Spectra of Molecular lons Isolated in Solid	PB89-201545 900,718	PB90-128133 901,474
Neon. 2. O4(1+) and O4(1-). PB90-128729 900,533	NIST (National Institute of Standards and Technology) Measurement Services: The Calibration of Thermocou-	Improved Low-Level Silicon-Avalanche-Photodiode Transfer Standards at 1.064 Micrometers.
IEAN	ples and Thermocouple Materials. PB89-209340 900,897	PB90-130303 900,736
Minimax Approach to Combining Means, with Practical	NIST (National Institute of Standards and Technology)	MEASUREMENT SCIENCE & TECHNOLOGY: POLICY & STATE-OF-THE-ART SURVEYS
Examples. PB89-171847 901,211	Measurement Services: AC-DC Difference Calibrations. PB89-222616 900,818	Metrology for Electromagnetic Technology: A Bibliogra- phy of NBS (National Bureau of Standards) Publications.
IEAN DENSITY APPROXIMATION	International Intercomparison of Neutron Survey Instru-	PB89-147847 900,871
Mean Density Approximation and Hard Sphere Expansion Theory: A Review.	ment Calibrations. PB89-229165 901,300	NBS (National Bureau of Standards) Laser Power and Energy Measurements.
PB89-228019 901,546 IEAN FREE PATH	Josephson Array Voltage Calibration System: Operational	PB89-171680 901,346
Calculations of Electron Inelastic Mean Free Paths for 31	Use and Venfication. PB89-230403 900,820	NBS (National Bureau of Standards) Calibration Services: A Status Report.
Materials. 900,341	Guideline for Work Station Design.	PB89-173934 900,878
Electron Mean Free Path Calculations Using a Model Di-	PB90-112418 900,643 Silicon Photodiode Self-Calibration.	Development of Electrophoresis and Electrofocusing Standards.
electric Function. PB89-177026 901,141	PB90-118159 900,734	PB89-175863 900,195
IEASUREMENT	NIST (National Institute of Standards and Technology) Calibration Services, Users Guide: Fee Schedule.	Laboratory Accreditation Systems in the United States, 1984.
Thin Film Thermocouples for Internal Combustion En- gines.	PB90-127820 900,913	PB89-176432 900,882
PB89-147094 900,607	MEASUREMENT SCIENCE & TECHNOLOGY: PHYSICAL STANDARDS & FUNDAMENTAL CONSTANTS	Optical Power Measurements at the National Institute of Standards and Technology.
Microwave Measurements of the Thermal Expansion of a Spherical Cavity.	Microwave Measurements of the Thermal Expansion of a	PB89-187579 900,918
PB89-147458 900,291	Spherical Cavity. PB89-147458 900,291	Group Index and Time Delay Measurements of a Standard Reference Fiber.
Techniques for Measuring the Electromagnetic Shielding Effectiveness of Materials. Part 2. Near-Field Source Sim-	Possible Quantum Hall Effect Resistance Standard.	PB89-189179 . 900,752
ulation. PB89-161533 900,681	PB89-149058 900,801 Measurement Standards for Defense Technology.	Progress in Vacuum Standards at NBS (National Bureau of Standards).
Gravity Tide Measurements with a Feedback Gravity	PB89-150965 901,270	PB89-201198 900,999
Meter. PB89-171755 901,310	Comment on 'Possible Resolution of the Brookhaven and Washington Eotvos Experiments'.	Thermophysical Properties for Bioprocess Engineering. PB89-228068 900,043
Measurement of Partial Discharges in Hexane Under DC	PB89-171581 901,504	International Cooperation and Competition in Materials
Voltage. PB89-173421 900,833	Gravity Tide Measurements with a Feedback Gravity Meter.	Science and Engineering. PB89-228332 901,191
Measurement of Regenerator Ineffectiveness at Low	PB89-171755 901,310	Faraday Effect Sensors: The State of the Art.
Temperatures. PB89-173884 901,006	Twenty Five Years of Accuracy Assessment of the Atomic Weights.	PB89-231153 900,823
Journal of Research of the National Institute of Stand-	PB89-174007 900,365	MEASUREMENT STANDARDS Measurement Ouality Assurance.
ards and Technology. Volume 94, Number 2, March-April 1989.	Study of Long-Term Stability of Atomic Clocks. PB89-174098 900,367	PB89-147508 901,298
PB89-184089 900,887 NIST (National Institute of Standards and Technology)	NBS (National Bureau of Standards) Standards for Opti-	MEASUREMENTS Measurement Standards for Defense Technology.
Calibration Services Users Guide. 1989 Edition.	cal Power Meter Calibration. PB89-176200 900,726	PB89-150965 901,270
PB89-200216 900,926 Dielectric Measurements for Cure Monitoring.	New Internationally Adopted Reference Standards of Voltage and Resistance.	MEASURING INSTRUMENTS Special Calibration Systems for Reactive Gases and
PB89-200430 900,567	PB89-184097 900,808	Other Difficult Measurements.
Standard Reference Materials for Dimensional and Physical Property Measurements.	Current Research Efforts at JILA (Joint Institute for Laboratory Astrophysics) to Test the Equivalence Principle at	PB89-149215 900,873 Computer Program for Instrument Calibration at State-
PB89-201164 900,892	Short Ranges.	Sector Secondary-Level Laboratories. PB89-173496 900,877
Drift Tubes for Characterizing Atmospheric Ion Mobility Spectra Using AC, AC-Pulse, and Pulse Time-of-Flight	PB89-185912 901,522 NIST (National Institute of Standards and Technology)	ANA (Automatic Network Analyzer) Measurement Results
Measurement Techniques. PB89-202543 900,438	Measurement Services: High Vacuum Standard and Its	on the ARFTG (Automatic RF Techniques Group) Travel-
Length Scale Measurement Procedures at the National	Use. PB89-193841 <i>900,891</i>	ing Experiment. PB89-173777 900,715
Bureau of Standards. PB89-209266 900,895	AC-DC Difference Calibrations at NBS (National Bureau of Standards).	Calibration with Randomly Changing Standard Curves. PB89-186381 900,888
Thermal Conductivity Measurements of Thin-Film Silicon	PB89-201560 900,816	Narrow-Angle Laser Scanning Microscope System for
Dioxide. PB89-212195 901,444	Stability of the SI (International System) Unit of Mass as Determined from Electrical Measurements.	Linewidth Measurement on Wafers. PB89-189344 900,782
Computation and Use of the Asymptotic Covariance	PB89-201818 900,894	Laboratory Evaluation of an NBS (National Bureau of
Matrix for Measurement Error Models. PB89-215321 901,214	History of the Present Value of 2e/h Commonly Used for Defining National Units of Voltage and Possible Changes	Standards) Polymer Soil Stress Gage. PB89-211973 901,291
Alternative Techniques for Some Typical MIL-STD-461/	in National Units of Voltage and Resistance. PB89-202154 901,535	Advances in NIST (National Institute of Standards and
462 Types of Measurements. PB89-235139 901,272	New International Temperature Scale of 1990 (ITS-90).	Technology) Dielectric Measurement Capability Using a Mode-Filtered Cylindrical Cavity.
Journal of Research of the National Institute of Stand-	PB89-202550 901,238	PB89-231146 900,907
ards and Technology, Volume 94, Number 4, July-August 1989.	Length Scale Measurement Procedures at the National Bureau of Standards.	Apparatus for Neutron Scattering Measurements on Sheared Fluids.
PB89-235634 900,908	PB89-209266 900,895	PB89-235667 901,335
Implementation of an Automated System for Measuring Radiated Emissions Using a TEM Cell.	Liquid-Supported Torsion Balance: An Updated Status Report on Its Potential for Tunnel Detection.	MECHANICAL ENGINEERING Report on Interactions between the National Institute of
PB90-117698 901,377	PB89-212062 901,542	Standards and Technology and the American Society of
Interactions between Two Dividers Used in Simultaneous Comparison Measurements.	High-Precision Absolute Gravity Observations in the United States.	Mechanical Engineers. PB89-172563 901,004

ECHANICAL PROPERTIES	MERCURY INORGANIC COMPOUNDS	PB89-157986 901,135
Performance of Alumina/Epoxy Thermal Isolation Straps. PB89-147078 901,070	Biotransformation of Mercury by Bacteria Isolated from a River Collecting Cinnabar Mine Waters.	Microbiological Metal Transformations: Biotechnological Applications and Potential.
Standard Reference Materials for Dimensional and Physical Property Magneton	PB89-229280 900,864 MERCURY IONS	PB89-175947 901,284
cal Property Measurements. PB89-201164 900,892	Atomic-Ion Coulomb Clusters in an Ion Trap.	Element-Specific Epifluorescence Microscopy In vivo Monitoring of Metal Biotransformations in Environmental
Effect of Chemical Composition on the 4 K Mechanical Properties of 316LN-Type Alloys.	PB89-157424 901,494 Recoilless Optical Absorption and Doppler Sidebands of	Matrices. PB89-177216 901,220
PB90-128554 901,110	a Single Trapped Ion. PB89-171631 901,505	In situ Observation of Particle Motion and Diffusion Inter-
Low Temperature Mechanical Property Measurements of Silica Aerogel Foam.	Ion Trapping Techniques: Laser Cooling and Sympathetic	actions during Coarsening. PB89-201982 901,151
PB90-128638 901,061	Cooling. PB90-128034 901,578	Numerical Simulation of Morphological Development
Tests of Adhesive-Bonded Seams of Single-Ply Rubber	Laser Cooling to the Zero-Point Energy of Motion.	during Ostwald Ripening. PB89-201990 901,152
Membranes. PB89-212120 900,138	PB90-128091 901,581 MERCURY (METAL)	Quality Assurance in Metals Analysis Using the Inductive- ly Coupled Plasma.
ECHANICS: DESIGN/TESTING/MEASUREMENT	Speed of Sound in a Mercury Ultrasonic Interferometer	PB89-202063 900,213
Local Brittle Zones in Steel Weldments: An Assessment of Test Methods.	Manometer. PB89-202220 901,319	Diffraction Effects Along the Normal to a Grain Boundary. PB89-202089 901,153
PB89-149082 901,092 Postweld Heat Treatment Criteria for Repair Welds in 2-	MERCURY SPACECRAFT Conceptual Design for a Mercury Relativity Satellite.	Mossbauer Spectroscopy.
1/4Cr-1Mo Superheater Headers: An Experimental Study. PB89-156160 901,094	PB89-234249 901,595	PB89-211932 901,189 Development of a Method to Measure In situ Chloride at
Dynamic Young's Modulus Measurements in Metallic Ma-	METAL ALLOYS Kinetics of Resolidification.	the Coating/Metal Interface.
terials: Results of an Interlaboratory Testing Program. PB89-157671 901,132	PB89-176457 901,138	PB89-235345 901,085 Microbiological Materials Processing.
Conventional and Quarter-Point Mixed Elements in Linear	Ignition Characteristics of the Iron-Based Alloy UNS S66286 in Pressurized Oxygen.	PB90-123712 901,261
Elastic Fracture Mechanics. PB89-157788 901,481	PB89-189336 901,104 METAL CARBONYLS	Journal of Research of the National Institute of Standards and Technology. November-December 1989.
Dynamic Microindentation Apparatus for Materials Char-	Time Resolved Studies of Vibrational Relaxation Dynam-	Volume 94, Number 6. PB90-163874 900,542
acterization. PB89-176911 901,140	ics of CO(v= 1) on Metal Particle Surfaces. PB89-203012 900,444	METEOROLOGICAL DATA
Ferrite Number Prediction to 100 FN in Stainless Steel Weld Metal.	METAL COMPLEXES	Probabilistic Models for Ground Snow Accumulation. PB89-186894 900,100
PB89-201586 901,106	Effect of pH on the Emission Properties of Aqueous tris (2,6-dipicolinato) Terbium (III) Complexes.	METHACRYLATES
Higher Order Beam Finite Element for Bending and Vibration Problems.	PB89-157135 900,250 Population Relaxation of CO(v = 1) Vibrations in Solution	Oligomers with Pendant Isocyanate Groups as Tissue Adhesives, 2. Adhesion to Bone and Other Tissues.
PB89-229124 901,484	Phase Metal-Carbonyl Complexes.	PB89-231245 900,056
On-Line Arc Welding: Data Acquisition and Analysis Using a High Level Scientific Language.	PB89-157291 900,315 Rate Constants for the Quenching of Excited States of	METHACRYLOXYETHYL TRIMELLITATE ANHYDRIDE Adsorption of 4-Methacryloxyethyl Trimellitate Anhydride
PB90-117391 900,972	Metal Complexes in Fluid Solution. PB89-227797 900,461	(4-META) on Hydroxyapátité and Its Role in Composite Bonding.
Measurement of Applied J-Integral Produced by Residual Stress.	METAL HYDRIDES	PB89-179220 900,041
PB90-117631 900,163 EETINGS	Neutron Vibrational Spectroscopy of Disordered Metal Hydrogen Systems.	METHANE Far-Infrared Laser Magnetic Resonance Spectrum of Vi-
Proceedings of the Celebratory Symposium on a Decade	PB89-157499 900,324	brationally Excited C2H(1). PB89-147474 900,292
of UV (Ultraviolet) Astronomy with the IUE Satellite, Volume 2.	METAL OXIDE SEMICONDUCTORS Numerical Analysis for the Small-Signal Response of the	Chemical Structure of Methane/Air Diffusion Flames:
N89-16535/1 900,014 Proceedings of the Workshop on Cement Stabilization of	MOS (Metal Oxide Semiconductors) Capacitor. PB89-186837 900,781	Concentrations and Production Rates of Intermediate Hydrocarbons.
Low-Level Radioactive Waste. Held at Gaithersburg, Maryland on May 31-June 2, 1989.	METAL OXIDE TRANSISTORS	PB89-171904 900,590
NUREG/CP-0103 901,302	High-Mobility CMOS (Complementary Metal Oxide Semi- conductor) Transistors Fabricated on Very Thin SOS	Very Large Methane Jet Diffusion Flames. PB89-175913 900,593
Wind and Seismic Effects. Proceedings of the Joint Meeting of the U.SJapan Cooperative Program in Natural Re-	Films. PB89-230460 <i>900,791</i>	Comprehensive Study of Methane + Ethane System. PB89-176747 900,841
sources Panel on Wind and Seismic Effects (20th) Held in Gaithersburg, Maryland on May 17-20, 1988.	METAL PARTICLE COMPOSITES	Analysis of Roto-Translational Absorption Spectra In-
PB89-154835 900,157	Methods for the Production of Particle Standards. PB89-201636 901,047	duced in Low Density Gases of Non-Polar Molecules: The Methane Case.
Report of the Invitational Workshop on Integrity Policy in Computer Information Systems (WIPCIS).	METAL RECOVERY Microbiological Materials Processing.	PB89-201800 900,427
PB89-168009 900,670 Fire Safety Science-Proceedings of the First International	PB90-123712 901,261	Isochoric (p,v,T) Measurements on CO2 and (0.98 CO2 + 0.02 CH4) from 225 to 400 K and Pressures to 35
Symposium. PB89-179261 900,596	METALLIC GLASSES Neutron Vibrational Spectroscopy of Disordered Metal	MPa. PB89-202493 <i>900,435</i>
Executive Summary for the Workshop on Developing a	Hydrogen Systems. PB89-157499 <i>900,324</i>	Evaluated Kinetics Data Base for Combustion Chemistry.
Predictive Capability for CO Formation in Fires. PB89-200091 900,134	METALLIZING	PB89-212096 900,601 Thermophysical Properties of Methane.
Laser Induced Damage in Optical Materials: 1987.	Electromigration Damage Response Time and Implica- tions for dc and Pulsed Characterization.	PB89-222541 900,450
PB89-221162 901,364 NBS/BAM (National Bureau of Standards/Bundesanstalt	PB89-212179 901,443	Tables for the Thermophysical Properties of Methane. PB89-222608 900,843
fur Materialprufung) 1986 Symposium on Advanced Ce-	METALLURGY Institute for Materials Science and Engineering: Metallur-	Measurements of Molar Heat Capacity at Constant Volume: Cv,m(xCH4+ (1-x)C2H6' T = 100 to 320 K, p
ramics. PB89-229074 901,055	gy, Technical Activities 1988. PB89-201321 901,147	< or = 35 MPa).
Conference Reports: National Computer Security Conference (11th). Held in Baltimore, MD. on October 17-20,	METALS	PB90-117896 900,844 METHYL ALCOHOL
1988. PB89-235675 900,672	Institute for Materials Science and Engineering, Fracture and Deformation: Technical Activities 1988.	Relative Acidities of Water and Methanol and the Stabilities of the Dimer Anions.
Sensors and Measurement Techniques for Assessing	PB89-148399 901,071	PB89-150981 900,299
Structural Performance. PB89-235865 900,162	Corrosion of Metallic Implants and Prosthetic Devices. PB89-150890 900,053	Detection of Gas Phase Methoxy Radicals by Resonance Enhanced Multiphoton Ionization Spectroscopy.
ELT VISCOSITY	Solutal Convection during Directional Solidification. PB89-150932 901,322	PB89-156764 900,307
Viscosity of Blends of Linear annd Cyclic Molecules of Similar Molecular Mass.	Institute for Materials Science and Engineering, Nonde-	METHYL ALCOHOL LASERS New FIR Laser Lines and Frequency Measurements for
PB89-172480 900,555	structive Evaluation: Technical Activities 1988. PB89-151625 900,917	Optically Pumped CD3OH. PB89-175731 <i>901,350</i>
EMBRANE PROTEINS Nonlinear Effect of an Oscillating Electric Field on Mem-	Casting Metals: Reactor Response.	METHYL RADICALS
brane Proteins PB90-123407 901,249	PB89-157143 900,054 Picosecond Study of the Population Lifetime of CO(v = 1)	Methyl Radical Concentrations and Production Rates in a Laminar Methane/Air Diffusion Flame.
EMBRANES	Chemisorbed on SiO2-Supported Rhodium Particles. PB89-157317 900,317	PB89-171912 900,591
Influence of Reaction Reversibility on Continuous-Flow Extraction by Emulsion Liquid Membranes.	Phase Equilibrium in Two-Phase Coherent Solids.	METHYLAMINE Far-Infrared Spectrum of Methyl Amine. Assignment and
PB89-176481 900,244 Tests of Adhesive-Bonded Seams of Single-Ply Rubber	PB89-157580 900,330 Influence of Dislocation Density on the Ductile-Brittle	Analysis of the First Torsional State. PB89-161574 900,346
Membranes. PB89-212120 900,138	Transition in bcc Metals. PB89-157804 901,133	METHYLATION
ASTM (American Society for Testing and Materials) Com-	ASM/NBS (American Society for Metals/National Bureau	Global Biomethylation of the Elements - Its Role in the Biosphere Translated to New Organometallic Chemistry
mittee Completes Work on EPDM Specification. PB89-212260 900,140	of Standards) Numerical and Graphical Database for Binary Alloy Phase Diagrams.	and Biotechnology. PB90-136854 901,232

ETHYLPEROXY RADICALS	PB89-235634	900,908	Crazes and Fracture in Polymers. PB89-176085	000 562
Temperature Dependence of the Rate Constant for the Hydroperoxy + Methylperoxy Gas-Phase Reaction.	In Search of the Best Clock. PB90-117367	900,632	Kinetics of Resolidification.	900,562
PB90-136375 900,534	Progress on Spin Detectors and Spin-F		PB89-176457	901,138
ETROLOGY Metrology for Electromagnetic Technology: A Bibliogra-	Scattering from Na at NIST. PB90-128299	901,583	Replacement of Icosahedral Al-Mr PB89-186332	by Decagonal Phase. 901,146
phy of NBS (National Bureau of Standards) Publications. PB89-147847 900,871	Fundamental Physical Constants - 1986		Metallurgical Evaluation of 17-4 P	*
Submicrometer Optical Metrology.	PB90-136474	900,535	ings. PB89-193262	901,105
PB89-150973 900,771	Critical Current Measurements of Nb3 tors: NBS (National Bureau of Standard		Numerical Simulation of Morph	*
Optical Sensors for Robot Performance Testing and Calibration.	the VAMAS (Versailles Agreement on	Advanced Maten-	during Ostwald Ripening.	-
PB89-157358 900,987	als and Standards) Interlaboratory Comp PB90-136748	901,480	PB89-201990 Microstructural Variations in Rapid	901,152
Strategic Defense Initiative Space Power Systems Metrology Assessment.	Journal of Research of the National In		PB90-123621	901,170
PB89-173405 901,268	ards and Technology. November-E Volume 94, Number 6.		Pathways for Microstructural Deve	
NBS (National Bureau of Standards) Calibration Services:	PB90-163874	900,542	PB90-123779 MICROWAVE ANTENNAS	901,173
A Status Report. PB89-173934 900,878	Reduction of Uncertainties for Absolution Pressure Measurements in the Atmo		Brief History of Near-Field Measur	rements of Antennas at
Emerging Technologies in Electronics and Their Meas-	Range. PB90-163882	900.030	the National Bureau of Standards. PB89-156863	900.703
urement Needs. PB89-189245 900,811	Journal of Research of the Institutes of		Efficient and Accurate Method for	/
Center for Electronics and Electrical Engineering: Techni-	Technology. September-October 198 Number 5.		senting Power Density in the Ne Antennas.	
cal Progress Bulletin Covering Center Programs, January to March 1989, with 1989 CEEE Events Calendar.	PB90-213687	900,673	PB89-157457	900,707
PB89-209225 900,786	MICELLES		MICROWAVE EQUIPMENT	
Center for Electronics and Electrical Engineering Techni- cal Publication Announcements. Covering Center Pro-	Concentration Dependence of the Com of Isotactic Polystyrene/Cis-Decalin Gels		Microwave Energy for Acid Deco Temperatures and Pressures Usin	omposition at Elevated a Biological and Botan-
grams, October/December 1988, with 1989 CEEE Events	PB89-172449	900,552	ical Samples. PB89-171961	
Calendar. PB89-209241 900,787	MICROANALYSIS Application of Synergistic Microanalysi	s Tochniques to	Safety Guidelines for Microwave	900,359 Systems in the Analyti-
Center for Electronics and Electrical Engineering Techni-	the Study of a Possible New Mineral	Containing Light	cal Laboratory.	
cal Publication Announcements. Covering Center Programs, January-March 1989, with 1989 CEEE Events Cal-	Elements. PB89-147037	901,277	PB90-118167	900,689
endar.	Computer-Aided Imaging: Quantitative	e Compositional	Introduction to Microwave Acid De PB90-118191	900,227
PB89-228308 900,789 NIST (National Institute of Standards and Technology)	Mapping with the Electron Probe Microal PB89-157754	nalyzer. 901,073	Comparison of Microwave Dryi	ing and Conventional
Calibration Services, Users Guide: Fee Schedule.	Micro-Analysis of Mineral Saturation		Drying Techniques for Reference f PB90-123464	Vlaterials. 900,229
PB90-127820 900,913	during Lactic Acid Demineralization. PB89-186373		MICROWAVE SPECTRA	,
Journal of Research of the National Institute of Standards and Technology. November-December 1989.	Continuum Radiation Produced in Pure	901,253 Flement Targets	Infrared and Microwave Spectra HF.	of OCO-HF and SCO-
Volume 94, Number 6. PB90-163874 900,542	by 10-40 keV Electrons: An Empirical Mo	odel.	PB89-179121	900,389
ETROLOGY: PHYSICAL MEASUREMENTS	PB89-201610	900,209	Microwave Spectrum and Molecul	
Interpretation of a between-Time Component of Error in	Performance Standards for Microanalysis PB89-201651	900,211	ylene-Ozone van der Waals Comp PB89-201735	lex. 900,424
Mass Measurements. PB89-149108 900,872	MICROBIOLOGY		MICROWAVE SPECTROSCOPY	
Institute for Materials Science and Engineering, Nonde-	Microbiological Metal Transformations: Applications and Potential.	Biotechnological	Electric-Dipole Moments of CH3OH-Formamide.	H2O-Formamide and
structive Evaluation: Technical Activities 1988. PB89-151625 900,917	PB89-175947	901,284	PB89-147375	900,288
Resonance Light Scattering from a Liquid Suspension of	Microbiological Materials Processing. PB90-123712	901,261	Microwave Spectrum and (14)N	Quadrupole Coupling
Microspheres. PB89-157887 901,340	MICROCOMPUTERS	001,201	Constants of Carbazole. PB89-157333	900,319
AC Electric and Magnetic Field Meter Fundamentals.	Allocating Staff to Tax Facilities: A	Graphics-Based	Ozonolysis of Ethylene. Microway	
PB89-173470 900,746	Microcomputer Allocation Model, PB90-129891	900,645	Structure, and Dipole Moment of I ide (1,2,3-Trioxolane).	Ethylene Primary Ozon-
Apparent Diurnal Effects in the Global Positioning System.	MICRODOSIMETRY		PB89-157440	900,323
PB89-174080 901,292	Refinement of Neutron Energy Deposition metry Calculations.	on and Microdosi-	Structure of the CO2-CO2-H2O vi Determined by Microwave Spectro	
Journal of Research of the National Institute of Standards and Technology, Volume 94, Number 1, January-	PB89-150791	901,264	PB89-230288	900,479
February 1989. Special Issue: Numeric Databases in Ma-	MICROEMULSIONS Overtitative Characterization of the Vice	soits of a Missos	Electric-Resonance Optothermal Microwave Spectrum of the K=	
terials and Biological Sciences. PB89-175194 901,186	Quantitative Characterization of the Visc mulsion.	-	E((+ or -)2) States.	
Feasibility of Detector Self-Calibration in the Near Infra-	PB90-123597	900,524	PB90-117433	900,497
red. PB89-176788 <i>900,384</i>	MICROSCOPY Standard Reference Materials: Descrip	tion of the SRM	Microwave Spectrum of Methyl A Analysis of the First Torsional Stat	e.
Remote Sensing Technique for Combustion Gas Temper-	1965 Microsphere Slide. PB89-153704		PB90-117839	900,509
ature Measurement in Black Liquor Recovery Boilers. PB89-179568 900,392	Resonance Light Scattering from a Liqu	901,390 id Suspension of	Microwave Spectral Tables. 3. C10H10.	Hydrocarbons, CH to
Computer Model of a Porous Medium.	Microspheres.	· ·	PB90-126269	900,530
PB89-179683 901,188	PB89-157887 Metallurgical Evaluation of 17-4 PH Stai	901,340	Microwave Electric-Resonance Op py of (H2O)2.	otothermal Spectrosco-
Journal of Research of the National Institute of Standards and Technology. Volume 94, Number 2, March-April	Metallurgical Evaluation of 17-4 PH Stai ings.		PB90-128141	900,531
1989.	PB89-193262	901,105	MICROWAVES	Shormal Evenesis of
PB89-184089 900,887 Automated Calibration of Optical Photomask Linewidth	MICROSPHERES Standard Reference Materials: Descrip	tion of the SRM	Microwave Measurements of the 1 Spherical Cavity.	
Standards at the National Institute of Standards and	1965 Microsphere Slide. PB89-153704	901,390	PB89-147458	900,291
Technology. PB89-186340 901,315	Resonance Light Scattering from a Liqu		Microwave Power Standards. PB89-149272	900,687
Accurate RF Voltage Measurements Using a Sampling	Microspheres.		NIST (National Institute of Stand	lards and Technology)
Voltage Tracker. PB89-201552 900,815	PB89-157887 Resonance Light Scattering from a Si	901,340	Automated Coaxial Microwave Pov PB89-176192	ver Standard. 900,807
Speed of Sound in a Mercury Ultrasonic Interferometer	crospheres.		Acoustic and Microwave Resonan	ces Applied to Measur-
Manometer. PB89-202220 901,319	PB89-176234	901,352	ing the Gas Constant and the The ture.	ermodynamic Tempera-
Journal of Research of the National Institute of Stand-	MICROSTRIP TRANSMISSION LINES Two-Layer Dielectric Microstrip Line Stru	cture: SiO2 on Si	PB89-228548	901,320
ards and Technology, Volume 94, Number 3, May-June	and GaAs on Si; Modeling and Measure PB89-156780	ment.	Microwave Digestion of Biologic	al Samples: Selenium
1989. PB89-211106 <i>901,441</i>	MICROSTRUCTURE	900,738	Analysis by Electrothermal Atomic etry.	
Interpolation of Silicon Photodiode Quantum Efficiency as	Critical Assessment of Requirements for	Ceramic Powder	PB89-229116	900,217
an Absolute Radiometric Standard. PB89-212245 901,445	Characterization. PB89-146849	901,016	Development of a Microwave Sus the Sterilization of Dental Instrume	stained Gas Plasma for ents.
Journal of Physical and Chemical Reference Data,	Experimental Observations on the Initiat	ion of DIGM (Dif-	PB89-231278	900,047
Volume 18, Number 2, 1989. PB89-222525 900,448	fusion Induced Grain Boundary Migration PB89-157630	901,130	Monitoring and Predicting Parame solution.	eters in Microwave Dis-
Journal of Research of the National Institute of Stand-		licrostructure of	PB90-118183	900,690
ards and Technology, Volume 94, Number 4, July-August 1989.	Ba2YCu3O(6+ x). PB89-171821	901,035	Frequency Standards Utilizing Pen PB90-128042	ning Traps. 901,379
	, !	507,005	. 500 .50075	301,373

Thermo-Optic Designs for Microwave and Millimeter- Wave Electric-Field Probes.	PB89-221154 901,286 MINING EQUIPMENT	PB89-201578 <i>901,530</i> MOLECULAR BIOLOGY
PB90-128588 900,691 Radiometer Equation and Analysis of Systematic Errors	Mining Automation Real-Time Control System Architecture Standard Reference Model (MASREM).	New Directions in Bioinformatics. PB89-175269 901,24s
for the NIST (National Institute of Standards and Technology) Automated Radiometers.	PB89-221154 901,286 MIRRORS	MOLECULAR COLLISIONS
PB90-130907 900,832 IGRATIONS	 Use of Focusing Supermirror Neutron Guides to Enhance Cold Neutron Fluence Rates. 	Dynamics of Molecular Collisions with Surfaces: Excita tion, Dissociation, and Diffraction.
Migration of Liquid Film and Grain Boundary in Mo-Ni Induced by W Diffusion.	PB89-171946 901,306	PB89-175996 900,375 MOLECULAR COMPLEXES
PB89-157614 901,128 Directional Invariance of Grain Boundary Migration in the	MISSILE WARHEADS Metallurgical Evaluation of 17-4 PH Stainless Steel Cast-	Spectroscopic Signatures of Floppiness in Molecula Complexes.
Pb-Sn Cellular Transformation and the Tu-Turnbull Hysteresis.	ings. PB89-193262 <i>901,105</i>	PB89-227979 900,46
PB89-157911 <i>901,134</i>	MIXING Mixing Motions Produced by Pipe Elbows.	MOLECULAR CONFIGURATIONS Kinetics of Electron Transfer from Nitroaromatic Radica
IL-STD-462 Proficiency Testing for MIL-STD 462 NVLAP (National	PB89-161871 901,326 Dielectric Mixing Rules for Background Test Soils.	Anions in Aqueous Solutions. Effects of Temperature and Steric Configuration.
Voluntary Laboratory Accreditation Program) Laboratories.	PB89-188585 901,289	PB89-156749 900,308 MOLECULAR ENERGY LEVELS
PB90-128612 901,381 ILITARY COMMUNICATION	Importance of Isothermal Mixing Processes to the Under- standing of Lift-Off and Blow-out of Turbulent Jet Diffu-	Semiclassical Way to Molecular Dynamics at Surfaces.
Secure Military Communications Can Benefit from Accurate Time.	sion Flames. PB89-201172 900,598	PB89-157713 900,33: Near-Threshold X-ray Fluorescence Spectroscopy of Mol
PB89-176507 901,274 ILITARY EQUIPMENT	MIXING CIRCUITS Measurement of Integrated Tuning Elements for SIS	ecules. PB89-176523 900,382
New Standard Test Method for Eddy Current Probes. PB89-187587 900,981	Mixers with a Fourier Transform Spectrometer. PB89-157051 900,706	Effects of Velocity and State Changing Collisions or Raman Q-Branch Spectra.
Alternative Techniques for Some Typical MIL-STD-461/	MM Wave Quasioptical SIS Mixers. PB89-214738 901,446	PB89-179196 900,39
462 Types of Measurements. PB89-235139 <i>901,272</i>	MIXTURES	Quenching and Energy Transfer Processes of Single Ro tational Levels of Br2 B triplet Pi(O(sub u)(+)) v'= 24
ILITARY FACILITIES Thermal and Economic Analysis of Three HVAC (Heat-	Phase Contrast Matching in Lamellar Structures Com- posed of Mixtures of Labeled and Unlabeled Block Co-	with Ar under Single Collision Conditions. PB89-179766 900,399
ing, Ventilating, and Air Conditioning) System Types in a Typical VA (Veterans Administration) Patient Facility.	polymer for Small-Angle Neutron Scattering. PB89-157119 901,182	Scheme for a 60-nm Laser Based on Photopumping of a High Level of $Mo(6+)$ by a Spectral Line of $Mo(11+)$.
PB89-188619 900,847	Semi-Automated PVT Facility for Fluids and Fluid Mixtures.	PB89-186415 900,40
False Alarm Study of Smoke Detectors in Department of Veterans Affairs Medical Centers (VAMCS). PB89-193288 900.093	PB89-157184 900,875	Energy Levels of Molybdenum, Mo 1 through 42. PB89-186472 900,41
ILITARY MOBILIZING	Determination of Binary Mixture Vapor-Liquid Critical Den- sities from Coexisting Density Data. PB89-202170 901,536	Spectroscopic Detection Methods. PB89-228100 901,549
Analyzing the Economic Impacts of a Military Mobilization.	Development of a Field-Space Corresponding-States	State Selection via Optical Methods.
PB90-128067 <i>901,273</i>	Method for Fluids and Fluid Mixtures. PB89-227995 901,331	PB89-228118 901,550 MOLECULAR ORBITAL THEORY
Antenna Measurements for Millimeter Waves at the National Bureau of Standards.	Mean Density Approximation and Hard Sphere Expansion Theory: A Review.	Qualitative MO Theory of Some Ring and Ladder Polymers.
PB89-150726 900,694	PB89-228019 901,546	PB89-156723 900,303
Thermo-Optic Designs for Microwave and Millimeter- Wave Electric-Field Probes.	Improved Conformal Solution Theory for Mixtures with Large Size Ratios. PB89-228563 900,477	MOLECULAR ORBITALS Infrared Spectrum of NeHF.
PB90-128588 900,691 Radiometer Equation and Analysis of Systematic Errors	Properties of Lennard-Jones Mixtures at Various Tem-	PB89-171227 900,35: Wavelengths and Energy Levels of the K I Isoelectronic
for the NIST (National Institute of Standards and Technology) Automated Radiometers.	peratures and Energy Ratios with a Size Ratio of Two. PB89-235204 900,493	Sequence from Copper to Molybdenum. PB89-179097 901,372
PB90-130907 900,832	MODE FIELD DIAMETERS Comparison of Far-Field Methods for Determining Mode	MOLECULAR PHYSICS
Millisecond Pulsar Rivals Best Atomic Clock Stability. PB89-185722 900,629	Field Diameter of Single-Mode Fibers Using Both Gaussian and Petermann Definitions.	Center for Atomic, Molecular, and Optical Physics Tech nical Activities, 1989.
INE WATERS	PB90-117474 900,756 MODELS	PB90-133158 901,586 MOLECULAR RELAXATION
Biotransformation of Mercury by Bacteria Isolated from a River Collecting Cinnabar Mine Waters.	Analytical Model for the Steady-State and Transient	Time Resolved Studies of Vibrational Relaxation Dynam
PB89-229280 900,864 INERAL DEPOSITS	Characteristics of the Power Insulated-Gate Bipolar Transistor. PB89-146880 900,767	ics of CO(v= 1) on Metal Particle Surfaces. PB89-203012 900,444
Microbiological Metal Transformations: Biotechnological Applications and Potential.	Simplified Discrete Event Simulation Model for an IEEE	Picosecond Vibrational Energy Transfer Studies of Sur face Adsorbates.
PB89-175947 901,284	(Institute of Electrical and Electronics Engineers) 802.3 Local Area Network.	PB90-136573 900,533
Interlaboratory Comparison of the Guarded Horizontal Pipe-Test Apparatus: Precision of ASTM (American Soci-	PB89-186829 900,617 AIRNET: A Computer Program for Building Airflow Net-	Far-Infrared Spectrum of Methyl Amine. Assignment and
ety for Testing and Materials) Standard Test Method C- 335 Applied to Mineral-Fiber Pipe Insulation.	work Modeling. PB89-193254 <i>900,076</i>	Analysis of the First Torsional State. PB89-161574 900,346
PB89-218341 901,011	Validated Furniture Fire Model with FAST (HEMFAST). PB89-215354 900,142	Laser Probing of Product-State Distributions in Thermal Energy Ion-Molecule Reactions.
INERALIZATION Liposome Technology in Biomineralization Research.	Vapor-Liquid Equilibrium of Binary Mixtures in the Ex-	PB89-171250 900,350 Effects of Velocity and State Changing Collisions or
PB90-128117 901,230	tended Critical Region. I. Thermodynamic Model. PB89-218374 901,544	Raman Q-Branch Spectra. PB89-179196 900,39
Application of Synergistic Microanalysis Techniques to the Study of a Possible New Mineral Containing Light	Experimental Investigation and Modeling of the Flow Rate of Refrigerant 22 Through the Short Tube Restric-	Rydberg-Klein-Rees Inversion of High Resolution van de
Elements. PB89-147037 901,277	tor. PB89-229041 <i>901,118</i>	Waals Infrared Spectra: An Intermolecular Potentia Energy Surface for Ar + HF (v = 1). PB89-227953 900,468
Twenty Five Years of Accuracy Assessment of the Atomic Weights.	MODULUS OF ELASTICITY Dynamic Young's Modulus Measurements in Metallic Ma-	Microwave Spectral Tables. 3. Hydrocarbons, CH to
PB89-174007 900,365	terials: Results of an Interlaboratory Testing Program. PB89-157671 901,132	C10H10. PB90-126269 900,530
Pahasapaite, a Beryllophosphate Zeolite Related to Synthetic Zeolite Rho, from the Tip Top Pegmatite of South	Bulk Modulus and Young's Modulus of the Superconduc-	MOLECULAR SPECTROSCOPY
Dakota. PB89-186431 <i>901,288</i>	tor Ba2Cu3YO7. PB90-123613 901,469	Technical Activities 1986-1988, Molecular Spectroscopy Division. PB89-175418 900,37
Biophysical Aspects of Lipid Interaction with Mineral: Liposome Model Studies.	Measuring In-Plane Elastic Moduli of Composites with Arrays of Phase-Insensitive Ultrasound Receivers.	Electric-Resonance Optothermal Spectrum of (H2O)2
PB90-117508 901,228 INESWEEPERS (SHIPS)	PB90-136672 900,970 MOISTURE CONTENT	Microwave Spectrum of the $K= 1-0$ Subband for the $E((+ \text{ or } -)2)$ States.
Tensile Tests of Type 305 Stainless Steel Mine Sweeping Wire Rope.	Experimental Validation of a Mathematical Model for Pre- dicting Moisture Transfer in Attics.	PB90-117433 900,49: Heterodyne Measurements on N2O Near 1635 cm(-1).
PB90-130287 <i>901,112</i>	PB89-150783 900,057	PB90-117797 900,500
INIMAX TECHNIQUE Minimax Approach to Combining Means, with Practical	MOLECULAR BEAM EPITAXY Surface Structure and Growth Mechanism of Ga on	MOLECULAR STRUCTURE Radiation-Induced Crosslinks between Thymine and 2-D
Examples. PB89-171847 <i>901,211</i>	Si(100). PB89-149181 <i>901,387</i>	Deoxyerythropentose. PB89-146682 900,243
INING Mining Automation Real-Time Control System Architec-	MOLECULAR BEAMS Influence of the ac Stark Effect on Multiphoton Transi-	Microwave Spectrum and (14)N Quadrupole Coupling Constants of Carbazole.
ture Standard Reference Model (MASREM).	tions in Molecules.	PB89-157333 900,318

NATIONAL INSTITUTES OF HEALTH RADIATION ONCOLOGY

Ozonolysis of Ethylene. Microwave Spectrum, Molecular Structure, and Dipole Moment of Ethylene Primary Ozonide (1,2,3-Trioxolane).	PB89-156897 901,217 MOLTEN SALT ELECTROLYTES Structural Study of a Metastable BCC Phase in Al-Mn	PB89-179816 900,749 MULTIMODE FIBERS
PB89-157440 900,323 Shimanouch, Takehiko and the Codification of Spectros-	Alloys Electrodeposited from Molten Salts. PB89-201040 901,064	Numerical Aperture of Multimode Fibers by Several Methods: Resolving Differences. PB90-117482 900,757
copic Information. PB89-157846 <i>900,335</i>	MOLYBDENUM Fundamental Configurations in Ma IV Spectrum	MULTIPLICATION
Electron and Photon Stimulated Desorption: Probes of	Fundamental Configurations in Mo IV Spectrum. PB89-147011 900,284	Wavefront Matrix Multiplication on a Distributed-Memory Multiprocessor.
Structure and Bonding at Surfaces. PB89-157960 901,116	Influence of Molybdenum on the Strength and Toughness	PB89-151807 900,646
Chemical Structure of Methane/Air Diffusion Flames:	of Stainless Steel Welds for Cryogenic Service. PB89-173512 901,100	MULTIPROCESSORS Wavefront Matrix Multiplication on a Distributed-Memory
Concentrations and Production Rates of Intermediate Hydrocarbons.	Scheme for a 60-nm Laser Based on Photopumping of a	Multiprocessor.
PB89-171904 900,590	High Level of Mo(6+) by a Spectral Line of Mo(11+). PB89-186415	PB89-151807 900,646 Performance Measurement of a Shared-Memory Multi-
Comparative Modeling of Protein Structure: Progress and Prospects.	Energy Levels of Molybdenum, Mo 1 through 42.	processor Using Hardware Instrumentation.
PB89-175285 901,247	PB89-186472 900,411 MOLYBDENUM IONS	PB89-173793 900,636
Computational Analysis of Protein Structures: Sources, Methods, Systems and Results.	4s(2) 4p(2)-4s4p(3) Transition Array and Energy Levels of	Hardware Instrumentation Approach for Performance Measurement of a Shared-Memory Multiprocessor.
PB89-175293 900,010	the Germanium-Like Ions Rb VI - Mo XI. PB89-201065 901,528	PB89-186852 900,638
Polymer Localization by Random Fixed Impurities: Gaus-	MOLYBDENUM OXIDES	Processing Rate Sensitivities of a Heterogeneous Multi- processor.
sian Chains. PB89-176044 900,559	Structure of V9Mo6O40 Determined by Powder Neutron Diffraction.	PB89-229017 900,641
Defocus Modeling for Compositional Mapping with Wave-	PB90-117995 900,515	MUON-CATALYZED FUSION Intrinsic Sticking in dt Muon-Catalyzed Fusion: Interplay
length-Dispersive X-ray Spectrometry. PB89-176150 900,378	MONEL	of Atomic, Molecular and Nuclear Phenomena.
Structure and Dynamics of Molecular Clusters via High	Temperature Hysteresis in the Initial Susceptibility of Rapidly Solidified Monel.	PB90-117565 <i>901,561</i> MURAMIDASE
Resolution IR Absorption Spectroscopy. PB89-185896 900,403	PB90-123423 901,164	Biological Thermodynamic Data for the Calibration of Dif-
Water Structure in Crystalline Solids: Ices to Proteins.	MONITORS Dielectric Measurements for Cure Monitoring.	ferential Scanning Calorimeters: Heat Capacity Data on the Unfolding Transition of Lysozyme in Solution.
PB89-186746 900,413	PB89-200430 900,567	PB90-117920 900,513
Water Structure in Vitamin B12 Coenzyme Crystals. 1. Analysis of the Neutron and X-ray Solvent Densities.	Texture Monitoring in Aluminum Alloys: A Comparison of Ultrasonic and Neutron Diffraction Measurements.	MUTATIONS
PB89-186803 901,222	PB90-117409 901,159	Generation of Oxy Radicals in Biosystems. PB90-117888 901,266
Water Structure in Vitamin B12 Coenzyme Crystals. 2. Structural Characteristics of the Solvent Networks.	MONOCHROMATORS	NATIONAL DEFENSE
PB89-186811 901,223	Apparatus Function of a Prism-Grating Double Monochro- mator.	Measurement Standards for Defense Technology. PB89-150965 901,270
Microwave Spectrum and Molecular Structure of the Eth- ylene-Ozone van der Waals Complex.	PB89-186282 901,359	NATIONAL INSTITUTE OF STANDARDS AND
PB89-201735 900,424	MONOCLONAL ANTIBODIES Anti-T2 Monoclonal Antibody Immobilization on Quartz	TECHNOLOGY
Heterodyne Measurements on OCS Near 1372 cm(-1). PB89-201743 900,425	Fibers: Stability and Recognition of T2 Mycotoxin. PB90-128760 901,267	National Engineering Laboratory's 1989 Report to the National Research Council's Board on Assessment of
Comparison of Two Highly Refined Structures of Bovine	MONOFILAMENTS	NIST (National Institute of Standards and Technology)
Pancreatic Trypsin Inhibitor.	Mechanical Property Enhancement in Ceramic Matrix	Programs. PB89-189294 900,004
PB89-202204 901,248 Spectroscopic Signatures of Floppiness in Molecular	Composites. PB89-189138 <i>901,076</i>	NIST (National Institute of Standards and Technology)
Complexes.	MONOMOLECULAR FILMS	Research Reports, March 1989.
PB89-227979 900,467 Multiple Scattering in the X-ray Absorption Near Edge	AES and LEED Studies Correlating Description Energies with Surface Structures and Coverages for Ga on	****
Structure of Tetrahedral Germanium Gases.	Si(100). PB89-171599 901,401	Publications of the National Institute of Standards and Technology, 1988 Catalog.
PB89-228480 900,474	MONTE CARLO METHOD	PB89-218382 900,006
Structure of the CO2-CO2-H2O van der Waals Complex Determined by Microwave Spectroscopy.	Polymer Localization by Random Fixed Impurities: Gaus-	Technical Activities 1986-1988, Molecular Spectroscopy
PB89-230288 900,479	sian Chains. PB89-176044 900,559	Division. PB89-175418 <i>900,372</i>
MOLECULAR VIBRATION Far-Infrared Laser Magnetic Resonance Spectrum of Vi-	MOSFET	Federal Software Engineering Standards Program.
brationally Excited C2H(1). PB89-147474 900,292	Radiation-Induced Interface Traps in Power MOSFETs. PB89-201974 900,784	PB89-211965 900,666
Laser Probing of Product-State Distributions in Thermal-	MOSFET SEMICONDUCTORS	NBS (National Bureau of Standards) Life-Cycle Cost (NBSLCC) Program (for Microcomputers).
Energy Ion-Molecule Reactions.	Power MOSFET Failure Revisited. PB89-231237 900,796	PB89-151211 900,849
PB89-171250 900,353 Effects of Velocity and State Changing Collisions on	MOSSBAUER EFFECT	NBS (National Bureau of Standards) Calibration Services:
Raman Q-Branch Spectra.	Mossbauer Imaging.	A Status Report.
PB89-179196 900,391 Frequency Measurements of High-J Rotational Transi-	PB89-176895 901,242 Mossbauer Hyperfine Fields in RBa2(Cu0.97Fe0.03)3	PB89-173934 900,878
tions of OCS and N2O.	O(7-x)(R=Y,Pr,Er).	Data Bases Available at the National Institute of Standards and Technology Research Information Center.
PB90-136946 900,541	PB89-201206 901,429	PB89-160014 900,932
MOLECULAR WEIGHT Resonant Raman Scattering of Controlled Molecular	Mossbauer Spectroscopy. PB89-211932 901,189	Report on Interactions between the National Institute of
Weight Polyacetylene. PB89-157093 900,548	Mossbauer Imaging: Experimental Results.	Standards and Technology and the American Society of Mechanical Engineers.
Synthesis and Characterization of Poly(vinylmethyl ether).	PB90-123415 900,922 MOTOR VEHICLES	PB89-172563 901,004
PB89-161616 900,551	Mobile Sources of Atmospheric Polycyclic Aromatic Hy-	New Realization of the Ohm and Farad Using the NBS (National Bureau of Standards) Calculable Capacitor.
Viscosity of Blends of Linear annd Cyclic Molecules of Similar Molecular Mass.	drocarbons: A Roadway Tunnel Study. PB90-123571 900,859	PB89-230445 901,557
PB89-172480 900,555	MOYDITE	National Bureau of Standards Message Authentication
Influence of Molecular Weight on the Resonant Raman Scattering of Polyacetylene.	Moydite, (Y, REE) (B(OH)4)(CO3), a New Mineral Species	Code (MAC) Validation System. PB89-231021 900,671
PB89-179246 900,564	from the Evans-Lou Pegmatite, Quebec. PB89-157747 900,186	NIST (National Institute of Standards and Technology)
MOLECULE COLLISIONS	MULTI-ELEMENT ANALYSIS	Research Reports, June 1989. PB89-235113 900,007
Collision Induced Spectroscopy: Absorption and Light Scattering.	Evaluation of Data on Higher Heating Values and Elemental Analysis for Refuse-Derived Fuels.	Working Implementation Agreements for Open Systems
PB89-21Ž252 901,363	PB90-136839 900,845	Interconnection Protocols. PB89-235931 900,642
MOLECULE STRUCTURE Use of an Imaging Proportional Counter in Macromolecu-	MULTI-PHOTON PROCESSES Resonance-Enhanced Multiphoton Ionization of Atomic	Experiences in Environmental Specimen Banking.
lar Crystallography.	Hydrogen.	PB90-123969 900,866
PB90-136599 900,538 MOLECULES	PB89-201073 901,529 MULTICHARGED IONS	NIST (National Institute of Standards and Technology) Calibration Services, Users Guide: Fee Schedule.
Biological Macromolecule Crystallization Database: A	Branching Ratio Technique for Vacuum UV Radiance	PB90-127820 900,913
Basis for a Crystallization Strategy. PB90-136722 901,250	Calibrations: Extensions and a Comprehensive Data Set. PB90-128257 901,582	Report on Interactions between the National Institute of Standards and Technology and the Institute of Electrical
Bioseparations: Design and Engineering of Partitioning	MULTIMETERS	and Electronic Engineers.
Systems. PB90-136763 901,231	Electrical Performance Tests for Hand-Held Digital Multi- meters.	PB90-130899 900,831
MOLLUSCA	PB89-162234 900,876	NATIONAL INSTITUTES OF HEALTH RADIATION ONCOLOGY BRANCH
Sequential Determination of Biological and Pollutant Elements in Marine Bivalves.	MULTIMODE FIBER Profile Inhomogeneity in Multimode Graded-Index Fibers.	Air Quality Investigation in the NIH (National Institutes of Health) Radiation Oncology Branch.

PB89-228977 900,079 NATIONAL VOLUNTARY LABORATORY ACCREDITATION PROGRAM	PB89-171946 901,306 NEUTRON CHOPPERS Use of Multiple-Slot Multiple Disk Chopper Assemblies to	Apparatus for Neutron Scattering Measurements on Sheared Fluids. PB89-235667 901,335
NVLAP (National Voluntary Laboratory Accreditation Program) Assessment and Evaluation Manual. PB89-228324 900,903	Pulse Thermal Neutron Beams. PB89-147466 901,485	Small Angle Neutron Scattering Studies of Single Phase Interpenetrating Polymer Networks.
Proficiency Testing for MIL-STD 462 NVLAP (National Voluntary Laboratory Accreditation Program) Laborato-	NEUTRON COUNTERS Monte Carlo Calculated Response of the Dual Thin Scintillation Detector in the Sum Coincidence Mode.	PB90-123456 900,577 Neutron Scattering and Its Effect on Reaction Rates in
ries. PB90-128612 <i>901,381</i>	PB89-176549 901,299 NEUTRON CROSS SECTIONS	Neutron Absorption Experiments. PB90-123738 901,569
NATURAL CONVECTION Interzonal Natural Convection for Various Aperture Configurations.	Measurements of the (235)U (n,f) Standard Cross Section at the National Bureau of Standards.	NEUTRON SOURCES 2.5 MeV Neutron Source for Fission Cross Section Measurement.
PB89-176499 900,066	PB89-176556 901,305 NEUTRON DETECTORS	PB89-176531 <i>901,512</i>
NATURAL GAS Speed of Sound in Natural Gas Mixtures. PB89-174031 900,840	Advances in the Use of (3)He in a Gas Scintillation Counter. PB90-123506 901,565	NEUTRON SPECTROMETERS Small Angle Neutron Scattering Spectrometer at the National Bureau of Standards.
NBSR REACTOR	NEUTRON DIFFRACTION	PB89-158158 901,396 NEUTRON SPECTROSCOPY
NBS (National Bureau of Standards) Reactor: Summary of Activities July 1987 through June 1988. PB9-168017 901,304	Neutron Powder Diffraction Structure and Electrical Properties of the Defect Pyrochlores Pb1.5M2O6.5 (M= Nb, Ta).	Neutron Vibrational Spectroscopy of Disordered Metal Hydrogen Systems.
NECKING Necking Phenomera and Cold Drawing.	PB89-172431 900,363	PB89-157499 900,324 Chemical Physics with Emphasis on Low Energy Excita-
PB89-201495 900,975	Repulsive Regularities of Water Structure in Ices and Crystalline Hydrates. PB89-186753 900,414	tions. PB89-179659 900,396
Methodology for Electron Stimulated Desorption Ion An-	Exchange and Magnetostrictive Effects in Rare Earth Su-	NICKEL SOU, 350
gular Distributions of Negative Ions. PB89-231310 900,486	perlattices. PB89-202667 901,438	Angle Resolved XPS (X-ray Photoelectron Spectroscopy) of the Epitaxial Growth of Cu on Ni(100).
NEODYMIUM BARIUM CUPRATES Pressure Dependence of the Cu Magnetic Order in	Low-Q Neutron Diffraction from Supercooled D-Glycerol. PB89-228001	PB89-150866 901,389 Dependence of Interface Widths on Ion Bombardment
RBa2Cu3O6 + x. PB90-123829 901,472	Structure of V9Mo6O40 Determined by Powder Neutron Diffraction.	Conditions in SIMS (Secondary Ion Mass Spectrometry) Analysis of a Ni/Cr Multilayer Structure.
NEON Infrared Spectrum of NeHF.	PB90-117995 <i>900,515</i>	PB89-172506 900,364
PB89-171227 900,351	Use of Focusing Supermirror Neutron Guides to Enhance	Mesh Monitor Casting of Ni-Cr Alloys: Element Effects. PB89-176077 900,040
Nonadiabatic Theory of Fine-Structure Branching Cross- Sections for Sodium-Helium, Sodium-Neon, and Sodium- Argon Optical Collisions.	Cold Neutron Fluence Rates. PB89-171946 901,306 NEUTRON GUIDES	Temperature-Dependent Radiation-Enhanced Diffusion in Ion-Bombarded Solids. PB89-179188 901,408
PB89-202162 900,433 Production and Spectroscopy of Molecular Ions Isolated	Calculations and Measurement of the Performance of Converging Neutron Guides.	Electron Transmission Through NiSi2-Si Interfaces.
in Solid Neon. PB90-117748 900,503	PB89-211999 901,541	PB89-231294 900,485 Adsorption of Water on Clean and Oxygen-Predosed
NEON COMPLEXES	Analytical Applications of Neutron Depth Profiling.	Nickel(110). PB90-123555 900,522
Calculation of Vibration-Rotation Spectra for Rare Gas- HCI Complexes.	PB89-146872 901,294 Effect of Neutrons on the Characteristics of the Insulated	NICKEL ALLOYS
PB89-228415 900,473 Weakly Bound NeHF.	Gate Bipolar Transistor (IGBT). PB89-157655 900,773	Migration of Liquid Film and Grain Boundary in Mo-Ni Induced by W Diffusion. PB89-157614 901,128
PB90-118100 900,519 Slit Jet Infrared Spectroscopy of NeHF Complexes: Inter-	Numerical Simulations of Neutron Effects on Bipolar Transistors.	Dynamic Young's Modulus Measurements in Metallic Ma-
nal Rotor and J-Dependent Predissociation Dynamics. PB90-118126 900,520	PB90-123589 900,797	terials: Results of an Interlaboratory Testing Program. PB89-157671 901,132
NEOPLASMS	International Intercomparison of Neutron Survey Instru-	Grain Boundary Structure in Ni3AI. PB89-201784 901,150
Two-Photon Laser-Induced Fluorescence of the Tumor- Localizing Photosensitizer Hematoporphyrin Derivative, PB89-157283 901,240	ment Calibrations. PB89-229165 901,300 NEUTRON REACTIONS	Ignition Characteristics of the Nickel-Based Alloy UNS N07718 in Pressurized Oxygen.
NETWORK ANALYZERS Calibrating Network Analyzers with Imperfect Test Ports.	Initial Spectra of Neutron-Induced Secondary Charged Particles.	PB89-218333 901,154 Grain Boundary Characterization in Ni3Al.
PB90-117680 900,825 NETWORKS	PB89-171862 <i>901,265</i>	PB89-229306 901,156 Grain Boundary Structure in Ni3Al.
Small Angle Neutron Scattering Studies of Single Phase Interpenetrating Polymer Networks.	Applications of Mirrors, Supermirrors and Multilayers at	PB89-229314 901,157
PB90-123456 900,577	the National Bureau of Standards Cold Neutron Research Facility, PB89-211981 901,540	Rapid Solidification and Ordering of B2 and L2 (sub 1) Phases in the NiAl-NiTi System. PB90-123639 901,171
NEURAL NETS Neural Network Approach for Classifying Test Structure	NEUTRON SCATTERING	NICKEL CHROMIUM STEELS
Results. PB89-212187 900,788	Application of SANS (Small Angle Neutron Scattering) to Ceramic Characterization.	Low-Temperature Phase and Magnetic Interactions in fcc Fe-Cr-Ni Alloys.
NEUTRON ABSORPTION DCTDOS: Neutron and Gamma Penetration in Composite	PB89-146856 901,017 Phase Contrast Matching in Lamellar Structures Com-	PB90-136771 901,113 NICKEL CONTAINING ALLOYS
Duct Systems. PB89-188809 901,275	posed of Mixtures of Labeled and Unlabeled Block Co- polymer for Small-Angle Neutron Scattering.	Formation of Dispersoids during Rapid Solidification of an Al-Fe-Ni Alloy.
Neutron Scattering and Its Effect on Reaction Rates in	PB89-157119 901,182	PB90-123647 901,172
Neutron Absorption Experiments. PB90-123738 901,569	Temperature, Composition and Molecular-Weight De- pendence of the Binary Interaction Parameter of Polysty- rene/Poly(vinylmethylether) Blends.	NICKEL HYDRIDES Detection of the Free Radicals FeH, CoH, and NiH by
NEUTRON ACTIVATION ANALYSIS Radiochemical Procedure for Ultratrace Determination of	PB89-157473 900,550	Far Infrared Laser Magnetic Resonance. PB90-117342 900,495
Chromium in Biological Materials. PB89-156913 900,179	Small Angle Neutron Scattering from Porosity in Sintered Alumina.	NICKEL ISOTOPES Absolute Isotopic Abundance Ratios and Atomic Weight
Neutron Activation Analysis of the NIST (National Insti- tute of Standards and Technology) Bovine Serum Stand-	PB89-157564 901,026 Uniaxial Deformation of Rubber Network Chains by Small	of a Reference Sample of Nickel. PB90-163890 900,543
ard Reference Material Using Chemical Separations. PB89-156921 900,180	Angle Neutron Scattering. PB89-175830 901,088	Absolute Isotopic Composition and Atomic Weight of Ter-
Role of Neutron Activation Analysis in the Certification of NBS (National Bureau of Standards) Standard Reference	Pore Morphology Analysis Using Small Angle Neutron Scattering Techniques.	restrial Nickel. PB90-163908 900,544
Materials. PB89-157879 900,187	PB89-175939 901,037	NICKEL OXIDES Electron Diffraction Study of the Faceting of Tilt Grain
Radiochemical and Instrumental Neutron Activation Anal-	Significance of Multiple Scattering in the Interpretation of Small-Angle Neutron Scattering Experiments.	Boundaries in NiO. PB89-201792 901,431
ysis Procedures for the Determination of Low Level Trace Elements in Human Livers. PB89-171953 901,236	PB89-179626 901,409 Magnetic Correlations in an Amorphous Gd-Al Spin	NICKEL SILICIDES Floction Transmission Through NiSi2-Si Interfaces
NEUTRON BEAMS	Glass. PB89-201693 <i>901,148</i>	Electron Transmission Through NiSi2-Si Interfaces. PB89-231294 900,485
Use of Multiple-Slot Multiple Disk Chopper Assemblies to Pulse Thermal Neutron Beams.	Neutron Scattering Study of the Spin Ordering in Amor-	NIOBIUM Stable and Metastable Ti-Nb Phase Diagrams.
PB89-147466 901,485 Basic Data Necessary for Neutron Dosimetry.	phous Tb45Fe55 and Tb25Fe75. PB89-201701 901,149	PB89-157432 901,125 NIOBIUM IONS
PB89-171854 901,241	Shear Effects on the Phase Separation Behaviour of a Polymer Blend in Solution by Small Angle Neutron Scat-	4s(2) 4p(2)-4s4p(3) Transition Array and Energy Levels of
Use of Focusing Supermirror Neutron Guides to Enhance Cold Neutron Fluence Rates.	tering. PB89-229264 900,574	the Germanium-Like Ions Rb VI - Mo XI. PB89-201065 901,528

NUCLEAR PHYSICS & RADIATION TECHNOLOGY

IOBIUM STANNIDES	PB89-156749 900,305	PB90-112392 901,207
Nb3Sn Critical-Current Measurements Using Tubular Fi- berglass-Epoxy Mandrels.	NITROGEN OXIDE NO/NH3 Coadsorption on Pt(111): Kinetic and Dynamical	Merit Functions and Nonlinear Programming. PB90-123944 901,208
PB89-200497 901,527	Effects in Rotational Accommodation. PB89-201123 900,423	NONLINEAR SYSTEMS
VAMAS (Versailles Project on Advanced Materials and Standards) Intercomparison of Critical Current Measure-	NITROGEN OXIDE (N2O)	Nonlinear Effect of an Oscillating Electric Field on Membrane Proteins.
ment in Nb3Sn Wires. PB89-202147 901,534	Vibrationally Resolved Photoelectron Studies of the 7(sigma) (-1) Channel in N2O.	PB90-123407 901,249
Critical Current Measurements of Nb3Sn Superconduc-	PB89-176945 900,257	NONPOLAR GASES Analysis of Roto-Translational Absorption Spectra In-
tors: NBS (National Bureau of Standards) Contribution to the VAMAS (Versailles Agreement on Advanced Materi-	Infrared Spectra of Nitrous Oxide-HF Isomers. PB89-228399 900,471	duced in Low Density Gases of Non-Polar Molecules:
als and Standards) Interlaboratory Comparison. PB90-136748 901,480	Heterodyne Measurements on N2O Near 1635 cm(-1).	The Methane Case. PB89-201800 900,427
IOBIUM TITANIUM	PB90-117797 900,506	NORTH AMERICA
Effect of Room-Temperature Stress on the Critical Cur- rent of NbTi.	Frequency Measurements of High-J Rotational Transitions of OCS and N2O.	Trends for Building Technology in North America. PB89-174106 900,104
PB89-179832 901,414	PB90-136946 900,541 NITROGEN OXIDE (NO)	NSLS
ITRAMINES Picosecond Laser Study of the Collisionless Photodisso-	Optically Driven Surface Reactions: Evidence for the	Performance of a High-Energy-Resolution, Tender X-ray Synchrotron Radiation Beamline.
ciation of Dimethylnitramine at 266 nm.	Role of Hot Electrons. PB89-157937 900,338	PB90-128083 901,580
PB89-172423 900,255 TRATE RADICALS	Non-Boltzmann Rotational and Inverted Spin-Orbit State	NUCLEAR CROSS SECTIONS Initial Spectra of Neutron-Induced Secondary Charged
Rate Constants for Reactions of Nitrogen Oxide (NO3)	Distributions for Laser-Induced Desorption of NO from Pt(111).	Particles.
Radicals in Aquecus Solutions. PB89-176242 900,379	PB89-157952 900,340	PB89-171862 901,265 NUCLEAR ENERGY LEVELS
TRIC ACID	Observation of Translationally Hot, Rotationally Cold NO Molecules Produced by 193-nm Laser Vaporization of	Determination of Short Lifetimes with Ultra High Resolu-
Effects of Purified Ferric Oxalate/Nitric Acid Solutions as a Pretreatment for the NTG-GMA and PMDM Bonding	Multilayer NO Films. PB89-234264 900,491	tion (n,gamma) S pectroscopy. PB90-123670 901,567
System. PB89-146716 900,034	Photoacoustic Measurement of Differential Broadening of	NUCLEAR FUSION
Voltammetric and Liquid Chromatographic Identification	the Lambda Doublets in NO(X (2)Pi 1/2, v= 2-0) by Ar. PB90-117656 900,500	Intrinsic Sticking in dt Muon-Catalyzed Fusion: Interplay of Atomic, Molecular and Nuclear Phenomena.
of Organic Products of Microwave-Assisted Wet Ashing of Biological Samples.	NITROGEN OXIDES	PB90-117565 901,561
PB89-157994 900,188	Vibrational Predissociation of the Nitric Oxide Dimer. PB89-147417 900,289	NUCLEAR MAGNETIC RESONANCE
Infrared Spectrum of the nu6, nu7, and nu8 Bands of HNO3.	Rate Constants for Reactions of Nitrogen Oxide (NO3)	Solid State (13)C NMR Investigation in Polyoxetanes. Effect of Chain Conformation.
PB89-172415 900,362	Radicals in Aqueous Solutions. PB89-176242 900,379	PB89-176036 900,558
Infrared Spectrum of the 1205-cm(-1) Band of HNO3. PB89-228514 900,475	NITROGENS	Fast Magnetic Resonance Imaging with Simultaneously Oscillating and Rotating Field Gradients.
Ferric Oxalate with Nitric Acid as a Conditioner in an Ad-	Quantum Mechanical Calculations on the Ar(1+) + N2 Charge Transfer Reaction.	PB89-176903 901,514 Magnetic Resonance of (160)Tb Oriented in a Terbium
hesive Bonding System. PB89-229272 900,045	PB89-228092 900,470	Single Crystal at Low Temperatures.
TRIC OXIDE	Ionization and Current Growth in N2 at Very High Electric Field to Gas Density Ratios.	PB89-179204 901,519
Photoacoustic Measurement of Differential Broadening of the Lambda Doublets in NO(X (2)Pi 1/2, v= 2-0) by Ar.	PB89-228381 901,552 NITROMETHANE	Deutenum Magnetic Resonance Study of Orientation and Poling in Poly(Vinylidene Fluoride) and Poly(Vinylidene
PB90-117656 900,500	Effects of Pressure on the Vibrational Spectra of Liquid	Fluoride-Co-Tetrafluoroethylene). PB89-186365 900,565
TRIDES Dissociation Lifetimes and Level Mixing in Overtone-Ex-	Nitromethane. PB89-158026 900,342	13C NMR Method for Determining the Partitioning of End
cited HN3 (X tilde (sup 1) A'). PB90-117425 900,263	NITROPYRENES	Groups and Side Branches between the Crystalline and Non-Crystalline Regions in Polyethylene.
TRILES	Facile Synthesis of 1-Nitropyrene-d9 of High Isotopic Purity.	PB89-202451 900,569
Preparation of Multistage Zone-Refined Materials for Thermochemical Standards.	PB90-123753 900,240	NUCLEAR PHYSICS & RADIATION TECHNOLOGY Radiation-Induced Crosslinks between Thymine and 2-D-
PB89-186795 900,203	NON-NEWTONIAN FLUIDS Shear Dilatancy and Finite Compressibility in a Dense	Deoxyerythropentose. PB89-146682 900,247
TROGEN Rate Constants for the Reaction HO2+ NO2+ N2->	Non-Newtonian Liquid. PB89-174023 901,328	Hydroxyl Radical Induced Cross-Linking between Pheny-
HO2NO2+ N2: The Temperature Dependence of the	Prediction of Shear Viscosity and Non-Newtonian Behav-	lalanine and 2-Deoxyribose. PB89-147029 900,547
Fall-Off Parameters. PB89-146658 900,278	ior in the Soft-Sphere Liquid. PB89-228035 901,548	Use of Multiple-Slot Multiple Disk Chopper Assemblies to
Experimental Thermal Conductivity, Thermal Diffusivity,	NONDESTRUCTIVE TESTS	Pulse Thermal Neutron Beams. PB89-147466 901,485
and Specific Heat Values of Argon and Nitrogen. PB89-148407 900,293	Optical Nondestructive Evaluation at the National Bureau of Standards.	Dichromate Dosimetry: The Effect of Acetic Acid on the
Vapor-Liquid Equilibrium of Nitrogen-Oxygen Mixtures and Air at High Pressure.	PB89-146740 900,976	Radiolytic Reduction Yield. PB89-147490 900,248
PB89-174932 900,368	Application of SANS (Small Angle Neutron Scattering) to Ceramic Characterization.	Measurement Quality Assurance.
Laser-Induced Fluorescence Study of Product Rotational	PB89-146856 901,017	PB89-147508 901,298
State Distributions in the Charge Transfer Reaction: Ar(1+)((sup 2 P)(sub 3/2)) + N2 -> Ar + N2(1+)(X) at 0.28 and 0.40 eV.	Ultrasonic Texture Analysis for Polycrystalline Aggregates of Cubic Materials Displaying Orthotropic Symmetry.	QCD Vacuum. PB89-149124 901,486
PB89-189823 900,420	PB89-146948 901,121 Ultrasonic Characterization of Surface Modified Layers.	Refinement of Neutron Energy Deposition and Microdosi-
Thermal Conductivity of Nitrogen and Carbon Monoxide	PB89-147409 901,115	metry Calculations. PB89-150791 901,264
in the Limit of Zero Density. PB89-222533 900,449	Local Brittle Zones in Steel Weldments: An Assessment of Test Methods.	Detection of Uranium from Cosmos-1402 in the Strato- sphere.
Reduction of Uncertainties for Absolute Piston Gage Pressure Measurements in the Atmospheric Pressure	PB89-149082 901,092	PB89-156962 901,592
Range.	Institute for Materials Science and Engineering, Nonde- structive Evaluation: Technical Activities 1988.	Activation Analysis Opportunities Using Cold Neutron Beams.
PB9-0163882 900,030 TROGEN ADDITIONS	PB89-151625 900,917	PB89-156970 900,183
Linear-Elastic Fracture of High-Nitrogen Austenitic Stain-	Optical Roughness Measurements for Industrial Surfaces. PB89-176655 900,979	Resonant Raman Scattering of Controlled Molecular Weight Polyacetylene.
less Steels at Liquid Helium Temperature. PB90-117623 901,108	Transmission Loss through 6061 T-6 Aluminum Using a	PB89-157093 900,548
Nitrogen in Austenitic Stainless Steels.	Pulsed Eddy Current Source. PB89-179840 901,143	Phase Contrast Matching in Lamellar Structures Com- posed of Mixtures of Labeled and Unlabeled Block Co-
PB90-117649 901,109 TROGEN DIOXIDE	Sensors for Intelligent Processing of Materials.	polymer for Small-Angle Neutron Scattering. PB89-157119 901,182
Rate Constants for the Reaction HO2+ NO2+ N2->	PB89-202006 900,920 Acoustic Emission: A Quantitative NDE Technique for the	Free-Electron-Like Stoner Excitations in Fe.
HO2NO2 + N2: The Temperature Dependence of the Fall-Off Parameters.	Study of Fracture.	PB89-158059 901,393
PB89-146658 900,278 High Resolution Spectrum of the pursub 1) pursub 2)	PB89-211924 900,921 NDE (Nondestructive Evaluation) Publications, 1985.	Recent Progress on Spectral Data for X-ray Lasers at the National Bureau of Standards.
High Resolution Spectrum of the nu(sub 1) + nu(sub 2) Band of NO2. A Spin Induced Perturbation in the Ground	PB89-229025 900,984	PB89-158091 901,341
State. PB89-187561 900,417	Institute for Materials Science and Engineering, Nonde- structive Evaluation: Technical Activities, 1989.	Atomic Transition Probabilities of Argon: A Continuing Challenge to Plasma Spectroscopy.
Synergistic Effects of Nitrogen Dioxide and Carbon Diox-	PB90-132739 900,925	PB89-158125 900,344
ide Following Acute Inhalation Exposures in Rats. PB89-214779 900,856	NONEQUILIBRIUM FLOW Non-Equilibrium Theories of Electrolyte Solutions.	NBS (National Bureau of Standards) Decay-Scheme Investigations of (82)Sr-(82)Rb.
TROGEN ORGANIC COMPOUNDS	PB89-174940 900,369	PB89-161558 901,498
Kinetics of Electron Transfer from Nitroaromatic Radical Anions in Aqueous Solutions. Effects of Temperature and	NONLINEAR PROGRAMMING FACTUNC: A User-Friendly System for Unconstrained	NBS (National Bureau of Standards) Reactor: Summary of Activities July 1987 through June 1988.
Steric Configuration.	Optimization.	PB89-168017 901,304

Basic Data Necessary for Neutron Dosimetry.	PB90-117995 900,515	OCTANOLS
PB89-171854 901,241	(109)Pd and (109)Cd Activity Standardization and Decay	Octanol-Water Partition Coefficients of Simple Organic
Initial Spectra of Neutron-Induced Secondary Charged Particles.	Data. PB90-123449 901,564	Compounds. PB90-126244 900,528
PB89-171862 901,265	Advances in the Use of (3)He in a Gas Scintillation	OCTREES
NBS (National Bureau of Standards) Radon-in-Water Standard Generator.	Counter. PB90-123506 901,565	Modeling Dynamic Surfaces with Octrees. PB90-112335 901,206
PB89-171888 901,295 Use of Focusing Supermirror Neutron Guides to Enhance	Electron Stopping Powers for Transport Calculations.	OFFICE BUILDINGS
Cold Neutron Fluence Rates.	PB90-123605 901,566 Neutron Scattering and Its Effect on Reaction Rates in	Progressive Collapse: U.S. Office Building in Moscow. PB89-175715 900,158
PB89-171946 901,306 Aluminumlike Spectra of Copper through Molybdenum.	Neutron Absorption Experiments.	Brick Masonry: U.S. Office Building in Moscow.
PB89-172365 900,360	PB90-123738 901,569 Neonlike Ar and Cl 3p-3s Emission from a theta-pinch	PB89-187504 900,160
Computer Program for Instrument Calibration at State- Sector Secondary-Level Laboratories.	Plasma.	Evaluating Office Lighting Environments: Second Level Analysis.
PB89-173496 900,877	PB90-123746 901,570 Applications of ETRAN Monte Carlo Codes.	PB89-189153 900,073
2.5 MeV Neutron Source for Fission Cross Section Measurement.	PB90-123902 901,574	Investigation of a Washington, DC Office Building. PB89-230361 900.081
PB89-176531 901,512	Cross Sections for Bremsstrahlung Production and Elec- tron-Impact Ionization.	Post-Occupancy Evaluation of Several U.S. Government
Monte Carlo Calculated Response of the Dual Thin Scintillation Detector in the Sum Coincidence Mode.	PB90-123910 901,575	Buildings. PB90-112384 900,088
PB89-176549 901,299	Overview of ETRAN Monte Carlo Methods. PB90-123928 901,576	Measured Air Infiltration and Ventilation Rates in Eight
Measurements of the (235)U (n,f) Standard Cross Section at the National Bureau of Standards.	Performance of a High-Energy-Resolution, Tender X-ray	Large Office Buildings. PB90-128158 900,090
PB89-176556 901,305	Synchrotron Radiation Beamline. PB90-128083 901,580	OFFICE EQUIPMENT
Characteristics of Ge and InGaAs Photodiodes. PB89-176796 900,729	Pattern Recognition Approach in X-ray Fluorescence	Guideline for Work Station Design. PB90-112418 900,643
Vibrationally Resolved Photoelectron Studies of the	Analysis. PB90-128786 900,234	OFFSHORE DRILLING
7(sigma) (-1) Channel in N2O. PB89-176945 900,257	Center for Radiation Research (of the National Institute	Alaska Arctic Offshore Oil Spill Response Technology
Vibrationally Resolved Photoelectron Angular Distribu-	of Standards and Technology) Technical Activities for 1989.	Workshop Proceedings. PB89-195663 900,842
tions for H2 in the Range 17 eV < or = h(nu) < or = 39 eV.	PB90-130279 901,307	OFFSHORE STRUCTURES
PB89-176952 900,385	Report on the 1989 Meeting of the Radionuclide Measurements Section of the Consultative Committee on	Local Brittle Zones in Steel Weldments: An Assessment of Test Methods.
Wavelengths and Energy Levels of the K I Isoelectronic Sequence from Copper to Molybdenum.	Standards for the Measurement of Ionizing Radiations:	PB89-149082 901,092
PB89-179097 901,372	Special Report on Standards for Radioactivity. PB90-163916 900,545	Hydrodynamic Forces on Vertical Cylinders and the Lighthill Correction.
Spectra and Energy Levels of the Galliumlike Ions Rb VII- Mo XII.	NUCLEAR WEAPONS	PB90-117417 901,313
PB89-179105 900,387	DCTDOS: Neutron and Gamma Penetration in Composite Duct Systems.	OHM
Significance of Multiple Scattering in the Interpretation of Small-Angle Neutron Scattering Experiments.	PB89-188809 901,275	Determination of the Time-Dependence of ohm NBS (National Bureau of Standards) Using the Quantized Hail Re-
PB89-179626 901,409	NUCLEATION Undercooling and Microstructural Evolution in Glass	sistance. PB89-230387 900,819
Oxygen Partial-Density-of-States Change in the YBa2Cu3Ox Compounds for x(Approx.)6,6.5,7 Measured	Forming Alloys.	OIL POLLUTION
by Soft X-ray Emission. PB89-186274 901,419	PB89-176465 901,139 Nucleation and Growth of Aperiodic Crystals in Aluminum	Alaska Arctic Offshore Oil Spill Response Technology Workshop Proceedings.
Comprehensive Dosimetry for Food Irradiation.	Alloys.	PB89-195663 900,842
PB89-186399 900,011	PB89-186324 901,145 NUCLEONS	OIL SPILLS
Scheme for a 60-nm Laser Based on Photopumping of a High Level of Mo(6+) by a Spectral Line of Mo(11+).	Comment on 'Feasibility of Measurement of the Electro-	Combustion of Oil on Water. PB89-149173 900,587
PB89-186415 900,407	magnetic Polarizability of the Bound Nucleon'. PB90-117730 901,563	Alaska Arctic Offshore Oil Spill Response Technology
Quasifree Electron Scattering on Nucleons in a Momentum-Dependent Potential.	NUMERICAL ANALYSIS	Workshop Proceedings. PB89-195663 900,842
PB89-186738 901,524	Error Bounds for Linear Recurrence Relations. AD-A201 256/5 901,192	OLIGOMERS
Dynamical Diffraction of X-rays at Grazing Angle, PB89-186886 901,421	Numerical Computation of Particle Trajectories: A Model	Oligomers with Pendant Isocyanate Groups as Adhesives for Dentin and Other Tissues.
Research Opportunities Below 300 nm at the NBS (National Bureau of Standards) Free-Electron Laser Facility.	Problem. PB89-158117 901,324	PB89-179253 900,042
PB89-192678 901,360	NUMERICAL DATA BASES	ON-LINE PROGRAMMING On-Line Concurrent Simulation in Production Scheduling.
4s(2) 4p(2)-4s4p(3) Transition Array and Energy Levels of the Germanium-Like lons Rb VI - Mo XI.	Journal of Research of the National Institute of Standards and Technology, Volume 94, Number 1, January-	PB89-172605 900,948
PB89-201065 901,528	February 1989. Special Issue: Numeric Databases in Ma-	ON LINE SYSTEMS
Resonance-Enhanced Multiphoton Ionization of Atomic Hydrogen.	terials and Biological Sciences. PB89-175194 901,186	Internal Structure of the Guide to Available Mathematical Software.
PB89-201073 901,529	Importance of Numeric Databases to Materials Science.	PB89-170864 900,927
Computation of the ac Stark Effect in the Ground State of Atomic Hydrogen.	PB89-175202 901,187 NIST (National Institute of Standards and Technology)/	OPEN SYSTEMS INTERCONNECTION Stable Implementation Agreements for Open Systems
PB89-202535 901,538	Sandia/ICDD Electron Diffraction Database: A Database	Interconnection Protocols. Version 2, Edition 1. December 1988.
Applications of Mirrors, Supermirrors and Multilayers at the National Bureau of Standards Cold Neutron Research	for Phase Identification by Electron Diffraction. PB89-175210 901,508	PB89-193312 900,618
Facility. PB89-211981 901,540	Numeric Databases in Chemical Thermodynamics at the National Institute of Standards and Technology.	User Guide for the NBS (National Bureau of Standards) Prototype Compiler for Estelle (Revised).
Simplified Shielding of a Metallic Restoration during Radi-	PB89-175228 900,371	PB89-196158 900,619
ation Therapy. PB89-229256 900,044	Numeric Databases for Chemical Analysis. PB89-175236 900,194	Working Implementation Agreements for Open Systems Interconnection Protocols.
Cross Section and Linear Polarization of Tagged Pho-	Structural Ceramics Database: Technical Foundations.	PB89-235931 900,642
tons. PB90-117292 <i>901,560</i>	PB89-175244 901,036	OPEN SYSTEMS INTERCONNECTIONS
Method for Evaluating Air Kerma and Directional Dose	Applications of the Crystallographic Search and Analysis System CRYSTDAT in Materials Science.	Ongoing Implementation Agreements for Open Systems Interconnection Protocols: Continuing Agreements.
Equivalent for Currently Available Multi-Element Dosemeters in Radiation Protection Dosimetry.	PB89-175251 901,402	PB89-166086 900,610
PB90-117532 901,301	NUTRITION NBS (National Bureau of Standards) Activities in Biologi-	OPERATING SYSTEMS (COMPUTERS) ZIP: The ZIP-Code Insulation Program (Version 1.0) Eco-
Intrinsic Sticking in dt Muon-Catalyzed Fusion: Interplay of Atomic, Molecular and Nuclear Phenomena.	cal Reference Materials.	nomic Insulation Levels for New and Existing Houses by Three-Digit ZIP Code. Users Guide and Reference
PB90-117565 901,561	PB89-157770 <i>901,219</i> O STARS	Manual.
Chlorine-like Spectra of Copper to Molybdenum. PB90-117706 900,501	Stellar Winds of 203 Galactic O Stars: A Quantitative Ul-	PB89-151765 900,058
Comment on 'Feasibility of Measurement of the Electro-	traviolet Survey. PB89-202626 900,022	OPERATIONS Assessment of Robotics for Improved Building Oper-
magnetic Polarizability of the Bound Nucleon'. PB90-117730 901,563	OCEAN WAVES	ations and Maintenance. PB89-189146 900,092
Analysis of Magnesiumlike Spectra from Cu XVIII to Mo	Wind and Seismic Effects. Proceedings of the Joint Meeting of the U.SJapan Cooperative Program in Natural Re-	OPTICAL ACTIVITY
XXXI. PB90-117821 900,508	sources Panel on Wind and Seismic Effects (20th) Held	Optical Rotation.
Use of Thorium as a Target in Electron-Spin Analyzers.	in Gaithersburg, Maryland on May 17-20, 1988. PB89-154835 900,157	PB89-149256 900,294 OPTICAL COMMUNICATION
PB90-117938 900,912	OCTACALCIUM PHOSPHATE	Waveguide Loss Measurement Using Photothermal De-
Structure of V9Mo6O40 Determined by Powder Neutron Diffraction.	Mechanism of Hydrolysis of Octacalcium Phosphate. PB89-201503 901,254	flection. PB89-157028 900,739

Fast Optical Detector Deposited on Dielectric Channel	PB89-147425 901,194	PB89-156772 900,308
Waveguides. PB89-171706 900,743	ORGANIC COMPOUNDS	Cr(110) Oxidation Probed by Carbon Monoxide Chemis-
System for Measuring Optical Waveguide Intensity Pro	Specimen Banking in the Netionel Status end Trends Progrem: Development of Protocols end First Year Re-	orption. PB89-228423 900,239
files.	sults.	OXYGEN SSO,255
PB89-188593 900,75	PB89-175855 901,308	Evaluated Chemical Kinetic Data for the Reactions of
OPTICAL DETECTION Optical Fiber Sensors for the Measurement of Electro	Octanol-Water Partition Coefficients of Simple Organic Compounds.	Atomic Oxygen O(3P) with Sulfur Containing Compounds. PB89-145122 900,269
magnetic Quantities.	PB90-126244 900,528	
PB89-176671 900,748	ORGANIC PHOSPHATES	Reections of Magnesium Prophyrin Radical Cations in Water. Disproportionation, Oxygen Production, and Com-
OPTICAL DETECTORS Picosecond Pulse Response from Hydrogenated Amor	Thermodynamic and Transport Properties of Cerbohy- drates and Their Monophosphetes: The Pentoses end	parison with Other Metalloporphyrins. PB89-151005 900,301
phous Silicon (a-Si:H) Optical Detectors on Channel Wa	Hexoses.	
veguides. PB89-176689 900,727	PB89-222574 900,453 ORGANIZATIONS	Semiconductor Measurement Technology: Automatic De- termination of the Interstitial Oxygen Content of Silicon
Blocked Impurity Band and Superlattice Detectors: Pros-	Directory of International end Regional Organizations	Wafers Polished on Both Sides. PB89-151831 900,772
pects for Rediometry. PB89-212161 900,730	Conducting Stendards-Related Activities. PB89-221147 900.008	Decey of High Valent Manganese Porphyrins in Aqueous
OPTICAL FIBERS	ORGANOMETALLIC COMPOUNDS	Solution and Catalyzed Formation of Oxygen.
Interferometric Dispersion Measurements on Small	Trace Speciation by HPLC-GF AA (High-Performance	PB89-156772 900,308
Guided-Wave Structures. PB89-173959 901,345	Liquid Chromatography-Graphite Furnace Atomic Absorp- tion) for Tin- and Lead-Bearing Organometallic Com-	Oxygen Isotope Effect in the Superconducting Bi-Sr-Ca- Cu-O System.
Optical Fiber Sensors for Electromagnetic Quantities.	pounds, with Signal Increases Induced by Transition-	PB89-157044 901,025
PB89-173967 900,725	Metal lons. PB89-157085 900,184	Synchrotron Radiation Study of BaO Films on W(001)
Optical Nevelty Filters	Global Biomethylation of the Elements - Its Role in the	and Their Interaction with H2O, CO2, and O2. PB89-157697 900,252
Optical Novelty Filters. PB89-228084 901,366	Biosphere Translated to New Organometallic Chemistry	Vapor-Liquid Equilibrium of Nitrogen-Oxygen Mixtures and
OPTICAL INTERFEROMETERS	and Biotechnology. PB90-136854 901,232	Air at High Pressure.
Microarcsecond Optical Astrometry: An Instrument and	ORIENTED NUCLEI	PB89-174932 900,368
Its Astrophysical Applications. PB89-171268 900,013	Magnetic Resonance of (160)Tb Oriented in a Terbium	Ignition Characteristics of the Iron-Based Alloy UNS S66286 in Pressurized Oxygen.
OPTICAL LENSES	Single Crystal at Low Temperatures. PB89-179204 901,519	PB89-189336 901,104
Fresnel Lenses Display Inherent Vignetting. PB89-157069 901,337	ORIFICE FLOW	Pure Rotational Far Infrared Transitions of (16)O2 in Its
DPTICAL MATERIALS	Effect of Pipe Roughness on Orifice Flow Measurement.	Electronic and Vibrational Ground State. PB89-202055 900,429
Group Index and Time Delay Measurements of a Stand-	PB89-231484 901,333 ORIFICE METERS	Fundamental Characterization of Clean and Gas-Dosed
ard Reference Fiber. PB89-189179 900,752	Measurements of Coefficients of Discharge for Concen-	Tin Oxide.
Laser Induced Damage in Optical Materials: 1987.	tric Flange-Tapped Square-Edged Onfice Meters in Water Over the Reynolds Number Range 600 to 2,700,000.	,
PB89-221162 901,364	PB89-235147 901,334	Oxygen Chemisorption on Cr(110): 1. Dissociative Adsorption.
OPTICAL MEASUREMENT	Optimum Location of Flow Conditioners in a 4-Inch Ori-	PB89-202980 900,441
Optical Nondestructive Evaluation et the National Bureau of Standards.	fice Meter. PB90-111675 900,911	Oxygen Chemisorption on Cr(110): 2. Evidence for Mo-
PB89-146740 900,976	ORION A	lecular O2(ads). PB89-202998 900,442
Optical Roughness Measurements for Industrial Surfaces. PB89-176655 900,975	Millimeter- and Submillimeter-Wave Surveys of Orion A	Semiconductor Measurement Technology: Database for
Spatial Filtering Microscope for Linewidth Measurements.	Emission Lines in the Ranges 200.7-202.3, 203.7-205.3, and 330-360 GHz.	and Statistical Analysis of the Interlaboratory Determina-
PB89-230346 901,366	PB90-123787 900,029	tion of the Conversion Coefficient for the Measurement of the Interstitial Oxygen Content of Silicon by Infrared
DPTICAL MEASUREMENTS	OSCILLATOR STRENGTHS	Absorption. PB89-221170 901,054
Submicrometer Optical Metrology. PB89-150973 900,771	Calculation of Tighter Error Bounds' for Theoretical Atomic-Oscillator Strengths.	Cross Sections for Collisions of Electrons and Photons
OPTICAL MEASURING INSTRUMENTS	PB89-158109 901,496	with Oxygen Molecules.
Opticel Sensors for Robot Performance Testing and Cali-	OSTWALD RIPENING	PB89-226575 900,457
bration. PB89-157358 900,987	In situ Observation of Particle Motion and Diffusion Inter- actions during Coarsening.	Interaction of Oxygen and Platinum on W(110). PB89-231302 901,158
Optical Fiber Sensors for Electromagnetic Quantities.	PB89-201982 901,151	Interlaboratory Determination of the Calibration Factor for
PB89-173967 900,725	Numerical Simulation of Morphological Development	the Measurement of the Interstitial Oxygen Content of
PTICAL MICROSCOPES Section Filtering Microscope for Linewidth Magguraments	during Ostwald Ripening. PB89-201990 901,152	Silicon by Infrared Absorption. PB90-117300 900,224
Spatial Filtering Microscope for Linewidth Measurements. PB89-230346 901,368	OVENS	Generation of Oxy Radicals in Biosystems.
OPTICAL MOLASSES	Analysis of High Performance Compensated Thermal En-	PB90-117888 901,266
Search for Optical Molasses in a Vapor Cell: Genera Analysis and Experimental Attempt.	closures. PB89-185748 <i>901,008</i>	OXYGEN IONS
PB90-163932 901,371	Comparison of Microwave Drying and Conventional	Vibrational Spectra of Molecular lons Isolated in Solid Neon. 2. O4(1+) and O4(1-).
OPTICAL PROPERTIES	Drying Techniques for Reference Materials. PB90-123464 900,229	PB90-128729 900,533
Field Measurement of Thermal and Solar/Optical Proper- ties of Insulating Glass Windows.	OXALATES 300,223	OZONATION
PB89-175905 900,064	Wheatleyite, Na2Cu(C2O4)2 . 2H2O, a Natural Sodium Copper Salt of Oxalic Acid.	Stopped-Flow Studies of the Mechanisms of Ozone-
Photoelastic Properties of Optical Materials.	Copper Salt of Oxalic Acid. PB89-179154 900,390	Alkene Reactions in the Gas Phase: Tetramethylethylene.
PB89-177208 901,355 OPTICAL SENSORS	Ferric Oxalate with Nitric Acid as a Conditioner in an Ad-	PB89-157515 900,326
Anti-T2 Monoclonal Antibody Immobilization on Quartz	hesive Bonding System.	OZONE
Fibers: Stability and Recognition of T2 Mycotoxin.	PB89-229272 900,045	Microwave Spectrum and Molecular Structure of the Eth- ylene-Ozone van der Waals Complex.
PB90-128760 901,267 DPTICAL SPECTRA	OXIDATION Rate Constants for One-Electron Oxidation by Methylper-	PB89-201735 900,424
High Resolution Optical Multiplex Spectroscopy.	oxyl Radicals in Aqueous Solutions.	OZONIZATION
PB89-185938 900,404	PB89-151013 900,302	Ozonolysis of Ethylene. Microwave Spectrum, Molecular Structure, and Dipole Moment of Ethylene Primary Ozon-
Towards the Ultimate Laser Resolution. PB89-186910 900,416	New Photolytic Source of Dioxymethylenes: Criegee Intermediates Without Ozonolysis.	ide (1,2,3-Tnoxolane).
OPTICAL WAVEGUIDES	PB89-156731 900,304	PB89-157440 900,323
Interferometric Dispersion Measurements on Smal	Sputtered Thin Film Ba2YCu3On. PB89-165427 901,029	PACKAGING MATERIALS Class Bettles for Carbonated Soft Drinks: Valuntary Brad
Guided-Wave Structures. PB89-173959 901,345	Chemical Kinetics of Intermediates in the Autoxidation of	Glass Bottles for Carbonated Soft Drinks: Voluntary Product Standard PS73-89.
OPTIMIZATION	SO2.	PB90-107046 900,012
Electronic Mail and the 'Locator's' Dilemma.	PB89-176754 900,256	PACKING
PB89-211957 901,205	Influence of Molecular Weight on the Resonant Raman Scattering of Polyacetylene.	Low Pressure, Automated, Sample Packing Unit for Dif- fuse Reflectance Infrared Spectrometry.
OPTOELECTRONIC DEVICES Photonic Electric-Field Probe for Frequencies up to 2	PB89-179246 900,564	PB90-135922 900,235
GHz.	OXIDATION REDUCTION REACTIONS	PAHASAPAITE
PB89-229207 900,732	Redox Chemistry of Water-Soluble Vanadyl Porphyrins. PB89-150999 900,300	Pahasapaite, a Beryllophosphate Zeolite Related to Synthetic Zeolite Rho, from the Tip Top Pegmatite of South
DRDER DISORDER TRANSFORMATION Polymerization of a Novel Liquid Crystalline Diacetylene	Reactions of Magnesium Prophyrin Radical Cations in	Dakota.
Monomer.	Water, Disproportionation, Oxygen Production, and Com-	PB89-186431 901,288
PB89-231286 900,578	panson with Other Metalloporphyrins. PB89-151005 900,301	PAINTS Relationship between Appearance and Protective Dura
ORDINARY DIFFERENTIAL EQUATIONS Mathematical Software: PLOD. Plotted Solutions of Dif	Decay of High Valent Manganese Porphyrins in Aqueous	Relationship between Appearance and Protective Durability of Coatings: A Literature Review.
ferential Equations.	Solution and Catalyzed Formation of Oxygen.	PB89-162598 901,063

ORDINARY DIFFERENTIAL EQUATIONS

Mathematical Software: PLOD. Plotted Solutions of Differential Equations.

		•
PALLADIUM 109 (109)Pd and (109)Cd Activity Standardization and Decay	PB89-185730 901,293	Gypsum-Water Systems. PB89-150759 901,022
Data. PB90-123449 901,564	PERMANENT MAGNETS Roles of Atomic Volume and Disclinations in the Magne-	Stable and Metastable Ti-Nb Phase Diagrams.
PANCREATIC JUICE	tism of the Rare Earth-3D Hard Magnets. PB89-202238 901,434	PB89-157432 901 125
Comparison of Two Highly Refined Structures of Bovine Pancreatic Trypsin Inhibitor.	PERMEAMETERS	Periodic Heat Conduction in Energy Storage Cylinders
PB89-202204 901,248	Trace Gas Calibration Systems Using Permeation Devices.	with Change of Phase. PB89-175897 900.852
PARALLEL PROCESSING Definitions of Granularity.	PB89-176580 900,883	Synthesis, Stability, and Crystal Chemistry of Dibarium
PB89-180012 900,650	PEROVSKITES Sputtered Thin Film Ba2YCu3On.	Pentatitanate. PB89-179741 901,041
PARALLEL PROCESSING (COMPUTERS) Design Factors for Parallel Processing Benchmarks.	PB89-165427 901,029	In situ Observation of Particle Motion and Diffusion Inter-
PB89-186845 900,637	PEROXYL RADICALS Absolute Rate Constants for Hydrogen Abstraction from	actions during Coarsening.
PARALLEL PROCESSORS Design Factors for Parallel Processing Benchmarks.	Hydrocarbons by the Trichloromethylperoxyl Radical.	PB89-201982 901,151 Ergodic Behavior in Supercooled Liquids and in Glasses.
PB90-117672 900,644	PB89-171532 900,357 PEROXYLMETHYL RADICALS	PB89-202444 901,435
PARTICLE SIZE Dynamic Light Scattering and Angular Dissymmetry for	Rate Constants for One-Electron Oxidation by Methylper-	Hysteretic Phase Transition in Y1Ba2Cu3O7-x Superconductors.
the In situ Measurement of Silicon Dioxide Particle Synthesis in Flames.	oxyl Radicals in Aqueous Solutions. PB89-151013 900,302	PB89-229082 901,454
PB89-179584 900,246	PERSONNEL DOSIMETRY	Amorphous Phase Formation in Al70Si17Fe13 Alloy. PB90-123522 901.167
PARTICLE SIZE DISTRIBUTION Critical Assessment of Requirements for Ceramic Powder	Method for Evaluating Air Kerma and Directional Dose Equivalent for Currently Available Multi-Element Dose-	PB90-123522 901,167 Quasicrystals and Quasicrystal-Related Phases in the Al-
Characterization.	meters in Radiation Protection Dosimetry. PB90-117532 901,301	Mn System.
PB89-146849 901,016 Ostwald Ripening in a System with a High Volume Frac-	PERTURBATION THEORY	PB90-123548 901,169 Rapid Solidification and Ordering of B2 and L2 (sub 1)
tion of Coarsening Phase.	Improved Conformal Solution Theory for Mixtures with	Phases in the NiAl-NiTi System.
PB89-157598 901,126 Model for Particle Size and Phase Distributions in Ground	Large Size Ratios. PB89-228563 900,477	PB90-123639 901,171
Cement Clinker.	PHASE DIAGRAMS	Low-Temperature Phase and Magnetic Interactions in fcc Fe-Cr-Ni Alloys.
PB90-136847 901,062 PARTICLE TRAJECTORIES	Synthesis and Characterization of Ettringite and Related Phases.	PB90-136771 901,113
Numerical Computation of Particle Trajectories: A Model	PB89-146963 900,238	Model for Particle Size and Phase Distributions in Ground Cement Clinker.
Problem. PB89-158117 901,324	Institute for Materials Science and Engineering, Ceramics: Technical Activities 1988.	PB90-136847 301,062
PARTICLES	PB89-148381 901,019	PHASED ARRAYS Measuring In-Plane Elastic Moduli of Composites with
Numerical Simulation of Morphological Development during Ostwald Ripening.	Multicritical Phase Relations in Minerals. PB89-150882 901,278	Arrays of Phase-Insensitive Ultrasound Receivers.
PB89-201990 <i>901,152</i>	Phase Equilibrium in Two-Phase Coherent Solids.	PB90-136672 900,970 PHASES
Mobile Sources of Atmospheric Polycyclic Aromatic Hydrocarbons: A Roadway Tunnel Study.	PB89-157580 900,330 ASM/NBS (American Society for Metals/National Bureau	Theory of Microphase Separation in Graft and Star Co-
PB90-123571 900,859	of Standards) Numerical and Graphical Database for	polymers. PB89-176028 <i>900,557</i>
Residential Wood Combustion: A Source of Atmospheric Polycyclic Aromatic Hydrocarbons.	Binary Alloy Phase Diagrams. PB89-157986 901,135	Microphase Separation in Blockcopolymer/Homopolymer.
PB90-128166 900,860	Three-State Lattice Gas as Model for Binary Gas-Liquid	PB89-176069 900,561
PARTICULATE COMPOSITES Creep Rupture of a Metal-Ceramic Particulate Composite.	Systems. PB89-171284 <i>900,354</i>	PHENYL RADICALS Reactions of Phenyl Radicals with Ethene, Ethyne, and
PB89-211825 901,077	Dynamics of a Spin-One Model with the Pair Correlation.	Benzene.
PARTITION COEFFICIENTS Determination of Hydrocarbon/Water Partition Coeffi-	PB89-171300 900,356	PB89-150908 900,297 PHENYLALANINE
cients from Chromatographic Data and Based on Solu- tion Thermodynamics and Theory.	Phase Relations between the Polytitanates of Barium and the Barium Borates, Vanadates and Molybdates.	Hydroxyl Radical Induced Cross-Linking between Pheny-
PB89-187538 900,205	PB89-171789 901,032	lalanine and 2-Deoxyribose. PB89-147029 900,547
PATHOLOGY Biological Evaluations of Zinc Hexyl Vanillate Cement	Phase Equilibria and Crystal Chemistry in the Ternary System BaO-TiO2-Nb2O5: Part 1.	PHOSPHATIDYLCHOLINE/DIALKYL
Using Two In vivo Test Methods.	PB89-171797 901,033	Biological Standard Reference Materials for the Calibration of Differential Scanning Calorimeters; Di-alkylphos-
PB89-157150 900,038 PATHS	Stable and Metastable Phase Equilibria in the Al-Mn System.	phatidylcholine in Water Suspensions.
Fast Path Planning in Unstructured, Dynamic, 3-D	PB89-172324 901,136 Vapor-Liquid Equilibrium of Nitrogen-Oxygen Mixtures and	PB89-186779 900,415 PHOTOABSORPTION
Worlds. PB89-177067 900,992	Air at High Pressure.	Marked Differences in the 3p Photoabsorption between
PATTERN RECOGNITION	PB89-174932 900,368 Algebraic Representation for the Topology of Multicom-	the Cr and Mn(1+) Isoelectronic Pair: Reasons for the Unique Structure Observed in Cr.
Pattern Recognition Approach in X-ray Fluorescence Analysis.	ponent Phase Diagrams.	PB90-117581 901,562
PB90-128786 900,234 PENNING TRAPS	PB89-177042 901,517 Computer Graphics for Ceramic Phase Diagrams.	PHOTOCHEMICAL REACTIONS
Frequency Standards Utilizing Penning Traps.	PB89-186290 901,043	Polymers Bearing Intramolecular Photodimenzable Probes for Mass Diffusion Measurements by the Forced
PB90-128042 901,379 PENTANES	Phase Diagrams for High Tech Ceramics. PB89-186308 901,044	Rayleigh Scattering Technique: Synthesis and Characterization.
Method for Improving Equations of State Near the Critical	PC-Access to Ceramic Phase Diagrams.	PB89-157101 901,181
Point. PB89-228027 901,547	PB89-211841 901,053	Dehydrogenation of Ethanol in Dilute Aqueous Solution Photosensitized by Benzophenones.
PENTOSES	TEM Observation of Icosahedral, New Crystalline and Glassy Phases in Rapidly Quenched Cd-Cu Alloys.	PB89-157556 900,251
Thermodynamic and Transport Properties of Carbohy- drates and Their Monophosphates: The Pentoses and	PB90-123514 901,166	Photodissociation of Methyl Iodide Clusters. PB89-171193 900,253
Hexoses. PB89-222574 900,453	PHASE EQUILIBRIA	Absolute Cross Sections for Molecular Photoabsorption,
PERFORMANCE EVALUATION	Phase Equilibria and Crystal Chemistry in the Ternary System BaO-TiO2-Nb2O5, Part 2. New Barium Polytitan-	Partial Photoionization, and Ionic Photofragmentation Process.
Results of a Survey of the Performance of EPDM (Ethylene Propylene Diene Terpolymer) Roofing at Army Facili-	ates with < 5 mole % Nb2O5. PB89-189815 900,419	PB89-186464 900,410
ties.	PHASE SPACE	Time-Resolved FTIR Emission Studies of Molecular Photofragmentation.
PB89-209316 900,136 Architecturally-Focused Benchmarks with a Communica-	Classical Chaos, the Geometry of Phase Space, and Semiclassical Quantization.	PB89-202642 900,261
tion Example. PB89-216477 900,640	PB89-172381 901,506	Evaluated Kinetic and Photochemical Data for Atmospheric Chemistry. Supplement 3.
PERFORMANCE STANDARDS	PHASE STUDIES Application of the Gibbs Ensemble to the Study of Fluid-	PB89-222582 900,454
Part Load, Seasonal Efficiency Test Procedure Evaluation of Furnace Cycle Controllers.	Fluid Phase Equilibrium in a Binary Mixture of Symmetric Non-Additive Hard Spheres.	Dissociation Lifetimes and Level Mixing in Overtone-Excited HN3 (X tilde (sup 1) A').
PB89-212146 900,848	PB90-117318 900,494	PB90-117425 900,263
PERFORMANCE TESTS Flectrical Performance Tests for Hand-Held Digital Multi-	PHASE TRANSFORMATION Formation and Stability Bange of the G Phase in the Alu-	PHOTOCHEMISTRY
Electrical Performance Tests for Hand-Held Digital Multi- meters.	Formation and Stability Range of the G Phase in the Aluminum-Manganese System.	New Photolytic Source of Dioxymethylenes: Criegee Intermediates Without Ozonolysis.
PB89-162234 900,876 Transport Layer Performance Tools and Measurement.	PB89-186316 901,144	PB89-156731 900,304
PB89-171326 Performance Tools and Measurement.	Development of a Field-Space Corresponding-States Method for Fluids and Fluid Mixtures.	PHOTOCHROMISM Polymers Bearing Intramolecular Photodimenzable
PERIODIC VARIATIONS Liging Multiple Reference Stations to Separate the Var-	PB89-227995 901,331	Probes for Mass Diffusion Measurements by the Forced Rayleigh Scattering Technique: Synthesis and Character-
Using Multiple Reference Stations to Separate the Variances of Noise Components in the Global Positioning	PHASE TRANSFORMATIONS Implications of Phase Equilibria on Hydration in the Tri-	ization.
System.	calcium Silicate-Water and the Tricalcium Aluminate-	PB89-157101 <i>901,181</i>

PHOTODETACHMENT	PB89-186340 901,315	PB90-111220 <i>900,910</i>
Three Dimensional Quantum Reactive Scattering Study of the I + HI Reaction and of the IHI(1-) Photodetach-	PHOTON CROSS SECTIONS Cross Section and Linear Polarization of Tagged Pho-	PIPES (TUBES)
ment Spectrum. PB89-227961 900,466	tons.	Interlaboratory Comparison of the Guarded Horizontal Pipe-Test Apparatus: Precision of ASTM (American Soci-
PHOTODIODES	PB90-117292 901,560	ety for Testing and Materials) Standard Test Method C-
Feasibility of Detector Self-Calibration in the Near Infra-	PHOTON-MOLECULE COLLISIONS Cross Sections for Collisions of Electrons and Photons	335 Applied to Mineral-Fiber Pipe Insulation. PB89-218341 901,011
red. PB89-176788 900,384	with Oxygen Molecules.	Effect of Pipe Roughness on Orifice Flow Measurement.
Characteristics of Ge and InGaAs Photodiodes.	PB89-226575 900,457	PB89-231484 901,333
PB89-176796 900,729	PHOTON STIMULATED DESORPTION Secondary-Electron Effects in Photon-Stimulated Desorp-	PISTON GAGES
Interpolation of Silicon Photodiode Ouantum Efficiency as an Absolute Radiometric Standard.	tion.	Non-Geometric Dependencies of Gas-Operated Piston Gage Effective Areas.
PB89-212245 901,445	PB89-157929 900,337 Photon-Stimulated Desorption as a Measure of Surface	PB89-231112 900,905
Silicon Photodiode Detectors for EXAFS (Extended X-ray Absorption Fine Structure).	Electronic Structure.	Observations of Gas Species and Mode of Operation Effects on Effective Areas of Gas Operated Pictor Gases
PB89-228498 900,731	PB89-231328 901,459	fects on Effective Areas of Gas-Operated Piston Gages. PB89-231120 900,906
High Accuracy Modeling of Photodiode Ouantum Efficien-	PHOTONIC PROBES Photonic Electric Field Probe for Frequencies up to 2	PLANCKS CONSTANT
cy. PB90-117599 <i>900,733</i>	GHz.	NBS (National Bureau of Standards) Determination of the
Silicon Photodiode Self-Calibration.	PB89-176184 900,683	Fine-Structure Constant, and of the Ouantized Hall Re- sistance and Josephson Frequency-to-Voltage Ouotient
PB90-118159 900,734	PHOTOSENSITIVITY Two-Photon Laser-Induced Fluorescence of the Tumor-	in SI Units. PB89-230437 901,556
Stability and Ouantum Efficiency Performance of Silicon Photodiode Detectors in the Far Ultraviolet.	Localizing Photosensitizer Hematoporphyrin Derivative.	PLANNING
PB90-128059 900,735	PB89-157283 901,240	Fast Path Planning in Unstructured, Dynamic, 3-D
Improved Low-Level Silicon-Avalanche-Photodiode Transfer Standards at 1.064 Micrometers.	PHOTOTHERMAL DEFLECTION Waveguide Loss Measurement Using Photothermal De-	Worlds.
PB90-130303 900,736	flection.	PB89-177067 900,992 Modular Process Planning System Architecture.
PHOTODISSOCIATION	PB89·157028 900,739 PHOTOVOLTAIC CELLS	PB90-128596 900,966
Picosecond Laser Study of the Collisionless Photodisso- ciation of Dimethylnitramine at 266 nm.	Lightning and Surge Protection of Photovoltaic Installa-	PLASMA
PB89-172423 900,255	tions. Two Case Histories: Vulcano and Kythnos.	Atomic Internal Partition Function.
Photodissociation Dynamics of C2H2 at 193 nm: Vibra-	PB89-229058 900,851 PHYSICAL CHEMISTRY	PB89-185904 901,373 PLASMA FREQUENCY
tional Distributions of the CCH Radical and the Rotational State Distribution of the A(010) State by Time-Resolved	Center for Atomic, Molecular, and Optical Physics Tech-	Chaos and Catastrophe Near the Plasma Frequency in
Fourier Transform Infrared Emission.	nical Activities, 1989.	the RF-Biased Josephson Junction.
PB89-179782 900,258 PHOTOELASTIC ANALYSIS	PB90-133158 901,586 PHYSICAL CONSTANTS	PB89-200463 901,424
Photoelastic Properties of Optical Materials.	CODATA (Committee on Data for Science and Technolo-	PLASMA PROTEINS Spectroscopic Ouantitative Analysis of Strongly Interact-
PB89-177208 901,355	gy) Recommended Values of the Fundamental Physical Constants, 1986.	ing Systems: Human Plasma Protein Mixtures.
PHOTOELECTRIC EMISSION Synchrotron Radiation Study of BaO Films on W(001)	PB89-145189 900,275	PB89-202576 901,225
and Their Interaction with H2O, CO2, and O2.	PHYSICAL PROPERTIES	PLASMAS (PHYSICS) Spectra and Energy Levels of the Galliumlike Ions Rb VII-
PB89-157697 900,252	Journal of Physical and Chemical Reference Data, Volume 17, Number 4, 1988.	Mo XII.
Semiclassical Way to Molecular Dynamics at Surfaces. PB89-157713 900,333	PB89-145114 900,268	PB89-179105 900,387
Surface Properties of Clean and Gas-Dosed SnO2 (110).	CODATA (Committee on Data for Science and Technolo-	Development of a Microwave Sustained Gas Plasma for the Sterilization of Dental Instruments.
PB89-179576 900,393	gy) Recommended Values of the Fundamental Physical Constants, 1986.	PB89-231278 900,047
Synchrotron Photoemission Study of CO Chemisorption on Cr(110).	PB89-145189 900,275	PLASTICIZERS
PB89-231336 900,262	Journal of Physical and Chemical Reference Data,	Adsorption of High-Range Water-Reducing Agents on Selected Portland Cement Phases and Related Materials.
PHOTOELECTRON SPECTROSCOPY	Volume 17, Number 1, 1988. PB89-186449 900,408	PB90-124306 Phases and Helated Materials.
Vibrationally Resolved Photoelectron Angular Distribu- tions for H2 in the Range 17 eV < or= h(nu) < or= 39	Journal of Physical and Chemical Reference Data,	PLASTICS
eV. PB89-176952 <i>900.385</i>	Volume 18, Number 3, 1989. PB90-126236 900,527	Smoke and Gas Evolution Rate Measurements on Fire-
PHOTOELECTRONS	PHYSICAL RADIATION EFFECTS	Retarded Plastics with the Cone Calorimeter. PB89-174890 900,868
Core-Level Binding-Energy Shifts at Surfaces and in	Effect of Neutrons on the Characteristics of the Insulated	PLATE TECTONICS
Solids. PB89-146898 900,282	Gate Bipolar Transistor (IGBT). PB89-157655 900,773	Rate of Change of the Quincy-Monument Peak Baseline
Angle Resolved XPS (X-ray Photoelectron Spectroscopy)	PHYSICS	from a Translocation Analysis of LAGEOS Laser Range Data.
of the Epitaxial Growth of Cu on Ni(100). PB89-150866 901,389	Technical Activities 1987, Center for Basic Standards.	PB89-234272 901,282
Vibrationally Resolved Photoelectron Studies of the	PB89-185615 901,521	PLATES (STRUCTURAL MEMBER)
7(sigma) (-1) Channel in N2O.	PICOSECOND PULSES Picosecond Vibrational Energy Transfer Studies of Sur-	Local Brittle Zones in Steel Weldments: An Assessment of Test Methods.
PB89-176945 900,257	face Adsorbates.	PB89-149082 901,092
PHOTOEMISSION Resonant Excitation of an Oxygen Valence Satellite in	PB90-136573 900,537	PLATES (STRUCTURAL MEMBERS)
Photoemission from High-T(sub c) Superconductors.	PIEZOELECTRIC CRYSTALS Photoelastic Properties of Optical Materials.	Ultrasonic Determination of Absolute Stresses in Alumi- num and Steel Alloys.
PB89-186860 901,420	PB89-177208 901,355	PB89-150957 901,124
PHOTOIONIZATION Vibrationally Resolved Photoelectron Angular Distribu-	Torsional Piezoelectric Crystal Viscometer for Com-	Preliminary Stochastic Model for Service Life Prediction
tions for H2 in the Range 17 eV < or= h(nu) < or= 39 eV.	pressed Gases and Liquids. PB89-228076 901,447	of a Photolytically and Thermally Degraded Polymeric Cover Plate Material.
PB89-176952 900,385	PINNING	PB89-173801 900,556
Autoionization Dynamics in the Valence-Shell Photoioni-	Reevaluation of Forces Measured Across Thin Polymer	Measurement of Applied J-Integral Produced by Residual
zation Spectrum of CO. PB89-176960 900,386	Films: Nonequilibrium and Pinning Effects. PB89-228589 900,573	Stress. PB90-117631 900,163
Resonance-Enhanced Multiphoton Ionization of Atomic	PIPE BENDS	PLATINUM
Hydrogen.	NBS' (National Bureau of Standards) Industry; Govern- ment Consortium Research Program on Flowmeter Instal-	Adsorption Properties of Pt Films on W(110).
PB89-201073 901,529 PHOTOLYSIS	lation Effects: Summary Report with Emphasis on Re-	PB89-146864 900,281
Picosecond Laser Study of the Collisionless Photodisso-	search January-July 1988. PB89-189120 901,010	Electronic Structure of Diammine (Ascorbato) Platinum(II) and the Trans Influence on the Ligand Dissociation
ciation of Dimethylnitramine at 266 nm. PB89-172423 900,255	PIPE FLOW	Energy.
Temperature Dependence of the Rate Constant for the	Mixing Motions Produced by Pipe Elbows.	PB89-147128 900,287
Hydroperoxy + Methylperoxy Gas-Phase Reaction.	PB89-161871 901,326	NO/NH3 Coadsorption on Pt(111): Kinetic and Dynamical Effects in Rotational Accommodation.
PB90-136375 900,534	NBS' (National Bureau of Standards) Industry; Govern- ment Consortium Research Program on Flowmeter Instal-	PB89-201123 900,423
Flash Photolysis Kinetic Absorption Spectroscopy Study of the Gas Phase Reaction HO2 + C2H5O2 Over the	lation Effects: Summary Report with Emphasis on Re-	Interaction of Oxygen and Platinum on W(110).
Temperature Range 228-380 K.	search January-July 1988. PB89-189120 901,010	PB89-231302 901,158
PB90-136565 900,536 Time-Resolved FTIR Emission Studies of Molecular Pho-	Prediction of Flowmeter Installation Effects.	PNEUMATIC LINES Scattering Parameters Representing Imperfections in Pre-
tofragmentation Initiated by a High Repetition Rate Ex-	PB89-211882 900,899	cision Coaxial Air Lines.
cimer Laser. PB90-136680 900,266	Prediction of Flowmeter Installation Effects. PB89-211890 900,900	PB89-184121 900,750
PHOTOMASKS	NBS' (National Bureau of Standards) Industry; Govern-	POLARIMETRY Semiconductor Measurement Technology: A Software
Automated Calibration of Optical Photomask Linewidth	ment Consortium Research Program on Flowmeter Instal-	Program for Aiding the Analysis of Ellipsometric Measure-
Standards at the National Institute of Standards and Technology.	lation Effects: Summary Report with Emphasis on Re- search July-December 1987.	ments, Simple Models. PB89-235923 <i>901,369</i>
-	· · · · · · · · · · · · · · · · · · ·	301,868

POLARITY Effect of Surface Ionization on Wetting Layers.	Thermal Degradation of Poly (methyl methacrylate) at 50C to 125C.	PB89-146724 900,546
PBS9-157259 901,323 Preparative Liquid Chromatographic Method for the Char-	PB89-157465 900,549 Temperature, Composition and Molecular-Weight De-	Polymers Bearing Intramolecular Photodimerizable Probes for Mass Diffusion Measurements by the Forced
acterization of Minor Constituents of Lubricating Base Oils.	pendence of the Binary Interaction Parameter of Polysty- rene/Poly(vinylmethylether) Blends.	Rayleigh Scattering Technique: Synthesis and Characterization. PB89-157101 901.181
PB89-175921 <i>901,114</i>	PB89-157473 900,550	PB89-157101 901,181 Phase Contrast Matching in Lamellar Structures Com-
POLARIZABILITY Comment on 'Feasibility of Measurement of the Electro-	Institute for Materials Science and Engineering, Polymers: Technical Activities 1988. PB89-166094 900.003	posed of Mixtures of Labeled and Unlabeled Block Co- polymer for Small-Angle Neutron Scattering.
magnetic Polarizability of the Bound Nucleon'. PB90-117730 901,563	Interim Criteria for Polymer-Modified Bituminous Roofing	PB89-157119 901,182 Temperature, Composition and Molecular-Weight De-
POLARIZATION Effects of Space Charge on the Poling of Ferroelectric	Membrane Materials. PB89-168025 900,114	pendence of the Binary Interaction Parameter of Polysty- rene/Poly(vinylmethylether) Blends.
Polymers. PB89-146708 <i>901,179</i>	Effects of Solvent Type on the Concentration Dependence of the Compression Modulus of Thermoreversible	PB89-157473 900,550 Concentration Dependence of the Compression Modulus
POLARIZATION (SPIN ALIGNMENT) Improved Low-Energy Diffuse Scattering Electron-Spin	Isotactic Polystyrene Gels. PB89-172456 900,553	of Isotactic Polystyrene/Cis-Decalin Gels. PB89-172449 900,552
Polarization Analyzer. PB89-229173 900,218	Measurement of the Torque and Normal Force in Torsion in the Study of the Thermoviscoelastic Properties of Poly-	Effects of Solvent Type on the Concentration Depend-
POLARIZATION (WAVES)	mer Glasses. PB89-172472 900.554	ence of the Compression Modulus of Thermoreversible Isotactic Polystyrene Gels. PB89-172456 900.553
Improved Polarization Measurements Using a Modified Three-Antenna Technique. PB89-156814 900.698	Viscosity of Blends of Linear annd Cyclic Molecules of Similar Molecular Mass.	Viscosity of Blends of Linear annd Cyclic Molecules of
Cross Section and Linear Polarization of Tagged Pho-	PB89-172480 900,555	Similar Molecular Mass. PB89-172480 900,555
tons. PB90-117292 <i>901,560</i>	Dynamics of Concentration Fluctuation on Both Sides of Phase Boundary, PB89-173942 901.183	Effects of Material Characteristics on Flame Spreading. PB89-212021 900,572
POLARIZED LIGHT Scattering of Polarized Light in Spectral Lines with Partial	Characterization of Organolead Polymers in Trace	POLYTOPES
Frequency Redistribution: General Redistribution Matrix. PB89-171607 901,344	Amounts by Element-Specific Size-Exclusion Chromatography.	Polytope Volume Computation. PB90-129982 901,203
POLISHING Epoxy Impregnation of Hardened Cement Pastes for	PBS-175962 900,196 Theory of Microphase Separation in Graft and Star Co-	PORE PRESSURE Pore-Water Pressure Buildup in Clean Sands Because of
Characterization of Microstructure. PB89-185573 901,042	polymers. PB89-176028 <i>900,557</i>	Cyclic Straining. PB89-175723 900,159
POLY (ETHER/VINYLMETHYL)	Solid State (13)C NMR Investigation in Polyoxetanes. Effect of Chain Conformation.	POROSITY
Synthesis and Characterization of Poly(vinylmethyl ether). PB89-161616 900,551	PB89-176036 900,558	Small Angle Neutron Scattering from Porosity in Sintered Alumina.
POLYATOMIC MOLECULES Time-Resolved FTIR Emission Studies of Molecular Pho-	Polymer Localization by Random Fixed Impurities: Gaussian Chains. PB89-176044 900.559	PB89-157564 901,026 Pore Morphology Analysis Using Small Angle Neutron
tofragmentation. PB89-202642 900,261	Polymeric Humidity Sensors for Industrial Process Appli-	Scattering Techniques. PB89-175939 901,037
POLYBUTADIENE More Polybusian Partitioning of Ethyl Propohog in Polybushul	cations. PB89-176424 900,563	Microporous Fumed-Silica Insulation as a Standard Reference Material of Thermal Resistance at High Tempera-
Morphological Partitioning of Ethyl Branches in Polyethyl- ene by (13)C NMR. PB89-176051 900,560	Influence of Molecular Weight on the Resonant Raman Scattering of Polyacetylene.	ture. PB90-130311 900,153
POLYCARBONATE RESINS	PB89-179246 900,564	POROUS MATERIALS
Thermal Analysis of VAMAS (Versailles Project on Advanced Materials and Standards) Polycarbonate-Polyeth-	Composites Databases for the 1990's. PB89-180376 901,075	Use of Dye Tracers in the Study of Free Convection in Porous Media.
ylene Blends. PB89-201487 900,568	Institute for Materials Science and Engineering, Polymers: Technical Activities 1987.	PB89-173918 901,327 Computer Model of a Porous Medium.
POLYCRYSTALLINE Ultrasonic Separation of Stress and Texture Effects in	PB89-188601 900,566 Versailles Project on Advanced Materials and Standards	PB89-179683 901,188 PORPHYRIN/VANADYL
Polycrystalline Aggregates. PB90-117557 900,499	Evolution to Permanent Status. PB89-201768 900,969	Redox Chemistry of Water-Soluble Vanadyl Porphyrins.
POLYETHYLENE Morphological Partitioning of Ethyl Branches in Polyethyl-	Polymer Phase Separation. PB69-202923 900,570	PB89-150999 900,300 PORTABLE EQUIPMENT
ene by (13)C NMR. PB89-176051 900,560	Surface-Interacting Polymers: An Integral Equation and	Draft International Document on Guide to Portable Instru- ments for Assessing Airborne Pollutants Ansing from
Thermal Analysis of VAMAS (Versailles Project on Advanced Materials and Standards) Polycarbonate-Polyeth-	Fractional Calculus Approach. PB89-202949 900,571	Hazardous Wastes. PB89-150775 900,855
ylene Blends. PB89-201487 900,568	Reevaluation of Forces Measured Across Thin Polymer Films: Nonequilibrium and Pinning Effects.	PORTLAND CEMENTS Adsorption of High-Range Water-Reducing Agents on Se-
13C NMR Method for Determining the Partitioning of End	PB89-228589 900,573 Shear Effects on the Phase Separation Behaviour of a	lected Portland Cement Phases and Related Materials. PB90-124306
Groups and Side Branches between the Crystalline and Non-Crystalline Regions in Polyethylene. PB89-202451 900,569	Polymer Blend in Solution by Small Angle Neutron Scattering.	Model for Particle Size and Phase Distributions in Ground
Charging Behavior of Polyethylene and Ionomers.	PB89-229264 900,574 Polymerization of a Novel Liquid Crystalline Diacetylene	Cement Clinker. PB90-136847 901,062
PB90-136813 900,578 POLYHEDRONS	Monomer. PB89-231286 900,575	POSITION ERRORS Iterative Technique to Correct Probe Position Errors in
Expected Complexity of the 3-Dimensional Voronoi Diagram.	Set Time Control Studies of Polymer Concrete. PB90-111238 901,057	Planar Near-Field to Far-Field Transformations. PB89-153886 900,695
PB89-209332 901,200 POLYISOPRENE	Off-Lattice Simulation of Polymer Chain Dynamics.	POSITION (LOCATION)
Uniaxial Deformation of Rubber Network Chains by Small Angle Neutron Scattering.	PB90-117524 900,576 Small Angle Neutron Scattering Studies of Single Phase	Optimum Location of Flow Conditioners in a 4-Inch Ori- fice Meter. PB90-111675 900,911
PB89-175830 901,088	Interpenetrating Polymer Networks. PB90-123456 900,577	POTASSIUM CHLORIDE
POLYMERIZATION Synthesis and Characterization of Poly(vinylmethyl ether).	Reaction of (Ir(C(3), N bpy)(bpy)2)(2+) with OH Radicals and Radiation Induced Covalent Binding of the Complex	Determination of the Absolute Specific Conductance of Primary Standard KCl Solutions.
PB89-161616 900,551 Microphase Separation in Blockcopolymer/Homopolymer.	to Several Polymers in Aqueous Solutions. PB90-123498 900,264	PB89-230320 900,481 POTASSIUM CHROMATES
PB89-176069 900,561 In vitro Investigation of the Effects of Glass Inserts on	POLYMETHYL METHACRYLATE	Dichromate Dosimetry: The Effect of Acetic Acid on the Radiolytic Reduction Yield.
the Effective Composite Resin Polymerization Shrinkage. PB90-117516 900.049	Thermal Degradation of Poly (methyl methacrylate) at 50C to 125C. PB89-157465 900,549	PB89-147490 900,248
POLYMERS	Measurement of the Torque and Normal Force in Torsion	Rydberg-Klein-Rees Inversion of High Resolution van der
In Situ Fluorescence Monitoring of the Viscosities of Particle-Filled Polymers in Flow.	in the Study of the Thermoviscoelastic Properties of Polymer Glasses. PB89-172472 900.554	Waals Infrared Spectra: An Intermolecular Potential Energy Surface for Ar + HF (v = 1). PB89-227953 900,465
PB89-146278 900,609 Effects of Space Charge on the Poling of Ferroelectric	Preliminary Stochastic Model for Service Life Prediction	Research for Electric Energy Systems: An Annual Report.
Polymers. PB89-146708 <i>901,179</i>	of a Photolytically and Thermally Degraded Polymeric Cover Plate Material.	PB90-112442 900,853 POWDER (PARTICLES)
Qualitative MO Theory of Some Ring and Ladder Polymers.	PB89-173801 900,556 Effects of Material Characteristics on Flame Spreading.	Critical Assessment of Requirements for Ceramic Powder Characterization.
PB89-156723 900,303 Resonant Raman Scattering of Controlled Molecular	PB89-212021 900,572 POLYSTYRENE	PB89-146849 901,016
Weight Polyacetylene. PB89-157093 900,548	Effect of Crosslinks on the Phase Separation Behavior of a Miscible Polymer Blend.	Institute for Materials Science and Engineering, Nonde- structive Evaluation: Technical Activities 1988. PB89-151625 900,917
2.5,010		. 300 .0.020

PROCESSING & PERFORMANCE OF MATERIALS

Co. L. I. V Differentian Deviden Defference from the	DD00 100000	000 200	DD00 102002	000 056
Standard X-ray Diffraction Powder Patterns from the JCPDS (Joint Committee on Powder Diffraction Stand-	PB90-123399 PRECISION	900,228	PB89-193882 PROCESSING	900,956
ards) Research Associateship. PB89-171763 900,190	Precision and Accuracy Assessment Derive bration Data.	ed from Cali-	Intelligent Processing of Material Workshop Conducted by the Na	
Solidification of Aluminum-Manganese Powders. PB89-172332 901,137	PB89-179162	900,886	ards and Technology. PB89-151823	900,942
Pore Morphology Analysis Using Small Angle Neutron	PRECISION MACHINING Preliminary Experiments with Three Identic	al Ultrapreci-	PROCESSING & PERFORMANCE O	
Scattering Techniques. PB89-175939 901,037	sion Machine Tools. PB89-150841	900,997	Ultrasonic Characterization of Su PB89-147409	
Process Control during High Pressure Atomization. PB89-179170 901,142	PRESERVATION	a Arabias	Cone Calorimeter Method for De	
Standard X-ray Diffraction Powder Patterns from the	Theory and Practice of Paper Preservation fo PB89-147052	900,934	ity of Composite Materials. PB89-149165	901,072
JCPDS (Joint Committee on Powder Diffraction Standards) Research Association.	PRESSURE PVT of Toluene at Temperatures to 673 K.		Solutal Convection during Directi	·
PB89-202246 900,214	PB89-157192	900,310	PB89-150932	901,322
OWDER TESTING Dynamic Poisson's Ratio of a Ceramic Powder during	PVT Measurements on Benzene at Tempera K.	atures to 723	Biological Evaluations of Zinc Using Two In vivo Test Methods.	
Compaction. PB89-177182 901,039	PB89-157200	900,311	PB89-157150 Adhesion to Dentin by Means of	900,038 Gluma Resin
OWER LINES	High Resolution Inverse Raman Spectrosco Q Branch.		PB89-157168	900,039
Measurement of Electrical Parameters Near AC and DC Power Lines.	PB89-171292 Thermal Conductivity of Refrigerants in a W	900,355	CO2 Separation Using Facilitation Change Membranes.	ated Transport Ion Ex-
PB89-173439 900,745 Coupling, Propagation, and Side Effects of Surges in an	Temperature and Pressure. PB89-226583	900,458	PB89-157374	900,321
Industrial Building Wiring System. PB89-173454 900,118	PRESSURE CONTROL	300,430	Thermal Degradation of Poly (50C to 125C.	
AC Electric and Magnetic Field Meter Fundamentals.	Experimental Fire Tower Studies of Elevato tion Systems for Smoke Control.	r Pressuriza-	PB89-157465	900,549
PB89-173470 900,746 National Institute of Standards and Technology (NIST) In-	PB90-117813	900,097	Metastable Phase Production a Ge Alloy Films by Rapid Cryst	
formation Poster on Power Quality.	PRESSURE GRADIENTS Note on Calculating Flows Through Vertice	cal Vents in	Treatments. PB89-157622	901,129
PB89-237986 900,754 Discussion of 'Steep-Front Short-Duration Voltage Surge	Zone Fire Models Under Conditions of Art Vent Pressure Difference.	itrary Cross-	Crystal Chemistry of Supercond	ductors: A Guide to the
Tests of Power Line Filters and Transient Voltage Suppressors.'	PB90-117573	900,147	Tailoring of New Compounds. PB89-171730	901,030
PB90-117326 900,755	PRESSURE MEASUREMENT NIST (National Institute of Standards and	Technology)	Laser Excited Fluorescence Stud PB89-176416	dies of Black Liquor. 900,243
OWER MEASUREMENT Measurement of Electrical Parameters Near AC and DC	Measurement Services: High Vacuum Stan Use.		Kinetics of Resolidification.	000,240
Power Lines. PB89-173439 900,745	PB89-193841	900,891	PB89-176457	901,138
Potential Errors in the Use of Optical Fiber Power Meters.	Non-Geometric Dependencies of Gas-Ope Gage Effective Areas.		Element-Specific Epifluorescend Monitoring of Metal Biotransform	ce Microscopy in vivo mations in Erivironmental
PB89-176697 900,728 Optical Power Measurements at the National Institute of	PB§9-231112 Observations of Gas Species and Mode of 0	900,905 Operation Ef-	Matrices. PB89-177216	901,220
Standards and Technology. PB89-187579 900,918	fects on Effective Areas of Gas-Operated Pis PB89-231120		Process Control during High Pres	
Performance Evaluation of Radiofrequency, Microwave,	Pressure Fixed Points Based on the Car		PB89-179170 Facilitated Transport of CO2 three	901,142
and Millimeter Wave Power Meters. PB89-193916 900,814	Vapor Pressure at 273.16 K and the H2O(I H2O(L) Triple-Point.) - H2O(III) -	Exchange Membranes: The Effe	ect of Hot Glycerine Pre-
Audio-Frequency Current Comparator Power Bridge: De-	PB89-231138	900,483	PB89-179618	900,395
velopment and Design Considerations. PB89-201537 900,717	Monitoring and Predicting Parameters in Missolution.		Ignition Characteristics of the \$66286 in Pressurized Oxygen.	Iron-Based Alloy UNS
OWER METERS	PB90-118183 PRESSURE SENSORS	900,690	PB89-189336	901,104
NBS (National Bureau of Standards) Laser Power and Energy Measurements.	Low Range Flowmeters for Use with Vacuu	ım and Leak	Automated Processing of Advar to Maintaining U.S. Industrial Co	
PB89-171680 901,346 NBS (National Bureau of Standards) Standards for Opti-	Standards. PB89-175707	900,374	als. PB89-201727	900,957
cal Power Meter Calibration. PB89-176200 900,726	PRESSURE TRANSDUCERS InSb as a Pressure Sensor.		Sensors for Intelligent Processing	g of Materials.
Performance Evaluation of Radiofrequency, Microwave,	PB89-231104	900,904	PB89-202006 Oligomers with Pendant Isocya	900,920
and Millimeter Wave Power Meters. PB89-193916 900,814	PRESSURE VESSELS Failure Analysis of an Amine-Absorber Press	ure Vessel.	Adhesives. 1. Synthesis and Cha	racterization.
International Comparison of Power Meter Calibrations Conducted in 1987.	PB89-173835	901,101	PB89-202212 Effect of Anisotropic Thermal (900,055 Conductivity on the Mor-
PB89-201545 900,718	Fracture Behavior of a Pressure Vessel Stee tile-to-Brittle Transition Region.	el in the Duc-	phological Stability of a Binary Al PB89-228985	lloy. 901,155
OWER SUPPLIES Power Quality Site Surveys: Facts, Fiction, and Fallacies.	PB89-189195	901,103	Ferric Oxalate with Nitric Acid as	
PB89-171656 900,805	PRIMARY STANDARDS Determination of the Absolute Specific Cor	nductance of	hesive Bonding System. PB89-229272	900,045
Battery-Powered Current Supply for Superconductor Measurements.	Primary Standard KCl Solutions. PB89-230320	900,481	Oligomers with Pendant Isocya	anate Groups as Tissue
PB89-200455 901,525	PROBES	ha dia.i	Adhesives. 2. Adhesion to Bone PB89-231245	and Other Tissues. 900,056
OWER TRANSMISSION LINES Characterizing Electrical Parameters Near AC and DC	Polymers Bearing Intramolecular Pho- Probes for Mass Diffusion Measurements by	y the Forced	Design and Synthesis of Prototypin BEP (Bureau of Engraving and	pe Air-Dry Resins for Use
Power Lines. 900,834 PB89-173462 900,834	Rayleigh Scattering Technique: Synthesis ar ization.		hicles.	0, 0
Power Frequency Electric and Magnetic Field Measurements: Recent History and Measurement Standards.	PB89-157101 PROBLEM SOLVING	901,181	PB90-112343 Directional Solidification of a Pla	901,068 nar Interface in the Pres-
PB89-176630 900,835	Mathematical Software: PLOD. Plotted Solu	utions of Dif-	ence of a Time-Dependent Elect PB90-112400	
DC Electric Field Effects during Measurements of Mono- polar Charge Density and Net Space Charge Density	ferential Equations. PB89-147425	901,194	Off-Lattice Simulation of Polymer	
Near HVDC Power Lines. PB90-128521 901,380	PROCEEDINGS Alaska Arctic Offshore Oil Spill Response	Toohnology	PB90-117524	900,576
OYNTING THEOREM	Workshop Proceedings.	•	Amorphous Phase Formation in A PB90-123522	Al70Si17Fe13 Alloy. 901,167
Optically Linked Electric and Magnetic Field Sensor for Poynting Vector Measurements in the Near Fields of Ra-	PB89-195663 PROCESS CONTROL	900,842	Solidification of an 'Amorphous'	Phase in Rapidly Solidi-
diating Šources. PB89-187595 900,712	Laser Induced Fluorescence for Measurem Concentrations in Pulping Liquors.	ent of Lignin	fied Al-Fe-Si Alloys. PB90-123530	901,168
RASEODYMIUM BARIUM CUPRATES	PB89-172530	901,184	Rapid Solidification and Orderin Phases in the NiAl-NiTi System.	ng of B2 and L2 (sub 1)
Magnetic Order of Pr in PrBa2Cu3O7. PB90-123803 901,471	Process Control during High Pressure Atomiz PB89-179170	ation. 901,142	PB90-123639	901,171
RASEODYMIUM IONS Magnetic Order of Pr in PrRa2Cu3O7	Automated Processing of Advanced Materia	ls. The Path	Pathways for Microstructural Dev PB90-123779	elopment in TiAl. 901,173
Magnetic Order of Pr in PrBa2Cu3O7. PB90-123803 901,471	to Maintaining U.S. Industrial Competitivene als.		Effect of a Crystal-Melt Interface	on Taylor-Vortex Flow.
REBREAKDOWN Effect of Pressure on the Development of Prebreakdown	PB89-201727 Sensors for Intelligent Processing of Material	<i>900,957</i> ls.	PB90-130261 Corrosion Behavior of Mild Ste	901,477 eel in High pH Aqueous
Streamers. PB90-128315 900,828	PB89-202006	900,920	Media. PB90-131152	901,086
RECIPITATION (CHEMISTRY)	PROCESS PLANNING NBS AMRF (National Bureau of Standards)	(Automated	Institute for Materials Science a	and Engineering, Nonde-
Calcium Hydroxyapatite Precipitated from an Aqueous Solution: An International Multimethod Analysis.	Manufacturing Research Facility) Proce System: System Architecture.	ss Planning	structive Evaluation: Technical A PB90-132739	

PROCUREMENT	Electronic Structure of the Cd Vecancy in CdTe. PB89-171318 901.398	Polymerizetion of e Novel Liquid Crystalline Diecetylene
Material Hendling Workstation, Recommended Technical Specifications for Procurement of Commercially Available Equipment.	PB89-171318 901,398 Magnetic Dipole Excitation of e Long Conductor in a Lossy Medium.	Monomer. PB89-231286 900,575
PB89-162564 900,998 PRODUCT DATA EXCHANGE SPECIFICATION	PB89-171664 900,742	Line Identifications end Redietive-Brenching Retios of Magnetic Dipole Lines in Si-like Ni, Cu, Zn, Ge, end Se. PB89-234165 901,558
Product Date Exchenge Specification: First Working Draft.	Stability of Birefringent Linear Retarders (Waveplates). PB89-171672 901,345	Magnetic Structure of Cubic Tb0.3Y0.7Ag.
PB89-144794 900,940	Neutron Powder Diffrection Structure end Electrical Properties of the Defect Pyrochlores Pb1.5M2O6.5 (M= Nb,	PB90-117789 901,466 Collisional Electron Detachment and Decomposition
Product Data Exchange: The PDES Project-Status end Objectives. PB90-112426 900,938	Te). PB89-172431 900,363	Collisional Electron Detachment and Decomposition Rates of SF6(1-), SF5(1-), end F(1-) in SF6: Implications for Ion Trensport end Electrical Discharges.
PRODUCT DEVELOPMENT	Solid State (13)C NMR Investigation in Polyoxetanes. Effect of Chain Conformation.	PB90-117862 900,511
Product Data Exchange Specification: First Working Draft.	PB89-176036 900,558 Photoelastic Properties of Optical Materiels.	Neutron Diffraction Determination of Full Structures of Anhydrous Li-X and Li-Y Zeolites, PB90-118001 900.516
PB89-144794 <i>900,940</i> PRODUCTION CONTROL	PB89-177208 901,355	PB90-118001 900,516 Nonlinear Effect of an Oscillating Electric Field on Mem-
On-Line Concurrent Simulation in Production Scheduling. PB89-172605 900,948	Magnetic Resonance of (160)Tb Oriented in a Terbium Single Crystal at Low Temperatures. PB89-179204 901,519	brane Proteins. PB90-123407 901,249
Real-Time Simulation and Production Scheduling Systems.	Influence of Molecular Weight on the Resonant Raman Scattering of Polyecetylene.	Mossbauer Imaging: Experimental Results. PB90-123415 900,922
PB89-183230 900,974 PRODUCTION ENGINEERING	PB89-179246 900,564	Temperature Hysteresis in the Initial Susceptibility of Rapidly Solidified Monel.
Publications of the Center for Manufacturing Engineering Covering the Period January 1978-December 1988.	Application of Magnetic Resonance Imaging to Visualizetion of Flow in Porous Media.	PB90-123423 901,164
PB90-130568 901,012	PB89-179592 901,329 Long-Range Incommensurate Magnetic Order in Dy-Y	Magnetization end Magnetic Aftereffect in Textured Ni/ Cu Compositionally-Modulated Alloys.
Emerging Technologies in Manufacturing Engineering. PB90-132747 901,013	Multilayers. PB89-179642 <i>901,411</i>	PB90-123431 901,165 TEM Observation of Icosahedral, New Crystalline and
PRODUCTION MODELS Use of GMAP (Geometric Modeling Applications Interface	Syntheses end Unit Cell Determination of Ba3V4O13 and Low- and High-Temperature Be3P4O13.	Glassy Phases in Rapidly Quenched Cd-Cu Alloys. PB90-123514 901,166
Program) Software as a PDES (Product Date Exchange Specification) Environment in the National PDES Testbed	PB89-179717 901,040	Charecterization of Structural and Magnetic Order of Er/
Project. PB89-215198 900,960	Synthesis and Magnetic Properties of the Bi-Sr-Ca-Cu Oxide 80- end 110-K Superconductors.	Y Superlattices. PB90-123662 901,470
PRODUCTION PLANNING	PB89-179725 901,412 Effect of Room-Tempereture Stress on the Critical Cur-	Megnetic Order of Pr in PrBa2Cu3O7. PB90-123803 901,471
Artificial Intelligence Techniques in Real-Time Production Scheduling. PB89-172571 900.945	rent of NbTi. PB89-179832 901,414	Vector Imaging of Magnetic Microstructure. PB90-128240 901.476
PB89-172571 900,945 Functional Approach to Designing Architectures for Com-	Alternative Approach to the Heuptman-Karle Determinantal Inequalities.	Mn-Mn Exchange Constants in Zinc-Manganese Chalco-
puter Integrated Manufacturing. PB89-172589 900,946	PB89-186241 901,416	genides. PB90-136706 <i>901,478</i>
PROFILES Profile Inhomogeneity in Multimode Graded-Index Fibers.	Repulsive Regularities of Water Structure in Ices and Crystalline Hydrates.	Neutron Diffraction Study of the Wurtzite-Structure Dilute Magnetic Semiconductor Zn0.45Mn0.55Se.
PB89-179816 900,749	PB89-186753 900,414 Current Capacity Degradation in Superconducting Cable	PB90-136714 901,479
PROGRAMMING MANUALS Internal Revenue Service Post-of-Duty Location Modeling	Strands. PB89-200471 901,526	Seerch for Optical Molasses in e Vapor Cell: Generel Analysis and Experimental Attempt.
System: Programmer's Manual for PASCAL Solver. PB89-161905 900,001	Magnetic Evaluation of Cu-Mn Matrix Material for Fine- Filament Nb-Ti Superconductors.	PB90-163932 901,371 PROPERTIES OF MATERIALS: STRUCTURAL/
PROJECT MANAGEMENT	PB89-200489 901,425	MECHANICAL
		In Situ Fluorescence Monitoring of the Viscositios of Par
Building Technology Project Summaries 1989. PB89-193213 900,131	Switching Noise in YBa2Cu3Ox 'Macrobridges'. PB89-200513 901,426	In Situ Fluorescence Monitoring of the Viscosities of Par- ticle-Filled Polymers in Flow. PR89-146278 900 600
PB89-193213 900,131 PROPELLANTS In Situ Fluorescence Monitoring of the Viscosities of Par-	PB89-200513 901,426 Magnetic Correlations in an Amorphous Gd-Al Spin	ticle-Filled Polymers in Flow. PB89-146278 900,609 Effects of Purified Ferric Oxalate/Nitric Acid Solutions as
PB89-193213 900,131 PROPELLANTS	PB89-200513 901,426 Magnetic Correlations in an Amorphous Gd-Al Spin Glass. PB89-201693 901,148	ticle-Filled Polymers in Flow. PB89-146278 Effects of Purified Ferric Oxalate/Nitric Acid Solutions as a Pretreatment for the NTG-GMA and PMDM Bonding System.
PB89-193213 900,131 PROPELLANTS In Situ Fluorescence Monitoring of the Viscosities of Particle-Filled Polymers in Flow. PB89-146278 900,609 PROPER MOTION	PB89-200513 901,426 Magnetic Correlations in an Amorphous Gd-Al Spin Glass. PB89-201693 901,148 Neutron Scattering Study of the Spin Ordering in Amorphous Tb45Fe55 and Tb25Fe75.	ticle-Filled Polymers in Flow. PB89-146278 Effects of Purified Ferric Oxalate/Nitric Acid Solutions as a Pretreatment for the NTG-GMA and PMDM Bonding System. PB89-146716 900,034
PB89-193213 900,131 PROPELLANTS In Situ Fluorescence Monitoring of the Viscosities of Particle-Filled Polymers in Flow. PB89-146278 900,609	PB89-200513 901,426 Magnetic Correlations in an Amorphous Gd-Al Spin Glass. PB89-201693 901,148 Neutron Scattering Study of the Spin Ordering in Amorphous Tb45Fe55 and Tb25Fe75. PB89-201701 901,149 Spin-Density-Wave Transition in Dilute YGd Single Crys-	ticle-Filled Polymers in Flow. PB89-146278 900,609 Effects of Purified Ferric Oxalate/Nitric Acid Solutions as a Pretreatment for the NTG-GMA and PMDM Bonding System. PB89-146716 900,034 Bonding Agents and Adhesives: Reactor Response. PB89-146732 900,035
PB89-193213 900,131 PROPELLANTS In Situ Fluorescence Monitoring of the Viscosities of Particle-Filled Polymers in Flow. PB89-146278 900,609 PROPER MOTION Proper Motion vs. Redshift Relation for Superluminal Radio Sources. PB89-157663 900,017 PROPERTIES OF MATERIALS: ELECTRONIC/MAGNETIC/	PB89-200513 901,426 Magnetic Correlations in an Amorphous Gd-Al Spin Glass. PB89-201693 901,148 Neutron Scattering Study of the Spin Ordering in Amorphous Tb45Fe55 and Tb25Fe75. PB89-201701 901,149	ticle-Filled Polymers in Flow. PB89-146278 Effects of Purified Ferric Oxalate/Nitric Acid Solutions as a Pretreatment for the NTG-GMA and PMDM Bonding System. PB89-146716 Bonding Agents and Adhesives: Reactor Response. PB89-146732 Defect Intergrowths in Barium Polytitanates. 1. Ba2Ti9O20.
PB89-I93213 900,131 PROPELLANTS In Situ Fluorescence Monitoring of the Viscosities of Particle-Filled Polymers in Flow. PB89-146278 900,609 PROPER MOTION Proper Motion vs. Redshift Relation for Superluminal Radio Sources. PB89-157663 900,017 PROPERTIES OF MATERIALS: ELECTRONIC/MAGNETIC/OPTICAL Electronic, Magnetic, Superconducting and Amorphous-	PB89-200513 901,426 Magnetic Correlations in an Amorphous Gd-Al Spin Glass. PB89-201693 901,148 Neutron Scattering Study of the Spin Ordering in Amorphous Tb45Fe55 and Tb25Fe75. PB89-201701 901,149 Spin-Density-Wave Transition in Dilute YGd Single Crystals.	ticle-Filled Polymers in Flow. PB89-146278 900,609 Effects of Purified Ferric Oxalate/Nitric Acid Solutions as a Pretreatment for the NTG-GMA and PMDM Bonding System. PB89-146716 900,034 Bonding Agents and Adhesives: Reactor Response. PB89-146732 Defect Intergrowths in Banum Polytitanates. 1.
PB89-193213 900,131 PROPELLANTS In Situ Fluorescence Monitoring of the Viscosities of Particle-Filled Polymers in Flow. PB89-146278 900,609 PROPER MOTION Proper Motion vs. Redshift Relation for Superfurninal Radio Sources. PB89-157663 900,017 PROPERTIES OF MATERIALS: ELECTRONIC/MAGNETIC/OPTICAL Electronic, Magnetic, Superconducting and Amorphous-Forming Properties Versus Stability of the Ti-Fe, Zr-Ru and Hf-Os Ordered Alloys.	PB89-200513 901,426 Magnetic Correlations in an Amorphous Gd-Al Spin Glass. PB89-201693 901,148 Neutron Scattering Study of the Spin Ordering in Amorphous Tb45Fe55 and Tb25Fe75. PB89-201701 901,149 Spin-Density-Wave Transition in Dilute YGd Single Crystals. PB89-202030 901,433 Roles of Atomic Volume and Disclinations in the Magnetism of the Rare Earth-3D Hard Magnets. PB89-202238 901,434	ticle-Filled Polymers in Flow. PB89-146278 900,609 Effects of Purified Ferric Oxalate/Nitric Acid Solutions as a Pretreatment for the NTG-GMA and PMDM Bonding System. PB89-146716 900,034 Bonding Agents and Adhesives: Reactor Response. PB89-146732 Defect Intergrowths in Barium Polytitanates. 1. Ba2Ti9O20. PB89-146823 Defect Intergrowths in Barium Polytitanates. 2. BaTi5O11. PB89-146831
PB89-193213 900,131 PROPELLANTS In Situ Fluorescence Monitoring of the Viscosities of Particle-Filled Polymers in Flow. PB89-146278 900,609 PROPER MOTION Proper Motion vs. Redshift Relation for Superluminal Radio Sources. PB89-157663 900,017 PROPERTIES OF MATERIALS: ELECTRONIC/MAGNETIC/OPTICAL Electronic, Magnetic, Superconducting and Amorphousforming Properties Versus Stability of the Ti-Fe, Zr-Ru and Hf-Os Ordered Alloys. PB89-146690 901,120 Effects of Space Charge on the Poling of Ferroelectric	PB89-200513 901,426 Magnetic Correlations in an Amorphous Gd-Al Spin Glass. PB89-201693 901,148 Neutron Scattering Study of the Spin Ordering in Amorphous Tb45Fe55 and Tb25Fe75. PB89-201701 901,149 Spin-Density-Wave Transition in Dilute YGd Single Crystals. PB89-202030 901,433 Roles of Atomic Volume and Disclinations in the Magnetism of the Rare Earth-3D Hard Magnets. PB89-202238 901,434 13C NMR Method for Determining the Partitioning of End Groups and Side Branches between the Crystalline and	ticle-Filled Polymers in Flow. PB89-146278 900,609 Effects of Purified Ferric Oxalate/Nitric Acid Solutions as a Pretreatment for the NTG-GMA and PMDM Bonding System. PB89-146716 900,034 Bonding Agents and Adhesives: Reactor Response. PB89-146732 Defect Intergrowths in Barium Polytitanates. 1. Ba2Ti9O20. PB89-146823 901,014 Defect Intergrowths in Barium Polytitanates. 2. BaTi5O11. PB89-146831 01,015 Critical Assessment of Requirements for Ceramic Powder Characterization.
PB89-193213 900,131 PROPELLANTS In Situ Fluorescence Monitoring of the Viscosities of Particle-Filled Polymers in Flow. PB89-146278 900,609 PROPER MOTION Proper Motion vs. Redshift Relation for Superluminal Radio Sources. PB89-157663 900,017 PROPERTIES OF MATERIALS: ELECTRONIC/MAGNETIC/OPTICAL Electronic, Magnetic, Superconducting and Amorphous-Forming Properties Versus Stability of the Ti-Fe, Zr-Ru and Hf-Os Ordered Alloys. PB89-146690 901,120 Effects of Space Charge on the Poling of Ferroelectric Polymers. PB89-146708 901,179	PB89-200513 901,426 Magnetic Correlations in an Amorphous Gd-Al Spin Glass. PB89-201693 901,148 Neutron Scattering Study of the Spin Ordering in Amorphous Tb45Fe55 and Tb25Fe75. PB89-201701 901,149 Spin-Density-Wave Transition in Dilute YGd Single Crystals. PB89-202030 901,433 Roles of Atomic Volume and Disclinations in the Magnetism of the Rare Earth-3D Hard Magnets. PB89-202238 901,434 13C NMR Method for Determining the Partitioning of End Groups and Side Branches between the Crystalline and Non-Crystalline Regions in Polyethylene. PB89-202451 900,569	ticle-Filled Polymers in Flow. PB89-146278 Effects of Purified Ferric Oxalate/Nitric Acid Solutions as a Pretreatment for the NTG-GMA and PMDM Bonding System. PB89-146716 Bonding Agents and Adhesives: Reactor Response. PB89-146732 Defect Intergrowths in Barium Polytitanates. 1. Ba2Ti9O20. PB89-146823 Boffect Intergrowths in Barium Polytitanates. 2. BaTi5O11. PB89-146831 Critical Assessment of Requirements for Ceramic Powder Characterization. PB89-146899 901,016 Application of SANS (Small Angle Neutron Scattering) to
PB89-I93213 900,131 PROPELLANTS In Situ Fluorescence Monitoring of the Viscosities of Particle-Filled Polymers in Flow. PB89-146278 900,609 PROPER MOTION Proper Motion vs. Redshift Relation for Superluminal Radio Sources. PB89-157663 900,017 PROPERTIES OF MATERIALS: ELECTRONIC/MAGNETIC/ OPTICAL Electronic, Magnetic, Superconducting and Amorphous-Forming Properties Versus Stability of the Ti-Fe, Zr-Ru and Hf-Os Ordered Alloys. PB89-146690 901,120 Effects of Space Charge on the Poling of Ferroelectric Polymers. PB89-146708 901,179 Optical Nondestructive Evaluation at the National Bureau of Standards.	PB89-200513 901,426 Magnetic Correlations in an Amorphous Gd-Al Spin Glass. PB89-201693 901,148 Neutron Scattering Study of the Spin Ordering in Amorphous Tb45Fe55 and Tb25Fe75. PB89-201701 901,149 Spin-Density-Wave Transition in Dilute YGd Single Crystals. PB89-202030 901,433 Roles of Atomic Volume and Disclinations in the Magnetism of the Rare Earth-3D Hard Magnets. PB89-202238 901,434 13C NMR Method for Determining the Partitioning of End Groups and Side Branches between the Crystalline and Non-Crystalline Regions in Polyethylene. PB89-202451 900,569 Antiferromagnetic Structure and Crystal Field Splittings in the Cubic Heusler Alloys HoPd2Sn and ErPd2Sn.	ticle-Filled Polymers in Flow. PB89-146278 Effects of Purified Ferric Oxalate/Nitric Acid Solutions as a Pretreatment for the NTG-GMA and PMDM Bonding System. PB89-146716 900,034 Bonding Agents and Adhesives: Reactor Response. PB89-146732 Defect Intergrowths in Barium Polytitanates. 1. Ba2Ti9O20. PB89-146823 901,014 Defect Intergrowths in Barium Polytitanates. 2. BaTi5O11. PB89-146831 Critical Assessment of Requirements for Ceramic Powder Characterization. PB89-146849 901,016
PB89-I93213 900,131 PROPELLANTS In Situ Fluorescence Monitoring of the Viscosities of Particle-Filled Polymers in Flow. PB89-146278 900,609 PROPER MOTION Proper Motion vs. Redshift Relation for Superluminal Radio Sources. PB89-157663 900,017 PROPERTIES OF MATERIALS: ELECTRONIC/MAGNETIC/OPTICAL Electronic, Magnetic, Superconducting and Amorphous-Forming Properties Versus Stability of the Ti-Fe, Zr-Ru and Hf-Os Ordered Alloys. PB89-146690 901,120 Effects of Space Charge on the Poling of Ferroelectric Polymers. PB89-146708 901,179 Optical Nondestructive Evaluation at the National Bureau of Standards. PB89-146740 900,976	PB89-200513 Magnetic Correlations in an Amorphous Gd-Al Spin Glass. PB89-201693 Neutron Scattering Study of the Spin Ordering in Amorphous Tb45Fe55 and Tb25Fe75. PB89-201701 Spin-Density-Wave Transition in Dilute YGd Single Crystals. PB89-202030 P01,433 Roles of Atomic Volume and Disclinations in the Magnetism of the Rare Earth-3D Hard Magnets. PB89-202238 13C NMR Method for Determining the Partitioning of End Groups and Side Branches between the Crystalline and Non-Crystalline Regions in Polyethylene. PB89-202451 Antiferromagnetic Structure and Crystal Field Splittings in the Cubic Heusler Alloys HoPd2Sn and ErPd2Sn. PB89-202659 Magnetic Structure of Y0.97Er0.03.	ticle-Filled Polymers in Flow. PB89-146278 Effects of Purified Ferric Oxalate/Nitric Acid Solutions as a Pretreatment for the NTG-GMA and PMDM Bonding System. PB89-146716 Bonding Agents and Adhesives: Reactor Response. PB89-146732 Defect Intergrowths in Barium Polytitanates. 1. Ba2Ti9O20. PB89-146823 Defect Intergrowths in Barium Polytitanates. 2. Ba15011. PB89-146831 Critical Assessment of Requirements for Ceramic Powder Characterization. PB89-146849 401,014 Application of SANS (Small Angle Neutron Scattering) to Ceramic Characterization. PB89-146856 901,017 Ultrasonic Texture Analysis for Polycrystalline Aggregates
PB89-I93213 900,131 PROPELLANTS In Situ Fluorescence Monitoring of the Viscosities of Particle-Filled Polymers in Flow. PB89-146278 900,609 PROPER MOTION Proper Motion vs. Redshift Relation for Superluminal Radio Sources. PB89-157663 900,017 PROPERTIES OF MATERIALS: ELECTRONIC/MAGNETIC/ OPTICAL Electronic, Magnetic, Superconducting and Amorphous- Forming Properties Versus Stability of the Ti-Fe, Zr-Ru and Hf-Os Ordered Alloys. PB89-146690 901,120 Effects of Space Charge on the Poling of Ferroelectric Polymers. PB89-146708 901,179 Optical Nondestructive Evaluation at the National Bureau of Standards. PB89-146740 900,976 Magnetic Field Dependence of the Superconductivity in Bi-Sr-Ca-Cu-O Superconductors.	PB89-200513 Magnetic Correlations in an Amorphous Gd-Al Spin Glass. PB89-201693 Neutron Scattering Study of the Spin Ordering in Amorphous Tb45Fe55 and Tb25Fe75. PB89-201701 Spin-Density-Wave Transition in Dilute YGd Single Crystals. PB89-202030 PB89-202030 PB89-202030 PB89-202238 Roles of Atomic Volume and Disclinations in the Magnetism of the Rare Earth-3D Hard Magnets. PB89-202238 13C NMR Method for Determining the Partitioning of End Groups and Side Branches between the Crystalline and Non-Crystalline Regions in Polyethylene. PB89-202451 Antiferromagnetic Structure and Crystal Field Splittings in the Cubic Heusler Alloys HoPd2Sn and ErPd2Sn. PB89-202659 Magnetic Structure of Y0.97Er0.03. PB89-202675	ticle-Filled Polymers in Flow. PB89-146278 900,609 Effects of Purified Ferric Oxalate/Nitric Acid Solutions as a Pretreatment for the NTG-GMA and PMDM Bonding System. PB89-146716 900,034 Bonding Agents and Adhesives: Reactor Response. PB89-146732 Defect Intergrowths in Barium Polytitanates. 1. Ba2Ti9O20. PB89-146823 901,014 Defect Intergrowths in Barium Polytitanates. 2. BaTi5O11. PB89-146831 Critical Assessment of Requirements for Ceramic Powder Characterization. PB89-146849 901,016 Application of SANS (Small Angle Neutron Scattering) to Ceramic Characterization. PB89-146856 901,017 Ultrasonic Texture Analysis for Polycrystalline Aggregates of Cubic Materials Displaying Orthotropic Symmetry. PB89-146948
PB89-193213 900,131 PROPELLANTS In Situ Fluorescence Monitoring of the Viscosities of Particle-Filled Polymers in Flow. PB89-146278 900,609 PROPER MOTION Proper Motion vs. Redshift Relation for Superluminal Radio Sources. PB89-157663 900,017 PROPERTIES OF MATERIALS: ELECTRONIC/MAGNETIC/OPTICAL Electronic, Magnetic, Superconducting and Amorphous-Forming Properties Versus Stability of the Ti-Fe, Zr-Ru and Hf-Os Ordered Alloys. PB89-146690 901,120 Effects of Space Charge on the Poling of Ferroelectric Polymers. PB89-146708 901,179 Optical Nondestructive Evaluation at the National Bureau of Standards. PB89-146740 900,976 Magnetic Field Dependence of the Superconductivity in Bi-Sr-Ca-Cu-O Superconductors. PB89-146815 901,385 High Resolution Imaging of Magnetization.	PB89-200513 Magnetic Correlations in an Amorphous Gd-Al Spin Glass. PB89-201693 Neutron Scattering Study of the Spin Ordering in Amorphous Tb45Fe55 and Tb25Fe75. PB89-201701 Spin-Density-Wave Transition in Dilute YGd Single Crystals. PB89-202030 P01,433 Roles of Atomic Volume and Disclinations in the Magnetism of the Rare Earth-3D Hard Magnets. PB89-202238 301,434 13C NMR Method for Determining the Partitioning of End Groups and Side Branches between the Crystalline and Non-Crystalline Regions in Polyethylene. PB89-202451 900,569 Antiferromagnetic Structure and Crystal Field Splittings in the Cubic Heusler Alloys HoPd2Sn and ErPd2Sn. PB89-202659 Magnetic Structure of Y0.97Er0.03. PB89-202675 Mossbauer Spectroscopy. PB89-211932	ticle-Filled Polymers in Flow. PB89-146278 900,609 Effects of Purified Ferric Oxalate/Nitric Acid Solutions as a Pretreatment for the NTG-GMA and PMDM Bonding System. PB89-146716 900,034 Bonding Agents and Adhesives: Reactor Response. PB89-146732 Defect Intergrowths in Barium Polytitanates. 1. Ba2Ti9O20. PB89-146823 901,014 Defect Intergrowths in Barium Polytitanates. 2. BaTi5O11. PB89-146840 Application of SANS (Small Angle Neutron Scattering) to Ceramic Characterization. PB89-146856 901,017 Ultrasonic Texture Analysis for Polycrystalline Aggregates of Cubic Materials Displaying Orthotropic Symmetry. PB89-146948 901,121 Synthesis and Characterization of Ettringite and Related Phases.
PB89-I93213 900,131 PROPELLANTS In Situ Fluorescence Monitoring of the Viscosities of Particle-Filled Polymers in Flow. PB89-146278 900,609 PROPER MOTION Proper Motion vs. Redshift Relation for Superluminal Radio Sources. PB89-157663 900,017 PROPERTIES OF MATERIALS: ELECTRONIC/MAGNETIC/OPTICAL Electronic, Magnetic, Superconducting and Amorphous-Forming Properties Versus Stability of the Ti-Fe, Zr-Ru and Hf-Os Ordered Alloys. PB89-146690 901,120 Effects of Space Charge on the Poling of Ferroelectric Polymers. PB89-146708 901,179 Optical Nondestructive Evaluation at the National Bureau of Standards. PB89-146740 900,976 Magnetic Field Dependence of the Superconductivity in Bi-Sr-Ca-Cu-O Superconductors. PB89-146815 901,385 High Resolution Imaging of Magnetization. PB89-147433 901,386 Oxygen Isotope Effect in the Superconducting Bi-Sr-Ca-	PB89-200513 Magnetic Correlations in an Amorphous Gd-Al Spin Glass. PB89-201693 Neutron Scattering Study of the Spin Ordering in Amorphous Tb45Fe55 and Tb25Fe75. PB89-201701 Spin-Density-Wave Transition in Dilute YGd Single Crystals. PB89-202030 PB89-202030 PB89-202030 PB89-202030 Golden and Disclinations in the Magnetism of the Rare Earth-3D Hard Magnets. PB89-202238 13C NMR Method for Determining the Partitioning of End Groups and Side Branches between the Crystalline and Non-Crystalline Regions in Polyethylene. PB89-202451 Antiferromagnetic Structure and Crystal Field Splittings in the Cubic Heusler Alloys HoPd2Sn and ErPd2Sn. PB89-202659 Magnetic Structure of Y0.97Er0.03. PB89-202675 Magnetic Structure of Y0.97Er0.03. PB89-211932 Measurement of Electrical Breakdown in Liquids. PB89-212229 900,447	ticle-Filled Polymers in Flow. PB89-146278 Effects of Purified Ferric Oxalate/Nitric Acid Solutions as a Pretreatment for the NTG-GMA and PMDM Bonding System. PB89-146716 Bonding Agents and Adhesives: Reactor Response. PB89-146732 Defect Intergrowths in Barium Polytitanates. 1. Ba2Ti9O20. PB89-146823 Defect Intergrowths in Barium Polytitanates. 2. BaTi5O11. PB89-146821 Defect Intergrowths in Barium Polytitanates. 2. BaTi5O11. PB89-146829 901,014 Application of SANS (Small Angle Neutron Scattering) to Ceramic Characterization. PB89-146849 PB89-146865 901,017 Ultrasonic Texture Analysis for Polycrystalline Aggregates of Cubic Materials Displaying Orthotropic Symmetry. PB89-146948 Synthesis and Characterization of Ettringite and Related Phases. PB89-146963 Stress Effects on III-V Solid-Liquid Equilibria.
PB89-193213 900,131 PROPELLANTS In Situ Fluorescence Monitoring of the Viscosities of Particle-Filled Polymers in Flow. PB89-146278 900,609 PROPER MOTION Proper Motion vs. Redshift Relation for Superluminal Radio Sources. PB89-157663 900,017 PROPERTIES OF MATERIALS: ELECTRONIC/MAGNETIC/OPTICAL Electronic, Magnetic, Superconducting and Amorphousforming Properties Versus Stability of the Ti-Fe, Zr-Ru and Ht-Os Ordered Alloys. PB89-146690 901,120 Effects of Space Charge on the Poling of Ferroelectric Polymers. PB89-146708 901,179 Optical Nondestructive Evaluation at the National Bureau of Standards. PB89-146740 900,976 Magnetic Field Dependence of the Superconductivity in Bi-Sr-Ca-Cu-O Superconductors. PB89-146815 901,385 High Resolution Imaging of Magnetization. PB89-147433 901,386	PB89-200513 Magnetic Correlations in an Amorphous Gd-Al Spin Glass. PB89-201693 Neutron Scattering Study of the Spin Ordering in Amorphous Tb45Fe55 and Tb25Fe75. PB89-201701 Spin-Density-Wave Transition in Dilute YGd Single Crystals. PB89-202030 PB89-202030 PB89-202030 Roles of Atomic Volume and Disclinations in the Magnetism of the Rare Earth-3D Hard Magnets. PB89-202238 13C NMR Method for Determining the Partitioning of End Groups and Side Branches between the Crystalline and Non-Crystalline Regions in Polyethylene. PB89-202451 Antiferromagnetic Structure and Crystal Field Splittings in the Cubic Heusler Alloys HoPd2Sn and ErPd2Sn. PB89-202659 Magnetic Structure of Y0.97Er0.03. PB89-202675 Mossbauer Spectroscopy. PB89-211932 Measurement of Electrical Breakdown in Liquids.	ticle-Filled Polymers in Flow. PB89-146278 Effects of Purified Ferric Oxalate/Nitric Acid Solutions as a Pretreatment for the NTG-GMA and PMDM Bonding System. PB99-146716 Bonding Agents and Adhesives: Reactor Response. PB89-146732 Defect Intergrowths in Barium Polytitanates. 1. Ba2Ti9O20. PB89-146623 Defect Intergrowths in Barium Polytitanates. 2. BaTi5O11. PB89-146821 Defect Intergrowths in Barium Polytitanates. 2. BaTi5O11. PB89-146821 Defect Intergrowths in Barium Polytitanates. 2. BaTi5O11. PB89-146829 901,015 Critical Assessment of Requirements for Ceramic Powder Characterization. PB89-146949 901,016 Application of SANS (Small Angle Neutron Scattering) to Ceramic Characterization. PB89-146896 901,017 Ultrasonic Texture Analysis for Polycrystalline Aggregates of Cubic Materials Displaying Orthotropic Symmetry. PB89-146946 Synthesis and Characterization of Ettringite and Related Phases. PB89-146963 Stress Effects on III-V Solid-Liquid Equilibria. PB89-146997
PR89-I93213 900,131 PROPELLANTS In Situ Fluorescence Monitoring of the Viscosities of Particle-Filled Polymers in Flow. P899-146278 900,609 PROPER MOTION Proper Motion vs. Redshift Relation for Superluminal Radio Sources. P899-157663 900,017 PROPERTIES OF MATERIALS: ELECTRONIC/MAGNETIC/OPTICAL Electronic, Magnetic, Superconducting and Amorphous-Forming Properties Versus Stability of the Ti-Fe, Zr-Ru and Hf-Os Ordered Alloys. P899-146690 901,120 Effects of Space Charge on the Poling of Ferroelectric Polymers. P899-146708 901,179 Optical Nondestructive Evaluation at the National Bureau of Standards. P899-146740 900,976 Magnetic Field Dependence of the Superconductivity in Bi-Sr-Ca-Cu-O Superconductors. P899-146815 901,385 High Resolution Imaging of Magnetization. P899-147433 901,386 Oxygen Isotope Effect in the Superconducting Bi-Sr-Ca-Cu-O System. P899-157044 901,025 Effect of pH on the Emission Properties of Aqueous tris	PB89-200513 Magnetic Correlations in an Amorphous Gd-Al Spin Glass. PB89-201693 Neutron Scattering Study of the Spin Ordering in Amorphous Tb45Fe55 and Tb25Fe75. PB89-201701 Spin-Density-Wave Transition in Dilute YGd Single Crystals. PB89-202030 PB89-202030 PB89-202030 PB89-202030 PB89-202238 Golf Atomic Volume and Disclinations in the Magnetism of the Rare Earth-3D Hard Magnets. PB89-202238 13C NMR Method for Determining the Partitioning of End Groups and Side Branches between the Crystalline and Non-Crystalline Regions in Polyethylene. PB89-202451 Antiferromagnetic Structure and Crystal Field Splittings in the Cubic Heusler Alloys HoPd2Sn and ErPd2Sn. PB89-202659 Magnetic Structure of Y0.97Er0.03. PB89-202675 Magnetic Structure of Y0.97Er0.03. PB89-212229 Measurement of Electrical Breakdown in Liquids. PB89-212229 Optical Novelty Filters. PB89-228084 FB89-228084 Evidence for the Superconducting Proximity Effect in	ticle-Filled Polymers in Flow. PB89-146278 Effects of Purified Ferric Oxalate/Nitric Acid Solutions as a Pretreatment for the NTG-GMA and PMDM Bonding System. PB89-146716 Bonding Agents and Adhesives: Reactor Response. PB89-146732 Defect Intergrowths in Barium Polytitanates. 1. Ba2Ti9O20. PB89-146823 Defect Intergrowths in Barium Polytitanates. 2. BaTi5O11. PB89-146831 Defect Intergrowths in Barium Polytitanates. 2. BaTi5O11. PB89-146831 Critical Assessment of Requirements for Ceramic Powder Characterization. PB89-146849 901,016 Application of SANS (Small Angle Neutron Scattering) to Ceramic Characterization. PB89-146949 VIltrasonic Texture Analysis for Polycrystalline Aggregates of Cubic Materials Displaying Orthotropic Symmetry. PB89-146963 Synthesis and Characterization of Ettringite and Related Phases. PB89-146963 Stress Effects on III-V Solid-Liquid Equilibria. PB89-146997 Prediction of Tensile Behavior of Strain Softened Composites by Flexural Test Methods.
PB89-193213 PROPELLANTS In Situ Fluorescence Monitoring of the Viscosities of Particle-Filled Polymers in Flow. PB89-146278 PROPER MOTION Proper Motion vs. Redshift Relation for Superluminal Radio Sources. PB89-157663 PROPERTIES OF MATERIALS: ELECTRONIC/MAGNETIC/OPTICAL Electronic, Magnetic, Superconducting and Amorphous-Forning Properties Versus Stability of the Ti-Fe, Zr-Ru and Hf-Os Ordered Alloys. PB89-146690 Effects of Space Charge on the Poling of Ferroelectric Polymers. PB89-146708 Optical Nondestructive Evaluation at the National Bureau of Standards. PB89-146740 Magnetic Field Dependence of the Superconductivity in Bi-Sr-Ca-Cu-O Superconductors. PB89-146815 High Resolution Imaging of Magnetization. PB89-147433 Oxygen Isotope Effect in the Superconducting Bi-Sr-Ca-Cu-O System. PB89-157044 Effect of PH on the Emission Properties of Aqueous tris (2,6-dipicolinato) Terbium (III) Complexes. PB89-157135	PB89-200513 Magnetic Correlations in an Amorphous Gd-Al Spin Glass. PB89-201693 Neutron Scattering Study of the Spin Ordering in Amorphous Tb45Fe55 and Tb25Fe75. PB89-201701 Spin-Density-Wave Transition in Dilute YGd Single Crystals. PB89-202030 PB89-202030 PB89-202030 PB89-202030 PB89-202030 PB89-202030 PB89-202030 PB89-202030 PB89-202030 PB89-202038 Golf Atomic Volume and Disclinations in the Magnetism of the Rare Earth-3D Hard Magnets. PB89-202238 JOHNA Method for Determining the Partitioning of End Groups and Side Branches between the Crystalline and Non-Crystalline Regions in Polyethylene. PB89-202451 Antiferromagnetic Structure and Crystal Field Splittings in the Cubic Heusler Alloys HoPd2Sn and ErPd2Sn. PB89-202659 Magnetic Structure of Y0.97Er0.03. PB89-202675 Mossbauer Spectroscopy. PB89-211932 Measurement of Electrical Breakdown in Liquids. PB89-212229 Optical Novelty Filters. PB89-212229 Optical Novelty Filters. PB89-228084 Evidence for the Superconducting Proximity Effect in Junctions between the Surfaces of YBa2CU3Ox Thin Films.	ticle-Filled Polymers in Flow. PB89-146278 Effects of Purified Ferric Oxalate/Nitric Acid Solutions as a Pretreatment for the NTG-GMA and PMDM Bonding System. PB89-146716 900,034 Bonding Agents and Adhesives: Reactor Response. PB89-146732 Defect Intergrowths in Barium Polytitanates. 1. Ba2Ti9O20. PB89-146823 901,014 Defect Intergrowths in Barium Polytitanates. 2. BaTi5O11. PB89-146831 Critical Assessment of Requirements for Ceramic Powder Characterization. PB89-146849 Application of SANS (Small Angle Neutron Scattering) to Ceramic Characterization. PB89-146946 GUItasonic Texture Analysis for Polycrystalline Aggregates of Cubic Materials Displaying Orthotropic Symmetry. PB89-146948 Synthesis and Characterization of Ettringite and Related Phases. PB89-146963 Stress Effects on III-V Solid-Liquid Equilibria. PB89-146997 Prediction of Tensile Behavior of Strain Softened Composites by Flexural Test Methods. PB89-147045 Sputter Deposition of Icosahedral Al-Mn and Al-Mn-Si.
PR89-193213 PROPELLANTS In Situ Fluorescence Monitoring of the Viscosities of Particle-Filled Polymers in Flow. PR89-146278 PROPER MOTION Proper Motion vs. Redshift Relation for Superluminal Radio Sources. PR89-157663 PROPERTIES OF MATERIALS: ELECTRONIC/MAGNETIC/OPTICAL Electronic, Magnetic, Superconducting and Amorphous-Forming Properties Versus Stability of the Ti-Fe, Zr-Ru and Hf-Os Ordered Alloys. PR89-146690 Effects of Space Charge on the Poling of Ferroelectric Polymers. PR89-146708 Optical Nondestructive Evaluation at the National Bureau of Standards. PR89-146740 Magnetic Field Dependence of the Superconductivity in Bi-Sr-Ca-Cu-O Superconductors. PR89-146815 High Resolution Imaging of Magnetization. PR89-147433 Oxygen Isotope Effect in the Superconducting Bi-Sr-Ca-Cu-O System. PR89-157044 Effect of pH on the Emission Properties of Aqueous tris (2,6-dipicolinato) Terbium (III) Complexes. PR89-157135 Molecular Dynamics Study of a Dipolar Fluid between Charged Plates. 2.	PB89-200513 Magnetic Correlations in an Amorphous Gd-Al Spin Glass. PB89-201693 Neutron Scattering Study of the Spin Ordering in Amorphous Tb45Fe55 and Tb25Fe75. PB89-201701 Spin-Density-Wave Transition in Dilute YGd Single Crystals. PB89-202030 Roles of Atomic Volume and Disclinations in the Magnetism of the Rare Earth-3D Hard Magnets. PB89-202238 13C NMR Method for Determining the Partitioning of End Groups and Side Branches between the Crystalline and Non-Crystalline Regions in Polyethylene. PB89-202451 Antiferromagnetic Structure and Crystal Field Splittings in the Cubic Heusler Alloys HoPd2Sn and ErPd2Sn. PB89-202659 Mossbauer Spectroscopy. PB89-211932 Measurement of Electrical Breakdown in Liquids. PB89-228084 Evidence for the Superconducting Proximity Effect in Junctions between the Surfaces of YBa2CU3Ox Thin Films. PB89-228449 Multiple Scattering in the X-ray Absorption Near Edge	ticle-Filled Polymers in Flow. PB89-146278 Effects of Purified Ferric Oxalate/Nitric Acid Solutions as a Pretreatment for the NTG-GMA and PMDM Bonding System. PB89-146716 900,034 Bonding Agents and Adhesives: Reactor Response. PB89-146732 Defect Intergrowths in Barium Polytitanates. 1. Ba2Ti9O20. PB89-146823 901,014 Defect Intergrowths in Barium Polytitanates. 2. BaTi5O11. PB89-146831 Critical Assessment of Requirements for Ceramic Powder Characterization. PB89-146849 401,016 Application of SANS (Small Angle Neutron Scattering) to Ceramic Characterization. PB89-146948 901,017 Ultrasonic Texture Analysis for Polycrystalline Aggregates of Cubic Materials Displaying Orthotropic Symmetry. PB89-146948 Synthesis and Characterization of Ettringite and Related Phases. PB89-146963 Stress Effects on III-V Solid-Liquid Equilibria. PB89-146997 Prediction of Tensile Behavior of Strain Softened Composites by Flexural Test Methods. PB89-147045 Sputter Deposition of Icosahedral Al-Mn and Al-Mn-Si. PB89-147102
PROPELLANTS In Situ Fluorescence Monitoring of the Viscosities of Particle-Filled Polymers in Flow. PB89-146278 PROPER MOTION Proper Motion vs. Redshift Relation for Superluminal Radio Sources. PB89-157663 PROPERTIES OF MATERIALS: ELECTRONIC/MAGNETIC/OPTICAL Electronic, Magnetic, Superconducting and Amorphous-Forming Properties Versus Stability of the Ti-Fe, Zr-Ru and Hf-Os Ordered Alloys. PB89-146690 Effects of Space Charge on the Poling of Ferroelectric Polymers. PB89-146708 Optical Nondestructive Evaluation at the National Bureau of Standards. PB89-146740 Magnetic Field Dependence of the Superconductivity in Bi-Sr-Ca-Cu-O Superconductors. PB89-146815 High Resolution Imaging of Magnetization. PB89-147433 Oxygen Isotope Effect in the Superconducting Bi-Sr-Ca-Cu-O System. PB89-157044 901,025 Effect of pH on the Emission Properties of Aqueous tris (2,6-dipicolinato) Terbium (III) Complexes. PB89-157135 Molecular Dynamics Study of a Dipolar Fluid between Charged Plates. 2. PB89-157218 Hydrodynamics of Magnetic and Dielectric Colloidal Dis-	PB89-200513 Magnetic Correlations in an Amorphous Gd-Al Spin Glass. PB89-201693 Neutron Scattering Study of the Spin Ordering in Amorphous Tb45Fe55 and Tb25Fe75. PB89-201701 Spin-Density-Wave Transition in Dilute YGd Single Crystals. PB89-202030 PB89-202030 Roles of Atomic Volume and Disclinations in the Magnetism of the Rare Earth-3D Hard Magnets. PB89-202238 13C NMR Method for Determining the Partitioning of End Groups and Side Branches between the Crystalline and Non-Crystalline Regions in Polyethylene. PB89-202451 Antiferromagnetic Structure and Crystal Field Splittings in the Cubic Heusler Alloys HoPd2Sn and ErPd2Sn. PB89-202659 Magnetic Structure of Y0.97Er0.03. PB89-202675 Massbauer Spectroscopy. PB89-219229 Optical Novelty Filters. PB89-228084 Evidence for the Superconducting Proximity Effect in Junctions between the Surfaces of YBa2CU3Ox Thin Films. PB89-228449 Multiple Scattering in the X-ray Absorption Near Edge Structure of Tetrahedral Germanium Gases. PB89-228480	ticle-Filled Polymers in Flow. PB89-146278 Effects of Purified Ferric Oxalate/Nitric Acid Solutions as a Pretreatment for the NTG-GMA and PMDM Bonding System. PB89-146716 900,034 Bonding Agents and Adhesives: Reactor Response. PB89-146732 Defect Intergrowths in Barium Polytitanates. 1. Ba2Ti9O20. PB89-146823 901,014 Defect Intergrowths in Barium Polytitanates. 2. BaTi5O11. PB89-146831 Critical Assessment of Requirements for Ceramic Powder Characterization. PB89-146849 Application of SANS (Small Angle Neutron Scattering) to Ceramic Characterization. PB89-146946 GUItasonic Texture Analysis for Polycrystalline Aggregates of Cubic Materials Displaying Orthotropic Symmetry. PB89-146948 Synthesis and Characterization of Ettringite and Related Phases. PB89-146963 Stress Effects on III-V Solid-Liquid Equilibria. PB89-146997 Prediction of Tensile Behavior of Strain Softened Composites by Flexural Test Methods. PB89-147045 Sputter Deposition of Icosahedral Al-Mn and Al-Mn-Si.
PR89-193213 PROPELLANTS In Situ Fluorescence Monitoring of the Viscosities of Particle-Filled Polymers in Flow. PB89-146278 PROPER MOTION Proper Motion vs. Redshift Relation for Superluminal Radio Sources. PB89-157663 PROPERTIES OF MATERIALS: ELECTRONIC/MAGNETIC/OPTICAL Electronic, Magnetic, Superconducting and Amorphous-Forming Properties Versus Stability of the Ti-Fe, Zr-Ru and Hf-Os Ordered Alloys. PB89-146690 Effects of Space Charge on the Poling of Ferroelectric Polymers. PB89-146708 Optical Nondestructive Evaluation at the National Bureau of Standards. PB89-146740 Magnetic Field Dependence of the Superconductivity in Bi-Sr-Ca-Cu-O Superconductors. PB89-146815 High Resolution Imaging of Magnetization. PB89-147433 Oxygen Isotope Effect in the Superconducting Bi-Sr-Ca-Cu-O System. PB89-157044 Effect of pH on the Emission Properties of Aqueous tris (2,6-dipicolinato) Terbium (III) Complexes. PB89-157135 Molecular Dynamics Study of a Dipolar Fluid between Charged Plates. 2. PB89-157218	PB89-200513 Magnetic Correlations in an Amorphous Gd-Al Spin Glass. PB89-201693 Neutron Scattering Study of the Spin Ordering in Amorphous Tb45Fe55 and Tb25Fe75. PB89-201701 Spin-Density-Wave Transition in Dilute YGd Single Crystals. PB89-202030 PB89-202030 PB89-202030 Roles of Atomic Volume and Disclinations in the Magnetism of the Rare Earth-3D Hard Magnets. PB89-202238 13C NMR Method for Determining the Partitioning of End Groups and Side Branches between the Crystalline and Non-Crystalline Regions in Polyethylene. PB89-202451 Antiferromagnetic Structure and Crystal Field Splittings in the Cubic Heusler Alloys HoPd2Sn and ErPd2Sn. PB89-202659 Magnetic Structure of Y0.97Er0.03. PB89-202675 Mossbauer Spectroscopy. PB89-218229 Optical Novelty Filters. PB89-212229 Optical Novelty Filters. PB89-228084 Evidence for the Superconducting Proximity Effect in Junctions between the Surfaces of YBa2CU3Ox Thin Films. PB89-228449 Multiple Scattering in the X-ray Absorption Near Edge Structure of Tetrahedral Germanium Gases. PB89-228480 Hydrogen Sites in Amorphous Pd85Si15HX Probed by Neutron Vibrational Spectroscopy.	ticle-Filled Polymers in Flow. PB89-146278 Effects of Purified Ferric Oxalate/Nitric Acid Solutions as a Pretreatment for the NTG-GMA and PMDM Bonding System. PB89-146716 900,034 Bonding Agents and Adhesives: Reactor Response. PB89-146732 Defect Intergrowths in Barium Polytitanates. 1. Ba2Ti9O20. PB89-146823 Defect Intergrowths in Barium Polytitanates. 2. BaTi5O11. PB89-146831 Defect Intergrowths in Barium Polytitanates. 2. BaTi5O11. PB89-146831 Critical Assessment of Requirements for Ceramic Powder Characterization. PB89-146849 901,016 Application of SANS (Small Angle Neutron Scattering) to Ceramic Characterization. PB89-146949 Synthesis and Characterization of Fettringite and Related Phases. PB89-146963 Stress Effects on III-V Solid-Liquid Equilibria. PB89-146997 Prediction of Tensile Behavior of Strain Softened Composites by Flexural Test Methods. PB89-147102 Quesicrystals with 1-D Trenslational Periodicity and e Ten-Fold Rotation Axis. PB89-147333 901,123 Metallographic Evidence for the Nucleation of Subsurface
PROPELLANTS In Situ Fluorescence Monitoring of the Viscosities of Particle-Filled Polymers in Flow. PROPER MOTION Proper Motion vs. Redshift Relation for Superluminal Radio Sources. PB89-146673 PROPERTIES OF MATERIALS: ELECTRONIC/MAGNETIC/OPTICAL Electronic, Magnetic, Superconducting and Amorphous-Forming Properties Versus Stability of the Ti-Fe, Zr-Ru and Hf-Oz Ordered Alloys. PB89-146690 Effects of Space Charge on the Poling of Ferroelectric Polymers. PB89-146708 Optical Nondestructive Evaluation at the National Bureau of Standards. PB89-146740 Magnetic Field Dependence of the Superconductivity in Bi-Sr-Ca-Cu-O Superconductors. PB89-14633 Oxygen Isotope Effect in the Superconducting Bi-Sr-Ca-Cu-O System. PB89-157044 Effect of pH on the Emission Properties of Aqueous tris (2,6-dipicolinato) Terbium (III) Complexes. PB89-157135 Molecular Dynamics Study of a Dipolar Fluid between Charged Plates. 2. PB89-157242 PB89-157242 PB89-157216 Re-Entrant Spin-Glass Properties of a-(FexCr1-x)75P15C10.	PB89-200513 Magnetic Correlations in an Amorphous Gd-Al Spin Glass. PB89-201693 Neutron Scattering Study of the Spin Ordering in Amorphous Tb45Fe55 and Tb25Fe75. PB89-201701 Spin-Density-Wave Transition in Dilute YGd Single Crystals. PB89-202030 Po1,433 Roles of Atomic Volume and Disclinations in the Magnetism of the Rare Earth-3D Hard Magnets. PB89-202238 13C NMR Method for Determining the Partitioning of End Groups and Side Branches between the Crystalline and Non-Crystalline Regions in Polyethylene. PB89-202451 Antiferromagnetic Structure and Crystal Field Splittings in the Cubic Heusler Alloys HoPd2Sn and ErPd2Sn. PB89-202659 Magnetic Structure of Y0.97Er0.03. PB89-202675 Mossbauer Spectroscopy. PB89-211932 Measurement of Electrical Breakdown in Liquids. PB89-228084 Evidence for the Superconducting Proximity Effect in Junctions between the Surfaces of YBa2CU3Ox Thin Films. PB89-228449 Multiple Scattering in the X-ray Absorption Near Edge Structure of Tetrahedral Germanium Gases. PB89-228480 Hydrogen Sites in Amorphous Pd85Si15HX Probed by Neutron Vibrational Spectroscopy. 901,456 Quantitative Problems in Magnetic Particle Inspection.	ticle-Filled Polymers in Flow. PB89-146278 Effects of Purified Ferric Oxalate/Nitric Acid Solutions as a Pretreatment for the NTG-GMA and PMDM Bonding System. PB89-146716 900,034 Bonding Agents and Adhesives: Reactor Response. PB89-146732 Defect Intergrowths in Barium Polytitanates. 1. Ba2Ti9O20. PB89-146823 901,014 Defect Intergrowths in Barium Polytitanates. 2. BaTi5O11. PB89-146831 Critical Assessment of Requirements for Ceramic Powder Characterization. PB89-146849 Application of SANS (Small Angle Neutron Scattering) to Ceramic Characterization. PB89-146846 QUI) Ultrasonic Texture Analysis for Polycrystalline Aggregates of Cubic Materials Displaying Orthotropic Symmetry. PB89-146948 Synthesis and Characterization of Ettringite and Related Phases. PB89-146963 Stress Effects on III-V Solid-Liquid Equilibria. PB89-146963 Stress Effects on III-V Solid-Liquid Equilibria. PB89-146965 Sputter Deposition of Icosahedral Al-Mn and Al-Mn-Si. PB89-147045 Sputter Deposition of Icosahedral Al-Mn and Al-Mn-Si. PB89-147045 Sputter Deposition of Icosahedral Periodicity and e Ten-Fold Rotation Axis. PB89-147381 901,123 Metallographic Evidence for the Nucleation of Subsurface Microcracks during Unlubricated Sliding of Metals. PB89-147391 901,001
PROPELLANTS In Situ Fluorescence Monitoring of the Viscosities of Particle-Filled Polymers in Flow. PB89-146278 PROPER MOTION Proper Motion vs. Redshift Relation for Superluminal Radio Sources. PB89-157663 PROPERTIES OF MATERIALS: ELECTRONIC/MAGNETIC/ OPTICAL Electronic, Magnetic, Superconducting and Amorphous-Forming Properties Versus Stability of the Ti-Fe, Zr-Ru and Hf-Os Ordered Alloys. PB89-146690 Effects of Space Charge on the Poling of Ferroelectric Polymers. PB89-146708 Optical Nondestructive Evaluation at the National Bureau of Standards. PB89-146740 Magnetic Field Dependence of the Superconductivity in Bi-Sr-Ca-Cu-O Superconductors. PB89-146815 High Resolution Imaging of Magnetization. PB89-147433 Oxygen Isotope Effect in the Superconducting Bi-Sr-Ca-Cu-O System. PB89-157044 Effect of pH on the Emission Properties of Aqueous tris (2,6-dipicolinato) Terbium (III) Complexes. PB89-157135 Molecular Dynamics Study of a Dipolar Fluid between Charged Plates. 2. PB89-157218 Hydrodynamics of Magnetic and Dielectric Colloidal Dispersions. PB89-157242 Re-Entrant Spin-Glass Properties of a-(FexCr1-x)757151C10. PB89-157481	PB89-200513 Magnetic Correlations in an Amorphous Gd-Al Spin Glass. PB89-201693 Neutron Scattering Study of the Spin Ordering in Amorphous Tb45Fe55 and Tb25Fe75. PB89-201701 Spin-Density-Wave Transition in Dilute YGd Single Crystals. PB89-202030 P01,433 Roles of Atomic Volume and Disclinations in the Magnetism of the Rare Earth-3D Hard Magnets. PB89-202238 13C NMR Method for Determining the Partitioning of End Groups and Side Branches between the Crystalline and Non-Crystalline Regions in Polyethylene. PB89-202451 Antiferromagnetic Structure and Crystal Field Splittings in the Cubic Heusler Alloys HoPd2Sn and ErPd2Sn. PB89-202659 Magnetic Structure of Y0.97Er0.03. PB89-202675 Mossbauer Spectroscopy. PB89-211932 Measurement of Electrical Breakdown in Liquids. PB89-212229 Optical Novelty Filters. PB89-228084 Evidence for the Superconducting Proximity Effect in Junctions between the Surfaces of YBa2CU3Ox Thin Films. PB89-22849 Multiple Scattering in the X-ray Absorption Near Edge Structure of Tetrahedral Germanium Gases. PB89-22840 Hydrogen Sites in Amorphous Pd85Si15HX Probed by Neutron Vibrational Spectroscopy. PB89-229140 Quantitative Problems in Magnetic Particle Inspection. 900,985	ticle-Filled Polymers in Flow. PB89-146278 Effects of Purified Ferric Oxalate/Nitric Acid Solutions as a Pretreatment for the NTG-GMA and PMDM Bonding System. PB89-146716 Bonding Agents and Adhesives: Reactor Response. PB89-146732 Defect Intergrowths in Barium Polytitanates. 1. Ba2Ti9O20. PB89-146823 Defect Intergrowths in Barium Polytitanates. 2. BaTi5O11. PB89-146821 Defect Intergrowths in Barium Polytitanates. 2. BaTi5O11. PB89-146829 901,015 Critical Assessment of Requirements for Ceramic Powder Characterization. PB89-146849 901,016 Application of SANS (Small Angle Neutron Scattering) to Ceramic Characterization. PB89-146849 901,017 Ultrasonic Texture Analysis for Polycrystalline Aggregates of Cubic Materials Displaying Orthotropic Symmetry. PB89-146948 901,121 Synthesis and Characterization of Ettringite and Related Phases. PB89-146997 Prediction of Tensile Behavior of Strain Softened Composites by Flexural Test Methods. PB89-147045 Sputter Deposition of Icosahedral Al-Mn and Al-Mn-Si. PB89-147045
PROPELLANTS In Situ Fluorescence Monitoring of the Viscosities of Particle-Filled Polymers in Flow. PROPER MOTION Proper Motion vs. Redshift Relation for Superluminal Radio Sources. PB89-146678 PROPER MOTION Proper Motion vs. Redshift Relation for Superluminal Radio Sources. PB89-157663 900,017 PROPERTIES OF MATERIALS: ELECTRONIC/MAGNETIC/OPTICAL Electronic, Magnetic, Superconducting and Amorphous-Forming Properties Versus Stability of the Ti-Fe, Zr-Ru and Hf-Os Ordered Alloys. PB89-146690 901,120 Effects of Space Charge on the Poling of Ferroelectric Polymers. PB89-146708 901,179 Optical Nondestructive Evaluation at the National Bureau of Standards. PB89-146740 900,976 Magnetic Field Dependence of the Superconductivity in Bi-Sr-Ca-Cu-O Superconductors. PB89-146815 High Resolution Imaging of Magnetization. PB89-147433 Oxygen Isotope Effect in the Superconducting Bi-Sr-Ca-Cu-O System. PB89-157044 Effect of pH on the Emission Properties of Aqueous tris (2,6-dipicolinato) Terbium (III) Complexes. PB89-157135 Molecular Dynamics Study of a Dipolar Fluid between Charged Plates. 2. PB89-157242 PB89-157242 PB89-157242 Re-Entrant Spin-Glass Properties of a-(FexCr1-x)75P15C10. PB89-157481 901,391 Small Angle Neutron Scattering from Porosity in Sintered Alumina.	PB89-200513 Magnetic Correlations in an Amorphous Gd-Al Spin Glass. PB89-201693 Neutron Scattering Study of the Spin Ordering in Amorphous Tb45Fe55 and Tb25Fe75. PB89-201701 Spin-Density-Wave Transition in Dilute YGd Single Crystals. PB89-202030 P01,433 Roles of Atomic Volume and Disclinations in the Magnetism of the Rare Earth-3D Hard Magnets. PB89-202238 13C NMR Method for Determining the Partitioning of End Groups and Side Branches between the Crystalline and Non-Crystalline Regions in Polyethylene. PB89-202451 Antiferromagnetic Structure and Crystal Field Splittings in the Cubic Heusler Alloys HoPd2Sn and ErPd2Sn. PB89-202659 Magnetic Structure of Y0.97Er0.03. PB89-202675 Mossbauer Spectroscopy. PB89-211932 Measurement of Electrical Breakdown in Liquids. PB89-228084 Evidence for the Superconducting Proximity Effect in Junctions between the Surfaces of YBa2CU3Ox Thin Films. PB89-228449 Multiple Scattering in the X-ray Absorption Near Edge Structure of Tetrahedral Germanium Gases. PB89-228480 Hydrogen Sites in Amorphous Pd85Si15HX Probed by Neutron Vibrational Spectroscopy. PB89-229140 Quantitative Problems in Magnetic Particle Inspection. PB89-229199 Low Field Determination of the Proton Gyromagnetic Ratio in Water.	ticle-Filled Polymers in Flow. PB89-146278 Effects of Purified Ferric Oxalate/Nitric Acid Solutions as a Pretreatment for the NTG-GMA and PMDM Bonding System. PB89-146716 900,034 Bonding Agents and Adhesives: Reactor Response. PB89-146732 Defect Intergrowths in Barium Polytitanates. 1. Ba2Ti9O20. PB89-146823 901,014 Defect Intergrowths in Barium Polytitanates. 2. BaTi5O11. PB89-146831 Critical Assessment of Requirements for Ceramic Powder Characterization. PB89-146849 Application of SANS (Small Angle Neutron Scattering) to Ceramic Characterization. PB89-146849 Q01,016 Ultrasonic Texture Analysis for Polycrystalline Aggregates of Cubic Materials Displaying Orthotropic Symmetry. PB89-146948 Synthesis and Characterization of Ettringite and Related Phases. PB89-146963 Stress Effects on III-V Solid-Liquid Equilibria. PB89-146997 Prediction of Tensile Behavior of Strain Softened Composites by Flexural Test Methods. PB89-147045 Sputter Deposition of Icosahedral Al-Mn and Al-Mn-Si. PB89-14702 Quesicrystals with 1-D Trenslational Periodicity and e Ten-Fold Rotation Axis. PB89-147381 Metallographic Evidence for the Nucleation of Subsurface Microcracks during Unlubricated Sliding of Metals. PB89-148118 901,087 Institute for Materiels Science and Engineering, Cerem-
PROPELLANTS In Situ Fluorescence Monitoring of the Viscosities of Particle-Filled Polymers in Flow. PB89-146278 PROPER MOTION Proper Motion vs. Redshift Relation for Superluminal Radio Sources. PB89-157683 900,017 PROPERTIES OF MATERIALS: ELECTRONIC/MAGNETIC/OPTICAL Electronic, Magnetic, Superconducting and Amorphous-Forming Properties Versus Stability of the Ti-Fe, Zr-Ru and Hf-Os Ordered Alloys. PB89-146690 Effects of Space Charge on the Poling of Ferroelectric Polymers. PB89-146708 Optical Nondestructive Evaluation at the National Bureau of Standards. PB89-146740 Magnetic Field Dependence of the Superconductivity in Bi-Sr-Ca-Cu-O Superconductors. PB89-146815 High Resolution Imaging of Magnetization. PB89-147433 Oxygen Isotope Effect in the Superconducting Bi-Sr-Ca-Cu-O System. PB89-157044 901,025 Effect of pH on the Emission Properties of Aqueous tris (2,6-dipicolinato) Terbium (III) Complexes. PB89-157135 Molecular Dynamics Study of a Dipolar Fluid between Charged Plates. 2. PB89-157218 Hydrodynamics of Magnetic and Dielectric Colloidal Dispersions. PB89-157481 Small Angle Neutron Scattering from Porosity in Sintered	PB89-200513 Magnetic Correlations in an Amorphous Gd-Al Spin Glass. PB89-201693 Neutron Scattering Study of the Spin Ordering in Amorphous Tb45Fe55 and Tb25Fe75. PB89-201701 Spin-Density-Wave Transition in Dilute YGd Single Crystals. PB89-202030 Roles of Atomic Volume and Disclinations in the Magnetism of the Rare Earth-3D Hard Magnets. PB89-202238 13C NMR Method for Determining the Partitioning of End Groups and Side Branches between the Crystalline and Non-Crystalline Regions in Polyethylene. PB89-202451 Antiferromagnetic Structure and Crystal Field Splittings in the Cubic Heusler Alloys HoPd2Sn and ErPd2Sn. PB89-202659 Magnetic Structure of Y0.97Er0.03. PB89-202675 Magnetic Structure of Y0.97Er0.03. PB89-212229 Optical Novelty Filters. PB89-212229 Optical Novelty Filters. PB89-228084 Evidence for the Superconducting Proximity Effect in Junctions between the Surfaces of YBa2CU3Ox Thin Films. PB89-228449 Multiple Scattering in the X-ray Absorption Near Edge Structure of Tetrahedral Germanium Gases. PB89-22840 Q00,474 Hydrogen Sites in Amorphous Pd85Si15HX Probed by Neutron Vibrational Spectroscopy. PB89-229199 Low Field Determination of the Proton Gyromagnetic	ticle-Filled Polymers in Flow. PB89-146278 Effects of Purified Ferric Oxalate/Nitric Acid Solutions as a Pretreatment for the NTG-GMA and PMDM Bonding System. PB89-146716 Bonding Agents and Adhesives: Reactor Response. PB89-146732 Defect Intergrowths in Barium Polytitanates. 1. Ba2Ti9O20. PB89-1468623 Defect Intergrowths in Barium Polytitanates. 2. BaTi5O11. PB89-146821 Defect Intergrowths in Barium Polytitanates. 2. BaTi5O11. PB89-146823 Defect Intergrowths in Barium Polytitanates. 2. BaTi5O11. PB89-146821 Defect Intergrowths in Barium Polytitanates. 2. BaTi5O11. PB89-146829 901,017 Critical Assessment of Requirements for Ceramic Powder Characterization. PB89-146849 Application of SANS (Small Angle Neutron Scattering) to Ceramic Characterization. PB89-146965 PB89-146965 Synthesis and Characterization of Polycrystalline Aggregates of Cubic Materials Displaying Orthotropic Symmetry. PB89-146963 Synthesis and Characterization of Ettringite and Related Phases. PB89-146963 Stress Effects on III-V Solid-Liquid Equilibria. PB89-146997 Prediction of Tensile Behavior of Strain Softened Composites by Flexural Test Methods. PB89-147045 Sputter Deposition of Icosahedral Al-Mn and Al-Mn-Si. PB89-147102 Quesicrystals with 1-D Trenslational Periodicity and e Ten-Fold Rotation Axis. PB89-147391 Metallographic Evidence for the Nucleation of Subsurface Microcracks during Unlubricated Sliding of Metals. PB89-147391 901,001

PROPERTIES OF MATERIALS: STRUCTURAL/MECHANICAL

Implications of Phase Equilibria on Hydration in the Tri- calcium Silicate-Water and the Tricalcium Aluminate- Gypsun-Water Systems.	PB89-175830 901,088 Pore Morphology Analysis Using Small Angle Neutron Scattering Techniques.	PB89-201792 901,431 Diffraction Effects Along the Normal to a Grain Boundary. PB89-202089 901,153
PB69-150759 901,022 Ultrasonic Determination of Absolute Stresses in Aluminum and Steel Alloys.	PB89-175939 901,037 Creep Cavitation in Liquid-Phase Sintered Alumina	Green Function Method for Calculation of Atomistic Structure of Grain Boundary Interfaces in Ionic Crystals.
PB89-150957 901,124	PB89-175954 901,038 Polymer Localization by Random Fixed Impurities: Gaus-	PB89-202105 901,050 Standard V ray Diffraction Rouder Patterns (rom the
Intelligent Processing of Materials: Report of an Industrial Workshop Conducted by the National Institute of Stand-	sian Chains. PB89-176044 900,559	Standard X-ray Diffraction Powder Patterns from the JCPDS (Joint Committee on Powder Diffraction Standards)
ards and Technology. PB89-151823 900,942	Morphological Partitioning of Ethyl Branches in Polyethyl-	ards) Research Association. PB89-202246 900,214
Structural Reliability and Damage Tolerance of Ceramic	ene by (13)C NMR. PB89-176051 900,560	Computer Simulation Studies of the Soliton Model. 3.
Composites for High-Temperature Applications. Semi- Annual Progress Report for the Period Ending September	Microphase Separation in Blockcopolymer/Homopolymer.	Noncontinuum Regimes and Soliton Interactions. PB89-202469 901,537
30, 1987. PB89-156350 <i>901,023</i>	PB89-176069 900,561	Liquid, Crystalline and Glassy States of Binary Charged
Structural Reliability and Damage Tolerance of Ceramic	Mesh Monitor Casting of Ni-Cr Alloys: Element Effects. PB89-176077 900,040	Colloidal Suspensions. PB89-202501 901,436
Composites for High-Temperature Applications. Semi- Annual Progress Report for the Period Ending March 31,	Undercooling and Microstructural Evolution in Glass	Polymer Phase Separation. PB69-202923 900,570
1988. PB89-156368 901,024	Forming Alloys. PB89-176465 901,139	Studies on Some Failure Modes in Latex Barrier Films.
Casting Metals: Reactor Response.	Wheatleyite, Na2Cu(C2O4)2 . 2H2O, a Natural Sodium Copper Salt of Oxalic Acid.	PB89-209308 901,089
PB89-157143 900,054 Neutron Vibrational Spectroscopy of Disordered Metal	PB89-179154 900,390	Brief Review of Recent Superconductivity Research at NIST (National Institute of Standards and Technology).
Hydrogen Systems.	Occurrence of Long-Range Helical Spin Ordering in Dy-Y Multilayers.	PB89-211114 900,766
PB89-157499 900,324 Structural Unit in Icosahedral MnAlSi and MnAl.	PB89-179634 901,410	Crack-Interface Traction: A Fracture-Resistance Mechanism in Brittle Polycrystals.
PB89-157648 901,131	Chemical Physics with Emphasis on Low Energy Excitations.	PB89-211817 901,051
Refinement of the Substructure and Superstructure of Romanechite.	PB89-179659 900,396	Creep Rupture of a Metal-Ceramic Particulate Composite. PB89-211825 901,077
PB89-157721 <i>901,392</i>	Synthesis, Stability, and Crystal Chemistry of Dibarium Pentatitanate.	Design Criteria for High Temperature Structural Applica-
Moydite, (Y, REE) (B(OH)4)(CO3), a New Mineral Species from the Evans-Lou Pegmatite, Quebec.	PB89-179741 901,041	tions. PB89-211833 901,052
PB89-157747 900,186	Acoustoelastic Determination of Residual Stresses. PB89-179808 901,318	PC-Access to Ceramic Phase Diagrams. PB89-211841 901.053
Universality Class of Planar Self-Avoiding Surfaces with Fixed Boundary.	Theoretical Models for High-Temperature Superconducti-	PB89-211841 901,053 Acoustic Emission: A Quantitative NDE Technique for the
PB89-157945 900,339 Effect of Coal Slag on the Microstructure and Creep Be-	vity. PB89-186266 <i>901,418</i>	Study of Fracture.
havior of a Magnesium-Chromite Refractory.	Formation and Stability Range of the G Phase in the Alu-	PB89-211924 900,921 Materials Failure Prevention at the National Bureau of
PB89-158034 901,027 Sayre's Equation is a Chernov Bound to Maximum Entro-	minum-Manganese System. PB89-186316 901,144	Standards. PB69-212237 901,190
py. PB89-158174 901,397	Nucleation and Growth of Aperiodic Crystals in Aluminum	Mechanism for Shear Band Formation in the High Strain
Synthesis and Characterization of Poly(vinylmethyl ether).	Alloys. PB89-186324 901,145	Rate Torsion Test. PB69-215370 900,901
PB89-161616 900,551	Replacement of Icosahedral Al-Mn by Decagonal Phase. PB89-186332 901,146	Development and Use of a Tribology Research-in-
Relationship between Appearance and Protective Durability of Coatings: A Literature Review.	Deuterium Magnetic Resonance Study of Orientation and	Progress Database. PB89-228274 901,002
PB69-162598 901,063 Toughening Mechanisms in Ceramic Composites: Semi-	Poling in Poly(Vinylidene Fluoride) and Poly(Vinylidene Fluoride-Co-Tetrafluoroethylene).	Computer-Controlled Test System for Operating Different
Annual Progress Report for the Period Ending September	PB89-186365 900,565	Wear Test Machines. PB89-228290 900,983
30, 1988. PB89-162606 901,028	Water Structure in Crystalline Solids: Ices to Proteins. PB89-186746 900,413	Fiber Coating and Characterization.
Institute for Materials Science and Engineering, Polymers:	Water Structure in Vitamin B12 Coenzyme Crystals. 1.	PB89-228571 901,067
Technical Activities 1988. PB89-166094 900,003	Analysis of the Neutron and X-ray Solvent Densities. PB89-186803 901,222	NBS/BAM (National Bureau of Standards/Bundesanstalt fur Materialprufung) 1986 Symposium on Advanced Ce-
Standard X-ray Diffraction Powder Patterns from the JCPDS (Joint Committee on Powder Diffraction Stand-	Computerized Materials Property Data Systems.	ramics. PB89-229074 901,055
ards) Research Associateship.	PB89-187512 901,312 Advanced Ceramics: A Critical Assessment of Wear and	Dependence of T(sub c) on the Number of CuO2 Planes
PB89-171763 900,190 Rising Fracture Toughness from the Bending Strength of	Lubrication.	per Cluster in Interplaner-Boson-Exchange Models of High-T(sub C) Superconductivity.
Indented Alumina Beams. PB89-171771 901,031	PB89-188569 901,045 Institute for Materials Science and Engineering, Polymers:	PB89-229132 901,455
Fracture Behavior of Ceramics Used in Multilayer Capaci-	Technical Activities 1987.	Effect of Heat Treatment on Crack-Resistance Curves in a Liquid-Phase-Sintered Alumina.
tors. PB89-171805 900,758	PB89-188601 900,566 Mechanical Property Enhancement in Ceramic Matrix	PB89-229231 901,056
Effect of Lateral Crack Growth on the Strength of Con-	Composites.	Shear Effects on the Phase Separation Behaviour of a Polymer Blend in Solution by Small Angle Neutron Scat-
tact Flaws in Brittle Materials. PB89-171813 901,034	PB89-189138 901,076 Ultrasonic Railroad Wheel Inspection Using EMATs	tering. PB89-229264 900,574
Densification, Susceptibility and Microstructure of	(Electromagnetic-Accoustic Transducers), Report No. 18. PB89-189229 901,596	Transient and Residual Stresses in Dental Porcelains as
Ba2YCu3O(6+ x). PB89-171821 901,035	Phase Equilibria and Crystal Chemistry in the Ternary	Affected by Cooling Rates. PB89-229298 900,046
Solidification of Aluminum-Manganese Powders. PB89-172332 901,137	System BaO-TiO2-Nb2O5. Part 2. New Barium Polytitan- ates with < 5 mole % Nb2O5.	Grain Boundary Characterization in Ni3Al. PB89-229306 901,156
Effects of Solvent Type on the Concentration Depend-	PB89-189815 900,419	PB89-229306 901,156 Grain Boundary Structure in Ni3Al.
ence of the Compression Modulus of Thermoreversible Isotactic Polystyrene Gels.	Metallurgical Evaluation of 17-4 PH Stainless Steel Castings.	PB89-229314 901,157
PB89-172456 900,553	PB89-193262 901,105	Thermomechanical Detwinning of Superconducting YBa2Cu3O7-x Single Crystals.
Measurement of the Torque and Normal Force in Torsion in the Study of the Thermoviscoelastic Properties of Poly-	Dielectric Measurements for Cure Monitoring. PB89-200430 900,567	PB89-231088 901,458
mer Glasses. PB89-172472 900,554	Structural Study of a Metastable BCC Phase in Al-Mn	Stainless Steel Weld Metal: Prediction of Ferrite Content. PB89-231260 901,107
Elevated Temperature Deformation of Structural Steel.	Alloys Electrodeposited from Molten Salts. PB89-201040 901,064	Toughening Mechanisms in Ceramic Composites. Semi-
PB89-172621 901,098 Role of Inclusions in the Fracture of Austenitic Stainless	Physics of Fracture, 1987. PB89-201107 901,428	Annual Progress Report for the Period Ending March 31, 1989.
Steel Welds at 4 K. PB89-173504 901,099	PB89-201107 901,428 Mossbauer Hyperfine Fields in RBa2(Cu0.97Fe0.03)3	PB89-235907 901,080
Influence of Molybdenum on the Strength and Toughness	O(7-x)(R = Y,Pr,Er). PB69-201206 901,429	Effect of Slag Penetration on the Mechanical Properties of Refractores: Final Report.
of Stainless Steel Welds for Cryogenic Service. PB89-173512 901,100	Institute for Materials Science and Engineering: Metallur-	PB90-110065 900,836 Comparison of Interplaner-Boson-Exchange Models of
Tensile Strain-Rate Effects in Liquid Helium.	gy, Technical Activities 1988. PB89-201321 901,147	High-Temperature Superconductivity - Possible Experi-
PB89-174882 901,102 NIST (National Institute of Standards and Technology)/	Necking Phenomena and Cold Drawing.	mental Tests. PB90-117334 901,462
Sandia/ICDD Electron Diffraction Database: A Database	PB89-201495 900,975 Commercial Advanced Ceramics.	Grain-Size and R-Curve Effects in the Abrasive Wear of Alumina.
for Phase Identification by Electron Diffraction. PB89-175210 901,508	PB89-201776 901,048	PB90-117383 <i>901,058</i>
Structural Ceramics Database: Technical Foundations. PB89-175244 901,036	Grain Boundary Structure in Ni3Al. PB89-201784 901,150	Fourth-Order Elastic Constants of beta-Brass. PB90-117607 901,160
Uniaxial Deformation of Rubber Network Chains by Small	Electron Diffraction Study of the Faceting of Tilt Grain	Gruneisen Parameter of Y1Ba2Cu3O7.
Angle Neutron Scattering.	Boundaries in NiO.	PB90-117615 901,465

Linear-Elastic Fracture of High-Nitrogen Austenitic Stainless Steels at Liquid Helium Temperature.	Grain Boundaries with Impurities in a Two-Dimensional Lattice-Gas Model.	PB89-234256 900,490
PB90-117623 901,108 Nitrogen in Austenitic Stainless Steels.	PB89-172407 901,507 Concentration Dependence of the Compression Modulus	PROSTHETIC DEVICES Corrosion of Metallic Implants and Prosthetic Devices.
PB90-117649 901,109	of Isotactic Polystyrene/Cis-Decalin Gels. PB89-172449 900,552	PB89-150890 900,053 Casting Metals: Reactor Response.
Tribochemical Mechanism of Alumina with Water. PB90-117722 901,059	Viscosity of Blends of Linear annd Cyclic Molecules of	PB89-157143 900,054
Formation of the Al-Mn Icosahedral Phase by Electrode- position.	Similar Molecular Mass. PB89-172480 900,555	PROTECTIVE COATINGS Relationship between Appearance and Protective Dura-
PB90-117763 900,504	Enthalpies of Desorption of Water from Coal Surfaces. PB89-173868 900,838	bility of Coatings: A Literature Review. PB89-162598 901,063
Calcium Hydroxyapatite Precipitated from an Aqueous Solution: An International Multimethod Analysis.	Speed of Sound in Natural Gas Mixtures. PB89-174031 900,840	Corrosion Induced Degradation of Amine-Cured Epoxy
PB90-123399 900,228 Neutron Study of the Crystal Structure and Vacancy Dis-	Latent Heats of Supercritical Fluid Mixtures.	Coatings on Steel. PB89-176291 901,084
tribution in the Superconductor Ba2Y Cu3 O(sub g-delta). PB90-123480 901,468	PB89-174908 900,242 Vapor-Liquid Equilibrium of Nitrogen-Oxygen Mixtures and	PROTECTIVE EQUIPMENT
Bulk Modulus and Young's Modulus of the Superconduc-	Air at High Pressure. PB89-174932 900,368	Simplified Shielding of a Metallic Restoration during Radiation Therapy. PB89-229256 900.044
tor Ba2Cu3YO7. PB90-123613 901,469	Comprehensive Study of Methane + Ethane System.	PROTECTORS
Microstructural Variations in Rapidly Solidified Alloys. PB90-123621 901,170	PB89-176747 900,841 Biodegradation of Tributyltin by Chesapeake Bay Microor-	Selecting Varistor Clamping Voltage: Lower Is Not Better. PB89-176648 900,760
Adhesive Bonding of Composites.	ganisms. PB89-177232 901,309	PROTEIN CONFORMATION
PB90-123696 900,050 EMATs (Electromagnetic Acoustic Transducers) for Roll-	Temperature-Dependent Radiation-Enhanced Diffusion in lon-Bombarded Solids.	Comparative Modeling of Protein Structure: Progress and Prospects.
By Crack Inspection of Railroad Wheels. PB90-123894 901,597	PB89-179188 <i>901,408</i>	PB89-175285 901,247 PROTEINS
Flaw Tolerance in Ceramics with Rising Crack Resistance Characteristics.	Thermal Conductivity of Liquid Argon for Temperatures between 110 and 140 K with Pressures to 70 MPa.	Structure of a Hydroxyl Radical Induced Cross-Link of
PB90-128026 901,060	PB89-179600 900,394 Phase Diagrams for High Tech Ceramics.	Thymine and Tyrosine. PB89-157838 901,244
Diffusion-Induced Grain Boundary Migration. PB90-128174 901,175	PB89-186308 901,044 Preparation of Multistage Zone-Refined Materials for	Use of Structural Templates in Protein Backbone Modeling.
Tensile Tests of Type 305 Stainless Steel Mine Sweeping Wire Rope.	Thermochemical Standards. PB89-186795 900,203	PB89-175277 901,246
PB90-130287 901,112	System for Measuring Optical Waveguide Intensity Pro-	Comparative Modeling of Protein Structure: Progress and Prospects.
Measurements of Tribological Behavior of Advanced Materials: Summary of U.S. Results on VAMAS (Versailles	files. PB89-188593 900,751	PB89-175285 901,247
Advanced Materials and Standards) Round-Robin No. 2. PB90-130295 901,003	In situ Observation of Particle Motion and Diffusion Inter- actions during Coarsening.	Computational Analysis of Protein Structures: Sources, Methods, Systems and Results.
Measuring In-Plane Elastic Moduli of Composites with Arrays of Phase-Insensitive Ultrasound Receivers.	PB89-201982 <i>901,151</i>	PB89-175293 900,010 Component Spectrum Reconstruction from Partially Char-
PB90-136672 900,970	Numerical Simulation of Morphological Development during Ostwald Ripening.	acterized Mixtures. PB89-202568 900,439
OPERTIES OF MATERIALS: THERMODYNAMIC/	PB89-201990 901,152 Electron Microscopy Studies of Diffusion-Induced Grain	PROTEINS CONFORMATION
Effect of Crosslinks on the Phase Separation Behavior of a Miscible Polymer Blend.	Boundary Migration in Ceramics. PB89-202097 901,049	Computational Analysis of Protein Structures: Sources, Methods, Systems and Results.
PB89-146724 900,546	Isochoric (p.v,T) Measurements on CO2 and (0.98 CO2 + 0.02 CH4) from 225 to 400 K and Pressures to 35	PB89-175293 900,010
Thermodynamics of Ammonium Scheelites. 6. An Analysis of the Heat Capacity and Ancillary Values for the Metabolish of the Metabolish and Analysis of the Metabolish and Met	MPa. PB89-202493 900,435	PROTOCOL (COMPUTERS) Ongoing Implementation Agreements for Open Systems
taperiodates KIO4, NH4IO4, and ND4IO4. PB89-147060 900,285	Interlaboratory Comparison of Two Types of Line-Source	Interconnection Protocols: Continuing Agreements. PB89-166086 900,610
Experimental Thermal Conductivity, Thermal Diffusivity, and Specific Heat Values of Argon and Nitrogen.	Thermal-Conductivity Apparatus Measuring Five Insulating Materials.	Prediction of Transport Protocol Performance through Simulation.
PB89-148407 900,293 Multicritical Phase Relations in Minerals.	PB89-218325 900,144 Interlaboratory Comparison of the Guarded Horizontal	PB89-171334 900,612
PB89-150882 901,278	Pipe-Test Apparatus: Precision of ASTM (American Society for Testing and Materials) Standard Test Method C-	PROTOCOLS Standardizing EMCS Communication Protocols.
Polymers Bearing Intramolecular Photodimerizable Probes for Mass Diffusion Measurements by the Forced	335 Applied to Mineral-Fiber Pipe Insulation. PB89-218341 901,011	PB89-172357 900,613
Rayleigh Scattering Technique: Synthesis and Characterization.	Low-Temperature Thermal Conductivity of Composites: Alumina Fiber/Epoxy and Alumina Fiber/PEEK.	Automatic Generation of Test Scenario (Skeletons) from Protocol-Specifications Written in Estelle. PB89-177125 900.615
PB89-157101 901,181 PVT of Toluene at Temperatures to 673 K.	PB89-218358 901,078	PB89-177125 900,615 Application of the ISO (International Standards Organiza-
PB89-157192 900,310	PVT Relationships in a Carbon Dioxide-Rich Mixture with Ethane.	tion) Distributed Single Layer Testing Method to the Con- nectionless Network Protocol.
PVT Measurements on Benzene at Temperatures to 723 K.	PB89-229181 900,478 Equilibrium Crystal Shapes and Surface Phase Diagrams	PB89-177133 900,616
PB89-157200 900,311 Effect of Surface Ionization on Wetting Layers.	at Surfaces in Ceramics. PB90-117755 901,162	Simplified Discrete Event Simulation Model for an IEEE (Institute of Electrical and Electronics Engineers) 802.3
PB89-157259 901,323	Measurements of Molar Heat Capacity at Constant	Local Area Network. PB89-186829 900,617
Stable and Metastable Ti-Nb Phase Diagrams. PB89-157432 901,125	Volume: Cv,m(xCH4 + (1-x)C2H6' T = 100 to 320 K, p < or = 35 MPa). PB90-117896 900,844	Stable Implementation Agreements for Open Systems Interconnection Protocols. Version 2, Edition 1. Decem-
Phase Equilibrium in Two-Phase Coherent Solids. PB89-157580 900,330	Small Angle Neutron Scattering Studies of Single Phase	ber 1988. PB89-193312 900,618
Ostwald Ripening in a System with a High Volume Frac-	Interpenetrating Polymer Networks. PB90-123456 900,577	User Guide for Wise: A Simulation Environment for Es-
tion of Coarsening Phase. PB89-157598 901,126	Quasicrystals and Quasicrystal-Related Phases in the Al- Mn System.	telle. PB89-196166 900,620
Migration of Liquid Film and Grain Boundary in Mo-Ni Induced by W Diffusion.	PB90-123548 901,169	User Guide for Wizard: A Syntax-Directed Editor and Translator for Estelle.
PB89-157614 901,128	Quantitative Characterization of the Viscosity of a Microe- mulsion.	PB89-196174 900,621
Experimental Observations on the Initiation of DIGM (Diffusion Induced Grain Boundary Migration).	PB90-123597 900,524 Formation of Dispersoids during Rapid Solidification of an	Free Value Tool for ASN.1. PB89-196182 900,622
PB89-157630 901,130 Directional Invariance of Grain Boundary Migration in the	Al-Fe-Ni Alloy. PB90-123647 901,172	Object-Oriented Model for Estelle and Its Smalltalk Implementation.
Pb-Sn Cellular Transformation and the Tu-Turnbull Hysteresis.	Pressure Dependence of the Cu Magnetic Order in RBa2Cu3O6+ x.	PB89-196190 900,623
PB89-157911 901,134	PB90-123829 901,472	Application of Formal Description Techniques to Conformance Evaluation.
ASM/NBS (American Society for Metals/National Bureau of Standards) Numerical and Graphical Database for Binary Alloy Phase Diagrams	Charging Behavior of Polyethylene and Ionomers. PB90-136813 900,578	PB89-211908 900,652 Object-Oriented Model for Estelle.
Binary Alloy Phase Diagrams. PB89-157986 901,135	Evaluation of Data on Higher Heating Values and Elemental Analysis for Refuse-Derived Fuels.	PB89-211916 900,653
Phase Relations between the Polytitanates of Barium and the Barium Borates, Vanadates and Molybdates.	PB90-136839 900,845 PROPORTIONAL COUNTERS	Working Implementation Agreements for Open Systems Interconnection Protocols.
PB89-171789 901,032 Phase Equilibria and Crystal Chemistry in the Ternary	Use of an Imaging Proportional Counter in Macromolecular Crystallography.	PB89-221196 900,624 Trial of Open Systems Interconnection (OSI) Protocols
System BaO-TiO2-Nb2O5: Part 1. PB89-171797 901,033	PB90-136599 900,538	Over Integrated Services Digital Network (ISDN). PB89-235576 900,625
Stable and Metastable Phase Equilibria in the Al-Mn	PROPYNE High-Resolution, Slit Jet Infrared Spectroscopy of Hydro-	Working Implementation Agreements for Open Systems
System. PRO0.172224	carbons: Quantum State Specific Mode Mixing in CH	Interconnection Protocols.

PROTON AFFINITY	PB89-177216 901,220	PB89-180020 900,779
Gas Phase Proton Affinities and Basicities of Molecules: A Comparison between Theory and Experiment. PB89-146674 900,280	Ouantitative Problems in Magnetic Particle Inspection. PB89-229199 900,985	Radiation-Induced Interface Traps in Power MOSFETs. PB89-201974 900,784
PROTON MAGNETIC RESONANCE Morphological Partitioning of Ethyl Branches in Polyethyl-	Interlaboratory Determination of the Calibration Factor for the Measurement of the Interstitial Oxygen Content of	Numerical Simulations of Neutron Effects on Bipolar Transistors.
ene by (13)C NMR. PB89-176051 900,560	Silicon by Infrared Absorption. PB90-117300 900,224	PB90-123589 900,797 RADIATION PATTERNS
PUBLIC BUILDINGS NBS (National Bureau of Standards) Life-Cycle Cost	Preconcentration of Trace Transition Metal and Rare Earth Elements from Highly Saline Solutions. PB90-118175 900,226	Optically Linked Electric and Magnetic Field Sensor for Poynting Vector Measurements in the Near Fields of Ra- diating Sources.
(NBSLCC) Program (for Microcomputers). PB89-151211 900,849	Ouantitative Characterization of the Viscosity of a Microe- mulsion.	PB89-187595 900,712
Post-Occupancy Evaluation of Several U.S. Government Buildings.	PB90-123597 900,524 Determination of Experimental and Theoretical k (sub	RADIATION PROTECTION Simplified Shielding of a Metallic Restoration during Radi-
PB90-112384 900,088 PUBLISHING	ASi) Factors for a 200-kV Analytical Electron Microscope. PB90-128653	ation Therapy. PB89-229256 900,044
Electronic Publishing: Guide to Selection. PB89-214753 PULPING	QUANTIZATION Classical Chaos, the Geometry of Phase Space, and	Method for Evaluating Air Kerma and Directional Dose Equivalent for Currently Available Multi-Element Dose- meters in Radiation Protection Dosimetry.
Laser Excited Fluorescence Studies of Black Liquor. PB89-176416 900,243	Semiclassical Quantization. PB89-172381 901,506	PB90-117532 901,301 RADIATION SHIELDING
PULSE TECHNIQUES	QUANTUM CHROMODYNAMICS OCD Vacuum.	DCTDOS: Neutron and Gamma Penetration in Composite
One-Electron Transfer Reactions of the Couple SO2/ SO2(1-) in Aqueous Solutions. Pulse Radiolytic and	PB89-149124 901,486 QUANTUM EFFICIENCY	Duct Systems. PB89-188809 901,275
Cyclic Voltammetric Studies. PB89-176093 900,376	Interpolation of Silicon Photodiode Ouantum Efficiency as	RADIATION THERAPY Basic Data Necessary for Neutron Dosimetry.
PULSE TUBE REFRIGERATORS Refrigeration Efficiency of Pulse-Tube Refrigerators.	an Absolute Radiometric Standard. PB89-212245 901,445	PB89-171854 901,241
PB89-173892 901,007	High Accuracy Modeling of Photodiode Ouantum Efficiency.	RADIATION TRANSPORT Applications of ETRAN Monte Carlo Codes.
PUMPING (ELECTRONICS) Alignment Effects in Electronic Energy Transfer and Re-	PB90-117599 900,733	PB90-123902 901,574
active Events. AD-A202 820/7 900,267	QUANTUM HALL EFFECT Possible Quantum Hall Effect Resistance Standard.	Overview of ETRAN Monte Carlo Methods. PB90-123928 901,576
PURIFICATION	PB89-149058 900,801 Determination of the Time-Dependence of ohm NBS (Na-	RADIO SOURCES (ASTRONOMY) Proper Motion vs. Redshift Relation for Superluminal
Design Principles for a Large High-Efficiency Sub-Boiling Still. PB89-187553 900,207	tional Bureau of Standards) Using the Ouantized Hall Resistance.	Radio Sources. PB89-157663 900,017
PB89-187553 900,207 PURITY	PB89-230387 900,819	RADIOACTIVATION ANALYSIS
Preparation of Multistage Zone-Refined Materials for Thermochemical Standards.	NBS (National Bureau of Standards) Determination of the Fine-Structure Constant, and of the Ouantized Hall Re-	Activation Analysis Opportunities Using Cold Neutron Beams.
PB89-186795 900,203	sistance and Josephson Frequency-to-Voltage Ouotient in SI Units.	PB89-156970 <i>900,183</i>
PYRENES Standard Chemical Thermodynamic Properties of Polycy-	PB89-230437 901,556 QUANTUM JUMPS	RADIOACTIVE CONTAMINANTS Air Ouality Investigation in the NIH (National Institutes of
clic Aromatic Hydrocarbons and Their Isomer Groups. 2. Pyrene Senes, Naphthopyrene Senes, and Coronene	Precise Test of Ouantum Jump Theory. PB89-157390 901,339	Health) Radiation Oncology Branch. PB89-228977 900,079
Series. PB89-226591 900,459	QUASARS	RADIOACTIVE ISOTOPES
PYROCHLORE Neutron Powder Diffraction Structure and Electrical Prop-	Proper Motion vs. Redshift Relation for Superluminal Radio Sources.	Single Particle Standards for Isotopic Measurements of Uranium by Secondary Ion Mass Spectrometry.
erties of the Defect Pyrochlores Pb1.5M2O6.5 (M= Nb, Ta).	PB89-157663 900,017 QUASIPARTICLE MIXERS	PB89-201669 901,297 Journal of Research of the National Institute of Stand-
PB89-172431 900,363	SIS Ouasiparticle Mixers with Bow-Tie Antennas. PB89-157036 900,705	ards and Technology. November-December 1989. Volume 94, Number 6.
PYROLYSIS Fundamental Aspects of Key Issues in Hazardous Waste	QUENCH HARDENING	PB90-163874 900,542
Incineration. PB89-212104 Upward Flame Spread on Vertical Walls.	Ouasicrystals with 1-D Translational Periodicity and a Ten-Fold Rotation Axis. PB89-147383 901,123	Report on the 1989 Meeting of the Radionuclide Meas- urements Section of the Consultative Committee on Standards for the Measurement of Ionizing Radiations:
PB89-214787 900,141	QUENCHING (COOLING) Metastable Phase Production and Transformation in Al-	Special Report on Standards for Radioactivity. PB90-163916 900,545
Experimental Study of the Pyrolysis of Pure and Fire Retarded Cellulose.	Ge Alloy Films by Rapid Crystallization and Annealing Treatments.	RADIOACTIVE WASTE MANAGEMENT
PB89-228316 901,090 QUALITATIVE ANALYSIS	PB89-157622 901,129	Service Life of Concrete. PB89-215362 901,303
Moydite, (Y, REE) (B(OH)4)(CO3), a New Mineral Species from the Evans-Lou Pegmatite, Ouebec.	Solidification of Aluminum-Manganese Powders. PB89-172332 901,137	RADIOACTIVITY NBS (National Bureau of Standards) Radon-in-Water
PB89-157747 900,186	Concentration Dependence of the Compression Modulus of Isotactic Polystyrene/Cis-Decalin Gels.	Standard Generator. PB89-171888 901,295
QUALITY ASSURANCE Measurement Ouality Assurance.	PB89-172449 900,552	Report on the 1989 Meeting of the Radionuclide Meas-
PB89-147508 901,298 Potential Applications of a Sequential Construction Ana-	RACETRACK MICROTRONS NBS/NRL (National Bureau of Standards/Naval Re-	urements Section of the Consultative Committee on Standards for the Measurement of Ionizing Radiations:
lyzer. PB89-191670 900,105	search Laboratory) Free Electron Laser Facility. PB89-175749 901,351	Special Report on Standards for Radioactivity. PB90-163916 900,545
Ouality Assurance in Metals Analysis Using the Inductive-	RADIANCE NBS (National Bureau of Standards) Scale of Spectral	RADIOASSAY
ly Coupled Plasma. PB89-202063 900,213	Radiance. PB89-201685 901,532	Sequential Determination of Biological and Pollutant Elements in Marine Bivalves.
QUALITY CONTROL Critical Assessment of Requirements for Ceramic Powder	RADIATION	PB89-156897 <i>901,217</i> RADIOBIOLOGY
Characterization. PB89-146849 901,016	Combustion Efficiency, Radiation, CO and Soot Yield from a Variety of Gaseous, Liquid, and Solid Fueled	Structure of a Hydroxyl Radical Induced Cross-Link of Thymine and Tyrosine.
QUANTITATIVE ANALYSIS	Buoyant Diffusion Flames. PB89-231179 900,604	PB89-157838 901,244
Determining Picogram Ouantities of U in Human Unine by Thermal Ionization Mass Spectrometry.	RADIATION CHEMISTRY Radiation-Induced Crosslinks between Thymine and 2-D-	RADIOLOGY Improved Standards for Real-Time Radioscopy.
PB89-146906 900,175 Comparison of Detection Limits in Atomic Spectroscopic	Deoxyerythropentose. PB89-146682 900,247	PB90-128679 900,923
Methods of Analysis. PB89-150858 900,176	RADIATION DAMAGE	Standards for Real-Time Radioscopy. PB90-128687 900,924
Trace Speciation by HPLC-GF AA (High-Performance	Electron and Photon Stimulated Desorption: Probes of Structure and Bonding at Surfaces.	RADIOLYSIS One-Electron Transfer Reactions of the Couple SO2/
Liquid Chromatography-Graphite Furnace Atomic Absorp- tion) for Tin- and Lead-Bearing Organometallic Com-	PB89-157960 901,116 Laser Induced Damage in Optical Materials: 1987.	SO2(1-) in Aqueous Solutions. Pulse Radiolytic and Cyclic Voltammetric Studies.
pounds, with Signal Increases Induced by Transition- Metal Ions. PB89-157085 900,184	PB89-221162 901,364	PB89-176093 900,376
Role of Standards in Electron Microprobe Techniques.	RADIATION EFFECTS Ultrasonic Characterization of Surface Modified Layers.	RADIOMETERS Radiometer Equation and Analysis of Systematic Errors
PB89-176143 900,197 Defocus Modeling for Compositional Mapping with Wave-	PB89-147409 901,115 Chemical Characterization of Ionizing Radiation-Induced	for the NIST (National Institute of Standards and Technology) Automated Radiometers.
length-Dispersive X-ray Spectrometry. PB89-176150 900,378	Damage to DNA. PB89-151922 901,235	PB90-130907 900,832
Element-Specific Epifluorescence Microscopy In vivo	Correlation between CMOS (Complementary Metal Oxide	Blocked Impurity Band and Superlattice Detectors: Pros-
Monitoring of Metal Biotransformations in Environmental Matrices.	Semiconductor) Transistor and Capacitor Measurements of Interface Trap Spectra.	pects for Radiometry. PB89-212161 900,730

RADIOPRESERVATION Comprehensive Dosimetry for Food Irradiation.	PB89-214779 900,856	PB89-149215 900,873
PB89-186399 900,011	RAY DIFFRACTION Molybdenum Effect on Volume in Fe-Cr-Ni Alloys.	REACTIVE SCATTERING Three Dimensional Quantum Reactive Scattering Study
RADIOSCOPY Typical Magazine of Padiagonaia Systems, Papilias to a	PB89-157796 901,095	of the I + HI Reaction and of the IHI(1-) Photodetach-
Typical Usage of Radioscopic Systems: Replies to a Survey.	RAY TRACING Computing Ray Trajectories between Two Points: A Solu-	ment Spectrum. PB89-227961 900,466
PB90-117664 <i>901,161</i>	tion to the Ray-Linking Problem.	REAL TIME OPERATIONS
Site Characterization for Radon Source Potential.	PB89-176929 901,354 RAYLEIGH SCATTERING	Real-Time Control System Modifications for a Deburning Robot. User Reference Manual.
PB89-209274 901,290	Polymers Bearing Intramolecular Photodimerizable	PB89-159669 900,990
NBS (National Bureau of Standards) Radon-in-Water	Probes for Mass Diffusion Measurements by the Forced Rayleigh Scattering Technique: Synthesis and Character-	Real Time Generation of Smooth Curves Using Local Cubic Segments.
Standard Generator.	ization. PB89-157101 <i>901,181</i>	PB89-171623 901,196
PB89-171888 901,295 RAILROAD CARS	REACTION KINETICS	Real-Time Simulation and Production Scheduling Systems.
Ultrasonic Railroad Wheel Inspection Using EMATs	Evaluated Chemical Kinetic Data for the Reactions of Atomic Oxygen O(3P) with Sulfur Containing Compounds.	PB89-183230 900,974
(Electromagnetic-Accoustic Transducers), Report No. 18. PB89-189229 901.596	PB89-145122 900,269	REAL-TIME RADIOSCOPY
RAINFALL	Rate Constants for the Reaction HO2+ NO2+ N2-> HO2NO2+ N2: The Temperature Dependence of the	Improved Standards for Real-Time Radioscopy. PB90-128679 900,923
Chemical Kinetics of Intermediates in the Autoxidation of SO2.	Fall-Off Parameters.	Standards for Real-Time Radioscopy.
PB89-176754 900,256	PB89-146658 900,278 Electronic Structure of Diammine (Ascorbato) Platinum(II)	PB90-128687 900,924 REAL TIME SYSTEMS
RALEIGH WAVES Ultrasonic Texture Analysis for Polycrystalline Aggregates	and the Trans Influence on the Ligand Dissociation Energy.	Mining Automation Real-Time Control System Architec-
of Cubic Materials Displaying Orthotropic Symmetry.	PB89-147128 900,287	ture Standard Reference Model (MASREM). PB89-221154 901,286
PB89-146948 901,121 RAMAN SPECTRA	Implications of Phase Equilibria on Hydration in the Tri-	RECALESCENCE
Micro-Raman Characterization of Atherosclerotic and Bio-	calcium Silicate-Water and the Tricalcium Aluminate- Gypsum-Water Systems.	Undercooling and Microstructural Evolution in Glass
prosthetic Calcification. PB89-149223 901,234	PB89-150759 901,022	Forming Alloys. PB89-176465 <i>901,139</i>
Stokes and Anti-Stokes Fluorescence of Er(3+) in the	Reactions of Phenyl Radicals with Ethene, Ethyne, and Benzene.	RECOMBINANT PROTEINS
Raman Spectra of Erbium Oxide and Erbium Glasses, PB89-149231 901,020	PB89-150908 900,297	Preliminary Crystallographic Study of Recombinant Human Interleukin 1beta.
Picosecond Coherent Anti-Stokes Raman Scattering	Rate Constants for One-Electron Oxidation by Methylper- oxyl Radicals in Aqueous Solutions.	PB90-136730 901,251
(CARS) Study of Vibrational Dephasing of Carbon Disul-	PB89-151013 900,302	RED SHIFT
fide and Benzene in Solution. PB89-176408 900,380	Kinetics of Electron Transfer from Nitroaromatic Radical Anions in Aqueous Solutions. Effects of Temperature and	Proper Motion vs. Redshift Relation for Superluminal Radio Sources.
Influence of Molecular Weight on the Resonant Raman	Stenc Configuration. PB89-156749 900,305	PB89-157663 900,017
Scattering of Polyacetylene. PB89-179246 900,564	Hyperconjugation: Equilibrium Secondary Isotope Effect	REDUCTION (CHEMISTRY) Dichromate Dosimetry: The Effect of Acetic Acid on the
RAMAN SPECTROSCOPY	on the Stability of the t-Butyl Cation. Kinetics of Near- Thermoneutral Hydride Transfer.	Radiolytic Reduction Yield. PB89-147490 900.248
High Resolution Inverse Raman Spectroscopy of the CO Q Branch.	PB89-156756 900,306	One-Electron Transfer Reactions of the Couple SO2/
PB89-171292 900,355	Decay of High Valent Manganese Porphyrins in Aqueous Solution and Catalyzed Formation of Oxygen.	SO2(1-) in Aqueous Solutions. Pulse Radiolytic and
Effects of Velocity and State Changing Collisions on Raman Q-Branch Spectra.	PB89-156772 900,308	Cyclic Voltammetric Studies. PB89-176093 900,376
PB89-179196 900,391	S2F10 Formation in Computer Simulation Studies of the Breakdown of SF6.	REFERENCE MATERIALS
RAPID QUENCHING (METALLURGY)	PB89-157523 900,327	Optical Rotation. PB89-149256 900,294
Temperature Hysteresis in the Initial Susceptibility of Rapidly Solidified Monel.	Critical Review of the Chemical Kinetics of Sulfur Tetra- fluoride, Sulfur Pentafluoride, and Sulfur Fluoride (S2F10)	REFINERIES
PB90-123423 901,164	in the Gas Phase.	Failure Analysis of an Amine-Absorber Pressure Vessel. PB89-173835 901,101
TEM Observation of Icosahedral, New Crystalline and Glassy Phases in Rapidly Quenched Cd-Cu Alloys.	PB89-161582 900,347 Rate Constants for Hydrogen Abstraction by Resonance	REFLECTION
PB90-123514 901,166	Stabilized Radicals in High Temperature Liquids.	Effect of Multiple Internal Reflections on the Stability of
Amorphous Phase Formation in Al70Si17Fe13 Alloy. PB90-123522 901,167	PB89-161608 900,348 Absolute Rate Constants for Hydrogen Abstraction from	Electrooptic and Magnetooptic Sensors. PB89-171722 900,724
Solidification of an 'Amorphous' Phase in Rapidly Solidi-	Hydrocarbons by the Trichloromethylperoxyl Radical.	REFLECTION COEFFICIENT
fied Al-Fe-Si Alloys. PB90-123530 <i>901,168</i>	PB89-171532 900,357 Methyl Radical Concentrations and Production Rates in a	Reflection Coefficient of a Waveguide with Slightly Uneven Walls.
Microstructural Variations in Rapidly Solidified Alloys.	Laminar Methane/Air Diffusion Flame.	PB89-201057 900,753
PB90-123621 901,170	PB89-171912 900,591	REFRACTORIES Effect of Slag Penetration on the Mechanical Properties
Formation of Dispersoids during Rapid Solidification of an AI-Fe-Ni Alloy.	Modeling Chemical Reaction Systems on an IBM PC. PB89-171920 900,358	of Refractories: Final Report.
PB90-123647 901,172	One-Electron Transfer Reactions of the Couple SO2/	PB90-110065 900,836
Pathways for Microstructural Development in TiAl. PB90-123779 901,173	SO2(1-) in Aqueous Solutions. Pulse Radiolytic and Cyclic Voltammetric Studies.	REFRACTORY MATERIALS Effect of Coal Slag on the Microstructure and Creep Be-
RARE EARTH ELEMENTS	PB89-176093 900,376	havior of a Magnesium-Chromite Refractory. PB89-158034 901.027
Roles of Atomic Volume and Disclinations in the Magne- tism of the Rare Earth-3D Hard Magnets.	lon Kinetics and Energetics. PB89-176101 900,377	Laser Induced Vaporization Time Resolved Mass Spec-
PB89-202238 901,434	Influence of Electronic and Geometric Structure on De- sorption Kinetics of Isoelectronic Polar Molecules: NH3	trometry of Refractones. PB90-136904 900,540
Exchange and Magnetostrictive Effects in Rare Earth Su- perlattices.	and H2O.	REFRIGERANTS
PB89-202667 901,438	PB89-176473 900,381 Mechanism and Rate of Hydrogen Atom Attack on Tolu-	Experimental Determination of Forced Convection Evaporative Heat Transfer Coefficients for Non-Azeotropic Re-
Preconcentration of Trace Transition Metal and Rare Earth Elements from Highly Saline Solutions.	ene at High Temperatures.	frigerant Mixtures.
PB90-118175 900,226	PB89-179758 900,398 Evaluated Kinetics Data Base for Combustion Chemistry.	PB89-186407 901,117
RARE EARTH MINERALS	PB89-212096 900,601	Thermal Conductivity of Refrigerants in a Wide Range of Temperature and Pressure.
Moydite, (Y, REE) (B(OH)4)(CO3), a New Mineral Species from the Evans-Lou Pegmatite, Quebec.	Evaluated Kinetic and Photochemical Data for Atmos-	PB89-226583 900,458
PB89-157747 900,186	pheric Chemistry. Supplement 3. PB89-222582 900,454	Experimental Investigation and Modeling of the Flow Rate of Refrigerant 22 Through the Short Tube Restric-
RARE GASES Stark Broadening of Spectral Lines of Homologous,	Rate Constants for the Quenching of Excited States of	tor. PB89-229041 901,118
Doubly Ionized Inert Gases. PB89-158083 900,343	Metal Complexes in Fluid Solution. PB89-227797 900,461	Thermophysical-Property Needs for the Environmentally
Process Control during High Pressure Atomization.	Polymerization of a Novel Liquid Crystalline Diacetylene	Acceptable Halocarbon Refrigerants. PB89-231054 900,482
PB89-179170 901,142	Monomer. PB89-231286 900,575	Vapor Pressures and Gas-Phase PVT Data for 1,1,1,2-
Triplet Dipoles in the Absorption Spectra by Dense Rare Gas Mixtures. 1. Short Range Interactions.	Temperature Dependence of the Rate Constant for the	Tetrafluoroethane. PB90-117987 900,514
PB90-136755 900,539	Hydroperoxy + Methylperoxy Gas-Phase Reaction. PB90-136375 900,534	REFUSE DERIVED FUELS
RATE CONSTANTS Rate Constants for Reactions of Nitrogen Oxide (NO3)	Flash Photolysis Kinetic Absorption Spectroscopy Study	Evaluation of Data on Higher Heating Values and Ele-
Radicals in Aqueous Solutions.	of the Gas Phase Reaction HO2 + C2H5O2 Over the Temperature Range 228-380 K.	mental Analysis for Refuse-Derived Fuels. PB90-136839 900,845
PB89-176242 900,379 RATS	PB90-136565 900,536	REGENERATORS
Synergistic Effects of Nitrogen Dioxide and Carbon Diox-	REACTIVE GASES Special Calibration Systems for Reactive Gases and	Ineffectiveness of Powder Regenerators in the 10 K Temperature Range.
ide Following Acute Inhalation Exposures in Rats.	Other Difficult Measurements.	PB89-173876 901,005

Measurement of Regenerator Ineffectiveness at Low	Rating Procedure for Mixed Air-Source Unitary Air Conditioners and Heat Pumps Operating in the Cooling Mode.	ROBOTICS Fast Path Planning in Unstructured, Dynamic, 3-D
Temperatures. PB89-173884 901,006	Revision 1. PB89-193247 900,075	Worlds.
EINFORCED CONCRETE Knowledge Based System for Durable Reinforced Con-	Proposed Methodology for Rating Air-Source Heat	PB89-177067 900,992 Assessment of Robotics for Improved Building Oper-
crete.	Pumps That Heat, Cool, and Provide Domestic Water Heating.	ations and Maintenance. PB89-189146 900,092
PB89-150734 900,110 ELATIVITY	PB90-112368 900,087	Visual Perception Processing in a Hierarchical Control
Conceptual Design for a Mercury Relativity Satellite.	RESIDUAL STRESS Ultrasonic Determination of Absolute Stresses in Alumi-	System: Level 1. PB89-221188 900,994
PB89-234249 901,595 ELIABILITY	num and Steel Alloys.	ROBOTS 300,334
Interpretation of a between-Time Component of Error in	PB89-150957 901,124 Acoustoelastic Determination of Residual Stresses.	Optical Sensors for Robot Performance Testing and Cali-
Mass Measurements. PB89-149108 900,872	PB89-179808 901,318	bration. PB89-157358 900,987
EMOTE SENSING Remote Sensing Technique for Combustion Gas Temper-	RESINS Adhesion to Dentin by Means of Gluma Resin.	Material Handling Workstation Implementation.
ature Measurement in Black Liquor Recovery Boilers.	PB89-157168 900,039	PB89-159644 900,988 Material Handling Workstation: Operator Manual.
PB89-179568 900,392 EPLICATING	In vitro Investigation of the Effects of Glass Inserts on the Effective Composite Resin Polymerization Shrinkage.	PB89-159651 900,989
Bootstrap Inference for Replicated Experiments.	PB90-117516 900,049	Real-Time Control System Modifications for a Deburring Robot. User Reference Manual.
PB90-128273 900,914 EPRODUCIBILITY	RESISTANCE Determination of the Absolute Specific Conductance of	PB89-159669 900,990
Quantitative Problems in Magnetic Particle Inspection.	Primary Standard KCI Solutions. PB89-230320 900,481	Precision Weight Calibration with a Specialized Robot. PB89-173975 900,879
PB89-229199 900,985 ESEARCH	RESISTANCE STANDARDS	Building Representations from Fusions of Multiple Views.
Center for Electronics and Electrical Engineering Techni-	Possible Quantum Hall Effect Resistance Standard. PB89-149058 900,801	PB89-177059 900,991
cal Publication Announcements Covering Center Programs, April-June 1986 with 1987 CEEE Events Calen-	NBS (National Bureau of Standards) Ohm: Past-Present-	Hierarchically Controlled Autonomous Robot for Heavy Payload Military Field Applications.
dar. PB89-185623 900,711	Future. PB89-149066 900,802	PB89-177075 901,271
Journal of Research of the National Institute of Stand-	Determination of the Time-Dependence of ohm NBS (Na-	Interfaces to Teleoperation Devices. PB89-181739 900,993
ards and Technology, Volume 94, Number 3, May-June 1989.	tional Bureau of Standards) Using the Quantized Hall Resistance.	NASA/NBS (National Aeronautics and Space Administra-
PB89-211106 901,441	PB89-230387 900,819	tion/National Bureau of Standards) Standard Reference Model for Telerobot Control System Architecture
Dental Materials and Technology Research at the National Bureau of Standards: A Model for Government-Private	RESISTIVITY PROBES Economical Ultrahigh Vacuum Four-Point Resistivity	(NASREM). PB89-193940 901,589
Sector Cooperation. PB90-128711 900,052	Probe. PB89-147086 900,870	Inventory of Equipment in the Turning Workstation of the
ESEARCH FACILITIES	RESONANCE	AMRF (Automated Manufacturing Research Facility). PB89-215339 900,961
NBS (National Bureau of Standards) Free Electron Laser Facility.	Using 'Resonant' Charge Exchange to Detect Traces of	Recommended Technical Specifications for Procurement
PB89-176515 901,353	Noble Gas Atoms. PB89-176770 901,296	of Equipment for a Turning Workstation. PB89-215347 900,962
ESEARCH MANAGEMENT Implications of Computer-Based Simulation Models,	RESONANCE ABSORPTION	Robot Crane Technology.
Expert Systems, Databases, and Networks for Cement	Autodetaching States of Negative Ions. PB89-150767 900,295	PB90-111667 900,146
Research. PB89-146989 900,581	RESONANCE ENHANCED MULTIPHOTON IONIZATION SPECTROSCOPY	Teleoperation and Autonomy for Space Robotics. PB90-123811 901,591
Technical Activities 1987, Center for Basic Standards. PB89-185615 901,521	Multiphoton Ionization Spectroscopy and Vibrational	ROLLING STOCK
National Engineering Laboratory's 1989 Report to the	Analysis of a 3p Rydberg State of the Hydroxymethyl Radical.	EMATs (Electromagnetic Acoustic Transducers) for Roll- By Crack Inspection of Railroad Wheels.
National Research Council's Board on Assessment of NIST (National Institute of Standards and Technology)	PB89-146666 900,279	PB90-123894 901,597
Programs. PB89-189294 900,004	RESONANCE IONIZATION MASS SPECTROSCOPY Detection of Gas Phase Methoxy Radicals by Resonance	ROMANECHITE Refinement of the Substructure and Superstructure of
Effects of Research on Building Practice.	Enhanced Multiphoton Ionization Spectroscopy. PB89-156764 900,307	Romanechite.
PB89-202584 900,168	Analytical Applications of Resonance Ionization Mass	PB89-157721 901,392 ROOFING
International Cooperation and Competition in Materials Science and Engineering.	Spectrometry (RIMS). PB89-161590 900,189	Interim Criteria for Polymer-Modified Bituminous Roofing
PB89-228332 901,191 ESEARCH PROGRAM ADMINISTRATION	RESONANCE LIGHT SCATTERING	Membrane Materials. PB89-168025 900,114
Institute for Materials Science and Engineering, Polymers:	Resonance Light Scattering from a Liquid Suspension of Microspheres.	Tests of Adhesive-Bonded Seams of Single-Ply Rubber
Technical Activities 1988. PB89-166094 900,003	PB89-157887 901,340	Membranes. PB89-212120 900, 138
Institute for Materials Science and Engineering, Polymers:	RESONANCE SCATTERING Resonance Light Scattering from a Suspension of Mi-	Strain Energy of Bituminous Built-Up Membranes: A New
Technical Activities 1987. PB89-188601 900,566	crospheres. PB89-176234 901,352	Concept in Load-Elongation Testing. PB89-212203 900,139
ESEARCH PROGRAMS	RESPUTTERING	ASTM (American Society for Testing and Materials) Com-
Technical Activities 1986-1988, Molecular Spectroscopy Division.	Universal Resputtering Curve. PB89-234314 901,460	mittee Completes Work on EPDM Specification. PB89-212260 900,140
PB89-175418 900,372	RETARDANTS	ROOFS
ESEARCH PROJECTS Technical Activities, 1988, Center for Analytical Chemis-	Interpretation of the Effects of Retarding Admixtures on Pastes of C3S, C3A plus Gypsum, and Portland Cement.	Experimental Validation of a Mathematical Model for Predicting Moisture Transfer in Attics.
try. PB89-151773 <i>900,177</i>	PB89-146971 900,580	PB89-150783 900,057
Center for Chemical Technology: 1988 Technical Activi-	RETARDERS (DEVICES) Stability of Birefringent Linear Retarders (Waveplates).	Corrosion of Metallic Fasteners in Low-Sloped Roofs: A Review of Available Information and Identification of Re-
ties. PB89-156376 900,241	PB89-171672 901,345	search Needs. PB89-162580 900,113
NIST (National Institute of Standards and Technology)	REVERSE PHASE LIQUID CHROMATOGRAPHY Preparation of Glass Columns for Visual Demonstration	Probabilistic Models for Ground Snow Accumulation.
Research Reports, March 1989. PB89-189310 900,005	of Reversed Phase Liquid Chromatography. PB89-187546 900,206	PB89-186894 900,100 Results of a Survey of the Performance of EPDM (Ethyl-
NIST (National Institute of Standards and Technology) Research Reports, June 1989.	REVIEWS	ene Propylene Diene Terpolymer) Roofing at Army Facili-
PB89-235113 900,007	Institute for Materials Science and Engineering, Nonde- structive Evaluation: Technical Activities 1988.	ties. PB89-209316 900,136
Center for Radiation Research (of the National Institute of Standards and Technology) Technical Activities for	PB89-151625 900,917	Report of Roof Inspection: Characterization of Newly-
1989. PB90-130279 901,307	NIST (National Institute of Standards and Technology) Research Reports, June 1989.	Fabricated Adhesive-Bonded S eams at an Army Facility. PB90-112376 900,107
ESIDENTIAL BUILDINGS	PB89-235113 900,007	ROOMS
Experimental Validation of a Mathematical Model for Pre- dicting Moisture Transfer in Attics.	REYNOLDS NUMBER Measurements of Coefficients of Discharge for Concen-	Fire Propagation in Concurrent Flows. PB89-151781 900,867
PB89-150783 900,057	tric Flange-Tapped Square-Edged Orifice Meters in Water Over the Reynolds Number Range 600 to 2,700,000.	ROTARY VALVES
ZIP: The ZIP-Code Insulation Program (Version 1.0) Economic Insulation Levels for New and Existing Houses by	PB89-235147 901,334	Multiple Actuator Hydraulic System and Rotary Control Valve Therefor.
Three-Digit ZIP Code. Users Guide and Reference Manual.	RISK ASSESSMENT Fire Risk Analysis Methodology: Initiating Events.	PATENT-4 838 145 900,995
PB89-151765 900,058	PB89-184527 900,125	ROTATIONAL SPECTRA Microwave Spectrum and (14)N Quadrupole Coupling

Summary of the Assumptions and Limitations in Hazard I. PB90-136821 900,606

ZIP: ZIP-Code Insulation Program (for Microcomputers). PB89-159446

Microwave Spectrum and (14)N Quadrupole Coupling Constants of Carbazole. PB89-157333 900,319

Frequency Measurement of the $J=1<-0$ Rotational Transition of HD (Hydrogen Deuteride).	Low Pressure, Automated, Sample Packing Unit for Dif- fuse Reflectance Infrared Spectrometry.	PB89-172506 900,364 SECURE COMMUNICATION
PB89-161566 901,499 High Resolution Spectrum of the nu(sub 1) + nu(sub 2)	PB90-135922 900,235 SAMPLERS	Secure Military Communications Can Benefit from Accurate Time.
Band of NO2. A Spin Induced Perturbation in the Ground State.	Tests of the Recalibration Period of a Drifting Instrument.	PB89-176507 901,274
PB89-187561 900,417	PB89-176275 900,199 SAMPLING	SEISMIC DESIGN
Laser-Induced Fluorescence Study of Product Rotational State Distributions in the Charge Transfer Reaction:	Sample Validity in Biological Trace Element and Organic Nutrient Research Studies.	Wind and Seismic Effects. Proceedings of the Joint Meet ing of the U.S. Japan Cooperative Program in Natural Re
$Ar(1+)((sup 2 P)(sub 3/2)) + N2 \rightarrow Ar + N2(1+$	PB89-156905 901,218	sources Panel on Wind and Seismic Effects (20th) Held in Gaithersburg, Maryland on May 17-20, 1988.
)(X) at 0.28 and 0.40 eV. PB89-189823 900,420	SAN ANDREAS FAULT Relationships between Fault Zone Deformation and Seg-	PB89-154835 900,157
Calculation of Vibration-Rotation Spectra for Rare Gas- HCl Complexes.	ment Obliquity on the San Andreas Fault, California. PB89-185953 901.279	SELENIUM Microwave Digestion of Biological Samples: Selenium
PB89-228415 900,473	Rate of Change of the Quincy-Monument Peak Baseline	Analysis by Electrothermal Atomic Absorption Spectrom etry.
Improved Rotational Constants for HF. PB90-117466 901,376	from a Translocation Analysis of LAGEOS Laser Range Data.	PB89-229116 900,217
ROTATIONAL STATES	PB89-234272 901,282	Determination of Selenium and Tellurium in Coppe Standard Reference Materials Using Stable Isotope Dilu
Spectroscopic Detection Methods. PB89-228100 901,549	SANDS Method to Measure the Tensile Bond Strength between	tion Spark Source Mass Spectrometry. PB90-123472 900,230
State Selection via Optical Methods.	Two Weakly-Cemented Sand Grains. PB89-166110 901,483	SELF AVOIDING SURFACES
PB89-228118 901,550	Pore-Water Pressure Buildup in Clean Sands Because of	Universality Class of Planar Self-Avoiding Surfaces with Fixed Boundary.
Rotational Energy Levels and Line Intensities for (2S+1)Lambda-(2S+1) Lambda and (2S+1)(Lambda+ or	Cyclic Straining. PB89-175723 <i>900,159</i>	PB89-157945 900,338
 -)-(2S+ 1)Lambda Transitions in a Diatomic Molecule van der Waals Bonded to a Closed Shell Partner. 	SATELLITE ANTENNAS	SELF SPUTTERING
PB90-117441 900,498	X-Band Atmospheric Attenuation for an Earth Terminal Measurement System.	Dynamical Simulation of Liquid- and Solid-Metal Self Sputtering.
ROUGHNESS Fractal-Based Description of the Roughness of Blasted	PB90-100736 900,626	PB89-228407 900,472 SEMICONDUCTING FILMS
Steel Panels. PB89-158018 901,096	SATELLITE SURVEYS Environmental Intelligence.	Laser Probing of the Dynamics of Ga Interactions or
Effect of Pipe Roughness on Orifice Flow Measurement.	PB89-201214 901,287	Si(100). PB89-186928 <i>901,42</i> 2
PB89-231484 901,333	SAYRE EQUATION Sayre's Equation is a Chernov Bound to Maximum Entro-	Thermal Conductivity Measurements of Thin-Film Silicon
ROUTING Real-Time Optimization in the Automated Manufacturing	py. PB89-158174 <i>901,397</i>	Dioxide. PB89-212195 <i>901,444</i>
Research Facility. PB89-172597 900,947	SCALE (RATIO)	SEMICONDUCTOR DEVICES
RUBIDIUM	Scaling Applications in Fire Research. PB90-118068 900,149	Semiconductor Measurement Technology: Automatic De termination of the Interstitial Oxygen Content of Silicor
Using 'Resonant' Charge Exchange to Detect Traces of Noble Gas Atoms.	SCANDIUM	Wafers Polished on Both Sides. PB89-151831 900,772
PB89-176770 901,296	Wavelengths and Energy Level Classifications of Scandi- um Spectra for All Stages of Ionization.	Center for Electronics and Electrical Engineering Techni
Wavelengths and Energy Levels of the K I Isoelectronic Sequence from Copper to Molybdenum.	PB89-145163 900,273	cal Progress Bulletin Covering Center Programs, July to September 1988, with 1989 CEEE Events Calendar.
PB89-179097 901,372	Journal of Physical and Chemical Reference Data, Volume 17, 1988, Supplement No. 3. Atomic Transition	PB89-168033 900,775
RUBIDIUM 82 NBS (National Bureau of Standards) Decay-Scheme In-	Probabilities Scandium through Manganese. PB89-145197 900,276	Feasibility of Detector Self-Calibration in the Near Infra- red.
vestigations of (82)Sr-(82)Rb. PB89-161558 901,498	SCANNING	PB89-176788 900,384
RUBIDIUM IONS	Precise Laser Frequency Scanning Using Frequency-Synthesized Optical Frequency Sidebands: Application to	Center for Electronics and Electrical Engineering Technical Progress Bulletin Covering Center Programs, October
4s(2) 4p(2)-4s4p(3) Transition Array and Energy Levels of	Isotope Shifts and Hyperfine Structure of Mercury. PB90-118134 901,370	to December 1988, with 1989 CEEE Events Calendar. PB89-193270 900,813
the Germanium-Like Ions Rb VI - Mo XI. PB89-201065 901,528	SCANNING LIGHT MICROSCOPY	Center for Electronics and Electrical Engineering: Technic
RUTHENIUM Floation Stimulated Description Ion Angular Distributions	Strategy for Interpretation of Contrast Mechanisms in Scanning Electron Microscopy: A Tutorial.	cal Progress Bulletin Covering Center Programs, January to March 1989, with 1989 CEEE Events Calendar.
Electron-Stimulated-Desorption Ion-Angular Distributions. PB89-201230 901,430	PB89-172498 900,192 SCATTERING CROSS SECTIONS	PB89-209225 900,786
Coadsorption of Water and Lithium on the Ru(001) Surface.	Cross Sections for K-Shell X-ray Production by Hydrogen	Center for Electronics and Electrical Engineering Technical Publication Announcements. Covering Center Pro-
PB89-202956 900,440	and Helium Ions in Elements from Beryllium to Uranium. PB89-226609 900,460	grams, October/December 1988, with 1989 CEEE Events Calendar.
RYDBERG-KLEIN-REES METHOD Rydberg-Klein-Rees Inversion of High Resolution van der	SCHEDULING	PB89-209241 900,787
Waals Infrared Spectra: An Intermolecular Potential	Artificial Intelligence Techniques in Real-Time Production Scheduling.	Center for Electronics and Electrical Engineering Technical Publication Announcements. Covering Center Pro-
Energy Surface for Ar + HF (v = 1). PB89-227953 900,465	PB89-172571 900,945	grams, January-March 1989, with 1989 CEEE Events Cal endar.
RYDBERG SERIES	Functional Approach to Designing Architectures for Computer Integrated Manufacturing.	PB89-228308 900,788
One-Photon Resonant Two-Photon Excitation of Rydberg Series Close to Threshold.	PB89-172589 900,946 Real-Time Optimization in the Automated Manufacturing	Effects of Doping-Density Gradients on Band-Gap Narrowing in Silicon and GaAs Devices.
PB89-171276 901,343 RYDBERG STATES	Research Facility.	PB89-228522 901,453
Multiphoton Ionization Spectroscopy and Vibrational	PB89-172597 900,947 Real-Time Simulation and Production Scheduling Sys-	SEMICONDUCTORS Surface Structure and Growth Mechanism of Ga or
Analysis of a 3p Rydberg State of the Hydroxymethyl Radical.	tems. PB89-183230 900,974	Si(100).
PB89-146666 900,279	SCIENTIFIC DATA	PB89-149181 901,38; Neural Network Approach for Classifying Test Structure
SMATRIX THEORY Spherical-Wave Source-Scattering Matrix Analysis of	Internal Structure of the Guide to Available Mathematical Software.	Results.
Coupled Antennas: A General System Two-Port Solution. PB89-156798 900,696	PB89-170864 900,927	PB89-212187 900,788 SEMICONDUCTORS (MATERIALS)
SAFETY	SCINTILLATION COUNTERS Monte Carlo Calculated Response of the Dual Thin Scin-	Standards and Test Methods for VLSI (Very Large Scale
Safety Guidelines for Microwave Systems in the Analytical Laboratory.	tillation Detector in the Sum Coincidence Mode. PB89-176549 901,299	Integration) Materials. PB89-158042 900,774
PB90-118167 900,689	Advances in the Use of (3)He in a Gas Scintillation	AES and LEED Studies Correlating Desorption Energies
SAFETY ENGINEERING Guidelines and Procedures for Implementation of Execu-	Counter. PB90-123506 901.565	with Surface Structures and Coverages for Ga or Si(100).
tive Order on Seismic Safety.	SEARCH STRUCTURING	PB89-171599 901,400 Narrow-Angle Laser Scanning Microscope System fo
PB89-148092 900,156 Effects of Research on Building Practice.	Automated Analysis of Operators on State Tables: A Technique for Intelligent Search.	Linewidth Measurement on Wafers.
PB89-202584 900,168	PB89-157366 900,669	PB89-189344 900,782 Semiconductor Measurement Technology: Database fo
Test Results and Predictions for the Response of Near- Ceiling Sprinkler Links in a Full-Scale Compartment Fire.	SEARCHING Automated Analysis of Operators on State Tables: A	and Statistical Analysis of the Interlaboratory Determina
PB89-231187 900,095	Technique for Intelligent Search. PB89-157366 900,669	tion of the Conversion Coefficient for the Measuremen of the Interstitial Oxygen Content of Silicon by Infrared
SAMPLE PREPARATION Introduction to Microwave Acid Decomposition.	SECONDARY ELECTRONS	Absorption. PB89-221170 901,054
PB90-118191 900,227	Secondary-Electron Effects in Photon-Stimulated Desorption.	SENSITIVITY
Comparison of Microwave Drying and Conventional Drying Techniques for Reference Materials.	PB89-157929 900,337	Ambiguity Groups and Testability. PB90-128703 900,722
PB90-123464 900,229	SECONDARY ION MASS SPECTROSCOPY Dependence of Interface Widths on Ion Bombardment	SENSORS
Experiences in Environmental Specimen Banking. PB90-123969 900,866	Conditions in SIMS (Secondary Ion Mass Spectrometry) Analysis of a Ni/Cr Multilayer Structure.	Sensors for Intelligent Processing of Materials. PB89-202006 900,920

900,920

EPARATION Neutron Activation Analysis of the NIST (National Insti-	PB89-209241 900,787 SIGNAL TO NOISE RATIO	Solidification of an 'Amorphous' Phase in Rapidly Solidified Al-Fe-Si Alloys.
tute of Standards and Technology) Bovine Serum Stand- ard Reference Material Using Chemical Separations.	Effect of Random Errors in Planar Near-Field Measure- ment.	PB90-123530 901,168 SILICON DIOXIDE
PB89-156921 900,180 CO2 Separation Using Facilitated Transport Ion Ex-	PB89-171839 900,708 SIGNALS AND SYSTEMS	Microporous Fumed-Silica Insulation Board as a Candidate Standard Reference Material of Thermal Resist-
change Membranes. PB89-157374 900,321	Center for Electronics and Electrical Engineering Techni- cal Publication Announcements. Covering Center Pro-	ance. PB89-148373 <i>901,018</i>
Theory of Microphase Separation in Graft and Star Co- polymers. PB89-176028 900,557	grams, January-March 1989, with 1989 CEEE Events Calendar. PB89-228308 900,789	Dynamic Light Scattering and Angular Dissymmetry for the In situ Measurement of Silicon Dioxide Particle Syn- thesis in Flames.
Microphase Separation in Blockcopolymer/Homopolymer. PB89-176069 900,561	SILANE	PB89-179584 900,246
Facilitated Transport of CO2 through Highly Swollen Ion- Exchange Membranes: The Effect of Hot Glycenne Pre- treatment.	Surface Reactions in Silane Discharges. PB89-185961 900,406 SILICON	Correlation between CMOS (Complementary Metal Oxide Semiconductor) Transistor and Capacitor Measurements of Interface Trap Spectra. PB89-180020 900,779
PB89-179618 900,395 EQUENTIAL ANALYSIS	Surface Structure and Growth Mechanism of Ga on Si(100). PB89-149181 901,387	Thermal Conductivity Measurements of Thin-Film Silicon Dioxide.
Potential Applications of a Sequential Construction Analyzer.	Indirect Energy Gap of Si, Doping Dependence. PB89-150833 901,388	PB89-212195 901,444 EXAFS (Extended X-ray Absorption Fine Structure) Study
PB89-191670 900, 105 ERVICE LIFE	Semiconductor Measurement Technology: Automatic De- termination of the Interstitial Oxygen Content of Silicon	of Buried Germanium Layer in Silicon. PB89-228472 901,452
Prediction of Service Life of Building Materials and Components.	Wafers Polished on Both Sides. PB89-151831 900,772	Microporous Fumed-Silica Insulation as a Standard Ref- erence Material of Thermal Resistance at High Tempera-
PB89-158000 900,112 Relationship between Appearance and Protective Dura-	Structural Unit in Icosahedral MnAISi and MnAI. PB89-157648 901,131	ture. PB90-130311 <i>900,153</i>
bility of Coatings: A Literature Review. PB89-162598 901,063	Application of Multiscattering Theory to Impurity Bands in Si:As.	SILICON HYDRIDES Surface Reactions in Silane Discharges.
Preliminary Stochastic Model for Service Life Prediction of a Photolytically and Thermally Degraded Polymeric Cover Plate Material.	PB89-157762 900,334 Surface Structures and Growth Mechanism of Ga on	PB89-185961 900,406 SILICON OXIDES
PB89-173801 900,556	Si(100) Determined by LEED (Low Energy Electron Dif- fraction) and Auger Electron Spectroscopy.	Standard Aggregate Materials for Alkali-Silica Reaction Studies.
Prediction of Service Life of Construction and Other Materials. PB89-175848 900,120	PB89-171342 901,399 AES and LEED Studies Correlating Desorption Energies	PB89-193221 901,046 Low Temperature Mechanical Property Measurements of
ETTING TIME Implications of Phase Equilibria on Hydration in the Tri-	with Surface Structures and Coverages for Ga on Si(100).	Silica Aerogel Foam. PB90-128638 <i>901,061</i>
calcium Silicate-Water and the Tricalcium Aluminate- Gypsum-Water Systems.	PB89-171599 901,401 Effects of a Gold Shank-Overlayer on the Field Ion Imag-	SILOXANES Reevaluation of Forces Measured Across Thin Polymer
PÉ89-150759 901,022 Set Time Control Studies of Polymer Concrete.	ing of Silicon. PB89-175988 901,404	Films: Nonequilibrium and Pinning Effects. PB89-228589 900,573
PB90-111238 901,057	Laser Probing of the Dynamics of Ga Interactions on Si(100).	SILVER Temperature-Dependent Radiation-Enhanced Diffusion in
Circular and Square Edge Effect Study for Guarded-Hot- Plate and Heat-Flow-Meter Apparatuses.	PB89-186928 901,422 Bond Selective Chemistry with Photon-Stimulated De-	lon-Bombarded Solids. PB89-179188 901,408
PB89-176135 900,881 Summary of Circular and Square Edge Effect Study for	sorption. PB89-201222 900,259	SIMULATION Control System Simulation in North America.
Guarded-Hot-Plate and Heat-Flow-Meter Apparatuses. PB89-176606 900,884	Infrared Absorption Cross Section of Arsenic in Silicon in the Impunity Band Region of Concentration. PB89-201750 900,426	PB89-157010 900,091 Real-Time Simulation and Production Scheduling Sys-
Equilibrium Crystal Shapes and Surface Phase Diagrams at Surfaces in Ceramics.	Chemisorption of HF (Hydrofluoric Acid) on Silicon Sur-	tems. PB89-183230 900,974
PB90-117755 901, 162 HEAR PROPERTIES	faces. PB89-212013 900,445	SINGLE CRYSTALS Exchange and Magnetostrictive Effects in Rare Earth Su-
Prediction of Shear Viscosity and Non-Newtonian Behavior in the Soft-Sphere Liquid. PB89-228035 901,548	Semiconductor Measurement Technology: Database for and Statistical Analysis of the Interlaboratory Determina- tion of the Conversion Coefficient for the Measurement	perlattices. PB89-202667 901,438
Apparatus for Neutron Scattering Measurements on Sheared Fluids.	of the Interstitial Oxygen Content of Silicon by Infrared Absorption.	Fundamental Characterization of Clean and Gas-Dosed Tin Oxide.
PB89-235667 901,335	PB89-221170 901,054 Silicon Photodiode Detectors for EXAFS (Extended X-ray	PB89-202964 900,785 EXAFS (Extended X-ray Absorption Fine Structure) Study
HEAR RATE Measurement of Shear Rate on an Agitator in a Fermentation Broth.	Absorption Fine Structure). PB89-228498 900,731	of Buried Germanium Layer in Silicon. PB89-228472 901,452
PB89-186720 901,009 HEAR TESTS	Effects of Doping-Density Gradients on Band-Gap Narrowing in Silicon and GaAs Devices.	Thermomechanical Detwinning of Superconducting YBa2Cu3O7-x Single Crystals.
Shear Dilatancy and Finite Compressibility in a Dense Non-Newtonian Liquid.	PB89-228522 901,453 AC Impedance Method for High-Resistivity Measure-	PB89-231088 901,458 SINGLE MODE FIBERS
PB89-174023 901,328 HIELDED ROOMS	ments of Silicon. PB89-231203 900,793	Comparison of Far-Field Methods for Determining Mode Field Diameter of Single-Mode Fibers Using Both Gaus- sian and Petermann Definitions.
Electromagnetic Fields in Loaded Shielded Rooms. PB89-180426 900,780	Electron Transmission Through NiSi2-Si Interfaces. PB89-231294 900,485	PB90-117474 900,756
HOCK ABSORBERS Static Tests of One-third Scale Impact Limiters.	Interlaboratory Determination of the Calibration Factor for the Measurement of the Interstitial Oxygen Content of Silicon by Infrared Absorption.	SINTERING Small Angle Neutron Scattering from Porosity in Sintered Alumina.
PB89-216469 901,000 HRINKAGE	PB90-117300 900,224 Photon-Stimulated Description of Fluorine from Silicon via	PB89-157564 901,026 Ostwald Ripening in a System with a High Volume Frac-
In vitro Investigation of the Effects of Glass Inserts on the Effective Composite Resin Polymerization Shrinkage. PB90-117516 900,049	Substrate Core Excitations. PB90-118027 900,517	tion of Coarsening Phase. PB89-157598 901,126
CK BUILDING SYNDROME Investigation of a Washington, DC Office Building.	Silicon Photodiode Self-Calibration. PB90-118159 900,734	Densification, Susceptibility and Microstructure of Ba2YCu3O(6+ x). PB89-171821 901,035
PB89-230361 900,081	Interaction of In Atom Spin-Orbit States with Si(100) Surfaces. PB90-128547 900,532	Creep Cavitation in Liquid-Phase Sintered Alumina.
GNAL ACQUISITION Center for Electronics and Electrical Engineering Technical Progress Rulletin Covering Center Programs, July to	SILICON CARBIDES	Effect of Heat Treatment on Crack-Resistance Curves in
cal Progress Bulletin Covering Center Programs, July to September 1988, with 1989 CEEE Events Calendar. PB89-168033 900,775	Novel Process for the Preparation of Fiber-Reinforced Ceramic-Matrix Composites. PB89-179733 901,074	a Liquid-Phase-Sintered Alumina. PB89-229231 901,056 SITE SELECTION
GNAL PROCESSING Center for Electronics and Electrical Engineering Techni-	Creep Rupture of a Metal-Ceramic Particulate Composite. PB89-211825 901,077	Internal Revenue Service Post-of-Duty Location Modeling System: Programmer's Manual for PASCAL Solver.
cal Progress Bulletin Covering Center Programs, October to December 1988, with 1989 CEEE Events Calendar. PB89-193270 900,813	Laboratory Measurement of the 1(sub 01)-0(sub 00) Transition and Electric Dipole Moment of SiC2.	PB89-161905 900,001 Internal Revenue Service Post-of-Duty Location Modeling
Center for Electronics and Electrical Engineering: Technical Progress Bulletin Covering Center Programs, January	Toughening Mechanisms in Ceramic Composites. Semi-	System: Programmer's Manual for FORTRAN Driver Version 5.0. PB89-161913 900,002
to March 1989, with 1989 CEEE Events Calendar. PB89-209225 900,786	Annual Progress Report for the Period Ending March 31, 1989. PB89-235907 901,080	SITE SURVEYS Power Quality Site Surveys: Facts, Fiction, and Fallacies.
Center for Electronics and Electrical Engineering Techni- cal Publication Announcements. Covering Center Pro- grams, October/December 1988, with 1989 CEEE Events	SILICON CONTAINING ALLOYS Amorphous Phase Formation in AI70Si17Fe13 Alloy.	PB89-171656 900,805
Calendar.	PB90-123522 901,167	Site Characterization for Radon Source Potential. PB89-209274 901,290

Tilt Observations Using Borehole Tiltmeters 1. Analysis of	PB89-151211 900,849	SOLITONS
Tidal and Secular Tilt. PB90-136649 901,283	ZIP: ZIP-Code Insulation Program (for Microcomputers). PB89-159446 900,060	Computer Simulation Studies of the Soliton Model. 3. Nonconfluent Regimes and Soliton Interactions.
SIZE DETERMINATION Circular and Square Edge Effect Study for Guarded-Hot-	HAZARD I Fire Hazard Assessment Method. PB89-215404 900,143	PB89-202469 901,537 SOLUBILITY
Plate and Heat-Flow-Meter Apparatuses. PB89-176135 900,881	SOFTWARE CONFIGURATION MANAGEMENT Software Configuration Management: An Overview.	Decorated Lattice Gas Model for Supercritical Solubility. PB89-175681 900,373
Summary of Circular and Square Edge Effect Study for Guarded-Hot-Plate and Heat-Flow-Meter Apparatuses. PB89-176606 900,884	PB89-193833 900,651 SOFTWARE ENGINEERING	Gas Solubility and Henry's Law Near the Solvent's Critical Point.
SIZE SEPARATION	Case History: Development of a Software Engineering Standard.	PB89-202485 900,434
Characterization of Organolead Polymers in Trace Amounts by Element-Specific Size-Exclusion Chromatog-	PB89-149116 900,665	NaCI-H2O Coexistence Curve Near the Critical Tempera- ture of H2O. PB89-202519 900,436
raphy. PB89-175962 <i>900,196</i>	Automated Documentation System for a Large Scale Manufacturing Engineering Research Project. PB89-150809 900,941	Evaluation of Data on Solubility of Simple Apolar Gases
SKEWED DENSITY FUNCTIONS Estimation of an Asymmetrical Density from Several	Software Configuration Management: An Overview.	in Light and Heavy Water at High Temperature. PB90-126251 900,529
Small Samples. PB89-201131 <i>901,212</i>	PB89-193833 900,651 Federal Software Engineering Standards Program.	SOLUTION MINING Novel Flow Process for Metal and Ore Solubilization by
SKIN EFFECT Scattering Parameters Representing Imperfections in Pre-	PB89-211965 900,666 Software Verification and Validation: Its Role in Computer	Aqueous Methyl Iodide. PB89-202113 901,285
cision Coaxial Air Lines. PB89-184121 900,750	Assurance and its Relationship with Software Project Management Standards.	SOLUTIONS Determination of the Absolute Specific Conductance of
SLAGS Effect of Coal Slag on the Microstructure and Creep Be-	PB90-111691 900,655 SOIL ANALYSIS	Determination of the Absolute Specific Conductance of Primary Standard KCI Solutions. PB89-230320 900,481
havior of a Magnesium-Chromite Refractory. PB89-158034 901,027	Site Characterization for Radon Source Potential.	SOLVATION SOLVATION
Effect of Slag Penetration on the Mechanical Properties	PB89-209274 901,290 SOIL GASES	Filling of Solvent Shells About Ions. 1. Thermochemical Criteria and the Effects of Isomeric Clusters.
of Refractories: Final Report. PB90-110065 900,836	Site Characterization for Radon Source Potential. PB89-209274 901,290	PB89-157549 <i>900,329</i>
SLIDING FRICTION Measurements of Tribological Behavior of Advanced Ma-	SOIL MECHANICS	Thermochemistry of Solvation of SF6(1-) by Simple Polar Organic Molecules in the Vapor Phase. PB89-202527 900,437
terials: Summary of U.S. Results on VAMAS (Versailles Advanced Materials and Standards) Round-Robin No. 2.	Laboratory Evaluation of an NBS (National Bureau of Standards) Polymer Soil Stress Gage. PB89-211973 901,291	SOLVENT EXTRACTION
PB90-130295 901,003 SMALL COMPUTER SYSTEM INTERFACE (SCSI) DEVICES	SOIL TESTS	Influence of Reaction Reversibility on Continuous-Flow Extraction by Emulsion Liquid Membranes.
Small Computer System Interface (SCSI) Command System: Software Support for Control of Small Computer	Dielectric Mixing Rules for Background Test Soils. PB89-188585 901,289	PB89-176481 900,244 SOLVENTS
System Interface Devices. PB89-151815 900,659	SOLAR CELL ARRAYS Lightning and Surge Protection of Photovoltaic Installa-	Gas Solubility and Henry's Law Near the Solvent's Criti-
SMOKE Light Scattering from Simulated Smoke Agglomerates.	tions. Two Case Histories: Vulcano and Kythnos. PB89-229058 900,851	cal Point. PB89-202485 <i>900,434</i>
PB89-157234 900,588	SOLAR FLARES	SOOT Aerodynamics of Agglomerated Soot Particles.
Computer Model of Smoke Movement by Air Conditioning Systems (SMACS).	Helium Resonance Lines in the Flare of 15 June 1973. PB90-118142 900,028	PB89-147482 900,586
PB89-157267 900,059 False Alarm Study of Smoke Detectors in Department of	SOLAR MAGNETIC FIELDS Solar and Stellar Magnetic Fields and Structures: Obser-	Soot Inception in Hydrocarbon Diffusion Flames. PB89-201966 900,599
Veterans Affairs Medical Centers (VAMCS). PB89-193288 900,093	vations. PB90-118118 900,027	SOS (SEMICONDUCTORS) Growth and Properties of High-Quality Very-Thin SOS
Outline of a Practical Method of Assessing Smoke Hazard.	SOLIDIFICATION Proceedings of the Workshop on Cement Stabilization of	(Silicon-on Sapphire) Films. PB90-128109 900,798
PB89-211858 900,078 SMOKE ABATEMENT	Low-Level Radioactive Waste. Held at Gaithersburg, Maryland on May 31-June 2, 1989.	SOUND TRANSDUCERS
Capabilities of Smoke Control: Fundamentals and Zone Smoke Control.	NUREG/CP-0103 901,302 Ultrasonic Characterization of Surface Modified Layers.	Vector Calibration of Ultrasonic and Acoustic Emission Transducers. PB99-202014 900,765
PB89-229157 900,080 Experimental Fire Tower Studies of Elevator Pressuriza-	PB89-147409 901,115	SOUND TRANSMISSION
tion Systems for Smoke Control. PB90-117813 900,097	Solutal Convection during Directional Solidification. PB89-150932 901,322	Speed of Sound in Natural Gas Mixtures. PB89-174031 900,840
SNOW Probabilistic Models for Ground Snow Accumulation.	Kinetics of Resolidification. PB89-176457 901,138	Speed of Sound in a Mercury Ultrasonic Interferometer Manometer.
PB89-186894 <i>900,100</i>	Undercooling and Microstructural Evolution in Glass Forming Alloys.	PB89-202220 901,319 SPACE HEATERS
SODIUM State Selection in Electron-Atom Scattering: Spin-Polar-	PB89-176465 901,139 Formation and Stability Range of the G Phase in the Alu-	Fire Risk Analysis Methodology: Initiating Events.
ized Electron Scattering from Optically Pumped Sodium. PB89-176572 901,513	minum-Manganese System. PB89-186316 901,144	PB89-184527 900,125 SPACE POWER REACTORS
Wheatleyite, Na2Cu(C2O4)2 . 2H2O, a Natural Sodium Copper Salt of Oxalic Acid.	Nucleation and Growth of Aperiodic Crystals in Aluminum	Detection of Uranium from Cosmos-1402 in the Strato- sphere.
PB89-179154 900,390 Nonadiabatic Theory of Fine-Structure Branching Cross-	Alloys. PB89-186324 <i>901,145</i>	PB89-156962 901,592 SPACE SHUTTLE MAIN ENGINE
Sections for Sodium-Helium, Sodium-Neon, and Sodium- Argon Optical Collisions.	Replacement of Icosahedral Al-Mn by Decagonal Phase. PB89-186332 901,146	Vortex Shedding Flowmeter for Fluids at High Flow Ve-
PB89-202162 900,433 Sodium Doppler-Free Collisional Line Shapes.	Effect of Anisotropic Thermal Conductivity on the Morphological Stability of a Binary Alloy.	locities. PB90-128661 900,608
PB89-234306 901,559	PB89-228985 901,155 Temperature Hysteresis in the Initial Susceptibility of	SPACEBORNE ASTRONOMY Proceedings of the Celebratory Symposium on a Decade
Exoergic Collisions of Cold Na*-Na. PB90-123761 901,571	Rapidly Solidified Monel. PB90-123423 901,164	of UV (Ultraviolet) Astronomy with the IUE Satellite, Volume 2.
SODIUM ATOMS Progress on Spin Detectors and Spin-Polarized Electron	TEM Observation of Icosahedral, New Crystalline and	N89-16535/1 900,014 SPACECRAFT ANTENNAS
Scattering from Na at NIST. PB90-128299 901,583	Glassy Phases in Rapidly Quenched Cd-Cu Álloys. PB90-123514 901,166	Development of Near-Field Test Procedures for Commu- nication Satellite Antennas, Phase 1, Part 2.
Superelastic Scattering of Spin-Polarized Electrons from Sodium.	Solidification of an 'Amorphous' Phase in Rapidly Solidified Al-Fe-Si Alloys.	PB89-156152 901,593
PB90-128307 901,584 SODIUM CHLORIDE	PB90-123530 901,168 Microstructural Vanations in Rapidly Solidified Alloys.	SPACECRAFT ELECTRONIC EQUIPMENT Expert Systems Applied to Spacecraft Fire Safety.
NaCl-H2O Coexistence Curve Near the Critical Temperature of H2O.	PB90-123621 901,170 Rapid Solidification and Ordering of B2 and L2 (sub 1)	PB89-231013 901,590 SPACECRAFT POWER SUPPLIES
PB89-202519 <i>900,436</i>	Phases in the NiAl-NiTi System. PB90-123639 901,171	Strategic Defense Initiative Space Power Systems Metrology Assessment.
SODIUM HYDRIDES Infrared Spectrum of Sodium Hydride.	Formation of Dispersoids during Rapid Solidification of an	PB̃89-173405 <i>901,268</i>
PB89-230296 900,480 SODIUM HYDROXIDE	AI-Fe-Ni Alloy. PB90-123647 901,172	SPATIAL DISTRIBUTION Numerical Simulation of Morphological Development
Experimental Study of the Pyrolysis of Pure and Fire Retarded Cellulose.	SOLIDS Electron and Photon Stimulated Desorption: Probes of	during Ostwald Ripening. PB89-201990 901,152
PB89-228316 901,090 SOFTWARE	Structure and Bonding at Surfaces. PB89-157960 901,116	SPECIAL RELATIVITY Fundamental Tests of Special Relativity and the Isotropy
NBS (National Bureau of Standards) Life-Cycle Cost (NBSLCC) Program (for Microcomputers).	Cross Sections for Inelastic Electron Scattering in Solids. PB89-202972 901,440	of Space. PB89-185920 901,523
,		50 1,525

		• · · · · · · · · · · · · · · · · · · ·
PECIFIC HEAT	PB89-185888 900,402	PB89-229009 900,094
Thermodynamics of Ammonium Scheelites. 6. An Analysis of the Heat Capacity and Ancillary Values for the Me-	SPECTRUM ANALYSIS Multiphoton Ionization Spectroscopy and Vibrational	Test Results and Predictions for the Response of Near- Ceiling Sprinkler Links in a Full-Scale Compartment Fire.
taperiodates KIO4, NH4IO4, and ND4IO4. PB89-147060 900,285	Analysis of a 3p Rydberg State of the Hydroxymethyl	PB89-231187 900,095
Development of Standard Measurement Techniques and	Radical. PB89-146666 900,279	SPUTTERING
Standard Reference Materials for Heat Capacity and Heat of Vaporization of Jet Fuels.	Ozonolysis of Ethylene. Microwave Spectrum, Molecular	Sputter Deposition of Icosahedral Al-Mn and Al-Mn-Si. PB89-147102 901,122
PB89-148100 900,837	Structure, and Dipole Moment of Ethylene Primary Ozon- ide (1,2,3-Trioxolane).	Sputtered Thin Film Ba2YCu3On.
Experimental Thermal Conductivity, Thermal Diffusivity,	PB89-157440 900,323	PB89-165427 901,029
and Specific Heat Values of Argon and Nitrogen. PB89-148407 900,293	Shimanouchi, Takehiko and the Codification of Spectros- copic Information.	Universal Resputtering Curve. PB89-234314 901,460
Specific Heat of Insulations.	PB89-157846 900,335	SQUEEZED LIGHT
PB89-172514 900,116 Specific Heat Measurements of Two Premium Coals.	Effects of Pressure on the Vibrational Spectra of Liquid Nitromethane.	Systems Driven by Colored Squeezed Noise: The Atomic
PB89-173900 900,839	PB89-158026 900,342	Absorption Spectrum. PB89-171185 901,500
Thermodynamic Properties of Dioxygen Difluoride (O2F2)	Atomic Transition Probabilities of Argon: A Continuing Challenge to Plasma Spectroscopy.	Generation of Squeezed Light by Intracavity Frequency
and Dioxygen Fluoride (O2F). PB89-222566 900,452	PB89-158125 900,344	Doubling. PB89-227938 <i>901,365</i>
Measurements of Molar Heat Capacity at Constant	Far-Infrared Spectrum of Methyl Amine. Assignment and Analysis of the First Torsional State.	SQUID DEVICES
Volume: Cv,m(xCH4+ (1-x)C2H6' T = 100 to 320 K, p < or = 35 MPa).	PB89-161574 900,346	Noise in DC SQUIDS with Nb/Al-Oxide/Nb Josephson Junctions.
PB90-117896 900,844	Aluminumlike Spectra of Copper through Molybdenum. PB89-172365 900,360	PB89-201032 900,763
PECIFICATIONS Standard Specifications for Cements and the Role in	Infrared Spectrum of the nu6, nu7, and nu8 Bands of	Impedance of Radio-Frequency Biased Resistive Super-
Their Development of Quality Assurance Systems for	HNO3.	conducting Quantum Interference Devices. PB89-201719 900,764
Laboratories. PB89-150742 <i>901,021</i>	PB89-172415 900,362 Dependence of Interface Widths on Ion Bombardment	STABILITY
Recommended Technical Specifications for Procurement	Conditions in SIMS (Secondary Ion Mass Spectrometry)	Elastic Interaction and Stability of Misfitting Cuboidal In- homogeneities.
of Equipment for a Turning Workstation. PB89-215347 900,962	Analysis of a Ni/Cr Multilayer Structure. PB89-172506 900,364	PB89-157903 901,482
PECTRA	Near-Threshold X-ray Fluorescence Spectroscopy of Mol-	Millisecond Pulsar Rivals Best Atomic Clock Stability.
Resonance Light Scattering from a Suspension of Microspheres.	ecules. PB89-176523 900,382	PB89-185722 900,629 In Search of the Best Clock.
PB89-176234 901,352	Luminescence Standards for Macro- and Microspectro-	PB90-117367 900,632
Drift Tubes for Characterizing Atmospheric Ion Mobility Spectra.	fluorometry. PB89-176598 900,383	STABILIZATION
PB90-128513 901,585	Structure and Dynamics of Molecular Clusters via High	Proceedings of the Workshop on Cement Stabilization of Low-Level Radioactive Waste. Held at Gaithersburg,
PECTRAL LINES	Resolution IR Absorption Spectroscopy. PB89-185896 900,403	Maryland on May 31-June 2, 1989. NUREG/CP-0103 901,302
Thermal Shifts of the Spectral Lines in the (4)F3/2 to (4)I11/2 Manifold of an Nd:YAG Laser.	High Resolution Optical Multiplex Spectroscopy.	Stabilization of Ascorbic Acid in Human Plasma, and Its
PB89-157382 901,338	PB89-185938 900,404	Liquid-Chromatographic Measurement.
Stark Broadening of Spectral Lines of Homologous, Doubly lonized Inert Gases.	Scheme for a 60-nm Laser Based on Photopumping of a High Level of Mo(6+) by a Spectral Line of Mo(11+).	PB89-179279 901,237
PB89-158083 900,343	PB89-186415 900,407	STAINLESS STEEL-305 Tensile Tests of Type 305 Stainless Steel Mine Sweeping
Atomic Transition Probabilities of Argon: A Continuing Challenge to Plasma Spectroscopy.	Chlorine-like Spectra of Copper to Molybdenum. PB90-117706 900.501	Wire Rope. PB90-130287 901,112
PB89-158125 900,344	Analysis of Magnesiumlike Spectra from Cu XVIII to Mo	
Scattering of Polarized Light in Spectral Lines with Partial	XXXI. PB90-117821 900,508	STANLESS-STEEL-316LN Effect of Chemical Composition on the 4 K Mechanical
Frequency Redistribution: General Redistribution Matrix. PB89-171607 901,344	Microwave Spectrum of Methyl Amine: Assignment and	Properties of 316LN-Type Alloys.
PECTRAL METHODS	Analysis of the First Torsional State. PB90-117839 900,509	PB90-128554 901,110
Elimination of Spurious Eigenvalues in the Chebyshev Tau Spectral Method.	Laser Induced Vaporization Time Resolved Mass Spec-	Fracture Behavior of 316LN Alloy in Uniaxial Tension at Cryogenic Temperatures.
PB89-209282 901,330	trometry of Refractories.	PB90-128562 <i>901,111</i>
PECTROMETERS Measurement of Integrated Tuning Elements for SIS	PB90-136904 900,540 Spectroelectrochemistry of a System Involving Two Con-	STAINLESS STEELS
Mixers with a Fourier Transform Spectrometer.	secutive Electron-Transfer Reaction.	Metallurgical Evaluation of 17-4 PH Stainless Steel Castings.
PB89-157051 900,706 PECTROPHOTOMETRY	PB90-136979 900,237 SPEECH	PB89-193262 901,105
Voltammetric and Liquid Chromatographic Identification	PCM/VCR Speech Database Exchange Format.	Ferrite Number Prediction to 100 FN in Stainless Steel Weld Metal.
of Organic Products of Microwave-Assisted Wet Ashing of Biological Samples.	PB89-176713 900,633	PB89-201586 901,106
PB89-157994 900,188	SPEECH RECOGNITION Compensating for Vowel Coarticulation in Continuous	Stainless Steel Weld Metal: Prediction of Ferrite Content.
Absolute Rate Constants for Hydrogen Abstraction from Hydrocarbons by the Trichloromethylperoxyl Radical.	Speech Recognition.	PB89-231260 901,107 Tensile and Fatigue-Creep Properties of a Copper-Stain-
PB89-171532 900,357	PB89-176721 900,634 SPHERICAL SCANNING	less Steel Laminate.
Chemical Calibration Standards for Molecular Absorption	Improved Spherical and Hemispherical Scanning Algo-	PB90-128646 901,083
Spectrometry. PB89-171938 900,191	rithms. PB89-156806 900,697	STANDARD REFERENCE DATA Journal of Physical and Chemical Reference Data,
Exploratory Research in Reflectance and Fluorescence	SPHERICAL SHELLS	Volume 17, Number 4, 1988. PB89-145114 900,268
Standards at the National Bureau of Standards. PB89-202022 900,428	Microwave Measurements of the Thermal Expansion of a Spherical Cavity.	Evaluated Chemical Kinetic Data for the Reactions of
PECTRORADIOMETERS	PB89-147458 900,291	Atomic Oxygen O(3P) with Sulfur Containing Compounds.
NBS (National Bureau of Standards) Scale of Spectral Radiance.	SPIN GLASS STATE	
PB89-201685 901,532	Re-Entrant Spin-Glass Properties of a-(FexCr1- x)75P15C10.	New International Skeleton Tables for the Thermodynamic Properties of Ordinary Water Substance.
PECTROSCOPIC ANALYSIS	PB89-157481 901,391	PB89-145130 900,270
Shimanouchi, Takehiko and the Codification of Spectros- copic Information.	SPIN ORBIT INTERACTIONS Neutron Scattering Study of the Spin Ordering in Amor-	Benzene Thermophysical Properties from 279 to 900 K at Pressures to 1000 Bar.
PB89-157846 900,335	phous Tb45Fe55 and Tb25Fe75.	PB89-145148 900,271
Spectroscopic Quantitative Analysis of Strongly Interacting Systems: Human Plasma Protein Mixtures.	PB89-201701 901,149 SPIN SPIN INTERACTIONS	Estimation of the Thermodynamic Properties of Hydrocarbons at 298.15 K.
PB89-202576 901,225	Dynamics of a Spin-One Model with the Pair Correlation.	PB89-145155 900,272
PECTROSCOPY Journal of Research of the National Institute of Stand-	PB89-171300 900,356	Wavelengths and Energy Level Classifications of Scandi-
Journal of Research of the National Institute of Standards and Technology, Volume 94, Number 4, July-August	SPIN WAVES Spin-Density-Wave Transition in Dilute YGd Single Crys-	um Spectra for All Stages of Ionization. PB89-145163 900,273
1989. PB89-235634 <i>900,908</i>	tals.	Atomic Weights of the Elements 1987.
Spectrum of Doubly Ionized Tungsten (W III).	PB89-202030 901,433 SPLINES	PB89-145171 900,274 CODATA (Committee on Data for Science and Tochnology
PB89-235659 900,223	Method for Fitting and Smoothing Digital Data.	CODATA (Committee on Data for Science and Technology) Recommended Values of the Fundamental Physical
PECTRUM ANALYSES Standard Reference Materials for the Determination of	PB90-128794 900,830	Constants, 1986. PB89-145189 900,275
Polycyclic Aromatic Hydrocarbons.	SPRINKLER SYSTEMS Estimating the Environment and the Response of Sprin-	Journal of Physical and Chemical Reference Data.
PB89-156889 900,178 One Is Not Enough: Intra-Cavity Spectroscopy with Multi-	kler Links in Compartment Fires with Draft Curtains and Fusible Line-Actuated Ceiling Vents. Part 2. User Guide	Volume 17, 1988, Supplement No. 3. Atomic Transition Probabilities Scandium through Manganese.
Mode Lasers.	for the Computer Code Lavent.	PB89-145197 900,276

Journal of Physical and Chemical Reference Data, Volume 17, 1988, Supplement No. 2. Thermodynamic and Transport Properties for Molten Salts: Correlation	Standard Reference Materials: Description of the SRM 1965 Microsphere Slide. PB89-153704 901,390	PB89-221147 900,000 Product Data Exchange: The PDES Project-Status and Objectives.
Equations for Critically Evaluated Density, Surface Tension, Electrical Conductance, and Viscosity Data. PB89-145205 900,277	Standard Reference Materials for the Determination of Polycyclic Aromatic Hydrocarbons.	PB90-112426 900,938
Chemical and Spectral Databases: A Look into the	PB89-156889 900,178 Neutron Activation Analysis of the NIST (National Insti-	Glossary of Standards-Related Terminology. PB90-130246 900,986
Future. PB89-180038 900,579	tute of Standards and Technology) Bovine Serum Standard Reference Material Using Chemical Separations.	STANDARDS Coding and Modulation Requirements for 4,800 Bits
Technical Activities 1987, Center for Basic Standards. PB89-185615 901,521	PB89-156921 900,180	Second Modems, Category: Telecommunications Standard.
Computer Graphics for Ceramic Phase Diagrams.	Long-Term Stability of the Elemental Composition in Biological Materials.	FIPS PUB 134-1 900,660
Journal of Physical and Chemical Reference Data,	PB89-156939 900,181 Status of Reference Data, Reference Materials and Ref-	General Aspects of Group 4 Facsimile Apparatus, Category: Telecommunications Standard.
Volume 17, Number 1, 1988. PB89-186449 900,408	erence Procedures in Surface Analysis. PB89-157705 900,332	FIPS PUB 149 900,666 Facsimile Coding Schemes and Coding Control Functions
Pressure and Density Series Equations of State for Steam as Derived from the Haar-Gallagher-Kell Formulation.	Preparation of Accurate Multicomponent Gas Standards of Volatile Toxic Organic Compounds in the Low-Partsper-Billion Range.	for Group 4 Facsimile Apparatus, Čategory: Telecommunications Standard. FIPS PUB 150 900,662
PB89-186456 900,409 Absolute Cross Sections for Molecular Photoabsorption, Partial Photoionization, and Ionic Photofragmentation Process.	PB89-157739 900,185 NBS (National Bureau of Standards) Activities in Biological Reference Materials. PB89-157770 901,219	High Speed 25-Position Interface for Data Termina Equipment and Data Circuit-Terminating Equipment, Cat egory: Telecommunications Standard. FIPS PUB 154 900,663
PB89-186464 900,410	Role of Neutron Activation Analysis in the Certification of	Data Communication Systems and Services User-Orient-
Energy Levels of Molybdenum, Mo 1 through 42. PB89-186472 900,411	NBS (National Bureau of Standards) Standard Reference Materials. PB89-157879 900.187	ed Performance Measurement Methods, Category: Tele- communications Standard. FIPS PUB 155 900,664
Standard Chemical Thermodynamic Properties of Polycyclic Aromatic Hydrocarbons and Their Isomer Groups 1.	Chemical Calibration Standards for Molecular Absorption	Standard Reference Materials for X-ray Diffraction. Part
Benzene Series. PB89-186480 900,412	Spectrometry. PB89-171938 <i>900,191</i>	 Overview of Current and Future Standard Reference Materials.
Thermal Conductivity of Nitrogen and Carbon Monoxide in the Limit of Zero Density.	Specific Heat of Insulations. PB89-172514 900.116	PB89-146799 901,384 Standards for the Interchange of Large Format Tiled
PB89-222533 900,449	Insulation Standard Reference Materials of Thermal Re-	Raster Documents. PB89-148415 900,668
Thermophysical Properties of Methane. PB89-222541 900,450	sistance. PB89-172548 <i>900,117</i>	Possible Quantum Hall Effect Resistance Standard.
Thermodynamic Properties of Argon from the Triple Point to 1200 K with Pressures to 1000 MPa.	Comparison of a Cryogenic Preconcentration Technique and Direct Injection for the Gas Chromatographic Analy-	PB89-149058 900,80% Case History: Development of a Software Engineering
PB89-222558 900,451	sis of Low PPB (Parts-per-Billion) (NMOL/MOL) Gas Standards of Toxic Organic Compounds.	Standard. PB89-149116 900,665
Thermodynamic Properties of Dioxygen Difluoride (O2F2) and Dioxygen Fluoride (O2F). PB89-222566 900,452	PB89-173843 900,193 High-Accuracy Differential-Pulse Anodic Stripping Voltam-	Microwave Power Standards.
Thermodynamic and Transport Properties of Carbohy-	metry Using Indium as an Internal Standard. PB89-176267 900,198	Standard Specifications for Cements and the Role in
drates and Their Monophosphates: The Pentoses and Hexoses.	Luminescence Standards for Macro- and Microspectro- fluorometry.	Their Development of Quality Assurance Systems for Laboratories.
PB89-222574 900,453 Evaluated Kinetic and Photochemical Data for Atmos-	PB89-176598 900,383	PB89-150742 901,023 Measurement Standards for Defense Technology.
pheric Chemistry. Supplement 3. PB89-222582 900,454	Biological Standard Reference Materials for the Calibration of Differential Scanning Calorimeters: Di-alkylphos-	PB89-150965 901,270
Journal of Physical and Chemical Reference Data, Volume 18, Number 1, 1989.	phatidylcholine in Water Suspensions. PB89-186779 900,415	Submicrometer Optical Metrology. PB89-150973 900,771
PB89-226559 900,455	Standard Reference Materials for Dimensional and Physical Property Measurements.	U.S. Organizations Represented in the Collection of Vol- untary Standards.
Standard Electrode Potentials and Temperature Coefficients in Water at 298.15 K.	PB89-201164 900,892 Development of New Standard Reference Materials for	PB89-154322 900,978 High-Accuracy Differential-Pulse Anodic Stripping Voltam-
PB89-226567 900,456 Cross Sections for Collisions of Electrons and Photons	Use in Thermometry. PB89-201180 900,893	metry with Indium as an Internal Standard. PB89-156947 900,182
with Oxygen Molecules. PB89-226575 900,457	Exploratory Research in Reflectance and Fluorescence Standards at the National Bureau of Standards.	Preparation of Accurate Multicomponent Gas Standards of Volatile Toxic Organic Compounds in the Low-Parts
Thermal Conductivity of Refrigerants in a Wide Range of Temperature and Pressure.	PB89-202022 900,428	per-Billion Range. PB89-157739 900,185
PB89-226583 900,458 Standard Chemical Thermodynamic Properties of Polycy-	Preparation of Standards for Gas Analysis. PB89-211940 900,215	Standards and Test Methods for VLSI (Very Large Scale
clic Aromatic Hydrocarbons and Their Isomer Groups. 2. Pyrene Series, Naphthopyrene Series, and Coronene	Development of the NBS (National Bureau of Standards) Beryllium Isotopic Standard Reference Material.	Integration) Materials. PB89-158042 900,774
Series. PB89-226591 900,459	PB89-231070 900,221 Determination of Trace Level Iodine in Biological and Bo-	Electrical Performance Tests for Hand-Held Digital Multi- meters.
Cross Sections for K-Shell X-ray Production by Hydrogen and Helium Ions in Elements from Beryllium to Uranium.	tanical Reference Materials by Isotope Dilution Mass Spectrometry.	PB89-162234 900,876 Guidelines for the Specification and Validation of IGES
PB89-226609 900,460	PB89-235642 900,222	(Initial Graphics Exchange Specification) Application Pro- tocols.
Rate Constants for the Quenching of Excited States of Metal Complexes in Fluid Solution.	Calcium Hydroxyapatite Precipitated from an Aqueous Solution: An International Multimethod Analysis. PB90-123399 900,228	PB89-166102 900,937
PB89-227797 900,461 Journal of Physical and Chemical Reference Data,	Comparison of Microwave Drying and Conventional	Effect of Chinese Standardization on U.S. Export Opportunities.
Volume 18, Number 3, 1989. PB90-126236 900,527	Drying Techniques for Reference Materials. PB90-123464 900,229	PB89-166128 900,172 Standard X-ray Diffraction Powder Patterns from the
Octanol-Water Partition Coefficients of Simple Organic Compounds.	Determination of Selenium and Tellunium in Copper Standard Reference Materials Using Stable Isotope Dilu-	JCPDS (Joint Committee on Powder Diffraction Standards) Research Associateship.
PB90-126244 900,528	tion Spark Source Mass Spectrometry. PB90-123472 900,230	PB89-171763 900,190 NBS (National Bureau of Standards) Radon-in-Water
Evaluation of Data on Solubility of Simple Apolar Gases in Light and Heavy Water at High Temperature. PB90-126251 900,529	Facile Synthesis of 1-Nitropyrene-d9 of High Isotopic Purity.	Standard Generator. PB89-171888 901,295
Microwave Spectral Tables. 3. Hydrocarbons, CH to	PB9Ó-123753 900,240 Improved Standards for Real-Time Radioscopy.	Standardizing EMCS Communication Protocols. PB89-172357 900,613
C10H10. PB90-126269 900,530	PB90-128679 900,923	Report on Interactions between the National Institute of
ANDARD REFERENCE MATERIALS Standard Reference Materials for X-ray Diffraction. Part	Microporous Fumed-Silica Insulation as a Standard Reference Material of Thermal Resistance at High Tempera-	Standards and Technology and the American Society of Mechanical Engineers.
Overview of Current and Future Standard Reference Materials.	ture. PB90-130311 <i>900,153</i>	PB89-172563 901,004 NBS (National Bureau of Standards) Calibration Services:
PB89-146799 901,384	Continine in Freeze-Dried Urine Reference Material. PB90-213703 900,675	A Status Report. PB89-173934 900,878
Microporous Furned-Silica Insulation Board as a Candidate Standard Reference Material of Thermal Resistance	STANDARDIZATION	NBS (National Bureau of Standards) Orifice-Flow Primary
ance. PB99-148373 <i>901,018</i>	Product Data Exchange Specification: First Working Draft.	High Vacuum Standard. PB89-175699 900,880
Environmental Standard Reference Materials - Present and Future Issues.	PB89-144794 900,940 Versailles Project on Advanced Materials and Standards	Low Range Flowmeters for Use with Vacuum and Leak Standards.
PB89-150940 900,865 Technical Activities, 1988, Center for Analytical Chemis-	Evolution to Permanent Status. PB89-201768 900,969	PB89-175707 900,372 Development of Electrophores and Electrofocusing
ry. PB89-151773 900,177	Directory of International and Regional Organizations Conducting Standards-Related Activities.	Standards. PB89-175863 900,195
	-	

Robe of Story and Story an			
Mousements of the CRUDU (In) Standard Cross Service and Plaques of Selection (1997) and the Service of Selection (1997) and the Selection (1997) a		·	
Personal Feature of Endower Manager Personal State of Endower Manager Pers			
photosphores of Magnetic Paul Measurements (1985-2504) Sancted Formal for the Exclusing of Physiphore Hotomark (1985-2504) Sancted Formal for the Exclusing of Physiphore Hotomark (1985-2504) Sancted Formal for the Exclusing of Physiphore Hotomark (1985-2504) Approximate Control of Tool Socients (1985-2504) Approximate Control of Tool Socients (1985-2504) Septiments (1985-2504) Sep	tion at the National Bureau of Standards.	PB89-235139 <i>901,272</i>	modynamic Equilibrium) Model Stellar Atmospheres.
Bender Finants or Echange of Finants or Echa			, , , , , , , , , , , , , , , , , , , ,
Signature for the Existancy of Prince of Topics (Selection) from Prince 1709 500-501 1975 500-50	ments: Recent History and Measurement Standards.	1989.	Spectral Type 09.5.
Authorise Conversión of Test Sorarios (Statebons hom Productive Special Confession Confe	, ———		
February Agreement on Trait Sorramin Standards at NSS (National Broads) February Agreement on Trait and Traid Standards (National Broads) February Agreement on Trait and Traid Standards (National Broads) February Agreement on Trait and Traid Standards (National Broads) February Agreement on Trait and Traid Standards (National Broads) February Agreement on Trait and Traid Standards (National Broads) February Agreement on Trait and Traid Standards (National Broads) February Agreement on Traits and Traid Standards (National Broads) February Agreement on Traits and Traid Standards (National Broads) February Agreement on Traits and Traid Standards (National Broads) February Agreement on Traits and Traid Standards (National Broads) February Agreement on Traits and Traid Standards (National Broads) February Agreement on Traits and Traid Standards (National Broads) February Agreement on Traits and Traid Standards (National Broads) February Agreement on Traits and Traid Standards (National Broads) February Agreement on Traits and Traid Standards (National Broads) February Agreement on Traits and Traid Standards (National Broads) February Agreement on Traits and Traid Standards (National Broads) February Agreement on Traits and Traid Standards (National Broads) February Agreement on Traits and Traid Standards (National Broads) February Agreement on Traits and Traid Standards (National Broads) February Agreement on Traits and Traid Standards (National Broads) February Agreement on Traits and Traid Standards (National Broads) February Agreement on Traits and Traid Standards (National Broads) February Agreement on Traits and Traid Standards (National Broads) February Agreement on Traits and Traid Standards (National Broads) February Agreement on Traits and Traid Standards (National Broads) February Agreement on Traits (National Broads) February Agreement	tion.	fice Meter.	
Postocopies Desiration Wittlen in Establish (Composite Databasis for the 1990). 2007. 1995-1907. 19		,	PB89-149199 900,015
Companions Delateauremonix. Page 1990-1995. Policy 1990-1995. Poli	Protocol-Specifications Written in Estelle.	PB90-112434 900,939	
PROS-10076	· · · · · · · · · · · · · · · · · · ·		Envelope Evolution.
Sacks and Technology, Volume St, Number 2, Monthy Appendence of Standards of Preparations of Standards of Sta	PB89-180376 901,075	PB90-118035 900,031	
Sandard Cherical Fateria Services and Servic	Journal of Research of the National Institute of Stand- ards and Technology, Volume 94, Number 2, March-April		Rotational Modulation and Flares on RS Canum Venati-
Now Internationally Adopted Relevance Standards of No. 2007. Whose and The Standards of Standards of Standards of No. 2007. Standard Advikes 1987, Centre for Basic Standards. 907.07		Standards for Real-Time Radioscopy.	corum and BY Draconis Stars X: The 1981 October 3 Flare on V711 Tauri (= HR 1099).
Visitings and fleesterine. 90.026 Fig8-9-156-15 Fig8-9-15			PB89-202618 900,02 *
Technical Apolites 1997, Centre for Taske Standards, 1997, 1998-1909 1909 1909 1909 1909 1909 1909 1909	Voltage and Resistance.		
PRISO-103003 Months and Technology and Control of Technology and Control of Technology and Control of Technology and Propagation of Multistage Zone-Refined Materials for Thermochanical Standards. Microprose propagation of Multistage Zone-Refined Materials for Thermochanical Standards. Microprose propagation of Multistage Zone-Refined Materials for Thermochanical Standards. Microprose propagation of Multistage Zone-Refined Materials for Thermochanical Standards. Microprose propagation of Multistage Zone-Refined Materials for Thermochanical Standards. Microprose propagation of Multistage Zone-Refined Materials for Thermochanical Standards. Microprose propagation of Multistage Zone-Refined Materials for Thermochanical Standards. Microprose propagation of Multistage Zone-Refined Materials for Thermochanical Standards. Microprose propagation of Multistage Zone-Refined Materials of Standards. Microprose propagation of Technology Law Standards. Microprose propagation o	Technical Activities 1987, Center for Basic Standards.	Improved Low-Level Silicon-Avalanche-Photodiode Trans-	vations.
Solicity Foundation of Marketings (1994) Proposation of Multistage Zone-Relined Materials for Proposation of Proposation o	1		
PERS-106469. PERS-	clic Aromatic Hydrocarbons and Their Isomer Groups 1.		Stellar Winds of 203 Galactic O Stars: A Quantitative UI-
Pegas allocal formation of Multislage Zone-Relined Materials for Thermochampian Standards and 20,000,000,000,000,000,000,000,000,000,	Benzene Series.	ture.	
and CALS (Gemputer-Acide Acquisition and Logistic Sup- Pissa 1975) and CALS (Gemputer-Acide Acquisition and Logistic Sup- Pissa 1975) and Carry (French and Tem Delay Measurements of a Stand- Fissa 1975) and Tem Delay Measurement of a Stand- ard Code Activities of the National Institute of Standards and Technology. Management on Trailis and Traile) Stand- ard Code Activities of the National Institute of Standards and Technology. Management of Management Standards. Management of Management Standards and Management Standards. Management of Management Standards and Management Standards. Management of Management Standards. Management of Management Standards and Management Standards. Management of Management Standards. Management Standards for Management Standards. Management Standards. Management S		·	,
PBB9-139167 STANK EFFECT Stark Broadering of Spectral Lines of Homologous, 1900,275 STANK EFFECT Stark Broadering of Spectral Lines of Homologous, 1900,275 STANK EFFECT Stark Broadering of Spectral Lines of Homologous, 1900,275 STANK EFFECT Stark Broadering of Spectral Lines of Homologous, 1900,275 STANK EFFECT Stark Broadering of Spectral Lines of Homologous, 1900,275 STANK EFFECT Stark Broadering of Spectral Lines of Homologous, 1900,275 STANK EFFECT Stark Broadering of Spectral Lines of Homologous, 1900,275 STANK EFFECT Stark Broadering of Spectral Lines of Homologous, 1900,275 STANK EFFECT Stark Broadering of Spectral Lines of Homologous, 1900,275 STANK EFFECT Stark Broadering of Spectral Lines of Homologous, 1900,275 STANK EFFECT Stark Broadering of Spectral Lines of Homologous, 1900,275 STANK EFFECT Stark Broadering of Spectral Lines of Homologous, 1900,275 STANK EFFECT Stark Broadering of Spectral Lines of Homologous, 1900,275 STANK EFFECT Stark Broadering Stark Stark Broad		and CALS (Computer-Aided Acquisition and Logistic Sup-	Development of a Microwave Sustained Gas Plasma for
Fig8-19567 (Group Index and Timo Delay Measurements of a Stanf. Effect of Circular Index and Timo Delay Measurements of a Stanf. Effect of Medical Index and Timo Delay Measurements of a Stanf. Effect of Medical Index and Timo Delay Measurements of Stanfards and Technology Measurement Stanfards and Technology Measurement Stanfards and Technology Measurement Stanfards of Stanfards and Technology Measurement Stanfards of Stanfards and Technology Measurement Stanfards (Measurement Stanfards) Stanfards (Me	New Standard Test Method for Eddy Current Probes.		
Doubly initized infert Gaises. 9.00,35 Chambergreed 9.00,36 Strokers 9.00,36 Strokers 9.00,36 Strokers 9.00,36 STORM WINDOWS 9.00,36 STORM	PB89-187587 900,981		
PBB8-15907 900.737 ATT (Carrant Agreement on Tarifs and Trade) Standards and Trachnology 1588. PBB8-191797 900.737 ATT (Standard Agreement on Tarifs and Trade) Standards and Trachnology 1588. PBB8-1918-191797 900.737 ATT (Standard Agreement on Tarifs and Trade) Standards and Trachnology 1588. PBB8-1918-191797 900.737 ATT (Standard Agreement Standards PBB8-1918-1917) 900.737 ATT (Standards Agreement Standards PBB8-1918-1917) 900.837 ATT (Standards Agreement Standards PBB8-1918-1918) 900.837 ATT (Standards PBB8-1918-1918) 900.837 ATT (Standards Agreement Standards PBB8-1918-1918) 900.837 ATT (Standards PBB8-1918-1918-1918-1918-1918-1918-1918-1	ard Reference Fiber.		Effect of an Electrically Large Stirrer in a Mode-Stirred Chamber.
ands Code Activities of the National Institute of Standards 90,177 NST (National Institute of Standards and Tochnology) Measurement Services: High Vacuum Standard and Its PBB-193641 PB		PB89-158083 900,343	
p889-201578 (akennal institute of Standards and 15 about 15 standards and 15	ards Code Activities of the National Institute of Standards		
NIST (National Institute of Standards and Technology) Measurement Services: High Yacum Standard and Its P889-193841 P889-193841 P889-193841 P889-193841 P889-193841 P889-193841 P889-193841 P889-193842 P889-193842 P889-193842 P889-193842 P889-193842 P889-193842 P889-193844 P889-19384	and Technology 1988.		
Measurement Services: Figh Vacuum Standard and lis 9688-19381 901-283	the state of the s		
FBBS 193841 90.089 (Salbation of Gamma-Ray-Emitting Brachytherapy PBBS 20164 Salbation of Gamma-Ray-Emitting Brachytherapy PBBS 19385 90.124 (Salbation of Mayor Document Interchange Sandards Description and Salbation of Mayor Document Interchange Sandards (Salbation of Particle Sa	Measurement Services: High Vacuum Standard and Its		(American Society of Heating, Refrigerating and Air-Con-
NBS (National Bureau of Standards) Measurement Services Calibration of Gamma-Ray-Fermiting Bitarytherapy pp. 391-7084 300,927 7ests of the Recalibration Period of a Drifting Instrument, 200,199 7ests of the Recalibration Period of a Drifting Instrument, 200,199 7ests of the Recalibration Period of a Drifting Instrument, 200,199 7ests of the Recalibration Period of a Drifting Instrument, 200,199 7ests of the Recalibration Period of a Drifting Instrument, 200,199 7ests of the Recalibration Period of a Drifting Instrument, 200,418 7ests of the Recalibration Data Analysis Program. LOGIT 200,418 7ests of the Recalibration Period of a Drifting Instrument, 200,418 7ests of the Recalibration Data Analysis of Experiments to Measure grighton of Cigarettes. Period Recalibration Period Standards at NBS (National Bureau Period Standards at NBS (National Bureau Period Standards) 7ests of the Production of Particle Standards. 200,484 7ests of the Production of Particle Standards. 200,484 7ests of the Production of Particle Standards 7ests of the Particle Partic			ditioning Engineers) Handbook - Fundamentals.
Sources Source		Software.	•
Document Interchange Standards. Description and Status of Majer Document and Graphics Standards. 900,329 (1987-1985) 19374. 900,329 (1987-1985) 19374. 900,329 (1987-1985) 19374. 900,329 (1987-1985) 19374. 900,329 (1987-1985) 19374. 900,329 (1987-1985) 1938-19395 (1987-1985) 1939-1939 (1987-1985) 1939-1939 (1987-1985) 1939-1939 (1987-1985) 1939-1939 (1987-1985) 1939-1939 (1987-1985) 1939-1939 (1987-1985) 1939-1939 (1987-1985) 1939-1939 (1987-1985) 1939-1939 (1987-1985) 1939-1939 (1987-1985) 1939-1939 (1987-1985) 1939-1939 (1987-1985) 1939-1939 (1987-1985) 1939-1939 (1987-1985) 1939-1939 (1987-1985) 1939-1939 (1987-1985) 1939-1939 (1987-1985) 1939-1939 (1987-1985) 1939-1939 (1987-1985) 1939-1939 (1987-198	Sources.	·	
of Major Document and Graphics Standards. PBB-1980-13937 Standard Reference Materials for Dimensional and Physical Property Measurements. 900,829 Development of New Standard Reference Materials for Use in Thermonium Standards at NBS (National Bureau of Standards). PBB-201190 Progress in Vacuum Standards at NBS (National Bureau of Standards). PBB-201190 PBB-201	·		
Standard Reference Materials for Dimensional and Physical Properties Massurements. 908.829 1186 90.839 90.839 Progress in Yacurum Standards at NBS (National Bureau of Standards) 90.839 97.839 90.839 97.839 90.839 97.839 90.839 97.839 90.839 97.839 90.839 97.839 90.839 97.839 90.839 97.839 90.839 97.839 90.839 97.839 90.839 97.839 90.839 97.839 90.839 97.839 90.839 97.839 90.839 97.839 90.839 97.839 90.839 97.839 90.839 97.839 90.839 97.839 97.839 90.839 97.839 90.839 97.839 90.839 97.839 90.839 97.839 90.839 97.839 90.839 97.839 90.839 97.839 90.839 97.839 90.839 97.839 90.839 97.839 90.839 97.839 90.839 97.839 90.839 97.839 90.839 97.839 90.839 97.839 90.839 97.83	of Major Document and Graphics Standards.		
Cigarettes. PBBs-201180 Development of New Standard Reference Materials for Development of New Standard Reference Materials for Joseph PBBs-201180 Porticipation of Particle Standards. PBBs-201198 PBBs-201198 PBBs-201198 PBBs-201198 PBBs-201198 PBBs-201519 PB		·	
Use in Thermometry, PBBS-201180 90,893 90,893 90,893 90,894 PBBS-201198 90,095	cal Property Measurements.	Cigarettes.	PB89-212203 900,139
Use in Thermometry, 900,893 Progress in Vacuum Standards at NBS (National Bureau of Standards) PBB9-201198 900,999 PBB9-201698 PBB9-201691 900,999 PBB9-178619 PBB9-178619 900,999 PBB9-178619 PBB9-178619 900,999 PBB9-178619 PBB9-178619 900,999 PBB9-178619 900,999 PBB9-178619 900,999 PBB9-178619 PBB9-178619 900,999 PBB9-178619		·	
STATISTICAL INFERENCE Bootstrap Interence for Replicated Experiments. 900,914 SPB9-201189 900,929 SPB9-201651 900,929 SPB9-201	Use in Thermometry.	System.	Stress.
of Slandards) 908-920196 900,999 Methods for the Production of Particle Standards. PB89-20187 Performance Standards for Microanalysis. PB89-20187 Stability of the SI (International System) Unit of Mass as Determined from Electrical Measurements. 900,894 Exploratory Research in Reflectance and Fluorescence Standards at the National Bureau of Standards. PB89-201819 PR89-20180 Properties of Steam. PB89-20282 Properties of Steam. PB89-20282 Properties of Steam. PB89-212153 Standard X-ray Diffraction Powder Patterns from the JoPDS. (Joint Committee on Powder Diffraction Standards and Sepsence) PB89-212153 PB89-212163 PB89-21216			•
Methods for the Production of Particle Standards PB89-201636 PB89-201651 PB89-101651 PB89-	of Standards).	Bootstrap Inference for Replicated Experiments.	Tensile Strain-Rate Effects in Liquid Helium.
PB89-201636 PB89-201651 PB89-201651 PB89-201651 PB89-201651 Stability of the SI (International System) Unit of Mass as Determined from Electrical Measurements. 90.894 Exploratory Research in Reflectance and Fluorescence Standards In Reflectance and Fluorescence Standards at the National Bureau of Standards. 90.428 PB89-200202 Properties of Steam. 90.428 PB89-200202 PR99-200203 PR99-2173 PR99-20048 PR99-21854 PR99-20048 PR99-21854 PR99-21854 PR99-21854 PR99-21854 PR99-21854 PR99-218554 PR99-218554 PR99-21857 PR99-218554 PR99-218554 PR99-218554 PR99-218554 PR99-218555 PR99-220042 PR99-218555 PR99-148504 PR99-218555 PR99-148504 PR99-218555 PR99-148504 PR99-218555 PR99-148504 PR99-218555 PR99-148504 PR99-220042 PR99-2200			
PB89-201618 Stability of the SI (International System) Unit of Mass as Derived from Electrical Measurements. 900,849 PB89-201618 PB89-201		Error Bounds for Linear Recurrence Relations.	
Pressure and Density Series Equations of State for Standards PBB9-201818 Properties of ton Electrical Measurements. 900,849 Properties of Stam. PBB9-202048 PBB9-202048 Properties of Stam. PBB9-202048 Properties of Stam. PBB9-202048 Properties of Stam. PBB9-202048 Properties of Stam. PB		· ·	
Steam as Derived from the Haar-Gallagher-Kell Formula-PB89-201619 900,894 Exploratory Research in Reflectance and Fluorescence Standards at the National Bureau of Standards PB89-202028 Poperties of Steam. PB89-202029 PSB9-202029 PSB9-202039 Standard X-ray Diffraction Powder Patterns from the JOPDS (Joint Committee on Powder Diffraction Standards) PSB9-219153 Standard X-ray Diffraction Powder Patterns from the JOPDS (Joint Committee on Powder Diffraction Standards) PSB9-219153 PSB9-21916 PSB9-21916 PSB9-219174 PSB9-21918 PSB9-21918 PSB9-14908 PSB	Stability of the SI (International System) Unit of Mass as	Pressure and Density Series Equations of State for	
Exploratory Research in Reflectance and Fluorescence Standards at the National Bureau of Standards. 900,428 Properties of Steam. 900,428 Properties of Steam. 900,533 Standard X-ray Diffraction Powder Patterns from the JCPDS (Joint Committee on Powder Diffraction Standards). PB89-20246 900,214 Gas Flow Measurement Standards. 900,214 Gas Flow Measurement Standards. 900,214 Gas Flow Measurement Standards Program. 900,214 Gas Flow Measurement Standards Program. 900,866 Update of U.S. Participation in International Standards Update of U.S. Participation in International Standards Update of U.S. Participation in International Standards Program. 900,902 PB89-228282 900,902 PB89-230387 900,829 PB89-18979 900,820 PB89-18979 900,820 PB89-18979 900,820 PB89-18979 900,820 PB89-18979 900,820 PB89-18979 900,820 PB89-2303087 900,820 PB89-18979 900,820 PB89-230409 PB89-18979 900,820 PB89-18979 PB89-18	Determined from Electrical Measurements. PB89-201818 900.894	tion.	ogy Assessment.
PB69-20202 Properties of Steam. PB69-202048 Properties of Steam. PB69-202049 Standard X-ray Diffraction Powder Patterns from the JCPDS (Joint Committee on Powder Diffraction Standards Association. PB69-202146 Gas Flow Measurement Standards. PB69-211874 Gas Flow Measurement Standards Program. PB69-211874 PB69-211874 Ultrasonic Texture Analysis for Polycrystalline Aggregates of Cubic Materials Displaying Orthotropic Symmetry. PB69-11879 PB69-20218 Ultrasonic Texture Analysis for Polycrystalline Aggregates of Cubic Materials Displaying Orthotropic Symmetry. PB69-11879 PB69-20218 Ultrasonic Texture Analysis for Polycrystalline Aggregates of Cubic Materials Displaying Orthotropic Symmetry. PB69-11879 PB69-20218 Ultrasonic Texture Analysis for Polycrystalline Aggregates of Cubic Materials Displaying Orthotropic Symmetry. PB69-11879 PB69-20219 Ultrasonic Texture Analysis for Polycrystalline Aggregates of Cubic Materials Displaying Orthotropic Symmetry. PB69-11879 PB69-20219 Ultrasonic Texture Analysis for Polycrystalline Aggregates of Cubic Materials Displaying Orthotropic Symmetry. PB69-11879 PB69-202113 STRESS ANALVSIS Laboratory Evaluation of an NBS (National Bureau of Standards) Polymer Soil Stress Gage. PB69-21979 PB69-21979 Material Displaying Orthotropic Symmetry. PB69-146948 Ultrasonic Texture Analysis for Polycrystalline Aggregates of Cubic Materials Displaying Orthotropic Symmetry. PB69-11879 PB69-202113 STRESS ANALVSIS Laboratory Evaluation of an NBS (National Bureau of Standards) Polymer Soil Stress Gage. PB69-21979 PB69-21979 Measurement of Applied J-Integral Produced by Residual Stress. PB69-118701 PB69-1989-203087 STRESS CORROSION TESTS PB69-17801 PB69-17801 PB69-17801 PB69-17801 PB69-17801 PB69-17801 PB69-17801 PB69-17801 PB69-17801 PB69-18802 PB69-17801	Exploratory Research in Reflectance and Fluorescence	·	
Properties of Steam. PB9-202048 Standard X-ray Diffraction Powder Patterns from the JCPDS (Joint Committee on Powder Diffraction Standards) Research Association. PB99-212153 STEELS STEELS Ultrasonic Texture Analysis for Polycrystalline Aggregates of Cubic Materials Displaying Orthotropic Symmetry. PB99-211874 Gas Flow Measurement Standards Program. PB99-211874 900,898 Federal Software Engineering Standards Program. PB99-211874 Ultrasonic Characterization of Surface Modified Layers. PB99-146948 Ultrasonic Characterization of Surface Modified Layers. PB99-146949 Ultrasonic Characterization of Surface Modified Layers. PB99-149090 Ultrasonic Determination of Absolute Stresses in Aluminum and Steel Alloys. PB99-19095 PB99-19095 PB99-19095 PB99-19096 PB99-19096 PB99-19096 PB99-19097 PB99-19098 PB99-19098 PB99-19098 PB99-19099	Standards at the National Bureau of Standards.		quirements of the Strategic Defense Initiative.
Standard X-ray Diffraction Powder Patterns from the JCPDS (Joint Committee on Powder Diffraction Standards) Research Association. BBS-202246 Gas Flow Measurement Standards. BBS-211874 Gas Flow Measurement Standards Program. BBS-2118674 PBSS-211867 Federal Software Engineering Standards Program. DBSS-211867 Determination of the Time-Dependence of ohm NBS (National Bureau of Standards) Using the Quantized Hall Resistance. DEBS-220887 BBSS-230987 PBSS-230987 PBSS-230987 PBSS-230987 PBSS-230989	Properties of Steam.	Activities of the International Association for the Proper-	•
JCPDS (Joint Committee on Powder Diffraction Standards) Research Association. PB89-202246 Gas Flow Measurement Standards. PB89-202248 Federal Software Engineering Standards Program. PB89-211965 PB89-211965 PB89-211965 JUltrasonic Characterization of Surface Modified Layers. PB89-147409 Local Brittle Zones in Steel Weldments: An Assessment of Test Methods. PB89-21802 J-Integral Values for Small Cracks in Steel Panels. PB89-149092 J-Integral Values for Small Cracks in Steel Panels. PB89-230387 Josephson Array Voltage Calibration System: Operational Use and Verification. PB89-230403 Measurement of the NBS (National Bureau of Standards) PB89-159018 PB89-159018 Fracture Behavior of a Pressure Vessel Steel in the Ducstrical Watt in SI Units. PB89-230403 National Bureau of Standards Message Authentication STEELS Ultrasonic Texture Analysis for Polycrystalline Aggregates of Cubic Materials Displaying Orthotropic Symmetry, 201,212 PB89-146948 Ultrasonic Texture Analysis for Polycrystalline Aggregates of Cubic Materials Displaying Orthotropic Symmetry, 201,212 PB89-146948 Ultrasonic Characterization of Surface Modified Layers. PB89-147909 J-Integral Values for Small Cracks in Steel Weldments: An Assessment of Test Methods. PB89-149082 J-Integral Values for Small Cracks in Steel Panels. PB89-149090 J-Integral Values for Small Cracks in Steel Panels. PB89-149090 J-Integral Values for Small Cracks in Steel Panels. PB89-150957 Josephson Array Voltage Calibration System: Operational Use and Verification. PB89-150918 PB89-150918 PB89-150918 Fracture Behavior of a Pressure Vessel Steel in the Ducstice-Transition Region. PB89-189195 Josephson Array Voltage Calibration System: Operational Use and Verification. PB89-152621 PB89-173835 STRESS ANALVSIS			Novel Flow Process for Metal and Ore Solubilization by
Ultrasonic Texture Analysis for Polycrystalline Aggregates of Cubic Materials Displaying Orthotropic Symmetry. PB89-202246 900,214 Gas Flow Measurement Standards. PB89-211874 900,898 Federal Software Engineering Standards Program. Update of U.S. Participation in International Standards Activities. PB89-147409 909.000 Determination of the Time-Dependence of ohm NBS (National Bureau of Standards) Using the Quantized Hall Resistance. PB89-230387 901,554 Improved Transportable DC Voltage Standard. PB89-230395 901,554 Desphson Array Voltage Calibration System: Operational Use and Verification. PB89-150018 900,820 Measurement of the NBS (National Bureau of Standards) Polymer Soil Stress Gage. PB89-17851 901,105 STRESS ANALYSIS Laboratory Evaluation of an NBS (National Bureau of Standards) Polymer Soil Stress Gage. PB89-211973 901,291 Measurement of Applied J-Integral Produced by Residual Stress. PB89-149082 901,092 Ultrasonic Determination of Strest Methods. PB89-149082 901,093 Ultrasonic Determination of Absolute Stresses in Aluminum and Steel Alloys. PB89-150957 901,124 Improved Transportable DC Voltage Standard. PB89-230395 901,096 Desphson Array Voltage Calibration System: Operational Use and Verification. PB89-178611 Use and Verification. PB89-178611 PB89-178612 PB89-17	JCPDS (Joint Committee on Powder Diffraction Stand-		
PB89-211874 PB89-211874 PB89-211875 PB89-211965 PB89-211965 PB89-21965 PB89-147409 PB89-147409 PB89-21965 PB89-147409 PB89-21965 PB89-147409 PB89-147409 PB89-21965 PB89-147409 PB89-21965 PB89-147409 PB89-21965 PB89-147409 PB89-21965 PB89-147409 PB89-21965 PB89-147409 PB89-21965 PB89-147609 PB89-147609 PB89-21965 PB89-147609 PB89-147609 PB89-21960 PB89-147609 PB89-147609 PB89-21960 PB89-147609 P		Ultrasonic Texture Analysis for Polycrystalline Aggregates of Cubic Materials Displaying Orthotropic Symmetry.	•-
Federal Software Engineering Standards Program. PB89-211965 900,666 Update of U.S. Participation in International Standards PB89-228282 PB89-228282 PB89-228282 Determination of the Time-Dependence of ohm NBS (National Bureau of Standards) Using the Quantized Hall Resistance. PB89-230397 PB89-230397 PB89-2503095 Measurement of Applied J-Integral Produced by Residual Stress. PB89-149080 PB89-268282 PB89-149080 PB89-270387 PB89-189189 PB89-172621 PB89-189189 PB89-172621 PB89-172621 PB89-189189 PB89-17262 PB89-172621 PB89-189189 PB89-17262 PB89-189189 PB89-17262 PB89-17262 PB89-189189 PB89-17262 PB89-17262 PB89-189189 PB89-17262 PB89-189189 PB89-17262 PB89-17262 PB89-189189 PB89-1891	Gas Flow Measurement Standards.	PB89-146948 901,121	
Determination of the Time-Dependence of ohm NBS (National Bureau of Standards) Determination of the Time-Dependence of ohm NBS (National Bureau of Standards) Determination of the Time-Dependence of ohm NBS (National Bureau of Standards) Determination of the Time-Dependence of ohm NBS (National Bureau of Standards) Determination of the Time-Dependence of ohm NBS (National Bureau of Standards) Determination of the Time-Dependence of ohm NBS (National Bureau of Standards) Determination of the Time-Dependence of ohm NBS (National Bureau of Standards) Determination of the Time-Dependence of ohm NBS (National Bureau of Standards) Determination of the Time-Dependence of ohm NBS (National Bureau of Standards) Determination of the Time-Dependence of ohm NBS (National Bureau of Standards) Determination of the Time-Dependence of ohm NBS (National Bureau of Standards) Determination of the Time-Dependence of ohm NBS (National Bureau of Standards) Determination of the Time-Dependence of ohm NBS (National Bureau of Standards) Determination of the Time-Dependence of ohm NBS (National Bureau of Standards) Determination of the Time-Dependence of ohm NBS (National Bureau of Standards) Determination of the Time-Dependence of ohm NBS (National Bureau of Standards) Determination of the Time-Dependence of ohm NBS (National Bureau of Standards) Determination of the Time-Dependence of ohm NBS (National Bureau of Standards) Determination of Standards NBS (National Bureau of Standards) Determination of Absolute Stresses in Alumination of Absolute Stresses in Alumination NBS (National Bureau of Standards) Determination of Absolute Stresses in Alumination of Absolute Stresses in Alumination NBS (National Bureau of Standards) Determination of the Roughness of Blasted Steel	· · · · · · · · · · · · · · · · · · ·	Ultrasonic Characterization of Surface Modified Layers. PB89-147409 901.115	
Update of U.S. Participation in International Standards PB89-149082 PB89-228282 PB89-228282 Determination of the Time-Dependence of ohm NBS (National Bureau of Standards) Using the Quantized Hall Resistance. PB89-230387 PB89-230387 PB89-149080 PB99-117631 Edge Stresses in Woven Laminates at Low Temperatures in Aluminations of Absolute Stresses in		Local Brittle Zones in Steel Weldments: An Assessment	Measurement of Applied J-Integral Produced by Residual
PB89-226282 90,902 Determination of the Time-Dependence of ohm NBS (National Bureau of Standards) Using the Quantized Hall Resistance. PB89-230387 900,819 Improved Transportable DC Voltage Standard. PB89-230395 901,554 Josephson Array Voltage Calibration System: Operational Use and Verification. PB89-158018 901,098 PB89-178621 901,098 STRESS CORROSION TESTS Failure Analysis of an Amine-Absorber Pressure Vessel. PB89-17865 901,098 PB89-17865 PB99-12865 STRESS CORROSION TESTS Failure Analysis of an Amine-Absorber Pressure Vessel. PB89-17861 PB89-178621 PB89-189189 PB89-178621 PB89-189189 PB89-178621 PB89-189189 PB89-178621 PB89-189189 PB89-178621 PB89-189189 PB89-189189 PB89-17861 PB89-189189 PB89	Update of U.S. Participation in International Standards		
Determination of the Time-Dependence of 6hm NBS (National Bureau of Standards) Using the Quantized Hall Resistance, PB89-230387 PB89-230387 PB89-230387 PB89-230387 PB89-230395 PB89-150957 Fractal-Based Description of the Roughness of Blasted Steel Panels. PB89-230395 Josephson Array Voltage Calibration System: Operational Use and Verification. PB89-230403 Measurement of the NBS (National Bureau of Standards) PB89-230403 Measurement of the NBS (National Bureau of Standards) PB89-230403 Measurement of the NBS (National Bureau of Standards) PB89-230403 Measurement of Standards PB89-230403 Measurement of the NBS (National Bureau of Standards) PB89-230403 Measurement of Standards PB89-230403 Measurement of the NBS (National Bureau of Standards) PB89-230403 Measurement of the NBS (National Bureau of Standards) PB89-230403 Measurement of the NBS (National Bureau of Standards) PB89-230403 Measurement of the NBS (National Bureau of Standards) PB89-230403 Measurement of the NBS (National Bureau of Standards) PB89-230403 Measurement of the NBS (National Bureau of Standards) PB89-230403 Measurement of the NBS (National Bureau of Standards) PB89-230403 Measurement of the NBS (National Bureau of Standards) PB89-230403 Measurement of the NBS (National Bureau of Standards) PB89-230403 Measurement of the NBS (National Bureau of Standards) PB89-230403 Measurement of the NBS (National Bureau of Standards) PB89-30403 Measurement of the NBS (National Bureau of Standards) PB89-30403 Measurement of the NBS (National Bureau of Standards) PB89-30403 Measurement of the NBS (National Bureau of Standards) PB89-30403 Measurement of the NBS (National Bureau of Standards) PB89-30403 Measurement of the NBS (National Bureau of Standards) PB89-30403 Measurement of the NBS (National Bureau of Standards) PB89-30403 Measurement of the NBS (National Bureau of Standards) PB89-30403 Measurement of the NBS (National Bureau of Standards) Measurement of the NBS (National Bureau of Standards) Measurement of the NBS (Nati		J-Integral Values for Small Cracks in Steel Panels.	Edge Stresses in Woven Laminates at Low Tempera-
sistance. PB89-230387 pB89-230385 pB89-172821 pB89-173835 pB89-189185 pB89-172821 pB89-189185 pB89-173835 pB89-173835 pB89-189185 pB89-173835 pB89-17	Determination of the Time-Dependence of ohm NBS (National Bureau of Standards) Using the Quantized Hall Bo	· ·	
Improved Transportable DC Voltage Standard. PB89-230395 Josephson Array Voltage Calibration System: Operational Use and Verification. PB89-230403 Measurement of the NBS (National Bureau of Standards) PB89-172621	sistance.	num and Steel Alloys.	
PB89-230395 901,554 Josephson Array Voltage Calibration System: Operational Use and Verification. PB89-158018 901,096 PB89-230403 900,820 Measurement of the NBS (National Bureau of Standards) PB89-172621 901,096 PB89-189195 901,003 PB89-230429 900,821 National Bureau of Standards Message Authentication PB89-230395 PB89-189195 901,003 Fracture Behavior of a Pressure Vessel Steel in the Ductille-to-Brittle Transition Region. PB89-21019 STRESS RELAXATION TESTS Far-Infrared Spectrum of Methyl Amine. Assignment and Analysis of the First Torsional State. PB89-189195 901,003 PB89-189195 901,003 STRESS WAVES			
Levated Temperature Deformation of Structural Steel. PB89-230403 Measurement of the NBS (National Bureau of Standards) PB89-230429 PB89-230420 Fracture Belavior of a Pressure Vessel Steel in the Ductile-to-Brittle Transition Region. PB89-230429 PB89-230429 PB89-212179 STRESS RELAXATION TESTS Far-Infrared Spectrum of Methyl Amine. Assignment and Analysis of the First Torsional State. PB89-16374 PB89-16374 PB89-212179 STRESS RELAXATION TESTS Far-Infrared Spectrum of Methyl Amine. Assignment and Analysis of the First Torsional State. PB89-16374 PB89-210439 PB89-210439 STRESS WAVES		Steel Panels.	Electromigration Damage Response Time and Implica-
PB99-230403 900,820 Measurement of the NBS (National Bureau of Standards) Electrical Watt in SI Units. PB89-172621 900,821 National Bureau of Standards Message Authentication PB89-189195 900,346 Quantitative Studies of Coatings on Steel Using Reflections (Coatings on Steel Using Reflections) STRESS RELAXATION TESTS Far-Infrared Spectrum of Methyl Amine. Assignment and Analysis of the First Torsional State. PB89-189195 900,346 STRESS WAVES	Josephson Array Voltage Calibration System: Operational Use and Verification.		
Electrical Watt in SI Units. PB89-230429 900,821 National Bureau of Standards Message Authentication Quantitative Studies of Coatings on Steel Using Reflections Analysis of the First Torsional State. PB89-161574 900,346 STRESS WAVES		PB89-172621 901,098	STRESS RELAXATION TESTS
PB89-230429 900,821 PB89-189195 901,103 PB89-161574 900,346 National Bureau of Standards Message Authentication Quantitative Studies of Coatings on Steel Using Reflections STRESS WAVES	Measurement of the NBS (National Bureau of Standards)	Fracture Behavior of a Pressure Vessel Steel in the Duc-	Far-Infrared Spectrum of Methyl Amine. Assignment and Analysis of the First Torsional State.
	PB89-230429 900,821		PB89-161574 900,346
		Quantitative Studies of Coatings on Steel Using Reflec- tion/Absorption Fourier Transform Infrared Spectroscopy.	STRESS WAVES Finite Element Studies of Transient Wave Propagation.

PB89-186902 <i>901,375</i>	PB89-157523 900,327	PB89-157077 901,492
STRONTIUM	Critical Review of the Chemical Kinetics of Sulfur Tetra- fluoride, Sulfur Pentafluoride, and Sulfur Fluoride (S2F10)	Sputtered Thin Film Ba2YCu3On. PB89-165427 901,029
Alignment Effects in Electronic Energy Transfer and Re- active Events.	in the Gas Phase.	Josephson-Junction Model of Critical Current in Granular
AD-A202 820/7 900,267	PB89-161582 900,347 Collisional Electron Detachment and Decomposition	Y1Ba2Cu3O(7-delta) Superconductors.
Wavelengths and Energy Levels of the K I Isoelectronic Sequence from Copper to Molybdenum.	Rates of SF6(1-), SF5(1-), and F(1-) in SF6: Implications	PB89-176978 901,406 Bean Model Extended to Magnetization Jumps.
PB89-179097 901,372	for Ion Transport and Electrical Discharges. PB90-117862 900,511	PB89-176994 901,407
NBS (National Bureau of Standards) Decay-Scheme In-	Electron-Energy Dependence of the S2F10 Mass Spec-	Synthesis and Magnetic Properties of the Bi-Sr-Ca-Cu Oxide 80- and 110-K Superconductors.
vestigations of (82)Sr-(82)Rb. PB89-161558 901,498	trum. PB90-117870 900,512	PB89-179725 901,412
STRONTIUM IONS	SULFUR HALIDES	High T(sub c) Superconductor/Noble-Metal Contacts with Surface Resistivities in the (10 to the Minus 10th Power)
4s(2) 4p(2)-4s4p(3) Transition Array and Energy Levels of	Thermochemistry of Solvation of SF6(1-) by Simple Polar Organic Molecules in the Vapor Phase.	Omega sq cm Range.
the Germanium-Like Ions Rb VI - Mo XI. PB89-201065 901,528	PB89-202527 900,437	PB89-179824 901,413 Theoretical Models for High-Temperature Superconducti-
STRUCTURAL ANALYSIS	SULFUR HEXAFLUORIDE Infrared Absorption of SF6 from 32 to 3000 cm(-1) in the	vity.
Progressive Collapse: U.S. Office Building in Moscow. PB89-175715 900,158	Gaseous and Liquid States.	PB89-186266 901,418 Oxygen Partial-Density-of-States Change in the
Brick Masonry: U.S. Office Building in Moscow.	PB89-157853 900,336 Electron-Transport, Ionization, Attachment, and Dissocia-	YBa2Cu3Ox Compounds for x(Approx.)6,6.5,7 Measured
PB89-187504 900,160	tion Coefficients in SF6 and Its Mixtures. PB89-171540 901,501	by Soft X-ray Emission. PB89-186274 901,419
Sensors and Measurement Techniques for Assessing Structural Performance.	Production and Stability of S2F10 in SF6 Corona Dis-	Resonant Excitation of an Oxygen Valence Satellite in
PB89-235865 900,162	charges.	Photoemission from High-T(sub c) Superconductors. PB89-186860 901,420
STRUCTURAL DESIGN Earthquake Hazard Mitigation through Improved Seismic	PB89-231039 900,822 Collisional Electron Detachment and Decomposition	Ag Screen Contacts to Sintered YBa2Cu3Ox Powder for
Design. PB89-149132 900,098	Rates of SF6(1-), SF5(1-), and F(1-) in SF6: Implications	Rapid Superconductor Characterization. PB89-200448 901,423
STRUCTURAL FORMS	for Ion Transport and Electrical Discharges. PB90-117862 900,511	Battery-Powered Current Supply for Superconductor
Damage Accumulation in Wood Structural Members Under Stochastic Live Loads.	SUPERCOMPUTERS	Measurements. PB89-200455 901,525
PB89-171748 900,115	Supercomputers Need Super Anthmetic. PB90-130253 900,657	Switching Noise in YBa2Cu3Ox 'Macrobridges'.
Design Criteria for High Temperature Structural Applications.	SUPERCONDUCTING CABLES	PB89-200513 901,426 Resistance Measurements of High T(sub c) Supercon-
PB89-211833 901,052	Current Capacity Degradation in Superconducting Cable Strands.	ductors Using a Novel 'Bathysphere' Cryostat.
STRUCTURE FACTORS	PB89-200471 901,526	PB89-228431 901,448
Alternative Approach to the Hauptman-Karle Determinan- tal Inequalities.	SUPERCONDUCTING DEVICES Superconducting Kinetic Inductance Bolometer.	Cryogenic Bathysphere for Rapid Variable-Temperature Characterization of High-T(sub c) Superconductors.
PB89-186241 901,416 Maximum Entropy Distribution Consistent with Observed	PB89-200505 900,762	PB89-228456 901,450 Hysteretic Phase Transition in Y1Ba2Cu3O7-x Supercon-
Structure Amplitudes.	SUPERCONDUCTING FILMS Evidence for the Superconducting Proximity Effect in	ductors.
PB89-186258 901,417 Low-Q Neutron Diffraction from Supercooled D-Glycerol.	Junctions between the Surfaces of YBa2CU3Ox Thin	PB89-229082 901,454 Dependence of T(sub c) on the Number of CuO2 Planes
PB89-228001 900,468	Films. PB89-228449 901,449	per Cluster in Interplaner-Boson-Exchange Models of
SUB-BOILING STILLS	SUPERCONDUCTING JUNCTIONS	High-T(sub C) Superconductivity. PB89-229132 901,455
Analysis of Ultrapure Reagents from a Large Sub-Boiling Still Made of Teflon PFA.	Evidence for the Superconducting Proximity Effect in Junctions between the Surfaces of YBa2CU3Ox Thin	Flux Creep and Activation Energies at the Grain Bound-
PB89-186357 900,202	Films. PB89-228449 901,449	anes of Y-Ba-Cu-O Superconductors. PB89-230353 901,457
Design Principles for a Large High-Efficiency Sub-Boiling Still.	SUPERCONDUCTING WIRES	Thermomechanical Detwinning of Superconducting
PB89-187553 900,207 SUBROUTINES	Effect of Room-Temperature Stress on the Critical Cur- rent of NbTi.	YBa2Cu3O7-x Single Crystals. PB89-231088 901,458
Creating CSUBs in BASIC.	PB89-179832 · 901,414	Reentrant Softening in Perovskite Superconductors.
PB89-176226 900,647 Creating CSUBs Written in FORTRAN That Run in	Nb3Sn Critical-Current Measurements Using Tubular Fi- berglass-Epoxy Mandrels.	PB90-117540 <i>901,464</i> Gruneisen Parameter of Y1Ba2Cu3O7.
BASIC.	PB89-200497 901,527	PB90-117615 901,465
PB90-128752 900,656 SUBSTITUTION REACTIONS	VAMAS (Versailles Project on Advanced Materials and Standards) Intercomparison of Critical Current Measure-	Neutron Study of the Crystal Structure and Vacancy Dis- tribution in the Superconductor Ba2Y Cu3 O(sub g-delta).
Qualitative MO Theory of Some Ring and Ladder Poly-	ment in Nb3Sn Wires. PB89-202147 901,534	PB90-123480 901,468
mers. PB89-156723 <i>900,303</i>	SUPERCONDUCTIVITY	Bulk Modulus and Young's Modulus of the Superconductor Ba2Cu3YO7.
SUBSTRATES	Electronic, Magnetic, Superconducting and Amorphous- Forming Properties Versus Stability of the Ti-Fe, Zr-Ru	PB90-123613 901,469
Effect of Surface Ionization on Wetting Layers. PB89-157259 901,323	and Hf-Os Ordered Alloys.	Offset Criterion for Determining Superconductor Critical Current.
SUBSURFACE INVESTIGATIONS	PB89-146690 901,120 Magnetic Field Dependence of the Superconductivity in	PB90-128133 901,474
Antennas for Geophysical Applications. PB89-179857 900,710	Bi-Sr-Ca-Cu-O Superconductors. PB89-146815 901,385	Critical Current Measurements of Nb3Sn Superconduc- tors: NBS (National Bureau of Standards) Contribution to
Clutter Models for Subsurface Electromagnetic Applica-	, , , , , , , , , , , , , , , , , , , ,	the VAMAS (Versailles Agreement on Advanced Materials and Standards) Interlaboratory Companison.
tions. PB89-229678 900,688	Crystal Chemistry of Superconductors: A Guide to the Tailoring of New Compounds. PB89-171730 901,030	PB90-136748 901,480
SUCROSE	Densification, Susceptibility and Microstructure of	SUPERCRITICAL FLOW Semi-Automated PVT Facility for Fluids and Fluid Mix-
Thermodynamics of the Hydrolysis of Sucrose. PB89-227904 901,227	Ba2YCu3O(6+ x). PB89-171821 901,035	tures.
SUGAR ALCOHOLS	Magnetic Evaluation of Cu-Mn Matrix Material for Fine-	PB89-157184 900,875 Decorated Lattice Gas Model for Supercritical Solubility.
Second Vinal Coefficients of Aqueous Alcohols at Elevat- ed Temperatures: A Calonmetric Study.	Filament Nb-Ti Superconductors. PB89-200489 901,425	PB89-175681 900,373
PB89-227896 900,462	Journal of Research of the National Institute of Stand-	SUPERCRITICAL FLUID CHROMATOGRAPHY Supercritical Fluid Chromatograph for Physicochemical
SUGARS Intramolecular H Atom Abstraction from the Sugar Moiety	ards and Technology, Volume 94, Number 3, May-June 1989.	Studies.
by Thymine Radicals in Oligo- and Polydeoxynucleotides.	PB89-211106 901,441	PB89-184105 900,201 Introduction to Supercritical Fluid Chromatography. Part
PB89-171870 901,263 SULFUR COMPOUNDS	Brief Review of Recent Superconductivity Research at NIST (National Institute of Standards and Technology).	Applications and Future Trends.
Evaluated Chemical Kinetic Data for the Reactions of	PB89-211114 900,766	PB89-230312 900,219 SUPERCRITICAL FLUIDS
Atomic Oxygen O(3P) with Sulfur Containing Compounds. PB89-145122 900,269	Companson of Interplaner-Boson-Exchange Models of High-Temperature Superconductivity - Possible Expen-	Latent Heats of Supercritical Fluid Mixtures.
SULFUR DIOXIDE	mental Tests. PB90-117334 901,462	PB89-174908 900,242 Supercritical Fluid Chromatograph for Physicochemical
One-Electron Transfer Reactions of the Couple SO2/ SO2(1-) in Aqueous Solutions. Pulse Radiolytic and	SUPERCONDUCTORS	Studies.
Cyclic Voltammetric Studies. PB89-176093 900,376	Institute for Materials Science and Engineering, Ceramics: Technical Activities 1988.	PB89-184105 900,201 SUPERHEATER HEADERS
Chemical Kinetics of Intermediates in the Autoxidation of	PB89-148381 <i>901,019</i>	Postweld Heat Treatment Criteria for Repair Welds in 2-
SO2. PB89-176754 900,256	Oxygen Isotope Effect in the Superconducting Bi-Sr-Ca-Cu-O System.	1/4Cr-1Mo Superheater Headers: An Experimental Study. PB89-156160 901,094
SULFUR FLUORIDES	PB89-157044 901,025	SUPERLATTICES

Current Ripple Effect on Superconductive D.C. Critical Current Measurements.

SUPERLATTICES
Characterization of Structural and Magnetic Order of Er/
Y Superlattices.

SULFUR FLUORIDES
S2F10 Formation in Computer Simulation Studies of the Breakdown of SF6.

				SURGES
PB90-123662	901,470	PB89-180046	901,415	Fundamental Characterization of Clean and Gas-Dosed
SUPPRESSORS		Photon-Stimulated Desorption as a Measure	of Surface	Tin Oxide. PB89-202964 900,785
Discussion of 'Steep-Front Short-Duration Vol- Tests of Power Line Filters and Transient Vol-	tage Surge oltage Sup-	Electronic Structure. PB89-231328	901,459	Oxygen Chemisorption on Cr(110): 1. Dissociative Ad-
pressors.' PB90-117326	900,755	SURFACES & INTERFACES		sorption. PB89-202980 900,441
SURFACE CHEMISTRY	300,733	Adsorption Properties of Pt Films on W(110). PB89-146864	900,281	Oxygen Chemisorption on Cr(110): 2. Evidence for Mo-
Picosecond Studies of Vibrational Energy 1	ransfer in	Core-Level Binding-Energy Shifts at Surface	•	lecular O2(ads). PB89-202998 900,442
Molecules on Surfaces. PB89-157309	900,316	Solids. PB89-146898	900,282	Stimulated Desorption from CO Chemisorbed on Cr(110).
Semiclassical Way to Molecular Dynamics at S	urfaces. 900,333	Surface Structure and Growth Mechanism		PB89-203004 900,443
PB89-157713 Technical Activities 1988, Surface Science Divi		Si(100). PB89-149181	901,387	Time Resolved Studies of Vibrational Relaxation Dynamics of CO(v= 1) on Metal Particle Surfaces.
PB89-161889	900,349	Angle Resolved XPS (X-ray Photoelectron Spe	•	PB89-203012 900,444
Surface Reactions in Silane Discharges. PB89-185961	900,406	of the Epitaxial Growth of Ću on Ni(100). PB89-150866	901,389	Thin Film Thermocouples for High Temperature Measure- ment.
Interaction of Water with Solid Surfaces: Fu		Final-State-Resolved Studies of Molecule-Sur		PB89-209290 901,065
Aspects. PB89-201081	900.421	actions. PB89-150916	900,298	Chemisorption of HF (Hydrofluoric Acid) on Silicon Surfaces.
Coadsorption of Water and Lithium on the Ru	(001) Sur-	Analytical Expression for Describing Auger Sp		PB89-212013 900,445
face. PB89-202956	900.440	Profile Shapes of Interfaces. PB89-157176	900,309	Dynamical Simulation of Liquid- and Solid-Metal Self- Sputtering.
Picosecond Vibrational Energy Transfer Studi	es of Sur-	Theoretical Study of the Vibrational Lineshap		PB89-228407 900,472
face Adsorbates. PB90-136573	900,537	Pt(111). PB89-157689	900,331	Cr(110) Oxidation Probed by Carbon Monoxide Chemis- orption.
SURFACE FINISHING	,,,,,	Synchrotron Radiation Study of BaO Films	•	PB89-228423 900,239
Kinetics of Resolidification. PB89-176457	901,138	and Their Interaction with H2O, CO2, and O2. PB89-157697	900,252	Improved Low-Energy Diffuse Scattering Electron-Spin Polarization Analyzer.
SURFACE MAGNETISM	001,100	Semiclassical Way to Molecular Dynamics at S		PB89-229173 900,218
Domain Images of Ultrathin Fe Films on Ag(100 PB89-158067	0). 901.394	PB89-157713	900,333	Electron Transmission Through NiSi2-Si Interfaces.
Magnetic Properties of Surfaces Investigated b		Secondary-Electron Effects in Photon-Stimulat tion.	ed Desorp-	PB89-231294 900,485 Interaction of Oxygen and Platinum on W(110).
larized Electron Beams. PB89-176564	901,405	PB89-157929	900,337	PB89-231302 901,158
SURFACE PROPERTIES	301,403	Optically Driven Surface Reactions: Evidend Role of Hot Electrons.	ce for the	Methodology for Electron Stimulated Desorption Ion Angular Distributions of Negative Ions.
Status of Reference Data, Reference Materials	s and Ref-	PB89-157937	900,338	PB89-231310 900,486
erence Procedures in Surface Analysis. PB89-157705	900,332	Electron and Photon Stimulated Desorption: Structure and Bonding at Surfaces.	Probes of	Photon-Stimulated Desorption as a Measure of Surface
Electron and Photon Stimulated Desorption:	Probes of	PB89-157960	901,116	Electronic Structure. PB89-231328 901,459
Structure and Bonding at Surfaces. PB89-157960	901,116	Calculations of Electron Inelastic Mean Free P Materials.	aths for 31	Universal Resputtering Curve.
Calculations of Electron Inelastic Mean Free Pa	aths for 31	PB89-157978	900,341	PB89-234314 901,460 Development of a Method to Measure In situ Chloride at
Materials. PB89-157978	900,341	Domain Images of Ultrathin Fe Films on Ag(10 PB89-158067	0). <i>901,394</i>	the Coating/Metal Interface.
Electron and Photon Stimulated Desorption: Be	enefits and	Technical Activities 1988, Surface Science Divi	sion.	PB89-235345 901,085
Difficulties. PB89-200745	901,427	PB89-161889	900,349	Structure of Cs on GaAs(110) as Determined by Scanning Tunneling Microscopy.
Surface-Interacting Polymers: An Integral Equ	uation and	Sputtered Thin Film Ba2YCu3On. PB89-165427	901,029	PB90-117490 901,463
Fractional Calculus Approach. PB89-202949	900,571	Surface Structures and Growth Mechanism	of Ga on	Resonance Enhanced Electron Stimulated Desorption. PB90-117771 900,505
Chemisorption of HF (Hydrofluoric Acid) on S	ilicon Sur-	 Si(100) Determined by LEED (Low Energy El fraction) and Auger Electron Spectroscopy. 	ectron Dif-	Cathodoluminescence of Defects in Diamond Films and
faces. PB89-212013	900,445	PB89-171342	901,399	Particles Grown by Hot-Filament Chemical-Vapor Deposition.
Equilibrium Crystal Shapes and Surface Phase	Diagrams	AES and LEED Studies Correlating Desorption with Surface Structures and Coverages for		PB90-117961 901,069
at Surfaces in Ceramics. PB90-117755	901,162	Si(100). PB89-171599	901.401	Influence of the Surface on Magnetic Domain-Wall Mi- crostructure.
Adsorption of Water on Clean and Oxyger Nickel(110).	-Predosed	Effects of a Gold Shank-Overlayer on the Field	, .	PB90-118019 901,467
PB90-123555	900,522	ing of Silicon. PB89-175988	901.404	Photon-Stimulated Desorption of Fluorine from Silicon via Substrate Core Excitations.
Ammonia Adsorption and Dissociation on a Iron(s) (100) Surface.	Stepped	Dynamics of Molecular Collisions with Surface	, .	PB90-118027 900,517
PB90-123563	900,523	tion, Dissociation, and Diffraction. PB89-175996	900,375	Magnetic Behavior of Compositionally Modulated Ni-Cu Thin Films.
SURFACE REACTIONS Final State Resolved Studies of Molecule Sur	food Intor	Influence of Electronic and Geometric Structi		PB90-118084 901,163
Final-State-Resolved Studies of Molecule-Sur actions.		sorption Kinetics of Isoelectronic Polar Molecand H2O.		Adsorption of Water on Clean and Oxygen-Predosed Nickel(110).
PB89-150916 Dynamics of Molecular Collisions with Surface	900,298	PB89-176473	900,381	PB90-123555 900,522
tion, Dissociation, and Diffraction.		Magnetic Properties of Surfaces Investigated blarized Electron Beams.	y Spin Po-	Ammonia Adsorption and Dissociation on a Stepped Iron(s) (100) Surface.
PB89-175996 SURFACE ROUGHNESS	900,375	PB89-176564	901,405	PB90-123563 900,523
Optical Roughness Measurements for Industria	Surfaces.	Surface Properties of Clean and Gas-Dosed St PB89-179576	nO2 (110). <i>900,393</i>	Initial Stages of Heteroepitaxial Growth of InAs on Si(100).
PB89-176655	900,979	Surface Reactions in Silane Discharges.	300,333	PB90-123878 901,473
Critical and Noncritical Roughening of Surface ment).	·	PB89-185961	900,406	Role of Adsorbed Gases in Metal on Metal Epitaxy. PB90-128125 901,174
PB89-180046	901,415	Laser Probing of the Dynamics of Ga Inter Si(100).	actions on	Direct Observation of Surface-Trapped Diffracted Waves.
Scattering Parameters Representing Imperfection Coaxial Air Lines.		PB89-186928	901,422	PB90-128216 901,475
PB89-184121	900,750	Electron and Photon Stimulated Desorption: B Difficulties.	enefits and	Interaction of In Atom Spin-Orbit States with Si(100) Surfaces.
Ultrasonic Sensor for Measuring Surface Rougl PB89-211809	900,679	PB89-200745	901,427	PB90-128547 900,532
Measuring the Root-Mean-Square Value of	a Finite	Interaction of Water with Solid Surfaces: For Aspects.	undamental	Picosecond Vibrational Energy Transfer Studies of Surface Adsorbates.
Record Length Periodic Waveform. PB90-163924	901,588	PB89-201081	900,421	PB90-136573 900,537
SURFACE STRUCTURE		NO/NH3 Coadsorption on Pt(111): Kinetic and Effects in Rotational Accommodation.	Dynamical	SURFACTANTS Substitutes for N-Phenylglycine in Adhesive Bonding to
Structure of Cs on GaAs(110) as Determined ning Tunneling Microscopy.	-	PB89-201123	900,423	Dentin. PB90-123795 900,051
PB90-117490	901,463	Bond Selective Chemistry with Photon-Stim sorption.	ulated De-	900,057 SURGES
SURFACES Universality Class of Planar Self-Avoiding Sur	faces with	PB89-201222	900,259	Tiger Tempering Tampers Transmissions.
Fixed Boundary. PB89-157945	900,339	Electron-Stimulated-Desorption Ion-Angular Dis PB89-201230	stributions. 901,430	PB89-157861 900,740 Coupling, Propagation, and Side Effects of Surges in an
Surface Structures and Growth Mechanism	of Ga on	Surface-Interacting Polymers: An Integral Eq		Industrial Building Wiring System.
Si(100) Determined by LEED (Low Energy El fraction) and Auger Electron Spectroscopy.	ectron Dif-	Fractional Calculus Approach. PB89-202949	900,571	PB89-173454 900,118 Selecting Varistor Clamping Voltage: Lower Is Not Better.
PB89-171342	901,399	Coadsorption of Water and Lithium on the Re		PB89-176648 900,760
Critical and Noncritical Roughening of Surfament).	ces (Com-	face. PB89-202956	900,440	Lightning and Surge Protection of Photovoltaic Installa- tions. Two Case Histories: Vulcano and Kythnos.
			,	

PB89-229058 900,851 Discussion of 'Steep-Front Short-Duration Voltage Surge Tests of Power Line Filters and Transient Voltage Sup-	Emerging Technologies in Manufacturing Engineering. PB90-132747 901,013 TECHNOLOGY INCENTIVES	TEMPERATURE SCALES New International Temperature Scale of 1990 (ITS-90), PB89-202550 901,238
pressors.' PB90-117326 900,755	Product Data Exchange Specification: First Working	TENSILE PROPERTIES
SURVEY MONITORS	Draft. PB89-144794 900,940	Prediction of Tensile Behavior of Strain Softened Com- posites by Flexural Test Methods.
International Intercomparison of Neutron Survey Instru- ment Calibrations.	Assessment of Robotics for Improved Building Operations and Maintenance.	PB89-147045 900,585
PB89-229165 901,300	PB89-189146 900,092	Necking Phenomena and Cold Drawing. PB89-201495 900,975
SURVEYS Advanced Ceramics: A Critical Assessment of Wear and	Promoting Technological Excellence: The Role of State and Federal Extension Activities.	TENSILE STRENGTH Elevated Temperature Deformation of Structural Steel.
Lubrication. PB89-188569 <i>901,045</i>	PB90-120742 900,171 TECHNOLOGY INNOVATION	PB89-172621 901,098
SUSPENDING (MIXING)	National Engineering Laboratory's 1989 Report to the National Research Council's Board on Assessment of	Tensile Strain-Rate Effects in Liquid Helium. PB89-174882 901,102
Liquid, Crystalline and Glassy States of Binary Charged Colloidal Suspensions.	NIST (National Institute of Standards and Technology)	Strain Energy of Bituminous Built-Up Membranes: A New Concept in Load-Elongation Testing.
PB89-202501 901,436 SWELLING	Programs. PB89-189294 900,004	PB89-212203 900,139
Facilitated Transport of CO2 through Highly Swollen Ion- Exchange Membranes: The Effect of Hot Glycenne Pre-	NIST (National Institute of Standards and Technology) Research Reports, March 1989.	Tensile and Fatigue-Creep Properties of a Copper-Stain- less Steel Laminate.
treatment. PB89-179618 900,395	PB89-189310 900,005	PB90-128646 901,083 TENSION TESTS
SYMPATHETIC COOLING	TECHNOLOGY TRANSFER Report on Interactions between the National Institute of	Method to Measure the Tensile Bond Strength between
Ion Trapping Techniques: Laser Cooling and Sympathetic Cooling.	Standards and Technology and the American Society of Mechanical Engineers.	Two Weakly-Cemented Sand Grains. PB89-166110 901,483
PB90-128034 <i>901,578</i> SYNCHROTRONS	PB89-172563 901,004 Materials Failure Prevention at the National Bureau of	Loading Rate Effects on Discontinuous Deformation in Load-Control Tensile Tests.
Bond Selective Chemistry with Photon-Stimulated De-	Standards. PB89-212237 901,190	PB89-171896 <i>901,097</i>
sorption. PB89-201222 900,259	Promoting Technological Excellence: The Role of State	Fracture Behavior of 316LN Alloy in Uniaxial Tension at Cryogenic Temperatures.
SYNTAX Free Value Tool for ASN.1.	and Federal Extension Activities. PB90-120742 900,171	PB90-128562 901,111 Tensile Tests of Type 305 Stainless Steel Mine Sweeping
PB89-196182 900,622	TEETH	Wire Rope. PB90-130287 901,112
SYNTHESIS Polymers Bearing Intramolecular Photodimerizable	Detection of Lead in Human Teeth by Exposure to Aqueous Sulfide Solutions.	TERBIUM
Probes for Mass Diffusion Measurements by the Forced Rayleigh Scattering Technique: Synthesis and Character-	PB89-201529 <i>901,256</i> TEFLON	Effect of pH on the Emission Properties of Aqueous tris (2,6-dipicolinato) Terbium (III) Complexes.
ization. PB89-157101 <i>901,181</i>	Analysis of Ultrapure Reagents from a Large Sub-Boiling Still Made of Teflon PFA.	PB89-157135 900,250
SYNTHESIS (CHEMISTRY)	PB89-186357 900,202	Neutron Scattering Study of the Spin Ordering in Amorphous Tb45Fe55 and Tb25Fe75.
Dynamic Light Scattering and Angular Dissymmetry for the In situ Measurement of Silicon Dioxide Particle Syn-	TELECOMMUNICATION Standardizing EMCS Communication Protocols.	PB89-201701 901,149 TERBIUM 160
thesis in Flames. PB89-179584 900,246	PB89-172357 900,613	Magnetic Resonance of (160)Tb Oriented in a Terbium Single Crystal at Low Temperatures.
Synthesis, Stability, and Crystal Chemistry of Dibanum	TELEOPERATORS Interfaces to Teleoperation Devices.	PB89-179204 901,519
Pentatitanate. PB89-179741 <i>901,041</i>	PB89-181739 900,993 TELLURIUM	TERNARY SYSTEM Phase Equilibria and Crystal Chemistry in the Ternary
Design and Synthesis of Prototype Air-Dry Resins for Use in BEP (Bureau of Engraving and Printing) Intaglio Ink Ve-	Determination of Selenium and Tellunium in Copper	System BaO-TiO2-Nb2O5: Part 1. PB89-171797 901,033
hicles. PB90-112343 901,068	Standard Reference Materials Using Stable Isotope Dilution Spark Source Mass Spectrometry.	TERNARY SYSTEMS
Synthesis and Characterization of Novel Bonded Phases	PB90-123472 900,230 TEMPERATURE	Quantitative Characterization of the Viscosity of a Microemulsion.
for Reversed-Phase Liquid Chromatography. PB90-128695 900,233	Thin Film Thermocouples for Internal Combustion Engines.	PB90-123597 900,524 TEST EQUIPMENT
SYNTHETIC RESINS Design and Synthesis of Prototype Air-Dry Resins for Use	PB89-147094 900,607	Use of Artificial Intelligence and Microelectronic Test
in BEP (Bureau of Engraving and Printing) Intaglio Ink Vehicles.	Isochoric (p,v,T) Measurements on CO2 and (0.98 CO2 + 0.02 CH4) from 225 to 400 K and Pressures to 35	Structures for Evaluation and Yield Enhancement of Microelectronic Interconnect Systems.
PB90-112343 901,068	MPa. PB89-202493 <i>900,435</i>	PB89-146955 900,768 Simple Apparatus for Vapor-Liquid Equilibrium Measure-
SYSTEMS Center for Electronics and Electrical Engineering Techni-	Thermal Conductivity of Refrigerants in a Wide Range of	ments with Data for the Binary Systems of Carbon Dioxide with n-Butane and Isobutane.
cal Progress Bulletin Covering Center Programs, October to December 1988, with 1989 CEEE Events Calendar.	Temperature and Pressure. PB89-226583 900,458	PB89-201115 900,422
PB89-193270 <i>900,813</i>	TEMPERATURE COEFFICIENT Standard Electrode Potentials and Temperature Coeffi-	Drift Tubes for Characterizing Atmospheric Ion Mobility Spectra Using AC, AC-Pulse, and Pulse Time-of-Flight
T-2 TOXIN Anti-T2 Monoclonal Antibody Immobilization on Quartz	cients in Water at 298.15 K. PB89-226567 900,456	Measurement Techniques. PB89-202543 900,438
Fibers: Stability and Recognition of T2 Mycotoxin. PB90-128760 901,267	TEMPERATURE CONTROL	TEST FACILITIES Combustion Testing Methods for Catalytic Heaters.
TABLES (DATA)	Analysis of High Performance Compensated Thermal Enclosures.	PB89-150924 900,846
Journal of Physical and Chemical Reference Data, Volume 17, 1988, Supplement No. 2. Thermodynamic	PB89-185748 901,008 TEMPERATURE DISTRIBUTION	Dynamic Young's Modulus Measurements in Metallic Materials: Results of an Interlaboratory Testing Program.
and Transport Properties for Molten Salts: Correlation Equations for Critically Evaluated Density, Surface Ten-	Performance Measurements of Infrared Imaging Systems	PB89-157671 901,132
sion, Electrical Conductance, and Viscosity Data. PB89-145205	Used to Assess Thermal Anomalies. PB89-179667 900,072	Laboratory Accreditation Systems in the United States, 1984. PB89-176432 900.882
Composites Databases for the 1990's. PB89-180376 901,075	TEMPERATURE MEASUREMENT Remote Sensing Technique for Combustion Gas Temper-	PB89-176432 900,882 Experimental Determination of Forced Convection Evapo-
TAGGED PHOTON METHOD	ature Measurement in Black Liquor Recovery Boilers. P889-179568 900,392	rative Heat Transfer Coefficients for Non-Azeotropic Re- frigerant Mixtures.
Cross Section and Linear Polarization of Tagged Photons.	Development of New Standard Reference Materials for	PB89-186407 901,117
PB90-117292 901,560 TARGETS	Use in Thermometry. PB89-201180 <i>900,893</i>	NBS (National Bureau of Standards)-Boulder Gas Flow Facility Performance.
Validation of Absolute Target Thickness Calibrations in a	New International Temperature Scale of 1990 (ITS-90), PB89-202550 901,238	PB89-186787 900,889 Use of GMAP (Geometric Modeling Applications Interface
QQQ Instrument by Measuring Absolute Total Cross-Sections of NE(1 +) (NE,NE)NE(1 +). PB89-157507 900,325	Acoustic and Microwave Resonances Applied to Measur-	Program) Software as a PDES (Product Data Exchange Specification) Environment in the National PDES Testbed
PB89-157507 900,325 TECHNICAL SOCIETIES	ing the Gas Constant and the Thermodynamic Tempera- ture.	Project. PB89-215198 <i>900,960</i>
Dental Materials and Technology Research at the National Bureau of Standards: A Model for Government-Private	PB89-228548 901,320 Monitoring and Predicting Parameters in Microwave Dis-	NIST (National Institute of Standards and Technology)
Sector Cooperation. PB90-128711 900,052	solution. PB90-118183 PB90-190-118183	Measurement Services: AC-DC Difference Calibrations. PB89-222616 900,818
TECHNOLOGICAL INTELLIGENCE	TEMPERATURE MEASURING INSTRUMENTS	NVLAP (National Voluntary Laboratory Accreditation Program) Program Handbook Construction Testing Services.
Measurement Standards for Defense Technology. PB89-150965 901,270	Performance Measurements of Infrared Imaging Systems Used to Assess Thermal Anomalies.	Requirements for Accreditation. PB90-112327 900,169
TECHNOLOGY ASSESSMENT Strategic Defense Initiative Space Bower Systems Matrol	PB89-179667 900,072	Center for Radiation Research (of the National Institute
Strategic Defense Initiative Space Power Systems Metrology Assessment.	Development of an Automated Probe for Thermal Conductivity Measurements.	of Standards and Technology) Technical Activities for 1989.
PB89-173405 901,268	PB89-209324 <i>900,896</i>	PB90-130279 901,307

900,117

TEST PORTS	THERMAL DIFFUSION	PB89-172548 900,117
Calibrating Network Analyzers with Imperfect Test Ports. PB90-117680 900,825	High Temperature Thermal Conductivity Apparatus for Fluids.	Thermal Resistance Measurements and Calculations of an Insulated Concrete Block Wall.
TESTS	PB89-174015 900,366	PB89-174916 900,119
Application of the ISO (International Standards Organization) Distributed Single Layer Testing Method to the Con-	THERMAL DIFFUSIVITY Experimental Thermal Conductivity, Thermal Diffusivity, and Specific Heat Values of Argon and Nitrogen.	IEEE (Institute of Electrical and Electronics Engineers) IRPS (International Reliability Physics Symposium) Tuton-
nectionless Network Protocol. PB89-177133 900,616	PB99-148407 900,293 Prediction of the Heat Release Rate of Douglas Fir.	al Thermal Resistance Measurements, 1989. PB89-231195 900,792
Proficiency Testing for MIL-STD 462 NVLAP (National Voluntary Laboratory Accreditation Program) Laboratories.	PB89-212039 901,185 THERMAL EFFICIENCY	THERMAL VOLTAGE CONVERTERS Recharacterization of Thermal Voltage Converters After
PB90-128612 901,381 Ambiguity Groups and Testability.	Structural Reliability and Damage Tolerance of Ceramic Composites for High-Temperature Applications. Semi-	Thermoelement Replacement. PB89-230452 900,720
PB90-128703 900,722	Annual Progress Report for the Period Ending September 30, 1987.	THERMISTORS Transient Response Error in Microwave Power Meters
TETRAFLUOROETHYLENE RESINS Deutenum Magnetic Resonance Study of Orientation and	PB89-156350 901,023 Structural Reliability and Damage Tolerance of Ceramic	Using Thermistor Detectors. PB89-173785 900,759
Poling in Poly(Vinylidene Fluoride) and Poly(Vinylidene Fluoride-Co-Tetrafluoroethylene). PB89-186365 900,565	Composites for High-Temperature Applications. Semi- Annual Progress Report for the Period Ending March 31,	Development of an Automated Probe for Thermal Conductivity Measurements.
TEXT PROCESSING	1988.* PB89-156368 901,024	PB89-209324 900,896 THERMO-OPTICS
Standard Generalized Markup Language (SGML). FIPS PUB 152 900,627	Refrigeration Efficiency of Pulse-Tube Refrigerators. PB89-173892 901,007	Thermo-Optic Designs for Microwave and Millimeter- Wave Electric-Field Probes.
TEXTILES Fire Properties Database for Textile Wall Covenings.	THERMAL ENERGY STORAGE EQUIPMENT Periodic Heat Conduction in Energy Storage Cylinders	PB90-128588 900,691
PB89-188635 900,126 TEXTURE	with Change of Phase. PB89-175897 900,852	THERMOCHEMICAL PROPERTIES Numeric Databases in Chemical Thermodynamics at the
Texture Monitoring in Aluminum Alloys: A Companson of	THERMAL INSULATION ZIP: The ZIP-Code Insulation Program (Version 1.0) Eco-	National Institute of Standards and Technology. PB89-175228 900,371
Ultrasonic and Neutron Diffraction Measurements. PB90-117409 901,159	nomic Insulation Levels for New and Existing Houses by Three-Digit ZIP Code. Users Guide and Reference	THERMOCHEMISTRY Hyperconjugation: Equilibrium Secondary Isotope Effect
Ultrasonic Separation of Stress and Texture Effects in Polycrystalline Aggregates.	Manual. PB89-151765 900,058	on the Stability of the t-Butyl Cation. Kinetics of Near- Thermoneutral Hydride Transfer.
PB90-117557 900,499	ZIP: ZIP-Code Insulation Program (for Microcomputers).	PB89-156756 900,306
THERMAL ANALYSIS Preparation of Multistage Zone-Refined Materials for Thermochemical Standards.	PB89-159446 900,060 Specific Heat of Insulations.	Thermochemistry of Solvation of SF6(1-) by Simple Polar Organic Molecules in the Vapor Phase.
PB89-186795 900,203	PB89-172514 900,116 Insulation Standard Reference Materials of Thermal Re-	PB89-202527 900,437 Thermodynamics of the Hydrolysis of Sucrose.
Thermal and Economic Analysis of Three HVAC (Heating, Ventilating, and Air Conditioning) System Types in a	sistance. PB89-172548 900,117	PB89-227904 901,227 PVT Relationships in a Carbon Dioxide-Rich Mixture with
Typical VA (Veterans Administration) Patient Facility. PB89-188619 900,847	Thermal Resistance Measurements and Calculations of	Ethane. PB89-229181 900,478
Considerations for Advanced Building Thermal Simulation Programs.	an Insulated Concrete Block Wall. PB89-174916 900,119	THERMOCOUPLES
PB®9-231047 900,084 THERMAL CONDUCTIVITY	U-Value Measurements for Windows and Movable Insula- tions from Hot Box Tests in Two Commercial Laborato-	Thin Film Thermocouples for Internal Combustion Engines.
Microporous Furned-Silica Insulation Board as a Candi-	nes. PB89-175889 <i>900,121</i>	PB89-147094 900,607 Thin Film Thermocouples for High Temperature Measure-
date Standard Reference Material of Thermal Resistance. PB89-148373 901,018	Friability of Spray-Applied Fireproofing and Thermal Insulations: Field Evaluation of Prototype Test Devices.	ment. PB89-209290 901,065
Experimental Thermal Conductivity, Thermal Diffusivity,	PB89-189328 900,130 Acoustical Technique for Evaluation of Thermal Insula-	NIST (National Institute of Standards and Technology) Measurement Services: The Calibration of Thermocou-
and Specific Heat Values of Argon and Nitrogen. PB89-148407 900,293	tion. PB89-193866 900,919	ples and Thermocouple Materials. PB89-209340 900,897
High Temperature Thermal Conductivity Apparatus for Fluids.	Interlaboratory Comparison of Two Types of Line-Source Thermal-Conductivity Apparatus Measuring Five Insulat-	THERMODYMANIC PROPERTIES
PB89-174015 900,366 Thermal Conductivity of Liquid Argon for Temperatures	ing Materials. PB89-218325 900,144	Journal of Physical and Chemical Reference Data, Volume 18, Number 1, 1989. PB89-226559 900,455
between 110 and 140 K with Pressures to 70 MPa. PB89-179600 900,394	Window U-Values: Revisions for the 1989 ASHRAE (American Society of Heating, Refingerating and Air-Con-	THERMODYNAMIC EQUILIBRIUM
Relation between Wire Resistance and Fluid Pressure in the Transient Hot-Wire Method.	ditioning Engineers) Handbook - Fundamentals. PB89-229215 900,145	Stress Effects on III-V Solid-Liquid Equilibria. PB89-146997 900,769
PB89-184113 901,520 Development of an Automated Probe for Thermal Con-	THERMAL MEASUREMENT	Phase Equilibrium in Two-Phase Coherent Solids. PB89-157580 900,330
ductivity Measurements. PB89-209324 900,896	Measurements of Molar Heat Capacity at Constant Volume: Cv,n(xCH4+ (1-x)C2H6' T = 100 to 320 K, p < or = 35 MPa).	Computer Program for Calculating Non-LTE (Local Thermodynamic Equilibrium) Model Stellar Atmospheres.
Thermal Conductivity Measurements of Thin-Film Silicon Dioxide.	< or = 35 MPa). PB90-117896 900,844 THERMAL MEASUREMENTS	PB89-171573 900,018
PB89-212195 901,444	Effects of Space Charge on the Poling of Ferroelectric Polymers.	Vapor-Liquid Equilibrium of Nitrogen-Oxygen Mixtures and Air at High Pressure. PB89-174932 900,368
Interlaboratory Comparison of Two Types of Line-Source Thermal-Conductivity Apparatus Measuring Five Insulat- ing Materials.	PB89-146708 901,179	Decorated Lattice Gas Model for Supercritical Solubility.
PB 89-218325 900,144	Review of Thermal Characterization of Power Transistors. PB89-150825 900,770	PB89-175681 900,373 Vapor-Liquid Equilibrium of Binary Mixtures in the Ex-
Interlaboratory Comparison of the Guarded Honzontal Pipe-Test Apparatus: Precision of ASTM (American Soci-	Thermal Resistance Measurements and Calculations of an Insulated Concrete Block Wall.	tended Critical Region. I. Thermodynamic Model. PB89-218374 901,544
ety for Testing and Materials) Standard Test Method C- 335 Applied to Mineral-Fiber Pipe Insulation. PB89-218341 901,011	PB89-174916 900,119 Analysis of High Performance Compensated Thermal En-	Equilibrium Crystal Shapes and Surface Phase Diagrams at Surfaces in Ceramics.
Low-Temperature Thermal Conductivity of Composites:	closures. PB89-185748 <i>901,008</i>	PB90-117755 901,162 THERMODYNAMIC PROPERTIES
Alumina Fiber/Epoxy and Alumina Fiber/PEEK. PB89-218358 901,078	Interlaboratory Comparison of Two Types of Line-Source Thermal-Conductivity Apparatus Measuring Five Insulat-	Benzene Thermophysical Properties from 279 to 900 K at
Thermal Conductivity of Nitrogen and Carbon Monoxide in the Limit of Zero Density.	ing Materials. PB89-218325 900,144	Pressures to 1000 Bar. PB89-145148 900,271
PB89-222533 900,449	THERMAL MEASURING INSTRUMENTS	Estimation of the Thermodynamic Properties of Hydrocarbons at 298.15 K.
Thermal Conductivity of Refrigerants in a Wide Range of Temperature and Pressure. P89-226583 900,458	High Temperature Thermal Conductivity Apparatus for Fluids.	PB89-145155 900,272
Simplified Representation for the Thermal Conductivity of	PB89-174015 900,366 Summary of Circular and Square Edge Effect Study for	Thermodynamic Values Near the Critical Point of Water. PB89-161541 901,497
Fluids in the Critical Region. PB89-228050 901,332	Guarded-Hot-Plate and Heat-Flow-Meter Apparatuses. PB89-176606 900,884	Standard Chemical Thermodynamic Properties of Polycy- clic Aromatic Hydrocarbons and Their Isomer Groups 1.
Effect of Anisotropic Thermal Conductivity on the Mor- phological Stability of a Binary Alloy.	THERMAL NEUTRONS Use of Multiple-Slot Multiple Disk Chopper Assemblies to	Benzene Series. PB89-186480 900,412
PB89-228985 901,155 Microporous Fumed-Silica Insulation as a Standard Ref-	Pulse Thermal Neutron Beams. PB89-147466 901,485	Development of New Standard Reference Materials for Use in Thermometry.
erence Material of Thermal Resistance at High Tempera- ture.	THERMAL RADIATION Upward Turbulent Flame Spread on Wood under External	PB89-201180 900,893
PB90-130311 900,153	Radiation. PB90-118050 PB90-118050	Thermal Analysis of VAMAS (Versailles Project on Ad- vanced Materials and Standards) Polycarbonate-Polyeth- ylene Blends.
THERMAL CYCLING TESTS	. 500 , 10000	, one pronds

THERMAL RESISTANCE

sistance.

Insulation Standard Reference Materials of Thermal Re-

THERMAL CYCLING TESTS

Low-Temperature Thermal Conductivity of Composites: Alumina Fiber/Epoxy and Alumina Fiber/PEEK. PB89-218358 901,078

ylene Blends. PB89-201487

Properties of Steam. PB89-202048

Activities of the International Association for the Proper-	PB89-157531 900,328	PB89-202048 901,533
ties of Steam between 1979 and 1984. PB89-212153 900,446	Filling of Solvent Shells About Ions. 1. Thermochemical	Pi-Electron Properties of Large Condensed Polyaromatic
Journal of Physical and Chemical Reference Data,	Critena and the Effects of Isomeric Clusters. PB89-157549 900,329	Hydrocarbons. PB89-202139 900,432
Volume 18, Number 2, 1989.	Dehydrogenation of Ethanol in Dilute Aqueous Solution	NaCl-H2O Coexistence Curve Near the Critical Tempera-
PB89-222525 900,448	Photosensitized by Benzophenones.	ture of H2O.
Thermodynamic Properties of Argon from the Triple Point to 1200 K with Pressures to 1000 MPa.	PB89-157556 900,251	PB89-202519 900,436
PB89-222558 900,451	Elastic Interaction and Stability of Misfitting Cuboidal In- homogeneities.	Thermochemistry of Solvation of SF6(1-) by Simple Polar Organic Molecules in the Vapor Phase.
Thermodynamic Properties of Dioxygen Difluoride (O2F2)	PB89-157903 901,482	PB89-202527 900,437
and Dioxygen Fluoride (O2F). PB89-222566 900,452	Van der Waals Equation of State Around the Van Laar	Evaluated Kinetics Data Base for Combustion Chemistry.
Thermodynamic and Transport Properties of Carbohy-	Point. PB89-158133 900,345	PB89-212096 <i>900,601</i>
drates and Their Monophosphates: The Pentoses and Hexoses.	Critical Review of the Chemical Kinetics of Sulfur Tetra-	Fundamental Aspects of Key Issues in Hazardous Waste Incineration.
PB89-222574 900,453	fluoride, Sulfur Pentafluoride, and Sulfur Fluoride (S2F10)	PB89-212104 900,861
Standard Chemical Thermodynamic Properties of Polycy-	in the Gas Phase. PB89-161582 900,347	Activities of the International Association for the Proper-
clic Aromatic Hydrocarbons and Their Isomer Groups. 2. Pyrene Senes, Naphthopyrene Senes, and Coronene	Rate Constants for Hydrogen Abstraction by Resonance	ties of Steam between 1979 and 1984.
Series.	Stabilized Radicals in High Temperature Liquids.	PB89-212153 900,446
PB89-226591 900,459	PB89-161608 900,348	Vapor-Liquid Equilibrium of Binary Mixtures in the Extended Critical Region. I. Thermodynamic Model.
Thermophysical-Property Needs for the Environmentally Acceptable Halocarbon Refrigerants.	Transient Cooling of a Hot Surface by Droplets Evapora- tion.	PB89-218374 901,544
PB89-231054 900,482	PB89-161897 900,971	Tables for the Thermophysical Properties of Methane.
THERMODYNAMICS	Absolute Rate Constants for Hydrogen Abstraction from	PB89-222608 900,843
Journal of Physical and Chemical Reference Data,	Hydrocarbons by the Trichloromethylperoxyl Radical. PB89-171532 900,357	Calorimetric and Equilibrium Investigation of the Hydrolysis of Lactose.
Volume 17, 1988, Supplement No. 2. Thermodynamic and Transport Properties for Molten Salts: Correlation	Electron-Transport, Ionization, Attachment, and Dissocia-	PB89-227888 901,226
Equations for Critically Evaluated Density, Surface Ten-	tion Coefficients in SF6 and Its Mixtures.	Second Virial Coefficients of Aqueous Alcohols at Elevat-
sion, Electrical Conductance, and Viscosity Data. PB89-145205 900,277	PB89-171540 <i>901,501</i>	ed Temperatures: A Calorimetric Study.
Numeric Databases in Chemical Thermodynamics at the	Development of Combustion from Quasi-Stable Tempera- tures for the Iron Based Alloy UNS S66286.	PB89-227896 900,462
National Institute of Standards and Technology.	PB89-173850 900,592	Thermodynamics of the Hydrolysis of Sucrose. PB89-227904 901,227
PB89-175228 900,371	Specific Heat Measurements of Two Premium Coals.	Asymptotic Expansions for Constant-Composition Dew-
Thermodynamics of Hydrolysis of Disaccharides. PB89-186761 901,221	PB89-173900 900,839	Bubble Curves Near the Critical Locus.
Biological Thermodynamic Data for the Calibration of Dif-	Dynamics of Concentration Fluctuation on Both Sides of	PB89-227987 <i>901,545</i>
ferential Scanning Calorimeters: Heat Capacity Data on	Phase Boundary. PB89-173942 901,183	Simplified Representation for the Thermal Conductivity of Fluids in the Critical Region.
the Unfolding Transition of Lysozyme in Solution. PB90-117920 900,513	Molecular Dynamics Investigation of Expanded Water at	PB89-228050 901,332
THERMODYNAMICS & CHEMICAL KINETICS	Elevated Temperatures.	Capillary Waves of a Vapor-Liquid Interface Near the Crit-
Rate Constants for the Reaction HO2+ NO2+ N2->	PB89-174957 900,370	ical Temperature.
HO2NO2+ N2: The Temperature Dependence of the Fall-Off Parameters.	Numeric Databases in Chemical Thermodynamics at the National Institute of Standards and Technology.	PB89-228555 900,476
PB89-146658 900,278	PB89-175228 900,371	Reevaluation of Forces Measured Across Thin Polymer Films: Nonequilibrium and Pinning Effects.
Gas Phase Proton Affinities and Basicities of Molecules:	Decorated Lattice Gas Model for Supercritical Solubility.	PB89-228589 900,573
A Comparison between Theory and Experiment. PB89-146674 900,280	PB89-175681 900,373	Pressure Fixed Points Based on the Carbon Dioxide
Evaporation of a Water Droplet Deposited on a Hot High	Theory of Microphase Separation in Graft and Star Co- polymers.	Vapor Pressure at 273.16 K and the H2O(I) - H2O(III) - H2O(L) Triple-Point.
Thermal Conductivity Solid Surface.	PB89-176028 900,557	PB89-231138 900,483
PB89-149157 901,487	One-Electron Transfer Reactions of the Couple SO2/	Properties of Lennard-Jones Mixtures at Various Tem-
Reactions of Phenyl Radicals with Ethene, Ethyne, and Benzene.	SO2(1-) in Aqueous Solutions. Pulse Radiolytic and Cyclic Voltammetric Studies.	peratures and Energy Ratios with a Size Ratio of Two. PB89-235204 900,493
PB89-150908 900,297	PB89-176093 900,376	Application of the Gibbs Ensemble to the Study of Fluid-
Relative Acidities of Water and Methanol and the Stabili-	Rate Constants for Reactions of Nitrogen Oxide (NO3)	Fluid Phase Equilibrium in a Binary Mixture of Symmetric
ties of the Dimer Anions. PB89-150981 900,299	Radicals in Aqueous Solutions. PB89-176242 900,379	Non-Additive Hard Spheres. PB90-117318 900,494
Redox Chemistry of Water-Soluble Vanadyl Porphynns.	Influence of Reaction Reversibility on Continuous-Flow	Biological Thermodynamic Data for the Calibration of Dif-
PB89-150999 900,300	Extraction by Emulsion Liquid Membranes.	ferential Scanning Calorimeters: Heat Capacity Data on
Reactions of Magnesium Prophyrin Radical Cations in Water. Disproportionation, Oxygen Production, and Com-	PB89-176481 900,244	the Unfolding Transition of Lysozyme in Solution.
parison with Other Metalloporphyrins.	Modelling of Impurity Effects in Pure Fluids and Fluid Mix-	PB90-117920 900,513
PB89-151005 900,301	tures. PB89-176739 <i>900,245</i>	Vapor Pressures and Gas-Phase PVT Data for 1,1,1,2- Tetrafluoroethane.
Rate Constants for One-Electron Oxidation by Methylper-	Chemical Kinetics of Intermediates in the Autoxidation of	PB90-117987 900,514
oxyl Radicals in Aqueous Solutions. PB89-151013 900,302	SO2.	Reaction of (Ir(C(3), N bpy)(bpy)2)(2+) with OH Radicals
New Photolytic Source of Dioxymethylenes: Criegee In-	PB89-176754 900,256	and Radiation Induced Covalent Binding of the Complex to Several Polymers in Aqueous Solutions.
termediates Without Ozonolysis.	Mechanism and Rate of Hydrogen Atom Attack on Tolu- ene at High Temperatures.	PB90-123498 900,264
PB89-156731 900,304 Kinetics of Electron Transfer from Nitroaromatic Radical	PB89-179758 900,398	Fluid Flow in Pulsed Laser Irradiated Gases; Modeling
Anions in Aqueous Solutions. Effects of Temperature and	Critical and Noncritical Roughening of Surfaces (Com-	and Measurement. PB90-123704 900,265
Steric Configuration.	ment). PB89-180046 901,415	Temperature Dependence of the Rate Constant for the
PB89-156749 900,305 Hyperconjugation: Equilibrium Secondary Isotope Effect	Van der Waals Fund, Van der Waals Laboratory and	Hydroperoxy + Methylperoxy Gas-Phase Reaction.
on the Stability of the t-Butyl Cation. Kinetics of Near-	Dutch High-Pressure Science.	PB90-136375 900,534
Thermoneutral Hydride Transfer. PB89-156756 900,306	PB89-185755 900,401	Flash Photolysis Kinetic Absorption Spectroscopy Study of the Gas Phase Reaction HO2 + C2H5O2 Over the
Detection of Gas Phase Methoxy Radicals by Resonance	Maximum Entropy Distribution Consistent with Observed Structure Amplitudes.	Temperature Range 228-380 K.
Enhanced Multiphoton Ionization Spectroscopy.	PB89-186258 901,417	PB90-136565 <i>900,536</i>
PB89-156764 900,307	Experimental Determination of Forced Convection Evapo-	Bioseparations: Design and Engineering of Partitioning
Decay of High Valent Manganese Porphyrins in Aqueous Solution and Catalyzed Formation of Oxygen.	rative Heat Transfer Coefficients for Non-Azeotropic Re- frigerant Mixtures.	Systems. PB90-136763 901,231
PB89-156772 900,308	PB89-186407 901,117	Instrument-Independent MS/MS Database for XQQ In-
Temperature, Composition and Molecular-Weight De-	Thermodynamics of Hydrolysis of Disaccharides.	struments: A Kinetics-Based Measurement Protocol.
pendence of the Binary Interaction Parameter of Polysty- rene/Poly(vinylmethylether) Blends.	PB89-186761 901,221	PB90-213695 900,674
PB89-157473 900,550	Biological Standard Reference Materials for the Calibra- tion of Differential Scanning Calonmeters: Di-alkylphos-	THERMOELEMENTS Recharacterization of Thermal Voltage Converters After
Validation of Absolute Target Thickness Calibrations in a	phatidylcholine in Water Suspensions.	Thermoelement Replacement.
QQQ Instrument by Measuring Absolute Total Cross-Sections of NE(1+) (NE,NE)NE(1+).	PB89-186779 900,415	PB89-230452 900,720
PB89-157507 900,325	Simple Apparatus for Vapor-Liquid Equilibrium Measure-	THERMOGRAPHY
Stopped-Flow Studies of the Mechanisms of Ozone-	ments with Data for the Binary Systems of Carbon Dioxide with n-Butane and Isobutane.	Fractal-Based Description of the Roughness of Blasted Steel Panels.
Alkene Reactions in the Gas Phase: Tetramethylethylene.	PB89-201115 900,422	PB89-158018 901,096
PB89-157515 900,326	Thermal Analysis of VAMAS (Versailles Project on Advanced Materials and Standards) Polycarbonate Polyeth	Thermographic Imaging and Computer Image Processing
S2F10 Formation in Computer Simulation Studies of the	vanced Materials and Standards) Polycarbonate-Polyeth- ylene Blends.	of Defects in Building Materials. PB89-176309 900,123
Breakdown of SF6. PB89-157523 900,327	PB89-201487 900,568	THERMOGRAVIMETRY
Ionic Hydrogen Bond and Ion Solvation. 5. OH(1-)O	Mechanism of Hydrolysis of Octacalcium Phosphate. PB89-201503 901,254	Thermal Analysis of VAMAS (Versailles Project on Ad-
Bonds. Gas Phase Solvation and Clustering of Alkoxide		vanced Materials and Standards) Polycarbonate-Polyeth-
and Carboxylate Anions.	Properties of Steam.	ylene Blends.

PB89-201487	900,568	THORIUM IONS	PB89-171862 <i>901,265</i>
THERMOMETERS		Laser-Produced Spectra and QED (Quantum Electrody- namic) Effects for Fe-, Co-, Cu-, and Zn-Like lons of Au,	Mossbauer Imaging. PB89-176895 901,242
Superconducting Kinetic Inductance Bolometer. PB89-200505	900,762	Pb, Bi, Th, and U. PB89-176010 901.510	PB89-176895 901,242 TITANATES
THERMOPHYSICAL PROPERTIES		THREE DIMENSIONAL MODELS	Synthesis, Stability, and Crystal Chemistry of Dibanum
Thermophysical Properties of Methane.	900,450	Modeling Dynamic Surfaces with Octrees.	Pentatitanate.
PB89-222541 Thermophysical Properties for Bioprocess Engin		PB90-112335 901,206	PB89-179741 <i>901,041</i>
PB89-228068	900,043	THYMINE Radiation-Induced Crosslinks between Thymine and 2-D-	Journal of Physical and Chemical Reference Data.
Measurements of Molar Heat Capacity at		Deoxyerythropentose.	Volume 17, 1988, Supplement No. 3. Atomic Transition Probabilities Scandium through Manganese.
Volume: $Cv_m(xCH4+ (1-x)C2H6' T = 100 to < or = 35 MPa)$.	320 K, p	PB89-146682 900,247 Structure of a Hydroxyl Radical Induced Cross-Link of	PB89-145197 900,276
PB90-117896	900,844	Thymine and Tyrosine.	TITANIUM ALLOYS
Spherical Acoustic Resonators. PB90-128505	901,321	PB89-157838 901,244 TIDES	Stable and Metastable Ti-Nb Phase Diagrams. PB89-157432 901,125
THERMOPLASTIC RESINS	001,021	Gravity Tide Measurements with a Feedback Gravity	TITANIUM INTERMETALLICS
Crazes and Fracture in Polymers.		Meter. PB89-171755 <i>901,310</i>	Rapid Solidification and Ordering of B2 and L2 (sub 1)
PB89-176085	900,562	TILTMETERS	Phases in the NiAl-NiTi System. PB90-123639 901,171
Effects of Thermal Stability and Melt Viscosity of plastics on Piloted Ignition.		Transducers in Michelson Tiltmeters.	Pathways for Microstructural Development in TiAl.
PB90-128232	900,151	PB89-185979 901,280 Tilt Observations Using Borehole Tiltmeters 1. Analysis of	PB90-123779 901,173
FHICKNESS Fiber Coating and Characterization.		Tidal and Secular Tilt.	TOKAMAK DEVICES
PB89-228571	901,067	PB90-136649 901,283	Chlorine-like Spectra of Copper to Molybdenum. PB90-117706 900,501
THIN FILMS		TIME STANDARDS Comparison of Time Scales Generated with the NBS	Analysis of Magnesiumlike Spectra from Cu XVIII to Mo
Adsorption Properties of Pt Films on W(110). PB89-146864	900,281	(National Bureau of Standards) Ensembling Algorithm. PB89-174072 900,628	XXXI. PB90-117821 900.508
Sputter Deposition of Icosahedral Al-Mn and Al-I		Calibration of GPS (Global Positioning System) Equip-	TOLERANCE LIMITS
PB89-147102	901,122	ment in Japan.	Problems with Interval Estimation When Data Are Adjust-
Sputtered Thin Film Ba2YCu3On. PB89-165427	901,029	PB89-212070 900,630	ed via Calibration. PB89-157812 901,209
Production of 0.1-3 eV Reactive Molecules by I		NBS (National Bureau of Standards) Calibration Service Providing Time and Frequency at a Remote Site by	TOLUENE
porization of Condensed Molecular Films: A		Weighting and Smoothing of GPS (Global Positioning System) Common View Data.	PVT of Toluene at Temperatures to 673 K.
Source for Beam-Surface Interactions. PB89-171201	900,254	PB89-212211 900,631	PB89-157192 900,310
Preliminary Stochastic Model for Service Life F	Prediction	TIME TRANSFER	TOMOGRAPHY Mossbauer Imaging.
of a Photolytically and Thermally Degraded I Cover Plate Material.	Polymeric	Apparent Diurnal Effects in the Global Positioning System.	PB89-176895 901,242
PB89-173801	900,556	PB89-174080 901,292	TOOTH DISEASES
Switching Noise in YBa2Cu3Ox 'Macrobridges'.		TIN	Quasi-Constant Composition Method for Studying the Formation of Artificial Caries-Like Lesions.
PB89-200513	901,426	Ostwald Ripening in a System with a High Volume Frac- tion of Coarsening Phase.	PB89-229249 901,259
Magnetic Correlations in an Amorphous Gd Glass.	I-AI Spin	PB89-157598 901,126	TOPOLOGY
PB89-201693	901,148	Directional Invariance of Grain Boundary Migration in the Pb-Sn Cellular Transformation and the Tu-Turnbull Hys-	Algebraic Representation for the Topology of Multicom-
Time-of-Flight Measurements of Hyperthermal Molecules Produced by UV Laser Vaporization	Cl(sub 2)	teresis.	ponent Phase Diagrams. PB89-177042 901,517
genic Chlorine Films.	-	PB89-157911 901,134	TORSION BALANCES
PB89-202634	900,260	TIN ALLOYS Effect of Anisotropic Thermal Conductivity on the Mor-	Liquid-Supported Torsion Balance: An Updated Status
Exchange and Magnetostrictive Effects in Rare I perlattices.	Earth Su-	phological Stability of a Binary Alloy.	Report on Its Potential for Tunnel Detection. PB89-212062 901,542
PB89-202667	901,438	PB89-228985 901,155 TIN/BUTYL	TORSION TESTS
Thin Film Thermocouples for High Temperature ment.	Measure-	Speciation Measurements of Butyltins: Application to	Measurement of the Torque and Normal Force in Torsion in the Study of the Thermoviscoelastic Properties of Poly-
PB89-209290	901,065	Controlled Release Rate Determination and Production of Reference Standards.	mer Glasses.
Studies on Some Failure Modes in Latex Barrier		PB89-146807 900,174	PB89-172472 900,554
PB89-209308	901,089	Determination of Ultratrace Concentrations of Butyltin Compounds in Water by Simultaneous Hydridization/Ex-	Mechanism for Shear Band Formation in the High Strain Rate Torsion Test.
Quantitative Studies of Coatings on Steel Using tion/Absorption Fourier Transform Infrared Speci		traction with GC-FPD Detection.	PB89-215370 900,901
PB89-212112	901,066	PB89-177224 901,311	TORSIONAL STRENGTH
Thermal Conductivity Measurements of Thin-Fili Dioxide.	m Silicon	TIN/DIBUTYL Speciation Measurements of Butyltins: Application to	Microwave Spectrum of Methyl Amine: Assignment and Analysis of the First Torsional State.
PB89-212195	901,444	Controlled Release Rate Determination and Production of	PB30-117839 900,509
Reevaluation of Forces Measured Across Thin	Polymer	Reference Standards. PB89-146807 900,174	TORUSES
Films: Nonequilibrium and Pinning Effects. PB89-228589	900,573	TIN OXIDES	Finite Unions of Closed Subgroups of the n-Dimensional Torus.
High-Mobility CMOS (Complementary Metal Oxi		Surface Properties of Clean and Gas-Dosed SnO2 (110). PB89-179576 900,393	PB89-143283 901,193
conductor) Transistors Fabricated on Very T Films,	hin SOS	Fundamental Characterization of Clean and Gas-Dosed	TOUGHNESS Role of Inclusions in the Erecture of Austonitia Stainless
PB89-230460	900,791	Tin Oxide.	Role of Inclusions in the Fracture of Austenitic Stainless Steel Welds at 4 K.
Interaction of Oxygen and Platinum on W(110). PB89-231302	901.158	PB89-202964 900,785 TIN/TETRABUTYL	PB89-173504 901,099
Cathodoluminescence of Defects in Diamond F		Speciation Measurements of Butyltins: Application to	Influence of Molybdenum on the Strength and Toughness of Stainless Steel Welds for Cryogenic Service.
Particles Grown by Hot-Filament Chemical-Vapo		Controlled Release Rate Determination and Production of Reference Standards.	PB89-173512 901,100
tion. PB90-117961	901,069	PB89-146807 900,174	TOXIC SUBSTANCES
Magnetic Behavior of Compositionally Modulate		TIN/TRIBUTYL	Comparison of a Cryogenic Preconcentration Technique and Direct Injection for the Gas Chromatographic Analy-
Thin Films. PB90-118084	001 160	Speciation Measurements of Butyltins: Application to Controlled Release Rate Determination and Production of	sis of Low PPB (Parts-per-Billion) (NMOL/MOL) Gas Standards of Toxic Organic Compounds.
Growth and Properties of High-Quality Very-T	901,163	Reference Standards.	PB89-173843 900, 193
(Silicon-on Sapphire) Films.		PB89-146807 900,174 Biodegradation of Tributyltin by Chesapeake Bay Microor-	TOXICITY
PB90-128109	900,798	ganisms.	Toxicity of Mixed Gases Found in Fires. PB89-212047 900,869
FINIOCARBAMATES Frequency Measurements of High-J Rotationa	d Transi-	PB89-177232 901,309 TISSUE ADHESIVES	Generation of Oxy Radicals in Biosystems.
tions of OCS and N2O.		Oligomers with Pendant Isocyanate Groups as Tissue	PB90-117888 901,266
PB90-136946 FHIRD ORDER SUSCEPTIBILITY	900,541	Adhesives. 1. Synthesis and Characterization.	TRACE AMOUNTS
Measurements of the Nonresonant Third-Order	Suscepti-	PB89-202212 900,055 Oligomers with Pendant Isocyanate Groups as Tissue	Preconcentration of Trace Transition Metal and Rare Earth Elements from Highly Saline Solutions.
bility. PB89-179212	901,357	Adhesives. 2. Adhesion to Bone and Other Tissues.	PB90-118175 900,226
FB09-179212	301,337	PB89-231245 900,056 TISSUE EXTRACTS	TRACE ELEMENTS
Progress on Spin Detectors and Spin-Polarized	Electron	Long-Term Stability of the Elemental Composition in Bio-	Sample Validity in Biological Trace Element and Organic Nutrient Research Studies.
Scattering from Na at NIST. PB90-128299	901,583	logical Materials. PB89-156939 <i>900,181</i>	PB89-156905 901,218
THORIUM 230 TARGET	,	TISSUES (BIOLOGY)	Radiochemical and Instrumental Neutron Activation Anal- ysis Procedures for the Determination of Low Level Trace
Use of Thorium as a Target in Electron-Spin Ana		Initial Spectra of Neutron-Induced Secondary Charged	Elements in Human Livers.
PB90-117938	900,912	Particles.	PB89-171953 901,236

Specimen Banking in the National Status and Trends	PB89-222574 900,453	PB90-118050 900,148
Program: Development of Protocols and First Year Results.	TRANSVERSE ELECTROMAGNETIC CELLS	TURBULENT FLOW
PB89-175855 901,308	Automated TEM (Transverse Electromagnetic) Cell for Measuring Unintentional EM Emissions.	Importance of Isothermal Mixing Processes to the Under- standing of Lift-Off and Blow-out of Turbulent Jet Diffu-
Determination of Ultratrace Concentrations of Butyltin Compounds in Water by Simultaneous Hydridization/Ex-	PB89-173769 900,682	sion Flames.
traction with GC-FPD Detection. PB89-177224 901,311	Theory and Measurements of Radiated Emissions Using a TEM (Transverse Electromagnetic) Cell.	PB89-201172 900,598 Assessment of Theories for the Behavior and Blowout of
Determination of Trace Level Iodine in Biological and Bo-	PB89-193890 900,761	Lifted Turbulent Jet Diffusion Flames.
tanical Reference Materials by Isotope Dilution Mass Spectrometry.	TRANSVERSE WAVES Implementation of an Automated System for Measuring	PB89-231096 900,603 TURNING (MACHINERY)
PB89-235642 900,222	Radiated Emissions Using a TEM Cell. PB90-117698 901,377	Recommended Technical Specifications for Procurement
TRACE GASES Trace Gas Calibration Systems Using Permeation De-	TRAPPING (CHARGED PARTICLES)	of Equipment for a Turning Workstation. PB89-215347 900,962
vices.	Laser Cooling. PB89-179147 901,518	TURNING (MACHINING)
PB89-176580 900,883 TRACER TECHNIQUES	TRENDS	Turning Workstation in the AMRF (Automated Manufacturing Research Facility).
Use of Dye Tracers in the Study of Free Convection in	Trends for Building Technology in North America. PB89-174106 900.104	PB89-185607 900,954
Porous Media. 901,327	TRIBOLOGY	Inventory of Equipment in the Turning Workstation of the AMRF (Automated Manufacturing Research Facility).
Integral Mass Balances and Pulse Injection Tracer Techniques.	Advanced Ceramics: A Critical Assessment of Wear and	PB89-215339 900,961
PB89-206833 900,077	Lubrication. PB89-188569 <i>901,045</i>	TWINNING Thermomechanical Detwinning of Superconducting
TRAINING Computer Security Training Guidelines.	Development and Use of a Tribology Research-in-	YBa2Cu3O7-x Single Crystals.
PB90-780172 900,677	Progress Database. PB89-228274 901,002	PB89-231088 901,458 TWO PHOTON ABSORPTION
TRANSDUCERS Automated Fringe Counting Laser Interferometer for Low	Computer-Controlled Test System for Operating Different Wear Test Machines.	Fundamental Tests of Special Relativity and the Isotropy
Frequency Vibration Measurements.	PB89-228290 900,983	of Space. PB89-185920 <i>901,523</i>
PB89-177190 900,885 TRANSFORMERS	Tribochemical Mechanism of Alumina with Water. PB90-117722 901,059	TYROSINE
Journal of Research of the National Institute of Stand-	Measurements of Tribological Behavior of Advanced Ma-	Structure of a Hydroxyl Radical Induced Cross-Link of Thymine and Tyrosine.
ards and Technology, Volume 94, Number 3, May-June 1989.	terials: Summary of U.S. Results on VAMAS (Versailles Advanced Materials and Standards) Round-Robin No. 2.	PB89-157838 901,244
PB89-211106 901,441	PB90-130295 901,003	Mechanisms of Free Radical Chemistry and Biochemistry of Benzene.
TRANSIENT RESPONSE Transient Response Error in Microwave Power Meters	TRIOXOLANE Ozonolysis of Ethylene. Microwave Spectrum, Molecular	PB90-117714 900,502
Using Thermistor Detectors. PB89-173785 900,759	Structure, and Dipole Moment of Ethylene Primary Ozon-	U VALUES Window U-Values: Revisions for the 1989 ASHRAE
Vector Calibration of Ultrasonic and Acoustic Emission	ide (1,2,3- [⊤] noxolane). PB89-157∴40 <i>900,323</i>	(American Society of Heating, Refrigerating and Air-Con-
Transducers. PB89-202014 900,765	TRIPLE POINT	ditioning Engineers) Handbook - Fundamentals. PB89-229215 900,145
TRANSISTORS	Thermodynamic Properties of Argon from the Triple Point to 1200 K with Pressures to 1000 MPa.	Origins of ASHRAE (American Society of Heating, Refrig-
Review of Thermal Characterization of Power Transistors. PB89-150825 900,770	PB89-222558 900,451	erating and Air-Conditioning Engineers) Window U-Value Data and Revisions for the 1989 Handbook of Funda-
Correlation between CMOS (Complementary Metal Oxide	Pressure Fixed Points Based on the Carbon Dioxide	mentals. PB89-231005 <i>900,083</i>
Semiconductor) Transistor and Capacitor Measurements of Interface Trap Spectra.	Vapor Pressure at 273.16 K and the H2O(I) - H2O(III) - H2O(L) Triple-Point.	ULTRAHIGH VACUUM
PB89-180020 900,779	PB89-231138 900,483	Economical Ultrahigh Vacuum Four-Point Resistivity Probe.
Specimen Biasing to Enhance or Suppress Secondary Electron Emission from Charging Specimens at Low Ac-	TRYPSIN INHIBITORS Comparison of Two Highly Refined Structures of Bovine	PB89-147086 900,870
celerating Voltages. PB89-228464 901,451	Pancreatic Trypsin Inhibitor. PB89-202204 901,248	ULTRAPRECISION MACHINE TOOLS Preliminary Experiments with Three Identical Ultrapreci-
IEEE (Institute of Electrical and Electronics Engineers)	TUBES	sion Machine Tools. PB89-150841 900,997
IRPS (International Reliability Physics Symposium) Tutonal Thermal Resistance Measurements, 1989.	Experimental Investigation and Modeling of the Flow Rate of Refrigerant 22 Through the Short Tube Restric-	ULTRASONIC FREQUENCIES
PB89-231195 900,792	tor. PB89-229041 901,118	Ultrasonic Texture Analysis for Polycrystalline Aggregates of Cubic Materials Displaying Orthotropic Symmetry.
TRANSITION METALS	TUNABLE LASERS	PB89-146948 901,121
Preconcentration of Trace Transition Metal and Rare Earth Elements from Highly Saline Solutions.	NBS (National Bureau of Standards) Free Electron Laser	Ultrasonic Sensor for Measuring Surface Roughness. PB89-211809 900,679
PB90-118175 900,226 Role of Adsorbed Gases in Metal on Metal Epitaxy.	Facility. PB89-176515 901,353	ULTRASONIC TESTING
PB90-128125 901,174	TUNERS	Ultrasonic Railroad Wheel Inspection Using EMATs (Electromagnetic-Accoustic Transducers), Report No. 18.
TRANSITION PROBABILITIES Journal of Physical and Chemical Reference Data,	Measurement of Integrated Tuning Elements for SIS Mixers with a Fourier Transform Spectrometer.	PB89-189229 901,596
Volume 17, 1988, Supplement No. 3. Atomic Transition	PB89-157051 900,706 TUNGSTEN	Ultrasonic Separation of Stress and Texture Effects in Polycrystalline Aggregates.
Probabilities Scandium through Manganese. PB89-145197 900,276	Adsorption Properties of Pt Films on W(110).	PB90-117557 900,499
TRANSITION TEMPERATURE	PB89-146864 900,281 Synchrotron Radiation Study of RaO Films on W001)	ULTRASONIC TESTS Ultrasonic Determination of Absolute Stresses in Alumi-
Dynamics of a Spin-One Model with the Pair Correlation. PB89-171300 900,356	Synchrotron Radiation Study of BaO Films on W(001) and Their Interaction with H2O, CO2, and O2.	num and Steel Alloys.
TRANSLATOR ROUTINES	PB89-157697 900,252 Interaction of Oxygen and Platinum on W(110).	PB89-150957 901,124 Dynamic Poisson's Ratio of a Ceramic Powder during
User Guide for Wizard: A Syntax-Directed Editor and Translator for Estelle.	PB89-231302 901,158	Compaction.
PB89-196174 900,621 TRANSMISSION ELECTRON MICROSCOPY	Spectrum of Doubly Ionized Tungsten (W III). PB89-235659 900,223	PB89-177182 901,039 Acoustoelastic Determination of Residual Stresses.
TEM Observation of Icosahedral, New Crystalline and	TUNNEL DETECTION	PB89-179808 <i>901,318</i>
Glassy Phases in Rapidly Quenched Cd-Cu Alloys. PB90-123514 901,166	Liquid-Supported Torsion Balance: An Updated Status Report on Its Potential for Tunnel Detection.	Measuring In-Plane Elastic Moduli of Composites with Arrays of Phase-Insensitive Ultrasound Receivers.
TRANSMISSION LINES	PB89-212062 <i>901,542</i>	PB90-136672 900,970
Tiger Tempering Tampers Transmissions. PB89-157861 900,740	Clutter Models for Subsurface Electromagnetic Applica- tions.	ULTRAVIOLET ASTRONOMY Proceedings of the Celebratory Symposium on a Decade
Magnetic Dipole Excitation of a Long Conductor in a	PB89-229678 900,688	of UV (Ultraviolet) Astronomy with the IUE Satellite, Volume 2.
Lossy Medium. PB89-171664 900,742	Electromagnetic Detection of Long Conductors in Tun- nels.	N89-16535/1 900,014
Measuring Fast-Rise Impulses by Use of E-Dot Sensors. PB89-173413 900,744	PB90-128190 900,827	ULTRAVIOLET DETECTORS Stability and Quantum Efficiency Performance of Silicon
Some Questions and Answers Concerning Air Lines as	TURBINE BLADES Measurement of Shear Rate on an Agitator in a Fermen-	Photodiode Detectors in the Far Ultraviolet.
Impedance Standards. PB89-176176 900,747	tation Broth. PB89-186720 901,009	PB90-128059 900,735 ULTRAVIOLET RADIATION
TRANSMISSION LOSS	TURBULENCE	Synchrotron Photoemission Study of CO Chemisorption
Waveguide Loss Measurement Using Photothermal De- flection.	NBS' (National Bureau of Standards) Industry; Govern- ment Consortium Research Program on Flowmeter Instal-	on Cr(110). PB89-231336 900,262
PB89-157028 900,739	lation Effects: Summary Report with Emphasis on Re- search July-December 1987.	ULTRAVIOLET SPECTRA
Thermodynamic and Transport Properties of Carbohy-	PB90-111220 , 900,910	Proceedings of the Celebratory Symposium on a Decade of UV (Ultraviolet) Astronomy with the IUE Satellite,
drates and Their Monophosphates: The Pentoses and Hexoses.	Upward Turbulent Flame Spread on Wood under External Radiation.	Volume 2. N89-16535/1 900,014

Spectra and Energy Levels of the Galliumlike Mo XII.	lons Rb VII-	PB89-230288 9000 VAN DER WAALS FORCES	479 Ventilation and Air Quality Investigation of the U.S. Geo- logical Survey Building.
PB89-179105	900,387	Rydberg-Klein-Rees Inversion of High Resolution van	PB89-229686 900,857
4s(2) 4p(2)-4s4p(3) Transition Array and Ene the Germanium-Like Ions Rb VI - Mo XI.		Waals Infrared Spectra: An Intermolecular Pote Energy Surface for Ar+ HF (v= 1).	Large Office Buildings.
PB89-201065 ULTRAVIOLET SPECTROSCOPY	901,528	PB89-227953 900,	
Scheme for a 60-nm Laser Based on Photog	oumping of a	VAN DER WAALS FUND Van der Waals Fund, Van der Waals Laboratory	VENTS
High Level of Mo(6+) by a Spectral Line of PB89-186415		Dutch High-Pressure Science. PB89-185755 900	Floor Vent.
UNITED STATES	000,101		1 500 10055
Update of U.S. Participation in International	al Standards	VAN LAAR POINT Van der Waals Equation of State Around the Van I	Note on Calculating Flows Through Vertical Vents in aar Zone Fire Models Under Conditions of Arbitrary Cross-
Activities. PB89-228282	900,902	Point.	Vent Pressure Difference.
UNITS OF MEASUREMENT	300,302	PB89-158133 900,	345 PB90-117573 900,147
U.S. Perspective on Possible Changes in t	he Electrical	VANADIUM Journal of Physical and Chemical Reference D	VERIFYING
Units.	901,491	Volume 17, 1988, Supplement No. 3. Atomic Transi	
PB89-157002	301,431	Probabilities Scandium through Manganese. PB89-145197 900,	DD90.235015 000.000
UPHOLSTERY Cigarette as a Heat Source for Smolder Init	iation in Up-	VANADIUM OXIDES	VERSAILLES PROJECT ON ADVANCED MATERIALS AND
holstery Materials. PB89-176762	900,595	Structure of V9Mo6O40 Determined by Powder Neu	ron STANDARDS
Fire Risk Analysis Methodology: Initiating Eve		Diffraction. PB90-117995 <i>900,</i>	Versailles Project on Advanced Materials and Standards 515 Evolution to Permanent Status.
PB89-184527	900,125	VANADIUM PORPHYRIN	PB89-201768 900,969
Flammability of Upholstered Furniture w	ith Flaming	Redox Chemistry of Water-Soluble Vanadyl Porphyrins	
Sources. PB90-136805	900,155	PB89-150999 900,	300 Standards and Test Methods for VLSI (Very Large Scale Integration) Materials.
URACILS	,	VAPOR CELLS Search for Optical Molasses in a Vapor Cell: Gen	PB89-158042 900 774
Intramolecular H Atom Abstraction from the S		Analysis and Experimental Attempt.	Silicon and GaAs Wire-Bond Cratering Problem.
by Thymine Radicals in Oligo- and Polydeoxy PB89-171870	901,263	PB90-163932 901,	
URANIUM	,	VAPOR PHASES Simple Apparatus for Vapor-Liquid Equilibrium Meas	VIBRATION METERS
Microbiological Metal Transformations: Biot	echnological	ments with Data for the Binary Systems of Carbon D	ox- Frequency Vibration Measurements.
Applications and Potential. PB89-175947	901,284	ide with n-Butane and Isobutane. PB89-201115 900,	PB89-177190 900,885
Single Particle Standards for Isotopic Meas		VAPOR PRESSURE	VIBRATIONAL SPECTRA
Uranium by Secondary Ion Mass Spectrometr	y. <i>901,297</i>	Pressure and Density Series Equations of State	for Multiphoton Ionization Spectroscopy and Vibrational Analysis of a 3p Rydberg State of the Hydroxymethyl
PB89-201669 URANIUM 235	901,297	Steam as Derived from the Haar-Gallagher-Kell Form tion.	Radical.
High Accuracy Determination of (235)U in No	ndestructive	PB89-186456 900,	
Assay Standards by Gamma Spectrometry. PB89-156954	900,249	Pressure Fixed Points Based on the Carbon Dio	ide Vibrational Predissociation of the Nitric Oxide Dimer. PB89-147417 900,289
Measurements of the (235)U (n,f) Standard		Vapor Pressure at 273.16 K and the H2O(I) - H2O(I H2O(L) Triple-Point.	Population Relaxation of CO(v= 1) Vibrations in Solution
tion at the National Bureau of Standards.		PB89-231138 900,	Phase Metal-Carbonyl Complexes.
PB89-176556	901,305	Vapor Pressures and Gas-Phase PVT Data for 1,1, Tetrafluoroethane.	
URANIUM 238 Determining Picogram Quantities of U in Hum	nan Urine by	PB90-117987 900,	Theoretical Study of the Vibrational Lineshape for CO/ Pt(111).
Thermal Ionization Mass Spectrometry.		VAPORIZING	PB89-157689 900,331
PB89-146906	900,175	Production of 0.1-3 eV Reactive Molecules by Laser ponzation of Condensed Molecular Films: A Poter	
Laser-Produced Spectra and QED (Quantur	n Flectrody-	Source for Beam-Surface Interactions.	PB89-158026 900.342
namic) Effects for Fe-, Co-, Cu-, and Zn-Like	lons of Au,	PB89-171201 900,	High Resolution Inverse Raman Spectroscopy of the CO
Pb, Bi, Th, and U. PB89-176010	901,510	Time-of-Flight Measurements of Hyperthermal Cl(sub Molecules Produced by UV Laser Vaporization of C	2) Q Branch. yo- PB89-171292 <i>900,355</i>
UREA		genic Chlorine Films. PB89-202634 900,	
Developing Definitive Methods for Human	Serum Ana-	Laser Induced Vaporization Time Resolved Mass Sp	(CARS) Study of Vibrational Dephasing of Carbon Disul-
lytes. PB89-146773	901,233	trometry of Refractories.	PR9-176408 000 380
URIC ACID		PB90-136904 900,	Vibrationally Resolved Photoelectron Studies of the
Developing Definitive Methods for Human lytes.	Serum Ana-	VARIABLE STARS Interpretation of Emission Wings of Balmer Lines in Lu	7(sigma) (-1) Channel in N2O.
PB89-146773	901,233	nous Blue Variables.	1 000-110040 900,207
URINE		PB89-212054 . 900,	Pure Rotational Far Infrared Transitions of (16)O2 in Its Electronic and Vibrational Ground State.
Determining Picogram Quantities of U in Hurr Thermal Ionization Mass Spectrometry.	nan Urine by	VARIANCE (STATISTICS) Variances Based on Data with Dead Time between	PR89-202055 900 429
PB89-146906	900,175	Measurements.	Time Resolved Studies of Vibrational Relaxation Dynam-
USER MANUALS (COMPUTER PROGRAMS)		PB89-174049 901,	ics of CO(v= 1) on Metal Particle Surfaces. PB89-203012 900,444
User's Reference Guide for ODRPACK: S Weighted Orthogonal Distance Regression Ve		VARISTORS Selecting Varistor Clamping Voltage: Lower Is Not Bet	
PB89-229066	901,215	PB89-176648 900,	760 HCI Complexes.
VACANCIES (CRYSTAL DEFECTS)		VATS	PB89-228415 900,473
Electronic Structure of the Cd Vacancy in Cd PB89-171318	1 e. <i>901,398</i>	Measurement of Shear Rate on an Agitator in a Ferm tation Broth.	en- Vibrational Spectra of Molecular Ions Isolated in Solid Neon. I. CO(sub 2, sup +) and CO(sub 2, sup -).
Neutron Study of the Crystal Structure and V	acancy Dis-	PB89-186720 901,	
tribution in the Superconductor Ba2Y Cu3 O(s PB90-123480	sub g-delta). 901,468	VELOCITY	Improved Rotational Constants for HF.
VACUUM APPARATUS	301,400	Effects of Velocity and State Changing Collisions Raman Q-Branch Spectra.	
Progress in Vacuum Standards at NBS (Nati	ional Bureau	PB89-179196 900,	14eon. 2. 04(17) and 04(14).
of Standards). PB89-201198	900,999	VELOCITY MEASUREMENT	PB90-128729 900,533
VACUUM DEPOSITED COATINGS	200,000	Spherical Acoustic Resonators in the Undergraduate L oratory.	VIDIATIONAL OF LOTTIC COOF 1
Thin Film Thermocouples for High Temperatu	re Measure-	PB89-179709 <i>901</i> ,	Hydrogen Systems.
ment. PB89-209290	901,065	VENTILATION Developments in the Heat Relance Method for Simula	PB89-157499 900,324
VACUUM ULTRAVIOLET RADIATION	,,,,,,,,	Developments in the Heat Balance Method for Simula Room Thermal Response.	VIDRATIONAL STATES
Branching Ratio Technique for Vacuum U	V Radiance	PB89-173926 900,	D62 Spectroscopic Detection Methods. PB89-228100 901,549
Calibrations: Extensions and a Comprehensiv PB90-128257	e Data Set. 901,582	Indoor Air Quality. PB89-176127 900,	- ·
VALIDATION		Ventilation Effectiveness Measurements in an Of	DR80_228118 001 550
Validated Furniture Fire Model with FAST (HE		Building.	VINYL ETHER RESINS
PB89-215354 VAN DER WAALS EQUATION	900,142	PB89-176614 900,	Lifect of Crossilliks off the Friase Separation behavior of
Van der Waals Equation of State Around th	ne Van Laar	Integral Mass Balances and Pulse Injection Tracer Teniques.	PB89-146724 900,546
Point. PB89-158133	900,345	PB89-206833 900,	remperature, Composition and Molecular-weight De-
	,	Air Quality Investigation in the NIH (National Institute	of nendence of the Rinary Interaction Parameter of Polysty-

Structure of the CO2-CO2-H2O van der Waals Complex Determined by Microwave Spectroscopy.

Air Quality Investigation in the NIH (National Institutes of Health) Radiation Oncology Branch.
PB89-228977 900,079

Temperature, Composition and Molecular-Weight Dependence of the Binary Interaction Parameter of Polystyrene/Poly(vinylmethylether) Blends. PB9-157473 900,550

KEYWORD INDEX

INVLIDENE FLUORIDE POLYMERS		,126 PB90-126251 900,529
Deuterium Magnetic Resonance Study of Orientation and Poling in Poly(Vinylidene Fluoride) and Poly(Vinylidene Fluoride-Co-Tetrafluoroethylene).		MATER ANALYSIS Determination of Ultratrace Concentrations of Butyltin
PB89-186365 900,565	WASTE DISPOSAL Draft International Document on Guide to Portable In	
ISCOMETERS Torsional Piezoelectric Crystal Viscometer for Compressed Gases and Liquids.	ments for Assessing Airbome Pollutants Arising Hazardous Wastes.	Biodegradation of Tributyltin by Chesapeake Bay Microor-
PB89-228076 901,447	PB89-150775 900 Fundamental Aspects of Key Issues in Hazardous W	,855 ganisms. PB89-177232 901,309
Prediction of Shear Viscosity and Non-Newtonian Behav-	Incineration. PB89-212104 900	,861 WATER DIMERS Microwave Electric-Resonance Optothermal Spectrosco-
ior in the Soft-Sphere Liquid. PB89-228035 901,548	WATER New International Skeleton Tables for the Thermodyr	py of (H2O)2.
Quantitative Characterization of the Viscosity of a Microe- mulsion.	ic Properties of Ordinary Water Substance.	WATER DISTRIBUTION
PB90-123597 900,524 ISIBLE SPECTRUM	Electric-Dipole Moments of H2O-Formamide	Transducers in Michelson Tiltmeters.
Dichromate Dosimetry: The Effect of Acetic Acid on the Radiolytic Reduction Yield.		9,288 WATER FLOW Application of Magnetic Resonance Imaging to Visualiza-
PB89-147490 900,248	Combustion of Oil on Water. PB89-149173 900	9,587 tion of Flow in Porous Media. PB89-179592 901,329
ISUAL PERCEPTION Visual Perception Processing in a Hierarchical Control	Relative Acidities of Water and Methanol and the St ties of the Dimer Anions.	abili- WATER POLLUTION
System: Level 1. PB89-221188 900,994		0,299 Combustion of Oil on Water. November 1987. PB89-185581 900,863
ITAMIN B 12 COENZYMES Water Structure in Vitamin B12 Coenzyme Crystals. 1.	Water. Disproportionation, Oxygen Production, and Opanison with Other Metalloporphyrins.	
Analysis of the Neutron and X-ray Solvent Densities. PB89-186803 901,222	PB89-151005 900	0,301 PB89-229280 900,864
Water Structure in Vitamin B12 Coenzyme Crystals. 2. Structural Characteristics of the Solvent Networks.	Synchrotron Radiation Study of BaO Films on W(and Their Interaction with H2O, CO2, and O2.	Specimen Banking in the National Status and Trends
PB89-186811 901,223	Thermodynamic Values Near the Critical Point of Wa	ter. Sults.
NBS (National Bureau of Standards) Activities in Biologi-	PB89-161541 901 Enthalpies of Desorption of Water from Coal Surface	WATER BOLL HTICH CAMPLING
cal Reference Materials. PB89-157770 901,219	PB89-173868 900	0,838 Designs for Assessment of Measurement Uncertainty: Experience in the Eastern Lake Survey.
OICE COMMUNICATION ACSB (Amplitude Companded Sideband): What Is Ade-	Molecular Dynamics Investigation of Expanded Wat Elevated Temperatures. PB89-174957 900	PB89-173827 900,862 0,370 WATER PRESSURE
quate Performance. PB89-176283 901,599	Influence of Electronic and Geometric Structure on	De- Pore-Water Pressure Buildup in Clean Sands Because of
OLATILE ORGANIC COMPOUNDS Preparation of Accurate Multicomponent Gas Standards	sorption Kinetics of Isoelectronic Polar Molecules: and H2O.	PB89-175723 900,159
of Volatile Toxic Organic Compounds in the Low-Parts- per-Billion Range.	PB89-176473 900 Water Structure in Crystalline Solids: Ices to Proteins	0,381 WATER REDUCING AGENTS Adsorption of High-Range Water-Reducing Agents on Se-
PB89-157739 900,185	PB89-186746 900 Repulsive Regularities of Water Structure in Ices	0,413 lected Portland Čement Phases and Related Materials.
Comparison of a Cryogenic Preconcentration Technique and Direct Injection for the Gas Chromatographic Analy- sis of Low PPB (Parts-per-Billion) (NMOL/MOL) Gas	Crystalline Hydrates.	WATT
Standards of Toxic Organic Compounds. PB89-173843 900,193	Water Structure in Vitamin B12 Coenzyme Crystal Analysis of the Neutron and X-ray Solvent Densities.	Wedsdrenient of the 1400 (14ational Dareau of Standards)
OLTAGE STANDARDS	PB89-186803 90	1,222 WAVEFORMS
Josephson Array Voltage Calibration System: Operational Use and Verification. PB89-230403 900,820	Water Structure in Vitamin B12 Coenzyme Crystal Structural Characteristics of the Solvent Networks. PB89-186811 90	s. 2. Improved Understanding for the Transient Operation of the Power Insulated Gate Bipolar Transistor (IGBT). PB89-231229 900,795
Voltammetric and Liquid Chromatographic Identification of Organic Products of Microwave-Assisted Wet Ashing	Determination of Hydrocarbon/Water Partition C cients from Chromatographic Data and Based on tion Thermodynamics and Theory.	
of Biological Samples. PB89-157994 900, 188	Effect of Water on Piloted Ignition of Cellulosic Mater	nals. Waveguide Loss Measurement Using Photothermal De-
One-Electron Transfer Reactions of the Couple SO2/ SO2(1-) in Aqueous Solutions. Pulse Radiolytic and	PB89-189187 900 Interaction of Water with Solid Surfaces: Fundam	flection.
Cyclic Voltammetric Studies. PB89-176093 900,376	Aspects.	9,421 Fast Optical Detector Deposited on Dielectric Channel Wavequides.
OLTMETERS High-Accuracy Differential-Pulse Anodic Stripping Voltam-	NaCI-H2O Coexistence Curve Near the Critical Tem ture of H2O.	pera- PB89-171706 <i>900,743</i>
metry with Indium as an Internal Standard. PB89-156947 900,182	PB89-202519 900	0,436 System for Measuring Optical Waveguide Intensity Pro- files. Sur- PB89-188593 900,751
/OLUME Microwave Measurements of the Thermal Expansion of a	Coadsorption of Water and Lithium on the Ru(001) face. PB89-202956 90	PB89-188593 900,751 0,440 Reflection Coefficient of a Waveguide with Slightly
Spherical Cavity. PB89-147458 900,291	Fundamental Characterization of Clean and Gas-D	Uneven Walls.
Measurement of the Torque and Normal Force in Torsion in the Study of the Thermoviscoelastic Properties of Poly-	1 200 20200 7	0,785 WAVELENGTHS Wavelengths and Energy Level Classifications of Scandi-
mer Glasses. PB89-172472 900,554	Standard Electrode Potentials and Temperature C cients in Water at 298.15 K.	um Spectra for All Stages of Ionization.
Polytope Volume Computation. PB90-129982 901,203	Second Virial Coefficients of Aqueous Alcohols at E	levat- WAVEPLATES
ORONOI DIAGRAMS	ed Temperatures: A Calorimetric Study. PB89-227896 90	Stability of Birefningent Linear Retarders (Waveplates). 901,345
Expected Complexity of the 3-Dimensional Voronoi Diagram.	Structure of the CO2-CO2-H2O van der Waals Cor Determined by Microwave Spectroscopy.	Metallographic Evidence for the Nucleation of Subsurface
PB89-209332 901,200 VORTICES	PB89-230288 90 Pressure Fixed Points Based on the Carbon Di	0,479 Microcracks during Unlubricated Sliding of Metals.
Solution for Diffusion-Controlled Reaction in a Vortex Field.	Vapor Pressure at 273.16 K and the H2O(I) - H2O H2O(L) Triple-Point.	
PB89-176622 900,594 VOWELS	PB89-231138 90 Electric-Resonance Optothermal Spectrum of (H	0,483 PB89-188569 901,045
Compensating for Vowel Coarticulation in Continuous Speech Recognition. PB89-176721 900,634	Microwave Spectrum of the $K=1-0$ Subband for $E((+ \text{ or } -)2)$ States.	Ollasonic Anilosu Wilest Inspection Sain Edwins (Electromagnetic-Accoustic Transducers), Report No. 18. PB89-189229 0,497
WALLBOARD	Tribochemical Mechanism of Alumina with Water.	Alumina.
Gypsum Wallboard Formaldehyde Sorption Model. PB90-132705 900,154	PB90-117722 90 Adsorption of Water on Clean and Oxygen-Pred	11,059 PB90-117383 901,058 dosed Measurements of Tribological Behavior of Advanced Ma-
WALLS Thermal Resistance Measurements and Calculations of	Nickel(110).	terials: Summary of U.S. Results on VAMAS (Versailles Advanced Materials and Standards) Round-Robin No. 2.
an Insulated Concrete Block Wall. PB89-174916 900,119	Octanol-Water Partition Coefficients of Simple Or Compounds.	
Brick Masonry: U.S. Office Building in Moscow. PB89-187504 900,160	PB90-126244 90	0,528 Computer-Controlled Test System for Operating Different
Fire Properties Database for Textile Wall Coverings.	Evaluation of Data on Solubility of Simple Apolar (in Light and Heavy Water at High Temperature.	PB89-228290 900,983

WEIGHT MEASUREMENT Precision Weight Calibration with a Specialized Robot. PB89-173975 900,879	WORKING FLUIDS Thermophysical-Property Needs for the Environmentally Acceptable Halocarbon Refrigerants.	PB89-201677 900,212 Pattern Recognition Approach in X-ray Fluorescence Analysis.
WELDED JOINTS	PB89-231054 900,482 WORKSTATIONS	PB9Ó-128786 900,234
Measurement of Applied J-Integral Produced by Residual Stress. PB90-117631 900,163	Material Handling Workstation Implementation. PB89-159644 900,988	X RAY LASERS Recent Progress on Spectral Data for X-ray Lasers at the National Bureau of Standards.
WELDING On-Line Arc Welding: Data Acquisition and Analysis	Material Handling Workstation: Operator Manual. PB89-159651 900,989	PB89-158091 901,341
Using a High Level Scientific Language. PB90-117391 900,972	Material Handling Workstation, Recommended Technical Specifications for Procurement of Commercially Available	X RAY LITHOGRAPHY Approach to Accurate X-Ray Mask Measurements in a Scanning Electron Microscope.
WELDMENTS Local Brittle Zones in Steel Weldments: An Assessment	Equipment. PB89-162564 900,998	PB89-172555 900,776
of Test Methods. PB89-149082 901,092	Vertical Machining Workstation of the AMRF (Automated Manufacturing Research Facility): Equipment Integration. PB89-176663 900,950	X RAY SPECTROSCOPY Role of Standards in Electron Microprobe Techniques. PB89-176143 900,197
Ultrasonic Determination of Absolute Stresses in Alumi- num and Steel Alloys.	Software for an Automated Machining Workstation.	Defocus Modeling for Compositional Mapping with Wave- length-Dispersive X-ray Spectrometry.
PB89-150957 901,124 Postweld Heat Treatment Criteria for Repair Welds in 2-	PB89-177109 900,953 Workstation Controller of the Cleaning and Deburning	PB89-176150 900,378
1/4Cr-1Mo Superheater Headers: An Experimental Study. PB89-156160 901,094	Workstation. PB89-189286 900,955	Near-Threshold X-ray Fluorescence Spectroscopy of Mol- ecules. PB89-176523 900,382
Role of Inclusions in the Fracture of Austenitic Stainless Steel Welds at 4 K.	Inventory of Equipment in the Cleaning and Deburring Workstation.	X RAYS
PB89-173504 901,099 Femite Number Prediction to 100 FN In Stainless Steel	PB89-209233 900,958 Recommended Technical Specifications for Procurement of Equipment for a Turning Workstation.	Cross Sections for K-Shell X-ray Production by Hydrogen and Helium lons in Elements from Beryllium to Uranium. PB89-226609 900,460
Weld Metal. PB89-201586 901,106	PB89-215347 900,962	XENON COMPLEXES
Stainless Steel Weld Metal: Prediction of Ferrite Content. PB89-231260 901,107	Guideline for Work Station Design. PB90-112418 900,643 WOVEN FIBER COMPOSITES	Calculation of Vibration-Rotation Spectra for Rare Gas- HCI Complexes. PB89-228415 900,473
WET METHODS Voltammetric and Liquid Chromatographic Identification	Edge Stresses in Woven Laminates at Low Temperatures.	YAG LASERS
of Organic Products of Microwave-Āssisted Wet Ashing of Biological Samples. PB89-157994 900,188	PB90-128265 901,082 X-RAY ABSORPTION	Thermal Shifts of the Spectral Lines in the (4)F3/2 to (4)I11/2 Manifold of an Nd:YAG Laser. PB89-157382 901,338
WETTING	Multiple Scattering in the X-ray Absorption Near Edge Structure of Tetrahedral Germanium Gases.	YTTERBIUM Characterization of Structural and Magnetic Order of Er/
Effect of Surface Ionization on Wetting Layers. PB89-157259 901,323	PB89-228480 900,474	Y Superlattices. PB90-123662 901,470
WHEELS EMATs (Electromagnetic Acoustic Transducers) for Roll-	X-RAY ANALYSIS Core-Level Binding-Energy Shifts at Surfaces and in	YTTRIUM
By Crack Inspection of Railroad Wheels. PB90-123894 901,597	Solids. PB89-146898 900,282	Moydite, (Y, REE) (B(OH)4)(CO3), a New Mineral Species from the Evans-Lou Pegmatite. Quebec.
WIND	Multiple Scattering in the X-ray-Absorption Near-Edge Structure of Tetrahedral Ge Gases.	PB89-157747 900,186
Assessment of Need for and Design Requirements of a Wind Tunnel Facility to Study Fire Effects of Interest to	PB89-146922 900,283	Occurrence of Long-Range Helical Spin Ordering in Dy-Y Multilayers.
DNA. PB89-200208 901,276	Angle Resolved XPS (X-ray Photoelectron Spectroscopy) of the Epitaxial Growth of Cu on Ni(100).	PB89-179634 901,410 Long-Range Incommensurate Magnetic Order in Dy-Y
WIND PRESSURE	PB89-150866 901,389 Structural Unit in Icosahedral MnAISi and MnAI.	Multilayers. PB89-179642 901,411
Wind and Seismic Effects. Proceedings of the Joint Meeting of the U.SJapan Cooperative Program in Natural Re-	PB89-157648 901,131	Exchange and Magnetostrictive Effects in Rare Earth Su-
sources Panel on Wind and Seismic Effects (20th) Held in Gaithesburg, Maryland on May 17-20, 1988.	Continuum Radiation Produced in Pure-Element Targets by 10-40 keV Electrons: An Empirical Model. PB89-201610 900,209	perlattices. PB89-202667 901,438
PB89-154835 900,157 WINDOW GLASS	Modeling of the Bremsstrahlung Radiation Produced in	YTTRIUM ALLOYS Spin-Density-Wave Transition in Dilute YGd Single Crys-
Field Measurement of Thermal and Solar/Optical Properties of Insulating Glass Windows.	Pure Element Targets by 10-40 keV Electrons. PB89-201644 901,531	tals. PB89-202030 901,433
PB89-175905 900,064 WINDOW GLAZING	X-RAY DETECTION High-Purity Germanium X-ray Detector on a 200 kV Ana-	Magnetic Structure of Y0.97Er0.03.
Window U-Values: Revisions for the 1989 ASHRAE	lytical Electron Microscope. PB89-201602 900,208	PB89-202675 901,439 YTTRIUM BARIUM CUPRATES
(American Society of Heating, Refrigerating and Air-Conditioning Engineers) Handbook - Fundamentals.	X-RAY DIFFRACTION	Magnetic Field Dependence of the Superconductivity in Bi-Sr-Ca-Cu-O Superconductors.
PB89-229215 900,145 WINDOWS	Standard Reference Materials for X-ray Diffraction. Part 1. Overview of Current and Future Standard Reference	PB89-146815 901,385
U-Value Measurements for Windows and Movable Insula- tions from Hot Box Tests in Two Commercial Laborato-	Materials. PB89-146799 <i>901,384</i>	Josephson-Junction Model of Critical Current in Granular Y1Ba2Cu30(7-delta) Superconductors.
ries. PB89-175889 900,121	Standard X-ray Diffraction Powder Patterns from the JCPDS (Joint Committee on Powder Diffraction Stand-	PB89-176978 901,406 High T(sub c) Superconductor/Noble-Metal Contacts with
Illumination Conditions and Task Visibility in Daylit	ards) Research Associateship. PB89-171763 900,190	Surface Resistivities in the (10 to the Minus 10th Power) Omega sq cm Range.
Spaces. PB89-189237 900,074	Wheatleyite, Na2Cu(C2O4)2 2H2O, a Natural Sodium Copper Salt of Oxalic Acid.	PB89-179824 901,413 Oxygen Partial-Density-of-States Change in the
Origins of ASHRAE (American Society of Heating, Refrig- erating and Air-Conditioning Engineers) Window U-Value	PB89-179154 900,390	YBa2Cu3Ox Compounds for x(Approx.)6,6.5,7 Measured by Soft X-ray Emission.
Data and Revisions for the 1989 Handbook of Fundamentals.	Syntheses and Unit Cell Determination of Ba3V4O13 and Low- and High-Temperature Ba3P4O13.	PB89-186274 901,419
PB89-231005 900,083 WIRE LINES	PB89-179717 901,040 Dynamical Diffraction of X-rays at Grazing Angle.	Resonant Excitation of an Oxygen Valence Satellite in Photoemission from High-T(sub c) Superconductors.
Tiger Tempering Tampers Transmissions. PB89-157861 900,740	PB89-186886 901,421 Standard X-ray Diffraction Powder Patterns from the	PB89-186860 901,420 Ag Screen Contacts to Sintered YBa2Cu3Ox Powder for
WIRE ROPE Tensile Tests of Type 305 Stainless Steel Mine Sweeping	JCPDS (Joint Committee on Powder Diffraction Standards) Research Association. PB89-202246 900,214	Rapid Superconductor Characterization. PB89-200448 901,423
Wire Rope. PB90-130287 901,112	Direct Observation of Surface-Trapped Diffracted Waves.	Evidence for the Superconducting Proximity Effect in Junctions between the Surfaces of YBa2CU3Ox Thin
WOOD	PB90-128216 901,475 Use of an Imaging Proportional Counter in Macromolecu-	Films. PB89-228449 901,449
Experimental Validation of a Mathematical Model for Predicting Moisture Transfer in Attics. PB89-150783 900,057	lar Crystallography. PB90-136599 900,538	Hysteretic Phase Transition in Y1Ba2Cu3O7-x Superconductors.
WOOD BURNING APPLIANCES	X RAY FLUORESCENCE	PB89-229082 <i>901,454</i> Gruneisen Parameter of Y1Ba2Cu3O7.
Residential Wood Combustion: A Source of Atmospheric Polycyclic Aromatic Hydrocarbons.	Sequential Determination of Biological and Pollutant Elements in Marine Bivalves.	PB90-117615 901,465
PB90-128166 900,860 WOOD PRODUCTS	PB89-156897 901,217 Near-Threshold X-ray Fluorescence Spectroscopy of Mol-	Neutron Study of the Crystal Structure and Vacancy Dis- tribution in the Superconductor Ba2Y Cu3 O(sub g-delta).
Damage Accumulation in Wood Structural Members Under Stochastic Live Loads.	ecules. PB89-176523 900,382	PB90-123480 901,468 YTTRIUM IONS
PB89-171748 900,115	X-RAY FLUORESCENCE ANALYSIS Near-Threshold X-ray Fluorescence Spectroscopy of Mol-	4s(2) 4p(2)-4s4p(3) Transition Array and Energy Levels of the Germanium-Like lons Rb VI - Mo XI.
Speciation Measurements of Butyltins: Application to	ecules. PB89-176523 900,382	PB89-201065 901,528
Controlled Release Rate Determination and Production of Reference Standards.	Uncertainties in Mass Absorption Coefficients in Funda-	YTTRIUM OXIDES Bulk Modulus and Young's Modulus of the Superconduc-
PB89-146807 900,174	mental Parameter X-ray Fluorescence Analysis.	tor Ba2Cu3YO7.

KEYWORD INDEX

PB90-123613 901,469

ZEOLITES

Neutron Diffraction Determination of Full Structures of Anhydrous Li-X and Li-Y Zeolites. PB90-118001 900,516

ZINC

Observations on Crystal Defects Associated with Diffusion Induced Grain Boundary Migration in Cu-Zn. PB89-157606 901,127

Experimental Observations on the Initiation of DIGM (Diffusion Induced Grain Boundary Migration).

PB89-157630

901,130

ZIRCONIUM IONS

4s(2) 4p(2)-4s4p(3) Transition Array and Energy Levels of the Germanium-Like Ions Rb VI - Mo XI. PB89-201065 901,526

SAMPLE ENTRY

Computer Viruses and Related Threats: A Management Guide

PB90-111683

900,654

PC A03/MF A01

Title

NTIS order number

Abstract number

Availablilty **Price Code**

2.5 MeV Neutron Source for Fission Cross Section Measurement. PB89-176531 901,512 Not available NTIS

4s(2) 4p(2)-4s4p(3) Transition Array and Energy Levels of the Germanium-Like Ions Rb VI - Mo XI. PB89-201065 901,528 Not available NTIS

(12)C(16)O Laser Frequency Tables for the 34.2 to 62.3 THz (1139 to 2079 cm(-1)) Region. PB89-193908 901,361 PC A03/MF A01

13C NMR Method for Determining the Partitioning of End Groups and Side Branches between the Crystalline and Non-Crystalline Regions in Polyethylene. PB89-202451 900,569 Not available NTIS

(109)Pd and (109)Cd Activity Standardization and Decay PB90-123449 901.564 Not available NTIS

Absolute Cross Sections for Molecular Photoabsorption, Partial Photoionization, and Ionic Photofragmentation Proc-

900,410 Not available NTIS Absolute Infrared Transition Moments for Open Shell Diatomics from J Dependence of Transition Intensities: Applica-

tion to OH 900.463 Not available NTIS

Absolute Isotopic Abundance Ratios and Atomic Weight of a Reference Sample of Nickel. PB90-163890 900,543

(Order as PB90-163874, PC A04)

Absolute Isotopic Composition and Atomic Weight of Terrestrial Nickel.
PB90-163908 900,544

(Order as PB90-163874, PC A04)

Absolute Rate Constants for Hydrogen Abstraction from Hydrocarbons by the Trichloromethylperoxyl Radical. PB89-171532 900,357 Not available NTIS

AC-DC Difference Calibrations at NBS (National Bureau of Standards).

PB89-201560

900.816 Not available NTIS

AC Electric and Magnetic Field Meter Fundamentals.
PB89-173470 900,746 Not available NTIS

AC Impedance Method for High-Resistivity Measurements of Silicon. PB89-231203 900,793 Not available NTIS

Accurate Determination of Planar Near-Field Correction Parameters for Linearly Polarized Probes.
PB89-156871 900,704 Not available NTIS

Accurate Energies of nS, nP, nD, nF and nG Levels of Neu-

PB89-202121 900,431 Not available NTIS Accurate RF Voltage Measurements Using a Sampling Voltage Tracker. PB89-201552 900.815 Not available NTIS

Acoustic and Microwave Resonances Applied to Measuring the Gas Constant and the Thermodynamic Temperature.
PB89-228548 901,320 Not available NTIS

Acoustic Emission: A Quantitative NDE Technique for the Study of Fracture. PB89-211924 900,921 Not available NTIS

Acoustical Technique for Evaluation of Thermal Insulation. PB89-193866 900,919 PC A03/MF A01

Acoustoelastic Determination of Residual Stresses. PB89-179808 901.318 Not available NTIS

ACSB (Amplitude Companded Sideband): What Is Adequate Performance.
PB89-176283 901,599 Not available NTIS 901,599 Not available NTIS

Activation Analysis Opportunities Using Cold Neutron Beams. PB89-156970 900,183 Not available NTIS

Activities of the International Association for the Properties of Steam between 1979 and 1984. PB89-212153 900,446 Not available NTIS

Adhesion to Dentin by Means of Gluma Resin.

PB89-157168

900.039 Not available NTIS

Adhesive Bonding of Composites.

900,050 Not available NTIS

Adsorption of High-Range Water-Reducing Agents on Selected Portland Cement Phases and Related Materials. PB90-124306 900,583 PC A03/MF A01

Adsorption of Water on Clean and Oxygen-Predosed Nickel(110). PB90-123555 900.522 Not available NTIS

Adsorption of 4-Methacryloxyethyl Trimellitate Anhydride (4-META) on Hydroxyapatite and Its Role in Composite Bond-

900.041 Not available NTIS

Adsorption Properties of Pt Films on W(110). PB89-146864 900,281 Not available NTIS

Advanced Ceramics: A Critical Assessment of Wear and Lubrication. PB89-188569 901,045 PC A06/MF A01

Advanced Heat Pumps for the 1990's Economic Perspectives for Consumers and Electric Utilities.
PB90-118043 900,089 Not available NTIS

Advances in NIST (National Institute of Standards and Technology) Dielectric Measurement Capability Using a Mode-Filtered Cylindrical Cavity.
PB89-231146 900,907 Not available NTIS

Advances in the Use of (3)He in a Gas Scintillation PB90-123506 901,565 Not available NTIS

Aerodynamics of Agglomerated Soot Particles. PB89-147482 900,586 Not available NTIS

AES and LEED Studies Correlating Desorption Energies with Surface Structures and Coverages for Ga on Si(100). PB89-171599 901,401 Not available NTIS

Ag Screen Contacts to Sintered YBa2Cu3Ox Powder for Rapid Superconductor Characterization.
PB89-200448 901,423 Not available NTIS

Air Quality Investigation in the NIH (National Institutes of Health) Radiation Oncology Branch.
PB89-228977 900,079 PC A07/MF A01

Airflow Network Models for Element-Based Building Airflow Modeling. PB89-230379 900,082 Not available NTIS

AIRNET: A Computer Program for Building Airflow Network Modeling. PB89-193254 900,076 PC A05/MF A01

Alaska Arctic Offshore Oil Spill Response Technology Workshop Proceedings. PR89-195663 900.842 PC A10/MF A01

Algebraic Representation for the Topology of Multicomponent Phase Diagrams. PB89-177042 901.517 Not available NTIS

Alignment Effects in Ca-He(5(sup 1)P(sub 1) - 5(sup 3)P(sub JI) Energy Transfer Collisions by Far Wing Laser Scattering.
PB89-179790 900,400 Not available NTIS

Alignment Effects in Electronic Energy Transfer and Reac-AD-A202 820/7 900,267 PC A03/MF A01

Allocating Staff to Tax Facilities: A Graphics-Based Microcomputer Allocation Model. PB90-129891 900,645 PC A03/MF A01

Alternative Approach to the Hauptman-Karle Determinantal Inequalities. PB89-186241 901.416 Not available NTIS

Alternative Techniques for Some Typical MIL-STD-461/462 Types of Measurements.
PB89-235139 901,272 PC A03/MF A01

Aluminumlike Spectra of Copper through Molybdenum. PB89-172365 900,360 Not available NTIS

Ambiguity Groups and Testability. PB90-128703 900,722 Not available NTIS

Ammonia Adsorption and Dissociation on a Stepped Iron(s) (100) Surface. PB90-123563 900,523 Not available NTIS

Amorphous Phase Formation in Al70Si17Fe13 Alloy. PB90-123522 901,167 Not available NTIS

AMRF (Automated Manufacturing Research Facility) Material Handling System Architecture.
PB89-177091 900,952 Not available NTIS

AMRF Part Model Extensions. PB90-129446 900,967 PC A03/MF A01

ANA (Automatic Network Analyzer) Measurement Results on the ARFTG (Automatic RF Techniques Group) Traveling Experiment.
PB89-173777 900.715 Not available NTIS

Analysis and Prediction of Air Leakage through Door Assemblies. PB89-231161 900,085 Not available NTIS

Analysis of Computer Performance Data. PB89-162614 900,635 PC A03/MF A01

Analysis of High Performance Compensated Thermal En-PB89-185748 901,008 Not available NTIS

Analysis of Magnesiumlike Spectra from Cu XVIII to Mo XXXÍ. PB90-117821 900,508 Not available NTIS

Analysis of Ridge-to-Ridge Distance on Fingerprints. PB89-230478 901,216 Not available NTIS

Analysis of Roto-Translational Absorption Spectra Induced in Low Density Gases of Non-Polar Molecules: The Meth-

PB89-201800 900,427 Not available NTIS

Analysis of Ultrapure Reagents from a Large Sub-Boiling Still Made of Teflon PFA.
PB89-186357 900,202 Not available NTIS Analytical Applications of Neutron Depth Profiling.
PB89-146872 901,294 Not available NTIS

Analytical Applications of Resonance Ionization Mass Spectrometry (RIMS).
PB89-161590 900,189 Not available NTIS 900,189 Not available NTIS

Analytical Expression for Describing Auger Sputter Depth Profile Shapes of Interfaces. PB89-157176 900,309 Not available NTIS

Analytical Methods for Firesafety Design. PB89-157275 900,111 Not available NTIS

Analytical Model for the Steady-State and Transient Characteristics of the Power Insulated-Gate Bipolar Transistor. PB89-146880 900,767 Not available NTIS

Analytical Modeling of Device-Circuit Interactions for the Power Insulated Gate Bipolar Transistor (IGBT).

PB89-176259 900,777 Not available NTIS Analyzing the Economic Impacts of a Military Mobilization. PB90-128067 901,273 Not available NTIS

Angle Resolved XPS (X-ray Photoelectron Spectroscopy) of the Epitaxial Growth of Cu on Ni(100). PB89-150866 901,389 Not available NTIS

Antenna for Laser Gravitational-Wave Observations in Space. PB89-234231 901,594 Not available NTIS

Antenna Measurements for Millimeter Waves at the National Bureau of Standards. PB89-150726 900,694 Not available NTIS

Antennas for Geophysical Applications. PB89-179857 900,710 Not available NTIS

Anti-T2 Monoclonal Antibody Immobilization on Quartz Fibers: Stability and Recognition of T2 Mycotoxin. PB90-128760 901,267 Not available NTIS

Antiferromagnetic Structure and Crystal Field Splittings in the Cubic Heusler Alloys HoPd2Sn and ErPd2Sn. PB89-202659 901,437 Not available NTIS

Apparatus for Neutron Scattering Measurements on Sheared Fluids. PB89-235667 901,335

(Order as PB89-235634, PC A04)

Apparatus Function of a Prism-Grating Double Monochromator. PB89-186282 901.359 Not available NTIS

Apparent Diurnal Effects in the Global Positioning System. PB89-174080 901,292 Not available NTIS

Apparent Spectroscopic Rigidity of Floppy Molecular Sys-PB90-123860 900.526 Not available NTIS

Application of Direct Digital Control to an Existing Building PB89-177141 900,068 Not available NTIS

Application of Formal Description Techniques to Conform-PB89-211908 900,652 Not available NTIS

Application of Magnetic Resonance Imaging to Visualization of Flow in Porous Media.
PB89-179592 901,329 Not available NTIS

Application of Multiscattering Theory to Impurity Bands in PR89-157762 900,334 Not available NTIS

Application of SANS (Small Angle Neutron Scattering) to Ceramic Characterization. PB89-146856 901.017 Not available NTIS

Application of Synergistic Microanalysis Techniques to the Study of a Possible New Mineral Containing Light Ele-PB89-147037 901 277 Not available NTIS

Application of the Gibbs Ensemble to the Study of Fluid-Fluid Phase Equilibrium in a Binary Mixture of Symmetric Non-Additive Hard Spheres. PB90-117318 900,494 Not available NTIS

Application of the ISO (International Standards Organiza-tion) Distributed Single Layer Testing Method to the Con-nectionless Network Protocol. PB69-177133 900,616 Not available NTIS 900,616 Not available NTIS

Applications of ETRAN Monte Carlo Codes. PB90-123902 901.574 No. Not available NTIS

Applications of Mirrors, Supermirrors and Multilayers at the National Bureau of Standards Cold Neutron Research Facility. PB89-211981 901,540 Not available NTIS

Applications of the Crystallographic Search and Analysis System CRYSTDAT in Materials Science.

PB89-175251

901.402

(Order as PB89-175194, PC A06) Approach to Accurate X-Ray Mask Measurements in a

Approach to Accurate Arity, Scanning Electron Microscope. 900,776 PC A03/MF A01

Approximate Formulation of Redistribution in the Ly(alpha), Ly(beta), H(alpha) System. PB90-123720 901,568 Not available NTIS

Architecturally-Focused Benchmarks with a Communication PB89-216477 900.640 PC A03/MF A01

Artificial Intelligence Techniques in Real-Time Production Scheduling. PB89-172571 900,945 PC A03/MF A01

ASM/NBS (American Society for Metals/National Bureau of Standards) Numerical and Graphical Database for Binary Alloy Phase Diagrams. PR89-157986 901.135 Not available NTIS Assessing the Flammability of Composite Materials. PB90-112996 901,081 PC A03/MF A01

Assessment of Need for and Design Requirements of a Wind Tunnel Facility to Study Fire Effects of Interest to DNA. PB89-200208 901.276 PC A10/MF A01

Assessment of Robotics for Improved Building Operations and Maintenance.
PB89-189146 900,092 PC A04/MF A01

Assessment of Space Power Related Measurement Requirements of the Strategic Defense Initiative. PB89-209357 901,269 PC A07/MF A01

Assessment of Theories for the Behavior and Blowout of Lifted Turbulent Jet Diffusion Fla PB89-231096 9 900,603 Not available NTIS

ASTM (American Society for Testing and Materials) Committee Completes Work on EPDM Specification. PB89-212260 900,140 Not available NTIS

Asymptotic Expansions for Constant-Composition Dew-Bubble Curves Near the Critical Locus. PB89-227987 901,545 Not available NTIS

Atomic Internal Partition Function PB89-185904 90 901,373 Not available NTIS

Atomic-lon Coulomb Clusters in an Ion Trap. PB89-157424 901,494 Not available NTIS

Atomic Transition Probabilities of Argon: A Continuing Chal-

lenge to Plasma Spectroscopy.
PB89-158125 900,344 Not available NTIS

Atomic Weights of the Elements 1987. PB89-145171 900.274 900,274 Not available NTIS

Audio-Frequency Current Comparator Power Bridge: Development and Design Considerations.

PB89-201537 900,717 Not available NTIS

Autodetaching States of Negative Ions. PB89-150767 900,295 Not available NTIS

Autoionization Dynamics in the Valence-Shell Photoionization Spectrum of CO. PB89-176960 900,386 Not available NTIS

AutoMan: Decision Support Software for Automated Manufacturing Investments. User's Manual. PB89-221873 900,963 PC A03/MF A01

Automated Analysis of Operators on State Tables: A Technique for Intelligent Search. PB89-157366 900,669 Not available NTIS

Automated Calibration of Optical Photomask Linewidth Standards at the National Institute of Standards and Technology. PB89-186340 901,315 Not available NTIS

Automated Documentation System for a Large Scale Manufacturing Engineering Research Project.
PB89-150809 900,941 Not available NTIS

Automated Fringe Counting Laser Interferometer for Low Frequency Vibration Measurements.

PB89-177190 900,885 Not available NTIS

Automated Processing of Advanced Materials. The Path to Maintaining U.S. Industrial Competitiveness in Materials. P889-201727 900,957 Not available NTIS

Automated TEM (Transverse Electromagnetic) Cell for Measuring Unintentional EM Emissions. PB89-173769 900,682 Not available NTIS

Automatic Generation of Test Scenario (Skeletons) from Protocol-Specifications Written in Estelle. PB89-177125 900,615 Not available NTIS

Basic Data Necessary for Neutron Dosimetry. PB89-171854 901,241 Not available NTIS

Battery-Powered Current Supply for Superconductor Meas-PB89-200455 901,525 Not available NTIS

Bean Model Extended to Magnetization Jumps. PB89-176994 901,407 Not available NTIS

Benzene Thermophysical Properties from 279 to 900 K at Pressures to 1000 Bar. 900.271 Not available NTIS

Bibliography of the NIST (National Institute of Standards and Technology) Electromagnetic Fields Division Publica-

PR89-189211 900,810 PC A06/MF A01

Biodegradation of Tributyltin by Chesapeake Bay Microorganisms. PB89-177232 901,309 Not available NTIS

Biological Evaluations of Zinc Hexyl Vanillate Cement Using Two In vivo Test Methods. 900,038 Not available NTIS PB89-157150

Biological Macromolecule Crystallization Database: A Basis for a Crystallization Strategy. PB90-136722 901,250 Not available NTIS

Biological Standard Reference Materials for the Calibration of Differential Scanning Calorimeters: Di-alkylphosphatidyl-choline in Water Suspensions. PB89-186779 900,415 Not available NTIS

Biological Thermodynamic Data for the Calibration of Differential Scanning Calorimeters: Heat Capacity Data on the Unfolding Transition of Lysozyme in Solution. PB90-117920 900,513 Not available NTIS

Biophysical Aspects of Lipid Interaction with Mineral: Liposome Model Studies.
PB90-117508 901,228 Not available NTIS

Bioseparations: Design and Engineering of Partitioning Sys-PB90-136763 901,231 Not available NTIS

Biotransformation of Mercury by Bacteria Isolated from a River Collecting Cinnabar Mine Waters.
PB89-229280 900,864 Not available NTIS

Blocked Impurity Band and Superlattice Detectors: Prospects for Radiometry. PB89-212161 900,730 Not available NTIS

Bond Selective Chemistry with Photon-Stimulated Desorp-PB89-201222 900,259 Not available NTIS

Bonding Agents and Adhesives: Reactor Response. PB89-146732 900,035 Not available NTIS

Bootstrap Inference for Replicated Experiments. PB90-128273 900,914 Not available NTIS

Branching Ratio Technique for Vacuum UV Radiance Calibrations: Extensions and a Comprehensive Data Set. PB90-128257 901,582 Not available NTIS

Brick Masonry: U.S. Office Building in Moscow. PB89-187504 900,160 Not available NTIS

Brief History of Near-Field Measurements of Antennas at the National Bureau of Standards.
PB89-156863 900,703 Not available NTIS

Brief Review of Recent Superconductivity Research at NIST (National Institute of Standards and Technology). PB89-211114 900,766

(Order as PB89-211106, PC A04)

Broadband, Isotropic, Photonic Electric-Field Meter for Measurements from 10 kHz to above 1 GHz.
PB90-128281 900,686 Not available NTIS

Building Economics in the United States. PB89-172399 900,102 Not available NTIS

Building Representations from Fusions of Multiple Views. PB89-177059 900,991 Not available NTIS

Building Technology Project Summaries 1989. PB89-193213 900,131 PC 900,131 PC A05/MF A01 Bulk Modulus and Young's Modulus of the Superconductor

Ba2Cu3YO7. PB90-123613 901,469 Not available NTIS

CAD (Computer Aided Design)-Directed Inspection. PB89-177018 900,980 Not available NTIS

Calcium Hydroxyapatite Precipitated from an Aqueous Solution: An International Multimethod Analysis.
PB90-123399 900,228 Not available NTIS

Calculable, Transportable Audio-Frequency AC Reference Standard. PB90-117854 900,721 Not available NTIS

Calculating Flows through Vertical Vents in Zone Fire Models under Conditions of Arbitrary Cross-Vent Pressure

Difference. PB89-148126 900,108 PC A03/MF A01

Calculation of the Flow Through a Horizontal Ceiling/Floor PB89-189252 900,128 PC A03/MF A01

Calculation of Tighter Error Bounds for Theoretical Atomic-Oscillator Strengths. PB89-158109 901.496 Not available NTIS

Calculation of Vibration-Rotation Spectra for Rare Gas-HCI Complexes. PB89-228415 900.473 Not available NTIS

Calculations and Measurement of the Performance of Con-

verging Neutron Guides. PB89-211999 901,541 Not available NTIS

Calculations of Electron Inelastic Mean Free Paths for 31 PB89-157978 900,341 Not available NTIS

Calibrating Antenna Standards Using CW and Pulsed-CW Measurements and the Planar Near-Field Method. PB89-149280 900,693 Not available NTIS

Calibrating Network Analyzers with Imperfect Test Ports. PB90-117680 900,825 Not available NTIS

Calibration of GPS (Global Positioning System) Equipment in Japan. PB89-212070 900.630 Not available NTIS

Calibration of Voltage Transformers and High-Voltage Capacitors at NIST.
PB89-211114 901.442

(Order as PB89-211106, PC A04)

Calibration Tables Covering the 1460- to 1550-cm(-1) Region from Heterodyne Frequency Measurements on the nu(sub 3) Bands of (12)CS2 and (13)CS2. PB93-157416 900,322 Not available NTIS

Calibration with Randomly Changing Standard Curves. PB89-186381 900,888 Not available NTIS

Calorimetric and Equilibrium Investigation of the Hydrolysis 901,226 Not available NTIS

Capabilities of Smoke Control: Fundamentals and Zone Smoke Control. PB89-229157 900.080 Not available NTIS

Capillary Waves of a Vapor-Liquid Interface Near the Critical Temperature. PB89-228555 900,476 Not available NTIS

Case History: Development of a Software Engineering PB89-149116 900.665 Not available NTIS

Casting Metals: Reactor Response. PB89-157143 900,054 Not available NTIS

Cathodoluminescence of Defects in Diamond Films and Particles Grown by Hot-Filament Chemical-Vapor Deposi-901,069 Not available NTIS

Center for Atomic, Molecular, and Optical Physics Technical Activities, 1989.
PB90-133158 901,586 PC A16/MF A02

Center for Chemical Technology: 1988 Technical Activities. PB89-156376 900,241 PC A08/MF A01

Center for Electronics and Electrical Engineering: Technical Progress Bulletin Covering Center Programs, January to March 1989, with 1989 CEEE Events Calendar. PB89-209225 900,786 PC A03/MF A01

Center for Electronics and Electrical Engineering Technical Progress Bulletin Covering Center Programs, July to Sep-tember 1988, with 1989 CEEE Events Calendar. PB89-168033 PC 403/MF A01

Center for Electronics and Electrical Engineering Technical Progress Bulletin Covering Center Programs, October to December 1988, with 1989 CEEE Events Calendar. PB89-193270 900,813 PC A03/MF A01

Center for Electronics and Electrical Engineering Technical Publication Announcements Covering Center Programs, April-June 1986 with 1987 CEEE Events Calendar. PB89-185623 PC 403/MF A01

Center for Electronics and Electrical Engineering Technical Publication Announcements. Covering Center Programs, January-March 1989, with 1989 CEEE Events Calendar. PB89-228308 900,789 PC A03/MF A01

Center for Electronics and Electrical Engineering Technical Publication Announcements: Covering Center Programs, July/September 1988, with 1989 CEEE Events Calendar. PB89-189302 PC A03/MF A01

Center for Electronics and Electrical Engineering Technical Publication Announcements. Covering Center Programs, October/December 1988, with 1989 CEEE Events Calen-PB89-209241 900.787 PC A03/MF A01

Center for Electronics and Electrical Engineering Technical Publication Announcements Covering Center Programs, October to December 1986, with 1987 CEEE Events Calendar, PB90-116195 900,824 PC A03/MF A01

Center for Radiation Research (of the National Institute of Standards and Technology) Technical Activities for 1989. PB90-130279 901,307 PC A09/MF A01

Chaos and Catastrophe Near the Plasma Frequency in the RF-Biased Josephson Junction. PB89-200463 901,424 Not available NTIS

Characteristics of Ge and InGaAs Photodiodes. PB89-176796 900,729 Not available NTIS

Characterization of Organolead Polymers in Trace Amounts by Element-Specific Size-Exclusion Chromatography. PB89-175962 900,196 Not available NTIS

Characterization of Structural and Magnetic Order of Er/Y 901,470 Not available NTIS

Characterizing Electrical Parameters Near AC and DC

PB89-173462 900,834 Not available NTIS

Charging Behavior of Polyethylene and Ionomers. PB90-136813 900,578 Not available NTIS

Chemical and Spectral Databases: A Look into the Future. PB89-180038 900,579 Not available NTIS

Chemical Calibration Standards for Molecular Absorption Spectrometry. PB89-171938 900,191 Not available NTIS

Chemical Characterization of Ionizing Radiation-Induced Damage to DNA.
PB89-151922 901,235 Not available NTIS

Chemical Kinetics of Intermediates in the Autoxidation of PB89-176754 900,256 Not available NTIS

Chemical Physics with Emphasis on Low Energy Excita-PB89-179659 900.396 Not available NTIS

Chemical Structure of Methane/Air Diffusion Flames: Concentrations and Production Rates of Intermediate Hydrocarhone

PB89-171904 900,590 Not available NTIS

Chemisorption of HF (Hydrofluoric Acid) on Silicon Sur-900,445 Not available NTIS PB89-212013

Chlorine-like Spectra of Copper to Molybdenum. PB90-117706 900,501 Not available NTIS

Cigarette as a Heat Source for Smolder Initiation in Upholstery Materials. PB89-176762 900,595 Not available NTIS

Circular and Square Edge Effect Study for Guarded-Hot-Plate and Heat-Flow-Meter Apparatuses. PB89-176135 900,881 Not available NTIS

Classical Chaos, the Geometry of Phase Space, and Semi-classical Quantization. PB89-172381 901,506 Not available NTIS

Clutter Models for Subsurface Electromagnetic Applica-PB89-229678 900,688 PC A03/MF A01

CO Laser Stabilization Using the Optogalvanic Lamb-Dip. PB89-179139 901,356 Not available NTIS

CO2 Separation Using Facilitated Transport Ion Exchange PB89-157374 900,321 Not available NTIS

Coadsorption of Water and Lithium on the Ru(001) Surface. PR89-202956 900,440 Not available NTIS

CODATA (Committee on Data for Science and Technology) Recommended Values of the Fundamental Physical Constants, 1986. 900,275 Not available NTIS PB89-145189

Coding and Modulation Requirements for 4,800 Bit/Second Modems, Category: Telecommunications Standard. FIPS PUB 134-1 900,660 PC A03/MF A01

Coherent Tunable Far Infrared Radiation.

PB90-117458

Collision Induced Spectroscopy: Absorption and Light Scattering. PB89-212252 901,363 Not available NTIS

900,684 Not available NTIS

Collisional Electron Detachment and Decomposition Rates of SF6(1-), SF5(1-), and F(1-) in SF6: Implications for Ion Transport and Electrical Discharges. PB90-117862 900,511 Not available NTIS

Collisional Losses from a Light-Force Atom Trap. PB90-123936 901,577 Not available NTIS

Combustion Efficiency, Radiation, CO and Soot Yield from a Variety of Gaseous, Liquid, and Solid Fueled Buoyant Diffusion Flames.

900.604 Not available NTIS PB89-231179 Combustion of Oil on Water.

PB89-149173 900,587 Not available NTIS

Combustion of Oil on Water. November 1987. PB89-185581 900,863 PC A04/MF A01

Combustion Testing Methods for Catalytic Heaters. PB89-150924 900,846 Not available NTIS

Comment on 'Feasibility of Measurement of the Electromagnetic Polarizability of the Bound Nucleon'. PB90-117730 901,563 Not available NTIS

Comment on 'Possible Resolution of the Brookhaven and Washington Eotvos Experiments'.
PB89-171581 901,504 Not available NTIS

Commercial Advanced Ceramics PB89-201776 901,048 Not available NTIS

Comparative Modeling of Protein Structure: Progress and Prospects. PB89-175285 901.247

(Order as PB89-175194, PC A06)

Comparison of a Cryogenic Preconcentration Technique and Direct Injection for the Gas Chromatographic Analysis of Low PPB (Parts-per-Billion) (NMOL/MOL) Gas Standards of Toxic Organic Compounds. PB89-173843 900,193 Not available NTIS

Comparison of Detection Limits in Atomic Spectroscopic Methods of Analysis. PB89-150858 900,176 Not available NTIS

Comparison of Far-Field Methods for Determining Mode d Diameter of Single-Mode Fibers Using Both Gaussian Petermann Definitions. 900.756 Not available NTIS PB90-117474

Comparison of Fluoride Uptake Produced by Tray and Flossing Methods In vitro. PB89-179238 901,252 Not available NTIS

Comparison of Interplaner-Boson-Exchange Models of High-Temperature Superconductivity - Possible Experimen-

FB90-117334 901.462 Not available NTIS

Comparison of Liquid Chromatographic Selectivity for Poly cyclic Aromatic Hydrocarbons on Cyclodextrin and C18 Bonded Phases. 900,231 Not available NTIS

Comparison of Measured and Calculated Antenna Sidelobe Coupling Loss in the Near Field Using Approximate Far-Field Data. PR89-156855 900,702 Not available NTIS

Comparison of Microleakage of Experimental and Selected Commercially Available Bonding Systems.
PB89-234223
901,079 Not available NTIS

Comparison of Microwave Drying and Conventional Drying Techniques for Reference Materials. PB90-123464 900,229 Not available NTIS

Comparison of Time Scales Generated with the NBS (Na-

tional Bureau of Standards) Ensembling Algorithm.
PB89-174072 900,628 Not available NTIS Comparison of Two Highly Refined Structures of Bovine

Pancreatic Trypsin Inhibitor. PB89-202204 901,248 Not available NTIS

Comparison of Two Transient Recorders for Use with the Laser Microprobe Mass Analyzer. PB89-176887 900,200 Not available NTIS

Comparisons of NBS/Harvard VI Simulations and Full-Scale, Multiroom Fire Test Data. PR90-128620 900,170 Not available NTIS

Compensating for Vowel Coarticulation in Continuous Speech Recognition. PB89-176721

900.634 Not available NTIS

Component Spectrum Reconstruction from Partially Characterized Mixtures. PB89-202568 900.439 Not available NTIS

Composites Databases for the 1990's. PB89-180376 901,075 PC A04/MF A01

Comprehensive Dosimetry for Food Irradiation. PB89-186399 900,011 Not available NTIS

Comprehensive Study of Methane nane + Ethane System. 900,841 Not available NTIS

PB89-176747 Computation and Use of the Asymptotic Covariance Matrix for Measurement Error Models.

PB89-215321 901.214 PC A03/MF A01 Computation of the ac Stark Effect in the Ground State of

Atomic Hydrogen. PB89-202535 901,538 Not available NTIS

Computational Analysis of Protein Structures: Sources, Methods, Systems and Results. PB89-175293 900,010

(Order as PB89-175194, PC A06)

Computer-Aided Imaging: Quantitative Compositional Mapping with the Electron Probe Microanalyzer. PB89-157754 901,073 Not available NTIS

Computer-Controlled Test System for Operating Different Wear Test Machines. PB89-228290 900,983 PC A03/MF A01

Computer Fire Models. PB89-173991

900,165 Not available NTIS

Computer Graphics for Ceramic Phase Diagrams. PB89-186290 901,043 Not available NTIS

Computer Model of a Porous Medium. PB89-179683 901,188 Not available NTIS

Computer Model of Smoke Movement by Air Conditioning Systems (SMACS).

PB89-157267 900,059 Not available NTIS

Computer Program for Calculating Non-LTE (Local Thermodynamic Equilibrium) Model Stellar Atmospheres.
PB89-171573 900,018 Not available NTIS

Computer Program for Instrument Calibration at State-Sector Secondary-Level Laboratories. PB89-173496 900,877 Not available NTIS

Computer Security Training Guidelines. PB90-780172 900,677 PC A03/MF A01

Computer Simulation Studies of the Soliton Model. 3. Non-continuum Regimes and Soliton Interactions. PB89-202469 901,537 Not available NTIS

Computer Viruses and Related Threats: A Management PB90-111683 900,654 PC A03/MF A01

Computerized Materials Property Data Systems. PB89-187512 901,312 Not available NTIS

Computing Ray Trajectories between Two Points: A Solution to the Ray-Linking Problem.
PB89-176929 901,354 Not available NTIS

Concentration Dependence of the Compression Modulus of Isotactic Polystyrene/Cis-Decalin Gels. PB89-172449 900,552 Not available NTIS

Conceptual Design for a Mercury Relativity Satellite. PB89-234249 901,595 Not available NTIS PB89-234249

Cone Calorimeter Method for Determining the Flammability of Composite Materials. PB89-149165 901,072 Not available NTIS

Conference Reports: National Computer Security Conference (11th). Held in Baltimore, MD. on October 17-20, 1988. PR89-235675 900,672

(Order as PB89-235634, PC A04)

Consensus Values, Regressions, and Weighting Factors. 901,213

(Order as PB89-211106, PC A04)

Considerations for Advanced Building Thermal Simulation 900,084 Not available NTIS

Considerations of Stack Effect in Building Fires. PB89-195671 900,133 PC A05/MF A01

Continuum Radiation Produced in Pure-Element Targets by 10-40 keV Electrons: An Empirical Model. PB89-201610 900,209 Not available NTIS

Control Strategies and Building Energy Consumption. PB89-172340 900,061 Not available NTIS

Control System Simulation in North America 900,091 Not available NTIS

Conventional and Quarter-Point Mixed Elements in Linear Elastic Fracture Mechanics. PB89-157788 901.481 Not available NTIS

Cool It. PB89-176986 901,516 Not available NTIS

Cooling and Trapping Atoms. PB89-176937 901,515 Not available NTIS

Cooling Effect Induced by a Single Evaporating Droplet on Infinite Body. a Semi-Infinite PB89-149249 901.488 Not available NTIS

Core-Level Binding-Energy Shifts at Surfaces and in Solids. 900,282 Not available NTIS

Correlation between CMOS (Complementary Metal Oxide Semiconductor) Transistor and Capacitor Measurements of Interface Trap Spectra.
PB99-180020 900,779 Not available NTIS

Corrosion Behavior of Mild Steel in High pH Aqueous PB90-131152 901.086 PC A03/MF A01

Corrosion Induced Degradation of Amine-Cured Epoxy Coatings on Steel. Coatings on S PB89-176291 901.084 Not available NTIS

Corrosion of Metallic Fasteners in Low-Sloped Roofs: A Review of Available Information and Identification of Research Needs 900.113 PC A06/MF A01

Corrosion of Metallic Implants and Prosthetic Devices. PB89-150890 900,053 Not available NTIS

Cotinine in Freeze-Dried Urine Reference Material. (Order as PB90-213687, PC A04)

Coupling, Propagation, and Side Effects of Surges in an Industrial Building Wiring System.
PB89-173454 900,118 Not available NTIS

Cr(110) Oxidation Probed by Carbon Monoxide Chemisorp-PB89-228423 900.239 Not available NTIS

Crack-Interface Traction: A Fracture-Resistance Mechanism

in Brittle Polycrystals. PB89-211817 901.051 Not available NTIS

Crazes and Fracture in Polymers. PB89-176085 900,562 Not available NTIS

Creating CSUBs in BASIC. PB89-176226 900,647 Not available NTIS

Creating CSUBs Written in FORTRAN That Run in BASIC. PB90-128752 900,656 Not available NTIS

Creation of a Fire Research Bibliographic Database PB89-174130 900,166 Not available NTIS

Creep Cavitation in Liquid-Phase Sintered Alumina. PB89-175954 901,038 Not available NTIS

Creep Rupture of a Metal-Ceramic Particulate Composite PB89-211825 901,077 Not available NTIS

Critical and Noncritical Roughening of Surfaces (Comment) PB89-180046 901,415 Not available NTIS

Critical Assessment of Requirements for Ceramic Powder PB89-146849 901 016 Not available NTIS

Critical Current Measurements of Nb3Sn Superconductors:

NBS (National Bureau of Standards) Contribution to the VAMAS (Versailles Agreement on Advanced Materials and Standards) Interlaboratory Comparison. PB90-136748 901,480 Not available NTIS

Critical Review of the Chemical Kinetics of Sulfur Tetrafluo-nide, Sulfur Pentafluoride, and Sulfur Fluoride (S2F10) in the Gas Phase.

PB89-161582 900,347 Not available NTIS

Cross Section and Linear Polarization of Tagged Photons. PB90-117292 901,560 Not available NTIS

Cross Sections for Bremsstrahlung Production and Electron-Impact Ionization. PB90-123910 901.575 Not available NTIS

Cross Sections for Collisions of Electrons and Photons with Oxygen Molecules.

PB89-226575 900,457 (Not available NTIS)

Cross Sections for Inelastic Electron Scattering in Solids. PB89-202972 901,440 Not available NTIS

Cross Sections for K-Shell X-ray Production by Hydrogen and Helium Ions in Elements from Beryllium to Uranium. PB89-226609 900,460 (Not available NTIS)

Cryogenic Bathysphere for Rapid Variable-Temperature Characterization of High-T(sub c) Superconductors. PB89-228456 901,450 Not available NTIS

Crystal Chemistry of Superconductors: A Guide to the Tailoring of New Compounds. PB89-171730 901.030 Not available NTIS

Crystal Structure of a Cyclic AMP (Adenosine Monophos-phate)-Independent Mutant of Catabolite Gene Activator Protein. PB89-201594 901,224 Not available NTIS

Current Capacity Degradation in Superconducting Cable PB89-200471 901,526 Not available NTIS

Current Research Efforts at JILA (Joint Institute for Laboratory Astrophysics) to Test the Equivalence Principle at Short Ranges. PB89-185912 901,522 Not available NTIS

Current Ripple Effect on Superconductive D.C. Critical Current Measurei PB89-157077 901,492 Not available NTIS

Damage Accumulation in Wood Structural Members Under Stochastic Live Loads. PB89-171748 900.115 Not available NTIS

Data Bases Available at the National Institute of Standards and Technology Research Information Center. 900,932 PC A06/MF A01 PB89-160014

Data Communication Systems and Services User-Oriented Performance Measurement Methods, Category: Telecommunications Standard. FIPS PUB 155 900.664 PC E11

Data Handling in the Vertical Workstation of the Automated Manufacturing Research Facility at the National Bureau of Standards.

900.943 PC A04/MF A01 PB89-159636

Data Management Strategies for Computer Integrated Manufacturing Systems. PB89-209258 900.959 PC A03/MF A01

DC Electric Field Effects during Meesurements of Monopolar Cherge Density end Net Spece Cherge Density Near HVDC Power Lines. PR90-128521 901.380 Not eveileble NTIS

DCTDOS: Neutron end Gamme Penetration in Composite PB89-188809 901,275 PC A05/MF A01

Decay of High Velent Menganese Porphyrins in Aqueous Solution end Catalyzed Formetion of Oxygen.
PB89-156772 900,308 Not eveilable NTIS

Decoreted Lattice Gas Model for Supercritical Solubility. PB89-175681 900,373 Not eveileble NTIS

Defect Intergrowths in Barium Polytitenetes. 1. Ba2Ti9O20. PB89-146823 901,014 Not evailable NTIS

Defect Intergrowths in Benum Polytitenetes. 2. BeTi5O11. PB89-146831 901,015 Not evailable NTIS

Definitions of Grenularity. PB89-180012

900,650 Not available NTIS

Defocus Modeling for Compositionel Mepping with Wevelength-Dispersive X-ray Spectrometry.

PB89-176150

900,378

Not aveilable NTIS

Dehydrogenation of Ethenol in Dilute Aqueous Solution Photosensitized by Benzophenones PB89-157556 900,251 Not aveilable NTIS

Densification, St Ba2YCu3O(6+ x). PB89-171821 Susceptibility and Microstructure of 901,035 Not available NTIS

Dental Materiels and Technology Research at the Netional Bureau of Standards: A Model for Government-Private Sector Cooperetion. 900,052 Not available NTIS PB90-128711

Dependence of Interface Widths on Ion Bombardment Conditions in SIMS (Secondary Ion Mass Spectrometry) Analysis of a Ni/Cr Multilayer Structure.
PB99-172506 900,364 Not evailable NTIS

Dependence of T(sub c) on the Number of CuO2 Planes per Cluster in Interplaner-Boson-Exchenge Models of High-T(sub C) Superconductivity, PB89-229132 901,455 Not available NTIS

Design and Synthesis of Prototype Air-Dry Resins for Use in BEP (Bureau of Engraving and Printing) Intaglio Ink Vehi-PR90-112343 901,068 PC A03/MF A01

Design Criteria for High Temperature Structural Applica-PB89-211833 901,052 Not available NTIS

Design Factors for Perellel Processing Benchmarks. PB89-186845 900,637 Not available NTIS PB90-117672 900,644 Not available NTIS

Design Principles for a Large High-Efficiency Sub-Boiling PB89-187553 900,207 Not available NTIS

Design Protocol, Part Design Editor, and Geometry Library of the Vertical Workstation of the Automated Manufacturing Research Facility at the National Bureau of Standards. 900,936 PC A06/MF A01

Design Quality through the Use of Computers. PB89-174114 900,063 Not available NTIS

Designs for Assessment of Measurement Uncertainty: Experience in the Eastern Lake Survey. PB89-173827 900,862 Not available NTIS

Detailed Description of the Knowledge-Based System for Physical Database Design. Volume 1. PB89-228993 900,929 PC A04/MF A01

Detailed Description of the Knowledge-Based System for Physical Database Design. Volume 2. 900,930 PC A09/MF A01 PB89-229033

Detection of Gas Phase Methoxy Radicals by Resonance Enhanced Multiphoton Ionization Spectroscopy. PB89-156764 900,307 Not available NTIS

Detection of Lead in Human Teeth by Exposure to Aqueous Sulfide Solutions. PB89-201529 901.256 Not available NTIS

Detection of the Free Radicals FeH, CoH, and NiH by Far

Detection of Uranium from Cosmos-1402 in the Strato-

sphere. PB89-156962 901.592 Not available NTIS

Determination of AC-DC Difference in the 0.1 - 100 MHz Frequency Range. PB89-228597 900,719 Not available NTIS

Determination of Binary Mixture Vapor-Liquid Critical Densities from Coexisting Density Data.
PB89-202170
901,536
Not available NTIS Determination of Experimental end Theoretical k (sub ASi) Factors for e 200-kV Anelytical Electron Microscope. PB90-128653 900,232 Not available NTIS

Determinetion of Hydrocarbon/Weter Partition Coefficients from Chrometogrephic Dete end Besed on Solution Thermodynemics end Theory. PB8-187538 900,205 Not evailable NTIS

Determinetion of Selenium and Tellurium in Copper Standard Reference Meteriels Using Stable Isotope Dilution Spark Source Mess Spectrometry. PB90-123472 900,230 Not eveileble NTIS

Determinetion of Serum Cholesterol by e Modification of the Isotope Dilution Mass Spectrometric Definitive Method. PB89-234181 901,239 Not eveileble NTIS

Determinetion of Short Lifetimes with Ultra High Resolution (n,gemme) Spectroscopy. PB90-123670 901,567 Not aveilable NTIS

Determination of the Absolute Specific Conductence of Primary Standard KCl Solutions. PB89-230320 900,481 Not available NTIS

Determination of the Time-Dependence of ohm NBS (Netional Bureau of Standards) Using the Quentized Hell Resistence PB89-230387 900,819 Not available NTIS

Determination of Total Cholesterol in Coconut Oil: A New NIST (Netional Institute of Standerds end Technology) Cholesterol Stenderd Reference Metenel. 901,262 Not eveilable NTIS

Determination of Trece Level lodine in Biological and Botenical Reference Materials by Isotope Dilution Mess Spectrometry. PB89-235642 900.222

(Order es PB89-235634, PC A04)

Determination of Ultretrace Concentrations of Butyltin Compounds in Water by Simultaneous Hydridization/Extraction with GC-FPD Detection. PB89-177224 901,311 Not eveilable NTIS

Determining Picogram Quentities of U in Humen Urine by Thermal Ionization Mass Spectrometry.
PB89-146906 900,175 Not evaileble NTIS

Deuterium Magnetic Resonance Study of Orientation end Poling in Poly(Vinylidene Fluonde) end Poly(Vinylidene Fluonde-Co-Tetrafluoroethylene). 900.565 Not available NTIS PB89-186365

Developing Definitive Methods for Human Serum Analytes. PB89-146773 901,233 Not evailable NTIS

Development and Use of a Tribology Research-in-Progress PB89-228274 901.002 PC A14/MF A01

Development of a Field-Space Corresponding-States Method for Fluids and Fluid Mixtures. 901.331 Not aveilable NTIS PB89-227995

Development of a Method to Measure In situ Chloride at the Coating/Metal Interface. PB89-235345 901,085 PC A03/MF A01

Development of a Microwave Sustained Gas Plasma for the Development of a minimum.

Sterilization of Dental Instruments.

900,047 Not available NTIS PB89-231278

Development of a Multiple Layer Test Procedure for Inclusion in NFPA (National Fire Protection Association) 701: Initial Experiments.
PB9-235673 900,096 PC A04/MF A01

Development of an Automated Probe for Thermal Conductivity Measurements. PB89-209324 900,896 PC A07/MF A01

Development of Combustion from Quasi-Stable Temperatures for the Iron Based Alloy UNS S66286.
PB89-173850 900,592 Not available NTIS

Development of Electrophoresis and Electrofocusing Stand-PB89-175863 900,195 Not available NTIS

Development of Near-Field Test Procedures for Communication Satellite Antennas, Phase 1, Part 2.
PB89-156152 901,593 PC A05/MF A01

velopment of New Standard Reference Materials for Use in Thermometry. PB89-201180 900.893 Not available NTIS

Development of Standard Measurement Techniques Standard Reference Materials for Heat Capacity and Heat of Vaporization of Jet Fuels. 900.837 PC A03/MF A01 PB89-148100

Development of the NBS (National Bureau of Standards) Beryllium Isotopic Standard Reference Meterial.
PB89-231070 900,221 Not available NTIS

Developments in the Heat Balance Method for Simulating Room Thermal Response. Room Thermal Response. PB89-173926 900,062 Not available NTIS

Dichromete Dosimetry: The Effect of Acetic Acid on the Radiolytic Reduction Yield. PB89-147490 900,248 Not eveilable NTIS

Dielectric Meesurements for Cure Monitoring. PB89-200430 900,567 Not aveileble NTIS

Dielectric Mixing Rules for Background Test Soils. PB89-188585 901,289 PC A03/MF A01

Differentiel Scanning Calorimetric Study of Brain Clathrin. PB90-117912 900,225 Not evailable NTIS

Diffrection Effects Along the Normal to a Grain Boundary 901,153 Not evailable NTIS PB89-202089

Diffusion-Induced Grein Boundary Migretion. PB90-128174 901,175 Not available NTIS

Dipole Moment Function and Vibretionel Transition Intensi-ties of OH. PB89-227920 900,464 Not available NTIS

Direct Observetion of Surface-Trapped Diffracted Waves. PB90-128216 901,475 Not available NTIS

Directionel Invarience of Grein Boundary Migration in the Pb-Sn Cellular Trensformation end the Tu-Turnbull Hystere-PB89-157911 901,134 Not available NTIS

Directional Solidification of a Planar Interface in the Presence of a Time-Dependent Electric Current.

901,461 PC A04/MF A01 PB90-112400

Directory of International and Regional Organizations Conducting Standards-Related Activities.
PB89-221147 900,008 PC A19/MF A01

Directory of NVLAP (National Voluntary Laboratory Accreditation Progrem) Accredited Laboratories, 1986-87. PB89-185599 900,933 PC A05/MF A01

Discussion of 'Steep-Front Short-Duration Voltage Surge Tests of Power Line Filters and Transient Voltage Suppres-PB90-117326 900, 755 Not available NTIS

Dissocietion Lifetimes and Level Mixing in Overtone-Excited HN3 (X tilde (sup 1) A'). PB90-117425 900,263 Not available NTIS

Document Interchenge Standards: Description and Status of Major Document and Graphics Standards. PB89-193874 900,928 PC A03/MF A01

Domein Imeges of Ultrathin Fe Films on Ag(100). PB89-158067 901,394 Not available NTIS

Doppler Imaging of AR Lacertae at Three Epochs PB89-149199 900,015 Not available NTIS

Draft International Document on Guide to Portable Instruments for Assessing Airborne Pollutants Arising from Hazardous Wastes. 900.855 Not available NTIS PB89-150775

Drift Tubes for Characterizing Atmospheric Ion Mobility PB90-128513 901.585 Not available NTIS

Drift Tubes for Characterizing Atmospheric Ion Mobility Spectra Using AC, AC-Pulse, and Pulse Time-of-Flight Measurement Techniques. PB89-202543 900,438 Not available NTIS

Dual Frequency P-Code Time Transfer Experiment. PB89-174064 900,614 Not available NTIS

Dynamic Light Scattering and Angular Dissymmetry for the In situ Measurement of Silicon Dioxide Particle Synthesis in PB89-179584 900,246 Not available NTIS

Dynamic Microindentetion Apparatus for Materials Charac-

PB89-176911 901,140 Not available NTIS Dynamic Poisson's Ratio of a Ceramic Powder during Com-

PB89-177182 901.039 Not available NTIS

Dynamic Young's Modulus Measurements in Metallic Materials: Results of an Interlaboratory Testing Program. PB89-157671 901,132 Not available NTIS

Dynamical Diffraction of X-rays at Grazing Angle. PB89-186886 901,421 Not available NTIS

Dynamical Simulation of Liquid- and Solid-Metal Self-Sputtering. PB89-228407 900,472 Not available NTIS

Dynamics of a Spin-One Model with the Pair Correlation. PB89-171300 900,356 Not available NTIS

Dynamics of Concentration Fluctuation on Both Sides of PB89-173942 901.183 Not available NTIS

Dynamics of Molecular Collisions with Surfaces: Excitation, Dissociation, and Diffraction.

900,375 Not available NTIS PB89-175996 Earthquake Hazard Mitigation through Improved Seismic Design. PB89-149132 900,098 Not available NTIS Earthquake Resistant Design Criteria. PB89-149140 900,099 Not available NTIS

Economical Ultrahigh Vacuum Four-Point Resistivity Probe. PB89-147086 900,870 Not available NTIS

Edge Stresses in Woven Laminates at Low Temperatures. PB90-128265 901,082 Not available NTIS

Effect of a Crystal-Melt Interface on Taylor-Vortex Flow. PB90-130261 901,477 PC A03/MF A01

Effect of an Electrically Large Stirrer in a Mode-Stirred PB90-117946 901,378 Not available NTIS

Effect of an Oil-Paper Interface Parallel to an Electric Field on the Breakdown Voltage at Elevated Temperatures. PB89-156988 901,490 Not available NTIS

Effect of Anisotropic Thermal Conductivity on the Morphological Stability of a Binary Alloy.
PB89-228985
901,155
PC A03/MF A01

Effect of Chemical Composition on the 4 K Mechanical Properties of 316LN-Type Alloys. PB90-128554 901,110 Not available NTIS

Effect of Chinese Standardization on U.S. Export Opportu-PB89-166128 900,172 PC A03/MF A01

Effect of Coal Slag on the Microstructure and Creep Behavior of a Magnesium-Chromite Refractory. PB89-158034 901,027 Not available NTIS

Effect of Crosslinks on the Phase Separation Behavior of a Miscible Polymer Blend. 900.546 Not available NTIS PR89-146724

Effect of Heat Treatment on Crack-Resistance Curves in a Liquid-Phase-Sintered Alumina.
PB89-229231 901,056 Not available NTIS

Effect of Lateral Crack Growth on the Strength of Contact

Flaws in Brittle Materials. PB89-171813 901,034 Not available NTIS

Effect of Multiple Internal Reflections on the Stability of Electrooptic and Magnetooptic Sensors. PB89-171722 900,724 Not available NTIS

Effect of Neutrons on the Characteristics of the Insulated Gate Bipolar Transistor (IGBT).
PB89-157655 900,773 Not available NTIS

Effect of pH on the Emission Properties of Aqueous tris (2,6-dipicolinato) Terbium (III) Complexes. PB89-157135 900,250 Not available NTIS

Effect of Pipe Roughness on Onfice Flow Measurement. PB89-231484 901,333 PC A04/MF A01

Effect of Pressure on the Development of Prebreakdown PB90-128315 900.828 Not available NTIS

Effect of Random Errors in Planar Near-Field Measurement. PB89-171839 900,708 Not available NTIS

Effect of Room-Temperature Stress on the Critical Current of NbTi. PB89-179832 901.414 Not available NTIS

Effect of Slag Penetration on the Mechanical Properties of Refractories: Final Report. PB90-110065 900,836 PC A07/MF A01

Effect of Surface Ionization on Wetting Layers. PB89-157259 901,323 Not available NTIS

Effect of Water on Piloted Ignition of Cellulosic Materials. PB89-189187 900,127 PC A09/MF A01

Effects of a Gold Shank-Overlayer on the Field Ion Imaging 901,404 Not available NTIS

Effects of Doping-Density Gradients on Band-Gap Narrowing in Silicon and GaAs Devices. .
PB89-228522 901,453 Not available NTIS

Effects of Grain Size and Cold Rolling on Cryogenic Properties of Copper PB90-128604 901,176 Not available NTIS

Effects of Material Characteristics on Flame Spreading. PB89-212021 900,572 Not available NTIS

Effects of Pressure on the Vibrational Spectra of Liquid Ni-

tromethane. PB89-158026 900,342 Not available NTIS

Effects of Purified Ferric Oxalate/Nitric Acid Solutions as a Pretreatment for the NTG-GMA and PMDM Bonding System. PB89-146716 900,034 Not available NTIS Effects of Research on Building Practice.
PB89-202584 900,168 Not available NTIS

Effects of Solvent Type on the Concentration Dependence of the Compression Modulus of Thermoreversible Isotactic Polystyrene Gels. 900.553 Not available NTIS

Effects of Space Charge on the Poling of Ferroelectric PR89-146708 901,179 Not available NTIS

Effects of Thermal Stability and Melt Viscosity of Thermoplastics on Piloted Ignition. 900.151 Not available NTIS

Effects of Velocity and State Changing Collisions on Raman Q-Branch Spectra. PB89-179196 900.391 Not available NTIS

Efficient Algorithms for Computing Fractal Dimensions. PB89-175871 901,198 Not available NTIS

Efficient and Accurate Method for Calculating and Representing Power Density in the Near Zone of Microwave Antennas. PB89-157457 900.707 Not available NTIS

Elastic Interaction and Stability of Misfitting Cuboidal Inho-PB89-157903 901,482 Not available NTIS

Electric-Dipole Moments of H2O-Formamide and CH3OH-Formamide. PB89-147375 900,288 Not available NTIS

Electric-Resonance Optothermal Spectrum of (H2O)2: Microwave Spectrum of the K=1-0 Subband for the E((+900,497 Not available NTIS

Electrical Performance Tests for Hand-Held Digital Multi-900.876 PC A13/MF A01 PR89-162234

Electrically Calibrated Silicon Bolometer for Low Level Optiand Energy Measurements.
714 901,348 Not available NTIS

Electrodeposition of Chromium from a Trivalent Electrolyte. PATENT-4 804 446 901,119 Not available NTIS

Electromagnetic Detection of Long Conductors in Tunnels. PB90-128190 900,827 Not available NTIS

Electromagnetic Fields in Loaded Shielded Rooms. PB89-180426 900,780 Not available NTIS

Electromagnetic Pulse Scattered by a Sphere. PB89-157895 901,495 Not available NTIS

Electromigration Damage Response Time and Implications for dc and Pulsed Characterization. PB89-212179 901.443 Not available NTIS

Electron and Photon Stimulated Desorption: Benefits and PB89-200745 901.427 Not available NTIS

Electron and Photon Stimulated Desorption: Probes of Structure and Bonding at Surfaces. PB89-157960 901,116 Not available NTIS

Electron Diffraction Study of the Faceting of Tilt Grain Boundaries in NiO. PB89-201792 901,431 Not available NTIS

Electron-Energy Dependence of the S2F10 Mass Spec-PB90-117870 900.512 Not available NTIS

Electron-Impact Excitation of Al(2+).
PB89-171565 901,503 Not available NTIS PB89-171565

Electron-Impact Excitation of the Resonance Transition in CA(1+). PB89-171557 901,502 Not available NTIS

Electron-Impact Ionization of La(q +) Ions (q = 1,2,3). PB90-123845 901,573 Not available NTIS

Electron Mean Free Path Calculations Using a Model Dielectric Function. PB89-177026 901.141 Not available NTIS

Electron Microscopy Studies of Diffusion-Induced Grain Boundary Migration in Ceramics.
PB89-202097 901,049 Not available NTIS

Electron-Stimulated-Desorption Ion-Angular Distributions. PB89-201230 901,430 Not available NTIS

Electron Stopping Powers for Transport Calculations. PB90-123605 901,566 Not available NTIS

Electron Transmission Through NiSi2-Si Interfaces. PB89-231294 900,485 Not available NTIS

Electron-Transport, Ionization, Attachment, and Dissociation Coefficients in SF6 and Its Mixtures.

PB89-171540

901,501

Not available NTIS

Electronic, Magnetic, Superconducting and Amorphous-Forming Properties Versus Stability of the Ti-Fe, Zr-Ru and Hf-Os Ordered Alloys. 901,120 Not available NTIS

Electronic Mail and the 'Locator's' Dilemma PB89-211957 901,205 Not available NTIS

Electronic Publishing: Guide to Selection. PB89-214753 900.935 PC A03/MF A01 PB89-214753

Electronic Structure of Diammine (Ascorbato) Platinum(II) and the Trans Influence on the Ligand Dissociation Energy. PB89-147128 900,287 Not available NTIS

Electronic Structure of the Cd Vacancy in CdTe. PB89-171318 901,398 Not available NTIS

Element-Specific Epifluorescence Microscopy In vivo Monitoring of Metal Biotransformations in Environmental Matri-PB89-177216 901,220 Not available NTIS

Elevated Temperature Deformation of Structural Steel. PB89-172621 901,098 PC A06/MF A01

Elimination of Spurious Eigenvalues in the Chebyshev Tau PB89-209282 901,330 PC A03/MF A01

EMATs (Electromagnetic Acoustic Transducers) for Roll-By Crack Inspection of Railroad Wheels.
PB90-123894 901,597 Not available NTIS 901,597 Not available NTIS

Emerging Technologies in Electronics and Their Measurement Needs.
PB89-189245 900,811 PC A05/MF A01

Emerging Technologies in Manufacturing Engineering. PB90-132747 901,013 PC A04/MF A01

Energy Levels of Molybdenum, Mo 1 through 42. PB89-186472 900,411 Not available NTIS

Energy Prices and Discount Factors for Life-Cycle Cost Analysis 1988: Annual Supplement to NBS (National Bureau of Standards) Handbook 135 and NBS Special Pub-900.850 PC A04/MF A01 PB89-153860

Engineering View of the Fire of May 4, 1988 in the First Interstate Bank Building, Los Angeles, California. PB89-183222 900,167 PC A03/MF A01

Enhancements to the VWS2 (Vertical Workstation 2) Data Preparation Software. PB90-132713 900,968 PC A04/MF A01

Enthalpies of Desorption of Water from Coal Surfaces. PB89-173868 900,838 Not available NTIS

Environmental Intelligence. PB89-201214 901.287 Not available NTIS

Environmental Standard Reference Materials - Present and Future Issues PB89-150940 900.865 Not available NTIS

Epoxy Impregnation of Hardened Cement Pastes for Characterization of Microstructure. 901.042 PC A03/MF A01 PB89-185573

Epoxy Impregnation Procedure for Hardened Cement Sam-PB89-147821 901,180 PC A03/MF A01

Equilibrium Crystal Shapes and Surface Phase Diagrams at Surfaces in Ceramics.
PB90-117755 901,162 Not available NTIS

Ergodic Behavior in Supercooled Liquids and in Glasses. PB89-202444 901,435 Not available NTIS

Error Analysis Techniques for Planar Near-Field Measurements PB89-156848 900,701 Not available NTIS

Error Bounds for Linear Recurrence Relations. AD-A201 256/5 901,192 PC A03/MF A01

Estimates of Confidence Intervals for Divider Distorted Waveforms. PB89-173447 900.806 Not available NTIS

Estimating the Environment and the Response of Sprinkler Links in Compartment Fires with Draft Curtains and Fusible Line-Actuated Ceiling Vents. Part 2. User Guide for the Computer Code Lavent.

PB89-229009 900,094 PC A03/MF A01

Estimation of an Asymmetrical Density from Several Small Samples. PB89-201131 901,212 Not available NTIS

Estimation of the Error Probability Density from Replicate Measurements on Several Items.
PB89-157820
901,210
Not available NTIS

Estimation of the Thermodynamic Properties of Hydrocarbons at 298.15 K. PB89-145155 900,272 Not available NTIS

Evaluated Chemical Kinetic Data for the Reactions of Atomic Oxygen O(3P) with Sulfur Containing Compounds. PB89-145122 900,269 Not available NTIS

Evaluated Kinetic and Photochemical Data for Atmospheric Chemistry. Supplement 3. PB89-222582 900.454 (Not Available NTIS)

Evaluated Kinetics Data Base for Combustion Chemistry. PB89-212096 900,601 Not available NTIS

Evaluating Emergency Management Models and Data Bases: A Suggested Approach.
PB89-189203 901,598 PC A10/MF A01

Evaluating Office Lighting Environments: Second Level Analysis. PB89-189153 900,073 PC A07/MF A01

Evaluation of Data on Higher Heating Values and Elemental Analysis for Refuse-Derived Fuels.
PB90-136839 900,845 Not available NTIS

Evaluation of Data on Solubility of Simple Apolar Gases in Light and Heavy Water at High Temperature. PB90-126251 900,529 Not available NTIS

Evaporation of a Water Droplet Deposited on a Hot High Thermal Conductivity Solid Surface.
PB89-149157 901,487 Not available NTIS

Evidence for the Superconducting Proximity Effect in Junctions between the Surfaces of YBa2CU3Ox Thin Films. PB89-228449 901,449 Not available NTIS

EVSIM: An Evaporator Simulation Model Accounting for Refrigerant and One Dimensional Air Distribution.
PB89-235881 900,086 PC A07/MF A01

EXAFS (Extended X-ray Absorption Fine Structure) Study of Buried Germanium Layer in Silicon. PB89-228472 901,452 Not available NTIS

Exchange and Magnetostrictive Effects in Rare Earth Su-901.438 Not available NTIS

Executive Summary for the Workshop on Developing a Predictive Capability for CO Formation in Fires. PB89-200091 900,134 PC A04/MF A01

Exoergic Collisions of Cold Na*-Na. PB90-123761 901.571 Not available NTIS

Expected Complexity of the 3-Dimensional Voronoi Dia-

gram. PB89-209332 901,200 PC A03/MF A01

Experience with IMDAS (Integrated Manufacturing Data Administration System) in the Automated Manufacturing Research Facility PB90-112350 900.964 PC \$63/MF \$01

Experiences in Environmental Specimen Banking. PB90-123969 900,866 Not available NTIS

Experimental Determination of Forced Convection Evaporative Heat Transfer Coefficients for Non-Azeotropic Refriger-

901,117 Not available NTIS

Experimental Fire Tower Studies of Elevator Pressurization Systems for Smoke Control. PB90-117813 900,097 Not available NTIS

Experimental Investigation and Modeling of the Flow Rate of Refrigerant 22 Through the Short Tube Restrictor. PB89-229041 901,118 PC A06/MF A01

Experimental Observations on the Initiation of DIGM (Diffusion Induced Grain Boundary Migration). PB89-157630 901,130 Not available NTIS

Experimental Study of Interpanel Interactions at 3.3 GHz. PB89-176218 900,709 Not available NTIS

Experimental Study of the Pyrolysis of Pure and Fire Retarded Cellulose.
PB89-228316 901,090 PC A07/MF A01

Experimental Thermal Conductivity, Thermal Diffusivity, and Specific Heat Values of Argon and Nitrogen. PB89-148407 900,293 PC A04/MF A01

Experimental Validation of a Mathematical Model for Predicting Moisture Transfer in Attics.
PB89-150783 900,057 Not available NTIS

Experimental Verification of the Relation between Two-Probe and Four-Probe Resistances. PB89-231211 900,794 Not available NTIS

Expert-Database System for Sample Preparation by Microwave Dissolution. 1. Selection of Analytical Descriptors. PB89-229108 900,216 Not available NTIS

Expert Systems Applied to Spacecraft Fire Safety. PB89-231013 901,590 Not available NTIS

Exploratory Research in Reflectance and Fluorescence Standards at the National Bureau of Standards. PB89-202022 900,428 Not available NTIS

External Representation of Product Definition Data.

900.939 PC A03/MF A01 PB90-112434

Facile Synthesis of 1-Nitropyrene-d9 of High Isotopic Punty. PB90-123753 900.240 Not available NTIS

Facilitated Transport of CO2 through Highly Swollen Ion-Exchange Membranes: The Effect of Hot Glycenne Pretreatment. 900,395 Not available NTIS

Facsimile Coding Schemes and Coding Control Functions for Group 4 Facsimile Apparatus, Category: Telecommunications Standard.

FIPS PUB 150 900.662 PC E08

FACTUNC: A User-Friendly System for Unconstrained Optimization. PB90-112392 901.207 PC A03/MF A01

Failure Analysis of an Amine-Absorber Pressure Vessel. PB89-173835 901,101 Not available NTIS

False Alarm Study of Smoke Detectors in Department of Veterans Affairs Medical Centers (VAMCS). PB89-193288 900,093 PC A11/MF A01

Far-Infrared Laser Magnetic Resonance Spectrum of the CD Radical and Determination of Ground State Parameters. PB90-117359 900,496 Not available NTIS

Far-Infrared Laser Magnetic Resonance Spectrum of Vibrationally Excited C2H(1). PB89-147474 900,292 Not available NTIS

Far-Infrared Spectrum of Methyl Amine. Assignment and Analysis of the First Torsional State.
PB89-161574 900,346 Not available NTIS

Faraday Effect Sensors: The State of the Art. PB89-231153 900.823 Not 900.823 Not available NTIS

Fast Magnetic Resonance Imaging with Simultaneously Oscillating and Rotating Field Gradients.
PB89-176903 901,514 Not available NTIS

Fast Optical Detector Deposited on Dielectric Channel Waveguides. PB89-171706 900.743 Not available NTIS

Fast Path Planning in Unstructured, Dynamic, 3-D Worlds. PB89-177067 900,992 Not available NTIS

Fast-Pulse Generators and Detectors for Characterizing Laser Receivers at 1.06 um. PB89-171698 901.347 Not available NTIS

Fatigue Resistance of a 2090-T8E41 Aluminum Alloy at Cryogenic Temperatures.
PB90-128737 901,177 Not available NTIS

Feasibility of Detector Self-Calibration in the Near Infrared. PB89-176788 900.384 Not available NTI 900.384 Not available NTIS

Federal Software Engineering Standards Program. 900,666 Not available NTIS

Ferric Oxalate with Nitric Acid as a Conditioner in an Adhesive Bonding System.

PB89-229272 900,045 Not available NTIS

Ferrite Number Prediction to 100 FN in Stainless Steel Weld Metal. PB89-201586 901,106 Not available NTIS

Fiber Coating and Characterization. PB89-228571 901, 901,067 Not available NTIS

Field Measurement of Thermal and Solar/Optical Properties of Insulating Glass Windows.

PB89-175905

900,064

Not available NTIS

lds of Horizontal Currents Located Above the Earth. 89-156830 900,700 Not available NTIS PB89-156830

Fields Radiated by Electrostatic Discharges. PB90-128778 901,382 Not available NTIS

Filling of Solvent Shells About Ions. 1. Thermochemical Criteria and the Effects of Isomeric Clusters.
PB89-157549 900,329 Not available NTIS

Final-State-Resolved Studies of Molecule-Surface Interac-PR89-150916 900,298 Not available NTIS

Finite Element Studies of Transient Wave Propagation PB89-186902 901,375 Not available NTIS

Finite Unions of Closed Subgroups of the n-Dimensional Torus. PB89-143283 901.193 PC A03/MF A01

Fire Growth and Development.

PB90-128570 900.152 Not available NTIS

Fire Induced Flows in Corridors: A Review of Efforts to Model Key Features. PB89-189260 900,129 PC A03/MF A01

Fire Propagation in Concurrent Flows. PB89-151781 900,867 PC A04/MF A01 PB89-188577 900,597 PC A03/MF A01

Fire Properties Database for Textile Wall Coverings. PB89-188635 900,126 PC A04/MF A01

Fire Research Publications, 1988 PB89-193304 900.132 PC A03/MF A01

Fire Risk Analysis Methodology: Initiating Events. PB89-184527 900,125 PC A08/MF A01

Fire Safety Science-Proceedings of the First International Symposium. PB89-179261 900,596 Not available NTIS

Flammability Characteristics of Electrical Cables Using the Cone Calorimeter. PB89-162572 900,741 PC A04/MF A01

Flammability of Upholstered Furniture with Flaming PB90-136805 900.155 Not available NTIS

Flammability Tests for Industrial Fabrics: Relevance and Limitations PB89-174122 901.091 Not available NTIS

Flash Photolysis Kinetic Absorption Spectroscopy Study of the Gas Phase Reaction HO2 + C2H5O2 Over the Temperature Range 228-380 K. PB90-136565 900,536 Not available NTIS

Flaw Tolerance in Ceramics with Rising Crack Resistance Characteristics. PB90-128026 901.060 Not available NTIS

Flow Coefficients for Interzonal Natural Convection for Vari-

900.069 Not available NTIS

low of Molecules Through Condoms 901,087 PC A03/MF A01 PB89-148118

Fluid Flow in Pulsed Laser Irradiated Gases: Modeling and 900,265 Not available NTIS

Flux Creep and Activation Energies at the Grain Boundaries of Y-Ba-Cu-O Superconductors. 901,457 Not available NTIS PB89-230353

Formation and Stability Range of the G Phase in the Aluminum-Manganese System.
PB89-186316 901.144 Not available NTIS

Formation of Dispersoids during Rapid Solidification of an

Al-Fe-Ni Alloy. PB90-123647 901,172 Not available NTIS

Formation of Hydroxyapatite in Hydrogels from Tetracal-cium Phosphate/Dicalcium Phosphate Mixtures. PB89-201511 901,255 Not available NTIS

Formation of the Al-Mn Icosahedral Phase by Electrodepo-PB90-117763 900.504 Not available NTIS

Fourth-Order Elastic Constants of beta-Brass. PB90-117607 901,160 Not available NTIS

Fractal-Based Description of the Roughness of Blasted Steel Panels PB89-158018 901,096 Not available NTIS

Fracture Behavior of a Pressure Vessel Steel in the Ductile-to-Brittle Transition Region. PB89-189195 901,103 PC A03/MF A01

Fracture Behavior of Ceramics Used in Multilayer Capaci-PB89-171805 900.758 Not available NTIS

Fracture Behavior of 316LN Alloy in Uniaxial Tension at Cryogenic Temperatures. PB90-128562 901,111 Not available NTIS

Free-Electron-Like Stoner Excitations in Fe. PB89-158059 901,393 Not available NTIS

Free Value Tool for ASN.1. PB89-196182 900,622 PC A04/MF A01

Frequency Measurement of the J=1< - 0 Rotational Transition of HD (Hydrogen Deuteride).

901,499 Not available NTIS PB89-161566 Frequency Measurements of High-J Rotational Transitions

of OCS and N2O. PB90-136946 900,541 Not available NTIS

uency Standards Utilizing Penning Traps. 0-128042 901,379 Not available NTIS PB90-128042

Fresnel Lenses Display Inherent Vignetting. PB89-157069 901,337 Not available NTIS

Friability of Spray-Applied Fireproofing and Thermal Insulations: Field Evaluation of Prototype Test Devices. PB89-189328 900,130 PC A04/MF A01

FT-IR (Fourier Transform-Infrared) Emission/Transmission Spectroscopy for In situ Combustion Diagnostics. PB89-211866 900,600 Not available NTIS

Functional Approach to Designing Architectures for Computer Integrated Manufacturing. PB89-172589 900,946 PC A03/MF A01 PB89-171755 901,310 Not available NTIS PB89-227946 901,281 Not available NTIS Green Function Method for Calculation of Atomistic Struc-High-Purity Germanium X-ray Detector on a 200 kV Analytical Electron Microscope.
PB89-201602 900,208 Not available NTIS ture of Grain Boundary Interfaces in Ionic Crystals.
PB89-202105 901,050 Not available NTIS Fundamental Aspects of Key Issues in Hazardous Waste PB89-202105 Incineration. PB89-212104 900,861 Not available NTIS Group Index and Time Delay Measurements of a Standard High Resolution Imaging of Magnetization.
PB89-147433 901,386 Not available NTIS Reference Fiber. PB89-189179 Fundamental Characterization of Clean and Gas-Dosed Tin 900,752 PC A03/MF A01 Oxide. PB89-202964 High Resolution Inverse Raman Spectroscopy of the CO Q Growth and Properties of High-Quality Very-Thin SOS (Silicon-on Sapphire) Films. PB90-128109 900,798 Not available NTIS 900.785 Not available NTIS PB89-171292 900,355 Not available NTIS Fundamental Configurations in Mo IV Spectrum.
PB89-147011 900,284 Not available NTIS High Resolution Optical Multiplex Spectroscopy.
PB89-185938 900,404 Not available NTIS Gruneisen Parameter of Y1Ba2Cu3O7. PB90-117615 901,465 Not available NTIS Fundamental Physical Constants - 1986 Adjustments. PB90-136474 900,535 Not available NTIS High-Resolution, Slit Jet Infrared Spectroscopy of Hydrocarbons: Quantum State Specific Mode Mixing in CH Stretch-Excited Propyne. Guide to Available Mathematical Software Advisory System. PB90-123654 901,201 Not available NTIS Fundamental Tests of Special Relativity and the Isotropy of Space. PB89-185920 900,490 Not available NTIS Guideline for Work Station Design. PB90-112418 900,643 PC A07/MF A01 PB89-234256 901,523 Not available NTIS High Resolution Spectrum of the $nu(sub\ 1) + nu(sub\ 2)$ Band of NO2. A Spin Induced Perturbation in the Ground Fundamentals of Enclosure Fire 'Zone' Models. Guidelines and Procedures for Implementation of Executive Order on Seismic Safety. PB89-176168 900,122 Not available NTIS 900,417 Not available NTIS Gain and Power Parameter Measurements Using Planar Near-Field Techniques.
PB89-156822 900,699 Not available NTIS PB89-148092 900.156 PC A03/MF A01 High Speed 25-Position Interface for Data Terminal Equipment and Data Circuit-Terminating Equipment, Category: Telecommunications Standard. Guidelines for Identification and Mitigation of Seismically Hazardous Existing Federal Buildings. PB89-188627 900,161 PC A03/MF A01 Gas Flow Measurement Standards. 900,898 Not available NTIS Guidelines for Implementing the New Representations of the Volt and Ohm Effective January 1, 1990. PB89-214761 900,817 PC A05/MF A01 High T(sub c) Superconductor/Noble-Metal Contacts with Surface Resistivities in the (10 to the Minus 10th Power) Omega sq cm Range. PB99-179824 901,413 Not available NTIS Gas Phase Proton Affinities and Basicities of Molecules: A Comparison between Theory and Experiment. PB89-146674 900,280 Not available NTIS Guidelines for the Specification and Validation of IGES (Initial Graphics Exchange Specification) Application Protocols. PB89-166102 900,937 PC A06/MF A01 901,413 Not available NTIS Gas Solubility and Henry's Law Near the Solvent's Critical High-Temperature Dental Investments PB89-202477 901,257 Not available NTIS PB89-202485 900,434 Not available NTIS um Wallboard Formaldehyde Sorption Model. -132705 900,154 PC A03/MF A01 Gypsum Wallb PB90-132705 High Temperature Thermal Conductivity Apparatus for GATT (General Agreement on Tariffs and Trade) Standards Code Activities of the National Institute of Standards and Technology 1988.
PB8-191977 900,173 PC A03/MF A01 Hand Calculations for Enclosure Fires. PB89-173983 900,164 Not available NTIS PB89-174015 900,366 Not available NTIS Higher Order Beam Finite Element for Bending and Vibration Problems. Hardware Instrumentation Approach for Performance Measurement of a Shared-Memory Multiprocessor.

PB89-186852 900,638 Not available NTIS General Aspects of Group 4 Facsimile Apparatus, Catego-PB89-229124 901,484 Not available NTIS ry: Telecommunications Standard. FIPS PUB 149 900,661 PC E08 Higher-Order Crossings: A New Acoustic Emission Signal Processing Method.
PB89-173488 900,678 Not available NTIS HAZARD I Fire Hazard Assessment Method. PB89-215404 900,143 CP **D05** General Methodology for Machine Tool Accuracy Enhancement by Error Compensation.
PB89-146781 900,996 Not available NTIS Heat Transfer in Compartment Fires Near Regions of Ceiling-Jet Impingement on a Wall.
PB90-118076 900,150 Not available NTIS History of the Present Value of 2e/h Commonly Used for Defining National Units of Voltage and Possible Changes in National Units of Voltage and Resistance. PB89-202154 901,535 Not available NTIS Generalized Mathematical Model for Machine Tool Errors PB89-150874 900,977 Not available N Not available NTIS Helium Resonance Lines in the Flare of 15 June 1973, PB90-118142 900,028 Not available NTIS Generation of Oxy Radicals in Biosystems. PB90-117888 901,266 Not available NTIS How to Estimate Capacity Dimension. PB89-172522 901,197 Not available NTIS Heterodyne Frequency and Fourier Transform Spectrosco-py Measurements on OCS Near 1700 cm(-1). PB90-117805 900,507 Not available NTIS Generation of Squeezed Light by Intracavity Frequency HVACSIM+, a Dynamic Building/HVAC/Control Systems Simulation Program.
PB89-177166 900,070 Not available NTIS Doubling. PB89-227938 901,365 Not available NTIS Heterodyne Frequency Measurements of (12)C(16)O Laser Generic Architecture for Computer Integrated Manufacturing Software Based on the Product Data Exchange Specification. Hybrid Representation of the Green's Function in an Over-moded Rectangular Cavity. PB90-117953 900,826 Not available NTIS PB89-229223 901,374 Not available NTIS cation. PB90-112459 900,826 Not available NTIS Heterodyne Measurements on N2O Near 1635 cm(-1). PB90-117797 900,506 Not available NTIS 900.965 PC A03/MF A01 Hybrid Structures for Simple Computer Performance Esti-Generic Liposome Reagent for Immunoassays. Heterodyne Measurements on OCS Near 1372 cm(-1). PB89-201743 900,425 Not available NTIS PB90-123886 901,229 Not available NTIS PB89-189161 900,639 PC A03/MF A01 Glass Bottles for Carbonated Soft Drinks: Voluntary Product Hydrodynamic Forces on Vertical Cylinders and the Lighthill Heuristic Analysis of von Kries Color Constancy. PB89-201099 901,362 Not available NTIS Standard PS73-89. PB90-107046 900.012 PC A03/MF A01 PB90-117417 901.313 Not available NTIS Hierarchically Controlled Autonomous Robot for Heavy Payload Military Field Applications.
PB89-177075 901,271 Not available NTIS Global Biomethylation of the Elements - Its Role in the Bio-sphere Translated to New Organometallic Chemistry and Biotechnology. PB90-136854 901,232 Not available NTIS Hydrodynamics of Magnetic and Dielectric Colloidal Disper-PB89-157242 900,314 Not available NTIS 901,232 Not available NTIS Hydrogen Sites in Amorphous Pd85Si15HX Probed by Neutron Vibrational Spectroscopy.
PB89-229140 901,456 Not available NTIS Glossary of Standards-Related Terminology. 900,986 PC A03/MF A01 Hierarchies for Computer-Integrated Manufacturing: A Functional Description. PB89-172613 900.949 PC A03/MF A01 High Accuracy Determination of (235)U in Nondestructive Assay Standards by Gamma Spectrometry. PB89-156954 900,249 Not available NTIS Government Open Systems Interconnection Profile Users' Hydroxyl Radical Induced Cross-Linking between Phenyla-Guide. PB90-111212 lanine and 2-Deoxyribose. PB89-147029 900.667 PC A07/MF A01 900.547 Not available NTIS High-Accuracy Differential-Pulse Anodic Stripping Voltam-metry Using Indium as an Internal Standard. PB89-176267 900,198 Not available NTIS Grain Boundaries with Impurities in a Two-Dimensional Lat-Hyperconjugation: Equilibrium Secondary Isotope Effect on the Stability of the t-Butyl Cation. Kinetics of Near-Thermoneutral Hydride Transfer. PB9-156756 900,306 Not available NTIS tice-Gas Model. PB89-172407 901,507 Not available NTIS High-Accuracy Differential-Pulse Anodic Stripping Voltam-metry with Indium as an Internal Standard. PB89-156947 900,182 Not available NTIS Grain Boundary Characterization in Ni3Al. PB89-229306 901,156 Not available NTIS Hysteretic Phase Transition in Y1Ba2Cu3O7-x Supercon-Grain Boundary Structure in Ni3Al. High-Accuracy Gas Analysis via Isotope Dilution Mass Spectrometry: Carbon Dioxide in Air. PB90-123951 900,032 Not available NTIS PB89-229082 901,454 Not available NTIS PB89-201784 901,150 Not available NTIS PR89-229314 901,157 Not available NTIS Identification of Carbonaceous Aerosols via C-14 Accelerator Mass Spectrometry, and Laser Microprobe Mass Spec-Grain-Size and R-Curve Effects in the Abrasive Wear of High Accuracy Modeling of Photodiode Quantum Efficiency. PB90-117599 900,733 Not available NTIS trometry. PB90-136540 Alumina. PB90-117383 900.236 Not available NTIS 901,058 Not available NTIS IEEE (Institute of Electrical and Electronics Engineers) IRPS (International Reliability Physics Symposium) Tutorial Thermal Resistance Measurements, 1989. PB9-231195 900,792 Not available NTIS High-Current Measurement Techniques. Part II. 100-kA Source Characteristics and Preliminary Shunt and Rogowski Coil Evaluations. Graphical Analyses Related to the Linewidth Calibration Problem 900,783 Not available NTIS 900,804 PC A04/MF A01 PB89-170872 High-Mobility CMOS (Complementary Metal Oxide Semi-conductor) Transistors Fabricated on Very Thin SOS Films. PB89-230460 900,791 Not available NTIS Graphics Application Programmer's Interface Standards and CALS (Computer-Aided Acquisition and Logistic Sup-Ignition and Flame Spread Measurements of Aircraft Lining PR89-172886 900,009 PC A04/MF A01 port). PB90-133091 900,658 PC A03/MF A01

High-Precision Absolute Gravity Observations in the United

Ignition Characteristics of the Iron-Based Alloy UNS

S66286 in Pressurized Oxygen.

Gravity Tide Measurements with a Feedback Gravity Meter.

901,104 PC A03/MF A01

Ignition Characteristics of the Nickel-Based Alloy UNS N07718 in Pressurized Oxygen. 901.154 PC A03/MF A01 PB89-218333

Illumination Conditions and Task Visibility in Daylit Spaces. PB89-189237 900,074 PC A04/MF A01

Impedance of Radio-Frequency Biased Resistive Superconducting Quantum Interference Devices. PB89-201719 900,764 Not available NTIS

Implementation of an Automated System for Measuring Radiated Emissions Using a TEM Cell.
PB90-117698 901,377 Not available NTIS

Implications of Computer-Based Simulation Models, Expert Systems, Databases, and Networks for Cement Research. PB89-146989 900,581 Not available NTIS

Implications of Phase Equilibria on Hydration in the Trical-cium Silicate-Water and the Tricalcium Aluminate-Gypsum-Water Systems. PB89-150759

901,022 Not available NTIS

Importance of Isothermal Mixing Processes to the Understanding of Lift-Off and Blow-out of Turbulent Jet Diffusion PB89-201172 900.598 Not available NTIS

Importance of Numeric Databases to Materials Science. PB89-175202 901

901,187

(Order as PB89-175194, PC A06)

Improved Conformal Solution Theory for Mixtures with Large Size Ratios. Large Size Ha PB89-228563 900.477 Not available NTIS

Improved Low-Energy Diffuse Scattering Electron-Spin Polarization Analyzer. 900 218 Not available NTIS PB89-229173

Improved Low-Level Sincorrections.
Standards at 1.064 Micrometers.
900,736 PC A03/MF A01 Improved Low-Level Silicon-Avalanche-Photodiode Transfer

Improved Polarization Measurements Using a Modified Three-Antenna Technique.
PB89-156814 900,698 Not available NTIS

Improved Rotational Constants for HF 901,376 PB90-117466 Not available NTIS

Improved Spherical and Hemispherical Scanning Algo-900.697 Not available NTIS

Improved Standards for Real-Time Radioscopy. PB90-128679 900,923 Not available NTIS

Improved Transportable DC Voltage Standard. PB89-230395 901,554 Not available NTIS

Improved Understanding for the Transient Operation of the Power Insulated Gate Bipolar Transistor (IGBT). PB89-231229 900,795 Not available NTIS

In Search of the Best Clock.

900,632 Not available NTIS

In Situ Fluorescence Monitoring of the Viscosities of Parti-cle-Filled Polymers in Flow. PB89-146278 900,609 PC A03/MF A01

In situ Observation of Particle Motion and Diffusion Interactions during Coarsening. PB89-201982 901,151 Not available NTIS

In vitro Investigation of the Effects of Glass Inserts on the Effective Composite Resin Polymerization Shrinkage.
PB90-117516 900,049 Not available NTIS

Incrementor: A Graphical Technique for Manipulating Pa-PB89-177000 900.648 Not available NTIS

Indirect Energy Gap of Si, Doping Dependence. PB89-150833 901,388 Not available NTIS Indoor Air Quality.

900,065 Not available NTIS Ineffectiveness of Powder Regenerators in the 10 K Temature Range.

PB89-173876 901,005 Not available NTIS

Inelastic Behavior of Full-Scale Bridge Columns Subjected to Cyclic Loading. PB89-174924 900.584 PC A12/MF A01

Influence of Dislocation Density on the Ductile-Brittle Transition in bcc Metals. PB89-157804

901,133 Not available NTIS Influence of Electronic and Geometric Structure on Desorption Kinetics of Isoelectronic Polar Molecules: NH3 and

PB89-176473 900,381 Not available NTIS

Influence of Molecular Weight on the Resonant Raman Scattering of Polyacetylene.

PB89-179246 900,564 Not available NTIS

Influence of Molybdenum on the Strength and Toughness of Stainless Steel Welds for Cryogenic Service. PB89-173512 901,100 Not available NTIS

Influence of Reaction Reversibility on Continuous-Flow Extraction by Emulsion Liquid Membranes.
PB89-176481 900,244 Not available NTIS

Influence of the ac Stark Effect on Multiphoton Transitions PB89-201578 901,530 Not available NTIS

Influence of the Surface on Magnetic Domain-Wall Micros-

PB90-118019 901,467 Not available NTIS

Infrared Absorption Cross Section of Arsenic in Silicon in the Impurity Band Region of Concentration.
PB89-201750
900,426 Not available NTIS

Infrared Absorption of SF6 from 32 to 3000 cm(-1) in the Gaseous and Liquid States.
PB69-157653 900,336 Not available NTIS

Infrared and Microwave Investigations of Interconversion Tunneling in the Acetylene Dime PB89-157341 96 900,320 Not available NTIS

Infrared and Microwave Spectra of OCO-HF and SCO-HF.
PB89-179121 900,389 Not available NTIS

Infrared Spectra of Nitrous Oxide-HF Isomers. PB89-228399 900.471 Not 900,471 Not available NTIS

Infrared Spectrum of D2HF. PB89-171219 900.350 Not available NTIS

Infrared Spectrum of NeHF. PB89-171227 900,351 Not available NTIS

Infrared Spectrum of Sodium Hydride. PB89-230296 900,480 Not available NTIS

Infrared Spectrum of the nu6, nu7, and nu8 Bands of PB89-172415 900.362 Not available NTIS

Infrared Spectrum of the 1205-cm(-1) Band of HNO3. PB89-228514 900,475 Not available NTIS

Initial Spectra of Neutron-Induced Secondary Charged Par-PR89-171862 901,265 Not available NTIS

Initial Stages of Heteroepitaxial Growth of InAs on Si(100). PB90-123878 901,473 Not available NTIS

InSb as a Pressure Sensor. PB89-231104 900.904 Not available NTIS

Institute for Materials Science and Engineering, Ceramics: Technical Activities 1988. PB89-148381 901,019 PC A05/MF A01

Institute for Materials Science and Engineering, Fracture and Deformation: Technical Activities 1988. PB89-148399 901,071 PC A05/MF A01

Institute for Materials Science and Éngineering: Metallurgy, Technical Activities 1988.
PB89-201321
901,147
PC A06/MF A01

Institute for Materials Science and Engineering, Nondestructive Evaluation: Technical Activities 1988. PB89-151625 900,917 PC A04/MF A01 PB89-151625

Institute for Materials Science and Engineering, Nondestructive Evaluation: Technical Activities, 1989. PB90-132739 900,925 PC A05/MF A01

Institute for Materials Science and Engineering, Polymers: Technical Activities 1987.
PB89-188601 900,566 PC A06/MF A01

titute for Materials Science and Engineering, Polymers: Technical Activities 1988.

PB89-166094 900,003 PC A06/MF A01

Instrument-Independent MS/MS Database for XQQ Instruments: A Kinetics-Based Measurement Protocol, PB90-213695

(Order as PB90-213687, PC A04)

Insulation Standard Reference Materials of Thermal Resist-PB89-172548 900,117 Not available NTIS

Integral Mass Balances and Pulse Injection Tracer Techniques. PB89-206833 900,077 PC A03/MF A01

Integrated Knowledge Systems for Concrete and Other Ma-PB89-176119 900.582 Not available NTIS

Integrated Manufacturing Data Administration System (IMDAS) Operations Manual. PB89-156384 900,916 PC A03/MF A01

Intelligent Processing of Materials: Report of an Industrial Workshop Conducted by the National Institute of Standards and Technology.

PB89-151823

900,942 PC A04/MF A01

900.031 Not available NTIS

Interaction of Cupric lons with Calcium Hydroxylapatite.
PB89-157127 900,037 Not available NTIS

Interaction of In Atom Spin-Orbit States with Si(100) Sur-PB90-128547 900,532 Not available NTIS

Interaction of Oxygen and Platinum on W(110). 901,158 Not available NTIS

Interaction of Water with Solid Surfaces: Fundamental Aspects. PB89-201081 900 421 Not available NTIS

Interactions between Two Dividers Used in Simultaneous Comparison Measurements. PB90-118035

Intercomparison of Load Cell Verification Tests Performed by National Laboratories of Five Countries. PB89-235915 900,909 PC A06/MF A01

Interfaces to Teleoperation Devices.

900,993 PC A03/MF A01

Interferometric Dispersion Measurements on Small Guided-Wave Structures. PB89-173959 901 349 Not available NTIS

Interim Criteria for Polymer-Modified Bituminous Roofing Membrane Materials. PB89-168025 900.114 PC A04/MF A01

Interlaboratory Comparison of the Guarded Horizontal Pipe-Test Apparatus: Precision of ASTM (American Society for Testing and Materials) Standard Test Method C-335 Ap-plied to Mineral-Fiber Pipe Insulation.

PB89-218341 901.011 PC A03/MF A01

Interlaboratory Comparison of Two Types of Line-Source Thermal-Conductivity Apparatus Measuring Five Insulating PB89-218325 900.144 PC A03/MF A01

Interlaboratory Determination of the Calibration Factor for the Measurement of the Interstitial Oxygen Content of Silicon by Infrared Absorption.

900.224 Not available NTIS PB90-117300

Internal Revenue Service Post-of-Duty Location Modeling System: Programmer's Manual for FORTRAN Driver Version 5.0. PB89-161913 900.002 PC A04/MF A01

Internal Revenue Service Post-of-Duty Location Modeling System: Programmer's Manual for PASCAL Solver. PB89-161905 900,001 PC A04/MF A01

Internal Structure of the Guide to Available Mathematical Software. PB89-170864 900,927 PC A04/MF A01

International Comparison of HV Impulse Measuring Sys-PB89-186423 900,809 Not available NTIS

International Comparison of Power Meter Calibrations Conducted in 1987. PB89-201545 900.718 Not available NTIS

International Cooperation and Competition in Materials Sci-

ence and Engineering. PB89-228332 901.191 PC A13/MF A01 International Intercomparison of Neutron Survey Instrument

Calibrations PB89-229165 901,300 Not available NTIS

Interpolation of Silicon Photodiode Quantum Efficiency as an Absolute Radiometric Standard.

PB89-212245

901,445

Not available NTIS

Interpretation of a between-Time Component of Error in Mass Measurements. PB89-149108 900,872 Not available NTIS

Interpretation of Emission Wings of Balmer Lines in Luminous Blue Variables.
PB89-212054 900,023 Not available NTIS

Interpretation of the Effects of Retarding Admixtures on Pastes of C3S, C3A plus Gypsum, and Portland Cement. PB89-146971 900,580 Not available NTIS

Interzonal Natural Convection for Various Aperture Configu-

rations. PB89-176499 900,066 Not available NTIS

Intramolecular Dynamics of van der Waals Molecules: An Extended Infrared Study of ArHF. 900,521 Not available NTIS

Intramolecular H Atom Abstraction from the Sugar Moiety by Thymine Radicals in Oligo- and Polydeoxynucleotides. PB89-171870 901,263 Not available NTIS

Intrinsic Sticking in dt Muon-Catalyzed Fusion: Interplay of Atomic, Molecular and Nuclear Phenomena. PB90-117565 901,561 Not available NTIS

Introduction to Microwave Acid Decomposition. PB90-118191 900,227 Not available NTIS

Introduction to Supercritical Fluid Chromatography. Part 2. Applications and Future Trends. PB89-230312 900,219 Not available NTIS

Inventory of Equipment in the Cleaning and Deburing Workstation. PB89-209233 900,958 PC A03/MF A01

Inventory of Equipment in the Tuming Workstation of the AMRF (Automated Manufacturing Research Facility). PB89-215339 900,961 PC A03/MF A01

Investigation of a Washington, DC Office Building. PB89-230361 900,081 Not available NTIS

Ion Kinetics and Energetics. PB89-176101

900,377 Not available NTIS

Ion Trapping Techniques: Laser Cooling and Sympathetic Cooling. PB90-128034 901.578 Not available NTIS

lonic Hydrogen Bond and Ion Solvation. 5. OH...(1-)O Bonds. Gas Phase Solvation and Clustering of Alkoxide and arboxylate Anions. 900.328 Not available NTIS PB89-157531

Ionization and Current Growth in N2 at Very High Electric Field to Gas Density Ratios. 901,552 Not available NTIS PB89-228381

| Isochoric (p,v,T) Measurements on CO2 and (0.98 CO2 + 0.02 CH4) from 225 to 400 K and Pressures to 35 MPa. PB89-202493 900,435 Not available NTIS

Isotope Dilution Mass Spectrometry for Accurate Elemental PB89-230338 900,220 Not available NTIS

Iterative Technique to Correct Probe Position Errors in Planar Near-Field to Far-Field Transformations. PB89-153886 900,695 PC A03/MF A01

IUE Observation of the Interstellar Medium Toward Beta PB89-228373 900,024 Not available NTIS

J-Integral Values for Small Cracks in Steel Panels. PB89-149090 901,093 Not available NTIS

Josephson Array Voltage Calibration System: Operational Use and Verification. PB89-230403 900,820 Not available NTIS

Josephson-Junction Model of Critical Current in Granular Y1Ba2Cu3O(7-delta) Superconductors. PB89-176978 901,406 Not available NTIS

Journal of Physical and Chemical Reference Data, Volume 17, 1988, Supplement No. 2. Thermodynamic and Transport Properties for Molten Salts: Correlation Equations for Critically Evaluated Density, Surface Tension, Electrical Conductance, and Viscosity Data.

PB89-145205 900,277 Not available NTIS Journal of Physical and Chemical Reference Data, Volume

17, 1988, Supplement No. 3. Atomic Transition Probabilities Scandium through Manganese. 900,276 Not available NTIS PB89-145197

Journal of Physical and Chemical Reference Data, Volume 17, Number 1, 1988. PB89-186449 900,408 Not available NTIS

Journal of Physical and Chemical Reference Data, Volume

17, Number 4, 1988. PB89-145114 900,268 Not available NTIS

Journal of Physical and Chemical Reference Data, Volume 18, Number 1, 1989.
PB89-226559 900,455 Not available NTIS

Journal of Physical and Chemical Reference Data, Volume 18. Number 2, 1989. PB89-222525 900,448 Not available NTIS

Journal of Physical and Chemical Reference Data, Volume 18, Number 3, 1989. PB90-126236 900.527 Not available NTIS

Journal of Research of the Institutes of Standards and Technology. September-October 1989. Volume 94, Number

PB90-213687 900.673 PC A04

Journal of Research of the National Institute of Standards and Technology. November-December 1989. Volume 94, Number 6.

PB90-163874 900.542 PC A04

Journal of Research of the National Institute of Standards and Technology, Volume 94, Number 1, January-February 1989. Special Issue: Numeric Databases in Materials and Biological Sciences. 901.186 PC A06 PB89-175194

Journal of Research of the National Institute of Standards and Technology. Volume 94, Number 2, March-April 1989. PB89-184089 900,887 PC **A04**

Journal of Research of the National Institute of Standards and Technology, Volume 94, Number 3, May-June 1989. PB89-211106 901,441 PC A04

Journal of Research of the National Institute of Standards and Technology, Volume 94, Number 4, July-August 1989. PB89-235634 900,908 PC A04

Kinetics of Electron Transfer from Nitroaromatic Radical Anions in Aqueous Solutions. Effects of Temperature and Steric Configuration.

PB89-156749

900,305

Not available NTIS

Kinetics of Resolidification. PB89-176457

901.138 Not available NTIS Knowledge Based System for Durable Reinforced Con-

PB89-150734 900,110 Not available NTIS

Laboratory Accreditation Systems in the United States, PB89-176432 900,882 Not available NTIS

Laboratory Evaluation of an NBS (National Bureau of Standards) Polymer Soil Stress Gage. PB89-211973 901,291 Not available NTIS PB89-211973

Laboratory Measurement of the 1(sub 01)-0(sub 00) Transition and Electric Dipole Moment of SiC2. PB89-228506 900,025 Not available NTIS

Laser Cooling. PB89-179147 901,518 Not available NTIS

aser-Cooling and Electromagnetic Trapping of Neutral PB89-176440 901,511 Not available NTIS

Laser Cooling to the Zero-Point Energy of Motion. PB90-128091 901,581 Not available NTIS

Laser Excited Fluorescence Studies of Black Liquor. PB89-176416 900,243 Not available Not available NTIS

Laser Induced Damage in Optical Materials: 1987. PB89-221162 901,364 PC A99/MF A01

Laser Induced Fluorescence for Measurement of Lignin Concentrations in Pulping Liquors.
PB89-172530
901,184
Not available NTIS

Laser-Induced Fluorescence Study of Product Rotational State Distributions in the Charge Transfer Reaction: $Ar(1+)((\sup 2 P)(\sup 3/2)) + N2 -> Ar + N2(1+)(X)$ at 0.28 and 0.40 eV. PB89-139823 900.420 Not available NTIS

Laser Induced Vaporization Time Resolved Mass Spectrometry of Refractories.
PB90-136904 900,540 Not available NTIS 900.540 Not available NTIS

Laser Microprobe Mass Spectrometry: Description and Selected Applications. PB89-201628 900,210 Not available NTIS

Laser-Noise-Induced Population Fluctuations in Two- and Three-Level Systems.
PB89-171235 901,342 Not available NTIS

Laser Probing of Ion Velocity Distributions in Drift Fields: Parallel and Perpendicular Temperatures and Mobility for Ba(1+) in He. PB89-171243 900,352 Not available NTIS

Laser Probing of Product-State Distributions in Thermal-Energy Ion-Molecule Reactions. PB89-171250 900,353 Not available NTIS

Laser Probing of the Dynamics of Ga Interactions on Si(100).
PB89-186928 901,422 Not available NTIS

Laser-Produced Spectra and QED (Quantum Electrodynamic) Effects for Fe-, Co-, Cu-, and Zn-Like lons of Au, Pb, Bi, Th, and U. PB98-176010 901,510 Not available NTIS

Laser Spectroscopy of Inelastic Collisions. PB89-185946 900,405 Not available NTIS

ate Stages of Close Binary Systems-Clues to Common Envelope Evolution. PB89-149207 900,016 Not available NTIS

Latent Heats of Supercritical Fluid Mixtures. PB89-174908 900,242 Not available NTIS

Length Scale Measurement Procedures at the National Bureau of Standards. PB89-209266 900,895 PC A04/MF A01

Light Scattering from Simulated Smoke Agglomerates. PB89-157234 900,588 Not available NTIS

Lightning and Surge Protection of Photovoltaic Installations. Two Case Histories: Vulcano and Kythnos. PB89-229058 900,851 PC A05/MF A01

Line Identifications and Radiative-Branching Ratios of Mag-netlc Dipole Lines in Si-like Ni, Cu, Zn, Ge, and Se. PB89-234165 901,558 Not available NTIS

Linear-Elastic Fracture of High-Nitrogen Austenitic Stainless Steels at Liquid Helium Temperature. 901.108 Not available NTIS PB90-117823

iposome-Enhanced Flow Injection Immunoanalysis. B89-146757 900,036 Not available NTIS PB89-146757

iposome Technology in Biomineralization Research. PB90-128117 901,230 Not available NTIS

Liquid, Crystalline and Glassy States of Binary Charged Colloidal Suspensions. PB89-202501 901.436 Not available NTIS

Liquid-Supported Torsion Balance: An Updated Status Report on Its Potential for Tunnel Detection. PB89-212062 901,542 Not available NTIS

Loading Rate Effects on Discontinuous Deformation in Load-Control Tensile Tests. PB89-171896 901,097 Not available NTIS

Local Brittle Zones in Steel Weldments: An Assessment of Test Methods. PB89-149082 901,092 Not available NTIS

Local Order In a Dense Liquid. PB89-157226 900,313 Not available NTIS

Logistic Function Data Analysis Program: LOGIT. PB89-189351 900,418 PC A05/MF A01

Long-Range Incommensurate Magnetic Order in Dy-Y Multilayers. PB89-179642

901,411 Not available NTIS Long-Term Stability of the Elemental Composition in Biological Materials.

PB89-156939 900,181 Not available NTIS

Low Field Determination of the Proton Gyromagnetic Ratio in Water. 901.555 Not available NTIS PB89-230411

Low Noise Frequency Synthesis. PB89-174056 96 900,716 Not available NTIS

Low Pressure, Automated, Sample Packing Unit for Diffuse Reflectance Infrared Spectrometry.
PB90-135922 900,235 Not available NTIS

Low-Q Neutron Diffraction from Supercooled D-Glycerol, PB89-228001 900,468 Not available NTIS

Low Range Flowmeters for Use with Vacuum and Leak 900,374 Not available NTIS PB89-175707

ow Temperature Mechanical Property Measurements of Silica Aerogel Foam. PB90-128638 901,061 Not available NTIS

Low-Temperature Phase and Magnetic Interactions in fcc Fe-Cr-Ni Alloys.
PB90-136771 901,113 Not available NTIS

Low-Temperature Thermal Conductivity of Composites: Alumina Fiber/Epoxy and Alumina Fiber/PEEK. PB89-218358 901,078 PC A04/MF A01

Luminescence Standards for Macro- and Microspectrofluorometry. PB89-176598 900.383 Not available NTIS

Machine-Learning Classification Approach for IC Manufacturing Control Based on Test Structure Measurements. PB89-228530 900,790 Not available NTIS

Magnetic Behavior of Compositionally Modulated Ni-Cu Thin Films. PB90-118084 901,163 Not available NTIS

Magnetic Correlations in an Amorphous Gd-Al Spin Glass. PB89-201693 901,148 Not available NTIS

Magnetic Dipole Excitation of a Long Conductor in a Lossy Medium. PB89-171664 900,742 Not available NTIS

Magnetic Evaluation of Cu-Mn Matrix Material for Fine-Filament Nb-Ti Superconductors. PB89-200489 901,425 Not available NTIS

Magnetic Field Dependence of the Superconductivity in Bi-Sr-Ca-Cu-O Superconductors. PB89-146815 901,385 Not available NTIS

Magnetic Order of Pr in PrBa2Cu3O7. PB90-123803 901,471 Not available NTIS PB90-123803

Magnetic Properties of Surfaces Investigated by Spin Polarized Electron Beams. PB89-176564 901,405 Not available NTIS

Magnetic Resonance of (160)Tb Oriented in a Terbium Single Crystal at Low Temperatures. PB89-179204 901,519 Not available NTIS

Magnetic Structure of Cubic Tb0.3Y0.7Ag. PB90-117789 901,466 Not available NTIS

Magnetic Structure of Y0.97Er0.03.

Magnetization and Magnetic Aftereffect In Textured Ni/Cu Compositionally-Modulated Alloys. PB90-123431 901,165 Not available NTIS

PR89-202675

901,439 Not available NTIS

PB90-123431 901,165 Not available NTIS

Magnetostatic Measurements for Mine Detection.

PB89-148365 900,685 PC A03/MF A01
Marked Differences in the 3p Photoabsorption between the

Marked Differences in the 3p Photoabsorption between the Cr and Mn(1+) Isoelectronic Pair: Reasons for the Unique Structure Observed in Cr. PB90-117581 901,562 Not available NTIS

Material Handling Workstation Implementation. PB89-159644 900,988 PC A04/MF A01

Material Handling Workstation: Operator Manual. PB89-159651 900,989 PC A03/MF A01

PB89-159651 900,989 PC A03/MF A

Material Handling Workstation, Recommended Technical Specifications for Procurement of Commercially Available Equipment. PB99-162564 900,998 PC A03/MF A01

Materials Failure Prevention at the National Bureau of Standards.
PB89-212237 901,190 Not available NTIS

Mathematical Software: PLOD. Plotted Solutions of Differential Equations.
PB89-147425 901,194 Not available NTIS

Maximum Entropy Distribution Consistent with Observed Structure Amplitudes.
PB99-186258 901,417 Not available NTIS

Mean Density Approximation and Hard Sphere Expansion Theory: A Review.
PB89-228019 901,546 Not available NTIS

PB89-228019 901,546 Not available NTIS

Measured Air Infiltration and Ventilation Rates in Eight

Measured Air Infiltration and Ventilation Rates in Eight Large Office Buildings.
PB90-128158 900,090 Not available NTIS

Measurement of Adapter Loss, Mismatch, and Efficiency Using the Dual Six-Port. PB89-147839 901,316 PC A10/MF A01

Measurement of Applied J-Integral Produced by Residual Stress.
PB90-117631 900,163 Not available NTIS

Measurement of Electrical Breakdown in Liquids. PB89-212229 900,447 Not available NTIS

Measurement of Electrical Parameters Near AC and DC

Power Lines. PB89-173439 900,745 Not available NTIS

Measurement of Integrated Tuning Elements for SIS Mixers with a Fourier Transform Spectrometer. PB89-157051 900,706 Not available NTIS

Measurement of Partial Discharges in Hexane Under DC Voltage.
PB99-173421 900.833 Not available NTIS

PB89-173421 900,833 Not available NTIS

Measurement of Regenerator Ineffectiveness at Low Tem-

peratures.
PB89-173884

901,006 Not available NTIS

Measurement of Shear Rate on an Agitator in a Fermenta-

PB89-186720 901,009 Not available NTIS

Measurement of the NBS (National Bureau of Standards) Electrical Watt in SI Units. PB89-230429 900,821 Not available NTIS

Measurement of the Torque and Normal Force in Torsion in the Study of the Thermoviscoelastic Properties of Polymer Glasses.

Glasses. 900,554 Not available NTIS

Measurement Procedures for Electromagnetic Compatibility Assessment of Electroexplosive Devices. PB89-146914 901,314 Not available NTIS

Measurement Quality Assurance. PB89-147508 901,298 Not available NTIS

Measurement Standards for Defense Technology. PB89-150965 901,270 Not available NTIS

Measurements of Coefficients of Discharge for Concentric Flange-Tapped Square-Edged Orifice Meters in Water Over the Reynolds Number Range 600 to 2,700,000. PB89-235147 PC A23/MF A01

Measurements of Molar Heat Capacity at Constant Volume: $Cv_rm(xCH4+(1-x)C2H6'T=100 \text{ to } 320 \text{ K, p} < \text{ or } = 35 \text{ MPa}).$ P890-117896 900.844 Not available NTIS

Measurements of the Nonresonant Third-Order Susceptibili-

ty. PB89-179212 *901,357* Not available NTIS

Measurements of the (235)U (n,f) Standard Cross Section at the National Bureau of Standards.
PB89-176556 901,305 Not available NTIS

Measurements of Tribological Behavior of Advanced Materials: Summary of U.S. Results on VAMAS (Versailles Advanced Materials and Standards) Round-Robin No. 2. PB90-130295 901,003 PC A05/MF A01

Measures of Effective Ergodic Convergence in Liquids. PB90-118092 900,518 Not available NTIS

Measuring Fast-Rise Impulses by Use of E-Dot Sensors. PB89-173413 900,744 Not available NTIS

Measuring In-Plane Elastic Moduli of Composites with Arrays of Phase-Insensitive Ultrasound Receivers. PB90-136672 900,970 Not available NTIS

Measuring the Root-Mean-Square Value of a Finite Record Length Periodic Waveform. PB90-163924 901,588

(Order as PB90-163874, PC A04)

Mechanical Property Enhancement in Ceramic Matrix Composites.
PB89-189138 901,076 PC A05/MF A01

Mechanism and Rate of Hydrogen Atom Attack on Toluene at High Temperatures.
PB89-179758 900.398 Not available NTIS

Mechanism for Shear Band Formation in the High Strain Rate Torsion Test.
PB89-215370 900,901 PC A03/MF A01

Mechanism of Hydrolysis of Octacalcium Phosphate. PB89-201503 901,254 Not available NTIS

Mechanisms of Free Radical Chemistry and Biochemistry of Benzene.
PB90-117714
900,502 Not available NTIS

Merit Functions and Nonlinear Programming. PB90-123944 901,208 Not available NTIS

Mesh Monitor Casting of Ni-Cr Alloys: Element Effects. PB89-176077 900,040 Not available NTIS

Metallographic Evidence for the Nucleation of Subsurface Microcracks during Unlubricated Sliding of Metals. PB89-147391 901,001 Not available NTIS

Metallurgical Evaluation of 17-4 PH Stainless Steel Castings.
PB89-193262 901,105 PC A03/MF A01

Metastable Phase Production and Transformation in Al-Ge Alloy Films by Rapid Crystallization and Annealing Treatments. 901,129 Not available NTIS

Method for Evaluating Air Kerma and Directional Dose Equivalent for Currently Available Multi-Element Dosemeters in Radiation Protection Dosimetry, PB90-117532 901,301 Not available NTIS

Method for Fitting and Smoothing Digital Data. PB90-128794 900,630 Not available NTIS

Method for Improving Equations of State Near the Critical Point.

PB89-228027

901.547 Not available NTIS

Method for Measuring the Effectiveness of Gaseous Contaminant Removal Filters.
PB89-235899 900,858 PC A04/MF A01

Method for Measuring the Stochastic Properties of Corona and Partial-Discharge Pulses.
PB90-128745 900,829 Not available NTIS

Method of and Apparatus for Real-Time Crystallographic Axis Orientation Determination.

PATENT-4 747 684

901,383

Not available NTIS

Method to Measure the Tensile Bond Strength between Two Weakly-Cemented Sand Grains.
PB89-166110 901,483 PC A03/MF A01

Methodology for Electron Stimulated Desorption Ion Angular Distributions of Negative Ions.
PB89-231310 900,486 Not available NTIS

Methods for the Production of Particle Standards.
PB89-201636 901,047 Not available NTIS

Methyl Radical Concentrations and Production Rates in a Laminar Methane/Air Diffusion Flame. PB89-171912 900,591 Not available NTIS

Metrology for Electromagnetic Technology: A Bibliography of NBS (National Bureau of Standards) Publications. PB89-147847 900,871 PC A04/MF A01

Micro-Analysis of Mineral Saturation Within Enamel during Lactic Acid Demineralization.
PB89-186373 901,253 Not available NTIS

Micro-Raman Characterization of Atherosclerotic and Bioprosthetic Calcification. PB89-149223 901,234 Not available NTIS

Microarcsecond Optical Astrometry: An Instrument and Its Astrophysical Applications. PB89-171268 900,013 Not available NTIS

Microbiological Materials Processing.
PB90-123712 901,261 Not available NTIS

Microbiological Metal Transformations: Biotechnological Applications and Potential.

PB89-175947

901,284

Not available NTIS

Microphase Separation in Blockcopolymer/Homopolymer. PB89-176069 900,561 Not available NTIS

Microporous Furned-Silica Insulation as a Standard Reference Material of Thermal Resistance at High Temperature. PB90-130311 900,153 PC A04/MF A01

Microporous Fumed-Silica Insulation Board as a Candidate Standard Reference Material of Thermal Resistance. PB89-148373 901,018 PC A03/MF A01

Microstructural Variations in Rapidly Solidified Alloys. PB90-123621 901,170 Not available NTIS

Microwave and Infrared Electric-Resonance Optothermal Spectroscopy of HF-HCl and HCl-HF.
PB89-234215 900,489 Not available NTIS

Microwave Digestion of Biological Samples: Selenium Analysis by Electrothermal Atomic Absorption Spectrometry. PB89-229116 900,217 Not available NTIS

Microwave Electric-Resonance Optothermal Spectroscopy of (H2O)2.
PB90-128141 900.531 Not available NTIS

Microwave Energy for Acid Decomposition at Elevated Temperatures and Pressures Using Biological and Botanical Samples.

PB89-171961 *900,359* Not available NTIS

Microwave Measurements of the Thermal Expansion of a Spherical Cavity.
PB89-147458 900,291 Not available NTIS

Microwave Power Standards.

PB89-149272 *900,687* Not available NTIS

Microwave Spectral Tables. 3. Hydrocarbons, CH to C10H10. PB90-126269 900,530 Not available NTIS

Microwave Spectrum and Molecular Structure of the Ethylene-Ozone van der Waals Complex.
PB89-201735 900,424 Not available NTIS

Microwave Spectrum and (14)N Quadrupole Coupling Constants of Carbazole.
PB89-157333 900,319 Not available NTIS

Microwave Spectrum of Methyl Amine: Assignment and Analysis of the First Torsional State.
PB90-117839 900,509 Not available NTIS

Microwave Spectrum, Structure, and Electric Dipole Moment of Ar-Ch3OH.
PB90-117847 900,510 Not available NTIS

Microwave Spectrum, Structure, and Electric Dipole Moment of the Ar-Formamide van der Waals Complex. PB89-157325 900,318 Not available NTIS

Migration of Liquid Film and Grain Boundary in Mo-Ni Induced by W Diffusion.
PB89-157614 901, 128 Not available NTIS

Millimeter- and Submillimeter-Wave Surveys of Orion A Emission Lines in the Ranges 200.7-202.3, 203.7-205.3, and 330-360 GHz.

PB90-123787 900,029 Not available NTIS
Millisecond Pulsar Rivals Best Atomic Clock Stability.
PB89-185722 900,629 Not available NTIS

Minimax Approach to Combining Means, with Practical Examples.
PB89-171847
901,211
Not available NTIS

Mining Automation Real-Time Control System Architecture Standard Reference Model (MASREM).
PB89-221154 901.286 PC A04/MF A01

PB89-221154 901,286 PC A04/MF A01

Mixing Motions Produced by Pipe Elbows.
PB89-161871 901,326 PC A03/MF A01

MM Wave Quasioptical SIS Mixers. PB89-214738 901,446 Not available NTIS

Mn-Mn Exchange Constants in Zinc-Manganese Chalco-

genides.
PB90-136706 901,478 Not available NTIS
Mobile Sources of Atmospheric Polycyclic Aromatic Hydro-

Mobile Sources of Atmospheric Polycyclic Aromatic Hydrocarbons: A Roadway Tunnel Study.
PB90-123571 900,859 Not available NTIS

Mode-Stirred Chamber for Measuring Shielding Effectiveness of Cables and Connectors: An Assessment of MIL-STD-1344A Method 3008.

PB89-149264

900,737

Not available NTIS

Model for Particle Size and Phase Distributions in Ground Cement Clinker.
PB90-136847 901,062 Not available NTIS

Modeling Chemical Reaction Systems on an IBM PC. PB89-171920 900,358 Not available NTIS

Modeling Dynamic Surfaces with Octrees PB90-112335 901,206 901,206 PC A03/MF A01

Modeling of the Bremsstrahlung Radiation Produced in Pure Element Targets by 10-40 keV Electrons. 901,531 Not available NTIS PB89-201644

Modelling of Impurity Effects in Pure Fluids and Fluid Mix-PB89-176739 900.245 Not available NTIS

Modular Process Planning System Architecture PR90-128596 900.966 Not available NTIS

Molecular Dynamics Investigation of Expanded Water at Elevated Temperatures. PB89-174957 900,370 Not available NTIS

Molecular Dynamics Study of a Dipolar Fluid between Charged Plate PB89-147441 900,290 Not available NTIS

Molecular Dynamics Study of a Dipolar Fluid between Charged Plates. 2. PB89-157218 900,312 Not available NTIS

lolybdenum Effect on Volume in Fe-Cr-Ni Alloys. B89-157796 *901,095* Not available NTIS PB89-157796

Monitoring and Predicting Parameters in Microwave Disso-PB90-118183 900,690 Not available NTIS

Monte Carlo Calculated Response of the Dual Thin Scintillation Detector in the Sum Coincidence Mode. PB89-176549 901,299 Not available NTIS

Monte Carlo Simulation of Domain Growth in the Kinetic Ising Model on the Connection Machine.

PB90-136797 901,587 Not available NTIS

Morphological Partitioning of Ethyl Branches in Polyethylene by (13)C NMR.
PB89-176051 900,560 Not available NTIS

Mossbauer Hyperfine Fields in RBa2(Cu0.97Fe0.03)3 O(7-

x)(R= Y,Pr,Er). PB89-201206 901,429 Not available NTIS Mossbauer Imaging.

Mossbauer Imaging: Experimental Results

901,242 Not available NTIS

PB90-123415 900,922 Not available NTIS Mossbauer Spectroscopy.

PB89-211932 901,189 Not available NTIS

Moydite, (Y, REE) (B(OH)4)(CO3), a New Mineral Species from the Evans-Lou Pegmatite, Quebec. PB89-157747 900,186 Not available NTIS

ulticritical Phase Relations in Minerals PB89-150882 901,278 Not available NTIS

Multiphoton Ionization Spectroscopy and Vibrational Analysis of a 3p Rydberg State of the Hydroxymethyl Radical. PB89-146666 900,279 Not available NTIS

Multiple Actuator Hydraulic System and Rotary Control 900,995 Not available NTIS PATENT-4 838 145

Multiple Scattering in the X-ray-Absorption Near-Edge Structure of Tetrahedral Ge Gases. 900,283 Not available NTIS PB89-146922

Multiple Scattering in the X-ray Absorption Near Edge Structure of Tetrahedral Germanium Gas 900,474 Not available NTIS PB89-228480

NaCI-H2O Coexistence Curve Near the Critical Tempera-PB89-202519 900,436 Not available NTIS

Narrow-Angle Laser Scanning Microscope System for Linewidth Measurement on Wafers. 900.782 PC A06/MF A01 PB89-189344

NASA/NBS (National Aeronautics and Space Administra-tion/National Bureau of Standards) Standard Reference Model for Telerobot Control System Architecture Model for (NASREM).

PB89-193940 901.589 PC A05/MF A01 National Bureau of Standards Message Authentication

Code (MAC) Validation System.
PB89-231021 900,671 Not available NTIS

National Engineering Laboratory's 1989 Report to the National Research Council's Board on Assessment of NIST (National Institute of Standards and Technology) Programs PBB9-189294 900,004 PC A03/MF A01

National Institute of Standards and Technology (NIST) In-Poster on Power Quality. 900,754 PC A02

Nb3Sn Critical-Current Measurements Using Tubular Fiber-glass-Epoxy Mandrels.

901,527 Not available NTIS PB89-200497

NBS AMRF (National Bureau of Standards) (Automated Manufacturing Resea System Architecture. PB89-193882 Research Facility) Process Planning System: 900.956 PC A06/MF A01

NBS/BAM (National Bureau of Standards/Bundesanstalt fur Materialprufung) 1986 Symposium on Advanced Ceram-901.055 PC A08/MF A01

NBS (National Bureau of Standards) Activities in Biological Reference Materials. PB89-157770 901,219 Not available NTIS

NBS (National Bureau of Standards)-Boulder Gas Flow Faerformance. PB89-186787 900.889 Not available NTIS

NBS (National Bureau of Standards) Calibration Service Providing Time and Frequency at a Remote Site by Weighting and Smoothing of GPS (Global Positioning System)
Common View Data. PB89-212211 900.631 Not available NTIS

NBS (National Bureau of Standards) Calibration Services: A Status Report. PB89-173934 900,878 Not available NTIS

NBS (National Bureau of Standards) Decay-Scheme Invesns of (82)Sr-(82)Rb. 901,498 Not available NTIS

NBS (National Bureau of Standards) Determination of the Fine-Structure Constant, and of the Quantized Hall Resistance and Josephson Frequency-to-Voltage Quotient in SI 901,556 Not available NTIS

NBS (National Bureau of Standards) Free Electron Laser Facility. PB89-176515 901.353 Not available NTIS

NBS' (National Bureau of Standards) Industry; Government Consortium Research Program on Flowmeter Installation Effects: Summary Report with Emphasis on Research January-July 1988.
PB89-189120 901,010 PC A04/MF A01

NBS' (National Bureau of Standards) Industry; Government Consortium Research Program on Flowmeter Installation Effects: Summary Report with Emphasis on Research July-PB90-111220 900.910 PC A05/MF A01

NBS (National Bureau of Standards) Laser Power and Energy Measurements. PB89-171680 901,346 Not available NTIS

NBS (National Bureau of Standards) Life-Cycle Cost (NBSLCC) Program (for Microcomputers).
PB89-151211 900,849 CP D99

NBS (National Bureau of Standards) Measurement Services: Calibration of Gamma-Ray-Emitting Brachytherapy Sources PB89-193858 901,243 PC A04/MF A01

NBS (National Bureau of Standards) Ohm: Past-Present-PB89-149066 900,802 Not available NTIS

NBS (National Bureau of Standards) Orifice-Flow Primary High Vacuum Standard. PB89-175699 900 880 Not available NTIS

NBS (National Bureau of Standards) Radon-in-Water Standard Generator. PB89-171888 901,295 Not available NTIS

NBS (National Bureau of Standards) Reactor: Summary of Activities July 1987 through June 1988.
PB89-168017 901,304 PC A11/MF A01

NBS (National Bureau of Standards) Scale of Spectral Radiance. PB89-201685

901.532 Not available NTIS NBS (National Bureau of Standards) Standards for Optical Power Meter Calibration. PB89-176200

900,726 Not available NTIS

901,570 Not available NTIS

NBS/NRL (National Bureau of Standards/Naval Research Laboratory) Free Electron Laser Facility.
PB89-175749
901,351
Not available NTIS

NDE (Nondestructive Evaluation) Publications, 1985. PB89-229025 900,984 PC A03/MF A01

ear-Field Detection of Buried Dielectric Objects. 390-128208 900,713 Not available NTIS PB90-128208

Near-Threshold X-ray Fluorescence Spectroscopy of Mole-PB89-176523 900.382 Not available NTIS

Necking Phenomena and Cold Drawing. PB89-201495 900,975 Not available NTIS Neonlike Ar and Cl 3p-3s Emission from a theta-pinch

Plasma. PB90-123746

Neural Network Approach for Classifying Test Structure Re-PB89-212187

900,788 Not available NTIS

Neutron Activation Analysis of the NIST (National Institute of Standards and Technology) Bovine Serum Standard Reference Material Using Chemical Separations. PB89-156921 900,180 Not available NTIS

Neutron Diffraction Determination of Full Structures of Anhydrous Li-X and Li-Y Zeolites.
PB90-118001 900,516 Not available NTIS

Neutron Diffraction Study of the Wurtzite-Structure Dilute Magnetic Semiconductor Zn0.45Mn0.55Se. PB90-136714 901,479 Not available NTIS

Neutron Powder Diffraction Structure and Electrical Properties of the Defect Pyrochlores Pb1.5M2O6.5 (M = Nb, Ta). 900,363 Not available NTIS

Neutron Scattering and Its Effect on Reaction Rates in Neutron Absorption Experiments. PB90-123738 901 569 Not available NTIS

Neutron Scattering Study of the Spin Ordering in Amorphous Tb45Fe55 and Tb25Fe75.
PB89-201701 901,149 Not available NTIS

Neutron Study of the Crystal Structure and Vacancy Distribution in the Superconductor Ba2Y Cu3 O(sub g-delta). 901,468 Not available NTIS PB90-123480

Neutron Vibrational Spectroscopy of Disordered Metal Hydrogen Systems. PB89-157499 900,324 Not available NTIS

New Cavity Configuration for Cesium Beam Primary Frequency Standards. PB89-171649 900,714 Not available NTIS

New Directions in Bioinformatics. PB89-175269

901,245 (Order as PB89-175194, PC A06)

New FIR Laser Lines and Frequency Measurements for Optically Pumped CD3OH. PB89-175731 901,350 Not available NTIS

New International Skeleton Tables for the Thermodynamic Properties of Ordinary Water Substance.

900,270 Not available NTIS PB89-145130

New International Temperature Scale of 1990 (ITS-90). PB89-202550 901,238 Not available NTIS

New Internationally Adopted Reference Standards of Voltage and Resistance. PB89-184097 900,808

(Order as PB89-184089, PC A04)

New Photolytic Source of Dioxymethylenes: Criegee Intermediates Without Ozonolysis. 900.304 Not available NTIS PB89-156731

New Realization of the Ohm and Farad Using the NBS (National Bureau of Standards) Calculable Capacitor 901,557 Not available NTIS

New Standard Test Method for Eddy Current Probes. PB89-187587 900,981 Not available NTIS

NIST Automated Computer Time Service. PB90-213711

(Order as PB90-213687, PC A04)

900.676

NIST (National Institute of Standards and Technology) Automated Coaxial Microwave Power Standard. PB89-176192 900,807 Not available NTIS

NIST (National Institute of Standards and Technology) Calibration Services, Users Guide: Fee Schedule.
PB90-127820 900,913 PC A04/MF A01

NIST (National Institute of Standards and Technology) Calibration Services Users Guide. 1989 Edition. PB89-200216 900,926 PC A10/MF A01

NIST (National Institute of Standards and Technology)
Measurement Services: AC-DC Difference Calibrations.
PB89-222616 900,818 PC A14/MF A01

NIST (National Institute of Standards and Technology) Measurement Services: High Vacuum Standard and Its Use 900.891 PC A04/MF A01 PB89-193841

NIST (National Institute of Standards Measurement Services: Mass Calibrations Standards and Technology)

PB89-153894 900.874 PC A05/MF A01

NIST (National Institute of Standards and Technology) Measurement Services: The Calibration of Thermocouples and Thermocouple Materials. PB89-209340 900.897 PC A10/MF A01

NIST (National Institute of Standards and Technology) Research Reports, June 1989. PB89-235113 900,007 PC A03/MF A01

NIST (National Institute of Standards and Technology) Rearch Reports, March 1989. PB89-189310 900,005 PC A03/MF A01

NIST (National Institute of Standards and Technology)/ Sandia/ICDD Electron Diffraction Database: A Database for Phase Identification by Electron Diffraction. 901.508 P389-175210

(Order as PB89-175194, PC A06)

Nitrogen in Austenitic Stainless Steels 901,109 Not available NTIS PB90-117649

NO/NH3 Coadsorption on Pt(111): Kinetic and Dynamical Effects in Rotational Accommodation PB89-201123 900,423 Not available NTIS

Noise in DC SQUIDS with Nb/Al-Oxide/Nb Josephson 900,763 Not available NTIS PB89-201032

Non-Aqueous Dental Cements Based on Dimer and Trimer PATENT-4 832 745 900,033 Not available NTIS

Non-Boltzmann Rotational and Inverted Spin-Orbit State Distributions for Laser-Induced Desorption of NO from Pt(111). PB89-157952 900,340 Not available NTIS

Non-Equilibrium Theories of Electrolyte Solutions.

PRR0_174940 . 900,369 Not available NTIS

Non-Geometric Dependencies of Gas-Operated Piston Gage Effective Areas. PB89-231112 900.905 Not available NTIS

Nonadiabatic Theory of Fine-Structure Branching Cross-Sections for Sodium-Helium, Sodium-Neon, and Sodium-Argon Optical Collisions. PB9-202162 900,433 Not available NTIS

Nonlinear Effect of an Oscillating Electric Field on Membrane Proteins. PB90-123407 901,249 Not available NTIS

Note on Calculating Flows Through Vertical Vents in Zone Fire Models Under Conditions of Arbitrary Cross-Vent Pressure Difference. 900.147 Not available NTIS

Note on the Capacitance Matrix Algorithm, Substructuring, and Mixed or Neumann Boundary Conditions. PB89-177034 901,199 Not available NTIS

Notion of Granularity. PB89-147003

900.915 Not available NTIS

Novel Flow Process for Metal and Ore Solubilization by Aqueous Methyl Iodide. PB89-202113 901,285 Not available NTIS

Novel Process for the Preparation of Fiber-Reinforced Ceramic-Matrix Composites. 901.074 Not available NTIS PR89-179733

Nucleation and Growth of Aperiodic Crystals in Aluminum

PB89-186324 901,145 Not available NTIS

Numeric Databases for Chemical Analysis. 900.194 PB89-175236 (Order as PB89-175194, PC A06)

Numeric Databases in Chemical Thermodynamics at the National Institute of Standards and Technology. 900.371 PB89-175228

(Order as PB89-175194, PC A06)

Numerical Analysis for the Small-Signal Response of the MOS (Metal Oxide Semiconductors) Capacitor.
PB89-186837 900,781 Not available NTIS

Numerical Aperture of Multimode Fibers by Several Methods: Resolving Differences. PB90-117482 900,757 Not available NTIS

Numerical Computation of Particle Trajectories: A Model

PB89-158117 901,324 Not available NTIS

Numerical Evaluation of Certain Multivariate Normal Inte-PB89-158166 901,195 Not available NTIS

Numerical Simulation of Morphological Development during Ostwald Ripening. PB89-201990 901,152 Not available NTIS

Numerical Simulations of Neutron Effects on Bipolar Tran-PB90-123589 900,797 Not available NTIS

NVLAP (National Voluntary Laboratory Accreditation Program) Assessment and Evaluation Manual.
PB89-228324 900,903 PC A03/MF A01 900.903 PC A03/MF A01

NVLAP (National Voluntary Laboratory Accreditation Program) Directory of Accredited Laboratories.
PB89-189278 900,890 PC A04/MF A01

NVLAP (National Voluntary Laboratory Accreditation Program) Program Handbook Construction Testing Services. Requirements for Accreditation. PB90-112327 900,169 PC A03/MF A01

Object-Oriented Model for ASN.1 (Abstract Syntax Notation One). PB89-177117 900.649 Not available NTIS

Object-Oriented Model for Estelle PB89-211916 900 900,653 Not available NTIS

Object-Oriented Model for Estelle and Its Smalltalk Implementation. PB89-196190 900,623 PC A05/MF A01

Observation of Translationally Hot, Rotationally Cold NO Molecules Produced by 193-nm Laser Vaporization of Multi-layer NO Films.
P889-234264 900,491 Not available NTIS

Observations of Gas Species and Mode of Operation Effects on Effective Areas of Gas-Operated Piston Gages.
PB89-231120 900,906 Not available NTIS

Observations on Crystal Defects Associated with Diffusion Induced Grain Boundary Migration in Cu-Zn. PB89-157606 901,127 Not available NTIS

Occurrence of Long-Range Helical Spin Ordering in Dy-Y Multilayers. PB89-179634 901,410 Not available NTIS

Octanol-Water Partition Coefficients of Simple Organic Compounds. PB90-126244 900,528 Not available NTIS

Off-Lattice Simulation of Polymer Chain Dynamics. PB90-117524 900,576 Not available NTIS

Offset Criterion for Determining Superconductor Critical Current. PB90-128133 901,474 Not available NTIS

Oligomers with Pendant Isocyanate Groups as Adhesives for Dentin and Other Tissues. PB89-179253 900.042 Not available NTIS

Oligomers with Pendant Isocyanate Groups as Tissue Adhesives, 1. Synthesis and Characterization PB89-202212 900,055 Not available NTIS

Oligomers with Pendant Isocvanate Groups as Tissue Adhesives. 2. Adhesion to Bone and Other Tissues.
PB89-231245 900,056 Not available NTIS

On-Line Arc Welding: Data Acquisition and Analysis Using a High Level Scientific Language.
PB90-117391 900,972 Not available NTIS

On-Line Concurrent Simulation in Production Scheduling. PB89-172605 900,948 PC A03/MF A01

One-Electron Transfer Reactions of the Couple SO2/ SO2(1-) in Aqueous Solutions. Pulse Radiolytic and Cyclic Voltammetric Studies. PB9-176093 900,376 Not available NTIS

One Is Not Enough: Intra-Cavity Spectroscopy with Multi-Mode Lasers. 900,402 Not available NTIS PR89-185888

One-Photon Resonant Two-Photon Excitation of Rydberg Series Close to Threshold. PB89-171276 901,343 Not available NTIS

Ongoing Implementation Agreements for Open Systems Interconnection Protocols: Continuing Agreements. PB89-166086 900,610 PC A09/MF A01

Operations Manual for the Automatic Operation of the Vertical Workstation. 900,973 PC A03/MF A01 PB89-183214

otical Fiber Sensors for Electromagnetic Quantities. 189-173967 900,725 Not available NTIS Optical Fiber PB89-173967

Optical Fiber Sensors for the Measurement of Electromagnetic Quantities. PB89-176671 900,748 Not available NTIS

Optical Nondestructive Evaluation at the National Bureau of Standards. PB89-146740 900.976 Not available NTIS

Optical Novelty Filters. PB89-228084 901,366 Not available NTIS

Optical Power Measurements at the National Institute of Standards and Technology. 900.918 Not available NTIS PB89-187579

Optical Rotation. PB89-149256 900,294 Not available NTIS

Optical Roughness Measurements for Industrial Surfaces. PB89-176655 900,979 Not available NTIS

Optical Sensors for Robot Performance Testing and Cali-PB89-157358 900.987 Not available NTIS

Optically Driven Surface Reactions: Evidence for the Role of Hot Electrons.

PB89-157937 900,338 Not available NTIS

Optically Linked Electric and Magnetic Field Sensor for Poynting Vector Measurements in the Near Fields of Radiating Sources.
PB89-187595 900.712 Not available NTIC

Optimum Location of Flow Conditioners in a 4-Inch Orifice PB90-111675 900,911 PC A05/MF A01

Origins of ASHRAE (American Society of Heating, Refrigerating and Air-Conditioning Engineers) Window U-Value Data and Revisions for the 1989 Handbook of Fundamentals. PB89-231005 900,083 Not available NTIS

Ostwald Ripening in a System with a High Volume Fraction of Coarsening Phase. PB89-157598 901,126 Not available NTIS

Outline of a Practical Method of Assessing Smoke Hazard. PB89-211858 900,078 Not available NTIS

Overview of ETRAN Monte Carlo Methods 901,576 Not available NTIS

Oxygen Chemisorption on Cr(110): 1. Dissociative Adsorp-PB89-202980 900.441 Not available NTIS

Oxygen Chemisorption on Cr(110): 2. Evidence for Molecu-PB89-202998 900.442 Not available NTIS

Oxygen Isotope Effect in the Superconducting Bi-Sr-Ca-Cu-PB89-157044 901,025 Not available NTIS

Oxygen Partial-Density-of-States Change in the YBa2Cu3Ox Compounds for x(Approx.)6,6.5,7 Measured by

Soft X-ray Emission. PB89-186274 901.419 Not available NTIS Ozonolysis of Ethylene. Microwave Spectrum, Molecular Structure, and Dipole Moment of Ethylene Primary Ozonide

(1,2,3-Trioxolane). PB89-157440 900,323 Not available NTIS

Pahasapaite, a Beryllophosphate Zeolite Related to Synthetic Zeolite Rho, from the Tip Top Pegmatite of South PB89-186431

901,288 Not available NTIS Parser That Converts a Boundary Representation into a Features Representation. PB89-160634

900,944 PC A03/MF A01 Part Load, Seasonal Efficiency Test Procedure Evaluation

of Furnace Cycle Controllers. PB89-212146 900,848 Not available NTIS Pathways for Microstructural Development in TiAl. PB90-123779 901,173 Not available NTIS

Pattern Recognition Approach in X-ray Fluorescence Analy-

PB90-128786 900,234 Not available NTIS

Access to Ceramic Phase Diagrams. 901,053 Not available NTIS PB89-211841

CM/VCR Speech Database Exchange Format. B89-176713 900,633 Not available NTIS PB89-176713

Performance Evaluation of Radiofrequency, Microwave, and Millimeter Wave Power Meters.
PB89-193916 900,814 PC A07/MF A01

Performance Measurement of a Shared-Memory Multi-processor Using Hardware Instrumentation. PB89-173793 900,636 Not available NTIS

Performance Measurements of Infrared Imaging Systems Used to Assess Thermal Anomalies

PB89-179667 900,072 Not available NTIS Performance of a High-Energy-Resolution, Tender X-ray Synchrotron Radiation Beamline. PB90-128083 901,580 Not available NTIS

Performance of Alumina/Epoxy Thermal Isolation Straps. PB89-147078 Not available NTIS PB89-147078

Performance of He II of a Centrifugal Pump with a Jet Pump Inducer PB89-229090 901.553 Not available NTIS

Performance Standards for Microanalysis. PB89-201651 900,211 Not available NTIS

Periodic Heat Conduction in Energy Storage Cylinders with Change of Phase. PB89-175897

900.852 Not available NTIS Perpendicular Laser Cooling of a Rotating Ion Plasma in a

Penning Trap. PB89-157408 901,493 Not available NTIS

Phase Contrast Matching in Lamellar Structures Composed of Mixtures of Labeled and Unlabeled Block Copolymer for Small-Angle Neutron Scattering, PB9-157119 901,182 Not available NTIS

Phase Diagrams for High Tech Ceramics. PB89-186308 901,044 Not available NTIS

Phase Equilibria and Crystal Chemistry in the Ternary System BaO-TiO2-Nb2O5: Part 1. PB89-171797 901,033 Not available NTIS

Phase Equilibria and Crystal Chemistry in the Ternary System BaO-TiO2-Nb2O5, Part 2. New Barium Polytitanates with < 5 mole % Nb2O5.
PB99-189815 900,419 Not available NTIS

Phase Equilibrium in Two-Phase Coherent Solids. PB89-157580 900,330 Not ava

900,330 Not available NTIS Phase Relations between the Polytitanates of Barium and

the Barium Borates, Vanadates and Molybdates. PB89-171789 901,032 Not available NTIS

Photoacoustic Measurement of Differential Broadening of the Lambda Doublets in NO(X (2)Pi 1/2, v= 2-0) by Ar. PB90-117656 900,500 Not available NTIS

Photodissociation Dynamics of C2H2 at 193 nm: Vibrational Distributions of the CCH Radical and the Rotational State Distribution of the A(010) State by Time-Resolved Fourier Transform Infrared Emission. PB89-179782 900,258 Not available NTIS

Photodissociation of Methyl Iodide Clusters. PB89-171193 900,253 Not available NTIS

Photoelastic Properties of Optical Materials.
PR89-177208 901,355 Not available NTIS

Photon-Stimulated Desorption as a Measure of Surface Electronic Structure. PB89-231328 901,459 Not available NTIS

Photon-Stimulated Desorption of Fluorine from Silicon via Substrate Core Excitations.
PB90-118027 900,517 Not available NTIS

Photonic Electric Field Probe for Frequencies up to 2 GHz. PB89-176184 900,683 Not available NTIS

PR89-229207 900,732 Not available NTIS

Photospheres of Hot Stars. 3. Luminosity Effects at Spectral Type 09.5 PB89-202592 900,020 Not available NTIS

Physics of Fracture, 1987. PB89-201107

901,428 Not available NTIS

Pi-Electron Properties of Large Condensed Polyaromatic PB89-202139 900.432 Not available NTIS

Picosecond Coherent Anti-Stokes Raman Scattering (CARS) Study of Vibrational Dephasing of Carbon Disulfide and Benzene in Solution. PB89-176408 900.380 Not available NTIS

Picosecond Laser Study of the Collisionless Photodissociation of Dimethylnitramine at 266 nm.
PB89-172423 900,255 Not available NTIS

Picosecond Pulse Response from Hydrogenated Amorphous Silicon (a-Si:H) Optical Detectors on Channel Waveguides. PB89-176689 900,727 Not available NTIS

Picosecond Studies of Vibrational Energy Transfer in Molecules on Surfaces. PB89-157309 900,316 Not available NTIS

Picosecond Study of the Population Lifetime of CO(v= 1) Chemisorbed on SiO2-Supported Rhodium Particles. PB89-157317 900,317 Not available NTIS

Picosecond Vibrational Energy Transfer Studies of Surface Adsorbates. PB90-136573 900 537 Not available NTIS

Polymer Localization by Random Fixed Impurities: Gaussian PB89-176044 900,559 Not available NTIS

Polymer Phase Separation. PB89-202923 900,570 Not available NTIS

Polymeric Humidity Sensors for Industrial Process Applica-PB89-176424 900,563 Not available NTIS

Polymerization of a Novel Liquid Crystalline Diacetylene Monomer. PB89-231286 900.575 Not available NTIS

Polymers Bearing Intramolecular Photodimerizable Probes for Mass Diffusion Measurements by the Forced Rayleigh Scattering Technique: Synthesis and Characterization. PBs9-157101 901,181 Not available NTIS

Polytope Volume Computation. 901,203 PC A03/MF A01

Population Relaxation of CO(v= 1) Vibrations in Solution Phase Metal-Carbonyl Complexes.
PB89-157291 900,315 Not available NTIS

Pore Morphology Analysis Using Small Angle Neutron Scattering Techniques.

PB89-175939 901.037 Not available NTIS

Pore-Water Pressure Buildup in Clean Sands Because of Cyclic Straining. PB89-175723 900,159 Not available NTIS

Possible Quantum Hall Effect Resistance Standard. PB89-149058 900,801 Not available NTIS

Post-Occupancy Evaluation of Several U.S. Government 900.088 PC A08/MF A01

Postweld Heat Treatment Criteria for Repair Welds in 2-1/4Cr-1Mo Superheater Headers: An Experimental Study. PB89-156160 901,094 PC A04/MF A01

Potential Applications of a Sequential Construction Analyz-PB89-191670 900,105 PC A03/MF A01

Potential Errors in the Use of Optical Fiber Power Meters. PB89-176697 900,728 Not available NTIS

Power Frequency Electric and Magnetic Field Measurements: Recent History and Measurement Standards.

PB89-176630 900,835 Not available NTIS

Power MOSFET Failure Revisited. PB89-231237 900,796 Not available NTIS

Power Quality Site Surveys: Facts, Fiction, and Fallacies. PB89-171656 900,805 Not available NTIS

Precise Laser Frequency Scanning Using Frequency-Synthesized Optical Frequency Sidebands: Application to Isotope Shifts and Hyperfine Structure of Mercury.
PB90-118134 901,370 Not available NTIS

Precise Test of Quantum Jump Theory. PB89-157390 901,339 Not available NTIS

Precision and Accuracy Assessment Derived from Calibra-PB89-179162 900,886 Not available NTIS

Precision Experiments to Search for the Fifth Force. PB89-228365 901,551 Not available NTIS

Precision Weight Calibration with a Specialized Robot. PB89-173975 900,879 Not available NTIS

Preconcentration of Trace Transition Metal and Rare Earth Elements from Highly Saline Solutions. PB90-118175 900,226 Not available NTIS

Predicting Formaldehyde Concentrations in Manufactured Housing Resulting from Medium-Density Fiberboard. PB89-148134 900,854 PC A03/MF A01

Prediction of Flowmeter Installation Effects. PB89-211882 900,899 Not available NTIS PB89-211890 900.900 Not available NTIS

Prediction of Service Life of Building Materials and Compo-PB89-158000 900.112 Not available NTIS

Prediction of Service Life of Construction and Other Materi-PB89-175848 900,120 Not available NTIS

Prediction of Shear Viscosity and Non-Newtonian Behavior in the Soft-Sphere Liquid. PB89-228035 901 548 Not available NTIS

Prediction of Tensile Behavior of Strain Softened Composites by Flexural Test Methods. PB89-147045 900,585 Not available NTIS

Prediction of the Heat Release Rate of Douglas Fir. PB89-212039 901,185 Not available NTIS

Prediction of Transport Protocol Performance through Simulation. PB89-171334 900,612 Not available NTIS

Preliminary Crystal Structure of Acinetobacter glutaminasificans Glutaminase-Asparaginase PB90-123381 9 901,260 Not available NTIS

Preliminary Crystallographic Study of Recombinant Human Interleukin 1 beta. PB90-136730 901,251 Not available NTIS

Preliminary Experiments with Three Identical Ultraprecision Machine Tools.
PB89-150841 900,997 Not available NTIS

Preliminary Performance Criteria for Building Materials, Equipment and Systems Used in Detention and Correctional Facilities.
PB89-148514 900,109 PC A08/MF A01

Preliminary Stochastic Model for Service Life Prediction of a Photolytically and Thermally Degraded Polymeric Cover Plate Material. 900,556 Not available NTIS

Preparation of Accurate Multicomponent Gas Standards of Volatile Toxic Organic Compounds in the Low-Parts-per-Billion Range.

PB89-157739

900.185 Not available NTIS

Preparation of Glass Columns for Visual Demonstration of Reversed Phase Liquid Chromatography. PB89-187546 900,206 Not available NTIS

Preparation of Multistage Zone-Refined Materials for Thermochemical Standards. PB89-186795 900.203 Not available NTIS

Preparation of Standards for Gas Analysis. PB89-211940 900,215 Not available NTIS

Preparative Liquid Chromatographic Method for the Characterization of Minor Constituents of Lubricating Base Oils. PB89-175921 901,114 Not available NTIS

Pressure and Density Series Equations of State for Steam as Derived from the Haar-Gallagher-Kell Formulation.
PB89-186456 900,409 Not available NTIS

Pressure Dependence of the Cu Magnetic Order in RBa2Cu3O6+ x. PB90-123829 901,472 Not available NTIS

Pressure Fixed Points Based on the Carbon Dioxide Vapor Pressure at 273.16 K and the H2O(I) - H2O(III) - H2O(L) Triple-Point. 900,483 Not available NTIS

Probabilistic Models for Ground Snow Accumulation. PB89-186894 900,100 Not available NTIS

Problems with Interval Estimation When Data Are Adjusted via Calibration. PB89-157812 901,209 Not available NTIS

Proceedings of the Celebratory Symposium on a Decade of UV (Ultraviolet) Astronomy with the IUE Satellite, Volume 2. N89-16535/1 900,014 PC A19/MF A01

Proceedings of the Workshop on Cement Stabilization of Low-Level Radioactive Waşte. Held at Gaithersburg, Maryland on May 31-June 2, 1989.

NUREG/CP-0103 901,302 PC A10/MF A02

Control during High Pressure Atomization. 9170 901,142 Not available NTIS PB89-179170

Processing Rate Sensitivities of a Heterogeneous Multiprocessor. PB89-229017 900,641 PC A03/MF A01

Product Data Exchange Specification: First Working Draft. PB89-144794 900,940 PC A99/MF E16

Product Data Exchange: The PDES Project-Status and Ob-PB90-112426 900.938 PC A03/MF A01

Production and Spectroscopy of Molecular lons Isolated in PB90-117748 900 503 Not available NTIS

Production and Stability of S2F10 in SF6 Corona Discharges. PB89-231039 900,822 Not available NTIS

Production of 0.1-3 eV Reactive Molecules by Laser Vaporization of Condensed Molecular Films: A Potential Source for Beam-Surface Interactions. 900,254 Not available NTIS PB89-171201

Proficiency Testing for MIL-STD 462 NVLAP (National Voluntary Laboratory Accreditation Program) Laboratories, PB90-128612 901,381 Not available NTIS

Profile Inhomogeneity in Multimode Graded-Index Fibers. PB89-179816 900,749 Not available NTIS

Progress in Understanding Atomic Structure of the Icosahe-dral Phase. PB89-171359 901.400 Not available NTIS

Progress in Vacuum Standards at NBS (National Bureau of Standards) PB89-201198 900.999 Not available NTIS

Progress on Spin Detectors and Spin-Polarized Electron Scattering from Na at NIST. PB90-128299 901,583 Not available NTIS

Progress Report of the Quality in Automation Project for FY88.
PB89-193296 900,982 PC A06/MF A01

Progressive Collapse: U.S. Office Building in Moscow. PB89-175715 900,158 Not available NTIS

Promoting Technological Excellence: The Role of State and Federal Extension Activities.
PB90-120742 900,171 PC A05/MF A01

Proper Motion vs. Redshift Relation for Superluminal Radio PB89-157663 900,017 Not available NTIS

Properties of Lennard-Jones Mixtures at Various Temperatures and Energy Ratios with a Size Ratio of Two. PB89-235204 900,493 PC A19/MF A01

Properties of Steam.

Publications of the Center for Manufacturing Engineering Covering the Period January 1978-December 1988. PB90-130568 901,012 PC A07/MF A01

Publications of the National Institute of Standards and Technology, 1988 Catalog. PB89-218382 900,006 PC A15/MF A01

Pulpal and Micro-organism Responses to Two Experimental Dental Bonding Systems. PB89-202931 901,258 Not available NTIS

Pure Rotational Far Infrared Transitions of (16)O2 in Its Electronic and Vibrational Ground State.
PB89-202055
900,429
Not available NTIS

PVT Measurements on Benzene at Temperatures to 723 K. PB89-157200 900,311 Not available NTIS

PVT of Toluene at Temperatures to 673 K. PB89-157192 900,310 Not available NTIS

PVT Relationships in a Carbon Dioxide-Rich Mixture with PB89-229181 900.478 Not available NTIS

QCD Vacuum. PB89-149124 901,486 Not available NTIS

Qualitative MO Theory of Some Ring and Ladder Polymers. PB89-156723 900,303 Not available NTIS

Quality Assurance in Metals Analysis Using the Inductively Coupled Plasr PB89-202063 900,213 Not available NTIS

Quantitative Characterization of the Viscosity of a Microemulsion. PB90-123597 900.524 Not available NTIS

Quantitative Problems in Magnetic Particle Inspection. PB89-229199 900.985 Not available NTIS

Quantitative Studies of Coatings on Steel Using Reflection/ Absorption Fourier Transform Infrared Spectroscopy. PB89-212112 901,066 Not available NTIS

Quantized Hall Resistance Measurement at the NML (National Measurement Laboratory).
PB89-179675 900,778 Not available NTIS

Quantum-Defect Parametrization of Perturbative Two-Photon Ionization Cross Sections. PB89-202600 901,539 Not available NTIS

Quantum Mechanical Calculations on the Ar(1+) + N2 Charge Transfer Reaction. PB89-228092

900.470 Not available NTIS

Quasi-Constant Composition Method for Studying the Formation of Artificial Caries-Like Lesions. PB89-229249 901,259 Not available NTIS

Quasicrystals and Quasicrystal-Related Phases in the Al-Mn System. PB90-123548 901,169 Not available NTIS

Quasicrystals with 1-D Translational Periodicity and a Ten-Fold Rotation Axis. PB89-147383 901,123 Not available NTIS

Quasifree Electron Scattering on Nucleons in a Momentum-Dependent Potential.

PB89-186738 901,524 Not available NTIS

Quenching and Energy Transfer Processes of Single Rotational Levels of Br2 B triplet Pi(O(sub u)(+)) v'= 24 with Ar under Single Collision Conditions. PB9-179766 900,399 Not available NTIS

Radiation-Induced Crosslinks between Thymine and 2-D-Deoxyerythropentose. PB89-146682 900,247 Not available NTIS

Radiation-Induced Interface Traps in Power MOSFETs. PB89-201974 900,784 Not available NTIS

Radiochemical and Instrumental Neutron Activation Analysis Procedures for the Determination of Low Level Trace Elements in Human Livers.
PB99-171953 901,236 Not available NTIS

Radiochemical Procedure for Ultratrace Determination of Chromium in Biological Materials.
PB89-156913 900,179 Not available NTIS

Radiometer Equation and Analysis of Systematic Errors for the NIST (National Institute of Standards and Technology) Automated Radiometers.

PB90-130907 900,832 PC A03/MF A01

Rapid Solidification and Ordering of B2 and L2 (sub 1) Phases in the NiAl-NiTi System. PB90-123639 901,171 Not available NTIS

Rate Constants for Hydrogen Abstraction by Resonance Stabilized Radicals in High Temperature Liquids.

900,348 Not available NTIS PB89-161608

Rate Constants for One-Electron Oxidation by Methylper-oxyl Radicals in Aqueous Solutions. PB89-151013 900,302 Not available NTIS

Rate Constants for Reactions of Nitrogen Oxide (NO3) Radicals in Aqueous Solutions. PB89-176242 900,379 Not available NTIS

Rate Constants for the Quenching of Excited States of Metal Complexes in Fluid Solution.
PB89-227797 900,461 (Not available NTIS)

Rate Constants for the Reaction HO2+ NO2+ N2->
HO2NO2+ N2: The Temperature Dependence of the FallOff Parameters. PB89-146658 900,278 Not available NTIS

Rate of Change of the Quincy-Monument Peak Baseline from a Translocation Analysis of LAGEOS Laser Range 901,282 Not available NTIS

Rating Procedure for Mixed Air-Source Unitary Air Conditioners and Heat Pumps Operating in the Cooling Mode. Revision 1 PB89-193247 900.075 PC A03/MF A01

Re-Entrant Spin-Glass Properties of a-(FexCr1-x)75P15C10. PB89-157481 901,391 Not available NTIS

Reaction of (Ir(C(3), N bpy)(bpy)2)(2+) with OH Radicals and Radiation Induced Covalent Binding of the Complex to Several Polymers in Aqueous Solutions. PB90-123498 900,264 Not available NTIS

Reactions of Magnesium Prophyrin Radical Cations in Water. Disproportionation, Oxygen Production, and Comparison with Other Metalloporphyrins. PB9-151005 900,301 Not available NTIS

Reactions of Phenyl Radicals with Ethene, Ethyne, and PB89-150908 900.297 Not available NTIS

Real-Time Control System Modifications for a Deburing Robot. User Reference Manual. PB89-159669 900,990 PC A03/MF A01

Real-Time Control System Software: Some Problems and 900,951 Not available NTIS

Real Time Generation of Smooth Curves Using Local Cubic PB89-171623 901,196 Not available NTIS

Real-Time Optimization in the Automated Manufacturing Research Facility.
PB89-172597 900,947 PC A03/MF A01

Real-Time Simulation and Production Scheduling Systems. PB89-183230 900,974 PC A03/MF A01

Recent Activities of the American Society for Testing and Materials Committee on Fire Standards.
PB89-180004 900,124 Not available NTIS

Recent Advances in Bonded Phases for Liquid Chromatography. PB89-187520 900,204 Not available NTIS

Recent Progress on Spectral Data for X-ray Lasers at the National Bureau of Standards.
PB89-158091 901,341 Not available NTIS

Recharacterization of Thermal Voltage Converters After Thermoelement Replacement.
PB89-230452 900,720 Not available NTIS

Recoilless Optical Absorption and Doppler Sidebands of a Single Trapped Ion.

PB89-171631

901.505 Not available ATTO

Recommended Technical Specifications for Procurement of Equipment for a Turning Workstation.
PB89-215347 900,962 PC A03/MF A01

Redistribution in Astrophysically Important Hydrogen Lines. PB90-128075 901,579 Not available NTIS

Redox Chemistry of Water-Soluble Vanadyl Porphyrins. PB89-150999 900,300 Not available NTIS

Reduced Dimensionality Quantum Reactive Scattering Study of the Insertion Reaction O(1D) + H2 -> OH + PB89-234280 900,492 Not available NTIS

Reduction of Uncertainties for Absolute Piston Gage Pressure Measurements in the Atmospheric Pressure Range. PB90-163882 900,030

(Order as PB90-163874, PC A04)

Reentrant Softening in Perovskite Superconductors. PB90-117540 901,464 Not available NTIS

Reevaluation of Forces Measured Across Thin Polymer Films: Nonequilibrium and Pinning Effects.
PB89-228589 900,573 Not available NTIS

Refinement and Experimental Verification of a Model for Fire Growth and Smoke Transport.

PB89-212005 900, 137 Not available NTIS

Refinement of Neutron Energy Deposition and Microdosimetry Calculations. PB89-150791 901.264 Not available NTIS

Refinement of the Substructure and Superstructure of Ro-PB89-157721 901,392 Not available NTIS

Reflection Coefficient of a Waveguide with Slightly Uneven Walls. PB89-201057 900.753 Not available NTIS

Refrigeration Efficiency of Pulse-Tube Refrigerators. PB89-173892 901,007 Not available NTIS

Relation between Wire Resistance and Fluid Pressure in the Transient Hot-Wire Method.

PB89-184113 901.520

(Order as PB89-184089, PC A04)

Relationship between Appearance and Protective Durability of Coatings: A Literature Review.
PB89-162598 901,063 PC A04/MF A01

Relationships between Fault Zone Deformation and Segment Obliquity on the San Andreas Fault, California. PB89-185953 901,279 Not available NTIS

Relative Acidities of Water and Methanol and the Stabilities of the Dimer Anions. PB89-150981 900,299 Not available NTIS

Remote Sensing Technique for Combustion Gas Tempera-ture Measurement in Black Liquor Recovery Boilers. PB89-179568 900,392 Not available NTIS

placement of Icosahedral Al-Mn by Decagonal Phase. 89-186332 901,146 Not available NTIS PB89-186332

Report of Roof Inspection: Characterization of Newly-Fabricated Adhesive-Bonded Seams at an Army Facility.
PB90-112376 900,107 PC A03/MF A01

Report of the Invitational Workshop on Integrity Policy in Computer Information Systems (WIPCIS).
PB89-168009 900,670 PC A09/MF A01

Report on Interactions between the National Institute of Standards and Technology and the American Society of Mechanical Engineers.
PB9-172563 901,004 PC A03/MF A01

Report on Interactions between the National Institute of Standards and Technology and the Institute of Electrical and Electronic Engineers. PB90-130899

900,831 PC A03/MF A01

Report on the 1989 Meeting of the Radionuclide Measurements Section of the Consultative Committee on Standards for the Measurement of Ionizing Radiations: Special Report on Standards for Radioactivity. PB90-163916

(Order as PB90-163874, PC A04)

Repulsive Regularities of Water Structure in Ices and Crystalline Hydrates. PB89-186753 900.414 Not available NTIS

Research as the Technical Basis for Standards Used in Building Codes. PB89-231062 900,101 Not available NTIS

Research for Electric Energy Systems: An Annual Report. PB90-112442 900,853 PC A06/MF A01

Research Opportunities Below 300 nm at the NBS (National Bureau of Standards) Free-Electron Laser Facility.
PB89-192678 901,360 Not available NTIS

Residential Wood Combustion: A Source of Atmospheric Polycyclic Aromatic Hydrocarbons. PB90-128166 900,860 Not available NTIS

Resistance Measurements of High T(sub c) Superconductors Using a Novel 'Bathysphere' Cryostat.

PB89-228431 901,448 Not available NTIS

Resonance Enhanced Electron Stimulated Desorption. PB90-117771 900,505 Not available NTIS

Resonance-Enhanced Multiphoton Ionization of Atomic Hy-

drogen. PB89-201073 901.529 Not available NTIS Resonance Ionization Mass Spectrometry of Mg: The 3pnd

Autoionizing Series. PB89-150817 900,296 Not available NTIS

Resonance Light Scattering from a Liquid Suspension of Microspheres. PB89-157887 901.340 Not available NTIS

Resonance Light Scattering from a Suspension of Microspheres. PB89-176234 901,352 Not available NTIS

Resonant Excitation of an Oxygen Valence Satellite in Photoemission from High-T(sub c) Superconductors. PB89-186860 901,420 Not available NTIS

Resonant Raman Scattering of Controlled Molecular Weight PR89-157093 900.548 Not available NTIS

Results of a Survey of the Performance of EPDM (Ethylene Propylene Diene Terpolymer) Roofing at Army Facilities. PB89-209316 900,136 PC A03/MF A01

of Thermal Characterization of Power Transistors. 50825 900,770 Not available NTIS PB89-150825

Rising Fracture Toughness from the Bending Strength of Indented Alumina Beams. PB89-171771 901.031 Not available NTIS

Robot Crane Technology.

PR90-111667 900,146 PC A04/MF A01

Role of Adsorbed Gases in Metal on Metal Epitaxy. PB90-128125 901,174 Not available NTIS

Role of inclusions in the Fracture of Austenitic Stainless PB89-173504 901,099 Not available NTIS

Role of Neutron Activation Analysis in the Certification of NBS (National Bureau of Standards) Standard Reference Materi PB89-157879 900,187 Not available NTIS

Role of Standards in Electron Microprobe Techniques. PB89-176143 900,197 Not available NTIS

Roles of Atomic Volume and Disclinations in the Magnetism of the Rare Earth-3D Hard Magnets. 901 434 Not available NTIS PB89-202238

Rotational Energy Levels and Line Intensities for (2S+1)Lambda-(2S+1) Lambda and (2S+1)(Lambda + or -)-(2S+1)Lambda Transitions in a Diatomic Molecule van der Waals Bonded to a Closed Shell Partner. PR90-117441 900,498 Not available NTIS

Rotational Modulation and Flares on RS Canum Venati-corum and BY Draconis Stars X: The 1981 October 3 Flare on V711 Tauri (= HR 1099). 900,021 Not available NTIS PB89-202618

Rotational Modulation and Flares on RS Canum Venati-corum and BY Draconis Stars. XI. Ultraviolet Spectral Images of AR Lacertae in September 1985. PB69-234298 900,026 Not available NTIS

Rotational Modulation and Flares on RS CVn and BY Dra Stars IX. IUE (International Ultraviolet Explorer) Spectroscopy and Photometry of II Peg and V711 Tau during February 1983.

PB89-171615 900.019 Not available NTIS

Rydberg-Klein-Rees Inversion of High Resolution van der Waals Infrared Spectra: An Intermolecular Potential Energy Surface for Ar+ HF (v= 1). 900,465 Not available NTIS

S2F10 Formation in Computer Simulation Studies of the

Breakdown of SF6. PB89-157523 900.327 Not available NTIS

Safety Guidelines for Microwave Systems in the Analytical Laboratory PB90-118167 900,689 Not available NTIS

Sample Validity in Biological Trace Element and Organic Nutrient Research Studies.
PB89-156905 901,218 Not available NTIS

Sayre's Equati PB89-158174 Equation is a Chernov Bound to Maximum Entropy. 58174 901,397 Not available NTIS

Scaling Applications in Fire Research PB90-118068 900,14 900,149 Not available NTIS

Scattering of Polarized Light in Spectral Lines with Partial Frequency Redistribution: General Redistribution Matrix. Frequency Re PB89-171607 901,344 Not available NTIS

Scattering Parameters Representing Imperfections in Precision Coaxial A PB89-184121 al Air Lines. 900,750

(Order as PB89-184089, PC A04)

Scheme for a 60-nm Laser Based on Photopumping of a High Level of Mo(6+) by a Spectral Line of Mo(11+). PB89-186415 900,407 Not available NTIS

Search for Optical Molasses in a Vapor Cell: General Analysis and Experimental Attempt. PB90-163932 901,371

(Order as PB90-163874, PC A04)

Second Virial Coefficients of Aqueous Alcohols at Elevated Temperatures: A Calorimetric Study. PB89-227896 900,462 Not available NTIS

Second Viscosity and Thermal-Conductivity Virial Coefficients of Gases: Extension to Low Reduced Temperature. PB89-179691 900,397 Not available NTIS

Secondary-Electron Effects in Photon-Stimulated Desorp-PB89-157929 900.337 Not available NTIS Secure Military Communications Can Benefit from Accurate PB89-176507 901,274 Not available NTIS

Selecting Varistor Clamping Voltage: Lower Is Not Better. PB89-176648 900,760 Not available NTIS

Semi-Automated PVT Facility for Fluids and Fluid Mixtures. PB89-157184 900,875 Not available NTIS

Semiclassical Way to Molecular Dynamics at Surfaces. PB89-157713 900,333 Not available NTIS

Semiconductor Measurement Technology: A Software Program for Aiding the Analysis of Ellipsometric Measurements, Simple Models. PR89-235923 901.369 PC A12/MF A01

Semiconductor Measurement Technology: Automatic Determination of the Interstitial Oxygen Content of Silicon Wafers Pollshed on Both Sides.

PB9-151831

900,772

PC A04/MF A01

Semiconductor Measurement Technology: Database for and Statistical Analysis of the Interlaboratory Determination of the Conversion Coefficient for the Measurement of the Interstitial Oxygen Content of Silicon by Infrared Absorption. PB89-221170 PC A09/MF A01

Sensors and Measurement Techniques for Assessing Structural Performance. PB89-235865 900,162 PC A04/MF A01

Sensors for Intelligent Processing of Materials. PB89-202006 900,920 Not available NTIS

Sequential Determination of Biological and Pollutant Elements in Marine Bivalves.
PB89-156897 901,217 Not available NTIS

ife of Concrete. 901.303 PC A07/MF A01 PR89-215362

Set Time Control Studies of Polymer Concrete. PR90-111238 901,057 PC A09/MF A02 PB90-111238

Shear Dilatancy and Finite Compressibility in a Dense Non-PB89-174023 901,328 Not available NTIS

Shear Effects on the Phase Separation Behaviour of a Polymer Blend in Solution by Small Angle Neutron Scattering. PB89-229264 900,574 Not available NTIS

Shear-Induced Angular Dependence of the Liquid Pair Correlation Function. PB89-228043 900,469 Not available NTIS

Induced Anisotropy in Two-Dimensional Liquids. -158141 901,325 Not available NTIS PB89-158141

Shimanouchi, Takehiko and the Codification of Spectrosco-PB89-157846 900,335 Not available NTIS

Shortest Paths in Simply Connected Regions in R2. PB90-123688 901,202 Not available NTIS

Significance of Multiple Scattering in the Interpretation of Small-Angle Neutron Scattering Experiments.
PB89-179626 901,409 Not available NTIS

Silicon and GaAs Wire-Bond Cratering Problem.
PB90-128182 900,799 Not available NTIS

Silicon Photodiode Detectors for EXAFS (Extended X-ray Absorption Fine Structure). PB89-228498 900,731 Not available NTIS

Silicon Photodiode Self-Calibration PR90-118159 900.734 Not available NTIS

Simple Apparatus for Vapor-Liquid Equilibrium Measurements with Data for the Binary Systems of Carbon Dioxide with n-Butane and Isobutane. 900,422 Not available NTIS PB89-201115

Simple F-Center Laser Spectrometer for Continuous Single Frequency Scans. PB89-179774 901,358 Not available NTIS

Simple Technique for Investigating Defects in Coaxial Con-PB89-146930 900,723 Not available NTIS

Simplified Discrete Event Simulation Model for an IEEE (Institute of Electrical and Electronics Engineers) 802.3 Local Area Network PB89-186829 900,617 Not available NTIS

Simplified Representation for the Thermal Conductivity of Fluids in the Critical Region.
PB89-228050 901,332 Not available NTIS

Simplified Shielding of a Metallic Restoration during Radiation Therapy. PB89-229256

900,044 Not available NTIS

Simulation of a Large Office Building System Using the HVACSIM+ Program.
PB89-177174 900,071 Not available NTIS

Simulation Study of Light Scattering from Soot Agglomer-PR89-212138 901,543 Not available NTIS

Single Particle Standards for Isotopic Measurements of Uranium by Secondary Ion Mass Spectrometry. PB89-201669 901,297 Not available NTIS

SIS Ouasiparticle Mixers with Bow-Tie Antennas. PB89-157036 900,705 Not ave 900,705 Not available NTIS

Site Characterization for Radon Source Potential PB89-209274 901,290 PC A04/MF A01

Slit Jet Infrared Spectroscopy of NeHF Complexes: Internal Rotor and J-Dependent Predissociation Dynamics.
PB90-118126 900,520 Not available NTIS

Small Angle Neutron Scattering from Porosity in Sintered PB89-157564 901,026 Not available NTIS

Small Angle Neutron Scattering Spectrometer at the National Bureau of Standards. PB89-158158 901,396 Not available NTIS

Small Angle Neutron Scattering Studies of Single Phase Interpenetrating Polymer Networks.

PB90-123456 900,577 Not available NTIS

Small Computer System Interface (SCSI) Command System: Software Support for Control of Small Computer System Interface Devices. 900.659 PC A06/MF A01 PB89-151815

Smoke and Gas Evolution Rate Measurements on Fire-Retarded Plastics with the Cone Calorimeter PB89-174890 900,868 Not available NTIS

Sodium Doppler-Free Collisional Line Shapes. PB89-234306 901,559 Not available NTIS

Software Configuration Management: An Overview. PB89-193833 900,651 PC A03/MF A01

re for an Automated Machining Workstation. 177109 900,953 Not available NTIS PB89-177109

Software Verification and Validation: Its Role in Computer Assurance and Its Relationship with Software Project Mangement Standards. PB90-111691 900.655 PC A03/MF A01

Solar and Stellar Magnetic Fields and Structures: Observa-PB90-118118 900,027 Not available NTIS

Solid State (13)C NMR Investigation in Polyoxetanes, Effect

of Chain Conformation. PB89-176036 900,558 Not available NTIS

Solidification of Aluminum-Manganese Powders. PB89-172332 901,137 Not available NTIS

Solidification of an 'Amorphous' Phase in Rapidly Solidified Al-Fe-Si Alloys. PB90-123530 901,168 Not available NTIS

Solutal Convection during Directional Solidification. PB89-150932 901,322 Not available NTIS

Solution for Diffusion-Controlled Reaction in a Vortex Field. PB89-176622 900,594 Not available NTIS

Some Ouestions and Answers Concerning Air Lines as Impedance Standards.
PB89-176176 900,747 Not available NTIS

Soot Inception in Hydrocarbon Diffusion Flames. PB89-201966 900,599 Not available NTIS

Spatial Filtering Microscope for Linewidth Measurements PB89-230346 901,368 Not available NTIS

Special Calibration Systems for Reactive Gases and Other Difficult Measurements.
PB89-149215 900,873 Not available NTIS

Speciation Measurements of Butyltins: Application to Controlled Release Rate Determination and Production of Reference Standards. 900,174 Not available NTIS

Specific Heat Measurements of Two Premium Coals. PB89-173900 900,839 Not available NTIS

Specific Heat of Insulations. PB89-172514 900,116 Not available NTIS

Specimen Banking in the National Status and Trends Program: Development of Protocols and First Year Results.
PB89-175855 901.308 Not available NTIS

Specimen Biasing to Enhance or Suppress Secondary Electron Emission from Charging Specimens at Low Accelerating Voltages.
PB89-228464
901,451
Not available NTIS

Spectra and Energy Levels of Br XXV, Br XXIX, Br XXX, PB89-176002 901,509 Not available NTIS

Spectra and Energy Levels of the Galliumlike Ions Rb VII-Mo XII. PB89-179105 900,387 Not available NTIS

Spectroelectrochemistry of a System Involving Two Consecutive Electron-Transfer Reaction.
PB90-136979 900,237 Not available NTIS

Spectroscopic Detection Methods. PB89-228100 901,549 Not available NTIS

Spectroscopic Quantitative Analysis of Strongly Interacting Systems: Human Plasma Protein Mixtures. PB89-202576 901,225 Not available NTIS

Spactroscopic. Signatures of Floppiness in Molecular Com-PB89-227979 900,467 Not available NTIS

Spectroscopy of Autoionizing States Contributing to Electron-Impact Ionization of Ions. PB90-123837 901,572 Not available NTIS

Spectrum and Energy Levels of Singly Ionized Cesium. 2. Interpretation of Fine and Hyperfine Structures. PB89-172373 900,361 Not available NTIS

Spectrum of Doubly Ionized Tungsten (W III). PB89-235659

900,223 (Order as PB89-235634, PC A04)

Speed of Sound in a Mercury Ultrasonic Interferometer Ma-PB89-202220 901,319 Not available NTIS

Speed of Sound in Natural Gas Mixtures. PB89-174031 900,840 Not available NTIS

Spherical Acoustic Resonators. PB90-128505 901,321 Not available NTIS

Spherical Acoustic Rasonators in the Undergraduate Laboratory. PB89-179709 901.317 Not available NTIS

Spherical-Wave Source-Scattering Matrix Analysis of Coupled Antennas: A General System Two-Port Solution.
PB89-156798 900,696 Not available NTIS

Spin-Density-Wave Transition in Dilute YGd Single Crystals. PB89-202030 901,433 Not available NTIS

Spin-Polarized Electron Microscopy.
901,395 Not available NTIS

Sputter Deposition of Icosahedral Al-Mn and Al-Mn-Si. PB89-147102 901,122 Not available NTIS

Sputtered Thin Film Ba2YCu3On PB89-165427 90

901.029 Not available NTIS

Stability and Quantum Efficiency Performance of Silicon Photodiode Detectors in the Far Ultraviolet. PB90-128059 900,735 Not available NTIS

Stability of Birefringent Linear Retarders (Waveplates). PB89-171672 901,345 Not available NTIS

Stability of the SI (International System) Unit of Mass as Determined from Electrical Measurements. PB89-201818 900,894 Not available NTIS

Stabilization and Spectroscopy of Free Radicals and Reac-Stabilization and Specificacy, the Molecules in Inert Matrices.

900,484 Not available NTIS

Stabilization of Ascorbic Acid in Human Plasma, and Its Liquid-Chromatographic Measurement. PB89-179279 901,237 Not available NTIS

Stable and Metastable Phase Equilibria in the Al-Mn System. PB89-172324 901,136 Not available NTIS

Stable and Metastable Ti-Nb Phase Diagrams. PB89-157432 901,125 Not available NTIS

Stable Implementation Agreements for Open Systems Inter-connection Protocols. Version 2, Edition 1. December 1988. PB89-193312 900,618 PC A22/MF A01

Stainless Steel Weld Metal: Prediction of Ferrite Content. PB89-231260 901,107 Not available NTIS PB89-231260

Standard Aggregate Materials for Alkali-Silica Reaction Studies. PB89-193221 901.046 PC A03/MF A01

Standard Chemical Thermodynamic Properties of Polycyclic Aromatic Hydrocarbons and Their Isomer Groups 1. Benzene Series.
PB9-186480 900,412 Not available NTIS

Standard Chemical Thermodynamic Properties of Polycyclic Aromatic Hydrocarbons and Their Isomer Groups, 2. Pyrene Series, Naphthopyrene Series, and Coronene Series. PB89-226591 900,459 (Not available NTIS)

Standard Electrode Potentials and Temperature Coefficients in Water at 298,15 K.
PB89-226567 900,456 (Not available NTIS)

Standard Format for the Exchange of Fingerprint Informa-PB89-176705 900.692 Not available NTIS

Standard Generalized Markup Language (SGML). FIPS PUB 152 900.627 PC E19

Standard Reference Materials: Description of the SRM 1965 Microsphera Slide. PB89-153704 901,390 PC A04/MF A01

Standard Reference Materials for Dimensional and Physical Property Measurements. PB89-201164 900,892 Not available NTIS

Standard Reference Materials for the Determination of Polycyclic Aromatic Hydrocarbons.
PB89-156889 900,178 Not available NTIS

Standard Reference Materials for X-ray Diffraction. Part 1. Overview of Current and Future Standard Reference Matenals. PB89-146799 901,384 Not available NTIS

Standard Specifications for Cements and the Role in Their Development of Quality Assurance Systems for Laborato-

PB89-150742 901,021 Not available NTIS Standard X-ray Diffraction Powder Patterns from the JCPDS (Joint Committee on Powder Diffraction Standards) Research Associateship.

900.190 Not available NTIS PB89-171763

Standard X-ray Diffraction Powder Patterns from the JCPDS (Joint Committee on Powder Diffraction Standards) Research Association.
PB89-202246 900,214 Not available NTIS

Standardizing EMCS Communication Protocols. PB89-172357 900,613 Not available NTIS

Standards and Test Methods for VLSI (Very Large Scale In-

tegration) Materials. PB89-158042 900,774 Not available NTIS

Standards for Real-Time Radioscopy. 900,924 Not available NTIS

Standards for the Interchange of Large Format Tiled Raster Documents. PB89-148415 900,668 PC A04/MF A01

Stark Broadening of Spectral Lines of Homologous, Doubly lonized Inert Gases. PB89-158083 900,343 Not available NTIS

State Selection in Electron-Atom Scattering: Spin-Polarized Electron Scattering from Optically Pumped Sodium. PB89-176572 901,513 Not available NTIS

State Selection via Optical Methods. PB89-228118 901,550 Not available NTIS

Static Tests of One-third Scale Impact Limiters 901,000 PC A04/MF A01

Statistical Analysis of Experiments to Measure Ignition of Cigarettes. PB89-201149 900,135 Not available NTIS

Statistical Descriptors in Crystallography: Report of the International Union of Crystallography Subcommittee on Statistical Descriptors. 901.432 Not available NTIS PB89-201826

Status of Reference Data, Reference Materials and Reference Proceduras in Surface Analysis.
PB89-157705 900,332 Not available NTIS

Stellar Winds of 203 Galactic O Stars: A Quantitative Ultra-900.022 Not available NTIS

Stimulated Desorption from CO Chemisorbed on Cr(110). PB89-203004 900,443 Not available NTIS

Stokes and Anti-Stokes Fluorescence of Er(3+) in the Raman Spectra of Erbium Oxide and Erbium Glasses. PB89-149231 901,020 Not available NTIS

Stopped-Flow Studies of the Mechanisms of Ozone-Alkene Reactions in the Gas Phase: Tetramethylethylene. PB89-157515 900,326 Not available NTIS

Strain Energy of Bituminous Built-Up Membranes: A New Concept in Load-Elongation Testing. PB89-212203 900,139 Not available NTIS

Strategic Defense Initiative Space Power Systems Metrology Assessment.
PB89-173405
901,268
Not available NTIS

Strategy for Interpretation of Contrast Mechanisms in Scanning Electron Microscopy: A Tutorial. PB89-172498 900, 192 Not available NTIS

Stress Effects on III-V Solid-Liquid Equilibria. PB89-146997 900,769 No Not available NTIS

Structural Ceramics Database: Technical Foundations. 901,036 (Order as PB89-175194, PC A06)

Structural Reliability and Damage Tolerance of Ceramic Composites for High-Temperature Applications. Semi-Annual Progress Report for the Period Ending March 31, 901,024 PC A03/MF A01 PB89-156368

Structural Reliability and Damage Tolerance of Ceramic Composites for High-Temperature Applications. Semi-Annual Progress Report for the Period Ending September 30, 1987. 901.023 PC A03/MF A01 PB89-156350

Structural Study of a Metastable BCC Phase in Al-Mn Alloys Electrodeposited from Molten Salts. PB89-201040 901,064 Not available NTIS

Structural Unit in Icosahedral MnAlSi and MnAl. PB89-157648 901,131 Not available NTIS

Structure and Dynamics of Molecular Clusters via High Resolution IR Absorption Spectroscopy. PB89-185896 900,403 Not available NTIS

Structure and Radiation Properties of Large-Scale Natural Gas/Air Diffusion Flames.

900.589 Not available NTIS PB89-157572 Structure of a Hydroxyl Radical Induced Cross-Link of Thy-

mine and Tyrosine. PB89-157838 901,244 Not available NTIS

Structure of Cs on GaAs(110) as Determined by Scanning Tunneling Microscopy.
PB90-117490 901,463 Not available NTIS

Structure of the CO2-CO2-H2O van der Waals Complex Determined by Microwave Spectroscopy.
PB89-230288 900,479 Not available NTIS

Structure of V9Mo6O40 Determined by Powder Neutron Diffraction. PB90-117995 900.515 Not available NTIS

Studies on Some Failure Modes in Latex Barrier Films. PB89-209308 901,089 PC A03/MF A01

Study of Long-Term Stability of Atomic Clocks. PB89-174098 900,367 Not a 900,367 Not available NTIS

Sub-Doppler Infrared Spectroscopy in Slit Supersonic Jets: A Study of all Three van der Waals Modes in v1-Excited ArHCl. PB90-123852 900,525 Not available NTIS

Submicrometer Optical Metrology.
900,771 Not available NTIS

Substitutes for N-Phenylglycine in Adhesive Bonding to PB90-123795 900,051 Not available NTIS

Summaries of Center for Fire Research In-House Projects and Grants: 1989. PB90-127101 900,605 PC A10/MF A02

Summary of Circular and Square Edge Effect Study for Guarded-Hot-Plate and Heat-Flow-Meter Apparatuses. PB89-176606 900,884 Not available NTIS

Summary of the Assumptions and Limitations in Hazard I 900,606 Not available NTIS

Supercomputers Need Super Arithmetic PB90-130253 900,65 900,657 PC A03/MF A01

Superconducting Kinetic Inductance Bolometer. PB89-200505 900,762 Not available NTIS

Supercritical Fluid Chromatograph for Physicochemical Studies PB89-184105 900,201

(Order as PB89-184089, PC A04)

Superelastic Scattering of Spin-Polarized Electrons from PB90-128307 901,584 Not available NTIS

Superlattice Magnetoroton Bands PB89-175970 901,403 Not available NTIS

Surface-Interacting Polymers: An Integral Equation and Fractional Calculus Approach. 900,571 Not available NTIS PB89-202949

Surface Properties of Clean and Gas-Dosed SnO2 (110). 900,393 Not available NTIS

Surface Reactions in Silane Discharges. PB89-185961 900,406 Not available NTIS

Surface Structure and Growth Mechanism of Ga on Si(100). PB89-149181 901,387 Not available NTIS

Surface Structures and Growth Mechanism of Ga on Si(100) Determined by LEED (Low Energy Electron Diffraction) and Auger Electron Spectroscopy.
PB89-171342
901,399
Not available NTIS

Survey of Selected Methods of Economic Evaluation for Building Decisions. PB89-173819 900, 103 Not available NTIS

Switching Noise in YBa2Cu3Ox 'Macrobridges'. PB89-200513 901.426 Not available NTIS

Synchrotron Photoemission Study of CO Chemisorption on Cr(110) PB89-231336 900,262 Not available NTIS

Synchrotron Radiation Study of BaO Films on W(001) and Their Interaction with H2O, CO2, and O2. PB89-157697 900,252 Not available NTIS

Synergistic Effects of Nitrogen Dioxide and Carbon Dioxide Following Acute Inhalation Exposures in Rats. PB89-214779 900,856 PC A03/MF A01

Syntheses and Unit Cell Determination of Ba3V4O13 and Low- and High-Temperature Ba3P4O13. PBs9-179717 901,040 Not available NTIS

Synthesis and Characterization of Ettringite and Related PB89-146963 900,238 Not available NTIS

Synthesis and Characterization of Novel Bonded Phases for Reversed-F PB90-128695

Synthesis and Characterization of Poly(vinylmethyl ether). PB89-161616 900,551 Not available NTIS

Synthesis and Magnetic Properties of the Bi-Sr-Ca-Cu Oxide 80- and 110-K Superconductors. PB89-179725 901,412 Not available NTIS

Synthesis, Stability, and Crystal Chemistry of Dibarium Pentatitanate PB89-179741 901,041 Not available NTIS

System for Measuring Optical Waveguide Intensity Profiles. PB89-188593 900,751 PC A04/MF A01

Systems Driven by Colored Squeezed Noise: The Atomic Absorption Spectrum. PB89-171185 901,500 Not available NTIS

Tables for the Thermophysical Properties of Methane. PB89-222608 900,843 PC A21/MF A01

Technical Activities 1986-1988, Molecular Spectroscopy Division. PB89-175418 900.372 PC A07/MF A01

Technical Activities 1987, Center for Basic Standards. PB89-185615 901,521 PC A13/MF A01

Technical Activities, 1988, Center for Analytical Chemistry. PB89-151773 900,177 PC A09/MF A01 PB89-151773

Technical Activities 1988, Surface Science Division. PB89-161889 900,349 PC A07/MF A01

Technical Examination, Lead Isotope Determination, and Elemental Analysis of Some Shang and Zhou Dynasty Bronze Vessels. PB90-136862 901,178 Not available NTIS

Technical Reference Guide for FAST (Fire and Smoke Transport) Version 18. PB89-218366 900,602 PC A07/MF A01

Techniques for Measuring the Electromagnetic Shielding Effectiveness of Materials. Part 1. Far-Field Source Simula-PR89-161525 900.680 Not available NTIS

Techniques for Measuring the Electromagnetic Shielding Effectiveness of Materials Part 2. Near-Field Source Simu-

900.681 Not available NTIS

Teleoperation and Autonomy for Space Robotics. PB90-123811 901,591 Not available NTIS

TEM Observation of Icosahedral, New Crystalline and Glassy Phases in Rapidly Quenched Cd-Cu Alloys. PB90-123514 901,166 Not available NTIS

Temperature, Composition and Molecular-Weight Dependence of the Binary Interaction Parameter of Polystyrene/Poly(vinylmethylether) Blends.
PB89-157473 900,550 Not available NTIS

Temperature Dependence of the Rate Constant for the Hydroperoxy + Methylperoxy Cas-Phase Reaction. PB90-136375 900,534 Not available NTIS Temperature-Dependent Radiation-Enhanced Diffusion in

Ion-Bombarded Solids PB89-179188 901,408 Not available NTIS

Temperature Hysteresis in the Initial Susceptibility of Rapidly Solidified Monel. PB90-123423 901,164 Not available NTIS

Tensile and Fatigue-Creep Properties of a Copper-Stainless Steel Laminate PB90-128646 901.083 Not available NTIS

Tensile Strain-Rate Effects in Liquid Helium. PB89-174882 901,102 Not available NTIS

Tensile Tests of Type 305 Stainless Steel Mine Sweeping Wire Rope.

PB90-130287 901.112 PC A03/MF A01

Test Results and Predictions for the Response of Near-Ceiling Sprinkler Links In a Full-Scale Compartment Fire. PB89-231187 900,095 Not available NTIS

Tests of Adhesive-Bonded Seams of Single-Ply Rubber PB89-212120 900,138 Not available NTIS

Tests of the Recalibration Period of a Drifting Instrument. PB89-176275 900,199 Not available NTIS

Texture Monitoring in Aluminum Alloys: A Comparison of Ultrasonic and Neutron Diffraction Measurements. PB90-117409 901,159 Not available NTIS

Theoretical Models for High-Temperature Superconducti-PB89-186266 901.418 Not available NTIS

Theoretical Study of the Vibrational Lineshape for CO/

900,331 Not available NTIS

Theory and Measurements of Radiated Emissions Using a TEM (Transverse Electromagnetic) Cell. PB89-193890 900,761 PC A03/MF A01

Theory and Practice of Paper Preservation for Archives. PB89-147052 900,934 Not available NTIS

Theory of Microphase Separation in Graft and Star Copolymers. PB89-176028 900.557 Not available NTIS

Thermal Analysis of VAMAS (Versailles Project on Advanced Materials and Standards) Polycarbonate-Polyethyl-900.568 Not available NTIS

Thermal and Economic Analysis of Three HVAC (Heating, Ventilating, and Air Conditioning) System Types in a Typical VA (Veterans Administration) Patient Facility. PB89-188619 PC A04/MF A01

Thermal Conductivity Measurements of Thin-Film Silicon Dioxide. PB89-212195 901,444 Not available NTIS

Thermal Conductivity of Liquid Argon for Temperatures between 110 and 140 K with Pressures to 70 MPa. PB89-179600 900,394 Not available NTIS

Thermal Conductivity of Nitrogen and Carbon Monoxide in the Limit of Zero Density.
PB89-222533 900,449 (Not available NTIS)

Thermal Conductivity of Refrigerants in a Wide Range of Temperature and Pressure. PB89-226583 900,458 (Not available NTIS)

Thermal Degradation of Poly (methyl methacrylate) at 50C PB89-157465 900,549 Not available NTIS

Thermal-Expansive Growth of Prebreakdown Streamers in 900.803 Not available NTIS

Thermal Resistance Measurements and Calculations of an Insulated Concrete Block Wall. PB89-174916 900,119 Not available NTIS

Thermal Shifts of the Spectral Lines in the (4)F3/2 to (4)I11/2 Manifold of an Nd:YAG Laser. PB89-157382 901,338 Not available NTIS

Thermo-Optic Designs for Microwave and Millimeter-Wave Electric-Field Probes. PB90-128588 900.691 Not available NTIS

Thermochemistry of Solvation of SF6(1-) by Simple Polar Organic Molecules in the Vapor Phase. PB9-202527 900,437 Not available NTIS

Thermodynamic and Transport Properties of Carbohydrates and Their Monophosphates: The Pentoses and Hexoses. PB89-222574 900,453 (Not available NTIS)

Thermodynamic Properties of Argon from the Triple Point to 1200 K with Pressures to 1000 MPa. PB89-222558 900,451 (Not Available NTIS)

Thermodynamic Properties of Dioxygen Diffuoride (O2F2) and Dioxygen Fluoride (O2F). PB89-222566 900,452 (Not Available NTIS)

Thermodynamic Values Near the Critical Point of Water. PB89-161541 901,497 Not available NTIS

Thermodynamics of Ammonium Scheelltes. 6. An Analysis of the Heat Capacity and Ancillary Values for the Metaperiodates KIO4, NH4IO4, and ND4IO4. PB89-147060 900,285 Not available NTIS

Thermodynamics of Hydrolysis of Disaccharides. PB89-186761 901,221 Not available NTIS

Thermodynamics of the Hydrolysis of Sucrose.
PB89-227904 901.227 Not available NTIS

Thermographic Imaging and Computer Image Processing of Defects in Building Materials.

PB89-176309 900,123 Not available NTIS

Thermomechanical Detwinr YBa2Cu3O7-x Single Crystals. Detwinning of Superconducting PB89-231088 901,458 Not available NTIS

Thermophysical Properties for Bioprocess Englneering. PB89-228068 900,043 Not available NTIS

Thermophysical Properties of Methane. PB89-222541 900.450 900,450 (Not Available NTIS)

Thermophysical-Property Needs for the Environmentally Acceptable Halocarbon Refingerants. PB89-231054 900,482 Not available NTIS

Thin Film Thermocouples for High Temperature Measure-PB89-209290 901.065 PC A03/MF A01

Thin Film Thermocouples for Internal Combustion Engines. PB89-147094 900,607 Not available NTIS PB89-147094

Three-Dimensional Atomic Spectra in Flames Using Stepwise Excitation Laser-Enhanced Ionization Spectroscopy. PB89-202071 900,430 Not available NTIS

Three Dimensional Quantum Reactive Scattering Study of the I $+\,$ HI Reaction and of the IHI(1-) Photodetachment Spectrum. PB89-227961 900,466 Not available NTIS

Three-State Lattice Gas as Model for Binary Gas-Liquid Systems. PB89-171284 900.354 Not available NTIS

Tiger Tempering Tampers Transmissions. PB89-157861 900.740 900.740 Not available NTIS

Tilt Observations Using Borehole Tiltmeters 1. Analysis of Tidal and Secular Tilt. PB90-136649 901.283 Not available NTIS

Time-of-Flight Measurements of Hyperthermal Cl(sub 2) Molecules Produced by UV Laser Vaporization of Cryogenic

Chlorine Films. 900.260 Not available NTIS

Time-Resolved FTIR Emission Studies of Molecular Photofragmentation. PB89-202642 900,261 Not available NTIS

Time-Resolved FTIR Emission Studies of Molecular Photofragmentation Initiated by a High Repetition Rate Excimer PB90-136680 900,266 Not available NTIS

Time Resolved Studies of Vibrational Relaxation Dynamics of CO(v= 1) on Metal Particle Surfaces.
PB89-203012 900,444 Not available NTIS

Torsional Piezoelectric Crystal Viscometer for Compressed nd Liquids. PB89-228076 901,447 Not available NTIS

Toughening Mechanisms in Ceramic Composites. Semi-Annual Progress Report for the Period Ending March 31, 1989. 901,080 PC A03/MF A01 PB89-235907

Toughening Mechanisms in Ceramic Composites: Semi-Annual Progress Report for the Period Ending September 30, 1988.

901,028 PC A03/MF A01 PB89-162606 Towards the Ultimate Laser Resolution. PB89-186910 900,416 Not available NTIS

Toxicity of Mixed Gases Found in Fires. PB89-212047 900,869 Not available NTIS

Trace Gas Calibration Systems Using Permeation Devices. PB89-176580 900,883 Not available NTIS

Trace Speciation by HPLC-GF AA (High-Performance Liquid Chromatography-Graphite Furnace Atomic Absorption) for Tin- and Lead-Bearing Organometallic Compounds, with Signal Increases Induced by Transition-Metal Ions. 900.184 Not available NTIS

Transducers in Michelson Tiltmeters 901,280 Not available NTIS

Transient and Residual Stresses in Dental Porcelains as Affected by Cooling Rates. PB89-229298 900,046 Not available NTIS

Transient Cooling of a Hot Surface by Droplets Evapora-PB89-161897 900.971 PC A04/MF A01

Transient Response Error in Microwave Power Meters

Using Thermistor Detectors. PB89-173785 900,759 Not available NTIS

Transmission Loss through 6061 T-6 Aluminum Using a Pulsed Eddy Current Source. PB89-179840 901,143 Not available NTIS

Tools and Measurement. 900,611 Not available NTIS Transport Layer Performance PB89-171326

Trapped lons and Laser Cooling 2: Selected Publications of the lon Storage Group, Time and Frequency Division, NIST, Boulder CO PB89-153878 901,489 PC A09/MF A01

Trends for Building Technology in North America. PB89-174106 900,104 Not available NTIS

Trial of Open Systems Interconnection (OSI) Protocols Over Integrated Services Digital Network (ISDN).
PB89-235576 900,625 PC A03/MF A01

Tribochemical Mechanism of Alumina with Water. PB90-117722 901,059 Not available NTIS

Triplet Dipoles in the Absorption Spectra by Dense Rare Gas Mixtures. 1. Short Range Interactions. PB90-136755 900,539 Not available NTIS

Turning Workstation in the AMRF (Automated Manufacturing Research Facility). PB89-185607 900,954 PC A10/MF A01

Twenty Five Years of Accuracy Assessment of the Atomic 900,365 Not available NTIS

Two-Layer Dielectric Microstrip Line Structure: SiO2 on Si and GaAs on Si; Modeling and Measurement. PB89-156780 900,738 Not available NTIS

Two-Photon Laser-Induced Fluorescence of the Tumor-Localizing Photosensitizer Hematoporphyrin Derivative. PB89-157283 901,240 Not available NTIS

Typical Usage of Radioscopic Systems: Replies to a 901,161 Not available NTIS

U.S. Organizations Represented in the Collection of Voluntary Standards.
PB89-154322 900,978 PC E06/MF E01

U.S. Perspective on Possible Changes in the Electrical PB89-157002 901,491 Not available NTIS

U-Value Measurements for Windows and Movable Insula-tions from Hot Box Tests in Two Commercial Laboratories. PB89-175889 900,121 Not available NTIS

Ultrasensitive Laser Spectroscopy and Detection. PB89-156996 901,336 Not available NTIS

Ultrashort-Pulse Multichannel Infrared Spectroscopy Using Broadband Frequency Conversion in LilO3. PB89-230304 901,367 Not available NTIS

Ultrasonic Characterization of Surface Modified Layers. PB89-147409 901,115 Not available NTIS

Ultrasonic Determination of Absolute Stresses in Aluminum and Steel Alloys. PB89-150957 901,124 Not available NTIS

Ultrasonic Railroad Wheel Inspection Using EMATs (Electromagnetic-Accoustic Transducers), Report No. 18. PB89-189229 901,596 PC A05/MF A01

Ultrasonic Sensor for Measuring Surface Roughness. PB89-211809 900,679 Not available NTIS

Ultrasonic Separation of Stress and Texture Effects in Polycrystalline Aggregates. PB90-117557 900,499 Not available NTIS

Ultrasonic Texture Analysis for Polycrystalline Aggregates of Cubic Materials Displaying Orthotropic Symmetry. PB89-146948 901,121 Not available NTIS

Uncertainties in Mass Absorption Coefficients in Fundamental Parameter X-ray Fluorescence Analysis.
PB89-201677 900,212 Not available NTIS

Undercooling and Microstructural Evolution in Glass Form-

ing Alloys. PB89-176465 901, 139 Not available NTIS

Uniaxial Deformation of Rubber Network Chains by Small Angle Neutron Scattering. PB89-175830 901,088 Not available NTIS

Unimolecular Dynamics Following Vibrational Overtone Excitation of HN3 v1 = 5 and v1 = 6:HN3(X tilde;v,J,K,) -> HN(K sup 3)(Sigma (1-));v,J,Omega) + N2(x sup 1)(Sigma sub g (1+) PB89-147110 900,286 Not available NTIS

Universal Resputtering Curve. PB89-234314 901,460 Not available NTIS

Universality Class of Planar Self-Avoiding Surfaces with Fixed Boundary. PB89-157945 900,339 Not available NTIS

Update of U.S. Participation in International Standards Ac-

PB89-228282 900,902 PC A03/MF A01

Upward Flame Spread on Vertical Walls. PB89-214787 900,141 PC A04/MF A01 Upward Turbulent Flame Spread on Wood under External

900,148 Not available NTIS

Use of an Imaging Proportional Counter in Macromolecular Crystallography. PB90-136599 900.538 Not available NTIS

Use of Artificial Intelligence and Microelectronic Test Structures for Evaluation and Yield Enhancement of Microelectronic Interconnect Systems. PB89-146955 900,768 Not available NTIS

Use of Artificial Intelligence Programming Techniques for Communication between Incompatible Building Information PB89-191985 900,106 PC A05/MF A01

Use of Dye Tracers in the Study of Free Convection in Porous Media. Porous Media. PB89-173918 901.327 Not available NTIS

Use of Focusing Supermirror Neutron Guides to Enhance Cold Neutron Fluence Rates. PB89-171946 901,306 Not available NTIS

Use of GMAP (Geometric Modeling Applications Interface Program) Software as a PDES (Product Data Exchange Specification) Environment in the National PDES Testbed

900,960 PC A03/MF A01 Use of Multiple-Slot Multiple Disk Chopper Assemblies to Pulse Thermal Neutron Beams.
PB89-147466 901,485 Not available NTIS

Use of N-Phenylglycine in a Dental Adhesive System. PB90-117375 900,048 Not available NTIS

Use of Structural Templates in Protein Backbone Modeling. PB89-175277 901,246

(Order as PB89-175194, PC A06)

Use of the IRDS (Information Resource Dictionary System) Standard in CALS (Computer-Aided Acquisition and Logistic Support). PB90-112467 900,931 PC A03/MF A01

e of Thorium as a Target in Electron-Spin Analyzers. 90-117938 900,912 Not available NTIS PB90-117938

User Guide for the NBS (National Bureau of Standards)
Prototype Compiler for Estelle (Revised).
PB89-196158 900,619 PC A05/MF A01

User Guide for Wise: A Simulation Environment for Estelle. PB89-196166 900,620 PC A03/MF A01

User Guide for Wizard: A Syntax-Directed Editor and Translator for Estelle. PB89-196174 900,621 PC A03/MF A01

User's Reference Guide for ODRPACK: Software for Weighted Orthogonal Distance Regression Version 1.7. PB89-229066 901,215 PC A05/MF A01

Using Multiple Reference Stations to Separate the Variances of Noise Components in the Global Positioning

901,293 Not available NTIS Using 'Resonant' Charge Exchange to Detect Traces of Noble Gas Atoms,

Validated Furniture Fire Model with FAST (HEMFAST). PB89-215354 900,142 PC A05/MF A01

901,296 Not available NTIS

PB89-176770

Validation of Absolute Target Thickness Calibrations in a QQQ Instrument by Measuring Absolute Total Cross-Sections of NE(1+) (NE,NE)NE(1+). PB99-157507 900,325 Not available NTIS 900,325 Not available NTIS

VAMAS (Versailles Project on Advanced Materials and Standards) Intercomparison of Critical Current Measurement in Nb3Sn Wires. 901,534 Not available NTIS PB89-202147

Van der Waals Equation of State Around the Van Laar PB89-158133 900,345 Not available NTIS

Van der Waals Fund, Van der Waals Laboratory and Dutch High-Pressure Science. PB89-185755 900,401 Not available NTIS

Vapor-Liquid Equilibrium of Binary Mixtures in the Extended Critical Region. I. Thermodynamic Model. PB89-218374 901,544 PC A04/MF A01

Vapor-Liquid Equilibrium of Nitrogen-Oxygen Mixtures and Air at High Pressure. PB89-174932 900.368 Not available NTIS

Vapor Pressures and Gas-Phase PVT Data for 1,1,1,2-Te-PB90-117987 900,514 Not available NTIS

Variances Based on Data with Dead Time between the PB89-174049 901.204 Not available NTIS

Vector Calibration of Ultrasonic and Acoustic Emission Transducers.

PB89-202014 900,765 Not available NTIS

Vector Imaging of Magnetic Microstructure PB90-128240 901,476 N 901,476 Not available NTIS

Ventilation and Air Quality Investigation of the U.S. Geological Survey Building. PB89-229686 900.857 PC A03/MF A01

Ventilation Effectiveness Measurements in an Office Build-PB89-176614 900,067 Not available NTIS

Versailles Project on Advanced Materials and Standards Evolution to Permanent Status. 900.969 Not available NTIS PB89-201768

Vertical Machining Workstation of the AMRF (Automated Manufacturing Research Facility): Equipment Integration. PB89-176663 900,950 Not available NTIS

Very Large Methane Jet Diffusion Flames. PB89-175913 900.593 Not available NTIS

Very Low-Noise FET Input Amplifier.

PB90-128224 900,800 Not available NTIS

Vibrational Exchange upon Interconversion Tunneling in (HF)2 and (HCCH)2. PB89-179113 900,388 Not available NTIS

Vibrational Predissociation in the H-F Stretching Mode of

PB89-234207 900.488 Not available NTIS

Vibrational Predissociation of the Nitric Oxide Dimer. 900,289 Not available NTIS

Vibrational Spectra of Molecular Ions Isolated in Solid Neon. I. CO(sub 2, sup +) and CO(sub 2, sup -). PB89-234199 900,487 Not available NTIS

Vibrational Spectra of Molecular Ions Isolated in Solid Neon. 2. O4(1+) and O4(1-). PB90-128729 900,533 Not available NTIS

Vibrationally Resolved Photoelectron Angular Distributions for H2 in the Range 17 eV < or= h(nu) < or= 39 eV. PB89-176952 900,385 Not available NTIS

Vibrationally Resolved Photoelectron Studies of the 7(sigma) (-1) Channel in N2O. PB89-176945 900,257 Not available NTIS

Viscosity of Blends of Linear annd Cyclic Molecules of Similar Molecular Mass. PB89-172480 900,555 Not available NTIS

Visual Perception Processing in a Hierarchical Control 900.994 PC A04/MF A01 PB89-221188

Voltammetric and Liquid Chromatographic Identification of Organic Products of Microwave-Assisted Wet Ashing of Biological Samples.

900,188 Not available NTIS PB89-157994

Vortex Shedding Flowmeter for Fluids at High Flow Veloci-900.608 Not available NTIS

Water Structure in Crystalline Solids: Ices to Proteins. PB89-186746 900,413 Not available NTIS

Water Structure in Vitamin B12 Coenzyme Crystals. 1. Analysis of the Neutron and X-ray Solvent Densities. PB89-186803 901,222 Not available NTIS

Water Structure in Vitamin B12 Coenzyme Crystals. 2. Structural Characteristics of the Solvent Natworks. PB89-186811 901,223 Not available NTIS

Wavefront Matrix Multiplication on a Distributed-Memory Multiprocesso PB89-151807 900.646 PC A04/MF A01

Waveguide Loss Measurement Using Photothermal Deflec-

PB89-157028 900,739 Not available NTIS

Wavelengths and Energy Level Classifications of Scandium Spectra for All Stages of Ionization.
PB89-145163 900,273 Not available NTIS

Wavelengths and Energy Levels of the K I Isoelectronic Sequence from Copper to Molybdenum.
PB89-179097
901,372
Not available NTIS

Weakly Bound NeHF. PB90-118100

900.519 Not available NTIS

Wheatleyite, Na2Cu(C2O4)2 . 2H2O, a Natural Sodium Copper Salt of Oxalic Acid. PB89-179154 900,390 Not available NTIS

Wind and Seismic Effects. Proceedings of the Joint Meeting of the U.S.-Japan Cooperative Program in Natural Resources Panel on Wind and Seismic Effects (20th) Held in Gaithersburg, Maryland on May 17-20, 1988. PB89-154835 900,157 PC A21/MF A01

Window U-Values: Revisions for the 1989 ASHRAE (American Society of Heating, Refrigerating and Air-Conditioning Engineers) Handbook - Fundamentals.

PB89-229215 900,145 Not available NTIS

Working Implementation Agreements for Open Systems Interconnection Protocols. PB89-221196 900,624 PC A10/MF A01

PB89-235931 900,642 PC A16/MF A01 Workstation Controller of the Cleaning and Deburring Work-

station. PB89-189286 900,955 PC A04/MF A01

X-Band Atmospheric Attenuation for an Earth Terminal Measurement System.
PB90-100736 900,626 PC A03/MF A01

ZIP: The ZIP-Code Insulation Program (Version 1.0) Economic Insulation Levels for New and Existing Houses by Three-Digit ZIP Code. Users Guide and Reference Manual. PB89-151765 900,058 PC A03/MF A01

ZIP: ZIP-Code Insulation Program (for Microcomputers). PB89-159446 900,060 CP **D01**

SAMPLE ENTRY

NIST/SP-500/166

Computer Viruses and Related Threats: A Management

Gulde

PB90-111683

900,654

PC A03/MF A01

Report or series number

Title

NTIS order number

Abstract number

Avallability Price Code

Report or series number

Title

NTIS order number

Abstract number

Avallability Price code

PB90-111683

Compuer Viruses and Related Threats: A Management

Gulde

PB90-111683

900.654

PC A03/MF A01

AD-A201 256/5

Error Bounds for Linear Recurrence Relations. AD-A201 256/5 901,192 PC A03/MF A01

AD-A202 820/7

Alignment Effects in Electronic Energy Transfer and Reactive Events. AD-A202 820/7 900,267 PC A03/MF A01

AFOSR-TR-88-1316

Alignment Effects in Electronic Energy Transfer and Reactive Events. AD-A202 820/7 900.267 PC A03/MF A01

ARO-20606.9-MA

Error Bounds for Linear Recurrence Relations. AD-A201 256/5 901,192 PC A03/MF A01

CAM-8901

Advanced Ceramics: A Critical Assessment of Wear and Lubrication. PB89-188569 901.045 PC A06/MF A01

EPRI-RP-2033-26

Proposed Methodology for Rating Air-Source Heat Pumps That Heat, Cool, and Provide Domestic Water Heating. PB90-112368 900,087 PC A06/MF A01

ESA-SP-281-V-2

Proceedings of the Celebratory Symposium on a Decade of UV (Ultraviolet) Astronomy with the IUE Satellite, Volume 2. N89-16535/1 900,014 PC A19/MF A01

FIPS PUB 134-1

Coding and Modulation Requirements for 4,800 Bit/Second Modems, Category: Telecommunications Standard.
FIPS PUB 134-1 900,660 PC A03/MF A01

FIPS PUB 149

General Aspects of Group 4 Facsimile Apparatus, Category: Telecommunications Standard.
FIPS PUB 149 900,661 PC E08 900,661 PC E08

FIPS PUR 150

Facsimile Coding Schemes and Coding Control Functions for Group 4 Facsimile Apparatus, Category: Telecommunications Standard. FIPS PUB 150 900,662 PC E08

FIPS PHR 152

Standard Generalized Markup Language (SGML). FIRS PUB 152 900,627 PC **E19**

FIPS PUB 154

High Speed 25-Position Interface for Data Terminal Equipment and Data Circuit-Terminating Equipment, Category: Telecommunications Standard.
FIPS PUB 154 900,663 PC E09

FIPS PUB 155

Data Communication Systems and Services User-Oriented Performance Measurement Methods, Category: Telecommunications Standard.
FIPS PUB 155 900,664 PC E11

GRI-88/0290

Advanced Ceramics: A Critical Assessment of Wear and PB89-188569 901,045 PC A06/MF A01

ICST/SNA-87/3

User Guide for the NBS (National Bureau of Standards)
Prototype Compiler for Estelle (Revised).
PB89-196158 900,619 PC A05/MF A01

ISBN-0-88318-585-7

Journal of Physical and Chemical Reference Data, Volume 17, 1988, Supplement No. 3. Atomic Transition Probabilities Scandium through Manganese. PB89-145197 900,276 Not available NTIS

ISBN-0-88318-587-3

Journal of Physical and Chemical Reference Data, Volume 17, 1988, Supplement No. 2. Thermodynamic and Transport Properties for Molten Salts: Correlation Equations for Critically Evaluated Density, Surface Tension, Electrical Conductance, and Viscosity Data.

PB89-145205 900,277 Not available NTIS

ISBN-1-55877-069-0

Promoting Technological Excellence: The Role of State and Federal Extension Activities.
PB90-120742 900,171 PC A05/MF A01

N89-16535/1

Proceedings of the Celebratory Symposium on a Decade of UV (Ultraviolet) Astronomy with the IUE Satellite, Volume 2.

N89-16535/1 900,014 PC A19/MF A01 PB90-116195 900,824 PC A03/MF A01 PB89-196190 900,623 PC A05/MF A01 NBS/SP-250/19 NBSIR-87/3625 NIST/BSS-166 NBS (National Bureau of Standards) Measurement Services: Calibration of Gamma-Ray-Emitting Brachytherapy Length Scale Measurement Procedures at the National Bureau of Standards.
PB89-209266 900,895 PC A04/MF A01 Inelastic Behavior of Full-Scale Bridge Columns Subjected to Cyclic Loading. Sources. PB89-174924 900,584 PC A12/MF A01 PR89-193858 901.243 PC A04/MF A01 NBSIR-88/3091 NIST/BSS-167 NBS/SW/DK-89/001 Group Index and Time Delay Measurements of a Standard Interim Criteria for Polymer-Modified Bituminous Roofing NBS (National Bureau of Standards) Life-Cycle Cost (NBSLCC) Program (for Microcomputers).
PB89-151211 900,849 CP D99 Reference Fiber. Membrane Materials. PB89-168025 PB89-189179 900,752 PC A03/MF A01 900,114 PC A04/MF A01 NBSIR-88/3092 NIST/GCR-89/557 NBS/SW/DK-89/003 System for Measuring Optical Waveguide Intensity Profiles. PB89-188593 900,751 PC A04/MF A01 ZIP: ZIP-Code Insulation Program (for Microcomputers). PB89-159446 CP **D01** Fire Propagation in Concurrent Flows. PB89-151781 900.867 PC A04/MF A01 NBSIR-88/3093 NIST/GCR-89/559 NBS/SW/DK-89/005 Development of Standard Measurement Techniques and Standard Reference Materials for Heat Capacity and Heat HAZARD I Fire Hazard Assessment Method. Transient Cooling of a Hot Surface by Droplets Evaporaof Vaporization of Jet Fuels. PB89-148100 PB89-215404 900.143 CP D05 PB89-161897 900.971 PC A04/MF A01 900,837 PC A03/MF A01 NBS/SW/DK-89/006A NIST/GCR-89/560 NBSIR-88/3095 AutoMan: Decision Support Software for Automated Manufacturing Investments. User's Manual. PB89-221873 900,963 PC A03/MF A01 Fire Propagation in Concurrent Flows PB89-188577 900, Dielectric Mixing Rules for Background Test Soils. PB89-188585 901,289 PC A03/MF A01 900,597 PC A03/MF A01 NBS/SW/MT-89/004A NBSIR-88/3096 NIST/GCR-89/561 User Guide for the NBS (National Bureau of Standards)
Prototype Compiler for Estelle (Revised).
PB89-196158 900,619 PC A05/MF A01 Measurement of Adapter Loss, Mismatch, and Efficiency Using the Dual Six-Port. PB89-147839 901,316 PC A10/MF A01 Effect of Water on Piloted Ignition of Cellulosic Materials. PB89-189187 900.127 PC A09/MF A01 NIST/GCR-89/562 NBS/SW/MT-89/004B NBSIR-88/3097 Fire Risk Analysis Methodology: Initiating Events. PB89-184527 900,125 PC A08/MF A01 Metrology for Electromagnetic Technology: A Bibliography of NBS (National Bureau of Standards) Publications. PB89-147847 900,871 PC A04/MF A01 User Guide for Wise: A Simulation Environment for Estelle. PB89-196166 900,620 PC A03/MF A01 NIST/GCR-89/563 NBS/SW/MT-89/004C Development of an Automated Probe for Thermal Conduc-NBSIR-88/3702 User Guide for Wizard: A Syntax-Directed Editor and Transtivity Measurements. PB89-209324 Epoxy Impregnation Procedure for Hardened Cement Samlator for Estelle. 900,896 PC A07/MF A01 PB89-196174 900.621 PC A03/MF A01 NIST/GCR-89/564 PB**8**9-147821 901.180 PC A03/MF A01 NBS/SW/MT-89/004D Validated Furniture Fire Model with FAST (HEMFAST), PB89-215354 900,142 PC A05/MF A01 NBSIR-88/3710 Free Value Tool for ASN.1. PB89-196182 Structural Reliability and Damage Tolerance of Ceramic Composites for High-Temperature Applications. Semi-Annual Progress Report for the Period Ending September 900,622 PC A04/MF A01 NIST/GCR-89/565 NBS/SW/MT-89/004E Upward Flame Spread on Vertical Walls. PB89-214787 900,141 PC A04/MF A01 Object-Oriented Model for Estelle and Its Smalltalk Imple-30, 1987. PB89-156350 mentation. 901,023 PC A03/MF A01 NIST/GCR-89/566 900.623 PC A05/MF A01 PR89-196190 NBSIR-88/3711 Experimental Study of the Pyrolysis of Pure and Fire Re-NBS/TN-1321 Guidelines and Procedures for Implementation of Executive tarded Cellulose. PB89-228316 (12)C(16)O Laser Frequency Tables for the 34.2 to 62.3 THz (1139 to 2079 cm(-1)) Region.'
PB89-193908 901,361 PC A03/MF A01 Order on Seismic Safety. PB89-148092 901.090 PC A07/MF A01 900,156 PC A03/MF A01 NIST/GCR-89-567 NBSIR-88/3721 NBSIR-86/3420 Promoting Technological Excellence: The Role of State and Federal Extension Activities. Flow of Molecules Through Condoms. PB89-148118 901.087 PC A03/MF A01 Combustion of Oil on Water. November 1987. PB89-185581 900,863 PC A04/MF A01 PB90-120742 900,171 PC A05/MF A01 NBSIR-88/3732 NBSIR-87/3075 NIST/SP-250/27 Calculating Flows through Vertical Vents in Zone Fire Models under Conditions of Arbitrary Cross-Vent Pressure NIST (National Institute of Standards and Technology)
Measurement Services: AC-DC Difference Calibrations.
PB89-222616 900,818 PC A14/MF A01 Postweld Heat Treatment Criteria for Repair Welds in 2-1/4Cr-1Mo Superheater Headers: An Experimental Study. PB89-156160 901,094 PC A04/MF A01 Difference PB89-148126 900.108 PC A03/MF A01 NBSIR-87/3081 NIST/SP-250/31 NBSIR-88/3743 Development of Near-Field Test Procedures for Communication Satellite Antennas, Phase 1, Part 2.
PB89-156152 901,593 PC A05/MF A01 Integrated Manufacturing Data Administration System (IMDAS) Operations Manual. PB89-156384 900,916 PC A03/MF A01 NIST (National Institute of Standards and Technology) Measurement Services: Mass Calibrations.
PB89-153894 900,874 PC A05/MF A01 PB89-153894 NRSIR-87/3504 NIST/SP-250/34 NBSIR-88/3749 Epoxy Impregnation of Hardened Cement Pastes for Characterization of Microstructure.
PB89-185573 901,042 PC A03/MF A01 NIST (National Institute of Standards and Technology) Measurement Services: High Vacuum Standard and Its Turning Workstation in the AMRF (Automated Manufacturing Research Facility). PB89-185607 llea 900,954 PC A10/MF A01 PB89-193841 NBSIR-87/3519 900,891 PC A04/MF A01 NBSIR-88/3761 Directory of NVLAP (National Voluntary Laboratory Accredi-NIST/SP-250/35 Predicting Formaldehyde Concentrations in Manufactured Housing Resulting from Medium-Density Fiberboard. PB89-148134 900,854 PC A03/MF A01 tation Program) Accredited Laboratories, 1986-87.
PB89-185599 900,933 PC A05/MF A01 NIST (National Institute of Standards and Technology)
Measurement Services: The Calibration of Thermocouples
and Thermocouple Materials. NBSIR-87/3529 NBSIR-88/3763 900,897 PC A10/MF A01 Use of Artificial Intelligence Programming Techniques for Communication between Incompatible Building Information PB89-209340 Data Handling in the Vertical Workstation of the Automated Manufacturing Research Facility at the National Bureau of NIST/SP-250/89ED Systems. PB89-191985 NIST (National Institute of Standards and Technology) Calibration Services Users Guide. 1989 Edition.
PB89-200216 900,926 PC A10/MF A01 Standards. 900.106 PC A05/MF A01 PR89-159636 900,943 PC A04/MF A01 NBSIR-87/3534 NBSIR-88/3773 Ignition and Flame Spread Measurements of Aircraft Lining Materials. DCTDOS: Neutron and Gamma Penetration in Composite NIST/SP-250-APP/89ED Duct Systems. PB89-188809 Materials. PB89-172886 NIST (National Institute of Standards and Technology) Cali-901,275 PC A05/MF A01 900,009 PC A04/MF A01 bration Services, Users Guide: Fee Schedule.
PB90-127820
900,913
PC A04/MF A01 NBSIR-87/3578 NBSIR-88/3784 Center for Electronics and Electrical Engineering Technical Material Handling Workstation Implementation NIST/SP-260/107 Publication Announcements Covering Center Programs, April-June 1986 with 1987 CEEE Events Calendar. PB89-185623 900,711 PC A03/MF A01 900,988 PC A04/MF A01 PB89-159644 Standard Reference Materials: Description of the SRM 1965 Microsphere Slide.
PB89-153704

901,390
PC A04/MF A01 NBSIR-88/3785 Material Handling Workstation: Operator Manual. NBSIR-87/3584 900,989 PC A03/MF A01 NIST/SP-305-SUPPL-20 Effect of Slag Penetration on the Mechanical Properties of Refractories: Final Report. **NBSIR-88/3786** Publications of the National Institute of Standards and Technology, 1988 Catalog. PB90-110065 900,836 PC A07/MF A01 Material Handling Workstation, Recommended Technical Specifications for Procurement of Commercially Available Technology, 1 PB**8**9-218382 900,006 PC A15/MF A01 NBSIR-87/3587 Equipment. PB89-162564 NIST/SP-400/81 Technical Activities 1987, Center for Basic Standards. PB89-185615 901,521 PC A13/MF A01 900,998 PC A03/MF A01 Semiconductor Measurement Technology: Automatic Determination of the Interstitial Oxygen Content of Silicon Wafers Polished on Both Sides.
PB89-151831 900,772 PC A04/MF A01 NBSIR-88/3832 NBSIR-87/3599 Real-Time Control System Modifications for a Deburing Robot. User Reference Manual. PB89-159669 900,990 PC A03/MF A01 Potential Applications of a Sequential Construction Analyz-NIST/SP-400/82 PB89-191670 900,105 PC A03/MF A01 NCSL/SNA-89/1 Semiconductor Measurement Technology: Database for and Statistical Analysis of the Interlaboratory Determination of the Conversion Coefficient for the Measurement of the Interstitial Oxygen Content of Silicon by Infrared Absorption. PB89-221170 901,054 PC A09/MF A01 NBSIR-87/3614 Free Value Tool for ASN.1. PB89-196182 Institute for Materials Science and Engineering, Polymers: Technical Activities 1987.
PB89-188601 900,566 PC A06/MF A01 900,622 PC A04/MF A01 NCSL/SNA-89/5 User Guide for Wizard: A Syntax-Directed Editor and Trans-NBSIR-87/3619 lator for Estelle. PB89-196174 NIST/SP-400/83 Thermal and Economic Analysis of Three HVAC (Heating, Ventilating, and Air Conditioning) System Types in a Typical VA (Veterans Administration) Patient Facility. PB99-188619 900,447 PC A04/MF A01 900,621 PC A03/MF A01 Semiconductor Measurement Technology: A Software Program for Alding the Analysis of Ellipsometric Measurements, Simple Models.
PB89-23923 901,369 PC A12/MF A01 NCSL/SNA-89/6

User Guide for Wise: A Simulation Environment for Estelle. PB89-196166 900,620 PC A03/MF A01

Object-Oriented Model for Estelle and Its Smalltalk Imple-

NIST/SP-500/160

Report of the Invitational Workshop on Integrity Policy in Computer Information Systems (WIPCIS).

NCSL/SNA-89/7

Center for Electronics and Electrical Engineering Technical

Publication Announcements Covering Center Programs, October to December 1986, with 1987 CEEE Events Calendar.

900,670 PC A09/MF A01 PB89-168009 NIST/SP-500/161

Software Configuration Management: An Overview. PB89-193833 900,651 PC A03/MF A01 NIST/SP-500/162

Stable Implementation Agreements for Open Systems Inter-connection Protocols. Version 2, Edition 1. December 1988. PB89-193312 900,618 PC A22/MF A01 NIST/SP-500/163

Government Open Systems Interconnection Profile Users'

Guide. PB90-111212 900.667 PC A07/MF A01 NIST/SP-500/164

Electronic Publishing: Guide to Selection. PB89-214753 900,935 900,935 PC A03/MF A01

NIST/SP-500/165 Software Verification and Validation: Its Role in Computer Assurance and Its Relationship with Software Project Management Standards.
PB90-111691 900,655 PC A03/MF A01

NIST/SP-500/166

Computer Viruses and Related Threats: A Management Guide. PB90-111683 900,654 PC A03/MF A01

NIST/SP-500/172

Computer Security Training Guidelines. PB90-780172 900,65 900,677 PC A03/MF A01 NIST/SP-753

Data Bases Available at the National Institute of Standards

and Technology Research Information Center.
PB89-160014 900,932 PC A06/MF A01

Laser Induced Damage in Optical Materials: 1987. PB89-221162 901,364 PC A99/MF A01 NIST/SP-760

Wind and Seismic Effects. Proceedings of the Joint Meeting of the U.S.-Japan Cooperative Program in Natural Resources Panel on Wind and Seismic Effects (20th) Held in Gaithersburg, Maryland on May 17-20, 1988. PB89-154835

NIST/SP-761 NIST (National Institute of Standards and Technology) Research Reports, March 1989. PB89-189310

900,005 PC A03/MF A01 NIST/SP-762

Alaska Arctic Offshore Oil Spill Response Technology Workshop Proceedings. PB89-195663 900,842 PC A10/MF A01 NIST/SP-765

NIST (National Institute of Standards and Technology) Research Reports, June 1989. PB89-235113 900,007 PC A03/MF A01

NIST/SP-766 NBS/BAM (National Bureau of Standards/Bundesanstalt fur Matenalprufung) 1986 Symposium on Advanced Ceram-

901.055 PC A08/MF A01 PR89-229074

NIST/SP-767 Directory of International and Regional Organizations Conducting Standards-Related Activities.
PB89-221147 900,008 PC A19/MF A01

NIST/SP-768

National Institute of Standards and Technology (NIST) Information Poster on Power Quality. PB89-237986 900.754 PC A02 NIST/TN-1235-89

NASA/NBS (National Aeronautics and Space Administra-tion/National Bureau of Standards) Standard Reference Model for Telerobot Control System Architecture (NASREM). PB89-193940

901,589 PC A05/MF A01 NIST/TN-1254 Interfaces to Teleoperation Devices.

900,993 PC A03/MF A01 NIST/TN-1257

NBS (National Bureau of Standards) Reactor: Summary of Activities July 1987 through June 1988.
PB89-168017 901,304 PC A11/MF A01

Assessment of Space Power Related Measurement Re-

quirements of the Strategic Defense Initiative.
PB89-209357
901,269
PC A07/MF A01 NIST/TN-1260

Visual Perception Processing in a Hierarchical Control System: Level 1. PB89-221188 900.994 PC A04/MF A01 NIST/TN-1261-VOL-1

Mining Automation Real-Time Control System Architecture Standard Reference Model (MASREM).
PB89-221154 901,286 PC A04/MF A01 NIST/TN-1262

Technical Reference Guide for FAST (Fire and Smoke Transport) Version 18.
PB89-218366 900,602 PC A07/MF A01

NIST/TN-1263 Guidelines for Implementing the New Representations of the Volt and Ohm Effective January 1, 1990.

PB89-214761 900,817 PC A05/MF A01 NIST/TN-1264

Measurements of Coefficients of Discharge for Concentric Flange-Tapped Square-Edged Orifice Meters in Water Over the Reynolds Number Range 600 to 2,700,000. PB89-235147 901,334 PC A23/MF A01

NIST/TN-1266

Development of a Method to Measure In situ Chloride at the Coating/Metal Interface.
PB89-235345

901,085

PC A03/MF A01

NIST/TN-1267

Robot Crane Technology. PR90-111667 900.146 PC A04/MF A01 NIST/TN-1310

Performance Evaluation of Radiofrequency, Microwave, and Millimeter Wave Power Meters.

900,814 PC A07/MF A01 PB89-193916 NIST/TN-1320 Alternative Techniques for Some Typical MIL-STD-461/462

Types of Measurements. PB89-235139 901,272 PC A03/MF A01 NIST/TN-1323

Iterative Technique to Correct Probe Position Errors in Planar Near-Field to Far-Field Transformations. PB89-153886 900,695 PC A03/MF A01

NIST/TN-1324

Trapped Ions and Laser Cooling 2: Selected Publications of the Ion Storage Group, Time and Frequency Division, NIST, Boulder, CO. PB89-153878 901,489 PC A09/MF A01 NIST/TN-1325

Tables for the Thermophysical Properties of Methane. PB89-222608 900,843 PC A21/MF A01 NIST/TN-1326

Theory and Measurements of Radiated Emissions Using a TEM (Transverse Electromagnetic) Cell. PB89-193890 900,761 PC A03/MF A01

NIST/TN-1327 Radiometer Equation and Analysis of Systematic Errors for the NIST (National Institute of Standards and Technology) Automated Radiometers.

PB90-130907 900.832 PC A03/MF A01 NIST/TN-1328

Vapor-Liquid Equilibrium of Binary Mixtures in the Extended Critical Region. I. Thermodynamic Model. PB89-218374 901,544 PC A04/MF A01

NIST/TN-1329 Effect of Pipe Roughness on Orifice Flow Measurement. PB89-231484 901,333 PC A04/MF A01

NIST/TN-1330 Optimum Location of Flow Conditioners in a 4-Inch Orifice Meter.
PB90-111675 900,911 PC A05/MF A01

NIST/TN-1331

Properties of Lennard-Jones Mixtures at Various Temperatures and Energy Ratios with a Size Ratio of Two.
PB89-235204 900,493 PC A19/MF A01 NISTIR-85/3273-3

Energy Prices and Discount Factors for Life-Cycle Cost Analysis 1988: Annual Supplement to NBS (National Bureau of Standards) Handbook 135 and NBS Special Publication 709.

PR89-153860 900,850 PC A04/MF A01 NISTIR-86/3472-1 Internal Revenue Service Post-of-Duty Location Modeling System: Programmer's Manual for PASCAL Solver. PB89-161905 900,001 PC A04/MF A01

NISTIR-86/3473-1 Internal Revenue Service Post-of-Duty Location Modeling System: Programmer's Manual for FORTRAN Driver Version 5.0.

PB89-161913 900,002 PC A04/MF A01 NISTIR-88/3098

Magnetostatic Measurements for Mine Detection. PB89-148365 PC A0 900,685 PC A03/MF A01 NISTIR-88/3099

Fracture Behavior of a Pressure Vessel Steel in the Ductile-to-Brittle Transition Region. PR89-189195 901,103 PC A03/MF A01

NISTIR-88/3717 Design Protocol, Part Design Editor, and Geometry Library of the Vertical Workstation of the Automated Manufacturing Research Facility at the National Bureau of Standards. PB89-151799 900,936 PC A06/MF A01

NISTIR-88/3722 Advanced Ceramics: A Critical Assessment of Wear and

Lubrication. PB89-188569 901.045 PC A06/MF A01 NISTIR-88/3744

Hierarchies for Computer-Integrated Manufacturing: A Functional Description. PB89-172613 900.949 PC A03/MF A01 NISTIR-88/3777

Finite Unions of Closed Subgroups of the n-Dimensional Torus. PB89-143283 901,193 PC A03/MF A01

NISTIR-88/3801 ZIP: The ZIP-Code Insulation Program (Version 1.0) Economic Insulation Levels for New and Existing Houses by Three-Digit ZIP Code. Users Guide and Reference Manual. PB89-151765 900,058 PC A03/MF A01

NISTIR-88/3803

Logistic Function Data Analysis Program: LOGIT. PB89-189351 900.418 PC A05/MF A01 NISTIR-88/3808

Narrow-Angle Laser Scanning Microscope System for Linewidth Measurement on Wafers. 900.782 PC A06/MF A01 PR89-189344 NISTIR-88/3810

Inventory of Equipment in the Turning Workstation of the AMRF (Automated Manufacturing Research Facility). PB89-215339 900,961 PC A03/MF A01

NISTIR-88/3811 Recommended Technical Specifications for Procurement of Equipment for a Turning Workstation.
PB89-215347 900,962 PC A03/MF A01

NISTIR-88/3817 Structural Reliability and Damage Tolerance of Ceramic Composites for High-Temperature Applications. Semi-Annual Progress Report for the Period Ending March 31,

901.024 PC A03/MF A01 PR89-156368

NISTIR-88/3824-2

Ongoing Implementation Agreements for Open Systems Interconnection Protocols: Continuing Agreements. PB89-166086 900,610 PC A09/MF A01

NISTIR-88/3826 Evaluating Emergency Management Models and Data Bases: A Suggested Approach.
PB89-189203 901,598 PC A10/MF A01

NISTIR-88/3828

NBS AMRF (National Bureau of Standards) (Automated Manufacturing Research Facility) Process Planning System:
System Architecture.
PB89-193882

900,956

PC A06/MF A01

NISTIR-88/3837 On-Line Concurrent Simulation in Production Scheduling. PB89-172605 900,948 PC A03/MF A01

NISTIR-88/3839

Institute for Materials Science and Engineering, Nondestructive Evaluation: Technical Activities 1988. PB89-151625 900,917 PC A04/MF A01 NISTIR-88/3840

Institute for Materials Science and Engineering, Ceramics: Technical Activities 1988. PB89-148381 901.019 PC A05/MF A01

NISTIR-88/3841 Institute for Materials Science and Engineering, Fracture and Deformation: Technical Activities 1988. PB89-148399 901,071 PC A05/MF A01

NISTIR-88/3842

Institute for Materials Science and Engineering, Polymers: Technical Activities 1988. PB89-166094 900,003 PC A06/MF A01

NISTIR-88/3843 Institute for Materials Science and Engineering: Metallurgy, Technical Activities 1988.

PB89-201321 901,147 PC A06/MF A01 NISTIR-88/3846

Guidelines for the Specification and Validation of IGES (Initial Graphics Exchange Specification) Application Protocols. PB89-166102 900,937 PC A06/MF A01 NISTIR-88/3851

Document Interchange Standards: Description and Status of Major Document and Graphics Standards.
PB89-193874

900,928

PC A03/MF A01

NISTIR-88/3853

NVLAP (National Voluntary Laboratory Accreditation Program) Assessment and Evaluation Manual. PB89-228324 900,903 PC A03/MF A01 NISTIR-88/3855

Integral Mass Balances and Pulse Injection Tracer Tech-PB89-206833 900,077 PC A03/MF A01

NISTIR 88/3864

Parser That Converts a Boundary Representation into a Features Representation.
PB89-160634 900,944 PC A03/MF A01 NISTIR-88/3865

Real-Time Optimization in the Automated Manufacturing Research Facility. PB89-172597 900.947 PC A03/MF A01

NISTIR-28/3872

Functional Approach to Designing Architectures for Computer Integrated Manufacturing. PB89-172589 900,946 PC A03/MF A01 900,946 PC A03/MF A01 NISTIR-88/3875

Technical Activities, 1988, Center for Analytical Chemistry. PB89-151773 900,177 PC A09/MF A01 NISTIR-88/3882

Acoustical Technique for Evaluation of Thermal Insulation. PB89-193866 900,919 PC A03/MF A01 PB89-193866

NISTIR-88/3883 Method to Measure the Tensile Bond Strength between Two Weakly-Cemented Sand Grains. PB89-166110 901 901,483 PC A03/MF A01

OR-3

NISTIR-88/3891 Artificial Intelligence Techniques in Real-Time Production Scheduling. PB89-172571 900.945 PC A03/MF A01 NISTIR-88/3892

In Situ Fluorescence Monitoring of the Viscosities of Particle-Filled Polymers in Flow. PB89-146278 900,609 PC A03/MF A01

NISTIR-88/3898

NBS' (National Bureau of Standards) Industry; Government Consortium Research Program on Flowmeter Installation Effects: Summary Report with Emphasis on Research July-December 1987. PB90-111220 900,910 PC A05/MF A01

NISTIR-88/3899

Elevated Temperature Deformation of Structural Steel. PB89-172621 901.098 PC A06/MF A01 NISTIR-88/3900

Bibliography of the NIST (National Institute of Standards and Technology) Electromagnetic Fields Division Publications.

PB89-189211 900.810 PC A06/MF A01 NISTIR-88/3901

Microporous Fumed-Silica Insulation Board as a Candidate Standard Reference Material of Thermal Resistance.
PB89-148373
901,018
PC A03/MF A01 NISTIR-88/3902

Experimental Thermal Conductivity, Thermal Diffusivity, and Specific Heat Values of Argon and Nitrogen. PB89-148407 900,293 PC A04/MF A01

NISTIR-88/3904

Ignition Characteristics of the Iron-Based Alloy UNS S66286 in Pressunzed Oxygen. 901.104 PC A03/MF A01 PB89-189336

NISTIR-88/3906

Ultrasonic Railroad Wheel Inspection Using EMATs (Electromagnetic-Accoustic Transducers), Report No. 18. PB89-189229 901,596 PC A05/MF A01 NISTIR-88/3907

Center for Chemical Technology: 1988 Technical Activities. PB89-156376 900.241 PC A08/MF A01 NISTIR-88/4000

Effect of Chinese Standardization on U.S. Export Opportu-PB89-166128 900.172 PC A03/MF A01

NISTIR-88/4001 Wavefront Matrix Multiplication on a Distributed-Memory Multiprocessor. PB89-151807 900,646 PC A04/MF A01

NISTIR-88/4002

Data Management Strategies for Computer Integrated Manufacturing Systems.
PB89-209258 900,959 PC A03/MF A01 NISTIR-88/4003

Flammability Characteristics of Electrical Cables Using the Cone Calonmeter.
PB89-162572 900,741 PC A04/MF A01

NISTIR-88/4004

Product Data Exchange Specification: First Working Draft. PB89-144794 900,940 PC A99/MF E16 NISTIR-88/4006

Assessment of Robotics for Improved Building Operations and Maintenance. PB89-189146 900,092 PC A04/MF A01 NISTIR-88/4008

Corrosion of Metallic Fasteners in Low-Sloped Roofs: A Review of Available Information and Identification of Reearch Needs.

PB89-162580 900,113 PC A06/MF A01 NISTIR-88/4010

Relationship between Appearance and Protective Durability of Coatings: A Literature Review.
PB89-162598 901,063 PC A04/MF A01

NISTIR-88/4012

Friability of Spray-Applied Fireproofing and Thermal Insulations: Field Evaluation of Prototype Test Devices.
PB89-189328 PC A04/MF A01 NISTIR-88/4014

Illumination Conditions and Task Visibility in Daylit Spaces. PB89-189237 900,074 PC A04/MF A01

NISTIR-88/4016

Composites Databases for the 1990's. PB89-180376 901,075 PC A04/MF A01 NISTIR-88/4017

Standards for the Interchange of Large Format Tiled Raster **Documents** PB89-148415 900,668 PC A04/MF A01 NISTIR-88/4018

Toughening Mechanisms in Ceramic Composites: Semi-Annual Progress Report for the Period Ending September 30, 1988 PB89-162606 901.028 PC A03/MF A01

NISTIR-88/4019 Analysis of Computer Performance Data. PB89-162614 900.635 PC A03/MF A01 NISTIR-88/4020

Center for Electronics and Electrical Engineering Technical Progress Bulletin Covering Center Programs, July to September 1988, with 1989 CEEE Events Calendar.

PB89-168033 900,775 PC A03/MF A01 NISTIR-88/4021

Electrical Performance Tests for Hand-Held Digital Multimeters. PB89-162234 900.876 PC A13/MF A01

NISTIR-89/3908 Interlaboratory Comparison of Two Types of Line-Source Thermal-Conductivity Apparatus Measuring Five Insulating

Materials. PB89-218325 900,144 PC A03/MF A01 NISTIR-89/3909

Clutter Models for Subsurface Electromagnetic Applica-PB89-229678 900,688 PC A03/MF A01

NISTIR-89/3911 Ignition Characteristics of the Nickel-Based Alloy UNS NO7718 in Pressurized Oxygen.

901.154 PC A03/MF A01 PB89-218333 NISTIR-89/3913

Interlaboratory Comparison of the Guarded Horizontal Pipe-Test Apparatus: Precision of ASTM (American Society for Testing and Materials) Standard Test Method C-335 Ap-plied to Mineral-Fiber Pipe Insulation. PB89-218341 PC A03/MF A01

NISTIR-89/3914 Low-Temperature Thermal Conductivity of Composites: Alumina Fiber/Epoxy and Alumina Fiber/PEEK.
PB89-218358 901,078 PC A04/MF A01

NISTIR-89/3917 Improved Low-Level Silicon-Avalanche-Photodiode Transfer Standards at 1.064 Micrometers.
PB90-130303 900,736 PC A03/MF A01

NISTIR-89/3918

X-Band Atmospheric Attenuation for an Earth Terminal Measurement System. PB90-100736 900,626 PC A03/MF A01

NISTIR-89/3919

Microporous Fumed-Silica Insulation as a Standard Reference Material of Thermal Resistance at High Temperature. PB90-130311 900.153 PC A04/MF A01

NISTIR-89/4023 Small Computer System Interface (SCSI) Command System: Software Support for Control of Small Computer System Interface Devices.

PB89-151815 900.659 PC A06/MF A01 NISTIR-89/4024

Intelligent Processing of Materials: Report of an Industrial Workshop Conducted by the National Institute of Standards and Technology. PB89-151823 900,942 PC A04/MF A01

NISTIR-89/4025 Technical Activities 1988, Surface Science Division.
PB89-161889 900,349 PC A07/MF A01

NISTIR-89/4026 Set Time Control Studies of Polymer Concrete. PB90-111238 901,057 PC A09/MF A02

NISTIR-89/4027 Preliminary Performance Criteria for Building Materials, Equipment and Systems Used in Detention and Correctional Facilities. PB89-148514 900.109 PC A08/MF A01

NISTIR-89/4028 Gypsum Wallboard Formaldehyde Sorption Model. PB90-132705 900,154 PC A03/MF A01 NISTIR-89/4029

Mixing Motions Produced by Pipe Elbows. PB89-161871 901,326 PC A03/MF A01 NISTIR-89/4031

Operations Manual for the Automatic Operation of the Vertical Workstation.

PB89-183214

900,973

PC A03/MF A01 900,973 PC A03/MF A01

NISTIR-89/4032 Assessing the Flammability of Composite Materials.
PB90-112996 901,081 PC A03/MF A01 NISTIR-89/4035

Considerations of Stack Effect in Building Fires.
PB89-195671 900,133 PC A05/MF A01 NISTIR-89/4037

Report on Interactions between the National Institute of Standards and Technology and the Institute of Electrical and Electronic Engineers. PB90-130899 900.831 PC A03/MF A01

NISTIR-89/4038 Report on Interactions between the National Institute of Standards and Technology and the American Society of Mechanical Engineers. 901.004 PC A03/MF A01 PB89-172563

NISTIR-89/4039 NVLAP (National Voluntary Laboratory Accreditation Program) Program Handbook Construction Testing Services. Requirements for Accreditation. 900,169 PC A03/MF A01

NISTIR-89/4040 High-Current Measurement Techniques. Part II. 100-kA Source Characteristics and Preliminary Shunt and Rogowski Coil Evaluations. 900,804 PC A04/MF A01

NISTIR-89/4041

International Cooperation and Competition in Materials Science and Engineering.
PB89-228332 901,191 PC A13/MF A01

NISTIR-89/4042

Internal Structure of the Guide to Available Mathematical PB89-170864 900,927 PC A04/MF A01 NISTIR-89/4045

Progress Report of the Quality in Automation Project for

PB89-193296 900,982 PC A06/MF A01 NISTIR-89/4046 Workstation Controller of the Cleaning and Deburing Work-

900,955 PC A04/MF A01

station. PB89-189236 NISTIR-89/4047

Approach to Accurate X-Ray Mask Measurements in a Scanning Electron Microscope. PB89-172555 900,776 PC A03/MF A01

NISTIR-89/4049

Assessment of Need for and Design Requirements of a Wind Tunnel Facility to Study Fire Effects of Interest to

PB89-200208 901.276 PC A10/MF A01 NISTIR-89/4050

Fire Induced Flows in Corridors: A Review of Efforts to Model Key Features. PB89-189260 900,129 PC A03/MF A01

NISTIR-89/4051

Technical Activities 1986-1988, Molecular Spectroscopy Di-PB89-175418 900,372 PC A07/MF A01

NISTIR-89/4052

Calculation of the Flow Through a Horizontal Ceiling/Floor Vent PB89-189252 900,128 PC A03/MF A01

NISTIR-89/4053

Architecturally-Focused Benchmarks with a Communication Example. PB89-216477 900,640 PC A03/MF A01

NISTIR-89/4055 Modeling Dynamic Surfaces with Octrees. PB90-112335 901.206

901,206 PC A03/MF A01 NISTIR-89/4056

NVLAP (National Voluntary Laboratory Accreditation Program) Directory of Accredited Laboratories.
PB89-189278 900,890 PC A04/MF A01

NISTIR-89/4057 Emerging Technologies in Electronics and Their Measurement Needs.
PB89-189245 900,811 PC A05/MF A01

NISTIR-89/4058 Standard Aggregate Materials for Alkali-Silica Reaction

PB89-193221 901,046 PC A03/MF A01 NISTIR-89/4059

Allocating Staff to Tax Facilities: A Graphics-Based Microcomputer Allocation Model.
PB90-129891
900,645
PC A03/MF A01

NISTIR-89/4060

National Engineering Laboratory's 1989 Report to the National Research Council's Board on Assessment of NIST (National Institute of Standards and Technology) Programs. PB89-189294 900,004 PC A03/MF A01

NISTIR-89/4061 Engineering View of the Fire of May 4, 1988 in the First Interstate Bank Building, Los Angeles, California.

PB89-183222

900,167

PC A03/MF A01

NISTIR-89/4062

Guidelines for Identification and Mitigation of Seismically Hazardous Existing Federal Buildings.
PB89-188627 900,161 PC A03/MF A01

NISTIR-89/4063 Hybrid Structures for Simple Computer Performance Esti-

PB89-189161 900,639 PC A03/MF A01 NISTIR-89/4065

Fire Properties Database for Textile Wall Coverings. PB89-188635 900,126 PC A04/MF A01

NISTIR-89/4067

Center for Electronics and Electrical Engineering Technical Publication Announcements: Covering Center Programs, July/September 1988, with 1989 CEEE Events Calendar, PB89-189302 900,812 PC A03/MF A01 NISTIR-89/4068

Building Technology Project Summaries 1989. PB89-193213 900,131 PC A05/MF A01 NISTIR-89/4069

Evaluating Office Lighting Environments: Second Level Analysis. PB89-189153 900,073 PC A07/MF A01

NISTIR-89/4070

Real-Time Simulation and Production Scheduling Systems. PB89-183230 900,974 PC A03/MF A01

NISTIR-89/4071

Rating Procedure for Mixed Air-Source Unitary Air Conditioners and Heat Pumps Operating in the Cooling Mode. PB89-193247 900.075 PC A03/MF A01

NISTIR-89/4072

AIRNET: A Computer Program for Building Airflow Network Modeling PB89-193254 900,076 PC A05/MF A01

NISTIR-89/4073

Mechanical Property Enhancement in Ceramic Matrix Composites. PB89-189138 901,076 PC A05/MF A01

NISTIR-89/4074

GATT (General Agreement on Tariffs and Trade) Standards Code Activities of the National Institute of Standards and Technology 1988. PB89-191977 900.173 PC A03/MF A01 MISTIR-89/4075

Metallurgical Evaluation of 17-4 PH Stainless Steel Castings. PB89-19**3**262 901.105 PC A03/MF A01

NISTIR-89/4076

Center for Electronics and Electrical Engineering Technical Progress Bulletin Covering Center Programs, October to December 1988, with 1989 CEEE Events Calendar. PB89-193270 900,813 PC A03/MF A01

MISTIR-89/4077

False Alarm Study of Smoke Detectors in Department of Veterans Affairs Medical Centers (VAMCS). PB89-193288 900,093 PC A11/MF A01

NISTIR-89/4080

NBS' (National Bureau of Standards) Industry; Government Consortium Research Program on Flowmeter Installation Effects: Summary Report with Emphasis on Research January-July 1988.
PB89-189120 901,010 PC A04/MF A01

NISTIR-89/4081

ISTIR-89/4061 Fire Research Publications, 1988. NISTIR-89/4082

Working Implementation Agreements for Open Systems Interconnection Protocols. PB89-221196 900,624 PC A10/MF A01

NISTIR-89/4084

Studies on Some Failure Modes in Latex Barrier Films. PB89-209308 901,089 PC A03/MF A01

NISTIR-89/4085 Results of a Survey of the Performance of EPDM (Ethylene Propylene Diene Terpolymer) Roofing at Army Facilities. PB89-209316 900,136 PC A03/MF A01

NISTIR-89/4086

Service Life of Concrete.

PB89-215362 901,303 PC A07/MF A01

NISTIR-89/4087

Thin Film Thermocouples for High Temperature Measurement. PB89-209290 901.065 PC A03/MF A01

NISTIR-89/4089

Static Tests of One-third Scale Impact Limiters. PB89-216469 901,000 PC A04/MF A01

NISTIR-89/4090

Elimination of Spunous Eigenvalues in the Chebyshev Tau Spectral Method. PB89-209282 901,330 PC A03/MF A01

NISTIR-89/4092

Inventory of Equipment in the Cleaning and Deburring Workstation. 900.958 PC A03/MF A01

PR89-209233 NISTIR-89/4093

Executive Summary for the Workshop on Developing a Predictive Capability for CO Formation in Fires. PB89-200091 900,134 PC A04/MF A01

NISTIR-89/4095

Center for Electronics and Electrical Engineering: Technical Progress Bulletin Covering Center Programs, January to March 1989, with 1989 CEEE Events Calendar. PB89-209225 900,786 PC A03/MF A01

NISTIR-89/4096

Center for Electronics and Electrical Engineering Technical Publication Announcements. Covering Center Programs, October/December 1988, with 1989 CEEE Events Calendar

PB89-209241 900,787 PC A03/MF A01 NISTIR-89/4100

Expected Complexity of the 3-Dimensional Voronoi Diagram. PB89-209332 901,200 PC A03/MF A01

NISTIR-89/4101

Intercomparison of Load Cell Verification Tests Performed by National Laboratories of Five Countries.
PB89-235915 900,909 PC A06/MF A01

NISTIR-89/4102

Computation and Use of the Asymptotic Covariance Matrix for Measurement Error Models.
PB89-215321 901,214 PC A03/MF A01 NISTIR-89/4103

User's Reference Guide for ODRPACK: Software for Weighted Orthogonal Distance Regression Version 1.7.

PB89-229066 NISTIR-89/4105 901,215 PC A05/MF A01

Synergistic Effects of Nitrogen Dioxide and Carbon Dioxide Following Acute Inhalation Exposures in Rats. PB89-214779 900,856 PC A03/MF A01 900,856 PC A03/MF A01

NISTIR-89/4106

Site Characterization for Radon Source Potential 901,290 PC A04/MF A01 PB89-209274 MISTIR-89/4107

Computer-Controlled Test System for Operating Different Wear Test Machines. 900 983 PC A03/MF A01 PB89-228290

NISTIR-89/4110

Design and Synthesis of Prototype Air-Dry Resins for Use in BEP (Bureau of Engraving and Printing) Intaglio Ink Vehi-PB90-112343 901,068 PC A03/MF A01

NISTIR-89/4111

Toughening Mechanisms in Ceramic Composites. Semi-Annual Progress Report for the Period Ending March 31, 1989 PB89-235907 901,080 PC A03/MF A01

NISTIR-89/4112

Development and Use of a Tribology Research-in-Progress Database. PB89-228274 901,002 PC A14/MF A01

NISTIR-89/4113

Lightning and Surge Protection of Photovoltaic Installations. Two Case Histories: Vulcano and Kythnos. PB89-229058 900,851 PC A05/MF A01

NISTIR-89-4116

AutoMan: Decision Support Software for Automated Manufacturing Investments. User's Manual. PB89-221873 900,963 PC A03/MF A01

NISTIR-89/4117

Use of GMAP (Geometric Modeling Applications Interface Program) Software as a PDES (Product Data Exchange Specification) Environment in the National PDES Testbed Project. PB89-215198 900,960 PC A03/MF A01

NISTIR-89/4118

Center for Electronics and Electrical Engineering Technical Publication Announcements. Covering Center Programs, January-March 1989, with 1989 CEEE Events Calendar. PB89-228308 900,789 PC A03/MF A01

MISTIR-89/4119

Method for Measuring the Effectiveness of Gaseous Contaminant Removal Filters. PB89-235899

900.858 PC A04/MF A01

MISTIR-89/4120

Experimental Investigation and Modeling of the Flow Rate of Refrigerant 22 Through the Short Tube Restrictor. PB89-229041 901,118 PC A06/MF A01

NISTIR-89/4121

Mechanism for Shear Band Formation in the High Strain Rate Torsion Test. 900 901 PC A03/MF A01 PB89-215370

NISTIR-89/4122

Estimating the Environment and the Response of Sprinkler Links in Compartment Fires with Draft Curtains and Fusible Line-Actuated Ceiling Vents. Part 2. User Guide for the Computer Code Lavent.

PB89-229009 900,094 PC A03/MF A01

NISTIR-89/4123 Polytope Volume Computation. PB90-129982 901,203 PC A03/MF A01

NISTIR-89/4124

Update of U.S. Participation in International Standards Ac-

PB89-228282 900.902 PC A03/MF A01

NISTIR-89/4126

Ventilation and Air Quality Investigation of the U.S. Geological Survey Building. PB89-229686 900.857 PC A03/MF A01

NISTIR-89/4128

Processing Rate Sensitivities of a Heterogeneous Multi-PB89-229017 900,641 PC A03/MF A01

NISTIR-89/4131

NDE (Nondestructive Evaluation) Publications, 1985. PB89-229025 900,984 PC A03/MF A01

NISTIR-89/4132

Experience with IMDAS (Integrated Manufacturing Data Administration System) in the Automated Manufacturing Re-PB90-112350 900,964 PC A03/MF A01

NISTIR-89/4133

EVSIM: An Evaporator Simulation Model Accounting for Refigerant and One Dimensional Air Distribution.
PB89-235881 900,086 PC A07/MF A01

NISTIR-89/4135

Supercomputers Need Super Arithmetic PB90-130253 900.65 900,657 PC A03/MF A01

NISTIR-89/4138

Development of a Multiple Layer Test Procedure for Inclusion in NFPA (National Fire Protection Association) 701: Initial Experiments.

PB89-235873 900,096 PC A04/MF A01

NISTIR-89/4139/1

Detailed Description of the Knowledge-Based System for Physical Database Design. Volume 1. PB89-228993 900,929 PC A04/MF A01

MISTIR-89/4139/2

Detailed Description of the Knowledge-Based System for Physical Database Design. Volume 2. PB89-229033 900.930 PC A09/MF A01

NISTIR-89/4140

Working Implementation Agreements for Open Systems Interconnection Protocols. 900.642 PC A16/MF A01

NISTIR-89/4143

Effect of Anisotropic Thermal Conductivity on the Morphological Stability of a Binary Alloy, PB89-228985 PC A03/MF A01

NISTIR-89/4145

Air Quality Investigation in the NIH (National Institutes of Health) Radiation Oncology Branch.
PB89-228977 900,079 PC A07/MF A01

NISTIR-89/4147

Institute for Materials Science and Engineering, Nondestructive Evaluation: Technical Activities, 1989. PB90-132739 900,925 PC A05/MF A01

NISTIR/89-4153

Sensors and Measurement Techniques for Assessing Structural Performance. PB89-235865 900,162 PC A04/MF A01

NISTIR-89/4154

Proposed Methodology for Rating Air-Source Heat Pumps That Heat, Cool, and Provide Domestic Water Heating. PB90-112368 900,087 PC A06/MF A01

NISTIR-89/4155

Report of Roof Inspection: Characterization of Newly-Fabricated Adhesive-Bonded Seams at an Army Facility.
PB90-112376 900,107 PC A03/MF A01

NISTIR-89/4159

FACTUNC: A User-Friendly System for Unconstrained Optimization. PB90-112392 901,207 PC A03/MF A01

NISTIR-89/4160

Trial of Open Systems Interconnection (OSI) Protocols Over Integrated Services Digital Network (ISDN).
PB89-235576 900,625 PC A03/MF A01

NISTIR-89/4161

Directional Solidification of a Planar Interface in the Pres-PB90-112400 901,461 PC A04/MF A01

NISTIR-89/4163

Guideline for Work Station Design. PB90-112418 900,643 PC A07/MF A01 NISTIR-89/4165

Product Data Exchange: The PDES Project-Status and Ob-

PB90-112426 900,938 PC A03/MF A01 NISTIR-89/4166

External Representation of Product Definition Data PB90-112434

900,939 PC A03/MF A01 NISTIR-89/4167

Research for Electric Energy Systems: An Annual Report. PB90-112442 900,853 PC A06/MF A01 NISTIR-89/4168

Generic Architecture for Computer Integrated Manufacturing Software Based on the Product Data Exchange Specifi-

PB90-112459 NISTIR-89/4169

Use of the IRDS (Information Resource Dictionary System) Standard in CALS (Computer-Aided Acquisition and Logistic Support). PB90-112467

900,965 PC A03/MF A01

900.931 PC A03/MF A01

NISTIR-89/4170

Measurements of Tribological Behavior of Advanced Materials: Summary of U.S. Results on VAMAS (Versailles Advanced Materials and Standards) Round-Robin No. 2. PB90-130295 901,003 PC A05/MF A01

NISTIR-89/4172

Adsorption of High-Range Water-Reducing Agents on Selected Portland Cement Phases and Related Materials. PB90-124306 900,583 PC A03/MF A01

NISTIR-89/4173

Corrosion Behavior of Mild Steel in High pH Aqueous 901,086 PC A03/MF A01

NISTIR-89/4174

Tensile Tests of Type 305 Stainless Steel Mine Sweeping PB90-130287 901,112 PC A03/MF A01

NISTIR-89/4175

Post-Occupancy Evaluation of Several U.S. Government Buildings. PB90-112384 900.088 PC A08/MF A01

NISTIR-89/4178

Proceedings of the Workshop on Cement Stabilization of Low-Level Radioactive Waste. Held at Gaithersburg, Maryland on May 31-June 2, 1989. NUREG/CP-0103 901,302 PC A10/MF A02

NISTIR-89/4180

Publications of the Center for Manufacturing Engineering Covering the Period January 1978-December 1988. PB90-130568 901,012 PC A07/MF A01

NISTIR-89/4183

Center for Radiation Research (of the National Institute of Standards and Technology) Technical Activities for 1989, PB90-130279 901,307 PC A09/MF A01

NISTIR-89/4184

Center for Atomic, Molecular, and Optical Physics Technical Activities, 1989. PB90-133158 901,586 PC A16/MF A02

NISTIR-89/4187

Emerging Technologies in Manufacturing Engineering. PB90-132747 901,013 PC A04/MF A01

NISTIR-89/4188

Summaries of Center for Fire Research In-House Projects and Grants: 1989. 900,605 PC A10/MF A02 PB90-127101

NISTIR-89/4189

AMRF Part Model Extensions. PB90-129446

900.967 PC A03/MF A01

NISTIR-89/4192

Effect of a Crystal-Melt Interface on Taylor-Vortex Flow. PB90-130261 901.477 PC A03/MF A01

NISTIR-89/4194

Glossary of Standards-Related Terminology. PB90-130246 900,986 PC A03/MF A01

NISTIR-89/4199

Graphics Application Programmer's Interface Standards and CALS (Computer-Aided Acquisition and Logistic Sup-

port). PB90-133091 900.658 PC A03/MF A01

NISTIR-89/4201

Enhancements to the VWS2 (Vertical Workstation 2) Data

Preparation Software. PB90-132713 900,968 PC A04/MF A01

NUREG/CP-0103

Proceedings of the Workshop on Cement Stabilization of Low-Level Radioactive Waste. Held at Gaithersburg, Maryland on May 31-June 2, 1989. NUREG/CP-0103 901,302 PC A10/MF A02

PAT-APPL-6-909 433

Electrodeposition of Chromium from a Trivalent Electrolyte. PATENT-4 804 446 901,119 Not available NTIS PAT-APPL-6-922 811 Non-Aqueous Dental Cements Based on Dimer and Trimer

ACIOS. PATENT-4 832 745

900,033 Not available NTIS PAT-APPL-7-063 558

Multiple Actuator Hydraulic System and Rotary Control Valve Therefor.
PATENT-4 838 145 900,995 Not available NTIS

PAT-APPL-7-089 893

Method of and Apparatus for Real-Time Crystallographic Axis Orientation Determination.
PATENT-4 747 684 901,383 Not available NTIS

PATENT-4 747 684

Method of and Apparatus for Real-Time Crystallographic Axis Orientation Determination. PATENT-4 747 684 901,383 Not available NTIS

PATENT-4 804 446

Electrodeposition of Chromium from a Trivalent Electrolyte. PATENT-4 804 446 901,119 Not available NTIS

PATENT-4 832 745 Non-Aqueous Dental Cements Based on Dimer and Trimer

Acids. PATENT-4 832 745 900.033 Not available NTIS

PATENT-4 838 145

Multiple Actuator Hydraulic System and Rotary Control Valve Therefor. PATENT-4 838 145 900.995 Not available NTIS

PB89-143283

Finite Unions of Closed Subgroups of the n-Dimensional Torus.

901.193 PC A03/MF A01

PB89-143283

PB89-144794 Product Data Exchange Specification: First Working Draft. PB89-144794 900,940 PC A99/MF E18

PB89-145114

Journal of Physical and Chemical Reference Data, Volume 17, Number 4, 1988. PB89-145114

900,268 Not available NTIS

PB89-145122

Evaluated Chemical Kinetic Data for the Reactions of Atomic Oxygen O(3P) with Sulfur Containing Compounds. PB89-145122 900,269 Not available NTIS

New International Skeleton Tables for the Thermodynamic Properties of Ordinary Water Substance.
PB89-145130 900,270 Not available NTIS PB89-145148

Benzene Thermophysical Properties from 279 to 900 K at Pressures to 1000 Bar. PB89-145148

PB89-145155

900,271 Not available NTIS

Estimation of the Thermodynamic Properties of Hydrocarbons at 298.15 K. 900,272 Not available NTIS

PB89-145155 PB89-145163

Wavelengths and Energy Level Classifications of Scandium Spectra for All Stages of Ionization. PB89-145163 900,273 Not available NTIS

PB89-145171

Atomic Weights of the Elements 1987. PB89-145171 900,274 Not available NTIS

PB89-145189

CODATA (Committee on Data for Science and Technology) Recommended Values of the Fundamental Physical Constants, 1986. PB89-145189 900,275 Not available NTIS

PB89-145197

Journal of Physical and Chemical Reference Data, Volume 17, 1988, Supplement No. 3. Atomic Transition Probabilities Scandium through Manganese.

900.276 Not available NTIS PB89-145197

PB89-145205

Journal of Physical and Chemical Reference Data, Volume 17, 1988, Supplement No. 2. Thermodynamic and Transport Properties for Molten Salts: Correlation Equations for Critically Evaluated Density, Surface Tension, Electrical Conductance, and Viscosity Data.

PB89-145205

900,277

Not available NTIS

PB89-146278

In Situ Fluorescence Monitoring of the Viscosities of Particle-Filled Polymers in Flow.
PB89-146278 900,609 PC A03/MF A01

PB89-146658

Rate Constants for the Reaction HO2+ NO2+ N2-> HO2NO2+ N2: The Temperature Dependence of the Fall-Off Parameters. 900,278 Not available NTIS

PB89-146666

Multiphoton Ionization Spectroscopy and Vibrational Analysis of a 3p Rydberg State of the Hydroxymethyl Radical. PB89-146666 900,279 Not available NTIS

PB89-146674

Gas Phase Proton Affinities and Basicities of Molecules: A Comparison between Theory and Experiment. PB89-146674 900,280 Not available NTIS

PB89-146682

Radiation-Induced Crosslinks between Thymine and 2-D-Deoxyerythropentose. PB89-146682 900,247 Not available NTIS

PB89-146690

Electronic, Magnetic, Superconducting and Amorphous-Forming Properties Versus Stability of the Ti-Fe, Zr-Ru and Hf-Os Ordered Alloys. 901,120 Not available NTIS

PB89-146708

Effects of Space Charge on the Poling of Ferroelectric Polymers. PB89-146708 901,179 Not available NTIS

PB89-146716

Effects of Punified Femic Oxalate/Nitric Acid Solutions as a Pretreatment for the NTG-GMA and PMDM Bonding System. PB89-146716 900.034 Not available NTIS

PB89-146724

Effect of Crosslinks on the Phase Separation Behavior of a Miscible Polymer Blend.
PB89-146724
900,546
Not available NTIS

PB89-146732

Bonding Agents and Adhesives: Reactor Response. PB89-146732 900.035 Not available NTIS

PB89-146740

Optical Nondestructive Evaluation at the National Bureau of Standards. PB89-146740 900.976 Not available NTIS

PB89-148757

Liposome-Enhanced Flow Injection Immunoanalysis. PB89-146757 900,036 Not available NTIS PB89-148773

Developing Definitive Methods for Human Serum Analytes. PB89-146773 901,233 Not available NTIS PB89-146781

General Methodology for Machine Tool Accuracy Enhancement by Error Compensation.
PB89-146781 900,996 Not available NTIS

PB89-148799

Standard Reference Materials for X-ray Diffraction, Part 1. Overview of Current and Future Standard Reference Materials. PB89-146799 901.384 Not available NTIS

PB89-146807

Speciation Measurements of Butyltins: Application to Controlled Release Rate Determination and Production of Reference Standards.

PB89-146807 900,174 Not available NTIS PR89-146815

Magnetic Field Dependence of the Superconductivity in Bi-Sr-Ca-Cu-O Superconductors. PB89-146815 901,385 Not available NTIS

PR89-146823

Defect Intergrowths in Barium Polytitanates. 1. Ba2Ti9O20. PB89-146823 901,014 Not available NTIS

PB89-146831

Defect Intergrowths in Barium Polytitanates. 2. BaTi**5**O11. PB89-146831 *901,015* Not available NTIS PB89-146849 Critical Assessment of Requirements for Ceramic Powder

naracterization.

PB89-146849 901,016 Not available NTIS PB89-146856

Application of SANS (Small Angle Neutron Scattering) to Ceramic Characterization.
PB89-146856 901,017 Not available NTIS

PB89-146864

Adsorption Properties of Pt Films on W(110). PB89-146864 900,281 Not available NTIS

PB89-146872

Analytical Applications of Neutron Depth Profiling. PB89-146872 901,294 Not available NTIS

PB89-146880

Analytical Model for the Steady-State and Transient Characteristics of the Power Insulated-Gate Bipolar Transistor. PB89-146880 900,767 Not available NTIS

PB89-146898

Core-Level Binding-Energy Shifts at Surfaces and in Solids. PB89-146898 900,282 Not available NTIS

PB89-146906

Determining Picogram Quantities of U in Human Urine by Thermal Ionization Mass Spectrometry. PB89-146906 900,175 Not available NTIS

PB89-146914

Measurement Procedures for Electromagnetic Compatibility Assessment of Electroexplosive Devices. PB89-146914 901,314 Not available NTIS

PB89-146922

Multiple Scattering in the X-ray-Absorption Near-Edge Structure of Tetrahedral Ge Gases. 900,283 Not available NTIS PB89-146922

PB89-148930

Simple Technique for Investigating Defects in Coaxial Con-PB89-146930 900,723 Not available NTIS

PB89-146948

Ultrasonic Texture Analysis for Polycrystalline Aggregates of Cubic Materials Displaying Orthotropic Symmetry. PB89-146948 901,121 Not available NTIS

PR89-146955

Use of Artificial Intelligence and Microelectronic Test Structures for Evaluation and Yield Enhancement of Microelectronic Interconnect Systems. PB89-146955 900,768 Not available NTIS

PB89-146963

Synthesis and Characterization of Ettringite and Related Phases. PB89-146963 900,238 Not available NTIS

PB89-146971

Interpretation of the Effects of Retarding Admixtures on Pastes of C3S, C3A plus Gypsum, and Portland Cement. PB89-146971 900,580 Not available NTIS

PR89-146989

Implications of Computer-Based Simulation Models, Expert Systems, Databases, and Networks for Cement Research. PB89-146989 900,681 Not available NTIS

PB89-146997

Stress Effects on III-V Solid-Liquid Equilibria. PB89-146997 900,769 Not available NTIS

PB89-147003

900.915 Not available NTIS

Notion of Granularity. PB89-147003

PB89-147011 Fundamental Configurations in Mo IV Spectrum. PB89-147011 900,284 Not available NTIS

PB89-147029

Hydroxyl Radical Induced Cross-Linking between Phenyla-lanine and 2-Deoxyribose. PB89-147029 900,547 Not available NTIS

PB89-147037

Application of Synergistic Microanalysis Techniques to the Study of a Possible New Mineral Containing Light Ele-PB89-147037 901.277 Not available NTIS

PB89-147045

Prediction of Tensile Behavior of Strain Softened Composites by Flexural Test Methods. PB89-147045 900.585 Not available NTIS

PB89-147052

Theory and Practice of Paper Preservation for Archives PB89-147052 900,934 Not available f 900,934 Not available NTIS PB89-147060

Thermodynamics of Ammonium Scheelites. 6. An Analysis of the Heat Capacity and Ancillary Values for the Metaperiodates KIO4, NH4IO4, and ND4IO4. PBB9-147060 900,285 Not available NTIS

PR89-147078

Performance of Alumina/Epoxy Thermal Isolation Straps. PB89-147078 901,070 Not available NTIS

PB89-147086 Economical Ultrahigh Vacuum Four-Point Resistivity Probe. PB89-147086 900,870 Not available NTIS

PB89-147094

Thin Film Thermocouples for Internal Combustion Engine PB89-147094 900,607 Not available N Not available NTIS PB89-147102

Sputter Deposition of Icosahedral Al-Mn and Al-Mn-Si, PB89-147102 901,122 Not available NTIS

PB89-147110

Unimolecular Dynamics Following Vibrational Overtone Excitation of HN3 v1 = 5 and v1 = 6:HN3(X tilde;v,J,K,) -> HN((X sup 3)(Sigma (1-));v,J,Omega) + N2(x sup 1)(Sigma sub g (1 +)). PB89-147110

900,286 Not available NTIS

PB89-147128

PB89-147433

Electronic Structure of Diammine (Ascorbato) Platinum(II) and the Trans Influence on the Ligand Dissociation Energy. PB89-147128 900,287 Not available NTIS PB89-147375

Electric-Dipole Moments of H2O-Formamide and CH3OH-Formamide. PB**8**9-147375

900,288 Not available NTIS PB89-147383

Quasicrystals with 1-D Translational Periodicity and a Ten-Fold Rotation Axis.

901,123 Not available NTIS PB89-147391

Metallographic Evidence for the Nucleation of Subsurface Microcracks during Unlubricated Sliding of Metals. PB89-147391 901,001 Not available NTIS

PB89-147409

Ultrasonic Characterization of Surface Modified Layers. PB89-147409 901,115 Not available NTIS

PB89-147417 Vibrational Predissociation of the Nitric Oxide Dimer

PB89-147417 900,289 Not available NTIS PB89-147425

Mathematical Software: PLOD. Plotted Solutions of Differential Equations. PB89-147425 901 194 Not available NTIS

High Resolution Imaging of Magnetization. PB89-147433 901,386 Not available NTIS PB89-147441

Molecular Dynamics Study of a Dipolar Fluid between Charged Plates.
PB89-147441 900,290 Not available NTIS

PB89-147458 Microwave Measurements of the Thermal Expansion of a Spherical Cavity.

PB89-147458 900,291 Not available NTIS

PR89-147466

Use of Multiple-Slot Multiple Disk Chopper Assemblies to Pulse Thermal Neutron Beams, PB89-147466 901,485 Not available NTIS PB89-147474

Far-Infrared Laser Magnetic Resonance Spectrum of Vibrationally Excited C2H(1).
PB89-147474 900,292 Not available NTIS PB89-147482

Aerodynamics of Agglomerated Soot Particles. PB89-147482 900.586 Not a

900,586 Not available NTIS PB89-147490

Dichromate Dosimetry: The Effect of Acetic Acid on the Radiolytic Reduction Yield.

PB89-147490

900,248

Not available NTIS 900,248 Not available NTIS PB89-147508

Measurement Quality Assurance. PB89-147508 901,298 Not available NTIS PB89-147821

Epoxy Impregnation Procedure for Hardened Cement Sam-

PB89-147821 901.180 PC A03/MF A01 PB89-147839

Measurement of Adapter Loss, Mismatch, and Efficiency Using the Dual Six-Port. PB89-147839 901,316 PC A10/MF A01

PB89-147847 Metrology for Electromagnetic Technology: A Bibliography of NBS (National Bureau of Standards) Publications. PB89-147847 900,871 PC A04/MF A01

PB89-148092

Guidelines and Procedures for Implementation of Executive Order on Seismic Safety.
PB89-148092
900,156
PC A03/MF A01

PB89-148100

Development of Standard Measurement Techniques and Standard Reference Materials for Heat Capacity and Heat of Vaporization of Jet Fuels.

PB89-148100 900.837 PC A03/MF A01 PB89-148118

Flow of Molecules Through Condoms. PB89-148118

901.087 PC A03/MF A01 PB89-148126

Calculating Flows through Vertical Vents in Zone Fire Models under Conditions of Arbitrary Cross-Vent Pressure Difference PB89-148126 900,108 PC A03/MF A01

PB89-148134

Predicting Formaldehyde Concentrations in Manufactured Housing Resulting from Medium-Density Fiberboard. PB89-148134 900,854 PC A03/MF A01

PB89-148365

Magnetostatic Measurements for Mine Detection. PB89-148365 900,685 PC A03/MF A01

PB89-148373

Microporous Fumed-Silica Insulation Board as a Candidate Standard Reference Material of Thermal Resistance.
PB89-148373 901,018 PC A03/MF A01 PB89-148373

PB89-148381

Institute for Materials Science and Engineering, Ceramics: Technical Activities 1988. PB89-148381 901,019 PC A05/MF A01

PB89-148399

Institute for Materials Science and Engineering, Fracture and Deformation: Technical Activities 1988. PB89-148399 901,071 PC A05/MF A01

PB89-148407

Experimental Thermal Conductivity, Thermal Diffusivity, and Specific Heat Values of Argon and Nitrogen. PB89-148407 900,293 PC A04/MF A01

PR89-148415

Standards for the Interchange of Large Format Tiled Raster Documents. PB89-148415 900.668 PC A04/MF A01

PB89-148514

Preliminary Performance Criteria for Building Materials, Equipment and Systems Used in Detention and Correctional Facilities PB89-148514 900,109 PC A08/MF A01

PB89-149058

Possible Quantum Hall Effect Resistance Standard. PB89-149058 900,801 Not available NTIS

PB89-149066

NBS (National Bureau of Standards) Ohm: Past-Present-Future. PB89-149066 900,802 Not available NTIS

PB89-149074

Thermal-Expansive Growth of Prebreakdown Streamers in Liquids. PB89-149074 900,803 Not available NTIS

PB89-149082

Local Brittle Zones in Steel Weldments: An Assessment of Test Methods. PB89-149082 901.092 Not available NTIS

PB89-149090

J-Integral Values for Small Cracks in Steel Panels. PB89-149090 901,093 Not available NTIS PB89-149090 PB89-149108

Interpretation of a between-Time Component of Error in Mass Measurements.
PB89-149108 900,872 Not available NTIS

PB89-149116

Case History: Development of a Software Engineering Standard. PB89-149116 900.665 Not available NTIS PB89-149124

QCD Vacuum. PB89-149124 901,486 Not available NTIS

PB89-149132

Earthquake Hazard Mitigation through Improved Seismic Design. PB89-149132 900,098 Not available NTIS PB89-149140

Earthquake Resistant Design Criteria. PB89-149140 900.05

900.099 Not available NTIS PB89-149157

Evaporation of a Water Droplet Deposited on a Hot High Thermal Conductivity Solid Surface.
PB89-149157 901,487 Not available NTIS

PB89-149165

Cone Calorimeter Method for Determining the Flammability of Composite Materials. PB89-149165 901.072 Not available NTIS

PB89-149173

Combustion of Oil on Water. PB89-149173 900,587 Not available NTIS PB89-149181

Surface Structure and Growth Mechanism of Ga on Si(100). PB89-149181 901,387 Not available NTIS PB89-149199

Doppler Imaging of AR Lacertae at Three Epochs. PB89-149199 900,015 Not available. 900,015 Not available NTIS

PB89-149207 Late Stages of Close Binary Systems-Clues to Common Envelope Evolution. PB89-149207 900.016 Not available NTIS

PB89-149215

Special Calibration Systems for Reactive Gases and Other Difficult Measurements. 900.873 Not available NTIS PB89-149215

PE89-149223 Micro-Raman Characterization of Atherosclerotic and Bio-

prosthetic Calcification. PB89-149223 901,234 Not available NTIS

PB89-149231

Stokes and Anti-Stokes Fluorescence of Er(3+) in the Raman Spectra of Erbium Oxide and Erbium Glasses.
PB89-149231 901,020 Not available NTIS

PB89-149249

Cooling Effect Induced by a Single Evaporating Droplet on a Semi-Infinite Body.
PB89-149249 901,488 Not available NTIS

PB89-149256 Optical Rotation.

900,294 Not available NTIS PB89-149264

Mode-Stirred Chamber for Measuring Shielding Effectiveness of Cables and Connectors: An Assessment of MIL-STD-1344A Method 3008. 900.737 Not available NTIS

PB89-149264 PB89-149272

Microwave Power Standards. PB89-149272

900.687 Not available NTIS

PB89-149280

Calibrating Antenna Standards Using CW and Pulsed-CW Measurements and the Planar Near-Field Method. PB89-149280 900,693 Not available NTIS

PB89-150726

Antenna Measurements for Millimeter Waves at the National Bureau of Standards. PB89-150726 900,694 Not available NTIS

PB89-150734

Knowledge Based System for Durable Reinforced Con-PB89-150734 900.110 Not available NTIS

PB89-150742

Standard Specifications for Cements and the Role in Their Development of Quality Assurance Systems for Laborato-PB89-150742 901.021 Not available NTIS

PB89-150759

Implications of Phase Equilibria on Hydration in the Tricalcium Silicate-Water and the Tricalcium Aluminate-Gypsum-Water Systems. PB89-150759 901,022 Not available NTIS

PB89-150767

Autodetaching States of Negative Ions. PB89-150767 900,295 Not available NTIS

PB89-150775

Draft International Document on Guide to Portable Instru-ments for Assessing Airborne Pollutants Arising from Haz-ardous Wastes. PB89-150775 900.855 Not available NTIS

PB89-150783

Experimental Validation of a Mathematical Model for Predicting Moisture Transfer in Attics.

PB89-150783 900,057 Not available NTIS

PB89-150791

Refinement of Neutron Energy Deposition and Microdosimetry Calculations. PB89-150791 901,264 Not available NTIS

PB89-150809

Automated Documentation System for a Large Scale Manufacturing Engineering Research Project.
PB89-150809 900,941 Not available NTIS

PB89-150817

Resonance Ionization Mass Spectrometry of Mg: The 3pnd Autoionizing Series. PB89-150817 900,296 Not available NTIS

PB89-150825

Review of Thermal Characterization of Power Transistors. PB**89**-150825 *900,770* Not available NTIS PR89-150833

Indirect Energy Gap of Si, Doping Dependence. PB89-150833 901,388 Not available NTIS PB89-150841

Preliminary Experiments with Three Identical Ultraprecision Machine Tools.
PB89-150841 900,997 Not available NTIS

PB89-150858

Comparison of Detection Limits in Atomic Spectroscopic Methods of Analysis.

PB89-150858 900,176 Not available NTIS PB89-150866

Angle Resolved XPS (X-ray Photoelectron Spectroscopy) of the Epitaxial Growth of Cu on Ni(100).

PB89-150866 901,389 Not available NTIS PB89-150874 Generalized Mathematical Model for Machine Tool Errors PB89-150874 900,977 Not available NT

Not available NTIS

PB89-150882

Multicritical Phase Relations in Minerals. PB89-150882 901,278 Not available NTIS PB89-150882

PB89-150890

Corrosion of Metallic Implants and Prosthetic Devices. PB89-150890 900,053 Not available NTIS

PB89-150908

Reactions of Phenyl Radicals with Ethene, Ethyne, and Benzene. PB89-150908 900,297 Not available NTIS

PB89-150916

Final-State-Resolved Studies of Molecule-Surface Interac-PB89-150916 900,298 Not available NTIS

PB89-150924

Combustion Testing Methods for Catalytic Heaters. PB89-150924 900,846 Not available NTIS

PB89-150932

Solutal Convection during Directional Solidification. PB89-150932 901,322 Not available NTIS PB89-150940

Environmental Standard Reference Materials - Present and Future Issues PB89-150940 900,865 Not available NTIS PB89-150957

Ultrasonic Determination of Absolute Stresses in Aluminum and Steel Alloys. PB89-150957 901,124 Not available NTIS

PB89-150965

Measurement Standards for Defense Technology. PB89-150965 901,270 Not available NTIS

PB89-150973

Submicrometer Optical Metrology. PB89-150973 900,771 Not available NTIS

PB89-150981

Relative Acidities of Water and Methanol and the Stabilities of the Dimer Anions. PB89-150981 900,299 Not available NTIS

PB89-150999

Redox Chemistry of Water-Soluble Vanadyl Porphyrins. PB89-150999 900,300 Not available NTIS

PB89-151005

Reactions of Magnesium Prophyrin Radical Cations in Water. Disproportionation, Oxygen Production, and Comparison with Other Metalloporphyrins.
PB89-151005 900,301 Not available NTIS

PB89-151013

Rate Constants for One-Electron Oxidation by Methylperoxyl Radicals in Aqueous Solutions.

PR89-151013 900,302 Not available NTIS

PB89-151211

NBS (National Bureau of Standards) Life-Cycle Cost (NBSLCC) Program (for Microcomputers).
PB89-151211 900,849 CP D99

PB89-151625

Institute for Materials Science and Engineering, Nonde-structive Evaluation: Technical Activities 1988. PB89-151625 900,917 PC A04/MF A01

PB89-151765

ZIP: The ZIP-Code Insulation Program (Version 1.0) Economic Insulation Levels for New and Existing Houses by Three-Digit ZIP Code. Users Guide and Reference Manual. 900,058 PC A03/MF A01

Technical Activities, 1988, Center for Analytical Chemistry. PB89-151773 900.177 PC A09/MF A01

PB89-151781

Fire Propagation in Concurrent Flows. PB89-151781 900,867 PC A04/MF A01

PB89-151799

Design Protocol, Part Design Editor, and Geometry Library of the Vertical Workstation of the Automated Manufacturing Research Facility at the National Bureau of Standards. PB89-151799 900,936 PC A06/MF A01

PR89-151807

Wavefront Matrix Multiplication on a Distributed-Memory Multiprocessor. PB89-151807 900,646 PC A04/MF A01

PB89-151815

Small Computer System Interface (SCSI) Command System: Software Support for Control of Small Computer System Interface Devices. PR89-151815 900 659 PC A06/MF A01

PB89-151823

Intelligent Processing of Materials: Report of an Industrial Workshop Conducted by the National Institute of Standards and Technology. 900,942 PC A04/MF A01

PB89-151831

Semiconductor Measurement Technology: Automatic Determination of the Interstitial Oxygen Content of Silicon Wafers Polished on Both Sides.
PB89-151831
900,772
PC A04/MF A01

PB89-151922

Chemical Characterization of Ionizing Radiation-Induced Damage to DNA

PB89-151922

PB89-153704 Standard Reference Materials: Description of the SRM 1965 Microsphere Slide.
PB89-153704

901,390
PC A04/MF A01

901,235 Not available NTIS

PB89-153860

Energy Prices and Discount Factors for Life-Cycle Cost Analysis 1988: Annual Supplement to NBS (National Bureau of Standards) Handbook 135 and NBS Special Publication 709. PB89-153860 900,850 PC A04/MF A01

PB89-153878

Trapped lons and Laser Cooling 2: Selected Publications of the lon Storage Group, Time and Frequency Division, NIST, Boulder, CO. PB89-153878 901,489 PC A09/MF A01

PB89-153886

Iterative Technique to Correct Probe Position Errors in Planar Near-Field to Far-Field Transformations. PB89-153886 900,695 PC A03/MF A01

PB89-153894

NIST (National Institute of Standards and Technology)
Measurement Services: Mass Calibrations.
PB89-153894 900,874 PC A05/MF A01

PB89-154322

U.S. Organizations Represented in the Collection of Voluntary Standards. PB89-154322 900,978 PC E06/MF E01

PB89-154835

Wind and Seismic Effects. Proceedings of the Joint Meeting of the U.S.-Japan Cooperative Program in Natural Resources Panel on Wind and Seismic Effects (20th) Held in Gaithersburg, Maryland on May 17-20, 1988, PB89-154835 900,157 PC A21/MF A01

PB89-156152

Development of Near-Field Test Procedures for Communication Satellite Antennas, Phase 1, Part 2.

PB89-156152

901,593

PC A05/MF A01

PB89-156160

Postweld Heat Treatment Criteria for Repair Welds in 2-1/4Cr-1Mo Superheater Headers: An Experimental Study. PB89-156160 901,094 PC A04/MF A01

PR89-156350

Structural Reliability and Damage Tolerance of Ceramic Composites for High-Temperature Applications. Semi-Annual Progress Report for the Period Ending September

PB89-156350 901,023 PC A03/MF A01

PB89-156368

Structural Reliability and Damage Tolerance of Ceramic Composites for High-Temperature Applications. Semi-Annual Progress Report for the Period Ending March 31, 1988. 901,024 PC A03/MF A01 PR89-156368

PB89-156376

Center for Chemical Technology: 1988 Technical Activities. PB89-156376 900,241 PC A08/MF A01

PB89-156384

Integrated Manufacturing Data Administration System (IMDAS) Operations Manual. PB89-156384 900,916 PC A03/MF A01

PB89-156723

Qualitative MO Theory of Some Ring and Ladder Polymers. PB89-156723 900,303 Not available NTIS

PB89-156731

New Photolytic Source of Dioxymethylenes: Criegee Intermediates Without Ozonolysis.
PB89-156731 900,304 Not available NTIS

PB89-156749

Kinetics of Electron Transfer from Nitroaromatic Radical Anions in Aqueous Solutions. Effects of Temperature and Steric Configuration. PB89-156749 900,305 Not available NTIS

PB89-156756

Hyperconjugation: Equilibrium Secondary Isotope Effect on the Stability of the t-Butyl Cation. Kinetics of Near-Thermoneutral Hydride Transfer.
PB89-156756 900,306 Not available NTIS

PB89-156764

Detection of Gas Phase Methoxy Radicals by Resonance Enhanced Multiphoton Ionization Spectroscopy. PB89-156764 900,307 Not available NTIS

PB89-156772

Decay of High Valent Manganese Porphyrins in Aqueous Solution and Catalyzed Formation of Oxygen.
PB89-156772 900,308 Not available NTIS

PB89-156780

Two-Layer Dielectric Microstrip Line Structure: SiO2 on Si and GaAs on Si; Modeling and Measurement. PB89-156780 900,738 Not available NTIS

PB89-156798

Spherical-Wave Source-Scattering Matrix Analysis of Coupled Antennas: A General System Two-Port Solution.
PB89-156798 900,696 Not available NTIS

PB89-156806

Improved Spherical and Hemispherical Scanning Algorithms. PB89-156806 900.697 Not available NTIS PB89-156814

Improved Polarization Measurements Using a Modified Three-Antenna Technique. Three-Antenna PB89-156814 900.698 Not available NTIS

PR89-156822

Gain and Power Parameter Measurements Using Planar Near-Field Techniques.

900,699 Not available NTIS

PB89-156822 PB89-156830

Fields of Horizontal Currents Located Above the Earth.
PB89-156830 900,700 Not available NTIS

PB89-156848

Error Analysis Techniques for Planar Near-Field Measure-PB89-156848 900,701 Not available NTIS

PB89-156855

Comparison of Measured and Calculated Antenna Sidelobe Coupling Loss in the Near Field Using Approximate Far-Field Data.
PB9-156855 900,702 Not available NTIS

PB89-156863

Brief History of Near-Field Measurements of Antennas at the National Bureau of Standards.
PB89-156863 900,703 Not available NTIS

PB89-156871

Accurate Determination of Planar Near-Field Correction Parameters for Linearly Polarized Probes.
PB89-156871 900,704 Not available NTIS

PB89-156889

Standard Reference Materials for the Determination of Polycyclic Aromatic Hydrocarbons. PB89-1568**89** 900,178 Not available NTIS

PB89-156897

Sequential Determination of Biological and Pollutant Elements in Marine Bivalves. PB89-156897 901,217 Not available NTIS

PB89-156905

Sample Validity in Biological Trace Element and Organic Nutrient Research Studies.
PB89-156905 901,218 Not available NTIS

PB89-156913

Radiochemical Procedure for Ultratrace Determination of Chromium in Biological Materials.
PB89-156913 900,179 Not available NTIS

PB89-156921

Neutron Activation Analysis of the NIST (National Institute of Standards and Technology) Bovine Serum Standard Reference Material Using Chemical Separations. 900,180 Not available NTIS

PB89-156939

Long-Term Stability of the Elemental Composition in Biological Materials.

PB89-156939 900.181 Not available NTIC

PB89-156947

High-Accuracy Differential-Pulse Anodic Stripping Voltammetry with Indium as an Internal Standard.
PB89-156947 900,182 Not available NTIS

PB89-156954

High Accuracy Determination of (235)U in Nondestructive Assay Standards by Gamma Spectrometry. PB89-156954 900,249 Not available NTIS

PB89-156962

Detection of Uranium from Cosmos-1402 in the Stratosphere. PB89-156962 901.592 Not available NTIS

PB89-156970

Activation Analysis Opportunities Using Cold Neutron PB89-15**6**970 900,183 Not available NTIS

PB89-156988

Effect of an Oil-Paper Interface Parallel to an Electric Field on the Breakdown Voltage at Elevated Temperatures. PB89-156988 901,490 Not available NTIS

PB89-156996

Ultrasensitive Laser Spectroscopy and Detection. PB89-156996 901,336 Not available NTIS

PB89-157002

U.S. Perspective on Possible Changes in the Electrical Units. PB89-157002 901,491 Not available NTIS

PB89-157010

Control System Simulation in North America. PB89-157010 900,091 Not available NTIS

PB89-157028

Waveguide Loss Measurement Using Photothermal Deflection. PB89-157**0**28 900,739 Not available NTIS

PB89-157036

SIS Quasiparticle Mixers with Bow-Tie Antennas. PB89-157036 900,705 Not available NTIS

PB89-157044

Oxygen Isotope Effect in the Superconducting Bi-Sr-Ca-Cu-O System. PB89-157044 901,025 Not available NTIS

PB89-157051

Measurement of Integrated Tuning Elements for SIS Mixers with a Fourier Transform Spectrometer.
PB89-157051 900,706 Not available NTIS

PB89-157069

Fresnel Lenses Display Inherent Vignetting. PB89-157069 901,337 Not available NTIS

PB89-157077

Current Ripple Effect on Superconductive D.C. Critical Current Measurements. PB**89**-157077 901,492 Not available NTIS

PB89-157085

Trace Speciation by HPLC-GF AA (High-Performance Liquid Chromatography-Graphite Furnace Atomic Absorption) for Tin- and Lead-Bearing Organometallic Compounds, with Signal Increases Induced by Transition-Metal Ions. PB83-157085 900,184 Not available NTIS

PB89-157093

Resonant Raman Scattering of Controlled Molecular Weight Polyacetylene. PB89-157093

900,548 Not available NTIS PB89-157101

Polymers Bearing Intramolecular Photodimerizable Probes for Mass Diffusion Measurements by the Forced Rayleigh Scattering Technique: Synthesis and Characterization. PBB9-157101 901,181 Not available NTIS

PB89-157119

Phase Contrast Matching in Lamellar Structures Composed of Mixtures of Labeled and Unlabeled Block Copolymer for Small-Angle Neutron Scattering.
PB89-157119
901,182
Not available NTIS

PB89-157127

Interaction of Cupric Ions with Calcium Hydroxylapatite. PB89-157127 900,037 Not available NTIS

PB89-157135

Effect of pH on the Emission Properties of Aqueous tris

(2,6-dipicolinato) Terbium (III) Complexes. PB89-157135 900,250 Not available NTIS

PB89-157143

Casting Metals: Reactor Response. PB89-157143 900,054 Not available NTIS

PB89-157150

Biological Evaluations of Zinc Hexyl Vanillate Cement Using Two In vivo Test Methods. PB89-157150 900,038 Not available NTIS

900,038 Not available NTIS PB89-157168

Adhesion to Dentin by Means of Gluma Resin. PB89-157168 900,039 Not available NTIS

Analytical Expression for Describing Auger Sputter Depth Profile Shapes of Interfaces.

PB89-157176 900,309 Not available NTIS

PB89-157184

Semi-Automated PVT Facility for Fluids and Fluid Mixtures. PB89-157184 900,875 Not available NTIS

PB89-157192

PVT of Toluene at Temperatures to 673 K PB89-157192 900,310 N

PVT Measurements on Benzene at Temperatures to 723 K. PB89-157200 900,311 Not available NTIS

PB89-157218

Molecular Dynamics Study of a Dipolar Fluid between Charged Plates. 2. PB89-157218 900.312 Not available NTIS

PB89-157226

Local Order in a Dense Liquid. PB89-157226

900.313 Not available NTIS

900,310 Not available NTIS

PB89-157234

Light Scattering from Simulated Smoke Agglomerates. PB89-157234 900,588 Not available NTIS

PB89-157242

Hydrodynamics of Magnetic and Dielectric Colloidal Disper-

PR89-157242

900,314 Not available NTIS PB89-157259

Effect of Surface Ionization on Wetting Layers. PB89-157259 901,323 Not available NTIS

PB89-157267

Computer Model of Smoke Movement by Air Conditioning Systems (SMACS). PB89-157267 900,059 Not available NTIS

PB89-157275

Analytical Methods for Firesafety Design. PB89-157275 900,111 Not available NTIS

PB89-157283

Two-Photon Laser-Induced Fluorescence of the Tumor-Lo-calizing Photosensitizer Hematoporphyrin Derivative. PB89-157283 901,240 Not available NTIS

PB89-157291

Population Relaxation of CO(v= 1) Vibrations in Solution Phase Metal-Carbonyl Complexes PB89-157291 900,315 Not available NTIS

PB89-157309

Picosecond Studies of Vibrational Energy Transfer in Molecules on Surfaces.

PR89-157309 900,316 Not available NTIS PB89-157317

Picosecond Study of the Population Lifetime of CO(v=1) Chemisorbed on SiO2-Supported Rhodium Particles. PB**89**-157317 900,317 Not available NTIS

PB89-157325

Microwave Spectrum, Structure, and Electric Dipole Moment of the Ar-Formamide van der Waals Complex. PB89-157325 900,318 Not available NTIS

PB89-157333

Microwave Spectrum and (14)N Quadrupole Coupling Constants of Carbazole.
PB89-157333 900,319 Not available NTIS

PB89-157341

Infrared and Microwave Investigations of Interconversion Tunneling in the Acetylene Dimer.
PB89-157341 900,320 Not available NTIS

PB89-157358

Optical Sensors for Robot Performance Testing and Calibration PB89-157358 900,987 Not available NTIS

PB89-157366

Automated Analysis of Operators on State Tables: A Technique for Intelligent Search.
PB89-157366 900,669 Not available NTIS

PR89-157374

CO2 Separation Using Facilitated Transport Ion Exchange PB89-157374 900.321 Not available NTIS

PB89-157382

Thermal Shifts of the Spectral Lines in the (4)F3/2 to (4)I11/2 Manifold of an Nd:YAG Laser.
PB89-157382 901,338 Not available NTIS

PB89-157390

Precise Test of Quantum Jump Theory. PB89-157390 901,339 Not available NTIS

PB89-157408

Perpendicular Laser Cooling of a Rotating Ion Plasma in a Penning Trap. PB89-157408 901.493 Not available NTIS

PB89-157416

Calibration Tables Covering the 1460- to 1550-cm(-1) Region from Heterodyne Frequency Measurements on the nu(sub 3) Bands of (12)CS2 and (13)CS2. 900,322 Not available NTIS

PB89-157424

Atomic-lon Coulomb Clusters in an Ion Trap. PB89-157424 901,494 Not available NTIS

PB89-157432

Stable and Metastable Ti-Nb Phase Diagrams. PB89-157432 901,125 Not available NTIS PB89-157440

Ozonolysis of Ethylene. Microwave Spectrum, Molecular Structure, and Dipole Moment of Ethylene Primary Ozonide (1,2,3-Troxolane).
PB8-157440 900,323 Not available NTIS

PB89-157457

Efficient and Accurate Method for Calculating and Representing Power Density in the Near Zone of Microwave An-

PB89-157457 PB89-157465

Thermal Degradation of Poly (methyl methacrylate) at 50C PB**89**-1574**6**5 900,549 Not available NTIS

900,707 Not available NTIS

PB89-157473

Temperature, Composition and Molecular-Weight Dependence of the Binary Interaction Parameter of Polystyrene/Poly(vinylmethylether) Blends.
PB99-157473 900,550 Not available NTIS

PB89-157481

Re-Entrant Spin-Glass Properties of a-(FexCr1-x)75P15C10. PB89-157481 901,391 Not available NTIS PB89-157499

Neutron Vibrational Spectroscopy of Disordered Metal Hydrogen Systems.
PB89-157499 900,324 Not available NTIS

PB89-157507

Validation of Absolute Target Thickness Calibrations in a QQQ Instrument by Measuring Absolute Total Cross-Sections of NE(1+) (NE,NE)NE(1+).
PB89-157507 900,325 Not available NTIS

PB89-157515

Stopped-Flow Studies of the Mechanisms of Ozone-Alkene Reactions in the Gas Phase: Tetramethylethylene. PB89-157515 900,326 Not available NTIS PB89-157523

\$2F10 Formation in Computer Simulation Studies of the Breakdown of SF6. PB89-157523 900,327 Not available NTIS

PB89-157531

Ionic Hydrogen Bond and Ion Solvation. 5. OH...(1-)O Bonds. Gas Phase Solvation and Clustering of Alkoxide and Carboxylate Anions. PB89-157531 900,328 Not available NTIS

PB89-157549

Filling of Solvent Shells About Ions. 1. Thermochemical Criteria and the Effects of Isomeric Clusters.

PB89-157549 900,329 Not available NTIS

PB89-157556

Dehydrogenation of Ethanol in Dilute Aqueous Solution Photosensitized by Benzophenones. PB89-157556 900,251 Not available NTIS

PB89-157564

Small Angle Neutron Scattering from Porosity in Sintered Alumina. PB89-157564 901,026 Not available NTIS

PB89-157572

Structure and Radiation Properties of Large-Scale Natural Gas/Air Diffusion Flames. PB89-157572 900,589 Not available NTIS

PB89-157580

Phase Equilibrium in Two-Phase Coherent Solids. PB89-157580 900.330 Not avai 900.330 Not available NTIS PB89-157598

Ostwald Ripening in a System with a High Volume Fraction of Coarsening Phase.
PB89-157598 901,126 Not available NTIS

PB89-157606

Observations on Crystal Defects Associated with Diffusion Induced Grain Boundary Migration in Cu-Zn.
PB89-157606 901,127 Not available NTIS

PB89-157614

Migration of Liquid Film and Grain Boundary in Mo-Ni Induced by W Diffusion. PB89-157614 901,128 Not available NTIS

PB89-157622

Metastable Phase Production and Transformation in Al-Ge Alloy Films by Rapid Crystallization and Annealing Treatments. PB89-157622 901,129 Not available NTIS

PB89-157630

Experimental Observations on the Initiation of DIGM (Diffusion Induced Grain Boundary Migration).
PB89-157630 901,130 Not available NTIS

PB89-157648

Structural Unit in Icosahedral MnAlSi and MnAl. PB89-157648 901,131 Not available NTIS

PB89-157655

Effect of Neutrons on the Characteristics of the Insulated Effect of Neutrons on the Gate Bipolar Transistor (IGBT).

900,773 Not available NTIS

PB89-157663

Proper Motion vs. Redshift Relation for Superluminal Radio 900.017 Not available NTIS

PB89-157663 PB89-157671

Dynamic Young's Modulus Measurements in Metallic Materials: Results of an Interlaboratory Testing Program. PB89-157671 901,132 Not available NTIS

PB89-157689

Theoretical Study of the Vibrational Lineshape for CO/ Pt(111). PB89-157689 900,331 Not available NTIS

PB89-157697

Synchrotron Radiation Study of BaO Films on W(001) and Their Interaction with H2O, CO2, and O2. PB89-157697 900,252 Not available NTIS PB89-157705

Status of Reference Data, Reference Materials and Reference Procedures in Surface Analysis.
PB89-157705
900,332
Not available NTIS

PB89-157713

Semiclassical Way to Molecular Dynamics at Surfaces. PB89-157713 900,333 Not available NTIS

PB89-157721

Refinement of the Substructure and Superstructure of Romanechite. PB89-157721 901.392 Not available NTIS

PB89-157739

Preparation of Accurate Multicomponent Gas Standards of

Volatile Toxic Organic Compounds in the Low-Parts-per-Billion Range. PB89-157739

900.185 Not available NTIS PB89-157747

Moydite, (Y, REE) (B(OH)4)(CO3), a New Mineral Species from the Evans-Lou Pegmatite, Quebec.
PB89-157747 900,186 Not available NTIS

PB89-157754 Computer-Aided Imaging: Quantitative Compositional Mapping with the Electron Probe Microanalyzer. PB89-157754 901,073 Not available NTIS

PB89-157762

Application of Multiscattering Theory to Impurity Bands in Si:As.
PB89-157762 900,334 Not available NTIS

PR89-157770 NBS (National Bureau of Standards) Activities in Biological Reference Materials. PB89-157770

901,219 Not available NTIS PR89-157788

Conventional and Quarter-Point Mixed Elements in Linear Elastic Fracture Mechanics. PR89-157788 901.481 Not available NTIS

PB89-158026 PB89-157796 900.342 Not available NTIS PB89-161541 901,497 Not available NTIS Molybdenum Effect on Volume in Fe-Cr-Ni Alloys. PB89-157796 901,095 Not available NTIS PB89-158034 PR89-161558 Effect of Coal Slag on the Microstructure and Creep Behav-NBS (National Bureau of Standards) Decay-Scheme Investigations of (82)Sr-(82)Rb.
PB89-161558 901,498 Not available NTIS ior of a Magnesium-Chromite Refractory.
PB89-158034 901,027 Not available NTIS PB89-157804 Influence of Dislocation Density on the Ductile-Brittle Transition in bcc Metals. PB89-158042 PB89-161566 Standards and Test Methods for VLSI (Very Large Scale Integration) Materials.
PB89-158042 900,774 Not available NTIS PR89-157804 901.133 Not available NTIS Frequency Measurement of the J = 1 < 0 Rotational Transition of HD (Hydrogen Deutende). PB89-161566 901,499 Not available NTIS PB89-157812 Problems with Interval Estimation When Data Are Adjusted via Calibration. PB89-158059 PB89-161574 Free-Electron-Like Stoner Excitations in Fe. PB89-158059 901,393 Not available NTIS PB89-157812 901,209 Not available NTIS Far-Infrared Spectrum of Methyl Amine. Assignment and Analysis of the First Torsional State.
PB89-161574 900,346 Not available NTIS PB89-157820 Estimation of the Error Probability Density from Replicate Measurements on Several Items.
PB89-157820 901,210 Not available NTIS PB89-158067 Domain Images of Ultrathin Fe Films on Ag(100). PB89-158067 901,394 Not available NTIS PB89-161582 Critical Review of the Chemical Kinetics of Sulfur Tetrafluo-ride, Sulfur Pentafluoride, and Sulfur Fluoride (S2F10) in the PB89-157838 PB89-158075 Structure of a Hydroxyl Radical Induced Cross-Link of Thymine and Tyrosine. Spin-Polarized Electron Microscopy. PB89-158075 901,395 Not available NTIS Gas Phase. PB89-161582 900.347 Not available NTIS mine and Tyrosine. PB89-157838 901,244 Not available NTIS PB89-161590 PB89-158083 PB89-157846 Stark Broadening of Spectral Lines of Homologous, Doubly lonized Inert Gases.
PB89-158083 900,343 Not available NTIS Analytical Applications of Resonance Ionization Mass Spectrometry (RIMS).
PB89-161590 900,189 Not available NTIS Shimanouchi, Takehiko and the Codification of Spectroscopic Information. PB89-157846 900,335 Not available NTIS PB89-158091 PB89-161608 Recent Progress on Spectral Data for X-ray Lasers at the National Bureau of Standards.
PB89-158091 901,341 Not available NTIS PB89-157853 Rate Constants for Hydrogen Abstraction by Resonance Stabilized Radicals in High Temperature Liquids. PB89-161608 900,348 Not available NTIS Infrared Absorption of SF6 from 32 to 3000 cm(-1) in the Gaseous and Liquid States. PB89-157853 900.336 Not available NTIS PB89-158109 PB89-161616 PB89-157861 Calculation of Tighter Error Bounds for Theoretical Atomic-Oscillator Strengths. Synthesis and Characterization of Poly(vinylmethyl ether). PB89-161616 900,551 Not available NTIS Tiger Tempering Tampers Transmissions. PB89-157861 900,740 PB89-158109 901,496 Not available NTIS 900,740 Not available NTIS PB89-161871 PB89-158117 PB89-157879 Mixing Motions Produced by Pipe Elbows. PB89-161871 901,326 Numerical Computation of Particle Trajectories: A Model 901.326 PC A03/MF A01 Role of Neutron Activation Analysis in the Certification of NBS (National Bureau of Standards) Standard Reference PB89-161889 PB89-158117 901.324 Not available NTIS Technical Activities 1988, Surface Science Division. PB89-161889 900,349 PC A07/MF A01 900 187 Not available NTIS PB89-158125 PR89-157879 Atomic Transition Probabilities of Argon: A Continuing Chal-PB89-157887 PB89-161897 lenge to Plasma Spectroscopy.
PB89-158125 900,344 Not available NTIS Resonance Light Scattering from a Liquid Suspension of Transient Cooling of a Hot Surface by Droplets Evapora-PB89-158133 PB89-157887 901.340 Not available NTIS PB89-161897 900.971 PC A04/MF A01 Van der Waals Equation of State Around the Van Laar PR89-157895 PB89-161905 Electromagnetic Pulse Scattered by a Sphere, PB89-157895 901,495 Not available NTIS Internal Revenue Service Post-of-Duty Location Modeling System: Programmer's Manual for PASCAL Solver. PB89-161905 900,001 PC A04/MF A01 PB89-158133 900.345 Not available NTIS PB89-158141 PB89-157903 Shear Induced Anisotropy in Two-Dimensional Liquids. PB89-158141 901,325 Not available NTIS Elastic Interaction and Stability of Misfitting Cuboidal Inho-PB89-161913 mogeneities. PB89-157903 Internal Revenue Service Post-of-Duty Location Modeling System: Programmer's Manual for FORTRAN Driver Ver-PB89-158158 901,482 Not available NTIS Small Angle Neutron Scattering Spectrometer at the National Bureau of Standards.
PB89-158158 901,396 Not available NTIS PB89-157911 sion 5.0. PB89-161913 Directional Invariance of Grain Boundary Migration in the Pb-Sn Cellular Transformation and the Tu-Turnbull Hystere-900,002 PC A04/MF A01 PB89-162234 PB89-158166 PB89-157911 Electrical Performance Tests for Hand-Held Digital Multi-901.134 Not available NTIS Numerical Evaluation of Certain Multivariate Normal Inte-PB89-157929 grals. PB89-158166 PB89-162234 900,876 PC A13/MF A01 901,195 Not available NTIS Secondary-Electron Effects in Photon-Stimulated Desorp-PB89-162564 PB89-158174 Material Handling Workstation, Recommended Technical Specifications for Procurement of Commercially Available PB89-157929 Sayre's Equation is a Chernov Bound to Maximum Entropy. PB89-158174 901,397 Not available NTIS 900.337 Not available NTIS PB89-157937 Equipment. PB89-162564 PB89-159446 Optically Driven Surface Reactions: Evidence for the Role 900 998 PC A03/MF A01 ZIP: ZIP-Code Insulation Program (for Microcomputers) of Hot Electrons. PR89-162572 PB89-159446 PB89-157937 900,338 Not available NTIS 900.060 CP D01 Flammability Characteristics of Electrical Cables Using the Cone Calorimeter. PB89-159636 PB89-157945 Universality Class of Planar Self-Avoiding Surfaces with Fixed Boundary. Data Handling in the Vertical Workstation of the Automated PB89-162572 900.741 PC A04/MF A01 ufacturing Research Facility at the National Bureau of PR89-162580 Standards. PB89-157945 900.339 Not available NTIS Corrosion of Metallic Fasteners in Low-Sloped Roofs: A Review of Available Information and Identification of Re-PR89-159636 900,943 PC A04/MF A01 PB89-157952 PB89-159644 Non-Boltzmann Rotational and Inverted Spin-Orbit State Distributions for Laser-Induced Desorption of NO from search Needs. Material Handling Workstation Implementation. PB89-159644 900,988 PC A04/MF A01 PB89-162580 900,113 PC A06/MF A01 Pt(111) PB89-162598 PB89-157952 900,340 Not available NTIS PB89-159651 Relationship between Appearance and Protective Durability of Coatings: A Literature Review.
PB89-162598 901,063 PC A04/MF A01 Material Handling Workstation: Operator Manual.
PR89-159651 900,989 PC A03/MF A01 PB89-157960 Electron and Photon Stimulated Desorption: Probes of Structure and Bonding at Surface PB89-159669 PB89-162606 PB89-157960 901,116 Not available NTIS Real-Time Control System Modifications for a Deburring Robot. User Reference Manual. PB89-159669 900,990 PC A03/MF A01 Toughening Mechanisms in Ceramic Composites: Semi-Annual Progress Report for the Period Ending September PB89-157978 Calculations of Electron Inelastic Mean Free Paths for 31 30, 1988 PB89-160014 Materials. PB89-162606 901,028 PC A03/MF A01 PB89-157978 900,341 Not available NTIS Data Bases Available at the National Institute of Standards PB89-162614 and Technology Research Information Center.
PB89-160014 900,932 PC A06/MF A01 PB89-157986 Analysis of Computer Performance Data. PB89-162614 900,635 ASM/NBS (American Society for Metals/National Bureau of Standards) Numerical and Graphical Database for Binary 900,635 PC A03/MF A01 PB89-160592 PB89-165427 Alloy Phase Diagrams. Electrodeposition of Chromium from a Trivalent Electrolyte. PATENT-4 804 446 901,119 Not available NTIS 901,135 Not available NTIS Sputtered Thin Film Ba2YCu3On. PB89-165427 901,029 Not available NTIS PB89-157994 PB89-160634 Voltammetric and Liquid Chromatographic Identification of Organic Products of Microwave-Assisted Wet Ashing of Biological Samples.
PB89-157994
900,188
Not available NTIS PB89-166086 Parser That Converts a Boundary Representation into a Features Representation.
PB89-160634

PC A03/MF A01 Ongoing Implementation Agreements for Open Systems Interconnection Protocols: Continuing Agreements. PB89-166086 900,610 PC A09/MF A01 PB89-161525 PB89-166094 PB89-158000 Techniques for Measuring the Electromagnetic Shielding Effectiveness of Materials. Part 1. Far-Field Source Simula-Institute for Materials Science and Engineering, Polymers: Technical Activities 1988. Prediction of Service Life of Building Materials and Compotion. PB89-161525 PB89-158000 900,003 PC A06/MF A01 900.112 Not available NTIS 900.680 Not available NTIS PB89-166094 PB89-158018 PB89-166102 PB89-161533 Fractal-Based Description of the Roughness of Blasted Guidelines for the Specification and Validation of IGES (Ini-Techniques for Measuring the Electromagnetic Shielding Effectiveness of Materials. Part 2. Near-Field Source Simu-

tial Graphics Exchange Specification) Application Protocols. PB89-166102 900,937 PC A06/MF A01

Method to Measure the Tensile Bond Strength between

Two Weakly-Cemented Sand Grains.

PB89-166110

Steel Panels PB89-158018

PB89-158026

tromethane.

901,096 Not available NTIS

Effects of Pressure on the Vibrational Spectra of Liquid Ni-

lation. PB89-161533

PB89-161541

900.681 Not available NTIS

Thermodynamic Values Near the Critical Point of Water.

901,483 PC A03/MF A01 PB89-171359 901,400 Not available NTIS PR89-171771 901,031 Not available NTIS PB89-166110 PB89-171532 PB89-166128 PB89-171789 Absolute Rate Constants for Hydrogen Abstraction from Hydrocarbons by the Trichloromethylperoxyl Radical. PB89-171532 900,357 Not available NTIS Effect of Chinese Standardization on U.S. Export Opportu-Phase Relations between the Polytitanates of Barium and the Barium Borates, Vanadates and Molybdates.
PB89-171789 901,032 Not available NTIS PB89-166128 900,172 PC A03/MF A01 PB89-171540 PB89-168009 PB89-171797 Electron-Transport, Ionization, Attachment, and Dissociation Coefficients in SF6 and Its Mixtures.
PB89-171540 901,501 Not available NTIS Report of the Invitational Workshop on Integrity Policy in Computer Information Systems (WIPCIS). PB89-168009 900,670 PC A09/MF A01 Phase Equilibria and Crystal Chemistry in the Ternary System BaO-TiO2-Nb2O5: Part 1.
PB89-171797 901,033 Not available NTIS PB89-171557 PB89-168017 PB89-171805 Electron-Impact Excitation of the Resonance Transition in NBS (National Bureau of Standards) Reactor: Summary of Fracture Behavior of Ceramics Used in Multilayer Capaci-Activities July 1987 through June 1988. PB89-168017 901,304 PC A11/MF A01 CA(1+). PB**8**9-**1**71**55**7 901,502 Not available NTIS tors. PB89-171805 900,758 Not available NTIS PB89-168025 PB89-171565 PB89-171813 Interim Criteria for Polymer-Modified Bituminous Roofing Electron-Impact Excitation of Al(2+). PB89-171565 901,503 Not available NTIS Effect of Lateral Crack Growth on the Strength of Contact Membrane Materials. PR89-168025 900,114 PC A04/MF A01 Flaws in Brittle Materials. PB89-171813 PB89-171573 901,034 Not available NTIS Computer Program for Calculating Non-LTE (Local Thermodynamic Equilibrium) Model Stellar Atmospheres. PB89-171573 900,018 Not available NTIS PB89-168033 Center for Electronics and Electrical Engineering Technical Progress Bulletin Covering Center Programs, July to September 1988, with 1989 CEEE Events Calendar. DR89-171821 Densification, Susceptibility and Microstructure of PB89-171581 Ba2YCu3O(6+ x). 900,775 PC A03/MF A01 Comment on 'Possible Resolution of the Brookhaven and Washington Eotvos Experiments'.
PB89-171581 901,504 Not available NTIS PB89-171821 901,035 Not available NTIS PB89-170864 PB89-171839 Internal Structure of the Guide to Available Mathematical Effect of Random Errors in Planar Near-Field Measurement. Software PB89-171599 PB89-171839 900,708 Not available NTIS PB89-170864 900.927 PC A04/MF A01 AES and LEED Studies Correlating Desorption Energies with Surface Structures and Coverages for Ga on Si(100). PB89-171599 901,401 Not available NTIS PB89-171847 PB89-170872 Minimax Approach to Combining Means, with Practical Ex-High-Current Measurement Techniques. Part II. 100-kA Source Characteristics and Preliminary Shunt and Rogowski Coil Evaluations. PB89-171607 amples. PB**8**9-**1**71**8**47 901,211 Not available NTIS Scattering of Polarized Light in Spectral Lines with Partial Frequency Redistribution: General Redistribution Matrix. PB89-171607 901,344 Not available NTIS PB89-170872 900.804 PC A04/MF A01 PB89-171854 PB89-171185 Basic Data Necessary for Neutron Dosimetry. PB89-171854 901,241 Not available NTIS Systems Driven by Colored Squeezed Noise: The Atomic Absorption Spectrum.
PB89-171185 901,500 Not available NTIS PB89-171615 Stars IX. IUE (International Ultraviolet Explorer) Spectroscopy and Photometry of II Peg and V711 Tau during February 1983. Rotational Modulation and Flares on RS CVn and BY Dra PR89-171862 Initial Spectra of Neutron-Induced Secondary Charged Par-PB89-171193 Photodissociation of Methyl Iodide Clusters. PB89-171193 900,253 Not available NTIS PB89-171862 901,265 Not available NTIS PB89-171615 900.019 Not available NTIS PB89-171870 PB89-171201 PB89-171623 Intramolecular H Atom Abstraction from the Sugar Moiety by Thymine Radicals in Oligo- and Polydeoxynucleotides. PB89-171870 901,263 Not available NTIS Production of 0.1-3 eV Reactive Molecules by Laser Vaporization of Condensed Molecular Films: A Potential Source for Beam-Surface Interactions. Real Time Generation of Smooth Curves Using Local Cubic Segments. PB89-171623 901,196 Not available NTIS 900,254 Not available NTIS PB89-171631 PB89-171888 PB89-171219 Recoilless Optical Absorption and Doppler Sidebands of a NBS (National Bureau of Standards) Radon-in-Water Stand-Single Trapped Ion. PB89-171631 Infrared Spectrum of D2HF. 901,505 Not available NTIS 900.350 Not available NTIS 901.295 Not available NTIS PB89-171219 PB89-171888 PB89-171649 PB89-171227 PB89-171896 New Cavity Configuration for Cesium Beam Primary Fre-Infrared Spectrum of NeHF. Loading Rate Effects on Discontinuous Deformation in Load-Control Tensile Tests. quency Standards. PB89-171649 PB89-171227 900,351 Not available NTIS 900,714 Not available NTIS PB89-171235 PB89-171896 901,097 Not available NTIS PB89-171656 Laser-Noise-Induced Population Fluctuations in Two- and Three-Level Systems.
PB89-171235
901,342
Not available NTIS PB89-171904 Power Quality Site Surveys: Facts, Fiction, and Fallacies. PB89-171656 900,805 Not available NTIS Chemical Structure of Methane/Air Diffusion Flames: Concentrations and Production Rates of Intermediate Hydrocar-PB89-171243 PB89-171664 Laser Probing of Ion Velocity Distributions in Drift Fields: Parallel and Perpendicular Temperatures and Mobility for Ba(1+) in He. PB8-171243 900,352 Not available NTIS Magnetic Dipole Excitation of a Long Conductor in a Lossy PB89-171904 900,590 Not available NTIS Medium. PB89-171664 PB89-171912 900,742 Not available NTIS Methyl Radical Concentrations and Production Rates in a PB89-171672 Laminar Methane/Air Diffusion Flame.
PB89-171912 900,591 Not available NTIS PB89-171250 Stability of Birefringent Linear Retarders (Waveplates). PB89-171672 901,345 Not available NTIS PB89-171912 Laser Probing of Product-State Distributions in Thermal-Energy Ion-Molecule Reactions. PB89-171250 900,353 Not available NTIS PB89-171920 PB89-171680 Modeling Chemical Reaction Systems on an IBM PC. PB89-171920 900,358 Not available NTIS NBS (National Bureau of Standards) Laser Power and Energy Measurements.
PB89-171680 901,346 Not available NTIS PB89-171268 Microarcsecond Optical Astrometry: An Instrument and Its PB89-171938 Astrophysical Applications. PB89-171268 PB89-171698 Chemical Calibration Standards for Molecular Absorption 900,013 Not available NTIS Fast-Pulse Generators and Detectors for Characterizing Spectrometry. PB89-171938 PB89-171276 Laser Receivers at 1.06 um. PB89-171698 900.191 Not available NTIS One-Photon Resonant Two-Photon Excitation of Rydberg 901,347 Not available NTIS PB89-171946 Series Close to Threshold. PB89-171276 PB89-171706 Use of Focusing Supermirror Neutron Guides to Enhance Cold Neutron Fluence Rates.
PB89-171946 901,306 Not available NTIS 901,343 Not available NTIS Fast Optical Detector Deposited on Dielectric Channel Wa-PB89-171284 veguides. PB89-171706 Three-State Lattice Gas as Model for Binary Gas-Liquid 900.743 Not available NTIS PB89-171953 PB89-171714 Systems. PB89-171284 Radiochemical and Instrumental Neutron Activation Analysis Procedures for the Determination of Low Level Trace Elements in Human Livers. 900,354 Not available NTIS Electrically Calibrated Silicon Bolometer for Low Level Opti-PR89-171292 cal Power and Energy Measurements. PB89-171714 901.34 High Resolution Inverse Raman Spectroscopy of the CO Q 901,348 Not available NTIS PB89-171953 901,236 Not available NTIS Branch. PB89-171722 PR89-171292 PB89-171961 900,355 Not available NTIS Effect of Multiple Internal Reflections on the Stability of Electrooptic and Magnetooptic Sensors. PB89-171722 900,724 Not available NTIS Microwave Energy for Acid Decomposition at Elevated Temperatures and Pressures Using Biological and Botanical PB89-171300 Dynamics of a Spin-One Model with the Pair Correlation. PB89-171300 900,356 Not available NTIS Samples. PB89-171961 PB89-171730 900.359 Not available NTIS PB89-171318 Crystal Chemistry of Superconductors: A Guide to the Tailoring of New Compounds.
PB89-171730 901,030 Not available NTIS PB89-172324 Electronic Structure of the Cd Vacancy in CdTe. PB89-171318 901,398 Not available NTIS Stable and Metastable Phase Equilibria in the Al-Mn

Damage Accumulation in Wood Structural Members Under Stochastic Live Loads.
PB89-171748 900,115 Not available NTIS

Gravity Tide Measurements with a Feedback Gravity Meter. PB89-171755 901,310 Not available NTIS

Standard X-ray Diffraction Powder Patterns from the JCPDS (Joint Committee on Powder Diffraction Standards) Research Associateship. PB9-171763 900,190 Not available NTIS

Rising Fracture Toughness from the Bending Strength of Indented Alumina Beams.

PB89-171748

PB89-171755

PB89-171763

PB89-171771

PB89-171326

PB89-171334

PB89-171342

PB89-171359

PB89-171326

ulation. PB**89-1**71334

Transport Layer Performance Tools and Measurement.

Prediction of Transport Protocol Performance through Sim-

Surface Structures and Growth Mechanism of Ga on Si(100) Determined by LEED (Low Energy Electron Diffraction) and Auger Electron Spectroscopy. PB9-171342 901,399 Not available NTIS

Progress in Understanding Atomic Structure of the Icosahedral Phase.

900,611 Not available NTIS

900 612 Not available NTIS

PB89-172332 Solidification of Aluminum-Manganese Powders. PB**89**-172332 *901,137* Not available NTIS PB89-172340 Control Strategies and Building Energy Consumption. PB89-172340 900,061 Not available NTIS

PB89-172340

System. PB89-172324

PB89-172357

Standardizing EMCS Communication Protocols. PB**89-172357** *900,613* Not available NTIS PB89-172365

Aluminumlike Spectra of Copper through Molybdenum. PB89-172365 900,360 Not available NTIS

901.136 Not available NTIS

901,098 PC A06/MF A01 PB89-173876 PB89-172621 PB89-172373 Spectrum and Energy Levels of Singly Ionized Cesium. 2. Interpretation of Fine and Hyperfine Structures. PB89-172373 900,361 Not available NTIS Ineffectiveness of Powder Regenerators in the 10 K Tem-PB89-172886 perature Range. PB89-173876 Ignition and Flame Spread Measurements of Aircraft Lining Materials.
PB89-172886 900,009 PC A04/MF A01 901,005 Not available NTIS PB89-173884 PB89-172381 Classical Chaos, the Geometry of Phase Space, and Semi-classical Quantization. PB89-173405 Measurement of Regenerator Ineffectiveness at Low Temperatures. PB89-173884 Strategic Defense Initiative Space Power Systems Metrolo-901,006 Not available NTIS 901.506 Not available NTIS PB89-172381 gy Assessment. PB89-173405 901,268 Not available NTIS PB89-173892 PB89-172399 Building Economics in the United States. PB89-172399 900,102 Not available NTIS PB89-173413 Refrigeration Efficiency of Pulse-Tube Refrigerators. PB89-173892 901,007 Not available NTIS Measuring Fast-Rise Impulses by Use of E-Dot Sensors. PB89-173413 900,744 Not available NTIS PB89-172407 PB89-173900 Grain Boundaries with Impurities in a Two-Dimensional Lat-PB89-173421 Specific Heat Measurements of Two Premium Coals. PB89-173900 900,839 Not available NTIS Measurement of Partial Discharges in Hexane Under DC tice-Gas Model. 901.507 Not available NTIS PB89-172407 Voltage. PB89-173421 PB89-173918 900.833 Not available NTIS PB89-172415 Use of Dye Tracers in the Study of Free Convection in Porous Media.
PB89-173918 901,327 Not available NTIS Infrared Spectrum of the nu6, nu7, and nu8 Bands of PB89-173439 HNO3. PB89-172415 Measurement of Electrical Parameters Near AC and DC Power Lines. PB89-173439 900,745 Not available NTIS 900,362 Not available NTIS PB89-173926 PB89-172423 Developments in the Heat Balance Method for Simulating Room Thermal Response.
PB89-173926 900,062 Not available NTIS Picosecond Laser Study of the Collisionless Photodissocia-tion of Dimethylnitramine at 266 nm. PB89-172423 900,255 Not available NTIS PB89-173447 Estimates of Confidence Intervals for Divider Distorted Waveforms. PB89-173447 PB89-173934 PB89-172431 900,806 Not available NTIS NBS (National Bureau of Standards) Calibration Services: A Neutron Powder Diffraction Structure and Electrical Properties of the Defect Pyrochlores Pb1.5M2O6.5 (M= Nb, Ta). PB89-172431 900,363 Not available NTIS PB89-173454 Status Report. PB89-173934 Coupling, Propagation, and Side Effects of Surges in an Industrial Building Wiring System.
PB89-173454 900,118 Not available NTIS 900.878 Not available NTIS PB89-173942 PB89-172449 Dynamics of Concentration Fluctuation on Both Sides of Phase Boundary. Concentration Dependence of the Compression Modulus of Isotactic Polystyrene/Cis-Decalin Gels. PB89-172449 900,552 Not available NTIS PB89-173462 Characterizing Electrical Parameters Near AC and DC 901,183 Not available NTIS PB89-173942 Power Lines. PB89-173462 PB89-173959 PB89-172456 900,834 Not available NTIS Interferometric Dispersion Measurements on Small Guided-Wave Structures. PB89-173959 901,349 Not available NTIS Effects of Solvent Type on the Concentration Dependence of the Compression Modulus of Thermoreversible Isotactic Polystyrene Gels.
PB89-172456 900,553 Not available NTIS PB89-173470 AC Electric and Magnetic Field Meter Fundamentals. 900,746 Not available NTIS PR89-173470 PB89-173967 PR89-173488 PB89-172472 Optical Fiber Sensors for Electromagnetic Quantities. PB89-173967 900,725 Not available NTIS Higher-Order Crossings: A New Acoustic Emission Signal Processing Method.
PB89-173488 900,678 Not available NTIS Measurement of the Torque and Normal Force in Torsion in the Study of the Thermoviscoelastic Properties of Polymer PB89-173975 Glasses Precision Weight Calibration with a Specialized Robot. PB89-173975 900,879 Not available NTIS PB89-172472 900.554 Not available NTIS PR89-173496 Computer Program for Instrument Calibration at State-Sector Secondary-Level Laboratories. PB89-173496 900,877 Not available NTIS PB89-172480 PB89-173983 Viscosity of Blends of Linear annd Cyclic Molecules of Similar Molecular Mass. PB89-172480 900,555 Not available NTIS Hand Calculations for Enclosure Fires. PB89-173983 900,164 Not available NTIS PB89-173504 PB89-173991 PB89-172498 Role of Inclusions in the Fracture of Austenitic Stainless Steel Welds at 4 K. PB89-173504 Strategy for Interpretation of Contrast Mechanisms in Scanning Electron Microscopy: A Tutorial.
PB89-172498 900,192 Not available NTIS Computer Fire Models. PB89-173991 901,099 Not available NTIS 900,165 Not available NTIS PB89-173512 PB89-174007 Influence of Molybdenum on the Strength and Toughness of Stainless Steel Welds for Cryogenic Service.
PB89-173512 901,100 Not available NTIS PB89-172506 Twenty Five Years of Accuracy Assessment of the Atomic Weights. PB89-174007 Dependence of Interface Widths on Ion Bombardment Conditions in SIMS (Secondary Ion Mass Spectrometry) Analysis of a Ni/Cr Multilayer Structure.
PB89-172506 900,364 Not available NTIS 900.365 Not available NTIS PB89-174015 High Temperature Thermal Conductivity Apparatus for Fluids. Automated TEM (Transverse Electromagnetic) Cell for PB89-172514 Measuring Unintentional EM Emissions.
PB89-173769 900,682 Not available NTIS PB**89-1**74015 Specific Heat of Insulations. 900,366 Not available NTIS PB89-172514 900.116 Not available NTIS PB89-173777 PB89-174023 Shear Dilatancy and Finite Compressibility in a Dense Non-Newtonian Liquid. PB89-174023 901,328 Not available NTIS PB89-172522 ANA (Automatic Network Analyzer) Measurement Results on the ARFTG (Automatic RF Techniques Group) Traveling How to Estimate Capacity Dimension. PB89-172522 901,197 Not available NTIS Experiment. PB89-173777 900,715 Not available NTIS PB89-172530 PB89-174031 Speed of Sound in Natural Gas Mixtures.

900,840 Not available NTIS PB89-173785 Laser Induced Fluorescence for Measurement of Lignin Transient Response Error in Microwave Power Meters Using Thermistor Detectors. PB89-173785 PB89-174049 900,759 Not available NTIS PB89-172548 Variances Based on Data with Dead Time between the PB89-173793 Insulation Standard Reference Materials of Thermal Resist-Measurements. Performance Measurement of a Shared-Memory Multi-PB89-174049 901,204 Not available NTIS 900.117 Not available NTIS processor Using Hardware Instrumentation.
PB89-173793 900,636 Not available NTIS PR89-172548 PB89-174056 PB89-172555 Low Noise Frequency Synthesis.

PRR9-174056 900,716 Not available NTIS PB89-173801 Approach to Accurate X-Ray Mask Measurements in a Scanning Electron Microscope. PB89-172555 900,776 PC A03/MF A01 Preliminary Stochastic Model for Service Life Prediction of a Photolytically and Thermally Degraded Polymeric Cover Plate Material. PB89-174064 Dual Frequency P-Code Time Transfer Experiment. PB89-174064 900,614 Not available NTIS PB89-172563 900.556 Not available NTIS Report on Interactions between the National Institute of Standards and Technology and the American Society of Mechanical Engineers. PB89-173801 PB89-173819 PB89-174072 Survey of Selected Methods of Economic Evaluation for Building Decisions.
PB89-173819 900,103 Not available NTIC Comparison of Time Scales Generated with the NBS (National Bureau of Standards) Ensembling Algorithm.
PB89-174072 900,628 Not available NTIS 901 004 PC A03/MF A01 PB89-172563 PR89-172571 Artificial Intelligence Techniques in Real-Time Production Scheduling. PB89-172571 900,945 PC A03/MF A01 PB89-173827 PB89-174080 Apparent Diurnal Effects in the Global Positioning System. PB89-174080 901,292 Not available NTIS Designs for Assessment of Measurement Uncertainty: Experience in the Eastern Lake Survey.
PB89-173827 900,862 Not available NTIS PB89-172589 PB89-174098 PB89-173835 Functional Approach to Designing Architectures for Com-Study of Long-Term Stability of Atomic Clocks. PB89-174098 900,367 Not available NTIS puter Integrated Manufacturing. PB89-172589 Failure Analysis of an Amine-Absorber Pressure Vessel. PB89-173835 901,101 Not available NTIS 900,946 PC A03/MF A01 PB89-174106 PB89-172597 PB89-173843 Trends for Building Technology in North America. PB89-174106 900,104 Not available NTIS Comparison of a Cryogenic Preconcentration Technique and Direct Injection for the Gas Chromatographic Analysis of Low PPB (Parts-per-Billion) (NMOL/MOL) Gas Standards of Toxic Organic Compounds.

PB89-173843

900,193

Not available NTIS Real-Time Optimization in the Automated Manufacturing Research Facility. PB89-174114 PB89-172597 900,947 PC A03/MF A01 Design Quality through the Use of Computers. PB89-174114 900,063 Not available NTIS PB89-172605 On-Line Concurrent Simulation in Production Scheduling. PB89-172605 900,948 PC A03/MF A01 PB89-173850 PB89-174122 Development of Combustion from Quasi-Stable Temperatures for the Iron Based Alloy UNS S66286.
PB89-173850 900,592 Not available NTIS Flammability Tests for Industrial Fabrics: Relevance and PR89-172613 Limitations Hierarchies for Computer-Integrated Manufacturing: A Func-901.091 Not available NTIS PB89-174122 tional Description. PB89-172613 900,949 PC A03/MF A01 PB89-173868 PB89-174130

Enthalpies of Desorption of Water from Coal Surfaces.

900,838 Not available NTIS

PB89-173868

Creation of a Fire Research Bibliographic Database. PB89-174130 900,166 Not available NTIS

PB89-172621

Elevated Temperature Deformation of Structural Steel.

PB89-174882

Tensile Strain-Rate Effects in Liquid Helium. PB89-174882 901,102 Not available NTIS

PB89-174890

Smoke end Gas Evolution Rate Measurements on Fire-Retarded Plastics with the Cone Calorimeter.
PB89-174890 900,868 Not available NTIS

PB89-174908

Latent Heats of Supercritical Fluid Mixtures. PB89-174908 900,242 Not available NTIS

PB89-174916

Thermal Resistance Measurements and Calculations of an Insulated Concrete Block Wall. PB89-174916 900,119 Not available NTIS

PB89-174924

Inelastic Behavior of Full-Scale Bridge Columns Subjected to Cyclic Loading. PB89-174924 900,584 PC A12/MF A01

PB89-174932

Vapor-Liquid Equilibrium of Nitrogen-Oxygen Mixtures and Air at High Pressure.
PB89-174932 900,368 Not available NTIS

PB89-174940

Non-Equilibrium Theories of Electrolyte Solutions. PB89-174940 900,369 Not aveilable NTIS

PB89-174957

Molecular Dynemics Investigation of Expanded Water at

Elevated Temperatures. PR89-174957 900.370 Not available NTIS

PR89-175194

Journal of Research of the National Institute of Standards and Technology, Volume 94, Number 1, January-February 1989, Special Issue: Numeric Databases in Materiels end iological Sciences.

901,186 PC A06 PB89-175194 PB89-175202

Importance of Numeric Databases to Materials Science. PB89-175202 901,

(Order as PB89-175194, PC A06)

PB89-175210

NIST (National Institute of Standards and Technology)/ Sandia/ICDD Electron Diffraction Database: A Database for Phase Identification by Electron Diffraction. 901,508

(Order as PB89-175194, PC A06)

PB89-175228

Numeric Databases in Chemical Thermodynamics at the National Institute of Standards and Technology. PB89-175228 900 371 (Order as PB89-175194, PC A06)

PR89-175236

Numeric Databases for Chemical Analysis.

(Order as PB89-175194, PC A06)

Structural Ceramics Database: Technical Foundations.

901.036 PR89-175244 (Order as PB89-175194, PC A06)

PB89-175251 Applications of the Crystallographic Search and Analysis System CRYSTDAT in Materials Science. PB89-175251 901,402

(Order as PB89-175194, PC A06)

PB89-175269

New Directions in Bioinformatics. PB89-175269

901 245 (Order as PB89-175194, PC A06)

PR89-175277

Use of Structural Templates in Protein Backbone Modeling. PB89-175277 901,246

901,246 (Order as PB89-175194, PC A06)

Comparative Modeling of Protein Structure: Progress and PB89-175285 (Order as PB89-175194, PC A06)

PR89-175293 Computational Analysis of Protein Structures: Sources, Methods, Systems and Results. PB89-175293 900,010

(Order as PB89-175194, PC A06)

PB89-175418

Technical Activities 1986-1988, Molecular Spectroscopy Division. PB89-175418 900,372 PC A07/MF A01

PB89-175681

Decorated Lattice Gas Model for Supercritical Solubility. PB89-175681 900,373 Not available NTIS

PB89-175699

NBS (National Bureau of Standards) Orifice-Flow Primary High Vacuum Standard. PB89-175699 900,880 Not available NTIS

PB89-175707

Low Range Flowmeters for Use with Vacuum and Leak Standards. PB89-1757**0**7 900,374 Not available NTIS

PB89-175715

Progressive Collapse: U.S. Office Building in Moscow. PB89-175715 900,158 Not available NTIS

PB89-175723

Pore-Water Pressure Buildup in Clean Sands Because of Cyclic Straining.
PB89-175723 900,159 Not available NTIS

PB89-175731

New FIR Leser Lines and Frequency Measurements for Optically Pumped CD3OH. PB89-175731 901,350 Not available NTIS

PR89-175749

NBS/NRL (National Bureau of Standards/Naval Research Laboratory) Free Electron Laser Facility. PB89-175749 901,351 Not available NTIS

PB89-175830

Uniaxial Deformation of Rubber Network Chains by Small Angle Neutron Scattering.
PB89-1.75830 901,088 Not evailable NTIS

PB89-175848

Prediction of Service Life of Construction and Other Materi-

PR89-175848 900.120 Not aveileble NTIS

PB89-175855

Specimen Banking in the National Status and Trends Program: Development of Protocols and First Year Results. PB89-175855 901,308 Not available NTIS

PR89-175863

Development of Electrophoresis and Electrofocusing Standards. PB89-175863 900.195 Not available NTIS

PB89-175871

Efficient Algorithms for Computing Fractal Dimensions. PB89-175871 901,198 Not available NTIS

PB89-175889

U-Value Measurements for Windows and Movable Insula-tions from Hot Box Tests in Two Commercial Laboratories. PB89-175889 900,121 Not available NTIS

PB89-175897

Periodic Heat Conduction in Energy Storage Cylinders with Change of Phase. PB89-175897 900,852 Not available NTIS

PB89-175905

Field Measurement of Thermal and Solar/Optical Properties of Insulating Glass Windows.

PB89-175905 900,064 Not available NTIS

PB89-175913

Very Large Methane Jet Diffusion Flames PB89-175913 900,593 900,593 Not available NTIS

PB89-175921

Preparative Liquid Chromatographic Method for the Characterization of Minor Constituents of Lubricating Base Oils. PB89-175921 901,114 Not available NTIS PB89-175939

Pore Morphology Analysis Using Small Angle Neutron Scattering Techniques.
PB89-175939 901,037 Not available NTIS

PB89-175947

Microbiological Metal Transformations: Biotechnological Applications and Potential. PB89-175947

901,284 Not available NTIS PB89-175954

Creep Cavitation in Liquid-Phase Sintered Alumina. PR89-175954 901,038 Not available NTIS PB89-175962

Characterization of Organolead Polymers in Trace Amounts by Element-Specific Size-Exclusion Chromatography. PB89-175962 900,196 Not available NTIS

PB89-175970

Superlattice Magnetoroton Bands. PB89-175970 901,403 Not available NTIS

PB89-175988

Effects of a Gold Shank-Overlayer on the Field Ion Imaging of Silicon. PB89-175988 901.404 Not available NTIS

PB89-175996

Dynamics of Molecular Collisions with Surfaces: Excitation, Dissociation, and Diffraction.
PB89-175996
900,375 Not available NTIS

PB89-176002

Spectra and Energy Levels of Br XXV, Br XXIX, Br XXX, and Br XXXI.
PB89-17**6002**901,509
Not available NTIS

PB89-176010

Laser-Produced Spectra and OED (Quantum Electrodynamic) Effects for Fe-, Co-, Cu-, and Zn-Like lons of Au, Pb, Bi, Th, and U. PB89-176010 901,510 Not available NTIS

PB89-176028

Theory of Microphase Separation in Graft and Star Copoly-PB89-17**6**0**2**8 900,557 Not available NTIS

PB89-176036

Solid State (13)C NMR Investigation in Polyoxetanes. Effect of Chain Conformation. PB89-176036 900,558 Not available NTIS

Polymer Localization by Random Fixed Impurities: Gaussian PB89-176044 900,559 Not available NTIS

PB89-176051

Morphological Partitioning of Ethyl Branches in Polyethylene by (13)C NMR.
PB89-176051 900.560 Not available NTC

PB89-176069

Microphase Separetion in Blockcopolymer/Homopolymer. PB89-176069 900,561 Not available NTIS

PB89-176077

Mesh Monitor Casting of Ni-Cr Alloys: Element Effects. PB89-176077 900,040 Not available NTIS

PB89-176085

Crazes and Fracture in Polymers. 900,562 Not available NTIS PB89-176085

PB89-176093

One-Electron Transfer Reactions of the Couple SO2/SO2(1-) in Aqueous Solutions, Pulse Radiolytic and Cyclic Voltammetric Studies.

900,376 Not available NTIS

PB89-176093 PB89-176101

Ion Kinetics and Energetics. PB89-176101

900,377 Not available NTIS

PB89-176119

Integrated Knowledge Systems for Concrete and Other Matena PB89-176119 900,582 Not available NTIS

PB89-176127

Indoor Air Ouality. PB89-176127 900,065 Not available NTIS

PB89-176135

Circular and Square Edge Effect Study for Guarded-Hot-Plate and Heat-Flow-Meter Apparatuses. PB89-176135 900,881 Not available NTIS

PB89-176143

Role of Standards in Electron Microprobe Techniques. PB89-176143 900,197 Not available NTIS

PB89-176150

Defocus Modeling for Compositional Mapping with Wave-length-Dispersive X-ray Spectrometry. PB89-176150 900,378 Not available NTIS

PB89-176168

Fundamentals of Enclosure Fire 'Zone' Models. PB89-176168 900,122 Not available NTIS PB89-176168

PB89-176176

Some Ouestions and Answers Concerning Air Lines as Impedance Standards.
PB89-176176 900,747 Not available NTIS

PB89-176184

Photonic Electric Field Probe for Frequencies up to 2 GHz. PB89-176184 900,683 Not available NTIS

PB89-176192

NIST (National Institute of Standards and Technology) Automated Coaxial Microwave Power Standard. PB89-176192 900,807 Not available NTIS

PB89-176200

NBS (National Bureau of Standards) Standards for Optical Power Meter Calibration. PB89-176200 900,726 Not available NTIS

PB89-176218

Experimental Study of Interpanel Interactions at 3.3 GHz PB89-176218 900.709 Not available N 900,709 Not available NTIS

PB89-176226

Creating CSUBs in BASIC. PB89-176226 900.647 Not available NTIS

PR89-176234

Resonance Light Scattering from a Suspension of Microspheres. PB**8**9-17**623**4 901.352 Not available NTIS

PB89-176242

Rate Constants for Reactions of Nitrogen Oxide (NO3) Radicals in Aqueous Solutions. PB89-176242 900,379 Not available NTIS

PB89-176259

Analytical Modeling of Device-Circuit Interactions for the Power Insulated Gate Bipolar Transistor (IGBT). PB89-176259 900,777 Not available NTIS

PB89-176267

High-Accuracy Differential-Pulse Anodic Stripping Voltam-metry Using Indium as an Internal Standard. PB89-176267 900,198 Not available NTIS

PB89-176275

Tests of the Recalibration Period of a Drifting Instrument. PB89-176275 900,199 Not available NTIS

PB89-176283

ACSB (Amplitude Companded Sideband): What Is Adequate Performance.
PB89-176283 901,599 Not available NTIS PB89-176291

Corrosion Induced Degradation of Amine-Cured Epoxy Coatings on Steel. PB89-176291 901,084 Not available NTIS

PB89-176309 PB89-176630 900.835 Not available NTIS PR89-176978 901,406 Not available NTIS Thermographic Imaging and Computer Image Processing of Defects in Building Materials. PB89-176309 900,123 Not available NTIS PR89-176648 PB89-176986 Selecting Varistor Clamping Voltage: Lower Is Not Better. PB89-176648 900,760 Not available NTIS Cool It. PR89-176986 901,516 Not available NTIS PR89-176408 PB89-176655 PB89-176994 Picosecond Coherent Anti-Stokes Raman Scattering Optical Roughness Measurements for Industrial Surfaces. PB89-176655 900,979 Not available NTIS (CARS) Study of Vibrational Dephasing of Carbon Disulfide and Benzene in Solution.

PB89-176408

900,380 Not available NTIS Bean Model Extended to Magnetization Jumps. PB89-176994 901,407 Not available NTIS PB89-176663 PB89-177000 Vertical Machining Workstation of the AMRF (Automated Manufacturing Research Facility): Equipment Integration. PB89-176663 900,950 Not available NTIS PB89-176416 Incrementor: A Graphical Technique for Manipulating Pa-Laser Excited Fluorescence Studies of Black Liquor.
PB89-176416 900,243 Not available NTIS PB89-177000 900,648 Not available NTIS PB89-176671 PB89-176424 PB89-177018 Optical Fiber Sensors for the Measurement of Electromag-Polymeric Humidity Sensors for Industrial Process Applica netic Quantities. PB89-176671 CAD (Computer Aided Design)-Directed Inspection. PB89-177018 900,980 Not available NTIS 900,748 Not available NTIS tions. PB89-176424 900.563 Not available NTIS PB89-176689 PB89-177026 PB89-176432 Electron Mean Free Path Calculations Using a Model Di-electric Function. PB89-177026 901,141 Not available NTIS Picosecond Pulse Response from Hydrogenated Amorphous Silicon (a-Si:H) Optical Detectors on Channel Wave-Laboratory Accreditation Systems in the United States, 1984. PB89-176432 guides. PB89-176689 900,882 Not available NTIS 900,727 Not available NTIS PR89-177034 PB89-176440 PB89-176697 Note on the Capacitance Matrix Algorithm, Substructuring, and Mixed or Neumann Boundary Conditions. PB89-177034 901,199 Not available NTIS Laser-Cooling and Electromagnetic Trapping of Neutral Potential Errors in the Use of Optical Fiber Power Meters. PB89-176697 900,728 Not available NTIS Atoms. PB89-176440 901,511 Not available NTIS PB89-176705 PB89-176457 PB89-177042 Standard Format for the Exchange of Fingerprint Informa-Kinetics of Resolidification. Algebraic Representation for the Topology of Multicomponent Phase Diagrams. 901.138 Not available NTIS PB89-176457 PB89-176705 900.692 Not available NTIS PR89-177042 901,517 Not available NTIS PB89-176465 PB89-176713 PB89-177059 Undercooling and Microstructural Evolution in Glass Form-PCM/VCR Speech Database Exchange Format. PB89-176713 900,633 Not available NTIS Building Representations from Fusions of Multiple Views. PB89-177059 900,991 Not available NTIS 901,139 Not available NTIS PB89-176721 PB89-176473 Compensating for Vowel Coarticulation in Continuous Speech Recognition. PB89-176721 900,634 Not available NTIS PB89-177067 Influence of Electronic and Geometric Structure on Desorp-PB89-177067 Past Path Planning in Unstructured, Dynamic, 3-D Worlds. PB89-177067 900,992 Not available NTIS tion Kinetics of Isoelectronic Polar Molecules: NH3 and PB89-176739 PB89-176473 900,381 Not available NTIS PB89-177075 Modelling of Impurity Effects in Pure Fluids and Fluid Mix-Hierarchically Controlled Autonomous Robot for Heavy Payload Military Field Applications.
PB89-177075
901,271
Not available NTIS PB89-176481 tures. PB89-176739 Influence of Reaction Reversibility on Continuous-Flow Ex-900,245 Not available NTIS traction by Emulsion Liquid Membranes.
PB89-176481

900,244

Not available NTIS PB89-176747 PB89-177083 Comprehensive Study of Methane + Ethane System. PB89-176747 900,841 Not available NTIS Real-Time Control System Software: Some Problems and Interzonal Natural Convection for Various Aperture Configu-PB89-176754 900.951 Not available NTIS PB89-176499 900,066 Not available NTIS Chemical Kinetics of Intermediates in the Autoxidation of PB89-177091 PB89-176507 PB89-176754 AMRF (Automated Manufacturing Research Facility) Materi-900,256 Not available NTIS Secure Military Communications Can Benefit from Accurate al Handling System Architecture.
PB89-177091 900,952 Not available NTIS PR89-176762 Time. PB89-176507 Cigarette as a Heat Source for Smolder Initiation in Upholstery Materials.
PB89-176762 900,595 Not available NTIS 901.274 Not available NTIS PB89-177109 PB89-176515 Software for an Automated Machining Workstation.
PB89-177109 900,953 Not available NTIS NBS (National Bureau of Standards) Free Electron Laser PB89-176770 Facility. PB89-176515 Using 'Resonant' Charge Exchange to Detect Traces of Noble Gas Atoms.

PB89-176770 901,296 Not available NTIS PB89-177117 901.353 Not available NTIS Object-Oriented Model for ASN.1 (Abstract Syntax Notation PB89-176523 Near-Threshold X-ray Fluorescence Spectroscopy of Mole-PB89-177117 900,649 Not available NTIS PB89-176788 cules. PB89-176523 Feasibility of Detector Self-Calibration in the Near Infrared. PB89-176788 900,384 Not available NTIS 900,382 Not available NTIS PB89-177125 PB89-176531 Automatic Generation of Test Scenario (Skeletons) from Protocol-Specifications Written in Estelle. PB89-177125 900,615 Not available NTIS PB89-176796 2.5 MeV Neutron Source for Fission Cross Section Measurement. PB89-176531 Characteristics of Ge and InGaAs Photodiodes. PB89-176796 900,729 Not available NTIS 901,512 Not available NTIS PR89-177133 PB89-176549 PB89-176887 Application of the ISO (International Standards Organiza-tion) Distributed Single Layer Testing Method to the Con-nectionless Network Protocol. PB9-177133 900,616 Not available NTIS Monte Carlo Calculated Response of the Dual Thin Scintil-Comparison of Two Transient Recorders for Use with the lation Detector in the Sum Coincidence Mode. PB89-176549 901,299 Not available NTIS Laser Microprobe Mass Analyzer. PB89-176887 900,200 Not available NTIS PB89-176556 PB89-176895 PB89-177141 Measurements of the (235)U (n,f) Standard Cross Section at the National Bureau of Standards. Mossbauer Imaging. Application of Direct Digital Control to an Existing Building Air Handler.
PB89-177141 900,068 Not available NTIS PB89-176895 901.242 Not available NTIS 901,305 Not available NTIS PB89-176556 PR89-176903 PB89-176564 Fast Magnetic Resonance Imaging with Simultaneously Oscillating and Rotating Field Gradients.
PB89-176903 901,514 Not available NTIS PR89-177158 Magnetic Properties of Surfaces Investigated by Spin Polarized Electron Beams. Flow Coefficients for Interzonal Natural Convection for Various Apertures. PB89-177158 901,405 Not available NTIS PB89-176564 PB89-176911 900.069 Not available NTIS PB89-176572 Dynamic Microindentation Apparatus for Materials Charac-State Selection in Electron-Atom Scattering: Spin-Polarized Electron Scattering from Optically Pumped Sodium. PB89-176572 901,513 Not available NTIS $\ensuremath{\mathsf{HVACSIM}}\xspace +$, a Dynamic Building/HVAC/Control Systems Simulation Program. PB89-176911 901,140 Not available NTIS PB89-176929 PB89-177166 900,070 Not available NTIS Computing Ray Trajectories between Two Points: A Solution to the Ray-Linking Problem.
PB89-176929 901,354 Not available NTIS PR89-176580 PB89-177174 Trace Gas Calibration Systems Using Permeation Devices. PB89-176580 900,883 Not available NTIS Simulation of a Large Office Building System Using the HVACSIM+ Program.
PB89-177174 900,071 Not available NTIS PB89-176598 PB89-176937 Cooling and Trapping Atoms. PB89-176937 901,515 Not available NTIS Luminescence Standards for Macro- and Microspectrofluor-PB89-177182 ometry Dynamic Poisson's Ratio of a Ceramic Powder during Com-PB89-176598 900,383 Not available NTIS PR89-176945 PB89-176606 ction Vibrationally Resolved Photoelectron Studies of the 7(sigma) (-1) Channel in N2O.
PB89-176945 900,257 Not available NTIS PB89-177182 901,039 Not available NTIS Summary of Circular and Square Edge Effect Study for Guarded-Hot-Plate and Heat-Flow-Meter Apparatuses. PB89-176606 900,884 Not available NTIS PB89-177190 Automated Fringe Counting Laser Interferometer for Low Frequency Vibration Measurements.

PB89-177190 900,885 Not available NTIS PB89-176952 PB89-176614 Vibrationally Resolved Photoelectron Angular Distributions for H2 in the Range 17 eV < or = h(nu) < or = 39 eV. PB89-176952 900,385 Not available NTIS Ventilation Effectiveness Measurements in an Office Build-PB89-177208 ing. PB89-176614 900,067 Not available NTIS PB89-176960 Photoelastic Properties of Optical Materials. Autoionization Dynamics in the Valence-Shell Photoionization Spectrum of CO. PB89-176960 900,386 Not available NTIS

PB89-177208

ces. PB89-177216

PB89-177216

901,355 Not available NTIS

901,220 Not available NTIS

Element-Specific Epifluorescence Microscopy In vivo Monitoring of Metal Biotransformations in Environmental Matri-

PB89-176622

Solution for Diffusion-Controlled Reaction in a Vortex Field. PB89-176622 900,594 Not available NTIS

Power Frequency Electric and Magnetic Field Measurements: Recent History and Measurement Standards.

PB89-176978

Josephson-Junction Model of Critical Current in Granular Y1Ba2Cu3O(7-delta) Superconductors.

PB89-177224

Determination of Ultratrace Concentrations of Butyltin Compounds in Water by Simultaneous Hydridization/Extraction with GC-FPD Detection.

PB89-177224 901,311 Not available NTIS

Biodegradation of Tributyltin by Chesapeake Bay Microorganisms. PB89-177232 901,309 Not available NTIS

PB89-179097

Wavelengths and Energy Levels of the K I Isoelectronic Sequence from Copper to Molybdenum.
PB89-179097 901,372 Not available NTIS

PR89-179105

Spectra and Energy Levels of the Galliumlike Ions Rb VII-

Mo XII. PR89-179105 900,387 Not available NTIS PB89-179113

Vibrational Exchange upon Interconversion Tunneling in (HF)2 and (HCCH)2.
PB89-179113 900,388 Not available NTIS

PR89-179121 Infrared and Microwave Spectra of OCO-HF and SCO-HF. PB89-179121 900,389 Not available NTIS

PB89-179139

CO Laser Stabilization Using the Optogalvanic Lamb-Dip PB89-179139 901,356 Not available N Not available NTIS PB89-179147

Laser Cooling. PB89-179147 PB89-179154

901,518 Not available NTIS

Wheatleyite, Na2Cu(C2O4)2 . 2H2O, a Natural Sodium Copper Salt of Oxalic Acid. PB89-179154 900,390 Not available NTIS PB89-179162

Precision and Accuracy Assessment Derived from Calibration Data. PB89-179162

900,886 Not available NTIS PB89-179170

Process Control during High Pressure Atomization. PB89-179170 901,142 Not available NTIS PB89-179188

Temperature-Dependent Radiation-Enhanced Diffusion in Ion-Bombarded Solids, 901,408 Not available NTIS PR89-179188

PB89-179196 Effects of Velocity and State Changing Collisions on Raman Q-Branch Spectra.

PB89-179196 900,391 Not available NTIS DRR9-179204

Magnetic Resonance of (160)Tb Oriented in a Terbium Single Crystal at Low Temperatures.
PB89-179204 901,519 Not available NTIS

PB89-179212

Measurements of the Nonresonant Third-Order Susceptibility. PB89-179212 901,357 Not available NTIS PB89-179220

Adsorption of 4-Methacryloxyethyl Trimellitate Anhydride (4-META) on Hydroxyapatite and Its Role in Composite Bond-

ing. PB89-179220 900.041 Not available NTIS PB89-179238

Comparison of Fluoride Uptake Produced by Tray and Flossing Methods In vitro. PB89-179238

901,252 Not available NTIS PB89-179246

Influence of Molecular Weight on the Resonant Raman Scattering of Polyacetylene. PB89-179246 900,564 Not available NTIS PB89-179253

Oligomers with Pendant Isocyanate Groups as Adhesives Oligomers with Pendaru 1907, 1

PB89-179261

Fire Safety Science-Proceedings of the First International 900,596 Not available NTIS

PB89-179279 Stabilization of Ascorbic Acid in Human Plasma, and Its

Liquid-Chromatographic Measurement.
PB89-179279
901,237
Not available NTIS PB89-179568

Remote Sensing Technique for Combustion Gas Temperature Measurement in Black Liquor Recovery Boilers.
PB89-179568 900,392 Not available NTIS

Surface Properties of Clean and Gas-Dosed SnO2 (110). PB89-179576 900.393 Not available N 900,393 Not available NTIS PB89-179584

Dynamic Light Scattering and Angular Dissymmetry for the In situ Measurement of Silicon Dioxide Particle Synthesis in Flames

PB89-179584 900,246 Not available NTIS PB89-179592

Application of Magnetic Resonance Imaging to Visualization of Flow in Porous Media.

PB89-179592 901,329 Not available NTIS PB89-179600

Thermal Conductivity of Liquid Argon for Temperatures between 110 and 140 K with Pressures to 70 MPa.

PB89-179600 900,394 Not available NTIS PB89-179618

Facilitated Transport of CO2 through Highly Swollen Ion-Exchange Membranes: The Effect of Hot Glycerine Pretreatment. PB89-179618

900.395 Not available NTIS PB89-179626

Significance of Multiple Scattering in the Interpretation of Small-Angle Neutron Scattering Experiments.
PB89-179626 901,409 Not available NTIS

PB89-179634

Occurrence of Long-Range Helical Spin Ordering in Dy-Y Multilayers. PB89-179634 901,410 Not available NTIS

PB89-179642 Long-Range Incommensurate Magnetic Order in Dy-Y Multilayers. PB89-179642 901,411 Not available NTIS

PB89-179659

Chemical Physics with Emphasis on Low Energy Excitations. PB89-179659 900,396 Not available NTIS

PB89-179667

Performance Measurements of Infrared Imaging Systems Used to Assess Thermal Anomalies.
PB89-179667 900,072 Not available NTIS

PB89-179675

Quantized Hall Resistance Measurement at the NML (National Measurement Laboratory).
PB89-179675
900,778
Not available NTIS

Computer Model of a Porous Medium. PB89-179683 901,188 Not available NTIS

PB89-179691

Second Viscosity and Thermal-Conductivity Virial Coefficients of Gases: Extension to Low Reduced Temperature. PB89-179691 900,397 Not available NTIS PB89-179709

Spherical Acoustic Resonators in the Undergraduate Laboratory. PB89-179709 901.317 Not available NTIS

PB89-179717 Syntheses and Unit Cell Determination of Ba3V4O13 and

Low- and High-Temperature Ba3P4O13.
PB89-179717 901,040 Not available NTIS PB89-179725

Synthesis and Magnetic Properties of the Bi-Sr-Ca-Cu Oxide 80- and 110-K Superconductors. PB89-179725 901,412 Not available NTIS PB89-179733

Novel Process for the Preparation of Fiber-Reinforced Ceramic-Matrix Composites. PR89-179733 901.074 Not available NTIS

PR89-179741 Synthesis, Stability, and Crystal Chemistry of Dibarium Pen-

tatitanate. PB89-179741 901,041 Not available NTIS PB89-179758

Mechanism and Rate of Hydrogen Atom Attack on Toluene at High Temperatures. PB89-179758 900.398 Not available NTIS

PB89-179766 Quenching and Energy Transfer Processes of Single Rotational Levels of Br2 B triplet Pi(O(sub u)(+)) v' = 24 with Ar under Single Collision Conditions.

PB89-179766 900,399 Not available NTIS

900,399 Not available NTIS PB89-179774

Simple F-Center Laser Spectrometer for Continuous Single Frequency Scans. PB89-179774 901,358 Not available NTIS

PB89-179782

Photodissociation Dynamics of C2H2 at 193 nm: Vibrational Distributions of the CCH Radical and the Rotational State Distribution of the A(010) State by Time-Resolved Fourier

Transform Infrared Emission. 900,258 Not available NTIS PB89-179782 PB89-179790

Alignment Effects in Ca-He(5(sup 1)P(sub 1) - 5(sup 3)P(sub J)) Energy Transfer Collisions by Far Wing Laser Scattering. PB89-179790

900.400 Not available NTIS PB89-179808

Acoustoelastic Determination of Residual Stresses. PB89-179808 901,318 Not available NTIS PB89-179816

Profile Inhomogeneity in Multimode Graded-Index Fibers. PB89-179816 900,749 Not available NTIS PB89-179824

High T(sub c) Superconductor/Noble-Metal Contacts with Surface Resistivities in the (10 to the Minus 10th Power) Omega sq cm Range. PB89-179824 901,413 Not available NTIS

PB89-179832 Effect of Room-Temperature Stress on the Critical Current

PB89-179832 901.414 Not available NTIS PB89-179840

Transmission Loss through 6061 T-6 Aluminum Using a Pulsed Eddy Current Source, PB89-179840 901,143 Not available NTIS

PB89-179857

Antennas for Geophysical Applications PB89-179857 900.710 900,710 Not available NTIS

PB89-180004

Recent Activities of the American Society for Testing and Materials Committee on Fire Standards. PB89-180004 900,124 Not available NTIS

PB89-180012

Definitions of Granularity. PB89-180012 900.650 Not available NTIS

PB89-180020

Correlation between CMOS (Complementary Metal Oxide Semiconductor) Transistor and Capacitor Measurements of Interface Trap Spectra.

PB9-180020 900,779 Not available NTIS

PB89-180038

Chemical and Spectral Databases: A Look into the Future. PB89-180038 900,579 Not available NTIS

PR89-180046

Critical and Noncritical Roughening of Surfaces (Comment). PB89-180046 901,415 Not available NTIS

PB89-180376

Composites Databases for the 1990's. PB89-180376 901,075 PC A04/MF A01

PB89-180426

Electromagnetic Fields in Loaded Shielded Rooms PB89-180426 900,780 Not availa 900,780 Not available NTIS PB89-181739

Interfaces to Teleoperation Devices. PB89-181739 900,993 PC A03/MF A01 PB89-183214

Operations Manual for the Automatic Operation of the Verti-Workstation. cal Workstatio PB89-183214

900.973 PC A03/MF A01 PB89-183222

Engineering View of the Fire of May 4, 1988 in the First Interstate Bank Building, Los Angeles, California. PB89-183222 900,167 PC A03/MF A01 PB89-183230

Real-Time Simulation and Production Scheduling Systems. PB89-183230 900,974 PC A03/MF A01

PB89-184089

Journal of Research of the National Institute of Standards and Technology. Volume 94, Number 2, March-April 1989. PB89-184089 900,887 PC A04

PB89-184097

PB89-184105

New Internationally Adopted Reference Standards of Voltage and Resistance.
PB89-184097 900,808

(Order as PB89-184089, PC A04)

Supercritical Fluid Chromatograph for Physicochemical Studie

PB89-184105 (Order as PB89-184089, PC A04)

PB89-184113 Relation between Wire Resistance and Fluid Pressure in

the Transient Hot-Wire Method. 901,520 (Order as PB89-184089, PC A04)

PB89-184121

Scattering Parameters Representing Imperfections in Precision Coaxial Air Lines. PB89-184121 900,750 (Order as PB89-184089, PC A04)

PB89-184527

Fire Risk Analysis Methodology: Initiating Events. PB89-184527 900,125 PC A08/MF A01

PB89-185573

Epoxy Impregnation of Hardened Cement Pastes for Characterization of Microstructure.
PB89-185573 901,042 PC A03/MF A01

PB89-185581

Combustion of Oil on Water. November 1987. PB89-185581 900,863 PC A04/MF A01

PB89-185599 Directory of NVLAP (National Voluntary Laboratory Accreditation Program) Accredited Laboratories, 1986-87.
PB89-185599 900,933 PC A05/MF A01

PB89-185607

Turning Workstation in the AMRF (Automated Manufacturing Research Facility). PB89-185607 900.954 PC A10/MF A01

PB89-185615 Technical Activities 1987, Center for Basic Standards. PB89-185615 901,521 PC A13/MF A01

PB89-185623

Center for Electronics and Electrical Engineering Technical Publication Announcements Covering Center Programs, April-June 1986 with 1987 CEEE Events Calendar.

PB89-185623 900 711 PC A03/MF A01 PB89-186357 PR89-186829 Analysis of Ultrapure Reagents from a Large Sub-Boiling Still Made of Teflon PFA.
PB89-186357 900,202 Not available NTIS PR89-185722 Simplified Discrete Event Simulation Model for an IEEE (Institute of Electrical and Electronics Engineers) 802.3 Local Millisecond Pulsar Rivals Best Atomic Clock Stability. PB89-185722 900,629 Not available NTIS Area Network. 900,617 Not available NTIS PB89-186365 PB89-185730 Deuterium Magnetic Resonance Study of Orientation and Poling in Poly(Vinylidene Fluoride) and Poly(Vinylidene Fluoride-Co-Tetrafluoroethylene). PB89-186837 Using Multiple Reference Stations to Separate the Variances of Noise Components in the Global Positioning Numerical Analysis for the Small-Signal Response of the MOS (Metal Oxide Semiconductors) Capacitor, PB89-186837 900,781 Not available NTIS System. PB89-185730 900,565 Not available NTIS PB89-186365 901,293 Not available NTIS PB89-186373 PB89-185748 PB89-186845 Analysis of High Performance Compensated Thermal En-Micro-Analysis of Mineral Saturation Within Enamel during Lactic Acid Demineralization. Design Factors for Parallel Processing Benchmarks. PB89-186845 900,637 Not available NTIS ciosures. PB89-185748 901,253 Not available NTIS PB89-186373 901,008 Not available NTIS PB89-186852 PB89-186381 PB89-185755 Hardware Instrumentation Approach for Performance Meas-Calibration with Randomly Changing Standard Curves. PB89-186381 900,888 Not available NTIS Van der Waals Fund, Van der Waals Laboratory and Dutch urement of a Shared-Memory Multiprocessor.
PB89-186852 900,638 Not available NTIS High-Pressure Science. PB89-185755 900.401 Not available NTIS PB89-186399 PB89-186860 PB89-185888 Comprehensive Dosimetry for Food Irradiation. Resonant Excitation of an Oxygen Valence Satellite in Photoemission from High-T(sub c) Superconductors.
PB89-186860 901,420 Not available NTIS 900,011 Not available NTIS One Is Not Enough: Intra-Cavity Spectroscopy with Multi-PB89-186399 Mode Lasers PB89-186407 PB89-185888 900.402 Not available NTIS Experimental Determination of Forced Convection Evaporative Heat Transfer Coefficients for Non-Azeotropic Refingerant Mixtures. DR89-186886 PB89-185896 Dynamical Diffraction of X-rays at Grazing Angle. PB89-186886 901,421 Not available NTIS Structure and Dynamics of Molecular Clusters via High PR89-186407 901.117 Not available NTIS Resolution IR Absorption Spectroscopy. PB89-185896 900,403 Not available NTIS PB89-186894 PB89-186415 Scheme for a 60-nm Laser Based on Photopumping of a High Level of Mo(6+) by a Spectral Line of Mo(11+). PB89-186415 900,407 Not available NTIS Probabilistic Models for Ground Snow Accumulation. PB89-186894 900,100 Not available NTIS PB89-185904 Atomic Internal Partition Function. PB89-185904 903 901,373 Not available NTIS PB89-186902 PB89-186423 PB89-185912 Finite Element Studies of Transient Wave Propagation. PB89-186902 901,375 Not available NTIS Current Research Efforts at JILA (Joint Institute for Laboratory Astrophysics) to Test the Equivalence Principle at Short Ranges.
PB9-185912

901,522

Not available NTIS International Comparison of HV Impulse Measuring Systems. PB89-186423 PB89-186910 900.809 Not available NTIS Towards the Ultimate Laser Resolution. PB89-186431 PB89-186910 900,416 Not available NTIS Pahasapaite, a Beryllophosphate Zeolite Related to Synthetic Zeolite Rho, from the Tip Top Pegmatite of South PB89-185920 PB89-186928 Fundamental Tests of Special Relativity and the Isotropy of Laser Probing of the Dynamics of Ga Interactions on Dakota. Space. PB89-185920 PB89-186431 901,288 Not available NTIS 901.523 Not available NTIS PB**89-18692**8 901,422 Not available NTIS PB89-186449 PB89-185938 Journal of Physical and Chemical Reference Data, Volume 17, Number 1, 1988.
PB89-186449 900,408 Not available NTIS PR89-187504 High Resolution Optical Multiplex Spectroscopy. PB89-185938 900,404 Not available NTIS Brick Masonry: U.S. Office Building in Moscow. PB89-187504 900,160 Not available NTIS PB89-185946 PB89-186456 PB89-187512 Laser Spectroscopy of Inelastic Collisions Pressure and Density Series Equations of State for Steam as Derived from the Haar-Gallagher-Kell Formulation.
PB89-186456 900,409 Not available NTIS Computerized Materials Property Data Systems. PB89-187512 901,312 Not available NTIS PB89-185946 900.405 Not available NTIS PB89-185953 Relationships between Fault Zone Deformation and Segment Obliquity on the San Andreas Fault, California.

PB89-185953 901,279 Not available NTIS PB89-187520 PB89-186464 Recent Advances in Bonded Phases for Liquid Chromatog-Absolute Cross Sections for Molecular Photoabsorption, Partial Photoionization, and Ionic Photofragmentation Procraphy. PB89-187520 900,204 Not available NTIS PB89-185961 Surface Reactions in Silane Discharges. PB89-185961 900,406 Not available NTIS PB89-187538 PB89-186464 900,410 Not available NTIS Determination of Hydrocarbon/Water Partition Coefficients from Chromatographic Data and Based on Solution Thermodynamics and Theory. PB89-186472 PB89-185979 Energy Levels of Molybdenum, Mo 1 through 42. PB89-186472 900,411 Not available NTIS Transducers in Michelson Tiltmeters. PB89-187538 900,205 Not available NTIS PB89-185979 901,280 Not available NTIS PB89-186480 PB89-187546 PB89-186241 Standard Chemical Thermodynamic Properties of Polycyclic Aromatic Hydrocarbons and Their Isomer Groups 1. Benzene Series. Preparation of Glass Columns for Visual Demonstration of Alternative Approach to the Hauptman-Karle Determinantal versed Phase Liquid Chromatography. 89-187546 900,206 Not available NTIS Inequalities PB89-187546 PB89-186241 PB89-186480 901,416 Not available NTIS 900.412 Not available NTIS PB89-187553 PB89-186258 PB89-186720 Maximum Entropy Distribution Consistent with Observed Structure Amplitudes. Measurement of Shear Rate on an Agitator in a Fermenta-Design Principles for a Large High-Efficiency Sub-Boiling Still. PB89-187553 tion Broth. 900,207 Not available NTIS PB89-186258 901,417 Not available NTIS PB89-186720 901,009 Not available NTIS PB89-186266 PB89-186738 PB89-187561 High Resolution Spectrum of the nu(sub 1) + nu(sub 2) Band of NO2. A Spin Induced Perturbation in the Ground Theoretical Models for High-Temperature Superconducti-Quasifree Electron Scattering on Nucleons in a Momentum-Dependent Potential. vity. PB89-186266 901.418 Not available NTIS PB89-186738 901.524 Not available NTIS State PB89-187561 900,417 Not available NTIS PB89-186274 PB89-186746 PB89-187579 Oxygen Partial-Density-of-States Change in the YBa2Cu3Ox Compounds for x(Approx.)6,6.5,7 Measured by Water Structure in Crystalline Solids: Ices to Proteins. PB89-186746 900,413 Not available NTIS Optical Power Measurements at the National Institute of Standards and Technology.
PB89-187579 900,918 Not available NTIS Soft X-ray Emission. PB89-186274 PB89-186753 901,419 Not available NTIS Repulsive Regularities of Water Structure in Ices and Crys-PB89-186282 PB89-187587 Apparatus Function of a Prism-Grating Double Monochro-PB89-186753 900,414 Not available NTIS New Standard Test Method for Eddy Current Probes. PB89-187587 900,981 Not available NTIS mator. PB89-186761 PB89-186282 901,359 Not available NTIS Thermodynamics of Hydrolysis of Disaccharides. PB89-187595 PB89-186290 901,221 Not available NTIS Optically Linked Electric and Magnetic Field Sensor for Poynting Vector Measurements in the Near Fields of Radiating Sources. PB89-186761 Computer Graphics for Ceramic Phase Diagrams. PB89-186290 901,043 Not available NTIS PB89-186779 Biological Standard Reference Materials for the Calibration of Differential Scanning Calorimeters: Di-alkylphosphatidyl-choline in Water Suspensions. 900,415 Not available NTIS PB89-186308 PB89-187595 900.712 Not available NTIS Phase Diagrams for High Tech Ceramics. PB89-186308 901,044 Not available NTIS PB89-188569 Advanced Ceramics: A Critical Assessment of Wear and PB89-186316 PB89-186787 Lubrication. PB89-188569 Formation and Stability Range of the G Phase in the Alumi-NBS (National Bureau of Standards)-Boulder Gas Flow Facility Performance. 901,045 PC A06/MF A01 num-Manganese System. PB89-186316 PB89-188577 901,144 Not available NTIS PB89-186787 900,889 Not available NTIS Fire Propagation in Concurrent Flows PB89-188577 900.3 PB89-186324 PB89-186795 900.597 PC A03/MF A01 Nucleation and Growth of Aperiodic Crystals in Aluminum Preparation of Multistage Zone-Refined Materials for Ther-PB89-188585 mochemical Standards. Dielectric Mixing Rules for Background Test Soils. PB89-188585 901,289 PC A03/MF A01 PB89-186324 901,145 Not available NTIS PB89-186795 900,203 Not available NTIS PB89-186332 PB89-186803 PB89-188593 Replacement of Icosahedral Al-Mn by Decagonal Phase. PB89-186332 901,146 Not available NTIS Water Structure in Vitamin B12 Coenzyme Crystals. 1. Anal-System for Measuring Optical Waveguide Intensity Profiles. PB89-188593 900,751 PC A04/MF A01 ysis of the Neutron and X-ray Solvent Densities. PB89-186803 901,222 Not available NTIS PB89-186340 PB89-186811 PB89-188601 Automated Calibration of Optical Photomask Linewidth Standards at the National Institute of Standards and Tech-Institute for Materials Science and Engineering, Polymers: Technical Activities 1987. Water Structure in Vitamin B12 Coenzyme Crystals. 2. Structural Characteristics of the Solvent Networks.

900.566 PC A06/MF A01

nology. PB89-186**3**40

901,315 Not available NTIS

PB89-186811

901,223 Not available NTIS

PB89-188601

PR89-188619

Thermal and Economic Analysis of Three HVAC (Heating, Ventilating, and Air Conditioning) System Types in a Typical VA (Veterans Administration) Patient Facility. PB89-188619 900,847 PC A04/MF A01

PB89-188627

Guidelines for Identification and Mitigation of Seismically Hazardous Existing Federal Buildings. PB89-188627 900,161 PC A03/MF A01

PB89-188635

Fire Properties Database for Textile Wall Coverings. PB89-188635 900,126 PC A04/MF A01 PB89-188809

DCTDOS: Neutron and Gamma Penetration in Composite 901,275 PC A05/MF A01

NBS' (National Bureau of Standards) Industry; Government Consortium Research Program on Flowmeter Installation Effects: Summary Report with Emphasis on Research January-July 1988. PB89-189120 901.010 PC A04/MF A01

PB89-189138

Mechanical Property Enhancement in Ceramic Matrix Composites. PB89-18**9**138 901,076 PC A05/MF A01

PB89-189146

Assessment of Robotics for Improved Building Operations and Maintenance. PB89-189146 900,092 PC A04/MF A01 PB89-189153

Evaluating Office Lighting Environments: Second Level

900.073 PC A07/MF A01 PB89-189161

Hybrid Structures for Simple Computer Performance Esti-900,639 PC A03/MF A01 PB89-189161

PB89-189179 Group Index and Time Delay Measurements of a Standard

Reference Fiber. PB89-189179 900,752 PC A03/MF A01 PB89-189187

Effect of Water on Piloted Ignition of Cellulosic Materials. PB89-189187 900,127 PC A09/MF A01 PB89-189195

Fracture Behavior of a Pressure Vessel Steel in the Ductileto-Brittle Transition Region. PB89-189195

901.103 PC A03/MF A01 PB89-189203

Evaluating Emergency Management Models and Data Bases: A Suggested Approach.
PB89-189203 901,598 PC A10/MF A01

PB89-189211 Bibliography of the NIST (National Institute of Standards

Technology) Electromagnetic Fields Division Publica-PB89-189211 900,810 PC A06/MF A01

PB89-189229

Ultrasonic Railroad Wheel Inspection Using EMATs (Electromagnetic-Accoustic Transducers), Report No. 18. PB89-189229 901,596 PC A05/MF A01 PB89-189237

Illumination Conditions and Task Visibility in Daylit Spaces. PB89-189237 900,074 PC A04/MF A01

PB89-189245 Emerging Technologies in Electronics and Their Measure-PB89-189245 900.811 PC A05/MF A01

PB89-189252 Calculation of the Flow Through a Horizontal Ceiling/Floor PB89-189252

900.128 PC A03/MF A01 PB89-189260 Fire Induced Flows in Corridors: A Review of Efforts to

Model Key Features. PB89-189260 900.129 PC A03/MF A01 PB89-189278

NVLAP (National Voluntary Laboratory Accreditation Program) Directory of Accredited Laboratories.
PB89-189278 900,890 PC A04/MF A01

PB89-189286 Workstation Controller of the Cleaning and Deburring Work-

PB89-18**9**286 900.955 PC A04/MF A01

National Engineering Laboratory's 1989 Report to the National Research Council's Board on Assessment of NIST (National Institute of Standards and Technology) Programs. PB99-189294 900,004 PC A03/MF A01 PB89-189302

Center for Electronics and Electrical Engineering Technical Publication Announcements: Covering Center Programs, July/September 1988, with 1989 CEEE Events Calendar. PB89-189302 900.812 PC A03/MF A01

PB89-189310 NIST (National Institute of Standards and Technology) Research Reports, March 1989.

PB89-189310 900,005 PC A03/MF A01 PB89-189328

Friability of Spray-Applied Fireproofing and Thermal Insulations: Field Evaluation of Prototype Test Devices. PB89-189328 900,130 PC A04/MF A01

Ignition Characteristics of the Iron-Based Alloy UNS \$66286 in Pressurized Oxygen.
PB89-189336 901,104 PC A03/MF A01

PB89-189344

PB89-189336

Narrow-Angle Laser Scanning Microscope System for Linewidth Measurement on Wafers.
PB89-189344 900,782 PC A06/MF A01

PB89-189351

Logistic Function Data Analysis Program: LOGIT. PB89-189351 900,418 PC A05/MF A01 PB89-189815

Phase Equilibria and Crystal Chemistry in the Ternary System BaO-TiO2-Nb2O5. Part 2. New Barium Polytitanates with < 5 mole % Nb2O5. PB99-189815 900,419 Not available NTIS

PB89-189823

Laser-Induced Fluorescence Study of Product Rotational State Distributions in the Charge Transfer Reaction: $Ar(1+)((\sup 2 P)(\sup 3/2)) + N2 -> Ar + N2(1+)(X)$ at 0.28 and 0.40 eV. and 0.40 eV. PB89-189823 900,420 Not available NTIS

PB89-191670 Potential Applications of a Sequential Construction Analyz-

PB89-191670 900,105 PC A03/MF A01

PB89-191977

GATT (General Agreement on Tariffs and Trade) Standards Code Activities of the National Institute of Standards and Technology 1988.
PB89-191977 900,173 PC A03/MF A01

PB89-191985

Use of Artificial Intelligence Programming Techniques for Communication between Incompatible Building Information Systems. PB89-191985 900,106 PC A05/MF A01

PB89-192678 Research Opportunities Below 300 nm at the NBS (National Bureau of Standards) Free-Electron Laser Facility.

PB89-192678 901,360 Not available NTIS PB89-193213

Building Technology Project Summaries 1989. PB89-193213 900,131 PC A05/MF A01

PB89-193221 Standard Aggregate Materials for Alkali-Silica Reaction

PB89-193221 901,046 PC A03/MF A01 PB89-193247

Rating Procedure for Mixed Air-Source Unitary Air Conditioners and Heat Pumps Operating in the Cooling Mode. Revision 1 900,075 PC A03/MF A01

PB89-193254 AIRNET: A Computer Program for Building Airflow Network Modeling. PB89-193254 900,076 PC A05/MF A01

PB89-193262 Metallurgical Evaluation of 17-4 PH Stainless Steel Cast-

ings. PB8**9**-1**9**32**6**2 901,105 PC A03/MF A01 PB89-193270

Center for Electronics and Electrical Engineering Technical Progress Bulletin Covering Center Programs, October to December 1988, with 1989 CEEE Events Calendar. PB89-193270 900,813 PC A03/MF A01

PR89-193288 False Alarm Study of Smoke Detectors in Department of Veterans Affairs Medical Centers (VAMCS). PB89-193288 900,093 PC A11/MF A01

PR89-193296

Progress Report of the Quality in Automation Project for FY88. PB89-193296 900,982 PC A06/MF A01 PR89-193304

Fire Research Publications, 1988. PB89-193304 900,132 PC A03/MF A01 PB89-193312

Stable Implementation Agreements for Open Systems Interconnection Protocols. Version 2, Edition 1. December 1988. PB89-193312 900,618 PC A22/MF A01 PB89-193833

Software Configuration Management: An Overview. PB89-193833 900,651 PC A03/MF A01

PB89-193841 NIST (National Institute of Standards and Technology) Measurement Services: High Vacuum Standard and Its llea

PB89-193841 900.891 PC A04/MF A01 PB89-193858 NBS (National Bureau of Standards) Measurement Services: Calibration of Gamma-Ray-Emitting Brachytherapy PB89-193858 901,243 PC A04/MF A01

PB89-193866 Acoustical Technique for Evaluation of Thermal Insulation. PB89-193866 900,919 PC A03/MF A01

PB89-193874

Document Interchange Standards: Description and Status of Major Document and Graphics Standards. PB89-193874 900,928 PC A03/MF A01

PB89-193882 NBS AMRF (National Bureau of Standards) (Automated

Manufacturing Research Facility) Process Planning System:
System Architecture.
PB89-193882

900,956

PC A06/MF A01 PB89-193890

Theory and Measurements of Radiated Emissions Using a TEM (Transverse Electromagnetic) Cell. PB89-193890 900,761 PC A03/MF A01

PR89-193890 PB89-193908

(12)C(16)O Laser Frequency Tables for the 34.2 to 62.3 THz (1139 to 2079 cm(-1)) Region.

901.361 PC A03/MF A01 PB89-193908 PR89-193916

Performance Evaluation of Radiofrequency, Microwave, and Millimeter Wave Power Meters. PR89-193916 900.814 PC A07/MF A01

PB89-193940

NASA/NBS (National Aeronautics and Space Administra-tion/National Bureau of Standards) Standard Reference Model for Telerobot Control System Architecture (NASREM) PB89-193940 901.589 PC A05/MF A01

PR89-195663 Alaska Arctic Offshore Oil Spill Response Technology Workshop Proceedings. PB89-195663 900,842 PC A10/MF A01

PR89-195671

Considerations of Stack Effect in Building Fires. PB89-195671 900,133 PC A05/MF A01 PB89-196158

User Guide for the NBS (National Bureau of Standards)
Prototype Compiler for Estelle (Revised).
PB89-196158 900,619 PC A05/MF A01

PB89-196166 User Guide for Wise: A Simulation Environment for Estelle. PB89-196166 900,620 PC A03/MF A01

PB89-196174 User Guide for Wizard: A Syntax-Directed Editor and Trans-

lator for Estelle PB89-196174 900,621 PC A03/MF A01 PB89-196182

Free Value Tool for ASN.1. PB89-196182 900.622 PC A04/MF A01

PB89-198190 Object-Oriented Model for Estelle and Its Smalltalk Implementation.

PB89-196190 900,623 PC A05/MF A01 PB89-200091

Executive Summary for the Workshop on Developing a Predictive Capability for CO Formation in Fires. PB89-200091 900,134 PC A04/MF A01 PB89-200208

Assessment of Need for and Design Requirements of a Wind Tunnel Facility to Study Fire Effects of Interest to

DNA. PB89-200208 901,276 PC A10/MF A01 PB89-200216

NIST (National Institute of Standards and Technology) Calibration Services Users Guide. 1989 Edition.
PB89-200216 900,926 PC A10/MF A01

PB89-200430 Dielectric Measurements for Cure Monitoring. PB89-200430 900,567 Not available NTIS

PB89-200448

Ag Screen Contacts to Sintered YBa2Cu3Ox Powder for Rapid Superconductor Characterization. PB89-200448 901,423 Not available NTIS PB89-200455

Battery-Powered Current Supply for Superconductor Meas-

PB89-200455 901.525 Not available NTIS PB89-200463

Chaos and Catastrophe Near the Plasma Frequency in the Chaos and Catastrophe Near III. RF-Biased Josephson Junction.

901,424 Not available NTIS

PB89-200471

Current Capacity Degradation in Superconducting Cable PB89-200471 901,526 Not available NTIS

PB89-200489 Magnetic Evaluation of Cu-Mn Matrix Material for Fine-Fila-Magnetic Evaluation of Control Magnetic Evaluation of Control PB89-200489

Nb3Sn Critical-Current Measurements Using Tubular Fiber-glass-Epoxy Mandrels. PB89-200497 901,527 Not available NTIS

PB89-201727 PB89-200505 PB89-201487 900.957 Not available NTIS Thermal Analysis of VAMAS (Versailles Project on Advanced Materials and Standards) Polycarbonate-Polyethyl-Superconducting Kinetic Inductance Bolometer. PB89-201735 900,762 Not available NTIS PB89-200505 Microwave Spectrum and Molecular Structure of the Ethylene-Ozone van der Waals Complex.
PB89-201735 900,424 Not available NTIS PB89-200513 PB89-201487 900,568 Not available NTIS Switching Noise in YBa2Cu3Ox 'Macrobridges'. PB89-200513 901,426 Not available NTIS PB89-201495 PB89-201743 Necking Phenomena and Cold Drawing. PB89-201495 900,975 Not available NTIS PB89-200745 Heterodyne Measurements on OCS Near 1372 cm(-1). PB89-201743 900,425 Not available NTIS Electron and Photon Stimulated Desorption: Benefits and PR89-201503 Difficulties PB89-201750 PB89-200745 901,427 Not available NTIS Mechanism of Hydrolysis of Octacalcium Phosphate. PB89-201503 901,254 Not availab Infrared Absorption Cross Section of Arsenic in Silicon in the Impurity Band Region of Concentration.
PB89-201750 900,426 Not available NTIS 901,254 Not available NTIS PB89-201032 PB89-201511 Noise in DC SQUIDS with Nb/Al-Oxide/Nb Josephson Formation of Hydroxyapatite in Hydrogels from Tetracal-cium Phosphate/Dicalcium Phosphate Mixtures. PB89-201511 901,255 Not available NTIS Junctions PB89-201768 PB89-201032 900,763 Not available NTIS Versailles Project on Advanced Materials and Standards Evolution to Permanent Status.
PB89-201768 900,969 Not available NTIS PB89-201040 PB89-201529 Structural Study of a Metastable BCC Phase in Al-Mn Alloys Electrodeposited from Molten Salts. Detection of Lead in Human Teeth by Exposure to Aqueous PB89-201776 PB89-201040 901.064 Not available NTIS Sulfide Solutions. Commercial Advanced Ceramics PB89-201529 901,256 Not available NTIS PR89-201057 901,048 Not available NTIS PB89-201776 PB89-201537 Reflection Coefficient of a Waveguide with Slightly Uneven PB89-201784 Audio-Frequency Current Comparator Power Bridge: Devel-Grain Boundary Structure in Ni3Al. PB89-201784 901 PB89-201057 900,753 Not available NTIS opment and Design Considerations PB89-201537 900 901,150 Not available NTIS 900,717 Not available NTIS PB89-201065 PB89-201545 PR89-201792 4s(2) 4p(2)-4s4p(3) Transition Array and Energy Levels of the Germanium-Like Ions Rb VI - Mo XI. PB89-201065 901,528 Not available NTIS Electron Diffraction Study of the Faceting of Tilt Grain Boundaries in NiO. PB89-201792 901,431 Not available NTIS International Comparison of Power Meter Calibrations Conducted in 1987. PB89-201545 900,718 Not available NTIS PB89-201073 PB89-201552 PR89-201800 Resonance-Enhanced Multiphoton Ionization of Atomic Hy-Analysis of Roto-Translational Absorption Spectra Induced in Low Density Gases of Non-Polar Molecules: The Methane Case. Accurate RF Voltage Measurements Using a Sampling Voltdrogen. PB89-2010**7**3 901.529 Not available NTIS age Tracker. PB89-201552 900,815 Not available NTIS PB89-201081 PB89-201800 900,427 Not available NTIS PB89-201560 Interaction of Water with Solid Surfaces: Fundamental As-PB89-201818 AC-DC Difference Calibrations at NBS (National Bureau of Standards). pects. PB89-201081 Stability of the SI (International System) Unit of Mass as Determined from Electrical Measurements. 900,421 Not available NTIS PB89-201560 900.816 Not available NTIS PB89-201099 PB89-201818 900,894 Not available NTIS PR89-201578 Heuristic Analysis of von Kries Color Constancy PB89-201826 PB89-201099 901,362 Not available NTIS Influence of the ac Stark Effect on Multiphoton Transitions Statistical Descriptors in Crystallography: Report of the International Union of Crystallography Subcommittee on Statistical Descriptors. PB9-201826 901,432 Not available NTIS PB89-201107 in Molecules. PB89-201578 901.530 Not available NTIS Physics of Fracture, 1987. PR89-201586 PB89-201107 901.428 Not available NTIS Ferrite Number Prediction to 100 FN in Stainless Steel Weld Metal. PB89-201115 PB89-201966 Simple Apparatus for Vapor-Liquid Equilibrium Measurements with Data for the Binary Systems of Carbon Dioxide PB89-201586 901,106 Not available NTIS Soot Inception in Hydrocarbon Diffusion Flames. PB89-201966 900,599 Not available NTIS PB89-201594 with n-Butane and Isobutane. PB89-201974 Crystal Structure of a Cyclic AMP (Adenosine Monophosphate)-Independent Mutant of Catabolite Gene Activator PB89-201115 900,422 Not available NTIS Radiation-Induced Interface Traps in Power MOSFETs. PB89-201974 900,784 Not available NTIS PB89-201123 NO/NH3 Coadsorption on Pt(111): Kinetic and Dynamical PB89-201594 901,224 Not available NTIS PB89-201982 Effects in Rotational Accommodation. PB89-201602 900,423 Not available NTIS In situ Observation of Particle Motion and Diffusion Interactions during Coarsening.
PB89-201982
901,151
Not available NTIS PB89-201123 High-Purity Germanium X-ray Detector on a 200 kV Analytical Electron Microscope. PB89-201131 901,151 Not available NTIS Estimation of an Asymmetrical Density from Several Small PB89-201602 900,208 Not available NTIS PB89-201990 PB89-201610 PB89-201131 901.212 Not available NTIS Numerical Simulation of Morphological Development during Continuum Radiation Produced in Pure-Element Targets by 10-40 keV Electrons: An Empirical Model. PB89-201610 900,209 Not available NTIS Ostwald Ripening. PR89-201149 PB89-201990 901,152 Not available NTIS Statistical Analysis of Experiments to Measure Ignition of PB89-202006 Cigarettes. PB89-201149 PB89-201628 900,135 Not available NTIS Sensors for Intelligent Processing of Materials. PB89-202006 900,920 Not available NTIS Laser Microprobe Mass Spectrometry: Description and Selected Applications.
PB89-201628 900,210 Not available NTIS PR89-201156 Graphical Analyses Related to the Linewidth Calibration Problem.
PB89-201156 900,783 Not available NTIS PB89-202014 Vector Calibration of Ultrasonic and Acoustic Emission PB89-201636 Methods for the Production of Particle Standards. PB89-201164 PB89-202014 900,765 Not available NTIS PB89-201636 901,047 Not available NTIS Standard Reference Materials for Dimensional and Physical PB89-202022 PB89-201644 Property Measurements. PB89-201164 Modeling of the Bremsstrahlung Radiation Produced in Pure Element Targets by 10-40 keV Electrons. PBR9-201644 901,531 Not available NTIS Exploratory Research in Reflectance and Fluorescence Standards at the National Bureau of Standards. 900,892 Not available NTIS PB89-201172 PB89-202022 900,428 Not available NTIS Importance of Isothermal Mixing Processes to the Understanding of Lift-Off and Blow-out of Turbulent Jet Diffusion PB89-202030 PB89-201651 PB69-201651 900,211 Not available NTIS Spin-Density-Wave Transition in Dilute YGd Single Crystals. PB89-202030 901,433 Not available NTIS Flames PB89-201172 900.598 Not available NTIS PB89-202048 PB89-201180 PB89-201669 Properties of Steam. PB89-202048 Single Particle Standards for Isotopic Measurements of Uranium by Secondary Ion Mass Spectrometry.
PB89-201669 901,297 Not available NTIS Development of New Standard Reference Materials for Use 901,533 Not available NTIS hermometry. PB89-202055 PB89-201180 900.893 Not available NTIS Pure Rotational Far Infrared Transitions of (16)O2 in Its PB89-201198 PB89-201677 Electronic and Vibrational Ground State.
PB89-202055
900,429
Not available NTIS Uncertainties in Mass Absorption Coefficients in Fundamental Parameter X-ray Fluorescence Analysis.
PB89-201677 900,212 Not available NTIS Progress in Vacuum Standards at NBS (National Bureau of Standards). PB89-201198 PB89-202063 900,999 Not available NTIS PB89-201206 PB89-201685 Quality Assurance in Metals Analysis Using the Inductively Coupled Plasma.
PB89-202063 900,213 Not available NTIS Mossbauer Hyperfine Fields in RBa2(Cu0.97Fe0.03)3 O(7-x)(R= Y,Pr,Er). PB89-201206 901,429 Not available NTIS NBS (National Bureau of Standards) Scale of Spectral Ra-900,213 Not available NTIS diance. PB89-201685 901,532 Not available NTIS PB89-202071 PB89-201214 PB89-201693 Three-Dimensional Atomic Spectra in Flames Using Stepwise Excitation Laser-Enhanced Ionization Spectroscopy. PB89-202071 900,430 Not available NTIS Magnetic Correlations in an Amorphous Gd-Al Spin Glass. PB89-201693 901,148 Not available NTIS Environmental Intelligence. PB89-201214 901,287 Not available NTIS PB89-201222 PB89-201701 PB89-202089 Neutron Scattering Study of the Spin Ordering in Amorphous Tb45Fe55 and Tb25Fe75.
PB89-201701 901,149 Not available NTIS Diffraction Effects Along the Normal to a Grain Boundary. PB89-202089 901,153 Not available NTIS Bond Selective Chemistry with Photon-Stimulated Desorp-PB89-201222 900,259 Not available NTIS PB89-202097 Electron Microscopy Studies of Diffusion-Induced Grain Boundary Migration in Ceramics.
PB89-202097 901,049 Not available NTIS PB89-201230 PB89-201719 Impedance of Radio-Frequency Biased Resistive Superconducting Quantum Interference Devices.
PB89-201719 900,764 Not available NTIS Electron-Stimulated-Desorption Ion-Angular Distributions. PB69-201230 901,430 Not available NTIS

PB89-202105

Green Function Method for Calculation of Atomistic Struc-

ture of Grain Boundary Interfaces in Ionic Crystals.

PB89-202105 901,050 Not available NTIS

PB89-201321

Technical Activities 1988. PB89-201321

Institute for Materials Science and Engineering: Metallurgy,

901.147 PC A06/MF A01

PB89-201727

Automated Processing of Advanced Materials. The Path to Maintaining U.S. Industrial Competitiveness in Materials.

PB89-202113

Novel Flow Process for Metal and Ore Solubilization by Aqueous Methyl lodide. PB89-202113

901,285 Not available NTIS

PB89-202121

Accurate Energies of nS, nP, nD, nF and nG Levels of Neutral Cesium 900,431 Not available NTIS PB89-202121

PB89-202139

Pi-Electron Properties of Large Condensed Polyaromatic Hydrocarbons. PB89-202139 900.432 Not available NTIS

PB89-202147

VAMAS (Versailles Project on Advenced Materials and Stendards) Intercomparison of Critical Current Measurement in Nb3Sn Wires. PB89-202147 901,534 Not available NTIS

PB89-202154

History of the Present Value of 2e/h Commonly Used for Defining National Units of Voltage and Possible Changes in National Units of Voltage and Resistance.

901,535 Not available NTIS

PB89-202162

Nonadiabatic Theory of Fine-Structure Branching Cross-Sections for Sodium-Helium, Sodium-Neon, and Sodium-Argon Optical Collisions. PB89-20162 900,433 Not available NTIS

PB89-202170

Determination of Binary Mixture Vapor-Liquid Critical Densities from Coexisting Density Data.
PB89-202170 901,536 Not available NTIS

PB89-202204

Comparison of Two Highly Refined Structures of Bovine Pancreatic Trypsin Inhibitor. PB89-202204 901,248 Not available NTIS

PB89-202212

Oligomers with Pendant Isocyanate Groups as Tissue Adhesives. 1. Synthesis and Characterization.
PB89-202212 900,055 Not available NTIS

PB89-202220

Speed of Sound in a Mercury Ultrasonic Interferometer Ma-PB89-202220 901.319 Not available NTIS

PB89-202238

Roles of Atomic Volume and Disclinetions in the Magnetism of the Rare Earth-3D Hard Megnets.
PB89-202238 901,434 Not available NTIS

PB89-202246 Standard X-ray Diffraction Powder Patterns from the JCPDS (Joint Committee on Powder Diffraction Standards) Re-

earch Association. PB89-202246 900,214 Not available NTIS

PB89-202444

Ergodic Behavior in Supercooled Liquids and in Glasses. PB89-202444 901,435 Not available NTIS

PB89-202451

13C NMR Method for Determining the Partitioning of End Groups and Side Branches between the Crystalline and Non-Crystalline Regions in Polyethylene. PB89-202451 900,569 Not available NTIS

PB89-202469

Computer Simulation Studies of the Soliton Model, 3, Noncontinuum Regimes and Soliton Interactions.
PB89-202469 901,537 Not available NTIS

PB89-202477

High-Temperature Dental Investments PB89-202477

901,257 Not available NTIS

PB89-202485

Gas Solubility and Henry's Law Near the Solvent's Critical Point PB89-202485 900,434 Not available NTIS

PB89-202493

Isochoric (p,v,T) Measurements on CO2 end (0.98 CO2 \pm 0.02 CH4) from 225 to 400 K end Pressures to 35 MPa. PB89-202493 900,435 Not available NTIS

PB89-202501

Liquid, Crystalline and Glassy States of Binary Charged Colloidal Suspensions.
PB89-202501 901,436 Not available NTIS 901,436 Not available NTIS

PB89-202519

NaCl-H2O Coexistence Curve Near the Critical Temperature of H2O. 900,436 Not available NTIS

PB89-202519 PB89-202527

> Thermochemistry of Solvation of SF6(1-) by Simple Polar Organic Molecules in the Vapor Phase PB89-202527 900.437 900,437 Not eveilable NTIS

PB89-202535

Computation of the ac Stark Effect in the Ground Stete of Atomic Hydrogen. PB89-202535 901,538 Not available NTIS

PB89-202543

Drift Tubes for Cheracterizing Atmospheric Ion Mobility Spectra Using AC, AC-Pulse, and Pulse Time-of-Flight Meesurement Techniques. PB89-202543 900,438 Not available NTIS

PB89-202550

New International Temperature Scale of 1990 (ITS-90).

PB89-202550 901,238 Not available NTIS

PB89-202568

Component Spectrum Reconstruction from Partially Characterized Mixtures. PB89-202568 900.439 Not available NTIS

PB89-202576

Spectroscopic Quantitative Analysis of Strongly Interacting Systems: Human Plasma Protein Mixtures.
PB89-202576 901,225 Not available NTIS PB89-202576

PB89-202584

Effects of Research on Building Practice.
PB89-202584 900,168 Not available NTIS PB89-202592

Photospheres of Hot Stars, 3, Luminosity Effects at Spec-

rai Type 09.5 PB89-202592 900,020 Not available NTIS PB89-202600

Quantum-Defect Parametrization of Perturbative Two-Photon Ionization Cross Sections. 901,539 Not available NTIS

PB89-202618

Rotational Modulation and Flares on RS Canum Venati-corum and BY Draconis Stars X: The 1981 October 3 Flare on V711 Tauri (= HR 1099). 900,021 Not available NTIS PB89-202618

PB89-202626

Stellar Winds of 203 Galactic O Stars: A Quantitative Ultraviolet Survey. PB89-202626 900.022 Not available NTIS

PB89-202634

Time-of-Flight Measurements of Hyperthermal Cl(sub 2) Molecules Produced by UV Laser Vaporization of Cryogenic Chlorine Films. PR89-202634 900,260 Not available NTIS

PRR9-202642

Time-Resolved FTIR Emission Studies of Molecular Photofragmentation. PB89-202642 900.261 Not available NTIS

PR89-202659

Antiferromagnetic Structure and Crystal Field Splittings in the Cubic Heusler Alloys HoPd2Sn and ErPd2Sn. PB89-202659 901,437 Not available NTIS

PR89-202667

Exchange and Magnetostrictive Effects in Rare Earth Superlattices.
PB89-202667 901,438 Not available NTIS

PR89-202675

Magnetic Structure of Y0.97Er0.03. PB89-202675 901. 901,439 Not available NTIS PB89-202923

Polymer Phase Separation. PB89-202923 900.570 Not available NTIS

PB89-202931 Pulpal and Micro-organism Responses to Two Experimental Dental Bonding Systems.

PB89-202931 901,258 Not evailable NTIS PB89-202949

Surface-Interacting Polymers: An Integral Equation and Fractional Calculus Approach. 900,571 Not available NTIS

PR89-202949 PB89-202956

Coadsorption of Water and Lithium on the Ru(001) Surface. PB89-202956 900,440 Not available NTIS

PB89-202964 Fundamental Characterizetion of Clean end Gas-Dosed Tin

PB89-202964 900,785 Not evailable NTIS PB89-202972

Cross Sections for Inelastic Electron Scattering in Solids. PB89-202972 901,440 Not available NTIS PB89-202980

Oxygen Chemisorption on Cr(110): 1. Dissociative Adsorp-PB89-202980 900,441 Not available NTIS

PB89-202998

Oxygen Chemisorption on Cr(110): 2. Evidence for Molecular O2(ads).
PB89-202998 900,442 Not evailable NTIS

PB89-203004

Stimuleted Desorption from CO Chemisorbed on Cr(110) PR89-203004 900,443 Not available NTIS PB89-203012

Time Resolved Studies of Vibrational Relaxetion Dynemics of CO(v= 1) on Metal Particle Surfaces.
PB89-203012 900,444 Not evailable NTIS

PB89-206833

Integrel Mess Balences and Pulse Injection Tracer Tech-PB89-206833 900.077 PC A03/MF A01

PB89-209225

Center for Electronics and Electrical Engineering: Technical Progress Bulletin Covering Center Programs, Januery to March 1989, with 1989 CEEE Events Celendar. PB89-209225 900,786 PC A03/MF A01

PB89-209233

Inventory of Equipment in the Cleaning and Deburring Workstation.

PB89-209233 900,958 PC A03/MF A01

PB89-209241

Center for Electronics and Electrical Engineering Technical Publication Announcements. Covering Center Programs, October/December 1988, with 1989 CEEE Events Calendar.

PB89-209241 900.787 PC A03/MF A01

PB89-209258

Data Management Strategies for Computer Integrated Manufacturing Systems.
PB89-209258 900,959 PC A03/MF A01

PB89-209266 Length Scale Measurement Procedures at the National

Bureau of Standards. PB89-209266 900,895 PC A04/MF A01

PB89-209274

Site Characterization for Radon Source Potential. 901,290 PC A04/MF A01 PB89-209282

Elimination of Spurious Eigenvalues in the Chebyshev Tau Spectral Method. PB89-209282 901,330 PC A03/MF A01

PB89-209290

Thin Film Thermocouples for High Temperature Measurement PB89-209290 901.065 - PC A03/MF A01

PB89-209308

Studies on Some Failure Modes in Latex Barrier Films. PB89-209308 901,089 PC A03/MF A01

PB89-209316

Results of a Survey of the Performance of EPDM (Ethylene Propylene Diene Terpolymer) Roofing at Army Facilities. PB89-209316 900,136 PC A03/MF A01

PB89-209324

Development of an Automated Probe for Thermal Conductivity Measurements. PB89-209324 900.896 PC A07/MF A01

PB89-209332

Expected Complexity of the 3-Dimensional Voronoi Diagram. PB89-209332 901.200 PC A03/MF A01

PB89-209340

NIST (National Institute of Standards and Technology) Measurement Services: The Calibration of Thermocouples and Thermocouple Materials. PB89-209340 900.897 PC A10/MF A01

PB89-209357

Assessment of Space Power Related Measurement Requirements of the Strategic Defense Initiative.

PB89-209357

901,269

PC A07/MF A01

PB89-211106

Journal of Research of the National Institute of Standards and Technology, Volume 94, Number 3, May-June 1989. PB89-211106 901,441 PC A04

PB89-211114

Brief Review of Recent Superconductivity Research at NIST (National Institute of Standards and Technology). PB89-211114 900,766 (Order as PB89-211106, PC A04)

PB89-211130

Consensus Values, Regressions, and Weighting Factors. PB89-211130 (Order as PB89-211106, PC A04)

PB89-211809

Ultrasonic Sensor for Measuring Surface Roughness. PB89-211809 900,679 Not aveilable NTIS PB89-211817

Crack-Interface Traction: A Frecture-Resistance Mechanism in Brittle Polycrystals. PB89-211817 901,051 Not available NTIS

PB89-211825

Creep Rupture of e Metal-Ceramic Particulate Composite. PB89-211825 901,077 Not available NTIS

PB89-211833 Design Criteria for High Tempereture Structural Applications

PB89-211**833** PB89-211841

PC-Access to Ceramic Phase Diegrams.

901,052 Not available NTIS

PB89-211841

901,053 Not aveileble NTIS PB89-211858 Outline of e Prectical Method of Assessing Smoke Hazard. PB89-211858 900,078 Not available NTIS

PB89-211868

FT-IR (Fourier Trensform-Infrared) Emission/Transmission Spectroscopy for In situ Combustion Diegnostics. PB89-211866 900,600 Not eveilable NTIS

PB89-211874

Gas Flow Measurement Stenderds. PB89-211874 900, 900,898 Not available NTIS PB89-211882

Prediction of Flowmeter Installetion Effects. PB89-211882 900,899 Not eveileble NTIS PB89-211890

Prediction of Flowmeter Instellation Effects.

OR-19

900,900 Not available NTIS PB89-211890 PB89-212161 900,730 Not available NTIS PB89-216477 900.640 PC A03/MF A01 PB89-211908 PB89-212179 PB89-218325 Electromigration Damage Response Time and Implications for dc and Pulsed Characterization.
PB89-212179 901,443 Not available NTIS Application of Formal Description Techniques to Conform-Interlaboratory Comparison of Two Types of Line-Source Thermal-Conductivity Apparatus Measuring Five Insulating ance Evaluation. PB89-211908 900,652 Not available NTIS Materials. PB89-218325 900,144 PC A03/MF A01 PB89-211916 PB89-212187 Object-Oriented Model for Estelle PB89-211916 90 PB89-218333 Neural Network Approach for Classifying Test Structure Re-900 653 Not available NTIS culte Ignition Characteristics of the Nickel-Based Alloy UNS NO7718 in Pressurized Oxygen. PB89-212187 900,788 Not available NTIS PB89-211924 PB89-218333 901,154 PC A03/MF A01 Acoustic Emission: A Quantitative NDE Technique for the Study of Fracture. PB89-211924 900,921 Not available NTIS PB89-212195 Thermal Conductivity Measurements of Thin-Film Silicon Di-PB89-218341 Interlaboratory Comparison of the Guarded Horizontal Pipe-Test Apparatus: Precision of ASTM (American Society for Testing and Materials) Standard Test Method C-335 Ap-plied to Mineral-Fiber Pipe Insulation. PB89-218341 PC A03/MF A01 oxide PB89-212195 901,444 Not available NTIS PB89-211932 PB89-212203 Mossbauer Spectroscopy. PB89-211932 901,189 Not available NTIS Strain Energy of Bituminous Built-Up Membranes: A New Concept in Load-Elongation Testing.
PB89-212203 900,139 Not available NTIS PB89-211940 PB89-218358 Preparation of Standards for Gas Analysis. PB89-211940 900,215 Not available NTIS Low-Temperature Thermal Conductivity of Composites: Alumina Fiber/Epoxy and Alumina Fiber/PEEK. PB89-212211 PB89-211957 NBS (National Bureau of Standards) Calibration Service Providing Time and Frequency at a Remote Site by Weighting and Smoothing of GPS (Global Positioning System)
Common View Data. 901.078 PC A04/MF A01 PB89-218358 Electronic Mail and the 'Locator's' Dilemma PB89-218366 PB89-211957 901,205 Not available NTIS Technical Reference Guide for FAST (Fire and Smoke Transport) Version 18. PB89-211965 PB89-212211 900.631 Not available NTIS Federal Software Engineering Standards Program.
PB89-211965 900,666 Not available NTIS PB89-212229 PB89-218366 900.602 PC A07/MF A01 Measurement of Electrical Breakdown in Liquids. PB89-218374 PB89-211973 900,447 Not available NTIS Vapor-Liquid Equilibrium of Binary Mixtures in the Extended Critical Region. I. Thermodynamic Model. PB89-218374 901,544 PC A04/MF A01 Laboratory Evaluation of an NBS (National Bureau of Standards) Polymer Soil Stress Gage.
PB89-211973 901,291 Not available NTIS PB89-212237 Materials Failure Prevention at the National Bureau of Standards PB89-218382 PB89-211981 PB89-212237 901,190 Not available NTIS Publications of the National Institute of Standards and Technology, 1988 Catalog. PB89-218382 900,006 PC A15/MF A01 Applications of Mirrors, Supermirrors and Multilayers at the National Bureau of Standards Cold Neutron Research Fa-PB89-212245 Interpolation of Silicon Photodiode Quantum Efficiency as an Absolute Radiometric Standard. 900,006 PC A15/MF A01 PB89-219281 PB89-211981 901,540 Not available NTIS PB89-212245 901,445 Not available NTIS PB89-211999 Non-Aqueous Dental Cements Based on Dimer and Trimer PB89-212252 Calculations and Measurement of the Performance of Con-PATENT-4 832 745 900,033 Not available NTIS Collision Induced Spectroscopy: Absorption and Light Scatverging Neutron Guides. PB89-211999 901,541 Not available NTIS tering. PB89-212252 PB89-221147 901.363 Not available NTIS Directory of International and Regional Organizations Conducting Standards-Related Activities.
PB89-221147 900,008 PC A19/MF A01 PB89-212005 PB89-212260 Refinement and Experimental Verification of a Model for ASTM (American Society for Testing and Materials) Committee Completes Work on EPDM Specification. Fire Growth and Smoke Transport. PB89-212005 900,137 Not available NTIS PB89-221154 900.140 Not available NTIS PB89-212260 PB89-212013 Mining Automation Real-Time Control System Architecture Standard Reference Model (MASREM). PB89-214738 Chemisorption of HF (Hydrofluoric Acid) on Silicon Sur-MM Wave Quasioptical SIS Mixers PB89-221154 901,286 PC A04/MF A01 PB89-214738 901,446 Not available NTIS PB89-212013 900,445 Not available NTIS PB89-221162 PB89-214753 Laser Induced Damage in Optical Materials: 1987. PB89-221162 901,364 PC A99/MF A01 PB89-212021 Electronic Publishing: Guide to Selection. Effects of Material Characteristics on Flame Spreading. PB89-212021 900,572 Not available NTIS 900,935 PC A03/MF A01 PB89-214753 PB89-221170 PB89-214761 Semiconductor Measurement Technology: Database for and Statistical Analysis of the Interlaboratory Determination of the Conversion Coefficient for the Measurement of the Interstitial Oxygen Content of Silicon by Infrared Absorption. PB89-221170 901,054 PC A09/MF A01 PB89-212039 Guidelines for Implementing the New Representations of the Volt and Ohm Effective January 1, 1990. PB89-214761 900,817 PC A05/MF A01 Prediction of the Heat Release Rate of Douglas Fir. PB89-212039 901,185 Not available NTIS PB89-212047 PB89-214779 Toxicity of Mixed Gases Found in Fires. PB89-212047 900,869 Not available NTIS Synergistic Effects of Nitrogen Dioxide and Carbon Dioxide Following Acute Inhalation Exposures in Rats. PB89-214779 900,856 PC A03/MF A01 PB89-221188 Visual Perception Processing in a Hierarchical Control System: Level 1.
PB89-221188 900,994 PC A04/MF A01 PB89-212054 Interpretation of Emission Wings of Balmer Lines in Lumi-PB89-214787 nous Blue Variables. PB89-212054 Upward Flame Spread on Vertical Walls. PB89-214787 900,141 PC A04/MF A01 PB89-221196 900.023 Not available NTIS Working Implementation Agreements for Open Systems Interconnection Protocols. PB89-212062 PB89-215198 Liquid-Supported Torsion_Balance: An Updated Status PB89-221196 Use of GMAP (Geometric Modeling Applications Interface Program) Software as a PDES (Product Data Exchange Specification) Environment in the National PDES Testbed 900,624 PC A10/MF A01 Report on its Potential for Tunnel Detection.

PB89-212062

901,542

Not available NTIS PB89-221873 AutoMan: Decision Support Software for Automated Manufacturing Investments. User's Manual. PB89-221873 900,963 PC A03/MF A01 PB89-212070 Calibration of GPS (Global Positioning System) Equipment PR89-215198 900,960 PC A03/MF A01 in Japan. PB**8**9-212070 PB89-215321 PB89-222368 900,630 Not available NTIS Computation and Use of the Asymptotic Covariance Matrix for Measurement Error Models. Multiple Actuator Hydraulic System and Rotary Control PB89-212096 Valve Therefor. PATENT-4 838 145 Evaluated Kinetics Data Base for Combustion Chemistry. PB89-212096 900,601 Not available NTIS PB89-215321 901,214 PC A03/MF A01 900,995 Not available NTIS PB89-215339 PB89-222525 PB89-212104 Inventory of Equipment in the Turning Workstation of the AMRF (Automated Manufacturing Research Facility). PB89-215339 900,961 PC A03/MF A01 Journal of Physical and Chemical Reference Data, Volume 18, Number 2, 1989. Fundamental Aspects of Key Issues in Hazardous Waste Incineration. PB89-222525 900,448 Not available NTIS PB89-212104 900.861 Not available NTIS PB89-215347 PB89-222533 PB89-212112 Recommended Technical Specifications for Procurement of Equipment for a Turning Workstation. Quantitative Studies of Coatings on Steel Using Reflection/ Absorption Fourier Transform Infrared Spectroscopy. PB89-212112 901,066 Not available NTIS Thermal Conductivity of Nitrogen and Carbon Monoxide in the Limit of Zero Density. 900.962 PC A03/MF A01 PB89-215347 PB89-222533 900,449 (Not available NTIS) PB89-215354 PB89-212120 PB89-222541 Validated Furniture Fire Model with FAST (HEMFAST) Thermophysical Properties of Methane. PB89-222541 900,450 (Not Available NTIS) Tests of Adhesive-Bonded Seams of Single-Ply Rubber PB89-215354 900,142 PC A05/MF A01 Membranes. PB89-212120 PB89-215362 900,138 Not available NTIS PB89-222558 Service Life of Concrete. PB89-212138 Thermodynamic Properties of Argon from the Triple Point to 1200 K with Pressures to 1000 MPa. PR89-215362 901,303 PC A07/MF A01 Simulation Study of Light Scattering from Soot Agglomer-PB89-222558 PB89-215370 900,451 (Not Available NTIS) PB89-212138 901,543 Not available NTIS Mechanism for Shear Band Formation in the High Strain PB89-222566 PB89-212146 Rate Torsion Test. Thermodynamic Properties of Dioxygen Difluoride (O2F2) and Dioxygen Fluoride (O2F).
PB89-222566 900,452 (Not Available NTIS) PB89-215370 900,901 PC A03/MF A01 Part Load, Seasonal Efficiency Test Procedure Evaluation of Furnace Cycle Controllers.
PB89-212146 900,848 Not available NTIS PB89-215404 HAZARD I Fire Hazard Assessment Metho PB89-215404 9 PB89-222574 900,143 CP D05 PB89-212153 Thermodynamic and Transport Properties of Carbohydrates and Their Monophosphates: The Pentoses and Hexoses. PB89-222574 900,453 (Not available NTIS) PB89-216469 Activities of the International Association for the Properties Static Tests of One-third Scale Impact Limiters of Steam between 1979 and 1984 901,000 PC A04/MF A01 PB89-212153 900,446 Not available NTIS PB89-216469 PB89-222582 PB89-212161 PB89-216477

Architecturally-Focused Benchmarks with a Communication

Example.

Evaluated Kinetic and Photochemical Data for Atmospheric

900,454 (Not Available NTIS)

Chemistry. Supplement 3. PB89-222582

Blocked Impurity Band and Superlattice Detectors: Prospects for Radiometry.

PB89-222608

Tebles for the Thermophysical Properties of Methane. PB89-222608 900,843 PC A21/MF A01

PB89-222618

NIST (Netional Institute of Standards and Technology)
Meesurement Services: AC-DC Difference Calibrations.
PB89-222616 900,818 PC A14/MF A01

PB89-228559

Journel of Physical and Chemical Refaranca Data, Volume 18, Number 1, 1989. PB89-226559 900,455 Not available NTIS

PB89-226587

Stenderd Electrode Potentiels end Temperature Coefficients in Water at 298.15 K.
PB89-226567 900,456 (Not available NTIS)

PB89-226575

Cross Sections for Collisions of Electrons end Photons with Oxygen Molecules. PB89-226575 900,457 (Not eveilable NTIS) PB89-226583

Thermal Conductivity of Refrigerents In a Wide Range of Tempereture end Pressure.
PB89-226583 900,458 (Not available NTIS)

PB89-226591

Stenderd Chemical Thermodynamic Properties of Polycyclic Arometic Hydrocarbons and Their Isomer Groups. 2. Pyrene Series, Naphthopyrene Series, and Coronene PB89-226591 900,459 (Not available NTIS)

PB89-226609

Cross Sections for K-Shell X-rey Production by Hydrogen and Helium lons in Elements from Beryllium to Uranium. PB89-226609 900,460 (Not aveileble NTIS)

PB89-227797

Rete Constents for the Quanching of Excited States of Metal Complexes in Fluid Solution.
PB89-227797 900,461 (Not available NTIS)

PB89-227888

Celorimetric and Equilibrium Investigation of the Hydrolysis of Lectose. PB89-227888 901,226 Not available NTIS

PB89-227896

Second Virial Coefficients of Aqueous Alcohols at Elevated Temperaturas: A Calorimetric Study. PB89-227896 Study. 900,462 Not available NTIS

PB89-227904

Thermodynamics of the Hydrolysis of Sucrose. PB89-227904 901,227 Not available NTIS

PB89-227912

Absolute Inferred Trensition Moments for Open Shell Diatomics from J Dependence of Transition Intensities: Application to OH. PB89-227912 900,463 Not available NTIS

PB89-227920 Dipole Moment Function end Vibretionel Trensition Intensities of OH.

PB89-227920

PB89-227938 Generation of Squeezed Light by Intracevity Frequency

900,464 Not available NTIS

Doubling. PB89-227938

901,365 Not available NTIS PB89-227946 High-Precision Absolute Grevity Observations in the United

PB89-227946 901,281 Not available NTIS PB89-227953

Rydberg-Klein-Rees Invarsion of High Resolution ven der Waals Infrared Spectra: An Intermolecular Potential Energy Surface for Ar+ HF (v= 1).
PB99-227953 900,465 Not available NTIS

PB89-227961

Three Dimensional Quantum Reactive Scattering Study of the I + HI Reaction and of the IHI(1-) Photodetechment Spectrum.

PB89-227961 900.466 Not eveilable NTIS PB89-227979

Spectroscopic Signatures of Floppiness in Moleculer Com-

plexes. PB89-227979 900.467 Not evaileble NTIS

PB89-227987

Asymptotic Expensions for Constant-Composition Dew-Bubble Curves Near the Critical Locus. PB89-227987 901,545 Not aveilable NTIS

PB89-227995

Development of a Field-Space Corresponding-States Method for Fluids end Fluid Mixtures. PB89-227995 901,331 Not available NTIS

PB89-228001

Low-Q Neutron Diffrection from Supercooled D-Glycerol. PB89-228001 900,468 Not available NTIS PB89-228019

Mean Density Approximation and Hard Sphere Expansion Theory: A Review.
PB89-228019 901,546 Not available NTIS

PB89-228027

Method for Improving Equations of State Near the Critical

PB89-228027

901,547 Not eveilable NTIS

PB89-228035 Prediction of Shear Viscosity end Non-Newtonien Behevior in the Soft-Sphere Liquid.

PB89-228035 901,548 Not eveileble NTIS 901,548 Not eveileble NTIS

PB89-228043

Sheer-Induced Anguler Dependence of the Liquid Pair Correletion Function. PR89-228043 900,469 Not eveileble NTIS

PB89-228050

Simplified Raprasentetion for the Thermal Conductivity of Fluids in the Critical Region. PB89-228050 901.332 Not aveileble NTIS

PB89-228068

Thermophysical Properties for Bioprocess Engineering. PB89-228068 900,043 Not eveileble NTIS PB89-228078

Torsional Piazoelectric Crystel Viscometer for Compressed Gases and Liquids. PB89-228076 901,447 Not eveilable NTIS

PB89-228084

Optical Novelty Filters. PB89-228084

901,366 Not availebla NTIS PB89-228092

Quentum Machenical Calculations on the Ar(1+) + N2 Charge Transfer Reection. PB89-228092 900,470 Not available NTIS

PB89-228100

Spectroscopic Detection Methods PB89-228100 901 901.549 Not eveileble NTIS

PB89-228118

Stete Selection via Optical Methods. PB89-228118 901,550 Not eveileble NTIS

PB89-228274

Development and Use of a Tribology Research-in-Progress Deteh PB89-228274 901.002 PC A14/MF A01

PB89-228282

Updete of U.S. Participation in International Standards Ac-PB89-228282 900.902 PC A03/MF A01

PB89-228290

Computer-Controlled Test System for Opereting Different Wear Test Machines.
PB89-228290 900,983 PC A03/MF A01

PB89-228308

Centar for Electronics and Electrical Engineering Technical Publication Announcements. Covering Center Programs, January-March 1989, with 1989 CEEE Events Calendar. PB89-228308 900,789 PC A03/MF A01

PB89-228316

Experimental Study of the Pyrolysis of Pure end Fire Retarded Cellulose. 901.090 PC A07/MF A01 PB89-228316

PB89-228324

NVLAP (National Voluntary Laboratory Accreditation Program) Assessment and Evaluation Manual.
PB89-228324 900,903 PC A03/MF A01

PB89-228332

International Cooperation and Competition in Materials Science and Engineering.
PB89-228332
901,191
PC A13/MF A01

PB89-228365

Precision Experiments to Search for the Fifth Force. PB89-228365 901,551 Not available NTIS

PB89-228373

IUE Observetion of the Intersteller Medium Toward Beta Geminorum. PB89-228373 900,024 Not available NTIS

PB89-228381

Ionizetion end Current Growth in N2 at Very High Electric Field to Ges Density Retios. PB89-228381 901,552 Not evailable NTIS

PB89-228399

Infrered Spectra of Nitrous Oxide-HF Isomers. PB89-228399 900 471 No. 900,471 Not aveilable NTIS

PB89-228407

Dynemical Simulation of Liquid- and Solid-Metal Self-Sputtenng. PB89-228407 900,472 Not available NTIS

PB89-228415

Celculation of Vibration-Rotation Spectra for Rare Gas-HCI Complexes. PB89-228415 900,473 Not available NTIS

PB89-228423

Cr(110) Oxidation Probed by Carbon Monoxide Chemisorp-PB89-228423 900,239 Not available NTIS

PB89-228431

Resistance Measurements of High T(sub c) Superconductors Using a Novel 'Bathysphere' Cryostat.
PB89-228431 901,448 Not available NTIS

PB89-228449

Evidence for the Superconducting Proximity Effect in Junctions between the Surfaces of YBa2CU3Ox Thin Films. PB89-228449 901,449 Not available NTIS

PB89-228456

Cryogenic Bethysphere for Rapid Veriable-Tempereture Cherecterizetion of High-T(sub c) Superconductors. PB89-228456 901,450 Not eveileble NTIS

PB89-228464

Specimen Biasing to Enhance or Suppress Secondary Electron Emission from Cherging Specimens et Low Accelereting Volteges. PB89-228464 901,451 Not aveileble NTIS

PB89-228472

EXAFS (Extended X-rey Absorption Fine Structure) Study of Burled Germenium Leyer in Silicon.
PB89-228472 901,452 Not evaileble NTIS PB89-228480

Multiple Scattering in the X-rey Absorption Neer Edge Structure of Tetrehedral Germanium Geses.
PB89-228480 900,474 Not evaileble NTIS

PB89-228498

Silicon Photodiode Detectors for EXAFS (Extended X-rey Absorption Fine Structure).
PB89-228498 900,731 Not availeble NTIS

PB89-228506

Leboratory Meesurement of the 1(sub 01)-0(sub 00) Trensition end Electric Dipole Moment of SiC2.
PB89-228506 900,025 Not availeble NTIS

PB89-228514

Infrared Spectrum of the 1205-cm(-1) Bend of HNO3. PB89-228514 900,475 Not available NTIS

PB89-228522

Effects of Doping-Density Gradients on Band-Gap Narrowing in Silicon end GaAs Devices.
PB89-228522 901,453 Not available NTIS

PB89-228530

Machine-Learning Clessification Approach for IC Manufacturing Control Based on Test Structure Measurements.
PB89-228530 900,790 Not available NTIS

PB89-228548

Acoustic end Microwave Resonances Applied to Measuring the Gas Constant and the Thermodynamic Temperature. PB89-228548 901,320 Not available NTIS

PB89-228555

Capillary Waves of a Vapor-Liquid Interface Near the Critical Temperature. PB89-228555 900,476 Not available NTIS

PB89-228563

Improved Conformal Solution Theory for Mixtures with Large Size Ratios. PB89-228563 900,477 Not available NTIS

PB89-228571

Fiber Coating and Characterization. PB89-228571 901. 901,067 Not available NTIS

PB89-228589

Reevaluation of Forces Measured Across Thin Polymer Films: Nonequilibrium and Pinning Effects. PB89-228589 900,573 Not available NTIS

PB89-228597

Determination of AC-DC Difference in the 0.1 - 100 MHz Frequency Range. PB89-228597 900,719 Not available NTIS

PB89-228977

Air Quality Investigation in the NIH (National Institutes of Health) Radiation Oncology Branch.
PB89-228977 900,079 PC A07/MF A01 PB89-228985

Effect of Anisotropic Thermal Conductivity on the Morphological Stability of a Binary Alloy.
PB89-228985

901,155
PC A03/MF A01

PB89-228993

Detailed Description of the Knowledge-Based System for Physical Database Design. Volume 1.
PB89-228993
900,929
PC A04/MF A01

PB89-229009

Estimating the Environment and the Response of Sprinkler Links in Compartment Fires with Draft Curtains and Fusible Line-Actuated Ceiling Vents. Part 2. User Guide for the Computer Code Lavent.

PB89-229009 900,094 PC A03/MF A01

PB89-229017 Processing Rate Sensitivities of a Heterogeneous Multi-

processor PB89-229017 PB89-229025

NDE (Nondestructive Evaluation) Publications, 1985. PB89-229025 900,984 PC A03/MF A01

PB89-229033

Detailed Description of the Knowledge-Based System for Physical Database Design. Volume 2. PB89-229033 900,930 PC A09/MF A01

PB89-229041

Experimental Investigation and Modeling of the Flow Rate of Refrigerant 22 Through the Short Tube Restrictor. PB89-229041 901,118 PC A06/MF A01

PB89-229058

Lightning and Surge Protection of Photovoltaic Installations. Two Case Histories: Vulcano and Kythnos.
PB89-229058 900,851 PC A05/MF A01

900.641 PC A03/MF A01

PB89-229066 PB89-229298 900 046 Not available NTIS PB89-230478 901,216 Not available NTIS User's Reference Guide for ODRPACK: Software for Weighted Orthogonal Distance Regression Version 1.7. PB89-229066 901,215 PC A05/MF A01 PB89-229306 PB89-231005 Origins of ASHRAE (American Society of Heating, Refrigerating and Air-Conditioning Engineers) Window U-Value Data and Revisions for the 1989 Handbook of Fundamentals. PB89-231005 900,083 Not available NTIS Grain Boundary Characterization in Ni3Al. PB89-229306 901,156 Not available NTIS PB89-229074 PB89-229314 NBS/BAM (National Bureau of Standards/Bundesanstalt Grain Boundary Structure in Ni3Al. fur Materialprufung) 1986 Symposium on Advanced Ceram-901 157 Not available NTIS PB89-231013 PB89-229314 Expert Systems Applied to Spacecraft Fire Safety. PB89-231013 901,590 Not available NTIS PB89-229678 901,055 PC A08/MF A01 PB89-229074 Clutter Models for Subsurface Electromagnetic Applica-PB89-229082 PB89-231021 tions. PB89-229678 Hysteretic Phase Transition in Y1Ba2Cu3O7-x Supercon-900,688 PC A03/MF A01 National Bureau of Standards Message Authentication Code (MAC) Validation System.
PB89-231021 900,671 Not available NTIS ductors. PB89-229082 PB89-229686 901,454 Not available NTIS Ventilation and Air Quality Investigation of the U.S. Geologi-PB89-229090 cal Survey Building. PB89-229686 PB89-231039 Performance of He II of a Centrifugal Pump with a Jet 900.857 PC A03/MF A01 Production and Stability of S2F10 in SF6 Corona Dis-Pump Inducer. PB89-229090 PB89-230148 901.553 Not available NTIS charges. PB89-231039 Method of and Apparatus for Real-Time Crystallographic Axis Orientation Determination.
PATENT-4 747 684 901,383 Not available NTIS 900,822 Not available NTIS PB89-229108 PB89-231047 Expert-Database System for Sample Preparation by Microwave Dissolution. 1. Selection of Analytical Descriptors. PB89-229108 900,216 Not available NTIS Considerations for Advanced Building Thermal Simulation PB89-230288 Programs. PB89-231047 Structure of the CO2-CO2-H2O van der Waals Complex Determined by Microwave Spectroscopy.

PB89-230288 900,479 Not available NTIS 900,084 Not available NTIS PB89-229116 PB89-231054 Microwave Digestion of Biological Samples: Selenium Analysis by Electrothermal Atomic Absorption Spectrometry. PB89-229116 900,217 Not available NTIS Thermophysical-Property Needs for the Environmentally Acceptable Halocarbon Refrigerants.
PB89-231054
900,482
Not available NTIS PB89-230296 Infrared Spectrum of Sodium Hydride PB89-230296 900,48 PB89-229124 900,480 Not available NTIS PB89-231062 Higher Order Beam Finite Element for Bending and Vibra-PB89-230304 Research as the Technical Basis for Standards Used in Building Codes.
PB89-231062 900,101 Not available NTIS tion Problems. 901,484 Not available NTIS Ultrashort-Pulse Multichannel Infrared Spectroscopy Using Broadband Frequency Conversion in LilO3. PB89-230304 901,367 Not available NTIS PR89-229124 PB89-229132 PB89-231070 Dependence of T(sub c) on the Number of CuO2 Planes per Cluster in Interplaner-Boson-Exchange Models of High-PB89-230312 Development of the NBS (National Bureau of Standards)
Beryllium Isotopic Standard Reference Material.
PB89-231070 900,221 Not available NTIS per Cluster in Interplaner-bo T(sub C) Superconductivity. Introduction to Supercritical Fluid Chromatography. Part 2. Introduction to Supercritical Parameters Applications and Future Trends.

900,219 Not available NTIS PB89-229132 901,455 Not available NTIS PB89-229140 PR89-231088 Hydrogen Sites in Amorphous Pd85Si15HX Probed by Neutron Vibrational Spectroscopy.
PB89-229140 901,456 Not available NTIS PB89-230320 Thermomechanical Detwinning of Superconducting YBa2Cu3O7-x Single Crystals. PB89-231088 901,458 Not available NTIS Determination of the Absolute Specific Conductance of Primary Standard KCI Solutions. PB89-230320 900,481 Not available NTIS PB89-229157 PR89-231096 PB89-230338 Capabilities of Smoke Control: Fundamentals and Zone Assessment of Theories for the Behavior and Blowout of Lifted Turbulent Jet Diffusion Flames. PB89-231096 900,603 Not available NTIS Isotope Dilution Mass Spectrometry for Accurate Elemental Smoke Control. PB89-229157 900.080 Not available NTIS PB89-230338 900,220 Not available NTIS PB89-229165 PB89-231104 PB89-230346 International Intercomparison of Neutron Survey Instrument InSb as a Pressure Sensor. PB89-231104 Spatial Filtering Microscope for Linewidth Measurements. PB89-230346 901,368 Not available NTIS 900,904 Not available NTIS PB89-229165 901,300 Not available NTIS PB89-231112 PB89-229173 PB89-230353 Flux Creep and Activation Energies at the Grain Boundaries of Y-Ba-Cu-O Superconductors.
PB89-230353 901,457 Not available NTIS Non-Geometric Dependencies of Gas-Operated Piston Gage Effective Areas. PB89-231112 900,905 Not available NTIS Improved Low-Energy Diffuse Scattering Electron-Spin Polarization Analyzer. PB89-229173 900,218 Not available NTIS PB89-229181 PB89-230361 PB89-231120 Observations of Gas Species and Mode of Operation Effects on Effective Areas of Gas-Operated Piston Gages. PB89-231120 900,906 Not available NTIS PVT Relationships in a Carbon Dioxide-Rich Mixture with Investigation of a Washington, DC Office Building. PB89-230361 900,081 Not available NTIS PB89-229181 900,478 Not available NTIS PB89-230379 PR89-231138 PB89-229199 Airflow Network Models for Element-Based Building Airflow Modeling.
PB89-230379 900,082 Not available NTIS Pressure Fixed Points Based on the Carbon Dioxide Vapor Pressure at 273.16 K and the H2O(I) - H2O(III) - H2O(L) Triple-Point. Quantitative Problems in Magnetic Particle Inspection. 900,985 Not available NTIS 900.082 Not available NTIS PB89-229199 PB89-230387 PB89-229207 PB89-231138 900,483 Not available NTIS Determination of the Time-Dependence of ohm NBS (National Bureau of Standards) Using the Quantized Hall Re-Photonic Electric-Field Probe for Frequencies up to 2 GHz. PB89-229207 900,732 Not available NTIS PB89-231146 Advances in NIST (National Institute of Standards and Technology) Dielectric Measurement Capability Using a Mode-Filtered Cylindrical Cavity.
PB99-231146 Not available NTIS PB89-229215 sistance. PB89-230387 900.819 Not available NTIS Window U-Values: Revisions for the 1989 ASHRAE (American Society of Heating, Refrigerating and Air-Conditioning Engineers) Handbook - Fundamentals. PB89-229215 900,145 Not available NTIS PB89-230395 Improved Transportable DC Voltage Standard. PB89-230395 901,554 Not available NTIS PB89-231153 Faraday Effect Sensors: The State of the Art. PB89-231153 900,823 Not available NTIS PB89-230403 PB89-229223 Josephson Array Voltage Calibration System: Operational Heterodyne Frequency Measurements of (12)C(16)O Laser PB89-231161 Use and Verification. PB89-230403 901,374 Not available NTIS 900,820 Not available NTIS Analysis and Prediction of Air Leakage through Door As-PB89-229231 PB89-230411 PB89-231161 900,085 Not available NTIS Effect of Heat Treatment on Crack-Resistance Curves in a Low Field Determination of the Proton Gyromagnetic Ratio in Water. Effect of Heat Treatment on Scale Liquid-Phase-Sintered Alumina.

901,056 Not available NTIS PB89-231179 PB89-230411 901,555 Not available NTIS Combustion Efficiency, Radiation, CO and Soot Yield from a Variety of Gaseous, Liquid, and Solid Fueled Buoyant Diffusion Flames PB89-229249 PB89-230429 Measurement of the NBS (National Bureau of Standards) Electrical Watt in SI Units. fusion Flames PB89-231179 Quasi-Constant Composition Method for Studying the For-Quasi-Constant Composition Includes mation of Artificial Caries-Like Lesions. 900.604 Not available NTIS PB89-230429 900.821 Not available NTIS PR89-231187 Test Results and Predictions for the Response of Near-Ceiling Sprinkler Links in a Full-Scale Compartment Fire.
PB89-231187 900,095 Not available NTIS PB89-230437 PB89-229256 NBS (National Bureau of Standards) Determination of the Fine-Structure Constant, and of the Quantized Hall Resist-Simplified Shielding of a Metallic Restoration during Radiation Therapy. PB89-229256 900,044 Not available NTIS ance and Josephson Frequency-to-Voltage Quotient in SI PB89-231195 Units. PB89-230437 IEEE (Institute of Electrical and Electronics Engineers) IRPS (International Reliability Physics Symposium) Tutorial Thermal Resistance Measurements, 1989. PB89-229264 901,556 Not available NTIS Shear Effects on the Phase Separation Behaviour of a Polymer Blend in Solution by Small Angle Neutron Scatter-PB89-230445 PB89-231195 New Realization of the Ohm and Farad Using the NBS (National Bureau of Standards) Calculable Capacitor.
PB89-230445 901,557 Not available NTIS 900,792 Not available NTIS ing. PB89-229264 900,574 Not available NTIS PB89-231203

Recharacterization of Thermal Voltage Converters After

High-Mobility CMOS (Complementary Metal Oxide Semi-conductor) Transistors Fabricated on Very Thin SOS Films. PB89-230460 900,791 Not available NTIS

Analysis of Ridge-to-Ridge Distance on Fingerprints.

900,720 Not available NTIS

PB89-230452

PB89-230460

Thermoelement Replacement. PB89-230452

AC Impedance Method for High-Resistivity Measurements

Experimental Verification of the Relation between Two-

Improved Understanding for the Transient Operation of the Power Insulated Gate Bipolar Transistor (IGBT). PB89-231229 900,795 Not available NTIS

900,793 Not available NTIS

900,794 Not available NTIS

of Silicon

PB89-231211

PB89-231229

PB89-231203

Probe and Four-Probe Resistances PB89-231211 900,

PB89-229272

PB89-229280

PB89-229298

PB89-229280

sive Bonding System. PB89-229272

Ferric Oxalate with Nitric Acid as a Conditioner in an Adhe-

Biotransformation of Mercury by Bacteria Isolated from a River Collecting Cinnabar Mine Waters.

Transient and Residual Stresses in Dental Porcelains as Affected by Cooling Rates.

900.045 Not available NTIS

900,864 Not available NTIS

PB89-231237

389-231237
Power MOSFET Failure Revisited.
900,796 Not available NTIS

PB89-231245

Oligomers with Pendant Isocyanate Groups as Tissue Adhesives, 2. Adhesion to Bone and Other Tissues.

PB89-231245

900,056

Not available NTIS

PB89-231252

Stabilization and Spectroscopy of Free Radicals and Reactive Molecules in Inert Matrices.
PB89-231252 900,484 Not available NTIS

PB89-231260

Stainless Steel Weld Metal: Prediction of Ferrite Content. PB89-231260 901, 107 Not available NTIS

PB89-231278

Development of a Microwave Sustained Gas Plasma for the Sterilization of Dental Instruments. PR89-231278 900.047 Not available NTIS

PR89-231286

Polymerization of a Novel Liquid Crystalline Diacetylene Monomer. PB89-231286 900.575 Not available NTIS

PB89-231294

Electron Transmission Through NiSi2-Si Interfaces. PB89-231294 900,485 Not available NTIS

PB89-231302

Interaction of Oxygen and Platinum on W(110).
PB89-231302 901,158 Not available NTIS

PB89-231310

Methodology for Electron Stimulated Desorption Ion Angular Distributions of Negative Ions.
PB89-231310 900,486 Not available NTIS

PB89-231328

Photon-Stimulated Desorption as a Measure of Surface Electronic Structure. PB89-231328 901,459 Not available NTIS

PB89-231336

Synchrotron Photoemission Study of CO Chemisorption on Cr(110).
PB89-231336 900,262 Not available NTIS

PB89-231484

Effect of Pipe Roughness on Orifice Flow Measurement PB89-231484 901.333 PC A04/MF A01

PB89-234165

Line Identifications and Radiative-Branching Ratios of Magnetic Dipole Lines in Si-like Ni, Cu, Zn, Ge, and Se. PB89-234165 901,558 Not available NTIS

PB89-234173 Determination of Total Cholesterol in Coconut Oil: A New NIST (National Institute of Standards and Technology) Cholesterol Standard Reference Material.

PB89-234173 901,262 Not available NTIS

PB89-234181

Determination of Serum Cholesterol by a Modification of the Isotope Dilution Mass Spectrometric Definitive Method. PB89-234181 901,239 Not available NTIS

PB89-234199

Vibrational Spectra of Molecular lons Isolated in Sclid Neon. I. CO(sub 2, sup +) and CO(sub 2, sup -).
PB89-234199 900,487 Not available NTIS

PB89-234207

Vibrational Predissociation in the H-F Stretching Mode of PB89-234207 900,488 Not available NTIS

PB89-234215

Microwave and Infrared Electric-Resonance Optothermal Spectroscopy of HF-HCl and HCl-HF.
PB89-234215 900,489 Not available NTIS

PB89-234223

Comparison of Microleakage of Experimental and Selected Commercially Available Bonding Systems. PB89-234223 901,079 Not available NTIS

PB89-234231

Antenna for Laser Gravitational-Wave Observations in

PB89-234231 901,594 Not available NTIS

PB89-234249

Conceptual Design for a Mercury Relativity Satellite. PB89-234249 901,595 Not available NTIS PB89-234256

High-Resolution, Slit Jet Infrared Spectroscopy of Hydrocarbons: Quantum State Specific Mode Mixing in CH Stretch-Excited Propyne. PB89-234256 900,490 Not available NTIS

PB89-234264

Observation of Translationally Hot, Rotationally Cold NO Molecules Produced by 193-nm Laser Vaporization of Multi-layer NO Films. 900,491 Not available NTIS

PB89-234272

Rate of Change of the Quincy-Monument Peak Baseline from a Translocation Analysis of LAGEOS Laser Range Data

PB89-234272 901,282 Not available NTIS

PB89-234280

Reduced Dimensionality Quantum Reactive Scattering Study of the Insertion Reaction O(1D) + H2 -> OH +

PB89-234280

900,492 Not available NTIS

PB89-234298

Rotational Modulation and Flares on RS Canum Venati-corum and BY Draconis Stars. XI. Ultraviolet Spectral Images of AR Lacertae in September 1985. PR89-234298 900,026 Not available NTIS

PR89-234306

Sodium Doppler-Free Collisional Line Shapes. PB89-234306 901,559 Not available NTIS

PB89-234314

Universal Resputtering Curve.
901,460 Not available NTIS PB89-235113

NIST (National Institute of Standards and Technology) Research Reports, June 1989. PB89-235113 900,007 PC A03/MF A01 PB89-235139

Alternative Techniques for Some Typical MIL-STD-461/462

Types of Measurements. PB89-235139 901,272 PC A03/MF A01

PB89-235147

Measurements of Coefficients of Discharge for Concentric Flange-Tapped Square-Edged Orifice Meters in Water Over the Reynolds Number Range 600 to 2,700,000. PB89-235147 901,334 PC A23/MF A01

PR89-235204

Properties of Lennard-Jones Mixtures at Various Temperatures and Energy Ratios with a Size Ratio of Two.
PB89-235204 900,493 PC A19/MF A01

PR89-235345

Development of a Method to Measure In situ Chloride at the Coating/Metal Interface.
PB89-235345

901,085

PC A03/MF A01

PR89-235576

Trial of Open Systems Interconnection (OSI) Protocols Over Integrated Services Digital Network (ISDN).

PB89-235576 PC A03/MF A01

PB89-235634

Journal of Research of the National Institute of Standards and Technology, Volume 94, Number 4, July-August 1989. PB89-235634 900,908 PC A04

PB89-235642

Determination of Trace Level Iodine in Biological and Botanical Reference Materials by Isotope Dilution Mass Spec-

PB89-235642

(Order as PB89-235634, PC A04)

PB89-235659

Spectrum of Doubly Ionized Tungsten (W III). PB89-235659

(Order as PB89-235634, PC A04)

900 223

PR89-235667

Apparatus for Neutron Scattering Measurements on Sheared Fluids heared Fluids. PB89-235667 (Order as PB89-235634, PC A04)

PB89-235675

Conference Reports: National Computer Security Conference (11th). Held in Baltimore, MD. on October 17-20, 1988.

PB89-235675

(Order as PB89-235634, PC A04)

PB89-235865

Sensors and Measurement Techniques for Assessing Structural Performance. PB89-235865 900.162 PC A04/MF A01

PB89-235873

Development of a Multiple Layer Test Procedure for Inclusion in NFPA (National Fire Protection Association) 701: Initial Experiments. PB89-235873 900.096 PC A04/MF A01

PB89-235881

EVSIM: An Evaporator Simulation Model Accounting for Refrigerant and One Dimensional Air Distribution.
PB89-235881 900,086 PC A07/MF A01

PB89-235899

Method for Measuring the Effectiveness of Gaseous Contaminant Removal Filters.
PB89-235899 900,858 PC A04/MF A01

PB89-235907

Toughening Mechanisms in Ceramic Composites. Semi-Annual Progress Report for the Period Ending March 31, 1989. PB89-235907 901,080 PC A03/MF A01

PB89-235915

Intercomparison of Load Cell Verification Tests Performed by National Laboratories of Five Countries. PB89-235915 900,909 PC A06/MF A01

PB89-235923

Semiconductor Measurement Technology: A Software Program for Aiding the Analysis of Ellipsometric Measurements, Simple Models.
PB89-235923 901,369 PC A12/MF A01

PB89-235931

Working Implementation Agreements for Open Systems Interconnection Protocols. PB89-235931 900,642 PC A16/MF A01 PB89-237986

National Institute of Standards and Technology (NIST) Information Poster on Power Quality. PB89-237986 900,754 PC A02

PB90-100736

X-Band Atmospheric Attenuation for an Earth Terminal Measurement System. PB90-100736 900.626 PC A03/MF A01

PB90-107046

Glass Bottles for Carbonated Soft Drinks: Voluntary Product Standard PS73-89, PB90-107046 900 012 PC A03/MF A01

PB90-110065

Effect of Slag Penetration on the Mechanical Properties of Refractories: Final Report. PR90-110065 900.836 PC A07/MF A01

PB90-111212

Government Open Systems Interconnection Profile Users' PB90-111212 900.667 PC A07/MF A01

PB90-111220

NBS' (National Bureau of Standards) Industry; Government Consortium Research Program on Flowmeter Installation Effects: Summary Report with Emphasis on Research July-December 1987. PB90-111220 900,910 PC A05/MF A01

PB90-111238

Set Time Control Studies of Polymer Concrete. PB90-111238 901,057 PC A09/MF A02

PR90-111667

Robot Crane Technology. PB90-111667 900,146 PC A04/MF A01

PB90-111675

Optimum Location of Flow Conditioners in a 4-Inch Orifice Meter. PB90-111675 900,911 PC A05/MF A01

PB90-111683

Computer Viruses and Related Threats: A Management Guide. PB90-111683 900.654 PC A03/MF A01

PB90-111691

Software Verification and Validation: Its Role in Computer Assurance and Its Relationship with Software Project Management Standards. PB90-111691 900,655 PC A03/MF A01

PB90-112327

NVLAP (National Voluntary Laboratory Accreditation Program) Program Handbook Construction Testing Services. Requirements for Accreditation. 900,169 PC A03/MF A01 PB90-112327

PB90-112335

Modeling Dynamic Surfaces with Octree PB90-112335 901,206 901,206 PC A03/MF A01

PB90-112343

Design and Synthesis of Prototype Air-Dry Resins for Use in BEP (Bureau of Engraving and Printing) Intaglio Ink Vehi-PB90-112343 901,068 PC A03/MF A01

PB90-112350

Experience with IMDAS (Integrated Manufacturing Data Administration System) in the Automated Manufacturing Research Facility.
PB90-112350 900,964 PC A03/MF A01

PB90-112368

Proposed Methodology for Rating Air-Source Heat Pumps That Heat, Cool, and Provide Domestic Water Heating. PB90-112368 900,087 PC A06/MF A01

PB90-112376

Report of Roof Inspection: Characterization of Newly-Fabricated Adhesive-Bonded Seams at an Army Facility.
PB90-112376 900,107 PC A03/MF A01

PB90-112384 Post-Occupancy Evaluation of Several U.S. Government

Buildings. PB**9**0-112384

900,088 PC A08/MF A01 PB90-112392 FACTUNC: A User-Friendly System for Unconstrained Opti-

PB90-112392

PB90-112400 Directional Solidification of a Planar Interface in the Presence of a Time-Dependent Electric Current.
PB90-112400 901,461 PC A04/MF A01

PB90-112418

B90-112418 Guideline for Work Station Design. 900,643 PC A07/MF A01

PB90-112426

Product Data Exchange: The PDES Project-Status and Objectives. PB90-112426 900,938 PC A03/MF A01

PB90-112434 External Representation of Product Definition Data PB90-112434

900,939 PC A03/MF A01 PB90-112442

Research for Electric Energy Systems: An Annual Report. PB90-112442 900,853 PC A06/MF A 900.853 PC A06/MF A01

901,207 PC A03/MF A01

PB90-112459 PB90-117482 900.757 Not available NTIS PB90-117748 900,503 Not available NTIS Generic Architecture for Computer Integrated Manufactur-ing Software Based on the Product Data Exchange Specifi-cation. PB90-112459 900,965 PC A03/MF A01 PB90-117490 PB90-117755 Structure of Cs on GaAs(110) as Determined by Scanning Equilibrium Crystal Shapes and Surface Phase Diagrams at Surfaces in Ceramics.
PB90-117755 901,162 Not available NTIS Tunneling Microscopy. PB90-117490 901,463 Not available NTIS PB90-112467 PB90-117508 PB90-117763 Use of the IRDS (Information Resource Dictionary System) Standard in CALS (Computer-Aided Acquisition and Logistic Biophysical Aspects of Lipid Interaction with Mineral: Liposome Model Studies.
PB90-117508 901,228 Not available NTIS Formation of the Al-Mn Icosahedral Phase by Electrodepo-Support). PB90-112467 sition. PB90-117763 900,504 Not available NTIS 900,931 PC A03/MF A01 PB90-117516 PB90-112996 PB90-117771 In vitro Investigation of the Effects of Glass Inserts on the Effective Composite Resin Polymerization Shrinkage. PB90-117516 900,049 Not available NTIS Assessing the Flammability of Composite Materials. PB90-112996 901,081 PC A03/MF A01 Resonance Enhanced Electron Stimulated Desorption. PB90-117771 900,505 Not available NTIS PB90-116195 PB90-117789 B90-117789

Magnetic Structure of Cubic Tb0.3Y0.7Ag.

901,466 Not available NTIS PB90-117524 Center for Electronics and Electrical Engineering Technical Publication Announcements Covering Center Programs, October to December 1986, with 1987 CEEE Events Calender. PB90-116195 900,824 PC A03/MF A01 Off-Lattice Simulation of Polymer Chain Dynamics. PB90-117524 900,576 Not available NTIS PB90-117797 PB90-117532 Method for Evaluating Air Kerma and Directional Dose Equivalent for Currently Available Multi-Element Dosemeters in Radiation Protection Dosimetry. PB90-117532 901,301 Not available NTIS Heterodyne Measurements on N2O Near 1635 cm(-1). PB90-117797 900,506 Not available NTIS PB90-117292 Cross Section and Linear Polarization of Tagged Photons. PB90-117292 901,560 Not available NTIS PB90-117805 Haterodyne Frequency and Fourier Transform Spectroscopy Measurements on OCS Near 1700 cm(-1).
PB90-117805 900,507 Not available NTIS PB90-117300 PB90-117540 Interlaboratory Determination of the Calibration Factor for the Measurement of the Interstitial Oxygen Content of Sili-Reentrant Softening in Perovskite Superconductors. PB90-117540 901,464 Not available NTIS con by Infrared Absorption. PB90-117300 PB90-117813 900,224 Not available NTIS PB90-117557 Experimental Fire Tower Studies of Elevator Pressurization Systems for Smoke Control. PB90-117318 Ultrasonic Separation of Stress and Texture Effects in Poly-Application of the Gibbs Ensemble to the Study of Fluid-Fluid Phase Equilibrium in a Binary Mixture of Symmetric Non-Additive Hard Spheres. PB90-117813 crystalline Aggregates. PB90-117557 900,097 Not available NTIS 900,499 Not available NTIS PB90-117821 PB90-117565 Analysis of Magnesiumlike Spectra from Cu XVIII to Mo XXXI. 900,494 Not available NTIS Intrinsic Sticking in dt Muon-Catalyzed Fusion: Interplay of Atomic, Molecular and Nuclear Phenomena. PB90-117565 901,561 Not available NTIS PB90-117326 PB90-117821 900,508 Not available NTIS Discussion of 'Steep-Front Short-Duration Voltage Surge Tests of Power Line Filters and Transient Voltage Suppres-PB90-117839 PB90-117573 Microwave Spectrum of Methyl Amine: Assignment and Analysis of the First Torsional State.
PB90-117839 900,509 Not available NTIS SOLS Note on Calculating Flows Through Vertical Vents in Zone Fire Models Under Conditions of Arbitrary Cross-Vent Pres-PR90-117326 900,755 Not available NTIS PB90-117334 Companison of Interplaner-Boson-Exchange Models of High-Temperature Superconductivity - Possible Experimen-PB90-117573 900.147 Not available NTIS Microwave Spectrum, Structure, and Electric Dipole Moment of Ar-Ch3OH. PB90-117581 tal Tests. Marked Differences in the 3p Photoabsorption between the Cr and Mn(1+) Isoelectronic Pair: Reasons for the Unique Structure Observed in Cr. PB90-117334 901,462 Not available NTIS PB90-117847 900,510 Not available NTIS PB90-117342 PB90-117854 Detection of the Free Radicals FeH, CoH, and NiH by Far Infrared Laser Magnetic Resonance. PB90-117342 900,495 Not available NTIS PB90-117581 901,562 Not available NTIS Calculable, Transportable Audio-Frequency AC Reference PB90-117599 Standard PB90-117854 900,721 Not available NTIS High Accuracy Modeling of Photodiode Quantum Efficiency. PB90-117599 900,733 Not available NTIS PB90-117359 PB90-117862 Far-Infrared Laser Magnetic Resonance Spectrum of the CD Radical and Determination of Ground State Parameters. PB90-117359 900,496 Not available NTIS Collisional Electron Detachment and Decomposition Rates of SF6(1-), SF5(1-), and F(1-) in SF6: Implications for Ion Transport and Electrical Discharges.
PB90-117862 900,511 Not available NTIS PB90-117607 Fourth-Order Elastic Constants of beta-Brass. PB90-117607 901,160 Not available NTIS PB90-117367 PB90-117615 In Search of the Best Clock. PB90-117367 PB90-117870 Gruneisen Parameter of Y1Ba2Cu3O7. 900.632 Not available NTIS 901,465 Not available NTIS Electron-Energy Dependence of the S2F10 Mass Spec-PB90-117375 PB90-117623 Use of N-Phenylglycine in a Dental Adhesive System. PB90-117870 900.512 Not available NTIS Linear-Elastic Fracture of High-Nitrogen Austenitic Stainless PR90-117375 900.048 Not available NTIS PB90-117888 Steels at Liquid Helium Temperature.
PB90-117623 901,108 Not available NTIS Generation of Oxy Radicals in Biosystems PB90-117888 901,266 PR90-117383 Grain-Size and R-Curve Effects in the Abrasive Wear of 901,266 Not available NTIS PB90-117631 Alumina. PB90-117383 PB90-117896 Measurement of Applied J-Integral Produced by Residual 901.058 Not available NTIS Measurements of Molar Heat Capacity at Constant Volume: Cv,m(xCH4+ (1-x)C2H6' T=100 to 320 K, p < or = 35 MPa). Stress. PB90-117631 PB90-117391 900,163 Not available NTIS On-Line Arc Welding: Data Acquisition and Analysis Using a High Level Scientific Language.
PB90-117391 900,972 Not available NTIS PB90-117649 PR90-117896 900,844 Not available NTIS Nitrogen in Austenitic Stainless Steels. PB90-117649 901,109 901,109 Not available NTIS PB90-117912 PB90-117409 Differential Scanning Calonmetric Study of Brain Clathrin. PB90-117912 900,225 Not available NTIS PB90-117656 Texture Monitoring in Aluminum Alloys: A Companson of Ultrasonic and Neutron Diffraction Measurements. Photoacoustic Measurement of Differential Broadening of the Lambda Doublets in NO(X (2)Pi 1/2, v= 2-0) by Ar. PB90-117656 900,500 Not available NTIS PB90-117409 901,159 Not available NTIS PB90-117920 Biological Thermodynamic Data for the Calibration of Differential Scanning Calorimeters: Heat Capacity Deta on the Unfolding Transition of Lysozyme in Solution. PB90-117920 900,513 Not evailable NTIS PB90-117417 PB90-117664 Hydrodynamic Forces on Vertical Cylinders and the Lighthill Typical Usage of Radioscopic Systems: Replies to a Correction. PB90-117417 901.313 Not available NTIS Survey. PB90-117664 901.161 Not available NTIS PB90-117425 PB90-117938 Use of Thorium as e Terget in Electron-Spin Analyzers. PB90-117938 900,912 Not available NTIS PB90-117672 Dissociation Lifetimes and Level Mixing in Overtone-Excited HN3 (X tilde (sup 1) A'). PB90-117425 Design Factors for Parellel Processing Benchmarks. PB90-117672 900,644 Not available NTIS 900,263 Not available NTIS PB90-117946 PB90-117433 PB90-117680 Effect of en Electricelly Large Stirrer in a Mode-Stirred Electric-Resonance Optothermal Spectrum of (H2O)2: Microwave Spectrum of the K= 1-0 Subband for the E((+ Calibrating Network Analyzers with Imperfect Test Ports. PB90-117680 900,825 Not available NTIS PB90-117946 901,378 Not aveileble NTIS PB90-117698 PB90-117953 PB90-117433 900,497 Not available NTIS Implementation of en Automated System for Measuring Radiated Emissions Using a TEM Cell.
PB90-117698 901,377 Not aveileble NTIS Hybrid Representation of the Green's Function in an Over-PB90-117441 moded Rectangular Cavity. Rotational Energy Levels and Line Intensities for (2S+1)Lambda-(2S+1) Lambda and (2S+1)(Lambda+ or -)-(2S+1)Lambda Transitions in a Diatomic Molecule van der Waals Bonded to a Closed Shell Pertner. PB90-117953 900,826 Not available NTIS PB90-117706 PB90-117961 Chlorine-like Spectre of Copper to Molybdenum. PB90-117706 900,501 Not evailable NTIS Cathodoluminescence of Defects in Diamond Films and Particles Grown by Hot-Filament Chemical-Vapor Deposi-PR90-117441 900,498 Not available NTIS PB90-117458 PB90-117714 tion. PB**9**0-1179**6**1 901,069 Not evailable NTIS Mechanisms of Free Radical Chemistry and Biochemistry of Coherent Tunable Far Infrared Rediation. PB90-117458 PB90-117987 900,684 Not available NTIS Benzene. PB90-117714 900,502 Not evailable NTIS Vapor Pressures and Gas-Phase PVT Data for 1,1,1,2-Te-trafluoroethane. PB90-117466 PB90-117722 Improved Rotational Constants for HF PB90-117466 901,376 Tribochemical Mechanism of Alumina with Water. PB90-117722 901,059 Not evailable NTIS 900.514 Not available NTIS PB90-117987 901,376 Not evaileble NTIS PB90-117995 PB90-117730 Structure of V9Mo6O40 Determined by Powder Neutron Diffrection.
PB90-117995 900,515 Not evaileble NTIS Comparison of Far-Field Methods for Determining Mode Field Diameter of Single-Mode Fibers Using Both Geussian and Petermann Definitions.

PB90-117474

900,756

Not evailable NTIS Comment on 'Feesibility of Measurement of the Electromagnetic Polarizebility of the Bound Nucleon'. PB90-117730 901,563 Not eveilable NTIS

PB90-117748

Solid Neon.

Production end Spectroscopy of Molecular lons Isoleted in

PB90-118001

Neutron Diffraction Determinetion of Full Structures of Anhydrous Li-X end Li-Y Zeolites.
PB90-118001 900,516 Not eveileble NTIS

ods: Resolving Differences.

Numerical Aperture of Multimode Fibers by Several Meth-

PB90-123423 901,164 Not aveilable NTIS PB90-123670 901,567 Not available NTIS PB90-118019 PB90-123431 PB90-123688 Influence of the Surfece on Magnetic Domein-Well Micros-Shortest Paths in Simply Connected Regions in R2.
PB90-123688 901,202 Not eveilable NTIS tructure. PB90-118019 Megnetizetion end Megnetic Aftereffect in Textured Ni/Cu Megnetizetion end megnetic restauration of the Megnetizetion end megnetic restauration of the Megnetizetion end megnetiz 901,467 Not eveileble NTIS PB90-118027 PB90-123696 PB90-123449 Adhesive Bonding of Composites.

PROP. 123696 900,050 Not available NTIS Photon-Stimuleted Desorption of Fluorine from Silicon vie Substrete Core Excitetions. PB90-118027 (109)Pd end (109)Cd Activity Stendardization and Decay Deta. PB90-123696 900,517 Not evailable NTIS PB90-123704 PB90-123449 901.564 Not available NTIS PB90-118035 Fluid Flow in Pulsed Laser Irrediated Gases; Modeling and PB90-123456 Interections between Two Dividers Used in Simultaneous Comperison Measurements. PB90-118035 Small Angle Neutron Scattering Studies of Single Phase Interpenetreting Polymer Networks.
PB90-123456 900,577 Not evaileble NTIS PB90-123704 900,265 Not available NTIS 900.031 Not eveilable NTIS PB90-123712 PB90-118043 Microbiologicel Materiels Processing. PB90-123712 901,261 Not evailable NTIS Advenced Heet Pumps for the 1990's Economic Perspectives for Consumers end Electric Utilities.
PB90-118043 900,089 Not aveileble NTIS PB90-123464 Comparison of Microweve Drying end Conventional Drying Techniques for Reference Meterials. PB90-123464 900,229 Not available NTIS PB90-123720 PB90-118050 Approximate Formuletion of Redistribution in the Ly(elphe), Ly(beta), H(alphe) System. PB90-123720 Upwerd Turbulent Fleme Spreed on Wood under External Determinetion of Selenium end Tellurium in Copper Standerd Reference Meterials Using Steble Isotope Dilution Sperk Source Mess Spectrometry. P890-123472 900,230 Not available NTIS 901,568 Not evelleble NTIS PB90-118050 900.148 Not eveileble NTIS PB90-123738 Neutron Scattering end Its Effect on Reection Rates in Neutron Absorption Experiments.
PB90-123738 901,569 Not eveilable NTIS PB90-118068 Scaling Applications in Fire Research. PB90-118068 900,149 PB90-123480 900,149 Not available NTIS Neutron Study of the Crystal Structure end Vacancy Distribution in the Superconductor Ba2Y Cu3 O(sub g-delta), PB90-123480 901,468 Not available NTIS PB90-118076 PB90-123746 Heet Transfer in Compartment Fires Neer Regions of Ceil-Neonlike Ar end Ci 3p-3s Emission from e theta-pinch ing-Jet Impingement on e Wall. PB90-118076 PB90-123498 Plasma. PB90-12374**6** 900,150 Not available NTIS 901.570 Not eveilable NTIS Reection of (Ir(C(3), N bpy)(bpy)2)(2+) with OH Redicals end Radietion Induced Covalent Binding of the Complex to PB90-118084 PB90-123753 Magnetic Behevior of Compositionally Moduleted Ni-Cu Severel Polymers in Aqueous Solutions.
PB90-123498 900,264 Not evailable NTIS Fecile Synthesis of 1-Nitropyrene-d9 of High Isotopic Purity. PB90-123753 900,240 Not evailable NTIS Thin Films. PB90-118084 901.163 Not eveileble NTIS PB90-123506 PR90-123761 PB90-118092 Advances in the Use of (3)He in a Gas Scintillation Exoergic Collisions of Cold Na*-Na. PB90-123761 901,3 Measures of Effective Ergodic Convergence in Liquids. PB90-118092 900,518 Not available NTIS 901,571 Not available NTIS PB90-123506 901,565 Not available NTIS PB90-123779 PB90-118100 PB90-123514 Pathweys for Microstructural Development in TiAl. PB90-123779 901,173 Not available NTIS Weekly Bound NeHF. TEM Observation of Icosahedral, New Crystalline and Glassy Phases in Rapidly Quenched Cd-Cu Alloys.
PB90-123514 901,166 Not available NTIS PB90-118100 900,519 Not eveileble NTIS PB90-123787 901,166 Not available NTIS PB90-118118 Millimeter- end Submillimeter-Wave Surveys of Orion A Emission Lines in the Ranges 200.7-202.3, 203.7-205.3, and 330-360 GHz. Soler end Stellar Megnetic Fields end Structures: Observe-PB90-123522 Amorphous Phase Formation in Al70Si17Fe13 Alloy. PB90-123522 901,167 Not available NTIS PB90-118118 900,027 Not available NTIS 900.029 Not available NTIS PB90-123787 PB90-118126 PB90-123530 PB90-123795 Slit Jet Infrared Spectroscopy of NeHF Complexes: Internal Rotor and J-Dependent Predissociation Dynamics. PB90-118126 900,520 Not availeble NTIS Solidification of an 'Amorphous' Phase in Rapidly Solidified Substitutes for N-Phenylglycine in Adhesive Bonding to Al-Fe-Si Alloys. PB90-123530 Dentin 901.168 Not available NTIS PB90-123795 900,051 Not available NTIS PB90-118134 PB90-123548 Precise Laser Frequency Scanning Using Frequency-Synthesized Optical Frequency Sidebands: Application to Isotope Shifts end Hyperfine Structure of Mercury.
PB90-118134 901,370 Not evailable NTIS PB90-123803 Quesicrystels end Quasicrystal-Related Phases in the Al-Megnetic Order of Pr in PrBa2Cu3O7. PB90-123803 901.47 Mn System. PB90-123548 901,169 Not available NTIS 901.471 Not available NTIS PB90-123555 PB90-123811 PB90-118142 Teleoperation and Autonomy for Space Robotics. PB90-123811 901,591 Not available NTIS Adsorption of Water on Clean and Oxygen-Predosed Helium Resonance Lines in the Flare of 15 June 1973. PB90-118142 900,028 Not available NTIS Nickel(110). PB90-123555 900.522 Not available NTIS PB90-123829 PB90-118159 PB90-123563 Pressure Dependence of the Cu Magnetic Order in RBa2Cu3O6+ x.
PB90-123829 901,472 Not available NTIS Silicon Photodiode Self-Calibration Ammonia Adsorption and Dissociation on a Stepped Iron(s) 900,734 Not available NTIS PB90-118159 (100) Surface. PB90-123563 900.523 Not available NTIS PB90-118167 PB90-123837 PB90-123571 Safety Guidelines for Microwave Systems in the Analytical Spectroscopy of Autoionizing States Contributing to Elec-Mobile Sources of Atmospheric Polycyclic Aromatic Hydrocarbons: A Roadway Tunnel Study.
PB90-123571 900,859 Not available NTIS Leboratory. PB90-118167 tron-Impact Ionization of Ions. PB90-123837 900.689 Not available NTIS 901,572 Not available NTIS PB90-118175 Preconcentration of Trace Transition Metal and Rare Earth Elements from Highly Saline Solutions. PB90-118175 900,226 Not available NTIS PB90-123845 PB90-123589 Electron-Impact Ionization of La(q +) Ions (q = 1,2,3). PB90-123845 901,573 Not available NTIS Numerical Simulations of Neutron Effects on Bipolar Transistors. PB90-123589 900,797 Not available NTIS PB90-123852 PB90-118183 Sub-Doppler Infrared Spectroscopy in Slit Supersonic Jets: A Study of all Three van der Waals Modes in v1-Excited ArHCl. PB90-123597 Monitoring and Predicting Parameters in Microwave Disso-Quantitative Characterization of the Viscosity of a Microelution PR90-118183 900 690 Not available NTIS mulsion. PB90-123597 PB90-123852 900.525 Not available NTIS 900,524 Not available NTIS PB90-118191 PB90-123605 PB90-123860 Introduction to Microwave Acid Decomposition. PB90-118191 900,227 Not available NTIS Electron Stopping Powers for Transport Calculations. PB90-123605 901,566 Not available NTIS PB90-118209 PB90-123860 Intramolecular Dynamics of van der Waals Molecules: An Extended Infrared Study of ArHF. PB90-123613 PB90-123878 Bulk Modulus and Young's Modulus of the Superconductor Ba2Cu3YO7. PB90-118209 900,521 Not available NTIS Initial Stages of Heteroepitaxial Growth of InAs on Si(100) PB90-123878 901,473 Not available NT PB90-123613 901,469 Not available NTIS PB90-120742 PB90-123621 Promoting Technological Excellence: The Role of State and Federal Extension Activities. PB90-123886 PB90-120742 900,171 PC A05/MF A01

Apparent Spectroscopic Rigidity of Floppy Molecular Sys-900,526 Not available NTIS 901,473 Not available NTIS Microstructural Variations in Rapidly Solidified Alloys. PB90-123621 901,170 Not available NTIS Generic Liposome Reagent for Immunoassays. PB90-123886 901,229 Not available NTIS PB90-123639

PB90-123902

PB90-123910

PB90-123928

PB90-123936

PB90-123894

Rapid Solidification and Ordering of B2 and L2 (sub 1) Phases in the NiAl-NiTi System. PB90-123639 901.171 Not available NTIS

PB90-123381

PR90-123399

PB90-123407

PB90-123415

PB90-123423

PB90-123415

PB90-123381

Preliminary Crystal Structure of Acinetobacter glutaminasifi-cans Glutaminase-Asparaginase.

Calcium Hydroxyapatite Precipitated from an Aqueous Solution: An International Multimethod Analysis.
PB90-123399 900,228 Not available NTIS

Nonlinear Effect of an Oscillating Electric Field on Membrane Proteins.
PB90-123407 901,249 Not available NTIS

Temperature Hysteresis in the Initial Susceptibility of Rapidly Solidified Monel.

Mossbauer Imaging: Experimental Results.

901,260 Not available NTIS

900,922 Not available NTIS

PB90-123647

Formation of Dispersoids during Rapid Solidification of an Al-Fe-Ni Alloy.
PB90-123647 901,172 Not available NTIS PB90-123654

Guide to Available Mathematical Software Advisory System. PB90-123654 901,201 Not available NTIS PB90-123662

Characterization of Structural and Magnetic Order of Er/Y Superlattices. PB90-123662 901,470 Not available NTIS

PB90-123670 Determination of Short Lifetimes with Ultra High Resolution (n.gamma) Spectroscopy.

Collisional Losses from e Light-Force Atom Trap. PB90-123936 901,577 Not available NTIS

EMATs (Electromagnetic Acoustic Transducers) for Roll-By Crack Inspection of Railroad Wheels.
PB90-123894 901,597 Not available NTIS

Applications of ETRAN Monte Carlo Codes. PB90-123902 901,574 Not available NTIS

Cross Sections for Bremsstrahlung Production and Electron-Impact Ionization.
PB90-123910 901,575 Not available NTIS

Overview of ETRAN Monte Carlo Methods. PB90-123928 901,576 Not available NTIS

PB90-123944 PB90-128182 900,799 Not available NTIS PB90-128620 900,170 Not available NTIS Merit Functions and Nonlinear Programming.

901,208 Not available NTIS PB90-128190 PB90-128638 Electromagnetic Detection of Long Conductors in Tunnels. PB90-128190 900,827 Not available NTIS Low Temperature Mechanical Property Measurements of PB90-123951 Silica Aerogel Foam. PB90-128638 High-Accuracy Gas Analysis via Isotope Dilution Mass Spectrometry: Carbon Dioxide in Air. PB90-123951 900,032 Not available NTIS PB90-128208 901,061 Not available NTIS Near-Field Detection of Buried Dielectric Objects. PB90-128208 900,713 Not available NTIS PB90-128646 Tensile and Fatigue-Creep Properties of a Copper-Stainless PB90-123969 PB90-128216 Steel Laminate. PB90-128646 Experiences in Environmental Specimen Banking. PB90-123969 900,866 Not available NTIS 901,083 Not available NTIS Direct Observation of Surface-Trapped Diffracted Waves. PB90-128216 901,475 Not available NTIS PR90-128653 PB90-124306 Determination of Experimental and Theoretical k (sub ASi) Factors for a 200-kV Analytical Electron Microscope, PB90-128653 900,232 Not available NTIS PB90-128224 Adsorption of High-Range Water-Reducing Agents on Selected Portland Cement Phases and Related Materials. PB90-124306 900,583 PC A03/MF A01 Very Low-Noise FET Input Amplifier. PB90-128224 900,800 Not available NTIS PB90-128661 PB90-128232 PB90-126236 Effects of Thermal Stability and Melt Viscosity of Thermo-Vortex Shedding Flowmeter for Fluids at High Flow Veloci-Journal of Physical and Chemical Reference Data, Volume 18, Number 3, 1989. plastics on Piloted Ignition. PB90-128232 ties. PB90-128661 900,151 Not available NTIS 900.608 Not available NTIS PB90-126236 900,527 Not available NTIS PB90-128679 PB90-128240 PR90-126244 Improved Standards for Real-Time Radioscopy. PB90-128679 900,923 Not available NTIS Vector imaging of Magnetic Microstructure.
PB90-128240 901,476 Not available NTIS Octanol-Water Partition Coefficients of Simple Organic Compounds. PB90-126244 PB90-128257 PB90-128687 900.528 Not available NTIS Standards for Real-Time Radioscopy. PB90-128687 900,924 Not available NTIS PB90-126251 Branching Ratio Technique for Vacuum UV Radiance Calibrations: Extensions and a Comprehensive Data Set. PB90-128257 901,582 Not available NTIS Evaluation of Data on Solubility of Simple Apolar Gases in Light and Heavy Water at High Temperature. PB90-126251 900,529 Not available NTIS PB90-128695 PB90-128265 Synthesis and Characterization of Novel Bonded Phases for Reversed-Phase Liquid Chromatography. PB90-128695 900,233 Not available NTIS Edge Stresses in Woven Laminates at Low Temperatures. PB90-128265 901,082 Not available NTIS PB90-126269 Microwave Spectral Tables. 3. Hydrocarbons, CH to PB90-128273 PB90-128703 PB90-126269 900,530 Not available NTIS Bootstrap Inference for Replicated Experiments. PB90-128273 900,914 Not available NTIS Ambiguity Groups and Testability. PB90-128703 900,722 Not available NTIS PB90-127101 Summaries of Center for Fire Research In-House Projects and Grants: 1989.
PB90-127101 900,605 PC A10/MF A02 PB90-128711 PB90-128281 Dental Materials and Technology Research at the National Bureau of Standards: A Model for Government-Private Sector Cooperation. PB90-128711 900,052 Not available NTIS Broadband, Isotropic, Photonic Electric-Field Meter for Measurements from 10 kHz to above 1 GHz. PB90-128281 900,686 Not available NTIS PB90-127820 NIST (National Institute of Standards and Technology) Calibration Services, Users Guide: Fee Schedule.
PB90-127820 900,913 PC A04/MF A01 PB90-128299 PB90-128729 Progress on Spin Detectors and Spin-Polarized Electron Scattering from Na at NIST.
PB**9**0-128299 901,583 Not available NTIS Vibrational Spectra of Molecular Ions Isolated in Solid Neon. 2. O4(1+) and O4(1-).
PB90-128729 900,533 Not available NTIS PB90-128026 901,583 Not available NTIS Flaw Tolerance in Ceramics with Rising Crack Resistance PB90-128307 Characteristics. PB90-128737 Superelastic Scattering of Spin-Polarized Electrons from PB90-128026 901,060 Net available NTIS Sodium. PB90-128307 Fatigue Resistance of a 2090-T8E41 Aluminum Alloy at PB90-128034 Cryogenic Temperatures. PB90-128737 901.584 Not available NTIS Ion Trapping Techniques: Laser Cooling and Sympathetic 901,177 Not available NTIS PB90-128315 Cooling. PB**9**0-128034 PB90-128745 Effect of Pressure on the Development of Prebreakdown 901,578 Not available NTIS Method for Measuring the Stochastic Properties of Corona and Partial-Discharge Pulses. Streamers. PB90-128315 PB90-128042 900.828 Not available NTIS Frequency Standards Utilizing Penning Traps. PB90-128042 901,379 Not available NTIS PB90-128745 900,829 Not available NTIS PB90-128505 PB90-128752 Spherical Acoustic Resonators. PB90-128505 PB90-128059 Creating CSUBs Written in FORTRAN That Run in BASIC PB90-128752 900,656 Not available NT 901,321 Not available NTIS Stability and Quantum Efficiency Performance of Silicon Photodiode Detectors in the Far Ultraviolet. PB90-128059 900,735 Not available NTIS PB90-128513 900,656 Not available NTIS PB90-128760 Drift Tubes for Characterizing Atmospheric Ion Mobility PB90-128059 Anti-T2 Monoclonal Antibody Immobilization on Quartz Fibers: Stability and Recognition of T2 Mycotoxin. PB90-128760 901,267 Not available NTIS Spectra. PB90-128513 PB90-128067 901,585 Not available NTIS Analyzing the Economic Impacts of a Military Mobilization. PB90-128067 901,273 Not available NTIS PB90-128521 DC Electric Field Effects during Measurements of Monopolar Charge Density and Net Space Charge Density Near PB90-128778 PB90-128075 Fields Radiated by Electrostatic Discharges. PB90-128778 901,382 Not available NTIS Redistribution in Astrophysically Important Hydrogen Lines. PB90-128075 901,579 Not available NTIS **HVDC** Power Lines. PB90-128521 901,380 Not available NTIS PB90-128786 PB90-128083 PB90-128539 Pattern Recognition Approach in X-ray Fluorescence Analy-Performance of a High-Energy-Resolution, Tender X-ray Synchrotron Radiation Beamline.
PB90-128083 901,580 Not available NTIS Comparison of Liquid Chromatographic Selectivity for Poly cyclic Aromatic Hydrocarbons on Cyclodextrin and C18 Bonded Phases. PB90-128786 900,234 Not available NTIS PB90-128794 PB90-128091 900,231 Not available NTIS Method for Fitting and Smoothing Digital Data. PB90-128794 900,830 Not available NTIS Laser Cooling to the Zero-Point Energy of Motion. PB90-128091 901,581 Not available NTIS Interaction of In Atom Spin-Orbit States with Si(100) Sur-PB90-129446 PB90-128109 faces PB90-128547 AMRF Part Model Extensions. 900,532 Not available NTIS Growth and Properties of High-Quality Very-Thin SOS (Silicon-on Sapphire) Films. PB90-128109 900,798 Not available NTIS PB90-129446 900,967 PC A03/MF A01 PB90-128554 Effect of Chemical Composition on the 4 K Mechanical Properties of 316LN-Type Alloys. PB90-128554 901,110 Not available NTIS PB90-129891 Allocating Staff to Tax Facilities: A Graphics-Based Microcomputer Allocation Model. PB90-128117 Liposome Technology in Biomineralization Research. PB90-128117 901.230 Not available PB90-129891 900.645 PC A03/MF A01 901,230 Not available NTIS PB90-128562 PB90-129982 PB90-128125 Fracture Behavior of 316LN Alloy in Uniaxial Tension at Polytope Volume Computation. PB90-129982 Role of Adsorbed Gases in Metal on Metal Epitaxy. PB90-128125 901,174 Not available NTIS Cryogenic Temperatures. PB90-128562 901,203 PC A03/MF A01 901,111 Not available NTIS PB90-128570 PB90-130246 PB90-128133 Fire Growth and Development, PB90-128570 900,152 Not available NTIS Glossary of Standards-Related Terminology. PB90-130246 900,986 PC A03/MF A01 Offset Criterion for Determining Superconductor Critical PB90-128133 901,474 Not available NTIS PB90-128588 PB90-130253 PB90-128141 Thermo-Optic Designs for Microwave and Millimeter-Wave Electric-Field Probes. Supercomputers Need Super Anthmetic. PB90-130253 900.655 Microwave Electric-Resonance Optothermal Spectroscopy 900,657 PC A03/MF A01 PB90-128588 900,691 Not available NTIS PB90-130261 PB90-128141 900,531 Not available NTIS PB90-128596 Effect of a Crystal-Melt Interface on Taylor-Vortex Flow. PB90-130261 901,477 PC A03/MF A01 PB90-128158 Modular Process Planning System Architecture. PB90-128596 900,966 Not available NTIS Measured Air Infiltration and Ventilation Rates in Eight PB90-130279 Large Office Buildings. PB90-128158 PB90-128604 Center for Radiation Research (of the National Institute of Standards and Technology) Technical Activities for 1989. PB90-130279 901,307 PC A09/MF A01 900.090 Not available NTIS Effects of Grain Size and Cold Rolling on Cryogenic Proper-PB90-128166 ties of Copper. PB90-128604 Residential Wood Combustion: A Source of Atmospheric 901,176 Not available NTIS PB90-130287 Polycyclic Aromatic Hydrocarbons.
PB90-128166
900,860
Not available NTIS PB90-128612 Tensile Tests of Type 305 Stainless Steel Mine Sweeping Proficiency Testing for MIL-STD 462 NVLAP (National Voluntary Laboratory Accreditation Program) Laboratories. PB90-128612 901,381 Not available NTIS Wire Rope. PB90-130287 PB90-128174 901,112 PC A03/MF A01 Diffusion-Induced Grain Boundary Migration. PB90-128174 901.175 Not available NTIS PB90-130295 PB90-128620 Measurements of Tribological Behavior of Advanced Materials: Summary of U.S. Results on VAMAS (Versailles Advanced Materials and Standards) Round-Robin No. 2.

Comparisons of NBS/Harvard VI Simulations and Full-

Scale, Multiroom Fire Test Data.

PB90-128182

Silicon and GaAs Wire-Bond Cratering Problem.

901,003 PC A05/MF A01 PB90-130295 PB90-130303

Improved Low-Level Silicon-Avalanche-Photodiode Transfer Standards at 1.064 Micrometers. PB90-130303 900,736 PC A03/MF A01

PB90-130311

Microporous Fumed-Silica Insulation as a Standard Reference Material of Thermal Resistance at High Temperature. PB90-130311 900,153 PC A04/MF A01

PB90-130568

Publications of the Center for Manufacturing Engineering Covering the Period January 1978-December 1988. PB90-130568 901,012 PC A07/MF A01

PB90-130899

Report on Interactions between the National Institute of Standards and Technology and the Institute of Electrical and Electronic Engineers. 900 831 PC A03/MF A01 PB90-130899

PB90-130907

Radiometer Equation and Analysis of Systematic Errors for the NIST (National Institute of Standards and Technology) Automated Radiometers. PB90-130907 900,832 PC A03/MF A01

PB90-131152

Corrosion Behavior of Mild Steel in High pH Aqueous Media. PB90-131152 901,086 PC A03/MF A01

PB90-132705

Gypsum Wallboard Formaldehyde Sorption Model. PB90-132705 900,154 PC A03/MF A01

PB90-132713

Enhancements to the VWS2 (Vertical Workstation 2) Data Preparation Software. 900,968 PC A04/MF A01 PB90-132713

PB90-132739

Institute for Materials Science and Engineering, Nonde-structive Evaluation: Technical Activities, 1989. PB90-132739 900,925 PC A05/MF A01

PB90-132747

Emerging Technologies in Manufacturing Engineering. PB90-132747 901,013 PC A04/MF A01

PB90-133091 Graphics Application Programmer's Interface Standards and CALS (Computer-Aided Acquisition and Logistic Sup-

port). PB**9**0-1**33**091 900,658 PC A03/MF A01

PB90-133158

Center for Atomic, Molecular, and Optical Physics Technical Activities, 1989.
PB90-133158 901,586 PC A16/MF A02

PB90-135922

Low Pressure, Automated, Sample Packing Unit for Diffuse Reflectance Infrared Spectrometry. PB90-135922 900,235 Not available NTIS

PB90-136375

PB90-136474

Fundamental Physical Constants - 1986 Adjustments. PB90-136474 900,535 Not available NTIS

PB90-136540

Identification of Carbonaceous Aerosols via C-14 Accelerator Mass Spectrometry, and Laser Microprobe Mass Spectrometry. PB90-136540 900,236 Not available NTIS

PB90-136565

Flash Photolysis Kinetic Absorption Spectroscopy Study of the Gas Phase Reaction HO2 + C2H5O2 Over the Tem-perature Range 228-380 K. PB90-136565 900,536 Not available NTIS

PB90-136573

Adsorbates

Picosecond Vibrational Energy Transfer Studies of Surface PB90-136573 900,537 Not available NTIS PB90-136599

Use of an Imaging Proportional Counter in Macromolecular Crystallography

PB90-136599 900.538 Not available NTIS PB90-136649

Tilt Observations Using Borehole Tiltmeters 1. Analysis of Tidal and Secular Tilt. PB90-136649 901,283 Not available NTIS

PB90-136672

Measuring In-Plane Elastic Moduli of Composites with Arrays of Phase-Insensitive Ultrasound Receivers. PB90-136672 900,970 Not available NTIS PB90-136680

Time-Resolved FTIR Emission Studies of Molecular Photofragmentation Initiated by a High Repetition Rate Excimer

Laser. PB90-136680 900,266 Not available NTIS

PB90-136706 Mn-Mn Exchange Constants in Zinc-Manganese Chalco-

gerilues. PB**9**0-1**3**6706 901.478 Not available NTIS PB90-136714

Neutron Diffraction Study of the Wurtzite-Structure Dilute Magnetic Semiconductor Zn0.45Mn0.55Se. PB90-136714 901,479 Not available NTIS

PB90-136722

Biological Macromolecule Crystallization Database: A Basis for a Crystallization Strategy.
PB90-136722 901,250 Not available NTIS

PB90-136730

Preliminary Crystallographic Study of Recombinant Human Interleukin 1beta.
PB90-136730 901,251 Not available NTIS

PB90-136748

Critical Current Measurements of Nb3Sn Superconductors: NBS (National Bureau of Standards) Contribution to the VAMAS (Versailles Agreement on Advanced Materials and Standards) Interlaboratory Comparison. PB90-136748 901,480 Not available NTIS

PB90-136755

Triplet Dipoles in the Absorption Spectra by Dense Rare Gas Mixtures. 1. Short Range Interactions. PB90-136755 900,539 Not available NTIS

PB90-136763

Bioseparations: Design and Engineering of Partitioning Systems. PB90-136763 901.231 Not available NTIS

PB90-136771

Low-Temperature Phase and Magnetic Interactions in fcc Fe-Cr-Ni Alloys. PB90-136771 901.113 Not available NTIS PB90-136797

Monte Carlo Simulation of Domain Growth in the Kinetic Ising Model on the Connection Machine.
PB90-136797 901,587 Not available NTIS

PB90-136805

Flammability of Upholstered Furniture with Flaming Sources. PB90-136805 900.155 Not available NTIS PB90-136813

Charging Behavior of Polyethylene and lonomers. PB90-136813 900,578 Not available NTIS

PB90-136821 Summary of the Assumptions and Limitations in Hazard PR90-136821 900,606 Not available NTIS

PB90-136839

Evaluation of Data on Higher Heating Values and Elemental Analysis for Refuse-Derived Fuels. PB90-136839 900,845 Not available NTIS PB90-136847

Model for Particle Size and Phase Distributions in Ground Cement Clinker.
PB90-136847

901,062

Not available NTIS

PB90-136854 Global Biomethylation of the Elements - Its Role in the Bio-

sphere Translated to New Organometallic Chemistry and Biotechnology.
PB90-136854
901,232
Not available NTIS

PB90-136862

Technical Examination, Lead Isotope Determination, and Elemental Analysis of Some Shang and Zhou Dynasty Bronze Vessels.

PR90-136862 901,178 Not available NTIS

PB90-136904

Laser Induced Vaporization Time Resolved Mass Spectrometry of Refractories. PB90-136904 900,540 Not available NTIS

PB90-136946

PB90-136946 900.541 Not available NTIS PB90-136979 Spectroelectrochemistry of a System Involving Two Consecutive Electron-Transfer Reaction.
PB90-136979 900,237 Not available NTIS

Frequency Measurements of High-J Rotational Transitions of OCS and N2O.

PB90-163874 Journal of Research of the National Institute of Standards and Technology. November-December 1989. Volume 94,

PB90-163874 900.542 PC A04 PB90-163882

Reduction of Uncertainties for Absolute Piston Gage Pressure Measurements in the Atmospheric Pressure Range. PB90-163882 900,030 (Order as PB90-163874, PC A04)

PB90-163890

Absolute Isotopic Abundance Ratios and Atomic Weight of Reference Sample of Nickel. PB90-163890

(Order as PB90-163874, PC A04)

PB90-163908

Absolute Isotopic Composition and Atomic Weight of Terrestrial Nickel. PB90-1**63**908 (Order as PB90-163874 PC A04)

PB90-163916

Report on the 1989 Meeting of the Radionuclide Measurements Section of the Consultative Committee on Standards for the Measurement of Ionizing Radiations: Special Report on Standards for Radioactivity. PB90-163916

(Order as PB90-163874, PC A04)

PB90-163924

Measuring the Root-Mean-Square Value of a Finite Record Length Periodic Waveform. PB90-163924

(Order as PB90-163874, PC A04)

PB90-163932

Search for Optical Molasses in a Vapor Cell: General Analysis and Experimental Attempt. PB90-163932

(Order as PB90-163874, PC A04)

PB90-213687

Journal of Research of the Institutes of Standards and Technology. September-October 1989. Volume 94, Number PB90-213687 900.673 PC A04

PB90-213695

Instrument-Independent MS/MS Database for XQQ Instruments: A Kinetics-Based Measurement Protocol. PB90-213695 (Order as PB90-213687, PC A04)

PB90-213703

Cotinine in Freeze-Dried Urine Reference Material. PB90-213703 (Order as PB90-213687, PC A04)

PB90-213711

NIST Automated Computer Time Service. PB90-213711 (Order as PB90-213687, PC A04)

PB90-780172

Computer Security Training Guidelines. 900,677 PC A03/MF A01

UDR-TR-88-136

Validated Furniture Fire Model with FAST (HEMFAST). PB89-215354 900,142 PC A05/MF A01



ALABAMA

Alexander City

Alexander City State Junior College Thomas D. Russell Library (1967)*

Auburn

Auburn University Ralph Brown Draughon Library (1907)

Birmingham

Birmingham Public Library (1895) Birmingham-Southern College Library (1932) Jefferson State Junior College James B. Allen Library (1970) Miles College C. A. Kirkendoll Learning Resource Center (1980) Samford University Library (1884)

Enterprise

Enterprise State Junior College Learning Resources Center (1967)

Fayette

Brewer State Junior College Learning Resources Center Library (1979)

Florence

University of North Alabama Collier Library (1932)

Gadsden

Gadsden Public Library (1963)

Huntsville

University of Alabama in Huntsville Library (1964)

Jacksonville

Jacksonville State University Houston Cole Library (1929)

Mobile

Mobile Public Library (1963) Spring Hill College Thomas Byrne Memorial Library (1937) University of South Alabama Library (1968)

Montgomery

Alabama Public Library Service (1984)

Alabama Supreme Court and State Law Library (1884)
Auburn University at Montgomery Library (1971) REGIONAL
Air University Library Maxwell Air Force Base (1963)

Normal

Alabama Agricultural and Mechanical University J. F. Drake Memorial Learning Resources Center (1963)

Troy

Troy State University Library (1963)

Tuscaloosa

University of Alabama Library (1860) REGIONAL University of Alabama School of Law Library (1967)

Tuskegee

Tuskegee University Hollis Burke Frissell Library (1907)

ALASKA

Anchorage

Anchorage Law Library (1973)
Anchorage Municipal Libraries Z. J. Loussac Public Library (1978)
University of Alaska at Anchorage Library (1961)
U.S. Alaska Resources Library (1981)
U.S. District Court Library (1983)

Fairbanks

University of Alaska Elmer E. Rasmuson Library (1922)

Juneau

Alaska State Library (1900) University of Alaska-Juneau Library (1981)

Ketchikan

Ketchikan Community College Library (1970)

AMERICAN SAMOA

Pago Pago

Community College of American Samoa Library (1985)

^{*}Year designated.

ARIZONA

Coolidge

Central Arizona College Instruction Materials Center (1973)

Flagstaff

Northern Arizona University Cline Library (1937)

Glendale

Glendale Public Library (1986)

Holbrook

Northland Pioneer College Learning Resources Center (1985)

Masa

Mesa Public Library (1983)

Phoenix

Department of Library Archives, and Public Records (unknown) REGIONAL Grand Canyon College Fleming Library (1978) Phoenix Public Library (1917)

Prescott

Yavapai College Library (1976)

Tempe

Arizona State University College of Law Library (1977) Arizona State University Library (1944)

Tucson

Tucson Public Library (1970) University of Arizona Library (1907) REGIONAL

U.S. Court of Appeals 9th Circuit Library (1984)

Yuma

Yuma City-County Library (1963)

ARKANSAS

Arkadelphia

Ouachita Baptist University Riley Library (1963)

Batesville

Arkansas College Library (1963)

Clarksville

University of the Ozarks Dobson Memorial Library (1925)

Conway

Hendrix College Olin C, Bailey Library (1903)

Fayetteville

University of Arkansas Mullins Library (1907) University of Arkansas School of Law Library (1978)

Little Rock

Arkansas State Library (1978) REGIONAL
Arkansas Supreme Court Library (1962)
Central Arkansas Library System Main Library (1953)
University of Arkansas at Little Rock Library Ottenheimer Library (1973)
University of Arkansas at Little Rock, School of Law Library (1979)

Magnolla

Southern Arkansas University Magale Library (1956)

Monticello

University of Arkansas at Monticello Library (1956)

Pine Bluff

University of Arkansas at Pine Bluff Watson Memorial Library (1976)

Russellville

Arkansas Tech University Tomlinson Library (1925)

Searcy

Harding University Beaumont Memorial Library (1963)

State University

Arkansas State University Dean B. Ellis Library (1913)

Walnut Ridge

Southern Baptist College Felix Goodson Library (1967)

CALIFORNIA

Anahelm

Anaheim Public Library (1963)

Arcadla

Arcadia Public Library (1975)

Arcata

Humboldt State University Library (1963)

Bakersfleld

California State College Bakersfield Library (1974) Kem County, Beale Memorial Library (1943)

Berkeley

University of California General Library (1907) University of California Law Library (1963)

Carson

California State University Dominguez Hills Educational Resources Center (1973) Carson Regional Library (1973)

Chico

California State University, Merriam Library (1962)

Claremont

Claremont Colleges' Libraries Honnold Library (1913)

Compton

Compton Public Library (1972)

Culver City

Culver City Library (1966)

Davis

University of California Shields Library (1953) University of California at Davis Law Library (1972)

Downey

Downey City Library (1963)

Fresno

California State University, Fresno, Henry Madden Library (1962) Fresno County Free Library (1920)

Fullerton

California State University at Fullerton Library (1963) Western State University College of Law Library (1984)

Garden Grove

Garden Grove Regional Library (1963)

Gardena

Gardena Public Library (1966)

Hayward

California State University, Hayward Library (1963)

Huntington Park

Huntington Park Library (1970)

Inglewood

Inglewood Public Library (1963)

irvine

University of California at Irvine Main Library (1963)

La Jolla

University of California at San Diego Central University Library (1963)

Lakewood

Angelo lacoboni Public Library (1970)

Lancaster

Lancaster Library (1967)

La Verne

University of La Verne College of Law Library (1979)

Long Beach

California State University at Long Beach Library (1962) Long Beach Public Library (1933)

Los Angeles

California State University at Los Angeles John F. Kennedy Memorial Library (1956)
Los Angeles County Law Library (1963)
Los Angeles Public Library (1891)
Loyola Marymount University Charles Von der Ahe Library (1933)
Loyola Law School Law Library (1979)
Occidental College Library (1941)
Southwestern University School of Law Library (1975)
University of California, University Research Library (1932)
University of California Los Angeles Law Library (1958)
University of Southern California Doheny Memorial Library (1933)
University of Southern California Law Library (1978)
U.S. Court of Appeals Ninth Circuit Library (1981)
Whittier College School of Law Library (1978)

Mallbu

Pepperdine University Payson Library (1963)

Menlo Park

Department of Interior Geological Survey Library (1962)

Montebello

Montebello Regional Library (1966)

Monterey

U.S. Naval Postgraduate School Dudley Knox Library (1963)

Monterey Park

Bruggemeyer Memorial Library (1964)

Northridge

California State University at Northridge Oviatt Library (1958)

Norwalk

Norwalk Regional Library (1973)

Oakland

Mills College Library (1966) Oakland Public Library (1923)

Ontario

Ontario City Library (1974)

Palm Springs

Palm Springs Public Library (1980)

Pasadena

California Institute of Technology Millikan Mernorial Library (1933) Pasadena Public Library (1963)

Pleasant Hill

Contra Costa County Library (1964)

Redding

Shasta County Library (1956)

Redlands

University of Redlands Armacost Library (1933)

Redwood City

Redwood City Public Library (1966)

Reseda

West Valley Regional Branch Library (1966)

Richmond

Richmond Public Library (1943)

Riverside

Riverside City and County Public Library (1947) University of California at Riverside Library (1963)

Sacramento

California State Library (1895) REGIONAL
California State University at Sacramento Library (1963)
Sacramento County Law Library (1963)
Sacramento Public Library (1880)
University of the Pacific McGeorge School of Law Library (1978)

San Bernardino

Don A. Turner County Law Library (1984) San Bernardino County Library (1964)

San Dlego

San Diego County Law Library (1973)

San Diego County Library (1973) San Diego Public Library (1895) San Diego State University Library (1962) University of San Diego Kratter Law Library (1967)

San Francisco

Golden Gate University School of Law Library (1979)
Hastings College of Law Library (1972)
San Francisco Public Library (1889)
San Francisco State University J. Paul Leonard Library (1955)
Supreme Court of California Library (1979)
U.S. Court of Appeals Ninth Circuit Library (1971)
University of San Francisco Richard A. Gleeson Library (1963)

San Jose

San Jose State University Library (1962)

San Leandro

San Leandro Community Library Center (1961)

San Luis Obispo

California Polytechnic State University Robert E. Kennedy Library (1969)

San Mateo

College of San Mateo Library (1987)

San Rafael

Marin County Free Library (1975)

Santa Ana

Orange County Law Library (1975) Santa Ana Public Library (1959)

Santa Barbara

University of California at Santa Barbara Library (1960)

Santa Clara

University of Santa Clara Orradre Library (1963)

Santa Cruz

University of California at Santa Cruz McHenry Library (1963)

Santa Rosa

Sonoma County Library (1896)

Stanford

Stanford University Libraries (1895) Stanford University Robert Crown Law Library (1978)

Stockton

Public Library of Stockton and San Joaquin County (1884)

Thousand Oaks

California Lutheran University Library (1964)

Torrance

Torrance Public Library (1969)

Turlock

California State University, Stanislaus Library (1964)

Vallejo

Solano County Library John F. Kennedy Library (1982)

Valencia

Valencia Regional Library (1972)

Ventura

Ventura County Library Services Agency (1975)

Visalia

Tulare County Free Library (1967)

Walnut

Mount San Antonio College Educational Resources Library Center (1966)

West Covina

West Covina Regional Library (1966)

Whittier

Whittier College Wardman Library (1963)

COLORADO

Alamosa

Adams State College Library (1963)

Aurora

Aurora Public Library (1984)

Boulder

University of Colorado at Boulder Norlin Library (1879) REGIONAL

Colorado Springs

Colorado College Tutt Library (1880) University of Colorado at Colorado Springs Library (1974) U.S. Air Force Academy Library (1956)

Denver

Auraria Library (1978)
Colorado Supreme Court Library (1978)
Denver Public Library (1884) REGIONAL
Department of the Interior Library (1962)
Regis College Dayton Memorial Library (1915)
U.S. Court of Appeals Tenth Circuit Library (1973)
University of Denver Penrose Library (1909)
University of Denver College of Law Westminster Law Library (1978)

Fort Collins

Colorado State University Libraries (1907)

Golden

Colorado School of Mines Arthur Lakes Library (1939)

Grand Junction

Mesa College Lowell Heiny Library (1978) Mesa County Public Library (1975)

Greeley

University of Northern Colorado James A. Michener Library (1966)

Gunnison

Western State College Leslie J. Savage Library (1932)

La Junta

Otero Junior College Wheeler Library (1963)

Lakewood

Jefferson County Public Library Lakewood Library (1968)

Pueblo

Pueblo Library District (1893) University of Southern Colorado Library (1965)

CONNECTICUT

Bridgeport

Bridgeport Public Library (1884)
University of Bridgeport School of Law Library Wahlstrom Library (1979)

Danbury

Western Connecticut State University Ruth A. Haas Library (1967)

Danlelson

Quinebaug Valley Community College Audrey P. Beck Library (1968)

Enfleld

Enfield Central Library (1967)

Hartford

Connecticut State Library (unknown) REGIONAL Hartford Public Library (1945) Trinity College Library (1895) University of Connecticut School of Law Library (1978)

Middletown

Wesieyan University Oiin Library (1906)

Mystic

Mystic Seaport Museum, Inc., G. W. Blunt White Library (1964)

New Britain

Central Connecticut State University Eiihu Burritt Library (1973)

New Haven

Southern Connecticut State University Hilton C. Buley Library (1968) Yale Law Library (1981) Yale University Seeiey G. Mudd Library (1859)

New London

Connecticut Coliege C. E. Shaln Library (1926) U.S. Coast Guard Academy Library (1939)

Stamford

Ferguson Library (1973)

Storrs

University of Connecticut Homer Babbidge Library (1907)

Waterbury

Post College Traurig Library and Learning Resources Center (1977) Silas Bronson Public Library (1869)

West Haven

University of New Haven Peterson Library (1971)

DELAWARE

Dover

Delaware State Coliege Wiiiiam C. Jason Library-Learning Center (1962)

State Law Library in Kent County (unknown)

Georgetown

Deiaware Technical and Community College Library (1968)

Newark

University of Delaware Library (1907)

Wilmington

Wider University School of Law Library (1976)

DISTRICT OF COLUMBIA

Washington

Administrative Conference of the United States Library (1972) Advisory Commission on Intergovernmental Relations Library (1977) American University Washington College of Law Library (1983) Catholic University of America Robert J. White Law Library (1979) Comptroller of the Currency Library (1986) Department of the Army Pentagon Library ANRAL(1969)

Department of Commerce Library (1955)

Department of Education (1988)

Department of Health and Human Services Library (1954) Department of Housing and Urban Development Library (1969) Department of the Interior Library Natural Resources Library (1895)

Department of Justice Main Library (1895) Department of Labor Library (1976) Department of the Navy Library (1895)

Department of State Library (1895)

Department of State Law Library (1966) Department of Transportation Main Library (1982)

Department of Transportation, U.S. Coast Guard Law Library (1982)

Department of the Treasury Library (1895)

District of Columbia Court of Appeals Library (1981)

District of Columbia Public Library (1943)

Equal Empioyment Opportunity Commission Library (1984)

Executive Office of the President, Office of Administration, Library & information Service Division (1965)

Federal Deposit Insurance Corporation Library (1972) Federal Election Commission Law Library (1975) Federal Energy Regulatory Commission Library (1983) Federal Labor Relations Authority Law Library (1982)

Federal Mine Safety & Health Review Commission Library (1979) Federal Reserve System Board of Governors Research Library

(1978)

Federal Reserve System Law Library (1976) General Accounting Office Technical Library (1974) General Services Administration Library (1975)

Georgetown University Library (1969)
Georgetown University Law Center Fred O. Dennis Law Library

George Washington University Melvin Gelman Library (1983)

George Washington University National Law Center Jacob Burns Law Library (1978)

Library of Congress Congressional Research Service (1978) Library of Congress Serial and Government Publications (1977)

Merit Systems Protection Board Library (1979) National Defense University Library (1895)

Pension Benefit Guaranty Corporation Legal Dept. Library (1984)

U.S. Court of Appeals Judges' Library (1975)
U.S. Court of Appeals for the Federal Circuit Library (1986)

U.S. information Agency Library (1984)

U.S. Office of Personnei Management Library (1963)

U.S. Postal Service Library (1895) U.S. Senate Library (1979)

U.S. Supreme Court Library (1978)

University of the District of Columbia Library Learning Resources Division (1970)

Veterans' Administration Central Office Library (1967)

FLORIDA

Boca Raton

Florida Atlantic University S. E. Wimberly Library (1963)

Clearwater

Clearwater Public Library (1972)

Coral Gables

University of Mlam! Otto G. Richter Library (1939)

Daytona Beach

Volusia County Library Center (1963)

De Land

Stetson University duPont-Ball Library (1887)

Fort Lauderdale

Broward County Library (1967) Nova University Law Library (1967)

Fort Plerce

Indian River Community College Library (1975)

Gainesville

University of Florida College of Law Library (1978) University of Florida Libraries (1907) REGIONAL

Jacksonville

Haydon Burns Public Library (1914) Jacksonville University Swisher Library (1962) University of North Florida Thomas G. Carpenter Library (1972)

Lakeland

Lakeland Public Library (1928)

Leesburg

Lake-Sumter Community College Library (1963)

Melbourne

Florida Institute of Technology Library (1963)

Miami

Florida International University Library Tamiami Trail (1970) Miami-Dade Public Library (1952)

North Mlami

Florida International University Bay Vista Campus Library (1977)

Opa Locka

St. Thomas University Library (1977)

Orlando

University of Central Florida Library (1966)

Palatka

Saint Johns River Community College Library (1963)

Panama City

Bay County Public Library (1983)

Pensacola

University of West Florida John C. Pace Library (1966)

Port Charlotte

Charlotte-Glades Library System (1973)

Saint Petersburg

Saint Petersburg Public Library (1965) Stetson University College of Law Charles A. Dana Law Library (1975)

Sarasota

Selby Public Library (1970)

Tallahassee

Florida Agricultural and Mechanical University Coleman Memorial Library (1936) Florida State University College of Law Library (1978) Florida State University Strozier Library (1941) Florida Supreme Court Library (1974) State Library of Florida (1929)

Tampa

Tampa-Hillsborough County Public Library (1965) University of South Florida Library (1962) University of Tampa Merl Kelce Library (1953)

Winter Park

Rollins College Olln Library (1909)

GEORGIA

Albany

Dougherty County Public Library (1964)

Americus

Georgia Southwestern College James Earl Carter Library (1966)

Athens

University of Georgia Libraries (1907) REGIONAL University of Georgia School of Law Library (1979)

Atlanta

Atlanta-Fulton Public Library (1880)
Atlanta University Center Robert W. Woodruff Library (1962)
Emory University School of Law Library (1968)
Emory University Woodruff Library (1928)
Georgia Institute of Technology Price Gilbert Memorial Library (1963)
Georgia State Library (unknown)
Georgia State University William Russell Pullen Library (1970)
Georgia State University College of Law Library (1983)
U.S. Court of Appeals 11th Circuit Library (1980)

Augusta

Augusta College Reese Library (1962) Medical College of Georgia Library (1986)

Brunswick

Brunswick-Glynn County Regional Library (1965)

Carrollton

West Georgia College Irvine Sullivan Ingram Library (1962)

Columbus

Columbus College Simon Schwob Memorial Library (1975)

Dahlonega

North Georgia College Stewart Library (1939)

Dalton

Dalton College Library (1978)

Macon

Mercer University Stetson Memorial Library (1964) Mercer University Walter F. George School of Law Library (1978)

Marletta

Kennesaw College Library (1968)

Milledgeville

Georgia College Ina Dillard Russell Library (1950)

Rome

Berry College Memorial Library (1970)

Savannah

Chatham-Effingham Liberty Regional Library (1857)

Statesboro

Georgia Southern College Zoah S. Henderson Library (1939)

Valdosta

Valdosta State College Library (1956)

GUAM

Agana

Nieves M. Flores Memorial Library (1962)

Mangllao

University of Guam Robert F. Kennedy Memorial Library (1978)

HAWAII

Hilo

University of Hawaii at Hilo Edwin H. Mookini Library (1962)

Honolulu

Hawaii Medical Library Incorporated (1968)
Hawaii State Library (1929)
Municipal Reference & Records Center (1965)
Supreme Court Law Library (1973)
University of Hawaii Hamilton Library (1907) REGIONAL
University of Hawaii William S. Richardson School of Law Library (1978)

Lale

Brigham Young University Hawaii Campus, Joseph F. Smith Library (1964)

Lihue

Lihue Public Library (1967)

Pearl City

Leeward Community College Library (1967)

Walluku

Maui Public Library (1962)

IDAHO

Bolse

Boise Public Library and Information Center (1929) Boise State University Library (1966) Idaho State Law Library (unknown) Idaho State Library (unknown)

Caldwell

College of Idaho Terteling Library (1930)

Moscow

University of Idaho College of Law Library (1978) University of Idaho Library (1907) REGIONAL

Nampa

Northwest Nazarene College John E. Riley Library (1984)

Pocatello

Idaho State University Eli Oboler Library (1908)

Rexburg

Ricks College Davis O. McKay Library (1946)

Twin Falls

College of Southern Idaho Library (1970)

ILLINOIS

Bloomington

Illinois Wesleyan University, Sheean Library (1964)

Bourbonnals

Olivet Nazarene University Benner Library & Learning Resource Center (1946)

Carbondale

Southern Illinois University at Carbondale Morris Library (1932) Southern Illinois University School of Law Library (1978)

Carlinville

Blackburn College Lumpkin Library (1954)

Carterville

Shawnee Library System (1971)

Champalgn

University of Illinois Law Library (1965)

Charleston

Eastern Illinois University Booth Library (1962)

Chicago

Chicago Public Library (1876)

Chicago State University Paul and Emily Douglas Library (1954)

DePaul University Law Library (1979)

Field Museum of Natural History Library (1963)

Illinois Institute of Technology Chicago-Kent College of Law Library

Illinois Institute of Technology Paul V. Galvin Library (1982)

John Marshall Law School Library (1981)

Loyola University of Chicago E. M. Cudahy Memorial Library (1966)

Loyola University School of Law Library (1979) Northeastern Illinois University Ronald Williams Library (1961)

Northwestern University School of Law Library (1978) University of Chicago Law Library (1964)

University of Chicago Library (1897)

University of Illinois at Chicago Library (1957)

William J. Campbell Library of the U.S. Courts (1979)

Decatur

Decatur Public Library (1954)

De Kalb

Northern Illinois University Founders' Memorial Library (1960) Northern Illinois University College of Law Library (1978)

Des Plaines

Oakton Community College Library (1976)

Edwardsville

Southern Illinois University at Edwardsville Lovejoy Memorial Library (1959)

Elsah

Principia College Marshall Brooks Library (1957)

Evanston

Northwestern University Library (1876)

Freeport

Freeport Public Library (1905)

Galesburg

Galesburg Public Library (1896)

Jacksonville

MacMurray College Henry Pfeiffer Library (1929)

Lake Forest

Lake Forest College Donnelley Library (1962)

Lebanon

McKendree College Holman Library (1968)

Lisle

Illinois Benedictine College Theodore F. Lownik Library (1911)

Macomb

Western Illinois University Government Publications & Legal Reference Library (1962)

Moline

Black Hawk College Learning Resources Center (1970)

Monmouth

Monmouth College Hewes Library (1860)

Mount Carmel

Wabash Valley College Bauer Media Center (1975)

Mount Prospect

Mount Prospect Public Library (1977)

Normal

Illinois State University Milner Library (1877)

Oak Park

Oak Park Public Library (1963)

Oglesby

Illinois Valley Community College Jacobs Memorial Library (1976)

Palos Hills

Moraine Valley Community College Learning Resources Center (1972)

Peorla

Bradley University Cullom-Davis Library (1963)

Peoria Public Library (1883)

River Forest

Rosary College Library Rebecca Crown Library (1966)

Rockford

Rockford Public Library (1895)

Romeoville

Lewis University Library (1952)

Springfield

Illinois State Library (unknown) REGIONAL

Streamwood

Poplar Creek Public Library (1980)

University Park

Governors' State University Library (1974)

Urbana

University of Illinois Documents Library (1907)

Wheaton

Wheaton College Buswell Memorial Library (1964)

Woodstock

Woodstock Public Library (1963)

INDIANA

Anderson

Anderson College Charles E. Wilson Library (1959) Anderson Public Library (1983) **Bioomington**

Indiana University Library (1881) Indiana University Law Library (1978)

Crawfordsville

Wabash College Lilly Library (1906)

Evansville

Evansville and Vanderburgh County Public Library (1928)

University of Southern Indiana Library (1969)

Fort Wayne

Allen County Public Library (1896) Indiana University-Purdue University at Fort Wayne (1965)

Franklin

Franklin College Library (1976)

Gary

Gary Public Library (1943) Indiana University Northwest Library (1966)

Greencastle

De Pauw University Roy O. West Library (1879)

Hammond

Hammond Public Library (1964)

Hanover

Hanover College Duggan Library (1892)

Huntington

Huntington College Richlyn Library (1964)

Indianapolis

Butler University Irwin Library (1965)
Indianapolis-Marion County Public Library (1906)
Indiana State Library (unknown) REGIONAL
Indiana Supreme Court Law Library (1975)
Indiana University School of Law Library (1967)

Indiana University Scriool of Law Library (1907)
Indiana University-Purdue University Library (1979)

Kokomo

Indiana University at Kokomo Learning Resource Center (1969)

Muncle

Ball State University Alexander M. Bracken Library (1959) Muncie Public Library (1906)

New Albany

Indiana University Southeast Library (1965)

Notre Dame

Notre Dame Law School Kresge Law Library (1985) University of Notre Dame Memorial Library (1883)

Rensselaer

Saint Joseph's College Library (1964)

Richmond

Earlham College Lilly Library (1964) Morrison-Reeves Library (1906)

South Bend

Indiana University at South Bend Library (1965)

Terre Haute

Indiana State University Cunningham Memorial Library (1906)

Vaiparaiso

Valparaiso University Moellering Memorial Library (1930) Valparaiso University Law Library (1978)

West Lafayette

Purdue University Libraries (1907)

IOWA

Ames

Iowa State University Library (1907)

Cedar Falls

University of Northern Iowa Library (1946)

Cedar Rapids

Cedar Rapids Public Library (1986)

Council Bluffs

Free Public Library (1885)
Iowa Western Community College Herbert Hoover Library (1972)

Davenport

Davenport Public Library (1973)

Des Moines

Drake University Cowles Library (1966) Drake University Law Library (1972) Public Library of Des Moines (1888) State Library of Iowa (unknown)

Dubuque

Carnegie-Stout Public Library (unknown) Loras College Wahlert Memorial Library (1967)

Fayette

Upper Iowa University Henderson-Wilder Library (1974)

Grinnell

Grinnell College Burling Library (1874)

lowa City

University of Iowa College of Law Library (1968) University of Iowa Libraries (1884) REGIONAL

Lamoni

Graceland College Frederick Madison Smith Library (1927)

Mason City

North Iowa Area Community College Library (1976)

Mount Vernon

Cornell College Russell D. Cole Library (1896)

Orange City

Northwestern College Ramaker Library (1970)

Sloux City

Sloux City Public Library (1894)

KANSAS

Atchison

Benedictine College North Campus Library (1965)

Baidwin City

Baker University Collins Library (1908)

Colby

Colby Community College H. F. Davis Memorial Library (1968)

Emporia

Emporia State University William Allen White Library (1909)

Hays

Fort Hays State University Forsyth Library (1926)

Hutchinson

Hutchinson Public Library (1963)

Lawrence

University of Kansas Law Library (1971) University of Kansas Spencer Research Library (1869) REGIONAL

Manhattan

Kansas State University Farrell Library (1907)

Plttsburg

Pittsburg State University Leonard H. Axe Library (1952)

Salina

Kansas Wesleyan University Memorial Library (1930)

Shawnee Mission

Johnson County Library (1979)

Topeka

Kansas State Historical Society Library (1877) Kansas State Library (unknown) Kansas Supreme Court Law Library (1975) Washburn University of Topeka Law Library (1971)

Wichita

Wichita State University Ablah Library (1901)

KENTUCKY

Ashland

Boyd County Public Library (1946)

Barbourville

Union College Abigail E. Weeks Memorial Library (1958)

Bowling Green

Western Kentucky University Helm-Cravens Library (1934)

Columbia

Lindsey Wilson College Katie Murrell Library (1987)

Crestylew Hills

Thomas More College Library (1970)

Danville

Centre College Grace Doherty Library (1884)

Frankfort

Kentucky Department of Libraries and Archives (1967) Kentucky State Law Library (unknown) Kentucky State University Blazer Library (1972)

Hazard

Hazard Community College Library (1988)

Highland Heights

Northern Kentucky University W. Frank Steely Library (1973)

Lexington

University of Kentucky Law Library (1968) University of Kentucky Libraries (1907) REGIONAL

Louisville

Louisville Free Public Library (1904) University of Louisville Ekstrom Library (1925) University of Louisville Law Library (1975)

Morehead

Morehead State University Camden-Carroll Library (1955)

Murray

Murray State University Waterfield Library (1924)

Owensboro

Kentucky-Wesleyan College Library Learning Center (1966)

Richmond

Eastern Kentucky University John Grant Crabbe Library (1966)

Williamsburg

Cumberland College Norma Perkins Hagan (1988)

LOUISIANA

Baton Rouge

Louisiana State Library (1976) Louisiana State University Middleton Library (1907) REGIONAL Louisiana State University Paul M. Hebert Law Center Library (1929) Southern University Law School Library (1979) Southern University Library (1952)

Eunice

Louisiana State University at Eunice LeDoux Library (1969)

Hammond

Southeastern Louisiana University Sims Memorial Library (1966)

Lafayette

University of Southwestern Louisiana Library (1938)

Lake Charles

McNeese State University Lether E. Frazar Memorial Library (1941)

Monroe

Northeast Louisiana University Sandel Library (1963)

Natchitoches

Northwestern State University of Louisiana Watson Memorial Library (1887)

New Orleans

Law Library of Louisiana (unknown)
Loyola University Government Documents Library (1942)
Loyola University Law Library (1978)
New Orleans Public Library (1883)
Our Lady of Holy Cross College Library (1968)
Southern University In New Orleans Leonard S. Washington Memorial
Library (1962)
Tulane University Law Library (1976)
Tulane University Howard-Tilton Memorial Library (1942)
U.S. Court of Appeals 5th Circuit Library (1973)

Pineville

Louislana College Richard W. Norton Memorial Library (1969)

University of New Orleans Earl K. Long Library (1963)

Ruston

Louisiana Technical University Prescott Memorial Library (1896) REGIONAL

Shreveport

Louisiana State University at Shreveport Library (1967) Shreve Memorial Library (1923)

Thibodaux

Nicholls State University Ellender Memorial Library (1962)

MAINE

Augusta

Maine Law and Legislative Reference Library (1973) Maine State Library (unknown)

Bangor

Bangor Public Library (1884)

Brunswick

Bowdoin College Library (1884)

Castine

Maine Maritime Academy Nutting Memorial Library (1969)

Lewiston

Bates College George and Helen Ladd Library (1883)

Orono

University of Malne Raymond H. Fogler Library (1907) REGIONAL

Portland

Portland Public Library (1884) University of Maine School of Law Garbrecht Law Library (1964)

Presque Isle

University of Maine at Presque Isle Library/Learning Resources Center (1979)

Sanford

Louis B. Goodall Memorial Library (1984)

Waterville

Colby College Miller Library (1884)

MARYLAND

Annapolis

Maryland State Law Library (unknown) U.S. Naval Academy Nimitz Library (1895)

Baltimore

Enoch Pratt Free Library (1887)
Johns Hopkins University Milton S. Eisenhower Library (1882)
Morgan State University Soper Library (1940)
University of Baltimore Langsdale Library (1973)
University of Baltimore Law Library (1980)
University of Maryland School of Law Marshall Law Library (1969)
U.S. Court of Appeals 4th Circuit Library (1982)

Bel Air

Harford Community College Library (1967)

Beitsville

Department of Agriculture National Agricultural Library (1895)

Bethesda

Department of Health and Human Services National Library of Medicine (1978)
Uniformed Services University of Health Sciences Learning Resource

Center (1983)

Catonsville

University of Maryland, Baltimore County Albin O. Kuhn Library & Gallery (1971)

Chestertown

Washington College Clifton M. Miller Library (1891)

College Park

University of Maryland McKeldln Library (1925) REGIONAL

Cumberland

Allegany Community College Library (1974)

Frostburg

Frostburg State University Library (1967)

Patuxent River

Patuxent River Central Library (1968)

Rockville

Montgomery County Department of Public Libraries (1951)

Sallsbury

Salisbury State College Blackwell Library (1965)

Towson

Goucher College Julia Rogers Library (1966) Towson State University Cook Library (1979)

Westminster

Western Maryland College Hoover Library (1886)

MASSACHUSETTS

Amherst

Amherst College Library (1884) University of Massachusetts University Library (1907)

Boston

Boston Athenaeum Library (unknown)
Boston Public Library (1859) REGIONAL
Boston University School of Law Pappas Law Library (1979)
Northeastern University Dodge Library (1962)
State Library of Massachusetts (unknown)
Suffolk University Law Library (1979)
Supreme Judicial Court Social Law Library (1979)
U.S. Court of Appeals First Circuit Library (1978)

Brookline

Public Library of Brookline (1925)

Cambridge

Harvard College Library (1860) Harvard Law School Library (1981) Massachusetts Institute of Technology Library (1946)

Chestnut Hill

Boston College Thomas P. O'Neill Jr., Library (1963)

Chicopee

College of Our Lady of the Elms Alumnae Library (1969)

Lowell

University of Lowell Lydon Library (1952)

Medford

Tufts University Wessel Library (1899)

Milton

Curry College Levin Library (1972)

New Bedford

New Bedford Free Public Library (1858)

Newton Centre

Boston College Law School Library (1979)

North Dartmouth

Southeastern Massachusetts University Library (1965)

North Easton

Stonehill College Cushing-Martin Library (1962)

Springfield

Springfield City Library (1966) Western New England College Law Library (1978)

Waltham

Brandeis University Library (1965) Waltham Public Library (1982)

Wellesley

Wellesley College Library (1943)

Wenham

Gordon College Jenks Learning Resource Center (1963)

Williamstown

William College Sawyer Library (unknown)

Worcester

American Antiquarian Society Library (1814) University of Massachusetts Medical Center Library (1972) Worcester Public Library (1859)

MICHIGAN

Albion

Albion College Stockwell-Mudd Library (1966)

Allendale

Grand Valley State College Zumberge Library (1963)

Alma

Alma College Library (1963)

Ann Arbor

University of Michigan Harlan Hatcher Graduate Library (1884) University of Michigan Law Library (1978)

Benton Harbor

Benton Harbor Public Library (1907)

Bloomfleld Hills

Cranbrook Institute of Science Library (1940)

Dearborn

Henry Ford Centennial Library (1969) Henry Ford Community College Library (1957)

Detroit

Detroit College of Law Library (1979)
Detroit Public Library (1868) REGIONAL
Marygrove College Library (1965)
Mercy College of Detroit Library (1965)
University of Detroit Library (1884)
University of Detroit School of Law Library (1978)
Wayne State University Purdy/Kresge Library (1937)
Wayne State University Arthur Neef Law Library (1971)

Dowaglac

Southwestern Michigan College Matthews Library (1971)

East Lansing

Michigan State University Documents Library (1907)

Farmington Hills

Oakland Community College Martin L. King Learning Resources Center (1968)

Flint

Flint Public Library (1967) University of Michigan-Flint Library (1977)

Grand Rapids

Calvin College & Seminary Library (1967) Grand Rapids Public Library (1876)

Houghton

Michigan Technological University Library (1876)

Jackson

Jackson District Library (1965)

Kalamazoo

Kalamazoo Public Library (1907) Western Michigan University Dwight B. Waldo Library (1963)

Lansing

Library of Michigan (unknown) REGIONAL Thomas M. Cooley Law School Library (1978)

Livonia

Livonia Public Library (1987) Schoolcraft College Library (1962)

Madison Heights

Madison Heights Public Library (1982)

Marquette

Northern Michigan University Lydia M. Olson Library (1963)

Monroe

Monroe County Library System (1974)

Mount Clemens

Macomb County Library (1968)

Mount Pleasant

Central Michigan University Library (1958)

Muskegon

Hackley Public Library (1894)

Petoskey

North Central Michigan College Library (1962)

Port Huron

Saint Clair County Library (1876)

Rochester

Oakland University Kresge Library (1964)

Royal Oak

Royal Oak Public Library (1984)

Saginaw

Hoyt Public Library (1890)

Sault Ste. Marle

Lake Superior State College Kenneth Shouldice Library (1982)

Traverse City

Northwestern Michigan College Mark Osterlin Library (1964)

University Center

Delta College Library (1963)

Warren

Warren Public Library Arthur J. Miller Branch (1973)

Ypsllantl

Eastern Michigan University Library (1965)

MICRONESIA

East Caroline Islands

Community College of Micronesia Library (1982)

MINNESOTA

Bemidil

Bernidji State University A.C. Clark Library (1963)

Blaine

Anoka County Library (1971)

Collegeville

Saint John's University Alcuin Library (1954)

Cottage Grove

Washington County Library-Park Grove Branch (1983)

Duluth

Duluth Public Library (1909) University of Minnesota Duluth Library (1984)

Eagan

Dakota County Library-Westcott Branch (1983)

Edina

Southdale-Hennepin Area Library (1971)

Mankato

Mankato State University Memorial Library (1962)

Marshall

Southwest State University Library (1986)

Minneapolis

Minneapolis Public Library (1893) University of Minnesota Law School Library (1978) University of Minnesota Wilson Library (1907) REGIONAL

Moorhead

Moorhead State University Livingston Lord Library (1956)

Morris

University of Minnesota, Morris, Rodney A. Briggs Library (1963)

Northfield

Carleton College Library (1930) Saint Olaf College Rolvaag Memorial Library (1930)

Saint Cloud

Saint Cloud State University, Learning Rescources Center (1962)

Saint Paul

Hamline University School of Law Library (1978)
Minnesota Historical Society Library (1867)
Minnesota State Law Library (unknown)
Saint Paul Public Library (1914)
University of Minnesota Saint Paul Campus Library (1974)
William Mitchell College of Law Library (1979)

Saint Peter

Gustavus Adolphus College Library (1941)

Winona

Winona State University Maxwell Library (1969)

MISSISSIPPI

Cleveland

Delta State University W. B. Roberts Library (1975)

Columbus

Mississippi University for Women John Clayton Fant Memorial Library (1929)

Hattlesburg

University of Southern Mississippi Joseph A. Cook Memorial Library (1935)

Jackson

Jackson State University Henry Thomas Sampson Library (1968)
Millsaps College Millsaps-Wilson Library (1963)
Mississippi College School of Law Library (1977)
Mississippi Library Commission (1947)
Mississippi State Law Library (unknown)

Lorman

Alcorn State University J. D. Boyd Library (1970)

Mississippi State

Mississippi State University Mitchell Memorial Library (1907)

University

University of Mississippi Library (1883) REGIONAL University of Mississippi James O. Eastland Law Library (1967)

MISSOURI

Cape Girardeau

Southeast Missouri State University Kent Library (1916)

Columbia

University of Missouri at Columbia Library (1862) REGIONAL University of Missouri-Columbia Law Library (1978)

Fulton

Westminster College Reeves Library (1875)

Hillsboro

Jefferson College Library (1984)

Jefferson City

Lincoln University Inman E. Page Library (1944) Missouri State Library (1963) Missouri Supreme Court Library (unknown)

Joplin

Missouri Southern State College Library (1966)

Kansas City

Kansas City Missouri Public Library (1881) Rockhurst College Greenlease Library (1917) University of Missouri at Kansas City General Library (1938) University of Missouri Kansas City Leon E. Bloch Law Library (1978)

Kirksviile

Northeast Missouri State University Pickler Memorial Library (1966)

Liberty

William Jewell College Charles F. Curry Library (1900)

Maryville

Northwest Missouri State University B. D. Owens Library (1982)

Rolla

University of Missouri-Rolla Curtis Laws Wilson Library (1907)

Saint Charles

Lindenwood College Margaret Leggat Butler Library (1973)

Saint Joseph

Saint Joseph Public Library (1891)

Saint Louis

Maryville College Library (1976)
Saint Louis County Library (1970)
Saint Louis Public Library (1866)
Saint Louis University Law Library (1967)
Saint Louis University Pius XII Memorial Library (1866)
U.S. Court of Appeals Eighth Circuit Library (1972)
University of Missouri at Saint Louis Thomas Jefferson Library (1966)
Washington University John M. Olin Library (1906)
Washington University Law Library (1978)

Springfield

Drury College, Walker Library (1874) Southwest Missouri State University Duane G. Meyer Library (1963)

Warrensburg

Central Missouri State University Ward Edwards Library (1914)

MONTANA

Billings

Eastern Montana College Library (1958)

Bozeman

Montana State University Renne Library (1907)

Butte

Montana College of Mineral Science and Technology Library (1901)

Havre

Northern Montana College Vande Bogart Library (1980)

Helena

Carroll College Library (1974) Montana State Library (1966) State Law Library of Montana (1977)

Missoula

University of Montana Maurene & Mike Mansfield Library (1909) REGIONAL

NEBRASKA

Blair

Dana College Dana-LIFE Library (1924)

Crete

Doane College Perkins Library (1944)

Fremont

Midland Lutheran College Luther Library (1924)

Kearney

Kearney State College Calvin T. Ryan Library (1962)

Lincoln

Nebraska Library Commission (1972)
Nebraska State Library (unknown)
University of Nebraska-Lincoln College of Law Library (1981)
University of Nebraska-Lincoln D. L. Love Memorial Library (1907)
REGIONAL

Omaha

Creighton University Reinert/Alumni Library (1964) Creighton University School of Law Library (1979) Omaha Public Library W. Dale Clark Library (1880) University of Nebraska at Omaha University Library (1939)

Scottsbluff

Scottsbluff Public Library (1925)

Wayne

Wayne State College U.S. Conn Library (1970)

NEVADA

Carson City

Nevada State Library (unknown) Nevada Supreme Court Library (1973)

Las Vegas

Clark County Law Library (1988) Las Vegas-Clark County Library (1974) University of Nevada at Las Vegas James Dickinson Library (1959)

Reno

National Judicial College Law Library (1979) Nevada Historical Society Library (1974) University of Nevada-Reno Library (1907) REGIONAL Washoe County Library (1980)

NEW HAMPSHIRE

Concord

Franklin Pierce Law Center Library (1973) New Hampshire State Library (unknown)

Durham

University of New Hampshire Library (1907)

Hanover

Dartmouth College Library (1884)

Henniker

New England College Danforth Library (1966)

Manchester

Manchester City Library (1884) New Hampshire College H. A. B. Shapiro Memorial Library (1976) Saint Anselm College Geisel Library (1963)

Nashua

Nashua Public Library (1971)

NEW JERSEY

Bayonne

Bayonne Free Public Library (1909)

Bloomfleld

Bloomfield Public Library (1965)

Bridgeton

Cumberland County Library (1966)

Camden

Rutgers University Camden Library (1966) Rutgers University School of Law Library (1979)

Convent Station

College of Saint Elizabeth Mahoney Library (1938)

East Brunswick

East Brunswick Public Library (1977)

East Orange

East Orange Public Library (1966)

Elizabeth

Free Public Library of Elizabeth (1895)

Glassboro

Glassboro State College Savitz Library (1963)

Hackensack

Johnson Free Public Library (1966)

Irvington

Irvington Public Library (1966)

Jersey City

Jersey City Public Library (1879) Jersey City State College Forrest A. Irwin Library (1963)

Lawrenceville

Rider College Franklin F. Moore Library (1975)

Madison

Drew University Library (1939)

Mahwah

Ramapo College Library (1971)

Mount Holly

Burlington County Library (1966)

New Brunswick

New Brunswick Free Public Library (1908) Rutgers University Alexander Library (1907)

Newark

Newark Public Library (1906) REGIONAL Rutgers-The State University of New Jersey John Cotton Dana Library (1966)

Ruigers University Law School Ackerson Law Library (1979) Seton Hall University Law Library (1979)

Newton

Sussex County Library (1986)

Passalc

Passaic Public Library (1964)

Phillipsburg

Phillipsburg Free Public Library (1976)

Plainfield

Plainfield Public Library (1971)

Pomona

Stockton State College Library (1972)

Princeton

Princeton University Library (1884)

Randolph

County College of Morris Sherman H. Masten Learning Resource

Center (1975)

Rutherford

Fairleigh Dickinson University Messler Library (1953)

Shrewsbury

Monmouth County Library (1968)

South Orange

Seton Hall University McLaughlin Library (1947)

Teaneck

Fairleigh Dickinson University Weiner Library (1963)

Toms River

Ocean County College Learning Resources Center (1966)

Trenton

New Jersey State Library (unknown) Trenton Free Public Library (1902)

Union

Kean College of New Jersey Nancy Thompson Library (1971)

Upper Montclair

Montclair State College Harry A. Sprague Library (1967)

Wayne

Wayne Public Library (1972)

West Long Branch

Monmouth College Guggenheim Memorial Library (1963)

Woodbridge

Woodbridge Public Library (1965)

NEW MEXICO

Albuquerque

University of New Mexico Medical Center Library (1973)
University of New Mexico School of Law Library (1973)
University of New Mexico General Library (1896) REGIONAL

Hobbs

New Mexico Junior College Pannell Library (1969)

Las Cruces

New Mexico State University Library (1907)

Las Vegas

New Mexico Highlands University Donnelly Library (1913)

Portales

Eastern New Mexico University Golden Library (1962)

Santa Fe

New Mexico State Library (1960) REGIONAL New Mexico Supreme Court Law Library (unknown)

Silver City

Western New Mexico University Miller Library (1972)

Socorro

New Mexico Institute of Mining & Technology Martin Speare Memorial Library (1984)

NEW YORK

Albany

Albany Law School Schaffer Law Library (1979) New York State Library (unknown) REGIONAL State University of New York at Albany University Library (1964)

Auburn

Seymour Library (1972)

Binghamton

State University of New York at Binghamton Glenn G. Bartle Library (1962)

Brockport

State University of New York at Brockport Drake Memorial Library (1967)

Bronx

Fordham University Library (1937)
Herbert H. Lehman College Library (1967)
New York Public Library (1973)
State University of New York Maritime College Stephen B. Luce Library (1947)

Bronxville

Sarah Lawrence College Esther Raushenbush Library (1969)

Brooklyn

Brooklyn College Library (1936)
Brooklyn Law School Library (1974)
Brooklyn Public Library Business Library (1984)
Brooklyn Public Library (1908)
Pratt Institute Library (1891)
State University of New York Health Center at Brooklyn Library (1958)

Buffalo

Buffalo and Erie County Public Library (1895)
State University of New York at Buffalo Charles B. Sears Law Library (1978)
State University of New York at Buffalo Lockwood Memorial Library (1963)

Canton

Saint Lawrence University Owen D. Young Library (1920)

Corning

Coming Community College Arthur A. Houghton Jr. Library (1963)

Cortland

State University of New York College at Cortland Memorial Library (1964)

Delhi

State University Agricultural and Technical College Library (1970)

East Islip

East Islip Public Library (1973)

Elmira

Elmira College Gannett Tripp Learning Center (1956)

Farmingdale

State University of New York at Farmingdale Greenley Library (1917)

Flushing

CUNY Law School at Queens College CUNY Law Library (1983) Queens College Paul Klapper Library (1939)

Garden City

Adelphi University Swirbul Library (1966)

Geneseo

State University of New York at Geneseo Milne Library (1967)

Greenvale

Long Island University B. Davis Schwartz Memorial Library (1964)

Hamilton

Colgate University, Everett Needham Case Library (1902)

Hempstead

Hofstra University Library (1964) Hofstra University School of Law Library (1979)

Huntington

Touro College Jacob D. Fuchsberg Law Center Library (1985)

Ithaca

Cornell University Library (1907) Cornell Law Library (1978) New York State College of Agriculture and Human Ecology Albert R. Mann Library (1943)

Jamaica

Queens Borough Public Library (1926) Saint John's University Library (1956) Saint John's University School of Law Library (1978)

Kings Point

U.S. Merchant Marine Academy Schuyler Otls Bland Library (1962)

Long Island City

Fiorello H. LaGuardla Community College Library (1981)

Middletown

Thrall Library (1986)

Mount Vernon

Mount Vernon Public Library (1962)

New Paltz

State University College at New Paltz Sojourner Truth Library (1965)

New York City

City College of City University of New York Cohen Library (1884) College of Insurance Library (1965) Columbia University Libraries (1882) Columbia University School of Law Library (1981)

Cooper Union for the Advancement of Science and Arts Library (1930) Fordham University School of Law Leo T. Kissam Memorial Library

Medical Library Center of New York (1976)

New York Law Institute Library (1909)

New York Law School Library (1979)

New York Public Library Astor Branch (1907)

New York Public Library Lenox Branch (1884)

New York University Law Library (1974)

New York University Elmer Holmes Bobst Library (1967)

U.S. Court of Appeals Second Circuit Library (1976)

Yeshiva University Chutick Law Library Cardozo School of Law (1979)

Yeshiva University Pollack Library (1979)

Newburgh

Newburgh Free Library (1909)

Niagara Falis

Niagara Falls Public Library (1976)

Oakdale

Dowling College Library (1965)

Oneonta

State University College at Onenonta James M. Milne Library (1966)

Oswego

State University of New York at Oswego Penfield Library (1966)

Plattsburgh

State University College at Plattsburgh Benjamin F. Feinberg Library (1967)

Potsdam

Clarkson University Harriet Call Burnap Memorial Library (1938) State University College at Potsdam Frederick W. Crumb Memorial Library (1964)

Poughkeepsle

Vassar College Library (1943)

Purchase

State University of New York at Purchase Library (1969)

Rochester

Rochester Public Library (1963) University of Rochester Rush Rhees Library (1880)

Saint Bonaventure

Saint Bonaventure University Friedsam Memorial Library (1938)

Saratoga Springs

Skidmore College Library (1964)

Schenectady

Union College Schaffer Library (1901)

Southampton

Long Island University Southhampton Campus Library (1973)

Sparkili

St. Thomas Aquinas College Lougheed Library (1984)

Staten Island

Wagner College Horrmann Library (1953)

Stony Brook

State University of New York at Stony Brook Main Library (1963)

Syracuse

Onondaga County Public Library (1978)
Syracuse University Bird Library (1878)
Syracuse University College of Law H. Douglas Barclay Law Library (1978)

Troy

Troy Public Library (1869)

Uniondale

Nassau Library System (1965)

Utica

Utica Public Library (1885) SUNY College of Technology Library (1977)

West Point

U.S. Military Academy Library (unknown)

White Plains

Pace University Law School Library (1978)

Yonkers

Yonkers Public Library Getty Square Branch (1910)

Yorktown Heights

Mercy College Library (1976)

NORTH CAROLINA

Asheville

University of North Carolina at Asheville D. Hiden Ramsey Library (1965)

Boiling Springs

Gardner-Webb College Dover Memorial Library (1974)

Boone

Appalachian State University Carol Grotnes Belk Library (1963)

Bules Creek

Campbell University Carrie Rich Memorial Library (1965)

Chapel Hill

University of North Carolina at Chapel Hill Davis Library (1884) REGIONAL University of North Carolina Law Library (1978)

Charlotte

Public Library of Charlotte and Mecklenburg County (1964) Queens College Everett Library (1927) University of North Carolina at Charlotte Atkins Library (1964)

Cullowhee

Western Carolina University Hunter Library (1953)

Davidson

Davidson College Library (1893)

Durham

Duke University School of Law Library (1978)
Duke University William R. Perkins Library (1890)
North Carolina Central University Law School Library (1979)
North Carolina Central University James E. Shepard Memorial Library (1973)

Eion College

Elon College Iris Holt McEwen Library (1971)

Fayetteville

Fayetteville State University Charles W. Chesnutt Library (1971)

Greensboro

North Carolina Agricultural and Technical State University F. D. Bluford Library (1937) University of North Carolina at Greensboro Walter Clinton Jackson Library (1963)

Greenville

East Carolina University J. Y. Joyner Library (1951)

Laurinburg

Saint Andrews Presbyterian College DeTamble Library (1969)

Lexington

Davidson County Public Library (1971)

Mount Olive

Mount Olive College Moye Library (1971)

Pembroke

Pembroke State University Mary H. Livermore Library (1956)

Raleigh

Department of Cultural Resources Division of State Library (unknown) North Carolina State University D. H. Hill Library (1923) North Carolina Supreme Court Library (1972)

Rocky Mount

North Carolina Wesleyan College Library (1969)

Sallsbury

Catawba College Library (1925)

Wilmington

University of North Carolina at Wilmington William M. Randall Library (1965)

Wilson

Atlantic Christian College Hackney Library (1930)

Winston-Salem

Forsyth County Public Library (1954) Wake Forest University Z. Smith Reynolds Library (1902)

NORTH DAKOTA

Bismarck

North Dakota State Library (1971)
North Dakota Supreme Court Law Library (unknown)
State Historical Society of North Dakota State Archives & Historical
Research Library (1907)
Veterans' Memorial Public Library (1967)

Dickinson

Dickinson State College Stoxen Library (1968)

Fargo

Fargo Public Library (1964) North Dakota State University Library (1907) REGIONAL

Grand Forks

University of North Dakota Chester Fritz Library (1890)

Minot

Minot State University Memorial Library (1925)

Valley City

Valley City State University Allen Memorial Library (1913)

NORTHERN MARIANA ISLANDS

Salpan

Northern Marianas College Olympio T. Boria Memorial Library (1988)

OHIO

Ada

Ohio Northern University J. P. Taggart Law Library (1965)

Akron

Akron-Summit County Public Library (1952) University of Akron Blerce Library (1963) University of Akron School of Law Library (1978)

Alliance

Mount Union College Library (1888)

Ashland

Ashland College Library (1938)

Athens

Ohlo University Alden Library (1886)

Batavia

University of Cincinnati Clermont College Library (1973)

Bluffton

Bluffton College Musselman Library (1951)

Bowling Green

Bowling Green State University Jerome Library (1933)

Canton

Malone College Everett L. Cattel Library (1970)

Chardon

Chardon Public Library (1971)

Cincinnati

Public Library of Cincinnati and Hamilton County (1884)
University of Cincinnati Central Library (1929)
University of Cincinnati College of Law Marx Law Library (1978)
U.S. Court of Appeals 6th Circuit Library (1986)

Cleveland

Case Western Reserve University Freiberger Library (1913)
Case Western Reserve University School of Law Library (1979)
Cleveland Public Library (1886)
Cleveland State University Cleveland-Marshall College of Law,
Joseph W. Bartunek III Law Library (1978)
Cleveland State University Library (1966)
Municipal Reference Library (1970)

Cleveland Heights

Cleveland Heights-University Heights Public Library (1970)

Columbus

Capital University Law School Library (1980)
Capital University Library (1968)
Ohio State University College of Law Library (1984)
Ohio State University Libraries (1907)
Ohio Supreme Court Law Library (1973)
Public Library of Columbus and Franklin County (1885)
State Library of Ohio (unknown) REGIONAL

Dayton

Dayton and Montgomery County Public Library (1909) University of Dayton Roesch Library (1969) Wright State University Library (1965)

Delaware

Ohio Wesleyan University L. A. Beeghly Library (1845)

Elyria

Elyria Public Library (1966)

Findiay

Findlay College Shafer Library (1969)

Gambler

Kenyon College Library (1873)

Granville

Denison University Libraries William H. Doane Library (1884)

Hiram

Hiram College Teachout-Price Memorial Library (1874)

Kent

Kent State University Libraries (1962)

Marietta

Marietta College Dawes Memorial Library (1884)

Marlon

Marion Public Library (1979)

Middletown

Miami University Middletown Gardner-Harvey Library (1970)

New Concord

Muskingum College Library (1966)

Oberlin

Oberlin College Library (1858)

Oxford

Miami University Libraries King Library (1909)

Portsmouth

Shawnee State University Library (1987)

Rio Grande

Rio Grande College and Community College Jeanette Albiez Davis Library (1966)

Springfield

Warder Public Library (1884)

Steubenville

Franciscan University of Steubenville John Paul II Library (1971) Public Library of Steubenville and Jefferson County (1950)

Tiffin

Heidelberg College Beeghly Library (1964)

Toledo

Toledo-Lucus County Public Library (1884) University of Toledo College of Law Library (1981) University of Toledo Library (1963)

University Heights

John Carroll University Grasselli Library (1963)

Westerville

Otterbein College Courtright Memorial Library (1967)

Wilmington

Wilmington College S. Arthur Watson Library (1986)

Wooster

College of Wooster Andrews Library (1966)

Worthington

Worthington Public Library (1984)

Youngstown

Public Library of Youngstown and Mahoning County (1923) Youngstown State University William F. Maag Library (1971)

OKLAHOMA

Ada

East Central Oklahoma State University Linscheid Library (1914)

Alva

Northwestern Oklahoma State University J. W. Martin Library (1907)

Bethany

Southern Nazarene University R. T. Williams Learning Resources Center (1971)

Durant

Southeastern Oklahoma State University Henry G. Bennett Memorial Library (1929)

Edmond

Central State University Library (1934)

Enid

Public Library of Enid and Garfield County (1908)

Langston

Langston University G. Lamar Harrison Library (1941)

Lawton

Lawton Public Library (1987)

Norman

University of Oklahoma Libraries Bizzell Memorial Library (1893) University of Oklahoma Law Library (1978)

Oklahoma City

Metropolitan Library System Main Library (1974) Oklahoma City University Dulaney Browne Library (1963) Oklahoma Department of Libraries (1893) REGIONAL

Shawnee

Oklahoma Baptist University Library (1933)

Stillwater

Oklahoma State University Library (1907) REGIONAL

Tahleguah

Northeastern Oklahoma State University John Vaughan Library (1923)

Tuisa

Tulsa City-County Library System (1963) University of Tulsa College of Law Library (1979) University of Tulsa McFarlin Library (1929)

Weatherford

Southwestern Oklahoma State University Al Harris Library (1958)

OREGON

Ashland

Southern Oregon State College Library (1953)

Bend

Central Oregon Community College Library/Media Service (1985)

Corvallis

Oregon State University Library (1907)

Eugene

University of Oregon Law Library (1979) University of Oregon Library (1883)

Forest Grove

Pacific University Harvey W. Scott Memorial Library (1897)

Klamath Falls

Oregon Institute of Technology Learning Resources Center-Library (1982)

La Grande

Eastern Oregon State College Walter M. Pierce Library (1954)

McMinnville

Linfield College Northup Library (1965)

Monmouth

Western Oregon State College Library (1967)

Pendleton

Blue Mountain Community College Library (1983)

Portland

Lewis and Clark College Aubrey R. Watzek Library (1967) Library Association of Portland (1884) Northwestern School of Law Lewis and Clark College Paul L. Boley Law Library (1979) Portland State University Millar Library (1963) REGIONAL Reed College Library (1912)

U.S Department of Energy Bonneville Power Administration Library (1962)

Salem

Oregon State Library (unknown)
Oregon Supreme Court Law Library (1974)
Willamette University College of Law Library (1979)
Willamette University Main Library (1969)

PENNSYLVANIA

Allentown

Muhlenberg College Haas Library (1939)

Altoona

Altoona Area Public Library (1969)

Bethel Park

Bethel Park Public Library (1980)

Bethlehem

Lehigh University Libraries Linderman Library (1876)

Blue Bell

Montgomery County Community College Learning Resources Center (1975)

Bradford

University of Pittsburgh at Bradford Bradford Campus Library (1979)

California

California University of Pennsylvania Louis L. Manderino Library (1986)

Carlisie

Dickinson College Boyd Lee Spahr Library (1947) Dickinson School of Law Sheeley-Lee Law Library (1978)

Cheyney

Cheyney University Leslie Pinckney Hill Library (1967)

Collegeville

Ursinus College Myrin Library (1963)

Coraopolis

Robert Morris College Library (1978)

Doylestown

Bucks County Free Library (1970)

East Stroudsburg

East Stroudsburg University Kemp Library (1966)

Erie

Erie County Library System (1897)

Greenville

Thiel College Langenheim Memorial Library (1963)

Harrisburg

State Library of Pennsylvania (unknown) REGIONAL

Haverford

Haverford College Magill Library (1897)

Hazieton

Hazleton Area Public Library (1964)

indiana

Indiana University of Pennsylvania Stapleton Library (1962)

Johnstown

Cambria County Library System Glosser Memorial Library Building (1965)

Lancaster

Franklin and Marshall College Shadek-Fackenthal Library (1895)

Lewisburg

Bucknell University Ellen Clarke Bertrand Library (1963)

Mansfield

Mansfield University Library (1968)

Meadville

Allegheny College Lawrence Lee Pelletier Library (1907)

Millersville

Millersville University Helen A. Ganser Library (1966)

Monessen

Monessen Public Library (1969)

New Castle

New Castle Public Library (1963)

Newtown

Bucks County Community College Library (1968)

Norristown

Montgomery County-Nomistown Public Library (1969)

Philadelphia

Drexel University W. W. Hagerty Library (1963)

Free Library of Philadelphia (1897)
Saint Joseph's University Drexel Library (1974)
Temple University Paley Library (1947)
Temple University Law Library (1979)
Thomas Jefferson University Scott Memorial Library (1978)
U.S. Court of Appeals Third Circuit Library (1973)
University of Pennsylvania Biddle Law Library (1974)
University of Pennsylvania Library (1886)

Pittsburgh

Allegheny County Law Library (1977)
Carnegie Library of Pittsburgh (1895)
Carnegie Library of Pittsburgh Allegheny Regional Branch (1924)
Duquesne University Law Library (1978)
La Roche College John J. Wright Library (1974)
U.S. Bureau of Mines Library (1962)
University of Pittsburgh Hillman Library (1910)
University of Pittsburgh Law Library (1979)

Pottsville

Pottsville Free Public Library (1967)

Reading

Reading Public Library (1901)

Scranton

Scranton Public Library (1895)

Shippensburg

Shippensburg University Ezra Lehman Memorial Library (1973)

Slippery Rock

Slippery Rock University Bailey Library (1965)

Swarthmore

Swarthmore College McCabe Library (1923)

University Park

Pennsylvania State University Libraries Pattee Library (1907)

Villanova

Villanova University Law School Pulling Law Library (1964)

Warren

Warren Library Association Warren Public Library (1885)

Waynesburg

Waynesburg College Library (1964)

West Chester

West Chester University Francis Harvey Green Library (1967)

Wilkes-Barre

King's College D. Leonard Corgan Library (1949)

Williamsport

Lycoming College Library (1970)

York

York College of Pennsylvania Schmidt Library (1963)

Youngwood

Westmoreland County Community College Learning Resources Center (1972)

PUERTO RICO

Mayaguez

University of Puerto Rico Mayaguez Campus Library (1928)

Ponce

Catholic University of Puerto Rico Encarnacion Valdes Library (1966) Catholic University of Puerto Rico School of Law Library (1978)

Rio Piedras

University of Puerto Rico J. M. Lazaro Library (1928)

REPUBLIC OF PANAMA

Balboa Heights

Panama Canal Commission Technical Resources Center (1963)

RHODE ISLAND

Barrington

Barrington Public Library (1986)

Kingston

University of Rhode Island Library (1907)

Newport

U.S. Naval War College Library (1963)

Providence

Brown University John D. Rockefeller Jr. Library (unknown)
Providence College Phillips Memorial Library (1969)
Providence Public Library (1884)
Rhode Island College James P. Adams Library (1965)
Rhode Island State Law Library (1979)
Rhode Island State Library (1895)

Warwick

Warwick Public Library (1966)

Westerly

Westerly Public Library (1909)

Woonsocket

Woonsocket Ham's Public Library (1977)

SOUTH CAROLINA

Charleston

Baptist College at Charleston L. Mendel Rivers Library (1967) The Citadel Military College Daniel Library (1962) College of Charleston Robert Scott Small Library (1869)

Clemson

Clemson University Cooper Library (1893)

Columbia

Benedict College Library Payton Learning Resources Center (1969) South Carolina State Library (1895) University of South Carolina Coleman Karesh Law Library (1983) University of South Carolina Thomas Cooper Library (1884)

Conway

University of South Carolina Coastal Carolina College Kimbel Library (1974)

Due West

Erskine College McCain Library (1968)

Florence

Florence County Library (1967) Francis Marion College James A. Rogers Library (1970)

Greenville

Furman University Library (1962) Greenville County Library (1966)

Greenwood

Lander College Larry A. Jackson Library (1967)

Orangeburg

South Carolina State College Miller F. Whittaker Library (1953)

Rock Hill

Winthrop College Dacus Library (1896)

Spartanburg

Spartanburg County Public Library (1967)

SOUTH DAKOTA

Aberdeen

Northern State College Beulah Williams Library (1963)

Brookings

South Dakota State University H. M. Briggs Library (1889)

Plerre

South Dakota State Library (1973) South Dakota Supreme Court Library (1978)

Rapid City

Rapid City Public Library (1963)
South Dakota School of Mines and Technology Devereaux Library (1963)

Sloux Falls

Augustana College Mikkelsen Library (1969) Sioux Falls Public Library (1903)

Spearfish

Black Hills State College Library Learning Center (1942)

Vermillion

University of South Dakota I. D. Weeks Library (1889)

TENNESSEE

Bristol

King College E. W. King Library (1970)

Chattanooga

Chattanooga-Hamilton County Bicentennial Library (1908) U.S. Tennessee Valley Authority Technical Library (1976)

Clarksville

Austin Peay State University Felix G. Woodward Library (1945)

Cleveland

Cleveland State Community College Library (1973)

Columbia

Columbia State Community College John W. Finney Memorial Library (1973)

Cookeville

Tennessee Technological University Jere Whitson Memorial Library (1969)

Jackson

Lambuth College Luther L. Gobbel Library (1967)

Jefferson City

Carson-Newman College Library (1964)

Johnson City

East Tennessee State University Sherrod Library (1942)

Knoxville

Knoxville County Public Library System Lawson McGhee Library (1973)

University of Tennessee at Knoxville John C. Hodges Library (1907) University of Tennessee Law Library (1971)

Martin

University of Tennessee at Martin Paul Meek Library (1957)

Memphis

Memphis-Shelby County Public Library and Information Center (1896) Memphis State University Cecil C. Humphreys School of Law Library (1979)

Memphis State University Libraries (1966)

Murfreesboro

Middle Tennessee State University Todd Library (1912)

Nashville

Fisk University Library (1965)
Public Library of Nashville and Davidson County (1884)
Tennessee State Library and Archives (unknown)
Tennessee State University Brown-Daniel Library (1972)
Vanderbilt University Alyne Queener Massey Law Library (1976)
Vanderbilt University Library (1884)

Sewanee

University of the South Jessie Ball duPont Library (1873)

TEXAS

Abllene

Abilene Christian University Margaret and Herman Brown Library (1978)

Hardin-Simmons University Rupert and Pauline Richardson Library (1940)

Arlington

Arlington Public Library (1970) University of Texas at Arlington Library (1963)

Austin

Texas State Law Library (1972)
Texas State Library (unknown) REGIONAL
University of Texas at Austin Perry-Castaneda Library (1884)
University of Texas at Austin Edie and Lew Wasserman Public Affairs
Library (1966)
University of Texas at Austin Tarlton Law Library (1965)

Baytown

Lee College Library (1970)

Beaumont

Lamar University Mary and John Gray Library (1957)

Brownwood

Howard Payne University Walker Memorial Library (1964)

Canyon

West Texas State University Cornette Library (1928)

College Station

Texas Agricultural and Mechanical University David G. Evans Library (1907)

Commerce

East Texas State University James Gilliam Gee Library (1937)

Corpus Christi

Corpus Christi State University Library (1976)

Corsicana

Navarro College Gaston T. Gooch Library (1965)

Dallas

Dallas Baptist University Vance Memorial Library (1967)
Dallas Public Library (1900)
Southern Methodist University Fondren Library (1925)
University of Texas Health Science Center-Dallas Library (1975)

Denton

North Texas State University Library (1948)

Edinburg

Pan American University Library (1959)

El Paso

El Paso Public Library (1906) University of Texas at El Paso Library Documents & Maps Library (1966)

Fort Worth

Fort Worth Public Library (1905)
Texas Christian University Mary Couts Burnett Library (1916)

Galveston

Rosenberg Library (1909)

Houston

Houston Public Library (1884)
North Harris County College Learning Resource Center (1974)
Rice University Fondren Library (1967)
South Texas College of Law Library (1981)
Texas Southern University Thurgood Marshall School of Law Library (1982)
University of Houston-Clear Lake Alfred R. Neumann Library (1980)
University of Houston-University Park Library (1957)
University of Houston School of Law Library (1979)

Huntsville

Sam Houston State University Newton Gresham Library (1949)

irving

Irving Public Library System (1974)

Kingsville

Texas Arts and Industries University Jernigan Library (1944)

Laredo

Laredo Junior College Harold R. Yeary Library (1970)

Longview

Longview Public Library (1961)

Lubbock

Texas Tech University Library (1935) REGIONAL Texas Tech University School of Law Library (1978)

Marshall

Wiley College Thomas Winston Cole Sr. Library (1962)

Nacogdoches

Stephen F. Austin State University Steen Library (1965)

Richardson

University of Texas at Dallas McDermott Library (1972)

San Angelo

Angelo State University Port Henderson Library (1964)

San Antonio

Saint Mary's University Academic Library (1964)
Saint Mary's University Sarita Kennedy East Law Library (1982)
San Antonio College Library (1972)
San Antonio Public Library (1899)
Trinity University Elizabeth Coates Maddux Library (1964)
University of Texas at San Antonio Library (1973)

San Marcos

Southwest Texas State University Library (1955)

Seguin

Texas Lutheran College Blumberg Memorial Library (1970)

Sherman

Austin College Abell Library (1963)

Texarkana

Texarkana College Paimer Memorial Library (1963)

Victoria

Victoria College/University of Houston Victoria Campus Library (1973)

Waco

Baylor University Law Library (1982) Baylor University Moody Memorial Library (1905)

Wichita Falls

Midwestern State University Moffett Library (1963)

UTAH

Cedar City

Southern Utah State College Library (1964)

Ephralm

Snow College Lucy A. Phillips Library (1963)

Logan

Utah State University Merrill Library and Learning Resources Center (1907) REGIONAL

Ogden

Weber State College Stewart Library (1962)

Provo

Brigham Young University Harold B. Lee Library (1908) Brigham Young University Law Library (1972)

Salt Lake City

University of Utah Eccles Health Sciences Library (1970)
University of Utah Law Library (1966)
University of Utah Marriott Library (1893)
Utah State Library (unknown)
Utah State Supreme Court Law Library (1975)

VERMONT

Burlington

University of Vermont Bailey/Howe Library (1907)

Castleton

Castleton State College Calvin Coolldge Library (1969)

Johnson

Johnson State College John Dewey Library (1955)

Lyndonville

Lyndon State College Samuel Reed Hall Library (1969)

Middlebury

Middlebury College Egbert Starr Library (1884)

Montpeller

Vermont Department of Libraries (1845)

Northfield

Norwich University Library (1908)

South Royalton

Vermont Law School Library (1978)

VIRGIN ISLANDS

Saint Croix

Florence Williams Public Library (1968)

Saint Thomas

College of the Virgin Islands Ralph M. Paiewonsky Library (1973) Enid M. Baa Library and Archives (1968)

VIRGINA

Alexandria

Dept. of the Navy Office of Judge Advocate General Law Library (1963)

Arlington

George Mason University School of Law Library (1981) U.S. Patent & Trademark Office Science Library (1986)

Blacksburg

Virginia Polytechnic Institute and State University Carol M. Newman Library (1907)

Bridgewater

Bridgewater College Alexander Mack Memorial Library (1902)

Charlottesville

University of Virginia Alderman Library (1910) REGIONAL University of Virginia Arthur J. Morris Law Library (1964)

Chesapeake

Chesapeake Public Library (1970)

Danville

Danville Community College Learning Resources Center (1969)

Emory

Emory and Henry College Kelly Library (1884)

Fairfax

George Mason University Fenwick Library (1960)

Fredericksburg

Mary Washington College E. Lee Trinkle Library (1940)

Hampden-Sydney

Hampden-Sydney College Eggleston Library (1891)

Hampton

Hampton University Huntington Memorial Library (1977)

Harrisonburg

James Madison University Carrier Library (1973)

Hollins College

Hollins College Fishburn Library (1967)

Lexington

Virginia Military Institute Preston Library (1874) Washington and Lee University University Library (1910) Washington and Lee University Wilbur C. Hall Law Library (1978)

Martinsville

Patrick Henry Community College Library (1971)

Norfolk

Norfolk Public Library (1895) Old Dominion University Library (1963) U.S. Armed Forces Staff College Library (1963)

Petersburg

Virginia State University Johnston Memorial Library (1907)

Quantico

Federal Bureau of Investigation Academy Library (1970)
Marine Corps Education Center MCDEC James Carson Breckinridge
Library (1967)

Reston

Department of the Interior Geological Survey Library (1963)

Richmond

U.S. Court of Appeals Fourth Circuit Library (1973)
University of Richmond Boatwright Memorial Library (1900)
University of Richmond Law School Library (1982)
Virginia Commonwealth University James Branch Cabell Library (1971)
Virginia State Law Library (1973)
Virginia State Library & Archives (unknown)

Salem

Roanoke College Library (1886)

Williamsburg

College of William and Mary Marshall-Wythe Law Library (1978) College of William and Mary Swem Library (1936)

Wise

Clinch Valley College John Cook Wylle Library (1971)

WASHINGTON

Bellingham

Western Washington University Mable Zoe Wilson Library (1963)

Cheney

Eastern Washington University JFK Library (1966)

Des Molnes

Highline Community College Library (1983)

Ellensburg

Central Washington University Library (1962)

Everett

Everett Public Library (1914)

Olympia

Evergreen State College Daniel J. Evans Library (1972) Washington State Law Library (1979) Washington State Library (unknown) REGIONAL

Port Angeles

North Olympic Library System (1965)

Pullman

Washington State University Holland Library (unknown)

Seattle

Seattle Public Library (1908)
University of Washington Suzallo Library (1890)
University of Washington Marian Gould Gallagher Law Library (1969)
U.S. Court of Appeals 9th Circuit Library (1981)

Spokane

Gonzaga University School of Law Library (1979) Spokane Public Library (1910)

Tacoma

Tacoma Public Library (1894)
University of Puget Sound Collins Memorial Library (1938)
University of Puget Sound School of Law Library (1978)

Vancouver

Fort Vancouver Regional Library (1962)

Walla Walla

Whitman College Penrose Memorial Library (1890)

WEST VIRGINIA

Athens

Concord College J. Frank Marsh Library (1924)

Bluefleld

Bluefield State College Hardway Library (1972)

Charleston

Kanawha County Public Library (1952) West Virginia Library Commission (1975) West Virginia Supreme Court Law Library (1977)

Elkins

Davis and Elkins College Library (1913)

Fairmont

Fairmont State College Library (1884)

Glenville

Glenville State College Robert F. Kidd Library (1966)

Huntington

Marshall University James E. Morrow Library (1925)

institute

West Virginia State College Drain-Jordon Library (1907)

Montgomery

West Virginia Institute of Technology Vining Library (1985)

Morgantown

West Virginia University Library (1907) REGIONAL

Salem

Salem College Library (1921)

Shepherdstown

Shepherd College Ruth Scarborough Library (1971)

Weirton

Mary H. Weir Public Library (1963)

WISCONSIN

Appleton

Lawrence University Seeley G. Mudd Library (1869)

Belolt

Beloit College Col. Robert H. Morse Library (1888)

Eau Claire

University of Wisconsin-Eau Claire William D. McIntyre Library (1951)

Fond du Lac

Fond du Lac Public Library (1966)

Green Bay

University of Wisconsin-Green Bay Learning Resources Center (1968)

La Crosse

La Crosse Public Library (1883)
University of Wisconsin-La Crosse Murphy Library (1965)

Madison

Madison Public Library (1965)
State Historical Society of Wisconsin Library (1870) REGIONAL University of Wisconsin-Madison Memorial Library (1939)
University of Wisconsin-Madison Law Library (1981)
Wisconsin State Law Library (unknown)

Milwaukee

Alverno College Library/Media Center (1971)
Marquette University Law Library (1987)
Medical College of Wisconsin, Inc. Todd Wehr Library (1980)
Milwaukee County Law and Reference Library (1934)
Milwaukee Public Library (1861) REGIONAL
Mount Mary College Haggerty Library (1964)
University of Wisconsin-Milwaukee Library (1960)

Oshkosh

University of Wisconsin-Oshkosh Forrest R. Polk Library (1956)

Platteville

University of Wisconsin-Platteville Karrman Library (1964)

Racine

Racine Public Library (1898)

Ripon

Ripon College Library (1982)

River Falls

University of Wisconsin-River Falls Chalmer Davee Library (1962)

Sheboygan

Mead Public Library (1983)

Stevens Point

University of Wisconsin-Stevens Point Library (1951)

Superior

Superior Public Library (1908) University of Wisconsin-Superior Jim Dan Hill Library (1935)

Waukesha

Waukesha Public Library (1966)

Wausau

Marathon County Public Library (1971)

Whitewater

University of Wisconsin-Whitewater Harold Anderson Library (1963)

WYOMING

Casper

Natrona County Public Library (1929)

Cheyenne

Wyoming State Law Library (1977) Wyoming State Library (unknown) REGIONAL

Glliette

Campbell County Public Library (1980)

Laramle

University of Wyoming, Coe Library (1907) University of Wyoming Law Library (1978)

Powell

Northwest Community College John Taggart Hinckley Library (1967)

Riverton

Central Wyoming College Learning Resources Center (1969)

Rock Springs

Western Wyoming Community College Library (1969)

Sherldan

Sheridan College Griffith Memorial Library (1963)

ALABAMA

Birmingham-2015 2nd Avenue North, 3rd Floor, Berry Building, 35203, Area Code 205 Tel 254-1331, FTS 8 229-1331

ALASKA

Anchorage-222 W. 7th Avenue, P.O. Box 32, 99513, Area Code 907 Tel 271-5041, FTS 8 271-5041

ARIZONA

Phoenix-Federal Building & U.S. Courthouse, 230 N. 1st Avenue, Room 3412, 85025, Area Code 602 Tel 261-3285, FTS 8 261-3285

ARKANSAS

Little Rock-Suite 811, Savers Federal Building, 320 W. Capitol Avenue, 72201, Area Code 501 Tel 378-5794, FTS 8 740-5794

CALIFORNIA

Los Angeles-Room 810, 11777 San Vicente Blvd., 90049-5076, Area Code 213 Tel 209-6616, FTS 8 793-6616

•San Diego-6363 Greenwich Drive, Suite 145, 92122, Area Code 619 Tel 557-5395, FTS 8 895-5395

San Francisco-Federal Building, Box 6013, 450 Golden Gate Avenue, 94102, Area Code 415 Tel 556-5860, FTS 8 556-5868

Santa Ana-116A W. 4th Street, Suite #1, 92701, Area Code 714 Tel 836-2461, FTS 8 799-2461

COLORADO

Denver-Room 119, U.S. Customhouse, 721 19th Street, 80202, Area Code 303 Tel 844-3246, FTS 8 564-3246

CONNECTICUT

Hartford-Room 610-B, Federal Office Building, 450 Main Street, 06103, Area Code 203 Tel 240-3530, FTS 8 244-3530

DISTRICT OF COLUMBIA

Room 1066, HCHB, Department of Commerce, 14th Street & Constitution Avenue, N.W., 20230, Area Code 202 Tel 377–3181, FTS 8 377–3181

FLORIDA

- •Clearwater-128 N. Osceola Avenue, 33515, Area Code 813 Tel 461-0011, FTS 8 826-3738
- JacksonvIIIe-Independence Square, Suite 200A, 32216, Area Code 904 Tel 791–2796, FTS 8 946–2796

Mlaml-Suite 224, Federal Building, 51 S.W. First Avenue, 33130, Area Code 305 Tel 536-5267, FTS 8 350-5267

 Orlando-Room 346, University of Central Florida, 32802, Area Code 305 Tel 648–1608, FTS 8 820–6235 •Tallahassee-Collins Building, Room 401, 107 W. Gaines Street, 32304, Area Code 904 Tel 488-6469, FTS 8 965-7194

GEORGIA

Atlanta-Room 625, 1365 Peachtree Street, N.E., 30309, Area Code 404 Tel 347-2271, FTS 8 257-2271

Savannah-120 Barnard Street, A-107, 31402, Area Code 912 Tel 944-4204, FTS 8 248-4204

HAWAII

Honolulu-4106 Federal Building, P.O. Box 50026, 300 Ala Moana Blvd., 96850, Area Code 808 Tel 541-1782, FTS 8 551-1785

IDAHO

Bolse (Denver, Colorado District)-700 W. State Street, 83720, Area Code 208 Tel 334-2470, FTS 8 554-9254

ILLINOIS

Chlcago-1406 Mid Continental Plaza Building, 55 E. Monroe Street, 60603, Area Code 312 Tel 353-4450, FTS 8 353-4450

- Palatine-W. R. Harper College, Algonquin & Rodelle Road, 60067, Area Code 312 Tel 397-3000, x532
- •Rockford-515 N. Court Street, P.O. Box 1747, 61110-0247, Area Code 815 Tel 987-8123, FTS 8 363-4347

INDIANA

Indianapolis-One N. Capitol, Suite 520, 46204, Area Code 317 Tel 269-6214, FTS 8 331-6214

ЮWA

Des Molnes-817 Federal Building, 210 Wainut Street, 50309, Area Code 515 Tel 284-4222, FTS 8 862-4222

KANSAS

•Wichita (Kansas City, Missouri District)—River Park Place, Suite 565, 727 North Waco, 67203, Area Code 316 Tel 269–6160, FTS 8 752–6160

KENTUCKY

Louisville-U.S. Post Office and Courthouse Building, 601 W. Broadway, 40202, Area Code 502 Tel 582-5066, FTS 8 352-5066

LOUISIANA

New Orleans-432 World Trade Center, No. 2 Canal Street, 70130, Area Code 504 Tel 589-6546, FTS 8 682-6546

[·]Denotes trade specialist at post or duty station

MAINE

 Augusta (Boston, Massachusetts District)-77 Sewell Street, 04330, Area Code 207 Tel 622-8249, FTS 8 633-6249

MARYLAND

Baltimore-415 U.S. Customhouse, Gay and Lombard Streets, 21202, Area Code 301 Tel 962-3560, FTS 8 922-3560

MASSACHUSETTS

Boston-World Trade Center, Suite 307, Commonwealth Pier Area, 02210, Area Code 617 Tel 565-8563, FTS 8 835-8563

MICHIGAN

Detroit-1140 McNamara Building, 477 Michigan Avenue, 48226, Area Code 313 Tel 226-3650, FTS 8 226-3650

•Grand Rapids-300 Monroe N.W., Room 409, 49503, Area Code 616 Tel 456-2411, FTS 8 372-2411

MINNESOTA

Minneapolls-108 Federal Building, 110 S. 4th St., 55401, Area Code 612 Tel 349-1638, FTS 8 777-1638

MISSISSIPPI

Jackson-328 Jackson Mall Office Center, 300 Woodrow Wilson Blvd., 39213, Area Code 601 Tel 965-4388, FTS 8 490-4388

MISSOURI

Kansas City-Room 635, 601 E. 12th Street, 64106, Area Code 816 Tel 426-3141, FTS 8 867-3141

St. Louis-7911 Forsyth Blvd., Suite 610, 63105, Area Code 314 Tel 425-3302-4, FTS 8 279-3302

NEBRASKA

Omaha-1133 O Street, 68137, Area Code 402 Tel 221-3664, FTS 8 864-3664

NEVADA

Reno-1755 E. Piumb Lane, Room 152, 89502, Area Code 702 Tel 784-5203, FTS 8 470-5203

NEW JERSEY

Trenton-3131 Princeton Pike Building, Suite 100, 08648, Area Code 609 Tel 989-2100, FTS 8 423-2100

NEW MEXICO

Albuquerque-5000 Marble Avenue, N.E., Suite 320, 87110, Area Code 505 Tel 262-6024, FTS 8 474-2386

NEW YORK

Buffalo-1312 Federal Building, 111 W. Huron Street, 14202, Area Code 716 Tel 846-4191, FTS 8 437-4191

New York-Federal Office Building, 26 Federal Plaza, Foley Square, 10278, Area Code 212 Tel 264-0634, FTS 8 264-0634

•Rochester-111 E. Avenue, Suite 220, 14604, Area Code 716 Tel 263-6480, FTS 8 963-6480

NORTH CAROLINA

Greensboro-203 Federal Building, 324 W. Market Street, P.O. Box 1950, 27402, Area Code 919 Tel 333-5345, FTS 8 699-5345

OHIO

Cincinnati-9504 Federal Office Building, 550 Main Street, 45202, Area Code 513 Tel 684-2944, FTS 8 684-2944

Cleveland-Room 600, 668 Euclid Avenue, 44114, Area Code 216 Tel 522-4750, FTS 8 942-4750

OKLAHOMA

Oklahoma City-5 Broadway Executive Park, Suite 200, 6601 Broadway Extension, 73116, Area Code 405 Tel 231-5302, FTS 8 736-5302

•Tulsa-440 S. Houston Steet, 74127, Area Code 918 Tel 581-7650, FTS 8 745-7650

OREGON

Portland-Room 618, 1220 S.W. 3rd Avenue, 97204, Area Code 503 Tel 221-3001, FTS 8 423-3001

PENNSYLVANIA

Phlladelphla-9448 Federal Building, 600 Arch Street, 19106, Area Code 215 Tel 597-2850, FTS 8 597-2850

Pttsburgh-2002 Federal Building, 1000 Liberty Avenue, 15222, Area Code 412 Tel 644-2850, FTS 8 722-2850

PUERTO RICO

San Juan (Hato Rey)-Room 659, Federal Building, Chardon Avenue, 00918, Area Code 809 Tel 753-4555, Ext. 555, FTS 8 753-4555

RHODE ISLAND

•Providence (Boston, Massachusetts District)—7 Jackson Walkway, 02903, Area Code 401 Tel 528–5104, Ext. 22, FTS 8 838–5104

SOUTH CAROLINA

•Charleston-17 Lockwood Drive, 29401, Area Code 803 Tel 724-4361, FTS 8 677-4361

Columbia-Strom Thurmond Federal Building, Suite 172, 1835 Assembly Street, 29201, Area Code 803 Tel 765-5345, FTS 8 677-5345

TENNESSEE

•Memphls-22 N. Front Street, Suite 200, 38101, Area Code 901 Tel 521-4137, FTS 8 222-4137

Nashville-Suite 1114, Parkway Towers, 404 James Robertson Parkway, 37219-1505, Area Code 615 Tel 736-5161, FTS 8 852-5161

TEXAS

AustIn-400 First City Center, 816 Congress Avenue, 78701, Area Code 512 Tel 472-5059, FTS 8 770-5939

Dallas-Room 7A5, 1100 Commerce Street, 75242, Area Code 214 Tel 767-0542, FTS 8 729-0542

Houston-2625 Federal Building, Courthouse, 515 Rusk Street, 77002, Area Code 713 Tel 229-2578, FTS 8 526-4578

UTAH

Salt Lake City-U.S. Customhouse, 350 S. Main Street, 84101, Area Code 801 Tel 524-5116, FTS 8 588-5116

VIRGINIA

Richmond-8010 Federal Building, 400 North 8th Street, 23240, Area Code 804 Tel 771-2246, FTS 8 925-2246

WASHINGTON

Seattle-3131 Elliott Avenue, Suite 290, 98121, Area Code 206 Tel 442-5616, FTS 8 399-5615

Spokane-West 808 Spokane Falls Boulevard, Room 650, 99201, Area Code 509 Tel 353-2922, FTS 8 439-2922

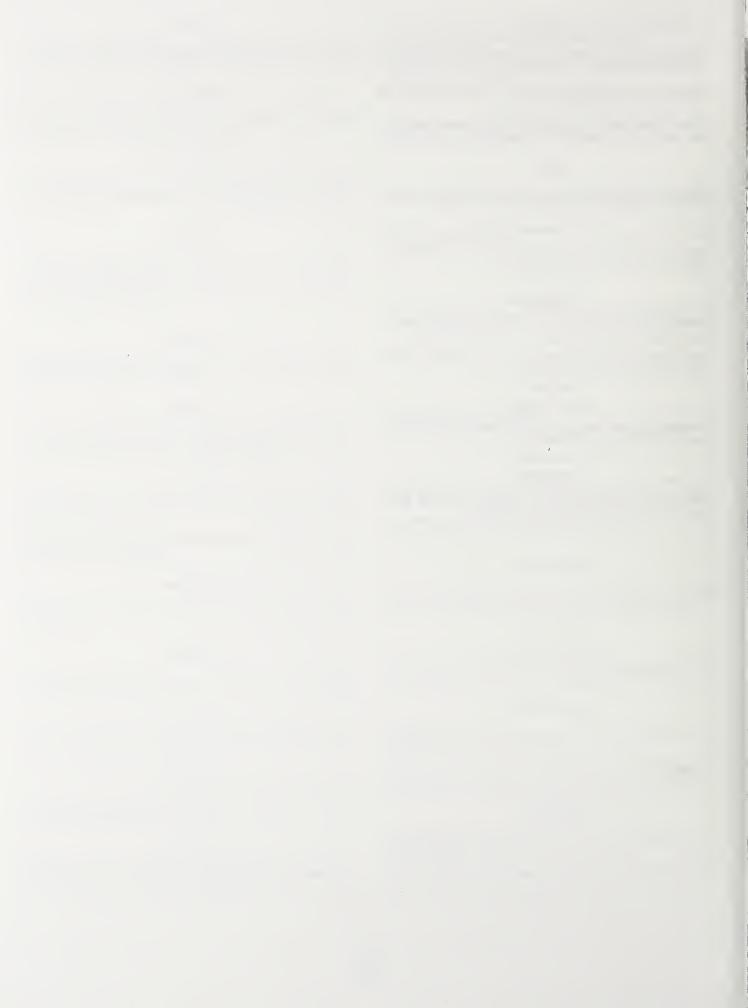
WEST VIRGINIA

Charleston-42 New Federal Building, 500 Quarrier Street, 26301, Area Code 304 Tel 347-5123, FTS 8 930-5123

WISCONSIN

Mllwaukee-605 Federal Building, 517 E. Wisconsin Avenue, 53202, Area Code 414 Tel 291-3473, FTS 8 362-3473

1997



NST-114A REV. 3-89)	U.S. DEPARTMENT OF COMMERCE NATIONAL INSTITUTE OF STANDARDS AND TECHNOLOGY	PUBLICATION OR REPORT NUMBER NIST/SP-305/21		
	BIBLIOGRAPHIC DATA SHEET	2. PERFORMING ORGANIZATION REPORT NUMBER		
	BIBLIOGRAFIIIC BATA SITEET	3. PUBLICATION DATE July 1990		
TITLE AND SUBT	ITLE	July 1990		
Publicatio	ns of the National Institute of Standards and Techr	ology, 1989 Catalog		
AUTHOR(S)				
Rebecca J.	Pardee and Ernestine T. Gladden, Editors			
PERFORMING OF	GANIZATION (IF JOINT OR OTHER THAN NIST, SEE INSTRUCTIONS)	7. CONTRACT/GRANT NUMBER		
NATIONAL INSTIT	IT OF COMMERCE FUTE OF STANDARDS AND TECHNOLOGY	8. TYPE OF REPORT AND PERIOD COVERED		
GAITHERSBURG,	MD 20899	January-December 1989		
SPONSORING OF	RGANIZATION NAME AND COMPLETE ADDRESS (STREET, CITY, STATE, ZIP)	Gandary December 1909		
Same as it				
. ABSTRACT (A 20	T DESCRIBES A COMPUTER PROGRAM; SF-185, FIPS SOFTWARE SUMMARY, IS ATTAC O-WORD OR LESS FACTUAL SUMMARY OF MOST SIGNIFICANT INFORMATION. IF DOC EVEY, MENTION IT HERE.)			
including (formerly National T papers pub catalog.)	supplement to Special Publication 305 contains full keywords and abstracts for National Institute of St National Bureau of Standards (NBS)) 1989 papers publicational Information Service (NTIS) collection. (Alished prior to 1989 but not reported in previous a Four indexes are included to allow the user to ideauthor, keywords, title, and NTIS order/report number	andards and Technology (NIST) Lished and entered into the Also included are NBS/NIST Supplements of this annual entify NBS/NIST papers by		
KEY WORDS (6 T				

FOR OFFICIAL DISTRIBUTION. DO NOT RELEASE TO NATIONAL TECHNICAL INFORMATION SERVICE (NTIS).

ORDER FROM SUPERINTENDENT OF DOCUMENTS, U.S. GOVERNMENT PRINTING OFFICE, WASHINGTON, DC 20402.

ORDER FROM NATIONAL TECHNICAL INFORMATION SERVICE (NTIS), SPRINGFIELD, VA 22161.

14. NUMBER OF PRINTED PAGES

15. PRICE

413

13. AVAILABILITY



ANNOUNCEMENT OF NEW PUBLICATIONS OF THE NATIONAL INSTITUTE OF STANDARDS AND TECHNOLOGY

Superintendent of Documents Government Printing Office Washington, DC 20402

Dear Sir:

Please add my name to the announcement list of new publications as issued by the National Institute of Standards and Technology.

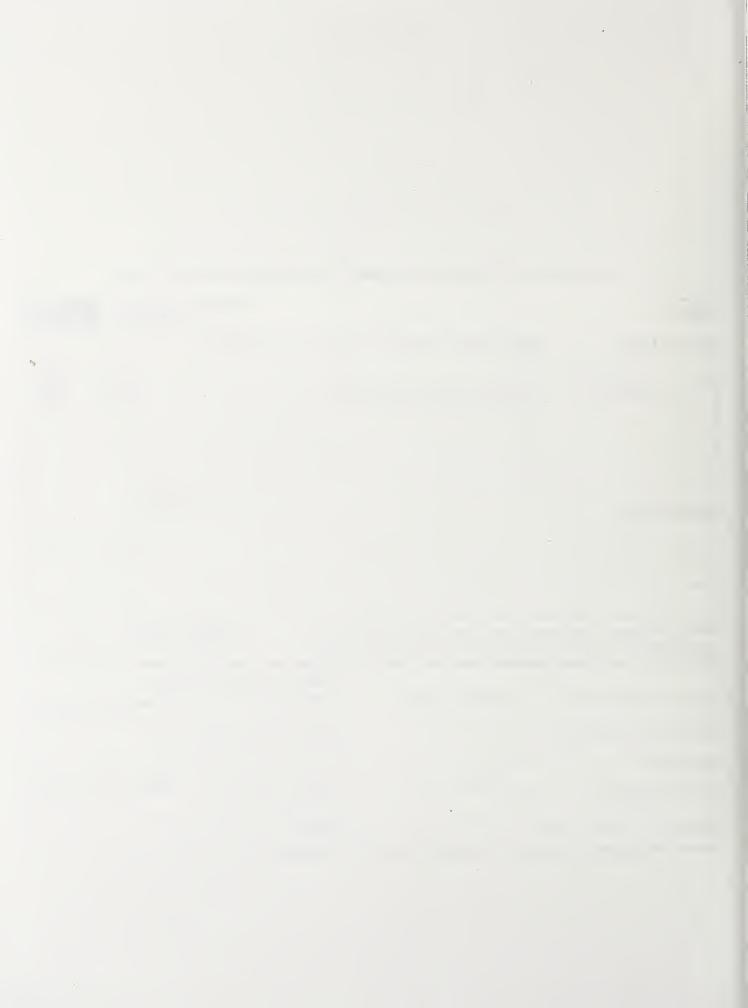
Name			
Company			
Address			
City	State	Zlp Code	

(Notification key N519)



Superintendent of Documents Publications and Subscriptions Order Form

*68	essing Cods 70	:			Charge your or It's e To fax your orders and	asy!	VISA 275-0019
PUBI	LICAT	CIONS	Please Type or Print (Form is	s aligned for typ		inquires (2	102, 216 0015
Qty.		Stock Nun	nber	Title		Price Each	Total Price
1	021-6	602-00001-9	Catalog-Bestselling Governmen	t Books		FREE	FREE
							·
SUBS	CRIP	TIONS			Total for Publicati	ons	
SUBSCRIPTIONS List Ditle		e		Price Each	Total Price		
					Total for Subscript	tions	
are go	od thro	ough 1/91. A	gular domestic postage and handling. Publ After that date, please call Order and Inform	ation Desk at	Total Cost of Orde	er	
202–78	33–323	8 to verify	prices. Subscription prices are subject to		time. International customore Method of Paymen		add 25%.
(Company or personal name) (Please type or print) (Additional address/attention line)			me) (Please type or print)	Check	payable to the Superinte		ocuments
			ion line)	=	VISA or MasterCard Account		
(Street	addre	ss)					
(City,	State,	ZIP Code)		(Credit card	expiration date) Than	k you for	your order!
((Dayti	me pho	one including	g area code)	(Signature)			7/89
Mail	To: Su	perintende	nt of Documents, Government Printing Of	ffice, Washingtor	n, DC 20402-9325		



U.S. DEPARTMENT OF COMMERCE **National Technical Information Service** SPRINGFIELD, VA 22161

ITS. ORDER FORM



TELEPHONE ORDERS

Call (703) 487-4650

TELEX 89-9405 Telecopier (703) 321-8547 Subscriptions: (703) 487-4630

(See reverse side for RUSH and EXPRESS ordering options) · HANDLING FEE: A handling fee is required for each order except for Express, Rush, Subscription, QuikORDER, or Pickup orders.

· SHIPPING: U.S.: Printed reports and microfiche copies are shipped First Class Mail or equivalent.

FOREIGN: Regular service: Printed reports and microfiche copies are shipped surface mail.

Air Mail service to Canada and Mexico: add \$3 per printed report; 75¢ per microfiche copy. Air Mail service to all other addresses: add \$6 per printed report; 75¢ per microfiche copy. SUBSCRIPTIONS and standing orders are sent surface mail; contact NTIS for air mail rates.

1 Address Information	C	TIC Users Co	de:	(Contract N	o	Tele William
PURCHASER: DATE:		DTIC Users Code: Contract No. Last ski SHIP TO (Enter ONLY if different from purchaser):			ok ugio		
Last Name	First Initial L	Last Name First Initia					tial
Title	T	Title					
Company/Organization		Company/Organization					
Address	Α	ddress					
City/State/ZIP		city/State/ZIP					
Attention	A	Attention					
Telephone number	elephone number Telephone number						
2 Method of Payment							
☐ Charge my NTIS Deposit Account _		Check/Mone	v order e	nclosed	for \$		
Charge my Amer. Express							restrictions):
Account No.	_	riease viii	MDD 41	o per o	idei (Se	, and the source of	restrictions)
		Purchas	e Order No				
Signature:(Required to validate a	all orders)						
3 Order Selection (For	computer products, see revers	e)	QUA	NTITY]		
Enter NTIS order number(s) (Ordering by title only will delay your order)		Customer†† Routing (up to 8 digits)	Printed Copy	Micro- fiche	UNIT PRICE	Foreign Air Mail	TOTAL PRICE
1.							
2.							
3.							
4.		1.1					
5.							
6.							
7.							
OVER - Order continued on r	'everse		SU	BTOTAL	From Ot	her Side	
† Billing Service: This service is restricted	to customers in the United States,		Regular Service Handling Fee per order				
Canada, and Mexico for an additional \$7.50 per order. A late payment charge will be applied to all billings more than 30 days overdue.			(\$3 U.S., Canada, and Mexico; \$4 others) Billing Fee if required (\$7.50)				
†† Customer Routing Code: NTIS can labe organization. If you want this service, put yo			GRAND TOTAL				

NTIS ORDER FORM - Side 2

3 Order Selection (Cont.)			NTITY			
Enter the NTIS order number(s) (Ordering by title only will delay your order)	Customer Routing	Printed Copy	Micro- fiche	UNIT	Foreign Air Mail	TOTAL PRICE
8.	-					
9.				_		
10.						
11.						
12.	*					
13.						
14.						
15.				-		
16.						
17.						
18.						
19.						
				S	ubtotal	

ENTER this amount on the other side of this form.



4 Computer Products

Enter the NTIS order number(s)

20.21.22.23.

(Ordering by title only will delay your order)

If you have questions about a particular computer product, please call our Federal Computer Products Center at (703) 487-4763.

TAPE DENSITY
(9 track)

Customer
Routing 1600 bpi 6250 bpi PRICE

Subtotal

All magnetic tapes are sent air mail or equivalent service to both U.S. and foreign addresses.

ENTER this amount on the other side of this form.



SPECIAL RUSH and EXPRESS ORDERING OPTIONS

RUSH SERVICE-Add \$10 per item: Orders are processed within 24 hours and sent First Class or equivalent. Available to U.S. addresses.

Telephone:

(800) 336-4700

in Virginia call (703) 487-4700 EXPRESS SERVICE-Add \$20 per item: Orders are processed within 24 hours AND delivered by overnight courier. Available to U.S. addresses only.

NIST Technical Publications

Periodical

Journal of Research of the National Institute of Standards and Technology — Reports NIST research and development in those disciplines of the physical and engineering sciences in which the Institute is active. These include physics, chemistry, engineering, mathematics, and computer sciences. Papers cover a broad range of subjects, with major emphasis on measurement methodology and the basic technology underlying standardization. Also included from time to time are survey articles on topics closely related to the Institute's technical and scientific programs. Issued six times a year.

Nonperiodicals

Monographs - Major contributions to the technical literature on various subjects related to the Institute's scientific and technical activities.

Handbooks—Recommended codes of engineering and industrial practice (including safety codes) developed in cooperation with interested industries, professional organizations, and regulatory bodies.

Special Publications—Include proceedings of conferences sponsored by NIST, NIST annual reports, and other special publications appropriate to this grouping such as wall charts, pocket cards, and bibliographies.

Applied Mathematics Series—Mathematical tables, manuals, and studies of special interest to physicists, engineers, chemists, biologists, mathematicians, computer programmers, and others engaged in scientific and technical work.

National Standard Reference Data Series—Provides quantitative data on the physical and chemical properties of materials, compiled from the world's literature and critically evaluated. Developed under a worldwide program coordinated by NIST under the authority of the National Standard Data Act (Public Law 90-396). NOTE: The Journal of Physical and Chemical Reference Data (JPCRD) is published quarterly for NIST by the American Chemical Society (ACS) and the American Institute of Physics (AIP). Subscriptions, reprints, and supplements are available from ACS, 1155 Sixteenth St., NW., Washington, DC 20056.

Building Science Series—Disseminates technical information developed at the Institute on building materials, components, systems, and whole structures. The series presents research results, test methods, and performance criteria related to the structural and environmental functions and the durability and safety characteristics of building elements and systems.

Technical Notes—Studies or reports which are complete in themselves but restrictive in their treatment of a subject. Analogous to monographs but not so comprehensive in scope or definitive in treatment of the subject area. Often serve as a vehicle for final reports of work performed at **NIST under the sponsorship** of other government agencies.

Voluntary Product Standards — Developed under procedures published by the Department of Commerce in Part 10, Title 15, of the Code of Federal Regulations. The standards establish nationally recognized requirements for products, and provide all concerned interests with a basis for common understanding of the characteristics of the products. NIST administers this program as a supplement to the activities of the private sector standardizing organizations.

Consumer Information Series—Practical information, based on NIST research and experience, covering areas of interest to the consumer. Easily understandable language and illustrations provide useful background knowledge for shopping in today's technological marketplace.

Order the above NIST publications from: Superintendent of Documents, Government Printing Office, Washington, DC 20402.

Order the following NIST publications—FIPS and NISTIRs—from the National Technical Information Service, Springfield, VA 22161.

Federal Information Processing Standards Publications (FIPS PUB) — Publications in this series collectively constitute the Federal Information Processing Standards Register. The Register serves as the official source of information in the Federal Government regarding standards issued by NIST pursuant to the Federal Property and Administrative Services Act of 1949 as amended, Public Law 89-306 (79 Stat. 1127), and as implemented by Executive Order 11717 (38 FR 12315, dated May 11, 1973) and Part 6 of Title 15 CFR (Code of Federal Regulations).

NIST Interagency Reports (NISTIR) — A special series of interim or final reports on work performed by NIST for outside sponsors (both government and non-government). In general, initial distribution is handled by the sponsor; public distribution is by the National Technical Information Service, Springfield, VA 22161, in paper copy or microfiche form.

ADMINISTRATION & MANAGEMENT

AERONAUTICS & AERODYNAMICS

AGRICULTURE & FOOD

ASTRONOMY & ASTROPHYSICS

ATMOSPHERIC SCIENCES

BEHAVIOR & SOCIETY

BIOMEDICAL TECHNOLOGY & HUMAN FACTORS ENGINEERING

BUILDING INDUSTRY TECHNOLOGY

BUSINESS & ECONOMICS

CHEMISTRY

CIVIL ENGINEERING

COMBUSTION, ENGINES, & PROPELLANTS

COMMUNICATION

COMPUTERS, CONTROL & INFORMATION THEORY

DETECTION & COUNTERMEASURES

ELECTROTECHNOLOGY

ENERGY

ENVIRONMENTAL POLLUTION & CONTROL

HEALTH CARE

INDUSTRIAL & MECHANICAL ENGINEERING

LIBRARY & INFORMATION SCIENCES

MANUFACTURING TECHNOLOGY

MATERIALS SCIENCES

MATHEMATICAL SCIENCES

MEDICINE & BIOLOGY

MILITARY SCIENCES

MISSILE TECHNOLOGY

NATURAL RESOURCES & EARTH SCIENCES

NAVIGATION, GUIDANCE, & CONTROL

NUCLEAR SCIENCE & TECHNOLOGY

OCEAN TECHNOLOGY & ENGINEERING

ORDNANCE

PHOTOGRAPHY & RECORDING DEVICES

PHYSICS

PROBLEM-SOLVING INFORMATION FOR STATE & LOCAL GOVERNMENTS

SPACE TECHNOLOGY

TRANSPORTATION

URBAN & REGIONAL TECHNOLOGY & DEVELOPMENT

